TRANSACTIONS
OF THE
AMERICAN INSTITUTE
OF
ELECTRICAL ENGINEERS

VOLUME 64
1945

PUBLISHED BY THE
AMERICAN INSTITUTE OF ELECTRICAL ENGINEERS
33 WEST 39TH STREET
NEW YORK 18, N. Y., U. S. A.

COPYRIGHT 1945
BY THE
AMERICAN INSTITUTE OF ELECTRICAL ENGINEERS

Printed in the United States of America by
The Mack Printing Company, Easton, Pa.

INDEX

1. Technical Subjects

Absorption Characteristics of Large A-C Stator Windings, Insulation Resistance and Dielectric-. Askey, Johnson....347–51; disc. 458

Absorption Tests in Drying Out Large Generators, Use of Dielectric-. Marcroft....56–60; disc. 415

Accelerometer—Vibrometer for Instrument-Gyroscope Testing, A Tachometer—. Laurenson, Long....593–6; disc. 960

Adjustable Speed, Central-Station Auxiliary-Drive Motors for Constant and. Gibson....746–50; disc. 976

Air-Blast Circuit Breaker for 138,000-Volt Service, A Three-Cycle 3,500-Megavolt-Ampere. Byrd, Beall....229–32; disc. 463

Air-Blast, Field Tests and Performance of Heavy-Duty High-Speed 138-Kv Circuit Breakers—Oil and. Sporn, St. Clair....401–10; disc. 463

Air Circuit Breakers in A-C Railway Service, Compressed-. Wilcox, Harker....141–5; disc 419

Air-Cooled Transformers, Dielectric Strength and Protection of Modern Dry-Type. Bellaschi, Beck....759–63; disc. 997

Air Gap for Various Magnetic Materials in Cores of Coils Subject to Superposed Direct Current, Optimum. Legg....709–12; disc. 969

Air Switch and the Principles Involved in Its Design, A New Outdoor. Graybill, Ferguson....583–6; disc. 953

(Air Transportation) An Interval and Dwell Tester for Bomb-Release Interval Controls. Long....648–51

(Air Transportation) Electrolytic Corrosion—Methods of Evaluating Insulating Materials Used in Tropical Service. Thompson, Mathes....295–9; disc. 443

(Air Transportation) Resonant-Circuit Constant-Current Regulators. Kevern....807–10; disc. 992

(Air Transportation) The Electrical Resistivity of Resin-Treated Wood and Laminated Hydrolyzed-Wood and Paper-Base Plastics. Weatherwax, Stamm....833–8

(Air Transportation) Treatment of High-Altitude Brushes by Application of Metallic Halides. Elsey....576–9

(Air Transportation) Vibration Insulation and Structural Rubber. Connon....324–9

Aircraft Alternator Drives, Governor Requirements for. Boice, Levoy....534–40; disc. 947

Aircraft Alternators, Constant-Speed Drives for. Breitwieser....763–8; disc. 991

Aircraft Applications, A Current-Limiting Fuse for Powell....541–5

Aircraft, Automatic Temperature Control for. Gund....730–4

Aircraft Cabin-Supercharger Drive, Speed-Control System for an. Godsey, Miner, Walley....37–40

Aircraft Circuit Breaker, A 208Y/120-Volt 120-Ampere Three-Pole 400-Cycle Electrically Operated. Titus, Reifschneider....551–5

Aircraft, 400-Cycle Inverters for Military. Hayes, Ray....233–7

Aircraft Generators, Parallel Operation of Main-Engine-Driven 400-Cycle. Levoy....811–16; disc. 987

Aircraft Ignition Cables and Connectors, Simulated-High-Altitude Testing of. Race, Ross....20–6

Aircraft Illumination. Davies....26–30

Aircraft Motor, A 400-Cycle. Schwandt....508–12; disc. 948

Aircraft, Preferred Practices for Electric Control Devices for. Hottenroth....197–200; disc. 444

Aircraft Systems, Instability in D-C. Bunce, Cunningham, Davidson....786–91

Aircraft Systems, Selenium Power Rectifiers for A-C. Embry....596–600

Aircraft, The Amplidyne Generator Applied to Speed-Controlled Electric Gun Turrets for. Zahorsky....221–5; disc. 436

Aircraft Transformers, Effect of Altitude on Temperature Rise of. Montsinger....251–2

Airplane-Engine-Testing Power Recovery, Dodge Chicago Plant's Electric-Power-Distribution Scheme With. Bailey....121–3; disc. 484

A-C Aircraft Systems, Selenium Power Rectifiers for. Embry....596–600

A-C Arc Welding, Power Supply for. Welch, Wyer....116–20; disc. 435

A–C Railway Service, Compressed-Air Circuit Breakers in. Wilcox, Harker....141–5; disc. 419

A-C Sheath Currents and Their Effect on Lead-Cable-Sheath Corrosion, Study of. Sherer, Granbois....264–8; disc. 483

A-C Stator Windings, Insulation Resistance and Dielectric-Absorption Characteristics of Large. Askey, Johnson....347–51; disc. 458

Alternator Drives, Governor Requirements for Aircraft. Boice, Levoy....534–40; disc. 947

Alternators, Constant-Speed Drives for Aircraft. Breitwieser....763–8; disc. 991

Altitude Brushes by Application of Metallic Halides Treatment of High-. Elsey....576–9

Altitude on Temperature Rise of Aircraft Transformers, Effect of. Montsinger....251–2

American Gas and Electric Company, Lightning Investigation on 132-Kv System of. Gross, Lippert....76–84; disc. 474

Ampere Air-Blast Circuit Breaker for 138,000 Volt Service, A Three-Cycle 3,500-Megavolt-. Byrd, Beall....229–32; disc. 463

Amplidyne Generator Applied to Speed-Controlled Electric Gun Turrets for Aircraft, The. Zahorsky....221–5; disc. 436

Amplidyne Generator, Fundamentals of the. Bower....873–81

Amplifier, The Resistance-Coupled. Cowles....359–65

Amplitude-Modulation, Frequency-Modulation, and Single-Side-Band Systems for Power-Line Carrier Transmission, A Comparison of the. Cheek....215–20; disc. 450

Analogy, Determination of Transient Shaft Torques in Turbine Generators by Means of the Electrical-Mechanical. McCann, Warren, Criner....51–6; disc. 492

Analysis and Design of a D-C Selsyn System. Manildi....512–16; disc. 946

Analysis of Arc-Welding Reactors. Wheeler....87–90; disc. 434

Anode-Circuit-Breaker Design and Performance Criteria. Boehne, Atwood....337–45; disc. 437

Apparatus Life Quality, Statistical Methods in the Development of. Ferrell....700–03; disc. 998

Apparatus, Lightning Arresters for Distribution. Beck, Forbes....719–24; disc. 970

Apparatus of Rectangular Cross Section, Formulas for Calculating Temperature Distribution in Transformer Cores and Other Electric. Higgins....190–4; disc. 493

Application of Capacitors for Power-Factor Improvement of Induction Motors. Bloomquist, Boice....274–8

Application of Electric Equipment for Ship-Propeller Milling Machine. Morton, Rutemiller....205–08; disc. 453

Application of Quality Control to Resistance Welding. Hobson, Inglis, McCants....573–5; disc. 951

Application of Silicone Resins to Insulation for Electric Machinery, The. DeKiep, Hill, Moses....94–8; disc. 460

Application, Selsyn Design and. Johnson....703–08; disc. 960

Applications, A Current-Limiting Fuse for Aircraft. Powell....541–5

Applications, and Economics, Frequency Changers—Characteristics. Crary, Easley....351–8; disc. 416

Arc-Backs in Rectifier Circuits—Artificial Arc-Back Tests. Evans, Maslin....303–11; disc. 439

Arc Duration, An Interval Timer for. Quill....237–40

Arc Rectifiers for Railroads, Mercury-. Watkins....84–6; disc. 419

Arc Welding, Power Supply for A-C. Welch, Wyer....116–20; disc. 435

Arc-Welding Reactors, Analysis of. Wheeler....87–90; disc. 434

Arc Welding, The Power-Distribution Problem in. Pierce, Smith....178–84; disc. 435

Armatures, Rewinding Commutator-Type Traction. Greene, Stafford, Gentilini....563–9; disc. 943

Arrester Blocks, Statistics as an Aid to Engineering Judgment in the Manufacture of Lightning-. Goffman....607–10; disc. 966

Arresters for Distribution Apparatus, Lightning. Beck, Forbes....719–24; disc. 970

Artificial Arc-Back Tests, Arc-Backs in Rectifier Circuits—. Evans, Maslin....303–11; disc. 439

Attenuation of Coaxial Radio-Frequency Cable, The S-Function Method of Measuring. Stewart....616–19, 938–9; disc. 966

Automatic Load Control for Turbine Generators. Crever, Jackson....656–60

Automatic Regulation of Turbine Generators to Relieve Power-Supply Systems of Steel-Mill Load Swings. Eberhardt, Harrison, Kohn, Darling....751–8

(Automatic Stations) Supervisory Control for New Chicago Subway. Derr, Buck, Stoos. 10–16; disc. 457

(Automatic Stations) The Combination of Supervisory Control With Other Functions on Power-Line Carrier Channels. Cheek, Derr....241–6

Automatic Temperature Control for Aircraft. Gund....730–4

Auxiliaries, Electric Drives for Steam-Electric Generating-Station. Brownlee, Elzi....741–5; disc. 976

Auxiliary-Drive Motors for Constant and Adjustable Speed, Central-Station. Gibson. 746–50; disc. 976

Auxiliary Drives in Steam-Electric Stations, Power Systems for. McClure, Whittlesey....844–51; disc. 976

Auxiliary Equipment and Systems, Modern Practice in Power-Plant. Muller....868–72; disc. 976

Auxiliary-Power Supply for Generating Stations. McCallum....693–5; disc. 976

Axis Equivalent Circuits of the Synchronous Machine, The Direct- and Quadrature. Rankin....861–8

B

Band Systems for Power-Line Carrier Transmission, A Comparison of the Amplitude-Modulation, Frequency-Modulation, and Single-Side. Cheek....215–20; disc. 450

Basic Concepts of Moving-Magnet-Instrument Rotors. Mendelsohn....529–34; disc. 947

(Basic Sciences) Eddy-Current Resistance of Multilayer Coils. Long....712–18

(Basic Sciences) Ferroinductance as a Variable Electric-Circuit Element. Ryder....671–8; disc. 962

(Basic Sciences) Formulas for Calculating Temperature Distribution in Transformer Cores and Other Electric Apparatus of Rectangular Cross Section. Higgins....190–4; disc. 493

(Basic Sciences) Power Geometry of General Transmission Systems. Altar....312–17; disc. 493

(Basic Sciences) Resistance and Capacitance Relations Between Short Cylindrical Conductors. ReQua....724–30; disc. 962

(Basic Sciences) The Self-Inductance of a Toroidal Coil Without Iron. Dwight....805–06; disc. 999

(Basic Sciences) Two-Phase Co-ordinates of a Four-Phase Network. Kimbark....7–9

Biased-Core-Current-Transformer Design Method. Specht....635–40

Bimetal, Tapered-Thickness. Elmer....661–5; disc. 962

Blocks, Statistics as an Aid to Engineering Judgment in the Manufacture of Lightning-Arrester. Goffman....607–10; disc. 966

Board of Directors, Report of the....1001–16

Bomb-Release Interval Controls, An Interval and Dwell Tester for. Long....648–51

Braking With Traction Motors, Dynamic. Riley, Woods....517–19

Breaker, A High-Capacity High-Voltage Three-Cycle Oil Circuit. Byrd, Rietz....160–3; disc. 463

Breaker, A 208Y/120-Volt 120-Ampere Three-Pole 400-Cycle Electrically Operated Aircraft Circuit. Titus, Reifschneider....551–5

Breaker Design and Performance Criteria, Anode-Circuit-. Boehne, Atwood....337–45; disc. 437

Breaker for 138,000-Volt Service, A Three-Cycle 3,500-Megavolt-Ampere Air-Blast Circuit. Byrd, Beall....229–32; disc. 463

Breaker, New Solenoid Mechanism for Magne-Blast. Wyman, Keagy....268–74; disc. 448

Breakers in A-C Railway Service, Compressed-Air Circuit. Wilcox, Harker....141–5; disc. 419

Breakers—Oil and Air-Blast, Field Tests and Performance of Heavy-Duty High-Speed 138-Kv Circuit. Sporn, St. Clair....401–10; disc. 463

Brush Performance, Maintenance of Good. Kalb....819–25; disc. 996

Brushes by Application of Metallic Halides, Treatment of High-Altitude. Elsey....576–9

Bus-Bar Industrial Distribution Systems: an Epitomization of Available Data, The Design of. Higgins....385–400; disc. 486

Bus-Tie Switches, Improving Stability by Rapid Closing of. Kimbark....61–4; disc. 456

Bushing Current Transformer for Metering, Orthomagnetic. Boyajian, Camilli....137–40; disc. 427

C

Cabin-Supercharger Drive, Speed-Control System for an Aircraft. Godsey, Miner, Walley....37–40

Pages 359–494 comprise the June 1945 "Supplement to Electrical Engineering—Transactions Section"; pages 873–1000 the December 1945 Supplement; pages beyond 1000 appear only in the 1945 Transactions volume.

Cable and Wire Spans Using Catenary Formulas, Sag and Tension Calculations for. Nash, Nash............685–92; disc. 984
Cable-Sheath Corrosion, Study of A-C Sheath Currents and Their Effect on Lead-. Sherer, Granbois............264–8; disc. 483
Cable, The S-Function Method of Measuring Attenuation of Coaxial Radio-Frequency. Stewart............616–19; disc. 966
Cables and Connectors, Simulated-High-Altitude Testing of Aircraft Ignition. Race, Ross........20–6
Cables, Electrolysis and Corrosion of Underground Power-System. Gorman........329–36; disc. 479
Cables, Report of Conference on Radio-Frequency............911–41
Calculating Fault Currents on Rural Distribution Systems, Graphical Method of. Linder............16–19; disc. 446
Calculating Temperature Distribution in Transformer Cores and Other Electric Apparatus of Rectangular Cross Section, Formulas for. Higgins............190–4; disc. 493
Calculations for Cable and Wire Spans Using Catenary Formulas, Sag and Tension. Nash, Nash............685–92; disc. 984
Calibrations, A Study of Wave Shapes for Radio-Noise-Meter. Frick................890–901; disc. 969
Canadian National Railways Terminal, Montreal, Canada, Electrification and Signaling of the. Gage............41–4; disc. 417
Capacitance Relations Between Short Cylindrical Conductors, Resistance and. ReQua............724–30; disc. 962
Capacitor Single-Phase Motor, A Generalized Circle Diagram for a Four-Terminal Network and Its Application to the. Tarboux....881–9; disc. 943
Capacitors for High-Frequency Induction-Heating Circuits. Clark, Scoville............791–6; disc. 995
Capacitors for Power-Factor Improvement of Induction Motors, Applications of. Bloomquist, Boice............274–8
Capacity—5,000,000 Kva, The Next Step in Interrupting. Hill, Leeds..............317–23; disc. 463
Capacity High-Voltage Three-Cycle Oil Circuit Breaker, A High-. Byrd, Rietz..160–3; disc. 463
Capacity Investment, Evaluation of Electric Distribution Losses in Terms of Generating-Station-. Mortara........................1–7; disc. 411
Carrier Channels, Power-Line. Brown.......246–51
Carrier Channels, The Combination of Supervisory Control With Other Functions on Power-Line. Cheek, Derr..............................241–6
Carrier-Current Relaying, Phase-Comparison. McConnell, Cramer, Seeley........825–33; disc. 973
Carrier Transmission, A Comparison of the Amplitude-Modulation, Frequency-Modulation, and Single-Side-Band Systems for Power-Line. Cheek............215–20; disc. 450
Case, Response Time and Lag of a Thermometer Element Mounted in a Protecting. Goodwin............665–70; disc. 959
Catenary Formulas, Sag and Tension Calculations for Cable and Wire Spans Using. Nash, Nash............685–92; disc. 984
Central-Station Auxiliary-Drive Motors for Constant and Adjustable Speed. Gibson..746–50; disc. 976
Changers—Characteristics, Applications, and Economics, Frequency. Crary, Easley............351–8; disc. 416
Channels, Power-Line Carrier. Brown.........246–51
Channels, The Combination of Supervisory Control With Other Functions on Power-Line Carrier. Cheek, Derr..........................241–6
Characteristics, Applications, and Economics, Frequency Changers—. Crary, Easley............351–8; disc. 416
Characteristics, Coincidence-Factor Relationships of Electric-Service-Load. Bary..............623–9
Characteristics of Large A-C Stator Windings, Insulation Resistance and Dielectric-Absorption. Askey, Johnson....................347–51; disc. 458
Characteristics of Oil-Insulated Transformers, Standards and Insulation. Vogel....167–71; disc. 431
Characteristics of Radio-Frequency Cables, Shielding. Fluharty..........................929–30
Chemical Contamination as Causes of Electrical-Insulation Failure. Braithwaite, Moses..580–3; disc. 945
Chicago Plant's Electric-Power-Distribution Scheme With Airplane-Engine-Testing Power Recovery, Dodge. Bailey................121–3; disc. 484
Chicago Subway, Supervisory Control for New. Derr, Buck, Stoos...................10–16; disc. 457
Circle Diagram for a Four-Terminal Network and Its Application to the Capacitor Single-Phase Motor, A Generalized. Tarboux.........881–9; disc. 943
Circuit Breaker, A High-Capacity High-Voltage Three-Cycle Oil. Byrd, Rietz..........160–3; disc. 463
Circuit Breaker, A 208Y/120-Volt 120-Ampere Three-Pole 400-Cycle Electrically Operated Aircraft. Titus, Reifschneider......................551–5
Circuit-Breaker Design and Performance Criteria, Anode-. Boehne, Atwood.........337–45; disc. 437
Circuit Breaker for 138,000-Volt Service, A Three-Cycle 3,500-Megavolt-Ampere Air-Blast. Byrd, Beall............229–32; disc. 463
Circuit Breakers in A-C Railway Service, Compressed-Air. Wilcox, Harker............141–5; disc. 419
Circuit Breakers—Oil and Air-Blast, Field Tests and Performance of Heavy-Duty High-Speed 138-Kv. Sporn, St. Clair................401–10; disc. 463
Circuit Constant-Current Regulators, Resonant-. Kevern........................807–10; disc. 992
Circuit Element, Ferroinductance as a Variable Electric-. Ryder..................671–8; disc. 962
Circuits—Artificial Arc-Back Tests, Arc-Backs in Rectifier. Evans, Maslin............303–11; disc. 439
Circuits of the Synchronous Machine, The Direct- and Quadrature-Axis Equivalent. Rankin......861–8
Circuits on Self-Propelled Vehicles, Grounding of. Ewing........................48–50; disc. 417
Circuits, Transient Response of Controlled Rectifier. Chin, Walter........................208–14
Closing of Bus-Tie Switches, Improving Stability by Rapid. Kimbark................61–4; disc. 456
Coaxial Radio-Frequency Cable, The S-Function Method of Measuring Attenuation of. Stewart............616–19, 938–9; disc. 966
Coil Without Iron, The Self-Inductance of a Toroidal. Dwight......................805–06; disc. 999
Coils, Eddy-Current Resistance of Multilayer. Long............712–18
Coils for Cylindrical Nonmagnetic Loads, Design of Induction-Heating. Vaughan, Williamson............587–92; disc. 965
Coils Subject to Superposed Direct Current, Optimum Air Gap for Various Magnetic Materials in Cores of. Legg....................709–12; disc. 969
Coincidence-Factor Relationships of Electric-Service-Load Characteristics. Bary...............623–9
Combination of Supervisory Control With Other Functions on Power-Line Carrier Channels, The. Cheek, Derr..........................241–6
(Committee Report) Guides for Operation of Transformers, Regulators, and Reactors............797–806; disc. 957
Committees for 1945-46, Officers and........1017–21
(Communication) Judging Mica Quality Electrically. Coutlee..............................735–41
(Communication) Optimum Air Gap for Various Magnetic Materials in Cores of Coils Subject to Superposed Direct Current. Legg....709–12; disc. 969
(Communication) Study of Wave Shapes for Radio-Noise-Meter Calibrations, A. Frick............890–901; disc. 969
(Communication) The Resistance-Coupled Amplifier. Cowles..............................359–65
(Communication) The S-Function Method of Measuring Attenuation of Coaxial Radio-Frequency Cable. Stewart...............616–19; disc. 966
(Communication) The Tapered Transmission Line. Milnor..............................345–6
Commutator-Type Traction Armatures, Rewinding. Greene, Stafford, Gentilini.......563–9; disc. 943
Comparison Carrier-Current Relaying, Phase-. McConnell, Cramer, Seeley.....825–33; disc. 973
Comparison of the Amplitude-Modulation, Frequency-Modulation, and Single-Side-Band Systems for Power-Line Carrier Transmission, A. Cheek............215–20; disc. 450
Comparison Testing, Winding-Fault Detection and Location by Surge-. Moses, Harter............499–503; disc. 945
Components as Applied to the Single-Phase Induction Motor, Symmetrical. Suhr......651–6; disc. 958
Components, Losses in Radio-Frequency-Cable. Ragan............927
Compounds for Insulating Electric Machines, Organo-Silicon. Kauppi, Moses..........90–3; disc. 457
Compressed-Air Circuit Breakers in A-C Railway Service. Wilcox, Harker............141–5; disc. 419
Concepts of Moving-Magnet-Instrument Rotors, Basic. Mendelsohn.................529–34; disc. 947
Conductors, Resistance and Capacitance Relations Between Short Cylindrical. ReQua............724–30; disc. 962
Conference on Radio-Frequency Cables, Report of............911–41
Connectors, Simulated-High-Altitude Testing of Aircraft Ignition Cables and. Race, Ross.......20–6
Considerations in Radio-Frequency-Cable Design, General. Wentz.......................925–6
Constant-Current Regulators, Resonant-Circuit. Kevern.......................807–10; disc. 992
Constant-Speed Drives for Aircraft Alternators. Breitwieser.......................763–8; disc. 991
Contamination as Causes of Electrical-Insulation Failure, Chemical. Braithwaite, Moses............580–3; disc. 945
Control Devices for Aircraft, Preferred Practices for Electric. Hottenroth.............197–200; disc. 444
Control for Aircraft, Automatic Temperature. Gund............730–4
Control for New Chicago Subway, Supervisory. Derr, Buck, Stoos...................10–16; disc. 457
Control for Turbine Generators, Automatic Load. Crever, Jackson..........................656–60
Control: Heating of Shunt-Motor Starting Resistors, Industrial. Leland, Rader.......695–9; disc. 961
Control of Electrical-Insulating Varnishes. Gibson, Braithwaite..........................520–4
Control of Load, Frequency, and Time of Interconnected Systems. Duff.................78–86; disc. 999
Control System for an Aircraft Cabin-Supercharger Drive, Speed-. Godsey, Miner, Walley.....37–40
Control to Resistance Welding, Application of Quality. Hobson, Inglis, McCants.........573–5; disc. 951
Control, Variable-Unbalanced-Voltage. Wickerham............98–102; disc. 449
Control With Other Functions on Power-Line Carrier Channels, The Combination of Supervisory. Cheek, Derr..........................241–6
Controlled Position Regulator for Propeller Milling Machine, Tracer-. Hanna, Osbon, Hartley............201–05; disc. 452
Controlled Rectification With Inductive and Generative Loads, Voltage and Current Relations for. Puchlowski......................255–60; disc. 442
Controlled Rectifier Circuits, Transient Response of. Chin, Walter..........................208–14
Controlling Quality, Statistical Tools for. Manuele, Goffman....................524–8; disc. 949
Controls, An Interval and Dwell Tester for Bomb-Release Interval. Long....................648–51
Co-ordinates of a Four-Phase Network, Two-Phase. Kimbark..............................7–9
Core-Current-Transformer Design Method, Biased-. Specht..............................635–40
Cores and Other Electric Apparatus of Rectangular Cross Section, Formulas for Calculating Temperature Distribution in Transformer. Higgins............190–4; disc. 493
Cores of Coils Subject to Superposed Direct Current, Optimum Air Gap for Various Magnetic Materials in. Legg....................709–12; disc. 969
Cores, Wound and Dummy-Rotor Methods of Quality Control and Trouble Shooting of Induction-Motor Windings and. Trickey........842–4; disc. 998
Corona-Initiation Measurements on Polyethylene and Rubber Cables. Depackh...............939–40
Corona Voltmeter, A. Widmer...............940–1
Corrosion—Methods of Evaluating Insulating Materials Used in Tropical Service, Electrolytic. Thompson, Mathes......................295–9; disc. 443
Corrosion of Underground Power-System Cables, Electrolysis and. Gorman..........329–36; disc. 479
Corrosion, Study of A-C Sheath Currents and Their Effect on Lead-Cable-Sheath. Sherer, Granbois............264–8; disc. 483
Corrosiveness of Soil Waters, Galvanic. Phelps, Kahn............156–9; disc. 482
Cost Studies of 69- to 230-Kv Underground Power-Transmission Systems and Tie Lines. Holm............852–60
Coupled Amplifier, The Resistance-. Cowles...359–65
Criteria, Anode-Circuit-Breaker Design and Performance. Boehne, Atwood.........337–45; disc. 437
Cross Section, Formulas for Calculating Temperature Distribution in Transformer Cores and Other Electric Apparatus of Rectangular. Higgins............190–4; disc. 493
Current-Limiting Fuse for Aircraft Applications, A. Powel..............................541–5
Current Relations for Controlled Rectification With Inductive and Generative Loads, Voltage and. Puchlowski.....................255–60; disc. 442
Current Resistance of Multilayer Coils, Eddy-. Long............712–18
Current-Transformer Design Method, Biased-Core-. Specht..............................635–40
Current Transformer for Metering, Orthomagnetic Bushing. Boyajian, Camilli.....137–40; disc. 427
Currents and Their Effect on Lead-Cable-Sheath Corrosion, Study of A-C Sheath. Sherer, Granbois............264–8; disc. 483
Currents on Rural Distribution Systems, Graphical Method of Calculating Fault. Linder............16–19; disc. 446
Currents, Rectifier Fault. Herskind, Kellogg............145–50; disc. 441
Cylindrical Conductors, Resistance and Capacitance Relations Between Short. ReQua............724–30; disc. 962
Cylindrical Nonmagnetic Loads, Design of Induction-Heating Coils for. Vaughan, Williamson............587–92; disc. 965

D

Damping and Synchronizing Torques of Power Selsyns. Concordia, Kron...............366–71; disc. 490
Damping Effect of D-C Marine Propulsion Motors on Vibrations Produced in Drive Shafts by Large Propellers. Litman..........................31–7
Data, The Design of Bus-Bar Industrial Distribution Systems: an Epitomization of Available. Higgins............385–400; disc. 486

Design, A New Outdoor Air Switch and the Principles Involved in Its. Graybill, Ferguson. 583–6; disc. 953
Design and Application, Selsyn. Johnson.......703–08; disc. 960
Design and Performance Criteria, Anode-Circuit-Breaker. Boehne, Atwood......337–45; disc. 437
Design Considerations of High-Frequency Twin-Conductor Cable. Greenfield.......932–3
Design, General Considerations in Radio-Frequency-Cable. Wents.......925–6
Design Method, Biased-Core-Current-Transformer. Specht.......635–40
Design of a D-C Selsyn System, Analysis and. Manildi.......512–16; disc. 946
Design of Bus-Bar Industrial Distribution Systems: an Epitomization of Available Data. Higgins.......385–400; disc. 486
Design of Induction-Heating Coils for Cylindrical Nonmagnetic Loads. Vaughan, Williamson.......587–92; disc. 965
Design of Sealed Ignitron Rectifiers for Three-Wire Service. Morack.......103–07
Detection and Location by Surge-Comparison Testing, Winding-Fault. Moses, Harter..499–503; disc. 945
Detection Methods as Applied to Distribution Transformers, Impulse-Failure-. Stewart, Holcomb.......640–44; disc. 956
Determination of Transient Shaft Torques in Turbine Generators by Means of the Electrical-Mechanical Analogy. McCann, Warren, Criner. 51–6; disc. 492
Development and Manufacture, Statistical Methods Applied to Insulator. Taylor.....495–9; disc. 952
Development of Apparatus Life Quality, Statistical Methods in the. Ferrell.......700–03; disc. 998
Devices, Dynamic Measurements on Electromagnetic. Norton.......151–6
Devices for Aircraft, Preferred Practices for Electric Control. Hottenroth.......197–200; disc. 444
Diagram for a Four-Terminal Network and Its Application to the Capacitor Single-Phase Motor, A Generalized Circle. Tarboux.......881–9; disc. 943
Diagrams, New Transmission-Line. Schwager, Wang.......610–15; disc. 955
Dielectric-Absorption Characteristics of Large A-C Stator Windings, Insulation Resistance and. Askey, Johnson.......347–51; disc. 458
Dielectric-Absorption Tests in Drying Out Large Generators, Use of. Marcroft.......56–60; disc. 415
(Dielectric Heating) Capacitors for High-Frequency Induction-Heating Circuits. Clark, Scoville.......791–6; disc. 995
Dielectric Heating, The Role of Frequency in Industrial. Scott.......558–62
Dielectric Strength and Life of Impregnated-Paper Insulation, The. Part IV. Whitehead, Kopper.......171–7; disc. 477, 942
Dielectric Strength and Protection of Modern Dry-Type Air-Cooled Transformers. Bellaschi, Beck.......759–63; disc. 997
Dielectric Strength of Polyethylene. Del Mar..918–19
Direct- and Quadrature-Axis Equivalent Circuits of the Synchronous Machine, The. Rankin......861–8
D-C Marine Propulsion Motors on Vibrations Produced in Drive Shafts by Large Propellers, Damping Effect of. Litman.......31–7
Direct Current, Optimum Air Gap for Various Magnetic Materials in Cores of Coils Subject to Superposed. Legg.......709–12; disc. 969
D-C Selsyn System, Analysis and Design of a. Manildi.......512–16; disc. 946
Distribution Apparatus, Lightning Arresters for. Beck, Forbes.......719–24; disc. 970
(Distribution) Electrolysis and Corrosion of Underground Power-System Cables. Gorman.......329–36; disc. 479
(Distribution) Galvanic Corrosiveness of Soil Waters. Phelps, Kahn.......156–9; disc. 482
(Distribution) Guides for Operation of Transformers, Regulators, and Reactors. (Committee Report).......797–806; disc. 957
Distribution Ideas as Applied in a Large War Plant, Modern Electric-Power-. Kaufmann, Kieb.......279–87; disc. 488
Distribution in Transformer Cores and Other Electric Apparatus of Rectangular Cross Section, Formulas for Calculating Temperature. Higgins.......190–4; disc. 493
Distribution Losses in Terms of Generating-Station-Capacity Investment, Evaluation of Electric. Mortara.......1–7; disc. 411
Distribution of Lightning Flashes to Transmission Lines, The Frequency of Occurrence and the. Golde.......902–10; disc. 982
(Distribution) Oil Stresses in Impregnated-Paper Insulation. Whitehead.......555–7; disc. 955
Distribution Power Supply, When the Welding Load Outgrows the. Clark, Stearns...645–8; disc. 964
Distribution Problem in Arc Welding, The Power-. Pierce, Smith.......178–84; disc. 435
(Distribution) Sag and Tension Calculations for Cable and Wire Spans Using Catenary Formulas. Nash, Nash.......685–92; disc. 984
Distribution Scheme With Airplane-Engine-Testing Power Recovery, Dodge Chicago Plant's Electric-Power-. Bailey.......121–3; disc. 484
(Distribution) Study of A-C Sheath Currents and Their Effect on Lead-Cable-Sheath Corrosion. Sherer, Granbois.......264–8; disc. 483
Distribution Systems: an Epitomization of Available Data, The Design of Bus-Bar Industrial. Higgins.......385–400; disc. 486
Distribution Systems, Graphical Method of Calculating Fault Currents on Rural. Linder..16–19; disc. 446
Distribution Systems, Improved Fault Protection for Rural. Van Ryan.......261–3
(Distribution) The Dielectric Strength and Life of Impregnated-Paper Insulation—Part IV. Whitehead, Kopper.......171–7; disc. 477, 942
Distribution Transformers, Impulse-Failure-Detection Methods as Applied to. Stewart, Holcomb.......640–44; disc. 956
Dodge Chicago Plant's Electric-Power-Distribution Scheme With Airplane-Engine-Testing Power Recovery. Bailey.......121–3; disc. 484
(Domestic and Commercial Applications) Coincidence-Factor Relationships of Electric-Service-Load Characteristics. Bary.......623–9
Drive Shafts by Large Propellers, Damping Effect of D-C Marine Propulsion Motors on Vibrations Produced in. Litman.......31–7
Drive, Speed-Control System for an Aircraft Cabin-Supercharger. Godsey, Miner, Walley......37–40
Drives, Governor Requirements for Aircraft Alternator. Boice, Levoy.......534–40; disc. 947
Drives in Steam-Electric Stations, Power Systems for Auxiliary. McClure, Whittlesey..844–51; disc. 976
Drop Produced by Resistance Welders, Line. Longini.......619–23; disc. 963
Dummy-Rotor Methods of Quality Control and Trouble Shooting of Induction-Motor Windings and Cores, Wound and. Trickey.......842–4; disc. 998
Duration, An Interval Timer for Arc. Quill....237–40
Dwell Tester for Bomb-Release Interval Controls, An Interval and. Long.......648–51
Dynamic Braking With Traction Motors. Riley, Woods.......517–19
Dynamic Measurements on Electromagnetic Devices. Norton.......151–6

E

Economics, Frequency Changers—Characteristics, Applications, and. Crary, Easley....351–8; disc. 416
Eddy-Current Resistance of Multilayer Coils. Long.......712–18
Effect of Altitude on Temperature Rise of Aircraft Transformers. Montsinger.......251–2
Effects in a Resistance-Type Thermometer, Heat-Flow. Millar.......678–85
Electric-Circuit Element, Ferroinductance as a Variable. Ryder.......671–8; disc. 962
Electric Control Devices for Aircraft, Preferred Practices for. Hottenroth.......197–200; disc. 444
Electric Distribution Losses in Terms of Generating-Station-Capacity Investment, Evaluation of. Mortara.......1–7; disc. 411
Electric Drives for Steam-Electric Generating-Station Auxiliaries. Brownlee, Elsi......741–5; disc. 976
Electric Equipment for Ship-Propeller Milling Machine, Application of. Morton, Rutemiller.......205–08; disc. 453
Electric Gun Turrets for Aircraft, The Amplidyne Generator Applied to Speed-Controlled. Zahorsky.......221–5; disc. 436
(Electric Machinery) A Generalized Circle Diagram for a Four-Terminal Network and Its Application to the Capacitor Single-Phase Motor. Tarboux.......881–9; disc. 943
(Electric Machinery) A Portable Instrument for Measuring Insulation Resistance at High Voltage. Atkinson, Taylor.......164–7; disc. 428
(Electric Machinery) Control of Electrical-Insulating Varnishes. Gibson, Braithwaite.......520–4
(Electric Machinery) Damping and Synchronizing Torques of Power Selsyns. Concordia, Kron.......366–71; disc. 490
(Electric Machinery) Dielectric Strength and Protection of Modern Dry-Type Air-Cooled Transformers. Bellaschi, Beck.......759–63; disc. 997
(Electric Machinery) Fundamentals of the Amplidyne Generator. Bower.......873–81
(Electric Machinery) Guides for Operation of Transformers, Regulators, and Reactors. (Committee Report).......797–806; disc. 957
(Electric Machinery) Impulse-Failure-Detection Methods as Applied to Distribution Transformers. Stewart, Holcomb.......640–44; disc. 956
(Electric Machinery) Industrial Control: Heating of Shunt-Motor Starting Resistors. Leland, Rader.......695–9; disc. 961
(Electric Machinery) Inherent Errors in the Determination of Synchronous-Machine Reactances by Test. Concordia, Maginniss.......288–94; disc. 491
(Electric Machinery) Insulation Resistance and Dielectric-Absorption Characteristics of Large A-C Stator Windings. Askey, Johnson......347–51; disc. 458
(Electric Machinery) Investigation of Hot-Spot Temperatures in Fractional-Horsepower Motors. Hirsch, Munier, Schmidt, Wightman, Himebrook, Lloyd, Coffman, Potter.......128–36; disc. 421
(Electric Machinery) Investigation of Hot-Spot Temperatures in Integral-Horsepower Motors. Hildebrand, Cain, Phillips, Hough, Rosswog, Potter.......124–8; disc. 421
(Electric Machinery) Maintenance of Good Brush Performance. Kalb.......819–25; disc. 996
(Electric Machinery) Measurement of Stray-Load Loss in Induction Motors. Ware......194–7; disc. 433
(Electric Machinery) Measurement of the Subtransient Impedances of Synchronous Machines. Tracy, Tice.......70–6; disc. 429
(Electric Machinery) Per-Unit Impedances of Synchronous Machines. Rankin
Part I.......569–73
Part II.......839–41
(Electric Machinery) Rating of High-Temperature Induction Motors. Alger, Jones...300–02; disc. 458
(Electric Machinery) Resonant-Circuit Constant-Current Regulators. Kevern....807–10; disc. 992
(Electric Machinery) Selsyn Design and Application. Johnson.......703–08; disc. 960
(Electric Machinery) Standards and Insulation Characteristics of Oil-Insulated Transformers. Vogel.......167–71; disc. 431
(Electric Machinery) Static Voltage Regulator for Rototrol Exciter. Harder, Valentine......601–06
(Electric Machinery) Symmetrical Components as Applied to the Single-Phase Induction Motor. Suhr.......651–6; disc. 958
(Electric Machinery) Synchronous Starting of Generator and Motor. Concordia, Crary, Kilbourne, Weygandt.......629–34; disc. 956
(Electric Machinery) Tapered-Thickness Bimetal. Elmer.......661–5; disc. 962
Electric Machinery, The Application of Silicone Resins to Insulation for. DeKiep, Hill, Moses.......94–8; disc. 460
(Electric Machinery) Transient Electrical Torques of Turbine Generators During Short Circuits and Synchronizing. Kirschbaum........65–70; disc. 492
(Electric Machinery) Variable-Unbalanced-Voltage Control. Wickerham..........98–102; disc. 449
(Electric Machinery) Winding-Fault Detection and Location by Surge-Comparison Testing. Moses, Harter.......499–503; disc. 945
(Electric Machinery) Wound and Dummy Rotor Methods of Quality Control and Trouble Shooting of Induction-Motor Windings and Cores. Trickey.......842–4; disc. 998
Electric Machines, Organo-Silicon Compounds for Insulating. Kauppi, Moses.........90–3; disc. 457
Electric-Power-Distribution Ideas as Applied in a Large War Plant, Modern. Kaufmann, Kieb.......279–87; disc. 489
Electric-Power-Distribution Scheme With Airplane Engine-Testing Power Recovery, Dodge Chicago Plant's. Bailey.......121–3; disc. 484
Electric Power in a Steel Plant. Graham.......816–18; disc. 994
Electric-Service-Load Characteristics, Coincidence-Factor Relationships of. Bary.......623–9
Electric Tachometers, Precision Testing of. Princi.......504–08; disc. 946
(Electric Welding) Analysis of Arc-Welding Reactors. Wheeler.......87–90; disc. 434
(Electric Welding) Line Drop Produced by Resistance Welders. Longini.......619–23; disc. 963
(Electric Welding) Power Supply for A-C Arc Welding. Welch, Wyer.......116–20; disc. 435
(Electric Welding) The Power-Distribution Problem in Arc Welding. Pierce, Smith.....178–84; disc. 435
(Electric Welding) When the Welding Load Outgrows the Distribution Power Supply. Clark, Stearns.......645–8; disc. 964
Electrical and Mechanical Testing of Radio-Frequency Cables at the Naval Research Laboratory, Methods of. Miller.......934–5
Electrical-Insulating Varnishes, Control of. Gibson, Braithwaite.......520–4
Electrical-Insulation Failure, Chemical Contamination as Causes of. Braithwaite, Moses..580–3; disc. 945
Electrical-Mechanical Analogy, Determination of Transient Shaft Torques in Turbine Generators by Means of the. McCann, Warren, Criner..51–6; disc. 492
Electrical Resistivity of Resin-Treated Wood and Laminated Hydrolyzed-Wood and Paper-Base Plastics. Weatherwax, Stamm.......833–8
Electrical Tests Over a Range of Frequencies. Fleming.......935–7
Electrical Torques of Turbine Generators During Short Circuits and Synchronizing, Transient. Kirschbaum.......65–70; disc. 492
Electrically Operated Aircraft Circuit Breaker, A 208Y/120-Volt 120-Ampere Three-Pole 400-Cycle. Titus, Reifschneider.......551–5

Electrification and Signaling of the Canadian National Railways Terminal, Montreal, Canada. Gage.......41–4; disc. 417
Electrolysis and Corrosion of Underground Power-System Cables. Gorman..........329–36; disc. 479
Electrolytic Corrosion—Methods of Evaluating Insulating Materials Used in Tropical Service. Thompson, Mathes..........295–9; disc. 443
Electromagnetic Devices, Dynamic Measurements on. Norton..........151–6
(Electronics) Arc-Backs in Rectifier Circuits—Artificial Arc-Back Tests. Evans, Maslin..303–11; disc. 439
(Electronics) Design of Sealed Ignitron Rectifiers for Three-Wire Service. Morack..........103–07
(Electronics) Rectifier Fault Currents. Herskind, Kellog..........145–50; disc. 441
(Electronics) Transient Response of Controlled Rectifier Circuits. Chin, Walter..........208–14
(Electronics) Voltage and Current Relations for Controlled Rectification With Inductive and Generative Loads. Puchlowski..........255–60; disc. 442
Element, Ferroinductance as a Variable Electric-Circuit. Ryder..........671–8; disc. 962
Element Mounted in a Protecting Case, Response Time and Lag of a Thermometer. Goodwin..........665–70; disc. 959
Engine-Driven 400-Cycle Aircraft Generators, Parallel Operation of Main-. Levoy.....811–16; disc. 987
Engine-Testing Power Recovery, Dodge Chicago Plant's Electric-Power-Distribution Scheme With Airplane-. Bailey..........121–3; disc. 484
Engineering Judgment in the Manufacture of Lightning-Arrester Blocks, Statistics as an Aid to. Goffman..........607–10; disc. 966
Epitomization of Available Data, The Design of Bus-Bar Industrial Distribution Systems: Higgins..........385–400; disc. 486
Equipment and Systems, Modern Practice in Power-Plant Auxiliary. Muller..........868–72; disc. 976
Equipment for Ship-Propeller Milling Machine, Application of Electric. Morton, Rutemiller..........205–08; disc. 453
Equivalent Circuits of the Synchronous Machine, The Direct- and Quadrature-Axis. Rankin....861–8
Errors in the Determination of Synchronous-Machine Reactances by Test, Inherent. Concordia, Magnniss..........288–94; disc. 491
Evaluating Insulating Materials Used in Tropical Service, Electrolytic Corrosion—Methods of. Thompson, Mathes..........295–9; disc. 443
Evaluation of Electric Distribution Losses in Terms of Generating-Station-Capacity Investment. Mortara..........1–7; disc. 411
Exciter, Static Voltage Regulator for Rototrol. Harder, Valentine..........601–06

F

Failure, Chemical Contamination as Causes of Electrical-Insulation. Braithwaite, Moses..........580–3; disc. 945
Failure-Detection Methods as Applied to Distribution Transformers, Impulse-. Stewart, Holcomb..........640–44; disc. 956
Fault Currents on Rural Distribution Systems, Graphical Method of Calculating. Linder..16–19; disc. 446
Fault Currents, Rectifier. Herskind, Kellogg..........145–50; disc. 441
Fault Detection and Location by Surge-Comparison Testing, Winding-. Moses, Harter..........499–503; disc. 945
Fault Protection for Rural Distribution Systems, Improved. Van Ryan..........261–3
Faults, Impedances Seen by Relays During Power Swings With and Without. Clarke..........372–84; disc. 471
Ferroinductance as a Variable Electric-Circuit Element. Ryder..........671–8; disc. 962
Field Tests and Performance of Heavy-Duty High-Speed 138-Kv Circuit Breakers—Oil and Air-Blast. Sporn, St. Clair..........401–10; disc. 463
5,000,000 Kva, The Next Step in Interrupting Capacity—. Hill, Leeds..........317–23; disc. 463
Formulas for Calculating Temperature Distribution in Transformer Cores and Other Electric Apparatus of Rectangular Cross Section. Higgins..........190–4; disc. 493
Formulas, Sag and Tension Calculations for Cable and Wire Spans Using Catenary. Nash, Nash..........685–92; disc. 984
400-Cycle Aircraft Motor, A. Schwandt..........508–12; disc. 948
400-Cycle Electrically Operated Aircraft Circuit Breaker, A 208Y/120-Volt 120-Ampere Three-Pole. Titus, Reifschneider..........551–5
400-Cycle Inverters for Military Aircraft. Hayes, Ray..........233–7
Four-Phase Network, Two-Phase Co-ordinates of a. Kimbark..........7–9
Four-Terminal Network and Its Application to the Capacitor Single-Phase Motor, A Generalized Circle Diagram for a. Tarboux.........881–9; disc. 943
Fractional-Horsepower Motors, Investigation of Hot-Spot Temperatures in. Hirsch, Munier, Schmidt, Wightman, Himebrook, Lloyd, Coffman, Potter..........128–36; disc. 421
Frequency, and Time of Interconnected Systems, Control of Load. Duff..........778–86; disc. 999
Frequency Cable, The S-Function Method of Measuring Attenuation of Coaxial Radio-. Stewart..........616–19, 938–9; disc. 966
Frequency Cables, Report of Conference on Radio-..........911–41
Frequency Changers—Characteristics, Applications, and Economics. Crary, Easley......351–8; disc. 416
Frequency in Industrial Dielectric Heating, The Role of. Scott..........558–62
Frequency-Modulation, and Single-Side-Band Systems for Power-Line Carrier Transmission, A Comparison of the Amplitude-Modulation. Cheek..........215–20; disc. 450
Frequency of Occurrence and the Distribution of Lightning Flashes to Transmission Lines, The. Golde..........902–10; disc. 982
Frequency System of Telemetering, A Modulated-. Renfro, Peterson..........45–7
Fundamentals of the Amplidyne Generator. Bower..........873–81
Fuse for Aircraft Applications, A Current-Limiting. Powell..........541–5

G

Galvanic Corrosiveness of Soil Waters. Phelps, Kahn..........156-9; disc 482
Gap for Various Magnetic Materials in Cores of Coils Subject to Superposed Direct Current, Optimum Air. Legg..........709–12; disc. 969
Generalized Circle Diagram for a Four-Terminal Network and Its Application to the Capacitor Single-Phase Motor, A. Tarboux.......881–9; disc. 943
Generating-Station Auxiliaries, Electric Drives for Steam Electric. Brownlee, Elzi...741–5; disc. 976
Generating-Station-Capacity Investment, Evaluation of Electric Distribution Losses in Terms of. Mortara..........1–7; disc. 411
Generating Stations, Auxiliary-Power Supply for. McCallum..........693–5; disc. 976
Generative Loads, Voltage and Current Relations for Controlled Rectification With Inductive and. Puchlowski..........255–60; disc. 442
Generator and Motor, Synchronous Starting of. Concordia, Crary, Kilbourne, Weygandt..........629–34; disc. 956
Generator Applied to Speed-Controlled Electric Gun Turrets for Aircraft, The Amplidyne. Zahorsky..........221–5; disc. 436
Generator, Fundamentals of the Amplidyne. Bower..........873–81
Generators, Automatic Load Control for Turbine. Crever, Jackson..........656–60
Generators by Means of the Electrical-Mechanical Analogy, Determination of Transient Shaft Torques in Turbine. McCann, Warren, Criner..........51–6; disc. 492
Generators During Short Circuits and Synchronizing, Transient Electrical Torques of Turbine. Kirschbaum..........65–70; disc. 492
Generators, Parallel Operation of Main-Engine-Driven 400-Cycle Aircraft. Levoy......811–16; disc. 987
Generators to Relieve Power-Supply Systems of Steel-Mill Load Swings, Automatic Regulation of Turbine. Eberhardt, Harrison, Kohn, Darling..751–8
Generators, Use of Dielectric-Absorption Tests in Drying Out Large. Marcroft..........56–60; disc. 415
Geometry of General Transmission Systems, Power. Altar..........312–17; disc. 493
Governor Requirements for Aircraft Alternator Drives. Boice, Levoy..........534–40; disc. 947
Graphical Method of Calculating Fault Currents on Rural Distribution Systems. Linder..16–19; disc. 446
Grounding of Circuits on Self-Propelled Vehicles. Ewing..........48–50; disc. 417
Guides for Operation of Transformers, Regulators, and Reactors. (Committee Report)..797–806; disc. 957
Gun Turrets for Aircraft, The Amplidyne Generator Applied to Speed-Controlled Electric. Zahorsky..........221–5; disc. 436
Gyroscope Testing, A Tachometer—Accelerometer—Vibrometer for Instrument-. Laurenson, Long..........593–6; disc. 960

H

Halides, Treatment of High-Altitude Brushes by Application of Metallic. Elsey..........576–9
Heat-Flow Effects in a Resistance-Type Thermometer. Millar..........678–85
Heating Circuits, Capacitors for High-Frequency Induction-. Clark, Scoville......791–6; disc. 995
Heating Coils for Cylindrical Nonmagnetic Loads, Design of Induction-. Vaughan, Williamson..........587–92; disc. 965
Heating of Moving Magnetic Strip, Induction. Baker..........184–9
Heating of Shunt-Motor Starting Resistors, Industrial Control. Leland, Rader........695–9; disc. 961
Heating, The Role of Frequency in Industrial Dielectric. Scott..........558–62
Heavy-Duty High-Speed 138-Kv Circuit Breakers—Oil and Air-Blast, Field Tests and Performance of. Sporn, St. Clair..........401–10; disc. 463
High-Altitude Brushes by Application of Metallic Halides, Treatment of. Elsey..........576–9
High-Altitude Testing of Aircraft Ignition Cables and Connectors, Simulated-. Race, Ross..........20–6
High-Capacity High-Voltage Three-Cycle Oil Circuit Breaker, A. Byrd, Rietz..........160–3; disc. 463
High-Frequency Induction-Heating Circuits, Capacitors for. Clark, Scoville..........791–6; disc. 995
High-Frequency Twin-Conductor Cable, Design Considerations of. Greenfield..........932–3
High-Speed 138-Kv Circuit Breakers—Oil and Air-Blast, Field Tests and Performance of Heavy-Duty. Sporn, St. Clair..........401–10; disc. 463
High-Temperature Induction Motors, Rating of. Alger, Jones..........300–02; disc. 458
High Voltage, A Portable Instrument for Measuring Insulation Resistance at. Atkinson, Taylor..........164–7; disc. 428
High-Voltage Three-Cycle Oil Circuit Breaker, A High-Capacity. Byrd, Rietz..........160–3; disc. 463
High-Voltage Transmission Lines, Nine Years' Experience With Ultrahigh-Speed Reclosing of. Sporn, Muller..........225–8; disc. 445
Horsepower Motors, Investigation of Hot-Spot Temperatures in Fractional-. Hirsch, Munier, Schmidt, Wightman, Himebrook, Lloyd, Coffman, Potter..........128–36; disc. 421
Horsepower Motors, Investigation of Hot-Spot Temperatures in Integral. Hildebrand, Cain, Phillips, Hough, Rosswog, Potter..........124–8; disc. 421
Hot-Spot Temperatures in Fractional-Horsepower Motors, Investigation of. Hirsch, Munier, Schmidt, Wightman, Himebrook, Lloyd, Coffman, Potter..........128–36; disc. 421
Hot-Spot Temperatures in Integral-Horsepower Motors, Investigation of. Hildebrand, Cain, Phillips, Hough, Rosswog, Potter..........124–8; disc. 421
Hydrolyzed-Wood and Paper-Base Plastics, The Electrical Resistivity of Resin-Treated Wood and Laminated. Weatherwax, Stamm..........833–8

I

Ignition Cables and Connectors, Simulated-High-Altitude Testing of Aircraft. Race, Ross..........20–6
Ignitron Rectifiers for Three-Wire Service, Design of Sealed. Morack..........103–07
Illumination, Aircraft. Davies..........26–30
Impedances of Synchronous Machines, Measurement of the Subtransient. Tracy, Tice.....70–6; disc. 429
Impedances of Synchronous Machines, Per-Unit. Rankin.
  Part I..........569–73
  Part II..........839–41
Impedances Seen by Relays During Power Swings With and Without Faults. Clarke....372–84; disc. 471
Impregnated-Paper Insulation, Oil Stresses in. Whitehead..........555–7; disc. 955
Impregnated-Paper Insulation, The Dielectric Strength and Life of. Part IV. Whitehead, Kopper..........171–7; disc. 477, 942
Improved Fault Protection for Rural Distribution Systems. Van Ryan..........261–3
Improvement of Induction Motors, Application of Capacitors for Power-Factor. Bloomquist, Boice..........274–8
Improving Stability by Rapid Closing of Bus-Tie Switches. Kimbark..........61–4; disc. 456
Impulse-Failure-Detection Methods as Applied to Distribution Transformers. Stewart, Holcomb..........640–44; disc. 956
Inductance of a Toroidal Coil Without Iron, The Self-. Dwight..........805–06; disc. 999
Induction-Heating Circuits, Capacitors for High-Frequency. Clark, Scoville.........791–6; disc. 995
Induction-Heating Coils for Cylindrical Nonmagnetic Loads, Design of. Vaughan, Williamson..........587–92; disc. 965
Induction Heating of Moving Magnetic Strip. Baker..........184–9
Induction Motor, Symmetrical Components as Applied to the Single-Phase. Suhr.......651–6; disc. 958
Induction-Motor Windings and Cores, Wound and Dummy-Rotor Methods of Quality Control and Trouble Shooting of. Trickey....842–4; disc. 998
Induction Motors, Application of Capacitors for Power-Factor Improvement of. Bloomquist, Boice..274–8
Induction Motors, Measurement of Stray-Load Loss in. Ware..........194–7; disc. 433
Induction Motors, Rating of High-Temperature. Alger, Jones..........300–02; disc. 458

Inductive and Generative Loads, Voltage and Current Relations for Controlled Rectification With. Puchlowski..........255–60; disc. 442
Industrial Control: Heating of Shunt-Motor Starting Resistors. Leland, Rader..........695–9; disc. 961
Industrial Dielectric Heating, The Role of Frequency in. Scott..........558–62
Industrial Distribution Systems: an Epitomization of Available Data, The Design of Bus-Bar. Higgins..........385–400; disc. 486
Inherent Errors in the Determination of Synchronous-Machine Reactances by Test. Concordia, Maginnis..........288–94; disc. 491
Instability in D-C Aircraft Systems. Bunce, Cunningham, Davidson..........786–91
Instrument for Measuring Insulation Resistance at High Voltage, A Portable. Atkinson, Taylor..........164–7; disc. 428
Instrument-Gyroscope Testing, A Tachometer—Accelerometer—Vibrometer for. Laurenson, Long..........593–6; disc. 960
Instrument Rotors, Basic Concepts of Moving-Magnet-. Mendelsohn..........529–34; disc. 947
(Instruments) A Modulated-Frequency System of Telemetering. Renfro, Peterson..........45–7
(Instruments) A Study of Wave Shapes for Radio-Noise-Meter Calibrations. Frick.....890–901; disc. 969
(Instruments) An Interval Timer for Arc Duration. Quill..........237–40
(Instruments) Analysis and Design of a D-C Selsyn System. Manildi..........512–16; disc. 946
(Instruments) Biased-Core-Current-Transformer Design Method. Specht..........635–40
(Instruments) Heat-Flow Effects in a Resistance-Type Thermometer. Millar..........678–85
(Instruments) Orthomagnetic Bushing Current Transformer for Metering. Boyajian, Camilli..........137–40; disc. 427
(Instruments) Precision Testing of Electric Tachometers. Princi..........504–08; disc. 946
(Instruments) Response Time and Lag of a Thermometer Element Mounted in a Protecting Case. Goodwin..........665–70; disc. 959
Insulating Electric Machines, Organo-Silicon Compounds for. Kauppi, Moses.......90–3; disc. 457
Insulating Materials Used in Tropical Service, Electrolytic Corrosion—Methods of Evaluating. Thompson, Mathes..........295–9; disc. 443
Insulating Varnishes, Control of Electrical-. Gibson, Braithwaite..........520–4
Insulation and Structural Rubber, Vibration. Connon..........324–9
Insulation Characteristics of Oil-Insulated Transformers, Standards and. Vogel..167–71; disc. 431
Insulation Failure, Chemical Contamination as Causes of Electrical-. Braithwaite, Moses..580–3; disc. 945
Insulation for Electric Machinery, The Application of Silicone Resins to. DeKlep, Hill, Moses..........94–8; disc. 460
Insulation, Oil Stresses in Impregnated-Paper. Whitehead..........555–7; disc. 955
Insulation Resistance and Dielectric-Absorption Characteristics of Large A-C Stator Windings. Askey, Johnson..........347–51; disc. 458
Insulation Resistance at High Voltage, A Portable Instrument for Measuring. Atkinson, Taylor..........164–7; disc. 428
Insulation, The Dielectric Strength and Life of Impregnated-Paper. Part IV. Whitehead, Kopper..........171–7; disc. 477, 942
Insulator Development and Manufacture, Statistical Methods Applied to. Taylor.....495–9; disc. 952
Integral-Horsepower Motors, Investigation of Hot-Spot Temperatures in. Hildebrand, Cain, Phillips, Hough, Rosswog, Potter..........124–8; disc. 421
Interconnected Systems, Control of Load, Frequency, and Time of. Duff..........778–86; disc. 999
Interrupting Capacity—5,000,000 Kva, The Next Step in. Hill, Leeds..........317–23; disc. 463
Interval and Dwell Tester for Bomb-Release Interval Controls. Long..........648–51
Interval Timer for Arc Duration, An. Quill...237–40
Inverters for Military Aircraft, 400-Cycle. Hayes, Ray..........233–7
Investigation of Hot-Spot Temperatures in Fractional-Horsepower Motors. Hirsch, Munier, Schmidt, Wightman, Himebrook, Lloyd, Coffman, Potter..........128–36; disc. 421
Investigation of Hot-Spot Temperatures in Integral-Horsepower Motors. Hildebrand, Cain, Phillips, Hough, Rosswog, Potter..........124–8; disc. 421
Investigation on 132-Kv System of American Gas and Electric Company, Lightning. Gross, Lippert..........76–84; disc. 474
Investigation on Transmission Lines, Lightning. Part VIII. Lewis, Foust..........107–15; disc. 472
Iron, The Self-Inductance of a Toroidal Coil Without. Dwight..........805–06; disc. 999

J

Judging Mica Quality Electrically. Coutlee....735–41

L

Lag of a Thermometer Element Mounted in a Protecting Case, Response Time and. Goodwin..........665–70; disc. 959
(Land Transportation) Dynamic Braking With Traction Motors. Riley, Woods..........517–19
(Land Transportation) Measurement of Railway-Motor Temperatures in Service. Teker..........545–50
(Land Transportation) Rewinding Commutator-Type Traction Armatures. Greene, Stafford, Gentilini..........563–9; disc. 943
Lead-Cable-Sheath Corrosion, Study of A-C Sheath Currents and Their Effect on. Sherer, Granbois..........264–8; disc. 483
Life Quality, Statistical Methods in the Development of Apparatus. Ferrell..........700–03; disc. 998
Lightning-Arrester Blocks, Statistics as an Aid to Engineering Judgment in the Manufacture of. Goffman..........607–10; disc. 966
Lightning Arresters for Distribution Apparatus. Beck, Forbes..........719–24; disc. 970
Lightning Flashes to Transmission Lines, The Frequency of Occurrence and the Distribution of. Golde..........902–10; disc. 982
Lightning Investigation on 132-Kv System of American Gas and Electric Company. Gross, Lippert..........76–84; disc. 474
Lightning Investigation on Transmission Lines—Part VIII. Lewis, Foust..........107–15; disc. 472
Lightning Investigations on 33-Kv Wood-Pole Lines. Andrews, McCann..........768–77; disc. 954
Limiting Fuse for Aircraft Applications, A Current-. Powell..........541–5
Line Diagrams, New Transmission-. Schwager, Wang..........610–15; disc. 955
Line Drop Produced by Resistance Welders. Longini..........619–23; disc. 963
Line, The Tapered Transmission. Milnor........345–6
Lines, Cost Studies of 69- to 230-Kv Underground Power-Transmission Systems and Tie. Holm..........852–60
Lines, Lightning Investigation on Transmission. Part VIII. Lewis, Foust..........107–15; disc. 472
Lines, Nine Years' Experience With Ultrahigh-Speed Reclosing of High-Voltage Transmission. Sporn, Muller..........225–8; disc. 445
Lines, The Frequency of Occurrence and the Distribution of Lightning Flashes to Transmission. Golde..........902–10; disc. 982
Load Characteristics, Coincidence-Factor Relationships of Electric-Service-. Bary..........623–9
Load Control for Turbine Generators, Automatic. Crever, Jackson..........656–60
Load, Frequency, and Time of Interconnected Systems, Control of. Duff..........778–86; disc. 999
Load Loss in Induction Motors, Measurement of Stray-. Ware..........194–7; disc. 433
Load Outgrows the Distribution Power Supply, When the Welding. Clark, Stearns.....645–8; disc. 964
Load Swings, Automatic Regulation of Turbine Generators to Relieve Power-Supply Systems of Steel-Mill. Eberhardt, Harrison, Kohn, Darling..751–8
Loads, Design of Induction-Heating Coils for Cylindrical Nonmagnetic. Vaughan, Williamson..........587–92; disc. 965
Loads, Voltage and Current Relations for Controlled Rectification With Inductive and Generative. Puchlowski..........255–60; disc. 442
Location by Surge-Comparison Testing, Winding-Fault Detection and. Moses, Harter..499–503; disc. 945
Loss in Induction Motors, Measurement of Stray-Load. Ware..........194–7; disc. 433
Losses in Radio-Frequency-Cable Components. Ragan..........927
Losses in Terms of Generating-Station-Capacity Investment, Evaluation of Electric Distribution. Mortara..........1–7; disc. 411

M

Machine, Application of Electric Equipment for Ship-Propeller Milling. Morton, Rutemiller..........205–08; disc. 453
Machine Reactances by Test, Inherent Errors in the Determination of Synchronous-. Concordia, Maginnis..........288–94; disc. 491
Machine, The Direct- and Quadrature-Axis Equivalent Circuits of the Synchronous. Rankin.......861–8
Machine, Tracer-Controlled Position Regulator for Propeller Milling. Hanna, Osbon, Hartley..........201–05; disc. 452
Machines, Organo-Silicon Compounds for Insulating Electric. Kauppi, Moses..........90–3; disc. 457
Machines, Per-Unit Impedances of Synchronous. Rankin.
  Part I..........569–73
  Part II..........839–41
Magne-Blast Breaker, New Solenoid Mechanism for. Wyman, Keagy..........268–74; disc. 448
Magnet-Instrument Rotors, Basic Concepts of Moving-. Mendelsohn..........529–34; disc. 947
Magnetic Materials in Cores of Coils Subject to Superimposed Direct Current, Optimum Air Gap for Various. Legg..........709–12; disc. 969
Magnetic Strip, Induction Heating of Moving. Baker..........184–9
Maintenance of Good Brush Performance. Kalb..........819–25; disc. 996
Manufacture of Lightning-Arrester Blocks, Statistics as an Aid to Engineering Judgment in the. Goffman..........607–10; disc. 966
Manufacture, Statistical Methods Applied to Insulator Development and. Taylor.......495–9; disc. 952
Manufacturing Methods, Radio-Frequency Cable. Odarenko..........922–5
Marine Propulsion Motors on Vibrations Produced in Drive Shafts by Large Propellers, Damping Effect of D-C. Litman..........31–7
Materials Used in Tropical Service, Electrolytic Corrosion—Methods of Evaluating Insulating. Thompson, Mathes..........295–9; disc. 443
Measurement of Railway-Motor Temperatures in Service. Taker..........545–50
Measurement of Stray-Load Loss in Induction Motors. Ware..........194–7; disc. 433
Measurement of the Subtransient Impedances of Synchronous Machines. Tracy, Tice..70–6; disc. 429
Measurements on Electromagnetic Devices, Dynamic. Norton..........151–6
Measurements on Polyethylene and Rubber Cables, Corona-Initiation. Depackh..........939–40
Measuring Attenuation of Coaxial Radio-Frequency Cable, The S-Function Method of. Stewart..........616–19; disc. 966
Measuring Insulation Resistance at High Voltage, A Portable Instrument for. Atkinson, Taylor..........164–7; disc. 428
Mechanism for Magne-Blast Breaker, New Solenoid. Wyman, Keagy..........268–74; disc. 448
Megavolt-Ampere Air-Blast Circuit Breaker for 138,000-Volt Service, A Three-Cycle 3,500-. Byrd, Beall..........229–32; disc. 463
Mercury-Arc Rectifiers for Railroads. Watkins..........84–6; disc. 419
Metallic Halides, Treatment of High-Altitude Brushes by Application of. Elsey..........576–9
Meter Calibrations, A Study of Wave Shapes for Radio-Noise-. Frick..........890–901; disc. 969
Metering, Orthomagnetic Bushing Current Transformer for. Boyajian, Camilli..........137–40; disc. 427
Method, Biased-Core-Current Transformer Design. Specht..........635–40
Method of Calculating Fault Currents on Rural Distribution Systems, Graphical. Linder..........16–19; disc. 446
Method of Measuring Attenuation of Coaxial Radio-Frequency Cable, The S-Function. Stewart..........616–19; disc. 966
Methods Applied to Insulator Development and Manufacture, Statistical. Taylor.......495–9; disc. 952
Methods as Applied to Distribution Transformers, Impulse-Failure-Detection. Stewart, Holcomb..........640–44; disc. 956
Methods in the Development of Apparatus Life Quality, Statistical. Ferrell..........700–03; disc. 998
Methods of Evaluating Insulating Materials Used in Tropical Service, Electrolytic Corrosion—. Thompson, Mathes..........295–9; disc. 443
Mica Quality Electrically, Judging. Coutlee...735–41
Military Aircraft, 400-Cycle Inverters for. Hayes, Ray..........233–7
Milling Machine, Application of Electric Equipment for Ship-Propeller. Morton, Rutemiller..........205–08; disc. 453
Milling Machine, Tracer-Controlled Position Regulator for Propeller. Hanna, Osbon, Hartley..........201–05; disc. 452
Modern Electric-Power Distribution Idea As Applied in a Large War Plant. Kaufmann, Kieb..........279–87; disc. 488
Modern Practice in Power-Plant Auxiliary Equipment and Systems. Muller..........868–72; disc. 976
Modulated-Frequency System of Telemetering, A. Renfro, Peterson..........45–7
Modulation, Frequency-Modulation, and Single-Side-Band Systems for Power-Line Carrier Transmission, A Comparison of the Amplitude-. Cheek..........215–20; disc. 450
Montreal, Canada, Electrification and Signaling of the Canadian National Railways Terminal. Gage..........41–4; disc. 417
Motor, A 400-Cycle Aircraft. Schwandt..........508–12; disc. 948
Motor, A Generalized Circle Diagram for a Four-Terminal Network and Its Application to the Capacitor Single-Phase. Tarboux..........881–9; disc. 943
Motor, Symmetrical Components as Applied to the Single-Phase Induction. Suhr....651–6; disc. 958
Motor, Synchronous Starting of Generator and. Concordia, Crary, Kilbourne, Weygandt..........629–34; disc. 956
Motor Temperatures in Service, Measurement of Railway-. Teker..........545–50

Motors, Application of Capacitors for Power-Factor Improvement of Induction. Bloomquist, Boice.........274–8
Motors, Dynamic Braking With Traction. Riley, Woods.........517–19
Motors for Constant and Adjustable Speed, Central-Station Auxiliary-Drive. Gibson..746–50; disc. 976
Motors, Investigation of Hot-Spot Temperatures in Fractional-Horsepower. Hirsch, Munier, Schmidt, Wightman, Himebrook, Lloyd, Coffman, Potter.........128–36; disc. 421
Motors, Investigation of Hot-Spot Temperatures in Integral-Horsepower. Hildebrand, Cain, Phillips, Hough, Rosswog, Potter.........124–8; disc. 421
Motors, Measurement of Stray-Load Loss in Induction. Ware.........194–7; disc. 433
Motors on Vibrations Produced in Drive Shafts by Large Propellers, Damping Effect of D-C Marine Propulsion. Litman.........31–7
Motors, Rating of High-Temperature Induction. Alger, Jones.........300–02; disc. 458
Moving-Magnet-Instrument Rotors, Basic Concepts of. Mendelsohn.........529–34; disc. 947
Moving Magnetic Strip, Induction Heating of. Baker.........184–9
Multilayer Coils, Eddy-Current Resistance of. Long.........712–18

N

Naval Research Laboratory, Methods of Electrical and Mechanical Testing of Radio-Frequency Cables at the. Miller.........934–5
Network and Its Application to the Capacitor-Single-Phase Motor, A Generalized Circle Diagram for a Four-Terminal. Tarboux.........881–9; disc. 943
Network, Two-Phase Co-ordinates of a Four-Phase. Kimbark.........7–9
New Solenoid Mechanism for Magne-Blast Breaker. Wyman, Keagy.........268–74; disc. 448
New Transmission-Line Diagrams. Schwager, Wang.........610–15; disc. 955
Next Step in Interrupting Capacity—5,000,000 Kva, The. Hill, Leeds.........317–23; disc. 463
Nine Years' Experience With Ultrahigh-Speed Reclosing of High-Voltage Transmission Lines. Sporn, Muller.........225–8; disc. 445
Noise-Meter Calibrations, A Study of Wave Shapes for Radio-. Frick.........890–901; disc. 969
Nonmagnetic Loads, Design of Induction-Heating Coils for Cylindrical. Vaughan, Williamson.........587–92; disc. 965

O

Occurrence and the Distribution of Lightning Flashes to Transmission Lines, The Frequency of. Golde.........902–10; disc. 982
Officers and Committees for 1945–46.........1017–21
Oil and Air-Blast, Field Tests and Performance of Heavy-Duty High-Speed 138-Kv Circuit Breakers—. Sporn, St. Clair.........401–10; disc. 463
Oil Circuit Breaker, A High-Capacity High-Voltage Three-Cycle. Byrd, Rietz.........160–3; disc. 463
Oil-Insulated Transformers, Standards and Insulation Characteristics of. Vogel.........167–71; disc. 431
Oil Stresses in Impregnated-Paper Insulation. Whitehead.........555–7, disc. 955
132-Kv System of American Gas and Electric Company, Lighting Investigation on. Gross, Lippert.........76–84; disc. 474
Operation of Main-Engine-Driven 400-Cycle Aircraft Generators, Parallel. Levoy.........811–16; disc. 987
Operation of Transformers, Regulators, and Reactors, Guides for. (Committee Report).........797–806; disc. 957
Optimum Air Gap for Various Magnetic Materials in Cores of Coils Subject to Superposed Direct Current. Legg.........709–12; disc. 969
Organo-Silicon Compounds for Insulating Electric Machines. Kauppi, Moses.........90–3; disc. 457
Orthomagnetic Bushing Current Transformer for Metering. Boyajian, Camilli.........137–40; disc. 427
Outdoor Air Switch and the Principles Involved in Its Design, A New. Graybill, Ferguson.........583–6; disc. 953
Outgrows the Distribution Power Supply, When the Welding Load. Clark, Stearns.........645–8; disc. 964

P

Paper-Base Plastics, The Electrical Resistivity of Resin Treated Wood and Laminated Hydrolyzed-Wood and. Weatherwax, Stamm.........833–8
Paper Insulation, Oil Stresses in Impregnated. Whitehead.........555–7; disc. 955
Paper Insulation, The Dielectric Strength and Life of Impregnated-. Part IV. Whitehead, Kopper.........171–7; disc. 477, 942
Parallel Operation of Main-Engine-Driven 400-Cycle Aircraft Generators. Levoy.........811–16; disc. 987
Per-Unit Impedances of Synchronous Machines. Rankin.
  Part I.........569–73
  Part II.........839–41
Performance Criteria, Anode-Circuit-Breaker Design and. Boehne, Atwood.........337–45; disc. 437
Performance, Maintenance of Good Brush. Kalb.........819–25; disc. 996
Performance of Heavy-Duty High-Speed 138-Kv Circuit Breakers—Oil and Air-Blast, Field Tests and. Sporn, St. Clair.........401–10; disc. 463
Phase-Comparison Carrier-Current Relaying. McConnell, Cramer, Seeley.........825–33; disc. 973
Plant, Electric Power in a Steel. Graham.........816–18; disc. 994
Plant, Modern Electric-Power-Distribution Ideas as Applied in a Large. Kaufmann, Kieb.........279–87; disc. 488
Plastics, The Electrical Resistivity of Resin-Treated Wood and Laminated Hydrolyzed-Wood and Paper-Base. Weatherwax, Stamm.........833–8
Pole 400-Cycle Electrically Operated Aircraft Circuit Breaker, A 208Y/120-Volt 120-Ampere Three-. Titus, Reifschneider.........551–5
Pole Lines, Lightning Investigations on 33-Kv Wood-. Andrews, McCann.........768–77; disc. 954
Polyethylene and Rubber Cables, Corona-Initiation Measurements on. Depackh.........939–40
Polyethylene as Cable Insulation. Maibauer, Myers.........916–18
Polyethylene, Dielectric Strength of. Del Mar.........918–19
Polyethylene, General Characteristics of. Shackleton.........912–16
Polyethylenes, Properties of Different. Clarke..919–21
Portable Instrument for Measuring Insulation Resistance at High Voltage, A. Atkinson, Taylor.........164–7; disc. 428
Position Regulator for Propeller Milling Machine, Tracer-Controlled. Hanna, Osbon, Hartley.........201–05; disc. 452
(Power Applications, Industrial) Application of Electric Equipment for Ship-Propeller Milling Machine. Morton, Rutemiller.........205–08; disc. 453
(Power Applications, Industrial) Design of Induction-Heating Coils for Cylindrical Nonmagnetic Loads. Vaughan, Williamson.........587–92; disc. 965
(Power Applications, Industrial) Design of Sealed Ignitron Rectifiers for Three-Wire Service. Morack.........103–07
(Power Applications, Industrial). Electric Power in a Steel Plant. Graham.........816–18; disc. 994
(Power Applications, Industrial) Induction Heating of Moving Magnetic Strip. Baker.........184–9
(Power Applications, Industrial) Maintenance of Good Brush Performance. Kalb.........819–25; disc. 996
(Power Applications, Industrial) The Design of Bus-Bar Industrial Distribution Systems: an Epitomization of Available Data. Higgins....385–400; disc. 486
(Power Applications, Industrial) Tracer-Controlled Position Regulator for Propeller Milling Machine. Hanna, Osbon, Hartley.........201–05; disc. 452
Power-Distribution Ideas as Applied in a Large War Plant, Modern Electric-. Kaufmann, Kieb.........279–87; disc. 488
Power-Distribution Problem in Arc Welding, The. Pierce, Smith.........178–84; disc. 435
Power-Distribution Scheme With Airplane-Engine-Testing Power Recovery, Dodge Chicago Plant's Electric-. Bailey.........121–3; disc. 484
Power-Factor Improvement of Induction Motors, Application of Capacitors for. Bloomquist, Boice.........274–8
(Power Generation) Automatic Load Control for Turbine Generators. Crever, Jackson.........656–60
(Power Generation) Auxiliary-Power Supply for Generating Stations. McCallum.....693–5; disc. 976
(Power Generation) Central-Station Auxiliary-Drive Motors for Constant and Adjustable Speed. Gibson.........746–50; disc. 976
(Power Generation) Control of Load, Frequency, and Time of Interconnected Systems. Duff.........778–86; disc. 999
(Power Generation) Electric Drives for Steam-Electric Generating-Station Auxiliaries. Brownlee, Elsi.........741–5; disc. 976
(Power Generation) Evaluation of Electric Distribution Losses in Terms of Generating-Station-Capacity Investment. Mortara.........1–7; disc. 411
(Power Generation) Frequency Changers—Characteristics, Applications, and Economics. Crary, Easley.........351–8; disc. 416
(Power Generation) Use of Dielectric-Absorption Tests in Drying Out Large Generators. Marcroft.........56–60; disc. 415
Power Geometry of General Transmission Systems. Altar.........312–17; disc. 493
Power in a Steel Plant, Electric. Graham.........816–18; disc. 994
Power-Line Carrier Channels. Brown.........246–51
Power-Line Carrier Channels, The Combination of Supervisory Control With Other Functions on. Cheek, Derr.........241–6
Power-Line Carrier Transmission, A Comparison of the Amplitude-Modulation, Frequency-Modulation, and Single-Side-Band Systems for. Cheek.........215–20; disc. 450
Power-Plant Auxiliary Equipment and Systems, Modern Practice in. Muller.........868–72; disc. 976
Power Ratings and Stability, Radio-Frequency-Cable. Biskeborn.........928–9
Power Rectifiers for A-C Aircraft Systems, Selenium. Embry.........596–600
Power Selsyns, Damping and Synchronizing Torques of. Concordia, Kron.........366–71; disc. 490
Power Supply for A-C Arc Welding. Welch, Wyer.........116–20; disc. 435
Power Supply for Generating Stations, Auxiliary-. McCallum.........693–5; disc. 976
Power Supply Systems of Steel-Mill Load Swings, Automatic Regulation of Turbine Generators to Relieve. Eberhardt, Harrison, Kohn, Darling.........751–8
Power Supply, When the Welding Load Outgrows the Distribution. Clark, Stearns.....645–8; disc. 964
Power Swings With and Without Faults, Impedances Seen by Relays During. Clarke..372–84; disc. 471
Power-System Cables, Electrolysis and Corrosion of Underground. Gorman.........329–36; disc. 479
Power Systems for Auxiliary Drives in Steam-Electric Stations. McClure, Whittlesey..844–51; disc. 976
Power-Transmission Systems and Tie Lines, Cost Studies of 69- to 230-Kv Underground. Holm....852–60
Practice in Power-Plant Auxiliary Equipment and Systems, Modern. Muller....... 868–72; disc. 976
Practices for Electric Control Devices for Aircraft, Preferred. Hottenroth.........197–200; disc. 444
Precision Testing of Electric Tachometers. Princi.........504–08; disc. 946
Preferred Practices for Electric Control Devices for Aircraft. Hottenroth.........197–200; disc. 444
Principles Involved in Its Design, A New Outdoor Air Switch and the. Graybill, Ferguson..583–6; disc. 953
Produced by Resistance Welders, Line Drop. Longini.........619–23; disc. 963
Propeller Milling Machine, Application of Electric Equipment for Ship-. Morton, Rutemiller.........205–08; disc. 453
Propeller Milling Machine, Tracer-Controlled Position Regulator for. Hanna, Osbon, Hartley.........201–05; disc. 452
Propellers, Damping Effect of D-C Marine Propulsion Motors on Vibrations Produced in Drive Shafts by Large. Litman.........31–7
Propulsion Motors on Vibrations Produced in Drive Shafts by Large Propellers, Damping Effect of D-C Marine. Litman.........31–7
Protecting Case, Response Time and Lag of a Thermometer Element Mounted in a. Goodwin.........665–70; disc. 959
Protection for Rural Distribution Systems, Improved Fault. Van Ryan.........261–3
(Protection) Lightning Investigations on 33-Kv Wood-Pole Lines. Andrews, McCann..768–77; disc. 954
Protection of Modern Dry-Type Air-Cooled Transformers, Dielectric Strength and. Bellaschi, Beck.........759–63; disc. 997
Protection, Rectifier Relay for Transformer. Michelson.........252–4
(Protective Devices) A High-Capacity High-Voltage Three-Cycle Oil Circuit Breaker. Byrd, Rietz.........160–3; disc. 463
(Protective Devices) A New Outdoor Air Switch and the Principles Involved in its Design. Graybill, Ferguson.........583–6; disc. 953
(Protective Devices) Anode-Circuit-Breaker Design and Performance Criteria. Boehne, Atwood.........337–45; disc. 437
(Protective Devices) Field Tests and Performance of Heavy-Duty High-Speed 138-Kv Circuit Breakers—Oil and Air-Blast. Sporn, St. Clair. 401–10; disc. 463
(Protective Devices) Graphical Method of Calculating Fault Currents on Rural Distribution Systems. Linder.........16–19; disc. 446
(Protective Devices) Lightning Arresters for Distribution Apparatus. Beck, Forbes...719–24; disc. 970
(Protective Devices) New Solenoid Mechanism for Magne-Blast Breaker. Wyman, Keagy.........268–74; disc. 448
(Protective Devices) Nine Years' Experience With Ultrahigh-Speed Reclosing of High-Voltage Transmission Lines. Sporn, Muller.........225–8; disc. 445
(Protective Devices) Phase-Comparison Carrier-Current Relaying. McConnell, Cramer, Seeley.........825–33; disc. 973
(Protective Devices) Rectifier Fault Currents. Herskind, Kellogg.........145–50; disc. 441
(Protective Devices) The Next Step in Interrupting Capacity—5,000,000 Kva. Hill, Leeds.........317–23; disc. 463
(Protective Devices) Three-Cycle 3,500-Megavolt-Ampere Air-Blast Circuit Breaker for 138,000-Volt Service. Byrd, Beall.........229–32; disc. 463

Q

Quadrature-Axis Equivalent Circuits of the Synchronous Machine, The Direct- and. Rankin........861–8
Quality Control and Trouble Shooting of Induction-Motor Windings and Cores, Wound and Dummy-Rotor Methods of. Trickey......842–4; disc. 998
Quality Control to Resistance Welding, Application of. Hobson, Inglis, McCants.........573–5; disc. 951
Quality Electrically, Judging Mica. Coutlee..735–41
Quality, Statistical Methods in the Development of Apparatus Life. Ferrell...........700–03; disc. 998
Quality, Statistical Tools for Controlling. Manuele, Goffman.......................524–8; disc. 949

R

Radio-Frequency Cable, The S-Function Method of Measuring Attenuation of Coaxial. Stewart...........616–19; disc. 966
Radio-Frequency Cables, Report of Conference on..........911–41
Radio-Noise-Meter Calibrations, A Study of Wave Shapes for. Frick.............890–901; disc. 969
Railroads, Mercury-Arc Rectifiers for. Watkins..........84–6; disc. 419
Railway-Motor Temperatures in Service, Measurement of. Teker..........................545–50
Railway Service, Compressed-Air Circuit Breakers in A-C. Wilcox, Harker...........141–5; disc. 419
Railways Terminal, Montreal, Canada, Electrification and Signaling of the Canadian National. Gage..........41–4; disc. 417
Rapid Closing of Bus-Tie Switches, Improving Stability by. Kimbark.................61–4; disc. 456
Rating of High-Temperature Induction Motors. Alger, Jones......................300–02; disc. 458
Ratings and Stability, Radio-Frequency-Cable Power. Biskeborn..............................928–9
Reactances by Test, Inherent Errors in the Determination of Synchronous-Machine. Concordia, Maginniss....................288–94; disc. 491
Reactors, Analysis of Arc-Welding. Wheeler..........87–90; disc. 434
Reactors, Guides for Operation of Transformers, Regulators, and, (Committee Report)..797–806; disc. 957
Reclosing of High-Voltage Transmission Lines, Nine Years' Experience With Ultrahigh-Speed. Sporn, Muller.......................225–8; disc. 445
Rectangular Cross Section, Formulas for Calculating Temperature Distribution in Transformer Cores and Other Electric Apparatus of. Higgins..........190–4; disc. 493
Rectification With Inductive and Generative Loads, Voltage and Current Relations for Controlled. Puchlowski.................255–60; disc. 442
Rectifier Circuits—Artificial Arc-Back Tests, Arc-Backs in. Evans, Maslin.............303–11; disc. 439
Rectifier Circuits, Transient Response of Controlled. Chin, Walter..........................208–14
Rectifier Fault Currents. Herskind, Kellogg..........145–50; disc. 441
Rectifier Relay for Transformer Protection. Michelson..................................252–4
Rectifiers for A-C Aircraft Systems, Selenium Power. Embry...............................596–600
Rectifiers for Railroads, Mercury-Arc. Watkins..........84–6; disc. 419
Rectifiers for Three-Wire Service, Design of Sealed Ignitron. Morack..........................103–07
(Regulation) Control of Load, Frequency, and Time of Interconnected Systems. Duff...778–86; disc. 999
(Regulation) Instability in D-C Aircraft Systems. Bunce, Cunningham, Davidson............786–91
Regulation of Turbine Generators to Relieve Power-Supply Systems of Steel-Mill Load Swings, Automatic. Eberhardt, Harrison, Kohn, Darling.........751–8
Regulator for Propeller Milling Machine, Tracer-Controlled Position. Hanna, Osbon, Hartley..........201–05; disc. 452
Regulator for Rototrol Exciter, Static Voltage. Harder, Valentine..............................601–06
Regulators, and Reactors, Guides for Operation of Transformers. (Committee Report)..797–806; disc. 957
Regulators, Resonant-Circuit Constant-Current. Kevern........................807–10; disc. 992
Relations Between Short Cylindrical Conductors, Resistance and Capacitance. ReQua..........724–30; disc. 962
Relations for Controlled Rectification With Inductive and Generative Loads, Voltage and Current. Puchlowski...................255–60; disc. 442
Relationships of Electric-Service-Load Characteristics, Coincidence-Factor. Bary...................623–9
Relay for Transformer Protection, Rectifier. Michelson..................................252–4
Relaying, Phase-Comparison Carrier-Current. McConnell, Cramer, Seeley.............825–33; disc. 973
Relays During Power Swings With and Without Faults, Impedances Seen by. Clarke....372–84; disc. 471
Release Interval Controls, An Interval and Dwell Tester for Bomb-. Long.........................648–51
Report of Conference on Radio-Frequency Cables..........911–41
Report of the Board of Directors.............1001–16
Requirements for Aircraft Alternator Drives, Governor. Boice, Levoy.................534–40; disc. 947
Resin-Treated Wood and Laminated Hydrolyzed-Wood and Paper-Base Plastics, The Electrical Resistivity of. Weatherwax, Stamm.................833–8
Resins to Insulation for Electric Machinery, The Application of Silicone. DeKiep, Hill, Moses..........94–8; disc. 460
Resistance and Capacitance Relations Between Short Cylindrical Conductors. ReQua..........724–30; disc. 962
Resistance and Dielectric-Absorption Characteristics of Large A-C Stator Windings, Insulation. Askey, Johnson.......................347–51; disc. 458
Resistance at High Voltage, A Portable Instrument for Measuring Insulation. Atkinson, Taylor..........164–7; disc. 428
Resistance-Coupled Amplifier, The. Cowles....359–65
Resistance of Multilayer Coils, Eddy-Current. Long..........712–18
Resistance-Type Thermometer, Heat-Flow Effects in a. Millar................................678–85
Resistance Welders, Line Drop Produced by. Longini..........619–23; disc. 963
Resistance Welding, Application of Quality Control to. Hobson, Inglis, McCants.........573–5; disc. 951
Resistivity of Resin-Treated Wood and Laminated Hydrolyzed-Wood and Paper-Base Plastics, The Electrical. Weatherwax, Stamm...........833–8
Resistors, Industrial Control: Heating of Shunt-Motor Starting. Leland, Rader........695–9; disc. 961
Resonant-Circuit Constant-Current Regulators. Kevern..........807–10; disc. 992
Response of Controlled Rectifier Circuits, Transient. Chin, Walter..........................208–14
Response Time and Lag of a Thermometer Element Mounted in a Protecting Case. Goodwin..........665–70; disc. 959
Rewinding Commutator-Type Traction Armatures. Greene, Stafford, Gentilini......563–9; disc. 943
Rise of Aircraft Transformers, Effect of Altitude on Temperature. Montsinger.....................251–2
Role of Frequency in Industrial Dielectric Heating, The. Scott................................558–62
Rotors, Basic Concepts of Moving-Magnet-Instrument. Mendelsohn..................529–34; disc. 947
Rototrol Exciter, Static Voltage Regulator for. Harder, Valentine..............................601–06
Rubber Cables, Corona-Initiation Measurements on Polyethylene and. Depackh..............939–40
Rural Distribution Systems, Graphical Method of Calculating Fault Currents on. Linder..........16–19; disc. 446
Rural Distribution Systems, Improved Fault Protection for. Van Ryan.........................261–3

S

S-Function Method of Measuring Attenuation of Coaxial Radio-Frequency Cable. Stewart..........616–19, 938–9; disc. 966
Sag and Tension Calculations for Cable and Wire Spans Using Catenary Formulas. Nash, Nash..........685–92; disc. 984
Sealed Ignitron Rectifiers for Three-Wire Service, Design of. Morack.......................103–07
Selenium Power Rectifiers for A-C Aircraft Systems. Embry..............................596–600
Self-Inductance of a Toroidal Coil Without Iron, The. Dwight.......................805–06; disc. 999
Self-Propelled Vehicles, Grounding of Circuits on. Ewing........................48–50; disc. 417
Selsyn Design and Application. Johnson..........703–08; disc. 960
Selsyn System, Analysis and Design of a D-C. Manildi..........512–16; disc. 946
Selsyns, Damping and Synchronizing Torques of Power. Concordia, Kron.......366–71; disc. 490
Service, Design of Sealed Ignitron Rectifiers for Three-Wire. Morack..........................103–07
Service-Load Characteristics, Coincidence-Factor Relationships of Electric-. Bary...............623–9
Service, Measurement of Railway-Motor Temperatures in. Teker..............................545–50
Sheath Currents and Their Effect on Lead-Cable-Sheath Corrosion, Study of A-C. Sherer, Granbois..........264–8; disc. 483
Shielding Characteristics of Radio-Frequency Cables. Fluharty..............................929–30
Ship-Propeller Milling Machine, Application of Electric Equipment for. Morton, Rutemiller..........205–08; disc. 453
Short Circuits and Synchronizing, Transient Electrical Torques of Turbine Generators During. Kirschbaum.....................65–70; disc. 492
Short Cylindrical Conductors, Resistance and Capacitance Relations Between. ReQua. 724–30; disc. 962
Shunt-Motor Starting Resistors, Industrial Control: Heating of. Leland, Rader......695–9; disc. 961
Signaling of the Canadian National Railways Terminal, Montreal, Canada, Electrification and. Gage..........41–4; disc. 417
Silicon Compounds for Insulating Electric Machines, Organo-. Kauppi, Moses.........90–3; disc. 457
Silicone Resins to Insulation for Electric Machinery, The Application of. DeKiep, Hill, Moses..........94–8; disc. 460
Simulated-High-Altitude Testing of Aircraft Ignition Cables and Connectors. Race, Ross.........20–6
Single-Phase Induction Motor, Symmetrical Components as Applied to the. Suhr.........651–6; disc. 958
Single-Phase Motor, A Generalized Circle Diagram for a Four-Terminal Network and Its Application to the Capacitor. Tarboux............881–9; disc. 943
Single-Side-Band Systems for Power-Line Carrier Transmission, A Comparison of the Amplitude-Modulation, Frequency-Modulation and. Cheek..........215–20; disc. 450
Soil Waters, Galvanic Corrosiveness of.. Phelps, Kahn..........156–9; disc. 482
Solenoid Mechanism for Magne-Blast Breaker, New. Wyman, Keagy...............268–74; disc. 448
Spans Using Catenary Formulas, Sag and Tension Calculations for Cable and Wire. Nash, Nash..........685–92; disc. 984
Specifications, Types of Radio-Frequency Cables and. Sheldon..................................930–2
Speed-Control System for an Aircraft Cabin-Supercharger Drive. Godsey, Miner, Walley.....37–40
Speed-Controlled Electric Gun Turrets for Aircraft, The Amplidyne Generator Applied to. Zahorsky..........221–5; disc. 436
Speed Reclosing of High-Voltage Transmission Lines, Nine Years' Experience With Ultrahigh-. Sporn, Muller.........................225–8; disc. 445
Stability by Rapid Closing of Bus-Tie Switches, Improving. Kimbark..................61–4; disc. 456
Stability, Radio-Frequency-Cable Power Ratings and Biskeborn..................................928–9
Standards and Insulation Characteristics of Oil-Insulated Transformers. Vogel......167–71; disc. 431
Starting of Generator and Motor, Synchronous. Concordia, Crary, Kilbourne, Weygandt..........629–34; disc. 956
Starting Resistors, Industrial Control: Heating of Shunt-Motor. Leland, Rader....695–9; disc. 961
Static Voltage Regulator for Rototrol Exciter. Harder, Valentine..................................601–06
Stations, Auxiliary-Power Supply for Generating. McCallum.....................693–5; disc. 976
Stations, Power Systems for Auxiliary Drives in Steam-Electric. McClure, Whittlesey..844–51; disc. 976
(Statistical Methods) Application of Quality Control to Resistance Welding. Hobson, Inglis, McCants..........573–5; disc. 951
Statistical Methods Applied to Insulator Development and Manufacture. Taylor.......495–9; disc. 952
Statistical Methods in the Development of Apparatus Life Quality. Ferrell...........700–03; disc. 998
Statistical Tools for Controlling Quality. Manuele, Goffman.......................524–8; disc. 949
Statistics as an Aid to Engineering Judgment in the Manufacture of Lightning-Arrester Blocks. Goffman........................607–10; disc. 966
Stator Windings, Insulation Resistance and Dielectric-Absorption Characteristics of Large A-C. Askey, Johnson.......................347–51; disc. 458
Steam-Electric Generating-Station Auxiliaries, Electric Drives for. Brownlee, Elzi.......741–5; disc. 976
Steam-Electric Stations, Power Systems for Auxiliary Drives in. McClure, Whittlesey..844–51; disc. 976
Steel-Mill Load Swings, Automatic Regulation of Turbine Generators to RelievePower-Supply Systems of. Eberhardt, Harrison, Kohn, Darling........751–8
Steel Plant, Electric Power in a. Graham..........816–18; disc. 994
Stray-Load Loss in Induction Motors, Measurement of. Ware.........................194–7; disc. 433
Strength and Life of Impregnated-Paper Insulation, The Dielectric. Part IV. Whitehead, Kopper..........171–7; disc. 477, 942
Stresses in Impregnated-Paper Insulation, Oil. Whitehead.........................555–7; disc. 955
Strip, Induction Heating of Moving Magnetic. Baker..........184–9
Structural Rubber, Vibration Insulation and. Connon.....................................324–9
Study of A-C Sheath Currents and Their Effect on Lead-Cable-Sheath Corrosion. Sherer, Granbois..........264–8; disc. 483
Study of Wave Shapes for Radio-Noise-Meter Calibrations, A. Frick...............890–901; disc. 969
Subtransient Impedances of Synchronous Machines, Measurement of the. Tracy, Tice..70–6; disc. 429
Subway, Supervisory Control for New Chicago. Derr, Buck, Stoos...................10–16; disc. 457
Supercharger Drive, Speed-Control System for an Aircraft Cabin-. Godsey, Miner, Walley......37–40
Superposed Direct Current, Optimum Air Gap for Various Magnetic Materials in Cores of Coils Subject to. Legg.........................709–12; disc. 969

Supervisory Control for New Chicago Subway. Derr, Buck, Stoos....................10–16; disc. 457
Supervisory Control With Other Functions of Power-Line Carrier Channels, The Combination of. Cheek, Derr............................241–6
Supply for A-C Arc Welding, Power. Welch, Wyer..116–20; disc. 435
Supply for Generating Stations, Auxiliary-Power. McCallum....................693–5; disc. 976
Supply, When the Welding Load Outgrows the Distribution Power. Clark, Stearns...645–8; disc. 964
Surge-Comparison Testing, Winding-Fault Detection and Location by. Moses, Harter..499–503; disc. 945
Switch and the Principles Involved in Its Design, A New Outdoor Air. Graybill, Ferguson..583–6; disc. 953
Switches, Improving Stability by Rapid Closing of Bus-Tie. Kimbark..................61–4; disc. 456
Symmetrical Components as Applied to the Single-Phase Induction Motor. Suhr.........651–6; disc. 958
Synchronizing Torques of Power Selsyns, Damping and. Concordia, Kron...............366–71; disc. 490
Sychronizing, Transient Electrical Torques of Turbine Generators During Short Circuits and. Kirschbaum..........................65–70; disc. 492
Synchronous-Machine Reactances by Test, Inherent Errors in the Determination of. Concordia, Maginniss..........................288–94; disc. 491
Synchronous Machine, The Direct- and Quadrature-Axis Equivalent Circuits of the. Rankin...861–8
Synchronous Machines, Measurement of the Subtransient Impedances of. Tracy, Tice..70–6; disc. 429
Synchronous Machines, Per-Unit Impedances of. Rankin.
  Part I..................................569–73
  Part II..................................839–41
Synchronous Starting of Generator and Motor. Concordia, Crary, Kilbourne, Weygandt..629–34; disc. 956
Systems, Control of Load, Frequency, and Time of Interconnected. Duff..........778–86; disc. 999
Systems, Improved Fault Protection for Rural Distribution. Van Ryan......................261–3

T

Tachometer—Accelerometer—Vibrometer for Instrument-Gyroscope Testing, A. Laurenson, Long..593–6; disc. 990
Tachometers, Precision Testing of Electric. Princi..504–08; disc. 946
Tapered-Thickness Bimetal. Elmer...661–5; disc. 962
Tapered Transmission Line, The. Milnor.......345–6
Telemetering, A Modulated-Frequency System of. Renfro, Peterson..........................45–7
Temperature Control for Aircraft, Automatic. Gund..730–4
Temperature Distribution in Transformer Cores and Other Electric Apparatus of Rectangular Cross Section, Formulas for Calculating. Higgins..................................190–4; disc. 493
Temperature Induction Motors, Rating of High-. Alger, Jones..................300–02; disc. 458
Temperature Rise of Aircraft Transformers, Effect of Altitude on. Montsinger.................251–2
Temperatures in Fractional-Horsepower Motors, Investigation of Hot-Spot. Hirsch, Munier, Schmidt, Wightman, Himebrook, Lloyd, Coffman, Potter.....................................128–36; disc. 421
Temperatures in Integral-Horsepower Motors, Investigation of Hot-Spot. Hildebrand, Cain, Phillips, Hough, Rosswog, Potter.........124–8; disc. 421
Temperatures in Service, Measurement of Railway-Motor. Teker..........................545–50
Tension Calculations for Cable and Wire Spans Using Catenary Formulas, Sag and. Nash, Nash..685–92; disc. 984
Tester for Bomb-Release Interval Controls, An Interval and Dwell. Long......................648–51
Testing, A Tachometer—Accelerometer—Vibrometer for Instrument Gyroscope. Laurenson, Long..593–6; disc. 960
Testing of Aircraft Ignition Cables and Connectors, Simulated-High-Altitude. Race, Ross.......20–6
Testing of Electric Tachometers, Precision. Princi..504–08; disc. 946
Testing of Radio-Frequency Cables at the Naval Research Laboratory, Methods of Electrical and Mechanical. Miller..........................934–5
Testing, Winding-Fault Detection and Location by Surge-Comparison. Moses, Harter..499–503; disc. 945
Tests and Performance of Heavy-Duty High-Speed 138-Kv Circuit Breakers—Oil and Air-Blast, Field. Sporn, St. Clair.................401–10; disc. 463
Tests, Arc-Backs in Rectifier Circuits—Artificial Arc-Back. Evans, Maslin..........303–11; disc. 439
Tests in Drying Out Large Generators, Use of Dielectric-Absorption. Marcroft.......56–60; disc. 415
Tests Over a Range of Frequencies, Electrical. Fleming..935–7
Thermometer Element Mounted in a Protecting Case, Response Time and Lag of a. Goodwin..665–70; disc. 959
Thermometer, Heat-Flow Effects in a Resistance-Type. Millar..............................678–85
Thickness Bimetal, Tapered-. Elmer...661–5; disc. 962
Three-Cycle Oil Circuit Breaker, A High-Capacity High-Voltage. Byrd, Rietz......160–3; disc. 463
Three-Cycle 3,500-Megavolt-Ampere Air-Blast Circuit Breaker for 138,000-Volt Service, A. Byrd, Beall..229–32; disc. 463
Three-Pole 400-Cycle Electrically Operated Aircraft Circuit Breaker, A 208Y/120-Volt 1.20-Ampere. Titus, Reifschneider......................551–5
Three-Wire Service, Design of Sealed Ignitron Rectifiers for. Morack......................103–07
Tie Lines, Cost Studies of 69- to 230-Kv Underground Power-Transmission Systems and. Holm..852–60
Time and Lag of a Thermometer Element Mounted in a Protecting Case, Response. Goodwin..665–70; disc. 959
Time of Interconnected Systems, Control of Load, Frequency, and. Duff............778–86; disc. 999
Timer for Arc Duration, An Interval. Quill...237–40
Tools for Controlling Quality, Statistical. Manuele, Goffman......................524–8; disc. 949
Toroidal Coil Without Iron, The Self-Inductance of a. Dwight......................805–06; disc. 999
Torques in Turbine Generators by Means of the Electrical-Mechanical Analogy, Determination of Transient Shaft. McCann, Warren, Criner..51–6; disc. 492
Torques of Power Selsyns, Damping and Synchronizing. Concordia, Kron...............366–71; disc. 490
Torques of Turbine Generators During Short Circuits and Synchronizing, Transient Electrical. Kirschbaum..........................65–70; disc. 492
Tracer-Controlled Position Regulator for Propeller Milling Machine. Hanna, Osbon, Hartley..201–05; disc. 452
Traction Armatures, Rewinding Commutator-Type. Greene, Stafford, Gentilini.......563–9; disc. 943
Traction Motors, Dynamic Braking With. Riley, Woods......................................517–19
Transformer Cores and Other Electric Apparatus of Rectangular Cross Section, Formulas for Calculating Temperature Distribution in. Higgins..190–4; disc. 493
Transformer Design Method, Biased-Core-Current-. Specht......................................635–40
Transformer for Metering, Orthomagnetic Bushing Current. Boyajian, Camilli.........137–40; disc. 427
Transformer Protection, Rectifier Relay for. Michelson......................................252–4
Transformers, Dielectric Strength and Protection of Modern Dry-Type Air-Cooled. Bellaschi, Beck..759–63; disc. 997
Transformers, Effect of Altitude on Temperature Rise of Aircraft. Montsinger.......................251–2
Transformers, Impulse-Failure-Detection Methods as Applied to Distribution. Stewart, Holcomb..640–44; disc. 956
Transformers, Regulators, and Reactors, Guides for Operation of. (Committee Report)..797–806; disc. 957
Transformers, Standards and Insulation Characteristics of Oil-Insulated. Vogel........167–71; disc. 431
Transient Electrical Torques of Turbine Generators During Short Circuits and Synchronizing. Kirschbaum..........................65–70; disc. 492
Transient Response of Controlled Rectifier Circuits. Chin, Walter..........................208–14
Transient Shaft Torques in Turbine Generators by Means of the Electrical-Mechanical Analogy, Determination of. McCann, Warren, Criner..51–6; disc. 492
(Transmission) Galvanic Corrosiveness of Soil Waters. Phelps, Kahn..................156–9; disc. 482
(Transmission) Impedances Seen by Relays During Power Swings With and Without Faults. Clarke..372–84; disc. 471
(Transmission) Improving Stability by Rapid Closing of Bus-Tie Switches. Kimbark.....61–4; disc. 456
(Transmission) Lightning Investigation of 132-Kv System of American Gas and Electric Company. Gross, Lippert......................76–84; disc. 474
(Transmission) Lightning Investigations on 33-Kv Wood-Pole Lines. Andrews, McCann..768–77; disc. 954
Transmission-Line Diagrams, New. Schwager, Wang..610–15; disc. 955
Transmission Line, The Tapered. Milnor.......345–6
Transmission Lines, Lightning Investigation on. Part VIII. Lewis, Foust............107–15; disc. 472
Transmission Lines, Nine Years' Experience With Ultra-high-Speed Reclosing of High-Voltage. Sporn, Muller......................225–8; disc. 445
Transmission Lines, The Frequency of Occurrence and the Distribution of Lightning Flashes to. Golde..902–10; disc. 982
(Transmission) Power-Line Carrier Channels. Brown..246–51
Transmission Systems and Tie Lines, Cost Studies of 69- to 230-Kv Underground Power-. Holm.852–60
Transmission Systems, Power Geometry of General. Altar..........................312–17; disc. 493
(Transmission) The Combination of Supervisory Control With Other Functions on Power-Line Carrier Channels. Cheek, Derr..................241–6
(Transportation, Air) A Current-Limiting Fuse for Aircraft Applications. Powell...................541–5
(Transportation, Air) A 400-Cycle Aircraft Motor. Schwandt......................508–12; disc. 948
(Transportation, Air) A 208Y/120-Volt 120-Ampere Three-Pole 400-Cycle Electrically Operated Aircraft Circuit Breaker. Titus, Reifschneider......551–5
(Transportation, Air) Aircraft Illumination. Davies..26–30
(Transportation, Air) An Interval and Dwell Tester for Bomb-Release Interval Controls. Long....648–51
(Transportation, Air) Automatic Temperature Control for Aircraft. Gund......................730–4
(Transportation, Air) Constant-Speed Drives for Aircraft Alternators. Breitwieser.....763–8; disc. 991
(Transportation, Air) Effect of Altitude on Temperature Rise of Aircraft Transformers. Montsinger..251–2
(Transportation, Air) Electrolytic Corrosion—Methods of Evaluating Insulating Materials Used in Tropical Service. Thompson, Mathes.....295–9; disc. 443
(Transportation, Air) 400-Cycle Inverters for Military Aircraft. Hayes, Ray......................233–7
(Transportation, Air) Governor Requirements for Aircraft Alternator Drives. Boice, Levoy..534–40; disc. 947
(Transportation, Air) Instability in D-C Aircraft Systems. Bune, Cunningham, Davidson.....786–91
(Transportation, Air) Parallel Operation of Main-Engine-Driven 400-Cycle Aircraft Generators. Levoy..811–16; disc. 987
(Transportation, Air) Preferred Practices for Electric Control Devices for Aircraft. Hottenroth..197–200; disc. 444
(Transportation, Air) Resonant-Circuit Constant-Current Regulators. Kevern.......807–10; disc. 992
(Transportation, Air) Selenium Power Rectifiers for A-C Aircraft Systems. Embry...............596–600
(Transportation, Air) Simulated-High-Altitude Testing of Aircraft Ignition Cables and Connectors. Race, Ross..20–6
(Transportation, Air) Speed-Control System for an Aircraft Cabin-Supercharger Drive. Godsey, Miner, Walley..37–40
(Transportation, Air) The Amplidyne Generator Applied to Speed-Controlled Electric Gun Turrets for Aircraft. Zahorsky.............221–5; disc. 436
(Transportation, Air) The Electrical Resistivity of Resin-Treated Wood and Laminated Hydrolyzed-Wood and Paper-Base Plastics. Weatherwax, Stamm..833–8
(Transportation, Air) Treatment of High-Altitude Brushes by Application of Metallic Halides. Elsey..576–9
(Transportation, Air) Vibration Insulation and Structural Rubber. Connon......................324–9
(Transportation, Land) Compressed-Air Circuit Breakers in A-C Railway Service. Wilcox, Harker..141–5; disc. 419
(Transportation, Land) Dynamic Braking With Traction Motors. Riley, Woods......................517–19
(Transportation, Land) Electrification and Signaling of the Canadian National Railways Terminal, Montreal, Canada. Gage............41–4; disc. 417
(Transportation, Land) Grounding of Circuits on Self-Propelled Vehicles. Ewing.......48–50; disc. 417
(Transportation, Land) Measurement of Railway-Motor Temperatures in Service. Teker..........545–50
(Transportation, Land) Mercury-Arc Rectifiers for Railroads. Watkins..................84–6; disc. 419
(Transportation, Land) Rewinding Commutator-Type Traction Armatures. Greene, Stafford, Gentilini..563–9; disc. 943
(Transportation, Marine) Damping Effect of D-C Marine Propulsion Motors on Vibrations Produced in Drive Shafts by Large Propellers. Litman.........31–7
Treatment of High-Altitude Brushes by Application of Metallic Halides. Elsey......................576–9
Tropical Service, Electrolytic Corrosion—Methods of Evaluating Insulating Materials Used in. Thompson, Mathes......................295–9; disc. 443
Trouble Shooting of Induction-Motor Windings and Cores, Wound and Dummy-Rotor Methods of Quality Control and. Trickey...842–4; disc. 998
Turbine Generators, Automatic Load Control for. Crever, Jackson..........................656–60
Turbine Generators by Means of the Electrical-Mechanical Analogy, Determination of Transient Shaft Torques in. McCann, Warren, Criner..51–6; disc. 492
Turbine Generators During Short Circuits and Synchronizing, Transient Electrical Torques of. Kirschbaum..................65–70; disc. 492
Turbine Generators to Relieve Power-Supply Systems of Steel-Mill Load Swings, Automatic Regulation of. Eberhardt, Harrison, Kohn, Darling....751–8

Turrets for Aircraft, The Amplidyne Generator Applied to Speed-Controlled Electric Gun. Zahorsky........221–5; disc. 436
Twin-Conductor Cable, Design Considerations of High-Frequency. Greenfield........932–3
208Y/120-Volt 120-Ampere Three-Pole 400-Cycle Electrically Operated Aircraft Circuit Breaker, A. Titus, Reifschneider........551–5
Two-Phase Co-ordinates of a Four-Phase Network. Kimbark........7–9
Types of Radio-Frequency Cables and Specifications. Sheldon........930–2

U

Ultrahigh-Speed Reclosing of High-Voltage Transmission Lines, Nine Years' Experience With. Sporn, Muller........225–8; disc. 445
Unbalanced-Voltage Control, Variable-. Wickerham........98–102; disc. 449
Underground Power-System Cables, Electrolysis and Corrosion of. Gorman........329–36; disc. 479
Underground Power-Transmission Systems and Tie Lines, Cost Studies of 69- to 230-Kv. Holm........852–60
United States, The Development of Radio-Frequency Cables in the. Neher........911–12
Use of Dielectric-Absorption Tests in Drying Out Large Generators. Marcroft........56–60; disc. 415

V

Variable Electric-Circuit Element, Ferroinductance as a. Ryder........671–8; disc. 962
Variable-Unbalanced-Voltage Control. Wickerham........98–102; disc. 449
Varnishes, Control of Electrical-Insulating. Gibson, Braithwaite........520–4
Vehicles, Grounding of Circuits on Self-Propelled. Ewing........48–50; disc. 417
Vibration Insulation and Structural Rubber. Connon........324–9
Vibrations Produced in Drive Shafts by Large Propellers, Damping Effect of D-C Marine Propulsion Motors on. Litman........31–7
Vibrometer for Instrument-Gyroscope Testing, A Tachometer—Accelerometer—. Laurenson, Long........593–6; disc. 960
Voltage and Current Relations for Controlled Rectification With Inductive and Generative Loads. Puchlowski........255–60; disc. 442
Voltage Control, Variable-Unbalanced-. Wickerham........98–102;-disc. 449
Voltage Regulator for Rototrol Exciter, Static. Harder, Valentine........601–06
Voltmeter, A Corona. Widmer........940–1

W

War Plant, Modern Electric-Power-Distribution Ideas, as Applied in a Large. Kaufmann, Kieb........279–87; disc. 488
Waters, Galvanic Corrosiveness of Soil. Phelps, Kahn........156–9; disc. 482
Wave Shapes for Radio-Noise-Meter Calibrations, A Study of. Frick........890–901; disc. 969
Welders, Line Drop Produced by Resistance. Longini........619–23; disc. 963
Welding, Application of Quality Control to Resistance. Hobson, Inglis, McCants........573–5; disc. 951
Welding Load Outgrows the Distribution Power Supply, When the. Clark, Stearns........645–8; disc. 964
Welding, Power Supply for A-C Arc. Welch, Wyer........116–20; disc. 435
Welding Reactors, Analysis of Arc-. Wheeler........87–90; disc. 434
Welding, The Power-Distribution Problem in Arc. Pierce, Smith........178–84; disc. 435
Winding-Fault Detection and Location by Surge-Comparison Testing. Moses, Harter........499–503; disc. 945
Windings and Cores, Wound and Dummy-Rotor Methods of Quality Control and Trouble Shooting of Induction-Motor. Trickey........842–4; disc. 998
Windings, Insulation Resistance and Dielectric-Absorption Characteristics of Large A-C Stator. Askey, Johnson........347–51; disc. 458
Wire Spans Using Catenary Formulas, Sag and Tension Calculations for Cable and. Nash, Nash........685–92; disc. 984
Wood and Laminated Hydrolyzed-Wood and Paper-Base Plastics, The Electrical Resistivity of Resin-Treated. Weatherwax, Stamm........833–8
Wood-Pole Lines, Lightning Investigations on 33-Kv. Andrews, McCann........768–77; disc. 954
Wound and Dummy-Rotor Methods of Quality Control Trouble Shooting of Induction-Motor Windings and Cores. Trickey........842–4; disc. 998

2. Authors

Adams, Patrick Henry. Disc........978
Adler, H. A. Disc........952
Alger, P. L.; H. A. Jones. Rating of High-Temperature Induction Motors........300–02; disc. 458
Altar, William. Power Geometry of General Transmission Systems........312–17
Anderson, Ernest H. B. Disc........455
Andrews, F. E.; R. O. Askey. Disc........447
Andrews, F. E.; G. D. McCann. Lightning Investigations on 33-Kv Wood-Pole Lines..768–77; disc. 954
Appleman, W. R. Disc........996
Archibald, C. G. Disc........994
Askey, J. S.; J. S. Johnson. Insulation Resistance and Dielectric-Absorption Characteristics of Large A-C Stator Windings........347–51; disc. 460
Askey, J. S.; J. S. Johnson. Disc........429
Askey, R. O.; F. E. Andrews. Disc........447
Atkinson, F. W.; R. B. Taylor. A Portable Instrument for Measuring Insulation Resistance at High Voltage........164–7; disc. 429
Atwood, W. A.; E. W. Boehne. Anode-Circuit-Breaker Design and Performance Criteria........337–45; disc. 438
Austen, A. E. W. Disc........942

B

Bailey, E. L. Dodge Chicago Plant's Electric-Power-Distribution Scheme With Airplane-Engine-Testing Power Recovery........121–3; disc. 485
Baker, B. F. Disc........464
Baker, R. M. Induction Heating of Moving Magnetic Strip........184–9
Baker, V. B. Disc........442
Barlow, E. P. Disc........444, 987
Bary, Constantine. Coincidence-Factor Relationships of Electric-Service-Load Characteristics.....623–9
Beall, Ben S.; H. L. Byrd. A Three-Cycle 3,500-Megavolt-Ampere Air-Blast Circuit Breaker for 138,000-Volt Service........229–32; disc. 469
Beall, Marsh F. Disc........985
Beattie, C. S.; S. C. Killian. Disc........953
Beck, Edward; P. L. Bellaschi. Dielectric Strength and Protection of Modern Dry-Type Air-Cooled Transformers........759–63; disc. 997
Beck, Edward; A. D. Forbes. Lightning Arresters for Distribution Apparatus........719–24; disc. 972
Beeuwkes, R. Disc........944
Bellaschi, P. L.; Edward Beck. Dielectric Strength and Protection of Modern Dry-Type Air-Cooled Transformers........759–63; disc. 998
Bennett, J. W.; F. R. Longley. Disc........970
Benson, I. C. Disc........956
Berberich, L. J. Disc........428, 457, 459, 995
Bisbee, R. F. Disc........950
Biskeborn, M. C. Radio-Frequency-Cable Power Ratings and Stability........928–9
Bliss, Philip. Disc........995
Bloomquist, W. C.; W. K. Boice. Application of Capacitors for Power-Factor Improvement of Induction Motors........274–8
Boehne, E. W.; W. A. Atwood. Anode-Circuit-Breaker Design and Performance Criteria........337–45; disc. 438
Boehne, E. W.; W. F. Skeats. Disc........419
Boice, W. K.; W. C. Bloomquist. Application of Capacitors for Power-Factor Improvement of Induction Motors........274–8
Boice, W. K.; L. G. Levoy, Jr. Governor Requirements for Aircraft Alternator Drives........534–40; disc. 948
Bower, J. L. Fundamentals of the Amplidyne Generator........873–81
Boyajian, A.; G. Camilli. Orthomagnetic Bushing Current Transformer for Metering...137–40; disc. 428
Brainerd, F. K. Disc........429
Braithwaite, C. H.; D. L. Gibson. Control of Electrical-Insulating Varnishes........520–4
Braithwaite, C. H., Jr.; G. L. Moses. Chemical Contamination as Causes of Electrical-Insulation Failure........580–3; disc. 945
Braley, H. D.; J. G. Noest, R. L. Webb. Disc.....979
Braun, H. B. Disc........948
Breitwieser, C. J. Constant-Speed Drives for Aircraft Alternators........763–8; disc. 992
Bretch, Edward. Disc........943, 958
Brown, C. Bradner. Disc........950
Brown, H. D. Disc........420
Brown, M. J. Power-Line Carrier Channels....246–51
Brownlee, Wm. R.; J. A. Elzi. Electric Drives for Steam-Electric Generating-Station Auxiliaries........741–5; disc. 981
Brumbaugh, Martin A. Disc........950, 966
Buck, C. J.; W. A. Derr, J. A. Stoos. Supervisory Control for New Chicago Subway........10–16
Bullard, W. R. Disc........412
Bunce, H. B. Disc........947
Bunce, H. B.; J. C. Cunningham. Disc........988
Bunce, H. B.; J. C. Cunningham, W. M. Davidson. Instability in D-C Aircraft Systems........786–91
Bunting, W. R. Disc........417
Burns, R. M. Disc........481, 482, 484
Byrd, H. L.; Ben S. Beall. A Three-Cycle 3,500-Megavolt-Ampere Air-Blast Circuit Breaker for 138,000-Volt Service........229–32; disc. 469
Byrd, H. L.; E. B. Rietz. A High-Capacity High-Voltage Three-Cycle Oil Circuit Breaker........160–3; disc. 470

C

Cain, B. M.; L. E. Hildebrand, F. D. Phillips, W. R. Hough, J. G. Rosswog, C. P. Potter. Investigation of Hot-Spot Temperatures in Integral-Horsepower Motors........124–8; disc. 425
Caldwell, G. A. Disc........452
Camilli, G.; A Boyajian. Orthomagnetic Bushing Current Transformer for Metering...137–40; disc. 428
Cecchetti, Felix. Disc........955
Cheek, R. C. A Comparison of the Amplitude-Modulation, Frequency-Modulation, and Single-Side-Band Systems for Power-Line Carrier Transmission........215–20; disc. 451
Cheek, R. C.; W. A. Derr. The Combination of Supervisory Control With Other Functions on Power-Line Carrier Channels........241–6
Chestnut, Harold. Disc........490
Chin, P. T.; G. E. Walter. Transient Response of Controlled Rectifier Circuits........208–14
Clark, C. N. Disc........435, 964, 965
Clark, C. N.; C. M. Stearns. When the Welding Load Outgrows the Distribution Power Supply........645–8; disc. 965
Clark, E. K. Disc........962
Clark, F. M.; M. E. Scoville. Capacitors for High-Frequency Induction-Heating Circuits........791–6; disc. 996
Clarke, Edith. Impedances Seen by Relays During Power Swings With and Without Faults....372–84
Clarke, W. J. Properties of Different Polyethylenes........919–21
Cliver, E. K. Disc........443
Coffman, O. G.; L. H. Hirsch, R. F. Munier, M. L. Schmidt, L. W. Wightman, F. S. Himebrook, T. C. Lloyd, C. P. Potter. Investigation of Hot-Spot Temperatures in Fractional-Horsepower Motors........128–36; disc. 425
(Committee Reports) See "Committee Reports" and other entries in Technical Subject Index
Conant, W. I. Disc........944
Concordia, C. Disc........962
Concordia, C.; S. B. Crary, C. E. Kilbourne, C. N. Weygandt, Jr. Synchronous Starting of Generator and Motor........629–34; disc. 956
Concordia, C.; Gabriel Kron. Damping and Synchronizing Torques of Power Selsyns........366–71; disc. 491
Concordia, C.; F. J. Maginniss. Inherent Errors in the Determination of Synchronous-Machine Reactances by Test........288–94; disc. 492
Connon, J. A. Vibration Insulation and Structural Rubber........324–9
Cooper, A. J. Disc........977
Coutlee, K. G. Judging Mica Quality Electrically........735–41
Cowles, Laurence G. The Resistance-Coupled Amplifier........359–65
Cox, J. H. Disc........420, 440
Craig, C. C. Disc........949, 967
Cramer, T. A.; A. J. McConnell, H. T. Seeley. Phase-Comparison Carrier-Current Relaying........825–33; disc. 975
Crary, S. B. Disc........445, 456, 490, 491
Crary, S. B.; C. Concordia, C. E. Kilbourne, C. N. Weygandt, Jr. Synchronous Starting of Generator and Motor........629–34; disc. 956
Crary, S. B.; R. M. Easley. Frequency Changers—Characteristics, Applications, and Economics........351–8
Crever, F. E.; R. L. Jackson. Automatic Load Control for Turbine Generators........656–60
Criner, H. E.; G. D. McCann, C. E. Warren. Determination of Transient Shaft Torques in Turbine Generators by Means of the Electrical-Mechanical Analogy........51–6
Crom, G. C. Disc........992
Cunningham, J. C. Disc........988
Cunningham, J. C.; H. B. Bunce, W. M. Davidson. Instability in D-C Aircraft Systems........786–91
Cushman, P. G.; R. W. Votaw. Disc........946

D

Darling, A. G. Disc........488
Darling, A. G.; W. W. Eberhardt, C. W. Harrison, E. J. Kohn. Automatic Regulation of Turbine Generators to Relieve Power-Supply Systems of Steel-Mill Load Swings........751–8.

Davidson, W. M.; H. B. Bunce, J. C. Cunningham. Instability in D-C Aircraft Systems..........786–91
Davies, W. W. Aircraft Illumination..........26–30
Deans, Wm. Disc..........487
DeKiep, J.; L. R. Hill, G. L. Moses. The Application of Silicone Resins to Insulation for Electric Machinery..........94–8; disc. 462
Del Mar, Wm. A. Dielectric Strength of Polyethylene..........918–19
Del Mar, Wm. A. Disc..........477, 955
Deming, W. Edwards. Disc..........967
Depackh, D. Corona-Initiation Measurements on Polyethylene and Rubber Cables..........939–40
Derr, W. A.; C. J. Buck, J. A. Stoos. Supervisory Control for New Chicago Subway..........10–16
Derr, W. A.; R. C. Cheek. The Combination of Supervisory Control With Other Functions on Power-Line Carrier Channels..........241–6
Desch, P. F.; J. G. Hutton. Disc..........989
Dickerson, P. M. Disc..........950
Dickinson, R. C. Disc..........437, 448
Dodge, H. F. Disc..........968
Drompp, A. F. Disc..........974
Duff, C. K. Control of Load, Frequency, and Time of Interconnected Systems..........778–86; disc. 1000
Dwight, H. B. The Self-Inductance of a Toroidal Coil Without Iron..........805–06; disc. 999

E

Easley, R. M.; S. B. Crary. Frequency Changers—Characteristics, Applications, and Economics..........351–8
Eberhardt, W. W.; C. W. Harrison, E. J. Kohn, A. G. Darling. Automatic Regulation of Turbine Generators to Relieve Power-Supply Systems of Steel-Mill Load Swings..........751–8
Elmer, William B. Tapered-Thickness Bimetal..........661–5; disc. 962
Else, H. D. Disc..........991
Elsey, Howard M. Treatment of High-Altitude Brushes by Application of Metallic Halides..........576–9
Elzi, J. A.; W. R. Brownlee. Electric Drives for Steam-Electric Generating-Station Auxiliaries..........741–5; disc. 981
Embry, Alvin L. Selenium Power Rectifiers for A-C Aircraft Systems..........596–600
Evans, R. D. Disc..........438
Evans, R. D.; A. J. Maslin. Arc-Backs in Rectifier Circuits—Artificial Arc-Back Tests..........303–11; disc. 441
Evans, R. D.; A. J. Maslin. Disc..........441
Ewing, D. D. Grounding of Circuits on Self-Propelled Vehicles..........48–50
Exner, D. W. Disc..........988
Eysenbach, H. A. Disc..........459

F

Faucett, M. A. Disc..........447
Ferguson, J. S. Disc..........968
Ferguson, J. S.; H. W. Graybill. A New Outdoor Air Switch and the Principles Involved in Its Design..........583–6; disc. 953
Ferrell, Enoch B. Statistical Methods in the Development of Apparatus Life Quality..........700–03
Fett, G. H. Disc..........434
Field, Robert F. Disc..........999
Fields, C. V. Disc..........995
Finlaw, John. Disc..........977
Fisher, Laurence E. Disc..........487
Fleming, C. C. Electrical Tests Over a Range of Frequencies..........935–7
Fluharty, R. G. Shielding Characteristics of Radio-Frequency Cables..........929–30
Forbes, A. D.; Edward Beck. Lightning Arresters for Distribution Apparatus..........719–24; disc. 972
Foster, L. W. Disc..........995
Foust, C. M.; N. Rohats. Disc..........945
Foust, C. M.; W. W. Lewis. Lightning Investigation on Transmission Lines—VII..........107–15; disc. 474
Frick, C. W. A Study of Wave Shapes for Radio-Noise-Meter Calibrations..........890–901; disc. 970
Fuller, John L. Disc..........458, 461

G

Gage, R. G. Electrification and Signaling of the Canadian National Railways Terminal, Montreal, Canada..........41–4
Gage, R. G. Disc..........421
Gallagher, E. I. Disc..........978
Ganzert, A. E. Disc..........944
Gay, F. W. Disc..........976
Geiger, J. M. Disc..........977
Gentilini, C.; N. J. Greene, D. E. Stafford. Rewinding Commutator-Type Traction Armatures..........563–9; disc. 944
George, E. E. Disc..........446
Gibson, D. L.; C. H. Braithwaite. Control of Electrical-Insulating Varnishes..........520–4
Gibson, Hal. Central-Station Auxiliary-Drive Motors for Constant and Adjustable Speed..........746–50
Gildner, H. H. Disc..........453
Godsey, F. W., Jr.; J. D. Miner, O. C. Walley. Speed-Control System for an Aircraft Cabin-Supercharger Drive..........37–40
Goffman, Casper. Statistics as an Aid to Engineering Judgment in the Manufacture of Lighting-Arrester Blocks..........607–10; disc. 968
Goffman, Casper. Disc..........998
Goffman, Casper; J. Manuele. Statistical Tools for Controlling Quality..........524–8; disc. 951
Golde, R. H. The Frequency of Occurrence and the Distribution of Lightning Flashes to Transmission Lines..........902–10; disc. 984
Goldsborough, S. L.; H. W. Lensner. Disc..........973
Goodwin, Harold, Jr. Disc..........412
Goodwin, W. N., Jr. Response Time and Lag of a Thermometer Element Mounted in a Protecting Case..........665–70; disc. 960
Gorman, L. J. Electrolysis and Corrosion of Underground Power-System Cables..........329–36; disc. 481
Graham, R. W. Electric Power in a Steel Plant..........816–18
Granbois, K. J.; C. M. Sherer. Study of A-C Sheath Currents and Their Effect on Lead-Cable-Sheath Corrosion..........264–8; disc. 484
Grant, Eugene L. Disc..........951
Graybill, H. W.; J. S. Ferguson. A New Outdoor Air Switch and the Principles Involved in Its Design..........583–6; disc. 953
Green, W. M.; A. F. Pelster. Disc..........989
Greene, N. J.; D. E. Stafford, C. Gentilini. Rewinding Commutator-Type Traction Armatures..........563–9; disc. 944
Greenfield, E. W. Design Considerations of High-Frequency Twin-Conductor Cable..........932–3
Gross, Eric T. B. Disc..........493
Gross, I. W.; G. D. Lippert. Lightning Investigation on 132-Kv System of American Gas and Electric Company..........76–84; disc. 476
Grosser, F. H., Jr.; R. C. Sherwood. Disc..........954
Grotzinger, J. Disc..........485
Gund, R. A. Automatic Temperature Control for Aircraft..........730–4

H

Haberl, H. W. Disc..........465
Hagenguth, J. H. Disc..........431, 472, 474, 954, 956, 982, 997
Halperin, Herman. Disc..........460, 477, 480, 482, 483
Hamilton, R. F. Disc..........411
Hamilton, W. S. H. Disc..........417
Hancock, Scott. Disc..........423
Hanna, C. R.; W. O. Osbon, R. A. Hartley. Tracer-Controlled Position Regulator for Propeller Milling Machine..........201–05; disc. 453
Hansson, E. Disc..........983
Harder, E. L.; C. E. Valentine. Static Voltage Regulator for Rototrol Exciter..........601–06
Harker, D. C.; H. M. Wilcox. Compressed-Air Circuit Breakers in A-C Railway Service..........141–5; disc. 419
Harrington, C. A. Disc..........976
Harrison, C. W.; W. W. Eberhardt, E. J. Kohn, A. G. Darling. Automatic Regulation of Turbine Generators to Relieve Power-Supply Systems of Steel-Mill Load Swings..........751–8
Harter, Earl F.; G. L. Moses. Winding-Fault Detection and Location by Surge-Comparison Testing..........499–503; disc. 945
Hartley, R. A.; C. R. Hanna, W. O. Osbon. Tracer-Controlled Position Regulator for Propeller Milling Machine..........201–05; disc. 453
Hatch, W. H. Disc..........971
Hatcher, C. T. Disc..........483
Hayes, C. P.; L. L. Ray. 400-Cycle Inverters for Military Aircraft..........233–7
Hedding, L. K. Disc..........999
Hemming, C. B. Disc..........996
Herskind, C. C. Disc..........417, 420, 439
Herskind, C. C.; H. L. Kellogg. Rectifier Fault Currents..........145–50; disc. 442
Heumann, G. F. Disc..........961
Heumann, G. W. Disc..........449
Hickernell, L. F. Disc..........486
Higgins, Thomas James. Formulas for Calculating Temperature Distribution in Transformer Cores and Other Electric Apparatus of Rectangular Cross Section..........190–4; disc. 494
Higgins, Thomas James. The Design of Bus-Bar Industrial Distribution Systems: an Epitomization of Available Data..........385–400; disc. 488
Higgins, Thomas James. Disc..........999
Hildebrand, L. E.; B. M. Cain, F. D. Phillips, W. R. Hough, J. G. Rosswog, C. P. Potter. Investigation of Hot-Spot Temperatures in Integral-Horsepower Motors..........124–8; disc. 425
Hill, A. W.; W. M. Leeds. The Next Step in Interrupting Capacity—5,000,000 Kva..........317–23; disc. 470
Hill, L. R.; J. DeKiep, G. L. Moses. The Application of Silicone Resins to Insulation for Electric Machinery..........94–8; disc. 462
Himebrook, F. S. Disc..........423
Himebrook, F. S.; L. H. Hirsch, R. F. Munier, M. L. Schmidt, L. W. Wightman, T. C. Lloyd, O. G. Coffman, C. P. Potter. Investigation of Hot-Spot Temperatures in Fractional-Horsepower Motors..........128–36; disc. 425
Hirsch, L. H.; R. F. Munier, M. L. Schmidt, L. W. Wightman, F. S. Himebrook, T. C. Lloyd, O. G. Coffman, C. P. Potter. Investigation of Hot-Spot Temperatures in Fractional-Horsepower Motors..........128–36; disc. 425
Hobbs, M. H. Disc..........463
Hobson, L. S.; R. S. Inglis, R. P. McCants. Application of Quality Control to Resistance Welding..........573–5
Hoffer, Irven S. Disc..........950
Holcomb, J. E.; H. C. Stewart. Impulse-Failure-Detection Methods as Applied to Distribution Transformers..........640–44; disc. 956
Holm, John G. Cost Studies of 69- to 230-Kv Underground Power-Transmission Systems and Tie Lines..........852–60
Holm, John G. Disc..........416, 447, 456, 463
Hotelling, Harold. Disc..........967
Hottenroth, F. W., Jr. Preferred Practices for Electric Control Devices for Aircraft..........197–200; disc. 444
Hough, W. R.; L. E. Hildebrand, B. M. Cain, F. D. Phillips, J. G. Rosswog, C. P. Potter. Investigation of Hot-Spot Temperatures in Integral-Horsepower Motors..........124–8; disc. 425
Howe, Donald W. Disc..........969
Hutchins, R. A. Disc..........943
Hutton, J. G.; P. F. Desch. Disc..........989

I

Inglis, R. S.; L. S. Hobson, R. P. McCants. Application of Quality Control to Resistance Welding..........573–5

J

Jackob, Max. Disc..........493
Jackson, J. G. Disc..........486
Johnson, J. S. Disc..........415
Johnson, J. S.; J. S. Askey. Insulation Resistance and Dielectric-Absorption Characteristics of Large A-C Stator Windings..........347–51; disc. 460
Johnson, J. S.; J. S. Askey. Disc..........429
Johnson, T. C. Selsyn Design and Application..........703–08
Jones, D. M. Disc..........466
Jones, H. A.; P. L. Alger. Rating of High-Temperature Induction Motors..........300–02; disc. 458

K

Kahn, Frank; H. S. Phelps. Galvanic Corrosiveness of Soil Waters..........156–9; disc. 483
Kalb, W. C. Maintenance of Good Brush Performance..........819–25
Kaufmann, R. H.; N. A. Kieb. Modern Electric-Power-Distribution Ideas as Applied in a Large War Plant..........279–87; disc. 489
Kauppi, T. A.; G. L. Moses. Organo-Silicon Compounds for Insulating Electric Machines..........90–3
Keagy, J. H.; B. W. Wyman. New Solenoid Mechanism for Magne-Blast Breaker..........268–74; disc. 448
Kellogg, H. L.; C. C. Herskind. Rectifier Fault Currents..........145–50; disc. 442
Kenefake, E. W. Disc..........450
Kennedy, L. F. Disc..........471
Kevern, G. M. Resonant-Circuit Constant-Current Regulators..........807–10
Kieb, N. A.; R. H. Kaufmann. Modern Electric Power-Distribution Ideas as Applied in a Large War Plant..........279–87; disc. 489
Kilbourne, C. E.; C. Concordia, S. B. Crary, C. N. Weygandt, Jr. Synchronous Starting of Generator and Motor..........629–34; disc. 956
Kilgore, L. A. Disc..........484
Kimbark, Edward W. Improving Stability by Rapid Closing of Bus-Tie Switches..........61–4; disc. 456
Kimbark, Edward W. Two-Phase Co-ordinates of a Four-Phase Network..........7–9
Kimbark, Edward W. Disc..........471
Kingsley, Charles, Jr.; W. V. Lyon. Disc..........958
Kirschbaum, H. S. Transient Electrical Torques of Turbine Generators During Short Circuits and Synchronizing..........65–70; disc. 493
Kohn, E. J.; W. W. Eberhardt, C. W. Harrison, A. G. Darling. Automatic Regulation of Turbine Generators to Relieve Power-Supply Systems of Steel-Mill Load Swings..........751–8
Komives, L. I. Disc..........479

Kopper, J. M.; J. B. Whitehead The Dielectric Strength and Life of Impregnated-Paper Insulation. Part IV..........171–7; disc. 479, 942
Kron, Gabriel; C. Concordia. Damping and Synchronizing Torques of Power Selsyns..........366–71; disc. 491

L

Lane, F. A. Disc..........957
Laurenson, R. M.; T. H. Long. A Tachometer—Accelerometer—Vibrometer for Instrument-Gyroscope Testing..........593–6; disc. 960
Leeds, W. M.; A. W. Hill. The Next Step in Interrupting Capacity—5,000,000 Kva....317–23; disc. 470
Legg, V. E. Optimum Air Gap for Various Magnetic Materials in Cores of Coils Subject to Superposed Direct Current..........709–12; disc. 969
Leland, G. F.; L. T. Rader. Industrial Control: Heating of Shunt-Motor Starting Resistors..........695–9; disc. 961
Lensner, H. W.; S. L. Goldsborough. Disc..........973
Levoy, L. G., Jr. Parallel Operation of Main-Engine-Driven 400-Cycle Aircraft Generators..........811–16; disc. 989
Levoy, L. G., Jr.; W. K. Boice. Governor Requirements for Aircraft Alternator Drives..........534–40; disc. 948
Lewis, W. S. Disc..........984
Lewis, W. W.; C. M. Foust. Lightning Investigation on Transmission Lines. Part VII. 107–15; disc. 474
Linder, F. W. Graphical Method of Calculating Fault Currents on Rural Distribution Systems..........16–19; disc. 447
Lippert, G. D.; I. W. Gross. Lightning Investigation on 132-Kv System of American Gas and Electric Company..........76–84; disc. 476
Litman, Bernard. Damping Effect of D-C Marine Propulsion Motors on Vibrations Produced in Drive Shafts by Large Propellers..........31–7
Liwschitz, M. M. Disc..........433
Lloyd, T. C.; L. H. Hirsch, R. F. Munier, M. L. Schmidt, L. W. Wightman, F. S. Himebrook, O. G. Coffman, C. P. Potter. Investigation of Hot-Spot Temperatures in Fractional-Horsepower Motors..........128–36; disc. 425
Lohman, R. W. Disc..........959
Long, T. H. An Interval and Dwell Tester for Bomb-Release Interval Controls..........648–51
Long, T. H. Eddy-Current Resistance of Multilayer Coils..........712–18
Long, T. H. Disc..........946
Long, T. H.; R. M. Laurenson. A Tachometer—Accelerometer—Vibrometer for Instrument-Gyroscope Testing..........593–6; disc. 960
Longini, R. L. Line Drop Produced by Resistance Welders..........619–23
Longini, R. L. Disc..........964
Longley, F. R.; J. W. Bennett. Disc..........970
Lukens, A. F. Disc..........460
Lusignan, J. T., Jr. Disc..........474
Lyon, W. V.; Charles Kingsley, Jr. Disc..........958

M

MacGuffie, C. I. Disc..........435
Macintyre, J. R. Disc..........947
Maginnis, F. J.; C. Concordia. Inherent Errors in the Determination of Synchronous-Machine Reactances by Test..........288–94; disc. 492
Maibauer, A. E; C. S. Myers. Polyethylene as Cable Insulation..........916–18
Manildi, Joseph. Analysis and Design of a D-C Selsyn System..........512–16; disc. 947
Manuele, Joseph; C. Goffman. Statistical Tools for Controlling Quality..........524–8; disc. 951
Marcroft, H. C. Use of Dielectric-Absorption Tests in Drying Out Large Generators.....56–60; disc. 416
Marcroft, H. C. Disc..........459
Marcy, H. Tyler. Disc..........988
Maslin, A. J.; R. D. Evans. Arc-Backs in Rectifier Circuits—Artificial Arc-Back Tests..........303–11; disc. 441
Maslin, A. J.; R. D. Evans. Disc..........441
Mathes, K. N. Disc..........457
Mathes, K. N.; B. H. Thompson. Electrolytic Corrosion—Methods of Evaluating Insulating Materials Used in Tropical Service..........295–9; disc. 444
McCallum, V. E. Auxiliary-Power Supply for Generating Stations..........693–5; disc. 982
McCann, G. D.; F. E. Andrews. Lightning Investigations on 33-Kv Wood-Pole Lines..768–77; disc. 954
McCann, G. D.; C. E. Warren, H. E. Criner. Determination of Transient Shaft Torques in Turbine Generators by Means of the Electrical-Mechanical Analogy..........51–6
McCants, R. P.; L. S. Hobson, R. S. Inglis. Application of Quality Control to Resistance Welding..........573–5
McCarty, W. R.; H. Weichsel. Disc..........992
McClure, J. R.; S. I. Whittlesey. Power Systems for Auxiliary Drives in Steam-Electric Stations..........844–51; disc. 981
McConnell, A. J. Disc..........472
McConnell, A. J.; T. A. Crámer, H. T. Seeley. Phase-Comparison Carrier-Current Relaying..........825–33; disc. 975
McCreary, H. J. Disc..........966
Mendelsohn, Lewis I. Basic Concepts of Moving-Magnet-Instrument Rotors..........529–34
Michelson, E. L. Rectifier Relay for Transformer Protection..........252–4
Michelson, E. L. Disc..........456
Mikina, Stanley J. Disc..........947
Millar, N. P. Heat-Flow Effects in a Resistance-Type Thermometer..........678–85
Miller, J. M. Methods of Electrical and Mechanical Testing of Radio-Frequency Cables at the Naval Research Laboratory..........934–5
Milnor, J. W. The Tapered Transmission Line..345–6
Miner, J D., Jr.; F. W. Godsey, O. C. Walley. Speed-Control System for an Aircraft Cabin-Supercharger Drive..........37–40
Monroe, W. P. Disc..........480
Montsinger, V. M. Effect of Altitude on Temperature Rise of Aircraft Transformers..........251–2
Montsinger, V. M. Disc..........460
Morack, M. M. Design of Sealed Ignitron Rectifiers for Three-Wire Service..........103–07
Moreton, Stuart D. Disc..........428
Morgan, Theo. H. Disc..........433
Mortara, M. Evaluation of Electric Distribution Losses in Terms of Generating-Station-Capacity Investment..........1–7; disc. 413
Morton, H. Earl; O. G. Rutemiller. Application of Electric Equipment for Ship-Propeller Milling Machine..........205–08
Moses, G. L.; C. H. Braithwaite, Jr. Chemical Contamination as Causes of Electrical-Insulation Failure..........580–3; disc. 945
Moses, G. L.; J. DeKiep, L. R. Hill. The Application of Silicone Resins to Insulation for Electric Machinery..........94–8; disc. 462
Moses, G. L.; Earl F. Harter. Winding-Fault Detection and Location by Surge-Comparison Testing..........499–503; disc. 945
Moses, G. L.; T. A. Kauppi. Organo-Silicon Compounds for Insulating Electric Machines......90–3
Muller, C. A; Philip Sporn. Nine Years' Experience With Ultrahigh-Speed Reclosing of High-Voltage Transmission Lines..........225–8; disc. 446
Muller, H. N., Jr. Disc..........445
Muller, H. N., Jr. Modern Practice in Power-Plant Auxiliary Equipment and Systems..........868–72; disc. 982
Munier, R. F. Disc..........998
Munier, R. F.; L. H. Hirsch, M. L. Schmidt, L. W. Wightman, F. S. Himebrook, T. C. Lloyd, O. G. Coffman, C. P. Potter. Investigation of Hot-Spot Temperatures in Fractional-Horsepower Motors..........128–36; disc. 425
Musselman, R. D. Disc..........436
Myers, C. S.; A. E. Maibauer. Polyethylene as Cable Insulation..........916–18

N

Nash, John F., Jr.; John F. Nash. Sag and Tension Calcuations for Cable and Wire Spans Using Catenary Formulas..........685–92; disc. 986
Nash, John F.; John F. Nash, Jr. Sag and Tension Calculations for Cable and Wire Spans Using Catenary Formulas..........685–92; disc. 986
Neher, J. H. The Development of Radio-Frequency Cables in the United States..........911–12
Noest, J. G. Disc..........461
Noest, J. G.; H. D. Braley, R. L. Webb. Disc......979
Norton, E. L. Dynamic Measurements on Electromagnetic Devices..........151–6
Nye, H. V. Disc..........465

O

Oace, R. J. Disc..........443
Odarenko, T. M. Radio-Frequency-Cable Manufacturing Methods..........922–5
Olney, F. D., Jr. Disc..........962
Osbon, W. O. Disc..........455
Osbon, W. O.; C. R. Hanna, R. A. Hartley. Tracer-Controlled Position Regulator for Propeller Milling Machine..........201–05; disc. 453
Ostman, H. F. Disc..........972

P

Parks, C. E.; J. J. Trainor. Disc..........457, 467
Pelster, A. F.; W. M. Green. Disc..........989
Perrin, L. M. Disc..........962
Peterman, L. C. Disc..........488
Peterson, Arthur Perry; H. E. Renfro. A Modulated-Frequency System of Telemetering..........45–7
Peterson, E. L. Disc..........984
Peterson, H. A.; C. A. Woodrow. Disc..........467
Peterson, William S. Disc..........979, 1000
Phelps, Howard S.; F. Kahn. Galvanic Corrosiveness of Soil Waters..........156–9, disc. 481
Phillips, F. D. Disc..........458
Phillips, F. D.; L. E. Hildebrand, B. M. Cain, W. R. Hough, J. G. Rosswog, C. P. Potter. Investigation of Hot-Spot Temperatures in Integral-Horsepower Motors..........124–8; disc. 425
Pierce, H. W.; C. E. Smith. The Power-Distribution Problem in Arc Welding..........178–84; disc 436
Potter, C. P.; L. E. Hildebrand, B. M. Cain, F. D. Phillips, W. R. Hough, J. G. Rosswog. Investigation of Hot-Spot Temperatures in Integral-Horsepower Motors..........124–8; disc. 425
Potter, C. P.; L. H. Hirsch, R. F. Munier, M. L. Schmidt, L. W. Wightman, F. S. Himebrook, T. C. Lloyd, O. G. Coffman. Investigation of Hot-Spot Temperatures in Fractional-Horsepower Motors..........128–36; disc. 425
Povery, E. H. Disc..........415
Powell, A. H. A Current-Limiting Fuse for Aircraft Applications..........541–5
Powell, A. H. Disc..........953
Prince, David C. Disc..........445
Princi, M. A. Precision Testing of Electric Tachometers..........504–08; disc. 946
Princi, M. A. Disc..........960
Puchlowski, K. P. Voltage and Current Relations for Controlled Rectification With Inductive and Generative Loads..........255–60; disc. 442

Q

Quill, J. S. An Interval Timer for Arc Duration..........237–40

R

Race, H. H.; A. M. Ross, Jr. Simulated-High-Altitude Testing of Aircraft Ignition Cables and Connectors..........20–6
Rader, L. T.; G. F. Leland. Industrial Control: Heating of Shunt-Motor Starting Resistors..........695–9; disc. 961
Ragan, G. L. Losses in Radio-Frequency-Cable Components..........927
Ramadanoff, D. Disc..........996
Ramey, B. B. Disc..........948
Rankin, A. W. Per-Unit Impedances of Synchronous Machines.
  Part I..........569–73
  Part II..........839–41
Rankin, A. W. The Direct- and Quadrature-Axis Equivalent Circuits of the Synchronous Machine..........861–8
Rankin, A. W. Disc..........431, 492
Ray, L. L.; C. P. Hayes. 400-Cycle Inverters for Military Aircraft..........233–7
Reed, G. M. Disc..........951
Reifschneider, P. J.; C. H. Titus. A 208Y/120-Volt 120-Ampere Three-Pole 400-Cycle Electrically Operated Aircraft Circuit Breaker..........551–5
Renfro, Harold E.; A. P. Peterson. A Modulated-Frequency System of Telemetering..........45–7
ReQua, F. L. Resistance and Capacitance Relations Between Short Cylindrical Conductors.....724–30
Richter, Walther. Disc..........999
Rietz, E. B.; H. L. Byrd. A High-Capacity High-Voltage Three-Cycle Oil Circuit Breaker..........160–3; disc. 470
Riley, L. G.; G. M. Woods. Dynamic Braking With Traction Motors..........517–19
Risler, C. B. Disc..........449
Rohats, N.; C. M. Foust. Disc..........945
Ross, A. M., Jr.; H. H. Race. Simulated-High-Altitude Testing of Aircraft Ignition Cables and Connectors..........20–6
Ross, M. D. Disc..........492
Rosswog, J. G.; L. E. Hildebrand, B. M. Cain, F. D. Phillips, W. R. Hough, C. P. Potter. Investigation of Hot-Spot Temperatures in Integral-Horsepower Motors..........124–8; disc. 425
Rothplex, Max W. Disc..........446
Rutemiller, Oren G.; H. E. Morton. Application of Electric Equipment for Ship-Propeller Milling Machine..........205–08
Ryan, John E. Disc..........962
Ryder, J. D. Ferroinductance as a Variable Electric-Circuit Element..........671–8; disc. 963

S

St. Clair, Harry P. Disc..........416
St. Clair, Harry P.; P. Sporn. Field Tests and Performance of Heavy-Duty High-Speed 138-Kv Circuit Breakers—Oil and Air-Blast..401–10; disc. 468
Schmidt, A., Jr. Disc..........420

Schmidt, M. L.; L. H. Hirsch, R. F. Munier, L. W. Wightman, F. S. Himebrook, T. C. Lloyd, O G. Coffman, C. P. Potter. Investigation of Hot-Spot Temperatures in Fractional-Horsepower Motors........128-36; disc. 425
Schwager, A. C. Disc........427
Schwager, A. C.; P. Y. Wang. New Transmission-Line Diagrams........610-15; disc. 955
Schwandt, G. O. A 400-Cycle Aircraft Motor........508-12; disc. 949
Scott, G. W., Jr. The Role of Frequency in Industrial Dielectric Heating........558-62
Scoville, M. E.; F. M. Clark. Capacitors for High-Frequency Induction-Heating Circuits........791-6; disc. 996
Seeley, H. T.; A. J. McConnell, T. A. Cramer. Phase-Comparison Carrier-Current Relaying........825-33; disc. 975
Shackleton, J. W. General Characteristics of Polyethylene........912-16
Sharpe, J. M. Disc........999
Sheldon, E. E. Types of Radio-Frequency Cables and Specifications........930-2
Sherer, C. M.; K. J. Granbois. Study of A-C Sheath Currents and Their Effect on Lead-Cable-Sheath Corrosion........264-8; disc. 484
Sherwood, R. C.; E. H. Groser, Jr. Disc........954
Shoemaker, R. W. Disc........487
Sholl, W. E. Disc........978
Silsbee, F. B. Disc........427
Skeats, W. F. Disc........468
Skeats, W. F.; E. W. Boehne. Disc........419
Small, Alvah. Disc........945
Smith, C. E.; H. W. Pierce. The Power-Distribution Problem Arc Welding........178-84; disc. 436
Smith, H. E. Disc........964
Specht, Theodore. Biased-Core-Current-Transformer Design Method........635-40
Sporn, Philip. Disc........467
Sporn, Philip; C. A. Muller. Nine Years' Experience With Ultrahigh-Speed Reclosing of High-Voltage Transmission Lines........225-8; disc. 446
Sporn, Philip; H. P. St. Clair. Field Tests and Performance of Heavy-Duty High-Speed 138-Kv Circuit Breakers—Oil and Air-Blast........401-10; disc. 468
Stafford, D. E ; N. J. Greene, C. Gentilini. Rewinding Commutator-Type Traction Armatures........563-9; disc. 944
Stamm, Alfred J.; R. C. Weatherwax. The Electrical Resistivity of Resin-Treated Wood and Laminated Hydrolyzed-Wood and Paper-Base Plastics..833-8
Stansel, N. R. Disc........965
Starr, E. C. Disc........972
Stearns, C. M.; C. N. Clark. When the Welding Load Outgrows the Distribution Power Supply........649-8; disc. 965
Stebbins, F. O. Disc........960
Steinberg, M. J. Disc........411
Stewart, Chandler, Jr. The S-Function Method of Measuring Attenuation of Coaxial Radio-Frequency Cable........616-19, 938-9; disc. 966
Stewart, H. C.; J. E. Holcomb. Impulse-Failure-Detection Methods as Applied to Distribution Transformers........640-44; disc. 956
Stirling, L. B. Disc........977, 1000
Stoos, J. A.; W. A. Derr, C. J. Buck. Supervisory Control for New Chicago Subway........10-16
Suhr, F. W. Symmetrical Components as Applied to the Single-Phase Induction Motor........651-6; disc. 958
Sunde, E. D. Disc........472

T

Tarboux, J. G. A Generalized Circle Diagram for a Four-Terminal Network and Its Application to the Capacitor Single-Phase Motor....881-9; disc. 943
Taylor, J. J. Statistical Methods Applied to Insulator Development and Manufacture........495-9
Taylor, Robert B.; F. W. Atkinson. A Portable Instrument for Measuring Insulation Resistance at High Voltage........164-7; disc. 429
Taylor, R. C. Disc........969
Teker, J. W. Measurement of Railway-Motor Temperatures in Service........545-50
Teker, J. W. Disc........944
Thompson, B. H.; K. N. Mathes. Electrolytic Corrosion—Methods of Evaluating Insulating Materials Used in Tropical Service........295-9; disc. 444
Thompson, J. D. Disc........436
Tice, William F.; G. F. Tracy. Measurement of the Subtransient Impedances of Synchronous Machines........70-6; disc. 431
Titus, C. H.; P. J. Reifschneider. A 208Y/120-Volt 120-Ampere Three-Pole 400-Cycle Electrically Operated Aircraft Circuit Breaker........551-5
Tracy, Gordon F.; W. F. Tice. Measurement of the Subtransient Impedances of Synchronous Machines........70-6; disc. 431
Trainor, J. J.; C. E. Parks. Disc........457, 467
Trickey, P. H., Wound- and Dummy-Rotor Methods of Quality Control and Trouble Shooting of Induction-Motor Windings and Cores........842-4
Tucker, Durward J. Disc........969

V

Valentine, C. E.; E. L. Harder. Static Voltage Regulator for Rototrol Exciter........601-06
Van Ryan, A. Improved Fault Protection for Rural Distribution Systems........261-3
Vaughan, J. T.; J. W. Williamson. Design of Induction-Heating Coils for Cylindrical Nonmagnetic Loads........587-92; disc. 966
Veinott, Cyril G. Disc........421
Vest, William L., Jr. Disc........974
Vogel, F. J. Standards and Insulation Characteristics of Oil-Insulated Transformers...167-71; disc. 433
Vogel, F. J. Disc........474, 997
Votaw, R. W.; P. G. Cushman. Disc........946

W

Wagner, C. H. Disc........985
Waldron, R. C. Disc........480
Wallace, J. M. Disc........447
Walley, O. C.; F. W. Godsey, J. D. Miner, Jr. Speed-Control System for an Aircraft Cabin-Supercharger Drive........37-40
Walter, G. E.; P. T. Chin. Transient Response of Controlled Rectifier Circuits........208-14
Wang, P. Y.; A. C. Schwager. New Transmission-Line Diagrams........610-15; disc. 955
Ware, D. H. Measurement of Stray-Load Loss in Induction Motors........194-7; disc. 434
Warren, C. E.; G. D. McCann, H. E. Criner. Determination of Transient Shaft Torques in Turbine Generators by Means of the Electrical-Mechanical Analogy........51-6
Watkins, S. S. Mercury-Arc Rectifiers for Railroads........84-6; disc. 421
Weatherwax, Richard C.; A. J. Stamm. The Electrical Resistivity of Resin-Treated Wood and Laminated Hydrolyzed-Wood and Paper-Base Plastics..833-8
Webb, R. L. Disc........416, 429, 458
Webb, R. L.; H. D. Braley, J. G. Noest. Disc.....979
Weichsel, H. Disc........421
Weichsel, H.; W. R. McCarty. Disc........992
Welch, A. U.; R. F. Wyer. Power Supply for A-C Arc Welding........116-20; disc. 435
Wents, E. C. Disc........427
Wents, J. F. General Considerations in Radio-Frequency-Cable Design........925-6
Weygandt, C. N., Jr.; C. Concordia, S. B. Crary, C. E. Kilbourne. Synchronous Starting of Generator and Motor........629-34; disc. 956
Wheeler, Charles M. Analysis of Arc-Welding Reactors........87-90; disc. 435
Whitehead, D. L. Disc........963
Whitehead, E. R. Disc........970
Whitehead, J. B. Oil Stresses in Impregnated-Paper Insulation........555-7; disc. 955
Whitehead, J. B.; J. M. Kopper. The Dielectric Strength and Life of Impregnated-Paper Insulation. Part IV........171-7; disc. 479, 942
Whitmer, E. W. Disc........415
Whitson, T. B. Disc........429
Whittlesey, S. I.; J. B. McClure. Power Systems for Auxiliary Drives in Steam-Electric Stations........844-51; disc. 981
Wickerham, W. R. Variable-Unbalanced-Voltage Control........98-102; disc. 450
Widmer, A. E. A Corona Voltmeter........940-1
Wieseman, R. W. Disc........415
Wightman, L. W.; L. H. Hirsch, R. F. Munier, M. L. Schmidt, F. S. Himebrook, T. C. Lloyd, O. G. Coffman, C. P. Potter. Investigation of Hot-Spot Temperatures in Fractional-Horsepower Motors........128-36; disc. 425
Wilcox, H. M.; D. C. Harker. Compressed-Air Circuit Breakers in A-C Railway Service........141-5; disc. 419
Williamson, J. W.; J. T. Vaughan. Design of Induction-Heating Coils for Cylindrical Nonmagnetic Loads........587-92; disc. 966
Withington, Sidney. Disc........419
Wolf, Edgar F. Disc........482
Woodrow, C. A.; H. A. Peterson. Disc........467
Woods, C. A., Jr. Disc........427
Woods, G. M.; L. G. Riley. Dynamic Braking With Traction Motors........517-19
Wright, W. L. Disc........485
Wyer, R. F. Disc........436
Wyer, R. F.; A. U. Welch. Power Supply for A-C Arc Welding........116-20; disc. 435
Wyman, B. W.; J. H. Keagy. New Solenoid Mechanism for Magne-Blast Breaker....268-74; disc. 448

Y

Young, Louis C. Disc........967

Z

Zahorsky, L. A. The Amplidyne Generator Applied to Speed-Controlled Electric Gun Turrets for Aircraft........221-5; disc. 436

Preface

This 64th volume of the TRANSACTIONS of the American Institute of Electrical Engineers contains all approved technical program papers and related discussions presented during the calendar year, in accordance with the improved publication procedure adopted in August 1940. Pages 1–358 and 495–872 comprise the papers published in the Transactions sections of the monthly issues of ELECTRICAL ENGINEERING, and pages 359–494 and 873–1000 contain papers and discussions that appeared in advance in the June and December 1945 "Supplements to Electrical Engineering—Transactions Section," respectively.

In compliance with a Government order restricting travel all AIEE national and District meetings, with the exception of the winter technical meeting, were abandoned in 1945. Instead spring, summer, and fall technical paper programs and pamphlet copies of the technical papers were distributed by mail, and written discussions were submitted.

The technical papers and discussion in this volume were presented as follows:

1. 1945 winter technical meeting, New York, N. Y., January 22–26, 1945.
2. Spring technical paper program, April 1945 issue of ELECTRICAL ENGINEERING.
3. Summer technical paper program, June 1945 issue of ELECTRICAL ENGINEERING.
4. Fall technical paper program, September 1945 issue of ELECTRICAL ENGINEERING.

In addition this volume contains:

1. 1945 annual report of the AIEE board of directors.
2. A complete listing of AIEE officers and committees for 1945–46.

Full correlation of all material in this volume has been accomplished by means of the multientry index beginning on page 1025. Reference to any of the several subject entries for a technical paper will lead directly to the paper and to any published discussion on that paper.

Statements and opinions given in papers and discussions published in TRANSACTIONS are the expressions of contributors for which the American Institute of Electrical Engineers assumes no responsibility.

Errata

1. Page 4, Table IV. The time of installation of unit 11 should be 28.5 years.

2. Page 6, Table V. The time of installation of unit 11 should be 28.5 years.

3. Pages 184–8. The parameter given as *K* should be *k*.

4. Page 395. Reference 224 is found in the AIEE JOURNAL not the *Journal* of the Institution of Electrical Engineers.

5. Page 288, Figure 1. The term, x_{ad} should be x_{afd} and x_{aq} should be x_{afq}.

6. Page 289, Table I. The term, x_{ad} should be x_{afd} and x_{aq} should be x_{afq}.

7. Page 290, column 2. The term x_{ad} should be x_{afd}.

8. Page 291, column 1. The term x_{ad} should be x_{afd}.

9. Page 294, Appendix III. The term x_{ad} should be x_{afd} and x_{aq} should be x_{afq}.

10. Page 609, Table III. In the first equation beginning "$t=$" the numeral 17 should be 0.17.

11. Pages 862 and 864, Figures 1 and 2. The following are corrected versions of these figures:

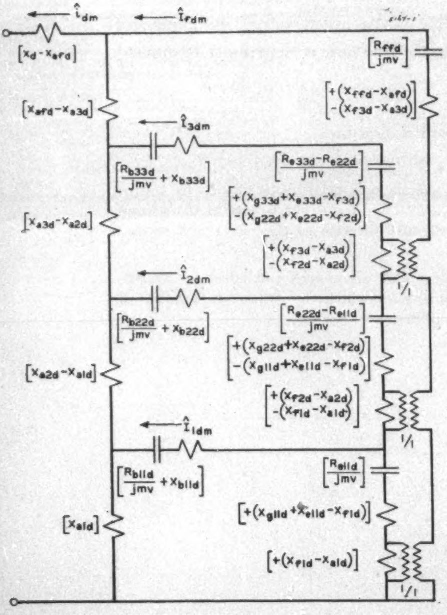

$\hat{i}_{dm}$
$\hat{i}_{fdm}$
$[x_d - x_{afd}]$
$\left[\frac{R_{ffd}}{jmv}\right]$
$\left[\begin{matrix}+(x_{ffd}-x_{afd})\\-(x_{f3d}-x_{a3d})\end{matrix}\right]$
$[x_{afd}-x_{a3d}]$
$\hat{i}_{3dm}$
$\left[\frac{R_{b33d}}{jmv}+x_{b33d}\right]$
$\left[\frac{R_{e33d}-R_{e22d}}{jmv}\right]$
$\left[\begin{matrix}+(x_{g33d}+x_{e33d}-x_{f3d})\\-(x_{g22d}+x_{e22d}-x_{f2d})\end{matrix}\right]$
$[x_{a3d}-x_{a2d}]$
$\left[\begin{matrix}+(x_{f3d}-x_{a3d})\\-(x_{f2d}-x_{a2d})\end{matrix}\right]$
1/1
$\hat{i}_{2dm}$
$\left[\frac{R_{b22d}}{jmv}+x_{b22d}\right]$
$\left[\frac{R_{e22d}-R_{e11d}}{jmv}\right]$
$\left[\begin{matrix}+(x_{g22d}+x_{e22d}-x_{f2d})\\-(x_{g11d}+x_{e11d}-x_{f1d})\end{matrix}\right]$
$[x_{a2d}-x_{a1d}]$
$\left[\begin{matrix}+(x_{f2d}-x_{a2d})\\-(x_{f1d}-x_{a1d})\end{matrix}\right]$
1/1
$\hat{i}_{1dm}$
$\left[\frac{R_{b11d}}{jmv}+x_{b11d}\right]$
$\left[\frac{R_{e11d}}{jmv}\right]$
$[+(x_{g11d}+x_{e11d}-x_{f1d})]$
$[x_{a1d}]$
$[+(x_{f1d}-x_{a1d})]$
1/1

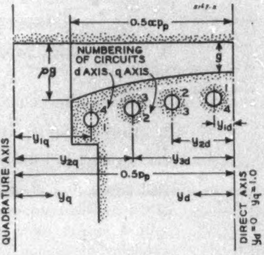

$0.5\alpha p_p$
NUMBERING OF CIRCUITS
d AXIS
q AXIS
ρg
g
1
2
3
4
y_{1q}
y_{2q}
y_{1d}
y_{2d}
y_{3d}
$0.5p_p$
y_q
y_d
QUADRATURE AXIS
$y_d=1.0 \quad y_q=0$
DIRECT AXIS
$y_d=0 \quad y_q=1.0$

Evaluation of Electric Distribution Losses in Terms of Generating-Station-Capacity Investment

M. MORTARA
MEMBER AIEE

ELECTRIC distribution losses affect the economy of a system in two ways: (*a*) by making it necessary to produce, over any period of time, in addition to the energy required by the load, the amount of energy absorbed by the losses during that same period, or "energy losses"; (*b*) by requiring, at the time of the peak, the availability of a generating capacity which exceeds the simultaneous value of total load by the coincident amount of power absorbed by the distribution losses, or "power losses." These two aspects both should be taken into consideration in planning a new electric system or in expanding an existing system.

When the unit cost of energy is known, the economic evaluation of factor *a* requires only the knowledge of the load curve at various times of the year, so that the yearly loss of energy may be determined with sufficient approximation. The economic evaluation of factor *b*, on the other hand, is much less definite, because it is affected by multiple and sometimes variable conditions, which must be properly considered. The purpose of the present paper is to indicate the principal among these conditions and to outline a procedure for the correct economic evaluation of power losses.

Conditions Affecting the Economic Value of Power Losses

The generation peak of an electric system independent from outside sources of power will coincide with the peak load; if, furthermore, the power is supplied by thermoelectric sources, it will be only necessary for the installed generating capacity at any time to be sufficient to take care of the expected peak load. It is obvious that, in a system of this type, a reduction of peak power losses would produce an equal reduction in the requirements of generating capacity.

The existence of interconnections with other systems capable of supplying energy during the period of the yearly peak, but not at other times, might change that condition, making the generation peak coincident with a lower load. In this case, the power losses affecting the requirements of generating capacity will be correspondingly lower, varying approximately as the square of the kilovolt-ampere load. A similar effect may come from the presence of mixed power sources, part thermoelectric and part hydroelectric, and conditions may be modified further if the hydroelectric plants are provided with storage ponds or reservoirs, capable of furnishing power to cover the daily peak at any time of the year.

It is clear that the economic value of peak power losses will be greater for the case mentioned first and that it may become relatively small in some of the other cases, where outside or mixed sources of power supply are available.

The cost of installation of new generating capacity, which is one of the factors determining the worth of power losses, is fairly uniform in the various stages of development, when a system is supplied by thermoelectric stations alone. In effect these stations can be built in unit sections, and complete new sections can be added as required.

In the case of hydroelectric supply, however, conditions are different, because there are certain parts of the plant, involving a major quota of the total cost, which have to be completed initially, regardless of the amount of generating capacity installed. The cost of this latter, therefore, will be generally much higher in the initial stage of a new project than for additions made later in order to reach the ultimate capacity for which the plant is designed. Another circumstance to be considered in the case of hydroelectric projects, is that the different and variable characteristics of river flow for various plants in the same system normally will require the total installed capacity to be appreciably higher than the generation peak. This adds to the difficulty of establishing the required time and cost of installation of generating units.

Table I

Interval of Development	Worth of Power Losses: From Equation 9	Worth of Power Losses: From Equation 9′
From G_0 to G_1	$s=1.53C$	$s=1.45C$
From G_0 to G_3	$s=2.40C$	$s=2.27C$
From G_0 to G_4	$s=3.72C$	$s=3.53C$

The basic case of an independent thermoelectric system and the procedures for approaching the problem in other cases are discussed in the following sections.

Worth of Power Losses in an Independent Thermoelectric System

PROCEDURE FOR THE ECONOMIC EVALUATION

The investigation of the problem and its solution are to be based upon the estimated effect of a variation of power losses on the future requirements of generating capacity. The initial step, therefore, will be the determination of a curve representing the expected growth of system load.

Analyses of statistical data of a number of public utilities show that the long-range trend of the yearly peak load, in a system serving a definite area, can be

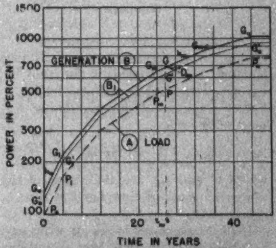

Figure 1. Trend curves of load and generation for an independent electric system, showing effect of different level of power losses on generation peak

---

Paper 45-4, recommended by the AIEE committee on power generation for presentation at the AIEE winter technical meeting, New York, N. Y., January 22–26, 1945. Manuscript submitted June 24, 1944; made available for printing November 3, 1944.

M. MORTARA is assistant to electrical engineer, Consolidated Gas Electric Light and Power Company, Baltimore, Md.

closely represented by a succession of segments of logarithmic parabolas or of exponential curves, with time as exponent. The latter curves, although somewhat less accurate than the former, are generally preferred in planning studies, having the practical advantage of becoming straight lines on semilogarithmic diagrams.

On any such diagram, the trend curve of the peak load will be a polygonal line A composed of rectilinear segments of progressively varying slope (see Figure 1). The equation of any one of the component segments is of the form

$$\log P = \log P_m + (t - t_m) \log h_m \tag{1}$$

where

t = time in years from the origin
t_m = initial time of the rectilinear portion under consideration
P = peak load at time t
P_m = peak load at time t_m
h_m = factor of growth or ratio between peaks in two consecutive years (constant for the portion of line under consideration)

When a system is designed and developed on the basis of constant percentage of peak power losses, the curve representing the generation peak will be also a polygonal line B, running above A (Figure 1) at constant vertical distance equal to the logarithm of the ratio between peak generation and peak load.

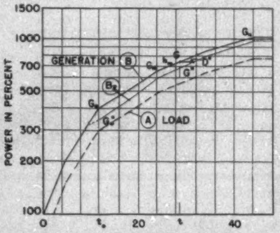

Figure 2. Trend curves of load and generation for an independent system, showing effect of individual power-loss reduction on generation peak

The equation of any rectilinear segment of line B is

$$\log G = \log G_m + (t - t_m) \log h_m \tag{2}$$

where G and G_m are the values of the generation peak at time t and at time t_m respectively.

If the peak power losses are expressed as a fraction of the peak load P, and d is the ratio between the two, the generation peak will be

$$G = P + dP = P(1+d)$$

For a lower ratio of losses d', the required generation will be reduced to

$$G' = P(1+d') = kG$$

where

$$k = \frac{1+d'}{1+d} \tag{3}$$

Over the time interval considered, the generation peak of a system having such lower loss ratio will be represented by the equation:

$$\log G' = \log G_m + (t - t_m) \log h_m + \log k \tag{4}$$

The representative curve is again a polygonal line B_1 located between A and B at constant vertical distance from each of them (Figure 1).

The horizontal distance between B and B_1 is equal to the time lag D_m in reaching a definite generation peak, caused by the power-loss reduction. Its value is constant during each period of uniform growth factor h_m and is obtained from equations 2 and 4 as

$$D_m = \frac{1}{\log h_m} \log \frac{1}{k} \tag{5}$$

If system conditions represented by B are assumed as basic reference plan, the afore-mentioned time lag will furnish the elements for determining the worth of savings of peak power losses that may be obtained by alternate plans. From equation 5 it is apparent that, for a definite ratio k, the time lag will be greater, the lower the rate of growth and vice versa.

To determine the economic value to be attributed to a reduction of peak power losses, two factors come under consideration:

(*a*). As noted before, a lower level of power losses causes a deferment D in reaching a certain generation peak, in comparison with the basic reference plan. This permits postponing, for that same interval D, the installation of each new generating unit and the outlay of fixed charges thereon.

(*b*). If W designates the capacity of one of the new units to be successively added during a period of growth factor h, the time T elapsing between unit additions in the reference plan, as deduced from equation 2, will be

$$T = \frac{1}{\log h} \log\left(1 + \frac{W}{G}\right) \tag{6}$$

If h and W remain constant while the peak G progressively increases, the interval T will correspondingly decrease and eventually become equal to the deferment interval D. This would indicate exactly one unit less to be required, at that time, in the lower-loss plan; which means that the installation of a unit would be saved because of the power-loss reduction. This occurrence, however, seldom materializes, since it would require the difference of power losses between the two plans to equal the capacity of a generating unit, within the time of ultimate development of the system. In view of the limitations on the percentages of power losses that can be practically considered, this condition is unlikely to obtain and therefore cannot, generally, be taken into account.

Consequently it appears that, in most cases, the worth of power losses can be evaluated solely on the basis of factor a, that is, the postponement in the outlay of fixed charges on each generating unit of future installation.

The money saving effected because of such deferment, on each of the units to be installed during any period for which a certain value h_n of the growth factor is valid, will be

$$S_n = CWD_n r = \frac{CWr}{\log h_n} \log \frac{1}{k} \tag{7}$$

where C is the cost per kilowatt of new installed capacity, W the capacity of the unit in kilowatts, D_n the deferment valid over that period, and r the yearly rate of fixed charges (in decimal). The total capacity to be installed during the interval under consideration may be assumed to be equal to the difference between final and initial generation peaks: $(G_{n+1} - G_n)$. Actually there will be some discrepancy, due to the fact that this difference may not be a multiple of the proposed capacity of generating units, but, over the various phases of development of the system, these discrepancies will compensate.

The total savings effected by the alternate plan of lower losses will be the summation of the various values of S_n or, if the index of ultimate development is designated by u:

$$S = \sum_{n=0}^{n=u-1} \frac{Cr(G_{n+1} - G_n)}{\log h_n} \log \frac{1}{k} \tag{8}$$

In the case under consideration, of uniformly lower percentage of power losses, k is constant and the total reduction of power losses is $(1-k)G_u$. Therefore, the saving per kilowatt of peak power-loss reduction, which can be considered as cost or worth of such losses, will be

$$s = \frac{S}{(1-k)G_u} = \frac{\log 1/k}{(1-k)G_u} \sum_{n=0}^{n=u-1} \frac{Cr(G_{n+1} - G_n)}{\log h_n} \tag{9}$$

If the values of $(h-1)$ and $(1-k)$ are smaller than 0.10 (as they usually will be in practice), expression 9 can be simplified, without appreciable error, as follows:

$$s = \frac{1}{G_u} \sum_{n=0}^{n=u-1} \frac{Cr(G_{n+1} - G_n)}{h_n - 1} \tag{9'}$$

Table II

Interval	Total Savings
G_0–G_2	$ 3,371,250
G_2–G_3	6,503,250
G_3–G_4	8,834,500
Total	$18,709,000

thus indicating that s is practically independent from the percentage of loss reduction.

These expressions are valid, as long as the ultimate reduction of power losses is smaller than the capacity of the generating unit assumed to be in use at that time, so that the same number of units is required on the alternate as on the reference plan of development. If there is elimination of one or more units, the corresponding savings should be adequately taken into account.

The value obtained from expressions 9 or 9′ is a weighted average of the costs of power losses in the successive phases, which vary in connection with the growth factor, as noted before.

In the preceding discussion, the effect of a lower level of power losses uniformly maintained, has been considered; but, for the complete solution of the proposed problem, it is necessary to investigate the effect of an individual reduction of such losses. Let it be assumed that in a system, originally designed to follow trend line B as shown on Figure 2, developments carried out in a certain phase bring down the power losses, so as to reduce the generation peak at time t_0 from G_0 to G_0''. The loss reduction of which the effects are to be determined is

$$g = G_0 - G_0'' = (1-k)G_0 \tag{10}$$

If no attempt is made to maintain the lower loss level, and the original loss ratio represented by line B is adopted again, the generation peak at time t, when the growth factor is h_m, can be derived from expressions 2 and 10. Its value G'' will satisfy the equation:

$$\log G'' = \log\left(G_m - \frac{g}{h_m^{\,t-t_m}}\right) + (t-t_m)\log h_m \tag{11}$$

represented by line B_3. The ratio between G'' and G is

$$\frac{G''}{G} = 1 - \frac{g}{G}$$

and becomes equal to unity only for G equal to infinity. The time lag between line B_3 and line B at time t can be determined considering that $\log h_m$ is the tangent of the angle of slope of trend line B, and that the vertical distance between the two lines is $\log [G/(G-g)]$; consequently, their horizontal distance, representing the time lag, will be

$$D'' = \frac{1}{\log h_m} \log \frac{G}{G-g} \tag{12}$$

This equation, with the data applicable at the time of installation of each future generating unit, gives the corresponding deferment in the outlay of fixed charges obtainable by the individual loss reduction. For the purpose of the following calculations, it can be assumed, without appreciable error, that units to be used are of uniform capacity, provided this is adequately chosen with regard to initial and ultimate system peak. If such capacity is designated by W and the first unit is assumed to be required in the reference plan at time t_0, the $(n+1)$th unit will be required when the generation peak reaches the value (G_0+nW). The corresponding deferment, due to the loss reduction g, will be

$$D_n'' = \frac{1}{\log h_m} \log \frac{G_0+nW}{G_0+nW-g}$$

If equation 10 is taken into account and it is posed $G_0/W = p$, the foregoing expression becomes

$$D_n'' = \frac{1}{\log h_m} \log \frac{p+n}{kp+n} \tag{13}$$

For values of (h_m-1) and $(1-k)$ smaller than 0.10, this equation can be simplified to

$$D_n'' = \frac{p(1-k)}{(h_m-1)(n+kp)} \tag{13'}$$

The effect of the individual loss reduction is still to produce a deferment in the installation of new generating units; but, over each period of uniform growth, the deferment, instead of being constant as in the case of uniformly lower loss level, has a gradually decreasing length. If C is the cost per kilowatt of new installed capacity, and r the yearly rate of fixed charges (in decimal), the money saving effected because of such deferment on the $(n+1)$th generating unit, *at the time this unit is required in the reference plan B*, is

$$(S_n'') = CWD_n''r \tag{14}$$

To determine the worth of this saving at time t_0, when the power-loss reduction is assumed to obtain, a factor of "present value" has to be applied to (S_n''). This factor is $1/(1+i)^{t_n}$, where i is the interest rate (in decimal) and t_n is the time of installation of the $(n+1)$th unit in the reference plan, counted in years from t_0. Therefore, the "present value" of the saving on the $(n+1)$th unit is

$$S_n'' = \frac{CWD_n''r}{(1+i)^{t_n}} \tag{15}$$

The total economic benefit produced by the individual loss reduction will be the summation of the "present values" applicable to each of the u generating units necessary to reach the expected ultimate capacity of the system. Consequently, this total benefit is given by the expression:

$$S_0'' + S_1'' + \ldots + S_u'' = \sum_{n=0}^{n=u-1} \frac{CWD_n''r}{(1+i)^{t_n}}$$

The money saving per kilowatt of peak power-loss reduction, which can be considered as the cost of such losses, is obtained by dividing the foregoing summation by the loss reduction $(1-k)G_0$ and is

$$s = \frac{1}{(1-k)G_0} \sum_{n=0}^{n=u-1} \frac{CWD_n''r}{(1+i)^{t_n}} \tag{16}$$

If the value derived from equations 13 or 13′ is substituted for D_n'', the foregoing expression can be written

$$s = \frac{1}{(1-k)p} \sum_{n=0}^{n=u-1} \frac{Cr}{(1+i)^{t_n} \log h_m} \log \frac{p+n}{kp+n} \tag{17}$$

or, in simplified form:

$$s = \sum_{n=0}^{n=u-1} \frac{Cr}{(1+i)^{t_n}(h_m-1)(kp+n)} \tag{17'}$$

The interval t_n to elapse for the installation of each unit, could be derived from equation 2 but is more readily and with sufficient approximation determined from the graphic of trend curve B. This same graphic also will indicate the value of the growth factor h_m applicable to the various units.

It appears that the worth s is influenced both by the percentage of loss reduction, which is a function of k and by the size of generating unit used for calculations, from which p is determined. However, it will be found that, with data corresponding to practical possibilities, the influence of variation of these two factors is very slight

Table III

Number of Unit	Present Value of Power Losses (at Time t_0)	
	Equation 17	Equation 17′
1	$s_1 = 0.548C$	$s_1 = 0.546C$
2	$0.365C$	$0.364C$
3	$0.263C$	$0.262C$
4	$0.191C$	$0.190C$
5	$0.183C$	$0.182C$
6	$0.141C$	$0.140C$
7	$0.111C$	$0.110C$
8	$0.089C$	$0.087C$
9	$0.073C$	$0.073C$
10	$0.118C$	$0.118C$
11	$s_{11} = 0.088C$	$s_{11} = 0.088C$

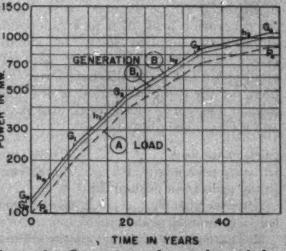

Figure 3. Comparison of two plans of development of an electric system, with different percentage of peak power losses

Table IV

Generating Units No.	n	Time of Installation t_n (Years)	Factor of Growth h_m	a $\frac{1}{\log h_m}$	b $\frac{1}{(1+i)^{t_n}}$ $i=0.06$	b $\frac{1}{(1+i)^{t_n}}$ $i=0.08$	c $\log \frac{p+n}{kp+n}$	d abc $i=0.06$	e abc $i=0.08$
1	0	0	1.05	47.2	1	1	0.02228	1.052	1.052
2	1	3.7	1.05	47.2	0.805	0.750	0.01848	0.702	0.654
3	2	6.9	1.05	47.2	0.680	0.580	0.01580	0.507	0.433
4	3	9.7	1.05	47.2	0.565	0.465	0.01379	0.368	0.303
5	4	12.1	1.04	58.7	0.490	0.390	0.01223	0.352	0.280
6	5	14.8	1.04	58.7	0.420	0.317	0.01100	0.271	0.204
7	6	17.3	1.04	58.7	0.363	0.260	0.00998	0.213	0.153
8	7	19.5	1.04	58.7	0.318	0.219	0.00914	0.171	0.118
9	8	21.5	1.04	58.7	0.285	0.187	0.00843	0.141	0.093
10	9	24.6	1.019	122.4	0.237	0.148	0.00783	0.227	0.142
11	10	26.5	1.019	122.4	0.190	0.110	0.00730	0.170	0.098
							Summation	4.174	3.530

and that normally the range of the consequent variation of s is well below ±5 per cent of its average.

As a rule, the simplified expression can be employed for calculations, and these may be accelerated further by the use of simple nomograms, as shown in the following paragraph.

Practical Application of the Method

Examples of application of the method will be given, both for the case of comparison of two alternate plans of system development with different level of peak power losses and for the case of evaluation of an individual reduction of peak power losses.

Example 1

For the former case, curves B and B_1 of Figure 3 will be assumed to represent the generation peak of a new independent system supplied solely by steam-power plants, respectively, in a basic reference plan and in an alternate lower-loss plan, for the complete period of development. The curve of the peak load is A, and the assumed data are:

Initial peak load.............. $P=100$ mw
Ultimate peak load........... $P_4=885$ mw
Initial generation peak in the reference plan B............ $G_0=120$ mw
Initial generation peak in the alternate plan B_1........... $G_0'=114$ mw
Factor of reduction of generation peak......... $G_0'/G_0=k=0.95$
Factors of growth....... $h_0=1.08$ $h_1=1.06$ $h_2=1.04$ $h_3=1.014$
Generation peaks in the reference plan B......... $G_1=260$ mw $G_2=465$ mw $G_3=870$ mw $G_4=1{,}060$ mw
Ultimate loss reduction by alternate plan B_1.... $(1-k)G_4=53$ mw
Capacity of generating units at ultimate development........ $W=80$ mw
Yearly rate of fixed charges: 13 per cent or, in decimal.......... $r=0.13$

The application of equations 9 and 9′ up to the end of successive phases of development gives the results shown in Table I (see appendix for detail calculations). The error of the simplified equation 9′ is −5 per cent and, for a problem of this nature, can be considered of no consequence; furthermore, it is on the conservative side, so that the use of this equation will be admissible in most cases.

It is apparent that the latest stages of development, with low growth factors, have the greatest influence on the amount of savings, because of the longer deferment then obtaining for the installation of new units. With the data of the example, on the basis of equation 9′ and a uniform cost C of $100 per kilowatt of new capacity assumed, the estimated savings in the various stages would be as shown in Table II. Compared with the ultimate installation cost of $106,000,000, this represents an over-all economy of 17.6 per cent which, together with the energy savings, might justify the adoption of the development plan with lower loss level.

Example 2

An example of comparison and evaluation of the individual loss reduction in an existing system of the same type as the foregoing is shown in the lower part of Figure 4, where line B is the trend curve of the reference plan and line B_2 is the trend curve obtained by an individual loss reduction at time t_0. The data assumed for this example are:

Generation peak at time t_0 in the reference plan........... $G_0=400$ mw
Loss reduction at time t_0, in the alternate plan................. $g=20$ mw
Generation peak at time t_0 in the alternate plan.......... $G_0''=380$ mw
Factor of reduction of generation peak at time t_0........ $G_0''/G_0=k=0.95$
Capacity of generating units.... $W=80$ mw
Ratio of initial generation peak to unit capacity....... $G_0/W=p=5$
Rate of interest: 6 per cent or, in decimal....................... $i=0.06$
Yearly rate of fixed charges: 13 per cent or, in decimal.......... $r=0.13$
Factors of growth.... $h_0=1.05$; $h_1=1.04$; $h_2=1.019$
Ultimate generation peak in the reference plan....... $G_3=1{,}280$ mw
Total number of units of capacity W to be installed................ $u=11$

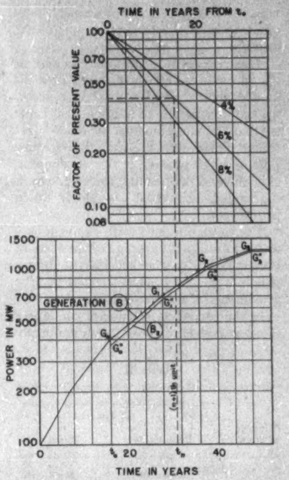

Figure 4. Comparison of two plans of development of an electric system, following an individual reduction of peak power losses

For the determination of factor $1+(1+i)^{t_n}$ appearing in equations 17 and 17′, the graphics of Figure 4 can be employed as follows: a vertical line is drawn from the point representing the $(n+1)$th unit on trend curve (B), to the straight radial line in the upper chart, labeled with the rate of interest to be used. The ordinate of the point of intersection, read on the scale at the left side of the chart, gives directly the value of $1/(1+i)^{t_n}$ applicable to that unit.

The partial values of power losses calculated by the two equations are given in Table III, which shows that the results of the exact formula 17 are practically identical to those of the simplified formula 17′. This latter will be used preferably, because it is of easier application, and calculations of its terms can be accelerated further by the use of nomogram Figure 5, which gives the value of factor $1/(h-1)(kp+n)$, as explained in the note on the figure. Detail calculations are given in the appendix.

If C is assumed to remain constant, the summation of the foregoing partial values gives $s=2.17$ C, but there is a considerable influence of the rate of interest upon this value. If the rate, instead of being six per cent as used in the preceding example, is eight per cent, the value of s is lowered to 1.83 C, a reduction of approximately sixteen per cent.

It may be observed that all values of peak power losses calculated are greater than the capital cost C of new generating capacity, contrary to assumptions frequently made.

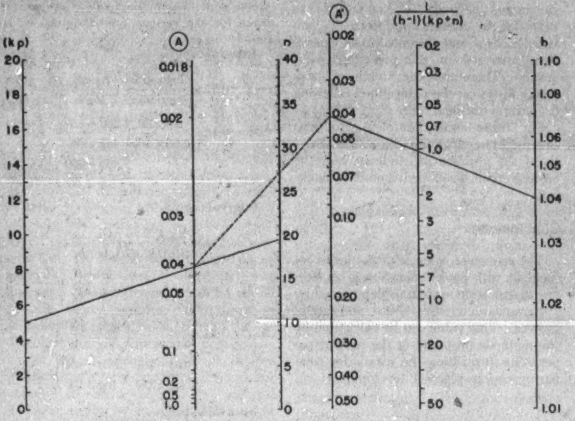

Figure 5. Nomogram for calculation of term $1/(h-1)(kp+n)$ in equation 17′

Given the quantities *h*, *k*, *p*, and *n*, draw a straight line from the value of *kp* on the scale so labeled to *n* on its own scale. Transfer the reading thus obtained on auxiliary scale *A* to auxiliary scale *A′*, as shown by dotted line, and draw a straight line from this point to the point representing *h* on its own scale. The intersection of this line with the scale labeled $1/(h-1)(kp+n)$ gives the requested quantity

A comparison between the economic value of an individual reduction of peak power losses and that of the corresponding reduction of energy losses will be interesting. The 20-megawatt reduction of the example can be assumed to reduce the annual energy losses by 50,000,000 kilowatt-hours: if the cost of energy is three mils per kilowatt-hour, the consequent money saving will be $150,000 per year, which, capitalized up to the time of ultimate development on the basis of the same interest rate of six per cent used previously, has a present value of $2,100,000. On the other hand, if it is assumed that the capital cost of new generating capacity *C* is $100 per kilowatt, the present value of the savings due to the reduction of peak power losses by 20,000 kw, is $4,340,000, or slightly more than twice the value of energy losses. Such ratio is almost unaffected by the rate of interest.

Outline of Procedure for the Economic Evaluation of Power Losses in Systems of Other Types

INDEPENDENT HYDROELECTRIC SYSTEMS

When the sources of power of a system consist solely of hydroelectric plants, these necessarily will include large reservoirs to permit regulation of the total output at any time, in accordance with load requirements. Unregulated plants usually will have installed capacity adequate to utilize such high flow as economically convenient, while regulated plants will have enough capacity to take care of the total load at the time of the lowest output of the former. Whether such condition is coincident with the yearly peak load or not, it will be found that, generally, the regulated plants are called upon to provide part of the generation to cover this peak, in years of low flow.

In such a system, the needs of new capacity will involve periodical construction of entirely new projects and their transmission facilities, with a possible graduation in the number of units and transmission lines installed. The time when each new project and its eventual complementary additions shall be ready for service in the basic reference plan will be derived from a trend curve of the generation peak similar to *B* on Figures 3 and 4. The deferments obtainable in the construction of the various projects, by reduction of peak power losses, then are determined, either by formula 12 or by formulas 13 and 13′, according to the proposed problem. On the basis of these deferments, the corresponding savings of fixed charges and their accrued or present value can be calculated, as required.

It should be noted that the capacity to be assigned to each hydroelectric plant is the net capacity available at the load centers, after deduction of transmission losses. The economy of the latter constitutes a separate problem from that of distribution losses.

INDEPENDENT SYSTEMS WITH COMBINED GENERATION

In a system where thermoelectric and hydroelectric generation are combined, conditions may vary widely, in connection with the relative importance of the two sources of supply.

When thermoelectric plants are only for stand-by purpose, their capacity will not be affected appreciably, as a rule, by possible reduction of power losses. Therefore, the procedure for determining the worth of peak power losses will be the same as previously outlined for a purely hydroelectric system.

On the other hand, if the two sources of supply are of approximately equivalent importance, the plan of development will call for alternate construction of either type of plant, and the methods of evaluation will be a combination of those already discussed.

A situation which may be encountered is that of a system having part of its supply provided by hydroelectric plants of fixed firm capacity, with no possibility or convenience of expansion and its main supply provided by thermoelectric stations. In this case there will be an estimated firm availability of hydroelectric power at the time of the yearly peak load and a minimum availability at the time of low flow, whenever the two conditions do not coincide.

Trend curves of the load and total generation should be plotted for these two conditions, and then the corresponding values of the hydroelectric contribution should be deducted from total generation, to obtain the trend curve of thermoelectric generation alone. The condition requiring higher values for this latter, will be selected for the application of the method previously discussed.

The segments of the trend line of the peak generation thus obtained are not, theoretically, rectilinear, but they can be considered as such without appreciable error. The value of the growth factor h_m' applicable to a segment between time t_m and time t_{m+1} is given by the relation:

$$\log h_m' = \frac{1}{t_{m+1}-t_m} \log \frac{G_{m+1}-G_e}{G_m-G_e}$$

where G_m and G_{m+1} represent total generation and G_e the fixed value of firm hydroelectric generation.

In this case, since the hydroelectric portion of generation is not affected by eventual reduction of power losses, in order to simplify calculations, the factor *k* by which the ratio of reduction is measured, should be referred to thermoelectric generation alone. The trend curves of peak thermoelectric generation in alternate plans, having lower loss level or involving an individual loss reduction, then will be obtained from the analogous trend curve representing the basic reference plan, with the procedure previously explained.

If thermoelectric generation peak and peak load coincide, the method for economic evaluation of peak power losses is exactly the same as described in the examples. In the other alternative, however, that the two peaks do not coincide, the following modifications are necessary:

(*a*). The power losses, to be deducted to obtain the trend curves of alternate plans, are only a fraction of the peak power losses. Namely, if q designates the ratio between the kilovolt-ampere values of the loads at the time of greatest thermoelectric generation and at the time of the yearly peak load, the ratio of the corresponding losses may be estimated to be very approximately q^2. For definite system characteristics, this ratio will be subject to minor variations over the whole period of development, so that it may be assumed to remain constant; consequently, if w and w_p are those two losses, it will be

$$w=q^2w_p$$

(*b*). If peak power losses are reduced, so as to obtain a constant ratio of reduction of total peak generation, the ratio of reduction applicable to the case under consideration will not be constant. Its average value applicable to any segment of the trend curve will have to be calculated on the basis of power losses, and used in the formulas where it appears.

(*c*). After the worth s_1 of power losses has been determined by application of the proper equations, the value s valid for the corresponding peak power losses will be derived from the relation:

$$s=q^2s_1$$

Since factor q is smaller than unity, it is evident that the worth of peak power losses may be reduced appreciably when there is no coincidence between yearly peak load and highest requirement of thermoelectric generation.

INTERCONNECTED SYSTEMS

Interconnected systems may belong to any of the types previously described, and the possibility of drawing power from interconnections will add a new element modifying the requirements of generating capacity within the system.

Power supply by interconnections may be divided broadly into two categories: firm and surplus (or secondary). The influence of each category upon system generating capacity is comparable to that due to certain conditions of combined hydro- and thermoelectric generation, analyzed in the preceding paragraph. Therefore, the worth of peak power losses can be determined following procedures outlined there.

For other more complex situations that might be encountered, a similar analysis of the problem will indicate how the basic method developed should be modified.

Conclusions

The economic value of power losses coincident with peak generation in an electric distribution system, is determined by system characteristics, setup, and rate of growth. This value can be calculated by the methods proposed in the present paper, thus furnishing the means for comparing various plans of development.

As in all problems of this nature, the mathematical solution is based on some simplified theoretical assumptions, from which actual conditions may more or less diverge. Such divergences can affect in a certain measure the absolute accuracy of the results, but, for the purpose of comparison, they will have, as a rule, negligible influence.

The worth of power losses is comparable to and in particular cases may be appreciably above that of the consequent energy losses.

Table V

Generating Units		Time of Installation	Factor of Growth	a $\frac{1}{h_m-1}$	b $\frac{1}{(1+i)^{t_n}}$		c $\frac{1}{kp+n}$	d abc	e
No.	n	t_n (Years)	h_m	h_m-1	i=0.06	i=0.08	kp+n	i=0.06	i=0.08
1	0	0	1.05	20	1	1	0.210	4.20	4.20
2	1	3.7	1.05	20	0.805	0.750	0.174	2.80	2.61
3	2	6.9	1.05	20	0.680	0.580	0.148	2.01	1.71
4	3	9.7	1.05	20	0.565	0.465	0.129	1.46	1.20
5	4	12.1	1.04	25	0.490	0.390	0.1145	1.40	1.11
6	5	14.8	1.04	25	0.420	0.317	0.1025	1.075	0.81
7	6	17.3	1.04	25	0.363	0.260	0.093	0.845	0.605
8	7	19.5	1.04	25	0.318	0.219	0.085	0.67	0.46
9	8	21.5	1.04	25	0.285	0.187	0.0785	0.56	0.365
10	9	24.6	1.019	52.7	0.237	0.148	0.0727	0.91	0.57
11	10	26.5	1.019	52.7	0.190	0.110	0.0678	0.68	0.39
							Summation	16.61	14.03

Appendix. Calculations of Worth of Power Losses for the Illustrative Examples

Detail Calculations for Example 1

1. By equation 9:

$$s=Cr\frac{\log 1/k}{(1-k)G_u}\sum_{n=0}^{n=u-1}\frac{G_{n+1}-G_n}{\log h_n}$$

If the foregoing expression is written for the three intervals considered in the example and the numerical values are substituted for the various symbols given, it is found:

Interval G_0 to G_2

$$s=C\times0.13\times\frac{\log 1/0.95}{(1-0.95)G_2}\left(\frac{G_1-G_0}{\log h_0}+\frac{G_2-G_1}{\log h_1}\right)$$

$$=C\times0.13\times\frac{0.02228}{0.05\times465}\left(\frac{260-120}{\log 1.08}+\frac{465-260}{\log 1.06}\right)=1.53C$$

Interval G_0 to G_3

$$s=C\times0.13\times\frac{\log 1/0.95}{(1-0.95)G_3}\left(\frac{G_1-G_0}{\log h_0}+\frac{G_2-G_1}{\log h_1}+\frac{G_3-G_2}{\log h_2}\right)$$

$$=C\times0.13\times\frac{0.02228}{0.05\times870}\left(\frac{260-120}{\log 1.08}+\frac{465-260}{\log 1.06}+\frac{870-465}{\log 1.04}\right)=2.40C$$

Interval G_0 to G_4

$$s=C\times0.13\times\frac{\log 1/0.95}{(1-0.95)G_4}\left(\frac{G_1-G_0}{\log h_0}+\frac{G_2-G_1}{\log h_1}+\frac{G_3-G_2}{\log h_2}+\frac{G_4-G_3}{\log h_3}\right)$$

$$=C\times0.13\times\frac{0.02228}{0.05\times1{,}060}\left(\frac{260-120}{\log 1.08}+\frac{465-260}{\log 1.06}+\frac{870-465}{\log 1.04}+\frac{1{,}060-870}{\log 1.014}\right)=3.72C$$

2. By equation 9′:

$$s=\frac{Cr}{G_u}\cdot\sum_{n=0}^{n=u-1}\frac{G_{n+1}-G_n}{h_n-1}$$

By analogous procedure as in the foregoing, it is found:

Interval G_0 to G_2

$$s=C\times\frac{0.13}{G_2}\left(\frac{G_1-G_0}{h_0-1}+\frac{G_2-G_1}{h_1-1}\right)$$

$$=C\times\frac{0.13}{465}\left(\frac{260-120}{1.08-1}+\frac{465-260}{1.06-1}\right)=1.45C$$

Interval G_0 to G_3

$$s=C\times\frac{0.13}{G_3}\left(\frac{G_1-G_0}{h_0-1}+\frac{G_2-G_1}{h_1-1}+\frac{G_3-G_2}{h_2-1}\right)$$

$$=C\times\frac{0.13}{870}\left(\frac{260-120}{1.08-1}+\frac{465-260}{1.06-1}+\frac{870-465}{1.04-1}\right)=2.27C$$

Interval G_0 to G_4

$$s=C\times\frac{0.13}{G_4}\left(\frac{G_1-G_0}{h_0-1}+\frac{G_2-G_1}{h_1-1}+\frac{G_3-G_2}{h_2-1}+\frac{G_4-G_3}{h_3-1}\right)$$

$$=C\times\frac{0.13}{1{,}060}\left(\frac{260-120}{1.08-1}+\frac{465-260}{1.06-1}+\frac{870-465}{1.04-1}+\frac{1{,}060-870}{1.014-1}\right)=3.53C$$

The total savings applicable to each of the three intervals, on the basis of a uniform

Two-Phase Co-ordinates of a Four-Phase Network

EDWARD W. KIMBARK
MEMBER AIEE

SUBSTITUTION of variables (voltage, current, impedance, and so forth) in order to simplify solution of problems on polyphase networks is a well-established practice. A polyphase network may be regarded as several single-phase networks which are coupled to one another in many places and all of which contain power sources. Simplification of network problems results from the replacement of the original phase networks by an equal number of single-phase substitute networks which are not coupled to one another or are coupled in fewer places or in a simpler manner than the phase networks, and which, preferably, have fewer power sources. In these substitute networks, the substitute currents and voltages exist.

Three-phase networks, because of their importance, have been given the most attention. The best-known and most widely used substitution is that of symmetrical components of a three-phase network, introduced by C. L. Fortescue[1] in 1918, and applied to many practical problems since that time.[2] The method of symmetrical components has the following useful properties:

1. The substitute networks (also called sequence networks) are independent of one another in all branches, including rotating machines, for which the three-phase network is balanced.
2. Certain unbalances, notably, short circuits, result in simple types of coupling between the sequence networks.
3. Normally only the positive-sequence network contains power sources.

A disadvantage of symmetrical components is that unbalances which are not symmetrical with respect to phase a of the three-phase network produce nonreciprocal coupling between the sequence networks. This type of coupling is difficult to represent on a calculating board.

Another useful substitution applicable to problems in three-phase networks is one called α, β, 0 components[3] or two-phase co-ordinates.[4] It has the following properties:

1. The substitute networks are independent of one another in all branches for which the three-phase network is balanced, except in rotating machines. They are independent also in rotating machines if the positive- and negative-sequence impedances of the machines are equal or are assumed to be equal.
2. Furthermore, one of the networks is independent of the other two for all unbalances which are symmetrical with respect to phase a, such, for example, as open-delta or T-connected transformers and simple short circuits.
3. There are power sources in two of the substitute networks. Their voltages are normally equal in magnitude and 90 degrees apart in phase.
4. All types of unbalance, except in rotating machines, in the three-phase network give reciprocal coupling between substitute networks.

Fortescue[1] stated the general principles of analysis of polyphase networks of any number of phases by means of symmetrical components. The properties of n-phase symmetrical components are similar to those stated previously for three phases. A recent paper by Boyajian[5] treats the analysis of four-phase networks by means of symmetrical components and gives equivalent circuits for several types of unbalance, including single-phase loads connected from line to neutral and from line to line.

The present paper describes a new method of analysis of four-phase networks, for which the name *two-phase co-ordinates* is proposed. In this method a four-phase five-wire network is regarded as two single-phase three-wire networks with common neutral. Each of these two networks is then replaced by its symmetrical-component networks, as described in the following. The properties of the resulting substitute variables are much like those listed previously for

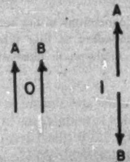

Figure 1. Symmetrical sets of current or voltage vectors of a single-phase three-wire system

---

Paper 45-1, recommended by the AIEE committee on basic sciences for presentation at the AIEE winter technical meeting, New York, N. Y., January 22–26, 1945. Manuscript submitted June 1, 1944; made available for printing November 2, 1944.

EDWARD W. KIMBARK is associate professor of electrical engineering at Northwestern University, Evanston, Ill. This paper was written while he was on leave to Massachusetts Institute of Technology, Cambridge, Mass., as visiting associate professor of electrical communications.

---

cost C of \$100 per kilowatt of new capacity, are determined as follows:

Interval G_0-G_2 Total loss reduction:

$(1-k)G_2=0.05\times465=23.25$ megawatts

Total savings:

$1.45\times100\times23{,}250=\$3{,}371{,}250$

Interval G_0-G_3 Total loss reduction:

$(1-k)G_3=0.05\times870=43.5$ megawatts

Total savings:

$2.27\times100\times43{,}500=\$9{,}874{,}500$

Interval G_0-G_4 Total loss reduction:

$(1-k)G_4=0.05\times1{,}060=53.0$ megawatts

Total savings:

$3.53\times100\times53{,}000=\$18{,}709{,}000$

The partial savings in the various stages of development are obtained as difference of the totals given.

Detail Calculations for Example 2

1. By equation 17:

$$s=\frac{Cr}{(1-k)p}\sum_{n=0}^{n=u-1}\frac{1}{(1+i)^{t_n}\log h_m}\log\frac{p+n}{kp+n}$$

The values of the component factors of the terms under summation sign, for each of the 11 units to be installed, are given in Table IV, taking into account that $k=0.95$ and $p=5$. The product of the factors of columns a, b, and c gives the individual summation terms. The time of installation of each unit, as well as the factor of present value, were derived from the graphics of Figure 4, taking into account that time t_n is measured assuming t_0 as origin. The worth of power losses applicable to each generating unit, given in Table III, is derived multiplying the individual values of column d by the factor:

$$\frac{r}{(1-k)p}C=\frac{0.13}{(1-0.95)5}C=0.52C$$

and is valid for the rate of interest six per cent. The total worth for the rate of interest eight per cent also mentioned in the example is obtained as product of the summation of column e by the same factor 0.52 C.

2. By equation 17′

$$S=Cr\sum_{n=0}^{n=u-1}\frac{1}{(1+i)^{t_n}(h_m-1)(kp+n)}$$

By similar procedure as previously explained, Table V can be established.

The worth of power losses applicable to each generating unit, given in Table III, is derived multiplying the individual values of column d by the factor:

$Cr=0.13C$

and is valid for the rate of interest six per cent. There is practical coincidence of the values of power losses obtained by equations 17 and 17′.

two-phase co-ordinates of a three-phase network.

Symmetrical Components of a Single-Phase Three-Wire Network

CURRENTS AND VOLTAGES

A symmetrical n-phase system has n voltages equal in magnitude and spaced $360°/n$ apart in phase. If n equals 2, the result is not a two-phase system, in the usual sense of that term, but rather a single-phase three-wire system. The characteristic angle is $360°/2=180°$. The two symmetrical sets of current or voltage vectors are shown in Figure 1: the zero-order set, differing in phase by $0\times180°=0$; and the first-order set, differing by $1\times180°=180°$. Zero-order currents are equal and in phase in the two outer wires, and return in the neutral wire or in the earth. They result from unbalanced line-to-neutral load or line-to-ground short circuits. First-order currents are equal and opposite in the two outer wires. They result from line-to-line loads or short circuits. The phase currents I_a and I_b in the outer conductors are given in terms of their symmetrical components I_0 and I_1 by the following equations:

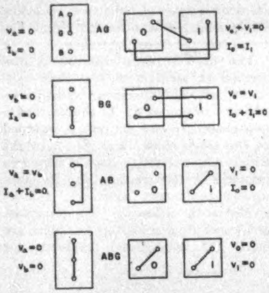

Figure 2. Connections of the sequence networks corresponding to four types of short circuit on a single-phase three-wire network

$$I_a=I_0+I_1 \tag{1}$$

$$I_b=I_0-I_1 \tag{2}$$

The inverse equations are:

$$I_0=(I_a+I_b)/2 \tag{3}$$

$$I_1=(I_a-I_b)/2 \tag{4}$$

Similar equations hold for voltages.

IMPEDANCES

Consider a circuit element, such as a transformer or line, for which the two phases, each consisting of an outer conductor with neutral or ground return, having equal self impedances Z_s and mutual impedance Z_m. The phase voltages, in terms of the phase currents and impedances, are:

$$V_a=Z_sI_a+Z_mI_b \tag{5}$$

$$V_b=Z_mI_a+Z_sI_b \tag{6}$$

The symmetrical components of voltage are:

$$V_0=(V_a+V_b)/2$$
$$=(Z_s+Z_m)(I_a+I_b)/2=Z_0I_0 \tag{7}$$

$$V_1=(V_a-V_b)/2$$
$$=(Z_s-Z_m)(I_a-I_b)/2=Z_1I_1 \tag{8}$$

where $Z_0=Z_s+Z_m$ and $Z_1=Z_s-Z_m$. For circuits of the type described, the two substitute circuits are independent. That, of course, is the advantage of the substitution.

SHORT CIRCUITS

There are four different types of short circuit on a single-phase three-wire circuit, as shown in Figure 2. The equivalent connections between substitute networks are also shown there.

TRANSFORMERS

The zero-order equivalent circuits of several transformer connections are shown in Figure 3. The zero-order impedance of a winding is measured by applying single-phase voltage from the two outer terminals, joined together, to the neutral tap, and by taking the ratio of applied voltage to the current in half the winding. The first-order circuit is the same for all the connections shown; it is the ordinary equivalent circuit of a transformer.

Four-Phase Networks

CURRENTS AND VOLTAGES

A four-phase network may be regarded as two single-phase three-wire networks, with the normal currents and voltages of one in quadrature with those of the other; and the substitutions described previously for such networks may be applied to each. The substitute currents (denoted by subscripts 4, 5, 6, 7) expressed in terms of phase currents (a, b, c, d) are then as follows:

$$I_4=(I_a+I_c)/2 \tag{9}$$

$$I_5=(I_a-I_c)/2 \tag{10}$$

$$I_6=(I_b+I_d)/2 \tag{11}$$

$$I_7=(I_b-I_d)/2 \tag{12}$$

The inverse equations are:

$$I_a=I_4+I_5 \tag{13}$$

$$I_c=I_4-I_5 \tag{14}$$

$$I_b=I_6+I_7 \tag{15}$$

$$I_d=I_6-I_7 \tag{16}$$

Similar equations hold for voltages. The computation required to go from phase quantities to two-phase co-ordinates and back is extremely simple.

TRANSFORMERS

Usually a four-phase network is fed from two transformers, the center taps of which are joined. When the substitution of variables, described by equations 9 to 16, is used, the two substitute networks of each transformer are independent, just as they are for one transformer on a single-phase three-wire system. Furthermore, the two transformers are independent of each other. Therefore, the substitution is suitable even if the two transformers of a bank differ in impedance, ratio, or both. If the transformers are Scott-connected, two-phase co-ordinates may be used for circuits on the three-phase side.[4]

SHORT CIRCUITS ON A FOUR-PHASE NETWORK

There are 16 different types of short circuit on a four-phase network, including double short circuits. These are listed in Figure 4, together with the equivalent connections between networks of four-phase symmetrical components. In Figure 5 are shown the equivalent connections between substitute networks of two-phase co-ordinates. In many cases the connections are simpler in the latter system than in the former. However, it should be remembered that both networks 5 and 7 contain generated electromotive forces (normally in quadrature), whereas, in symmetrical components only the positive-sequence network (number 1) has them.

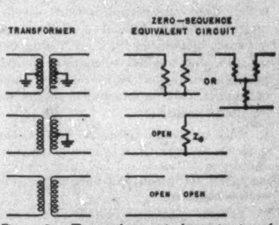

Figure 3. Zero-order equivalent circuits of single-phase transformers

MODIFIED SYMMETRICAL COMPONENTS

It is a familiar fact in symmetrical components of a three-phase system that the equations and the equivalent circuits of faults or other unbalances are simplest if the unbalance is symmetrical with respect to the reference phase (phase a). For example, a line-to-line short circuit is usually assumed to be on phases b and c for this reason. Otherwise, phase shifts would be required in the connections between sequence networks.

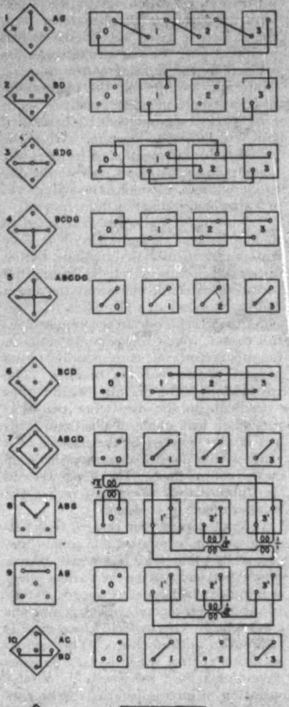

Figure 4. Connections of the sequence networks corresponding to 16 types of short circuit on a four-phase network

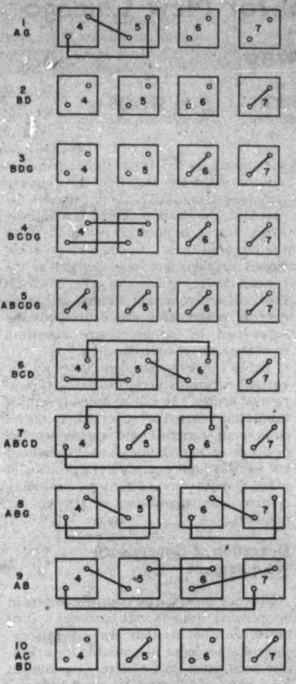

Figure 5. Connections of the substitute networks of two-phase co-ordinates corresponding to 16 types of short circuit on a four-phase network

In a four-phase system some faults are symmetrical with respect to phase *a*, but there are others, such as a short circuit between adjacent lines, which cannot be made so. Most such faults, however, are symmetrical about an axis midway between two phases. The following modified symmetrical components have the reference phase midway between phases *a* and *b*:

$$I_0=(I_a+I_b+I_c+I_d)/4 \tag{17}$$

$$I_1'=(I_a\underline{/-45^\circ}+I_b\underline{/45^\circ}+I_c\underline{/135^\circ}+I_d\underline{/-135^\circ})/4 \tag{18}$$

$$I_2'=(I_a\underline{/-90^\circ}+I_b\underline{/90^\circ}+I_c\underline{/-90^\circ}+I_d\underline{/90^\circ})/4 \tag{19}$$

$$I_3'=(I_a\underline{/-135^\circ}+I_b\underline{/135^\circ}+I_c\underline{/45^\circ}+I_d\underline{/-45^\circ})/4 \tag{20}$$

The inverse equations are:

$$I_a=I_0+I_1'\underline{/45^\circ}+I_2'\underline{/90^\circ}+I_3'\underline{/135^\circ} \tag{21}$$

$$I_b=I_0+I_1'\underline{/-45^\circ}+I_2'\underline{/-90^\circ}+I_3'\underline{/-135^\circ} \tag{22}$$

$$I_c=I_0+I_1'\underline{/-135^\circ}+I_2'\underline{/90^\circ}+I_3'\underline{/-45^\circ} \tag{23}$$

$$I_d=I_0+I_1'\underline{/135^\circ}+I_2'\underline{/-90^\circ}+I_3'\underline{/45^\circ} \tag{24}$$

The modified symmetrical components are used in those parts of Figure 4 where the four-phase networks are indicated by squares with vertical and horizontal sides; regular symmetrical components are used where the networks are indicated by squares with sloping sides.

The unbalance shown in part 16 of Figure 4 does not have either type of symmetry. Consequently, the connection made between sequence networks for representing this unbalance requires transformers of complex ratio. When two-phase co-ordinates are used, however, none of the connections between substitute networks require such transformers.

References

1. METHOD OF SYMMETRICAL CO-ORDINATES APPLIED TO THE SOLUTION OF POLYPHASE NETWORKS, C. L. Fortescue. AIEE TRANSACTIONS, volume 37, 1918, pages 1027–1140.

2. SYMMETRICAL COMPONENTS AS APPLIED TO THE ANALYSIS OF UNBALANCED ELECTRICAL CIRCUITS (book), C. F. Wagner, R. D. Evans. McGraw-Hill Book Company, Inc., New York, N. Y., 1933.

3. PROBLEMS SOLVED BY MODIFIED SYMMETRICAL COMPONENTS, Edith Clarke. *General Electric Review,* volume 41, 1938, pages 488–94, 545–9. CIRCUIT ANALYSIS OF A-C POWER SYSTEMS (book), volume 1, SYMMETRICAL AND RELATED COMPONENTS, Edith Clarke. Chapter X, Alpha, Beta, and Zero Components of Three-Phase Systems, John Wiley and Sons, Inc., New York, N. Y. 1943.

4. TWO-PHASE CO-ORDINATES OF A THREE-PHASE CIRCUIT, Edward W. Kimbark. AIEE TRANSACTIONS, volume 58, 1939, pages 894–910.

5. SYMMETRICAL-COMPONENTS ANALYSIS OF THE FOUR-PHASE SYSTEM, A. Boyajian. AIEE TRANSACTIONS, volume 63, 1944, February section, pages 48–51.

Supervisory Control for New Chicago Subway

W. A. DERR
ASSOCIATE AIEE

C. J. BUCK
NONMEMBER AIEE

J. A. STOOS
NONMEMBER AIEE

THE FIRST SECTION of the long-planned Chicago subway was opened to the public October 17, 1943. The section of subway which now is in daily operation extends along State Street and is 4.9 miles in length. This is but the first step in a program which ultimately may comprise as much as 50 miles of subway in the city of Chicago.

The necesssity of having the complete electric system under the control of a single operator resulted in the application of supervisory-control equipment. The supervisory-control dispatching-office equipment is located in the Chicago Rapid Transit Company office on the 12th floor of the Edison Building in downtown Chicago. Remote-station supervisory-control equipment is located at eight control centers in the subway. Figure 1 shows the location of the dispatching office with respect to the eight control centers. The Visicode type of supervisory-control equipment which was applied operates over a single pair of wires between the dispatching office and each of the remote control centers. There is also a pair of spare line wires for the control centers located north of the dispatcher's office and another pair for the centers south of the dispatcher's office. At each control center there is a toggle switch which is used to connect that center to the normal or the spare line.

The electric distribution system for the subway is shown in Figure 2. It will be noted from this figure that traction power is fed directly to the subway from three Commonwealth-Edison Company substations, namely, South State, East Lake, and Sedgwick, and in addition power is fed from the distribution system of the elevated lines by means of remotely controlled circuit breakers located at the extremities of the subway where track connections are made with the elevated lines. In some cases, these circuit breakers are located right at the control center, whereas in other cases the breakers are remotely located from the control center and are controlled and supervised by a direct-wire extension from the nearest control center.

Table I. Operations Performed by the Supervisory Control Equipment at a Typical Control Center

Supervise low battery voltage, battery ground, and line wire ground.
Control and supervise four circuit breakers in the control center.
Control and supervise station fans, low-speed forward, high-speed forward, and high-speed reverse.
Control and supervise five reclosing circuit breakers at a Commonwealth Edison Company substation.
Supervise normal- and emergency-service feeder voltage at each of two a-c switchboard rooms.
Supervise high-water and motor-overload trip at each of two pump rooms.
Control and supervise tunnel-fan high speed and tunnel-fan low speed or ventilating-louvre positions.
The supervisory control equipment provides space and wiring for the addition of seven future functions.

Table I gives a complete list of all the various functions performed at a typical control center. It will be noted from this tabulation that the supervisory-control equipment controls and supervises the position of ventilating fans throughout the subway and supervises the position of other devices in addition to providing control and supervision of the circuit breakers.

Operation of Supervisory Equipment

Visicode supervisory-control equipment is operated from 48-volt batteries. Batteries are used so that the supervisory-control equipment is available for operation even when no a-c power is available. Two number 14 wires are used between the dispatching office and each remote control center for operation of the supervisory-control equipment.

The supervisory equipment operates by means of coded d-c impulses. Each unit controlled has a particular code associated with it. In case of a selection initiated by the dispatcher, the associated code is sent to the remote control center, from where the selected relay returns a duplicate code, as a check, to the dispatching office. When the check code is received at the dispatching office, the associated selection lamp on the control desk, as well as that on the diagram board, is lighted. The returned check code must agree exactly with the code initially sent out or no further operation is possible. Thus the selection of a particular unit is positively checked before it is possible to perform an operation. Actually to perform an operation the dispatcher turns the associated twist key to the desired position, after having proper selection verified by the lighting of the selection lamp, and then presses the master control push button. This operation sends the closing or tripping code to the selected unit, causing it to operate. When the breaker changes position, it initiates the sending of a supervision code to the dispatching office, changing the red, green, or amber lamp indication to correspond.

An automatic operation is reported in similar fashion. When a circuit breaker trips automatically, its auxiliary switch causes its selecting code to be transmitted to the dispatching office and the alarm bell to be sounded. The office relay returns the check code to the remote control center, which immediately sends in the supervision code corresponding to the tripped position of the breaker. The green lamp on the diagram board flashes to indicate to the dispatcher that that particular unit changed position. This fact is also denoted by the flashing of a white-with-black-dot disagreement lamp on the control desk. The dispatcher can then immediately select and reclose the breaker should he so desire.

Visicode supervisory control is an all-relay system composed of simple mechanically uniform telephone relays, which send and receive the various selection and control codes at approximately 14 impulses per second. Each selection is automatically checked and the control is inherently antipumping. The coded-operation control which is used provides protection against the possibility of false operation of any apparatus due to foreign voltages on the line wires.

New Features

This particular installation has several new features which have not been used on previous supervisory-control installations. These are: the amber-lamp indication, the blinking-lamp indication, and the supervision of the direct-wire extensions from the control centers.

A description of these features is included in the two following sections.

Dispatching Office Supervisory Control Equipment

In the dispatching office on the 12th floor of the Edison Building, there is a control desk on which is mounted all of the necessary control keys and push buttons for controlling all of the apparatus in the eight remote control centers.

A diagram board with indicating lamps to designate the positions of the various devices supervised is located behind the control desk in a position to be viewed readily by the dispatcher. Figure 3 shows the control desk and the diagram board for the State Street subway.

Paper 45-7, recommended by the AIEE committee on automatic stations for presentation at the AIEE winter technical meeting, New York, N. Y., January 22–26, 1945. Manuscript submitted September 20, 1944; made available for printing November 9, 1944.

W. A. Derr is design engineer, switchboard engineering department, Westinghouse Electric and Manufacturing Company, East Pittsburgh, Pa.; C. J. Buck is with the Chicago Rapid Transit Company, Chicago, Ill.; J. A. Stoos is with the department of subways and superhighways, City of Chicago.

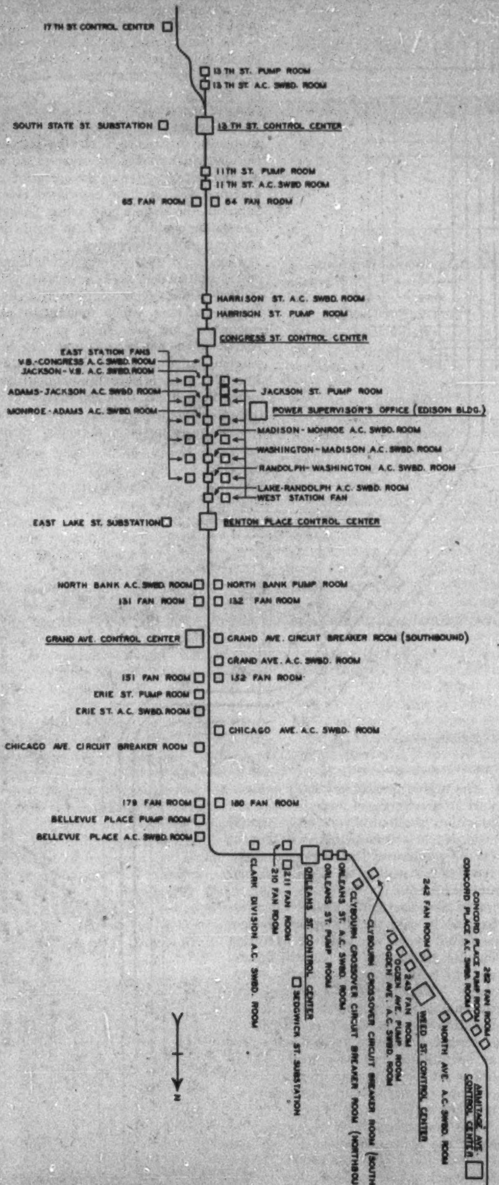
17 TH ST. CONTROL CENTER
13 TH ST. PUMP ROOM
13 TH ST. A.C. SWBD. ROOM
SOUTH STATE ST. SUBSTATION
13 TH ST. CONTROL CENTER
11TH ST. PUMP ROOM
11 TH ST. A.C. SWBD ROOM
65 FAN ROOM
64 FAN ROOM
HARRISON ST. A.C. SWBD. ROOM
HARRISON ST. PUMP ROOM
CONGRESS ST. CONTROL CENTER
EAST STATION FANS
V.B.-CONGRESS A.C. SWBD. ROOM
JACKSON - V.B. A.C. SWBD. ROOM
ADAMS-JACKSON A.C. SWBD ROOM
JACKSON ST. PUMP ROOM
MONROE - ADAMS A.C. SWBD. ROOM
POWER SUPERVISOR'S OFFICE (EDISON BLDG.)
MADISON - MONROE A.C. SWBD. ROOM
WASHINGTON - MADISON A.C. SWBD. ROOM
RANDOLPH- WASHINGTON A.C. SWBD. ROOM
LAKE-RANDOLPH A.C. SWBD. ROOM
WEST STATION FAN
EAST LAKE ST. SUBSTATION
BENTON PLACE CONTROL CENTER
NORTH BANK A.C. SWBD. ROOM
NORTH BANK PUMP ROOM
131 FAN ROOM
132 FAN ROOM
GRAND AVE. CONTROL CENTER
GRAND AVE. CIRCUIT BREAKER ROOM (SOUTHBOUND)
GRAND AVE. A.C. SWBD. ROOM
151 FAN ROOM
152 FAN ROOM
ERIE ST. PUMP ROOM
ERIE ST. A.C. SWBD. ROOM
CHICAGO AVE. A.C. SWBD. ROOM
CHICAGO AVE. CIRCUIT BREAKER ROOM
179 FAN ROOM
180 FAN ROOM
BELLEVUE PLACE PUMP ROOM
BELLEVUE PLACE A.C. SWBD. ROOM
CLARK DIVISION A.C. SWBD. ROOM
210 FAN ROOM
211 FAN ROOM
ORLEANS ST. CONTROL CENTER
SEDGWICK ST. SUBSTATION
ORLEANS ST. PUMP ROOM
ORLEANS ST. A.C. SWBD. ROOM
CLYBOURN CROSSOVER CIRCUIT BREAKER ROOM (NORTHBOUND)
CLYBOURN CROSSOVER CIRCUIT BREAKER ROOM (SOUTHBOUND)
OGDEN AVE. A.C. SWBD. ROOM
OGDEN AVE. PUMP ROOM
243 FAN ROOM
242 FAN ROOM
WEED ST. CONTROL CENTER
NORTH AVE. A.C. SWBD. ROOM
CONCORD PLACE A.C. SWBD. ROOM
CONCORD PLACE PUMP ROOM
262 FAN ROOM
ARMITAGE AVE. CONTROL CENTER
N

Figure 1. Locations in subway where supervisory-control functions are performed

The supervisory-control dispatching-office relay equipment is mounted in cases on the swinging panels of cabinets behind the diagram board.

The control desk is divided into eight sections corresponding to the eight control centers remotely controlled. There is a molded control-key plate or escutcheon for each piece of apparatus remotely controlled. There is space in each of the eight control-center sections of the control desk for mounting 24 of these control escutcheons. For the positions not now equipped there are molded blank plates. Wiring is installed in the control desk for all positions so an added function can be provided readily by replacing a blank plate with a control escutcheon.

Figure 4 shows a supervisory-control relay and a control-desk escutcheon. It will be noted that the escutcheon is equipped with a push-type selection key, a twist-type control key, a small white lamp, and a small white-with-black-dot lamp, as well as with two engraved name plates.

The small white lamp is the selection lamp. It is used to inform the dispatcher that the supervisory-control equipment has completed the selection of that particular unit and that the equipment is ready for further operation.

The white-with-black-dot lamp is the disagreement lamp which is used to indicate to the dispatcher that the setting of the individual twist-type control key disagrees with the position of the apparatus unit at the control center. For example, assume that the dispatcher has operated the individual twist-type control key to the "close" position and has closed a circuit breaker and this breaker opens due to the operation of protective devices at the remote control center. The disagreement lamp will then be lighted in addition to the green supervisory indicating lamp on the diagram board to inform the dispatcher that the particular unit has undergone a change and that the setting of the control key does not agree with the lamp indication.

The twist-type control key affords the dispatcher the means for selecting a "trip" or "close" operation. The setting of this key determines what operation is to be performed.

The nonlocking push-type selection key enables the dispatcher to set the supervisory-control equipment into operation to select a definite apparatus unit. Thus the dispatcher may cause the supervisory-control equipment to select any individual unit at the remote control center.

In addition to the individual control escutcheons just described, the control desk is equipped with four nonlocking push-type master control keys for each control center, designated as follows:

Master control key.
Zone reset key.
Zone check key.
Blinker reset key.

The master control key must be operated after selection of an individual unit to initiate the control code. The control code which is transmitted is dependent on the position of the individual twist-type control key on the associated control escutcheon.

The zone reset key is used to cancel selections in case the dispatcher changes his mind before sending the operation impulse, to acknowledge line-wire failure, and to acknowledge automatic operations. This key is also associated with the audible alarm circuit. When an automatic operation occurs, the alarm bell is energized to notify the dispatcher that an operation is being recorded. If the bell is set for continuous ringing, it will continue to give an alarm until the zone reset key is momentarily depressed.

The zone check key is operated to check the lamp indication of each and every device in a control center. If the zone check key is depressed after a selection has been made, the selected unit only is checked. Thus, the zone check key serves as an individual as well as a master check.

The blinker reset key is used to stop the flashing of red, green, or amber lights on the diagram board and of disagreement lights of the control desk. Any automatic operation which takes place at a control center results in a flashing light to enable the dispatcher to readily pick out the unit which changed position. That is, if a breaker trips due to the operation of a protective relay, the associated green lamp at the dispatching office flashes. The lamp continues to flash until the blinker reset key is operated.

There are a total of four station lamps on the control desk, associated with each control center. One of these is a line supervision lamp which is normally extinguished and only lights in case of trouble on the line wires between the dispatching office and the control center. The pilot lamp is normally extinguished and is lighted any time the supervisory-control equipment is not normal. The zone-alarm lamp is a normally extin-

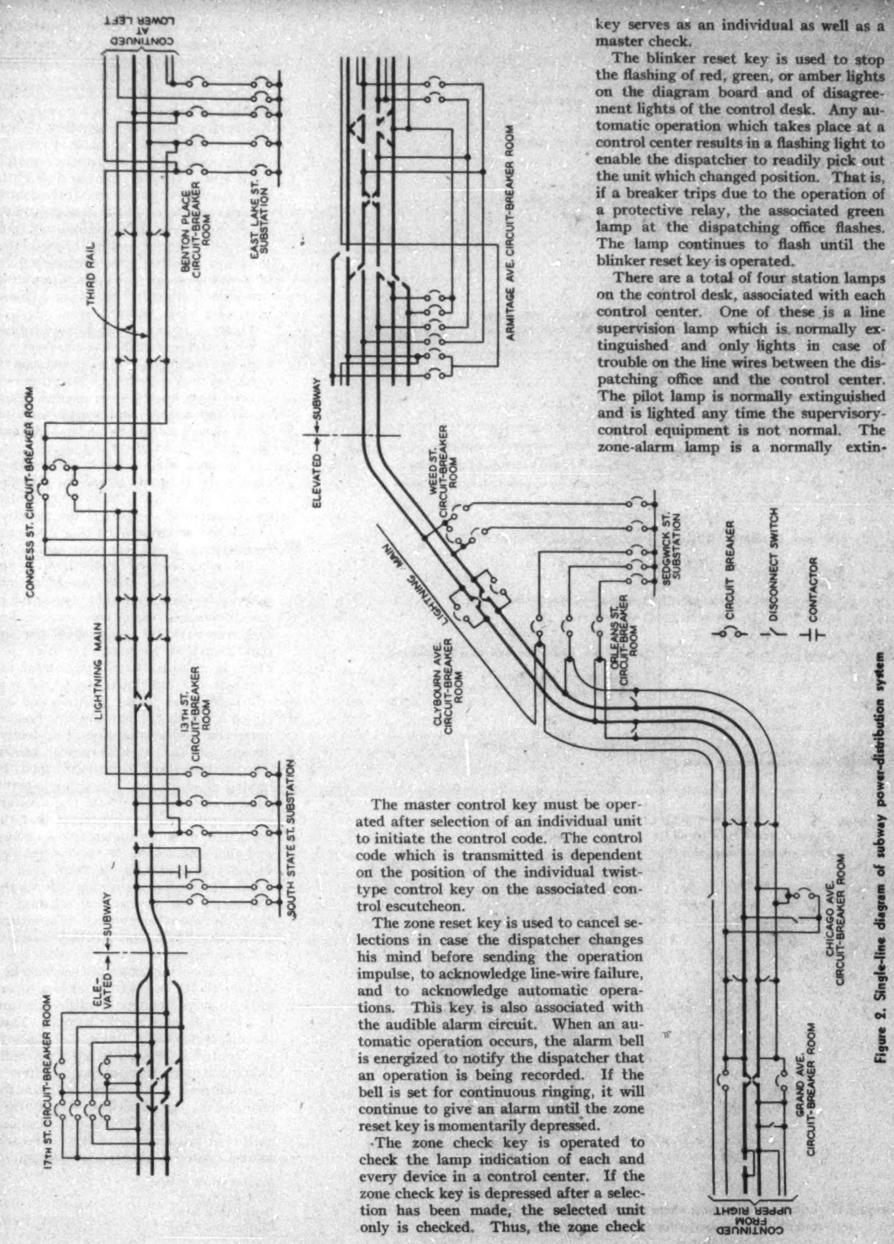
CONTINUED AT LOWER LEFT
BENTON PLACE CIRCUIT-BREAKER ROOM
EAST LAKE ST. SUBSTATION
THIRD RAIL
CONGRESS ST. CIRCUIT-BREAKER ROOM
LIGHTNING MAIN
13TH ST. CIRCUIT-BREAKER ROOM
SOUTH STATE ST. SUBSTATION
ELE-VATED
SUBWAY
17TH ST. CIRCUIT-BREAKER ROOM
ARMITAGE AVE. CIRCUIT-BREAKER ROOM
SUBWAY
ELEVATED
WEED ST. CIRCUIT-BREAKER ROOM
SEDGWICK ST. SUBSTATION
LIGHTNING MAIN
CLYBOURN AVE. CIRCUIT-BREAKER ROOM
ORLEANS ST. CIRCUIT-BREAKER ROOM
CIRCUIT BREAKER
DISCONNECT SWITCH
CONTACTOR
CHICAGO AVE. CIRCUIT-BREAKER ROOM
GRAND AVE. CIRCUIT-BREAKER ROOM
CONTINUED FROM UPPER RIGHT

Figure 2. Single-line diagram of subway power-distribution system

guished lamp which is lighted whenever an automatic operation takes place. Each zone has a zone-alarm lamp on the diagram board which is in parallel with the one on the control desk. The fourth common lamp is used to indicate low control-center battery voltage, battery ground, or line-wire ground. This is a normally extinguished lamp which is lighted only to indicate trouble. The control desk is also equipped with jacks which are used to insert testing instruments into the line circuits.

The diagram board is divided into eight sections, one for each control center. Each section consists of four removable panels. There are dustproof doors on the rear which provide access to the panel wiring. The panels are finished in gray and are equipped with Vinylite plastic mimic bus of various colors. The lamps on the diagram board may be operated from an a-c supply or from the 48-volt battery.

The circuit-breaker indicating lamps are arranged in a layout depicting the actual track routing as can be seen from Figure 3. There is a red, green, and white lamp for each of the subway breakers. The red lamp indicates a closed breaker and the green lamp indicates an open breaker. The white lamp is a selection lamp which operates in parallel with the selection lamp on the control desk.

An additional amber lamp is furnished on the diagram board for each of the power-supply breakers located in the Commonwealth Edison substations at South State Street, East Lake Street, and Sedgwick Street. These breakers are arranged for automatic reclosing when they trip due to a fault if the d-c load-measuring equipment indicates that reclosing is permissible. When the breakers are tripped by supervisory control they are locked out and will not reclose automatically. The fact that one of these breakers may be tripped and locked out or tripped and not locked out makes it necessary to have two separate indications for an open breaker. An amber lamp indicates that the breaker is open but not locked out and that it will automatically reclose if the fault is removed. A green lamp indicates that the breaker is open and locked out. If one of these breakers trips due to the operation of protective devices an amber-lamp indication is the result at the dispatching office. The dispatcher may then lock this breaker out if he desires by selecting the point, setting the associated twist-type control key in the "trip" position, and operating the master control key. This results in the breaker being locked out and the green lamp being lighted at the dispatching office.

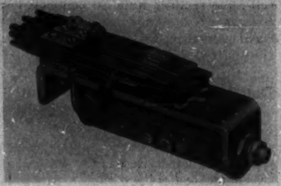

Figure 4a (left). Typical supervisory-control relay

Figure 4b (right). Typical dispatcher's control and supervision escutcheon

Just below the sections containing the breaker indicating lamps are the sections containing the red, green, and white lamps for the ventilating fans. The fans are divided into two types, tunnel fans and station fans. Each tunnel fan can be controlled by two supervisory control points. One point is used to start and stop the fan on high speed. The other point starts and stops the fan on low speed, and can also be used to open and close the independent louvres. The supervisory equipment is transferred from low speed fan control to louvre control by a transfer switch in the fan-control cabinet. The station fans are divided into two groups, one of six and the other of seven fans. Each group is controlled by three supervisory-control points. One point starts and stops the fans on low-speed forward operation. The other two points control the fans on high-speed forward and high-speed reverse operation respectively. Each fan is equipped with a transfer switch to transfer the control of that individual fan from supervisory to local push-button control. For each fan group, there is a lamp on the diagram board which indicates whether all the fans in that group have responded to the control operation. In all cases, a red lamp indicates that the fan is running, a green lamp indicates that the fan is stopped, and the white lamp is a selection lamp paralleling the selection lamp on the control-desk escutcheon.

The lamp indications for subway-pump alarms and the indications of a-c service are located on the lower sections of the diagram board. There is no remote control associated with these indications and hence there is no control escutcheon on the control desk associated with these indications. Only a red and a green lamp are used for these indications, no white selection lamp being required since no control of these units is provided from the control desk.

Figure 3. Supervisory-control desk and diagram board in Edison Building power dispatcher's office

Control-Center Supervisory-Control Equipment

The control-center supervisory equipment is mounted on the swinging panels of cabinets suitable for mounting against the wall. On one swinging panel the supervisory-control relays are mounted in four cases. Relay equipment is provided for all of the present functions performed and there is space and wiring available to provide additional functions which it may be desirable to perform by the supervisory-control equipment in the future. The interposing relays which are under the control of the supervisory relays and which operate into the control circuits of the breakers located in the control-center room are mounted on the other swinging panel. Figure 5 shows the 13th Street control center with the supervisory-control panels in the background.

The interposing relays for the control of the units which are located at some distance from the control center and which are controlled by a direct-wire extension are located with the units controlled. These interposing relays are under control of the supervisory relays over wires extending between the supervisory-control relay equipment and the interposing-relay location.

Relays are provided in the supervisory-

Figure 5. View of 13th Street control center showing rear view of circuit-breaker panels with supervisory-control panels in the background

control relay cases to provide an indication of low supervisory-control battery voltage. These relays operate at 45 volts so as to give an indication to the dispatcher before the battery voltage gets too low for operation of the supervisory equipment. The voltage-indication relays automatically restore when the voltage is raised to normal.

Grounds are detected on the control-center supervisory battery, the supervisory-control line wires between the dispatching office and the control center, and on all of the wires used for direct-wire extension from the control-center location by means of a Rectox ground detector. The Rectox ground detector is a full-wave rectifier unit, so connected as to cause a relay to operate when a ground occurs, resulting in an indication being transmitted to the dispatching office.

Table II

	Red Lamp	Green Lamp
Breaker closed by supervisory control	On	Off
Breaker opened by supervisory control	Off	On
Breaker in open position due to automatic tripping	Off	Flashing
Breaker closed locally	Flashing	Off

Table III

	Red Lamp	Green Lamp
Unit closed by supervisory control	On	Off
Unit opened by supervisory control	Off	On
Unit in open position due to automatic opening	Off	Flashing
Unit closed locally	Flashing	Off
Control and supervision wire broken	Flashing	Flashing

Detailed Description of Different Types of Control and Supervision

The fact that all of the equipment controlled and supervised is not located in the control center itself made it necessary to employ several different types of circuits for controlling and supervising the apparatus units involved. There are essentially four different circuit arrangements used, as will be described under the following subheadings.

A. Control and Supervision of Units Located in Control Center

For the control of units located right in the control center, there are two interposing relays on the control center panel for performing the "trip" and "close" operations. For all of these units, a single *a* auxiliary switch is used to obtain the red- and green-lamp indications at the dispatching office.

There are only two supervision codes associated with these units, a "trip" code of three impulses and a "close" code of five impulses.

Table II gives the lamp indications which are obtained at the dispatching office for manual and automatic operations on these units.

B. Single-Wire Extension Control and Supervision

The control of all fans and breakers not located right at the control center, with the exception of the automatic-reclosing Commonwealth Edison Company breakers, is arranged so that control and supervision is obtained over a single wire between the control center and the remote unit.

Figure 6 shows the elements of this direct-wire extension between the control center and the location of the remote unit. It will be noted from Figure 6 that an *a* and a *b* auxiliary switch are used for supervision purposes. The *a* auxiliary switch is connected to the negative side of the supervisory-control battery and the *b* auxiliary switch is connected to the positive side of the supervisory-control battery. The other sides of the *a* and *b* auxiliary switches connect to the coils of the "trip" and "close" interposing relays with the other side of the two interposing relays being connected to the single wire which extends to the control center. The two interposing relays which performed the control functions are energized by causing the proper polarity to be placed on the single control and supervision wire at the control center

The coils of the relays designated as *A* and *B* in Figure 6 are both connected to the single control and supervision wire at the control center. The resistance of this circuit is of such magnitude that approximately 20 milliamperes of current passes over the single control and supervision wire for supervision purposes. This current passes through the interposing-relay coil, but is only approximately 15 per cent of the current required for operation of the interposing relay. Thus the interposing relay does not operate until direct supervisory battery potential is placed on the control and supervision wire at the control center.

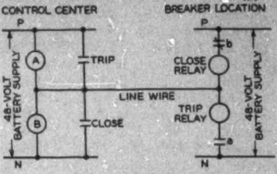

Figure 6. Schematic diagram showing essentials of single-wire control scheme

Either relay *A* or relay *B* will normally be energized at the control center due to either the *a* or the *b* switch of the breaker being closed. However, if the single control and supervision wire should become open, relays *A* and *B* will be energized in series. This fact makes it possible to supervise both positions of the remote breaker and also to supervise the continuity of the single control and supervision wire with relays *A* and *B*.

Table IV

	Red Lamp	Green Lamp
Unit in open position due to automatic opening	Off	Flashing
Unit closed locally	Flashing	Off
Supervision wire broken	Flashing	Flashing

Table V

	Red Lamp	Green Lamp	Amber Lamp
Breaker closed by supervisory control	On	Off	Off
Breaker opened by supervisory control	Off	On	Off
Breaker in open position due to automatic tripping	Off	Off	Flashing
Breaker locked out by supervisory control after automatic tripping	Off	On	Off
Breaker locked out by emergency alarm	Off	Flashing	Off
Breaker reclosed automatically	Flashing	Off	Off
Either or both control wires open	Flashing	Flashing	Off

Figure 7. View of typical pump room

The supervisory cabinet is the middle cabinet on the wall

There are three supervision codes associated with these units, a "trip" code of three impulses, a "close" code of five impulses, and a code of four impulses to indicate loss of the single-wire control and supervision circuit.

Table III gives the lamp indications which are obtained at the dispatching office on manual and automatic operations on these units.

C. Single-Wire-Extension Supervision

The supervision of a-c service voltage is arranged to operate over a single wire extending from the unit supervised to the control center. These units are arranged exactly as the single-wire control and supervision described in section B except that the interposing relays are omitted.

There are three supervision codes just as given in section B.

Table IV gives the lamp indications which are obtained at the dispatching office on automatic operations on these units.

Each of the pump rooms is supervised by a loop circuit which is opened in case of high water or motor overload trip. The lamp indications are the same as those listed above except that there is no indication for a broken wire. Figure 7 illustrates a typical pump room. The supervisory-control equipment is located in the center cabinet.

D. Two-Wire Extension Control and Supervision

Two wires are used between each of the automatic-reclosing Commonwealth Edison Company breakers and the control center for complete control and supervision of this breaker.

Figure 8 shows the elements of this direct-wire extension between the control center and the automatic-reclosing-breaker location. It will be noted from Figure 8 that one of the two wires is connected to the "trip" interposing relay. The other side of the "trip" interposing-relay coil connects to a make and a break contact of a toggle-type lockout relay. These contacts are designated as *MXC* and *MXT* on Figure 8.

If the breaker is tripped by operation of the supervisory-control "trip" interposing relay, the lockout relay is operated. This relay opens one of its contacts which is in series with the operating coil of the recloser, thus locking out the recloser. The supervisory-control "trip" interposing relay is operated either by having positive supervisory battery potential connected to the control wire by the supervisory-control equipment or by having this potential connected to the line wire by an emergency-alarm-relay contact located at the control center. The emergency-alarm system consists of pull boxes located at intervals along the track. These pull boxes are tied in with the supervisory-control relays at the control centers. When a pull box is operated, the breakers supplying that section of track are tripped and locked out.

If one of the automatic-reclosing breakers is tripped through the operation of protective equipment, the lockout relay is not operated, and hence the breaker will reclose as soon as the fault has cleared.

It will be noted from Figure 8 that the coils of relays *A* and *B* are both connected to the single trip wire at the control center and that relays *C* and *D* are both connected to the single close wire at the control center. The use of these four relays makes it possible to denote whether a breaker is closed, tripped but not locked out, or tripped and locked out, and also to supervise the continuity of the two control and supervision wires.

There are four supervision codes associated with the automatic-reclosing-breaker points—a "trip" code of three impulses if the breaker is tripped and locked out, a "trip" code of two impulses if the breaker is tripped but not locked out, a "close" code of five impulses, and code of four impulses to indicate trouble on either of the two control and supervision wires extending from the control center to the breaker.

Table V shows the lamp indications which are obtained at the dispatching office for manual and automatic operations of the automatic reclosing breakers.

Conclusion

The Visicode supervisory-control equipment used to control power for the State Street subway was designed to furnish all necessary information to the dispatcher in as small a space as feasible. This is of particular importance due to the future expansion of the subway system.

On supervisory-control systems built in the past, the change in position of a device has been indicated by the lighting of a disagreement lamp. This installation marked the advent of a new type of indication to indicate an automatic operation—the flashing of the red, green, or amber position-indicating lamp. The flashing-lamp signal has proved to be a definite improvement in locating a unit which has changed position, where a large number of units are involved.

The use of the single- and two-wire control schemes described has provided reliable operation with a minimum of conductors throughout the subway. The supervision of the wires involved in the direct-wire extensions from the control center is a unique feature.

Having the control of power circuits and ventilating means of the subway at the fingertips of one man provides fast and efficient operation.

The subway project was financed jointly by the city and the Public Works Administration of the federal government,

Figure 8. Schematic diagram showing essentials of control scheme for reclosing breakers

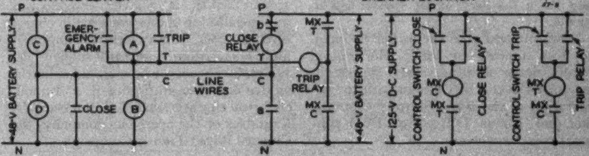

Graphical Method of Calculating Fault Currents on Rural Distribution Systems

F. W. LINDER
ASSOCIATE AIEE

IN the application of fuses, oil circuit reclosers, or any other type of sectionalizing device on a distribution system, a considerable amount of time and effort is usually spent in calculating fault currents at various locations on the system. The purpose of this paper is to describe a graphical method of calculating the fault currents which simplifies the task of making the calculations. The advantages of the graphical method, over other methods commonly used to make fault-current calculations, are:

1. A visual picture is obtained of the possible fault currents at any location on the system.
2. There is less chance for error.
3. Considerable time and effort are saved in making the calculations.
4. A compact permanent record is obtained.
5. It provides an easy method of quickly calculating the fault currents on new extensions added to the system after the original fault-current study has been completed.

The graphical method outlined in this paper is an exact method of calculating the fault currents. The accuracy obtained depends upon the scale chosen for the calculation diagrams and the care taken by the person making the calculations.

Line-to-ground, line-to-line, and three-phase types of faults will be considered in the following discussion. The illustrations and examples used to describe the graphical method were designed for rural distribution lines of the multigrounded neutral type, having a nominal voltage of 7,200/12,470 volts. However, the fundamental principles of the graphical method can be applied to any distribution system.

Description of Method

Fault-current calculations are made on current diagrams which are designed for a specific system voltage. A separate current diagram is used for line-to-ground, line-to-line, and three-phase faults. Typical current diagrams are shown in Figures 1 and 2, which are 7,200-volt diagrams for use on 7,200/12,470-volt multigrounded-neutral systems. The current diagrams in Figures 1 and 2 are exactly the same except for the line-mileage scales. The line-mileage scales in Figure 1 are for calculating line-to-ground faults and the line-mileage scales in Figure 2 are for calculating three-phase fault currents. A similar current diagram for calculating line-to-line fault currents would have line-mileage scales designed for line-to-line faults.

From the practical standpoint, the positive- and negative-sequence impedances of the power source may be assumed to be equal. If the further assumption is made that the equivalent spacing on two-phase lines is equal to the equivalent spacing on three-phase lines, then the line-to-line fault currents are equal to $\sqrt{3}/2$ times the three-phase fault currents. Therefore, for all practical purposes, line-to-line current diagrams are not absolutely necessary. Knowing the three-phase fault currents, the line-to-line fault currents can be calculated by a simple slide-rule operation.

The background of the current diagram in either Figure 1 or 2 is a rectangular co-ordinate system with resistance R in ohms along the horizontal axis and reactance X in ohms along the vertical axis. These resistance and reactance scales are for the total resistance and reactance values of the circuit from the power source to any point on the system where it is desired to know the fault current. The impedance of the circuit is

$$Z=\sqrt{R^2+X^2}$$

which is in the form of the equation of a circle where Z is the radius and R and X are co-ordinates for any point on the circle. The quarter circles on the current diagrams are impedance circles, each circle representing a value of impedance for corresponding values of R and X on the resistance and reactance scales. Instead of indicating the value of impedance that each circle represents, the circles are calibrated in terms of current in amperes based on the system line to neutral voltage. The line-to-neutral voltage is used as the base voltage for line-to-ground, line-to-line, and three-phase current diagrams. Fault currents can be read on the circles at the intersection of the total resistance and total reactance values of the circuit from the power source to the fault location on the system. It should be remembered that in the case of voltage transformations in the circuit, the resistance and reactance values must be referred to the voltage base for which the current diagram is designed.

In the lower right-hand corner of each current diagram, there is a group of scales called "line-mileage scales," each scale representing a different copper equivalent conductor size. Each scale is calibrated in miles, starting from zero at the left end of the scale, which refers to the length of a section of distribution line. The slope and calibration of each scale is governed by the per mile resistance and reactance values of the distribution line. Therefore, to design a line-mileage scale for line-to-ground faults, it is necessary to know the per phase resistance and reactance of the line for line-to-ground faults and for the conductor used. It is necessary to know the resistance and reactance values of the system for line-to-line and for three-phase faults to design mileage scales for these respective types of faults.

To design a line-mileage scale, choose a convenient point on the diagram for the zero point of the scale. Using the same scale as the resistance and reactance scales on the current diagram, lay off a distance horizontally to the right, equal to the resistance of one mile of line. From the point just located, lay off a distance vertically upward equal to the reactance of one mile of line forming two legs of a right triangle, the hypotenuse of which is equal to the impedance of one mile of line on the bases of the scale used for the current diagram. Draw the hypotenuse and extend it upward to the right,

---

Paper 45-8, recommended by the AIEE committee on protective devices for presentation at the AIEE winter technical meeting, New York, N. Y., January 22–26, 1945. Manuscript submitted April 24, 1944; made available for printing November 10, 1944.

F. W. LINDER is in the design and construction division of the Rural Electrification Administration, United States Department of Agriculture, St. Louis, Mo.

---

the latter contributing $23,130,000 of the $57,400,000 total cost. The city's share, $34,270,000, was obtained from the traction fund, thus eliminating the necessity for a tax levy or for special assessments.

Planning and construction of the project was directed by Philip Harrington, commissioner of subways and superhighways for the city of Chicago with the co-operation of the PWA Subway Commission and Joshua D'Esposito, PWA subway project engineer.

The portion of the work covered by this paper was financed by the city alone. The city is to be reimbursed by the operating company when unification of local transit facilities is achieved. Engineering and installation of this work was in charge of C. W. Post, subway electrical engineer, and J. A. Stoos, assistant subway designer, for the city, who were aided by the advice and co-operation of E. A. Imhoff, electrical engineer, and C. J. Buck and G. Krambles of the operating company, the Chicago Rapid Transit Company.

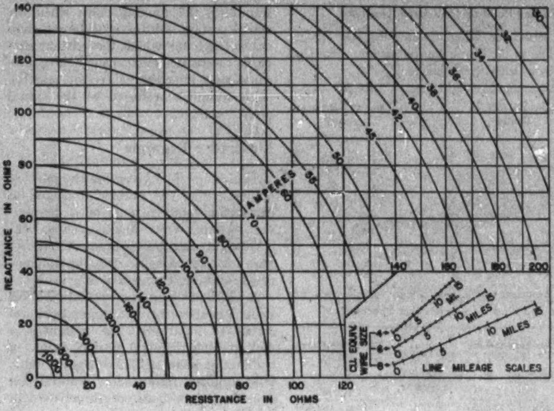

Figure 1. Typical 7,200-volt current diagram with line-mileage scales for calculating line-to-ground fault currents

forming the desired line-mileage scale. The scale can then be calibrated in miles by marking off distances equal to the length of the hypotenuse of the small impedance triangle. The use of the line-mileage scales in making fault current calculations will be explained farther on in this paper.

The line-mileage scales on the current diagrams shown in Figures 1 and 2 are for rural distribution lines constructed to the specifications of the Rural Electrification Administration. Values of resistance and reactance per mile for REA lines, which were used in designing the line-mileage scales, are given in Table I, which are average values for the various types of conductor used. The resistance and reactance of Copperweld, aluminum conductor steel reinforced, hard-drawn copper, and other types of conductor differ slightly for the same copper equivalent conductor size. However, the impedances of the various types of conductor are approximately the same for corresponding sizes and the error is negligible if average values for each copper equivalent conductor size are used in designing the line-mileage scales.

Use of Current Diagrams

In using the current diagrams for determining the fault currents on a distribution system, the starting point is at the source end of the system which is usually the load side of a substation feeding the system. It is necessary to know the equivalent total resistance and total reactance of the system from the generators to the starting point of the distribution system, for the type of fault being calculated and for both maximum and minimum fault-current conditions. All resistance and reactance values must be referred to the voltage base of the current diagrams. In many cases, the impedance of the supply system up to the distribution substation, which is referred to as the source impedance, is negligible and only the impedance of the substation need be considered. When the source impedance is appreciable, data is usually available on either the short-circuit kilovolt-amperes, fault currents, or positive-sequence impedance of the power source at the supply side of the distribution substation. From these data the equivalent source impedance for use in determining the starting points on the current diagrams can be calculated by use of formulas given in Table II, which apply to the most common types of rural distribution systems. Formulas are also given in Table II for determining the equivalent substation impedance which must be added to the source impedance. To determine the starting point on the current diagram, multiply the total source and substation impedance by 0.20 to determine the resistance component and by 0.98 to determine the reactance component. Other proportionate values may be assumed, based on judgment.

The formulas in Table II apply to four-wire wye multigrounded-neutral distribution systems supplied from a three-phase power source through a delta–wye transformer bank, which is the most common type of rural distribution system. The formulas for line-to-ground faults have no significance on delta distribution systems. However, the impedance formulas in Table II for line-to-line and three-phase faults apply to delta distribution systems supplied by a delta-delta substation. Other cases which are less common than those discussed above will not be considered in this paper. The relationship between the formulas in Table II should be noted. Each of the source and substation impedance formulas for line-to-line faults is $2/\sqrt{3}$ times the corresponding formula for three-phase faults. Each of the source impedance formulas for line-to-ground faults is two-thirds times the corresponding formula for three-phase faults and the substation impedance formula for line-to-ground faults is the same as the formula for three-phase faults.

When a fault occurs on the system, there may be some resistance in the fault, which should be considered. The fault resistance could be any value; however, it has been found that 40 ohms is a reasonable value to assume. An assumed value of fault resistance should be added to the resistance of the circuit in calculating minimum fault currents. From the practical standpoint, it is not necessary to consider the fault resistance for each type of fault. On multigrounded-neutral systems, the fault resistance need be considered only on line-to-ground faults because line-to-ground faults are usually used for minimum currents and line-to-ground faults are the only type of fault which can occur at any location on systems containing single-phase lines. On systems where line-to-line or three-phase faults are used for minimum currents, the fault resistance should be considered.

Table I. Impedance of REA Lines In Ohms Per Circuit Mile

Average Values for Copperweld, Aluminum Conductor Steel-Reinforced, and Hard-Drawn Copper; Standard REA Spacing; Earth Resistivity—100 Meter-Ohms

Copper Equivalent Conductor Size	For Line-to-Ground Faults; Single-Phase Impedance With Multigrounded-Neutral Wire		For Line-to-Line Faults; $2/\sqrt{3}$ Times Impedance to Positive- or Negative-Sequence Currents		For Three-Phase Faults; Impedance to Positive- or Negative-Sequence Currents	
	Resistance	Reactance	Resistance	Reactance	Resistance	Reactance
1/0	0.723	1.124	0.643	0.847	0.556	0.733
2	1.00	1.22	1.014	0.890	0.877	0.770
4	1.63	1.31	1.605	0.928	1.388	0.803
6	2.45	1.46	2.546	0.969	2.202	0.838
8	3.74	1.55	4.069	1.001	3.520	0.866
9½	5.04	1.67				
11	7.36	1.704				

Table II. Formulas for Determining the Starting Point on the Current Diagrams

Formulas for Determining the Equivalent Source Impedance When Given Either $I_{3\phi}$, $I_{(L-L)}$, $va_{3\phi}$, or Z_1, of the Power Source at the Supply Side of the Distribution Substation. (For Use on Distribution Systems Supplied by a Delta-Wye Substation)*

Given	For Line-to-Ground Faults	For Line-to-Line Faults	For Three-Phase Faults
$I_{3\phi}$	$Z_s=\frac{2E_n^2}{\sqrt{3}I_{3\phi}E_{(L-L)}}$	$Z_s=\frac{2E_n^2}{I_{3\phi}E_{(L-L)}}$	$Z_s=\frac{\sqrt{3}E_n^2}{I_{3\phi}E_{(L-L)}}$
$I_{(L-L)}$	$Z_s=\frac{E_n^2}{I_{(L-L)}E_{(L-L)}}$	$Z_s=\frac{\sqrt{3}E_n^2}{I_{(L-L)}E_{(L-L)}}$	$Z_s=\frac{3E_n^2}{2I_{(L-L)}E_{(L-L)}}$
$va_{3\phi}$	$Z_s=\frac{2E_n^2}{va_{3\phi}}$	$Z_s=\frac{2\sqrt{3}E_n^2}{va_{3\phi}}$	$Z_s=\frac{3E_n^2}{va_{3\phi}}$
Z_1	$Z_s=\frac{2Z_1E_n^2}{E_{(L-L)}^2}$	$Z_s=\frac{2\sqrt{3}Z_1E_n^2}{E_{(L-L)}^2}$	$Z_s=\frac{3Z_1E_n^2}{E_{(L-L)}^2}$

Formulas for Determining Substation Transformer Impedance in Ohms When Given $\%Z_T$ of Transformer. (For Use on Distribution Systems Supplied by a Delta-Wye Substation)*

Given	For Line-to-Ground Faults	For Line-to-Line Faults	For Three-Phase Faults
$\%Z_T$	$Z_T=\frac{\%Z_TE_n^2}{kva_{1\phi}\ 100{,}000}$	$Z_T=\frac{\%Z_T2E_n^2}{\sqrt{3}kva_{1\phi}\ 100{,}000}$	$Z_T=\frac{\%Z_TE_n^2}{kva_{1\phi}\ 100{,}000}$

Multiply Z_s and Z_T by 0.20 to obtain resistance components and by 0.98 to obtain reactance components. Other proportionate parts of resistance and reactance may be assumed, based on judgment.

List of Symbols

$E_{(L-L)}$ = Line-to-line voltage in volts on supply side of substation.
E_n = Line-to-ground voltage in volts on load side of substation.
$I_{3\phi}$ = Three-phase fault current in amperes on supply side of substation.
$I_{(L-L)}$ = Line-to-line fault current in amperes on supply side of substation.
Z_s = Equivalent impedance in ohms per phase of source at load voltage.
Z_1 = Positive-sequence impedance in ohms of source at substation.
Z_T = Equivalent impedance in ohms per phase of substation transformers.
$\%Z_T$ = Per cent impedance of substation transformers.
$va_{3\phi}$ = Three-phase short-circuit power in volt-amperes on supply side of substation.
$kva_{1\phi}$ = Substation transformer capacity in kilovolt-amperes per phase.

* Formulas for line-to-line and three-phase faults also apply to delta distribution systems supplied by a delta-delta substation. Formulas for line-to-ground faults have no significance on delta systems.

The procedure for calculating fault currents on the current diagrams is as follows:

1. Locate the point for the equivalent total impedance of the source and distribution substation by laying off the resistance along the horizontal scale and the reactance along the vertical scale. Locate the total impedance for both maximum and minimum fault-current conditions. Read the fault currents on the circles.

2. Draw a line from the points located in step 1 to the right, parallel to the line-mileage scale for the conductor size in the first section of line away from the substation. These lines can be drawn by manipulation of two drafting triangles, a rule and a triangle, or any other graphical means.

3. Using a compass, or dividers, and the mileage scale for the proper conductor size, set the instrument to the number of miles from the substation to the first point out on the system where it is desired to know the fault currents. Lay this distance off from the points located in step 1 along the lines drawn in step 2.

4. Read the fault currents on the circles.

5. Repeat the above procedure for the next point farther out on the system where it is desired to know the fault current. If the conductor size on the line changes, draw a new line on the diagram from the point for the end of the first conductor size, parallel to the proper mileage scale. Repeat until all points on the system, at which fault current values are desired, have been plotted on the diagram.

Although a current diagram is designed for a specific system voltage, it can be used for any system voltage provided the physical characteristics of the system are such that the impedance per mile of line is the same as the impedance used in designing the line-mileage scales. The fault current is directly proportional to the system line-to-neutral voltage. Therefore, fault currents read on a current diagram for a specific voltage can be converted to another voltage by multiplying them by the ratio of the line-to-neutral voltage of the system being studied to the line-to-neutral voltage for which the diagram was designed. In determining the starting point when the actual system voltage is different than the voltage for which the current diagrams were designed, the source and substation impedances to the starting point should be referred to the actual system voltage.

Illustrative Example

This example is given for the purpose of illustrating the graphical method of calculating fault currents on a distribution system. Only line-to-ground fault currents are calculated because the procedure for calculating each of the different types of fault currents is the same.

A one-line diagram of a hypothetical system is shown in the upper left-hand corner of Figure 3. The system is a multigrounded-neutral system, having a nominal voltage of 7,200/12,470 volts. It is supplied from a 33-kv transmission line through a bank of three 150-kva single-phase 33-kv to 7.2-kv transformers, each having an impedance of five per cent. The short-circuit kilovolt-amperes on the transmission line at the location of the substation is 20,000 kva. The problem is to determine the maximum and minimum fault currents at the points indicated on the diagram of the system.

Using the proper formula from Table II, the source impedance is:

$$Z_s=\frac{2\times(7{,}200)^2}{20{,}000{,}000}=5.2\text{ ohms}$$

The substation impedance is

$$Z_t=\frac{5\times(7{,}200)^2}{150\times100{,}000}=17.3\text{ ohms}$$

The total equivalent impedance of the source and substation referred to the distribution-system voltage is 22.5 ohms. Assuming the resistance component to be 0.20 times total equivalent impedance and the reactance component to be 0.98 times the total equivalent impedance, the total resistance to the load side of the substation is 4.5 ohms and the total reactance is 22.1 ohms which are the values used for the starting point on the current diagram for maximum fault current. Assuming a 40-ohm fault resistance, the starting point for minimum fault currents is 44.5 ohms resistance and 22.1 ohms reactance.

Table III. Data for Illustrative Example

Point	Preceding Point on Line Toward Substation	Miles From Previous Point on Line Toward Substation	Copper Conductivity Size—Section From Previous Point	Maximum Line-to-Ground Fault Current, Amperes	Minimum Line-to-Ground Fault Current, Amperes
Substation				320	145
A	Substation	13	4	153	94
B	*A*	7	6	110	75
C	*A*	10	6	98	60
D	*C*	5	8	79	58
E	*A*	19	6	73	55
F	*E*	9	6	59	46
G	*F*	8	8	47	38

The distance between the points on the system at which fault-current values are desired and the copper equivalent-conductor size in each section are given in Table III. The graphical calculation of the fault currents is shown on the current diagram in Figure 3 and the fault current values are tabulated in Table III.

Alternate Design for Line Mileage Scales

There is an alternate design for the line-mileage scales which some engineers may prefer to use. Instead of putting the mileage scales on the current diagrams, a right triangle similar to a drafting triangle can be constructed for each line-mileage scale. A separate triangle is necessary for each conductor size and for each type of fault. The triangles should be designed as described previously for designing the line-mileage scales on the current diagrams with the hypotenuse of each triangle calibrated in miles. These triangles can be used directly on the current diagram to draw lines between points at the proper slope and to lay off mileage distances between points.

Change in Source or Substation Impedance

If the source or substation impedance is changed, as in the case of installing additional generating capacity or installing larger transformers in the distribution substation, it is easy to determine the new fault currents on the distribution system, if a fault-current study of the system has been previously made by the graphical method. It is necessary to calculate the new equivalent resistance and reactance up to the beginning of the distribution system and locate the new starting points on a current diagram. Lay the new current diagram over the old current diagram and line up the starting points. Then trace the old fault current points and lines between the points onto the new current diagram. The new fault current values can then be read from the new current diagram.

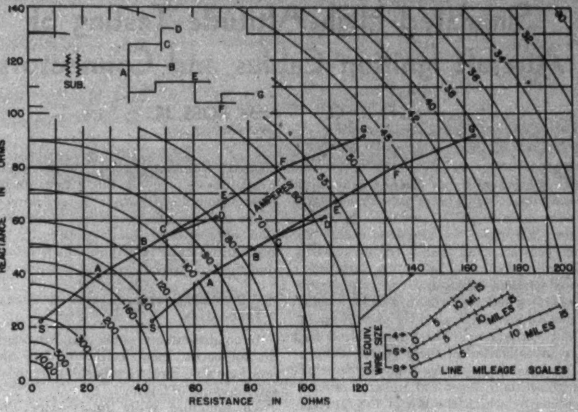

Figure 3. Illustrative example showing one-line diagram of a 7,200/12,470-volt system and graphical calculation of line-to-ground fault currents

Calculations above the current scale are for maximum fault currents and calculations below the current scale are for minimum fault currents. Refer to Table III for other data

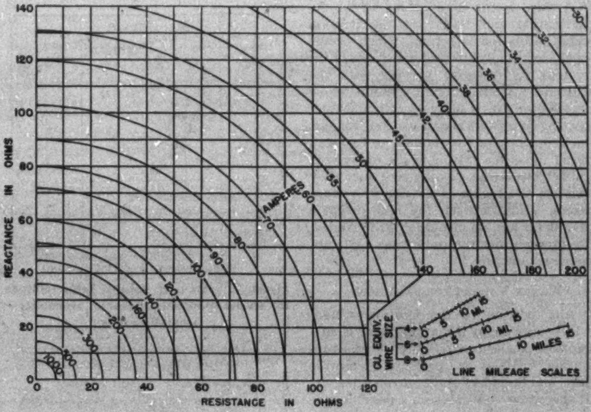

Figure 2. Typical 7,200-volt current diagram with line-mileage scales for calculating three-phase fault currents

Conclusion

The accuracy desired depends largely upon the scale chosen for designing the current diagrams. It is believed that sufficient accuracy can be obtained if the diagrams are prepared on standard $11^1/_2$-by-17-inch graph paper calibrated ten to the inch. A scale of one-half inch equals ten ohms can be used. If the system consists mainly of conductor sizes larger than number 4 copper equivalent, it is recommended that a scale of one inch equals ten ohms be used.

Separate current diagrams should be used for each substation. In cases where the distribution system is large and there are a large number of locations on the system where it is desired to know the fault currents, it is suggested that separate current diagrams be used for each one of the main feeder lines, in order to prevent confusion which may result from too many points on the same current diagram.

When the fault currents on a system have been calculated by the graphical method, the current diagrams will prove to be valuable in the operation of the system. Each current diagram gives a visual picture of fault current conditions at any location on the system.

References

1. Procedure for Making a Sectionalizing Study on Rural Electric Systems, B. O. Watkins. Technical Standards Bulletin 4, United States Department of Agriculture, Rural Electrification Administration.

2. Graphical Method of Calculating Fault Currents on REA Lines, F. W. Linder. United States Department of Agriculture, Rural Electrification Administration.

Simulated-High-Altitude Testing of Aircraft Ignition Cables and Connectors

H. H. RACE
FELLOW AIEE

A. M. ROSS, JR.
NONMEMBER AIEE

PROGRESS in flying to ever increasing altitudes has brought with it a host of problems of which none have been more urgent than those involving the distribution of magneto energy to the aircraft spark plug. Highly stressed even under more favorable conditions, conventional cables and connectors have exhibited failures in high-altitude operation whose origin called for prompt study and correction. This paper describes an investigation of these causes using a simulated high-voltage high-temperature high-altitude tester and presents several means by which the life of the ignition system may be appreciably extended.

The Problems

1. Arc-over at Connectors

In order to fly aircraft with high-voltage ignition systems to altitudes greater than about 30,000 feet, one of the technical problems which must be solved is the prevention of arc-over at any point in the ignition system, since such arc-overs prevent the plugs from firing. The conventional ignition system is assembled with at least three components—magneto, ignition wire, and spark plug—with detachable connectors between them. In general these connectors are not gas tight so that any spaces not filled with solid dielectric contain air at a pressure determined by the altitude. The effect of this is illustrated in Figure 1 by curve 1 which shows how the arc-over voltage of a number of types of connectors decreases as the air pressure is decreased to simulate high altitude. This effect represents an inherent limitation of the conventional high voltage ignition system.

The engine manufacturers have stated that the maximum voltage which may be required at the plug for the most severe conditions of engine operation is of the order of 12.7 kv peak. Figure 1 shows that this voltage cannot be obtained with conventional connectors above 20,000 to 25,000 feet altitude. However, if the engine requires only nine kv peak, standard connectors will not arc-over up to 40,000 feet.

Apart from temporarily reducing the available voltage to the spark plugs, intermittent high-altitude arc-overs may cause serious and permanent deterioration of connectors and cable ends by tracking, a type of failure which is not remedied by descent to lower altitudes.

2. Thermal Deterioration of Cable Insulation

If conditions are such that arc-overs do not occur, then deterioration of the ignition-cable insulation is the next most serious cause of failure.

To minimize radio interference the ignition cables must be completely encased in a metal shield (called the harness) from the distributor to the spark plug. Figure 2 shows a conventional spark-plug connection, at which point the highest temperatures are reached.

Engine manufacturers have stated that the temperature at the bottom of the spark plug well may be as high as 400 degrees Fahrenheit and in the elbow between 250 and 350 degrees Fahrenheit. Accelerated chemical decomposition at these temperatures causes deterioration of all conventional organic insulation. However, since there are large differences in the rates of oxidative and thermal decomposition among available rubber-like insulating materials, a proper choice of cable insulation and sheath materials is very important.

3. Corona Cutting of Cable Insulation

A third factor contributing to the deterioration and failure of the ignition cable insulation is corona, which occurs in all electrically stressed gas spaces of the system, its intensity varying with the altitude. Conventional ignition cable (see Figure 3A) is supplied with a lacquer coating to protect the insulation from attack, but mechanical damage to this may result in corona cutting of the underlying rubber insulation. Moreover, since they exist in the region of maximum voltage stress, voids between the ignition-cable conductor and its insulation will give rise to intensely destructive corona and subsequent puncture.

4. Water-Vapor Condensation

Any portion of the ignition system which is open to the atmosphere is susceptible to the condensation of moisture during changes in pressure, temperature, and humidity of the surrounding air. If this water condenses on a possible arc-over or creepage path of the insulation, as in connectors or spark-plug wells, the arc-over voltage will be greatly reduced.

Possible Solutions

Supercharging (to Correct 1, 3, and 4)

Although arc-over, corona, and entrance of moisture could be eliminated by supercharging the entire ignition system, this is not desirable if other solutions can be found because of the large supercharger capacity required and the likelihood of leaks or mechanical damage at any one of the many connections. A single break would destroy the high-altitude performance of the entire system. Furthermore, supercharging the harness appears unnecessary because of other possibilities listed below.

Filling of Manifold (to Correct 3 and 4)

Complete and permanent filling of the harness manifold with a void-free dielectric will eliminate corona and moisture difficulties. This has been made possible by the development of polymerizable liquids suitable for impregnating completely wired manifolds. One of these is at first sufficiently fluid to permit ready vacuum filling, and is converted by a brief bake at moderate temperatures to a soft elastic infusible gel of excellent electrical properties. Several thousand units of one make of this type have been put in service with no failures of manifold cables as yet reported.

Filling of Detachable Leads (to Correct 3 and 4)

Similarly, improved leads (from manifold to spark plug) have been developed. These are detachable from the manifold proper and carry an ignition cable and connectors completely molded into a Neoprene-filled flexible shielding con-

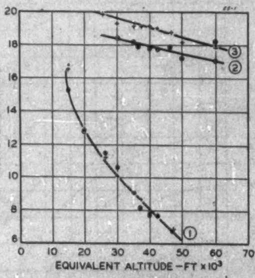

Figure 1. Arc-over voltage versus altitude for several spark-plug-connector assemblies—short-time tests

1—{ Textolite sleeve only—⊙
  { Mycalex sleeve only—+
2—Mycalex sleeve—+short grommet
3—Short ceramic sleeve—+long grommet

Paper 45-5, recommended by the AIEE committee on air transportation for presentation at the AIEE winter technical meeting, New York, N. Y., January 22–26, 1945. Manuscript submitted April 12, 1944; made available for printing November 3, 1944.

H. H. Race is research engineer, General Electric Company, Schenectady, N. Y., and A. M. Ross, Jr., is chemist in the works laboratory of the same company at Bridgeport, Conn.

duit. Tests are described in the section "Experimental—Results on Standard Cycle."

FILLING OF CONNECTORS (TO CORRECT 1, 3, AND 4)

By filling all spaces in the spark-plug well and connector with a plastic semisolid dielectric, arc-over may be made more difficult even at high altitudes. A compound of suitable electrical characteristics and excellent heat stability has recently been made available for this purpose.

INORGANIC TERMINAL SLEEVES (TO CORRECT 1 AND 2)

Until recently organic terminal sleeves have been generally used. These have very poor arc resistance so that if arc-over of appreciable intensity occurs the insulation becomes carbonized and is permanently destroyed. Recently inorganic terminal sleeves made from porcelain and Mycalex have been introduced. These do not change the arc-over characteristic of an open assembly at high altitude (see Figure 1), but the inorganic materials are not damaged by this arcing and will function satisfactorily again below the critical arc-over altitude. Another very important characteristic is that these inorganic materials do not deteriorate with time at the high temperatures existing in spark-plug wells.

NEOPRENE SEALING GROMMETS (TO CORRECT 1 and 4)

Neoprene is a synthetic rubber of greatly enhanced resistance to corona and can be compounded to have excellent heat resistance. It is, therefore, an excellent gasket material to seal connectors against water vapor from without or loss of pressure from within, thus improving the arc-over voltage characteristics of the sealed assembly as indicated in Figure 1, curves 2 and 3. This advantage is not always retained permanently in service as will be brought out in the discussion of our experiments, but it is helpful within the expected life between necessary disassemblies.

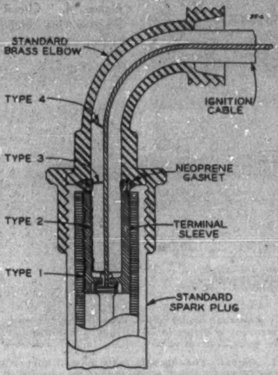

Figure 2. Cross section of plug-elbow-terminal-cable assembly (seven-millimeter cable)

Jagged lines denote possible paths of failure

INORGANIC ELBOWS (TO CORRECT 2 AND 3)

Solid spark-plug elbows have been made with Mycalex-insulated cores. These accomplish the desirable result that no organic material be located in the high temperature region of the spark-plug well.

Table I

Forty-Two Lacquered-Braid Cables

	Test Variations	Effect
Operating conditions:		
1. Voltage	12.7 kv peak; three sources: (*a*). 60 cycle transformer (*b*). aircraft magneto (*c*). electronic interrupter	No significant differences
2. Altitude	47,000 feet, constant (ten centimeters pressure)	
3. Temperature	270–400 F maximum (at plug elbow)	Longer life below 300 F; differences slight above 300 F
4. Cycling	Irregular or hourly, temperature only	Most failures occur in first cooling period
Components:		
1. Cables	All lacquered-braid: 7 mm (2 types) 5 mm (1 type)	No significant differences
2. Terminal sleeves	One inch Mycalex 9/16 inch Mycalex 9/16 inch porcelain	No significant differences
3. Grommets and boots*	Appropriate to terminal sleeves and cables above*	No significant differences*
4. Filling compounds	None, or one of seven types organic semisolid	Slight differences; type 7 has superior heat stability
5. Spark plugs**	1 type aircraft plug**	

*The necessity of having grommets to seal the connector was shown by four additional tests in which grommets were omitted: at 47,000 feet two assemblies failed at once; at 35,000 feet one failed at once, another lasted 1.7 hours. These tests are not included in Figure 10, curve 1.

**Plug electrodes were spread and 400 pounds pressure of nitrogen was admitted to electrode chamber to prevent plug from firing.

COMPOSITE TERMINALS (TO CORRECT 1, 2, 3, AND 4)

A neoprene boot of one millimeter wall-thickness, approximately the length of the elbow, is slipped over the end of five-millimeter cables to adapt them to seven-millimeter connector assemblies. During the course of our investigation a new terminal was developed in which the neoprene adapter-boot, a neoprene grommet, and a Mycalex terminal sleeve were molded integrally with the addition of a molded-in copper ring for the gasketing surface. This is a marked improvement and will be discussed in detail in connection with our test results.

IMPROVED IGNITION CABLES (TO CORRECT 1, 2, 3, AND 4)

This major improvement will be discussed in detail. The simulated flight tester, to be described, has very clearly demonstrated the superiority of the new constructions.

Simulated Altitude Testing—Apparatus and Procedures

The urgency of the problem of determining the causes of cable and connector failures and of developing improved assemblies required the adoption of a laboratory apparatus for reproducing, in at least some of its essential respects, the operation of an actual aircraft ignition system. This was not intended to replace individual property tests on construction materials but rather to provide laboratory information in advance of engine tests in the field.

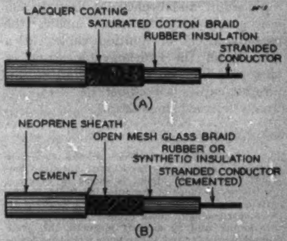

Figure 3. Conventional lacquered-braid ignition cable (A) and improved high-altitude ignition cable (B)

Essentially the test apparatus developed consists of: a means of applying a controlled, pulsating voltage to a shielded cable-connector-spark-plug assembly, a means of heating the spark plug to a controlled temperature, and a

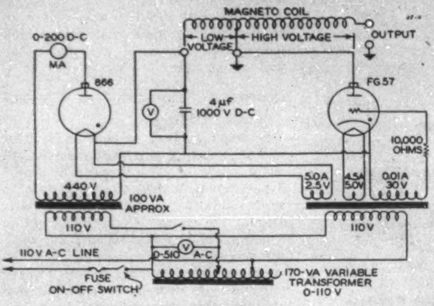
MAGNETO COIL
0-200 D-C
MA
LOW VOLTAGE
HIGH VOLTAGE
OUTPUT
866
FG 57
V
4 μf
1000 V D-C
10,000 OHMS
440 V
100 VA APPROX
5.0A 2.5V
4.5A 5.0V
0.01A 30V
110V
110V
V
110V A-C LINE
0-510 A-C
FUSE
ON-OFF SWITCH
170-VA VARIABLE TRANSFORMER 0-110 V

Figure 4. Circuit diagram for electronic interrupter

means for maintaining the system at a controlled external pressure. Early in our experimentation, it was noticed that certain types of assemblies failed more rapidly when the temperature and pressure were varied than they did under constant conditions. Repeated expansion and contraction caused leaks to develop after which electric discharges resulted in failure. Since fluctuation in these variables is characteristic of actual flight conditions a cyclic procedure was adopted and appropriate equipment installed.

Standard Test Conditions and Equipment

The original apparatus and procedures were varied during the course of the investigation and eventually fixed in accordance with discussions among the manufacturers of ignition cables at a meeting of the ignition-cable group of the technical advisory committee for aircraft cables, December 15, 1943. As finally selected these are:

(*a*). Voltage:

1. *Source.* The construction of the electronic interrupter, designed by the Electric Autolite Company, Port Huron, Mich., is shown in Figure 4 and the wave shape of the pulse (as drawn from a cathode-ray oscilloscope) is exhibited in Figure 5 in comparison with those produced by a 60-cycle transformer and an aircraft magneto, the other voltage sources tested. The pulse from this device is somewhat similar to that from the aircraft magneto but is higher in energy and would therefore be more destructive to partially failed specimens.

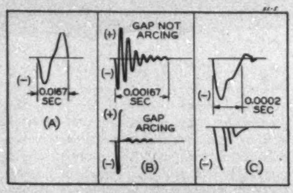

Figure 5. Wave shapes for three voltage sources sketched from high-voltage cathode-ray oscilloscope

A—Sixty-cycle ignition transformer
B—Thermionic interrupter
C—Aircraft magneto

2. *Output.* The output from the pulser is adjusted to 12.5 ± 0.5 kv peak at the start of the test and is permitted to fall as it will. A failure is considered to have occurred when the voltage falls to 5 kv peak.

(*b*). *Pressure.* The vacuum regulator is adjusted so that the minimum pressure reached is 10 ± 0.5 centimeters of mercury.

(*c*). *Temperature.* The input to the heaters is such as to raise the temperature of the spark plug (measured at the copper gasket) to 500 ± 10 degrees Fahrenheit and the elbow (measured at its midpoint) to 325 ± 5 degrees Fahrenheit, these being the maximum temperatures measured in vacuo.

(*d*). *Cycling.* The following switching schedule is used:

Time (Minutes)	Heat	Vacuum	Voltage
0	On	On	On
45		Off	
90		On	
120	Off		
135		Off	
180	On	On	On

The nature of the equipment is well illustrated by our most recent setup. A simplified block diagram for this is given in Figure 6 which indicates its construction and operation. It will be noted that the equipment is entirely automatic, the vacuum and heat cycling being controlled with an electric clock by cam-operated switches, and the voltage, temperature, and pressure being recorded automatically. A special contact on the voltage recorder shuts down the equipment when the failure voltage (five kilovolts peak) is reached.

Figures 7 and 8 are photographs of part of this equipment. In Figure 7 the electronic interrupter can be seen in the right-hand corner of the cage. At the top is the capacitance divider from which crest voltage readings can be taken on a vacuum-tube voltmeter.[1]

The right-hand plate shows the spark

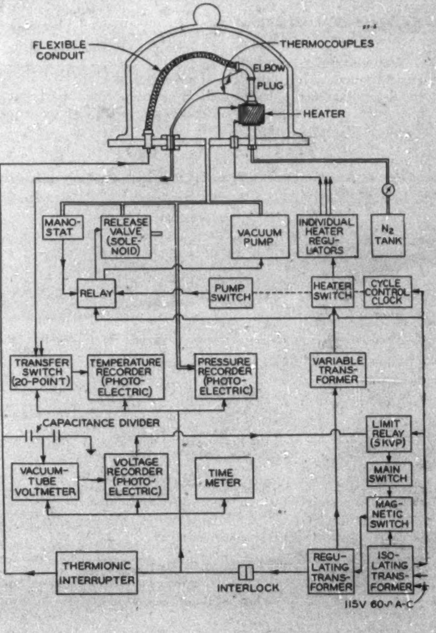
FLEXIBLE CONDUIT
THERMOCOUPLES
ELBOW
PLUG
HEATER
MANO-STAT
RELEASE VALVE (SOLE-NOID)
VACUUM PUMP
INDIVIDUAL HEATER REGU-LATORS
N₂ TANK
RELAY
PUMP SWITCH
HEATER SWITCH
CYCLE CONTROL CLOCK
TRANSFER SWITCH (20-POINT)
TEMPERATURE RECORDER (PHOTO-ELECTRIC)
PRESSURE RECORDER (PHOTO-ELECTRIC)
VARIABLE TRANS-FORMER
CAPACITANCE DIVIDER
LIMIT RELAY (5 KVP)
VACUUM-TUBE VOLTMETER
VOLTAGE RECORDER (PHOTO-ELECTRIC)
TIME METER
MAIN SWITCH
MAG-NETIC SWITCH
THERMIONIC INTERRUPTER
INTERLOCK
REGU-LATING TRANS-FORMER
ISO-LATING TRANS-FORMER
115V 60∿ A-C

Figure 6. Block diagram of automatic cycling and recording simulated-high-altitude-test equipment

Figure 7. Laboratory installation showing two three-sample test units, high-voltage power supply, and capacitance divider

Figure 8. Laboratory installation showing recording and control instruments

plugs inserted in their blocks (with heaters removed). In order to prevent sparking these plugs have their outer electrodes machined back and a pressure of 20 pounds per square inch of nitrogen is applied to the block. On the left the bell jar is completely set up with cables and shields in place and heaters and thermocouples connected.

Figure 8 exhibits the working bench, showing from right to left:

1. Electronic relay, operated from contact on voltage recorder to shut down the entire set up at failure.
2. Voltage recorder.
3. Vacuum-tube voltmeter.
4. Pressure recorder.
5. Temperature recorder.[3]
6. Motor-driven thermocouple transfer switch which scans each of 20 thermocouples every five minutes ($12^1/_2$ seconds reading, $2^1/_2$ seconds in transit between couples).

Voltage regulators, presssure regulator, heater-current adjustments, and so forth, are underneath this bench.

An example of the voltage-temperature-pressure records produced by this equipment is given in Figure 9.

EXAMINATION OF SAMPLES AFTER FAILURE

It was found early in the investigation that failures may occur in several ways. The importance of making and recording "post-mortem" examinations in such a study cannot be overemphasized as a means of learning how and why failures occur.

For convenience failures are grouped into four types:

Type 1 represents arc-over or creepage failure between the inside surface of the spark plug well and the outside surface of the terminal sleeve.

Type 2 represents arc-over or creepage failure between the inside surface of the terminal sleeve and the surface of the ignition cable.

Type 3 represents puncture of the cable under the gasket.

Type 4 represents puncture of the cable anywhere back of the gasket.

These failure types are illustrated in Figure 2. When the track or puncture is not visible, it can often be detected very readily by the use of a high-frequency spark coil (such as glass blowers use for detecting leaks in high-vacuum systems); the discharge from this travels visibly but harmlessly to any conducting path or puncture.

Table II

Forty-Six Neoprene-Sheathed Cables

	Test Variations	Effect
Operating conditions:		
1. Voltage	12.7 kv peak; electronic interrupter	
2. Altitude	47,000 feet (ten centimeters pressure)	
3. Temperature	350 F maximum (at plug elbow)	
4. Cycling	Hourly, heat only	
Components:		
1. Cables	All neoprene-sheathed: Five mm (six types) Seven mm (eight types)	Some types markedly superior
2. Terminal sleeves	One inch Mycalex $^9/_{16}$ inch Mycalex	No significant differences
3. Grommets and boots*	Appropriate to cables and terminal sleeves*	No significant differences
4. Filling compounds	None, or one of three types organic semisolid	No significant differences
5. Spark plugs**	One type aircraft plug**	

*One additional sample (not plotted) run without grommet lasted 1.2 hours.

**In the course of running this group the nitrogen pressure was reduced from 400 pounds to 25 pounds and the plug electrodes machined off to prevent firing.

Experimental—Early Results

The major problem facing the investigation at its inception was the fixing of the many variables involved in test conditions and component parts of the simulated ignition assembly. The early results, all obtained before the standard cycling procedure was finally devised, fall naturally into two groups.

LACQUERED-BRAID CABLES

The first tests were made on conventional ignition cables of the construction represented in Figure 3A. During this group of runs many variations of procedure and assembly components were used. These are summarized in Table I and the results on test life are plotted in Figure 10, curve 1.

No lacquered-braid cable withstood more than 22 hours of this treatment, as Figure 10, curve 1, indicates. In general, the failed samples exhibited very close resemblance to samples which had failed in actual high-altitude engine tests, the cotton braid being badly charred and the lacquer coating blistered and decomposed in the high-temperature region of the plug well. It was evident that this decomposition was caused by tracking as much as by the externally applied heat. Of all failures, approximately 60 per cent were due to arc-over and tracking, and 40 per cent to cable punctures.

NEOPRENE-SHEATHED CABLES

Because of the results summarized in Table I, subsequent experiments were

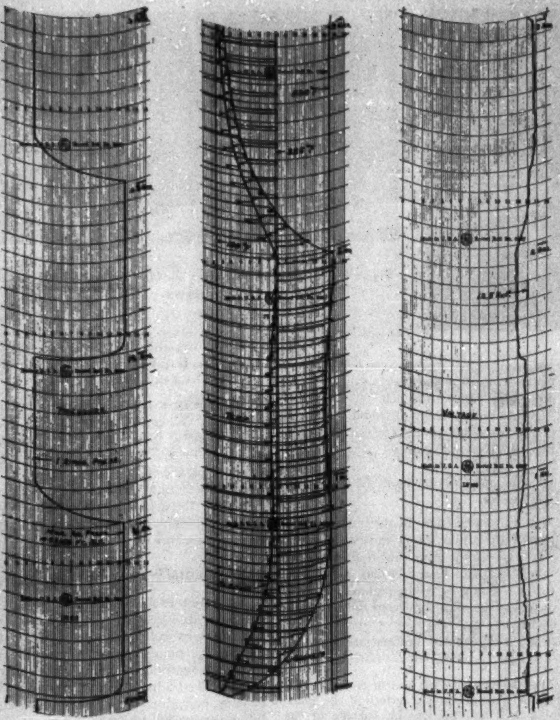

Figure 9. Pressure, temperature, and voltage records for automatically controlled simulated-high-altitude tester

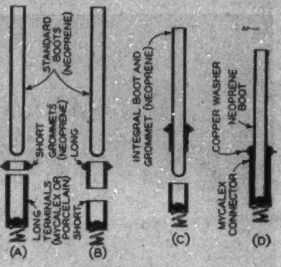
STANDARD BOOTS (NEOPRENE)
SHORT
GROMMETS (NEOPRENE)
LONG
LONG
TERMINALS (MYCALEX OR PORCELAIN)
SHORT
(A)
(B)
INTEGRAL BOOT AND GROMMET (NEOPRENE)
(C)
COPPER WASHER
NEOPRENE BOOT
MYCALEX CONNECTOR
(D)

Figure 11

A and B—Standard five-millimeter terminal assemblies

C—Integral boot and grommet connector assembly

D—Improved composite terminal assembly

run at constant voltage (12.7 kv peak) from a single source (electronic interrupter) and at constant altitude (47,000 feet). The maximum temperature measured at the elbow was set at 350 degrees Fahrenheit and a time switch installed to turn the heaters on for one hour then off for an hour continuously. This cycling, producing expansion and contraction of the connector assemblies, is a severe test of the effectiveness of connector sealing.

The neoprene-sheathed cables, though varying from type to type, immediately exhibited their inherent superiority. The variables of operation during this second group of tests is summarized in Table II, and the results plotted in Figure 10, curve 2. Most of the cables conform to the construction pictured in Figure 3B.

The superiority of the neoprene-sheathed cables, exhibited strikingly in Figure 10, curve 2, is the result of three major factors. First is the elimination of the cotton braid, which, we have seen, is a notable source of tracking failures, either through moisture absorption or gradual carbonization from arc-over or external heat. It is of interest in this connection that cables lacquered directly over the rubber insulation behave rather well on this test, one sample lasting 65 hours. However, this construction is mechanically undesirable, the lacquer pulling loose from the rubber on bending or stretching. It would seem best to eliminate braids altogether, but this is not satisfactory for other reasons. In particular, a braid is required to strengthen the cable against horizontal tension encountered in re-wiring harness. Seventeen samples of neoprene-sheathed cable without braid were tested with promising results on electrical life, but these are all subject to injury on pulling, the insulation tending to stretch loose from the core. The open-mesh glass braid shown in Figure 3B appears to be the best compromise.

Figure 10. Test life of lacquered-braid and neoprene-sheathed cables—early results

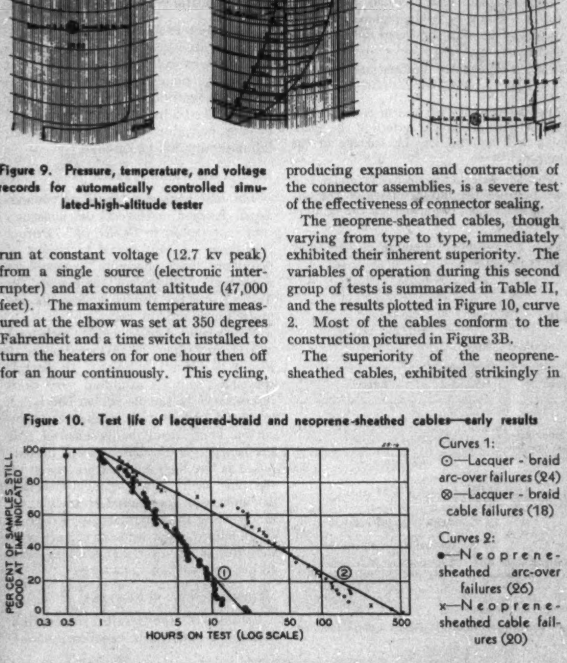

In the second place, the inherent heat and ozone resistance of the best quality neoprene sheaths exhibits itself to advantage in this set of tests.

Finally, the construction of this cable is better suited to proper sealing of the spark-plug well. The open-mesh glass braid is well imbedded in the insulation during the vulcanization process and in some makes was found to be thoroughly sealed.

Other matters, for example the problem of sealing the insulation to the conductor to prevent internal voids and consequent corona, are common to both cable types. The details of their construction have been discussed elsewhere.[8]

Discussion

We may conclude, then, from this survey, that the simulated-altitude test is capable of producing rapid failures of

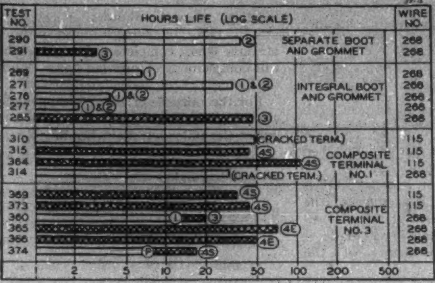

Figure 12. Test life of five-millimeter lacquered-braid cables

Standard cycling procedure

inferior ignition assemblies which resemble those found in actual operation; that the electronic interrupter used is a satisfactory substitute for the aircraft magneto (which would require excessive servicing for continuous laboratory operation); and that cycling of temperature is essential in reproducing one of the drastic conditions of aircraft operation.

Although there are marked differences between different makes, a good neoprene-sheathed cable should outlive the best lacquered-braid cable by a large margin. Sealing of the connector by some type of grommet is essential, and there is room for considerable improvement in the effective life of available grommets. This is demonstrated by the wide scattering of arc-over failures (types 1 and 2) exhibited in Figure 10. The nature of this sealing compound or its absence seems to be secondary to the effectiveness of the seal and more or less independent of it (the two best assemblies using neoprene-sheathed cable had no filling compound). All terminal sleeves tested were inorganic, and no differences could be demonstrated between the various types. It was noticed, incidentally, that many spark plugs were found to leak air at the conclusion of the test period. This is said, however, not to occur very frequently in actual operation.

Experimental—Results on Standard Cycle

Composite Terminals

The experiments previously discussed have demonstrated that with all types of available connector assemblies the majority of failures are caused by arc-over (types 1 and 2). To eliminate the type-2 failures a terminal was designed for five-millimeter cables in which the neoprene adapter boot, the grommet, and the Mycalex terminal sleeve were molded integrally, the boot being firmly bonded to the interior of the inorganic sleeve. Later this was improved by including a copper-ring washer molded into the grommet to give better electrical contact (for better radio shielding) and to relieve the soft neoprene grommet of abuse caused by cycling of temperature or by removing and replacing the connector incidental to inspection and service. This improved design is shown in Figure 11 in comparison with three other types of connector assembly. As subsequent data demonstrate, it materially reduces the number of arc-over failures.

Five-Millimeter Cables

Both lacquered-braid and neoprene-sheathed types were tested according to the standard cycling procedure, using four different types of terminal:

(*a*). Standard adapter boot plus grommet (Figure 11A and B).

(*b*). Boot and grommet molded integrally (Figure 11C).

(*c*). Composite terminal.

(*d*). Composite terminal with copper gasket (Figure 11D).

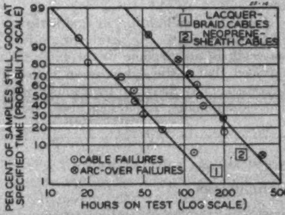

Figure 14. Distribution plots—test life of five-millimeter lacquered-braid and neoprene-sheathed cables with composite terminals

1—Lacquer-braid cables
2—Neoprene-sheath cables
⊙—Cable failures
⊗—Arc-over failures

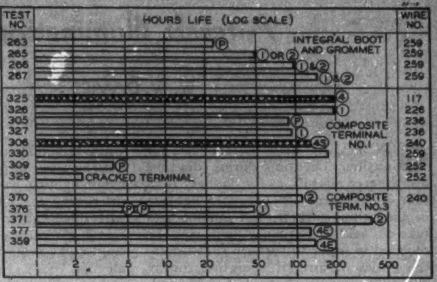

Figure 13. Test life of five-millimeter neoprene-sheathed cables

Standard cycling procedure

The results of the tests for lacquered-braid cables are given in Figure 12 and for neoprene-sheathed cables in Figure 13.

In these charts the length of each bar is proportional to the logarithm of the test life for the sample numbered in the left-hand column. The type of failure is indicated by a number at the end of the bar, these having the same significance as the failure types indicated in Figure 2. Type *P* represents a spark-plug failure.

In several of these assemblies, it was possible to continue testing after a spark-plug failure by replacing the defective plug, and after a type 1 failure by cleaning the terminal sleeve and plug well and renewing the filling compound. Tests marked "cracked terminal" were made with defective experimental terminals and actually failed by tracking along a crack in the Mycalex sleeve.

The superiority of the neoprene-sheathed cables is indicated by examination of Figures 12 and 13, and there is a striking improvement of the lacquered-braid cables when made up with composite terminals. A comparison of neoprene-sheathed and lacquered-braid cables assembled with composite terminals may be made by plotting the life times of all samples tested to completion (omitting those which failed because of cracked terminals) as in Figure 14. The two curves are linear and parallel so that their displacement (0.52 log units) permits us to say that the life expectancy of a neoprene-sheathed cable is approximately $3^1/_2$ times that of a lacquered-braid cable under these conditions.

Seven-Millimeter Cables

The results of 18 tests on seven-millimeter cables (which are too large in cross section to permit the use of boots or composite terminals) give an equally favorable comparison for neoprene-sheathed cables as against lacquered-braid cables.

Aircraft Illumination

W. W. DAVIES
NONMEMBER AIEE

GENERALLY little use is found for auxiliary lighting during daytime operation of aircraft, as the daylight is all that is necessary for adequate lighting of the cabin, cockpit, and landing and take-off fields. Artificial light may be required in order to perform successfully the duties of aircraft operation during about 60 per cent of the 24-hour period. Though normal daylight may be effective for more than 50 per cent of the day throughout the year, actually artificial lighting is required at the dawn and dusk periods inasmuch as the normal amount of daylight is not adequate. It is obvious of course that it is highly impractical to provide over-all lighting to duplicate daylight. Therefore, localized artificial lighting is the best approach to the problem. With proper illumination in the cockpit, however, normal operating conditions are carried out equivalent to those of daylight hours. Artificial lighting is definitely needed so that all functions can be accomplished without delay during the hours of darkness.

When the air-transport industry was in its infancy, night operation was a thing talked about but not accomplished On the early airplanes landing lights or cabin lighting were not installed. It is interesting to look back at some of the early history. In several of the periodicals of the early days much was made of the night-flying experiments of the air mail.

An early attempt at night flying was made between Cheyenne and Chicago in 1921 by pilot Jack Knight of the air-mail service. The first night-flying section of the air mail was set up in 1923 in order to complete a regular coast-to-coast operation without interruption for darkness. The night route was between Chicago and Cheyenne. It is interesting to note that much is made in the historical records of the fact that Air-Mail Pilot H. T. Lewis spent considerable time with General Electric Company engineers devising and producing a new and satisfactory type of "wing headlight" (which was carried on the tip of the airplane wing) for the use of airplanes about to make a landing at night. Of further interest, in 1926 one of the highlights of one manufacturer's description of the characteristics of his craft was that it was "complete with night-flying equipment including landing lights, running lights, etc. . . ."

Even of cabin lighting we find little use in the early days. An interesting advertisement of an airplane in the early 20's advised that, "the cabin is an inclosed limousine body fitted up luxuriously with individual chairs, a spacious aisle, 'dome lighting,' curved windows of celluloid, etc." Today, of course, to most of us an airplane is not complete unless it has the full complement of running lights, landing lights, cockpit, and cabin lighting.

For the purpose of this paper, general aircraft illumination will be considered under the following main headings:

A. Flight operations
1. Landing lights.
2. Navigation lights.

B. Cockpit
1. Instruments.
2. Over-all.

C. Cabin
1. Passenger comfort.
2. Attendant service.

D. Ground servicing
1. Loading and unloading—passengers and cargo.
2. Aircraft servicing.

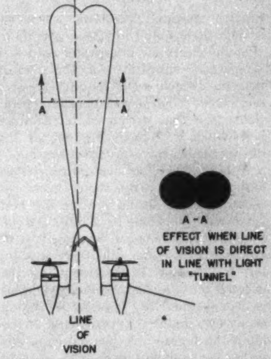
A
A
A - A
EFFECT WHEN LINE OF VISION IS DIRECT IN LINE WITH LIGHT "TUNNEL"
LINE OF VISION

Figure 1. Present nose landing lights

Paper 45-6, recommended by the AIEE committee on air transportation for presentation at the AIEE winter technical meeting, New York, N. Y., January 22–26, 1945. Manuscript submitted June 1, 1944; made available for printing November 4, 1944.

W. W. DAVIES is research engineer, United Air Lines, Inc., Municipal Airport, Chicago, Ill.

The author is indebted to W. J. Addems, director of flight operations, and to R. D. Kelly, superintendent of engineering development, both of United Air Lines, Inc., for their time and help given in the preparation of this paper.

The majority of the failures (12 out of 15) were arc-over types but four of the neoprene-sheathed assemblies had not failed after 400 hours and two were still running after 500 hours of test. The longest-lived lacquered-braid cable ran 92.2 hours.

FILLED LEADS

Twelve sets of this type were tested according to the standard procedure. One group of six gave entirely arc-over failures between 23.5 and 84.0 hours. Another group of three (with other terminal assemblies) had excellent test lives, one failing by puncture after 252 hours, the other two still running at 675 hours when the test was discontinued. Only one short-time puncture (37.7 hours) was encountered. Evidently with suitable terminal fittings these leads have considerable promise.

Conclusions

The simulated-altitude test equipment is a means for reproducing certain aspects of actual flight conditions. In this way it has exposed weaknesses in cables and connector assemblies which might not otherwise have been so readily understood or remedied. It has shown the necessity for sealing spark-plug wells and has led to an improved terminal construction. The superiority of neoprene-sheathed over lacquered-braid ignition cables has been amply demonstrated.

Even for the best types of assembly prepared so far the variability of results is great (roughly a ten-to-one ratio in test life), and this indicates a need for new insulating and gasketing materials and for improved design of component parts.

The simulated-altitude test is not a substitute for regular specification testing for acceptance or manufacturing control, but, rather, a useful adjunct to them. However, its most valuable function is to give information on newly designed assemblies in advance of actual engine tests. The development of new insulating materials or of new cable or connector constructions can certainly be accelerated through its use.

References

1. DIELECTRIC STRENGTH OF INSULATING LIQUIDS IN A CONTINUOUSLY CIRCULATING SYSTEM, Hubert H. Race. AIEE TRANSACTIONS, volume 59, 1940, pages 730–7.

2. D. F. Hang, *General Electric Review*, volume 46, 1943, pages 623–5.

3. HIGH-VOLTAGE-IGNITION-CABLE DESIGN FOR AIRCRAFT, H. H. Wermine. AIEE TRANSACTIONS, volume 62, 1943, November section, pages 716–19.

Flight Operation

LANDING LIGHTS

The present functions of the landing lights are:

(*a*). To aid the performance of the landing by lighting the immediate landing path for the pilot.

(*b*). To identify the airplane in the maneuver and approach by means of the lighted landing lights. These are turned on several miles from the field to avoid collision with other aircraft.

Landing lights generally have been positioned in either the nose or the wing. Although the positioning of the lights in the nose satisfies both of the aforementioned desired functions, there is a definite objection to their use in fog, or snow, or rain. The light is reflected from the individual particles and in effect detracts from what can be seen through the beam, that is, when one is looking directly down the beam or "tunnel of light." See Figure 1. This is very undesirable, and the author knows of no satisfactory solution which is immediately available. Actually, in many cases an approach has been made in bad weather conditions, and the pilot has been able to see a good portion of the surrounding obstructions and outline of the major objects about the field with the lights off. However, as soon as the lights have been snapped on, he is unable to see more than a few feet beyond the airplane. It has been found, however, that this condition can be improved materially when the lights are located in the wing some distance outboard from the fuselage. This can be explained best by reference to Figure 2. When the pilot is making the landing, if the left landing light is shut off, he in effect looks through and not down the opposite beam of light and does not get the direct reflection of light upon the particles of snow, fog, or rain. By passing the line of vision then, across the light beam, the runway and small objects on it can be seen with less difficulty than when one is looking straight down a "tunnel of light" which normally would be formed by the nose lights.

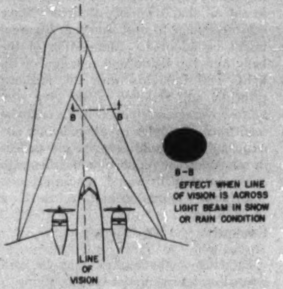
B
B
B-B
EFFECT WHEN LINE OF VISION IS ACROSS LIGHT BEAM IN SNOW OR RAIN CONDITION
LINE OF VISION

Figure 2. Present wing landing lights

Experience has indicated that probably the best direction for the beams of wing landing lights is as shown in Figure 2, that is, with the left landing light, or pilot's light, pointing ahead so that light is best for the pilot, and the right landing light, or copilot's light, converging on the same spot. The main advantage of this is to protect the pilot's vision for all conditions of the operation. As example, in the event of a failure of either light, the lighted portion of the runway would be the same in either case. It is appreciated, however, that this is a compromise condition as this is an undesirable situation from the standpoint of the copilot. Several cases have been encountered, however, of lights burning out at the time of landing, and some protection must be given. One possibility is to direct both lights as shown in Figure 3 giving a wider spot on the runway; giving good landing light for both the pilot's and copilot's position; and incorporating within each landing light an automatic lamp changer of the type that is used in airway beacons at the present time. The unit could be such that it incorporates two lamps located on a rotary device, so that at the time one lamp would give out a control circuit would be closed automatically, actuating the device and swinging the second lamp into position.

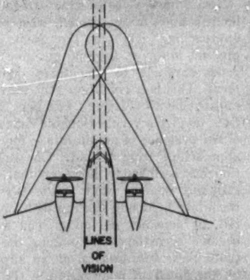

Figure 3. Proposed wing landing lights (with lamp burnout protection)

United Air Lines has felt for some time that the use of a sealed-beam-type landing light would afford some major benefit and have suggested this to the Civil Aeronautics Authority for further study. At the present time with the normal filament and parabolic reflector it is difficult to obtain a sharp cutoff or channel of light, as there is considerable dispersion around the outside of the beam of light. Channeling could be accomplished, of course, by the means of a long cylinder projecting forward from the landing light, but this is impractical. The engineering section of United Air Lines has conducted some tests using a grid close to the lens of the light itself, with the grid surface blackened to prevent reflection and thus limit the dispersion. The grid used in this manner channels the light so that the beam itself has a sharp cutoff and projects directly to the place to be illuminated. There are cases, however, where dispersed light or a general over-all effect may be desirable. By utilizing the sealed-beam principle the two filaments could be placed in the landing light where one could be used with a grid or some similar unit for positive channeling, and the other used as a dispersed light. These could be controlled individually from the cockpit so that the pilot could choose between a sharp channeled light for both landing lights or a dispersed one, or could have one landing light with the positive channel beam and the other with a dispersed light.

Intensity of illumination of the present landing lights probably has been adequate in the past. However, with increased operation both in terms of volume and number of aircraft, coming into an airport, and with the possibility of improved landing equipment permitting operation in more inclement weather, considerable comment has been expressed as to the need of landing lights with greater intensity. The author cannot agree with this statement in its entirety. Discussions with many pilots have indicated that the need for additional illumination for the landing operation is required simply because there is a lack of adequate illumination on the ground. Therefore, it appears that a better solution would be found by completely lighting up the runway so that it glowed as a ribbon with no reflections. The general characteristics of the landing lights with respect to intensity, then, could remain as they are at the present. See Figure 4. This would eliminate the need of carry-

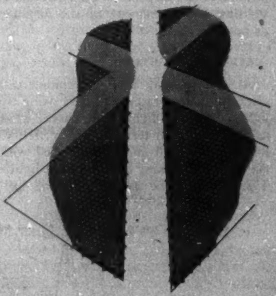

Figure 4. Positive ribbon lighting for airport runway

ing added weight in the form of additional electric power and larger landing lights aboard the aircraft.

Rotating-type landing lights or landing lights that may be swung fore and aft as the means of locating the light just where it is desired have been suggested and used. Although there may be some advantage in some special operations or conditions for such a light, it is believed there is one major disadvantage as compared to the stationary type. With the stationary landing lights, which are always in the same position with respect to the airplane, a pilot in landing can judge his distance above the ground and in effect get a rough measure of the attitude of his airplane to aid him in making the landing. With the rotatable light, unless it is stopped at the same place all of the time, he can establish no definite relationship between the light spot on the runway and the airplane.

Suggestions have been made that a taxi light, that is, a light essentially in the fuselage or in the wing that would illuminate objects on either side of the airplane would be desirable. One thought advanced was to incorporate additional elements in the main landing light which could be designed to act as a taxi light and could be controlled individually from the cockpit. Although in principle this may be a good idea, it still appears that the sounder approach would be to illuminate all of the objects on the ground at the airport, and keep as much lighting equipment out of the airplane as possible.

Navigation Lights

At the present time all commercial aircraft incorporate standard wing-tip lights and taillights. Further, what might have been termed "safety lights" have been added and incorporated with the existing running or navigation lights. This includes the addition of one taillight, one belly light, and one top light. All of these lights are actuated with a mechanism which causes them to flash on and off at frequent intervals. They were installed primarily for the purpose of identity and recognition in order to avoid possible collisions, and, although they have been fraternally referred to as "Christmas-tree" lights, it is the opinion of the author that they serve a very definite useful purpose and contribute considerably to the safety of night flying. Reference to Figure 5 shows the general characteristics of the running lights on the average commercial transport.

The actual value of the flashing lights is to avoid collision, and their real use comes in contact flying and slight overcast conditions, particularly in a heavily trafficked area about an airport. In instrument weather aircraft normally are controlled at greater distances from each other, and the flashing lights are not so much needed then. Actually no equipment is available to make such lights capable of penetrating overcast conditions.

The wing-tip lights give satisfactory identification for an airplane when one is approaching it from the front. At present, however, they do not give very good coverage to the three quarters rear. This is a condition that warrants improvement. Flashing taillights, however, do give a very reasonable indication of the presence of an aircraft to any one approaching from behind. One suggestion has been made, however, that, if a standard spacing were made between the white light and the red light on the tail, by constant use pilots soon would become accustomed to judging the distance they were away from an airplane by the apparent relationship of the two lights; that is, if the lights appeared to be very close together, they would know they were a far distance apart; and, contrary, if the lights were a considerable distance apart, they would know they were close upon the heels of another craft. This may have an advantage in formation flying, but it does not appear that approach and landing operations would be scheduled so closely as to warrant such an installation. In addition the use of single, twin, and triple rudders might confuse the establishment of a reasonably standard distance between lights.

One objection to the flashing lights has been the effect in mist or overcast. When the airplane is being operated in an overcast condition with the belly and top lights flashing, there is intermittent light and darkness in the cockpit and cabin, due to the reflection of the flashing light on the overcast. This, of course, is not all that might be desired. Some scheme similar to that shown in Figure 6 might be adopted. Elimination of the belly and top lights and redesign of tip lights and taillights with the flashing principle still retained would give adequate coverage, so that the lights could be seen from all angles by approaching aircraft, and yet would keep the glow effect in an overcast condition far enough away so that it would not affect too greatly the cabin or cockpit.

Cockpit

Lighting of the cockpit may be considered under two major classifications.

General or Ground Check

There is a general need for over-all illumination of the cockpit primarily for use in checking the controls and the instruments prior to takeoff and after landing. There may be some use for general over-all lighting in en-route operation, but it is infrequent, and its prime use will be prior to actual flight. It is important that the installation of over-all lighting satisfy the full sense of the definition, that is, illuminate ade-

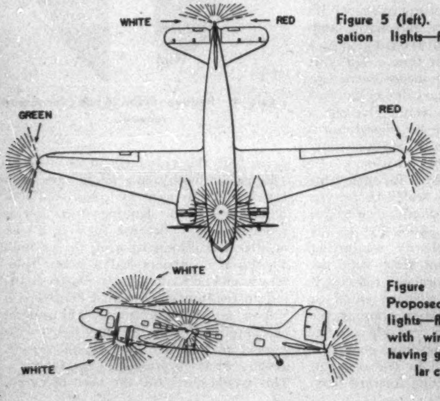

Figure 5 (left). Present navigation lights—flashing type

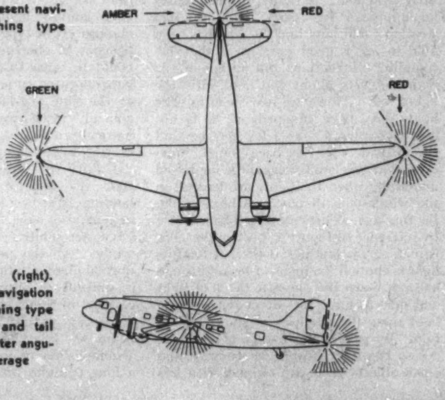

Figure 6 (right). Proposed navigation lights—flashing type with wing and tail having greater angular coverage

quately every portion of the cockpit where any controls, knobs, dials, instruments, or equipment of similar nature are located. Present cockpits have lights located at various points which, although they may give adequate light within a short distance of the source, do not give the necessary amount of light to another section of the cockpit that might well justify a minute inspection prior to operation of the aircraft. Further, there is a certain amount of paper work in the form of charts, records, and logs which the crew must fill in or refer to, and adequate light must be available for this purpose.

EN-ROUTE OPERATION

In en-route operation there are two considerations, namely:

(*a*). Adequate lighting of the instruments at all times.

(*b*). Auxiliary or spot lighting for the purpose of recording data, reading charts, or plotting of the course by either the pilot or copilot.

With respect to instrument lighting, it is very definitely desired that some form of indirect lighting of the instruments be accomplished. At present, with the dimming type of partial over-all lights which throw the light directly on several instruments the degree of illumination is not the same for each particular instrument. This is undesirable, because some of the instruments then become easier to read than others. It is essential that all instruments be lighted to the same degree and that the intensity can be changed by means of a suitable rheostat control to either "full off" or "full on," or, to any desired degree of illumination between the two extreme points. Figure 7 shows a tone relationship or an illumination relationship between instrument lighting in an existing transport cockpit. Figure 8 shows what is desired. It is appreciated that the use of individual instrument lighting by means of direct methods adds considerable complication to the electric system in the cockpit, and service experience to date has not been very good on the individual elements of such installations. However, it is believed that in principle this method is sound and that efforts to accomplish these desired results should not be relaxed.

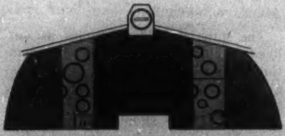

Figure 7. Average lighting relationship of existing instrument panels

One of the objections to the partial type of over-all lights which have been used for lighting the instrument panel has been the bad reflection on the instrument-panel glass, and on the cockpit windshield as well. Tests conducted using a special coating on instrument glasses and on the windshield have indicated that this condition is well along toward being corrected. Such an improvement would eliminate one of the objections of partial over-all lighting of the instruments.

At the present time many commercial cockpits are equipped with an auxiliary source of light such as a spotlight. This light is for the purpose of controlling a spot of light for use by either the pilot or copilot, so that accurate reading of charts, plotting of course, or other necessary paper work can be accomplished. This may be done either by the pilot or copilot and should be so designed that it does not interfere with the other's vision in flying the craft. It appears relatively simple to shield the source of light so that it does not attract the attention of the crew member not using it, but no satisfactory means has yet been found for controlling the illumination of the cockpit or glare caused by the reflection of the spotlight on the light-colored charts or papers being studied or analyzed.

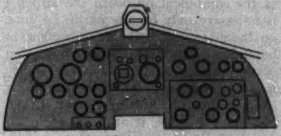

Figure 8. Desired even lighting relationship of instrument panel

In order to eliminate some of these difficulties of spot lighting as well as to improve over-all cockpit lighting, considerable study has been made with the use of fluorescent lights. This may offer very definite advantages and spot sources of ultraviolet perhaps can be used for lighting charts and records, outlined or drawn with fluorescent active material. Some experiments have indicated that this may give adequate legibility to the charts or course maps and still not cause undesirable illumination for the member of the cockpit crew who is not using the chart. It is also believed that by intelligent positioning of the spotlights they could serve a dual purpose of giving both adequate over-all light when desired and the ultraviolet spot as needed. This can be accomplished simply by using an ultraviolet filter (as already has been accomplished in many places) in conjunction with the main source of light. Such a scheme offers the optional use of full lighting or a control spot lighting.

Still another problem in this consideration of cockpit lighting has been that of having satisfactory illumination within the cockpit and still not adversely affecting vision outside of the cockpit during night operation. At the present during night operation and even with the cockpit instrument lights at a low level so that just the indications are discernible, it still takes the pilot a short time to acclimatize his eyes that he can have adequate night vision when looking out of the cockpit. Many studies are being made at the present in an effort to improve this situation such as the use of red light which will give good illumination to the instruments themselves and still not affect the so-called night vision, thus permitting the pilot to see equally well inside the cockpit and outside of the cockpit.

Although present experiments using ultraviolet light for activating fluorescent materials or instruments have not proved entirely successful to date, this may offer a means of obtaining adequately lighted instruments without the need of complicated indirect-lighting means for each individual instrument. It must be borne in mind, however, that it is very desirable to be able to change the degree of brilliancy of the instrument lighting dependent upon the particular conditions en route.

Cabin

Although passenger-cabin lighting has improved considerably over that in the past, much of the same problem still exists as in the cockpit lighting, and that is the matter of getting the available light in the right places and eliminating undesirable glare. With overhead lighting or what has sometimes been referred to as dome lighting, bright source spots can be reduced materially and probably can be eliminated altogether by the use of indirect or alcove lights. This is very definitely desirable. The main light in the cabin is then dependent upon reflection from light-colored surfaces in the cabin interior. This is also advantageous from the point of adequate light in the daytime, and much is to be gained from this arrangement. Over-all lighting at night is primarily for loading and unloading of passengers and ground operation and has a value at the start of the flight to permit the stewardesses and passengers to get generally settled before the beginning of the flight. In addition it is necessary when meals are being served.

In a day airplane or sleeper airplane, particularly when the latter does not have full partitions, some of the passengers may desire to sleep while others may desire to read or talk with one another. Some means of auxiliary or spot lighting, which we have called reading lights in the past, is necessary. One of the biggest objections has been that both the source of light and the projection of light to the paper or book being

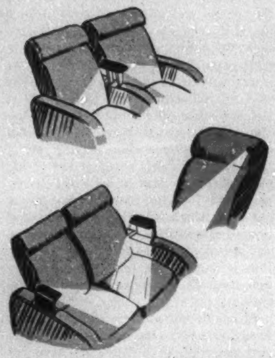

Figure 9. Possibilities for reading lights

read cause undesirable reflections to the individual not using the light. Another objection has been that the positioning of the source of light has not always been made so as to give the most efficient utilization of it for the person who wishes to use it.

Some suggestions as to possibilities with auxiliary or reading lights in the cabin are shown in Figure 9. It is appreciated that any one of these suggestions does not solve all of the difficulties. However, it should be pointed out that passenger business is still to be an important source of revenue of the air-transport companies for some time to come, and an intelligent solution to this problem is definitely needed.

An additional type of lighting required in the cabin is that for servicing, or, stated in another manner, the furnishing of additional light at the crew attendant's quarters so that the attendant's work can be accomplished properly. Use of lights in some present commercial transports, although properly shielded at the light source, have still been so located that they have permitted a considerable amount of reflection, which has the effect of indirectly lighting a good portion of the cabin close to the service quarters. This has proved very undesirable to those people who are seated close to the service quarters. It is appreciated that this problem is further complicated, because usually at service quarters light-covered shiny surfaced materials are used. It is believed, however, that attention again should be paid to the use of over-all or indirect lighting in the service quarters when the entire section is being used for the serving of food or handling of equipment. A separate source for auxiliary or spot lighting should be provided for the use of the attendant to accomplish paper work or other jobs that do not require the full utilization of the service quarters.

It is realized that as airplanes become larger separate quarters both for passenger lounges and the service section probably will be used, segregating them entirely by means of partitions. This will aid in keeping light from disturbing other passengers. It is believed, however, that the same general principles still apply.

Ground Servicing

Loading and Unloading—Passengers and Cargo

It is believed that in general a sound principle of aircraft design is to develop the airplane to be a self-sufficient unit independent as much as possible of ground equipment. There are several places, however, where it is desirable to make exceptions to this rule, particularly where the weight or complication of the equipment on board the airplane is necessary only for the job to be done on the ground, and therefore becomes a handicap toward the efficient operation of the airplane in flight. If the equipment is necessary, however, for flight as in the case of a heating system, it then becomes desirable, if at all possible, to design the system so that it can handle the ground problems adequately.

In the case of lighting, however, for loading and unloading of passengers and cargo, this does not hold true for the operation performed outside of the airplane. If the cabin is lighted adequately for operation in flight, there is no need for special lights being installed in or at the airplane door which would be used for the purpose of lighting the platform of the loading stand. This latter type of light is used only when passengers are getting on and off the airplane and undoubtedly would have no use while en route. Therefore, it is more practical to put the light itself on the passenger loading stand. Spotlights or small floods (which have been suggested), placed in the door or lower portion of the door jamb of the airplane and utilized only at the time of loading and unloading passengers, are unsatisfactory, and a finer job can be done when the same lights are built into the loading stand.

The same principle applies with respect to loading and unloading cargo from the door of the airplane to the loading equipment. The light should be placed on the loading equipment, not in the door of the airplane or on the door jamb. However, it is definitely necessary and desirable that adequate light be provided within the cargo compartment of the airplane itself, as this is necessary to permit proper stowing of cargo. Also to identify and read waybills on individual shipments. Such lighting cannot be accomplished satisfactorily from an outside ground source, and can best be done by design within the airplane. One point of interest here is that on passenger loading and unloading equipment, lights should be so low as to light the path adequately and yet not have the passenger's shadow block the vision of steps and ground or loading ramp obstructions. In cargo loading and unloading equipment, and in the cargo compartments themselves, it is desirable that the light source be both high and low, that is, in the form of flood or indirect lighting, so that adequate light will be available so that all obstructions, steps, and so forth, can be seen, in addition to giving adequate light at any height for the proper handling and stowing of cargo. See Figure 10.

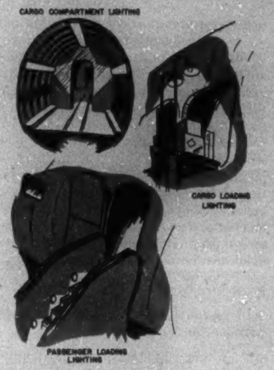

Figure 10. Cargo-compartment lighting, cargo-loading lighting, and passenger-loading lighting

Aircraft Servicing

The same general principles as outlined for loading and unloading operations apply to the servicing of airplanes at the terminal station. The lighting should be accomplished on the ground, and the airplane should not be handicapped with the weight of lighting equipment to satisfy the ground operation. It is believed that one of the best methods is to incorporate low-powered floodlights which in effect would "bathe" with a relatively low illumination those portions of the airplane normally requiring service. This would be adequate for inspection and simple servicing procedures, but not bright enough to cause glare or make working about the craft difficult. It is further believed that these lights should be of a lower intensity than the lighting required for cargo-handling equipment.

It has been suggested that these lights be of the flush type built directly into the ramp or apron about the terminal. Although this is most desirable from a functional or operating point of view, it is appreciated that there are many problems, such as adequate sealing, that must be overcome. The principle, however, is considered as being worthy of further study.

Damping Effect of D-C Marine Propulsion Motors on Vibrations Produced in Drive Shafts by Large Propellers

BERNARD LITMAN
ASSOCIATE AIEE

Synopsis: D-c machines often are employed in ship-propulsion drives where maneuverability and a wide speed range are required. The d-c machine also has the advantage of serving as a source of damping if propeller pulsation should coincide with the natural frequency at some speed. This damping force arises because of the fact that any change in speed of the motor will cause a corresponding change in load current and torque. This torque change acts to oppose the original speed change, thus providing an effective damping force. The necessary equations and circuits are developed for calculating this damping effect and an illustrative calculation is included with actual test values for comparison.

IT IS occasionally necessary to determine the magnitude of torsional vibration in a system running at one of its critical speeds. To do so requires a knowledge of all the damping sources within the system and their magnitudes. Typical damping sources are hysteresis damping in the shaft and friction and viscous damping in the system. If the system includes a d-c machine, this will also serve as an important damping source and limit the vibration magnitudes. An example of such a system is an electric ship-propulsion drive. Here the d-c machine is frequently used because of its ease of speed control over a wide range. However, operation may occur at the natural frequency, where propeller vibrations may set up abnormal stresses in the shafting. If investigation shows the damping to be large enough, the necessity of changing the natural frequency by an uneconomical redesign of the mass–elastic system may be avoided.

The damping force in a d-c machine is similar in behavior to a viscous damping force, being proportional to the speed, though the origin of this force is somewhat different. Assume, for example, that the speed of the machine has dropped below its mean value at some point of its vibration cycle. This causes a corresponding drop in the countervoltage of the motor so that a larger load current will tend to flow. This load current and the corresponding load torque will tend to speed up the motor, thus opposing the drop in speed which we have assumed. If we neglect the inductance of the armature circuit and consider only the resistance, then torque changes will be in phase with and proportional to speed changes, so that these torque changes act as a true damping torque. When the inductance of the armature circuit is considered, we no longer have pure damping since the current and torque changes are not in phase with the speed variation. Thus, during part of the cycle the damping torque may actually aid the oscillation while during the rest of the cycle it opposes the oscillation. The vibrational energy imparted by the propeller is absorbed partly by the propeller itself as in any case of viscous damping. The remainder of the energy is absorbed by the motor by means of the mechanism described above. The magnitude of vibration in the different parts of the system will rise to the point where the energy absorbed is equal to the energy imparted by the propeller.

Actual solutions are most simply made by setting up equivalent electrical circuits which have the same differential equations as the mechanical system we are considering. The source of pulsating torque becomes an applied voltage at some point in the system. Shaft elements become capacitors, masses become inductances, and damping elements become resistances. When the inductance of the armature circuit is included, our equivalent circuit becomes somewhat more elaborate, containing negative resistance and inductance terms.

The standard electrical symbols for these elements are used in the figures which follow. These circuits are solved by using the standard methods of complex algebra as for any steady-state a-c network. The circuit may be solved for any operating speed by using the corresponding value of the applied pulsating frequency. The maximum values of shaft torque are most conveniently determined by first finding the natural speeds with damping neglected. These will be very near the speeds at which maximum torques occur when damping is considered. For a more accurate calculation, one or two other speeds near this natural speed may be checked and a curve drawn through these points so as to estimate the peak.

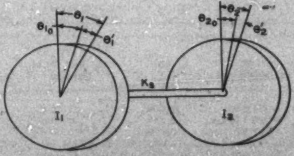

Figure 1. Physical system of two masses and connecting shaft

The Two-Mass System Without Damping

Refer to Figure 1 for which the following symbols apply:

θ_1 = actual angular position of rotor—radians
θ_{1_0} = uniformly moving angular vector which would be the position of the rotor if there were no torque pulsations and the rotor moved uniformly
$\theta_1' = \theta_1 - \theta_{1_0}$ = rotor displacement above or below mean position
Similarly for θ_2.
I_1 = moment of inertia—pound-feet squared divided by g
Similarly for I_2.
K_s = shaft spring constant—foot-pounds per radian

The natural frequency of this system will then be given by

$$f=\frac{1}{2\pi}\sqrt{K_s\left(\frac{1}{I_1}+\frac{1}{I_2}\right)} \tag{1}$$

This familiar result may be obtained from the differential equations or the equivalent circuit which we give now. In order to determine the effect of torque variations, we shall assume the second mass to be absorbing the torque transmitted from the first but doing so nonuniformly by having a mean torque T_0 and a smaller superimposed sinusoidal

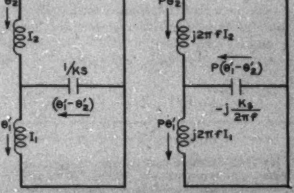

Figure 2a (left). Equivalent electric circuit for two-mass system without damping

Figure 2b (right). Equivalent circuit with proper values of admittance and susceptance at frequency *F*

Paper 45-2, recommended by the AIEE committee on marine transportation for presentation at the AIEE winter technical meeting, New York, N. Y., January 22–26, 1945. Manuscript submitted May 9, 1944; made available for printing November 2, 1944.

BERNARD LITMAN is mechanical engineer, d-c generator engineering department, Westinghouse Electric and Manufacturing Company, East Pittsburgh, Pa.

torque T' (hence total torque $T=T_0+T'$), while the first mass has supplied to it a constant torque T_0.

Let p represent the differential operator $\frac{d}{dt}$. Taking torques applied to the first mass, we have:

$$T_0-K_s(\theta_1-\theta_2)=I_1p^2\theta_1 \tag{2}$$

For the second mass

$$K_s(\theta_1-\theta_2)-T=I_2p^2\theta_2 \tag{3}$$

If our absorbed torque were not pulsating and the motion were uniform, these equations would reduce to

$$T_0-K_s(\theta_{1_0}-\theta_{2_0})=0 \tag{4}$$

$$K_s(\theta_{1_0}-\theta_{2_0})-T_0=0 \tag{5}$$

By subtraction of these from the first set of equations, we have

$$I_1p^2\theta_1'+K_s(\theta_1'-\theta_2')=0 \tag{6}$$

$$I_2p^2\theta_2'-K_s(\theta_1'-\theta_2')+T'=0 \tag{7}$$

where the primed quantities are angle and torque variations above (or below) mean value. It is these quantities in which we are interested since they represent oscillations or displacements from the mean position.

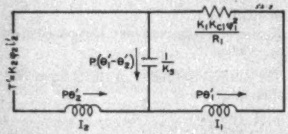

Figure 3. Equivalent circuit for two-mass system with motor resistance damping in one mass

Figure 2a shows an equivalent circuit which by inspection is seen to have the same differential equations 6 and 7 and hence will give the same solution Since we are considering sinusoidal variations we can set up Figure 2b with impedances and find the response by using the complex vector notation.

f = frequency of the applied torque T'

$p\theta_1$ and $p\theta_2$ = "currents" flowing in the circuit

If T' is the maximum torque variation, then the "voltage" across the capacitor is the maximum value of $K_s(\theta_1-\theta_2)$ or the maximum value of shaft torque. If T' is expressed in per unit (that is, as a fractional part of the mean torque, T_0), then the shaft torque will likewise be in per unit. Thus if we obtain a value of 0.5 for shaft-torque variation, the actual maximum shaft torque (and stress) will be 1.5 times the normal design value.

From Figure 2b it is seen that the total impedance is

$$\frac{1}{\frac{1}{j2\pi fI_1}-\frac{2\pi f}{jK_s}}+j2\pi fI_2$$

which will equal zero when the frequency is given by

$$f=\frac{1}{2\pi}\sqrt{K_s\left(\frac{1}{I_1}+\frac{1}{I_2}\right)}$$

This verifies equation 1.

It is evident at resonance that the magnitude of the oscillation is infinitely large; hence we must include damping to obtain the true behavior of the system.

Inclusion of Resistive Damping

When we include resistive damping we must consider the variation of electrical torque within the machines—hence we add another set of differential equations to our previous set. With reference to Figure 1, we have for body number 1:

$$K_1\phi_1 i_1-K_s(\theta_1-\theta_2)=I_1p^2\theta_1 \tag{8}$$

$$E_1=i_1R_1+K_{c1}\phi_1p\theta_1 \tag{9}$$

where

$K_1\phi_1$ = motor-torque constant in pound-feet per ampere

$K_{c1}\phi_1$ = motor counterelectromotive force constant in volts per radian per second

E_1 = applied line voltage to machine number 1 in volts

R_1 = machine-armature-circuit resistance in ohms

i_1 = machine-armature-circuit current in amperes

We may write again the equations for uniform (nonpulsating) motion, and obtain

$$K_1\phi_1 i_{1_0}-K_s(\theta_{1_0}-\theta_{2_0})=0 \tag{10}$$

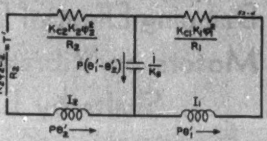

$\frac{K_{c2}K_2\varphi_2^2}{R_2}$
$\frac{K_{c1}K_1\varphi_1^2}{R_1}$
$\frac{K_2\varphi_2E_2'}{R_2}=T'$
$P(\theta_1'-\theta_2')$
$\frac{1}{K_s}$
I_2
I_1
$P\theta_2'$
$P\theta_1'$

Figure 4. Equivalent circuit for two-mass system with motor resistance damping in both masses

$$E_1=i_{1_0}R_1+K_{c1}\phi_1p\theta_{1_0} \tag{11}$$

and by subtraction we obtain equations in terms of the variation from mean values:

$$K_1\phi_1 i_1'-K_s(\theta_1'-\theta_2')=I_1p^2\theta_1' \tag{12}$$

$$i_1'R_1+K_{c1}\phi_1p\theta_1'=0 \tag{13}$$

We may eliminate i_1' from equations 12 and 13 and obtain

$$\frac{-K_1\phi_1K_{c1}\phi_1p\theta_1'}{R_1}-K_s(\theta_1'-\theta_2')=I_1p^2\theta_1' \tag{14}$$

For the second machine we assume the torque absorbed, $K_2\phi_2 i_2$, is made up of a mean torque $K_2\phi_2 i_{2_0}$ and a sinusoidally varying torque $K_2\phi_2 I_2'$ (which is the same as T' given in the previous section); and that this pulsating load being absorbed by the second machine causes the pulsations which we are considering. We therefore may write for the second motor:

$$K_s(\theta_1-\theta_2)-K_2\phi_2 i_2=I_2p^2\theta_2 \tag{15}$$

and under nonpulsating conditions we have:

$$K_s(\theta_{1_0}-\theta_{2_0})-K_2\phi_2 i_{2_0}=0 \tag{16}$$

Hence by subtraction, we obtain:

$$K_s(\theta_1'-\theta_2')-K_2\phi_2 i_2'=I_2p^2\theta_2' \tag{17}$$

Since we assume that i_2' is a known load-current variation, we may replace $K_2\phi_2 i_2'$ by a known torque variation T' and we may now set up the equivalent circuit of Figure 3 whose differential equations are seen to be the same as equations 14 and 17.

As before, for a given frequency we may insert a complex impedance and solve for the "voltage" or torque across the "capacitance" or shaft in terms of the pulsating applied torque T'. We notice

Table I

Propeller Damping Only—See Figure 13

(1) Rpm	(2) ω Third Harmonic	(3) $3K_{p\omega}\omega_{p0}$	(4) $j\omega I_p$	(5) $-jK_s/\omega$	(6) $j\omega I_m$	(7) (5) and (6) in Parallel	(8) Total Impedance	(9) (7)/(8) Magnitude Only	(10) (9) times $(\text{Rpm}/250)^3$
100	31.4	770	$j14,030$	$-j34,650$	$j8,460$	$j11,220$	$770+j25,250$	0.495	0.071
150	47.2	1,154	$j21,100$	$-j23,100$	$j12,700$	$j28,200$	$1,154+j49,300$	0.572	0.206
200	62.8	1,540	$j28,000$	$-j17,320$	$j16,900$	$j650,000$	$1,540+j678,000$	0.960	0.612
230	72.4	1,770	$j32,300$	$-j15,050$	$j19,480$	$-j66,000$	$1,770-j33,700$	1.950	1.650
250	78.6	1,925	$j35,100$	$-j13,850$	$j21,160$	$-j40,000$	$1,925-j4,900$	7.61	7.81
256	80.5	1,970	$j35,900$	$-j13,540$	$j21,660$	$-j36,100$	$1,970-j200$	18.20	19.
275	86.5	2,115	$j38,600$	$-j12,600$	$j23,300$	$-j27,400$	$2,115+j11,200$	2.40	2.9

that our circuit now has a resistance term which, as might be expected, varies inversely as the actual armature resistance R_1. Thus with a smaller armature resistance, a given speed change will result in a larger load current and torque variation so that the resistance damping term in our circuit must increase.

One might ask why the damping term appears only in the branch of the circuit pertaining to machine number 1 and why there is not a similar term for machine number 2. The answer lies in the fact that we are assuming the load-current variation i_2', to have a known value. Actually this quantity would be difficult to determine without actual measurement since it depends not only upon the nature of the pulsating load but also upon the characteristics of machine number 2 which is supplying this load. We, therefore, may carry our analysis a step further by assuming that it is the line voltage E_2 whose variation is known and that the load current I_2 does not vary directly with E_2 because we must include the damping effects of motor number 2.

We can then write for machine number 2

$$K_{e2}\phi_2 p\theta_2 - i_2R_2 = E_2 \qquad (18)$$

and in terms of the variation from mean values we obviously will have

$$K_{e2}\phi_2 p\theta_2' - i_2'R_2 = E_2' \qquad (19)$$

We may now eliminate i_2' from equations 17 and 19 and obtain

$$K_s(\theta_1'-\theta_2') - \frac{K_{e2}K_{t2}\phi_2^2}{R_2}p\theta_2' - I_2p^2\theta_2' + \frac{K_{t2}\phi_2E_2'}{R_2} = 0 \qquad (20)$$

We may again set up an equivalent circuit from equations 14 and 20 and obtain Figure 4.

Now it is apparent that we have a resistance term in both branches of our circuit. This analysis might be carried further to the ultimate source of torque pulsations. Thus if the load being supplied by machine number 2 were a motor-driven air compressor, we might add another branch to our circuit to include the characteristics of the third machine and apply our pulsating torque from the air compressor to this branch. This more complete circuit is not developed here since the damping features of d-c machines are more easily demonstrated with a simple circuit and the simpler circuits can usually be applied to most cases with a fair degree of accuracy.

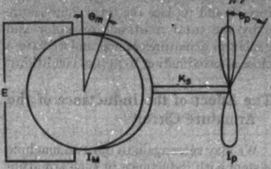

Figure 5. Physical system for ship-propulsion drive

If, as is the case in most systems, the torque pulsations are not sinusoidal, we may still resolve them into their harmonic components, treat each harmonic separately, and superimpose the responses to each harmonic torque pulsation in order to obtain the complete solution.

A Case of Combined Electrical and Mechanical Damping

Before including the effects of the inductance of the armature circuit we shall show how the simplified damping circuits already presented may be applied to a specific case which will be treated numerically in the appendix. This is the case of the ship-propulsion drive shown in Figure 5. The differential equations for the motor remain as before but we must also include the damping introduced by the propeller itself since its torque changes with speed changes.

The propeller torque under steady conditions varies nearly as the square of the speed. Assuming for the moment that this holds even when the speed is undergoing oscillations, we may write

Propeller torque $= K_p\omega_p^2$ pound-feet

where ω_p is given in radians per second. Then:

$$K_s(\theta_m-\theta_p) - K_p\omega_p^2 = I_pp^2\theta_p \qquad (21)$$

and under nonoscillating conditions:

$$K_s(\theta_{m0}-\theta_{p0}) - K_p\omega_{p0}^2 = 0 \qquad (22)$$

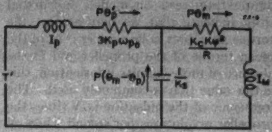

Figure 6. Equivalent circuit for ship-propulsion drive

Hence

$$K_s(\theta_m'-\theta_p') - K_p(\omega_p^2-\omega_{p0}^2) = I_pp^2\theta_p' \qquad (23)$$

But

$$\omega_p^2-\omega_{p0}^2 \doteq 2\omega_{p0}(\omega_p-\omega_{p0}) = 2\omega_{p0}\omega_p' = 2\omega_{p0}p\theta_p' \qquad (24)$$

Hence

$$K_s(\theta_m'-\theta_p') - 2K_p\omega_{p0}p\theta_p' = I_pp^2\theta_p' \qquad (25)$$

Equation 25 has a damping term whose coefficient is $2K_p\omega_{p0}$, but actually with the ship moving forward at constant speed, changes in angular speed of the propeller will cause larger changes in propeller torque than we have anticipated from the "square of the speed" law. Thus we can see that the propeller need not drop to zero speed in order to have zero torque, for if it drops sufficiently it will screw freely through the water without putting out any torque. Hence our damping term should be increased, the exact amount of the increase depending somewhat on the propeller design characteristics. A fairly close approximation, and the one which is generally used is to increase the damping by 50 per cent. Hence we may rewrite equation 25 thus:

$$K_s(\theta_m'-\theta_p') - 3K_p\omega_{p0}p\theta_p' = I_pp^2\theta_p' \qquad (26)$$

Combining this with the equation for the motor (see equation 14), we can set up an equivalent circuit which can be solved without difficulty for steady-state sinusoidal pulsations. This circuit is shown in Figure 6.

These torque pulsations arise because of the oscillating torque of the propeller as it passes through the varying wake of the ship and the obstructions of the stern frame. The magnitude of this pulsation is a quantity which is practically impossible of calculation but approximate

Table II

Propeller and Motor Resistance Damping—See Figure 14

(1) Rpm	(2) ω Third Harmonic	(3) $3K_p\omega_{p0}$	(4) $j\omega I_p$	(5) $-jK_s/\omega$	(6) $j\omega I_m$ + Resistance	(7) (5) and (6) in Parallel	(8) Total Impedance	(9) Ratio, (7)/(8)	(10) (9) × (Rpm/250)^2
100	31.4	770	j14,030	−j34,650	11,100+j8,460	16,500+j4,200	17,270+j18,230	0.670	0.108
150	47.2	1,154	j21,100	−j23,100	11,100+j12,700	25,600+j850	26,754+j21,950	0.740	0.266
200	62.8	1,540	j28,000	−j17,320	11,100+j16,900	28,400−j17,100	29,940+j10,900	1.040	0.665
230	72.4	1,770	j32,300	−j15,050	11,100+j19,480	17,500−j22,000	19,270+j10,300	1.290	1.09
250	78.6	1,925	j35,100	−j13,650	11,100+j21,160	12,100−j21,800	14,035+j13,300	1.29	1.29
256	80.5	1,970	j35,900	−j13,540	11,100+j21,660	11,000−j21,800	12,970+j14,100	1.27	1.33
275	86.5	2,115	j38,600	−j12,600	11,100+j23,300	7,400−j19,800	9,515+j17,060	1.08	1.30

figures from tests on models and actual ships indicate that we may assume the torque pulsation to be ten per cent of the mean torque of the propeller and in the absence of more definite information, this is the value that is commonly used. The frequency of the pulsation is N times the propeller revolutions per second where N is the number of blades in the propeller.

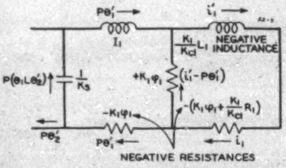

Figure 7. Equivalent circuit when motor inductance is included

Figure 6 tacitly assumes that the propulsion motor is connected to an infinite bus, whereas it is actually connected to a generator whose effects should be considered. This may be done in either of two ways:

1. Elaborate the equivalent circuit to include a branch for the generator.
2. Make an assumption that the internal generated voltage of the generator is constant.

This is very nearly true since from Figure 6 we see that the propeller damping term absorbs much of the vibration because it is directly in series with the torque pulsation, and the remaining pulsations in the motor circuit are reduced. Hence the speed oscillations which are transmitted to the generator are quite small and the internal generated voltage may be assumed as practically constant. We therefore should replace the term R_1 in Figure 6 by the total resistance of motor and generator armature circuits and we have a close approximation to actual conditions.

The Effect of the Inductance of the Armature Circuit

We may refer again to our two-machine system with inductance in each armature circuit being considered this time. This inductance is principally that of the machine itself but should also include that of the lines connecting it to the power supply. We assume as before that machine number 1 is on an infinite bus while machine number 2 is supplying a system whose line voltage E_2 is pulsating periodically.

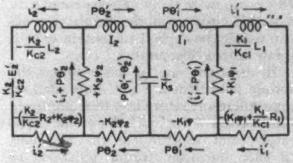

Figure 8. Complete circuit for two motors with inductance of both included

Considering machine number 1 first we may write our torque equation as before:

$$K_1\phi_1 i_1 - K_s(\theta_1 - \theta_2) = I_1 p^2\theta_1 \tag{27}$$

Our voltage equation includes an inductive term, $-L\dfrac{di}{dt}$, and becomes:

$$E_1 = i_1 R_1 + K_{e1}\phi_1 p\theta_1 + L_1 p i_1 \tag{28}$$

Under steady nonpulsating conditions, these equations will reduce to the same simpler expressions given in equations 10 and 11 and by subtraction we obtain equations in terms of the variation from mean values, thus:

$$K_1\phi_1 i_1' - K_s(\theta_1' - \theta_2') = I_1 p^2\theta_1' \tag{29}$$

and

$$R_1 i_1' + K_{e1}\phi_1 p\theta_1' + L_1 p i_1' = 0 \tag{30}$$

Equations 29 and 30 are sufficient for setting up an equivalent network but in order to do so we must first modify them somewhat by adding and subtracting certain terms and we thus obtain equations 31 and 32 which are seen to be the same as the first set of equations.

$$K_1\phi_1(i_1' - p\theta_1') - K_1\phi_1 p\theta_1' - K_s(\theta_1' - \theta_2') = I_1 p^2\theta_1' \tag{31}$$

$$\left[K_1\phi_1 + \frac{K_1}{K_{e1}} R_1\right] i_1' + \frac{K_1}{K_{e1}} L_1 p i_1' - K_1\phi_1(i_1' - p\theta_1') = 0 \tag{32}$$

These two equations can be set up into an equivalent circuit which is shown in Figure 7. Comparison of the circuit with equations 31 and 32 shows that the two agree.

The open end of this circuit will be tied on to a similar one for machine number 2. We see that this circuit is somewhat more elaborate than our previous circuits and has smaller damping because there are negative resistance terms as well as a negative inductive term; this latter being equivalent to a capacitance. If we let L_1 approach zero our circuit can be simplified and will reduce to our previous circuits with a single resistive term of magnitude $K_{e1}K_1\phi_1^2/R_1$ as before. On the other hand, if we let L_1 approach infinity it is seen that all our resistance terms drop out and we have a circuit with no damping at all.

For machine number 2 we will have a similar pair of equations except that the terms in the voltage equation will not be placed equal to zero but equal to E_2' which is the pulsation in the line voltage E_2. Thus we have:

$$E_2' = K_{e2}\phi_2 p\theta_2' - i_2' R_2 - L_2 p i_2' \tag{33}$$

$$K_s(\theta_1' - \theta_2') - K_2\phi_2 i_2' = I_2 p^2\theta_2' \tag{34}$$

These can then be expanded into equations similar to equations 31 and 32 so that an equivalent circuit may be set up. Figure 8 shows the complete equivalent

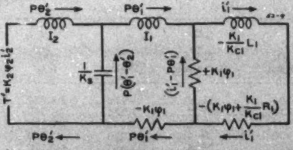

Figure 9. Equivalent circuit with damping considered in one motor only

Table III. Ship-Propulsion Drive—Tabulated Calculations

Inductive Case—See Figure 15

Rpm	ω Third Harmonic	$3K_p\omega_{p3}$	$j\omega I_p$	$-jK_s/\omega$	$j\omega I_m$	$-12.9 - j\omega L$
100	31.4	770	j14,030	−j34,650	j8,460	−12.9−j0.0202
150	47.2	1,154	j21,100	−j23,100	j12,700	−12.9−j0.0304
200	62.8	1,540	j28,000	−j17,320	j16,900	−12.9−j0.0404
230	72.4	1,770	j32,300	−j15,050	j19,480	−12.9−j0.0466
250	78.6	1,925	j35,100	−j13,850	j21,160	−12.9−j0.0507
256	80.5	1,970	j35,900	−j13,540	j21,660	−12.9−j0.0518
264	83.0	2,035	j37,000	−j13,120	j22,350	−12.9−j0.0539
275	86.5	2,115	j38,600	−j12,600	j23,300	−12.9−j0.0557

Rpm	Unit A	Unit B	Unit C	Total Impedance	Unit C Total Impedance	$\times\left(\frac{\text{Rpm}}{250}\right)^2$
100	3,960−j5,300	3,947+j 3,160	4,720+j 2,890	5,490+j16,920	0.31	0.05
150	2,180−j4,400	2,167+j 8,300	5,150+j12,200	6,300+j33,300	0.39	0.14
200	1,355−j3,600	1,342+j13,300	22,500+j50,200	24,040+j78,200	0.67	0.43
230	1,110−j3,220	1,097+j16,260	93,000−j117,500	94,800−j85,200	1.18	1.00
250	910−j3,020	897+j18,140	9,050−j56,400	10,975−j21,300	2.38	2.38
256	870−j2,950	857+j18,710	5,700−j48,000	7,670−j12,100	3.34	3.50
264	810−j2,880	797+j19,470	3,500−j37,000	5,600−j0	6.70	7.50
275	760−j2,790	747+j20,510	1,870−j32,300	3,985+j10,400	2.92	3.53

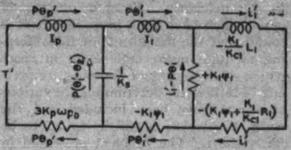

Figure 10. Complete circuit for ship-propulsion drive with motor inductance included

circuit including the branch we have already developed for machine number 1.

If for E_2' we use the maximum value of the line-voltage pulsation, then the "voltage" across the capacitor will be the maximum value of $K_s(\theta_1'-\theta_2')$ which is the maximum value of shaft torque. Similarly, we can determine the amount of load-current variation in both machines.

Other Cases With Inductance Included

From Figure 8 we see that at higher frequencies the armature-circuit inductance will reduce the damping but the load-current pulsation, i_2', will also be reduced since it must pass through an inductance. If we wish, we may assume that it is the load current i_2' and hence the pulsating torque applied to machine number 2 which remains constant while frequency changes. Such an assumption would enable us to see more clearly how the damping becomes less effective at higher frequencies. The circuit for this case is shown in Figure 9.

We may also set up an equivalent circuit for cases of combined electrical and mechanical damping as in the ship-propulsion drive which was treated by means of the simpler circuit, considering armature resistance only. By now it is apparent what form this circuit will take without rewriting all the differential equations and this circuit is shown in Figure 10. This circuit will be used in the appendix for the sample calculation of an actual system.

Determination of Machine Constants

A SHAFT SPRING CONSTANT K_s IN FOOT-POUNDS PER RADIAN

For unit torque of one foot-pound the angular twist in radians of a shaft section is given by

$$\theta=\frac{32\times 12\times L}{E_s d^4} \tag{35}$$

L = Length of section—inches
d = Diameter of section—inches
E_s = Shear modulus of elasticity—pounds per square inch

For steel shafting this may be rewritten:

$$\theta=1.036\times 10^{-5}L/d^4 \text{ radian per foot-pound} \tag{36}$$

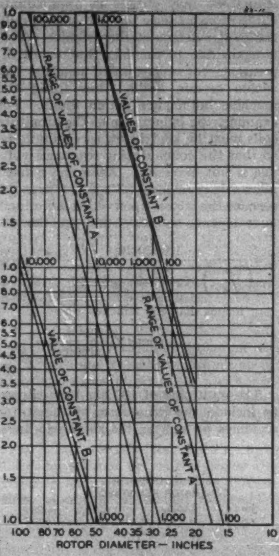

Figure 11. Standard values of WR^2 for d-c machines

$WR^2=A+B'$ in pound-feet squared
l = Rotor core length in inches

With a number of shaft sections of different diameter and length, the formula is applied to each in turn and the summation $\Sigma\theta$ obtained. Then $K_s=1/\Sigma\theta$ in foot-pounds per radian.

B. MOMENT OF INERTIA I

The usual electric machine can be broken down into a number of cylindrical sections such as: coils, core, spider hub, spider arms, end plates, commutator bars, commutator V-rings. The moment of inertia of any such section may be calculated if the detail weights and dimensions are known. Note that the WR^2 must be divided by g—(32.2 feet per second per second) in order to obtain moment of inertia I as used in the preceding equations.

In the absence of detail drawings of the machine a fairly close approximation to the WR^2 may be obtained from a knowledge of the rotor diameter and core length. This is due to the fact that for a given frame size, economical designs generally lead to approximately the same proportions for the various parts of the machine.

For a given rotor diameter the WR^2 varies directly with the core length so that we may write:

$$WR^2=A+BL \tag{37}$$

where A is the WR^2 for zero length and is due to the end plates, end winding, commutator, and so forth and B is the additional WR^2 per inch of core length. Both A and B are functions of the rotor diameter, varying approximately as the cube of the diameter so that we may draw a straight-line curve on logarithmic paper. This has been done in Figure 11 where the variation is shown for a wide range of standard d-c machines. For any given frame size the maximum and minimum WR^2 values differ by about ±8 per cent from the mean value, which is not too large a range for approximate calculations.

C. MOTOR-TORQUE CONSTANT $K\phi$ IN POUND-FEET PER AMPERE

This may be obtained from the nameplate rating of the machine and is given by:

$$K\phi=\frac{\text{horsepower}}{\text{rpm}}\times\frac{5{,}250}{I} \tag{38}$$

where I is rated armature current in amperes.

If the machine is not operating at rated conditions, the actual operating conditions should be substituted in the equation. This constant is proportional to the field flux and will vary inversely as the speed if field control is used but will remain constant if armature-voltage control of speed is used.

D. MOTOR COUNTERELECTROMOTIVE FORCE CONSTANT $K_e\phi$ IN VOLTS PER RADIAN PER SECOND

This likewise is obtained from the name-plate rating and is given by

$$K_e\phi=\frac{E\times 60}{\text{Rpm}\times 2\pi} \tag{39}$$

where E is the counterelectromotive force of the machine. This may be taken

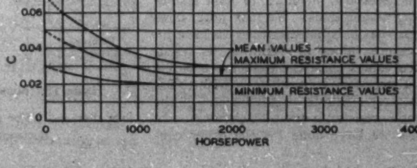

Figure 12. Standard values of armature-circuit resistance for d-c machines

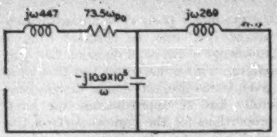

Figure 13. Numerical circuit values

Propeller damping only

as practically equal to the line voltage or for greater accuracy it may be corrected for IR drop. As with the torque constant, the counter electromotive force constant is proportional to the field flux.

E. Resistance of Motor-Armature Circuit R in Ohms

This may be determined from a knowledge of the conductor size, total conductor length, and number of parallel paths in the armature and in the series, commutating, and compensating field windings. The resistance of the connecting power lines may also be included but in most cases where all the equipment is located in physical proximity, the resistance of the lines is not large.

Where the design details are not available, an approximate estimate of the resistance may be obtained by comparison with standard machines. Economical designs require that the resistance loss be as small as possible and yet that the amount of copper used not be excessively large. Hence the per cent I^2R loss which is the same as the per cent voltage drop ($I^2R/IE = IR/E$) has roughly a constant value for a given-size machine. These values are plotted in Figure 12 for a wide range of machines and enable the determination of the resistance as:

$R = CE/I$ ohms

where C is obtained from the curve of Figure 12 and E and I are taken from the name-plate reading.

When more accurate calculations are desired, the actual resistance of the machine should be obtained, since the magnitude of the damping depends principally on the value of the resistance which is used.

Inductance of the Armature Circuit L in Henrys

The inductance of the armature circuit is not capable of accurate calculation since it requires the determination of magnetic fields in all parts of the circuit. It is necessary, therefore, to make simplifying assumptions. We may note, however, that it is not necessary to have inductance values as accurately as resistance values since the inductance enters as a secondary term when we wish to use the more accurate circuit instead of the simpler resistance damping circuit.

As we have done for the other constants, we may obtain an approximate value of inductance without knowing all the design details of the machine. This is again due to the fact that detail dimensions for a given-size machine fall within certain limits, thus fixing the machine inductance within limits. For example, the inductance of the armature coils must be kept below a certain value so that the commutating reactance voltage is not excessive. Assuming a fixed allowable reactance voltage, we may determine the factors upon which the inductance depends and we obtain equation 40.

$$L = \frac{100 \times \text{volts}}{\left(\frac{\text{Rpm}}{100}\right)^2 \times \text{poles} \times \text{amperes} \times \text{inches diameter} \times \text{inches core length} \times \left(\frac{\text{poles}}{\text{circuits}}\right)} \text{ henrys} \tag{40}$$

The multiplier of 100 has been chosen to include the inductance of the stator windings as well as the rotor windings.

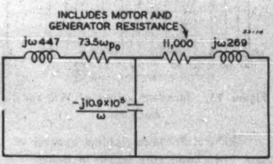
INCLUDES MOTOR AND GENERATOR RESISTANCE
jω447
73.5ω$_{p_0}$
11,000
jω269
$-\frac{j10.9\times10^5}{\omega}$

Figure 14. Numerical circuit values

Propeller and motor-resistance damping

This formula involves constants which may be taken from the name-plate reading and a knowledge of the rotor diameter and length. Comparison with more accurate calculations and with measurements indicates a fair agreement, and the error to be expected is generally less than 20 per cent.

Conclusions

Methods have been presented for determining the amount of damping present in d-c machines. From a number of cases which have been investigated, it is found that the magnitude of this damping is quite appreciable even in cases where other sources of damping are present. Methods for determining the various constants have been included and the work of calculation will be found to be fairly short. The problem presented in the appendix includes calculations for several assumptions and a range of speeds, whereas only one operating point (at the critical speed) need actually be calculated.

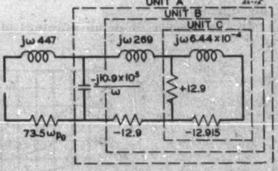

Figure 15. Numerical circuit values

Propeller and motor damping with motor inductance included

The question arises as to whether it is necessary to utilize the more elaborate inductive circuit. Usually it will be necessary to do so since it makes an appreciable difference in the results. A rough criterion which may be used is as follows:

Take the reactance voltage due to the armature inductance L, at the critical frequency F, and full-load current I. If this is less than three per cent of the rated machine voltage the simplified circuit may be used with fair accuracy. If it is any larger, the more elaborate circuit must be used in order to obtain satisfactory results.

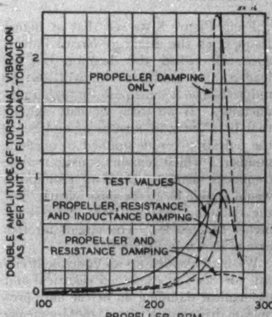

Figure 16. Comparative plot of calculated and test values of vibration amplitude, ship-propulsion drive

In order to determine the relative damping contribution of the propeller and the propulsion motor for an actual installation, sample calculations are presented in the appendix for such an installation. This drive was on board the Coast Guard cutter *Naugatuck* and oscillographic records of electrical and mechanical pulsations were taken. Torque pulsations in the shaft were recorded with a torsional strain gauge mounted on a calibrated section of the drive shaft. The cutter is driven by a single-screw three-bladed propeller. The motor is a 500-volt d-c machine rated 800 horsepower at 250 rpm and is powered by two 400-kw generators.

It is apparent from the comparative

plot of Figure 16 that only the complete equivalent circuit will give a fair approach to actual results. Considering the propeller damping alone leads to far too large a pulsation. On the other hand, considering only the resistance of the motor leads to far too large a damping force in the motor. The complete circuit gives a much better approach to actual conditions but it, too, deviates from the experimental curve due principally to the fact that propeller pulsations and propeller damping do not truly follow the simplified laws we have postulated for them.

Appendix

Calculation of ship-propulsion-drive constants:

$$K_s = \frac{6^4 \times 10^5}{1.036 \times 114.6} = 10.9 \times 10^5 \text{ foot-pounds per radian}$$

WR^2 of motor = 8,670 pound-feet^2

WR^2 of propeller plus 25 per cent added on account of entrained water = 14,400 pound-feet^2

Critical speed

$$= \frac{1}{2\pi}\sqrt{10.9 \times 10^5 \left(\frac{32.2}{8,670} + \frac{32.2}{14,400}\right)}$$

$= 12.8$ vibrations per second

which is 256 rpm for the third harmonic pulsation of the three-bladed propeller.

$$K\phi = \frac{800}{250} \times \frac{5,250}{1,300} = 12.9 \text{ pound-feet per ampere}$$

$$K_e\phi = \frac{500 \times 60}{250 \times 2\pi} = 19.1 \text{ volts per radian per second}$$

K_p = Propeller torque constant for use in circuit of Figure 6

$$= \frac{\text{Torque}}{(w_{p0})^2} = \frac{16,800}{(26.2)^2} = 24.5 \text{ pound-feet per (radian per second)}^2$$

$R = 0.01109$ ohm at 75 degrees centigrade—from design details

$$\frac{K_e\phi \times K\phi}{R} = 22,200 \text{ pound-feet per radian per second—resistive damping constant}$$

Inductance $= L = 4.77 \times 10^{-4}$ henry

In making the calculations, the propeller-torque pulsation has been assumed at six per cent of the mean torque rather than the more commonly assumed value of ten per cent, since it is more nearly correct in this case. A verification of this is obtained by employing the equivalent circuit to calculate the armature load-current variation at the critical speed. This amounts to five per cent of rated current and checks rather closely with experimental values obtained by an oscillographic test.

The last column in Tables I, II, and III gives the vibration in per unit of full-load torque pulsation. Actually in plotting these results we assume a six per cent torque pulsation.

References

1. Mechanical Vibrations (book), J. P. Den Hartog.

2. Practical Solution of Torsional-Vibration Problems (book), W. K. Wilson.

3. Test of Transient Conditions in Maneuvering a Coast Guard Harbor Cutter, H. H. Curry, J. C. Fink. Society of Naval Architects and Marine Engineers *Transactions*, volume 46, 1941, page 100.

Speed-Control System for an Aircraft Cabin-Supercharger Drive

F. W. GODSEY, JR.
MEMBER AIEE

J. D. MINER, JR.
MEMBER AIEE

O. C. WALLEY
ASSOCIATE AIEE

Synopsis: Cabin supercharging is becoming extremely important as flight ceilings for military aircraft are extended upward. Many different schemes have been worked out for using main-engine power to drive variable-speed blowers at speeds which will maintain the desired air-flow and cabin pressure at various altitudes. Two fundamental problems are

1. Providing a variable-ratio transmission between the engine and the blower.
2. Controlling the blower speed to maintain the required air delivery.

In some cases a third problem arises because the point of air delivery is at a considerable distance from the engine, necessitating either a long transmission of power or the use of long air ducts. Requirements for remote supercharger drives of moderate power may be met by means of a variable-voltage electric coupling. By using suitable motor characteristics the air delivery of a blower connected to such an electric coupling can be controlled by a simple regulator designed to vary current in proportion to voltage. Requirements for the electric equipment are developed, and laboratory tests on a nine-horsepower model are presented to demonstrate that the equipment meets the specified performance.

Aircraft cabin-supercharger devices are required to deliver an increasing volume of air as the altitude increases. It usually is desired to maintain outside pressure up to 8,000 feet; to maintain the pressure equivalent of 8,000 feet from 8,000 to 30,000 feet; and then to let the cabin pressure decrease at higher altitudes to maintain safe pressure differentials. A certain minimum air delivery is necessary to meet the oxygen requirements of the crew, so that the usual conditions of operation will be a constant weight of air flowing from the blower each minute, cabin pressure fixed at the pressure equivalent to 8,000 feet, and inlet pressure varying according to altitude. A variable-speed centrifugal blower provides a suitable source of air delivery but requires a means of coupling it to the main engine to permit operation of the blower at the speed corresponding to altitude requirements, regardless of the speed at which the engine may be operating.

General Requirements

This paper presents an all-electric approach to the problem and is based entirely upon specifications for blower input issued by Wright Field as shown in Figure 1. An *electric coupling* is used which consists of a d-c generator driving a d-c motor. This arrangement permits any desired location of the blower. The principal purpose of this paper is to investigate the possibility of devising a suitable method of speed control to maintain automatically the desired rate of mass air delivery.

It will be noted from Figure 1 that the required power range is approximately ten to one, and the required speed range is approximately the square root of ten to one. The drive takes power from a standard high-speed engine take-off and must operate over a generator speed range of 5,000 to 10,000 rpm. By specification the electric coupling must be entirely independent of the 24-volt bus on the airplane.

A variable-voltage d-c generator driving a separately excited motor would offer a practical and flexible system of speed control, if some source of motor excitation were available. Investigation is necessary, therefore, to determine whether some simple method of speed control can be worked out using shunt, compound, or series excitation for the motor and either variable or constant voltage from the generator. A further object of the investigation is to determine whether

---

Paper 45-3, recommended by the AIEE committee on air transportation for presentation at the AIEE winter technical meeting, New York, N. Y., January 22–26, 1945. Manuscript submitted June 16, 1944; made available for printing November 2, 1944.

F. W. Godsey, Jr., is staff assistant of the new products division of the Westinghouse Electric and Manufacturing Company, East Pittsburgh, Pa. J. D. Miner, Jr., is engineering manager of the aviation engineering department and O. C. Walley is design engineer with the Westinghouse Company in Lima, Ohio.

the specified speed control may be accomplished simply by controlling the relation between speed and torque or whether a pressure-sensitive device must be used to control speed in order to obtain the specified speed for each altitude.

Motor Characteristics

Specifications of horsepower and speed versus altitude as given in Figure 1 may be converted into a speed–torque curve to facilitate investigation of motor performance requirements. The speed–torque curve is plotted in Figure 2 and proves to be a straight line which may be expressed as

$$n = 2{,}100\,T \tag{1}$$

where n represents speed in rpm and T represents torque in pound-feet.

The internal torque which must be developed by the motor will be considerably more than the value indicated by equation 1 because of friction, windage, and rotational iron loss. An approximate expression for the internal torque would be

$$n = 1{,}700\,T \tag{2}$$

In this expression the losses in torque have been assumed proportional to speed; that is, brush and bearing friction at standstill and also the nonlinear components of windage and iron loss have been neglected.

When other conditions remain constant, the torque required to drive a centrifugal blower varies with the square of the speed of the impeller. A series of speed–torque curves for the blower has been added to Figure 2 for each 5,000 feet of altitude. These curves are constructed easily by selecting the appropriate speeds from Figure 1, and setting the torque proportional to the square of the speed through the same speed–torque points on Figure 2. It will be observed that a motor having a speed–torque curve meeting the specified values will operate the blower at the correct speeds, because the intersections of the speed–torque curves are single-valued and at low speeds motor torque is always greater than the blower torque.

Perhaps this explanation needs emphasis. If the motor can be made to provide the speed–torque relation shown in Figure 2, it will operate at the specification speed and only at this speed at any altitude within the range covered by the specification, *and no other altitude-sensitive control is required.*

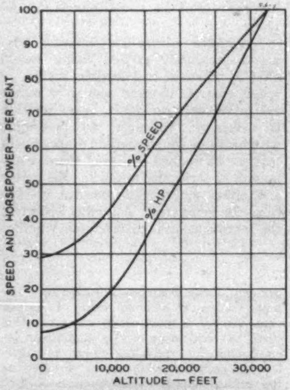

Figure 1. Specification of speed and horsepower versus altitude for the input to the blower of the supercharger

100 per cent speed = 10,000 rpm
100 per cent horsepower = 9 horsepower

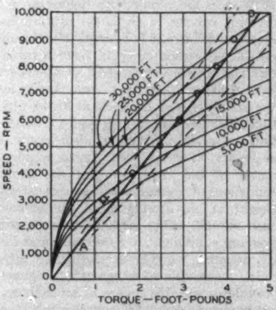

Figure 2. The specifications of Figure 1 converted to a conventional speed–torque curve

Superimposed are the speed–torque curves of the blower for each 5,000 feet of altitude and also test points obtained with the model equipment

O—Test points
A—Specified speed–torque curve with 15 per cent speed band

The proposal that a motor be designed with deliberate intent to have speed increase with increasing torque is startling to a motor designer. A motor with only a slight rising characteristic may hunt violently on a load having appreciable inertia, and here it is proposed that the speed increase directly with torque. The curves of Figure 2 are reassuring, however; no instability will result from any straight-line speed–torque curve passing through the origin. It remains then to devise some way to produce the unconventional speed–torque curve required.

A d-c motor responds only to voltage, current, and flux, and the desired motor performance must be expressed in terms of these quantities. The fundamental equations for speed and torque are

$$e = n\,k\,\phi \tag{3}$$

where e equals counterelectromotive force, n equals rpm, ϕ equals flux per pole in kilolines, and

$$k = \text{conductors} \cdot \frac{\text{poles}}{\text{circuits}} \cdot 10^{-8} \cdot \frac{1}{60} \tag{4}$$

$$T = 7.03 k\phi I_a \tag{5}$$

where I_a equals armature amperes, and T equal torque in pound-feet.

By substitution

$$e = 1.192\,k^2\phi^2 I_a \cdot 10^4 \tag{6}$$

Equation 6 gives the relations between induced voltage, flux, and armature current for any motor operating on the assumed speed–torque curve in equation 2. A preliminary study of these relations may be made by assuming voltage, flux, and current to be held constant in turn as shown in Table I.

Table I. Range of e, ϕ, and I_a From Minimum to Maximum Altitude

e	ϕ	I_a
Constant	$\sqrt{10}$ to 1	10 to 1
1 to $\sqrt{10}$	Constant	1 to $\sqrt{10}$
1 to 10	1 to $\sqrt{10}$	Constant

Analysis of Table I indicates that the generator will be of the same size for all three arrangements; that is, the maximum output is ten times the minimum output, if the increase is all in current equally, divided between current and voltage, or all in voltage. This is a natural consequence of the fact that the load on the generator is completely independent of generator speed. However, this condition does not obtain for the motor. If cooling considerations are neglected, the motor would be about three times as large for constant voltage as it would for either constant flux or constant current. A constant-voltage motor would have to deliver maximum power with less than 30 per cent of its maximum flux capacity being utilized. Also, a constant-voltage system would require two regulators: the first to maintain constant voltage, and the second to keep the flux in the motor in inverse proportion to the armature current. Needless to say, the flux regulator would be a difficult instrument to devise.

Constant-flux operation with voltage directly proportional to current results in a motor of reasonable weight but involves some difficult control problems. Again, two regulators would be required: one to hold field current constant regardless of voltage, and the second to vary voltage in proportion to current. The field winding would be likely to overheat at low speeds, since field losses would remain at full value while ventilation would fall off rapidly.

Constant-current operation with voltage varying over a ten-to-one range appears somewhat more practical, although it also presents a difficult ventilation problem at low speed, since the copper losses remain as high at minimum speed as they are at maximum output. Examination of equation 6 indicates that for constant-current operation the flux must vary as the square root of the voltage. This condition may be approached over a limited range by careful design of the magnetic circuit, by using shunt excitation, and by using pole-face windings to prevent field distortion under load. The regulation problem would be simple, as a standard voltage regulator could be used by replacing the potential coil with a current coil.

From these considerations it appears that the ideal condition is a compromise approaching the constant-current condition but with some change in current with load to reduce the range of voltage required and to reduce copper losses at low speeds. Further examination of equation 6 will show that, if the relation between current and voltage is of the form:

$$I = I_0 + Ae \tag{7}$$

the relation of flux and voltage will be

$$\phi^2 = \frac{e}{1.192\,k^2(I_0 + Ae)} \tag{8}$$

This is a promising equation, since, if Ae is small compared to I_0, the flux will be proportional to the square root of the voltage (as before) for small values of voltage but will approach a saturation value as e approaches infinity. A voltage regulator to meet the requirements of equation 6 is very simple; it requires a current coil to balance the spring forces at current I_0 and a differential potential coil to bias the regulator, so that each increment in voltage requires a proportional increment in current for equilibrium.

Before one proceeds to the actual design of a motor, equation 6 must be modified to include brush drop, armature-circuit resistance drop, and shunt-field amperes. The armature current becomes

$$I_a = \frac{V - (1.0 + R_a I_a)}{1.192\,k^2\phi^2 \cdot 10^4} \tag{9}$$

where V is terminal voltage, R_a is the resistance of the entire armature circuit, and the brush potential drop is assumed constant at one volt.

The total line current is

$$I_L = I_a + \frac{V}{R_f} \tag{10}$$

where I_L equals line current and R_f is the hot resistance of the shunt field.

At this point it is necessary to make a tentative motor design and then to determine whether operation within the specified limits will be possible by means of a regulator working to equation 7. For the model designed to meet the specifications of Figure 1, a four-pole motor with provisions for generous pole-face windings was selected. Accurate compensation of armature ampere turns is used to prevent field distortion. The armature has 82 conductors and two circuits, so that k is $2.74 \cdot 10^{-4}$. The total resistance of the armature circuit is 0.013 ohm. Curvature was introduced into the saturation characteristic of the motor at low excitations by notching the backs of the poles to provide thin sections of restricted area. These thin sections saturate at low values of flux and then behave like an increasing air-gap length at higher values of flux. The actual saturation curve is plotted in Figure 3, and it will be noted that the curve does not deviate greatly from a square curve. The hot-field resistance is ten ohms.

Various values of V may be assumed, and corresponding values of ϕ taken from curve 1 of Figure 3. Equations 9 and 10 are then used to find the relation between V and I_L. This relation has been plotted as curve 3 of Figure 3. It will be noted that this curve is not linear; the actual shape varies with the shape of the saturation curve and may be modified considerably by slight changes in this curve. Over the principal operating range, however, the relation of I_L and V is reasonably close to the linear curve:

$$I_L = 140 + 0.75\,V \tag{11}$$

shown as curve 2 on Figure 3.

It is obvious that very careful precautions must be taken in the design and construction of the motor to minimize the effects of residual voltage, as otherwise, the performance of the system will differ widely between ascending and descending tests.

A nine-horsepower motor was built to these specifications and tested with a regulator which controlled current and speed per the test points shown in Figure 3. Speed-versus-voltage readings are shown in Figure 3, and speed-versus-torque readings are shown in Figure 2. The test points are well within specification limits except for the relatively unimportant points at the extreme low end of the speed range.

Generator Characteristics

No special characteristics are necessary for the generator insofar as meeting the requirements of the regulating system. Any generator capable of delivering the required range of voltage and the required range of current will be satisfactory so long as it meets general specifications for aircraft generators. For the model built and tested for this investigation the stacking was lengthened on a 5,000-rpm 30-volt generator, so as to provide a maximum output of 50 volts at 185 amperes. The generator is compensated fully to provide good commutation over a wide range of output at any speed from 5,000 to 10,000 rpm. A four-pole design with 51 commutator bars provides a very conservative value of volts per bar for high-altitude operation. Aside from voltage rating, the generator is of conventional design.[1,2]

Regulator

A schematic diagram of the regulator is shown in Figure 4 and a photograph of the regulator in Figure 6. The basic principle of the regulator is very simple. The operating coils consist of

1. A heavy coil of a few turns carrying the entire line current.
2. A differential-potential coil carrying current in proportion to system voltage.

This regulator will adjust the generator field until sufficient current flows, so that the algebraic sum of the ampere turns in the current coil and the opposing ampere turns in the potential coil will produce enough flux to balance the regulator spring. Each time the regulator acts to increase the current, it does so by raising the system voltage. With increasing voltage it takes higher and higher values of current to produce equilibrium.

A decrease in torque, such as is produced by an increase in altitude, tends to reduce the current drawn by the motor in proportion to the reduction in torque required to operate the blower. The

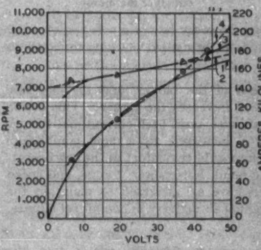

Figure 3

1—Motor saturation curve, flux versus volts

2—Test volt-ampere curve for regulator, $I_L = 140 + 0.75V$

3—Calculated volt-ampere curve for regulator,

$$I_L = \frac{V - (1 + 0.013I_a)}{8.95\phi^2 \cdot 10^{-6}} + \frac{V}{10}$$

4—Test speed-voltage curve, revolutions per minute versus test voltage regulator, however, cannot permit a decrease in current; instead it operates to raise the excitation on the generator. The increased system voltage increases speed of the blower, and the increased speed increases the torque. This action continues, until both current and voltage have increased to a new equilibrium point for the regulator; at the new operating point, horsepower, torque, and speed will have all increased to maintain the original air delivery in pounds per minute.

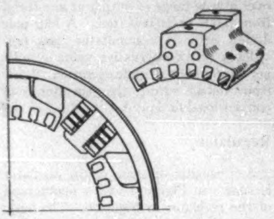

Figure 4. A quarter section of the magnetic circuit of the motor

Inset shows the restricted pole section which produces the desired saturation characteristics

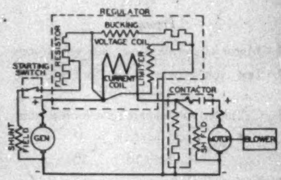

Figure 5. Schematic diagram of the electric coupling system

Two refinements are necessary to make the regulator entirely satisfactory. In the first place, a shunt-wound generator never would build up voltage with a low-resistance motor across its terminals. For this reason, a starting contactor is provided which will open the motor circuit until the generator has built up to a low voltage. During starting the current regulator necessarily acts as a current limiter, preventing currents in excess of the regulator setting by inserting the control resistance in the generator-field circuit. The drop in voltage will cause the starting contactor to open, and the system will cycle several times as the blower motor comes up to speed. This is not harmful in any way, as the line current is practically zero at the instant the contactor opens, and the only effect is to increase the time required for acceleration to full speed. A series coil is provided to hold the contactor in at low voltages.

The second device which must be added to the basic regulator is a voltage-limiting device which acts to prevent the voltage from exceeding about 55 volts. This device is necessary because the system tends to be self-destructive in the event of loss of load for any reason. The device acts on the armature of the regulator as soon as the calibration voltage is reached and destroys regulator equilibrium in such a way as to make it regulate for 55 volts. Since the motor is shunt wound, motor speed is limited to a value only slightly over the maximum rated speed of 10,000 rpm.

Figure 6. The generator (left) and motor (right) of the electric coupling

Figure 7. The regulator which controls the relation of current to voltage

The voltage-limiting device may be seen to the back and right of the main regulator

Conclusions

It has been demonstrated that it is possible to design a motor with characteristics such as will result in a speed–torque curve with torque directly proportional to speed over an appreciable range of output, when the motor is operated from a system having voltage and current control of the form $I = I_o + AV$. It also has been shown that a motor with such a speed–torque curve will meet the requirements of specifications intended to assure a constant rate of mass air delivery at any altitude between 8,000 and 30,000 feet when used with a centrifugal blower operating to supercharge an airplane cabin. A simple regulator to control current and voltage has been described.

A model has been built and tested, and found to meet the specified speed–torque requirements within narrow limits. It was found during the tests that the steepness of the speed–torque curve could be adjusted readily by changing the ratio of current-coil ampere turns to potential-coil ampere turns and that the entire power-output level could be raised or lowered by adjusting the spring tension on the regulator. No tests were made of actual altitude performance.

The chief difficulties with the system appear to lie in the accuracy required of the motor characteristics, particularly in regard to control of the magnetic circuit. Elimination of residual effects requires careful selection of magnetic materials and elaborate annealing; the accuracy usually built into a regulator must, to a lesser degree, be built into the motor, since the motor characteristics form an important part of the regulating system. Some minor difficulties also may arise from temperature effects, but these do not appear important so long as the permissible speed variation is 15 per cent.

The speed-limiting action which takes place at maximum altitude appears in line with recent proposals to allow cabin pressure to decrease at altitudes above 30,000 feet to lessen danger to personnel in the event of rupture of the airplane cabin.

The project was a very interesting experiment, its future possibilities must be exploited by the experimental section of the Army Air Forces at Wright Field.

References

1. Design Relationships for D-C Generators for Use in Aircraft, S. R. Bergman. AIEE Transactions, volume 62, 1943, October section, pages 613–16.

2. Design Considerations for D-C Aircraft Generators, J. D. Miner. AIEE Transactions, volume 63, 1944.

Electrification and Signaling of the Canadian National Railways Terminal, Montreal, Canada

R. G. GAGE
NONMEMBER AIEE

THE development of the Montreal Terminal of the Canadian National Railways, which was started in 1931 and lay dormant all during the depression years, was revived as an unemployment relief measure and continued as a wartime measure in 1939. The project consisted of centralizing the four passenger stations, the construction of a new station, and the alteration of existing freight yards and facilities.

The Canadian National Railways' facilities at Montreal are a combination of those of the Grand Trunk Railway and Canadian Northern Railway, both of which, together with the Canadian Government Railways, were combined to form the Canadian National Railways System in Canada. The use of Bonaventure station, the old and outmoded terminal of the Grand Trunk Railway and Canadian Government Railways, for many years had been the cause of congestion and, owing to the numerous grade crossings of city streets involved, had been a source of serious city complaints.

During its construction, the only way the Canadian Northern Railway could enter Montreal for its eastern terminus was by way of a three-mile double-track tunnel under Mount Royal, terminating in a passenger station at Lagauchetière Street, adjacent to the uptown retail business district of the city. Having to operate through this long tunnel, the Canadian Northern Railway was forced to electrify its lines for a distance of about ten miles, including the tunnel, and one of the then (1914) modern and popular systems, namely 2,400-volt d-c, was adopted. Six 1,000-horsepower locomotive units were built by the General Electric and the Canadian General Electric companies and eight multiple-unit car equipments were provided, two of which were subsequently installed.

After an exhaustive study just prior to 1930, it was decided to develop the new terminal on an enlargement of the original Canadian Northern station site. This now comprises 14 passenger- and three express-station tracks, of which the four through tracks in the center have platforms long enough to accommodate 20-car trains. These station tracks connect with the double track of the Mount Royal Tunnel on the north and with six main tracks, tapering down to two, on a viaduct extending southward to the Victoria Bridge. The station building is centrally located in relation to the platforms, reducing to the minimum the distance which passengers must cover in boarding or leaving trains. The platforms are of car floor height and are served by two broad stairways and an escalator leading directly on to the center line through the station concourse, immediately above. The subtrack area, extending throughout the station area, provides the express, baggage, mail, and customs facilities and is accessible by motor or truck directly from Lagauchetiere Street, one of the main thoroughfares. Access to the station proper by taxi and private automobile is from two plazas located on the north and south sides, connecting directly to the adjacent streets. Direct access for pedestrians is by means of stairs and escalators at both the east and west sides from Dorchester Street. The two upper floors of the station building are occupied by the railway operating staff.

As will be gathered, the entire station area is below the adjoining street levels, primarily on account of the elevation of the tracks in the Mount Royal Tunnel which is also the elevation of the track on Victoria Bridge leading across the St. Lawrence River. The tracks between these two points are constructed on a viaduct, thereby securing grade separation of all intervening city streets. The entire project has been laid out in such a way that the overhead rights for office buildings, hotel, auditorium, and so forth may be built without interfering with any of the existing structures as provision has been made for the necessary supporting foundations for such buildings. It is felt well within the realm of possibility that, with the normal growth of Montreal, this terminal area will develop in a similar manner to that of Grand Central Terminal in New York.

Electrification

Power for the Montreal Terminal is purchased from the Quebec Hydro Commission at three phase, 12,000 volts, being received from two independent substations which, together with six other substations, are connected to the 66,000-volt ring of the power distribution system. The two supply lines terminate in a railway transformer substation, located below the tracks in the station area, each line having capacity to carry the total terminal load of approximately 6,000 kva. The main circuit breakers on each of these supply cables are equipped with an automatic change-over device ensuring the continuity of service in case of trouble arising in the cable itself or in the substation feeding it. This 12,000-volt supply is stepped down to 4,000 volts, three phase for general distributions; 208/120 volts, three phase, four wire for general lighting and car charging purposes; and 575 volts, three phase for station elevators, fan motors, pumps, and so forth. Two independent three-phase 4,000-volt circuits are run in conduit from this substation to the central control tower at the Lachine

---

Paper 45-10, recommended by the AIEE committee on land transportation for presentation at the AIEE winter technical meeting, New York, N. Y., January 22-26, 1945. Manuscript submitted October 25, 1944; made available for printing November 20, 1944.

R. G. Gage is chief electrical engineer, Canadian National Railways, Montreal, Quebec, Canada.

Electric locomotives and trolley feeder breakers were manufactured by the English Electric Company, London, England, and purchased from the Montreal Harbour Commission. Glass-bulb rectifiers and rectifier transformers were supplied by the Hewittic Electric Company Ltd., Hersham (Walton-on-Thames) Surrey, England, through the Northern Electric Company at Montreal. Overhead trolley fittings were supplied by the Ohio Brass Company, Mansfield, whose engineers were also consulted in the design and application.

Signal equipment for the Montreal area was purchased from the Union Switch and Signal Company, Pittsburgh, Pa., who are also responsible for the detail engineering and construction. Signal equipment for the St. Lambert area was purchased from the General Railway Signal Company, Rochester, N. Y., who are also responsible for the detail engineering and construction.

All of the above work was carried out by the chief engineer of the Canadian National Railways, under the immediate supervision of the chief electrical engineer and his staff.

Canal lift bridge to supply energy for the operation of the lift bridge over the canal and for the terminal signaling.

The feature of the power system for the terminal which is of special interest is the use of glass-bulb mercury-arc rectifiers for supplying the 2,400-volt direct current for traction. Although these are used to a considerable extent for traction purposes in England and in other parts of the Commonwealth, it is their first use in Canada and probably any place in 2,400-volt service.

Two independent 12,000-volt three-phase circuits are run from the transformer station and, protected by main circuit breakers connected with two 2,156-kva 12,000/2,200-volt 3- to 12-phase rectifier transformers. Each transformer feeds a bank of four glass-bulb rectifiers whose capacity under normal rating is 1,500 kw per bank and 3,000 kw on a five-minute peak rating. The 12 phases in each transformer are connected in two three-phase groups joined at their neutral points by an interphase transformer; these two six-phase groups are in turn connected together at their neutral points by a third interphase transformer. The rectifiers are operated in pairs connected in parallel across six phases. Bulbs *A* and *B* are connected to the six phases comprising group one and bulbs *C* and *D* to the six phases comprising group two. Each bank is protected by a 2,400-volt d-c breaker with a normal time lag set to take care of the normal operating short-period peak loads but with a very high-speed setting for reverse current, protecting against reverse flow between banks in case of a backfire in the bulb.

The chief reasons for the selection of glass-bulb rectifiers instead of the more familiar steel-tank type were the decidedly lower cost to install; a much better delivery date under wartime conditions; the advantage of having the installed capacity in eight equal units instead of two; the elimination of all vacuum and cooling auxiliaries; and the excellent reported record in service on British railways.

The rectifiers consist of vacuum-sealed glass bulbs fitted with six operating anodes, each protected with a fuse, two exciting anodes, and an auxiliary automatic-starting anode. A pool of mercury covers the cathode located in the base of the bulb. The bulbs are mounted in steel cabinets with open grille doors for purposes of ventilation and are cooled by a fan located immediately beneath the bulb and connected so that its speed increases with the total current in the rectifier. The life of the tubes, as indicated by the records in other railway installations, is a matter of years. Individual failures, of course, occur as a result of defective workmanship or material as in all types of equipment.

The rectifier is started by energizing the 120-volt auxiliary circuit, which operates a magnetic contactor whose function is to cause a flexible contact to dip into the mercury pool and, when withdrawn, to strike an arc. This arc energizes the exciting circuit and maintains continuous arcing on the exciter electrodes which in turn is automatically transferred to the load anodes upon the application of load. Inasmuch as the rectifier has a permanent vacuum, no preliminary time is required for auxiliaries and the rectifier can take on its load immediately upon demand. It can, therefore, be thrown on or off the line from remote control points, or could be controlled by a time switch if desired. By the use of a large number of anodes in multiple, 24 in this case; and the reduction of current concentration on the anodes, backfiring is eliminated, or at least none has taken place to date.

The transformers are of the oil-insulated self-cooled type, 3-to-12 phase, housing the interphase transformers, the auxiliary starting transformer, and a choke in the main rectifier circuit which controls the cooling-fan speed in proportion to the load.

The rectifier station is designed for remote control and to be operated without continuous attendance. The rectifier banks can be put on or off the line independently from manually operated remote-control points from the substation or at the interlocking control tower at the Lachine Canal.

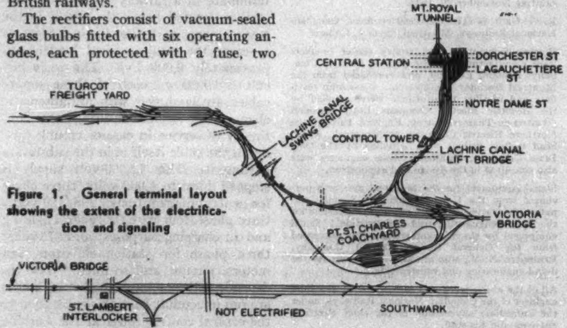

Figure 1. General terminal layout showing the extent of the electrification and signaling

Figure 2. Rectifier station showing the two banks of rectifiers, one on each side of the center aisle, with three of the trolley section breakers in the far end

In order to overcome interference with telegraph and telephone communications, corrective equipment was installed consisting of a coil of 30 turns and 1.115 millihenries inductance in the negative return and four tuned shunts between the positive and negative to eliminate the 360, 720, 1,080, and 1,440 frequencies. The rectifiers are operated without interference with existing communication circuits.

In addition to the mercury-arc rectifier station, direct current is supplied from a motor generator substation originally installed by the Canadian Northern Railway in 1918. This station consists of two three-unit sets composed of a 12,000-volt synchronous motor and two 1,200-volt 1,500 kw d-c generators connected in series. This station is being held as a reserve and will, undoubtedly, be replaced by modern rectifiers when the electrification is extended.

The catenary system throughout the terminal consists of steel bridges spanning the main line tracks spaced on an average of 180 feet apart, carrying copper conductors of approximately 800,000 circular mils equivalent copper conductivity per track, made up of a Copperweld and copper main messenger, copper auxiliary messenger, and two bronze grooved trolley wires. The trolley system is divided into 12 sections, each provided with a feeder breaker. Seven of these breakers, with an auxiliary for emergency use, are installed in the rectifier substation, and the balance in the switching room of the interlocking tower at the canal. All the breakers are remotely controlled by push-button switches mounted on the signal control panel in the operating tower. The signal levermen, under the direction of the train controller, are thus able to

Figure 3. Interior of rectifier cubicle

energize or de-energize any trolley section as called for by the exigencies of the service. They also control the rectifier station, putting either or both banks on or off the line as required.

There are no special engineering features in the overhead system. It conforms to recognized good practice for heavy-duty electrification. Owing to the steel shortage under war conditions, the catenary bridges are lacking in uniformity. At first they were designed and fabricated from new material, then from second-hand bridge steel removed from railway bridges and, finally, from creosoted timber when steel became unprocurable.

The additional electric locomotives necessary for an enlarged electrical operation, together with the feeder breakers for the 12 trolley sections, were obtained from the Montreal Harbour Commission as a result of their termination of electrical operation. The electrical characteristics of the Harbour installation were by design the same as those of the original Canadian Northern installation, so that it would be possible for the Canadian Northern to operate on the Harbour trackage in the interchange service.

Throughout the electrified zone, one rail of each track is bonded for propulsion return currents and the several return rails in parallel tracks are cross bonded together for conductivity. Owing to the use of direct current for propulsion, it was necessary to install a-c signal track circuits. Complications in the layout in some of the tracks, as well their cost, made it desirable to avoid the use of impedance bonds as frequently used with signal systems on electrified lines. This bonded return rail is used as a common rail for both signaling and traction, the other rail being insulated and retained for signaling.

A new coachyard was built at Point St. Charles consisting of 32 tracks, 19 of which were electrified, lighted, and equipped with battery-charging, vacuum, and steam-heating facilities. The overhead consists of the lightest type of street-railway construction with the trolley carried from single cross messengers spaced at 80-foot centers. Thirty-three-foot 85-pound scrap rails, with the ends embedded about five feet in concrete, are used as the trolley supports. The stresses in the trolley wires, as well as in the cross spans, are taken care of by dead-end guying. On each alternate support in the longitudinal rows, and staggered as between rows, is mounted a 6,000-lumen 20-ampere series lamp for lighting the yard. The lamps are supported in a hoop-type bracket mounted on the top of the trolley supporting poles giving a height above rail of about 28 feet. The lamps are fitted with symmetric refractors and are arranged in four regulated circuits. Very satisfactory and uniform lighting throughout the yard area has been obtained.

A rather novel feature in this yard is the arrangement of the car-charging facilities. The constant-potential system is used, supplemented by portable chargers to take care of the occasional car requiring special attention, such as those fitted with Edison batteries requiring a higher charging voltage.

Owing to the large variations in the total car-charging load, the usual practice of having two car-charging generator sets, with which at least one relatively large set would be running with a very light load for a considerable portion of the day, it was decided to install 16 500-ampere 50-volt motor generator sets located on the midway through the center of the platforms and at the approximate center of the loads. Owing to the relatively narrow platforms, these sets were mounted in small houses about 15 feet above the platforms, thus permitting the ordinary use of platform trucks necessary in the servicing of trains.

The houses, which also accommodate the regulating equipment, are accessible through a trap door in the floor. Windows provide ventilation in the summer and heat generated by the sets themselves provides the necessary heat in winter. The wiring for each platform is the three-wire return-loop system with the operating coils of the voltage regulator connected across, thus maintaining a constant potential at all charging outlets. Each generator is protected by a current regulator, a fuse, and a reverse-current relay. There is also a magnetic starter with start-stop push-button control at the base of each house support. A series relay is connected to the d-c side which serves to automatically stop the set when the last car is taken off charge. This relay also makes it necessary to have at least one car on the circuit before the motor generator set will run.

Signaling

The signaled area is divided into two parts, that on the south or east side of the St. Lawrence River—comprising two main tracks with connections to a large freight yard at Southwark—extends from St. Lambert for four route miles eastward and represents 108 controlled functions; the balance on the north or west side of the river extends from the west end of Turcot freight yard through the station area into the Mount Royal Tunnel and includes main tracks varying from two to six and their connections to the 17 station tracks. This latter installation covers about eight route miles and comprises 607 controlled functions. The former, which is controlled from the tower at St. Lambert, is what is known as wire-controlled relay interlocking and is divided into four zones. Inasmuch as this territory is not electrified, but is in close proximity to electrified lines, two-rail a-c track circuits are used. The Montreal side consists of relay interlocking laid out in ten zones, each of which is connected with the operating tower at the Lachine Canal lift bridge by means of polar code control. As all of this area is electrified, single-rail a-c track circuits are used throughout.

All main-line tracks throughout the aforementioned entire areas are provided with signals for movements in both directions and trains are governed by signal

Figure 4. Control panel of the St. Lambert interlocker showing signal buttons in the tracks and switch levers below

Figure 5. Operating panel and track diagram of Montreal interlocker showing the switch and signal push-turn buttons on the panel. Those in the triangular portions control the arc rectifiers and the trolley-feeder-section breakers

indication only. All relay racks and panels were wired in the factory before shipment and all relays are of the plug-in type which permits replacement without interfering with the permanent wiring and with minimum interruption to the service.

All signals are of the searchlight type using ten-watt ten-volt precision-based lamps, giving a strong parallel light beam which is clearly seen in bright daylight. This signal consists of a relay mechanism carrying three small colored screens on its armature, so arranged to show green with one polarity on the relay, yellow on the opposite polarity, and red when the relay is de-energized. The signal also includes a well-designed lens system producing a well-defined light beam. The signals at St. Lambert are of the standard interlocking type mounted on high ground masts or bridges for main-track movements and single-light dwarf signals for inferior-track movements, whereas all signals on the Montreal side are of the two-unit, low, ground type. The color aspects as shown by the signals are the usual: *green*—"proceed"; *yellow*—"proceed, expecting to find the next signal at stop"; and *red*—"stop." On the Montreal side, and at some points on the St. Lambert side, an aspect of red over yellow is displayed with the meaning to "proceed expecting to find the immediate block occupied." This means that an engineer accepting a red over yellow signal moves upon his own responsibility. This signal is necessary in terminal operation to enable locomotives to enter a block to connect with a train either in switching or in engine-changing operation. Dwarf, that is, low ground-type, signals are used in the Montreal interlocker throughout in order to utilize the trackage to the fullest extent and also to enable the signal to be located at the point at which it governs. The use of the low signals at Montreal also very greatly simplifies construction by separating the signals from interference with the electrified overhead system.

The interlocking machine at St. Lambert is made of a black-on-white laminated-plastic panel with the tracks milled out, showing a permanently white track diagram on a black background. All the switches are equipped with point indicators, which correspond to the operation of switch points in the track and offer a continuous broad white line, indicating the route which has been set up for a train movement. Signals are shown by illuminated push buttons located in the track where the signal is located. A green light in this button indicates that the signal is in the "proceed" position. The switches are controlled by small key switches located on the panel directly below the function. Miniature lamps located in each track section show by a red light the position of all trains throughout the interlocked area.

The Montreal interlocking machine, owing to the number of functions controlled by it, consists of an operating panel and a track diagram. The operating panel is of the desk type with an inclined top, similar to the control panel in many a-c power stations. The switches and signals are controlled by miniature push-and-turn type switches on the panel, located in convenient groups in relation to the functions controlled and as shown on the track diagram. The track diagram is a large elevated vertical panel on which is painted in colors the various track circuits throughout the controlled area. Each track section is fitted with a lamp which shows by a red light when the track is occupied. Signal locations are indicated by lamps adjacent to the track governed which, when lighted with a green light, show that the signal is in the "proceed" position. All signal lights are put out when passed by a train and the red track-occupancy lamp goes out as soon as a train passes the immediate track section. It will thus be seen that the progress of a train throughout the interlocked territory can easily be followed by the train controller. This is very different from former times. Now, regardless of the distance a train is from the tower, or of the weather conditions prevailing along the track, the controller is continuously informed as to the position of all trains in his territory.

In two respects the Montreal installation is of particular interest to the engineering profession. The first is the area over which the control of the track switches and signals is centralized in this one machine. This perhaps is unique at the present moment, as the ten controlled zones comprising the interlocker would formerly have been controlled by perhaps five or six independent interlockers. The second point, and one which made this centralization of control possible, is the use of a high-speed code connecting the control machine with a bungalow or control point in each of the ten zones. The coding is performed over a set of six wires, three of which are reserved for the outgoing control code and three for the incoming indication code. The code itself consists of a series of d-c pulses, in which two line wires are alternately energized and de-energized. During the energized periods the line circuit may be of either positive or negative polarity. Only two wires are used during coding, the three wires being used to determine the polarity of the line circuit.

When the signalman depresses a switch or signal-control button on the control panel, he initiates a control code, which, after passing through the proper interlocking relay group, passes over the control-code line circuit to a control-reception panel in the zone bungalow, then to the function-control relays and finally to the wayside relays and apparatus, that is, to the switch-point operating mechanism or signal. When the function has operated in accordance with the code sent out from the control tower, the completion of such operation initiates a corresponding indication code which runs through corresponding relay groups and over the indication-line circuit, back to the control machine in the case of a switch-point operation, and to the track diagram in the case of a signal operation, thus, by means of indication lamps, informing the signalman that his instruction has been completed. This code is unique in the speed with which it operates, namely 35 pulses per second.

The fact that the entire Montreal Terminal area has been equipped with signals so that trains may run in either direction on all the main tracks and that train operation is entirely by signal indication, without the use of train orders, has resulted in a very great reduction in freight-train delays. The operation of the terminal since the opening of the Central Station in July 1943 would indicate that the centralizing of signal control over a relatively large terminal area is feasible and economical, and that the combination of the duties of signalmen in controlling the movements of trains, as well as controlling by remote operation the trolley-feeder switches of the electrified zones, is also practicable, and that the men readily learn and appreciate the functions of the equipment which they are asked to control.

A Modulated-Frequency System of Telemetering

HAROLD E. RENFRO
NONMEMBER AIEE

ARTHUR PERRY PETERSON
ASSOCIATE AIEE

WITH today's centralized control and supervision of power systems, it is essential that the man at the controls knows what is going on at all outlying stations and interconnection points. Telemetering equipment keeps him informed of load changes, transfer of power from one system to another, variations in voltage, and all other values that are necessary for efficient operation.

No one system of telemetering can meet all requirements. The speed of indication, accuracy, number of separate channels available, dependability, ease of totalizing, freedom from interference, the availability and need of repair parts, and the initial cost, as well as maintenance cost, are factors that determine the design of any system of remote metering. A résumé of the telemetering practice up to 1941 will be found in the report of the joint committee of the AIEE committee on automatic stations and the AIEE committee on instruments and measurements, published in October 1941. That report also contains an excellent bibliography on telemetering systems and methods.

When the Department of Lighting of the City of Seattle wanted a telemetering system which would operate over a carrier-current channel they were unable to locate such a system that would give them continuous and instantaneous readings. They felt that, for their purposes, an impulse system which provided readings at regular intervals was not the answer to their problem. Furthermore, they wanted a system that would permit several readings simultaneously over a single set of conductors. It was this need that led to the development of a modulated-frequency system of carrier telemetering.

The telemetering system herein described was designed to give continuous and almost instantaneous readings which are independent of supply voltage and are not affected by wide variations in remote-line characteristics. It was designed to operate with a high degree of dependability during emergencies, to permit a large number of channels on one pair of conductors, to give very fast response, and to incorporate certain other desirable features.

The transmitter generates its own carrier frequency making it unnecessary to provide a separate carrier-current system. Standard radio receiver tubes are used throughout and all parts subject to wear or breakdown are easily replaceable standard radio parts.

General

The block diagram, Figure 4, illustrates the principle of operation and this will be described briefly. In the telemeter transmitter is incorporated the primary instrument, such as a wattmeter, which determines the values to be transmitted. This primary instrument controls the frequencies of two high-frequency oscillators whose outputs are converted into a single beat frequency. The beat frequency, which varies with the magnitude of the quantity being measured, is amplified and transmitted over the line, whether it be a transmission line or a telephone line. Normally, capacitive coupling is used with a transmission line whereas inductive coupling, with a band-pass filter to separate the carrier frequencies from the voice frequencies, is used with a telephone line. Only telephone-line applications will be described here.

At the receiving point the incoming signal from the line is amplified and then mixed with the output of a local oscillator of constant frequency. This converter stage is followed by a low-pass filter which attenuates all but the beat frequency. The current at this beat frequency is then amplified and fed into a frequency meter, of which the final indicating instrument is a part.

Transmitter

The schematic diagram of the telemeter transmitter is shown in Figure 6. The primary instrument actuates two variable capacitors, C_1 and C_2, which, in turn, simultaneously control the frequencies of the two oscillators. The variable capacitors form part of the capacitance of the frequency-determining resonant circuit of each oscillator.

The greatest difficulty with instruments of this type that have been tried in the past has been that a variable capacitor on the shaft of the primary instrument develops a torque of its own that varies with the potential applied to it. A variable inductance develops a somewhat similar torque due to current through it. This destroys the calibration of the instrument and makes a reliable system impossible, unless counter measures are taken.

An analysis of the torque developed by a variable capacitor with a voltage across its plates shows the following to be true: two conductors separated by an insulator tend to move toward each other when a difference of potential exists between them. With parallel-plane conductors of infinite area, this force is perpendicular

Figure 1. Front view of the assembled telemeter transmitter

The two wrought-iron tanks at the bottom house the oscillatory circuits

Figure 2. Telemeter receiver

The indicating instrument is not shown

Paper 45-19, recommended by the AIEE committee on instruments and measurements for presentation at the AIEE winter technical meeting, New York, N. Y., January 22-26, 1945. Manuscript submitted May 8, 1944; made available for printing December 1, 1944.

Harold E. Renfro is an engineer in the Department of Lighting of the City of Seattle, Wash., and Arthur Perry Peterson is president of the Control Corporation, Minneapolis, Minn.

to the planes of the conductors. In a rotary variable air capacitor having two identical semicircular parallel fixed plates with a single semicircular rotor midway between them, a difference of potential causes several forces which are listed below. Figure 5 illustrates these forces and also shows the manner in which the two capacitors are formed by the stationary plates and damping disk of the primary instrument.

1. Forces between the rotor and upper stator which are balanced by forces between the rotor and lower stator. These forces, which are not shown on Figure 5, are parallel to the shaft and do not tend to rotate it.

2. Forces between the stator plates and the extended parts of the rotor, shaft, and so forth, which are symmetrical about the axis. These forces, shown as A_1, A_2, A_3, and A_4, are radial and do not tend to produce rotation.

3. Forces between the diametrical edge of the rotor and the stators when the rotor is not fully meshed. These forces, shown as B_1, B_2, B_3, and B_4, are tangential and tend to turn the rotor in a direction that will mesh it deeper between the plates of the stator.

Thus, the only rotary electrostatic force is due to edge effect so that, with plates so shaped that the edge exposure is constant with any angle of rotation, the torque produced is dependent only on difference of potential and is entirely independent of angular position except near zero mesh and full mesh. Throughout practically the whole angle of rotation, the torque may be kept constant with constant applied potential. Currents flow radially and so do not produce any torque.

Two variable capacitors having a common rotor are incorporated in the transmitting instrument in such a manner that increasing the mesh of one capacitor decreases the mesh of the other. At the time that one capacitor is at maximum mesh the other is at minimum mesh so that the two oscillator frequencies approach or recede from each other with rotation of the common rotor. The two capacitors have a common rotor which is formed by the damping disk of the wattmeter. Each of the two stators consists of two parallel aluminum plates spaced 0.083 inch apart and mounted so the damping disk passes between them. The four plates are identical and have the same voltage applied between each plate and the rotor, thus neutralizing any torque which is produced.

Figure 3. Indicating instruments at the receiving end of six telemetering systems

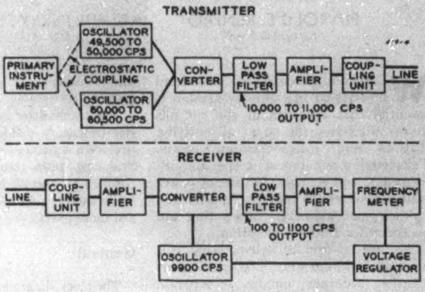

Figure 4. Block diagram of the modulated-frequency system of telemetering

Since the two capacitors formed by the plates and damping disk are of small capacitance, the oscillator frequencies must be high in order to obtain the desired frequency change with a given angle of rotation of the instrument shaft. A fast response to changes in measured values is obtained since no mechanical connection is made to the shaft and all torques due to electrostatic forces are eliminated through cancellation.

Various oscillator frequencies can be used and, in the case of several metering sets operating over a common line, the frequencies must be separated sufficiently in order to provide the required number of channels. A remote-metering arrangement using typical oscillator frequencies will be described.

One of the variable capacitors described herein is in an oscillator circuit arranged to generate 50,000 cycles per second at minimum mesh of the capacitor plates and 49,500 cycles per second at maximum mesh. The other variable capacitor is in an oscillator circuit which generates 60,000 cycles per second at maximum mesh and 60,500 cycles per second at minimum mesh. At the time one capacitor is at maximum mesh the other is at minimum mesh so that the two oscillator frequencies approach or recede from each other with rotation of the transmitting instrument shaft. The oscillator tubes are *A* and *B* in Figure 6.

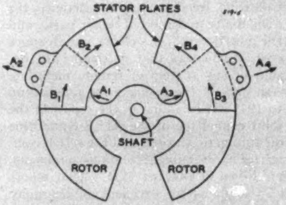

Figure 5. Electrostatic forces in two rotary variable air capacitors, each having two identical semicircular parallel fixed plates

A single semicircular rotor midway between the fixed plates is common to both capacitors

In order to insure an accuracy of two per cent, the maximum frequency variation of each of the three oscillators used in the system cannot vary more than two thirds of one per cent, assuming zero error in other components. Investigation showed that electron-coupled oscillators, tuned by a combination of positive- and negative-temperature-coefficient ceramic fixed capacitors plus a very small variable capacitor, have excellent stability over long periods of time. All oscillator circuits used in this system of telemetering are stabilized in this manner. The amount of negative-temperature-coefficient capacitor capacitance necessary to compensate for the coil and positive-temperature-coefficient capacitors in the set as described here was 10.71 per cent of the total capacity. Coils and mountings were developed that repeated their temperature-frequency characteristics faithfully.

The two voltages which are generated by the oscillators are fed into a converter tube (tube *C* in Figure 6) where the difference or beat frequency, which varies between 10,000 and 11,000 cycles per second, is produced.

The output of the converter is fed into a low-pass filter which attenuates the high frequencies and all harmonics and

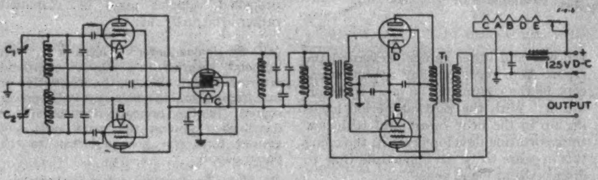

Figure 6. Schematic diagram of the telemeter transmitter

passes only the beat frequency to an amplifier which is arranged in push-pull. In Figure 6 the amplifier tubes are *D* and *E*.

The amplifier feeds the line through an inductive coupling unit (T_1) which has laminated phenolic-sheet insulation between the primary and secondary windings and is capable of withstanding the highest voltage exposure of the line. A single-stage low-pass filter with a cutoff frequency of 4,500 cycles per second prevents the carrier power from entering the telephone instrument circuit where it would be wasted. This filter is not shown in Figure 6.

Receiver

The schematic diagram of the telemeter receiver is shown in Figure 7. At the receiving point the telephone line connects to a coupling unit similar to that at the transmitter. Voice frequencies are passed on to the telephone unit and the carrier frequency goes to the metering receiver.

The receiver consists of one 10,000 to 11,000-cycle amplifier stage, local oscillator, detector, low-pass filter, audio amplifier, frequency meter with indicating instrument, and a voltage regulator. The high-frequency amplifier stage (tube *A* and associated circuits) is fixed in frequency and is adjusted to 10,490 cycles per second. This frequency is approximately the geometric mean between 10,000 and 11,000 cycles per second. The local oscillator (tube *F*) has a constant output frequency of 9,900 cycles per second. The oscillator output and the high-frequency output are fed into the converter stage (tube *B*) where a beat frequency is produced. This beat frequency varies between 100 and 1,100 cycles per second. The high frequencies and all harmonics are eliminated by the low-pass filter which follows the converter stage. The output of the low-pass filter (100 to 1,100 cycles per second) is then amplified by the audio amplifier (tube *C*) which feeds the frequency meter. Incorporated as a part of the frequency meter is the final indicating instrument. Its pointer is at the left end of the scale with 100-cycle input and at the right end of the scale with 1,100-cycle input.

The frequency meter consists of two triode tubes, *D* and *E*, connected in series; that is, the plate of *E* is connected to the positive line, its cathode is connected to the plate of the other triode, *D*, and the other cathode is connected to the negative line. A fixed capacitor is shunted across the plate and cathode of each tube. These capacitors are shown as C_3 and C_4. The grids in normal operation are biased beyond cutoff so that no plate current flows except that due to a-c grid excitation. At the time one grid is made more positive, the other is made more negative so that both tubes cannot conduct at the same time. Both tubes may be nonconducting at once but conduction is alternate. When either tube becomes conducting, it discharges the capacitor across its plate-cathode circuit and charges the capacitor which is connected across the nonconducting tube. When the grid polarities change, the opposite capacitors charge and discharge. A d-c milliammeter in series with the d-c supply shows the average current used to charge the capacitors. With a constant direct voltage each charge requires a definite current for a definite time. The time of discharge and charge is shorter than the period of one input alternation at the highest frequency used and therefore the d-c milliammeter reading is a definite indication of the number of charges per second. The number of charges is controlled by the input frequency and is independent of the input voltage and wave form within wide limits.

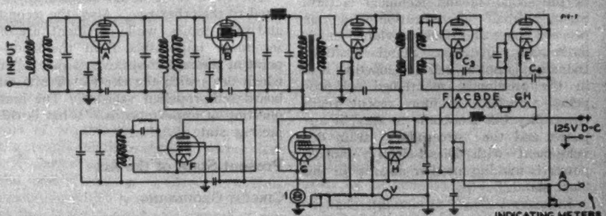

Figure 7. Schematic diagram of the telemeter receiver

The frequency meter and oscillator in the receiver are supplied from an electronic voltage regulator which is of a type frequently used and will not be described here. The neon-glow tube, *I*, and vacuum tubes *G* and *H* with their associated circuits comprise the voltage regulator. The actual output potential remains constant at 80 volts with the line voltage between 100 and 130.

Zero current in the indicating instrument puts the pointer off scale to the left. Such a condition indicates that the d-c power supply is off at the receiver or that the frequency-meter tubes have failed. If the transmitter power is off, or if the line is in trouble so that no carrier current is received, the bias is removed from the frequency-meter tubes and the indicating instrument goes off scale on the upper end. In this case the current is limited by degenerative resistors in the cathodes of the frequency-meter tubes. If the indicating instrument pointer is on its scale, the observer knows that none of the troubles just mentioned are being experienced.

Totalizing at the transmitter may be accomplished by a multiple-wound current transformer in the a-c circuits to the wattmeter. Totalizing at the receivers may be done in the frequency-meter output circuits by adding the direct current in a lead common to several instruments. Strip chart recording d-c milliammeters are available for continuous records at the receiving point.

Six complete sets of this system of telemetering are now in continuous service and have been for the past few years. The experience thus gained definitely indicates that the equipment has met the requirements expected of it. It provides almost instantaneous indications with standard accuracy. It permits a large number of readings to be transmitted over a single circuit and it is a simple matter to totalize readings from several transmitters. It is dependable and free from interference. It has proved easy to maintain at a minimum of expense.

Grounding of Circuits on Self-Propelled Vehicles

D. D. EWING
FELLOW AIEE

SOME years ago a prominent member of a group of engineers, who at that time called themselves "efficiency" engineers, had for a pet slogan the expression "whatever is, is wrong." For the present purpose any objections to this saying from the standpoint of syntax will be passed by but it has been observed that methods and procedures that for years have been refined in the crucible of practice usually have survived because they do have merit. Nevertheless the field of technology is anything but a quiescent one and it is desirable, therefore, that long existing methods, procedures, and standards be subject to constant scrutiny in the light of new developments.

For over 50 years the electric circuits and equipment on board electric railway cars have been in process of development and many of the electrical features of design and construction have long been pretty well standardized. For a similar period of time the electric circuits on automobiles have been undergoing a similar procedure and with a similar end result. At the turn of the century many enthusiastic electrical engineers believed that "the last stand" of the steam engine, namely, the steam locomotive, was about to be wiped out. Apparently these enthusiasts did not take into account all of the economic and technical factors. Steam-railroad electrification did not proceed apace and there developed much individuality in design. Standardization, therefore, is not as well developed as it is in the previously mentioned self-propelled vehicles. In more recent years the trolley bus has come to stay, it appears, and the "streamliner" train development with Diesel-electric motive power is making another assault on the "last stand."

In heavy railroad service interchangeability of equipment comes high in the list of the "must" requirements. A number of engineers have, for some years, been feeling that there should be a new scrutiny of existing electric-circuit and equipment standards and practices with the objective of setting up standards and recommended practices which, at least in the heavy transportation field, will further equipment interchangeability and promote efficient maintenance and repair methods and practices.

A few years ago a subcommittee of the committee on land transportation of the Institute was appointed to study this problem. A report was formulated but the war and other causes prevented the report from receiving any attention except in the committee on land transportation. With the postwar period looming up in the near future and with new transportation developments in the offing this appears to be an opportune time to discuss the problem again.

This paper is largely abstracted from the report of the subcommittee and the writer is indebted to the members of the subcommittee and the general committee for many of the ideas here presented. It is not expected that all engineers interested in the subject will agree with everything stated here. Frankly, it is hoped that they will not and that this paper will serve as a target to bring out constructive criticism and also new viewpoints so that in the end there may be some clarification and also some crystallization of the ideas now extant on the subject.

An analysis of the problems originally assigned to the subcommittee indicated that three topics were involved:

1. Grounding of circuits on vehicles.
2. Current leakage in self-propelled rubber-tired vehicles.
3. Static charges on vehicles.

The third topic is not necessarily related to the other two. Also, the second and third topics, while pertinent, are of secondary importance from the standpoint of the main objective of this paper which deals with the electric circuits on board self-propelled vehicles. The first question of importance is, "What is the present state of the art?"

Present State of the Art

CIRCUIT GROUNDING

A study of the National Electrical Code and other safety regulations with reference to circuit grounding indicates that inside circuits are grounded to limit the voltage which may be impressed on a circuit by exposure to lightning; or by exposure to, or conflict with, higher voltage lines; or to limit the maximum potential to ground which may result from the normal operating voltage.

These limitations, which grounding is supposed to impose, are sought primarily in an endeavor to reduce the hazards from fire and electric shock or burn. A secondary objective is to minimize the hazards to service; for example, service interruptions Also, circuits may be grounded to facilitate trouble indication and location, to provide for more accurate and reliable circuit protection, and, in some cases, to simplify the circuit layout and to allow a more economical construction.

The circuits which are used in self-propelled vehicles may be classified rather arbitrarily. as:

(*a*). Single-conductor circuits with "ground" returns. In a vehicle the ground return is a path through the locomotive or bus frame from the motors to the power source. In the ordinary electric-railway distribution system the track rails and ground form the ground return to the power supply.

(*b*). Two-conductor circuits with both conductors insulated.

(*c*). Two-conductor circuits with one conductor grounded. The "ground" may be at one point or at several points. It may be a "dead" or solid ground, a ground through a resistance, a fuse or a protective relay of some sort, or through a combination of these components.

As used here the term "vehicles" includes electric locomotives, steam-electric locomotives, Diesel-electric locomotives, storage-battery locomotives, streetcars, electric motorcars, trolley busses, gas-electric busses, Diesel-electric busses and gas busses, and automobiles used in public transportation service. Also, the foregoing classification covers only d-c and single-phase a-c circuits.

In the selection of the proper circuit for a given service the engineer does not always have a free choice. For example, the power circuits of electric motorcars and locomotives which operate on rails and receive their power from an outside source ordinarily must use the class (*a*) circuit. Similarly, for practical reasons, the main circuits in a trolley bus must belong to class (*b*).

The choice is not so restricted, however, for the following circuits:

1. Traction motor circuits on steam-electric, Diesel-electric, and conversion-type electric locomotives.
2. Main power circuits on gas-electric and Diesel-electric busses and trucks.
3. Starting, lighting, and other auxiliary services on busses, trucks, and automobiles.
4. Auxiliary circuits on electric motorcars, locomotives, and trolley busses.
5. Electric circuits on railroad passenger cars.

This lack of restriction has resulted in a considerable diversity of opinion among

---

Paper 45-11, recommended by the AIEE committee on land transportation for presentation at the AIEE winter technical meeting, New York, N. Y., January 22-26, 1945. Manuscript submitted October 14, 1944; made available for printing November 22, 1944.

D. D. EWING is professor of electrical engineering, Purdue University, Lafayette, Ind.

engineers with a corresponding diversity of practice among equipment users. One user insists that all low-voltage circuits on self-propelled vehicles shall be ungrounded and another desires that his auxiliary equipment use the "ground-return" type of circuit. Many railroad passenger cars are lighted with a d-c axle-type generator and storage-battery system, other cars use three-phase 220-volt power service to operate their air conditioning apparatus. There is a discernible trend toward the use of even higher-voltage three-phase systems.

Common questions which arise are: Should the main power circuit on a Diesel-electric or gas-electric bus or locomotive be grounded or kept well insulated? If grounded, should the ground be a solid ground or a resistance ground? Should the circuit be grounded through a fuse or a relay? Should control, lighting, and other auxiliary services use grounded or ungrounded circuits?

These questions cannot be answered haphazardly. Often there is more than one good answer to a question. At any rate, the evidence available indicates that circuit design for self-propelled vehicles at present is not a universally standardized procedure.

In the selection of the proper circuit, the engineer should be guided by such considerations as safety, technical requirements, economy in first cost, and continuity of operation. Mostly the choice is, perforce, a compromise.

The outstanding advantages of the single-conductor ground-return system are simplicity of circuit layout, low first cost, and the quick detection and ease of location of faults. Its disadvantages are the lack of constancy in circuit resistance and the fact that a fault on the single conductor may render the circuit inoperative at some time when operation of some sort is absolutely necessary. Circuit-resistance variations are caused by loose rivets, bolts, joints, and so forth, in the mechanical parts. These poor contacts may result in burning and corrosion of the metal frames and leakage through bearings may cause serious bearing trouble.

In automotive equipment this circuit is used almost universally and the apparatus and accessories necessary in its application are highly developed and very economical in cost.

The system of employing two insulated conductors has the advantage of making possible a high degree of circuit insulation and isolation. It is practically the only choice for all circuits fed by trolley voltage in the trolley bus. Circuit resistance is easy to maintain at a constant level and the likelihood of failure is less since there must be a fault on each line before complete circuit failure can occur. This advantage becomes a real disadvantage, however, when the matters of fault indication and location are considered. This circuit costs more and there seems to be a trend toward its increased use in the better class of vehicles. In some services, where a common return wire is used, the insulated circuit is at a disadvantage as compared with the ground-return circuit. This is notably true in the case of certain control and signal circuits where an opening in the common return wire might cause false indications or false operation.

Circuits of the third class (those with two conductors, one of which is grounded) have a wide field of application, potentially at least. They are high in first cost and maintenance but provide current paths of constant resistance and a ready means of fault indication and location. Such circuits appear to be particularly applicable to the traction motor circuits on a-c and Diesel-electric locomotives and, in general, wherever a circuit path of high integrity is required.

The preceding discussion applies only to d-c and single-phase services.

The heavy power demands on modern railway trains have resulted in the installation of three-phase generating units on some trains. Voltages up to 220 volts are in use and higher voltages have been given some consideration. The circuits used require a minimum of three conductors. As the 220-volt three-phase circuits used for supplying the air conditioning apparatus on some railway passenger cars must be operated from the standby power services in the yards, grounding of the circuits on the cars is not feasible because of the possibility of neutral or other grounds on standby services. Where the 220 volts is transformed within the car to some lower voltage for lighting or other low-voltage service it seems to be customary to ground one side of the low-voltage service.

CURRENT LEAKAGE IN SELF-PROPELLED RUBBER-TIRED VEHICLES

A number of years ago, when someone took some streetcars off the tracks and mounted them on wheels suitable for operation over street pavements, a new sort of trouble developed. People on the street sometimes received severe electric shocks when they stepped aboard the new "trackless trolleys." Circuit insulation which never gave any trouble in the old single-conductor ground-return streetcar circuits developed electrical leaks. The early equipment was adapted streetcar equipment and was not suitable for use on a vehicle where the body could not be solidly grounded. Considerable investigation was done on this problem by equipment users and manufacturers as well as by the American Transit Engineering Association and its predecessor organization. It was found that if all circuits, power and auxiliary, were very carefully insulated from the bus body, "hot" body trouble was no longer a major worry. Busses gave little or no trouble from current leakage when insulated to meet specifications[3] calling for the following minimum insulation resistances:

1. Power circuits (without motors) in parallel with other circuits	8 megohms
2. Individual motors	10 megohms
3. Assembled control apparatus	5 megohms

One operator tries to maintain at all times the bus-body-to-trolley resistance greater than three megohms.

Procedures for the mitigation of current leakage troubles have also included, in some cases, the use of insulated steps, door handles, stanchions, and grab handles.

All in all, the problems that arise from current leakage are so well in hand that the subject would not have been discussed here were it not for the fact that current leakage is often blamed for shocks that have a very different cause; namely, static charges.

STATIC CHARGES

In modern busses and automobiles static charges have been the source of no little trouble under certain atmospheric conditions. Present-day upholstery materials and modes in wearing apparel have combined to accentuate the difficulty.

The electron theory has afforded the physicists an easy explanation of the accumulation of static charges. These charges are often spoken of as frictional electricity although friction itself seems to have little to do with the matter. When two dissimilar materials such as wool and rubber or silk and glass are pressed tightly together or are rubbed together some of the electrons stray from one material to the other. For example, electrons will stray from the wool to the rubber leaving the wool positively charged and the rubber with a negative charge. When silk and glass come in contact some electrons leave the glass and go to the silk so that the glass becomes positively charged and the silk negative. Charges so produced are common causes of trouble in printing presses, grain elevators, textile elevators, textile mills, moving belts, gasoline filling stations, and so forth.

As far as vehicles are concerned, two types of trouble are encountered. These may be arbitrarily designated as "inside" and "outside" troubles.

The modern seat cushion with a mohair or woolen-cloth cover and a rubber-cushion filling becomes really quite an ideal electrostatic generator when someone with rubber-soled shoes sits on the cushion. The passenger's body rapidly acquires a positive charge by conduction from the seat cushion if the air is dry enough to prevent leakage of the charge. When the passenger touches the signal button to indicate his stopping place, he receives a shock which he is quite likely to attribute to the signal circuit. The shock is identical to the one the passenger would receive in his own home if, after walking over a woolen carpet or waxed floor, he should happen to touch a metal object. Other causes of "inside" shock are scuffing of feet on rubber floor mattings and sliding on rubber-fabric seat coverings. These shocks are not in themselves dangerous but they may cause passengers to injure themselves in some other way. There seems to be no easy way of mitigating this trouble. Proper combinations in upholstery and the covering of all metal objects easily accessible to passengers afford some relief. Fortunately, meteorological conditions are only occasionally favorable to the production of static charges.

"Outside" shocks are those received by persons standing on the pavement and touching the vehicle body. The bus body is insulated from the earth by rubber tires and in some cases by the paving, as, for instance, dry concrete or asphalt. A charge may accumulate on the vehicle body by the body moving through the air or as a result of the wheels running over dry pavement. As the bus body is a rather large capacitor, a charge of considerable magnitude may be collected. When a person who is standing on the ground touches the car body there is a discharge which may produce quite a shock. These charges are never bothersome except in dry, frosty weather or at times when both air and pavement are very dry. Busses running on gravel roads have very little trouble with them. They are worst on asphalt-covered streets and with new or cleanly washed tires. Dirty tires help conduct the accumulated charges to earth. This process can be furthered by painting the inner sides of the tires with some form of conducting paint. Recent improvements in the way of "conducting" tires undoubtedly will be available after the war. Keeping the wheels perfectly aligned so as to avoid the slippage of rubber over asphalt is helpful. Some companies use drag chains or some similar devices during periods when static is troublesome. Some simple means of discharging the static charges as fast as they are developed is needed. Possibly the development of new surfacing materials will be hastened by the war effort. In any event the problem is a complex one and needs much further study.

Conclusions

Giving due consideration to matters of economy, circuit requirements from a power standpoint, and to the reasons underlying circuit grounding, the following conclusions may be drawn:

1. All circuits on trolley busses which operate at trolley potential must be of the two-conductor type with all wires and apparatus well insulated from the bus body and other parts accessible to passengers or street traffic.

2. All low-voltage circuits on small busses and automobiles used in passenger service may be of the one-insulated-conductor ground-return type.

3. All circuits carrying small currents at low voltages (6 to 32 volts) which are thoroughly isolated from possible exposure to, or conflict with, higher voltages and which are accessible in any way to passengers or street traffic may be of the one-insulated-conductor ground-return type.

4. Ground-return circuits should not be used on trucks or other vehicles carrying gasoline, oil, or other highly inflammable or explosive materials.

5. All so-called "ground-return" circuits, where there is possibility of a loose mechanical joint in part of the return circuit, should have the return of bare copper conductors electrically connected to the mechanical parts at a number of points.

6. All internal circuits carrying heavy currents at both low and high voltages (starter-motor circuits on automobiles and small busses excepted) may be of the two-insulated-conductor type with one conductor grounded. The two conductors here serve as a guarantee of circuit integrity and the ground connection is of assistance in fault indication and location, keeps static charges drained off, and otherwise assists in protecting apparatus and service. This classification is not intended to include circuits which are fed from an external source such as a trolley wire or third rail.

7. All circuits on rail vehicles connected to external sources of power such as trolley wires and third rails are necessarily of the one-conductor-with-ground-return type or of the two-conductor-with-one-conductor-grounded type.

8. Control and signal circuits using a common return wire may have this common return grounded on car or truck frames at a number of points whenever other circuit conditions are such as to permit grounding. The grounding of the common return will tend to reduce false indications or operations in case of return-wire breakage.

9. Three-phase 220-volt circuits used on railroad cars to supply air-conditioning equipment should not be grounded. However, the structural parts of the cars should be solidly grounded.

10. All a-c and d-c circuits on railroad cars with voltage ratings of 64 to 120 volts should be of the insulated-conductor type. If an a-c circuit is fed through a transformer from a higher-voltage circuit then the lower-voltage circuit should have one conductor grounded. Also, if such a circuit is exposed to static from belts or moving air streams, one side of the circuit should be grounded.

It does not seem feasible to make a complete classification of all the circuits used in vehicular service and categorically state that such and such circuits should always be grounded and certain others should not be. The safety, economic, and technical factors are somewhat different in the different transportation fields, and these factors should be given some weight in the consideration of any recommendations relative to standardization.

Recommendation

Standards in some of the operating fields have been set up by the American Association of Railroads, in others by the Society of Automotive Engineers, and in still others by the American Transit Association. In those fields where these several associations have what for convenience may be called primary jurisdiction, the standardization problems have on the whole been cared for promptly and effectively. Under present conditions there is a considerable amount of overlapping. For example, the power equipment on a Diesel-electric locomotive from one viewpoint may be considered as just overgrown Diesel-electric bus equipment. The question arises as to who shall set up the needed equipment standards in such a case? Shall they be set up by manufacturer's associations, by professional engineering groups, or associations of operating companies? The question is a difficult one. Obviously some things belong in one place and some in another. In this case it is possible that better end results will be produced if the work is done by joint committees working under the sponsorship of a professional engineering group. It would seem to be a proper recommendation, therefore, that the Institute act as sponsor in this instance and set up the necessary mechanism for working out the desired standards and recommended practices.

References

1. The Application of Electricity for the Auxiliaries of Railroad Trains, J. E. Gardner. AIEE Transactions, volume 60, 1941, January section, pages 34–6.

2. National Electrical Code.

3. Acceptance Tests for Insulation Resistance of Trolley Busses. Manual Section *E*132–36. American Transit Engineering Association.

4. Eliminating Current Leakage on Electric Coaches, W. S. Rainville, Jr. *Traction Shop and Roadway*, February 1932, page 31, and *AREA* for February 1932, page 860.

5. Economic Factors in Design of Modern Trolley Busses, Charles Guernsey. *Traction Shop and Roadway*, August 1931, page 234.

6. Single-Motor Trolley Coaches, R. H. Sjoberg. *Mass Transportation*, August 1937, page 239.

7. Finding Current Leakage, R. S. Beers. *Transit Journal*, June 1940, page 202.

8. Static Shock to Bus Passengers, *AREA* September 1928, page 560.

9. Static Electricity, *Transit Journal*, March 1940, page 101.

10. Static Electricity in Automobiles, *Chevrolet Service News*, volume 14, July 1940.

11. Static Electricity on Rubber-Tired Vehicles, Robin Beach. Electrical Engineering, volume 60, May 1941, pages 202–08.

12. Detecting the Saboteur "Static Electricity" in Gasoline Fires, Robin Beach. Electrical Engineering, volume 61, October 1942, pages 501–08.

Determination of Transient Shaft Torques in Turbine Generators by Means of the Electrical–Mechanical Analogy

G. D. McCANN
MEMBER AIEE

C. E. WARREN
ASSOCIATE AIEE

H. E. CRINER
NONMEMBER AIEE

Synopsis: A brief description is given of the mechanical-transients analyzer and its application to the determination of the shaft torques in turbine generators during transient disturbances, such as electric short circuits and synchronizing out of phase. This device employs the principle of the electrical–mechanical analogy with analogous electric circuits to represent a given mechanical system and special electric circuits for producing the desired transient excitation functions. With the analyzer a detailed study has been made of the shaft torques that can occur in turbogenerators with mechanical systems having both one and two modes of vibration. The relative severity of various types of faults has been determined together with the effect of external system or fault resistance and generator loading. Short circuits produce rotor air-gap torques containing damped unidirectional, fundamental electrical frequency, and second-harmonic frequency components. In the practical range of machine design, the fundamental-frequency component has the dominant effect on the resulting transient shaft torques for the more severe types of disturbances. The types of short circuits studied include three-phase, line-to-line, single-line-to-ground, and double-line-to-ground faults from no load and full load and with varying amounts of external resistance. It was found that for short circuits at no load with no external resistance a line-to-line fault results in the most severe shaft torques. For faults with low external resistance (of the order of one per cent per phase), a double-line-to-ground fault produces the highest shaft torques which for mechanical systems of low natural frequency may exceed the torques produced by a line-to-line fault with zero resistance. However, for values of external resistance as high as the machine subtransient reactance, the shaft torques are lower than with zero resistance. The most severe fault torques are produced by line-to-line short circuits from full load with no external impedance. Synchronization at angles greater than 30 degrees can produce transient shaft torques which in some cases are more severe than those resulting from short circuits.

THE determination of transient shaft torques in turbogenerators during short circuit or synchronization out of phase is representative of a large group of problems encountered in the design of mechanical or electromechanical apparatus. Stated in general terms, the problem is to determine the transient response of a physical system to a suddenly applied excitation. In a large majority of the cases which arise, the motion of the system can be specified, with sufficient accuracy, by a set of linear constant-coefficient differential equations. The solution of these equations, by classical or operational methods, is well known and does not present any difficulties of a theoretical nature. However, if the system being studied contains two or more degrees of freedom and the suddenly applied excitation is at all complicated, the work involved in the numerical solution of the equations of motion soon becomes prohibitive. Under these conditions it becomes highly desirable to seek other means of solution. Several methods are available. These include mechanical calculators, such as the differential analyzer, measurements on full-scale models, or some equivalent dynamic system. This may be a simplified equivalent mechanical system or its analogous electric circuits.

Table I. Electrical–Mechanical Analogy Used With Mechanical-Transients Analyzer for the Study of Turbine-Generator Shaft-Torque Problems

Inertia–Inductance Torque–Voltage Analogy

Inertia (I)	**Inductance (L)**
Torque = inertia × angular acceleration	**Voltage** $= L\frac{di}{dt}$
$T = I\frac{d\omega}{dt}$	
Spring constant (K)	**Capacitance (C)**
$T = K \times$ **angular displacement**	$V = \frac{q}{C} = \frac{1}{C}\int i\,dt$
$T = K\theta = K\int\omega\,dt$	
Velocity damping (G) $T = G\omega$	**Resistance (R)** $V = Ri$

The method of the electrical–mechanical analogy is particularly well suited for solving problems of this nature. The analogy between electric and mechanical systems has been well known for many years[1] and is based on the identity in the form of the differential equations representing the two systems. The particular analogy used in this paper is given in Table I. This is classified as the inertia–inductance torque–voltage analogy. This is not the only one possible. For example, the dual of the afore-mentioned circuit may be used in which inertia and capacitance are analogous quantities, and torque may be analogous to current. The inertia–inductance analogy and its dual represent the two possible analogies between the physical constants of the electric and mechanical systems for each of which there is an infinite number of possible analogies between the electrical and mechanical variables. For example, in the inertia–inductance analogy torque may be analogous to voltage, rate of change of voltage, and so forth; while in the inertia–capacitance analogy torque may be analogous to current, rate of change of current, and so forth. The significance of these analogies is discussed in greater detail in reference 2.

It is evident from the foregoing discussion that the complex cumbersome mechanical system may be replaced by its analogous electric circuit consisting of simple inductors, capacitors, and resistors. The required excitation is applied to the analogous electric system by means of special electric circuits, and the transient response is measured directly as voltages and currents. This method has the advantages of simplicity, low cost, and flexibility. A new device, the mechanical-transients analyzer, has been developed[3] for solving a wide range of transient vibration problems by this means.

Nature of the Transient Short-Circuit Torque Problem

When a generator is suddenly short-circuited or synchronized out of phase, a transient torque consisting of unidirectional and alternating components suddenly is impressed on the generator rotor. Each component of this torque decays exponentially to a value determined by the steady-state terminal conditions of the machine. In the case of a salient-pole generator, there is an infinite series of alternating components at harmonic electrical frequencies; whereas, for the turbogenerator, the only alternating torques of appreciable magnitude are those at fundamental and second-harmonic electrical frequencies. Equations for the calculation of these torques for a turbogenerator under various terminal conditions are given in a companion paper.[3] A simplified form of the rotor air-gap torque for turbogenerators is illustrated by the following equation:

$$T_r = A\epsilon^{-at} + B\epsilon^{-bt}\sin\omega t - C\epsilon^{-ct}\sin 2\omega t \qquad (1)$$

A typical turbogenerator on which these electrical torques are impressed is shown by the tandem unit at the top of

---

Paper 45-15, recommended by the AIEE committee on electrical machinery for presentation at the AIEE winter technical meeting, New York, N. Y., January 22–26, 1945. Manuscript submitted November 8, 1944; made available for printing November 25, 1944.

G. D. McCANN, C. E. WARREN, and H. E. CRINER all are with Westinghouse Electric and Manufacturing Company, East Pittsburgh, Pa.; Doctor McCann is transmission engineer, central-station engineering department, and Mr. Warren is in the industry engineering department.

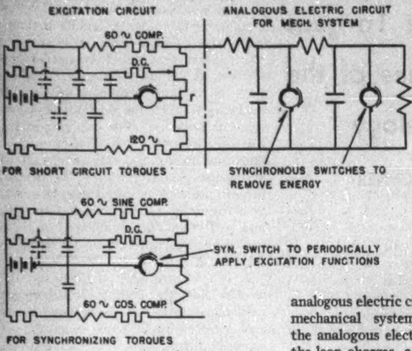
EXCITATION CIRCUIT
60 ∿ COMP.
D.C.
r
120 ∿
FOR SHORT CIRCUIT TORQUES
ANALOGOUS ELECTRIC CIRCUIT FOR MECH. SYSTEM
SYNCHRONOUS SWITCHES TO REMOVE ENERGY
60 ∿ SINE COMP.
D.C.
SYN. SWITCH TO PERIODICALLY APPLY EXCITATION FUNCTIONS
60 ∿ COS. COMP.
FOR SYNCHRONIZING TORQUES

Figure 1. Simplified circuit diagrams of the mechanical-transients analyzer as used for determining turbine-generator shaft torques

Figure 3A. The mechanical constants of this system are the inertias of the generator and turbine rotors (I_1, I_2, I_3), the spring constants of the generator and turbine shafts (k_1, k_2) and equivalent velocity-damping factors, resulting largely from hysteresis loss in the shaft materials and energy absorption in couplings, bearings, and fits. As a result of the suddenly impressed rotor air-gap torque (T_r) the mechanical system will oscillate at forced and natural frequencies producing abnormal torques in the generator and turbine shafts. A knowledge of the peak shaft torques resulting from these oscillations is desirable in the design of the shafts and their associated couplings and keyways. The equations of motion for the mechanical system, for the generator load torque T_L with no mechanical damping assumed, are the following:

$$\left.\begin{aligned} T_r-\Delta T_L&=I_1\ddot{\theta}_1+k_1(\theta_1-\theta_2)\\ 0&=k_1(\theta_2-\theta_1)+I_2\ddot{\theta}_2+k_2(\theta_2-\theta_3)\\ 0&=k_2(\theta_3-\theta_2)+I_3\ddot{\theta}_3\end{aligned}\right\} \quad (2)$$

The angular displacements (θ) of the respective rotors are measured from the average position of the rotors at $t=0$; that is, the constant velocity of rotation does not appear in the equations. The quantity ΔT_L is the change in load due to the terminal fault on the machine. The change in load depends on the type of fault and other system conditions. It is usually assumed that this change in load takes place instantly on occurrence of the fault. The actual torque on each shaft is then the torque as determined from the preceding equations plus the initial torque on the shaft at $t=0$.

Analogous Electric System

A simplified circuit diagram of the mechanical-transients analyzer as used for the solution of the foregoing problem is shown in Figure 1. The two principal parts of the analyzer are the excitation circuits, which produce the voltages proportional to the components of T_r, and the analogous electric circuits representing the mechanical system. The equations of the analogous electric circuit in terms of the loop charges, q_1, q_2, and q_3, are as follows:

$$\left.\begin{aligned} E_r-\Delta E_L&=L_1\ddot{q}_1+\frac{1}{C_1}(q_1-q_2)\\ 0&=\frac{1}{C_1}(q_2-q_1)+L_2\ddot{q}_2+\\ &\qquad\frac{1}{C_2}(q_2-q_3)\\ 0&=\frac{1}{C_2}(q_3-q_2)+L_3\ddot{q}_3\end{aligned}\right\} \quad (3)$$

where E_r is a voltage whose components are analogous to the components of T_r and ΔE_L is analogous to the change in load ΔT_L. A comparison of equations 2 and 3 shows immediately the similarity of the equations of motion of the two systems, which is the basis of the analogy.

The voltage E_r is generated in the resistor r connected across the terminals of the analogous circuit. The various components of E_r are produced as follows. The unidirectional or d-c component results from the discharge of a capacitor through a resistor. The capacitor shown in the d-c circuit is charged by a constant-voltage source and is then discharged through a portion of r when the rotating switch closes. The capacitor recharges during the time the switch is open and the cycle is repeated when the switch again closes. By driving the switches at synchronous speed, the voltages may be viewed as a standing image on the screen of a cathode-ray oscillograph. This is a method that was developed for studying transients in electric power systems.[4] The alternating components of torque are generated in a similar manner, except that the capacitors are discharged through an inductor and resistor in series. The resulting oscillatory current will be a damped sinusoidal wave, and the voltage drop across r will be analogous to the damped sinusoidal components in T_r. By adjusting the capacitance, inductance, and resistance in this circuit, any desired frequency and damping may be obtained. Components of opposite polarity are obtained by discharging through the lower section of r. When it is desired to obtain a damped cosine function of time, the resistor r is replaced by a small inductor (see lower half of Figure 1). The voltage across this inductor will be a cosine function provided its losses are low. However, it is always possible to balance out the inphase component of the inductor by an inphase component of opposite polarity.

It is necessary that the currents in the analogous circuit produce no appreciable voltage across the coupling resistor r or coupling inductor. The current in the excitation circuits must be very large compared to the current in the analogous circuit that flows through r. This condition will be satisfied provided the coupling impedance is at all times small compared to the impedance looking in at the terminals of the analogous circuit. Since the analogous circuit always contains a slight amount of resistance, which represents the damping of the mechanical system, it is possible to make r sufficiently small so that the foregoing conditions are satisfied, even though the analogous circuit may be resonant at the frequency of the excitation circuit. This has been proved experimentally by measuring the voltage drop across r as the analogous circuit was made to approach resonance.

As discussed in detail in reference 2, special inductors were developed for the analogous circuits of the mechanical-transients analyzer so that the circuits provide damping as low as that found in practical mechanical systems. These coils have a Q in excess of 100 in the range of 200 to

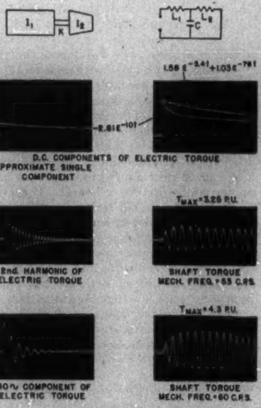

Figure 2. Mechanical-transients-analyzer oscillograms of rotor air-gap torques and resulting shaft torques on single-frequency turbo-generator unit for line-to-line short circuit from no load

$R_e=1$ per cent per phase
$I_1=1$; $I_2=0.16$; $K=1.54\times10^4$

1,000 cycles per second, which corresponds to an amplitude decay factor of less than three per cent per cycle. An illustration of the effect of Q on the crest per unit torque is illustrated by Figure 5. It should be noted that the peak torque is changed by only 8.5 per cent with a Q variation of 100 to 50 (respective decrements three and seven per cent) in the region of resonance and that the effect of the Q change is entirely negligible in the practical range of mechanical-system frequency.

The required relationships between the dynamic constants of the mechanical system and the electrical constants of the analogue are given in reference 2.

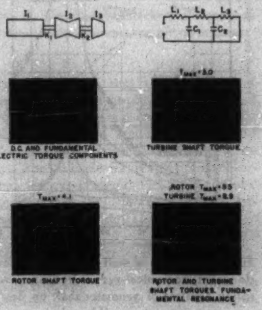

A. Three-phase short circuit from no load with no external resistance

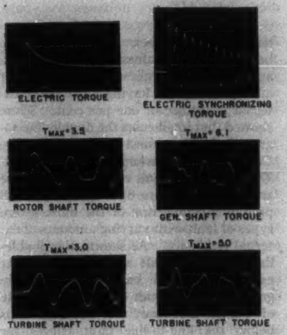

B. Three-phase short circuit from no load $R_e=X_d''$ per phase

C. Synchronizing 90 degrees out of phase System reactance $X_s=X_d''$

Figure 3. Mechanical-transients-analyzer oscillograms of rotor air-gap and shaft torques on double-frequency turbogenerator unit

$I_1=1$ $K_1=1.35\times10^4$
$I_2=0.821$ $K_2=1.09\times10^4$
$I_3=0.821$

Mechanical Systems and Types of Disturbances Studied

The wide variation of possible mechanical-system constants and types of short circuits and synchronizing torques makes it impractical to present a completely comprehensive analysis of this problem. However, general conclusions can be drawn with regard to certain factors, such as the relative severity of various types of faults and the effect of external impedance and generator load. With these as a basis the mechanical-transients analyzer provides a ready means of studying a given unit for the particular system condition under which it is to operate.

Two types of units were chosen for detailed study, a single-frequency unit consisting of a generator and one turbine element and a double-frequency unit with a generator and two turbine elements. The dynamic mechanical systems and their analogous electric circuits for the mechanical-transients analyzer are shown in Figures 2 and 3A. The same generator was assumed for both units. Its electrical constants are listed at the bottom of Table II, which also gives the equations for the types of short circuits and synchronizing torques studied. The derivation of these equations is presented in a companion paper.[3] The electrical constants of the assumed machine result in air-gap torques which are representative of the upper range of severity.

Typical Torque Oscillograms

In Figures 2 to 4 are shown typical oscillograms of the rotor air-gap torques and the resulting shaft torques obtained with the mechanical-transients analyzer. Figures 2 and 3 apply to the two units chosen for detailed study. Figure 4 illustrates the use of the analyzer for more complex problems. In this system two generators are driven by a geared turbine. The generator being short-circuited has salient poles, and the air-gap torque consists of a damped unidirectional component and a series of damped sinusoidal components of fundamental and harmonic electrical frequencies. However, the effects of all components above the fourth harmonic are negligible. The equation for the air-gap torque as used with the analyzer is given in the caption of Figure 4.

Torque-Frequency Curves

For the two units chosen for detailed study fixed relationships between the various inertia constants were assumed and the effect of varying the shaft spring constants determined. In this way curves were obtained of the maximum shaft torques resulting from each type of disturbance. Such curves provide a complete analysis of the dynamic mechanical system of a single-frequency unit, because for such a system the torques resulting from a given disturbance are a function only of the mechanical-system frequency and the ratio of the two inertia constants. The resulting crest torque for a given system frequency is directly proportional to the ratio $I_2/(I_1+I_2)$. Thus for a given electrical torque, the crest-torque curves for the single-frequency unit studied (Figures 5 and 7) therefore can be applied to any other single-frequency unit by proper adjustment of the torque magnitudes. However, for the double-frequency unit the larger number of system elements makes it impractical to present a general analysis of all possible systems. For this case it was found that the more important conclusions can be illustrated by a single set of curves of crest torque plotted as a function of the dominant one of the two system frequencies: that is, the frequency containing most of the mechanical energy. The curves for this unit were obtained by varying the spring constant of only one shaft (the generator-turbine shaft). For this condition the less important system frequency ranged between 12 and 22 cycles per second. Crest-torque curves as obtained in this manner are given in Figures 6 and 8. It should be realized that the magnitudes of the crest torques shown on these curves do not apply to all designs, since absolute magnitude is a function of the relation between the various inertia constants.

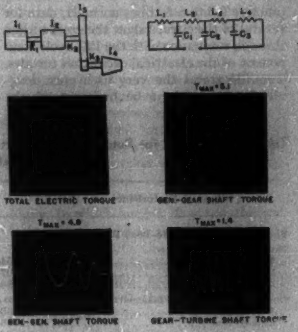

Figure 4. Typical gear-driven-generator problem

Three-phase short circuit on salient-pole generator from no load with no external resistance

$$T_r=\epsilon^{-4.8t}(6.2\sin\omega t+4.65\sin 3\omega t)-\epsilon^{-3t}(2.13\sin 2\omega t+1.95\sin 4\omega t)+1.2\epsilon^{-3t}$$

Fundamental frequency is 25 cycles per second

$I_2=1$ $K_1=1.065\times10^4$
$I_1=0.965$ $K_2=3.72\times10^4$
$I_3=1.45$ $K_3=18.22\times10^4$
$I_4=2.52$

Although as shown by the curves the practical design range should place the dominant natural frequency appreciably below 60-cycle resonance (usual design practice 2.5 to 6.5 times normal), data for several of the curves show the crest torque through resonance with the 120-cycle component of the electrical excitation torques. This illustrates the very high crest magnitudes that might be built up if the natural frequencies were allowed to approach resonance with the excitation frequencies.

Table II. Equations for Rotor Air-Gap Short Circuit and Synchronizing Torques as Used for Transient-Shaft-Torque Study

Type of Disturbance	Per Unit Rotor Air-Gap Torque
Short Circuits From No-Load Rated Voltage	
No external impedance:	
Three-phase	$1.54\epsilon^{-7.9t}+10.3\epsilon^{-10t}\sin\omega t$
Line-to-line	$2.07\epsilon^{-8.2t}+10.4\epsilon^{-6.9t}\sin\omega t-5.18\epsilon^{-6.7}\sin 2\omega t$
Line-to-ground	$1.88\epsilon^{-7.0t}+9.50\epsilon^{-9.3t}\sin\omega t-4.75\epsilon^{-6.3t}\sin 2\omega t$
One per cent per phase external resistance (R_e) — zero external reactance:	
Three-phase	$2.60\epsilon^{-15t}+10.3\epsilon^{-48t}\sin\omega t$
Line-to-line	$1.58\epsilon^{-5.4t}+1.03\epsilon^{-79t}+10.4\epsilon^{-46t}\sin\omega t-5.18\epsilon^{-6.7t}\sin 2\omega t$
or	$2.61\epsilon^{-10t}+10.4\epsilon^{-48t}\sin\omega t-5.18\epsilon^{-6.7t}\sin 2\omega t$
Line-to-ground	$2.55\epsilon^{-9.3t}+9.50\epsilon^{-63t}\sin\omega t-4.75\epsilon^{-6.3t}\sin 2\omega t$
Double-line-to-ground	$3.16\epsilon^{-15t}+10.4\epsilon^{-48t}\sin\omega t-1.39\epsilon^{-9.0t}\sin 2\omega t$
External resistance $=X_d''$ per phase—zero external reactance:	
Three-phase	$5.19(\epsilon^{-40t}-\epsilon^{-440t})+5.19\epsilon^{-400t}\sin\omega t$
Synchronizing Torque at Rated Voltage	
Three phase 90 degrees out of phase	$5.16+5.16\sin\omega t-5.16\cos\omega t$
System reactance $X_s=X_d''$	

Per Unit Electric-Machine Constants

X_d''	X_d'	X_d	X_2	X_0	T_{do}''	T_{do}'	R_1	R_2	R_a
0.097	0.152	1.17	0.096	0.0177	0.055 second	6.65 second	0.0048	0.025	0.00105

Short Circuits at No Load—No External Impedance

Figure 5 gives the crest torque on the single-frequency unit resulting from three types of fault at no-load rated voltage and with no external impedance. Figure 6 gives the effect of the various components of the electrical excitation torque for a line-to-line fault on the double-frequency unit. As shown by Table II, it would be expected that the line-to-line fault would produce the most severe shaft torque, since it has both the highest d-c and 60-cycle components of the air-gap torque. In the practical range of system frequencies the effect of its larger negative 120-cycle component should not be important. This is borne out by the solutions. As illustrated in Figure 6, the 60-cycle component of the rotor air-gap torque has the dominant effect upon the crest shaft torque, except at the lower range of mechanical-system frequencies. Although the variation of crest shaft torque is not very great for the three types of faults (see Figure 5), the line-to-line fault gives the most severe condition when no external impedance is present.

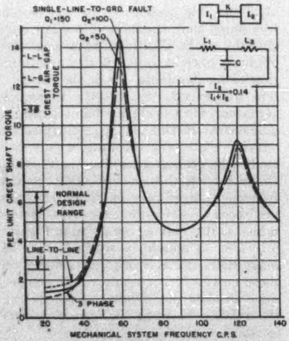

Figure 5. Curves of shaft torque as a function of mechanical-system frequency for short circuits on single-frequency unit from no load and with no external resistance

Effect of External Resistance

The presence of external-system reactance decreases the magnitude of the fault currents and, therefore, the rotor air-gap torque. However, the addition of external resistance without increasing the reactance (which may occur for certain types of faults with appreciable resistance) can increase some components of the air-gap torque The effect of external resistance on the rotor air-gap torques is shown on Table II. It increases the crest magnitude of the d-c component, increases rapidly the damping of the 60-cycle component, and increases more slowly the damping of the d-c component. This can readily be seen by comparison of the electrical-torque oscillograms in Figures 2 and 3A. Also (as shown by Table I of reference 3), the relative magnitude of the more highly damped of the two decrement factors of the d-c component is increased so that a less accurate representation is obtainable with only one equivalent decrement factor. However, this latter factor is not important for small values of external resistance. Representative solutions (see Figure 2) were obtained, using the two forms of the d-c component listed in Table II for a line-to-line fault with one per cent per phase external resistance. No appreciable difference was found in the resulting shaft torques.

Since the addition of external resistance increases the magnitude of the d-c component of electrical torque, it might be thought that such a condition will produce more severe shaft torques at the lower system frequencies where the d-c component has its greatest effect. This was found to be true for low values of external resistance. Torque data were obtained for all types of faults having a per phase external resistance of one per cent. These showed that in all cases the double-line-to-ground fault is most severe since (see Table II) it has the largest d-c component Typical crest-torque curves for this case are given in Figure 6. Figures 7 and 8 present a comparison of the most severe types of fault with varying amounts of external resistance. As shown, the double-line-to-ground fault with one per cent external resistance can produce slightly greater crest torques at the lower range of system frequency but rapidly drops below the line-to-line fault curves for no external resistance as 60-cycle resonance is approached.

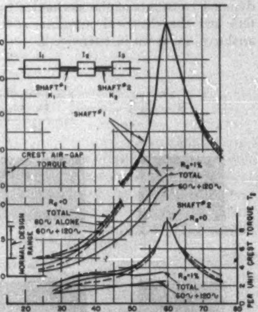

Figure 6. Curves of shaft torque as function of dominant mechanical-system frequency when spring constant of generator shaft on double-frequency unit is varied

Line-to-line faults from no load

$I_1=1$; $I_2=I_3=0.821$; $K_2=1.09\times10^4$

To show that the further increase of the d-c component with greater amounts of external resistance is more than offset by increased damping, torque curves were obtained for the case of a three-phase fault with the per phase external resistance equal to (X_d''). These are shown in Figures 7 and 8. For this case the resistance is sufficiently large to affect materially the fault currents and machine

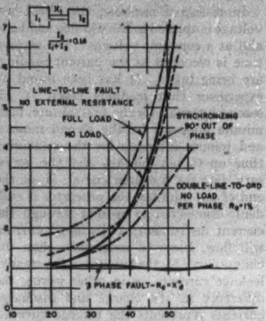

Figure 7. Shaft-torque—mechanical-frequency curves for single-frequency turbogenerator

time constants so that the equations of reference 3 do not apply. The electrical torque for this case was calculated directly from fundamental machine equations.[8] A solution for this case is shown in Figure 3B. The 60-cycle component of the electrical torque is negligible, and the d-c component is the difference of two exponentials (see Table II).

Short Circuits From Full Load

The transient rotor air-gap torques for short circuits from load are of the same form as those from no load (T_r) with the addition of a transient term (ΔT_L) to represent the rapid dropping of part of the load (see equation 2). The total shaft torque is the transient response torque to these excitation functions as determined with the mechanical-transients analyzer plus the initial steady-state load torque. The transient-torque components (T_r) are very nearly proportional to the square of the voltage behind subtransient reactance. For this machine at unity power factor these components are only about one per cent higher than for short circuits from no load. The most severe shaft torques for this machine are produced by a short circuit from unity power factor at full load. It is difficult to determine in general the form of the component representing dropping of load, since this is affected by such factors as electric-system conditions and fault impedance. To simplify this problem it was assumed that the load is suddenly dropped. Total load was assumed to be dropped for three-phase and double-line-to-ground faults and half load for line-to-line and single-line-to-ground faults. Both turbine elements of the double-frequency unit were assumed to have equal outputs so that the turbine-turbine shaft carries half the steady-state load. For the foregoing assumptions the most severe shaft torques are produced by line-to-line faults from full load with no external resistance. Curves for the crest torques resulting from such a fault are shown in Figures 7 and 8. These are about one per unit higher than the corresponding fault from no load, showing that the effect of the negative component representing dropping of load is not very great and a more detailed treatment of the manner of dropping load is not too important.

It might be thought that a high-resistance fault from full load could be more severe if the external resistance is high enough actually to increase the machine load. Then the added load-changing component will be positive. However, Figures 7 and 8 show that except at very low values of the mechanical-system frequency the system response to the other rotor-air-gap-torque components (T_r) will be so low that the net effect cannot be as severe as the case of a line-to-line fault with no external resistance, since the (ΔT_L) term has only a small effect on the net shaft torques. At the lower range of mechanical-system frequencies the difference between the torques produced under these two conditions will be small. In general the most severe case is a line-to-line short circuit from full-load unity power factor with no external resistance.

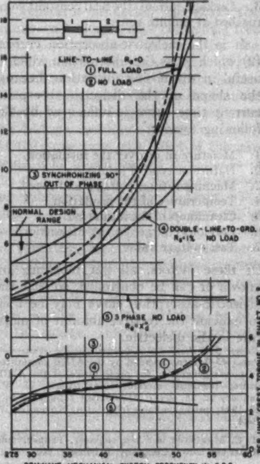

Figure 8. Shaft-torque—dominant-mechanical-frequency curves for double-frequency turbogenerator

$I_1=1$; $I_2=I_3=0.821$; $K_2=1.09\times10^6$

Time to Crest Shaft Torque

The time required for the shaft torque to reach its crest is of some importance if greater than the minimum circuit-breaker interrupting time. Under this condition full crest torque might not be reached. As would be expected for systems of this nature, the time to crest torque is relatively short at low system frequencies and increases as resonance with an excitation frequency is approached. This effect is shown by the shaft-torque oscillograms of Figures 2 and 3A, which also show the decrease of time to crest as the decrement of the rotor air-gap torque is increased. Curves of time to crest torque are given in Figure 9, which further illustrate these effects. If there were no damping in the mechanical system, the maximum time to crest would be infinite, assuming infinite duration for the fault. However, as shown by Figure 9, the maximum time to crest is about eight cycles of 60-cycle frequency if the mechanical system has 60-cycle resonance. For natural frequencies below 50 cycles, the time to crest is below three cycles of 60-cycle frequency so that the full crest torque in general should be used for all considerations.

Synchronizing Out of Phase

In Figure 2 of reference 3 is presented an analysis of the crest synchronizing torque as a function of system reactance and angle of synchronization. For a given value of system reactance, the crest-synchronizing-torque increase is roughly proportional to angle of synchronization, being about 12 per unit at an angle of 90 degrees for a system reactance ($X_s=X_d''$). It increases with decreasing X_s. For a synchronizing angle of 30 degrees, it is also about 12 per unit when $X_s=0$. Shaft torques for synchronization 90 degrees out of phase with $X_s=X_d''$ are shown in Figures 7 and 8. This provides a fair basis for the more severe synchronizing torques that normally might be expected. The resulting shaft torques are as

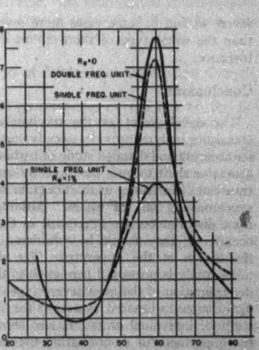

Figure 9. Curves showing time to crest shaft torque as a function of turbogenerator mechanical-system frequency

severe as and in some cases more severe than the worst type of short-circuit disturbance.

Conclusions

The development of the mechanical-transients analyzer provides a ready means for accurate and detailed study of turbine-generator shaft torques produced by such transient disturbances as short circuits and synchronizing out of phase. Although these disturbances are infrequent in their occurrence, they should be considered in the design of the apparatus. The detailed analysis presented here enables the determination of the most severe types of disturbance to be used as a basis for the study of individual units. It also shows the importance of co-ordinating the mechanical design of both turbine and generator. For instance the torque-frequency curves show that an increase in shaft stiffness in all cases increases the shaft torques. Thus, simply increasing shaft diameter need not necessarily provide a decrease in maximum shaft stress, and an accurate determination of the results requires a co-ordinated analysis.

References

1. Dynamical Analogies, Harry F. Olsen. D. Van Nostrand Company, Inc., New York, N. Y., 1943.

2. A New Device for the Solution of Transient-Vibration Problems by the Method of Electrical–Mechanical Analogy, H. E. Criner, G. D. McCann, C. E. Warren. Scheduled for publication in *Journal of Applied Mechanics*, 1945.

3. Transient Electrical Torques of Turbine Generators During Short Circuits and Synchronizing, H. S. Kirschbaum. AIEE Transactions, volume 64, 1945, February section, pages 65–70.

4. System Recovery Voltage Determination by Analytical and A-C Calculating-Board Methods, R. D. Evans, A. C. Monteith. AIEE Transactions, volume 56, 1937, June section, pages 695–705.

5. Two-Reaction Theory of Synchronous Machines—I, R. H. Park. AIEE Transactions, volume 48, 1929, pages 716–27.

Use of Dielectric-Absorption Tests in Drying Out Large Generators

H. C. MARCROFT
ASSOCIATE AIEE

DIELECTRIC absorption is the name commonly given to the effect which takes place in electrical insulation when it is subjected to a direct potential, with reference particularly to the manner in which the resulting charging current into the insulation decreases with time. The time rate of change and the magnitude of the observed current are indications of the amount of absorbed moisture (among other things) existing in the insulation of large generators, which apparatus affords a practical application of the dielectric absorption phenomenon. A newly wound generator or a generator long idle contains moisture in the insulation which should be removed before full operating voltage is applied to the winding insulation.[1] The method of using the dielectric absorption effect to determine the state of dryness of large generators is presented as a new means of measurement and one better adapted to giving more information than methods previously used.

Dielectric Absorption

When a direct potential is suddenly applied to a generator armature winding, the current flowing into the winding will have three components:[2]

1. A capacitance current, resulting from the capacitance of the winding to the generator core.

2. Dielectric-absorption current, continuing much longer in time than the capacitance current and having a characteristic diminishing value.

3. Leakage current, the final constant value reached at infinite time.

It is the dielectric-absorption current (2) which gives the information which is useful in diagnosing insulation, because the shape of the dielectric-absorption current–time curve is influenced by the following factors:

1. Moisture in or over the insulation.
2. Nature or type of insulation.
3. Machine rating, voltage, and speed.
4. Temperature of the insulation.
5. Cleanliness of the insulation.
6. Previous charges in the dielectric.
7. Test-voltage value.

Of these factors, all but moisture are known or can be controlled, so that the dielectric-absorption curve may be used to indicate the relative amount of moisture in the dielectric.

In testing a machine, the direct test voltage is applied to the winding suddenly and at a constant voltage. The elapsed time is recorded as the current readings are being taken. It has been found by experience that readings taken at 15-second intervals for the first minute, half-minute intervals for the second minute, and minute intervals for the remaining time up to ten minutes give the necessary data for a charge curve. If, at the end of ten minutes, the generator is suddenly connected to ground through the current instrument, a discharge current will flow, lesser in magnitude than the charge curve by the amount of the steady-leakage current; or in other words, the difference in the charge and discharge currents represents the leakage current, which is equal to the charge current at infinite time. In practice, the current and voltage readings are expressed in megohms.

It is necessary to have a steady supply of direct current in order to run a dielectric-absorption curve because the relatively large capacitance of the generator winding is able to store a sufficient electrical charge so that the normal commercial voltage fluctuations will result in the test current surging and even reversing. Some method must, therefore, be used to smooth the supply voltage. The curves which are discussed here were obtained by using a special testing set employing small dry cells as the voltage supply. The resulting curves are consequently very smooth.

The data taken on a test made on a nominally dry 10,000-kva turbogenerator are shown in Figure 1. The effect of dielectric absorption is shown in the decline of the charging current. Even at ten minutes time, the current is seen to be diminishing at a noticeable rate. It is this effect which has been neglected so often in previous practice in which short-time tests are made, frequently lasting less than 30 seconds. Such short-time tests result in values which are unreliable, since the tests are discontinued at a time when the resistance indication is changing with time at a fast rate. This effect is not sufficiently noticeable at the time of test because the scales of instruments usually used become crowded at increasing resistance values. In the case of instruments with manually generated power, the personal element of tiring of the operator frequently dictates the shorter test.

The first absorption test made on the generator of Figure 1 was at a potential of 500 volts, shown in curve 1. The discharge of this absorbed charge is indicated by curve 2. This sequence of tests was followed immediately by a charge test at 1,000 volts (curve 3), and the discharge of this charge (curve 4), which followed immediately.

The difference between the charge and discharge curves is shown by the dotted

---

Paper 45-9, recommended by the AIEE committee on power generation for presentation at the AIEE winter technical meeting, New York, N. Y., January 22–26, 1945. Manuscript submitted July 25, 1944; made available for printing November 17, 1944.

H. C. Marcroft is a test engineer, Pennsylvania Water and Power Company, Baltimore, Md.

Table I. Drying Generator Winding Showing Increase in Slope Factor

Generator *A*—13.3 Kv, 31,000 Kva, Three Phase, 60 Cycle

Test No.	Temp, C	Slope Factor	Drying Time, Hrs
1	26	0.22	0
2	58	0.30	15
3	76	0.41	27
4	75	0.62	39
5	75	0.72	51
6	75	0.90	63
7	75	1.12	75
8	75	1.44	87
9	35.7	1.88	87

line in both cases and is approximately the final leakage current for the 500-volt test. For the 1,000-volt test, the dotted curve is not a true leakage value because the charge curve 3 has a lower value, and the discharge curve 4 has a higher value than would be the case if the test had been made on a winding not having an absorbed charge still remaining in the dielectric. Error in insulation-resistance measurements is introduced when the measurements are made on a generator insulation which is not completely discharged. On a large generator, the discharge time has been found to be an hour or more to drain a 500-volt charge of ten-minutes duration. The discharge time is not proportional to the charge voltage but increases faster than the voltage, within limits observed in these recorded tests.

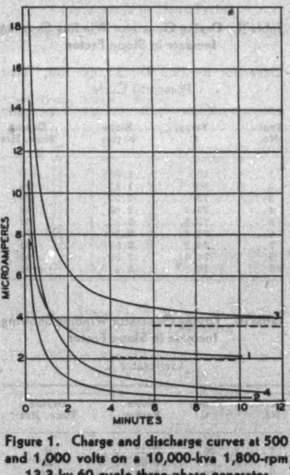

Figure 1. Charge and discharge curves at 500 and 1,000 volts on a 10,000-kva 1,800-rpm 13.3-kv 60-cycle three-phase generator

1. Charge at 500 volts
2. Discharge of run 1
3. Charge at 1,000 volts
4. Discharge of run 3

Both positive and negative charges can exist at the same time in a generator insulation. One interesting example of this effect was demonstrated on a dielectric-absorption test in which a charge of positive polarity was followed immediately by a shorter charge of negative polarity. When the generator was grounded and the discharge current was being observed, the negative charge was found to leave the generator first followed by the positive charge. The meter indicated a definite and rather abrupt reversal of current during the discharge.

Moisture Effects

The amount of absorbed moisture in the generator insulation will affect the number of leakage paths containing free ions; the resistance is lower for the greater number of such paths. When this moisture is driven out of the insulation, as it is on a dry-out run, the number of leakage paths is greatly reduced and the leakage resistance becomes greater. At the same time, the effect of the ions being held bound on the boundaries of the surfaces separating dissimilar insulating substances is made apparent. The effect may be likened to the charging of many small capacitors joined together by countless ties of very high resistance. The charges which these capacitors take are recoverable by grounding the generator winding, in which case they will flow in the opposite direction to that of the charge. Interfacial polarization[4] is the term often used to describe the condition of the insulation containing charges resulting from applied voltage across the insulation.

The degree of dryness of the insulation is reflected in the shape of the dielectric-absorption charging-current curve taken over a period of time.

Effect of Test Voltage

Moisture in insulation decreases its resistance on d-c measurements. The apparent resistance of hygroscopic insulation containing water decreases with an increase in the test voltage used. This was noticeable to a certain extent on dielectric-absorption tests made on a number of large generators. The mechanism by which this change in resistance occurs is explained by a theory, confirmed by experiments, given by S. Evershed[3] in 1913. He calls this effect "endosmosis." According to this theory, the water in insulation which causes leakage paths is a very minute fraction of the water in the insulation. Under increasing voltage stress, the so-called dormant water is forced out of the cross channels and into the direct resistance paths, enlarging the conducting water films and thus lowering the resistance. The practical difficulty in using this effect on tests is the requirement of a large voltage range of d-c supply having a very steady voltage and being sufficiently portable. The testing time and especially the time consumed in discharging the insulation is often prohibitive.

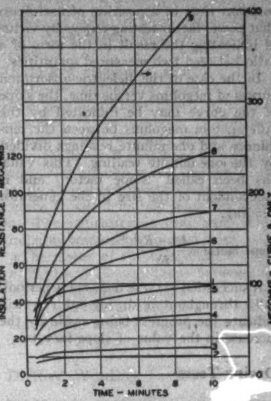

Figure 2. Insulation-resistance–time curves for generator *A*—31,000 kva, 13.3 kv, 60 cycle, 109 rpm

1. Cold, before dryout
2. Drying run started, 15 hours, 58 degrees centigrade
3. Drying continued, 27 hours, 76 degrees centigrade
4. Drying continued, 39 hours, 75 degrees centigrade
5. Drying continued, 51 hours, 75 degrees centigrade
6. Drying continued, 63 hours, 75 degrees centigrade
7. Drying continued, 75 hours, 75 degrees centigrade
8. Drying ended, 87 hours, 75 degrees centigrade
9. Cold, after dryout, 35.7 degrees centigrade

Use of Dielectric-Absorption Curves

The steepness of the rise of the resistance curve with time indicates the relative amount of moisture present in the insulation. However, all generator insulations do not have the same curves. For example, some generators are wound with coils having the end turns treated with a conducting paint to control the corona which otherwise might exist in the end-turn spaces. Such a machine has a lower and flatter absorption curve than a generator without end-turn corona control treatment. The larger and slower-speed generators have more coils and lower resistance than smaller high-speed machines yet the shapes of the absorption curves would be the same, all other things being unchanged. This is a fortunate circumstance as it puts the dielectric-absorption tests in a position of usefulness that power factor testing enjoys by virtue of indicating the result in the form of a ratio between two measured quantities.

In the case of the dielectric-absorption curves of megohms versus time, the slope of the curve may be indicated by the difference in megohms between the ten-minute and one-minute readings divided by the one-minute reading. This value has been called "slope factor" and is independent of the size of the generator winding.

$$\text{Slope factor} = \frac{R_{10}-R_1}{R_1}$$

A succession of these tests made periodically throughout a drying-out run will indicate the progress being made by the increase in the value of slope factor.

Drying Tests

The drying-out progress of a 31,000-kva three-phase 60-cycle hydro generator (generator *A*) is shown in Figure 2. This machine has mica-tape insulation throughout the entire coil, the coil-end connections, and pole leads or group leads. The tie cords on the coils are linen but on the end connections and phase-collector busses they are fiber glass. This generator was out of service two months during which time moisture was absorbed. There is no resistance varnish used on these coils. The curves show the resistance of the insulation for 500 volts impressed and for a charging time of ten minutes. The corresponding values of temperature of the insulation and slope factor, as the drying run progressed, are given in Table I. The slope factor increased from 0.22 at the start to 1.44 at the end of drying run which was of 87 hours' duration. A value of 1.25 slope factor has been arbitrarily set as a satisfactory dry value for this class of generator at 75 degrees centigrade approximately. The increase in slope factor to 1.88 after the generator had cooled is caused principally by the fact that the resistance-temperature curves for one-minute and ten-minute values do not have the same slope.

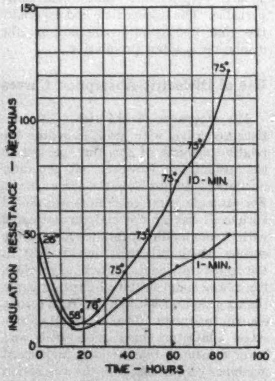

Figure 3. One-minute and ten-minute resistance values during drying run on generator *A*

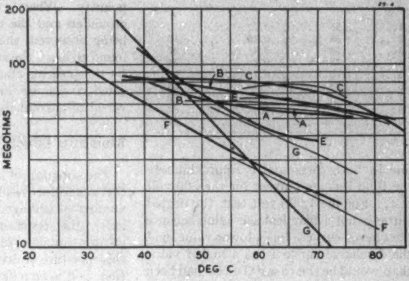

Figure 4. One-minute resistance–temperature curves for six large water-wheel generators showing changes in resistance between 1938 and 1940

Light lines, 1938 tests

Heavy lines, 1940 tests

The two curves of Figure 3 show the one-minute and ten-minute resistance values obtained from Figure 2 during the dryout time of 87 hours. The divergence of the two curves indicates graphically the increasing drying of the insulation. Obviously, the slope factor will continue to rise beyond the end of the curve with further drying. A generator of this type in steady service will have a value of slope factor in the order of two or three at 60 degrees centigrade.

Sufficient outage time was not available to allow the continuation of the dry-out curves to a steady state at this time. However, the drying was continued beyond the time at which the ohmmeter method indicated the machine to be dry, that is, when two successive insulation readings are constant with a drying period between readings. This was also true of other generators which were tested.

In Tables II and III are shown the results obtained in drying two additional generators of the same characteristics and rating as generator *A* of Table I. The course of drying of a 37,500-kva 25-cycle single-phase 13.3-kv hydro generator is shown in Table IV, in which the drying run was of 97 hours' duration. This was the initial dry-out following the erection of the machine. Similar curves are obtained on these machines as for generator *A*, Figures 2 and 3. For reasons discussed in the following heading, constant temperature should be maintained during a dry-out run.

Temperature Effects

There is a marked temperature effect on generator-insulation resistance as may be seen from Figures 4 and 5. Tests were made at 500 volts in 1938 and in 1940 on a number of large 13.3-kv hydro generators for the purpose of comparing the resistance–temperature curves over a period of time.

In order to minimize the effect of humidity, all tests were made only after the generators had been carrying a good load for at least two weeks prior to the tests. The first test point was always at the highest temperature and, as the generator cooled, the points at lower temperature were obtained. This procedure usually required 24 hours for a test.

Temperature of the insulation was obtained from the embedded resistance detectors; the average of the six was used for the nominal temperature. It is desirable to raise the generator temperature considerably above the tempera-

Table II. Drying Generator Winding Showing Increase in Slope Factor

Generator *B*—13.3 Kv, 31,000 Kva, Three Phase, 60 Cycle

Test No.	Temp, C	Slope Factor	Drying Time, Hrs
1	15	1.83	0
2	69	1.82	24
3	75	2.32	36
4	73.2	2.63	48
5	73.5	2.85	60
6	75.8	2.86	72
7	74.2	2.91	84
8	74.4	3.06	96
9	73.8	3.1	108

Table III. Drying Generator Winding Showing Increase in Slope Factor

Generator C

Test No.	Temp, C	Slope Factor	Drying Time, Hrs
1	26	0.17	0
2	38	0.33	22
3	70	0.323	34
4	70	0.60	46
5	70.2	0.78	55
6	71.4	1.06	70
7	74.5	1.09	83
8	70	1.26	94
	74	2.77	In steady service

ture of the first test point in order to allow the temperature gradient of the insulation to become a minimum for the first test point.

Figure 4 gives the values obtained from the dielectric-absorption curves at one minute time; Figure 5 gives the values from the dielectric-absorption curves at ten minutes time.

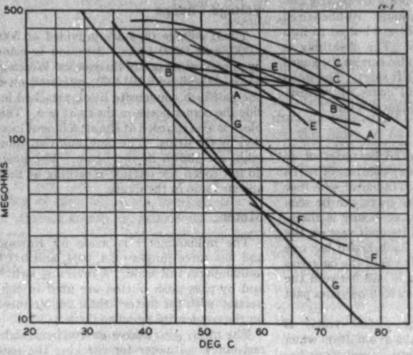

Figure 5. Ten-minute resistance–temperature curves for same conditions as in Figure 4

The heavy curves are the tests made in 1940; the lighter curves are for the 1938 tests.

Table IV. Drying Generator Winding Showing Increase in Slope Factor

Generator *D*—13.3 Kv, 37,500 Kva, One Phase, 25 Cycle

Test No.	Temp, C	Slope Factor	Drying Time, Hrs	Winding Condition
1	30	0.27	0	Cold—before drying
2	49	0.30	16	Warming up
3	72	0.14	29	Warming up
4	72	0.43	41	Warming up
5	75	0.52	47	Up to final temp
6	75	0.62	53	
7	74	1.0	65	
8	75	1.25	77	
9	75	1.41	89	
10	75	1.5	97	Dryout run stopped
11	25	1.57		Cold—after drying

Table V. Slope-Factor Values for Dry Generators in Daily Operation

These Values Are Obtained From Figures 4 and 5, 1940 Tests

		Slope Factor		
		1940		1938
Generator	Manufacturer	75 C	60 C	60 C
A	*A*	1.55	2.3	2.8
B	*A*	1.86	2.2	2.8
C	*A*	1.78	2.0	3.7
E	*A*		3.1	2.7
F	*B*	0.69	0.65	0.71
G	*B*	0.44	0.65	1.20

The generator number is shown on each curve. Generators *A*, *B*, *C*, and *E* are made by one manufacturer; generators *G* and *F* are made by another manufacturer. There is a noticeable difference in the two machines in the slopes of the temperature curves. Both kinds of generators have mica insulation as the slot insulation. The difference in the shape and magnitude of the curves is caused by the different manner of insulating the coil sections by the two manufacturers.

Table V gives the slope factors of these machines at 60 degrees centigrade and 75 degrees centigrade for generators in daily operation under normal load.

These figures are therefore typical for nominally dry generators. The 1940 curves of Figures 4 and 5 were used for data in Table V. The slope factor generally increases with decreased temperature, caused by the ten-minute value of resistance increasing at a faster rate than the one-minute value.

From these results, it is evident that at a temperature of 60 degrees centigrade, slope factor values of over 2.0 may be regularly obtained from generators with mica-tape insulation and no end-section corona treatment. Generators *F* and *G* have the end sections protected with varnished cambric, which apparently has lower resistance than the other generators, and which is reflected in the slope factor figures. This class of winding would appear to be dry with a slope factor value of 0.50 or more. Thus it becomes desirable to know the type of the coil insulation in applying the method of dielectric-absorption curves to the dryout tests, in cases where the slope factor is of the lower order.

The temperature–resistance curves (Figure 5) show that generators of different manufacture (and consequently a certain difference in insulation) have temperature curves which may differ in slope. There is even in some cases a change of slope in these curves for the same machine from year to year. Generators *A*, *B*, *C*, *F*, *G* are three-phase, 31,111-kva machines; generator *E* is a one-phase, 35,000-kva machine. All of these generators have closed ventilation. Generator *G* has had some trouble with oil film on the winding, which may explain the lowered resistance for the 1940 test. Not enough is yet known of the yearly changes of resistance–temperature curves to say definitely what the reason is. The indication is that humidity is probably responsible in most cases.

The slopes of the temperature curves of Figure 5 lie anywhere between the extremes of eight degrees to 33.5 degrees centigrade to double the resistance. The former applies to generator *G* and the latter to generator *B*.

Divided-Winding Tests

The foregoing tests were all made with the whole winding connected together and energized between winding and ground. On generators *A* and *C*, dielectric-absorption curves were made later with the winding separated into the three phases, so that by energizing one phase at a time, with the other two grounded, an indication of interphase-insulation resistance was obtained. These values are given in Table VI.

The values of slope factor for tests between phase windings are not necessarily the same as for the entire winding to core. The leakage paths are very different and depend not only upon the coil-insulation material but also upon additional materials such as cording of various types and supporting blocks. Also, the kind of varnish used on the end-coil sections becomes very important whereas this has much less effect on the measurement of resistance between the total winding and the core. For the purpose of determining the dryness of a generator, the dielectric-absorption curve of the total winding to the core is the one best adapted to the purpose. Where a generator winding is suspected of being damaged, a test between phases may be employed to determine whether or not all phases have deteriorated equally. A

Table VI. Slope-Factor Values for Tests Between Phase Windings

		Megohms			
Generator	Phase	One Minute	Ten Minutes	Slope Factor	Temp, C
A	*A*	69.5	114	0.64	81.2
	B	78.0	125	0.60	80.6
	C	70.2	109	0.56	79.5
	All	50.6	141	1.8	83.8
C	*A*	104	192	0.84	77.6
	B	100	177	0.77	79
	C	113	208	0.84	76
	All	81	306	2.3	74

high-voltage d-c absorption test should prove of more value in such a case than the low-voltage test because of the possibility of finding concentrated faults more readily by high leakage current.[5]

Conclusion

The use of dielectric-absorption curves in drying out large generators is an improvement over previous practices. More information is obtained by these curves than can be gained from spot readings which are taken at short charging times. The record of the dry-out run has been put on an exact basis. The condition of a generator with respect to moisture can be expressed in terms of slope factor. Dielectric-absorption curves taken periodically during a drying run will give the data necessary to observe the progress of the moisture removal as indicated by the rise in slope factor. It is desirable that constant temperature be maintained throughout the run.

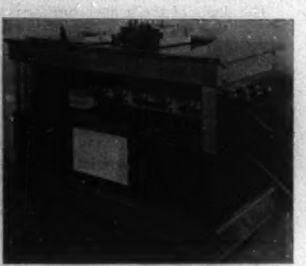

Figure 6. Generator-insulation-test table

The value of the slope factor will vary over a considerable range depending upon the type of insulation and its treatment.

The accumulation of temperature-resistance curves, at ten-minute time, over a period of years, should provide a good indication of changes in or over the insulation of the generator winding.

Appendix. Description of Insulation-Test Table

General Construction

The table is constructed of fir wood and measures 19 by 40 inches by 32 inches high, including wheels. The posts are two by two inches, bolted to the frame. Rubber-tired truck casters (four-inch) are bolted to iron plates across the ends. The sheathing is ¼-inch bakelite which also carries the guard and ground terminals (left side). The wood is finished with several coats of varnish. The table is shown in Figures 6 and 7.

Batteries

The support for the 35 batteries of 45 volts each (Burgess 5308) consists of seven trays of white pine boiled in paraffin for four hours. The ends of the trays can be seen in Figure 6. The bottom board is three-quarter-inch stock and its ends rest on the table cross members. Each board has one side and two end pieces to hold the batteries in place. A strip of tin is laid between the trays and the cross-rails which becomes part of the guard circuit.

The battery voltage (1,500 volts) is broken up into sections to avoid drain when not in use and for safety. Each tray becomes a group (235 volts) separated by six switches. The switch mounting board is boiled in paraffin and is guarded at the point of attachment to the corner posts by tin strips. At the left end of this board, a metal box is attached, which contains three batteries (Burgess 5540). Each three-volt tap is brought out to a point on a rotary switch on the top panel for voltage adjustment. Nine steps are available to take care of any voltage adjustment. The "5308" batteries have taps at 22.5 volts.

Charge–Discharge Switch

The main "charge–discharge" switch is built from a Trumbull 3821½ 500-volt 30-ampere switch. The slate base and fiber crosspiece on the blades were discarded, and the metal parts were mounted on three "condensite" blocks which were mounted on an iron V frame. This was done for several reasons:

1. The separation between blades carrying opposite potentials was increased.
2. Condensite is a much better insulator than slate and fiber.
3. The frame of one-fourth by one-inch strap iron could be bent so that the throw from charge to discharge position was short and easily done.
4. The iron framework made possible an ideal guard circuit between switch elements. The handle of the switch extends through the top condensite panel which is slotted for that purpose. Figure 6 shows this switch mounted under the left corner of the table.

Voltage Change

Three voltage taps are provided at 500, 1,000, and 1,500 volts. Selection is made by plugging into one of three jacks (Westinghouse 591496 and 591497), mounted on a one-half-inch condensite block attached inside the corner posts on the right end. This block is also guarded at the attachment location by tin strips. The plug, and two dummies, are shown in the figure. The plugs do not touch the outside sheathing as they appear to do in the figure.

Meter

The milliammeter is made by Rawson and has three ranges—0.4, 0.04, and 0.004 milliamperes full scale. A reversing switch and by-pass push button are used in connection with the meter; these are mounted on the condensite panel at the left.

The meter also makes an excellent high-resistance voltmeter for checking the batteries when used with a standard ten-megohm resistor. The batteries should not be checked with an ordinary voltmeter as such procedure depletes the battery faster than testing would do.

Wiring

The wiring is shown in Figure 7 and is done with benchboard wire. Wiring support blocks are of bakelite and guarded with tin strips under the blocks. A fuse block is provided in the negative battery lead to guard against internal trouble. Another fuse is located in the positive lead to guard against external faults. This fuse is rated 1,000 volts, one-sixteenth ampere, and is sufficient for tests at 500 volts; tests at higher voltages generally require a larger rating for large generator testing. The protective resistor of 2,870 ohms limits a possible short-circuit current to a reasonable value.

The high-voltage cable lead is single-conductor number 4 "superservice" flexible rubber-covered and is 25 feet long.

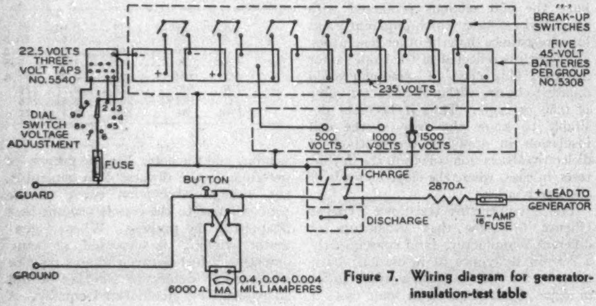

Figure 7. Wiring diagram for generator-insulation-test table

References

1. Field Testing of Generator Insulation, Edison Electric Institute subject committee on generator insulation and testing. AIEE Transactions, volume 60, 1941, December section, page 1003.

2. Insulation Resistance of Armature Windings, R. W. Wieseman. AIEE Transactions, volume 53, 1934, June section, pages 1010–21.

3. The Characteristics of Insulation Resistance, S. Evershed. *Journal* of the Institution of Electrical Engineers (London, England), volume 52, 1913, number 224.

4. The Basis for the Nondestructive Testing of Insulation, R. F. Field. AIEE Transactions, volume 60, 1941, September section, pages 890–5.

5. Progress Report of D-C Testing of Generators in the Field, E. R. Davis, M. F. Leftwich. AIEE Transactions, volume 61, 1942, January section, pages 14–18.

Improving Stability by Rapid Closing of Bus-Tie Switches

EDWARD W. KIMBARK
MEMBER AIEE

RAPID opening of circuit breakers on faulted lines has been recognized for many years as one of the most effective ways of improving power-system stability. Rapid opening followed by rapid reclosing has been used more recently and gives further improvement in stability if the fault is transitory. Rapid closing of normally open breakers offers yet another means of improving stability—a means which has never been put into practice, so far as the author is aware, but which promises to have a field of usefulness.

This paper presents the results of calculations of the power limit of a particular two-machine power system, both with the proposed switching scheme and, for comparison, with various other switching schemes which are in common use.

Figure 1, which is reprinted from an AIEE committee report[1] published in 1937, shows the effect of the presence or absence of high-voltage bussing at the ends of a double-circuit line over which power is being transmitted from a hydroelectric station to a large receiving system when a two-wire-to-ground fault occurs near the sending end of one circuit and is cleared by simultaneous opening of the breakers at both ends of that circuit. Two curves of power limit versus fault duration are drawn in this figure: curve *A* for the transmission system without high-voltage busses, curve *B* for the system with high-voltage busses. High-voltage bussing is detrimental to stability as long as the fault is on the line because the fault then pulls down the voltage of both circuits instead of only one and thus impairs their capacity to transfer power. After clearing of the fault, however, the bussing is beneficial because it lowers the reactance between generators by connecting two banks of transformers in parallel at each end of the remaining transmission circuit. With slow clearing of the fault, the detrimental effect of bussing during the fault predominates over the beneficial effect after clearing the fault. With rapid clearing, the opposite is true. As a result, curve *B* is below curve *A* at long fault durations and is above curve *A* at short durations. The curves cross at a fault duration of about 0.15 second (nine cycles on the basis of 60 cycles per second), which is the time of clearing if standard eight-cycle circuit breakers and one-cycle relays are used.

The thought naturally occurs: Inasmuch as high-voltage bussing is detrimental during the fault but beneficial after the fault, why not use bus-tie switches which are normally open but which close simultaneously with the opening of the breakers which disconnect the faulted line? The same protective relays which open each line circuit breaker could be used to close the nearby bus-tie switch.

When such switching is used on the power system of Figure 1, the calculated power limit as a function of fault duration is as shown by curve *C* of Figure 2. Curves *A* and *B* are the same in Figure 2 as in Figure 1 except that they have been recalculated using voltages behind transient reactance at each end of 1.00 unit instead of some higher value.

If the fault is cleared instantly, the power limit does not depend on whether the bus-tie switches are open or closed before and during the fault, but it does depend on the position of these switches after clearing the fault. Therefore, curve *C* intersects curve *B* at zero fault duration because both curves represent switching schemes in which the bus-tie switches are closed after clearing of the fault. However, if the fault persists a long while, the power limit is determined chiefly by conditions during the fault and very little by conditions after clearing. Therefore, curve *C* approaches curve *A* as the fault duration increases since both curves represent switching schemes in which the bus-tie switches are open during the fault. At intermediate values of clearing time curve *C* is above both curves *A* and *B*, showing that the power limit has been raised by closing the bus-tie switches simultaneously with the opening of the line breakers. The increase in power limit over that obtainable with the better of the first two arrangements (bus ties always open or always closed) is greatest for clearing times in the neighborhood of those afforded by modern high-speed relays and breakers. With 0.15-second (nine-cycle) clearing the power limit is increased from 0.87 to 0.98 per unit—an increase of 12 or 13 per cent over the first-named value. With 0.10-second (six-cycle) clearing the power limit is increased from 0.98 to 1.05 per unit—an increase of seven per cent. The improvement attainable in this case through rapid closing of bus-tie switches in conjunction with eight-cycle breakers is just equal to the improvement attainable through replacing eight-cycle breakers with five-cycle breakers.

The transient power limits calculated for 0.10-second, 0.15-second, and 0.20-second clearing of a two-wire-to-ground fault are listed in Table I for the three kinds of switching which have been considered already (*A*, *B*, *C*) and for other kinds of switching (*D* to *N*) which are to be considered subsequently. The steady-state power limit for the final circuit condition is also tabulated for each kind of switching.

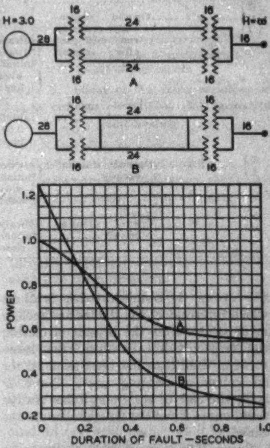

Figure 1. Effect of bussing arrangement on stability limits, double line-to-ground fault at sending end (reprinted from reference 1)

A—Low-voltage bussing
B—High-voltage bussing
System reactance shown in per cent; inertia constant H = kilowatt-seconds per kilovolt-ampere

Rapid Reclosing

It is interesting to compare the improvement in stability obtainable through the use of rapidly closed ties with that obtainable through rapid reclosing of the line breakers. Curves *D* and *E*, Figure 3, show calculated power limit versus fault duration if the breakers are closed 0.25 second (15 cycles) after interrupting fault current. This value of dead time

---

Paper 45-13, recommended by the AIEE committee on power transmission and distribution for presentation at the AIEE winter technical meeting, New York, N. Y., January 22–26, 1945. Manuscript submitted July 8, 1944; made available for printing November 24, 1944.

EDWARD W. KIMBARK is an associate professor in the department of electrical engineering, Northwestern University, Evanston, Ill. This paper was written while he was visiting associate professor of electrical communications, Massachusetts Institute of Technology, Boston, Mass.

Table I. Comparison of Power Limits for Various Kinds of Switching

Two-Wire-to-Ground Fault at Sending End of One Line of the Power System of Figure 1

Curve	No. of High-Voltage Switching Stations	Kind of Switching		Transient Power Limit in Per Unit if Clearing Time of First Breaker Is:			Steady-State Power Limit of Final Condition (Per Unit)
		Line Breakers	Tie Switches	0.10 Sec	0.15 Sec	0.20 Sec	
A	2	Opened simultaneously	Always open	0.88	0.84	0.79	0.93
B			Always closed	0.98	0.87	0.76	1.09
C			Initially open; close when line breakers open	1.05	0.98	0.91	1.09
D	2	Opened simultaneously and reclosed 0.25 sec later	Always open	0.98	0.90	0.83	1.25
E			Always closed	1.00	0.88	0.77	1.25
F			Initially open; close when line breakers open	1.08	0.99	0.91	1.25
G	2	Opened sequentially, receiving end 0.30 sec after sending end	Always open	0.78	0.74	0.71	0.93
H			Always closed	0.78	0.70	0.63	1.09
I			Initially open; close when adjacent line breakers open	0.85	0.80	0.76	1.09
J	2	Opened simultaneously	Initially open; close 0.05 sec after line breakers open		0.94		1.09
K	3	Opened simultaneously	Always closed	1.04	0.91	0.78	1.17
L			Initially open; close when adjacent line breakers open	1.12	1.03	0.94	1.17
M	∞	Opened simultaneously	Always closed	1.10	0.95	0.83	1.25
N			Initially open, then closed	1.21	1.09	0.99	1.25

(15 cycles) is obtained with breakers which interrupt in five cycles and reclose in 20 cycles after the instant of closing the trip circuit; however, the same value of dead time has been assumed for all values of clearing time. Curve *D* is for the case of the tie switches always open, curve *E* for the tie switches always closed.

Curve *D* lies considerably above curve *A*, particularly at short fault durations, because of the effect of reclosure; at long fault durations, however, *D* approaches *A*. Curve *E* lies above curve *B* for the same reason, though the difference between *E* and *B* is less than the difference between *D* and *A*. However, neither *D* nor *E* lies much above *B* at the usual clearing times. At 0.10-second fault duration *D* coincides with *B*, and *E* is only 0.02 per unit above *B*. At 0.15-second fault duration *D* is only 0.03 above *B*, and *E* is only 0.02 above *B*. These results are in general agreement with conclusions previously reached by others,[3] to the effect that rapid reclosing is of little benefit after two-wire-to-ground or three-phase faults on a sectionalized double-circuit line, especially if the generators have low inertia for the amount of power transmitted (as is true of hydroelectric generators with little local load).

Curve *D* is below curve *C* at all values of fault duration and *E* is below *C* except for fault durations less than four cycles. Accordingly, rapid reclosing of the line breakers is less effective than rapid closing of the bus-tie switches unless the fault can be cleared with extreme rapidity (requiring three-cycle or faster breakers).

The assumption of a shorter dead time than 0.25 second (15 cycles) would raise curves *D* and *E*, especially at short fault durations. If the dead time is decreased too much, however, the fault arc is likely to restrike when the line breakers reclose. The dead time should be about 10 or 12 cycles at 138 kv and longer at higher voltages. Therefore the possibility of raising the power limit by faster reclosing has decided limits. Zero dead time (if such were possible) would raise curve *E* at zero fault duration to the transient power limit 1.39, which considerably exceeds the steady-state power limit of 1.25, but curve *E* would still approach curve *B* rapidly as the fault duration increased. The steep slope at short fault durations of curves such as *E* for rapid reclosing as compared with the slope of curves such as *B* for no reclosing, has been pointed out previously.[2]

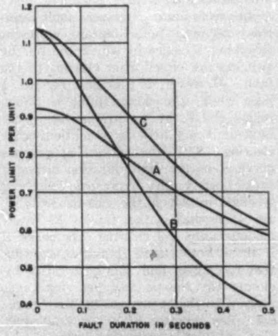

Figure 2. Effect of the rapid closing of bus-tie switches on stability of the power system of Figure 1

A—Bus-tie switches always open
B—Bus-tie switches always closed
C—Bus-tie switches initially open but close simultaneously with opening of line breakers

The use of rapid closing of bus-tie switches followed by reclosing of the line breakers 0.25 second later gives a slightly higher power limit than does the closing of bus ties alone. This is shown by curve *F*, Figure 3, which lies above curve *C*, especially at short fault durations. The improvement due to reclosing is slight at fault durations of 0.10 and 0.15 second.

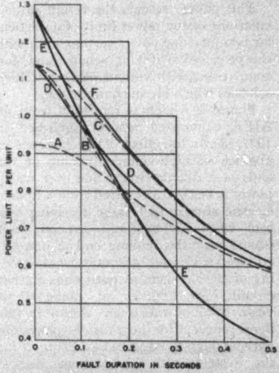

Figure 3. Effect of the rapid reclosing of the line breakers on stability

A, *B*, *C*—Same as in Figure 2: no reclosing
D, *E*, *F*—With reclosing after 0.25-second dead time
D—Bus-tie switches always open
E—Bus-tie switches always closed
F—Bus-tie switches initially open but close simultaneously with opening of line breakers

Intermediate Switching Stations

A common method of improving the stability of a power system like that shown in Figure 1 is to add one or more high-voltage switching stations at intermediate points of the line. The effect of one intermediate switching station at the center of the transmission line, in addition to the two high-voltage terminal switching stations, is shown in Figure 4. Curves *B* and *C*, as in previous figures, are for terminal bussing only. Curves *K* and *L* are for an additional switching station at the center. Curves *B* and *K* are for permanent bussing at all three switching stations; while *C* and *L* are for rapidly closed bus-tie switches at all stations. If solid bussing at the terminals (curve *B*) be taken as the original condition, the improvement due to the addition of rapid closing of bus-tie switches at the two terminals (curve *C*) is greater than the improvement due to the intermediate switching station (curve *K*) at clearing times of 0.10 second (six cycles) or more. The addition of two circuit-closing switches at the ends of the lines is more effective than addition of four circuit breakers at the middle of the line.

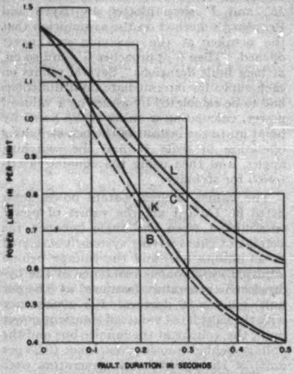

Figure 4. Effect of one intermediate high-voltage switching station on stability

B, *C*—Same as in Figure 2; high-voltage bussing at terminals only

K, *L*—One intermediate switching station added

B, *K*—Bus-tie switches at all stations always closed

C, *L*—Bus-tie switches at all stations initially open but close simultaneously with opening of line breakers

Even if the intermediate switching station is used (curve *K*), a considerable additional improvement is effected by the addition of three rapidly closed bus-tie switches (curve *L*). Again the use of rapidly closed bus-tie switches in conjunction with eight-cycle line breakers gives as much increase of power limit as does the replacement of eight-cycle breakers by five-cycle breakers.

The greatest possible improvement due to the addition of intermediate switching stations would occur if a very great number of such stations was used, spaced very closely together. (If faults occurred nowhere but at the sending end, one additional station very near the sending end would have the same effect.) Curves for this condition are not given, but values of power limit are entered in Table I, lines *M* and *N*. These values show that an infinite number of intermediate switching stations (line *M*) are more effective than rapidly closed bus-tie switches at the terminals only (line *C*) for a clearing time of 0.10 second but are less effective at 0.15 second and longer clearing times, and even if a large number of switching stations are used, the provision of rapidly closed bus-tie switches at all stations (line *N*) raises the power limit further. Once again the use of the bus-tie switches with eight-cycle breakers is as effective as replacing eight-cycle breakers with five-cycle breakers.

Sequential Switching

Rapid reclosing is of negligible aid to stability unless the breakers at both ends of the faulted line are opened rapidly and almost simultaneously. If a relaying scheme is used which requires time delay in the opening of the breaker at one end of the line in case of a fault near the other end, neither breaker can be reclosed successfully until the required dead time has elapsed after the opening of the second breaker. It is then too late to do much good.

Closing of bus ties, on the other hand, is of some benefit in conjunction with sequential fault clearing. When the line breaker at the end near the fault opens, the adjacent bus tie simultaneously closes, paralleling the two banks of transformers. The bus tie at the other end is still open, so the fault is connected to the sound part of the system through high reactance. Later, when the second line breaker opens, the second bus tie simultaneously closes, paralleling the transformers at that end.

Curves *G*, *H*, and *I*, Figure 5, show the calculated power limit of the system of Figure 1 for a two-wire-to-ground fault at the sending end cleared sequentially. Power limit is plotted as a function of the time required to open the breaker at the sending end (including relay time). The breaker at the receiving end is assumed to open 0.30 second (18 cycles) after the breaker at the sending end. Curve *G*, for bus ties always open, and curve *H*, for bus ties always closed, cross at 0.10 second. Curve *I*, for bus ties closed simultaneously with opening of the adjacent line breakers, lies above both *G* and *H*. The power limit is raised from 0.78 to 0.85 per unit with 0.10-second clearing at the sending end, and from 0.74 to 0.80 per unit with 0.15-second clearing. These increases are nine and eight per cent, respectively. The improvement attainable through synchronized closing of bus-tie switches in conjunction with eight-cycle breakers is slightly greater than that attainable through replacing eight-cycle breakers with five-cycle breakers.

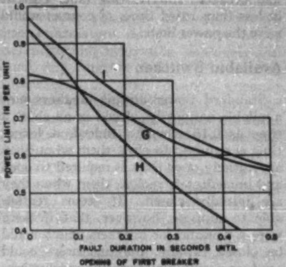

Figure 5. Effect of the rapid reclosing of bus-tie switches on stability with sequential fault clearing

G—Bus-tie switches always open

H—Bus-tie switches always closed

I—Bus-tie switches initially open; each closed simultaneously with opening of adjacent line breaker

However, much greater improvement can be effected through the addition of pilot relaying to obtain simultaneous high-speed opening of the breakers at both ends than can be obtained through the addition of synchronized bus-tie switches. Curve *B* is 26 per cent higher than either curve *G* or *H* at 0.10 second and 18 per cent higher at 0.15 second. Nevertheless, it is of interest to know that some benefit would be obtained in the event of a fault by leaving synchronized bus-tie switches in service during the outage of a pilot channel.

Imperfect Synchronization

It is obvious that, for the greatest effectiveness, each bus-tie switch should close simultaneously with the opening of the associated line circuit breaker. Even though not perfectly timed, however, these switches can still improve stability. In order to obtain an idea of the effect of imperfect synchronization, the power limit was calculated for the case in which the fault was cleared in 0.15 second and both bus-tie switches were closed 0.05 second later. The power limit was found to be 0.94 per unit as compared with 0.98 for perfect synchronization. Thus an increase of 37.5 per cent in the closing time of the switch (from 8 to 11 cycles) gives four per cent decrease in power limit. The decrease is the same as that caused by delaying the opening of the line breakers half as long, or 0.025

second, with simultaneous closing of the tie switches (curve *C*). Early closing of the tie switches would probably decrease the power limit more than late closing, but would be less likely to occur. Any lack of synchronization due to the line breakers interrupting fault current in less than rated time, of course, would raise the power limit.

Available Switches

Standard power circuit breakers now available cannot be closed in as short a time as 0.15 second. Indeed, a longer time is required to close them when they are initially open than is required to open and immediately reclose them when they are initially closed. It seems reasonable to suppose, however, that if there were a demand for breakers which could be closed rapidly, manufacturers could produce a suitable operating mechanism.

Rapid-closing bus-tie switches could be so operated that they would never be required to interrupt short-circuit current or, perhaps, even load current. For such service an air-break switch might be suitable.

Conclusions

The following conclusions may be drawn from this study regarding the suitability of rapid closing of bus-tie switches for raising the power limit of the power transmission system of Figure 1 (based on the clearing of a two-wire-to-ground fault at the sending end of one circuit):

1. With 0.15-second (nine-cycle) fault clearing, the power limit is increased 12 per cent by rapid closing of the bus-tie switches; with 0.10-second (six-cycle) clearing, seven per cent.

2. The increase in power limit due to the addition of rapid-closing bus-tie switches to 0.15-second fault clearing is the same as the increase produced by speeding up the fault clearing from 0.15 to 0.10 second (changing eight-cycle breakers to five-cycle breakers).

3. The increase in power limit due to rapid closing of bus-tie switches is greater than the increase attainable through rapid reclosing of the line breakers with 0.25-second dead time for all fault-clearing times except those under 0.07 second (four cycles), and with 0.10-second or 0.15-second fault clearing, the increase is three or four times as great.

4. Rapid closing of bus-tie switches is effective even with permanent faults, whereas rapid reclosing is beneficial only with transitory faults and is detrimental with permanent faults. Therefore, rapid closing of bus-tie switches is applicable to underground cable systems.

5. Rapid reclosing is effective with double-circuit transitory faults, whereas closing of bus ties is not. However, the power limit with double-circuit faults is much lower than that with single-circuit faults.

6. The increase in power limit due to rapid closing of bus-tie switches at the line terminals is greater than the increase attainable through the addition of an intermediate high-voltage switching station at the middle of the line for all fault-clearing times except those under 0.08 second (five cycles).

7. Even if rapid reclosing or additional switching stations are used to increase the power limit, considerable further increase can be obtained through use of rapidly closed bus-tie switches.

8. Rapid closing of bus-tie switches can be employed in conjunction with sequential clearing of faults and when so employed it raises the power limit eight or nine per cent whereas reclosing is applicable only with simultaneous clearing. However, changing from sequential to simultaneous clearing gives two or three times as much improvement as the addition of rapid-closing bus-tie switches.

9. For best results, each bus-tie switch should close simultaneously with the opening of an adjacent line circuit breaker. Exact synchronization is not necessary, however.

Although the calculated results have been limited to the rapid closing of bus-tie switches on a double-circuit line, the principle proposed in this paper is not so limited. Stability will be improved by the closing of any switch simultaneously with the clearing of a fault, provided the transfer reactance between synchronous machines during the fault is lower with the switch open than with it closed and after clearing of the fault is lower with the switch closed than with it open.

Appendix. Methods of Calculation

In the power system of Figure 1, resistance and capacitance were neglected. Negative-sequence inductive reactances were assumed equal to the corresponding positive-sequence reactances given in the figure. Zero-sequence inductive reactances of the transmission lines were assumed to be twice as great as the positive-sequence values. The internal voltage of each generator (voltage behind transient reactance) was assumed always to be 1.00 per unit.

Curves of transient-power limit versus fault duration for kinds of switching which involved only one instant of switching after the inception of the fault (curves *A*, *B*, *C*, *K*, *L*, *M*, and *N*) were calculated by the rapid method of Byrd and Pritchard.[3] For kinds of switching which involved two instants of switching (curves *D* to *J* inclusive), a more laborious method had to be used, as follows: The point for zero fault duration was read from an auxiliary curve calculated by Byrd and Pritchard's method; the abscissa of the auxiliary curve was the time of the second switching operation (reclosing of line breakers for curves *D*, *E*, and *F*, opening of second line breaker for curves *G*, *H*, and *I*). For long fault durations the curve was known to approach closely some previously calculated curve; for example, curve *D* approaches curve *A*. In case of curves *G*, *H*, and *I*, auxiliary curves *G′*, *H′*, and *I′* were plotted by Byrd and Pritchard's method on the assumption that the breaker at the receiving end never opened. Then *G* approaches *G′*, and so on, at long fault durations. Several points on each curve for intermediate fault durations had to be calculated by assuming a value of power, calculating a swing curve point by point up to the instant of the last switching operation in order to find the switching angles, and then using the equal-area criterion for stability.

The values of steady-state power limit listed in Table I are the values of power transmitted when the angle between the voltage of the receiving system (considered as an infinite bus) and the voltage behind adjusted synchronous reactance of the hydroelectric generators (assumed as 0.84 per unit) reaches 90 degrees. For consistency with the calculated values of transient power limit, the voltage of the infinite bus and the voltage behind transient reactance (0.28 per unit) of the hydroelectric generators were both taken as 1.00 per unit. In every case the steady-state power limit thus computed for the final condition of the circuit exceeds the transient power limit for fault-clearing time of 0.10 second or longer.

References

1. First Report of Power-System Stability, AIEE subcommittee on interconnection and stability factors. AIEE Transactions, volume 56, 1937, February section, pages 261–82.

2. Analysis of the Application of High-speed Reclosing Breakers to Transmission Systems, S. B. Crary, L. F. Kennedy, C. A. Woodrow. AIEE Transactions, volume 61, 1942, June section, pages 339–48.

3. Solution of the Two-Machine Stability Problem, H. L. Byrd, S. R. Pritchard, Jr. *General Electric Review*, volume 36, February 1933, pages 81–93.

Transient Electrical Torques of Turbine Generators During Short Circuits and Synchronizing

H. S. KIRSCHBAUM
ASSOCIATE AIEE

THE calculation of shaft and frame stresses in turbine generators during short circuits or synchronizing is dependent upon a knowledge of the electrical torque developed at the rotor air gap. This torque generally contains unidirectional, fundamental-frequency, and second-harmonic components, all of which are damped. It is the steady components of torque which are of interest in the calculation of system stability, while all the components are of interest to the turbine generator designer.

The torques have been calculated on the assumption of an "ideal" synchronous machine[1] and the equations will not be applicable to all types of synchronous machines. The turbine generator and salient-pole machines with connected dampers are close approximations during subtransient and transient periods. The salient-pole machine with unconnected dampers or no dampers at all is furthest removed in its characteristics from the ideal machine and will have torques containing all odd and even harmonics.[2] The unidirectional torque would be extremely difficult to calculate for such machines.

Various authors have presented torque equations derived by different approaches.[2,3,4,11] Nickle, Pierce, and Henderson thoroughly treated the alternating torques during single-phase short circuits by a combination of the constant-flux-linkages theorem and Park's torque equation.[5] They did not consider loss torques. Stone and Kilgore, in calculating the unidirectional torques during short circuit, assumed that all ohmic losses in the machine would appear as torque. This resulted in much too high a value of unidirectional torque. Whitney and Criner presented equations for single-phase,[3] three-phase, and double-line-to-ground faults; these equations contained both the unidirectional and alternating components of torque. However, several terms of the equation for the double-line-to-ground fault were in error and require modification. No treatment was made of armature time constants during this type of fault.

In this paper a semi-empirical method is presented for deriving the short-circuit and synchronizing-torque equations, using the method of symmetrical components. The equations are valid only to the extent that the assumptions made in their derivations are valid.

Basic Assumptions

In the first approach to the problem it is necessary to make certain simplifying assumptions in regard to the arrangement and electrical characteristics of the component parts of the machine. The closeness of agreement between assumed and actual conditions will determine how nearly the computed and actual performances of the machine will compare. A synchronous machine idealized to the following extent will be considered:

A. The air gap is uniform. The presence of slots on the quadrature axis of the machine and none on the direct axis does not invalidate this assumption to any great extent.

B. Saturation and hysteresis are neglected in calculating the alternating components of torque.

C. The field has distributed symmetrical windings on both axes. During the subtransient period this assumption is justified. In the actual machine there is no winding on the quadrature axis. However, the transient reactance on both axes are usually sufficiently close together to justify this assumption.

D. The stator has a sinusoidally distributed three-phase winding.

E. The air-gap flux is sinusoidally distributed in space.

Short-Circuit Torques

When the armature is short-circuited, there is trapped in the armature circuit a portion of normal armature flux, that portion being dependent upon the time of application and the type of short circuit. The decay of the trapped flux depends upon the time constant of the armature circuit containing the flux. It is this flux which manifests itself as a d-c component in the short-circuit current. If the short circuit is unbalanced, the armature current will contain, in addition to the d-c component, positive- and negative-sequence components of fundamental frequency. These components of current will set up positive- and negative-sequence armature magnetomotive forces and, neglecting saturation, positively and negatively rotating fields. The sudden appearance of the positive-sequence armature magnetomotive force over the direct axis of the rotor causes the rotor currents to rise suddenly, counterbalancing this additional direct-axis excitation. This follows from the fact that the flux linking the rotor circuits cannot change instantly. The additional rotor currents, induced by the sudden appearance of the positive-sequence field, are unsupported by exciter voltage and they decay with decrements which are dependent upon the short-circuit rotor time constants and the type of fault. The net excitation on the direct axis decays and, as a consequence, the air-gap flux also decays. This subject is treated very thoroughly in the papers of Doherty and Nickle.[6,7]

The alternating torque acting on the rotor (and also the stator) is proportional to the product of rotor and stator fields times the sine of the angle between them, thus there will be only fundamental-frequency and second-harmonic alternating torques. The fundamental-frequency torque results from the interaction of the unidirectional-armature field with the rotor field and the second-harmonic torque results from the interaction of the negative-sequence armature field with the rotor field. It can be shown[8] that these two components can be calculated by taking the sum of the instantaneous-phase powers as determined by the product of induced-phase voltage and instantaneous-armature current.

In addition to these alternating torques, there are also present unidirectional torques caused by losses in the machine. However, not all the ohmic losses will appear as torque. It is possible to determine (neglecting windage and friction) the unidirectional torque from the general relation applied to the average power.

Power output equals power input to the shaft plus the rate of decrease of stored kinetic energy in the machine plus the rate of decrease of stored magnetic energy in the machine minus the total ohmic losses in the machine. The sum of the first two terms on the right-hand side of the equation are proportional to the unidirectional torque acting on the rotor (the changes in rotor velocity are usually quite small). During a short circuit, the power output is zero and the unidirectional torque is equal to the sum of the average ohmic losses minus the rate of decrease of average stored magnetic energy in the machine. In other words, some of the ohmic losses are supplied by

---

Paper 45-14, recommended by the AIEE committee on electrical machinery for presentation at the AIEE winter technical meeting, New York, N. Y., January 22–26, 1945. Manuscript submitted November 8, 1944; made available for printing November 25, 1944.

H. S. KIRSCHBAUM is central station engineer, Westinghouse Electric and Manufacturing Company, East Pittsburgh, Pa.

The author wishes to acknowledge the many helpful suggestions made by C. B. Warren of the central station department of the Westinghouse Electric and Manufacturing Company.

decaying magnetic fields. Of the losses in the machine, two components are so supplied; the loss caused by the flow of direct current in the short-circuited armature, and the loss caused by the flow of the additional direct current in the rotor circuits. The remainder of the d-c ohmic loss in the rotor field is supplied by the exciter. Therefore, the only machine losses which appear as unidirectional torque are those which are caused by the flow of alternating current in the various machine circuits.

Assuming a solid rotor structure, the rotor resistance and reactance vary very closely as the square root of the frequency of the rotor current.[8] At double frequency the rotor resistance is $\sqrt{2}$ times as great as it is at fundamental frequency. If R_2 is the negative-sequence resistance of the machine as measured with double-frequency rotor currents flowing, the rotor resistance is $2(R_2-R_1)$ at double frequency and at fundamental frequency it is $\sqrt{2}(R_2-R_1)$. In turbine generators, it has been determined that the rotor losses vary very closely as the 1.8 power of the rotor current.[9] Since the rotor circuits are assumed to be identical on both axes of the rotor, the rotor currents will be balanced polyphase currents and there will be no second- or fourth-harmonic components of rotor loss; only the average loss will appear. Because transients of short duration in the rotor body are neglected, the rotor-loss torques appear as a suddenly applied unidirectional torque. The ohmic loss resulting from the flow of 60-cycle current in the stator has a double-frequency component during unbalanced short circuits. This double-frequency torque is usually negligible in comparison with the other alternating torques present during the short circuit, hence only the average value of this loss is retained in the computation of the unidirectional component. The total alternating- and unidirectional-rotor torques are derived for the line-to-line-to-line short circuit in Appendix II.

Table I

Type of Fault	Short-Circuit Torque
Line-to-ground on phase a	$T=\frac{E^2}{(X_d''+X_2+X_0)}\left[2FA\sin(\omega t+\alpha)-F^2\sin 2(\omega t+\alpha)\right]+2\left[\frac{EF}{X_d''+X_2+X_0}\right]^{1.8}\cdot(R_2-R_1)+$ $\sqrt{2}\left[\frac{\sqrt{2}EA}{X_d''+X_2+X_0}\right]^{1.8}(R_2-R_1)+3\left[\frac{EF}{X_d''+X_2+X_0}\right]^2 R_1$ per unit torque $F=\left[\frac{X_d''+X_2+X_0}{X_d+X_2+X_0}+\frac{(X_d''+X_2+X_0)(X_d-X_d')}{(X_d'+X_2+X_0)(X_d+X_2+X_0)}\epsilon^{-\frac{t}{T_{do}'}\frac{X_d+X_2+X_0}{X_d'+X_2+X_0}}+\frac{(X_d'-X_d'')}{(X_d'+X_2+X_0)}\epsilon^{-\frac{t}{T_{do}''}\frac{X_d'+X_2+X_0}{X_d''+X_2+X_0}}\right]$ $A=(\cos\alpha)\epsilon^{-2\pi f\frac{3R_a}{X_d''+X_2+X_0}t}$, α = angle between direct axis of rotor and phase a
Line-to-line on phases b to c	$T=\frac{E^2}{(X_d''+X_2)}\left[2FA\sin(\omega t+\alpha)-F^2\sin 2(\omega t+\alpha)\right]+2\left[\frac{EF}{X_d''+X_2}\right]^{1.8}(R_2-R_1)+$ $\sqrt{2}\left[\frac{\sqrt{2}EA}{X_d''+X_2}\right]^{1.8}(R_2-R_1)+2\left[\frac{EF}{X_d''+X_2}\right]^2 R_1$ per unit torque $F=\left[\frac{X_d''+X_2}{X_d+X_2}+\frac{(X_d''+X_2)(X_d-X_d')}{(X_d'+X_2)(X_d+X_2)}\epsilon^{-\frac{t}{T_{do}'}\frac{X_d+X_2}{X_d'+X_2}}+\frac{(X_d'-X_d'')}{(X_d'+X_2)}\epsilon^{-\frac{t}{T_{do}''}\frac{X_d'+X_2}{X_d''+X_2}}\right]$ $A=(\cos\alpha)\,\epsilon^{-2\pi f\frac{2R_a}{X_d''+X_2}t}$, α = angle between quadrature axis of rotor and phase a
Three phase	$T=\frac{E^2}{X_d''}FA\sin\omega t+\sqrt{2}\left[\frac{\sqrt{2}EA}{2X_d''}\right]^{1.8}\cdot(R_2-R_1)+\left[\frac{EF}{X_d''}\right]^2 R_1$ per unit torque $F=\left[\frac{X_d''}{X_d}+\frac{X_d''(X_d-X_d')}{X_d'X_d}\epsilon^{-\frac{t}{T_{do}'}\frac{X_d}{X_d'}}+\frac{(X_d'-X_d'')}{X_d'}\epsilon^{-\frac{t}{T_{do}''}\frac{X_d'}{X_d''}}\right]$ $A=\epsilon^{-2\pi f\frac{R_a}{X_d''}t}$
Line-to-line-to-ground on phases b and c	$T=\frac{E^2}{\left[X_d''+\frac{X_2X_0}{X_2+X_0}\right]}\left[2A_1F\sin(\omega t+\alpha)-2A_2F\cos(\omega t+\alpha)-F^2\frac{X_0}{X_2+X_0}\sin 2(\omega t+\alpha)\right]+$ $2\left[\frac{EF}{X_d''+X_2+\frac{X_d''X_2}{X_0}}\right]^{1.8}\cdot(R_2-R_1)+\sqrt{2}\left\{\left[\frac{\sqrt{2}EA_1}{X_d''+\frac{X_2X_0}{X_2+X_0}}\right]^{1.8}+\left[\frac{\sqrt{2}EA_2}{X_d''+\frac{X_2X_0}{X_2+X}}\right]^{1.8}\right\}\times$ $(R_2-R_1)+2\left[\frac{EF\sqrt{X_2^2+X_2X_0+X_0^2}}{X_d''X_2+X_2X_0+X_0X_d''}\right]^2 R_1$ per unit torque $F=\left[\frac{X_d''X_2+X_2X_0+X_0X_d''}{X_dX_2+X_2X_0+X_0X_d}+\frac{(X_d''X_2+X_2X_0+X_0X_d'')(X_2+X_0)(X_d-X_d')}{(X_d'X_2+X_2X_0+X_0X_d')(X_dX_2+X_2X_0+X_0X_d)}\epsilon^{-\frac{t}{T_{do}'}\frac{X_dX_2+X_2X_0+X_0X_d}{X_d'X_2+X_2X_0+X_0X_d'}}+\right.$ $\left.\frac{(X_2+X_0)(X_d'-X_d'')}{(X_d'X_2+X_2X_0+X_0X_d')}\epsilon^{-\frac{t}{T_{do}''}\frac{X_d'X_2+X_2X_0+X_0X_d'}{X_d''X_2+X_2X_0+X_0X_d''}}\right]$ $A_1=\left[\frac{(X_2+2X_0)\cos\alpha}{2(X_2+X_0)}\right]\epsilon^{-2\pi f\frac{2R_a}{X_d''+X_2}t}$, $A_2=\left[\frac{X_2\sin\alpha}{2(X_2+X_0)}\right]\epsilon^{-2\pi f\frac{6R_a}{X_d''+X_2+4X_0}t}$, α = angle between quadrature axis of rotor and phase a

Table II

Type of Synchronizing	Synchronizing Torques
Three phase	$T=\frac{E^2\sin\delta}{(X_d''+X_s)}\left[1-\cos\omega t+\tan\frac{\delta}{2}\sin\omega t\right]$.
Single phase (a phase not connected)	$T=\frac{E^2\sin\delta}{(X_d''+X_2+2X_s)}\left[1-\cos 2(\omega t+\alpha)-\tan\frac{\delta}{2}\sin 2(\omega t+\alpha)-\frac{2\sin\left(\frac{\alpha+\beta}{2}\right)}{\cos\left(\frac{\alpha-\beta}{2}\right)}\sin(\omega t+\alpha)\right]$

$e_a=E\cos(\omega t+\alpha)$, $e_s=E\cos(\omega t+\beta)$, $\delta=(\alpha-\beta)$

Decrements

The subject of rotor and armature decrements has been very ably handled elsewhere for single-phase and three-phase faults and will not be discussed here.[6,7] However, except for the work of Smith and Weygandt,[12] the armature decrements for the double-line-to-ground fault have not been treated as extensively. Because the armature has two coupled circuits which are short-circuited, the direct currents in the armature will, in general, have two decrements. Therefore, there will be two decrements on the fundamental-frequency rotor torque and on the unidirectional torque resulting from the flow of fundamental-frequency current in the rotor. These decrements are derived in Appendix III, however space does not permit the full derivation of the rotor torques during a double-line-to-ground fault.

External Impedance

If the external impedance is predominantly reactance (or resistance so low as not to affect the short-circuit current) the torques can be calculated from the equations in Table I by replacing the machine reactances by the total reactances in the various sequence networks. In calculating the loss torques (R_2-R_1) will remain unchanged but R_1 in the calculation of the stator loss must be replaced by (R_1+R_e). In the factor A, R_a is replaced by (R_a+R_e') where R_e' is the d-c resistance per phase of the external impedance.

If the external impedance is predominantly resistance of a large enough magnitude to affect the fault current, the time constants of the fundamental-frequency torque and the unidirectional torque resulting from the flow of fundamental-frequency current in the rotor will be very low (in the order of one or two cycles or less). In most cases these components may be neglected in calculating shaft stresses. The stator loss, which will be quite high, has time constants which are determined by the decay of rotor flux, and for external resistances in the order of subtransient reactance the rotor time constants are but little affected by the presence of the external resistance. The methods which have been presented in Appendixes II and III can be extended to the calculation of faults containing appreciable resistance by the inclusion of the resistance in the sequence networks. This type of fault is of importance in those types of mechanical systems where the contribution of the unidirectional torque to shaft torque is appreciable. This is discussed at greater length in a companion paper.[10]

Short Circuits From Load

It is more probable for a short circuit to occur from load than from no load, but for this condition the equations of Table I can be applied by making several approximations. The alternating components of torque can be calculated fairly accurately by using the derived equations with the voltage behind subtransient reactance. When the short circuit is three phase, the entire external load is dropped and the only unidirectional torque will be that given by the equations in Table I. This is also true in the case of a double-line-to-ground fault on a machine with very low zero-sequence reactance.

Assuming a static load, the machine will rapidly drop about a half load on a line-to-line fault. In this case, the total unidirectional torque on the machine is the sum of the loss torque plus half the initial load on the machine. On a line-to-ground fault, the amount of load dropped will depend upon the zero-sequence reactance of the machine but may be calculated by symmetrical components. The remaining load is then added to the loss torque to get the total unidirectional torque. In both of these cases, the load which the machine carries will have a decrement equal to the decrement of the ohmic loss in the machine. In a companion paper[10] the effect of short circuiting the machine from load is discussed in relation to the resultant stresses.

Synchronizing

If a machine is synchronized considerably out of phase with a low-reactance system, the resulting torques may reach values greater than those encountered during a short circuit. If the synchronizing takes place with all three circuit-breaker poles closing at the same in-

Table III

Type of Short Circuit	Unidirectional Torque	Sin ($\omega t+\alpha$)	Cos ($\omega t+\alpha$)	Sin 2($\omega t+\alpha$)
Three phase, $R_e=0$	$1.54\epsilon^{-7.92t}$	$10.3\epsilon^{-10.3t}$	Negligible	0
Three phase, $R_e=0.01$	$1.57\epsilon^{-10.3t}+1.03\epsilon^{-78t}$	$10.3\epsilon^{-48.5t}$	Negligible	0
Line to line, $R_e=0$, $\alpha=0°$	$2.07\epsilon^{-6.32t}$	$10.4\epsilon^{-8.93t}$	Negligible	$-5.18\epsilon^{-5.66t}$
Line to line, $R_e=0.01$, $\alpha=0°$	$1.58\epsilon^{-6.38t}+1.03\epsilon^{-78t}$	$10.4\epsilon^{-46.0t}$	Negligible	$-5.18\epsilon^{-5.66t}$
Line to ground, $R_e=0$, $\alpha=0°$	$1.88\epsilon^{-7.62t}$	$9.50\epsilon^{-8.26t}$	Negligible	$-4.75\epsilon^{-8.34t}$
Line to ground, $R_e=0.01$, $\alpha=0°$	$1.66\epsilon^{-8.10t}+0.89\epsilon^{-107t}$	$9.50\epsilon^{-62t}$	Negligible	$-4.75\epsilon^{-5.34t}$
Double line to ground, $R_e=0$, $\alpha=0°$	$1.77\epsilon^{-8.06t}$	$10.4\epsilon^{-8.61t}$	Negligible	$-1.39\epsilon^{-9.08t}$
Double line to ground, $R_e=0.01$ $\alpha=0°$,	$2.14\epsilon^{-9.02t}+1.02\epsilon^{-27.6t}$	$10.4\epsilon^{-47.7t}$	Negligible	$-1.39\epsilon^{-9.03t}$
Double line to ground, $R_e=0$ $\alpha=90°$,	$1.33\epsilon^{-13.5t}$	Negligible	$-7.54\epsilon^{-13.3t}$	$-1.39\epsilon^{-9.03t}$

Machine constant	X_d''	X_d'	X_d	X_2	X_0	T_{d0}''	T_{d0}'	R_1	R_2	R_a
Value (per unit)	0.097	0.152	1.170	0.096	0.0177	0.055 sec	6.65 sec	0.00480	0.0250	0.00105

stant, there will exist unidirectional synchronizing and loss torques and, in addition, a fundamental-frequency torque resulting from the trapped armature flux. However, if only two of the poles close (the other pole not closing at all), there will be, in addition to the above torques, a double-frequency torque developed by the negative-sequence armature current.

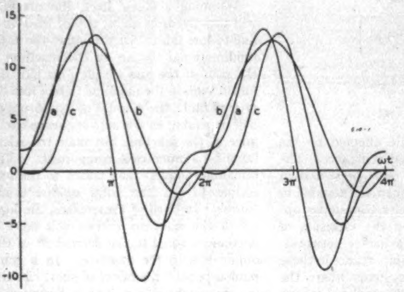

Figure 1. Short-circuit and synchronizing torques

(a). Line-to-line short circuit, $\alpha = 0°$

(b). Three-phase synchronizing, $\delta = 90°$, $X_s = X_d''$

(c). Single-phase synchronizing, $\delta = 90°$, $\alpha = 135°$, $\beta = 45°$, $X_s = X_d''$

Because of the complexity of the synchronizing problem, additional simplifying assumptions have been made to supplement those already made.

For faulty synchronizing, the loss torque is generally much less than the synchronizing torques and may be neglected.

If synchronization takes place with the machine either leading or lagging the system, the armature current will have a direct axis component which will tend to demagnitize the main poles causing the direct axis rotor flux to decay. This results in the problem of calculating the current in a circuit having one voltage fixed (the source) and one voltage varying with time (the internal machine voltage). Since, in a great many mechanical systems, the maximum stresses are reached in the first or second cycle, the problem can be greatly simplified by neglecting the rotor decrements.

Finally, it is assumed that the angle between the system and machine remains sufficiently unchanged during the first two or three cycles to permit the calculation of the synchronizing currents without having to take into account the oscillation of the machine with respect to the system.

In Appendix IV the synchronizing-torque equation is derived on the above assumptions for single-phase synchronizing. The torque equations presented in Table II are applicable to only the first two or three cycles of the synchronization. If it is desired to calculate the torque beyond two or three cycles, the decrements of rotor flux may be included as shown under short-circuit torques.

Illustrations

In Table III there are listed the various torque components for a typical turbine generator short-circuited from no load. The tabulation includes short circuits with and without an external resistance of 0.01 per unit. The field-decrement factor was calculated using an average decrement which gave the correct initial and sixth-cycle values. This is pessimistic but, as shown by McCann, Warren, and Criner,[10] the shaft torques are but slightly affected using this approximation. In those cases where the fault was through an external resistance, the loss torques contained two components with such widely different decrements that they were not combined as above.

In Figure 1 there are shown the electrical torques for a line-to-line short circuit and two conditions of synchronizing. Although the three-phase synchronizing torque does not reach as high a peak as the line-to-line short-circuit torque, its components are only unidirectional and fundamental-frequency ones. These components will produce much more serious shaft stress than would second-harmonic torque. As shown in Figure 2 (which was plotted for the same machine as in Table III) synchronizing considerably out of phase is especially dangerous. The peak shaft torque will be approximately proportional to the peak electrical torque. All other conditions being equal, the electrical torque for single-phase synchronizing (only two poles closing) is not as severe as for three-phase synchronizing.

Conclusions

As a result of the analysis made in this paper the following conclusions can be drawn regarding the various factors affecting transient torques in synchronous machines.

Short circuits on low-reactance turbine generators will produce electrical torques acting on the rotor which may reach peaks of 15 to 20 times normal torque.

The effect of external resistance during a fault is twofold, the unidirectional torque is increased, and the decrement of the fundamental-frequency torque is also increased. This may, or may not, result in increased shaft stress, depending upon the masses and spring constants of the turbine generator.

The negative-sequence resistance of the machine is a very important constant in determining the unidirectional torque during unbalanced faults. At the present time this constant is not known very accurately for values of rotor current in the order of short-circuit currents.

Synchronizing out of phase can produce electrical torques in excess of those encountered during short circuit. This is especially true for low-reactance machines connected to low-reactance systems.

Appendix I. List of Symbols

Per phase machine constants (all constants are per unit unless noted otherwise):

X_d''—Direct-axis subtransient reactance
X_d'—Direct-axis transient reactance
X_d—Direct-axis synchronous reactance
X_2—Negative-sequence reactance
X_0—Zero-sequence reactance
L—Self-leakage inductance of any stator phase
M—Mutual inductance between any two stator phases
R_1—Positive-sequence resistance

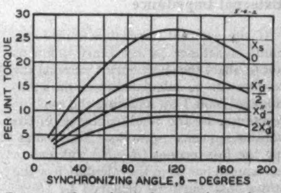

Figure 2. Crest electrical torque during three-phase synchronizing as a function of synchronizing angle and system reactance

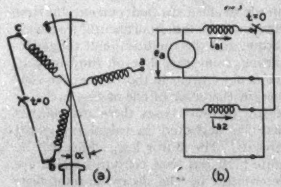

Figure 3. Line-to-line short circuit on a synchronous machine

R_2—Negative-sequence resistance
R_a—D-c resistance of stator
T_{do}''—Subtransient-open-circuit time constant in direct axis—seconds
T_{do}'—Transient-open-circuit time constant in direct axis—seconds

Machine and system quantities (per unit unless noted otherwise):

e—Instantaneous machine (or system) voltage
i—Instantaneous-phase current
E—Effective machine (or system) voltage
X_s—System reactance
R_e—External resistance
α, β, δ—Angles defined in Tables I and II
f—Fundamental frequency in cycles per second
ω—$2\pi f$
t—Time in seconds after the initiation of the circuit transient

Appendix II. Line-to-Line Short Circuit

During a line-to-line short circuit, Figure 3a, the alternating armature currents can be calculated by using the method of symmetrical components. With the positive- and negative-sequence networks connected as shown in Figure 3b, the sequence components of armature current can be determined, and from these the armature current.

The instantaneous voltage of phase a before the short circuit is

$$e_a = E\cos(\omega t+\alpha)$$

This voltage is proportional to the rotor flux, which, after the short circuit, decays because of the demagnetizing effect of the armature current. The decrement factor for this flux has been derived by Doherty and Nickle and is

$$F=\frac{X_d''+X_2}{X_d+X_2}+\frac{(X_d''+X_2)(X_d-X_d')\epsilon^{-\frac{t}{T_{do}'}\frac{X_d+X_2}{X_d'+X_2}}}{(X_d'+X_2)(X_d+X_2)}+\frac{(X_d'-X_d'')\epsilon^{-\frac{t}{T_{do}''}\frac{X_d'+X_2}{X_d''+X_2}}}{(X_d'+X_2)} \quad (1)$$

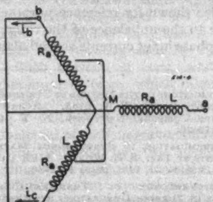

Figure 4. Flow of direct current in the armature of a synchronous machine during a double-line-to-ground fault

$$L \doteq \frac{1}{3}[X_d''+X_2+X_0] \text{ in per unit}$$

$$M \doteq \frac{1}{6}[X_d''+X_2-2X_0] \text{ in per unit}$$

The a-c symmetrical components of current are

$$i_{a1}=-i_{a2}=\frac{EF\sin(t+\alpha)}{(X_d''+X_2)} \text{ instantaneous per unit amperes} \quad (2)$$

From these, the alternating phase currents are

$$i_b=-i_c=\frac{-\sqrt{3}EF\cos(t+\alpha)}{(X_d''+X_2)} \text{ instantaneous per unit amperes} \quad (3)$$

At zero time, the phase current must be zero, therefore, there is in each phase a d-c component of current which has a decrement determined by the armature circuit.

The total phase currents are

$$i_b=-i_c=\frac{\sqrt{3}E}{(X_d''+X_2)}[A-F\cos(\omega t+\alpha)] \quad (4)$$

where

$$A=(\cos\alpha)\epsilon^{-2\pi f\frac{2R_a}{X_d''+X_2}t} \quad (5)$$

The power transferred across the air gap can be determined by taking the sum of the instantaneous products of the phase currents and phase voltages.

$$P=\frac{2}{3}[i_ae_a+i_be_b+i_ce_c] \quad (6)$$

$$P=\frac{2}{3}[0+i_b(e_b-e_c)]=\frac{2}{3}\frac{\sqrt{3}E}{(X_d''+X_2)}\times [A-F\cos(\omega t+\alpha)]\sqrt{3}EF\sin(\omega t+\alpha) \quad (7)$$

$$P=\frac{E^2}{(X_d''+X_2)}[2AF\sin(\omega t+\alpha)-F^2\times \sin 2(\omega t+\alpha)] \quad (8)$$

In per unit, the torque acting in the rotor is equal to the power transferred across the air gap.

The unidirectional torque acting on the rotor can be written as the sum of the a-c ohmic losses in the machine. The initial unidirectional field has twice the value that the initial negative-sequence field has, resulting in equal induced rotor voltages. Since the impedance of the solid rotor varies very closely as the square root of frequency, the fundamental-frequency rotor currents are $\sqrt{2}$ times the second-harmonic rotor currents. Because of the effect of rotor saturation on the depth of current penetration in the rotor, the rotor losses vary as the 1.8 power of the rotor current.

The a-c ohmic losses in the machine are

$$P_L=2\left[\frac{EF}{X_d''+X_2}\right]^{1.8}(R_2-R_1)+\sqrt{2}\left[\frac{\sqrt{2}EA}{X_d''+X_2}\right]^{1.8}(R_2-R_1)+2\left[\frac{EF}{X_d''+X_2}\right]^2R_1 \quad (9)$$

The total torque acting on the rotor is

$$T=\frac{E^2}{(X_d''+X_2)}[2FA\sin(\omega t+\alpha)-F^2\sin 2(\omega t+\alpha)]+2\left[\frac{EF}{X_d''+X_2}\right]^{1.8}\times(R_2-R_1)+\sqrt{2}\left[\frac{\sqrt{2}EA}{X_d''+X_2}\right]^{1.8}(R_2-R_1)+2\left[\frac{EF}{X_d''+X_2}\right]^2R_1 \quad (10)$$

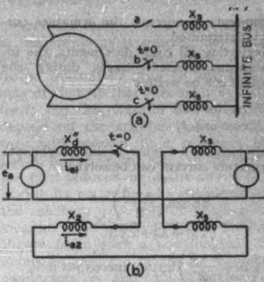

Figure 5. Single-phase synchronizing

Appendix III. Armature Decrements During Double-Line-to Ground Fault

The machine windings have approximately the self-leakage and mutual reactances shown in Figure 4.

The differential equations for the direct armature currents can be written as follows:

$$\begin{cases}(R_a+Lp)i_b-(Mp)i_c=0 & (11)\\ -(Mp)i_b+(R_a+Lp)i_c=0 & (12)\end{cases}$$

from which the determinental equation can be written

$$D(p)=(R_a+Lp)^2-(Mp)^2=0 \quad (13)$$

The roots of this equation will give the decrements of the d-c components of armature current. They are

$$p_1=-\frac{R_a}{(L+M)}=-\frac{2R_a}{X_d''+X_2} \text{ in per unit} \quad (14)$$

$$p_2=-\frac{R_a}{(L-M)}=-\frac{6R_a}{X_d''+X_2+4X_0} \text{ in per unit} \quad (15)$$

Converting to second instead of per unit time measure, the direct currents generally will have the following forms

$$i_b=A_1\epsilon^{-2\pi f\frac{2R_a}{X_d''+X_2}t}+A_2\epsilon^{-2\pi f\frac{6R_a}{X_d''+X_2+4X_0}t} \quad (16)$$

$$i_c=A_3\epsilon^{-2\pi f\frac{2R_a}{X_d''+X_2}t}+A_4\epsilon^{-2\pi f\frac{6R_a}{X_d''+X_2+4X_0}t} \quad (17)$$

where the constants can be determined by initial conditions.

Appendix IV. Single-Phase Synchronizing Out of Phase

During single-phase synchronizing, Figure 5a, the sequence components of armature currents can be found by connecting the sequence networks as in Figure 5b. From the positive- and negative-sequence components of current, the armature current is determined.

Neglecting all rotor decrements, the instantaneous phase voltages during the transient can be written

$$e_a = E\cos(\omega t+\alpha)$$
$$e_b = E\cos(\omega t+\beta)$$

from which the a-c symmetrical components of armature current can be solved.

$$i_{a1} = -i_{a2} = \frac{2E\sin\left(\frac{\alpha-\beta}{2}\right)}{(X_d''+X_2+2X_s)}\times \cos\left(\omega t+\frac{\alpha+\beta}{2}\right) \text{instantaneous per unit amperes} \quad (18)$$

The alternating phase currents are

$$i_b = -i_c = \frac{2\sqrt{3}\,E\sin\left(\frac{\alpha-\beta}{2}\right)}{(X_d''+X_2+2X_s)}\times \sin\left(\omega t+\frac{\alpha+\beta}{2}\right) \quad (19)$$

Since the currents must start from zero, there is a d-c component present in the current. The total phase currents are therefore

$$i_b = -i_c = \frac{2\sqrt{3}E\sin\left(\frac{\alpha-\beta}{2}\right)}{(X_d''+X_2+2X_s)}\times \left[\sin\left(\omega t+\frac{\alpha+\beta}{2}\right)-\sin\left(\frac{\alpha+\beta}{2}\right)\right] \quad (20)$$

The instantaneous power is

$$P = \frac{2}{3}\left[i_ae_a+i_be_b+i_ce_c\right] \quad (21)$$

$$P = \frac{2}{3}\left[i_b(e_b-e_c)\right] = \frac{2}{3}\cdot\frac{2\sqrt{3}E\sin\left(\frac{\alpha-\beta}{2}\right)}{(X_d''+X_2+2X_s)}\times \left[\sin\left(\omega t+\frac{\alpha+\beta}{2}\right)-\sin\left(\frac{\alpha+\beta}{2}\right)\right]\times \sqrt{3}E\sin(\omega t+\alpha) \quad (22)$$

Since in per unit the rotor torque is equal to the power transferred across the gap

$$T = P = \frac{E^2\sin\delta}{(X_d''+X_2+2X_s)}\left[1-\cos 2(\omega t+\alpha)-\tan\frac{\delta}{2}\sin 2(\omega t+\alpha)-2\frac{\sin\left(\frac{\alpha+\beta}{2}\right)}{\cos\left(\frac{\alpha-\beta}{2}\right)}\times \sin(\omega t+\alpha)\right] \quad (23)$$

where

$$\delta = (\alpha-\beta) \quad (24)$$

References

1. Definition of an Ideal Synchronous Machine and Formula for the Armature Flux Linkages, R. H. Park. *General Electric Review*, volume 31, 1928, pages 332–4.

2. Single-Phase Short-Circuit Torque of a Synchronous Machine, C. A. Nickle, C. A. Pierce, M. L. Henderson. AIEE Transactions, volume 51, 1932, pages 966–71.

3. Transient Torques in Synchronous Machines, L. A. Kilgore, M. Stone. AIEE Transactions, volume 52, 1933, pages 945–52.

4. Determination of Short-Circuit Torques in Turbine Generators by Test, E. C. Whitney, H. E. Criner. AIEE Transactions, volume 59, 1940, pages 885–9.

5. Two-Reaction Theory of Synchronous Machines, Generalized Method of Analysis—Part I, R. H. Park. AIEE Transactions, volume 48, 1929, pages 716–27.

6. Synchronous Machines—V, Three-Phase Short Circuit of Synchronous Machines, R. E. Doherty, C. A. Nickle. AIEE Transactions, volume 49, 1930, pages 700–14.

7. Synchronous Machines—IV, Single-Phase Short Circuits, R. E. Doherty, C. A. Nickle. AIEE Transactions, volume 47, 1928, pages 457–87.

8. Applications of the Method of Symmetrical Components (book), W. V. Lyon. McGraw-Hill Publishing Company, New York, N. Y., 1937, pages 412–20.

9. Determination of Synchronous Machine Constants by Test, S. H. Wright. AIEE Transactions, volume 31, 1931, pages 1331–50.

10. Determination of Transient Shaft Torques in Turbine Generators by Means of the Electrical–Mechanical Analogy, G. D. McCann, C. E. Warren, H. E. Criner. AIEE Transactions, volume 64, 1945, February section, pages 51–6.

11. Short-Circuit Torques in Synchronous Machines Without Damper Windings, G. W. Penney. AIEE Transactions, volume 48, 1929, pages 1230–40.

12. Double-Line-to-Neutral Short Circuit of an Alternator, J. B. Smith, C. N. Weygandt. AIEE Transactions, volume 56, 1937, pages 1149–55.

Measurement of the Subtransient Impedances of Synchronous Machines

GORDON F. TRACY
ASSOCIATE AIEE

WILLIAM F. TICE
NONMEMBER AIEE

A METHOD of measuring the direct-axis and the quadrature-axis subtransient impedances of a synchronous motor or generator by impressing three-phase voltages on the machine at standstill is described in this paper. With respect to the two methods at present prescribed in the Test Code for Synchronous Machines and elsewhere,[1,2,3] the proposed method for measuring the subtransient impedances has the advantages that it does not involve the taking of oscillograms and the consequent uncertainties in their analyses, nor does it require that the rotor of the machine under test be set in certain definite positions. This latter requirement, called for in the single-phase test, is frequently troublesome, particularly if the machine is large. Moreover, as three-phase, rather than single-phase voltages are impressed, the measurements are made under conditions more nearly simulating those of normal operation

The proposed method consists, briefly, of making two tests on the machine at standstill with the rotor in any position whatsoever. In the first test a three-phase voltage is impressed on the stator terminals and appropriate instrument readings are taken from which the positive-sequence and negative-sequence components of both the voltage and the current are obtained. In the second test a single-phase alternating voltage is applied to the field terminals with the stator terminals disconnected, readings being taken of the corresponding voltages induced in the stator. This latter test yields the angular position of the field structure with respect to the reference phase. The data obtained from these tests are then substituted into two equations, shown later in this paper as equations 37 and 38, which yield the subtransient impedances.

Development of the Equations

Rotor Magnetomotive Forces

The basic principles of this development were suggested by a paper on the calculation of the starting characteristics of synchronous motors by H. V. Putman.[4] The general case of a cylindrical rotor carrying an unbalanced two-phase winding and a stator carrying a balanced three-phase winding will first be discussed, then the treatment will be modified to apply to a synchronous machine.

In Figure 1a the conductors A and A' represent one phase of the rotor while B and B' represent the other phase. These two windings are assumed to be unbalanced, not only with respect to their impedances, but also with respect to the number of turns in each. In addition, the magnetic axes are not 90 degrees apart. The magnetic axis of stator phase a is also shown for reference purposes.

Due to the unbalance of the rotor, the three-phase input currents are unbalanced

---

Paper 45-12, recommended by the AIEE committee on electrical machinery for presentation at the AIEE winter technical meeting, New York, N. Y., January 22–26, 1945. Manuscript submitted October 30, 1944; made available for printing November 24, 1944.

G. F. Tracy is associate professor of electrical engineering, University of Wisconsin, Madison, Wis., and W. F. Tice is with the Barber-Colman Company, Rockford, Ill.

The authors wish to acknowledge the courtesy of S. H. Mortensen and his associates of the Allis-Chalmers Manufacturing Company in furnishing test data, and the assistance of C. G. Hagensick of the Westinghouse Electric and Manufacturing Company and former student at the University of Wisconsin in the preparation of data.

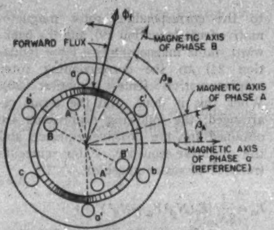

Figure 1a. Cylindrical-rotor machine with balanced three-phase stator and unbalanced two-phase rotor

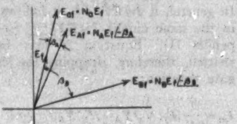
$E_{af}=N_aE_f$
$E_{Af}=N_AE_f\underline{/-\beta_A}$
E_f
β_A
β_B
$E_{Bf}=N_BE_f\underline{/-\beta_B}$

Figure 1b. Vector diagram showing relative phase positions of voltages due to forward flux

and are considered, therefore, to consist of a positive-sequence and a negative-sequence set of components. Corresponding to the positive-sequence currents is a forward-rotating magnetomotive force and air-gap flux, and corresponding to the negative-sequence currents is a backward-rotating magnetomotive force and air-gap flux. These two air-gap fluxes are considered to be constant in magnitude as they rotate, and, at standstill, they rotate forward and backward, respectively, at synchronous speed.

Two voltages, corresponding to the two components of air-gap flux, are induced in each rotor phase. Let E_{Af} be the voltage induced in phase A by the forward flux and E_{Ab} be that induced in phase A by the backward flux. Since the rotor circuits are closed each voltage produces a current. In phase A these currents will be designated by I_{Af} and I_{Ab}. Each current, in turn, sets up a magnetomotive force which alternates along the magnetic axis of the phase. Using a well-known analysis, the space fundamental of each magnetomotive force may be replaced by two component traveling space sinusoids moving in opposite directions at synchronous speed, each having an amplitude equal to one-half of the peak amplitude of the original magnetomotive force. The vector expression for the forward-moving component of magnetomotive force due to I_{Af} is†

$$\boldsymbol{M}_{Af}' = -j\,0.9\,N_A\boldsymbol{I}_{Af}\underline{/\beta_A} \tag{1}$$

while that for the backward-moving component of magnetomotive force due to I_{Af} is

$$\boldsymbol{M}_{Af}'' = +j\,0.9\,N_A\hat{\boldsymbol{I}}_{Af}\underline{/\beta_A} \tag{2}$$

where

N_A = effective turns in phase A (including pitch and breadth factors).
$\boldsymbol{I}_{Af}$ = vector value* of I_{Af}.
$\hat{\boldsymbol{I}}_{Af}$ = conjugate of $\boldsymbol{I}_{Af}$.
β_A = angle of displacement of rotor phase A from the reference axis.

In equations 1 and 2, as well as all which follow, the single prime indicates a forward-rotating magnetomotive force and the double prime indicates a backward-rotating magnetomotive force. The subscripts refer to the current component producing the magnetomotive force; the first indicating the phase, and the second showing whether produced by the forward or the backward flux.

Two expressions, similar to equations 1 and 2, may be written for the magnetomotive force components due to current I_{Ab} in phase A corresponding to the backward flux. Likewise, four more expressions may be written for the magnetomotive force components due to the currents in phase B. There will be a total, therefore, of eight traveling waves of magnetomotive force, four moving forward along the air gap at synchronous speed and four moving backward at synchronous speed.

Before finding the resultant magnetomotive force it is convenient to express each current in terms of the corresponding voltage and the admittance of the circuit on which the voltage acts. Since, in general,

$$\boldsymbol{I} = \boldsymbol{E}\boldsymbol{Y} \tag{3}$$

and**

$$\hat{\boldsymbol{I}} = \hat{\boldsymbol{E}}\hat{\boldsymbol{Y}} \tag{4}$$

equations 1 and 2 become

$$\boldsymbol{M}_{Af}' = -j\,0.9\,N_A\boldsymbol{E}_{Af}\boldsymbol{Y}_A\underline{/\beta_A} \tag{5}$$

$$\boldsymbol{M}_{Af}'' = +j\,0.9\,N_A\hat{\boldsymbol{E}}_{Af}\hat{\boldsymbol{Y}}_A\underline{/\beta_A} \tag{6}$$

The two components of phase A magnetomotive force corresponding to the backward flux are

$$\boldsymbol{M}_{Ab}' = -j\,0.9\,N_A\boldsymbol{E}_{Ab}\boldsymbol{Y}_A\underline{/\beta_A} \tag{7}$$

$$\boldsymbol{M}_{Ab}'' = +j\,0.9\,N_A\hat{\boldsymbol{E}}_{Ab}\hat{\boldsymbol{Y}}_A\underline{/\beta_A} \tag{8}$$

The four components of phase B magnetomotive force are

$$\boldsymbol{M}_{Bf}' = -j\,0.9\,N_B\boldsymbol{E}_{Bf}\boldsymbol{Y}_B\underline{/\beta_B} \tag{9}$$

$$\boldsymbol{M}_{Bf}'' = +j\,0.9\,N_B\hat{\boldsymbol{E}}_{Bf}\hat{\boldsymbol{Y}}_B\underline{/\beta_B} \tag{10}$$

$$\boldsymbol{M}_{Bb}' = -j\,0.9\,N_B\boldsymbol{E}_{Bb}\boldsymbol{Y}_B\underline{/\beta_B} \tag{11}$$

$$\boldsymbol{M}_{Bb}'' = +j\,0.9\,N_B\hat{\boldsymbol{E}}_{Bb}\hat{\boldsymbol{Y}}_B\underline{/\beta_B} \tag{12}$$

Since the forward flux, ϕ_f, is constant in magnitude as it rotates, the voltage induced by it in any turn of any winding (rotor or stator) will be identical in magnitude with that induced in any other turn; but the phase of the voltage will depend on the angular position of the turn with respect to a reference axis. Let $\boldsymbol{E}_f$ be the vector value of the voltage *per turn* induced by ϕ_f in any winding having its magnetic axis coincident with the reference axis. Stator phase a is so located. The forward flux is shown in Figure 1a in such a position that it is about to generate maximum voltage in conductors a and a'. Therefore the vector $\boldsymbol{E}_f$, Figure 1b, will be nearly vertical at this instant. Later in time, when the forward flux has moved through β_A degrees, maximum voltage will be generated in rotor phase A. Hence the vector $\boldsymbol{E}_{Af}$ lags $\boldsymbol{E}_f$ by β_A degrees. Likewise $\boldsymbol{E}_{Bf}$ lags $\boldsymbol{E}_f$ by β_B degrees. The magnitude of each is equal to that of $\boldsymbol{E}_f$ multiplied by the respective number of turns. The voltages due to the forward flux, expressed in terms of $\boldsymbol{E}_f$ are

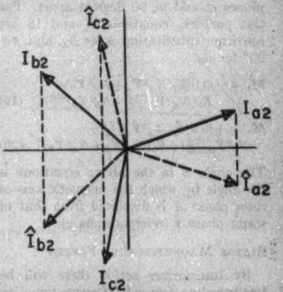

Figure 2. Relations between the negative-sequence currents and their conjugates

$$\boldsymbol{E}_{Af} = N_A\boldsymbol{E}_f\underline{/-\beta_A} \tag{13}$$

$$\boldsymbol{E}_{Bf} = N_B\boldsymbol{E}_f\underline{/-\beta_B} \tag{14}$$

Similarly,

$$\boldsymbol{E}_{Ab} = N_A\boldsymbol{E}_b\underline{/+\beta_A} \tag{15}$$

$$\boldsymbol{E}_{Bb} = N_B\boldsymbol{E}_b\underline{/+\beta_B} \tag{16}$$

where $\boldsymbol{E}_b$ is the vector value of the voltage per turn induced by the backward flux in any winding having its magnetic axis coincident with the reference axis.

The resultant forward rotor magnetomotive force is the vector sum of equations 5, 7, 9, and 11, and this sum is shown below after appropriate substitution of equations 13 to 16.

$$\begin{aligned}\boldsymbol{M}_r' = -j\,0.9\,[&\boldsymbol{E}_f(N_A^2\boldsymbol{Y}_A+N_B^2\boldsymbol{Y}_B)+\\ &\boldsymbol{E}_b(N_A^2\boldsymbol{Y}_A\underline{/2\beta_A}+N_B^2\boldsymbol{Y}_B\underline{/2\beta_B})]\end{aligned} \tag{17}$$

Similarly, the resultant backward rotor

---

† See Appendix I for the derivation of equations 1 and 2.

* A vector quantity is designated by a bold-face symbol and a conjugate is designated by a circumflex over the symbol.

** See Appendix II for verification of equation 4.

magnetomotive force is the vector sum of equations 6, 8, 10, and 12, which, upon substitution of equations 13 to 16, yields:

$$\boldsymbol{M}_r'' = +j\,0.9[\hat{\boldsymbol{E}}_f(N_A^2\hat{\boldsymbol{Y}}_A\underline{/2\beta_A} + N_B^2\hat{\boldsymbol{Y}}_B\underline{/2\beta_B}) + \hat{\boldsymbol{E}}_b(N_A^2\hat{\boldsymbol{Y}}_A + N_B^2\hat{\boldsymbol{Y}}_B)] \quad (18)$$

It is to be observed, in making the substitutions leading to equation 18, that the conjugate of $\boldsymbol{E}_f\underline{/-\beta_A}$ is $\hat{\boldsymbol{E}}_f\underline{/+\beta_A}$; that is, the reversal in sign applies not only to the angle included in the vector $\boldsymbol{E}_f$ but also to the attached angle $-\beta_A$.

While equations 17 and 18 are written for a rotor with only two phases, it is evident that they may be made to apply to a rotor with any number of phases by adding terms of the form $N_c^2\boldsymbol{Y}_c$, $N_c^2 \times \boldsymbol{Y}_c\underline{/2\beta_c}$, and so forth. In applying this analysis to a synchronous machine, however, where phase A is to represent the direct-axis circuits and phase B the quadrature-axis circuits, only two phases are necessary, and the magnetic axes of these phases should be 90 degrees apart. For this purpose, equations 17 and 18 are rewritten substituting β for β_A, and $\beta + 90°$ for β_B.

$$\boldsymbol{M}_r' = -j0.9[\boldsymbol{E}_f(N_A^2\boldsymbol{Y}_A + N_B^2\boldsymbol{Y}_B) + \boldsymbol{E}_b(N_A^2\boldsymbol{Y}_A\underline{/2\beta} - N_B^2\boldsymbol{Y}_B\underline{/2\beta})] \quad (19)$$

$$\boldsymbol{M}_r'' = +j0.9[\hat{\boldsymbol{E}}_f(N_A^2\hat{\boldsymbol{Y}}_A\underline{/2\beta} - N_B^2\hat{\boldsymbol{Y}}_B\underline{/2\beta}) + \hat{\boldsymbol{E}}_b(N_A^2\hat{\boldsymbol{Y}}_A + N_B^2\hat{\boldsymbol{Y}}_B)] \quad (20)$$

The angle β in the above equations is the angle by which the magnetic axis of rotor phase A is displaced from that of stator phase a (reference phase).

STATOR MAGNETOMOTIVE FORCES

By transformer action there will be two traveling sinusoids of magnetomotive force produced by the stator, a forward-moving magnetomotive force corresponding to $\boldsymbol{M}_r'$ and a backward-moving magnetomotive force corresponding to $\boldsymbol{M}_r''$. Since the stator windings are three-phase symmetrical windings, each traveling sinusoid is produced by a set of *balanced* currents in the stator windings; the first set being the positive-sequence set, and the second, the negative-sequence set.

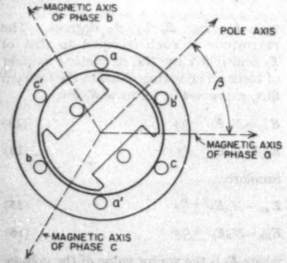

Figure 3. Synchronous machine with its pole axis displaced β degrees from the axis of phase a

Using the expressions for magnetomotive force as a space vector from Appendix I, the forward-rotating magnetomotive-force wave due to the positive-sequence currents in the stator is

$$\boldsymbol{M}_s' = -j0.9(N_a\boldsymbol{I}_{a1}\underline{/0°} + N_b\boldsymbol{I}_{b1}\underline{/120°} + N_c\boldsymbol{I}_{c1}\underline{/240°}) \quad (21)$$

The angles shown in equation 21 express the direction in *space* of the magnetic axes of the three phases. In equation 21 substitute $\boldsymbol{I}_{b1} = \boldsymbol{I}_{a1}\underline{/-120°}$, and $\boldsymbol{I}_{c1} = \boldsymbol{I}_{a1}\underline{/-240°}$; also $N_a = N_b = N_c = N_s$ (effective stator turns per phase). Then

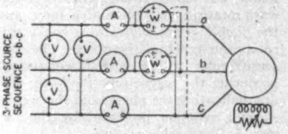

Figure 4. Connection diagram for test I

$$\boldsymbol{M}_s' = -j0.9(3N_s\boldsymbol{I}_{a1}) \quad (22)$$

The negative-sequence currents produce a backward magnetomotive force:

$$\boldsymbol{M}_s'' = +j0.9N_s(\hat{\boldsymbol{I}}_{a2}\underline{/0°} + \hat{\boldsymbol{I}}_{b2}\underline{/120°} + \hat{\boldsymbol{I}}_{c2}\underline{/240°}) \quad (23)$$

Since the conjugates of the currents are involved (see Figure 2)

$$\hat{\boldsymbol{I}}_{b2} = \hat{\boldsymbol{I}}_{a2}\underline{/-120} \text{ and } \hat{\boldsymbol{I}}_{c2} = \hat{\boldsymbol{I}}_{a2}\underline{/-240}$$

$$\therefore \boldsymbol{M}_s'' = j0.9(3N_s\hat{\boldsymbol{I}}_{a2}) \quad (24)$$

Expressions 22 and 24 are similar to the familiar expression for the peak height of the fundamental of armature magnetomotive force of a three-phase winding, with the exception that 22 and 24 show not only the magnitudes but also the space positions of the peaks with respect to the magnetic axis of phase a.

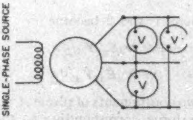

Figure 5. Connection diagram for test II

A development, similar to that above, for the backward component of magnetomotive force due to the positive-sequence currents, and the forward component due to the negative-sequence currents, would yield zero in each case, as would be expected.

STATOR-CURRENT EQUATIONS

The next step is to equate the forward stator magnetomotive force (equation 22) to the corresponding rotor magnetomotive force (equation 19), and the backward stator magnetomotive force (equation 24) to the corresponding rotor magnetomotive force (equation 20). When this is done, and the terms rearranged, the following expressions are obtained for the positive-sequence and the negative-sequence stator currents (referred to stator phase a):

$$\boldsymbol{I}_{a1} = \frac{1}{3N_s}[\boldsymbol{E}_f(N_A^2\boldsymbol{Y}_A + N_B^2\boldsymbol{Y}_B) + \boldsymbol{E}_b(N_A^2\boldsymbol{Y}_A - N_B^2\boldsymbol{Y}_B)\underline{/2\beta}] \quad (25)$$

$$\hat{\boldsymbol{I}}_{a2} = \frac{1}{3N_s}[\hat{\boldsymbol{E}}_f(N_A^2\hat{\boldsymbol{Y}}_A - N_B^2\hat{\boldsymbol{Y}}_B)\underline{/2\beta} + \hat{\boldsymbol{E}}_b(N_A^2\hat{\boldsymbol{Y}}_A + N_B^2\hat{\boldsymbol{Y}}_B)] \quad (26)$$

In general, if $\hat{\boldsymbol{I}} = \hat{\boldsymbol{E}}\hat{\boldsymbol{Y}}\underline{/+\delta}$, it follows that in the same circuit $\boldsymbol{I} = \boldsymbol{E}\boldsymbol{Y}\underline{/-\delta}$ (see appendix II). Equation 26 may be rewritten, therefore, dropping the conjugate notation:

$$\boldsymbol{I}_{a2} = \frac{1}{3N_s}[\boldsymbol{E}_f(N_A^2\boldsymbol{Y}_A - N_B^2\boldsymbol{Y}_B)\underline{/-2\beta} + \boldsymbol{E}_b(N_A^2\boldsymbol{Y}_A + N_B^2\boldsymbol{Y}_B)] \quad (26a)$$

Equations 25 and 26a can be simplified by multiplying both sides of each by $2/N_s$. The admittances now appear as

$$\frac{2}{3}\frac{N_A^2}{N_s^2}\boldsymbol{Y}_A \text{ and } \frac{2}{3}\frac{N_B^2}{N_s^2}\boldsymbol{Y}_B$$

These are seen to be the values of the two rotor admittances referred to the stator. A further simplification is effected if the magnetizing reactance of each rotor phase, considered as a susceptance, be combined vectorially with the corresponding expression for rotor admittance, as in the equivalent circuit of a transformer. In Figure 1a, where the air gap is uniform, the magnetizing reactance is the same for both phases; but in the synchronous machine, shown in Figure 3, the magnetizing reactance along the pole axis is much larger than that along the interpolar axis. Let $\boldsymbol{Y}_A'$ and $\boldsymbol{Y}_B'$ be the admittances of phases A and B, respectively, referred to the stator, it being understood that each includes its own magnetizing reactance. Then

$$\boldsymbol{I}_{a1} = \frac{N_s}{2}[\boldsymbol{E}_f(\boldsymbol{Y}_A' + \boldsymbol{Y}_B') + \boldsymbol{E}_b(\boldsymbol{Y}_A' - \boldsymbol{Y}_B')\underline{/2\beta}] \quad (27)$$

$$\boldsymbol{I}_{a2} = \frac{N_s}{2}[\boldsymbol{E}_f(\boldsymbol{Y}_A' - \boldsymbol{Y}_B')\underline{/-2\beta} + \boldsymbol{E}_b(\boldsymbol{Y}_A' + \boldsymbol{Y}_B')] \quad (28)$$

With $\boldsymbol{Y}_A'$ and $\boldsymbol{Y}_B'$ as defined above, $\boldsymbol{I}_{a1}$ and $\boldsymbol{I}_{a2}$ are the symmetrical components of the *total* input current including the magnetizing components.

THE STATOR-VOLTAGE EQUATIONS

Defining $\boldsymbol{V}_1$ and $\boldsymbol{V}_2$ to be the positive-sequence and the negative-sequence components, respectively, of the line-to-neutral voltage impressed on stator phase a, and Z_a to be the leakage impedance of phase a, then

$$V_1 = E_{af} + I_{a1}Z_a = N_sE_f + I_{a1}Z_a \tag{29}$$

$$V_2 = E_{ab} + I_{a2}Z_a = N_sE_b + I_{a2}Z_a \tag{30}$$

Solving for E_f and E_b from equations 27 and 28 and substituting in equations 29 and 30 yields

$$V_1 = I_{a1}\left(\frac{Y_A'+Y_B'}{2Y_A'Y_B'}+Z_a\right)+ I_{a2}\left(\frac{Y_B'-Y_A'}{2Y_A'Y_B'}\right)\underline{/2\beta} \tag{31}$$

$$V_2 = I_{a1}\left(\frac{Y_B'-Y_A'}{2Y_A'Y_B'}\right)\underline{/-2\beta}+ I_{a2}\left(\frac{Y_A'+Y_B'}{2Y_A'Y_B'}+Z_a\right) \tag{32}$$

But

$$\frac{Y_A'+Y_B'}{2Y_A'Y_B'}=\frac{1}{2}(Z_A'+Z_B')$$

and

$$\frac{Y_B'-Y_A'}{2Y_A'Y_B'}=\frac{1}{2}(Z_A'-Z_B')$$

Therefore

$$V_1 = I_{a1}\left(\frac{Z_A'+Z_B'}{2}+Z_a\right)+I_{a2}\left(\frac{Z_A'-Z_B'}{2}\right)\underline{/2\beta} \tag{33}$$

$$V_2 = I_{a1}\left(\frac{Z_A'-Z_B'}{2}\right)\underline{/-2\beta}+ I_{a2}\left(\frac{Z_A'+Z_B'}{2}+Z_a\right) \tag{34}$$

APPLICATION TO SYNCHRONOUS MACHINE

In the synchronous machine to which Figure 1a corresponds, phase A represents the field circuit and all damper-bar circuits having their magnetic axes coincident with the pole axis, while phase B represents all circuits having their magnetic axes in the interpolar axis. Equations 33 and 34 are in a form where the direct-axis impedance and the quadrature-axis impedance appear directly. The direct-axis subtransient impedance is

$$Z_d'' = Z_a + Z_A'$$

that is, Z_d'' is the sum of the stator leakage impedance and the impedance which rotor phase A represents (including its magnetizing reactance). Similarly, the quadrature-axis subtransient impedance is

$$Z_q'' = Z_a + Z_B'$$

Equations 33 and 34 now become

$$V_1 = I_{a1}\left(\frac{Z_d''+Z_q''}{2}\right)+I_{a2}\left(\frac{Z_d''-Z_q''}{2}\right)\underline{/2\beta} \tag{35}$$

$$V_2\underline{/2\beta} = I_{a1}\left(\frac{Z_d''-Z_q''}{2}\right)+I_{a2}\left(\frac{Z_d''+Z_q''}{2}\right)\underline{/2\beta} \tag{36}$$

The subscript a of I_{a1} and I_{a2} need not be carried further. By taking the sum and difference of equations 35 and 36, Z_d'' and Z_q'' are readily obtained:

$$Z_d'' = \frac{V_1+V_2\underline{/2\beta}}{I_1+I_2\underline{/2\beta}} \tag{37}$$

$$Z_q'' = \frac{V_1-V_2\underline{/2\beta}}{I_1-I_2\underline{/2\beta}} \tag{38}$$

Z_d'' and Z_q'' are expressed in terms of the symmetrical components of the voltage to neutral and of the line current in stator phase a (reference phase) and of the angle by which rotor phase A (that is, the pole axis of a synchronous machine) is displaced forward from the magnetic axis of phase a.

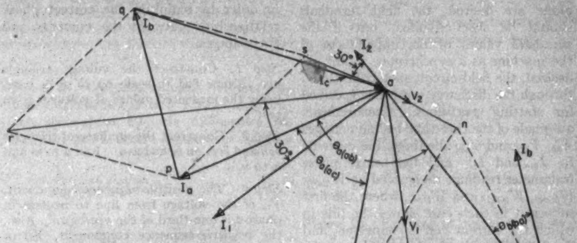

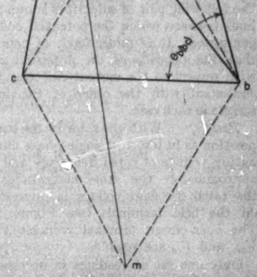

Figure 6a. Graphical solution for sequence components of voltages and currents

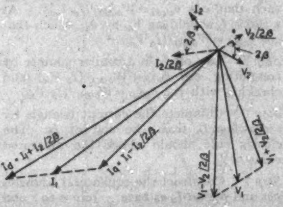

I_2
2β
$V_2\underline{/2\beta}$
2β
$I_2\underline{/2\beta}$
V_2
$I_d = I_1+I_2\underline{/2\beta}$
I_1
$I_q = I_1-I_2\underline{/2\beta}$
$V_1-V_2\underline{/2\beta}$
V_1
$V_1+V_2\underline{/2\beta}$

Figure 6b. Graphical procedure for evaluating numerators and denominators of equations 37 and 38

Determination of Angle β

The angle β is the angle by which the axis of rotor phase A (pole axis) is displaced from the magnetic axis of stator phase a. It is considered positive when the displacement is toward the magnetic axis of phase b; that is, in the direction in which the machine would rotate when the sequence of the impressed voltages is abc.

Assume that the field circuit in Figure 3 is excited with alternating current and that the flux distribution along the air gap is essentially sinusoidal and symmetrical about the pole axis. The voltage induced in phase a at standstill by transformer action will then be proportional to the cosine of the angle between the pole axis and the magnetic axis of phase a; that is, to the cosine of the angle β. Likewise, the voltage induced in phase b will be proportional to cos $(120-\beta)$ and that in phase c to cos $(120+\beta)$. Therefore

$$V_a = V\cos\beta$$
$$V_b = V\cos(120-\beta)$$
$$V_c = V\cos(120+\beta)$$

With a wye connection, the voltages between terminals will be

$$V_{ab} = V_a - V_b = V[\cos\beta - \cos(120-\beta)] = \sqrt{3}\,V\cos(\beta+30)$$

$$V_{bc} = V_b - V_c = V[\cos(120-\beta) - \cos(120+\beta)] = \sqrt{3}\,V\sin\beta$$

$$V_{ca} = V_c - V_a = V[\cos(120+\beta) - \cos\beta] = \sqrt{3}\,V\cos(\beta-30)$$

whence

$$\frac{V_{ab}}{V_{bc}} = \frac{\cos(\beta+30)}{\sin\beta} \tag{39}$$

$$\frac{V_{bc}}{V_{ca}} = \frac{\sin\beta}{\cos(\beta-30)} \tag{40}$$

$$\frac{V_{ca}}{V_{ab}} = \frac{\cos(\beta-30)}{\cos(\beta+30)} \tag{41}$$

These three ratios are plotted with respect to β in Figure 7; and, with the ratios computed from readings of the open-circuit voltages at the terminals, the value of β is readily obtained from the curves. Each ratio yields two values of β, one of which will be common to all three ratios. This common value is the true value of β.

Test Procedure

Test I. The connection diagram for this test is shown in Figure 4. With the field structure blocked in any position whatsoever, three-phase voltages are applied to the stator terminals, these voltages being of such a magnitude that approximately rated current flows in the stator. The sequence of these voltages must be *a–b–c*. If the subtransient impedances of the machine alone are desired, the field terminals should be short-circuited, but if the standstill values of the impedances of the machine as a synchronous motor are desired, the field circuit should be closed through the discharge resistance specified for starting conditions. Measurements are made of the three line-to-line voltages V_{ab}, V_{bc}, and V_{ca}, the three line currents I_a, I_b, and I_c; and four single-phase wattmeter readings designated as $W_{a(ab)}$, $W_{a(ac)}$, $W_{b(bc)}$, and $W_{b(ba)}$, where the first subscript in each case shows the line in which the current coil is connected, and the following pair of subscripts shows the lines between which the potential coil is connected. It is understood, of course, that the polarity of the potential coil with respect to the current coil must be consistent with the order of the subscripts in each case.

Test II. With the rotor in the same position as in test I, a single-phase alternating voltage of rated frequency and of approximately the same magnitude as the rated d-c field voltage is impressed on the field terminals (see Figure 5). The open-circuit terminal voltages V_{ab}, V_{bc}, and V_{ca} are read.

Only one set of readings is necessary in each of the two tests. If a check should be desired, the rotor may be moved to some other position (no particular position being necessary) and a second set of readings taken for both tests I and II.

Calculation Procedure

The vector values (referred to a common reference) of the sequence components of the voltages and currents of test I must be obtained for substitution in equations 37 and 38. Of the several methods available[5,6] one of the most direct is used without proof in the following calculation procedure, in which the diagram for the solution of the currents is superimposed on that for the voltages in order to maintain the correct phase relationships between the currents and the voltages.

Step 1. Construct the voltage triangle *abc* (Figure 6a) to scale on *cb* as a base, using the measured values of voltages from test I.

Step 2. Construct the equilateral triangles *bcn* and *bcm* on *bc* as base. Join *a* to *m* and *a* to *n*.

Step 3. The positive-sequence component, V_1, of the voltage from line to neutral in phase *a* is one-third of the vector *am*. Also, the negative-sequence component, V_2, of the voltage from line to neutral in phase *a* is one-third of the vector *an*.

Step 4. Lay off the current I_a to scale from point *a*, lagging *ab* by an angle $\theta_{a(ab)}$ such that $\cos \theta_{a(ab)} = W_{a(ab)}/(I_a V_{ab})$. As a check, I_a should lag V_{ac} by $\theta_{a(ac)}$ such that $\cos \theta_{a(ac)} = W_{a(ac)}/(I_a V_{ac})$.

Step 5. Lay off I_b in a similar manner by computing $\cos \theta_{b(bc)} = W_{b(bc)}/(I_b V_{bc})$ and checking with $\cos \theta_{b(ba)} = W_{b(ba)}/(I_b V_{ba})$.

Step 6. Complete the current triangle by redrawing I_b from the end of I_a. The closing side should check the measured value of I_c.

Step 7. Construct the equilateral triangles *pqr* and *pqs* on I_b as base. Join *a* to *r* and *a* to *s*.

Step 8. The positive-sequence component, I_1, of the current in line *a* is found by drawing a vector whose length is $1/\sqrt{3}$ times that of *ar* and which is rotated 30° counter clockwise from *ar*. The negative-sequence component, I_2, of the current in line *a* is found by drawing a vector whose length is $1/\sqrt{3}$ times that of *as* and which is rotated 30° clockwise from *as*.

Step 9. Calculate the three ratios V_{ab}/V_{bc}, V_{bc}/V_{ca}, and V_{ca}/V_{ab}, using data from test II.

Step 10. Read angle β from Figure 7. The three ratios will each yield two values of β, but the true value is that which is common to all three cases.

All the necessary information is now available for solving for Z_d'' and Z_q'' from equations 37 and 38. Each of the quantities V_1, V_2, I_1, and I_2 is a vector quantity and must carry its appropriate phase angle with respect to a common reference. The most reasonable common reference is the vector V_1. The magnitude of each vector is scaled from Figure 6a, and also its phase position with respect to the common reference. Equations 37 and 38 may then be solved by the usual procedures of complex algebra.

An alternative graphical procedure for evaluating the numerators and denominators of equations 37 and 38 is outlined in the following additional steps, and is illustrated in Figure 6b, in which the vectors V_1, V_2, I_1, and I_2 have been redrawn from Figure 6a.

Step 11. Rotate V_2 forward through 2β and add it to V_1. The resultant is the numerator of equation 37.

Step 12. Rotate V_2 forward through 2β and subtract it from V_1. The resultant is the numerator of equation 38.

Steps 13 and 14. Proceed as in steps 11 and 12 with the vector I_2. The resultant vectors are the denominators of equations 37 and 38.

It is obvious that Figure 6b may be combined with Figure 6a where the scale is sufficiently large to avoid undue complication.

A complete sample solution, using data from actual tests on a 7,500-kva machine, is shown in Figure 8. It will be observed that V_2 is negligible. This should be so in most cases. V_2 will be appreciable only when the machine under test has a value of Z_q'' widely different from Z_d'', and at the same time the machine being used as a source is relatively small or is feeding in its power through lines of relatively high impedance.

Experimental Verification

Several tests carried out on machines whose characteristics differed widely from one another showed that the values of Z_d'' and Z_q'' as found from equations 37 and 38 agreed satisfactorily with those found from the single-phase test as prescribed in the Test Code for Synchronous Machines. In most cases the corresponding values were within two or three per cent of each other. A second series of tests consisted of taking several sets of readings on each of three machines with the field structures blocked in many different positions in order to verify the

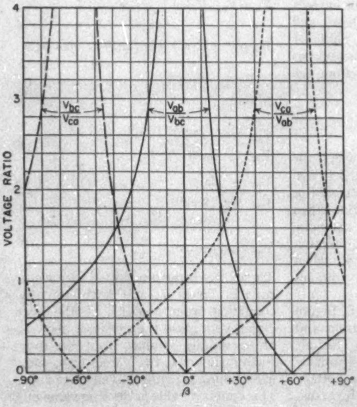

Figure 7. Curves for determining angle β of a wye-connected machine using data of test II

premise of the method that correct values of Z_d'' and Z_q'' can be found with the rotor in any position whatsoever. The results again were satisfactory, the greatest deviation from the mean value being about seven per cent. This corresponds to an error in the per unit value of impedance of about 0.03 on an average machine. In order to check the accuracy with which the angular displacement, β, of the field structure may be found by the use of the curves of Figure 7, a protractor scale was affixed to the end of the shaft in each case so that the displacement could be measured mechanically as well as electrically. The agreement in all tests was very good, the greatest difference between the values of the angle as found by the two methods being two and one-half electrical degrees.

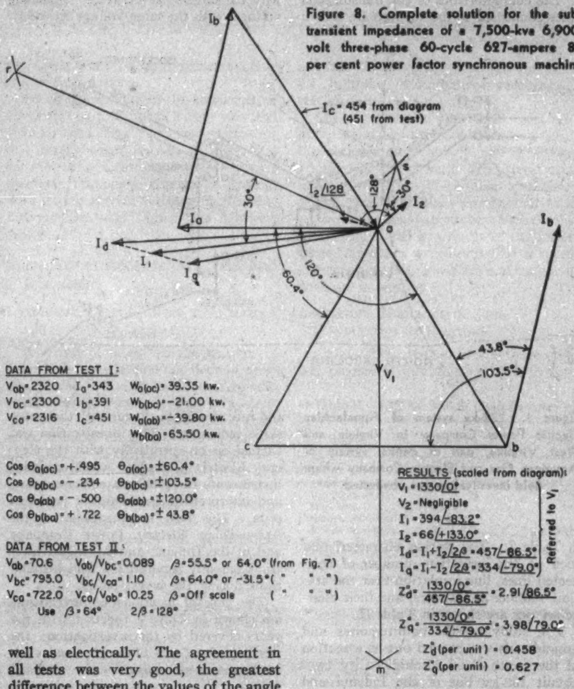
Figure 8. Complete solution for the subtransient impedances of a 7,500-kva 6,900-volt three-phase 60-cycle 627-ampere 80 per cent power factor synchronous machine

I_b
r
I_c = 454 from diagram
(451 from test)
s
$I_2\underline{/128}$
128°
30°
I_2
I_a
30°
I_d
I_1
I_q
o
120°
60.4°
I_b
43.8°
103.5°
V_1
c
b
m
DATA FROM TEST I:
V_{ab} = 2320 I_a = 343 $W_{a(ac)}$ = 39.35 kw.
V_{bc} = 2300 I_b = 391 $W_{b(bc)}$ = −21.00 kw.
V_{ca} = 2316 I_c = 451 $W_{a(ab)}$ = −39.80 kw.
$W_{b(ba)}$ = 65.50 kw.
Cos $\theta_{a(ac)}$ = +.495 $\theta_{a(ac)}$ = ±60.4°
Cos $\theta_{b(bc)}$ = −.234 $\theta_{b(bc)}$ = ±103.5°
Cos $\theta_{a(ab)}$ = −.500 $\theta_{a(ab)}$ = ±120.0°
Cos $\theta_{b(ba)}$ = +.722 $\theta_{b(ba)}$ = ±43.8°
DATA FROM TEST II:
V_{ab} = 70.6 V_{ab}/V_{bc} = 0.089 β = 55.5° or 64.0° (from Fig. 7)
V_{bc} = 795.0 V_{bc}/V_{ca} = 1.10 β = 64.0° or −31.5° (" " ")
V_{ca} = 722.0 V_{ca}/V_{ab} = 10.25 β = Off scale (" " ")
Use β = 64° 2β = 128°
RESULTS (scaled from diagram):
$V_1 = 1330\underline{/0°}$
V_2 = Negligible
$I_1 = 394\underline{/-83.2°}$
$I_2 = 66\underline{/+133.0°}$
$I_d = I_1 + I_2\underline{/2\beta} = 457\underline{/-86.5°}$
$I_q = I_1 - I_2\underline{/2\beta} = 334\underline{/-79.0°}$
Referred to V_1
$Z_d'' = \frac{1330\underline{/0°}}{457\underline{/-86.5°}} = 2.91\underline{/86.5°}$
$Z_q'' = \frac{1330\underline{/0°}}{334\underline{/-79.0°}} = 3.98\underline{/79.0°}$
Z_d''(per unit) = 0.458
Z_q''(per unit) = 0.627

Appendix I

Magnetomotive Force as a Space Vector

The magnetomotive force due to an alternating current in a concentrated coil on a cylindrical rotor, as in Figure 9, alternates up and down the magnetic axis of the coil, and has a peak height (with respect to time) at all points along the gap of $\sqrt{2}\,NI$, where N is the number of turns and I is the rms current. The fundamental of this "square wave" of magnetomotive force has a peak height, with respect to *time* and *space*, of $(\sqrt{2}\,NI)4/\pi$. For a distributed and short pitch winding the same expression holds provided N includes the breadth and pitch factors.

Using a well-known analysis, the alternating magnetomotive force may be replaced by two traveling space sinusoids, moving in opposite directions around the air gap at synchronous speed, the peak height (in space) of each being $(\sqrt{2}\,NI)2/\pi = 0.9NI$. In a two-pole machine there will be but one space cycle of each component of magnetomotive force. Let the two waves be represented by the vectors $\boldsymbol{M_f}$ and $\boldsymbol{M_b}$ each of which is considered to pass through the positive peak of the wave which it represents. At the instant that the current is zero the net magnetomotive force is zero; and, to represent this condition, the two vectors lie oppositely directed along a line perpendicular to the magnetic axis. At this same instant the conventional vector representing the current in the winding lies along the horizontal reference axis. A moment later, when the current vector has moved forward through α degrees, $\boldsymbol{M_f}$ will also have moved counterclockwise α degrees, and $\boldsymbol{M_b}$ will have moved clockwise α degrees, as shown in Figure 9. At this instant the vector expressions for $\boldsymbol{M_f}$ and $\boldsymbol{M_b}$ are

$$\boldsymbol{M_f} = 0.9NI\underline{/\beta - 90 + \alpha}$$

$$\boldsymbol{M_b} = 0.9\,NI\underline{/\beta + 90 - \alpha}$$

where β is the angular position of the magnetic axis with respect to an arbitrary reference axis.

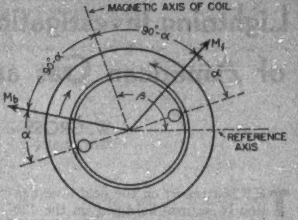
Figure 9. Component magnetomotive-force vectors of a concentrated coil

MAGNETIC AXIS OF COIL
90°−α
90°−α
M_f
α
M_b
β
α
REFERENCE AXIS

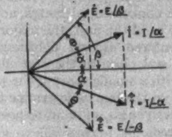
Figure 10. Relations of current and voltage vectors to their conjugates

$\dot{E} = E\underline{/\beta}$
$\dot{I} = I\underline{/\alpha}$
θ
α
β
α
θ
$\hat{I} = I\underline{/-\alpha}$
$\hat{E} = E\underline{/-\beta}$

By regrouping we obtain

$$\boldsymbol{M_f} = 0.9N(I\underline{/\alpha})\,\underline{/\beta - 90}$$

$$\boldsymbol{M_b} = 0.9N(I\underline{/-\alpha})\,\underline{/\beta + 90}$$

But $I\underline{/\alpha}$ is the vector expression for the current vector at the instant considered and $I\underline{/-\alpha}$ is the vector expression for the conjugate of the current vector. Therefore

$$\boldsymbol{M_f} = 0.9N\boldsymbol{I}\underline{/\beta - 90} = -j0.9N\boldsymbol{I}\underline{/\beta} \tag{42}$$

$$\boldsymbol{M_b} = 0.9N\hat{\boldsymbol{I}}\underline{/\beta + 90} = +j0.9N\hat{\boldsymbol{I}}\underline{/\beta} \tag{43}$$

Appendix II

Conjugate Vector Relationships

Let the voltage and current in a circuit having an admittance of Y mhos be as shown by the vectors $\boldsymbol{E}$ and $\boldsymbol{I}$ of Figure 10. The current is expressible as

$$\boldsymbol{I} = \boldsymbol{EY}$$

or

$$I\underline{/\alpha} = (E\underline{/\beta})(Y\underline{/-\theta}) = EY\underline{/\beta - \theta}$$

But, by definition of conjugates,

$$\hat{\boldsymbol{I}} = I\underline{/-\alpha}$$

Therefore

$$\hat{\boldsymbol{I}} = EY\underline{/-(\beta - \theta)} = (E\underline{/-\beta})(Y\underline{/\theta}) = \hat{\boldsymbol{E}}\hat{\boldsymbol{Y}}$$

This means that the conjugates of current, voltage, and admittance are related by an

Lightning Investigation on 132-Kv System of American Gas and Electric Company

I. W. GROSS
FELLOW AIEE

G. D. LIPPERT
ASSOCIATE AIEE

THE last report on the field investigation of natural lightning on the 132-kv transmission system of the American Gas and Electric Company was presented in a paper by the authors in 1942.[1] Since that time the field research work has been continued, although not as extensively as in the past, the major project being centered around lightning conditions at and close to the stations themselves, with a smaller part of the work being done on the line to determine the relative effectiveness of counterpoises and ground rods.

The objective of this investigation was to determine lightning conditions at major stations where expensive electric equipment is located, the failure of which might have serious effects on equipment, system operation, and electric service. With a better knowledge of the behavior of lightning at stations, it should be possible more adequately to protect important equipment from insulation damage.

The results of the field study from 1942 to, and including part of, 1944 are presented and discussed in this paper. The data have been combined in most cases with that previously obtained, in order to offer a composite picture of all records to date on the particular features studied.

Plan and Scope of Field Work

The major part of the investigation was carried out on a section of the Appalachian Electric Power Company division of the central system of the American Gas and Electric Company which is shown in Figure 1. The isokeraunic levels of the section of country where this part of the system is located range from 40 to 50.

The characteristics of the transmission lines connected to the stations are shown in Table I. The station characteristics such as bus insulation, number of connected lines, line insulation near the station, number of arresters, and their characteristics are shown in Table II.

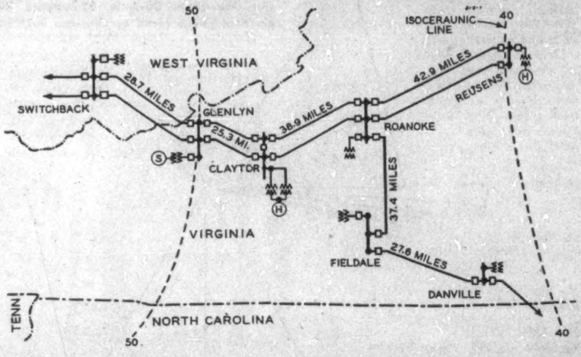

Figure 1. 132-kv system of Appalachian Electric Power Company in Virginia and West Virginia, part of central system of American Gas and Electric Company where field investigation was conducted

The study on the counterpoises and ground rods was carried out on a section of the South Bend–Michigan City two-circuit 132-kv line of the Indiana and Michigan Electric Company in Indiana, which has previously been described.[2]

In planning the field setup instruments were installed to measure currents and voltages as follows:

A. Lightning currents in line conductors, in ground wires, in leads to transformers, and in lightning arresters.

B. Lightning voltages at station busses.

C. Rates of lightning and switching-surge voltage change at stations.

D. Currents in counterpoises, ground rods, and tower footings in one section of a 132-kv line.

All lightning currents were measured with the surge-crest ammeter;[3] lightning voltages with the surge-voltage recorder;[4] and rate of voltage change with the wave-slope indicator.[1] The investigation was carried on co-operatively with the General Electric Company which supplied instruments and collaborated in analyzing and interpreting the results of field records. The field organizations of the Appalachian Electric Power Company and of the Indiana and Michigan Electric Company serviced the field installations during the investigation.

The general locations of instruments are shown in Table I together with the years covered by the investigation; the number of records obtained; and their maximum, minimum, and median* values.

In Table IV is shown the instrument sensitivity or measurement range. The instrument arrangements were designed to cover a range of lightning values which previous experience indicated as most likely to be encountered in the particular circuits in which they were installed. In the case of surge-crest ammeters on line conductors and transformer leads, it was necessary to design the instrument, so as to minimize the demagnetizing effect of 60-cycle fault currents; this resulted in

---

Paper 45-18, recommended by the AIEE committee on power transmission and distribution for presentation at the AIEE winter technical meeting, New York, N. Y., January 22–26, 1945. Manuscript submitted October 31, 1944; made available for printing December 1, 1944.

I. W. Gross is electrical research engineer and G. D. Lippert is in the engineering department of the American Gas and Electric Service Corporation, New York, N. Y.

* The median value is the value which 50 per cent of the records exceed.

---

expression which is identical in form with that relating the current, voltage, and admittance themselves.

References

1. Test Code for Synchronous Machines, Preliminary Report. AIEE Standards, January 1937.

2. The Reactances of Synchronous Machines. R. H. Park, B. L. Robertson. AIEE Transactions, volume 47, 1928, pages 514–36.

3. Determination of Synchronous-Machine Constants by Test, S. H. Wright. AIEE Transactions, volume 50, 1931, pages 1331–51.

4. Starting Performance of Synchronous Motors, H. V. Putman. AIEE Transactions, volume 46, 1927, pages 39–57.

5. Applications of the Method of Symmetrical Components (book), W. V. Lyon. McGraw-Hill Book Company, New York, N. Y., 1937. Page 53.

6. Symmetrical Components (book), C. F. Wagner, R. D. Evans. McGraw-Hill Book Company, New York, N. Y., 1933. Chapter 13.

7. Starting Performance of Salient-Pole Synchronous Motors, T. M. Linville. AIEE Transactions, volume 49, 1930, pages 531–47.

Table I. 132-Kv Transmission-Line Characteristics—Appalachian Electric Power Company Division

	Glen Lyn–Switchback	Glen Lyn–Claytor	Claytor–Roanoke	Roanoke–Reusens	Roanoke–Fieldale	Fieldale–Danville
Length of line—miles	28.7	25.3	38.9	42.9	37.4	27.6
Number of towers	128	104	167	200	164	136
Number of circuits	2	2	2	2	1	1
Number of ground wires	1	1	1	1	1	1
Arrangement of conductors	Vertical	Vertical	Vertical	Vertical	Vertical	Vertical
Insulator spacing—inches	$5^1/_8$	Suspension $4^3/_4$ Strain 5	Suspension $4^3/_4$ Strain 5	Circuit 1 $4^3/_4$ & 5 Circuit 2 $5^3/_8$	$5^1/_8$	$5^1/_8$
Number of units—suspension T-M-B	11-11-10	10-10-10	10-10-10	Circuit 1 12-12-10 Circuit 2 10-10-10	10-10-10	10-10-10
Number of units—strain T-M-B	12-12-12	12-12-12	12-12-12	12-12-12	12-12-12	12-12-12
Flashover (kilovolts) of	10($5^1/_8$) 930	10($4^3/_4$) 790	10($4^3/_4$) 790	10($4^3/_4$) 790	10($5^1/_8$) 930	10($5^1/_8$) 930
Insulators—$1^1/_2$ x 40	11($5^1/_8$) 1,010	12(5) 980	12(5) 980	10(5) 840	12($5^1/_8$) 1,080	12($5^1/_8$) 1,080
Positive wave	12($5^1/_8$) 1,080			12($4^3/_4$) 910 12(5) 980 10($5^1/_8$) 930		
Protector tubes	None	Circuit 1 only	Circuit 1 only	None	Yes	Yes
Discharge kilovolts of tubes						
Positive		680	680		680	680
Negative		760	760		760	760

the lower limit of measurements being higher than desired.

All instruments were in service from about May 1 to October 1 each year and were serviced about every two weeks during the lightning season. Instruments for measuring lightning-arrester currents and rate of voltage change at stations were left in service throughout the year but serviced only during the lightning season.

Summary of Records, Analysis, and Discussion

LIGHTNING DISTURBANCES AT STATIONS AND ARRESTER OPERATIONS

In Table V is shown the number of years this investigation has been in progress at the five stations on the Appalachian Electric Power Company's system. There has been a total of 21 station years of experience. In this table is also shown the number of times lightning-arrester discharges have been measured at stations. There has been a total of 115 disturbances during this time, or an average of 5.5 lightning disturbances per station per year as indicated by the measurement of lightning currents at the stations. There has been an average of 2.3 times per station per year when lightning arresters discharged. This analysis indicates that on the average one lightning-arrester discharge has occurred for each 2.4 lightning disturbances reaching a station.

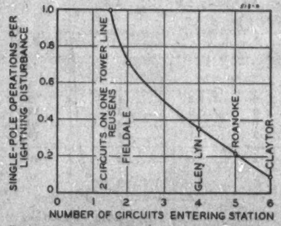

Figure 2. Effect of number of circuits at 132-kv stations on lightning-arrester operations (1939–43 inclusive)

The effect of the number of lines terminating at a station on arrester operation is given in Table V and is shown graphically in Figure 2. The trend of a marked reduction in arrester operations as the number of lines terminating at a station increases is apparent. This checks with theory, and is a result of the lower surge impedance encountered by a surge entering a station where several outgoing lines are in parallel.

LIGHTNING CURRENTS IN LINE CONDUCTORS AT STATIONS

From 1939 to 1943 inclusive, there were 302 records of lightning currents in line conductors at stations, and 130 records of current in single-pole arresters. These data are all shown as magnitude–frequency curves in Figure 3. These magnitude–frequency curves show not only a summary of all conductor and lightning-arrester currents at the five stations, but also the currents at each separate station. The maximum line-conductor current obtained at a station was 11,500 amperes. Ten per cent of the currents were 3,500 amperes or greater, and 50 per cent of the currents were at least 2,000 amperes.

CURRENTS INTO AND OUT OF STATIONS

Of the 302 lightning currents in conductors at stations, 143 were flowing toward the station and 159 were flowing away from the station.

Table II. 132-Kv Station Characteristics—Appalachian Electric Power Company Division

Station	Glen Lyn	Claytor	Roanoke	Reusens	Fieldale
Number of suspension insulator units on station bus	12	12	12	12	12
Flashover kilovolts of bus insulators	980–1,080	980	910–980	910–980	1,080
Number of connected circuits	4	6**	5	2	2
Reduced line insulation at station entrance	All except Claytor number 1 which is tube-equipped	Roanoke number 2 and Glen Lyn number 2—Roanoke number 1 and Glen Lyn number 1 are tube-equipped	All except Claytor number 1 and Fieldale which are tube-equipped	Yes	No—tube-equipped
Number of towers in reduced section	5	5	5	5	
Number of suspension and strain insulators in reduced section	9	9	9	9	
Flashover kilovolts of reduced section ($1^1/_2$x40 positive wave)	720–850	720–765	720–850	720–850	
Number of 3-pole lightning arresters	4	4	3	3	
Kilovolt maximum 60-cycle rating	106	109	106-100-121	106–109	109
Arrester-gap breakdown*	635	388	635-388-430	635–388	388
IR at 5,000 amperes*	353	363	353-363-403	353–363	363

* Average industry values.

** Including two circuits of 1,000 feet.

Table III. Lightning-Measuring Instruments, Locations, and Number and Magnitude of Records Obtained on 132-Kv System

Reference	Instrument Location	Instrument Years	Years of Operation	Number of Records	Record Magnitude Maximum	Record Magnitude Median	Record Magnitude Minimum**
1.	Tower legs above ground	456	1939–44	123	15,100	2,400	1,000
2.	Tower legs below ground	378	1939–44	66	6,800	1,650	1,000
3.	250-foot counterpoises	126	1939–44	55	11,000	2,700	200
4.	Ground rods at towers	393	1939–44	121	20,000	1,200	200
5.	Ground wires at towers near stations	136	1940–43	41	36,000	2,400	1,000
6.	Ground wires at stations*	100	1940–43	60	10,300	1,700	1,000
7.	Conductors at towers near stations	228	1941–42	171	14,600	2,200	1,000
8.	Conductors at stations	210	1939–43	302	11,500	2,000	1,000
9.	Conductors at transformers	23	1944	0			
10.	Wave-scope indicators at stations	115	1939–9/1/44	1,025	810	115	10
11.	Arresters at stations	288†	1936–43	261‡	4,100	500	200
12.	Voltage recorders at stations	33	1939–43	429	525	165	100

*Where three ground wires are in parallel.
**Lower limit of link registration—trace records.
†Single-pole years.
‡Single-pole records.

Table VI. Simultaneous Line-Conductor Currents Into and Out of Stations With Accompanying Arrester Currents

24 Selected Records (3,000 Amperes or Greater—Either Incoming or Outgoing)

Station	Total Current Into Station, Amperes	Total Current Out of Station, Amperes	Arrester Current, Amperes	Arrester Poles Discharging
Glen Lyn	11,200	8,700	N*	
Glen Lyn	7,500	1,000	N	
Glen Lyn	5,000	1,000	N	
Glen Lyn	2,800	3,600	N	
Glen Lyn	3,400	2,400	300	1
Glen Lyn	2,300	3,400	N	
Claytor	3,000	1,000	N	
Claytor	2,000	3,200	N	
Claytor	2,000	3,800	N	
Claytor	2,400	3,400	N	
Claytor	3,700	2,700	N	
Claytor	3,000	2,000	N	
Claytor	1,000	4,200	N	
Claytor	5,000	1,000	N	
Claytor	8,200	1,000	850	2
Claytor	1,000	4,000	1,750	2
Claytor	4,600	3,000	N	
Roanoke	1,000	5,300	1,750	2
Roanoke	2,000	3,200	350	1
Roanoke	1,000	3,000	200	1
Roanoke	3,000	2,000	450	1
Roanoke	3,000	2,000	N	
Roanoke	4,800	8,000	N	
Roanoke	2,000	5,800	N	

* N indicates no record obtained.

In Table VI are shown simultaneously obtained currents flowing toward and away from stations and the accompanying station arrester current, all three recorded on the same phase wire. In each case the current values given are the summation of all currents measured in line wires and arresters. Of the 58 cases showing simultaneous line currents into and out of the station, 24 of the highest records were selected for analysis in Table VI. From the table it appears that there is no characteristic trend between the magnitudes of currents entering and leaving a station, nor between these currents and the arrester current. However, as there were other station current paths where no instruments were installed and as the instrument sensitivity does not permit measurement of low values of current, the comparison of currents by the above method may not be significant. The question may well arise as to why lightning arresters in some cases show no discharge current with currents in line conductors of 3,000 amperes or more. A line current of 3,000 amperes and line surge impedance of 400 ohms would produce a line voltage of 1,200 kv, which should cause arrester operation. The explanation may be that recorded line currents are the addition of several lightning surges—not merely one. Again, the current measured may be the result of reflection at a transition point where the surge impedance becomes lower and the line voltage at the station likewise lower.

Table IV. Instrument Measurement Range

Surge-crest ammeters	
On tower legs	1,000 to 55,000 amperes
On ground wires	1,000 to 72,000 amperes
On line conductors	1,000 to 55,000 amperes
On lightning arresters	200 to 14,400 amperes
On ground rods	200 to 24,000 amperes
On counterpoises	200 to 24,000 amperes
Wave-slope indicator	10 to 10,000 kv per microsecond
Surge-voltage recorder	100 to 1,300 kv

CURRENT ATTENUATION AND REFLECTION ADJACENT TO STATIONS

During 1941 and 1942 surge-crest ammeters were in service on line conductors at the five stations and on all circuits at intervals of approximately one-half mile and one mile distant from the station. By this arrangement it was planned to obtain data on attenuation and reflection of lightning currents in line conductors. Of the 58 records obtained, 23 were of low magnitude or of inconsistent direction of current flow and were rejected in the tabulation. In Table VII are shown the 35 records selected for analysis. The averages of currents flowing toward the station were 2,800 amperes, 2,600 amperes, and 2,810 amperes, respectively, at the station, one-half mile out, and one mile out. Individual cases, however, varied considerably from the average results, and the data do not indicate any definite trend. If the currents attenuated to any extent, the results are obscured by possible reflection at the station where a change of surge impedance is encountered.

In the case of currents flowing away from a station it was believed that, if appreciable attentuation took place, it would not be obscured by reflection from the station. An average of all the records indicated currents at the station of

Table V. Lightning Disturbances at 132-Kv Stations, 1939–43 Inclusive

	Roanoke	Glen Lyn	Claytor	Reusens	Fieldale	Totals
Station years of investigation	5	4	4	4	4	21 station years
All lightning disturbances*						
1939	4					4
1940	8	6	7	3	4	28
1941	6	6	5	5	3	25
1942	8	3	4	5	5	25
1943	9	5	7	7	5	33
Total	35	20	23	20	17	115
Average disturbance per year	7.0	5.0	5.8	5.0	4.3	
Disturbance per station per year—1939–43 inclusive						
Experience years (1939–43 inclusive)						21
Disturbances						115
Disturbances per station per year						5.5
Lightning arrester discharges						
1939	2					2
1940	3	2	0	3	1	9
1941	1	3	0	5	3	12
1942	0	1	0	5	4	10
1943	2	1	2	7	4	16
Total	8	7	2	20	12	49
Number of lines entering station	5	4	6	1 1/2**	2	
Lightning-arrester operations per lightning disturbance	0.228	0.350	0.087	1.00	0.710	0.425 avg
Average discharges per station per year						49/21 = 2.3

* Indicated by measurement of lightning current in conductors and/or arresters.

** Based on two circuits entering station on same towers.

2,670 amperes; at one-half mile out of 2,520 amperes; and one mile out of 2,450 amperes. Although the average values indicated a slight attenuation, individual cases vary considerably from the average, and there appears to be no pronounced trend.

There were eight instances where currents of 2,000 amperes or more were measured at the station entrance, one-half mile out, and one mile out, in which the direction of current flow at one of these points was reversed with respect to that at the other two. A tabulation of these cases is shown in Table VIII. The explanation for this may be that either a lighting stroke or a line flashover occurred between measurement points. This seems to indicate that some strokes and line flashovers have occurred within a mile of the stations without causing any arrester operation or damage to station apparatus.

Lightning-Arrester Currents at 132-Kv Stations

Measurements were obtained of currents in lightning arresters at the five stations from 1936 to 1944 inclusive. The maximum current obtained during this period was 4,100 amperes. This record, however, was obtained at a time when no other instruments were in service at the station, and therefore no correlation with other lightning data was possible.

The arrester records shown in Figure 3 (1940–43 inclusive) include only those obtained when instruments were in service to measure line-conductor currents. However, the inclusion of data obtained from 1936 to 1939 inclusive on arresters only does not alter the shape of the magnitude–frequency curve, except to increase the maximum value of current to 4,100 amperes. Of the lightning-arrester records obtained simultaneously with line-conductor currents, ten per cent were 1,500 amperes or higher, and 50 per cent were 500 amperes or higher. Although the maximum value of arrester current measured in this investigation was only 4,100 amperes, on another part of the system a maximum arrester current of

Table VII. Attenuation of Lightning Currents in 132-Kv-Line Wires Near Stations (1941–1942)

Currents (Amperes) Flowing					
Toward Station			From Station		
At Station	1/2 Mile Out	1 Mile Out	At Station	1/2 Mile Out	1 Mile Out
2,400	2,400	2,500	2,800	1,000	2,400
3,400	3,900	3,800	2,700	2,800	3,000
1,000	1,000	2,000	3,500	7,400	3,800
2,300	2,700	2,700	2,900	2,200	2,000
3,000	2,800	3,500	3,200	3,100	3,600
8,500	5,300	7,300	3,400	4,400	3,400
3,200	2,300	3,000	2,000	3,000	2,200
2,300	2,000	1,000	3,200	2,400	2,800
2,700	2,600	3,200	2,900	3,400	2,400
1,000	2,000	2,000	2,100	1,000	2,000
2,000	2,000	1,000	1,000	1,000	2,000
1,000	1,000	2,000	1,000	1,000	2,000
5,000	3,700	3,600	2,100	2,600	2,600
1,000	2,300	2,300	2,000	2,600	2,100
3,200	2,900	3,200	1,000	2,100	1,000
			2,600	2,400	2,400
			2,000	2,000	2,400
			2,700	2,000	3,400
			2,200	2,000	2,400
			2,000	2,000	1,000
Average 2,800	2,600	2,810	2,670	2,520	2,450

Figure 3. Lightning currents in conductors and arresters at 132-kv stations (1939–43 inclusive)

I—Arrester currents
II—Conductor currents
A—Roanoke station—126 conductor records, 23 arrester records
B—Fieldale station—24 conductor records, 26 arrester records
C—Reusens station—10 conductor records, 66 arrester records
D—Claytor station—76 conductor records, 6 arrester records
E—Glen Lyn station—66 conductor records, 9 arrester records
F—All records—302 conductor records, 130 arrester records

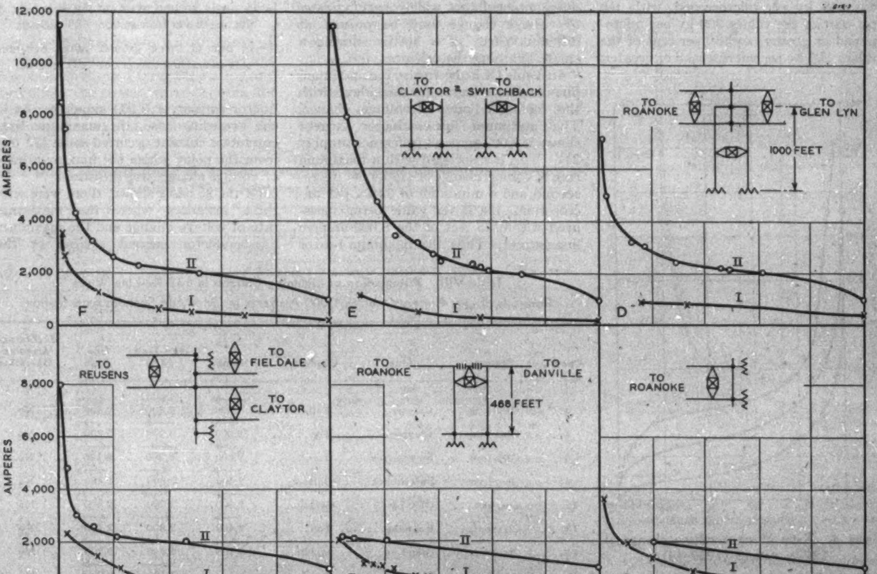

16,000 amperes was measured in an arrester on the 132-kv system—the result of a stroke within 400 feet of the station.

RATES OF VOLTAGE CHANGE AT STATIONS

In a previous paper[1] the authors presented data on the rate of surge-voltage change at stations comprising 539 wave-slope indicator records for 1939 to 1941 inclusive. In the past three years there have been obtained 486 additional wave-slope-indicator records making a total of 1,025. These six years' records have been analyzed and the results are presented here.

Of the 1,025 records, 353 were rejected because they did not lend themselves readily to accurate analysis. The 672 records selected for analysis have been segregated into three groups. The first group consists of 348 surges believed to be attributable to switching only; the second group, 291 records which were the result of lighting and switching; and the third group of 33 surges interpreted as resulting from lightning only. These three groups of records are shown as magnitude–frequency curves in Figure 4. The maximum rate of voltage change caused by lightning only was 810 kv per microsecond, with ten per cent of the records 475 kv per microsecond or greater, and 50 per cent of the records 220 kv per microsecond or greater. In the lightning and switching group, the maximum value was 648 kv per microsecond, with ten per cent of the values 300 kv per microsecond or greater, and 50 per cent of the values 150 kv per microsecond or greater.

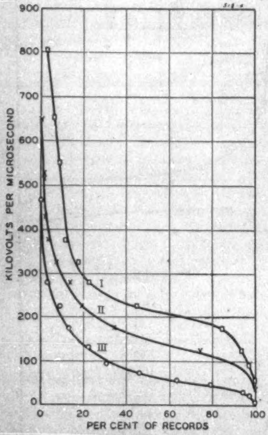

Figure 4. Rates of surge-voltage change at 132-kv stations (1939–44)

I—Lightning only—33 surges

II—Lightning and switching surges

III—Switching only—348 surges

In the switching group, the rates of voltage change were a maximum of 470 kv per microsecond, ten per cent being 200 kv per microsecond or greater and 50 per cent being 115 kv per microsecond or greater.

At the Roanoke 132-kv substation, wave-slope indicators were installed on phases one and three of all connected lines. The wave-slope indicators were located on carrier-current capacitors which are connected to the incoming line ahead of all other station apparatus and are some 70 circuit feet from the station bus. The maximum distance between measuring locations was approximately 280 circuit feet. In Table IX are shown 25 simultaneously obtained records of the rate of voltage change at different locations in the station.

From the data it is seen that the rate of voltage change due to a surge may vary widely between different points in the same station. An extreme case is shown in reference 14 of Table IX. Here a rate of voltage change of 470 kv per microsecond was recorded at the line entrance of Reusens number 2, whereas at the line entrance of Reusens number 1, some 200 circuit feet distant, the rate of voltage change was below the minimum sensitivity of the wave-slope indicator (ten kilovolts per microsecond). Numerous similar occurrences are shown in this same table. Thus it appears from the data obtained that widely varying rates of voltage change may be present at different parts of a station during a single lightning disturbance.

In Table IX is shown also the maximum line-conductor currents coincident with the measured rate of voltage change. The maximum line-conductor current shown is 8,000 amperes (reference number 24). This is associated with a maximum rate of voltage change of 412 kv per microsecond and a minimum of 33 kv per microsecond, the latter value being measured within 25 feet of the 8,000-ampere line current. Thus, the maximum rate of voltage change in this case was recorded at some distance (250 feet approximately) from where the maximum line-conductor current was measured. In reference number 14 of this same table, the rate of voltage change of 470 kv per microsecond was measured adjacent to a line-conductor current of 2,000 amperes. As in the preceding case, the maximum line-conductor current occurred some 175 feet from the point where the maximum rate of voltage change was measured.

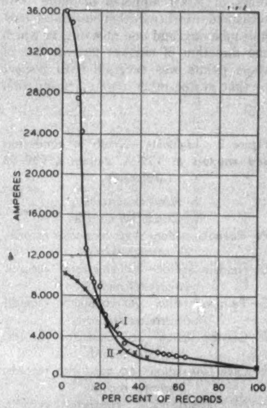

Figure 5. Lightning currents in overhead ground wires at 132-kv stations

I—In single ground wire on the line side of the first tower from station—41 records

II—In one of three ground wires between station and first tower out—60 records

Of the 25 cases shown, there were only three instances where the maximum rate of voltage change and the maximum line-conductor current existed at the

Table VIII. Attenuation of Lightning Currents in 132-Kv-Line Wires

Reversals of Line Currents Above 1,000 Amperes in One-Mile Sections From Station

Case	Station	Line	Conductor	Station	One-Half Mile	One Mile	Lightning-Arrester Operation
4	Glen Lyn	Claytor	Bottom	→ 3,600	← 9,300	← 9,300	No
4	Glen Lyn	Claytor	Top	← 5,000	→ 3,900	→ 3,300	No
6	Glen Lyn	Switchback	Top	→ 2,000	← 2,200	← 8,100	No
6	Glen Lyn	Switchback	Bottom	→ 2,400	← 2,800	← 2,400	No
11	Claytor	Glen Lyn	Middle	→ 2,000	→ 2,000	← 2,000	No
13	Claytor	Roanoke	Top	→ 2,400	← 2,800	← 2,400	No
14	Claytor	Glen Lyn	Middle	← 3,400	→ 2,800	→ 2,200	No
17	Roanoke	Claytor	Bottom		← 2,100	→ 2,000	No
24	Roanoke	Claytor	Middle	→ 1,000	← 2,500	← 2,700	No

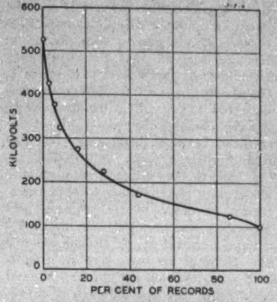

Figure 6. Surge voltages on 132-kv station busses (1940–43 inclusive)

same point. If it be assumed that the maximum line-conductor currents are records obtained nearest to the lightning stroke initiating the disturbance, it would appear that the highest rates of voltage change are not caused by the initiating surge but by other conditions within the station, possibly voltage reflections from apparatus terminals, and similar causes. If this be true, it dictates the necessity of placing protective devices close to the apparatus to be protected.

GROUND-WIRE CURRENTS AT STATIONS

In Figure 5 is shown a comparison of ground-wire currents obtained on the line side of the first tower from the station and currents in the ground wires between the first tower and the station structure. The maximum current on the line side of the first tower was 36,000 amperes, and the maximum in any one of the three parallel ground wires adjacent to the station structure was 10,300. In general, the current divided equally between the three parallel ground wires, although there were some exceptions to this at lower values of current. Although the two curves in Figures 5 do not have the same general shape, it is believed that this is not particularly significant.

The ground-wire current distribution at the first tower out from a station for the three different ground-wire arrangements investigated is shown in Table X. Though it might be expected that the sum of currents in multiple-ground wires between station and the first tower out nearly would equal the ground-wire current on the line side of the tower, this is not always true. The reason, no doubt, is that no account has been taken of the unmeasured tower current itself.

LIGHTNING VOLTAGES AT 132-KV STATIONS

A total of 429 bus-voltage records were obtained during 1940 to 1943 inclusive from surge-voltage recorders. These were in service at the Roanoke, Fieldale, and Claytor stations during 1940 and 1941, and at the Roanoke station only during 1942, 1943, and 1944. As records of appreciable magnitude were not obtained during 1944, they have not been included here. The maximum voltage obtained was 525 kv, 50 per cent of the records being 165 kv or greater. These voltage records are shown as a magnitude-frequency curve in Figure 6. These are all below the safe impulse strength of modern equipment used on 132-kv systems.

Table IX. Coincident Rates of Voltage Change and Maximum Lightning Line Currents at Roanoke 132-Kv Substation (1940–1943 Inclusive)

Reference	Maximum Line Amperes	Phase	Kv/µs					Lightning-Arrester Discharge
			Claytor		Reusens			
			Number 1	Number 2	Number 1	Number 2	Fieldale	
1	2,500	1		115	64	168	102*	No
2	2,000	1		126		212	136*	Yes
3	2,200	3	94		172	155	150*	Yes—2
4	2,400	1	27	300		52	80*	No
5	2,000	1		230	72	186	55*	Yes
6	2,400	1		40	10	72	92*	Yes
7	2,800	3	164	110	116		45*	No
8	2,000	1			168	288	97*	No
9	2,000	1	17	270	228*	108	76*	No
10	3,200	3		42	24		67*	No
11	2,000	1		320		80	64*	No
12	2,600	3	44	37	156		13*	No
13	2,900	3	132		24		53*	No
14	2,000	1				470	82*	No
15	2,000	3			235*		245	No
16	2,000	1		155		64	71*	No
17	2,200	1	*	332	95	245		No
18	2,000	1		150			*	No
19	2,000	1		145	*		210	Yes
20	2,700	1		380	*	64	310	No
21	2,000	3		35	80*	10	146	No
22	3,800	1		120		212*		No
23	2,000	1		290	*		178	No
24	8,000	1		412	33*	216	133	No
25	2,000	1		36		64	179*	No

* Circuit on which maximum current was measured.

LIGHTNING CURRENTS IN TRANSFORMER LEADS

During the 1944 lightning season, instruments were in service on all three leads of seven 132-kv transformer banks to measure lightning currents to the transformers. No records have been obtained from these instruments this year.

GROUND ROD, COUNTERPOISE, AND TOWER-FOOTING CURRENTS

Surge-crest ammeters were installed on the South Bend–Michigan City 132-kv line to obtain a complete record of current flowing in counterpoises, ground rods, and tower legs in order to determine which of these members was most effective in carrying lightning currents.

Magnitude–frequency curves of all currents measured in tower legs, counterpoises, and ground rods are shown in Figure 7.

A total of 29 cases was obtained during 1939 to 1944 inclusive, where currents were measured in two or more members. In Table XI are shown ten cases where a comparison is made between simultaneously obtained measurements in three members—tower footings, ground rods, and counterpoises. In all cases except one (case 10), the tower footing was most effective in carrying lightning current, based on d-c conductances. The average of the ten cases indicates the counter-

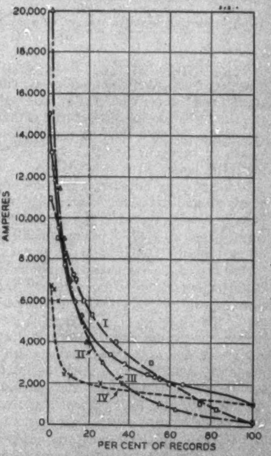

Figure 7. Lightning currents in tower legs, counterpoises, and ground rods—South Bend–Michigan City 132-kv line (1939–44)

I—52 currents in 250-foot counterpoises
II—115 currents in tower legs above ground
III—111 currents in ground rods (10 to 120 feet)
IV—65 currents in tower legs below ground

Table X. Lightning Current in Ground Wires at 132-Kv Stations, 1940–1944

(Only Records Where 3,000 Amperes or Above Were Measured in at Least One Wire)

Type 1. Glen Lyn, Claytor, Roanoke			Type 2. Reusens			Type 3. Fieldale		
Amperes*								
Line Side	Station Side	Total Station Side	Line Side	Station Side	Total Station Side	Line Side	Station	Line Side
−2,500	2,000 1,000 3,000	6,000	17,200	10,000 5,800	15,800	−1,000	−4,300	−1,000
						1,000	−11,700	
36,000	8,400 10,300 9,000	27,700	12,200	12,500 33,000	45,500	−2,400	5,800	21,000
9,500	1,000 1,000 1,000	3,000	3,000				3,000	2,000
						−4,000	20,600	20,100
				4,100 3,500	7,600		2,900	3,400
4,500	9,700 4,600 9,500	23,800	5,000	2,000	2,000	−4,800		
−9,400	−2,000 −2,400	−4,400				2,900	3,400	−1,000
						2,900	7,100	12,000
35,000	8,500 7,400 8,300	24,200						
24,300	5,000 6,000 7,300	18,300						
6,000	1,000 1,000 2,100	4,100						
12,700	4,600 3,300 3,300	11,200						
4,200 −3,000	−1,000 −1,000	−2,000						
27,500	8,500 7,000 10,250	25,750						
3,400 9,750	2,400 1,000 2,000	5,400						

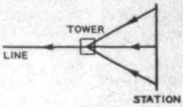

Type 1

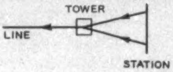

Type 2

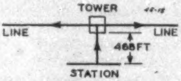

Type 3

* Current direction as shown in figure, otherwise shown (−).

poise as carrying 70 per cent of the current expected from its d-c conductances, the ground rod 115 per cent of that expected, and the tower footing 302 per cent of that expected. Though there is considerable variation between the individual cases, the trend indicated is quite definite.

In other cases not shown in the table, where ground-rod and tower-footing currents only were recorded, the ground rod (eight cases) carried 83 per cent and the tower footing 180 per cent of that expected by d-c conductance. Similarly where counterpoise (four cases) and tower-footing currents only were measured, the counterpoises carried 71 per cent of the current and the tower footing 393 per cent of the current that normally would be expected. A similar comparison between counterpoise and ground-rod currents only (eight cases) indicated that the counterpoise was carrying only 81 per cent and the ground rod 162 per cent of the current expected by d-c conductance.

Summarizing the data presented here, the tower footing is most effective in carrying lightning current; the ground rods less effective; and the counterpoise least effective. In this location the efficiency of ten-foot ground rods is very low. The maximum ground-rod efficiency is shown for ground rods of 40 to 60 feet in length. The type of soil was sandy loam of moderately high resistivity; the ground rods ranged from 10 to 120 feet in length; and the counterpoises were 2/0 copper 250 feet long, buried 18 inches. Tower footings were of the grillage type about five feet square and ten feet deep.

Discussion of Special Records

In studying a large quantity of summarized data such as has been obtained during this investigation, an analysis of a typical case may be of interest. In Figure 8 are shown typical records of a lightning disturbance at the Roanoke 132-kv station. During the servicing period of approximately two weeks, two lightning storms were reported in the general vicinity of the station. From a study of the lightning currents recorded (Figure 8), it appears that there were five lightning strokes to the 132-kv system in the general vicinity of the station. Three of these strokes were on the Claytor circuit: one between the first and fifth towers of 26,000 amperes or more; one between the fifth and seventh towers of possibly 36,000 amperes; and one stroke beyond the seventh tower of 42,000 amperes or higher. Conductor currents measured in the Fieldale circuit indicate a possible stroke beyond tower 8 of this line. The absence of any ground wire records on this line suggests that the stroke may have been several spans past tower 8. One stroke of at least 65,000 amperes was indicated by currents in the ground wire on the Reusens circuit. This stroke occurred between 3,500 and 9,300 feet from the station.

During this disturbance, the maximum line current recorded was 2,700 amperes; the maximum rate of voltage change was 440 kv per microsecond; the maximum voltage recorded at the station was 413 kv. None of the three three-pole lightning arresters at the station showed measurable currents, although it is possible that the arresters operated but the current was below the measurement range of the instruments.

In view of the records obtained in this one case the following statements seem justified:

1. Where lightning strokes occur some 1,500 feet or more from a station, if the line conductors are shielded, maximum lightning currents in the line wires at the station are in the order of 2,700 amperes or less.

2. Under the same conditions the incoming lightning voltages are not sufficient to cause arrester operation in the station.

3. Rates of voltage change at the station resulting from these nearby surges ranged as high as 440 kv per microsecond, although the nearest stroke was probably 1,500 feet distant. This feature may be significant in indicating that higher rates of voltage change at the station may occur, if the strokes are nearer the station.

Summary and Conclusions

From the results of this investigation, the summary data of which have been presented above, the following conclusions are drawn:

1. Lightning disturbances at five stations over a four-year period averaged 5.5 per station per year. Of these, 2.3 per station per year were of sufficient magnitude to cause arrester operation.

2. Lightning currents in conductors at stations showed a median value of 2,000 amperes. Seven per cent were 4,000 amperes or above and the highest was 11,500 amperes. All lines were shielded with overhead ground wires terminating on the station structure.

3. There appears to be no appreciable attenuation of lightning currents in line conductors within the first mile of the station.

4. The highest lightning-arrester current measured was 4,100 amperes, although elsewhere on the 132-kv system one current of 16,000 amperes was recorded.

Based on these results and similar records of arrester current obtained by the authors and others, it appears that the AIEE Standards for distribution and station-type arresters of 65,000- and 100,000-ampere lightning-current discharges are consider-

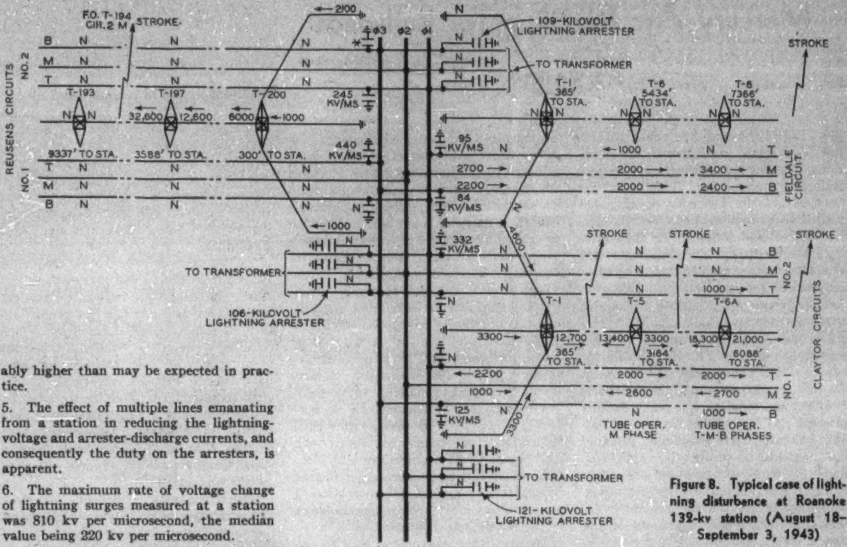
F.O. T-194
CIR. 2 M
STROKE
REUSENS CIRCUITS
NO. 2
NO. 1
B
M
T
N
T-193
T-197
T-200
32,600
12,600
6000
1000
2100
9337' TO STA.
3588' TO STA.
300' TO STA.
245 KV/MS
440 KV/MS
95 KV/MS
84 KV/MS
332 KV/MS
125 KV/MS
φ3
φ2
φ1
109-KILOVOLT LIGHTNING ARRESTER
TO TRANSFORMER
106-KILOVOLT LIGHTNING ARRESTER
121-KILOVOLT LIGHTNING ARRESTER
T-1
365' TO STA.
T-6
5434' TO STA.
T-8
7366' TO STA.
2700
2200
2000
3400
2400
4600
FIELDALE CIRCUIT
T-5
T-6A
3300
12,700
13,400
3164' TO STA.
18,300
21,000
6088' TO STA.
2600
2700
TUBE OPER. M PHASE
TUBE OPER. T-M-B PHASES
CLAYTOR CIRCUITS

Figure 8. Typical case of lightning disturbance at Roanoke 132-kv station (August 18–September 3, 1943)

ably higher than may be expected in practice.

5. The effect of multiple lines emanating from a station in reducing the lightning-voltage and arrester-discharge currents, and consequently the duty on the arresters, is apparent.

6. The maximum rate of voltage change of lightning surges measured at a station was 810 kv per microsecond, the median value being 220 kv per microsecond. The maximum rate of voltage change due to switching surges was 470 kv per microsecond and the median value was 115 kv per microsecond. When allowances are made for a reasonable factor of safety, the present generally accepted 1,000 kv per microsecond rate of rise for test specifications on apparatus seems reasonable.

7. The rates of voltage change measured within a station varied considerably at different points. Rates of change as high as 470 kv per microsecond were observed at one point in the station, whereas the rate of voltage change at other points was below the range of measurement (ten kilovolts per microsecond). This indicates clearly the necessity of keeping protective devices close to the equipment to be protected.

8. No consistent ratio was observed between lightning currents in conductors and the rates of voltage change at station entrances.

9. The maximum lightning voltage measured at any substation was 525 kv with 50 per cent of the records 165 kv or greater. This maximum voltage value is well below the safe insulation strength of modern 132 kv station equipment and within the range expected from the arrester protection.

10. In this investigation no consistent relationship was found between lightning currents and voltages at a station. Lightning currents in line conductors of 11,500, 8,500, 8,000, 7,500, and 6,500 amperes were recorded without any arrester operations recorded. These were accompanied by measured maximum rates of voltage rise of 100 to 160 kv per microsecond. The arresters at the station where these high-current records were obtained have a gap breakdown of 635 kv. In other instances arresters discharged where the

Table XI. Division of Lightning Current Between Counterpoises, Ground Rods, and Tower Footings, South Bend–Michigan City 132-Kv Line

Case 1	Member 2	Length, Feet 3	Resistance, Ohms 4	Measured Amperes 5	Per Cent Conductivity 6	Per Cent Current 7	Relative Efficiency Ratio 7/6 8
1	Counterpoise	250	15	7,800	82.3	64.5	0.78
	Ground rod	60	110	2,500	11.4	20.5	1.80
	Tower footing	10	200	1,800	6.3	15.0	2.37
2	Counterpoise	250	14	3,300	69.5	51.0	0.73
	Ground rod	10	100	200	9.8	3.0	0.31
	Tower footing	10	48	3,000	20.7	46.0	2.23
3	Counterpoise	250	10	5,100	61.0	43.5	0.72
	Ground rod	40	25	3,300	26.2	28.3	1.08
	Tower footing	10	48	3,300	12.8	28.2	2.20
4	Counterpoise	250	14	3,300	63.7	50.7	0.80
	Ground rod	10	45	200	19.5	3.1	0.16
	Tower footing	10	48	3,000	16.8	46.2	2.75
5	Counterpoise	250	9	3,000	71.8	52.2	0.73
	Ground rod	100	32	1,250	20.2	21.7	1.07
	Tower footing	10	80	1,500	8.0	26.1	3.14
6	Counterpoise	250	8	9,000	75.2	42.5	0.55
	Ground rod	49	32	5,400	18.8	25.5	1.36
	Tower footing	10	100	6,800	6.0	32.0	5.34
7	Counterpoise	250	14	6,300	67.6	66.3	0.99
	Ground rod	32	48	200	26.5	2.1	0.08
	Tower footing	10	160	3,000	5.9	31.6	5.35
8	Counterpoise	250	10	5,100	69.4	44.8	0.65
	Ground rod	40	40	3,300	17.4	29.0	1.67
	Tower footing	10	48	3,000	13.2	26.2	1.98
9	Counterpoise	250	9	4,600	71.8	61.4	0.85
	Ground rod	100	32	1,400	20.2	18.7	0.92
	Tower footing	10	80	1,500	8.0	20.0	2.50
10	Counterpoise	250	10	800	71.2	13.7	0.192
	Ground rod	65	36	3,550	19.8	60.7	3.06
	Tower footing	10	80	1,500	9.0	25.6	2.84
Average values							
	Counterpoise						0.70
	Ground rod						1.15
	Tower footing						3.02

Mercury-Arc Rectifiers for Railroads

S. S. WATKINS
MEMBER AIEE

DURING the past five years, because of wartime restrictions, few additional mercury-arc rectifiers have been installed for railroad use. This period has been notable for intensive development and mass production of rectifiers for electrochemical industries where they have been operated to produce concentrations of current output greatly exceeding those required by railroad loads.

The purpose of this paper is to examine those developments in mercury-arc rectifiers and associated equipment that deserve consideration in future plans for the supply of direct current for moving trains. To this end, experience of operators has been studied for data of value. Results of space and cost studies for typical 700-volt substations are presented, prepared on the basis of present-day apparatus designs. Study of apparatus characteristics is not limited to the conditions chosen for typical substations but is extended to include their significance in the design of d-c power-supply systems in general.

Operation, Control, and Maintenance

The majority of mercury-arc rectifier substations for transit and railroad service are nonattended with automatic starting and protective equipment. Direct-wire remote control or supervisory control[1] to the nearest suitably attended location, or supervisory control of a group of substations from a load dispatcher's office, are methods commonly used. The operating advantages of a central supervisory-control system should cause its increasing use. As a minimum, supervisory control must provide remote starting and stopping of the rectifier, with indication of running or stopped condition, and remote indication of rectifier automatic shutdown and lockout. Telemetering of output often is included. Indication of running condition of control-battery charger or telemetering of battery voltage often is used. Abnormal temperature or vacuum conditions such as to cause rectifier shutdown and lockout[2] usually are not separately indicated by supervisory control, but are registered on operation indicators or annunciators in the substation.

Daily visits of one-quarter hour to one hour to each substation are the practice of several organizations maintaining a large number of unattended mercury-arc rectifiers of the 650-volt class and predominantly of the multianode type, but including a few single-anode multitank units. Practices for cleaning and complete inspection of rectifiers and all substation equipment vary in these organizations from six hours once per week to eight hours once per month. Complete overhauls are made at intervals of once per year or longer. Maintenance-cost figures for rectifiers vary widely but were placed at about half that of synchronous converters where comparative data were available.

Recent records of arc-back frequency ranged from two to five per year per rectifier. Increase of arc-back rate above the average for any rectifier has usually indicated some abnormal condition which required correction. Systematic records of arc-backs for each rectifier, by date, have been a valuable assistance in efficient maintenance. Following arc-backs, rectifiers usually are restarted by remote control immediately. D-c feeder short circuits that are cleared with normal speed usually have no adverse effect on rectifier operation.

Experience with multianode rectifiers and single-anode multitank rectifiers on the same system indicates that a maintenance crew should cover about 50 per cent more rectifiers of the latter type in an equal time.

Space and Cost of Rectifier Substations

Preliminary studies of space and cost have been made for several typical substations to determine the effect of the number and size of rectifier units. Dimensions, characteristics, and estimating prices of present-day rectifiers and other substation equipment were obtained. The studies were made on the basis of the following assumed conditions:

Power supply to be at 13,200 volts, 60 cycles. Short-circuit current from the 60-cycle system to be within the interrupting capacity of 500,000-kva circuit breakers on the 13,200-volt side of the rectifier transformers. Direct current to be supplied at 700 volts. Substations to be nonattended and supervisory controlled. Rectifiers, auxiliaries, d-c switching and control equipment, to be in a brick building. Transformers and high-voltage switchgear to be outdoors.

Minimum width of substation was sought by placing the rectifiers and the transformers as close as possible to the end walls for connection through wall bushings. A narrow substation design aids in finding available locations along a railroad right of way. This sort of design applies particularly to suburban transportation. The space limitations of city transit systems often require that all equipment be indoors and that transformers be water-cooled.

Paper 45-17, recommended by the AIEE committee on land transportation for presentation at the AIEE winter technical meeting, New York, N. Y., January 22–26, 1945. Manuscript submitted November 8, 1944; made available for printing December 1, 1944.

S. S. Watkins is electrical engineer, Gibbs and Hill, Inc., New York, N. Y.

---

accompanying line-conductor currents were as low as 2,000 amperes.

11. Where three ground wires were in parallel between the station structure and the first line tower, the lightning currents divided nearly equally between the three wires. The maximum lightning current measured in a single ground wire at stations where three ground wires were in parallel was 10,300 amperes. The maximum current on the line side of the tower where there was only one ground wire was 36,000 amperes.

12. Based on the measured d-c resistance of tower footings, ground rods, and counterpoises, the tower footing is most efficient, 40- to 120-foot ground rods less efficient, and the 250-foot counterpoise least efficient in carrying lightning currents. This conclusion is based on results where the soil is sandy loam and of moderately high resistance.

13. At stations having a large number of connected lines, it appears that comparatively high line-conductor currents rarely are accompanied by sufficient potential to cause arrester operation. At the stations having only two connected lines, numerous instances occurred where arresters operated, but currents in the line conductors were below the limit of registration (1,000 amperes). It is therefore concluded that the presence of several lines at a station reduces the severity of lightning conditions to which apparatus can be subjected.

14. Although the records indicate direct lightning strokes to the transmission system within a mile of the station, there was no case of failure of equipment within the station. It therefore is concluded that the present method of protection by shielding incoming lines and limiting the voltage by lightning arresters at the station has been fully adequate.

References

1. Lightning Investigation on 132-Kv Transmission System of the American Gas and Electric Company, I. W. Gross, G. D. Lippert. AIEE Transactions, volume 61, 1942, April section, pages 178–85.

2. Lightning Experience on 132-Kv Transmission Lines of the American Gas and Electric Company System, 1930–31, Philip Sporn. AIEE Lightning Reference Book, 1918–35. Pages 1147–54, 1163.

3. Direct Measurement of Surge Currents, C. M. Foust, J. T. Henderson. AIEE Lightning Reference Book, 1918–35. Pages 1432–6, 1440.

4. Measurement of Surge Voltages on Transmission Lines Due to Lightning, E. S. Lee, C. M. Foust. AIEE Lightning Reference Book, 1918–35. Pages 230–9.

The rectifiers on which the studies were based were in all cases six-phase rectifier assemblies of single-anode tanks. It does not appear that the multitank rectifier design has caused much change in the over-all space requirements of substations. Comparative figures for several sizes and numbers of rectifiers are shown in Table I. Comparison of rectifiers of the same capacity of different manufacture showed considerable differences in over-all dimensions. Space allowances were made to take the largest equipment. Final designs for specific equipment might produce more compact arrangements. However, the space economy of the 3,000-kw rectifiers as compared with the 1,000-kw units is apparent.

Table I. Estimated Space Requirements for Rectifier Substations

Number and Size of Rectifier Units	Building Floor Space			Substation Total Ground Space		
	Width and Length	Sq Ft	Sq Ft Per Kw	Width and Length	Sq Ft	Sq Ft Per Kw
1—1,000 kw	24 by 25	600	0.60	31 by 60	1,860	1.86
2—1,000 kw	24 by 36	864	0.43	31 by 90	2,790	1.40
3—1,000 kw	24 by 49	1,176	0.39	31 by 120	3,720	1.24
1—3,000 kw	24 by 34	816	0.27	31 by 75	2,325	0.78
2—3,000 kw	24 by 61	1,464	0.25	31 by 130	4,030	0.67

Preliminary estimates were made for typical substations exclusive of real-estate cost. To establish a common basis of comparison, a single 60-cycle supply feeder and four d-c feeders were used for each substation, although the number of feeders is apt to be greater in varying amounts in case of application to actual power-supply systems. Cost study results are shown in Figure 1.

Ratings of Rectifiers

Rectifier and transformer combinations are manufactured as co-ordinated designs. Transformers are designed for primary voltage as required by the incoming power supply. Increases in primary-voltage rating affect the cost of rectifier transformers by about the same percentages as in the case of power transformers.

The following overload ratings of rectifier and transformer combinations are generally accepted:

Light duty; 100 per cent load continuously, followed by 150 per cent load for two hours, or 200 per cent load for one minute without injury.

Normal railroad service; 100 per cent load continuously, followed by 150 per cent load for two hours, or 300 per cent load for one minute.

Heavy-duty main-line service; 100 per cent continuously, followed by 150 per cent load for two hours, or 300 per cent load for five minutes.

Transformers are not to exceed 60 degrees centigrade at the end of the two-hour load in these ratings.

Some instances have been noted in operating experience with rectifiers of older design where heavy starting-current swings lasting 15 to 20 seconds have caused arc-back rates to increase. Although rectifier designers are confident that improvements in rectifier design have made those of present manufacture less affected by load swings, it is recommended that load curves and expected swings of starting current be fully discussed with rectifier manufacturers when the capacities of rectifiers for new installation are being determined.

Although rectifier groups of 36 or more phases have been used on heavy-load concentrations in the electrochemical industry, 6-phase and 12-phase rectifiers have been used for railroad service. On only a few railroad installations has interference with communication circuits required the use of filters. D-c filters are relatively inexpensive, filters for the a-c supply circuits are expensive. Rectifiers of more than 12 phases would seldom be justified for railroad service. Six phases are favored unless 12 can be shown to be necessary.

Single-Anode and Multiple-Anode Rectifiers

Single-anode rectifier tanks, assembled as six-phase rectifiers, have been in operation on railroad load of the 650-volt class for about five years. Because of lower arc-drop, single-anode type rectifiers of this class have from one to one and one-half per cent better efficiency than those of the multianode type. The limited amount of railroad experience with single-anode rectifiers favors this type for greater reliability and less maintenance than the multianode type.

Because of wartime regulations, railroad installations have been restricted and therefore railroad experience with single-anode rectifiers has been limited. Greatest experience with this type has been in the electrochemical industry. Here, mass production has stimulated design improvement of single-anode rectifiers. For new installations on railroad load at 700 volts or lower, only the single-anode type is likely to be offered although many years of efficient and reliable operation may be expected of those multianode rectifiers that are now in use.

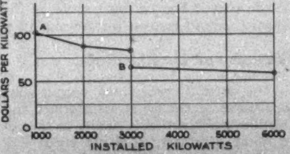

Figure 1. Estimated installed cost of mercury-arc rectifier substations, exclusive of real estate

A. With 1,000-kw units
B. With 3,000-kw units

At 1,500 or 3,000 volts the improvement in efficiency is relatively small for single-anode type rectifiers as compared with the multianode type. Reduced tendency to arc-back, localization of trouble and ability to remove a single-anode tank are advantages remaining in favor of the single-anode type at higher voltage. Opinion is general that the single-anode type will be extended to higher-voltage classes but the degree of present development in that direction varies. For 3,000-volt service, single-anode as well as multianode rectifiers now can be furnished.

Present-day single-anode type rectifiers consist of 6 or 12 tanks assembled on an insulated structural base with vacuum pumps, manifold, and circulating-water pumps common to the assembly. A separate vacuum valve between each tank and the manifold permits any tank to be removed without loss of vacuum in the remaining tanks. It has been found that a 12-tank rectifier can be shut down, a tank removed, a spare tank installed, and the rectifier placed back in operation in about one hour. In some cases, depending upon the recommendations of the manufacturer, a tank may be opened and inspected and returned to normal operation after the establishment of normal vacuum, without the necessity of a bake-out. A desirable feature of some designs is the use of water-cooling on the connection between each tank and the vacuum valve that connects it to the manifold and on the connection between the mercury-vapor vacuum pump and the manifold. Any mercury vapor tending to transfer from either the tank or the pump condenses and drains back to its respective source.

Sealed Steel-Tube Rectifiers

Sealed steel-tube single-anode rectifiers, being permanently evacuated, require no vacuum pumping equipment but are provided with water-cooling to maintain the proper operating temperature. The tubes are assembled in groups of 3, 6, or 12. Connections are three-phase or six-phase, depending on the capacity. They are available as factory-built substations. Sealed-tube rectifiers have had increasing use in industrial and mining applications, with the greatest volume in the 250-volt class where the single-anode design has a substantial advantage in efficiency over other conversion equipment. The simplicity of these rectifiers, without vacuum equipment and in most cases with raw tap-water connections for cooling, has recommended them in their main fields of application.

These rectifiers are now available for 600-volt service in a six-phase assembly for as high as 1,000-kw total capacity. The simplicity of the sealed tube in the present stage of development is achieved at a sacrifice of operating life of the tube since the internal pressure gradually increases because of effects of the arc. On heavy city transit or suburban service the present maximum size of 1,000 kw is small and tube replacement cost probably would not compare favorably with the maintenance cost of vacuum-pumped equipment where skilled personnel is available.

However, the possibilities of sealed-tube rectifiers deserve some consideration in the case of lighter transit systems. It has been suggested that these rectifiers have a field of application on 600-volt trolley-coach systems requiring small power-supply units. Steel cubicles containing the tubes might be placed outdoors and provided with heaters and outdoor cooling equipment for keeping operating temperatures within proper limits. The cost of such a design, assembled with the transformer and the a-c and d-c switching as a unit outdoor substation, in ratings up to 1,000 kw, might compare favorably with that of conventional arrangements of indoor equipment in a building.

Switching Equipment

Switching equipment on the high-voltage side of the rectifier transformers is of conventional types. Circuit-breaker voltage class and interrupting rating are determined by the characteristics of the supply system. One high-voltage circuit breaker is required for each rectifier unit. The number of additional incoming feeder circuit breakers depends on considerations of service continuity and over-all system design. Connection of each rectifier transformer through a single circuit breaker direct to the power-supply system may be used to advantage where the latter system is sufficiently reliable. The transformer supplying the substation and rectifier auxiliaries must be connected so that its supply is not interrupted by opening of the rectifier-transformer circuit breaker. When power supply is at 13,200 volts or less, outdoor metal-clad switchgear makes an effective switching arrangement.

High-speed (one-cycle) air circuit breakers between the rectifier cathode and the d-c bus are used in 3,000- and 1,500-volt substations and in many substations of the 650-volt class. These circuit breakers are automatic on reverse current and, in case of arc-back, interrupt the reverse feed from the d-c system. There is a tendency, at present, to use semi-high-speed air circuit breakers in the cathode connection where the total continuous capacity on a 650-volt bus is less than 9,000 amperes but to use high-speed switching wherever the capacity on the bus is above 9,000 amperes or where synchronous converters operate in parallel with rectifiers on the same bus.

The choice of high-speed switching for the 650-volt rectifier has been widened by the development of high-speed air circuit breakers for connection between rectifier anodes and transformer secondary. These circuit breakers usually are six-pole, consisting of six single poles each with individual reverse-current tripping device. The six poles operate together as a unit on closing. The location of these circuit breakers is such that all current contributions to an arc-back are interrupted by the opening of one circuit-breaker pole. Tests of these circuit breakers on arc-backs have shown that reduction of current magnitude starts in less than one half cycle and that interruption is complete in less than one cycle. Previous to the use of high-speed anode circuit breakers, although back feed from the d-c bus to an arc-back was interrupted within one cycle, the current contributed by other phases of the same rectifier was not interrupted until about eight cycles later by the circuit breaker on the high voltage side of the transformer. Anode circuit breakers have been a product of necessity for protection against the possible destructive effects of short circuits in the electrochemical industry where the concentrations of current on a single bus are many times those encountered in railroad service.

When high-speed anode circuit breakers are used, semi-high-speed circuit breakers may be used in the cathode connection. This combination should be favorably considered wherever high-speed switching is required for rectifiers in the 650-volt class. High-speed anode circuit breakers afford ideal protection.

Wherever, in the over-all design of the incoming power supply system, it is possible to eliminate circuit breakers on the high-voltage side of the transformers the anode circuit breaker may serve as the starting circuit breaker for the rectifier.

Voltage and Load Control

The natural unregulated output-voltage curve of the usual transformer and rectifier combination is similar to that of a shunt generator, drooping about five per cent. This characteristic assists in division of load between substations and has been preferred on a majority of installations. Where a flat-compound characteristic is desired, it can be accomplished by delaying the start of current conduction through each anode to the extent necessary to counteract the rise of output voltage with decreasing load. In this case the transformer and rectifier must be designed with a natural characteristic to provide a voltage above that for which the rectifier is to be regulated. Delayed conduction, called phase control, increases d-c ripple and increases distortion of the voltage wave of the a-c supply. Power factor is decreased by about the same percentage as the reduction in voltage below the unregulated value. Both these effects are greatest at the lightest loads when phase control is used for compounding.

Phase control may be accomplished by timing the removal of negative bias from a control grid located in the arc path. In an ignitron type of single-anode rectifier employing the saturable-reactor ignition circuit, operation of a rheostat in a d-c coil circuit changes the time characteristic of the circuit and controls the timing of rectifier ignition. In standard designs a range up to 15 per cent voltage reduction is available by adjustment. Circuits can be designed for greater than 15 per cent voltage reduction but this is not usually advisable or necessary.

Voltage control by the methods described may be accomplished manually by a load dispatcher if the control rheostat is motor-operated through the medium of supervisory control. By this means, rectifier output voltages may be adjusted for a desired division of load between different sources of a-c supply.

If automatic regulation is desired, a voltage regulator may be used to operate the ignition-timing rheostat. The compounding characteristic may be designed for similarity with that of existing compound-wound apparatus where parallel operation is required. Where automatic load limiting is required, the ignition-timing rheostat may be put under the supervision of an output-current relay so as to reduce output voltage as a limiting load is approached. This feature may serve power-purchase policy in avoidance of demands above a given limit or it may be used to prevent overloading particular substations above a set limit.

References

1. TELEMETERING, SUPERVISORY CONTROL, AND ASSOCIATED CIRCUITS, joint subcommittee of the AIEE committees on automatic stations and on instruments and measurements. AIEE report, revised edition, October 1941.

2. AUTOMATIC CONTROL FOR MERCURY-ARC RECTIFIERS, H. Bany, M. E. Reagan. AIEE TRANSACTIONS, volume 55, 1936, pages 100–09.

3. IGNITRONS FOR THE TRANSPORTATION INDUSTRY, J. H. Cox, G. F. Jones. AIEE TRANSACTIONS, volume 58, 1939, December section, pages 618–24.

4. EXCITRON MERCURY-ARC RECTIFIERS, O. K. Marti. AIEE TRANSACTIONS, volume 59, 1940, pages 927–30.

Analysis of Arc-Welding Reactors

CHARLES M. WHEELER
NONMEMBER AIEE

Synopsis: It is the purpose of this paper to examine the need and design of arc-welding reactors for d-c arc-welding sets. The inductance useful in stabilizing welding arcs is defined, and methods for calculating and measuring this quantity are suggested. Further, criteria for designs which make most effective use of material are established. Finally, a recent development in reactor design is described.

REACTORS used in d-c arc-welding circuits often have been likened in their action to that of flywheels on engines. Both absorb energy during periods of unwanted energy surplus and release this stored energy to the system during periods when the energy is low. Through this added inertia their respective systems are stabilized; for, whereas the flywheel reduces mechanical pulsations, the welding reactor smooths fluctuations in current. The presence of self-inductance in d-c arc-welding circuits is, therefore, highly desirable—it is, in fact, often essential to the satisfactory operation of single-operator arc-welding generators.

Questions concerning means of procuring this inductance immediately arise. Why are reactors sometimes used, whereas at other times they are not? Fundamentally, what is the nature of welding inductance? How much is required? These questions are important to both designers and users of d-c arc-welding sets, because their answers are reflected in terms of quality of characteristics, and compact efficient equipment.

This paper therefore is concerned not only with the application of welding reactors as a means for improving arc characteristics, but also with methods for arriving at compact efficient designs in which the material is used to best advantage. Finally, a recent development in arc-welding reactors is described.

Are Reactors Required?

A basic consideration confronting the designing engineer is whether the required amount of self-inductance can be incorporated more advantageously in the electromagnetic design of the generator, or whether an external device is more practical. The former alternative may complicate the design and construction of the generator with a resultant increase in weight, whereas the latter, of course, requires that a reactor be used. The alternative which the designer chooses is generally the one resulting in the more effective over-all use of electromagnetic material and the simpler construction.

At one time it was standard practice to use large welding reactors with most generators, but through subsequent refinements in the design of the generators and improvements in welding electrodes the usual reactor accompanying arc-welding generators practically disappeared.

However, the comparatively recent introduction and wide application of 3,600-rpm welding sets have placed a new emphasis on the use of external reactors, because these high-speed generators have inherently less self-inductance than their 1,800-rpm predecessors of similar design. In many cases well-balanced designs require the use of external reactors. The design of reactors for these units merits special attention, for their size and weight must bear a favorable relationship to that of the rest of the equipment.

The Arc-Welding Reactor

The essential elements of a welding reactor (a coil having N turns, a magnetic core with cross section A and length l, and an effective air gap G) are shown in Figure 1. A direct current I, establishes flux ϕ in the core. This reactor supplements a welding generator's characteristics through the addition of self-inductance to the welding circuit.*

Nature of Welding Inductance

It is a characteristic of a d-c arc that the current fluctuates about an average value and may die out suddenly if there is not sufficient stability in the source of power. The function of the reactor is to oppose these fluctuations through a self-induced voltage which is proportional to the rate of change of current. This voltage also supplements that supplied by the generator in establishing a "restriking" voltage when the arc tends to "pop out." The inductance useful in welding, or "welding inductance," should be defined in terms of its effectiveness in stabilizing changes above and below an average current. It should be expressed as the *rate of change* of flux linkages per ampere** as in equation 1.

$$L_w = N\frac{d\phi}{dI}\times 10^{-8} \text{ henrys} \tag{1}$$

Welding inductance as defined by this equation is a function of current since it is influenced to a large extent by saturation in the magnetic circuit of the reactor. It is a quantity, however, which may be readily calculated in the manner to be described.

Calculation of Welding Inductance

Welding inductance may be calculated directly from the saturation curve for a given reactor as indicated in Figure 2. For any assumed value of current the inductance is proportional to the slope of the saturation curve as indicated. Figure 3 shows the welding-inductance characteristic calculated from the saturation curve in Figure 2.

In this method of calculation, as well as in the analysis of reactor-design con-

---

Paper 45-29, recommended by the AIEE committee on electric welding for presentation at the AIEE winter technical meeting, New York, N. Y., January 22–26, 1945. Manuscript submitted November 30, 1944; made available for printing December 11, 1944.

CHARLES M. WHEELER is with General Electric Company, West Lynn, Mass.

* There is a second type of separate electromagnetic device, sometimes called a "d-c transformer," whose elements are the same as those of a reactor, except that a second winding, connected in series with the generator's shunt field, is added. Its function is to apply, through mutual coupling, a forcing voltage on the shunt field of the generator which is proportional to the rate of change of welding current. As a result, the inductance it adds to the welding circuit is relatively low, for the apparent inductance of its series coil is proportional to its leakage flux. The "d-c transformer," therefore, serves principally to improve the dynamic characteristics of the generator with which it is used, rather than add to the stored energy in the welding circuit. Designs often are modified for the purpose of increasing the leakage flux in order to increase the effective series inductance.

The transforming reactor, so called because it performs the functions of a "d-c transformer" and a reactor, is designed with a separate magnetic path for the leakage flux. See reference 1. Whether a d-c transformer or transforming reactor is used depends largely on the inherent dynamic characteristics of the generator and its inherent self-inductance.

** Inductance of coils having iron cores may be variously defined, depending on the basic concept of this quantity. It has also been evaluated in terms of total stored energy and total flux linkages per ampere. See reference 2.

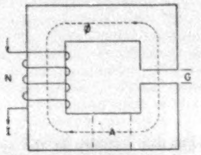

Figure 1. Essential elements of an arc-welding reactor

siderations which follows, the effects of hysteresis and eddy currents on welding inductance are assumed to be insignificant. It has been found from experience that in many applications these factors truly can be neglected, because conventional welding-reactor designs have laminated cores, their air gaps are relatively large, and frequencies associated with the rate of change of flux are fairly low. However, the effects of "stray" flux on welding inductance may be appreciable and should be calculated. Here, "stray" flux is defined as that flux which is established by the coil but does not pass across the air gap of the magnetic circuit. Its paths may lie in the window which accommodates the coil or through parallel magnetic paths near the coil.

Measurement of Welding Inductance

A straightforward method for measuring welding inductance, and one which gives good qualitative values, lies in recording the voltage induced in the reactor winding by current surges from the generator itself. This is easily accomplished in practice by means of a search coil* wound between reactor turns. The search-coil winding should assume, insofar as possible, the same space occupied by the reactor winding in order to include the effects of stray flux on inductance. If the number of search-coil turns is the same as the number of reactor turns, the welding inductance may be calculated directly from an oscillogram by dividing instantaneous values of search-coil voltage, E_s, by the rate of change of current.**

$$L_w = \frac{E_s}{dI/dt} \text{ henrys} \qquad (2)$$

Figure 4 shows data plotted from a representative oscillogram taken on a sample reactor (Figure 2) when the welding generator was suddenly short-circuited. The inductance characteristic determined directly from the oscillogram is shown in Figure 3 for comparison with the characteristic calculated from the saturation curve. It will be noted that the test and calculated welding-inductance characteristics agree very well up to the point where the reactor core saturates. Thereafter the test inductance is appreciably higher. The reason for this apparent discrepancy is that this particular reactor had a parallel magnetic path for stray flux, the effects of which are not included in the saturation curve.

Determination of Welding-Inductance Requirements

The necessary amount of welding inductance in a reactor to be designed for a given generator is best determined from actual welding tests. These tests are conducted at all practical welding currents within the range of the generator using various types of electrodes. Welding-inductance requirements may be determined by inserting a laboratory reactor in the circuit and adjusting its inductance to whatever amount may be required for satisfactory welding characteristics at each value of welding current. The inductance characteristic of the laboratory reactor should, of course, be substantially uneffected by saturation for the range of currents used.

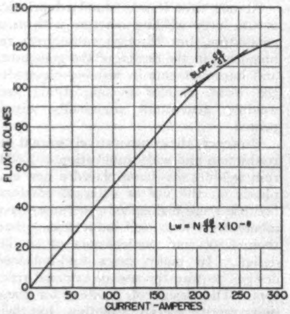

Figure 2. Saturation curve of a representative reactor showing method of calculating welding inductance

These tests provide welding-inductance values required as indicated by points 1, 2, 3, and so on, in Figure 5. In this particular example, it is noted that point 5 defines the required inductance L_w', at a limiting welding current I_w'. These are the values of inductance and average welding current about which a reactor should be designed for satisfactory overall welding performance. There is, however, a steady current I', somewhat higher than I_w', which should be used in design formulas, because the required welding inductance must be effective during current surges above the average as well as at average values. The ratio I'/I_w' can best be determined from experience and analysis of oscillograms taken during actual welding.

Thus the welding reactor for this example should be designed to have 1.1 millihenrys inductance (L_w') at a limiting steady current of 190 amperes (I') as indicated in Figure 5.

The following analysis is a review of design requirements for compact efficient arc-welding reactors, based on the specification that a known value of welding inductance is required at a limiting steady current.

Design of Welding Reactors

The design of coils and of magnetic circuits for series reactors is contingent in a large measure upon each other, for the mechanical configuration of one affects that of the other. The coil design, for example is dependent upon the cross-sectional area of the core and the number of ampere turns specified by the magnetic circuit. Other factors, such as degree of ventilation, heat-dissipating ability of the type of winding used, type of insulation, and duty cycle for which the coil is intended, fix its design when the current, turns, and dimensions of the core are known.

In general, welding inductance may be expressed by the equation,

$$L_w = \frac{3.19 N^2 A}{G} x f(I, G/1) \times 10^{-8} \text{ henrys} \qquad (3)$$

in which $f(I, G/l)$ is an expression for the shape of the inductance characteristic. It varies from almost 1.0 for small values of current to practically zero for very large currents. It is immediately apparent that there is an infinite number of combinations of N, A, and G (and l) which will give a desired value of welding inductance at a required limiting current. But relatively few designs will accomplish this end without some extravagance

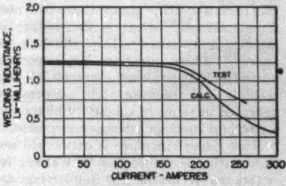

Figure 3. Welding-inductance characteristic

Curve "calc." is from saturation curve, Figure 2. Curve "test" is from oscillogram, Figure 4

---

* The oscillograph element may be connected directly across the reactor winding and the induced voltage determined by subtracting instantaneous values of IR drop.

** A second method for determining welding inductance experimentally lies in superimposing a small alternating current on various values of direct magnetizing current. The a-c inductance so measured is "the welding inductance." The oscillograph method is generally to be preferred, however, for the latter usually presents circuit problems.

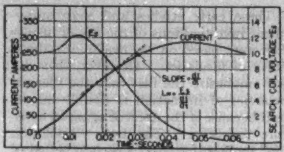

Figure 4. Plot of current and search-coil voltage from oscillogram of open-circuit to short-circuit test, showing method for determining welding inductance

in the use of electromagnetic material. Such a waste would be without advantage to either the designer or the user.

The general problem of design, therefore, is to find not so much *some combination* of materials which will give the desired characteristics as certain *specific combinations* in which the materials are used most effectively for obtaining those characteristics. For the former method of approach is little more than a process of trial and error, whereas the latter is synthesis of design leading to compact efficient apparatus in which unused and unuseful material is eliminated. Through synthesis the product is "tailored" to the requirements of the user.

Now, in welding reactors the performance requirements are that the useful amount of inductance, L_w' shall be obtainable at a limiting current, I'. For most effective use of materials these values should be obtained at a point on the reactor characteristic where the maximum energy useful for welding is available. Just as welding inductance requires specific definition, the energy associated with this inductance must be defined in terms of its stabilizing influence on fluctuations above and below an average welding current. This means that the energy useful in welding is actually incremental energy—the rate of change of energy per ampere. An expression for incremental energy dW/dI, may be determined in the following manner.

Energy stored in magnetic circuits is defined as

$$W = \int EI\,dt \text{ joules}$$

Since

$$E = L_w \frac{dI}{dt} \text{ (from equation 2)}$$

then

$$\frac{dW}{dI} = L_w I \text{ joules per ampere} \tag{4}$$

For most effective use of materials the maximum incremental energy should occur at the limiting values of inductance and current, or

$$\left.\frac{dW}{dI}\right|_{\max.} = L_w' I' \text{ joules per ampere} \tag{5}$$

The significance of this concept is shown graphically in Figure 6, in which P is a typical welding-inductance characteristic and p is the incremental-energy characteristic as determined from equation 4. Curves Q and R are the inductance characteristics for the same reactor showing, respectively, the effects of increasing and decreasing the air gap 15 per cent. From these curves it is apparent that a change of air gap in either direction results in the loss of welding inductance at I' with a consequent sacrifice in welding characteristics at this current. This loss results from the occurrence of the maximum incremental energy at some current other than I' (see curves of q and r), even though the value of maximum incremental energy is substantially unaffected by changes in air gap.

It is apparent from this analysis that there are specific relationships between turns, core dimensions, and air gap for the most effective use of material. A departure from these relationships results in a sacrifice in performance or an ineffective use of materials. There are, of course, many possible variations in synthesized designs to meet a specified performance characteristic. Each has a different number of turns and different core dimensions. For example, one has the fewest number of turns and another the lowest weight, but the material in each is used most effectively when the maximum welding energy available is obtained at the limiting performance requirements. From this range of possibilities the designer chooses one which is best adapted to the welding generator.

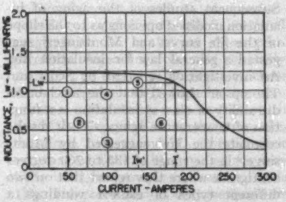

Figure 5. Method for determining welding-inductance requirements from welding tests

L_w' is limiting welding inductance, I_w' limiting average welding current, and I' limiting steady current

A New Arc-Welding Reactor

A new arc-welding reactor embodying the principles of most effective use of materials has a unique feature which improves the transient characteristics of the welding generator. This reactor, consisting solely of a U-shaped core and a winding, is mounted on the generator in such a manner that the magnet frame completes its magnetic circuit. In Figures 7 and 8 it is shown in combination with a Bergman split-pole welding generator.

Figure 7 shows the general distribution of flux in the machine at open circuit. It is noted that the magnet frame flux for this condition is confined principally to the top and bottom quadrants. But when current is caused to flow from the generator, the flux in these sections is transferred to the right and left quadrants. This exchange of flux progresses until, at short circuit, the generator flux in the magnet frame is confined principally to the right and left quadrants as shown in Figure 8. During sudden changes in current, it is normally necessary for the generator to supply energy for accomplishing this redistribution of flux.

The flux established by the reactor, on the other hand, increases from zero at no load to a maximum at short circuit. It thus serves to maintain substantially constant flux in the section of frame spanned by the reactor core, eliminating the energy normally required to change the flux in this section. The transient response of the generator is thereby improved proportionately.

A second benefit from this arrangement is the saving in space and weight made possible through the elimination of a large section of the reactor core.

Thus, while its prime function is to supply welding inductance, this reactor is integrated with the welding generator in such a manner that its transient characteristics are improved, and smaller lighter-weight designs are made possible.

Conclusion

The desirability of self-inductance in d-c arc-welding circuits has been established through long experience. Although improvements in generator design have made it practical to include the required inductance in the electromagnetic material of the generator, the recent trend toward smaller lighter-weight 3,600-rpm

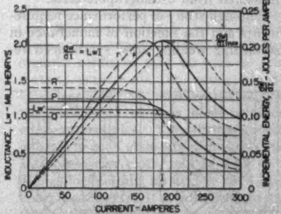

Figure 6. Welding-inductance and incremental-energy characteristics (curves *P* and *p*), showing effects of increasing the effective air gap 15 per cent (curves *Q* and *q*), and effects of decreasing the effective air gap 15 per cent (curves *R* and *r*)

Organo-Silicon Compounds for Insulating Electric Machines

T. A. KAUPPI
ASSOCIATE AIEE

G. L. MOSES
MEMBER AIEE

Synopsis: The general problem of electrical insulation is reviewed in relation to silicone insulating materials. Silicone compounds are described and their chemical and physical characteristics discussed. Thermal stability and moisture resistance of silicone insulation are compared to that of conventional class-*A* and class-*B* insulation. Predictions are made as to the field of usefulness of silicones in electrical insulation. Recommendations are made for widespread investigation to evaluate the over-all advantages of this new type of insulation.

THE aging of insulating materials is an important factor in the life of electric machines. It is the organic components which age and therefore the deterioration of class-*B* insulation is largely determined by the bonds and varnish rather than by the inorganic components, which have indefinite life. Arnold and Frost[1] indicate that insulating varnish is the most important factor from the standpoint of insulation aging. The permissible operating temperature limits[2] imply this as they permit only a 20-degree-centigrade increase in observable temperature for class *B* over class *A* when inorganic materials such as mica, asbestos, and fiber glass are used in combination with organic resins.

Very early in the development of electric machinery the relation between the life of machine insulation and the operating temperature was recognized. In 1898 discussions of this occurred in meetings of the AIEE.[3] In 1913 Lamme and Steinmetz[4] said, "The problem of permissible temperature limits in electric apparatus is largely that of durability of the insulation" and proposed the idea of a curve expressing the life of insulation. Subsequent studies of the aging of insulation modified opinions as to the shape of the life curve and Montsinger[5] suggested a general law for insulation life. An investigation reported by Scott and Thompson[6] showed that the mechanical durability of class *A* insulation is a function of temperature aging. Their results correlate the law suggested by Montsinger[5] in the range of 135 to 200 degrees centigrade where they report that on two different types of class-*A* windings a temperature increment of 10 to 11 degrees centigrade reduced the time to failure to half.

These early studies and most subsequent investigations of the life of insulation were based on the mechanical durability of insulation. However, they did not emphasize the fact that the thermal behavior of insulation is doubly important because of the effect of aging on moisture resistance. The term "insulation life" implies that after a certain period of aging the useful life of the insulation is expended or that there is a fairly definite end point. However, life is a variable thing and it is preferable to consider that the actual value of insulation life in the laboratory depends on the tests or criteria used to determine the end point. Likewise, service conditions determine the life in normal operation. The use of very severe tests, or severe operating conditions, will result in a minimum life which may be only a fraction of the maximum-life end point obtained by less rigorous conditions. Since one of the most important functions of an insulating varnish is to exclude moisture from the electric windings, it is the opinion of the authors that minimum life of a varnish film may be taken as the point at which a hazardous reduction in moisture resistance occurs.

This general line of reasoning has been applied to the development and evaluation of a totally new group of insulating varnishes, known as silicones. The first silicone varnishes made in the laboratory exhibited remarkable heat stability and waterproofness when compared to organic varnishes. However, it was found necessary to modify the original resins to suit them to the handling requirements of electric-machinery manufacture, and to develop new silicone resins for use in different types of insulation. In this development it was imperative to retain the heat stability and moistureproofness of the original silicones, and therefore it was necessary to have tests which would evaluate these properties.

It is the purpose of this paper to give a brief account of the development of the materials known as silicones, a description of their properties as applied to electrical insulating problems, and a report on some of the results obtained to date and on the work now in progress.

Development of Silicones

Silicones as a new class of high polymeric materials[7] resulted from fundamental research in the field of polymer chemistry bounded by the glasses and

---

Paper 45-30, recommended by the AIEE committee on electric machinery for presentation at the AIEE winter technical meeting, New York, N. Y., January 22-26, 1945. Manuscript submitted November 24, 1944; made available for printing December 12, 1944.

T. A. KAUPPI is manager of product engineering for the Dow Corning Corporation, Midland, Mich., and G. L. MOSES is section engineer, development insulation section, a-c generator engineering, Westinghouse Electric and Manufacturing Company, East Pittsburgh, Pa.

---

welding sets has placed a new emphasis on the desirability of external reactors.

There is a particular kind of inductance, termed "welding inductance" in this paper, which is effective in producing desired welding characteristics. This inductance, defined as the rate of change of flux linkages per change in current, may be calculated by graphical means and measured from oscillographic tests.

Through study of performance requirements and the function of inductance in stabilizing welding arcs, synthesized reactor designs take full advantage of electromagnetic material. They are thus "tailored" to the requirements of the user through the elimination of unused and unuseful weight.

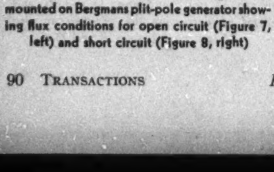

Figures 7 and 8. New arc-welding reactor mounted on Bergmans plit-pole generator showing flux conditions for open circuit (Figure 7, left) and short circuit (Figure 8, right)

Nomenclature

L_w = welding inductance, henrys
I = current, amperes
ϕ = flux, webers
t = time, seconds
E_s = search-coil voltage (at time t), volts
W = energy, joules
N = number of turns
A = area of magnetic circuit, square inches
l = length of magnetic circuit, inches
G = effective air gap, inches

$$= \text{air gap} \times \frac{\text{area of magnetic circuit}}{\text{effective area of air gap}}$$

References

1. A NEW SYSTEM FOR D-C ARC WELDING, S. R. Bergman. AIEE TRANSACTIONS, volume 50, 1931, pages 678-80.

2. SOME ASPECTS OF INDUCTANCE WHEN IRON IS PRESENT, L. T. Rader, E. C. Litscher. AIEE TRANSACTIONS, volume 63, 1944, March section, pages 133-9.

silicates on the one hand and by the organic plastics on the other. Interest was stimulated by the development of fibrous glass for electrical insulation, since insulating resins and varnishes of a high order of heat resistance were needed before the maximum advantage could be taken of the thermal stability of fiber glass. It soon became apparent that silicones were natural complements to glass, mica, and asbestos in bonding, filling voids, and excluding moisture.

Silicones are derived from sand, brine, coal, and oil as ultimate-source materials. However, like certain of the organic high polymers which are said to come from coal, air, and water, their synthesis involves a number of steps and a considerable amount of industrial and chemical technology as indicated in Figure 1. Sand provides the source of silicon and when heated with coke from coal and chlorine from brine, forms silicon tetrachloride. Organic chlorides, made from hydrocarbons derived from coal and oil by treatment with chlorine from brine are attached to silicon through the use of magnesium metal, also from brine. This reaction[8] replaces one or more chlorine atoms in silicon tetrachloride with a hydrocarbon radical as shown in Figure 1 to produce a variety of organo-silicon chlorides. These are then treated with water to remove all the chlorine and by-product magnesium chloride. The silanols so formed condense with each other to build up large molecules in a manner similar to the hardening of a silicic acid gel or the setting of a phenol-formaldehyde resin.

Liquid Silicones

One of the first groups of silicone polymers to reach commercial production was the liquid silicones. Several families of these silicone fluids are now available in a wide range of viscosities. They are characterized in general by the properties of low change of viscosity with temperature, low freezing point, unusual inertness, and stability to heat. The silicone fluids are finding application as gauge liquids, damping fluids, and in various hydraulic applications. An interesting application is the use of a dilute solution of silicone fluid for treating ceramic surfaces to render them water repellent.

Liquid silicones fall into two groups based on the range of viscosity and service temperature to be covered. Fluids for use down to −55 degrees centigrade and below are listed in Table I for one type covering viscosity grades up to 100 centistokes. The viscosity grades above 20 centistokes are nonvolatile and useful as liquid dielectrics. Their temperature coefficient of viscosity is very low. Fluids for use down to −40 degrees centigrade and up to 200 degrees centigrade are listed in Table II for another type of fluid silicones covering viscosity grades from 100 centistokes upward. All viscosity grades in this type are nonvolatile-liquid dielectrics with an even lower rate of viscosity change with temperature than the lighter-viscosity fluids of Table I. The liquid silicones in Tables I and II are further characterized by their heat stability, their general inertness, and oxidation resistance. They are noncorrosive to metals and are nonsolvents for rubber, synthetics, and other organic plastics. Their flash points are considerably higher than petroleum oils of equivalent viscosity and they will burn, when once ignited, to form silica, carbon dioxide, and water. Their surface tension is low, about 20 dynes per centimeter, and they readily wet clean, dry surfaces of glass, ceramics, and metals, making them water repellent. They are insoluble in water, and are unaffected by water, dilute acids, or salt solutions. They are soluble in most organic solvents including carbon tetrachloride and aromatic naphthas, but are insoluble in alcohol and acetone.

The dielectric constants of the nonvolatile types of the silicone fluids listed range from 2.7 to 2.8 at room temperature depending on the viscosity grade. The dielectric constant of these fluids decreases with increase in temperature. The change is about that which would be expected from the expansion data from Tables I and II. The dielectric constant of liquid silicones changes very little with frequency as shown in Table III. The power factors of these fluids are unusually low, being less than 0.0001 at ordinary frequencies. They do not increase appreciably with increased frequency up to 10^7 and 10^8 cycles as the data of Table III show. At higher frequencies, there is evidence of a more rapid rise in power factor. The power factor increases with temperature but remains lower than a typical transformer oil. Their dielectric strength at 60 cycles is 250–300 volts per mil at 100 mils. Their volume resistivity is in the order of 10^{14} and does not drop below 10^{12} at 200 degrees centigrade. The low dissipation factors of these liquid silicones at elevated temperatures or at high frequencies and their inertness to moisture indicate them for use in liquid-filled capacitors.

Silicone Greases

A translucent silicone grease having a consistency like petroleum jelly has been developed for use as a lubricant for ignition cables to reduce corona cutting of the insulation and permit easy wiring of ignition harnesses. It is stable to heat and retains the consistency of a soft grease from −40 to 200 degrees centigrade. Although it is a soft grease in appearance, it has the unusual property of not melting on exposure to heat. This material also is inert and oxidation resistant. It has no solvent effect upon synthetic insulations or rubber, and tends to prevent the hardening of these materials when heated in contact with air.

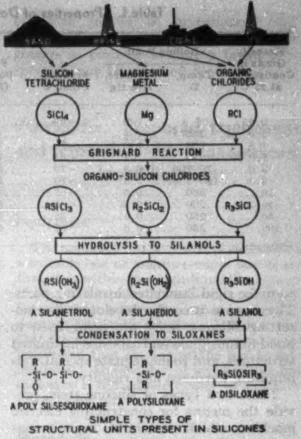

Figure 1. The general chemical processes for the formation of silicones from sand, brine, coal, and oil

Other greases under development are being used for lubricating ball and roller bearings. One type can be used at temperatures as low as −60 degrees Fahrenheit and has high-temperature stability at least as good as the best available organic greases. Another type of silicone lubricating grease is showing stability in ball bearings several times as great as organic greases at the same temperature.

Silicone Resins

Silicone resins are available in two principal types. The first is the insulating-varnish type, which is comparable in physical properties to organic oleoresinous varnishes. The baking temperatures required to cure the currently available silicone varnishes are sufficiently high (200–250 degrees centigrade) to prohibit their use on organic materials; whereas organic varnishes may be used to coat cotton, paper, silk, or wood, silicone varnishes must be used with inorganic materials, such as glass fiber, asbestos, mica, or ceramics. The silicone varnish is used to coat glass-served magnet wire and fiber-glass cloth, and is used as a binder for building up flexible mica-glass laminated sheet. It is also used as the final impregnating and coating varnish to bind together the individual machine components and waterproof the complete assembly.

The second type of silicone resin corresponds in general behavior to the organic thermosetting resins normally used

Table I. Properties of Dow Corning Type-500 Fluid

Viscosity Grade in Centistokes at 25 C	Boiling Point Temp, C	Boiling Point Pressure, Mm Hg	Freezing Point, C	Flash Point, F (Min)	Sp Gr at 25 C/25 C	Refractive Index at 25 C	Expansion Coef, $C \times 10^3$ per C, 25 to 100 C
0.65	99.5	760	−68	30	0.7606	1.3748	1.598
1.0	152	760	−86	100	0.8182	1.3822	1.451
1.5	192	760	−76	160	0.8516	1.3872	1.312
2.0	230	760	−84	195	0.8710	1.3902	1.247
3.0	70–100	0.5	−70	225	0.896	1.394	1.170
5.0	120–160	0.5	−70	270	0.918	1.397	1.095
10	200	0.5	−67	350	0.940	1.399	1.035
20	200	0.5	−60	520	0.950	1.400	1.025
50	250	0.5	−55	540	0.955	1.402	1.000
100	250	0.5	−55	600	0.966	1.403	0.994

to make rigid laminated insulating parts. These more recently developed thermosetting silicone resins are being used to bond fibrous glass and asbestos laminated structures, and to impregnate special coils requiring hardness and rigidity.

These two types of silicone resin provide the means for constructing electric machines which contain no organic materials. The thermal limitations of the complete insulation may be raised to such an extent that thermal aging of the insulation can be ignored in the design process. Factors other than insulation aging will then ordinarily establish the normal operating temperature of the machine at a point well below the temperatures which could be permitted if silicone insulation were used.

Typical Material Tests

Numerous laboratory tests have been made comparing the thermal endurance of silicone resins with many of the organic resins. The most common test is for flexing life on metal panels. This test corresponds to the ASTM "heat endurance" test for varnishes[9] except that elevated temperatures are used. For the tests reported a film 0.002 inch thick is coated on each side of an aluminum panel 0.005 inch thick. After aging at temperature, the end point is determined by bending around a definite mandrel (one-eighth inch diameter is standard).

The results of a series of tests to determine the flexibility life for a silicone resin and for one of the better organic synthetic resin (phenolic alkyd) varnishes are shown in Figure 2. These tests clearly indicate the different order of magnitude of the thermal endurance of the silicone resin. It is of particular interest to note the tests indicate that the life follows the general form of law suggested by Montsinger.[5] This is of considerable significance if it can be demonstrated that the life of insulation on apparatus follows the same law over a wide spread in temperature as it will permit extrapolation of highly accelerated thermal-aging-test data.

Tests on Stator Coils

Tests on sample a-c stator coils show comparable results to those on materials and varnish films. A typical series of tests compares standard class-*B* stator coils and similar silicone-insulated coils which are identical in all respects except the bonding resins, impregnating varnish, and surface film. The coils use glass-insulated wire, glass-backed mica wrapper on the slot section, glass-backed mica tape on the diamonds, and are taped all over with glass tape. In the series of tests reported in Figure 3 the moisture resistance of the two groups of coils is compared during aging at 200 degrees centigrade in air. The initial insulation resistances as well as the values after aging were determined with the coils half immersed in tap water. The values were all measured with a 500-volt d-c megohm bridge one minute after voltage application after one hour in water. The curve clearly indicates the considerable improvement obtained in thermal endurance of the moisture resistance through the substitution of silicone resins for high-grade phenolic-alkyd resins. The difference in the initial insulation resistance is indicative of the superior moisture resistance of silicone resins.

Tests on Complete Apparatus

The final criterion of insulation life is its ability to endure under actual operating conditions in service. Laboratory tests on insulation specimens are useful for purposes of comparison but correlation between such tests and actual performance is always difficult and often impossible. It therefore appears desirable to parallel laboratory tests on materials with tests on complete apparatus, simulating severe service conditions so far as possible. Such tests should be made at several different temperature conditions so that the temperature slope of the thermal endurance can be established.

Special tests have been devised to provide a common basis for such appraisal of the insulation characteristics of motors having high-temperature silicone insulation. These tests were drawn up by a group of engineers representing several companies interested in this development. The primary yardstick used in these tests is the moistureproofness of the insulation. The equipment and procedure for these humidity tests are detailed in the appendix. Windings are exposed to humidity (usually for 24 hours) to determine their resistance to moisture both initially as a bench mark and after some degree of accelerated aging or other damaging test.

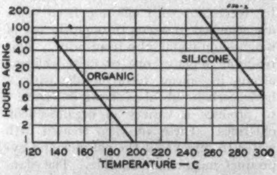

Figure 2. Comparison of the heat endurance of organic and silicone varnishes

Aging to the point of flexing failure is shown on aluminum panels for several temperatures

To establish the initial condition for a bench mark the windings are humidified by this method for 24 hours and the insulation resistance is then measured be-

Table II. Properties of Dow Corning Type-200 Fluid

Viscosity Grade in Centistokes at 25 C	Flash Point, F (Min)	Sp Gr at 25 C/25 C	Lbs/Gal at 25 C	Refractive Index at 25 C	Expansion Coef $C \times 10^3$ Per Deg C: —25 to 0 C	Expansion Coef $C \times 10^3$ Per Deg C: 25 to 100 C	Viscosity in Centistokes at —40 F	Viscosity in Centistokes at 100 F	Viscosity in Centistokes at 210 F
100	600	0.968	8.08	1.4030	0.926	0.969	650	82	32
200	615	0.971	8.10	1.4031	0.921	0.968	1,300	160	65
350	625	0.972	8.11	1.4032	0.917	0.966	1,950	260	135
500	625	0.972	8.11	1.4033	0.909	0.965	3,300	370	190
1,000	640	0.973	8.12	1.4035	0.900	0.963	6,500	735	260

tween winding and frame. Immediately thereafter a five-minute high-potential test is applied between winding and frame using a test-voltage value the same as the rated line-to-line voltage of the machine. Finally, the machine is operated at normal voltage with no load for five minutes.

As a damaging test of thermal endurance it has been recommended that motors be operated at 240 degrees centigrade as observed by resistance of the winding. The motor should be shut down at least once a day to permit thermal cycling. At periods of 200 hours elapsed time (at temperature) the humidity test should be made to include taking insulation resistance data, five-minute high-potential test, and five-minute no-load run. Where similar tests are to be made at different temperatures to explore the slope of the temperature-aging curve, it is suggested that the length of the running period between humidity tests be halved for each 12-degree centigrade increase or doubled for each 12-degree centigrade decrease in observed temperature by resistance. Such tests are now underway by several investigators comparing silicone and standard insulations. It is suggested by the authors that experimental data from these tests be discussed before the Institute as the data become available to permit rapid evaluation of silicone types of insulation.

Conclusions

It is important to recognize that the use of silicone resins in electrical insulation need not represent any radical departures from well-established practices. Inorganic components of high-temperature insulation have long been available and their characteristics proved. It was the organic bonds, impregnants, and surface treatments which limited the thermal endurance of composite insulation containing mica, asbestos, and fibrous glass. References made in this paper to silicone insulation imply the substitution of silicone resins for all the organic resins in the better grades of class-*B* insulation and do not refer to the use of silicone resins as mica substitutes in any way.

Innumerable tests in the laboratory and over 50 years of service experience have demonstrated that thermal aging is the most important single factor in insulation life. Only after such aging occurs does good insulation become vulnerable to the other ills which plague it. Differences in the thermal endurance of various types of insulation have been clearly demonstrated to be a function of the stability of their essential components. Therefore, the recent development of silicone resins promises great improvement in thermal stability of insulation for electric machines as it improves the weakest link in the insulation system. This improvement properly utilized by designers can be a great asset to the industry. There is no point in increasing operating temperature unless some useful economic purpose is served, but where electric machinery must operate at elevated temperatures silicone resins and high-temperature insulation offer a solution to a previously unsolved problem.

Table III. Dielectric Properties of Typical Dow Corning Silicone Fluids

(At 25 C and 50 Per Cent Relative Humidity)

	3 Centistokes, Type 500		350 Centistokes, Type 200	
Frequency, Cycles	Dielectric Constant	Power Factor	Dielectric Constant	Power Factor
10^3	2.412	0.0001	2.74	0.0001
10^5	2.41	0.0001	2.73	0.0001
10^6	2.405	0.0002	2.72	0.0002
10^7	2.40	0.0002	2.71	0.0002
10^8	2.39	0.0002	2.70	0.0006

Silicone resins have been demonstrated to have thermal stability far beyond that of the best of the conventional organic materials. It therefore appears timely to re-examine the thermal endurance requirements for insulation of electric machinery, to evaluate the possibile advantages from the use of these more heat-resistant materials, and to seek means for utilizing them for the improvement of electric machinery where their use is justified. These general problems should be investigated and tests made by as many interested engineers as possible so that a broad perspective may be obtained promptly.

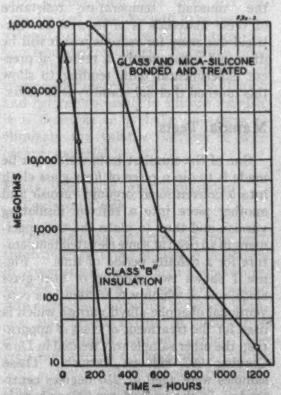

Figure 3. Comparison of the moisture resistance of class-*B* and silicone-treated insulations on typical a-c generator coils during aging at 200 degrees centigrade

Insulation resistance values were taken after one hour immersion in tap water for each point

Appendix. Proposed Equipment and Procedure for Standardized Humidity Test

Equipment

The apparatus to be tested is enclosed in a suitable box or moisture-vapor barrier so that it is within the high-humidity atmosphere. The top should be slanting or peaked (or otherwise arranged) so that condensate does not drip on the winding. It is desirable that the sides of the box have thermal insulation and that the top of the box be uninsulated. An open pan of water within the enclosure is heated electrically to humidify the enclosed air.

Procedure

The relative humidity is maintained at 100 per cent by heating the open pan of water within the enclosure to five or ten degrees centigrade above the ambient air temperature in the enclosure. This should be sufficient to produce minute droplet condensate on the frame and insulation surfaces of the apparatus. However, it must not produce sufficiently severe condensation to form puddles or streams of water on the insulation. The test equipment should preferably be located in a room whose ambient temperature is between 25 and 30 degrees centigrade. Apparatus not open for the free circulation of air must have one end bracket removed to permit free access of the humidified air to all parts of the winding.

References

1. Service Requirements of Insulating Varnishes, R. H. Arnold, L. E. Frost. *Industrial and Engineering Chemistry*, volume 25, 1933, page 133.

2. AIEE Standard 1, General Principles Upon Which Temperature Limits Are Based in the Rating of Electrical Machinery and Apparatus.

3. The Standardizing of Generators, Motors, and Transformers, AIEE Transactions, volume 15, 1898, pages 3–22.

4. Temperature and Electrical Insulation, C. P. Steinmetz, B. G. Lamme. AIEE Transactions, volume 32, 1913, pages 79–89.

5. Loading Transformers by Temperature, V. M. Montsinger. AIEE Transactions, volume 49, 1930, pages 776–92.

6. Temperature-Aging Tests on Class-*A*-Insulated Fractional-Horsepower Motor Stators, J. A. Scott, B. H. Thompson. AIEE Transactions, volume 61, 1942, pages 499–501.

7. Silicones, a New Class of Polymers, S. L. Bass, J. F. Hyde, E. C. Britton, R. R. McGregor, *Modern Plastics*, volume 21, 1944, page 124.

8. Organic Derivatives of Silicon Preparation of Alkysilicon Chlorides, F. S. Kipping, *Proceedings* Chemical Society (London, England), volume 20, 1904, page 15.

9. American Society for Testing Materials *Standards*, *D*-115–41, paragraphs 17–19.

The Application of Silicone Resins to Insulation for Electric Machinery

J. DeKIEP
MEMBER AIEE

L. R. HILL
NONMEMBER AIEE

G. L. MOSES
MEMBER AIEE

Synopsis: Experience with the application of silicone resins is described, including laboratory tests on materials and coils, as well as laboratory tests on rotating apparatus. Practical problems regarding the use of these materials are discussed and recommendations made for obtaining an adequate high-temperature insulation. Thermal aging tests are reported and recommendations made as to tentative temperature limits for general rating and application purposes.

THE thermal endurance of insulation has long been recognized as an important limiting factor in electric-machine design. The investigations of numerous engineers[1,2] and the electrical-industry standards[3] have clearly indicated that operating temperature is the determining factor for insulation thermal endurance and is, therefore, the primary basis for establishing general machine ratings. It must be recognized, however, that there are frequently other design considerations which outweigh temperature limitation.

The advent of silicone resins is an important milestone in insulation development as these resins in combination with inorganic insulations such as mica, asbestos, and fiber glass have unusually high thermal endurance. It appears that designers may utilize this excellent temperature resistance in three important ways, when permitted by AIEE Standards:

1. To reduce size and weight of some apparatus through increase in operating temperature.

2. To permit operation in a high ambient temperature.

3. To obtain increased insulation service life or reliability where it is desired to maintain conventional size, weight, and temperature.

Silicone-Resin Development

Recent developments have made possible the production of a new class of materials known as silicones having certain unusual properties which are of vital interest to the electrical industry. Some silicone materials have physical properties which are comparable to conventional organic materials such as varnishes, oils, greases, plastic resins, and film-forming materials. They are, however, characterized by a chemical structure in which silicon takes the place of carbon in certain portions of the molecule. They have mechanical and electrical stability when exposed to elevated temperature. Based upon recent work by the Dow Corning Corporation, it is now apparent that the silicone materials can be produced so that they duplicate many of the better known organic materials with respect to most physical properties. Silicones can be "tailor made" for specific applications in the same way that organic compounds have been developed in the past. Since the unusual temperature resistance of these materials is of interest to electrical designers for reasons which will be discussed subsequently, a review of present experimental data tending to show this unusual thermal stability is in order.

Material Tests

One of the simplest tests which can be made is to dip a piece of fiber-glass cloth into a conventional organic varnish and another piece into a silicone insulating varnish and then to place the two specimens in an oven at some elevated temperature for a definite period of time. Figure 1 shows two samples of fiber-glass cloth, one of which was treated in a conventional phenolic-alkyd varnish which is used for the treatment of class *B* apparatus; the other sample was treated in Dow Corning 993 silicone varnish. These samples were aged at 250 degrees centigrade. In the unaged condition there is very little difference in the mechanical properties of the two samples. They are both good electrical insulators, are not seriously affected by immersion in transformer oil, and are quite moisture resistant. After only two hours' aging, the sample which was treated in organic varnish was seriously affected and after 20 hours' aging had completely deteriorated and under no circumstances could be considered as a dielectric material, while the silicone-treated sample had undergone no observable deterioration.

A more quantitative evaluation of the relative thermal stability of conventional organic varnishes and silicone varnish can be obtained by making the standard ASTM flexing life test (frequently called heat endurance) for insulating varnishes. It has been found that the use of copper panels as recommended by ASTM is not satisfactory since the copper is prone to rapid oxidation and it is desirable to substitute either cadmium plated copper or aluminum for the test panels. Figure 2 shows the relative ASTM flexing life of a conventional phenolic-alkyd varnish and one of the silicone varnishes. It is well known that these flexing life tests do not indicate the point at which varnish films would fail on an electric machine, but they are useful for comparing the relative order of magnitude of heat endurance. The end point of this test corresponds roughly to a 14 per cent elongation of the film. It is of interest to examine the rate at which the maximum elongation for failure changes with time and temperature. Figure 3 gives the percentage elongation for failure ont he modified ASTM flexing life test plotted against the number of hours aging. At 200 degrees centigrade a good phenolic-alkyd organic varnish will last about two hours before failure occurs at 14 per cent elongation. One silicone varnish under the same condition will last about 1,000 hours. At seven per cent elongation and 200 degrees centigrade the organic varnish will last about 40 hours while the silicone varnish will last about 1,500 hours. These data indicate that at the same temperature, the silicone varnish may last from 40 to 500 times as long as an organic varnish.

A very sensitive test on the relative thermal stability of two materials can be made by coating copper wire with the resins and making elongation tests at periodic intervals after aging at elevated temperature. Figure 4 gives a detailed comparison between a wire enameled with an oleoresinous varnish, a synthetic organic resin enamel, and one of the silicone insulating varnishes. At 150 degrees centigrade the silicone-enameled wire was aged for 6,964 hours before it failed at an elongation of nine per cent while the synthetic-organic-resin-insulated wire failed at a nine per cent elongation after only 240 hours. At 200 degrees centigrade the synthetic-organic-resin-insulated wire failed at an elongation of three per cent in two hours while the silicone-insulated wire was aged for 216 hours before failure at the same elongation.

A critical analysis of all the relative data on aging of organic materials and silicone materials leads to the conclusion that the silicones are highly stable with respect to thermal aging; however, since

---

Paper 45-23, recommended by the AIEE committee on electric machinery for presentation at the AIEE winter technical meeting, New York, N. Y., January 22–26, 1945. Manuscript submitted November 22, 1944; made available for printing December 8, 1944.

The authors are all associated with the Westinghouse Electric and Manufacturing Company, East Pittsburgh, Pa. J. DeKiep is manager, a-c motor engineering; L. R. Hill is section engineer, insulation section, feeder engineering; and G. L. Moses is section engineer, development insulation section, a-c generator engineering.

The authors gratefully acknowledge the co-operative work of numerous members of the Dow Corning organization which made this development possible. In addition, acknowledgment is made for continued interest and helpful guidance of Messrs. R. C. Bergvall, J. G. Ford, C. F. Hill, and J. Swiss, all of the Westinghouse Electric and Manufacturing Company.

Figure 1. Samples of fiber-glass cloth coated with organic resin and silicone resin varnishes showing effect of aging at 250 degrees centigrade

the rate of deterioration with respect to different temperatures is not a constant factor for either the organic materials or the silicone materials, it is necessary to compare the two at a specific temperature if a comparison of their relative heat stability is to be made. It is the opinion of the authors that silicone varnishes which are now available will protect electric apparatus for 20 to 100 times as long as conventional organic materials at the same temperature, or to put the matter another way, operating temperatures may be raised 50 to 75 degrees centigrade when these resins are used.

Since the silicone resins are characterized by extreme heat stability, it would be reasonable to suppose that they would also require higher temperatures for drying and processing. At the present time this is the case for most of these. It has been found that electric machines insulated with silicone varnishes must be baked at temperatures from 200 to 250 degrees centigrade for times which are comparable to standard processes using organic varnishes. There is some indication, from recent experimental work, that this condition will not always exist.

Tests on moisture permeability using a Payne cup indicate that the moisture transmission through films of cured silicone varnishes is comparable to that obtained through the better grades of organic insulating varnishes and materials such as soft vulcanized rubber, molded phenolics, or asphalt sealing compounds. These tests might lead to the belief that very little improvement in the moisture resistance of electric machines could be obtained by using silicone insulation. Actual tests on insulated coils, however, indicate that silicone-insulated coils maintain their insulation resistance under high-humidity conditions for a much longer period of time than do coils insulated with organic varnishes.

High-Temperature Insulating Materials

Extensive tests have indicated that materials deteriorate under the influence of heat due to two effects which are apparently independent of each other and differ in relative magnitude depending on the specific materials. One of these effects is caused by oxidation and can be prevented to a certain extent by minimizing the presence of oxygen. The second effect, sometimes called thermal decomposition, is primarily a function of time and temperature. Since most conventional organic materials show rapid thermal deterioration below the processing temperatures for silicone resins, it is desirable that all such materials be eliminated from the coils, filling strips, wedges, and other insulating structures of a machine. Therefore, it has been necessary to develop a complete line of insulating materials based on silicone resins which replace the conventional materials containing organic matter susceptible to thermal decomposition. Silicone-varnished-glass cloth, silicone–glass–mica wrappers, silicone–glass-covered wire, silicone filling cements, silicone–glass–mica tape, silicone-sized glass tape, and silicone-treated asbestos cloth have been developed for limited use in high-temperature insulated machines. In certain cases it is difficult to eliminate thin layers of tissue paper on composite mica insulation and before processing in silicone varnish, it is desirable to prebake apparatus to eliminate the volatile portions of such organic material.

Heat, Vibration, and Expansion Tests on Coils

Tests were run on armature coils with three different types of class *B* insulation in comparison with high-temperature-silicone insulation. These were wound into a core and subjected to severe vibration and thermal cycling in combination with accelerated thermal aging. The coils were typical d-c generator armature coils and each coil consisted of two single coils per slot composed of four strands of 0.114 by 0.229-inch copper ribbon. All groups had mica ground insulation, but numbers 2 and 4 used glass-backed mica. Groups 1 and 3 were finished with asbestos tape and were treated with a high-grade organic thermosetting varnish and groups 2 and 4 with glass tape. Groups 1, 2, and 3 were treated with thermosetting varnish and group 4 with silicone varnish. There were nine coils from each group wound in a core as shown in Figure 5. A fractional-horsepower high-speed motor operated on an unbalanced flywheel to provide severe vibration. All the coils were connected in series and energized through a cycle drum and a timer so that the coils were heated for 12 minutes and cooled by a blower for 18 minutes. The test ran 16 hours a day for 36 days, during which the coil temperatures were between 209 and 230 degrees centigrade. The asbestos finishing tape in groups 1 and 3 showed serious thermal deterioration and the glass tape in group 2 became hard and brittle, while the glass finishing tape of group 4 (high-temperature-silicone insulated) was still soft and flexible. Mica treated with silicone resin retained considerable more flexibility than the class-*B* mica insulation. The glass-covered conductor insulation was in usable condition on both groups 2 and 4 but the insulation on the wire with silicone treatment had better flexibility than that treated with organic resin.

Thermal Aging Test of Totally Enclosed Induction Motor

It is believed that the first motor successfully treated with silicone resins was a totally enclosed fan-cooled induction motor on which tests were started early in April 1942. For this test it was designed for ten horsepower, three phases, 60 cycles, 440 volts, four poles, 1,690 rpm. It was insulated with the best available grade of class-*B* insulating materials using glass and mica and the finished winding treated with silicone varnish. (Composite high-temperature-silicone insulating materials were not used as at that time they were not available.)

SUMMARY OF TESTS

1. Complete engineering tests were made including full-load temperature run at rated horsepower (100 degrees centigrade rise by thermocouple).

2. The motor was overloaded, the temperature reaching 416 degrees centigrade in $1^1/_2$ hours.

3. The load was reduced until the temperature stabilized at 300 degrees centigrade.

4. The motor was heavily overloaded for a

period of 45 minutes, the temperature of the windings reaching 506 degrees centigrade.

5. After the foregoing tests the motor was retreated and then given a thermal endurance test at a load producing 210 degrees centigrade rise by resistance. This test continued for a total of 3,376 hours at an estimated hot-spot temperature of approximately 250 degrees centigrade.

6. Periodically the motor was dismantled for examination and exposed to high humidity and various insulation tests.

DETAIL DISCUSSION

After thermal endurance test of 920 hours the silicone-varnish treatment was in generally good condition. The windings stood high-potential and high-frequency tests at 2,000 volts, insulation-resistance tests, and high-potential tests after exposure to humidity without failure. After a severe humidity test with end bells removed, the insulation resistance was reduced but was adequate for operation. The motor was again examined and given humidity and insulation resistance tests after 2,250 hours aging. The varnish showed slight signs of deterioration but remained reasonably good. After 3,376 hours of operating on the accelerated aging test the motor stalled due to bearing failure. The rotor conductors melted and flowed over the windings as is shown in Figure 6. The silicone varnish and insulation were in relatively the same conditions as when last examined. It was evident that the bearing was the cause of failure. On the basis of this evidence it may be concluded that the winding and insulation were suitable for further operation. To examine the condition of the insulation, the motor was stripped. The resin was found to be brittle and to powder as the winding was stripped. At places the glass tape in the end windings broke easily. Loosening of the glass was more frequent in the end windings than in the slots, but glass-backed mica cells were still solid and flexible to a considerable degree. In most places the glass wire covering still retained adhesion to the conductors. It must be recognized that in this first silicone-treated motor other resins and bonds were used, the silicone varnish being used only for final treatments.

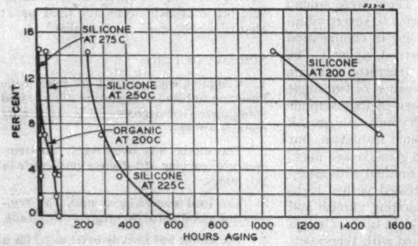

Figure 2. Comparison of flexing life of 0.002-inch-thick films of organic resin and silicone varnishes on copper panels aged at various temperatures

Thermal Aging Test of Medium-Size Three-Phase Generator

The stator winding of this generator was completely insulated with high-temperature-silicone insulation. This included silicone resins for treatment of the glass-covered wire, mica bond, treatment of glass cloth and tape, impregnation of the coils, and surface dipping of the wound stator. All ground insulation was glass-backed mica wrapper or tape. Treated glass was used only as a separator or binder. Slot wedges were of the best available grade of phenolic-bonded asbestos laminate plus a few made of phenolic-bonded glass cloth.

WATER-SPRAY TEST

An initial water spray was made to check the moisture resistance of the winding. During a 48-hour spray test the insulation resistance (one-minute value) of the winding fell from 28,000 megohms to 2,600 megohms.

THERMAL AGING TESTS

While heating the stator, the generator was driven at normal speed with the stator winding short-circuited. Field current was adjusted to produce a stator current of $2^1/_2$ times normal, resulting in approximately 210 degrees centigrade rise by resistance. Thermal cycling of the winding was obtained by operating the stator on short circuit on alternate days only. At other times the stator was operated on open circuit with the field overexcited. This resulted in approximately 40 per cent above normal voltage being generated in the stator winding producing the effect of overpotential test on turn and ground insulation. A further purpose was to provide thermal cycling of the windings on these alternate days.

The following temperatures in degrees centigrade were observed on the stator and are representative:

Ambient air temperature	25
Winding rise (by resistance)	211
Core rise (by thermometer)	94
Frame rise (by thermometer)	42
Outgoing air rise (by thermometer)	69

Periodically during the thermal aging test the machine was examined. The visual aging of the outer varnish film was very slight during the whole test. The machine operated for 2,966 hours with the stator winding at the conditions previously described. Based on 211 degrees centigrade rise by resistance with a 25-degree-centigrade ambient temperature and a 15-degree-centigrade hot-spot allowance, this is equal to approximately 250 degrees centigrade hot-spot temperature. At the end of this thermal aging test the winding was humidified, by maintaining exposed water surfaces heated above the ambient temperature in an enclosure. The generator was covered with a double thickness of waterproof paper and a tarpaulin. Water was evaporated at the rate of approximately three quarter gallon per 24 hours within this enclosure and the following values of insulation resistance observed:

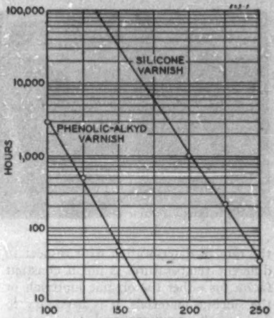

Figure 3. Comparison by elongation of silicone varnish film 0.002-inch thick and organic varnish film 0.002-inch thick after thermal aging

Time of Humidification	Stator Winding Megohms (One-Minute Value)
Start	4,900
3 days	2,800
16 days	1,300
19 days	380

FINAL INSULATION TESTS

Immediately upon completion of the final humidification test a series of tests was made on the stator winding (without dryout) as follows:

1. High-potential test to ground at 1.4 times rated voltage (60 cycles) for five minutes.

2. Operation open-circuited at normal speed with maximum field excitation (40 per cent overvoltage) for one hour.

3. Short circuit applied to stator terminals with field excitation set for normal open-circuit voltage. Applied for two minutes, with no evidence of loosening of winding.

4. Insulation resistance—10,200 megohms; dissipation factor—3.2 per cent.

5. Intentional destruction by high-potential test (without drying out winding). Held 1,000 volts and failed at 1,600 volts in 12 seconds. (Rated operating alternating voltage = 440 volts.)

Laboratory Tests on General-Purpose Induction Motors

Numerous totally enclosed fan-cooled induction motors have been made using high-temperature-silicone insulation and subjected to operation at high temperature. None of these motors as yet show any marked deterioration of the insulation as indicated by insulation-resistance readings and all motors have been subjected to high-potential tests with no breakdowns. The motors listed in Table I with the operating temperature and time of operation up to date were still under test at the time of preparation of this paper.

The table indicates that the use of silicone varnish and materials will make it possible to operate electric apparatus at a higher temperature than has been used previously. It must be recognized that in the use of higher operating temperatures, other problems must be studied. Air gaps may have to be larger to allow for more expansion of the rotor, bearings will have to allow for more shaft expansion, and bearings and lubricants must operate at higher temperatures.

High-Temperature Lubricants

From the standpoint of machine construction and operation, it is obvious that if the greater temperature stability of silicone resins and insulating materials is to be utilized it is necessary on certain apparatus to obtain lubricants which will function at higher temperatures. The development of silicone oils and greases has advanced to the point where it appears that these materials enjoy the same superiority over organic lubricants as silicone varnishes enjoy over organic varnishes. Tests on actual motors have indicated that the better grade of organic lubricants cannot be operated for extended periods of time above 90 degrees centigrade. Comparable tests on silicone greases lead to the belief that bearings lubricated with these materials can be operated at about 50 degrees centigrade above conventional limits. Extensive tests are now in progress and it appears likely that machines will be in service which have not only silicone treated and bonded insulation but silicone lubrication as well.

Table I

Motor (Hp)	Winding Temperature	(Deg C) Hours
2	170	3,486
2	165	3,486
4	140	3,996
4	160	3,996
7$^1/_2$	320	1,907
7$^1/_2$	320	1,907
15	185	3,506
15	170	3,506
25	160	3,291
25	135	3,291
6	285	4,500
10	250	3,400
10	250	3,400
25	240	3,300
10	200	5,200
10	185	3,200

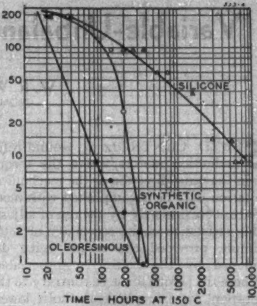

Figure 4. Elongation failure versus time for resin films on number 18 copper wire

Review of Design Factors

A large number of general-purpose induction motors have been wound using silicone-treated materials and silicone as an impregnating varnish. On open, splashproof, and semienclosed motors where the performance of the motor rather than the temperature determines the amount of material used, the use of high-temperature insulation gives no advantage. The size of these motors is determined by the pull-out torque, starting torque and starting current, efficiency, and power factor and it is found that when the above factors are maintained at values acceptable to the users, the temperature rise is such that present class *B* insulation has sufficient thermal stability to give life comparable to present class-*A*-insulated motors.

Silicone materials may have a use on totally enclosed and totally enclosed fan-cooled motors, as the present allowable temperature limits definitely determine the amount of material used. The design of these motors for maximum use of the electric parts, keeping the performance acceptable as stated above, gives temperatures somewhat in excess of the allowable class *B* temperature. For this type motor, the use of silicone materials with the higher temperatures may be advantageous.

Several totally enclosed and fan-cooled motors have been made and tested experimentally. The performance of these motors is not the ultimate performance as the electric parts used were those currently in use in class-*A*-insulated machines. For a true high-temperature motor for maximum use of the material it will be necessary to change the relation of copper to iron, the quality of the iron, length of air gap, and so forth. Further studies of this problem are now under way.

Special Considerations and Limitations

There has been considerable discussion of some of the limitations of silicone resins; for example, mechanical fragility, low abrasion resistance, and poor oil and solvent resistance. In this connection it must be recognized that there are many of these materials with varying physical characteristics. It is true that some, particularly the early forms, were considerably inferior to the better organic resins in some of these characteristics. However, there is considerable difference between silicone resins in this respect. More recently developed resins have been even better, and are now readily usable. That essential silicone characteristic, thermal stability, tends to make the resins difficult to cure. As a consequence, full physical characteristics, such as abrasion resistance, may not be developed unless proper processing is obtained. In using high-temperature-silicone insulating materials it is important that precautions be taken in every stage of manufacture to develop the essential physical and chemical characteristics of the silicone resins.

The high baking temperatures (usually 200 degrees centigrade to 250 degrees centigrade) necessary for curing silicone resins, in the present state of the art make it imperative that composite insulations contain little if any organic materials. All bonding resins for composite insulations should be silicone and an absolute

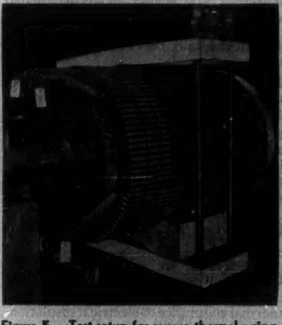

Figure 5. Test setup for severe thermal aging, thermal cycling, and vibration test

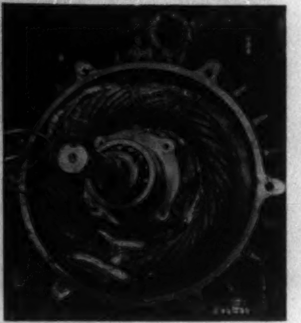

Figure 6. First silicone-treated motor after bearing failure

Operated 3,376 hours at 250 degrees centigrade hot-spot temperature

minimum of cellulose materials should be used for structural purposes. Before applying silicone treatment, either by impregnation or dipping, the coil or apparatus should be baked out, at a temperature at least equal to the final baking temperature, to drive cut all gas from decomposition of organic materials such as is contained in small percentages of cellulose.

It should be recognized that there is much to be learned regarding these new silicone compounds and their application to electric apparatus Furthermore, the high-temperature-silicone insulating materials are available in limited quantities. It, therefore, appears advisable to restrict the use of high-temperature-silicone materials to a few specific applications so that this development will be carried out in an orderly and progressive manner.

Interpretation of Tests

Tests on silicone resins, silicone-treated materials, and wound apparatus treated with silicone varnishes demonstrate that:

1. An unusually high order of thermal endurance is obtained.
2. The materials are usable with relatively minor variations in conventional processes (mainly in baking temperature).
3. That on some types of electric apparatus an appreciable advantage may be obtained in rating through operating at the higher temperatures when such are permitted by AIEE Standards.

Conclusions and Recommendations

Silicone resins and composite high-temperature-silicone insulation materials promise considerable improvement in the thermal endurance of electrical insulation. The exact improvement is difficult to evaluate and will require much additional experience and test work. It is believed conservative to state that the silicone materials with which the authors are familiar have from 50 to 75 degrees centigrade advantage over conventional class *B* insulations.

It is the recommendation of the authors that the availability of this new type of insulation be recognized at once by the assignment of some classification or designation to differentiate it from class *B* and *C*. It is further suggested that a tentative limit be established for this insulation at 40 degrees centigrade above the present observable temperature (by resistance) for class *B*. Furthermore, an increase of five degrees centigrade in hot-spot allowance is suggested. On this basis, it is suggested that the limiting hot-spot temperature for high-temperature-silicone insulation (corresponding to the 130 degrees centigrade limit for class *B* insulation in AIEE Standard 1) be set, at 175 degrees centigrade. It is recognized that certain industries have special standards and that only experience and further tests will demonstrate what their limits should be. It is the opinion of the authors that these recommendations are conservative but that the proposed temperature limits will give designers a significant advantage over class *B* temperature limits.

References

1. Temperature and Electrical Insulation, C. P. Steinmetz, B. G. Lamme. AIEE Transactions, volume 32, 1913, pages 79–80.

2. Loading Transformers by Temperature, V. M. Montsinger. AIEE Transactions, volume 49, 1930, pages 776–92.

3. AIEE Standard 1, General Principles Upon Which Temperature Limits Are Based in the Rating of Electrical Machinery and Apparatus.

4. New Silicone Resins Boost Insulation Temperature Limits, G. L. Moses. *Westinghouse Engineer*, September 1944, pages 138–41.

Variable-Unbalanced-Voltage Control

W. R. WICKERHAM
NONMEMBER AIEE

SPEED CONTROL of wound-rotor induction motors where the torque is in the same direction as the mechanical rotation may be accomplished with moderate success merely by the use of adjustable resistance in the secondary or rotor circuit, provided the torque being developed by the motor is appreciable. Where the torque must be contrary to the rotation, for example, crane-hoist lowering, the problem of control at less than synchronous speed becomes much more complex, and special consideration in control design is required. Such refined subsynchronous speed control can be attained, provided the torque is in excess of possibly 35 per cent of full load, by exciting the motor stator with direct current and adjusting rotor resistance in the ordinary way. For those applications where the countertorque is less than 50 per cent normal, or absent altogether, satisfactory speed control is provided by application of adjustable unbalanced polyphase voltage to the motor primary. Neither of these systems is entirely satisfactory for the complete speed–torque range, since the former does not provide low torque at high speeds and the latter does not provide rated torque at slow speeds. Both require considerably greater input current than the motor would require to develop an equivalent countertorque with balanced polyphase voltage applied. It is possible, of course, to control the countertorque in the orthodox manner by an adjustable rotor resistor. This system has been used extensively, but is considered satisfactory only for certain applications involving predetermined loads.

The performance characteristics of the polyphase induction motor, when operating with unbalanced primary voltage, have long been understood, and literature on the subject has appeared from time to time. Reaction to the use of unbalanced voltage generally has been pessimistic because of the associated phenomena of relatively high input current for a given output torque. It is the purpose of this paper to describe briefly a system of control which incorporates a new feature, namely, variable unbalanced primary voltage automatically responsive to speed. Introduction of variable unbalance has made it possible to:

1. Employ unbalanced voltage without the excessive input current which might be expected.
2. Obtain characteristics providing any degree of starting torque from zero to 75 per cent full load without adjustment of rotor resistance.
3. Obtain less than synchronous speed with no load.
4. Obtain characteristics providing re-

Paper 45-27, recommended by the AIEE committee on electrical machinery for presentation at the AIEE winter technical meeting, New York, N. Y., January 22–26, 1945. Manuscript submitted November 24, 1944; made available for printing December 11, 1944.

W. R. Wickerham is with the Westinghouse Electric and Manufacturing Company, East Pittsburgh, Pa.

tarding torques which are zero at zero speed, and which cover a speed range of 0 to 35 per cent at light or no load, and 10 per cent to 150 per cent at full load.

The essential elements of the control system are shown in Figure 10, and include a variable impedance reactor, a phase shifter, and a speed detector with amplifier, in addition to the parts composing a standard reversing controller.

Performance With Unbalanced Voltage

The familiar mental conception of the reactions taking place in an induction motor pictures a single revolving magnetic field on the stator, the rotor following at somewhat lessened speed, with voltage and frequency existing in the rotor windings in proportion to the slip. If the applied polyphase voltage happens to be unbalanced, the revolving field becomes unsymmetrical, that is, it does not have the same magnitude for all positions on the stator. This unsymmetrical field can be analyzed by the method of symmetrical components. By this means this unsymmetrical field can be replaced by two symmetrical fields, one of which revolves in the same direction as the rotor (positive sequence) and the other of which revolves in the opposite direction (negative sequence). The relative magnitude of negative sequence increases with the degree of unbalance. The net output torque of the motor is, of course, the algebraic summation of the component positive- and negative-sequence torques which are developed in the rotor due to the positive- and negative-sequence stator fields.

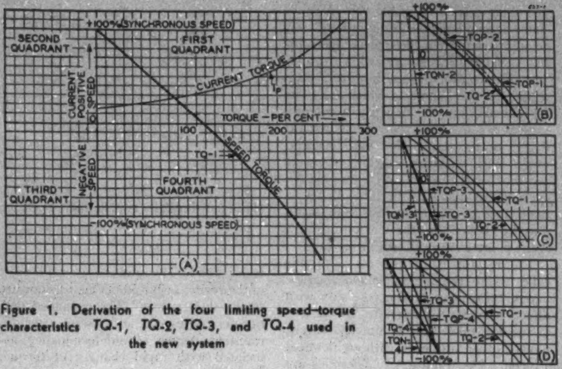

Figure 1. Derivation of the four limiting speed–torque characteristics *TQ-1*, *TQ-2*, *TQ-3*, and *TQ-4* used in the new system

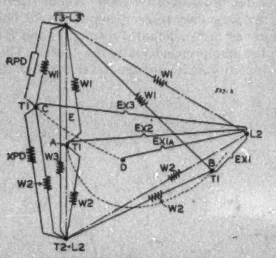

Figure 2. Vector relations for voltages across motor windings *W*1 and *W*2, for the four conditions of unbalance producing the limiting speed–torque characteristics of Figure 1

High Secondary Resistance—Limited Input Current

A fundamental of the new system, and one of prime importance, consists in the use of a single relatively high value of external rotor resistance for all subsynchronous speed control which will produce the speed–torque characteristic *TQ*-1 in Figure 1A. The curve *TQ*-1 shows that within the operating range in the fourth quadrant the motor operation is stable, that is, an increase in speed is always accompanied by an increase in retarding torque. Curve I_p shows the current input for balanced voltage, corresponding to *TQ*-1.

From the viewpoint of symmetrical components, *TQ*1 may be considered to be the positive-sequence torque component, where the negative-sequence component is zero. The new system uses a minimum unbalance in voltage as caused by the displacement voltage vector *EX*1 in Figure 2, where *EX*1 equals 0.23*E*. For the minimum unbalance illustrated the positive-sequence speed–torque characteristic is shown by curve *TQP*2, and the negative-sequence component by *TQN*2 in Figure 1B. The positive component is quite similar to the positive component *TQ*1 for balanced voltage, except that the magnitude is reduced along the torque axis. The loss in torque is caused by a net reduction in primary voltage (winding *W*1 96 per cent normal and winding *W*2 80 per cent normal).

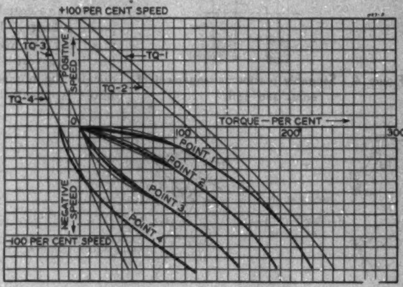

Figure 3. Speed–torque characteristics for motor with speed-responsive variable unbalanced voltage

As the torque changes from 0 to maximum for points 1–2–3, the corresponding unbalance varies as *T*1 moves along the locus from *A* toward *B* in Figure 2. For point 4, *T*1 moves along the locus from *C* toward *D*

The negative-sequence component is similar to the positive component, except the magnitude is lower since the unbalance is not great, and it is inverted on the speed axis since the slip for this field is opposite to that for the positive field. The motor shaft torque is the algebraic sum of the two components, or the characteristic *TQ*2.

If the motor primary voltage is further unbalanced by increasing the displacement vector *EX*2 (Figure 2) to 0.866*E*, single phase is essentially applied to the motor. The positive (*TQP*-3) and negative (*TQN*-3) sequence components are equal in magnitude for equal degrees of relative slip, and therefore the shaft torque characteristic *TQ*3 passes through zero torque at zero speed and the shaft torque opposes the rotation at all speeds.

If *EX* is increased in magnitude still further, as shown by *EX*3, the phase sequence at the motor terminals is reversed and the negative-sequence torque component becomes predominant as shown by a comparison of *TQP*-4 and *TQN*-4. The corresponding motor shaft torque passes through zero at minus 35 per cent speed and shows that negative torque is developed at zero speed.

Speed-Responsive Variable Unbalance

The four speed–torque characteristics *TQ*-1, *TQ*-2, *TQ*-3, and *TQ*-4, each resulting from the application of different values of fixed unbalanced voltage and with input current limited, do not cover effectively the area of the fourth quadrant (Figure 3) and are therefore unsuitable in themselves for speed control at all loads. The new system provides the necessary coverage by effecting an automatic transfer in response to speed from either of the characteristics *TQ*-3 or *TQ*-4 at zero speed toward or to the characteristic *TQ*-2 at any selected negative speed. The curves are of the general shape shown in Figure 3. They are quite different, particularly in the low-torque regions, than any speed–torque characteristics heretofore attained. There may be as many intermediate curves as desired, and they may originate from either *TQ*-3 or *TQ*-4 at zero speed.

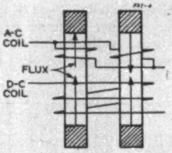

Figure 4. Saturable reactor—arrangement of cores and coils

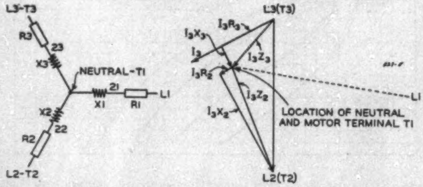

Figure 5. Hypothetical equivalent circuit and vectors for combination consisting of motor windings and the phase shifter *RPD-XPD* (Figure 2)

Variable-Impedance Reactor

The vector voltages $EX1$ and $EX2$ and any intermediate value shown between $L1$ and $T1$ in Figure 2 are produced by a single-phase variable-impedance reactor connected between these points. The vector voltage $EX3$ and $EX1A$ and all intermediate values are produced by the same reactor in combination with a phase shifter. It may be argued that with anything less than infinite impedance, the reactor drop $EX2$ from $L1$ to $T1$ cannot equal $0.866E$. This is true, but if the impedance in ohms is not less than $0.026E^2$ motor horsepower there is no effective phase rotation at the motor terminals and no torque is developed at the shaft. It is desirable that $EX1$ be made as small as possible in order closely to approach normal three-phase operation for developing high retarding torque. Practical considerations, however, place a limit on the degree to which $EX1$ can be reduced, and the design is a compromise between size of the reactor and the degree of unbalance that can be tolerated. With a reactor weighing about 20 per cent of the weight of a six-pole 60-cycle motor and capable of a change in impedance of 55 to 1, $EX1$ can be reduced to $0.23E$ and the maximum result is the point 1 curve shown in Figure 3.

The reactor is of the d-c saturable type, where the a-c impedance can be varied by control of the core flux with direct current. Physically it consists of two identical cores mounted adjacent to each other, and each with an identical a-c coil. (See Figure 4.) The coils are connected in parallel but in reversed relation such that the flux in the two cores is always of equal magnitude but of opposite polarity. Both cores are enclosed in a third coil, which is unaffected by a-c flux in the cores since their summation, due to the opposite polarity, is always zero. Application of direct current to this third coil introduces undirectional flux and thus reduces the capacity for alternating flux and accordingly the reactance of the a-c coils. The d-c energy required for excitation of the reactor is quite small compared to the a-c energy that may be controlled. Considering the maximum a-c volt-amperes at 100 per cent, the minimum will be eight per cent and the direct current energy to cause this change will be 0–1.5 per cent, for the reactor as designed for this control system. The solid curves in Figure 3 in the region below 50 per cent torque are steady-state values. The expanded portions of curves 1, 2, and 3 show a certain transient degree of indeterminancy associated with rapid changes of torque. This is caused by the time constant of the d-c exciting circuit of the reactor. The motor performance is affected only when low flux densities and the associated slower time response is involved.

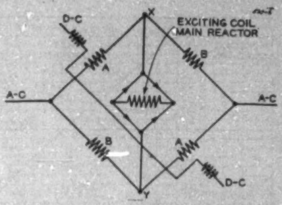

Figure 6. Circuit for amplification of detector output

Phase Shifter

The phase shifter is a series reactor and resistor combination, indicated by XPD and RPD in Figure 2. As connected, the resistor RPD and motor winding $W1$ form one element of a wye-connected three-phase load. The second element is the reactor XPD and winding $W3$, and the third is the reactor (voltage drop $EX3$). The neutral of the wye-connected load is therefore the motor terminal $T1$, and the displacement of the neutral with respect to $L1$–$L2$–$L3$ determines the unbalance of voltages applied to the motor windings. Each of the elements contains reactance and resistance, and each may be resolved into hypothetical equivalent circuits per Figure 5, where the three elements are $Z1$, $Z2$, $Z3$. By choice of values for XPD and RPD, so that the hypothetical impedance of $Z2$ and $Z3$ are about half the hypothetical impedance of the motor winding with the secondary resistor connected, $Z2$ becomes preponderantly reactance, and $Z3$ becomes preponderantly resistance. The quantity $Z1$ is much greater than either $Z2$

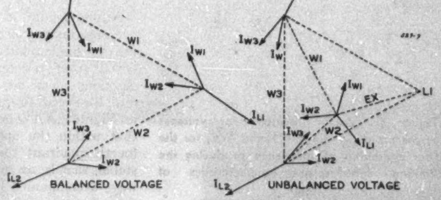

Figure 7. Comparison of balanced- and unbalanced-motor-current vectors

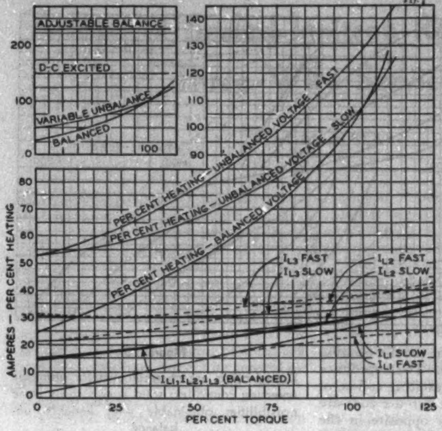

Figure 8. Current input and per cent average heating of the three motor primary windings for ten-horsepower six-pole wound-rotor motor

"Fast" and "slow" refer to speed, and the former is accompanied by high unbalance, the latter by low unbalance when developing a given torque. The insert shows a comparison of average winding heating associated with four different systems of control, when exerting full-load torque at the lowest possible speed

or $Z3$ when the reactor is unexcited, therefore its effect on the position of the hypothetical neutral can be neglected, and the approximate location can be determined by a vector analysis of $Z2$ and $Z3$ in series across the voltage $L2$–$L3$. A vector diagram of the component voltages through $Z2$ and $Z3$ appear in Figure 5, showing how the neutral of this system is displaced with respect to the reference voltages $L1$–$L2$–$L3$, to produce the vector $EX3$ shown in Figure 2, and reversed phase sequence.

Speed Detector and Secondary-Voltage Phenomena

Direct current for control of the reactor impedance must vary, not necessarily directly, but at least as a function of motor speed. The source of power for control of this direct current is the motor secondary voltage, and particularly the high-frequency modulations that exist therein.

When operating the motor with unbalanced primary, the secondary terminal voltage is the summation of the positive- and negative-sequence voltages being generated in the rotor coils. For normal operation with balanced primary voltage, only the positive sequence exists, and the secondary voltage has a perfectly finite magnitude and frequency for any selected speed (slip). Thus in the increasing speed range 0 to minus 100 per cent the magnitude increases from Es to $2Es$, and the frequency increases from 60 to 120 cycles for 60-cycle applications. The appearance of the negative-sequence component, with its descending magnitude and frequency (60 to 0 cycles) in the same speed range, produces modulation in magnitude of the predominating positive-sequence component but does not affect its fundamental frequency. Besides these modulations there is still another variable in the secondary voltage, resulting from the variable unbalance. This variable is indirectly associated with speed in such a way that a rise in speed is accompanied by a rise in secondary voltage, however only in proportion to the torque being developed. Thus as the speed rises from 0 to minus 100 per cent the magnitude of the secondary voltage is largely indeterminate, but its frequency has a perfectly definite value for any speed. The speed detector therefore has been designed for minimum response to magnitude of impressed voltage, and maximum response to the frequency thereof.

The detector itself consists simply of a three-phase transformer operating at high flux density, a capacitor in series with each primary coil, and a rectifier to convert the output to direct current. The impedance of a capacitor varies inversely

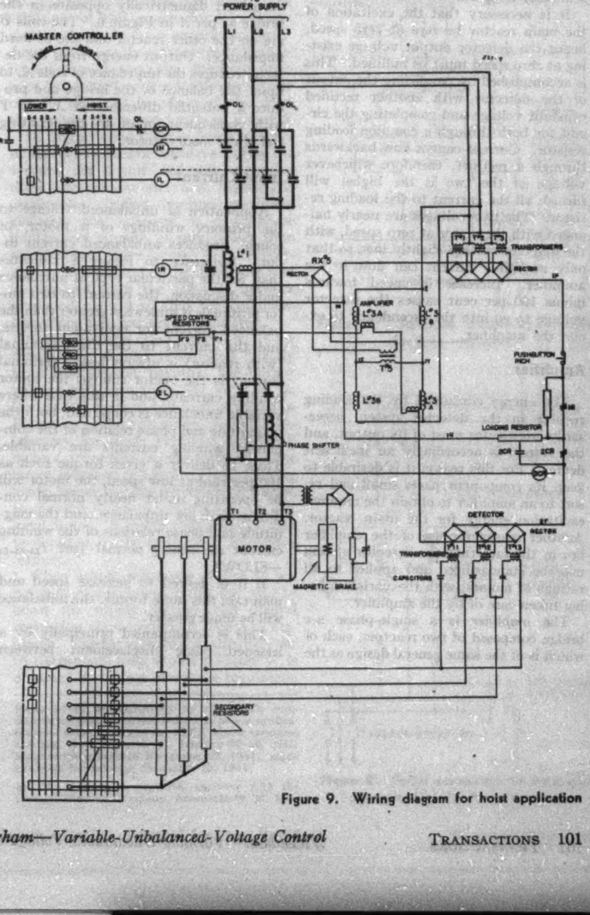

Figure 9. Wiring diagram for hoist application

with the applied frequency, therefore the terminal voltage on the transformer primary will increase as the frequency rises from 60 to 120 cycles. The wave form of the transformer secondary voltage is peaked rather than sine form due to the core saturation, and the increased primary voltage increases the amplitude of the peaks because of increased time rate of flux reversal. The increase in amplitude is accompanied by lessened duration, so that the energy per peak remains about constant. As the frequency rises there are more peaks per unit time, hence the output of the system varies directly as the frequency, except as modified by the relatively minor motor secondary voltage variations from other causes. The increase due to the presence of the capacitors can be made to transcend that due to other causes with the result that the output of the detector system responds fairly well to frequency and consequently to speed.

It is necessary that the excitation of the main reactor be zero at zero speed, hence the detector output voltage existing at zero speed must be nullified. This is accomplished by paralleling the output of the detector with another rectified constant voltage and completing the circuit for both through a common loading resistor. Current cannot flow backwards through a rectifier, therefore whichever voltage of the two is the higher will furnish all the current to the loading resistor. The two voltages are nearly balanced with the motor at zero speed, with the detector voltage slightly low, so that only negligible current can flow to the amplifier. Increase in speed towards minus 100 per cent causes the detector voltage to go into the ascendency to excite the amplifier.

Amplifier

The energy consumed by the loading resistor in the detector system necessarily constitutes most of its output, and the system is accordingly an inefficient device. For this reason it is desirable to keep its component parts small and resort to an amplifier to obtain the required excitation energy for the main reactor. Another reason for use of the amplifier lies in the fact that the detector system may be standardized and applied to all ratings of motors, with the variables being taken care of by the amplifier.

The *amplifier* is a single-phase a-c bridge composed of two reactors, each of which is of the same general design as the main reactor, except that the d-c exciting coil is omitted from one. The impedance of the reactor with the exciting coil is, of course, variable and its two a-c coils are connected diametrically opposite in the bridge as per A in Figure 6. The coils B are on the other reactor and are of fixed impedance. Output energy from the detector reduces the impedance of coils A, to upset the balance of the bridge and produce a potential difference at X and Y with consequent input to the exciting coil of the main reactor.

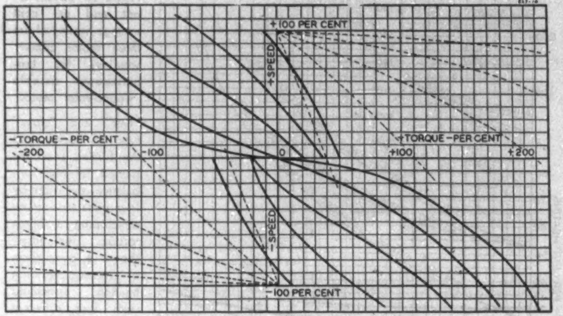

Figure 10

Dotted curves are characteristics for orthodox reversing controller; solid curves show some possibilities obtainable with variable unbalance

Input Current

Application of unbalanced voltage to the primary windings of a motor, of course, produces unbalanced current input. Reference to Figure 8 indicates that, for the particular type of unbalance under discussion, the current to two motor terminals is somewhat greater than the balanced current for equivalent torque, and the current to the third terminal (with reactor) is always less. Terminal current is the vector sum of the motor winding currents, and in this case where variable unbalance is concerned, both the magnitude and phase relation of the component winding currents are variable. Thus, to deliver a given torque such as 100 per cent at low speed, the motor will be operating under nearly normal conditions with low unbalance, and the magnitude and phase relations of the winding current are nearly normal (see I_{L_1,L_2,L_3}—SLOW).

If it is desired to increase speed and maintain this same torque, the unbalance will be made greater.

This is accompanied principally by a lessened phase displacement between component winding currents, and some increase in magnitude. The terminal current changes to I_{L_1,L_2,L_3}—FAST, as shown in Figure 8. The effect of such changed displacement angles for the current in the three windings of Figure 2 will be appreciated by study of the typical vector diagrams in Figure 7.

Conclusions

A wiring diagram for this control system, as it would be applied to a crane hoist, is shown in Figure 8. The above description has stressed fourth-quadrant performance and the test curves shown were taken with the average primary current limited to 125% at rated load. These conditions should not be regarded as limitations but rather as particular values for a particular application. It is self-evident that with the large number of control elements available many combinations of values may be used giving equivalent variations and modifications in performance.

A simple reversal of motor terminal connections produces performance in the first and second quadrants equal to that developed in the third and fourth. Figure 9 then shows how this new system has produced speed–torque curves filling in a much needed portion of the speed–torque area, supplying a valuable tool for the design engineer.

Design of Sealed Ignitron Rectifiers for Three-Wire Service

M. M. MORACK
MEMBER AIEE

IN the past four years, the many constructional and operational advantages of sealed ignitron rectifiers have greatly aided the war effort by saving critical materials and manufacturing facilities. Two-wire sealed ignitron rectifiers[1] have met industry's urgent need for efficient d-c power and have found wide application in the range of 75- to 1,000-kw capacity, at voltages ranging between 250 and 600 volts direct current for general industrial, railway, mining, and electrochemical service.

The field of application of the ignitron rectifier is considerably enlarged by the introduction of equipments for three-wire service, and it is the purpose of this paper to describe the design, characteristics, and performance of these units.

The Field for the Three-Wire Rectifier

One field of usefulness of the three-wire rectifier is for supplying d-c power to industrial three-wire systems. There is another application to be found in metropolitan districts where steps are being taken to retire the Edison three-wire d-c system and existing building generating plants. In many cases it will not be economical to rewire buildings for a 208-volt three-phase 60-cycle supply or to replace d-c motors and control for a-c operation. The problem of supplying d-c power for three-wire systems without the installation of rotating apparatus has long delayed the conversion in many districts.

Three-wire sealed ignitron rectifiers offer several distinct advantages when compared with other forms of converting equipment. The rectifier is largely static, thus eliminating special foundation and space requirements. Rectifiers are quiet in operation and easy to operate. The no-load losses are small and the efficiency is fairly constant and reasonably high over the entire load range. Rectifier equipments are factory assembled as unit d-c substations thereby minimizing installation time and expense.

Design and Operating Characteristics

POWER CIRCUITS

Three-wire service can be furnished by rectifiers in a number of ways: Large industrial three-wire requirements may be met by standard two-wire rectifiers operating at 250 volts in conjunction with a balancer set as shown in Figure 1. The alternating voltage of factory distribution systems will be above the 208-volt level so that rectifier transformers will be required. Noise levels and space requirements are not determining factors.

Another class of three-wire service is offered by dry-dock applications where 250/125-volt equipment is required for 100 per cent unbalanced operation or for double current capacity at 125 volts. Here the series or parallel operation of two 125-volt rectifiers is preferable. The efficiency of this power-circuit arrangement is about the same as rotating equipment, but it has the advantage of flexibility and ease of operation. For higher ratings, two delta six-phase double-wye power circuits are used in place of the delta three-phase single-way[2] units of Figure 2.

In larger cities, where programs are under way to limit or retire the Edison d-c system, the simple and less expensive three-wire rectifier shown in Figure 3 is applicable. Sealed ignitron rectifying elements are arranged in a six-phase double-way circuit[3] to take power from the 208-volt three-phase 60-cycle network. The neutral of the three-wire load is obtained from the 208-volt network grounded neutral so that the complication of the balancer set is eliminated.

Tests indicate that when a 75-kw double-way rectifier is supplied directly from the 208-volt network, the output voltage will vary from 247 volts at no load to 237 volts at full load as shown in Figure 4a. This voltage regulation is satisfactory for single elevators and small motors connected to one rectifier. For larger numbers of elevators and lighting loads, better voltage regulation is needed to prevent rough elevator operation and lamp flicker. Suitable voltage ratios may be obtained by the addition of autotransformers.

When autotransformers of five to ten per cent of equipment rating are used to boost the supply voltage, the natural regulation characteristic is shown in Figure 4b. The flat voltage characteristic out to 100 per cent load, shown in Figure 4c, is obtained by the use of voltage regulators. Regulated output characteristics may be had without the use of autotransformers when a line-to-neutral voltage below 125 volts is acceptable.

The double-way power circuit is capable of supplying 100 per cent current to a completely unbalanced load on the basis of rectifying element rating; however, such loads produce d-c components in the network transformer and thereby tend to increase exciting current. For partially balanced loads, the line-to-line component gives six-phase current wave shapes while the unbalanced portion is three-phase single-way. Figure 5 shows the network high-voltage current wave shape for balanced and for 50 per cent unbalanced load conditions for a rectifier.

Tests made on a 75-kw three-wire recti-

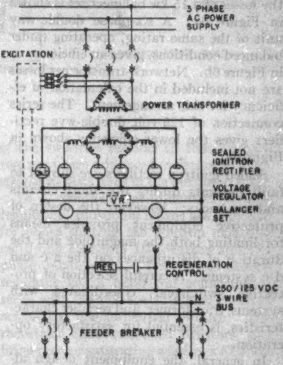

Figure 1. Six-phase double-wye rectifier for three-wire service

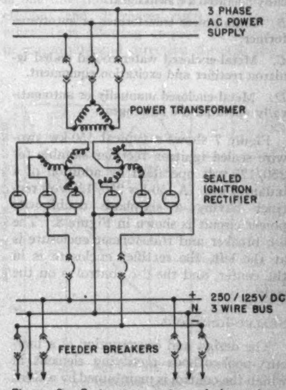

Figure 2. Series connection of three-phase zigzag rectifiers for three-wire service

---

Paper 45-35, recommended by the AIEE committees on electronics and industrial power applications for presentation at the AIEE winter technical meeting, New York, N. Y., January 22–26, 1945. Manuscript submitted November 22, 1944; made available for printing December 13, 1944.

M. M. MORACK is electrical engineer with the General Electric Company, Schenectady, N. Y.

fier operating on a 600-kva delta–wye transformer bank indicate that the difference in temperature rise for the two load conditions is due chiefly to the increase in core loss. The difference in temperature rise for two eight-hour heat runs made with balanced and fully unbalanced load was about three degrees centigrade.

In large network transformers, the d-c component would have less effect on the core loss than shown in the test run since the relative size of transformers would be greater. Also, the unbalanced condition created for test is greater than would be encountered in practice where the rectifier would seldom be called upon to furnish more than 25 per cent unbalance.

Relative efficiencies for the foregoing power-circuit arrangements are shown in Figure 6. The efficiency of a 150-kw six-phase double-wye equipment including the losses of a 15-kw balancer set is shown in Figure 6a. A six-phase double-way unit of the same rating, operating under balanced conditions, gives an efficiency as in Figure 6b. Network-transformer losses are not included in the calculation of efficiency for this arrangement. The series connection of 125-volt double-wye rectifiers gives the lower efficiency shown in Figure 6c.

Sealed ignitron rectifiers are subject to fault currents during d-c short circuits and arc-backs; however, the design of protective equipment provides means for limiting both the magnitude and the duration of disturbances on the a-c and d-c systems. A careful selection of protective switchgear, co-ordinated with systems, transformer, and rectifier characteristics, is essential for satisfactory operation.

In general, the equipment design allows factory-assembled unit substations consisting of the following components:

A. Metal-enclosed manually or automatically operated a-c switchgear.

B. Main power transformer or autotransformer.

C. Metal-enclosed water-cooled sealed ignitron rectifier and excitation equipment.

D. Metal-enclosed manually or automatically operated d-c switchgear.

Figure 7 shows a typical 150-kw two-wire sealed ignitron rectifier suitable for 250/125-volt operation by addition of a balancer set. A 150-kw 250/125-volt rectifier having a six-phase double-way power circuit is shown in Figure 8. The a-c breaker and transformer enclosure is at the left, the rectifier enclosure is in the center, and the d-c control is on the right.

SEALED IGNITRONS

The design and construction of a mercury-pool-cathode rectifying element in which the control is maintained by a third electrode, or ignitor, is shown in Figure 9. Elements of the ignitron are a seamless steel water-jacketed resistance-welded vacuum chamber containing a main graphite anode, an auxiliary anode, two ignitor tips, deionization baffles, and a mercury-pool cathode.

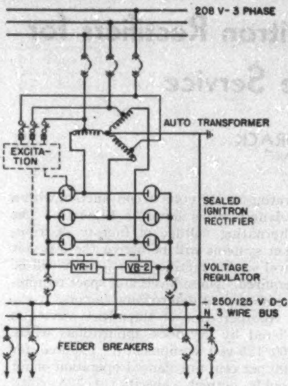

Figure 3. Six-phase double-way three-wire rectifier

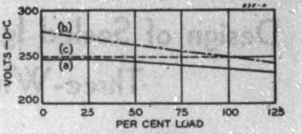

Figure 4. Output-voltage characteristics of six-phase double-way rectifier

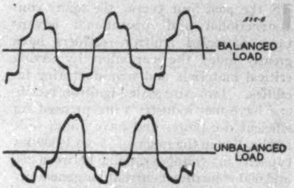

Figure 5. Network-line-current wave shapes with rectifier load

Ignitor tips are made of boron carbide, a refractory material having high specific resistance. The function of the ignitor is to control the time at which the anode current begins to flow. Once the ignitor has initiated the discharge, it has no further effect on the anode current. Control is restored to the ignitor when the main-anode and auxiliary-anode currents cease long enough for the mercury to become sufficiently deionized.

The flexible stranded anode lead, with its pressed-copper terminal, is silver-soldered to a steel stud which supports the graphite anode. This entire assembly is insulated from the cylinder, which is at cathode potential, by means of a glass-to-metal-alloy seal. These last materials have practically the same coefficient of expansion over a wide temperature range, and their use results in vacuum-tight operation.

After the cathode spot has been created by the ignitor, the auxiliary anode functions to maintain the spot for the remainder of the main anode period. This provides sufficient ionization to enable the main anode to carry the load current, even at small percentages of rating.

Uniform cooling of all parts of the vacuum chamber is accomplished with water. Water flow is directed upward by helical vanes to avoid air pockets or hot spots.

MAGNETIC EXCITATION EQUIPMENT

Each anode of an ignitron rectifier is associated with an ignitor which requires a positive impulse current once each cycle to start the arc. In order to fire the ignitors at the correct predetermined time, the magnetic-excitation circuit[4] shown in Figure 10 is used extensively for two-wire rectifiers. The phase position of the ignitor impulses can be adjusted by controlling the saturation in the phase-shifting reactor *PL*. A direct current of 1.5 amperes furnished by a regulator may be used to vary the firing point of the ignitor over an angle of approximately 50 degrees as shown in Figure 11.

For double-way three-wire rectifiers, ignitors which are 180 degrees apart in phase relation operate at different cathode potentials and an insulating transformer is used in the circuit. In addition, a phase shift between 180-degree ignitors is required for line-to-neutral regulation. The excitation circuit is arranged as in Figure 12.

The operation of the circuit is similar to that of Figure 10 except that a presaturating winding is provided on the nonlinear reactor *FL* for shifting the 180-degree ignitor peaks with respect to each other. When a direct saturating current is applied in one direction, the positive peak advances and the negative peak retards. When the saturating current is reversed the peaks shift the opposite way. In this manner a ten-degree dissymmetry can be used for the line-to-neutral voltage regulation.

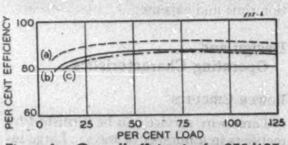

Figure 6. Over-all efficiencies for 250/125-volt 150-kw ignitron rectifiers

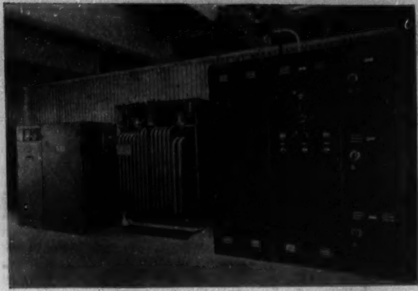

Figure 7 (above). Metal-enclosed sealed ignitron rectifier rated 150 kw, 250 volts direct current

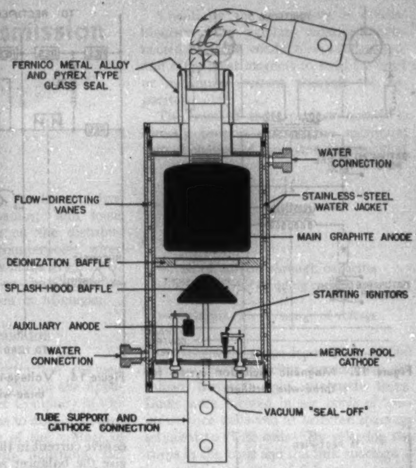
FERNICO METAL ALLOY AND PYREX TYPE GLASS SEAL
WATER CONNECTION
STAINLESS-STEEL WATER JACKET
FLOW-DIRECTING VANES
MAIN GRAPHITE ANODE
DEIONIZATION BAFFLE
SPLASH-HOOD BAFFLE
STARTING IGNITORS
AUXILIARY ANODE
WATER CONNECTION
MERCURY POOL CATHODE
VACUUM "SEAL-OFF"
TUBE SUPPORT AND CATHODE CONNECTION

Figure 9 (right). Section of a sealed ignitron

VOLTAGE-REGULATING EQUIPMENT

Rectifiers in common with other electric apparatus have regulation. To mitigate the drop in direct voltage, and to compensate for variations in the rectifier supply voltage, the phase position of the ignitor voltage is varied with respect to the positive half-cycle of anode voltage by a direct voltage regulator as shown in Figure 13.

The regulator consists of a rheostatic element, and a magnetic voltage-sensitive element connected by a spring-balanced mechanical link. In the regulator circuit, the rheostatic element forms one arm of a resistance bridge connected across the output of the rectifier. The saturating-current windings of the phase-shifting reactors *PL* in the excitation circuit of Figure 10 are connected between the midpoints of the bridge. When the d-c output rises, the carbon stacks forming the rheostatic element are tilted, and their resistance increases. This change of resistance in one arm of the bridge results in decreased current flow in the saturating windings of the phase-shifting reactors, thus phase retarding the ignitors, and decreasing the direct voltage. The rheostat is provided for adjustment of the voltage to be held. The regulator will maintain the selected voltage from no load to full load within plus or minus one per cent, within the range of 15 per cent voltage control imposed by the limitations of the excitation circuit. For parallel operation of two or more rectifiers, an equalizer connection is made by joining the equalizing coils in series across the opposing voltage drops of the cathode shunts of the two machines.

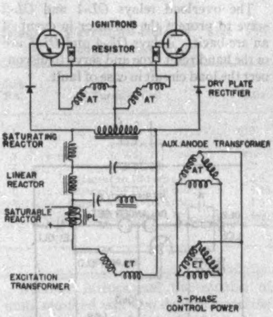
IGNITRONS
RESISTOR
DRY PLATE RECTIFIER
AT
AT
SATURATING REACTOR
AUX. ANODE TRANSFORMER
AT
LINEAR REACTOR
SATURABLE REACTOR
PL
ET
ET
EXCITATION TRANSFORMER
3-PHASE CONTROL POWER

Figure 10. Magnetic excitation system for two-wire rectifiers

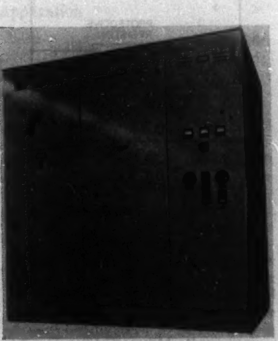

Figure 8. Metal-enclosed sealed ignitron rectifier rated 150 kw, 250/125 volts direct current

The voltage-regulating equipment for the six-phase double-way three-wire rectifier uses two regulators, one to maintain line-to-line voltage, and the other to regulate the line-to-neutral voltage at one-half the line-to-line value. From Figure 14 it will be noted that the line-to-line regulator is similar to the bridge regulator of the two-wire rectifier in that all ignitors are phase advanced or retarded in response to variations in the output voltage.

To accomplish line-to-neutral voltage regulation, additional means are provided for phase shifting the ignition points of rectifying elements 180 degrees apart in phase relationship. The line-to-neutral regulator has a main coil connected in series with the voltage-adjusting rheostat across the line-to-neutral voltage. The rheostatic elements, fixed resistors, and firing reactor saturating windings *FL* form a bridge connected across line-to-neutral voltage. Two rheostatic elements are normally open and two are normally closed, so that movement of the linkage in one direction increases current in one element and decreases current in the other, thus allowing current to change in magnitude and direction through the

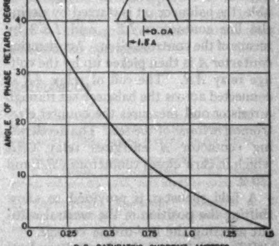

Figure 11. Phase-shift characteristics of magnetic excitation circuit

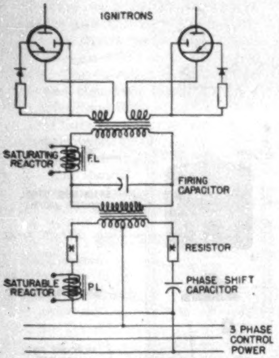
IGNITRONS
SATURATING REACTOR
FL
FIRING CAPACITOR
RESISTOR
SATURABLE REACTOR
PL
PHASE SHIFT CAPACITOR
3 PHASE CONTROL POWER

Figure 12. Magnetic excitation system for three-wire rectifiers

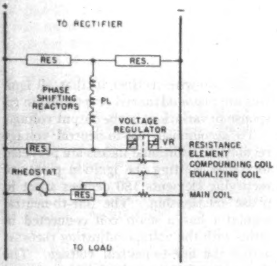
+
−
TO RECTIFIER
RES
RES.
PHASE SHIFTING REACTORS
PL
VOLTAGE REGULATOR
VR
RES.
RESISTANCE ELEMENT
COMPOUNDING COIL
EQUALIZING COIL
RHEOSTAT
RES.
MAIN COIL
TO LOAD

Figure 13. Voltage-regulating equipment for two-wire rectifier

saturating windings in accordance with the line-to-neutral voltage.

BALANCER SET

Three-wire service is provided from two-wire rectifiers by a balancer set connected across the 250-volt d-c output to furnish the neutral connection. A typical balancer-set control circuit is shown in Figure 15. With rectified voltage available, the balancer set is started by closing the line contactors *LE*-1 and *LE*-2 by means of the control switch. Accelerating contactor *A* is then picked up by the voltage relay *AR*. The coil of relay *AR* is connected across the balancer set through a resistor and measures the counter electromotive force of the set. The accelerating contactor *A* energizes relay *CBR* which in turn closes contactors *CB*-1 and *CB*-2.

A field rheostat is provided to allow shifting the position of the neutral without affecting the line-to-line voltage.

Relay *OL*-3 is of the thermal-overload type and serves to protect the balancer set against excessive unbalanced load. Excessive current in the neutral will de-energize the balancer set and disconnect all load from the rectifier.

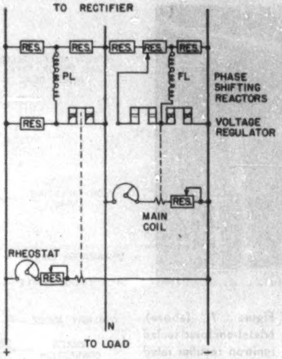
TO RECTIFIER
RES.
RES.
RES.
RES.
RES.
PL
FL
PHASE SHIFTING REACTORS
RES.
VOLTAGE REGULATOR
RES.
MAIN COIL
RHEOSTAT
RES.
N
TO LOAD
+

Figure 14. Voltage-regulating equipment for three-wire rectifier

The overload relays *OL*-1 and *OL*-2 serve to protect the balancer in event of an arc-back. Relays *OL*-4 and *OL*-5 are of the hand reset type and serve to disconnect the load circuit in case of fault.

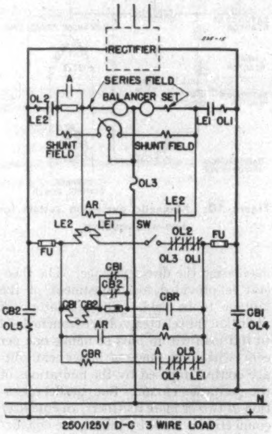
RECTIFIER
SERIES FIELD
BALANCER SET
A
OL2
LE2
LE1
OL1
SHUNT FIELD
SHUNT FIELD
OL3
LE2
AR
LE2
LE1
SW
OL2
FU
FU
OL3
OL1
CB1
CB2
CBR
CB1
CB2
CB2
OL5
CB1
OL4
AR
A
CBR
A
OL5
OL4
LE1
N
+
250/125V D-C 3 WIRE LOAD

Figure 15. Balancer-set circuit for two-wire rectifiers

A—Accelerating contactor
AR—Accelerating relay
CB—Circuit-breaker contactor
CBR—Auxiliary relay
OL—Overload relay
*—Resistor
SW—Switch
FU—Fuse

The rating of the balancer set is determined by the requirements of the application. A balancer set of 25 per cent of the rectifier rating is sufficient for most applications.

REGENERATIVE-BRAKING PROTECTIVE EQUIPMENT

A rectifier operating under normal conditions will not carry reverse current, and any load which tends to regenerate will cause the d-c bus voltage to rise. Protection must be provided by a "pump-back" resistor, connected across the bus by a contactor whenever reverse power is encountered, and removed when the regeneration ceases. The resistor is usually designed to absorb about ten per cent of the rectifier rating and is sufficient for cranes, elevators, and other similar loads where regeneration occurs at infrequent intervals.

The operation of the protective equipment may be understood by reference to Figure 16. Whenever regeneration is present the bus voltage will rise rapidly provided there is no other load which can absorb the regenerative power. A fast-acting relay *VR* is adjusted to operate at a voltage slightly higher than the normal rectifier rating. The coil of *VR* is energized through the timing-relay contacts *TR*. The coil circuit *TR* is completed through the normally closed interlock on the main contactor *M*.

The operation of *VR* closes *M*, connecting the protective resistor across the line. The bus voltage is maintained by the rectifier and *VR* remains closed until the contacts *TR* open after a time delay obtained by the long time constant of the circuit and a copper-jacketed coil. If re-

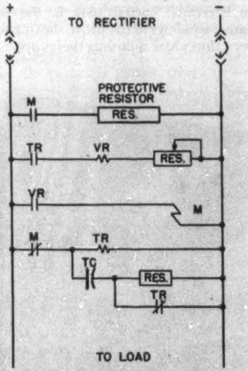
+
−
TO RECTIFIER
PROTECTIVE RESISTOR
M
RES.
TR
VR
RES.
VR
M
M
TR
TC
RES.
TR
TO LOAD

Figure 16. Regeneration-control circuit

M—Main contactor
VR—Voltage relay
TR—Time relay
TC—Timing capacitor

Lightning Investigation on Transmission Lines—VIII

W. W. LEWIS
FELLOW AIEE

C. M. FOUST
MEMBER AIEE

PREVIOUS papers of this series gave data on a lightning investigation carried on co-operatively by a number of power companies and the General Electric Company, and the seventh paper of the series[1] brought the data up to and including 1938. Additional papers[2,3] covered special angles of the investigation.

The present paper discusses an investigation, under the joint sponsorship of the American Gas and Electric Service Corporation, of voltages, currents, and rates of change of voltage at five stations of the Appalachian Electric Power Company in Virginia; data on currents in towers and strokes on the lines of five different power companies; and some additional information on the distribution of current in counterpoise wires and driven rods, and voltage gradient in the vicinity of towers on the Consumers Power Company system in Michigan.

The Wave-Slope Indicator

The wave-slope indicator first was used in 1939 on the 132-kv lines of the Appalachian Electric Power Company in Virginia.[4] The object was to obtain an idea of the rate of change of the voltage of transient waves from lightning and switching traveling into the stations.

Table I. Wave-Slope-Indicator Link Arrangement and Ratio

Link No.	Turns in Coil	Ratio
1	35	610
2	10	246
3	3.5	98
4	1.5	39
5	Adjacent to 10-turn coil	15.6
6	Adjacent to 10-turn coil	6.25
7	Adjacent to 10-turn coil	2.5
8	Adjacent to 10-turn coil	1.0

Essentially the instrument is a combination of a coupling capacitor, connected between conductors and ground, and surge-crest magnets to read the crest or maximum current through the capacitor.

The crest of the capacitor current is directly proportional to the maximum rate of change of capacitor voltage, that is,

$$I=C\frac{de}{dt}$$

in which

I = crest of current through capacitor
C = capacitance of coupling capacitor
$\frac{de}{dt}$ = maximum rate of change of voltage

A measuring range from 10 to 10,000 amperes crest capacitor current was obtained through eight magnetic links. Links were located in air cores of low-inductance coils and at selected spacings adjacent to these coils. By selecting the turns in the coils and the link spacings, a magnetization ratio of 2.5 was obtained between adjacent links, thus giving a ratio between links 1 and 8 of about 610. These ratios were verified by laboratory tests with the cathode-ray oscillograph, in which current surges of known magnitude and wave shape were used.

Links were installed in the cores of 35-, 10-, 3.5-, and 1.5-turn coils; also four additional links were placed adjacent to the 10-turn coil. The numbering of the links and the approximate ratios were as shown in Table I.

The original arrangement was continued during the years 1939, 1940, and

---

Paper 45-26, recommended by the AIEE committee on power transmission and distribution for presentation at the AIEE winter technical meeting, New York, N. Y., January 22–26, 1945. Manuscript submitted October 30, 1944; made available for printing December 11, 1944.

W. W. Lewis is with the central-station engineering divisions and C. M. Foust with the general engineering laboratory, both with General Electric Company, Schenectady, N. Y.

The authors acknowledge the co-operation in this investigation of I. W. Gross and G. D. Lippert of the American Gas and Electric Service Corporation; J. G. Hemstreet and C. C. Tanner of the Consumers Power Company; L. M. Robertson of the Public Service Company of Colorado; and R. F. McAtee and J. G. Hutton of the general engineering laboratory and D. D. MacCarthy and W. N. Neiman of the lightning-arrester engineering division of General Electric Company.

---

generation still persists when *TR* opens, the circuit will recycle.

Application

The design of sealed-ignitron-rectifier equipment for three-wire operation is determined to a large extent by the nature of the application. The six-phase double-wye power circuits offer the best efficiency and output wave form but require the added complications and losses of a balancer set. Series connection of 125-volt rectifiers eliminates the balancer equipment, provides flexibility, and is suitable for 100 per cent current unbalance, but gives six per cent lower efficiency and higher no-load losses.

The six-phase double-way power circuit offers the best solution to the change-over problem. Such equipment is economical to build and requires a minimum of space which is usually hard to find in existing buildings. The rectifier provides a medium efficiency of 86 per cent. Satisfactory voltage regulation can be provided by autotransformers and voltage regulators.

Rectifier ratings and the number of units required will also depend upon the application. For elevator loads, particularly in hotels, apartment houses, and office buildings it is good practice to have a 100 per cent reserve or stand-by unit, which will permit the rectifier in service to be removed. For reasons of safety, such service must continue under all conditions and a satisfactory solution to the problem is to provide two complete independent rectifiers with provisions for rapid change-over in case of direct-voltage failure. Simple switching provides preselection of normally operating and reserve rectifiers. Where requirements are less severe and where units may be removed for maintenance and inspection, it is not necessary to provide a stand-by unit.

Conclusions

The basic problems of sealed ignitron rectifiers for three-wire service have been solved and the equipments are highly reliable when properly applied, installed, and serviced. The type of power circuit is dependent on the requirements of the application. Tests show that the additional heating in network transformers resulting from the unbalanced load on the six-phase double-way circuit will be negligible and that the circuit offers an efficient, economical, three-wire rectifier where 208-volt power is available. The equipment is semiautomatic in operation, so that periodic inspection and cleaning is all that is necessary to insure continuous and reliable operation.

References

1. SEALED-TUBE IGNITRON RECTIFIERS, M. M. Morack, H. C. Steiner. AIEE TRANSACTIONS, volume 61, 1942, August section, pages 594–9.

2. RECTIFIER TERMINOLOGY AND CIRCUIT ANALYSIS, C. H. Willis, C. C. Herskind. AIEE TRANSACTIONS, volume 61, 1942, July section, pages 496–9.

3. THREE-PHASE RECTIFIER CIRCUITS, A. J. Maslin. *Electronics*, volume 9, December 1936, page 28.

4. IGNITOR EXCITATION CIRCUITS AND MISFIRE INDICATION CIRCUITS, A. H. Mittag, A. Schmidt, Jr. AIEE TRANSACTIONS, volume 61, 1942, August section, pages 574–7.

Table II. Wave-Slope-Indicator Calibration

Undamped-Surge Oscillatory Calibration

									Wave Slopes			
		SCA Scale Reading							Link			
1 Surge-Generator Excitation, Volts	2 Link Position	3 Group 1	4 Group 2	5 Group 3	6 Average	7 Ratio	8 Per Cent Oscillation	9 Capacitor Current	10 Kv Per μsec	11 Average	12 CRO Kv Per μsec	13 Deviation, Per Cent
32	2	*R*10	*R*5	*R*16	10.3							
	3	*R*53	*R*46	*R*41	46.7	1.30	15	400	240	222	228	−2.6
	4	*R*36	*R*36	*R*36	36.0	2.37	15	344	205			
	5	*R*16	*R*15	*R*14.5	15.2							
38	2	*D*28	*D*23	*D*18	23.0							
	3	*R*46	*R*38	*R*33.5	39.2	0.92	15	487	290	272	270	+0.7
	4	*R*46	*R*41.5	*R*41	42.8	2.24	14	430	255			
	5	*R*20	*R*19	*R*15	19.0	2.04						
	6	*R*10	*R*8	*R*10	9.3							
44	2	*D*33	*D*30	*D*26	29.7							
	3	*R*41	*R*33	*R*26	33.3	0.72	13	624	380	340	312	+9.0
	4	*R*51	*R*44	*R*44	46.3	2.07	15	500	300			
	5	*R*23.5	*R*21.5	*R*22	22.5	2.06						
	6	*R*10.5	*R*10	*R*12	10.8							
	7	0	*Rtr*	*Rtr*								
50	2	*D*38	*D*41	*D*34	37.7							
	3	*R*36	*R*28	*R*24	29.3	0.62	15	624	380	355	355	0
	4	*R*53	*R*44	*R*45	47.3	1.95	15	550	330			
	5	*R*26	*R*22	*R*24.5	24.2	2.02						
	6	*R*12	*R*11	*R*13	12.0	3.00						
	7	*Rtr*	*R*5	*R*5	4.0							
56	2	*D*49	*D*38	*D*30	35.0							
	3	*R*31	*R*24	*R*19	28.0	0.60	15	610	375	378	398	−5
	4	*R*54	*R*44	*R*42	46.7	1.75	16	620	380			
	5	*R*28.5	*R*26	*R*26	26.8	2.14						
	6	*R*12	*R*11.5	*R*14	12.5	3.10						
	7	*Rtr*	*Rtr*	*R*5	4.0							
62	2	*D*50	*D*41	*D*52	47.7							
	3	*R*22.5	*D*10	*R*11	14.5	0.31	15	630	390	425	440	−3.4
	4	*R*52	*R*42	*R*46	46.7	1.47	16	750	460			
	5	*R*34	*R*30	*R*31	31.7	2.07						
	6	*R*14	*R*16	*R*16	15.3	2.19						
	7	*R*5	*R*8	*R*8	7.0							

D = direct reading on surge-crest ammeter (*SCA*) *R* = reverse reading on surge-crest ammeter *CRO* = cathode-ray oscillograph *tr* = trace

1941, modified somewhat in 1942, and again in 1943. The 35-turn coil and link 1 of the original installation were omitted. The final connections were as shown in Figure 1.

Carrier-current coupling capacitors of 0.00025, 0.0005, 0.001, and 0.0015 microfarad which were on the system were utilized. A total of 26 instruments was located on ten circuits at Glenlyn, Claytor, Roanoke, Reusens, and Fieldale.

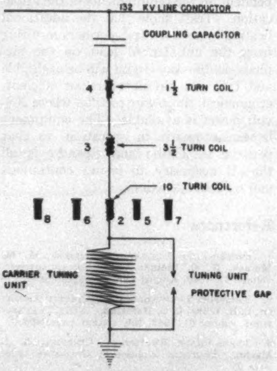

Figure 1. Final wave-slope-indicator arrangement of 1943

Numbered capsules represent magnetic links

A typical calibration curve of one of the coils is shown in Figure 2, and Figure 3 shows the relation between maximum-voltage wave slope and crest capacitor current for each value of capacitor used. A range of voltage steepness of from 10 to 10,000 kv per microsecond was covered by the arrangement.

SPECIMEN LABORATORY CALIBRATION

The arrangement of coupling capacitor, coils, and magnetic links, as used on the transmission line and shown in Figure 1, was calibrated in the laboratory with surge-generator discharges of differing voltage wave shapes. These wave shapes were of three general types as to polarity—unidirectional, oscillatory, and repeated unidirectional of mixed polarities. Representative of these calibrations is one which included the application of both damped and undamped oscillations and provided a direct comparison of numerical values of voltage wave slopes recorded by cathode-ray oscillograph with those indicated by the magnetic links.

For both the damped and undamped circuits the wave slope was varied over a considerable range by varying the surge-generator excitation voltage. Magnetic links occupied all link positions from 2 to 8 as shown on Figure 1, and three groups of links were used for checking purposes. Tables II and III summarize data collected for these calibrations and show the several steps involved in interpretation of wave-slope values. As both the damped and undamped waves were oscillatory, a two-link oscillatory calibration was used, such as shown in Figure 5 of reference 5.

In Tables II and III, column 1 gives the surge-generator excitation voltage, which was increased progressively to provide for some range of wave slopes. Column 2 is the reference number for individual link positions as indicated in

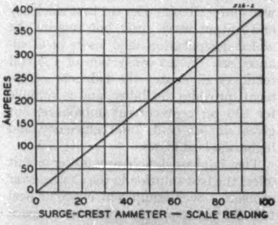

Figure 2. Typical calibration curve for one of the wave-slope-indicator coils

Calibration of 3.5-turn coil, link 3, ammeter reading versus amperes

Table III. Wave-Slope-Indicator Calibration

Damped-Surge Oscillatory Calibration

1 Surge-Generator Excitation, Volts	2 Link Position	3 SCA Scale Reading Group 1	4 SCA Scale Reading Group 2	5 SCA Scale Reading Group 3	6 SCA Scale Reading Average	7 Ratio	8 Per Cent Oscillation	9 Capacitor Current	10 Wave Slopes, Link, Kv Per μsec	11 Wave Slopes, Link, Average	12 Wave Slopes, CRO Kv Per μsec	13 Deviation Per Cent
32	2	*R*100+	*R*100+	*R*90	97+	1.33						
	3	*R*80	*R*69	*R*70	73	2.28	6	300	180	193	188	−2.5
	4	*R*32	*R*34	*R*30	32	2.41	14	344	207			
	5	*R*14	*R*13.5	*R*13	13.5	3.50						
	6	*Rtr*	*R*5	*Rtr*	4							
38	2	*R*100+	*R*83	*R*80	88	1.12						
	3	*R*88	*R*76	*R*73	79.0	1.84	6	436	265	245	232	+5.6
	4	*R*44	*R*44	*R*43	43.7	2.71	0	368	225			
	5	*R*17	*R*15	*R*16	16.0	2.00						
	6	*R*5	*R*10	*R*10	8.0							
44	3	*R*100	*R*79	*R*75	84.7	1.65	5	530	320	290	270	+7.4
	4	*R*52	*R*52	*R*50	51.3	2.90	0	432	260			
	5	*R*49	*R*17	*R*17	17.7	1.77						
	6	*R*10	*R*10	*R*10	10.0							
50	3	*R*100+	*R*78	*R*74	84	1.44	6	610	370	335	308	+9.0
	4	*R*64	*R*58	*R*56	59.3	2.96	0	500	300			
	5	*R*22	*R*19	*R*19	20.0	1.97						
	6	*R*10	*R*10	*R*11	10.3							
	7	0	*Rtr*	*Rtr*								
56	4	*R*72	*R*67	*R*61	66.6	2.86	0	559	340	340	345	−1.5
	5	*R*25.5	*R*25.5	*R*22	23.3	2.09						
	6	*R*10.5	*R*11	*R*12	11.2							
	7	0	*Rtr*	*R*5								
62	4	*R*78	*R*68	*R*68	71.3	2.55	0	605	370	370	382	−3.1
	5	*R*29	*R*24.5	*R*30	27.8	2.32						
	6	*R*12	*R*12	*R*12	12.0							
	7	0	*Rtr*	*R*5								

D = direct reading on surge-crest ammeter (*SCA*) *R* = reverse reading on surge-crest ammeter *CRO* = Cathode-ray oscillograph *tr* = trace

Figure 1. Columns 3, 4, and 5 are three groups of magnetic-link records, each obtained by the application of a single surge of the same wave shape as obtained at each excitation voltage of column 1. These three groups of links were used to check link variations on the same surge. In column 6 are given the average values for each link position for the three groups of links. In the measurement setup magnetization of links 2, 3, and 4 is normally opposite from that of links 5, 6, 7, and 8. For convenience in analysis, however, records from links 5, 6, and 7 have been put down in these tables in reverse to their actual polarity.

In the interpretation of wave slopes the oscillatory-calibration method requires the calculation of an inner-link–outer-link ratio as given in column 7. This ratio is the same as that for a normal surge-crest-ammeter two-magnetic-link station, as used extensively for tower leg, line conductor, and down-leads in previously reported field lightning investigations. In this wave-slope method the inner link is the link operating in the next stronger magnetic-field position to any other link. For instance, link 2 of Figure 1 in the 10-turn coil is inner link to link 3 in the $3\frac{1}{2}$-turn coil. Relative field intensities between link positions is 2.5 to 1. In the tables the inner–outer-link ratio is entered on the corresponding inner-link line. If we refer now to the appropriate oscillatory-calibration curve, the per cent oscillation and capacitor currents of column 8 and 9 are read directly. This is done similarly for each inner-link–outer-link combination of adjacent links. The current values of column 9 are translated to wave-slope values, column 10, by use of a curve such as shown in Figure 3. When more than one value of wave slope for a single surge application can be derived from the magnetic links, the values should check and be averaged for the final wave-slope value. Such averages are given in column 11, and in column 12 are recorded wave-slope values derived from cathode-ray oscillograms. A percentage comparison of magnetic-link values and cathode-ray oscillograph values is given in column 13.

Table IV. Wave-Slope-Indicator Records—Analysis by Link Position, 1939 to 1943, Inclusive

Appalachian Electric Power Company 132-Kv System

Range, Kv Per Microsecond	Links 2–3	Links 3–4	Links 4–5 and 5–6	Total No.	No. at or Above Level	Percentage at or Above Level
11–20	7	0	0	7	589	100.0
21–30	9	0	0	9	582	98.8
31–40	51	0	0	51	573	97.3
41–50	45	2	0	47	522	88.6
51–60	54	1	0	55	475	80.6
61–80	43	20	0	63	420	71.4
81–100	19	43	1	63	357	60.6
101–150	33	104	3	140	294	49.9
151–200	11	44	12	67	154	26.15
201–250	19	11	3	33	87	14.77
251–300	8	19	5	32	54	9.17
301–350		12	2	14	22	3.74
351–400		2	0	2	8	1.36
401–450		2	0	2	6	1.02
451–500		1	0	1	4	0.68
520		1	0	1	3	0.51
524		1	0	1	2	0.34
550			1	1	1	0.17
Total	299	263	27	589		

The deviations for these tests range up to nine per cent which is the measurement accuracy of the magnetic links as commonly used for crest surge currents. In deriving wave-slope values from the magnetic links, some measure of experience in weighting of values from different link positions is required. In general, surge-crest ammeter readings below 10 and above 90 on the instrument scale were rejected as possibly affected by small residuals and saturation levels.

The basic calibration curves on which all the field interpretations are made were

Table V. Surge Voltages on Station Busses, 1940–1943, Inclusive

Appalachian Electric Power Company 132-Kv System

Range of Voltage, Kv	1940*	1941*	1942†	1943**	Total	No. at or Above Level	Percentage at or Above Level
0–100			7	55	62	429	100.00
101–150		58	120	1	179	367	85.6
151–200		17	50	2	69	188	43.8
201–250	5	12	33	3	53	119	27.7
251–300	4	19	6	6	35	66	15.4
301–350	2	3	0	1	6	31	7.23
351–400	4	3	2	5	14	25	5.83
401–450	0	4	3	1	8	11	2.56
451–500	1			1	2	3	0.70
525	1				1	1	0.23
Total	17	116	221	75	429		
Maximum	525	428	420	473			

* Roanoke and Claytor stations.

† Roanoke, Claytor, and Fieldale stations.

** Roanoke station only.

Table VI. Insulation Flashover Strength of Lines and Stations Under Investigation on 132-Kv System of Appalachian Electric Power Company

Number of lines	6
Number of circuits	10
Number of overhead ground wires	1 per line
Number of stations	5
Number of connected lines at stations	2 to 5
Number of insulator units in line suspension strings (spaced $4^{3}/_{4}$, 5, and $5^{1}/_{8}$ inches)	10 to 12
Flashover of line-insulator strings (1.5x40 positive wave)	790 to 1,080 kv
Number of circuits equipped with protector tubes	4
Discharge voltage of protector tubes	
1.5x40 positive wave	680 kv
1.5x40 negative wave	760 kv
Number of insulator units in reduced line insulation (spaced $4^{3}/_{4}$, 5, and $5^{1}/_{8}$ inches), 5 towers adjacent to station (on all except tube-equipped lines)	9
Flashover of reduced line insulation (1.5x40 positive wave)	720 to 890 kv
Bus-insulation flashover strength	
1.5x40 positive wave	590 kv
1.5x40 negative wave	770 kv
Number of three-phase lightning arresters	16
Rating of arresters, 60-cycle rms	106, 109, 121 kv
Arrester-gap breakdown (1.5x40 voltage wave) or *IR* drop at 5,000 amperes (10x20 current wave)	350 to 425 kv

Table VIA. Comparison of Insulator Units Spaced 5¾ Inches Apart

No. of Insulator Disks	Flashover Kv 1.5x40 Positive Wave	Flashover Kv 1.5x40 Negative Wave
8	780	760
9	860	845
10	945	930
11	1,025	1,015
12	1,105	1,105

built up similar to the calibration checks of Tables II and III, requiring, of course, the use of generated wave shapes including a wide range of damping factors.

WAVE-SLOPE-INDICATOR RECORDS

The analysis of the wave-slope-indicator records was made by two methods. The first method of analysis consisted of classifying the records according to the ratio of adjacent-link readings and using an appropriate set of calibration curves. The purpose of this method was to determine the rates of voltage change from surges due to all causes.

The second method of analysis consisted of grouping the records according to link position. The purpose of this method was to determine the origin of the surges; that is, whether due to lightning, switching, or a combination of both.

ANALYSIS BY FIRST METHOD

The classification by the first method is as follows:

Class 1—Unidirectional surges only.

Class 2*A*—Oscillatory surges from three-link readings.

Class 2*B*—Oscillatory surges from two-link readings.

Class 3—Superimposed repeated surges. Rate of voltage change doubtful.

Class 4—Single-link readings. Surge characteristics uncertain; calibrated as unidirectional.

Class 5—Adjacent link polarities reversed. Surge characteristics uncertain.

During the years 1929 to 1943, inclusive, there were 979 records in all, with one class-5 record of 810 kv per microsecond in the year 1942.

ANALYSIS BY SECOND METHOD

The records in classes 3, 4, and 5, comprising about 40 per cent of all the records, are somewhat uncertain, and there is some doubt as to their correct interpretation. These records, therefore, have been rejected in making the analysis by the second method. In this analysis of the wave-slope records it was found by specially staged tests made in 1939, that the links nearest the current-carrying coils of the wave-slope indicator are always affected by switching surges. As the distance between the links and the coils increased, the effect diminished rapidly, and links 5 and 6 did not appear to be affected appreciably by switching surges. Records from links 2 and 3 therefore were considered to be due principally to switching; records from links 3 and 4 were considered to be due to switching or lightning or a combination of both; records from links 4 and 5 or 5 and 6 were considered to be due to lightning only.

A summary of the 589 records, according to the second method of analysis, for the five years, 1939 to 1943, inclusive, is given in Table IV.

In Figure 4 are plotted as abscissas the percentage of records at least equal to the kilovolts per microsecond as ordinates. The kilovolts per microsecond are given in zones, and in each case the bottom figure of the zone is plotted as ordinate, except for the three highest figures of 520, 524, and 550, which are plotted individually. Abscissas are plotted logarithmically. By this method of plotting a logarithmic curve will appear as a straight line, which permits ready extrapolations.

The sensitivity of the method does not lend itself to readings under about ten kilovolts per microsecond. Probably there are a large number of surges below this value which are not recorded. If these had been recorded, the percentage value for all other ranges would be reduced somewhat and the whole curve lowered.

Based on the data plotted, it would appear that surges were recorded about in the following order:

One in 2 (50 per cent)—at least 100 kv per microsecond.

One in 10 (10 per cent)—at least 225 kv per microsecond.

One in 100 (1 per cent)—at least 415 kv per microsecond.

One in 1,000 ($^{1}/_{10}$ per cent)—at least 605 kv per microsecond.

One in 10,000 ($^{1}/_{100}$ per cent)—at least 795 kv per microsecond.

Surge Voltages at Stations

Surge voltages were measured at Roanoke and Claytor stations of the Appalachian Electric Power Company in 1940; at Roanoke, Claytor, and Fieldale in 1941 and 1942; and at Roanoke only in 1943. The surge-voltage recorder with insulator string potentiometer was used. One instrument is used per phase and gives direct and reverse readings for each surge.[6]

As shown in Table V, 429 surges were recorded. The highest voltage recorded was 525 kv, and 50 per cent of all the surges were at least 145 kv.

Table VI gives the flashover strength

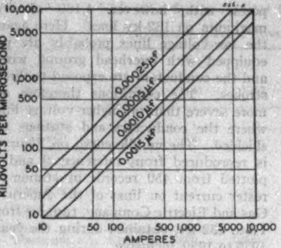

Figure 3. Relation between amperes and wave slope for various coupling capacitors

Figure 5 (right). Station-arrester currents at 132-kv stations of the Appalachian Electric Power Company, 124 records, 1940 to 1943, inclusive, and for comparison 1,608 records from distribution circuits,[8] and 459 records of station arresters 11 to 132 kv[9]

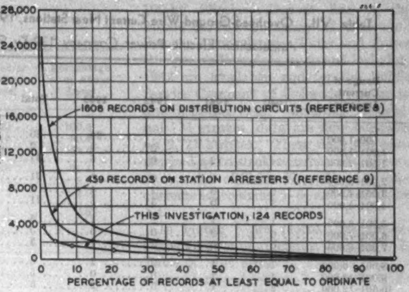

of the transmission-line and station insulation for the lines and stations at which instruments were located. The line insulation varies both in number and spacing of disks, so that the flashover ranges between 790 and 1,080 kv for the 1.5x40 positive wave. The negative-wave flashover with the 1.5x40 wave is not appreciably different from the positive, as will be seen from the comparison of insulator units spaced 5¾ inches apart,[7] given in Table VI*A*.

All lines, exept those equipped with expulsion protector tubes, have reduced insulation for five towers (approximately one mile) out from the station. Nine disks of various spacings are used in this section, both in suspension and strain, with a flashover ranging from 720 to 850 kv. On the tube-equipped lines the incoming voltage is held to 680 kv with the 1.5x40 positive wave and 760 kv with the negative wave. The bus insulators will flash over at 590 kv with the 1.5x40 positive wave and 770 kv with the negative wave. Three types and ratings of station arresters are used, and it is estimated that with the 1.5x40 voltage wave or the 10x20 current wave, the arresters will hold voltages ranging from 350 to 425 kv.

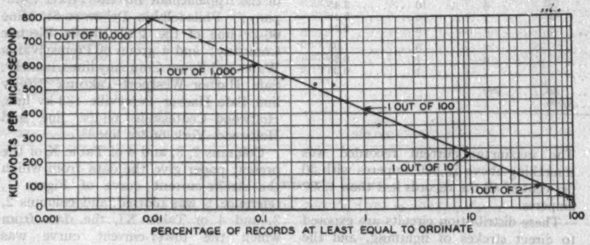

Figure 4. Rates of change of voltage at 132-kv stations of the Appalachian Electric Power Company, 589 records, 1939 to 1943, inclusive

With the line arrangement, that is, one or two circuits vertically arranged and one overhead ground wire, it is not likely that very many strokes will make direct contact with the conductors, but in most cases the voltage will get onto the conductor by insulator flashover or expulsion-protector-tube operation. The voltage reaching the station will therefore be limited to the reduced line-insulation flashover or tube-discharge voltage of the order of 680 to 850 kv. The waves will have some chance to attenuate in traveling to the station and then will be limited by the bus insulation to 590 to 770 kv and further by the arresters to 350 to 425 kv.

All of the measured voltages are well within the reduced line insulation, or expulsion-protector-tube, or bus-insulator flashover, and all but about six per cent are under the voltage assigned to the arresters.

In this investigation when a surge enters a station from a line it has anywhere from one to four other outgoing lines on which to dissipate itself, and also from one to four power transformer banks and from two to five banks of lightning arresters. If a surge impedance of 500 ohms is assumed for the lines and 3,000 ohms for the power transformers, and if the arresters which do not come into play until the arrester gap breaks down are neglected, the incoming surge encounters a surge impedance all the way from about 125 to 430 ohms. This decrease in station surge impedance compared to the incoming line surge impedance will cause the voltage surge to decrease to four tenths to nine tenths of the incoming surge. If the incoming surge is assumed to be limited to 680 to 850 kv by the reduced line insulation or expulsion protector tubes, then the bus voltage will be reduced to about 275 to 765 kv by the station surge impedance. The basic-impulse insulation level[10] for 138-kv apparatus is 650 kv, and in some of the most favorable station arrangements a voltage well below this value is held by the station impedance alone.

Current in Overhead Ground Wires and Line Conductors and in Station Arresters

In Table VII are summarized the overhead-ground-wire currents measured near stations in 1940 to 1943, inclusive, a total of 133 readings. The maximum current recorded was 36,000 amperes with 50 per

Figure 6 (right). Currents in lightning strokes, 2,721 records from 11 lines 66 to 220 kv on five systems, 1933 to 1943, inclusive, and for comparison, data on 734 strokes from seven lines on four systems, 1933 to 1936, inclusive[1]

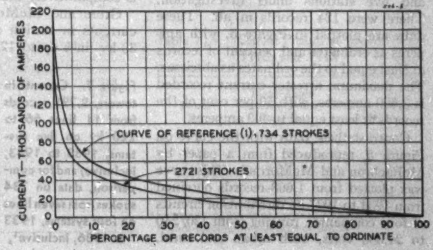

Table VII. Overhead-Ground-Wire Current Near Stations, 1940–1943, Inclusive

Appalachian Electric Power Company 132-Kv System

Range of Current, Amperes	1940	1941	1942	1943	Total	No. at or Above Level	Percentage at or Above Level
500–1,000				20	20	133	100.0
1,001–1,500			2	0	2	113	85.0
1,501–2,000	24	12	0	5	41	111	83.6
2,001–3,000	6	6	0	9	21	70	52.6
3,001–4,000	2	0	2	4	8	49	36.8
4,001–5,000	3	0	3	5	11	41	30.8
5,001–6,000	1	1	2	1	5	30	22.5
6,001–7,000	0	0	0	0	0	25	18.8
7,001–8,000	0	0	2	1	3	25	18.8
8,001– 9,000	1	1	2	2	6	22	16.5
9,001–10,000	4	1	0	0	5	16	12.03
10,001–12,000	2	1	0	2	5	11	8.28
12,001–15,000	0	0	0	0	0	6	4.51
15,001–20,000	0	1	0	0	1	6	4.51
20,001–30,000	1		1	1	3	5	3.76
33,000	0		1		1	2	1.50
36,000	1				1	1	0.75
Total	45	23	15	50	133		
Maximum	36,000	17,200	33,000	27,500			

Table VIII. Line-Conductor Current at Stations, 1940–1943, Inclusive

Appalachian Electric Power Company 132-Kv System

Range of Current, Amperes	1940	1941	1942	1943	Total	No. at or Above Level	Percentage at or Above Level
500–1,000				43	43	290	100.0
1,001–1,500			30	0	30	247	85.2
1,501–2,000	65	23	0	14	102	217	74.8
2,001–3,000	29	20	19	11	79	115	39.7
3,001–4,000	3	7	3	6	19	36	12.4
4,001–5,000	1	1	2	3	7	17	5.86
5,001–6,000	0		0	0	0	10	3.45
6,001–7,000	2		0	0	2	10	3.45
7,001–8,000	2		0	3	5	8	2.76
8,001–9,000	1		1		2	3	1.04
9,001–10,000	0				0	1	0.35
11,500	1				1	1	0.35
Total	104	51	55	80	290		
Maximum	11,500	5,000	8,500	8,000			

cent of all records at least equal to 2,200 amperes.

In the four years 1940 to 1943, inclusive, 290 records were obtained of line-conductor current adjacent to stations. The data are given in Table VIII. The maximum current recorded was 11,500 amperes, and 50 per cent of all the records were at least equal to 1,800 amperes.

In Table IX are given the records of station-arrester current for the four years and five stations under investigation. There were 124 records in all. These data are plotted in Figure 5, with amperes as ordinates and per cent of records at least equal to the ordinates as abscissas. The maximum arrester current recorded is 3,600 amperes, with 50 per cent of the records at least equal to 400 amperes.

Contrast these data with the curve on Figure 5, reproduced from a paper by McEachron and McMorris.[8] This curve was plotted from 1,608 records obtained from 1934 to 1937 on distribution circuits of four companies, ranging from 120/240 to 24,000 volts, both urban and rural. The maximum current recorded was something above 25,000 amperes with 50 per cent of all the records less than 1,300 amperes.

These distribution circuits are exposed to direct strokes of lightning, and the arresters are as a rule near the stroke. On the other hand, the stations in our investigation are shielded from direct strokes and are only subject to traveling waves, so that the duty on the arresters is comparatively mild.

Gross and McMorris[9] have recorded currents in station arresters of 22- and 33-kv lines up to 12,000 and 15,000 amperes, with, however, 4,100 amperes maximum on 132-kv lines. Here again, the low-voltage lines probably are not equipped with overhead ground wires, and the conductors are exposed to direct strokes. The conditions therefore are more severe than on higher-voltage lines where the conductors and stations are shielded. The middle curve on Figure 5 is reproduced from reference 9 and is plotted from 459 records of station-arrester current on lines of the American Gas and Electric Company, ranging from 11 to 132 kv, obtained during the years 1936 to 1939, inclusive.

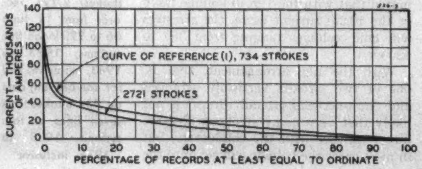

Figure 7. Currents in towers, 2,721 records from 11 lines 66 to 220 kv on five systems, 1933 to 1943, inclusive; and for comparison, data on 734 strokes from seven lines on four systems, 1933 to 1936, inclusive[1]

Hansson and Waldorf[14] report the results of an investigation of current in 26 banks of arresters at 66-, 132-, and 220-kv stations, during the years 1935 to 1942, inclusive. A total of 53 records was obtained, the maximum current being 7,400 amperes through one of the 66-kv arresters. Six per cent of the discharges exceeded 2,700 amperes, and 66 per cent were less than 1,000 amperes.

Lightning Current in Towers and Strokes

In Figure 1 of reference 1, cumulative curves of tower and probable stroke current were given for 734 strokes, occurring during the years 1933 to 1936, inclusive. These data were secured on the Wallenpaupack–Siegfried 220-kv line of the Pennsylvania Power and Light Company;[11] Glenlyn–Roanoke 132-kv line of the Appalachian Electric Power Company;[12] Philadelphia–Delaware Stateline 66-kv line of the Philadelphia Electric Company; and a group of Pennsylvania Water and Power Company lines, namely: Safe Harbor–Westport–Takoma 220-kv line, Safe Harbor–Perryville 132-kv line, Holtwood–Coatesville 66-kv line and Holtwood–York 66-kv line.[13]

Columns 2, 3, and 4 of Table X of the present paper give the data from which the stroke-current curve of Figure 1, reference 1, was plotted, and columns 2, 3, and 4 of Table XI, the data from which the tower-current curve was plotted.

Since 1936 a large amount of additional data have been accumulated on the Pennsylvania Water and Power Company's lines, including, in addition to the lines previously listed, the Safe Harbor–Riverside 220-kv, the Holtwood–Baltimore 66-kv, and the Philadelphia Road–Gunpowder 110-kv lines;[14] also, on the

Table IX. Station-Arrester Current, 1940–1943, Inclusive

Appalachian Electric Power Company 132-Kv System

Range of Current, Amperes	1940	1941	1942	1943	Total	No. at or Above Level	Percentage at or Above Level
150–250	8	1	2	2	13	123	100.0
251–500	7	12	12	28	50	110	89.4
501–1,000	5	1	6	13	25	51	41.5
1,001–1,500	2	3	5	5	15	26	21.1
1,501–2,000	0	2	1	3	6	11	8.94
2,001–3,000	1	3			4	5	4.07
3,600		1			1	1	0.81
Total	23	23	26	51	123		
Maximum	2,100	3,600	1,700	1,950			

Table X. Currents in Lightning Strokes

Eleven Lines of Five Systems, 66 to 220 Kv, 1933 to 1943, Inclusive

1 Range of Current, Amperes	2 No. of Strokes in Range 1933–1936[1]	3 No. at or Above Level, 1933–1936	4 Percentage at or Above Level, 1933–1936	5 No. of Strokes in Range, 1933–1943	6 No. at or Above Level, 1933–1943	7 Percentage at or Above Level, 1933–1943
1,000–5,000	72	734	100	567	2,721	100
5,001–10,000	121	662	90.2	611	2,154	79.2
10,001–20,000	167	541	73.7	640	1,543	56.7
20,001–30,000	115	374	51.0	296	903	33.2
30,001–40,000	92	259	35.3	227	607	22.3
40,001–50,000	62	167	22.8	140	380	14.0
50,001–60,000	30	105	14.3	80	240	8.82
60,001–70,000	24	75	10.2	61	160	5.88
70,001–80,000	8	51	6.95	22	99	3.64
80,001–90,000	11	43	5.86	21	77	2.83
90,001–100,000	6	32	4.36	11	56	2.06
100,001–110,000	5	26	3.54	11	45	1.65
110,001–120,000	5	21	2.86	9	34	1.25
120,001–130,000	7	16	2.18	9	25	0.918
130,001–140,000	5	9	1.23	7	16	0.588
140,001–150,000	0	4	0.545	2	9	0.331
150,001–160,000	2	4	0.545	3	7	0.257
160,001–170,000	0	2	0.273	0	4	0.147
170,001–180,000	0	2	0.273	1	4	0.147
180,001–190,000	0	2	0.273	0	3	0.110
190,001–200,000	1	2	0.273	1	3	0.110
200,001–210,000	0	1	0.136	0	2	0.073
212,400	0	1	0.136	1	2	0.073
218,000	1	1	0.136	1	1	0.037
Total	734			2,721		
Maximum negative	218,000			218,000		
Maximum positive	193,000			212,000		

Table XI. Currents in Towers

Eleven Lines of Five Systems, 66 to 220 Kv, 1933 to 1943, Inclusive

1 Range of Current, Amperes	2 No. of Currents in Range, 1933–1936[1]	3 No. at or Above Level, 1933–1936	4 Percentage at or Above Level, 1933–1936	5 No. of Currents in Range, 1933–1943	6 No. at or Above Level, 1933–1943	7 Percentage at or Above Level, 1933–1943
1,000–5,000	78	734	100	617	2,721	100
5,001–10,000	182	656	89.4	816	2,104	77.6
10,001–20,000	171	474	64.6	589	1,288	47.3
20,001–30,000	133	303	41.3	300	699	25.7
30,001–40,000	110	170	23.2	248	399	14.7
40,001–50,000	33	60	8.2	81	151	5.55
50,001–60,000	11	27	3.7	33	70	2.57
60,001–70,000	7	16	2.2	21	37	1.36
70,001–80,000	4	9	1.22	5	16	0.588
80,001–90,000	0	5	0.68	4	11	0.404
90,001–100,000	3	5	0.68	5	7	0.257
100,001–110,000	0	2	0.27	0	2	0.074
110,001–120,000	1	2	0.27	1	2	0.074
120,001–130,000	0	1	0.14	0	1	0.037
132,000	1	1	0.14	1	1	0.037
Total	734			2,721		
No. negative	685			2,235		
No. positive	49			486		
Maximum negative	132,000			132,000		
Maximum positive	100,000			100,000		

100-kv Shoshone–Denver line of the Public Service Company of Colorado.[2] For the Pennsylvania Water and Power Company's lines data up to and including 1942 are available, and for the Public Service Company of Colorado line up to and including 1943. Including the original 734 strokes, data are now available on 2,721 strokes. These data are summarized as to stroke currents in columns 5, 6, and 7 of Table X, and as to tower currents in columns 5, 6, and 7 of Table XI.

In Figure 6 are plotted the stroke-current curve of reference 1 (column 4, Table X, 734 strokes), and the stroke-current curve of column 7, Table X, 2,721 strokes; and in Figure 7 the tower-current curve of reference 1 (column 4, Table XI, 734 strokes), and the tower-current curve from column 7, Table XI, 2,721 strokes.

In reference 1, the average of each 10,000-ampere range was plotted as ordinate, whereas in the present paper the lower limit of each range is plotted. It will be noted that the new curves fall somewhat under the old curves.

In the data of reference 1, of the 734 strokes 685 or 93.3 per cent were negative, and 49 or 6.7 per cent were positive. In the more extensive data of the 2,721 strokes, 2,235 or 82.1 per cent were negative and 486 or 17.9 per cent positive.

The maximum negative-stroke current in both the old and present data was 218,000 amperes. The maximum positive-stroke current in the old data was 193,000 amperes, and in the more extensive data 212,000 amperes. The maximum current in individual towers in both the old and present data is 132,000 amperes negative, and 100,000 amperes positive. While the percentage of positive strokes is small, occasionally there is a positive stroke of very high magnitude.

Distribution of Current in Counterpoise and Driven Rods

In a paper by the present authors, in collaboration with J. G. Hemstreet,[3] a comparison was made between the current picked up under lightning-surge conditions by driven rods and by counterpoise wires, both parallel to the line and at right angles to the line. The results of

Table XIA. Current Pickup at Towers 7717, 7716, and 7718

Tower No.	Right-Angle Counterpoise, Amperes	Driven Rod, Amperes
7716	0*	3,400
7717	5,200	14,300
7718	2,300*	9,600
Total	7,500+	27,300

* Link missing on east side of tower.

six strokes to the Consumers' Power Company 140-kv *N*-14 line occurring in the years 1937 to 1941, inclusive, were analyzed. In the years 1942 and 1943 three additional strokes took place to this line. These will be discussed briefly.

Stroke 14. Some time prior to May 5, 1942, a stroke hit the ground near tower 7666 in section *A*, equipped with parallel continuous counterpoise and right-angle counterpoise. Current flowed into the stroke over the continuous counterpoise and overhead ground wire from two spans each side of tower 7666. At tower 7666 the following conditions prevailed:

Toward tower 7666:	
From overhead ground wire	8,600 amperes
From continuous counterpoise	7,300 amperes
From right-angle counterpoise	1,000 amperes
Total	16,900 amperes
Away from tower 7666:	
In west right-angle counterpoise toward stroke to ground	—16,000 amperes

Similar occurrences have been noted from time to time on the Pennsylvania Power and Light Company 220-kv line and the 100-kv line of the Public Service Company of Colorado. The transmission system, that is, overhead ground wire and counterpoise or counterpoise alone, has acted as a carrier to gather in the current for the stroke at one side of the transmission line.

Stroke 15. This stroke occurred in April 1943 in section *C*, equipped with right-angle counterpoise and driven rods. The stroke contacted the overhead ground wire just north of tower 7717, and current was picked up and fed into the stroke at this tower and the adjacent towers 7716 and 7718. Table XIA shows the current pickup at these towers.

As in the previously reported strokes, the driven rod picked up about 80 per cent of the current, with the other 20 per cent coming in on the right-angle counterpoise.

Stroke 16. This stroke occurred on September 6, 1943, in section *C* (right-angle counterpoise and driven rods). The stroke occurred to the overhead ground wire between towers 7717 and 7718, and the overhead ground wire brought in current from a distance of five to six towers each side of the point of stroke. The total pickup by the counterpoise and driven-rod system was about 111,000 amperes, of which 82,000 amperes, or 74 per cent, came in by way of the driven rods, and 29,000 amperes, or 26 per cent, by way of the right-angle counterpoise, neglecting the small amount via the tower footings.

Voltage Gradient in Vicinity of Towers

There were no strokes in 1942 to the section of the 140-kv *T*-20 line of the Consumers' Power Company equipped to measure voltage gradient in the vicinity of towers. Two strokes occurred in this section on September 6, 1943, stroke 17 to the overhead ground wire between towers 4405 and 4406 and stroke 18 at tower 4411. Readings were obtained at five towers in each stroke, but good correlation between tower current and the potential from tower to probe rod six feet away from the tower was secured only at two towers in stroke 18.

Table XII repeats the information for six strokes and nine towers first given in Table XVI of reference 3, and also gives the information for the two towers in stroke 18. In addition, there are given data for eight towers in strokes 7 and 8, in which the readings of voltage between the tower and probe rod were uncertain, because the lightning-stroke-recorder film flashed over. However, since we know the flashover voltage of the film, we can put this voltage down as a minimum value and figure out the ratio of R_s/R_N, knowing that the actual ratio is somewhat greater than the value given. Data also are included on one additional tower for stroke 7 and two additional towers for stroke 11, which were omitted previously, because the lightning-stroke-recorder reading in each case was just a trace. Values of five and seven kilovolts have been assigned to the traces and the readings included.

This gives a total of 22 readings, which can be considered good data or supporting data. Seventy-seven readings were rejected because either the current or voltage readings were missing or doubtful.

Figure 2 of reference 3 is redrawn as Figure 8 in this paper, with the nine original points, five additional good points, and eight points which are uncertain as to ratio of R_s/R_N, except that we know the ratio is greater than the plotted value. The drawn curve is actually the same as that given in Figure 2 of reference 3, the additional points only serving to tie the curve down a little more firmly.

Table XII. Surge Resistance of Tower Footings

Consumers Power Company 140-Kv, *T*-20 Line

1 Date	2 Stroke No.	3 Tower No.	4 R_N, Tower-Footing Resistance, Ohms	5 I_T Total Tower Current, Amperes	6 R_NI_T, Tower Potential (4)x(5), Kv	7 V_M, Tower-to-Probe Potential, Kv	8 V_T, Tower Potential, (7)x(2.5) Kv	9 R_S, Surge Resistance, (8)/(5), Ohms	10 R_S/R_N, (9)/(4), Ratio
9/15/1936	7	4393	33	2,000	66	7	17.5	8.75	0.265
		4394	35	6,000	210	27	67.5	11.25	0.322*
		4395	51	3,000	153	30+	75+	25 +	0.49 +
		4396	56	2,300	129	30+	75+	32.6 +	0.582 +
		4403	1,260	9,200	11,592	40+	100+	10.88+	0,0086+
		4404	816	12,900	10,526	40+	100+	7.77+	0.0095+
		4405	1,187	12,300	14,600	40+	100+	6.86+	0.0058+
		4408	75	7,700	578	30+	75+	9.75+	0.13 +
6/4/1937	8	4407	266	9,500	2,527	100+	250+	26.35+	0.099 +
		4408	76	50,000	3,750	100+	250+	5 +	0.067 +
		4410	15	3,300	50	5	12.5	3.8	0.254*
5/27/1938	9	4408	75	11,700	878	190	475	40.6	0.542*
5/27/1938	10	4400**	1,299	13,700	17,796	280	700	51.1	0.039*
		4401	942	6,800	6,406	170	425	62.5	0.066*
5/27/1938	11	4392	22	2,000	44	5	12.5	6.25	0.284
		4393	33	3,400	122.2	5	12.5	3.68	0.112
		4394	35	6,600	231	40	100	15.15	0.433*
		4395	51	16,000	816	170	425	26.6	0.522*
		4396	56	11,000	616	140	350	31.8	0.568*
7/30/1940	13	4412	13	45,600	593	222	555	12.15	0.935*
9/6/1943	18	4411	14	10,400	145.6	18.0	45	4.33	0.31
		4412	13	11,900	154.7	37.8	94.5	7.95	0.612

Total tower current (column 5) assumed 1.5 times measured current in tower legs, to take care of cross-member current.

* From Table XVI of reference 3. ** Flashover all three phases.

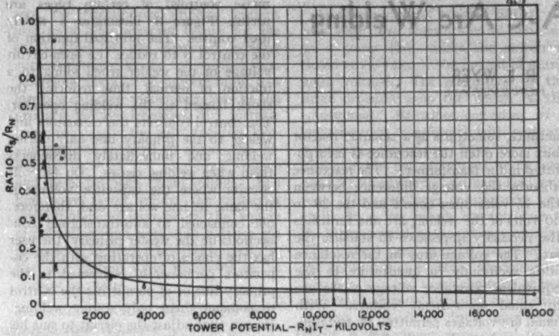

Figure 8. Ratio of surge resistance during natural lightning strokes to normal tower-footing resistance plotted against product of current and normal footing resistance

○ (9) Original points, Figure 2, reference 3
● (5) Additional good points
δ (8) Points which are probably low because lightning-stroke recorder flashed over

Additional probe rods were driven in 1943 at a distance of 12 feet from the tower. These, like the original rods six feet from the tower, were driven five feet deep. Lightning-stroke recorders were mounted on the first set of probe rods and coupled by voltage divider between the rods, so that surge voltages between the rods would be read.

Two good records were obtained in 1943. Several other simultaneous readings were obtained of voltage between tower and first probe rod and between first and second probe rods, but no readings or uncertain readings of tower current. No attempt will be made to analyze these readings until further reliable data have been accumulated.

Conclusions

1. Rate of change of voltage has been measured at five stations on the 132-kv system of the Appalachian Electric Power Company over a five-year period. The highest measured rate of change was 550 kv per microsecond, with 50 per cent at least equal to 100 kv per microsecond. These data should have an important bearing on fixing a reasonable front-of-wave test for apparatus.

2. Voltages up to 525 kv were measured on 132-kv station busses over a four-year period. This voltage is limited by the line and bus insulation, the lightning arresters, and the station surge impedance.

3. Currents up to 36,000 amperes were measured in overhead ground wires near stations and up to 11,500 amperes in line conductors of 132-kv lines over a four-year period. On a well shielded line, direct strokes are intercepted by the overhead ground wires, and current gets onto the conductors only through flashover of the line insulators or the protective tubes. The conductor-current magnitude is further modified by the outgoing lines and arresters.

4. Currents up to 3,600 amperes were measured in station arresters on 132-kv lines over a four-year period. This value should be contrasted with a current of 25,000 amperes measured in distribution-circuit arresters,[8] and 15,000 amperes in low-voltage-transmission-circuit arresters.[9] It appears that in stations with well-shielded incoming lines both voltage and current magnitudes are of very moderate values.

5. Stroke-current and tower-current data are available from 11 lines of five companies, gathered during a period of 11 years and totaling 2,721 strokes. The maximum stroke current was 218,000 amperes and the maximum tower current 132,000 amperes. Of the total strokes 82 per cent were negative and 18 per cent positive.

6. A few additional readings are available from the setup on the 140-kv system of the Consumers' Power Company, designed to evaluate the surge resistance of towers. These data tend to anchor somewhat more firmly the curve first given as Figure 2 of reference 3 and to reinforce the conclusions previously drawn that the ratio of surge tower-footing resistance to normal tower-footing resistance decreases with increased current and increased resistance, and that this ratio may be as low as 0.04 for the sandy soil conditions and the magnitude of resistance and current encountered.

A paper by I. W. Gross and G. D. Lippert gives further details of the investigation on the American Gas and Electric Company system;[15] another recent paper is pertinent to our present investigation in that it discusses the impulse characteristics of various types of soils and electrodes.[16]

References

1. Lightning Investigation on Transmission Lines—VII, **W. W. Lewis, C. M. Foust.** AIEE Transactions, volume 59, 1940, April section, pages 227–32.

2. Lightning Investigation at High Altitudes in Colorado, **L. M. Robertson, W. W. Lewis, C. M. Foust.** AIEE Transactions, volume 61, 1942, April section, pages 201–08.

3. Study of Driven Rods and Counterpoise Wires in High-Resistance Soil on Consumers' Power Company 140-Kv System, **J. G. Hemstreet, W. W. Lewis, C. M. Foust.** AIEE Transactions, volume 61, 1942, September section, pages 628–34.

4. Lightning Investigation on 132-Kv Transmission System of the American Gas and Electric Company, **I. W. Gross, G. D. Lippert.** AIEE Transactions, volume 61, 1942, April section, pages 178–85.

5. Direct Measurement of Surge Currents, **C. M. Foust, J. T. Henderson.** AIEE Transactions, volume 54, 1935, April section, pages 373–8.

6. Instruments for Lightning Measurements, **C. M. Foust.** *General Electric Review*, April 1931.

7. Flashover Characteristics of Rod Gaps and Insulators, Edison Electric Institute and National Electrical Manufacturers' Association Joint Subcommittee on Correlation of Laboratory Data. AIEE Transactions, volume 56, 1937, June section, pages 712–14.

8. Discharge Current in Distribution Arresters—II, **K. B. McEachron, W. A. McMorris.** AIEE Transactions, volume 57, 1938, June section, pages 307–12.

9. Lightning Current in Arresters at Stations, **I. W. Gross, W. A. McMorris.** AIEE Transactions, volume 59, 1940, August section, pages 417–22.

10. Standard Basic Impulse Insulation Levels Joint Committee on Co-ordination of Insulation, EEI publication *H8*, NEMA publication 109, January 1941.

11. Lightning Investigation on a 220-Kv System—III, **Edgar Bell.** AIEE Transactions, volume 59, 1940, pages 822–8.

12. Lightning Current in 132-Kv Lines, **Philip Sporn, I. W. Gross.** AIEE Transactions, volume 56, 1937, February section, pages 245–52, 259–60.

13. Probable Outages of Shielded Transmission Lines, **S. K. Waldorf.** AIEE Transactions, volume 56, 1937, May section, pages 597–600.

14. An Eight-Year Investigation of Lightning Currents and Preventive Lightning Protection on a Transmission System, **E. Hansson, S. K. Waldorf.** AIEE Transactions, volume 63, 1944, May section, pages 251–8.

15. Lightning Investigation on 132-Kv System of American Gas and Electric Company, **I. W. Gross, G. D. Lippert.** AIEE Transactions, volume 64, 1945, February section, pages 76–84.

16. Impulse Characteristics of Electrical Connections to the Earth, **J. R. Eaton.** *General Electric Review*, October 1944, pages 41–50.

Power Supply for A-C Arc Welding

A. U. WELCH
ASSOCIATE AIEE

R. F. WYER
NONMEMBER AIEE

THE rapid growth of a-c arc welding in the last ten years has resulted in a-c welding becoming a large fraction of all arc welding rather than a negligible proportion. As power loads due to a-c arc welding become larger, questions arise in the minds of users and power-supply authorities about power requirements of a-c welders and the effect of a-c welders on power circuits. In some instances arc welding has been confused with resistance welding, although the two are entirely different from the standpoint of power supply. This paper presents data useful for determining the effects of a-c arc-welding loads on electric power circuits.

A-c arc welders may be divided into two general types—industrial welders and utility welders. For industrial service, welders must be suitable for high-speed high-quality welding, must be designed for quick and easy arc starting, and must be usable with long welding leads. This requires fairly high open-circuit voltage for easy arc starting and stability of current. Industrial welders generally include capacitors for power-factor correction. Utility welders are built in low-current ratings, usually 200 amperes and below and are characterized by low open-circuit voltage, low kilovolt-ampere demand, simplicity of construction, and low cost. They are intended for use in small shops for repair work where their slow arc starting, slow operation, and current variation with arc length are not too objectionable.

High-reactance transformer-type single-operator welders are used almost universally for a-c welding. They are two-winding transformers, not autotransformers, for obvious reasons of safety. A-c arc welders are rated in terms of welding amperes rather than kilovolt-amperes.

Industrial-Duty Welders

Industrial-duty welders are built for primary power circuits of 220-, 440-, or 550-volt rating and step down the voltage to approximately 75. Although voltages as high as 100 have been used, industrial-duty welders generally range from 70 to 80 volts open circuit. Included in the welder is an adjustable reactance, sometimes as a separate reactor but more often the reactance is incorporated in the transformer. The reactance absorbs the voltage difference between the 75 volts open circuit and the 20 to 40 volts of the welding arc and furnishes the necessary impedance to stabilize the arc. The voltage drop in the reactance adds vectorially in quadrature to the equivalent resistance voltage of the arc to equal open-circuit voltage. With usual arc voltages permitted by metallic-welding electrodes and with the usual open-circuit voltages, the reactance voltage is 75 to 85 per cent of open-circuit voltage and, during the start of a weld with the electrode short-circuited, is equal to 100 per cent. Adjustment of the reactance therefore permits accurate control of welding current because the reactance is the largest impedance in the circuit.

The usual ampere ratings for industrial hand welding are 200, 300, 400, and 500 amperes. The usual range of output is from 20 per cent to 125 per cent of the rating. The adjustment above 100 per cent not only permits occasional short jobs to be done at higher than rated current, but, even more important, it permits welding to be done at rated current with welding leads as long as 150 feet.

Figure 1 shows a simple equivalent circuit of an arc-welding transformer. The capacitors, shown dotted, generally are included in heavy-duty industrial welders to improve power factor and reduce current demand from the primary circuit. The vector diagram of primary voltage and current in an a-c arc welder illustrates the effect of capacitors in reducing current and improving power factor. Figure 2 shows kilovolt-ampere input and power factor of 300-ampere a-c welders with and without power-factor correction.

Welders with built-in power-factor correction generally are designed to operate at 0.75 to 0.85 power factor at rated load. The power factor becomes unity at approximately half load, and the primary current is leading at lighter loads and at no load. This leading current is often useful for improving the over-all power factor of the primary circuit when other low-power-factor equipments such as motors are connected to the same circuit.

Where large numbers of high-power-factor welders are connected to a single circuit and where welding loads are such that the majority operate idle or lightly loaded, the total leading current may become undesirably high. In such cases automatic voltage-reducing controls(Idlematic controls) of certain types are useful. Figure 3 illustrates a widely used control. The principal function of the control is to reduce the open-circuit voltage of the welder when idling to a fraction of normal, thus reducing the shock hazard to the welding operator. The control connects the capacitors and welder to the primary line only during welding and immediately disconnects them when welding ceases. On 440-volt circuits where the capacitor voltage is the same as line voltage and, therefore, not connected to autotransformer connections on the welder primary, the user has the choice of operating with the capacitors permanently connected to the primary line or of permitting the control to connect them only during welding. He can thus adjust the circuit to suit his operating conditions. The data given later in the paper under duty factor may be used as a guide to determine the preferable connection.

Figure 4 shows secondary volt-ampere curves of a typical industrial a-c arc welder. Each curve applies for one setting of the control reactance. Most industrial welders have stepless adjustment of reactance so that there is an infinite number of these curves between minimum and maximum.

EFFECT OF PRIMARY-VOLTAGE VARIATION

A-c welder rated input current and kilovolt-amperes are based upon operation at rated primary voltage: 220, 440, or 550 volts. Many industrial circuits actually operate at average levels higher than these nominal values, often at 110 per cent. Figure 5 shows how the primary kilovolt-ampere input is increased by overvoltage. The curves are based on maintained rated secondary load. The arc voltage will stay constant as determined by the electrode and length of arc, but with increasing primary voltage it will be necessary to readjust the current control to prevent current from increasing. With constant secondary cur-

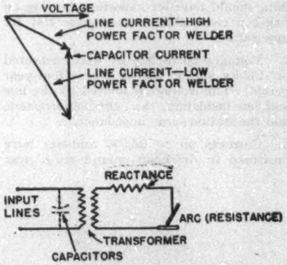

Figure 1. A-c-arc-welder equivalent circuit and vector diagram

---

Paper 45-28, recommended by the AIEE committee on electric welding for presentation at the AIEE winter technical meeting, New York, N. Y., January 22-26, 1945. Manuscript submitted November 22, 1944; made available for printing December 11, 1944.

A. U. WELCH and R. F. WYER are engineers with the General Electric Company, Mr. Welch in Pittsfield, Mass., and Mr. Wyer in Schenectady, N. Y.

rent the transformer primary current also must stay constant except for the small effect of the increased exciting current required by the transformer core. Therefore, the kilovolt-ampere input to a low-power-factor welder increases as the primary voltage increases, the increase being principally the extra reactive kilovolt-amperes required to absorb the difference between the fixed-load voltage and the higher open-circuit voltage. In a high-power-factor welder the capacitor kilovolt-amperes increase as the square of the voltage and more than balance the increase of inductive kilovolt-amperes so that the current input decreases as the voltage increases.

NO-LOAD SWITCHING TRANSIENTS IN A-C ARC WELDERS

Figure 6 shows transient primary voltages and currents which occur when applying or removing excitation with no load on the secondary circuit. These tests were made on a standard welder rated 550 primary volts, 500 amperes secondary current, rated welder with and without power factor correcting capacitors. Switching was done with a standard 600-volt safety switch of snap-action type. Power supply was one-phase of a 550-volt two-phase 60-cycle 600-kva shop circuit used principally for power supply to motor-driven machine tools in a machine shop. The impedance of the supply circuit was such that the voltage drop at the welder primary terminals, when loaded at 500 amperes secondary current, measured approximately two per cent.

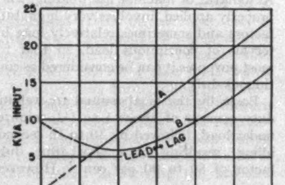

Figure 2. Input kilovolt-amperes and power factor of an industrial 300-ampere a-c welder at standard 40-volt load

A—Low-power-factor welder
B—High-power-factor welder

An inrush surge of exciting current occurs when any transformer is switched on a power line, unless the switch is closed at very nearly the instant of maximum voltage. The magnitude of the surge depends upon the design of the transformer. A welder consisting of a low-reactance transformer with separate secondary reactor may have very large instantaneous-current surges up to perhaps 20 times normal primary-load current. High-reactance transformers generally draw low inrush currents due to the high reactance of the primary winding. The highest crest current measured on the high-reactance welder previously referred to was two times the crest of normal rated current, although calculations indicate as much as three times might occur, if the circuit were closed at exactly voltage zero. Inrush-current peaks of this magnitude die down rapidly and have usually no noticeable effect on the primary circuit. They cause much less voltage drop in primary circuits than the starting of an equivalent motor.

When a high-power-factor welder is switched on the line, a surge current may flow in the capacitors as shown in the oscillogram of Figure 6B. Currents approaching five times normal have been measured, but the duration of the current flow is so short—generally less than 0.001 second—that the effect on the primary circuit is negligible. Instantaneous overvoltages of 25 per cent above normal have been measured of the same short duration.

Switching-off excitation of a low-power-factor welder may result in a transient-voltage rise as will be seen in Figure 6A. This voltage depends upon the speed at which the switch can interrupt the exciting current. High-speed snap-action switches may cut off current so rapidly that the inductive kick can cause considerable voltage rise. A rise 84 per cent above normal was measured on this welder.

Oscillograms of switching-off excitation from a high-power-factor welder show that, as would be expected, the capacitors completely eliminate overvoltage. (See Figure 6B.) The energy storage capacity of the capacitors is so high that any stored inductive energy in the transformer core cannot affect the capacitor voltage measurably. After removal of excitation, the capacitors discharge slowly through the transformer winding, oscillating at a decreasing frequency because of the nonlinear characteristic of the transformer core.

SWITCHING OF ARC WELDERS WHEN LOADED

Starting and finishing a weld switches the load on the secondary side of the welder. It will be seen from the curves of Figure 4 that a reactance-controlled industrial welder limits the short-circuit current at the start of a weld to a value not much higher than normal welding current. There also may be a transient overcurrent for one or two cycles of the type caused by switching a reactive load on an a-c line. However, the resistance of the electrode, its contact resistance, and the resistance of the welding cable and transformer are large enough to hold the transient overcurrent to a low value, usually much less than 1.5 times the steady-state current. Therefore, starting a welding arc does not result in large current surges. A typical oscillogram of welding current and arc voltage in Figure 7 shows that neither starting nor extinguishing a welding arc causes objectionable transients. Starting the arc can cause momentary currents seldom exceeding approximately 1.5 times normal. Extinguishing the welding arc by withdrawing the electrode is a slow process requiring several cycles, so that the current and voltage in the reactance decrease gradually and no overvoltage occurs.

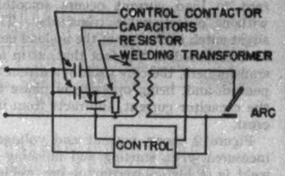

Figure 3. A-c arc welder with automatic voltage-reducing (Idlematic) control

The additional oscillograms of Figure 8 show primary and secondary voltages and currents occurring when a welding arc is started and stopped at various loads. Figure 8A shows start and finish of a 300-ampere welding load on a low-power-factor welder. Figure 8B shows a 500-ampere load on a high-power-factor welder. Figure 8C is included to show that at loads less than half rating the load current of a high-power-factor welder may be less than no-load current. This also is shown by the curves of Figure 2. As will be seen from these oscillograms, the transition from leading no-load cur-

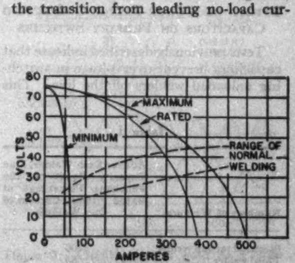

Figure 4. Output volt-ampere curves of 300-ampere industrial welder

rent to load current occurs smoothly without objectionable transients. The slight notch in the top of the no-load current is caused by the fact that, as in all transformers, the core exciting current is peaked, and, being opposite in phase to the capacitor current, subtracts from its crest.

Figure 9 shows current and voltages measured when starting and finishing a weld in a high-power-factor arc welder with Idlematic control. The action of the control is illustrated clearly by these oscillograms. Before starting the weld the contactor is open, leaving the capacitors and the welder primary winding disconnected. The welder secondary is excited from the control at reduced voltage—approximately 30 volts. When the electrode is touched to the work, the welder secondary voltage becomes nearly zero, and the control voltage is impressed on the contactor coil. When the contactor closes, it connects the welding load and the capacitors simultaneously to the line. The control is designed so that the contactor holds in, as long as welding load is maintained. When the welding arc is extinguished, normal open-circuit voltage appears on the secondary circuit for about two cycles at which time the contactor drops out disconnecting the capacitors and welder primary and reducing secondary voltage to normal idling voltage. The capacitors are discharged automatically through a discharge resistor. Overvoltage from switching off the welder exciting current is prevented by the control circuit which connects the welder secondary terminals to a resistor before disconnecting the welder primary terminals.

The two oscillograms in Figure 9 were not taken at the same time or set up, which accounts for the different scales of voltages and currents. The somewhat rounded top of the secondary voltage in the first oscillogram is caused by the impedance voltage drop in the long secondary leads used in this test, as voltage measurement was made at the transformer not at the arc. The actual wave shape of any a-c metallic-welding arc voltage is very flat-topped.

EFFECT OF POWER-FACTOR-CORRECTING CAPACITORS ON PRIMARY SWITCHES

Tests previously described indicate that capacitors prevent overvoltage in switching unloaded welders off the line. This would indicate that the interrupting duty on the switch is reduced by the presence of the capacitors. Although no comparative tests are available on loaded welders, the following facts may be indicative: There have been reported instances of primary-switch failure on low-power-factor welders occurring when the welding electrode froze to the work, maintaining a secondary short circuit, which had to be interrupted by opening the primary switch. In this case the load voltage is zero and the power factor of the primary current is very low—five to ten per cent. Therefore, the inductance built into the welder for the purpose of making the welding arc stable makes the arc in the switch very difficult to interrupt. On the other hand, a series of tests made on several types of commercial horsepower-rated switches connected to a short-circuited power-factor-corrected welder indicated that the switches cleared the circuit with less disturbance than was normal for the same current and power factor without capacitors. Apparently, the capacitors hold switching-surge voltages so low that they lessen switch interrupting duty considerably.

Table I

Numbers of Welders	Add for Each Welder, Line Capacity Equal to the Following Percentage of Rated Primary Current of One Welder
First and second welder	100
Third welder	85
Fourth welder	70
All additional	60

Capacitor current itself is interrupted easily by a switch. Capacitor-current surge on closing the switch has not been found to cause trouble, as switches used with arc welders are capable of closing on several times as much current as that caused by the amount of capacitance used in a welder.

EFFECT OF CAPACITORS ON EXTERNALLY CAUSED SURGE VOLTAGES

Switching-surge overvoltages occur on all types of electric power circuits, but they are of comparatively high frequency and extremely short duration—a few thousandths of a second. Although no evidence is available to indicate that they present a shock hazard to the welding operator, it is interesting to note that the power-factor-correcting capacitors on a welder present a very effective barrier to high-frequency voltage.

PHASE UNBALANCE

The question of phase unbalance due to the application of single-phase welding transformer loads occasionally is encountered. This is usually an academic question; cases where phase unbalance from this source have proved actually troublesome are very rare. Perhaps the interest in this question arises from confusion of a-c arc welders, having relatively low kilovolt-ampere input, with resistance welders having relatively large kilovolt-ampere input. A good rule of thumb says that even without the balancing effect of polyphase motors running on the same line, no troublesome voltage unbalance will occur, if the kilovolt-ampere input to the arc-welding transformer does not exceed approximately half the kilovolt-ampere rating of the three-phase distribution-transformer bank to which it is connected. When a number of a-c welders are supplied by a polyphase line, they may be connected to different phases in order to balance their load, except when the transformers are to be operated in parallel.

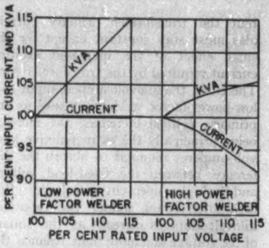

Figure 5. The effect of higher-than-rated input voltage on a-c arc welders operating at rated current

DUTY FACTOR

The arc-welding duty cycle varies widely, not only from plant to plant, but also from hour to hour in the same plant. (In this paper the term "duty cycle" will mean a group of specified intervals of arc time and idle time; for example, five minutes on and five minutes off. Duty factor is the ratio of arc time to the total time under consideration.) The majority of welders are used in manual-welding duty, and the following comments are confined to this class of service. Automatic, or machine arc welding, when properly applied, involves very high duty factors and sometimes relatively long intervals of continuous load, so that for most purposes it can be considered as continuous duty.

Basically, the usual manual-arc-welding duty consists of about 1 to $1^1/_2$ minutes under load, followed by 10 to 15 seconds idling, resulting in a short-time duty factor of 80 to 90 per cent. However,

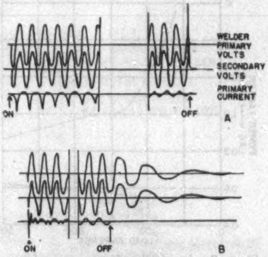

Figure 6. No-load switching of arc-welding transformers

A—Low-power-factor welder
B—High-power-factor welder

this cycle is rarely repeated more than eight or ten times before a longer idling interval takes place, so that all-day duty factors may run as low as ten per cent or as high as 50 or 60 per cent, depending on the nature of the work.

Advantage may be taken of these facts in providing electric service for groups of arc welders. Table I lists a conservative method of calculating primary-line capacity to supply a group of welders.

This table is usable for either low-power-factor welders or power-factor-corrected welders, using in either case the actual primary current input when delivering rated welding current. Wiring according to this table will carry, without being overloaded, the current from 50 per cent of welders operating at full load and 50 per cent idling, when low-power-factor welders are used, and will carry the current from 60 per cent of the welders at full load and 40 per cent idling, when power-factor-corrected welders with permanently connected capacitors are used.

Table I also can be used when welders are distributed among the phases of a three-phase circuit by the following procedure: Consider each group of three welders connected to the three phases as a single unit of current rating 1.73 times the primary rating of an individual welder and use the table as though the three were a single welder.

A single high-power-factor welder without Idlematic control, or its equivalent, will draw considerable leading-power-factor kilovolt-amperes while the welder is idling. The maximum 15-minute kilovolt-ampere demand will depend to a considerable extent on the duty factor, as well as on the amount of the capacitive kilovolt-ampere drawn by the capacitors, since it will involve a base load drawn by the capacitors during idling, plus intervals of somewhat higher kilovolt-ampere load during actual welding. The peak demand of a single welder will occur during the very short intervals when the welder is short-circuited in striking the arc and usually will have a maximum possible value of less than twice the kilovolt-ampere input at normal rated load.

When idlematic control is used, the capacitors usually are switched off, along with the welder primary, whenever the arc is broken. This eliminates the no-load capacitive kilovolt-ampere as a factor in the maximum kilovolt-ampere demand, which then will be some lower value, depending on the duty factor.

If a large number of welders without power-factor correction operate as a group, diversity begins to influence both maximum demand and peak demand. Figure 10 shows the shape of the welding-load curve for a group of 238 operators in a shipyard. (The recording ammeter from which this curve was derived actually measured one-seventh of the total load, which accounts for the relatively low currents indicated.) The average load was one-quarter of the connected load, indicating an average all-day duty factor of 25 per cent. (In this case connected load is assumed to be the total rated input of the number of welders equal to the number of operators working that day.) The 15-minute maximum demand was 26 per cent of the connected load, and the short-time peak indicated on the original ammeter record was only 30 per cent of the connected load.

Studies of the load imposed by smaller groups of welders show that diversity may be expected to reduce the 15-minute maximum demand drastically when more than four or five units are operating. Five units may have only 77 per cent as much maximum demand per unit as a single machine, and 20 units only 65 per cent as much.

Likewise, the peak short-time demand per unit will be reduced when sufficient numbers of welders are involved. In one case it was found that the expected peak demand per unit began to decrease when the number of welders reached six or seven and decreased fairly uniformly to about 80 per cent of the single-unit peak demand when 50 welders were included in the group.

With high-power-factor welders not equipped with Idlematic control, it is possible that the maximum demand may be the capacitive no-load kilovolt-amperes of the machines. Unless the duty factor is unusually high, the maximum demand of the group when operating under load will be reduced, because the leading kilovolt-amperes of those units which are idling will cancel all or a part of the lagging kilovolt-amperes drawn by the loaded units. But the capacitive kilovolt-amperes of the entire group may be drawn all at once during meal hours or rest periods, and this frequently will be the determining factor in the 15-minute maximum demand. The peak demand per unit will be reduced slightly (at normal duty factors) by the leading kilovolt-amperes of idling units.

POWER FACTOR

In the matter of power factor to be expected from groups of high-power-factor welders, duty factor again plays an important part. Unless the capacitors are disconnected automatically when welding stops, the capacitive kilovolt-amperes of the idling units is available to improve the power factor of the system on which they are connected.

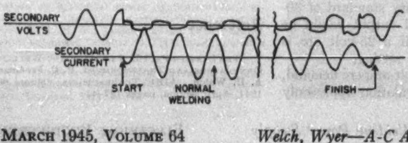

Figure 7. Secondary voltage and current in a-c arc-welding transformer

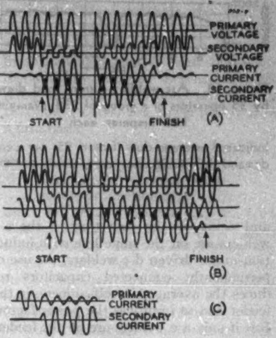

Figure 8. Oscillograms of currents and voltages during start and finish of a-c arc welds

A—300-ampere weld on a low-power-factor welder

B—500-ampere weld on a high-power-factor welder

C—150-ampere weld on a 500-ampere high-power-factor welder

Figure 11 illustrates how power factors on various feeders will vary, depending on whether or not the capacitors are switched off at no load. These data are calculated for current designs of 300-ampere welders, the a-c units being equipped with ten kilovolt-amperes in capacitors and the d-c units being ordinary three-phase motor-driven generator sets without power-factor correction. In the calculations the welders are assumed to be operating on a load of 200 amperes at 30 volts with a 45 per cent duty factor. If the duty factor were higher, the power factor of the d-c units would be higher and that of the a-c units more lagging.

By comparing the figure for feeders *A*

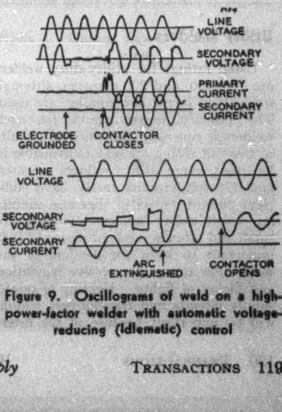

Figure 9. Oscillograms of weld on a high-power-factor welder with automatic voltage-reducing (Idlematic) control

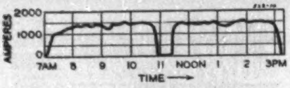

Figure 10. Arc-welding-current load drawn by 35 operators of a group of 238, averaging 160 amperes each

Indicated average-duty factor 25 per cent, demand factor 26 per cent, peak demand 1,700 amperes (30 per cent)

and C, it can be seen that, if the a-c welders are on the same line with induction-motor-driven d-c welders, the use of permanently connected capacitors reduces the average kilovolt-amperes in the feeder and so improves the power factor. But if only a-c welders are on the feeder, then automatic disconnection of the capacitors is preferable. The latter is also true from the point of view of the total load drawn by all three of the feeders illustrated.

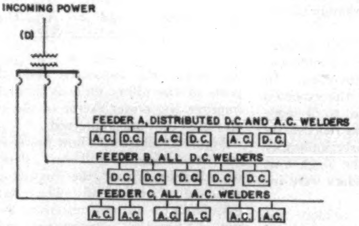
INCOMING POWER
(D)
FEEDER A, DISTRIBUTED D.C. AND A.C. WELDERS
A.C.
D.C.
A.C.
D.C.
A.C.
D.C.
FEEDER B, ALL D.C. WELDERS
D.C.
D.C.
D.C.
D.C.
D.C.
FEEDER C, ALL A.C. WELDERS
A.C.
A.C.
A.C.
A.C.
A.C.
A.C.

AVERAGE K.V.A. INPUT AND POWER FACTOR

		FEEDER A		FEEDER B		FEEDER C		SUBSTATION (D)	
		k.v.a.	p.f.	k.v.a.	p.f.	k.v.a.	p.f.	k.v.a.	p.f.
WITH CAPACITORS PERMANENTLY CONNECTED	LOAD	33.	0.91	66	0.6	32.	0.67*	99.	0.91
	NO LOAD (NOON HOUR)	12.	*0.90	53.	0.34	60.	0*	34.	*0.90
WITH AUTOMATIC DISCONNECTION OF CAPACITORS	LOAD	42.5	0.69	66.	0.60	21.	0.9	127.5	0.69
	NO LOAD (NOON HOUR)	26.5	0.34	53.	0.34	0		79.5	0.34

* POWER FACTOR LEADING

Figure 11. Typical load conditions on feeders supplying 300-ampere welders operating at 200 amperes 30 volts, 0.45 duty factor from one load-center substation

Utility Welders

Usual ratings for utility-duty welders are 100, 150, and 200 amperes, although some, both larger and smaller, are used. The primary power source for such welders is generally 230 volts, as circuits of 460-volt rating are seldom available in locations where utility welders are used and 115-volt circuits rarely have sufficient current capacity. Because circuits on which utility welders are used are small and often serve lighting loads, it is important to keep the demand of the welder low to avoid excessive regulation and flicker of lights. Heating of power supply circuits and transformers seldom will be important because of the intermittent nature of the load. These factors indicate that the first principle in design of utility welders should be lowest possible primary kilovolt-ampere demand. Also, it is desirable to keep the power factor high. The use of very low open-circuit voltage accomplishes both ends by reducing the kilovolt-ampere demand and by increasing the ratio of arc voltage to open-circuit voltage, thus increasing the power factor. Open-circuit voltages in the range of 40 to 60 volts are adequate for maintenance of a stable welding arc at low currents with present-day heavily coated a-c welding electrodes, although arc starting may be difficult and time-consuming, particularly when welding on clean smooth sheet steel. Another desirable design feature is strict limitation of the maximum obtainable output to prevent overload on the power circuit. The overtravel of current adjustment normally included in industrial welders is not necessary in utility welders, because there is less need for long welding leads and high output. Large welds for repair of heavy metal sections always can be made by multiple passes.

The characteristics of a design which might be suggested by the preceding discussion are shown in Figure 12. Such a welder would be suitable for operating standard one-eighth-inch a-c steel welding electrodes, and thus would be suitable for most repair welding. Its nominal rating probably would be 100 amperes based on the customary standard of 30-volt arc. The actual output would be about 120 amperes, if a 25-volt arc is held on the maximum setting.

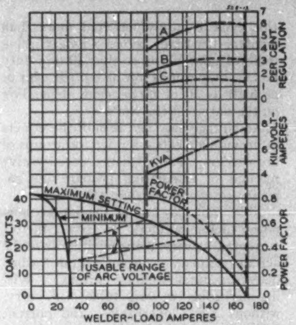

Figure 12. Utility-welder volt-ampere curves with curves of regulation of power source, welder kilovolt-amperes, and power factor when welder is operating at maximum setting

A—Three-kilovolt-ampere distribution transformer

B—Five-kilovolt-ampere distribution transformer

C—42-mile 6,900-volt rural line of 30 miles of number 6 conductor, ten miles of number 8 conductor, and two miles of number 11 conductor

The curves of kilovolt-ampere demand, power factor, and regulation apply only to the maximum setting of the welder; demand and regulation will, of course, decrease at reduced current settings. The line-regulation curve is based on a line likely to be found in rural areas. Power lines in urban areas would have less regulation.

It should be appreciated that the points shown by the curves at zero-load volts occur only momentarily, when the electrode is touched to the work to start the arc.

The maximum 15-minute demand of a welder of this design would not exceed 3.5 kva. A consumer supplied at 230 volts from an individual distribution transformer large enough to handle an electric range would not require additional transformer capacity to supply the welder. This is based on the assumption that the consumer will tolerate light flicker on his premises caused by his own welding load, since he is not likely to operate the welder many hours per year during hours that lights are on. It is not feasible at present to generalize upon regulation problems on systems where several consumers are served from a common distribution secondary circuit because of variation of circuit design used in different localities.

Reference

1. The Service Factor Rating of Arc-Welding Generators and Transformers, R. C. Freeman, A. U. Welch. AIEE Transactions, volume 60, 1941, April section, pages 137–41.

Dodge Chicago Plant's Electric-Power-Distribution Scheme With Airplane-Engine-Testing Power Recovery

E. L. BAILEY
FELLOW AIEE

THE Dodge Chicago plant was built to manufacture airplane engines for superbombers and the entire project was designed exclusively for that one purpose. The plan called for much more than the usual assembly of parts, as it was the intent that this plant make practically everything from castings on through to the finished motor. Accordingly, there are aluminum and magnesium foundries, forge, heat-treat, and machine shops as well as assembly and testing buildings. There are 19 principal buildings with their particular use broadly indicated by their names. The site covers over a square mile.

A list of the equipment in these buildings gives us the connected load, but the use factors for this equipment in each area had to be determined and assigned in order to obtain the power required. Fortunately, when the illumination level and type of lamp were selected for an area, it was straightforward arithmetic to determine the lighting load, as it is considered 100 per cent load factor; but the power demand was much more difficult to determine. The machine shop, our building 4, for example, being the largest one-floor building in the world, covers over 80 acres and contains over 6,000 production machine tools as well as heat-treat, plating, battery charging, conveyors, air-conditioning, building utilities and countless other special features. The estimate for machine demand for all of the buildings is shown in Table I.

At the center of each area of approximately 2,000 kva a double-ended unit substation is placed consisting of two 1,000-kva three-phase 12,000/480-volt transformers and their associated circuit breakers, each feeding a group of radial distribution circuits of approximately 400 to 600 amperes. The 480-volt bus may be paralleled to give service on any circuit in case of emergency by opening one secondary line breaker and closing a tie breaker. The transformers with their associated feeder circuits normally are operated with the tie breaker open, as one approaches very close to the limit of the rupturing capacity on the circuit breakers when the tie breaker is closed. The primary feeds for the two transformers in one substation come from different cables, but there are five transformers on each cable. By this means a dual primary feed on each substation area is obtained, but a separate primary-switch position is not tied up for each transformer. There is some variation from this plan as some locations did not warrant the installation of two transformers, in which case only one was installed with a throw-over primary feed where the operation of the circuit was considered important. The lighting of about 12,000 kw is supplied from the same substations through 50-kva air-cooled transformers (480 volt to 120/240 volt) properly disposed throughout the areas. Combination high-intensity tungsten units are used for the general lighting of about 25 foot-candles, augmented by fluorescent or individual tungsten units for the more critical visual tasks. Fluorescent lamps are used in the offices.

From all these data approximately 90,000-kva connected load was estimated with 39,000-kw probable maximum demand for the plant. However, originally it was provided with only 30,000-kva feed from two 15,000-kva 33-kv circuits in order that it would not be overequipped for power supply. A curve of the estimated load per month was laid out for contact with the public utility company so that it could provide facilities required for the plant as the load grew. It was with some temerity that such a curve was given, but subsequent experience has been gratifying, as there was not too much divergence from it for many months. About a year ago, however, loads indicated that a third 15,000-kva line would be required. It is now installed along with step-type voltage regulators so that now a 45,000-kva power supply is on a firm basis.

Power-Recovery Engine Test

When the production engine-test equipment was being considered, it was immediately evident that the output of these engines, being over 2,200 horsepower, would require very substantial equipment. Further, the amount of power seemed worthwhile salvaging if possible. The engine test requires that the engine be loaded under all conditions of speed and torque that might be expected in flight.

There are at least four commonly accepted plans for loading airplane engines for test. One is simply to install a special propeller or club on to the engine and arrange suitable air-control ducts or tunnels to direct and control the air and noise so that speed–torque curves can be taken. Such a scheme generally is known as a club test. This involves no electric connections other than some scheme for starting the engine and some blowers to carry away the excess fumes and create conditions similar to those in flight surrounding the motor. The actual horsepower developed by an engine while driving a club propeller has to be determined by calibration.

There are three common electrical schemes available; the simplest is what is known as an inductor-type absorption machine, which is simply a short-circuited water-cooled armature mounted in a frame, hung on bearings with a beam scale to measure the torque. This is quite satisfactory and is used by several of the engine builders. The engine has to be cranked for starting by auxiliary equipment as the inductor alternator will not develop torque as a motor.

The second electrical method makes use of an a-c generator connected to the en-

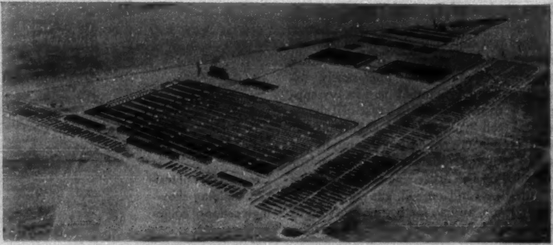

Figure 1. General view of Dodge Chicago plant

Paper 45-21, recommended by the AIEE committee on industrial power applications for presentation at the AIEE winter technical meeting, New York, N. Y., January 22–26, 1945. Manuscript submitted October 30, 1944; made available for printing December 5, 1944.

E. L. BAILEY is staff electrical engineer in the staff master mechanic's department, Chrysler Corporation, Highland Park, Mich.

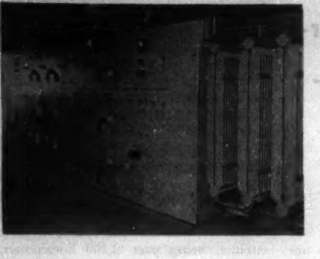

Figure 2 (left). Typical 2,000-kva 12,000/460-volt unit substation

Figure 3 (right). Power-absorption generators

gine through some sort of slip coupling, either a fluid or magnetic type. Both of these schemes are used. The results obtained from these hookups also are quite satisfactory. An excellent power factor is maintained on these circuits as the generators are all synchronous type. The power output of the engine is determined by the electric output of the generators plus the generator losses and the slip-coupling losses. This all can be figured out quite simply with the calculated curves of generator losses plus slip-coupling losses and the electric-power measurements. Load can be determined within plus or minus $1^1/_2$ per cent which is quite satisfactory for commercial purposes.

The last scheme for loading the engine is by making use of the variable-speed generators. Here the slip couplings are eliminated. The generator operates over the testing-speed range of the engine output shaft. The calibration of the electric meters may include the generator losses so that direct readings can be taken for use in a simple equation that will give correct engine horsepower output.

In the variable-speed generator the slip losses all are dissipated in an air-cooled resistor so that no problem arises regarding coolant supply.

It seemed that the simplicity of the slip-ring induction generator solidly coupled to the engine without any expensive and troublesome slip coupling would make the most suitable device for loading these high-power-output variable-speed engines. Experience with this type has been most satisfactory from both operating and maintenance point of view.

Description of Typical Test Cell

The test-cell operation is understood most clearly by referring to the cut-away drawing (Figure 4). The newly assembled engine mounted on a heavy supporting frame is run into a test cell shown as test cell 32 where the engine-output shaft is connected by a simple coupling (not a slip coupling) directly to the generator installed on the other side of the cell (see Figure 3). Ignition, oil, gas supply, carburetor, air, and so forth are connected to the engine by means of quick connectors, and the engine is ready to run when the soundproof door of the cell is closed. Since this is an air-cooled engine which exhausts into the cell, exhaust and supply fans are required to produce air movement similar to flight conditions. (These are marked clearly in the drawing.) A forced-air-cooled grid resistor with drum-type control is located on the roof of the building for dissipating the slip losses from the generator secondary circuits.

In using the slip-ring induction generator, the excitation, of course, comes from the supply line. Accordingly, the power factor will not be any better on this generator circuit than that of any normal induction motor of this horsepower and speed, so power-factor correction must be made for the circuit, preferably by a synchronous motor or capacitor, or both, associated with the test stand. By using a 300-horsepower synchronous motor to drive the cooling fan plus 180 kva of static capacitor, it is possible to supply sufficient leading current to give a minimum operating condition of approximately 90 per cent power factor.

Immediately below the generator room is located a switching and transformer room containing also the shunt and series capacitors and various devices for operation of the cell.

Refer to Figure 5 for the sequence of operations for a typical test run as follows:

The remotely controlled air circuit breaker in the test building substation is closed by the test operator from his control booth connecting the slip-ring generator, synchronous-motor-driven supply fan, and a shunt-type static capacitor to the bus of a 2,500-kva 12,000/2,300-volt 60-cycle transformer which, in turn, is connected through a series capacitor to the 12-kv plant system bus.

When the switch is closed, the engine is cranked at low speed, as full secondary or rotor resistance is placed in the circuit, while the supply-fan motor, being thrown across the line, quickly comes up to speed. The shunt-type capacitor helps reduce the current inrush, and together with the synchronous motor, when up to speed and properly excited, brings the

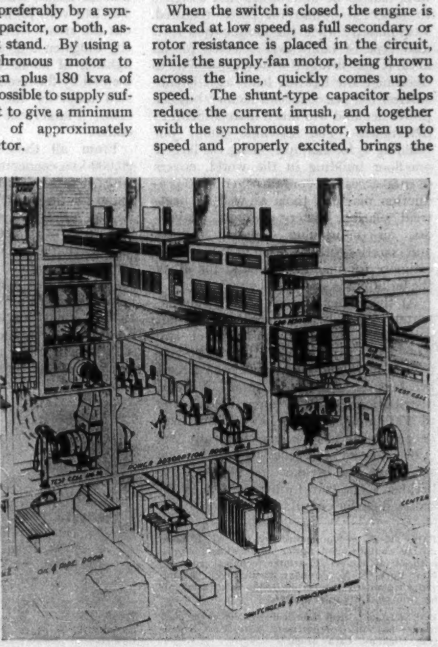

Figure 4. Test-cell building number 5

Cross section of test-cell building showing location of equipment

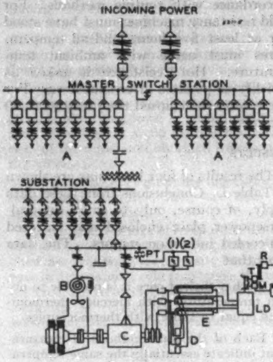

Figure 5. Wiring diagram of test-cell electric elements

1—Kilowatt-hour meter
2—Torque instrument
A—High-voltage feeders
B—Supply fan
C—Induction generator
D—Vernier resistors
E—Leading resistors
R—Receiver
T—Transmitter
LD—Loading drum
M—Drum motor
PS—Position selector
PI—Position indicator
PT—Power transformer

Table I. Tabulation of Connected Loads, Load Factors, and Totals for Estimating Plant Demand

Building	Building Name	Connected Power, Kilovolt-Amperes	Load Factor	Maximum Power Demand, Kilovolt-Amperes	Lighting, Kilovolt-Amperes	Maximum Demand, Light and Power
1	Tool shop	500	0.6	300	120	420
2	Office	500	0.5	250	1,200	1,450
3	Personnel	100	0.5	50	100	150
4	Machine shop					
	Machine tools (6,000)	30,000	0.4	12,000	8,500	20,500
	Heat treat	7,500	0.7	5,250		5,250
	Plating	800	0.7	560		560
	Battery charging	760	0.4	300		300
	Maintenance	300	0.4	120		120
	Assembly power	750	0.2	100		150
	High-cycle power	50	0.8	40		40
	Utilities	7,400	1.0	7,400		7,400
	Ventilating fans—roof	4,000	1.0	4,000		4,000
	Ventilating fans—basement	480	1.0	480		480
	Ventilating fans—cafeteria	170	1.0	170	200	370
	Mechanical handling and the like	1,000	1.0	1,000		1,000
6	Oil and chip disposal	700	0.5	350	50	400
7	Aluminum-foundry compressor	3,000	0.4	1,200	900	2,100
		700	1.0	700		700
8	Magnesium-foundry compressor	3,000	0.4	1,200	900	2,100
		500	1.0	500		500
9	Heating plant 1	3,900	0.98	3,800	50	3,850
10	Light forge	1,460	0.6	870	150	1,020
11	Tool and die shop	5,630	0.6	3,400	300	3,700
12	Heavy forge	3,100	0.6	1,860	150	2,010
13	Propeller test	500	1.0	500	30	530
14	Heating plant 2	1,350	0.98	1,300	50	1,350
	Miscellaneous outside lighting and power			500	100	600
		78,150		48,200	12,800	61,000

power factor of the group to a satisfactory value for all loads and speeds.

The series capacitor shown in the supply line to the 2,500-kva transformer eliminates the voltage drop due to the reactance loss in the transformer, so that there is no disturbance on the 2,300-volt bus when one of these units is started. This use of a series capacitor is believed to be the first large-scale application of such a device in an industrial plant, and it is gratifying to report trouble-free performance.

After a short period of motoring, to be sure that air and oil are as required, the ignition on the engine is closed, the throttle opened, and the resistor adjusted to give the speeds and loads specified by the engineers for the test. An indicating kilowatt meter connected in the stator circuit indicates the power flow back to the a-c system and also is used to indicate the engine brake horsepower as:

$$\text{Engine brake horsepower} = \frac{(\text{stator power} + \text{stator losses}) \times \text{actual speed}}{\text{synchronous speed}}$$

A factory curve gives losses at all outputs, with conversion factor applied so that a value K from the curve times actual speed = brake horsepower.

The power recovery from this system is completely automatic. Engines are started, tested, and removed from the cells with no disturbance of any kind.

Examining the wiring diagram, it will be noted that several test cells are grouped on a 2,300-volt bus. Feeders extend to various plant loads from this bus, including all the cell auxiliaries. This was designed so that the recovery power would operate these associated loads with minimum loss and also reduce the capacity of the transformer that connects to the 12-kv system bus.

Conclusion

Although the electric power system was designed and installed during the war, it has met adequately the exacting requirements of this large manufacturing project, and the power recovery system for the engine test not only has given us very reliable easily operated trouble-free testing facilities, but also enabled us to supply from an otherwise wasted source over 4,000,000 kilowatt-hours per month or 20 per cent of the electric power required for the project.

Investigation of Hot-Spot Temperatures in Integral-Horsepower Motors

L. E. HILDEBRAND
MEMBER AIEE

B. M. CAIN
ASSOCIATE AIEE

F. D. PHILLIPS
MEMBER AIEE

W. R. HOUGH
MEMBER AIEE

J. G. ROSSWOG
ASSOCIATE AIEE

C. P. POTTER
FELLOW AIEE

THE revision of American Standard C50, "Rotating Electrical Machinery," resulted in various suggestions for changing the method of measuring the temperature rise of motors and for establishing temperature-rise limits to be used with these methods. A review of the temperature tests taken in the past indicated that they are of little value for comparing the various methods. Few tests included temperature measurements by more than one method, and none of them had enough embedded detectors to measure accurately the hot-spot temperature. In order to obtain accurate data, the authors were asked to make and report the results of temperature tests on integral-horsepower motors. It was believed that the data thus obtained would be valuable to the standardizing committees of the AIEE, the American Standards Association, and the National Electrical Manufacturers' Association, as well as to motor users.

Scope of Tests

Temperature tests were made on open, plain enclosed (nonventilated), and totally enclosed fan-cooled polyphase integral-horsepower motors. The temperature rise of the stator windings was measured by four methods:

1. Mercury thermometer.
2. Surface thermocouples on the hottest accessible part of the winding.
3. Resistance.
4. Embedded thermocouples (using enough to locate the hot spot).

First Set of Tests*

DESCRIPTION OF MOTORS TESTED

In order to obtain a comparison between the temperature rise by thermometer, surface thermocouple resistance, and embedded detector, continuous temperature tests were made on a three-horsepower 1,750 rpm three-phase squirrel-cage induction motor in the 225 frame. One set of readings was taken with the parts assembled as a totally enclosed fan-cooled motor. The other set was taken with the external fan and fan cover removed.

LOCATION OF TEMPERATURE INDICATORS

A single thermometer for taking coil temperatures was inserted under a felt pad cemented to the outside surface of the end windings on the end opposite the fan. It was impractical to attempt to place a thermometer on the fan end of the motor. A hole was drilled in the end shield to admit the thermometer. The hole was closed around the thermometer with putty. The felt-pad method of mounting the thermometer required more time for preparation than the usual putty method, but the results are considered more reliable.

Thermocouples for taking coil surface temperature were attached to the outside surface of the windings with felt pads and cemented in place. Two thermocouples were used on each end of the winding, one at the top and one at the side; making a total of four.

Thermocouples for taking internal coil temperatures were put in place with the windings. These were located in the center of the slot portion in both top and bottom coils. Five thermocouples were used, two in one slot and one each in three other slots. Two other thermocouples were placed between the slot insulation and the core iron.

TEST PROCEDURE

Resistances of the windings were measured with a Kelvin double bridge. Cold and hot resistance were taken in accordance with routine methods. For cold resistance machines must have stood for at least five hours, and all temperatures must agree with ambient temperature. Hot resistance is taken as quickly as possible after shutdown. For these tests the elapsed time was 30 to 40 seconds.

RESULTS

The results of four heat runs are shown in Table I. Conclusions from these data apply, of course, only to small integral-horsepower plain enclosed and enclosed fan-cooled induction motors. The data show that

1. With sufficient care it is possible to obtain temperatures with mercury thermometers equal to those with thermocouples.
2. Each of the four methods of measurement indicate essentially the same temperature.

Any one of them, therefore, may be considered as representing the temperature of the hottest spot within a small margin.

It can be assumed safely that if the highest observed rise by resistance or by one of four thermocouples or one of four carefully installed thermometers is 65 degrees centigrade, then the temperature of the hottest spot is between 65 and 70 degrees centigrade.

DISCUSSION AND CONCLUSIONS

Conclusions from the three investigations can be applied only to induction motors, since further testing is necessary to establish relationships for d-c machines. From the data already obtained it is evident however, that the relationship between observed surface temperatures and the temperature of the hottest spot for induction motors is quite different from that for d-c motors.

For all classes of machines the point of reference is the temperature of the hottest spot. This temperature, of course, cannot be determined except on a basis of probability, even though one were to take many more temperature readings than are possible on commercial machines. A practical method of measurement, therefore, must be chosen, considering expediency and availability of measuring apparatus. The necessary sacrifice in probable range between the observed temperature and the true hot spot should be consistent with sound economics based on expected useful life of the insulation.

For induction motors in small integral-horsepower sizes of the following, conclusions appear to be sound, based on data from this paper.

(*a*). *Temperature by Resistance.* Temperature by resistance at the moment of shutdown obtained by extrapolating a cooling curve is very close to the temperature of the hottest spot. The temperature so obtained does not differ greatly from that which would be obtained if a large number of temperature measurements were taken, in-

---

* Data reported by General Electric Company, Lynn, Mass.

Paper 45-33, recommended by the AIEE committee on electric machinery for presentation at the AIEE winter technical meeting, New York, N. Y., January 22-26, 1945. Manuscript submitted November 17, 1944; made available for printing December 13, 1944.

L. E. HILDEBRAND and B. M. CAIN are electrical engineers with General Electric Company, Lynn, Mass. F. D. PHILLIPS is assistant designing engineer, General Electric Company, Schenectady, N.Y. W. R. HOUGH is engineer in charge of a-c motor design, and J. G. ROSSWOG is electrical engineer, engineering department, both with Reliance Electric and Engineering Company, Cleveland, Ohio. C. P. POTTER is manager, large-motor engineering division, Wagner Electric Corporation, St. Louis, Mo.

This paper, a summary of four conference papers presented at the conference on temperature measurements at the summer technical meeting, St. Louis, Mo., June 26-30, 1944, was prepared by a subcommittee composed of W. R. Hough, F. D. Phillips, and C. P. Potter.

The committee apologizes for having made various changes in the original reports. In order to follow the same form throughout it was necessary to rearrange some of the material, and, in order to conserve paper, it was necessary to omit some of the more detailed information.

cluding embedded detectors. This is for both open and totally enclosed machines, although the difference between the observed temperature and the hot spot is undoubtedly greater for open machines.

Temperature by resistance obtained from a single hot-resistance reading taken within 50 seconds after shutdown is within eight per cent (five degrees at 65 degrees centigrade rise) of the maximum obtained from a cooling curve.

Since cooling curves require more effort to obtain and interpret, their use does not appear to be justified.

The chief advantage of temperature measurement by resistance is its simplicity. The chief disadvantages are necessity for extreme care in determining cold resistance, the need for accurate resistance bridges, and the uncertainty of relying on a single reading which must be taken with extreme care.

(*b*). *Temperature by Thermocouples on End Windings.* Temperature by thermocouples on the end winding is very close to the temperature of the hottest spot. This is true for both open and totally enclosed machines, although the maximum difference between the highest observed temperature and the hottest spot is undoubtedly greater for open machines. Using more thermocouples reduces the average value of this difference so that more margin must be permitted for a single reading than when four or more readings are taken.

The chief advantages of thermocouples for temperature measurement on end windings are:

1. They are easy to install.
2. They can be installed without interfering with the normal ventilation of the machine.
3. They can be installed on coil surfaces not readily accessible to mercury thermometers.
4. Because they are easy to install, a relatively large number of thermocouples can be used with less time required to prepare the machines for the heating test than when using a smaller number of thermometers.

The disadvantage of the thermocouple is that its use requires a thermocouple potentiometer which must be kept in good calibration to be reliable.

(*c*). *Temperature by Mercury Thermometer on End Windings.* Temperature by thermometer on the end windings is the same as that obtained by thermocouple, if special care is used in installing the thermometer and if the size of the machine permits making a good application of the thermometers.

The chief advantage of thermometers for temperature measurement on end windings is that they are readily obtainable. The chief disadvantages of thermometers are:

1. Because of their apparent simplicity, they are likely to be used carelessly.
2. Greater skill is required to obtain accurate readings than is required with thermocouples.
3. Thermometers are difficult to install, because they are not readily accommodated by the mechanical structure.
4. Because they are difficult to install, the tendency is to use too few.

Table I

			Temperature Rise						
			By Mercury Thermometer		By Surface / Thermocouple		By Resistance		
Phase	Enclosure	Speed, Rpm	Degrees Centigrade, Actual	Per Cent of Hot Spot	Degrees Centigrade, Actual	Per Cent of Hot Spot	Degrees Centigrade, Actual	Per Cent of Hot Spot	Degrees Centigrade, Hot Spots by Embedded Detector
3	Plain enclosed	1,800	58	98	56	95	61	104	59
3	Plain enclosed	1,800	58	94	57½	93	62	100	62
3	Enclosed fan-cooled	1,800	57	94	64	105	61	100	61
3	Enclosed fan-cooled	1,800	58½	98	62	103	62	103	60

Highest of four thermocouples on outside surface of end windings.

Resistance measured 30 to 40 seconds after shutdown.

Highest of five thermocouples embedded in various places in slot portion of coil.

Table II

			Temperature Rise						
			Laminations		Winding by Surface Thermocouple		Winding by Resistance		
Horsepower	Speed	Cycles	Degrees Centigrade, Actual	Per Cent of Hot Spot	Degrees Centigrade, Actual	Per Cent of Hot Spot	Degrees Centigrade, Actual	Per Cent of Hot Spot	Degrees Centigrade, Hot-Spot by Embedded Detectors
Open Motors									
150	1,200	60	41	89	29	63	31	68	46
60	500	25	39	89	36	82	41	93	44
50	1,000	50	48	89	49	91	43	80	54*
20	500	25	37	88	34	81	35	83	42*
25	1,800	60	37	77	32	67	37	77	48
10	750	25	46	88	46	88	52	100	52
Splashproof Motors									
50	1,800	60	44	79	39	70	43	77	56
25	750	25	56	85	58	88	63	95	66
250	1,800	60	26	87	25	83	26	87	30
250	1,500	50	32	97	29	88	29	88	33
125	750	25	34	90	33	87	32	84	38
Enclosed Motors									
10	1,800	60	69	102	65	95	67	98	68
5	900	30	65	100	64	98	63	97	65
5	750	25	58	94	60	97	58	94	62*
Fan-Cooled Motors									
15	1,800	60	39	71	55	100	53	96	55
15	1,800	60	39	72	53	98	54	100	54
7½	750	25	34	72	48	102	48	98	47
7½	750	25	34	72	48	102	48	98	47
30	600	60	45	75	54	90	53	88	60
25	500	50	47	78	53	88	57	95	60
10	250	25			57	93	58	95	61

* High-slip motors.

Second Set of Tests†

Description of Motors Tested

As wide a variety of motors as possible was selected from motors in current production, and it was possible to obtain open, dripproof, enclosed, and enclosed ventilated motors in a wide range of speeds and horsepowers. All were three-phase squirrel-cage motors, both normal and high torque, normal and high slip; all were insulated before test, and the majority were random-wound, though the larger sizes have form-wound coils insulated before insertion in the slot.

Location of Temperature Indicators

In order to obtain the hot spot, thermocouples were installed in the slots at various points, since it was found, by previous tests, that the hottest spot was located in the slot. Sixteen or more were used and were distributed, four near the bottom of the motor, four near the top, and four at each side, and were located next to the iron, between the two coils, in the coils, and under the wedge. The hottest temperature was obtained between the coils or next to the wedge.

Thermocouples were located in eight places on the coil ends—at the top, bottom, and sides on each end of the motor, and care was taken to install them in the locations giving the highest temperatures. Lamination temperatures were taken in 8 to 12 locations on open or splashproof motors and in two or more locations (through holes bored in the frame) on enclosed motors.

Test Procedure

Temperature rises were measured by surface thermometer (thermocouple), sta-

---

† Data reported by General Electric Company, Schenectady, N. Y.

Table III

			Temperature Rise (Running)						
			Winding by Thermometer		Winding by Surface Thermocouple		Winding by Resistance		
Enclosure	Type of Heat Run	Per Cent Load	Degrees Centigrade, Actual	Per Cent of Hot Spot	Degrees Centigrade, Actual	Per Cent of Hot Spot	Degrees Centigrade, Actual	Per Cent of Hot Spot	Degrees Centigrade, Hot Spot by Embedded Detector
Fan cooled	Continuous	75	31.2	89.1	31.6	90.4	32.5	93.0	35.0
Fan cooled	Continuous	100	48.5	90.3	49.4	92.0	53.5	99.6	53.7
Fan cooled	Continuous	125	82.0	89.5	84.4	93.1	88.0	96.0	91.6
Fan cooled	60 minutes	150	89.0	85.6	93.8	90.2	97.5	93.7	104.0
Fan cooled	30 minutes	170	97.0	80.9	104.8	87.3	115.0	95.7	120.0
Plain enclosed	Continuous	75	36.7	92.2	38.1	95.7	40.5	102.0	39.8
Plain enclosed	Continuous	100	57.0	91.0	60.0	95.9	60.5	96.7	62.6
Plain enclosed	Continuous	115	76.0	91.0	77.0	92.3	82.5	98.8	83.5
Plain enclosed	60 minutes	166	50.0	86.6	53.5	92.7	55.5	96.2	57.7
Plain enclosed	30 minutes	250	67.0	85.2	69.5	88.5	78.5	99.8	78.6
Open	Continuous	100	30.5	82.3	33.8	91.1	32.0	86.3	37.1
Open	Continuous	125	51.5	80.9	59.6	93.6	61.5	96.5	63.7
Open	60 minutes	145	60.5	72.2	77.7	92.8	79.5	94.9	83.8
Open	30 minutes	170	62.0	56.6	96.0	87.8	95.5	87.2	109.3

Table IV

			Temperature Rise (After Shutdown)						
			Winding by Thermometer		Winding by Surface Thermocouple		Winding by Resistance		
Enclosure	Type of Heat Run	Per Cent Load	Degrees Centigrade, Actual	Per Cent of Hot Spot	Degrees Centigrade, Actual	Per Cent of Hot Spot	Degrees Centigrade, Actual	Per Cent of Hot Spot	Degrees Centigrade, Hot Spot by Embedded Detector
Fan cooled	Continuous	75	33.0	94.3	31.6	90.4	32.5	93.0	35.0
Fan cooled	Continuous	100	50.8	94.5	49.5	92.2	53.5	99.6	53.7
Fan cooled	Continuous	125	86.0	93.9	84.4	93.1	88.0	96.0	91.6
Fan cooled	60 minutes	150	96.0	92.2	93.8	90.2	97.5	93.7	104.0
Fan cooled	30 minutes	170	105.5	86.1	109.0	88.9	115.0	93.8	122.5
Plain enclosed	Continuous	75	38.5	95.5	38.1	94.5	40.5	100.5	40.3
Plain enclosed	Continuous	100	59.2	94.5	60.0	95.9	60.5	96.7	62.6
Plain enclosed	Continuous	115	78.5	94.0	77.0	92.3	82.5	98.8	83.5
Plain enclosed	60 minutes	166	54.0	93.6	54.6	94.5	55.5	96.2	57.7
Plain enclosed	30 minutes	250	74.0	90.0	75.8	92.2	78.5	95.5	82.2
Open	Continuous	100	32.5	87.6	33.8	91.1	32.0	86.3	37.1
Open	Continuous	125	58.5	91.8	59.6	93.6	61.5	96.5	63.7
Open	60 minutes	145	73.5	87.8	78.8	94.0	79.5	94.9	83.8
Open	30 minutes	170	94.0	86.0	104.4	95.5	95.5	87.2	109.3

tor-winding resistance, and embedded temperature detector (thermocouple). No mercury thermometers were used, as our practice is to use thermocouples only in obtaining temperatures on heat runs, particularly on enclosed motors, since we have found thermocouples more convenient and easier to install properly than thermometers, as well as easier to read.

Cold resistance and temperature of the motor were carefully measured to obtain the correct base for determining the temperature by resistance. After shutdown, resistance readings were taken as soon as possible and continued for 30 minutes. Cooling curves were plotted for each run and extrapolated to shutdown time to determine temperature rise by resistance. Failure to begin readings quickly and to carry them far enough to determine the slope of the curve would result in large error in the temperature as observed.

The results of the temperature tests are shown in Table II.

DISCUSSION AND CONCLUSIONS

For open motors the conventional hot-spot allowance for thermometer measurement is given in AIEE Standard 1 as 15 degrees centigrade. The tests recorded in Table II indicate that this allowance is adequate. The same standard gives a conventional hot-spot allowance by resistance measurement of five degrees centigrade. American Standard C-50 gives a limiting temperature rise for general-purpose open motors as 50 degrees centigrade and for other motors as 60 degrees centigrade. Tests indicate that the temperature difference between hot spot and rise by resistance is variable, depending on motor speed and the intensity of ventilation over the coil ends. For open motors it appears that rise by resistance is not a satisfactory method of arriving at hot-spot temperatures.

For enclosed motors and enclosed fan-cooled motors, the conventional hot-spot allowance for thermometer measurements is ten degrees centigrade, and for temperatures by resistance measurements five degrees centigrade. These tests show that coil-end surface temperatures, hot-spot temperatures, and temperatures by resistance measurements are equal within fairly narrow limits. This is due to the fact that intense ventilation of coil ends does not take place in motors of these types. The heat generated is dissipated through the enclosure, and the temperatures of the various internal parts of the motor are quite uniform. The hot-spot allowance of five degrees centigrade between rise by resistance and hot spot is adequate. Because of the convenience of the rise-by-resistance method for motors of these types, this method is strongly recommended for enclosed motors.

Third Set of Tests**

DESCRIPTION OF MOTORS TESTED

The motors tested were NEMA frame 254, five horsepower, three phase, four pole, 60 cycle, of fan-cooled, plain enclosed, and open construction; windings in all cases were semienclosed slot, random-wound, with class-*A* insulation, and untaped coils, varnish impregnated. Temperature tests included continuous 60-minute duty and 30-minute duty for each enclosure. Fan-cooled motors had one outer fan at the end opposite the drive end which forced air across the outer surface of the stator. Plain enclosed motors were of the type having the

Table V

			Temperature Rise					
			Thermometer, Per Cent of Hot Spot		Thermocouple, Per Cent of Hot Spot		Resistance, Per Cent of Hot Spot	
Tests	Enclosure	Time	Running	Maximum	Running	Maximum	Running	Maximum
3	Fan cooled	Continuous	89.6	94.2	91.8	91.9	96.2	96.2
3	Plain enclosed	Continuous	91.4	94.6	94.6	94.2	98.5	98.6
2	Open	Continuous	81.6	89.7	92.3	92.3	91.4	91.4
1	Fan cooled	60 minutes	85.6	92.2	90.2	90.2	93.7	93.7
1	Plain enclosed	60 minutes	86.6	93.6	92.7	94.5	96.2	96.2
1	Open	60 minutes	72.2	87.8	92.8	94.0	94.9	94.9
1	Fan cooled	30 minutes	80.9	86.1	87.3	88.9	95.7	93.8
1	Plain enclosed	30 minutes	85.2	90.0	88.5	92.2	99.8	95.5
1	Open	30 minutes	56.6	94.0	87.8	95.5	87.2	87.2

** Data reported by Reliance Electric and Engineering Company, Cleveland, Ohio.

outer surface of the stator core exposed. Open motors were of the double end ventilation construction. The stators were of the dripproof type with air discharge from the lower half of the stator only.

LOCATION OF TEMPERATURE INDICATORS

Temperatures of cores and windings were obtained while running, and after shutdown by means of thermometers, surface thermocouples, and embedded thermocouples. The location of thermometers and thermocouples for all motors is shown in Figure 1, reference 1, which represents an axial cross section of the motor in the vertical plane. In addition to the thermocuples shown, the open motor included 14 additional thermocouples. These were spotted in every third coil to determine the temperature distribution circumferentially around the stator.

TEST PROCEDURE

The conventional method of measuring resistance of the windings, terminal to terminal, was used following shutdown and included a series of readings which could be plotted against time, and the curve extended to the instant of shutdown. Tests were taken at various percentages of rated load to produce a relatively wide spread in resulting temperature rise.

RESULTS

The pertinent information obtained from these tests is given on Tables III and IV. Both tables give the conditions of test, including enclosure, time, and load. Table III gives maximum temperature rises observed during running and including the instant of shutdown, and, in addition, the temperature rise by resistance as determined within approximately one minute or less after shutdown. The hot-spot temperature rise is the highest observed temperature rise by embedded thermocouple during running. The percentage of the maximum observed rise to the hot-spot rise is given in each case. Table IV differs from Table III only in that the values of maximum temperature rise are those observed either during running or after shutdown, depending on which were higher. Table V is a summary of the average results of like conditions of enclosure and time and includes only the percentage relation to the hot-spot temperature.

DISCUSSION AND CONCLUSIONS

1. *Temperature Rise During Running and After Shutdown*

(*a*). There is a substantial difference between temperature rises by thermometer during running and after shutdown. The temperature rises increase after shutdown in practically all cases.

(*b*). There is no significant change in temperature rise by surface thermocouple after shutdown except in the case of intermittent ratings. In the case of 60-minute ratings, the change is minor. In the case of 30-minute ratings, it may be substantial.

(*c*). In all cases the rise by resistance did not increase after the instant of shutdown. The rise by resistance by the conventional method as determined within one minute after shutdown in all cases was within six per cent of the rise at the instant of shutdown. On the average, it was within three per cent.

(*d*). There is no significant change in temperature of the hot spot after shutdown except in the case of intermittent ratings of less than one hour.

Table VI

Enclosure	Winding	Per Cent Load	Temperature Rise: By Mercury Thermometer: Degrees Centigrade, Actual	By Mercury Thermometer: Per Cent of Hot Spot	By Surface Thermocouple: Degrees Centigrade, Actual	By Surface Thermocouple: Per Cent of Hot Spot	By Resistance: Degrees Centigrade, Actual	By Resistance: Per Cent of Hot Spot	Degrees Centigrade, Hot Spot by Embedded Detector
Fan cooled	Treated	75	24.2	70	26.8	77	29.9	86	34.8
Fan cooled	Treated	100	41.1	71	46.0	80	49.1	85	57.8
Fan cooled	Treated	115	52.0	71	57.1	78	63.5	87	73.1
Fan cooled	Treated	125	63.3	70	71.3	79	77.5	86	90.3
Fan cooled	Treated	100	49.0	73	52.9	79	58.3	87	66.8
Open	Treated	100	21.1	56	27.2	72	31.6	83	37.9
Open	Treated	125	28.8	54	35.1	66	45.8	86	53.2
Open	Treated	144	34.5	48	48.4	68	61.5	86	71.6
Open	Treated	160	43.1	46	65.4	69	78.2	83	94.4

Table VII. Summary of Tests on Integral-Horsepower A-C Motors

Manufacturer	Enclosure	Temperature Rise: Thermometer, Per Cent of Hot Spot	Surface Thermocouple, Per Cent of Hot Spot	Resistance, Per Cent of Hot Spot
General Electric, Schenectady	Open		61–91	68–100
Reliance	Open	88–92	91–94	86–97
Wagner	Open	46–56	66–72	83–86
All tests	Open	46–92	63–94	68–100
General Electric, Lynn	Plain enclosed	94–98	93–95	100–104
General Electric, Schenectady	Plain enclosed		95–98	94–98
Reliance	Plain enclosed	94–96	92–96	97–101
All tests	Plain enclosed	94–98	92–98	94–104
General Electric, Lynn	Enclosed fan cooled	94–98	103–105	100–103
General Electric, Schenectady	Enclosed fan cooled		88–102	88–100
Reliance	Enclosed fan cooled	94–95	90–93	93–100
Wagner	Enclosed fan cooled	70–73	77–80	85–87
All tests	Enclosed fan cooled	70–98	77–105	85–103

2. *Location of Hot Spot*

(*a*). On the fan-cooled motors the hot spot was always near the ends of the stator coils between the upper and lower coil sides. In all cases except one it was at the end opposite the outer cooling fan. The position varied between the top and bottom of the stator.

(*b*). On plain enclosed motors the hot-spot location varied with the degree of load. Under normal loads the hot spot was in the coil nearest the air gap in the slot portion. During overload conditions including intermittent duty the hot spot was near the end of the stator coils between the upper and lower coil sides. In all cases the hot spot was at the top of the stator.

(*c*). On open motors the hot spot in all cases was in the coil side farthest from the air gap at the top of the stator. The position varied between the center of the core and the end of the core.

3. *Relation of Rise by Resistance to Rise by Embedded Thermocouple*

With the number and distribution of the embedded thermocouples, it might be expected that there would be close agreement between the average rise by embedded thermocouples and the rise by resistance. Actually, this was not the case. In practically all cases the rise by resistance was higher than the average of the rise by embedded thermocouples.

4. *Relation of Hot-Spot Allowance to Motor Enclosure and Time Rating*

The results show that the hot-spot allowance should consider both enclosure and time rating.

DEDUCTIONS

1. Thermometer, surface thermocouple, and resistance methods all can give suffi-

ciently cousistent results to be recognized as approved methods.

(a). The resistance method most nearly approaches hot-spot temperatures and consequently should be the preferred method.

(b). The surface thermocouple next to the resistance method most nearly approaches hot-spot temperatures and should be the next preferred method.

(c). The thermometer method should be the least preferred method. If it is used, the maximum rise during running or after shutdown should be the basis of measurement rather than maximum rise during running.

2. The allowable temperature rise in each case should be based on determination as follows:

(a). Resistance method—the temperature rise to be determined by resistance measurement within one minute after shutdown.

(b). Surface thermocouple—the temperature rise to be determined by the maximum observed reading during running or after shutdown.

(c). Thermometer method—the temperature rise to be determined by the maximum observed reading during running or after shutdown.

Fourth Set of Tests‡

Description of Motors Tested

Two 40-horsepower 1,750-rpm three-phase squirrel-cage motors were tested at various loads as reported in AIEE Transactions[1] pages 468–72, September 1939. One of these motors was an open motor, and the other was a totally enclosed fan-cooled motor.

Location of Temperature Indicators

In order to be sure of finding the hot spot 40 embedded detectors were installed in the totally enclosed fan-cooled motors, as shown in Figure 1 of reference 1. A mercury thermometer extended through a slot in the end plate and the bulb of the thermometer was immediately adjacent to a surface thermocouple. There were 34 embedded detectors in the open motor, as shown in Figure 2, reference 1, and again the bulb of the mercury thermometer was immediately adjacent to a surface thermocouple. The surface thermocouples and the thermometer bulbs were on the outside of the tape which covers the free ends of the windings and were covered with a small amount of sealing compound. The embedded detectors were located in various parts of the slots and in various parts of the free ends; a complete record of their location may be found in paper referred to.

Test Procedure

Continuous temperature tests were made at various loads, and the temperature readings were taken while the motors were running. A double bridge was used to measure the resistance of the stator winding. At the end of each run the rotor was stopped very quickly, and the stator resistance was measured in a minute or less.

The results of nine heat runs are shown in Table VI.

---

‡ Data reported by Wagner Electric Corporation, St. Louis, Mo.

Investigation of Hot-Spot Temperatures in Fractional-Horsepower Motors

L. H. HIRSCH
NONMEMBER AIEE

R. F. MUNIER
ASSOCIATE AIEE

M. L. SCHMIDT
MEMBER AIEE

L. W. WIGHTMAN
NONMEMBER AIEE

F. S. HIMEBROOK
MEMBER AIEE

T. C. LLOYD
ASSOCIATE AIEE

O. G. COFFMAN
NONMEMBER AIEE

C. P. POTTER
FELLOW AIEE

THE revision of American Standard C50, "Rotating Electrical Machinery," resulted in various suggestions for changing the method of measuring the temperature rise of motors and for establishing temperature-rise limits to be used with these methods. A review of the temperature tests taken in the past indicated that they are of little value for comparing the various methods. Few tests included temperature measurements by more than one method, and none of them had enough embedded detectors to measure accurately the hot-spot temperature. In order to obtain accurate data the authors were asked to make temperature tests on fractional-horsepower motors and to report the results. It was believed that the data thus obtained would be valuable to the standardizing committees of the AIEE, the American Standards Association, and the National Electrical Manufacturers Association, as well as to motor users.

Scope of Tests

Temperature tests were made on open and totally enclosed (nonventilated), single-phase, polyphase, and d-c fractional-horsepower motors, with treated and untreated windings. The temperature rise of the stator windings was measured by four methods:

1. Mercury thermometer.
2. Surface thermocouples on the hottest accessible part of the winding.
3. Resistance.
4. Embedded thermocouples (using enough to locate the hot spot).

First Set of Tests*

Description of Motors Tested

In selecting motors for tests, three types were chosen. They were a one-

---

* Data reported by Century Electric Company, St. Louis, Mo.

Discussion and Conclusions

While it is possible to obtain fairly accurate measurements of temperature using mercury thermometers in motors which are so constructed that a thermometer can be placed in the right location, it should be borne in mind that many motors have mechanical features which prevent the satisfactory use of mercury thermometers without mutilating the motors. In such cases the temperatures taken are quite likely to be lower than the true values, and the actual operating temperatures of such motors are a good deal higher than the observed readings.

On the other hand, thermocouples are flexible and may readily be placed on the hottest parts of windings so that readings taken using surface thermocouples are more nearly correct than those which are obtained by using mercury thermometers. It is, suggested therefore, that the use of mercury thermometers be discouraged. This might be done by specifying the use of thermocouples and eliminating the use of mercury thermometers, or by specifying a new method which would consist in the determination of temperatures by means of thermocouples applied to the hottest part of the machine accessible to thermocouples.

Summary of Data Reported by All Companies

A brief summary of the preceding data is given in Table VII. In this table, as in the preceding tables, the maximum temperature obtained by embedded detector is considered the hot spot. When temperatures by surface thermocouple or resistance exceed those obtained by means of the embedded detector, either one of two conclusions may be reached; either the embedded detector was not placed in the hottest part of the winding, or an error was made in the measurements.

Reference

1. Measurement of Temperature in General-Purpose Squirrel-Cage Induction Motors, C. P. Potter. AIEE Transactions, volume 58, 1939, September section, pages 468–78.

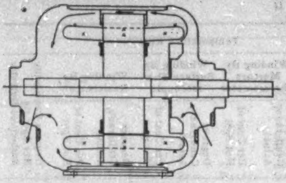

Figure 1. Sectional view showing ventilation and location of thermocouples in Century single-phase motors

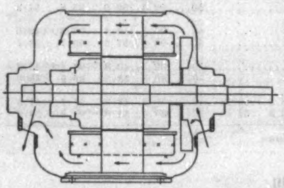

Figure 2. Sectional view showing ventilation and location of thermocouples in Century d-c motors

fourth-horsepower 60-cycle 1,750-rpm single-phase capacitor-start motor, a one-half-horsepower 60-cycle 1,750-rpm, repulsion-start induction-run motor, and a one-half-horsepower, 1,750-rpm d-c compound motor. These motors were tested first as open motors and then as nonventilated enclosed motors. The windings of all motors were given an insulating-varnish treatment before tests were made.

LOCATION OF TEMPERATURE INDICATORS

Thermocouples were placed at various positions in the stator coils at the time the coils were put in the slots. Figures 1 and 2 show the location of the thermocouples in the a-c and d-c motors respectively. Thermocouples were placed on the stator-coil extensions as shown. Thermometers were placed as close to the thermocouples on the extensions as practical.

TEST PROCEDURE

Each motor was loaded and run until temperatures had become constant. Readings of all thermocouples and thermometers were taken while the motor was running. Resistance readings were taken as soon after shutdown as practical, and the time was recorded. Several more resistance readings were taken over a period of five minutes, and a curve was drawn with ordinates as resistances and abscissas as time. The extension of this curve to zero time gives an approximate value of resistance at the instant of shutdown. This value was used in calculating the temperature rise by resistance shown in the accompanying tables.

Temperatures of the repulsion start and the d-c wound rotors were taken by resistance method and by thermometers after the motor was shutdown. To obtain thermometer readings the motor was rerun and disassembled. The time after shutdown for recording thermometer temperatures was approximately three minutes.

RESULTS

The hot-spot temperatures in both the open-type a-c motors occurred in the winding extension on the air-exhaust end. In the enclosed a-c motors the hot spot occurred at the center of the slot midway between the ends of the core, although the embedded detectors in the coil ends were within a few degrees of the hot spot. In the d-c motor the hot spot occurred in the center of the shunt coil on both the open and enclosed motors.

A comparison of temperatures is shown in Table I, which also presents the relation of thermometer, thermocouple, and resistance values as a percentage of the hot spot. From the table there seems to be a definite relation between temperatures as taken by hot-spot and resistance methods. The average ratio between resistance and hot spot for both the open motors and enclosed motors is 94 per cent. Comparison of temperatures by surface thermocouples and thermometers shows fairly consistent results, but not so close as hot spot and resistance. For thermometer readings the bulbs were placed on the extension close to the thermocouples and readings taken without disturbing the motor assembly. The difference between these two methods probably is caused by the difficulty of holding the thermometer bulb in place due to its size and shape, whereas the thermocouple can be tied in place with little chance of its shifting.

The difference between surface indicators and hot-spot or resistance methods is quite large on the d-c motor. The ratio between hot-spot and resistance temperature was 92 per cent for the open motor and 96 per cent for the enclosed motor. However, the ratio between hot-spot and coil-surface temperatures was 51 per cent for the open motor and 76 per cent for the enclosed motor. This shows that the movement of ventilating air over the field coils plays a great part in reducing the temperature of the coil surface, but a tightly wound coil completely enclosed with heavy wrappings of insulating materials is a very poor radiator for the heat generated within the coil.

DISCUSSION AND CONCLUSIONS

In general the relation between hot-spot and resistance measurements in open and enclosed fractional-horsepower motors tested is a fixed value.

Measurement of temperatures by resistance is simple and, if done carefully with reliable instruments, is quite accurate. In taking resistance measurements a definite interval of time after shutdown should be established or the results extrapolated back to the time of shutdown.

Table I

					Temperature Rise						
					By Mercury Thermometer		By Surface Thermocouple		By Resistance		
Type Motor	Frame Size	Enclosure	Horsepower	Rpm	Degrees Centigrade, Actual	Per Cent of Hot Spot	Degrees Centigrade, Actual	Per Cent of Hot Spot	Degrees Centigrade, Actual	Per Cent of Hot Spot	Degrees Centigrade Hot Spot By Embedded Detector
Capacitor start—single phase	65	Open	1/4	1,750	43	84	47	92	48	94	51
		Plain enclosed			64	97	65	98.5	62	94	66
Repulsion-start induction-run—single phase	81	Open	1/2	1,750	36	92	37	95	38	97	39
		Plain enclosed			66	90.5	67	92	69	94	73
Direct current	81	Open	1/2	1,750	25	51	25	51	45	92	49
		Plain enclosed			63	76	63	76	80	96	83

Paper 45-32, recommended by the AIEE committee on electric machinery for presentation at the AIEE winter technical meeting, New York, N. Y., January 22-26, 1945. Manuscript submitted November 17, 1944; made available for printing December 13, 1944.

L. H. HIRSCH is electrical engineer with the Century Electric Company, St. Louis, Mo.; R. F. MUNIER is chief motor engineer with the Emerson Electric Manufacturing Company, St. Louis; M. L. SCHMIDT is section engineer and L. W. WIGHTMAN is electrical engineer with the General Electric Company, Fort Wayne, Ind.; F. S. HIMEBROOK is electrical engineer with The Master Electric Company, Dayton, Ohio; T. C. LLOYD is chief engineer and O. G. COFFMAN is engineer with Robbins and Myers, Inc., Springfield, Ohio; C. P. POTTER is manager of the motor engineering department of the Wagner Electric Corporation, St. Louis, Mo.

This paper, a summary of six conference papers presented at the conference on temperature measurements at the summer technical meeting, St. Louis, Mo., June 26-30, 1944, was prepared by a subcommittee composed of W. R. Hough, F. D. Phillips, and C. P. Potter.

The committee apologizes for having made various changes in the original reports. In order to follow the same form, it was necessary to rearrange some of the material, and, in order to conserve paper, it was necessary to omit some of the more detailed information.

Measuring resistances of wound rotors presents problems, especially in small motors. The inaccessibility makes it difficult to get good contact to the windings and can be a serious source of error. For this reason resistance measurements of wound rotors cannot be relied upon.

The relation between the resistance method and surface temperatures for d-c motors is different from that for the a-c motors tested.

The values for temperature by resistance are the instant of shutdown values and were obtained by plotting the resistance–time curves and extrapolating back to the instant of shutdown. All temperatures were taken while the motor was running.

Second Set of Tests*

Tests were conducted on five standard open-protected motors having four-, six-, and eight-inch stator-punching diameters and rated as follows:

DESCRIPTION OF MOTORS TESTED

$^1/_{20}$ horsepower, 115 volts, 60 cycles, single phase, 1,725 rpm, split phase, general purpose.

$^1/_6$ horsepower, 115 volts, 60 cycles, single phase, 1,725 rpm, capacitor start, general purpose.

$^1/_4$ horsepower, 115 volts, 60 cycles, single phase, 1,725 rpm, split phase, short-hour service.

$^1/_4$ horsepower, 220 volts, 60 cycles, three phase, 1,725 rpm, polyphase, general purpose.

$^1/_2$ horsepower, 115 volts, 60 cycles, single phase, 1,725 rpm, capacitor start, general purpose.

All of the single-phase motors had the main winding placed in the bottom of the slots with the auxiliary winding on top of it and displaced 90 electrical degrees. The polyphase motor had a symmetrical winding. All windings were treated with a standard grade of commercial varnish. Ventilating openings were located in the lower quadrant of the front and back end shields, beneath the oil reservoirs. The ventilation of the general-purpose motors is shown in Figure 3 and the ventilation of the short-hour-service motor is shown in Figure 4. The centrifugal starting-switch mechanisms were located in the front end of the single-phase motors.

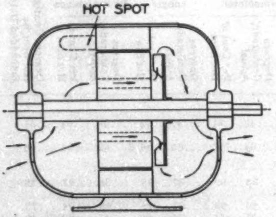

Figure 3. Sectional view showing ventilation in Emerson general-purpose motors

Table II

Open Motors			Temperature Rise								
			Frame By Thermocouple		Winding By Mercury Thermometer		Winding By Surface Thermocouple		Winding By Resistance*		
Type Motor	Horsepower	Rpm	Degrees Centigrade, Actual	Per Cent of Hot Spot	Degrees Centigrade, Actual	Per Cent of Hot Spot	Degrees Centigrade, Actual	Per Cent of Hot Spot	Degrees Centigrade, Actual	Per Cent of Hot Spot	Degrees Centigrade Hot Spot By Embedded Detector
Split phase—general purpose	$^1/_{20}$	1,725	35.1	75.8			40	86.5	43.5	93.9	46.3
			44.0	77.6			50	88.2	53.5	94.3	56.7
Capacitor start—general purpose	$^1/_6$	1,725	29.0	66.4			40	91.8	41.7	95.5	43.6
			35.8	65.9			50	92.1	52.0	95.8	54.3
Split phase—short hour service	$^1/_4$	1,725	28.0	66.7			40	95.3	40.4	96.3	42.0
			32.5	60.5			50	93.0	51.9	96.7	53.7
Polyphase—general purpose	$^1/_4$	1,725	27.7	64.1			40	92.5	40.3	93.4	43.2
			36.3	64.8			50	89.3	53.5	95.5	56.0
Capacitor start—general purpose	$^1/_2$	1,725	28.2	63.7	28.5	65.3	40	90.2	43.3	97.7	44.3
			36.0	64.1	36.3	64.6	50	89.0	53.0	94.3	56.2

* Resistance readings taken within one minute of shutdown.

Table III

Plain Enclosed Motors			Temperature Rise								
			Frame By Thermocouple		Winding By Mercury Thermometer		Winding By Surface Thermocouple		Winding By Resistance*		
Type Motor	Horsepower	Rpm	Degrees Centigrade, Actual	Per Cent of Hot Spot	Degrees Centigrade, Actual	Per Cent of Hot Spot	Degrees Centigrade, Actual	Per Cent of Hot Spot	Degrees Centigrade, Actual	Per Cent of Hot Spot	Degrees Centigrade Hot Spot By Embedded Detector
Capacitor start—general purpose	[illegible]	1,725	40.9	73.0			55	98.2	54.0	96.4	56.0
			47.8	71.8			65	97.8	64.0	96.3	66.5
Split phase—short hour	$^1/_4$	[illegible]	[illegible]	73.6			55	98.0	54.6	97.4	56.1
			[illegible]	72.8			65	98.0	65.0	98.0	66.3
Polyphase—general purpose	$^1/_4$	1,725	43.2	72.2			55	91.8	59.7	99.7	59.9
			50.2	70.4			65	91.2	70.0	98.3	71.2
Capacitor start—general purpose	$^1/_2$	1,725	42.9	75.9	49.0	86.8	55	97.3	56.0	99.2	56.5
			51.2	76.4	57.6	86.0	65	97.1	66.0	98.5	67.0

* Resistance readings taken within one minute of shutdown.

LOCATION OF TEMPERATURE INDICATORS

The frame temperatures were obtained from thermocouples placed at approximately the middle of the frame, on the top of the motor. It was possible to obtain the winding temperature by thermometer for the eight-inch stator motor only. The thermometer was placed against the outermost part of the stator winding, at the end of the motor from which the ventilating air was exhausted. The bulb of the thermometer was covered as specified in American Standard C50-1943, paragraph 2.056. The temperatures by surface thermocouples were obtained from thermocouples placed among the outer conductors of the stator winding end wire, at the end of the motor from which the ventilating air was exhausted. The resistance readings that were used in determining the temperature value from differences of resistances were taken using a Wheatstone bridge. For the purpose of determining the hot-spot temperature value, thermocouples were placed at various locations within and around the windings, as these wind-

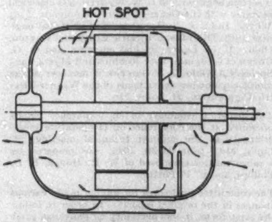

Figure 4. Sectional view showing ventilation in Emerson short-hour-service motors

---

* Data reported by Emerson Electric Manufacturing Company, St. Louis, Mo.

Table IV

Enclosure	Horsepower	Rpm	Phases	Temperature Rise						Degrees Centigrade Hot Spot by Embedded Detector
				By Mercury Thermometer		By Surface Thermocouple		By Resistance		
				Degrees Centigrade, Actual	Per Cent of Hot Spot	Degrees Centigrade, Actual	Per Cent of Hot Spot	Degrees Centigrade, Actual	Per Cent of Hot Spot	
Plain enclosed and impregnated	1/20	1,725	1	43	75	54	95	53	93	57
	1/4	1,725	1	51	85	60	100	54	90	60
	1/3	1,725	3	52	90	56	97	57	98	58
	3/4	1,725	1	66	92	72	100	68	95	72
Plain enclosed preimpregnated	1/20	1,725	1	43	78	54	98	54	98	55
	1/4	1,725	1	55	82	64	96	66	98	67
	1/3	1,725	3	51	85	57	95	58	97	60
	3/4	1,725	1			76	96	73	93	79
Open and impregnated	1/20	1,725	1	34	79	42	98	41	95	43
	1/4	1,725	1	33	80	38	93	39	95	41
	1/3	1,725	3	40	80	49	98	50	100	50
	3/4	1,725	1	42	79	51	96	47	89	53
Open and preimpregnated	1/20	1,725	1	34	77	43	98	43	98	44
	1/4	1,725	1	34	76	40	89	42	93	45
	1/3	1,725	3	27	79	33	97	32	94	34
	3/4	1,725	1			55	93	55	93	59

ings were placed in the stator core. The highest reading obtained from each test was considered the hot-spot value.

Test Procedure

The motors were tested first as open-protected machines. A set of four or more temperature tests were made at different loads for each motor, so that curves could be drawn to obtain temperature values at desired intermediate load points. Final thermocouple and thermometer readings were taken while the motors were still running, after constant values had been reached. Resistance readings were obtained within one minute after shutdown. Motors in the six- and eight-inch frames then were tested in the same manner as totally enclosed machines. The various temperature indicators were not disturbed when the motors were changed from open-protected to totally enclosed conditions. The internal ventilating fans were retained when the motors were totally enclosed.

Results

As a result of this investigation it was found that in all instances, for open-protected motors, the hottest spot was at the air-exhaust end of the motor at approximately the center of the stator winding, in the end wire about one-half inch outside of the lamination stacking. In all of the motors that were tested, the air entered and left by way of openings in the lower quadrant of the end shields. The highest temperature was always approximately 180 degrees from the center of these openings.

For totally enclosed motors, this location also provided the maximum temperature, though frequently there were other locations equally hot.

Curves were drawn making it possible to determine the load and the frame and thermometer (when taken), resistance-method, and hot-spot temperature rises corresponding with thermocouple temperature rises of both 40 degrees centigrade and 50 degrees centigrade for open-protected motors, and 55 degrees centigrade and 65 degrees centigrade for totally enclosed motors.

These final data are tabulated for open-protected motors in Table II and for totally enclosed motors in Table III.

For the open-protected motors, the values of the thermocouple and resistance temperature rises, as a per cent of the hot-spot value, are as follows:

Thermocouple: Average, 90.8; minimum, 86.5.

Resistance: Average, 95.3; minimum, 93.4.

For totally enclosed motors, the percentage values are as follows:

Thermocouple: Average, 96.3; minimum, 91.2.

Resistance: Average, 98.4; minimum, 96.3.

Discussion and Conclusions

From these tests, it is concluded that it is possible to determine the hot-spot temperature-rise values in fractional-horsepower a-c motors either by means of thermocouple readings as described herein, or by determining the temperature rise from differences of resistances. It is thought that, if the minimum ratio of temperature rises be used, there would exist little probability that the estimated values would not be on the safe side, yet would be sufficiently close to the actual values so as not to provide an overconservative figure.

The resistance method appears to be the more valuable, since the difference between the average and minimum ratios of temperature rises, as given under the heading of "Results," is only about two percentage points. The corresponding ratio based on thermocouple readings is about five per cent.

It is concluded that it is safe, for open-protected motors, to consider a temperature-rise value by thermocouple as representing 85 per cent of the hot-spot value and to consider a temperature-rise value determined from differences of resistances as representing 92 per cent of the hot-spot value.

For totally enclosed motors, it is concluded that it is safe to consider a temperature-rise value by thermocouple as representing 90 per cent of the hot-spot value and to consider a temperature-rise value determined from differences of resistances as representing 95 per cent of the hot-spot value.

Third Set of Tests*

Description of Motors Tested

The motors tested were rated 1/20, 1/4, 1/3, and 3/4 horsepower at 1,725 rpm. The polyphase motors were all one-third horsepower and were approximately the same physical size as the one-fourth-horsepower single-phase motors. The windings of half of the motors were impregnated with an insulating varnish in the conventional manner. The rest of the motors were built with preimpregnated insulation and did not have the conventional varnish impregnation after winding.

Both the open and totally enclosed motors had fans on both ends of the rotor. In the open motors both fans draw air in at the bearing and expel it through openings in the periphery of the end shield. In the totally enclosed motors the fans merely stir up the air. The open motors were protected to such an extent that

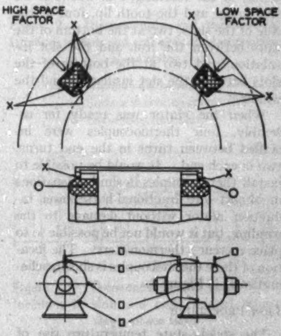

Figure 5. Schematic location of temperature indicators in General Electric motors

□ Mercury thermometers
x Surface thermocouple
O Embedded detectors

---

* Data reported by General Electric Company, Fort Wayne, Ind.

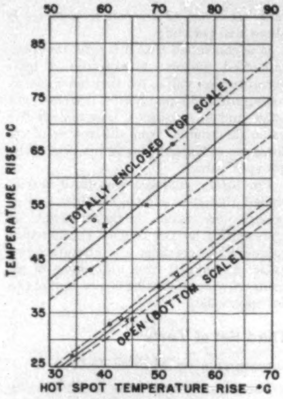

Figure 6. Temperature rise by mercury thermometer of General Electric motors

o Impregnated winding
x Preimpregnated winding

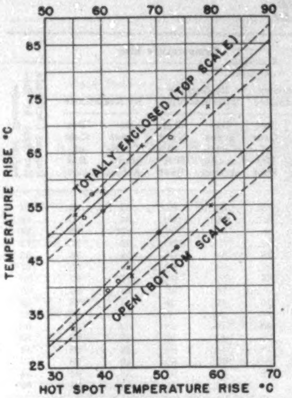

Figure 7. Temperature rise by resistance of General Electric motors

o Impregnated winding
x Preimpregnated winding

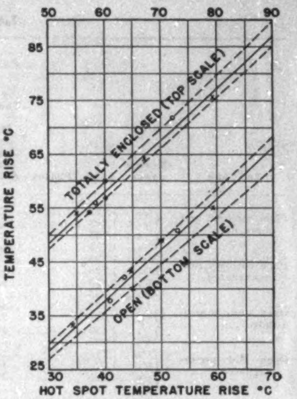

Figure 8. Temperature rise by surface thermocouple of General Electric motors

o Impregnated winding
x Preimpregnated winding

mercury thermometers could not be placed on the windings without disassembly.

LOCATION OF TEMPERATURE INDICATORS

Twenty thermocouples were embedded in the winding of each motor in an endeavor to locate the hot spot and determine the magnitude of the temperature gradients in the winding. Four were embedded in the approximate center of the end turns, two on each end. Four were embedded in the center of slots, two in the slot having the highest space factor and two in the slot having the lowest space factor. Twelve were distributed around the periphery of the slots at the center of the stacking, four between the slot wedge and the tooth lip, four at the side of the slots, two at the bottom of the slots between the iron and the slot insulation, and two at the bottom of the slots between the slot insulation and the winding.

When the stator was ready for assembly, four thermocouples were installed between turns in the end turns, two in each end. It would be possible to install thermocouples in similar locations in almost any fractional-horsepower induction motor without damage to the winding, but it would not be possible so to place mercury thermometers. The location of these thermocouples is shown schematically in Figure 5.

TEST PROCEDURE

The steady-state temperature rise of the stator windings was measured by four methods: embedded detector, resistance, thermocouple at the hottest spot accessible in the completed stator, and mercury thermometer.

Cold resistance was measured after "soaking" the motors for approximately 12 hours in a closed room. At least six measurements of resistance were made during the first three minutes after shutdown to establish a cooling curve. In almost every test, the first reading was within 30 seconds of shutdown. The cooling curve was plotted on semilogarithmic paper and extrapolated to shutdown time to determine the temperature rise by resistance.

After the first two heat runs, holes were drilled in the motor shells so that two mercury thermometers could be placed permanently on the windings. It normally would not be possible to place mercury thermometers in an equally good position on motors intended for service, but it would be possible on motors selected as representative of a lot.

All tests were taken at an ambient temperature of 25 to 35 degrees centigrade in substantially still air. A dynamometer load was used to obtain approximately 55-degrees-centigrade rise on totally enclosed motors and 40-degrees-centigrade rise on open motors by mercury thermometer.

The maximum temperatures obtained by four methods in 16 heat runs are shown in Table IV.

DISCUSSION AND CONCLUSIONS

In the following discussion, hot-spot temperature is defined as the highest temperature measured by embedded thermocouple. Analysis of the complete test data indicates that it is very improbable that the true hot spot is significantly higher in the motors covered by this report.

The temperature rise (highest reading) by mercury thermometer, resistance, and end-turn thermocouple is plotted against hot-spot temperature in Figures 6, 7, and 8. The curves, which are straight lines through the origin, show average-, maximum-, and minimum-temperature rise as a function of hot-spot-temperature rise. A wide spread between curves indicates poor co-ordination with true hot-spot temperature; that is, a poor method.

In actual testing, the measured temperature rise is, of course, the independent variable, and the hot-spot temperature which is to be controlled is the dependent variable. Table V shows the range of hot-spot temperatures which would be obtained with certain arbitrarily selected measured temperature-rise limits.

The principal advantages and disadvantages of the three methods used are as follows:

Mercury Thermometer:

Advantages: Equipment availability; established practice.

Disadvantages: Large difference between measurement and hot spot; extreme difficulty in properly placing thermometers in small and in totally enclosed motors.

Table V

	Measured		Range of Hot Spot	
Test Method	Temperature Open, Degrees	Rise Totally Enclosed, Degrees	Temperature Open, Degrees	Rise Totally Enclosed, Degrees
Mercury thermometer	50	55	62–66	60–73
Resistance	60	65	60–68	66–72
Thermocouple	60	65	61–68	65–69

Table VI

				Temperature Rise						
				By Thermometer		By Thermocouple		By Resistance		
Phase	Enclosure	Horse-power	Winding	Degrees Centigrade, Actual	Per Cent of Hot Spot	Degrees Centigrade Actual	Per Cent of Hot Spot	Degrees Centigrade Actual	Per Cent of Hot Spot	Degrees Centigrade Hot Spot by Embedded Detector
3	Dripproof	3/4	Untreated	39.0	94	39.5	95	40.0	96	41.5
3	Dripproof	3/4	Treated	38.5	93	39.5	95	40.0	96	41.5
3	Plain enclosed	3/4	Untreated	59.5	95	60.0	96	62.0	99	62.5
3	Plain enclosed	3/4	Treated	55.5	94	56.0	95	57.5	97	59.0
3	Enclosed fan-cooled	3/4	Untreated	48.0	83	49.0	85	52.5	91	58.0
3	Enclosed fan-cooled	3/4	Treated	39.5	73	48.0	88	53.0	97	54.5
1	Dripproof	3/4	Untreated	36.0	74	45.5	94	43.4	90	48.5
1	Dripproof	3/4	Treated	38.0	79	45.0	94	43.5	91	48.0
1	Plain enclosed	3/4	Untreated	65.0	95	67.0	98	65.5	96	68.5
1	Plain enclosed	3/4	Treated	59.0	93	61.5	97	60.5	95	63.5
1	Enclosed fan-cooled	3/4	Untreated	44.0	75	52.5	89	53.5	91	59.0
1	Enclosed fan-cooled	3/4	Treated	42.0	79	49.5	93	50.0	94	53.5
1	Dripproof	1/4	Untreated	40.5	90	43.0	96	42.0	93	45.0
1	Dripproof	1/4	Treated	38.0	84	44.0	97	41.5	91	45.5
1	Plain enclosed	1/4	Untreated	63.0	91	68.5	98	64.0	92	69.5
1	Plain enclosed	1/4	Treated	59.0	88	64.0	96	64.0	96	67.0

Resistance:
Advantages: Equipment availability; usually no disassembly or damage; good co-ordination with hot spot.

Disadvantages: Requires more skill and care, since only one reading is obtained.

Thermocouple:
Advantages: Easy to measure temperature at several places, good co-ordination with hot spot, continuous readings during run.

Disadvantages: Relative scarcity of instruments; disassembly before and after test; same low temperatures as mercury thermometers, if end turns are heavily taped or puttied.

The characteristic which it is desired to control is the hot-spot temperature. It generally is agreed that the hot-spot temperature is not directly measurable on normal commercial machines by simple methods. Since a secondary measurement is necessary, the quantity measured should be related closely to hot-spot temperature so that, first, the user will be protected adequately and, second, the average motor will not have an unnecessarily large size.

According to this criterion, the measurements of temperature rise by resistance and by thermocouple in the end turns are equally good. Both methods measure a temperature considerably closer to hot-spot temperature than mercury thermometers do, and, at least in totally enclosed motors, the measurement is a more consistent indication of hot-spot temperature. Since measurement by resistance and by end-turn thermocouple appear to be equally accurate and, depending on testing conditions, either may be more convenient than the other for a particular motor, both methods should be recognized in the standards. The mercury-thermometer method, which is both less accurate and less convenient, should be discontinued.

In determining the standard temperature rise by any method, the tests showing the most difference between temperature rise by this method and hot-spot temperature rise should be given the most weight. According to this criterion, 65-degrees-centigrade rise by resistance or end-turn thermocouple is equivalent to 55-degrees-centigrade rise by mercury thermometer for totally enclosed motors, and 60-degrees-centigrade rise by resistance or end-turn thermocouple is equivalent to 50-degrees-centigrade rise by mercury thermometer in open motors.

Fourth Set of Tests*

DESCRIPTION OF MOTORS TESTED

The test motors were built using all standard parts except the stators. The stators were the standard ones used for dripproof motors of their rating, except that they were wound with a number of thermocouples embedded in the slots and in the end turns. The same stators were used for all tests of a given rating regardless of the effect of the enclosure on the temperature rise at rated load.

Three different four-pole 60-cycle induction motors were tested, a three-fourths-horsepower polyphase squirrel-cage motor, a three-fourths-horsepower single-phase repulsion-start motor, and a one-fourth-horsepower, single-phase repulsion-start motor. Each of the three-fourths-horsepower motors was tested with the following constructions:

1. Dripproof.
2. Totally enclosed nonventilated.
3. Totally enclosed fan-cooled.

The one-fourth-horsepower motor was tested only in the dripproof and totally enclosed nonventilated constructions.

Ventilation of the dripproof motors was obtained by the use of a single fan mounted inside the end shield at the shaft-projection end of the rotor or armature. The totally enclosed nonventilated motors were entirely self-cooled. Motors using totally enclosed, fan-cooled construction were cooled in the conventional manner by a fan mounted on a shaft projection opposite the normal projection. Such motors had no internal fan.

Dripproof end shields were used rather than the old-style open shields, because most present-day fractional-horsepower open motors are practically dripproof motors.

LOCATION OF TEMPERATURE INDICATORS

For the determination of the hot spot, thermocouples were placed in the winding when the conductors were being inserted in the slots. The locations of these indicators are shown in Figures 9 and 10. In addition an indicator was placed beneath the slot insulation to allow the measurement of the iron temperature.

It should be noted that it is a simpler problem to locate the hot spot in a polyphase stator than in a single-phase stator, because the heat is generated uniformly in a polyphase stator, whereas the usual single-phase stator has regions of greater and lesser heat generation, depending upon the distribution of the winding.

The hottest accessible spot in the polyphase motor was determined by tests to be between stator coil ends at the end of the winding opposite the shaft projection. In subsequent tests a thermometer was

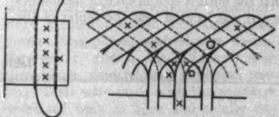

Figure 9. Thermocouple and thermometer locations in slots and coil ends of Master polyphase stator

□ Mercury thermometer
x Surface thermocouples
o Embedded detectors

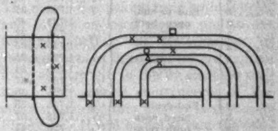

Figure 10. Thermocouple and thermometer locations in slots and coil ends of Master single-phase stator

□ Mercury thermometer
x Surface thermocouples
o Embedded detectors
Δ Hottest spot accessible to surface thermocouple

---

* Data reported by The Master Electric Company, Dayton, Ohio.

inserted here (see Figure 9) and the exposed portion of its bulb covered with modeling clay as recommended in AIEE Standard 9. A thermocouple was tied in place as close to the thermometer bulb as was possible.

The construction of the single-phase motors was such that the thermometer (see Figure 10) had to be placed on the outside of the coil-end extension. In this type of motor a much more desirable place was available for the location of a thermocouple, namely in the interstice formed where the coils were tied on the ends. A surface thermocouple was placed at this point.

TEST PROCEDURE

Motors were loaded until the temperature rises were approximately 40 degrees centigrade for the dripproof construction and 55 degrees centigrade for the totally enclosed constructions. Each test was continued until all temperature indicators remained constant for at least four consecutive readings spaced 15 minutes apart. After shutdown the resistance of the stator was measured several times in a period of approximately five minutes to permit extrapolation of the time–resistance curve back to the time of shutdown.

The same stator and temperature indicators were used for all tests of a given rating and were in exactly the same locations.

Results of these tests are shown in Table VI.

DISCUSSION AND CONCLUSIONS

Hottest Spot in Stator. It was found that the hottest spot in each of the motors tested was located near the center of the end turns, at the top of the winding opposite the shaft-projection end of the stator. In the case of totally enclosed motors there were often several spots at the maximum temperature, but the location just described was always one of these.

Hottest Normally Accessible Spot in Stator. An examination of the data for the three-fourths-horsepower polyphase motor shown in Table VI indicates that when thermometers and thermocouples are placed identically there is relatively little difference between their indications. In cases where construction is such that the thermometer can have only a limited contact with the winding, the use of properly placed thermocouples gives a definite advantage because of the ease with which a surface-thermocouple may be inserted in a desirable location.

All of the data shown herein indicate that the hottest accessible spot in an induction-motor stator which is ventilated by a single internal fan is at an interstice in the coil-end connections at the end opposite the fan.

Temperature Rise as Indicated by Change in Stator Resistance. The temperature rise calculated from the change in stator resistance can be seen to provide a dependable means for determining the temperature rise of stators.

For greatest accuracy the resistance should be measured at suitable intervals up to about five minutes after shutdown, the curve of resistance versus time after shutdown plotted, the curve extrapolated back to zero time, or time of shutdown, and the stator resistance at this time determined. This curve may be plotted on ordinary co-ordinate paper. Usually it will be almost linear, unless the final temperature reading is less than 85 per cent of the shutdown value.

In general for fractional-horsepower motors there is less than one per cent error in the resistance value, if it has been measured in less than one minute after shutdown.

Comparison of Results. Examination of the data shows that for plain totally enclosed motors all three of the methods of temperature measurement used provide consistent results which do not differ greatly from the hot-spot temperature. The data also indicate that for dripproof and totally enclosed fan-cooled motors the thermometer method is considerably less consistent than either of the other two methods.

Fifth Set of Tests

DESCRIPTIONS OF MOTORS TESTED

Tests were made on fractional-horsepower motors employing laminations in common use. These had four flats forming four open sectors between core and shell. Other designs used completely round laminations with better opportunity for heat conduction from laminations to outer shell. Ventilation with such construction was by fans at both ends.

In all cases the slots were insulated by 0.010-inch insulating paper. Formvar or enamel-insulated wires were used, and the windings were not varnish treated.

No attempt was made to use windings representing commercially acceptable temperature rises. The enclosed motors were not intended for such service and in some cases the load was reduced to prevent excessive final temperatures.

Past experience indicated that the fans used with this line of motors differed in their effects with direction of rotation. For that reason many of the tests were repeated with reversed rotation, forming a convenient check on results.

LOCATION OF TEMPERATURE INDICATORS

Approximately 64 thermocouples were used with a potentiometer. Embedded thermocouples were placed in the centers of all coils and on the centerline of the field cores at the time of winding insertion. Thermocouples on the surfaces of the end coils were held in place by fuller's earth and sodium silicate.

TEST PROCEDURE

Although it would be a comparatively simple matter to arrange a series of heat runs, measuring the rise by various methods, such a procedure still could leave unanswered several questions which might possibly have affected the results. For this reason, possible influential factors were listed and a series of tests arranged

Table VII

Core Length, Feet	Coils	Ventilation	Horsepower	Rpm	Temperature Rise: By Mercury Thermometer: Degrees Centigrade, Actual	Temperature Rise: By Mercury Thermometer: Per Cent of Hot Spot	Temperature Rise: Surface Thermocouple: Degrees Centigrade, Actual	Temperature Rise: Surface Thermocouple: Per Cent of Hot Spot	Temperature Rise: By Resistance: Degrees Centigrade, Actual	Temperature Rise: By Resistance: Per Cent of Hot Spot	Degrees Centigrade Hot Spot by Embedded Detector
2 5/8	4	End to end, open both rotations	1/3	1,725	42	85.5	49	100	50.5	103	49
2 5/8	4		1/3	1,725	42.5	87	48	98	47.5	97	49
2 5/8	3		1/3	1,725	37	71.2	48	92	47.3	91	52
2 5/8	3		1/3	1,725	40	74	50	92.5	49.8	92.5	54
1 5/8	3		1/6	1,725	27	93	29	100	26.5	91.5	29
1 5/8	3		1/6	1,725	25	86.4	28	96.5	28.5	98.3	29
1 5/8	4		1/6	1,725	25	86.4	28	96.5	28.8	99.4	29
1 5/8	4		1/3	1,725	24	82.7	27	93	27.5	94.9	29
2 5/8	4	End-ventilated, open both rotations	1/3	1,725	37	90	42	102	40.5	99	41
2 5/8	4		1/3	1,725	40	89	45	100	45	100	45
2 5/8	3		1/3	1,725	38	90.5	43	102	39.5	94	42
2 5/8	3		1/3	1,725	37	88	42	100	39.4	94	42
2	3		1/4	1,725	41	91.1	44	98	39.5	87.7	45
2	3		1/4	1,725	39	97.5	39	97.5	40.5	101	40
2	4		1/4	1,725	40	93	41	95	40.7	94.8	43
2	4		1/4	1,725	40	91	42	95.5	43.5	98.8	44
2 5/8	4	Plain enclosed	1/4	1,725	71	91	79	101	76.5	98	78
2 5/8	3		1/4	1,725	69	85.4	78	96	76.5	94.5	81
1 5/8	3		1/6	1,725	67	90.7	73	99	71.5	96.7	74
2 5/8	4		1/3	1,725	57	87.8	65	100	68.8	105.7	65
2 5/8	3		1/3	1,725	60	90	68	101	67.5	101	67
2	3		1/4	1,725	62	85	72	99	65.2	89.4	73
2	4		1/4	1,725	62	90	67	97	65.5	95	69
1 5/8	4		1/4	1,725	60	82.3	71	97	68.8	94.2	73

---

*Data reported by Robbins and Myers, Inc., Springfield, Ohio.

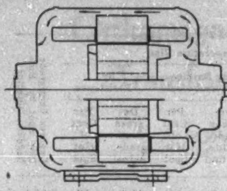

Figure 11. Sectional view showing ventilation of Wagner one-sixth-horsepower single-phase and polyphase motors

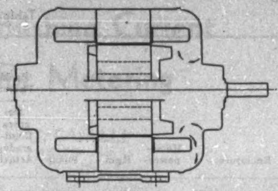

Figure 12. Sectional view showing ventilation of Wagner one-half-horsepower polyphase motors

so that the effect of these factors might be shown up, if present.

The amount of cooling air and the manner in which it is passed over and about the cores and windings are of importance in determining the final temperature rise of open motors. However, practical considerations limit air-delivery and heat-dissipation facilities. Within such limits it would appear that the general *pattern* of temperatures throughout an open motor would be unaffected by the amount of cooling air. For this reason changes in fans and amounts of cooling air were not planned as factors in these tests. In the fully enclosed motor, heat-transfer and dissipating facilities influence the final temperatures. However, the general pattern of temperatures throughout a closed motor was believed to remain unchanged by such features.

Tests investigating possible ventilation effects, therefore, neglected the above factors and considered instead only the following conditions:

1. Open motors: end-to-end ventilation; end ventilation.
2. Closed motors: no special heat-dissipating methods employed.

The ratio of slot area to slot length might influence temperature gradient and hot-spot values. Or in other words, it is conceivable that a change in core length, for the same laminations, might result in a similar change in hot-spot and end-coil temperature differentials. To investigate this possible effect, tests were made with motors having different lengths of core.

In designing single-phase motors, the extent of the distribution of the concentric stator coils frequently affects the final temperature rise. Some designs show a reduced rise through distributing the field in more slots. The possible effect of this distribution of coils and heat on hot-spot temperatures was investigated by repeating tests with three coils per pole and four coils per pole in the stator winding.

It was assumed at the outset of these tests that, even if the possible items listed previously should prove to be of no influence on the final pattern of temperatures, the repetitive nature of the tests would prove of value as a check on results. These items formed the key shown on the test sheets by which individual heat runs can be identified.

The motor under test was clamped to a metal bedplate on the dynamometer stand. Some heat flow to the bedplate resulted, but it was thought unnecessary to attempt to eliminate or minimize this effect.

Results of these tests are shown in Table VII.

DISCUSSION AND RECOMMENDATIONS

One disconcerting result noted at once in the tabulation, is the tendency for resistance measurements to indicate temperatures higher than the hot-spot values. (Percentage greater than 100.) Since resistance measurements presumably represent an average, this shows an average greater than its highest component. There are three possible explanations:

1. The true hot-spot was higher than that read. Had only a few thermocouples been used, it would be likely that such a spot could be missed. Under the circumstances it seems unlikely.
2. The rotor was considerably hotter than the stator copper, and immediately on shutdown the stator copper increased in temperature by reflected heat. Such a phenomenon is frequently observed. Such an explanation would not hold here as the repeat test with opposite rotation then should have shown the same effect with the ratio also over 100 per cent. It will be noted that this never occurred.
3. The third, inescapable conclusion is that all temperatures by resistance showing this ratio greater than 100 per cent represent incorrect and, hence, useless readings.

This point is mentioned because it shows up one defect in the rise-by-resistance method. The writers and the organization with which they are connected have used resistance measurements for years as an indication of temperature rise. It has been used in those cases where it:

1. Is the only practicable method.
2. Forms a useful check on other measurements.

To the writers it appears to be a one-shot method, with little chance for a check on human or instrumental error. The possible improvement by taking a series of resistance measurements, after shutdown at accurately determined intervals, does not appear to overcome the difficulties, because such points may rise or fall with time, depending upon reflected rotor heat. Hence extrapolation of points to determine exact shutdown temperature appears as a dubious improvement.

A few statements might be of interest:

1. The hottest spot measured by any embedded detector was never more than four degrees from that measured on the end coils of the same motor by thermocouples. Generally they were only one or two degrees apart.
2. The general pattern of temperatures for the various motors was very similar for end thermocouples versus embedded detectors versus hot spots. In contrast, thermometer readings displayed the greatest range.
3. Reduced stack did not result in a more uniform pattern of temperature with lower hot-spot increase. It must be remembered, however, that any one stack was provided with other variable elements, such as numbers of coils and changes in ventilation method.
4. It would appear that the introduction of cooling air into one end of the motor only, results in hot spots considerably higher than the average temperature. Ventilating both ends of the motor gives more uniform temperature rises.

Sixth Set of Tests*

DESCRIPTION OF MOTORS TESTED

The ratings tested consisted of a one-sixth-horsepower single-phase capacitor-start induction motor, one-sixth-horsepower three-phase, squirrel-cage induction motor, and a one-half-horsepower three-phase, squirrel-cage induction motor. Tests were made with the windings untreated both as open and totally enclosed motors. The windings then were treated with insulating varnish, and the tests were repeated both as open and totally enclosed motors. The reason for making tests with the stator windings both treated and untreated was to determine whether the temperature rise might be affected by the varnish treatment. The reason for making tests both as open and totally enclosed motors was to determine whether the temperatures in various parts of open motors are as uniform as they are in totally enclosed motors. The general construction of the one-sixth-horsepower motors is shown in Figure 11. It will be noted that the one-sixth-horsepower motors have ventilating spaces between the stator core iron and the frame, and the rotor is of cast aluminum construction with blower blades on only one end. The construction of the one-half-horsepower motor is shown in

---

* Data reported by Wagner Electric Corporation, St. Louis, Mo.

Figure 12. It will be noted that it does not have ventilating spaces between the frame and the core but that the rotor is of cast aluminum with blower blades on only one end.

Location of Temperature Indicators

Sixteen thermocouples were placed in each of these motors in various slots midway between the two ends of the core stack and distributed uniformly around the circumference. Some of these thermocouples were damaged during the winding operating, and, therefore, all of them could not be used. The minimum number of thermocouples which were used in any of the motors is nine in the one-sixth-horsepower single-phase motor. It is believed that enough thermocouples were used in all of the motors to obtain a fair approximation of the hot-spot temperature. Surface thermocouples were placed on the hottest accessible part of the free ends of the winding, and mercury thermometers also were placed in the hottest places which were accessible to the thermometers.

Test Procedure

Continuous temperature tests were made on all three motors both open and totally enclosed with the windings treated and untreated. Particular care was taken to obtain accurate resistance readings, and the cold-resistance readings were taken after the motors had remained in a room of practically constant temperature for a period of several hours. Hot resistances were taken within ten seconds after shutdown. This was done by using three more so as to obtain the hot resistance in the shortest possible time. The temperature readings were taken on the thermometers and thermocouples while the motor was operating and were not continued after shutdown. The same stator thermocouples and embedded detectors were used for all four tests on a given rating.

The results are summarized in Table VIII.

Table VIII

Enclosure	Horsepower	Rpm	Phase	Temperature Rise: By Mercury Thermometer: Degrees Centigrade, Actual	By Mercury Thermometer: Per Cent of Hot Spot	By Surface Thermocouple: Degrees Centigrade, Actual	By Surface Thermocouple: Per Cent of Hot Spot	By Resistance: Degrees Centigrade, Actual	By Resistance: Per Cent of Hot Spot	Degrees Centigrade Hot Spot by Embedded Detector
Open untreated	1/2	1,750	3	37.7	70	53.0	98	49.9	92	54.1
	1/6	1,750	3			43.2	92	44.1	94	47.1
	1/6	1,750	1	40.0	75	45.8	86	50.8	95	53.3
Open treated	1/2	1,750	3	37.4	78	48.8	102	47.3	99	48.0
	1/6	1,750	3	35.7	89	38.6	96	39.0	97	40.0
	1/6	1,750	1	35.1	79	37.7	84	43.5	97	44.6
Plain enclosed untreated	1/2	1,750	3	42.7	82	52.6	100	48.8	93	52.3
	1/6	1,740	3	48.6	90	48.3	89	52.7	98	54
	1/6	1,750	1	49.1	85	52.8	91	54.3	94	58.0
Plain enclosed treated	1/2	1,750	3	45.4	83	56.0	102	52.0	95	54.8
	1/6	1,750	3	50.2	96	50.2	96	52.0	100	52.2
	1/6	1,750	1	46.2	90	47.4	92	50.8	99	51.5

Table IX. Summary of Tests on Fractional-Horsepower A-C Motors

Manufacturer	Enclosure	Temperature Rise: Thermometer, Per Cent of Hot Spot	Surface Thermocouple, Per Cent of Hot Spot	Resistance, Per Cent of Hot Spot
Century	Open	84–92	92–95	94–97
Emerson	Open	61–78*	87–95	93–98
General Electric	Open	76–80	89–98	89–100
Master	Open	74–94	94–97	90–96
Robbins and Myers	Open	71–98	92–102	88–103
Wagner	Open	70–89	84–102	92–99
All tests	Open	61–98	84–102	88–103
Century	Plain enclosed	91–97	92–99	94–94
Emerson	Plain enclosed	70–76*	91–98	96–100
General Electric	Plain enclosed	75–92	95–100	90–98
Master	Plain enclosed	88–95	95–98	92–99
Robbins and Myers	Plain enclosed	82–91	96–101	80–106
Wagner	Plain enclosed	82–96	89–102	93–100
All tests	Plain enclosed	70–97	89–102	89–106
Master	Enclosed fan-cooled	73–83	85–93	91–97

* Frame temperature.

Discussion and Conclusions

Although it is possible to obtain fairly accurate measurements of temperatures, using mercury thermometers, in motors which are so constructed that a thermometer can be placed in the right location, it should be borne in mind that many motors have mechanical features which prevent the satisfactory use of mercury thermometers without mutilating the motors. In such cases the temperatures taken are quite likely to be lower than the true values, and the actual operating temperatures of such motors are a good deal higher than the observed readings.

On the other hand, thermocouples are flexible and may be placed readily on the hottest parts of windings so that readings taken using surface thermocouples are more nearly correct than those which are obtained by using mercury thermometers. It is, therefore, suggested that the use of mercury thermometers be discouraged. This might be done by specifying the use of thermocouples and eliminating the use of mercury thermometers, or by specifying a new method which would consist in the determination of temperatures by means of thermocouples applied to the hottest part of the machine accessible to thermocouples.

Summary of Data Reported by All Companies

A brief summary of the preceding data is given in Table IX. In this table, as in the preceding tables, the maximum temperature obtained by embedded detector is considered the hot spot. When temperatures by surface thermocouple or resistance exceed those obtained by means of the embedded detector, either one of two conclusions may be reached: either the embedded detector was not placed in the hottest part of the winding, or an error was made in the measurements.

Orthomagnetic Bushing Current Transformer for Metering

A. BOYAJIAN
FELLOW AIEE

G. CAMILLI
FELLOW AIEE

BUSHING current transformers are ideal for many reasons. They are compact, convenient, economical, and, from the operator's standpoint, they eliminate a separate piece of equipment. But they have one inherent limitation, namely, an accuracy generally not satisfactory for metering. Many efforts therefore have been made in the past to overcome this inherent limitation of the conventional design, with considerable success in the laboratory but limited success in practice.

The factor that causes inaccuracy in current transformers is a minute nuisance burden (1–10 volt-ampere excitation loss) consumed in the core. The bushing-type current transformer is handicapped particularly in this matter because its exciting ampere turns are necessarily very few, the primary winding consisting of but a single turn, a through conductor, and, therefore, for a given instrument burden into which a given current is to be transformed, the volts per turn, the flux density, and the volt-amperes consumed by the core have to be correspondingly higher. It may well surprise one that in all these years some way has not been found to deliver these few volt-amperes from the powerhouse by some means that will relieve the primary from this nuisance burden. A significant step now has been taken in this direction. The device is called orthomagnetic for reasons explained below.

Principle

If a core is excited from an a-c source and then a higher-frequency excitation superimposed on it through a separate winding of suitable design, maintaining the original excitation unchanged, it will be observed that the volt-ampere input by the original (lower-frequency) circuit is diminished by the superposition, although the total losses in the core may be considerably increased. That is, the higher-frequency source furnishes more than what might be considered its proper share of the total volt-amperes consumed by the core; the lower-frequency source, less than its share. Thus, toward the lower-frequency source, the iron behaves as an improved material; toward the higher-frequency source, as a degraded material. That this cannot be a matter of one circuit delivering power to the other circuit in the ordinary way will be appreciated by remembering the mathematical law that voltage at one frequency cannot produce power with current of another frequency. In fact, in the practical application of the principle under discussion, the two circuits are designed with their mutual inductances balanced out (Figure 1), so that the higher-frequency circuit cannot induce any current in the lower-frequency circuit, and vice versa. It will be seen in Figure 1 that the connections of coil $b2$ are reversed, making the mutual induction between coils a_2 and b_2 opposite to that between a_1 and b_1, and therefore the mutual induction between circuits A and B will be zero. With only ordinary care used in making the two cores and windings alike in the current transformers here reported, no appreciable current of higher-frequency could be detected in the lower-frequency (primary and secondary) circuits (Figure 6).

Some understanding of the rationale of the phenomenon perhaps may be gained from the following elementary discussion.

Referring to Figure 2, let a-b-c-d-e represent the hysteresis loop corresponding to the 60-cycle excitation in the absence of any other excitation. If the state of affairs at the point a is considered, it is seen that the magnetizing current is zero, and there is a residual magnetism a-a'. If, now, a high-frequency excitation is superimposed on the core (the higher the frequency the better for this explanation), this residual magnetism will be eliminated after several cycles of the high-frequency excitation, and a will move up to a': that is, while the low-frequency current is still the same, the flux density corresponding to it will be changed.

If the low-frequency ampere-turns are equal to the abscissa of b, then normally, in the absence of any other excitation, the flux density will be the ordinate of b, representing a residual magnetism b-b', where b' is some intermediate value between the ordinates of the ascending and the descending portions of the loop for the given abscisssa. If, now, a high-frequency excitation is superimposed, this residual magnetism is eliminated, and b moves up to b'.

Similarly to the foregoing, under the residual demagnetizing action of the high-frequency excitation, c moves to c', and so forth, and thus the low-frequency magnetization moves along a', b', c', d, c', b', a', and so on, instead of a, b, c, d, e. Thus, theoretically, the low-frequency hysteresis loss can be eliminated with the aid of simultaneous high-frequency excitation. The low-frequency eddy-current loss, however, cannot be affected materially by the high-frequency excitation.

That the hysteresis loss associated with a d-c loop is reduced, if simultaneously an a-c excitation is superimposed, seems to have been observed first by Gerosa and Finzi in Italy more than half a century ago.[1] Later investigators observed that, if two a-c excitations are applied simultaneously, the higher frequency excitation tends to furnish a larger fraction of the hysteresis loss.[2] In the late '20's the present authors discovered or redis-

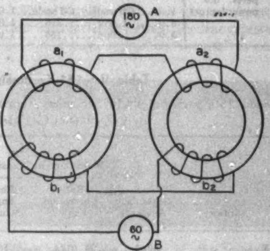

Figure 1. Diagram of connection to study the excitation characteristics of magnetic cores simultaneously excited at two different frequencies

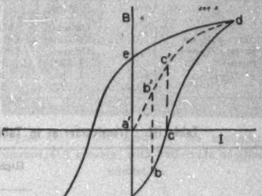

Figure 2. Performance of the auxiliary high-frequency excitation in reducing the residual flux due to the lower-frequency excitation

---

Paper 45-24, recommended by the AIEE committee on instruments and measurements for presentation at the AIEE winter technical meeting, New York, N. Y., January 22–26, 1945. Manuscript submitted November 6, 1944; made available for printing December 8, 1944.

A. BOYAJIAN and G. CAMILLI are in the power transformer engineering division of the General Electric Company, Pittsfield, Mass.

The authors are indebted for the current-transformer tests and adjustments to the General Electric Company engineers W. B. Connover and J. M. Camerlengo of the works laboratory, Pittsfield; and for the excitation data to engineers B. M. Smith and B. D. Templer of the general engineering laboratory, Schenectady, N. Y.

covered that not only the hysteresis loss but also the reactive volt-amperes can be reduced in this way, and they proposed to utilize this principle to reduce the exciting current and thereby improve the accuracy of the bushing-type current transformer.[3] Outwardly the device was somewhat similar to the one here reported, but it could not be reduced to commercial practice for several reasons. First, the frequency of the auxiliary excitation would have to be about seven times that of the circuit to be metered, and so, since there was no commercially feasible means of securing such frequency, the idea could not be exploited commercially. Second, even if this frequency were provided, only borderline cases could be improved to good accuracy by this means, because the reduction would be fractional at best, and the scope of the application of the principle would be very limited.

The new factor in the situation which makes the auxiliary higher-frequency excitation a success where it had failed before is the discovery that the volt-ampere characteristic curve can be linearized by proper choice of auxiliary excitation, that the benefits derived from this principle may be many times those from a mere reduction of either the watt losses or of the exciting current, and that, if advantage is taken of this fact, triple-frequency instead of sevenfold frequency auxiliary excitation may be used.

Table I. 69-Kv Current Transformer

100:5 Amperes (20 Secondary Turns); Two Cores, Each $10^5/_8$ Inches Inside Diameter by $12^5/_8$ Inches Outside Diameter by $5^1/_4$ Inches High; Total Core Weight=100 Pounds

		Plain Current Transformer		Triple Frequency Excitation Added		Impeder (Z) Added		Complete With Autotransformer	
Burden	Secondary Amperes	Ratio Correction Factor	Phase Angle, Minutes	Ratio Correction Factor	Phase Angle, Minutes	Ratio Correction Factor	Phase Angle, Minutes	Ratio Correction Factor	Phase Angle, Minutes
Y (15 volt-amperes, 0.9 power factor)	0.5	Off scale	Off scale	1.0215	+25	1.0184	+3	1.0005	+5
	1.0	Off scale	Off scale	1.0216	+26	1.0184	+3	1.0004	+4
	3.0	1.082	216	1.0211	+21	1.0180	−1	1.0003	+1
	5.0	1.068	156	1.0212	+16	1.0180	−5	1.0004	−2

Table II. 161-Kv Bushing-Type Current Transformer

Ratio 150/5 Amperes (30 Secondary Turns); Two Cores, Each 20 Inches Inside Diameter by $24^3/_4$ Inches Outside Diameter by 2 Inches High

		Plain Current Transformer		High-Frequency Excitation Added		With Impeder and Autotransformer	
Burden	Secondary Amperes	Ratio Correction Factor	Phase Angle, Minutes	Ratio Correction Factor	Phase Angle, Minutes	Ratio Correction Factor	Phase Angle, Minutes
X (2.5 volt-amperes, 0.9 power factor)	0.5	1.0174	103	1.0022	3		
	1.0	1.0154	81	1.0027	4		
	2.0	1.0138	64	1.0028	4		
	3.0	1.0130	59	1.0031	4		
	5.0	1.0119	43	1.0033	5		
Y (15 volt-amperes, 0.9 power factor)	0.5	1.0665	262	1.0149	12	1.0056	+ 4
	1.0	1.0591	196	1.0156	13	1.0050	+ 3
	2.0	1.0510	134	1.0157	13	1.0047	+ 2
	3.0	1.0463	103	1.0158	13	1.0045	+ 1
	5.0	1.0400	72	1.0158	13	1.0043	0
2 (50 volt-amperes, 1.0 power factor)	0.5	Off scale	Off scale	1.0443	125	1.0020	+18
	1.0	Off scale	Off scale	1.0439	120	1.0014	+10
	2.0	Off scale	Off scale	1.0433	106	1.0008	+ 2
	3.0	1.086	350	1.0433	100	1.0012	− 4
	4.0	1.081	300	1.0440	100	1.0018	− 7
	5.0	1.077	250	1.0442	100	1.0019	−14

Table III. Transformer as in Table II But Wound for 300/5 Amperes

		High-Frequency Excitation Added		With Impeder and Autotransformer	
Burden	Secondary Amperes	Ratio Correction Factor	Phase Angle, Minutes	Ratio Correction Factor	Phase Angle, Minutes
Y (15 volt-ampere, 0.9 power factor)	0.5	1.0046	+3	1.0003	+3
	1	1.0045	+2	1.0002	+2
	3	1.0043	+2	1.0000	+2
	5	1.0041	−1	0.9998	−1

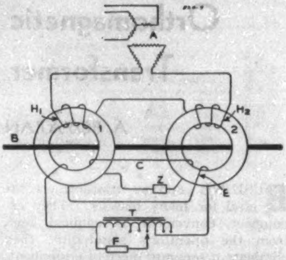

Figure 3. Diagram of connection of a bushing-type current transformer with auxiliary triple-frequency excitation

A=triple-frequency transformers
B=primary conductor
1 and 2=cores
H_1 and H_2=winding for the triple-frequency excitation
C=auxiliary winding
Z=compensating burden
E=main secondary winding
T=autotransformer
F=burden

A device incorporating a core of which the magnetization has been rendered straight, by auxiliary higher-frequency excitation, has been christened by the authors orthomagnetic (having straight-line magnetic characteristics).

Current-Transformer Circuit

In Figure 3, B is the through conductor of a bushing and constitutes the primary winding; 1 and 2 are duplicate wound-strip cores; E is the secondary winding; H_1-H_2, the 180-cycle excitation winding; T, an autotransformer inserted between the secondary winding and the burden, with a number of small tap-steps to make precise adjustment of the current ratio; Z, a phase-angle compensating impeder; and F, the burden.

The need for the autotransformer will be appreciated, if it be remembered that the primary being only one turn and the secondary 10–50 turns, one secondary turn may represent a two–ten per cent step which would not be fine enough. The autotransformer and the impeder are a separate piece of equipment from the current transformer and may be mounted apart from it.

The equipment to furnish the 180-cycle excitation to the current transformer is shown in Figures 3 and 7, consisting of a wye-delta bank of three small single-phase transformers, with the corner of the delta opened for connection to the terminals of winding H_1-H_2 as a single-phase system, while the wye-winding is excited from a three-phase 60-cycle source.

As the theory of static third-harmonic generators (also called frequency-multipliers) is well known, we shall be satisfied here with a reference[2] to the subject.

The capacity of the 180-cycle static generator shown in Figure 7 is 400 volt-amperes and weighs about 25 pounds. The 180-cycle power input into the 69-kv current transformers of Table I is 42 watts at about 90 per cent power factor, and that into the 161-kv unit of Table II 70 watts. The harmonic generator therefore can supply excitation to a number of current transformers.

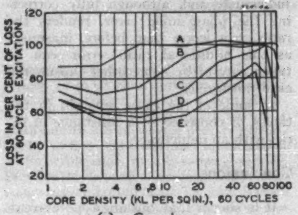

(a). Core loss

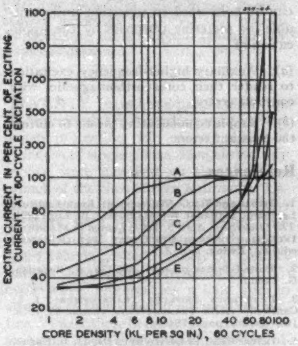

(b). Exciting current

Figure 4. Excitation characteristics of magnetic cores (wound strip) when excited simultaneously at different flux densities at 60-cycles and at triple frequency

Core density (kilolines per square inch), 60 cycles

A—2,500 lines per square inch, 180 cycles
B—7,500 lines per square inch, 180 cycles
C—15,000 lines per square inch, 180 cycles
D—25,000 lines per square inch, 180 cycles
E—32,250 lines per square inch, 180 cycles

The harmonic generator is too large a load for potential transformers installed for metering service.

Accuracy Characteristics

The ratio and phase-angle characteristics of two such bushing-current transformers, one for 69-kv and the other for 161-kv circuits, are exhibited in detail in Tables I–III.

The significance of these exhibits as to the improvements accomplished may be gathered from a few of the items listed. For instance, for the 161-kv unit for 150/5 amperes with wye-burden, the following figures are found in Table II:

	At 0.5 Ampere		At 5.0 Amperes	
	Ratio Error, Per Cent	Phase Angle, Minutes	Ratio Error, Per Cent	Phase Angle, Minutes
Plain current transformer	−6.7	+262	−4	72
180-cycle excitation added	−1.5	+ 12	−1.6	13
Z and autotransformer also added	−0.56	+ 4	−0.43	0

The maximum ratio error is seen to have been cut down from 6.7 per cent to 0.56 per cent; the phase-angle error, from 262 minutes to 4 minutes. In the final result, as the ratio error varies between −0.43 per cent and −0.56 per cent, it follows that if the measurements are multiplied by 1.005, the maximum ratio error of the result will be no more than 0.05 per cent, that is, about $^1/_{20}$ of one per cent.

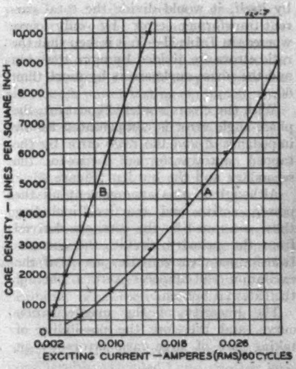

Figure 5. Exciting current of wound-strip magnetic cores with and without auxiliary triple-frequency excitation

A—60 cycles
B—60 cycles plus 180 cycles (32,250 lines per square inch)

Effect of Voltage Fluctuations

Variations in the current-transformer accuracy under fluctuations of the supply voltage to the harmonic generator also were investigated, and it was found that a ten per cent range of voltage fluctuation made a difference of 0.1 per cent in the ratio error and one minute in the phase-angle error.

Wave Shape

Figure 6 shows oscillograms of primary and secondary currents. In order to make the higher-frequency component more conspicuous in case it should find its way into the 60-cycle circuits, the higher-frequency excitation was furnished at 540 cycles for these oscillograms. No trace of such a harmonic was visible in any of the oscillograms taken.

In one test, in order to determine accurately any possible induced harmonic current in the secondary circuit unmixed with any fundamental-frequency current, the secondary current was measured under full triple-frequency excitation and *no primary current*, and it was found to be about one-tenth of one per cent of the rated current of the winding. Needless to add, no matter how large the harmonic current, it cannot affect the wattmeter indications unless a corresponding harmonic voltage, inphase with the harmonic current, also is impressed across the potential coils of the meters.

Freedom From Residual Magnetism

Those familar with this subject know that current-transformer accuracy tests do not always reproduce themselves on account of varying values of residual magnetism, unless the core is demagnetized carefully before each test.[5] The present type, with a constant demagnetizing excitation, is free from this uncertainty.

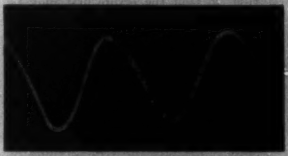

Figure 6a. Wave shape of the primary current with 0.5-ampere secondary current, no high frequency

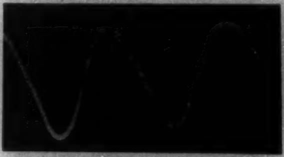

Figure 6b. Wave shape of the secondary current, 0.5 ampere, with 540-cycle auxiliary excitation

Magnetization Curves

Figure 4 gives typical magnetization data taken on a wound-core unit made up of silicon-steel strip and subjected to 60-cycle and 180-cycle excitations simultaneously. Figure 4a gives the watt-loss data and Figure 4b, the exciting-current data. To bring out the benefit of dual excitation more clearly and quantitatively, ordinates give the losses (watt or exciting current) as a percentage of the corresponding values in the absence of auxiliary excitation. It is seen that in the range of the flux densities to be encountered in bushing-transformer practice (1–10 kilolines per square inch), impressive reductions in watt losses and exciting current are accomplished when a 180-cycle excitation is superimposed at a density of 25–30 kilolines per square inch: the watt losses are cut down to a half, and the exciting current to a third. Other test data, not reproduced here, show that, up to about 60-kiloline 60-cycle density, the benefit of this auxiliary excitation is practically unaffected by the phase displacement between the two excitations.

Impressive as these curves may be, they exhibit only one factor in the improved accuracy of the current transformer through such auxiliary excitation. The more important factor, as intimated above, is the possibility of the conversion of the nonlinear magnetization curve into a linear one by appropriate auxiliary excitation, so that the errors first may be rendered constant and then be compensated for by other means. Any reduction is, of course, a gain, insofar as it reduces the necessary compensation to that extent, but the possible error reduction by the linearization-and-compensation method is many times that by the exciting-current reduction method.

Figure 5 exhibits the straightening of the magnetization curve very clearly. Curve *A* applies to the normal 60-cycle volt-ampere characteristic of the core without auxiliary excitation, curve *B* to the 60-cycle characteristic with the benefit of a 180-cycle auxiliary excitation maintained at about 30 kilolines per square inch.

So far as the absolute value of the exciting current is concerned, curve *B* is only about 50 per cent better than *A*. It is not so good as what might have been obtained with seventh harmonic or with higher triple-frequency excitation; and, by itself, it would divide the total current-transformer error by only two, whereas in Table II—*Y*, it is seen that the ratio errors are divided by more than ten and the phase-angle errors by more than 60.

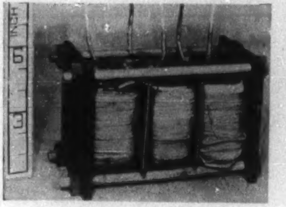

Figure 7. View of a frequency-tripling transformer; rated output 400 volt-amperes

Primary voltage = 240 volts; secondary voltage, 120 volts

With the errors rendered constant, the phase-angle error is compensated for by impedance *Z* and the ratio error by the tapped autotransformer between the secondary and the burden (Figure 3).

Although in this arrangement all the power, active and reactive, including those consumed by the core, are derived from the primary circuit, the current-transformer characteristics are as if the excitation volt-amperes were a part of the external burden.

The linearity of the magnetization curve, and therefore the possibility of taking care of large ratio errors by an autotransformer, greatly simplifies the problem of correcting the phase-angle error by the impedance *Z*. This impedance may be chosen conveniently over a surprisingly wide range of power factor and magnitude, because it is not a serious matter if *Z* is chosen somewhat injudiciously and, although fully correcting the phase-angle error, renders the ratio error worse than before, inasmuch as this additional ratio error can be taken care of by some other tap on the autotransformer.

In some of the cases reported in the tables, *Z* consisted of a resistance in series with an inductance.

Conclusions

It is shown that bushing-type current transformers, which in their simple form would not be good enough for metering, can be converted to precision units suitable for metering purposes by the application of

(*a*). Auxiliary higher-frequency excitation to render their cores orthomagnetic, with constant errors.

(*b*). Simple compensating means to correct the constant errors.

References

1. **Gerosa and Finzi.** *Rendiconti* del Regio Instituto Lombardo (Milano), volume 24, fasc. 10, April 1891; *The Electrician*, April 3, 1891; quoted in Magnetic Induction in Iron and Other Metals (second edition), **Ewing**, page 317.

2. United States patent 1,706,139, **A. Boyajian, G. Camilli.**

3. Frequency Tripling Transformers, **J. L. Cantwell.** AIEE Transactions, volume 55, 1936, July section, pages 784–90.

4. Instrument Transformers (book), **B. Hague.** Sir Isaac Pitman and Sons, London, England. Pages 95–103.

5. The Effect of Current-Transformer Residual Magnetism on Balanced-Current or Differential Relays, **H. T. Seeley.** AIEE Transactions, volume 62, 1943, April section, pages 164–8. Discussion page 384.

6. Transformer Losses Due to Simultaneous Excitation at Two Different Frequencies, **F. Schroeter.** *Archiv fuer Elektrotechnik* (Berlin), volume 13, March 31, 1924.

Compressed-Air Circuit Breakers in A-C Railway Service

H. M. WILCOX
MEMBER AIEE

D. C. HARKER
ASSOCIATE AIEE

Synopsis: The increasing interest in compressed air as an interrupting and operating medium for circuit breakers in central-station and industrial service, together with its gratifying record in service periods extending up to five years, warrants investigation of its application to a-c railway service. Previous developments leading up to present standards of requirement for this service are reviewed, and a description is given of a compressed-air breaker designed for high-speed interruption of short circuits on contact line feeders in single-phase 25-cycle railway service at 12,000 volts to ground. Application of the principle to other railway service is discussed.

TWENTY years have passed since the first circuit breakers designed to afford speed protection for contact lines in 11,000-volt single-phase 25-cycle railway service were installed on the Danbury branch of the New Haven Railroad.[1] Using oil as an interrupting medium, these breakers were designed to detect and interrupt, in conjunction with high-speed relaying, short circuits on contact lines in 0.04 second, one cycle on a 25-cycle wave, representing a long step in advance of then existing oil-breaker practice. These three breakers are still in service today in their original application, although increased power to meet the demands of heavier traffic may necessitate their replacement by breakers with rupturing ability beyond their moderate rating in the foreseeable future.

Tests made with these breakers in their service position demonstrated their ability to meet specified time requirements and indicated that this performance might be expected to reduce damage to overhead installations and motive equipment to a minimum, as well as insure satisfactory continuity of service on parallel signal and communication circuits. Accordingly, this specification as to time performance, 0.04 second or less, has remained standard up to the present day. It should be stated, however, that high-speed equipment in railway service shows a considerable proportion of interruptions after a single loop of short-circuit current when the zero point in the a-c wave is favorably located.

In the years immediately following this installation another important electrification project required the provision of high-speed breakers with interrupting ability up to 50,000 amperes at 12,000 volts to ground, and in 1928 two new designs; one an air-insulated breaker,[2] the other an oil-insulated breaker,[3] were installed in considerable numbers on the four-track main-line electrified zone of the Pennsylvania Railroad from Philadelphia to Wilmington,[4] later extended to Washington. Both designs followed earlier practice in their own fields, the air breaker being an extension to moderate alternating voltages of the magnetic-blowout principle then in operation for a number of years in d-c railway service, and the oil breaker following fundamentals of the original New Haven breaker but with considerably improved mechanical details. Both breakers were developed with the aid of high-power testing equipment then becoming available with sufficient power to demonstrate their performance.

Preparatory to this large main-line project, an exhaustive investigation of requirements for relay protection had been made,[5] and the results were here put into practical effect. One noticeable result of this investigation may be noted in the conclusion reached that the use of a d-c shunt tripping magnet for opening the high-speed breaker tends toward greater flexibility in protective relaying, and this form of tripping is now regarded with favor for the service.

By 1930 this electrified zone had been considerably extended,[6] and another air-insulated high-speed breaker had appeared, operating on the then newly developed deion theory of arc rupture. This breaker was demonstrated by test to be the equal in service ability of previous designs and was installed in considerable numbers on further extensions of the system. Essentially of the indoor class of construction, it represented a forward step in application, considering the amount of organic material incorporated at critical points of insulation in its interrupting chamber with possibilities of deterioration in outdoor service. As protection against such possibility, the breaker structure was enclosed in a weatherproof steel housing with double walls, interposing an annular air space around the breaker to minimize the effects of condensation. Space heaters were provided further to reduce this effect. Breakers of this class have now been in continuous service adjacent to the Jersey Meadows for 12 years without more than the normal deterioration to be expected for that period in any service. This experience has demonstrated effectively the feasibility of applying organic insulation in outdoor service when adequate protection is afforded.

By 1935 concentrations of power at rail-junction points on this system had increased to such extent that the previously accepted interrupting rating of 50,000 amperes for high-speed breakers was clearly inadequate for certain feeder positions. It became evident that, as an alternative to a rather extensive rearrangement of feeders, a costly operation at the best, breakers of greater interrupting capacity must be developed for this service, and the new interrupting specification was set at 65,000 amperes as meeting all requirements in the foreseeable future. This demand brought out a fourth design, another oil-insulated breaker of the impulse type,[7] now in service at various points on the system.

As a result of the service experience obtained with the varying types of equipment on this electrified system in the years since full-scale operation was put into effect, together with the information obtained from several years of trial operation preceding it,[6] the requirements for

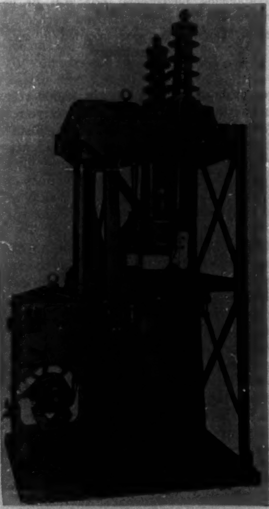

Figure 1. An early form of high-speed breaker

This oil breaker was the first high-speed interrupter to be placed in service at 12,000 volts

---

Paper 45-31, recommended by the AIEE committee on land transportation for presentation at the AIEE winter technical meeting, New York, N. Y., January 22-26, 1945. Manuscript submitted November 27, 1944; made available for printing December 12, 1944.

H. M. WILCOX is section engineer, and D. C. HARKER is engineer, both in the switchgear engineering department of Westinghouse Electric and Manufacturing Company, East Pittsburgh, Pa.

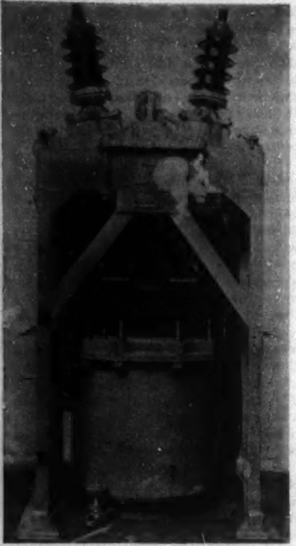

Figure 2. A more modern high-speed oil breaker

Incorporating fundamental principles of its predecessor, but with improved mechanical details, this breaker was installed in considerable numbers

protection of contact lines in 12,000-volt railway service, the type of protective relaying,[6] and the arrangement of substation equipment had become clearly identified, and standards of performance had been fixed. Development of new lines of apparatus for this service must then consist largely of adaptation of more modern devices to its use.

Outstanding among interrupting mediums today is compressed air, applied in the form of a transverse blast for maximum current interruption at voltages in the powerhouse class. Five years of experience in service operation with conventional-speed breakers in powerhouse duty, together with a laboratory-testing record which has made the compressed-air breaker the most completely tested device in the upper range of current interruption ever offered to the trade, render it most desirable for application to heavy-duty a-c railway service.

Even more desirable, such application does not involve extreme exploration into untried avenues of development. The breaker parts proper, including the contact elements, arc chute, muffler, blast tube, and blast valve, may be taken bodily from conventional-speed breakers service-proved for the equivalent interrupting duty in other applications. Since a latched-in type of mechanism is best adapted to a rapid start of acceleration of the moving contact on opening, the design of high-speed latch and d-c tripping magnet proved by 15 years of service in previous designs of high-speed breakers for railway service may be utilized in its present form. The high-speed linkage with its accelerating device and contact connecting rod may be substantially the same as in earlier breakers, modified only to adapt it to a new position in the breaker structure. Compressed air being available as an interrupting medium, it is logical to utilize it for the conventional-speed closing function; hence a conventional air-closing cylinder. There remains, then, only to co-ordinate these features into a single operating unit.

Figure 4 shows a breaker of such design meeting the present specification of 65,000 amperes interrupting capacity at 12,000 volts to ground, single phase, 25 cycles, with an interrupting time of 0.04 second or less in conjunction with high-speed relaying, and with a potential withstanding test of 65,000 volts for one minute. Mounted in a weatherproof steel housing with double walls, incorporating the annular air space of earlier designs, the complete structure is divided into three compartments. The lowermost compartment carries the air reservoirs, operating mechanism, and all low-voltage control equipment. Immediately above it, isolated by a horizontal grounded barrier, is the main breaker compartment enclosing the high-potential breaker parts. At the top of the structure is an expansion or diffusion chamber, enclosed by the cupola form of roof construction and isolated from the main breaker compartment by a horizontal insulating barrier. The arc chute discharges the air blast with its heated arc products through a muffler into this diffusion chamber from which it is vented to atmosphere through louvered openings. Conductors are brought through the roof of the housing to the breaker terminals by conventional condenser bushings of 34.5-kv rating.

Doors are provided at the front and rear of the housing allowing full access to all parts of the breaker. The doors of the two main compartments are separated, permitting access to mechanism and controls without exposure to high-potential parts. Footings have been designed to permit installation on the same foundation as earlier designs of high-speed breaker, facilitating replacement of those breakers in positions where breakers of lower rupturing ability have become inadequate, because of increased power requirements. The condenser bushings, while incorporating refinements of modern design, are interchangeable with those of earlier breakers.

The contact details and their arrangement with respect to the air blast and arc chute conform to the conventional practice previously presented before the Institute.[9] The conventional blade and finger type of contact is used on this design in contrast to the butt-type contacts of earlier high-speed breakers to provide the overlapping contact travel necessary to insure full amplitude of blast air at the time of contact parting. The blast valve is of the conventional metal-to-metal-seat poppet type, mechanically operated by a

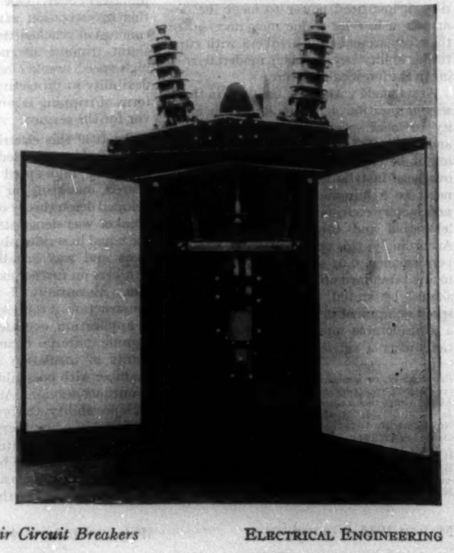

Figure 3. The deion high-speed breaker

Incorporating the deion principle of arc rupture, this breaker is rendering valuable interrupting service up to 50,000 amperes

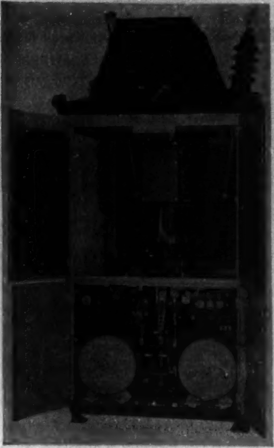

Figure 4. Compressed-air high-speed breaker

Embodiment of a modern compressed-air interrupting device renders this breaker capable of handling the heaviest railway service

cam surface on the trip-free lever when opening, but arranged to be inoperative on the breaker closing stroke since the air blast is not essential in circuit closing.

Application of accelerating force to the moving contact on opening differs slightly in this breaker from the practice in previous high-speed breakers with their short follow-up of butt-type contacts. There it was necessary to concentrate the accelerating force at the start of motion in order to obtain the highest speed possible at contact parting, and to continue this acceleration in order to insure a contact gap sufficient to withstand voltage when the arc has been swept onto arcing horns in the extinguishing process.

In the compressed-air breaker a somewhat more moderate accelerating force with the longer contact follow will produce the same contact speed at parting and, while the arc is maintained on the contacts, interruption may be allowed to occur at a shorter contact gap since the presence of blast air increases the dielectric strength of the gap. This increase in dielectric strength of the contact gap reduces the possibility of arc re-establishment on voltage restoration. As a further advantage the decelerating force may be applied earlier in the opening stroke, bringing the contact to rest more easily and reducing stresses on the mechanism.

Table I shows the results of a single series of interrupting tests made in the high-power laboratory with a compressed-air high-speed breaker. Power was obtained from two 60,000-kva generators operating in parallel at 11,000 volts, 25 cycles. Current values were limited by the station reactors. The tests were made phase to phase, ungrounded, this circuit having recovery rates varying with the currents interrupted from 500 to 810 volts per microsecond, giving an interrupting condition somewhat more severe than the bonded-rail return circuit in railway service. The shunt tripping magnet of the breaker was energized by a high-speed relay actuated in turn by the bushing-type current transformers supplied as a part of the breaker.

Figure 6A shows the interrupting performance of the breaker at moderate short-circuit-current values, 14,800 amperes, on a rather highly asymmetrical wave. On this test the contacts parted just at or slightly before the end of the first loop but had not reached a gap sufficient for interruption, and current continued to flow through the second loop, completing interruption in one full cycle. Because of the offset wave, this cycle, measured on the zero line, actually required 0.041 second to complete. Voltage disturbance at the final zero was quite limited. The tripping coil was energized in approximately 0.006 second after the start of flow of short-circuit current and remained energized for about one cycle, being interrupted by a mechanically operated cutout contactor during the opening stroke of the breaker. Blast air continued for 1.5 cycles after interruption, thus insuring complete deionization of the arc path.

In order to insure that the breaker has reserve rupturing ability beyond its current rating of 65,000 amperes, interrupting tests were made with short-circuit currents up to 20 per cent above this rating. Figure 6B shows its performance when interrupting 79,500 amperes. The magnetic effect of the current loop through the breaker increased the speed of contact travel on this test, and parting occurred sufficiently early to permit interruption at the first current zero, resulting in a single loop of short-circuit current of 0.031-second duration. No voltage disturbance accompanied the interruption. The oscillographic record of blast air shows some effect of the pressure of arc gases in a single peak during the period immediately preceding interruption, but the rapid drop from this peak at the current zero shows how completely these gases were scavenged before current could flow in the reverse direction.

The cathode-ray record, Figure 7, shows the voltage condition accompanying the interruption of 41,000 amperes on one of these tests. The circuit-recovery rate was 810 volts per microsecond with a frequency of 12,500 cycles. This is not a particularly high recovery rate from the viewpoint of switching experience on 60-cycle utility and industrial-distribution circuits, but it is believed to be appreciably higher than any to be encountered in 25-cycle contact-line-feeder circuits. It will be noted that the first peak of recovery voltage is only slightly above normal restored voltage, whereas the high-frequency oscillations are damped out into natural frequency after approximately 0.003 second. On no test did the first peak of recovery voltage reach a value of twice normal voltage.

Air-compressing equipment for a supply of air to these breakers is installed in a separate housing designed for mounting on any foundation for the breakers.

Figure 5. Air-compressing equipment

Motor-driven compressors, automatic-control, cooling coils, and storage reservoirs are assembled in a compact unit

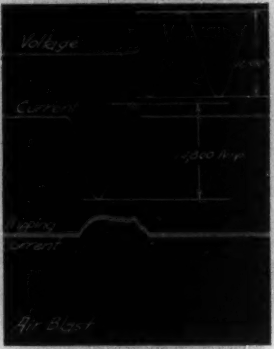

A. Interrupting 14,800 amperes

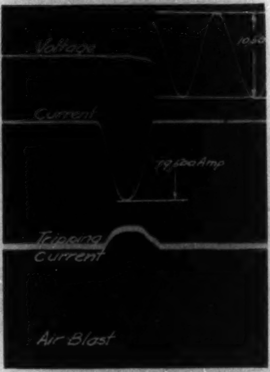

B. Interrupting 79,500 amperes

Figure 6. Oscillographic records of high-speed compressed-air-breaker tests

The air-supply unit shown in Figure 5 is designed for installations of one or two breakers where there is little prospect of future additions. This unit is equipped with two belt-driven two-stage air-cooled compressors, each with a delivery of approximately 4.4 cubic feet per minute of free air, permitting use of one compressor for service while the other is out for inspection or maintenance. Normally both compressors are running. For a larger bank of breakers requiring two or more supply units, a single compressor per unit with a higher delivery rating is recommended.

Normal operating pressure for air-storage reservoirs in the supply unit is 250 pounds per square inch, a reducing feed valve automatically maintaining a working pressure of 150 pounds per square inch in the air-delivery system to the circuit-breaker reservoirs. Compressors and motors with their control are located in an enclosed portion of the housing with double walls, supplied with space heaters to insure that they will be operative under the most severe temperature conditions. The storage reservoirs are located in an open portion of the housing, protected only by expanded metal panels. Air intakes for the compressors are carried to the outside of the enclosure.

Operation of the air-supply unit is controlled automatically by a pressure governor set to cut off the compressor motor when storage pressure reaches 250 pounds per square inch, and to cut it in again when pressure has been reduced to some predetermined lower value. An additional pressure switch is set to operate an alarm if pressure becomes reduced to a point requiring attention of an attendant.

Special care has been taken in the design of the air-supply unit to reduce the moisture content of the air before it is delivered to the circuit breakers. In addition to an intercooler between stages of compression, air from the discharge valve of the high-compression cylinder of the compressor passes through an aftercooler of finned copper tubing to the first storage reservoir, whence it passes through a second aftercooler to the second storage reservoir, carrying the outlet to the air-delivery system. Both reservoirs operate at a normal pressure of 250 pounds per square inch.

These coolers are designed to reduce the air from its high temperature on leaving the compressor to ambient temperature at the outlet to the delivery lines, condensing the vapor content of the air in the process and depositing it in the storage reservoirs where provision is made for its drainage. Since the storage reservoirs themselves are exposed to ambient temperature, little or no further condensation takes place after the air leaves the supply unit, and adequately dry air for circuit breaker operation is assured.

For other railway service, not requiring high-speed interruption, such as generator or transformer breakers in powerhouse or substation duty, conventional-speed indoor breakers are available for operating voltages from 11,000 to 33,000 in three-pole (three-phase) or two-pole (single-phase) form for interrupting duty from 500,000 kva upward. These breakers, normally designed for eight-cycle interruption on a 60-cycle basis, may be expected to complete interruption in three cycles after a tripping impulse when applied in 25-cycle service. Following conventional powerhouse practice, compressed air is used in these breakers for both closing and opening breaker operations, air being admitted on either side of the main operating piston as desired.

Table I. A Series of Interrupting Tests With a High-Speed Compressed-Air Circuit Breaker

11,000 Volts, 25 Cycles, Single Phase

Test No.	Initial Voltage, Kv	Current Interrupted, Amperes	Duration of Short Circuit, Seconds	Restored Voltage, Kv
1	11.0	14,900	0.042	11.2
2	11.0	14,700	0.043	11.2
3	11.0	14,650	0.044	11.2
4	11.0	18,900	0.041	11.1
5	11.0	19,300	0.040	11.2
6	11.0	18,800	0.041	11.3
7	11.0	30,600	0.033	11.1
8	11.0	30,600	0.033	11.1
9	11.0	30,400	0.033	11.1
10	11.0	44,000	0.033	11.1
11	11.0	43,400	0.031	10.8
12	11.0	44,000	0.033	10.8
13	11.0	44,600	0.031	10.85
14	11.0	58,000	0.031	10.7
15	11.0	57,800	0.029	10.7
16	11.0	56,500	0.030	10.5
17	11.0	68,500	0.034	10.4
18	11.0	67,000	0.032	10.5
19	11.0	68,500	0.031	10.5
20	11.0	78,000	0.029	10.4
21	11.0	80,000	0.030	10.5
22	11.0	79,500	0.031	10.5

Conclusions

The use of compressed-air circuit breakers in powerhouse and substation duty has advanced sufficiently far in the United States to assure its reliability for service. The extension of this interrupting medium to high-speed equipment for protection of contact line feeders in 12,000-volt 25-cycle single-phase railway service has now been accomplished, and its ability to meet reliably the specified time requirements for this service has been demonstrated by full-scale tests.

References

1. OPERATING EXPERIENCE WITH HIGH-SPEED OIL CIRCUIT BREAKERS, B. F. Bardo. AIEE TRANSACTIONS, volume 47, 1928, pages 1293–6.

2. HIGH-SPEED CIRCUIT BREAKERS, J. W. McNairy. AIEE TRANSACTIONS, volume 47, 1928, pages 1276–84.

3. HIGH-SPEED CIRCUIT BREAKERS FOR RAILWAY ELECTRIFICATION, H. M. Wilcox. AIEE TRANSACTIONS, volume 47, 1928, pages 1285–92.

4. ARRANGEMENT OF FEEDERS AND EQUIPMENT FOR ELECTRIC RAILWAYS, R. B. Morton. AIEE TRANSACTIONS, volume 47, 1928, pages 1297–1301.

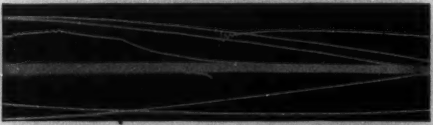

Figure 7. Typical cathode-ray oscillogram of test with compressed-air high-speed breaker

Rectifier Fault Currents

C. C. HERSKIND
MEMBER AIEE

H. L. KELLOGG
ASSOCIATE AIEE

CURRENTS in excess of normal, or fault currents, flow in rectifier circuits under conditions of arc-back or d-c short circuit. In normal service, faults are imposed on rectifiers by both the arc-backs that occur in the rectifier itself and the short circuits that occur in the external d-c system. Rectifier units must, therefore, include suitable protective switchgear to limit the magnitude and duration of the fault currents in order to

1. Prevent damage to the rectifier, transformer, and other parts.
2. Limit the disturbance on the a-c and d-c systems.

The determination of the fault currents in power rectifiers is essential to the design of rectifier and transformer equipment capable of withstanding the short-circuit forces, the selection of suitable protective switchgear, and the setting of relay and breaker trip mechanisms.

A wide variety of circuit combinations may be obtained under fault conditions, and many are of such complexity that accurate calculation of the instantaneous fault currents is difficult, if not impracticable. However, a complete determination of the instantaneous fault currents under all the possible conditions is not essential. Sufficient information for the design and application of rectifier equipment may usually be obtained from maximum values of the instantaneous and sustained currents.

This paper presents fault-current analyses for the widely used delta double-wye connection. The methods are also applicable to other connections. Three basic types of rectifier faults are considered in the analyses. Most rectifier faults can be resolved into one of these types, which are:

1. D-c short circuit.
2. Arc-back in a wye.
3. Arc-back with d-c feed.

Power rectifiers of the single-way type usually employ a rectifier transformer having interlaced secondary windings. Windings on the same leg of the transformer core are interlaced to obtain minimum losses and optimum reactance relationships. Various types of construction may be used; for example, two windings may be interlaced by winding the two coil conductors side by side in a single structure, by alternating pancake coils in a stack, or by alternating concentric coils. Many modifications are possible which meet the essential requirement that the current sheaths produced by the interlaced coils occupy essentially the same space distribution with respect to the primary so that they have common leakage-flux paths.

The usual rectifier circuit has negligible reactance in the transformer secondary circuit as the transformer secondary windings are interlaced, the anode leads are generally short, and anode reactors of appreciable reactance are seldom used. Under these conditions, all the circuit reactance may be considered to be located in the transformer primary and supply line.

The short-circuit analysis which follows treats the general case with primary reactance. The special case where all the reactance is located in the secondary leads has been treated in previous analyses.[1]

D-C Short Circuit

SUSTAINED D-C SHORT-CIRCUIT CURRENT

A typical double-wye rectifier circuit is shown in Figure 1a and the usual transformer construction is indicated in Figure 1b. When such a rectifier is short-circuited at its d-c terminals the fault currents have the characteristic forms shown in Figure 2.

The transformer secondary currents (per phase) on sustained d-c short circuit are the same as on a-c short-circuit impedance test when all the reactance is located in the transformer primary and supply line. Under these conditions each rectifying element carries a current wave of sinusoidal form and 180 degrees duration, one of the two secondary coils on each phase carrying the positive half cycle of current, while the other carries the negative half cycle. The a-c short-circuit current may be calculated as for a standard power transformer, and the sustained d-c short-circuit current is obtained by changing rms to average values.

The rms short-circuit current, I_s', per pair of interlaced secondary coils on each phase is

$$I_s' = \frac{E_s}{X} \tag{1}$$

where

E_s = transformer secondary line-to-neutral voltage in rms volts
X = reactance per phase in ohms line to neutral

The average d-c short-circuit current in amperes, I_{sc}, obtained by averaging the current for the three phases is

$$I_{sc} = 3\frac{2\sqrt{2}}{\pi} I_s' \tag{2}$$

The ohmic reactance, X, may be expressed in terms of the per unit transformer reactance, $\underline{X}$, referred to the volt-ampere base, VA.

$$X = \frac{3E_s^2}{VA} \underline{X} \tag{3}$$

When the necessary substitutions in equation 2 are made,

$$I_{sc} = \frac{2\sqrt{2}}{\pi} \frac{VA}{E_s} \frac{1}{\underline{X}} \tag{4}$$

In calculating the sustained short-circuit current the reactance of the a-c supply $\underline{X}_L$ may be added directly to that of the transformer $\underline{X}_T$ to obtain the total reactance, that is, $\underline{X} = \underline{X}_T + \underline{X}_L$.

The resistance of the transformer windings is generally small in comparison with their reactance and does not alter the circuit action appreciably. The effect of resistance of the transformer windings therefore may be included readily in the short-circuit calculations by substituting the impedance for the reactance in equation 4. If $\underline{R}$ is the per unit resistance per phase, the per unit impedance is

$$\sqrt{\underline{R}^2 + \underline{X}^2}$$

An approximate correction for the effect of arc drop may be made by assuming that the arc drop during short circuit is a sinusoidal voltage of constant rms value, E_b, which is in phase with the current and subtracts from the applied voltage. The voltage relations are then as shown in the vector diagram in Figure 3 and the net voltage acting in the circuit is E_s'. The short-circuit current is reduced in the

---

Paper 45-51, recommended by the AIEE committees on electronics and protective devices for presentation at the AIEE winter technical meeting, New York, N. Y., January 22-26, 1945. Manuscript submitted November 25, 1944; made available for printing December 19, 1944.

C. C. Herskind is electrical engineer and H. L. Kellogg is student engineer, both in the power rectifier department, General Electric Company, Schenectady, N. Y.

---

5. Discussion by H. C. Graves of papers on Electrified Railways. AIEE Transactions, volume 47, 1928, pages 1311-13.

6. The Pennsylvania Railroad Electrification, J. V. B. Duer. AIEE Transactions, volume 50, 1931, pages 101-05.

7. Design and Test of High-Speed High-Interrupting-Capacity Railway Circuit Breaker, W. F. Skeats. AIEE Transactions, volume 57, 1938, July section, pages 359-63.

8. An Electrified-Railway Substation of the Pennsylvania Railroad, J. V. B. Duer. AIEE Transactions, volume 48, 1929, pages 1147-9.

9. A 2,500,000-Kva Compressed-Air Powerhouse Breaker, L. R. Ludwig, H. M. Wilcox, B. P. Baker. AIEE Transactions, volume 61, 1942, May section, pages 235-41.

ratio E_s'/E_s because of the arc drop. The solution for this ratio is

$$\frac{E_s'}{E_s}=\sqrt{1-\left(\frac{E_b}{E_s}\frac{\underline{X}}{\sqrt{\underline{R}^2+\underline{X}^2}}\right)^2}-\frac{E_b}{E_s}\frac{\underline{R}}{\sqrt{\underline{R}^2+\underline{X}^2}} \tag{5}$$

The final expression for the sustained d-c short-circuit current including the effect of resistance and arc drop is then

$$I_{sc}=\frac{2\sqrt{2}}{\pi}\frac{VA}{E_s\sqrt{\underline{R}^2+\underline{X}^2}}\frac{E_s'}{E_s} \tag{6}$$

If the volt-ampere base, VA, is equal to the rated input volt-amperes of the double-wye rectifier transformer with theoretical current wave shape, that is,

$$VA=\frac{\pi}{3}E_{do}I_{dn}=\frac{\sqrt{3}}{\sqrt{2}}E_sI_{dn} \tag{7}$$

where

E_{do} = theoretical direct voltage
I_{dn} = direct current at rated output

The expression for sustained short-circuit direct current may be written:

$$I_{sc}=\frac{2\sqrt{3}}{\pi}\cdot\frac{I_{dn}}{\sqrt{\underline{R}^2+\underline{X}^2}}\cdot\frac{E_s'}{E_s} \tag{8}$$

Equation 8 holds only for the double-wye circuit, but equation 6, which is expressed in terms of volt-amperes, applies to any single-way circuit with a three-phase supply. For a double-way circuit, I_{sc} will be equal to one-half the value given by equation 6.

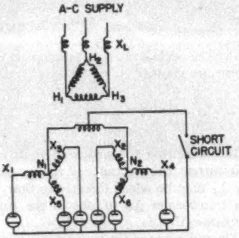

(a)—Circuit diagram

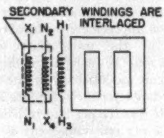

(b)—Transformer construction

Figure 1. Double-wye rectifier

Rate of Rise of D-C Short-Circuit Current

The rate of rise of d-c short-circuit current immediately following the time of fault depends on: the number of phases feeding into the fault, the inductance L of each phase, the inductance L_0 of the fault path, and the arc drop E_a of the rectifying elements. The maximum rate of rise for a double-wye rectifier is obtained when three phases, 60 degrees apart, conduct. The crest value of the average voltage of the three phases in parallel is equal to $(2\sqrt{2}/3)E_s-E_a$. If this voltage is impressed on the rectifier inductance $L/3$ and the fault path inductance, the maximum rate of rise is obtained.

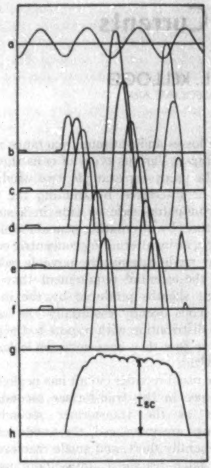

Figure 2. D-c short-circuit oscillogram

(a)—Timing wave
(b) to *(g)*—Anode currents
(h)—Short-circuit current

$$\left(\frac{di}{dt}\right)_{\max}=\frac{(2\sqrt{2}/3)E_s-E_a}{(L/3)+L_0} \tag{9}$$

In system studies involving short-circuit conditions it is often helpful to represent a rectifier unit by a simple machine having equivalent voltage, inductance, and resistance such that its action approximates the average behavior of the rectifier. While the rectifier circuit action does not remain the same throughout the range of operation from normal load to short circuit, representative values for the equivalent voltage, inductance, and resistance may be selected on the following basis:

The output voltage of a double-wye rectifier at no load is

$$E_{do}=\frac{3\sqrt{3}}{\pi\sqrt{2}}E_s=1.17E_s \tag{10}$$

and is obtained with an anode conduction period of 120 degrees. The conduction period increases with load, very rapidly at first and more slowly as short-circuit conditions are approached. Under sustained d-c short circuit the anode conduction period is 180 degrees and the average voltage is

$$E_{do}'=\frac{2\sqrt{2}}{\pi}E_s=0.90E_s \tag{11}$$

This voltage does not appear at the rectifier terminals, but is the internal electromotive force of the rectifier. Under conditions approaching short circuit the anode conduction period is nearly 180 degrees and the equivalent voltage of the rectifier unit may therefore be assumed to be 0.90 E_s.

Since two anodes are normally conductive in a double-wye rectifier at light load, the equivalent inductance of the rectifier unit is $L/2$. Under sustained d-c short circuit three anodes are normally conductive. However, at any instant one secondary wye has one anode conductive while the other secondary wye has two anodes conductive. The interphase transformer tends to maintain parallel operation between these two dissimilar circuits as at light load. It has been found that good agreement between calculated and tested values of rate of rise of current on d-c short circuit is obtained if the equivalent inductance of the rectifier unit under transient conditions is assumed to be $L/2$. Similarly, the equivalent resistance may be assumed to be $R/2$.

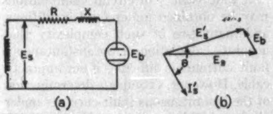

Figure 3. Arc-drop correction for sustained d-c short circuit

(a)—Circuit diagram
(b)—Vector diagram

Using the foregoing empirical relations, the rate of rise of short-circuit current of the equivalent unit is

$$\frac{di}{dt}=\frac{0.90E_s-E_a}{(L/2)+L_0} \tag{12}$$

This formula is used to determine the calculated values of the rate of rise of short-circuit direct current referred to in the section on comparison of calculated and test results.

Arc-Back in a Wye

The fault conditions covered by this case are obtained when an arc-back occurs on a single-wye rectifier operating with d-c circuit open or connected to a pure resistance load and is sustained after steady-state conditions are reached. The fault circuit is shown in Figure 4a.

The arc-back current under steady-state conditions in a delta double-wye rectifier without d-c feed arises principally from the other two anodes in the same wye as the faulty anode. The cur-

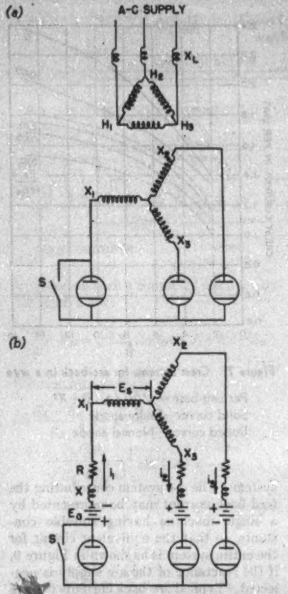

Figure 4 (left). Arc-back in a wye

(a)—Circuit diagram

(b)—Equivalent circuit

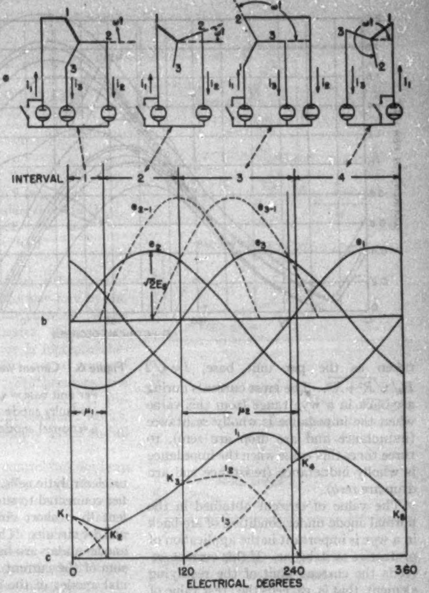

Figure 5 (right). Arc-back in a wye

(a)—Circuit diagrams

(b)—Voltages

(c)—Currents

rent contribution of the anodes on the other wye is limited to a low value by the impedance of the interphase transformer and the interlacing of the two secondary coils of each phase of the rectifier transformer.[3] Another factor in limiting this contribution is the long conduction period of the anodes of the faulted wye. The analysis of arc-back current when there is no d-c feed, therefore, reduces to an analysis of the current in a single wye with one anode arcing back and two normal anodes. The equivalent circuit is shown in Figure 4b.

In the equivalent circuit the open-circuit voltages of the three phases of the wye are assumed to be sinusoidal voltages 120 degrees apart having maximum values equal to $\sqrt{2}\,E_s$. Each phase of the transformer is assumed to have an inductance L and a resistance R and each rectifying element to have a constant arc drop E_a, which may be represented by a counter electromotive force.

Each cycle may be divided into four intervals having different combinations of conducting phases. The vector relations and circuit arrangement for each of these intervals are shown in Figure 5a, where the cycle is assumed to start at a time such that the open-circuit secondary voltages are

$$\left.\begin{aligned} e_1&=\sqrt{2}E_s \sin\left(\omega t+\frac{2\pi}{3}\right)\\ e_2&=\sqrt{2}E_s \sin \omega t\\ e_3&=\sqrt{2}E_s \sin\left(\omega t-\frac{2\pi}{3}\right)\end{aligned}\right\} \tag{13}$$

The secondary voltages on open circuit and the secondary currents under arc-back are shown in Figures 5b and 5c, respectively, where i_1 is the instantaneous current in the faulted phase and i_2 and i_3 are the currents in the two normal phases.

The instantaneous current during each interval may be calculated by the application of Kirchhoff's laws to the network and the solution of the resulting differential equations.

If the cycle is assumed to start when the voltage e_2 is equal to zero, the following relations may be written for the first interval:

$$e_3-e_1-L\left(\frac{di_3}{dt}+\frac{di_1}{dt}\right)-R(i_3+i_1)-2E_a=0 \tag{14}$$

and

$$e_2-e_1-L\left(\frac{di_2}{dt}+\frac{di_1}{dt}\right)-R(i_2+i_1)-2E_a=0 \tag{15}$$

as

$$e_1+e_2+e_3=0$$

and

$$i_1=i_2+i_3$$

By substitution

$$\frac{di_1}{dt}+\frac{R}{L}i_1=\frac{\sqrt{2}E_s}{L}\sin\left(\omega t-\frac{\pi}{3}\right)-\frac{4}{3}\frac{E_a}{L} \tag{16}$$

whose solution is

$$i_1=\frac{\sqrt{2}E_s}{\sqrt{R^2+L^2\omega^2}}\left[\sin\left(\omega t-\frac{\pi}{3}-\gamma\right)+\epsilon^{-\frac{Rt}{L}}\sin\left(\frac{\pi}{3}+\gamma\right)\right]-\frac{4}{3}\frac{E_a}{R}\times\left[1-\epsilon^{-\frac{Rt}{L}}\right]+K_1\epsilon^{-\frac{Rt}{L}} \tag{17}$$

where

$$\gamma=\tan^{-1}\frac{L\omega}{R}$$

Similar expressions may be derived for the current during each interval. The current equations for all four intervals are summarized in the appendix.

In order to determine the crest value of the current in both the faulty and the normal phases under steady-state conditions it is necessary to construct the current waves. The construction of the current waves may be made by choosing values of the ratios X/R and $E_a/\sqrt{2}E_s$, assuming a value for the initial current, K_1, and making successive trial solutions of the equations until the condition $K_1=K_5$ is satisfied. Figure 6 shows the fault-current waves calculated from the above equations when $E_a/\sqrt{2}E_s=0.05$.

The crest values of the fault currents under steady-state conditions are plotted as a function of X/R on Figure 7 for $E_a/\sqrt{2}E_s=0$, 0.05, and 0.10. The crest current obtained with the three terminals of the wye short-circuited directly is

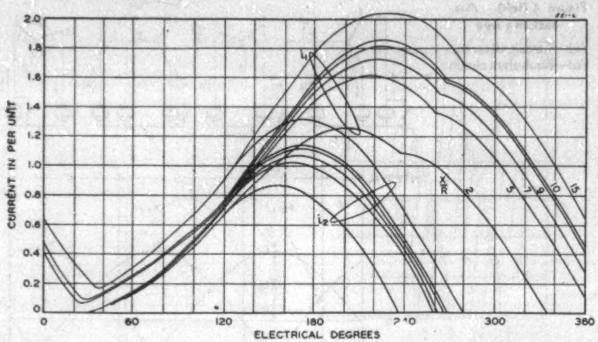

Figure 6. Current waves for arc-back in a wye

Per unit base $= \sqrt{2}E_s/\sqrt{R^2+X^2}$
i_1 = faulty anode current
i_2 = normal anode current

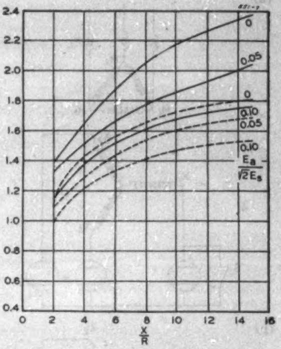

Figure 7. Crest currents for arc-back in a wye

Per unit base $= \sqrt{2}E_s/\sqrt{R^2+X^2}$
Solid curves—Faulty anode
Dotted curves—Normal anode

taken as the per unit base, $I = \sqrt{2} E_s/\sqrt{R^2+X^2}$. The crest currents during arc-back in a wye range from this value when the impedance is wholly resistance (inductance and arc drop are zero), to three times this value when the impedance is wholly inductance (resistance and arc drop are zero).

The value of current obtained in the normal anode under condition of arc-back in a wye is important in the application of protective switchgear. If this current exceeds the current limit of the rectifying element, that is, exceeds the crest value of current which the rectifying element can carry without arc-back during the succeeding inverse period, simultaneous arc-backs will be obtained on several anodes. Under such conditions, the benefits accruing from the use of selective individual anode breakers would be largely lost and excessive duty would be incurred on the rectifier equipment.

Arc-Back With D-C Feed

In many applications rectifiers are arranged to operate in parallel with other converting equipment, such as d-c generators, synchronous converters, or other rectifiers; or to supply power to counter-electromotive-force loads, such as motors or electrolytic cells. Arc-back in a rectifier connected to such a system is equivalent to a short circuit on both the a-c and d-c circuits. The current in the faulty anode under arc-back conditions is the sum of the current delivered by the normal anodes of the rectifier and the current feedback from the d-c system.

A typical rectifier installation with several double-wye-connected rectifiers operating in parallel is shown in Figure 8. Under arc-back conditions with the usual circuit constants the two normal anodes on the same wye with the faulted anode, are the only ones in the rectifier delivering appreciable current into the faulted anode as the current from the anodes connected to the other wye is limited by the impedance of the interphase transformer and the effect of the interlacing of transformer windings.[2] The d-c feed-back current is supplied by the normal rectifiers connected in parallel with the rectifier which is arcing back, together with the other converting equipment and counter-electromotive force-load connected to the d-c system. The d-c system contributing the feed-back current may be represented by a single machine having suitable constants, so that the equivalent circuit for the entire system is as shown in Figure 9, if the reactance of the a-c supply is neglected. Typical arc-back currents flowing in such a circuit are indicated in Figure 10.

Where several rectifiers operate in parallel on a common bus the current in the faulty anode during arc-back is substantially equal to the feed-back current, as the inductance of the equivalent machine supplying the feed-back current is low in comparison with the inductance of the winding connected to the faulted anode and the current contribution from the normal anodes on the same wye may be neglected. If the current contribution from the normal anodes on the same wye is neglected, the system may be represented by a series circuit with a direct voltage E_d', an alternating voltage $\sqrt{2}\ E_s \sin(\omega t+\beta)$, an arc drop E_a, a total inductance L_d, and a total resistance R_d as shown in Figure 11. The formulas which follow

Table I. Comparison of Calculated Versus Test Values of Rectifier Fault Currents

Rectifier Rating		Circuit Constants				D-C Short Circuit				Arc-Back in a Wye		Arc-Back With D-C Feed			
						Sustained Amp		Rate of Rise Amp Per μsec		Faulty Anode Crest Amp		Amp at One-Half Cycle		Rate of Rise Amp Per μsec	
Kw	Volts	Transformer Kva	X	R	E_s	Calc	Test	Calc	Test	Calc	Test	Calc	Test	Calc	Test
150	240	184	0.126	0.027	240	5,200	4,720	0.99	1.23						
1,500	3,000	1,590	0.073	0.008	2,640	7,260	7,100*	1.78	2.18*	6,060	7,100†§				
3,000	3,000	3,210	0.082	0.005	2,366	14,700	11,800	1.44	1.53	14,300	10,600†				
1,675	515	1,685	0.037	0.008	568	65,000	47,000	11.4	8.6						
1,675	515	1,925	0.071	0.006	500	47,000	43,900**	8.65	7.15**	41,600	41,300	62,000	46,000‡	10.0	8.42‡
3,250	650	7,500	0.115	0.006	612							83,200	54,200	11.8	8.18
3,250	650	7,500	0.079	0.006	612							92,700	79,400∥	14.2	14.2∥

* Figure 12.

** Figure 2.

§ See Figure 13.

† Includes contribution of all normal anodes.

‡ Feed-back current in cathode.

∥ Figure 14.

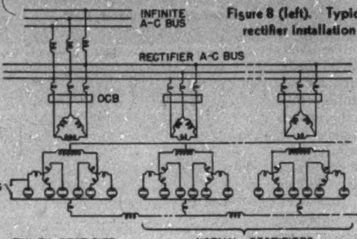

Figure 8 (left). Typical rectifier installation

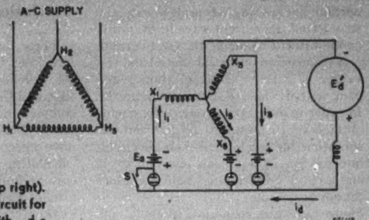

Figure 9 (top right). Equivalent circuit for arc-back with d-c feed

are based on such a simplified circuit. By Kirchhoff's law:

$$L_d\frac{di}{dt}+R_di=\sqrt{2}E_s\sin(\omega t+\beta)+E_d'-E_a \tag{18}$$

Solution for i yields

$$i=\frac{E_d'-E_a}{R_d}\left[1-\epsilon^{-\frac{R_d}{L_d}t}\right]+\frac{\sqrt{2}E_s}{\sqrt{R_d^2+L_d^2\omega^2}}\left[\sin(\omega t+\beta-\gamma)-\epsilon^{-\frac{R_d}{L_d}t}\sin(\beta-\gamma)\right] \tag{19}$$

where

$$\gamma=\tan^{-1}\frac{L_d\omega}{R_d}$$

In these formulas, the angle β is the phase angle of the line-to-neutral voltage of the faulty phase at the time of arc-back.

Maximum fault currents are obtained when the arc-back occurs immediately following conduction. As most double-wye rectifiers operating without phase control have an angle of overlap between 20 and 25 degrees at rated load, β will have negative values of five to ten degrees. However, in determining maximum fault currents no appreciable error will be incurred by assuming $\beta=0$.

Comparison of Calculated and Test Results

In order to check the validity of the assumptions made in the derivation of the foregoing formulas and determine the accuracy with which fault currents may be calculated by these formulas, a number of comparisons between tests and calculated values have been made. The results of these checks are shown in Table I. Typical oscillograms showing fault current obtained under a number of the conditions are shown in Figures 2, 12, 13, and 14.

With reference to the results given in Table I, the fault currents obtained in test are generally lower than the calculated values. One reason for this is that the reactance and resistance of the interphase transformer, anode leads, d-c bus bars, and the short-circuiting loop are neglected in most calculations as these quantities are difficult to determine and are usually small. Another is the effect of saturation of the transformer core by the d-c components of fault current. When the transformer saturates, the voltage drop in the supply line is increased because of the high exciting current required by the transformer. Furthermore, the actual supply-system reactance is frequently higher than the assumed values, as such values are generally based on full generating capacity.

The effect of phase control has not been considered in these analyses as the most severe fault currents are obtained when operating with no phase control. The effect of phase control depends upon the kind of rectifier excitation employed and the part of the cycle during which it permits the start of anode conduction, as the voltage across the rectifying element is shifted in phase under fault conditions.

The effects of arc-drop must be included in the calculation of fault currents if accurate results are desired, particularly for rectifiers at 600 and 250 volts. The value of the arc-drop under fault conditions depends upon the type of rectifying element employed and the magnitude of the fault current.

An average arc drop of 100 volts has been assumed in the calculations for the 600- and 3,000-volt rectifiers given in Table I, and an average arc drop of 50 volts for the 250-volt rectifier.

Typical d-c short-circuit currents are shown in Figures 2 and 12. Both these oscillograms show an initial transient current exceeding the sustained value. The effect is particularly pronounced in Figure 12. This high initial fault current is caused by a displacement of the transformer currents similar to that obtained on three-phase a-c short-circuit tests.

A typical oscillogram of the current in the faulty anode during arc-back in a wye is shown in Figure 13. This test was made on a six-anode rectifier and the fault current therefore includes the contribution of all five normal anodes. The current wave form should be compared with the calculated waves shown in Figure 6.

With five normal anodes feeding into the faulty anode, some current will flow through the interphase as the fault is maintained. The effect of this current is to lower the current contribution of the

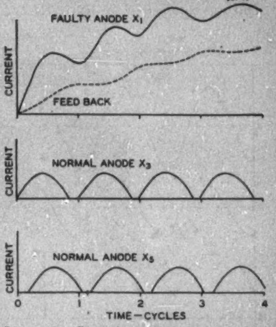

Figure 10. Typical current waves for arc-back with d-c feed

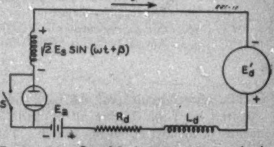

Figure 11. Simplified circuit for arc-back with d-c feed

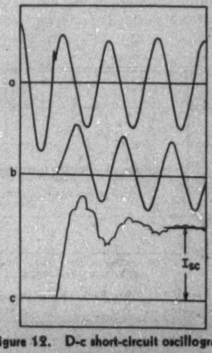

Figure 12. D-c short-circuit oscillogram

(a)—A-c supply voltage
(b)—A-c supply current
(c)—Short-circuit current

normal anodes in the faulty wye and smooth out the current wave in the faulty anode without changing the crest current.

A comparison of the calculated and test values of current obtained during arc-back with d-c feed is shown in Figure 14. In order to avoid the severe overcurrents obtained with sustained feed under this condition, the anode breakers begin circuit interruption in less than one half cycle and a check on ultimate sustained values cannot be obtained. In the case shown in Figure 14 some reduction in fault current was obtained in one half cycle.

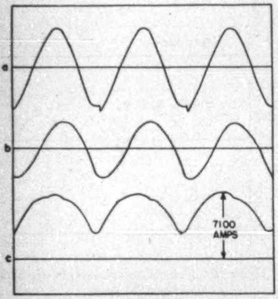

Figure 13. Arc-back in a wye oscillogram

(a)—A-c supply voltage
(b)—A-c supply current
(c)—Arc-back current

The short-circuit and arc-back tests covered by Table I were all applied by means of a short-circuiting switch. The current values obtained during arc-back with d-c feed are therefore higher than would be obtained under actual arc-back conditions because of the absence of the arc drop of the faulty rectifying element.

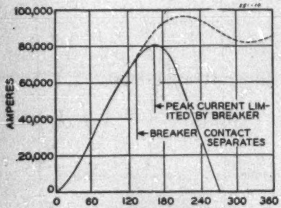

Figure 14. Arc-back with d-c feed

Solid curve—Measured current
Dotted curve—Calculated current

Conclusions

Three basic types of rectifier faults have been treated in the foregoing analyses. While other arrangements are possible and the analyses do not suffice for the complete determination of fault currents under all conditions, the formulas which have been derived provide a means for calculating the maximum values of fault current under certain limiting conditions usually encountered in service. Inasmuch as the duty on the rectifier, transformer, and switchgear depends in large measure upon the maximum current, the determination of the instantaneous current throughout the duration of the fault is usually not essential. The expressions for fault current which have been derived are based on a number of assumptions and are therefore only approximate. However, they afford a better understanding of the circuit action during faults and provide means for predicting fault-current magnitudes with greater accuracy than heretofore has been possible.

Appendix I. Symbols

I_{sc} = sustained d-c short-circuit current in average amperes
I_{dn} = rated direct current of rectifier in average amperes
E_s = transformer-secondary line-to-neutral voltage in rms volts
E_{do} = theoretical direct voltage in average volts, assuming no overlap, no phase control, and zero arc drop
E_d' = open-circuit voltage of the equivalent d-c machine
E_a = average arc drop, in volts
E_b = sinusoidal voltage equal to the fundamental component of E_a, in rms volts
X = line-to-neutral reactance at the transformer-secondary terminals in ohms
$\underline{X}$ = per unit reactance
$L = X/\omega$
$\omega = 2\pi f$, where f = frequency of a-c supply
L_d = inductance of simplified circuit for arc-back with d-c feed in henrys
R = line-to-neutral resistance at the transformer secondary terminals in ohms
$\underline{R}$ = per unit resistance
R_d = resistance of simplified circuit for arc-back with d-c feed in ohms
VA = per unit volt-ampere base
K = current constant in amperes

Appendix II. Arc-Back in a Wye (Current Equations)

Let $X = L\omega$, $I = \sqrt{2}E_s/\sqrt{R^2+L^2\omega^2}$, and $\gamma = \tan^{-1}\frac{L\omega}{R}$.

Interval 0 to u_1 where $\theta_1 = \omega t$:

$$i_1 = I\left[\sin\left(\omega t - \frac{\pi}{3} - \gamma\right) + \epsilon^{-\frac{R\theta_1}{X}}\sin\left(\frac{\pi}{3}+\gamma\right) - \frac{4}{3}\frac{E_a}{\sqrt{2}E_s}\sqrt{1+\left(\frac{X}{R}\right)^2}\left(1-\epsilon^{-\frac{R\theta_1}{X}}\right) + K_1\epsilon^{-\frac{R\theta_1}{X}}\right] \quad (20)$$

and

$$i_2 = I\left[\sin\left(\omega t + \frac{\pi}{3} - \gamma\right) + \epsilon^{-\frac{R\theta_1}{X}}\sin\left(\frac{\pi}{3}-\gamma\right) - \frac{2}{3}\frac{E_a}{\sqrt{2}E_s}\sqrt{1+\left(\frac{X}{R}\right)^2}\left(1-\epsilon^{-\frac{R\theta_1}{X}}\right) + K_1\epsilon^{-\frac{R\theta_1}{X}}\right] \quad (21)$$

Interval u_1 to $\frac{2\pi}{3}$: where $\theta_2 = (\omega t - u_1)$:

$$i_1 = I\left[\frac{\sqrt{3}}{2}\sin\left(\omega t - \frac{\pi}{6} - \gamma\right) - \frac{\sqrt{3}}{2}\epsilon^{-\frac{R\theta_2}{X}}\sin\left(u_1 - \frac{\pi}{6} - \gamma\right) - \frac{E_a}{\sqrt{2}E_s}\sqrt{1+\left(\frac{X}{R}\right)^2}\left(1-\epsilon^{-\frac{R\theta_2}{X}}\right) + K_2\epsilon^{-\frac{R\theta_2}{X}}\right] \quad (22)$$

Interval $\frac{2\pi}{3}$ to $\left(\frac{2\pi}{3}+u_2\right)$ where $\theta_3 = \left(\omega t - \frac{2\pi}{3}\right)$:

$$i_1 = I\left[\sin\left(\omega t - \frac{\pi}{3} - \gamma\right) - \epsilon^{-\frac{R\theta_3}{X}}\sin\left(\frac{\pi}{3}-\gamma\right) - \frac{4}{3}\frac{E_a}{\sqrt{2}E_s}\sqrt{1+\left(\frac{X}{R}\right)^2}\left(1-\epsilon^{-\frac{R\theta_3}{X}}\right) + K_3\epsilon^{-\frac{R\theta_3}{X}}\right] \quad (23)$$

and

$$i_3 = I\left[\sin(\omega t - \gamma) - \epsilon^{-\frac{R\theta_3}{X}}\sin\left(\frac{2\pi}{3}-\gamma\right) - \frac{2}{3}\frac{E_a}{\sqrt{2}E_s}\sqrt{1+\left(\frac{X}{R}\right)^2}\left(1-\epsilon^{-\frac{R\theta_3}{X}}\right) + K_3\epsilon^{-\frac{R\theta_3}{X}}\right] \quad (24)$$

Interval $\left(\frac{2\pi}{3}+u_2\right)$ to 2π where

$$\theta_4 = \left(\omega t - \frac{2\pi}{3} - u_2\right):$$

$$i_1 = I\left[-\frac{\sqrt{3}}{2}\cos(\omega t - \gamma) + \frac{\sqrt{3}}{2}\epsilon^{-\frac{R\theta_4}{X}} \times \cos\left(\frac{2\pi}{3}+u_2-\gamma\right) - \frac{E_a}{\sqrt{2}E_s}\sqrt{1+\left(\frac{X}{R}\right)^2} \times \left(1-\epsilon^{-\frac{R\theta_4}{X}}\right) + K_4\epsilon^{-\frac{R\theta_4}{X}}\right] \quad (25)$$

References

1. MERCURY ARC POWER RECTIFIERS (book), O. K. Marti, H. Winograd, pages 66–80.

2. A NEW MULTIPLE HIGH-SPEED AIR CIRCUIT BREAKER FOR MERCURY-ARC-RECTIFIER ANODE CIRCUITS AND ITS RELATION TO THE ARC-BACK PROBLEM, J. W. Seaman, L. W. Morton. AIEE TRANSACTIONS, volume 61, 1942, November section, pages 788–96.

Dynamic Measurements on Electromagnetic Devices

E. L. NORTON
NONMEMBER AIEE

FOR the investigation of relays and similar electromagnetic apparatus, data giving the variation of current and flux as well as the motion of the armature during the operating cycle are of great value. The rapid-record oscillograph[1] has been used extensively for current measurements and, where a moderate accuracy is sufficient, is very satisfactory. Data on the flux also may be obtained by graphical integration of oscillographic data, but such a process is laborious and, unless great care is taken, is of doubtful accuracy. The development of a shadowgraph attachment[2] for the oscillograph provided a means of measuring armature motion at the same time and with the same order of accuracy as the current measurements.

The method to be described has been developed to take current-time, flux-time, displacement-time, and velocity-time data by point by point readings on a d-c microammeter. By careful design and operation of the apparatus, it is possible to measure current and flux with an accuracy determined chiefly by that of the ammeter which in the better-grade instruments is ±1/2 per cent of full scale. The accuracy of displacement and velocity measurements, which depend upon the use of a photoelectric cell and amplifier, is not as good but is still sufficient for most work and is probably better than other methods of comparable simplicity and ease of operation, such, for example, as high-speed motion pictures or the shadowgraph method.

Although intended primarily for dynamic measurements, the apparatus also provides a rapid, accurate, and sensitive method for obtaining other magnetic data, such as the magnetization curve, where the variation with time is not of interest. It is not suitable for measurements involving extremely slow changes in magnetism, but for apparatus similar to that used in the telephone plant, where such changes usually take place within a half second or less, it is entirely satisfactory.

Measurement of Flux With a Search Coil

The principle upon which all of the measurements are based may be understood from an explanation of the measurement of flux by the use of a search coil.

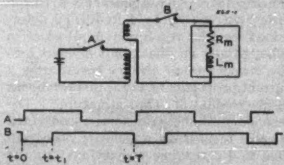

Figure 1. Circuit for the measurement of flux by a search coil

As in Figure 1, the relay or other structure is connected to the supply voltage through a contact known as the *A* contact. A search coil is connected to a d-c instrument through the *B* contact. Contact *A* is opened and closed with about 50 per cent make and break at such a rate that the flux in the relay has sufficient time to reach a substantially steady state during both the closed and the open intervals. Contact *B* operates in synchronism with contact *A*. It always opens just before the *A* contact closes at which point the flux has dropped to its minimum point, or substantially the residual value. The point of closure of the *B* contact may be adjusted to occur at any time during the cycle.

Let the flux linking the search coil of N turns at any time be Φ, The resistance of the search coil and wiring is R_c. Assume that the ammeter has a resistance R_m and inductance L_m the current flowing is then given by

$$N\frac{d\Phi}{dt}+L_m\frac{di}{dt}+(R_m+R_c)i=0 \tag{1}$$

The instrument will read the average value of current for the cycle. Let the period of the cycle be T and let the time of closing the B contact be t_1, measured from the time of the previous open period. The direct current read by the instrument will then be

$$\begin{aligned}I_0&=\frac{1}{T}\int_{t_1}^{T}idt\\&=-\frac{1}{(R_m+R_c)T}\int_{t_1}^{T}\frac{d}{dt}(N\Phi+L_mi)dt\\&=\frac{(N\Phi+L_mi)_{t_1}-(N\Phi+L_mi)_T}{(R_m+R_c)T}\end{aligned} \tag{2}$$

Now the product L_mi at t_1, when the B circuit is closed, must be zero. Furthermore, if the period T is long in comparison with the time of decay of the flux Φ and with the time constant L/R of the measuring circuit, the product L_mi is also negligible at $t=T$. We may write then

$$\Phi_{t_1}-\Phi_T=\frac{RTI_0}{N}\times10^8 \tag{3}$$

where R is now the total resistance of the measuring circuit. The factor 10^8 has been added to reduce the units to the common ones. The flux ΦT is the residual flux so that, if this is taken as a reference value, the value of the flux at the time of closing the B contact is simply

$$\Phi=\frac{RTI_0}{N}\times10^8 \tag{4}$$

There are available relatively rugged commercial instruments of the pivot type with 10-ohms resistance and a full-scale reading of 0.2×10^{-3} amperes. If then $T=0.1$, a full-scale deflection would be obtained for a value of $\Phi=2{,}000$ with a ten-turn search coil of negligible resistance. If more sensitive instruments of the suspension type be used or a lower value of T, the sensitivity may be increased still further. With commercial instruments and $T=0.1$ second, the method is being used for measurements with a sensitivity approximately 100 times as great as that of a fluxmeter of comparable ruggedness.

It may be objected that the flux in equation 1 is made up not only of the flux to be measured but also of a component due to the current in the measuring circuit. This is true, and the flux

---

Paper 45-65, recommended by the AIEE committee on instruments and measurements for presentation at the AIEE winter technical meeting, New York, N. Y., January 22-26, 1945. Manuscript submitted November 16, 1944; made available for printing December 26, 1944.

E. L. NORTON is engineer with the Bell Telephone Laboratories, Inc., New York, N. Y.

threading the search coil is different during the time the B contact is closed from what it would be without this circuit. Note, however, that we are not concerned with how the flux varies between times t_1 and T but only with its value at the limits. Since the flux at t_1 is that which has been established with the search-coil circuit open, the one requirement is that the constants be such that the current in the measuring circuit be substantially zero at the time T.

Measurement of Current

The instantaneous value of current is measured by connecting the primary of an air-core transformer in series with the circuit and connecting the secondary in place of the search coil. Under these conditions the instantaneous current at time t_1 is given by

$$i=\frac{RT}{M}I_0 \qquad (5)$$

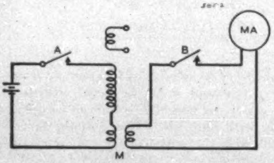

Figure 2. Circuit for the measurement of current

where M is the mutual inductance of the air-core coil and the other symbols have the same significance as before. The circuit is shown in Figure 2.

Measurement of Flux Using Bridge Circuit

In many cases, it is desired to measure the flux linkages in the magnetizing winding itself, either because the use of a search coil is inconvenient or because the data are desirable for other reasons. For such purposes, the circuit in Figure 3 is used. The relay or other device to be measured together with the primary of an air-core inductance, if current readings are also desired, is made one arm of a bridge which is balanced to direct current by closing both the A and B contacts and adjusting R_d for no deflection of the meter. If the contacts then are operated with the period T, the instrument will read a current I_0, and the flux turns of the relay at time t_1 will be

$$N\Phi\times10^8=R_mI_0T\times\left[1+K\left(1+\frac{R_o}{R_m}+\frac{R_d}{R_m}\right)\right]-L_1i \qquad (6)$$

where $N\Phi$ is the flux linkage of the winding, or N the number of turns and Φ the average flux per turn (the other quantities being indicated on the drawing). The term L_1i is a correction term, usually negligible, involving the self-inductance L_1 of the primary of the air-core coil and i the instantaneous current at time t_1; i is determined by a separate measurement as previously described. If its value be not needed, the air-core coil is omitted from the circuit.

If the bridge circuit be used to measure the flux during the decay part of the cycle, after A has opened, a slight error is introduced because of the presence of the shunt $(1+K)R_o$ across the circuit. To avoid this, the connections are modified for measurements on decay to that shown in Figure 4. When this circuit is used, B is never closed until A has opened. The resistance $K(R_o+R_m)$ is placed in series with the meter to make the expression for flux linkages the same as before.

Measurements have been made using the bridge method on apparatus having a flux of from less than one maxwell to over 50,000 maxwells and taking currents of from a fraction of a milliampere to over an ampere.

Measurement of Displacement and Velocity

An optical system is arranged such that the illumination falling on a photoelectric cell is proportional to the displacement of the armature. An amplifier effective from direct current up to a frequency determined by the resolution required with substantially no phase shift delivers into the primary of an air-core transformer a current proportional to the instantaneous displacement of the armature. The secondary of this transformer connected to the measuring apparatus then will give a d-c reading proportional to the armature displacement at the time the B contact closes.

If the amplifier be changed to one in which the output current is proportional to the rate of change of input voltage, or, in other words, to one in which the voltage gain is proportional to the frequency with a 90-degree phase shift, the instrument then will read a value proportional to the rate of change of displacement or to the instantaneous velocity. Under these conditions, the amplifier differentiates the input voltage once, the output transformer differentiates the second time, and the d-c instrument integrates once, leaving a net result of one differentiation.

Apparatus

Figure 5 shows the instrument designed to take the measurements described. In the center is the flux machine. It consists of a small synchronous motor with a gear-shift mechanism allowing a choice of five accurately held pulse rates varying from one to ten a second, the A and the B contacts with provision for accurately setting the time t_1 to any part of the cycle, a built-in bridge with the choice of a wide range of ratio arms, and a set of keys by which any of a number of test circuits may be quickly set up.

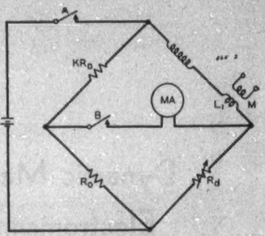

Figure 3. Bridge circuit for the measurement of flux linkages in a relay winding

In addition to applying an on-and-off battery condition, the instrument is designed to supply battery reversals to the apparatus under test. This is used in testing core materials to eliminate residual effects and for polar relays and similar structures.

The method used to control the time of closure of the B or meter circuit is adapted from the usual form of pulse machine.[3] As in Figure 6 two contacts are provided, each closed for 50 per cent of the cycle. One is fixed in phase and is set to open just before the A or battery circuit is closed. The second contact may be adjusted in phase through 360 degrees and may be connected either in parallel or series with the first. When the two contacts are exactly out of phase and in parallel, the circuit is closed at all times as illustrated in position 1. If the second contact now be shifted in phase to position 2, the contacts still being in parallel, the circuit will be closed for three-fourths of the time, and, if shifted to position 3, for half the time. The contacts then are connected in series. In position 4, the circuit still is closed for half the time. A further shift to position 5 gives closure for one-fourth of the cycle, and, finally, in position 6 a shift of 360 degrees from

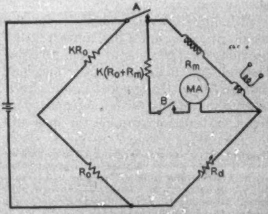

Figure 4. Modification of Figure 3 used to measure decay of flux

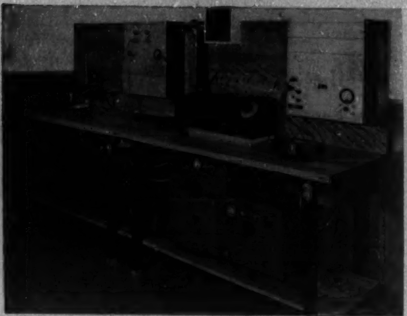

Figure 5. Apparatus assembled for use

the start gives no closure. Note that in all conditions the circuit is opened by the fixed contact, which maintains a fixed phase relation with the *A* contact and is closed by the movable contact.

In practice, it is more convenient to supply two movable contacts 180 degrees apart in phase, one for the parallel connection and one for the series, and to shift their phase through only 180 degrees. The ordinary pulse machine uses only a single movable contact and 180 degrees shift but has not the feature of opening the circuit at a fixed phase.

In the instrument shown, the *B* contacts are bronze brushes bearing on silver segments on a seven-inch disk. The conducting segments cover half of the circumference so that one contact per revolution is made. The movable brushes are adjusted by a worm-drive dial of the type used for precision condensers, one division corresponding to 1/1,000 of a cycle. The *A* or battery circuit is opened and closed by relatively heavy cam-driven platinum–iridium contacts with provision for ease of cleaning and adjustment.

The gear-shifting mechanism consists of two shafts each carrying five gears, the first shaft geared to the motor, the second to the commutator disk. Between the shafts is a carriage carrying five idler gears, which is raised and lowered by a rack and pinion from a knob on the front of the apparatus. For each revolution of the knob, the successive idler gears are brought into mesh with the successive pairs of gears on the two shafts allowing a choice of five speeds to be obtained.

The elements of the bridge circuit of Figure 3 are built into the instrument. The resistances are held accurately and are of ample current-carrying capacity. The value of R_0 is 250 ohms, the decade resistance R_d has a maximum resistance of 111 ohms with an 0.2-ohm rheostat for accurate balance, and the value of K may be selected from five values from 1 to 120. Provision is made to connect an external resistance in place of R_d, if the decade boxes have insufficient range or current-carrying capacity. For a typical 1,000-ohm relay, a value of $K=40$ would be used so that the circuit constants would be: $R_0=250$, $KR_0=10{,}000$, $R_d=25$. A pulse rate of $T=0.25$ ordinarily would be used.

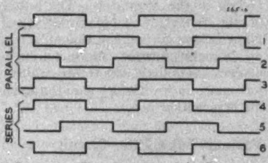

Figure 6. The operation of the *B* contact

For the measurement of current, three large toroidal air-core mutual inductances are provided, having mutual inductances of 0.02, 0.10, and 0.50 henry. These make it possible to measure currents of from less than one milliampere to several amperes. The coils are selected by means of a three-position key and a plug provided to short-circuit the primary, if current measurements are not required.

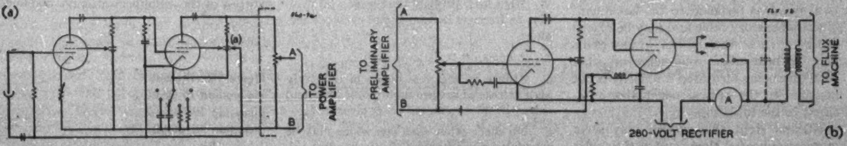

Figure 7. The amplifier for displacement and velocity measurements

Apparatus for Displacement and Velocity Measurements

The optical system and amplifier used for the measurement of displacement and velocity are shown at the left of Figure 5.

Preliminary experiments indicated that the type of amplifier required for displacement measurements, that is one with uniform gain and substantially no phase shift extending down to direct current, presented no serious difficulties because of the relatively low net gain required and the relatively high output voltage of the photoelectric cell. The amplifier for velocity measurements, however, where the voltage gain was required to increase linearly with frequency presented more practical difficulties. The indicated maximum gain required was well over 100 decibels at a frequency of 1,000 or 2,000 cycles, and, moreover, the phase characteristic required was one which increased the difficulties of avoiding self-oscillation.

From many theoretical and practical considerations it was decided to make the amplifier in two sections, each with feedback and each with two stages. The first or preliminary amplifier is shown in Figure 7a.

This is a two-stage feed-back amplifier, but the feedback may be either a capacitance for velocity measurements or a resistance for displacement measurements. The capacitances are of mica and the resistances of a precision type, and the gain is sufficient so that the net gain is substantially independent of everything but the feed-back impedance over the range of interest. This permits absolute measurement of displacement and velocity to be made, if a single constant which is ordinarily the total motion of the armature is known. The contacts of a small relay operated from the heater circuit are placed at *a* to avoid the drain on the plate battery, if the feed-back switch is left on a resistance terminal.

For measuring displacement the switch is placed on one of the six resistance contacts and for measuring velocity on one of the four capacitance contacts. The successive values of capacitance and resistance change in the ratio of three, or three and one third, to one so that a wide range of gain is obtainable. The circuit is operated at as high a feedback as is consistent with the required sensitivity. Finer adjustment of the gain may be made by the potentiometer on the right which is a part of the second or power amplifier shown in Figure 7b. This is also a two-

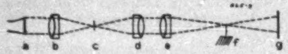

Figure 8. The optical system for displacement and velocity measurements

a—Lamp
b—Condensing lens
c—Slit
d, e—Objectives
f—Moving vane
g—Photoelectric cell

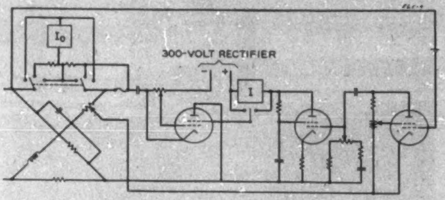

Figure 9. The filter circuit to smooth the data to the measuring instrument

stage feed-back amplifier with a resistance feedback modified by the network shown to compensate for the distributed capacitance of the air-core output transformer.

The first three stages of the amplifier are high-gain pentodes and the output a power pentode. The first tube is mounted in the same container which holds the photoelectric cell, which is shielded electrostatically and magnetically except for a small window by a permalloy shell. The lamp is a nine-volt, two-ampere bulb, which is operated normally at five to six volts, a range of 2–12 volts being available by a rheostat.

The Optical System

Most of the features of the optical system are due to the advice and assistance of associates who have been connected with the sound-motion-picture development. The fundamental design is similar to the film-reproducing system with certain necessary changes in dimensions.[4]

In Figure 8, *a* is the lamp, *b* the condensing lens, *c* a slit, *d* and *e* objective lenses, *f* a vane on the part whose motion is to be studied, or the sharp edge of the part itself, and *g* is the photoelectric cell. The lamp and the condensing lens are the same as those used in the film reproducer. The slit is the same except that its width has been increased to 0.005 inch and a feature added permitting its length to be adjusted from zero to about 0.10 inch. The objective lenses are inexpensive Bausch and Lomb achromatic lenses. Lens *e* is interchangeable for different focal lengths and may be moved back and forth in the supporting tube for precisely focusing the image of the slit on the moving part.

The three lenses and slit are mounted in a tube fastened to the lamp housing, which in turn is fastened to a short optical bench which also supports the photoelectric-cell container. The lamp housing contains provision for bringing the lamp filament to the proper position. The optical bench is fastened to the backboard of the laboratory table and may be placed at any angle so that motion in any plane may be measured. The relay or other structure being measured ordinarily is not fastened to the optical bench but is secured to the table top.

At first sight this system may seem more complicated than is necessary. Its advantage is that it provides a rectangular beam of light of constant width and adjustable length at the point to be measured. The necessity for numerous light shields and screens is done away with, although it is advisable to throw a black cloth over the whole apparatus, when once adjusted, to keep out the overhead illumination.

The reason for this last is of interest. The flux machine is driven by a synchronous motor on the same 60-cycle mains as the overhead lights, so that the contacts on the machine operate in synchronism with the fluctuations in light intensity. Any measurements made with overhead illumination getting into the cell will, therefore, have a superimposed 120-cycle ripple. For the same reason extreme care had to be taken to avoid any 60-cycle pickup in the apparatus. The heaters of the tubes are supplied with well-filtered direct current and cannot be used on alternating current. Noise not due to 60 cycles is of little importance, which is fortunate, since with high gain the amplifier is somewhat noisy.

Vacuum-Tube Filter Circuit

It has been assumed tacitly in the foregoing theory that it is possible to read the direct component of a complex wave simply by placing a d-c instrument in the circuit. This is true if a sluggish instrument is used with a relatively high pulse rate. Many measurements, however, require a slow pulse rate, and the more convenient rapid-reading types of instruments will follow the pulses to such an extent that an accurate reading is impossible.

On the right of the photograph is the apparatus which serves as a very efficient low-pass filter. This filter must fulfill a variety of very stringent requirements, chief of which may be listed:

1. Low loss to direct current.
2. High loss, probably exceeding 30 decibels to frequencies above one cycle per second.
3. A constant-resistance input.
4. Ability to suppress peaks of relatively high voltage of several hundred or thousand times the direct voltage being measured.
5. No effect other than one which may be calculated accurately on the d-c reading.
6. The circuit should not increase greatly the time required for the instrument to reach a steady reading.

Requirement 3 may call for some comment. It was pointed out earlier that the method requires the time constant of the measuring circuit to be small in comparison with the period of the pulses. A filter built in the ordinary way to have high suppression to pulses of period T would not have a time constant small in comparison with this figure. The requirement of constant-resistance input is a convenient way of expressing the necessity of fulfilling this condition.

The original work on the system used was done by R. F. Wick, and many of the features to be described are attributed to him. The circuit diagram is shown in Figure 9. From left to right the elements are as follows: a balanced impedance bridge containing the ammeter in one arm, a blocking capacitor, a vacuum tube used as a plate-supply impedance for the power tube, and a two-stage amplifier with an interstage phase-adjusting circuit. The three-point double-pole key when in the normal position removes the meter (50 ohms) and substitutes a 50-ohm resistance. When off normal the meter is connected in either polarity.

The operation of the circuit is best understood by assuming the reactance elements to be omitted from the bridge and the contact on the potentiometer forming one diagonal to be at the lower left. The input to the amplifier is then directly across the line, and any feedback is eliminated, since the bridge is balanced. Any alternating component applied will be amplified and sent back through the meter in the opposite polarity from that coming directly from the line. If then the gain in the amplifier is correct and its phase shift nearly zero, the alternating component through the meter will be greatly reduced.

The bridge provides the constant-resistance feature at the input, since the output of the amplifier can have no effect

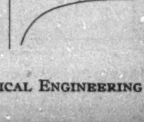

Figure 10. Illustrating method of compensating for phase distortion in amplifier

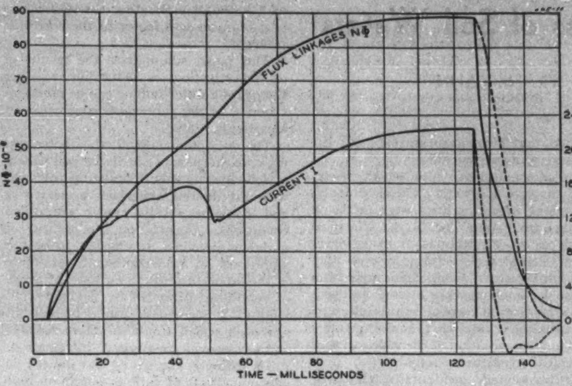

Figure 11. Current and flux variation in central-office-type relay

Dashed lines—Decay with resistance
Capacitor protective circuit

on the input impedance. It does however necessitate a loss from both line and amplifier to the measuring instrument.

Practically, the difficulty in design is in securing an amplifier with enough peak-output capacity and negligible phase shift at frequencies from one cycle up. This has been accomplished by a combination of several methods. Most of the phase shift is introduced by the plate capacitor in the last stage. The effect of this is reduced by using as a plate-supply resistance to the 6*L*6 used as a power stage, a second 6*L*6 operated with a plate potential of about 50 volts and a screen of 300 volts. The equivalent resistance in so far as voltage drop is concerned is about 1,600 ohms, but the resistance to fluctuations in the plate current is many times this figure.

The gain of the amplifier is controlled by feedback secured by the potentiometer in the diagonal arm of the bridge. The gain is sufficient so that a substantial amount of feedback may be used with a consequent further reduction in phase shift.

The final phase compensation is secured by the interstage potentiometer. The effect of this is illustrated in Figure 10. The lower curve is the net phase shift of the amplifier without the interstage circuit. The upper curve is the phase shift, which may be introduced before the grid of the second stage. By proper adjustment these may be made to compensate each other down to a frequency of one or two cycles. The circuit constants are such that the final adjustment of low-frequency phase may be made with a negligible effect on high-frequency gain. It may be of interest that, if the bridge be unbalanced by short-circuiting the lower 50-ohm resistance, an error of 20 per cent or more is introduced in the d-c reading because of the extremely large effective reactance of the feed-back amplifier. If the bridge be unbalanced by short-circuiting the meter, the amplifier is quite likely to motor-boat and blow the fuse used to protect the meter. It is for this reason that the meter key is made to replace the meter by a 50-ohm resistance. When in this position, the fuse also is short-circuited to avoid needlessly blowing fuses with the high surges which frequently occur when the amplifier is turned on and the capacitors start to charge.

The filter, as described, omitting the reactance elements from the bridge, would be entirely satisfactory within the power capacity of the amplifier. With certain measurements, notably those of velocity, the peaks of the wave as applied to the filter, which in this case would be proportional to acceleration, are so high that no reasonable amplifier would be able to follow them. These knifelike peaks, however, are so sharp that they may be removed easily by reactance elements added to the bridge as shown. It will be noted that the bridge is still of constant resistance and still is balanced at all frequencies.

Three adjustments are provided on the amplifier, one controls the feedback, a second the phase correction, and the third the plate current. A plate milliammeter is provided to measure either plate current or the sum of plate and screen currents, as will be clear from the diagram. The amount of suppression is controlled by a three-position key, which may be used to cut down the sizes of the capacitors in the circuit in a ratio of two and four to one. In cases where one of the higher pulse rates is used, adequate suppression and somewhat faster readings may be secured by using smaller capacitors. With the maximum suppression, two cycles may be reduced to such an extent that it has no detectable effect on the meter pointer. Accurate measurements at one cycle may be made, although there is a slight motion of the pointer.

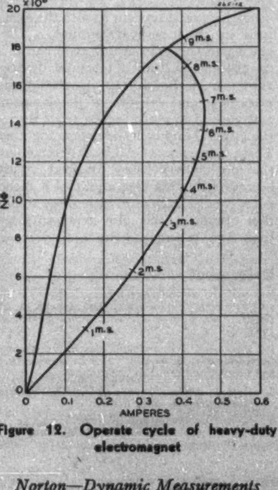

Figure 12. Operate cycle of heavy-duty electromagnet

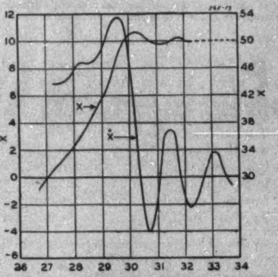

Figure 13. Relative motion of armature and core of relay at the end of its stroke when striking stop pins

x—In mils
$\dot{x}$—In inches per second

Abscissas—Time in milliseconds after closing contact

Analytical studies have indicated that the transient response of the circuit depends to a large extent on the ratio of the interstage coupling capacitor to the output capacitor and, moreover, that there is an optimum ratio of the phase-compensating capacitor to the other two. In altering the amount of suppression, therefore, the ratios of the three capacitors are held constant.

Galvanic Corrosiveness of Soil Waters

HOWARD S. PHELPS
ASSOCIATE AIEE

FRANK KAHN
ASSOCIATE AIEE

Synopsis: Results are presented of a study of the relation of pH of soil waters to galvanic action between couples of lead, copper, iron, and carbon. Galvanic-cell tests were made using as electrolytes actual soil waters or soil extracts from 31 locations at which trouble had been experienced. The following conclusions apparently can be drawn from this investigation:

1. Galvanic corrosiveness on lead, copper, and iron appears generally more severe for soil waters of low pH than for those of high pH.
2. Indications are that the static potentials of lead and iron are practically constant in soil electrolytes of pH up to approximately ten; as pH is increased above ten, lead becomes more negative and iron more positive. The potential of copper becomes more negative in substantially straight-line relation with increasing pH. Carbon potentials appear to be practically independent of pH of soil waters.
3. For electrodes of lead, copper, iron, and carbon in soil waters, the relation of degree of polarization to pH of electrolyte seems to show definite trends.

PLANNING an underground plant which includes metals initially or eventually to be exposed to contact with soil waters involves consideration of the deteriorating effects of corrosion. In wet environments, lead-sheathed cables, iron pipes, and other underground metallic structures are often subjected to corrosion caused by direct earth currents. In many such cases, it has been determined that current producing the electrolysis is of galvanic origin.

In an attempt to evaluate relative corrosiveness of soil waters, chemical analyses along orthodox lines were made on waters from many locations. Chemical analyses of electrolytes from environments considered severely corrosive often did not appear to differ significantly from those for environments classed as inert. Also, no definite correlation was observed between the corrosiveness of these waters and any combination of the wide range of chemical constituents found.

It was noted, incidentally, that the hydrogen-ion concentration of the waters varied from approximately pH 2 to pH 12. Also, experimental data in hand indicated a possible relation between galvanic corrosiveness and pH of electrolyte. Because of the ease with which the pH of a water sample can be determined, such a relation could prove of great value as a basis for estimating the seriousness of galvanism as a factor in the corrosion problem.

This paper summarizes the results of an investigation to determine whether the pH of a water sample can be used as a criterion of the galvanic corrosiveness at a particular site.

The only obvious method of determining corrosiveness of particular soil waters or soil extracts was to make up test cells with the desired materials as electrodes and compare results under controlled conditions. Considering the number of variables involved, it was felt to be too ambitious an undertaking to simulate in the laboratory anything like the range of conditions provided by field environments. It seemed desirable to seek an approach which would be more feasible and yet provide instructive information.

Accordingly, the study was limited to galvanic effects of various waters on four materials commonly occurring as electrodes in underground installations. The electrodes selected were lead (from commercial lead sheathing), copper (electrolytic), iron (low-carbon steel), and carbon (arc-lamp electrode or core of a dry cell).

Thirty-one samples of manhole waters, soil waters, and distilled-water extracts from soil specimens, collected from various locations where trouble had been experienced, were used as electrolytes. Several of the waters used were from sources hundreds of miles apart. For comparison, municipally-supplied tap water was also included.

Galvanic-corrosion behavior was investigated by studying the "current versus potential" relations of pairs of the electrodes on the various electrolytes, following the suggestion of Burns.[1] The test cell comprised a beaker containing 200 milliliters of electrolyte with two test electrodes immersed for two and one-half square inches of surface. A saturated calomel electrode was used as a reference electrode, connection being made through a salt bridge. The test and reference electrodes were disposed in a triangle with the opening of the salt bridge ap-

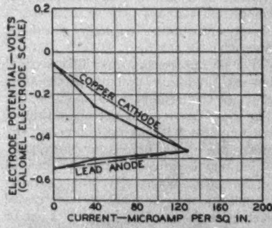

Figure 1. Current-versus-potential characteristic of lead–copper galvanic couple in soil-water electrolyte of pH 7

Dashed lines show polarization slopes

Paper 45-60, recommended by the AIEE committee on power transmission and distribution for presentation at the AIEE winter technical meeting, New York, N. Y., January 22–26, 1945. Manuscript submitted November 29, 1944; made available for printing December 27, 1945.

HOWARD S. PHELPS is engineer in charge, special investigation and testing division, and FRANK KAHN is senior technical assistant, testing section, both in the engineering department of the Philadelphia Electric Company, Philadelphia, Pa.

Measurements

The results of a few typical measurements are given in Figures 11, 12, and 13.

Figure 11 shows the build-up and decay during operation and release of a central-office telephone relay having a number of contact springs. The scalloped effect in the current build-up curve is due to the sudden changes in load on the armature as successive contact springs are picked up. The more rapid build-up of the current at the start of the cycle as compared with the flux is caused by the presence of eddy currents in the core.

Two decay curves are shown, one with a resistance-capacitor protective shunt across the operating contacts and the second with no protection. The voltage tending to produce a spark across the contacts is equal to the slope of the flux curve and this is reduced substantially by the addition of the shunt. The finite rate of decay of flux with no shunt is due to the presence of eddy currents.

Figure 12 shows similar data taken for a heavy-duty laminated-core electromagnet but plotted in a different manner. This is effectively a dynamic magnetization curve of instantaneous flux plotted against instantaneous current during the operating cycle. The top curve is the usual magnetization curve with the armature in the operated position. Data plotted in this way are of great value in the theoretical study of magnetic devices.

Figure 13 shows data on relative displacement and velocity of the armature and core of a central-office relay during the interval in which they come together. These data are used chiefly in determining the maximum velocity attained by the armature, in this case about 11.8 inches per second. To give an idea of the resolution obtained, this plot represents less than three per cent of the total cycle.

References

1. AN OSCILLOGRAPH FOR 10,000 CYCLES, A. M. Curtis. *Bell System Technical Journal*, January 1933.

2. VIBRATION STUDIES WITH THE RAPID RECORD OSCILLOGRAPH, H. E. Hill. *Bell Laboratories Record*, September 1937.

3. United States patent 1,543,813, Impulse Generating Device, G. F. Atwood.

4. A SOUND PROJECTOR SYSTEM FOR USE IN MOTION PICTURE THEATERS, E. O. Scriven. *Bell System Technical Journal*, January 1929.

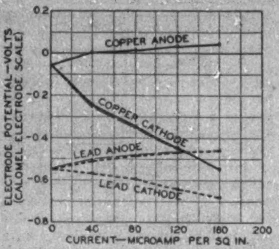

Figure 2. Current-versus-potential characteristics for two cells with current supplied externally; one cell having two copper electrodes and the other cell (broken lines) having two lead electrodes

Light dashed lines show galvanic-couple characteristic reproduced from Figure 1

proximately at half the depth of immersion of the test electrodes. All potentials were measured with a null potentiometer, and short-circuit currents were determined by an ammeter with potential drop compensated with an external voltage source as suggested by Denison.[3] The cell tests were made at an ambient temperature of 75 degrees Fahrenheit ±5 degrees Fahrenheit.

Previous experience having indicated a knowledge of the chemical constituents to be of little help in evaluating corrosiveness, chemical analyses of these waters were not made except for electrometric determination of hydrogen-ion concentrations.

In Figure 1 is shown a typical "current versus potential" characteristic for the lead–copper couple in one of the soil waters. This characteristic shows how the potential differences between each test electrode and the calomel electrode vary with magnitude of current flow between electrodes as the cell is gradually short circuited. The individual curve for each electrode is known as its polarization curve. The dashed straight lines shown in Figure 1 were drawn by connecting the points representing the open-circuit conditions for each electrode and the point representing the short-circuit condition. Each dashed line is a fair approximation of the actual anodic or cathodic polarization curve for the respective electrode and its slope will be referred to as the "polarization slope." It will be observed that anodic polarization slopes will be positive and cathodic polarization slopes, negative.

From preliminary tests, it became apparent that one of the most critical aspects of these test cells was the technique of cleaning the electrodes before each test to give reproducible potentials. Various treatments were tried and it was found simplest to remove a surface layer of metal with nitric acid and wash thoroughly with tap water followed by distilled water. This proved effective except in the case of the carbon electrodes which were difficult to depolarize. However, it was found that heating in a Bunsen flame to approximately 250 degrees Fahrenheit followed by soaking in nitric acid and washing generally restored the initial condition.

The cells were permitted to reach a substantially steady state before taking final readings. On open circuit several minutes were required to reach steady state in a number of instances. On short circuit, however, considerably more time generally was required to reach approximate stabilization.

Another approach to the electrolytic behavior of the electrodes in the various electrolytes was made by observing the "current versus potential" relation of two electrodes of the same material when direct current was supplied to the cell from an outside source. This method produces simultaneously the anodic and cathodic polarization curves for the particular electrode material. In order to determine the galvanic relation of any two materials in the electrolyte, it is not necessary to set up the actual cell. For all practical purposes, the proper curves can be combined to show what galvanic action will result.

Figure 2 illustrates this relation for lead and copper electrodes in the same electrolyte used in the tests shown in Figure 1. A galvanic cell comprised of a lead and a copper electrode in this electrolyte should give the characteristic indicated by the combination of the anodic curve of the lead and the cathodic curve of the copper. This is substantiated by reproducing by light dashed lines in Figure 2 the characteristic for this cell shown in Figure 1.

Figure 3 shows static electrode potentials to the calomel electrode scale for lead, copper, iron, and carbon plotted against pH of the electrolyte. Because of scattering of the points representing the data, envelopes have been drawn to show the general trends. It is seen that the potentials of lead and iron seem to be substantially constant in electrolytes of pH up to ten. As the pH is increased above ten, lead becomes more negative and iron more positive. The potential of copper becomes increasingly negative in practically linear relation with pH as the pH increases. The potential of carbon appears to be practically independent of pH of electrolyte.

Figure 4 shows envelopes for open-circuit electromotive force and short-circuit currents, plotted against pH of electrolyte, for galvanic cells of the six combinations of the electrodes: lead-copper, lead–iron, copper–iron, lead–carbon, copper–carbon, and iron–carbon, respectively.

The electromotive forces shown by the dotted envelopes in Figure 4 are obviously what would be expected from the appropriate combinations of the static electrode potentials shown in Figure 3. Of particular interest is the reversal of polarity of the lead–iron couple in soil waters above approximately pH 10 as shown in Figure 4B.

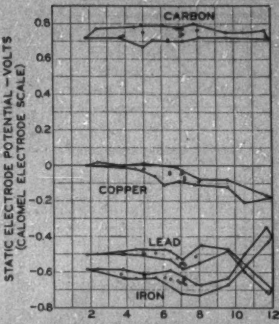

Figure 3. Static electrode potential versus pH of soil-water electrolyte for electrodes of lead, copper, iron, and carbon

The envelope of short-circuit currents versus pH for the lead–copper couple, shown in Figure 4A, does not appear to evidence any characteristic trend. However, the maximum current for this couple (400 microamperes per square inch at pH 5.0) is of the order of half the maxima found for the lead–iron and copper–iron couples. With carbon as one electrode of the couple, current maxima were of the order of 20 to 40 times this magnitude.

The envelope of short-circuit currents for the lead–iron couple, Figure 4B, shows highest values of current below pH 7. Thereafter, as the pH increases, the current diminishes to zero at pH approximately 10 to 11 and then increases gradually with polarity reversed.

The short-circuit current envelope for the lead–carbon couple, Figure 4D, appears to have a minimum at approximately pH 8, with the highest value of current magnitude at pH 11.7.

The short-circuit currents for copper–iron, copper–carbon, and iron–carbon couples apparently have maximum values below neutral pH (pH 7) tapering down to low values at pH of approximately 12. In the copper–iron couple in particular (Figure 4C) in the soil-water electrolyte of pH 12, the short-circuit current was only 2 microamperes per square inch.

Figure 5 shows slopes of the anodic and cathodic polarization curves versus pH for the lead, carbon, copper, and iron electrodes, respectively.

From Figure 5A it appears that lead is practically nonpolarizing at both extremes of pH with increased polarization occurring between approximately pH 7 to 10.

As shown in Figure 5C, copper as an anode is nonpolarizing at low pH and rises to a peak in the region of pH 12.

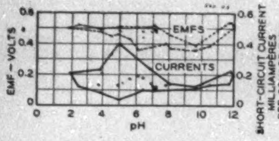

(A). Lead–copper couple

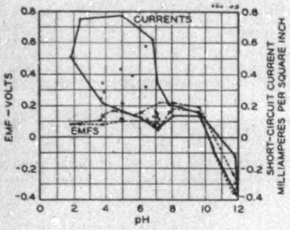

(B). Lead–iron couple

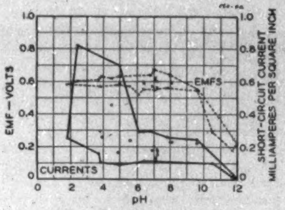

(C). Copper–iron couple

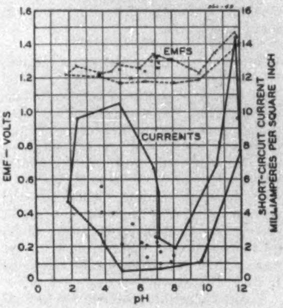

(D). Lead–carbon couple

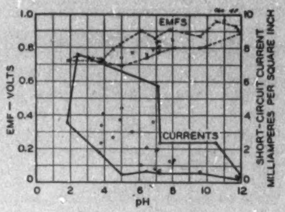

(E). Copper–carbon couple

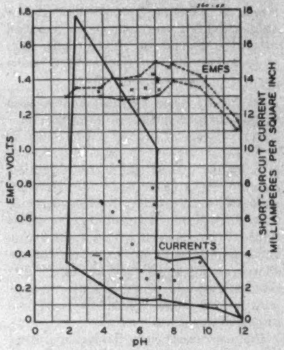

(F). Iron–carbon couple

Figure 4. Open-circuit electromotive force and short-circuit current versus pH of soil-water electrolyte for galvanic-couple combinations of lead, copper, iron, and carbon electrodes

There appears to be considerable scattering of degree of polarization below pH 7 for copper as a cathode, but a pronounced peak of high magnitude was obtained for the soil water of pH 12.

Iron as an anode polarizes little in soil waters of pH less than approximately ten. Above this value, as shown in Figure 5D, polarization is very marked. As a cathode, iron appears to polarize increasingly with increase in pH.

The polarization slopes for carbon, as both anode and cathode, shown in Figure 5B, indicate low values at the extremes of pH with a hump in the region approximately pH 7 to 10. Although carbon may not be of special interest as a galvanic electrode in virgin soils, it often becomes of importance in urban fills. The uniformly high positive potential of carbon will tend to cause severe anodic corrosion of practically any other metallic underground structure when such structure and the carbon are related to their environment as a short-circuited galvanic couple. This is particularly true where the soil waters are at extremes of pH. When voltage measurements between metallic earth substructures show a constant potential difference of the order of one volt, an open-circuited galvanic cell, involving carbon as a cathode, is strongly indicated. Bonding together of such structures is contraindicated.

A test was made to determine the influence of the ohmic resistance of the electrolytes on the results obtained. A galvanic cell of one of the pairs of electrodes in a representative electrolyte was set up as usual and permitted to stabilize for a dynamic condition. Electrode potentials were carefully observed while one of the electrodes was moved about in the beaker. No changes in the dynamic electrode potentials were observed during this test, although the electrode spacing was varied from a separation of approximately two inches to closest proximity possible without actual contact. It was therefore concluded that the ohmic resistance drops in the electrolyte could be neglected. As a matter of interest, the resistivity of the soil waters tested ranged from a few hundred to several thousand ohm-centimeters at 25 degrees centigrade.

It should be thoroughly understood that this study has been confined to galvanic effects on actual soil waters. This means that, for the conclusions drawn, corrosion by direct chemical attack or by microbiological organisms is expressly excepted. Also, it is emphasized that the effects observed in this study were obtained for soil waters which very probably have somewhat related chemical characteristics. In other words, soil waters probably contain many salts in common with the likelihood of similarity of galvanic behavior, despite variations in concentration and acidity. It is not intended to generalize the conclusions drawn beyond soil-water environments.

It is appreciated that underground environments introduce many variables not taken into account here, such as surface films, movement of electrodes, flow of electrolytes, and so forth. The authors did not attempt the comprehensive investigation which would be required to determine the effects of these factors. Although having no counterpart in field occurrences, the cleaning of the electrodes by chemical removal of surface layers eliminated an important cause of variation in results. Conceding that this procedure produces results which are not completely representative of practical effects, it is still believed the data are indicative of the relative order of severity of galvanic corrosion.

The polarization slope is a direct ratio of voltage to current density and can be considered to be a measure of the current density which would result from a given dynamic electrode potential. With known magnitudes of voltages between identified structures in an underground electrolysis circuit, and provided local galvanic effects could be satisfactorily taken into account, it may prove possible to estimate the current-density distribution on the structures concerned.

It may also prove feasible to determine relative severity of corrosion on electrically-interconnected metallic underground structures of different materials. This is illustrated by the following example.

Assume a composite anode of copper and lead in an underground electrolysis circuit energized from a d-c source (for example a lead-cable sheath with copper-bonding conductors in a wet manhole and at a potential positive to the surrounding environment). Assume also that the local galvanic current between the lead and the copper can be neglected. Consider first that the electrolyte is of pH 8. From Figures 5A and 5C it is observed that the average value of polarization slopes for both lead and copper at pH 8 is approximately 0.8 volt per milliampere per square inch. The densities of anodic current flowing from the two metals into the electrolyte would therefore be comparable and electrolytic corrosion of the two metals would be of similar severity.

Next, consider conditions the same except the electrolyte to be at pH 12 instead of pH 8. Figures 5A and 5C indicate that at pH 12 the anodic polarization slope for lead is down to approximately 0.1 volt per milliampere per square inch while the anodic polarization slope for copper has increased to the order of two volts per milliampere per square inch.

The significance of this difference in polarization slopes is that to maintain equal dynamic potentials to the environment at pH 12, the current flow from the lead anode must be of the order of 20 times that from the copper. As a consequence, anodic corrosion of the lead component of a composite lead–copper electrode will be many times as severe as for the copper. Preliminary tests appear to corroborate this analysis.

It is hoped that the material which has been presented will stimulate interest to the extent that others may be induced to contribute data to provide a better understanding of this subject.

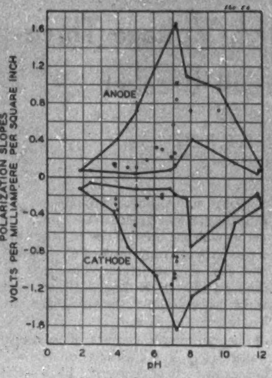

(A). Lead electrodes

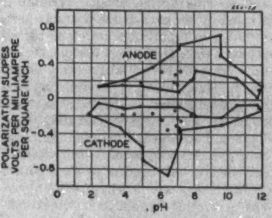

(B). Carbon electrodes

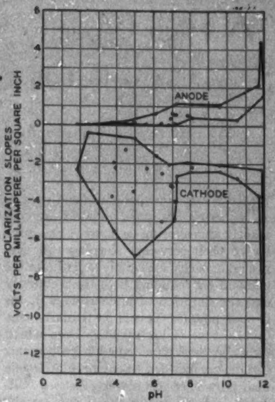

(C). Copper electrodes

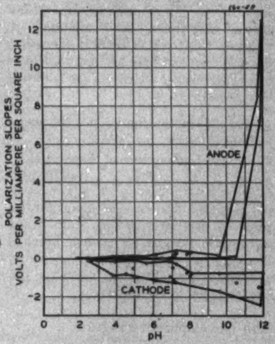

(D). Iron electrodes

Figure 5. Slopes of anodic and cathodic polarization curves versus pH of soil-water electrolytes for lead, carbon, copper, and iron

Conclusions

Assuming that the waters which were used are representative soil electrolytes, it is believed the following conclusions are indicated by the data presented.

1. Galvanic corrosiveness on lead, copper, and iron appears generally more severe for soil waters of low pH than for soil waters of high pH.

2. The static potentials of these electrodes have the following relationships to pH of soil waters:

(*a*). The static potential of lead is practically constant at about −0.5 volt (calomel electrode scale, e_c) in soil electrolytes of pH up to approximately ten. Above this, lead becomes more negative with increase of pH.

(*b*). As the pH of the soil waters increases, the potential of copper becomes more negative in substantially straight-line relation with pH. It changes in potential from approximately zero volts (e_c) at pH 2, to approximately −0.2 volt (e_c) at pH 12.

(*c*). The potential of iron is substantially constant at approximately −0.6 volt (e_c) in soil waters of pH up to approximately ten. Above this value, iron becomes increasingly more positive with increase of pH.

(*d*). Carbon potential appears to be practically independent of pH of soil waters at approximately +0.75 volt (e_c).

3. The degree of polarization of these electrodes apparently shows the following relationships to pH of soil electrolytes:

(*a*). Lead is practically nonpolarizing at both extremes of pH with a possibility of increased polarization occurring between approximately pH 7 to 10.

(*b*). Copper as an anode is nonpolarizing at low pH and rises to a peak in the region of pH 12. For copper as a cathode there also appears to be a peak of high polarization at pH 12.

(*c*). Iron as an anode polarizes little in soil waters of pH less than ten. Above this value, polarization is very marked. As a cathode, iron appears to polarize increasingly with increase in pH.

(*d*). Carbon appears to be practically nonpolarizing at extremes of pH, with slight polarization occurring in the region approximately pH 7 to 10.

References

1. **R. M. Burns.** *Bell System Technical Journal,* volume 15, 1936, page 20.

2. **I. A. Denison.** Electrochemical Society *Transactions,* volume 81, 1942, page 233.

3. GALVANIC CORROSIVENESS OF SOIL FOUND BY SIMPLE PH TEST, H. S. Phelps, Frank Kahn. *Electrical World,* volume 122, August 19, 1944, pages 93–6.

A High-Capacity High-Voltage Three-Cycle Oil Circuit Breaker

H. L. BYRD
ASSOCIATE AIEE

E. B. RIETZ
ASSOCIATE AIEE

POWER-system designers and operating engineers quite properly are constantly endeavoring to improve the quality of their services. Increases in connected capacity inevitably accentuate the demand for reducing both the frequency and the duration of interruptions in the flow of power. This is particularly true in the case of high-voltage lines which form the "backbone" of all large systems. Circuit-breaker-design engineers welcome their portion of this problem in the fulfillment of the requirement for circuit breakers having higher interrupting ratings, shorter interrupting times, and faster reclosing times. An outstanding example of this trend is found in the recent development and field testing of a 138-kv oil circuit breaker which had the following new requirements:

1. An interrupting rating of 3,500 megavolt-amperes.
2. An interrupting time of three cycles.
3. A reclosing time of less than 20 cycles.

This paper discusses the important features of the interrupting contact and mechanism designs for such a breaker. It also covers a comparison of laboratory and field test results which prove the ratings assigned to the breaker.

The Development Program

The development of the new breaker involved four major considerations:

1. The type of interrupting contacts.
2. The operating mechanism for the breaker.
3. The breaker-mechanism linkage.
4. Proof that the breaker in its over-all performance would meet the new requirements.

The Interrupting Contacts

Multibreak interrupters for five-cycle breakers were developed some years ago and were subjected to exhaustive field tests at that time.[1,2] These tests and subsequent operating experience have shown the current-interrupting characteristics of these interrupters to be so satisfactory that the new problem evidently was one of further development of this principle rather than one of new fundamental research.

This development resulted in the new multibreak interrupter for three-cycle tank-type breakers as shown in Figure 1. Although the oil-blast principle of arc interruption was applied in the same manner as with the original design, there was a complete rearrangement of the contacts and enclosing structure. This gave an improved flow of oil through the arc path which substantially shortened the arc lengths.

The interrupter consists of a heavy-walled Herkolite enclosing tube which houses two sets of contacts. Each set of contacts comprises a pressure-generating and an interrupting break. Pressure is created by the arcs as the contacts part, resulting in rapid interruption as the oil is forced through the port openings in the tube adjacent to the interrupting break. Arcing plates made of arc-resisting material are mounted on the stationary contacts at the pressure-generating side. These are arranged with a definite clearance to the moving contacts so that high-current arcs will transfer to them with a resultant decrease in length of the pressure-generating arcs and an improved control of the pressure within the interrupter results. Earlier tests demonstrated that more than adequate oil-blast action was always present on higher currents. Therefore, the reduction in the length of the pressure-generating arc does not jeopardize good interrupting performance. Light current-interrupting performance is not compromised since the arc initially starts from the main contact surfaces. The fact that satisfactory oil-blast action is available throughout the interrupting range is clearly demonstrated by the test results which are discussed later.

The enclosing tube is adequately secured to an adapter at the upper end, and it is secured to the support for the moving-contact assembly at the lower end. The stationary contacts are mounted on the tube or bolted to the end supports. The moving contacts are assembled on an insulation rod which forms part of the moving-contact assembly. This assembly can be removed from the bottom of the interrupter without dismantling of the contacts. This permits the complete inspection of all of the contact and insulation parts without changes of adjustment. Corona shields at the top and bottom ends of the interrupter improve the electrostatic-field distribution.

Each interrupter has mounted on it and connected in parallel with the interrupting contacts a resistor for use primarily during the interruption of capacitance current. The resistors limit to safe values overvoltages due to restriking when long transmission lines are de-energized. The effectiveness of these resistors has been fully demonstrated by field tests and operating experience in the last three years.[3] The complete assembly of interrupters, resistors, and moving

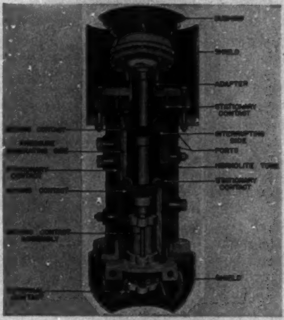

Figure 1. View of a cutaway 138-kv multibreak interrupter

The moving contacts are in the closed position and move downward when the breaker opens. Short-circuit currents are interrupted before the end of their travel

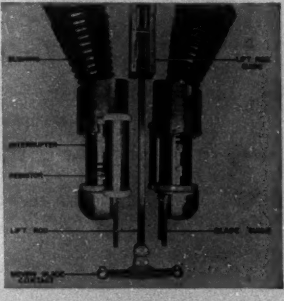

Figure 2. Pole-unit assembly of 138-kv multibreak interrupters showing resistors and lightweight moving-blade contact

---

Paper 45-45, recommended by the AIEE committee on protective devices for presentation at the AIEE winter technical meeting, New York, N. Y., January 22–26, 1945. Manuscript submitted November 28, 1944; made available for printing December 21, 1944.

H. L. Byrd is managing engineer and E. B. Rietz is section engineer of the power-circuit-breaker division, both with General Electric Company, Philadelphia, Pa.

The authors thank the American Gas and Electric Service Corporation and the Ohio Power Company for making the field tests possible and the engineers of these companies for their co-operation during the tests.

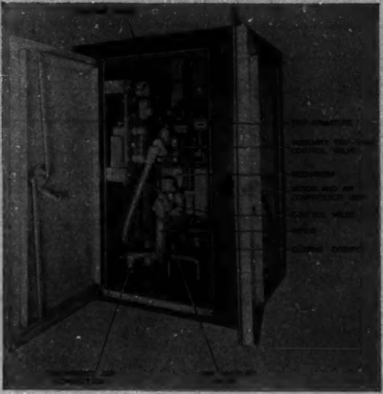
TRIP ARMATURE
AUXILIARY TRIP-FREE CONTROL VALVE
MECHANISM
MOTOR AND AIR COMPRESSOR UNIT
CONTROL VALVE
PIPING
CLOSING DASHPOT

Figure 3 (left). The pneumatic operating mechanism for a three-cycle breaker

The unit is self-contained with its own air system and is mounted directly on the first-pole-unit tank

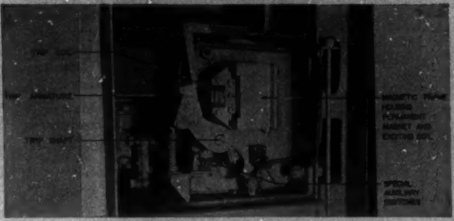
TRIP COIL
TRIP ARMATURE
TRIP SHAFT
MAGNETIC FRAME HOUSING PERMANENT MAGNET AND EXCITING COIL
SPECIAL AUXILIARY SWITCHES

Figure 4. Enlarged view of the high-speed trip on the three-cycle operating mechanism

This reduces the breaker dead time

blade contact for a single-pole unit is shown in Figure 2.

OPERATING MECHANISM FOR THE BREAKER

The high-speed opening and reclosing requirements for this breaker necessitated an operating mechanism of the stored-energy type with performance not met by existing designs. High-speed opening could possibly have been obtained by the use of heavy opening springs and large trip currents with existing mechanisms, but this would be conducive to short life and excessive maintenance on both the operating mechanism and the breaker. To attain the required opening speed without encountering these difficulties, a new high-speed trip latch was developed for the pneumatic operating mechanism which already had proved adequate for high-speed reclosing. This mechanism with its simplified linkage, low energy consumption, and satisfactory operating record made it a logical selection.

The operating mechanism is shown in Figure 3. It is of the pneumatically trip-free type. The construction of the power unit, compressed-air system, storage reservoir, and controls is essentially the same as described in a previous paper before the Institute.[4] All of these parts with the exception of the storage reservoir are assembled in a weatherproof housing which is mounted as an integral part on the front-pole-unit tank. The storage reservoir is mounted underneath and attached directly to the housing. For trip-free operations, so that there may be no delay in the opening of the breaker contacts, an auxiliary air connection is made to the top of the cylinder above the piston. This admits air above the piston on such an operation and speeds the reversal of piston motion so that the breaker contacts are free to open as fast as on a normal opening operation. An emergency air connection with suitable shutoff valves permits the use of an auxiliary air supply with a minimum of inconvenience.

Figure 4 shows a close-up view of the high-speed trip latch. This consists of an armature attached directly to the trip shaft and held by a permanent magnet housed in a magnetic frame while the breaker is closed. The mechanism linkage is arranged so that at all times when the breaker is closed there is a positive force tending to pull the armature away from the face of the magnet. The trip impulse is applied to a coil built into the magnetic circuit. Flux from the coil cancels the holding force of the permanent magnet by shifting its flux out of the armature circuit and the armature is released. Therefore, there is a minimum of time between the trip impulse and the start of movement of the breaker. An exciting coil is used to supplement the magnet during the closing operation to prevent the possibility of jarring out from the shock of the closing operation.

BREAKER MECHANISM LINKAGE

The breaker pole-unit linkage is shown in Figure 5. All of the main fulcrum points are equipped with antifriction bearings and are marked *X*. These are used to reduce the breaker dead time after the operating mechanism is unlatched.

Low-friction bearings throughout the breaker linkage give two advantages:

1. The energy requirement for the operating mechanism is reduced.

2. Greater acceleration at the start of the opening stroke is produced without increasing the velocity during the arcing period.

The reduced friction losses permit the use of lighter opening springs, thus reducing

Figure 5. Pole-unit linkage of the three-cycle breaker showing relationship of parts, low-friction bearings (X), and provisions for decelerating moving parts at ends of stroke

A—Stop
B—Stop clearance
C—For travel-recorder connector
D—Buffer
E—Lever
F—Crank
G—Link
H—Beam
I—Link rod
J—Dashpot

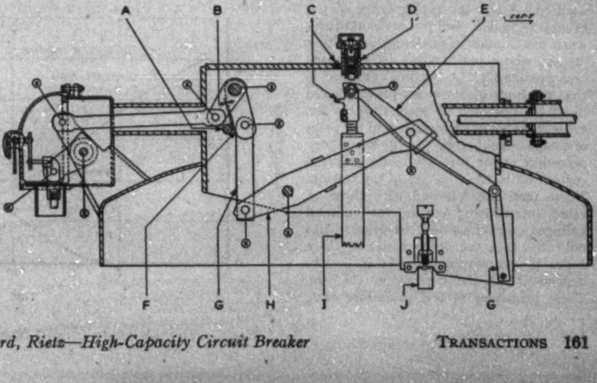

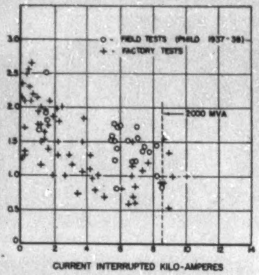

Figure 6. Interrupting performance of original 138-kv multibreak interrupters showing arc duration in cycles at various currents

Field tests made on triple-pole breaker at 138 kv. Factory tests made on a single-pole-breaker unit at voltages of 110, 88, 66, 44, 22, and 14.5 kv

the energy required to charge these springs on closing as well as the energy over the entire closing stroke. This reduces the forces on the linkage parts and permits modifications to reduce the inertia of these parts, thus further accelerating the opening operation.

With the conventional toggle arrangement of the linkage to obtain increased mechanical advantage as the contacts engage, the low-friction bearings are of greatest advantage when the toggle is closed. Therefore, they give greater acceleration during the time that the contacts are parting.

PROOF OF PERFORMANCE

Performance Demonstrated in Laboratory Tests. It has long been evident that it would be difficult to provide test stations with short-circuit capacities equal to the ever increasing interrupting ratings of high-voltage circuit breakers. This has led to the development of empirical procedures for making tests with reduced power which experience indicates are fully adequate for design purposes. Laboratory tests at reduced power can be used to predict the performance of the breakers under full-power conditions when use is made of modern interrupting devices whose performance is consistent and predictable. A further requisite is that the interrupting principle employed must be subjected at some time to the ultimate proof of performance in the form of complete field tests. In the laboratory procedure, tests first are made at rated voltage up to the capacity of the station. These tests are followed with those at rated interrupting current at reduced voltages. Previous test experience has indicated that the performance of these types of interrupting devices is largely dependent on the current in the arc. These principles of test procedure have been substantiated by years of laboratory-test experience and by field tests. The 1937–38 Philo field tests on multibreak interrupters are a good example.[2] Figure 6 shows the results of those field tests as compared with the laboratory tests. The arc durations are in the same order of magnitude for like currents in both laboratory and field tests.

A summary of a complete series of laboratory tests made on the new interrupter is represented by Figures 7 and 8. Figure 7 shows interrupting tests made up to currents of 23,000 amperes. The arc durations are well within a limit of 1.5 cycles except on the very low end of the current range. This limit was established in conjunction with a contact parting time of 1.5 cycles for the operating mechanism. The arc durations for different voltages are of the same order of magnitude, illustrating that the interrupter performance is not primarily dependent on applied test voltage. Pressures were measured within the interrupter, and their values were well below the safe working strength of the structure.

Figure 7. Interrupting performance of new 138-kv multibreak interrupters during laboratory tests

Tests made on a single interrupter at voltages of 66, 55, 44, 22, and 14.5 kv

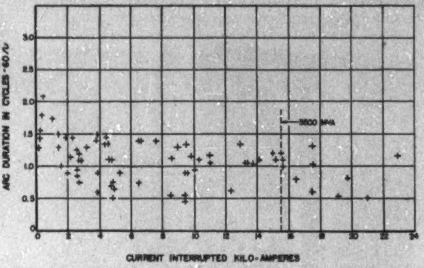

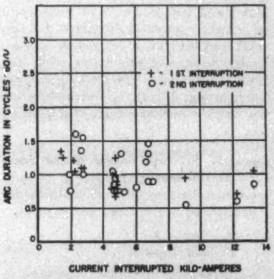

Figure 8. Interrupting performance of new 138-kv multibreak interrupters during laboratory tests on high-speed reclosing, showing comparative performance of first and second interruptions of the duty cycle

Tests made on a single interrupter at voltages of 66, 55, 22, and 14.5 kv

Ultrahigh-speed-reclosing tests were made under identical conditions, and the performances on the first and second interruptions are shown by the plotted results in Figure 8. These show equivalent interrupting performances, based on substantially the same arc durations, and demonstrate that the interrupter always is left with a sufficient quantity of oil for adequate interruption on the second operation for such short reclosing times as 20 cycles or less.

Figure 9 shows the no-load operating tests on a triple-pole breaker including opening, closing, reclosing, and trip-free

Figure 9. Time–travel curves of the three-cycle 20-cycle-reclosing breaker showing opening, closing, reclosing, and trip-free operations under no-load conditions

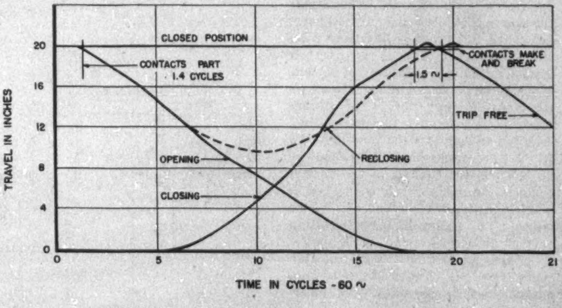

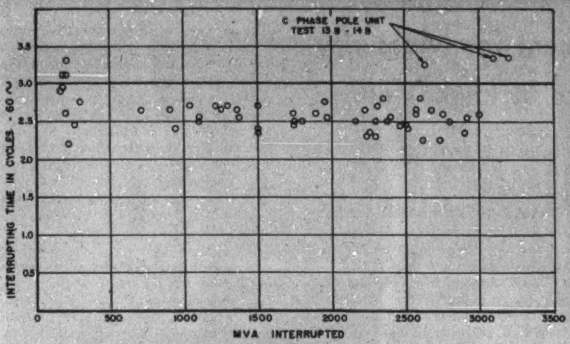

Figure 10. Interrupting performance of three-cycle breaker on field tests showing breaker interrupting times at various duties

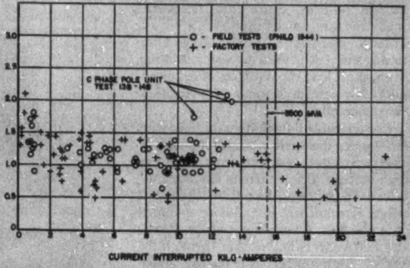

Figure 11. Interrupting performance of 3,500-megavolt-ampere three-cycle interrupters showing arc duration in cycles at various currents

Field tests made on triple-pole breaker at 139 kv. Factory tests made on single interrupter at voltages of 66, 55, 44, 22, and 14.5 kv

operations. A contact parting time of 1.4 cycles was obtained. The reclosing time of less than 20 cycles indicated an operating mechanism with adequate power to perform under load conditions.

Performance Demonstrated in Field Tests. The final proof of performance was demonstrated during two series of field tests that were made at the Philo station of the Ohio Power Company on the weekends of July 22 and August 5, 1944. This represented the largest concentration of power ever made available for full-scale circuit-breaker testing. A full description of the test setup and test results is contained in a paper presented at the 1945 winter meeting by Philip Sporn and Harry P. St. Clair entitled "Field Tests and Performance of Heavy-Duty High-Speed 138-Kv Circuit Breakers—Oil and Air-Blast."[6]

The satisfactory results of these tests were predicted by the laboratory tests. Straight opening tests, *CO*-15 second–*CO* duty-cycle tests and high-speed-reclosing duty-cycle tests were handled without disturbance or signs of distress up to the limits of available short-circuit capacity. The breaker interrupting times are well below three cycles, except in several tests of the second series when one pole of the breaker slightly exceeded this time of interruption. A summary of these times is shown in Figure 10 which includes all phases. The reclosing times were less than 20 cycles, and on the highest duty there was satisfactory performance with a reclosing time of $15^1/_2$ cycles.

A comparison of the breaker interrupting performance on these full-scale field tests with its performance on laboratory tests is illustrated in Figure 11 which shows the arc durations from the field tests superimposed on arc durations of the laboratory tests. Because of the similarity of results, there is a direct confirmation of the laboratory-test procedure.

The line-de-energizing tests demonstrated the same principle as laboratory tests had shown that only moderate overvoltages, up to 1.4 times normal, were present when interrupting lumped capacitances up to 10,000 kva on a single-pole unit.

Conclusions

1. The performance of the breaker in opening, closing, and reclosing on short circuits approximating 3,500 megavolt-amperes under actual operating conditions justifies the assigned breaker ratings.

2. The field-test results confirmed the testing laboratory procedures imperative to circuit-breaker designers.

3. Actual confirmation of laboratory-test results up to 3,500 megavolt-amperes enables designers to build upon these foundations in the development of 5,000-megavolt-amperes breakers. Although the laboratory-test interruption at 23,000 amperes in Figure 7 corresponds to approximately 5,500 megavolt-amperes at 138 kv, it is fully recognized that the final design of a 5,000-megavolt-ampere breaker would require further development but the present available data give the assurance that such a breaker is practical and can be built when the need exists.

References

1. A New Multibreak Interrupter for Fast-Clearing Oil Circuit Breakers, R. M. Spurck, H. E. Strang. AIEE Transactions, volume 57, 1938, December section, pages 705–10.

2. Tests on and Performance of a High-Speed Multibreak 138-Kv Oil Circuit Breaker, Philip Sporn, H. P. St. Clair. AIEE Transactions, volume 57, 1938, December section, pages 696–705.

3. Switching Overvoltage Hazard Eliminated in High-Voltage Oil Circuit Breakers, L. F. Hunt, E. W. Boehne, H. A. Peterson. AIEE Transactions, volume 62, 1943, March section, pages 98–100.

4. A Pneumatic Mechanism for Outdoor Oil Circuit Breakers, L. J. Linde, E. B. Rietz. AIEE Transactions, volume 63, 1944, July section, pages 543–6.

5. Ultrahigh-Speed Reclosing of High-Voltage Transmission Lines, D. C. Prince, Philip Sporn. AIEE Transactions, volume 56, 1937, January section, pages 81–90.

6. Field Tests and Performance of Heavy-Duty High-Speed 138-Kv Circuit Breakers—Oil and Air-Blast, Philip Sporn, H. P. St. Clair. AIEE Transactions, volume 64, 1945.

A Portable Instrument for Measuring Insulation Resistance at High Voltage

F. W. ATKINSON
MEMBER AIEE

ROBERT B. TAYLOR
NONMEMBER AIEE

THERE has been an increasing trend toward measuring insulation resistance of high-voltage machines and cables at or above their rated voltage by the use of direct current. The advantage of high voltage lies in its ability to detect leakage paths which do not occur at lower voltages.[1] D-c tests are advantageous because of the elimination of capacitance-current effects. Since the resistances measured are usually quite high—of the order of megohms—if high-voltage alternating current is used to test insulation, even small load capacitances offer impedances low enough to mask the insulation-resistance effect.

Considerable information on insulation resistance, dielectric absorption, and dielectric strength resulting from the use of high-voltage direct current has been obtained from large heavy rectifier sets either permanently installed or mounted on a truck.[2] A ten-year study by Davis and Leftwich[3] indicates that through the use of high-voltage d-c testing much knowledge can be gained concerning the cause of high-voltage generator insulation failures. They report that a majority of generator failures are traceable to mechanical defects, many of which were detected and located before failure in service. Other investigations have explored the field with lower voltages of the order of 500 to 1,000 volts direct current.[4,5]

The study of insulation resistance at high voltages has been restricted by the type of equipment available, which has involved transportation problems and has been very costly. There is considerable evidence that the availability of a portable tester of suitable characteristics would greatly stimulate collection of such data throughout the industry. A suitable portable instrument of rugged construction recently has been made possible by the development of a new cold-cathode rectifier tube. Because a cold-cathode tube requires no cathode heating power, it is well adapted to those applications.

New Cold-Cathode Rectifier Tube

Rectifier tubes employed in this test instrument belong to a new family of high-voltage rectifiers which do not require heated cathodes.[6] They are gas-filled diodes in which the cathodes are composed of an array of fine wire points. The cathode, when negative, discharges to the anode which consists of a fired-on graphite coating on the interior of the Pyrex-glass envelope.

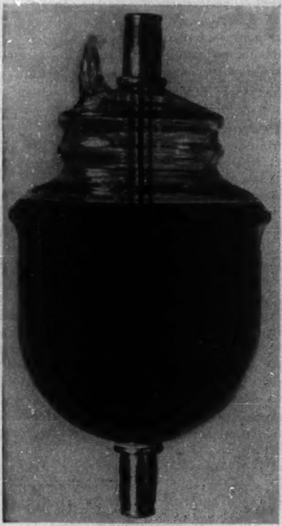

Figure 1 (above). Takktron type 60.8 high-voltage rectifier tube (cold-cathode)

By controlling the pressure and composition of the gas, the number of points in the cathode, and the anode–cathode spacing, it is possible to provide a wide range of rectifying characteristics. Present standardized tube models will provide d-c outputs up to 25 kv and currents up to ten milliamperes in half-wave circuits.

These tubes are particularly suited for cascade voltage-multiplying circuits since no filament-transformer insulation problems are encountered.[7] Also it is possible to reverse the high-voltage output polarity merely by reversing each tube in its mounting. By use of such voltage-multiplying circuits, practical power units producing up to 200 kv have been built. Even higher voltages are feasible. Such high-voltage power units are characterized by light weight, compactness, and air insulation in the high-voltage portion of the unit. Small high-voltage transformers are used since the maximum alternating voltage required is 30 kv rms.

These tubes are not damaged if their maximum inverse peak voltages are exceeded. Under this condition soft diffuse discharges take place between the cathode and the anode without damaging the tube or its characteristics. Complete short-circuiting of the output of this type of tube, or of a power unit employing the tube, likewise has no harmful effects. The absence of a hot cathode implies no deterioration during idle periods and the ability of the tube to start instantly upon the application of power.

These desirable self-protective properties are gained from the internal resistance of the tube. This resistance has little effect on the output-voltage regulation for load currents within the current rating of the tube. Beyond this value, however, the tube resistance becomes large enough to protect both the tube and the high-voltage transformer. This tube resistance is also advantageous in that it

Figure 2. Voltage–current characteristics of Takktron type 60.8 tube

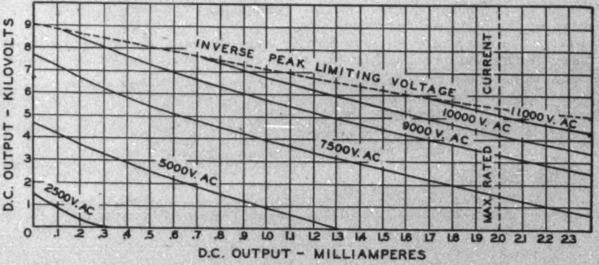

Paper 45-66, recommended by the AIEE committees on electric machinery and instruments and measurements for presentation at the AIEE winter technical meeting, New York, N. Y., January 22–26, 1945. Manuscript submitted November 24, 1944; made available for printing December 22, 1944.

F. W. Atkinson is president and Robert B. Taylor is director of research of the TAKK Corporation, Newark, Ohio.

The authors acknowledge the assistance and criticism of J. S. Askey, J. S. Johnson, and G. L. Moses, engineers of the Westinghouse Electric and Manufacturing Company.

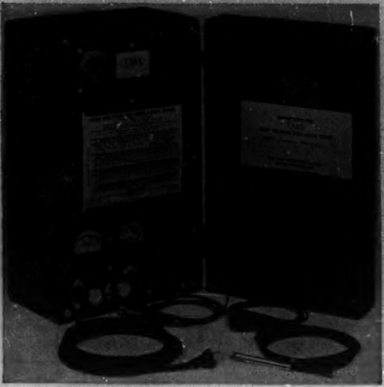

Figure 3 (left). Panel view of aircraft-ignition-cable tester

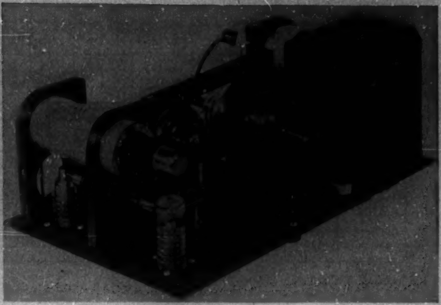

Figure 4. Interior view of tester illustrating ample clearances, rugged construction, and inherent simplicity

aids the filtering of the output voltage, and only small filter capacitances are needed for low-output ripple voltage.

The Takktron type 60.8 rectifier tube shown in Figure 1 has a maximum inverse peak-voltage rating of 21 kv. Its direct output current and voltage characteristics for various alternating input voltages are shown in Figure 2. This tube is designed for a maximum output current of two milliamperes and at this current will provide a direct voltage of five kilovolts. At "no load" the tube will deliver nine kilovolts direct current.

The tube is air-cooled and is mounted in an insulating ring support by means of three rubber *V* blocks equally spaced around the periphery of the enlarged section of the envelope. The tube terminals and the terminal connectors are designed to be free of corona at the tube potentials.

The physical dimensions of the Takktron type 60.8 tube are as follows:

(*a*). Over-all length...........$6^{1}/_{4}$ inches
(*b*). Length of envelope........$4^{1}/_{2}$ inches
(*c*). Maximum diameter of envelope...............$3^{1}/_{4}$ inches

Use in Testing Aircraft-Ignition Cable

To assist in evaluating the performance of aircraft-ignition systems, the instrument shown in Figure 3 was developed to measure the insulation resistance of cables and other ignition parts such as magnetos, distributor blocks, heads, fingers, sleeves, and plates at or above their operating voltages. The range of the instrument is 10 to 10,000 megohms measured at any voltage between 2,500 and 15,000 volts. The outside dimensions of the instrument are 10 by $11^{1}/_{2}$ by $18^{1}/_{2}$ inches, and it weighs 31 pounds.

An interior view shown in Figure 4 illustrates the rugged construction of the unit. A schematic diagram is shown in Figure 5. The input to the high-voltage transformer is controlled by a variable autotransformer. The secondary voltage is fed into a voltage-doubling circuit, which is filtered by a 15,000-volt 0.02-microfarad-output capacitor. An adjustable spark gap is provided to prevent overstressing of component parts as well as to limit the output voltage. In series with the gap is a 10,000-ohm resistor to reduce high current surges during flashover. The kilovoltmeter is connected across the high-voltage output of the rectifier.

In series with the grounded terminal is a current instrument with 0–100- and 0–500-microampere scales. A neon glow lamp is shunted across the current-instrument circuit in such a manner that leakage currents in excess of either current range will cause it to flash. This also will occur when current pulses in excess of 100 microamperes or 500 microamperes are of such short duration that the current-instrument pointer is not deflected because of its mechanical inertia. In addition the neon glow lamp serves to protect the sensitive current instrument against short-circuit currents encountered with faulty insulation.

Two high-voltage output terminals are provided, one connected directly to the power supply and the other through a 100-megohm series resistor. The output voltage of the directly connected terminal is indicated by the kilovoltmeter. Figure 6 shows a typical voltage-regulation curve from no load to short-circuit current without adjustment of the voltage control. Because of the tube characteristics the instrument is not damaged when this output terminal is short-circuited at full voltage. The "off–on" switch also may be operated under short-circuit conditions without harm. This terminal is especially useful in both dielectric-absorption and dielectric-breakdown tests. Insulation resistance in megohms may be determined from the expression:

$$\frac{\text{Kilovolt reading} \times 1{,}000}{\text{microamperes}}$$

The value of the neon-lamp resistor may be neglected since it is approximately 0.5 megohm.

The other high-voltage output terminal is used where it is desirable to limit the current in the test specimen. With the internal 100-megohm resistor the voltage across the test specimen is inversely proportional to the leakage current. Figure 7 shows the voltage-regulation curve of this circuit. If the insulation is in perfect condition and therefore has low leakage current, the test voltage is approximately that indicated by the kilovoltmeter. Since aircraft-ignition harness usually is tested at voltages between 10 and 12 kv, the instrument is calibrated in megohms in this voltage

Figure 5. Circuit diagram of aircraft-ignition-cable testers

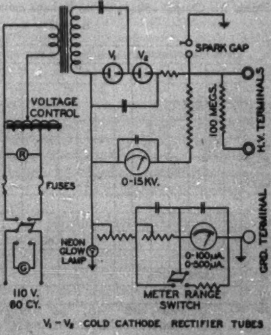

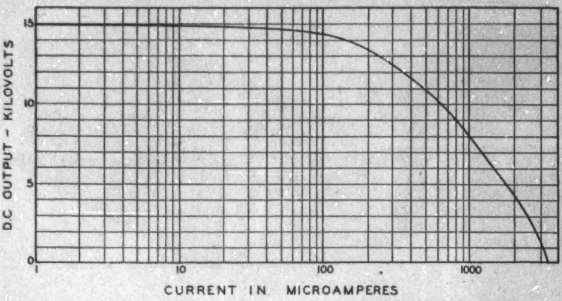

Figure 6. Voltage-regulation curve of aircraft-ignition-cable tester when series resistor is not used

Voltage adjustment unchanged

range. To determine the insulation resistance, the voltage is raised to the test value (indicated by a red dot on the voltmeter scale), the leakage current is noted, and the corresponding resistance is read on the calibration chart on the face of the instrument. Figure 8 shows a typical calibration curve. For other test voltages insulation resistance in megohms may be calculated from the expression:

$$\frac{\text{Kilovolt reading} \times 1{,}000}{\text{microamperes}} - 100$$

Since the rectifier tubes are not in the instrument circuit, it is not necessary to readjust these instruments when replacing tubes.

The series resistance increases the personal safety to the operator, and for this reason instruments with this circuit only are recommended for use by airplane mechanics or others not familiar with high-voltage testing procedures.

Where it is desired to operate the unit from a storage battery, a self-contained vibrator–inverter has been designed to supply 110 volts alternating current from a 12- or 24-volt d-c source. Since no filament power is required, the inverter and the battery drain are small.

Exploratory Work in Industrial Field

Although this instrument now is used primarily for testing aircraft-ignition cable, some exploratory work with it has been done in the industrial field to determine test requirements there. Insulation-resistance and dielectric-absorption measurements have been made on sections of a 25,000-kva 6,900-volt-class vertical water-wheel generator. The winding-to-ground capacitance of this generator is approximately 0.13 microfarad per section or 0.4 microfarad for the entire machine.

Figure 9 shows the dielectric-absorption curves at 10,000 volts for each section and for the entire machine.

Testing Cable

Insulation resistance of a 350,000-circular-mil three-conductor impregnated-paper compound-filled lead-sheath cable, rated at 15 kv, 18,385 feet long ($3^1/_2$ miles), was measured with the instrument shown in Figure 3. Test results were as shown in Table I.

Table I. Insulation Resistance of 350,000-Circular-Mil Three-Conductor Impregnated-Paper Compound-Filled Lead-Sheath Cable Rated at 15 Kv, 18,385 Feet ($3^1/_2$ Miles) Long

AT-13	Voltage, Kv	TAKK Tester (Current, Microamperes)	Resistance, Megohms
Phase *A* to ground	14.8	60	246
Phase *B* to ground	14.0	62	226
Phase *C* to ground	13.8	42	328
A to *B*	14.5	74	196
B to *C*	14.0	57	246
C to *A**	14.5	70	206

* Nothing grounded.

These and other tests indicate that for the industrial field other current–instrument ranges would be desirable. Possible ranges might include a unit for measuring insulation resistance at 2,500, 5,000, 10,000, and 15,000 volts with current ranges of 0–25 microamperes, 0–250 microamperes, and 0–2,500 microamperes. This would result in a unit with an insulation-resistance range from one-half to 30,000 megohms. Other portable testers

Figure 7. Output voltage versus leakage current when series resistor is used

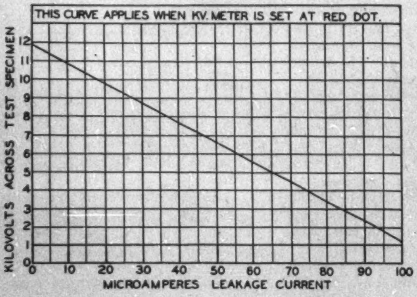

Figure 8. Typical instrument-calibration curve of aircraft-ignition-cable tester when protective resistance is used

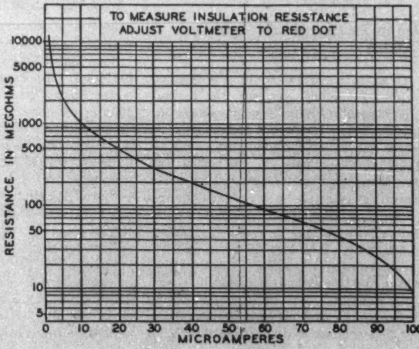

have been developed for operation at 60,000 and 100,000 volts at currents up to five milliamperes.

Conclusion

The TAKK d-c high-voltage insulation tester and insulation-resistance instrument fills a need in the study of numerous types of electrical insulation. Limited experience indicates that it is useful in testing high-voltage cable, aircraft-ignition systems, and high-voltage generating apparatus. It is the belief of the authors that there are many other applications in the electrical industry where a device of this type will be found useful and economical. It is hoped that the availability of this device will encourage the collection of considerable data on insulation testing and insulation resistance which will contribute to a better understanding of the subject and further developments in the art.

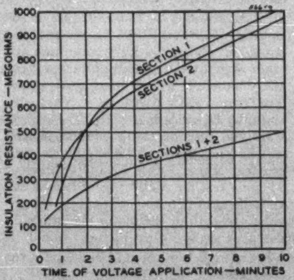

Figure 9. Dielectric-absorption curves for a 25,000-kva 6,900-volt water-wheel generator taken at 10,000 volts

References

1. Testing Electrical Insulation, Graham Lee Moses. *Railway Mechanical Engineer*, May 1944, pages 235–9.

2. Insulation Resistance of Armature Windings, R. W. Wieseman. AIEE Transactions, volume 53, 1934, June section, pages 1010–21.

3. Progress Report on D-C Testing of Generators in the Field, E. R. Davis, M. F. Leftwich. AIEE Transactions, volume 61, 1942, January section, pages 14–18.

4. Electrical Maintenance of Large Rotating Machinery, John S. Askey. *Power Plant Engineering*, volume 46, July 1942, pages 82–4.

5. Field Testing of Generator Insulation, Edison Electric Institute committee report. AIEE Transactions, volume 60, 1941, December section, pages 1003–11.

6. United States patent 2,250,451, Methods and Apparatus for Electric Discharge, W. H. Bennett.

7. United States patent 2,285,402, Rectification System, W. H. Bennett, June 9, 1942.

Standards and Insulation Characteristics of Oil-Insulated Transformers

F. J. VOGEL
MEMBER AIEE

THE STRENGTH of the insulation in transformers to resist various types of voltage stress is very important. The service and life of the transformer is partially dependent on the insulation strength, and in recognition of this fact standards for insulation strength long have been established. In the course of time improvements have taken place in design, new applications have been created, and more has been learned about the nature of stresses which arise in service. Service conditions, too, probably will change in the future, which will require changes in insulation requirements. Therefore it is natural that gradual changes in the standards, and additions to them, have taken place, with the result that sometimes they are not entirely consistent. It is desired in this paper to point out some inconsistencies and propose certain changes in the standards which might be given consideration.

Partial History of Insulation Requirements

For the purpose of this paper, it is necessary to recall that at one time the standards required a test on the major insulation of two times the rated voltage plus 1,000 volts, and an induced test of two times the winding voltage, with minimum values specified. One of the additions to the standards arose from the electrification of railroads. Railroads use a grounded single-phase system, which led to the use of transformers with relatively little insulation on the grounded end. Without going into detail about the reasoning involved, only an induced test was used replacing both the applied test on the major insulation and the induced test on the winding insulation for this apparatus. The magnitude of the test was specified as 2.73 times the normal operating voltage to ground and was extended to any transformer with one end of the winding grounded, such as transformers for three-phase service with grounded neutral. This procedure was later abandoned and replaced by induced tests at specified levels; more nearly approaching an induced test of 3.46 times the voltage to neutral.

During the period from 1920 to 1930, the effects of lightning on transmission lines, particularly on transformers, became of special interest to utility and manufacturers' engineers. In the early 20's when transformers were damaged, the matter was dismissed on the basis that transformers were struck by lightning, an act of God, and that nothing could be done about it. The transformer designer used extra insulation between turns at the line end as dictated by experience and his own judgment. The major insulation of low-voltage transformers was in excess of that needed for the specified tests, partly because it was not difficult to obtain more insulation and partly because experience showed it necessary. At the end of the 20's, some customers were specifying levels for surge strength, requiring transformers to be stronger than specified lengths of insulator strings, gaps, bushings, and so forth. At that time, transformer designers generally did not have design information on the magnitude of service stresses nor knowledge of the strength of insulating materials to withstand them.

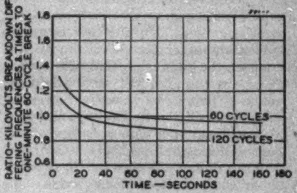

Figure 1

From Figure 23 of reference 1

In order to help clarify this situation impulse testing of transformers was started and levels were established, which were changed several times. It is of interest that these levels were lower than those specified in the late 20's, even though transformers actually were improved greatly in insulation strength in the early 30's.

In a period of such development, where levels often were based on what was expedient at the time, it is to be expected that everything would not be exactly perfect. When machines by one manufacturer are being built with certain claimed design features, it is not always possible

---

Paper 45-41, recommended by the AIEE committee on electric machinery for presentation at the AIEE winter technical meeting, New York, N. Y., January 22–26, 1945. Manuscript submitted October 18, 1944; made available for printing December 27, 1944.

F. J. Vogel is professor of electrical engineering, Illinois Institute of Technology, Chicago, Ill.

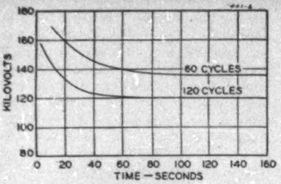

Figure 2

From Figures 13 and 14 of reference 2

to make changes in standards effective at once. This has been recognized more than once by making such changes effective at some later date. Sometimes levels determined are not consistent and unnecessarily effect the design, and it is believed that this situation is partially the case today for transformers. In order to see if this condition exists, I believe the best procedure would be to enumerate all of the service requirements and determine how much insulation would be required to meet them.

Requirements for Transformer Insulation

In the solution of any design problem it is necessary to determine the service requirements and use materials which will withstand them. In the case of transformers and other electric machinery, it is of course the intent to specify tests which are above the expected service requirements. This is to assure a margin of safety that will give good service and good quality of material. A comparison of service conditions and specified tests is useful both as a design criterion and in showing any inconsistencies that may exist.

One of the service requirements for insulation is that it withstand the steady-state voltage to ground from all parts of the winding. In the case of three-phase transformers, this is 57.7 per cent of the line-to-line voltage at the terminals. Since the test required to indicate this strength is the one-minute test, a comparison of the actual strength required, probable one-minute 60-cycle strength, and the tests specified by the standards can be made (Table I).

Table I. Comparison of Normal Service Requirements With Standard Specifications for Insulation

System Voltage	Maximum Normal Service Stress to Ground	One-Minute 60-Cycle Test Equivalent to Service Stress	Specified One-Minute 60-Cycle Test Applied	Specified One-Minute 120-Cycle Test Induced	60-Cycle Test Equivalent to 120-Cycle Induced Test
138 kv	79.8 kv	88 kv	275 kv	275 kv	300 kv

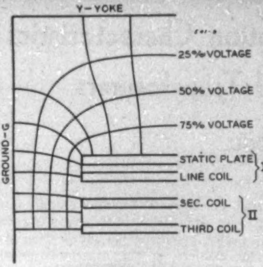

Figure 3. Dielectric field of core-type transformer with all coils at approximately line voltage

I—100 per cent voltage
II—Practically 100 per cent voltage

The equivalent one-minute 60-cycle strength is obtained from reference to Figures 1 and 2 taken from papers by Montsinger[1] and Vogel.[2] The 60-cycle-test voltage equivalent to the high-frequency induced test also is obtained from Figures 1 and 2.

Table I clearly shows that normal service voltages would not require the present test levels. It also shows that the present 60-cycle applied- and 120-cycle induced-test levels are not equivalent.

Another requirement is that transformer insulation withstand line fault conditions. In the case of delta-connected transformers, one line could be grounded, giving full line voltage to ground. In the case of star-connected transformers, depending on line conditions, various voltages could exist. Such data, available in a paper by R. D. Evans and Sherwin H. Wright,[3] are required in the application of lightning arresters and often are calculated for specific applications. In some cases, generator overspeed and other factors enter into the problem. Usually, where further consideration to the question is not merited, it is considered that the maximum voltage from any line to ground may be equal to normal line-to-line voltage or slightly more on ungrounded neutral systems. On grounded systems, 80 per cent of normal line-to-line voltage is assumed as the maximum voltage from any line to ground. On this basis, the comparison in Table II might be made.

The reason for giving these tabulations is to show the big margins now available. It would seem that the major insulation is not stressed greatly under normal or fault conditions. Indeed these are not limiting features. This has been recognized by some operators, where willingness to use lower-than-standard voltage tests and insulation levels has been expressed, provided impulse protection was afforded.

Another consideration is that of switching surges and arcing grounds,[4,5,6] giving overvoltage values anywhere from $2^1/_2$ to 5 or 6 times the normal voltage to neutral. The higher voltage values in the range are apparently rare occurrences. In the case of a 138-kv system, switching surges would be anything from 280-kv up to 680-kv crest. These surges, generated in the transformer and line reactance and the capacitance of the system, have frequencies of oscillation low enough so that reasonably uniform voltage distributions will be obtained in the transformer windings.

No standard test to simulate switching surges or even to verify the strength of transformers against these surges has been made commercially, although experiments have been conducted which determine the probable strength of transformers for switching surges.[5] Very few, if any, transformer failures attributed to switching surges ever have occurred. Even those transformers built before 1930 with low levels of impulse-voltage strength have had few, if any, switching-surge failures. Many of the transformers of the 138-kv class had levels of 500-kv and less, instead of the 750-kv now standard. This fact confirms that the voltage distribution of switching surges in windings is fairly uniform as inferred previously.

The conclusions from the above are that transformers will withstand switching surges as limited by the lightning protection used, since the voltage distribution in the windings approaches uniformity, and the impulse and switching surge strength of the transformer insulation to ground are approximately equal.

The last factor to be considered is that of impulse or lightning surges. The impulse test levels now specified for transformers are intended to be values not exceeded in service.

The test levels for impulse strength are standardized and for the 138-kv class are 750 kv for a chopped wave of three-microseconds duration and 650 kv for a full wave. Several observers[5,7,8] have determined the impulse ratio of oil-impregnated insulation as 2.1 or better. If a fair average be 2.1, the 60-cycle one-minute strength required for the major insulation would be $750/\sqrt{2}\times 2.1$ or 250 kv rms. However, 275 kv is the specified strength. Since 750 kv is minimum and exact regulation on the impulse test is not easily possible, a test margin of 10 per cent, from 750 kv to 820 kv, is reasonable and may be needed.

In the case of the grounded neutral transformer, however, the margin is much greater. From Table II, the equivalent 60-cycle test for such transformers is 305 kv instead of 275 kv. Therefore, the impulse strength of the major insulation, in the absence of other factors, would be $305\times\sqrt{2}\times 2.1$ or about 915 instead of the 750 specified.

However, such specified levels do not necessarily insure the ability of a transformer to withstand all service conditions.

Even if lightning arresters are mounted on the units and as close to the terminals as possible, some very high overvoltages can occur but for very short times. If the arrester be 25 or 30 feet from the terminals and the wave front is steep, an appreciable voltage reflection may take place at the bushing terminals. A transformer will withstand such higher voltages if of short enough duration. For example, typical oil-impregnated transformer insulation can withstand 125 per cent of the three microsecond strength for one microsecond. No test is made to prove this fact for the transformer as a unit at the present time, although it is stated in the literature.[8]

If we summarize the above requirements and tests, we see from Tables I and II that the applied 60-cycle dielectric tests and 120-cycle induced tests are far more severe than any steady 60-cycle fault or switching-surge voltage to be expected in service for ordinary transformers and might safely be reduced. We also see that the 120-cycle induced test of approximately 3.46 times the voltage to neutral for grounded-neutral transformers is more severe than the two times normal line voltage for transformers for ungrounded service, although probably the service is more severe, both for the major insulation and the winding insulation, for transformers for ungrounded service. Apparently also we can dismiss the effect of switching surges, since, even if they were of the same magnitude as impulse test waves, they would be more uniformly distributed through the winding. The major insulation for grounded-neutral transformers is higher than required to meet impulse tests. This is another inconsistency in the present rules. Also, no test is specified to insure high impulse strengths for short times or for steep waves, even though such strength may be desirable and may be available.

Since impulse levels determine the insulation provided for both grounded-neutral and ungrounded-neutral service, it would be interesting to see what comparison there would be between two extreme types of transformers built to the same impulse strength.

Strength of Different Types of Transformer

Shielded Transformer for 138-Kv Service

If we define a shielded transformer to be one in which the distribution of voltage in the dielectric field adjacent to the high-voltage-line coils is the same both for impulse voltages and 60-cycle voltages, then we can draw the following conclusions:

1. The 60-cycle strength of the major insulation is in the order of 275 kv, which is greater than required for service.

2. The strength against switching surges is ample.

Table II. Comparison of Fault Requirements With Standard Specifications for Insulation

System Voltage	Maximum 60-Cycle Fault Stress to Ground	One-Minute 60-Cycle Strength—Equivalent to Fault Stress to Ground	Specified One-Minute 60-Cycle Test, Applied	Specified One-Minute 120-Cycle Test, Induced	60-Cycle Test—Equivalent to 120-Cycle Induced Test
138-kv ungrounded neutral	138 kv	154 kv	275 kv		
138-kv grounded neutral	110 kv	122 kv		275 kv	305 kv

3. The impulse strength for waves chopped after three microseconds is higher than test levels.

4. The steep-front-wave voltage strength should be higher than the three-microsecond strength and at least 1.25 times that value.

Unshielded Transformer for 138-Kv Service

Figures 3 and 4 show the coil arrangement for typical circular-coil-type transformers. The figures show only the outer part of the coils, and *G* represents the outer leg of the iron circuit and *Y* the top yoke. *G* could be either the outer leg of the core or an approximation to the adjacent winding stack. The figures are sections of the windings and show only the outside of the coils. There is a connection on the outer turn of the line coil to static plate and between the outer turns of coils 3 and 4, 4 and 5, and so on. The inner turns of coils 1 and 2, 3 and 4, and so on are not shown.

In Figure 4, a design has been chosen with less than three per cent of the winding between the finishes of the line and second coil. Hence there would be about three per cent of the induced voltage between coils on the induced test. Likewise on steep-wave-front tests we could have as much as 50 per cent of the surge voltage between these coils. In order for the stress between coils to be 50 per cent of the total surge voltage, a poor distribution factor would be required. This factor is a function of the capacitance of the entire column of coils to ground and the coil-to-coil capacitance along the stack. This poor factor was chosen to give an extreme condition.

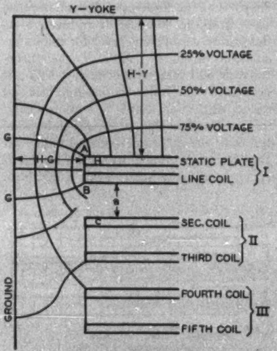

Figure 4. Dielectric field of core-type transformer with extreme voltage concentration at line end

I—100 per cent voltage
II—50 per cent voltage
III—25 per cent voltage

In Figure 4, *A* and *B* are corners of the static plate and line coil respectively and are connected together to form the line terminal. In order to determine the strength of such an assembly, and to determine the clearance necessary, a study of the voltage gradients at *A* and *B* was made. The conditions were that *HY* was 4, *H-H* was 2, and *A-B* was $^3/_4$ inches, which are common proportions. The distance from *B* to *C*, and the voltage from *B* to *C* are variable. In the first test, the gradients along *AG* and *BG* were kept alike and the distance and voltage from *B* to *C* varied. The results of this test are as shown on Figure 5; also, one test was made where the distance *a* was kept at unity, the voltage varied, and the gradients measured at both *A* and *B*. The results are shown on Figure 6. The tests were made by placing electrodes in a water tray and measuring the voltage drop from the corners of the electrodes to a fixed radius. Vacuum-tube voltmeters were used.

Figure 5 shows that, if *a* is four inches the same as *HY*, the stress at *A* and *B* would be alike with the same voltage across both *HY* and *a*. On the other hand, if the voltage at *a* is about 50 per cent of that across *HY*, a distance of $1^1/_2$ inches would be required. Further, it was found that the actual strength to ground for all conditions of Figure 4 was some 93 to 94 per cent of what it would be with a

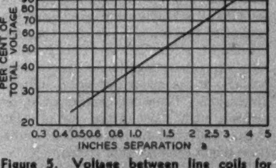

Figure 5. Voltage between line coils for different coil-to-coil clearances and for equal gradients at static plate and line coil

Table III. Relative Strengths of Typical Transformers

	Insulation Strength of Transformers—138-Kv Class					
	Fully Shielded Transformers		Unshielded Transformers I*		Unshielded Transformers II**	
Type of Stress	Transformer for 120-Cycle Induced Test, Kilovolts	Transformer for 60-Cycle Applied Test, Kilovolts	Transformer for 120-Cycle Induced Test, Kilovolts	Transformer for 60-Cycle Applied Test, Kilovolts	Transformer for 120-Cycle Induced Test, Kilovolts	Transformer for 60-Cycle Applied Test, Kilovolts
60 cycles	302 rms	275 rms	302 rms	275 rms	302 rms	275 rms
Full-wave impulse	650–900 crest	650–820 crest	650–900 crest	820 crest	<840 crest	<760 crest
Three-microsecond impulse	900 crest	820 crest	900 crest	820 crest	<840 crest	<760 crest
One-microsecond impulse	1,120 crest	1,020 crest	<1,050 crest	<950 crest	<1,050 crest	<950 crest

* Unshielded I has line coils with few turns so that the impulse penetrates into the winding when the front is $1\frac{1}{2}$ to $2\frac{1}{2}$ microseconds.

** Unshielded II has line coils with turns so that the distribution for even $1\frac{1}{2}$-microsecond fronts is wholly due to the capacitance between coils and turns.

uniform distribution as in Figure 3. In other words, if we had a uniform distribution, we would have an impulse strength of about 820 kv with a 275-kv 60-cycle one-minute test and an impulse strength of about 760 kv for conditions similar to Figure 4.

In a previous paper,[9] the use of "form factors" to estimate the strength of insulation arrangements in terms of a standard arrangement was used. Therefore, the form factor is a measure of the relative strength of the parts and without further consideration of exact values can be used to determine the relative strength of different parts of the winding. This form factor may vary when showing the relations of the stresses under 60-cycle and surge conditions in the same transformer. As an example of this, the form factors for the perfectly shielded transformer are the same for both 60-cycle and impulse stresses, and the stresses are relatively the same for both conditions. For the transformer of Figure 4 and under conditions of 60-cycle stress, the form factor would be 0.93 and the highest stress at *A*. Under surge conditions, if similar to those shown in Figure 5, the form factor would be 0.87 for steep wave fronts.

From Figure 6, conditions could be even worse, since, if the stress from *A* to *B* is large, the stress at *B* increases rapidly. For example, if the distance *a* is one inch and the stress across *a* is 70 per cent of the voltage from *H* to *Y* or *A* to *G*, the form factor at *B* is 0.70 which shows that failure would occur at *B* and at a relatively low value. The form factor for uniform distribution was 0.93 and is 0.70 for the condition given. From the results of this study, it is seen that the breakdown stress between coils is not a function of the voltage and distance alone but also of the major insulation and coil dimensions. The worst conditions, as described, might exist in the case of steep fronts, and good or even excellent conditions might exist for slow fronts.

There is still one other point which must not be overlooked. Even were the form factors the same at points *A* and *B*, if the strength of the insulating materials used is lower at *B* than *A*, the actual strength of the assembly under impulse conditions will be lowered. If we grant, however, that the insulation materials used at *A* and *B* are the same, we can determine the relative strengths of some typical transformers as shown in Table III.

In order to make the information in the Table III clear, let us consider the transformers designated as unshielded II.

The grounded-neutral transformer might be tested at 120 cycles for one minute at 275 kv or the equivalent of 302 kv, if tested at 60 cycles. Its impulse strength if the stress at both *A* and *B* were alike, would be $302\times\sqrt{2}\times2.1\times0.87/0.93$ or 840 kv. Likewise, at one microsecond, the strength would be 1.25 times 840 kv or 1,050. Actually values less than these are to be expected.

This table is quite interesting in that it shows that the three-microsecond impulse tests and the 60-cycle or induced tests determine a sufficient level for major insulation strength. Also, if the three-microsecond value is specified, it does not necessarily determine the one-microsecond value, but, if an ample one-microsecond value were specified, it would determine not only the three-microsecond value but the 60-cycle strength as well. To see if this is true, let us study what would happen if a 1,050-kv test were specified at one-microsecond. If this were specified for both grounded-neutral and fully insulated transformers, a 60-cycle level of at least 275 kv would be required for all types, and the 750- to 820-kv three-microsecond level would be automatically obtained. The inconsistency between the 120-cycle and 60-cycle tests would be removed. The latter would be true also, if the three-microsecond values were specified.

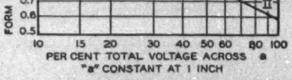

Figure 6. Variation in gradient at static plate and line coil for constant clearance between line coils and varying voltage between coils

I—Form factor at *A*
II—Form factor at *B*

At the present time, 650 kv is specified for the full-wave value. This is an independent and arbitrary value and determines the winding strength in the middle and grounded end.

Experience has shown that ability to withstand the applied 60-cycle test or 120-cycle induced test is no proof of a transformer's ability to withstand impulse tests. Therefore, it would be desirable to apply impulse tests to all transformers as a specified commercial test. It would be desirable to change the present tests, if any economies would result and if the testing procedure would be simplified. It is suggested that a three-microsecond, a one-microsecond, or a steep-front impulse test might be substituted for the present applied or induced tests. Since the full-wave test is necessary, it should be retained. Probably it would be desirable also to retain a two times induced test as a last test for all transformer windings. If the one-microsecond test at the correct level were used, it would ensure the three-microsecond value without making another test.

Incidentally, it is believed that very few failures are caused by 60-cycle or induced test at the factory, and practically all insulation troubles are found on either the steep-front or full-wave tests. Practically no failures are found on the three-microsecond chopped test.

Conclusions

It has been shown that an adequate one-microsecond or steep-wave-front strength of transformers also ensures both an adequate value of three-microsecond strength and 60-cycle strength, and avoids inconsistencies existing at the present time. It should, therefore, be possible to substitute impulse tests on transformers giving either a one-microsecond or three-microsecond value for the present 60-cycle applied or the high-frequency induced tests.

The present full-wave values still should be specified to ensure adequate strength against this type of surge. As further insurance, it is suggested that all overpotential tests at low frequencies should not be abandoned, and that a test of two times normal voltage be induced in all transformers. It is suggested that the tests recommended here be studied by the AIEE transformer subcommittee with a view to changing the present standards.

The Dielectric Strength and Life of Impregnated-Paper Insulation—IV

J. B. WHITEHEAD
FELLOW AIEE

J. M. KOPPER
MEMBER AIEE

STUDIES of the causes and mechanism of the failure of impregnated-paper insulation are commonly obscured by the burning due to the final complete breakdown. In a number of years of study of the more accessible properties of impregnated paper and their relation to stability and breakdown, constant attention has been given to the restriction of this burning and a nearer view of the beginnings of failure. Simple fuses and even rapid circuit breakers in the primary circuit of the testing transformer are of no avail. Some improvement is obtained by the use of a thyratron in the grounded lead of the sample with suitable connection to a rapid circuit breaker in the primary. But by far the best results, and indeed very complete success, have been reached by a method for detecting the first occurrence of gaseous ionization within the test specimen. This method is a development of the pioneer work of Paine[1] and the subsequent applications of Arman and Starr and of Whitehead and Shaw,[2] using resonance methods for following the oscillations which arise in the ionization of gas spaces in the insulation wall. New features which have been added are increased sensitivity, improved balancing of the Schering bridge for the frequency of maximum oscillations, the use of greater amplification, and a sensitive recording instrument for registering the first occurrence of internal ionization. The complete setup, as described in this paper, is called the "ionization recorder." With this instrument it is possible to detect the beginnings of failure in a completely impregnated specimen initially free of gas spaces or voids, often to within one layer of the impregnated structure, and also to follow its growth, with interruption at any desired stage on the way to complete breakdown. So far, the instrument has been applied only to the study of the influence of paper density on dielectric strength and stability, and the comparative behavior of two types of paper and two types of oil. From the results it will be seen that a very intimate picture of breakdown and its causes is presented.

Purpose

Earlier studies[3,4] on paper density showed clearly that for four papers ranging in specific gravity from 0.74 to 1.18, and for two oils, one light and one heavy, there is for each oil a pronounced decrease in dielectric strength with increasing paper density. A sound rational explanation of this result is found in much evidence that failures begin in the oil channels, and in the fact that the stress in these channels increases with increasing paper density due to the differences in the values of dielectric constant in paper and in oil.

Notwithstanding these clear-cut experimental results, many cable engineers state that experience has shown that the use of high-density paper in certain high-voltage cables increases dielectric strength. However, there is little or no published evidence in support of this view, except perhaps as regards breakdown tests of impulse type, and even in that case the picture is not clear.[5]

In possible explanation of this conflict of evidence it should be noted that in our specimens no gas pockets or bubbles are present, and in other respects they resemble the insulation of oil-filled cables far more closely than that of the solid cable. As a consequence no gaseous ionization is present in our tests, and breakdown stresses are well above those encountered in cable practice.

In the earlier studies referred to[3,4] an accelerated step-voltage test was used, the specimens being immersed in the oil under study at a constant temperature of 40 degrees centigrade. Breakdown occurred after two to four days at stresses up to 900 volts per mil. The chief purpose of the tests now reported has been to check the results of the earlier relatively long-time step-voltage tests, with others in which high stress is applied rapidly (two minutes) with resulting breakdown in a few minutes, thereby greatly reducing the influence of time as a possible factor in the earlier studies. For this purpose it was deemed sufficient to use only two grades of paper, namely, grades *B* and *D* of the earlier work.

Other results of interest are the stress-time curves of each paper impregnated with each oil, for short ranges in the neighborhood of breakdown; noticeable differences in two lots of supposedly identical paper from the same manufacturer; and further observations on the causes and mechanism of failure, based on careful dissection and oil extraction of numerous specimens suffering partial failure at various stages up to complete breakdown.

Test Specimens and Materials

The test specimens consisted of 16 layers of five-mil cable paper one inch wide, spiralled cable fashion on a smooth

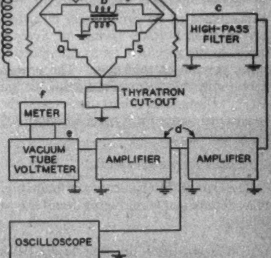

Figure 1. The ionization recorder

Paper 45-58, recommended by the AIEE committee on power transmission and distribution for presentation at the AIEE winter technical meeting, New York, N. Y., January 22–26, 1945. Manuscript submitted October 17, 1944; made available for printing December 21, 1944.

J. B. WHITEHEAD is professor of electrical engineering in school of engineering and J. M. KOPPER is junior instructor in electrical engineering, The Johns Hopkins University, Baltimore, Md.

Thanks are extended to the AIEE, the Engineering Foundation, and to various manufacturers and utilities companies, and to the advisory committee under the chairmanship of H. H. Race.

References

1. EFFECTS OF TIME AND FREQUENCY ON INSULATION TEST OF TRANSFORMERS, V. M. Montsinger. AIEE TRANSACTIONS, volume 43, 1924, pages 337–47.

2. INSULATION TESTS OF TRANSFORMERS AS INFLUENCED BY TIME AND FREQUENCY, F. J. Vogel; AIEE TRANSACTIONS, volume 43, 1924, pages 348–55.

3. POWER-SYSTEM VOLTAGES AND CURRENTS UNDER FAULT CONDITIONS, EFFECT OF SEQUENCE IMPEDANCES, R. D. Evans, S. H. Wright. ELECTRICAL ENGINEERING, volume 50, June 1931, pages 415–20.

4. KLYDONOGRAPH SURGE INVESTIGATIONS, J. H. Cox, P. H. McAuley, L. G. Huggins. AIEE TRANSACTIONS, volume 46, 1927, pages 315–29.

5. CO-ORDINATION OF INSULATION, V. M. Montsinger, J. E. Clem, W. L. Lloyd. AIEE TRANSACTIONS, volume 52, 1933, pages 417–27.

6. VOLTAGES INDUCED BY ARCING GROUNDS, J. F. Peters, Joseph Slepian. AIEE TRANSACTIONS, volume 42, 1923, pages 478–93.

7. FACTORS INFLUENCING THE INSULATION CO-ORDINATION OF TRANSFORMERS, F. J. Vogel. AIEE TRANSACTIONS, volume 52, 1933, pages 411–27.

8. BREAKDOWN CURVE FOR SOLID INSULATION, V. M. Montsinger. AIEE TRANSACTIONS, volume 54, 1935, December section, pages 1300–1.

9. CORONA VOLTAGES OF TYPICAL TRANSFORMER INSULATIONS UNDER OIL, II, F. J. Vogel. AIEE TRANSACTIONS, volume 57, 1938, September section, pages 531–4.

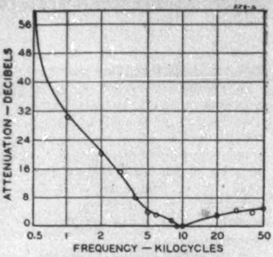

Figure 2. Filter characteristic

brass tube, one inch diameter, 48 inches long, with $33^1/_3$ per cent overlap and nominal $^3/_{64}$-inch channel width. The lead-foil central electrode (16.5 inches long) was flanked by overlapping guard electrodes extending halfway up the narrow-angle reinforcing end cones.[6]

The paper was furnished by a well-known manufacturer in two values of density; nominal values of specific gravity were: type *B* paper, 0.86; type *D* paper, 1.10.

Two oils were studied; one (5314) was a thin oil as used in oil-filled cables, having values of viscosity at 40, 60, and 100 degrees centigrade of 17, 8.2, and 3 centipoises, respectively, while the other (5317) was a heavier oil as used in solid cables, having values of viscosity at 40, 60, and 100 degrees centigrade of 480, 120, and 18.3 centipoises, respectively.

In general from three to nine identical specimens were tested for each combination of paper and oil, or for other variables studied.

For other details of the experimental equipment, methods of drying, impregnation, temperature control, and electrical measurements, the earlier papers[3] may be consulted.

The Measuring Equipment

Schering Bridge

This bridge of unsymmetrical type, and completely screened, has been described in earlier papers.[7] Power factor and capacitance at 60 cycles were measured up to 52,000 volts, giving an average stress in the specimen up to 650 effective volts per mil of thickness. The power-factor sensitivity was of the order 10^{-4} to 10^{-6}. During the short-time tests the maximum stress on a specimen was 725 volts per mil.

The Ionization Recorder

The essential elements of the ionization recorder are shown in Figure 1 and are as follows:

(*a*). The modified Schering bridge with test specimen in place.

(*b*). A bridge output transformer with electrostatic shield between primary and secondary, and with both windings balanced as to capacitance to ground, permitting the grounding of one terminal of the secondary coil without upset of the symmetry of the bridge circuit.

Table I

Cell Number	Thickness of Film, Cm	Area of Film, Sq Cm	Deflection Scale Divisions	Deflection Per Sq Cm
1	0.021	10.96	8.50	0.78
2	0.022	2.85	2.25	0.79
4	0.014	1.27	1.25	0.98

(*c*). An attenuator and a high-pass filter, whose characteristics are shown in Figure 2, matches as to impedance with the bridge transformer.

(*d*). A three-stage vacuum-tube amplifier.

(*e*). A bridge-type vacuum-tube voltmeter.

(*f*). A d-c recording milliammeter giving full-scale deflection for one milliampere, connected across the output terminals of the vacuum-tube voltmeter.

With the recorder connected, a specimen in place in the bridge, and a stress of 400 volts per mil applied, a small reading was found on the recorder. Its magnitude, from one to three per cent of the maximum reading encountered in the tests, showed no appreciable variation within the range of stresses used. With the specimen replaced by an air capacitor the small reading was still present and was found due to minute discharge points on the disconnecting switches and other parts of the high-voltage circuit. Since these discharges could not be eradicated completely, all recorder readings are based on this zero disturbance as datum line. Further, they were found useful for balancing the bridge, obviating the necessity of an auxiliary discharge gap for this purpose.

As shown in Figure 2 the filter effectively cuts out all frequencies below 3,000 cycles. The complete recorder circuit was found to be most sensitive in the region of 9,000 cycles. This is within the range of dominant frequencies of the gaseous discharge in cable insulation as found by Bennett, Paine,[1] and others. Thus the recorder receives the amplified, rectified, and integrated d-c record of frequencies above 3,000 and up to 16,000 cycles per second arising in a gaseous discharge in the specimen under test, and appearing at the output terminals of the bridge, the latter being balanced for minimum zero reading. The initial sensitivity of the bridge and recorder at 9,000 cycles was one division of the recorder scale per 18 microvolts at the transformer input terminals.

The initial sensitivity of the recorder was also measured in terms of the first discharge over a small air gap between plane surfaces. The gaps consisted of thin sheets of mica or lead foil with circular holes cut in them, mounted between thin sheets of glass. The gap was placed in parallel with an air capacitor, in place of the test specimen in the bridge circuit. On raising the voltage, visual discharge of the gap takes place at a sharply marked voltage, and with an immediate reading on the recorder. Table I gives the recorder readings for these initial discharges for three sizes of gap. From these simple data it appears that the recorder gives a response of about 0.8 to 0.9 division per square centimeter area of a 0.2-millimeter gap, and that the response is roughly proportional to the area of the gap.

Experimental Results

Initial Gaseous Ionization

In using the ionization recorder for the study of breakdown in impregnated paper the approach to failure is usually seen to be divided into three well-defined stages. The first is a slow (one minute) rise of the trace of the needle above the zero line. This indicates the beginning and slow growth of a spot of internal ionization. It is best observed at from 50 to 100 volts per mil below the maximum rapid breakdown value. With no further increase of stress the record flattens out into a second stage of constant value of internal ionization which may continue for hours, indicating a temporarily stable condition. However, something progressive is obviously taking place, for there comes a time when with no further increase in stress the

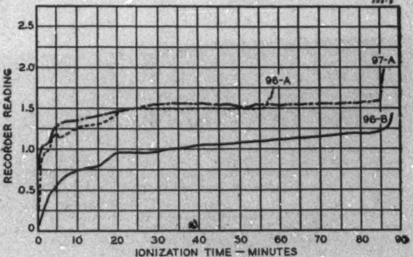

Figure 3. Ionization curves showing three stages in the variation of ionization with time

Paper *D* and oil 5317 at 600 volts per mil

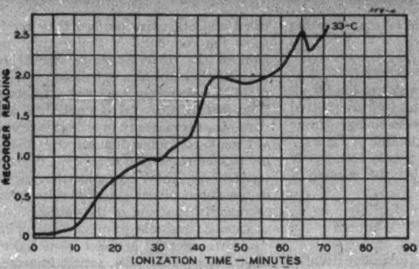

Figure 4. Ionization curve showing the nearly uniform rate of increase of ionization with time at very high stress

Paper *E* and oil 5314 at 800 volts per mil

record begins another rise which ultimately leads to breakdown, sometimes within a few minutes or even seconds. The boring action of the ionization has advanced so far that equilibrium is upset, and cumulative increase of stress on the still-undamaged portion of the insulating wall sets in. Figure 3 shows three good examples of the three stages, taken at 600 volts per mil on three identical specimens of *D* paper and oil 5317. Although there is some spread in shape and values the three stages are clearly seen in each case.

The duration of each stage is shortened rapidly with increase of applied stress. As the rapidly applied (two minutes from 100 volts per mil to full value) stress is increased, stages 1 and 2 disappear, ionization begins at once, and failure follows soon in stage 3. Figure 4 shows such a case, *E* paper,[3] 5314 oil, 800 volts per mil. This type of record is chiefly of interest as showing that even short-time failures are progressive with rapidly increasing volume of internal ionization. Thus for shorter and shorter duration of stress application, and ultimately impulse test, higher and higher values of stress are indicated for complete penetration over the ionization path.

If complete breakdown is allowed to occur the recorder needle goes off scale and the transformer primary circuit is interrupted by the thyratron circuit. In this case there is considerable burning in the path of the failure, although the thyratron usually interrupts before complete puncture has taken place. The ionization recorder, however, provides at once an indication of approach to breakdown and the circuit may be opened at any stage. In this way partial failures only are allowed to occur, and the growth of the internal gaseous ionization and its attack on the oil–paper structure may be closely followed by subsequent examination of the specimens. In most cases the failures extend through from four to six layers, but many instances in which only one or two layers are involved have been encountered.

New *B* and *D* Papers

It was necessary to obtain new lots of both *B* and *D* papers; they were furnished by the same manufacturer as the earlier lots, and on the same specifications. They agreed closely, in both density and thickness with the earlier papers, but certain differences were noticed in handling and assembling, principally in the matters of springiness or stiffness. Both the new papers were tested therefore with the same program of accelerated step tests as the old, using 5314 oil. The results of these check tests on six specimens of the new *B* paper and three of the new *D* paper are given in Table II. Comparison with the earlier tests shows that the earlier *B* paper had an average maximum-life stress of 713 volts per mil, and the later *B* paper 652 volts per mil, that is, the former 61 volts per mil or 9.3 per cent the better. There was no appreciable difference in the results on the two lots of *D* paper.

Influence of Paper Density

The approximate breakdown value of each type of present specimen was known from the earlier step tests, and from preliminary ionization-record tests. However, in order to lessen the uncertainty caused by the inherent spread of observed short-time intervals, it was decided to extend the range of observations over several values of stress in the neighborhood of the nominal maximum breakdown value. In this way breakdown stress-time curves are obtained with clearer pictures of the differences, if any, in the behavior of the two papers as the time of application of breakdown stress becomes shorter and shorter. Consequently, breakdown tests were made on each paper impregnated with each oil, at three values of stress, with results as indicated in Figures 5 and 6, and with accompanying ionization-time records. Table III gives the results of nine tests on *D* paper impregnated with the heavier oil. Table IV gives the average values for all tests on both papers and both oils. The curves of Figures 5 and 6 are plotted from the values in Table IV.

The sequence of observations was as follows: On switch closure a stress of 100 volts per mil was applied immediately, and then increased uniformly so as to reach the test value within two minutes. The ionization recorder was then cut in and its record followed, noting the condition of the specimen as regards the volume of internal ionization, and the successive stages marking the approach to failure. Immediate approach to failure is indicated by a rapid rise of the ionization record in the third stage of the curve of Figure 3. Most of the tests were interrupted a few seconds before complete puncture to avoid burning and to obtain a "partial" failure, yielding a much clearer picture on subsequent dissection of the specimen.

The curves of Figures 5 and 6 show that the influence of paper density reported in the earlier paper,[4] using a voltage step test, is confirmed by the present short-time tests, namely, breakdown stress and life are lower for the denser paper. If the two curves for the *B* paper are raised by 60 volts per mil to correct for its difference with the old *B* paper, the amount of the lowering is seen to be closely the same as in the earlier work. In the case of the 5314 oil the amount of lowering is practically the same for the lower stresses and longer times, becoming somewhat less as the test stress is raised. Using 5317 oil the amount of lowering is more or less uniform at the value found in the earlier work, except perhaps for the highest stresses where there is some indication that the curves may approach each other at still higher stresses.

Table II. Comparison of Old and New *B* and *D* Papers

Paper	Specific Gravity	Breakdown Stress, Volts Per Mil	Life, Hours
Old *B*	0.83	713	75.5
New *B*	0.86	652	63.6
Old *D*	1.14	573	48.9
New *D*	1.10	564	47.0

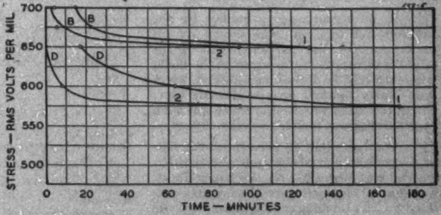

Figure 5. Variation of life and time to start ionization

Papers *B* and *D* impregnated with oil 5314

1—Life
2—Time to start ionization

POWER FACTOR

The increase of power factor with increasing paper density noted in the earlier work is also found in the present tests. Of particular interest are the observations of power factor (measured at 300 volts per mil) before and during the course of the tests which show that the effects of foregoing ionization have little effect in increasing power factor until well into the neighborhood of failure. In one case in which the ionization stress was 600 volts per mil, the power factor over the range 200 to 500 volts per mil was substantially constant at 0.0032; after 75 minutes at 600 volts per mil and very copious ionization for 7.5 minutes and breakdown imminent, the power factor was found to be 0.0041. In another step-voltage test the power factor at 400 volts per mil was 0.00449; after 28 hours at 482 volts per mil the value was 0.00430; after 39 hours at 529 volts per mil the value was 0.00510. The specimen failed at 529 volts per mil and 39.43 hours; a power factor reading was taken two minutes before failure, with value 0.00685. Thus even in the neighborhood of failure the value of power factor remains very low. The deterioration due to ionization in the approaching failure must be confined to very small volumes of insulation and ionized gas.

POST-MORTEM EXAMINATIONS

In a foregoing paper[4] the results of the examinations of 117 cases of failure were reported, with very clear evidence that initial failure usually occurs in oil channels or films. Similar evidence has been found in the post-mortem examinations of 65 failures in the present work. Of special interest are 6 incipient failures, involving only one or two layers, and reaching neither electrode, or only showing wax on paper edges of oil channels. In all these cases ionization as indicated on the recorder was well advanced before interruption of the test.

The important facts about the failures are:

(*a*). Of the 54 punctures reaching an electrode, 88 per cent terminated in an oil channel, 79 per cent of these at the central brass conductor.

(*b*). Microscopic examination of many burned areas disclosed the presence of removable carbonized oil particles on and among the paper fibers, with scorching of the fibers only at the edge of the puncture.

(*c*). In numerous cases examined by the magenta-dye test, wax was always present at the puncture and particularly along the edges of the tapes in the region of the burn, where the outline of the channel of one layer was clearly marked on an adjacent tape. The presence of wax in specimens where no tape burning was found is worthy of note.

(*d*). The facts that 88 per cent of the failures terminated in oil channels, that carbonized oil was deposited on the paper fibers, and that oil channels were often clearly outlined by wax on adjacent tapes point to the beginning of breakdown in the oil rather than in the paper fibers.

STRESS–LIFE CURVES

When the average values of life for all combinations of paper and oil are plotted against the values of stress on logarithmic co-ordinates, the straight line of Figure 7 results, indicating an inverse 12th-power stress–life variation in the range of stresses studied.

The Mechanism of Breakdown

The certainty that initial failure usually occurs in the oil channels greatly facilitates the drawing of the picture of the mechanism of complete failure. The properties of insulating liquids, and especially of petroleum oils, have been widely studied and their behavior under various conditions of electric stress, pressure, and temperature, are well known. For our present purpose we need only invoke three conspicuous properties of insulating oils, namely:

1. **Electrical conductivity and the d-c volt-ampere curve.**
2. **Space charge accumulation and its influence on potential gradient.**
3. **The influence of pressure and of temperature.**

THE VOLT–AMPERE CURVES OF OILS

There are illustrated in Figure 8 volt–ampere curves (a) for a high-grade insulating oil, (b) for the same oil carefully purified, and (c) the effect of successive redistillations in a closed system. Obviously the regions of rapid current increase are due to secondary ionization in the oil, that is, a progressive liberation of more free liquid ions. In the purest states the curves are identical in shape with the corresponding curves for a gas (although the ranges of values are different), and as in gases so in liquids the upturn of the curve is due to ionization by collision of electrons with neutral atoms and molecules of the oil. Cable oils, especially after contact with the paper and copper, have rather the characteristics of type (a) than of types (b) and (c); unless redistilled and otherwise purified they rarely show the horizontal or "saturation" region of the current–voltage curve. In purified oils ionization by collision and the rapid rise of current begins at a stress of from 250 to 300 volts per mil.[8] In less pure oils, the current curve begins to rise at even lower values of stress, due probably to dissociation, or other type of ionic separation. Above the saturation region in the purest oils the current rises as an exponential function of the voltage. As an extreme example, in toluol with an increase in potential gradient from 300 to 1,000 volts per mil the current increases 20,000 times.[8] In the less pure oil of type (a), ionization is well under way at 250 volts per mil and the current has already a relatively high value and increases four times as the stress rises from 250 to 300 volts per mil.

The ions of the saturation region are most commonly due to residual dissociated impurities. These are increased by contact with other materials, for example, paper and copper in the impregnation process, thus accounting for a change of the oil to type (a). The upturn of the current curve is due to collision of electrons liberated in the oil and at the electrodes, and moving with high velocities, with the neutral atoms and molecules of the oil, thereby causing a cumulative increase in the number of ions of both signs.

SPACE CHARGES

The accumulation of space charges near the electrodes in a gas at low pressure in which electrons are being liberated is well understood. A similar phenomenon takes place in a liquid under high electric stress. However, the mass of the liquid ion is so great and its specific velocity so small, that it appears more likely that the well-known accumulation of ions, and consequent high potential gradients at the electrodes of an insulating oil are due to clouds of ions surrounded by neutral molecules, and unable to escape to the electrodes.[9] As the stress or temperature rises, more and more of these ions are liberated from the enveloping neutral molecules, with corresponding contributions to the increase in current.

Table III. *D* Paper, 5317 Oil

Specimen	Breakdown Stress, Volts Per Mil	Time to Start Ionization, Minutes	Duration of Ionization, Minutes	Life, Minutes
98-*A*	650	0	33.0	33.0
98-*B*	650	0	19.0	19.0
98-*C*	650	0	18.5	18.5
Average	650	0	23.5	23.5
96-*A*	600	0	59	59
96-*B*	600	2	86	88
97-*A*	600	0	86	86
Average	600	0.7	77	77.7
96-*C*	500	55	378	433
97-*B*	500	614	32	646
97-*C*	500	648	790	1,438
Average	500	439	400	839

Table IV. Average Values, All Tests

Breakdown Stress, Volts Per Mil	Time to Start Ionization, Minutes		Duration of Ionization, Minutes		Life, Minutes	
	B	D	B	D	B	D
Oil 5314						
700	4.5		10.3		14.8	
675	5.5		17.2		22.7	
650	95	0	34	17.1	129	17.1
600		7.9		54.9		62.8
575		95.1		77.4		172.5
Oil 5317						
650	0	0	29.6	23.5	29.6	23.5
600	11.3	0.7	125.7	77	137	77.7
500	617	439	293	400	910	839

Under alternating stresses below say 200 volts per mil, in the oil channels of impregnated paper, these space-charge layers oscillate back and forth with the frequency of the applied stress. At very low stress the amplitudes of oscillation are small. With increasing stress the amplitudes increase, until ultimately some of the ions reach the boundary of the channel. Motion is arrested, and space charges accumulate, with increase of potential gradient over the oil–paper interface. The velocities of ions in cable oils at 20 to 30 degrees centigrade are of the order 10^{-4} centimeter per second per volt per centimeter; at the stresses here in question the velocities are quite high enough to permit practically complete passage of the ions back and forth over the whole thickness of the channel, in one 60-cycle period. In the lower range of stress this oscillating motion of space charges causes the component of loss due to the oil and contributes to the measured values of capacitance and power factor as already described in earlier papers.[4,8] The increase of stress at the surface of separation of oil and paper is not yet high enough to cause breakdown of the oil. As the stress increases further the number of free ions in the oil increases rapidly, due to internal ionization. Thus, the volume of space charge increases and the local stress at the interface between oil and paper rises rapidly to values far above the overall average measured values, and initial gas formation and gaseous ionization occur, leading on to breakdown in a short time.

Pressure and Temperature

Over a wide range of pressure above and below atmospheric value, the volt-ampere characteristic of the oil is not affected in either position or shape. However, with decrease of pressure below atmospheric, breakdown occurs at lower and lower voltages and for very low pressures may take place in the saturation region of an oil of type (b). Increase of temperature causes an exponential increase of the value of the saturation current, and corresponding increases in the ordinates of the curve above the saturation region; the curve retains its shape but moves upward in exponential relation to the temperature increase. These relations are in accord with the theory of secondary ionization in liquids.[8] As related to the present problem, it may be noted that in a certain cable oil under constant value of stress, an increase in the temperature from 15 to 83 degrees centigrade causes the current to increase 40 times, and for a temperature of 102 degrees centigrade, 150 times. Increase of temperature decreases viscosity and increases ionic velocities and current. Up to about 50 degrees centigrade the product of conductivity and viscosity is approximately constant, indicating that the "free-ion content" of the oil is constant.[11] At higher temperatures further dissociation sets in with large increases in the number of free ions, current, and loss.

Ionization, Space Charge, and Power Factor

The normal power factor–stress curves[3] of Figure 9 may be explained somewhat as follows: The in-phase component of the current is due principally to the motion of ionic charges through the mass of the oil, and this motion causes an energy loss due to friction. The magnitudes of current and loss are thus very sensitive to the number of ions present, to their specific velocities (mobilities), and to the applied stress. In the initial or low-stress regions of the curves the first stirrings of oscillatory motion of the sluggish ions begins. With increasing stress excursions are longer, more ions begin to move, and the ionic current increases faster than the capacitance-charging current; the power factor rises. With increase of temperature, the same sequence occurs, but the power factor rises more rapidly and to higher values due to the thermal increase in the number of dissociated ions.

In the lower range of temperatures and for stresses between say 30 and 300 volts per mil the power factor–stress curves are flat. This is the region in which all of the liquid ions have been set in motion. Their excursions (with frictional loss) are unrestricted, and like the charging component of the current, are proportional to the stress; the power factor remains constant. These conditions obtain over the range 20 to 50 or 60 degrees centigrade, though the constant value of power factor increases with the temperature owing to the increase in the number of free ions.

With further increase of temperature the power factor maxima at low stresses appear. The increasing maxima are due to the thermal increase in the number of dissociated free ions. But the increase of temperature also causes a decrease in viscosity; ionic mobilities increase, and with increasing stress ionic oscillations reach the paper barriers of the oil spaces. Thus ionic motion is restricted, the loss component of current no longer increases linearly with stress; the capacitance component maintains its linear increase; the power factor decreases with increasing stress.

At stresses beyond say 300 volts per mil all these curves again enter regions of power factor increase at first gradual and then more rapid. This increase is caused by the rise in conductivity of the oil due to ionization by collision attendant upon the increase of stress. Ultimately these increases lead on to breakdown, space charge playing its part in increasing the internal oil stress as described above.

Original differences in oil power factor are also reflected in the constant-power-factor values of the impregnated insulation; but a lower oil power factor does not necessarily lead to a higher breakdown strength. Oil power factor is usually measured at low stress (say 25 volts per mil), and is due to the original free ion content and conductance of the oil. In the higher range of stress toward breakdown, however, the conductance of the oil is enormously increased by secondary ionization, rising to hundreds or even thousands of times the low stress value. The original difference is negligible in the greatly increased values of each. Aside from certain inherent properties of the oil itself, breakdown is largely dependent on space charge formation, in its turn related to the total number of mobile ions present. Consequently, it is not normal to find any correlation in oils between power factor and dielectric strength.

Breakdown

In the light of the foregoing the process of failure in the insulation here studied is readily explained as follows.

The original state of the insulation comprises thoroughly impregnated paper and completely filled oil channels, that is, entire absence of visible gas pockets or bubbles. The type then is that of the best oil-filled cable insulation.

Under increasing stress the first disturbance of the original condition is the liberation of small gas bubbles in the oil channels. This occurs when the crest

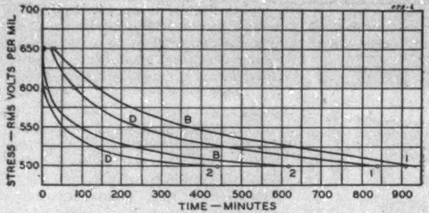

Figure 6. Variation of life and time to start ionization

Papers *B* and *D* impregnated with oil 5317

1—Life
2—Time to start ionization

value of the a-c stress wave reaches the breakdown (electron avalanche, or disruptive spark) stress of the oil. The computed value of the stress in the oil channels at final failure of the specimen in the paper density studies is from 1,000 to 1,500 volts per mil. The maximum disruptive strength of the purest hydrocarbon liquids is about 3,000 volts per mil,[8] that of a good cable oil substantially lower. The difference between these figures and those computed is to be found in the free ion content of the oil after impregnation, and, more important, in the consequent increase in stress near the paper surface by the accumulation of space charges in each half cycle.

Initial or crest gaseous ionization may not be detected at once on the recorder unless it occurs in a large number of places at the same initial critical stress. Nor does it necessarily result in a permanent gas bubble, if the stress rises no further. A minute gas bubble at the crest of the wave readily might be absorbed by the oil in the following half cycle during which the stress is below the critical value. However, if even crest ionization is allowed to continue it will liberate at each recurrence more liquid ions, the volume of the bubble and its attendant gas discharge will increase, attack the paper, and finally lead on to failure, with corresponding indications on the ionization recorder. Evidence of these conditions is found in the examination of several specimens removed from test at various stages of internal ionization. In these there was no gas formation or other evidence of approaching failure except a slight odor of burnt oil. However, on oil extraction and magenta staining clear wax deposits were found in every case, usually along the paper edges.

Some of the tests clearly indicate that for stresses as low as 400 volts per mil sufficient time will lead to the appearance of ionization and ultimately to breakdown. Figures 5 and 6 show that a time element is involved both before and after copious ionization begins. An explanation of the time element in the preionization (recorder reading zero) period is offered in the foregoing paragraph. In the postionization period time is obviously necessary for the gaseous discharge to burn its way through the adjacent paper tapes. Figure 3 gives a good idea of the growth of ionization in the average case; from post-mortem examinations of a number of specimens it appears that the central constant values of these curves is maintained while the ionization discharge is working through from one to three layers of the 16 layer specimen; from then on the failure proceeds with a rush. Obviously, as the rapidly applied stress is increased the time interval before ionization becomes shorter and finally disappears (in this work at from 600 to 700 volts per mil). Still further increase of stress reduces the time during which sustained ionization is evident. The shortest such time intervals observed in these tests were from three to nine minutes, at 700 volts per mil.

THE INFLUENCE OF PAPER DENSITY ON BREAKDOWN

The decrease in breakdown strength with increasing paper density found in these and preceding tests clearly is due to the increase of stress shifted to the oil channels by the increase in the dielectric constant of the denser papers. This and other behavior in the matters of conductance, capacitance, power factor, loss, and oil density have been explained in preceding papers, with particular reliance on the variation of ionic content and space-charge phenomena in oils.

The present tests, with increasing single values of stress rapidly applied and with failures occurring after intervals down to three minutes after the application of stress, show the same decrease in breakdown stress with increasing paper density as found in the earlier voltage step tests, which ranged over life values from two to four days. No attempt was made to shorten the life further by stresses above 700 volts per mil. It should also be noted that for both oils, stresses for immediate ionization are more than 12 per cent higher for the lighter than for the heavier paper.

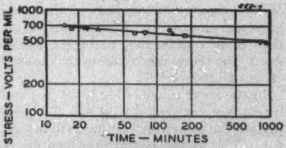

Figure 7. Life versus stress for four combinations of oil and paper

○—Paper *B*, oil 5314 △—Paper *B*, oil 5317
□—Paper *D*, oil 5314 ▽—Paper *D*, oil 5317

As to tests of impulse type, that is, durations of stress of the order of microseconds, the time intervals requisite for ionization to begin and to increase disappear, and breakdown takes on the character of disruptive discharge or so-called pure electric breakdown. If the medium is uniform this type of breakdown should occur at higher stress the denser the medium, as based on theory and confirmed by experiment. Cable insulation is not uniform, and the mechanism of failure pictured in these studies makes it a matter of progressive action first in the oil and then in the paper. Under impulse test the influence of time is practically excluded, and it may well be that the over-all density is the controlling factor. The results of Foust and Scott[6] give some support to this view; and as already noted Figure 6 suggests that for the heavier oil the curves for *B* and *D* paper may coincide or cross each other at still higher stresses.

There remains the question of the apparent contradiction between these studies and cable manufacturers' informal reports that the use of high-density paper results in higher dielectric strength. A possible answer suggests itself as follows.

If the comparison is that between a cable insulated completely with low-density paper and the same cable insulated completely with high-density paper, then the present studies indicate strongly that the former would have the higher dielectric strength in tests such as here reported, excepting possibly those of impulse types. However, if the cable-conductor insulation is made up in part with high-density paper next to the conductor, and in part with low-density paper outside, two conflicting conditions enter as follows:

(*a*). The electric stress at the surface of the conductor is reduced due to the increased capacitance of the inside-high density paper.

(*b*). The ratio of the dielectric constants of the denser paper and of the oil is increased, and so tends to increase the stress in the oil channel, and thus offset the lowering of stress of condition (*a*).

Approximate analysis in terms of cable dimensions and dielectric constants leads to equations which show that under certain conditions, for the same dimensions and the same value of applied voltage, the value of the oil stress in the channels of the inside high-density paper, may fall below that in the inside oil channels of the same specimen insulated throughout with low-density paper. Thus for a single conductor with cable insulation compounded of high- and low-density papers, a gain of dielectric strength up to 11 per cent over that of the low-density paper

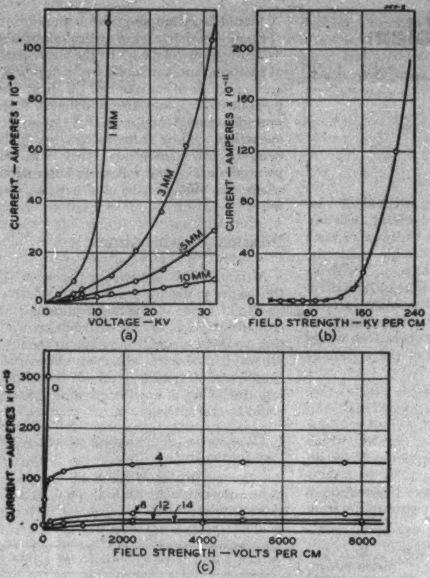

Figure 8. Current-voltage curves in insulating oils

(a). Commercial insulating oils

(b). Further purified

(c). Successive distillations

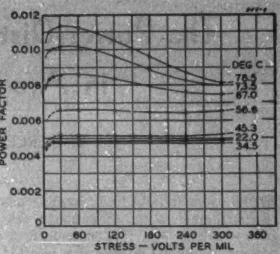

Figure 9. Power factor versus stress at different temperatures

alone is indicated, depending on the dimensions and relative values of paper density and dielectric constants of paper and of oil.

Gas-Filled Cables

It is interesting to ask whether these results have any bearing on the conditions in gas-filled cables. There being no free oil in the channels it appears that the mechanism of a short-time test failure may be of different type; space-charge and surface-layer effects are probably lower in value and of less effect; the cumulative oil ionization leading to failures at lower stresses and longer times in oil-filled channels has no obvious counterpart in gas-filled insulation. On the other hand two important facts stand out:

1. The ratio of values of stress in paper and oil noted are more than doubled for the paper and gas of the gas-filled cable.

2. Local ionization in gas-filled insulation may not be reflected in an over-all measurement of power factor of even a short sample, and such local ionization once started must be a serious menace even to wax-covered paper.

It would be interesting to know the values of stress at which local ionization, as distinct from that indicated by power-factor curves may first be detected in gas-filled insulation, and its rate of growth if any, as a factor in ultimate failure.

Conclusions

1. High-stress short-time constant-temperature tests of completely impregnated cable-paper insulation, approximating that in oil-filled cables, show that a higher-density paper has a lower breakdown strength. The results confirm those of earlier tests in which a step-voltage test over longer times was used. The behavior is much the same for both a light and a heavy oil.

2. A method is described for detecting the first occurrence of gaseous ionization in impregnated-paper insulation and for taking a continuous record of its growth up to breakdown. Interruptions of the tests at various stages as revealed by the ionization recorder show that ionization and failure almost invariably begin in the oil channels of cable insulation, and that a time element enters in both preionization and subsequent ionization periods.

3. Breakdown stress-time curves have been plotted for low- and high-density papers, each impregnated with a light and a heavy oil, for stresses between 700 and 500 volts per mil, and corresponding time intervals between 3 minutes and 900 minutes. A time variation as the inverse 12th power of the stress is suggested.

4. The mechanism of breakdown and power-factor and capacitance variation as related to paper density are discussed and explained in terms of fundamental conductance phenomena in insulating oils.

References

1. Investigation of Cable Ionization Characteristics With Discharge Detection Bridge, H. A. Brown, J. T. Tykociner, E. B. Paine. Bulletin 260, engineering experiment station, University of Illinois, August 15, 1933, page 6.

2. The Measurement of Discharges in Dielectrics, A. N. Arman, A. T. Starr. Institution of Electrical Engineers *Journal* (London, England) volume 79, July 1936, pages 67–81.

The Detection of Initial Failure in High-Voltage Insulation, J. B. Whitehead, M. R. Shaw, Jr. AIEE Transactions, volume 60, 1941, June section, pages 267–72.

3. The Dielectric Strength and Life of Impregnated-Paper Insulation—I, J. B. Whitehead. AIEE Transactions, volume 59, 1940, pages 715–20.

4. The Dielectric Strength and Life of Impregnated-Paper Insulation—III, J. B. Whitehead. AIEE Transactions, volume 61, 1942, August section, pages 618–22.

5. Some Impulse-Voltage Breakdown Tests on Oil-Tested Paper-Insulated Cables, C. M. Foust, J. A. Scott. AIEE Transactions, volume 59, 1940, July section, page 389.

6. Residual Air and Moisture in Impregnated-Paper Insulation—III, J. B. Whitehead, F. Hamburger, Jr. AIEE Transactions, volume 50, 1931, pages 1430–40.

7. The Influence of Residual Air and Moisture in Impregnated-Paper Insulation, J. B. Whitehead, F. Hamburger, Jr. AIEE Transactions, volume 47, 1928, pages 314–33.

8. Das Flussige Dielektrikum (book), A. Nikuradse. Julius Springer, Berlin, Germany, 1934.

9. The Conductivity of Insulating Oils, J. B. Whitehead, R. H. Marvin. AIEE Transactions, volume 49, 1930, pages 647–55.

10. Residual Air and Moisture in Impregnated-Paper Insulation—II, J. B. Whitehead, W. B. Kouwenhoven, F. Hamburger, Jr. AIEE Transactions, volume 47, 1928, pages 826–36.

11. The Dielectric Losses in Impregnated Paper, J. B. Whitehead. AIEE Transactions, volume 52, 1933, pages 667–81.

The Power-Distribution Problem in Arc Welding

H. W. PIERCE
NONMEMBER AIEE

C. E. SMITH
ASSOCIATE AIEE

THE extent to which arc welding has contributed to the shipbuilding program is well known. The consequent expansion of welding in shipyards resulted in various problems: the training of operators, production of the materials used, and by no means least, the development of satisfactory power-distribution systems. It is the intent of this paper to discuss briefly the general principles of power distribution for arc welding and to illustrate the application of these principles in the provision of an adequate, flexible, and economical distribution system in a typical shipyard. Although many conditions in shipbuilding are peculiar to the industry, it is believed that similar reasoning can be applied to any metal-fabricating plant making use of arc welding on a like scale.

Background

In the period between World War I and World War II, the plant of the New York Shipbuilding Corporation consisted essentially of five large covered building ways, a wet slip, outfitting piers, and the usual shipyard fabricating and outfitting shops. The corporation had commenced building operations in 1900 and therefore had a background of long experience in riveted ships of all classes. Arc welding was introduced in the yard prior to World War I on a very small scale; as late as 1930 equipment for this work consisted of only a score of individual d-c motor-generator sets and one constant-potential multiple-operator set with half a dozen outlet panels. Power for most of the welding machines and other power applications was provided by a 2,300-volt distribution system supplying various substations, transforming to 440-volt three-phase 60-cycle power for the shipways and fabricating shops. Some use was made of d-c power distribution in the case of the latter.

Applications of arc welding increased steadily from 1930 to 1939, particularly in the naval vessels then building, and the number of operators employed reached a peak of 300. Power for these growing operations was provided by moderate increase in the regular 440-volt distribution system, and some addition of both single-operator and portable multiple-operator motor-generator sets. A-c drive was made standard, and the old d-c-drive sets were replaced. It became increasingly evident that further extension of welding in shipbuilding operations would require radical revision of the system of power distribution.

Expansion

The magnitude of the problem which had to be solved in connection with the increase of activity from 1939 on is best understood by reference to the records of employment and power consumption from that time to the present. The power consumption and demand curves shown in Figure 1 are, of course, for all power used in the yard, as it is not possible to separate that used for welding operations except in certain areas. Records at these points established the correlation between electrode consumption and power, and these, when applied to the yard as a whole, indicate that at the peak in 1943 arc welding accounted for at least 1,250,000 kilowatt-hours per month.

Figure 1. Power and man-load record, New York Shipbuilding Corporation, 1939–44

A—Total man-load
B—Kilowatt-hours monthly
C—Maximum demand
D—Welding man-load

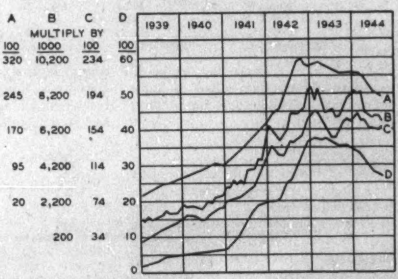

In 1939, moreover, the contracts under negotiation only partially indicated the requirements of the future, but it was realized that a basic plan of distribution would have to be selected which would be highly flexible and which could be expanded as increased demands were placed upon it. At no time during this expansion period was it possible to predict the welding requirements with any degree of accuracy for more than the next 12 months. It should be noted also that at the outset of expansion shortages of critical materials had not yet developed. In the latter part of the program, availability of equipment and materials became one of the most important factors, and time of delivery took precedence over first cost or economy in operation. Since these factors are incident to war emergency, they will be pointed out in the following discussion where they dictated the choice of any detail.

Principal Considerations

Although it is not within the scope of this paper to discuss in detail the relative merits of types of welding equipment, a bare description of the distribution system would be meaningless without the reasons which led to its selection. The principal questions which required answer before the layout of any distribution system could be started were:

1. Was direct or alternating current to be used for the arc?
2. Was generation of d-c welding current to be accomplished with individual or multiple-operator units?
3. What was the maximum current and range of current to be supplied each operator?
4. What was the total power to be delivered to each specified area of operation?

The first two items are highly controversial; furthermore, technological improvements present a constantly changing picture. Decision can be made only on the basis of close examination of all factors involved in a specific application.

Primary Factors

The selection of equipment and, therefore, the determination of the main features of the distribution system rest with the following factors:

1. Position in which welding is done.
2. Size and types of electrodes used.
3. Average current demand per operator.

Paper 45-48, recommended by the AIEE committee on electric welding for presentation at the AIEE winter technical meeting, New York, N. Y., January 22–26, 1945. Manuscript submitted November 27, 1944; made available for printing December 26, 1944.

H. W. Pierce is assistant general manager and C. E. Smith is plant electrical engineer with the New York Shipbuilding Corporation, Camden, N. J.

4. Total number of operators.
5. Area covered by welding operations; distances involved.
6. Space limitations.
7. Cost of installation.
8. Operating costs, including maintenance.
9. Safety.

Many of these factors are interdependent: the size and type of electrode is partly dependent upon the position in which welding is to be done, and items 4 and 5 taken together form a most important factor—the degree of concentration of force.

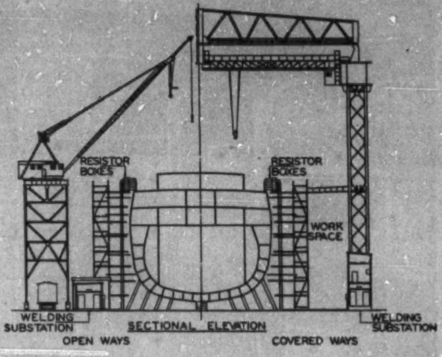

Figure 2. Sectional elevation of building ways, showing both covered and open types

General Conditions

Shipyards and shipyard practices are not necessarily alike, depending on the size and type of ship built by any yard. In the case of New York Shipbuilding Corporation for the past five years, the output has been naval construction exclusively and almost entirely large combatant vessels: cruisers, aircraft carriers, and battleships. Even under the pressure of wartime, such vessels require from ten months upwards on the ways and from four to eight months outfitting. Because of the complication of structure, the amount of shape, and rate of production, there is comparatively less opportunity for subdivision of the work, and, consequently, the necessity to do a high proportion of welding on the ways. The welding force increases with the steel erected, reaching a maximum at launching. It then drops to zero until the next keel is laid down, when the cycle starts over again.

Following launching, the ship moves into the wet slip where heavy weights, such as turrets, are installed and finally to an outfitting pier for completion. The welding load drops only momentarily following launching and, as a rule, equals or frequently exceeds previous peaks during the outfitting period, decreasing sharply as the delivery date approaches.

Welding conditions in the shops are quite different from those in the wet slip, and there is considerable variation between shops, depending upon functions. Insofar as welding operations are concerned, we deal principally with the plate and angle, boiler, copper, pipe, machine, and turret shops. The subassembly areas or slabs are quite similar to the plate- and angle-fabricating shop, in regard to welding.

In illustrating the application of factors which led to the choice of the distribution system, it is therefore convenient to deal with the ways, the outfitting piers, and the shops separately.

As previously noted, the entire system developed over a period of several years. The first step was the provision of adequate power on the five permanent and covered ways, the wet slip, piers then in use, and the shops. Subsequent expansion added five open temporary ways and required additional pier facilities. In the main, this expansion was an extension of the systems previously adopted, but some additional problems, notably availability of materials, were involved.

Covered-Ways Equipment

At the time the power system was developed for this area, there was little choice in the type of power for welding. A large percentage of the welding must be done in the vertical and overhead positions, and electrodes for alternating current, which would operate as easily and give comparable speeds and weld quality, were not available. Even now, with great improvement in a-c electrodes, the use of alternating current for ship work on the ways is debatable. It is necessary to have moderately long lines from the machine or panel to the work. This line lies on and across great masses of steel and leads through openings and hatchways, resulting in large and variable inductive drops. Although alternating current has been used on the ways in a number of European shipyards, direct current is almost always used in the United States.

The relative advantages and disadvantages of the two methods of generating the d-c power, the single-operator or the constant-potential multiple-operator set, require more consideration. Both types were available, both had been in use in this yard. The peak load on one shift on one way was estimated at 120 production operators and 80 tackers, therefore, requiring some 200 welding machines or panels per ship during the last months on the ways. This represents a high concentration of force. Space in the way area is at a premium, even if the machines or panels could be located at ground level. The length of welding cable actually handled by each operator had been standardized at 200 feet, made up of 100 feet of 2/0 cable attached to machine or panel, and 100 feet of 1/0, permanently spliced. This represented a compromise between minimum voltage drop and a length which would permit a reasonable working radius with minimum weight. Reference to a sketch showing a typical sectional elevation of the ways, Figure 2, shows the necessity, even with a 200-foot lead, for keeping the current control as close to the ship and to the level of the top deck as possible. This may be done by locating the machines either on deck or in the staging. The former method is very unsatisfactory on ships with a number of decks or much subdivision, since all machines have to be moved as additional steel is erected. Even when a group of machines is nested in a cradle there is still interference and loss of valuable deck space. The use of the staging space is a far better solution. One or two vertical moves keeps the outlet close enough to the top of structure yet is relatively independent of erection. Leads are very little longer than when placed on deck and there is no interference with cranes or other services.

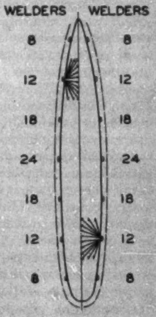

Figure 3. Typical resistor-box grouping of panels to provide 200 operators per ship

It is our usual practice to group machines or outlets at stations along the

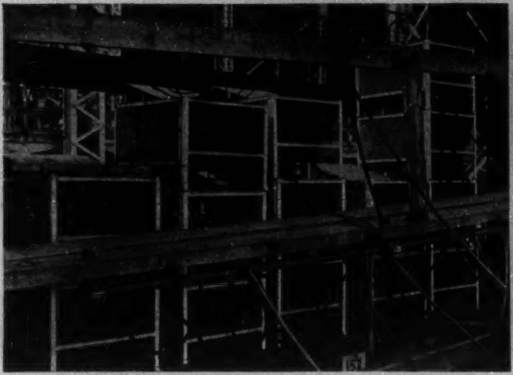

Figure 4. Front view of stack of resistor panels for ship welding

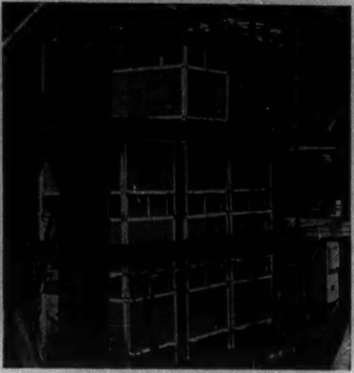

Figure 5. Rear view of stack of resistor panels for ship welding

ship's side, spacing these groups at intervals so that the effective working radii of leads overlap, thereby affording coverage for all jobs. Since the bulk of work is amidship, the grouping at these points is heavy and, in a typical case, takes the form shown in Figure 3.

Most ship welding on the ways is done with electrodes of $^3/_{16}$-inch or less diameter, using less than 200 amperes, due to the fact that so much welding is done in either the vertical or overhead positions. Tack welding requires much less, besides having an extremely low duty factor. There is, however, enough heavy deck and armor work requiring 300 to 400 amperes per operator to demand some heavy equipment at all stations. Individual motor-generator sets are available in standard sizes from 100 to 600 amperes. Though 200-ampere units have been found satisfactory in some cases, the 24-hour operation under shipyard conditions has made it advisable to use 300-ampere units as a minimum together with a lesser number of 400-ampere machines. As the work load is constantly shifting, it becomes a major problem to maintain a proper balance of equipment. The weight of some 20 to 30 such units requires special towers or staging units, and their movement is a major rigging operation.

Considerable experience with constant-potential motor-generator sets in the past had established, to our satisfaction, the following points:

1. A 1,500-ampere constant-potential set would carry 15 operators and ten tack welders on this type of work.
2. Parallel operation of such machines increased the number of production operators which could be carried to 120 when six units were in parallel.
3. At these loads, interference was nil or negligible.
4. Reactors were unnecessary to stabilize the welding circuit.

This led the way to our own design of a very compact and lightweight resistor panel, providing 30 to 200 amperes, in steps of ten amperes, independently, for each of two operators. In jobs requiring more than 200 amperes, a paralleling switch could be closed, permitting only one welder to work but giving 60 to 400 amperes. The total weight of this double-outlet panel is 180 pounds against 872 pounds for two standard 200-ampere individual units or 1,700 pounds for two 300-ampere units. The double panel is designed for stacking as shown by Figures 4 and 5, and the total weight of a group of 12 panels or 24 outlets is, therefore, only 2,160 pounds. Due to this light weight, it is possible to place these stacks on ordinary staging, which means being able to place them in the most desirable location and to shift them easily as conditions change.

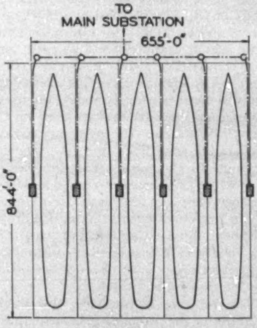

Figure 6. Plan of ways showing location of substations

▨—Welding substation
○—Underground manhole
—···Duct system
—·— 2,300-volt feeder

These considerations alone would have lead to the adoption of the constant-potential system for way's work. First cost was, as a matter of fact, lower for the entire system, and, from a safety standpoint, all portable cable and connections were thus handling 70 volts maximum instead of 440 volts. From a maintenance standpoint, oiling and upkeep of some 200 small motor-generator units would prove considerably more costly than would the six large units favorably located in a substation. A temporary-light station is placed adjacent to the substation, and the man in charge of temporary lights and service at that point is the operator of the welding substation, starting and cutting in machines as required. Since the panels are of simple and rugged construction, they withstand misuse and rough handling to a surprising degree.

There was, in this case, no disadvantage in the fact that all machines must work on the same polarity. The electrodes used for medium-steel structure, as well as the chrome-nickel austenitic electrodes, all either were designed for d-c reverse polarity or operated satisfactorily on either polarity.

Power Distribution on Covered Ways

The estimated man load per shift per ship was 120 production welders averaging 180 amperes per arc with an estimated operating time of 30 per cent, requiring, therefore, a capacity of approximately 7,000 amperes per way. The largest standard motor-generator set available was the 1,500-ampere size rated at 1,200 amperes continuous or 1,500 amperes for one hour. Six machines would, therefore, carry the estimated load. As previously stated, this had been checked by experience, and it was found that the 60 to 80 tack welders required per ship per shift also could be carried without overloading, because of the extremely low operating time required in tacking.

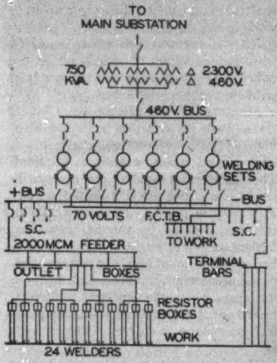

Figure 7. Single-line diagram of a typical welding substation and distribution to operators

F.C.T.B.—Full-capacity terminal bar
S.C.—Similar circuits

It is common practice to locate welding substations of this nature at the head of the ways. In this case, such space was not available, and, secondly, due to the length of the ways, it appeared highly desirable to locate the machines at approximately mid-length to reduce line drop and the amount of copper required. Accordingly, six welding substations were installed as shown in Figure 6. A single-line diagram of typical welding substation is shown in Figure 7. Under the covered ways, due to the column arrangements supporting the crane ways and roof, an area of 10 by 30 feet was available at each location.

On account of this small space a two level substation was designed, the upper level housing the switchgear and transformers, the lower level housing six constant-potential welding machines (Figure 2). To co-operate with the manufacturer, it was decided to mount the control equipment for both motor and generator above the motor-generator set, all supported on a common base, thus shortening the set and giving a very compact unit. A 440-volt driving motor was selected because of the use of 440-volt supply for miscellaneous power in ship construction and also because control equipment would be much smaller and less expensive than with 2,300 volts. From the standpoint of portability, such sets then could be used throughout the yard.

Synchronous motors on other power application had accomplished satisfactory correction of the yard power factor; therefore, induction motors were chosen for welding, again resulting in lower cost. The final machine adopted consisted of a 440-volt, 150-horsepower induction motor driving a 1,500-ampere 70-volt generator with an over-all length of $7^{1}/_{2}$ feet. This size permitted six machines to be located in the space assigned, giving a total capacity of 9,000 amperes for one hour or 7,200 amperes continuously, which was safely above the estimated load. A typical interior view is shown in Figure 8.

The machine described made a compact portable unit permitting a ready transfer of machines between stations as the work load built up on a particular way, thereby eliminating the possibility of idle machines and greatly reducing the number required.

From the main substation, where switchgear with adequate short-time and interrupting capacities could be provided, a 2,300-volt cable was installed to each welding substation, directly connected to a 750-kva bank of air-cooled transformers stepping down to 440 volts. Air-cooled rather than oil-cooled transformers were selected because of fire hazard adjacent to the ships under construction. Each motor circuit was connected to the 440-volt bus through air circuit breakers to the welder motor below. The generators are paralleled through a ring bus with positive and negative feeders taken off at opposite ends of their respective rings. This places all units equidistant from point of take-off and insures equal distribution of load between machines. This is of great importance, when it is considered that the load reaches a maximum of 9,000 amperes, and, in one station where ten machines are used, it reaches a maximum of 15,000 amperes. From the positive bus four 2,000,000-circular-mil feeders are connected through 2,000-ampere single-pole air circuit breakers, the feeders running parallel to the shipways. These feeders branch out, two in each direction, overlapping at the midship area or in heavy-load center (see Figure 9). Connected to these feeders are 18 outlet boxes spaced along each side of the shipways to give flexibility and to shorten the portable cables connected to the resistor boxes shown in Figures 3, 4, and 5.

Figure 8. Interior lower level of typical six-machine substation

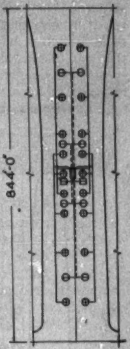

Figure 9. Typical substation, feeder and, outlet-box arrangement

▮—Welding substation
⊟—Full-capacity negative terminal
⊕—Outlet box
⊖—Terminal bar
——Positive feeder
- - -Negative feeder

This is the end of the permanent installation. To these outlet boxes there are connected four portable cables which run to the ship where 12 200- to 400-ampere duplex resistor panels are connected supplying a total of 24 welders.

Tack welders, who use small electrodes and comparatively low currents, could use a much smaller panel. Special tacker's panels are, in fact, in use in some yards. We have not adopted this for various reasons. It is common to have the heaviest tacking force on the day shift, working with other crafts in the erection and fitting of structure. Succeeding shifts carry a higher proportion of welders who perform the production work. When tackers finish, their lines are left on the job, and are taken over by the welding operator, with consequent saving of time and effort. To conserve on the number of panel outlets where an unusually large force of tackers is assigned to a shift, we have found it practicable to work two on a single outlet. The duty cycle is so low that there is little interference between the two, even when they are not in the same vicinity or in direct communication.

Particular attention is paid to the ground or return system. From the negative bus or ground return there are connected four 2,000,000-circular-mil cables each terminating at four equidistant points along the shipways. At these points there are heavy copper terminal bars to which the hulls of the ships are well bonded with portable cables. In addition there is installed a full-capacity negative ground terminal connected directly to the generator bus located amidship, or in the heavy-load center, to which the ships' hulls are connected with portable cables. These also are shown in Figure 7. In the early stages of ship construction the four feeders are necessary because various joints, seams, and so forth of the hull have not been completed, which offers a poor path for the return currents. As the ship nears completion the hull becomes a relatively good path for the return currents, far better, in fact, than all the cables that could be installed in a practical and economical manner. As this condition is reached, cables are added between the full-capacity negative bus and the ship's hull, until practically all the return currents are returning to the substation at this point.

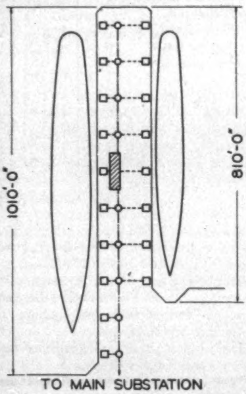

Figure 10. Welding substation and distribution system on typical outfitting pier

▨—Welding substation
○—Underground manhole
□—Outlet box
—· ·—Duct system
– – –Conduit system

Outfitting Piers

Insofar as the selection of welding equipment for the outfitting piers is concerned the factors are very similar to those considered for the covered ways. The outfitting piers are long and narrow with gantry cranes spanning practically the entire width. Thus, very little space was available between the crane rails and the side of the pier for location of welding equipment. As on the ways, consideration of space and weight requirements led to the adoption of the constant-potential system with, however, provision of sufficient power for a few individual-operator machines to cover any special job in the course of outfitting which might require a different polarity or special equipment.

A welding substation was installed between the crane tracks spanned by the gantry cranes. From the substation's cable vault an underground-duct system was installed to outlet boxes located on each side above ground between the crane rails and the sides of the piers, as shown in Figure 10. These outlet boxes are connected to the underground manholes with metallic conduits running under the crane rails. The resistor boxes are stacked in groups on the decks of the ships and are connected by portable cables to the outlet boxes (see Figure 11). With this method no interference was experienced among the cranes, material handling, ship mooring cables, and the welding outlet boxes and cables.

On the outfitting pier, where ships are moored one on each side after launching, an extremely heavy welding area was created. Based on an estimated manload peak of 160 welders per ship with two large ships outfitting simultaneously, or 320 welders per shift, using 150 amperes per man with an operating time of 25 per cent, a capacity of 12,000 amperes was required.

The same type and size of multiple-welding machines are used as on the ways for interchangeability between stations. A ten-machine station was installed having a total capacity of 15,000 amperes one hour or 12,000 amperes continuous. The one-hour rating takes care of all additional power required for tacking service. The ten welding generators were paralleled on a ring bus with the positive and negative cables taken off at opposite ends of their respective rings. From the positive ring ten 2,000,000-circular-mil insulated feeder cables were connected through ten 2,000-ampere single-pole air circuit breakers, these cables running underground through the duct system to 20 outlet boxes (two boxes per cable). From the negative ring ten 2,000,000-circular-mil bare cables were installed, these cables running underground through the duct system to the same outlet boxes. This shipyard is located in a fresh-water area, and, with the ship well-bonded to heavy negative-ground return cables, no pitting of ships' hulls due to electrolytic corrosion has been experienced.

Shops

Welding conditions in most of the fabricating shops are very different from those discussed under ways and outfitting piers. The operators are either in relatively small groups or are widely distributed over a considerable area, so that the concentration of force is low. More positioning for downhand welding is done, hence the average current used is much higher. Many shop operations require special electrodes, and more or less frequent changes in polarity are necessary. Space is usually ample for locating machines, and, as work loads are uniform and steady, there is little occasion to move or transfer equipment. An individual machine can, therefore, be selected which can be used to capacity and which is particularly suited to the operation at that point, whereas the multiple-operator set is at a serious disadvantage.

In many instances full advantage can be taken of a-c welding, particularly in the turret and boiler shops where heavy work in the downhand position predominates. The shops therefore are equipped with individual units, either a-c or d-c motor-generator sets or transformer-type welders, as the work dictates.

All units take power from the 440-volt three-phase 60-cycle shop feeders with fused outlet boxes and safety switches at all locations where welding is required. The transformer welders are necessarily single phase and are distributed equally over the three phases. Expansion of facilities was handled by running new shop feeders, or reinforcing old ones. A number of outlet boxes ample to cover anticipated needs were provided, and, in those few cases where the load was underestimated or radically shifted, it was comparatively simple to modify the 440-volt feeders.

The five temporary ways, which concluded the expansion problem, presented a similar electrical problem to that on the permanent covered ways, except that the former were intended for slightly smaller ships, and there was no overhead crane structure, as shown in left-hand side of Figure 2. These ways were built on the site previously occupied by two wide ways in World War I. This resulted in an arrangement permitting a very narrow space between pairs of ships and prevented installation of machines or outlets between each ship. On the other hand, this close coupling permitted a ship to be serviced for welding entirely from one side, assuming adequate generating capacity.

Three six-machine substations were, therefore, installed for the five ways (Figure 12), the compact design permitting the station to be located between the ship and the gantry space and actually under the staging. Since length was not restricted, but height had to be kept down the machines, transformers, and switchgear were all located on the same level with an underground-duct system branching out from each substation to the various outlet boxes located on both sides of the pairs of ways. All cables were run underground to the outlet boxes with portable cables connecting these boxes to the resistor units located on the staging at the side of the ship.

The estimated welding man-load per ship

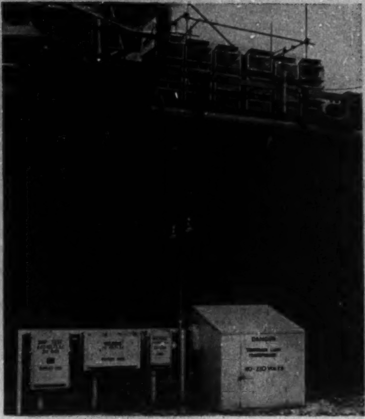

Figure 11 (left). View of power-distribution outlets on pier with welding resistor panels on ship

Figure 13 (right). Arrangement of single - operator welding machines for shipways use

per shift was 90 welders using 180 amperes per arc with an operating time of 30 per cent. This meant a peak load of approximately 4,860 amperes. The fact that two adjacent ships would not be expected to be in the same construction stage at the same time allowed sufficient margin whereby two ships could be supplied from a six-machine station. This condition proved satisfactory, until a ship was held up due to change in design. This caused a welding peak to develop beyond the capacity of the substations.

Normally, an additional substation would have been installed on the open side of the fifth ship to supply the additional welding capacity. As it was impossible to obtain either the large constant-potential motor-generator sets or the transformers and switchgear in time, it was necessary to use items on hand. Eighty 200-ampere individual motor-generator sets were found to be immediately available; accordingly, five towers were installed on the side of the ship way and five 440-volt circuits were run, one to each tower, from existing 440-volt outlets in the vicinity. These also are shown on Figure 12. Sixteen welding machines were located on a platform on each tower permitting the 16 machines to be lifted as a unit as erection progressed on the ship. See Figure 13. A standard welder's lead was run from each machine to the working locations on the ship. The negative or ground-return cables were connected to a heavy bus bar which was mounted on each tower and bonded to the hull of the ship.

It is interesting to note that the system used at this particular way was one of the alternatives considered and discarded in deciding the principal power-distribution system for welding on the ways. Experience with the system wholly justified the original decision where time of delivery or a lack of critical materials did not apply. Although some of the difficulties encountered were due to the fact that 200-ampere machines rather than 300-ampere machines had to be used, the lack of flexibility and portability in this emergency setup was keenly felt. Both operators and supervisors in welding, as well as other departments affected, are in unanimous agreement on this point.

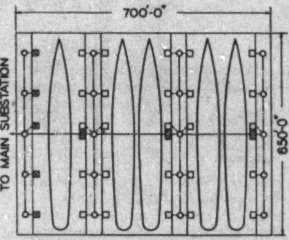

Figure 12. Plan of open ways showing location of substations and distribution system

▮—Welding substation
o—Underground manhole
□–··–Duct system
- - -Conduit system
☒—Tower for single-operator welding sets

Incidental Power

In conclusion, there remain substantial power demands for items incidental to, but not included in the foregoing discussion of welding power. Electric arc welding releases various fumes and gases, which have been proved low in toxicity but which are irritating and, like all metal fumes and smoke, dangerous, if inhaled in concentrations easily reached in confined spaces in ship's compartments and tanks. Removal of these fumes and the provision for a supply of fresh air, therefore, are problems of welding and another problem for the plant electrical engineer.

Use is made of two principal types of ventilating equipment at the New York Shipbuilding Corporation:

(*a*). A two-horsepower individual exhauster, handled by the welding operator and taking the fumes directly from the arc, designed for use on the 240-volt 180-cycle system provided primarily for drilling and reaming operations aboard ship and in the shops.

(*b*). Fifteen-horsepower exhausters with multiple 4-inch suction lines which can be led to various working locations, exhausting fumes outside the ship.

These operate from the 440-volt, three-phase 60-cycle system provided for general power. The extent to which ventilating apparatus for welding increases the power requirements can be appreciated, when it is compared to the power actually consumed in welding operations. Depending upon the degree to which the ship has been closed in, the concentration of work, and many other factors, from one-third to one-half as much power may be used in ventilation as in actual welding.

The use of welding in fabricating extremely heavy sections as in stern posts, rudder crossheads, and in joining high tensile and ballistic steels with moderate to high hardenability, has added the necessity of extensive preheating. Though this can be accomplished in some instances in a furnace, as by gas or oil torch, electric preheating is by far the most satisfactory form for most applications. Both induction and resistance types are in use, but

Induction Heating of Moving Magnetic Strip

R. M. BAKER
MEMBER AIEE

Synopsis: The general problem of heating iron or steel strip by induction is analyzed to arrive at equations for power-factor efficiency and density of heating under all conditions. Certain general curves are shown to illustrate the limitations of strip thickness, frequency, and density of heating.

MANY engineers are already familiar with the application of radio-frequency power to the brightening of electrolytic tin plate in continuous-line production. In this process, induction heating raises the temperature of the iron strip to the melting point of tin, causing the tin surface to melt and flow into a uniform tightly adhering layer while the strip is traveling at speeds up to 1,000 feet per minute or more. This application required the use of vacuum-tube oscillator equipment (frequency about 200 kilocycles) because of the thinness of strip to be heated: (0.007 inch to 0.014 inch approximately). There are, however, many possible applications of induction heating to thicker iron or steel strip, which may be accomplished by rotating machines (inductor alternators) having an upper practical frequency of about 10,000 cycles per second (9,600 cycles standard). This paper is written to show when and how iron strip may be heated at machine frequencies (9,600 cycles) and to show when it is necessary to use higher frequencies supplied by industrial vacuum-tube oscillators or generators.

There is practically no limitation on the thickness of strip which can be heated by induction, but, since a continuous-line process is considered, the most likely thickness range is from 0.003 inch to 0.032 inch. Strip widths up to four or five feet can be satisfactorily handled.

This treatment is limited to iron or steel strip which is ferromagnetic. Paramagnetic materials like copper, aluminum, brass, and such cannot be heated satisfactorily by the usual process of induction heating. Iron and steel lose their ferromagnetism between 700 and 800 degrees centigrade and cannot be heated economically above this temperature.

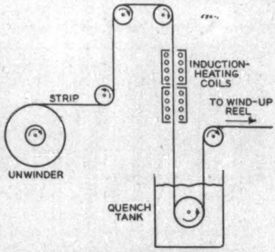

Figure 1. Simplified arrangement for induction heating of continuous moving strip

A much simplified handling and heating equipment is shown in Figure 1. The heating coils usually are wound in a single layer from hollow copper tubing about one-half-inch outside diameter and with the turns spaced one-eighth inch to one-half inch, depending on the frequency and the job to be done. The turns make complete loops around the strip and conform to the strip as closely as electrical and mechanical considerations permit. The coil may be made in several sections as indicated and extend from one foot to ten or more feet along the strip. Suitable support and insulation must, of course, be supplied.

Figure 2 shows typical circuits for feeding power to the work coil; circuit *a* using a vacuum-tube generator (200 kilocycles or higher) and circuit *b* using an inductor-type alternator (3,000 to 9,600 cycles).

Nomenclature

W_w = total watts required or induced in strip
N = strip speed (feet per minute)
c = specific heat
A_s = area of strip cross section (square centimeters)
θ = temperature rise of strip (degrees centigrade)
l_c = length of coil (centimeters)
μ = effective magnetic permeability of strip
H = peak magnetizing force (oersteds)
f = frequency (cycles per second)
t = strip thickness (centimeters)
K = a parameter (see equation 3)
ρ = electrical resistivity of strip (ohm centimeters)
$G(Kt)$ = a function of Kt (Figures 3 and 5)
W = watts per cubic centimeter in strip
K_1 = a constant (see equation 5)
B = flux density corresponding to magnetizing force, H; for H greater than 60, $B = 18{,}000$ gauss
I = coil current (rms) amperes
V = coil voltage (rms) volts
n = turns per centimeter in coil
W_c = copper loss in coil (watts)
b_c = width of coil (centimeters)
b_s = width of strip (centimeters)
h_c = smaller dimension of coil opening (centimeters)
K_L = voltage factor of coil
$(VI)_a$ = coil volt-amperes due to flux in the air
$(VI)_i$ = coil volt-amperes due to flux in the iron
δ_f = depth of flux penetration (centimeters)

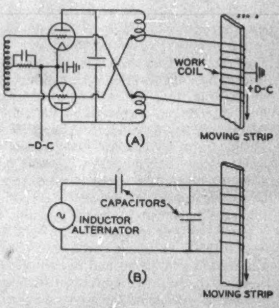

Figure 2. Electric circuits for induction heating of moving strip

---

Paper 45-80, recommended by the AIEE committee on industrial power applications for presentation at the AIEE winter technical meeting, New York, N. Y., January 22–26, 1945. Manuscript submitted November 25, 1944; made available for printing December 26, 1944.

R. M. BAKER is section engineer in the electrophysics department of the research laboratories of the Westinghouse Electric and Manufacturing Company, East Pittsburgh, Pa.

---

preference here is toward the resistance method, using strip heaters attached to the work. Aboard ship the 440-volt power is stepped down to 115-volts through $37^1/_2$-kva portable air-cooled transformers for ship-lighting circuits. Preheating makes use of this power, the strip heaters being connected up in very much the same manner as temporary lighting.

In the heavy fabricating shops, where preheating is an even heavier load, use was made of existing 230-volt d-c power feeders no longer needed for power tools, which had been converted in the course of several years, to a-c. Had such d-c power and shop feeders not been available, preheating in these shops would have been handled as aboard ship and would have required further reinforcement of the 440-volt shop feeders.

Power Required to Heat Moving Strip

The power required to heat strip depends on the weight of strip passed through the coil in unit time, its specific heat, and the temperature rise desired. It is expressed conveniently as

$$W_w = 16.6\, NcA_s\theta \text{ watts} \qquad (1)$$

where

N = strip speed (feet per minute)
c = specific heat
A_s = cross section of strip (square centimeters)
θ = temperature rise (degrees centigrade)

The equation for the watts per cubic centimeter which must be generated in the strip for a given speed and temperature rise is

$$W = \frac{16.6N\theta}{l_c} \text{ watts per cubic centimeter} \qquad (2)$$

l_c = length of coil (centimeters)

Power Generated in Strip

Because of the complications introduced by magnetic saturation, the mathematical problem of calculating the power input to a magnetic strip by a certain magnetizing force and frequency never has been accurately solved. The problem has been solved mathematically on the assumption that the permeability (μ) is constant in the strip and depends only on the peak magnetizing force at the surface. This solution gives

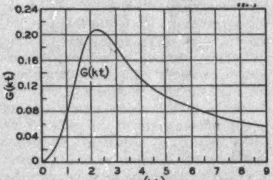

Figure 3. Strip heating by induction G(kt) versus (kt)

$$W = {}^1/_2\, \mu H^2 f G(kt) 10^{-7} \ \frac{\text{watts}}{(\text{cm})^3}$$

$$k = \sqrt{\frac{4\pi^2\mu f}{\rho}\, 10^{-9}}$$

For large values of kt, $G(kt) = \dfrac{1}{2kt}$

$$W = {}^1/_2\, \mu H f G(Kt) \times 10^{-7} \text{ watts per cubic centimeter} \qquad (3)$$

where

μ = magnetic permeability
H = peak magnetizing force at the surface of the strip (oersteds)
f = frequency (cycles per second)

$$K = \sqrt{\frac{4\pi^2 2\mu f 10^{-9}}{\rho}}$$

t = thickness of strip (centimeters)
ρ = electrical resistivity of strip (ohm centimeters)
$G(Kt)$ = a function of Kt, involving hyperbolic functions and plotted for convenient use in Figure 3

It can be shown for the nonferrous metals ($\mu = 1$) that $1/K$ is equal to the effective depth of current penetration. The same is approximately true for the ferromagnetic metals (iron and steel) below the Curie point (750 degrees centigrade), if (μ) is given the proper value.

For large values of Kt, corresponding to small depths of current penetration in the strip, the function $G(Kt)$ becomes equal to $1/2Kt$, and equation 3 for values of $Kt > 3$ may be written

$$W = \frac{1.26 \times 10^{-4}}{t} H^2 \sqrt{\mu f \rho} \text{ watts per cubic centimeter} \qquad (4)$$

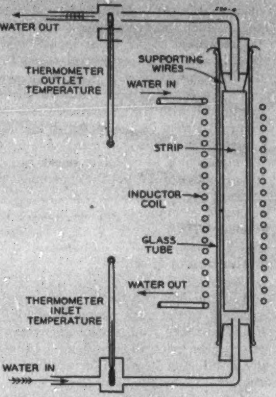

Figure 4. Schematic arrangement for measuring power input to strip

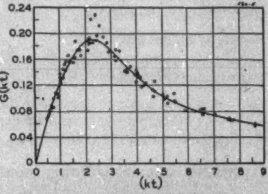

Figure 5. Experimental curve G(kt)

Summary of data for all strip thicknesses and all frequencies of tin plate

0.0095 inch—193 kilocycles
0.007 inch—77 kilocycles, 193 kilocycles
0.003 inch—77 kilocycles, 168 kilocycles, 300 kilocycles
0.00115 inch—88 kilocycles, 300 kilocycles, 490 kilocycles
9.6 kilocycles—0.32 inch, 0.028 inch, 0.005 inch, 0.007 inch

Table 1. Power Factor and Efficiency at 9,600 Cycles

Five-Foot Active Coil Length

Strip Thickness, Centimeters	Coil Power Factor	Per Cent Coil Efficiency	Over-All Efficiency
0.02			
0.04	0.03	44	33
0.08	0.14	89	66

If it be assumed that the effective or proper value of permeability to substitute in equations 3 and 4 bears a constant ratio to the peak permeability (B/H) at the surface of the strip, it may be written

$$\mu = K_1\left(\frac{B}{H}\right)$$

and substituting in equation 4 gives

$$W = \frac{1.26 \times 10^{-4}}{t} \sqrt{K_1 B H^3 f \rho} \text{ watts per cubic centimeter} \qquad (5)$$

The equation was first tested by the writer in this form and was found to agree well with experimental measurements on tin plate 0.010 inch thick induction heated with frequencies of several hundred kilocycles (large Kt values), when the constant K_1 was given the value 1.8. Thus, for this condition it is found that the effective value of permeability to be substituted in the power equation is 1.8 times (B/H), the permeability at the surface of the strip corresponding to the peak magnetizing force, H.

It was only natural to question whether or not this value of μ determined at high Kt values could be used satisfactorily in equation 3 with the curve of Figure 3 to calculate power input at low Kt values. To check this a series of tests was made using magnetic strip (tin-plate stock) ranging in thickness from 0.00115 inch to 0.032 inch and frequencies ranging from 9.6 kilocycles to 490 kilocycles. These tests are described later.

Experimental Check of Equation 3

Although induction heating is often applied to strip 36 inches or more wide, it was decided in view of the large number of measurements necessary to use for the test a section of strip 1.25 centimeters wide by 45 centimeters long, supported in a glass tube (two-centimeters inside diameter) as shown in Figure 4. The coil to carry the high-frequency current and produce the desired heating was five cen-

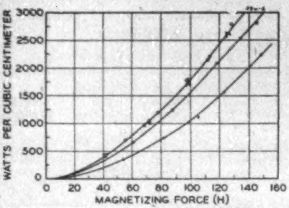

Figure 6. Power generated in 0.0095-inch-thick tin plate with various coil lengths

Frequency—196 kilocycles
Coil lengths:
o—39.3 centimeters
x—29.5 centimeters
Δ—20.8 centimeters
□—12.0 centimeters
▽— 4.8 centimeters

timeters in diameter and 39 centimeters long. It was wound with 61 turns of $^3/_{16}$-inch outside diameter hollow copper tubing and was water-cooled. The power input to the strip was determined from the rate of flow of water through the glass tube and its temperature rise. The temperature of the strip, which in most tests was near or slightly above the boiling point of water, was measured with a thermocouple.

Calculation of Data

In order to correlate the experimental results of many tests it was decided to assume that the form of equation 3 was correct as written with the possible exception that the $G(Kt)$ function of equation 3 might not agree with the theoretical curve of Figure 3 at low values of Kt. Solving equation 3 for this function gives

$$G(Kt)=\frac{2W10^7}{\mu Hf} \tag{6}$$

By determining W by measurement, calculating H from the current and coil dimensions, evaluating $\mu=1.8$ (B/H), and inserting the value of measured frequency, one can calculate the value of $G(Kt)$ which makes equation 3 agree with the measured power input in any test. In this way an experimental curve for $G(Kt)$ was determined and is shown in Figure 5. It is seen that this curve agrees well with the theoretical curve of Figure 3 except in the region of low Kt values. Thus, it is shown that one may use equation 3 to calculate power input for any value of Kt, but the experimental curve of Figure 5 instead of the theoretical curve of Figure 3 should be used to evaluate $G(Kt)$.

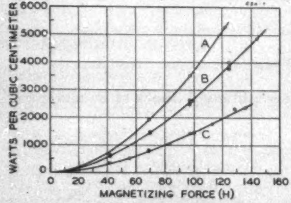

Figure 7. Power generated in 0.007-inch-thick tin plate at various frequencies

A—335 kilocycles
B—193 kilocycles
C— 77 kilocycles

Evaluation of B and H

B is the flux density in gauss corresponding to the peak magnetizing force H and is taken from the magnetization curve of the material to be heated. Usually in induction heating it is necessary to make H greater than 60 to obtain the desired power input so that B may be given a constant (near saturation) value of 18,000.

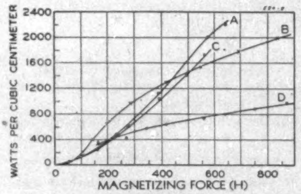

Figure 8. Induction heating of iron strip, 9,600 cycles

A—0.028 inch thick
B—0.014 inch thick
C—0.032 inch thick
D—0.007 inch thick

The magnetizing force was calculated in all cases from the equation,

$H=0.4\pi\sqrt{2}nI$ oersteds
$n=$ turns per centimeter in coil
$I=$ rms amperes in coil (7)

This equation is accurate only when the coil is long in comparison to its diameter or minimum cross-section dimension.

Experimental Curves of Power Input

The ranges of strip thickness and frequency used in obtaining the composite curve of Figure 5 is illustrated by the curves of Figures 6 to 13 inclusive.

The curves of Figure 6 show the effect of coil length and indicate simply that for short coils, the value of H is not calculated accurately by equation 7. It is seen that the error is negligible for coil lengths greater than 20 centimeters, and all subsequent tests were made with a coil length of 29 centimeters (46 turns).

The curves of Figure 7 show the effect of varying H and frequency. The frequency, strip thickness, and H in these curves correspond to large Kt values, and, as indicated by equation 5, the power input, W, increases with the $^3/_2$ power of H. Recent tests with a single-turn coil heating iron pipe indicate this law to be valid for values of H as great as 1,000.

Figure 8 shows that the shape of the power curves is quite different for thin strip and lower frequencies (low Kt values).

Figures 9 to 13 inclusive show experiment points determined on the $G(Kt)$ curve for various strip thicknesses and frequencies. In each case the theoretical curve is shown dotted for comparison with the experimental points. Most of the points were calculated from measurements for which H was greater than 60. Where points were taken from tests in which H was less than 60, the points are marked with a number corresponding to the H value. In general these points do not correlate as well as points taken at higher values of H.

Limitation of Power Input to Strip

The curves of Figure 14 show the power input to strips of various thicknesses calculated from equation 3, and the experimental curve of Figure 5. These curves are plotted in terms of W', the watts per square centimeter of strip $(W'=tW)$. As long as the depth of current penetration $(1/K)$ is less than about one third the strip thickness $(Kt>3)$, the current in each face of the strip is equal to the ampere turns of the coil and the power input at constant frequency (9,600 cycles) increases as the $^3/_2$ power of H. This condition is maintained for the 0.16-centimeter-thick strip even up to the highest values of H indicated. When the depth of current penetration becomes greater, due to increasing H, than one third the strip thickness, $Kt<3$, the currents on the two sides of the strip begin to counteract, and the power input goes up less rapidly than the $^3/_2$ power of H. This is illustrated by the curve for the 0.08-centimeter-thick strip, which begins to drop off at $H=400$. The curves for the 0.04-centimeter-thick and 0.02-

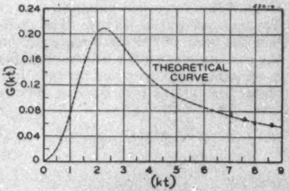

Figure 9. Experimental values G(kt). 0.0095-inch-thick tin plate

Frequency 193 kilocycles

centimeter-thick strips drop off at much lower values of H. In fact the curve for the 0.02-centimeter-thick strip shows very little increase in power input above $H=500$. The copper loss and reactive volt-amperes of the coil increase approximately with the square of H so that, as the power curve begins to flatten, the power factor and efficiency of the induction-heating coil become very low. Thus it is evident that there is a definite practical limit to the power which may be put into a strip of given thickness at any frequency. If the frequency be increased, this limiting value of power is, of course, increased. This is described in more detail in the next section.

Table II. Power Factor and Efficiency at 9,600 Cycles

Ten-Foot Active Coil Length

Strip Thickness, Centimeters	Coil Power Factor	Per Cent Coil Efficiency	Over-All Efficiency
0.02			
0.04	0.08	81	59.5
0.08	0.23	95	71.0

Power Factor and Efficiency

The power factor of the induction-heating coil is given by the equation

$$\mathrm{Pf}=\frac{W_w+W_c}{VI} \tag{8}$$

where

W_w = total power induced in the strip (watts)
W_c = total copper loss in the coil (watts)
V = coil voltage (rms volts)
I = coil current (rms amperes)

The coil efficiency is given by the equation

$$\text{Coil efficiency}=\frac{W_w\times 100}{W_w+W_c} \tag{9}$$

To determine the value of the factors entering into these equations consider a coil arrangement as shown in Figure 15.

l_c = length of coil (centimeters)
b_c = width of coil (centimeters)
b_s = width of strip (centimeters)
h_c = smaller dimension of coil opening (centimeters)
t = strip thickness (centimeters)

From equation 3 the total power into the strip is

$$W_w={}^1/_2\mu H^2ftl_cb_sG(Kt)10^{-7}\text{ watts} \tag{10}$$

Or if H is greater than 60 one may substitute

$$\mu=\frac{1.8\times 18{,}000}{H}$$

in equation 10 to obtain

$$W_w=1.62\times 10^{-3}fHtl_cb_sG(Kt)\text{ watts} \tag{11}$$

It is shown in Appendix I that the copper loss in the coil will be approximately

$$W_c=2.31\times 10^{-7}\,l_cb_cH^2\sqrt{f}\text{ watts} \tag{12}$$

It is also shown that the volt-amperes in the empty coil (no strip) are given by the equation,

$$(\mathrm{VI})_a=2.5K_LfH^2h_cl_cb_c\times 10^{-8}\text{ volt-amperes} \tag{13}$$

where

K_L = inductance factor of coil

The total volt-amperes of the coil is made up of two components: the volt-amperes $(VI)_a$ due to air flux and $(VI)_i$ due to flux in the iron. This latter is the most difficult and uncertain factor to evaluate, but luckily its value usually will represent a small part of the total volt-amperes of the coil. The writer has chosen to calculate $(VI)_i$ by a method suggested by Rosenberg's work[3] on eddy-current heating. Although the assumptions made by Rosenberg seem very crude, they produce a power equation almost identical with equation 5 of this paper when $K_1=1.8$.

It is assumed that the flux density penetrates from each surface of the strip at the constant value, B, to a depth (δ_f) at which point it suddenly drops to zero.

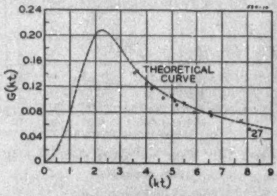

Figure 10. Experimental values G(*kt*). 0.007-inch-thick tin plate

o—77 kilocycles
x—1.93 kilocycles

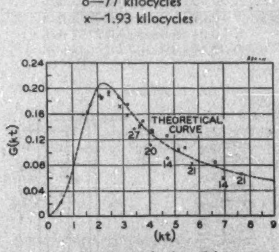

Figure 11. Experimental values G(*kt*). 0.003-inch-thick tin plate

o— 77 kilocycles
x—168 kilocycles
□—130 kilocycles

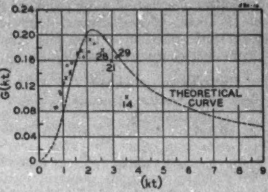

Figure 12. Experimental values G(kt). 0.00115-inch-thick tin plate

o— 88 kilocycles
x—300 kilocycles
Δ—490 kilocycles

This depth of flux penetration is given by the equation,

$$\delta_f=5{,}040\sqrt{\frac{\rho H}{Bf}}\text{ centimeters} \tag{14}$$

It is also assumed that the total flux varies sinusoidally in time and is in phase with the magnetizing force at the surface of the strip.

On these assumptions Appendix II shows that for the condition $\delta_f < t/2$ volt-amperes in the coil due to flux in the iron is given by

$$(VI)_i=5HfB\delta_fb_sl_c\times 10^{-8}\text{ volt-amperes} \tag{15}$$

If δ_f be greater than $t/2$, equation 15 may still be used, but δ_f must be replaced by $t/2$. That is, the flux in the strip cannot increase more after the depth of flux penetration becomes equal to one half the strip thickness. For convenient reference the depth of flux penetration is plotted as a curve in Figure 16.

Because the primary resistance drop in the coil is negligible and because of the way $(VI)_i$ has been obtained, the total volt-amperes in the coil is represented by

$$VI=(VI)_a+(VI)_i \tag{16}$$

and one has all the factors necessary to calculate power factor and efficiency from equations 8 and 9.

Typical Curves of Power Factor and Efficiency at 9,600 Cycles

If it be assumed that the strip and coil are of equal width (a condition which only can be approached in practice) one may calculate W_w, W_c, and VI per square

Table III. Power Factor and Efficiency at 200 Kilocycles

Five-Foot Active Coil Length

Strip Thickness, Centimeters	Coil Power Factor	Per Cent Coil Efficiency	Over-all Efficiency
0.02	0.13	98	59
0.04	0.11	97	58
0.08	0.09	96	57.5

centimeter of strip and using equations 8 and 9 obtain general curves of power factor and efficiency. This was done for the following set of conditions:

$f = 9{,}600$ cycles per second
$\rho = 22 \times 10^{-6}$ ohm centimeters
$K_L = 0.7$ (equation 12)
$B = 18{,}000$
$h_c = 7.5$ centimeters

The resulting equations obtained from equations 11, 12, 13, and 15 and based on one square centimeter of strip are

$$W_c = 0.226 \times 10^{-4} H^2 \qquad (17)$$

$$W_w = 15.5 H t G(Kt) \qquad (18)$$

$$(VI)_a = 12.6 \times 10^{-4} H^2 \qquad (19)$$

$$(VI)_s = 8.62 H \delta_f \qquad (20)$$

From these equations and equation 8, values of power factor were calculated and plotted in Figures 17 and 18. Coil efficiency was calculated from these equations and equation 9 and is plotted as curves in Figure 19. These curves indicate in a general way what power density, power factor, and coil efficiency can be obtained at 9,600 cycles when heating strips of various thicknesses.

Consider now the possibility of using 9,600-cycle power to brighten tin plate. This now is being accomplished with 200-kilocycle power under the following conditions:

$N = 1{,}000$ feet per minute
$\rho = 22 \times 10^{-6}$ ohm centimeters
$c = 0.12$
$l_c = 152$ centimeters (five feet)
$t = 0.018$ centimeters to 0.03 centimeters
$\theta = 250$ degrees centigrade

By substitution in equation 2 it is found that the power density necessary is 3,300 watts per cubic centimeter of strip. Values of power factor and efficiency obtainable with this input, taken from the curves of Figures 18 and 19, are listed in Table I. The over-all efficiency is calculated assuming an efficiency of 75 per cent for the motor-generator set. No values are shown for the 0.02-centimeter-thick strip, because it appears impossible to put the necessary power into this strip under any condition. Even for the 0.04-centimeter-thick strip, which is thicker than most tin-plate stock, the efficiency and power factor are still too low to be practical. The 0.08-centimeter-thick strip could, however, be heated quite satisfactorily.

In any case capacitors will be connected in parallel with the coil or in a series–parallel arrangement, as shown in Figure 2, to bring the power factor at the terminals of the generator essentially to 100 per cent.

Conditions could be improved somewhat by making the active length of coil twice as long (ten feet), as shown in Table II. It is still impractical to heat the 0.02-centimeter-thick strip although the 0.04-centimeter-thick strip can be heated with this longer coil at an efficiency comparable to that obtained with the present 200-kilocycle tin-brightening line.

Since most tin-plate production is for a strip thickness of about 0.025 centimeters, it is easy to see why the present installations were set up to use the higher frequency (200 kilocycles). One would not need to jump all the way from 9,600 cycles to 200 kilocycles from the standpoint of the work coil efficiency and power factor, but radio-frequency generators are cheaper and easier to operate at 200 kilocycles than at some lower frequency.

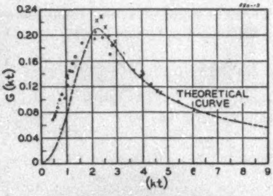

Figure 13. Experimental values of G(*kt*) for tin plate of various thicknesses

Frequency—9.6 kilocycles

o—0.032 inch thick
x—0.028 inch thick
□—0.014 inch thick
△—0.007 inch thick

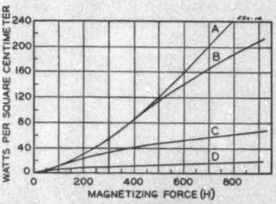

Figure 14. Watts per square centimeter of strip versus *H*

Frequency—9,600 cycles

Strip thicknesses:

A—0.16 centimeter = 0.063 inch
B—0.08 centimeter = 0.0315 inch
C—0.04 centimeter = 0.0157 inch
D—0.02 centimeter = 0.0078 inch

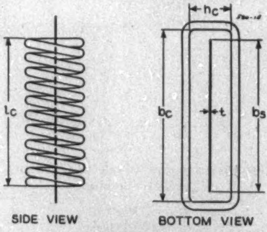

Figure 15. Induction-heating coil

Coil Power Factor and Efficiency at 200 Kilocycles

The same equations used in calculating the curves of Figures 17, 18, and 19 were applied to the problem of heating the same strip thicknesses at 200 kilocycles. The results are shown by the two curves of Figure 20. Since the depth of penetration of flux and current at this higher frequency is less than half the strip thickness, even at the highest power inputs (high values of *H*), a single curve of power factor and a single curve of efficiency is obtained for all three strip thicknesses when plotting against watts per square centimeter of strip. The crosses on the curves indicate the condition of operation for each strip thickness with a strip speed of 1,000 feet per minute and a temperature rise of 250 degrees centigrade. The values of efficiency and power factor are listed in Table III. The over-all efficiencies are calculated on an assumed efficiency of 60 per cent for the radio-frequency generator (vacuum-tube oscillator). Comparing Tables I and III one sees that, whereas the 0.02-centimeter-thick strip could not be heated at 9,600 cycles, it can be heated more efficiently than thicker strips at 200 kilocycles. The 0.04-centimeter-thick strip can be heated more efficiently at 200 kilocycles than at 9,600 cycles with an active coil length of five feet; however, by going to a coil twice as long this strip can be heated about equally well at both frequencies. The 0.08-centimeter-thick strip can be heated more efficiently at 9,600 cycles than at 200 kilocycles.

Coil Voltage and Current

The equations in the body of this paper have been kept in terms of volt-amperes in the coil rather than considering voltage and current separately. Knowing

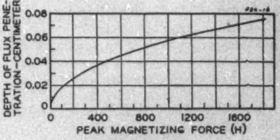

Figure 16. Depth of flux penetration in iron at 9,600 cycles

$\rho = 22 \times 10^{-6}$ ohm-centimeters

$$\delta = 5{,}040 \sqrt{\frac{\rho H}{Bf}}$$

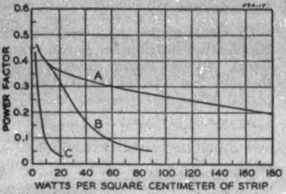

Figure 17. Coil power factor versus watts per square centimeter of strip, 9,600 cycles

Strip thicknesses:

A—0.08 centimeter = 0.0315 inch
B—0.04 centimeter = 0.0157 inch
C—0.02 centimeter = 0.0079 inch

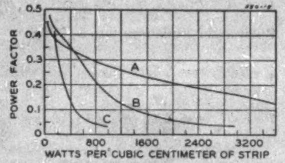

Figure 18. Coil power factor versus watts per cubic centimeter of strip, 9,600 cycles

Strip thicknesses:

A—0.08 centimeter = 0.0315 inch
B—0.04 centimeter = 0.0157 inch
C—0.02 centimeter = 0.0079 inch

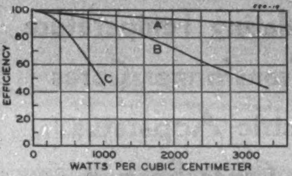

Figure 19. Coil efficiency versus watts per cubic centimeter of strip, 9,600 cycles

Strip thickness:

A—0.08 centimeter = 0.0315 inch
B—0.04 centimeter = 0.0157 inch
C—0.02 centimeter = 0.0079 inch

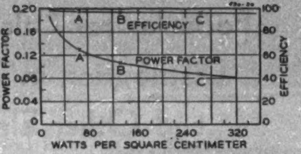

Figure 20. Coil power factor and efficiency versus watts per square centimeter of strip, 200 kilocycles

A—t = 0.02 centimeter (1,000 feet per minute)
B—t = 0.04 centimeter (1,000 feet per minute)
C—t = 0.08 centimeter (1,000 feet per minute)

the total volt-amperes of the coil, one may, after fixing on the number of turns per centimeter, determine the coil current from the value of H necessary to obtain the desired power density in the strip. The volt-amperes of the coil divided by this current will give the voltage across the coil with this current flowing.

Conclusions

Some heat can be generated in magnetic strip at even low frequencies, but there is for every strip thickness and frequency a definite practical limit to the density of heating possible. For any strip thickness and frequency the power factor and coil efficiency drop off with increasing power density as shown by the curves of Figures 17 to 20 inclusive. At strip speeds of 1,000 feet per minute and a temperature rise of 250 degrees centigrade, strips thicker than 0.04 centimeters (0.0157 inch) can be heated satisfactorily at 9,600 cycles. For thinner strips vacuum-tube or other type of generator must be used to supply a higher frequency. If the temperature rise be increased, the strip speed must be reduced proportionately to keep the power density constant.

Iron or steel strip cannot be heated economically above the Curie point (700 to 800 degrees centigrade) by induction heating as described in this paper.

Appendix I

Coil Copper Loss

Consider a coil consisting of a single wide sheet of copper forming a turn around the strip to be heated. Current supplied to this turn will concentrate almost entirely on the inside surface, and, if the current be adjusted to give a magnetizing force, H, in the space between the coil and the strip, the copper loss in watts per square centimeter of inside surface will be just that which would be produced by induction heating a sheet of copper in a magnetic field of strength, H. This can be shown to be[3]

$$W = 0.63\times10^{-4}H^2\sqrt{\rho f}\text{ watts per square centimeter} \quad (21)$$

Substituting the value $\rho = 2\times10^{-6}$ ohm centimeters for copper and multiplying by the total inner surface area of the coil, $2b_cl_c$, gives for the total power

$$W_c' = 1.78\times10^{-7}b_cl_cH^2\sqrt{f}\quad\text{watts} \quad (22)$$

Experience indicates that with a turn spacing of from one fourth to one conductor diameter, the actual loss is approximately 1.3 times that indicated by equation 22 or the total copper loss is

$$W_c = 2.31\times10^{-7}l_cb_cH^2\sqrt{f}\text{ watts} \quad (23)$$

The number of turns obviously does not enter into the calculation of total loss.

Volt-Amperes in Coil Due to Air Flux

The strip usually will occupy such a small fraction of the total volume of the coil that the volt-amperes due to air flux may be considered equal to the volt-amperes of the empty coil.

If the ratio of coil section length to the minimum dimension of coil opening (l_c/h_c) be greater than four, the heating observed seems to justify the use of the equation,

$$H = 0.4\pi\sqrt{2}nI\text{ oersteds} \quad (24)$$

to calculate the peak value of magnetizing force in the coil. However only part of the total flux b_ch_cH cuts all the turns of the coil. The voltage induced in the coil is

$$V_a = \sqrt{2}\pi fnl_cK_Lb_ch_cH\,10^{-8}\text{ volts (rms)} \quad (25)$$

where K_L = voltage factor of coil and has a value of about 0.7 when the ratio l_c/h_c is between four and six. K_L will approach unity for a long coil.

The current in the coil from equation 24 is

$$I = \frac{H}{0.4\pi\sqrt{2}n}\text{ amperes (rms)} \quad (26)$$

Multiplying equations 25 and 26 the volt-amperes of the coil due to air flux is found to be

$$(VI)_a = 2.5K_LfH^2h_cl_cb_c\times10^{-8}\quad\text{volt-amperes} \quad (27)$$

Appendix II. Volt-Amperes in Coil Due to Flux in the Iron

If flux penetrates at density B to a depth δ_f from each surface of the strip, the total flux in the iron is $2b_s\delta_fB$. The voltage induced in the coil by this flux is

$$V_i = \sqrt{2}\pi fnl_c2b_s\delta_fB\times10^{-8} \quad (28)$$

Multiplying this by the coil current from equation 26 gives for the coil volt-amperes due to flux in the iron,

$$(VI)_i = 5HfB\delta_fb_sl_c\times10^{-8}\text{ volt-amperes} \quad (29)$$

It is obvious, as indicated in the body of the paper, that, if δ_f becomes greater than one half the strip thickness it must be replaced by $t/2$.

References

1. ALTERNATING CURRENTS (book), **Alexander Russell.** Harvard University Press, Cambridge, Mass., 1914. Volume I, chapter XX.

2. EDDY CURRENTS IN IRON MASSES, **E. Rosenberg.** *Electrician*, August 24, 1923, pages 188–99.

3. HEATING OF NONMAGNETIC CONDUCTORS BY MAGNETIC INDUCTION, **R. M. Baker.** AIEE TRANSACTIONS, volume 63, 1944, June section, pages 273–8.

Formulas for Calculating Temperature Distribution in Transformer Cores and Other Electric Apparatus of Rectangular Cross Section

THOMAS JAMES HIGGINS
ASSOCIATE AIEE

THIS paper comprises solution of a very general problem in the mathematical theory of heat; application of it to effect formulas for the temperature distribution T, the maximum temperature T_m, and the average temperature T_a in transformer cores; and indication of its use with reference to other electric apparatus of rectangular cross section and of such general shape that the temperature distribution is essentially two dimensional. As theory indicates and experiment confirms that this condition is often fulfilled in practice, these formulas ought to be of considerable interest to designers of such equipment. For, commonly, the maximum electric loading of an electric device is determined by the permissible maximum or hot-spot temperature in it. Hence knowledge of this maximum temperature and of the temperature distribution in general is desired by the designer faced with making up new designs, improving operating performance of existing designs, or deciding upon maximum, yet safe, overload limits for apparatus already in service.

This work falls naturally into two parts. The first encompasses statement of the problem in the theory of heat; mathematical formulation of this problem, solution for the general temperature distribution, T, by the well-known method of expansions in infinite series, and derivation therefrom of formulas for the maximum and average temperatures, T_m and T_a and expression of special forms for T, T_m, and T_a. The second part embraces interpretation of the formulas derived in the first in reference to application to transformer cores; illustration of use thereto through calculation of the maximum temperature in a specified core and comparison with the corresponding experimental value; discussion of application to calculating temperatures in toroidal electric coils of rectangular cross section; and mention of other uses.

Derivation of Formulas

STATEMENT OF PROBLEM

The axis of a homogeneous infinite rectangular cylinder coincides with the z axis of a system of rectangular coordinates; the sides of the rectangular cross section, S, of width $2a$ and height $2b$ are directed parallel to the x and y axes (Figure 1). The thermal conductivities in the x and y direction are k_x and k_y. The rate of internally generated heat density is $q_0(1+\alpha_0 T)$, where of q_0 and α_0 are arbitrary constants. From the face of the cylinder f_i ($i=1, 2, 3, 4$) heat is transferred to the adjacent medium according to the relationship, $T-T_i=-K_i\partial T/\partial n$; where of n denotes the outward drawn normal to f_i; $K_i=R_ik_n$, wherein R_i designates the surface thermal resistivity of f_i and k_n the thermal conductivity in the direction of n; and regarding a point in f_i, T and T_i are respectively the corresponding temperatures in the cylinder and in the immediately adjacent ambient medium. No restriction is made as to the distribution of T_i over f_i except that it be expressible in a generalized Fourier series. What is required is the temperature distribution $T(x, y)$, the maximum temperature T_m, and the average temperature T_a of the cylinder.

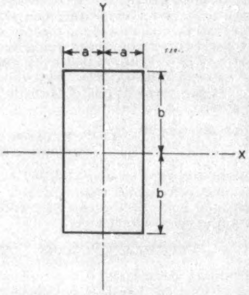

Figure 1

SOLUTION FOR T

By virtue of the given conditions the temperature distribution is two dimensional. By well-known theory we have, then, to find $T(x, y)$ that satisfies the partial differential equation

$$k_x\partial^2T/\partial x^2+k_y\partial^2T/\partial y^2=-q_0(1+\alpha_0T) \qquad (1)$$

over S, and the boundary conditions

$$T-T_1=-K_1\partial T/\partial x \qquad x=a \qquad (2)$$

$$T-T_2=\ \ K_2\partial T/\partial x \qquad x=-a \qquad (3)$$

$$T-T_3=-K_3\partial T/\partial y \qquad y=b \qquad (4)$$

$$T-T_4=K_4\partial T/\partial y \qquad y=-b \qquad (5)$$

Rearranging equation 1 yields

$$\partial^2T/\partial x^2+k\partial^2T/\partial y^2+C^2T=-C' \qquad (6)$$

wherein

$$k=k_y/k_x;\ \ C^2=q_0\alpha_0/k_x;\ \ C'=q_0/k_x \qquad (7)$$

Rearranging equations 2 to 5 yields

$$T+K_1\partial T/\partial x=\sum_{i=1}^{\infty}S_i\cos(s_iy+s_i') \qquad x=a \qquad (8)$$

$$T-K_2\partial T/\partial x=\sum_{i=1}^{\infty}S_i'\cos(s_iy+s_i') \qquad x=-a \qquad (9)$$

$$T+K_3\partial T/\partial y=\sum_{i=1}^{\infty}P_i\cos(p_ix+p_i') \qquad y=b \qquad (10)$$

$$T-K_4\partial T/\partial y=\sum_{i=1}^{\infty}P_i'\cos(p_ix+p_i') \qquad y=-b \qquad (11)$$

wherein the right-hand members are respectively the generalized Fourier expansions of T_1 and T_2 over $-b\leq y\leq b$ and of T_3 and T_4 over $-a\leq x\leq a$.

The procedure for solving equation 6 pursuant to equations 8 to 11 is: Symbolize the left-hand member of equation 6 as an operator $\nabla=(\partial^2/\partial x^2+k\partial^2/\partial y^2+C^2)$ operating on T, and find a particular solution of equation 6. Add to this functions F involving arbitrary constants so related that $\nabla F=0$, whence the resulting sum is also a solution of equation 6. Substitute this resulting expression in equations 8 to 11. Solve the resulting set of equations for values of the constants, whence T is now determined.

Thus, we assume T to be of the form

$$\begin{aligned}T=&\sum_{i=1}^{\infty}A_i\cos(m_ix+m_i')\cosh(n_iy+n_i')+\\&\sum_{i=1}^{\infty}B_i\cos(p_ix+p_i')\cosh(q_iy+q_i')+\\&\sum_{i=1}^{\infty}C_i\cosh(r_ix+r_i')\cos(s_iy+s_i')+\\&\qquad\qquad\sum_{i=1}^{\infty}D_i\cos(m_ix+m_i')\end{aligned} \qquad (12)$$

Substituting equation 12 in equation 6 yields

$$\begin{aligned}&\sum_{i=1}^{\infty}A_i(-m_i^2+kn_i^2+C^2)\cos(m_ix+m_i')\times\\&\qquad\qquad\cosh(n_iy+n_i')+\\&\sum_{i=1}^{\infty}B_i(-p_i^2+kq_i^2+C^2)\times\\&\qquad\qquad\cos(p_ix+p_i')\cosh(q_iy+q_i')+\end{aligned}$$

Paper 45-39, recommended by the AIEE committee on basic sciences for presentation at the AIEE winter technical meeting, New York, N. Y., January 22-26, 1945. Manuscript submitted November 13, 1944; made available for printing December 27, 1944.

THOMAS JAMES HIGGINS is associate professor of electrical engineering, Illinois Institute of Technology, Chicago, Ill.

$$\sum_{i=1}^{\infty} C_i(r_i^2-ks_i^2+C^2)\cosh(r_ix+r_i')\times \cos(s_iy+s_i')+$$

$$\sum_{i=1}^{\infty} D_i(-m_i^2+C^2)\cos(m_ix+m_i')=-C' \quad (13)$$

Assuming

$$n_i=[(m_i^2-C^2)/k]^{1/2} \quad (14)$$

$$q_i=[(p_i^2-C^2)/k]^{1/2} \quad (15)$$

$$r_i=(ks_i^2-C^2)^{1/2} \quad (16)$$

we have from equation 13

$$\sum_{i=1}^{\infty} D_i(-m_i^2+C^2)\cos(m_ix+m_i')=-C' \quad (17)$$

Now as derived in the appendix, the generalized Fourier expansion of $-C'$ is

$$-C'=-\sum_{i=1}^{\infty}(4C'\sin m_ia\cos m_i')(2m_ia+\sin 2m_ia\cos 2m_i')^{-1}\cos(m_ix+m_i') \quad (18)$$

Comparing corresponding coefficients of the cosine terms in the left-hand member of equation 17 and the right-hand member of equation 18 we find for D_i

$$D_i=(4C'\sin m_ia\cos m_i')(m_i^2-C^2)^{-1}\times(2m_ia+\sin 2m_ia\cos 2m_i')^{-1} \quad (19)$$

Accordingly, equation 12 satisfies equation 6 pursuant to equations 14, 15, 16, and 19. We proceed to determine values of the remaining constants such that equation 12 will satisfy the boundary conditions.

Substituting equation 12 in equations 8 to 11 yields

$$\sum_{i=1}^{\infty} A_i[\cos(m_ia+m_i')-K_1m_i\times \sin(m_ia+m_i')]\cosh(n_iy+n_i')+$$

$$\sum_{i=1}^{\infty} B_i[\cos(p_ia+p_i')-K_1p_i\times \sin(p_ia+p_i')]\cosh(q_iy+q_i')+$$

$$\sum_{i=1}^{\infty} C_i[\cosh(r_ia+r_i')+K_1r_i\times \sinh(r_ia+r_i')]\cos(s_iy+s_i')+$$

$$\sum_{i=1}^{\infty} D_i[\cos(m_ia+m_i')-K_1m_i\times \sin(m_ia+m_i')]=\sum_{i=1}^{\infty} S_i\cos(s_iy+s_i') \quad (20)$$

$$\sum_{i=1}^{\infty} A_i[\cos(m_ia-m_i')-K_2m_i\times \sin(m_ia-m_i')]\cosh(n_iy+n_i')+$$

$$\sum_{i=1}^{\infty} B_i[\cos(p_ia-p_i')-K_2p_i\times \sin(p_ia-p_i')]\cosh(q_iy+q_i')+$$

$$\sum_{i=1}^{\infty} C_i[\cosh(r_ia-r_i')+K_2r_i\times \sinh(r_ia-r_i')]\cos(s_iy+s_i')+$$

$$\sum_{i=1}^{\infty} D_i[\cos(m_ia-m_i')-K_2m_i\times \sin(m_ia-m_i')]=\sum_{i=1}^{\infty} S_i'\cos(s_iy+s_i') \quad (21)$$

$$\sum_{i=1}^{\infty} A_i[\cosh(n_ib+n_i')+K_3n_i\times \sinh(n_ib+n_i')\cos(m_ix+m_i')+$$

$$\sum_{i=1}^{\infty} B_i[\cosh(q_ib+q_i')+K_3q_i\times \sinh(q_ib+q_i')]\cos(p_ix+p_i')+$$

$$\sum_{i=1}^{\infty} C_i[\cos(s_ib+s_i')-K_3s_i\times \sin(s_ib+s_i')]\cosh(r_ix+r_i')+$$

$$\sum_{i=1}^{\infty} D_i\cos(m_ib+m_i')=\sum_{i=1}^{\infty} P_i\cos(p_ix+p_i') \quad (22)$$

$$\sum_{i=1}^{\infty} A_i[\cosh(n_ib-n_i')+K_4n_i\times \sinh(n_ib-n_i')]\cos(m_ix+m_i')+$$

$$\sum_{i=1}^{\infty} B_i[\cosh(q_ib-q_i')+K_4q_i\times \sinh(q_ib-q_i')]\cos(p_ix+p_i')+$$

$$\sum_{i=1}^{\infty} C_i[\cos(s_ib-s_i')-K_4s_i\times \sin(s_ib-s_i')]\cosh(r_ix+r_i')+$$

$$\sum_{i=1}^{\infty} D_i\cos(m_ix+m_i')=\sum_{i=1}^{\infty} P_i'\cos(p_ix+p_i') \quad (23)$$

When we take in equation 20

$$\tan(m_ia+m_i')=1/K_1m_i \quad (24)$$

$$\tan(p_ia+p_i')=1/K_1p_i \quad (25)$$

the first, second, and fourth terms of the left-hand member disappear and we have, on equating coefficients of corresponding cosine terms,

$$C_i[\cosh(r_ia+r_i')+K_1r_i\sinh(r_ia+r_i')]=S_i' \quad (26)$$

Similarly, if in equation 21 we take

$$\tan(m_ia-m_i')=1/K_2m_i \quad (27)$$

$$\tan(p_ia-p_i')=1/K_2p_i \quad (28)$$

we obtain

$$C_i[\cosh(r_ia-r_i')+K_2r_i\sinh(r_ia-r_i')]=S_i' \quad (29)$$

From equation 22, providing

$$\tan(s_ib+s_i')=1/K_3s_i \quad (30)$$

$$A_i[\cosh(n_ib+n_i')+K_3n_i\sinh(n_ib+n_i')]+D_i=0 \quad (31)$$

we obtain

$$B_i[\cosh(q_ib+q_i')+K_3q_i\sinh(q_ib+q_i')]=P_i \quad (32)$$

Finally, from equation 23, providing

$$\tan(s_ib-s_i')=1/K_4s_i \quad (33)$$

$$A_i[\cosh(n_ib-n_i')+K_4n_i\sinh(n_ib-n_i')]+D_i=0 \quad (34)$$

we obtain

$$B_i[\cosh(q_ib-q_i')+K_4q_i\sinh(q_ib-q_i')]=P_i' \quad (35)$$

Solving equations 24 and 27 simultaneously yields the values of m_i and m_i'; similarly the values of p_i and p_i' and of s_i and s_i' are furnished by simultaneous solution of equations 25 and 28 and of equations 30 and 33. Nomograms affording graphical solution of these pairs of equations are to be found in reference 2. Inasmuch as m_i, p_i, and s_i are determined, equations 14, 15, and 16 respectively yield n_i, q_i, and r_i. But n_i now being known, n_i^1 and A_i are the only unknowns in equations 31 and 34. Accordingly, equating the right-hand members, canceling D_i and then A_i, expanding the hyperbolic terms, and solving for $\tanh n_i'$ and thence n_i', we have

$$n_i'=\tanh^{-1}(K_4-K_3)[(2/n_i)+(K_3+K_4)\coth n_ib]^{-1} \quad (36)$$

In equations 31 and 34 A_i is now the only unknown. Thus, from equation 31

$$A_i=-D_i[\cosh(n_ib+n_i')+K_3n_i\sinh(n_ib+n_i')]^{-1} \quad (37)$$

Again, r_i being known in equations 26 and 29, r_i' and C_i are the only unknowns. Thus, dividing left and right-hand members of equations 26 and 29 to eliminate C_i, expanding the hyperbolic terms, solving for $\tanh r_i'$ and thence r_i', we have

$$r_i'=\tanh^{-1}\frac{[(\cosh r_ia+K_1r_i\sinh r_ia)S_i'-(\cosh r_ia+K_2r_i\sinh r_ia)S_i]}{[(\sinh r_ia+K_1r_i\cosh r_ia)S_i'-(\sinh r_ia+K_2r_i\cosh r_ia)S_i]} \quad (38)$$

In equations 26 and 29 C_i is now the only unknown. Thus from equation 26

$$C_i=S_i[\cosh(r_ia+r_i')+K_1r_i\sinh(r_ia+r_i')]^{-1} \quad (39)$$

In analogous fashion we obtain from equations 32 and 35

$$q_i'=\tanh^{-1}\frac{[(\cosh q_ib+K_3q_i\sinh q_ib)P_i'-(\cosh q_ib+K_4q_i\sinh q_ib)P_i]}{[(\sinh q_ib+K_3q_i\cosh q_ib)P_i'-(\sinh q_ib+K_4q_i\cosh q_ib)P_i]} \quad (40)$$

and

$$B_i=P_i[\cosh(q_ib+q_i')+K_3q_i\sinh(q_ib+q_i')]^{-1} \quad (41)$$

Accordingly, all constants in equation 12 being determined, we have the complete solution for T.

SOLUTION FOR T_m

T is a function of two variables. The form of T—the sum of four infinite series—renders unfeasible determination of the maximum temperature by application of the rules of the calculus for determining maxima and minima of functions of two variables. In general, the maximum temperature is to be ascertained by plotting the temperature distribution over that region of the cross section which a preliminary calculation, or consideration of given physical conditions, indicates as encompassing T_m. If, however, the temperature distribution be symmetrical about each of the co-ordinate axes (that is, $K_1=K_2$, $K_3=K_4$, $S_i=S_i'$, $P_i=P_i'$), T_m occurs at $x=0$, $y=0$. Hence, for this case, which, in fact, is that usually encountered in practice

$$T_m=\sum_{i=1}^{\infty} A_i \cos m_i' \cosh n_i' + \sum_{i=1}^{\infty} B_i \cos p_i' \times$$
$$\cosh q_i' + \sum_{i=1}^{\infty} C_i \cosh r_i' \cos s_i' +$$
$$\sum_{i=1}^{\infty} D_i \cos m_i' \tag{42}$$

Solution for T_a

The average temperature T_a over the cross section is given by

$$T_a=(^1/_4ab)\int_{-a}^{a}\int_{-} T\,dx\,dy \tag{43}$$

Substituting equation 12 in equation 43 and integrating yields

$$T_a=(1/ab)[\sum_{i=1}^{\infty} A_i \sin m_ia \cos m_i' \sinh \times$$
$$n_ib \cosh n_i'/m_in_i +$$
$$\sum_{i=1}^{\infty} B_i \sin p_ia \cos p_i' \sinh \times$$
$$q_ib \cosh q_i'/p_iq_i +$$
$$\sum_{i=1}^{\infty} C_i \sin s_ib \sin s_i' \sinh \times$$
$$r_ia \cosh r_i'/r_is_i +$$
$$\sum_{i=1}^{\infty} D_ib \sin m_ia \cos m_i'/n_i] \tag{44}$$

Special Forms

For reasons which will follow it is convenient to have the equations that stem from expressing the temperature in the form

$$T=T'+T_s;\ T_i=T_i'+T_s \tag{45}$$

wherein T_s is an arbitrary constant.

Substituting equation 45 in equation 1 yields

$$\partial^2T'/\partial x^2+k\partial^2T'/\partial y^2+C^2T'=-C'' \tag{46}$$

wherein

$$C''=q_0(1+\alpha_0T_s)/k_x \tag{47}$$

Substituting equation 45 in equations 2 to 5 yields

$$T'-T_1'=-K_1\partial T'/\partial x \qquad x=a \tag{48}$$
$$T'-T_2'=K_2\partial T'/\partial y \qquad y=-a \tag{49}$$
$$T'-T_3'=-K_3\partial T'/\partial y \qquad y=b \tag{50}$$
$$T'-T_4'=K_4\partial T'/\partial y \qquad y=-b \tag{51}$$

wherein

$$T_j'=T_i-T_s \quad (i=1, 2, 3, 4) \tag{52}$$

By virtue of the formal identity of equation 46 with equation 6 and of equations 48 to 51 with equations 2 to 5 we have at once that the solution for T' is afforded by that for T, if therein we replace C' by C'' and interpret S_i, S_i', P_i, and P_i' as the coefficients of the generalized Fourier expansions of, respectively, T_1', T_2', T_3', and T_4'. A similar conclusion holds for T_m' and T_m and for T_a' and T_a, whence

$$T_m=T_m'+T_s;\ T_a=T_a'+T_s \tag{53}$$

The transformations indicated by equations 45 and 53 are of particular interest because they afford very rapid solution of T for the practically important case of $T_1=T_2=T_3=T_4=T_s$. For then, interpreted as the Fourier coefficients of $T_1'=T_2'=T_3'=T_4'=0$, $S_i=S_i'=P_i=P_i'=0$; and the boundary equations for T' are much simpler than the corresponding equations for T. Whence T', and thus $T=T'+T_s$, can be found more quickly than could T, if this latter were to be evaluated directly from the equations given in stating the problem.

Application of Formulas

Transformer Cores

Formulas for calculating temperature distribution in transformer cores of rectangular cross section have been derived by Cockroft,[1] Roth,[2] and Buchholz.[3] Their procedures are alike: determination of the desired formulas is posed as a boundary-value problem in the mathematical theory of heat (in fact, as a special case of that treated in stating the problem). Solution of this problem is effected in some well-known fashion. That the assumptions enabling pose of temperature determination as a boundary-value problem in heat theory are valid under appropriate geometrical conditions is confirmed by the excellent agreement obtained by Roth between corresponding experimentally and analytically (from his formula) determined values of the temperature at points in the cross section of a small single-phase transformer. That the boundary conditions of practice are as indicated by equations 2 to 5 is substantiated by Cockroft's plots of data obtained from transformer-core temperature investigations sponsored by the Metropolitan-Vickers Company.

Cockroft considers the case of uniform generated heat density with thermal resistivity different on adjacent sides but identical over opposite sides in the adjacent ambient medium. Roth extends Cockroft's solution to encompass thermal resistivity different on each side; additionally, he advances the solution for nonuniform generated heat density with thermal resistivity different on each side. This latter work encompasses Buchholz's consideration of nonuniform generated heat density and boundary conditions of thermal resistivity identical over all sides and uniform temperature of adjacent ambient medium. Yet Roth's solutions, the most general available, do not encompass such practically important cases as that of a core with oil duct through the cross section (hence a nonconstant temperature distribution in the ambient medium along the lower edge of the upper half of the cross section) and of such area of cross section that the influence of the nonuniform generated heat density due to change of electric resistivity of the iron with temperature cannot be neglected.

The solution of this case—and of yet more general problems—is, however, afforded by the formulas derived in the first part of this paper. We need only interpret k_x and k_y as the thermal conductivities in the core, α_0 as the temperature coefficient of resistance at zero degrees centigrade of the core iron, q_0 as the generated heat density due to core losses in the iron at zero degrees centigrade, and R_i $(i=1, 2, 3, 4)$ as the surface thermal resistivities of the core faces; express the temperature distribution in the ambient medium as a generalized Fourier series; and through appropriate substitution of these data obtain T, T_m, and T_a.

Values of the just mentioned physical constants for typical materials are to be found in the papers of Cockroft, Roth (exhaustive treatment), and Buchholz. The value of q_0, the rate of generated heat density due to eddy currents and hysteresis losses, can be calculated from well-known formulas.

A Numerical Example

To illustrate application of the formulas derived in the first part of this paper to calculation of transformer temperatures we consider the following problem: to calculate the maximum temperature rise in the single-phase transformer tested by Roth.

Given Data. Single-phase transformer with rectangular cross section, $a=4$ cm, $b=6.75$ cm, laminations parallel to edges $2a$; measured maximum temperature rise equals 85 degrees centigrade above temperature of ambient medium; transformer gives up heat to ambient medium, which is air at temperature T_s; core loss $=0.0678$ watt per cubic centimeter.

Derived Data. We have $k_x=0.32$ watt per centimeter per degree centigrade; $k_y=0.005$ watt per centimeter per degree centigrade; $k=^1/_{64}$; $R_1=R_2=1{,}000/3$ square centimeter per watt per degree centigrade; $R_3=R_4=1{,}000/1.92$ square centimeter per watt per degree centigrade—values given by Roth as typical for the transformer tested. Hence, $K_1=K_2=R_1k_x=106.6$ centimeters; $K_3=K_4=R_3k_y=2.6$ centimeters. Inasmuch as no specific statement is made, we assume that the given core loss is the steady-state or hot core loss per unit volume of core. Necessarily, therefore, we consider it the average operating core loss and neglect nonuniformity due to temperature distribution. This assumption implies, as reference to equations 1 and 7 substantiates, that $q=q_0(1+\alpha_0T)\approx 0.0678$ watt per cubic centimeter; whence $C^2=0$ and $C''=q/k=0.212$. It is to be expected that in this instance no appreciable error is introduced by the neglect of nonuniformity of core loss due to temperature distribution: for the cross section is small; only the eddy-current losses are affected by variation in the temperature coefficient of resistance; the slight error introduced may be compensated by other small errors, for example, the effect of the not exactly uniform magnetic field on the distribution of hysteresis losses and so forth.

Formula for T_m'. Making use of the special forms already given, we have $P_t=P_t'=S_t=S_t'=0$; from given data, $K_1=K_2$, $K_3=K_4$, $C^2=0$. When these values are used equations 36, 39, and 41 yield $n_t'=C_t=B_t=0$. Accordingly, by equation 12 we need determine further only m_t, m_t', n_t, A_t and B_t. Equations 24 and 27 yield $m'=0$ and $\tan m_ta=(K_1m_t)^{-1}$, and from equation 14 we obtain $n_t=m_t/k^{1/2}$. With these values we obtain from equations 19 and 37

$$D_t=4C''\sin m_ta/m_t^3(2m_ta+\sin 2m_ta)$$

$$A_t=-4C''\sin m_ta/m_t^3(2m_ta+\sin 2m_ta)\times (\cosh n_tb+K_3n_t\sinh n_tb)$$

Finally, substituting appropriately in equation 12 and taking $x=y=0$, we have for T_m'

$$T_m'=4C''\sum_{t=1}^{\infty}[\sin m_ta/m_t^3(2m_ta+\sin 2m_ta)][1-(\cosh n_tb+K_3n_t\times\sinh n_tb)^{-1}] \quad (54)$$

Numerical Values of T_m and T_a. Using the above derived values of q, k_x, k_y, K_1, and K_3, we find by direct calculation

$m_1a=0.1925$; $m_1=0.0481$; $n_1=0.3848$; $n_1b=2.605$

$m_2a=3.1535$; $m_2=0.7884$; $n_2=6.3072$; $n_2b=42.57$

$\sin m_1a=0.1913$; $\sin 2m_1a=0.3756$; $\cosh n_1b=6.802$; $\sinh n_1b=6.728$

$\sin m_2a=-0.0124$; $\sin 2m_2a=0.0248$; $\cosh n_2b=\sinh n_2b>10^{18}$

Substituting appropriately in equation 54, we obtain

$$T_m'=85.3°-0.00216°+\ldots=85.3°$$

This value is but 0.3 degrees centigrade greater than the measured value.

Note that the infinite series of equation 54 converges so rapidly that it is necessary to use only the first term! All computations were performed on a 20-inch slide rule; values of trigonometric and hyperbolic functions are taken from standard tables having arguments in radian measure.

ELECTRIC COILS

A current-carrying toroidal coil of rectangular cross section, comprised of many turns of insulated wire of circular or of rectangular cross section, is an important component of many electric devices. Commonly, the coil is either exposed to the atmosphere—as, for example, are the field coils of a dynamo—or is submerged in a liquid—as, for example, are the coils of a transformer. Usually, conditions are such that the temperature distribution in the coil is substantially independent of the angular co-ordinate of a system of cylindrical co-ordinates, the longitudinal axis of which is the axis of the coil. If so, the temperature distribution is two-dimensional, that is, it is the same over any cross section of the coil.

In use the heat generated in the coil results in a general temperature rise throughout the coil. In consequence, a point of maximum temperature is to be found in the cross section. By virtue of the assumed angular symmetry this maximum temperature is the maximum temperature in the coil. Now, in that the permissible maximum coil current is that which produces a specified maximum temperature in the coil, and in that the hot or operating resistance of the coil depends on (and can be calculated from) the average temperature of the coil, formulas for predetermining the temperature distribution, maximum temperature, and average temperature are of considerable interest to the designer of toroidal coils.

A comprehensive discussion of the physical bases underlying derivation of such formulas comprises a recent lengthy paper by the writer.[4] For explicit details the reader is referred to this paper. For present purposes it suffices to remark that following epitomization of the work of Binder,[5] Humburg,[6] Jakob,[7,8] Ott,[9] Punga,[10] Rogowski,[11,12] and Vidmar,[13] a careful consideration of the individual and collective effects of the various physical and geometric factors involved leads to the conclusion that, if a toroidal coil, *i*, is comprised of many turns of thinly insulated wire of comparatively small cross section, *ii* is of rectangular cross section, and *iii* is of a ratio of outer to inner radius greater than (roughly) two, determination of T, T_a, and T_m for the coil—internally generated heat and change of wire resistance with temperature being taken into account—can be posed as a more or less complex two-dimensional boundary-value problem in the mathematical theory of heat, capable of solution by known methods. Illustratively, the solution for the boundary-value condition of constant surface temperature is obtained and it is shown that this solution encompasses, as special cases, the earlier analytic solutions of Humburg,[6] Jakob,[7,8] and Rogowski.[11,12]

The more important problems that arise in practice are, however, not encompassed in the comparatively simple boundary condition of constant temperature. Experiment shows that the boundary condition is commonly that of equations 2 to 5. Solutions for such a boundary condition have been advanced by Roth[3] and Buchholz.[14] The latter takes into account variation of wire resistance with temperature but considers only the case of constant temperature in the adjacent ambient medium with the same thermal resistivity on opposite sides of the rectangular cross section. On the other hand, though Roth encompasses a thermal resistivity and a (constant) temperature of adjacent medium different for each of the four sides of the rectangular cross section, he has not—because (as he states) of the analytic difficulties involved—taken into account the change in resistance of the wire with temperature. Thus, though the formulas of Buchholz and Roth cover a number of problems actually encountered in practice, they do not cover problems of such practical importance as that of calculating the temperature in a rectangular toroidal coil wound in the slot of a spool, wound around a heat-conducting core, or otherwise so disposed that the thermal resistances on the sides are such that they are not encompassed in Buchholz's solution and whereof the electric loading is such that change of wire resistivity with temperature has a marked effect on the temperature distribution over the cross section (the considerable influence of even small variations over the cross section in wire resistivity is strikingly illustrated by the curves contained in Jakob's paper).

The solutions of such cases and of many others are, however, afforded by the formulas derived in the first part of the paper. Thus, we need only interpret k_x and k_y as the equivalent thermal conductivities of the coil (analytic methods of calculating these and physical data essential thereto are to be found in References 2 and 8); α_0 as the temperature coefficient of resistance at zero degrees centigrade of the coil wire; $q_0=I^2R_0/V$ whereof I is the coil current, V the coil volume, R_0 the resistance of the coil at zero degrees centigrade; and R_s the appropriate surface thermal resistance of the coil (numerical values for various materials are to be found in Reference 2). Then we express the temperature distribution in the ambient medium adjacent to each of the four edges in terms of its equivalent generalized Fourier series and through appropriate substitution of these data obtain T, T_m, and T_a from equations 12, 42 (if applicable), and 44 or from the equivalent equations 45 and 53.

In that calculation of the temperature distribution in electric coils by the formulas mentioned involves nothing not already demonstrated by the numerical example given, it does not seem desirable to take space for additional calculations on electric coils. The interested reader is referred to the numerical examples to be found in the writer's[4] first paper on temperature distribution in electric coils and in an unpublished paper wherein formulas, expressed in Fourier–Bessel series, are derived for coils of such radii that the toroidal geometry must be taken into account. In each example calculated values are found to be in close agreement with corresponding values determined by experiment.

OTHER APPLICATIONS

The formulas derived in the first part of the paper are applicable to the determination of temperature distribution in bus bars of rectangular cross section, in conductors of rectangular cross section lying in the armature slots of large rotating machines, and to problems in other physical domains that are defined by equations 1 to 5 and proper interpretation of the symbols therein.

Appendix

Over the range $-a \leq x \leq a$ a function $f(x)$ that satisfies certain necessary conditions (usually fulfilled by functions encountered in actual practice) can be expanded in a generalized Fourier series

$$f(x) = \sum_{i=1}^{\infty} M_i \cos(m_i x + M_i')$$

whereof

$$\tan(m_i a + m_i') = C_1/m_i$$

$$\tan(m_i a - m_i') = C_2/m_i$$

C_1 and C_2 are arbitrary constants, and M is given by

$$M_i = 2m_i(2m_i a + \sin 2m_i a \cos 2m_i')^{-1} \times \int_{-a}^{a} f(x) \cos(m_i x + m_i')dx$$

Illustratively, if $f(x) = -C'$, we have

$$\begin{aligned} M_i &= -2m_i' C'(2m_i a + \sin 2m_i a \times \cos 2m_i')^{-1} \int_{-a}^{a} \cos(m_i x + m_i')dx \\ &= -4C' \sin m_i a \cos m_i' \times (2m_i a + \sin 2m_i a \cos 2m_i')^{-} \end{aligned}$$

and

$$-C' = -\sum_{i=1}^{\infty} 4C' \sin m_i a \cos m_i'(2m_i a + \sin 2m_i a \cos 2m_i')^{-1} \cos(m_i x + m_i')$$

References

1. The Temperature Distribution in a Transformer or Other Laminated Core of Rectangular Cross Section in Which Heat Is Generated at a Uniform Rate, J. D. Cockroft. *Proceedings* of the Cambridge Philosophical Society (London, England), volume 22, 1923–25, pages 759–72.

2. Introduction a l'Étude Analytique de l'Echauffement des Machines Electriques, E. Roth. *Bulletin* Société Française des Electriciens (Paris, France) (2), volume 7, 1927, pages 840–922.

3. Die Zweidimensionale Warmeströmung des Beharrungszustande in Rechteckigem Querschnitt Geblätterter Eisenkörper bei Flächenhaft, Unsteig Oder Steig Verteilten Wärmequellen, H. Buchholz. *Zeitschrift für Angewandte Mathematik und Mechanik* (Berlin, Germany), volume 14, 1934, pages 285–94.

4. Formulas for Calculating the Temperature Distribution in Electrical Coils of General Rectangular Cross Section, T. J. Higgins. American Society of Mechanical Engineers *Transactions*, volume 66, 1944, pages 665–70.

5. Über die Berechnung der Temperaturen im Innern von Magnetspulen, L. Binder. *Archiv für Elektrotechnik* (Berlin, Germany), volume 2, 1913, pages 131–48.

6. Die Temperaturverteilung im Innern von Magnetspulen mit Rechteckigem Querschnitt, K. Humburg. *Elektrotechnik und Maschinenbau* (Vienna, Austria), volume 27, 1909, pages 677–81, 696–703.

7. Die Temperaturverteilung in Einer Elektrischen Wicklung von Rechteckigem Querschnitt, M. Jakob. *Archiv für Elektrotechnik* (Berlin, Germany), volume 8, 1919, pages 117–26.

8. Influence of Nonuniform Development of Heat Upon the Temperature Distribution of Electrical Coils and Similar Heat Sources of Simple Form, M. Jakob. American Society of Mechanical Engineers *Transactions*, volume 65, 1913, pages 593–602.

9. Untersuchungen zur Frage der Erwärmung Elektrischer Maschinen, L. Ott. *Mitteilungen* über Forschungarbeiten auf dem Gebiete des Ingenieurwesens, Heft 35 und 36, 1906, pages 53–107.

10. Die Maximale Temperatur von Feldspulen, F. Punga. *Archiv für Elektrotechnik* (Berlin, Germany), volume 21, 1928, pages 97–105.

11. Erganzung der Erwarmungsvorschriften: Zum Vorschlag des Herrn Vidmar, W. Rogowski. *Archiv für Elektrotechnik* (Berlin, Germany), volume 7, 1918–19, pages 41–7.

12. Hochsttemperatur Stromdurchflossener Spulen, W. Rogowski, V. Viewig. *Archiv für Elektrotechnik* (Berlin, Germany), volume 8, 1919–20, pages 329–331.

13. A Suggested Addition to the Test Codes on Temperature Rise, M. Vidmar. *Elektrotechnik und Maschinenbau* (Vienna, Austria), volume 36, 1918, pages 49–52, 64–6.

14. Die Verteilung der Beharrungstemperatur in Einer Stromdurchflossenen Spule mit Rechteckigem Querschnitt bei Temperaturabhangigen Widerstand, H. Buchholz. *Archiv fur Elektrotechnik* (Berlin, Germany), volume 28, 1934, pages 122–30.

Measurement of Stray-Load Loss in Induction Motors

D. H. WARE
NONMEMBER AIEE

Synopsis: This paper is written to present test data confirming the accuracy of the reverse-rotation test for stray-load loss[24] in polyphase induction motors. This method is the most convenient yet proposed for direct measurement of stray-load losses in squirrel-cage motors, and it is recommended that it be included in the AIEE Test Code for Polyphase Induction Machines.[27] Proposals for this revision are made.

THE efficiency of an induction motor may be determined by one of several methods. One method is to load the motor to normal load and measure the electric input and mechanical shaft output power. This is the so-called input-output method. Another method, usually termed the segregated-loss method, is to determine each loss separately and to calculate the efficiency from their sum.

The input-output method is the precise method of determining efficiency but is often very difficult to perform. Precise technique[19,21,22] is required, regardless of how the motor is loaded. When input and output are measured, the difference of these two quantities of nearly equal magnitude is the result required. Accuracy is reduced by the subtraction. Often the necessary power supply and loading equipment are not available to load fully large motors under conditions where accurate measurements may be taken.

Consequently, it is very important to have dependable methods available to determine efficiency by the segregated-loss method. Not only is it important to know the sum of the losses, but also, from the designer's point of view, it is important to know the value of each loss. The losses that must be determined are the primary copper loss, the secondary copper loss, the core loss, friction and windage loss, and stray-load loss. The first four of these may be measured quite accurately by comparatively direct methods.

Stray-load loss, however, is more difficult to measure. Before methods were available for direct measurement, stray-load loss often was called the unknown loss to distinguish it from the four components of the total loss that could be measured directly. It is similar to the short-circuit core loss in transformers and synchronous machines and is caused by leakage flux.

It is to be expected that stray-load loss in induction machines could be measured in a manner similar to that used to measure short-circuit core loss in synchronous machines. One member could be excited with direct current of such value to give full-load current in the other member, which would be short-circuited. At the same time the shaft would be driven at normal speed. By measuring shaft input and determining the copper loss in the short-circuited member, the stray-load loss or short-circuited core loss could be calculated.

This method is the one now in the test code for direct measurement of stray-load loss of induction motors. It is very satis-

---

Paper 45-42, recommended by the AIEE committee on electric machinery for presentation at the AIEE winter technical meeting, New York, N. Y., January 22–26, 1945. Manuscript submitted November 21, 1944; made available for printing December 16, 1944.

D. H. Ware is with the General Electric Company, Schenectady, N. Y.

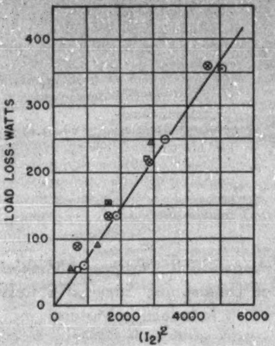

Figure 1. Stray-load loss tests on 25-horsepower 1,800-rpm motor

⊙ Stray-load loss by reverse rotation
⊗ Stray-load loss by dynamometer efficiency test, number 1
▲ Stray-load loss by dynamometer efficiency test, number 2
□ Stray-load loss by dynamometer efficiency test, number 3

factory for wound-rotor motors, where the direct current may be applied to the secondary winding, generating normal frequency in the primary winding. However, squirrel-cage motors can be excited only from the primary winding. The secondary copper loss must be measured by applying the equivalent alternating current to the primary winding and measuring the torque at standstill. This test, which is described on page 12 of the "AIEE Test Code for Polyphase Induction Machines," has not proved practicable for factory use.

In 1939, T. H. Morgan, W. E. Brown, and A. J. Schumer presented the reverse-rotation method of measuring stray-load loss.[24] This test is more direct and easier to perform on squirrel-cage motors. Considerable care must be taken to get accurate results by the reverse-rotation method, since the load loss is the difference between measured quantities. However, it is easier to obtain a certain degree of accuracy with this method than with the input-output method because the quantities measured are so much smaller in the reverse-rotation test.

In the discussion following Professor Morgan's paper it was pointed out that the stray-load losses that occur in the stator at fundamental frequency are not included in the test he proposed. Such losses are caused by leakage flux penetrating the conductors, binding bands, finger flanges, and other structural parts.

It is the purpose of this paper to show that, if these losses are measured separately and properly considered in the calculations, dependable and accurate results will be obtained. These losses may be large or small depending on the design of the motor but usually are not appreciable in small motors. However, large motors, rated 500 to 1,000 horsepower and larger, cannot be tested correctly without considering these losses. This is especially true of two-pole motors.

Test Procedure

The reverse-rotation test is performed by applying balanced polyphase voltage to the stator terminals of the motor while driving the rotor at synchronous speed in the direction opposite to that of the rotation of the magnetic field. If the motor is a wound-rotor motor, the rotor should be short-circuited. The mechanical power required to drive the rotor and the electric power input to the stator each is measured. Let W_r represent the electric-power input to the stator and P_r represent the mechanical power required to drive the rotor. W_r includes the following losses:

1. I^2R loss in the stator.
2. Stray losses in all structural parts, conductors, and so forth occurring at fundamental frequency in the stator.
3. Core loss in the stator that occurs at fundamental frequency.
4. One half the losses in the rotor caused by the fundamental flux. Since the rotor is rotating in the direction opposite that of the magnetic field, these losses occur at a frequency twice that applied to the stator. They include I^2R loss, fundamental core loss, and stray losses in the conductors and structural parts in the rotor.

The quantity P_r includes:

1. Stray losses in the rotor and stator caused by tooth-frequency fluxes.
2. One half the losses in the rotor caused by the fundamental flux
3. Friction and windage losses.

The friction and windage loss may be measured by removing the voltage from the motor terminals and again measuring the mechanical power required to drive the rotor. Let P_f represent this power.

Table I

Motor	Stray-Load Loss by Dynamometer (Watts)	Stray-Load* Loss by Reverse Rotation (Watts)
A	637	650
B	230	245
C	400	335
D	195	230
E	487	450
F	712	620
G	130	215
H	1,003	800
I	355	520
J	747	670
K	224	350
L	184	157
M	255	260

* Fundamental stator loss was considered to be negligible.

The I^2R loss in the stator, the stray losses occurring in the stator at fundamental frequency, and some fundamental core loss may be measured by applying the same polyphase current to the stator with the rotor removed. Let this quantity be represented by W_s. The core loss under this condition may be slightly different from that during the reverse-rotation test, since the voltage applied will be somewhat different. However, this core loss has been found to be a negligible quantity in either case. The stray loss in the rotor and stator caused by the tooth-frequency fluxes may be represented by

$$LL_r = (P_r - P_f) - (W_r - W_s)$$

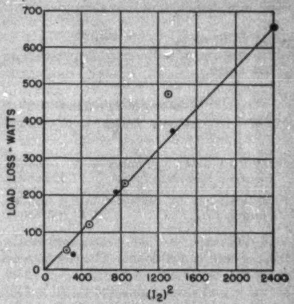

Figure 2. Stray-load loss tests on 30 horsepower 1,200-rpm motor

⊙ Stray-load loss by reverse rotation
● Stray-load loss by dynamometer efficiency test

The stray loss in the stator due to the fundamental frequency is represented by

$$LL_s = W_s - I^2R_s$$

where R_s is the d-c stator resistance at the temperature conditions of the test with the rotor removed. This loss is caused by the stator current and is proportional to the square of the stator current. However, that portion caused by the magnetizing current is included in the measurement of the no-load core loss and should be omitted in the determination of stray-load losses. Consequently, this loss should be determined at a value of current,

$$I_s = \sqrt{I_1^2 - I_m^2}$$

where I_1 represents the primary current when the motor is loaded, and I_m represents the magnetizing current.

It has been shown[13] that the tooth-frequency loss, LL_r, varies with the square of the rotor current. Since the rotor current is approximately equal to I_2, the tooth-frequency loss also should be determined at current I_2.

The reverse-rotation test and the stator-impedance test may be taken at different temperatures. In order that a correction for copper temperature can be made, it is best to keep LL_s separate from I^2R. If R_r represents the d-c resistance at the temperature of the reverse-rotation test, the formula for the tooth-frequency loss becomes

$$LL_r=(P_r-P_f)-(W_r-I_2^2R_r-LL_s)$$

The total stray-load loss equals

$$LL_t=LL_r+LL_s$$

The completed formula is then

$$LL_t=P_r-P_f-W_r+I_2^2R_r+2LL_s$$

Test Data

The following data were obtained on a squirrel-cage motor rated 1,750 horsepower 3,600 rpm.

Stray-load loss by pump-back between identical motors............11,800 watts

Stray-load loss by reverse-rotation test including LL_s...............13,100 watts

The difference of 1,300 watts represents 0.1 per cent of full load. The fundamental-frequency stray-load loss in the stator was measured as 5,400 watts. The reverse-rotation test as originally proposed neglected the fundamental stator loss, but this test clearly indicates that it must not be neglected. Without this correction, which is twice LL_s or 10,800 watts, the stray-load loss would have been calculated to be 2,300 watts from the test data.

A squirrel-cage motor rated 500 horsepower at 1,800 rpm was tested with the following results:

Stray-load loss by pump-back between identical motors.............2,500 watts

Stray-load loss by reverse-rotation test including LL_s................2,800 watts

The two methods differ by 300 watts or 0.08 per cent of full load. The fundamental loss in the stator was tested to be 320 watts. Here consideration of the fundamental stator loss is not so important.

The tests that follow were taken before it was thought necessary to consider the fundamental stator loss. However, motors of similar size and design were tested for this loss and were found to have a negligible amount.

Three methods were used to test a wound-rotor motor rated 150 horsepower at 900 rpm. The following values were obtained for rated load.

Stray-load loss by pump-back between identical motors..............615 watts

Stray-load loss by reverse-rotation test (LL_s neglected)...................600 watts

Stray-load loss by d-c excitation of rotor.. ....600 watts

A squirrel-cage motor rated 25 horsepower at 1,800 rpm was tested by reverse-rotation test. Dynamometer efficiency was measured three times. Figure 1 gives the results of these tests. The fundamental stator loss was neglected.

A 30-horsepower squirrel-cage motor, rated 1,200 rpm, was tested by the reverse-rotation method and by dynamometer efficiency. Figure 2 shows the results. Here also, the fundamental stator loss was neglected.

Thirteen motors, all rated 25 horsepower at 1,800 rpm, of the squirrel-cage type were tested by dynamometer efficiency and by the reverse-rotation test. These motors were built by 11 different manufacturers and varied considerably in their characteristics. Table I gives the results.

These data should be considered by examining the error in load loss as a per cent of full load, not as a per cent of the load loss. The probable error in measurement is about the same quantity in watts for a given size motor, whether the load loss is large or small. Consequently, the error expressed as a percentage of full load is a better measure of the value of a stray-load loss test. This is true whether the load loss is determined by pump-back between identical motors, by a dynamometer, by the reverse-rotation test, or by d-c excitation of the rotor.

Conclusion

It is now six years since the publication of Professor Morgan's paper. This seems sufficient time for all concerned to evaluate his method of direct measurement of stray-load loss.

This paper indicates how his method may be brought into agreement with the input-output test by making the test and correction for fundamental stator-load loss in large motors. This correction is unnecessary in testing small motors. With this correction, where necessary, the reverse-rotation test is accurate for all sizes and speeds of motors and is easily performed.

It appears desirable, therefore, to consider Professor Morgan's method for inclusion in the "AIEE Test Code for Polyphase Induction Machines."

Appendix I. Nomenclature

W_r = power input to stator during reverse-rotation test
P_r = power input to shaft during reverse-rotation test
P_f = power input to shaft with no power applied to stator terminals
W_s = power input to stator during stator-impedance test with rotor removed
LL_t = total stray-load loss
LL_r = stray-load loss due to rotation
LL_s = stray-load loss in stator with rotor removed
I_1 = primary current at load for which stray losses are to be determined
I_m = magnetizing current
I_2 = primary current value at which stray-load loss tests are made
R_s = primary d-c resistance during stator-impedance test with rotor removed
R_r = primary d-c resistance during reverse-rotation test

Appendix II. Proposed Method of Determining Stray-Load Loss in Induction Motors

Measure stray loss in the stator with the rotor removed by applying balanced polyphase current to the terminals of the primary winding. The value of watts measured, less the primary I^2R current, is designated by LL_s. This loss should be measured at a value of current I_2 where

$$I_2=\sqrt{I_1^2-I_m^2}$$

I_1 is the primary-load current and I_m is the magnetizing current.

With the rotor and stator assembled, apply balanced polyphase current to the stator terminals. Drive the rotor at synchronous speed in a direction opposite to that of the phase rotation of the stator. Measure shaft input designated by P_r and the stator input designated by W_r. These measurements should be made at the value of current I_2.

Remove the power from the stator and determine the mechanical power required to drive the rotor at synchronous speed in the same direction. Designate this power by P_f.

The stray-load loss is then equal to

$$P_r-P_f-W_r+I_2^2R_r+2LL_s$$

References

1. NOTE SUR L'ESSAI DES MOTEURS ASYCHRONES, **P. Meunier.** *L'Eclairage Electrique*, volume 34, 1903, pages 228–31.

2. THE DISTRIBUTION OF MAGNETIC INDUCTION AND HYSTERESIS LOSS IN ARMATURES, **W. M. Thornton.** *Journal* of Institution of Electrical Engineers (London, England), 1906, volume 37, pages 125–37.

3. POLE-FACE LOSSES, **C. A. Adams, A. C. Lanier, C. C. Pope, C. O. Schooley.** AIEE TRANSACTIONS, volume 28, 1909, pages 1133–56.

4. INDUCTION-MOTOR LOAD LOSSES, **H. G. Reist, A. E. Averett.** AIEE TRANSACTIONS, volume 32, 1913, pages 423–7.

5. STRAY LOSSES IN INDUCTION MOTORS, **A. M. Dudley.** AIEE TRANSACTIONS, volume 32, 1913, pages 429–34.

6. NOTES ON INDUCTION-MOTOR LOSSES, **R. W. Davis.** AIEE TRANSACTIONS, volume 32, 1913, pages 435–7.

7. THE UNSYMMETRICAL HYSTERESIS LOOP, **J. D. Ball.** AIEE TRANSACTIONS, volume 34, 1915, pages 2693–715.

8. A METHOD OF SEPARATING NO-LOAD LOSSES IN ELECTRICAL MACHINERY, **C. J. Fechheimer.** AIEE TRANSACTIONS, volume 39, 1920, pages 291–9.

Preferred Practices for Electric Control Devices for Aircraft

F. W. HOTTENROTH, JR.
NONMEMBER AIEE

THE devices required for controlling electric equipment on airplanes include pressure switches, thermostats, control relays, contactors, switching mechanisms, and various combinations of these devices. These controls must operate correctly under the extremely severe conditions encountered on airplanes and, at the same time, must be smaller, lighter, and more reliable than similar devices produced for other applications.

In order to design properly to meet the requirements, it is necessary first of all to set up standards which describe accurately the conditions under which the devices must operate. Test equipment is built which simulates these conditions and is used to check the operation of devices in accordance with the standards.

The results of these tests provide additional standards such as electrical creepages and clearances and, in addition, they indicate desirable design features which should be incorporated in devices to make them suitable for operation on airplanes.

It is regrettable that at this late date there are no general standards for electric devices used on airplanes. There are many standards set by governmental agencies for specific devices but these standards are not consistent with those of other agencies, or even with other standards set by the same agency.

The purpose of this paper is two-fold:

1. To suggest that the AIEE set up standards of preferred practices for electric control equipment used on aircraft. A set of standards is included as a sample of the type of standards which are considered necessary.

2. To describe design features which have definite advantages under conditions encountered on aircraft.

Altitude

One of the first requirements for a device which is used on an airplane is that it must operate satisfactorily at the altitudes which will be encountered by the airplane. Not many years ago, an altitude of 25,000 feet was considered the ultimate in airplane performance. The altitude record in 1929 was less than 42,000 feet. Today, we speak of 40,000-foot service ceilings for present-day airplanes and of 50,000-foot service ceilings for airplanes that will be built in the near future. In order that the electric devices of today will operate satisfactorily on the airplanes of tomorrow, standards for altitude should be 50,000 feet.

An altitude of 50,000 feet is equivalent to an absolute pressure of 3.4 inches of mercury. This pressure is readily obtainable with a small vacuum pump. The majority of tests on devices to determine the effect of altitudes can be run on equipment consisting of the compressor from a small household refrigerator connected as a vacuum pump to a bell jar equipped with terminal connections for handling various types of control and load circuits.

The greatest effect of altitude on electric control devices is the effect upon the electrical rating of contacts, due to the increased difficulty of extinguishing an arc at the low pressures encountered at high altitudes.

A large number of tests have been run to determine the effect of altitude upon contact-interruption ratings at various voltages and with various forms of contact mechanisms. Much of these test data have been described in detail in a paper presented by J. S. Rader and L. T. Quill at the Los Angeles meeting of AIEE held in August 1944.[2] From a design viewpoint, the comparison of 12- to 24-volt operation and the advantages of double-break contact construction should be stressed. When most airplanes were equipped with 12-volt systems there was little difficulty in extinguishing arcs, even at high altitude. When airplane voltages were increased to 24 volts, arcing troubles were encountered. Figure 1 shows that a contact break of only $^1/_{32}$ inch will extinguish a 12-volt 40-ampere inductive arc but it will extinguish only four amperes if the voltage is increased to 24 volts.

However, reference to Figure 2 shows that use of double-break contacts practically eliminates the handicap of the 24-volt system. The contact gap for 24 volts with double-break contacts is practically the same as that required for 12 volts with single-break contacts. The close relationship between the curves in Figures 1 and 2 indicates the operation of some physical law or a remarkable coincidence.

The reduction of ratings of contact devices due to altitude is clearly shown in Figure 3. Sea-level ratings must be divided by three to obtain ratings for high altitude. Fortunately the rating curve takes an upward turn at altitudes above those under discussion. The extreme case is the high rating of the vacuum switch.

Another important factor to be considered in high-altitude design work is the necessity for greater creepages and clearances due to lower potential breakdown values at high altitudes. M. J. DeLerno's paper[1] on potential breakdown

---

Paper 45-74, recommended by the AIEE committee on air transportation for presentation at the AIEE winter technical meeting, New York, N. Y., January 22-26, 1945. Manuscript submitted November 25, 1944; made available for printing December 30, 1944.

F. W. Hottenroth is in the industrial control engineering division, General Electric Company, Schenectady, N. Y.

---

9. Induction-Motor Core Losses, P. L. Alger, R. Eksergian. AIEE Journal, volume 39, October 1920, pages 906–20.

10. Tooth Frequency Iron Losses in Slip-Ring Induction Motors, D. B. Hoseason. *The Electrician* (London, England), volume 91, 1923, pages 240–2.

11. Tooth Pulsation in Rotating Machinery, T. Spooner. AIEE Transactions, volume 43, 1924, pages 252–61.

12. Surface Iron Losses With Reference to Laminated Materials, T. Spooner, I. F. Kinnard. AIEE Transactions, volume 43, 1924, pages 262–81.

13. Zusatzliche Verluste in Kleinen Drehstrommotoren, W. Rogowski, V. Vieweg. *Archiv für Elektrotechnik* (Berlin, Germany), 1925.

14. Squirrel-Cage-Induction-Motor Core Losses, T. Spooner, AIEE Transactions, volume 44, 1925 pages 155–63.

15. No-Load Copper Eddy-Current Losses, T. Spooner. AIEE Transactions, volume 45, 1926, pages 231–9.

16. AIEE Standard, 1, 1925; 9, 1927.

17. Measurement of Stray-Load Loss in Polyphase Induction Motors, C. J. Koch. AIEE Transactions, volume 51, 1932, pages 756–63.

18. Determination of the Additional Losses in Three-Phase Asynchronous Motors, H. E. Linckh. *Archiv für Elektrotechnik* (Berlin, Germany), volume 23, 1929, pages 19–39.

19. Modern Equipment for the Precise Testing of Motors, E. A. Emmerling. *General Electric Review*, volume 37.

20. Power Losses in Induction Machines, Paul M. Narbutovskih. AIEE Transactions, volume 53, 1934, November section, pages 1466–71.

21. Efficiency Tests of Induction Machines, C. C. Leader, F. D. Phillips. AIEE Transactions, volume 53, 1934, December section, page 1628–32.

22. Stray-Load-Loss Test on Induction Machines, T. H. Morgan, Paul M. Narbutovskih. AIEE Transactions, volume 53, 1934, February section, pages 286–90.

23. Stray-Load-Loss Tests on Induction Machines—II, T. H. Morgan, Victor Siegfried. AIEE Transactions, volume 55, 1936, May section, pages 493–7.

24. Reverse-Rotation Test for the Determination of Stray-Load Loss in Induction Machines, T. H. Morgan, W. E. Brown, A. J. Schumer, AIEE Transactions, volume 58, 1939, July section, pages 319–24.

25. Induction-Motor Characteristics at High Slip, T. H. Morgan, W. E. Brown, A. J. Schumer. AIEE Transactions, volume 59, 1940, August section, pages 464–68.

26. Calorimetric Method for Determining Efficiencies of Electrical Machines, Victor Siegfried, Charles W. Thulin. AIEE Transactions, volume 61, 1942, July section, pages 530–32.

27. AIEE Test Code for Polyphase Induction Machines, AIEE Standard 500, 1937.

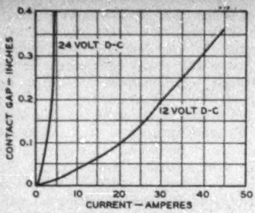

Figure 1. Comparison of single-break contact gaps required for 12- and 24-volt inductive loads at altitudes to 50,000 feet

These curves show conservative ratings for inductance equivalent to motor loads and are about 50 per cent of maximum interrupted test values

at high altitude indicates that high potential tests made at sea level on devices to be used at high altitude should be three times the normal values.

Vibration

Devices should operate satisfactorily under any conditions of vibration encountered on an airplane. However, there still is no definite figure to express accurately the maximum vibration conditions actually encountered on all types of airplanes.

There has been a rule of thumb which states that a device should not be damaged by vibration having simple harmonic motion, with an amplitude of 1/32 inch which is equivalent to a total travel of 1/16 inch. This vibration should vary in frequency from 5 to 55 cycles per second, with the frequency continuously varying. If the device is not damaged by this vibration for a period of five hours, it is considered that it will not be damaged by the vibration it will encounter during the life of the device. This requirement was amplified by some to such an extent that devices had to operate satisfactorily even under these extreme conditions of vibration. We believe that this was never the intent of the requirement. Many devices are built to operate within certain specified tolerances. Under these extreme conditions of vibration they will not operate within those tolerances. Furthermore, under those conditions they may actually operate incorrectly. It seems that there should be a difference between the values for a shakedown test during which a device will not become inoperative and operational test during which a device should operate within prescribed limits. A shakedown test should be equivalent to an accelerated life test. This principle has been carried out in the new specifications set up by Wright Field covering requirements for 400-cycle apparatus. Standards have been set up which require that a device should not be damaged by vibration for five hours with a 1/32-inch amplitude. A second standard for operation requires that a device must operate satisfactorily during vibration of 1/32 inch total travel at frequencies from 5 to 55 cycles per second.

Test equipment for checking devices under these conditions of vibration is now readily obtainable from many sources. Some types of testing equipment have been made extremely heavy and rugged to withstand the vibration set up by their own moving masses. This has necessitated fastening of the equipment to large masses of concrete and has made it extremely difficult to measure correctly vibration amplitudes. Other forms of vibration machines are inherently balanced and are, therefore, lighter weight and have longer life. They are particularly well suited for life testing.

Tests on various devices on the vibration machine show the importance of balanced construction. Pivoted parts should have equal masses on each side of the pivot. Furthermore, tests on the vibration machine show that parts should be rigid and, at the same time, have as light weight as possible.

Figure 4 shows an extremely sensitive relay which is equipped with a balanced armature and which is ideally suited for operation under vibration conditions. This is a polarized relay with a dead center position. When no current is applied, the armature is in a central position and contacts are both open. These contacts remain open even if the relay is subjected to vibration of 1/32 inch total travel at any frequency up to 60 cycles per second. Then, if the relay is energized by current flowing in either direction, one pair of contacts will close and will stay closed under the same vibration conditions. The amount of power necessary to close the contacts and hold them against this vibration is only one half milliwatt. The design of a relay with such a low-power input, able to withstand such extreme vibrations, would be extremely difficult if the principle of balanced construction were not observed.

Temperature

Temperature conditions encountered by aircraft are far more severe than are encountered in ordinary applications of other devices. The higher an airplane flies the lower the temperature it encounters until it reaches the stratosphere. Then the temperature begins to increase. But at an altitude of 60,000 feet above the equator, the temperature may be as low as 112 degrees Fahrenheit. However, the Army Air Forces, in their winterization program, have set −65 degrees Fahrenheit as the minimum temperature for design requirements.

On the other hand, it has been found advisable to design devices to withstand temperatures as high as 200 degrees Fahrenheit for 48 hours. It is, therefore, necessary that the designs for devices for aircraft be suitable for a total range of 265 degrees Fahrenheit. The main item of interest in covering this wide temperature range is the proper choice of materials to insure correct operation of devices over this temperature range. Tests on pressure switches which had rubber diaphragms showed the differentials might become 20 to 30 times as great when the rubber was stiffened by low temperatures as it would when operating at normal temperatures. On the other hand, pressure switches equipped with metal bellows are practically unaffected by temperature.

In designing devices for aircraft, the kinds of material used should be carefully chosen so that different expansion coefficients of materials will not cause wide variations in operation. A piece of aluminum one inch long will shrink two thousandth's of an inch more than a piece of iron one inch long in going from the top temperature at 200 degrees Fahrenheit to the bottom temperature of −65 degrees Fahrenheit. This change in dimension may be the cause of faulty operation in many devices.

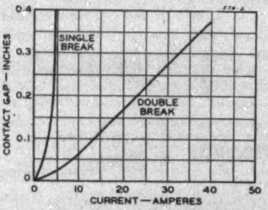

Figure 2. Comparison of single-break contact ratings to double-break contact ratings for 24-volt d-c inductive loads at altitudes to 50,000 feet

These curves show conservative ratings for inductance equivalent to motor loads and are about 50 per cent of maximum interrupted test values

A wide range of temperature makes it essential that any timing devices operating on a thermal principle must be compensated for temperature. This may be done as is shown in Figure 5, by having two pieces of bimetal which oppose each other. Change of ambient temperature increases the forces between the two pieces of bimetal. Heating of one bimetal with relation to the other will operate the contact mechanism after a definite time. Due to the compensation principle used, the timing is practically unaffected by change of temperature.

On the other hand, it should be noted that common forms of timing relays operating on the flux-decay principle are considerably affected by temperature. The curve shown in Figure 6 is representative of the temperature effect upon this type of relay. Most of the change in timing is due to the increased conductivity of the copper slug at low temperatures. This characteristic should be taken into account in applying timing devices so that the increased timing at low temperatures will not be a source of trouble.

Salt Atmosphere and Humidity

A commonly accepted standard for salt atmosphere is that a device must pass satisfactorily a 200-hour salt-spray test. This is an accelerated test which is generally imposed upon a device after it has satisfactorily passed all other tests. There is considerable difference in opinion as to whether it is necessary for a device to operate satisfactorily immediately after being taken from the salt-spray test, or whether it is permissible to clean the salt off the device and then have it operate satisfactorily. There seems to be no firm standard on this subject. It appears reasonable to set up as a standard that a device must operate satisfactorily after it has been cleaned, following exposure for 200 hours to the salt-spray test. When a small electric control which has contacts as part of its mechanism is exposed to the salt-spray test and is left uncovered in the salt spray for a period of 200 hours, it is certain that particles of salt will evaporate out of solution on the contacts. When the device is removed from the salt spray and the salt has thoroughly dried on the contacts, it is quite unlikely that the contacts will operate. If, however, the salt is removed, the contacts should operate properly. The condition of 200 hours of steady exposure to salt spray is an accelerated testing condition which is not actually met in service. It is more intended to prove that the device will not corrode and become inoperable due to corrosion resulting from the salt atmosphere encountered by airplanes operating near the ocean. We, therefore, feel that the above interpretation of the standard is fully justified by the actual application of the devices.

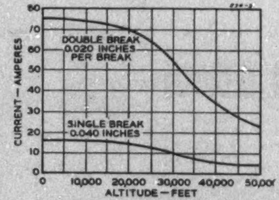

Figure 3. Comparison of 0.020-inch double-break contact rating to 0.040-inch single-break contact rating for 24-volt d-c inductive loads

Contact ratings are approximately 50 per cent of maximum interrupted-current test values. For rating purposes, inductive loads are considered to be motor loads with *L/R* ratio about 0.03

In addition to the salt atmosphere, there is an atmospheric condition of high humidity which often is encountered by devices. This humidity condition is far more severe than has been ordinarily encountered by devices manufactured for use in the United States. In the tropics, it is often possible to have high temperatures and, at the same time, high humidities. In order to simulate this condition with an accelerated test, we have set as our standard for humidity requirements that a device must operate satisfactorily after being subjected to a 95 per cent humidity at 100 degrees Fahrenheit for a period of 168 hours.

The test equipment for salt-spray testing is fully described in Army-Navy Specification AN-QQ-S-91. This type of equipment has been used for some time for corrosion-resistance tests. For the testing of devices under conditions of humidity, an easy way to maintain correct humidity is to place the devices in a bell jar together with certain salts which automatically maintain a correct percentage of humidity. Potassium-sulphate crystals hold a humidity of 96 per cent at 100 degrees Fahrenheit.

In order to design devices which are suitable for uses under the conditions of corrosive atmosphere and humidity, there seem to be three major items which have to be kept constantly in mind. The first of these is that when dissimilar metals are used close together they must be properly chosen so that they are not far apart on the electromotive series or, if they are far apart, they must be properly plated. For instance, a designer who is accustomed to using parts made of brass must be particularly careful to see that they are not fastened directly to aluminum parts, unless the brass parts are plated by a coating such as nickel plate. Secondly, it is essential that all steel parts must be plated with a corrosion-resisting plating or the parts must be made of a type of stainless steel. This does not work an undue hardship on the designer in the case of structures, but it is often difficult to protect properly stampings made from thin spring steel or wire springs made from spring wire having diameters of less than approximately $^1/_{32}$ inch. Ordinary plating methods are very likely to produce faulty springs since the nascent hydrogen produced in the plating process may attack the spring steel and cause hydrogen embrittlement. Reputable spring manufacturers have developed properly controlled techniques for taking care of this condition but it is still an item which must be watched carefully.

One of the most severe effects of humidity on materials is the expansion of plastic parts on which changes in dimension may cause difficulty. Some molded parts are entirely satisfactory for ordinary domestic applications but may change dimensions by as much as $^1/_{64}$ inch per inch when subjected to the extreme humidity conditions encountered by our airplanes. This by no means prohibits the use of molded parts on airplane devices but does warrant extreme care in their use wherever dimensional stability is essential for correct operation. Of course, this condition is even more amplified in the case of fibre parts which will expand two to three times as much as common plastic parts.

Voltage

Designers of aircraft controls have had difficulty in finding out just what the standards of voltage are which must be met by devices when used on airplanes. Normally, the planes of today have 24-volt systems. Actually, this means that the battery furnishes 26.4 volts at full charge at the battery terminals. When the generator is operating properly, it supplies a regulated voltage of 28.5 plus or minus 0.5 volt at the voltage regulator terminals. A designer, therefore, has a choice of a number of voltages to consider as standard. On the basis of the nominal voltage the standard practice for d-c systems allows ten per cent over and 20 per cent under. Therefore, he could design a device to operate at 26.4 volts maximum and 19.2 volts minimum. This is obviously incorrect since the top voltage may go as high as 29 volts on a properly regulated system. Starting from the maximum voltage of 29 volts and using the same spread of plus ten per cent and minus 20 per cent, we work backwards to a minimum value of 21 volts. This seems like a reasonable spread of voltage and indicates that a device should operate satisfactorily at voltages as low as 21 volts and should not overheat at voltages as high as 29 volts. However, it is possible that the generators may be shot away and all important devices must operate satisfactorily on the battery voltage.

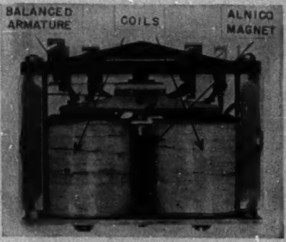

Figure 4. Balanced-armature design of polarized relay operates correctly even under extreme conditions of vibration with only one-half-milliwatt coil input

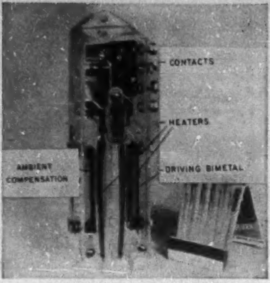

Figure 5. Thermal timing relay with ambient-temperature compensation

Sample in transparent housing

This indicates that there may be a minimum voltage of 19 volts. However, the batteries are probably highly overloaded when generators are inoperative, so it seems advisable that an even lower value should be used. A standard of 18 volts seems reasonable thereby allowing a one-volt additional safety factor over the 19 volts given above. However, it should be noted that some of the Air Corps standards call for correct operation at 20 volts.

A standard stating that devices must operate correctly at 18 volts is incomplete unless temperatures are also taken into consideration. A device which may function properly at 18 volts with ambient temperatures of 70 degrees Fahrenheit may not operate at 18 volts at 200 degrees Fahrenheit. And even though it may operate at 18 volts at 200 degrees Fahrenheit for a short period of time, its own self-heat over a longer period of time may make it inoperable at the same values. Fortunately, the temperature of 200 degrees Fahrenheit cannot exist for any long period of time after the airplane is in operation so the possible condition of operation for an extended period of time at temperatures above 70 degrees Fahrenheit may be assumed to be nonexistent. This is the basis of the standard that devices must operate correctly at 18 volts and 200 degrees Fahrenheit with no self-heating and at 18 volts at 70 degrees Fahrenheit with full self-heat.

Conclusions

Lieutenant Colonel Holliday, head of the electrical equipment laboratory at Wright Field, has emphasized the fact that a device which is not completely reliable has no place on an airplane. At the same time, he points out that weight is the prime consideration in choosing between two devices which are equally reliable.

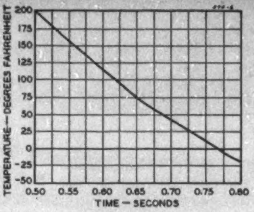

Figure 6. Effect of temperature on dropout time of flux-decay relays

In order to meet both of these requirements it is essential that the designer of devices for aircraft must have clear-cut definitions of the requirements of devices for aircraft in the form of design standards. There are no such standards at the present time.

Should not the AIEE and the National Electrical Manufacturers Association fill this need by setting up standards of preferred practices for electric devices used on aircraft? As a concrete foundation for such a program the following suggestions are offered for discussion and consideration as standards to cover electric control devices.

Appendix. Standards for Electric Control Devices Used on Aircraft

A. Devices must operate satisfactorily under the following conditions or any combination of these conditions.

1. Acceleration to ten *g*.

2. Altitudes to 50,000 feet.

3. Vibration at amplitude of 0.015 inch with frequencies of 0 to 55 cycles per second

4. Temperatures from —70 degrees Fahrenheit to +70 degrees Fahrenheit for continuous operation.

5. Voltages from 18 to 29 volts for 24-volt systems.

B. Devices must withstand the following conditions without being damaged. If operating characteristics are affected to the point where the device does not operate satisfactorily it will be considered damaged.

1. Vibration for five hours in each of the two worst airplanes at an amplitude of 0.030 inch and with frequencies from 0 to 55 cycles at normal room ambient temperature.

2. Temperatures from —70 degrees Fahrenheit to 200 degrees Fahrenheit for 48 hours at the worst temperatures.

3. Humidity of 95 per cent at 100 degrees Fahrenheit ambient temperature for 168 hours with rated coil voltage applied from coil terminal to ground.

4. Salt spray for 200 hours. Salt crystals may be washed off before rechecking operation.

5. High-potential test:

	High Potential A-C Rms Volts Applied for One Second	
Rated Voltage	Sea Level	50,000-Foot Altitude
Up to 50 volts direct current	600	250
Up to 208 volts direct current	3,000	1,000

C. Ratings

1. Magnet coils.

Must pick up at 200 degrees Fahrenheit ambient temperature with no self-heat in coil at 18 volts for 24-volt system.

Coil temperatures must not exceed 325 degrees Fahrenheit with maximum volts and 200 degrees Fahrenheit ambient temperature with device mounted on aluminum plate in accordance with reasonable design practice.

2. Contact ratings.

Devices with motor ratings must be able to make and break six times their normal rating with $L/R=0.03$.

D. Spacings (inches)

		Potential in Volts	
		0 to 30	31 to 300
Between any uninsulated live part and an uninsulated part of opposite polarity,* uninsulated grounded part other than the enclosure or exposed metal part	Through air	1/16	1/8
	Over surface	1/8	1/4
Between any uninsulated live part and the walls of a metal enclosure		1/8	1/4
Between wiring terminals		1/8	1/4

A barrier of 1/32-inch-thick insulation may be used in lieu of these spacings.

* Parts of opposite polarity are those which may be so connected in a circuit that a direct connection between the parts would produce a short circuit.

References

1. POTENTIAL BREAKDOWN OF SMALL GAPS UNDER SIMULATED HIGH-ALTITUDE CONDITIONS, M. J. DeLerno. AIEE TRANSACTIONS, volume 63, 1944, March Section, pages 109–12.

2. D-C ARC INTERRUPTION FOR AIRCRAFT, J. S. Quill, L. T. Rader. AIEE TRANSACTIONS, volume 63, 1944, December Section, pages 883–8.

3. WHY TOMORROW'S PLANES WILL HAVE A-C ELECTRICAL SYSTEMS, T. B. Holliday. *Electrical Manufacturing*, July 1943.

4. Underwriters' Laboratories Standard for Industrial Control.

Tracer-Controlled Position Regulator for Propeller Milling Machine

C. R. HANNA
FELLOW AIEE

W. O. OSBON
MEMBER AIEE

R. A. HARTLEY
ASSOCIATE AIEE

IN a companion paper by Rutemiller and Morton[1] the electrical control of an automatic machine for milling ship propellers up to 24 feet in diameter is described. The outstanding features of this machine, which is illustrated in Figure 1, are the speed and accuracy with which it can generate the desired blade contours in conformity with scale models. These features permit enormous savings in time over previous methods of propeller machining. This superior performance is made possible largely by the use of two tracer-controlled regulators to control the positioning of milling cutters which machine both faces of the blades simultaneously. It is the purpose of this paper to describe the design features and performance characteristics of the regulators and to indicate by means of a typical stability calculation in an appendix some of the theoretical considerations involved in their development. Although the regulating system described was designed specifically for the propeller milling machine, it may be used, with some modifications, in other machine-tool applications, as well as in other fields.

General Description

The control required for contour following comes under the classification of position regulators and presents a much more difficult problem than most other types of regulators, such as speed governors or electric voltage or current regulators. In position regulators a follow member not only must accelerate at the proper rate and move at the right speed, but also must be in the correct position. In an electric system using a fixed-field motor whose armature is supplied with variable voltage from a generator, the current must be controlled for proper acceleration, the voltage must be regulated for proper speed, and the accumulated motion must at every instant be such as to position the follow member accurately. It should be apparent, therefore, that such regulators are of necessity more involved than most other regulators.

In the propeller milling machine, two identical position regulators are needed—one normally being used to control the suction-face drive motor, and the other the pressure-face drive motor. As illustrated in Figure 2, each regulator consists essentially of a standard variable-voltage drive with the exciter for the main generator energized by a single-stage d-c amplifier which derives its positioning stimulus from a Silverstat tracer unit. The unidirectional output of the exciter is applied to the generator field in series with an independent constant potential so as to obtain a drive-motor rotation that is continuously variable from a maximum in one direction through zero to a maximum in the opposite direction. Each motor drives a small saddle carrying the associated tracer unit and also a large saddle carrying one of the two milling cutters.

A detailed description of the operation of the machine is given in the companion paper already referred to. Consequently, the following brief explanation will suffice to describe the functioning of the regulators. As the model table rotates relative to the tracer unit, the tracer probe will be deflected as it traverses the model. This causes a corresponding deflection of the tracer Silverstat,[2] resulting in a proportional change in the Silverstat voltage. This voltage change is amplified by the amplifier and exciter and results in a change in generator voltage which causes the drive motor to move the tracer saddle in the direction to return the tracer probe and Silverstat to their original positions, relative to the saddle. Errors are minimized and hunting is prevented by circuits which are described later.

The ratio of the tracer-saddle speed to the cutter-saddle speed is adjusted by means of gearing to equal the scale ratio of the model. Also the work arbor supporting the propeller is rotated in unison with the model table. Consequently, the milling cutters move proportionately across the blade faces in contours similar to those being traced by the corresponding probes. The Silverstat steps are sufficiently small and the stability of the regulating system is sufficiently great to produce continuously smooth and stepless motion of the cutter saddles.

Following each cutting stroke the propeller blade and models are returned automatically at high speed to the starting position, preparatory to the next cut. During this return traverse the main saddles attain velocities several times the normal cutting speed, and, although there is no requirement for accurate following during the return stroke, because the cutting tools are withdrawn from the work, it is necessary that the regulators retain control throughout this interval to avoid severe transient disturbances during reversals of direction at the ends of the strokes.

The Tracer Unit

The tracer unit is illustrated in Figures 3 and 4. It consists essentially of a small Silverstat operated by a double-lever system. These elements together with the Silverstat resistors are compactly assembled within a cylindrical steel case. A probe whose shape conforms to that of the cutting tool is mounted on the tapered nose of the primary lever.

The ratio of the lever system is adjustable so that the motion of the probe required to produce full Silverstat deflection can be made to correspond approximately to the ratio of the size of the model to that of the propeller being machined. This adjustment in the tracer sensitivity provides means for maintaining the stiffness* of the regulator constant as the model ratio is changed. In other words, when a particular size of model is used, the absolute magnitude of the error is independent of the model ratio, and a 24-foot propeller can be machined with no greater absolute error than a ten-foot one. Since this adjustment affects only the magnitude of the error and does not of itself determine the model ratio, it does not need to be continuous. Accordingly, four positions of the ratio-adjusting pin, corresponding to blade-to-model ratios of 2, 3, 4, and 5, provide adequate range.

The spring and gravitational forces acting on the levers are such that the maximum force on the probe need never exceed two pounds. Thus, with probes of reasonable weight the force exerted on the model is sufficiently low to permit the use of even moderately soft materials such as plaster or soft wood. Ball-bearing pivots provide definite fulcrums with minimum friction for both levers.

A pair of contacts built into the tracer unit serves as a limit switch to shut down the machine when the Silverstat operating lever is deflected beyond its normal range. This feature protects the propeller blade, the tracer unit, and the machine, from damage due to mechanical or electrical failures. A time-delay relay in the limit-switch control circuit prevents shutdown during minor transient conditions which result in only moderately excessive accelerations. During these transients

---

Paper 45-47, recommended by the AIEE committee on industrial power applications for presentation at the AIEE winter technical meeting, New York, N. Y., January 22–26, 1945. Manuscript submitted November 2, 1944; made available for printing December 28, 1944.

C. R. Hanna is associate director, and W. O. Osbon is research engineer, both with the research laboratories, Westinghouse Electric and Manufacturing Company, East Pittsburgh, Pa. R. A. Hartley, now with Adel Precision Products Corporation, Burbank, Calif., formerly was with the research laboratories of Westinghouse Electric and Manufacturing Company.

* The stiffness of the regulator is defined as the force developed on the main saddle by unit main-saddle displacement.

Figure 1. A general view of the propeller milling machine

The model table is in the left foreground. The propeller mounted on the work arbor is about 12 feet in diameter

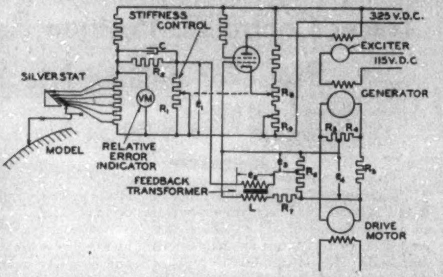

Figure 2. Schematic wiring diagram of the regulating system

damage to the tracer is prevented by adequate overtravel in the lever system.

The Regulator Circuit

Because of time delays inherent in the regulating system a stable regulator capable of only mediocre accuracy can be realized by applying only the Silverstat positioning stimulus to the amplifier input. Sustained oscillations in this simple low-accuracy regulator would be prevented by the inherent damping of the motor-armature circuit. The maximum practical stiffness, and hence the accuracy, of such a system is restricted to relatively low values by fundamental design limitations on the ratio of motor-circuit damping to system inertia and also by the time delays which have the effect of introducing phase shifts that reduce the effective damping of the system. Any attempt to increase the regulator stiffness to improve the accuracy would result in hunting. In the system illustrated in Figure 2 there are three principal time delays: namely, the exciter-field delay, the generator-field delay, and the motor- and generator-armature-circuit delay. Consequently, in order to obtain a regulating system with adequate stiffness to insure high accuracy and at the same time provide sufficient damping to insure rapid decay of free oscillations, it is necessary to introduce strong antihunting influences which will now be described.

In reference to Figure 2, the voltage e_1 appearing across the sensitivity or stiffness-adjusting rheostat R_1 is derived from the Silverstat and has an average value corresponding to the normal zero-error position of the tracer probe. At this normal operating point half of the Silverstat resistance is short-circuited out. Variations from this average voltage value, corresponding to displacement of the probe from its zero-error position, can be considered as made up of two components. One of these is the drop due to the component of current which flows through R_2 and is proportional to the probe deflection or positional error. This component constitutes the positioning stimulus for the regulator. The other component is due to the part of the current which flows through the capacitor C. By making R_1 small compared to R_2, and by proper choice of the value of C, this component can be made proportional to the rate of change or first derivative of the probe displacement. It is well known[2,3] that the inclusion in the input to a regulator of a stimulus proportional to the rate of change of the quantity being regulated exerts a powerful stabilizing effect. When the tracer probe is deflected from its normal position this component of voltage appears ahead of the positioning stimulus. Thus a large restoring force is produced which tends to correct for the error before it can attain its maximum value. For this reason this component may be considered as anticipating the positioning voltage, and the circuit comprised of R_1, R_2, and C therefore is referred to as an anticipator circuit. Because it is not feasible to make R_1 negligibly small compared to R_2, the anticipator does not give perfect differentiation, with the result that an additional small time delay acting upon the anticipator output is introduced into the regulating system. This effect is shown analytically in the appendix.

A further stabilizing voltage, e_2, is obtained from the feedback transformer connected into the generator–motor-armature circuit. The bridge circuit consisting of R_3, R_4, R_5 and the motor-armature resistance are balanced so that the voltage across R_6 is strictly proportional to the back electromotive force of the motor and independent of load and accelerating currents. Since the back electromotive force is proportional to speed, this voltage is thus proportional to the output velocity. The time constant L/R_7 of the primary circuit of the transformer is made low so that the primary current is essentially in phase with the voltage across R_6 and the output velocity. The transformer secondary voltage e_2 is proportional to the rate of change of the primary current and hence is proportional to the output acceleration. This voltage is applied to the amplifier input with a polarity such that the torque due to it opposes rapid acceleration of the drive motor. It is therefore antihunting in its effect. Because it is not feasible to make the time constant of the transformer primary circuit negligibly small, the differentiation of velocity to obtain acceleration is not perfect, and the consequence here also is the introduction of another small time delay, acting in this case only upon the acceleration component of the amplifier input voltage.

With the regulator input voltages described thus far, it is possible to increase the stiffness to a point where the positioning accuracy at very low speeds is more than adequate. However, when the drive motor is running at some constant speed, the steady-state excitation required by the main generator must be produced entirely

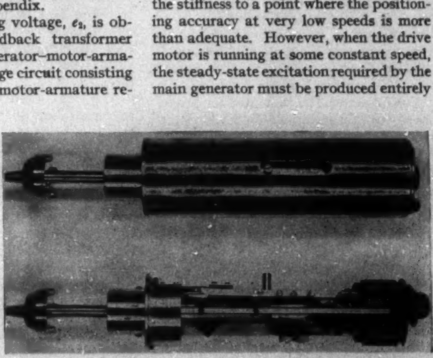

Figure 3. The tracer units

The lower unit is removed from its cylindrical housing

Table I

Machine Constants	Accuracy Constants	Stability Constants
$M=1.2\times10^3$ lbs per (ft per sec^2)	$s=60\times10^3$ lbs per ft	$m=10.8\times10^3$ lbs per (ft per sec^2)
$r=2.7\times10^3$ lbs per (ft per sec)	$r_0=2.5\times10^4$ lbs per (ft per sec)	$T_a=0.5$ sec
$T_1=0.01$ sec	$k_1=8$	$T_4=0.02$ sec
$T_2=0.7$ sec		
$T_3=0.05$ sec		

by the positioning voltage. This means that when the motor is running at top speed the Silverstat must be deflected by the probe far enough from the mid-position to produce full excitation of the generator. In other words a high output speed can be obtained only at the expense of a proportional deviation or error in the tracer probe position, and at top speed this error may be several times the normal acceleration error.

It is the function of the voltage e_3 to minimize these errors proportional to speed. This voltage being part of the drop across R_4 is proportional to the output velocity and is applied to the amplifier input in series with e_1 and e_2 in such a direction as to tend to maintain the output velocity which produced it. Most of the main generator excitation required to produce the output speed is thus provided by e_3, relieving the Silverstat of the major portion of this duty. By this means the velocity error is reduced to a small fraction of what it otherwise would be. The portion of the velocity excitation provided by the Silverstat is just sufficient to insure that the tracer unit retains control of the regulator. Instead of improving the stability of the regulator, however, the feedback for velocity-error correction has exactly the opposite effect. Fortunately though, the reduction in damping is small, and it is readily compensated for by a slight increase in the derivative component of the anticipator-circuit output voltage.

The Amplifier

The use of a vacuum-tube amplifier greatly simplifies the attainment of adequate anticipation, acceleration feedback, and velocity-error correction with circuit components of small physical size and low power consumption. Its almost infinite input impedance permits a wide flexibility in circuit arrangement and makes it possible to eliminate completely undesirable loading of the anticipator circuit by the feedback circuits and vice versa. A further advantage of the amplifier is that it permits the use of very low-wattage Silverstat resistors, making it feasible to mount these within the limited space inside the tracer housing, thus avoiding a large number of electric connections to the tracer unit.

Although only a single tube is indicated in Figure 2, there are actually three tubes connected in parallel. This improves the reliability of the equipment, since the regulators still will operate with somewhat greater error on only two tubes. The tubes, which are of a standard radio type obtainable in any radio shop, are very conservatively loaded so as to insure a long useful life.

A potentiometer R_6 in the cathode-biasing circuit is ganged to the stiffness control R_1 for the purpose of compensating for the change in average drop across R_1 as the stiffness of the regulating system is varied. This makes it possible to change the regulator stiffness without causing any disturbance in the system. Control R_6 is used to adjust the regulator to the center of its range during the setting-up process.

A voltmeter connected across the Silverstat is calibrated in terms of relative error and provides a means of constantly checking the operating condition of the regulator and the accuracy of the milling operation. One of these instruments is located at the control station for each of the two regulators. A vernier centering adjustment, not indicated in the schematic diagram, but connected in series with R_6, is mounted alongside the relative-error indicator on the control pedestal. This serves as a relative-error control and may be used by the operator, if desired, to "monitor" the error during the milling strokes. It also facilitates adjustment during the setting-up operation and provides a means of correcting for possible drifting during the initial warming-up period.

Performance

The performance of the propeller-milling machine as a whole is capable of greatly exceeding the specification requirement of 200 square inches of blade surface milled per hour. This is due both to the inherent cutting capacity of the machine and to the ability of the regulators to maintain a high degree of accuracy at speeds higher than needed. A practical cutting speed for face milling is of the order of 30 inches per minute, and at this speed the regulators hold the accuracy to better than ±0.004 inch at the work. During the high-speed return stroke the velocity reaches 100 inches per minute and the corresponding error is of the order of ±0.012 inch. As mentioned previously there is no necessity for maintaining high accuracy during the return stroke so that the latter figure has no particular significance in the operation of the machine. It is indicative, however, of the capabilities of the regulators.

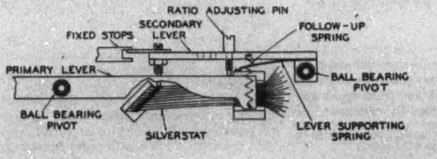

Figure 4. Schematic diagram of the tracer mechanism

The rates of acceleration and deceleration at the ends of the strokes are limited to values of the order of ten inches per minute per second, and during these intervals the error is held to well within the specification requirement of ±0.020 inch.

Conclusion

In designing the regulators much consideration was given to features which insure reliability and ease of operation. No unusual skill is required either to operate or to service the equipment.

Although the regulating system described was developed specifically for the propeller milling machine, the fundamental principles involved are of such a general nature that they will find useful application in a wide variety of regulator problems.

Appendix I

The Anticipator

If we refer to Figure 2, the ratio of e_1 to the Silverstat voltage in operational form is

$$\frac{R_1}{R_1+\dfrac{R_2/Cp}{R_2+1/Cp}}=\frac{(1+T_ap)/(k_1+1)}{1+T_ap/(k_1+1)}$$

where

$T_a=R_2C=$ the anticipator time constant
$k_1=R_2/R_1$
$p=$ the differential operator d/dt

It is apparent from this expression that the anticipator output contains two components, one proportional to the Silverstat voltage, and one proportional to the rate of change of this voltage. Both components are delayed, however, as indicated by the time-delay operator[3] $[1+T_ap/(k_1+1)]$.

Any departure in e_1 from its average value is due to a displacement of the main saddle from its correct position and results in a force on the saddle tending to reduce the displacement. The appearance of this force, however, is subject successively to the delays of the exciter field, the generator field, and the generator–motor-armature circuit. The expression for the force due to e_1 in terms of the displacement x is thus

$$F_s=\frac{s(1+T_ap)x}{(1+T_1p)(1+T_2p)(1+T_3p)[1+T_ap/(k_1+1)]} \tag{1}$$

where the proportionality constant s is the regulator stiffness, and T_1, T_2, and T_3 are, respectively, the three delays previously listed.

Acceleration Feedback

The feedback transformer voltage may be written as

$$e_2=k_2Lpi=\frac{k_2Lpe_4}{R_7+Lp}=\frac{k_2T_tpe_4}{1+T_tp}$$

where i is the primary current, k_2 is the transformer ratio, and T_t is the primary time constant L/R_7. The voltage e_2 is thus proportional to the rate of change of e_4 and is delayed by the time lag of the transformer primary circuit. Since e_4 in turn is proportional to the output velocity or rate of change of displacement, e_2 is proportional to the second derivative of displacement or acceleration. The voltage e_2 also results in a force on the main saddle which is likewise delayed by the times T_1, T_2, and T_3. If we follow the foregoing reasoning, this force, which tends to reduce the acceleration, may be expressed in terms of the displacement as follows:

$$F_a=\frac{mp^2x}{(1+T_1p)(1+T_2p)(1+T_3p)(1+T_tp)} \tag{2}$$

where m is the force per unit acceleration and has the dimensions of a mass.

Velocity-Error Correction

In a similar manner the force due to the velocity-error-correction voltage e_3 may be written as

$$F_v=\frac{-r_0px}{(1+T_1p)(1+T_2p)(1+T_3p)} \tag{3}$$

where r_0 is the force per unit velocity having the dimensions of damping. The negative sign in equation 3 signifies that the damping is negative or that the force F_v is tending to maintain the velocity px rather than to reduce it.

Characteristic Equation

The three forces acting on the saddle due to regulator action are opposed by the inertia of the mechanical system and the electrical damping of the generator–motor-armature circuit. The appearance of the latter opposing force, however, is delayed by the armature-circuit time delay T_3. Expressed algebraically the relationship is

$$-Mp^2x-\frac{rpx}{(1+T_3p)}=F_s+F_a+F_v \tag{4}$$

where r and M are, respectively, the slope of the speed–force curve and the mass of the mechanical system, both referred to the saddle. Substitution of equations 1, 2, and 3 in this equation, and reduction of the right-hand side to a common denominator give the following as the characteristic equation of the complete regulator system:

$$-Mp^2-\frac{rp}{(1+T_3p)}=\frac{s(1+T_ap)(1+T_tp)+mp^2[1+T_ap/(k_1+1)]-r_0p[1+T_ap/(k_1+1)](1+T_tp)}{(1+T_1p)(1+T_2p)(1+T_3p)(1+T_tp)\times[1+T_ap/(k_1+1)]} \tag{5}$$

The constants M, r, T_1, T_2, and T_3 are fixed by the design of the rotating machines,* and constants s, r_0, and k_1 are determined by the accuracy requirements of the regulator. The problem is then to determine values of m, T_a, and T_t, which will result in stable operation with a high rate of decay of free oscillations. A typical set of values is given in Table I.

By substituting these values into equation 5, clearing of fractions, collecting terms, and dividing by the coefficient of p^7, the following equation is obtained:

$$p^7+189.3p^6+11{,}400p^5+268.5\times10^3p^4+380.7\times10^4p^3+314.6\times10^5p^2+67.96\times10^6p+12.97\times10^7=0 \tag{6}$$

The approximate factoring of this equation by the method described in Appendix II is

$$(p+16.2)(p+63.94)(p+95.0)(p^2+2.16p+5.58)(p^2+12.04p+235.4)=0 \tag{7}$$

The three linear factors in equation 7 represent nonoscillatory motions of the saddle of the form $x=x_0\epsilon^{p_1t}$ where p_1 is the root of the appropriate factor. The quadratic factors of the form $p^2+\beta p+\gamma$ correspond to oscillatory motions of the saddle which may be represented by the general equation

$$x=\epsilon^{-\Delta t}(A\cos 2\pi ft+B\sin 2\pi ft)$$

where f is the frequency of oscillation and Δ is the decrement. In terms of the trinomial coefficients β and γ,

$$f=\frac{1}{2\pi}\sqrt{\gamma-\beta^2/4}$$

and

$$\Delta=\beta/2$$

The fractional decay per cycle is given by

$$(1-\epsilon^{-\Delta/f})$$

The oscillation frequencies obtained by this means from the two quadratic factors in equation 7 are 0.336 and 2.24 cycles per second, respectively, and the corresponding rates of decay are 96 per cent per cycle and 93.1 per cent per cycle. These rates of decay represent very high damping. If either of these figures were smaller (of the order of 60 per cent or less) it would be necessary to change one or more of the stability constants listed previously and repeat the solution of the characteristic equation. If even the optimum values of the stability constants still yield too low a rate of decay, it is necessary to reduce the regulator stiffness and accept the correspondingly lower accuracy.

Appendix II

In the solution of high-order linear equations such as equation 6 in Appendix I, the means of finding linear factors by Horner's method or by successive trials using synthetic division are well known. The determination of quadratic factors which represent complex roots presents greater difficulty. A form of synthetic division for quadratic factors was devised by one of the authors for facilitating rapid approximation by successive trials and is shown in this appendix. It was found later that the method was given by M. Liwschitz, formerly with the Westinghouse Electric and Manufacturing Company, in an unpublished report.

Equation 6 after depression by the removal of the three linear factors becomes

$$p^4+14.2p^3+267p^2+575p+1{,}317=0$$

The method is best illustrated by performing the long division by one of the actual quadratic factors.

$$\begin{array}{l|l}
\underline{p}^4+\underline{14.2}p^3+\underline{267.00}p^2+\underline{575}p+\underline{1{,}317} & p^2+\ \underline{2.16}p+\underline{5.58} \\ \cline{2-2}
\underline{p^4+\underline{2.16}p^3+\ \ \underline{5.58}p^2} & p^2+12.04p+235.4, \\
\quad \underline{12.04}p^3+261.42p^2+575p & \\
\quad \underline{12.04p^3+\ \underline{26.02}p^2+\ \underline{67}p} & \\
\qquad\quad 235.4p^2+508p+1{,}317 & \\
\qquad\quad \underline{235.4p^2+\underline{508}p+\underline{1{,}317}} &
\end{array}$$

In the foregoing, the important figures are underlined. The process is greatly simplified by tabulating only these figures as follows:

$$\begin{array}{cccccl}
1 & 14.2 & 267.0 & 575 & 1{,}317 & \big|\,\underline{2.16+5.58} \\
 & & 5.58 & 67 & 1{,}317 & \\
 & 2.16 & 26.02 & 508 & & \\ \hline
1 & 12.04 & 235.4 & \dots & \dots &
\end{array}$$

The upper of the two rows under the dividend coefficients are the successive products of the differences by the last coefficient of the divisor. The lower of the two rows are the successive products of the differences by the middle coefficient of the divisor. The differences are obtained readily by subtracting two numbers simultaneously from the dividend coefficients. The differences, of course, are the coefficients of the quotient.

This compact tabulation of only the necessary figures greatly facilitates the estimation of more accurate coefficients for use in succeeding trials. It is easily possible to make sufficiently accurate approximations of the two unknown coefficients in the divisor for equations of the sixth order with fewer than ten trials. For fourth-order equations

---

* The mass of the saddle is negligible compared to the equivalent mass of the drive motor.

Application of Electric Equipment for Ship-Propeller Milling Machine

H. EARL MORTON
NONMEMBER AIEE

OREN G. RUTEMILLER
MEMBER AIEE

THE ship screw propeller, introduced a little over a century ago, is now used almost universally.[1] Large high-speed passenger and naval vessels of the present day use propellers as large as 22 feet in diameter. These screws must transmit very large amounts of power which causes them to erode and pit rapidly. Erosion and cavitation can be minimized and the efficiency of power transmission increased by the use of smooth accurately finished blades.

The methods used in finishing ship propellers did not keep pace with the art of machining metals and have been a laborious time-consuming job. The excess metal that had to be removed from the rough casting to produce the desired contour was taken away by hand chipping, grinding, and polishing. The large size and cost of a suitable machine tool undoubtedly discouraged its early development. The first attempts were made about 17 years ago by using modified planers and shapers arranged to generate a helix. In 1937 the Morton Manufacturing Company designed and built a special machine for shaping the pressure face side of propeller blades, and two additional machines of this design have been built since.[2] This machine generates the helix through the action of pitch gears much like a screw-cutting lathe. It is not capable of machining the back or suction-face side of the blade, because this surface is not a true helix. Furthermore, it cannot be used on pressure-face sides of blades on which the pitch is not constant from hub to tip.

The machines just described are limited in their application, and the need for a machine that would generate any contour accurately and quickly was increased by the rapidly expanding ship-building program. In 1940 the Morton Manufacturing Company and the Westinghouse Electric and Manufacturing Company undertook the development of such a machine for the United States Navy.

The general arrangement of the machine is shown in the side elevation and plan view, Figure 1, and in the picture of the final installation, Figure 2. The machine is equipped with two cutting heads so that it can be arranged to operate on both sides of a blade simultaneously, thus speeding up the operation and equalizing the pressure of the cutters and reducing the deflection of the work. This arrangement is clearly shown in Figure 3.

The machine is equipped with 11 motors and three motor generator sets. Practically all of these motors operate in a definite sequence when the machine is performing in an automatic cycle. Full magnetic control is provided for all motors.

Position Regulators

The machine is of the form-following type, that is, one that reproduces the contour of a pattern or model in the metal of the propeller casting. This provides for the machining of any contour on either side of the blade and the machining of any number of propellers with either right- or left-hand pitch from the same model. Since all blades on a given propeller are duplicates, a pattern of only one blade is required, and the propeller is indexed for each succeeding blade.

The models are made of some soft material such as wood, so that they can be made easily by hand. Therefore, the form-following device must apply only a very small pressure to the model. Because of the size of the work, it is desirable to use reduced-size models. Machines of the pantograph type have been built for machining airplane propellers, but the limitations of pressure and the extreme complication of a magnifying pantograph for a machine of this size make such an arrangement impractical. A position-regulating system of the servo type, therefore, is used on this machine.

The accuracy of the machine depends primarily upon the position regulators, and the speed of operation is determined by their ability to follow changes in contour rapidly.

The regulators used on this machine are entirely electrical. They control the speed of the saddle-feed motors from 1,000 rpm forward to 1,000 rpm reverse without any apparent loss of control in the region around zero speed. These regulators are described in another paper.[3]

Cutter Drive

The cutters are driven by adjustable-speed constant-voltage d-c motors, which provide the speed adjustment that is necessary to suit cutters of different diameters. The motors are reversed by manually operated switches on the control panel so that cutters of either hand can be accommodated. The magnetic controllers do not provide dynamic braking, as it is desirable to have the cutters rotate from the momentum of the drive in case of a voltage failure so they will cut themselves clear.

Relieving Mechanisms

The cutter saddles are each provided with relieving mechanisms that move the cutters clear of the work during the return stroke and into position for cutting during

---

Paper 45-71, recommended by the AIEE committee on industrial power applications for presentation at the AIEE winter technical meeting, New York, N. Y., January 22–26, 1945. Manuscript submitted November 3, 1944; made available for printing December 28, 1944.

H. EARL MORTON is president of the Morton Manufacturing Company, Muskegon Heights, Mich. OREN G. RUTEMILLER now with Crosley Corporation, Cincinnati, Ohio, formerly was with Westinghouse Electric and Manufacturing Company.

The authors acknowledge the able assistance given on this project by Commander Gold, Commander Mumma, Captain W. C. Wade, and L. V. Calhoun, of the United States Navy; R. H. Patrick and R. E. Morton of the Morton Manufacturing Company; and C. R. Hanna, R. A. Hartley, W. O. Osbon, W. R. Harding, W. H. Formhals, and G. E. King, of Westinghouse Electric and Manufacturing Company.

---

as illustrated, four or five trials usually suffice, making the method more rapid than the usual Ferrari-Cardan method. A further advantage over the latter and other more or less formal methods is that there is no chance of carrying an error through the complete solution since each trial is a check on the preceding one.

The number of trials required is reduced, of course, if one can start with coefficients close to the final values. A quick and convenient first approximation to the correct value of the last coefficient of the divisor is obtained by factoring the original equation with the odd-powered terms omitted. For the example given the expression

$$p^4+267p^2+1,317$$

is factored approximately into

$$(p^2+5)(p^2+260)$$

giving either 5 or 260 as one coefficient of the first trial divisor. This method is exact if the damping in the system is zero, in which case the odd-powered coefficients are absent to begin with. The approximation is quite good, however, for dampings as great as 50 per cent of critical.

References

1. THE APPLICATION OF ELECTRIC EQUIPMENT TO THE SHIP-PROPELLER MILLING MACHINE, H. Earl Morton, Oren G. Rutemiller. AIEE TRANSACTIONS, volume 64, 1945, April section, pages 205–08.

2. RECENT DEVELOPMENTS IN GENERATOR VOLTAGE REGULATION, C. R. Hanna, K. A. Oplinger, C. E. Valentine. AIEE TRANSACTIONS, volume 58, 1939, pages 838–44.

3. RECENT DEVELOPMENTS IN SPEED REGULATION, C. R. Hanna, K. A. Oplinger, S. J. Mikina. AIEE TRANSACTIONS, volume 59, 1940, pages 692–700.

the cut stroke. These mechanisms are driven by compound-wound d-c motors provided with full magnetic reversing control, in order that they will operate in the proper sequence during the automatic cycle.

At the beginning of the cutting stroke, the cutter is positioned with respect to the work by this mechanism. This positioning must be consistent and accurate. The relief-drive motors drive the cutter saddles against a positive stop, at which time the motor stalls. The mechanism is self-locking in this position, and the motor is de-energized by a timing relay.

Ram-Feed Drive

The ram-feed motion, that is, the motion of the cutter radially along the blade is driven by a constant-speed constant-voltage d-c motor. This motor provides movement at traverse speeds for setting up the machine and also movement in definite increments to position the cutter into a new path for each successive cut during automatic operation.

This motor is controlled by a reversing dynamic-braking controller which is governed by a measuring relay. The measuring relay is a device that measures motor revolutions and stops the motor after a definite movement has been accomplished. The increment of movement is adjustable, thus providing a means of adjusting the amount of feed for each stroke. This device, when operating in conjunction with a properly designed controller, consistently can measure increments of one-half motor revolution and can then be adjusted to give any increment of movement up to 20 revolutions.

Saddle-Feed Drive

The saddle-feed screws are each driven by adjustable-voltage d-c drives. These drives are controlled by the position regulators when the tracers are in operation. They are provided with full-magnetic reversing regenerative-braking controllers so that they may be operated from push buttons at high or low fixed speeds for setting-up purposes.

The entire speed range of these motors is obtained by generator voltage control. Consequently, the voltage impressed on the motor armature is an approximate measure of the saddle speed. Voltmeters are provided to indicate this voltage at all times; these are calibrated in terms of saddle speed in inches per minute and provide the operator with a continuous indication of the cutter saddle speed.

Work-Arbor and Model-Table Drive

The work arbor and model table are coupled together mechanically, and, while their relative position may be changed for indexing the blades, they are always moved as a unit during the machining operation.

This is the primary feed motion. When the model table is rotated by the work-arbor motor, the movement of the model changes the position of the probes from their neutral or center position, thus causing the saddle-feed motors to move in the proper direction and at the proper speed to bring the tracer probes back to the center position by moving the tracer saddle. The cutter saddles also are moved a proportionate amount since they are driven by the same motor. Models of different ratios are accommodated by changing the gear ratio between the cutter and tracer saddle; thus the rate of work-arbor rotation controls the rate of motion of the saddles.

There is a certain maximum rate of acceleration that can be accommodated by the position-regulating system. The work-arbor drive is arranged to provide controlled acceleration and retardation so that the ability of the regulator system is not exceeded. The rate of acceleration is controlled by a motor-operated rheostat that is driven by an adjustable-speed d-c motor. This rheostat controls the fields of the work-arbor motor and its associated adjustable voltage generator.

On most machine tools, it is desirable to maintain a certain optimum surface cutting speed. This speed depends upon the size and type of cutter and the material being machined and the geometry of the machine. The construction of this machine is such that the surface speed of the cutter across the work depends primarily upon two variable factors: the pitch of the blade which may vary from six to 30 feet, and the radius of the cut which may vary from one to $12^1/_2$ feet. The work-arbor drive, therefore, must provide an adjustable-speed range in excess of 60 to one.

Since the work-arbor drive is the primary feed motion, it must be stable at any operating speed over its entire speed range. This means that the speed regulation with changing loads must be practically flat over the entire speed range.

The Rototrol regulated adjustable-speed drive was selected for this motion, because it provides all of these features.[4,5]

The work-arbor motor also may be operated from jogging or inching push

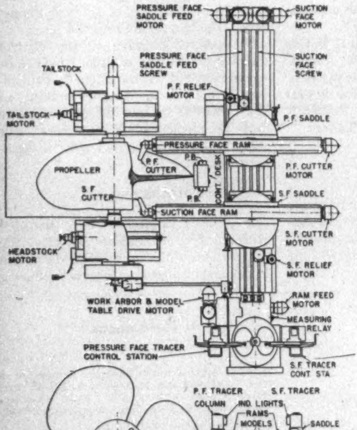

Figure 1 (left). Side elevation and plan view of propeller milling machine giving names of various parts as used in test

Figure 2 (below). General view of machine as installed

The control cubicle is at the left. The operator is stationed on the pit balcony. The control desk is also located here

buttons at a high or low fixed speed to facilitate setting up the machine.

Work-Arbor and Saddle-Feed Control

There is, naturally, a maximum limit to the speed at which the position regulators can follow and maintain the required accuracy of positioning. A speed of 50 inches per minute was set on this machine as the maximum usable feed speed for the cutter saddles. This corresponds to 500 rpm of the saddle-feed motors and is the maximum speed at which the position-regulating system must follow accurately.

During the return stroke when the cutters are in the relieved position, high accuracy is not necessary and, consequently, the saddle-feed motors can operate at their maximum speed of 1,000 rpm at this time. To insure that these limits will not be exceeded, a speed-regulating system is provided for the work-arbor motor. Two voltage relays are connected so as to be responsive to the voltage generated by the saddle-feed generators, and these relays are, therefore, responsive to the saddle-feed motor speed. These relays are set with a small differential in pickup voltage, and their contacts are arranged to control the motor-operated rheostat.

When the pickup voltage of the first relay is reached, the motor-operated rheostat is stopped if it has not already accelerated the work-arbor motor to maximum speed. If the position regulator calls for a greater speed from the saddle-feed motors than that allowed for by the differential setting of the two relays, the second relay will pick up causing the rheostat to decrease the work-arbor speed. The dropout point of the second relay is naturally higher than that of the first; consequently it will drop out and stop the rheostat before the voltage drops low enough to drop out the first relay.

The pickup voltage of both of these relays may be set by means of a rheostat that is located on the operator's control desk. This rheostat is used to set the speed of operation of the feeds.

The amount of metal to be removed may be much greater in some places than in others, and, therefore, the depth of cut may vary considerably. A cutter load-regulating arrangement is therefore provided. This consists of two additional relays similar to those already described but connected so as to be responsive to cutter motor current. The contacts of these relays control the work-arbor motor rheostat in the same manner as the voltage relays previously described. These relays also are provided with calibrating rheostats mounted on the control desk. Through the action of these relays, the work-arbor motor speed is regulated in accordance with the cutter load, slowing down when deep cuts or hard spots are encountered and speeding up again when the cutter load returns to normal.

Figure 3. View from control desk showing a propeller being machined

This shows the two cutters in cutting position

The saddle speed-limiting regulators and the cutter load regulators provide safety features which protect the machine and cutters automatically, thus relieving the operator from this responsibility while the machining operation is going on.

Push-Button Control for Setting Up

The contour of a ship propeller blade is a very irregular surface. There are few reference points available to use as datum points when setting up the machine. In setting up, the operator must position the rough propeller with respect to the model so that there will be enough stock at all points on each blade. This involves a rather tedious setting-up operation during which the various parts of the machine must be moved individually and, in some cases, several motions simultaneously and in synchronism.

Momentary-contact push buttons in portable push-button stations are provided for this purpose. These push buttons give an inching or jogging operation in which the motor rotates only so long as the push button is held depressed, and the motor is stopped quickly by dynamic or regenerative braking when the button is released.

Two fixed speeds are provided for the jogging operation. A fast speed is used to move the machine cutting elements rapidly into approximate position and a very slow speed for accurately positioning these members.

The jogging push buttons are contained in portable push-button stations provided with handles for easy portability, and long flexible cables enable the operator to carry these stations about so that he can take them to any necessary location while setting up the machine. Brackets are provided on the operator's desk which hold these portable push-button stations in an accessible position when they are not in use.

Automatic Operation

After the setting-up operation is completed, the electric circuits are arranged for automatic operation by means of selector switches on the various control stations. This prevents movement of any part by use of the jog buttons and makes the machine ready for full automatic operation.

The position regulators must be in operation and properly adjusted, the cutter motors must be running, and the relieving mechanism control must be set for automatic operation before the automatic cycle may be started. The automatic cycle always is started in the return direction. Depressing the "Auto-Return" push button starts the work-arbor motor and the motor-operated rheostat. The rheostat accelerates the motor until it reaches its maximum speed or until one of the tracer-controlled saddle-feed motors reaches its selected maximum speed, and the speed regulators take control. The work-arbor motor then continues to operate under control of the speed regulators, and the saddles operate under control of the position regulators which follow the model.

As the cutters approach the edge of the blade, the dogs on the model table operate the return-limit switch which starts the motor-operated rheostat in the direction to decrease the speed of the work-arbor motor. When the rheostat reaches its minimum speed position, the work-arbor motor is stopped. The relief-drive motors then move the cutter saddles into cutting position, and the work-arbor motor is started in the opposite direction. This motor again is accelerated by the motor-operated rheostat. There is a separate saddle-speed-limit control rheostat on the operator's desk so that the maximum speed of the saddle may be set for different speeds in each direction. This permits the operator to set the cutting speed for the best cutting condition while the return stroke may be made at a much faster rate. The motor-operated rheostat therefore stops when the saddle speed reaches the maximum determined by the setting of the saddle-speed-limit control rheostat for the cutting direction. During the remainder of the cutting stroke, the work-arbor motor speed is under control of both the speed-limit control and the cutter load-limit control. The cutter saddles are controlled by the position regulators.

When the cutters approach the other edge of the blade, the dogs on the model table operate the cut-limit switch, which starts deceleration of the work-arbor motor through the action of the motor-operated rheostat, and again this motor stops when the rheostat reaches the minimum speed position. The relief-drive motors then move the saddle so that the cutters are clear of the work, and the work-arbor motor again is started in the return direction. At this same time, the ram-feed motor is started, and it operates for a definite number of revolutions as determined by the measuring relay; thus the rams are moved ahead a definite amount and the cutters will follow in a new path across the blade during the next cut stroke.

The machine will continue to follow this automatic cycle without further attention from the operator except the occasional adjustment of the model-table dogs which adjust the length of stroke to conform approximately to the outline of the blade.

The automatic cycle may be stopped at any time by depressing the "Stop" push button. This will cause relieving mechanisms to move the cutters clear of the work and the work-arbor motor to be decelerated just as is done at the end of the stroke. The work-arbor motor will stop when the motor-operated rheostat reaches the minimum-speed position and will not start again until a "Start" push button is depressed. The cutter motors will continue to run, and the position regulators will remain in operation.

An "Emergency-Stop" push button is provided which is intended for use only in an emergency such as might be caused by the breaking of a cutter or the like. When this button is depressed, the relieving mechanisms move the cutters away from the work, and the work-arbor motor and both saddle-feed motors are stopped quickly by regenerative braking. The position regulators are thrown out of operation. It is then necessary to synchronize the tracers with the cutters again and pick up the cut by adjustment.

Protective Devices

In addition to the protective features previously described, overtravel-limit switches are provided to protect against inadvertent movement of any part of the machine beyond its normal limit of travel.

If the tracer probes strike an obstruction, or if they fall off the model because the stroke-limit switches are not set correctly, limit switches that are built into the tracer head are operated. The operation of any of these limit switches has the same effect as depressing the "Emergency-Stop" push button.

There is a number of setup clutches on the machine which provide for different mechanical arrangements for various operations. To insure that these are set in their proper relative positions, various interlocking limit switches are arranged to be operated by these levers. These limit switches are connected into the control circuits in such a manner that the proper mechanical setup must be made before the machine can be operated.

Conclusion

The electric equipment applied on this machine provides reliable means, by the use of proved apparatus, for performing all of the functions required on a machine of this type. Several new problems of regulation, interlocking, and sequence control were encountered in the design of this equipment. Standard equipment was employed throughout with minor modifications to make it better suited for its particular use.

The successful completion of a machine tool of this type requires not only a consideration of the structural design of the machine parts to insure rigidity and accuracy, but also a co-ordination of design between the electrical engineer and the machine designer in arriving at the best solution for the kinematics of the machine. The proper operation of the mechanisms involved depend so much upon co-operative action between the electrical and mechanical devices, that the design of both must be considered simultaneously. It would have been very difficult to select and design electric equipment for this machine after the mechanical design had been completed. We believe that the outstanding machines of the future will be the co-operative efforts of electric-application engineers and the machine designers.

References

1. The First Twenty Years of Screw Propulsion, Edgar C. Smith. *Transactions* of the Newcomen Society, volume 19, 1938–39, page 145.

2. Propeller Planer or Shaping Machine, H. Earl Morton, O. G. Rutemiller. *Transactions*, Westinghouse Machine-Tool Forum, 1938.

3. Tracer-Controlled Position Regulator for Propeller Milling Machine, C. R. Hanna, W. O. Osbon, R. A. Hartley. AIEE Transactions, volume 64, 1945, April section, pages 201–05.

4. Electrical Drives for Wide Speed Ranges, G. A. Caldwell, W. H. Formhals. AIEE Transactions, volume 61, 1942, February section, pages 54–6.

5. Wide Speed-Range Control With the Rototrol, W. H. Formhals. *Westinghouse Engineer*, May 1942, page 51.

6. Propellers for Driving the Victory Merchant Fleet, S. W. Randolph. *Machinery*, November 1942, pages 154–63.

Transient Response of Controlled Rectifier Circuits

P. T. CHIN
ASSOCIATE AIEE

G. E. WALTER
ASSOCIATE AIEE

Synopsis: Transients in circuits supplied by controlled rectifiers using gas- or mercury-vapor-filled electron tubes are found analytically by an extended superposition method. Loads containing resistance, inductance, and a counter electromotive force are studied, and results are obtained for both rectification and inversion. Examples are based on the half-wave biphase rectifier, while the appendix contains an analysis of a *p*-phase rectifier. The assumptions include constant-circuit parameters, a fixed firing angle during transients, continuous load current, and no-leakage reactance in the supply transformer.

DESPITE the increasing use of rectifiers in industry, most of the analyses and reports in technical literature cover only the steady-state aspects of their operation. Little has been written about their performance with suddenly applied loads, with abrupt changes in operating conditions, or even with relatively common switching procedures.

As the field of their application has been widened and as more exact characteristics have been specified for them in these applications, the need for complete knowledge of their behavior has increased also. For instance, the rate at which the field in an eddy-current clutch can be strengthened affects the performance of a synchronous motor driving a wind-tunnel propeller through that clutch. Similarly, the transient characteristic of a motor or exciter field supplied from a rectifier is important when the field must be de-energized in an emergency. And much of the action during the reversing of a thyratron-controlled motor by inversion depends on the transient performance of the motor and the rectifier.

This paper has two main purposes. The first is to extend the existing published theory beyond steady-state analyses. The second is to call attention to an analytical method which is valuable as much for its simplicity as for its generality.

Paper 45-40, recommended by the AIEE committee on electronics for presentation at the AIEE winter technical meeting, New York, N. Y., January 22–26, 1945. Manuscript submitted November 22, 1944; made available for printing December 22, 1944.

P. T. Chin and G. E. Walter are both with General Electric Company Schenectady, N. Y., Mr. Chin in the electronics section of the industrial-control engineering division, and Mr. Walter in the engineering general division.

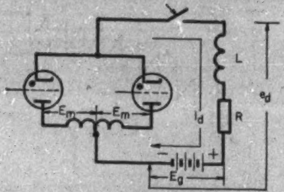

Figure 1. The equivalent circuit of a biphase half-wave controlled rectifier supplying a load containing resistance, inductance, and a counter electromotive force

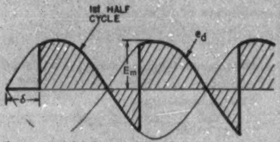

Figure 2. Voltage output of the circuit in Figure 1

Both rectification and inversion will be discussed.

Some simplifications are necessary, of course, to permit any analysis at all. The complete problem of finding responses in automatic control and regulating systems employing rectifiers is complicated immediately by the continuously changing firing angle of the rectifier tubes. To make a beginning, a constant firing angle is assumed throughout this paper. Most of the time this involves only a reasonable approximation, and part of the time it is an exact statement.

In addition, the load current is assumed to be continuous. Discontinuous conduction, in which the current pulses succeeding the first one are identical and in which no transient response lasts beyond each pulse, has already been discussed.[1]

To keep the analysis specific, only rectifiers using grid-controlled gas- or mercury-vapor-filled electron tubes will be mentioned. For simplicity, the half-wave biphase rectifier is studied exclusively in the main portion of this paper. Appendix II contains the general analysis of a *p*-phase rectifier.

Method of Analysis

If the switch in the circuit of Figure 1 is closed after the instantaneous voltage across the transformer winding passes through zero and before the firing point of the first tube is reached, the total voltage across the load, e_d, will appear as in Figure 2. The transient-current response to this voltage could be found by using ordinary differential equations, with successive boundary conditions to be evaluated tediously, or else by a Fourier series method, where the current responses to the d-c component and the fundamental and harmonic a-c components are determined separately.

Operational calculus, with either the Heaviside or Laplacian transform method, has at least two disadvantages. Most engineers have not had an opportunity to become proficient in its use, and frequently the problem of determining the proper operational forms is almost as difficult as the problem they are to solve.

Instead, the method suggested here is based on the superposition theorem and an extension of the Duhamel integral.[2,3] It states merely that the total current in a linear circuit can be found at any time by superposing all the currents produced by separate voltage sources in the circuit, regardless of whether transient or steady-state responses are considered and despite the fact that each of the component currents may have started at a different time.

Figure 3 shows how a typical rectifier circuit, supplying a load containing resistance, inductance, and a counter electromotive force (pictured as a battery), can be studied as the sum of two circuits. The circuit in Figure 3B yields the current i_1, which is the component produced by the rectifier output voltage shown in Figure 2. In Figure 3C, only the current i_2 produced by the counter electromotive force is considered. Together, i_1 and i_2 comprise the total current response in the complete circuit.

Since the exponential rise of i_2 in Figure 3C is a relatively familiar phenomenon, finding i_1 as the result of the serrated rectifier output voltage presents the major difficulty. The first step, illustrated in Figure 4, is to decompose this voltage into continuous sine waves of the same frequency which start at regular intervals. Each voltage, moreover, is introduced at the same angle on its sinusoidal wave shape.

The first sine wave has the same peak value as the rectifier output voltage, and the sine waves thereafter have peak values twice as large and start at half-cycle intervals. When these waves are superposed, the resulting voltage wave is the original rectifier output voltage for which the response is desired.

If the beginning of the *n*th voltage wave is chosen as the zero axis of time, this wave can be expressed as

$$e_n = 2E_m \sin (\omega t + \delta) \tag{1}$$

in the interval $0 < \omega t < \pi$. Since each of the component waves begins π radians before the following one, the expressions for all of the components during this same interval will be

$$\left.\begin{array}{l} e_{n-1} = 2E_m \sin (\omega t + \delta + \pi) \\ e_{n-2} = 2E_m \sin (\omega t + \delta + 2\pi) \\ \cdots\cdots\cdots\cdots\cdots\cdots\cdots\cdots \\ e_3 = 2E_m \sin [\omega t + \delta + (n-3)\pi] \\ e_2 = 2E_m \sin [\omega t + \delta + (n-2)\pi] \\ e_1 = E_m \sin [\omega t + \delta + (n-1)\pi] \end{array}\right\} \tag{2}$$

The current response to each of these components is simply the transient resulting when it is switched at the specified time into a circuit containing resistance and inductance. This response has the general form:[4]

$$i = (E/Z) \sin (\theta - \delta)\epsilon^{-t/T} + (E/Z) \sin (\omega t - \theta + \delta) \tag{3}$$

for an applied voltage of

$$e = E \sin (\omega t + \delta) \tag{4}$$

If E in equation 3 is replaced by $2E_m$, the general current expression becomes the exact response to the *n*th component wave. For the exact response to any of the component waves, it is necessary only to notice that, during the interval $0 < \omega t < \pi$, the existing component current produced by a voltage wave which started r half cycles earlier is identical with the current which will exist r half cycles later as the result of the *n*th component voltage.

If we let t_1 be the time for a half cycle, the current response to any of the component voltages can be found by substituting $(t + rt_1)$ for t in the expression for the current response to the voltage wave which precedes it by r half cycles. The currents in the interval $0 < \omega t < \pi$ thus appear as follows:

$$\left.\begin{array}{l} i_n = (2E_m/Z) \sin (\theta - \delta)\epsilon^{-t/T} + \\ \qquad (2E_m/Z) \sin (\omega t - \theta + \delta) \\ i_{n-1} = (2E_m/Z) \sin (\theta - \delta)\epsilon^{-(t+t_1)/T} + \\ \qquad (2E_m/Z) \sin (\omega t - \theta + \delta + \pi) \\ i_{n-2} = (2E_m/Z) \sin (\theta - \delta)\epsilon^{-(t+2t_1)/T} + \\ \qquad (2E_m/Z) \sin (\omega t - \theta + \delta + 2\pi) \\ \cdots\cdots\cdots\cdots\cdots\cdots\cdots\cdots \\ i_3 = (2E_m/Z) \sin (\theta - \delta)\epsilon^{-[t+(n-3)t_1]/T} + \\ \qquad (2E_m/Z) \sin [\omega t - \theta + \delta + (n-3)\pi] \\ i_2 = (2E_m/Z) \sin (\theta - \delta)\epsilon^{-[t+(n-2)t_1]/T} + \\ \qquad (2E_m/Z) \sin [\omega t - \theta + \delta + (n-2)\pi] \\ i_1 = (E_m/Z) \sin (\theta - \delta)\epsilon^{-[t+(n-1)t_1]/T} + \\ \qquad (E_m/Z) \sin [\omega t - \theta + \delta + (n-1)\pi] \end{array}\right\} \tag{5}$$

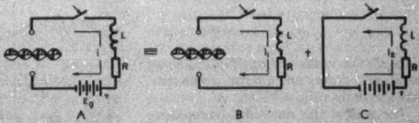

Figure 3. Equivalent representation of the circuit in Figure 1

A. Original circuit, with the rectifier replaced by a source supplying the proper voltage

B. Circuit responding only to the rectifier voltage

C. Circuit responding only to the counter electromotive force

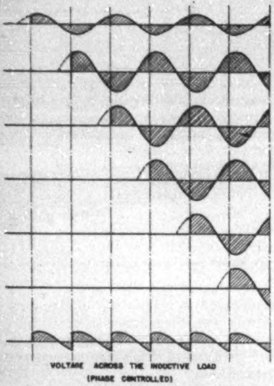

Figure 4. Decomposition of the output voltage of a biphase half-wave controlled rectifier into sinusoidal components

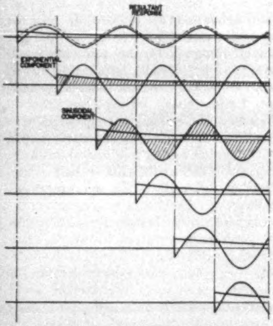

Figure 5. Current responses to the sinusoidal voltage components of Figure 4

The total current response, i_t, during the interval concerned is

$$i_t = i_1 + i_2 + i_3 \ldots i_{n-2} + i_{n-1} + i_n \qquad (6)$$

Since each component current in equation 5 consists of an exponential and a sinusoidal term, i_t is composed of an n-term group of exponentials and an n-term group of sinusoids.

By adding and subtracting $(E_m/Z)\times \sin(\theta-\delta)\epsilon^{-[t+(n-1)t_1]/T}$, the sum of the exponential terms in i_t can be rewritten as

$$\begin{aligned} i_{t(\text{exp})} = {} & (2E_m/Z)\sin(\theta-\delta)\epsilon^{-t/T}\times \\ & [(1-\epsilon^{-nt_1/T})/(1-\epsilon^{-t_1/T})]- \\ & (E_m/Z)\sin(\theta-\delta)\epsilon^{-[t+(n-1)t_1]/T} \end{aligned} \qquad (7)$$

since all the terms having $(2E_m/Z)$ as a coefficient form an n-term geometric series with the ratio $\epsilon^{-t_1/T}$.

The sum of the sinusoidal terms in i_t can always be expressed as

$$i_{t(\text{sin})} = (E_m/Z)\sin(\omega t-\theta+\delta) \qquad (8)$$

in the interval $0<\omega t<\pi$, whether n is even or odd.

On this basis,

$$\begin{aligned} i_t = {} & i_{t(\text{exp})} + i_{t(\text{sin})} \\ = {} & (E_m/Z)\sin(\omega t-\theta+\delta)+(2E_m/Z)\times \\ & \sin(\theta-\delta)\epsilon^{-t/T}[(1-\epsilon^{-nt_1/T})/(1-\epsilon^{-t_1/T})]- \\ & (E_m/Z)\sin(\theta-\delta)\epsilon^{-[t+(n-1)t_1]/T} \end{aligned} \qquad (9)$$

Equation 9 is valid in the interval $0 \leqq \omega t \leqq \pi$ and gives the exact load current in the circuit of Figure 3B for the nth half cycle after the closing of the switch. The complete transient response can be found by letting n assume all the integral values from one to infinity, or to a number that brings the exponential terms as closely as desired to their limiting values.

A "physical picture" of this transient response can be obtained by considering the voltage components in Figure 4 as actual voltages which are switched into the load circuit at regular intervals. With linear circuit elements, each transient caused by the inclusion of another voltage source in the circuit behaves exactly as though it were the only transient present, and the total response at any instant is simply the sum of all the previously started transients. A convenient mathematical relation between these transients then makes it possible to express their sum in three terms.

Assumptions

The analysis presented in this paper is based on the following assumptions:

1. The load circuit contains only resistance, inductance, and possibly a counter electromotive force in series.
2. The resistance and inductance are constant.
3. If it is present, the counter electromotive force remains constant during the interval analyzed.
4. Leakage reactance in the rectifier supply transformer is negligible.
5. The arc drop of a rectifier tube is constant.
6. Ionization and deionization times in the rectifier tubes are negligible.
7. The angle of retard, δ, remains fixed during a transient.
8. Load current is continuous.

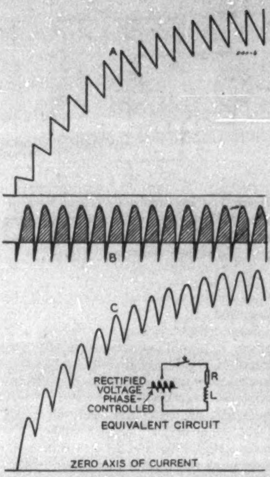

Figure 6. Current build-up in an inductive circuit supplied by a biphase half-wave controlled rectifier

A—Sum of the exponential components of the successive current responses

B—Sum of the sinusoidal components of the successive current responses

C—Total current response

9. The rectifying elements are grid-controlled gas- or mercury-vapor-filled electron tubes.

In general, these are standard assumptions, and the errors introduced are small compared to the main response.

Only resistance and inductance are considered in the load circuit, since shunt capacitance is ordinarily insignificant at power frequencies in industrial loads. When the counter electromotive force is generated in the armature of a d-c motor, assuming it to be constant requires that the speed of the motor remain unchanged during the transient period. It is usually an accurate assumption, depending only on the relative magnitudes of the electrical time constant, L/R, of the motor's armature circuit and the mechanical time constant, J/D (moment of inertia divided by the damping torque), of the shaft load. In a fully loaded one-horsepower 230-volt

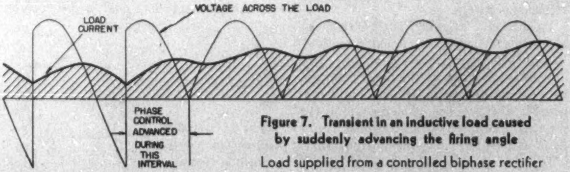

Figure 7. Transient in an inductive load caused by suddenly advancing the firing angle

Load supplied from a controlled biphase rectifier

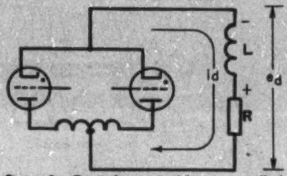

Figure 8. Equivalent circuit for a controlled biphase half-wave rectifier momentarily operating as an inverter from the energy stored in its inductive load

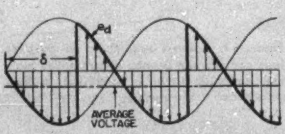

Figure 9. The output of a controlled biphase rectifier operating as an inverter

1,150-rpm d-c shunt motor, for instance, L/R may be in the order of 0.01 second whereas J/D, even assuming that the shaft load consists entirely of friction with no inertia, may be in the order of 0.4 second. With load inertia considered, J/D may easily exceed 1.0 second. If a series inductance is intentionally added for filtering purposes, however, this assumption must be studied carefully.

Rectification With no Counter Electromotive Force Present

If the arc drop of the rectifier tubes is neglected, transient currents in such loads as motor and clutch fields can be found from the circuit in Figure 3B by using equation 9. The transient-current responses to the sinusoidal voltage components of Figure 4, mentioned only briefly in the previous analysis, are illustrated in detail in Figure 5. Each one contains the sinusoidal and exponential currents which can be added, as in Figure 6, to obtain the total current response beginning with the closing of the switch.

Figure 6A shows the build-up of the exponential component expressed in equation 7, and Figure 6B, the sinusoidal component of equation 8.

The steady-state current can be obtained from equation 9 by letting n approach infinity.

$$i_{t-ss}=(E_m/Z)\sin(\omega t-\theta+\delta)+(2E_m/Z)\times \sin(\theta-\delta)[\epsilon^{-t/T}/(1-\epsilon^{-t_1/T})] \quad (10)$$

If $T \gg t_1$, as it may be if the load is heavily inductive, the first term in equation 10 will be very nearly equal to the ripple component of the load current, and the second term will closely approximate the d-c component.

Finally, if the load inductance, L is assumed to increase without limit, the ripple component of load current approaches zero and equation 10 becomes

$$i_{t-ss}=(2/\pi)(E_m/R)\cos\delta \quad (10a)$$

which is the well-established expression for the load current in a biphase half-wave rectifier supplying an infinitely inductive load.

This method of analysis is not limited to starting transients but applies equally well when the firing angle of the tubes is suddenly advanced as in Figure 7. Here the rectifier output voltage which formerly produced a certain load current is abruptly and completely replaced by a new output voltage. As far as the previous load current is concerned, the voltage causing it becomes zero, and it decays exponentially from the value i_0 that it had at the instant the new firing angle became effective. The component of the load current from the new output voltage begins, of course, from zero just as though there were no other component present; and the complete expression for the transient in Figure 7 is

$$i_t=i_0\epsilon^{-[t+(n-1)t_1]/T}+(E_m/Z)\times \sin(\omega t-\theta+\delta)+(2E_m/Z)\sin(\theta-\delta)\epsilon^{-t/T}\times [(1-\epsilon^{-nt_1/T})/(1-\epsilon^{-t_1/T})]-(E_m/Z)\times \sin(\theta-\delta)\epsilon^{-[t+(n-1)t_1]/T} \quad (9a)$$

in which δ is the new angle of retard.

Inversion With no Counter Electromotive Force Present

When a rectifier is supplying power to its load, it is operating as a rectifier in the normal sense; when it is absorbing power from the load, it is operating as an inverter. Current can pass through the rectifier tubes, however, in only one direction, and load current thus flows in the same direction for both rectification and inversion.

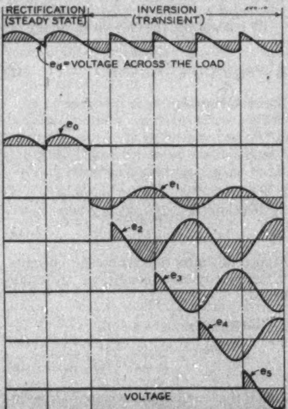

Figure 10. Decomposition of the output voltage wave of a controlled biphase rectifier suddenly transferring from rectifier to inverter operation

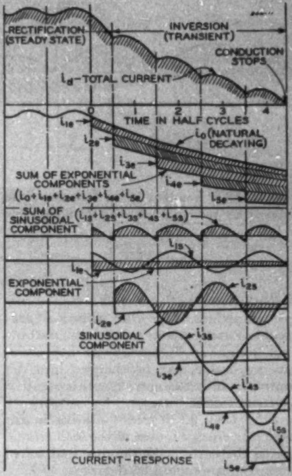

Figure 11. Total and component current responses in an inductive load supplied by a controlled biphase rectifier following an abrupt change from rectifier to inverter operation

To absorb power from some source in the load circuit, a rectifier therefore must have an output voltage which is either negative itself or, if positive, at least lower than the value necessary to keep the existing load current flowing through the load. In both cases, some energy source in the load circuit must supply power to keep the load current flowing.

A rectifier supplying an inductive load such as a field winding will operate momentarily as an inverter if the firing angle of the tubes is increased suddenly. While the current is dropping to its new level, the energy stored in the magnetic field will provide the power for inverter action. The equivalent circuit for the rectifier under these conditions is given in Figure 8, where the polarity markings by the inductance, L, show the induced voltage that maintains the flow of current.[5]

Since there is no external source of energy in the load circuit, continuous inversion is impossible, and the load current will drop either to a value that can be supplied by the rectifier with the new firing angle or to zero if the output voltage of the rectifier is negative. This characteristic provides rapid control of the current in inductive loads with no danger of excessive voltages. The stored energy is removed by delivering it through the rectifier back to the a-c supply lines.

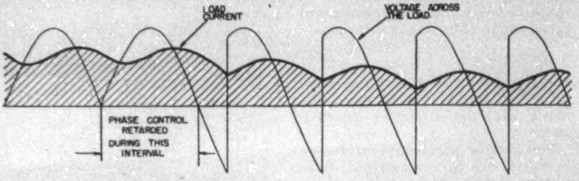

Figure 12. Transient in an inductive load caused by suddenly retarding the firing angle

Load supplied from a controlled biphase rectifier

Negative rectifier output voltages may seem startling. However, if the load current is somehow kept continuous, the output voltage in Figure 2, with a positive average value, can be changed into the output voltage of Figure 9, with a negative average value, merely by making δ greater than 90 degrees. During inversion, the energy source in the load circuit keeps the current continuous, and δ frequently does exceed 90 degrees.

Figure 10 illustrates this inverter action when firing is retarded. The top diagram shows how the output voltage changes as the firing angle is increased. In the decomposition of this output-voltage wave in the lower diagrams, e_0, the former output voltage as a rectifier, becomes zero at the instant inversion begins and is replaced by the succession of sinusoidal voltages, $e_1, e_2, e_3, e_4, \ldots$.

If the transient response to each of these voltages is obtained, the total current during inversion can be expressed as the sum of an exponentially decaying component and the exponential and sinusoidal components of the current responses to each of the successive voltages. These component currents are shown in Figure 11. In the interval between the appearances of e_1 and e_2 in Figure 10, the current response is

$$i_t = i_0\epsilon^{-t/T} - (E_m/Z)\sin(\omega t-\theta+\delta_1) - (E_m/Z)\sin(\theta-\delta_1)\epsilon^{-t/T} \quad \text{(11a)}$$

in which the time t is measured from the beginning of e_1, i_0 is the load current when $t=0$, and δ_1 is the previous angle of retard for operation as a rectifier.

In the succeeding half cycles, time is measured from the instant of appearance of the sinusoidal voltage component for that half cycle, and δ_2 is the new angle of retard for inverter operation. If the interval between the appearances of e_2 and e_3 in Figure 10 is considered as the second half cycle, the current in the nth half cycle will be

$$i_t = i_0\epsilon^{-[t+(\delta_2-\delta_1)/\omega+(n-2)t_1]/T} + (E_m/Z)\sin(\omega t-\theta+\delta_2) + (2E_m/Z)\times \sin(\theta-\delta_2)\epsilon^{-t/T}[(1-\epsilon^{-(n-1)t_1/T}) \div (1-\epsilon^{-t_1/T})] - (E_m/Z)\sin(\theta-\delta_1)\times \epsilon^{-[t+(\delta_2-\delta_1)/\omega+(n-2)t_1]/T} \quad \text{(11b)}$$

Because the new angle of retard, δ_2, produces a negative rectifier output voltage, the top diagram in Figure 11 shows that conduction stops after several half cycles. (Actually, the current would become discontinuous with a very small average value rather than stopping altogether.) It illustrates how a motor or clutch field can be completely de-energized by sufficiently retarding the firing angle. If δ_2 is less than 90 degrees, however, the load current, instead of becoming zero, will merely drop to a new value as in Figure 12, and equations 11a and 11b still will apply.

Nothing has been said about the additional requirements for successful operation of the rectifier circuit during inversion since that subject is beyond the intent of this paper. It is well covered in technical literature and has been mentioned in at least one recent article in AIEE TRANSACTIONS.[6] The work in this paper is based on the tacit assumption that none of these requirements is violated.

Rectification With a Counter Electromotive Force Present

This is the original case illustrated in Figure 3A. The circuit in Figure 3B has already been analyzed; all that remains is a study of the circuit in Figure 3C and the addition of this result to equation 9.

By inspection, the current in Figure 3C is

$$i_2 = (E_b/R)(1-\epsilon^{-t/T}) \quad \text{(12)}$$

The total current, i_t, is therefore

$$i_t = i_{t(\text{exp})} + i_{t(\sin)} - i_2 = (E_m/Z)\sin(\omega t-\theta+\delta) + (2E_m/Z)\times \sin(\theta-\delta)\epsilon^{-t/T}[(1-\epsilon^{-nt_1/T}) \div (1-\epsilon^{-t_1/T})] - (E_m/Z)\sin(\theta-\delta)\times \epsilon^{-[t+(n-1)t_1]/T} - (E_b/R)(1-\epsilon^{-[t+(n-1)t_1]/T}) \quad \text{(13)}$$

Figure 13 shows the component currents. When steady-state conditions are established,

$$i_{t-ss} = (E_m/Z)\sin(\omega t-\theta+\delta) + (2E_m/Z)\sin(\theta-\delta)[\epsilon^{-t/T} \div (1-\epsilon^{-t_1/T})] - E_b/R \quad \text{(14)}$$

and, if the load inductance approaches infinity,

$$i_{t-ss} = (2/\pi)(E_m/R)\cos\delta - E_b/R \quad \text{(15)}$$

The arc drop of a rectifier tube may be considered as the counter electromotive force, E_b, if a more accurate solution is desired for the transient response in a load containing only resistance and inductance. E_b can also be an actual battery, the speed voltage in the armature of a d-c motor, or the sum of the tube drop and a counter-voltage in the load circuit.

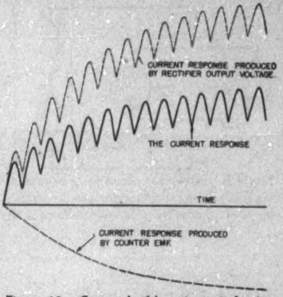

Figure 13. Current build-up in an inductive load containing a counter electromotive force and supplied from a controlled biphase rectifier

Equation 13 assumes that conduction begins when the first rectifier tube is fired after the switch in the load circuit is closed. Actually, this is true only when $E_m \times \sin\delta > E_b$, because conduction will not begin unless there is a positive-anode voltage across the incoming tube. If $E_m \sin\delta < E_b$, as illustrated in Figure 14, a slight correction is necessary in equation 13 to recognize that the first half cycle of current begins when $E_m \sin\omega t = E_b$.

Inversion With a Counter Electromotive Force Present

An equivalent circuit for inversion with a counter electromotive force in the load circuit depends on the polarity of that counter electromotive force. Figure 1 can be used if the counter electromotive force opposes the load current and the inverter action occurs as the angle of retard is increased to lower the value of the load current. The rectifier output voltage then will appear as in Figure 2, or possibly as in Figure 9 if the current is to be brought rapidly to zero.

From the equivalent circuit of Figure 1, the transient response can be determined immediately by adding the current rise caused by the counter electromotive force

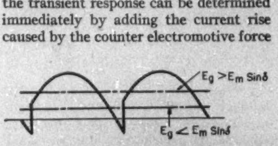

Figure 14. Possible relations between transformer voltage and counter electromotive force at the instant of firing a tube in a biphase rectifier

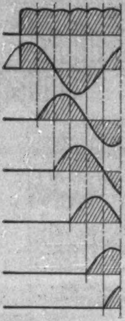

Figure 15 (left). Decomposition of the output voltage wave of a six-phase uncontrolled rectifier

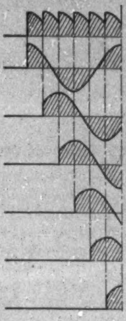

Figure 16 (right). Decomposition of the output voltage wave of a six-phase controlled rectifier

to equations 11a and 11b. In the first half cycle,

$$i_t = i_0\epsilon^{-t/T} - (E_m/Z)\sin(\omega t-\theta+\delta_1) - (E_m/Z)\sin(\theta-\delta_1)\epsilon^{-t/T} - (E_b/R)(1-\epsilon^{-t/T}) \quad (16a)$$

In the succeeding half cycles,

$$i_t = [i_0 - (E_m/Z)\sin(\theta-\delta_1) + E_b/R]\epsilon^{-[t+(\delta_2-\delta_1)/\omega+(n-2)t_1]/T} + (E_m/Z)\sin(\omega t-\theta+\delta_2) - E_b/R + (2E_m/Z)\sin(\theta-\delta_2)\epsilon^{-t/T}\times[(1-\epsilon^{-(n-1)t_1/T})/(1-\epsilon^{-t_1/T})] \quad (16b)$$

When the counter electromotive force aids instead of opposes the flow of load current, it supplies energy to the circuit and continuous inversion is possible. If the transient is produced by retarding the firing angle in a circuit which is already operating as an inverter, the current response can be obtained directly from equations 16a and 6b by changing the sign of E_b wherever it appears. Then E_b becomes (E_g-E_t) instead of (E_g+E_t), since arc drop always opposes load current.

However, when the transient is caused by closing the main switch in the load circuit, the complete solution can be found from equations 13, 14, and 15, by reversing the sign of E_b and using $E_b = E_g - E_t$.

Polyphase Rectifier Circuits

To illustrate the generality of the method, Figures 15 and 16 show how the components of the voltage output of a six-phase rectifier are obtained. The transient current for controlled or uncontrolled operation can be determined as the sum of the responses to these voltage components.

Special Circuits and Abnormal Operation

Although the biphase rectifier output voltages studied so far are typical of the majority of such rectifiers, their uniform peak values and constant firing angles make them all special cases. The general case is shown in Figure 17 and could result from an unbalanced supply transformer winding, from dissimilar tube characteristics, or from both simultaneously as illustrated.

Despite the differences in peak transformer voltage and angle of retard, this output voltage can be resolved as before into sinusoidal components. All of these components, beginning with the second half cycle, have the same magnitude, $E_{m1}+E_{m2}$, although the moments of their entries depend on the firing angle, δ_1 or δ_2, in the corresponding half cycle of the complete output voltage. Appendix III contains the complete analysis of this general biphase case. For engineering work, the output voltages already used, while admittedly special cases, give sufficiently accurate results.

However, two special rectifier circuits deserve mention since transient responses in them can be obtained from the general biphase case. If one of the thyratrons in Figure 1 is replaced by a phanotron, which has no control grid, the result is sometimes called the "horse-and-ox" circuit, for reasons which become apparent on studying the output voltage in Figure 18. While the peak voltage is the same for all the half cycles, δ_1 definitely differs from δ_2. From the voltage components shown, the transient response is obtained as before.

The other special circuit, which has been termed the "free-wheeling" circuit, can be made by removing one half of the transformer winding in Figure 1 and replacing the corresponding thyratron by a phanotron. Its output voltage is given in Figure 19.

In addition to these variations of the biphase rectifier, certain abnormalities can occur also in polyphase circuits. For instance, if one anode in a six-phase rectifier supplying an exciter field were to become inoperative, it would be practical as well as desirable to know if the field current would remain continuous. This could be accomplished readily by decomposing the output voltage of Figure 20 and determining whether the current response during the interval of missing anode voltage is theoretically negative at any point. If it is, conduction will be discontinuous, for a reverse current cannot pass through a rectifier.

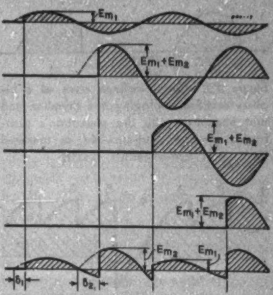

Figure 17. Decomposition of the generalized output voltage wave of a biphase rectifier, considering unequal anode voltages and firing angles

Appendix I. Nomenclature

R = resistance of load circuit, ohms
L = inductance of load circuit, henrys
ω = line frequency, radians per second
Z = load-circuit impedance at line frequency $=(R^2+\omega^2L^2)^{1/2}$
T = time constant of load circuit, seconds $=L/R$
θ = load-circuit power-factor angle at line frequency $=\tan^{-1}\omega L/R$
E_m = peak value of the alternating voltage impressed on the load circuit
E_g = counter electromotive force in the load circuit, volts
E_t = rectifier-tube arc drop, volts
$E_b = E_g+E_t$ for rectification $=E_g-E_t$ for inversion
p = number of rectifier phases
t_1 = nominal conduction time per phase (for continuous conduction), seconds $=2\pi/\omega p$
α = nominal conduction angle per phase (for continuous conduction), radians $=\omega t_1=2\pi/p$
β = firing angle for uncontrolled rectification with continuous conduction, radians $=(\pi-\alpha)/2=\pi(p-2)/2p$
δ = angle by which firing is retarded beyond β, radians
γ = angle, in a p-phase rectifier, by which the firing of the first anode is retarded beyond δ due to closing of the switch to the load, radians
e = general symbol for an applied voltage which is a function of time, usually accompanied by an identifying subscript but used without one in equation 4
E = peak value of the general sinusoidal voltage in equations 3 and 4
t = time, seconds

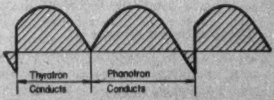

Figure 18. Output-voltage wave of a biphase rectifier employing one thyratron and one phanotron ("horse-and-ox" circuit)

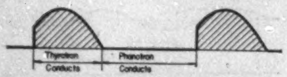

Figure 19. Output-voltage wave of a biphase rectifier employing one thyratron and one phanotron with the phanotron's transformer winding short-circuited or removed ("free-wheeling" circuit)

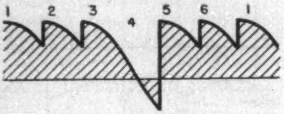

Figure 20. Output voltage of a controlled six-phase rectifier with one rectifying element inoperative

Appendix II. The p-Phase Rectifier

Figure 21 shows the rectifier output voltage of a p-phase rectifier. The immediate problem is to find the voltage that can be added to $\sin \omega t$ to obtain $\sin(\omega t-\alpha)$.

$$E_m \sin \omega t+f(t)=E_m \sin(\omega t-\alpha)$$
$$f(t)=-2E_m \sin(\alpha/2)\cos[\omega t-(\alpha/2)] \quad (17)$$

Thus $2E_m \sin(\alpha/2)$ is the peak value of the successive component voltages. These components can be summarized as follows, letting $t=0$ at the beginning of the nth component:

$$\left.\begin{array}{l} e_n=2E_m \sin(\alpha/2)\sin(\omega t+\delta) \\ e_{n-1}=2E_m \sin(\alpha/2)\sin(\omega t+\delta+\alpha) \\ e_{n-2}=2E_m \sin(\alpha/2)\sin(\omega t+\delta+2\alpha) \\ \cdots\cdots\cdots\cdots\cdots\cdots\cdots\cdots \\ e_2=2E_m \sin(\alpha/2)\sin[\omega t+\delta+(n-2)\alpha] \\ e_1=E_m \sin[\omega t+\delta+(n-1)\alpha+\beta] \end{array}\right\} \quad (18)$$

Equation 18 holds for $0<\omega t<\alpha$. The corresponding current responses are

$$\left.\begin{array}{l} i_n=2(E_m/Z)\sin(\alpha/2)\sin(\omega t-\theta+\delta)+ \\ \quad 2(E_m/Z)\sin(\alpha/2)\sin(\theta-\delta)\epsilon^{-t/T} \\ i_{n-1}=2(E_m/Z)\sin(\alpha/2)\sin(\omega t-\theta+ \\ \quad \delta+\alpha)+2(E_m/Z)\sin(\alpha/2)\times \\ \quad \sin(\theta-\delta)\epsilon^{-(t+t_1)/T} \\ i_{n-2}=2(E_m/Z)\sin(\alpha/2)\times \\ \quad \sin(\omega t-\theta+\delta+2\alpha)+2(E_m/Z)\times \\ \quad \sin(\alpha/2)\sin(\theta-\delta)\epsilon^{-(t+2t_1)/T} \\ \cdots\cdots\cdots\cdots\cdots\cdots\cdots\cdots \\ i_2=2(E_m/Z)\sin(\alpha/2)\sin[\omega t-\theta+\delta+ \\ \quad (n-2)\alpha]+2(E_m/Z)\sin(\alpha/2)\times \\ \quad \sin(\theta-\delta)\epsilon^{-[t+(n-2)t_1]/T} \\ i_1=(E_m/Z)\sin[\omega t-\theta+\delta \\ \quad +(n-1)\alpha+\beta]+(E_m/Z) \\ \quad \sin(\theta-\beta-\delta-\gamma)\epsilon^{-[t+(n-1)t_1-\gamma/\omega]/T} \end{array}\right\} \quad (19)$$

The total current response is

$$\left.\begin{array}{l} i_t=i_1+i_2+\ldots+i_{n-2}+i_{n-1}+i_n \\ \quad =(E_m/Z)\sin(\omega t-\theta+\delta+\beta)+ \\ \quad 2(E_m/Z)\sin(\alpha/2)\times \\ \quad \sin(\theta-\delta)\epsilon^{-t/T}[(1-\epsilon^{-(n-1)t_1/T})/ \\ \quad (1-\epsilon^{-t_1/T})]+(E_m/Z)\times \\ \quad \sin(\theta-\beta-\delta-\gamma)\epsilon^{-[t+(n-1)t_1-\gamma/\omega]/T} \end{array}\right\} \quad (20)$$

Figure 21. Output voltage of the general p-phase rectifier

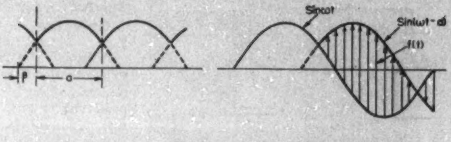

for $0\leqq t\leqq t_1$.

In steady state, equation 20 becomes

$$i_t=(E_m/Z)\sin(\omega t-\theta+\delta+\beta)+2(E_m/Z)\times$$
$$\sin(\alpha/2)\sin(\theta-\delta)[\epsilon^{-t/T}/(1-\epsilon^{-t_1/T})] \quad (21)$$

If a counter electromotive force, E_b, is present, the steady-state solution is

$$i_t=(E_m/Z)\sin(\omega t-\theta+\delta+\beta)-E_b/R+$$
$$2(E_m/Z)\sin(\alpha/2)\sin(\theta-\delta)\times$$
$$[\epsilon^{-t/T}/(1-\epsilon^{-t_1/T})] \quad (22)$$

Appendix III. The General Biphase Rectifier

The voltage components shown in Figure 17 may be summarized in two ways. If n is odd,

$$\left.\begin{array}{l} e_n=(E_{m1}+E_{m2})\sin(\omega t+\delta_1) \\ e_{n-1}=(E_{m1}+E_{m2})\sin(\omega t+\delta_1+\pi) \\ e_{n-2}=(E_{m1}+E_{m2})\sin(\omega t+\delta_1+2\pi) \\ \cdots\cdots\cdots\cdots\cdots\cdots\cdots\cdots \\ e_3=(E_{m1}+E_{m2})\sin[\omega t+\delta_1+(n-3)\pi] \\ e_2=(E_{m1}+E_{m2})\sin[\omega t+\delta_1+(n-2)\pi] \\ e_1=E_{m1}\sin[\omega t+\delta_1+(n-1)\pi] \end{array}\right\} \quad (23a)$$

for $0<\omega t<(\pi+\delta_2-\delta_1)$.

If n is even,

$$\left.\begin{array}{l} e_n=(E_{m1}+E_{m2})\sin(\omega t+\delta_2) \\ e_{n-1}=(E_{m1}+E_{m2})\sin(\omega t+\delta_2+\pi) \\ e_{n-2}=(E_{m1}+E_{m2})\sin(\omega t+\delta_2+2\pi) \\ \cdots\cdots\cdots\cdots\cdots\cdots\cdots\cdots \\ e_3=(E_{m1}+E_{m2})\sin[\omega t+\delta_2+(n-3)\pi] \\ e_2=(E_{m1}+E_{m2})\sin[\omega t+\delta_2+(n-2)\pi] \\ e_1=E_{m1}\sin[\omega t+\delta_2+(n-1)\pi] \end{array}\right\} \quad (23b)$$

for $0<\omega t<(\pi+\delta_1-\delta_2)$.

Finding the current responses is complicated somewhat by the difference between δ_1 and δ_2. If n is odd, the current components are

$$\left.\begin{array}{l} i_n=[(E_{m1}+E_{m2})/Z]\sin(\omega t-\theta+\delta_1)+ \\ \quad [(E_{m1}+E_{m2})/Z]\sin(\theta-\delta_1)\epsilon^{-t/T} \\ i_{n-1}=[(E_{m1}+E_{m2})/Z]\sin(\omega t-\theta+ \\ \quad \delta_1+\pi)+[(E_{m1}+E_{m2})/Z]\times \\ \quad \sin(\theta-\delta_2)\epsilon^{-[t+t_1+(\delta_1-\delta_2)/\omega]/T} \\ i_{n-2}=[(E_{m1}+E_{m2})/Z]\times \\ \quad \sin(\omega t-\theta+\delta_1+\pi)+[(E_{m1}+ \\ \quad E_{m2})/Z]\sin(\theta-\delta_1)\epsilon^{-(t+2t_1)/T} \\ \cdots\cdots\cdots\cdots\cdots\cdots\cdots\cdots \\ i_3=[(E_{m1}+E_{m2})/Z]\sin[\omega t-\theta+\delta_1+ \\ \quad (n-3)\pi]+[(E_{m1}+E_{m2})/Z]\times \\ \quad \sin(\theta-\delta_1)\epsilon^{-[t+(n-3)t_1]/T} \\ i_2=[(E_{m1}+E_{m2})/Z]\sin[\omega t-\theta+ \\ \quad \delta_1+(n-2)\pi]+[(E_{m1}+E_{m2})/Z]\times \\ \quad \sin(\theta-\delta_2)\epsilon^{-[t+(n-2)t_1+(\delta_1-\delta_2/\omega]/T} \\ i_1=(E_{m1}/Z)\sin[\omega t-\theta+\delta_1+ \\ \quad (n-1)\pi]+(E_{m1}/Z)\times \\ \quad \sin(\theta-\delta_1)\epsilon^{-[t+(n-1)t_1]/T} \end{array}\right\} \quad (24a)$$

for $0<\omega t<(\pi+\delta_2-\delta_1)$.

If n is even, the current components are

$$\left.\begin{array}{l} i_n=[(E_{m1}+E_{m2})/Z]\sin(\omega t-\theta+\delta_2)+ \\ \quad [(E_{m1}+E_{m2})/Z]\sin(\theta-\delta_2)\epsilon^{-t/T} \\ i_{n-1}=[(E_{m1}+E_{m2})/Z]\times \\ \quad \sin(\omega t-\theta+\delta_2+\pi)+[(E_{m1}+E_{m2})/Z]\times \\ \quad \sin(\theta-\delta_1)\epsilon^{-[t+t_1+(\delta_2-\delta_1)/\omega]/T} \\ i_{n-2}=[(E_{m1}+E_{m2})/Z]\sin(\omega t-\theta+ \\ \quad \delta_2+2\pi)+[(E_{m1}+E_{m2})/Z]\times \\ \quad \sin(\theta-\delta_2)\epsilon^{-(t+2t_1)/T} \\ \cdots\cdots\cdots\cdots\cdots\cdots\cdots\cdots \\ i_3=[(E_{m1}+E_{m2})/Z]\sin[\omega t-\theta+ \\ \quad \delta_2+(n-3)\pi]+[(E_{m1}+E_{m2})/Z]\times \\ \quad \sin(\theta-\delta_1)\epsilon^{-[t+(n-3)t_1+(\delta_2-\delta_1)/\omega]/T} \\ i_2=[(E_{m1}+E_{m2})/Z]\sin[\omega t-\theta+\delta_2+ \\ \quad (n-2)\pi]+[(E_{m1}+E_{m2})/Z]\times \\ \quad \sin(\theta-\delta_2)\epsilon^{-[t+(n-2)t_1]/T} \\ i_1=(E_{m1}/Z)\sin[\omega t-\theta+\delta_2+ \\ \quad (n-1)\pi]+(E_{m1}/Z)\times \\ \quad \sin(\theta-\delta_1)\epsilon^{-[t+(n-1)t_1+(\delta_2-\delta_1)/\omega]/T} \end{array}\right\} \quad (24b)$$

for $0<\omega t<(\pi+\delta_1-\delta_2)$.

The sum of the responses, when n is odd, is

$$i_t=(E_{m1}/Z)\sin(\omega t-\theta+\delta_1)+$$
$$[(E_{m1}+E_{m2})/Z]\sin(\theta-\delta_1)\epsilon^{-t/T}\times$$
$$[(1-\epsilon^{-(n+3)t_1/T})/(1-\epsilon^{-2t_1/T})]-(E_{m2}/Z)\times$$
$$\sin(\theta-\delta_1)\epsilon^{-[t+(n-1)t_1]/T}+[(E_{m1}+$$
$$E_{m2})/Z][\sin(\theta-\delta_2)\epsilon^{-[t+(\delta_1-\delta_2)/\omega]/T}]\times$$
$$[(1-\epsilon^{-(n+1)t_1/T})/(1-\epsilon^{-2t_1/T})] \quad (25a)$$

for $0\leqq\omega t\leqq(\pi+\delta_2-\delta_1)$.

When n is even, the total current is

$$i_t=(E_{m2}/Z)\sin(\omega t-\theta+\delta_2)+$$
$$[(E_{m1}+E_{m2})/Z][\epsilon^{-t/T}]\times$$
$$[(1-\epsilon^{-(n+2)t_1/T})/(1-\epsilon^{-2t_1/T})]\times$$
$$[\sin(\theta-\delta_2)+\epsilon^{-(\delta_2-\delta_1)/\omega T}\sin(\theta-\delta_1)]-$$
$$(E_{m2}/Z)\sin(\theta-\delta_1)\epsilon^{[t+(n-1)t_1+(\delta_2-\delta_1)/\omega]/T} \quad (25b)$$

for $0\leqq\omega t\leqq(\pi+\delta_1-\delta_2)$.

References

1. Theory of Rectifier—D-C Motor Drive, E. H. Vedder, K. P. Puchlowski. AIEE Transactions, volume 62, 1943, pages 863–9.

2. Operational Circuit Analysis (book), V. Bush. John Wiley and Sons, Inc., New York, N. Y., 1929. Page 56.

3. Circuit Response to Nonsinusoidal Wave Forms, P. T. Chin. *Electronics*, October 1944, pages 138–41.

4. Introduction to Electric Transients (book), E. B. Kurtz, G. F. Corcoran. John Wiley and Sons, Inc., New York, N. Y., 1935. Page 151.

5. A Graphical Analysis of the Voltage and Current Wave Forms of Controlled Rectifier Circuits, P. T. Chin, E. E. Moyer. AIEE Transactions, volume 63, 1944, July section, pages 501–08.

6. Inverter Action on Reversing of Thyratron Motor Control, H. L. Palmer, H. H. Leigh. AIEE Transactions, volume 63, 1944, April section, pages 175–84.

A Comparison of the Amplitude-Modulation, Frequency-Modulation, and Single-Side-Band Systems for Power-Line Carrier Transmission

R. C. CHEEK
ASSOCIATE AIEE

MANY utility engineers interested in increasing the applications of power-line carrier on their systems are confronted today with the difficult problem of finding space for additional channels in an already crowded carrier spectrum. This is a problem, not only for large utilities which have extensive carrier systems of their own, but also for smaller companies interconnected into large groups in which the total number of carrier installations is large.

Other problems that arise in some power-line carrier applications are the high attenuation of some long-haul communication and telemetering circuits, particularly those which include several by-pass points, and the high interference and noise levels that exist on some lines.

In general, increasing the power of ordinary amplitude-modulation equipment does not provide a satisfactory solution to these problems. This fact has led to a consideration of the possibilities in the power-line carrier field of two systems of transmission fundamentally different from the amplitude-modulation system, namely, the frequency-modulation system and the single-side-band system.

The ability of a frequency-modulation power-line carrier system to provide gains in signal-to-noise ratio over the amplitude-modulation system with certain types of noise has been reported in a previous paper.[1] The channel width which must be provided for a frequency-modulation system in order to obtain appreciable gains in this respect was not clearly brought out, however. It is the purpose of the present paper to consider more fully this limitation of the frequency-modulation system for power-line carrier work, and to furnish a comparison of the amplitude-modulation, frequency-modulation, and single-side-band systems on the basis of their channel-width requirements, their ability to work through attenuation, and their susceptibility to interference and noise. Since the amplitude-modulation system is used in this paper as a basis of comparison for the other two systems, it will be considered first.

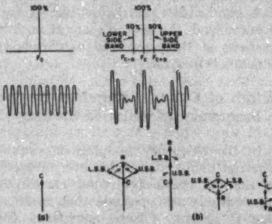

Figure 1. Amplitude-modulation system

(a). Unmodulated conditions, in spectrum, wave, and vector representation

(b). Complete modulation

Width of Channel Required by the Amplitude-Modulation System

Conditions are shown in Figure 1a for the amplitude-modulation system when no modulation is present, that is, when there is no speech or telemetering impulse on the channel. The only component in the frequency spectrum is the carrier, a constant-amplitude single-frequency sine wave, which is shown in vector form as a single vector of constant length. This vector is assumed to be rotating counterclockwise at carrier frequency. Its length can be taken as unity or 100 per cent.

Conditions for 100-per-cent amplitude modulation of the carrier wave by a sinusoidal audio tone are shown for comparison in Figure 1b. In addition to the carrier-frequency wave of 100-per-cent amplitude, two additional high-frequency waves are introduced into the frequency spectrum, one of a frequency equal to carrier frequency plus modulating frequency, and one of frequency equal to carrier frequency minus modulating frequency. The amplitude (voltage) of each of these additional components, which are called the side-band components, is 50 per cent of the carrier amplitude. The power in each side-band component therefore is 25 per cent of the carrier power. This gives a total average power during complete modulation of 1.5 times the unmodulated carrier power. This power is the average of the variations in total transmitted power as the carrier and side-band components combine to give a wave whose power varies between the limits of zero and four times the unmodulated carrier power during an audio cycle.

A vector representation is given in Figure 1b of the way in which the side-band components combine with each other and with the carrier component to produce a resultant whose amplitude varies between zero and twice carrier amplitude and whose frequency is always carrier frequency. The vector diagrams are drawn for successive intervals of time during an audio cycle. The vectors representing the upper and lower side-band components revolve about the carrier vector in opposite directions at audio frequency, because their frequencies are carrier frequency plus audio frequency and carrier frequency minus audio frequency, respectively. The two side-band vectors are always of just the proper phase to produce a resultant which directly aids or opposes the carrier vector.

In the foregoing discussion, modulation by a single audio frequency was assumed. This produced one pair of side-band components. If more than one audio frequency were present, a pair of side-band components for each, of frequency equal to carrier plus audio frequency and carrier minus audio frequency, would be produced. In such a case the sum of the amplitudes of the upper side-band components would equal 50 per cent of the carrier amplitude, and the sum of the lower side-band components would equal

---

Paper 45-68, recommended by the AIEE committee on power transmission and distribution for presentation at the AIEE winter technical meeting, New York, N. Y., January 22-26, 1945. Manuscript submitted November 8, 1944; made available for printing December 28, 1944.

R. C. Cheek is central-station engineer, Westinghouse Electric and Manufacturing Company, East Pittsburgh, Pa.

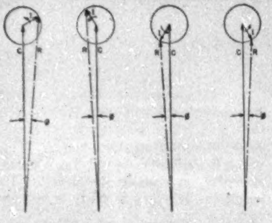

Figure 2. Amplitude and phase modulation of a carrier by an interfering wave

50 per cent of the carrier amplitude for complete modulation.

In the amplitude-modulation system the carrier and all side-band components are transmitted, and an amplitude-modulation receiver must accept a frequency band sufficiently wide to accommodate the lowest and highest side-band components produced. The channel width required is therefore twice the frequency of the highest audio frequency to be transmitted. In power-line carrier work this normally means a band of six kilocycles to accomodate speech frequencies and audio tones as high as three kilocycles.

Effects of Interference and Noise on an Amplitude-Modulated Signal

In the amplitude-modulation system, the receiver responds only to changes in the amplitude of the carrier; changes in the phase or slight changes in the frequency of the carrier produce no audible output from the receiver. Interference with an amplitude-modulated signal occurs when an undesired wave is passed by the tuned circuits of the receiver (which must accept all frequencies in a six-kilocycle band in the system under discussion) and adds to the carrier wave in much the same manner as the desired side-band components add to it, producing variations in its amplitude. If the undesired signal is another carrier wave, the familiar beat-note type of interference is the result. The frequency of the audio output of the receiver for this type of interference is the difference between the frequencies of the carrier and the interfering wave. The amplitude of the audio output is the same for all interfering waves of equal amplitude applied to the detector, whether their frequency is close to that of the desired carrier or close to the edge of the band accepted by the receiver.

Vector diagrams showing the effect of interference on an amplitude-modulated carrier are given in Figure 2, in which the amplitude of the interfering wave is assumed to be ten per cent of the amplitude of the desired carrier. Assuming that no side-band components are present, that is, that the carrier is not intentionally being modulated, the carrier vector is again a vector of constant length, rotating at carrier frequency. The vector representing the interfering wave adds to the carrier vector and revolves about it at a frequency equal to the difference in frequency between the two. The resultant vector varies in amplitude and phase at this difference frequency. The amplitude variations are equivalent to ten-per-cent modulation of the carrier amplitude, and the receiver detects them as such.

The foregoing discussion was based on interference from a single-frequency wave. Random noise consists of a large number of such waves of all frequencies, distributed throughout the band accepted by the receiver. The effective noise voltage output of the receiver is the effective value of the noise produced by all the random noise components accepted by the receiver. Assuming that noise components of all frequencies are present, and that they have equal amplitudes, the rms noise output of an amplitude-modulation receiver is

$$E_{rms} = \sqrt{\int_{-f_{max}}^{f_{max}} k^2 d(F_n - F_c)} = k\sqrt{2f_{max}} \quad (1)$$

where k represents the amplitude of the noise produced by each individual noise component, f_{max} is the highest audio frequency to be transmitted by the system, that is, the cutoff point of the receiver pass band above and below carrier frequency, and F_n and F_c are the frequencies of the noise and carrier components, respectively.

Width of Channel Required by the Frequency-Modulation System

In the frequency-modulation system[2] a carrier signal, identical in every respect to the amplitude-modulated carrier, is transmitted during periods when modulation is absent. These conditions are shown in Figure 3a. The only quantity transmitted is a constant-amplitude single-frequency sine wave, represented by a single vector of constant length.

When modulation is present the conditions shown in Figure 3b are obtained in a particular frequency-modulation system. The transmitted wave has the same amplitude as the original carrier, but its frequency varies above and below the original carrier frequency. This variation in frequency takes place at a rate corresponding to the audio frequency being transmitted. It is caused by the presence of side-band components, as in the amplitude-modulation system. However, several important differences exist. Instead of a single pair of side-band components for a single modulating frequency, as in amplitude-modulation, an infinite number of side-band pairs is produced in frequency modulation. These side-band pairs are spaced in the spectrum above and below carrier frequency at multiples of the audio frequency. The first side-band pair occurs at carrier plus audio frequency and carrier minus audio frequency, as in amplitude modulation. The second pair occurs at carrier plus and minus twice audio frequency, the third at carrier plus and minus three times audio frequency, and so on. Although there are an infinite number of side-band pairs in a frequency-modulated signal, the amplitude of each pair is generally different, and at a certain distance in each direction from carrier frequency the amplitudes of higher- and lower-frequency side-band components become negligible.

Another important difference between frequency modulation and amplitude modulation is that in frequency modulation the amplitude of the carrier-frequency component is always reduced during modulation, and the vector representing it changes in length accordingly. However, the resultant obtained by adding the new carrier vector and the side-band vectors is always in true frequency modulation a vector of length equal to the original length of the vector representing the carrier. The intelligence is transmitted, not by a change in the amplitude of the resultant vector, but by a continuous oscillation in its phase position. This oscillation in the phase position of the resultant vector introduces a modulation of the frequency, because during the process of a change in phase a change takes place in the speed of rotation of the vector, which of course means a change in frequency. The frequency deviation from normal at any instant is proportional to the rate at which the phase of the resultant vector is changing at that instant.

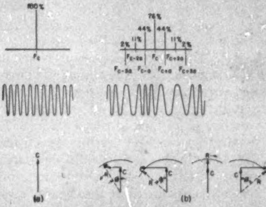

Figure 3. Frequency-modulation system

(a). Unmodulated conditions, in spectrum, wave, and vector representation

(b). Modulation with unity deviation ratio

The ratio of the maximum resultant frequency deviation to the highest audio frequency to be transmitted in a frequency-modulation system is called the deviation ratio. The conditions shown in Figure 3b are those obtained with a maximum carrier-frequency deviation of three kilocycles above and below normal with a modulating frequency of three kilocycles. If three kilocycles is the highest audio frequency to be transmitted in this system, as is assumed to be the case in all systems considered in this discussion, the deviation ratio of the system is unity. A system with unity deviation ratio has been chosen for illustration because, as will be shown later, it is only with a deviation ratio of at least unity that the frequency-modulation system offers appreciable gains in signal-to-noise ratio over amplitude modulation.

The vector diagrams of Figure 3b show at successive intervals of time how with unity deviation ratio the resultants of each pair of side-band vectors add to the carrier vector to maintain the amplitude but to produce a change in the phase of the transmitted wave. The two vectors representing the first side-band pair revolve about the carrier vector in opposite directions at audio frequency. Their resultant is always of such a phase as to add in quadrature with the carrier vector. The vectors representing the second side-band pair revolve about the resultant of the first side-band pair at twice the audio frequency, producing by themselves a resultant always in phase with the carrier vector. The vectors of the third side-band pair revolve about the resultant of the second side-band pair at three times the audio frequency, producing by themselves a resultant always in quadrature with the carrier vector. There are successively higher and lower side-band pairs, but they are small and their resultants are not shown. The total effect of all the vectors is to produce a resultant vector whose length is always that of the vector representing the original carrier, but whose phase varies in accordance with the transmitted audio frequency. This phase oscillation produces an oscillation in the frequency of the transmitted wave.

It can be seen in Figure 3b that, although the frequency swing of the resultant wave is only three kilocycles above and below carrier frequency, the side-band components that must be transmitted in order to obtain this frequency swing actually occupy a band width greater than six kilocycles. According to Hund,[8] good engineering practice requires that the side-band components in a band 50 per cent greater than the maximum resultant frequency swing above and below normal carrier frequency be transmitted, that is, all side-band components in a band of width $1.5 \times 2\Delta F$, where ΔF is the maximum frequency deviation from normal. Narrowing the transmitted or received band width to less than this figure will introduce excessive audio distortion into the channel.

Suppose, for example, an attempt were made in the system under consideration to reduce the channel width occupied by the transmitted signal by transmitting only those side-band components in a frequency band three kilocycles above and below carrier frequency. For modulation by any audio frequency from three kilocycles down to 1.5 kilocycles, the carrier and only a single pair of side-band components would be transmitted. At successively lower frequencies in this range, the amplitude of the carrier component becomes successively less, the amplitudes of the suppressed side-band components become greater, and the distortion of the apparent swing of the resultant signal increases. The distortion is greatest just below the point at which the second side-band pair comes within the transmitted band of frequencies, that is, at a modulating frequency of 1.5 kilocycles. The resultant frequency swing, as it appears to a discriminator with center frequency tuned to carrier frequency, is shown in Figure 4 for several modulating frequencies between 1.5 and 3 kilocycles. The curves of Figure 4 were plotted from relations derived in the appendix.

Effects of Interference and Noise on a Frequency-Modulated Signal

The frequency swing of a frequency-modulated signal above and below normal frequency depends upon two factors: the loudness of the modulating signal, and the frequency swing the system is designed to have for a signal of that loudness. The frequency swing in a given frequency-modulation system is the same for any audio frequency of a given loudness. This means that the phase swing must be inversely proportional to the modulating frequency. If the lower modulating frequencies are to produce the same frequency change as the higher modulating frequencies, the resultant vector representing the signal must travel through a greater phase change during a low-frequency audio cycle than during a higher-frequency audio cycle. In other words, the speed of swing of the resultant vector is the same at a given point on the audio cycle, whether the audio frequency is high or low. The resultant vector has a longer time to change in phase during a low-frequency audio cycle; so the actual phase swing is greater than for a higher-frequency audio cycle. This fact is important to an understanding of the way in which frequency modulation can provide gains in signal-to-noise ratio over amplitude modulation.

The deviation ratio in frequency modulation expresses in radians the maximum phase swing when the signal is modulated by a wave of maximum loudness and of the highest audio frequency the system is intended to transmit. In the system under consideration, which has unity-deviation ratio, the phase swing is one radian when a three-kilocycle tone of maximum loudness is being transmitted. This phase swing varies inversely with the audio frequency if the audio amplitude is kept constant and becomes enormous with very low modulating frequencies.

Consider the effect of adding to the unmodulated frequency-modulation carrier the same interfering signal assumed in the discussion of amplitude modulation in Figure 2. If the interfering wave has ten per cent of the amplitude of the desired carrier and has a frequency three kilocycles away from carrier frequency, the vector representing it will revolve around the carrier vector as before, producing a resultant whose amplitude varies ten per cent above and below normal amplitude and whose phase oscillates with a maximum swing of 5.7 degrees or 0.1 radian. Amplitude limiters in the frequency-modulation receiver remove the amplitude variations, but the receiver responds to the phase variations. The phase swing is one tenth of the swing produced when the system is modulated by a three-kilocycle tone of maximum loudness; therefore the interfering signal causes the same amount of interference it caused to the amplitude-modulation carrier.

If the interfering signal is removed only 1.5 kilocycles in frequency from the carrier, however, conditions are somewhat different. Assuming again that the amplitude of the interfering wave is ten per cent of normal carrier amplitude, the same 0.1-radian phase oscillation occurs,

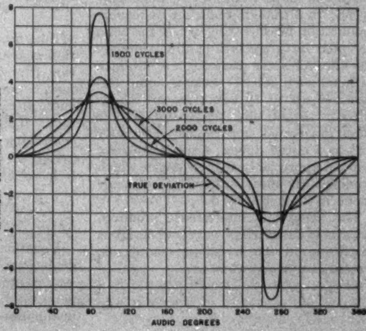

Figure 4. Distortion of a frequency - modulated signal when all except the first pair of side-band components are suppressed

Unity deviation ratio, highest audio frequency three kilocycles

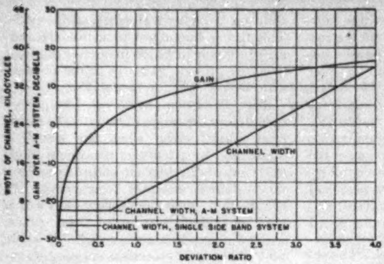

Figure 5. Decibel gain of frequency modulation over amplitude modulation and channel width required by frequency-modulation system as deviation ratio is increased

Maximum audio frequency three kilocycles

this time at a frequency of 1.5 kilocycles. This swing is only $^1/_{20}$ of the phase swing for a desired 1.5-kilocycle modulation of maximum loudness. The result is that, although the amplitude of the interfering wave is the same as before, the amount of audio output it causes is only half as much. As the interfering signal gets closer and closer in frequency to the carrier, the audio output it produces becomes less and less, reaching zero at carrier frequency.

It has been shown that in order to obtain reasonably distortion-free reproduction of the signal, the receiver in this system will have to accept a band of frequencies greater than three kilocycles above and below carrier frequency. Interfering waves in this band removed more than three kilocycles from the carrier will cause more interference in the frequency-modulation receiver than they would cause in the corresponding amplitude-modulation receiver, even if the latter were required to accept such frequencies. Actually the radio-frequency circuits in an amplitude-modulation receiver normally are designed to pass a band of width equal to twice the maximum audio frequency, or six kilocycles in this case. The same effect could be obtained in the frequency-modulation receiver under consideration by passing the required band of frequencies in the radio-frequency circuits but designing the audio circuits so that they cut off sharply at the maximum audio frequency of three kilocycles. In ultrahigh-frequency frequency-modulation broadcasting, where the band accepted by a receiver is approximately 225 kilocycles, the same effect is obtained without such filters, because audio frequencies up to 15 kilocycles are transmitted. Practically the entire audible range is covered, and the ear inherently acts as a cutoff device, since it does not respond appreciably to interference which produces an audio output of frequency above 15 kilocycles.[3]

The amount of interference produced by single interfering waves of a given amplitude in the frequency-modulation system can be expressed as

$$E_t = k\,\frac{F_t - F_c}{\Delta F} \tag{2}$$

in which $F_t - F_c$ is the difference between the interfering frequency and the carrier frequency, and k is the interference produced when this difference is equal to ΔF, the maximum deviation of frequency of the system. The factor k in equation 2 is the same as the factor k which appears in equation 1 for the amplitude-modulation system, if it is assumed that the frequency ΔF is in the audible range and is passed by the audio circuits of the receiver.

The effect of random noise upon a frequency-modulation signal can be found by integrating to determine the rms noise output, as before. Assuming that a band width of 1.5 × 2 ΔF is passed by the frequency-modulation receiver, we have

$$E_{rms} = \sqrt{\int_{-1.5\Delta F}^{1.5\Delta F} k^2 \left[\frac{F_n - F_c}{\Delta F}\right]^2 d(F_n - F_c)} = 1.5k\sqrt{\Delta F} \tag{3}$$

if it is assumed that ΔF is within the range of audible frequencies and that no low-pass filter is provided in the audio circuits of the receiver. If such a filter is provided, the maximum gain in signal-to-noise ratio is obtained when its cutoff frequency is f_{max}, the highest audio frequency to be handled by the system. The limits of integration in equation 3 in this case become $-f_{max}$ and f_{max}, and we have

$$E_{rms} = \frac{k f_{max}\sqrt{2 f_{max}}}{\sqrt{3}\,\Delta F} \tag{4}$$

Equation 4 for the frequency-modulation system is exactly equivalent to equation 1 for the amplitude-modulation system, assuming that the same maximum audio frequency is to be transmitted by each. This provides a basis for directly comparing the performance of the two systems. Dividing equation 4 by equation 1, we have

$$\frac{E_{F-M}}{E_{A-M}} = \frac{f_{max}}{\sqrt{3}\,\Delta F} \tag{5}$$

Equation 5 shows that with unity-deviation ratio, the frequency-modulation system provides a gain in rms signal-to-noise ratio of 4.8 decibels over amplitude modulation. Larger-deviation ratios provide larger gains, but these gains can be obtained only at the expense of channel width. Figure 5 shows, for systems in which the maximum audio frequency is three kilocycles, a curve of the decibel gain afforded by the frequency-modulation system as the deviation ratio is increased. A curve giving the channel width required by the system as the deviation ratio is increased is also shown for comparison. The latter curve is based on the requirement that the channel width be 1.5 × 2 ΔF for reasonably distortion-free reproduction.

The Single-Side-Band System

In the amplitude-modulation system, the carrier-frequency component of the signal is unchanged during modulation, as shown in Figure 1. Modulation merely introduces additional components, which act upon the carrier in such a way that the amplitude of the resultant signal varies above and below carrier amplitude. It can be seen from the vector diagrams of Figure 1b that it would be possible to communicate with one of the side-band components suppressed. The remaining component still would produce amplitude variations in the resultant signal at the modulating frequency, and these variations could be detected by an ordinary amplitude-modulation receiver. It is possible to go a step further and suppress the carrier itself as well as the components of one of the side bands. If this is done in a low-power stage of an amplitude-modulation transmitter, the entire power capability of the transmitter can be used to amplify and transmit the components of a single side band. The carrier-frequency component, upon which the side-band components act to produce amplitude variations, can be supplied by a small oscillator at the receiving end of the channel; thus, instead of using a comparatively large amount of power at the transmitting end to generate a constant-frequency constant-amplitude sine wave, which contains no intelligence, and subjecting it to all the attenuation and losses involved in transmitting it to the receiving end of the channel, it is possible to produce the equivalent of this wave with very little power at the receiving point. The power which ordinarily is used at the sending end to transmit the carrier component then can be used to transmit intelligence-bearing components of a single side band. In the remainder of this paper, the single-side-band system referred to is the type in which the carrier as well as one of the side bands is suppressed.

The conditions for no modulation in the single-side-band system are shown in Figure 6a. The frequency spectrum contains no components of any frequency under these conditions, and the constant-frequency constant-amplitude carrier common to the amplitude-modulation and frequency-modulation systems is absent.

When modulation is present, again assuming modulation by a single audio frequency, a single component of frequency appears in the spectrum, as shown in Figure 6b. This quantity is a pure sine wave, of constant amplitude, and of constant frequency equal to nominal carrier frequency plus audio frequency, assuming that the upper side-band component is being transmitted. Actually, either the upper or the lower side-band component could be used. No carrier-frequency component is transmitted under any conditions.

The vector diagrams of Figure 6b represent conditions at the receiving end of a single-side-band channel when modulation is present. The locally generated carrier wave is shown as a dotted vector, to which the incoming side-band vector is added. The frequency of the side-band wave differs from the locally generated carrier frequency; therefore the vector representing it revolves about the carrier vector. This variation takes place at audio frequency, and the resultant vector varies in amplitude at the audio frequency. The resultant wave, produced by adding the local carrier and the received side-band wave, is a wave very similar to that which would have been obtained had the carrier and both side-band components been transmitted from the sending end. This resultant wave can be applied to an ordinary amplitude-modulation detector and rectified in the usual manner.

The width of the channel required by the single-side-band system is exactly half that required by the amplitude-modulation system. In other words, the space in the spectrum occupied by a single-side-band transmitter and the band of frequencies which must be accepted by the receiver are equal to the maximum audio frequency to be transmitted, or three kilocycles for ordinary power-line carrier work.

Gains in Signal-to-Noise Ratio With the Single-Side-Band System

A single-side-band receiver must accept only half the band width required in an amplitude-modulation receiver. The lower limit of the integral of equation 1 is zero for the single-side-band system, and we have

$$E_{rms} = \sqrt{\int_0^{f_{max}} k^2 d(F_n - F_c)} = k\sqrt{f_{max}} \quad (6)$$

Halving the band width therefore eliminates half of the noise power and provides an immediate gain of three decibels for the single-side-band system. Other gains can be realized, depending upon the characteristics of the transmitter used to amplify the single-side-band signal.

In the amplitude-modulation system the average power transmitted during complete modulation is 1.5 times the unmodulated carrier power. The extra power required during modulation can be supplied in several different ways. In one system, the output stage of the transmitter is capable of handling only the normal carrier power, and the additional 50 per cent is supplied by power-type modulator tubes. In another system, the output stage of the transmitter operates at a relatively low efficiency during periods of no modulation. The modulator supplies no appreciable power but acts to change the efficiency of the transmitter during modulation, increasing the average output by 50 per cent. In both cases, the 1.5 times normal power during modulation is the average power transmitted as the instantaneous power varies between the limits of zero and four times normal during the audio cycle, and an amplitude-modulation transmitter of the efficiency-modulated type must be able to produce this four times normal power at its peak efficiency, which it reaches for an instant during each audio cycle.

When an amplitude-modulation transmitter of the efficiency-modulated type is used to amplify a single-side-band component, it can operate at peak efficiency throughout the audio cycle, because the signal is a constant-amplitude radio-frequency wave without the peaks and "troughs" of an amplitude-modulation signal. The amplitude of the single-side-band component transmitted therefore is twice the amplitude of the carrier which is transmitted by the same equipment in the amplitude-modulation system. This signal, added to the locally generated carrier-frequency wave at the receiving end of the channel, produces a variation in the amplitude of the resultant wave twice as great as the variation in the amplitude of the signal transmitted by the same apparatus in amplitude modulation.

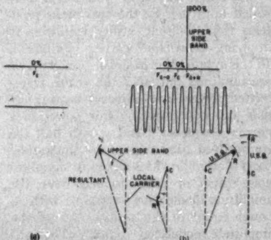

Figure 6. Single-side-band system, in spectrum, wave, and vector representation

(a). Unmodulated conditions

(b). Modulation producing side-band power of four times unmodulated carrier power in amplitude-modulation system

This is an additional gain of six decibels, which added to the three decibels gained by reducing the channel width gives a total gain for the single-side-band system of nine decibels over the amplitude-modulation system, with the same apparatus and the same peak transmitted power. In other words, the single-side-band system provides the equivalent of an amplitude-modulation system of eight times the carrier power and occupies only half the amplitude-modulation channel width.

Equations 4 and 6 provide a means of comparing directly the performance of the frequency-modulation and single-side-band systems in the presence of random noise. Dividing equation 4 by equation 6 we get

$$\frac{E_{F-M}}{E_{SSB}} = \frac{f_{max}}{\Delta F}\sqrt{\frac{2}{3}} \quad (7)$$

The two systems cannot be compared on the basis of the same required channel width, because at least the first pair of side-band components must be transmitted in the frequency-modulation system. Even though the peak-to-peak frequency swing $2\Delta F$ of the frequency-modulation signal is limited to the band width of the single-side-band signal, the first pair of side-band components required to produce the swing occur at carrier frequency plus and minus audio frequency, as in the amplitude-modulation system. For a maximum audio frequency of three kilocycles, a comparison can be made between the single-side-band system with a three-kilocycle band width and the frequency-modulation system with the minimum band width of six kilocycles. The requirement that the frequency-modulation band width be at least $1.5 \times 2\Delta F$ gives a maximum value of two kilocycles for ΔF, for which equation 7 shows a gain of 1.8 decibels for the single-side-band system, with a peak power which is reached only intermittently during conversation, equal to the continuously transmitted power of the frequency-modulated signal. If advantage is taken of the power capability of an efficiency-modulated amplitude-modulation transmitter to amplify the single-side-band signal, as discussed in the previous paragraph, the additional gain of six decibels brings the total gain to 7.8 decibels. In all cases the frequency-modulated signal requires at least twice the band width of the single-side-band signal.

Other Advantages of the Single-Side-Band System

Reduction in channel width and gains in signal-to-noise ratio in the presence of random noise are by no means the only advantages offered by the single-side-band system in power-line carrier work. A severe type of interference occasionally encountered on power systems is the type known as corona modulation,[4] a phenomenon in which the amplitude and phase of an amplitude-modulated or a frequency-modulated carrier are modulated in a complex manner by the presence of space charge due to corona. This space charge varies the effective shunt conductance of the line, periodically changing its attenuation and phase-shift constants. It has been found that increasing the power of the carrier fails to alleviate this condition, because the relative amount of modulation apparently stays the same, maintaining the same signal-to-noise ratio. The single-side-band system offers an ideal solution of this problem, because the carrier is supplied at the receiving end of the channel and therefore is not subjected to this type of modulation.

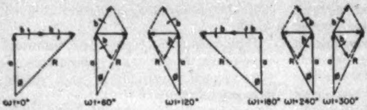

Figure 7. Addition of carrier and first side-band pair in a frequency-modulation system at successive intervals during an audio cycle

One of the most important features of the single-side-band system is that the absence of the carrier signal permits many applications that are impossible with the amplitude-modulation and frequency-modulation systems, in which a continuous carrier is transmitted. Elimination of the carrier permits a single receiver to receive signals from several different transmitting points simultaneously. For example, different telemetering tones can be used to modulate single-side-band transmitters at each of several locations, all on the same nominal carrier frequency. These transmitters can all be received simultaneously on a single receiver, because there is no beat-note interference and elimination of weak signals by strong ones as is the case with the amplitude-modulation or frequency-modulation systems.

Elimination of the carrier wave also permits repetition of carrier frequencies for separate-tone telemetering and load-control channels, even though these channels may be physically near each other on the power system. All that is required is that the strength of the desired signal be comparable to that of the undesired signal at the receiving point. It is not even necessary that the desired signal be as strong as the undesired one. Separate-tone frequencies must be used for each function, of course, but the nominal carrier frequencies can be the same.

An outstanding feature of the single-side-band system results from its similarity to the amplitude-modulation system. Basic amplitude-modulation transmitter and receiver units, with the unit type of rack-and-panel construction,[5] can be designed so that they can be converted in the field to single-side-band operation by the addition of single-side-band panel units. This makes it possible for utilities which do not at present have spectrum-crowding or interference problems to install suitably designed basic amplitude-modulation equipment for their present purposes, with the assurance that should such problems arise later they can be coped with by conversion of the amplitude-modulation equipment to the single-side-band system.

Conclusions

It is possible with the frequency-modulation system to obtain large gains over the amplitude-modulation system in signal-to-noise ratio. However, these gains are proportional to the deviation ratio employed and can be obtained only at the expense of channel width in the carrier-frequency spectrum. In the presence of random noise, a frequency-modulation system of unity deviation ratio provides a gain of 4.8 decibels in signal-to-noise ratio over an amplitude-modulation system of the same carrier power but requires a channel width at least 50 per cent greater for reasonably distortion-free audio reproduction.

The single-side-band system is a more sound approach to the two main problems that confront utility engineers in applying power-line carrier equipment. In this sytem gains in signal-to-noise ratio are obtained by using the entire transmitted power for intelligence-bearing signals and concentrating this power in a narrow frequency band. With half the transmitted band width, the single-side-band system provides a gain in signal-to-noise ratio of nine decibels over the amplitude-modulation system, with a power equal to the peak power of the amplitude-modulated signal. The absence of a continuous carrier in the single-side-band system makes possible the repetition of carrier frequencies for some applications and further increases the gains in channel space it provides. The similarity of the single-side-band system to the amplitude-modulation system makes it possible to convert to the single-side-band system present and future installations of amplitude-modulation equipment of suitable design.

Appendix. Distortion of a Frequency-Modulated Signal Caused by Suppression of All Except the First Pair of Side-Band Components

In a frequency-modulation system, the resultant of the first pair of side-band components is always in quadrature with the carrier component. The magnitude of this resultant varies at the modulating frequency between the limits of plus and minus twice the amplitude of the individual side-band components. These relations are shown in Figure 7 in vector form for successive points on an audio cycle. The vector obtained by adding the carrier vector to the resultant of the side-band vectors has with respect to the carrier vector a phase position ϕ which can be expressed for any instant of time as

$$\phi = \arc\tan \frac{2b \cos \omega t}{a} \qquad (8)$$

where b is the amplitude of each side-band component, ω is 2π times the modulating frequency, and a is the amplitude of the carrier component. If the amplitude variations of the resultant are removed by limiters, the discriminator of a frequency-modulation receiver responds only to the rate of change of phase of the resultant signal, that is, to

$$\frac{d\phi}{dt} = \frac{-(2b\omega/a) \sin \omega t}{1+(4b^2/a^2) \cos^2 \omega t} \text{ radians per second} \qquad (9)$$

Dividing equation 9 by 2π, we get the equivalent instantaneous frequency deviation,

$$F_t = \frac{-(2bf/a) \sin \omega t}{1+(4b^2/a^2) \cos^2 \omega t} \text{ cycles} \qquad (10)$$

in which f is the modulating frequency in cycles. The curves of Figure 4 were obtained by substituting the proper values for a and b from a table of Bessel functions, assuming a frequency-modulation system with unity deviation ratio and three kilocycles maximum audio modulating frequency.

References

1. FREQUENCY MODULATION FOR POWER-LINE CARRIER CURRENT, E. W. Kenefake. AIEE TRANSACTIONS, volume 62, 1943, October section, pages 616–19.

2. FREQUENCY MODULATION, W. L. Everitt AIEE TRANSACTIONS, volume 59, 1940, November section, pages 613–25.

3. FREQUENCY MODULATION (book), August Hund. McGraw-Hill Book Company, Inc., New York, N. Y., 1942.

4. PROBLEMS IN POWER-LINE CARRIER TELEPHONY, W. V. Wolfe, J. D. Sarros. AIEE TRANSACTIONS, volume 48, 1929, pages 107–13. Also closure by J. D. Sarros, pages 115–16.

5. A VERSATILE POWER-LINE CARRIER SYSTEM, H. W. Lensner, J. B. Singel. AIEE TRANSACTIONS, volume 63, 1944, March section, pages 129–32.

The Amplidyne Generator Applied to Speed-Controlled Electric Gun Turrets for Aircraft

L. A. ZAHORSKY
ASSOCIATE AIEE

THE PURPOSE of this paper is to explain the action of a particular type of Amplidyne generator in terms of its relationship to the turret performance and to attempt to separate its characteristics from those of the turret.

Development of this Amplidyne generator and the outbreak of the war were concurrent, and, due to incomplete knowledge of the requirements of this type of generator, it was expedient to define the characteristics of the turret control system as a whole. This caused difficulties in applying the Amplidyne to other systems. The characteristics of the Amplidyne can be defined independently of the system. Some effects of the variations in the Amplidyne characteristics and changes in circuit constants on the over-all performance of the turret will be shown.

Function of the Turret Power Drive

Most turrets using these Amplidynes are powered in both elevation and azimuth, by means of two separate control systems each consisting of a turret motor, an Amplidyne, and a control circuit.

The Amplidyne is part of a motor-generator set driven from the electric system of the airplane and makes available readily controlled power to operate the turret motor. By varying the adjustment of certain potentiometers connected in the control-field circuit of the Amplidyne, its output, and hence the performance of the turret, may be controlled by the operator.

The control circuit is used to combine properly the characteristics of the Amplidyne with those of the turret motor to produce the desired over-all performance of the system.

An important characteristic of the power drive is that of constant speed for a given potentiometer setting, independent of the gun position with respect to the wind. Another very important requirement of the power-drive system is that it be capable of driving the turret smoothly at very low speed. In direct contrast to this characteristic is the necessity for the turret power system to be capable of turning the turret rapidly from one target to another.

Description of the Amplidyne

The Amplidyne under consideration constitutes the generator end of a two-bearing motor-generator set. The 27-volt d-c driving motor is on the same shaft as the Amplidyne generator and drives it at about 8,300 rpm. The driving motor is an eight-pole compound-wound motor with one series turn to obtain quick starting and decrease the inrush current. This enables the unit to start and attain 85 per cent of its rated no-load speed in less than one second. The generator is rated at 60-volts 8.8-amperes output for ten minutes on and 20 minutes off. Figure 1 shows a complete Amplidyne set; Figure 2 is a sectionalized view showing the internal construction.

The generator has a two-pole stator with a control-field winding, *F* (see Figure 3), and compensating-field winding, *H*, acting in the load axis. Two rheostats are shunted across the compensating field for adjustment. An additional control field, *G*, acting in the same axis is provided for antihunt purposes. There is also a winding in the quadrature axis. The generator has four brushes mounted on an adjustable mechanism and spaced 90 degrees apart. Two diametrically opposite brushes, *C*, are connected in series with the compensating winding and the output terminals of an *AN* connector to constitute the load axis. The other two brushes, *D*, are short-circuited to complete the quadrature circuit. The operation is, briefly, as follows. Full-field excitation of the order of 0.1 watt in the control-field winding causes a small flux in the load axis which generates an electromotive force of about ten volts acting in the quadrature axis. This voltage then causes current to flow through the quadrature brushes, which in turn sets up a quadrature magnetic field. This field then causes an electromotive force of approximately 90 volts to be generated across the load brushes. As soon as a load current is allowed to flow, the compensating winding more than compen-

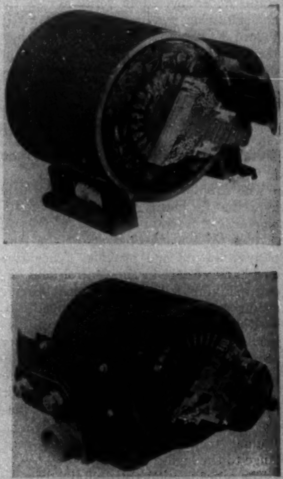

Figure 2. Cut-away views showing the internal construction of the Amplidyne

The upper illustration is the generator end and the lower is the motor end

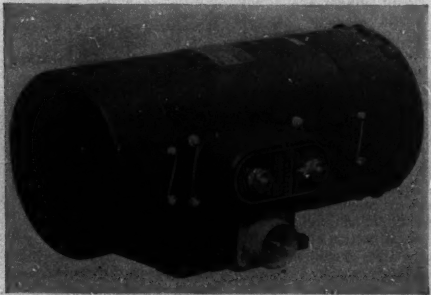

Figure 1. A typical aircraft Amplidyne for turret control

Paper 45-81, recommended by the AIEE committee on air transportation for presentation at the AIEE winter technical meeting, New York, N. Y., January 22-26, 1945. Manuscript submitted November 17, 1944; made available for printing January 2, 1945.

L. A. Zahorsky is student test engineer with the General Electric Company, Fort Wayne, Ind.

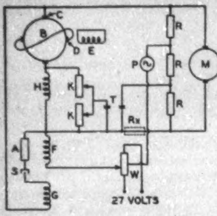

Figure 3. A typical elementary circuit diagram with fixed feedback

A —Antihunt resistor
B —The Amplidyne rotor
C —Amplidyne load brushes
D —Amplidyne quadrature brushes
E —Short-circuited quadrature winding
F —Control field
G —Antihunt field
H —Compensating winding
K —Compensating adjusting rheostats
M—Turret-motor armature
N—Turret-motor shunt field
P —Vibrator inverter transformer
R —Fixed-feedback resistors
S —Capacitor for antihunt
T —Normally open contactors operated simultaneously
W—Control potentiometer

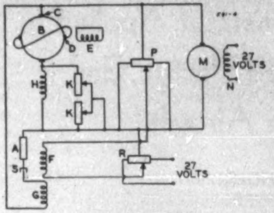

Figure 4. A typical elementary circuit diagram with variable feedback

A —Antihunt resistor
B —The Amplidyne rotor
C —Amplidyne load brushes
D —Amplidyne quadrature brushes
E —Short-circuited quadrature winding
F —Control field
G —Antihunt field
H —Compensating winding
K —Compensation-adjusting rheostats
M—Turret-motor armature
N—Turret-motor shunt field
P —Variable-feedback potentiometer
R —Control potentiometer coupled to variable-feedback potentiometer
S—Antihunt capacitor

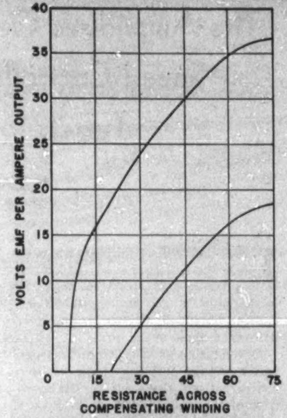

Figure 5. Curves showing generated electromotive force per ampere of load current versus resistance across compensating winding

The two curves differ by three per cent of compensating-winding turns

sates for its armature-reaction effect. The amount of overcompensation, measured in volts per ampere output, is readily adjustable by means of the two rheostats, *K*, connected in series across the compensating winding, *H*, as shown in Figure 3. The curves in Figure 5 show the effectiveness of the rheostats. The difference between the two curves is the effect obtained by changing the compensating winding on one pole by approximately 3.0 per cent.

Detailed Operation of the Amplidyne

The Amplidyne-generator control field is excited by means of a control potentiometer. A resistor used as a voltage divider, *R*, is connected across the Amplidyne output and provides a negative feed-back voltage in the control-field circuit. Figure 3 shows a typical circuit arrangement. The amount of feedback is adjustable by a contactor, *T* as in Figure 3, or in some cases by a potentiometer as in Figure 4. When a contactor is used, two ranges of turret operation are obtained, a low or normal range for tracking and a high-speed range for sluing. The circuit in Figure 4 gives a gradual transition from the low-speed range to the high-speed range.

The amplification thus obtained is extremely great for d-c generators with very low time constants, and therefore special consideration has been given to maintaining a stable system. The following three methods are used to help prevent instability in the system: First, there is a short-circuited quadrature winding (*E* in Figure 3) to decrease irregularities in the output voltage caused by commutation irregularities of the quadrature brushes. Without the short-circuited winding to dissipate the energy thus generated, the irregularities may be amplified by the quadrature flux and be apparent as unsteady output voltage. Second, there is a capacitor and resistor in series with an antihunt field intended primarily to prevent the turret motor from overshooting the desired speed. When the excitation of the Amplidyne is changed, the Amplidyne will attempt to establish very quickly the new output desired. Since it has a turret-motor load which furnishes a back electromotive force, the output current of the Amplidyne often is reversed completely when the control handles are moved so as to decrease the speed of the turret. The antihunt circuit admits a current through the antihunt windings in proportion to the rate of change of voltage across the turret-motor armature. Therefore, when the turret motor is changing speed rapidly, the antihunt field is furnishing the Amplidyne an excitation to oppose this change. Third, there is the feed-back voltage connected in series with the control potentiometers. The action of the voltage from this feedback approaches that of a voltage regulator. If the control field were connected completely across the Amplidyne output voltage, instead of just over a portion of the output voltage, the system would approach a voltage-regulator system. Therefore, the output voltage would be nearly independent of the output current, if the control fields were connected completely across the Amplidyne output. The magnitude of the effect of the feedback is shown in Figure 6. Curve *A* is the characteristic obtained with no feedback, whereas curve *B* is with 6.0 per cent feedback. Per cent feedback is the per cent of the resistance across the Amplidyne output that is in series with the control field.

A rising characteristic with increase in load is needed to obtain constant turret-motor speed. This is obtained by

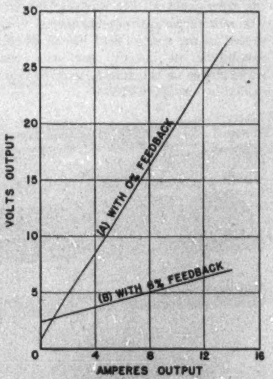

Figure 6. Volt–ampere characteristic curve with and without feedback

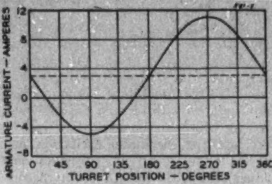

Figure 7. Armature current versus turret position measured from forward position

the compensating winding which, as mentioned above, more than compensates for the armature reaction and the *IR* drop in the Amplidyne.

Figure 7 shows an idealized curve of turret-motor armature current versus the angular position of the turret. It is apparent from inspection of the curve that it is a sine curve plus a constant. The constant is the turret friction measured in armature amperes of the turret motor. The magnitude of the sine curve is the torque exerted on the gun turret due to the wind load.

The typical turret motor is a separately excited shunt-wound machine the speed-torque characteristic of which is shown in Figure 8. Figure 9 shows the characteristic of speed versus input ampere to an enlarged scale starting at 200 rpm no load. For easy operation of the turret it is desirable that the speed regulation of the turret motor be less than 30 per cent from no load to full load for all speeds down to as low as 200 rpm. This demonstrates the need for the rising characteristic of the Amplidyne shown in Figure 6 previously discussed. By combining in the right proportions the rising characteristic of the Amplidyne with the falling characteristic of the turret motor, the results shown in Figure 10 are obtained. These results are obtained in a circuit with a switch to change from normal tracking-speed range to sluing-speed operation by changing the feed-back ratio. Figure 11 shows the results obtained in a circuit using the variable feedback as shown in Figure 4. In the system with variable feedback, if the compensation be adjusted correctly with the controls set to run the motor at 600 rpm, this adjustment will be incorrect when running the motor at 200 rpm, and the motor will stall before full load is reached. If adjusted for flat regulation similar to Figure 10 at 200 rpm, the compensation will be too great at 600 rpm and above, and the turret motor will speed up under load. This is true of a particular combination of circuit, turret motor, and Amplidyne. If a fixed resistance be added in series with the center tap on the feed-back potentiometer (*P* in Figure 4), very nearly flat compensation can be obtained over the entire speed range.

The system is very critical with respect to resistance added in series with the turret-motor armature and Amplidyne. Figure 12 shows the result of test taken where per cent of regulation was plotted versus series resistance added in the control circuit as R_s in Figure 3 between the Amplidyne and the turret motor. Very nearly the same effect is obtained by changing the armature resistance of the turret motor. The armature resistance of the turret motors which have been used by various manufacturers of turrets has varied over the range from 0.29 ohm to 0.90 ohm. These Amplidynes were not successful in being adjustable over this wide range and still able to meet other performance requirements of the turret. This range in resistance of turret motors has been decreased to approximately 0.29 ohm to 0.60 ohm. All tests and users reports indicate that the Amplidynes are capable of being adjusted with the rheostats on the Amplidynes over a range wide enough to compensate for this much resistance change in the turret motors.

In Figure 10, it is noticed that the speed versus ampere input to the turret motor, when used in the turret control circuit, is not a line but a closed loop. The curve was taken as follows: The turret motor was set at full-load current input, then this load was gradually decreased to the no-load current value. The speed was noted, and then the load was increased gradually while recording values of speed until full load again was obtained. Then the load was decreased slowly, recording speed values until the no-load speed again was obtained. The hysteresis lag in the stator iron of the Amplidyne causes the two curves not to coincide. The drop in speed as the load increases is caused by the lag between the magnetizing effect of the load current in the compensating winding, and the flux in the iron. As the magnetizing current in the compensating winding becomes greater, the percentage flux lag becomes much less, and therefore the curve begins to flatten out. In decreasing the load, the flux does not decrease immediately with the decrease in magnetizing current in the compensating winding, thus giving the rising characteristic on decreasing load. If a true one-half hysteresis curve were taken by this method, an open curve with two different speeds at the no-load end of the curve would result. Since, however, the curve was started at full load and carried through to no load, the turret motor had to return to the same no-load speed it started from the first time. Therefore the closed curve shown is obtained.

This objectionable change in speed can be eliminated by preventing the occurrence of residual voltage in the Amplidyne generator. A source of 60-cycle alternating voltage connected in series with the control field will decrease materially this speed change, as is apparent in Figure 13. This has been accomplished in some instances by a vibrator-type inverter transformer and is illustrated by *P* in Figure 3.

As an interesting sideline, it is apparent

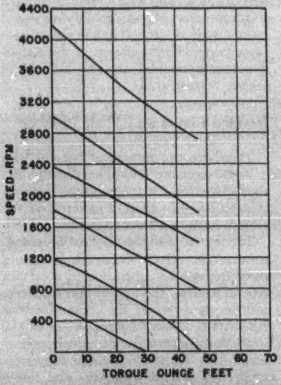

Figure 8. Curves of turret-motor speed versus output torque with constant voltages at 10-volt intervals from 10 to 60 volts

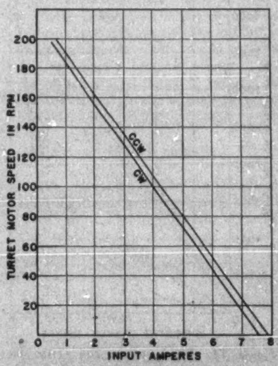

Figure 9. A typical turret-motor-speed-versus-input-ampere curve at approximately five per cent of rated no-load speed

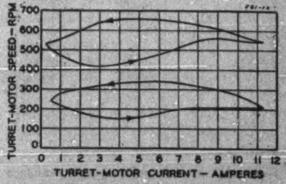

Figure 10. Turret-motor speed versus turret-motor armature current in a typical turret not using a vibrator inverter

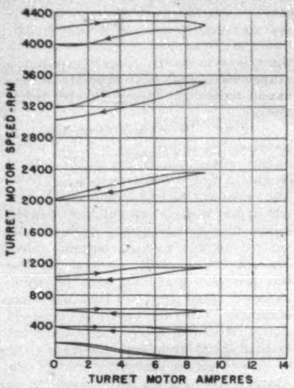

Figure 11. Turret-motor speed versus turret-motor armature current for the circuit shown in Figure 4

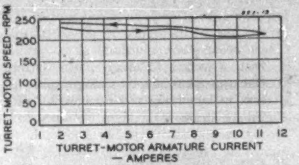

Figure 13. Turret-motor speed versus turret-motor armature current for the same turret circuit as in Figure 10, except that a vibrator inverter has been added and the Amplidyne compensation readjusted

that tests taken with the inverter used with the Amplidyne can show the compensation characteristics more nearly than tests with the inverter left out. Some of these Amplidynes have an undeserved reputation for being inconsistent in test. If the unit be warmed up thoroughly and the inverter used, very consistent test results can be obtained. Without the alternating current it is very difficult to repeat compensation readings, as is evident from inspection of the characteristics without it.

The curves of Figure 14 are presented to show the wide range of performance that may be obtained with different control-circuit arrangements. The two circuits given in Figures 3 and 4 were used to obtain these curves. The solid lines are the no-load speed versus potentiometer position, and the dashed lines are the full-load speed versus potentiometer position. These curves illustrate that the speed regulation of the system is practically zero throughout the entire rheostat travel in the low-speed range and is practically flat up to about 40 per cent of maximum speed in the high-speed range. With the variable feedback there are two places at which the compensation is correct. The first place is at the low speed at which the compensation is adjusted. The second place is at a higher speed where the Amplidyne has begun to saturate. The overcompensating effect is decreased as a result of this saturation until the drooping characteristic of the turret motor equals the overcompensation of the Amplidyne.

Some turret specifications require that the turret have a maximum speed less than a certain value to prevent failure of some mechanical part, whereas other turret specifications require that the maximum turret speed be over a certain value in order to meet speed requirements. This maximum speed is reflected in the Amplidyne as maximum voltage output. The maximum output voltage can be adjusted by brush shift, except in cases where the control circuit completely saturates the Amplidyne. Some turrets are equipped with taps on the feed-back resistor which can be used to increase or decrease the maximum excitation furnished to the Amplidyne. This gives some adjustment of the turret speed in the systems where control does not completely saturate the Amplidyne.

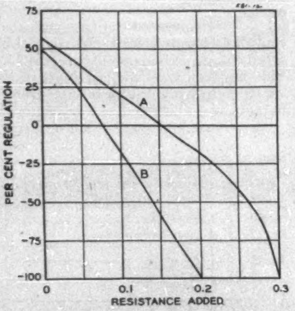

Figure 12. Speed regulation versus resistance added in series with the turret-motor armature

A—15 ohms feed-back resistance
B—75 ohms feed-back resistance

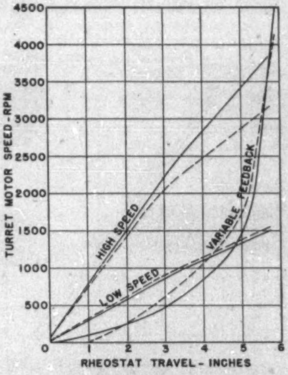

Figure 14. Turret-motor speed versus the control-potentiometer travel

———No-load speed
— — —Full-load speed

Present Specifications for the Amplidyne

The present specifications for Amplidynes are in terms of the performance of a complete turret control system. Most of the test limits that are used to adjust the Amplidyne are based on the speed of the turret motor at various loads and control potentiometer settings. A particular set of limits follows for a 530-watt Amplidyne and 3,000-rpm motor for use in the circuit shown in Figure 3.

Circuit Condition of Contactor, T	Turret Motor Rpm	
	No Load	Full Load
Closed	200	200 ± 20%
Closed	3,400	3,400 ± 26%
Open	200	200 ± 20%
Open	1,200	1,200 ± 20%

To prevent instability in the system due to the brushes of the Amplidyne being shifted too far against rotation, a limit of six volts is imposed as the maximum residual output voltage allowed with zero control-field excitation.

The irregularities of the Amplidyne voltage output at one quarter of its rated output voltage and with no load are limited to three volts. Most Amplidynes would meet a limit of one volt and in many cases (approximately 30 per cent of the Amplidynes manufactured) show no variation in output voltage at all.

Revised Limits and Their Purpose

There are two important reasons why it would be more desirable to define the characteristics of an Amplidyne in terms of itself alone instead of in terms of the performance of a turret system.

The first is from the application standpoint. When all the engineering data are given in terms of operation of a certain type of system, the application engineers and the users receive the impression that the Amplidyne must be used in a circuit of only one type and has no other application. Also the Amplidyne has been misapplied in several instances, and limits have been placed on the operation of a turret which are correlated in no way with the actual performance of the Amplidyne and its range of adjustment. If the characteristics of the Amplidyne be given as a unit, the allowable variations on these values listed, the application engineer can apply the Amplidyne to any circuit he wishes and know what to expect the system to do.

The second is for complaint and trouble shooting. When a turret manufacturer or an ultimate user experiences some difficulty meeting his specifications, it is difficult to determine whether or not the Amplidyne is at fault. If the characteristics of the Amplidyne were defined in terms of the Amplidyne alone, the machine could be set up on a test bench and tested. There are many possible defects in a turret which might affect its over-all characteristics and which could be attributed incorrectly to the Amplidyne, because the performance of the Amplidyne alone was not known.

Each value in a specification should have a definite purpose so far as the machine being described is concerned without reference to the system operation as a whole. The specification should describe how the Amplidyne should be adjusted and should limit the adjustments directly in terms of the Amplidyne characteristics. The following gives in brief form the type of specification needed to adjust an Amplidyne properly:

1. No-load saturation-curve slope should be specified to limit the position of the brushes. Shifting the brushes against rotation of the Amplidyne increases the voltage output for a given excitation.

2. The compensation should be adjusted to a curve similar to the zero feed-back curve of Figure 6 by adjusting the rheostats and the taps on the compensating winding to obtain zero-per-cent voltage regulation with a given increase in field current opposing the output current.

3. The residual voltage should be specified for those applications where a vibrator inverter is not used.

4. Commutator-film-breakdown excitation should be limited to minimize the dead spot in response to the control signal. It takes a finite value of excitation to break down the brush film on the commutator in the quadrature circuit before output voltage is obtained.

5. Maximum output voltage should be specified to maintain all machines alike.

6. Maximum output watts with a given load resistance should be checked to be sure the unit will withstand the peak loads.

Typical Specification

The following sample specifications are numbered in correspondence with the foregoing paragraphs.

1. One-half voltage (30 volts) no load must be obtained with an excitation of 0.020 ampere to 0.040 ampere in the control field.

2. The voltage regulation shall be 2.0 volts rise per ampere output starting at 4.0 volts no load.

3. The residual voltage shall be less than six volts with zero field after saturation of the field.

4. Increasing excitation from 0 to 0.006 ampere shall produce a change in no-load output volts from 5 to 12 volts starting from a negative residual voltage.

5. The no-load output voltage of the unit with 0.250-ampere excitation shall be 85 to 95 volts.

6. The unit shall be capable of operating for five seconds with a load of 925 watts at 15.4 amperes output.

Nine Years' Experience With Ultrahigh-Speed Reclosing of High-Voltage Transmission Lines

PHILIP SPORN
FELLOW AIEE

C. A. MULLER
MEMBER AIEE

Synopsis: Data covering nine years' operating experience with 91 ultrahigh-speed-reclosing breaker installations mainly on a large interconnected and integrated high-voltage system are presented and analyzed: out of 635 cases of flashover cited, 570 reclosures were successful and 65 cases of reclosure were unsuccessful, a record of 89.8-per-cent successful reclosure. Double-circuit lines show a record of unsuccessful reclosure double the average but 80 per cent of the apparently unsuccessful reclosures resulted in successful reclosure of one circuit. The conclusions drawn are that ultrarapid reclosure has proved itself a tool of major importance for use in improving high-voltage line reliability; that its use can, and should be, extended to lower-voltage lines, and that further improvements are in sight as a result of recent improvements in circuit-breaker opening and reclosure time.

SINCE the last publication[1] of operating experience with ultrahigh-speed reclosing of high-voltage transmission lines, four more years of operating experience have been gathered on lines of the American Gas and Electric Company systems. This experience is of so much more extensive a nature than that available previously that it now makes possible not only more thorough checking of ideas and conclusions previously entertained but not entirely proved, but, in fact, it appears that sufficient data now have been made available to serve as a basis for definite and final conclusions as to a number of important aspects of ultrarapid reclosure and the benefits inherent therein. It is the object of this paper to present and analyze these data and to draw these conclusions.

Systems on Which Installed

The principal system on which the equipments under discussion are installed is the central system of the American Gas and Electric Company. This is shown diagrammatically in Figure 1 in its most up-to-date form. This integrated system operates in seven states and consists of 45 circuit miles of 154-kv, 2,818 circuit miles of 132-kv, 64 circuit miles of 110-kv, 304 circuit miles of 88-kv, and 695 circuit miles of 66-kv high-voltage circuits. Most of the 132-kv circuits are of double-circuit steel-tower construction. It is to be noted that neither the 88-kv nor the 66-kv lines are indicated in Figure 1. However, there are only three terminals installed on the 88-kv circuits and only six terminals on the 66-kv circuits; as against that there are installed 72 terminals on the 154- and 132-kv circuits.

The load which the central system serves has had a maximum one-hour integrated peak of over 1,450,000 kw. As pointed out previously, the system is a predominantly steam-electric system with a small portion of hydroelectric generating capacity. Extensive and important foreign interconnections exist on several portions of the system through which diversity and other capacity exchanges are carried out with adjacent systems. Because of the fact that practically all the energy served on the system travels over considerable transmission distance before reaching the load and because of sudden changes in power flow, it has been found particularly important to maintain maximum continuity in the operation of transmission networks. Obviously this in turn results not only in the rendering of the utmost in high continuity of service, but also makes possible the operation of the system in a most co-ordinated manner

Paper 45-57, recommended by the AIEE committee on protective devices for presentation at the AIEE winter technical meeting, New York, N. Y., January 22–26, 1945. Manuscript submitted December 6, 1944; made available for printing December 27, 1944.

PHILIP SPORN is vice-president and chief engineer and C. A. MULLER is protection engineer, both of the American Gas and Electric Service Corporation, New York, N. Y.

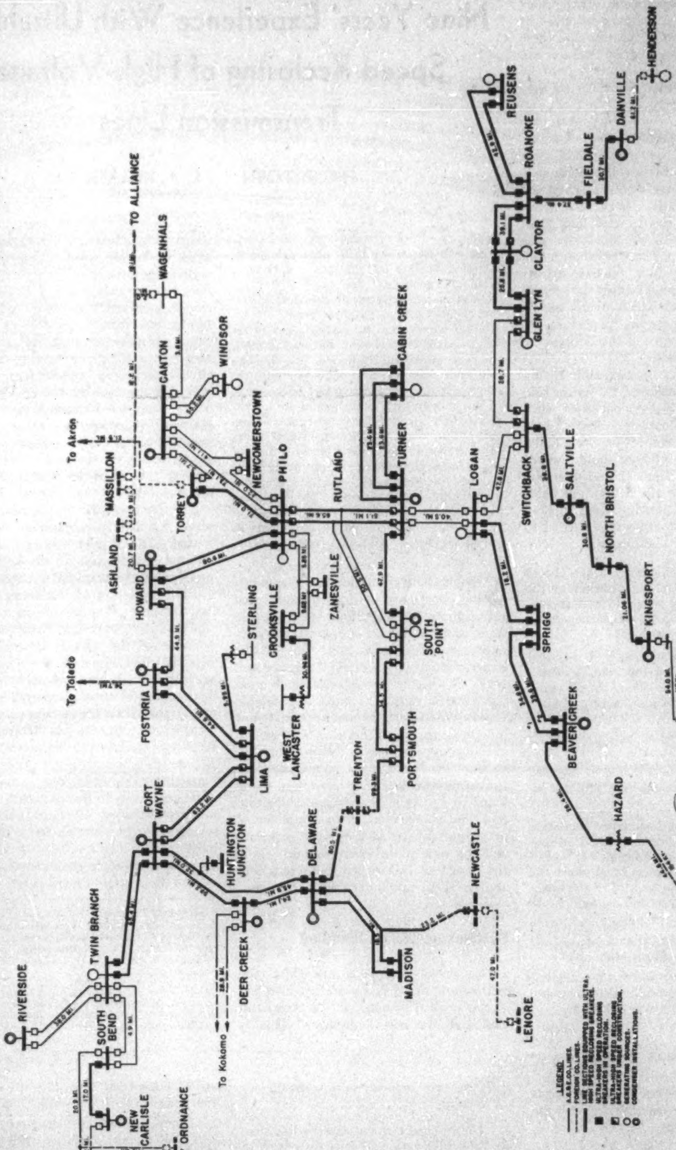
RIVERSIDE
SOUTH BEND
TWIN BRANCH
NEW CARLISLE
MICHIGAN CITY
KINGSBURY ORDNANCE
To Kokomo
DEER CREEK
FORT WAYNE
HUNTINGTON JUNCTION
DELAWARE
MADISON
NEWCASTLE
LENORE
LIMA
FOSTORIA
To Toledo
HOWARD
ASHLAND
MASSILLON
To Akron
TORREY
CANTON
WAGENHALS
TO ALLIANCE
WINDSOR
NEWCOMERSTOWN
PHILO
STERLING
CROOKSVILLE
ZANESVILLE
WEST LANCASTER
RUTLAND
TRENTON
PORTSMOUTH
SOUTH POINT
TURNER
CABIN CREEK
LOGAN
SPRIGG
BEAVER CREEK
HAZARD
PINEVILLE
SWITCHBACK
GLEN LYN
CLAYTOR
ROANOKE
REUSENS
FIELDALE
DANVILLE
HENDERSON
SALTVILLE
NORTH BRISTOL
KINGSPORT
WATERVILLE
LEGEND
A.G.&E.CO. LINES.
FOREIGN CO. LINES.
LINE SECTIONS EQUIPPED WITH ULTRA-HIGH SPEED RECLOSING BREAKERS.
ULTRA-HIGH SPEED RECLOSING BREAKERS IN OPERATION.
ULTRA-HIGH SPEED RECLOSING BREAKERS UNDER CONSTRUCTION.
GENERATING SOURCES.
CONDENSER INSTALLATIONS.

Figure 1. Ultrahigh-speed-reclosing oil-circuit-breaker installations on the 132-kv transmission system of the central system of the American Gas and Electric Company

Table I. Summary of Actual Operations of Ultrahigh-Speed-Reclosing Oil Circuit Breakers, May 1936 to November 1944

Line	Line Voltage (Kv)	Length of Line (Circuit-Miles)	Number of Terminals	Date of Installation	Ultrahigh-Speed Oil-Circuit-Breaker Operations																													
					Number of Operations										Number of Successful Reclosures										Number of Unsuccessful Reclosures									
					1936	1937	1938	1939	1940	1941	1942	1943	1944	Total	1936	1937	1938	1939	1940	1941	1942	1943	1944	Total	1936	1937	1938	1939	1940	1941	1942	1943	1944	Total
Hazard–Pineville	154	45.0	2	4/11/42							1	2	2	5							1	1	2	4								1		1
Fort Wayne–Deer Creek	132	50.2	2	5/17/36	4	5	3	1	3	4	2	4	1	27	3	4	3	1	3	3	2	3		22	1	1				1		1	1	5
South Bend–New Carlisle	132	17.0	2	1/29/38			1	1		2			2	6			1	1		2			1	5									1	1
No. 1 Twin Branch–Fort Wayne	132	65.4	2	8/31/38				1	2	2	5	8	5	23				1	2	2	5	8	4	22									1	1
No. 2 Twin Branch–Fort Wayne	132	65.4	2	7/25/38			2	3	1		2	3	1	12			2	3	1		1	3	1	11							1			1
No. 1 and No. 2 Twin Branch–Fort Wayne	132		4	8/31/38				2			4	3	2	11				1			4	2	2	9				1				1		2
North Bristol–Kingsport	132	21.1	3	3/20/40					6	8	1	4	5	24					4	8	1	4	5	22					2					2
Saltville–North Bristol	132	30.8	2	3/22/40					6	9	1	11	4	31					6	9	1	8	2	26								3	2	5
Roanoke–Fieldale	132	37.4	2	4/28/40					12	6	10	14	7	49					12	6	9	13	7	47							1	1		2
No. 1 Roanoke–Reusens	132	42.9	2	5/ 1/40						2	7	10	6	25						2	7	98	6	24								1		1
No. 2 Roanoke–Reusens	132	42.9	2	5/ 1/40					3	1		2	1	7					3	1		2	1	7										
No. 1 and No. 2 Roanoke–Reusens	132		4	5/ 1/40					6	7	14	14	7	48					4	4	12	9½	5	34½					2	3	2	4½	2	13½
No. 1 Philo–Howard	132	80.6	2	5/ 2/40					3	4	3	1	4	15					3	4	3	1	4	15										
No. 2 Philo–Howard	132	80.6	2	5/20/40					3	3		2	4	82					3	3		2	4	12										
No. 1 and No. 2 Philo–Howard	132		4	5/20/40							1		3	4						4	1		3	4										
Fort Wayne–Delaware	132	77.9	3	5/26/40					1	5	5	8	5	24					1	8	5	6	4	20						1		2	1	4
Turner–South Point	132	47.9	2	8/ 1/40						8	10	26	12	56							10	268	128	56										
Fostoria–Lima	132	44.6	2	10/ 3/40							2		4	6							2		2	4									2	2
Delaware–Newcastle	132	41.7	3	1/ 9/41						1	5	3	3	12						1	4	2	3	10							1	1		2
No. 1 Cabin Creek–Turner	132	23.6	2	5/ 1/41						2	1		5	8						2	1		5	8										
No. 2 Cabin Creek–Turner	132	23.6	2	5/ 1/41							2	2	2	6							2	2	2	6										
No. 1 and No. 2 Cabin Creek–Turner	132		4	5/ 1/41						3	4	3	5	15						3	3	3	5	14							1			1
No. 3 Cabin Creek–Turner	132	23.6	2	5/12/43								2		2								2		2										
Delaware–Trenton	132	80.3	2	8/26/41							1	4	1	6							1	3	1	5								1		1
Philo–Torrey	132	70.7	2	1/ 8/42							2	2	5	9							2	2	5	9										
Delaware–Madison	132	18.5	2	1/23/42							1	4		5							1	4		5										
Beaver Creek–Hazard	132	28.4	2	2/ 1/42							5	11	2	18							5	11	2	18										
No. 1 Glen Lyn–Claytor	132	25.8	2	3/22/42							5	3	8	16							5	3	8	16										
No. 2 Glen Lyn–Claytor	132	25.8	2	3/22/42							2		2	4							2		2	4										
No. 1 and No. 2 Glen Lyn–Claytor	132		4	3/22/42							1		1	2							1		½	1½									½	½
No. 1 Claytor–Roanoke	132	39.1	2	5/ 1/42							5	9	2	16							5	9	1	15									1	1
No. 2 Claytor–Roanoke	132	39.1	2	5/ 1/42							1	8	2	11								6	2	8							1	2		3
No. 1 and No. 2 Claytor–Roanoke	132		4	5/ 1/42								3		3								2½		2½								½		½
Deer Creek–Delaware	132	24.1	2	6/25/42							1	2	1	4							1	2	1	4										
Lima–Sterling	132	5.95	1	1/ 6/43								1		1								1		1										
No. 1 Logan–Sprigg	132	18.1	2	3/ 5/43									1	1									1	1										
No. 2 Logan–Sprigg	132	18.1	2	3/ 5/43								1	3	4								1	2	3									1	1
No. 1 and No. 2 Logan–Sprigg	132		4	3/ 5/43								2	9	11								2	5½	7½									3½	3½
Sprigg–Beaver Creek	132	39.6	2	3/17/43								13	12	25								13	7	20									5	5
Fieldale–Danville	132	30.8	2	6/27/43								3	8	11								3	8	11										
Crooksville–West Lancaster	132	30.96	2	8/ 8/43										0										0										
Switchback–Saltville	132	38.8	3	6/22/44										0										0										
Baileysville–Coalwood	88	15.9	3	12/ 5/43									4	4									2	2									2	2
No. 1 Deepwater–Atlantic City	66	63.1	2	6/27/40						2	1	1	8	12						2	1	1	7	11									1	1
No. 2 Deepwater–Atlantic City	66	63.1	2	6/27/40					3	6	1		4	14					3	6	1		3	13									1	1
No. 1 and No. 2 Deepwater–Atlantic City	66		4	6/27/40					1	2	1	2	4	10					1	2	1	2	4	10										
No. 1 Stanton–Suburban	66	10.9	3	6/29/40									2	2									2	2										
No. 2 Stanton–Suburban	66	10.9	3	6/29/40									1	1									1	1										
No. 1 and No. 2 Stanton–Suburban	66		6	6/29/40										0										0										
No. 2 Crooksville–Newark	66	32.7	2	8/ 8/43								3	5	8								3	5	8										
Newark–Lancaster	66	30.74	2	8/ 8/43								2	7	9								2	5	7									2	2
West Lancaster–Anchor Hocking	66	1.34	2	8/ 8/43										0										0										
Total		1,634.1	91		4	5	6	8	50	77	107	196	172	635	3	4	6	7	46	72	100	177	155	570	1	1		1	4	5	7	19	27	65

Sporn, Muller—Ultrahigh-Speed Reclosing and the utilization at all times of the most efficient combination of generating sources regardless of their location.

In addition to equipments on the central system, four terminals have been in operation on 66-kv lines of the Atlantic City Electric Company and six terminals on 66-kv lines of The Scranton Electric Company, bringing the total of terminals in service of the latest date to 91.

Operating Experience

A summary of the total operating experience since the first installation is given in Table I. Referring to that table, it will be seen that a total of 91 terminals involving 43 line sections have been covered and that these 43 line sections cover approximately 1,634 circuit miles of line, 1,360 miles of which operate at 132,000 volts. In the period May 1936 to November 1944, covering substantially nine lightning years, 635 cases of flashover resulting in line opening occurred. Of these, 531 cases were single-line trouble and 104 cases were two-line trouble. Out of the same number of 635 cases of flashover, 570 reclosures were successful and 65 cases of reclosures were unsuccessful. This is a record of 10.2-per-cent unsuccessful reclosures. In this connection it needs to be pointed out that in eight of these cases a permanent fault existed on the line and that under such conditions obviously successful reclosure was a physical impossibility, since nothing but a permanent outage could clear the trouble. These permanent faults were caused by either lines being on the ground, physical damage to steel tower, failure of a lightning arrester, or a string of insulators pulling loose because of ice loading. If one chooses to disregard these eight cases, the total unsuccessful reclosures were 57, representing 9.0 per cent. It is interesting to note that for the 104 cases of two-line trouble, 21 unsuccessful reclosures were experienced, giving an unsuccessful percentage of 20.2 per cent for simultaneous trouble on two lines. The method of scoring employed for recording unsuccessful reclosures for two-line trouble was this: in cases where only one line of the two reclosed successfully, the operation was credited with one-half unsuccessful reclosure, and in cases where neither line reclosed successfully, the operation was credited with a full unsuccessful reclosure. Since in 80 per cent of the cases of reclosures on two-line trouble which were not fully successful one of the two lines reclosed successfully, it is evident that the scoring method adopted reflects, if anything, a pessimistic version of the effect of reclosure. From Table I it will be seen that number one and number two Roanoke–Reusens lines experienced 48 cases of two-line trouble of which $13^{1}/_{2}$ were unsuccessful reclosures during the period from May 1940 to November 1944. The unsuccessful reclosures consisted of 19 cases where only one line of the two failed to reclose successfully and four cases where both lines failed to reclose successfully. An investigation of the large percentage of unsuccessful reclosures experienced on these lines for two-line trouble was made and it was found that apparently cascading of breaker-tripping operations was occurring on these lines which resulted in unsuccessful reclosing operation. At the Reusens end of these lines no source of ground current is available, since the transformer banks are connected delta on the 132,000-volt side and, further, the amount of phase-to-phase short-circuit current available from the Reusens generation is very limited. In some cases of two-line trouble on these lines, both breakers at Roanoke station and only one breaker at Reusens would trip simultaneously on the initial fault and the second breaker at Reusens would trip some eight cycles later after the breakers at Roanoke had opened; this resulted in a dead time of only three to four cycles on one of the lines thus causing a restrike on this line. In some cases both breakers at Roanoke only would open on the initial fault, the Reusens breakers staying in, and would retrip on reclosure due to the arc being maintained by the small amount of generating capacity at Reusens. These operations account for the high number of unsuccessful reclosures on these lines for two-line trouble and further account for the high percentage of unsuccessful reclosures on the total number of two-line trouble operations. The locus for solution of the Roanoke–Reusens line difficulties is obviously beyond the zone of switching and relaying.

The seven unsuccessful reclosing operations for the Saltville–North Bristol and North Bristol–Kingsport lines partially can be accounted for as a result of the systems having drifted so far out of synchronism at the instant of reclosure as to cause the breakers to retrip when low hydroelectric generating capacity is in operation at Waterville. In all seven of these cases all three-phase relays operated at both stations, indicating an apparent three-phase fault; this, however, appears most unlikely on a single-circuit line. The more probable reason for the three-phase relays operating is the interchange of current flow between the two systems at the instant of reclosure on account of the two systems being sufficiently out of synchronism.

Perhaps the most interesting record to note is that of number one and number two Philo–Howard lines which experienced 27 cases of single-line faults and four cases of two-line trouble during the period from May 1940 to November 1944. Here, successful reclosures were obtained in all cases giving the two lines a perfect record for these four years. Before the installation of ultrahigh-speed-reclosing breakers on these lines was made, when two-line trouble occurred it was almost impossible to resynchronize the two systems tied together by them without first dropping load. The installation of ultrahigh-speed-reclosing breakers was thus a perfect solution to the serious difficulty brought about by simultaneous trouble on both circuits.

Conclusions

The data obtained in the course of nine years' experience with ultrarapid reclosure of high-voltage circuits and here presented and analyzed are complete enough to warrant the following definite conclusions:

1. On high-voltage lines, properly insulated and provided with ground-wire protection, 90-per-cent successful reclosure has been and can be obtained by the use of ultrarapid reclosing as now developed.

2. While the experience obtained with double-circuit lines indicates a record of apparently unsuccessful reclosure approximately double that of the average, the significant fact is that in these cases 80 per cent of the apparently unsuccessful reclosure resulted in successful reclosure of one of the two circuits.

3. Ultrarapid reclosure has proved itself a tool of major importance in planning and building any overhead high-voltage transmission system or transmission circuit. It is without question the most economical and reliable means of improving high-voltage-transmission reliability.

4. The confirmed and highly successful result obtained on high- and medium-high-voltage lines again points clearly to benefits obtainable from application to lower-voltage lines. The only barrier to the extension of such application is economic: simpler and lower cost reclosing mechanisms and, if possible, relaying are needed.

5. There is excellent reason to believe that single-circuit, and particularly double-circuit, reclosure performance can be improved by decreasing time of fault duration and thus speeding up the reclosure cycle. The recent successful development of three-cycle breakers,[2] making possible 12-cycle reclosure,[3,4] will open the way for exploring this.

References

1. Five Years' Experience With Ultrahigh-Speed Reclosing of High-Voltage Transmission Lines, **Philip Sporn, C. A. Muller.** AIEE Transactions, volume 60, 1941, pages 241–6.

2. A High-Capacity High-Voltage Three-Cycle Oil Circuit Breaker, **H. L. Byrd, E. B. Rietz.** AIEE Transactions, volume 64, 1945, April section, pages 160–3.

3. A Three-Cycle 3,500-Megavolt-Ampere Air-Blast Circuit Breaker for 138,000-Volt Service, **H. L. Byrd, B. S. Beall, III.** AIEE Transactions, volume 64, 1945, May section, pages 229–32.

4. Field Tests and Performance of Heavy-Duty High-Speed 138-Kv Circuit Breakers—Oil and Air-Blast, **Philip Sporn, Harry P. St. Clair.** AIEE Transactions, volume 64, 1945.

A Three-Cycle 3,500-Megavolt-Ampere Air-Blast Circuit Breaker for 138,000-Volt Service

H. L. BYRD
ASSOCIATE AIEE

BEN S. BEALL, III
ASSOCIATE AIEE

Synopsis: Early investigation of the air-blast principle of arc interruption clearly indicated that this principle was based on sound fundamentals and that continued research and development would lead to an economical and practical design. Preliminary studies indicated that the axial-flow interrupter was admirably suited to the high-voltage breakers with their lower current ratings, while the high current of the low-voltage equipments could be handled best by an interrupter comprising a cross-blast principle. Outdoor axial-blast breakers having interrupting ratings as high as 1,500 megavolt-amperes for service up to 138 kv have been in service for the past few years. Circuit-breaker designers and operating engineers have expended many years of diligent effort in the development of high-voltage oil circuit breakers to their present high degree of dependability and performance. Although the development of high-voltage air-blast breakers is of much more recent origin, the rate of progress has been relatively so rapid that the air-blast breaker described in this paper has exhibited performance characteristics so outstanding as to merit careful attention.

A DISCUSSION of the early field test of a complete high-voltage air-blast circuit breaker developed in this country and tested in the field under actual service conditions was presented before the AIEE in January 1942.[1,3] Two breakers of this design were placed in service at the Turner substation of the Appalachian Electric Power Company in 1942. There are also other installations of outdoor air-blast circuit breakers of similar design but for lower-voltage service, namely 69 and 34.5 kv. These initial installations of outdoor air-blast circuit breakers have verified the sound judgment of the early conclusions regarding the advantages of air-blast interruption, but at the same time have revealed that considerable attention must be paid to the mechanical construction and electrical insulation of outdoor air-blast breakers.

Operating experiences with these breakers have been such as to confirm the following basic desirable qualities characteristic of the air-blast principle:

1. Even at comparatively low pressures, air has a high dielectric strength. Figure 1 shows, graphically, the relative dielectric strength of air and oil for rod gaps having dimensions closely approximating the contact rods used on the air-blast breaker described herein.

2. Air provides an excellent means for transmitting mechanical energy in a device such as a circuit breaker. When used for such purposes, air is the equivalent of an infinitely rugged insulator of high dielectric strength and having practically negligible inertia.

3. Air-blast action, or air flow from a pressure chamber, is extremely effective in carrying away the products of an arc and establishing a space of high dielectric strength in order to effect interruption of an a-c arc.

4. The interrupting time of the air-blast circuit breaker is essentially independent of current magnitude within the range of the breaker rating. The constant interrupting time is explained by the fact that the energy required to interrupt the circuit is stored in the form of high-pressure air in the breaker air receiver and the interrupting time is a function of the mechanical time to release the energy and to move the breaker contacts the required distance.

The operating experience has fully justified the development of a new air-blast breaker for 138-kv service rated 3,500 megavolt-amperes with an interrupting time of three cycles and a reclosing time of 20 cycles measured from the time of energizing trip on the initial short circuit to re-establishment of the circuit.

General Construction of Breaker

Each pole unit consists of the following essential elements with their auxiliaries arranged as shown schematically in Figure 2:

1. Interrupting unit.
2. External switch blade.

Interrupting Unit

Early compressed-air breakers used a jet of air at one terminus of the arc. The air jet was directed around the cylindrical-shaped stationary contact which was partially enclosed in a nozzle-shaped hood. The air exhausted from the nozzle-shaped hood to the atmosphere. The other terminus of the arc was drawn along with the moving contact into an area which was essentially at atmospheric pressure. Since the moving contact was in such a comparatively low-pressure region, it was natural that there should be a pronounced tendency toward progressive electrical breakdown from this point immediately after initial interruption.

The 138-kv air-blast breakers described in references 1 and 3 made use of a construction which permitted the moving contact to remain in a region of pressure approximating 100 pounds. This greatly increased the dielectric strength of the air surrounding the moving contact and consequently increased the efficacy of the earlier air-blast interrupters.

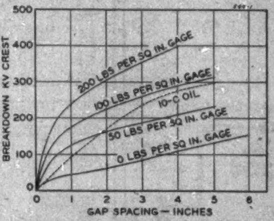

Figure 1. Breakdown of $1^{1}/_{4}$-inch rod gaps in air at various pressures and in oil

The air-blast interrupters developed for the breaker described herein employ a design which:

(*a*). Permits the moving contact to be drawn into the region of maximum pressure and thus assures surrounding air of highest dielectric strength to withstand potential gradient stresses immediately after initial interruption.

(*b*). The air blast is directed in such a manner as to carry the ionized gases generated by the arc away from each contact, thus further improving the ability of the contacts to withstand the high-potential gradient stresses immediately after the initial interruption.

(*c*). Provides excellent voltage distribution across the elements of the interrupter during and after interruption.

A cross section of the entire interrupting unit is shown in Figure 3A. The interrupter has two moving contact rods which complete the electrical circuit through the interrupter by engaging the stationary contact which is located at the center of the assembly. The contact rods normally are held closed under the action of the heavy compression springs shown at upper and lower ends of the assembly. The contact rods are operated

---

Paper 45-44, recommended by the AIEE committee on protective devices for presentation at the AIEE winter technical meeting, New York, N. Y., January 22–26, 1945. Manuscript submitted December 2, 1944; made available for printing December 28, 1944.

H. L. Byrd and Ben S. Beall, III, are both with the General Electric Company, Philadelphia, Pa.

The authors express their appreciation to the American Gas and Electric Company and the Ohio Power Company who made possible the final testing of this air-blast breaker.

by pistons which serve to open the contacts against the action of the springs when air is admitted to the interrupter. Each contact moves a distance of eight inches. Each of the stationary contacts is provided with an orifice of slightly smaller diameter than the contact rod tips. These orifices, when uncovered by the opening movement of the contact rods, permit air in the interrupter to be exhausted to the atmosphere.

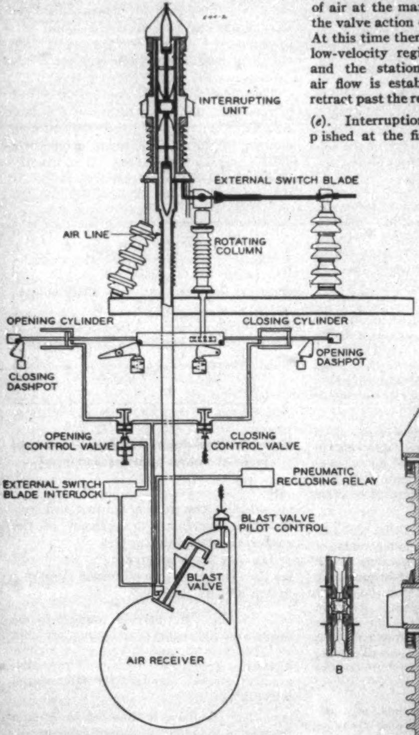

Figure 2 (left). Schematic arrangement of complete pole unit

The sequential operation of the interrupter is as follows:

(*a*). High pressure enters the lower end of the interrupter through the air-line insulator and travels upward through the vertical passages, filling both the upper and lower half of the interrupter.

(*b*). The high-pressure air acts on the pistons to move the contacts apart uncovering the exhaust ports in the stationary contact plates.

(*c*). As the contacts part, an arc is momentarily drawn between the moving contact rod and the stationary contact plate as shown in Figure 3B.

(*d*). The air flow is increased as the contacts leave the throats and, under the action of the air flow carrying the arc products toward a common point, the two arcs transfer from the stationary contacts and establish between the two moving contacts as shown in Figure 3C. During the portion of the stroke in which the contact tips are in the restrictions of the throats, the contacts prevent the escape of the maximum amount of air at the maximum velocity because of the valve action of the contacts themselves. At this time there is a relative low-pressure low-velocity region between the movable and the stationary contacts. Maximum air flow is established when the contacts retract past the restriction in the throats.

(*e*). Interruption is consistently accomplished at the first current zero occurring after the contact rods leave the restriction section of the throats at which time the arc is acted upon by the full force of the air blast.

Figure 3 (below). Sectional view of air-blast interrupter

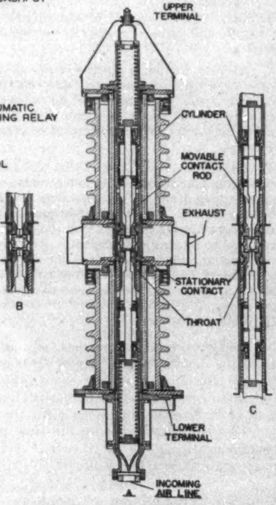

The interrupting units are controlled by individual blast valves as shown in Figure 2. The valves are of simple construction utilizing pilot control on differential pressure for operation of the main valve. The pilot valve is attached directly to the opening solenoid plunger thus eliminating the necessity of an operating linkage and consequently reducing friction to a minimum. The solenoid, pilot, and main valve have a total operating time of slightly over one cycle. The contacts in the interrupter part in approximately one and one half cycles after the opening solenoid is energized. The contacts reach the end of the restriction in the throats in approximately $2^{1}/_{4}$ cycles after the opening solenoid is energized and interruption takes place at the subsequent current zero.

EXTERNAL SWITCH BLADE

The external switch blades are provided for a dual purpose:

1. To maintain the open position of the breaker.
2. To establish the circuit on the closing operation.

The operation of external switch blades is described best from the following description of the sequential operation of the breaker.

OPENING OPERATION

With the breaker in the closed position and with normal air pressure in the air receiver, the trip circuit is set up. The three solenoid coils of the blast-control valves are energized in series initiating the operation of the interrupter units, previously described.

The operation of the external switch blades is interlocked pneumatically to prevent motion of the disconnect unless all three blast valves have operated. The external switch-blade opening valve is pneumatically operated by the interlock and when opened admits air to the opening cylinder. The opening piston drives three racks which engage spur gears attached to the lower end of the rotating insulators, which drive the external switch blade through a beveled-gear arrangement mounted at the hub of the disconnect. When the external switch blades have opened sufficiently to prevent flashover due to system voltage, the trip circuit is de-energized, allowing the interrupter contacts to return to their normally closed position. The typical operation curve, Figure 4A, shows the opening of the interrupter head and the subsequent opening of the external switches after the power circuit has been interrupted.

CLOSING OPERATION

During a normal closing operation only the external switch blades are operated. The closing valve coil is energized which opens the valve thus charging the closing cylinder which drives the racks and gears in the direction to rotate the operating porcelain to close the switch blades. The closing time of the breaker is approximately 20 cycles. The design of the external stationary contacts and the switch-contact shoe is such that burning of the current-carrying parts is almost eliminated and the contact parts will be in a serviceable condition after closing repeatedly 25,000 amperes, the momentary rating of the breaker.

Reclosing Operation

The high-speed reclosing operation is performed by the interrupting heads alone. The blast valves are opened as in a normal trip operation and are immediately closed to allow the interrupter head contacts to reclose and re-establish the power circuit. During the first operation of a reclosing duty cycle, the external switch blades are blocked to prevent motion and the trip circuit is de-energized by means of the pneumatic reclosing relay. The reclosing relay is essentially a pneumatically operated auxiliary switch, the contacts of which control the sequential operation of the reclosing cycle. The reclosing relay is operated by the pressure from the downstream side of the blast valve. By de-energizing the trip circuit at approximately the same time as the interrupter contacts reach their full stroke, the interrupter heads will close to a position where full-line voltage will strike over and re-energize the power circuit through the breaker in approximately 14 cycles. If the fault persists and the trip circuit is again energized, the breaker will go through a normal opening operation. Figure 4B shows a typical no-load reclosing operation with the second trip being energized at approximately 14 cycles.

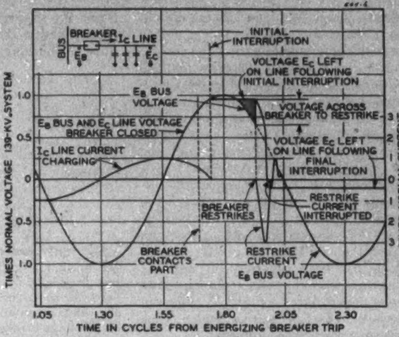

Figure 6. Effect of low-voltage restrikes in breaker-opening capacitance or line-charging currents

Laboratory-Test Results

The results of laboratory and field tests on earlier air-blast breakers[1,3] formed a basis for establishing the laboratory-test procedures employed during the development testing of the new breaker.

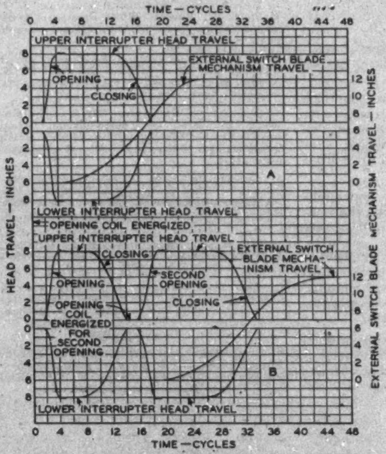

Figure 4. Time–travel curve on interrupter contacts and external switch blade—(A) opening operation and (B) reclosing operation

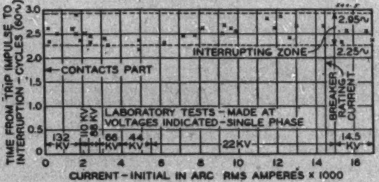

Figure 5. Interrupting performance of breaker during laboratory tests

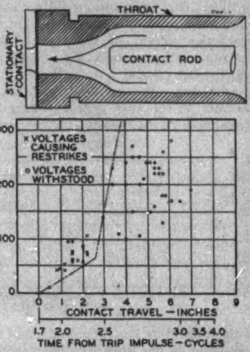

Figure 7. Restrike characteristic of air-blast breaker in opening line-charging current

Figure 5 shows the results of one of the final series of laboratory interrupting tests made prior to shipment of the breaker. It will be noted that the breaker operated with remarkable consistency between the limits of 2.25 to 2.95 cycles corresponding to the first current zero occurring after the contacts leave the constricted section of the throats. This characteristic is one of the primary advantages of interruption by means of an independent source of power. The tests at higher currents were made at reduced voltages. However, it will be noted that the performance of this breaker, in common with other low-arc-voltage interrupters, was essentially independent of the applied test voltage.

The laboratory reclosing tests indicated that the breaker was fully capable of meeting the unusually high-speed reclosing duty for which it was designed. The breaker operated to interrupt all faults within its rating and re-establish the circuit within approximately 14 cycles.

Laboratory tests were made with capacitors simulating line-charging switching. These tests were made over a wide range of values extending up to an equivalent of 25,500 kva, or approximately 200 miles of 138-kv line. These tests indicated that the breaker evidenced no tendency toward restriking except at very low contact separation while the contacts were in the restricted section of the throat. These restrikes occurred at comparatively low voltages since the dielectric strength of the gap between the contacts was low. The restrikes had the effect of discharging the capacitors rather than building up in the manner which has been observed on restrikes occurring when opposite polarity exists across the restriking contacts.[2,7] Figure 6 shows the effect of restrikes which occur under the conditions outlined.

Where final interruptions did not occur until the contacts reached the end of the restricted section of the throat thus leaving a comparatively high charge on the capacitors, the tests indicated that the breaker withstood the high voltages incident to the next system voltage reversal because the high dielectric strength of the interrupter had been established by this point in the stroke. These results are shown in Figure 7.

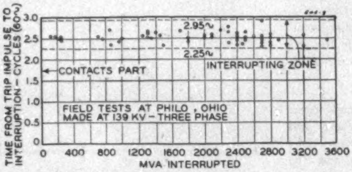

Figure 8. Interrupting performance of breaker during field tests at 138 kv

Field-Test Results

The performance of the breaker during full-scale field tests made at the Philo station of the Ohio Power Company is covered by another paper.[8]

Conclusions

1. The field-test results again confirmed the testing-laboratory procedures. Figure 9 shows a comparison of the breaker interrupting performance on full-scale field tests with results obtained on one series of laboratory tests made just prior to shipment of the breaker. Confirmation of laboratory-test procedures by actual field tests is indispensable to circuit-breaker designers who are called upon to meet the demands for high-voltage breakers of higher interrupting ratings.

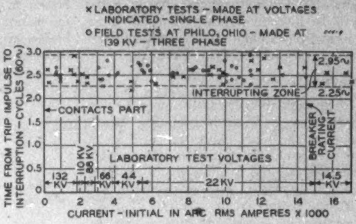

Figure 9. Interrupting performance of breaker, showing composition of laboratory and field tests

2. The precision with which the breaker performed during the entire series of open, closing, and reclosing 138-kv three-phase faults of 260 to 3,500 megavolt-amperes confirms the desirable operating characteristics which have been ascribed to breakers employing an independent source of power for arc interruption. This characteristic of the breaker is shown in Figure 8 on which has been plotted the fault-clearing time for each one of the field tests made on this breaker. The graph shows the fault duration and megavolt-amperes (on three-phase basis) for each pole unit.

3. The reclosing performance under full-power test conditions suggests that deionization time of line-insulator flashovers soon may represent the sole limitation to the speed with which high-voltage circuits may be reclosed.[4,5] The three-cycle operating time of breakers such as this will probably require that we recast our previous concepts on minimum time for deionization.

4. The over-all performance of the breaker has been most gratifying. However, it would be irrational to infer that the developmental task on high-voltage air-blast breakers is completed. Although there are ample data and operating experience on compressed-air systems as used for the performance of purely mechanical operations, use of these data in many cases has been found pernicious where problems of insulation and arc interruption were encountered. More operating experience with high-voltage outdoor air-blast breakers is needed. From the practical viewpoint, more economical solutions to problems of providing adequate current transformers and air-supply systems must be found.

References

1. Field Tests and Performance of a High-Speed 138-Kv Air-Blast Circuit Breaker, Philip Sporn, H. E. Strang. AIEE Transactions, volume 61, 1942, January section, pages 1–6.

2. Switching Overvoltage Hazard Eliminated in High-Voltage Oil Circuit Breakers, L. F. Hunt, E. W. Boehne, H. A. Peterson. AIEE Transactions, volume 62, 1943, February section, pages 98–106.

3. A Conserved-Pressure Air-Blast Circuit Breaker for High-Voltage Service, W. K. Rankin, R. M. Bennett. AIEE Transactions, volume 60, 1941, May section, pages 193–7.

4. Five Years' Experience With Ultrahigh-Speed Reclosing of High-Voltage Transmission Lines, Philip Sporn, C. A. Muller. AIEE Transactions, volume 60, 1941, May section, pages 241–6.

5. Experience With Ultrahigh-Speed Reclosing of High-Voltage Transmission Lines. Philip Sporn, C. A. Muller. AIEE Transactions, volume 58, 1939, December section, pages 625–36.

6. Tests on High- and Low-Voltage Oil Circuit Breakers, Philip Sporn, H. P. St. Clair. AIEE Transactions, volume 46, 1927, pages 289–314.

7. Tests and Analysis of Circuit-Breaker Performance When Switching Large Capacitor Banks, T. W. Schroeder, E. W. Boehne, J. W. Butler. AIEE Transactions, volume 61, 1942, November section, pages 821–31.

8. Field Test and Performance of Heavy-Duty High-Speed 138-Kv Circuit Breakers—Oil and Air Blast, Philip Sporn, H. P. St. Clair. AIEE Transactions, volume 64, 1945.

400-Cycle Inverters for Military Aircraft

C. P. HAYES
ASSOCIATE AIEE

L. L. RAY
ASSOCIATE AIEE

Synopsis: Certain equipment on modern military aircraft requires a-c power with a high standard of quality. Good wave shape, very small voltage variations, fairly close frequency range, freedom from radio-noise interference, and reliability over a wide range of operating conditions are required of the power supply. A review of the authors' experiences in design and development of such power supplies is offered with some suggestions for future explorations.

WITH THE ADVENT of World War II, demands for automatic controls, radio, and other types of intricate equipment for military aircraft increased rapidly. In general, this type of equipment requires an a-c power supply having extreme freedom from wave distortion, modulation, and transient disturbances. Nearly all such devices require very close control of voltage, and many require control of frequency to variations of plus or minus five per cent. The main electric system of the airplane consists of 28-volt engine-driven d-c generators and storage batteries. In the parlance of the service laboratories, an inverter is a device for converting d-c power to a-c power and that definition will be used throughout this paper. The purpose of this paper is to point out some of the problems in the design of suitable inverters for such exacting service. Such a discussion would not be complete without a look at the future with some suggestions for improvement by careful co-ordination between designers of airplanes, auxiliary equipment, and auxiliary power supplies.

Standardization of Frequency and Number of Phases

Even after the beginning of hostilities there were conflicting schools of thought regarding the proper frequency and the most desirable number of phases to obtain the lowest weight of the over-all system. Designers of radio and similar equipment proposed an 800-cycle single-phase source as the power supply which would enable them to design the lightest equipment. They maintained that, although a three-phase design would result in a lighter inverter, loads could not be divided to maintain the necessary balance between phases. Another group pointed out that increasing power requirements on larger airplanes indicated an early trend to alternating current as the main power supply with the load predominantly motors. If a two-pole motor is assumed to be the lightest design, this would result in motor speeds far above existing practical limits. Naturally, this group desired three-phase supply because of the resulting savings in weight of both motors and generators. Pressure for standardization and its obvious advantages finally forced agreement to 400-cycle three-phase supply for large systems. However, the problems of balanced loading under all conditions of component-load operation presented such an obstacle to the three-phase system that single phase was soon adopted for most inverters.

Types of Inverters

There are many devices to obtain alternating current from a d-c source. Among these devices are mechanical vibrators, electronic inverters, dynamotors, motor alternators, and various special combinations and variations of these types.[1]

The vibrator inverter relies on mechanical interruption of the direct current at the desired frequency. Although these devices have given excellent performance on many applications at 60 cycles, higher frequencies are limited because of mechanical difficulties. Such devices have found wide use in aircraft[2] for small power ratings and frequencies below 200 cycles (see Figure 1).

The electronic inverter always has been difficult to apply where the transformation must be effected from a low-voltage high-current source. This is because tube size is largely a function of current and because efficiency decreases with operating voltage as a result of the relatively constant internal voltage drop of the tube. The electronic inverter is inherently unstable and usually requires elaborate control to maintain stability. All these factors have precluded its use on aircraft.

The dynamotor inverter may be described as a d-c motor with taps, or an additional rotor winding, connected to slip rings. A-c power may be drawn from the slip rings. In other words, input and output windings have a common magnetic circuit like a transformer, and voltage output is proportional to voltage input as in the transformer. Control of the field current will change the frequency but will have little effect on the voltage. Since the direct-voltage supply is subject to considerable variation, the output voltage also varies over too wide a range for many applications. This limitation, in addition to the adverse effect of low-power-factor loads on commutation, has prevented very extensive use of the dynamotor inverter on recent military aircraft.

The motor alternator, as its name implies, consists of a d-c driving motor and an alternator which supplies the a-c power output. It is inherently heavier than the dynamotor, but its operating characteristics are much more adaptable to the requirements of aircraft inverters. The separate magnetic circuits provide the maximum isolation of the output from disturbances on the d-c supply system. Independent control of frequency and voltage is easily obtained. Considerable investigation at the outset of development work on aircraft inverters has resulted in the conclusion that the lightest type of alternator is the salient-pole alternator with excitation supplied from the d-c line. Various types of inductor generators and permanent-magnet generators have been investigated; but, for equal output, heating, power factor, and inherent stability, the salient-pole machine has proved to be lighter.

Power Packages

Early inverters were furnished with separate voltage regulators, filters, and starting systems. Demands from the armed services led to incorporation of more and more of these devices into the same structure. The advantages of simplicity of design, ease of installation, ease of servicing, and better co-ordination of the various elements were obviously desirable. Later designs have followed this pattern and have proved very satisfactory. One of the more recent examples of this design philosophy is described in detail.

Frequency Control

Frequency control of vibrator and electronic inverters is not within the scope of this paper. Frequency control of dynamotors and motor alternators is much the same, since both involve the variation of

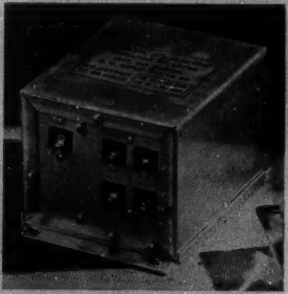
Figure 1. Vibrator-type inverter

Paper 45-82, recommended by the AIEE committee on air transportation for presentation at the AIEE winter technical meeting, New York, N. Y., January 22-26, 1945. Manuscript submitted November 18, 1944; made available for printing January 2, 1945.

C. P. HAYES and L. L. RAY are both in the fractional-horsepower motor engineering division of the General Electric Company, Fort Wayne, Ind.

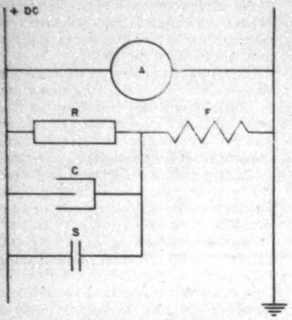

Figure 2. Elementary circuit of centrifugal contact-speed regulator

A—Motor armature
C—Capacitor
F—Motor field
R—Regulator resistor
S—Regulator contacts

the field current to maintain the necessary rotational speed. Of the several methods of frequency control available, none is free from objectionable features. All methods depend on control of the current in one or more field windings of the motor or dynamotor. For success, each method depends on a motor design which is co-ordinated very carefully with the requirements and with the limitations of the control to be used.

One simple light control consists of centrifugally operated contacts in parallel with a fixed resistor. This resistor is placed in series with the motor field (see Figure 2). In the simplest form, this contact remains open until regulating speed is reached, being held open by the leaf spring to which the movable contact is secured. When the control speed is reached, centrifugal force on the contact becomes greater than the spring force, and the contacts close. This allows more field current to flow, reducing the motor speed. As soon as the speed falls to a value such that the spring force again exceeds the centrifugal force, the contacts open again, reducing the field current and increasing the speed. In most cases, speed can be maintained within plus or minus two per cent by this means. However, there is some deterioration of commutation, and some troubles have been experienced with the contacts. A small capacitor usually is required across the contacts to assist in breaking the field current. The wide temperature, voltage, and load variations encountered in such applications require a large difference between the minimum field current and the maximum field current. Therefore, the resistor, R, must be a large percentage of the total field-circuit resistance. Operation of the contacts, in effect, shifts the motor back and forth between widely divergent speed–torque curves. The resultant armature current pulsations cause variation in the d-c terminal voltage. This voltage variation is reflected into the alternator excitation, producing an objectionable modulation of the a-c output voltage. Modulation as low as one half of one per cent has caused trouble on some apparatus.

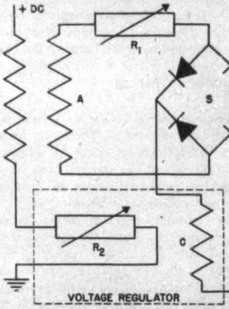

Figure 4. Elementary voltage-regulator circuit

A—Alternator output winding
C—Voltage-regulator actuating coil
F—Alternator field winding
R_1—Calibrating resistor
R_2—Field-control resistor
S—Rectifier

Another basic type of frequency control makes use of a resonant circuit which is supplied from the inverter output. Variation in frequency causes a large change in voltage across one of the elements. This change in voltage may be used directly to vary a control field of the motor, or it may be amplified by one of several means. Without amplification, the elements of the resonant circuit may be quite large and heavy. If amplification be used, either electronic or some other means, the resonant circuit can be small, but the amplifier adds weight. Some work has been done using the resonant circuit with electronic amplification. Amplification also has been accomplished very successfully using a standard aircraft carbon-pile voltage regulator. All of these methods, though giving continuous smooth control, are heavy. In addition, if electronic amplifiers be used, high-voltage fine-wire field windings are required, which introduce additional hazards to reliability.

Another method, which appears to have good possibilities, is the carbon-pile-type speed regulator, which is operated centrifugally. Speed variations are translated into force by a centrifugal mechanism. The force controls resistance of the carbon pile, which in turn controls the motor field current. However, no great amount of operating experience has yet been obtained. It is feared that this device probably will be subject to the same troubles as the carbon-pile voltage regulator, which will be discussed later.

Voltage Control

Early types of d-c regulators for aircraft first were used to control inverter output by rectifying the a-c output and feeding this direct current into the actuating coil of the regulator. Temperature compensation of the circuits was not difficult, but these early regulators consisted of tapped resistors, which were successively short-circuited, tap by tap, to control the alternator field current. Severe modulation difficulties were experienced due to hunting between the nearest taps above and below the voltage actually required to satisfy the actuating coil of the regulator. The device, including the necessary rectifier and temperature compensation, required shock mounting and was considered to be bulky and heavy. A picture of the regulator element is shown in Figure 3.

The carbon-pile voltage regulator has been adopted widely in this country (see Figure 5). It has been adapted to control of inverters, in the same way as the

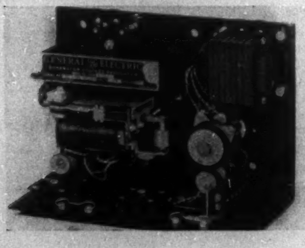

Figure 3 (left). Early type of tapped-resistor voltage regulator

Figure 5 (right). Experimental electronic voltage regulator (American Time Products, Inc.) compared with a carbon-pile voltage regulator (Leland Electric Company) and its rectifier

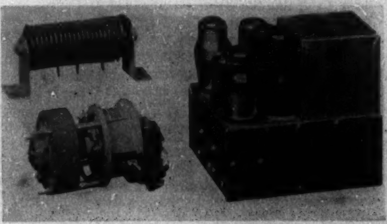

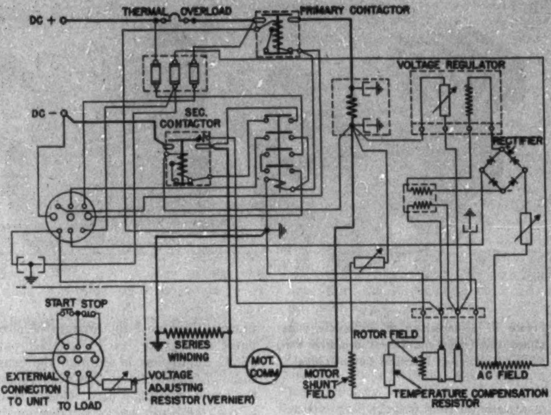

Figure 7. Wiring diagram of inverter

tapped-resistor type just described (see Figure 4). It has the advantage of continuity of control but requires a high degree of skill to adjust in the field. It is also somewhat unstable, which has caused considerable trouble due to modulation of the output voltage. The good performance of the carbon pile disks under short-time loading conditions provides a temptation to give them a higher service rating than practical, especially in view of the insistent demand for reduced weight. However, the minute arcing which occurs when the pressure is reduced on the disk to secure maximum resistance, causes pitting and cumulative burning, so that the device is soon inoperative if it is overloaded. Only experience can tell what the proper limit of rating these carbon-pile regulators should be. The aforementioned delicate adjustment which must be repeated after the simplest of servicing operations is a considerable hazard to reliable operation.

Some work has been done with electronic control devices (Figure 5), where a bridge circuit compares output voltage with a standard-voltage tube. Output of the bridge circuit is amplified by electronic tubes and fed into a control field of the alternator. Here again, high voltages and fine-wire windings are objectionable from the standpoint of reliability, as compared with other types of control. So far, devices of this type are both heavy and bulky, compared to the carbon-pile type.

Present requirements of certain inverter loads are too severe to be satisfied with any existing regulators. Considerable experience in this field indicates that either regulators must be improved or the load device must be made less sensitive to modulation and voltage variation.

Radio-Noise Requirements

Most equipment is quieted by suitable filters installed on the airplane at the point of manufacture. Since inverters are frequently installed after manufacture and delivery of the airplane to the armed services, they usually are required to meet radio-noise limits. This means that radio-noise filters are built in as part of the machine. Most specifications require standard limits of noise over a standard frequency band, but requirements appear to be increasing in severity at this writing.

Brush Life

Early d-c motors and inverters for aircraft encountered considerable difficulty because of the extremely short life of the brushes when operating at high altitudes. The reasons for the condition were several. Brushes used on early machines were those selected by designers based on their experience with ground-level performance. At the same time, in their desire to meet pressing demands by the armed services for lighter equipment, compromises occasionally were made with designs which were later proved inadvisable. Finally, the effects of commutation on brushes and commutators at high altitudes where extremely small quantities of moisture are present had not been investigated. This last factor, the most important, required time to prove and longer to overcome. Rapid strides were made to develop brushes suitable for high-altitude operation, once equipment was available for high-altitude testing.[3,4] Radical improvements also have been made in brush cooling, as will be described later.

Cooling

Lightweight high-speed devices for aircraft must dissipate most of their heat by forced convection, because natural convection and radiation cannot dissipate successfully the losses generated in such machines. When altitudes representing one quarter of an atmosphere (approximately 40,000 feet) are encountered, the volume flow of cooling air remains constant, but its weight flow drops to one fourth that obtained at sea level. This means that the ventilating air is much less effective under these conditions. This effect is compensated for, to some degree, by the lower temperatures at such altitudes. Smithsonian tables[5] indicate an average temperature of −55 degrees centigrade at 40,000 feet. However, inverters and similar equipment usually are installed in the main fuselage, and flight tests indicate that the unheated cabin temperature is normally 25 to 35 degrees centigrade warmer than outside air. The designer's problem would be greatly simplified, if more data on operating conditions were known. However, from the data indicated, it readily may be seen that the worst condition for cooling is that of

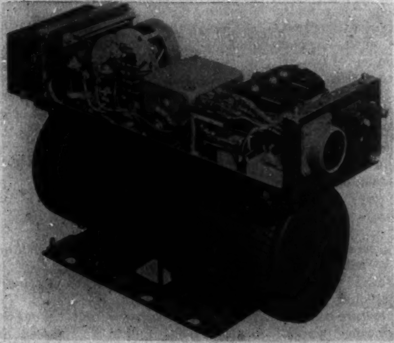

Figure 6. Power-package inverter—1.5 kva, 360/500 cycle

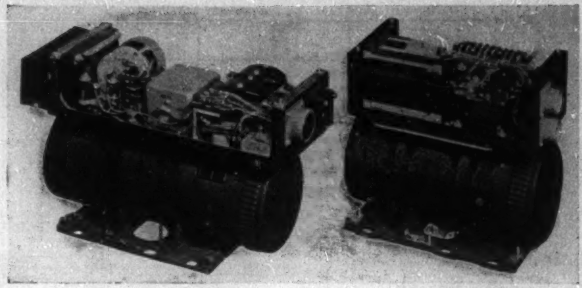

Figure 8. Comparison of 400-cycle three-phase drive (right) and 28-volt d-c drive (left) for inverters of identical output rating

maximum altitude with highest expected machine ambient temperature. Early machines were designed for temperature corresponding to Smithsonian values, which meant that performance suffered when higher ambient temperatures were encountered. Newer designs have taken into account these higher ambient temperatures at high altitudes.

Later machines have been designed to obtain better cooling of the brushes and, at the same time, maintain adequate cooling of the windings.

Maintenance

Because of misconceptions of expected service procedures and requirements, many early designs did not give sufficient emphasis to ease of servicing the equipment. This shortcoming, combined with the short brush life mentioned, resulted in vigorous complaints by service personnel. Later designs have been improved vastly in this regard, particularly with respect to brush inspection and replacement.

Typical Inverter

A recent design which has been used widely in Army aircraft is shown in Figure 6. An interesting feature of this inverter is that all structural parts, with a few exceptions, are of steel. This feature was dictated by the extreme shortage of aluminum and magnesium at the time of its development. By careful design, an over-all weight penalty of only five per cent was involved.

The right-hand side of the machine, as viewed in Figure 6, is the drive motor. Brushes may be removed for inspection without the use of any tools and can be replaced with new brushes by a few turns of one screw on each stud. The removable brush caps are part of a carefully designed cooling system for the brushes. The fan expels air from the machine, drawing fresh cool air through the alternator and motor, and a parallel path allows air to flow in through the brush caps. A restriction of flow occurs along the brush, creating a high velocity of air to cool the brush and to impinge on the commutator surface for further cooling benefits. This system has greatly increased brush life without resorting to reduced current density in the brushes. This factor, coupled with improved brush materials and improved commutation, resulted in high-altitude brush life which was startling compared to previous experience. The brush life of this machine far exceeded any obtained previously. Recent improvements on drive motors for other types of equipment, where duty is not so severe and where the same basic type of brush rigging and cooling is used, indicate an expected high-altitude brush life equal to or better than that expected at normal altitude.

The left-hand side of the machine consists of the alternator. The wave shape is extremely good, having a harmonic content below four per cent. It consists of a six-pole salient-pole rotor excited through slip rings from the d-c supply. The 400-cycle output is generated in the stator windings.

The control box is mounted on top with heavy stud terminals for the d-c input. A standard aircraft connector provides easily removable connections for output, remote vernier voltage setting, remote push-button starting, and one or two circuits not directly related to this discussion.

If viewed from left to right, the control box includes voltage regulator elements, radio-noise filter, contactors, and interlock relay for motor starting. All elements of the control are mounted for ease in servicing and replacement in the event of combat damage. A diagram of the circuit is shown in Figure 7. Provision is made for temperature compensation of the motor field circuit to minimize frequency variation. No other frequency control is provided. The voltage-regulator network is also temperature compensated. Tests indicate a change in regulated voltage of less than one volt over a range of −40 degrees centigrade to +65 degrees centigrade.

This machine, though made obsolete by more recent armed service specifications requiring closer frequency limits, still represents many desirable features for this type of equipment. With the addition of frequency control with a suitable driving motor, it would conform closely to present-day specifications for future applications.

It represents a partial retreat from the extreme "bone cutting" weight reduction of earlier designs. It has operated continuously at altitudes above 35,000 feet at ambient temperatures of +15 degrees centigrade for long periods of time. With increasing experience regarding types of installation, it is believed that the margin of safety in this machine, though much greater than foregoing designs, is none too great. Since these inverters usually are installed after all other equipment, compromises made with ventilation upon installation are frequently startling.

For future applications on aircraft with a-c power supplies, it may still be necessary to isolate certain fussy loads from the main system. Figure 8 shows an interesting comparison between two machines designed to identical specifications, except that the drive motor for the machine on the right is designed to operate on a 400-cycle, three-phase supply while the machine on the left is identical to that in Figure 6, for d-c supply. The simplification of control and weight reduction are quite obvious.

Recommendations

In view of the considerable weight required for control, it appears reasonable to suggest a review of present specification limits with the following points in mind.

Inherent speed regulation without the use of speed-control devices appears to be limited to about plus or minus ten per cent. Current developments in permanent-magnet excitation indicate a possibility of five-to-seven-per-cent voltage regulation for a given frequency and voltage proportional to frequency for any fixed load impedance. If the load devices could be designed for such a spread in frequency and voltage with less increase in weight than that saved in the control, over-all weight would be reduced. More important, much of the complexity of the inverter would be eliminated, resulting in less field servicing, greater dependability, and longer life.

In general, new electronic devices have been very demanding in regard to quality of the power supply. Usually, later designs can tolerate more variation, and this trend should be encouraged, if it result in lower over-all weight, greater simplicity of the system, or both.

If this approach does not yield satisfactory results, radical improvement in

An Interval Timer for Arc Duration

J. S. QUILL
ASSOCIATE AIEE

IN DEVELOPMENT work leading to new and improved designs of equipment involving arc interruption the success of the work is to a large extent influenced by the quality of the instruments used for measurement. The arc-interruption problem is one that has been in existence since the first electric installation. Nevertheless, progress continually is being made in developing smaller and more efficient devices for stopping the flow of electric current. One of the most promising ways of furthering this progress lies in the development of new methods of measurement.

Scope of This Paper

This paper describes a laboratory electronic instrument which was developed for the purpose of measuring in milliseconds the time during which arcing exists when an electric circuit is opened. The need for such an instrument and the type of investigation for which it is best suited also are discussed. Examples are presented to illustrate the usefulness of the instrument for timing both a-c and d-c arcs.

The interruption devices referred to in this paper are those commonly found in industrial-control applications: contactors, relays, push buttons, and so forth. In some respects the problem of arc interruption for control applications is similar to that found in switchgear and other related applications. The illustrations given will be, for the most part, on a-c applications, but similar illustrations could be given for d-c interruption.

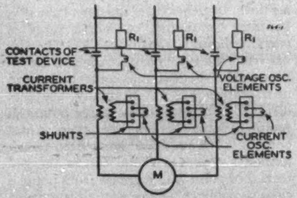

Figure 1. Circuit-connection elementary diagram for a three-phase arc-interruption test, showing connections for magnetic-oscillograph elements to record current and voltage traces for each phase

M—Locked-rotor motor load

Development Testing on Arc-Interrupting Devices

Arcing tests on industrial-control devices can be classified as

1. Interruption tests.
2. Life tests on the contact tips.

The two are somewhat interrelated. Because it takes several months to conduct a single tip-life test, some means of predicting the outcome of these tests is essential, and, in many cases, the interruption tests serve this purpose.

Interruption tests sometimes are made in order to determine whether a device will interrupt a particular load, but more often they are made to compare designs and to find out which is the most efficient. The tests consist of operating the contactor making and breaking the current of a prescribed load. A locked-rotor motor frequently is used for load, because, in general, it is the most severe load that the contactor will be required to interrupt. The arc-interruption transient usually lasts 50 milliseconds or less for a-c applications and 100 milliseconds or less for d-c applications. There is little commercially available measuring equipment that will measure during so short an interval.

Measuring Equipment

The magnetic oscillograph frequently is used to obtain arc-interruption information. The circuit connections used for this purpose are shown in Figure 1. The current and voltage traces for one phase resulting when the contactor is closed and opened, are shown in Figure 2. Elements may also be used to record arc-energy traces, or the energy may be calculated for each interruption from the voltage and current traces. The information obtained from an oscillogram, then, is the arc time in milliseconds, the wave-shape of the arc voltage and current, and the arc energy.

It is not feasible to take oscillograms of all operations, because an interruption test may consist of several hundred operations. Even if the records were taken and developed, the time required to transcribe the information from them would be prohibitive. Therefore, it is necessary to base conclusions on a few oscillograms and hope that the information obtained is representative. Furthermore, since the oscillograph element and its external resistor, R_1, must be placed in parallel with the arcing tips, the quantities to be measured are affected by the measuring equipment. Figure 3 shows the effect of this arc-shunt resistance on the average arc time. The oscillograph circuit resistance shunting the arc usually ranges between 5,000 and 15,000 ohms for 550-volt interruption. The average arc time is 70 to 90 per cent shorter when the oscillograph is connected, the data recorded on oscillograms being optimistic. It would be impractical to use a more sensitive oscillograph element because of its limitations of frequency response.

Information on arcing can be obtained by means of high-speed moving pictures. In some cases the information obtained is excellent, but in analyzing the results obtained the modifications that were necessary so that the arc could be photographed should be kept in mind. A fact not well known about this technique is that, if an auxiliary light source is used, the amount of light required for the high-speed pictures may obscure the arc on low-current interruptions for several milliseconds both at the beginning and at the end of the arcing period. The expense and time required to obtain data are additional limitations of this method.

An instrument has been developed to measure the arcing time for d-c interruptions as well as the time of bounce of contacts when closing.[1] With this instrument the contacts under observation can be tested only on direct current. Concerning a-c interruption, the paper describing the instrument states that, because of the additional variables involved, readings of arc time will vary widely. The article continues "If the test is made with direct current, the latter can be adjusted to any value, thus simulating any desired 'instantaneous' value of alternat-

---

Paper 45-64, recommended by the AIEE committee on instruments and measurements for presentation at the AIEE winter technical meeting, New York, N. Y., January 22–26, 1945. Manuscript submitted November 14, 1944; made available for printing December 28, 1944.

J. S. Quill is electrical engineer, General Electric Company, Schenectady, N. Y.

---

devices for the control of frequency and voltage is needed. The prime requirements of such devices are light weight and continuity of control. In other words, discontinuities, such as finite resistance steps or vibrating contacts, should be avoided.

References

1. Aircraft Inverter Construction, C. T. Button. AIEE Transactions, volume 62, 1943, September section, pages 598–602.

2. Aircraft Transformers—Small and Light, O. Kiltie. AIEE Transactions, volume 62, 1943, pages 899–902.

3. The Testing of Brushes for Life and Performance Under Various Altitude Conditions, C. J. Herman. AIEE Transactions, volume 63, 1944, December section, pages 929–33.

4. New Test Chambers for Aircraft Electric Apparatus With Particular Reference to Carbon Brushes, E. R. Summers, J. F. Settle. AIEE Transactions, volume 63, 1944, pages 1205–12.

5. Smithsonian Physical Tables (book), eighth edition. Smithsonian Institution, Washington, D. C., 1934. Table 695.

Figure 2. Oscillograph traces of voltage and current transients produced during a single-phase arc interruption

The E_v signal is the voltage signal from across the contacts of the interrupting device while the E_i signal is proportional to the interrupted current

ing current." Actually, a-c interrupters are seldom tested on direct current, since the interruption phenomena involved are quite different. The fact that arcing time varies over a wide range emphasizes the need for some means of easily obtaining a large number of readings to insure proper analysis.

The Electronic Arc Timer

A laboratory electronic instrument for measuring the length of time that an arc persists when an electric circuit is opened has been developed. The instrument requires two input signals, one obtained from the arc voltage, and the second from the circuit current. Typical arc-voltage and circuit-current signals are shown on Figure 2. Timing is initiated when the voltage signal appears, and it is stopped when the current goes to zero. During the interim, a capacitor is charged linearly with time, and the voltage on the capacitor is inversely proportional to the arc time. The instrument consists of a regulated power supply, a timing circuit, a voltage-signal circuit, and a current-signal circuit. These circuits are shown on Figures 4, 5, 6, and 7 which are drawn so that the position of a line on a diagram is indicative of the potential of the element represented. Point 5 is at the lowest potential and is drawn at the lowest position on the circuit diagram, whereas point 1 is at the highest potential and is drawn at the top of the circuit diagram. This method of drawing the diagrams should be kept in mind for the following explanation of the operation of the instrument.

The power supply and timing circuit are shown in Figure 4. The power supply is of the conventional type used to provide constant direct voltages independent of a-c line voltage fluctuations. The timing circuit consists of capacitor $3C$ charged by a constant current through pentode $9VT$. The charging current is controlled by the variable cathode resistor $5VAR$. The maximum time interval measured can be varied either by changing the size of the capacitor $3C$, or by changing the charging current. The voltage across the timing capacitor $3C$ controls the grid of a cathode-follower circuit in which a d-c voltmeter is used as the cathode resistor. The voltage across the voltmeter is therefore inversely proportional to the voltage on the capacitor. This unique method of measuring the voltage across the capacitor reduces the leakage current to a minimum. The timing circuit is turned on and off by means of the bias voltage that is placed on the screen-grid of the pentode at point 7. The following is an explanation of how the arc voltage and circuit current are used to start and stop the timing circuit.

The voltage-signal circuit that starts the timing circuit is shown in Figure 5. E_v and C are connected across the tips of the device on which the arc time is to be measured. When the tips of the test device are closed, current is flowing through the tips, but the voltage across them is practically zero. With zero voltage between E_v and C, point 16 (plate of $17VT$) is adjusted by means of the potentiometer $3VAR$ to the level of point 2 in potential. As soon as the contacts part and arcing begins, a voltage appears between E_v and C. E_v may be either positive or negative with respect to C. The change in potential between point 10 and point 4 is proportional to the change between E_v and C. Point 10 controls the potential of point 16, which controls the current through the peaking transformer V. If E_v becomes more than five-volts positive with respect to C, point 16 drops close to point 18 in potential. When E_v becomes more than five-volts negative with respect to C, point 16 becomes close to point 1 in potential. In either case, the neon tube $2Ne$ becomes conducting causing a surge of current through transformer V. The signal from the secondary winding of transformer V is rectified and controls the grid of thyratron $11VT$. Normally, the grid of $11VT$ is biased to a negative potential (point 9) somewhere between point 4 and point 5. The rectified signal from transformer V fires $11VT$ and causes the potential of point 8 to increase from point 4 close to point 18. Since negligible current passes through resistor $7R$, point 7 is maintained at the same potential as point 8. Therefore, if a positive or negative voltage signal of five volts or more is placed between E_v and C, the pentode ($9VT$) in the timing circuit is made conducting.

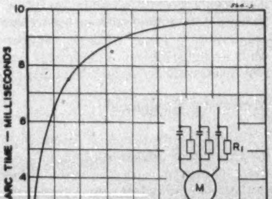

Figure 3. Average arc time versus arc-shunt resistance for arc interruption by a commercially available size-2 contactor

100 readings of arc time taken for each point. One third of readings taken on each phase

M—550-volt 305-ampere 50-horsepower locked-rotor induction motor

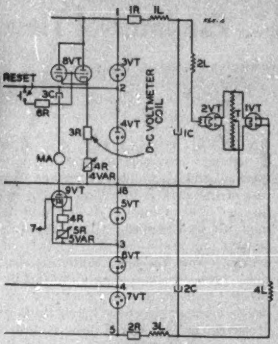

Figure 4. Power supply and timing circuit for arc-interval timer

The current-signal circuit that stops the timing circuit is shown in Figure 6. The input signal, proportional to current, is placed between E_i and C. With zero signal input, $1VAR$ and $2VAR$ are adjusted so that $13VT$ and $14VT$ are not conducting, but, if either point 14 or point 15 increases in potential, $13VT$ or $14VT$ will start conducting. With the contacts of the test device closed, E_i is fluctuating with respect to point C. When E_i is five volts or more positive with respect to C, point 12 is close to point 18 in potential, and point 13 is close to point 1 in potential. When E_t is negative with respect to point C, the reverse is true. Therefore, when the current signal is oscillating, points 12, 13, 14, and 15 also are oscillating. Thyratrons 13*VT* and 14*VT* are alternately conducting. When either tube is conducting, point 11 is close to point 18 in potential. During the interim in which neither tube is conducting, point 11 is held down in potential by means of the capacitor 4*C*. When the current signal between E_t and C goes to zero and remains zero for a short time, point 11 will increase in potential enough to cause neon tube 1*Ne* to become conducting which results in a surge of current through transformer *I*. The resulting signal from the secondary winding of transformer *I* is rectified by 10*VT* and controls the grid of thyratron 12*VT*. Normally, the grid of 12*VT* is biased negatively. The rectified signal from transformer *I* fires 12*VT* and thereby removes the positive bias on the grid of pentode 9*VT* and prevents it from conducting.

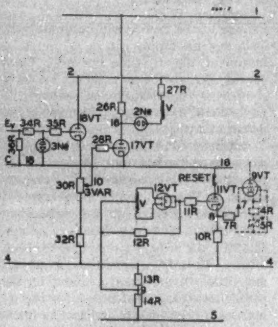
1
2
27R
26R
2Ne
V
18VT
16
Ey
34R
35R
3Ne
36R
C
18
28R
17VT
30R
10
3VAR
12VT
V
RESET
11VT
9VT
11R
8
7
7R
4R
5R
12R
10R
32R
4
13R
9
14R
5

Figure 5. Voltage signal circuit for arc-interval timer

This circuit starts the timing circuit when a voltage is placed between E_y and C

The complete circuit for the timer is shown in Figure 7. E_y, C, and E_t are connected to the test contactor as shown on Figure 8. The current signal can be obtained from a small amount of series resistance or from current transformers. With Figure 7 as reference, the operation of the circuit can be summarized as follows. When a voltage signal appears between E_y and C, thyratron 11*VT* is made to conduct. This increases the potential of point 7 and starts the timing circuit. When the signal between E_t and C goes to zero and remains zero for a short interval, 12*VT* is made conducting. This removes the positive voltage from point 7 and stops the timing circuit. The methods of resetting the timer and means of calibrating are given in the following paragraphs.

Reset

Before each reading the timer must be reset while the contacts of the test device are closed and current is flowing. The reset consists of removing the plate voltage from the thyratrons and discharging the timing capacitor. A small relay is used for this purpose. Reset may be accomplished by hand, by means of an external reset, or automatically. When hand reset is used, the procedure is as follows:

1. Close the contacts of the device being tested.
2. Close and open the contacts of the reset relay.
3. Open the contacts of the test device.
4. Read the output voltmeter.

In many cases this process is too slow, and it is not desirable to have current flowing into the load for the length of time required for hand reset. In this case an external relay can be used to reset the instrument. This relay should have two sets of contacts, one of which closes before the second. When this relay is energized, the first contacts to close energize the test contactor and the second reset the timer. When the relay is de-energized, the reset relay is de-energized before the coil of the contactor. This method insures the proper sequencing of events and permits having the test contactor closed for only a few cycles. The third method of reset requires no external relay. The timer is normally held in reset. When the current signal appears, the timer is dropped out of reset, and it is again reset after a definite time delay. The time delay can be adjusted to allow for the operation of the test contactor and for reading the output voltmeter.

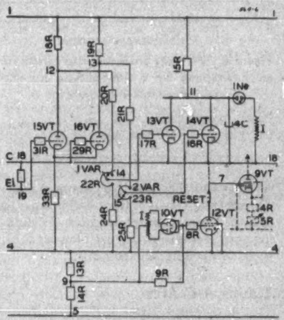
1
18R
19R
15R
12
13
20R
21R
11
1Ne
15VT
16VT
13VT
14VT
4C
I
31R
29R
17R
16R
C
18
El
19
1VAR
14
22R
2VAR
23R
33R
15
RESET
24R
25R
10VT
12VT
9VT
7
4R
5R
8R
4
13R
9
9R
14R
5

Figure 6. Current-signal circuit for arc-interval timer

This circuit stops the timing circuit when the voltage between E_t and C, proportional to current, goes to zero

Calibration

The arc timer can be calibrated by several methods. Two voltage signals are required for calibration; one to start and the second to stop the timing. If the time interval between the voltage signals can be controlled accurately, a calibration curve of time interval between these two voltage signals versus voltage to which the timing capacitor is charged can be obtained. The voltage signals can be obtained from an electronic circuit or from motor-driven commutators. In the first case the time can be varied by changing the frequency standard, whereas in the second case, the speed of the motor controls the time interval. Calibration also can be accomplished by taking an oscillographic record of an actual arc interruption. Here the timer-output-voltage trace can be put on the same film with the arc voltage and circuit current. From such a record the slope of the timer output voltage in volts per millisecond can be obtained. The time delay caused by the capacitor 4*C* can be measured. By checking a few points in this manner, a complete calibration curve can be obtained. Although the timer possibly could be made into a precision instrument, for arc-interruption work this is not necessary. For

Figure 7. Complete circuit diagram for arc-interval timer

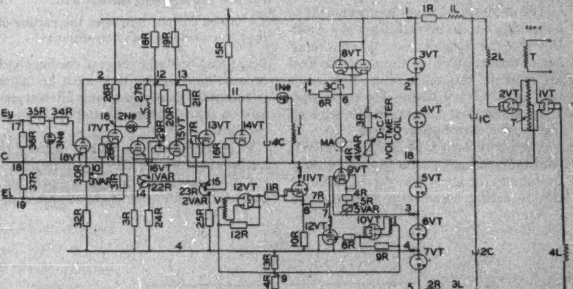
1
1R
1L
2L
T
18R
19R
15R
8VT
3VT
2
12
13
28R
27R
20R
21R
11
1Ne
3C
6R
6
2
2VT
1VT
Ey
35R
34R
16
2Ne
17VT
29R
15VT
17R
13VT
14VT
4C
I
1C
T
17
36R
3Ne
26R
16R
MA
3R
4R
4VAR
D-C VOLTMETER COIL
4VT
C
18
18VT
10
3VAR
31R
16VT
1VAR
22R
11VT
9VT
18
EL
37R
19
14
23R
2VAR
15
12VT
11R
7R
4R
5R
5VAR
5VT
32R
3R
24R
25R
V
12R
8
7
12VT
10R
8R
10VT
3
6VT
4
9R
4
7VT
2C
4L
13R
9
14R
5
2R
3L

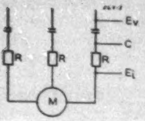

Figure 8. Elementary diagram showing how input signals for the arc-interval timer actually are obtained

M—Locked-rotor motor load

this application, one is interested primarily in comparative results. For this reason, an accuracy of plus or minus one millisecond has been considered satisfactory.

Advantages of the Timer

There are a number of characteristics of the timer that make it well suited for arc-interruption work. It reads directly and thereby eliminates expensive and time-consuming photographic processes. Only a few minutes are required to set up the instrument for a test, and no readjustments are required when the voltage or current to be interrupted is changed, providing the input signals are greater than the minimum five volts. Readings of arc time can be obtained very rapidly, and it requires only a few minutes to complete a test of 100 interruptions with the arc time recorded for each operation. Because its input impedance is several megohms, the timer does not alter the interruption transient. The instrument can be used to time either a-c or d-c interruptions, a feature that distinguishes it from any other device so far reported.

The usefulness of the timer is not limited to the measurement of arc time. It can be used to measure the interval between two voltage signals; either signal can be above five volts and suddenly go to zero or be zero and jump to five volts or more. In this manner the timer has been used to measure the opening and closing travel time of contactors, the sequencing of devices, and for many similar applications. It is especially useful in the range from several milliseconds to 200 milliseconds.

Timing D-C Arcs

The arc-interval timer has been used to advantage for the investigation of d-c arc-interruption phenomena.[2] When a number of interruptions of the same d-c load are repeated the range of arc-time readings usually is not large. For this reason 10 or 20 readings of arc time at each load insure good distribution curves.

A series blowout-type contactor often is used to handle d-c power loads. In these contactors the arc is transferred from the tips to arcing horns soon after the tips part. Figure 9 shows a curve of average arc time versus current for interruption by this type of contactor. The long arc time in the low-current region and the practically constant time for loads above 100 amperes are characteristic of d-c blowout contactors. It should be noticed in Figure 9 that the series blowout field of the usual number of turns is not effective for low currents. For this reason low-current relays and interlocks for control circuits usually do not have a series blowout coil, but rely upon gap or a permanent-magnet field to stretch the arc until the current ceases. For these devices curves of average arc time versus current can be used to find the effect upon interruption of changing gap, permanent-magnet blowout field, speed of opening, and so forth.

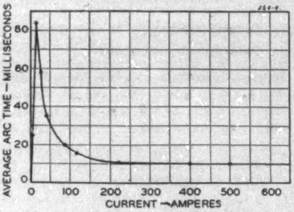

Figure 9. Average arc time versus current for arc interruption by a blowout-type commercially available d-c contactor

Load: inductive, 250 volts
30 readings of arc time taken at each point

Timing A-C Arcs

The range of arc-time readings for a-c interruption is much greater than for d-c interruption. The principal reason for the difference is that alternating current goes to zero two times each cycle. Interruption occurs at or near the normal current zero. The arc time therefore depends upon

1. The time between the parting of the tips and the following current zero.
2. Which current zero after the parting of the tips completes the interruption.

Because of the large range of readings and because data on arc time must be taken from each of three phases, it is often necessary to take as many as 100 readings at each load.

It is difficult to generalize concerning a-c interruptors, for they are quite different in design and principle of operation. The average arc time is about four milliseconds for loads on which interruption always occurs at the first current zero after the parting of the tips, providing the tips part at random.[3] For larger loads the shape of the arc-time-versus-current curve depends primarily upon

1. The design of the interrupting device.
2. The applied voltage.
3. The type of load.

Failure of the device will occur at some load, and the failure can be predicted by means of the arc-time curves. These curves also provide an excellent means of comparing the operation of several contactors and of evaluating changes in the design of a single contactor.

Data can be obtained by use of the instrument described that cannot be obtained by other means.[3] The results shown on Figure 3 are a good example of this type of information. It is well known that the oscillograph-circuit resistance shunting the arc has some influence upon arcing. Specific information about the magnitude of the change caused by the parallel resistance and how large the resistance can be without influencing interruption has been lacking. The information in Figure 3 was obtained in a few hours.

Conclusion

There has been a definite need for measuring instruments that can supply information concerning the transient produced by circuit interruption. An instrument is described that is especially suited for the measurement of the length of time that an arc-transient exists. The new instrument has been a valuable aid in conducting both a-c and d-c arc-interruption studies. The instrument has been in use for approximately a year, during which time over a quarter of a million readings of arc time have been taken. Data are being accumulated on the performance of interrupting devices, the relative severity of loads, the correlation of single-phase and three-phase interruption tests, and on many other aspects of the interruption problem. This kind of information is of great value to designers of arc-interrupting devices.

References

1. **An Instrument for the Determination of Contact Making and Breaking Time, W. Richter, W. H. Elliott. AIEE Transactions, volume 62, 1943, January section, pages 14–16.**

2. **D-C Arc Interruption for Aircraft, J. S Quill, L. T. Rader. AIEE Transactions, volume 63, 1944, December section, pages 883–8.**

3. **Measuring Arc Duration, J. S. Quill. *General Electric Review*, volume 47, November 1944, pages 22–4.**

The Combination of Supervisory Control With Other Functions on Power-Line Carrier Channels

R. C. CHEEK
ASSOCIATE AIEE

W. A. DERR
ASSOCIATE AIEE

THE PRACTICE of using a single power-line carrier channel to perform several different functions is becoming increasingly common. This practice is encouraged by the savings in equipment and in carrier-channel space that can be effected when a single carrier transmitter and receiver are used jointly by some combination of relaying, telemetering, communication, load control, and supervisory-control equipment. The recent introduction of a wide line of individual rack-mounted carrier components[1] makes it possible to select exactly the apparatus necessary for the combination of functions to be performed and further encourages the use of a single carrier assembly for several co-ordinated functions.

Certain combinations of functions on carrier channels have been described in previous papers.[1,2] These papers generally have described functions on point-to-point channels and have considered mainly such functions as relaying, communication, and telemetering, mentioning supervisory control only briefly. As a result, methods of combining carrier communication and relaying are relatively well known. The channel requirements of telemetering and load control are comparatively simple, and the combination of these functions with others offers no especially difficult problems. However, the channel requirements of supervisory-control systems, particularly those of the multistation type, are relatively more strict than those for most functions. The application of such systems in combination with other carrier functions requires an understanding of these requirements if correct and dependable operation is to be secured. These requirements have not been previously described in detail.

It is the purpose of this paper to point out what conditions must be satisfied for proper operation of a standard supervisory-control system; to tell why some combinations of carrier supervisory control with other functions, which on the surface appear workable, may be subject to undesirable limitations; and to describe methods of co-ordinating certain acceptable combinations so that reliable operation of the supervisory control system is assured.

Principles of Operation of Supervisory Control

Supervisory control is a system of controlling and supervising from a central point the operation of equipment at one or more remote locations. Control and supervision of a number of separate pieces of equipment are accomplished with relatively few conductors or channels. In the Visicode supervisory-control system, which is the system considered in all further discussion in this paper, only a single pair of wires or a single carrier channel is required.

In the Visicode supervisory-control system, supervision and control of a large number of individual pieces of equipment are obtained by selective relay systems, which automatically generate and receive impulses in coded groups to perform the functions of selecting the apparatus to be controlled, performing the desired operation, and indicating that an operation has taken place. The latter function is performed whether the operation is initiated through the supervisory system or not.

In this system, a group of units to be controlled is assigned a group number. Individual units within the group are assigned point numbers. These numbers represent the number of impulses in the two series of impulses which must be sent from the dispatching point to select the group and point desired. Selection is accomplished by a system somewhat similar to an all-relay automatic-telephone system, with the following two main exceptions:

1. The operator does not operate a telephone dial to select the remote unit he desires to control. Each remote unit has its corresponding selection button on the operator's control board, and the operator merely depresses the proper button momentarily. The proper group and point selection impulses are sent automatically.
2. After each set of impulses is sent, the receiving equipment at the remote location must send back the same number of impulses before operation can proceed. This provides a positive check at each step of the sequence of operation.

For a complete control operation, the operator presses a point-selection button. The dispatching equipment automatically sends a series of impulses corresponding to the desired group number. The supervisory equipment at the remote station sends back a series of impulses called the group check code, indicating that correct group selection has been made. Reception of the group check code at the controlling point causes the point selection code to be sent. This code also is repeated by the receiving equipment, and the reception of this point check code at the controlling point lights an indicating lamp to signify that the desired unit has been selected and that the remote supervisory equipment is ready to perform a controlling function on that unit. The operator then turns a two-position twist key to the desired operation, for example, to "trip" if a circuit breaker is being controlled. This lights a "disagreement" lamp, indicating that the condition of the controlled equipment does not correspond to that indicated by the position of the twist key. The operator then presses momentarily another button, which causes his

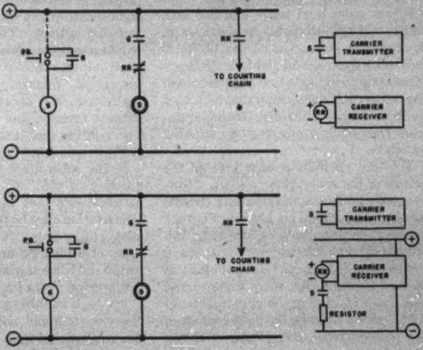

Figure 1. Fundamental supervisory-control impulsing circuits for carrier operation

A (above). External stepping

B (right). Internal stepping

Paper 45-77, recommended by the AIEE committees on automatic stations and power transmission and distribution for presentation at the AIEE winter technical meeting, New York, N. Y., January 22-26, 1945. Manuscript submitted November 8, 1944; made available for printing December 29, 1944.

R. C. Cheek is central-station engineer, and W. A. Derr is design engineer, switchboard engineering department, both with Westinghouse Electric and Manufacturing Company, East Pittsburgh, Pa.

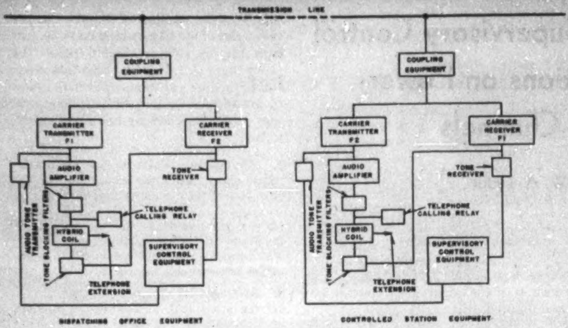

Figure 2. Block diagram showing essential components for combination of point-to-point two-frequency duplex carrier communication with single-station supervisory control

supervisory equipment to send a third series of impulses. These impulses, when received at the remote station, cause the supervisory equipment to close the necessary circuits to perform the desired operation. Operation of the controlled equipment in the desired manner then causes the remote supervisory apparatus to send back the "supervision" code. Reception of this code at the controlling point changes the indication of the red and green position-indicating lamps and extinguishes the disagreement lamp. The supervisory equipment at the controlling point then automatically sends a long impulse which resets the entire supervisory system to normal.

Operation of the supervisory system to indicate an automatic operation of controlled equipment at a remote point is somewhat similar, except that group- and point-selection codes automatically are initiated from the remote point and checked back from the dispatching point. Reception of the supervision code at the dispatching point, after group and point selection have been made and checked, rings an alarm bell, lights an alarm lamp, changes the indication of the position-indicating lamps, and lights a disagreement lamp to indicate that the position of the remote unit differs from that indicated by the twist key. The dispatching equipment then sends a long resetting impulse, as before.

It is not possible to show here all the details of the supervisory system. However, the fundamental impulsing circuits for carrier operation are given in Figure 1 to show how impulses are generated. Impulsing through the carrier set is shown in Figure 1A. When the push button is pressed momentarily, relay 6 closes and seals itself in, closing the circuit to time-delay relay 5 through the back contact of the receiver relay *RR*. Relay 5 closes, starting the carrier transmitter. Reception of the transmitter by the local receiver causes relay *RR* to operate, opening the circuit to relay 5. After a slight time delay, relay 5 releases. This cycle of operation constitutes one impulse. Impulsing continues automatically until proper number of impulses for the desired group are sent, whereupon counting relays open the circuit to relay 6 through contacts not shown. This stops impulsing and prepares the equipment for reception of the check-back code. This type of impulsing is called external stepping.

It is possible in some cases to operate the receiver relay directly from the carrier power source by placing an additional contact of relay 5, in series with a suitable dropping resistor, across the plate circuit of the receiver detector. Impulsing then can take place, even though the transmitted signal is not received locally. This is called internal stepping.

Channel Requirements of Supervisory-Control Systems

The rate of impulsing of the supervisory equipment is from 9 to 14 impulses per second, comparable to the speed of impulsing of a telephone dial. This rate of impulsing is considerably higher than the highest rate of any standard impulse telemetering system. The fastest such system in use at the present time has a maximum impulse rate of approximately 3.5 per second. In an impulse-rate telemetering system, it is necessary only that the channel preserve the rate of impulsing. The relative duration of the "on" and "off" periods is not important.

In the supervisory-control system the duration of the "on" period is approximately twice that of the "off" period. This relation must be preserved in order to allow proper sequential relay operations, some of which occur during the "on" period and some of which occur during the "off" period of the impulse cycle.

The high impulsing speed of the supervisory system and the requirement that the relative duration of the "on" and "off" periods be preserved make it undesirable to use more than one relaying point to retransmit mechanically supervisory impulses received from a distant point.

When the supervisory system operates on an audio-frequency tone channel modulating a carrier transmitter, the tone frequency and the speed of operation of the tone receiver must be such that the supervisory impulses can be handled without appreciable distortion of the "on" and "off" periods. In the line of tone equipment described in reference 1, a number of tones suitable for supervisory operation are available. This makes it possible to combine supervisory control with telephone communication, with suitable filters to prevent interference between the two functions. The filters are inserted into the speech circuits and eliminate the supervisory tone frequency from the speech frequencies transmitted.

There are two types of Visicode supervisory control, one in which all the equipment to be controlled is located at a single point, and one in which the equipment is in several groups at different locations. These two types are referred to as the single-station and multistation systems, respectively.

A fundamental requirement of the multistation system is that a control or supervision function in progress between the dispatching office and a controlled station should not be interfered with by supervisory signals from other controlled stations. This requirement is met by assigning different group codes to each station and arranging each station so that reception of a group code not associated with it locks out the supervisory equipment at that station. Initiation of a supervisory function by any station is prevented before completion of the first impulse of a received group-selection code, which is the first series of impulses transmitted for either a control or supervision function. Complete lockout is effected at the end of this series of impulses. After complete lockout, stations not involved in the function in progress can neither send nor respond to supervisory impulses until the reset signal is received. Any automatic operations of equipment that occur while a supervisory function is in progress are reported as soon as the channel is cleared by the reset signal.

There is a possibility that two or more controlled stations will start transmitting almost simultaneously to report automatic operations. In such a case it is necessary that the impulses from all such stations be synchronized with each other, so that the dispatching office and other stations will receive a coherent code. The actual code received by the dispatching office in such a case will be the longest code of those being sent, and those stations which send shorter codes will be locked out by the extra impulses. When the channel is cleared by the reset signal, they will again start reporting by repeating their group-selection codes.

These requirements can be met by using external stepping and arranging the system so that every station receives its own signals as well as the signals of every other station. In this way synchronism of impulses is assured, because the impulsing of any station is governed by impulses which may be sent simultaneously from other stations.

In general, multistation supervisory control can be combined only with other noncontinuous carrierfunctions. Continuous functions, such as telemetering and load control, are excluded by the requirement that all stations receive all signals. Transmission of a continuous carrier from any station would prevent that station from receiving supervisory signals in a single-frequency system and might prevent other stations from receiving them in a two-frequency system.

When supervisory control is combined with communication on a multistation channel, the system must be arranged so that when one function is in progress it locks the other out. Communication must be locked out at all stations by the first supervisory impulse from any station. Lockout must continue until the supervisory operation is completed. Furthermore, the supervisory system at all stations must be locked out by communication from the moment the carrier is placed on the channel for ringing until the channel is released.

For single-station supervisory systems on point-to-point carrier channels, the requirements are somewhat less strict than for multistation systems, and the number of possible combinations is greater. Internal stepping can be used in single-station systems, and it is necessary only that a signal transmitted from one station be received at the other station. It is not essential that the transmitting station receive its own signals.

When supervisory control is operated over a carrier channel provided for its exclusive use, external impulsing with an unmodulated carrier signal normally is used. For this type of operation the transmitters and receivers at all locations operate on the same frequency, and all stations receive each other. Modifications of this arrangement must be made in some cases in order to combine the supervisory system with other functions.

Combination of Single-Station Supervisory Control With Other Functions on Point-to-Point Carrier Channels

1. *Supervisory Control and Relaying.* Carrier relaying normally is operated on an unmodulated carrier, with the carrier transmitter and receiver at each terminal set at the same frequency; thus all carrier signals from either station are received at both stations. It is possible to combine supervisory control with relaying on such a carrier channel without making any fundamental changes in either the carrier equipment or the relaying equipment. Since the channel issued for relaying only during fault conditions, it is normally free for use by the supervisory system. The relaying circuits must be arranged to take preference over any supervisory operation which may be in progress when a fault occurs.

This arrangement provides a simple method of combining relaying and supervisory control. However, the two functions are not entirely independent. The fact that both the relaying and the supervisory-control systems operate on straight carrier means that all relaying impulses are received by the supervisory equipment. If the supervisory system is at rest when the relaying equipment operates, it will be stepped off normal, making it necessary for the operator to reset it after each relaying operation. Likewise, if an automatic operation is being reported by the supervisory system when the relaying system operates, the supervisory signal will not be completed, and the operator must reset the equipment before the automatic operation can be reported. Starting of the carrier transmitter at either station for testing also must be followed by resetting of the supervisory equipment.

2. *Supervisory Control and Communication.* Supervisory control can be combined with communication of either the single-frequency push-to-talk or the two-frequency duplex type. The simplest way to make this combination is to make the communication function a point on the supervisory system. A contact in the telephone hook switch takes the place of the point-selection key which normally appears on the operator's supervisory-control board. Picking up of the telephone at either end sets the supervisory system into operation to select the corresponding telephone point at the other end of the channel. This rings the telephone bell at the other end. When the call is answered, circuits are set up through the hook switches to lock out the supervisory equipment until the telephones are restored. This system requires no audio-tone equipment but is suitable only for applications where telephone extensions are short, because of the number of separate circuits required in such extensions.

Standard two-frequency duplex carrier-communication assemblies use hybrid coils to combine receiver-output and transmitter-input circuits so that two-wire telephone extensions can be used. Supervisory control can be combined with such a system in such a way that the two systems are completely independent. This can be done by operating the supervisory system on an audio tone with tone-blocking filters to eliminate the supervisory tone frequency from the speech on the channel. A block diagram of this arrangement is shown in Figure 2.

3. *Supervisory Control and Telemetering.* The combination of supervisory control with continuous telemetering requires two carrier frequencies. The telemetering equipment is operated on an audio tone, modulating the carrier frequency, and at the station where the telemetering impulses orginate the supervisory system also must operate on an audio tone. At the other station, the supervisory equipment can operate on unmodulated carrier. This arrangement permits telemetering to continue during a supervisory operation. A number of different quantities can be telemetered continuously by using a different tone frequency for each.

The supervisory system itself can provide telemetering of one quantity at a time for short periods without the use of audio tones. In this case each telemetering function is made a point on the supervisory system and is selected by the operator in the same way a point is selected for a control function. After the operator has taken the required readings, he must reset the supervisory system so that automatic operations can be reported. This

Figure 3. Combination of supervisory control with carrier relaying, communication, continuous telemetering, and load control

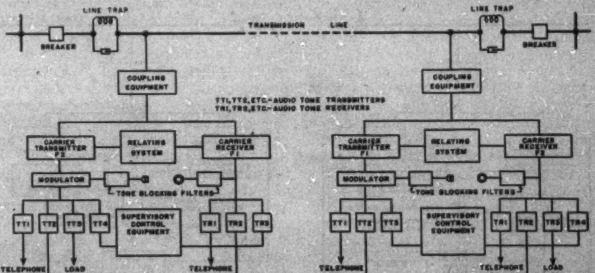

system, called selective telemetering, requires no audio tones in single-station supervisory systems and can operate on a single-frequency channel.

4. *Supervisory Control and Load Control.* The system described for continuous telemetering can be used for load control. The channel requirements are very similar, except that load control is necessarily a continuous function.

5. *Supervisory Control, Relaying, and Communication.* A limited form of carrier communication often is provided with carrier relaying equipment. Supervisory control best can be combined with these two functions by making the communication function a point on the supervisory system, as has been described for the combination of supervisory control with communication only. With some relaying systems a two-frequency duplex arrangement can be used, although the single-frequency system usually is used with carrier relaying.

6. *Supervisory Control, Relaying, and Continuous Telemetering or Load Control.* The requirements for this combination are the same as those described for the combination of supervisory control with continuous telemetering, that is, a separate carrier frequency must be used for transmission in each direction. This requires that the relaying system be capable of operating on such a channel.

7. *Supervisory Control, Communication, and Continuous Telemetering or Load Control.* Two carrier frequencies are required for this combination. The telephone ringing function can be performed either through the supervisory system or by using a separate tone frequency for the purpose. If the supervisory system is used for ringing, audio-tone transmitters are required for the supervisory system at the station at which telemetering and load-control impulses originate but not at the other station. Tone transmitters are required also for the telemetering or load-control function. If a separate audio tone is used for ringing, the supervisory system requires a separate tone transmitter and receiver at each station, regardless of the requirements imposed by the transmission of continuous telemetering and load-control impulses. In all cases, high-pass filters must be used to eliminate from the channel those voice frequencies which would interfere with the proper operation of the functions which use audio tones.

Figure 4. Multistation communication and supervisory control, with communication through a point on the supervisory-control system

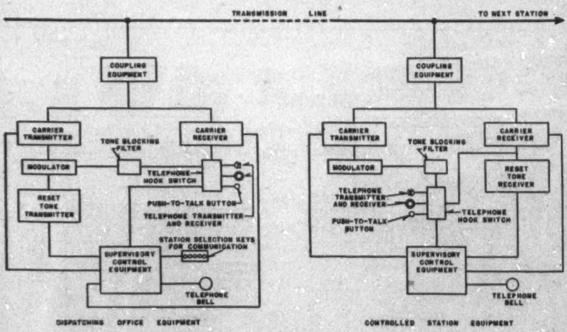

8. *Supervisory Control, Relaying, Communication, and Continuous Telemetering or Load Control.* The requirements for this combination are the same as those described for combination 7, with the additional requirement that the relaying system be capable of operating on a two-frequency channel. The relaying system, of course, must be arranged so that it can take control of the carrier from all other functions when a fault occurs.

This combination includes all the functions that have been considered. The block diagram of Figure 3 shows all the important components required to perform these functions with a single carrier transmitter and receiver at each terminal.

Combination of Multistation Supervisory Control With Other Functions

It has been pointed out that it is not possible to have continuous telemetering or load control in combination with multistation supervisory control on a single carrier channel. Certain considerations also make it inadvisable to consider the combination of multistation supervisory control with relaying on consecutive relaying channels. A separate carrier channel is required for each line section for carrier relaying, in order to prevent the possibility of false blocking of relaying signals. This means that any combination of supervisory control with relaying, in which the supervisory system extends beyond the line section protected by the relaying channel, requires the use of electronic or mechanical repeaters. The complexity of any such repeaters that would meet the requirements outlined for multistation supervisory control makes it preferable to use an entirely separate carrier channel for the supervisory-control system. It would be possible, however, to use a single set of coupling equipment for both the relaying and supervisory transmitters and receivers at each station.

1. *Single-Frequency Communication Through a Point of the Supervisory System.* Push-to-talk communication between the controlling or dispatching office and any controlled station on the supervisory system can be obtained by using a point on the supervisory system to provide selective ringing to each controlled station, and from controlled stations to the dispatching office. Since the supervisory-control system is intended only for selective functions between the dispatching office and controlled stations, and not between controlled stations, this system is limited to communication between the dispatching office and controlled stations only. Controlled stations cannot communicate with each other. This is no disadvantage, because the controlled stations of a supervisory system normally are unattended, and there would be no necessity for establishing communication other than that provided between the dispatching office and a controlled station.

In this system, the use of the supervisory equipment to perform the communication functions assures that the supervisory equipment is locked out at all stations until the conversation is completed.

The main components of this system are shown in the block diagram of Figure 4. A tone transmitter is used at the dispatching office for transmitting the reset signal. The usual method of resetting the supervisory system is the transmission of a long carrier impulse. This method cannot be used in a multistation system with communication because the placing of carrier in the channel for communication would be recognized by the supervisory equipment at all stations as a resetting impulse. The use of a tone to modulate the carrier for resetting provides a means of discrimination between a reset signal and carrier placed on the channel for communication. The tone-blocking filters are used to eliminate the resetting tone frequency from the speech before it is placed on the channel.

To call any one of the remote stations from the dispatching office, the operator picks up the telephone handset and operates the telephone selection key for the station to be called. The supervisory system transmits the group-selection code, which is returned by the remote station. The point-selection code is then transmitted from the dispatching office. Reception of this code at the called station rings the bell at that station. The point check code is not returned from the called station until the handset at that location is picked up. Reception of the point check code at the dispatching office indicates that the call is completed and establishes the push-to-talk communication circuits.

When the telephones are restored at the conclusion of the conversation, the resetting tone automatically is transmitted to reset the entire system to normal. Any automatic operations that have taken place at any point on the system during conversation then will be reported.

Communication is established in a similar manner from controlled stations. These stations communicate only with the dispatching office, and individual selection keys for calling are unnecessary. The telephone hook switch can be used to initiate operation of the supervisory system to call the dispatching office. Reception of the group- and point-selection codes at the dispatching office rings the telephone bell. When the operator picks up his handset, the point check code is transmitted, establishing the push-to-talk circuits at both stations. Resetting at the end of conversation is accomplished as before.

It is possible to obtain selective telemetering with this system without additional carrier equipment. The telemetering impulses are transmitted by unmodulated carrier, and resetting is accomplished by a modulated carrier impulse as before.

2. Two-Frequency Duplex Communication Through a Point of the Supervisory System. A two-frequency duplex form of communication can be obtained with a system very similar to that described under item 1. The equipment required is the same as that shown in Figure 4. The limitations given with regard to communication among controlled stations apply also to this system. In this case, the dispatching-office transmitter operates on a frequency F_1, which is received at all controlled stations. Internal stepping is used at the dispatching office. All controlled stations transmit on a second frequency F_2, which is received at the dispatching office. The requirment that all stations receive all signals is met by allowing the receiver at the dispatching office to key the dispatching-office transmitter; thus a signal sent from any controlled station is received at all stations, and external stepping can be used at the controlled stations. The procedure for establishing communication is the same as for the single-frequency system.

3. Semi-Independent Supervisory-Control and Two-Frequency Duplex Communication. The systems described under items 1 and 2 provide the combination of communication and supervisory control with a minimum of equipment. These systems are subject to the limitation that telephone extensions must consist of a number of conductors and be continuous metallic circuits. This limits the length of the extensions that can be used. It is occasionally desirable to use long two-wire telephone extensions, and such extensions may include insulating transformers which would interrupt d-c control paths.

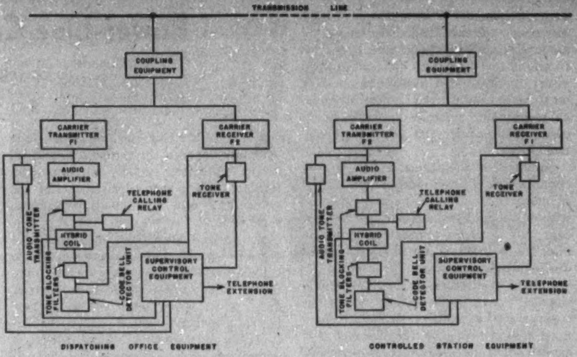

Figure 5. Semi-independent multistation supervisory-control and two-frequency duplex communication

The block diagram of Figure 5 shows the component parts necessary to combine supervisory control with a standard two-frequency duplex carrier communication assembly to provide semi-independent operation of the communication and supervisory systems. Two-wire telephone extensions are used. This system, like the others described, provides for communication between controlled stations and the dispatching station only, and not for communication among controlled stations.

The system is arranged so that the use of the carrier assembly for communication locks out the supervisory system at all stations, and vice versa. The supervisory system operates on an audio tone, which is received from a controlled station on frequency F_2 at the dispatching station and retransmitted on frequency F_1 to other stations on the system. Tone filters remove the supervisory-tone frequency from the voice frequencies transmitted.

When carrier is placed on the channel on either frequency for telephone ringing and subsequent communication, a relay at each location prevents the supervisory equipment from starting. Lockout continues until communication is completed. On the other hand, reception of the first supervisory impulse at all stations opens the telephone extension circuits to lock out all communication until the supervisory operation is completed.

The addition of selective telemetering to this system requires the use of a separate tone transmitter at the dispatching office and a separate tone receiver at each controlled station for resetting.

4. Multistation Single-Frequency Communication and Supervisory Control. In automatic simplex carrier-communication assemblies, the receiver is blocked during periods when the transmitter is in operation.[3] The fundamental requirement that external stepping be used in multistation supervisory-control systems makes it necessary to provide an additional carrier receiver at each station for the use of the supervisory equipment when this type of communication is combined with supervisory control. A tone transmitter and receiver are required for the operation of the supervisory system at each station in order to provide discrimination between carrier placed on the channel for communication and that placed on the channel for supervisory control. The use of tone equipment requires that tone-blocking filters be used in all speech circuits to prevent speech frequencies from impulsing the supervisory system.

With the equipment described, a combined system could be provided in which the presence of a carrier signal on the channel for communication purposes would lock out the supervisory system at all stations until the carrier is removed after a pause in speech. The system would have to be arranged so that when the supervisory equipment begins to transmit impulses, communication is locked out at all stations until the supervisory function is completed. The latter requirement would make it necessary to provide special means to lock out communication at all stations on the communication system that are not part of the supervisory system.

In general, automatic simplex communication equipment is intended for high-quality communication, and it is undesirable to modify the audio channels in such equipment by the addition of tone-blocking filters. Furthermore, the amount of additional equipment required to adapt the system to combined supervisory control and communication in most cases would make it more economical to provide a separate single-frequency carrier channel for the supervisory-control system.

Similar considerations apply to the combination of semi-independent single-frequency manual simplex communication with multistation supervisory control, except that in such communication assemblies the receiver is not always disabled during transmission.

In both the automatic and the manual simplex systems, the locking out of the supervisory equipment would depend upon the presence on the channel of a carrier not modulated by the supervisory tone. At each pause in conversation this carrier would be removed, unlocking the supervisory control until transmission is resumed for communication. The possibility would exist that the supervisory system at one station would start transmitting at the same time that another station places carrier on the channel during communication. The latter station would not receive the supervisory impulses under these circumstances and might prevent proper reception of the impulses at one or more other stations. The supervisory equipment at some stations would not be locked out by the first group code under these conditions, a fundamental requirement for multistation operation.

Consideration has been given to means of locking out the supervisory equipment at all stations continuously during an entire communication period, irrespective of the presence of carrier on the channel. However, the amount of equipment involved in such schemes is considerable, and the arrangements are complicated.

These considerations lead to the general conclusion that, although multistation simplex communication and supervisory control can be combined in a single channel, it is advisable to use separate channels for these functions with joint use of coupling equipment only.

Conclusions

Single-station supervisory-control systems on point-to-point carrier channels can be combined in almost any desired combination with relaying, telemetering, load control, or communication. Internal stepping of the supervisory system can be used. Two-frequency carrier channels are required for the combination of supervisory control with continuous functions, such as telemetering or load control.

In multistation supervisory control systems, all stations must receive all signals, and external stepping of the supervisory system is required at all controlled stations. Continuous carrier functions cannot be combined with supervisory control on single-frequency carrier channels. Certain combinations of multistation supervisory control with relaying and communication equipment are not practical, for reasons that have been given. Methods of combining multistation supervisory control and certain types of communication in practical systems have been described.

References

1. A Versatile Power-Line Carrier System, H. W. Lensner, J. B. Singel. AIEE Transactions, volume 63, 1944, March section, pages 129–32.

2. Possibilities and Methods of Extending a Carrier-Current Relaying Channel to Other Uses, R. M. Smith, S. L. Goldsborough. AIEE Transactions, volume 60, 1941, January section, pages 23–7.

3. Electronic Switching Simplifies Power-Line Communication, J. D. Booth. *Electronics*, volume 15, May 1942, pages 44–7.

Power-Line Carrier Channels

M. J. BROWN
MEMBER AIEE

A POWER-LINE carrier channel as the link between the transmitter and receiver of a carrier system, determines, by its losses, the power requirements of the transmitter and the sensitivity of the receiver.

An understanding of the operation of carrier channels and an approach to the calculation of losses to be expected were set forth early in the application of carrier currents to power lines. However, experience with power-line carrier installations has added much to our knowledge of actual line losses. Likewise, the methods used to apply carrier to the lines follow uniform practice, and the devices employed are reliable in performance. The losses introduced by their use are well understood.

As the art progresses, new applications are made, involving factors not previously of importance. Practical experience gained in these applications supplement the initial calculations, but the calculations must come first, and both theory and empirical data are of importance.

At the present time a stimulus has been given power-line carrier activities by the introduction of audio-frequency tones for extended use of a single-channel frequency modulation as a means of limiting effects of interference, and single-sideband transmission as a method of increasing the number of useful channels. Channels will be established on lower-voltage lines to an increasing extent.[1,2,3]

In the interest of a better understanding of the factors which must be considered in the extension of power-line carrier applications, the following discussion of theoretical and practical experience is offered.

High-Frequency Transmission-System Losses

The transmission lines of a power system become high-frequency transmission lines when power-line carrier is applied to them. Factors which are not a consideration at power frequencies become important to a degree that they must be taken into consideration at carrier frequencies if an entirely workable system is to be designed.

Transmission losses are proportioning functions. That is, the received signal strength is only a fraction of the transmitted signal strength, and that fraction is numerically equal to the product of fractions expressing the transmission characteristics of the various components in the circuit. If the logarithm of these fractions, based on the ratio of power in to power out, is used instead of the actual ratio itself, these logarithms may be added to obtain a logarithm representing total loss. This is a convenience, because the addition of these figures is simpler than the multiplication of loss ratios. The decibel is the unit used in these calculations and is numerically expressed as follows:

$$\text{db} = 10 \log_{10} \frac{P_1}{P_2}$$

where

db = decibels loss (attenuation)
P_1 = power into a device
P_2 = power out of a device

If the loss encountered in each series device of a transmission system is expressed in decibels, then the total loss in decibels is the sum of the losses in decibels. Therefore, if it is known that a transmitter–receiver combination works successfully through an attenuation of a specific number of decibels, the system will be workable if the total losses encountered are less than this value. As the transmitter power is increased, the number of decibels that it will work

---

Paper 45-78, recommended by the AIEE committee on power transmission and distribution for presentation at the AIEE winter technical meeting, New York, N. Y., January 22–26, 1945. Manuscript submitted November 25, 1944; made available for printing January 2, 1945.

M. J. Brown is design engineer, switchboard engineering department, Westinghouse Electric and Manufacturing Company, East Pittsburgh, Pa.

through, with a given receiver, increases. Likewise, as receiver sensitivity is increased, the attenuation through which it will operate successfully with a given transmitter increases.

Obviously there are economical limits of transmitter size and limits on interference-free receiver sensitivity. Thus transmitter–receiver combinations in practical use are not numerous. The lower-powered combinations are designed to operate through losses up to 30 decibels, and the more elaborate equipment is rated correspondingly higher.

High-Frequency Transmission Lines

A transmission line for high frequency can be considered ideally as an infinitely long pair of equally spaced wires of the same diameter throughout, supported in free space without inductive or capacitive coupling to other circuits. Lines of this type have been treated mathematically on the basis that they are composed (Figure 4) of an infinite number of resistors and inductors in series and having an infinite number of capacitors and resistors shunting the lines at equally spaced points along the lines.[4]

Several important concepts are derived from this treatment. One is that an infinitely long transmission line, because it cannot reflect energy back toward the transmitting end, displays a characteristic impedance that is a function of the resistance, inductance, leakage, and capacitance of a unit length. Quantitatively this impedance is as follows:

$$Z_0=\sqrt{\frac{R+j\omega L}{G+j\omega C}}$$

where

R = ohms resistance per unit length
L = henrys inductance per unit length
G = mhos conductance of leakage per unit length
C = farads capacity per unit length
$\omega = 2\pi f$ where f is frequency in cycles

Now if the transmission-line conductors are severed at a finite distance from the sending end, the impedance displayed by the remaining infinite section is still the characteristic impedance of the line. It follows then that if we terminate a finite length of transmission line with an impedance equal to the characteristic impedance of the line, then no reflections will be received at the sending end, since this was the case when the finite section was terminated with the infinite line. This is another important concept employed in power-line carrier systems. The impedance of the receiving system must be equal to the characteristic impedance of the line if the sending end is to be free of received reflections.

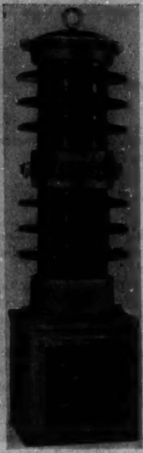

Figure 1 (left). Terminal equipment for two single-line-to-ground power-line carrier channels on a 69-kv line

Figure 3 (right). A single-phase suspension-mounting by-pass unit for bridging an autotransformer in a line

It is an interesting commentary at this point to note that the transmitter internal impedance, as viewed from the line through the transmitter output transformer is also related, in best practice, to the characteristic impedance of the line although for a different reason. The transmitter operates most efficiently from the standpoint of high carrier output and low harmonic output when its internal impedance and its load impedance are properly proportioned. A ratio of load impedance to tube impedance of 2 to 1 was shown by Hanna, Sutherland, and Upp, as being most efficient for triodes, whereas Pidgeon shows that ratios of 1 to 3 to 1 to 10 are common practice for pentodes.[5,6]

Since the R and G terms in the formulas for characteristic impedance are negligible in open-construction power lines, because the resistance and leakage are low compared to the reactance components, the

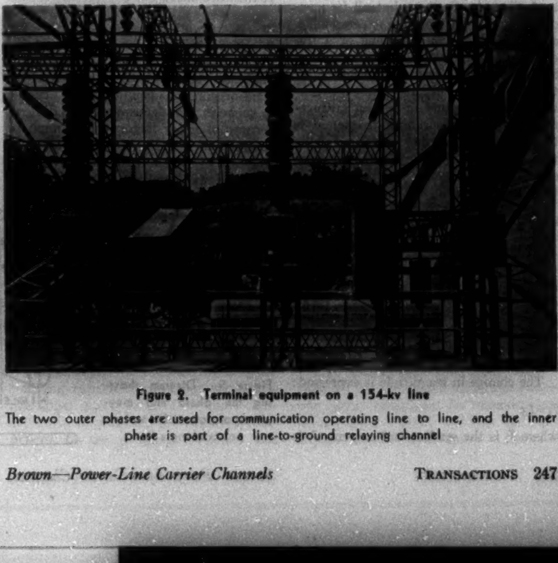

Figure 2. Terminal equipment on a 154-kv line

The two outer phases are used for communication operating line to line, and the inner phase is part of a line-to-ground relaying channel

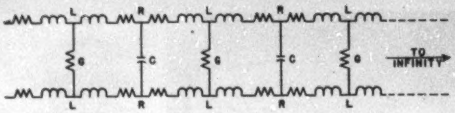

Figure 4. The equivalent diagram of the infinite line

formula for characteristic impedance simplified into

$$Z_0=\sqrt{\frac{}{C}}=276\log_{10}\frac{2D}{d}$$

where D is the distance between conductors, and d is the diameter of the conductor.[7]

Ordinary high-voltage transmission lines display characteristic impedances of 800 to 850 ohms for line-to-line channels and about 500 ohms for line-to-ground channels. Power cable will display an impedance in the order of 25 ohms. Even lower impedances are encountered in some special carrier installations, such as train communication, where track to ground leakage is high, and impedances in the order of 3.5 to 7 ohms are experienced.[8]

It long has been standard practice to isolate spur lines by series line traps to prevent attenuation due to reflections received from the end of the spur line.

Therefore, an attempt is made to terminate each carrier channel in the characteristic impedance of the line, and on spur lines where it is not possible to do so the line is isolated.

While this may appear to be an ideal treatment, it is approached in practice on relaying channels which extend from only one end of a transmission-line section to another. Channels used for communication, telemetering, and supervisory control, however, may be carried through a considerable network and have many terminals. Such systems often cannot be made free of reflections, but all frequencies of transmission are not affected alike, and a selection can be made of a frequency least affected by reflection losses. System switching operations which alter the carrier channels also must be considered in the study of system arrangement when the optimum frequency is being selected. Further, undesired paths through parallel lines and into spur lines should be eliminated by putting line traps in series with such lines.

The Attenuation of Carrier Frequencies in Transmission Lines

A further study of the infinite transmission line reveals that carrier current which is applied at the transmitting end of the line changes in both phase and magnitude as it progresses along the line.

The change in magnitude is expressed:

$$I_2=I_1\epsilon^{-\alpha X}$$

where I_1 is the sending-end current, I_2 is the current at a point X distance in miles from the sending end, and α is the attenuation constant.

The phase position is shifted backwards as the distance from the sending end increases. The position is given by the equation:

$$I_2=I_1\epsilon^{-j\beta X}$$

where β is the wave-length constant. It is the number of radians per mile which the current vector is shifted backwards. These may be combined to give the complete expression:

$$I_2=I_1\epsilon^{-X(\alpha+j\beta)}=I_1\epsilon^{-Px}$$

and, since the characteristic impedance is a pure resistance, the voltages may be expressed as

$$E_2=E_1\epsilon^{-X(\alpha+j\beta)}=E_1\epsilon^{-Px}$$

where E_1 is the sending-end voltage, E_2 is the voltage at a point X miles from the sending end, and P is the propagation constant which is equal to $(\alpha+j\beta)$. Figure 5 is a graphical representation of conditions along a transmission line carrying a high-frequency current.

Of particular interest in estimating the expected losses due to line attenuation is the attenuation constant, α. Its more complete form is simplified for the transmission-line case when leakage is considered negligible compared to resistance and both leakage and resistance are considered negligible compared to reactance. It then becomes:

$$\alpha=\frac{R}{2Z_0}=\frac{R}{2}\sqrt{\frac{C}{L}}$$

The resistance R is the resistance of the transmission-line conductor at carrier frequencies. Its determination is difficult because of many factors which must be considered in skin-effect calculations. The case of solid and tubular conductors has been well studied, and reliable formulas have been developed for determining radio-frequency resistance.[9] B. R. Teare and Josephine R. Webb have shown that copper-clad steel conductors have a resistance substantially equal to the tubular copper portion alone for frequencies up to 160 kilocycles.[10] However, stranded transmission-line conductors introduce many factors, such as number and size of strands, that all have an effect on high-frequency resistance. Unfortunately, the solid conductors about which the skin-effect literature has been most concerned is the exception rather than the rule in transmission-line construction, and thus the formulas offered do not apply in many cases. Experience with concentric stranded cable has shown that new cable with bright conductors shows a definitely lower high-frequency resistance than that with weathered conductors. It has been suggested that in the first case the current travels from conductor to conductor in a direction parallel to the axis of the conductor and in the latter case must spiral around the axis of the cable, following the convolutions of the outer conductors, since corrosion prevents passage from one conductor to another.

Literature dealing with power-line carrier attenuation has repeatedly indicated that attenuation experienced on lines has been in excess of the calculated attenuation. Boddie and Curtis stated that measurements on a number of lines indicated that the actual line resistance was about 250 per cent of the calculated value. Their calculations assumed that stranded conductors were equivalent to solid conductors of the same copper cross section. Likewise, Laughlin, Pakala, and Reagan reported losses on the Boulder Dam lines of five times calculated losses.[11] The latter reference used the formula for tubular conductors in determining the high-frequency resistance of the line conductors. Actually the Boulder Dam conductors are tubes made of flat interlocking segments spiraled along the axis of the conductor. Some variation from the tubular-conductor formula results should be expected in this case; however, it seems doubtful that the entire discrepancy between calculated loss and actual loss was due to an error in the determination of conductor resistance. The authors point to the possibility of losses in

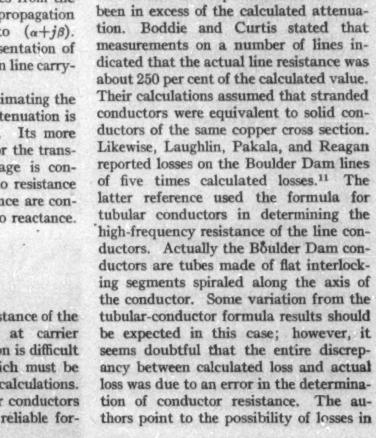

Figure 5. Diagram showing the phase and magnitude of potential at various points along a line

other phase conductors and the ground circuits being responsible.

While an exact evaluation of attenuation by calculation has not proved to be entirely successful, empirical data have been accumulated that allow the engineer to estimate the attenuation to be expected on ordinary lines. One simple formula that can be applied with reasonable accuracy for attenuation of power-line carrier in the 50- to 150-kilocycle range on lines of 34.5 kv and above is as follows:

$$\text{db per mile} = k[0.01 + (\text{kc} \times 10^{-3})]$$

where kc is the frequency in kilocycles and *k* is a multiplying factor of 1.6 for line-to-ground coupling and 1.3 for line-to-line coupling. This expression will predict higher losses than will be encountered in most instances and thus afford a factor of safety in its use. Rives offers curves for attenuation in the range from 30 to 200 kilocycles.[12]

Although it was pointed out that the best practice dictates terminating a line in its characteristic impedance to prevent reflections, the complex nature of the receiver circuit impedances makes it difficult to be assured that a line is so terminated. Consequently, attenuation curves run on actual installations will not show a smooth variation in attenuation with frequency.

Coupling Losses

The carrier energy in flowing from the transmitter terminals to the power line encounters losses in the coaxial cable, coupling capacitor, and line-tuning units, and upon arrival on the line is offered a shunt path through the line trap to a return circuit of widely varying characteristics. It is, therefore, of interest to determine losses in the coupling equipment, since these losses at both the transmitting and receiving end must be added to the line losses.

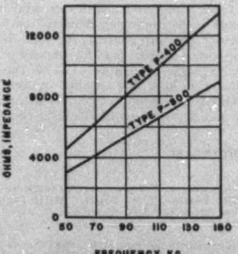

Figure 6. Impedance at resonance for typical single-frequency line traps

Double-frequency tuning reduces the peak impedance about 50 per cent. Values taken from this curve are used directly with either the single- or double-frequency impedance curves of Figure 7. Type *P*-400 is 400-ampere size, and type *P*-800 is 800-ampere size

The line-tuning unit and coupling capacitor are adjusted on installation to be resonant with each other at the operating frequency. Therefore, the losses in the line-tuning unit are related to the capacitance value of the coupling capacitor, because this value determines how much inductance is required. If constant *Q* for the line-tuning unit is assumed, the coil losses are proportional to its inductance. In the range from 15 to 345 kv, the capacitive reactance of standard coupling capacitors varies from 320 to 4,250 ohms at 50 kilocycles, and correspondingly less at the higher frequencies. Table I shows the approximate total resistive component of standard-size coupling capacitors and their resonating inductances. The values of capacitor power factor and coil *Q* generally will differ in actual practice for a specific application from those used in the table. Therefore, the table should be used only for estimating purposes.

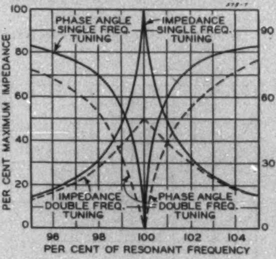

Figure 7. Resonance curves for typical line traps

The losses of the coil and capacitor add in this circuit to give a resistive component of about six per cent of the capacitive reactance; consequently, the equivalent series resistance for these two devices is between 20 ohms at 50 kilocycles for a 15-kv capacitor and 320 ohms at 50 kilocycles for a 345-kv capacitor.

Obviously, the losses will be negligible if the ratio of this resistive component to the characteristic impedance of the line is small, as it is in most cases. If the ratio does not exceed 1 to 5, the loss will be one decibel or less. However, coupling into a cable which has a low characteristic impedance, through a high-voltage capacitor, will introduce losses that must be taken into account.

For example, in the case of a 69-kv coupling capacitor operating through a line tuner into a cable of 25 ohms characteristic impedance, the resistive component of the coupling capacitor and tuner will be 70 ohms, and the losses will be six decibels.

Table I. Approximate Equivalent Resistance of Resonated Coupling-Capacitor Circuits

Line Couplers or By-Pass Equipment
Capacitor Power Factor = 4 Per Cent

$$\text{Coil } Q = \frac{\omega L}{R} = 50$$

$$R = X_C(\text{Power Factor} + 1/Q)$$

System Voltage, Kv	Coupling-Capacitor Value, μf	Reactance at 50 Kc	Approximate Equivalent Resistance R, Ohms at 50 Kc
15	0.01	320	20
23	0.0075	430	25
34.5	0.005	640	38
46	0.004	800	48
69	0.00275	1,160	70
92	0.002	1,600	96
115	0.00187	1,700	104
138	0.00137	2,320	139
161	0.00125	2,550	153
196	0.00094	3,390	203
230	0.00094	3,390	203
287.5	0.00075	4,250	255
345	0.0006	5,300	320

By-Pass Equipment

A by-pass unit is simply one or more coupling capacitors with their associated line-tuning units.

If an autotransformer in a line must be by-passed, only one capacitor and line-tuning unit are required; however, if a breaker is to be by-passed, a coupling capacitor and line-tuning unit on each side of the breaker are required with drain coils to ground at the interconnection between the line-tuning units. The drain coil avoids power-frequency charging current being put on a de-energized line.

The losses will be the same as for an equivalent number of coupling capacitors and line-tuning units, and like coupling capacitors will be of added importance on lines of low characteristic impedance.

Coaxial Transmission Lines

Coaxial cable is used in many installations as the means of carrying transmitter power through the switchyard to the line-tuning equipment and coupling capacitor. Likewise, it serves as a channel for the received signal coming into the receiver and as an interconnection between units of a by-pass arrangement.

Such runs occasionally are in excess of 1,000 feet but usually only a fraction of this. The cable losses increase with frequency. At 150 kilocycles the loss is 0.5 decibel per 1,000 feet in the type of cable in ordinary use.

The transformer equipment that is supplied by the manufacturers of power-line carrier equipment for matching into these cables is highly efficient and fully adjustable, so that the input to the cable

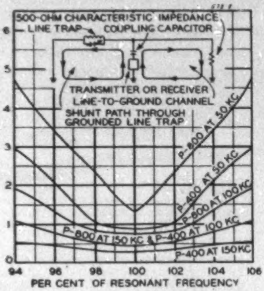

Figure 8. Losses in 400-ampere (type-*P*-400) and 800-ampere (type-*P*-800 single-frequency line traps when a line-to-ground carrier channel of 500 ohms characteristic impedance is short-circuited through line trap

and output from it can be matched properly to the cable characteristic impedance, and no loss is encountered from mismatch conditions.

Power-Line Carrier-Line Traps

The attenuation due to line traps varies with the type of trap, the method of tuning (single or double frequency), the relation between the frequency being transmitted and the resonant frequency of the trap, and the conditions of the line beyond the trap.

The high-frequency current, after leaving the transmitter and the line-tuning unit, passes through the coupling capacitor to the transmission line as shown in Figure 8. The current is divided into two parts, one part continuing down the line toward the distant terminal and the other part passing through the line trap. In Figure 8 it is assumed that the line beyond the trap has zero impedance. Actually, the line beyond the trap can be any impedance from zero to nearly infinity and can be either resistive, capacitively reactive, or inductively reactive. The total reactance of the shunt path is the vector sum of the line-trap impedance and return-path impedance.

The line trap being a parallel resonant circuit displays an impedance which is a complex quantity whose components vary with frequency. The peak impedance at resonance increases with frequency as shown in Figure 6. On either side of resonance the impedance drops off as shown in Figure 7. The phase angle of the impedance also is shown on Figure 7. The impedance of the trap is inductively reactive below resonance and capacitively reactive above.

Consequently the sum of the line-trap impedance and the return-path impedance conceivably can be any combination of reactance and resistance within the limits of these two elements. It can be conceived that the reactive component of the line trap can resonate with an equal reactive component of opposite sign displayed by the return circuit, thereby cancelling out the reactive components and leaving only the resistive components. If the line showed low resistance, this condition would produce a shunt path of low impedance with high attenuation. While theoretically possible, it is unlikely that this condition will be experienced in practice. However, the condition where the return path is of zero impedance can be approached and for practical purposes may be considered as the extreme condition.

The attenuation of the carrier signal by the shunt path through the line trap is shown in Figures 8 and 9. It will be seen that, as the carrier frequency departs from the resonant frequency of the trap, it suffers more attenuation. Likewise, the double-frequency line traps do not offer so much impedance as the single-frequency traps, and therefore the attenuation is higher. The 400-ampere traps because of their higher impedance show less attenuation than the 800-ampere traps.

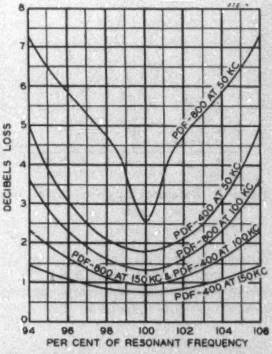

Figure 9. Losses in 400-ampere (type-*PDF*-400) and 800-ampere (type *PDF*-800) double-frequency line traps when a line-to-ground carrier channel of 500 ohms characteristic impedance is short-circuited through line trap

These curves are based on the assumption that the transmitter is a constant-current generator, operating into a load impedance consisting of the line trap in parallel with the 500-ohm characteristic impedance of the line. The power into the 500-ohm branch decreases as the impedance of the line trap decreases. The constant-current characteristic is approached closely by a transmitter whose internal impedance is high compared to the load impedance, as is the case with transmitters having pentodes in the output stage.

Examination of the circuit of Figure 8 will show that, if a receiver is considered instead of a transmitter, the results will be the same, and the curves are valid for the receiving end as well as the transmitting end. In this case, the line is the current source, and the receiver can be assumed to be a 500-ohm load paralleled by the line trap.

It should be noted that these curves are not for normal operating conditions but for a condition which for practical purposes may be considered as producing the most attenuation. This condition is of importance in carrier relaying, because the channel over which a blocking signal must be transmitted is paralleled by a path through the line trap and an external fault.

Conclusions

1. Although the phenomena of high-frequency transmission are understood, there is still a lack of quantitative information on the high-frequency resistance of transmission-line conductors and ground paths and the losses in the impedance introduced into a channel by coupling with other phase conductors. Power-line carrier-channel losses therefore are more reliably computed from formulas and curves based on empirical data, than from the basic formulas.

2. Coupling capacitors, line-tuning units, and by-pass units normally are of such high efficiency in their operation that their losses may be neglected or appraised at some nominal low value in the order of one or two decibels. However, in special cases such as the operation into lines or cables of low characteristic impedance, consideration of losses in the coupling capacitor, line-tuning units, and by-pass units is required.

3. Line traps ordinarily function with very little loss, but if the channel is short-circuited beyond the line trap, the attenuation becomes appreciable and of increasing magnitude as the frequency departs from resonance. The attenuation for side bands therefore is greater than for the carrier frequency. The calculation of losses through a line trap at a line terminal or spur line should be based on the condition that the channel is short-circuited beyond the trap

References

1. A Versatile Power-Line Carrier System. H. W. Lensner, J. B. Singel. AIEE Transactions, volume 63, 1944, March section, pages 129-33.

2. Frequency Modulation for Power-Line Carrier Current, E. W. Kenefake. AIEE Transactions, volume 62, 1943, October section, pages 616–19.

3. A Comparison of the Amplitude-Modulation, Frequency-Modulation, and Single Side-Band Systems, R. C. Cheek. AIEE Transactions, volume 64, 1945, May section, pages 215–20.

4. Communication Engineering (book), W. L. Everitt. McGraw-Hill Book Company, Inc., New York, N. Y.

5. Development of a New Power Amplifier Tube, C. R. Hanna, L. Sutherlin, C. B. Upp.

Effect of Altitude on Temperature Rise of Aircraft Transformers

V. M. MONTSINGER
FELLOW AIEE

THE PURPOSE of this paper is to present a method of calculating the effect of altitude on the temperature rise of various designs of aircraft transformers which are required to operate at extremely high altitudes.

So far as is known the tests reported in Mr. Kiltie's[1] paper are the first ones that have been made under conditions representing such a wide range in altitude—up to 40,000 feet—on an actual transformer. The fact that there is very close agreement between the calculated values and observed values lends confidence in our ability to calculate the effect of altitude on the temperature rise of other types of electric apparatus, provided, as pointed out later, that the percentages of the loss of heat by convection and by radiation at sea level are known.

The effect of altitude on temperature rise of a simple piece of apparatus like a self-cooled transformer can vary as much as 2.5:1, depending on the per cent of the loss of heat by radiation (dependent on outside envelope of the cooling surface) and the loss by convection (dependent on the total developed area of cooling surfaces), because only the loss by convection is affected by altitude. It is for this reason that no two types of apparatus will be affected alike by altitude.

The effect of altitude on transformers is of course least for one with a plain tank for which at sea level approximately 45 per cent of the total loss is dissipated by convection and 55 per cent by radiation, and greatest where all loss of heat is by convection as from the inside of ventilated windings of dry-type natural-draft transformers.

As the aircraft transformer used for Mr. Kiltie's tests had no ventilating ducts in the winding and whereas most, if not all, of the losses were dissipated to the air from the outside surface, it should follow quite closely the behavior of a plain-tank surface. This is particularly true of the outer coil, since the temperature rises reported were those of the outside surface.

Figure 1 shows temperature rise versus loss of heat by convection and by radiation as calculated by equations shown with Figure 1. The barometric pressures used for ρ were based on equation 11 of reference 2.

As a basis for selecting the tested temperature rises of the coils, it is believed that the average of the rises obtained with and without the Durel mounting plate should be used to compare with the calculated rises. There is not very much difference—the calculated rise being slightly higher than the tested when the mounting plate was used and slightly lower when the plate was not used.

Table I shows a comparison of the tested and calculated rises for the outer coil. The calculated values were obtained by finding the total losses W_c and W_r from Figure 1 that correspond to the sea level temperature rise, and then finding by trial the temperature rise at the higher altitudes that gave the same total losses, the copper loss being corrected for the higher rise at the higher altitude. For example: for 150 degrees-centigrade rise at sea level, Figure 1 gives a total loss of W_c and $W_r = 1.91$ watts per square inch. For 25,000 feet the loss is $1.91 \times 1.055 = 2.02$. A temperature rise of 173 degrees gives, by Figure 1, a total watts per square inch of 2.01.

Table I

Altitude, Feet	Surface Temperature Rise of Outer Coil, Degrees Centigrade: Test*	Calculated	Ratio of Copper Loss
Sea level	150	150 (base)	1.0
12,000	161.5	161.5	1.03
25,000	172.5	173.0	1.055
40,000	180.5	185.0	1.10

*Average of coil rises with and without Durel mounting plate.

There is some uncertainty as to how to calculate the temperature rise of the inner coil, since the internal temperature drop should not be affected by air density to the same extent as the outside surface rise over air is affected. Unless low air pressure affected the internal temperature drop, the increase in temperature rise of the inner coil should be approximately the same number of degrees as found for the outer coil, since most of its loss was probably dissipated to the air from the outside surface of outer coil, some from the edges of the inner coil, and perhaps some by the core.

In Table II are the tested and calculated temperature rises of the inner coil based on the assumption that its rise was increased by altitude the same number of degrees as the outer coil was increased.

Table II

Altitude, Feet	Temperature Rise of Inner Coil, Degrees Centigrade: Test*	Sea-Level Test**	Calculated
Sea level	196.5	196.5+ 0	=196.5
12,000	209.5	196.5+11.5	=208.0
25,000	225	196.5+23	=219.5
40,000	230	196.5+35	=231.5

*Average of rises with and without Durel mounting plate.

**Calculated temperature rise of outer coil over rise at sea level.

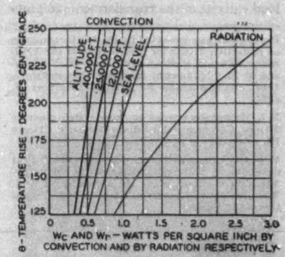

Figure 1. Loss by convection and by radiation

$W_c = 1.4 \times 10^{-3} \times \theta^{1.25} \rho^{0.5}$

ρ = relative air density to sea-level density

$W_r = 3.68 \times 10^{-11} e(T_2^4 - T_1^4)$

e = 0.95 (emissivity factor)

$T_2 = 273+30+\theta$

T_1 = 273+30-degrees-centigrade ambient temperature

Altitude, feet:	Sea level	12,000	25,000	40,000
Relative air density:	1.0	0.662	0.425	0.254

Table II indicates that the internal

Paper 45-75, recommended by the AIEE committee on air transportation for presentation at the AIEE winter technical meeting, New York, N. Y., January 22-26, 1945. Manuscript submitted November 27, 1944; made available for printing January 2, 1945.

V. M. Montsinger is research engineer with the General Electric Company, Pittsfield, Mass.

Proceedings of the Institute of Radio Engineers, 1928.

6. Theory of Multielectrode Vacuum Tubes, H. A. Pidgeon. AIEE Transactions, volume 53, 1934, pages 1485-98.

7. C. A. Boddie. Institute of Radio Engineers *Transactions*, June 1927.

8. Train Communication, L. O. Grondahl, P. W. Bossart. AIEE Transactions, volume 62, 1943, July section, pages 493-500.

9. Bureau of Standards circular 74.

10. Skin Effect in Bimetallic Conductors, B. R. Teare, Jr., Josephine R. Webb. AIEE Transactions, volume 62, 1943, June section, pages 297-302.

11. Carrier-Current Losses Measured and Interference Minimized on Boulder-Los Angeles Transmission Line, J. D. Laughlin, W. E. Pakala, M. E. Reagan. AIEE Transactions, volume 59, 1940, January section, pages 4-10.

12. Application of Carrier to Power Lines, F. M. Rives. AIEE Transactions, volume 62, 1943, pages 835-44.

temperature drop through the insulation and air interstices was increased slightly by low air densities as would be expected.

The important point to remember is that these tests gave the minimum effect of altitude on the temperature rise of air-cooled transformers, because the losses were dissipated from a plain surface in which the loss of heat by radiation (unaffected by altitude) in percentage of total loss was the maximum possible.

Calculations indicate that, if the copper loss of this transformer had been dissipated entirely by convection air currents, the temperature rise at 40,000 feet probably would have been (when taking into account the increased copper loss due to temperature rise) in the order of 350 degrees centigrade instead of 189.5 degrees centigrade.

References

1. Aircraft Transformers—Small and Light, O. Kiltie. AIEE Transactions, volume 62, 1943, pages 897–902.

2. Effect of Barometric Pressure on Temperature Rise of Self-Cooled Stationary Induction Apparatus, V. M. Montsinger. AIEE Transactions, volume 35, 1916, pages 599–626.

Rectifier Relay for Transformer Protection

E. L. MICHELSON
MEMBER AIEE

THE BASIC PRINCIPLE of differential protection of electric equipment consists of measuring the sum of the currents at the various terminals of the generator, transformer, or bus. If the vector sum of these currents is substantially zero, there is no fault; if the vector sum is not zero, a fault condition is indicated.

In the case of transformer protection, the effect of the exciting current plays an important role, inasmuch as exciting current is equivalent to fault current from the standpoint of differential protection. Under normal conditions of operation, when the exciting current is less than ten per cent of full-load current, the exciting current easily can be provided for in the setting of the relay. However, because of the high value of exciting current which may flow at the instant a transformer is energized, unnecessary operations of the differential relay may occur when a transformer is being energized.

The excessive exciting current which may occur at the instant of energizing a transformer, commonly known as the inrush current, is due to the combined effects of transformer saturation, residual magnetism, and the transient d-c component in the current wave.[1] Inrush currents are a random phenomenon and can vary in magnitude from practically normal exciting current to several times full-load current of the transformer. In practice, heavy inrush currents can be expected in a large percentage of energizing operations, since the conditions required for low inrush currents are rather limited. An example of a heavy inrush current is shown in Figure 1. In this case, the first peak has a value equal to approximately three times the full-load current of the transformer.

Methods to Prevent Relay Operations Resulting from Inrush Currents

The need to prevent operation of transformer differential relays due to inrush current has been accentuated greatly by the use of sensitive high-speed relays. With slow-speed and insensitive relays, the rapid decrement of the exciting current eliminates unnecessary relay operations. With sensitive high-speed relays, which trip in one to three cycles, a special method must be provided to prevent operations due to inrush current. Some of the methods which have been used for this purpose consist briefly of the following arrangements:

1. One method makes use of the fact that inrush current contains a high percentage of harmonic currents and a large d-c component. The direct and harmonic currents are separated by means of filters from the fundamental current and are used to restrain relay action. On actual faults, the harmonic currents will be small compared to the total fault current and sensitive action is obtained.[2]

2. In another method, voltage relays are used to block the tripping action of the differential relay, if there is no appreciable reduction in bus voltage at the instant of energizing the transformer. This blocking action exists only long enough to permit the inrush current to decline to normal value. If a fault exists in the transformer circuit at the time it is energized, the bus voltage decreases and the tripping action of the differential relay is not blocked.

3. In a third method, the operating coil of the differential relay is desensitized for a short time after the transformer is energized. This is accomplished by partially short-circuiting the operating coil of the relay by the manual switch used for closing the transformer breaker. It has been found that on induction-type percentage differential relays with a minimum operating current of two amperes, a desensitized setting of four to five amperes gives satisfactory results.

Principle of the Rectifier Relay

This paper describes a new principle which has been applied for the purpose of eliminating incorrect relay operations resulting from inrush currents. The method used does not decrease the sensitivity of the relay at the instant the transformer is energized. This principle of the new relay is based on the fact that the inrush current is a pulsating direct current of positive or negative polarity. Figure 2 shows the method used for taking advantage of this situation. Two relays are used in series with dry-type rectifiers, so that one relay functions on positive current and the other on negative current. In order to close the tripping circuit, both relays must be energized. In the case of an inrush current, only one relay will be energized and no tripping will result. In the event of a fault with substantially equal positive and negative currents, both relays will trip and the transformer will be cleared from the system.

While the foregoing describes the principle of the rectifier relay from the theoretical point of view, a very important practical situation must be taken into account. As shown on Figure 1, the inrush current is by no means a direct current with respect to the secondary circuit, although the primary current is substantially direct. Within approximately five cycles after the transformer of Figure 1 is energized, an appreciable a-c component of current appears in the secondary circuit. This alternating current is a result of current-transformer saturation caused by the flow of direct current through the current transformer, a phenomenon which has been discussed and analyzed in recent AIEE papers.[3,4] The magnitude of the a-c component and the time required for it to appear in the circuit will vary principally with the construction of the current transformer and the resistance of the secondary circuit.

In order to prevent tripping due to the false a-c component, a time-delay auxiliary relay was added which functions in the following manner. As shown in Figure 3, if either of the two primary relays trip, the auxiliary relay *A* is energized. After 1.5 cycles, the relay trips, contact *A* is closed, and a resistor *R* is connected across the current circuit of the primary relays. The effect of this resistor is to desensitize the primary relays, thus re-

---

Paper 45-55, recommended by the AIEE committee on protective devices for presentation at the AIEE winter technical meeting, New York, N. Y., January 22–26. Manuscript submitted November 15, 1944; made available for printing December 28, 1944.

E. L. Michelson is senior engineer, system planning division, Commonwealth Edison Company, Chicago Ill.

P. N. Sandstrom, deceased, was responsible for the development of the relay described in this paper. The author acknowledges the assistance of R. I. Ward in the development of the relay and preparation of the paper.

Figure 1. Typical example of transformer inrush current. First peak of lower wave is approximately three times full load current of transformer

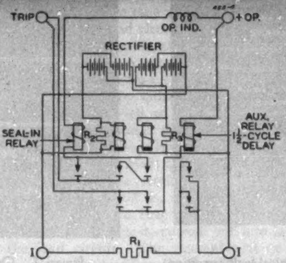

Figure 4. Connections of completed relay

quiring a heavier current to trip. When the inrush current subsides to a value below the tripping value for the primary relay, the auxiliary relay drops out and the sensitive setting is re-established. In an application discussed later, it was found that a sensitive setting of 2.5 amperes and a desensitized setting of 5.0 amperes gave satisfactory operation.

If a fault occurs with a symmetrical current wave, the two primary relays will trip in approximately one cycle and the auxiliary relay plays no part in the operation. If a fault occurs with a displaced current wave, the action will depend upon the degree of asymmetry, the magnitude of the fault current, and the d-c decrement. In many cases, the fault current will be sufficiently high and the d-c decrement sufficiently fast so that the speed of tripping will not be affected by the desensitizing action. For faults with displaced waves of low magnitude and a relatively slow decrement of the d-c component, the desensitizer will take effect and a fault current higher than the desensitized setting will be required for tripping. For the applications being considered, this latter condition did not appear to be very important, since even the desensitized setting of the relay was lower than the setting of comparable relays.

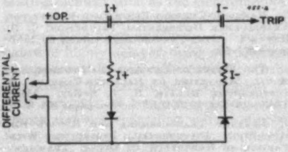

Figure 2. Basic connections of rectifier relay

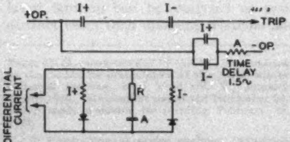

Figure 3. Connection diagram showing use of time-delay relay for desensitizing primary relay

One limitation arises in regard to the dropout value for the primary relays. It is necessary for the dropout current with the desensitized setting to be lower than the pickup value with the sensitive setting. If this condition is not obtained, it is possible for the breaker to be tripped at the instant when the primary relay drops out and sensitizes the relay. In the application described later, the pickup for the sensitive condition was 2.5 amperes and the dropout for the desensitized condition 2.3 amperes.

Application of Rectifier Relay

A number of laboratory tests were made with the relay described above with satisfactory results. Figure 4 shows the connections for the completed relay. This diagram shows three resistors; R_1 is the shunting resistor of the foregoing discussion, while R_2 and R_3 are connected across the coils of the primary relays. These latter resistors are used to set the primary relays and to obtain smoother operation of the primary relays on the half-wave current. Telephone-type relays with copper slugs were used which further improved their operation on half-wave current. Selenium-rectifier elements were used, four stacks being connected in series to provide for the maximum reverse voltage which could be obtained. Figure 5 shows the completed relay. Figure 6 is an oscillogram for a symmetrical fault condition and shows the relay contacts of both primary relays closing within 1.14 cycles after the circuit was energized. Figure 7 is an oscillogram for a condition of inrush current, and shows the contacts of one relay closing, but no action on the second relay.

This relay scheme was put in service for the differential protection of a transformer which had been giving considerable trouble due to unnecessary operations of the differential relay on inrush currents. The setting used was 2.5 amperes for the primary relays with the desensitizer increasing the setting to 5.0 amperes. This relay has been giving satisfactory service and has eliminated unnecessary tripping due to inrush current and at the same time has provided a more sensitive setting for actual fault conditions.

It appears that the new relay described in this paper could be used advantageously in any application where saturation of current transformers may cause false tripping, such as bus differential and residual overcurrent relaying. Figure 8 shows a typical example of the effect of current-transformer saturation on residual relays. In this case, a residual relay was used on the 12-kv leads to a delta-

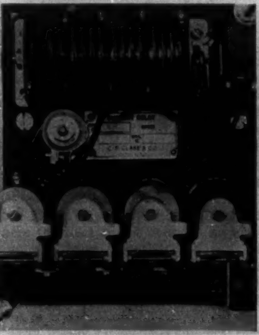

Figure 5. Completed relay

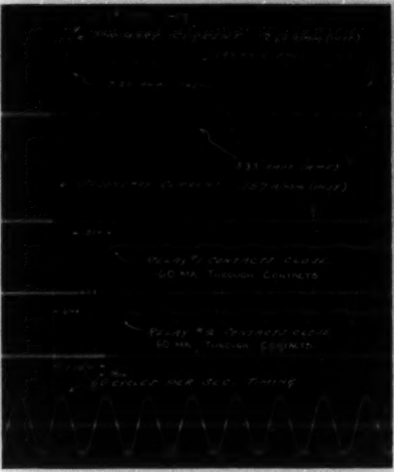

Figure 6. Operation of rectifier relay for symmetrical fault condition

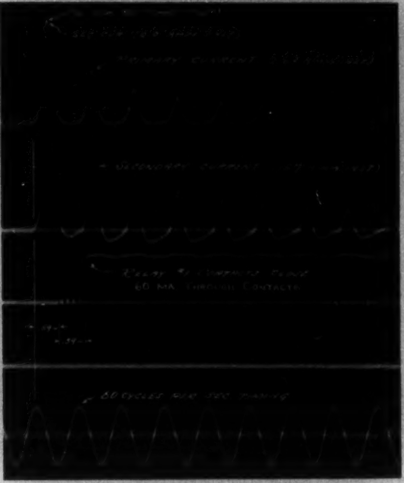

Figure 7. Operation of rectifier relay for inrush current

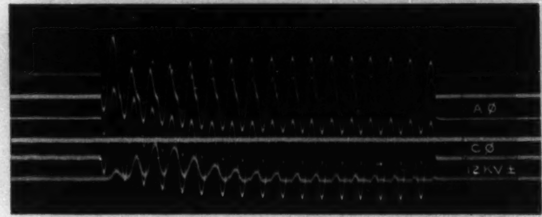

Figure 8. Oscillogram showing direct current through residual relay, with displaced fault current flowing in current transformers on *A* and *C* phases

connected transformer. When a phase-to-ground fault was placed on the high-voltage star-connected winding, a heavy displaced current appeared in two of the phase leads on the 12-kv side of the transformer. Unequal saturation of the two current transformers caused by the d-c component resulted in a considerable d-c residual current, as shown in the bottom trace of Figure 8. The rectifier relay would permit the use of an instantaneous sensitive setting without danger of tripping falsely for uses exemplified by Figure 8.

Conclusion

This paper describes a new relay for transformer protection and other applications, which will not operate on the pulsating direct current that appears to be caused by transformer inrush currents and other causes. This action is obtained by using two primary relays, one operating only on positive currents and the other only on negative currents. Under fault conditions, both relays operate and the faulted unit is tripped. If the current flows only in one direction, only one primary relay will operate and no tripping results.

References

1. Transformer Engineering (book), L. F. Blume. John Wiley and Son, Inc., New York, N. Y.

2. Harmonic-Current-Restrained Relays for Transformer Differential Protection, C. D. Hayward. AIEE Transactions, volume 60, 1941, pages 377–82.

3. The Effect of Current-Transformer Residual Magnetism on Balanced-Current or Differential Relays, H. T. Seeley. AIEE Transactions, 1943, April section, pages 164–8.

4. Current Transformers and Relays for High-Speed Differential Protection, With Particular Reference to Offset Transient Currents, E. C. Wentz, W. K. Sonnemann. AIEE Transactions, 1940, August section, pages 481–8.

Voltage and Current Relations for Controlled Rectification With Inductive and Generative Loads

K. P. PUCHLOWSKI
ASSOCIATE AIEE

ELECTRONIC RECTIFIERS with controlled point of ignition are now used widely in various industrial-control and power-conversion systems. Although the principle of operation of thyratron and ignitron rectifiers is generally known, the analytical methods for calculation of d-c output voltages of rectifiers have been surprisingly incomplete. For example, the calculation of a d-c output voltage of a polyphase rectifier with no delay of the angle of ignition or with a slight delay only is a conventional matter, since the necessary formulas can be found in standard textbooks. When, however, the point of ignition of a polyphase rectifier is delayed beyond a certain critical value, the conventional formulas for d-c output voltages do not apply any more.

A problem of somewhat similar nature is encountered in the case of a single-phase half-wave rectifier where the conventional expression for the rectifier output voltage $E_{dc}=\sqrt{2}E_s/\pi$ applies to rectifiers with resistive loads only and is not valid in the case of an inductive load. An attempt to calculate the average value of the d-c load-terminal voltage for a single-phase half-wave rectifier with an inductive load becomes a rather complicated affair.

If in addition to a resistance and an inductance the load circuit of a polyphase rectifier with considerably delayed firing also includes a direct-voltage generating element such as the electromotive force of a running d-c motor, the relations become even more involved. The significance of highly delayed firing of rectifiers is apparent if one will consider their application to control and regulation of field currents of various rotating machines and as a controlled voltage supply for armatures of d-c motors in electronic adjustable-speed drives.

The problem of determining the output voltages of a p-phase rectifier with delayed ignition can be analyzed as two distinct cases with different relations involved in each case. The first is the rather well-known case where the current flowing in the load circuit has a continuous character: that is, at no time it drops to zero although it may contain a more or less pronounced a-c component. This is the case usually encountered in polyphase rectifiers with no delayed firing or when the firing is only slightly delayed.

If the firing, however, is delayed beyond a certain critical point, the current in any polyphase rectifier will become discontinuous: that is, it will consist of separate pulses so that within a certain portion of the cycle no current will flow in the load circuit. The conventional expressions for rectifier direct voltages are not valid in this case, and very little can be found in technical literature about the proper manner of attack of such a problem. This surprising gap undoubtedly is caused by the apparent complexity of relationships involved and the difficulty in adapting these relations to practical problems.

This paper presents an outline of generalized relations for average values of direct voltages of a p-phase rectifier for both cases of continuous and discontinuous conduction. The very natural question how to determine the critical point of ignition which separates the two cases is, of course, of particular interest, and this problem is given special consideration. A relatively simple method of calculation of direct voltages and currents described in this paper is illustrated by two examples.

Case of Continuous Conduction

The basic diagram of connections of a symmetrical p-phase rectifier with controlled point of ignition is shown in Figure 1, and the graph of the anode supply voltage and the d-c load voltage is given in Figure 2.

For a p-phase rectifier the phase displacement of two consecutive anode voltage waves (Figure 2) is

$$\varphi=\frac{2\pi}{p} \tag{1}$$

If the transformer leakage reactance is neglected, an instantaneous commutation will be obtained, and each rectifying element will conduct over the period from x_f to $x_f+2\pi/p$, where x_f is the point of ignition, and the average value of the rectifier output voltage (Figure 2) will be

$$E_{dc}=\frac{1}{\left(\frac{2\pi}{p}\right)}\int_{x_f}^{x_f+\frac{2\pi}{p}}\sqrt{2}E_s\sin x dx$$

or, after the integration,

$$E_{dc}=\frac{pE_s}{\sqrt{2}\pi}\left[\cos x_f-\cos\left(x_f+\frac{2\pi}{p}\right)\right] \tag{2}$$

Expression 2 is a different form of a well-known formula for the rectifier output voltage which can be found in textbooks. The introduction of the angle of ignition x_f in expression 2 seems advisable from the point of view of unification of different formulas for rectifier output voltages.

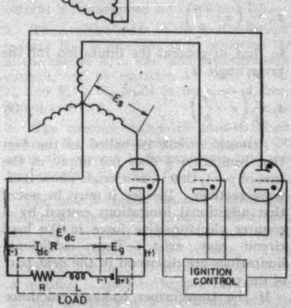

Figure 1. Power circuit of a controlled polyphase rectifier shown for the case $p=3$

If the arc drop of the rectifier E_e is taken into account, the rectifier output voltage will become

$$E_{dc}=\frac{pE_s}{\sqrt{2}\pi}\left[\cos x_f-\cos\left(x_f+\frac{2\pi}{p}\right)\right]-E_e \tag{3}$$

or

$$E_{dc}=\frac{pE_s}{\sqrt{2}\pi}\left[\cos x_f-\cos\left(x_f+\frac{2\pi}{p}\right)-a_e\frac{2\pi}{p}\right] \tag{3A}$$

where

$$a_e=\frac{E_e}{\sqrt{2}E_s}$$

Equation 3 also represents the direct voltage at the load terminals of the rectifier E_{dc}'. This is true also in the case where the load circuit contains an electromotive force opposing the flow of current. This apparently self-evident fact is mentioned here because, as it will be seen later, it does not apply to all cases of rectification.

From Figure 2 it becomes apparent that if the arc drop is neglected the minimum

---

Paper 45-53, recommended by the AIEE committee on electronics for presentation at the AIEE winter technical meeting, New York, N. Y., January 22-26, 1945. Manuscript submitted November 24, 1944; made available for printing February 29, 1945.

K. P. Puchlowski is design engineer, industrial-control engineering department, Westinghouse Electric and Manufacturing Company, East Pittsburgh, Pa.

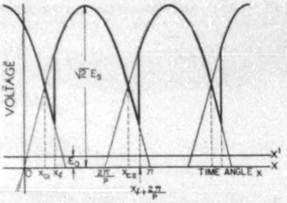

Figure 2. Anode supply voltage and d-c output voltage of a polyphase rectifier ($p=3$) with delayed ignition

Transformer leakage reactance neglected

theoretically possible value of the angle of ignition is

$$x_{cl}=\frac{1}{2}\left(\pi-\frac{2\pi}{p}\right)$$

so that in general the limitation for the firing angle is

$$x_f>\frac{1}{2}\left(\pi-\frac{2\pi}{p}\right) \tag{4}$$

Attention must be called to the fact that limitation 4 does not apply in the case of $p=1$, that is, to a single-phase half-wave rectifier. Besides, it must be noted that additional limitations caused by a counter electromotive force in the load circuit may exist. These additional limitations are discussed in the next part of the paper.

If the transformer leakage reactance is taken into account the extinction of arc in the outgoing rectifying element (anode) will be delayed so that a definite commutation period will exist during which the two rectifying elements will conduct current simultaneously, and during this commutation period the load voltage will follow the average of the two anode voltages.[1] In this case the graph of the rectifier output voltage is as shown in Figure 3.

The effect of transformer reactance is part of the voltage regulation of the rectifier transformer and lowers the voltage output of the rectifier. This internal voltage drop of the transformer is directly proportional to the load current and to the reactance of the transformer, and is represented by the expression:[1]

$$\Delta E_{dc}=\frac{I_{dc}X_tE_{dc}}{2\sqrt{2E_s}\sin(\pi/p)} \tag{5}$$

where

I_{dc} = d-c load current
X_t = leakage reactance of transformer
E_s = a-c supply voltage (transformer secondary)
p = number of phases

It is evident from expressions 3 and 5 that in the case of continuous conduction the output voltage of the rectifier, that is, the voltage at the load terminals does not depend upon the inductance of the load nor upon any counter electromotive force which may be part of the load circuit (motor, battery).

Case of Discontinuous Conduction

If the angle of ignition is delayed beyond a certain critical point the current in the load circuit of the rectifier will become discontinuous: that is, it will drop to zero in the outgoing rectifying element before the incoming rectifying element will start conducting, so that there will be a definite period during which no current at all will flow in the load circuit.

This case has a particular significance wherever controlled rectifiers are used to supply a very wide range of load voltages such as in different control and regulating systems, rectifier motor drives, and the like.

Figure 4 represents a positive half of the anode supply voltage of a rectifier without any reference to the number of phases. It can be well understood that since no commutation in an ordinary sense will exist between the rectifying elements it is immaterial for the analysis of the individual current pulse whether it has been produced by a one-, two-, three-, or a p-phase rectifier.

Figure 4 is of particular importance since it illustrates a number of basic designations used in subsequent parts of this paper. All the electrical angles are referred to the initial 0 point as shown in the graph so that the equation of the anode supply voltage (with respect to zero line X) is

$$e=\sqrt{2}E_s\sin x$$

where E_s is the rms value of the a-c supply voltage and $x=\omega t$ the variable time angle.

The sum of the electromotive force (E_g) present in the load circuit and opposing the flow of current (Figure 4), such as the electromotive force generated in the armature of a rotating d-c motor, and of the constant arc drop of the rectifier E_o is represented by E_d

$$E_d=E_g+E_o \tag{6}$$

Obviously, the current flow in the load can be produced only by that portion of the anode supply voltage which rises above the constant voltage E_d so that in effect all the values of load current i and of the voltage drop caused by this current must be referred to a new zero line X'' shifted by E_d with respect to zero line X.

The angle of ignition, that is, the point at which the rectifying element starts conducting, is designated by x_f. The angle of extinction of the arc or the point at which the rectifier stops conducting is designated by x_s.

If for the sake of simplification it is assumed that the minimum starting voltage of the rectifier is equal to the arc drop, then it becomes apparent from Figure 4 that the range of the angles of ignition is

$$x_1<x_f<x_2 \tag{7}$$

If the voltage coefficient a is introduced,

$$a=\frac{E_d}{\sqrt{2}E_s}=\frac{E_g+E_o}{\sqrt{2}E_s} \tag{8}$$

the expressions for x_1 and x_2 will be as follows:

$$x_1=\sin^{-1}a \tag{9}$$

$$x_2=\pi-\sin^{-1}a \tag{10}$$

and the range of angles of ignition will be

$$\sin^{-1}a<x_f<\pi-\sin^{-1}a \tag{11}$$

When there is no electromotive force in the load circuit ($E_g=0$)

$$a=a_0=\frac{E_o}{\sqrt{2}E_s}$$

In this case the load voltages must be referred to the zero line X' (Figure 4).

For an ideal rectifier without any arc drop,

$$a=a'=\frac{E_g}{\sqrt{2}E_s}$$

and if there is no electromotive force in the load circuit, then $a=0$, and the maximum possible theoretical range of firing angles is

$$0<x_f<\pi$$

The analytical relationship between the angle of ignition x_f and the angle of extinction x_s as derived by Vedder and Puchlowski[2] is

$$\cos\theta\sin(x_s-\theta)-a+\left[a-\cos\theta\sin(x_f-\theta)\right]\epsilon^{-\frac{x_s-x_f}{\tan\theta}}=0 \tag{12}$$

where θ is the impedance angle of the load circuit that is

$$\tan\theta=\frac{\omega L}{R} \tag{13}$$

$$\cos\theta=\frac{R}{\sqrt{R^2+\omega^2L^2}} \tag{14}$$

R = resistance of the load circuit
L = inductance of the load circuit
$\omega=2\pi f$ (f = supply line frequency)

Although the equation 12 cannot be solved explicitly for x_s, the value of the angle of extinction can be calculated with satisfactory degree of accuracy for given values of x_f, θ, and a in accordance with the relatively simple method of gradual approximations which will be presented later in this paper.

Values of x_s as a function of x_f calculated from equation 12 are plotted in the form of several families of graphs in Figure 5.

All the curves of $x_s=f(x_f)$ for the same value of the coefficient a converge at a point corresponding to $x_s=x_f=x_3$, as can be understood easily from Figure 4. All these points of convergence lie, of course, on the straight line A-C (Figure 5) which determines the maximum possible value x_2 of the angle of ignition x_f for a given value of coefficient a (expression 10). The straight line A-B determines the minimum possible value x_1 (expression 9) of the angle of ignition x_f for a given a.

It may be interesting to note that for the border case of a purely resistive load $L=0$ ($\cos\theta=1$) the angle of extinction x_s is solely a function of the coefficient a and is independent of x_f:

$$x_s=x_2=\pi-\sin^{-1}a \tag{15}$$

as can be understood from Figure 4 or derived directly from equation 12.

For another border case of a purely inductive load $R=0$ ($\cos\theta=0$) equation 12 cannot be used to calculate x_s since, though it is fulfilled also in that case, it becomes an identity.

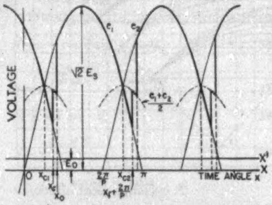

Figure 3. Anode supply voltage and d-c output voltage of a polyphase rectifier ($p=3$) with delayed ignition

Transformer leakage reactance considered

For $\cos\theta=0$ the value of x_s can be obtained from the following relationships:

For $a=0$ (rectifier without arc drop),

$$x_s=2\pi-x_f \tag{16}$$

For $a>0$,

$$\cos x_s+ax_s=\cos x_f+ax_f \tag{17}$$

Equation 17 can be obtained directly from equation 20 for the condition $\cos\theta=0$, $I_{dc}R=0$.

Relationship 16 is represented in Figure 5 by the straight line C-D. Relationship 17 is also plotted in Figure 5 as part of each family of curves for a given value of coefficient a.

Figure 5 gives a clear picture of the maximum possible range of angles of ignition and angles of extinction for different coefficients a. As an example the maximum range of points of ignition x_f for $a=0$ is represented by B-C and for $a=0.8$ by M-N. Similarly, the maximum range of angles of extinction x_s for $a=0$ is represented by B-D and for $a=0.8$ by M-K. For $a=1$ the whole operating area of angles of ignition and extinction contracts into point A.

The average value of the rectifier output voltage E_{dc} can be calculated directly from Figure 4 by integrating the anode-voltage function with respect to zero line X' (taking into account the arc drop of the rectifier) over the period of conduction x_s-x_f and averaging the result over the entire phase cycle $2\pi/p$,

$$E_{dc}=\frac{1}{\left(\frac{2\pi}{p}\right)}\int_{x_f}^{x_s}(\sqrt{2}\,E_s\sin x-E_0)dx$$

$$E_{dc}=\frac{pE_s}{\sqrt{2}\pi}[\cos x_f-\cos x_s-a_0(x_s-x_f)] \tag{18}$$

$$a_0=\frac{E_0}{\sqrt{2}E_s} \tag{19}$$

If the load circuit contains an electromotive force E_g opposing the direction of current flow (Figure 1) the average value of the $I_{dc}R$ voltage drop in the load (armature-voltage drop, for instance) can be calculated by integrating the voltage function with respect to zero line X'' (Figure 4) over the conduction period of the rectifier x_s-x_f, and averaging the result over the phase cycle $2\pi/p$,

$$I_{dc}R=\frac{1}{\left(\frac{2\pi}{p}\right)}\int_{x_f}^{x_s}(\sqrt{2}\,E_s\sin x-E_d)dx$$

$$I_{dc}R=\frac{pE_s}{\sqrt{2}\pi}[\cos x_f-\cos x_s-a(x_s-x_f)] \tag{20}$$

where

$$a=\frac{E_d}{\sqrt{2}E_s}=\frac{E_g+E_0}{\sqrt{2}E_s}$$

The average direct voltage at the load terminals then will become

$$E_{dc}'=I_{dc}R+E_g$$
$$=\frac{pE_s}{\sqrt{2}\pi}[\cos x_f-\cos x_s-a(x_s-x_f)]+E_g$$

$$E_{dc}'=\frac{pE_s}{\sqrt{2}\pi}\left[\cos x_f-\cos x_s-a(x_s-x_f)+a'\frac{2\pi}{p}\right] \tag{21}$$

$$a'=\frac{E_g}{\sqrt{2}E_s} \tag{22}$$

When the load circuit does not contain any generative element, that is, $E_g=0$, then from expression 8 $a=a_0=E_0/\sqrt{2}E_s$, from expression 22 $a'=0$ and expressions 20 and 21 become identical with the expression 18. Hence, for $E_g=0$ the average direct voltage across the load terminals E_{dc}' is equal to the average direct-voltage drop in the load $I_{dc}R$ and equal to the rectifier output voltage E_{dc}

$$E_{dc}'=E_{dc}=I_{dc}R \tag{23}$$
for $E_g=0$

General Remarks on Voltage Relations

The comparison of expression 18 for the rectifier output voltage in the case of discontinuous current with expression 3A for the rectifier output voltage in the case of continuous current reveals that expression 3A can be regarded as a particular case of the general expression 18. Obviously, when the load current becomes continuous the angle of extinction x_s for a given rectifying element becomes equal to the commutation angle $x_f+2\pi/p$ (Figure 2):

$$x_s=x_f+\frac{2\pi}{p} \tag{24}$$

By substituting expression 24 for x_s in equation 18, equation 3A is obtained.

Thus on the basis of previous considerations a following generalized scheme of relations can be set up:

1. The average value of the rectifier output voltage E_{dc} is represented by the general equation 18, which in the case of continuous current is transformed into equation 3A.

2. The average value of the load-terminal voltage E_{dc}' is represented by equation 18 in the case of R, L load and discontinuous current, and by equation 3A both for R, L, and R, L, E_g loads in the case of continuous current.

3. The average value of load-terminal voltage E_{dc}' is represented by equation 21 when the current is discontinuous and the load contains R, L, and E_g.

The case 3 stands out as a rather peculiar case in rectifier practice since here the load-terminal voltage is not equal to the rectifier output voltage. This situation normally is encountered where a rectifier is used to supply the voltage to the armature of a d-c motor, and to control the speed of the motor within a wide range by controlling the armature voltage. In general, the technical literature contains very little on the analytical aspects of this subject,[2] apparently because until recently the rectifier–motor drives had been in the stage of infancy, and only quite recent developments have aroused considerable interest in such systems.[4,5,6]

The fact that in the case of a generative load with discontinuous current the

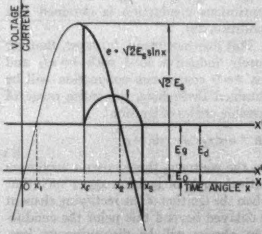

Figure 4. Anode supply voltage, load-terminal voltage, and load current referred to a single rectifying element

General case of a generative load (E_g)

load-terminal voltage is not equal to the rectifier output voltage can be understood even without any reference to analytical relations. Figure 4 shows clearly that during the nonconductive period of the rectifier the voltage at the load terminals is equal to the electromotive force generated in the load. On the other hand, the rectifier output voltage during the nonconductive period is equal to zero.

Thus, for the discontinuous conduction of a rectifier with load containing a countervoltage

$$E_{dc}' > E_{dc} \tag{25}$$

Critical Point of Ignition

When the point of ignition of a rectifying element of a polyphase rectifier (Figure 2) is delayed beyond the firing point which may be called "critical point of ignition," the current in the load will become discontinuous; that is, each rectifying element will conduct an individual pulse of current, and there will be no commutation from one anode to the next anode.

It is apparent from Figures 2 and 4 that this critical point x_{fc} must satisfy the following equation:

$$x_s = x_{fc} + \frac{2\pi}{p} \tag{26}$$

$$x_{fc} = x_s - \frac{2\pi}{p} \tag{27}$$

and continuous conduction will be obtained when

$$x_f < x_s - \frac{2\pi}{p} \tag{28}$$

while the condition for discontinuous conduction is

$$x_f > x_s - \frac{2\pi}{p} \tag{29}$$

The higher is the value of the impedance angle of the load, the higher are the values of x_s (Figure 5) and x_{fc} (equation 27), and, consequently, the wider is the range of points of ignition for which continuous conduction is obtained (see condition 28).

This does not mean, however, that for purely inductive load with $\theta = \pi/2$ and $\cos\theta = 0$ continuous conduction will be obtained throughout the entire range of possible angles of ignition:

$$\sin^{-1} a < x_f < \pi - \sin^{-1} a$$

On the contrary, there exists a maximum critical angle of ignition $x_{fc\max}$ such that when the ignition of the rectifying element is delayed beyond this point the conduction always will be discontinuous, irrespective of how high the load inductance may be, that is, even for $\cos\theta = 0$.

This maximum critical point of ignition can be calculated under the assumption of purely inductive load ($\cos\theta = 0$) from equation 17 by substituting x_s from expression 26 into equation 17:

$$\cos\left(x_{fc\max} + \frac{2\pi}{p}\right) + a\left(x_{fc\max} + \frac{2\pi}{p}\right) = \cos x_{fc\max} + a x_{fc\max}$$

Hence,

$$x_{fc\max} = \sin^{-1}\frac{\pi a}{p\sin(\pi/p)} - \frac{\pi}{p} \tag{30}$$

where

$$\frac{\pi}{p} < \sin^{-1}\frac{\pi a}{p\sin(\pi/p)} \leq \pi \tag{31}$$

Equation 30 does not apply to $p=1$, that is to single-phase half-wave rectifiers, since for these rectifiers the conduction is discontinuous for any possible firing angle.

For an ideal rectifier ($E_o = 0$) $a = 0$ (for an R, L load). Also, in many practical cases a is so small that it may be assumed equal to zero.

Then from expressions 30 and 31

$$x_{fc\max} = \pi - \frac{\pi}{p}$$

Since the range of possible firing angles is represented by the limitation 11 it is evident that when

$$x_{fc\max} \leq \sin^{-1} a \tag{32}$$

the current in the load will be discontinuous even for a purely inductive load ($\cos = 0$) for any possible angle of ignition of the rectifier. From the relationship 32 one can calculate the critical value a_c of the coefficient a such that when $a > a_c$ the current always will be discontinuous for any possible angle of ignition.

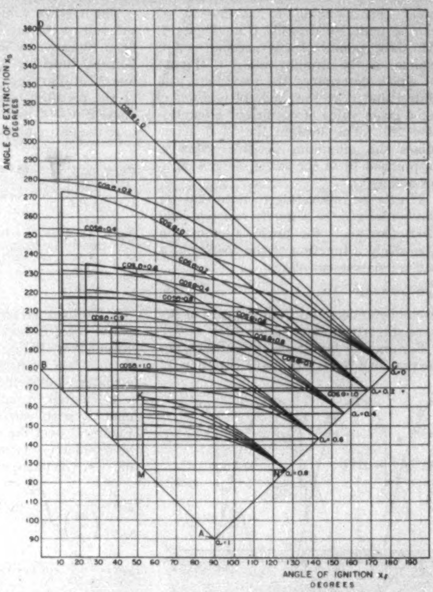

Figure 5. System of graphs representing $x_s = f(x_f)$ for different values of parameters a and $\cos\theta$

From the relationships 32 and 30 the following equation for a_c is obtained:

$$\sin^{-1}\frac{\pi a_c}{p\sin(\pi/p)} - \sin^{-1} a_c = \frac{\pi}{p} \tag{33}$$

Hence

$$a_c = \frac{\sin(\pi/p)}{\sqrt{\sin^2(\pi/p) + \left(\cos(\pi/p) - \dfrac{\pi/p}{\sin(\pi/p)}\right)^2}} \tag{34}$$

where

$$p \neq 1$$

Calculations of the Angle of Extinction—Method of Gradual Approximations

In the course of previous considerations the significance of the concept of the angle of extinction was fully emphasized. In order that fundamental expressions 18, 20, 21, and 27 can be used directly as practical formulas for calculations of the load-terminal voltage and for determination whether discontinuous or continuous conduction of the rectifier is obtained, a relatively simple and accurate method to determine x_s is necessary.

The basic equation 12 which represents the relationship between the angles of ignition and extinction, transformer voltage and circuit constants, is a theoretically accurate analytical relationship, but it has the disadvantage that x_s cannot be expressed as an explicit function of x_f, a, and θ.

However, the following method of gradual approximations will permit to calculate x_s in a relatively simple manner with any required degree of accuracy.

The family of graphs shown in Figure 5 where x_s is plotted as a function of x_f for a set of values of a and $\cos\theta$ covering the entire range of $0<a<1$ and $0<\cos\theta<1$ can be used to determine directly by interpolation the first approximation x_s' of the angle of extinction.

Equation 12 can be represented as

$$\sin(x_s-\theta)=\frac{a-[a-\cos\theta\sin(x_f-\theta)]\epsilon^{-\frac{x_s-x_f}{\tan\theta}}}{\cos\theta} \qquad (35)$$

Introducing the following designations:

$$A=a-\cos\theta\sin(x_f-\theta) \qquad (36)$$

$$B=\epsilon^{-\frac{\pi(x_s-x_f)}{180\tan\theta}} \qquad (37)$$

$$M=\sin(x_s-\theta) \qquad (38)$$

$$N=\frac{a-AB}{\cos\theta} \qquad (39)$$

we obtain from equation 35

$$x_s=\sin^{-1}N+\theta \qquad (40)$$

where $x_s \geqq \pi-\sin^{-1}a$.

On the basis of the first approximation x_s' obtained from Figure 5 the values M' (equation 38), N' (equation 39), and x_{s1} (equation 40) are calculated. Then the second approximation of the angle of extinction x_s'' will be obtained from one of the three formulas, for one of the four possible conditions as specified in Table I.

The significance of expressions for x_s'' shown in Table I can be understood if attention is called to the fact that for $M'>N'$ the actual solution x_s of equation 35 is

$$x_s>x_s'$$

and for $M'<N'$

$$x_s<x_s'$$

and also that the value x_{s1} as compared to that of x_s' is indicative of the necessary degree of correction.

Very often the second approximation x_s'' will represent a sufficiently accurate solution of equation 12 (or 35). Usually, if the conditions are such that formula $x_s''=(x_s'+x_{s1})/2$ (Table I) was used to determine x_s'', the latter may be assumed to be a fairly close approximation of x_s. Otherwise, it is recommended to determine the third approximation x_s''' using x_s'' as a basis for calculation of M'' (equation 38), B'' (equation 37), N'' (equation 39), and x_{s2} (equation 40). Then, the third approximation x_s''' will be obtained from one of the three formulas as shown in Table II, analogous to Table I.

Obviously, this procedure can be carried on until the required degree of accuracy is obtained. In most practical cases, however, the second or third approximation yields sufficiently accurate results. For many estimating purposes even the first approximation x_s' obtained directly from Figure 5 may prove entirely adequate.

Examples

Two examples of calculations will be given here in order to emphasize the practical significance of previous considerations and illustrate the application of several basic formulas.

Example 1. Calculate the direct voltage at the load terminals and load current of a single-phase half-wave phanotron rectifier (no grid control) for the following set of conditions:

Rectifier supply voltage	$E_s=110$ volts
Resistance of the load	$R=10$ ohms
Inductance of the load	$L=52$ millihenrys
Line frequency	$f=60$ cycles per second
Rectifier arc-voltage drop	$E_0=15$ volts

From equation 13,

$$\tan\theta=\frac{377\times0.052}{10}=1.96$$

$$\theta=62°58', \cos\theta=0.4545$$

From equation 8,

$$a=a_0=\frac{15}{\sqrt{2}\times110}=0.0964$$

The angle of ignition from equation 9 (the rectifier without delayed ignition):

$$x_f=x_1=\sin^{-1}0.0964=5°32'$$

From Figure 5 the first approximation of the angle of extinction for $a=0.0964$, $\cos\theta=0.4545$ and $x_f=5°32'$ is $x_s'=242°$. From equations 36, 37, 38, 39, and 40,

$$A=0.0964-0.4545\sin(5°32'-62°58')=0.4791$$

$$B'=\epsilon^{-\frac{\pi\times(242-5.53)}{180\times1.96}}=0.122$$

$$M'=\sin(242°-62°58')=0.0169$$

$$N'=\frac{0.0964-0.4791\times0.122}{0.4545}=0.0835$$

$$x_{s1}=\sin^{-1}0.0835+62°58'=238°11'$$

$$M'<N' \qquad x_{s1}<x_s'$$

Thus, the second and sufficient approximation (from Table I),

$$x_s''=\frac{x_s'+x_{s1}}{2}=\frac{242+238°11'}{2}=240°6'$$

The load-terminal voltage (from equation 21 for $a'=0$),

$$E_{dc}'=\frac{110}{\sqrt{2}\pi}\left[\cos 5°32'-\cos 240°6'-0.0964\left(\frac{\pi\times240.1}{180}-\frac{\pi\times5.53}{180}\right)\right]=27.2 \text{ volts}$$

and the load current ($E_{dc}'=I_{dc}R$ for $a'=0$),

$$I_{dc}=\frac{E_{dc}'}{R}=\frac{27.2}{10}=2.72 \text{ amperes}$$

Example 2. A three-phase controlled rectifier is supplying the power to the armature of a one-horsepower 230-volt four-ampere 850-rpm d-c motor. Calculate the armature current, the armature voltage, and the theoretical rectifier output voltage, assuming that the ignition of the rectifier is delayed to be $x_f=110°$ and that the motor is running at the rated speed.

The following figures are known:

Transformer voltage	$E_s=350$ volts
	$\omega=377$
Armature resistance	$R=3$ ohms
Armature inductance	$L=70$ millihenrys
Rectifier arc drop	$E_0=15$ volts

Table I

	M′>N′	M′<N′
$x_{s1}>x_s'$	$x_s''=\frac{x_s'+x_{s1}}{2}$	$x_s''=x_s'-\frac{x_{s1}-x_s'}{2}$
$x_{s1}<x_s'$	$x_s''=x_s'+\frac{x_s'-x_{s1}}{2}$	$x_s''=\frac{x_s'+x_{s1}}{2}$

Table II

	M″>N″	M″<N″
$x_{s2}>x_s''$	$x_s'''=\frac{x_s''+x_{s2}}{2}$	$x_s'''=x_s''-\frac{x_{s2}-x_s''}{2}$
$x_{s2}<x_s''$	$x_s'''=x_s''+\frac{x_s''-x_{s2}}{2}$	$x_s'''=\frac{x_s''+x_{s2}}{2}$

At rated speed the electromotive force of the motor,

$$E_g = 230 - 4\times 3 = 218 \text{ volts}$$

From equation 13,

$$\tan\theta = \frac{377\times 0.07}{3} = 8.8$$

$$\theta = 83°32', \quad \cos\theta = 0.1126$$

From equation 8,

$$a = \frac{218+15}{\sqrt{2}\times 350} = 0.471$$

From equation 19,

$$a_0 = \frac{15}{\sqrt{2}\times 350} = 0.0303$$

From Figure 5 the first approximation of the angle of extinction for $a = 0.471$, $\cos\theta = 0.1126$ and $x_f = 110°$ is

$$x_s' = 183°$$

Thus, from equations 36, 37, 38, 39, and 40,

$$A = 0.471 - 0.1126 \sin(110° - 83°32') = 0.4209$$

$$B' = \epsilon^{-\frac{\pi\times(183-110)}{180\times 8.8}} = 0.865$$

$$M' = \sin(183° - 83°32') = 0.9864$$

$$N' = \frac{0.471 - 0.4209\times 0.865}{0.1126} = 0.95$$

$$x_{s1} = \sin^{-1} 0.95 + 83°32' = 191°43'$$

Since

$$M' > N', \quad x_{s1} > x_s'$$

then from Table I the second approximation

$$x_s'' = \frac{x_s' + x_{s1}}{2} = \frac{183° + 191°43'}{2} = 187°21'$$

The corrected values B'', $M,''$ N'', and x_{s2} are

$$B'' = \epsilon^{-\frac{\pi\times(187.35-110)}{180\times 8.8}} = 0.858$$

$$M'' = \sin(187°21' - 83°32') = 0.9711$$

$$N'' = \frac{0.471 - 0.4209\times 0.858}{0.1126} = 0.9775$$

$$x_{s2} = \sin^{-1} 0.9775 + 83°32' = 185°42'$$

Here $M'' < N''$ and $x_{s2} < x_s''$ and from Table II the third approximation,

$$x_s''' = \frac{x_s'' + x_{s2}}{2} = \frac{187°21' + 185°42'}{2} = 186°32'$$

The critical point of ignition (equation 27),

$$x_{fc} = 186°32' - \frac{180\times 2\times\pi}{\pi\times 3} = 66°32'$$

Hence, it is apparent that $x_f > x_{fc}$ and a discontinuous conduction is obtained.

To calculate the armature current one must refer to formula 20 or 21.

From formula 20,

$$I_{dc}R = \frac{3\times 350}{\sqrt{2}\pi}\left[\cos 110° - \cos 186°32' - 0.471\left(\frac{\pi\times 186.53}{180} - \frac{\pi\times 110}{180}\right)\right] = \frac{3\times 350\times 0.02}{\sqrt{2}\pi} = 4.72 \text{ volts}$$

Hence the armature current,

$$I_{dc} = \frac{4.72}{3} = 1.57 \text{ amperes}$$

The armature voltage (load-terminal voltage),

$$E_{dc} = E_g + I_{dc}R = 218 + 4.72 = 222.72 \text{ volts}$$

Obviously, the value of E_{dc}' could be calculated directly from equation 21, and the same result would be obtained.

The rectifier output voltage from equation 18,

$$E_{dc} = \frac{3\times 350}{\sqrt{2}\pi}\left[\cos 110° - \cos 186°32' - 0.0303\left(\frac{\pi\times 186.53}{180} - \frac{\pi\times 110}{180}\right)\right] = 144.3 \text{ volts}$$

This voltage, of course, is a purely theoretical one and cannot be measured directly. Thus the relationship 25 is confirmed.

If in the course of calculations the angle of ignition would be found smaller than the critical angle of ignition x_{fc}, it would mean that continuous conduction is obtained, and the armature voltage, equal to the rectifier output voltage, would be calculated from equation 3 or 3A.

Usually, the conditions for continuous or discontinuous current 28 and 29 can be checked by using the first approximation of the angle of extinction taken directly from graphs in Figure 5.

Conclusions

The generalization of expressions for the rectifier output voltage and load-terminal voltage to cover all cases of controlled rectification for both continuous and discontinuous conduction and for any number of phases seems to be of particular significance. Clear distinction between the concepts of the rectifier output voltage and the load-terminal voltage is necessary, particularly in the case of discontinuous conduction with a generative load. The determination of the critical angle of ignition, separating the cases of continuous and discontinuous conduction, is of great importance when dealing with rectifiers with a wide range of firing.

Circuit constants have a predominant effect on both load-terminal voltage and the output voltage of a rectifier operating with discontinuous conduction.

The method of calculation of angles of extinction discussed in this paper enables to use relatively simple formulas for average values of direct voltages. As the examples have shown, this method permits to perform the calculations efficiently and without any reference to complicated relationships.

List of Symbols

A = term (equation 36)
a = voltage coefficient (equation 8)
a_0 = voltage coefficient (equation 19)
a' = voltage coefficient (equation 22)
a_c = critical value of voltage coefficient (equation 34)
B = term (equation 37)
E_s = rms supply voltage (transformer secondary)
E_{dc} = rectifier output voltage (average value)
E_{dc}' = load-terminal voltage (average value)
E_g = direct voltage generated in load circuit (opposing electromotive force)
E_0 = arc-voltage drop of rectifier
$E_d = E_g + E_0$
e = instantaneous value of anode supply voltage
I_{dc} = rectifier load current (average value)
L = inductance of load circuit (in henrys)
M = term (equation 38)
M', M'', M''' = intermediate values of term M
N = term (equation 39)
N', N'', N''' = intermediate values of term N
p = number of phases (secondary)
R = resistance of load circuit
$x = \omega t$ = variable time angle
x_f = angle of ignition (firing)
x_1 = minimum possible angle of ignition
x_2 = maximum possible angle of ignition
x_{fc} = critical angle of ignition
$x_{fc\,\max}$ = maximum critical angle of ignition
x_s = angle of extinction
x_s', x_s'', x_s''' = first, second, third approximations of the angle of extinction
x_{s1}, x_{s2}, x_{s3} = intermediate values of the angle of extinction (equation 40)
θ = impedance angle of load circuit
$\omega = 2\pi f$ = angular line frequency
$\pi = 3.1416$
$\epsilon = 2.7183$

References

1. GASEOUS CONDUCTORS, J. D. Cobine. McGraw-Hill Book Company, Inc., New York, N. Y., and London, England, 1941. Pages 494–9.

2. THEORY OF RECTIFIER—D-C MOTOR DRIVE, E. H. Vedder, K. P. Puchlowski. AIEE TRANSACTIONS, volume 62, 1943, pages 863–70.

3. RECTIFIER-CIRCUIT DUTY, C. C. Herskind. AIEE TRANSACTIONS, volume 63, 1944, March section, pages 123–8.

4. ELECTRONIC CONTROL OF D-C MOTORS, K. P. Puchlowski. AIEE TRANSACTIONS, volume 62, 1943, pages 870–7.

5. THYRATRON MOTOR CONTROL, E. E. Moyer, H. L. Palmer. AIEE TRANSACTIONS, volume 62, 1943, November section, pages 706–12.

6. BEHAVIOR FACTORS OF RECTIFIER-DRIVEN D-C MOTORS, Victor Siegfried. AIEE TRANSACTIONS, volume 63, 1944, July section, pages 530–2.

7. APPLIED ELECTRONICS, electrical engineering staff of Massachusetts Institute of Technology. John Wiley and Sons, Inc., New York, N. Y., 1943.

Improved Fault Protection for Rural Distribution Systems

A. VAN RYAN
ASSOCIATE AIEE

Synopsis: The use of automatic oil circuit reclosers on rural distribution lines has resulted in improved continuity of service as well as reduced maintenance cost. However, automatic circuit reclosers now in use are limited in application because of their inability to co-ordinate properly with fuses on the load side of the reclosers. An improved oil circuit recloser has been designed to incorporate the advantages of minimum time-delay opening on the first and second operations to clear all transient faults on the protected section, and greater time-delay opening on the third and fourth operations to allow the blowing of a sectionalizing or transformer fuse to isolate a permanent fault without causing a lockout of the recloser. A description is given of the design, operation, and advantages of this recloser which permits clearing of all transient line faults and isolates permanent faults by properly co-ordinating with sectionalizing fuses.

Improved Equipment Is Required

RURAL distribution systems with their long lines and small loads scattered over large areas depend, for their economical operation, upon low cost of installation, minimum cost of maintenance, and maximum continuity of service.

With the expansion of these systems and the consequent greater cost of service trips, the need has arisen for improved low-cost equipment which is capable of decreasing the number of outages thereby reducing the maintenance cost.

Experience has proved that approximately 85 per cent of all faults occurring on rural systems are of a temporary nature; consequently, the desired protective equipment not only must be able to clear all faults but also should be able to restore service completely after all temporary faults and to isolate the permanent faults to the smallest possible localities.

While automatic circuit reclosers, if properly designed to co-ordinate with one another, can be used advantageously at all sectionalizing points, the low revenue of most of the short branches usually will prohibit such universal use, and it is therefore desirable that inexpensive fuse cutouts be retained on the system.

The ideal combination of protective equipment thus will permit the use of simple fuse cutouts on the smaller branches to isolate the permanent faults occurring there and will make use of automatic circuit reclosers at the feeders and more important sectionalizing points to clear all temporary faults and to isolate permanent faults occurring between the recloser and the fuses.

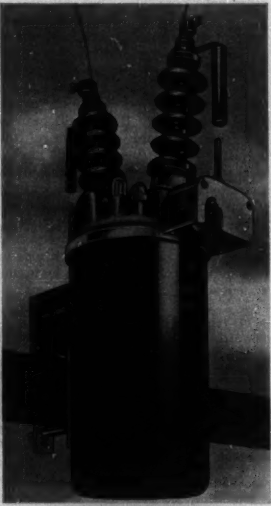

Figure 1. Single-pole automatic oil circuit recloser

To make this selective action possible, the automatic circuit recloser must be of an improved design and meet the following requirements:

1. It must have at least a first operation with a time–current characteristic which is faster than that of the fuse or fuses which it protects, so that the fault will not damage the fuses.

2. It must have at least one subsequent operation with a time–current characteristic which is considerably slower than that of the fuses which it protects, so that the fuse protecting the faulted line will blow.

3. It must, after a minimum of these two operations, lock out in the open position so that, if a permanent fault occur on that part of the system protected only by a recloser, the recloser will isolate this fault from the system.

4. It must be reliable in its operation, light in weight, and low in cost in order to hold the maintenance and installation costs to a minimum.

To meet the foregoing requirements a new automatic oil circuit recloser has been developed as shown in Figure 1.

General Construction

This automatic circuit recloser consists of an aluminum cover and a steel tank, which may be grounded in a conventional manner. A steel hanger welded to the tank permits single-bolt pole mounting, and a simple bracket provides for crossarm mounting. Two conventional porcelain bushings are used so that the line terminals are the only external live parts. Spark gaps are mounted beside each bushing so that surge voltages cannot damage the recloser. The operating handle and the counter are covered by a hood to protect them from sleet. The position of the handle is up when the recloser is closed and down when the recloser is open. All operations are recorded on a counter, and all but the lockout operations are independent of the operating handle, which, in a downward position, indicates that the recloser is permanently locked out. An oil-level gauge is located on the cover.

Operational Features

This automatic circuit recloser requires four consecutive operations to lock out.

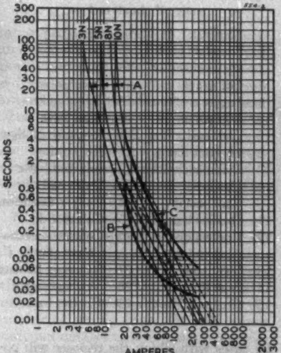

Figure 2. Clearing-time–current curves for ten-ampere automatic oil circuit recloser and melting- and clearing-time–current curves for co-ordinating fuse links

A—100-per-cent-rated fuse links
B—First and second operations
C—Third and fourth operations

Paper 45-54, recommended by the AIEE committee on protective devices for presentation at the AIEE winter technical meeting, New York, N. Y., January 22–26, 1945. Manuscript submitted November 13, 1944; made available for printing December 27, 1944.

A. VAN RYAN is chief engineer of the Kyle Corporation, South Milwaukee, Wis.

The first two of these have a time–current characteristic which is considerably faster than that of fuses having the same rating. The last two operations are time delayed and have a time–current characteristic which is approximately the same as that of fuses having the same rating.

Clearing time–current curves for a ten-ampere automatic circuit recloser and melting and clearing time–current curves for fuses with which the recloser will co-ordinate are shown in Figure 2. It can be seen that properly selected fuses will remain undamaged upon the occurrence of a fault and that the recloser will open the circuit to clear the fault. If the fault exist after reclosing, the recloser will open the circuit again in the same manner. If the fault exist after the second reclosure, the recloser will operate after a greater time delay and will blow the properly selected fuse, thus isolating the fault to the smallest protected section. The recloser can operate still a fourth time to be certain the fuse will clear, and, if the fault is not protected by a fuse, the recloser will open and lock out to clear the fault from the system.

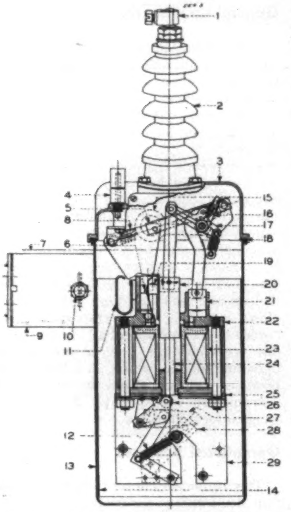

Figure 3. Sectional view of complete automatic oil circuit recloser

1—Terminal
2—Porcelain bushing
3—Metal cover
4—Oil gauge
5—Toggle mechanism
6—Trip piston
7—Oil level
8—Lockout spring
9—Mounting bracket
10—Ground connector
11—Thermal trip
12—Contact operating spring
13—Steel tank
14—Tank liner
15—Operating handle
16—Operating mechanism
17—Hand trip mechanism
18—Cover gasket
19—Slide valve
20—Solenoid plunger
21—Pump piston
22—Solenoid frame
23—Series coil
24—Plunger extension
25—Coil shield
26—Contact - mechanism roller
27—Stationary contact
28—Moving contact
29—Contact frame

Automatic circuit reclosers of different ratings will co-ordinate with one another as well as with fuses.

Figure 3 shows in sectional view the main elements of this automatic circuit recloser. Essentially, these consist of three assemblies, namely: the operating mechanism with lockout spring-and-toggle mechanism mounted in the cover, the hydraulic mechanism and the series coil suspended below the cover, and the contact mechanism mounted below the series coil.

It will be seen that the upward movement of the operating handle elongates the lockout spring while at the same time it permits the toggle mechanism to arrive at an over-center position thus storing the energy of the lockout spring for the lockout operation. It also will be seen that the downward movement of the operating handle trips the toggle mechanism to release the stored energy in the lockout spring and open the recloser until the operating handle is again moved upward.

Figure 4 is a schematic cross section of the hydraulic mechanism, which aids in explaining its operation. The hydraulic system serves four separate functions:

1. It trips the recloser to the lockout position after the fourth operation in any group of successive operations.
2. It accounts for the time delay of inverse characteristic on the third and fourth successive operations.
3. It introduces a reclosing delay of one second between operations to insure the complete dissipation of ionized gasses.
4. It recycles the recloser when the fault is cleared or isolated.

The hydraulic system operates as follows. Upon the occurrence of an overload or fault, the solenoid plunger is drawn into the series coil. The plunger extension acts upon the contact-mechanism roller and, through a set of links, extends the two contact operating springs. When the solenoid plunger arrives at its nearly final position, the contact-mechanism roller imparts a blow to the movable contacts and at the same time brings the hinge point of the contact operating springs to an over-center position so as to cause a rapid contact separation. During this first downward movement of the solenoid plunger the entrapped oil escapes through an escape port by lifting a slide valve in the hydraulic mechanism, as can be seen in Figure 4. Simultaneously with the downward movement of the solenoid plunger a pump piston is moved within a cylinder to force a predetermined quantity of oil below a trip piston.

During the second operation of the recloser, the entrapped oil below the solenoid plunger again escapes freely through the escape port, while the trip piston rises to such a position as to close this escape opening at the finish of the second operation.

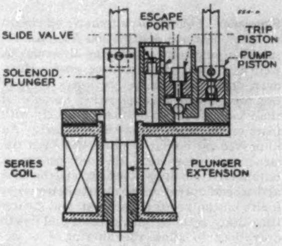

Figure 4. Sectional view of hydraulic mechanism

With the escape port closed off during the third and fourth operations, the downward travel of the solenoid plunger is retarded, because the escape of entrapped oil is possible only by leakage along the solenoid plunger. As the trip-out piston rises higher with each successive operation of the breaker, it not only closes the escape port at the end of the second operation but also continues to rise during the third and fourth operations, and at the end of the fourth operation it contacts the insulated toggle link to trip the toggle and thus release the energy stored in the lockout spring, which causes the recloser to open and lock out.

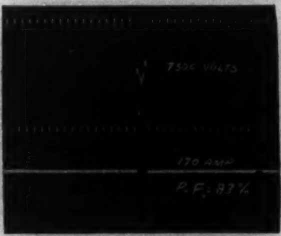

Figure 5. Interruption of 170 amperes at 7,500 volts and power factor of 83 per cent on five-ampere recloser

The energy stored in the contact operating springs during the downward movement of the plunger is not consumed entirely in separating the contacts. It also

Figure 6. Four interruptions of 75 amperes at 7,500 volts and power factor of 82.5 per cent on ten-ampere recloser

acts to return the solenoid plunger to its uppermost position and, after doing this, returns the moving contact to the closed position with a snap action. The upward movement of the plunger therefore constitutes the time delay between successive operations. It is retarded, because the slide valve in the hydraulic mechanism closes off the escape port and only permits oil to enter through a small opening in its top.

It will be noted from Figure 4 that the trip piston is provided with a valve which permits a slight leakage of oil so that this piston slowly will resettle to its original position. Thus, if a fault be cleared after any operation, the recloser automatically will reset itself for a complete cycle of successive operations. The total time for this to take place after a lockout operation has occurred is approximately one minute and thus approximately 15 seconds per operation.

The oil used in the automatic circuit recloser is of a low viscosity which will not change greatly with decrease in temperature. As the time required for the blowing of a fuse link is also dependent upon ambient temperatures, the retardation of the oil circuit recloser by lower temperatures will be minimized. While extremely low temperatures will have an effect upon the time–current curves of the automatic oil circuit recloser, this deficiency is well offset by the advantages of the hydraulic mechanism, in that it can take great shock and eliminates ratchets, gears, and latches which are less sturdy and dependable. It constitutes a simple means to vary the time delay by allowing the free escape of oil during the first and second operations and by restricting the escape of oil during the third and fourth operations.

The contact mechanism is a unitary structure which is removed readily and replaced. It employs a double set of contacts to eliminate the use of braids or flexible leads. As previously explained, the opening or closing of these contacts can be effected only by a complete downward or upward stroke of the solenoid plunger, consequently, partial opening of the contacts, or so-called telegraphing, is impossible. The separating of the contacts is initiated by the final downward movement of the plunger, which imparts a blow to them in proportion to the current value to be interrupted, while the total separation of the contacts is accomplished by the contact operating springs. After the return of the solenoid plunger to its uppermost position, the contacts reclose with a snap action. Contacts are made of copper tungsten which insures long life by its ability to withstand arcing.

The recloser coils are so designed that minimum tripping current for any size recloser produces the same number of ampere turns and thus the same force upon the plunger. This permits changing reclosers to any rating merely by changing coils. As will be noted in Figure 3, replacement of coils requires no loosening of linkages or disturbing of the contact mechanism. Coils are made in normal ratings of 5, 10, 15, 25, and 50 amperes for minimum trip-current values of 10, 20, 30, 50, and 100 amperes. The interrupting capacities are 150, 250, 375, 600, and 1,200 amperes respectively.

Time current values have been obtained from oscillographic records of interruptions. Figure 5 shows an oscillogram of a single interruption at 7,500 volts and 170 amperes on a five-ampere recloser at a power factor of 83 per cent. Figure 6 shows an oscillogram of four operations with lockout on a ten-ampere recloser at 7,500 volts with a 75-ampere fault current at a power factor of 82.5 per cent.

It will be noted that a thermal trip is provided which will, upon excessive oil temperature, move the insulated toggle link and trip the toggle to release the stored energy of the lockout spring, thus causing a recloser lockout operation.

In the design of this recloser it was found possible to reduce the total weight to approximately 65 pounds and the quantity of oil to approximately $2^1/_2$ gallons, while the required internal and external flashover values were maintained.

Summary

The important improvement of this automatic circuit recloser is its double time–current characteristic. As previously explained, this will permit the use of fuses on small branches of the system so as to keep the initial cost to a minimum. Upon the occurrence of a temporary fault this new recloser will clear the fault and restore service immediately afterwards, and upon the occurrence of a permanent fault will cause the fuse link to blow.

If reclosers are used on feeders and main branches, and if fuses are used for all short branches, the use of this improved-type automatic circuit recloser will result in considerable saving in maintenance cost, because it will reduce the number of service trips. It will reduce customer outages to a minimum and confine the fault to the smallest practical locality.

Study of A-C Sheath Currents and Their Effect on Lead-Cable-Sheath Corrosion

C. M. SHERER
ASSOCIATE AIEE

K. J. GRANBOIS
ASSOCIATE AIEE

Synopsis: The destruction of lead sheaths on underground cables by electrolysis usually is caused by the action of direct currents which originate from one or several well-defined sources. Little information is available concerning a-c electrolysis, and since the extent of its destructive action is less widespread than that produced by direct current it is considered generally to be relatively less important in the field of cable-sheath corrosion. This paper discusses two cases of electrolysis in which the lead sheaths on single-conductor power cables were corroded through, causing cable breakdowns; and describes field observations and laboratory tests which show that at first the corrosive action was accelerated greatly by rectified alternating currents which were induced in the sheaths by the load current. A method of protecting the sheaths against such electrolytic corrosion also is described.

THE GENERAL PROBLEM of lead-cable-sheath corrosion is a familiar one to any industrial organization whose field of activity involves the extensive use of lead-covered cables. This is particularly true of communication and electric-power companies. One of the earlier and most common forms of electrolytic corrosion is that caused by the accumulation of stray direct currents by underground cables traversing areas served by transit lines which are discharged back to earth in sections where the cables are positive with respect to ground. Destruction of the cable sheaths in the positive areas where current leaves the cable is known as anodic corrosion. Other factors, more recently recognized, include chemically developed earth potentials resulting from unfavorable soil conditions, galvanic potentials produced by dissimilar metals, and irregularities in the lead sheath itself.

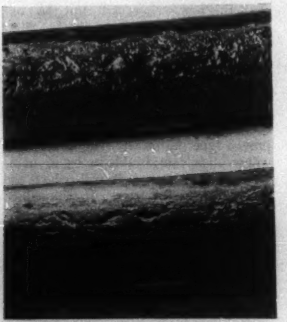

Figure 1. Two specimens of corroded lead sheaths

Electrolysis caused by alternating current has never received widespread consideration, and the consensus of opinion among many authorities has been that it is a complicated phenomenon and is usually unimportant, particularly where sheath sectionalization, with single grounding point, is used.

Two Cable Failures

That a-c corrosion can be of considerable importance is demonstrated by the fact that the case histories of two insulation failures on 13-kv single-conductor lead-covered power cables show that the breakdowns were the result of corrosion produced by a combination of galvanic current and rectified alternating sheath currents. In both cases a one-eighth-inch lead sheath was corroded through, permitting water which was present in the cable ducts to enter and eventually cause insulation failure. Neighboring cables were badly pitted and it was necessary to either replace these or provide protection against further corrosion.

The phenomenon of a-c corrosion was found by extensive field and laboratory tests to be attributable to a process of rectification in which alternating voltages of low value induced in the sheaths by the load current in the cables resulted in alternating currents between sheaths and ground; these were converted to direct currents which produced anodic corrosion. The initial failure occurred in 1937 on a 1,750,000 circular mils paper-insulated single-conductor power cable which was one of eight used to connect a 13,300-volt 25-cycle single-phase 35,000-kva generator in the main generating station at Safe Harbor to the 13-kv bus in adjacent Conestoga substation. The cables are connected four in multiple per phase and are approximately 1,600 feet long. They normally carry a total load of about 2,600 amperes. Each lead sheath is sectionalized at three locations; this results in four approximately equal lengths which are insulated from each other with sheath insulators to prevent the circulation of sheath currents. Individual sheath sections are bonded at only one point to a nearby copper ground bus and sheath voltages are limited to 12 volts per section at normal loading. The cables are installed in eight individual fibre ducts, in a concrete bulkhead. Seven hundred feet of the cable run lie within a tunnel cut through a rock formation of mica schist, which is stratified and porous, permitting water to seep into the tunnel and subsequently into the cable ducts. This provides a low-resistance path to ground from the sheaths and facilitates the action of corrosion. Figure 1 shows two specimens of pitted cables.

The second and most recent failure occurred in November 1943, on a single-conductor 13,200-volt paper-insulated 1,500,000 circular mils cable connecting a 33,750-kva three-phase 60-cycle outdoor transformer to the 13-kv bus in the Holtwood plant of the Pennsylvania Water and Power Company. The cable is one of a group of six, each approximately 290 feet long, connected two per phase. Each cable is installed in a separate fiber

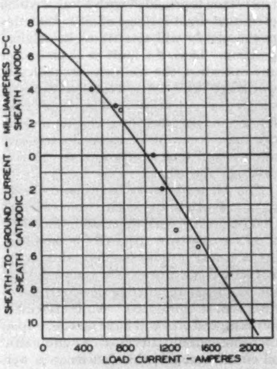

Figure 2. Curve plotted from actual field measurements showing reversal of d-c polarity with increasing load current

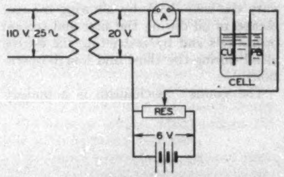

Figure 3. Circuit used for tests on corrosion cells

Paper 45-61, recommended by the AIEE committee on power transmission and distribution for presentation at the AIEE winter technical meeting, New York, N. Y., January 22–26, 1945. Manuscript submitted April 6, 1944; made available for printing January 3, 1945.

C. M. SHERER is assistant chief of tests, Pennsylvania Water and Power Company, Holtwood, Pa., and K. J. GRANBOIS is test engineer, Safe Harbor Water Power Corporation, Safe Harbor, Pa.

duct laid in a concrete envelope surrounded by a solid wall of porous rock or earth fill. Here again seepage water drains into the ducts and creates a condition of low resistance from sheath to ground, which, in effect, shunts the single metallic ground connection on the lead sheath at the outdoor-cable pothead and forms a path for corrosion currents to flow from the sheath to ground for the entire duct length.

Field Observations

Samples of water removed from the ducts at both Safe Harbor and Holtwood were high in alkalinity, having pH values from 9.5 to 11.6. Analyses showed that sodium carbonate, sodium bicarbonate, calcium carbonate, and sodium hydroxide were present. In solution these chemicals provide an excellent electrolyte for the generation of galvanic currents between the sheaths and the nearby copper ground wire, and because of their low resistance the magnitude of both the galvanic and rectified currents was increased. A water sample from the ducts at Holtwood had a specific resistance of only 115 ohms per cubic centimeter as compared with 7,800 ohms for Baltimore city water. Resistance of individual cable sheaths to station ground was as low as 2.7 ohms with the metallic ground connection removed. In a dry installation of fiber duct a resistance to ground of the order of megohms may be expected.

The cables at Safe Harbor lie within several feet of a copper ground bus which runs parallel to them embedded in the tunnel concrete. The water-soaked concrete and fiber duct act as an electrolyte between the lead cables and copper ground wire, so that with no power flow through the cables a small direct potential is present; in effect lead sheath and copper ground constitute a galvanic cell with the copper ground wire as the positive electrode. That is, the copper is positive with respect to the sheaths at the grounding points outside the ducts, with the metallic ground connection removed. There are no stray direct currents in the areas to complicate the situation, and the nearest street-car lines are many miles distant. With the cables de-energized, direct currents up to eight milliamperes were measured flowing between one cable sheath and ground, with the cable anodic, that is, current flow was away from the cable into the wet concrete. This was galvanic current produced by the potential difference between lead sheath and copper ground wire.

Table I

Section	Cables De-energized	Cables Carrying 2,600 Amperes Total Current
1	0.85 milliampere, sheath −	0.3 milliampere, sheath −
2	1.1 milliamperes, sheath −	1.85 milliamperes, sheath +
3	0.1 milliampere, sheath −	0.7 milliampere, sheath −
4	2.7 milliamperes, sheath −	12.0 milliamperes, sheath −

Further observations showed that the direct currents varied in magnitude when varying load current flowed in the cables, and even in some instances reversed their polarity as the load current increased above a certain value. The measurements shown in Table I made at the normal grounding points between sheath and ground bus are representative of direct currents in the four individual sections of the faulted cable, after repairs were made, section 4 now being new cable.

It is seen that the load current had the effect of increasing the direct current in two cases, reducing it in one case, and actually reversing it in another.

Figure 2 represents graphically a case at Safe Harbor in which the sheaths of eight cables were tied together and the direct current measured through the common wire to ground. It is seen that at no load the current is 7.5 milliamperes with the sheaths anodic, and above 1,000 amperes total load the polarity reverses making the sheaths cathodic.

In searching for a possible cause for the variation of the direct currents the most significant clue was the change in their magnitude with changes in load current, and consequently with the induced alternating sheath currents. It was decided to investigate the possibility of these alternating currents being converted into direct current through some process of rectification. Accordingly, a series of laboratory tests were undertaken which extended over a period of nearly a year, and it was found that alternating currents are rectified in lead–copper electrolytic cells using water from the cable ducts as an electrolyte, with resultant destruction of the lead. Such cells are believed to be laboratory analogies of field conditions.

Laboratory Studies

Laboratory experiments were conducted on lead–copper cells to observe the effectiveness of the counter-potential method for preventing sheath corrosion, and to study the factors which affect the rectification phenomenon found on the cables. The experiments were divided into two main groups:

(*a*). A-c corrosion studies.
(*b*). Rectification studies.

CORROSION STUDY

Electrolytic cells were constructed of glass laboratory jars $2^1/_4$ by 4 inches by 6 inches deep, with lead and copper electrodes in an electrolyte of water from the cable ducts. Samples of water were used having pH values from 8.2 to 9.5, and specific resistance of 450 ohms per cubic centimeter. In these tests the loss of weight of the electrode was used as a measure of the degree of corrosion. Cell *A* was energized continuously at low voltage with 25-cycle current only, using one-half ampere initially and reducing later to one-tenth ampere. Two other cells were energized with 25-cycle current, with ten milliamperes direct current superimposed. In one of these, cell *B*, the direct current was applied in the direction to

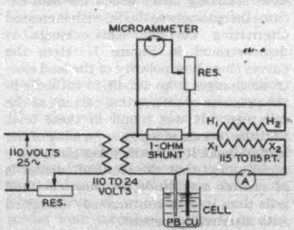

Figure 4. Circuit used for measuring rectified current

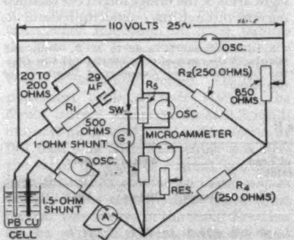

Figure 5. Circuit used for taking oscillograms of rectified current

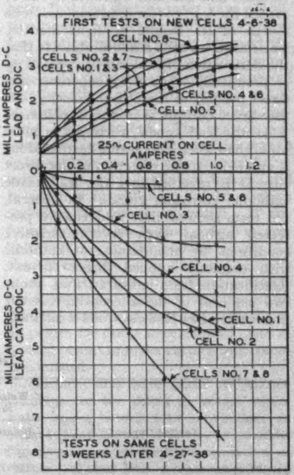

Figure 6. Rectified current versus applied alternating current on new and aged cells

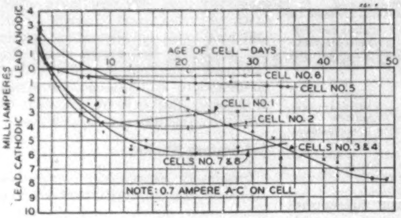

Figure 7 (above). Effect of aging on rectification in test cells

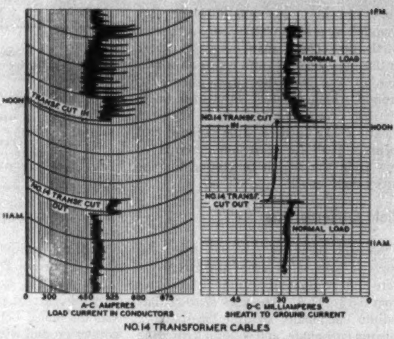

Figure 8 (right). Synchronized charts showing effect of changes in load current on d-c sheath-to-ground current

make the lead electrode cathodic; in cell *C* the lead was made anodic. The magnitude of alternating and direct currents was held at the same value on all cells. Porous alundum cups were placed over the anodes to keep the corrosion products near the corroding surfaces, thus simulating conditions of the cables in the ducts. It was not possible to maintain the value of alternating current at one-half ampere because the porous cups became clogged and increased the cell resistance, therefore after about four months of operation the current was reduced to one-tenth ampere on all cells. The circuit used for these tests is shown in Figure 3.

Results of the tests, after continuous operation for eight months, are summarized in Table II.

These figures show that the combined rectified and galvanic currents of cell *A* caused the lead to lose approximately one fourth of its weight in eight months. The results on cells *B* and *C* indicate that the destruction of lead can be speeded up or practically stopped by superimposing direct current of the proper polarity. If the direct current is in the direction to make the lead anodic, corrosion is more rapid than when alternating current alone is applied. If the direction of the direct current is reversed and the lead made cathodic, corrosion ceases. In general, the tests showed that lead can be protected against even severe corrosive conditions by maintaining it cathodic with correctly applied direct current. Rectification tests indicated that about two per cent of the alternating current present at a new lead electrode is rectified, and to maintain the lead cathodic an amount of direct current slightly above this must be applied.

Rectification Study

The factors which affect rectification, and the characteristics of the phenomenon, were studied on eight lead–copper cells using four different samples of water for electrolyte which were obtained from widely separated sections of the Safe Harbor cable ducts. Duplicate cells were made with each type of electrolyte. The cells were continuously short-circuited except for a short period each day when they were energized with 25-cycle current for making observations of the rectifying action. With the circuit* shown in Figure 4 it was possible to measure fractions of a milliampere direct current in the presence of several amperes of alternating current. The transformer neutralized the alternating current in the measuring circuit, and the rectified current was measured on a microammeter shunted by one ohm.

Oscillograms of the alternating and direct currents were obtained by means of the bridge circuit shown in Figure 5. With a desired value of alternating current on a cell, the bridge was balanced by adjusting resistance R_1 until the galvanometer was at minimum deflection. The relatively high resistance of the two right arms of the bridge forced the rectified current through the oscillograph shunt R_3 and the left side of the bridge. Records obtained in this manner agreed with results obtained by the use of indicating instruments shown in Figure 4.

It was found that the rectifying action of the cells was a function of the surface of the lead electrode, and that rectification characteristics changed with the aging of the lead in the electrolyte, even to the extent of causing reversal of polarity of the rectified current. The curves of Figure 6 show the manner in which the age of the cell affected rectification for the eight cells used in the experiment. Direct current is plotted against increasing values of applied alternating current. The group of curves above the reference abscissa were obtained when the cells were new, with fresh electrolyte and cleaned and scraped electrodes. The lower group of curves are representative of the same cells three weeks later, with the cells having been short-circuited during the interval. All the curves show a small galvanic current in the absence of applied alternating current; under this condition lead is always anodic because of its position with respect to copper in the electromotive-force series of elements. When the cells were new, an increase in the amount of alternating current caused the lead to become increasingly anodic; but during the three-week period in which the cells were short-circuited, the rectifying characteristic of the lead underwent a change, after which the lead became increasingly cathodic with increased alternating current. This change is demonstrated in Figure 7. Here the curves show how polarity of the lead electrode changes from anodic to cathodic in the presence of alternating current as the cells age. It was found in these tests that the process of aging or forming of the lead to make it cathodic takes place more rapidly, and that the rectified current is of greater magnitude, in short-circuited cells than in cells continuously energized with alternating current.

Tests made with cells using water from the Holtwood cable ducts confirmed the

Table II

Cell	Applied Current	Weight of Lead in Grams		Per-Cent Change	Weight of Copper in Grams		Per-Cent Change
		Before	After		Before	After	
A	25 cycles only	119.7	90.2	−24.8	47.7	47.7	
B	Alternating plus direct—lead cathodic	116.8	116.3	− 0.4	48.8	20.0	−59.0
C	Alternating plus direct—lead anodic	112.8	52.5	−53.5	47.7	47.8	

---

* Acknowledgment is made to E. F. Wolfe and Charles Wasserman of the Consolidated Gas Electric Light and Power Company of Baltimore for this circuit.

earlier results at Safe Harbor that rectified currents in new cells are of the same polarity as the galvanic currents and add to the latter to make the lead increasingly anodic.

A number of experiments to determine the factors affecting rectification were carried out by varying the conditions under which the cells were tested. The conclusion was reached that rectification depends on the condition of the surface of the lead; polarity of the rectified current is dependent upon the pH of the electrolyte and the length of time the lead has been in the electrolyte. Newly cleaned and scraped electrodes placed in cells with fresh and with used electrolyte respectively indicate that age of the electrolyte does not affect rectification. However, when new clean lead electrodes were substituted for aged ones, polarity changed from cathodic to anodic. Changing old copper electrodes for new ones made no difference in rectification. A ten-per-cent increase in rectified current resulted from an increase in temperature from 5 degrees to 50 degrees centigrade. Irrespective of whether the lead electrodes were tarnished, scraped, greased, oxidized, or rough surfaced, they were always anodic when first placed in a cell with a copper electrode and always became cathodic at a later time. Cells with two lead electrodes showed no rectification when the surfaces of the two were identical, but if one was new and the other cell-aged, as much as two per cent of the applied alternating current was rectified.

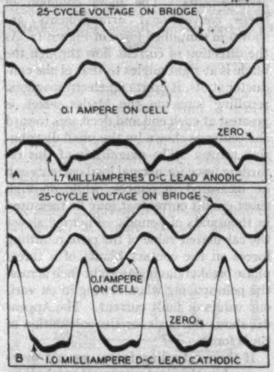

Figure 9. Rectification tests on lead–copper cells. Oscillograms showing wave form and polarity of rectified current on a new and an aged cell

A—Fresh electrolytic cell
pH is 8.2
Resistance is 630 ohms per cubic centimeter at 25 degrees centigrade
Cell age is $2^{1}/_{2}$ minutes

B—Aged electrolytic cell
pH is 8.3
Resistance is 2,200 ohms per cubic centimeter at 25 degrees centigrade
Cell age is $2^{1}/_{2}$ months

Inasmuch as the rectification apparently is due to the surface condition or film formation and the element of time, it is interesting to observe this effect in the field. A synchronized recording was made at Holtwood of the load current and the direct current in the ground connection of six cable sheaths in parallel. In Figure 8 the direct current is seen to be maximum at zero load current and in general decreases with an increase in load. The load swings produce corresponding changes in the direct current. However, a polarizing effect because of time is also present, particularly when the load current suddenly is reduced to zero or when suddenly applied.

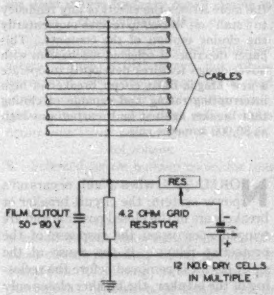

Figure 10. Method of applying counter potential for corrosion prevention

As a matter of general interest, the wave form and polarity of the rectified current in the laboratory cells is shown in the oscillograms of Figures 9A and 9B for a new cell and an aged cell.

Correlation of Laboratory Tests and Field Observations

As previously discussed, field observations made following the cable failures disclosed that load current affected the magnitude of direct currents flowing between sheaths and ground. On the replacement cable at Safe Harbor, the direct current increased from 2.7 milliamperes at no load to 12 milliamperes at full load. Because this cable was new the large increase of current correlates with the results obtained on new cells in the laboratory tests in which the rectified current was always in the same direction as the galvanic current, with the lead anodic. Referring again to Figure 2, the reversal of the direct current with load current above a certain value agrees with the characteristics found on aged cells, in which polarity of the direct current reverses to make the lead cathodic for alternating currents above given values. Since the rectified currents on aged lead oppose the galvanic currents and are in the direction to make lead cathodic, it might be expected that rectification would make the sheaths self-protecting above a critical load current, and this is no doubt true after the lead is sufficiently formed or aged. Since this process of forming is a function of several variable factors such as continuity and magnitude of load current, time, and quantity and character of water in the ducts, it is not possible to determine when the self-protecting condition will be attained. One method to provide definite protection to lead cables in wet ducts is the application of direct current in the direction to maintain the sheaths always cathodic.

Corrosion-Prevention Measures Applied to Cables

Inasmuch as the rectified currents in the field were, in some cases, in the direction to produce corrosion of the cable sheaths, and the galvanic currents always in this direction, the most obvious remedy was to apply a counter potential of a slightly higher order from an external source to force a flow of current in the opposite direction. The method adopted at Safe Harbor consisted of an application of a bank of 12 number 6 dry cells in multiple, connected across a resistor between the cable sheaths and ground bus as shown in Figure 10. Operating rules require that the sheaths must have a positive ground connection, and it was, therefore, not permissible simply to insert the batteries between sheaths and ground. The eight cable sheaths were connected together, then grounded through a 4.2-ohm grid resistor across which the batteries were operated. The resistor performs two functions. It provides a path to ground for any currents that might result from a cable-insulation failure, and in addition furnishes an *IR* drop which serves as the counter potential. It was found experimentally that a drop of one-half volt across the resistor made the sheaths cathodic to the duct and concrete at all points where they were accessible for observation. Since it was important that the sheaths be definitely cathodic at all points the ducts were chipped open at several places to make certain this condition existed.

Measures also were taken to provide drainage for the ducts at places where water had a tendency to accumulate, in order to keep the cables as dry as possible. Finally, an experimental installation of rubber-jacketed lead cable was made in the area where corrosion was most severe.

The possibility of increasing the resistance of the cable sheaths to ground by flushing the ducts with clean water was investigated. The duct of one sheath section whose resistance to ground was 1.75 ohms was flushed continuously for seven days with the expectation that removal of the accumulated impurities would result in an improvement in resistance. After flushing, compressed air was blown through the duct for several weeks to dry it out. Results were disappointing; a slight decrease rather than an increase in resistance was effected, the final value being 0.9 ohm.

The failure at Safe Harbor occurred after the cables had been in service less than three years. The protective measures were applied immediately following the failure, and during the period of more than seven years which has elapsed since then no more failures have taken place.

The breakdown at the Holtwood plant occurred after the cable had been in service 12 years, indicating a much slower rate of corrosion. Corrosion-prevention measures taken here are similar to those employed at Safe Harbor, except that copper-oxide rectifiers instead of dry cells are used as a source of counter potential.

Conclusions

From the laboratory tests and field observations, it is reasonable to conclude that the cable failures described were the result of rectified induced alternating sheath currents in combination with galvanic currents, plus possibly a small amount of chemical action. The destructive effects of a-c corrosion were most pronounced when the cables were new and the ducts first became wet with alkaline seepage water. Evidence appears to indicate that the destructive effects of rectification decrease with time and eventually cease entirely as a result of a reversal of polarity.

It is important that in new installations of single-conductor lead cables in underground-duct systems caution be observed to guard against the effects of water seepage into the ducts. Galvanic currents may be expected to flow from the lead sheath to the usual metallic ground system, and when the ducts first become wet destructive effects also may be expected from the rectified induced sheath currents.

Data on laboratory cells showing how the rectification phenomena and corrosion change with respect to time cannot be used to predict changes in the field. They serve only to demonstrate the phenomena in a qualitative way. On short-circuited test cells, for instance, the rectified current reversed its polarity within several days after the cells were made; in contrast with this, on some of the cables in the field it was still in the anodic direction several years after the cables were installed.

New Solenoid Mechanism for Magne-Blast Breaker

B. W. WYMAN
ASSOCIATE AIEE

J. H. KEAGY
ASSOCIATE AIEE

Synopsis: The existence of relatively high electromagnetic forces in circuit breakers when subjected to fault currents of appreciable magnitude has long been recognized. One of the problems in the design of a circuit-breaker operating mechanism is to provide smooth and effective closing performance, even though the breaker be closed against a short circuit and is thereby subjected to these high electromagnetic retarding forces during the final portion of the closing stroke. The greater the magnitude of the short-circuit current, the higher these electromagnetic retarding forces become and the more serious the effects of any tendency to "stall" or, worse, to reverse momentarily the closing motion of the contacts. This paper describes a solenoid mechanism with novel design features developed to operate a new Magne-Blast circuit breaker of high interrupting rating and capable of closing that breaker against fault currents as high as 80,000 amperes rms.

NORMALLY, when a fault occurs on a power system, the circuit breaker or breakers are in the closed position and are tripped open upon the response of the protective relays. If the cause of the short circuit is removed before the reclosing of the breaker, the breaker closes only the load current of the circuit. If, however, the cause of the short circuit is not removed before the reclosing of the breaker, the fault current is re-established as soon as the circuit-breaker contacts touch. This may occur frequently on systems which are reclosed automatically after fault operations, if the faults happen to be of a persistent nature. This re-establishment of short-circuit current by the touching of the circuit-breaker contacts sets up electromagnetic retarding forces, which, for the more simple contact arrangements, oppose the closing motion of the breaker. The magnitude of these opposing forces is proportional to the square of the short-circuit current, and in circuit breakers having high momentary and interrupting current ratings they may be very high. Any tendency of the circuit breaker to "stall" or reverse momentarily its closing motion at such high values of fault current easily might result in excessive contact burning or other undesirable disturbances in the breaker during the brief interval between establishment of the fault current and the subsequent tripping operation of the breaker.

The electromagnetic retarding forces responsible for this "stalling" action arise from the U-shaped loop circuit which is formed by the contacts and the conductor studs in most of the conventional contact arrangements. The more common of these conventional arrangements are shown in simplified form in Figure 1. As the direction of current flow through the blade is at right angles to that of the conductor studs, it exerts an electromagnetic repelling force on the blades which is greatest at each end and decreases toward the center as shown by the small distribution arrows. The magnitude of this retarding force for normal load currents can be measured in ounces, while on high short-circuit currents it may be measured in thousands of pounds. Figure 2 shows the calculated value of the peak retarding forces on the contact blades of a three-phase breaker having an eight-inch across-the-pole spacing when closing in on various values of fault current. The Appendix shows the basis for the calculation of these forces.

If these retarding forces are not overcome by the instantaneous-mechanism output force plus the forces from kinetic energy stored in the moving parts, "stalling" may occur. Figure 3A shows the contact stalling which occurs in an actual test breaker operated by a conventional solenoid mechanism when closing in against various values of short-circuit current. The stalling which occurred in

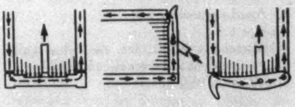

(A) (B) (C)

Figure 1. Contact arrangements on conventional small and intermediate ratings of circuit breakers

Dashed lines show U-shaped current path that produces the electromagnetic forces which are shown by the small arrows tending to open the contact blades

A. Oil circuit breaker
B. Low-voltage air circuit breaker
C. Magne-Blast power circuit breaker

Paper 45-56, recommended by the AIEE committee on protective devices for presentation at the AIEE winter technical meeting, New York, N. Y., January 22–26, 1945. Manuscript submitted November 24, 1944; made available for printing December 27, 1944.

B. W. WYMAN is in the power-circuit-breaker department and J. H. KEAGY is development engineer, both with General Electric Company, Philadelphia, Pa.

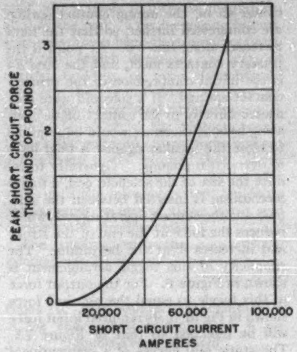

Figure 2. Peak magnetic retarding forces acting to retard closing motion of three-phase breaker closing against various short-circuit currents

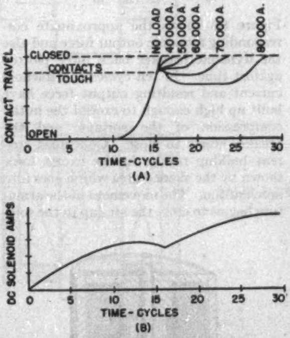

Figure 3. The effect of short-circuit magnitude upon stalling tendency during closing in conventional breaker

A. Conventional breaker closing travel versus time, closing against various values of short-circuit currents showing how stalling increases at contact making when breaker is closing higher short-circuit currents. After stalling breaker completes its closing stroke when solenoid builds up to a sufficiently high value to overcome retarding forces

B. Solenoid current buildup associated with A

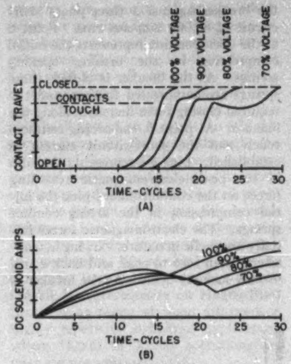

Figure 4. The effect of reduced control voltage upon stalling tendency during closing in conventional breaker

A. Conventional breaker travel-versus-time curves closing 50,000-ampere three-phase short circuit with various percentages of rated control voltage sustained at solenoid terminals, showing increased amounts of stalling which occurs with lower percentages of rated control voltage

B. Solenoid-current buildup curves for tests shown in A

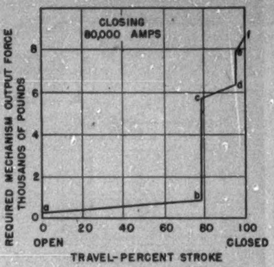

Figure 5. Variation of force at breaker contacts throughout closing stroke

0-*a* = initial compression in breaker opening springs

a-*b* = the increase in force as these springs are compressed

b-*c* = peak electromagnetic retarding forces of short circuit plus initial compression in arcing-contact springs

c-*d* = increase in arcing-contact-spring pressure as these springs are compressed

d-*e* = initial compression in primary-contact springs

e-*f* = increase in primary-contact-spring pressure as these springs are compressed

these tests when closing currents of 60,000 amperes or above resulted in contact arcing and disturbance in the breaker. The duration of the stalling period increased with the short-circuit current, becoming as high as 12 cycles at 80,000 amperes. After stalling occurs, the solenoid current continues to build up as shown in Figure 3B and, when the solenoid output force finally exceeds the short-circuit retarding force, the breaker completes its closing stroke. Any advantageous utilization of kinetic energy has been lost.

This stalling tendency for conventional solenoid-mechanism designs is aggravated greatly if we reduce the d-c control voltage maintained at the solenoid terminals. Figure 4A shows the amount of stalling obtained when closing against a 50,000-ampere short circuit with various percentages of rated control voltage maintained at the coil terminals. The progressively lower d-c solenoid-current buildup rate for each of these voltages is shown in Figure 4B and results in

1. Longer time delay before starting to close.
2. Lower closing speed.
3. Increased stalling at contact making.

In recognition of these effects, recommended practice requires at least 90-percent rated control voltage to be maintained at the coil terminals of any breaker that may be required to close in against a short circuit. As further insurance against the effects of possible stalling, application recommendations for some time have required instantaneous tripping relays, which are operative only during the breaker closing operation, to be included as part of the essential equipment in all locations where the short-circuit current may exceed a stipulated value. As these relays are operative only when the closing control circuit is energized, they do not interfere with the selective relays used to trip the breaker from its normally closed position. These relays limit the duration of any possible "stalling" to a value of the order of two to four cycles. However, it has been realized that it is highly desirable, in new designs, to eliminate completely stalling over the entire operating range of control voltage. Accordingly, an improved mechanism design with greater instantaneous output force has been developed.

This mechanism design, applied to a 500,000-kva Magne-Blast breaker has demonstrated the ability to close and latch that breaker, without stalling, against three-phase short-circuit currents in excess of 80,000 amperes rms, that is, in excess of the momentary current rating of the breaker. Any adverse effects of "stalling" such as sustained contact arcing or other disturbances in the breaker thus are eliminated, and the provision of the instantaneous overcurrent tripping relays previously referred to is no longer required.

The remainder of this paper describes the development and construction of new solenoid mechanisms of this design, which employ a flux-shifting principle of operation.

Analysis of Problem

In the development of a mechanism to eliminate stalling when closing against

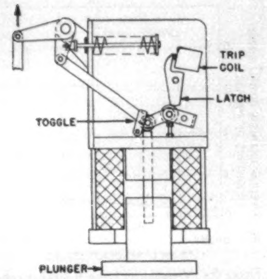

Figure 6. Toggle mechanism used to reduce required solenoid force at closed position on Magne-Blast breaker showing simplicity of linkage

high short circuits, it is necessary first to analyze the forces involved. Figure 5 shows how the breaker closing forces vary through the stroke. Curve *a-b-c-d-e-f* represents the closing-force curve which the mechanism must supply when closing the breaker against a three-phase short circuit of 80,000 amperes rms. Point *a* at the open position represents the initial compression in the breaker opening springs. As the breaker is closed, these springs are compressed further, and the required closing force increases along the line *a-b*. At point *b*, the arcing contacts touch and the short-circuit current is established. Line *b-c* represents the sum of the peak electromagnetic retarding forces on the contact blades plus the initial compression in the arcing contact springs. The electromagnetic forces initially are cyclic in nature, varying in magnitude from zero to peak and back again to zero once per cycle. As the breaker is closed on in, the arcing contact springs are compressed further, so that the force increases along line *c-d*. At point *d* the primary contacts meet, and the step *d-e* is the initial compression in the primary contact springs. If a solenoid were connected directly to the contact-blade operating rods, it therefore would be required to close the breaker against a final force of over 8,000 pounds. Generally to reduce the size of the solenoid coil, a toggle mechanism is inserted between the solenoid and the contact operating rods which reduces the force at the end of the stroke and increases it at the beginning. The simplicity of this toggle arrangement is shown in Figure 6. For the output force of this toggle to equal the required force shown in Figure 5, its required input force will be modified to that of Figure 7A. The static pull curves of a conventional solenoid capable of producing sufficient output force to close this breaker are shown in Figure 7B. Although this conventional solenoid ultimately will close the breaker against 80,000 amperes, it will result in serious stalling at the time contacts meet as the coil current will not yet have built up to a high enough value to exceed point *c* and close the breaker. This can be seen from Figures 8A, 8B, and 8C. Figure 8A shows the d-c solenoid-coil-current buildup versus time which, when eddy currents are neglected, follows the equation:

$$E=Ri+\frac{d(Li)}{dt}=Ri+L\frac{di}{dt}+\frac{dL}{dt}$$

Figure 8B shows the approximate corresponding dynamic output force and also the dynamic breaker back force plotted against time. In ten cycles the solenoid current and resulting output force have built up high enough to exceed the initial compression of the springs, and the breaker starts to close. Continued current buildup results in the excess force shown by the shaded area which goes into acceleration. The movement of the armature begins to close the air gap in the sole-

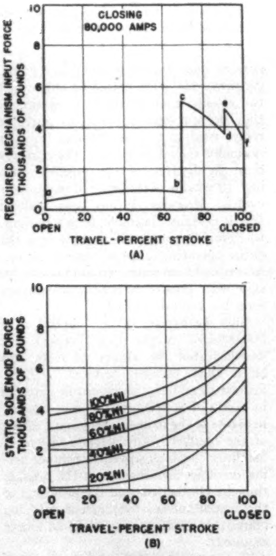

Figure 7. Mechanism input forces as modified by toggle linkage

A. Input force to mechanism in Figure 6 to equal output force required in Figure 5 at breaker contacts with magnetic force included

B. Static-pull curves of conventional solenoid capable of producing output forces required in Figure 7A to close breaker at 70-per-cent rated current

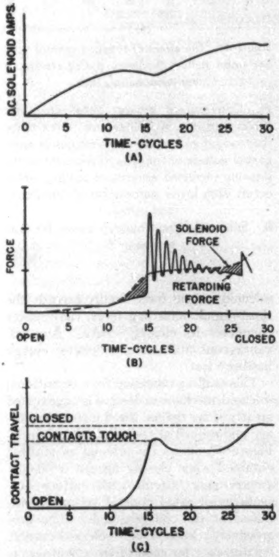

Figure 8. Conventional solenoid-current buildup, dynamic output force, and stalling when closing 80,000-ampere short circuit

A. D-c solenoid-current buildup versus time with closing operation for breaker with conventional solenoid mechanism when closing against 80,000-ampere three-phase short circuit

B. Dynamic-solenoid-output-force buildup versus time associated with solenoid-current buildup shown in A plotted over required static-force curve to close breaker. Shaded area equals excess of solenoid output force which goes into accelerating breaker contacts

C. Closing travel versus time resulting for breaker closing against 80,000-ampere three-phase short circuit showing stalling due to short-circuit magnetic forces at time of contact touching

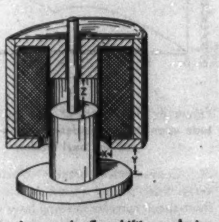

Figure 9. Improved flux-shifting closing solenoid-coil design with bottom plate on plunger

X = air gap around circumference of plunger

Y = air gap to bottom plate which short-circuits gap X as plunger closes

Z = normal air gap at top of plunger

noid, which tends to increase the inductance of the coil. This increasing inductance generates a back electromotive force, $[i(dL/dt)]$ which decreases the rate of current buildup, or even momentarily may cut the current down. Figure 8C shows the associated breaker-contact travel. In 15 cycles the contacts touch, though the solenoid output force has not yet built up to the required short circuit plus contact force, and so the breaker stalls until the solenoid current builds up high enough to exceed these forces and complete the closing stroke.

The stalling with the conventional solenoid can be reduced somewhat by increasing the amount of toggle which raises the required force at the open position but decreases it faster as the stroke progresses. This action holds the breaker back until the coil current has built up to a higher value before it can start closing. There is a limit, however, to this hold-back action, as it results in a higher excess force all the way through the stroke, and this greatly increases acceleration and speed so that abnormal dashpots or closing buffers may be required to absorb the impact of closing this breaker against no load. Excessive closing speeds are to be avoided if possible to increase the mechanical life of the breaker. An extremely long maintenance-free operating life is a prerequisite on Magne-Blast breakers, as many of them are used on highly repetitive industrial applications where 15,000 to 30,000 operations per year are not unusual.

Figure 10. Flux paths for various positions in *A* the conventional solenoid, and *B* the double-air-gap solenoid

In the open position, the flux path in the two types of solenoids is the same, but, as the plunger nears the closed position, more and more of the flux in the double-air-gap solenoid is shifted from the nonpulling annular gap to the pulling gap of the bottom plate, as shown in the half-closed and closed positions

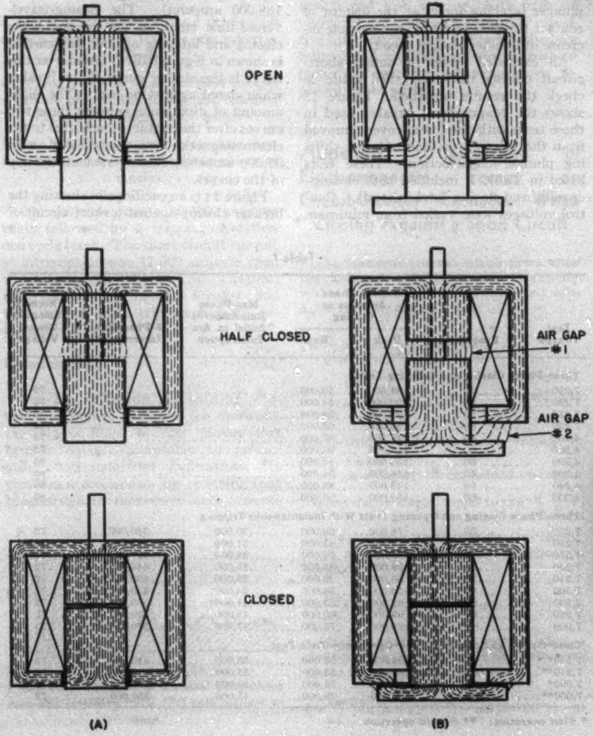

Improved Solenoid Design

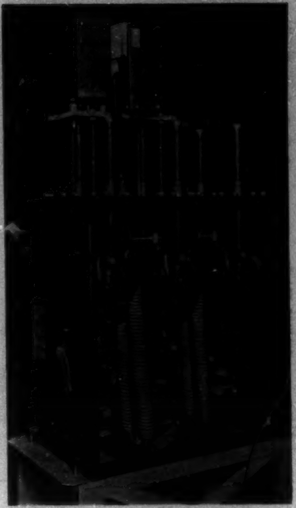

Figure 11. Rear of Magne-Blast breaker with arc chutes removed and tension springs connected through lost-motion linkage to operating rod shaft simulating short-circuit retarding forces

To avoid high closing speed and still close against high currents without stalling, the solenoid mechanism should provide a normal dynamic output pull in the early part of its stroke of about the same magnitude as the conventional solenoid. When the contacts meet, however, the output force should rise rapidly without delay to pull the breaker contacts closed without waiting for the coil current to increase in value. The total pull from a conventional solenoid plunger depends on the total flux across the pulling gap into the plunger. It is impossible to increase quickly the total amount of flux in the magnetic circuit on account of the inductance of its path, but it is possible to

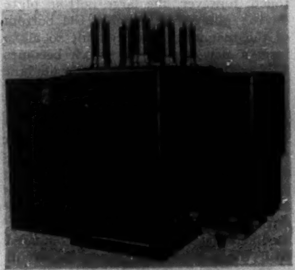

Figure 12. A 500,000-kva Magne-Blast circuit breaker with lower cover removed from solenoid to show flux-shifting plunger construction

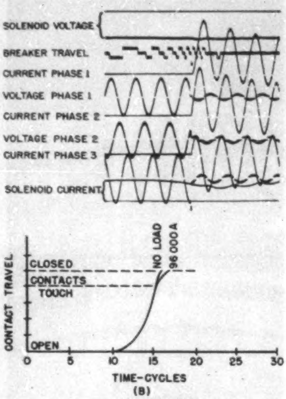

Figure 13. Improved flux-shifting solenoid closing against 96,000-ampere three-phase short circuit

A. Oscillogram showing breaker closing and latching on 96,000-ampere rms three-phase short circuit with 70-per-cent rated control voltage sustained at solenoid terminals

B. Flux-shifting-solenoid closing-travel-versus-time curve when closing and latching against no load and when closing and latching against 96,000 amperes as determined from the oscillogram in A

shift its path so that the same flux crosses two pulling gaps.

Figure 9 shows a plunger solenoid design in which the initial flux path in the open position is across the annular gap *X* up through the cylindrical plunger and through the pulling gap *Z* to the pole piece and down through the return circuit. The plunger, however, is fitted with the large bottom plate *B*. In the early part of the stroke practically all the flux flows across gap *X*. As the plunger closes in to the point where the breaker contacts touch, however, the large bottom plate on the plunger approaches the bottom of the magnetic return circuit so as to form a new gap at *Y*, which becomes shorter than gap *X*. The major amount of the flux therefore will have shifted by this time from the nonuseful gap *X* to the additional pulling gap *Y* which adds its force to that of *Z*. With no increase in total flux, therefore, this flux-shifting design exerts a greater pulling force at the end of the stroke. Figure 10B shows how this flux path shifts for various positions during the stroke for a solenoid with the modified magnetic circuit as compared with the conventional magnetic circuit in Figure 10A.

The original development tests on this double air-gap type of solenoid were made by simulating the short-circuit forces with heavy tension springs fastened through a partial-stroke lost-motion connection to the mechanism output shaft. Figure 11 is the rear view of a breaker resting on a framework with arc chutes removed to show these tension springs. A Cincinnati analyzer is mounted on top of the breaker to measure contact travel. By varying the tension in these springs, it is possible to simulate various magnitudes of short-circuit currents. Dynamic flux measurements made during these tests determine the optimum air gap and bottom-plate dimensions for the solenoid magnetic circuit.

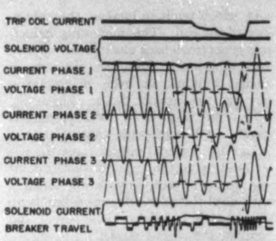

Figure 14. Oscillogram showing breaker closing against 75,000 amperes tripped instantly, interrupting 540,000 kva at 7,250 volts

The conventional solenoid plunger construction first tested in this manner was shown to be capable of closing against a spring load equivalent to a 50,000-ampere three-phase short circuit with 90-per-cent control voltage. In contrast, the modified flux-shifting solenoid using the same coil-and-mechanism toggle construction closed successfully against a spring load equivalent to 95,000 amperes without stalling even when the control voltage was reduced to approximately 70 per cent of rated voltage. This represented an increase of over 1,800 pounds (peak oscillating force of 3,600 pounds) in plunger latching force, at the instant of contact touching, with no appreciable increase in breaker closing speed.

An extended series of actual short-circuit closing tests was then made to check the results obtained. Figure 12 shows the Magne-Blast breaker used in these tests with the lower cover removed from the solenoid to show the flux-shifting plunger construction. These tests listed in Table I, included both closing–opening and closing–latching tests. Control voltages were varied from minimum to 100-per-cent normal and the short-circuit current exceeded 80,000 amperes rms in a number of tests. No stalling occurred on any tests, and there was no disturbance at the breaker. The positive no-stalling closing action reduced contact erosion to a negligible amount.

Figure 13A is an oscillogram showing the breaker closing and latching against 96,000 amperes rms (peak current = 158,000 amperes). The closing-travel-versus-time curve of the breaker when closing and latching against this current is shown in Figure 13B. Plotted over this curve is the closing curve of the breaker when closed against no load. The slight amount of divergence between these two curves after the contacts touch, due to the electromagnetic forces associated with 96,000 amperes, can be seen at the top of the curves.

Figure 14 is an oscillogram showing the breaker closing against a short circuit of

Table I

Test Voltage	Frequency	Max Phase Amperes on Closing		Max Phase Rms Amperes Initial in Arc Interruption	3-Phase Kva Interruption	Per-Cent Normal Solenoid Control Voltage
		Peak	Rms			
Three-Phase Closing and Latching Tests						
7,250	60	84,000	50,000			72
7,250	60	90,000	54,000			72
7,250	60	92,000	53,000			72
7,250	60	112,000	66,000			72
4,200	60	147,000	87,000			72
4,200	60	158,000	95,000			72
4,200	60	155,000	92,000			95
4,200	60	158,000	94,000			95
4,200	60	148,000	88,000			80
4,200	60	158,000	96,000			80
Three-Phase Closing and Opening Tests With Instantaneous Tripping						
7,250	30	76,000	50,000	30,000	380,000	72
7,250	30	75,000	45,000	31,000	390,000	72
7,250	30	57,000	34,000	34,000	430,000	72
7,250	30	59,000	35,000	35,000	440,000	72
7,250	30	66,000	39,000	39,000	490,000	72
7,500	60	56,000	34,000	24,000	310,000	72
7,500	60	92,000	55,000	41,000	530,000	72
7,250	60	99,000	60,000	43,000	540,000	72
7,000	60	120,000	73,000	47,000	570,000	72
Close–Open + 15 Seconds + Close–Open Duty-Cycle Test						
7,250*	60	92,000	56,000	33,000	420,000	72
7,250**	60	89,000	53,000	35,000	440,000	72
7,000*	60	100,000	59,000	39,000	470,000	72
7,000**	60	120,000	70,000	45,000	550,000	72

* First operation. ** Second operation.

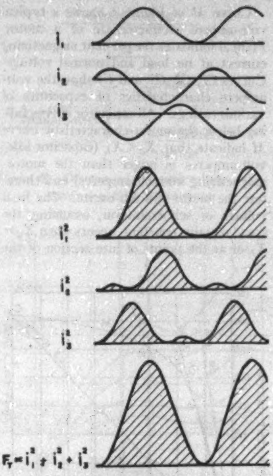

Figure 15

i_1, i_2, and i_3 are the three-phase short-circuit currents when closing 100-per-cent inductive circuit

i_1^2, i_2^2, and i_3^2 are the squares of these currents which are proportional to magnetic retarding forces on individual switch blades

$F_T \propto i_1^2 + i_2^2, + i_3^2$ is the total three-phase magnetic retarding force for the three phases of breaker

73,000 amperes rms (120,000 amperes peak) followed by a tripping operation one cycle later. The short-circuit current at interruption was 47,000 amperes rms; which represented 570,000 kva. The total interrupting time of the breaker was three cycles from trip impulse to interruption.

Conclusions

The double-air-gap flux-shifting solenoid mechanism designed for operating the Magne-Blast breaker makes this breaker equally adaptable to public-utility and industrial applications. It provides a mechanism for reclosing that breaker against maximum fault currents with minimum control voltage maintained at the coil terminals, without stalling and without damage to the contacts. For industrial applications it provides a positive mechanism of extremely simple design and few moving parts with an operating speed fitting it for highly repetitive applications such as steel-mill motor control and arc-furnace control, without requiring excessive adjustment or replacement of parts.

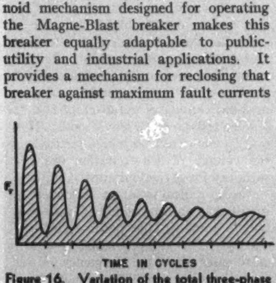

Figure 16. Variation of the total three-phase magnetic retarding force (F_t) with respect to time

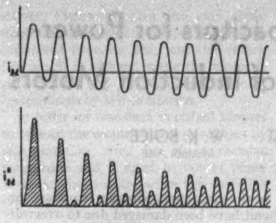

Figure 17

i_{l-l} is the single-phase fault current when switch is closed at zero voltage point on voltage wave

i_{l-l}^2 is the square of single-phase fault current which is proportional to magnetic retarding force on blade

Appendix. Calculation of Electromagnetic Forces on Circuit-Breaker Contacts When Closing Against a Short Circuit

The transient current which flows upon the closing of a switch in an inductive circuit with a sinusoidally varying impressed voltage is given by the equation:

$$i = \frac{E_m}{\sqrt{R^2+(\omega L)^2}} \left[\sin(\omega t+\theta-\phi) - \epsilon^{-\frac{Rt}{L}} \sin(\theta-\phi)\right] \quad (1)$$

where

θ = electrical angle from zero voltage to making of circuit

ϕ = angle of lag of current behind voltage or power-factor angle $\left[\text{equal to } \tan^{-1}\left(\frac{\omega L}{R}\right)\right]$

If we neglect resistance in the circuit, $R=0$, and $\phi=90$ degrees, and the equation becomes

$$i = \frac{E_m}{\omega L}\left[\sin(\omega t+\theta-90°) - \sin(\theta-90°)\right] \quad (2)$$

Closing a three-phase switch upon a three-phase a-c short circuit similarly gives rise to three currents equal to

$$i_1 = \frac{E_m}{\omega L}\left[\sin(\omega t+\theta-90°) - \sin(\theta-90°)\right] \quad (3)$$

$$i_2 = \frac{E_m}{\omega L}\left[\sin(\omega t+\theta-90°-120°) - \sin(\theta-90°-120°)\right] \quad (4)$$

$$i_3 = \frac{E_m}{\omega L}\left[\sin(\omega t+\theta-90°-240°) - \sin(\theta-90°-240°)\right] \quad (5)$$

θ being measured in all cases from the instantaneous voltage zero in the first phase.

If these switch blades bridge at right angles two parallel conductors as shown in Figure 1 of the paper, the instantaneous magnetic force tending to open each switch blade is equal to

$$F = 4.5 i^2 K\, 10^{-8} \text{ pounds*} \quad (6)$$

where

i = the current in that blade

K = a constant determined by switch proportions

$= \log_e \frac{S}{0.779R} \frac{l+\sqrt{l^2+R^2}}{l+\sqrt{l^2+S^2}}$

S = distance between parallel conductor centers—inches

R = radius of parallel conductors—inches

l = length of parallel conductors—inches

The total instantaneous magnetic force then acting upon the three switch blades is equal to

$$F_t = 4.5(i_1^2+i_2^2+i_3^2)K\, 10^{-8} \text{ pounds} \quad (7)$$

When i_1, i_2, and i_3 are squared and added together, it will be found that all the terms involving the closing angle θ cancel out, and

$$i_1^2+i_2^2+i_3^2 = \frac{E_m^2}{(\omega L)^2} 3(1-\cos \omega t) \quad (8)$$

The sum of the squares of the three instantaneous currents therefore are independent of the closing angle θ.

The total instantaneous magnetic retarding forces on the blades of a switch closing on a zero-power-factor three-phase short circuit are equal to

$$F_t = 4.5\left(\frac{E_m}{\omega L}\right)^2 3(1-\cos \omega t)K\, 10^{-8} \text{ pounds} \quad (9)$$

This force starts at zero and reaches a crest of $\frac{27(E_m)^2}{(\omega L)^2} K\, 10^{-8}$ in 180 degrees and drops to zero again in 360 degrees as shown in Figure 15. If the circuit contained zero resistance, this force would continue to oscillate indefinitely, as all three of the phase currents each would retain its original amount of displacement. Because of the resistance in any actual circuit, however, these currents eventually will become symmetrical, after which the sum of the magnetic forces has a constant value one-fourth its original peak magnitude as shown in Figure 16.

As previously shown the total of the three magnetic retarding forces for a three-phase

---

*This equation is based upon the switch blades being spaced far enough apart so that each blade is not acted upon by the currents in the other two phase parallel conductors. It does not hold with very close phase spacings.

Application of Capacitors for Power-Factor Improvement of Induction Motors

W. C. BLOOMQUIST
ASSOCIATE AIEE

W. K. BOICE
MEMBER AIEE

POWER-FACTOR improvement of induction-motor loads by means of shunt capacitors has been a common practice for many years. Recently, the practice of connecting the capacitors directly at the motor terminals has developed in order to permit switching of the capacitors and motor as a unit. This will not result in adverse motor operation if the number of capacitors is selected properly. There is very little written material regarding operating experience, although capacitor and motor manufacturers have accumulated some experience.[1,2,3,4] This experience has shown that frequently too large a capacitor rating was used, resulting in overvoltage due to self-excitation when the motor starter was opened; in some cases the voltage rose to 200 per cent causing failure of motor insulation, indicating lamps, and other devices. In several instances, the motor coupling and shaft were damaged when too large a capacitor bank was used and the motor switched by a reduced-voltage autotransformer-type starter. In some cases, motors have been damaged from overload because allowance was not made in the overload setting for the reduction in line current due to the capacitors. In other cases, instruments and meters connected in the current-transformer secondary circuit have been damaged due to overvoltage.[5]

The purpose of this paper is to discuss these problems and their solution. A useful application table is included which lists the maximum capacitor rating for use with motors and the reduction in line current with the recommended capacitor rating. This latter information is useful for selecting the proper overload-relay setting.

Overvoltage Due to Self-Excitation

Self-excitation refers to the action of an induction motor operating as an induction generator with excitation supplied by capacitors, such as may occur when the switch is opened and the running motor is disconnected from the power source or when the motor is driven by an external means.

The mathematical theory of self-excitation is involved[6] and here only a simplified graphical solution will be given. If resistance is neglected, self-excitation will occur when

$X_C \leqq X_L$

X_C = capacitive reactance

X_L = magnetizing reactance

(A small value of X_C corresponds to a large capacitor kilovolt-ampere rating.) For practical purposes $X_C = X_L$ when the capacitor kilovolt-ampere rating is equal to the magnetizing kilovolt-ampere of the motor. This is very nearly the reactive kilovolt-amperes or kilovars at no load.

Curve *M* of Figure 1 shows a typical volt-ampere characteristic of a motor. Point *A* indicates the per cent magnetizing current at no load and normal voltage. Curves *C1*, *C2*, *C3*, and *C4* show the volt-ampere characteristics of capacitors of various ratings. All capacitor curves falling below the motor-characteristic curve *M* indicate that $X_C < X_L$ (capacitor kilovolt-amperes is larger than the motor-magnetizing kilovolt-amperes) and therefore the motor will self-excite. The final voltage of self-excitation, assuming the speed remains constant, occurs when $X_C = X_L$ or at the points of intersection of the capacitor curve with the motor-characteristic curve (points *A*, *B*, and *C*). Capacitor curves above the motor curve, such as curve *C4*, indicate that the capacitor kilovolt-amperes is less than the motor magnetizing requirements, and the motor will not self-excite. Self-excitation can be checked by connecting a voltmeter across the motor terminals and reading the voltage after the switch is opened.

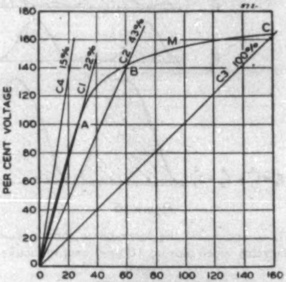

Figure 1. Motor-excitation curve and capacitor volt-ampere characteristic curves

Curve *C2* of Figure 1 is for the case where the capacitor kilovolt-amperes is sufficient to improve the motor full-load power factor to 100 per cent. Note that the voltage of self-excitation is 143 per cent; this will vary among motors and may be considerably higher for some.

In the usual motor application, the motor slows down rapidly after the switch is opened and the voltage rapidly decreases; a 15- to 20-per-cent reduction in speed eliminates self-excitation so the voltage collapses in a few seconds. However, in a few cases with high-inertia loads the voltage of self-excitation has been sustained for several minutes.

The graphical solution described assumes that the frequency of self-excitation is equal to the power-system frequency. This is approximately true in most cases since the frequency of self-excitation corresponds to the motor speed which is very nearly synchronous speed.

Overvoltage may be reduced by means

Paper 45-72, recommended by the AIEE committee on industrial power applications for presentation at the AIEE winter technical meeting, New York, N. Y., January 22–26, 1945. Manuscript submitted December 5, 1944; made available for printing December 28, 1944.

W. C. Bloomquist and W. K. Boice are both in the industrial power section, industrial engineering division, General Electric Company, Schenectady, N. Y.

---

short circuit is independent of the closing angle of the circuit. For a single-phase fault current, however, the crest value of these forces will vary 4 to 1, and their average over a cycle will vary 3 to 1 depending upon the closing angle of the circuit. The highest value is obtained when a line-to-line fault occurs beyond the breaker at a zero point on the voltage wave. In this case, a full-offset current wave flows through two poles of the breaker simultaneously.

$$i_{l-l} = \frac{E_{m\,l\ to\ l}}{2\sqrt{R^2+(\omega L)^2}}\left[\sin(\omega t+\theta-\phi) - \epsilon^{-\frac{Rt}{L}}\sin(\theta-\phi)\right] \quad (10)$$

where

$E_{m\,l\ to\ l}$ = line-to-line voltage = $1.73E_m$

If we neglect resistance and close at 0 degrees to this line voltage,

$$i_{l-l} = \frac{1.73E_m(1-\cos\omega t)}{2\omega L} \quad (11)$$

The magnetic retarding force associated with this current is equal to

$$F_{tl-l} = 4.5K\frac{3E_m^2(1-\cos\omega t)^2}{4(\omega L)^2}10^{-8} \quad (12)$$

The peak of this force is equal to that for the three-phase fault condition in equation 9.

As this short-circuit current becomes symmetrical, this force dies down to a double-frequency oscillating force as shown in Figure 17. If the switch had been closed at peak voltage, the current would have been symmetrical in the first loop, and the forces would have started out at their final value.

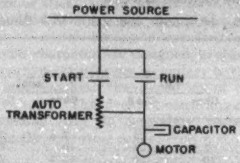

Figure 2. Diagram of reduced-voltage autotransformer-type motor starter

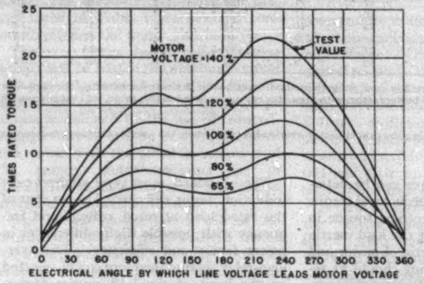

Figure 3. Peak electrical torque versus switching angle

of a series or shunt resistance in the capacitor circuit but generally such devices are not used because of the continuous losses or the complication of switching the resistor to avoid the losses.

Overvoltage alone may not be the sole criterion for selecting the amount of capacitors to use; the listings of Table I consider both transient torque and voltage.

Transient Torques

When a running induction motor with shunt capacitors is connected to a power source, a high transient torque may be developed. This may occur when a motor is transferred to the line from the reduced-voltage tap of an autotransformer-type starter, Figure 2. This also may occur when a running motor temporarily is disconnected from its line, and the switch (Figure 5) is reclosed while the motor is still running and maintaining voltage at its terminals by self-excitation.

In order for transient electrical torques to appear, the motor voltage developed by self-excitation must be of appreciable magnitude and it must be out of phase with the line voltage when the switch is closed. The torque is similar to that caused by connecting two synchronous generators together which are out of phase.

If there is no load connected to the motor shaft, the torque will be absorbed by the motor inertia and will result merely in a momentary acceleration or deceleration of the motor, lasting for a few cycles.

If the inertia of the load connected to the shaft is appreciable, some of the torque will be transmitted by the shaft to cause acceleration or deceleration of the load. If the load inertia is several times the inertia of the motor rotor, most of the transient electrical torque will be transmitted as transient mechanical torque by the shaft and coupling. In some cases this has caused fracture of couplings and twisting of shafts.

The peak value of the electrical torque is determined primarily by the magnitudes of the line and motor voltage, the electrical angle between them, and the reactance and resistance of the motor. High transient torques are accompanied by high transient line currents. The transient torque is of an oscillating character, lasting only for a few cycles and usually having its maximum value in a decelerating direction. The values of peak torque obtainable for a typical motor are shown by Figure 3.

A series of tests was made to verify the expected values of transient torque. Figure 4 is an oscillogram of a test made on a 100-horsepower motor with 40 kva of capacitors connected to its terminals. This amount of capacitors improved the full-load motor power factor to substantially 100 per cent. The motor and capacitor bank were switched as a unit from reduced voltage to full voltage by means of a manual reduced-voltage autotransformer-type starter. No load (except a tachometer) was connected to the motor shaft. The maximum torque developed

Figure 4. Oscillogram of test for transient torque of induction motor with shunt capacitors

Motor rating: 100 horsepower, 1,800 rpm, 2,200 volts, 24 amperes. Capacitor rating: 40 kva

Motor started with manual reduced-voltage autotransformer starter. No load connected to motor shaft

Maximum electrical torque (from slope of speed trace and motor inertia) = 21 times motor rated torque

Tachometer deceleration trace not used, since peak went off film. This trace obtained from oscillograph element in series with capacitor across tachometer. Harmonics in this trace are due to commutator ripple and slight misalignment in tachometer coupling

Line-voltage trace obtained from special circuit which shows only the peaks of the voltage wave

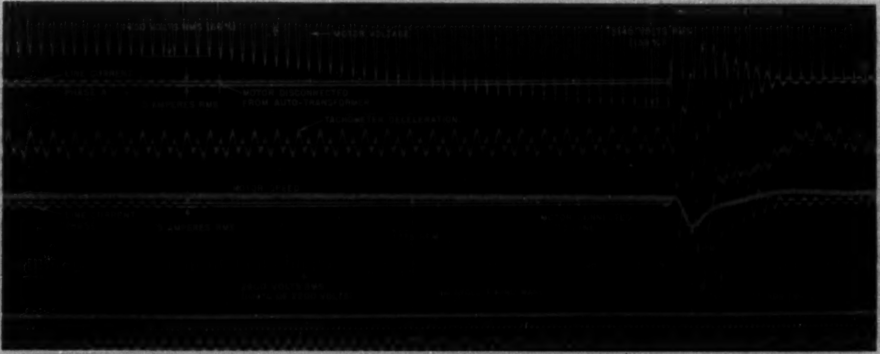

Table I. Recommended Maximum Capacitor Rating When Capacitor and Motor Are Switched as a Unit*

Representative Data for Three-Phase 60-Cycle General-Purpose Open-Type Induction Motors of 220-, 440-, 550-, and 2,300-Volt Rating

Induction-Motor Horsepower Rating	Motor Speed in Rpm											
	3,600		1,800		1,200		900		720		600	
	Ckva**	%AR#	Ckva	%AR	Ckva	%AR	Ckva	%AR	Ckva	%AR	Ckva	%AR
10	2.5	9	4	11	4	12	5	17	5	23	7.5	28
15	2.5	9	5	11	5	11	7.5	16	7.5	21	10	26
20	5	9	5	10	5	11	7.5	15	10	20	12.5	24
25	5	9	7.5	10	7.5	10	10	14	10	19	15	22
30	7.5	9	10	9	10	10	10	13	12.5	18	15	21
40	10	9	10	9	10	10	12.5	12	15	16	17.5	19
50	12.5	9	12.5	9	12.5	9	15	12	20	15	22.5	17
60	15	9	15	8	15	9	17.5	11	22.5	14	25	16
75	17.5	9	17.5	8	17.5	8	20	11	27.5	13	30	15
100	22.5	9	22.5	8	22.5	8	25	10	35	12	37.5	14
125	25	9	27.5	8	27.5	8	30	9	40	11	47.5	13
150	32.5	9	35	8	35	8	37.5	9	47.5	11	55	13
200	42.5	9	42.5	8	42.5	8	45	9	60	10	67.5	12

* When manual reduced-voltage autotransformer-type starter such as shown in Figure 2 is used, refer to method described in the text for selecting the capacitor rating if load data is appreciably higher than that of the motor. The motor full-load power factor, with capacitor ratings as listed in this table, will range from 95 to 98 per cent.

** CKVA is rated kilovolt-amperes of capacitors connected at motor terminals.

# %AR is per cent reduction in line current due to capacitors and is helpful for selecting the proper motor-overload setting when the overload relay is located as shown in Figure 5.

was determined from measurement of the maximum rate of change of motor speed and a calculated value of motor inertia. In the case shown by Figures 3 and 4, there was a delay of approximately 0.7 second from the time the motor was disconnected from the 65-per-cent autotransformer tap until it was connected to the line. During this interval, the motor voltage built up to 138 per cent by self-excitation and became about 252 degrees out of phase. The resulting high torque is apparent from the rapid momentary deceleration of the motor after transfer to the line. The measured torque was 21 times rated torque. This measured value is plotted on Figure 3, from which the good agreement between calculated and test results can be seen.

In order to prevent transient mechanical torques from damaging the shaft and coupling, the peak mechanical torque should not be permitted to exceed about six times normal. In general, if the connected capacitor kilovolt-amperes does not exceed the value given by Table I, excessive torques will not result from switching occasioned by the use of electrically operated reduced-voltage starters. This is true because the switching time is so short that a high motor voltage and electrical angular difference does not appear.

If manual switching is employed, and the load inertia is appreciably higher than that of the motor, excessive shaft torques may develop. It is suggested that such cases be given special consideration, taking the particular motor characteristics and load inertia into account before selecting a value of capacitor kilovolt-amperes to be connected to the motor terminals to be switched with the motor. This may be done as follows: By the graphical method outlined in this paper, the maximum motor voltage from self-excitation by a trial selection of capacitors can be determined. From Figure 3 for this motor voltage, the maximum electrical torque can be determined. The maximum mechanical torque will be less than the electrical torque in the same proportion that the load inertia is less than the total inertia of motor and load. The capacitor rating should be selected by trial such that the maximum mechanical torque in the shaft and coupling, determined in this manner, does not exceed six times normal. As previously indicated, this procedure is not necessary if the switching time is less than about 0.3 second, as would be the case for most electrically operated motor starters.

Thermal-Overload Protection of the Motor

When capacitors are connected to the motor terminals they supply some of the motor-magnetizing requirements so the actual line current is less than it would be without capacitors. If the capacitors are connected to the motor starter on the load side of the thermal-overload device as shown in Figure 5, the overload relay will not provide proper protection to the motor if it is selected for the uncorrected motor full-load current. The relay should be selected for a smaller current rating commensurate with the reduced line current due to the effect of the capacitors.

The per cent reduction in line current due to capacitors is shown in Table I. Note the large reduction in line current for the slow-speed motors.

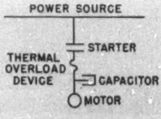

Figure 5. Location of capacitors and thermal-overload relay

The standard open-type squirrel-cage induction motor will carry 115 per cent of the rated load at rated voltage and frequency with possible slight differences in power factor and efficiency. The overload-relay setting therefore can be selected on the basis of the 1.15 service factor. The reduction in current as listed in Table I applies for either the 100- or 115-per-cent loading. Examination of data for motors of various horsepower and speed ratings has shown this to be true.

Overvoltage Protection for Current-Transformer Secondary Windings

Excessive overvoltages (several thousand volts) have been observed in current-transformer secondary circuits of motor circuits with shunt capacitors for rotating-machine protection or power-factor improvement. The analysis of this was described in a recent paper.[5]

Referring to Figure 6, when a de-energized capacitor is switched on to the bus it appears initially as a short circuit since the capacitor voltage cannot be changed instantaneously. Therefore, the instant the switch is closed the system voltage is distributed in the impedance from the bus to the capacitor, and since the impedance of the current transformer may constitute a major portion of this circuit impedance, it may assume the major part of the voltage drop. The voltage as viewed from the transformer secondary winding will be increased by the turn ratio. The magnitude of this voltage also will depend upon the volt-ampere burden in the transformer secondary circuit; the larger the burden in volt-amperes the higher the voltage. The amount of capacitors at the motor terminals has very little effect on the magnitude of the voltage.

Many types of protective devices can be used in the current-transformer secondary circuit, such as a shunting resistor, cutout, or filter. Very effective protection is provided by a by-pass device of a ceramic material having a nonlinear-resistance characteristic designed to shunt the current-transformer secondary terminals and thus limit the magnitude of the overvoltage. This does not cause any objectionable error in secondary current within the operating range.

Basis of Application Table

How many capacitors can be safely applied? The recommended capacitor ratings listed in Table I are selected conservatively for the motor and its drive.

The overvoltage due to self-excitation usually will be within the maximum value (110 per cent) normally permitted for continuous motor operation. The transient torque occasioned by the use of reduced-voltage starters will be held to a reasonable value, with the possible exception of the manual autotransformer-type of starter, for which a suggested application procedure has been outlined.

The no-load power factor will be approximately 100 per cent and the motor full-load power factor will range from 95 to 98 per cent which gives sufficient power-factor improvement in most cases. The capacitor rating will range from 20 to 40 per cent of the full-load motor kilovolt-amperes; the smaller value applies to the high-speed motors which inherently have a higher power factor than slow-speed motors.

The data are confined to a single table for simplicity for the most common motor sizes in the 220-, 440-, 550-, and 2,300-volt rating. Some of the capacitor kilovolt-ampere values given in Table I do not conform to the present standard capacitor ratings for all voltage classes, but in such cases the next lower standard rating may be selected. The standard capacitor ratings for the common voltage classes are given in Table II.

Individual-Motor Power-Factor Improvement Versus the Group-Capacitor Method

The use of a common motor controller for switching the motor and the capacitor as a unit has become increasingly popular because of the elimination of one switching device and because of the operating convenience. The capacitor is switched in and out of service with its associated motor and therefore tends to eliminate overvoltage usually associated with light-load conditions in a plant. This unit-switching arrangement is economically attractive when only a few motors are involved or when there is no diversity among motors. In those plants having a large number of motors and diversity among motors in operation, such as is common in industrial plants with a large number of motor-driven equipments, group capacitors automatically switched in several steps are usually more economical than individual-motor power-factor improvement. Operation with automatic control results in the functional equivalent of individual-motor power-factor improvement since the capacitors may be switched in blocks as dictated by the load requirements. Several papers have been written recently describing various types of control and their application for automatically switching capacitors.[7,8]

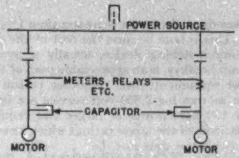

Figure 6. Circuit arrangement producing overvoltage in current-transformer secondary circuit

Several studies were made to determine the relative economics of plant power-factor improvement by means of capacitors with individual motors and the group-capacitor method.

The price comparisons were on the basis of the *same amount of total power-factor improvement*. For example, when all motors are connected to the line at the same time, so that the motor-diversity factor is one, the capacitor kilovolt-amperes required is the same for the two methods. When 50 per cent of the motors are on at the same time, corresponding to a motor-diversity factor of two, the group-capacitor rating need be only 50 per cent of the total capacitor kilovolt-amperes connected to all motors. The motor-diversity factor is the total motor-connected horsepower as related to the total horsepower of motors in operation.

The price ratio of individual capacitors to group capacitors was almost equal for the 220-, 440-, and 550-volt equipments for the same percentage of motors on the bus so the average price ratio for this voltage range was used. The price data were based on standard noninflammable liquid-filled capacitors used for power-factor improvement.

EXAMPLE 1. POWER-FACTOR IMPROVEMENT OF INDIVIDUAL MOTORS VERSUS GROUP METHOD OF POWER-FACTOR IMPROVEMENT FOR SERVICE BELOW 600 VOLTS

The price ratio of individual versus group capacitors for typical plants with motors from 3 to 50 horsepower is shown on Figure 7, plotted as a function of the per cent of motors in operation.

Note from curve *A* of Figure 7 that the group-capacitor method with manual switching is more economical than the individual-motor method even for the 100-per-cent condition when all motors are in operation. This is true because the price of capacitors in dollars per kilovolt-ampere is higher for small units than for larger units such as are commonly used with the group-capacitor method.

Curve *B* shows the price ratio when the automatic control and switching feature is incorporated with the group-capacitor method. (This is the operating equivalent of the individual-motor-capacitor method.) Note that even with the automatic control feature the group-capacitor method is economically more attractive than the individual-motor method.

Curve *C* shows the price relationship on the basis of the same capacitor cost, in dollars per kilovolt-ampere, for the two methods and clearly indicates the effect of diversity in the motors in operation.

Curve *A* will be very nearly correct for all applications. Low-voltage manual-switching devices are inexpensive so the cost of the

Table II. Standard Capacitor Ratings for Three-Phase 60-Cycle Units

	Individual Units			Standard Rack-Type Equipments*		
	Volts			Volts		
Capacitor Kva	230	460 and 575	2,400	230	460 and 575	2,400
0.5	x					
1.0	x	x				
2.0		x				
2.5	x					
5.0	x	x				
7.5	x					
10.0		x	x			
15.0		x	x			
15				x		
30				x	x	x
45				x		
60				x	x	x
90				x	x	
120				x	x	x
135				x		
180				x	x	x
240					x	
270					x	x
360					x	x

* Standard rack-type equipment as commonly used for group-capacitor installations. Larger banks are available for 2,400-volt service if more capacity is required. This listing is for standard racks of full capacity. Units may be removed in 7.5-kva units for 230-volt service and 15-kva units for 460-, 575-, and 2,400-volt service.

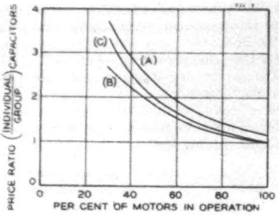

Figure 7. Price ratio (individual/group) capacitors versus per cent of motors in operation (for service voltages below 600 volts)

Curve A—Group capacitors with manual switching
Curve B—Group capacitors with automatic control and switching
Curve C—Equal capacitor cost in dollars per kilovolt-ampere for individual-motor and group-capacitor methods

switching device is a small part of the total capacitor-equipment cost. Curve *B* is representative for medium- and large-size industrial plants. For small plants or plants having a small connected motor load the price ratio will be lower since the cost of the automatic-control and switching feature becomes a large part of the capacitor-equipment cost when small capacitor banks are used. Generally, however, the automatic-control feature is not necessary in the small plants.

Example 2. Group Capacitors for Diversified Motor Load and Individual Capacitors for Selected Large Motors for Service Below 600 Volts

In those applications involving a large number of small motors and some large motors it is good practice to use group capacitors for the diversified motor load and individual capacitors for selected large motors. Large motors require large capacitor units which have a low unit price approaching that of the group-capacitor method. A low diversity factor among the large motors favors the individual method of power-factor improvement. If the motor-diversity factor is greater than about 1$^1/_2$, the group-capacitor method is generally more economical.

The combination of group capacitors for the diversified load and individual capacitors for selected large motors offers the operating benefits associated with unit switching and thus helps prevent overvoltage during light-plant-load conditions. Consequently, automatic control usually is not required for the group capacitors used in such cases.

Example 3. 2,300-Volt Service

The group-capacitor method may not be economically attractive for 2,300-volt (or higher voltage) equipments unless the motor-diversity factor is greater than 1$^1/_2$ to 2. This is true because the cost of the capacitor-switching device, usually a power circuit breaker, is an appreciable part of the total equipment cost. Another reason is that motors for 2,300-volt service are usually 100 horsepower or larger and require capacitors of the larger ratings which have a relatively low unit cost.

Applications involving 2,300-volt equipments should be considered individually.

Conditions Favorable to Individual-Motor Power-Factor Improvement

1. Capacitors automatically switched. Capacitors will be on only when needed and therefore will minimize plant-voltage rise at no load.

2. Application engineering simplified. Capacitor rating may be selected from Table I.

3. Flexibility for plant rearrangements. When plant changes require rearrangement of equipment the capacitor and motor can be moved together thus insuring proper power-factor improvement of the motor at any location.

4. Simplified installation. The capacitor and motor starter may be in a unit housing.

Conditions Unfavorable to Individual-Motor Power-Factor Improvement

1. Price higher for equipments below 600 volts. This is shown in Figure 7. The price comparisons are on the basis of actual selling price and not on the installed basis. If the installation cost were included, the relationship would probably be even more unfavorable to the individual-motor method since, generally, many small units cannot be installed as cheaply as a few large racks in a group. This is particularly true when the type of equipment furnished for group-capacitor installations is shipped complete as a unit ready for service. Even though the unit-type capacitor and starter is used, which does not require any additional installation expense for the capacitors, the group-capacitor method is cheaper.

2. Poor use of investment. This is true when all motors are not on at the same time. In the average industrial plant only 25–75 per cent of the motors are connected to the bus at the same time.

3. Lack of interchangeability of motor equipment. Usually 220-volt motors can be recommended for 440 volts but capacitors cannot. It is possible to use a 460-volt capacitor on 220 volts, but resulting in approximately 25 per cent of the rated kilovolt-amperes. A 230-volt capacitor cannot be used with a 440-volt motor, although two 230-volt capacitors can be connected in series for 440-volt motor service.

4. Limitations in location. Capacitors for power-factor improvement of 5- to 25-horsepower motors for 220-, 440-, or 550-volt service are relatively large compared with the motor and may require special consideration to location and mounting. However, this limitation may be avoided if the capacitor is located in the motor starter.

5. Improvement in over-all plant power factor limited. Power-factor improvement of individual motors has the limitation of improvement of the motor load only. The full-load motor power factor is improved to 95 to 98 per cent for the capacitor values recommended in Table I. If additional power-factor improvement is necessary for the plant, the additional capacitors required should not be switched with the motors. With the group-capacitor method, the entire plant power factor may be improved to the desired level.

Conclusions

1. In applying shunt capacitors to the terminals of induction motors for power-factor improvement, care should be exercised in selecting the capacitor rating to avoid:

(*a*). Overvoltage due to self-excitation.

(*b*). Transient torques.

(*c*). Overvoltage in current-transformer secondary circuits.

(*d*). Improper motor-overload protection.

2. The data in Table I are a practical guide in selecting the amount of capacitors to be switched with a motor.

3. Generally, economic considerations favor the group-capacitor installation for plant power-factor improvement when the service voltage is below 600 volts, the individual motors are small, and the motor-diversity factor is large. For other conditions individual comparisons should be made. For maximum operating benefits the group-capacitor method usually will consist of several blocks of capacitors automatically switched.

References

1. WHY NOT SWITCH CAPACITORS WITH THE LOAD? J. W. Butler, E. B. Pope. *General Electric Review*, volume 41, August 1938, pages 366–9.

2. SELF-EXCITATION OF INDUCTION MOTORS, C. F. Wagner. AIEE TRANSACTIONS, volume 58, 1939, February section, pages 47–51.

3. INSTALLING POWER-FACTOR CONDENSERS. *The Engineer*, December 4, 1942, pages 462–3.

4. CAN CAPACITORS CONNECTED TO INDUCTION MOTORS CAUSE DANGEROUS OVERVOLTAGES? Ivar Herlitz. *Asea Tidning*, volume 27, November 1935, pages 174–5.

5. OVERVOLTAGE PROTECTION OF CURRENT-TRANSFORMER SECONDARY WINDINGS AND ASSOCIATED CIRCUITS, R. H. Kaufmann, G. Camilli. AIEE TRANSACTIONS, volume 62, 1943, July section, pages 467–72.

6. ANALYSIS OF SERIES CAPACITOR APPLICATION PROBLEMS, J. W. Butler, C. Concordia. AIEE TRANSACTIONS, volume 56, 1937, August section, pages 975–88.

7. AUTOMATIC CONTROL AND SWITCHING EQUIPMENT FOR CAPACITOR BANKS AND ITS APPLICATION, T. W. Schroeder, W. C. Bloomquist. AIEE TRANSACTIONS, volume 63, 1944, September section, pages 649–54.

8. EXTENDING THE USE OF SHUNT CAPACITORS BY MEANS OF AUTOMATIC SWITCHING, W. H. Cuttino. AIEE TRANSACTIONS, volume 63, 1944, September section, pages 674–8.

Modern Electric-Power-Distribution Ideas as Applied in a Large War Plant

R. H. KAUFMANN
MEMBER AIEE

N. A. KIEB
MEMBER AIEE

IT now becomes possible to reveal the composition of a typical war-plant electric distribution system (aircraft-engine manufacture). It is the hope of the authors that many of the principles and practices which have been embodied in this electric system can be adopted by others to effect the simplification and economies in power distribution that have been done in this instance.

In December 1941 this nation was plunged into the present world conflict. Participation was no longer optional. In this, a mechanized war, there arose an immediate demand for almost every conceivable type of machine for use on land, on the sea, and in the air in unheard of quantities. It became essential that every man-hour of effort and every pound of material be made to yield the greatest return.

The direct objectives considered foremost in the creation of the electric system herein described included:

1. Speedy completion.
2. High utilization efficiency of material, particularly copper and steel.
3. Conservation of man-hours in manufacture, installation, and operation.
4. An electric system as nearly independent of building structure as possible.
5. The incorporation of an acceptable degree of electrical service reliability.
6. Assured safety to equipment and personnel.

In the interest of speeding the work and securing the maximum degree of co-ordination and economic balance, the entire electric distribution system was negotiated as a single project. The co-operative efforts of the Pratt and Whitney Aircraft Corporation; Albert Kahn, Architects and Engineers; the General Electric Company; together with the Defense Plant Corporation, were enlisted to that end. Paul R. Olson of the East Hartford Pratt and Whitney organization deserves particular credit for his untiring efforts in expediting this project.

The Electric Distribution System

A bird's-eye view of the complete distribution system is presented by the overall one-line diagram, Figure 1. The several component parts as portrayed in this diagram represent the approximate geographical arrangement.

In immediate evidence is the application of the load-center principle of power distribution which has been publicized quite widely: "Transmit power at the highest practical voltage to relatively small distributed substations". In this instance, primary distribution is accomplished at 13.8 kv.

Reliability of electric service is incorporated in the form of the secondary selective arrangement in which each individual load circuit has access to an alternate independent source of low-voltage power. This system has met its expectations with flying colors, possessing the following outstanding advantages:

1. Both normal and emergency operation incorporate the simplicity of radial distribution.
2. All circuit equipment normally shares in carrying the total load resulting in low power and reactive kilovolt-ampere loss, as well as better maintained delivered voltages.
3. Emergency operation entails merely the opening of the low-voltage circuit breaker in the de-energized source and closing the tie breaker.

It will be observed that effective duplication of electric service is carried through to the incoming 110-kv supply system. The two co-ordinating primary feeders at each and every substation originate from different 13.8-kv busses. Both of the latter in turn may be energized by either or both main transformers and, should a second 115-kv feeder be added, from either or both incoming high-voltage lines.

In the belief that the most logical presentation will parallel the sequence followed in initial planning, the several specific load areas will be described first and be followed by a description of the primary-feeder arrangement and main incoming-power substation.

Main Factory Building

The main factory building encloses under a single roof a ground area of 1,000 feet by 2,000 feet. Operations are conducted on a single floor at ground level, with the exception of a mezzanine floor over about ten per cent of the area, making a total working floor space of about 2,250,000 square feet. Of this total area, approximately 70 per cent is devoted to active manufacture; 15 per cent to rough stores; ten per cent to finished parts receiving, assembly, and shipping; and five per cent to inspection. The mezzanine floor is allocated to inspection and a portion of the active manufacture.

Supplying general-purpose power and light to this area are 16 load-center unit substations aggregating 30,000 kva, representing about 13.3 volt-amperes per square foot of working floor space. In one load area, an additional load-center substation has been installed because of a high concentration of power in the form of heat-treating equipment. In general, the area served by a single substation is about 250 feet by 500 feet, but is somewhat larger in areas characterized by lower power-utilization densities. In the rough-stores area the supply substation capacity is reduced by the application of 750-kva transformer units, in contrast with 1,000-kva units used elsewhere.

The substations are installed in enclosures forming a part of ventilating-fan houses located on the building roof. The reasons for this selection are: 13.8-kv feeder cables are supported on racks close to the building roof; the bulk of the power is distributed to plug-in bus also located closer to the roof than to the floor; and the fact that the enclosures could be integrated with houses there located for other purposes.

Equipment was hoisted through a large hatchway later closed with a removable wood cover. Each substation was handled in three pieces (the two Pyranol-filled transformers and the switchgear section) using a portable A frame above the hatchway. The A frame has been retained for possible future use. The installation procedure was carried

---

Paper 45-79, recommended by the AIEE committee on industrial power applications for presentation at the AIEE winter technical meeting, New York, N. Y., January 22–26, 1945. Manuscript submitted November 27, 1944; made available for printing January 2, 1945.

R. H. KAUFMANN is in the industrial engineering department of the General Electric Company, Schenectady, N. Y., and N. A. KIEB is electrical engineer with the Pratt and Whitney Aircraft Corporation of Missouri, Kansas City, Mo.

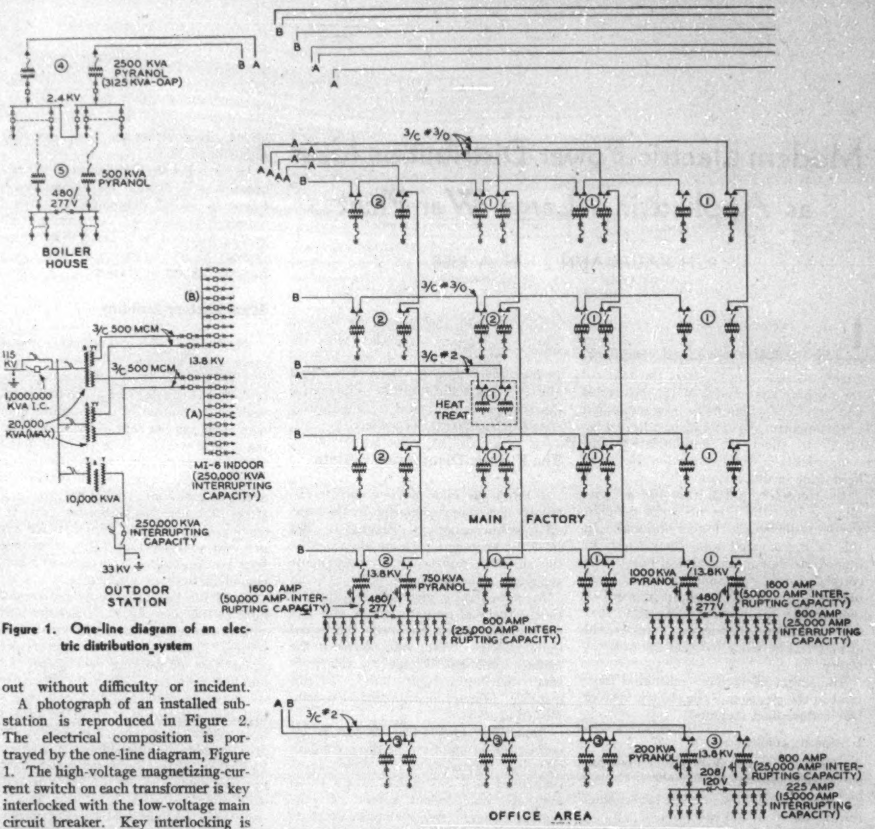
④
2500 KVA
PYRANOL
(3125 KVA-OAP)
2.4 KV
B A
B
B
A
A
⑤
500 KVA
PYRANOL
480/
277 V
BOILER
HOUSE
(B)
3/C 500 MCM
13.8 KV
115
KV
3/C 500 MCM
1,000,000
KVA I.C.
20,000
KVA(MAX)
(A)
MI-6 INDOOR
(250,000 KVA
INTERRUPTING
CAPACITY)
10,000 KVA
250,000 KVA
INTERRUPTING
CAPACITY
33 KV
OUTDOOR
STATION
3/C #3/0
A
A
A
A
AAAAA
B
②
①
3/C #3/0
B
3/C #2
B
A
HEAT
TREAT
MAIN FACTORY
13.8KV
750 KVA
PYRANOL
1600 AMP
(50,000 AMP INTERRUPTING CAPACITY)
480/
277 V
600 AMP
(25,000 AMP INTERRUPTING CAPACITY)
1000 KVA
PYRANOL
13.8KV
480/
277V
1600 AMP
(50,000 AMP INTERRUPTING CAPACITY)
600 AMP
(25,000 AMP
INTERRUPTING
CAPACITY)
A B
3/C #2
③
200 KVA
PYRANOL
13.8 KV
208/
120V
600 AMP
(25,000 AMP INTERRUPTING CAPACITY)
225 AMP
(15,000 AMP
INTERRUPTING
CAPACITY)
OFFICE AREA

Figure 1. One-line diagram of an electric distribution system

out without difficulty or incident.

A photograph of an installed substation is reproduced in Figure 2. The electrical composition is portrayed by the one-line diagram, Figure 1. The high-voltage magnetizing-current switch on each transformer is key interlocked with the low-voltage main circuit breaker. Key interlocking is included to permit closure of the low-voltage tie circuit breaker only when one of the transformer secondary circuit breakers is open.

Both power and light are served by common load-center unit substations using a 460—265 four-wire grounded-neutral system to supply 440-volt polyphase motors in the normal manner and 265-volt fluorescent lighting units from line to neutral potential. Plug-in bus is used to distribute power to the major portion of the load, consisting of distributed machine tools, so as to obtain the flexibility needed to accept fairly frequent rearrangement of machine tools for production efficiency, improvement, or changed requirements.

Factory Power Distribution

The manner in which low-voltage power is distributed from the load-center unit substations to the plug-in bus sections for a typical unit load area is illustrated in Figure 3. Two adjacent 230-foot lengths of 250-ampere War Production Board approved plug-in bus are fed from their center point by an individual power feeder from the substation. To avoid operation at undue temperature on the plug-in bus, should the load be badly disproportioned among the four radial extensions, a temperature alarm (including bell and lamp) is installed adjacent to the feeder tap on each bus section which will sound an alarm upon reaching an 80-degree centigrade operating temperature. A typical feeder tap to a plug-in bus section is illustrated in Figure 4. Each power feeder consists of three single-line conductors plus one bare neutral conductor, which conductors are spaced symmetrically by means of trisected porcelain support blocks. Individual conductors are kept taut by straining them in the horizontal direction to structural members of the building. The manner in which this is accomplished will be evident by inspection of Figures 4 and 8.

Factory Lighting Distribution

Fluorescent lighting was adopted in the interest of economy. On first thought, the copper and steel in fluorescent ballasts might indicate that incandescent lighting would have the advantage. But the greater light efficiency of fluorescent lamps reduces the power requirement of the factory area by some 6,000 to 7,000 kw. The copper and steel which would be required in the complete electric system from prime mover to lamp to supply this additional load would exceed the copper and steel needed in the fluorescent-lamp ballasts. The material requirement

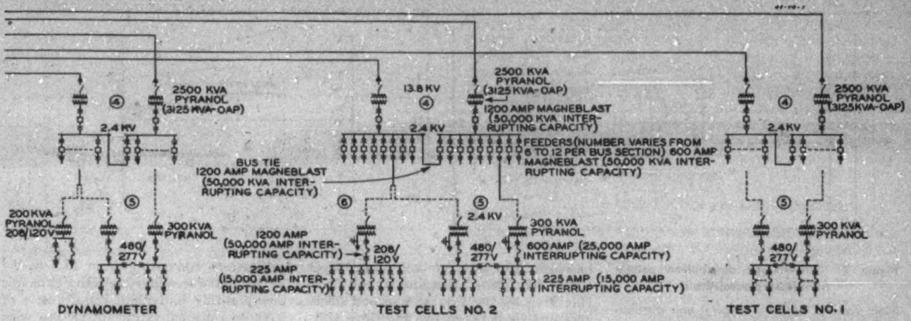
2500 KVA
PYRANOL
(3125 KVA-OAP)
④
2.4 KV
13.8 KV
④
2500 KVA
PYRANOL
(3125 KVA-OAP)
1200 AMP MAGNEBLAST
(50,000 KVA INTERRUPTING CAPACITY)
2.4 KV
FEEDERS (NUMBER VARIES FROM 6 TO 12 PER BUS SECTION) 600 AMP MAGNEBLAST (50,000 KVA INTERRUPTING CAPACITY)
BUS TIE
1200 AMP MAGNEBLAST
(50,000 KVA INTERRUPTING CAPACITY)
④
2500 KVA
PYRANOL
(3125 KVA-OAP)
2.4 KV
⑤
200 KVA
PYRANOL
208/120 V
300 KVA
PYRANOL
480/277 V
⑥
⑤
2.4 KV
1200 AMP
(50,000 AMP INTERRUPTING CAPACITY)
208/120 V
225 AMP
(15,000 AMP INTERRUPTING CAPACITY)
300 KVA
PYRANOL
480/277 V
600 AMP (25,000 AMP INTERRUPTING CAPACITY)
225 AMP (15,000 AMP INTERRUPTING CAPACITY)
⑤
300 KVA
PYRANOL
480/277 V
DYNAMOMETER
TEST CELLS NO. 2
TEST CELLS NO. 1

Figure 1 (continued)

of the 265-volt design are much less than for the 120- or 208-volt design. Also the supply of both light and power from common load-center unit substations results in further economy of materials. An ingenious innovation is represented by the suspension of a series of fluorescent units from an overhead messenger cable. A single number-12 conductor, in combination with the messenger as a ground return, serves a four-kilowatt lighting load.

A sketch showing the fundamental aspects of factory lighting distribution is included in Figure 3. Ten 400-watt fluorescent fixtures are supported from one overhead horizontal messenger cable. Each fluorescent fixture taps the number 12 feeder line carried horizontally directly below the messenger through the fuse. Three such adjacent strings of fluorescent lights are fed from a three-phase tap from the main lighting feeder through circuit breakers located in a building column five feet above floor level.

The resulting lighting in this plant is excellent. The relatively low intrinsic brilliance of fluorescent lamps, together with their location about 16 feet above floor level, produces the effect of a ceiling of soft light and almost complete absence of shadow. It has been observed that this ceiling of light tends to obscure equipment mounted above that level and effectively hides the maze of pipes, cableways, vertical suspension members, and the like, which had been expected would constitute an eyesore. Experience to date indicates that an average fluorescent lamp life in excess of 7,000 hours is being obtained.

To supply a relatively small amount of 120-volt power to column receptacles for miscellaneous hand tools, portable lights, and so forth, and for lighting and receptacle power in basement washrooms, small air-cooled transformers are distributed over the factory area, taking single-phase power from the 480-volt system and converting it to 240–120 volt. This power is distributed by branch circuits of relatively short length.

Capacitor Application

About 10,000-kva in capacitors have been applied to the 480-volt distribution system, in 90-kva blocks directly adjacent to the feeder tap in the plug-in bus. The principal reason for the capacitive kilovolt-amperes is a power-contract power-factor clause limiting the power factor to not less than 0.975 lagging. By absorbing the reactive kilovolt-amperes near its origin (machine-tool load), the reactive kilovolt-amperes and power loss which would be incurred by transmission through the distribution system is avoided.

Capacitor application constitutes an extremely flexible means of enhancing the load-carrying ability of a particular load-center unit substation. Figure 5 defines the increase in load which may be accepted in combination with a particular amount of capacitor kilovolt-amperes, for a basic load power factor of 0.6 and 0.8 lagging. With a load power factor of 0.6 lagging (typical of machine-tool load), it will be observed that the amount of such load which can be accepted by a 1,000-kva substation without exceeding its rating can be increased to 1,300 kva by the application of 420 kva in capacitors. *Thus an excess machine-tool load of 300 kva could be accepted, as needed at an investment cost of $11 per kilovolt-ampere (420 kva of capacitors at $8 per kilovolt-ampere installed), which is no greater than the cost of increased capacity in the basic power-distribution system.*

Grounding System

Considerable study was given to the attainment of an adequate grounding system, which assumes particular significance in reinforced-concrete building construction. The unintentional transfer of ground current between various metallic members or structures is to be avoided. It is particularly important that there exist a positive direct path to the supply transformer neutral to conduct ground-fault current during the existence of a circuit ground fault to avoid sputtering or arcing between metallic members which may be in light contact and to avoid differences of potential between exposed metallic bodies, which might constitute a hazard to personnel.

Beneath each substation are driven four $^3/_4$-inch diameter, ten-foot-long Copperweld ground rods interconnected with the associated substation neutral bus. At each station these are bonded to heavy water mains, which in general traverse the plant in the north–south direction. Between adjacent unit load areas in the east–west direction, the 4/0 neutral cable of the outermost power feeder is continued and joined to the corresponding neutral in the next adjacent load area, and the lighting messenger cables are interconnected electrically from one load

Figure 2. Typical 2,000-kva 13,800-to-480–277-volt secondary selective factory load-center unit substation

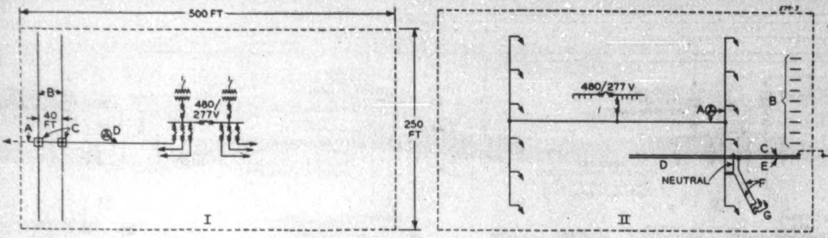

Figure 3. Low-voltage distribution pattern from factory substations

Main factory building: typical unit distribution

I. Typical power-distribution feeder
A—4/0 neutral to next area
B—250-ampere plug-in bus
C—Power-factor capacitors applied
D—Three 350,000-circular-mil conductors; one 4/0 neutral

II. Typical lighting-distribution feeder
A—Three number-four conductors; one number-six neutral
B—Messengers spaced approximately 15 feet
C—Steel messengers
D—Ten 400-watt fluorescent units suspended from this messenger
E—Number-12 copper
F—Three number-12 in conduit
G—Column switches at floor level

area to the next. This entire grounding system is interconnected with the main substation grounding system by way of the main water-piping system and the metallic sheaths of the multiplicity of power feeder cables.

Office Building

The office building covers an area of 80 feet by 2,000 feet and is in contact with the long dimension of the main factory building. This portion of the structure incorporates a basement, a first, and a second floor. The basement, devoted to storage and a small amount of miscellaneous machinery and with fairly low illumination levels, represents an area of low electric-load density. The first and second floors are devoted to active office service, including normal illumination intensities, column-mounted fans, and the usual array for electrically operated business machines.

This load area is served by four load-center unit substations of secondary selective design, functionally equivalent to those located in the factory, differing in that the low-voltage service is 208–120 volt and individual Pyranol transformers are rated 200 kva. The aggregate substation capacity of 1,600 kva can accommodate an electric-load density of two volt-amperes per square foot in the basement area and four volt-amperes per square foot on the first and second floor. (Lighting on the first and second floors accounts for between two and three volt-amperes per square foot.)

These substations are located in houses (wood construction) on the factory roof directly adjacent to the office building. An illustration of one installation appears in Figure 6. The low-voltage feeders from each substation drop through the factory roof and then are carried horizontally, and the same type of construction is used as for factory feeders. At appropriate points, branch circuits are carried through the wall to the office building and dropped vertically in conduit to supply distribution cabinets at the second, first, and basement floor levels. The detail arrangement of this low-voltage feeder system is portrayed schematically by the sketch, Figure 7. A section of the horizontal feeder array beneath the factory roof adjacent to the office building is shown in Figure 8.

From the wall distribution cabinets, conventional distribution practice is followed using conduit for permanent installation, such as lighting fixtures and Walker underfloor duct for flexible installation of business machine and other electrical outlets.

Engine Test and Dynamometer Area

This section of the plant is devoted to production and experimental engine testing and occupies an area of 250 by 900 feet. Each production test cell requires a 250-horsepower blower motor together with several small motors, driving fans and pumps, and special interior lighting of explosion-proof character. There are associated areas requiring illumination equivalent to that provided in the factory area with relatively low power load density. That portion devoted to experimental engine test involves electric power requirements similar to those of the production test area but in addition incorporates electrical-test dynamometer equipment of which the present equipment utilizes two 1,250-kva and one 750-kva synchronous rotating machines. There are also a number of motors of 300- and 600-horsepower rating.

Serving this load area are three unit substations converting from 13.8 to 2.4 kv, using the secondary selective principle incorporating individual transformers of 2,500-kva normal rating (3,125 kva with supplementary cooling) in combination with metal-clad vertical-lift switchgear sections utilizing Magne-blast circuit breakers of 50,000-kva interrupting capacity. The two complementary sections of the substation are installed face to face, as illustrated in Figure 9. The tie breaker is installed in one lineup, and the bus from the other section is extended by means of 500,000-circular-mil three-conductor five-kilovolt cable.

The stator circuit of each 2,300-volt machine is connected directly with its respective switching position in the metal-clad lineup by means of three-conductor five-kilovolt cable. In general, the normal control of each motor circuit breaker is from a control panel adjacent to the controlled machine. Figure 10 shows a group of synchronous-motor field cubicles on each of which is mounted the control switch which actuates the circuit breaker in the metal-clad structure. The metal-clad circuit-breaker position contains a permissive control switch, which allows

Figure 4. Typical construction employed for factory 480–277-volt feeders

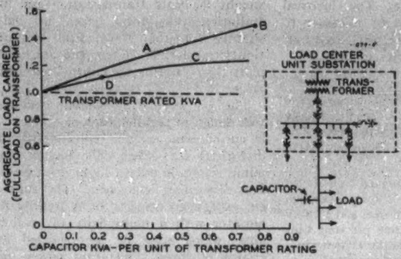

Figure 5. Chart showing increased machine-tool load permissible with capacitor assistance

A—Load power factor = 0.6
B—Net power factor = 0.9
C—Load power factor = 0.8
D—Net power factor = 0.9

the circuit breaker to be tripped locally and can be positioned to prevent closing the breaker from the remote station.

Small motors and general-purpose lighting are served by load-center unit substations supplying 460–265-volt service, which closely resemble those employed in the factory area, except that they are of smaller rating and are served at 2.4-kv from the main stations. A typical unit is illustrated in Figure 11. For the special test-cell lighting and some other miscellaneous load demanding 120-volt service, there are provided small load-center unit substations delivering 208–120-volt service. A consideration of these several auxiliary load-center unit substations as to unit capacity, switching, and protection requirement, indicated that they could be served more economically at 2.4 kv through the larger substations than directly at 13.8 kv.

Boilerhouse Area

The electric-load demands in the boilerhouse closely resemble those of the engine-test and dynamometer area. A substantial number of motors with ratings in excess of 100 horsepower are employed for powering cooling-tower fans, air compressors, water-circulating pumps, and fire pumps which were most effectively served at 2.4 kv. In addition, there exists the usual array of boilerhouse small auxiliaries in the form of fans, blowers, and pumps, which are best adapted to low-voltage service.

Figure 6. Typical 400-kva 13,800-to-208–120-volt secondary selective office load-center unit substation

Serving this load is one secondary selective substation converting from 13.8 kv to 2.4 kv with component parts duplicating those employed in the test-area substations. Considerations of floor area made an end-to-end installation arrangement preferable, as illustrated in Figure 12. Low-voltage power is supplied by a load-center unit substation delivering 460–265-volt service in the same manner as was done in the test area.

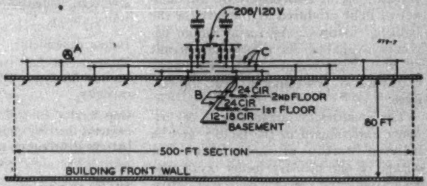

Figure 7. Low-voltage distribution pattern from office substations

Typical unit distribution for office building

A—Three 4/0 conductors; one 1/0 neutral
B—To each floor: three number four, one number-six neutral in conduit
C—Strained horizontally along office wall in the factory area

The electrical demands in the boilerhouse area are at their maximum level during the summer months, when the refrigerating plant assumes its maximum demand. During that season the substation is loaded to its rated capacity.

To insure the maintenance of an adequate ground system for the boilerhouse area, which is physically set apart from the remainder of the plant building, ground cables are installed interconnecting the local boilerhouse ground system with the main substation ground network paralleling the interconnection formed by the 13.8-kv-feeder cable sheaths. A multiplicity of water pipes also interconnects the boilerhouse and factory ground systems.

13.8-Kv Feeder Cable System

All power is distributed from the main substation by means of three-conductor 15-kv leaded cables with asbestos tape and red flameproof paint. The majority of feeder cables are composed of 3/0 conductor, representing an economical balance between copper and sheath-metal requirements. Several cables employ a number 2 conductor, which represents about the smallest size which can be employed safely with a 250,000-kva short-circuit level at the source end. Instantaneous attachments on these feeder-cable protective relays are applied and required to avoid the attainment of damaging copper temperature due to primary-circuit fault-current flow.

Except for circuits leading to the boiler house, the 13.8-kv cables are supported on wood lattice* racks or troughs suspended from the building roof above the level of the illumination fixtures. This method of handling cable runs possesses many admirable qualities, which can be used advantageously in future applications. Practically no advance preparation of building structure is needed. Cables are easily pulled into place. In the present instance, full reel lengths of 1,000 feet were pulled into place without the slightest difficulty. To assist in pulling around corners, a jig was prepared which forms a 24-inch radius arc, around the periphery of which a number of wood rollers were arranged. By temporarily clamping this jig at a corner, the cable was swung around a 90-degree turn with a very small amount of drag. Splices can be made at any spot along the trough. Cables are cut only when a point of termination is reached. The entire length of cable is accessible after installation. Repairs can be made with no

---

* It is recognized that this does not comply with the National Electrical Safety Code requirements, but it is applicable as a method of meeting wartime conditions.

DANGER 13800 VOLTS

Figure 8. Typical view of office main 208–120-volt feeders showing branch-circuit tap

waste of cable and without disturbing any section of the cable other than a damaged portion. Permissible current load levels are no less and may be greater than those permitted in underground runs. Typical views of the installed cable way are included in Figures 4 and 8. Though the appearance of the cable trench itself is not particularly pleasant, it is, as installed, obscured effectively by the blanket of light produced at the level of the lighting fixtures. As metal again becomes available, its use would permit efficient lightweight compact trough construction possessing a neat appearance.

The quadrature arrangement of primary feeders used in the factory area is believed worthy of note. Should an outage of one primary feeder occur, the several affected stations each will derive its emergency load from different primary feeders. Thus the emergency load resulting from the loss of one primary feeder is distributed among four other feeders. It also will be evident that the two feeder cables, to any one substation, traverse entirely different routes and thus are unlikely to be disrupted simultaneously.

Main Incoming-Power Substations

The incoming-power substation accepts power at 110 kv, converts to and distributes at 13.8 kv, to the various unit substations previously described. Provision also is included for interconnection with 33-kv service. The electrical features will be evident by reference to the over-all one-line diagram, Figure 1. Principal equipment items include:

Outdoor equipment:

Two 20,000-kva forced-oil air-pressure-cooled three-phase transformers, 110-kv delta high voltage, 13.8-kv wye low voltage, with four $2^{1}/_{2}$ per cent taps below normal in the 110-kv winding.

One 10,000-kva oil-immersed self-cooled three-phase transformer, 110-kv wye high voltage 33-kv wye low voltage, and 13.8-kv delta tertiary with two five per cent taps above and below normal in the 110-kv winding.

One 115-kv oil circuit breaker with isolating and by-pass disconnect switches.

One 33-kv oil circuit breaker with isolating and by-pass disconnect switches.

Three 115-kv transformers, high-voltage disconnect switches, horn gap.

One substation structure, wood construction.

Grounding resistor for the 13.8-kv system.

Auxiliary equipment including lightning arresters, potential devices and current transformers.

Indoor equipment:

Two metal-clad switchgear assemblies, vertical-lift type, 250,000-kva interrupting capacity.

One duplex control board, control power battery, battery-charging equipment, and battery distribution panel.

Main 20,000-Kva Transformers

Forced-oil air-pressure cooling of the main 20,000-kva transformers was adopted primarily as a material conservation means. Subsequent experience indicates that it merits extensive use at attended stations. The smaller size and lighter weight facilitate transportation and installation. The total losses are only slightly more than those of the conventional transformer design, and are much more than offset by the reduced purchase price.

The oil circulating system contains two pumps in parallel, each of which can be cut off, removed, and replaced without disturbing the other. The loss of one pump results in only a slight decrease in heat-dissipating efficiency. The oil-to-air exchanger consists of a multibank radiator with a multiplicity of cooling fans, which may be sectionalized in groups of three. Operating power for fans and pumps is derived from control power transformers included in the indoor metal-clad structure.

The split 13.8-kv winding design as employed in the main transformers accomplishes the following:

1. Each transformer serves as a source to two bus sections, permitting continued operation of both busses with one transformer out of service; without the aid of external reactors or bus-tie circuit breakers.

2. Short-circuit interrupting requirements are controlled by inherent transformer reactance. The internal winding configuration is such as to make the external characteristics equivalent to two independent 10,000-kva units.

3. All circuit breakers are of identical rating (600 amperes).

4. A change in voltage ratio of the main power transformers is accomplished easily without de-energizing either bus section. One transformer may be de-energized, its ratio changed by one tap, and then restored to the system, following which the same procedure would be repeated on the second transformer. The temporary circulating current in the transition stage will be limited to a small fraction of rated value.

The neutrals of both 13.8-kv winding sections are interconnected and brought out to permit grounding. The high-voltage winding is connected in delta to stabilize magnetically the three-phase transformer and also to make the grounding systems of the 13.8-kv and the 110-kv system independent. Each transformer 13.8-kv neutral is grounded through an outdoor-service grounding resistor, limiting the ground fault current to a low

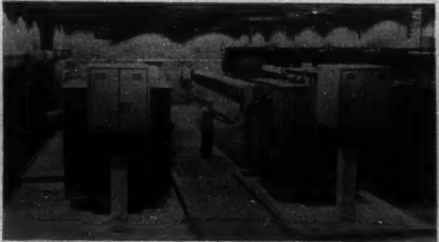

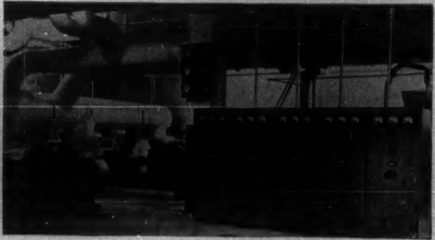

Figure 9 (left). View of typical 5,000-kva 13.8- to 2.4-kv secondary selective test-area unit substation with the two sections mounted face to face

Figure 10 (right). A group of typical synchronous-motor field cubicles from which motor control is effected

Figure 11. View of typical 600-kva 2,400 to-480-277-volt secondary selective load-center unit-substation

value, (not exceeding 1,000 amperes). Grounding of the 13.8-kv neutral in this manner maintains the system voltage normally symmetrical with respect to ground, provides a source of ground current for fast ground-fault relaying, minimizes transient-voltage surges resulting from switching operations, and is free from excessive overvoltages of repetitive restrike origin.

Auxiliary 10,000-Kva Transformer

The size and design of the 10,000-kva auxiliary transformer was worked out in conjunction with the affiliated power utility company. The 110-kv and 33-kv windings are connected in wye to provide means of grounding these neutrals and to establish zero-phase shift between the 110- and 33-kv terminal voltages. A necessary tertiary winding was wound for 13.8 kv and connected so that the resulting terminal voltage agrees in phase with that derived from the main transformers.

The function of this transformer is threefold:

1. To supply 13.8-kv power on a temporary basis from the 33-kv system for initial plant operation (3,500 kva maximum).
2. To serve permanently as a means of securing emergency power, in limited amounts, from the 33-kv system should the 110-kv supply be interrupted.
3. To provide means of transferring power from the 110-kv to the 33-kv system.

Prior to the availability of 110-kv power, this transformer served a number of unit substations in a temporary toolshop area, enabling the manufacture of tools and jigs to be initiated. About 400,000 square feet of working area was being served in this manner at the time primary power became available, although power-load levels were subnormal as would be expected (about 1,000-kva power load and approximately 400-kva lighting load).

Grounding System

The grounding system at this station involves a multiplicity of driven Copperweld ground rods distributed over the outdoor substation site. The installation of an inverted tile, flush with the ground surface and equipped with a wood cover at each ground rod, serves to keep the ground-rod terminal clamps out of contact with the earth, thus minimizing corrosion, and makes each connection accessible for inspection or measurement of resistance. Ground cables are installed leading to the indoor station, paralleling the incoming 13.8-kv power cable sheaths and integrating the grounding system of the entire plant.

Indoor Station

The indoor station, located along the factory end wall, includes two sections of 15-kv vertical-lift metal-clad switchgear (250,000-kva interrupting capacity), through which the 13.8-kv power is directed to plant feeders. Between these two sections is located a duplex board at which the primary control of the station is affected.

The front of the duplex board is devoted to the control of the 110-kv, 33-kv, and 13.8-kv transformer circuits; primary station metering and indicating instruments; and the master annunciator; arranged as shown in Figure 13. The rear of the duplex board is devoted to relays associated with incoming-power circuit protection up to the 13.8-kv metal-clad busses; and switching equipment for the station a-c auxiliary power, the appearance of which is illustrated in Figure 14.

Both sections of the metal-clad switchgear are assembled to be symmetrical with respect to the central duplex board. Incoming-power circuits are adjacent to the duplex board, and feeders for the various services appear in successive order. One switchgear section is illustrated in Figures 15 and 16. Circuit-breaker controls, indicating instruments, and relays for each feeder circuit are located on the corresponding metal-clad unit, although the opening of any feeder breaker will be announced and identified by an annunciator drop at the duplex board.

Outgoing feeder cables leaving the metal-clad structure are racked in a cable trench with a removable cover (see Figure 16), from which they pass through the adjoining wall into the factory build-

Figure 12. View of 5,000-kva 13.8- to 2.4-kv boilerhouse unit substation with the two sections mounted end to end

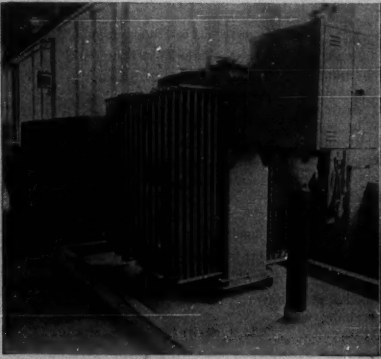

Figure 13. Front view of main substation duplex control board

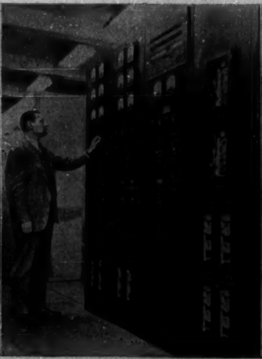

Figure 14. Rear view of main substation duplex control board

Figure 15 (left). Front view of one section of the 13.8-kv main substation vertical-lift metal-clad switchgear

Figure 16 (right). Rear view of metal-clad switchgear section shown in Figure 15

ing. They then are run up to the overhead cable troughs as illustrated in Figure 17.

Auxiliary a-c control power for main-transformer auxiliaries, indoor and outdoor station lighting, and control-battery charging is supplied by one 25-kva transformer, with a 208–120-volt low-voltage winding, incorporated in one unit of each metal-clad assembly. The auxiliary load normally is proportioned between the two units, but provision is made for switching the total load to either transformer in an emergency. Essential station lights are equipped with an automatic transfer relay, by which they are energized from the control battery, should the normal source fail. The emergency lighting circuit is fused separately at the battery distribution panel. The control battery, associated charging equipment, and distribution panel are installed in an adjacent room.

Interlocking

The electrically operated high-voltage horn-gap disconnect switches associated with the 20,000-kva transformers are interlocked electrically, with their respective low-voltage circuit breakers permitting them to be opened only when both low-voltage circuit breakers are open. The manually operated ratio-adjuster switches on these transformers also are interlocked to permit operation only when both the high-voltage disconnect switch and the two low-voltage circuit breakers are open. An inherent feature of vertical-lift metal-clad switchgear is an interlock, which prevents the circuit breaker from being moved to the disconnect position with the circuit-breaker element closed.

Relaying

All 13.8-kv feeder units are equipped individually with inverse-time overcurrent line and ground trip relays, the former co-ordinated to be selective with unit substation switching equipment. Instantaneous attachments, set above the current level obtained with a unit substation low-voltage bus fault, also are applied to avoid damaging internal temperature on the number-2-conductor feeder cables by shortening the clearing time in the presence of high fault-current magnitudes.

The 13.8-kv incoming-power circuits are equipped individually with inverse-time overcurrent line and ground relays co-ordinated to be selective with feeder-circuit line- and ground-relay protection.

Transformer differential-relay protection is applied to each of the 20,000-kva and the auxiliary 10,000-kva transformers. While the absence of individual high-voltage circuit breakers requires that the entire system be de-energized, the differential protective relays minimize internal damage by promptly interrupting the source of power, and, by relay targets, identifies the unit in trouble, enabling it to be isolated immediately and service restored promptly on remaining equipment.

The 110-kv incoming-line circuit is provided with inverse-time overcurrent line and ground relays, the former selectively co-ordinated with 13.8-kv switching equipment and the latter co-ordinated with ground relaying at the source end of the line. Power directional relays directed outward are applied to obtain automatic opening of the 110-kv oil circuit breaker as a result of external trouble on the 110-kv line.

The 33-kv incoming-line circuit is equipped with inverse-time overcurrent line and ground relays, together with power directional relays, selectively co-ordinated with remotely located 33-kv protective equipment.

A few words might be devoted appropriately to an explanation of how the 13.8-kv neutral grounding improves the fault protective picture. The 13.8-kv ground-relaying system involves only those circuit elements intervening between the transformer low-voltage neutral and the terminals of the 13.8-kv feeders. All circuit faults within this zone involving ground can be isolated correctly more rapidly, and with a greater margin of selectivity. Except for transitory surges of very short duration, no ground current flows in healthy feeder circuits. Feeder ground relays may be made sensitive and fast. Circuit faults involving only ground during the clearing interval will be subjected to only the limited ground fault current, thus further limiting the energy liberated at the fault. In the system here used, the flow of ground fault current in the 13.8-kv system does not result in ground current flow in circuits operating at other voltages. Neither will ground current flow elsewhere cause current flow in the 13.8-kv ground-relaying system.

Metering

The main substation incorporates the following instrument and metering equipment:

Ammeter in the 110-kv incoming line.

Ammeter in the 33-kv line circuit.

Voltmeter for each 13.8-kv bus.

Ammeter in each 13.8-kv incoming line.

Wattmeter for each 13.8-kv bus.

Watt-hour meter for each 13.8-kv bus with totalizing demand meter.

Reactive kilovolt-ampere-hour meter for each 13.8-kv bus with totalizing demand meter.

Ammeter in each 13.8-kv outgoing feeder.

Watt-hour demand meter in each 13.8-kv outgoing feeder.

Annunciator

To expedite station operation, a 30-drop annunciator with audible alarm signal is installed on the duplex board and duplicated in the office of chief of maintenance, which serves to announce and identify any of the following occurrences:

Oil-circulating-pump stoppage or auxiliary-power failure at transformers 1 or 2.

Transformer differential or back-up ground-relay operation of transformers 1, 2, or the auxiliary 10,000 kva.

Low oil level in transformers 1, 2, or the auxiliary 10,000 kva.

Overtemperature in transformers 1, 2, or the auxiliary 10,000 kva.

Opening of the following circuit breakers, if the control switch was moved to the close position last:

110-kv incoming oil circuit breaker.

33-kv incoming circuit breaker.

Each of the 13.8-kv incoming-power circuit breakers.

Each of the 13.8-kv feeder breakers (the four factory-feeder circuit breakers on each bus section operate a common annunciator drop).

Operating Experience

Operating experience with this electric system has been remarkably good. The few exceptions to an otherwise perfect record were not of serious character and occasioned no loss of sleep.

Initially, some trouble was encountered in the 13.8-kv cable terminal potheads requiring that the circuits be de-energized successively, the potheads opened, and modifications made. The advantages of the secondary selective system became clearly evident during this procedure. The necessary modification work was carried out without the loss of power at any station and without the use of auxiliary makeshift power supply equipment.

A number of faults have occurred in the plug-in bus resulting from the accidental insertion of wire or small diameter rod through the expanded metal side barriers.

Figure 17. View of the 13.8-kv cable feeders as they leave the main substation and pick up overhead troughs

Substation electric loads consistently are approaching closely the present installed capacity. A number of stations are operating at substantially full rated value while others at present generally are loaded to between 50 and 75 per cent of their ratings, but subsequent increases of 10 to 15 per cent are expected.

Summary

It may be concluded, without reservation, that the application of load-center distribution principles as herein described was responsible for an amazing reduction in material investment, principally copper and steel, compared with that which would have been required by power-distribution methods employed only a short time ago. In the planning of this project, the greatest emphasis constantly was placed on conservation of materials.

The use of compact, repetitively manufactured metal-clad, load-center unit substations do realize good economy in materials and man-hours, and at the same time incorporate simplicity and safety.

Unusual features incorporated in this system, which in themselves are responsible for large savings in material, man-hours, or both, include:

1. The application of forced-oil air-pressure cooling to the main incoming service transformers.

2. The use of overhead high-voltage feeder-cable troughs.

3. The use of spaced single-conductor low-voltage feeder design with moderate unit copper cross sections.

4. The use of 265-volt fluorescent lighting in combination with common load-center unit substations for serving power and light. (This feature alone accounts for a saving of five tons of copper and ten tons of steel compared with the most economical method of applying 120-volt fluorescent lighting.

The secondary selective system design offers a well-balanced combination of simplicity and service reliability.

The negotiation of the entire distribution system as a single unit proved highly beneficial in reducing the time of execution and insuring the best co-ordination between the several component portions.

As the supply of steel becomes less critical, it would seem reasonable to return to the use of steel construction in the outdoor station and to more effective metal-clad construction in low-voltage feeder circuits and plug-in bus.

It is the sincere hope of the authors that some of the features herein described, which have proved so beneficial in this installation, may in some small measure assist others to realize an improved more economical industrial distribution system in the future.

Inherent Errors in the Determination of Synchronous-Machine Reactances by Test

C. CONCORDIA
MEMBER AIEE

F. J. MAGINNISS
ASSOCIATE AIEE

As PROGRESS in the design and in the calculation of performance of synchronous machines has been made it has become necessary to specify their characteristics with continually greater accuracy. The predetermination of short-circuit currents, voltage dip on sudden application of load, stability characteristics during system disturbances, excitation requirements, and many other characteristics has been made possible by the development of an adequate theory, confirmed and refined by operating and test experience. The machine characteristics commonly used to predict performance usually are specified in terms of various reactances and time constants. As the number of these quantities and the accuracy to which they must be known has increased, certain inconsistencies among methods of definition, calculation, and test have become apparent. These should ideally all result in the same value. If they differ, one naturally would be inclined to consider the test value as the true reactance. In any case in which a reactance of a particular machine is specified, a method of testing for that reactance also must be specified, and any other definition of the reactance has little practical significance. In this sense the criterion of a good method of calculating the reactance is that it predict as nearly as possible the value which will be found by the specified test method. It, of course, can be asked legitimately whether the specified reactance is the proper one in view of the use to which it is to be put, and the definition is intended to describe the reactance so as to answer this question.

The reactance found by test will be affected by errors in the method of test (as for example, nonsimultaneous short circuit of all three phases in case of three-phase short-circuit tests), by the conditions of the machine under test (as for example, the degree of saturation corresponding to the voltage used), by errors of measurement and calibration, and by the technique of measurement.

The purpose of this paper is to present the results of a comparison of the values of reactance which might be found by recommended test procedures with the values calculated by well-established formulas, as affected by the machine characteristics, and by nonsimultaneous closing of the test circuit-breaker contacts. A three-phase short-circuit test on a salient-pole synchronous machine was simulated by setting up the proper equations on the differential analyzer. The effect of saturation was not considered, and the precision of measurement of the current curves was undoubtedly greater than would be possible for an actual oscillogram so that the variations obtained were inherent in the method.

Only two of the several reactances, the direct-axis transient reactance and the direct-axis subtransient reactance, have been studied. The direct-axis short-circuit transient and subtransient time constants also have been considered but in less detail.

Definition of Machine Quantities

In the AIEE Test Code for Synchronous Machines (January 1944 revision), the definition of direct-axis transient reactance (x_d') is given as[1]

> "1.840 The direct axis transient reactance is the ratio of the fundamental component of reactive armature voltage, due to the fundamental direct-axis a-c component of the armature current, to this component of current under suddenly applied load conditions and at rated frequency, the value of current to be determined by the extrapolation of the envelope of the a-c component of the current wave to the instant of the sudden application of load, neglecting the high-decrement currents during the first few cycles."

In this definition the transient reactance is defined both in terms of the fundamental component of armature current and of the envelope of the a-c component of the current. The phase currents obtained after the three-phase short circuit even of an idealized machine contains second harmonics which may have appreciable magnitudes. In an actual machine having saturation, hysteresis, and eddy currents, the current may contain other harmonics as well. Even in the ideal case, with only second harmonics present, it would be extremely difficult and impractical to determine the amount of fundamental in the transient wave as is required by the first part of the definition.

Two direct-axis transient reactances are defined, the rated current value and the rated voltage value, which will differ because of saturation. However, this paper does not investigate this classification of transient reactance, as saturation effects have been neglected.

The definition of direct-axis subtransient reactance is[1]

> "1.860 The direct axis subtransient reactance is the ratio of the fundamental component of reactive armature voltage, due to the initial value of the fundamental direct axis a-c component of armature current, to this component of current under suddenly applied load conditions and at rated frequency."

Measurement of Machine Reactances

Testing and measuring procedures for the determination of the direct-axis transient and subtransient reactances have been given in reference 1 and are reproduced as follows:

> "DIRECT AXIS TRANSIENT REACTANCES (x_d'); DETERMINATION BY TEST
>
> "1.843 The direct axis transient reactance is determined from the current waves of a three-phase short circuit suddenly applied to the machine operating at no load and rated speed. The direct axis transient reactance is equal to the ratio of the no load voltage to the corresponding value of the armature current given by the extrapolation of the envelopes of the a-c components of the armature current waves to the instant of the sudden application of the short circuit neglecting the high decrement currents during the first few cycles. Figures 26 and 27 (Figures 26 and 27 of the Test Code are Figures 14 and 15 of this paper) illustrate this method of determining the direct axis transient reactance.
>
> "1.844 In plotting the current values from the oscillogram, the first peak should be plotted at the abscissa 1, and subsequent peaks numbered consecutively. The positive

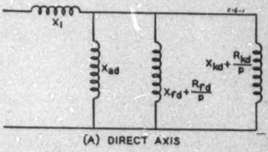

(A) DIRECT AXIS

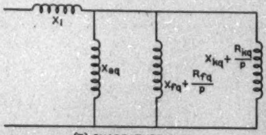

(B) QUADRATURE AXIS

Figure 1. Synchronous-machine equivalent circuits

Paper 45-16, recommended by the AIEE committee on electric machinery for presentation at the AIEE winter technical meeting, New York, N. Y., January 22-26, 1945. Manuscript submitted October 27, 1944; made available for printing December 7, 1944.

C. CONCORDIA and F. J. MAGINNISS are both in the analytical division, central-station engineering divisions, General Electric Company, Schenectady, N. Y.

The authors wish to acknowledge the assistance of R. F. Simon and Mrs. D. R. Stupp of the General Electric Company, and of Ensign W. Ridgway, United States Navy, formerly of the General Electric Company.

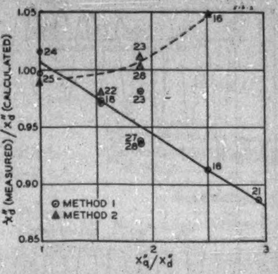

Figure 2. Effect of x_q''/x_d'' on measured subtransient reactance

peaks will be odd numbers, and the negative peaks will be even numbers or vice versa. The current values from the oscillograms should be plotted first, and then the median line and the a-c component. These curves are usually plotted on standard rectangular coordinates, and are most conveniently analyzed if the currents are expressed in per-unit values, with the unit value equal to the peak value of the rated current wave. (See Figure 26.)

"1.845 The a-c component should then be replotted on semi log scales with the current on the logarithmic scale together with a plot of the a-c component minus the sustained short-circuit current* (Curve *B*, Figure 27). These curves should pass through the ordinates for peak 1. Since the first peak is plotted at abscissa 1, the abscissa for the time of application of the short [circuit] is usually not at zero, but at a time which can be readily determined from the oscillogram. This zero-time line should be plotted on the semi log plot, and extrapolations of the current curves are extended to this line. It is important in plotting the first several cycles of the (AC component minus the sustained value) to choose current and time scales that will avoid a steep slope during the first three or four cycles. It will usually be found that curve *B* can be very closely represented by a straight line and a curve for several cycles at the beginning of the short circuit. The curves for the tests and analysis should be carried out for sufficient cycles to establish definitely the straight-line part of curve *B*. The difference *A* (see Figure 27) between curve *B* and the extension of the straight part to $t=O$, when plotted on the semi log scales, will also be closely represented by a straight line. (This straight line should always be plotted to pass through the ordinate for peak 1.)

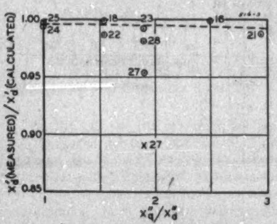

Figure 3. Effect of x_q''/x_d'' and of r_a on measured transient reactance

Case 27 has low armature resistance r_{al} lower value obtained from first 15 cycles

"1.846 The ordinate for curve *B* at $t=O$ is equal to the sum of the ordinates at $t=O$ from the two straight lines. The ordinate for the a-c component at $t=O$ is then determined by adding the sustained short circuit current to the ordinate of curve *B* at $t=O$. The curve for the transient component plus the sustained value of the current is determined by adding the sustained short circuit current to the extended straight line part of curve *B*.

$$x_d'=\frac{e}{I'}\text{(per unit value)}$$

where

e = the open-circuit voltage of the machine immediately before the short circuit, expressed in per unit based on rated voltage

I' = per unit current from the transient component plus the sustained value at $t=O$. (Figure 27; Figure 15 of this paper)

"DIRECT AXIS SUBTRANSIENT REACTANCE (x_d''); DETERMINATION BY TEST, METHOD (1)

"1.863 The direct axis subtransient reactance is determined from the sudden short-circuit test described in paragraph 1.843

$$x_d''=\frac{e}{I''}\text{ (per unit value)}$$

See paragraph 1.846 for "e". I'' = per-unit current from the a-c component curve at $t=O$ (Figure 27).

"1.864 Method (2). An alternate method of evaluating subtransient reactance, which may be used when the three phases are known to be short circuited simultaneously or at least within approximately ten degrees, is that based on the maximum possible asymmetrical component. Plot the three asymmetrical components (median line Figure 26 represents one of these components) on semi log scales with currents on the logarithmic scale. The peaks may be

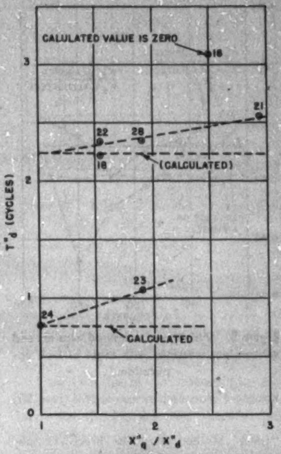

Figure 4. Effect of ratio x_q''/x_d'' on measured subtransient time constant

numbered as in paragraph 1.844 and the line for $t=O$ located as described in paragraph 1.845 for plotting Figure 27. Extrapolate the curves back to zero time thereby obtaining three initial values, which may be designated a, b, c. Lay these components off (uniform scale) along three radial lines 60° apart radiating from a point O, the largest of the three values being laid off on the middle line. Draw perpendiculars through the end points of each of the three lines, and the point where these perpendiculars meet determines the point M. In case the perpendiculars do not meet in a point, but form a small triangle, locate M in the approximate center of the triangle. Then the distance OM represents the maximum possible asymmetrical component, to the same scale as the three components on the radial lines.

$$x_d''=\frac{e}{OM}\text{ (per unit value)}$$

See paragraph 1.846 for "e". OM is expressed as a per unit value, with the base equal to the peak value of the rated current wave. The ampere value of OM is equal to the peak value of the normal current wave multiplied by the per unit value of OM.

Table I. Machine Physical Reactances and Resistances

Case	R_a	x_l	x_{ad}	x_{fd}	x_{kd}	R_{fd}	R_{kd}	x_{aq}	x_{fq}	x_{kq}	R_{fq}	R_{kq}
22	0.00694	0.0557	1.068	0.1507	0.496	0.00068	0.037	0.414		0.3556	∞	0.035
23	0.00694	0.0557	1.068	0.1942	0.1356	0.00068	0.037	0.414		0.3556	∞	0.035
24	0.00694	0.0577	1.068	0.1942	0.1356	0.00068	0.037	0.414		0.0906	∞	0.035
18	0.00694	0.0557	1.068	0.1507	0.496	0	0.037	0.414		0.3556	∞	0.035
21	0.00694	0.0557	1.068	0.1507	0.496	0.00068	0.037	0.414			∞	∞
16	0.00694	0.0557	1.068	0.1507		0	∞	0.414			∞	∞
25	0.00694	0.0557	1.068	0.1507		0	∞	1.068	0.1507		0	∞
27	0.00231	0.0557	1.068	0.1942	0.1356	0.00068	0.01223	0.414		0.3556	∞	0.035
28	0.00694	0.0557	1.068	0.1942	0.1356	0.00068	0.01223	0.414		0.3556	∞	0.035

---

* The sustained short-circuit current is determined from the direct-axis synchronous impedance curve, using the armature current corresponding to the steady-state field current immediately before the machine is short-circuited.

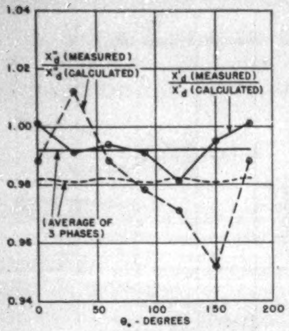

Figure 5. Variation of measured transient and subtransient reactance with angle of fault application

Reactance from each phase current (case 23)

"1.865 Method (3). The direct axis subtransient reactance may also be determined for three phase machines from a static impedance test in which a single phase voltage is impressed across two armature phase windings in series (connected for 120° phase displacement) with the field short circuited. The rotor is placed in the angular position for maximum induced field current. The subtransient reactance equals the ratio of half the applied voltage to the resulting armature current."

Several comments may be made with regard to these recommended test procedures even before the results of the present study are examined.

In this paper the envelope is taken as a smooth curve drawn through the extreme maximum and minimum points of the current-versus-time curve. This would seem to be so obvious as not to require comment except for the fact that the envelope has been defined in a different way in a previously published paper[2] on this subject.

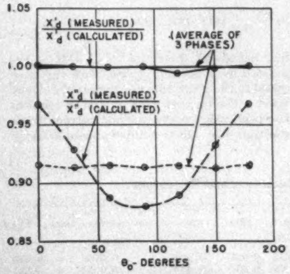

Figure 6. Variation of transient and subtransient reactance with angle of fault application

Reactance found from each phase current; case 16 (no amortisseur)

The median line is defined only by a curve of Figure 14. This comment is again pertinent because in reference 2 the midpoint of the envelopes as there defined has been used. In the present paper the midpoint of the envelope as here defined is taken as the median line.

In the static line-to-line test for the determination of subtransient reactance the current will be sinusoidal if the voltage is sinusoidal, aside from the effect of saturation. Thus without saturation the result found from test will differ from the nominal calculated value only by the inclusion of the stator and rotor resistances. This does not imply of course that it is a better test, since in the first place saturation effects may be very important and in the second place additional test equipment is required since the short-circuit test is necessary for the transient reactance anyway.

Calculation of Machine Quantities

When the per-unit mutual reactances between armature and field, armature and amortisseur, and field and amortisseur are all the same, as is assumed in the present case, it is possible to use direct- and quadrature-axes equivalent circuits for the calculation of the synchronous machine constants. These circuits are shown in Figure 2 of reference 3 and in Figure 1 here in slightly more complete form; the field resistance is not assumed zero and an additional winding is considered in the quadrature axis (see Appendix III).

The calculation of subtransient and transient reactances and time constants from these equivalent circuits is made as follows:

1. *The direct-axis subtransient reactance* x_d'' is the input impedance of the direct-axis equivalent circuit with $R_{fd}/p = R_{kd}/p = 0$. Thus x_d'' is equal to x_l in series with the paralleled value of x_{ad}, x_{fd} and x_{kd}

$$x_d'' = x_l + \frac{x_{ad}x_{fd}x_{kd}}{x_{ad}x_{fd}+x_{ad}x_{kd}+x_{fd}x_{kd}}$$

2. *The direct-axis transient reactance,* x_d, is the input impedance of the direct-axis equivalent circuit with $R_{fd}/p = 0$ and $R_{kd}/p = \infty$. Thus x_d' is equal to x_l in series with the paralleled value of x_{ad} and x_{fd}.

$$x_d' = x_l + \frac{x_{ad}x_{fd}}{x_{ad}+x_{fd}}$$

3. *Direct-axis subtransient short-circuit time constant,* T_d''. The direct-axis equivalent circuit is assumed broken in the amortisseur branch; R_{fd}/p is assumed zero; the input terminals of the equivalent circuit are short circuited. The reactance of the circuit as viewed from the terminals in the amortisseur branch is divided by R_{kd} to give T_d''.

$$T_d'' = \frac{x_{kd} + \dfrac{x_l x_{ad} x_{fd}}{x_l x_{ad} + x_l x_{fd} + x_{ad} x_{fd}}}{2\pi f\, R_{kd}} \text{ (seconds)}$$

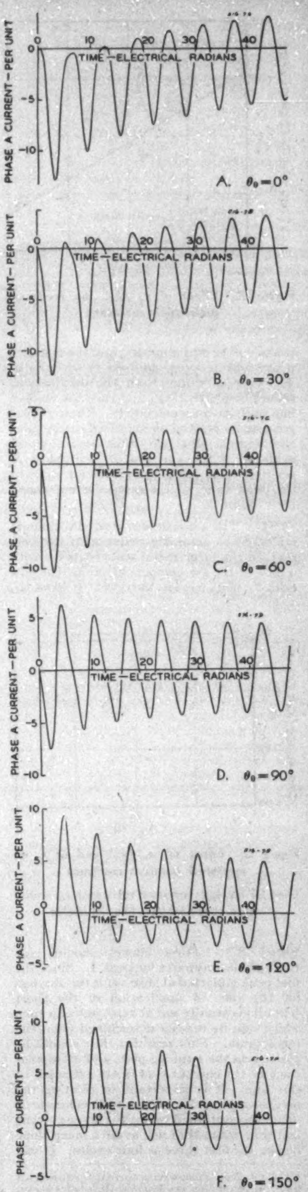

A. $\theta_0 = 0°$

B. $\theta_0 = 30°$

C. $\theta_0 = 60°$

D. $\theta_0 = 90°$

E. $\theta_0 = 120°$

F. $\theta_0 = 150°$

Figure 7. Phase-*A* current versus time; case 23

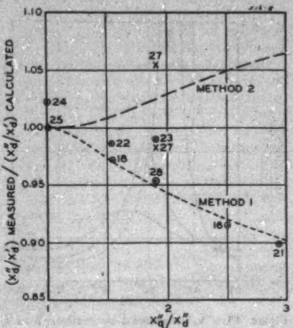

Figure 8. Variation of measured x_d''/x_d' with x_q''/x_d''

Curves are from calculations for cases of very small decrements. Points are from method 1

4. *Direct-axis transient short-circuit time constant, T_d'.* The amortisseur branch of the direct-axis equivalent circuit is assumed open circuited and the circuit is assumed broken in the field branch. The input terminals are short circuited. The reactance of the circuit as viewed from the terminals in the field circuit divided by the field resistance, R_{fd}, gives T_d'.

$$T_d' = \frac{x_{fd} + \dfrac{x_l x_{ad}}{x_l + x_{ad}}}{2\pi f\, R_{fd}} \text{ (seconds)}$$

Analysis; Simultaneous Closing

On the basis of the preceding sections of this paper it is seen that no exact comparison can be made between the defined transient and subtransient reactances and the calculated or measured values of these quantities. It is possible, however, to determine the correspondence that is to be expected between the calculated values of the reactances and the values determined by an ideal short-circuit test.

Park's equations[8] of an idealized synchronous machine (see Appendix I) were set up on the differential analyzer and the phase *A* current obtained for a three-phase short circuit on a machine initially running open circuited. All three phases were short circuited simultaneously; the effect of sequential closing is considered in the next section.

This *A*-phase current record takes the place of the oscillogram described in the sections on measurement and was analyzed as there described, giving values of x_d', x_d'', T_d', and T_d''.

For each machine studied, six solutions were obtained. These were the *A*-phase current for short circuits applied at each of six rotor angles, varying from 0 degrees to 150 degrees with respect to the axis of phase *A* in 30-degree steps. The *A*-phase current for a fault at 0 degrees from the axis of phase *A* is the negative of the current in the *C* phase for a fault at 60 degrees, and is also the current in the *B* phase for a fault at 120 degrees. It is seen then that the six solutions obtained contain all three-phase currents for each angle specified (30-degree steps). Moreover the average values of the reactances (average of the three phases for any one test) will be repeated every 60 degrees. Thus if there is a variation of this average reactance with angle of application of the fault, it is periodic with a period of 60 degrees.

The machines studied are defined in terms of the reactances and resistances of the individual stator and rotor circuits. Values of these quantities, as well as of the transient and subtransient reactances and time constants calculated from them, are given in Tables I and II.

Case 22 represents the characteristics of a machine having a rather high ratio of calculated subtransient to transient reactance, $x_d''/x_d' = 0.16/0.1878 = 0.852$, so that the equivalent amortisseur-leakage reactance $x_{kd}(=0.496)$ is large. This makes the subtransient time constant large.

Case 23 was studied to show the effect of a much smaller ratio of calculated subtransient to transient reactance, $x_d''/x_d' = 0.13/0.22 = 0.591$. One effect of the smaller x_d'' is to make x_{kd} and thus T_d'' much smaller.

Case 24 was studied to show the effect of making the rotor symmetrical for subtransient effects. The quadrature-axis subtransient reactance x_q'' (calculated) was reduced to $x_q'' = 0.13$ so that it was equal to x_d'' of case 23. In case 23 the ratio of x_q''/x_d'' was 1.9, which is rather large.

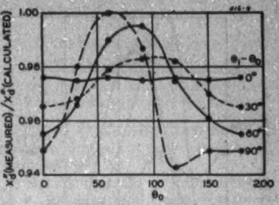

Figure 9. Effect of θ_0 and of $(\theta_1-\theta_0)$ on measured value of x_d'', method 1

$x_q''/x_d'' = 1.5$

Case 18 is like the first case (22) except $R_{fd}=0$. This was considered in order to show the effect of the field transient time constant T_d'.

Case 21 was considered in order to show the effect of a large ratio of x_q''/x_d''. The quadrature-axis amortisseur was removed entirely so that $x_q''/x_d'' = 2.94$. It is otherwise the same as case 22.

In cases 16 and 25 there are no rotor resistances; the amortisseur has been completely removed and the field resistance made zero. Case 16 has an effective ratio $x_q''/x_d'' = x_q'/x_d' = 0.4697/0.1878 = 2.5$, while in case 25 $x_q''/x_d'' = x_q'/x_d' = 0.1878/0.1878 = 1.00$.

Cases 27 and 28 are to show the effect of increasing the armature and subtran-

Table II. Calculated Machine Constants

Case	x_d'	x_d''	x_d''/x_d'	x_q''	x_q''/x_d''	Cycles T_a	 T_d'	 T_d''
22	0.1878	0.1600	0.852	0.247	1.54	4.45	47.7	2.3
23	0.2200	0.1300	0.591	0.247	1.90	3.90	57.8	0.76
24	0.2200	0.1300	0.591	0.130	1.00	2.98	57.8	0.76
18	0.1878	0.1600	0.852	0.247	1.54	4.45	∞	2.3
21	0.1878	0.1600	0.852	0.4697	2.94	5.47	47.7	2.3
16	0.1878	0.1878	1.00	0.4697	2.50	6.15	∞	0.0
25	0.1878	0.1878	1.00	0.1878	1.00	4.30	∞	0.0
27	0.2200	0.1300	0.591	0.247	1.90	11.90	57.8	2.3
28	0.2200	0.1300	0.591	0.247	1.90	3.90	57.8	2.3

Table III. Average Measured Machine Constants

Case	x_d'	x_d''	x_d''/x_d'	T_d'	T_d''
22	0.1851	0.1557	0.841	49.9	2.35
		0.1568*	0.840*		
23	0.2183	0.1276	0.585	59.8	1.08
		0.1314*	0.602*		
24	0.2188	0.1321	0.604	60.5	0.76
18	0.1873	0.1555	0.830	∞	2.22
21	0.1855	0.1419	0.765	56.0	2.55
16	0.1876	0.1718	0.916	∞	3.09
		0.1954*	1.042*		
25	0.1872	0.1872	1.0	∞	0
		0.1859*	0.993*		
27	0.1958**	0.1215**	0.621**		
	0.2089	0.1225	0.586		
28	0.2158	0.1217	0.564	61.2	2.34
		0.1306*	0.605*		

* Denotes median method (method 2). ** Only first 15 cycles measured.

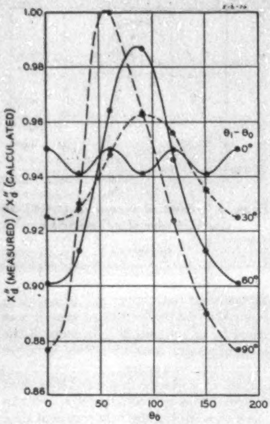

Figure 10. Effect of θ_0 and of $(\theta_1-\theta_0)$ on measured value of x_d'', method 1

$x_q''/x_d''=2.0$

sient time constants. Case 28 is like case 23 except for a smaller direct-axis amortisseur resistance, designed to give a calculated subtransient time constant equal to that of case 22. Case 27 has the small direct-axis amortisseur resistance and also a small armature resistance.

Some of the results of the analyses of the short-circuit-current curves obtained on the differential analyzer for these cases are shown in Table III. This table shows the average of all six-phase currents for each case. The measured values of x_d'', x_d', and T_d'' are plotted against the calculated ratio x_q''/x_d'' in Figures 2, 3, and 4, respectively.

Figure 2 shows that for method 1 there is a tendency for the measured direct-axis subtransient reactance to decrease if the quadrature-axis subtransient reactance is increased even though no change has been made in the direct-axis rotor circuits. If the median method (method 2 of the AIEE Test Code) is used, there is no such tendency. Instead, the reactance increases slightly. As the ratio x_q''/x_d'' approaches 1.0 the measured x_d'' approaches the calculated value. All of these observations are confirmed by the results of calculations for the idealized case in which all decrements are neglected (see Figure 8).

Figure 3 shows that the ratio x_q''/x_d'' has practically no effect on the measured value of x_d'. On the other hand, the armature resistance appears to have a considerable effect. When the armature resistance is low, as in case 27, x_d' is low, presumably because of the slow decay of the second-harmonic component of current.

Figure 4 shows a slight tendency for the measured subtransient time constant T_d'' to increase with increasing x_q''/x_d'', which may be caused by the decaying second harmonic modifying the apparent subtransient decay. A striking example of this effect is shown in case 16, where there is no amortisseur, and the whole subtransient effect is produced by the second harmonic, the magnitude of the fundamental remaining constant. Case 16 also shows that the ratio of subtransient to transient reactance may be considerably less than unity even though a machine has no amortisseur.

Table IV shows the reactances obtained from the individual-phase currents and from the two sets of three-phase short circuits. Since the effects of angle should be appreciable only when $x_d'' \neq x_q''$ it is evident that the effects of the ratio x_q''/x_d'' as shown in Figures 2, 3, and 4 would be somewhat greater if the average of only three phases had been used instead of the data of Table III. However, the latter is believed to be more representative, especially in view of possible measurement errors.

Figure 5 shows measured results for the individual current waves for case 23. Figure 6 is a similar curve for case 16. The variation indicates that it is highly desirable to measure all three-phase currents and possibly to take more than one test even if there were no theoretical differences among the phases. Figure 7 shows the actual current waves for the case of Figure 5.

Figure 8 is a summary of the effect on the ratio of subtransient to transient reactance of variation in x_q''/x_d''. Since Figure 3 showed no appreciable effect of x_q''/x_d'' on x_d', Figure 8 may be considered to represent also the effect of x_q''/x_d'' on x_d''. The calculated variation of x_d'' neglecting decrements also is shown on Figure 8, and is seen to be in reasonably good agreement with the differential-analyzer results.

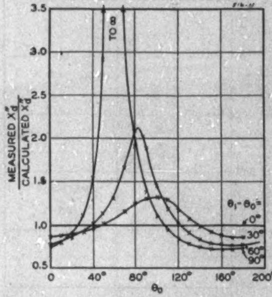

Figure 11. x_d'' measured by method 2 as a fraction of its calculated value versus θ_0

$x_q''/x_d''=1.5$

Analysis; Sequential Switching

On the basis of certain simplifying assumptions, the effect of sequential switching on the measured value of direct-axis subtransient reactance has been determined. In addition to the usual ideal synchronous machine assumptions, all machine resistances are considered to be

Table IV. Ratio of Measured to Calculated Machine Reactances

Case		θ_0						Three-Phase Average for Fault at		
		0°	30°	60°	90°	120°	150°	$\theta_0=0$	30°	Average
22	x_d'	0.988	0.996	0.980	*	0.976	0.989	0.981	0.993	0.986
	x_d''	0.988	0.970	0.959	*	0.962	0.988	0.970	0.979	0.973
								0.983**	0.976**	0.980**
23	x_d'	1.001	0.991	0.994	0.991	0.981	0.995	0.992	0.992	0.992
	x_d''	0.988	1.012	0.988	0.978	0.971	0.952	0.982	0.981	0.982
								1.013**	1.008**	1.011**
24	x_d'	0.992	0.992	0.996	0.990	1.001	0.995	0.996	0.992	0.994
	x_d''	0.985	1.069	1.036	1.002	1.004	1.002	1.008	1.024	1.016
18	x_d'	0.997	1.000	1.002	0.997	1.001	0.995	1.000	0.997	0.999
	x_d''	0.998	0.979	0.960	0.951	0.960	0.979	0.973	0.970	0.971
21	x_d'	1.014	0.991	0.971	0.970	0.970	1.008	0.985	0.990	0.987
	x_d''	0.904	0.909	0.868	0.859	0.874	0.906	0.882	0.891	0.887
16	x_d'	1.001	1.000	1.000	1.000	0.995	0.999	0.999	1.000	0.999
	x_d''	0.968	0.929	0.887	0.880	0.890	0.932	0.915	0.914	0.914
								1.014**	1.081**	1.048**
25	x_d'	1.000	1.000	1.000	0.997	0.992	0.992	0.997	0.996	0.997
	x_d''	1.000	1.000	1.000	0.997	0.992	0.992	0.997	0.996	0.997
								0.995**	0.981**	0.988
27	x_d'***	0.951	0.893	0.854	0.839	0.857	0.947	0.887	0.893	0.890
	x_d'	0.973	0.963	0.961	0.924	0.931	0.973	0.955	0.953	0.954
	x_d''	0.983	0.975	0.934	0.908	0.880	0.950	0.932	0.944	0.938
28	x_d'	0.975	0.974	0.991	0.991	0.990	0.964	0.985	0.976	0.981
	x_d''	0.997	0.948	0.922	0.901	0.909	0.940	0.943	0.930	0.936
								0.998**	1.008**	1.003

* Results for this point are questionable and are not included in average values.

** Denotes method 2.

*** Only first 15 cycles measured.

zero. The three-phase currents[4] (see Appendix II) have been plotted for values of θ_0, the angle at which the first two phases are short circuited, and of $\theta_1-\theta_0$, the angle of delay between the short circuiting of the first two phases and of the third phase. Since there is no decay of current, the peak-to-peak phase currents may be used to determine the direct-axis subtransient reactance. As in the previous section of this paper, the direct-axis subtransient reactance has been determined by the two methods described there.

Method 1

Figures 9 and 10 give the ratio of measured reactance[*] (differential-analyzer results), to calculated reactance for values of x_q''/x_d'' of 1.5 and 2.0, respectively. (Sequential switching will not affect the measured reactance for $x_q''/x_d''=1$.) For a delay in closing of the third phase of 60 electrical degrees, the maximum variations in measured reactance can be four per cent for $x_q''/x_d''=1.5$ and 8.5 per cent for $x_q''/x_d''=2.0$. These variations are much larger than those due to the subtransient saliency alone as discussed under simultaneous switching.

Method 2

The theoretical discrepancy ratio as defined in reference 4 is the ratio of x_d'' measured by method 2, except that only the direct component of current is used, to its defined value. This neglects the effect of the second-harmonic current on the measured value of the asymmetrical component. In this paper x_d'' is measured by method 2 considering the total current. Figures 11 and 12 show the ratio of measured to calculated reactance for values of x_q''/x_d'' of 1.5 and 2.0, respectively for various values of θ_0 and $\theta_1-\theta_0$. A similar set of curves for $x_q''/x_d''=1.0$ is given in Figure 3 of reference 4.

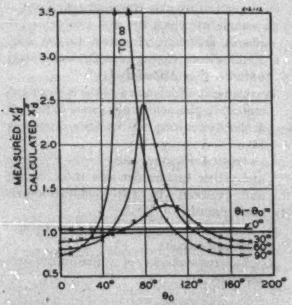

Figure 12. x_d'' **measured by method 2 as a fraction of its calculated value versus** θ_0

$x_q''/x_d''=2.0$

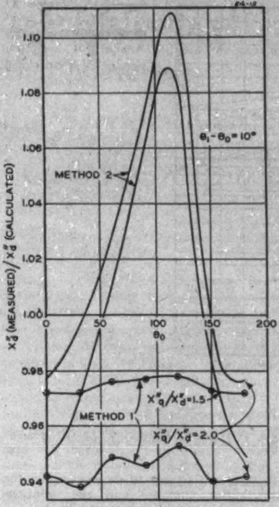

Figure 13. Effect of θ_0 **and of** x_q''/x_d'' **on measured value of** x_d''

It has been noted in the section of this paper on simultaneous switching that in general method 2 gives results somewhat closer to the calculated subtransient reactance than does method 1. From this it should not be inferred that method 2 is generally superior. The difficulty in adjusting the circuit breaker to close the three phases within ten degrees as required by the standards as well as the difficulty in determining from the oscillogram whether or not this angle is less than ten degrees are both considerable. Moreover, it is seen from Figure 13 that even for so small a delay angle as ten degrees, the results obtained by this method are far inferior to those obtained by method 1.

Conclusions

From the results obtained in this study the following conclusions may be drawn:

1. The direct-axis subtransient reactance and time constant as measured by any short-circuit test method so far proposed depends not only on the characteristics of the direct-axis rotor circuits, but also on those of the quadrature axis.
2. Method 1 of the AIEE Test Code should be used in the measurement of direct-axis subtransient reactance to the exclusion of method 2, the asymmetrical method.
3. There may be a considerable variation of the magnitude of the individual-phase currents with angle of fault application. This, in conjunction with possible measurement errors, makes it very important to use the average obtained from all three-phase currents of any one test, and highly desirable to use the results of more than one test.
4. Since the measured subtransient reactance may be low and the measured transient reactance may be about right in comparison with calculated values, the ratio of subtransient to transient reactance may be low. In particular, even with no amortisseur the measured ratio x_d''/x_d' is appreciably smaller than unity.
5. It often may be necessary to use considerably more than 15 cycles in order to obtain the correct value of transient reactance, especially if the armature resistance is low.
6. The maximum difference in closing angle should be limited to as low a value as possible.
7. The short-circuit test methods given in the AIEE Test Code approach, but are not in entire agreement with, the definition of subtransient reactance. It would, moreover, be impracticable if not impossible to test directly for the defined subtransient reactance.

Appendix I

On the assumption of constant unit rotor speed, Park's equations[5] for an ideal synchronous machine may be written

$$e_d=p\psi_d-ri_d-\psi_q \tag{1}$$

$$e_q=p\psi_q-ri_q+\psi_d \tag{2}$$

$$\psi_d=G(p)E-x_d(p)i_d \tag{3}$$

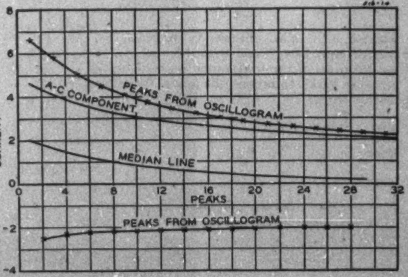

Figure 14. Figure 26 of Test Code

Peak values of instantaneous short-circuit currents and deviation of a-c component

---

[*] By measured reactance is meant that value which would be obtained by analysis of an oscillogram of the short-circuit current of an ideal synchronous machine with characteristics corresponding to the assumptions.

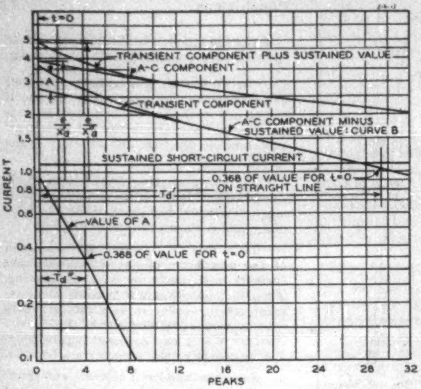

Figure 15. Figure 27 of Test Code

[redacted]

Analysis of a-c component of short-circuit current

$$\psi_q=-x_q(p)i_q \tag{4}$$

If a simultaneous three-phase short circuit is applied at the terminals of a machine initially running open-circuited with no change in the applied field voltage, these equations reduce to

$$0=p\psi_d-ri_d-\psi_q \tag{5}$$

$$-e_{q0}=p\psi_q-ri_q+\psi_d=-1.0 \tag{6}$$

$$\psi_d=-x_d(p)i_d \tag{7}$$

$$\psi_q=-x_q(p)i_q \tag{8}$$

where $x_d(p)$ and $x_q(p)$ are the operational input impedances of the circuits of Figure 1.

After reduction to suitable form for the differential analyzer, these become

$$p\psi_d=\psi_q+ri_d \tag{9}$$

$$\psi_d=\int p\psi_d dt \tag{10}$$

$$p\psi_q=-1.0-\psi_d+ri_q \tag{11}$$

$$\psi_q=\int p\psi_q dt \tag{12}$$

$$pi_d=ap\psi_d+b\psi_d+ci_d+\int(di_d+e\psi_d)dt \tag{13}$$

$$i_d=\int pi_d dt \tag{14}$$

$$pi_q=fp\psi_q+g\psi_q+hi_q+\int(ji_q+k\psi_q)dt \tag{15}$$

$$i_q=\int pi_q dt \tag{16}$$

where $a, b, \ldots k$ are obtained in the reduction of equations 7 and 8 to 13 and 15. By definition of the transformation used to arrive at Park's equations, the phase A current is written

$$i_a=i_d\cos\theta-i_q\sin\theta \tag{17}$$

Since

$$p\theta=1$$

$$\begin{aligned}pi_a&=-i_d\sin\theta+pi_d\cos\theta-i_q\cos\theta-pi_q\sin\theta\\&=-(i_d+pi_q)\sin\theta+(pi_d-i_q)\cos\theta\end{aligned} \tag{18}$$

Then

$$i_a=\int(i_d+pi_q)d\cos\theta+\int(pi_d-i_q)d\sin\theta \tag{19}$$

Equations 9–16 and 19 were set up on the differential analyzer and the solutions referred to in the text were obtained.

Appendix II

In determining direct-axis subtransient reactance for cases of nonsimultaneous switching, peak-to-peak values of the three-phase currents have been obtained by numerical substitution in equations 1 of reference 4. These are

$$i_1=\frac{I_0}{x_d''}\left\{\cos\theta-\frac{k_0}{\sqrt{3}n}[(1+n)-(1-n)\cos 2\theta]-\frac{k_1}{\sqrt{3}n}\left[\frac{1+n}{2}+(1-n)\cos(2\theta+120°)\right]\right\}$$

$$i_2=\left\{\frac{I_0}{x_d''}\cos(\theta-120°)+\frac{k_0}{\sqrt{3}n}\left[\frac{1+n}{2}+(1-n)\cos(2\theta-120°)\right]-\frac{k_1}{\sqrt{3}n}\times\left[\frac{1+n}{2}+(1-n)\cos 2\theta\right]\right\}$$

$$i_3=\frac{I_0}{x_d''}\left\{\cos(\theta+120°)+\frac{k_0}{\sqrt{3}n}\times\left[\frac{1+n}{2}+(1-n)\cos(2\theta+120°)\right]+\frac{k_1}{\sqrt{3}n}[(1+n)-(1-n)\cos(2\theta-120°)]\right\}$$

where

$$n=x_q''/x_d''$$

and

$$k_0=\sin(\theta_0+120°)$$

$$k_1=\sin\theta_1+[\sin(\theta_1+120°)-\sin(\theta_0+120°)]\times\frac{\frac{1+n}{2}+(1-n)\cos(2\theta_1+120°)}{1+n-(1-n)\cos(2\theta_1-120°)}$$

and where the phase rotation is 1, 2, 3, and line 3 is the last one short-circuited, at $\theta=\theta_1$, after previous short circuit of lines 1 and 2 at $\theta=\theta_0$.

It will be noted that a typographical error in these equations in the reference has been corrected.

Appendix III. Nomenclature

See also Figure 1 and Appendixes I and II.

x_d'' = direct-axis subtransient reactance
x_d' = direct-axis transient reactance
x_l = armature-leakage reactance
x_{ad} = mutual reactance between the armature and field, field and direct-axis amortisseur, and armature and direct-axis amortisseur
x_{fd} = field-leakage reactance
x_{kd} = direct-axis amortisseur leakage reactance
R_{fd} = field resistance
R_{kd} = direct-axis amortisseur resistance
T_d'' = direct-axis subtransient short-circuit time constant
T_d' = direct-axis transient short-circuit time constant
x_q'' = quadrature-axis subtransient reactance
x_d' = quadrature-axis transient reactance
θ_0 = angle at which the first two armature phases are short circuited, in the nonsimultaneous closing of a short-circuiting switch. (See Appendix II)
θ_1 = angle at which third phase is short-circuited, in the nonsimultaneous closing of a short-circuiting switch (See Appendix II)
x_{aq} = mutual reactance between the armature and either quadrature-axis rotor circuit and between the two quadrature-axis rotor circuits
x_{kq}, x_{fq} = leakage reactances of quadrature-axis rotor circuits
R_{kq}, R_{fq} = resistances of quadrature-axis rotor circuits

References

1. AIEE TEST CODE FOR SYNCHRONOUS MACHINES, January 1944 revision.

2. ANALYSIS OF SHORT-CIRCUIT OSCILLOGRAMS, **W. W. Kuyper.** AIEE TRANSACTIONS, volume 60, 1941, April section, pages 151–3; discussion, page 753.

3. OVERVOLTAGES CAUSED BY UNBALANCED SHORT CIRCUITS, **Edith Clarke, C. Concordia, C. N. Weygandt.** AIEE TRANSACTIONS, volume 57, 1938, August section, pages 453–66, 468.

4. EFFECT OF SEQUENTIAL SWITCHING ON SHORT-CIRCUIT CURRENTS IN SYNCHRONOUS MACHINES, **Frank von Roeschlaub.** *General Electric Review*, volume 43, number 6, June 1940, pages 256–61.

5. TWO-REACTION THEORY OF SYNCHRONOUS MACHINES—GENERALIZED METHOD OF ANALYSIS, **R. H. Park.** AIEE TRANSACTIONS, volume 48, 1929, pages 716–27, 729.

Electrolytic Corrosion—Methods of Evaluating Insulating Materials Used in Tropical Service

B. H. THOMPSON
NONMEMBER AIEE

K. N. MATHES
MEMBER AIEE

Synopsis: The selection of insulating materials to guard against electrolytic corrosion has become increasingly important as the use of electric devices in the tropics has increased. Moisture conditions in the tropics are described, and means for producing such conditions in the laboratory are considered. The visual, corrosion-current, and water-extract conductivity methods for studying electrolytic corrosion are described. Typical results for a number of different materials are given.

THE EFFECT of moisture on electric windings is a factor to be considered for successful performance in the field. In some cases moisture absorption in the insulating material produces a direct dielectric failure between turns, between phases, or to ground. In others moisture absorption may produce leakage currents which electrolytically decompose the conductor and result in open rather than in short-circuited windings. This destructive effect has been named electrolytic corrosion. Electrolytic corrosion accounts for a large proportion of failures caused by moisture in apparatus containing fine wire.[1]

Humidity Conditions in Service

Because absorption of atmospheric moisture is responsible for electrolytic corrosion, a study of humidity conditions is important. Relative humidity in the continental United States seldom rises above 95 per cent, and extended periods above 90 per cent are uncommon, except possibly on the Gulf Coast. In the tropics moisture conditions are much more severe. During the rainy season relative humidity above 95 per cent is common. Table I gives values obtained for Rangoon, Burma. The figures for the worst month, August, can be summarized as follows:

1. For eight hours a day the relative humidity is 97 per cent or higher.
2. For 13 hours a day the relative humidity is 95 per cent or higher.

Since these are average figures, it is obvious that the air very often must be saturated completely with moisture and that exposed apparatus will be covered with dew. Rangoon is probably not the wettest place in the tropics. It is, however, a location in the tropics for which humidity values have been recorded officially. Reports from the tropics of 30 feet of rainfall in two months and seas of mud are frequent. It is not surprising that electric apparatus often is soaked completely with water for long periods of time. The windings often dry out only when heated or when exposed directly to the sun.

Even in temperate climates moisture condensation may occur on apparatus chilled during aircraft flight at high altitudes. This water may be forced even into electric windings by pressure changes resulting from subsequent changes in altitude. Serious damage may occur, if this absorbed water freezes and cracks the insulation.

Aircraft apparatus will be exposed to high humidities caused by changes in altitude for only relatively short periods of time, unless the apparatus operates in closed containers in which moisture collects. Consequently, flight conditions in temperate climates are much less severe than tropical conditions. Of course, aircraft in the tropics will be exposed to tropical conditions of moisture while grounded. The wet apparatus then would, in subsequent flight, be exposed to the temperature and pressure changes accompanying changes in altitude.

Humidity Conditions in the Laboratory

Laboratory moisture tests should approximate service conditions as closely as possible.

To simulate the worst tropical conditions, a laboratory condition of 100-per-cent relative humidity, plus dew at 35 degrees centigrade (95 degrees Fahrenheit) has been adopted. This condition is reproducible and is obtained easily with inexpensive equipment. Water in the bottom of a heat-insulated box is heated

Figure 1. Refrigerator box used for obtaining a humidity of 100 per cent plus dew at 35 degrees centigrade

Figure 2. Glass-rod samples used in the visual method of evaluating the corrosiveness of insulating materials

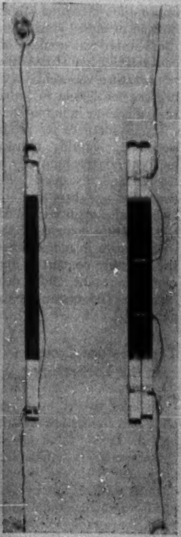

Paper 45-73, recommended by the AIEE committee on air transportation for presentation at the AIEE winter technical meeting, New York, N. Y., January 22–26, 1945. Manuscript submitted November 24, 1944; made available for printing January 5, 1945.

B. H. THOMPSON and K. N. MATHES are in the general engineering laboratory, General Electric Company, Schenectady, N. Y.

The authors acknowledge the assistance of B. W. Erikson of the industrial control division of the General Electric Company.

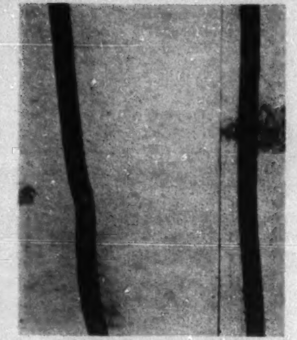

Figure 3. Photomicrograph of electrolytic corrosion of copper wire

with an immersion heater. The water vapor rising from the surface of the warm water will condense as a fine dew throughout the slightly cooler space in the box. A large refrigerator box (Figure 1) is tipped back sufficiently to hold water in the bottom and at the same time to allow condensed water to run off the top surface without dripping. The box is located in a room held at 25±1 degree centigrade, and sufficient heat is supplied at a constant rate to the water to maintain an air temperature of 35 degrees centigrade. This equipment has been used for most of the work to be described.

Lower humidities were obtained with appropriate saturated salt solutions in the bottom of closed glass desiccators. Distilled water was used to obtain 100-per-cent relative humidity without dew. The temperature was held very closely at 25 degrees centigrade to prevent condensation or change in humidity.

Cyclic methods for producing condensation by varying temperature at 95-per-cent relative humidity have been considered and discarded. Periods of condensation are short and erratic. Such a cycle is also artificial. With this method the moisture content of the air changes with change in temperature. In service the moisture content of the air tends to remain constant, and a decrease in temperature produces an increase in relative humidity.

Temperature Cycles in the Laboratory

At least two types of temperature cycling and immersion tests have been suggested. One of these uses salt water and, consequently, is applicable only to sealed apparatus. In the other test the apparatus receives five cycles between plus 85 degrees centigrade and minus 65 degrees centigrade, followed by immersion in water which is cycled five times between room temperature and 71 degrees centigrade in 24 hours. This test is difficult to interpret.

A number of tests have been made in which simple temperature cycles preceded exposure to 100-per-cent relative humidity plus dew. Such temperature cycles will open up brittle insulation subject to thermal shock. It is the authors' opinion that subsequent exposure to 100-per-cent relative humidity plus dew is sufficiently severe and easier to interpret than water immersion.

Corrosion Tests on Insulating Materials

It has been recognized that the best approach to corrosion-free apparatus lies in the use of insulating materials which will be as free as possible of corrosion effect.[1] Factors influencing electrolytic corrosion are discussed in the appendix. The following sections describe three methods developed to evaluate corrosion-inducing characteristics of insulating materials.

VISUAL TEST

Two types of glass-rod samples are used for the visual evaluation of corrosiveness. One uses a single rod and the other two rods. The single rods are wrapped with the sheet material to be tested. They also may be used for testing varnish films by forming the varnish film on the rod. A sheet material like cellulose acetate, however, tested at 100-per-cent relative humidity plus dew may collect a pool of water at the edge of the sheet. To help overcome this condition the double-rod sample is used (right side of Figure 2). The sheet material is wrapped around the two rods in the form of a figure eight so that no edge appears at the surface. Two windings of three close turns of 0.010-inch bare copper wire around the rods are spaced approximately one inch apart at the center of the rods. The sample is hung vertically at the required humidity and 120-volts direct current applied between windings. The condition of the positive wire is examined periodically with a microscope.

The test is run for seven days. The test is discontinued in a shorter time, if the positive wire corrodes completely open Corrosion usually starts with slight marking of the copper or slight discoloration of the insulating material, followed by mechanical roughening, which leads eventually to deep pitting. The initial marking on the wire is difficult to photograph, but surface roughening and a deep pit are shown in Figure 3.

The following method of comparing corrosion resistance of insulating materials has been found convenient:

Appearance Under a 20-Power Microscope	Rating
Coloring or corrosion first appears in 1 day	Very corrosive
Coloring or corrosion first appears in 2 days	Poor
Coloring or corrosion first appears in 3 days	Fair
Coloring or corrosion first appears in 7 days	Good

At the end of seven days the plus electrode wire is removed and examined under a 20-power microscope. If only faint markings are visible on the surface of the wire, the material is rated excellent. Such results should be obtained at a test humidity representing expected service humidities. Extrapolation from a lower to a higher humidity has been found to be misleading, for example, a rating of excellent at 95-per-cent relative humidity has with our present knowledge, little meaning at tropical conditions of 100-per-cent humidity plus dew. Tests on materials, of course, are only comparative and cannot be used to predict life of assembled apparatus.

The physical appearance of the positive wire is, of course, only a qualitative measurement, and the rating depends somewhat upon the judgment of the observer. Our efforts to use the wire breaking strength as a quantitative measure at a humidity of 100 per cent plus dew have been unsuccessful for the following reasons.

1. When sufficient corrosion has been obtained to affect breaking strength significantly, the wire may be pitted severely at one place or less severely at several places.

Figure 4. Holder for corrosion-current measurements

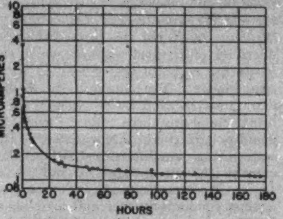

Figure 5. Corrosion-current–time curve for cellulose-acetate cloth adhesive tape

Glass-rod-type specimen. Volts—120 direct current on continuously. Humidity—100 per cent (no dew). Temperature—25 degrees centigrade

Consequently, a large number of samples will be needed to give a significant result.

2. A very long time on test may be needed to produce a measurable decrease in the breaking strength of the wire. It is estimated that three months would be required to produce a detectable change in breaking strength for a sample that would just make the rating of excellent by the visual method.

An adaptation of the glass-rod test is used for rigid insulating materials—the copper wire electrodes are wrapped directly on the sample. It has been found desirable to roughen or cut at least one edge of molded material to remove the "skin." The roughened edge represents the machined or sanded surfaces often encountered in use.

Corrosion-Current Method

Electrolytic corrosion occurs when current flow makes available ionic constituents to attack the metal. Therefore it should be possible to obtain an indirect measure of electrolytic corrosion by measuring the magnitude of the corrosion current providing that:

1. All the current measured does contribute to corrosion—the ions carried to the positive wire are able to attack it. (Platinum wire resists such attack.)

2. The decomposition products of corrosion at the wire do not form a tight insulating surface, which would eventually prevent current flow.

Actual tests have shown that copper wire on a large number of different insulating materials fulfills the above conditions.

All tests on insulating materials are made with copper. Aluminum, silver, nickel, and nichrome are known to be attacked, but a different rate may be expected for different metals.

Guarded sample holders (Figure 4) have been constructed to make current measurements on sheet insulating materials. (Varnishes have been evaluated by testing them as coatings on films known to be low in corrosiveness by previous test.) The sample is exposed to the desired humidity for a sufficient length of time to obtain equilibrium (usually 24 hours). The current resulting from 120-volts direct current across the sample is measured with a galvanometer capable of detecting 0.0001 microampere. When voltage is applied to a sample of sheet insulating material, the current decreases rapidly at first and then more slowly as a function of time (Figure 5). A series of current–time curves are plotted in Figure 6. The decrease in current after the voltage has been applied and the recovery after the voltage has been removed seem to be typical polarization and appear to be functions of the amount of corrosion that has taken place. The more corrosive materials show the largest initial current and the greatest decrease of current with time. At first thought it seems necessary to obtain the current–time curve in order to make a comparison between materials. However, the initial current is influenced only by the characteristics of the material, and that which follows is reduced by polarization. The initial current is, therefore, the value giving the comparison between materials. Since it is rather difficult to measure the initial current, the current value 15 seconds after the voltage has been applied is used instead.

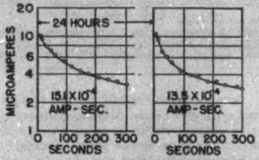

Figure 6. Corrosion current during five-minute applications of voltage at 24-hour interval

Cellulose-acetate cloth adhesive tape. Glass-rod-type specimen. Volts—120 direct current. Temperature—25 degrees centigrade. Humidity—100 per cent (no dew)

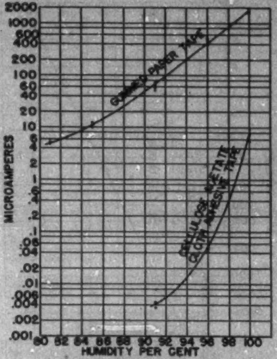

Figure 7. Effect of humidity at 25 degrees centigrade on corrosion current

Glass-rod-type of specimen

Because the corrosion-current method is indirect, it becomes necessary to calibrate it in terms of the visual-corrosion test. Table II shows a comparison of initial-corrosion current and integrated actual corrosion current–time with visual corrosion. Time was adjusted by trial to obtain a point at which pitting or roughening of the wire had just become visible microscopically. The similarity between the current–time values for a definite amount of corrosion is striking

Table I. Monthly Mean of the Relative Humidity (Per Cent) for Each Hour at Rangoon

Values Obtained From India Meteorological Department, Poona, India

Hour	January	February	March	April	May	June	July	August	September	October	November	December
Midnight	85	81	83	82	90	96	96	97	97	96	93	90
1	86	83	86	84	91	97	96	97	96	97	93	90
2	86	86	88	85	92	97	97	97	97	97	94	91
3	88	86	90	88	92	97	97	97	97	97	94	92
4	89	87	92	90	93	97	97	98	97	97	94	92
5	89	91	93	90	93	97	97	97	98	97	94	93
6	89	91	93	91	94	97	97	98	98	97	95	93
7	90	91	93	88	91	96	97	97	97	97	93	92
8	83	85	87	81	86	93	95	96	94	93	89	84
9	73	73	75	70	80	89	91	93	90	87	82	77
10	64	63	63	61	73	87	88	91	88	83	77	69
11	53	49	49	53	69	85	86	88	85	80	71	61
Noon	47	40	41	48	68	85	84	88	85	78	68	59
13	43	36	35	45	68	84	82	88	84	75	66	57
14	41	34	35	46	68	83	83	88	83	75	66	58
15	40	34	37	48	70	85	86	89	84	74	66	57
16	43	38	43	53	73	85	87	89	86	75	69	60
17	48	44	48	57	75	88	91	90	89	81	77	67
18	61	53	59	65	79	91	92	93	91	88	86	76
19	68	63	67	71	83	93	93	94	93	91	89	82
20	74	71	73	74	86	94	94	95	94	93	91	88
21	79	75	76	77	87	95	95	96	95	94	92	87
22	82	78	77	79	88	95	95	96	96	95	92	89
23	84	80	79	80	89	96	95	96	96	96	93	90
Mean	70	67	69	71	82	92	92	94	92	89	84	79

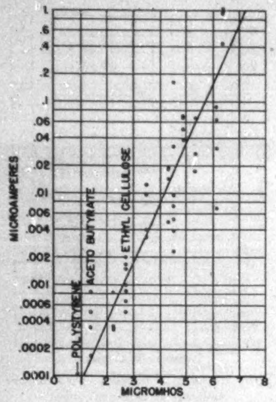

Figure 8. Comparison of corrosion current with conductivity of water extract for films

The corrosion current was measured at a humidity of 100 per cent plus dew at 35 degrees centigrade. The conductivity of water extract is in micromhos per centimeter for 100 square inches per liter of water. All films are cellulose acetate except the three marked otherwise

in view of the wide difference between conditions and samples shown in Table II.

We have found that 0.02-microampere initial current with the holder shown in Figure 4 compares with the grade of excellent of the visual method.

Table III shows typical results for a number of sheet and fabric insulations at 100-per-cent relative humidity plus dew at 35 degrees centigrade. Conclusions can be drawn as follows:

1. A single class of materials such as cellulose acetate may possess a wide range of corrosion-inducing characteristics.

2. The materials which are wet by water—cloth, paper, and cellophane—are considerably more corrosive than the water-resistant foils like acetates and polystyrene.

3. No great difference between the various untreated fabrics is apparent at 100-percent relative humidity plus dew.

The above conclusions apply for a humidity of 100 per cent plus dew at 35 degrees centigrade. The relative corrosiveness for the various materials may be widely different at lower humidities.

Table IV and Figure 7 have been included to show the reliability and the range of the corrosion-current method. Corrosion currents for a gummed-paper tape and an adhesive-backed cellulose-acetate fabric have been compared as a function of humidity. Conclusions follow.

1. The consistency of results is good—except for two values, one of which was obviously in error, maximum and minimum values were within two to one.

2. The ratio between the gummed paper and the acetate adhesive tape is not constant with change in humidity. The following tabulation illustrates the danger of predicting corrosion results at higher humidity from results at a low humidity or vice versa.

Corrosion Current—Microamperes

	A—Cellulose-Acetate Fabric Adhesive Tape	B—Gummed-Paper Tape	Ratio B/A
100-per-cent relative humidity	7.79	1,690.0	217
91-per-cent relative humidity	0.00499	63.7	12,800

3. The corrosion-current method has great sensitivity and can be used to evaluate corrosion characteristics in cases which would take a long time by the visual method. It has been estimated that corrosion detectable by the current method would require nearly four years exposure to be detected by the visual method.

WATER-EXTRACT CONDUCTIVITY TEST

The magnitude of the corrosion current depends upon the quantity of free ions available for carrying the current. A measure of the relative amounts of ionizable constituents in the insulating material should, therefore, be a measure of the relative corrosiveness of the material. We have measured the increase in conductivity of distilled water in which the insulating material was stirred at room temperature. The conductivity of the extract was measured with a conductivity bridge (applying three volts, 60 cycles to avoid polarization). A correlation of the water-extract conductivity with corrosion current is given in Figures 8 and 9. In Figure 8 corrosion current is plotted against conductivity per unit area, since both current and extract conductivity depend in this case primarily on area. The current per mil thickness and the extract conductivity per unit volume are the controlling factors for materials which wet easily. The correlation would be expected to hold only at 100-per-cent relative humidity plus dew.

The water-extract conductivity test requires relatively little apparatus. The method should be useful in quality control, particularly if care is used to insure reasonable accuracy.

Conclusions

High relative humidity with moisture condensation is a characteristic tropical condition. This condition can be simulated easily in the laboratory and should be used to test insulation materials designed for tropical application. Materials should be tested, of course, in the form in which they are used in the completed device.

Table II. Correlation of Corrosion Ampere-Seconds and Extent of Corrosion of Plus Electrode Wire on Glass-Rod Type of Corrosion Specimen

Material	Humidity, Per Cent	Temperature, Degrees Centigrade	Initial Current, Microamperes	Duration of Test, Hours	Ampere-Second	Extent of Corrosion of Plus Wire With 40 Times Magnification
Black cellulose-acetate fabric adhesive tape	100+dew	35	120	1.0	0.18	Scattered small pits visible
White cellulose-acetate fabric adhesive tape	100+dew	35	92	7.0	0.18	Color in tape just visible; small pits all along the plus wire visible
Gummed-paper tape	96	24	420	0.33	0.23	Color in paper visible; depth in corrosion visible
Gummed-paper tape	96	24	410	0.33	0.21	Color in paper visible; depth in corrosion visible

Table III. Corrosiveness of Various Materials at a Humidity of 100 Per Cent Plus Dew at 35 Degrees Centigrade. Measured by the Corrosion-Current Method

Material	Thickness, Mils	Corrosion Current, Microamperes		
		Average	Minimum	Maximum
Polystyrene film	1.1	<0.0001		
Cellulose-acetate film *A*	1.1	0.0005	0.0002	0.0008
Cellulose-acetate film *B*	5.0	0.056	0.039	0.070
Cellulose-acetate film *C*	10.0	0.86	0.43	1.07
Continuous-filament glass cloth	4.3	340	240	420
Cellulose-acetate cloth	7.0	290	240	340
Cotton cloth	9.6	420	310	500
Cellophane film	0.75	680	500	800
Kraft paper *A*	0.6	200	180	220
Kraft paper *B*	6.5	1,470	1,360	1,600

Three types of test have proved useful in evaluating corrosiveness of insulating materials.

1. The visual test gives qualitative results. Microscopic examination is used to increase sensitivity. The rating depends somewhat upon the judgment of the observer. The visual test may be used at any humidity.

2. The corrosion-current test is quantitative and the most sensitive method. Corrosion, which may take considerable time to show up under a microscope, can be quickly evaluated. The corrosion-current method is also applicable at any humidity.

3. The water-extract test is quantitative but limited in correlation to corrosion tests made at 100-per-cent relative humidity plus dew. Considerable care is necessary to obtain accurate results.

The corrosive nature of insulating materials differs widely. In fact a single class of materials may possess a wide range of corrosion-inducing characteristics. No class of materials yet has been found to be completely noncorrosive. Consequently, corrosion characteristics should be determined and controlled by test. Such tests form a basis for design.

Table IV. Corrosion Currents for an Acetate-Fabric Tape and a Paper Tape at Various Humidities

Specimens on Glass Rods, Spacing Between Copper-Wire Electrodes One Inch, Voltage 120 Volts Direct Current. Current Measured 15 Seconds After Application of Voltage. Current in Microamperes

Humidity, Per Cent Degrees Centigrade	100 Plus Dew 35	100 25	96 25	91 25	85 25	81 25
Cellulose-acetate fabric adhesive tape						
	192	5.37	0.0415	0.00344		
	165	7.50	0.0552	0.00420		
	144	7.67	0.0679	0.00789		
	116	9.23	0.0532	0.00445		
	51.9*	7.14	0.0457			
	226	9.81	0.0503			
Average	169	7.79	0.0523	0.00499		
Gummed-paper tape						
	4,480	1,630	464	57.0	12.6	4.74
	5,140	1,720	503	72.1	10.9	4.89
	5,340	1,740	512	51.1	10.9	4.82
	5,910	1,660	372	68.4	9.5	5.32
				68.7		
				64.7		
Average	5,220	1,690	463	63.7	10.8	4.94

* Not used in obtaining the average.

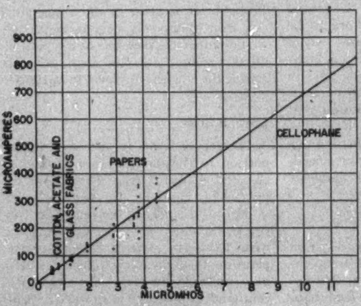

Figure 9. Comparison of corrosion current with conductivity of water extract for fabrics, paper, and cellophane

Corrosion current is in microamperes per mil thickness for a humidity of 100 per cent plus dew at 35 degrees centigrade. Conductivity of water extract is in micromhos per centimeter per mil thickness for 100 square inches per liter of water

Appendix. Factors Influencing Electrolytic Corrosion

If a direct potential be applied between two copper wires separated by an insulating material, current will flow. At low humidities this current is usually exceedingly small. As humidity is increased, moisture may be absorbed within the insulating material and adsorbed on the surface. In the presence of the free water the current increases markedly for most insulating materials. If the air become saturated with moisture, the water may condense on the surface to form an additional path for current flow. As current flows, the copper at the positive wire is ionized and combines with the acidic or oxidizing component of the electrolyte.

Pure water is a good insulator, but water will dissolve avidly at least small amounts of a great variety of substances. These materials ionize to form an electrolyte. The sources of electrolyte in insulation can be listed as follows:

1. Water-soluble constituents on the surface or in the body of the material.

2. Chemical hydrolysis, for example, of glue.

3. Electrochemical decomposition to give water soluble constituents—cellulose, for example, may be oxidized to give acidic components.[2]

4. Change due to heat:

(*a*). To give water-soluble decomposition products

(*b*). To produce sweating of water-soluble constituents to the surface.

(*c*). To permit penetration of water into the body of the material which may contain soluble materials.

5. Presence of fungus, which produces water-soluble products in their growth process.

When liquid water condenses on the surface, it may tend to form tiny drops or spread to a continuous film as shown schematically in Figure 10. The angle of contact at the interface between water and the solid insulating material is called the contact angle. This angle is a measure of the tendency of water to spread or to collect in droplets (the tendency to collect in droplets is associated with high-contact angle). Disconnected droplets, even though they contain an electrolyte possess relatively high resistance to current flow. In contrast a continuous water film containing electrolytes will conduct current readily.

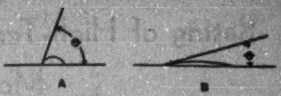

Figure 10. Diagram showing the angles of contact, θ, of a drop of water to an insulating material

A.—A high angle
B.—A low angle

Insulation in devices which have been varnish treated or coated may not reach a moisture content in service corresponding to the atmospheric humidity because:

1. The length of the period of idleness for the insulation to reach a stable moisture condition increases with the delay in the entrance of moisture.

2. Varnished-treated insulation, even though poorly treated, will not take on as much moisture as the untreated material.

In other words, when voltage is applied in service the insulation is at a moisture condition corresponding to some humidity below the atmosphere humidity to which the device is exposed. For such applications it may be desirable to make the corrosion test on the insulation at a humidity below the service conditions of humidity.

Since so many factors may produce electrolytic corrosion, only actual test can be the deciding factor.

References

1. Corrosion Causes and Remedies in Fine Wire Magnet Coils, B. W. Erikson. *Product Engineering*, March 1943, page 158.

2. Causes of Corrosion of Fine Copper Wire Carrying a Potential, H. N. Stephens, G. B. Gehrenbech. AIEE Transactions, volume 59, 1940, June section, pages 357–60.

Rating of High-Temperature Induction Motors

P. L. ALGER
FELLOW AIEE

H. A. JONES
NONMEMBER AIEE

Synopsis: The advent of new high-temperature insulating materials, such as the silicones, gives new freedoms to the motor designer. It is probable, however, that factors other than insulation will limit the desirable motor-temperature rise to values well below the endurance limits of these materials. It is, therefore, desirable to recognize that the size of an induction motor is measured electrically by its breakdown torque, and mechanically by the size of shaft and bearings, the temperature rise being only a secondary factor. Calculations are presented, based on idealized assumptions, which indicate that the optimum temperature rise for continuous rated induction motors is below 80 degrees centigrade, whatever the insulating materials used.

SOME NEW synthetic insulating materials, such as the silicones, have much higher temperature endurance than any flexible insulations heretofore known. It is probable that coil windings insulated with these new materials will have fully as long a useful life at a continuous temperature of 175 to 200 degrees centigrade as present class *A* or class *B* insulations have at their standard hot-spot temperature limits of 105 and 130 degrees centigrade, respectively. Presumably AIEE Standard 1[1] will be revised, to recognize these new materials, with a permitted temperature rise by resistance of the order of 120 degrees centigrade; on the same basis as the 60- and 80-degree-centigrade rise values now recognized for class *A* and class *B* materials.

These materials will open the way to smaller and lighter motors for many special applications, where intermittent operation, frequent starting, or restricted ventilation make small frames and high temperatures necessary. Also, they will have an insurance value because they will enable motors to withstand stalling and exposure to high ambient temperatures for longer periods. The silicones, therefore, will be welcomed by motor designers.

It is well known, however, that a large proportion of the general-purpose motors now produced in a highly competitive market have temperatures well below those permitted by the present rules.[2] Also, despite the availability of class *B* insulations, the lower temperature class *A* insulation is used for most low-cost electric apparatus.

It, therefore, appears that the high temperatures permitted by the new materials will not be utilized in many applications, even when the materials themselves are employed.

Two questions, therefore, arise:

1. What is the optimum temperature rise for general-purpose electric equipment, such as an induction motor, for example?
2. How should the method of rating be changed, if the operating temperature is not limited by insulation life?

Effects of High Temperatures

There are several ways in which temperature affects the operation of a motor, besides the thermal life of the insulation.

BEARINGS

The organic bearing lubricants deteriorate rapidly at temperatures above 80 to 90 degrees centigrade. A very rough rule for general-purpose induction motors is that the temperature rise of the bearings is half that of the windings. With a 40-degree-centigrade ambient temperature, therefore, a higher continuous temperature rise of the winding than 80 degrees centigrade generally will require special provisions for cooling the bearings. There is hope, however, that synthetic lubricants will be developed to withstand much higher temperatures.

It should be noted also that motors must have shafts and bearing diameters suited to the torques, pulley sizes, and belt pulls required to transmit their rated horsepower loads. If motors are to be built in radically smaller sizes, these smaller motors must have shafts and bearings materially larger in proportion to their frame diameters than now customary. Hence, existing motor frames generally must be redesigned mechanically, if they are to carry higher horsepower ratings. For a given horsepower, speed, and type of drive, the shaft diameter should be the same.

METALLURGY

A number of the metals ordinarily used in motors are affected by high temperatures. Pure tin solder melts at 232 degrees centigrade, and the tin–lead babbitts and solders soften at temperatures of the order of 150 degrees centigrade. The highest practicable temperature for soldering binding wire without affecting its strength is about 300 degrees centigrade. The hardened steel races of ball bearings gradually soften if kept at temperatures of 200 degrees centigrade or more. Pure copper under stress is subject to brittle fracture at temperatures above 160 degrees centigrade. However, by using silver solder, silver bearing copper, bronze or silver bearing alloys, and other special features, these temperature limits can be raised, if there is sufficient economic incentive.

THERMAL EXPANSION

Thermal expansion occurs in differing amounts for copper, iron, and insulating materials. The higher the temperature, and the larger the machine, the greater is the risk of insulation cracking, and other types of mechanical failure. This factor is limiting in such large machines as turbine alternators, with temperature-rise values below 100 degrees centigrade, but is not important in small motors. Its importance when the new synthetic insulations are used will be measured inversely by the flexibility of these insulations. This still is being investigated.

Table I

Temperature Rise Above a 40-Degree-Centigrade Ambient Temperature	Relative Resistance of Copper
0	0.82
60	1.00
120	1.18
180	1.36
240	1.54

IRON LOSS

The core losses are slightly reduced at increased temperatures because of the increased resistivity of the iron, and consequently lowered eddy currents. This factor is not important, however, as the iron loss itself is not controlling, and the eddy current loss is only a part of this. Probably an increase of the temperature rise from 60 to 120 degrees centigrade would reduce the core loss of a typical induction motor by less than a tenth; raising the efficiency by perhaps a third of a point.

COPPER LOSS

The copper losses are increased in proportion to the increase in resistivity at elevated temperatures. This law is expressed by Table I.

On this account, 18 per cent more copper section must be used in a given motor, with 160-degree-centigrade copper temperature, to secure a given efficiency, than in a similar motor with only 100-degree-centigrade copper temperature. Eight-

---

Paper 45-50, recommended by the AIEE committee on electric machinery for presentation at the AIEE winter technical meeting, New York, N. Y., January 22–26, 1945. Manuscript submitted December 1, 1944; made available for printing January 4, 1945.

P. L. ALGER is staff assistant to the vice-president in charge of design engineering, General Electric Company, Schenectady, N. Y., and H. A. JONES does appliance project engineering for the General Electric Company, Bridgeport, Conn.

een per cent of the full-load copper loss represents between one and one and one-half points in efficiency for a general-purpose induction motor, or rather more than ten per cent of the total losses.

Overload Capacity

The overload capacity of the motor is markedly reduced, when the full-load temperature rise is increased. Assume, for example, that two similar motors in a 40-degree-centigrade ambient temperature are compared at 1.25 times rated load, motor *A* having 60 degrees centigrade, and motor *B*, 120-degree-centigrade rise at rated load; both motors having the same component losses at rated load. In each case, the copper losses at 1.25 load will be roughly 1.56 times the copper losses at rated load, since they vary as the square of the current.

Since the temperature rise at overloads is nearly proportional to the copper loss, motor *A* will have an apparent temperature rise at 1.25 load of about 1.56×60, or 94 degrees centigrade, while *B* will have about 1.56×120, or 188 degrees centigrade rise. With these increases in temperature, the copper resistance increases also, causing higher losses and still further rise of temperature. This causes the phenomenon of "temperature creep," whereby the temperature goes on increasing for a long time after the application of an overload, in extreme cases becoming unstable and rising to destructive values.

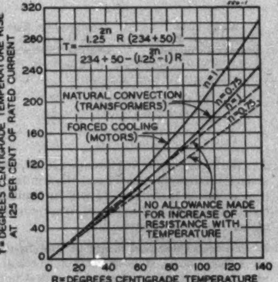

Figure 1. 125-per-cent versus 100-per-cent current temperature rise for electric apparatus with an ambient temperature of 50 degrees centigrade

Temperature rise assumed proportional to the nth power of the I^2R loss

In the case of natural convection, as for a transformer, the heat dissipation rate increases faster than the temperature rise, so partially offsetting the effect of increased copper resistivity. In the case of forced convection, as for a high-speed motor, the heat-dissipation rate is proportional to the temperature rise.

These effects are illustrated in Figure 1, from which the net additional temperature at 1.25 load can be estimated as a function of the rise at rated load. It is interesting to note also that the thermal time constant of the motor with 120-degree-centigrade rise is 16 per cent greater on overloads than that of the motor with 60-degree-centigrade rise, due to this temperature-creep effect.

All of the effects discussed under previous headings are produced by the extra temperature rise on overload, their magnitudes increasing rapidly as the rated-load temperature rise is increased.

It is a general rule that the life of organic insulation is halved for each ten-degree-centigrade rise in temperature, approximately. The effects of temperature on lubricants, expansion, and so forth, also increase exponentially. Therefore, even if the materials in motor *B* have the same life at 160 degrees centigrade as those in motor *A* have at 100 degrees centigrade, it is probable that motor *B* will have a life at its ultimate 1.25 load temperature of 285 degrees centigrade (Figure 1) only a small fraction of the life of motor *A* at its 1.25 load temperature of 147 degrees centigrade (Figure 1).

If the ten-degree-centigrade law for half life holds for the insulating materials in motor *A*, they will last only about four per cent of the time at 1.25 load that they would last at rated load. Even if the materials in motor *B* are so much more heat resistant that they follow a 15-degree-centigrade law for half life, this motor will still last only one-third per cent as long at 1.25 load as at rated load. Other estimates of the life at one and one-fourth load for different full-load temperature rises are given in Table II.

Thus, the magnitude and duration of overloads must be considered very carefully before a high temperature rise is selected for electric equipment.

Selection of Optimum Temperature

The urge to use a higher temperature is, of course, the advantage gained in reduced size, weight, or cost. There must be some optimum temperature rise, therefore, which strikes a balance between these advantages and the disadvantages mentioned above.

A series of calculations were made to determine this optimum temperature rise for a general-purpose induction motor of about 30-horsepower rating. These calculations were based upon several assumptions, as follows:

1. The ratio of motor length to diameter was held constant.
2. The over-all weight of the motor varied as the cube of the diameter.
3. The air-gap length varied as the square root of the motor diameter.
4. The maximum torque of the motor was held constant, which in turn signified that the motor reactance remained at one value.
5. The flux densities of the stator teeth and core were held at a specified constant value.
6. The core loss and windage and friction were held constant.
7. The space factor of the stator slots was held constant until the 60-degree-centigrade temperature-rise point was reached. At this rise, the space factor changed as a result of changing from class *A* to present class *B* insulating materials.
8. The temperature rise of the motor was assumed to be directly proportional to the heating losses, and inversely proportional to the square of the motor diameter.
9. With the motor running continuously at name-plate temperature rise, the motor life was taken to be seven years. In order to evaluate the overload life of the motor, the following duty cycle was assumed:

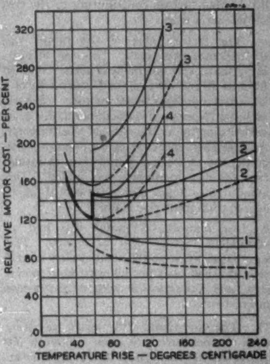

Figure 2. Effect of rated-load temperature rise on motor cost for 30-horsepower induction motor

Solid curves give costs with insulation allowances now in use. Dotted extensions show cost with allowances and insulation costs equivalent to class *A*

The break in the solid curves is a result of changing from class *A* to class *B* insulation costs and allowances

Curve 1—Direct factory cost of motor
Curve 2—Factory cost plus efficiency cost
Curve 3—Factory plus efficiency plus replacement cost
Curve 4—Factory plus efficiency plus additional fan cost

Two hours per day at three-fourths load
Four hours per day at full load
Two hours per day at one and one-fourth load

In addition, it was assumed that the temperature rise necessary to halve insulation life became greater as the name-plate rise increased, as given in Table III.

With the assumptions of a duty cycle and the temperature rise necessary to halve insulation life, it was possible to evaluate a motor-replacement cost. This cost of re-

Table II Reduction in Motor Life on Overload

Temperature Rise From Figure 1		Ratio of Life at 125-Per-Cent Current to Life at Rated Current	
At Rated Current, Degrees Centigrade	At 1.25 Current, Degrees Centigrade	Life Halved for Each Ten-Degree-Centigrade Temperature Increase	Life Halved for Each 15-Degree-Centigrade Temperature Increase
40	68	0.14	0.26
60	107	0.038	0.114
80	149	0.0083	0.041
100	194	0.0015	0.013
120	245	0.00017	0.0031
140	305	0.00001	0.0005

placing worn-out motors indefinitely was amortized at a ten-per-cent interest rate.

10. Other factors contributing to the cost of the motor were:

a. The factory cost of the motor was divided into two parts. The cost of bearings, shaft, and mechanical parts remained fixed at 25 per cent of the factory cost of a 50-degree-centigrade rise motor. The remaining 75 per cent of the direct motor costs varied directly as the cube of the diameter. At a temperature rise of 60 degrees centigrade, the additional cost of class *B* insulation (as now available) was added. This amounted to 20 per cent of the cost of the 50-degree-centigrade rise motor.

b. One kilowatt of motor loss had an equivalent factory cost of $40.00. This was based upon 2,000 hours yearly operation, one-half cent per kilowatt hour power cost, and amortization with a 25-per-cent interest rate.

11. The additional I^2R losses resulting from temperature rise alone (above a 50-degree-centigrade rise) were given an equivalent factory cost, and this amount was spent on extra ventilating equipment. The cost of fans for the 50-degree-centigrade rise motor was taken as five per cent of the direct factory cost. The heat dissipation varied as the fourth root of the amount spent on fans.

Figure 2 shows results obtained based upon the foregoing assumptions. The solid curves indicate the effects of going to higher-temperature motors with present-day insulation costs and space allowances. The distinct break at 60-degree-centigrade rise is caused by the additional cost of installing class *B* insulating materials, and the additional insulation-space allowance which must be made in the stator slots. The dotted extensions above 60 degrees centigrade indicate characteristics that could be obtained if, in the future, the cost and space allowance for class *B* materials could be brought down to present-day class *A* standards.

It will be noted that curve 2, showing the cost of the bare motor plus losses, has a minimum at 80-degree-centigrade rated-temperature rise, even though the motor is assumed to operate only 2,000 hours a year.

If additional cooling is provided, as indicated by curve 4, to increase the overload capacity, the minimum cost occurs at a little lower temperature, and this effect would be accentuated if the motor were operated for more than 2,000 hours.

Curve 3, which adds the replacement costs on the basis of continuous operation throughout the year, 25 per cent of the time at 1.25 load, shows a further reduction of the temperature rise for minimum cost. The significance of this curve lies in its shape rather than the actual values, since it is based on quite arbitrary assumptions.

Discussion

The foregoing indicates that although there is no single answer to the question, the optimum general-purpose motor temperature rise at rated load is below 80 degrees centigrade by resistance.

One point that stands out in the above analysis is that the space required for the insulation is of great importance. For example, glass fiber and varnish-insulated wire, as used in class *B* insulated induction motors, has roughly ten-per-cent larger diameter than resin-insulated wire, as now commonly used in class *A* motors, requiring an increase of roughly one half a frame size, or about 15 per cent in equivalent rating, for the same motor performance.

A second point that stands out from the analysis is the importance of efficiency in the case of motors operating for extended periods. As the curves in Figure 2 illustrate, even if a motor is designed for a high-temperature rise, it may be economical to provide extra cooling simply because of the reduced losses and greater overload capacity thereby obtained at a relatively low cost.

It seems clear, therefore, that the temperature rise of continuous rated motors will continue to be a useful measure of their performance, and that the present usual values will not be changed materially by the advent of the new high-temperature insulations.

For the short-time-rated and intermittent-duty motors, where the temperature often has been limiting, the temperature rise will become less important, and the breakdown torque of the motor will assume a greater importance as a measure of motor size.

There are, therefore, three distinct measures of motor capacity:

1. The breakdown torque.
2. The shaft and bearing sizes.
3. The rated-load temperature rise (inverse).

All of these must be chosen to suit the application. In a particular case, any one of these may be limiting.

Conclusions

The following conclusions are reached from this analysis:

1. The silicones and other new high-temperature insulating materials will give new freedom to the motor designer, permitting lighter weights, more severe duty cycles, and more difficult applications of motors in many cases.

Table III

Name-Plate Temperature Rise, Degrees Centigrade	Temperature Rise to Halve Life, Degrees Centigrade
50	10
60	12
100	15
200	20

2. With these new high-temperature materials, the temperature rise of the windings of continuous rated motors will be limited by the efficiency and overload requirements rather than by insulation life.

3. To keep these new motor developments on a sound basis, it is important to recognize that high temperature in itself is not a virtue. The best motor for any job is the one that has the right combination of breakdown torque, efficiency, and shaft size, with the lowest temperature rise that can be secured at a reasonable cost.

References

1. GENERAL PRINCIPLES UPON WHICH TEMPERATURE LIMITS ARE BASED IN THE RATING OF ELECTRIC MACHINERY AND APPARATUS, AIEE Standard 1, June 1940.

2. THE RATING OF ELECTRIC MACHINERY AND APPARATUS, **R. E. Hellmund.** AIEE TRANSACTIONS, volume 58, 1939, October section, pages 499–503.

3. RATING OF GENERAL-PURPOSE INDUCTION MOTORS, **P. L. Alger, T. C. Johnson.** AIEE TRANSACTIONS, volume 58, 1939, September section, pages 445–56.

4. REPORT ON GENERAL PRINCIPLES FOR RATING OF ELECTRIC APPARATUS FOR SHORT-TIME, INTERMITTENT, OR VARYING DUTY, AIEE Standard 1A, September 1941.

Arc-Backs in Rectifier Circuits
Artificial Arc-Back Tests

R. D. EVANS
FELLOW AIEE

A. J. MASLIN
ASSOCIATE AIEE

THE enormous development in the use of rectifiers for the electrolytic reduction of light metals has been an outstanding development of World War II. One important problem in this rectifier development has been the performance at the time of rectifier arc-back. Currents of between 50,000 to 100,000 amperes may be encountered on an individual rectifier and associated transformer. Still higher currents would obtain if back feed from other units on the same bus were not eliminated by prompt isolation from the circuit or d-c bus.

This development in rectifiers has presented the need for more basic information on the performance of rectifier circuits under arc-back conditions. Knowledge of arc-back currents is important in the design and operation of rectifiers, transformers, and circuit breakers used for their control. The scope of the present paper is limited to a general discussion of arc-back phenomena and the results of artificial arc-back tests, particularly as to the magnitude–time characteristics of the arc-back currents.

Arc-back of a rectifier is a term that refers to the phenomena that occur when current flows from the cathode to an anode, the reverse from normal direction of flow. In effect, an arc-back provides

1. Short circuit on one phase of a rectifier-transformer circuit.
2. Paths for the flow of direct current or pulsating current from other rectifier phases and from the d-c bus.

Consequently, the arc-back currents under these conditions are greater than the sustained currents corresponding to a three-phase short circuit on the rectifier-transformer secondaries of the star group subjected to arc-back.

Arc-back phenomena contain many factors that are as yet but imperfectly understood. Commercial rectifiers are subject to occasional arc-backs, the frequency of which is known to increase as functions of the rectifier current and output voltage. The tendency to arc-back is also known to increase as the amount of phase control is increased. It is common experience that the frequency of arc-back decreases after a unit becomes "seasoned." The frequency of arc-back also increases if severe loads are applied on a cold rectifier or one that has been carrying a very light load. These factors have been recited as a matter of general background because the mechanism of arc-back was not within the scope of the present investigation.

Artificial Arc-Back Tests

In studying the character of arc-back phenomena,[1,2] the most desirable method, of course, is to observe actual arc-backs under service conditions. Records of arc-backs that have occurred under service conditions have been obtained by means of an instrument especially devised for this purpose, called the memnoscope.[3] This investigation, however, did not make use of that method because it was undesirable to take all the necessary recording apparatus to the field and because it was undesirable to await arc-backs as they occur in practice. For this reason the investigation was made in the laboratory with some field tests for corroboration of the chief results.

There are two principal methods for the artificial representation of arc-back phenomena, namely,

1. Short-circuiting switches.
2. Reverse-connected ignitrons or single-tube rectifiers.

The simplest method of simulating an arc-back is to connect the anode to the cathode by a short-circuiting switch. In particular, the short-circuiting switch was provided with a high-speed mechanism which was electronically controlled so as to initiate the arc-back close to the desired point of the voltage wave.

The second method of simulating arc-backs is to use a reverse-connected rectifier in parallel with the ignitron or other rectifier element to be subjected to an artificial arc-back. In practice a reversed ignitron was used and it provided an easy method for controlling the initiation of the artificial arc-back. However, the reversed ignitron presents some important differences from the actual ignitron subjected to arc-back. In the actual arc-back, current flows from the cathode to the anode, whereas in the reversed ignitron it flows from the anode to the cathode. Another difference is that a loaded ignitron subjected to actual arc-back is operating at normal temperatures and has normal ionization, whereas the reversed ignitron is initiated from a no-load condition. However, the test data, subsequently given under the heading of "Arc-Drop Characteristics of Arc-Back Currents," show that for the same current flow there is little actual difference in the arc drop of a reverse-connected ignitron from that of a normally connected ignitron under arc-back conditions.

In comparison of the two methods of representation of an arc-back, it will be evident that the short-circuiting switch offers too small a resistance because the effect of the arc drop in the ignitron is not taken into account. Compensation for this arc drop might be approximated by the addition of a resistance in series with the short-circuiting switch. However, the simplicity of the scheme using a short-circuiting switch commends itself, and the resulting slightly pessimistic test condition is not objectionable.

Factors Affecting Arc-Back Current

In the study of arc-back currents, it is convenient to refer to the schematic diagrams of rectifier circuits that are illustrated in Figure 1. In the two parts of this figure are shown the two principal methods used for clearing arc-backs.

The principal factors that affect the arc-back current magnitudes for either the initial or subsequent peaks are as follows:

1. Characteristics of the a-c supply system, including the reactance of the rectifier transformer and source.
2. Characteristics of the d-c back-feed system, including the breakers used to interrupt back-feed current.
3. Method of clearing arc-backs.
4. Arc-drop characteristics of arc-back currents.
5. Rectifier firing conditions, including the use of phase control.
6. The time of initiation of the arc-back.
7. Sympathetic arc-backs in associated rectifier elements and their possible recovery for subsequent normal nonconducting periods.

1. CHARACTERISTICS OF A-C SUPPLY SYSTEM

The basic factors in the determination of arc-back current are, of course, the circuit voltage and the reactance of the rectifier transformer and the source. In most large rectifiers the size of the individual transformer is fairly definite, corresponding approximately to an output

---

Paper 45-20, recommended by the AIEE committee on electronics for presentation at the AIEE winter technical meeting, New York, N. Y., January 22–26, 1945. Manuscript submitted November 14, 1944; made available for printing December 5, 1944.

R. D. EVANS is consulting transmission engineer, Westinghouse Electric and Manufacturing Company, East Pittsburgh, Pa., and A. J. MASLIN is design engineer in the transformer engineering department of the same company at Sharon, Pa.

The authors acknowledge the co-operation of F. S. Glaza, electrical superintendent of the Dow Chemical Company, Texas division, who made the arrangements for the field tests at Velasco, Texas. They also acknowledge the assistance of L. A. Casanova, H. S. Kirschbaum, J. H. Cox, and G. F. Jones.

of 10,000 amperes, or 6,000 kw at 600 volts. Such transformers are normally built on a three-phase core with two groups of windings, which operate substantially as independent units. Frequently each secondary winding supplies through a balance coil a second ignitron tube in parallel with the first, but for simplicity these are not shown. The equivalent impedance diagram for one of these transformers with each group having one three-phase primary winding and two three-phase secondary windings is shown in Figure 2. Examination will show that the two secondary windings of each group are very closely coupled. Because of the close coupling between the secondary windings, the equivalent-star diagram has a branch connected to the high-voltage terminal that constitutes most of the transformer reactance. In small systems supplying a single rectifier transformer, the source reactance may be quite appreciable in comparison to the transformer reactance. However, in the case of large rectifier stations the reactance of the source becomes small in comparison with the reactance of an individual transformer, so that the currents would be increased by only 5 to 15 per cent if there were an infinite bus at the high-voltage terminals.

An arc-back causes heavy direct currents to flow through the transformer-secondary windings, the effect of which is to saturate the core. However, because the arc-back is in effect a short circuit, the increased exciting currents that flow as a result of the saturation in the cores do not appreciably increase the total alternating current. This result is shown in an oscillogram included in the discussion of laboratory tests.

2. CHARACTERISTICS OF D-C BACK-FEED SYSTEM

Rectifiers may feed into load circuits supplied by motor generators, synchronous converters, or other rectifiers. However, in large stations, the characteristics of the d-c circuit are usually relatively unimportant in determining the magnitude of the back-feed current. This results from the circumstances

1. That the inductance of the back-feed system is high.
2. That high-speed anode or cathode breakers are used which are capable of isolating the arc-back before the back-feed currents reach large magnitudes.

The magnitude of back-feed current is usually limited in large rectifier stations to from 40,000 to 50,000 amperes, the amount varying somewhat with the point of initiation of the arc-back.

3. METHOD OF CLEARING ARC-BACKS

Two methods for clearing of arc-backs are in common use; these are known as "cathode-breaker clearing" and "anode-breaker clearing"[4,5] and are illustrated schematically in Figure 1. This illustration applies to larger rectifier installations used in the electrochemical industry for which two rectifier sections are supplied from single transformers. With the system of Figure 1a the isolation of an arc-back in a rectifier element of one star group requires

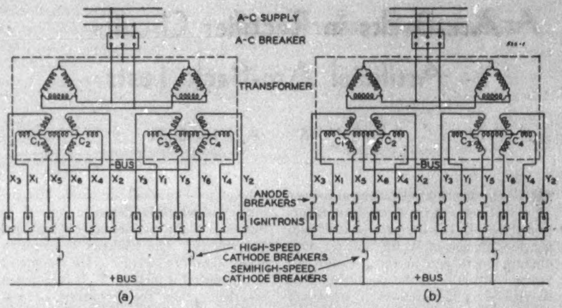

Figure 1. Schematic diagram illustrating the two principal methods of clearing rectifier arc-backs

(a). Cathode-breaker clearing
(b). Anode-breaker clearing

1. The opening of the corresponding high-speed cathode breaker, normally operating in one-half cycle (on a 60-cycle basis).
2. The opening of the a-c supply breaker, normally operating in eight to ten cycles.

With the system of Figure 1b the isolation of an arc-back in a rectifier element of one star group requires the opening of the associated anode-breaker pole, operating in about one-half cycle. It will be observed that the arc-backs are isolated from the d-c bus by the cathode breaker in one case and by the anode breaker in the other, circumstances from which are derived the terms which designate the method of clearing. Of course, with cathode-breaker clearing, the opening of the a-c supply breaker is required to isolate the arc-back from the a-c supply. With anode-breaker clearing, the opening of the a-c breaker is not required for isolating the a-c supply; consequently, one a-c breaker may be used in the supply to several rectifier units. A semihigh-speed cathode breaker operating in two or three cycles is used for disconnecting the rectifier from the bus; it also serves as a backup for the anode breaker. In the anode-breaker scheme the individual poles may be operated separately and restored* separately or operated as a group as a result of the operation of an individual pole. In the small rectifier installations each rectifier section is supplied from a separate transformer and cathode-breaker clearing has been the method generally employed. The principal difference between these two methods of clearing an arc-back is in the duration of the arc-back condition, which with (1) cathode-breaker clearing is one-half cycle for disconnecting the d-c back feed and eight to ten cycles for disconnecting the a-c feed, and (2) with anode-breaker clearing is one-half to two cycles.

4. ARC-DROP CHARACTERISTICS UNDER ARC-BACK CURRENTS

Arc drop of a rectifier element, as is well known, increases as a function of the current carried. However, the magnitude of this voltage drop depends upon the particular design of the rectifier and upon the magnitude of the current. The arc-drop data shown in Figure 3 were taken from measurements on the ignitron tube, which is the most widely used unit in commercial service. Figure 3 shows arc-drop data obtained for several different conditions of current flow, including normal forward-flow current for the first and subsequent cycles of heavy current resulting from artificial arc-backs. Figure 3 also shows arc-back data obtained from some natural arc-backs which were the result of an artificial arc-back on some other anode. In general, the arc drops obtained under natural arc-backs have magnitudes corresponding closely to those

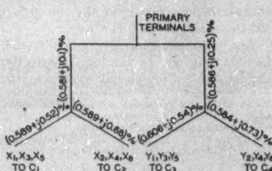

Figure 2. Equivalent impedance diagram for typical rectifier transformer used in large electrochemical installations

Diagram applies to transformer with double-delta primary and quadruple-wye secondary as in Figure 1. Impedances expressed in per cent on total transformer kilovolt-amperes obtained for artificial arc-backs with a reverse-connected ignitron. The arc-drop data also do not show any important difference in the arc-drop magnitude for currents on the first cycle or for subsequent cycles for heavy current flow when compared on the basis of the same maximum current. It was somewhat surprising that the arc drop under arc-back conditions became so large in comparison with the normal full-load arc drop which is also shown in the figure.

The arc-drop data shown in Figure 3 would not permit drawing a simple curve to represent average performances. The data suggest

1. A slow increase in voltage drop for currents up to 20,000 amperes.

2. A rapid increase in the range between 20,000 and 40,000 amperes.

3. A reduced rate of increase for the range between 40,000 and 80,000 amperes, the maximum for which arc drop was observed during arc-back tests.

The presence of arc drop reduces considerably the magnitude of maximum arc-back current. The difference between maximum arc-back currents on artificial arc-back tests with a reversed ignitron and on tests with a short-circuiting switch is about 15 per cent, and this may be attributed to the effect of additional arc drop in one phase. Because of the arc-drop characteristics under heavy currents, it is evident that arc-back simulation by means of a short-circuiting switch slightly increases the arc-back currents.

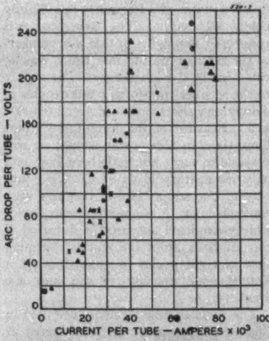

Figure 3. Arc-drop characteristics of standard ignitron tube under different conditions

Normal conduction, anode to cathode:

⊡—Arc drop under full-load conditions.

Reverse-connected ignitron in parallel with normal-connected unit:

△—First cycle ▲—Subsequent cycles.

Reverse-connected ignitron in place of normal-connected unit:

⊙—First cycle ●—Subsequent cycles

Reverse conduction, cathode to anode:

x—Natural arc-back

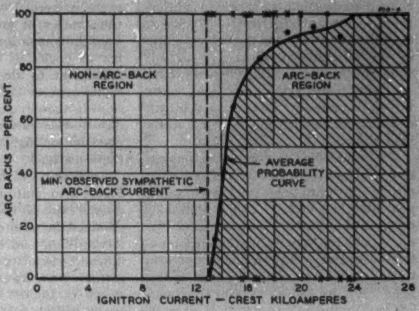

Figure 4. Probability of arc-back—plotted as a function of previous values of forward-flow fault current in crest amperes per tube

●—Average for laboratory tests, using 2,000-ampere steps Minimum arc-back current and maximum non-arc-back current observed for individual tubes, plotted on 100 per cent and 0 per cent probability lines, respectively: x—Different tubes, laboratory tests o—Different tubes, field test

5. Rectifier Firing Conditions

The method and time of firing each rectifier element has an important effect on the magnitude–time characteristic of arc-back currents. The general effect of phase control is to reduce the magnitude of arc-back currents. In the continuously excited rectifiers without phase control each incoming anode starts carrying current as soon as the proper difference of potential is reached, that is, when a slight positive potential appears on the incoming anode. In rectifiers with phase control obtained by grid or igniter delay, the start of conduction is correspondingly delayed. If the supply to the grid or igniter circuit is not affected by the arc-back currents, the firing will normally take place at definite points on the a-c supply wave. In this investigation only ignitrons under normal firing conditions were investigated; tests in the laboratory were made without delayed firing or phase control; tests in the field were made under actual operating conditions and these included some phase delay.

6. Initiation of the Arc-Back

The magnitude of the initial crest of the arc-back current is importantly controlled by the time of initiation of the arc-back, this magnitude being the maximum when the arc-back follows immediately after the end of normal conduction and a minimum when the arc-back occurs just before the end of the nonconducting period. If the arc-back occurs shortly before normal conduction begins, there is a small first cycle followed by a high second cycle which approaches the magnitude of current corresponding to the crest of an arc-back occurring at the end of normal conduction. The magnitude of the initial arc-back current crest is of principal importance when anode breakers are used, since the subsequent arc-back current cycles are not experienced because of the isolation of the phase subjected to arc-back. With cathode-breaker clearing the back feed is quickly interrupted, but the current tends to reach the same crest at the end of eight or ten cycles, regardless of the point of initiation of the arc-back. There is, however, the difference that if the arc-back occurs late in the cycle there are fewer cycles of high current.

7. Sympathetic Arc-Backs

By a sympathetic arc-back is meant one which occurs as the result of a natural or artificial arc-back in another anode circuit. The causes of such sympathetic arc-backs are not fully known. However, the tendencies toward sympathetic arc-backs are importantly affected by the magnitude of the arc-back current and previous load conditions in the rectifier unit. If the arc-back tests are made under conditions approximating the severity of arc-back current encountered in the usual commercial operation, the arc-back current magnitudes can reach 50,000 to 70,000 amperes or even higher. Under these conditions the forward-flow current in units of the same star group as the anode subjected to arc-back become very large. In the laboratory tests subsequently described, efforts were made to load the ignitrons so as to approximate the temperatures and ionization condi-

Table I. Crest Values of Anode Currents in Field Tests

Test	Current Direction*	Kiloamperes in Various Anodes X_1	X_2	X_3	X_4	X_5	X_6
1	F	48	36	41	26	0	39
	R	0	0	31	34	68	0
2	F	37	24	43	26	0	27
	R	0	0	0	0	67	0
3	F	35	21	41	25	0	26
	R	0	0	0	0	65	0
4	F	37	37	43	25	0	39
	R	0	0	0	40	62	0
5	F	36	22	44	26	0	27
	R	0	0	0	0	62	0

* F, forward flow, R, reverse flow on arc-back. Artificial arc-back placed on anode X_5.

tions corresponding to service conditions prior to the arc-back tests. Because of the differences between the "green" tubes in the laboratory and the "seasoned" tubes in the field and the difference in the operating-temperature conditions, there was less tendency toward sympathetic arc-backs on tests in the field than in the laboratory.

The controlling factor in the production of sympathetic arc-backs is the magnitude of forward-flow fault current in the preceding half cycle.[6] This is shown by the probability-of-arc-back curve of Figure 4, which is based on extensive laboratory tests and a limited number of field tests described in a later section of this paper. Figure 4 shows that for the standard ignitron tube there are

1. A non-arc-back region (or more precisely, a low-arc-back region) for forward-flow currents of less than 13,000 amperes crest.
2. An arc-back region for forward-flow currents greater than 24,000 amperes crest.
3. An intermediate region for which sympathetic arc-backs occur with high probability.

For this intermediate region an average probability curve is plotted from the results of tests using relatively narrow current ranges. Also on Figure 4 are plotted for individual tubes, whenever justified by the data,

1. The highest forward-flow current without arc-back.
2. The lowest forward-flow current with arc-back.

Figure 4 is based on 100 artificial arc-back tests in the laboratory and each test may provide data on 5 or 11 ignitron tubes. It will be observed that the results from the five field tests are not inconsistent with data obtained from the extensive laboratory tests.

In connection with Figure 4, it may be observed that the probability curve should show a definite but negligibly small value for low currents, since arc-backs do occur in normal operation, even though the number of arc-backs is exceedingly small in comparison with the total number of cycles in operation. From the standpoint of arc-back phenomena, the significance of the probability curve resides in the circumstance of whether the forward-flow current will result in an appreciable or high probability of sympathetic arc-back.

Application of the rectifier data from Figure 4 to ignitrons under arc-back conditions explains the wide range of results obtained in service. The magnitude of forward-flow current varies widely in different installations and the results are further complicated by probability, as shown in Figure 4. In some cases no anode will be subjected to sympathetic arc-back. In other cases, all anodes will be subjected to sympathetic arc-backs so that the anode-current records look like those of polyphase short circuits. An anode subjected to a sympathetic arc-back for several cycles may recover its normal characteristics as a rectifier and may even subsequently develop a second sympathetic arc-back. Oscillograms of various conditions will be shown later in connection with the discussion of artificial arc-back tests in the laboratory and in the field.

The presence of sympathetic arc-backs has an important bearing on the arc-back phenomena in general. The presence of sympathetic arc-backs tends to reduce the maximum current to be carried by the ignitron unit or the particular transformer winding associated with the initial arc-back. If the second arc-back occurs on the other winding on the same core with the winding supplying the rectifier unit initially subjected to arc-back, the sum of the two anode currents approaches approximately the original value. From an examination of Figure 2, it will become apparent that when both windings are short-circuited, the total short-circuit current will be about the same as for a short circuit on one winding, with the current divided between the two secondary windings. When anode breakers are used, sympathetic arc-backs may increase the number of poles operated and the time required completely to isolate the arc-backs, since the second arc-back must be cleared by a second breaker operation, a process that may be repeated in sequence.

Table II. Magnitude of Arc-Back Currents

	Laboratory Test, 8,500-Kva Transformer; Primary, Double-Delta; Secondary, Quadruple-Wye With Interphase Transformers		Field Test, 6,550-Kva Transformer; Primary, Double-Delta; Secondary, Quadruple-Wye With Interphase Transformers	Laboratory Test, 250-Kva Transformer; Primary, Delta; Secondary, Double-Wye With Interphase Transformers
Arc-Back Simulation	Reversed Ignitron	Short-Circuiting Switch	Short-Circuiting Switch	Short-Circuiting Switch
I_{AB}—Maximum arc-back current (amperes)	81,500	95,000	67,800	12,500
*I_{BF}—Back-feed current (amperes)	25,000	25,000	22,000	2,500
E_0/X—Symmetrical short-circuit current (crest amperes)	52,000	52,000	38,000	8,000
$\frac{I_{AB}}{E_0/X}$	1.59	1.83	1.78	1.56
$\frac{I_{AB}-I_{BF}}{E_0/X}$	1.1	1.35	1.21	1.25

*I_{BF}—This is the current fed out the neutral point of the star group subjected to arc-back; it includes current from the other star groups of the same or other transformers.

Artificial Arc-Back Tests in the Laboratory

The characteristics of the particular ignitron tube have an important effect on arc-back phenomena, since these determine the actual arc drop and the tendency to produce sympathetic arc-backs. All arc-back tests referred to in this paper were made on the standard ignitron tube, which is used widely, particularly in the larger electrochemical installations.

An extensive series of artificial arc-back tests was made in the laboratory on the setup illustrated in Figure 5. The power supply for these arc-back tests was obtained from the number 2 high-power laboratory. The high-power-laboratory generator was driven by an induction motor at a frequency but slightly below 60 cycles. The generator was connected through suitable a-c breakers to the rectifier transformer which was located in the d-c laboratory. The supply to the rectifier transformer was capable of delivering a short circuit of over 1,000,000 kva. Because of the long-time–current limitations in this power supply, it was possible to carry but little base load, and only momentary loads of 4,000 d-c amperes. The supply circuit breakers were controlled by a sequence-drum device which permitted varying the duration of the arc-back from the normal tripping time of eight cycles to approximately a simultaneous opening of a-c and d-c breakers.

The main rectifier transformer used in this set of laboratory tests was rated at 8,500 kva and provided with double delta-primary windings for 13,800 volts with quadruple-wye secondaries of 712 volts from line-to-neutral terminals, and with interphase transformers. This main power transformer was designed to deliver 780-volt d-c service when used with two sets of ignitron tubes, each set delivering 5,000 amperes continuously. This transformer employs a core constructed of Hipersil, the new high-permeability core material. It has the same weight and physical dimensions, and substantially the same losses, as the older 6,550-kva transformer mentioned later in the discussion of field tests. The core-and-coil assembly, after the completion of the laboratory arc-back test program, is shown in Figure 6. This transformer was designed to withstand the stresses attending arc-back currents of 100,000 amperes, thus the laboratory tests furnished an experimental verification of the design.

Two rectifier frames, each with six ig-

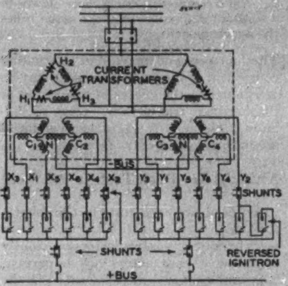

Figure 5. Schematic diagram for artificial arc-back tests on a large rectifier installation

Arc-back on phase Y_2 with simulation by reversed ignitron in parallel with normally connected unit. In many tests the reversed ignitron was replaced by a short-circuiting switch. Locations of shunts and current transformers for oscillograph measurements are shown

nitron tubes, were provided for the tests. In addition, a single tube was provided to initiate an artificial arc-back in some tests. Special auxiliary transformers were used for the supply of the excitation circuits. Reactor-firing circuits were provided for the two six-tube frames. A phase-shifting transformer was used for the control of the tube which was used to simulate an arc-back. Two high-speed d-c breakers, which trip in approximately one-half cycle on heavy reverse current, were provided. The laboratory motor generator sets, including four 1,500-kw 750-volt d-c generators, were connected through high-speed breakers to the d-c busses of the *X* and *Y* sections of the transformer. A short-circuiting breaker, equipped with electronic control, was also used in many tests for simulating an arc-back. Anode breakers were used in the leads of the *X* section of the transformer during some tests.

Figure 7 shows an interesting record obtained during the laboratory tests with the setup just described. This test gave the highest arc-back current obtained with a reverse-connected ignitron and the amount was 81,500 amperes. It will be noted that during this particular test the application of an artificial arc-back on anode circuit Y_5* caused every ignitron on the other phases to arc-back until the circuit was opened by the a-c supply breakers. The *X*-section anode-current records (not shown) included a single loop of current, the current flow being limited by the operation of the high-speed cathode breaker. It will be noted that the current flow corresponds to a three-phase short circuit on the secondaries of the transformer for the *Y* section. The back feed to the *Y* section represented a maximum of 36,500 amperes and had a maximum rate of rise of 5,270,000 amperes per second.

With the same setup but with the reverse-connected ignitron replaced by a short-circuiting switch and with the arc-back being initiated at the end of the normal-conducting period, a maximum arc-back current of 95,000 amperes was recorded.

The oscillogram of Figure 8 is of particular interest. This test was made with the two sets of ignitron tubes connected to the *X* group, leaving the *Y* group of the transformer disconnected. In this case an artificial arc-back with simulation by a short-circuiting switch was placed on anode X_5 and was initiated close to the end of normal-conduction period. In this test the ignitrons of the star group consisting of anodes X_2, X_4, and X_6 were not subjected to sympathetic arc-backs. However, the ignitrons for anodes X_1 and X_3 arced back for four cycles. On the fifth cycle all anodes recovered leaving only the single arc-back on anode X_5, the one subjected to artificial arc-back. It is of interest that the maximum arc-back current for anode X_5 has a first-cycle crest magnitude of 76,700 amperes and about equal magnitude on the fifth cycle. On the following cycle the ignitrons for anodes X_1 and X_3 were subject to sympathetic arc-backs and did not recover again until the primary circuit was interrupted. The primary current on phase *C* of the *X* section, the delta winding associated on the same core with the secondary winding for anode X_5, shows an almost fully displaced a-c wave which was quickly reduced in magnitude because of sympathetic arc-backs. However, on the cycle corresponding to the recovery from arc-back conditions of all anode circuits, the primary-current crest reaches a crest about equal to the initial crest.

With the test setup corresponding with that of Figure 8 but with anode breakers connected in the leads to *X* section, oscillograms of Figure 9 were obtained. In this case also, arc-back simulation was by a short-circuiting switch and the arc-back was initiated at the end of the normal-conducting period. The artificial arc-back was impressed on the circuit of anode X_5. Current flow is shown for anodes X_1, X_3, and X_4. In this case anode X_1 arced back at the end of its normal-conducting period and this necessitated the opening of the anode breaker for phase X_1 as well as for phase X_5, the phase subjected to artificial arc-back. On other tests with anode breakers the number of sympathetic arc-backs varied, involving in some cases a maximum of five phases. The first-cycle maximum anode current for any of the tests with anode breakers was 66,000 amperes, a value that is appreciably below the maximum crest obtained without the anode breakers. The difference may be explained in part by the fact that high-speed cathode breakers were used as well as anode breakers, and that both of these breakers were capable of introducing important arc drop within a half cycle from the inception of the artificial arc-back. Consequently, the actual arc-back current crest was appreciably reduced when high-speed cathode breakers were used with anode breakers. It has been estimated for this case that if semihigh-speed cathode breakers were used, the first-cycle crest would have amounted to about 70,000 amperes.

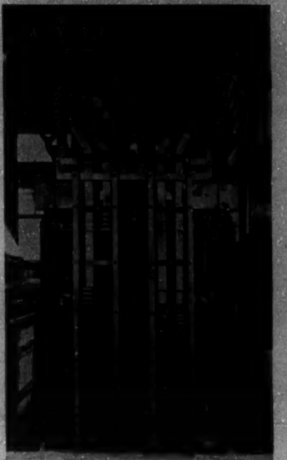

Figure 6. Core and coil assembly of 8,500-kva transformer as it appeared after detanking at the end of the laboratory tests

In another series of tests, six ignitron tubes were supplied from a bank of 250-kva transformers arranged in the usual double-wye secondary with interphase connection to produce 250 volts direct current. The rectifiers were adjusted to carry an initial load of 900 amperes and were fed into a d-c system consisting of a large motor generator set. The artificial arc-backs were applied by means of a short-circuiting switch; the arc-backs were isolated by the operation of a high-speed cathode breaker and by operation of the a-c supply breaker.

Oscillograph measurements during the artificial arc-back tests included the six anode currents obtained from shunts and the three primary-delta currents obtained from especially designed current transformers. A typical oscillogram of artificial arc-back is shown in Figure 10. In this test the artificial arc-back was placed on anode 5 and was initiated substantially at the end of the normal conducting period, the time that produces the maximum first cycle of anode current, which reached a value of 12,200 amperes. This initial current was slightly reduced by disconnection of the back feed, and this slightly reduced value was maintained substantially constant on successive peaks throughout the arc-back condition which lasted for about 11 cycles. Examination of the other anode currents shows that they were also substantially constant throughout the arc-back conditions. The primary currents, however, show a considerable reduction in the d-c component. The alternating component of the primary current increases but slightly during the arc-back condition. The envelope of the primary current of phase *C* has been drawn in on the oscillogram and it shows the difference between the alternating components corresponding to 1,380 amperes at the beginning of the second cycle and to 1,430 amperes at the end of the arc-back condition. Analysis for phase *C* shows that the resultant magnetization (in ampere-turns) is composed of

---

* Note that in Figures 7, 8, and 9 the anodes are designated as 5-*Y* instead of Y_5 and so on, as used elsewhere in text.

1. An a-c component reaching a substantially constant value in a few cycles.
2. A d-c component rising more slowly to a constant magnitude of about seven times the a-c component.

The four-per-cent increase in alternating component of the primary current may be attributed to the effects of saturation of the rectifier transformer. The oscillogram of Figure 10 is typical of an artificial arc-back involving only one anode.

Artificial Arc-Back Tests in the Field

Artificial arc-back tests in the laboratory may vary from field service conditions because of various factors previously discussed. These factors include particularly the use of "seasoned" tubes in the field which have normal operating temperatures and normal ionization prior to the arc-back. Accordingly, it was arranged to make a series of artificial arc-back tests at the Velasco, Tex. plant of the Dow Magnesium Corporation. The particular rectifier station used contains 12 ignitron-type rectifier sections supplied from six transformers with quadruple wye-connected secondaries. These six transformers are arranged to provide a 36-phase rectifier station which is accom-

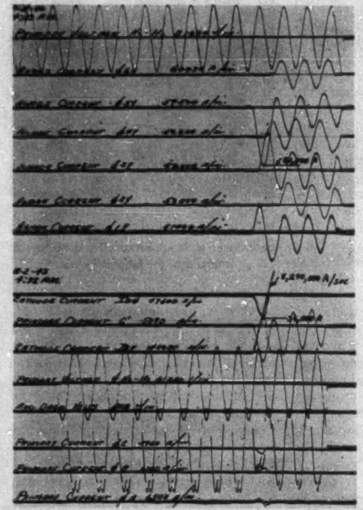

Figure 7 (left). Oscillogram of artificial arc-back tests in the laboratory

Simulation by reversed ignitron on anode Y_5, similar to Figure 5. Sympathetic arc-backs occur on all anodes of the *Y* group. Cathode-breaker clearing

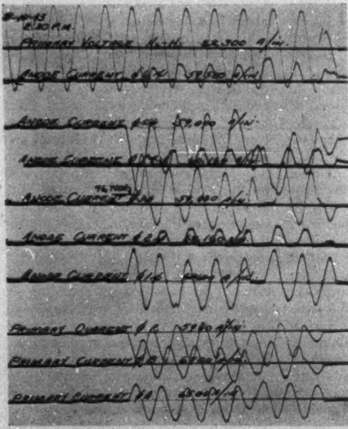

Figure 8 (lower left). Oscillogram of artificial arc-back tests in the laboratory

Simulation by short-circuiting switch. Test setup similar to Figure 5, except *Y*-section ignitrons placed in parallel with the *X*-section units. Sympathetic arc-backs occur in all ignitrons of the *X* group, and all recover on the fifth cycle and then reoccur. Cathode-breaker clearing

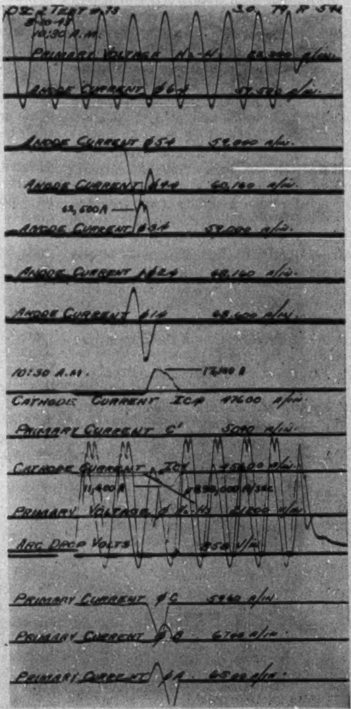

Figure 9 (right). Oscillogram of artificial arc-back tests in the laboratory

Simulation by short-circuiting switch. Setup identical with that of Figure 8, except anode-breaker clearing

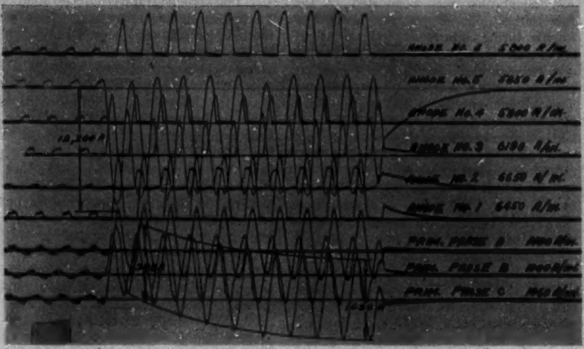

Figure 10. Oscillogram of artificial arc-back tests in the laboratory

Simulation by short-circuiting switch. Cathode-breaker clearing. Typical oscillogram of artificial arc-back tests without sympathetic arc-backs. (Certain lines retouched)

plished by using three delta-primary transformers and three wye-primary transformers and using four phase-shifting transformers. The tests were made on the transformer with delta primary that is connected to the source without phase-shifting transformer.

The artificial arc-back tests were made on rectifier section 3*B*, which is supplied by rectifier transformer number 3 rated at 6,550 kva with an equivalent impedance diagram similar to that shown in Figure 2. The schematic diagram of the main-circuit connections for the tests is essentially the same as that in Figure 5. An electronically controlled, short-circuiting switch was connected so as to short-circuit one ignitron tube. The currents flowing in the cathode and in the anode circuits of the 3*B* section were measured by a magnetic oscillograph with elements operated from shunts. During the artificial arc-back tests, the rectifier station was supplied from the Dow company's own power house, which was delivering 104,000 kw and 111,000 kva; a tie with the Houston Lighting Company was also in service. At the time of the tests, all rectifier sections in the station were carrying a load of 5,250 amperes per section at 648 volts direct current. The ignitor controls for each of the 12 rectifiers were carefully adjusted so that the sections carried 5,250 amperes each. All units were operating with some ignitor delay. All artificial arc-back tests were made from the same initial power-circuit conditions. However, the individual tests differ because the closing breaker applied the artificial arc-back at different points of the cycle.

Five artificial arc-back tests were made with this setup. Two oscillograms obtained during these tests are shown in Figures 11 and 12 which are representative of records with and without sympathetic arc-backs, respectively. The oscillograms show that each artificial arc-back was cleared by proper breaker operation. The d-c feedback was cleared by operation of the high-speed cathode breaker in a half cycle. The a-c circuit was cleared by the transformer primary-side breaker in nine to ten cycles from the inception of the artificial arc-back to the end of arcing between breaker contacts.

The characteristics of the d-c back feed, as given by these oscillograms, show a maximum rate of rise of current of 8,600,000 amperes per second, as defined by a tangent line from the beginning of reverse current to a high value of current before limitation by cathode-breaker operation. The maximum d-c back-feed current was 41,100 amperes, which was reached at a rate of 6,300,000 amperes per second.

Examination of the anode currents showed that artificial arc-backs of tests 1 and 4 produced sympathetic arc-backs but that those of tests 2, 3, and 5 did not. These conditions are shown in somewhat greater detail in Table I. On test 1, the ignitron of anode X_3 arced back in the first cycle but recovered and did not arc back again during the tests. Also on test 1 the ignitron of anode X_4 arced back at the end of the fifth cycle and did not recover until the end of the ninth cycle. On test 4, anode X_4 arced back at the end of the fourth cycle and did not recover again during the test. The crest values of anode currents in both forward and reverse directions for the different tests are also shown in Table I.

The oscillograms gave additional evidence that the highest initial arc-back current occurs when the arc-back is initiated at the end of the normal-conducting period, such as was obtained on tests 1 and 3. When an artificial arc-back occurs at this point and sympathetic arc-backs are not produced, the high initial crest of anode current on the first cycle is maintained at approximately constant value on succeeding cycles throughout the arc-back condition, that is, until cleared by

Figure 11. Oscillogram of artificial arc-back tests at Dow Magnesium Corporation, Velasco, Tex.

Simulation by short-circuiting switch. Artificial arc-back on phase 5. No sympathetic arc-backs encountered. Table II, test 3. See Figure 5

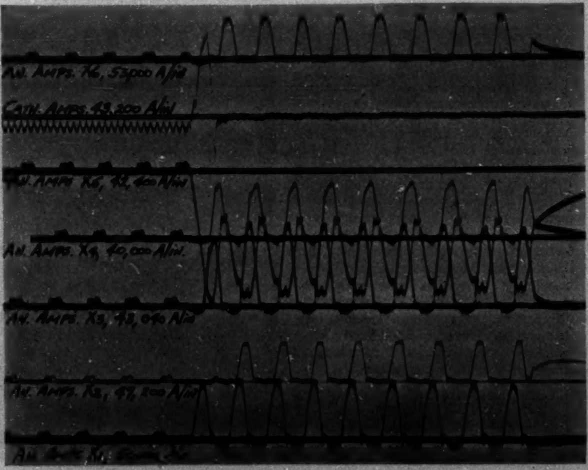

the a-c breaker. If the artificial arc-back occurs after the end of normal conduction and if a sympathetic arc-back does not occur, the anode current is initially considerably smaller but rises to approximately the same ultimate value as is obtained when the arc-back occurs at the end of normal conduction. If a sympathetic arc-back occurs, the anode that is subject to the initial arc-back subsequently has currents considerably below the initial arc-back value. Sympathetic arc-backs frequently increase the currents flowing in the anodes not subjected to arc-back.

Magnitude of Arc-Back Currents

A summary of the arc-back test data has been listed in Table II. This list is of particular interest in giving the ratios of the observed maximum arc-back current to the crest of the symmetrical three-phase short circuit on the particular star group subjected to arc-back. Of interest also is the ratio of the difference between the arc-back current and the back-feed current expressed as a ratio to the crest of the symmetrical three-phase short-circuit current on the particular star group subjected to arc-back. It will be observed that the arc-back current experienced in the field is appreciably lower than that in the laboratory. This is the result of the operating conditions which included an appreciable amount of voltage reduction by phase control.

Voltage Surges in Rectifier Circuits

One speculative problem of rectifier operation is the production of voltage surges. Theories for explaining rectifier surges[7] are based on the inability of the rectifier to provide the ionization necessary for current flow under two conditions, namely,

1. Heavy current as under short circuit or arc-back.
2. Light current when the current "snaps out" on approaching zero value.

The tendency of rectifier circuits to produce surges is known to vary with the type and design of the rectifier itself.

Experience has shown that the standard ignitron tubes have favorable characteristics from the standpoint of overvoltage. However, the arc-back test just described provided opportunity for gathering additional data on overvoltage. Accordingly, provision was made for surge voltage-measuring equipment including klydonographs and cathode-ray oscillographs. Five multielement klydonographs were connected to measure voltages between following terminals:

X_1, X_3, X_5, and C_1 to C_2
X_2, X_4, X_6, and N to C_1
Y_1, Y_3, Y_5, and C_2 to C_4 (See Figure 5)
Y_2, Y_4, Y_6, and N to C_3
H_1, H_2, H_3 to ground

Klydonographs were connected to the low-voltage side of the rectifier transformer during eight short circuits, 146 artificial arc-backs, 14 arc-backs in normal operation, and in addition a somewhat greater number of energizing operations. The klydonograph on the high-voltage side was connected for about 120 tests. Cathode-ray-oscillograph measurements were made for 21 tests between the high-voltage terminal and ground and for 47 tests on the low-voltage side either in parallel with klydonograph terminals or between anode terminals and ground.

Transient voltages below twice normal are of no importance and have been neglected in this investigation. On the high-voltage side one artificial arc-back test and the subsequent switching operation gave transient voltages of 4.8, 2.7, and 1.7 times normal on the three phases; two other tests gave voltages of 2.7 times normal on one phase and another test gave a voltage of 2.5 times normal on one phase. None of the cathode-ray oscillograms gave transient voltages on the high-voltage side to ground greater than 2.0 times normal. The cathode-ray oscillograph was connected for only a part of the total number of tests and by chance was not connected during the tests that gave the highest voltage. During one set of switching operations separate from an arc-back test, a transient voltage of 2.55 times normal was obtained on one phase.

On the low-voltage side the klydonograms showed voltages of 3.1 times normal between terminals X_4 and C_1 and between X_6 and C_1 on one test, and a voltage of 3.1 times normal between terminals X_1 and C_2 on another test. Cathode-ray oscillograms showed a voltage of 2.2 times normal between terminals X_1 and ground on one test, and a voltage of 2.1 times normal between terminals X_5 and C_2. The klydonograph is not well adapted for measuring the lower overvoltages on rectifier circuits for 600-volt output because it does not produce measurable voltages below about three kilovolts and may fail to record at all for voltages of about two kilovolts. The klydonograph, however, is capable of recording overvoltages as high as about 15 kv, and, therefore, should have recorded high surges had they been encountered. The cathode-ray oscillograms showed many records in the vicinity of twice normal but no records inconsistent with the klydonograms.

One of the possible methods of producing voltage surges in a transformer obtains when circuit breakers on the a-c and d-c sides are switched simultaneously. Fifteen artificial arc-back tests were made with the a-c breaker pretripped by a sequence drum so as to approximate simultaneous operation of a-c and d-c breakers. In none of these tests was any appreciable overvoltage recorded on either klydonograms or cathode-ray oscillograms. Possibly one reason for the absence of overvoltages arises from the fact that an artificial arc-back provides a path for the discharge of reactive energy in the rectifier transformer, and sympathetic arc-backs provide additional paths. Current flows in these paths after d-c and a-c breakers are opened as shown by several of the oscillograms, such as Figures 8 or 10. In view of the absence of overvolt-

Figure 12. Oscillogram of artificial arc-back tests at Dow Magnesium Corporation, Velasco, Tex.

Simulation by short-circuiting switch. Artificial arc-back on phase X_6. Sympathetic arc-backs encountered on phases X_3 and X_4. Table II, test 1. See Figure 5

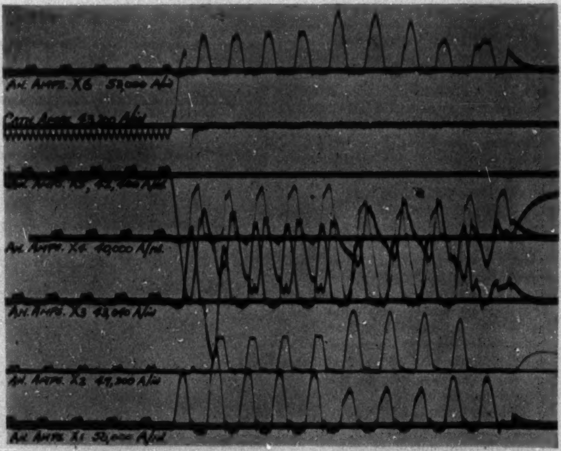

ages during these tests and the improbability of simultaneous switching operations occurring in practice, it is apparent that voltage surges from this cause are unlikely to be of practical importance with ignitrons.

Another series of laboratory tests was made to determine whether abnormal operating conditions would cause the standard ignitron tank to show a tendency for the production of surges. Six short-circuit tests were made with a normal 3,000-kw 600-volt rectifier starting with cooling water at the normal temperature of 52 degrees centigrade. Three of these tests started from a load of 1,000 amperes and three from no load. Of these, four were cleared on the d-c side by a semihigh-speed breaker and two by a high-speed breaker. No arc-backs were encountered during these tests. Eleven short-circuit tests then were made with the rectifier cooling water starting at the unusually low temperature of 19 degrees centigrade. Of these tests, four started from an initial load of 1,000 amperes and the remainder from no load. Because of the unusually low cooling-water temperature the short circuits in many cases were accompanied by arc-backs, particularly when starting from no load. On none of these tests were any surges recorded by klydonographs connected to the low-voltage side of the rectifier transformer in the manner previously described.

Surge-voltage measurements were also made in the field and klydonographs were installed in two electrochemical plants to measure the transient voltages on the low-voltage side of one rectifier transformer in a manner similar to that previously described in connection with the laboratory tests. In a plant equipped with anode-breaker switching, operated by the Aluminum Company of America at Alcoa, Tenn., no surges were recorded by the klydonographs during a month's operation in which two arc-backs, one miscellaneous automatic operation, and nine energizing and de-energizing operations took place. In a plant equipped with cathode-breaker clearing operated by the Dow Chemical Company at Velasco, Tex., no surges were recorded by klydonographs during a period in which 15 arc-backs and a corresponding number of energizing and de-energizing operations took place.

This investigation of voltage surges on rectifier circuits has included voltage measurements during a large number of arc-backs accompanied by energizing and de-energizing operations. In none of these tests were voltages greater than 3.3 times normal obtained on the low-voltage side. The highest transient voltages measured were 3.3 times normal measured with a cathode-ray oscillograph; the three next highest voltages of 3.1 times normal were measured with klydonographs. Only five tests gave transient voltages in excess of three times normal and none of the remaining measurements exceeded either 2.2 times normal or exceeded three kilovolts (the minimum definitely measurable voltage of the klydonograph). Out of over 100 artificial arc-back tests, transient voltages measured on the high-voltage side of the rectifier transformer showed only one case with a voltage as high as 4.8 times normal and only five cases greater than 2.5 times normal.

The switching surges on the high-voltage side of the transformer are believed to have resulted from the disconnection of the circuit following the arc-back. This is shown from the character of the oscillograms. Additional evidence along this line is also given by one switching operation separate from an arc-back test which caused a surge of 2.55 times normal. While a switching surge of 4.8 times normal is relatively high, it is within the usual limits of four to six times normal to be expected occasionally on switching surges.[8,9] All these transient voltages are well below the basic insulation levels of normal transformer design.

With phenomena that are believed to occur but seldom or never, it is, of course, difficult to reach conclusions from tests which give negative results. Nevertheless, results of this investigation of rectifier surges are reassuring.

Conclusions

This paper has presented the results of an extensive series of artificial arc-back tests that have provided additions of value to the published information on the magnitude and character of arc-back currents.

The artificial arc-back tests have shown that the arc drop in the ignitrons used in the larger electrochemical installations constitutes an important factor in limiting arc-back currents.

These artificial arc-back tests provided extensive measurements of transient voltages experienced on rectifier circuits without giving evidence of surge voltages other than those normally associated with the switching operations incident to the disconnection of the a-c supply to the transformer associated with a rectifier under arc-back conditions. The results of this investigation for voltage surges while negative in character are, nevertheless, reassuring from the standpoint of practical operating experience.

The nature and cause of sympathetic arc-backs have been analyzed and shown to be dependent upon the previous magnitudes of forward-flow current. Data are presented on this current limit for a standard ignitron tube.

References

1. Backfires in Mercury-Arc Rectifiers, J. Slepian, L. R. Ludwig. AIEE Transactions, volume 61, 1932, pages 92–104.

2. Backfiring in Mercury-Arc Rectifiers, J. E. White. *Journal of Applied Physics*, July 1940, page 507.

3. Memory Attachments for Oscilloscopes, W. E. Pakala. AIEE Transactions, volume 57, 1938, December section, pages 682–4.

4. A Fast Circuit Breaker, D. I. Bohn, Otto Jensen. AIEE Transactions, volume 61, 1942, March section, pages 165–8.

5. A New Multiple High-Speed Air Circuit Breaker for Mercury-Arc Rectifier Anode Circuits in Its Relation to the Arc-Back Problem, J. W. Seaman, L. W. Morton. AIEE Transactions, volume 61, 1942, November section, pages 788–96.

6. The Testing of Mercury-Arc Rectifiers, H. L. Kellogg, C. C. Herskind. AIEE Transactions, volume 62, 1943, December section, pages 765–73.

7. The Cause of High-Voltage Surges in Rectifier Circuits, A. W. Hull, F. R. Elder. *Journal of Applied Physics*, 1942, pages 372–8.

8. Overvoltages in Transmission Lines Due to Ground Faults as Affected by Neutral Impedances, Engineering Report Number 30, November 15, 1934, Joint Subcommittee on Development and Research, Edison Electric Institute-Bell Telephone System, Engineering Reports, volume 4.

9. Power System Transients Caused by Switching and Faults, R. D. Evans, A. C. Monteith, R. L. Witzke. AIEE Transactions, volume 58, 1939, August section, pages 386–94.

Power Geometry of General Transmission Systems

WM. ALTAR
ASSOCIATE AIEE

IN its present known form[1-6] the power-circle diagram of a transmission system applies to operating conditions where constant voltages are maintained at both the sender and the receiver. While this is by far the most frequent type of operation, instances are numerous where the designer or analyst is confronted with conditions requiring only one of these two voltages to be constant. This is true particularly when the concept of a transmission system is taken in a broader sense as applied to a generator, motor, transmission line, or generally speaking, to any part of a composite transmission system. To mention but one example, the induction motor may be considered a transmission system which supplies power in varying amounts to an equivalent electric load of unity power factor, and its circle diagram accordingly is of a different character. From a viewpoint which looks at all equipment having input and output terminals as general transmission systems, it seemed desirable to formulate on a broader basis the relations between sender and receiver power as exemplified by the constant-voltage circles of the conventional sender and receiver charts. Moreover, a more general relation will permit the translation from one chart to the other, not only of actual power loci of operation, but also of efficiency contours, contours of loss, power factor, receiver wattage and amperage, and other concepts of interest. As it happens, all these cases fall into the wider class where

(*a*). The voltage is maintained constant at one terminal point of the system.

(*b*). The operating locus or contour is a circle for this terminal point.

For the sake of brevity, the sender end through most of the following will be considered as the terminal point with constant voltage, a restriction which is merely one of nomenclature and sign convention.

While the extension of the theory to this wider class of loci was being studied a simple geometrical relationship was established between coexisting diagrams in the two charts. Its existence is obscured in the conventional presentation of power circles, because it is customary to plot sender and receiver charts either separately, or else in one and the same reference frame. For the formulation of the new relation, on the other hand, it is obligatory that the charts be plotted in two different co-ordinate systems which are tilted and displaced against one another to an extent computable from the circuit properties of the system. We shall use the term "power-chart transformation" for the geometrical procedure which carries points of the sender chart collectively into their coexisting points in the properly placed receiver chart. The transformation is such as to transform circles into ellipses. Fortunately, these elliptical receiver loci degenerate in all cases of practical interest into a circle, a parabola, or a terminated straight line, all of which can be constructed easily because of the adopted choice of receiver chart axes. No equally simple and direct procedure exists when the two charts are plotted in the conventional manner.

By resorting to a third dimension one can interpret the power-chart transformation as a projective relation, similar in character to the so-called stereographic projection which in a different way already has proved useful in other branches of circuit theory.[7] This makes the relationship between the charts exceedingly simple to visualize and at times points an easier way for graphical procedure in the chart plane.

The proposed choice of receiver axes proves its advantage most strikingly when it enables us to trace an operating locus or contour on one, say the receiver chart, with the help of points from the other chart. This may be illustrated by the so-called envelope which is the boundary on the receiver chart of the accessible load range.[8] As explained in the section on limiting parabola, the parabola has the open-circuit point as its focus and its directrix is the line which bisects the distance between open- and short-circuit points. This statement involves two points of the sender chart and a curve on the receiver chart, and its meaning is clearly contingent upon the particular choice of reference frames.

It is gratifying that the graphical procedure thus resolves itself into two distinct steps, one exclusively concerned with the circuit properties of the system, the other exclusively with specified operating conditions or contours. The circuit properties determine the manner in which the sender and receiver frame are laid out, but do not enter explicitly into that part of the procedure where the sender or the receiver locus is found graphically from the other. In fact, the second step follows a standard pattern no matter whether one deals with the simplest conceivable case of an impedance line in series with the load, or with the most elaborate four-terminal network.

Before discussing the general procedure as applied to an arbitrary sender circle, contours of practical interest likely to occur in actual problems are discussed, beginning with the familiar power-circle diagram and its modification. All numerical illustrations are derived from a balanced three-phase transmission system, one phase of which is represented in Figure 1 by its equivalent π-circuit. In assuming numerical values, the real part of Y_1 has been exaggerated in order to emphasize the asymmetry of the network. It is not actually a necessary part of the procedure to reduce a given system to its π-circuit because the characteristic chart points can be computed directly, or found by measurement.

Points S and O, recurring in Figures 3 to 9, are the end points of the two vectors of complex sender power $(P+jQ)$ when rated voltage $E_s = 240$ kv line-to-line is applied to the sender terminals, and the receiver end is short-circuited or, respectively, open; thus

$$\left.\begin{aligned}(P+jQ)_{s1} &= \frac{240^2}{768-576j}+\frac{240^2}{23.6+160j}\\ &= (100-316.3j)\text{ mva}\\ (P+jQ)_{o1} &= \frac{240^2}{768-576j}+\frac{240^2}{23.6-1{,}440j}\\ &= (54.5+76.0j)\text{ mva}\end{aligned}\right\} \qquad (1)$$

Reversing the direction of transmission one obtains the receiver-end short-circuit power

$$(P+jQ)_{s2} = \frac{240^2}{-1{,}600j}+\frac{240^2}{23.6+160j} = (52.0-316.3j)\text{ mva}$$

Point N (Figure 4) is obtained by plotting in the sender chart the difference $(P+jQ)_{s1}-(P+jQ)_{s2}$ and, for symmetric sys-

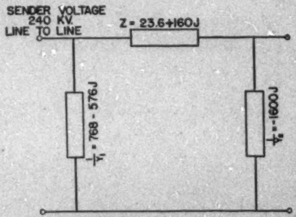

Figure 1. Equivalent circuit representing one phase of balanced transmission system

---

Paper 45-38, recommended by the AIEE committee on basic sciences for presentation at the AIEE winter technical meeting, New York, N. Y., January 22-26, 1945. Manuscript submitted November 8, 1944; made available for printing December 28, 1944.

WM. ALTAR is in the research laboratories, Westinghouse Electric and Manufacturing Company, East Pittsburgh, Pa.

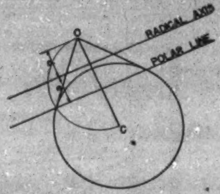

Figure 2. Radical and polar axes of a circle and a point *O*

tems, coincides of course with the origin of the sender chart.

With the help of these points the receiver chart is laid out with its origin at *O*, and the orientation of its axes is obtained by rotating the sender axes through that angle 2δ, and in that sense, by which the vector **SN** would be tilted into the direction **SO** (Figure 4). The axes so obtained are subdivided in divisions equal to the units of the sender scale.

With the two frames thus laid out, it is quite generally true that all lines connecting a pair of coexisting points on the two charts are parallel to line *SO;* a rule which greatly simplifies the identification of such pairs.

The only geometrical concept likely to strike the reader as unfamiliar is the so-called radical axis[6] of a circle and a point *O*. The radical axis is the straight line *r* (Figure 2) which passes halfway between the point *O* and the polar axis of *O* and the circle. Figure 2 indicates how *r* may be determined graphically. Frequent reference will be made to the straight line which perpendicularly bisects the distance *SO*, and for which we shall use the letter *b*.

It sometimes is preferable to represent the system by its three characteristic points *O*, *S*, and *M* instead of *O*, *S*, and *N*. To find *M* (Figure 4) one draws a line through *S*, bisecting the angle between vectors **SN** and **SO**, thus obtaining the direction of vector **SM**. Its length is the geometrical mean of *SN* and *SO*. Or algebraically

$$\begin{aligned} \mathbf{SM} &= \sqrt{\mathbf{SO}\,\mathbf{SN}} \\ &= \sqrt{(45.5-392.3j)(52-316.3j)} \qquad (2) \\ &= 356.3e^{-j82^\circ\,2'} \end{aligned}$$

The Conventional Diagram and Its Modification

For purposes of comparison, Figure 3 shows the sender and receiver circle constructed in the customary manner[5] for the system of Figure 1, operated at constant sender voltage $E_s = 240$ kv line-to-line, and constant receiver voltage $E_r = 200$ kv. In the conventional procedure, provision is made for identifying pairs of coexisting points by locating the pair for which Θ_v is zero, that is, where sender and receiver voltage are in phase. Other pairs then can be identified by laying off equal angles Θ_v on the two circles.[2]

If we now move the receiver circle, together with its reference frame, to their new positions as previously described, we have the following changes (Figure 4). Centers *S* and *s* fall on a straight line with point *O;* the radical axis *r* of the sender circle and *O* is an axis of symmetry for the two circles; coexisting point pairs lie on straight lines parallel to *SO*, so that the quantity Θ_v; and the construction of a reference pair is no longer needed. When needed, the reference pair with $\Theta_v = O$ can be found easily since the sender point is the intersection of the sender circle and line *SM*. More specifically, the vector **SM** may serve as a reference vector representing E_s. For an arbitrary load condition, represented by point *P* in the sender chart, the vector $\boldsymbol{E_r}$ is then represented by vector **SP** both in magnitude and phase.* Consequently, for a receiver voltage $E_r = 200$ kv, both the sender and receiver circle have a radius

$$\overline{SM}\,\frac{200}{240} = \frac{356.3}{1.20} = 296.9 \text{ mva}$$

The center of the sender circle is *S*, while that of the receiver circle may be found graphically by drawing the radical axis *r* of the sender circle and *O*, which one knows to be an axis of symmetry for points *S* and *s*. Comparing Figures 3 and 4, it will be noted that vector **SM** is identical with E_s^2/Z of Figure 3.

The Limiting Parabola

In the manner of the preceding section, a number of receiver circles of different radii may be found, each representing a different value of E_r. The envelope of these circles, which is of occasional interest in connection with system stability, is a parabola. When plotted in the properly placed receiver frame (Figure 5), the parabola has the point *O* as its focus, and the line *b* as its directrix, and thus may be traced easily as the locus of all points having equal distances from point *O* and line *b*. Line *b* marks the coexisting locus on the sender chart, and transmission systems operate exclusively above this line. Also shown on Figure 5 is the receiver circle of Figure 4, tangent to the parabola at two points.

Contours of Load Power Factor

Unlike the preceding cases, this requires the determination of the sender locus from the given receiver locus, which is a straight line *g* through the receiver origin. Consequently,** the sender locus is a circle through *O* and *S* and tangent to *g* (Figure 6). It is more accurate to describe the receiver locus *g*, not as a straight line, but as an ellipse collapsed into a straight-line section, the terminating points being points of the parabola of Figure 5 or, alternatively, the extreme points on *g* to be reached by projecting points of the circle in the direction *SO*. From Figure 6 it will be seen that any two points on the sender chart which are situated symmetrically relative to line *b* give rise to the same receiver power, and so the two halves of the sender plane each equally are transformed by the power-chart transformation into the receiver-chart region which lies inside the parabola.

In Figure 6 is shown the sender locus for a load power factor 0.90 lagging. Its center *C* is the intersection of *b* and a

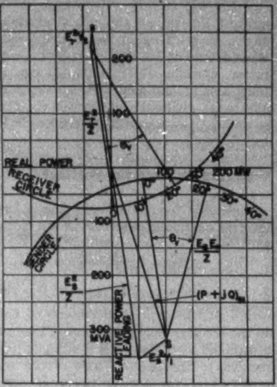

Figure 3. Conventional circle diagram for system of Figure 1, when receiver voltage is maintained at 200 kv line to line

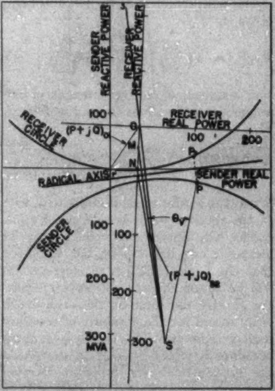

Figure 4. Modified form of circles for constant sender and receiver voltage

---

* See Appendix I. The proof of the statement is contained in equation 8.

** See Appendix II, case 3.

straight line drawn through O at right angles to g. To find the sender power when delivering 100,000 kva at 0.9 power factor, a distance $OP_r = 100,000$ kva is taken along g, and a line PP_r is drawn parallel to OS, giving the intersection P. The second intersection with the sender circle has no practical significance.

Contours of Receiver Wattage

Generally, for any straight line in the receiver chart, the sender locus is a circle such that:

1. Its center lies on line b.
2. Its radical axis with respect to O is the receiver locus.*

In the receiver chart, the contour line for a specified watt output is a straight line parallel to the reactive axis of the receiver chart, the one for 100 megawatts being shown in Figure 7. Accordingly, all sender contours are concentric circles, their center C being the intersection of line b and the real axis of the receiver chart (not shown in Figure 7). To find the radius, draw a semicircle over OC, and a line p parallel to the receiver locus r at twice the distance (200 megawatts) from O. Line p is the polar axis of O and the desired circle; its intersection with the semicircle is A. The radius of the wanted sender circle is CA. Shown in Figure 7 is the pair of points which was used previously in different connection in Figure 4. The receiver locus is again an ellipse collapsed into a terminated straight line and extending across the inner region of the limiting parabola.

Contours of Receiver Amperage

In the sender chart the contours of constant receiver current I_r are concentric circles with center at O, their radius being given by**

$$R = E_s I_r \sqrt{3} \left(\frac{\overline{\overline{SO}}}{\overline{\overline{SM}}} \right) = E_s I_r \sqrt{3} \sqrt{\frac{\overline{\overline{SO}}}{\overline{\overline{SN}}}} \qquad (3)$$

For instance, a receiver current of 200 amperes per line gives the radius (Figure 8)

$$R = 240 \cdot 200 \cdot \sqrt{3} \cdot \frac{356.3}{320.6} 10^{-3} = 92.5 \text{ megavolt-amperes}$$

When the sender circle is concentric with O, the receiver locus is a circle of equal radius, the center C of which may be located along line OS by the condition that the angle (SDC) is 90 degrees. It will be noted that these receiver circles are exactly the same as the ones previously found for the contours of constant receiver voltage. This is only as it must be, since it is not difficult to show that the sender locus for constant receiver voltage V is the mirror image relative to line b, of the sender locus for constant receiver current I_r when the latter is numerically equal to the short-circuit current I_{12} obtained when voltage V is placed at terminals 2 and terminals 1 are short circuited.

The contours of receiver voltage and of receiver amperage are the only ones giving circles in both charts.

The General Relation Between the Two Charts

These illustrations will suffice to give an idea of the possible use of the procedure for graphical analysis. It will not be necessary to produce individual proofs of the rules stated in foregoing sections, since they are all special cases, or corollaries, of the general theorem which gives the receiver locus (an ellipse in general) for a sender circle of arbitrary position and radius (Figure 9).

In order to determine the receiver ellipse, the radical axis r of the sender circle and point O is drawn, and point $\bar{C}$ is placed symmetrically to C with respect to line r. Next the center C' of the ellipse is found by means of the requirement that the two point triples (O, S, C) and $(C, \bar{C}, C')$ form similar triangles. Inspection shows that points O, S, and C are respectively homologous to points C, $\bar{C}$, and C', and follow each other in opposite sense (that is, O, S, C clockwise; C, $\bar{C}$, and C' counterclockwise in Figure 9). Other points P_r on the ellipse can be found by a variety of methods, for instance, by choosing an arbitrary point G on r and using the similarity of triangles (G, C, C') and (H, P, P_r); homologous lines being parallel to each other. However, the usefulness of Figure 9 lies principally in its general validity which permits the derivation of the specific rules given in the preceding sections. This will be shown in the appendix.

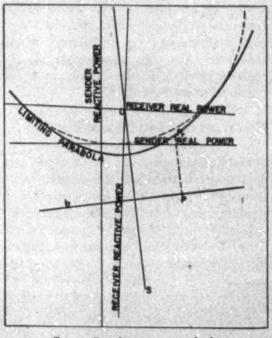

Figure 5. Limiting parabola

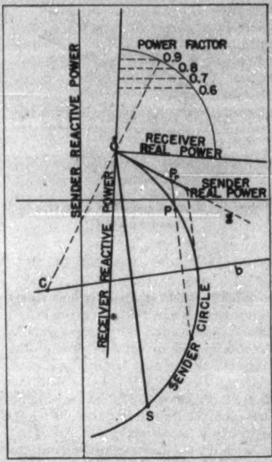

Figure 6. Sender contour of constant load power factor 0.9, lagging

The general character of the power-chart transformation as applied to a sender circle may be visualized by imagining that Figure 9 shows in perspective two boards in space, meeting at an angle along line r. A circular hole in the lower board, representing the sender circle, when illuminated by a distant source in the direction SO will throw an elliptical shadow of the kind shown in the figure.

Another way of visualizing the relationship is preferable, because it represents at once the entire charts instead of just one circle at a time. In Figure 10 is shown the chart plane with its two reference systems in perspective. A sphere of arbitrary radius is placed in contact with the sender chart, point O being the point of tangency and the south pole of the sphere. Points of the sender chart then can be projected on the sphere in the direction toward the north pole A, thus representing the sender chart on the sphere by what is known as stereographic projection. In particular, the image of the short-circuit point is thus obtained on the sphere, and through it and through point O a straight line is drawn up to point B, that is, to its intersection with another horizontal plane tangent to the sphere at its north pole A.

Now, in order to determine the receiver point from the given sender point, it is only necessary to transfer the latter to the sphere by stereographic projection from A, and to project the obtained images back from the sphere into the receiver chart using point B as the center of projection, as shown in Figure 10. Proof that this procedure is mathematically equivalent to the two-dimensional procedure (as embodied in Figure 9) will be found in the last part of the appendix. Lacking a better name, it will be referred to as the

---

* See Appendix II, case 2.

** See Appendix I. The proof of the statement is contained in equations 8.

"modified stereographic projection." A simple mechanical or optical device could be built on the basis of the projective relation, for example, one providing two arms hinged to *A* and *B* respectively, and so linked with each other that one arm automatically traces the receiver locus while the other is guided along any desired sender locus in the chart plane. More important, perhaps, the modified stereographic projection affords a concise formulation of the peculiarities of the power-chart transformation. For instance, we see why circular sender curves must give rise to ellipses in the receiver chart. This is so because sender circles are always stereographically represented as circles on the sphere which are then subjected to reprojection from the center *B*. Again, the general rule that the direction sender–receiver point is always parallel to *SO* follows geometrically from the fact that corresponding point pairs lie in a plane with *A* and *B*, as do points *S* and *O*. Line *AB* is parallel to *SO* and to PP_r, thus proving our rule.

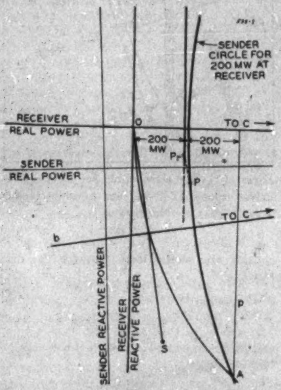

Figure 7. Sender contour of constant receiver wattage (200 megawatts)

The limiting parabola permits a neat visualization in terms of the modified stereographic projection, being the border line of the shadow which the sphere will cast on the receiver chart when illuminated by a point source at *B*. The shadow clearly must be a conic section, and more specifically a parabola since the light source *B* is at the same height as the north pole *A*. It becomes a simple problem in geometry to verify its exact location and the fact that the borderline of the illuminated region on the sphere is the stereographic projection of line *b*.

It also will be seen that any straight line in the sender chart gives a circle through *A* by stereographic projection on the sphere, and in the receiver chart a parabola by reprojection from *B*. Occasionally, it may be helpful to know that the radical axis of an arbitrary sender circle and *O* lies in the same plane as the stereographic image of the circle on the sphere.

Operation With Constant Receiver, Variable Sender Voltage

The power-chart transformation also can be established if the receiver terminals instead of the sender terminals are operated at constant voltage. To reformulate our statements for this case, it is merely necessary to interchange the words "sender" and "receiver" whenever they occur and to reverse the signs of all power vectors, for example, by rotating the diagram of sender and receiver chart as a whole through 180 degrees. The letters *S* and *O* now mean short-circuit and open-circuit power measured "looking backward," that is, with rated voltage at receiver terminals and the sender end short circuited or, respectively, open. As an illustration, Figure 11 shows the diagram for the system of Figure 1, operating with constant receiver voltage of 240 kv line-to-line and constant real power at the sender. (If the circuit of Figure 1 included the generator synchronous impedance, assumed constant for the sake of arguments, this would give the receiver contours of prime-mover $HP=2.0\times10^5$.) Points *S* and *O* are determined by plotting on the receiver chart the two vectors $-(P+jQ)_{rs}$ and $-(P+jQ)_{ro}$, respectively, the latter being

$$-\left(\frac{240^2}{-1{,}600j}+\frac{240^2}{791.6-416j}\right)=-57.0-66.0j$$

Point *N* has the same position on the receiver chart which it previously (Figure 4) had in the sender chart. The angles $2\delta'$ and 2δ are not equal. Otherwise, the construction is very much like the one outlined in Figure 7 except that the words "sender" and "receiver" are reversed; a circular receiver locus now corresponds to the sender locus *g*, the latter being the radical axis of the receiver locus relative to the point *O*.

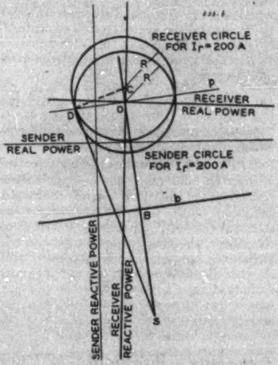

Figure 8. Sender and receiver contours of receiver current (200 amperes per line)

Appendix I. Power-Chart Transformation Applied to a General Sender Circle

The construction embodied in Figure 9 will be established by first deriving a generally valid complex vector equation for sender and receiver power. The fundamental line equations

$$E_r=E_s(ZY_1+1)-IZ \tag{4a}$$

$$I=-E_s(ZY_1Y_2+Y_1+Y_2)+I(ZY_2+1) \tag{4b}$$

can be reduced to a form not involving the circuit elements Z, Y_1, Y_2. Thus, one avoids the need for representing given transmission systems by equivalent circuits. Setting E_r in equation 4a and I_r in equation 4b alternatively zero, one finds the short-circuit current and, respectively, the open-circuit current of the system

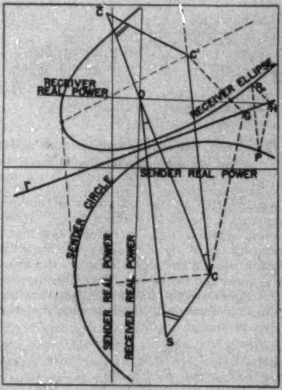

Figure 9. Receiver locus for an arbitrary sender circle

$$I_{s1}=E_s\frac{ZY_1+1}{Z}\text{ and }I_{o1}=E_s\left(Y_1+\frac{Y_2}{ZY_2+1}\right) \tag{5}$$

To eliminate the circuit elements we introduce the quantity I_m, meaning the current which flows in the short-circuiting strap at short circuit. Thus

$$I_{sm}=E_s/Z=\sqrt{I_{s2}(I_{s1}-I_{o1})}=\sqrt{I_{s1}(I_{s2}-I_{o2})} \tag{6}$$

n terms of which

$$Z=E_s/I_m,\ E_sY_1=I_{s1}-I_m,\quad E_sY_2=I_{s2}-I_m \qquad (7)$$

Introducing equation 7 into equation 4 we have

$$E_r=E_s\frac{I_{s1}-I}{I_m}\text{ and }I_r=I_m\frac{I-I_{o1}}{I_{s1}-I_{o1}} \qquad (8)$$

from which the receiver power vector is obtained by complex multiplication

$$(P+jQ)_r=\hat{E}_rI_r=\hat{E}_s\frac{(\hat{I}_{s1}-\hat{I})(I-I_{o1})}{(I_{s1}-I_{o1})}\frac{I_m}{\hat{I}_m} \qquad (9)$$

Since the sender voltage is constant, each current vector on the right hand of equation 9 is turned into a complex power vector by multiplication with $\hat{E}_s$. Using the short notation $\boldsymbol{P}$ for $(P+jQ)=\hat{E}_sI$, and similarly $\boldsymbol{P}_r=(\boldsymbol{P}+j\boldsymbol{Q})_r$, $\boldsymbol{P}_{s1}=\hat{E}_sI_{s1}$, $\boldsymbol{P}_m=E_sI_m$, and so forth, equation 9 is changed to

$$\boldsymbol{P}_r=\frac{(\hat{\boldsymbol{P}}_{s1}-\hat{\boldsymbol{P}})(\boldsymbol{P}-\boldsymbol{P}_{o1})}{(\hat{\boldsymbol{P}}_{s1}-{}_{o}\hat{\boldsymbol{P}}_{1})}\frac{\boldsymbol{P}_m}{\hat{\boldsymbol{P}}_m} \qquad (10)$$

Equation 10 could be interpreted as a complex equation between points P, P_r if both were plotted as the end points of complex vectors in the same reference frame. However, equation 10 can be reduced to a much simpler form by displacing the receiver frame against the sender frame in the manner described in the text, that is by moving its origin through a distance P_{o1} and rotating the axes through an angle 2δ such that the unit vector

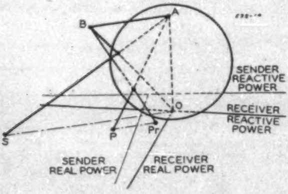

Figure 10. Power-chart transformation represented as a projective relation in space

$$e^{2j\delta}=\frac{(\boldsymbol{P}_{s1}-\boldsymbol{P}_{o1})}{(\hat{\boldsymbol{P}}_{s1}-\hat{\boldsymbol{P}}_{o1})}\frac{\hat{\boldsymbol{P}}_m}{\boldsymbol{P}_m} \qquad (11)$$

With reference to this new receiver frame, points which in the sender chart represent a power vector $\boldsymbol{P}$ are then represented by $\boldsymbol{P}'$

$$\boldsymbol{P}'=(\boldsymbol{P}-\boldsymbol{P}_{o1})e^{-2j\delta} \qquad (12)$$

$$\boldsymbol{P}_{s1}'=(\boldsymbol{P}_{s1}-\boldsymbol{P}_{o1})e^{-2j\delta}\text{ and }\boldsymbol{P}_{o1}'=\text{zero} \qquad (12a)$$

while points representing receiver power are, of course, still given by $\boldsymbol{P}_r$. Introducing equations 11, 12, and 12a, into equation 10 changes this equation to

$$\boldsymbol{P}_r=\frac{(\hat{\boldsymbol{P}}_{s1}-\hat{\boldsymbol{P}})(\boldsymbol{P}-\boldsymbol{P}_{o1})}{(\hat{\boldsymbol{P}}_{s1}-\hat{\boldsymbol{P}}_{o1})}e^{-2j\delta}=\left(\boldsymbol{P}-\frac{\hat{\boldsymbol{P}}\boldsymbol{P}}{\boldsymbol{P}_{s1}}\right)'$$

or

$$\boldsymbol{P}'-\boldsymbol{P}_r=\frac{\overline{\boldsymbol{P}}'^2}{\boldsymbol{P}_{s1}'} \qquad (13)$$

Equation 13 has formally the simplicity which equation 10 would have when applied to an impedance line. Omitting primes for this case, one finds equation 13 reduces to

$$\boldsymbol{P}-\boldsymbol{P}_r=\bar{I}^2(R-jX)$$

As equation 13 is quite general, one can borrow the circle diagrams of the impedance line for use in the general case.

Proof of the geometrical relation embodied in Figure 9 rests on equation 13. We shall use the symbol $\overline{OS}$ to indicate the vector pointing from S to O and so forth, so that $\overline{PP}_r=(P'-P_r)$, $\overline{OS}=P_{s1}'$ and so forth. Now it is a known property of the radical axis that its distance x from an arbitrary point P on the circle is proportional to the square of distance $\overline{OP}$, thus

$$\overline{OP}^2=2x\overline{OC}$$

or in complex notation, using vectors in the receiver chart

$$\boldsymbol{P}'\hat{\boldsymbol{P}}=2\boldsymbol{x}\hat{\boldsymbol{c}} \qquad (14)$$

where $\boldsymbol{x}$ is the vectorial distance from line r to P, and $\boldsymbol{c}$ is the vector from O to center C (Figure 9). Combining this with equation 13 one has a proportionality between complex vectors

$$(\boldsymbol{P}'-\boldsymbol{P}_r):2=\hat{\boldsymbol{c}}:\boldsymbol{P}_{s1}' \qquad (15)$$

This can be interpreted as stating similarity of two triangles, one formed by the two vectors $\overline{\boldsymbol{PP}}_r$ and $\overline{\boldsymbol{PP}}$, and the others by the two vectors $\overline{\boldsymbol{OC}}$ and $\overline{\boldsymbol{OS}}$. The conjugate signs on the right of equation 15 signify that it is a similarity with inverted clock-sense as stated in the text. To find the center C' of the ellipse, the construction by similar triangles may be used, identifying points P and P_r with C and C', respectively. (This notwithstanding, C' is not the receiver point coexisting with sender point C.)

Appendix II. Proof of the Corollaries Used in This Paper

Case 1. Contours of Constant Receiver Voltage. Since the sender circles have their center at S, points S and C in Figure 9, and consequently points P_r and P, coincide. This means that sender and receiver points are symmetrically situated with respect to r.

Case 2. Contours of Constant Receiver Wattage. The sender circle has its center on b, making the triangles (OSC) and (PP_rP) of Figure 9 isosceles, so that point P_r lies on a line which perpendicularly bisects $\overline{PP}$, that is, on the radical axis r. Conversely, whenever the receiver locus is a straight line, it is the radical axis of the sender circle and point O.

Case 3. Contours of Load Power Factor. The straight line of case 2 passes through O, reducing the radical axis to the tangent at O. The sender circle passes through O and, having its center on b, through S also.

Case 4. Contours of Receiver Amperage. The sender circle has its center at O so that the quantity P' of equation 13 is of constant amount. The receiver locus is obtained by shifting the sender locus through the distance

$$\frac{\overline{P'}^2}{P_{s1}}=\frac{(\text{radius})^2}{\overline{OS}}$$

and this is in accordance with the construction of Figure 8.

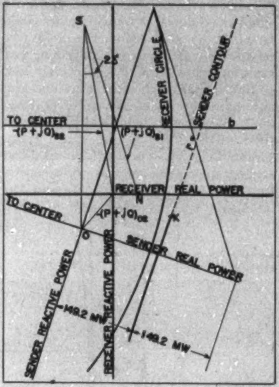

Figure 11. Receiver circle for constant receiver voltage (240 kv) and constant sender real power

Appendix III. Proof of the Modified Stereographic Projection

As shown in the text, the modified stereographic projection gives correctly the direction from sender to receiver point as parallel to SO. Since any arbitrary sender point can be defined as the intersection of one such line with a sender circle of constant load power factor, it will be sufficient to show that these sender circles are correctly given by the modified stereographic projection.* Now referring to Figure 10, if the receiver locus is a straight line g through O, the corresponding circle on the sphere lies on a plane through line g and point B, a plane which also contains the stereographic image of point S. It follows that the sender circle, obtained by projection from A, must pass through O and S, and be tangent to g, which was to be demonstrated.

References

1. CIRCLE DIAGRAMS FOR TRANSMISSION SYSTEMS, R. D. Evans, H. K. Sels. *Electric Journal,* 1922, page 550.

2. SOME THEORETICAL CONSIDERATIONS OF POWER TRANSMISSION, C. L. Fortescue, C. F. Wagner. AIEE TRANSACTIONS, volume 43, 1924, pages 16–23.

3. FERNÜBERTRAGUNGSMÖGLICHKEITEN GROSSER ENERGIEMENGEN, Ossanna. *Elektrotechnische* Zeitschrift 43, page 1025, 1922.

4. ZUR ABLEITUNG DER NEUEN ARBEITSDIA-

---

* See Appendix II, case 2.

The Next Step in Interrupting Capacity—5,000,000 Kva

A. W. HILL
MEMBER AIEE

W. M. LEEDS
MEMBER AIEE

Synopsis: Serious consideration is being given to large power-system interconnections which could develop short circuits at certain locations in excess of 3,500,000 kva. High-voltage oil-circuit-breaker capabilities for such heavy duty are reviewed in this paper, the fundamental design requirements outlined, and results of high-power laboratory tests presented which demonstrate that interrupting capacity ratings as high as 5,000,000 kva are feasible. Laboratory test methods for demonstrating these extremely high arc rupturing ratings are evaluated. The importance of verifying high-speed reclosing performance with high-power tests is emphasized, and on the basis of data already obtained, standard reclosing time intervals considerably less than 20 cycles are foreseen.

THE interconnection of large electric-power systems has resulted in such heavy concentration of power at certain points that the possibility of short circuits in excess of 3,500,000 kva must be considered. Whether advantages of solidly tied together "super-power" systems are to be fully realized may depend in considerable measure on the adequacy of the protective equipment. This paper reviews the present status of high-voltage oil circuit-breaker design and development, with particular emphasis on the requirements for interrupting capacity ratings as high as 5,000,000 kva in the 138-kv, 161-kv, and 230-kv voltage classes.

Performance Requirements for 5,000,000-Kva Oil Circuit Breakers

In the rating of high-voltage oil circuit breakers for 5,000,000 kva, the item which demands the most critical attention is the interrupting capacity. Insulation tests, continuous and short-time current carrying ratings, and mechanical operating speeds need not involve any serious departure from conventional practices. However, the arc-rupturing ability cannot be predicted accurately, and assurance of adequacy requires actual short-circuit testing along the following lines:

1. Voltage interrupting ability should be demonstrated to at least 87 per cent of line-to-line voltage across a single pole at whatever current values are available. For the 138-, 161-, and 230-kv ratings under consideration, these minimum test voltages would be 115-, 140-, and 200-kv respectively. Interrupters which show very little increase in arcing time as the voltage is raised are particularly favorable to methods of extrapolation where full rated short-circuit power is not available for testing.

2. Voltage-recovery rate may be an important consideration, depending on how sensitive the interrupting device is to the rate of rise of recovery voltage.[1] Most high-power laboratory circuits have a recovery rate in excess of 1,000 volts per microsecond for the higher current range. However, it should be pointed out that verification tests on a power system will have a very much lower rate because of the added capacitance of transmission lines and the overvoltage damping effect of parallel loads connected to the bus at the time of test.

3. Current-interrupting ability should be shown by short-circuit tests up to the full current values of 21,000, 18,000, and 12,500 amperes for 5,000,000-kva ratings at 138, 161, and 230 kv respectively, using the highest test voltages at which these currents may be obtained. Still better are tests in which the rated short-circuit currents are interrupted by a subdivision, such as a half pole of the breaker, across which normal voltage for that particular section can be applied, as discussed under test methods.

4. High-speed reclosing of oil circuit breakers is generally recognized as involving additional severity in short-circuit interrupting duty when there must be a second interruption after an interval of only a fraction of a second. For two operations in such close succession, it has been customary to use an interrupting rating factor of 75 per cent for ratings between 10,000 and 20,000 amperes, and 65 per cent for ratings between 20,000 and 40,000 amperes. If these factors are applied to 5,000,000-kva breakers the interrupting capacity at 161 kv and 230 kv would be reduced to 3,750,000 kva for rapid reclosing duty, and at 138 kv to 3,250,000 kva. Since intervals of 20 or 30 cycles do not, in general, allow time for the gas produced by one operation to be completely replaced by oil in the interrupting units before the next operation, it is essential that full voltage and current per unit be used in demonstrating the adequacy of the breaker for high-speed reclosing duty.

High-Voltage Oil-Circuit-Breaker Design

There are a number of factors which affect the interrupting capacity of a high-voltage oil circuit breaker. It is taken for granted that modern oil circuit breakers require some type of arc extinguishing device in order to provide sufficiently effective arc-rupturing action to meet present day high-speed interrupting time ratings. High effectiveness is indicated by low tank pressures and small quantities of gas generated. For a given contact velocity and current to be interrupted, it is evident that the total amount of gas generated will be proportional to the arc energy, and in turn to the arc voltage per inch of contact separation and time of arcing.

A number of arc-rupturing devices which use self-generated arc extinguishing power have the characteristic of reduced arcing time as the current increases. If the short-circuit current is raised higher and higher, eventually one of two things will result to set a limit on the interrupting capacity. In the first place, the interrupting effectiveness may be impaired by insufficient oil supply in the arc chamber, or choking of the vent passages may leave too much ionized gas in the arc space with the result that the arc is not interrupted and failure occurs. On the other hand, the internal pressure generated during the arcing period may reach values sufficient to rupture the arc chamber so that the ability to function on subsequent operations would be lost even if arc interruption should occur on the operation during which damage occurred. If prompt back-up protection is not provided, continued arcing may result in splitting open the tank itself.

It has been found experimentally that, not only is the internal pressure proportional to the total arc energy, but superimposed high-pressure impulses are present which are a function of the rate of arc energy liberation, in other words to the instantaneous arc power. It is evident, therefore, that excessive speed of arc lengthening, either by magnetic looping

---

Paper 45-46, recommended by the AIEE committee on protective devices for presentation at the AIEE winter technical meeting, New York, N. Y., January 22-26, 1945. Manuscript submitted November 27, 1944; made available for printing December 26, 1944.

A. W. Hill and W. M. Leeds are both in the switchgear engineering department, Westinghouse Electric and Manufacturing Company, East Pittsburgh, Pa.

---

gramme, E. Gross. *Elektrotechnik und Maschinenbau*, 1926.

5. Electrical Transmission and Distribution Reference Book. Westinghouse Electric and Manufacturing Company, 1942. Page 43 ff.

6. Theorie der Wechselstromubertragung (book), H. Grunholz. Springer, 1928.

7. Principles of Microwave Radio, E. U. Condon. *Reviews of Modern Physics*, volume 14, page 341.

8. Projective Geometry (book), O. Veblen, J.W. Young. Ginn and Company. Volume 2, page 159.

9. A Semi-Graphical Method of Determining the Power Limits of an Interconnector, H. Rissik. *Journal* of the Institution of Electrical Engineers, (London, England) volume 88 II, 1941, page 568.

Figure 1. 115-kv oil circuit breaker rated 1,500,000 kva with five-cycle interrupting time

Oil volume reduced to only 60 per cent of superseded eight-cycle breaker by using multiflow deion-grid interrupters

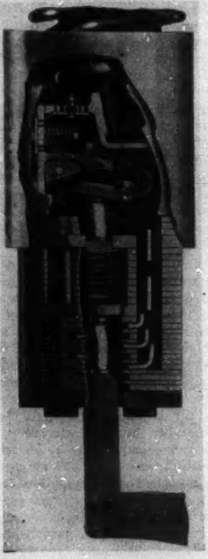

Figure 2. Cut-away view of 138-kv multiflow deion grid showing oil flow produced by upper pressure-generating arc

Lower arc is subjected to deionizing flow from three pairs of converging oil jets. Gases are exhausted through two pairs of vents at intermediate levels

of the arc, blasting of the arc through ports or around splitter plates, or by extremely high contact velocities, will tend toward raising the pressure peak and, therefore, influence the ultimate short-circuit capacity. Those arc rupturing devices which are relatively freely vented, avoid unnecessary arc lengthening, and utilize moderate contact opening speeds, will be most suited to application in circuit breakers of maximum interrupting rating.

Although the effectiveness of modern circuit-interrupting devices has resulted in making the tank diameters of the high-voltage breakers more dependent on insulation clearances than on interrupting capacity, there are still certain considerations of physical dimensions which must not be neglected in the design of breakers having rupturing capacity as high as 5,000,000 kva. In the first place, the gas vented from the arc-extinguishing structures momentarily substitutes a weaker dielectric for the oil usually maintained between live parts and the grounded tank and also between the live parts on adjacent terminals. Insulating shields on the interrupting structures, and possibly insulating tank liners, can be used to maintain adequate dielectric strength, both by the introduction of the solid dielectric and by the baffling effects which maintain a layer of relatively undisturbed oil adjacent to the metal parts where the voltage gradient is a maximum. Well-rounded metallic shields covering all live parts are of particular benefit in keeping down excessive localized voltage gradients from which breakdown streamers might start.

Sufficient air space is usually provided above the oil level in the large breakers so that even if all exhaust pipe openings were closed the amount of gas generated during a maximum kilovolt-ampere interruption would raise the static pressure only a fraction of an atmosphere. However, circuit-breaker tanks are known to have a tendency to jump during heavy short-circuit interruptions due to transient pressure effects. These have been analyzed[2] and shown experimentally to be due to unbalanced vertical forces. As the gas is rapidly expelled from the arc-extinguishing structures, a considerable mass of oil must be lifted to make room for the expanding gases. A strong downward pressure impulse is transmitted to the bottom of the tank whereas the upward force is utilized in accelerating the moving oil mass and is not directly applied to the breaker structure. As a result, the entire breaker moves downward by elastic deformation of mounting supports, frame, and foundation, and then rebounds upward.

It is doubtful whether in the larger circuit breakers the upward moving oil strikes the cover or dome with sufficient force to produce appreciable mechanical pressure. Pressure records taken at the bottom of the tank indicate repeated pressure impulses due to oscillations of

Figure 3. Circuit-breaker test connections and equivalent three-phase interrupting capacity obtainable

Half-pole test and three-phase test on single pole assumes equal division of voltage between halves of pole unit under normal conditions

	A THREE POLE TEST	B SINGLE POLE TEST	C HALF POLE TEST	D 3ϕ ON 1 POLE TEST
TEST CIRCUIT	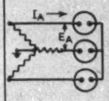	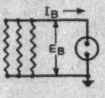	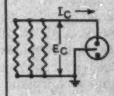	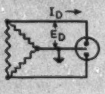
TEST KVA	$\sqrt{3}\,E_A I_A$ *	$E_B I_B = \frac{E_A}{\sqrt{3}} I_B$	$E_C I_C = \frac{E_A}{2\sqrt{3}} I_C$	$\sqrt{3}\,E_D I_D$ *
EQUIVALENT 3ϕ KVA AT VOLTAGE E_A	$\sqrt{3}\,E_A I_A$	$3 E_B I_B$	$6 E_C I_C$	$6 E_D I_D$ x
EQUIV. 3ϕ KVA / 3ϕ LAB. CAP	1.0	1.8 +	3.6	3.46

* MAXIMUM CURRENT IN ANY ONE PHASE
+ BASED ON SINGLE-PHASE LABORATORY CAPACITY, 80% OF THREE-PHASE CAPACITY
x BASED ON SIX TIMES MAXIMUM DUTY ON HALF POLE

Figure 4. Two 60,000-kva high-power laboratory generators capable of producing three-phase short circuits of more than 2,000,000 kva at 13,200 volts

Each rotor weighs approximately 250 tons

the oil mass continuing for an appreciable time following arc interruption. In fact, the collapse of the gas bubble due to cooling immediately after arc rupture often results in a pressure impulse to the bottom of the tank at the moment of downward return of the oil mass which is actually of greater magnitude than the initial rise of pressure during arcing. Because of the pressure shocks on the breaker, it is well to have the tanks bolted firmly to the foundation. However, it has been found that the design of more effective arc-rupturing devices with resulting lower pressure impulses has more than kept up with the increase in breaker ratings so that stresses during the interruption of 3,000,000 to 5,000,000 kva in modern breakers are actually less than when interrupting 1,000,000 to 2,500,000 kva in the earlier designs.

The multiflow deion grid for high-voltage oil circuit breakers has been described before the Institute in previous papers.[3,4] The high degree of arc-rupturing effectiveness obtained with those interrupters has made possible a very substantial reduction in tank diameter and oil volume for standard ratings. For instance, the 1,500,000-kva breaker for 115-kv service shown in Figure 1 uses tanks only 50 inches in diameter with an oil volume 60 per cent of the breaker which it supersedes. It may be well to review the features which make the multiflow grids particularly suitable for circuit breakers of high rupturing capacity.

A cross section of a 138-kv five-cycle grid assembly which has been tested to nearly 5,000,000 kva is shown in Figure 2. The upper contact gap for producing oil-driving pressure is opened slightly in advance of the main contact gap by downward movement of the spring-biased intermediate contact and the main moving contact and cross bar. The oil under pressure flows toward the main arc through three pairs of inlet channels at different levels, passing through orifice openings in close proximity to the arc which is thereby cooled and deionized. The carbonized oil and arc products are then exhausted through two pairs of ports alternated between the inlet passages. By this means, the complete length of arc is acted upon, and arc rupture is accomplished without unnecessary lengthening and with surprisingly low pressure within the main body of oil, even at the highest short-circuit interrupting duty.

Even for three-cycle interrupting time ratings it has been found necessary to provide only two interrupting units per pole, the additional speed being obtained by faster tripping of the breaker mechanism and by increasing the speed of opening of the lower contact in the grid with a multiplying linkage. By eliminating extra pairs of multibreaks within the breaker, the total arc length, arc energy, and resulting pressure are kept within reasonable limits. The arcing time is so short that the silver tungsten arcing tips show relatively small amount of wear and burning during even the heaviest short circuit. Furthermore, the principle of bringing oil radially inward from opposite sides of the arc tends to center the arc in the orifices which are, therefore, protected by flowing oil from burning, and thus maintain their original dimensions very closely for a large number of short-circuit interruptions.

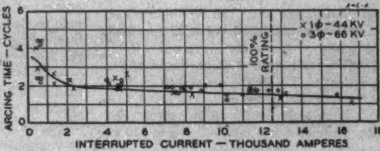

Validity of single-phase testing demonstrated by same performance under two conditions

Figure 5. Comparison of arcing time on single-phase 44-kv tests and three-phase ungrounded 66-kv tests verifying 1,500,000-kva rating on standard deion grids

High-Power Laboratory Test Methods

Without a high-power testing laboratory, the development of modern circuit-interrupting devices to their present state of high effectiveness would have been virtually impossible. In the laboratory the voltage, current, and circuit conditions may be varied at will and repeated as often as necessary to obtain the desired amount of design and performance data.

Final verification of a new design by field tests on an actual power system has, of course, certain advantages both to the manufacturer and operating company, particularly where the short-circuit capacity available is in excess of that provided by the testing laboratory. Thus, a confirmation of the methods of extrapolation in laboratory testing is obtained while the operator gains assurance as to the operation he may expect on his particular system. It should be recognized, however, that because of hazards involved in subjecting a power system to these heavy short circuits, the number of repeated tests necessarily is rather limited. Also, the low recovery rate usually associated with an extensively interconnected system makes it unlikely that the most severe circuit conditions to which the breaker might be exposed, perhaps in other locations, will be obtained during the tests.

Four methods of high-power laboratory testing applicable to high-voltage oil circuit breakers are illustrated in Figure 3. Method *A* is the standard three-phase connection from the power transformer bank to the test breaker with the fault ungrounded. This is rarely used for verifying the large outdoor floor-mounted oil circuit breakers which are tested more conveniently single phase, and which, in general, have ratings exceeding the three-phase short-circuit capacity of the laboratory. For instance, the two 60,000-kva testing generators of the Westinghouse High-Power Laboratory,[5] shown in Figure 4, will develop together a three-phase first-cycle symmetrical short circuit of over 2,000,000 kva at the generator voltage of 13,200 volts. However, the impedance of the step-up transformers limits the maximum three-phase short-circuit current at these higher voltages to 1,600,000 kva. By pretripping the test breaker so that the circuit breaker contacts will part in the first cycle of short circuit, the total rms current measured in the most asymmetrical phase will reach a value approximately 50 per cent greater than the symmetrical value. Calculating the

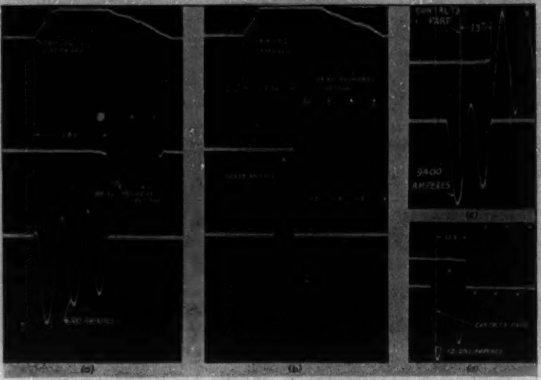

Figure 6. 230-kv multiflow deion-grid short-circuit tests

(a). Three-cycle grid, 198 kv single-phase equivalent to 2,500,000 kva at 230 kv three phase

(b). Three-cycle grid, 132 kv single phase, equivalent to 4,300,000 kva at 230 kv three phase

(c). Five-cycle grid, 132 kv single phase, equivalent to 3,700,000 kva at 230 kv three phase

(d). Three-cycle grid, 66 kv across half pole, equivalent to 4,800,000 kva at 230 kv three phase

three-phase kva on the basis of initial voltage and the maximum rms current in any one phase, the resulting short circuit may be considered to demonstrate an interrupting capacity of 2,400,000 kva. The shorter the arcing time, the more valid this test becomes, since the current decrement during the arcing period will be somewhat greater than under average power-system short-circuit conditions.

Method *B* of applying a single-phase fault at normal line-to-ground voltage to a single breaker pole is the most common method of laboratory testing of high-voltage breakers. With minimum transformer impedance obtained by paralleling all transformers, about 60 per cent of the three-phase capacity is developed in the single pole, the equivalent three-phase power, therefore, being 1.8 times the laboratory capacity. Thus, the two Westinghouse generators feeding six single-phase transformers in parallel will produce a first-cycle symmetrical single-phase short circuit of nearly 1,000,000 kva, corresponding to a three-phase grounded fault of 3,000,000 kva. Pretripping to obtain greater asymmetry during the arcing period will raise the equivalent three-phase power to well over 4,000,000 kva.

The question often is raised in connection with single-phase tests at line-to-ground voltage as to whether the adequacy of a breaker to interrupt a three-phase ungrounded fault has been demonstrated. In the latter case, the first pole to clear must interrupt 87 per cent of line voltage instead of 58 per cent, while the other two poles divide the duty in opening the line-to-line fault which remains. The discrepancy is not nearly so great as might be imagined, however, since, on a three-phase ungrounded test, each pole takes its turn in succession to try to be the first pole to clear the circuit. This follows from the fact that the currents in each of the three phases do not go through zero value at the same time but at approximately 60 electrical degree intervals. Failure to perform satisfactorily actually would mean that no one of the three poles had the ability to open the short-circuit current at 87 per cent of line voltage. It is not surprising, therefore, that a test at this 87 per cent voltage applied directly to a single breaker pole, which has no choice but to clear or fail, should impose a more severe condition than a three-phase ungrounded fault on the full three-pole breaker. For this reason, a circuit breaker which has been demonstrated to have the ability to interrupt short circuits of at least moderate power at 87 to 100 per cent of line voltage may be tested single phase at 58 per cent of line voltage up to its rated interrupting current with considerable assurance of demonstrating the ability of the breaker to handle not only grounded short circuits but three-phase ungrounded short circuits as well.

Confirmation of this analysis is given by the test data plotted in Figure 5 showing the arcing time in a 69-kv oil circuit breaker being tested for a 1,500,000-kva rating by both single-phase tests at 44 kv and three-phase ungrounded tests at 66 kv. The average arcing time was almost identical under the two test conditions which were carried to short-circuit currents well above the breaker rating.

To demonstrate interrupting capacity at still higher kva, at least two other methods are available. By cutting out one half of the interrupting elements in a single pole as shown in method *C* of Figure 3, and testing at one-half line-to-

Figure 7. 138-kv multiflow deion-grid short-circuit tests

(a) Five-cycle grid, 88-kv single phase, equivalent to 4,200,000 kva at 152 kv three phase

(b) Five-cycle grid, 132-kv single phase, equivalent to 4,500,000 kva at 230 kv three phase

(c) Five-cycle grid, 44 kv across each grid, equivalent to 4,800,000 kva at 152 kv three phase

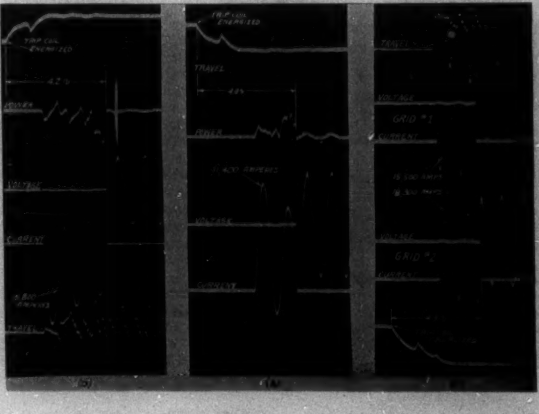

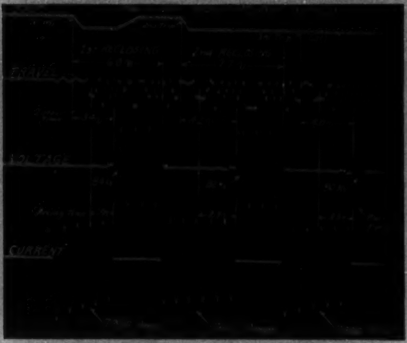

Figure 8 (above left). 35-cycle reclosing duty on 161-kv multiflow deion grids

Interruption of 12,200 amperes at 88 kv to ground, equivalent to 3,200,000 kva three phase, reclosed in 29.5 cycles, second interruption of 9,500 amperes. Both operations within three cycles each

Figure 9 (left). 20-cycle reclosing duty on 161-kv multiflow deion grids

Interruption of 11,100 amperes at 88 kv to ground, equivalent to 2,900,000 kva three phase, reclosed in 20 cycles, second interruption of 10,000 amperes. Both operations within four cycles each

Figure 10 (above right). Eight-cyle double reclosing duty on 161-kv multiflow deion grids

Three interruptions averaging 7,500 amperes at 88 kv to ground, equivalent to 2,000,000 kva three phase, reclosed in 6.9 and 7.7 cycles. All operations within five cycles each

ground voltage, it is theoretically possible to subject the half pole to twice as much duty as would be the case when testing the complete pole unit. However, this test may be deficient in three respects. In the first place, the voltage distribution at the time of interruption is such that more than half of the recovery voltage appears across one of two breaks in a grounded steel-tank breaker. In the second place, the voltage between the energized terminal and the tank under this special test condition is only one half of normal and, therefore, the possibility of flashover through gas bubbles is not adequately checked. In the third place, the total stress on the pole unit with regard to physical shocks and total volume of gas produced is only one half the value to be expected with the whole pole unit functioning at full power.

The question of voltage distribution can be minimized if some controlling means such as a suitable resistor is used across each of the interrupters so as to assure a substantially equal division of voltage between the two halves of the breaker. Then, insofar as the ability of the half pole to interrupt its rated voltage and current is concerned, this type of test may be considered valid.

The fourth test method, connection *D* of Figure 3, of applying a three-phase short circuit to the single-test pole unit has been used in European high-power laboratories for many years.[6] Two phases from the power transformers are connected to the main terminals and the third phase grounded and connected by a flexible shunt inside the breaker to the moving contact cross arm. Line-to-line test voltage is thus applied to each half of the pole unit, although it should be recognized that the currents are out of phase and also that the first pole to clear only gets 87 per cent of the value which the second pole clears. Nevertheless, this test has the advantage of developing the full amount of arc energy in the single-pole unit. Also, the electromagnetic stresses and the expulsion effect on the tip of the moving contact are more equally balanced. Instead of calculating the equivalent three-phase short-circuit duty as three times the three-phase laboratory output, it seems reasonable to apply the same criterion used in method *C* of six times the maximum duty on the most highly stressed half of the pole unit which gives a three-phase equivalent factor of $6\sqrt{3}$, or 3.46.

Short-Circuit Tests Above 3,500,000 Kva

A number of very high power interruptions have been made during the development and verification of high-voltage breakers for 3,500,000 kva using the test methods outlined here. For instance, the three-cycle 230-kv breaker for 3,500,000 kva was given a single-phase test at normal line-to-ground voltage of 132 kv interrupting a total asymmetrical current of 10,900 amperes. This is a direct test of 1,440,000 kva on the single test pole, equivalent to 4,300,000 kva three phase. As a further check on the interrupting ability of this breaker, 87 per cent of line voltage or 198 kv was applied to the single-pole unit, and a short-circuit current of 6,300 amperes cleared satisfactorily. This is equivalent to 2,500,000 kva on the basis of current alone, but if the 50 per cent additional voltage is included, the equivalent kva for a three-phase short circuit on a 345-kv

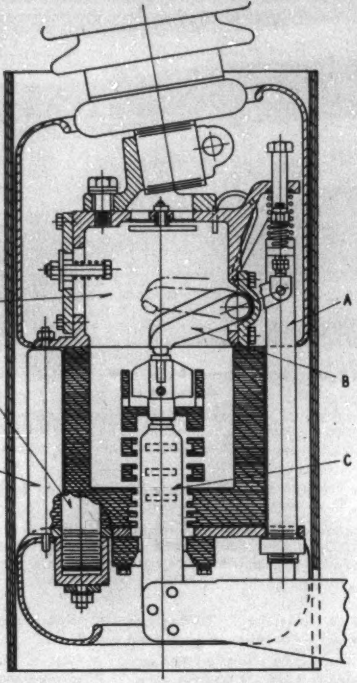

Figure 11 (left). 5,000,000-kva multiflow deion grid design for five-cycle interrupting time

Side operating rod *A* opens upper contact *B* simultaneously with opening of main contact *C*. Large oil reserve in pressure chamber *D*; strong tie rods *E*; resistor *F* for voltage distribution control

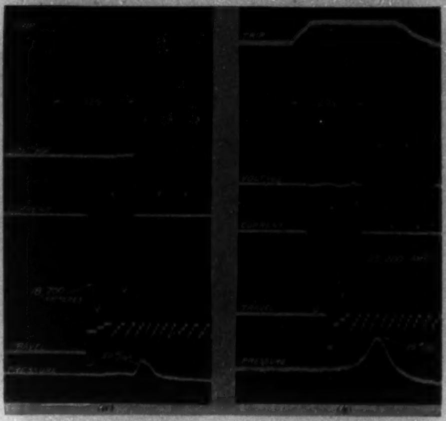

Figure 13 (above). High-power interrupting tests on multiflow deion grids using half-pole test method

(a). 230-kv interrupter, 18,700 amperes at 66 kv across half pole, equivalent to 7,400,000 kva three phase

(b). 161-kv interrupter, 25,200 amperes at 44 kv across half pole, equivalent to 6,600,000 kva three phase

system may be considered to be 3,750,000 kva. A still higher current of 12,200 amperes was interrupted with one half of the pole unit shunted out and 66 kv applied to the other half. Assuming that all six similar units of the complete three-pole breaker were handling the same duty, this would be equivalent to 4,800,000 three phase kva.

A design of 230-kv five-cycle multiflow grids was tested up to 9,400 amperes with 132 kv across the single pole, which is a direct test equivalent to 3,700,000 kva. The oscillogram for this test and the three 230-kv tests mentioned in the previous paragraph are shown in Figure 6.

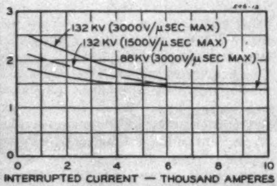

Figure 12. Arcing time in high-voltage multiflow deion grid fairly constant over wide range of voltage, interrupted current, and voltage recovery rate

Although 138-kv breakers could be tested at the line-to-ground voltage of 76 kv, maximum power can be obtained at the standard laboratory test voltage of 88 kv, and the slightly higher voltage demonstrates some additional factor of safety and voltage-interrupting ability. Three high-power tests are shown in Figure 7 on a 138-kv breaker. The maximum current of 15,800 amperes at 88 kv corresponds to 3,800,000 kva at rated voltage and 4,200,000 kva at the actual test voltage. The exceptional interrupting ability of this particular multiflow deion grid was demonstrated by interrupting the maximum capacity of the laboratory with full-line voltage across the single pole. This test of 11,400 amperes with 132 kv on a single pole was interrupted satisfactorily, being actually equivalent to a 230-kv three-phase short circuit of 4,500,000 kva. A three-phase short-circuit test applied to the single pole with 44 kv across each grid also was obtained, clearing 18,300 and 15,500 amperes in the two interrupters. For this test, the short-circuit power on a three-phase basis at rated voltage corresponds to 4,800,000 kva.

Ultrahigh-Speed Reclosing

The value of high kilovolt-ampere laboratory interrupting capacity tests is unusually important in the case of high-speed reclosing. Under these conditions, the gas generated from the first operation might be expected to produce conditions that would affect the interrupting ability on a succeeding operation after an interval as short as 20 or 30 cycles. It is, therefore, very hazardous to extrapolate from low-kva tests on high-speed reclosing duty cycles to estimate the interrupting ability at high kva. It has been found that the multiflow deion grids are readily applied to ultrahigh-speed reclosing duty cycles, as illustrated in the following examples of tests made with a 161-kv five-cycle multiflow grid design.

The first test illustrated in Figure 8 is an interruption of 12,200 amperes at 88 kv across the single pole on a 35-cycle reclosure which corresponds to an interrupting duty of 3,200,000 kva. With the timing altered to give a 20-cycle reclosing operation, the next film in Figure 9 illustrates the interruption of 11,100 amperes at 88 kv across a single pole.

During an experimental test aimed at

approximately ten-cycle reclosing, a double reclosure was obtained with only seven to eight cycles for the reclosing intervals as shown in Figure 10. The current cleared was 7,900 amperes at 88 kv, corresponding to a three-phase fault of 2,100,000 kva, and, in spite of the extraordinarily heavy duty of three operations at such close intervals, every interruption was accomplished within five cycles and the external demonstration on the breaker did not appear much greater than was to have been expected on a normal 20-cycle reclosing duty. This test gives evidence of a large factor of safety in interrupting ability of the multiflow deion grid, both for standard interrupting operations and for high-speed reclosing duty cycles. It has become evident that, while the interrupting capacity is reduced by very rapid reclosing operations, there is no inherent limitation on the rapidity with which a circuit breaker can be reclosed and interrupt a second fault. With such an effective circuit interrupter, the design problem becomes one of providing an adequate mechanism and control scheme for these rapid duty cycles. The real limit will be set by the minimum time which must elapse after the first interruption for deionization of the line flashover to avoid re-establishment of the fault when voltage is reapplied, unless the fault is permanent.

A 5,000,000-Kva Circuit-Breaker Design

As a result of confirmation gained from these and many hundreds of other high-power laboratory tests on a variety of high-voltage circuit interrupters, some showing good performance and others failing completely, the principal design features of a high-voltage oil circuit breaker capable of meeting an interrupting capacity rating of 5,000,000 kva have become fairly clear. With substantially constant arcing time in the high short-circuit current range, the gas generation and tank pressure become almost directly proportional to interrupting rating. This means that the tank volume should be increased in proportion to the rating in order to keep adequate electrical clearances during arc rupture. Other than an increase in the size and strength of the steel tanks, there need be relatively few differences in the main structural features as compared to present day 2,500,000- and 3,500,000-kva designs.

The heart of the circuit breaker is, however, the arc-extinguishing device. Figure 11 shows a sectional view of a multiflow deion grid designed for a 5,000,000-kva rating with five-cycle interrupting time. The four insulating tie rods have been increased in strength and the volume of the upper pressure chamber enlarged substantially. This assures a sufficient quantity of oil for high-speed reclosing where the interval between operations is too short to permit refilling. No appreciable change is required in the interrupting section other than a slight increase in size of the fibre plates to accommodate the large tie rods. The resistor of about $1^{1}/_{2}$ megohms connected between the top and bottom of the stack assures approximately equal division of voltage between the pair of interrupting units in each pole of the breaker.

The suitability of the multiflow deion grid interrupters for extrapolation to higher powers is shown by the characteristic curves of Figure 12. The arcing time, particularly at the higher currents, is very nearly the same for tests at voltages of either 88 kv and 132 kv. Also, a change in voltage-recovery rate of two to one made only a slight change in the arcing time, indicating positive arc-interrupting action.

In order to determine the arc-rupturing performance at extremely high currents, the half-pole test method was applied to experimental units of a design similar to Figure 11, one built for a 230-kv five-cycle rating and one for a 161-kv five-cycle rating. Oscillograms of two tests are shown in Figure 13, the first being an interruption of 18,700 amperes with 66 kv across one grid unit, this being one half the normal line-to-ground voltage for a 230-kv system. The corresponding three-phase short-circuit power is 7,400,000 kva. There was very little external evidence of this tremendous power being interrupted, the maximum impulse pressure being only 50 pounds per square inch. The laboratory circuit on which this test was made had the very high recovery rate of 3,100 volts per microsecond. Test *B* of Figure 12 was made with 44 kv across a single 161-kv grid unit, corresponding to one half the line-to-ground voltage for a 154-kv system, the circuit-voltage recovery rate being 2,500 volts per microsecond. The interrupted current of 25,200 amperes amounts to 6,600,000 kva on a three-phase basis.

These and other tests indicate that 5,000,000-kva ratings for high-voltage oil circuit breakers equipped with multiflow deion grids are entirely practical.

Conclusion

By utilizing special high-power laboratory test methods such as the application of short circuits to only one half of a single breaker pole, sufficient information has been obtained concerning the performance of modern oil circuit breakers to indicate interrupting ability considerably above present ratings. Certain high-speed reclosing breakers have been shown apparently to have no inherent limitation in the shortness of the time interval between successive operations, although there is some reduction in interrupting capacity. The accumulation of considerable short-circuit test data at very high powers on high-voltage oil circuit breakers equipped with multiflow deion grids gives considerable assurance that, when needed, circuit breakers having ratings of 5,000,000 kva can be made available.

References

1. Transient Recovery Voltages and Circuit-Breaker Performance, R. C. VanSickle. AIEE Transactions, volume 61, 1942, November section, pages 804–13.

2. Arc Energy Fixes Circuit-Breaker Pressures, W. M. Leeds. *Electrical World*, volume 98, December 26, 1931, pages 1138–41.

3. A Multiorifice Interrupter for High-Voltage Oil Circuit Breakers, L. R. Ludwig, W. M. Leeds. AIEE Transactions, volume 62, 1943, March section, pages 119–25.

4. High-Voltage Oil Circuit Breakers for Rapid Reclosing Duty, A. W. Hill, W. M. Leeds. AIEE Transactions, volume 63, 1944, March section, pages 113–18.

5. High-Capacity Circuit-Breaker Testing Station, J. B. MacNeill, W. B. Batten. AIEE Transactions, volume 61, 1942, February section, pages 49–53.

6. High-Power Oil Circuit Breakers, J. Biermans. *Elektro Journal*, number 4, February 10, 1929, pages 31–36.

Vibration Insulation and Structural Rubber

J. A. CONNON
NONMEMBER AIEE

SENSITIVE electric and electronic devices are what might be termed the "nerve centers" of modern war equipment. The men in airplanes, ships, and tanks depend upon them for communication, for fire and direction control, and for the detection of enemy targets. The role of these devices in nonmilitary applications is familiar.

To ensure accurate functioning and prolonged life, these units must be protected from damaging vibration and shock. It is the purpose of this paper to present to the engineer concerned with the protection of delicate equipments a compilation of information, on the fundamentals of mechanical vibrations and the properties of structural rubber, which otherwise could be obtained only through critical study of a large volume of existing data.

Vibration is, in general, a periodic motion essentially sinusoidal in character. It is practically always objectionable and its elimination or insulation is desirable. The term vibration elimination, it is to be borne in mind, is not synonomous with vibration insulation. Vibration elimination connotes correction of the condition causing vibration, whereas vibration insulation deals with diminishing the amount of transmitted vibrational energy.

Vibration-insulation problems can be classified in two categories:

1. Problems involving the insulation, from its surroundings, of a unit originating vibratory disturbances, for example, an airplane engine.

2. Problems involving the protection of a delicate unit from external vibratory disturbances, for example, a radio set, an instrument panel.

Problems in either category can be solved by supporting the unit on a correctly designed, resilient suspension. Rubber mountings, or rubber springs as they are in reality, are used extensively for this purpose; they are both practical and economical.

Requisite to the proper appraisal and solution of vibration-insulation problems is an understanding of the fundamentals and theory of mechanical vibrations.

Fundamentals of Mechanical Vibrations

Consider a system consisting of a mass supported on a spring and constrained by guides so that only vertical movements are possible (Figure 1). A mechanical system of this sort, the geometrical position of which can be expressed at any instant by one number only, is said to have one degree of freedom. Assume that damping is absent and that the spring deflects according to Hooke's Law (within the elastic limit of any body the ratio of the stress to the strain produced is constant).

The deflection of the spring due to the weight of the mass is known as the *static deflection* (*d*). If the force required to deflect the spring a given amount is relatively great, the spring is said to be "stiff." Spring stiffness is denoted by the *spring constant* (*k*) defined as the number of pounds required to deflect the spring one linear inch.

If the mass be displaced by a single push or pull and then released, it will oscillate in free vibration above and below its equilibrium position (the original rest point) at a frequency known as the *natural frequency*. The natural frequency of a spring system is a function of the static deflection.

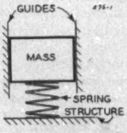

Figure 1. A single-degree-of-freedom system

$$f_n = \frac{188}{\sqrt{d}} \qquad (1)$$

f_n = natural frequency (cycles per minute)
d = static deflection (inches)

It can be seen immediately that high natural frequencies correspond with small deflections (refer "natural frequency versus static deflection" curve, Figure 2).

Assume now that the mass in Figure 1 is a machine in which a certain amount of unbalance exists. When the machine is running, it is acted upon by a vertical periodic force (deriving from the unbalance) which causes it to vibrate (a problem in category 1). This impressed force, one of three acting on the mass (the others are inertia force of the mass and the spring force) has a maximum value F and a frequency f_f. The vibration causes the already statically deflected spring alternately to be compressed and elongated a small amount below and above its equilibrium position, hence it exerts on, or transmits to, the supporting structure a force whose maximum value it can be shown is

$$X = F\frac{1}{1-\left(\frac{f_f}{f_n}\right)^2} \qquad (2)$$

X = transmitted force
F = impressed force
f_f = impressed frequency
f_n = natural frequency

The ratio of the transmitted force to the impressed force is known as transmissibility.

$$\text{Transmissibility} = \frac{\text{transmitted force}}{\text{impressed force}} = \frac{X}{F} \qquad (3)$$

The ideal, of course, is to have transmissibility equal to zero (the practical aim is to make it as small as possible). It is evident that the value of transmissibility depends solely upon the relative values of the impressed and natural frequencies,

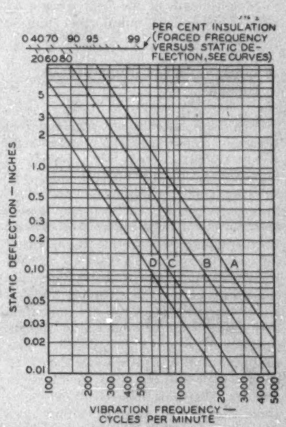

Figure 2. The relationship between natural frequency and static deflection, and per-cent insulation for various combinations of forced frequency and static deflection in an undamped, single-degree-of-freedom system

Curve *A*—Forced frequency versus static deflection for 93-per-cent insulation
Curve *B*—Forced frequency versus static deflection for 81-per-cent insulation
Curve *C*—Forced frequency versus static deflection for 0-per-cent insulation
Curve *D*—Natural frequency versus static deflection

Paper 45-76, recommended by the AIEE committee on air transportation for presentation at the AIEE winter technical meeting, New York, N. Y., January 22–26, 1945. Manuscript submitted November 15, 1944; made available for printing January 4, 1945.

J. A. CONNON is product engineer, war products division, United States Rubber Company, Los Angeles, Calif.

The author acknowledges the assistance of his associates in the preparation of this paper and expresses his appreciation for the permission granted by the United States Rubber Company to publish photographs of its products and the results of tests carried on in its laboratories.

and that, fundamentally, vibration insulation does not entail "absorption" of vibratory energy in the spring but is achieved through the "mismatching" of frequencies.

A plot of transmissibility against *frequency ratio* (f_f/f_n) is given in Figure 3. Examination of this curve reveals that when $(f_f/f_n) < \sqrt{2}$, the transmissibility is greater than unity. Theoretically, infinite transmitted forces (and displacement amplitudes) can occur at resonance $(f_f/f_n = 1)$. Insulation, or reduction of transferred vibration, prevails only when $(f_f/f_n) > \sqrt{2}$.

The value of ***per-cent insulation*** is given by the following expression:

$$\text{Per-cent insulation} = (1 - \text{transmissibility}) \times 100 \qquad (4)$$

The 0-, 81-, and 93-per-cent insulation curves in Figure 2 are plots of arbitrarily selected solutions of equation 4.

In the preceding section a system acted upon by a single external force and having only vertical motion was considered. The forces acting on, and the motions of, a real system are considerably more complex. A rubber mounting, too, is a more complex entity than a hypothetical spring chosen for the first illustration.

Imagine a device, such as a radio set, that must be mounted protectively in an airplane (a problem in category 2). Assume, for the sake of simplicity, that it is a rectangular mass whose center of gravity is located at its geometric center. Assume, too, that identical resilient mountings are installed under the set, one at each of the four base corners (Figure 4A). A unit mounted in this manner has six degrees of freedom, that is, six motions are possible at any instant: translational motion along each of three mutually orthogonal axes (for convenience these axes can be labelled X, Y, and Z, and considered to have their origin (O), at the neutral position of the center of gravity of the mass), and rotational motion around each of these axes.

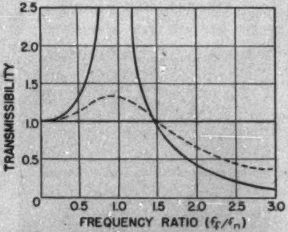

Figure 3. Values of transmissibility for various values of (f_f/f_n) in an undamped system (solid line); the effect of damping on transmissibility (dash line)

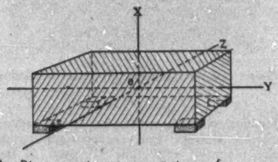

A—Diagrammatic representation of a mass mounted on springs

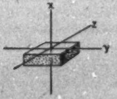

B—Diagrammatic representation of a rubber spring

Figure 4

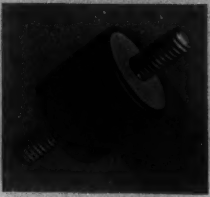

Figure 7 (left). Cylindrical mounting

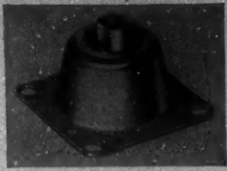

Figure 8 (right). Cylindrical mounting enclosed in safety cup

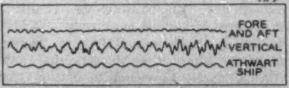

Figure 5. A record of the translational displacement components of a rigidly mounted unit

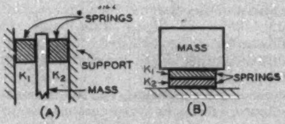

Springs in parallel

Springs in series

Figure 6

The motions of a mounted unit of given mass and moments of inertia are dependent upon:

1. Character of the excitation.
2. Elastic constants and damping of the mountings.
3. Location of the mountings.

In general, the vibratory forces at any location in a structure occur in several directions at different frequencies and with different amplitudes. These forces are both translatory and rotary in nature. The curves shown in Figure 5 are illustrative. They represent the translational-displacement components (simultaneously measured along three axes) of a rigidly mounted unit. (Displacements and accelerations rather than forces ordinarily are measured.) The data were taken from the study of a particular problem. It is to be noted that the vertical amplitude is considerably greater than either the athwartship or fore and aft amplitudes and that the fore and aft frequency differs considerably from the vertical and athwartship frequencies. A similar record (not shown) of the rotational displacements was made in this study.

The characteristics of a structure have a great deal to do with determining the nature of the vibratory forces at any particular location. The principal frequencies usually are related, simply, to those of rotating or reciprocating mechanisms installed elsewhere in the structure. The amplitudes of, and the directions in which the vibratory forces occur are, in the general case, not in accordance with any simple relationship and are not readily predictable.

Attention now will be given to the elastic properties of rubber mountings. A rubber mounting (Figure 4B) can be considered to have three mutually orthogonal elastic axes, x, y, and z, the origin located at the neutral position of the point of application of the load. In the general case, the rectilinear elastic constants, or spring rates, along these axes are unequal. (The torsional constants around them, ordinarily neglected, are also unequal.) The relationship among the constants is dependent primarily upon the design of the mounting.

Since the elastic constants differ, the deflections corresponding to a given load applied successively along each axis will differ. A rubber mounting, therefore, for any given loading has three different, rectilinear, natural frequencies, one along each axes.

In a normal installation the load on a mounting is applied in the direction of one axis; the x axis, for example. The natural or resonant frequency in this direction can be calculated from the observed deflection. The coexistent resonant frequencies in each of the other directions can be computed by substituting for d in equation 1 the amount the mounting would deflect if the load, actually applied along the x axis, were applied successively along the y and z axes.

It is perhaps well to point out that if springs are combined in parallel (Figure 6A), or in series (Figure 6B), the combined or over-all spring constants of the combinations are as follows:

In a parallel system

$$K = k_1 + k_2 + k_3 + \dots k_n$$

In a series system

$$K = \frac{1}{\frac{1}{k_1} + \frac{1}{k_2} + \frac{1}{k_3} + \dots + \frac{1}{k_n}}$$

K = over-all spring constant

$k_1, k_2, k_3, \dots k_n$ = spring constants of the individual springs

The deflections, hence the natural frequencies, of such combinations are functions of the over-all constant.

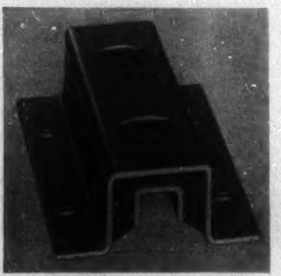

Figure 9. Safety channel mounting

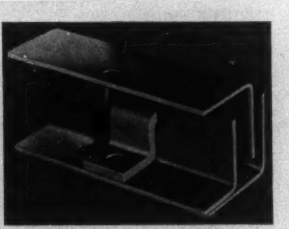

Figure 10. Heavy-duty three-angle mounting

In any rubber-suspension vibration system there is a damping force which originates in the mountings and acts on the mass. The effect of this damping force is to prevent the build-up of large forces and amplitudes at or near resonance and to decrease the efficiency of mountings at frequency ratios greater than $\sqrt{2}$. Damping rounds off the peak of the transmissibility curve and moves it everywhere closer to the value one (Figure 3). The amount of damping, therefore, must be a compromise between the good low-frequency effects and the poor high-frequency effects. It is desirable ordinarily to have the minimum damping that satisfactorily will limit resonant vibration.

It must be remembered that the rapidity with which a mechanism is brought through resonances as its speed is changed has an influence on the amount of build-up. Restricting the operation at or near resonances to a short-duration transient obviously is recommended.

Several representative rubber mountings are shown in Figures 7 through 13. It will be observed that, to facilitate its application as an elastic support, rubber generally is adhered to metal. The mounting in Figure 7 is the simplest type; a cylinder of rubber with studs adhered to the ends. It can support a load in either compression, that is, normal to its ends, or in shear, parallel to the end planes. This type of mounting has relatively low spring rates in all directions parallel to the end planes. Figure 8 illustrates a refinement of this type incorporating a safety cup; it is designed to support a load in compression. It is well in most cases to arrange the rubber supports so that in case of complete failure of the rubber, due to accident or fire, the mounted unit still will be supported by some sort of interlocking metal device. Figures 9 and 10 are, respectively, illustrations of channel, and three-angle-type mountings. These mountings have relatively low spring constants along their longitudinal and vertical axes. In either mounting, the longitudinal and vertical spring rates are equal. An unusual disk-type mounting which has low and substantially equal spring rates along all three elastic axes is shown in Figure 11. A special-purpose variant of this design is the meter mounting shown in Figure 12. Figure 13 illustrates a nonadhered, corrugated-disk mounting suited for relatively high frequencies.

Since, as was stated, the translational vibratory forces in a structure may occur in several directions and at different frequencies, it is expedient:

1. To use mountings which provide the greatest deflections commensurate with stability.
2. To install mountings whose highest natural frequency is sufficiently far below the lowest expected impressed frequency, to ensure adequate insulation in all directions.
3. To install the "softest" axis or axes of the mountings parallel to the direction or plane in which the greatest disturbance occurs.

In a given excited system, the elastic constants of the springs, together with their disposition with respect to the neutral position of the center of gravity of the mounted unit and the moments of inertia of the unit, determine the frequencies at which rotational, or rocking, resonances occur. The distances of the mounts from the axes of the unit are the arms of the moments tending to produce angular motion about them. The moments of inertia of the unit express, of course, the rotational properties of the mass.

The calculation of the frequencies at which rocking resonances occur will not be dealt with in this paper. Suffice it to say that in most practical systems:

1. The frequencies at which the three rotational resonances occur are in the neighborhood of the translational resonances.
2. In general, their presence tends to extend the range of frequencies over which transmissibility exceeds a value of one. The accelerations arising from them can be as destructive as those related to translational resonances. Hence, their insulation or prevention is desirable.
3. If rotary excitation is negligible, the rocking modes ordinarily can be prevented by means of a symmetrical center-of-gravity suspension, that is, one in which the mountings are so chosen and so located in a plane passing through the center of gravity of the mounted unit that the sum of the moments about the center of gravity, around the X, Y, and Z axes, equals zero. In such a system, translational excitation does not cause angular motion, and vice versa. A center-of-gravity suspension possesses, too, stability advantages.
4. In a noncenter-of-gravity suspension, rotary excitation is not a necessary condition for rocking.

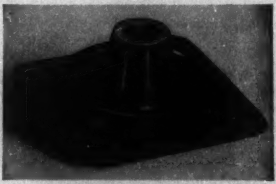

Figure 11. Disk mounting

Figure 12. Meter or instrument mounting

5. In a noncenter-of-gravity suspension in which the mountings are located beneath the unit, diminution of the range over which rocking resonances occur can be achieved through the use of mountings having substantially lower elastic constants along horizontal axes.

An indication of the effects some of the factors just discussed can have on a system may be obtained from an examination of Figures 14, 15, and 16. The transmissibility curves in these figures were plotted from shake-table data. It can be seen that superior insulation was achieved in the case in which mountings having relatively-lower natural frequencies in the horizontal directions were used under the unit (Figure 15). Even more marked improvement in insulation was obtained when these same mountings were placed in a plane through the center of gravity of the unit (Figure 16).

It may be concluded that the best method of vibration mounting any type of unit is a center of gravity suspension on mountings, of suitable capacity, having equal and low natural frequencies along all three elastic axes.

Structural Rubber

The word "rubber" when used in this section refers to natural rubber.

The following information is primarily qualitative rather than quantitative. It is presented with the belief that familiarity, in a general way, with the properties of rubber compounds is helpful to the engineer concerned with the use of rubber mountings.

Rubber, when used as mechanical building material to support a load, is known as structural rubber. In this capacity it can be stressed in the following five ways: shear, compression, tension, torsion, and flexure.

It is to be noted that rubber, like water, is practically incompressible (Figure 17). It is said to be stressed in compression when supporting a load which tends to squeeze it.

Most vibration mountings are designed to be loaded in either compression or shear. Tension is not employed extensively, because a slight tear or cut in rubber stressed in tension can produce rapid failure. Torsion may be considered a special case of shear. Flexure can involve compression, shear, and tension.

The stress-strain relationships for a rubber compound are given by the shear (Table I), compression, and tension moduli. These moduli are not, strictly, constants. Because of this fact, and because of other properties of rubber to be described, calculations in accordance with the theoretical formulas given in the first part of this paper will be slightly in error when rubber is the spring material under consideration.

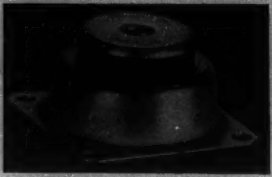

Figure 13. Cup mounting

It is well to discuss "durometer" and its significance with respect to modulus. The durometer values of compounds of the type used in mountings range normally between 30 and 70. These values are ascertained by means of the Shore durometer (type A), an instrument which measures the hardness of a rubber surface in terms of the indentation produced in the surface by a small, flat-tipped, tapering needle subjected to a practically constant indenting force. The arbitrary scale of this instrument runs with increasing hardness from 0 to 100. The relationship connecting durometer hardness with modulus is at best only approximate. Although useful for roughly determining the modulus of a stock, durometer is strictly a measure of only local surface hardness. The moduli of a stock provide the more accurate statement of its load carrying, or structural characteristics.

The shear deflection of rubber is inversely proportional to the shear modulus.

The compression deflection is a function of shape, expressed by area ratio, as well as of the compression modulus. The area ratio of a slab of rubber is the ratio of the load-bearing area to the area free to bulge. Slabs having high (2.50) area ratios deflect a smaller percentage of their thickness than slabs of the same compound having low (0.25) area ratios.

The moduli of rubber compounds vary small amounts with temperature and with the amplitude and frequency of impressed vibration as well as with the static strain to which the rubber is subjected.

At low temperatures rubber stocks stiffen. For a given compound the temporary changes in moduli due to chilling depend upon the chill temperature, the duration of the chill, and the strain during the chill. The temperature at which the moduli increase rather suddenly is generally between −40 degrees Fahrenheit and −60 degrees Fahrenheit, depending upon the compound.

At temperatures above 170 degrees Fahrenheit ordinary structural rubber compounds begin to soften. The effect of heat aging becomes pronounced and, under strain, rubber acquires a permanent set or deformation.

The static moduli decrease with increased strain.

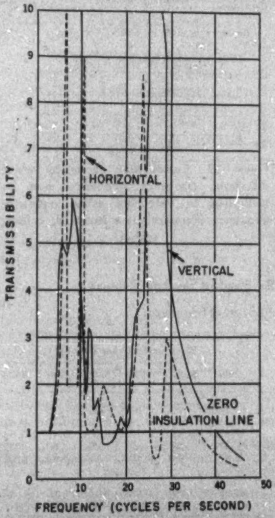

Figure 14. Shake-table performance of a unit mounted on rubber springs installed underneath the unit; the ratio of the horizontal elastic constants to the vertical was approximately 2:1

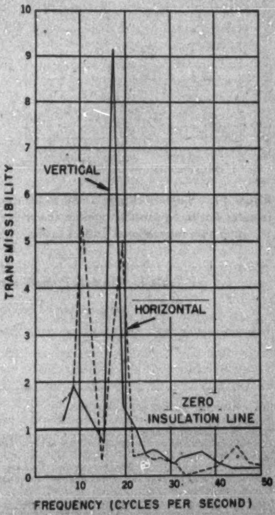

Figure 15. Shake-table performance of a unit mounted on rubber springs installed underneath the unit; the ratio of the horizontal elastic constants to the vertical was approximately 1:1

The moduli of rubber are greater for vibratory stress than for static (0 frequency stress). It is interesting to note that for mountings operating at low temperatures, the stiffness, and consequently the natural frequency, will be greater than that indicated by the increased static moduli alone, for the dynamic moduli are more sensitive to temperature changes than are the static.

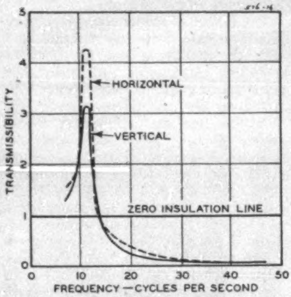

Figure 16. Shake-table performance of a unit mounted on rubber springs installed in a horizontal plane passing through the center of gravity; the ratio of the horizontal elastic constants to the vertical was approximately 1:1

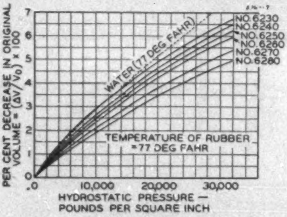

Figure 17. Volume change of 30 to 80 durometer stocks, hydrostatic pressure (curve for water from International Critical Tables)

For exact prediction of the natural frequency of a rubber mounting under load, the value calculated from the static deflection in equation 1 has to be adjusted. The frequency-factor curves in Figure 18 show the factor by which the calculated natural frequency should be multiplied in order to obtain the actual natural frequency. In most calculations this refinement can be neglected, particularly when dealing with the softer rubbers.

Damping is usually expressed as the ratio of the actual damping force, C, to the critical damping force C_c. The critical damping force is that force which is just sufficient to prevent oscillatory motion of a particular system when disturbed. The values of the ratio C/C_c for structural rubber compounds are in the neighborhood of 0.08.

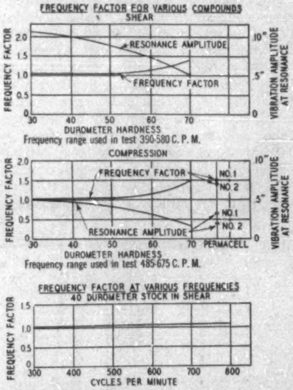

Figure 18. Curves show factor by which calculated resonance frequency must be multiplied to determine actual resonance frequency (Permacell is a structural, cellular rubber)

Damping ordinarily limits the build-up of displacement amplitude at resonance to eight or ten times that of the impressed amplitude; it is possible for magnifications of from 15 to 20 to occur.

The damping forces exerted by rubber mountings derive from a property of the material known as hysteresis or internal friction. When rubber is deformed and allowed to return to its original position the load–deflection curve is not strictly a single line but a loop similar in shape to that shown in Figure 19. The area within the loop represents energy transformed into heat; "absorbed" by the mounting. This quantity is known as the hysteresis loss. Since rubber is a poor conductor of heat, its temperature will rise when it is excessively, repeatedly, and rapidly deformed.

Because of hysteresis, the amplitude of vibration of a system set into free vibration will become less with each successive oscillation. It has been found that each successive amplitude, measured on the same side of the equilibrium position, will be less than the former by a factor which is approximately constant

$$\frac{A_1}{A_0}=\frac{A_2}{A_1}=\frac{A_3}{A_2}=\frac{A_4}{A_3}\ldots\ldots=10^{-\kappa}$$

The quantity κ is called the logarithmic decrement of amplitude. Values for logarithmic decrement, successive-amplitude ratio, and per-cent energy loss due to hysteresis are given in Table I for rubber at 70 degrees Fahrenheit. These quantities decrease at higher temperatures.

When rubber is under load, there is a gradual increase in deflection which is referred to as drift. If the load is removed it is found that it has caused a permanent change in the unstressed dimensions of the rubber which is referred to as permanent set. Drift increases rapidly for a short time (a matter of hours) after the load is first applied and then the curve levels off to practically a horizontal line. The drift of rubber supporting a vibrating load will be greater than that for the same com-

Table I. Physical Properties of Six Standard Structural Rubbers

Temperature of Rubber, 70 Degrees Fahrenheit

	Structural Rubber Number					
	5709	5133	5638	5235	5691	5623
Shear modulus, pounds per square inch	50	70	95	140	195	
*Logarithmic decrement of amplitude (referred to base 10)	0.041	0.055	0.14	0.23	0.35	0.47
*Successive amplitude ratio	0.91	0.88	0.72	0.59	0.45	0.34
Per-cent energy loss due to hysteresis, per cycle of vibration	17	22	47	65	80	89
Specific heat	0.47	0.43	0.40	0.38	0.35	0.33
Thermal conductivity in Btu, per square foot per hour for a temperature gradient of one degree Fahrenheit per inch thickness	0.97	1.04	1.08	1.15	1.26	1.33
Velocity of sound in rubber rods, feet per second	115	165	210	345	750	

* The logarithmic decrement given here represents the negative of the power to which 10 must be raised in order to obtain the ratio of any two consecutive amplitudes (on the same side of zero deflection) as unexcited vibration dies out. For instance, if the logarithmic decrement is 0.2, the ratio of one amplitude to the preceding one is $10^{-0.2}=\frac{1}{10^{0.2}}=\frac{1}{1.585}=0.631=$ successive amplitude ratio.

(Ordinarily logarithmic decrement is referred to Napierian log base e and, if such values are required, they would be 2.30 times the values given here.)

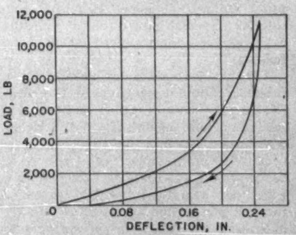

Figure 19. Hysteresis loop for a typical rubber compound

pound supporting a static load at the same temperature. Drift is greater for severe vibration than for mild vibration; it is greater at high temperatures than at low.

The failure of a rubber mounting, in time, partly is due to the fact that the rubber member is under load during service and partly is due to the fact that it is fatigued by vibration. The dynamic-fatigue life of a rubber part, defined as the total number of repeated cycles of vibration required to rupture it, is dependent on the initial strain, the amplitude of vibration, the temperature of the rubber, the ingredients and state of cure of the rubber, and external destructive variables such as sunlight, ozone, and oil.

Since, at the present time, synthetic-rubber compounds must be substituted for natural-rubber compounds in some mounting applications, their structural properties are being explored intensively. To date they have not exhibited the versatility of natural-rubber compounds as structural materials.

References

1. Mechanical Vibrations, J. P. Den Hartog. Second edition, 1940.

2. Vibration Problems in Engineering, S. Timoshenko. Second edition, 1937.

3. Some Physical Properties of Rubber, United States Rubber Company. Second edition, 1941.

4. Rubber Springs, Walter C. Keys. *Mechanical Engineering*, May 1937.

Electrolysis and Corrosion of Underground Power-System Cables

L. J. GORMAN
MEMBER AIEE

ELECTROLYTIC CORROSION is recognized universally as a major problem in the maintenance of underground metallic structures. This is particularly true in the case of underground cable and piping systems. The subject is of a primary interest to cable- and pipe-operating utilities, and a great deal of study and research is being devoted to electrolytic corrosion by utility engineers throughout the country.

The following is a summary of the principles and methods which are the outgrowth of long experience with the mitigation of electrolysis and corrosion on the power-system cables of the Consolidated Edison Company of New York, Inc. This system comprises approximately 22,000 miles of underground lead-covered cable operating under a wide variety of soil and duct conditions. Although system experience include both the cable and the gas-piping systems, this paper will deal more particularly with the conditions affecting the cable system.

Practically all of the essential factors involved in present-day problems of electrolysis and corrosion were recognized in the early work on this subject, and presented in the 1921 "Report of the American Committee on Electrolysis" and in other publications of that period.[1,2] In this earlier work emphasis was placed on electrolysis caused by stray electric currents, and little attention was given to the other factors influencing corrosion. During the past 15 or 20 years, the importance of these other factors, notably the influence of various galvanic or electrolytic cells which originate on the metal surface or in its environment, has been more clearly realized. Furthermore, a great deal has been added to our knowledge of the various corrosion processes and their control. Consequently, there has been a considerable change in point of view with respect to electrolysis, particularly in the evaluation of the various factors involved. This has led to important changes in the procedures for electrolysis testing and in the methods used for the mitigation of corrosion.

Electrolytic Corrosion

It is well established that the corrosion of metal in the presence of moisture occurs extensively through electrochemical reactions which are essentially electrolytic processes occurring in various forms of the electrolytic cell. These processes are recognized as an important cause of widespread corrosion on underground structures and as constituting, in many instances, more serious problems than stray electric current or other forms of corrosion. The electrolytic-cell-corrosion processes should be distinguished from stray-current electrolysis where the source of current is external to the system. In the electrolytic cell the corroding current results from electrochemical reactions at the surface of the metal or in its immediate environment and is frequently referred to as galvanic corrosion. Like stray current, the electrolytic-cell processes involve the flow of electric current through an electrolyte and may be treated under the general subject of electrolysis.

The electrochemical theory of corrosion has been covered in detail in the numerous publications on that subject.[3,4,5,6,7] It is desired, however, to call attention to certain of the factors which relate more particularly to electrolytic corrosion of underground cable systems and which appear to have the most influence on the corrosion problems affecting the system under consideration.

Galvanic Potential and Current

In general the rate of corrosion in an electrolytic process depends on the magnitude of the current and the electrochemical equivalent of the metal. With the current densities and other conditions usually found in practice the rate of corrosion of metal may be calculated approximately by Faraday's law. The voltage has no effect on the corrosion except insofar as it determines the current strength. There is no minimum voltage below which electrolysis does not occur. Corrosion by electrolysis usually is localized and results in the characteristic pitting observed in the electrolysis of lead-cable sheath or iron pipe. The pitting is characteristic of both stray-current electrolysis and the electrolytic-cell type of corrosion, and the type of action cannot be distinguished by the appearance of the metallic surface.

The potential and current involved in the corrosion process may originate externally as in the stray-current electrolysis, or they may originate within an electrolytic cell. In the latter case, the cell potential is the algebraic sum of the voltages due to the electrode potentials which result from the relative anode and cathode reactions of the metal electrodes in the particular solution constituting the electrolyte.

The standard electrode potentials for the various metals are given in the well-known electrochemical series. The order of nobility in which the metals appear in the series and their values of potential are determined in standard solutions and under standard conditions which are not usually obtainable in practice. Electrode potentials vary considerably in soil water and frequently the order of nobility is reversed. This is particularly true of metals which are near together in the series. For this reason, the standard electromotive-force series is not directly applicable to the corrosion of metals in contact with soil moisture. The electrode potentials of various metals in sea water have been determined.[8]

Paper 45-59, recommended by the AIEE committee on power transmission and distribution for presentation at the AIEE winter technical meeting, New York, N. Y., January 22-26, 1945. Manuscript submitted November 20, 1944; made available for printing January 4, 1945.

L. J. Gorman is assistant engineer in the electrical engineering department, Consolidated Edison Company of New York, Inc., New York, N. Y.

The author thanks F. E. Kulman, H. F. Koester, and H. C. Wilner for their valuable assistance in conducting the tests and compiling the data used in this paper and acknowledges the work done on the duct surveys by H. P. Simonson, who has since died in the war at sea.

The potential of an electrolytic cell occurring on the surface of a metal in contact with an electrolyte will vary, depending on the condition of the surface, impurities, mechanical strains, and so forth which result in the formation of local cells. If uniformly distributed and closely associated, these cells tend to neutralize each other. Furthermore, the potential of a given metal will vary in different solutions or with different ion concentrations in the same solution. Galvanic potentials also may be produced by differential aeration, that is, by variations in the supply of oxygen to adjacent parts of the same metal surface. This type of cell may occur, for example, in a cable duct where the degree of aeration varies from point to point in the duct because of the accumulation of mud or sediment, or in a congested cable system where the supply of air to the cables in the bottom ducts is more or less restricted. Under these conditions the metal surfaces to which the oxygen supply is restricted will be anodic to the surfaces that are better aerated. Dissimilar metals and dissimilar soils are included as important sources of galvanic potential.

The potentials resulting from such causes as differential aeration, concentration cells, mechanical injuries, and so forth are local in character and usually small, ranging from a few hundredths of a volt to 0.1 volt or 0.2 volt in severe cases. These potentials do not cause serious corrosion under favorable duct conditions. However, severe corrosion has been experienced in ducts where the resistance to the corroding current is low. These local cells may be expected in any duct. Their activity will depend on the duct conditions.

The potentials caused by variations in the soil external to the duct bank may be considerable, depending on the relative characteristics of the soils concerned. For example, anodic potentials amounting to from 0.8 to 1.0 volt have been obtained between the cable sheath and the duct wall, where the duct bank passed through cinder-filled soil. These potentials may be local or extend over a considerable section of the duct bank and may cause severe corrosion in ducts where, otherwise, the conditions are favorable. It is important to distinguish between the purely local type of cell and the type of cell resulting from differences in the characteristics of relatively large masses of soil in which ducts are laid.

Electrolytic cells of the dissimilar-metal type frequently occur between the cable sheath and copper bond wires or bronze splice filling nipples, phase tags, and so forth. Serious local corrosion of the lead sheath may occur where cables with these attachments are exposed to manhole water, or where the sheath and attachments are in contact with wet cement or other covering used to protect the cables. Severe cases of galvanic corrosion have been experienced in water-filled manholes between the lead sheath and zinc-coated oil reservoirs and galvanized manhole hardware. The zinc is anodic to lead, and, when immersed in water with a large quantity of lead, the galvanic action removes the zinc, thus exposing the iron to natural corrosion. Numerous cases of galvanic corrosion of lead have been experienced in iron ducts because of galvanic potentials between the lead and rusted iron. In severe cases, potentials amounting to 0.4 volt have been measured between lead and iron rust to which the lead is anodic under the conditions usually found on the system.

CONTROLLING FACTORS

In a corrosion cell of given open circuit, or static voltage, the current flow will depend upon a multitude of factors, such as polarization, relative anode and cathode areas, circuit resistance, film formation, passivity, hydrogen overvoltage, hydrogen-ion concentration (pH), oxidation, and other chemical reactions in the electrolyte. Some of the factors tend to retard the corrosion process and others tend to increase the corrosion cell activity.

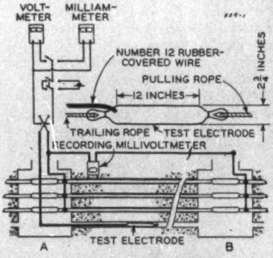

Figure 1. Method and equipment for surveying cable ducts

Of the several factors mentioned the most important in the control of underground corrosion appear to be polarization, hydrogen-ion concentration, circuit resistance and the relative anode and cathode areas. The rate of corrosion under most soil conditions appears to be controlled chiefly by the resistivity of the environment in contact with the cable and the rate at which hydrogen is depolarized or otherwise removed from the cathode areas.

Polarization is a general term used to group the various factors which influence the potential of the electrolytic cell with the passage of current. Polarization may include such factors as the effects of ion concentration at the electrodes, resistance changes resulting from the electrolytic processes, and certain electrode effects which depend on the composition and character of the electrodes. Polarization occurs, in varying degree, at both the anode and the cathode but usually is most pronounced at the cathode. When cathode polarization is predominant, the corrosion process is said to be cathode controlled, and, when anode polarization is predominant, the process is anode controlled. Hydrogen depolarization is effected by its combination with oxygen, or the hydrogen may be removed as a gas. Any agency tending to increase the oxygen available for depolarization will accelerate anode corrosion. Agitation of the electrolyte tends to increase the supply of depolarizing oxygen as well as aids in the removal of hydrogen gas bubbles.

The resistivity of the environment in immediate contact with the cable or pipe seems to be the principal factor in controlling cable-sheath and pipe corrosion. In the case of cable occupying ducts, the resistivity of the duct walls and any water or sediment contained in the duct will determine to a very large extent the amount of corrosion experienced on lead-covered cables. In practice, the contact resistance between the cable and its duct wall and through the duct wall may vary between wide limits in a single duct section, and the severity of the corrosion will be most pronounced at points of low resistance. In most cases a direct correlation has been found between this resistance and cable-sheath corrosion. The influence of duct resistance will be discussed further in another section of this paper.

In the usual case of cable-sheath corrosion, the major component of the resistance exists at the surface of the sheath, and any film formation that will increase this surface resistance is an important factor in controlling the corroding current. The use of certain chemical inhibitors, such as silicates, phosphates, chromates, and so forth, in the formation of protective films on lead sheath has been discussed by Radley and Richards[9] and other investigators. The protective effect of chemical inhibitors artificially applied to cable sheaths and ducts has not been investigated on the system of the Consolidated Edison Company. However, in the usual type of soil and duct water found on the system the natural formation of films does not appear to have any important influence on corrosion.

Wesley[10] has shown that the relative anode and cathode areas have an important influence on cathode polarization. If the cathode area be relatively large, the hydrogen polarization will be correspondingly weak, and anode corrosion will occur at a higher rate than under conditions where the cathode area is equal to or less than the anode area. This factor is of particular importance in selecting metals to be used together in sea water or soil. For example, in the selection of bolts or rivets the metal should be slightly cathodic to that of the structure to which they are attached. Likewise, the solder used in cable splices should have as nearly as possible the same electrode potential as the lead sheath. The relative area effects are most pronounced where attempts are made to protect the cable sheath against dissimilar-metal corrosion by coating the sheath. Any imperfections in the coating will restrict the area of lead exposed and concentrate the corrosion. Furthermore, cement or other coatings used to arcproof cables appear to limit the relative area effect and to concentrate galvanic corrosion of the lead near the point of contact with the cathode metal.

A considerable amount of cable-sheath corrosion has been associated with alkaline soil and duct water. In most cases, the alkalinity is due to the presence of green concrete and frequently occurs in poorly drained ducts in which the accumulated duct water is evaporated slowly by the heat of the cables. This produces a concentration of the alkaline salts dissolved from the duct walls and surrounding soil, and pH values amounting to 11 or 12 have been obtained in severe cases. The action on the cable sheath appears to be chiefly chemical, producing the red or brown oxides of lead. In the usual case the action is aided by small positive potentials acting through a low-resistance electrolyte. In such cases the duct conditions can be improved by flushing the duct with fresh water. In manholes, the alkaline attack occurs most frequently under the cement arcproofing on the cables and splices where the protection used under the arcproofing is inadequate.

In further reference to hydrogen-ion concentration (pH) laboratory experiments indicate that soils having relatively high pH values are anodic to soils of lower pH and that cable passing from one type of soil to the other will tend to discharge current into the more alkaline soil. The potential differences appear to be approximately 0.06 volt for a difference of one in pH value, and the variation with pH seems to be a straight line function. These laboratory tests have been confirmed largely by field observations in which cables passing from a neutral or slightly acid soil into an alkaline soil have been found to be slightly negative with respect to the duct wall in the neutral or acid soil and definitely positive in the alkaline soil.

Stray-Current Electrolysis

The principles underlying stray-current electrolysis are too well known to require a further explanation at this time. The stray-current problem is mentioned, however, to call attention to the status of stray current as a factor in cable-sheath corrosion.

In Greater New York electrolysis from stray railway current has been reduced to minor proportions through the co-operative efforts of the several electric transit systems and the cable- and pipe-operating utilities concerned. However, the problem still exists, potentially, and to avoid serious consequences its control must be exercised through the continued supervision and maintenance of the various measures that have been installed for electrolysis mitigation. On the Consolidated Edison system this control is obtained through approximately 120 drainage connections to the railway negative returns at various locations throughout the area.

In certain parts of the territory the trolley service virtually has been discontinued, and many of the elevated-railway structures have been removed. The outstanding effect has been the removal of cathodic protection in sections where the rails and structures normally were positive with respect to the cable and piping systems. In consequence, the electrolytic-cell type of corrosion has appeared in many localities formerly protected through cathodic action by the railway structures. Moreover the removal of the elevated- and street-railway structures has upset, to a considerable extent, the balance that formerly existed and has necessitated a major readjustment in many of the drainage connections and other measures used for protection in the anodic areas.

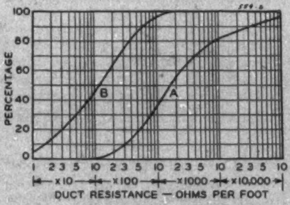

Figure 2. Cumulative percentage curves showing the results of duct-resistance surveys

A—Plotted from 9,500 tests at random locations on the system

B—Duct resistance associated with sheath corrosion

Cathodic corrosion has not been serious on the power-cable system in this territory. However, this type of corrosion is a matter of constant concern, and negative potentials are limited as much as possible, particularly in areas where the decomposition of sodium chloride or other salt and the deposition of their hydroxides on the cable sheath is likely to occur. Two or three severe cases of this type of corrosion have been experienced.

To date, there have been no cases of corrosion that could be identified with a-c electrolysis, although there are a number of single-conductor cross-bonded feeders operating on the systems with eight- to ten-volts alternating current from sheath to ground and 12 to 15 volts between sheaths of the phases. In some instances, the cables occupy ducts considered unfavorable, and some corrosion has been experienced. However, in all cases, this corrosion could be accounted for by small direct potentials or other duct conditions.

Electrolysis Surveys and Tests

The protection of the cable system depends primarily on the adequate supervision and control of all the factors involved and the maintenance of the measures adopted for the mitigation of electrolysis and corrosion. This supervision and maintenance is accomplished through systematically planned electrolysis surveys and tests which can be conveniently divided into three general classifications, namely,

1. Maintenance tests.
2. General surveys.
3. Special investigations.

Maintenance Tests. They are scheduled on a periodic basis to cover the inspection of existing installations for electrolysis protection and to check periodically the electrolysis conditions existing on the system. The installations include drainage connections, insulating joints, cathodic protection installations, and any other measures installed for electrolysis protection on either the cable or piping system. Usually maintenance tests are scheduled on an annual basis. Some installations such as those involving drainage switches, rectifiers, and other special equipment are inspected more frequently. In other cases where the conditions are well stabilized an inspection every two or three years is sufficient.

General Electrolysis Surveys. Made for the purpose of locating corrosion areas and obtaining general information on electrolysis conditions affecting the system, the general surveys may be supplemented by special tests to determine the protective measures to be installed in areas subject to electrolysis and corrosion. The general surveys are planned to cover systematically the various parts into which the system is divided for the purpose of survey. Consideration is given in particular to the localities in which changes in the electrolysis conditions are likely as the result of changes in the electric transit lines or important modifications in the cable system.

Special Tests. Made in situations which require a more or less extended investigation, frequently they involve the underground structures of other companies and may be initiated by either company depending on what structures are involved. The special work includes the investigation of the conditions incidental to corrosion failures and the surveys and tests made in connection with important new cable installations.

TEST METHODS: THE DUCT SURVEY

The test methods employed for stray-current-electrolysis surveys have been fairly well standardized, and the test procedures are described in detail in the various publications on that subject.[1,2] In situations involving only stray currents, these procedures continue to give satisfactory results. However, the usual stray-current-electrolysis tests do not yield information on the local electrolytic-cell conditions existing between the test points because of the wide variations in the soil and duct conditions from point to point along the cable ducts. For this reason, other test methods are required for the electrolytic-cell types of corrosion. Considerable experimental work has been done to develop a test method that would yield test data that could be correlated with actual cable-sheath corrosion. This work has resulted in the present duct survey.

During the past ten years or more, the duct survey has been used on the cable system to explore the electrolysis conditions existing in duct sections between manholes, and particularly to investigate the duct conditions incidental to corrosion failures. The duct survey also is used to advantage where it is desired to explore the electrolysis conditions in ducts prior to the installation of new cable. Furthermore, statistical studies of a sufficient number of duct-survey data, obtained in connection with actual cable failures, will yield information and criteria which can be used as a basis for estimating the severity of particular electrolysis situations.

The duct survey is made by pulling an electrode through a vacant duct which is adjacent to the ducts carrying cable. Instruments are connected between this electrode and the lead sheath of the adjacent cables, and measurements of potential, current, and resistance are made at frequent intervals (five to ten feet) throughout the duct. The arrangement and connections for the test are shown in Figure 1. The test electrode most generally used consists of a piece of cable 12 inches long and 2.75 inches in diameter fitted with a pulling eye and test leads. A small galvanic potential may exist between the cable sheath and the test electrode, although the material in both is the same. This difference, however, is small (0.01 volt or less) and does not affect seriously the results. The surface of the electrode should be maintained in good condition, and its electrode potential with respect to cable sheath should be checked periodically using manhole or duct water as the electrolyte. Various nonpolarizing and other special types of electrode have been investigated. However, the most satisfactory results under the usual field conditions have been obtained with the short length of lead cable sheath. An essential requirement is that the electrode be as simple and as rugged as possible.

The potential existing between the duct wall and the adjacent cable sheath is measured by the voltmeter connection shown in Figure 1. A high-resistance voltmeter should be used to minimize the errors due to electrode-contact resistance. Voltmeters having a resistance of 400,000 ohms per volt or more are satisfactory for this purpose. Because of the high resistance of the voltmeter circuit, the potential of the test electrode will be substantially that of the duct wall, and the measurements thus obtained give an approximation of the potential of the cable sheath with respect to the duct wall from point to point through the duct. The potential survey is supplemented by a time record of potential taken at a selected point in the duct to determine the characteristic of the potential. A 24-hour recorder, having a resistance of 10,000 ohms per volt, is used for this purpose. The characteristic of the record will indicate whether the condition is caused by an external source of potential, such as in stray-current electrolysis or by electric-cell conditions set up by variations in the environment.

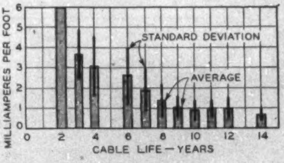

Figure 3. Age of cable versus average current discharged through test electrode

Data obtained in connection with corrosion failures

To determine the magnitude and direction of the current picked up from or discharged to the duct wall through the test electrode, a low resistance milliammeter is connected in place of the voltmeter. Since the resistance of the milliammeter circuit is relatively low, the potential of the test electrode will be substantially that of the adjacent cables, and it may be assumed that the current discharge per foot of cable at the point of test is approximately in the same order of magnitude as that measured. This current, when flowing into the duct wall, will cause anodic corrosion, and it may, when flowing to the cable sheath, result in cathodic corrosion.

In the measurement of potential or current at points within the duct it is important to correct for the *IR* drop due to any stray current flowing on the cable sheaths. Where the cables are carrying appreciable stray current, for example, from manhole *A* to manhole *B* in Figure 1, there will be a potential drop along the sheath, and a reading taken at some mid-position in the duct and referred to the sheath in manhole *A* will not give an accurate reading of the potential and current at the point of test. To correct for sheath current the usual practice is to record the magnitude and direction of the current flowing on the sheath and to compute the *IR* drop to the point of test. The appropriate correction then can be applied to the readings of potential and current measured between the cable sheath and the test electrode. In most cases the *IR* drop between *A* and *B* can be measured directly by a recording millivoltmeter as shown in Figure 1.

The resistance between the test electrode as one terminal and the adjacent cable as the other is measured at each test point as a part of the survey. The measurement can be made conveniently by connecting a low-voltage battery (1.5-volt dry cell) in series with a sensitive milliammeter between the cable sheath and the test electrode. The resistance is computed from the battery voltage and the measured current. The milliammeter should have a sensitivity in the order of 0.05 milliampere per division, and its resistance should not exceed two or three ohms. Suitable shunt resistances can be used to vary the range as required. The same instrument can be used for both the current and the resistance measurements. A reversing switch is required to reverse the potential on the test electrode to minimize any errors due to small d-c sheath potentials, polarization, or other effects. The battery current in this test is usually small and does not appreciably influence the battery voltage. However, it is a good practice to check this voltage from time to time during the progress of the survey.

The resistance as measured in the foregoing is somewhat arbitrary and is mostly the contact resistance between the surface of the electrode in contact with the duct and the duct wall and represents, approximately, the contact resistance per duct foot of cable. The area of contact will vary, depending on the duct conditions. In dry ducts the contact area will be small, whereas in ducts containing mud and water the contact may be an appreciable part of the total electrode area. The relation between contact area and resistance and its influence on the interpretation of the test data is explained in the following section. The resistance of the duct bank, the earth, and the contact resistance between the duct walls and the cable sheath in the occupied ducts also are included in the measurement. However, these resistances are relatively low compared with the electrode resistance and apparently do not appreciably influence the results.

In new installations, where it is desired to explore the duct conditions prior to installing cable, or where cables are not available in the duct bank under test, the adjacent water pipe or other pipe or cable system can be used for a resistance survey. However, in such cases, the potential and current measurements, if made, will have no very significant meaning.

In any type of survey it must be realized that there are numerous points throughout the cable duct where the cable sheath is subject to small local potentials due to such causes as differential aeration, concentration cells, and so forth. With the cable in place these potentials are inaccessible for measurement, and, if the cable be removed, the original conditions no longer exist. The potential of these local cells are usually small but in aggravated cases may be in the order of 0.1 to 0.2 volt. In general, it may be assumed that these small local potentials exist, to a greater or less extent, in all ducts containing cable. Their effectiveness in causing cable-sheath corrosion will depend upon the resistance of the environment in immediate contact with the cable sheath and the polarizing effects due to the flow of current. This emphasizes the importance of duct resistance and its influence on cable-sheath corrosion.

Analysis of Duct-Survey Data

An accurate evaluation of an electrolysis condition can be obtained only through the proper analysis and interpretation of the test data. Readings of potential and current have no particular significance, unless they can be translated into terms of corrosion on the cable or piping system concerned. The desired interpretation of test data can be obtained best through the systematic investigation of the conditions incidental to corrosion cases and through studying the accummulated data in accordance with appropriate statistical methods.

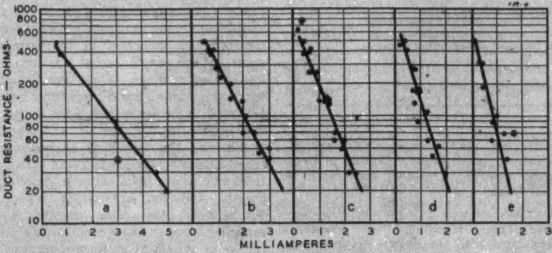

Figure 4. Electrode current versus duct resistance for cable in five age groups

The data are those used in Figure 3, but recognition is given to duct resistance

a—Six years
b—Eight years
c—Nine and ten years
d—11 and 12 years
e—13 and 14 years

Electrolysis test data serve two general purposes:

1. For individual cases, they serve to identify the cause and furnish the information required for the application of suitable remedial measures to the particular case concerned.

2. When properly classified and analyzed, together with other similar data taken systematically over the system, they constitute the basis for statistical studies of the conditions existing on the system as a whole.

For these reasons, the systematic taking and recording of data by trained observers in accordance with a well-developed plan is of first importance in making electrolysis surveys and in planning for over-all improvements on the system.

The foregoing general principles have been applied to the analysis of the duct-survey data obtained over a period of years with a view to showing the relationship between the data and actual cable-sheath corrosion. The results of the duct-resistance surveys made uniformly over the system are given in Figure 2. Curve *A* shows the duct resistance plotted on a cumulative percentage basis for approximately 9,500 duct-resistance tests made at random but well-distributed points on the system. This curve shows, for example, that in 65 per cent of the tests the duct resistance was above 1,000 ohms and less than 1,000 ohms in 35 per cent of the tests, curve *B* of the figure is a similar percentage curve of duct resistance obtained in connection with approximately 200 cable failures. From this curve it will be noted that only five per cent of the corrosion failures occurred in ducts having resistance of 1,000 ohms or more. Further it will be noted that 70 per cent of the corrosion failures occurred in ducts in which the resistance was 250 ohms or less, whereas in curve *A* only six per cent of the total tests was under 250 ohms. These results indicate that the greater portion of the corrosion is occurring on a relatively small part of the system, that is, 70 per cent of the corrosion is occurring in approximately six per cent of the ducts. In general the curves show the importance of duct resistance as a factor in rating ducts with respect to corrosion. On the basis of the data, ducts in which resistances of 250 ohms or less are measured are rated unfavorably from the standpoint of corrosion.

To relate test data with actual corrosion and to establish a basis for the interpretation of the duct survey, studies were made of the potential, the current, and the resistance data obtained in the investigation of approximately 100 corrosion failures for which complete and consistent data were obtained.

Figure 3 shows the distribution of cable life as related to the average current discharged from the test electrode to the duct wall at or near the point of failure. For this purpose the cable life, from the date of installation to the date of failure, was grouped into yearly periods, that is, all failures falling within *N* years minus five months and *N* years plus six months were grouped under *N* years. The vertical columns in the figure show the averages of the current measured for the failures in each of the yearly groups. The standard deviation from the mean value of current was computed and shown by the vertical line associated with each of the columns. The magnitude of the deviations and other elements in the data show that the variations for any period are more than can be attributed to chance and prohibit a correlation between corrosion and the average current as measured. Furthermore, the lack of correlation is also evident from the fact that the contact area of electrode varies considerably under different duct conditions, thus introducing the question of duct resistance.

In order to incorporate duct resistance as a factor in the analysis, the data were grouped, for convenience, into two-year periods and the current plotted with respect to duct resistance on semilog paper as shown in Figures 4*a* to 4*e*. Straight lines were drawn to show the best averages between current and duct resistance in each of the groups. From these figures curves were constructed showing the relations between cable life and current for four values of duct resistance as shown by the curves in Figure 5. In comparing Figure 5 with Figure 3 it will be seen that the deviations from the average in Figure 3 readily can be accounted for by variations in the duct resistance. Although there is some variation in the resistivity of the duct contents and the duct wall, it is believed that the duct resistance depends primarily on the area of contact. Consequently, for a given total discharge per foot of cable, the current per unit area is relatively less in the low resistance ducts, that is, one milliampere measured in a 50-ohm duct represents a much lower current density than the same current measured in a 400-ohm duct.

The relationship shown in Figure 5 between cable life, discharge current and duct resistance has been confirmed in numerous surveys. For example, in a recent case involving a 13.2-kv oil-filled tie feeder, the survey showed a duct resistance of approximately 500 ohms and a discharge of 0.9 milliampere at a point where corrosion had penetrated the cable sheath. By interpolation from Figure 5, the probable life of the cable was estimated at four to five years. Corrosion also had penetrated the sheath at a second point in the same duct where the duct resistance amounted to 200 ohms, the current was 2.4 milliamperes, and the estimated cable life was slightly less than four years. The feeder had been in service four years and two months at the time of failure. The corrosion in this case was caused by soil potentials resulting from the cinder-filled soil adjacent to the duct bank. Typical duct surveys are shown in Figure 6.

Classification of Cable-Sheath Corrosion

A consideration of the foregoing emphasizes the necessity for a procedure to identify the various corrosion factors concerned and to permit their classification or grouping with respect to the various types of attack. For this purpose the corrosion on the underground cables of the Consolidated Edison system is divided for convenience into three general categories:

1. Direct chemical attack.
2. Stray-current electrolysis.
3. Electrolytic-cell (galvanic) corrosion.

In the case of cables occupying a duct system, it is important to distinguish between corrosion occurring in the ducts and corrosion occurring in manholes, pull boxes, service boxes, and so forth. Duct corrosion results from certain factors in the soil or duct over which the operating company has only partial control, whereas manhole corrosion usually occurs under the arcproofing or at bond wires, splice-filling nipples, and other dissimilar metal attachments where installation methods do not provide adequate protection. The importance of treating manhole and duct corrosion separately has been recognized on the Consolidated Edison system and the methods for protecting manhole cables and splices have been modified to insure adequate protection in the future.

When the classification of corrosion is considered with a view to the identification of the various factors under field conditions and the practical application of protective measures, the following grouping of causes has been found convenient and workable.

1. Stray-Current Anodic Corrosion. The corrosion caused by the electrolytic action of direct current picked up from foreign sources and discharged into an environment which acts as an electrolyte. The action occurs at the anode or point from which the current is discharged.

2. Stray-Current Cathodic Corrosion. This type of corrosion is caused by the secondary reactions of the cathodic products of electrolysis. The action occurs when direct current flows to the cable sheath from an environment containing dissolved salts, which are corrosive to lead.

3. A-C Electrolysis. The corrosion caused by alternating currents flowing between underground structures and earth is negligible at the usual current densities encountered in practice.

4. Soil Corrosion (Electrolytic-Environment Type). Corrosion resulting from electrolytic-cell potentials originating in the environment due principally to differences in the characteristics of the soil external to the duct bank.

5. Duct Corrosion (Electrolytic-Environment Type). Corrosion due to conditions existing in the duct and usually associated with low duct resistance. Differential-aeration, concentration cells, and so forth, when occurring in the duct, are included in this group.

Table I

	Per Cent (Approximate)
Duct Failures	
Stray current (anodic)	7.0
Stray current (cathodic)	1.0
A-c electrolysis	0.0
Soil corrosion	6.0
Duct corrosion	24.0
Self-corrosion (sheath scoring)	10.0
Galvanic corrosion (iron-pipe ducts)	7.0
Chemical corrosion	4.0
Unclassified	6.0
Subtotal	65.0
Manhole Failures	
Galvanic corrosion (filling nipples, bonds, and so forth)	23.0
Chemical attack (under arcproofing)	9.0
Unclassified	3.0
Subtotal	35.0

6. Self-Corrosion (Electrolytic Metal-Surface Type). Resulting from conditions associated with the surface of the metal, such as scoring or other mechanical injuries which may set up local galvanic cells on the surface of the metal.

7. Galvanic Corrosion (Dissimilar Metals). Resulting from the contact of dissimilar metals in the presence of an electrolyte in manholes and ducts.

8. Chemical Corrosion. Corrosion which results from the direct chemical action of certain acids and alkalies on lead-cable sheath in manholes and ducts.

The application of the foregoing classification to the corrosion failures for a four-year period on the high-voltage cables of the Consolidated Edison system gives, approximately, the percentages listed in Table I.

The corrosion rate for 1943, per 100 miles of occupied duct, amounted to approximately 0.82 for the high-voltage cable system. Furthermore, approximately 30 per cent of the corrosion failures occurred in certain corrosive areas representing less than 1.0 per cent of the duct system. Manhole corrosion failures are less restricted to areas and are distributed more widely than those occurring in ducts. The corrosion rate has been reduced from 1.13 in 1940 to the present rate by the application of protective measures in the areas identified as corrosive.

Mitigation of Cable-Sheath Corrosion

ELECTROLYSIS DRAINAGE

Electrolysis drainage is used extensively for the mitigation of stray-current electrolysis on the cable system. Drainage consists essentially in providing a connection between the cable sheath and the negative bus or negative returns of the railway system involved. The object is to provide a metallic return for stray railway currents picked up by the cable system and thus to lower the potential of the sheath below that of the surrounding earth in the normally positive areas. Where the cables thus are maintained at a negative potential they also are protected by cathodic action against the galvanic types of corrosion.

The drainage of a power system presents more difficult problems than are encountered in the drainage of communication cables or railway cables which are not included in a distribution system. In the power system the sheaths of the primary and secondary cables normally are bonded together and connected to the system neutral of the wye-connected transformer low-voltage windings. These transformer windings provide a low d-c resistance connection with the live copper of the secondary cable. In the case of a 500-kva transformer this resistance amounts to approximately 0.00013 ohm and constitutes an effective bond between the cable sheaths and the low-voltage copper. Furthermore, the cable sheaths are grounded through the system neutral to the water system at customers' services. Consequently, when an attempt is made to drain the power system, the drainage not only applies to the cable sheaths, but also includes the system neutral, the copper in the low-voltage cables, and the water system. This very greatly reduces the effectiveness of drainage, and in the average situation it is estimated that only 30 to 40 per cent of the drainage current is effective in reducing the potential of the cable sheaths.

Where the power-system cables closely parallel communication cables or a railway cable system, there may be a considerable difference of potential between the cable systems resulting from the difference in the effectiveness of drainage on the respective systems. This constitutes an important problem in reducing the effects of stray-current electrolysis on the power system. Where practical, control drainage is used, that is, resistors are connected in the drainage cables and adjusted to limit the current to that required to maintain the cable sheaths concerned slightly negative with respect to the duct wall. In some cases the power cables are bonded to the communication or railway cables to reduce potential differences between the systems.

CATHODIC PROTECTION

In certain instances, where applicable, the cathodic scheme of protection is used. There are several of these installations in operation on the power cable system in New York City. The scheme is used principally, where the electrolytic-cell type of electrolysis is the influencing factor.

Cathodic protection consists essentially in placing earth electrodes properly arranged with respect to the cable ducts concerned and in applying a positive potential for the purpose of raising the duct or earth potential sufficiently to render the cable sheath negative with respect to the earth. In this arrangement, current flowing through the earth to the cable sheath tends to neutralize any positive sheath potentials likely to cause corrosion. Current at the required potential is supplied by motor generators or suitable rectifiers. The principles underlying cathodic protection have been described in several papers on the subject.[11,12,13]

In some installations of cathodic protection on the cable system, the anode consists of scrap cable installed in a vacant duct with its sheath connected through a rectifier to the cables under protection. Car rails buried adjacent to the duct bank have proved satisfactory in other installations where the current requirements are small. In cases where considerable current is required, the car rail should be imbedded in coke breeze, or specially designed carbon electrodes should be used. In one of our installations plain car rail has been in service for approximately six years, discharging an average of ten milliamperes per foot of rail.

The cathodic scheme of protection has met with considerable success on long pipe lines and cables where other structures are not seriously involved, and where there is sufficient right of way for the proper installation of the earth electrodes. Under the congested conditions found in New York City, the cathode method has but limited application. Where used, precautions must be taken to avoid discharging current to other structures which are not included in the protective scheme. Moreover, the current discharged from individual short electrodes or from sections of a long electrode laid parallel to the cables will vary between wide limits from point to point, depending on the soil conditions. There is danger in supplying too much current in some sections in order to obtain protection in others. In such cases there is grave danger of cathodic corrosion in the sections receiving an excessive amount of current. To avoid the possibility of cathodic reaction, the current should be limited to only that required to give protection, and its uniformity over the duct section should be checked by a duct survey.

PROTECTIVE COVERINGS

Protective coverings are used on the cable sheaths in certain areas, where corrosion is caused by local soil and duct conditions and where drainage or other electrical methods for protection are impractical. The protective covering which has been most generally used on the Consolidated Edison system consists of coating the cable sheath with an asphalt compound and applying two layers of canvas tape saturated with the compound. This covering has afforded adequate protection for ten years or more under the most severe corrosive conditions existing on the system. However, considerable difficulty has been experienced in pulling this type of cable into or out of the cable ducts, because of the increased over-all diameter of the cable and the tendency of the compound to cement to the duct walls. In some cases where an attempt was made to remove the cable, it was found that the disintegrated fabric clogged the duct so as to make removal of the cable impossible. In such cases the ducts have to be abandoned.

Because of these difficulties, a special rubber-faced tape has been used in some of the recent installations. The rubber tape is applied to the cable in two layers after which the tape is vulcanized and mica dust is applied. The surface has a smooth finish which is of considerable aid in pulling. A quantity of the rubber-covered cable was installed, on an experimental basis, in 1940 to determine its durability and characteristics as a protective coating. To date there have been no failures in this type of coating.

CABLE-GREASE PROTECTION

A special cable grease is being used extensively on the cable system for protection in areas subject to the environmental types of corrosion. This type of protection has been used on the power cables in New York City for the past four years. Another company has had ten to 15 years of experience with grease-coated cable. The results reported to date have been generally satisfactory.

The grease compound used is a heavy tacky petroleum grease very similar to axle grease. A little light oil is added by the manufacturer to make the grease workable. The grease is applied to the cable sheath by hand as it is pulled into the duct, care being taken to have the grease rubbed on all parts of the cable. The quantity applied amounts to approximately 25 pounds per 100 feet on cable having an outside diameter of three inches and proportionately less for smaller cable. In the use of grease for cable-sheath protection, it is important that the cable be installed in clean ducts. Any sand or mud in the duct will mix with the grease and leave a flaky coating without protective value.

CLEANING AND FLUSHING CABLE DUCTS

In cases where the cable sheaths are subject to chemical corrosion, or in ducts in which alkaline or acid conditions exist, very beneficial results have been obtained by flushing the duct with hydrant water before installing the cable. Several corrosive conditions have been cleared up by this process. In one case, where ducts enter a substation through a massive concrete envelope, the ducts were flushed every three months for approximately one year before the recurrence of an alkaline condition finally was stopped.

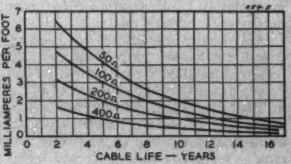

Figure 5. Age of cable versus current and duct resistance

Curves derived from the current–resistance data given in Figure 4

THE USE OF ZINC FOR CATHODIC PROTECTION

Zinc electrodes are used in several system transformer manholes to provide cathodic protection to the transformer tanks. The electrodes, consisting of zinc bars 36 inches long and $^1/_2$ inch x 4 inches cross section, are placed on the walls of the manholes, bonded together and connected to the transformer tanks.

The zinc installations in question have not been in service for sufficient time to determine their effectiveness. The potential between the electrodes and the steel tank amounts to approximately 0.45 volt. The zinc is anodic and there is a definite flow of current from the electrodes to the tanks, which are painted so that this current reaches the metal through the pores and small defects in the paint coating. The current amounts to approximately 0.4 ampere for each transformer tank.

In a recent paper on the use of zinc for cathodic protection Wahlquist[14] calls attention to the advantages of this type of protection. He also points out that zinc may not be applicable for use in locations where high resistivity limits the current output. Attention also is called to the formation of high-resistance films on the surface of the zinc and the use of chemical treatment for the reduction of these films.

Summary and Conclusion

The corrosion of metal underground is, to a large extent, the product of electrochemical processes. Electrolytic corrosion may result from stray current or from electrolytic cells associated with the metal or with its environment. Electrolytic corrosion may result from dissimilar metals in contact, or more usually from concentration cells set up in the environment by such factors as differential aeration or dissimilarity in the soils in contact with the metal.

Chemical corrosion is experienced most frequently under green concrete, in wooden ducts, and in service boxes or manholes on cable sheath buried under decomposing organic matter.

Stray-current electrolysis has been reduced to minor proportions by the measures installed for its mitigation and through the co-ordinated efforts of all the utilities concerned. Electrolysis drainage is used extensively for stray-current-electrolysis mitigation on the cable system. Continued supervision and maintenance are required for all measures installed for stray-current-electrolysis protection.

Corrosion from environmental conditions has increased in certain sections where the operation of trolley lines has been discontinued and where the cathodic protection afforded by the rails has been removed. The environment types of corrosion occur most frequently in soils of a heterogeneous nature and under conditions where the resistivity of the environment in contact with the cable is relatively low. Protection against environmental corrosion is obtained through the use of protective coatings or through the application of cathodic protection.

Electrolysis surveys are conducted on schedules arranged to give the required supervision and to detect, insofar as possible, new situations that may arise. The manhole tests usually made in connection with stray-current electrolysis do not give adequate information on the environmental types of corrosion. This has necessitated the development of a duct survey which will yield information on the conditions in the duct and furnish data by which the severity of corrosion conditions can be estimated.

A large percentage of the corrosion failures on the cable system occur in a few more or less well-defined areas comprising a small percentage of the total system. The failure rate has been reduced appreciably in the past five years.

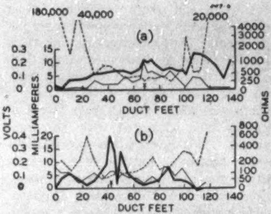

Figure 6. Typical duct surveys showing corrosion failures at points of low duct resistance

The further mitigation of existing electrolysis conditions can be accomplished best by the application of corrective measures in the areas subject to environmental corrosion. In such areas the plans for new work should provide for the best possible duct construction and adequate manhole and duct drainage. In existing installations and in situations where it is impractical to control the environment, provisions should be made for the application of cathodic protection or the use of protective coatings.

Future development and research in electrolysis mitigation should include, as major projects, field studies of environmental conditions and the further development of existing and new types of protective coatings. Further study also should be given to the application of cathodic protection to both cable and piping systems in congested areas.

References

1. Report of the American Committee on Electrolysis, 1921 (book). AIEE.

2. Electrolysis Testing, Burton McCullom, R. H. Logan. Technologic papers of the Bureau of Standards, number 355, 1927.

3. Corrosion, Causes and Prevention (second edition), Frank N. Speller. McGraw-Hill Book Company, Inc., New York, N. Y., 1935. Chapter 2, Nature and Mechanism of Corrosion, pages 8–52.

4. Corrosion of Metals—I Mechanism of Corrosion Processes, R. M. Burns. *Bell System Technical Journal*, volume 15, 1936, number 1, pages 20–38.

5. The Electrochemistry of Corrosion, R. H. Brown, R. B. Mears. *Transactions*, Electrochemical Society, volume 74, 1938, pages 495–517.

6. The Velocity of Corrosion From the Electrochemical Standpoint, Part II, N. R. Evens, T. P. Hoar. *Proceeding*, Royal Society London, England), volume 137, Series *A*, 1931, page 343.

7. Galvanic Corrosion, R. H. Brown. American Society for Testing Materials *Bulletin*, number 126, January 1944, pages 21–6.

8. Some Observations of the Potentials of Metals and Alloys in Sea Water, F. L. Laque, G. L. Cox. *Proceedings*, American Society for Testing Materials, volume 40, 1940, pages 670–87.

9. The Corrosion of Underground Cables, W. G. Radley, C. E. Richards. *Journal* of the Institution of Electrical Engineers (London, England), volume 85, December 1939, pages 685–703.

10. Controlling Factors in Galvanic Corrosion, W. A. Wesley. *Proceedings*, American Society for Testing Materials, volume 40, 1940, pages 690–702.

11. A Theory of Cathodic Protection, R. B. Mears, R. H. Brown. *Transactions* of the Electrochemical Society, volume 74, 1938, pages 519–31.

12. Cathodic Protection Interference, A. V. Smith. *American Gas Association Monthly*, volume 25, October 1943, pages 421–7.

13. Cathodic Protection of Buried Metals, M. C. Miller. *Electric Light and Power*, volume 25, June 1944, pages 92–6.

14. Use of Zinc for Cathodic Protection, H. W. Wahlquist. *Proceedings*, first annual meeting of the National Association of Corrosion Engineers, April 1944, pages 61–73.

Anode-Circuit-Breaker Design and Performance Criteria

E. W. BOEHNE
FELLOW AIEE

W. A. ATWOOD
NONMEMBER AIEE

THE rapidly expanding use of mercury-arc rectifiers, both as to total installed capacity and the relatively large number of units operating in parallel, emphasizes the importance of suitable switchgear to provide over-all satisfactory rectifier operation. The necessity for such switchgear, particularly for a high-speed air circuit breaker in the rectifier anode circuit, has been outlined in previous papers before the Institute.[1,2] During the past several years, considerable progress has been made in the reduction of arc-backs in power rectifiers. Anode circuit breakers, although subject to less frequent duty as a result of this progress, are required to operate at higher voltages and interrupt greater arc-back currents as indicated by recorded rates of rise of current in excess of 11,000,000 amperes per second. At this rate of rise in a large 650-volt (d-c) rectifier installation, the anode-breaker interrupting duty is equivalent to that of the first phase to clear a 130,000-kva fault in a three-phase 1,400-volt a-c system.

These power-duty requirements in the unique single-phase a-c–d-c circuit of the rectifier under arc-back dictate a further careful re-examination of the circuital requirements of the anode breaker which may assist in obtaining design and performance criteria. Such a study has been made and is presented herein, together with the performance of the General Electric Company's six-pole 1,600-ampere 750-volt type-*AG*-2 air circuit breaker under such requirements.

Summary

The arc voltage E_B developed by the anode-breaker, together with its early introduction into the circuit following current reversal, constitute the most essential performance criteria. It is shown that a current zero, the first prerequisite for interruption, can be created in the arc-back circuit only by developing a counter current (i_B) which neutralizes the arc-back current (I). This helpful concept is developed in a rigorous quantitative manner. The electromotive force for this counter current is the arc drop of the anode breaker (E_B).

Contrary to general belief, the arc energy (k) developed by the anode breaker does not necessarily decrease as the arc voltage is introduced earlier in the circuit For each arc-voltage characteristic there exists a particular time of introduction, (θ_e), which gives maximum arc energy. Neither can the point of minimum energy be accepted as the desirable objective due to the relatively high initial recovery voltage (E_1) associated with this point. Optimum anode-circuit-breaker performance, in circuits having high rates of current rise, requires establishing the final current zero during the inverse-voltage period (E_1 negative) together with arc energies (k) which avoid the peak of the energy characteristic.

The modification of these results as affected by the ratio of the reactive ohms (ωL) to the resistance ohms (R) of the circuit is discussed on a quantitative basis. Quantitative variations in the various parameters are presented to study their effect. Certain unique characteristics of anode breakers are explained. An example of an anode-circuit-breaker malperformance, observed when testing a developmental breaker at elevated voltages, is presented with corrective measures indicated.

The entire study is carried out on a clearly defined per unit basis which permits the numerical values on all the graphs to be applied to any voltage system at 25, 50, or 60 cycles. All arc energies (k) are given on a 60-cycle basis in watt hours per megavolt-ampere, the latter being the product of the kilovolts of the effective alternating voltage and the corresponding symmetrical zero-power-factor kiloamperes produced in the inductive ohms of the equivalent circuit.

The embodiment of these principles in the high-speed *AG*-2 air circuit breaker is demonstrated with numerous field oscillograms. The new design features of this breaker are described.

The Circuit

The actual circuit of the arc-back current in a rectifier[1,3] is of an inherently complex nature which fortunately has

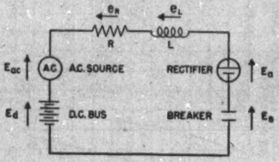

Figure 1 (above). Equivalent arc-back circuit of rectifier which is useful in the study of the performance of anode breakers

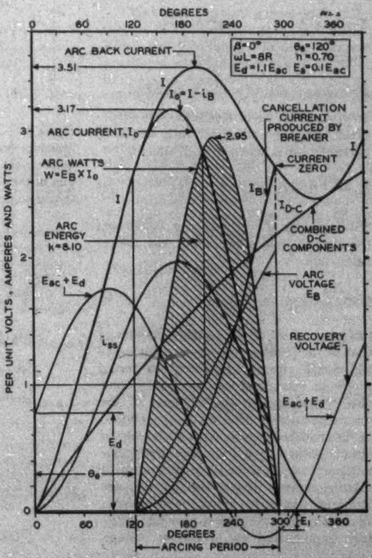

Figure 2. Sample calculation of the circuit of Figure 1 under practical condition of anode-breaker performance

The arc voltage of the breaker (E_B) produces the current (i_B) which neutralizes the arc-back current I, thus producing a current zero. The effect of rectifier arc drop has already been considered in the computation of I (see equation 6). The shaded area is the arc energy k released by the anode breaker

---

Paper 45-52, recommended by the AIEE committee on protective devices for presentation at the AIEE winter technical meeting, New York, N. Y., January 22–26, 1945. Manuscript submitted November 27, 1944; made available for printing December 16, 1944.

E. W. Boehne and W. A. Atwood are both with the General Electric Company, Philadelphia, Pa.

been reduced[3] to the simple approximate and practical equivalent circuit shown in Figure 1. Here are found the well-known parameters of inductance (L) and resistance (R) both of which may be considered linear. Under arc-back, the current (I) is supplied by two separate sources of voltage, namely, an a-c and a d-c source designated respectively as E_{ac} and E_d. The analysis of this circuit is enhanced by considering each of the several voltages to act one at a time and to add the resulting currents to obtain the final result.

The Currents

The current produced by the direct voltage (E_d) acting alone is

$$I_d=\frac{E_d}{R}\left\{1-\epsilon^{-\left(\frac{R}{\omega L}\right)\omega t}\right\} \tag{1}$$

The current produced by the alternating voltage acting alone is given by the general expression for the short-circuit current in the R, L circuit. Since the contribution of the direct voltage given by equation 1 is already defined in its simplest terms, it becomes profitable to express the d-c component of the alternating current in a similar form, giving for the total a-c contribution

$$I_{ac}=\frac{E_m}{Z}[\sin(\gamma-\beta)+\sin(\omega t+\beta-\gamma)]-\frac{E_m}{Z}\sin(\gamma-\beta)\left\{1-\epsilon^{-\left(\frac{R}{\omega L}\right)\omega t}\right\} \tag{2}$$

where

$Z=\sqrt{R^2+\overline{\omega L}^2}$; $E_m=\sqrt{2}E_{ac}$

$\gamma=\tan^{-1}\left(\frac{\omega L}{R}\right)$

β = voltage angle of arc-back initiation

In equation 2 when R is zero, $\gamma = 90$ degrees, and the undamped, fully displaced current results when $\beta = 0$, namely

$$I_{ac}=\frac{E_m}{\omega L}[1-\cos\omega t] \tag{3}$$

Similarly, for $R = 0$ and $\beta = 90$ degrees the symmetrical short-circuit current results, namely

$$i_{ac}=\frac{E_m}{\omega L}\sin\omega t \tag{4}$$

The arc drop of the rectifier, as well as that of the breaker, may be considered as additional circuit electromotive forces which in turn produce currents of their own which oppose the currents of the source voltages.[5] The arc drop produced by the rectifier is essentially a flat-top or direct voltage which remains practically constant in spite of the large fluctuation in circuit current. Even though this arc drop may fluctuate slightly or differ from this exact characteristic it may be faithfully represented by a direct voltage ($-E_a$) of an average constant magnitude. On this basis, the rectifier drop may be considered to produce its own current, namely

$$i_a=-\frac{E_a}{R}\left\{1-\epsilon^{-\left(\frac{R}{\omega L}\right)\omega t}\right\} \tag{5}$$

The total arc-back current (I), including the effect of rectifier drop ($-E_a$), may now be written as the sum of equations 1, 2, and 5

$$I=\left[\left(\frac{E_d-E_a}{R}\right)-\frac{E_m}{Z}\sin(\gamma-\beta)\right]\times\left\{1-\epsilon^{-\left(\frac{R}{\omega L}\right)\omega t}\right\}+\frac{E_m}{Z}[\sin(\gamma-\beta)+\sin(\omega t+\beta-\gamma)] \tag{6}$$

or $I=I_{DC}+I_{SS}$ (see Figure 2)

This grouping of all the transient components in one term (I_{DC}) simplifies the quantitative and graphical presentations and affords a clearer visualization of the effect of the various factors involved.

The majority of arc-backs initiate in the inverse period and create arc-backs at the end of the conducting period with the failure, for one reason or another, of rectification. The instantaneous value of the alternating voltage at the time of current reversal determines the value of β. It is a function of the angle of overlap of the rectifier which, in turn, is dependent upon the rectifier loading. For very light loading, including no load, the angle β may be as low as -30 degrees, or 30 degrees prior to a normal alternating-voltage zero. This condition would give the maximum arc-back currents. As the loading is increased, however, the angle of overlap is increased and the point of current reversal occurs close to a normal alternating-voltage zero or when β is zero. Since arc-backs are more frequent under load, it will be found practical to consider values of β close to zero. A simplification in the final arc-back current of equation 6 of practical significance

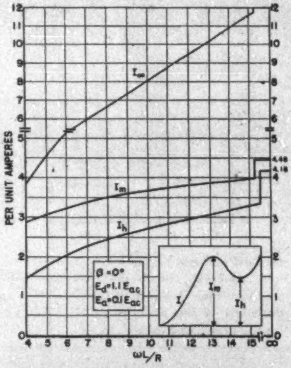

Figure 3. Curves showing the effect of circuit resistance upon the relative magnitude of arc-back current at the initial peak and at the bottom of the first dip, and the ultimate current should no protective equipment be employed

Rectifier drop is included

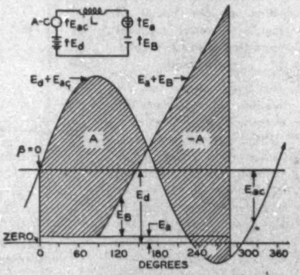

(a). The circuit voltages

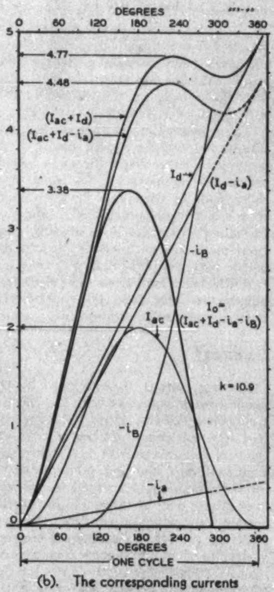

(b). The corresponding currents

Figure 4. The voltages and the corresponding currents which would flow in the circuit of Figure 1 when resistance is zero

Each current is proportional to the area under the corresponding voltage, the net current I_0 being proportional at all times to the net shaded area as indicated in Figure 4a results when the initiating angle β is made slightly negative so that $(\gamma-\beta)=90$ degrees. This results in a value of $\beta=-14$ degrees for a circuit whose ratio of $\omega L/R$ is as low as 4; -7.1 degrees for a $\omega L/R$ of 8; and for a ratio of $\omega L/R$ of 15, the value of β to satisfy this condition is only -3.8 degrees. These values fall between the practical limits of arc-back initiation of -30 degrees and 0 degrees. When $(\gamma-\beta)$ is made 90 degrees in equation 6, and the close approximation of ωL to Z is absorbed, there results

$$I=\left[\left(\frac{E_d-E_a}{R}\right)-\frac{E_m}{\omega L}\right]\left\{1-\epsilon^{-\left(\frac{R}{\omega L}\right)\omega t}\right\}+\frac{E_m}{\omega L}[1-\cos\omega t] \qquad (7)$$

This practical division places all the variables in the transient term and affords easy determination of the total current.

Quantitative Values and the Per Unit System

The numerical work in this paper is presented on a per unit basis and therefore is applicable to any system regardless of voltage, kilowatt capacity, or frequency.

Per unit voltage is $E_m=\sqrt{2}E_{ac}$

Per unit current is $I_m=E_m/\omega L$

Hence, ωL is unity on the per unit system

Per unit watts, $W=E_m \cdot I_m$

Per unit arc energy (k) is expressed as the watt hours per megavolt-ampere where the base megavolt-amperes is $0.5\times10^{-6}\ E_m \cdot I_m$. All values of k are expressed on a 60-cycle basis. For 25-cycle systems all values of k should be multiplied by 2.4 and for 50-cycle systems the value of k should be multiplied by 1.20 to obtain true values.

The ratio of the effective direct voltage (E_d) to alternating voltage (E_{ac}) in the rectifier circuit under arc-back may vary from 0.90 to 1.17, depending upon the number of rectifiers on the bus[3] and to a smaller extent upon the regulation of the a-c system. The value of 1.17 assumes an infinite d-c and a-c bus and is the upper limit. This condition is approached in large electrochemical installations where a large a-c source supplies the rectifier transformers. A value of 1.10 is chosen for this ratio for the numerical work in this paper. It is fairly indicative of large existing circuits in the electrochemical industry. Thus

$$E_d=1.10E_{ac} \qquad (8)$$

Likewise the arc drop of the rectifier (E_a) depends upon the type of rectifier employed. Expressing this direct voltage in per unit of the rms value of the alternating voltage facilitates the numerical presentations on a per unit basis. A rectifier drop under arc-back of ten per cent of the alternating voltage is chosen as being indicative of the higher voltage systems. This percentage is slightly pessimistic and, if used, will be more pessimistic for the lower voltage systems. The equations and method of attack permit the use of any value of rectifier drop. For the numerical cases presented in this paper

$$E_a=0.1E_{ac} \qquad (9)$$

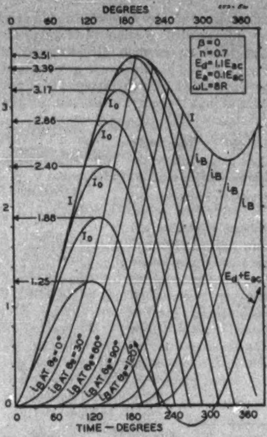

(a). The breaker generated current (i_B) produced by a linearly rising arc voltage, E_B ($n=0.70$), is introduced at 30-degree intervals, the corresponding arc currents (I_o) being shown ($I_o=I-i_B$)

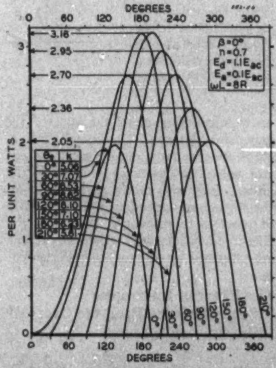

(b). The corresponding wattage curves of Figure 5a. ($W=E_B \cdot I_o$). The area under each curve is the arc energy and is tabulated on the figure and plotted in Figure 6

Figure 5. Arc currents and their corresponding wattages for various contact parting times from $\theta_e=0$ degrees to $\theta_e=210$ degrees. The composite results of these values are plotted in Figure 6

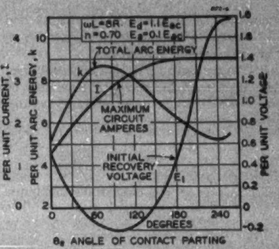

Figure 6. Master arc-interruption criteria resulting as the time of introduction (θ_e) of the arc voltage (E_B) is varied from zero to 210 degrees following the initiation of a high-capacity arc-back ($\beta=0$)

The composite data for these curves are presented in Figure 5

Adopting the ratios given in equations 8 and 9 as being indicative of the large rectifier installations, equation 7 becomes

$$I=\left[0.707\left(\frac{\omega L}{R}\right)-1\right]\left\{1-\epsilon^{-\left(\frac{R}{\omega L}\right)\omega t}\right\}+\{1-\cos\omega t\} \qquad (10)$$

When the ratio $\omega L/R$ is taken as eight (used on many of the curves) the numerical equation for the arc-back current becomes

$$I=4.65\{1-\epsilon^{-0.125\,\omega t}\}+\{1-\cos\omega t\} \qquad (11)$$

This current has an initial peak of 3.6 (Figure 10) and an ultimate peak of 6.65. When β is zero instead of -7.1 degrees, associated with an $\omega L/R$ of eight, the initial peak is reduced 2.5 per cent to a per unit current of 3.51. The total arc-back current for the case of $\beta=0$ is shown in Figure 2. The relative magnitude of the initial current peaks (I_m) and the magnitude at the initial current dip (I_h) for $\beta=0$ is described in Figure 3 as a function of the ratio of $\omega L/R$. The top curve describes the relative magnitude of the ultimate current peak, I_a.

The Interrupter

An inspection of the total arc-back current in Figure 2 reveals an inherently d-c characteristic in that no natural current zeros are present to afford an opportunity for interruption. It is imperative that an interrupter be employed which is capable of producing a current zero. This is only possible by producing an arc voltage in the interrupter which is capable of causing a current to flow which will neutralize the circuit current (I) of the arc-back. This in turn demands a circuit breaker capable of developing sufficient arc drop and thus inherently avoids an oil breaker as the latter functions on the low-arc-voltage principle and is hence only adaptable to circuits which afford a natural current zero.

The arc drop (E_B) of a self-contained air breaker of the magnetic type may be represented by a linearly rising voltage having an equation

$$-E_B = n \cdot E_m \cdot \omega t \qquad (12)$$

where n is the slope of the linearly rising arc voltage in per unit of the maximum slope of the per unit a-c source. When $n=1.0$, $E_B=E_m$ at one radian ($\omega t=1$ or 57.3 degrees). This is defined graphically in the lower left-hand corner of Figure 7.

The current produced by this linearly rising voltage in the L, R circuit is

$$i_B = \frac{nE_m}{R}\left[\omega t - \frac{\omega L}{R}\left(1-\epsilon^{-\left(\frac{R}{\omega L}\right)\omega t}\right)\right] \qquad (13)$$

This current is not admitted to the circuit until the contacts of the breaker part θ_e degrees later and permit the rapidly expanding arc to develop the linearly rising arc voltage of equation 12. This current is shown in Figure 2, introduced by a breaker which parts its contacts in one third of a cycle ($\theta_e=120$ degrees or $\omega t=2\pi/3$) and which develops an arc voltage which rises linearly at a rate of 0.70 of the maximum slope of the a-c source ($n=0.70$). The actual net circuit current I_e is the difference between these two currents and is also plotted in Figure 2 as the oscillograph would record this current. It follows that the peak available current will be lowered and will occur earlier as the arc voltage of the interrupter is introduced earlier in the circuit.

A clearer visualization and working knowledge of these various relationships which avoid the apparent complexity of the equations which appear above is to consider the same circuit without resistance ($R=0$). In this case, which is a close approximation for large rectifiers, each of the several currents will be proportional at all times to the volt-time area under the respective voltages. This comes about in any pure inductive circuit since

$$i = \frac{\int e\,dt}{L}$$

which is merely another way of expressing the fact that

$$e = L\frac{di}{dt}$$

The currents in the pure inductive arc-back circuit [zero power factor, ($R=0$)] are shown in Figure 4b. Each in turn is proportional to the area under the corresponding voltage in Figure 4a. The net current is hence proportional to the net volt–time area acting on the inductance. It follows that from the initial current zero to the final current zero, the net area under the voltage is zero[5] as indicated by the shaded portion of Figure 4a. The resulting current, I_e, is shown in Figure 4b and at all times is proportional to the shaded area in Figure 4a. Peak current must occur as the sum of the arc-voltage drops equal the sum of the generated voltages. The above relationships are true for a purely inductive circuit only. As resistance is added to the circuit these area relations do not hold, the departure depending upon the ratio of reactive to resistance ohms ($\omega L/R$). The true relations with resistance present are expressed by equations already given.

Figure 7. The solid lines portray the resulting malperformance associated with the fast introduction of an arc voltage which rises too slowly ($n=0.2$) to create a current zero before the arc-back current starts for the second major peak. The resulting current (I_0) is double-humped and results in the creation of excess energy

Also indicated are the corresponding phenomena for different arc-voltage slopes varying from n equal to 1.0 to 0.10. The corresponding breaker energies are tabulated on the figure. Figure 8 is a composite of these results. Figure 9 shows a typical case of the malperformance similar to $n=0.20$

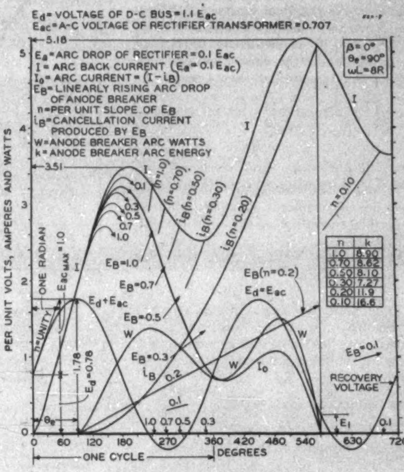

The Effect of Interrupter Characteristics Upon the Over-All Interruption Problem

The determination, of the total arc-back circuit current, by superimposing the separate contributions, enables the effect of variations of any particular voltage to be studied easily. Of particular interest is the examination of the effect of various anode-breaker arc-voltage characteristics upon the total current as well as other important circuit-breaker interruption criteria.

The three primary considerations which have a direct bearing upon the successful interruption of the arc-back current are:

1. The creation of a current zero.
2. The instantaneous recovery voltage at current zero and the resulting recovery-voltage characteristic.
3. The total arc energy liberated just prior to current zero and its distribution.

The exact interrelation between items 2 and 3 above is complex and will vary depending upon the interrupter. Nevertheless, it becomes obvious that low arc energy followed by a current zero which occurs at a time when the instantaneous recovery voltage is low is a desirable combination for good interrupter performance. In Figure 2 is shown a complete sample calculation on a per unit basis which determines these factors for the following conditions:

1. $E_d=1.10E_{ac}$
2. $E_a=0.1E_{ac}$
3. $(E_d-E_a)=E_{ac}$
4. $\beta=0$
5. $\theta_e=120$ degrees
6. E_B = linearly rising
7. $n=0.70$
8. $R=\omega L/8$
9. $\gamma=82.9°$
10. $Z=1.008\omega L$

The maximum per unit value of the initial current peak is 3.51 which is limited to 3.17 by the arc voltage. The arc-wattage curve (W) is the product of the arc voltage and the arc current. It is computed graphically. Its area is the arc energy (k) in watt hours per megavolt-ampere on the base previously defined. For example, in a 650 volt (d-c) rectifier installation (alternating voltage 590) having a ratio of ωL to R of eight, which initiates an arc-back as the alternating voltage passes through zero ($\beta=0$) and produces an initial rate of rise of current of 11,000,000 amperes per second to an initial crest of 90,000 amperes, the value of

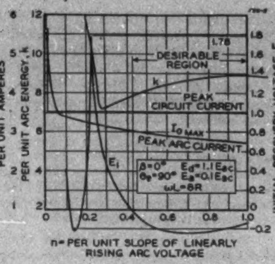

Figure 8 (left). Master arc-interruption criteria resulting as the slope (n) of the linearly rising arc voltage (E_B) is varied from 1.0 to 0.10

The individual cases are indicated in Figure 7. The arc-voltage initiating angle θ_e is constant at 90 degrees

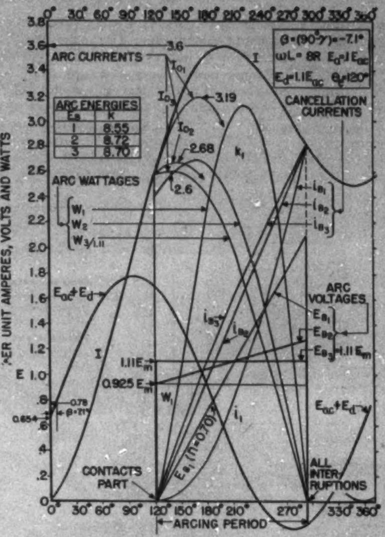

E_B	k
1	8.55
2	8.72
3	8.70

Figure 10. Arc currents and wattages resulting from three separate shapes of arc voltages, all of which are initiated at the same time ($\theta_e=120$ degrees) and which produce current zeros simultaneously. Arc energies are tabulated on the figure

Note for this case the value of β is chosen as -7.1 degrees which permits I to be expressed by equation 7 of the text

the per unit current would be 90,000/3.51 = 25,600 amperes = I_{ac} maximum. The symmetrical alternating current would then be 18,100 and produced by an alternating voltage of 590 volts or a megavolt-ampere of 10.7 on a single-phase basis. Hence, the total arc energy having these values, developed as described by Figure 2, would be: 8.1×10.7 or 86.5 watt-hours. This is approximately the energy released by the anode breaker in clearing such arc-backs which take place following the conducting period. During such an interruption, the peak circuit current of 90,000 amperes would be limited to only 81,000 amperes, which occurs at 0.46 cycle, and current zero would take place during the inverse-voltage period as desired and indicated by Figure 2. An oscillogram closely approaching these conditions is shown in Figure 14.

Effect of Breaker Speed

It is of interest now to examine the corresponding results of Figure 2 when the arc voltage is initiated at various intervals, θ_e, following the current reversal. The results of this variation are presented in Figure 5. In Figure 5a are shown the breaker-generated currents (i_B) and the resulting current-limiting action as the angle θ_e is taken to zero in 30-degree-steps (the latter case would require instantaneous tripping of an anode breaker having no mechanical time). In Figure 5b are shown the corresponding arc-wattage curves together with their areas tabulated on a per unit energy basis on the figure. These characteristics are plotted in Figure 6 and show the interesting fact that, for the particular representative arc-voltage characteristic chosen, the arc energy reaches a crest when θ_e is about 75 degrees. The current zero, however, occurs at a very favorable point to assist the interruption, and the external circuit is benefited by additional current-limiting action. When the same arc voltage is admitted at 150 degrees, however, the energy is reduced to 82 per cent of the maximum value and current zero is still in a favorable region. The peak current on the other hand is 19 per cent in excess of the peak current at the maximum energy point.

Effect of Rate of Rise of Anode-Breaker Voltage

In a similar manner, it is of interest to vary the slope (n) of the linearly rising anode-breaker arc voltage (E_B), keeping a fixed value of its point of initiation (θ_e). Such a study is sketched in Figure 7 by indicating the performance for values of n of 1.0, 0.7, 0.5, 0.3, 0.2, and 0.1 and all for a value of θ_e of 90 degrees. The case of $n=0.2$ is shown in detail to exhibit the phenomena resulting when the arc voltage is so low that its cancellation current (i_B) does not neutralize the arc-back current before the latter rises toward the second current peak. Note the double-peaked current I_o. Figure 9 exhibits an oscillogram of such an occurrence. This was obtained when a 650-volt developmental anode breaker was tested at 1,030 volts.

In spite of the large increase in arc energy associated with this case ($n=0.2$) an opportunity to clear is presented by the fact that the ultimate current zero at 570 degrees occurs at a low value of recovery voltage (E_1) and is followed by a relatively

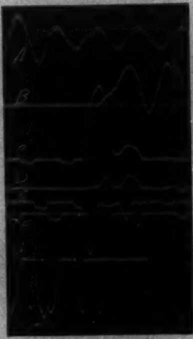

Figure 9. Oscillogram showing a malperformance which occurs should the developed arc voltage of the breaker rise too slowly to create a current zero during the dip in arc-back current following the initial peak

See Figure 7 ($n=0.2$) for a graphical interpretation of this phenomenon. This record was obtained by testing a 650-volt developmental anode breaker at 1,030 volts

Curve *A*. Sixty-cycle timing wave

Curve *B*. Anode-breaker voltage (E_B) and recovery voltage ($E_{ac}+E_d$)

Curve *C*. Anode current of faulted pole as limited by anode breaker (I_o) (see Figure 7)

Curve *D*. Anode-breaker watts (*W*)

Curve *E*. Forward current of anode circuit of another pole on same wye

Curve *F*. Forward current of anode circuit of remaining pole on same wye

Curve *G*. Voltage across the *MC-5* air circuit breaker used to short-circuit the rectifier to create the simulated arc-back current long interval before the recovery voltage rises to a threatening magnitude. The arc voltage which rises at half this rate ($n=0.1$) produces still more energy and the current zero is located at 692 degrees which suggests the possibility of failure. When $n=0.3$, on the other hand, the arc energy is less than half the energy at $n=0.1$, although the initial recovery voltage is in the same relative position. The master characteristics for this variation in n are presented in Figure 8. This study reveals that, for a given time of introduction of the arc voltage of the anode breaker, the energy characteristic increases as the slope of the linearly rising voltage is increased. The current zeros, however, are more desirably located in the inverse-voltage period for the higher values of n.

Effect of Arc-Voltage Shape

Although a linearly rising arc voltage of the anode breaker was chosen to demonstrate the various performance characteristics, the method is applicable to any type of arc-voltage wave shape. In Figure 10, for example, are shown three arc-voltage characteristics which start simultaneously and produce current zeros simultaneously in a circuit having a ratio of $\omega L/R$ of eight. The flat-top arc voltage is particularly easy to analyze since it produces a current (i_B) of the form $(1-\epsilon^{-(R/\omega L)\omega t})$ as shown. The special trapezoidal arc voltage (E_{B3} of Figure 10) having the equation

$$E_{B3}=n\left[1+\left(\frac{R}{\omega L}\right)\omega t\right]E_m \qquad (14)$$

produces a linearly rising current (i_{B3}) in the R, L circuit. This current reaches a per unit value of n in one radian ($\omega t=1$ or 57.3 degrees) and hence crosses the rectangular portion of the trapezoidal voltage at that point. It is also particularly easy to consider. The peak arc currents are merely indicated in Figure 10. It is particularly significant that, in spite of the difference in arc-voltage shape, the arc energies (k), as shown in Figure 10, differ by only two per cent. Space does not permit the modulation of these other arc-voltage characteristics with respect to magnitude and point of initiation.

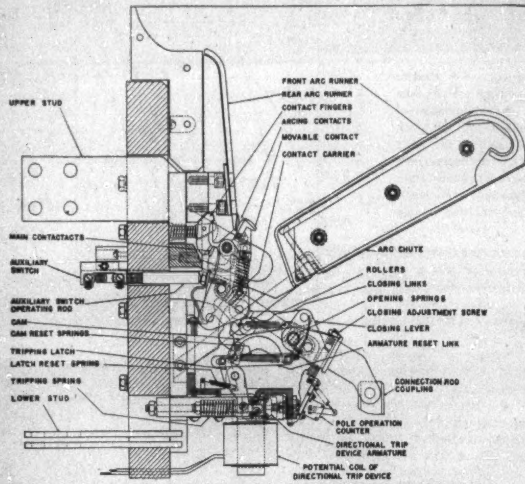
UPPER STUD
FRONT ARC RUNNER
REAR ARC RUNNER
CONTACT FINGERS
ARCING CONTACTS
MOVABLE CONTACT
CONTACT CARRIER
MAIN CONTACTS
AUXILIARY SWITCH
AUXILIARY SWITCH OPERATING ROD
CAM
CAM RESET SPRINGS
TRIPPING LATCH
LATCH RESET SPRING
TRIPPING SPRING
LOWER STUD
ARC CHUTE
ROLLERS
CLOSING LINKS
OPENING SPRINGS
CLOSING ADJUSTMENT SCREW
CLOSING LEVER
ARMATURE RESET LINK
CONNECTION ROD COUPLING
POLE OPERATION COUNTER
DIRECTIONAL TRIP DEVICE ARMATURE
POTENTIAL COIL OF DIRECTIONAL TRIP DEVICE

Figure 11a (above). Type *AG*-2 anode-circuit-breaker contacts, arc chute, directional trip mechanism, and auxiliary switch

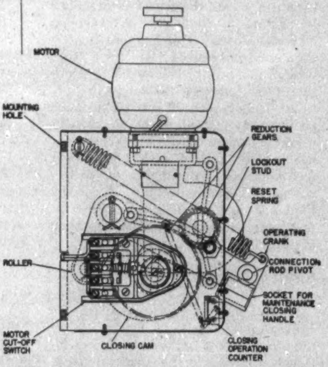
MOTOR
MOUNTING HOLE
REDUCTION GEARS
LOCKOUT STUD
RESET SPRING
OPERATING CRANK
CONNECTION ROD PIVOT
ROLLER
SOCKET FOR MAINTENANCE CLOSING HANDLE
MOTOR CUT-OFF SWITCH
CLOSING CAM
CLOSING OPERATION COUNTER

Figure 11b (right). Motor-operated closing mechanism for type *AG*-2 anode circuit breaker

Conclusions From Analytical Study

It follows from the foregoing that the anode-circuit-breaker designer has the opportunity of selecting the most desirable combination of the three primary characteristics:

(*a*). Point of introduction of arc voltage.

(*b*). Arc-voltage shape.

(*c*). Arc-voltage magnitude which will best fulfill the requirements for satisfactory anode-breaker performance.

There are numerous combinations of these variables which will achieve comparable performance. It also can be shown that the optimum characteristics will not hold the same interrelationship for circuits which differ widely in rates of rise of arc-back current or for circuits differing widely in the ratio of $\omega L/R$. In general, the field may be divided into two general classifications:

1. Systems having high rates of rise of arc-back current (above 8,000,000 amperes per second) which in turn are associated with large rectifier installations having high ratios of $\omega L/R$, requiring large kilovolt-ampere interrupting capacity breakers.

2. Systems having low rates of rise of arc-back current (below 8,000,000 amperes per second) which in turn are associated with smaller rectifier installations having lower ratios of $\omega L/R$ and requiring breakers of smaller kilovolt-ampere interrupting capacity.

Two breaker characteristics are thus indicated. It is the purpose now to describe a breaker developed for the higher-duty requirements.

A High-Capacity Anode Circuit Breaker

The General Electric Company's six-pole 1,600-ampere 750-volt type *AG*-2 air circuit breaker is quite similar in general appearance and much of the detail structure remains as it was in the breaker described in the Seaman-Morton paper[1] presented in November 1942.

To meet the increased interrupting capacity at the higher rates of rise of current, changes have been incorporated in the latest anode breaker to achieve improved operating characteristics, performance, and life. Advantage has been taken of the trends indicated by the analytical study presented in the early portions of this paper.

The most noticeable changes lie in the upper stud, contacts, and interrupter unit construction (see Figure 11). Field tests with this open-chute construction have demonstrated that blowout coils contributed little to the over-all performance and as a result have been eliminated. Rapid arc motion following contact separation is enhanced by the hairpin loop in the current path to the arcing tips, the use of silver–molybdenum arcing tips, and steel arc runners. The back steel runner is mounted directly on the breaker upper stud and the stationary silver–molybdenum arcing tip is secured directly on the runner. The front runner is connected from its lower end to the lower stud of the breaker.

The arc chute has been somewhat increased in size and better insulation has been provided between the two arc runners in the chute by using Mycalex insulation and bushings to separate the front runner from the sides of the arc chute. Inside the arc chute there is practically no material to carbonize (see Figure 12). Only the steel runners, a small area of Mycalex, and the treated asbestos-board sides are exposed to the arc. The steel arc runners, because of the blowout effect established by the arc current which causes the arc to travel very rapidly along the runners, remain relatively cool and give up a minimum of metal to find its way into the arc stream. The minimizing of metal vapor in the arc stream works toward the establishment of an arc path of high resistance which is capable of creating and maintaining the arc-voltage characteristic required for optimum performance.

Curved ends on the arc runners are an aid in keeping metal vapor out of the arc stream because the point of arc contact on the runner does not hold to any one spot until interruption occurs. In a straight runner ending abruptly, an arc generally plays off one point until interruption, thereby raising the temperature of the runner to the melting point and feeding metal into the arc until the arc is broken. The arc-chute materials have been given standard treatments used on arc chutes of 15-kv air circuit breakers.[4] These treatments improve the arc-voltage characteristics of the chute and afford an increase in the dielectric strength of the open breaker.

The upper studs are redesigned so that the front portion carrying the back arc runner with its attached silver–molybdenum arcing tip may be removed as a unit to permit ready access to the primary contact fingers. The upper studs may have either vertical or horizontal bars extending through the panel to the rear for ease in making main connections. Each primary contact finger, of which there are three, has pivoted therein a spring guide through which a strong compression spring acts on the contact finger rather than seating the stiff spring directly on the finger, as was done formerly.

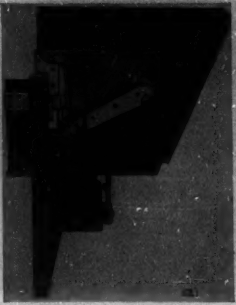

Figure 12a (left). One pole of AG-2 anode circuit breaker with new open-type arc chute with side plate removed. The curved steel runners permit rapid arc motion and keep metal vapor to a minimum

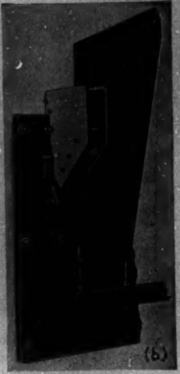

Figure 12b (right). End pole of type AG-2 anode circuit breaker. End and front barriers removed

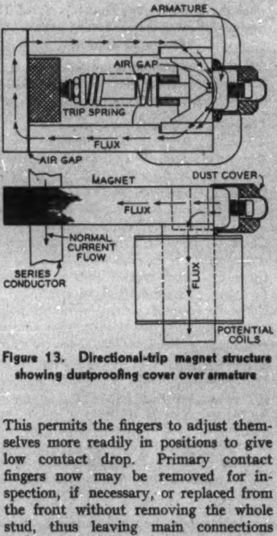

Figure 13. Directional-trip magnet structure showing dustproofing cover over armature

This permits the fingers to adjust themselves more readily in positions to give low contact drop. Primary contact fingers now may be removed for inspection, if necessary, or replaced from the front without removing the whole stud, thus leaving main connections undisturbed, an improvement over the original construction.

From the primary fingers, main current is carried through silver contacts to the bridge to the lower stud. Advantage is taken of the magnetic forces set up by the current being carried through the breaker to increase pressure at all contacts, but as further insurance against pitting at the lower contact, the bridge is connected by a flexible copper braid to the lower stud. The pivot in the bridge carrier which supports the bridge is also the pivot for a new arcing tip arm with a silver–molybdenum tip. This arcing tip is connected directly to the lower stud by an extension of the copper braid, previously mentioned, which connects the main bridge and lower stud. The arcing tip arm is adjustable for position, to secure proper operating sequence of main and arcing contacts. A strong spring biases the arcing tip toward the contact making position.

Certain additional improvements have been made in breaker-pole mechanism which are the result of excellent field experience. Notable among these is the addition of a dustproofing cover (Figure 13) which protects the armature and pole faces of the directional trip device.

Field Tests

When anode-circuit-breaker tests are made at the site of a rectifier installation, arc-back currents are created by short-circuiting the rectifier by a suitable short-circuiting breaker; namely, one free from arcing during the closing stroke. The drop created by such a breaker is small and cannot be considered as representing the arc drop in the rectifier during actual arc-back. As a result, the simulated arc-back current is increased and rises at a higher rate than the natural arc-back. But more important, the rectifier's interrupting capacity is not made available to divide the resulting recovery voltage with the anode breaker. In other words, the entire burden of interruption, under slightly more severe conditions, is placed squarely upon the anode breaker under test. The ability of the anode breaker consequently is tested under quite pessimistic conditions.

A typical test made at a large 650-volt (d-c) rectifier installation is shown in Figure 14. Curve *F* is the arc-back current of full magnitude which rises to 79,000 amperes at a rate of 11,400,000 amperes per second. The arc voltage is shown in curve *B* while the arc wattage is recorded in curve *E* which, measured, represents 82 watt-hours of energy. The crest current of the test circuit is 88,000 amperes. The per unit megavolt-ampere of the circuit as described in the early

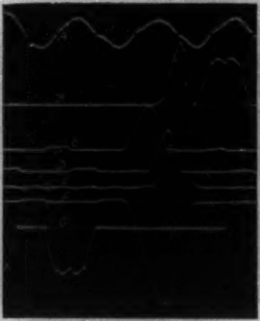

Figure 14. Typical simulated arc-back test of the type *AG-2* anode breaker on a large 650-volt rectifier installation

Curve *A*. Sixty-cycle timing wave

Curve *B*. Anode-breaker voltage which shows the arc voltage (E_B) and the recovery voltage $(E_{ac}+E_d)$

Curves *C* and *D*. Forward currents in the other anodes on the same wye

Curve *E*. Anode-breaker watts. The peak wattage of this curve is 80,000 kw. The area under this curve represents 82 watt-hours $(k=7.5)$

Curve *F*. Simulated arc-back current as limited by anode breaker. This current has a crest of 79,000 amperes in a circuit capable of 88,000 amperes at the initial peak

Curve *G*. Voltage across the *MC*-5 air circuit breaker used to short the rectifier to create the simulated arc-back current. Same scale as curve *B*.

part of the paper is 10.9. The energy constant k for the test is 82/10.9 or 7.5 which may be compared with computed values of k shown on the figures.

A simulated arc-back is shown in Figure 15 where the value of β was determined by the random closing of the rectifier short-circuiting breaker. Here $\beta=$ 75 degrees. Interruption occurs promptly. Note the low arc wattage represented by trace *E*. Curve *F* exhibits a sympathetic arc-back on another phase of the same wye with maximum current of 75,500.

A case not uncommon during such a series of tests is shown in Figure 16. Here the arc-back is simulated by the random closing of the rectifier short-circuiting breaker at $\beta=153$ degrees, thus giving rise to a small current peak which is sufficient to trip the breaker. Prior to contact parting, however, the current has started for the first major peak where it is throttled by the action of the arc voltage to an early current zero. Peak current = 42,700. Arc energy = 67 watt-hours.

During such tests, simulated arc-backs are sometimes initiated later than 170 degrees thus causing only a small reverse current to flow which trips the breaker producing only the smallest spark. Such cases are recorded under actual arc-back conditions. Frequently on test, because of the absence of the rectifier in the circuit, such breaker trippings are followed by simulated arc-back currents after the intervening conducting period which are interrupted by the "pretripped" breaker under conditions representing a breaker having zero mechanical time. Such conditions are believed to be improbable during normal operation because of the healing provided by the rectifier during the intervening conducting period which prevents such "hyphenated" arc-backs.

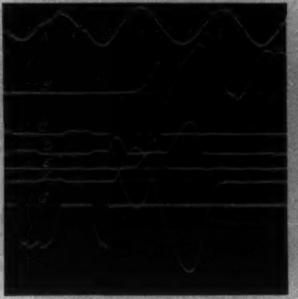

Figure 15. Performance of the *AG-2* anode circuit breaker under simulated arc-back test when the short-circuiting breaker is closed 75 degrees following the conducting period. (β close to 75 degrees)

Same circuit conditions as in Figure 14 except different pole under test. Same calibrations as in Figures 14 and 16

Curve *A*. Sixty-cycle timing wave

Curve *B*. Anode-breaker voltage which shows the arc voltage (E_B) and the recovery voltage $(E_{ac}+E_d)$

Curve *C*. Simulated arc-back current as limited by anode breaker. This current has a crest of 51,700 amperes

Curve *D*. Forward current in another pole of the same wye

Curve *E*. Anode-breaker watts on the same scale as Figure 14

Curve *F*. Forward current in another pole of the same wye which developed into a sympathetic arc-back of 75,500-ampere peak which was cleared by the same pole tested in Figure 14. Effect of rectifier drop is present in this curve

Curve *G*. Voltage across the *MC*-5 air circuit breaker used to short-circuit the rectifier to create the simulated arc-back current. Same scale as curve *B*. The 75-degree delay is measured easily from this trace

Conclusions From Tests

A six-pole 750-volt anode breaker of simplified construction, embodying improved chutes of open construction, has demonstrated its ability to interrupt safely, repeated arc-back currents rising to 90,000 amperes at rates of rise in excess of 11,000,000 amperes per second. Peak currents in all cases have occurred in less than one-half cycle. After more than 100 tests at such currents, the contacts have been found in relatively good condition and the breaker required no imperative maintenance.

A contact of simple sturdy construction, employing no blowout coils, and assisted by a streamlined arc chute of high dielectric strength, enabled the development of a rapidly rising arc-voltage characteristic of high magnitude which is extremely stable. Properly introduced into the circuit by the action of a magnetic trip and a high-speed mechanism, this arc-voltage characteristic creates an over-all performance having optimum qualities with respect to established criteria of circuit interruption. A new and fundamental approach to the anode-breaker problem has been presented which enables the effect of controllable factors to be visualized and weighed with respect to over-all performance. In each

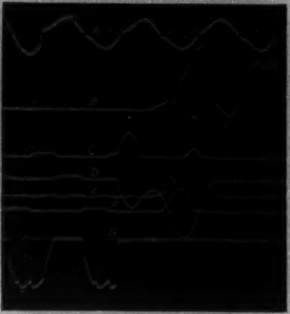

Figure 16. Simulated arc-back test in which the short-circuiting breaker closed 153 degrees following conduction resulting in a small initial current which tripped the breaker prior to the major rise of current

The rapid introduction of the arc voltage throttled this current to a 42,700-ampere peak. Arc energy, 67 watt-hours. All calibrations same as Figures 14 and 15

Curve *A*. Sixty-cycle timing wave

Curve *B*. Anode-breaker voltage which shows the arc voltage (E_B) and the recovery voltage $(E_{ac}+E_d)$

Curves *C* and *F*. Forward current in other poles on the same wye

Curve *D*. Simulated arc-back current in pole under test

Curve *E*. Anode-breaker watts

Curve *G*. Voltage across the *MC*-5 air circuit breaker used to short-circuit the rectifier to create the simulated arc-back current. Same scale as curve *B*

The Tapered Transmission Line

J. W. MILNOR
FELLOW AIEE

SEVERAL general mathematical solutions have been published dealing with the tapered transmission line as applied to communication service. These solutions [1–5] are in the form of a series or in Bessel functions, and are rather unwieldy for purposes of design.

Certain special plans of tapering, of which the exponential[6] is one, permit relatively simple solutions. It is the purpose of this paper to illustrate the applicability of such plans to practical wire-line tapering and to provide working formulas for design.

The tapering of loaded-wire lines and of lines for radio frequencies is useful, because of its transformer properties, in coupling points in a circuit which have different impedances. In submarine cable telegraph practice tapering has been applied as an aid to duplex balancing to obtain two-way working.[7] For this purpose the central portion of the cable is heavily loaded, with the portion near each end nonloaded and the intermediate cable taper-loaded.

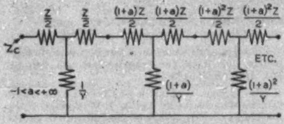

Figure 1. Lumped-tapered line showing impedance of each branch

Exponential Tapering

The subject of tapering may be developed most simply by first presenting the solutions for the exponential plan. It is assumed here that the line parameters, for sinusoidal currents, follow:

$$\left.\begin{array}{l}\text{Line series impedance per unit} \\ \text{of length} = Z_x = R_x + j\omega L_x = Z_0\epsilon^{ax} \quad (1) \\ \text{Line shunt admittance per unit} \\ \quad \text{of length} = Y_x = G_x + j\omega C_x = Y_0\epsilon^{-ax}\end{array}\right\} \quad (1)$$

in which x is the distance along the line, and a, Y_0, and Z_0 are constants; a may be positive or negative, corresponding to impedance which increases or decreases with distance from the origin.

At any point along the line, the voltage and the current bear the relation

$$-\frac{dE}{dx} = Z_0\epsilon^{ax}I \text{ and } -\frac{dI}{dx} = Y_0\epsilon^{-ax}E \quad (2)$$

The solution of these is

$$\left.\begin{array}{l}E = \dfrac{b_1(\theta+a/2)\epsilon^{(-\theta+a/2)x}}{Y_0} + \\ \qquad\qquad \dfrac{b_2(-\theta+a/2)\epsilon^{(\theta+a/2)x}}{Y_0}\end{array}\right\} \quad (3)$$

$$I = b_1\epsilon^{(-\theta-a/2)x} + b_2\epsilon^{(\theta-a/2)x}$$

in which b_1 and b_2 are constants, and $\theta = \sqrt{Y_0Z_0 + a^2/4}$

From these the next expressions follow directly: The characteristic impedance at any point x, looking away from the origin, is

$$Z_c = \frac{\theta + a/2}{Y_0}\epsilon^{ax} \quad (4)$$

In a line of length x terminated in its characteristic impedance, the ratios of received to sent voltages and currents are

$$\frac{E_r}{E_s} = \epsilon^{(-\theta+a/2)x} \text{ and } \frac{I_r}{I_s} = \epsilon^{(-\theta-a/2)x} \quad (5)$$

If the line be terminated by an impedance Z_r at the distance x, with sending from the origin, the line impedance looking from the origin is

$$Z_s = \frac{Z_0 + Z_r\epsilon^{-ax}(\theta \coth \theta x + a/2)}{\theta \coth \theta x - a/2 + Y_0Z_r\epsilon^{-ax}} \quad (6)$$

The ratio of received to sent voltages is

$$\frac{E_r}{E_s} = \frac{\theta Z_r\epsilon^{ax/2}}{\theta Z_r \cosh \theta x + (Z_0\epsilon^{ax} + aZ_r/2) \sinh \theta x} \quad (7)$$

Application to Wire-Line Tapering

Since the exponential tapering consists of a specified changing with distance of both the series impedance and the shunt admittance, it is not directly applicable to the usual wire line. However, complete freedom may be obtained as to the manner in which either the shunt admittance or the series impedance (but not both) vary along the line, while retaining the advantages of exponential tapering, by the expedient of assigning x to represent a suitable function of the distance along the line rather than the distance itself. If the function be analytical, the resulting differential equations are capable of solution, or in any case the performance may be determined by proper substitutions in the results given for the exponential tapering. The determination of the proper function is facilitated by noting, by integration of equations 1,

$$\left.\begin{array}{r}\text{Total series impedance from origin to} \\ \text{point } x = \dfrac{Z_0}{a}(\epsilon^{ax} - 1) \\ \text{Total shunt admittance from origin} \\ \text{to point } x = \dfrac{Y_0}{a}(1 - \epsilon^{-ax})\end{array}\right\} \quad (8)$$

Tapering of Line-Series Impedance Only

In wire-line or submarine-cable communication the most usual requirement is that in which the shunt admittance is unvarying with distance. This condition is met by equating the second of equations 8 to $Y_l l = Y_0 l$. Then

$$x = \frac{1}{a}\log\frac{1}{1-al} \quad \text{or} \quad \epsilon^{ax} = \frac{1}{1-al} \quad (9)$$

in which l now represents the distance along the line, and a may be positive or negative. The line parameters follow the rule:

$$Z_l = Z_0/(1-al)^2 \text{ and } Y_l = Y_0 \quad (10)$$

The characteristic impedance at a point l, looking away from the origin, is

$$Z_c = \frac{\theta + a/2}{Y_0} \cdot \frac{1}{1-al} \quad (11)$$

where

$$\theta = \sqrt{Y_0Z_0 + a^2/4}$$

Paper 45-70, recommended by the AIEE committee on communication for presentation at the AIEE winter technical meeting, New York, N. Y., January 22–26, 1945. Manuscript submitted November 11, 1944; made available for printing January 4, 1945.

J. W. MILNOR is a consulting engineer, Maplewood, N. J.

Inasmuch as standard definitions applicable to tapered lines have not been established, the author has used the term "characteristic impedance" as a general expression to indicate the impedance of a line of infinite length, whether the elements of the line are smooth or lumped.

---

case it enables the designer as well as the industrial engineer to interpret oscillograph records properly and to understand with greater assurance the performance of this important protective equipment.

References

1. A NEW MULTIPLE HIGH-SPEED AIR CIRCUIT BREAKER FOR MERCURY-ARC-RECTIFIER ANODE CIRCUITS AND ITS RELATION TO THE ARC-BACK PROBLEM, J. W. Seaman, L. W. Morton. AIEE TRANSACTIONS, volume 61, 1942, November section, pages 788–96.

2. A FAST CIRCUIT BREAKER, D. I. Bohn, Otto Jensen. AIEE TRANSACTIONS, volume 61, 1942, March section, pages 165–8.

3. RECTIFIER FAULT CURRENTS, C. C. Herskind, H. L. Kellogg. AIEE TRANSACTIONS, volume 64, 1945, March section, pages 145–50.

4. A MAGNETIC-TYPE AIR CIRCUIT BREAKER FOR 15,000-VOLT SERVICES, L. J. Linde, B. W. Wyman. AIEE TRANSACTIONS, volume 63, 1944, March section, pages 140–44.

5. GEOMETRY OF ARC INTERRUPTION, E. W. Boehne. AIEE TRANSACTIONS, volume 60, 1941, pages 524–32.

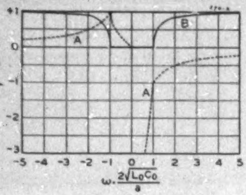

Figure 2. Characteristic impedance of smooth-taper-loaded line ignoring losses

A—Imaginary component
B—Real component

In a line of length *l* terminated in its characteristic impedance, the ratios of received to sent voltages and currents are

$$\frac{E_r}{E_s}=(1-al)^{\frac{\theta}{a}-\frac{1}{2}} \text{ and } \frac{I_r}{I_s}=(1-al)^{\frac{\theta}{a}+\frac{1}{2}} \qquad (12)$$

Values of the sending-end impedance and of the ratio of received to sent voltage, when a line of length l is terminated in an impedance Z_r, may be obtained by inserting in equations 6 and 7 the value of x obtained from equation 9.

Lumped-Tapered Line

The foregoing equations developed for the smooth-tapered transmission line, are applicable also to the lumped-tapered line at the lower frequencies, if the line is loaded. Such a line exhibits the usual cutoff at a higher frequency. To obtain the complete solution of the lumped-tapered line it is necessary to follow a different method.

A lumped-tapered line which permits ready mathematical solution may be built up of a succession of units in which the impedances increase in geometric progression. Such a line made up of *T* units is shown in Figure 1. The performance is determined by solving the first unit only, which for the purpose is considered to be terminated in an impedance equal to $(1+a)Z_c$. The coefficient of tapering a of the lumped line may take any value between -1 and $+\infty$. The resulting characteristic impedance at the head of the line is

$$Z_c=\frac{\left[\frac{a}{2}\left(1+\frac{YZ}{2}\right)+\sqrt{YZ(1+a)\left(1+\frac{YZ}{4}\right)+\frac{a^2}{4}\left(1+\frac{YZ}{2}\right)^2}\right]}{Y(1+a)} \qquad (13)$$

The ratios of received to sent voltages and currents across each unit in a long line are

$$\frac{E_r}{E_s}=(1+a)\frac{I_r}{I_s} \qquad (14)$$

$$\frac{I_r}{I_s}=\frac{1}{\left[\left(1+\frac{a}{2}\right)\left(1+\frac{YZ}{2}\right)+\sqrt{YZ(1+a)\left(1+\frac{YZ}{4}\right)+\frac{a^2}{4}\left(1+\frac{YZ}{2}\right)^2}\right]} \qquad (15)$$

Properties of the Tapered Line

The plans of tapering described herein, as well as others which may be derived from the exponential taper, are preferred forms. Aside from the comparative ease of mathematical analysis, they have the advantage that the tapering does not cause reflections of energy from points within the section, and the transfer of energy is therefore relatively efficient.

The tapering results in a transformer action which may step up or down, as is evident from equations 5, 12, 14, and 15.

A long taper-loaded line does not transmit frequencies below that where $\omega=\pm a/(2\sqrt{L_0C_0})$. This condition may set a limit to the permissible rate of taper. The characteristic impedance is largely capactitive or inductive, depending upon the sign of a, near and below the cutoff. This is illustrated in Figure 2.

Where the tapered line is lump loaded, the line, if long, behaves like a band-pass filter. The lower frequencies are lost because of the tapering; the higher frequencies because of the lumping.

References

1. Propagation des Courants Sinusoidaux sur des Lignes Quelconques, C. Revut. *Revue Générale de l'Electricité*, volume 7, May 8, 1920, number 19, page 611.

2. Propagation of Periodic Currents over Nonuniform Lines, J. R. Carson. *The Electrician*, volume 86, March 4, 1921, number 10, page 272.

3. Nonuniform Lumped Electric Lines, S. Ballantine. *Journal* of the Franklin Institute, volume 203, April 1927, page 561.

4. Sinusoidal Currents in Linearly Tapered Loaded Transmission Lines, J. W. Arnold, P. F. Bechberger. *Proceedings* of the Institute of Radio Engineers, volume 19, February 1931.

5. The Nonuniform Transmission Line, A. T. Starr. *Proceedings* of the Institute of Radio Engineers, volume 20, June 1932.

6. Transmission Lines With Exponential Taper, H. A. Wheeler. *Proceedings* of the Institute of Radio Engineers, volume 27, January 1939. A useful bibliography is included.

7. The Newfoundland–Azores High-Speed Duplex Cable, J. W. Milnor, G. A. Randall. AIEE Transactions, volume 50, 1931, pages 380–96.

Insulation Resistance and Dielectric-Absorption Characteristics of Large A-C Stator Windings

J. S. ASKEY
MEMBER AIEE

J. S. JOHNSON
ASSOCIATE AIEE

THERE HAS BEEN considerable discussion and differences of opinion relative to the significance of insulation-resistance measurements. Numerous investigations have been made and investigators have placed varying degrees of importance on their findings.[1,2,3,4] Nevertheless, insulation-resistance measurements are used widely as a nondestructive insulation test to aid in judging the suitability of machine windings for proof test or for service. Therefore, data on average values and normal spread of the insulation resistance of new insulation are of general interest. It is the belief of the authors that in order to interpret properly insulation-resistance data, a sufficiently large number of machines must be examined to permit statistical analysis.[5,6] Furthermore, insulation studied must be segregated according to detailed construction since broad insulation classifications such as AIEE class *A* or class *B* do not specify necessarily the order of insulation resistivity. Also, the effect of other important factors such as temperature and physical-design characteristics must be considered.

Many of the data that have been presented heretofore have been obtained from machines in service. Many of these machines were of older vintage and the insulation-resistance data thus obtained therefore have been on older-type insulations at an advanced stage of the insulation life expectancy. Although these data are of value, they cannot be used properly as a basis for arriving at conclusions relative to newer-type insulation, particularly on such insulation in the earlier stages of its operating life. A need was felt, therefore, for an investigation of the insulation-resistance characteristics of new machines before leaving factory. Accordingly, data are given on approximately 1,000 new a-c synchronous and induction machines of ratings 1,000 horsepower and above.

Insulation resistance of rotating machines is known to vary over what appears to be relatively wide limits and depends on a number of factors. Certain of these factors are related to the manner in which the measurements are made, and others depend upon the nature of the insulation material and its structure. The absorptive nature of machine insulation, the effects of temperature and moisture generally are recognized. Attempts have been made to standardize testing technique, to take into account the nature of the insulating material and design characteristics of machines. This was done with the hope that when correction was made for these variables, other factors which might give a clue to insulation condition would be apparent. The ultimate aim of work of this kind is to enable one to obtain by measurements of insulation resistance and study of dielectric-absorption characteristics useful information relative to the possible existence of conditions in the insulation which might lead to eventual failure in service. Present indications are that insulation-resistance measurements are useful principally for determining moisture condition of the insulation.

Scope of Work

As a necessary preliminary to such an effort it is essential to analyze insulation-resistance data on a large number of machines to determine normal variations. These data must be taken in a consistent manner and an attempt should be made to correct for known factors which affect the insulation resistance. The scope of this work has been to obtain and analyze such data on a large number of stator windings, all of the same general class.

The slot or ground insulation of all the machines studied was mica. It was, however, applied in such a manner as to present four types of insulation as:

1. Paper-backed sheet-form mica slot insulation, with end turns insulated with treated cloth tapes.
2. Glass-backed sheet-form mica slot insulation, with end turns insulated with mica tapes.
3. Mica tape applied continuously over all portions of coils, impregnated in synthetic varnish.
4. Asphaltum-bonded mica tape applied continuously over all portions of coils, impregnated with an asphaltum compound.

In the foregoing grouping, number 1 represents class *A* insulation for which cotton tape is used for a coil binder. The other groups, 2, 3, and 4, are class *B* insulation for which coil binding tape is of fiber glass.

Temperature Corrections

There is a need for more insulation resistance–temperature data since measurements in general may be made over a wide range of temperatures and for purposes of comparison, must be referred to a common temperature. Also, present standards do not specify how insulation temperature shall be determined. Insulation-resistance measurements with insulation at a uniform temperature of 75 degrees centigrade would not be expected to be the same as measurements made with machine at an operating temperature of 75 degrees centigrade because of temperature gradient existing in the insulation. Either some uniform method of determining insulation temperature applicable to all machines or the practice of making measurements at ambient temperature conditions and correcting to a base temperature seems desirable. Examination of machine temperature–insulation resistance data available shows an approximate logarithmic variation of resistance with temperature. Synthetic varnish-impregnated mica insulation shows a change in

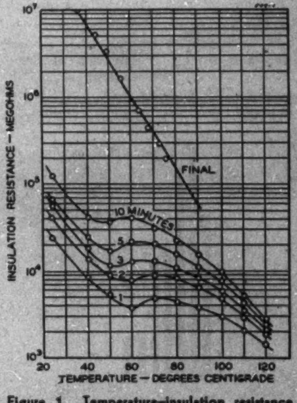

Figure 1. Temperature–insulation resistance characteristics of asphalt-bonded mica-tape insulation

Volume resistivity at 25 degrees centigrade after one minute of voltage application equals 1.7×10^9 megohm inches

Ratio-volume resistivity after ten and one minutes of voltage application at 25 degrees centigrade equals five

---

Paper 45-49, recommended by the AIEE committee on electric machinery for presentation at the AIEE winter technical meeting, New York, N. Y., January 22-26, 1945. Manuscript submitted November 3, 1944; made available for printing January 4, 1945.

J. S. ASKEY is section manager, commercial insulation section, and J. S. JOHNSON is an engineer in the development insulation section, both of the a-c generator engineering department, the Westinghouse Electric and Manufacturing Company, East Pittsburgh, Pa.

The authors wish to acknowledge the assistance and helpful criticism of P. H. McAuley, L. J. Berberich, and G. L. Moses.

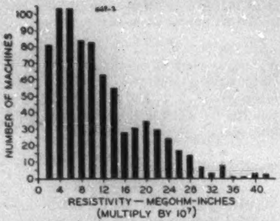

Figure 2. Frequency distribution of volume resistivity measured after one minute of voltage application; groups 1, 2, 3, and 4

Average volume resistivity equals 10.6×10^7 megohm-inches

Standard deviation is 7.4×10^7 megohm-inches

resistance from 25 degrees centigrade to 75 degrees centigrade of approximately ten to one. Asphalt-bonded continuous mica tape has a ratio of approximately 14 to 1. Since all insulation-resistance data reported here were obtained at or close to room conditions, temperature corrections were made to 25 degrees centigrade. This temperature was chosen because the temperature differences for which correction was necessary would then be small and chances of error due to inexact correction factors were minimized.

Of interest in connection with temperature–insulation resistance data are results of tests made on some asphalt-bonded mica coils. These coils had been conditioned in an oven for several months at approximately 100 degrees centigrade before temperature–insulation resistance data were obtained. Insulation resistance was measured at 500 volts direct current and a microammeter with a stabilized negative feed-back amplifier was used for current measurement. As shown in Figure 1, instead of straight logarithmic variation with temperature, a changing slope with a double inflection in the range of 40 to 80 degrees centigrade is obtained on measurements made after one to ten minutes of voltage application. Temperature–insulation resistance slope at steady-state conditions (after 15 hours of voltage application) is a straight logarithmic function as shown. Hill and Berberich reported that the ratio of ten-minute to one-minute resistivity on this type of insulation increases with temperature reaching a maximum in the range of 60 to 80 degrees centigrade and then decreases with further increase in temperature.[7]

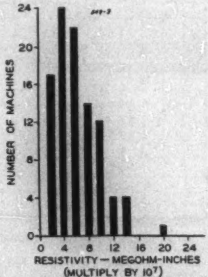

Figure 3. Frequency distribution of volume resistivity (one-minute value); group 1—class *A* with mica slot insulation

Average volume resistivity equals 6.0×10^7 megohm-inches

Standard deviation is 3.3×10^7 meghom-inches

Effects of Machine Size

In order to put insulation-resistance measurements of all machines on a comparable basis, effective insulation area and thickness data were obtained from the design information. Based on the effective area and thickness data, the insulation resistance of all the stator windings was expressed on a resistivity per megohm inch of insulation basis. In making the corrections for physical size, effect of leakage over end windings was neglected. All measurements were from three phases in parallel to ground.

Analysis of Data

Frequency-distribution curves of insulation resistance as measured after one minute of voltage application for all machines surveyed and groups 1, 2 3, and 4 separately are represented in Figures 2, 3, 4, 5, and 6. All resistance measurements were made at 500 volts direct current using an electronic-type megohm bridge. Distributions obtained are approximately normal.

Average resistivity and standard deviation for above groups are as follows:

Groups	Average Volume Resistivity, Megohms ×10^7	Standard Deviation, Megohms ×10^7	Per-Cent Dispersion
1, 2, 3, and 4	10.6	7.4	70
1	6.0	3.3	55
2	13.5	5.6	42
3	5.8	3.7	64
4	15.0	8.4	56

Groups 2 and 3 both represent data on a large number of identical machines, whereas group 4 represents machines of widely different physical size and voltage rating. Whether the relatively larger standard deviation of resistivity values of group 4 results from this fact or is naturally inherent in the type of insulation it represents is not obvious. In any event, it is evident that even after corrections are made for temperature and physical-design characteristics there is a considerable spread in the insulation resistivity. Furthermore, the average resistivities of mica insulations having somewhat different form or treated differently vary by as much as 2.5 to 1. Identical machines built in the same factory have a range of 20 to 1. The machines of group 2 were segregated into two groups according to their season of manufacture (Figure 7). This segregation narrows the dispersion somewhat but it is still relatively broad. As shown, the ratio between winter- and summer-built average is approximately two to one. That a considerable part of this spread is due to small amounts of moisture in the insulation is evident from the fact that during the summer months when moisture conditions are more severe, resistivities are appreciably lower.

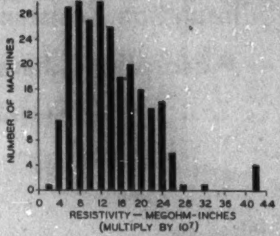

Figure 4. Frequency distribution of volume resistivity (one-minute value); group 2—class *B* with glass-reinforced slot insulation

Average volume resistivity equals 13.5×10^7 megohm-inches

Standard deviation is 5.6 by 10^7 megohm-inches

Dielectric-Absorption Characteristics

As is generally recognized, the insulation resistance of a stator winding will in-

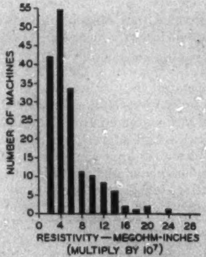

Figure 5. Frequency distribution of volume resistivity (one-minute value); group 3—class *B*, continuous mica tape with synthetic-varnish impregnation

Average volume resistivity equals 5.8×10^7 megohm-inches

Standard deviation is 3.7×10^7 megohm-inches

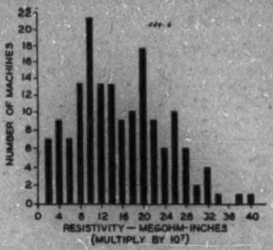

Figure 6. Frequency distribution of volume resistivity (one-minute value), group 4—class B, asphalt-bonded continuous mica tape with asphalt impregnation

Average volume resistivity equals 15.0×10^7 megohm-inches

Standard deviation is 8.4×10^7 megohm-inches

crease with time of application of voltage. This variation is caused by the electrification or "dielectric-absorption" effect in the insulation and is a function of the nature and condition of the insulation.

The shape of this absorption curve was studied on the machines surveyed and it was found that in general the first part of the curve plots as an approximate straight line on log-log paper and would therefore have an equation of the form:

$R_t = R_1 t^n$

where

R_t = insulation resistance after t minutes of voltage application
R_1 = insulation resistance after one minute of voltage application.
t = time in minutes
n = slope of curve on log-log paper

If t is taken as ten minutes, $n = \log \dfrac{R_{10}}{R_1}$ or the logarithm of the ratio of the ten and one minute readings of insulation resistance. The insulation resistance finally becomes constant and the slope of the absorption curve then is, of course, zero.

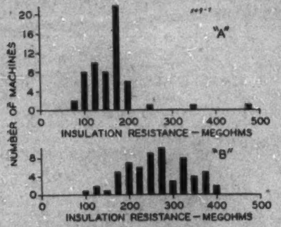

Figure 7. Frequency distribution of insulation resistance (one minute), group 2

A—Summer-built machines
Average is 146 megohms
Standard deviation is 42 megohms
B—Winter-built machines
Average is 265 megohms
Standard deviation is 80 megohms

The ratio of the ten to the one minute insulation-resistance values at 25 degrees centigrade was obtained. Figures 8, 9, and 10 show the frequency distribution of the ratio R_{10}/R_1. Figures 2, 3, 4, 5, and 6 previously referred to give the frequency distribution of R_1. As shown in Table I, the dispersion of this ratio is considerably less than the dispersion in the value of R_1.

It is thought generally that the steepness of the slope of the absorption curve as well as the magnitude of the one-minute resistance is an indication of the dryness of a winding and that the steeper the slope the drier the insulation. Figure 11 shows the variation of the average ratio R_{10}/R_1 with insulation resistivity for machines of group 2. This group consisted of approximately 120 3,300-horsepower 2,400-volt synchronous machines having fiber-glass-reinforced mica slot insulation with impregnation in synthetic varnish. The ratio R_{10}/R_1 is seen to increase steeply at first and then flatten out and remain substantially constant over a wide range of insulation resistivity. This sort of variation seems to be characteristic at least of the insulations studied. Even coils of Figure 1 which were extremely dry, having an insulation resistivity of approximately 2×10^9 megohms, have a ratio of five at 25 degrees centigrade. Although it is true that average values of R_{10}/R_1 are constant over a wide range in resistivity, individual values vary from approximately two to six over the whole range. Figure 12 shows average absorption curves at 25 degrees centigrade plotted on logarithmic paper for ratios R_{10}/R_1 of 2, 4, and 6.

In general, study of absorption characteristics shows that new machines as built with mica ground insulation have:

1. Insulation resistivities at 25 degrees centigrade of the order of 10^7 to approximately 4×10^9 megohms.

2. Insulation resistivities in the range of one to ten minutes which vary approximately as a power function of time having an equation of the form $R_t = R_1 t^n$.

3. Ratios of R_{10}/R_1 at 25 degrees centigrade vary from one to six over the complete range of resistivity.

4. Average values of the ratio R_{10}/R_1 are substantially constant over a wide range in resistivity and decrease rather sharply for lower values of resistivity.

Minimum Insulation Resistance

Insulation-resistance measurements are used widely and are considered necessary to give assurance that the condition of insulation is such that proof voltage test can be made, to determine relative dryness of the insulation and to locate possible weak spots resulting from operation or from application of proof voltage test. Insulation resistance–time curves or, correlated periodic one-minute readings on a given machine, have more significance in judging suitability of the insulation for test or operation. At the present time, the specification of precise safe minimum values of insulation resistance does not appear possible, particularly on broad general classes of insulation. As is evident from data presented here, which involves only one general class of machines and one general type of insulation (mica), there is not only a wide spread in individual values of insulation resistance but also a spread of as much as two to one in the average resistivity, depending upon the specific type of mica insulation used. In addition to these factors, the specifica-

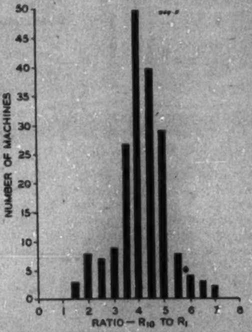

Figure 8. Frequency distribution, ratio of insulation resistance as measured after ten and one minutes of voltage application (group 2)

Average ratio is 4.0
Standard deviation is 1.0

Table I

Group	Volume Resistivity After One Minute of Voltage Application—Megohms $\times10^7$ at 25 Degrees Centigrade			Ratio-Volume Resistivity After 10 and 1 Minutes of Voltage Application at 25 Degrees Centigrade		
	Average	Standard Deviation	Per-Cent Dispersion	Average	Standard Deviation	Per-Cent Dispersion
2	13.5	5.6	42	4.0	1.0	25
3	5.8	3.7	64	3.1	0.9	29
4	15.0	8.4	56	2.6	1.0	38

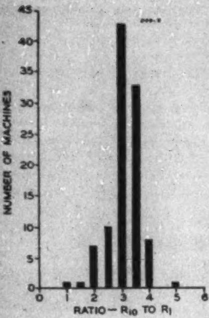

Figure 9 (left). Frequency distribution, ratio of insulation resistance as measured after ten and one minutes of voltage application, group 3

Average ratio is 3.1
Standard deviation is 0.9

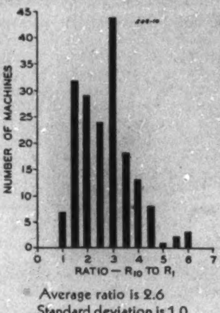

Figure 10 (right). Frequency distribution, ratio of insulation resistance as measured after ten and one minutes of voltage application, group 4

Average ratio is 2.6
Standard deviation is 1.0

tion of a safe minimum is further complicated by the following factors:

1. Even assuming the dielectric strength of an insulating material generally decreases with decrease in resistivity, the voltage breakdown–resistivity relation is not the same for all materials and even for the same material is subject to rather wide variation.
2. It cannot be assumed safely that the insulation resistivity of a machine is uniform so that in setting up safe minimums, an allowance must be made for possible nonuniform distribution of resistivity.

The present AIEE formula which gives the order of insulation resistance to be expected is:[8,9]

$$R_t = \frac{\text{rated voltage}}{\dfrac{\text{rated kva}}{100} + 1{,}000}$$

where

R_t = insulation resistance at 75 degrees centigrade

Other formulas have been proposed by Wieseman which attempt to take into account type of insulation, average physical-design factors, and which give insulation resistance in terms of voltage, kilovolt-ampere rating, and speed of machines. The formula suggested for class *B* synchronous and induction machines over 1,000 kva is as follows:

$$R_t = 0.1\,\frac{(\text{voltage}+3{,}600)\ (\text{rpm})^{1/3}}{\text{kva}^{3/8}}$$

These formulas have a more logical basis than the present AIEE formula and in a general way do take into account physical-design factors. They do not take into account in general the type of insulation, since class *A* or class *B* does not define necessarily the insulation with reference to insulation-resistivity characteristics. Various types of class *B* insulations can have different resistivities and, as is shown in this paper, even mica insulations with different fabrication as regards physical reinforcing material and treatment have different resistivities. These formulas, however, do give a better picture of the order of insulation resistance to be expected. One criticism which has been made is that the formulas are more complicated involving fractional powers, and that this would necessitate in general the reference to charts or nomographs for the calculation of resistance. For the average maintenance man, this appears to be a valid criticism.

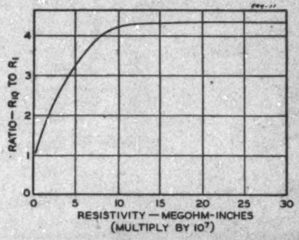

Figure 11. Average ratio of insulation resistance (ten-minute value/one-minute value) as a function of insulation resistance measured one minute after voltage application, group 2

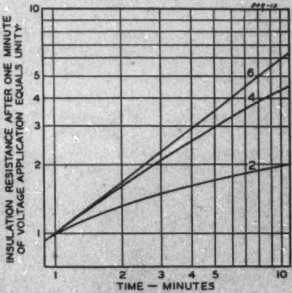

Figure 12. Average insulation-resistance–time curves as a function of ratio of insulation resistance measured after ten and one minutes of voltage application, group 2

Examination of insulation-resistance data such as is presented here leads to the conclusion that for large a-c machines there is merit in a formula which takes into account, at least in a general way, type of insulation and physical-design characteristics. However, normal variations existing in insulation resistivities, physical-design factors, and other uncertainties are such that a simpler linear approximation is completely adequate and is actually as descriptive of the order of insulation resistance to be expected, as more complicated formula. For class B synchronous and induction machines over 1,000 kva, the following formula is suggested:

$$R_t = 0.006\,\frac{(E+3{,}600)\ (\text{rpm}+1{,}400)}{(\text{kva}+5{,}000)}$$

Figure 13 gives a comparison of the Wieseman formula and the suggested linear approximation.

Summary

Insulation-resistance and dielectric-absorption data have been presented which give a comprehensive picture of average and normal spread in insulation characteristics of new large a-c synchronous and induction machines having mica insulation. Dielectric-absorption characteristics have been analyzed. Average curves and normal variations are given. Ratio of insulation resistance at 25 degrees centigrade as measured after ten minutes and after one minute of voltage application has been found to increase from one, for relatively moist windings, to approximately four, for moderately dry windings, and then to remain substantially constant over a wide range in insulation resistivity. Ratio for well-dried insulation is of the same order.

Average temperature–insulation resistance characteristics for machines based on data available are given. Temperature–insulation resistance characteristics

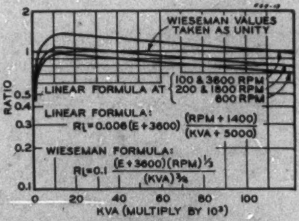

Figure 13. Comparison of Wieseman formula and suggested linear approximation

Ratio of proposed linear approximation to Wieseman formula for minimum insulation resistivity

A-c synchronous machines 1,000 kva and above of well-dried asphalt-bonded mica insulation are given as a function of various times of voltage applications. Indications are that variation of absorptive current with temperature for asphaltic-bonded mica insulation does not even approximate a simple logarithmic function. Considerations involved in the proper selection of a safe minimum value of insulation resistance are discussed. A linear formula which takes into account effects of speed, kilovolt-ampere rating, and voltage rating, with adequate precision when consideration is given to other variations involved, is suggested for large class *B* a-c induction and synchronous machines.

Work is being continued on the study of variations involved and significance which may be attached to insulation-resistance measurements. Others should be encouraged to engage in similar activity with emphasis on obtaining a sufficient amount of data to permit statistical evaluation of results since spot readings have proved of little value in the past. Such data, obtained from a number of manufacturers and correlated with periodic data obtained on machines during service life, would aid in a better understanding of the nature and significance of insulation resistance measurements.

References

1. INSULATION RESISTANCE OF ARMATURE WINDING, R. W. Wieseman. AIEE TRANSACTIONS, volume 53, 1934, June section, pages 1010–21.

2. FIELD TESTING OF GENERATOR INSULATION, EEI Subject Committee on Generator Insulation and Testing. AIEE TRANSACTIONS, volume 60, 1941, December section, pages 1003–11.

3. EFFECT OF TEMPERATURE ON INSULATION RESISTANCE, J. L. Rylander. *Electric Journal*, August 1935, September 1937.

4. PROGRESS REPORT OF D-C TESTING OF GENERATORS IN THE FIELD, E. R. Davis, M. F. Leftwich. AIEE TRANSACTIONS, volume 61, 1942, January section, pages 14–18.

5. THE APPLICATION OF STATISTICS TO DIELECTRICS, C. M. Summers, K. E. Ross. ELECTRICAL ENGINEERING, November 1944, pages 405–07.

6. AN ENGINEER'S MANUAL OF STATISTICAL METHODS, Leslie E. Simon. John Wiley and Son, Inc., 1941.

7. Discussion by C. F. Hill and L. J. Berberich of FIELD TESTING OF GENERATOR INSULATION. AIEE TRANSACTIONS, volume 60, 1941, pages 1318–19.

8. PROPOSED TEST CODE FOR SINGLE-PHASE MOTORS, AIEE Standard 502, November 1941.

9. TEST CODE FOR POLYPHASE INDUCTION MACHINES, AIEE Standard 500, August 1937.

Frequency Changers—Characteristics, Applications, and Economics

S. B. CRARY
MEMBER AIEE

R. M. EASLEY
NONMEMBER AIEE

FREQUENCY CHANGERS have been discussed at various times during the past 20 years.[1,2] At the 1944 AIEE summer technical meeting there was presented a thorough analysis of the design and operating characteristics of a new 20,000-kw electronic frequency changer.[3-7] Its installation, together with increasing interest in railroad electrification for the immediate postwar period, has resulted in a renewed interest in frequency changers.

A survey[8] of a-c public-utility generating capacity as of January 1, 1941 indicates that there exist in the United States 3,250,000 kw at other than 60 cycles or about eight per cent of the 40,000,000 kw of total installed generating capacity. Of this odd-frequency capacity (other than 60 cycles) about 70 per cent is at 25 cycles. There also exist in this country 4,000,000 kw of public-utility-owned frequency-changer capacity of which about 80 per cent is 25-cycle. These odd-frequency systems are in general decreasing in size except for additions to large existing industrial 25-cycle systems, particularly steel mills, and for new capacity for a-c railroad electrification. The steel mills and railroad electrifications represent the greatest potential users of large frequency-changer equipment.

Frequency-changing equipment falls into two general classifications as shown by Table I, synchronous tie and nonsynchronous tie. The general classification, synchronous or nonsynchronous, determines the essential *system* power-flow characteristics. As shown, there are available different types of frequency-changer equipment for obtaining either type of system performance. It then becomes a matter of engineering, amenable to analysis, as to which is the best type of frequency changer to use for a given application. It is the purpose of this paper to outline the important features of the different types including relative costs and losses.

Synchronous Tie

The synchronous-tie type of equipment provides a link between the two systems which responds to kilowatt load changes on either system similar to that of a transmission tie line. That is, if a load change occurs on one system, a kilowatt change occurs through the frequency-changer set which is dependent upon the relative governor and supplementary-governor control regulation of both systems. For example, if two systems of equal size are tied together by a synchronous–synchronous tie and each system has the same capacity in generation under governor control with equal governor regulation and load characteristics, a load

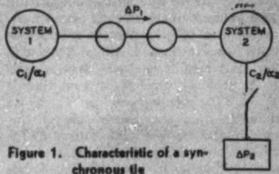

Figure 1. Characteristic of a synchronous tie

$$\Delta P_1 = \frac{\left(\frac{C_1}{\alpha_1}\right)}{\left(\frac{C_1}{\alpha_1}\right)+\left(\frac{C_2}{\alpha_2}\right)}\Delta P_2$$

where

α_1 = system speed regulation of system 1
α_2 = system speed regulation of system 2
C_1 = generating capacity of system 1 in kilowatts
C_2 = generating capacity of system 2 in kilowatts

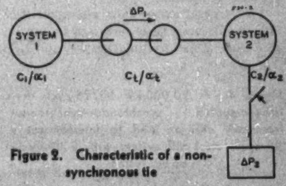

Figure 2. Characteristic of a nonsynchronous tie

$$\Delta P_1 = \frac{\left(\frac{C_1}{\alpha_1}\right)}{\left(\frac{C_1}{\alpha_1}\right)+\left(\frac{C_2}{\alpha_2}\right)+\left(\frac{C_1}{\alpha_1}\right)\left(\frac{C_2}{\alpha_2}\right)\left(\frac{\alpha_t}{C_t}\right)}\Delta P_2$$

where

α_1 = system speed regulation of system 1
α_2 = system speed regulation of system 2
α_t = speed regulation of tie
C_1 = generating capacity of system 1 in kilowatts
C_2 = generating capacity of system 2 in kilowatts
C_t = tie capacity in kilowatts

Paper 45-34, recommended by the AIEE committee on power generation for presentation at the AIEE winter technical meeting, New York, N. Y., January 22–26, 1945. Manuscript submitted November 25, 1944; made available for printing December 13, 1944. Presented originally at a meeting of the AIEE New York Section, New York, N. Y., October 18, 1944.

S. B. CRARY is in the central station engineering divisions and R. M. EASLEY is in the central station divisions, General Electric Company, Schenectady, N. Y.

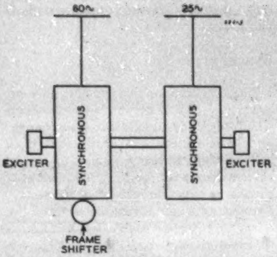

Figure 3. Synchronous–synchronous

increase on one of the systems will result in about 50 per cent of the load increase being transferred through the synchronous tie. If the load change is relatively slow, automatic or manual supplementary control of the governors of both systems—one system holding frequency, the other holding tie load—may be used to control the amount of load change through the synchronous tie. This is no different from the present use of frequency and tie line load controllers for transmission lines. If the ratio of the system sizes is, for example, ten to one with the same percentage system speed regulation for each system, the smaller system representing the 25-cycle system, and the larger system the 60-cycle system, a load change on the 25-cycle system will result in about nine-tenths of the load change being transferred through the synchronous frequency-changer set to the 60-cycle system. However, if there is in the smaller system sufficient generating capacity provided with adequate supplementary control, the load change through the synchronous-tie frequency-changer set may be limited.

The general power-flow characteristic of a synchronous tie is shown in Figure 1. The system speed regulation (α_1 and α_2) may be taken as either the inherent governor regulation or the governor supplementary control regulation depending upon the time after the load change has occurred. If the change is relatively rapid, the power flow before the governors have had time to effect a change can be determined simply by

$$\Delta P_1 = \frac{C_1}{C_1 + C_2}\ \Delta P_2$$

when the same effective inertia per kilowatt of generating capacity is assumed.

The control of power through the synchronous tie is determined by the relative generating capacity under governor control of the two systems, the size and rate of application of a load change, and whether or not supplementary control is used for control of the frequency-changer load.

Where the loads are not highly variable, it has been found possible to use synchronous-tie frequency-changer capacity of only ten per cent of the smaller system and to obtain satisfactory operation by manual control or load dispatching of the governors of the smaller system. However, when the loads are large and vary rapidly, it becomes more difficult to keep a synchronous tie in synchronism, particularly one whose capacity is small relative to the magnitude of the suddenly applied load change. For any given case, performance may be predetermined with good engineering accuracy by analysis.

Nonsynchronous Tie

The nonsynchronous tie is one which is capable of confining large and rapid load changes to one system. If the load variations are large so that they would be objectionable, for example, to the larger system, they may be confined to the smaller system by a nonsynchronous tie. On the other hand, the smaller system which has the objectionable load is subjected to a considerably larger frequency deviation and greater change in its generator loading than if the tie were synchronous. Although operating companies object to large rapidly varying loads, the design of interconnected systems has progressed so as to permit taking on these varying loads with less and less difficulty.

The characteristic of an asynchronous tie is shown in Figure 2. The different types of frequency changers are characterized by a different speed regulation α_t. The synchronous tie can be represented as a special case with $\alpha_t = 0$.

Summarizing, there are these essential and important differences between the synchronous and the nonsynchronous ties:

(*a*). With the synchronous tie, the rapidly varying load changes are shared by both systems, the larger system taking the greater part of the variation.

(*b*). With the nonsynchronous tie, the rapidly varying load changes can be confined to where they originate. The type of nonsynchronous tie determines the degree of this isolation for different rates of load application.

An essential characteristic to keep in mind is that it is simpler to parallel synchronous-tie equipment with the same type of tie capacity. Similarly, the use of nonsynchronous tie equipment tends to perpetuate the use of this equipment when additional tie capacity is needed at a future time, since it is desirable to keep the inherent speed regulation of the paralleled ties similar. This is particularly true for rapidly varying loads.

Essential Features

The essential features of the five types of frequency changers listed in Table I are as follows:

Synchronous–synchronous[9, 10] (synchronous tie). Figure 3.

(*a*). This type consists of a synchronous motor and synchronous generator with their individual exciters. It may be provided with a pilot exciter in the larger sizes and may have a starting motor. For 60 to 25 cycles the speed is 300 rpm, while for 60 to 50 cycles the speed may be 600 or 300 rpm.

(*b*). A frame shifter is usually provided on the 60-cycle end for parallel load division between frequency-changer sets. Frame

Figure 4. A 20,000-kw 60/25-cycle hydrogen-cooled synchronous–synchronous frequency changer used to interconnect a 25-cycle steel-mill system with a 60-cycle power system

Figure 5. A 30,000-kw 60-cycle three-phase to 25-cycle single-phase air-cooled synchronous–synchronous frequency changer used to supply a single-phase 25-cycle railroad system from a 60-cycle power system

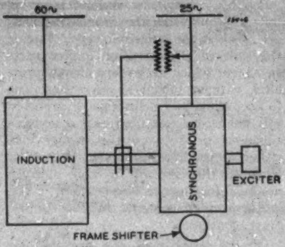

Figure 6. Induction frequency converter

shifters can be provided which allow for a shift of 16 to 24 mechanical degrees for a 300-rpm set. This is sufficient range for synchronizing and paralleling. The angle can be changed over its complete range at a rate of one mechanical degree (12 electrical degrees) in nine seconds.

(*c*). Voltage regulators and excitation systems are usually provided so as to obtain sufficient pull-out torque and kilovars to meet normal and emergency system requirements for the maintenance of system voltages. Under regulator control the pull-out power exceeds considerably the nominal synchronous-machine pull-out power, approaching 200 to 300 per cent of normal depending on system conditions.

(*d*). Sufficient kilovar capacity can be provided to meet the load and system requirements at a relatively low cost per kilovar.

(*e*). A single-phase generator may be provided at one end to supply single-phase load. In this case the stator of the single-phase generator is spring-mounted to reduce the transmission of vibration to the foundation and to reduce the magnitude of the alternating component of stator-bolt stresses.

Figure 4 shows a 20,000-kw 60/25-cycle hydrogen-cooled synchronous–synchronous frequency changer used to interconnect a 25-cycle steel-mill system with a 60-cycle power system.

Figure 5 shows a 30,000-kw 60-cycle three-phase to 25-cycle single-phase air-cooled synchronous–synchronous frequency changer used to supply a single-phase 25-cycle railroad system from a 60-cycle power system.

Induction frequency converter–synchronous[14] (synchronous tie). Figure 6.

(*a*). This type consists of an induction machine for the 60-cycle end and a synchronous machine for the 25-cycle end which has 35/60 of the kilowatt capacity of the 60-cycle induction machine. The rotor of the induction machine is connected by slip rings through a transformer to the 25-cycle system. This provides an electrical as well as mechanical tie between the 60- and 25-cycle systems. A direct-connected exciter is usually provided for the synchronous machine. The 60–25-cycle set has a speed of 300 rpm.

Figure 7. A 40,000-kw 60/25-cycle air-cooled induction frequency converter used to interconnect 60- and 25-cycle three-phase metropolitan systems

(*b*). The synchronous machine may be used to provide kilovars and regulate the voltage at the 25-cycle end. A tap-changing transformer may be used for a limited amount of regulation of the 60-cycle bus voltage.

(*c*). The kilovar capacity of this set is limited compared with the synchronous–synchronous set. Under fault or emergency conditions, however, this set is able to transfer kilovars from one system to another. It is, therefore, well suited for connecting together closely coupled systems so that one system can support the other in case of a fault or overload. This type of frequency changer found application in the days of synchronous converters and before generator voltage regulators were so generally used.

Table I. Classification of Important Types of Frequency Changers

Type	Approximate Kilowatt Capacity Installed in United States Since 1928
Synchronous tie	
Synchronous–synchronous	585,000
Induction frequency converter—synchronous	15,000
Nonsynchronous tie	
Induction–synchronous load-regulating	110,000
Electronic load-regulating	26,600
Induction-synchronous	Negligible

(*d*). This type of set may be provided with a frame shifter for parallel load division.

(*e*). It is not well suited for supplying single-phase loads as a phase unbalance would be reflected into the three-phase system.

Figure 7 shows a 40,000-kw 60/25-cycle air-cooled induction frequency converter used to interconnect 60- and 25-cycle three-phase metropolitan systems.

Induction–synchronous load-regulating[11,12,13] (nonsynchronous tie). Figure 8.

(*a*). This type of set consists of a synchronous machine connected to one system with an induction machine connected to the other system. The induction machine receives slip-frequency excitation from a regulating exciter which is in turn excited from a frequency-changing exciter. The induction end may be at either frequency. This type of set has, in general, the same speeds as the synchronous–synchronous sets for a given frequency ratio, although it is not as rigidly limited in possible speeds. Installations up to 10,000 kw capacity have been made with rated speeds in the range of 500 to 514 rpm.

(*b*). Control of voltage and kilovar supply can be obtained at either end. It is somewhat easier to obtain low power factor at the synchronous end.

(*c*). Load control can be made sufficiently fast to meet the most severe requirements usually met in practice.

(*d*). It can be used to supply single-phase load from the synchronous end.

(*e*). Controlled frequency range is usually about plus or minus two per cent.

Figure 9 shows a 10,000-kw induction synchronous load-regulating air-cooled 60/25-cycle frequency changer set used for supplying an industrial 25-cycle system.

Electronic load-regulating[3–7] (nonsynchronous tie). Figure 10.

(*a*). This type of frequency changer consists of rectifier and inverter elements with transformers, switches, and control.

(*b*). Load through the frequency changer can be controlled so as to hold power through the frequency changer with rapid changes in system frequency and therefore this equipment is capable of isolating load changes of one system from another.

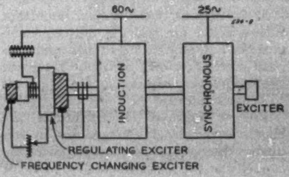

Figure 8. Induction–synchronous load-regulating

(*c*). System kilovar requirements as well as the excitation kilovar requirements of the frequency changer set must be supplied by synchronous condensers or from system sources.

(*d*). Because this set is excited from a system it requires system synchronous capacity to maintain the voltage and frequency within limits for proper rectifier and inverter excitation.

(*e*). Recent improvements include use of

Figure 9. A 10,000-kw induction–synchronous load-regulating air-cooled 60/25-cycle frequency changer set used for supplying an industrial 25-cycle system

high-voltage pentode ignitrons[8] with automatic clearing and re-energization following inverter "shoot throughs."

(*f*). In case of power failure on one or both systems, the service may be quickly re-established by reclosing the line circuit breakers, provided the system voltages have returned to the range required for commutation. No resynchronization is needed as with many types of rotating equipment.

(*g*). This type of frequency changer, being a static equipment, is well suited to a design of an unattended station.

Figure 12 of reference 3 shows a cross-section elevation af a 20,000-kw electronic load-regulating frequency changer.

Induction–synchronous (nonsynchronous tie). Figure 11.

(*a*). Consists of induction motor with a synchronous generator and exciter.

(*b*). Allows for a departure in frequency from one system to another with change in loading. Load transfer depends on departure from synchronous-frequency ratio and is not independent as in case of II-1 and II-2 types.

(*c*). Induction motor requires system kilovars for excitation.

Important Applications

It so happens that the most important future fields for the use of frequency-changer equipment, steel mills, and railroad electrification, probably represent the most severe rapidly fluctuating loads to be encountered.

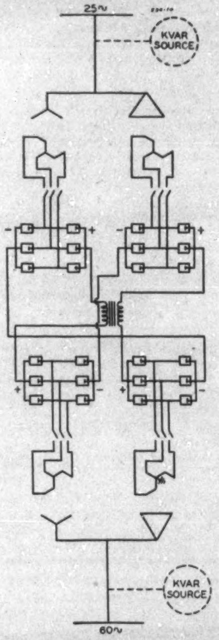

Figure 10. Electronic load-regulating

Present railroad electrifications are characterized by large capacity in frequency changers relative to the generating capacity at the lower frequency. On the other hand, the steel-mill 25-cycle system may be relatively large compared to the frequency-changer capacity. This may be said to be the essential difference between these two types of frequency-changer applications aside from the distinction that the railroad electrification is usually single-phase. The distance traversed by railroad as compared with the concentration of load and availability of waste heat energy in the steel mill is one of the essential reasons why it becomes more economical in the former case to use a large capacity in frequency-changer sets relative to generating capacity at the lower frequency. In the case of the railroad this allows a better utilization of the railroad kilowatt diversity by high-voltage transmission of the power with the location of the 25-cycle supply not being dependent on sites having generating plant facilities.

In the case of railroad electrification which uses a large frequency-changer capacity relative to the generation at the lower frequency, there is no particular problem in keeping the sets in synchronism in spite of the severe railroad load changes provided the 60-cycle supply system has adequate transmission-line capacity. The synchronous–synchronous set has the advantage of being separately excited by direct-connected exciters. This provides better voltage conditions along the 25-cycle transmission system following load changes than can be provided by a frequency changer receiving its excitation from the alternating voltage, such as the electronic type. In case the railroad electrification interconnects two areas which are independently operated, without adequate interconnections to keep them in synchronism, it probably will be necessary to provide a nonsynchronous tie between the two systems either at the lower or higher frequency. However this case will be more unlikely in the future as the development of the interconnected systems in the United States continues.

On the other hand, the steel-mill 25-cycle system may be relatively large compared with the magnitude of the load change that is suddenly applied which in turn may be large compared with the frequency-changer capacity, particularly if there is a large strip mill. This case represents the most severe type for the use of a synchronous tie, since the total load change, if the 60-cycle system is large, will be practically all transmitted through the synchronous tie. In the case of a steel mill this load may be suddenly applied and removed in a few seconds (20,000 to 30,000 kw may be applied in 8 to 12 seconds), so that supplementary control of the 25-cycle steel-mill generation would, only with difficulty, regulate the flow of power through the tie. This is an ideal case for making use of the rotating energy of the system if a relatively large frequency change can be tolerated on the 25-cycle system. Also, a small amount of the total load may be controlled by allowing the frequency to change within the control limits of the nonsynchronous tie, when the 25-cycle system includes a large rotating load. This case represents, therefore, an ideal situation for the use of a nonsynchronous tie. Either the induction synchronous load-regulating or electronic type may be used, whichever most satisfactorily meets the requirements of the particular case. The electronic frequency changer's requirement of receiving its excitation from the a-c supply system need not be a limitation in this case, although it would be in the case of railroad electrification where there does not exist a relatively cheap source of kilovar capacity.

For conditions as outlined the large strip-mill load of a steel mill because of its character may be interconnected with a large system by a nonsynchronous tie with the principal advantage of insulating the 60-cycle system from the load changes of the steel mill. On the other hand, the railroad electrification can be supplied through a synchronous tie provided, of course, that the 60-cycle supplying systems are sufficiently well interconnected so as to remain in synchronism.

Economic Discussion

It seems in order to consider these same classes of equipment from an eco-

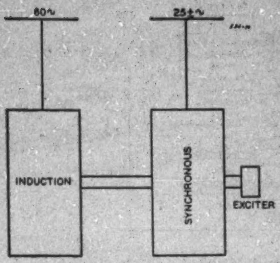

Figure 11. Induction–synchronous

nomic standpoint and an attempt is made herein to cover such factors as relative first costs and losses. Such factors as costs of foundations, costs of buildings, and the amount of first cost to be considered as offset by evaluated loss savings may vary within rather wide limits, depending on local conditions, customer's ideas as to types of structures, load factors, and so forth. Therefore, any figures set up by a manufacturer are open to question and can be right only for one set of conditions.

It is expected that the cost of installation and foundation should favor the electronic equipment. If, however, the latter requires the use of synchronous condensers for system excitation the total installation cost with the electronic frequency changer may be higher than with a rotating equipment.

Since it is felt that the difference in switchgear will not decisively affect the comparisons, it will be left out of this discussion for the sake of simplifying the picture.

It is further recognized that within the scope of this paper it is impossible to cover completely all variations which may be encountered in actual practice. This refers to cases where excess kilovars may be available, where various types of starting are required for rotating equipment, and so forth. Such data as are given hereafter will be given in such detail as to permit considerable flexibility in applying them to individual cases in order to make them most useful.

Figure 12 has been prepared to show the relative costs of the various types of frequency-changer sets at 20,000 kw for operation between 13,800-volt three-phase 60-cycle bus and 13,800-volt three-phase 25-cycle bus. It is assumed that power flow in either direction will be required with full set kilowatt output, but that the generators of rotating equipments will be permitted to operate at increased power factor when motoring in order to stay within rated kilovolt-amperes. In representing the various pieces of equipment going into the makeup of the rotating sets, the percentage is shown adjacent thereto in order to give a comparison. Similar percentages are not shown for the electronic set because it is expected that these may change appreciably relative to the rotating sets. Such figures, however, can be made available by the manufacturers when needed on a current basis. Thus it is possible from the figures to arrive at different combinations more applicable to individual problems. It will be noted that the synchronous–synchronous set has been chosen as 100 per cent (this without the starting motor included) and all other equipment is shown on this same base. A starting motor can be added to this set as shown in part A of Figure 12 at 3.4 per cent, or the coolers, exciters, and frame-shifting device may be omitted at the figures indicated.

Transformers for stepping up from 13.8 kv can be added directly to the rotating equipment at either end. At a capacity of 20,000 kw for the electronic equipment and below high-voltage values of 138 kv, it will be somewhat cheaper to combine these step-up transformers with the transformer reactor combination already included for 13.8 kv. At this kilowatt capacity the net effect of requiring transformers on the 60-cycle end of the rotating equipment will be to increase its cost relative to that of the electronic equipment approximately ten per cent at 23 kv and 1.0 per cent at 115 kv. Adding transformers to the 25-cycle end will result in differences about 50 per cent more than these. Larger sets will be slightly more favorable than this to the rotating equipment and smaller ones to the electronic.

SYNCHRONOUS–SYNCHRONOUS (AIR-COOLED)

The synchronous–synchronous set shown in Figure 12A consists of the following:

One 25,000-kva 0.8-power-factor 13,800-volt three-phase 25-cycle synchronous generator.

One 23,500-kva 0.9-power-factor 13,800-volt three-phase 60-cycle synchronous motor.

One generator exciter with motor-operated rheostat.

One motor exciter with motor-operated rheostat.

One common pilot exciter with manually operated rheostat.

Surface air coolers (no duct work) and frame-shifting device for the 60-cycle unit.

This represents 100 per cent.

The starting motor shown as an added item at 3.4 per cent is a low-voltage machine (2,200 volts or less).

SYNCHRONOUS–SYNCHRONOUS (HYDROGEN-COOLED)

The hydrogen unit shown in Figure 12B has main machines of the same rating as the air-cooled unit (although of smaller physical dimensions in order to take advantage of improved cooling with hydrogen as the cooling medium), does not have a frame-shifting device, but does have built-in surface gas coolers. It will be minus direct-connected exciters but it will be noted that an induction-motor-driven exciter set is shown separately, consisting of driving motor, two main exciters, and

Table II. Summary of Frequency-Changer Characteristics

			Type of Frequency Changer				
			Air-Cooled Synchronous–Synchronous	Induction Frequency Converter—Synchronous	Induction–Synchronous Load-Regulating	Electronic Load-Regulating	Induction–Synchronous
Type of tie			Synchronous	Synchronous	Nonsynchronous	Nonsynchronous	Nonsynchronous
Effective kilowatt-speed regulation of tie	Sudden changes		0	0	0.005 to 0.01	0 to ∞	0.005 to 0.01
	Rapid changes		0	0	0 to ∞	0 to ∞	0.005 to 0.01
	Slow changes	†	0	0	0 to ∞	0 to ∞	0.005 to 0.01
		‡	0 to ∞	0 to ∞	0 to ∞	0 to ∞	0 to ∞
Excitation			Independent, both ends	Independent, one end; system, one end	Independent, one end; system, one end	System, both ends	Independent, one end; system, one end
Relative cost (20,000 kw)**			1.0	1.34	1.30	*	
Relative full-load losses (20,000 kw)***			1.0		1.47	1.65**	

† Without supplementary governor control of system prime movers.
‡ With supplementary governor control of system prime movers.
* Greater than Scherbius plus transformers.
** Includes synchronous condensers for kilovar supply.
*** Three-phase 60-cycles to three-phase 25 cycles.

pilot exciter suitable for supplying both main exciters. It will be noted that the total for frequency changer set and exciter set is 108.2 per cent.

Since a starting motor would unduly complicate the hydrogen enclosure a starting autotransformer is shown on the chart at 2.6 per cent as a separate item. It will be noted that this has a price of the same order of magnitude as the starting motor.

SYNCHRONOUS–SYNCHRONOUS (AIR-COOLED SINGLE-PHASE)

Figure 12C shows a synchronous–synchronous set rated and furnished same as the unit shown in A except that the 25-cycle generator is a single-phase unit having special amortisseur winding and spring mounting to damp out mechanical vibrations due to the pulsations of the single-phase current. The third leg of the winding is omitted as is usual. It will be noted that this equipment has a price of 120.5 per cent. A starting motor or autotransformer may be added.

INDUCTION–SYNCHRONOUS LOAD-REGULATING

Figure 12D shows the variable-ratio rotating equipment and again the kilovolt-amperes, voltage, and power-factor ratings are the same as for Figure 12A, the a-c excitation equipment being designed to give 0.8 power factor overexcited. This equipment also provides for a limiting relative spread between 25- and 60-cycle system frequencies of plus or minus one per cent. Additional spread will increase the cost. Blowers are required for properly ventilating the induction machine and these are included.

The equipment has a price of 129.7 per cent. A starting motor or autotransformer may be added.

INDUCTION FREQUENCY CONVERTER—SYNCHRONOUS

Figure 12E shows the induction frequency converter-synchronous set. The 60-cycle induction unit is designed for unity power factor but there is included a synchronous condenser to bring this to 0.9 power factor. Therefore the over-all equipment is again comparable with Figure 12A since the 25-cycle generator is made 0.52 power factor to bring this end of the equipment to 0.8 power factor over-all.

The total is 135.4 per cent. A starting motor or autotransformer may be added.

ELECTRONIC LOAD-REGULATING

Figure 12F shows the electronic equipment consisting of the necessary 25- and 60-cycle transformers, the electronic converter, or rectifier, and the inverter, together with synchronous-condenser equipment to correct the 60-cycle power factor to approximately 0.9 overexcited and the 25-cycle power factor to approximately 0.8 overexcited. (There is in addition sufficient kilovar capacity to allow for approximately a five per cent drop in voltage on either system.) This equipment is actually two 10,000-kw units and therefore for some installations may have definite operating advantages in that either half may be shut down and the other operated independently.

It is recognized that the power factor correction as provided may not be required but this is included to bring all equipments to a comparable basis. At the present time, if it is assumed that the necessary 25- and 60-cycle reactive kilovolt-amperes is available and need not be charged against the electronic equipment,

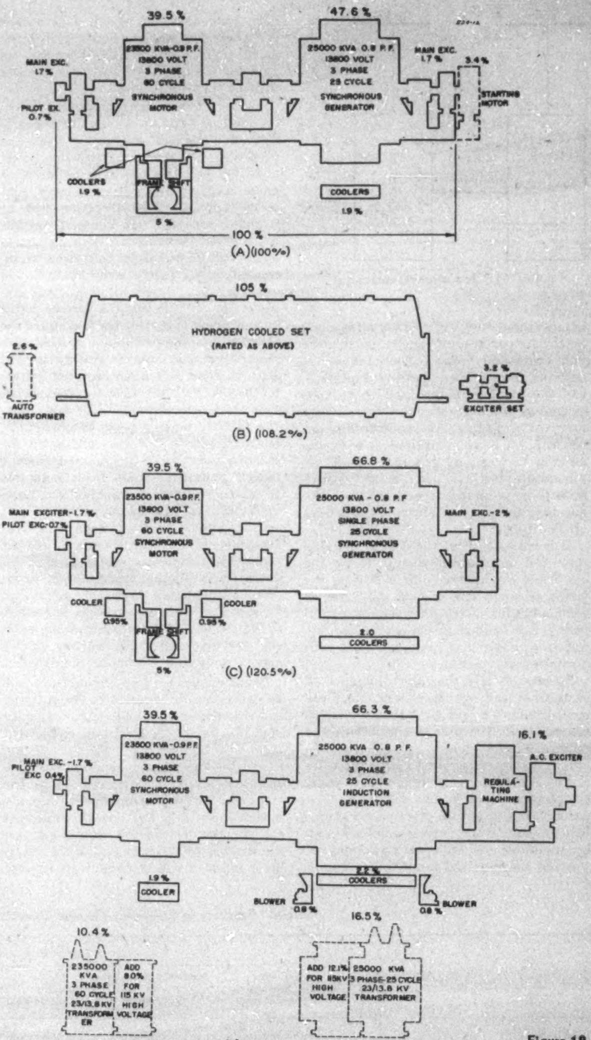
39.5 %
47.6 %
23500 KVA-0.9 P.F.
13800 VOLT
3 PHASE
60 CYCLE
SYNCHRONOUS MOTOR
25000 KVA 0.8 P.F.
13800 VOLT
3 PHASE
25 CYCLE
SYNCHRONOUS GENERATOR
MAIN EXC. 1.7 %
PILOT EX. 0.7 %
MAIN EXC. 1.7 %
3.4 %
STARTING MOTOR
COOLERS 1.9 %
FRAME SHAFT
5 %
COOLERS
1.9 %
100 %
(A)(100%)
105 %
HYDROGEN COOLED SET
(RATED AS ABOVE)
2.6 %
AUTO TRANSFORMER
3.2 %
EXCITER SET
(B) (108.2%)
39.5 %
66.8 %
23500 KVA-0.9 P.F.
13800 VOLT
3 PHASE
60 CYCLE
SYNCHRONOUS MOTOR
25000 KVA - 0.8 P.F.
13800 VOLT
SINGLE PHASE
25 CYCLE
SYNCHRONOUS GENERATOR
MAIN EXCITER-1.7 %
PILOT EXC-0.7 %
MAIN EXC.-2 %
COOLER
0.95 %
COOLER
0.95 %
FRAME SHAFT
5 %
2.0
COOLERS
(C) (120.5%)
39.5 %
66.3 %
23500 KVA-0.9 P.F.
13800 VOLT
3 PHASE
60 CYCLE
SYNCHRONOUS MOTOR
25000 KVA 0.8 P.F.
13800 VOLT
3 PHASE
25 CYCLE
INDUCTION GENERATOR
MAIN EXC. -1.7 %
PILOT EXC 0.4 %
16.1 %
A.C. EXCITER
REGULATING MACHINE
1.9 %
COOLER
2.2 %
COOLERS
BLOWER
0.8 %
BLOWER
0.8 %
10.4 %
23500 KVA
3 PHASE
60 CYCLE
23/13.8 KV
TRANSFORMER
ADD 8.0 % FOR 115 KV HIGH VOLTAGE
16.5 %
ADD 12.1 % FOR 115 KV HIGH VOLTAGE
25000 KVA 3 PHASE 25 CYCLE 23/13.8 KV TRANSFORMER
(D) (129.7%)

Figure 12

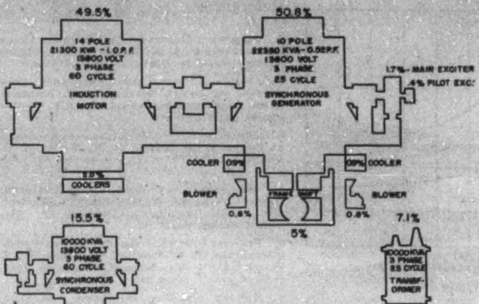
49.5%
14 POLE
21300 KVA - 1.0 P.F.
13800 VOLT
3 PHASE
60 CYCLE
INDUCTION
MOTOR
50.8%
10 POLE
22380 KVA - 0.52 P.F.
13800 VOLT
3 PHASE
25 CYCLE
SYNCHRONOUS
GENERATOR
1.7% - MAIN EXCITER
.4% PILOT EXC.
COOLER
0.9%
0.9%
COOLER
COOLERS
BLOWER
BLOWER
0.8%
0.8%
5%
15.5%
10000 KVA
13800 VOLT
3 PHASE
60 CYCLE
SYNCHRONOUS
CONDENSER
7.1%
10000 KVA
3 PHASE
25 CYCLE
TRANSFORMER

(E) (135.4%)

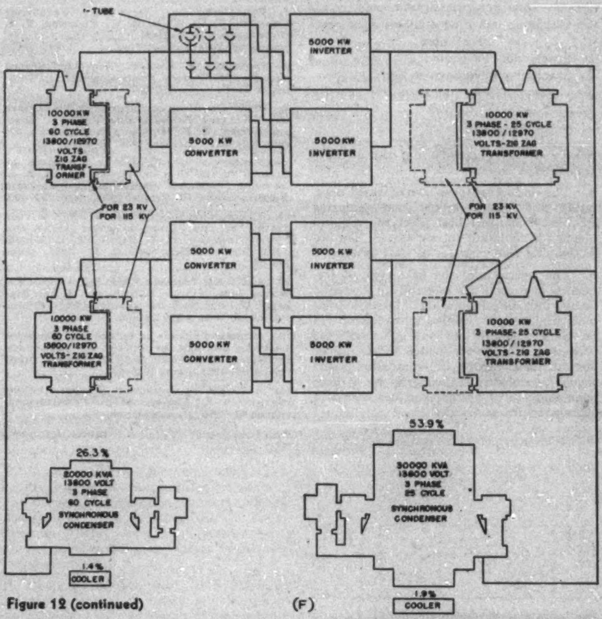
1-TUBE
5000 KW
INVERTER
10000 KW
3 PHASE
60 CYCLE
13800/12970
VOLTS
ZIG ZAG
TRANSFORMER
5000 KW
CONVERTER
5000 KW
INVERTER
10000 KW
3 PHASE - 25 CYCLE
13800/12970
VOLTS-ZIG ZAG
TRANSFORMER
FOR 23 KV
FOR 115 KV
FOR 23 KV
FOR 115 KV
5000 KW
CONVERTER
5000 KW
INVERTER
10000 KW
3 PHASE
60 CYCLE
13800/12970
VOLTS - ZIG ZAG
TRANSFORMER
5000 KW
CONVERTER
5000 KW
INVERTER
10000 KW
3 PHASE - 25 CYCLE
13800/12970
VOLTS - ZIG ZAG
TRANSFORMER
53.9%
30000 KVA
13800 VOLT
3 PHASE
25 CYCLE
SYNCHRONOUS
CONDENSER
26.3%
20000 KVA
13800 VOLT
3 PHASE
60 CYCLE
SYNCHRONOUS
CONDENSER
1.4%
COOLER
1.9%
COOLER

Figure 12 (continued) (F)

the cost of the electronic equipment and transformers is greater than that of the rotating variable-ratio equipment plus its transformers.

It might be noted that if reverse flow of power is not required a saving in the converter equipment is possible. Such a condition is rarely visualized in system interconnection but might be reasonable in supplying an isolated load.

It should be kept in mind that the engineering problems involved in design and manufacture of rotating equipment have had the benefit of many years of study so that the probabilities of substantial cost improvements are not very great. On the contrary, the electronic equipment is at a much earlier stage of development. Therefore, it is fair to assume that substantial improvements and cost reductions may be possible in this type of equipment in the near future.

Comparative Costs and Losses Versus Capacity

At the present it is believed that rotating equipment will be even more advantageous in sizes above 20,000 kw and somewhat less so in the smaller sizes, with electronic most competitive at about 5,000-kw sets.

Figure 13 is largely self-explanatory. Again the three-phase to three-phase air-cooled synchronous-synchronous set is considered 100 per cent. Shown thereon are relative per cent full load losses over the range of 5,000 kw to 35,000 kw for synchronous-synchronous, synchronous-synchronous hydrogen-cooled, rotating variable-ratio, and electronic frequency-changer equipment. It will be noted that for the electronic a curve is shown for the equipment itself exclusive of condenser losses and at 20,000 kw a higher point which includes losses in condensers used to correct power factor to overexcited values comparable to those of the rotating sets.

Figure 14 shows relative per cent no-load losses for the same sets.

If it is assumed that 23-kv transformers are required on both ends of a 20,000-kw rotating variable-ratio frequency-changer set the relative per cent full-load losses including transformer losses would increase to 1.79 and the no-load to 0.794. These points are shown on the figures.

In evaluating losses some consideration may also need to be given to cooling-water requirements. Lower losses mean less cooling water if coolers are used and may be an economic factor if water is purchased.

It is recognized that there are other ex-

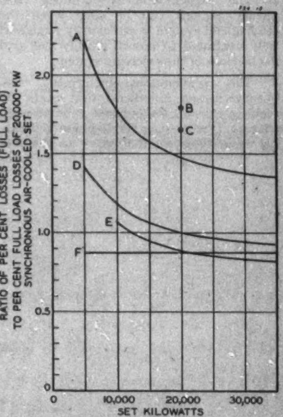

Figure 13

A—Variable ratio—rotating
B—Variable ratio—rotating, including 23-kv transformer losses at both ends
C—Electronic including equipment for reactive supply
D—Synchronous air-cooled
E—Synchronous hydrogen-cooled
F—Electronic (less equipment for reactive supply)

penses which manufacturers are not in a position to evaluate definitely, such as operation, maintenance, supervision, and, in the case of the electronic equipment, tube replacement. Experience with these particular tubes is not sufficient to give actual operating data on life. For several years similar heavy-duty power tubes have been sold with a three-year operating warranty and it is expected that experience with these tubes will be comparable or in the order of three to five years' operating life.

The electronic frequency changer described in references 3, 4, 5, and 7 illustrates a case most favorable to this type of equipment: the power supplies were 69 kv and 44 kv, respectively; sufficient kilovars were already available at both the 60-cycle and 25-cycle systems; an unattended station was called for; because of flood conditions in the proposed location the frequency changer had to be located high above ground, a fact which favored a static equipment. These conditions may or may not be duplicated elsewhere and, therefore, the choice can be made only individually for each case.

Conclusions

1. There are now available several different types of frequency changers with a wide range of characteristics (Table II), which have been proved in service to meet the requirements of differing applications.

2. The synchronous-synchronous frequency changer can be used when the sending-end system is sufficiently large and well integrated to absorb readily the load fluctuations of the receiving system.

3. The synchronous-synchronous frequency changer, in general, best meets the requirements for single-phase railroad electrification, where the single-phase generating capacity is small relative to the frequency-changer capacity and the distance traversed is large.

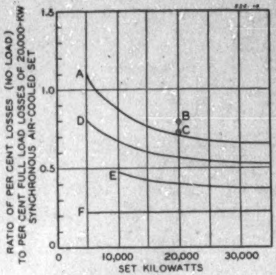

Figure 14

A—Variable ratio—rotating

B—Variable ratio—rotating, including 23-kv transformer losses at both ends

C—Electronic including equipment for reactive supply

D—Synchronous air-cooled

E—Synchronous hydrogen-cooled

F—Electronic (less equipment for reactive supply)

4. The induction synchronous load-regulating and the electronic load-regulating frequency changers best meet the requirements for confining to one system the objectionable load changes of that system.

5. The selection of the best type of frequency changer while affected by economic factors including evaluation of losses, availability and cost of reactive kilovolt-amperes on each system, and special conditions obtaining at the site which might affect normal relationships of foundation costs should be determined primarily by a thorough analysis of system and set electrical characteristics.

References

1. Frequency Converter Ties Between Large Power Systems, J. W. Dodge. *General Electric Review*, volume 26, June 1923, pages 435–44.

2. Application of Large Frequency Converters to Power Systems, E. J. Burnham. AIEE Transactions, volume 47, 1928, October section, pages 1070–80.

3. The Electronic Converter for Exchange of Power, F. W. Cramer, L. W. Morton, A. G. Darling. AIEE Transactions, volume 63, 1944, pages 1059–69.

4. Switchgear and Control for an Electronic Power Converter, W. N. Gittings, A. W. Bateman. AIEE Transactions, volume 63, 1944, August section, pages 585–9.

5. Pentode Ignitrons for Electronic Power Converters, H. C. Steiner, J. L. Zehner, H. E. Zuvers. AIEE Transactions, volume 63, 1944, October section, pages 693–7.

6. History and Development of the Electronic Power Converter, E. F. W. Alexanderson, E. L. Phillipi. AIEE Transactions, volume 63, 1944, September section, pages 654–7.

7. Design of an Electronic Frequency Changer, C. H. Willis, R. W. Kuenning, E. F. Christensen, B. D. Bedford. AIEE Transactions, volume 63, 1944, pages 1070–8.

8. Directory of Electric Generating Plants, January 1941, Federal Power Commission, Washington D. C.

9. 30,000-Kw Outdoor Frequency Converters for Supplying Pennsylvania Railroad Electrification, W. B. Morton. *General Electric Review*, volume 35, October 1932, pages 510–16.

10. Economics of Frequency Changers as Applied to the Chicago Power System, E. L. Michelson. National Electric Light Association *Bulletin*, volume 19, October 1932, pages 595–600.

11. Interconnection of the 25- and 60-Cycle System of the Union Electric Light and Power Company, L. V. Nelson, E. L. Hough. AIEE Transactions, volume 51, 1932, pages 113–20.

12. 40,000-Kw Variable-Ratio Frequency-Converter Installation, E. S. Bundy, A. Van Niekerk, W. H. Rodgers. AIEE Transactions, volume 49, 1930, pages 245–56.

13. Interconnection of Power and Railroad Traction Systems by Means of Frequency Changers, L. Encke. AIEE Transactions, volume 47, 1928, pages 1056–69.

14. A 35,000-Kw Induction Frequency-Converter, O. E. Shirley. AIEE Transactions, volume 43, 1924, pages 1011–24.

The Resistance-Coupled Amplifier

LAURENCE G. COWLES
ASSOCIATE AIEE

VACUUM-TUBE amplifiers for audio- and low-frequency applications are commonly resistance-coupled, and their design is an everyday problem for engineers in many different fields of application. The published information on the resistance-coupled amplifier is not only widely scattered and confusing but also inadequate. No convenient method is available for predicting the required electrode voltages and the correspondingly changed dynamic constants of a vacuum tube having a resistor in its plate circuit. Furthermore, no really practical method is available for designing a coupling network or for determining the phase and amplitude characteristics of both the tuned and wide-band resistance-coupled amplifier.

This paper describes methods and charts which have proved to be of extremely practical value for solving the main problems confronting an engineer working on the design and application of resistance-coupled amplifiers. The material presented includes:

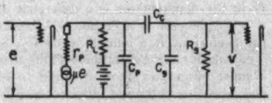

Figure 1. Complete resistance-coupled amplifier

1. The classical network solution of the resistance-coupled amplifier rearranged and simplified but without approximations.

2. A new and simple method employing an equivalent circuit and charts for determining the phase and amplitude characteristics of the resistance-coupled amplifier, the entire procedure being exact, even when applied to the narrow band or "tuned resistance-coupled amplifier."

3. A set of rules and charts for determining suitable operating voltages and the corresponding dynamic constants of any vacuum tube operated class *A* with a resistor in its plate circuit.

4. A simple bridge circuit with which the dynamic constants of a vacuum tube, as used in resistance coupling, can be measured either to check or to replace the graphical method. The bridge is useful also for studying the gain and wave form obtainable from different tubes under different operating conditions.

The Conventional Resistance-Coupled-Amplifier Network

The conventional representation of the resistance-coupled-amplifier network is shown in Figure 1. Several solutions of this network have been published, and details of the process will not be repeated. The solution, however, is rearranged and condensed in this section for a more rapid calculation of the essential constants which are used later in the equivalent circuit.

The amplifier discussed in this paper must be of such a type that it can be represented as a number of independent stages composed of the elements shown in Figure 1. The vacuum tubes are assumed to be linear and to have a negligible grid-plate capacitance, although the input impedance of the tube, including that determined by the grid-plate capacitance, is to be included in the grid-cathode resistance and capacitance shown in Figure 1. For most audio-frequency applications this reflected input impedance may be assumed to be a capacitance $(1+\mu'')C_{gp}$ having a negligible conductance, where μ'' is the actual grid-to-plate amplification of the tube in its circuit. The capacitors C_p and C_g shown in the circuit include the output and input capacitances of the first and second tubes, respectively, plus whatever additional capacitance has been added to increase the amplifiers' interstage high-frequency cutoff.

If one stage of the amplifier is considered, the solution of the network equations for the circuit of Figure 1 gives the voltage v available for the succeeding stage in terms of the voltage e applied to the grid of the tube in the stage under discussion. The tube shown in the figure has its plate voltage applied through a plate resistor R_L so that the actual plate voltage is less than that of the battery supply.

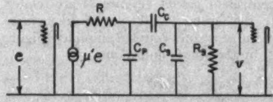

Figure 2. Condensed resistance-coupled amplifier

A later section presents a chart for selecting a suitable plate resistor R_L and for determining the correct value of the internal plate resistance r_p from values given in the tube handbook. The amplification constant μ, for reasons given later, can be taken at the value given in the handbook. (If preferred, the constants of the tube can be measured in the bridge circuit described in the final section of this paper.)

The circuit of Figure 1 may be simplified easily to the circuit of Figure 2 in accordance with Thevenin's theorem, by making the substitutions:

$$\mu' = \frac{\mu R_L}{r_p + R_L} \tag{1}$$

and

$$R = \frac{r_p R_L}{r_p + R_L} \tag{2}$$

The new constant μ' is the effective grid-to-plate amplification of the tube when working into the external plate resistor R_L. The effective plate-circuit resistance R is the parallel combination of R_L and r_p.

If one solves the equations for the (complex) grid-to-grid amplification v/e in Figure 2, one obtains

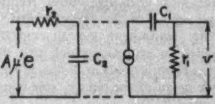

Figure 3. Equivalent circuit

$$\frac{v}{e} = \mu' \frac{-ja\omega}{d\omega^2 - jb\omega - 1} \tag{3}$$

where ω is the angular frequency, and

$$\left.\begin{aligned} a &= C_c R_g \\ b &= C_c R_g + (C_c + C_p)R + C_g R_g \\ C^2 &= C_c C_p + (C_c + C_p)C_g \\ d &= C^2 R R_g \end{aligned}\right\} \tag{4}$$

The complex coupling loss

$$F(\omega) = \frac{-ja\omega}{d\omega^2 - jb\omega - 1} \tag{5}$$

has a maximum and is real for

$$F(\omega_0) = a/b$$

when

$$\omega_0 = \sqrt{1/d} \tag{6}$$

Therefore

$$d = 1/\omega_0^2$$

It will be convenient to define the cutoff frequencies used in this paper as those for which the amplitude is reduced to 0.707 of the maximum. The actual high and low cutoff frequencies, ω_b and ω_a, of the resistance-coupled-amplifier stage under discussion are roots of the equation:

$$|F(\omega_a;\ \omega_b)| = 0.707a/b$$

Paper 45-69, recommended by the AIEE committee on communication for presentation at the AIEE winter technical meeting, New York, N. Y., January 22-26, 1945. Manuscript submitted August 24, 1944; made available for printing December 21, 1944.

LAURENCE G. COWLES is development engineer, geophysical laboratory, The Texas Company, Houston, Tex.

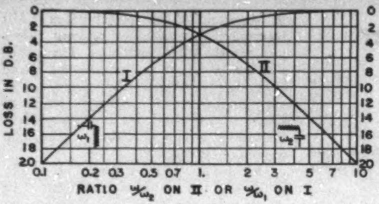

Figure 4 (left). Relative loss-frequency curves

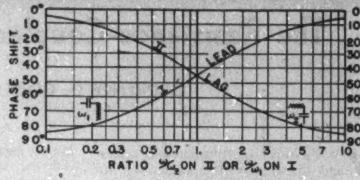

Figure 5 (right). Phase – frequency curves

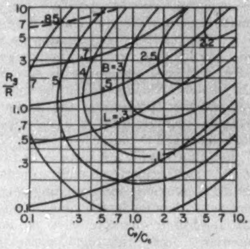

Figure 6. Coupling band width *B* and peak-frequency loss *L* when $C_g=0$

The grid-to-grid amplification may be expressed in terms of the amplifier cutoff frequencies ω_a and ω_b as follows:

$$\frac{v}{e}=\mu'\frac{-j\frac{a}{b}(\omega_b-\omega_a)\omega}{\omega^2-j(\omega_b-\omega_a)\omega-\omega_a\omega_b} \tag{7}$$

The frequency of maximum gain and zero phase shift, ω_0, is useful in a number of ways as a design parameter. In a given design it is usually a specified constant. The amplifier's phase and frequency characteristics when expressed on log–log paper are symmetrical about ω_0 so that ω_0 is the geometric mean of the actual high and low cutoff frequencies ω_b and ω_a. It is also the geometric mean of the equivalent circuit cutoff frequencies ω_2 and ω_1, which are defined later. From equation 6 $1/\omega_0$ is the geometric mean of the circuit time constants *CR* and CR_g.

The methods used by Luck,[1] Johnson,[2] and Seletzky[3] for the design of the resistance-coupled amplifier or for the calculation of its phase and amplitude characteristic are based on equations 3 and 4 or their equivalents. It is well recognized that these methods either present difficulties and are time-consuming when applied to the narrow-band amplifier or must be restricted to the wide-band amplifier. A simple equivalent circuit, which clarifies and expedites the entire problem, can be introduced to represent all of the characteristics of the resistance-coupled amplifier network of Figure 2.

The Equivalent Circuit

The important problems of calculating the phase and amplitude characteristics of a given amplifier coupling circuit or of circuit design to meet given characteristics can be understood better and solved much more easily by employing an equivalent circuit which is introduced in this section to represent the interstage elements of the amplifier.

The simplicity of the equivalent circuit to be described lies in the fact that the phase and amplitude characteristics of an amplifier composed of a number of stages of the type represented in Figure 1 can be determined by the superposition of the well-known phase and amplitude characteristics of the simple resistance–capacitance structures shown in Figure 3. The cutoff frequencies of the equivalent circuit are related very simply to the cutoff frequencies of the resistance-coupled amplifier, and the equivalence is exact at all frequencies for which the elements (including grid and plate tube impedances) of Figure 1 remain unchanged.

Subject to the following interpretation, the circuit in Figure 3 is equivalent to the circuit in Figures 1 and 2 at all frequencies. The high-frequency cutoff resistance–capacitance filter on the left is driven by the alternating voltage $A\mu'e$. The low-frequency cutoff resistance–capacitance filter on the right is driven by a (zero-impedance) voltage exactly equal to the voltage across the capacitor c_2 in the first resistance–capacitance filter. The dotted lines connecting c_2 with the second driving voltage are to suggest this unilateral transfer of the instantaneous voltage on c_2 to the following resistance–capacitance filter. Accordingly, we have

$$\frac{v}{e}=\mu'\frac{-jA\omega_2\omega}{\omega^2-j(\omega_1+\omega_2)\omega-\omega_2\omega_1} \tag{8}$$

where the low and high cutoff frequencies of the equivalent-circuit sections are $\omega_1 = 1/r_1c_1$ and $\omega_2 = 1/r_2c_2$. The output voltage of the network in Figure 3 can be made equal at all frequencies to the v in Figure 2 by adjusting the constant A and by selecting suitable values of r_1c_1 and r_2c_2.

A comparison of equations 3, 7, and 8 shows that the cutoff frequencies in the equivalent circuit (Figure 3) are related to the actual (0.707) cutoff frequencies in the resistance-coupled amplifier (Figure 2) by the simple equations:

$$\omega_1+\omega_2=\omega_b-\omega_a=b\omega_0^2 \tag{9}$$

$$\omega_1\omega_2=\omega_b\omega_a\quad=\omega_0^2 \tag{10}$$

and

$$A\omega_2=\frac{a}{b}(\omega_b-\omega_a)=a\omega_0^2 \tag{11}$$

The solution of equations 9 and 10 for the cutoff frequencies leads to a quadratic equation, but it is simpler and quicker to solve the equations by testing a few trial frequencies on a slide rule. As for equation 11, it is seldom necessary to carry through the calculation indicated, because one usually is interested only in the maximum gain of the equivalent circuit which is $\mu'(a/b)$.

Equations 7 and 8 are not of exactly the same form in that the coefficient of $j\omega$ in the denominator is a difference of two frequencies in equation 7, whereas the coefficient is a sum in equation 8. A calculation using equation 4 shows that b^2 must be greater than or equal to $4d$ and, because b and d are necessarily positive, $b \geqq 2\sqrt{d}$ so that

$$b\omega_0\geqq 2 \tag{12}$$

It follows from equations 9 and 12 that the band width of the resistance-coupled amplifier never can be less than twice the mean or peak frequency, and all possible values of $(\omega_b - \omega_a)$ range from $2\omega_0$ upward.

Because of the symmetry of ω_1 and ω_2 in equation 8 and because A may be adjusted at will, it always can be assumed that $\omega_2 \geqq \omega_1$. The minimum value of $(\omega_1 + \omega_2)$ is $2\omega_0$ when $\omega_1 = \omega_2$ as $\omega_1\omega_2 = \omega_0^2$. It is now obvious that positive equivalent-circuit cutoff frequencies ω_2 and ω_1 always can be found such that equations 9 and 10 are satisfied and $\omega_2 \geqq \omega_1$. Hence, it is always possible to find an equivalent at all frequencies to the resistance-coupled amplifier of Figure 1. Conversely, except for certain practical limitations,* an amplifier always can be constructed to duplicate the frequency characteristics of any equivalent circuit, provided that $A\omega_2$ in equation 11 does not exceed $0.5\,(\omega_b - \omega_a)$, ω_b and ω_a being determined by equations 9 and 10.

---

* For example the band width $2\omega_0$ cannot be obtained in a practical amplifier having $C_g=0$ unless $R_g\gg R$. For $R_g=MR$ the minimum band width is $2\sqrt{\frac{M+1}{M}}\,\omega_0$ for which $\frac{a}{b}=\frac{1}{2}\,\frac{M}{M+1}$ and $C_p=(M+1)C_e$.

The relative amplitude and phase characteristics of a given single-stage amplifier can be calculated by computing b and d in equation 4 from the amplifier circuit constants, or by using the measured (actual) low and high cutoff frequencies. This information in equations 9 and 10 gives ω_1 and ω_2 for the equivalent circuit. The phase and amplitude characteristics introduced by the low-frequency and high-frequency cutoffs in the equivalent circuit then are obtained separately from the well-known curves of simple resistance–capacitance filters having cutoff frequencies ω_1 and ω_2. These curves are reproduced for convenience in Figures 4 and 5. For an amplifier composed of a number of stages it is necessary only to continue adding, at each frequency, two phase angles and two amplitude losses (expressed in decibels) for each stage in the amplifier (and adding 180° phase shift if the number of stages is odd).

It is interesting to observe that the band width of a single-stage resistance-coupled amplifier is always the *sum* of the equivalent-circuit cutoff frequencies. Furthermore, the narrowest band obtainable is equal to $2\omega_0$ when $\omega_1 = \omega_2 = \omega_0$. This leads to useful relations for the actual cutoff frequencies of the narrow band amplifier:

$$\omega_a=0.41\omega_0;\quad \omega_b=2.41\omega_0;\quad b\omega_0=2$$

Coupling-Circuit Design

The design of amplifier interstage elements to produce a given frequency characteristic has been treated by others but not in a form permitting the selection of circuit constants directly from a specified band width and peak-frequency coupling loss. The problem is easy if the band width is large compared to the mid-band frequency, but difficulties arise when the band width and mid-band frequency are of the same order of magnitude.

A given frequency characteristic, specified by the mid-band frequency ω_0 and the relative band width

$$B\equiv\frac{\omega_b-\omega_a}{\omega_0} \tag{13}$$

is sufficient to determine two of the constants in equation 5. A specified peak-frequency coupling loss L gives the third, for example,

$$d=1/\omega_0^2,\quad b=B/\omega_0,\quad a=bL$$

Unfortunately, however, given a, b, and d, the simultaneous solution of equations 4 for the required circuit constants not only is unwieldy but more often than not leads to impractical or imaginary circuit elements.

An entirely different approach is more expedient and allows a better understanding of the coupling problem. Curves of constant relative band width B and peak-frequency coupling loss L can be plotted against the ratios R_g/R and $(C_p+C_g)+C_c$ when for any one set of curves the ratio C_p/C_g is constant. One set of these curves is shown on Figure 6 for $C_g = 0$, another set on Figure 7 for $C_p = C_g$, and a third on Figure 8 for $C_p = 0$. Additional curves could be prepared for other ratios of C_p/C_g, but this is hardly necessary as one can interpolate between figures with an accuracy sufficient for practical purposes.

The charts are used to select ratios of R_g/R, C_p/C_c, and C_g/C_c which give the desired band width B and an acceptable peak-frequency coupling loss L. Thereafter it is a simple matter to complete the design using the frequency relation 6, in the following form, to find C_c:

$$\frac{1}{C_c^2}=\omega_0^2RR_g\left(\frac{C_p}{C_c}+\frac{C_p}{C_c}\frac{C_g}{C_c}+\frac{C_g}{C_c}\right) \tag{14}$$

The usefulness of the charts is shown most easily by an example. Consider an interstage network for which $R = 0.25$ megohm, $R_g = 0.5$ megohm, $C_g = 0$, and $\omega_0 = 1{,}000$. As is usually the case, the ratios R_g/R and C_p/C_c are restricted to some extent because of vacuum-tube considerations and because of the convenience of certain resistor and capacitor sizes. Reference to Figure 6 shows that, for $R_g/R = 2$, B is a minimum and equals 2.45 when $C_p/C_c = 3$. Therefore, the minimum band is 2,450 radians per second with a coupling loss of ten decibels when $C_p/C_c = 3$. On the other hand the band width is increased only ten per cent and the peak-frequency coupling loss is decreased to six decibels if C_p/C_c is decreased to one.

From equation 14 the peak frequency is 1,000 radians per second for $C_c = \sqrt{8\frac{C_c}{C_p}}\times 10^{-3}$ and convenient capacitor sizes result if C_p/C_c is 2. This, the logical choice, results in a band width of 2,500 radians per second with a coupling loss of eight decibels at the peak frequency. A study of Figures 6, 7, and 8 shows that this is about the best narrow-band low-loss coupling circuit that can be designed without increasing the ratio R_g/R.

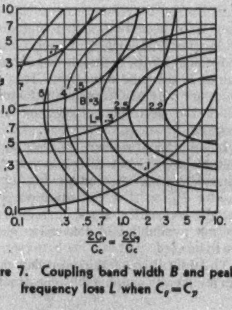

Figure 7. Coupling band width B and peak-frequency loss L when $C_g=C_p$

If we substitute $B = 2.5$ and $\omega_0 = 1{,}000$ in

$$\omega_1+\omega_2=\omega_b-\omega_a=B\omega_0 \tag{15}$$

and

$$\omega_1\omega_2=\omega_b\omega_a=\omega_0^2 \tag{10}$$

then the cutoff frequencies are $\omega_a=350$, $\omega_b = 2{,}850$, and the equivalent-circuit cutoff frequencies are $\omega_1=500$ and $\omega_2=2{,}000$ radians per second.

Vacuum-Tube Operation With a Resistor in the Plate Circuit

In many applications of vacuum tubes it is common practice to use a resistor in the plate (or screen) battery circuit. The designer usually employs a static characteristic to select a suitable resistor, determine the voltage drop in the resistor, and determine voltages for the other electrodes that will result in a suitable operating point. The chief difficulty in a problem of this kind arises because the static characteristic curves are not conveniently at hand. This is especially the case for pentodes, because data rarely are published for operating points at reduced electrode voltages. There has been a definite need for methods and charts sufficiently universal so that a designer could predict the electrode voltages and dynamic constants of any ordinary vacuum-tube operated with an external plate or screen resistor. In this section practical rules are presented for changing the operating point of a vacuum tube, and a chart based on these rules and the three-halves power law is given which permits one to select a plate resistor consistent with maximum gain, maximum voltage, or other requirements of the design, and to determine the actual reduced plate voltage of a triode, or the screen voltage of a multielectrode tube. Then, with the remaining electrode voltages reduced in direct proportion to the reduced plate (or screen) voltage, the plate current, internal impedance, and mutual conductance of the tube can be obtained, using extrapolation curves and values of these constants given in the tube handbooks.

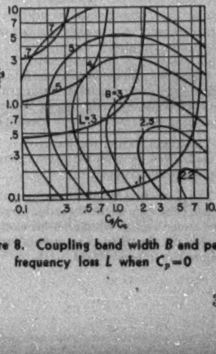

Figure 8. Coupling band width B and peak-frequency loss L when $C_p=0$

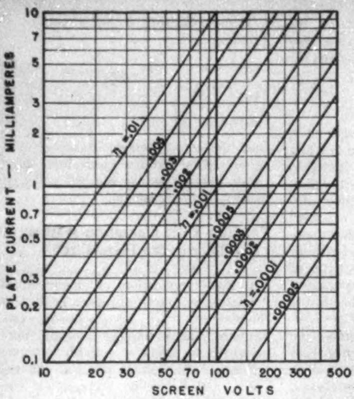

Figure 9 (left). Plate-current–screen-voltage chart

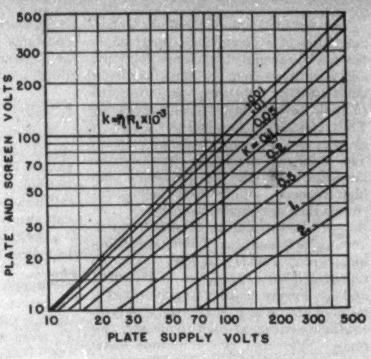

Figure 10 (right). Screen-voltage–plate-supply-voltage chart

The selection of a plate resistor and bias voltages for a triode in resistance coupling is not difficult, nor are the optimum values critical. With pentodes the situation is somewhat similar if the screen voltage can be supplied through a properly chosen series resistor, but difficulties arise, especially when the screen voltage is fixed, or if one wishes to know the plate current and dynamic constants.

The problem is greatly simplified, and operating points close to the optimum are obtained simply by reducing all electrode voltages proportionally from the values specified in the handbook. If all of the electrode voltages are reduced proportionally, then, as will be shown, the static and dynamic constants can be obtained for the new operating point by extrapolating on suitable conversion charts.

For convenience and clarity the material in this section is developed in detail for the screen grid types of vacuum tubes without specific mention of the triodes. The entire analysis applies equally well to the triodes, and it is a simple matter to include them, once the method has been explained for the other types.

We begin by stating four practical rules which can be used to govern a change in operating point and to determine the dynamic characteristics of a vacuum tube changed from one class-*A* operating point to another similar operating point; namely:

1. **A suitable class-*A* operating point can be changed to another (reasonably) similar operating point by reducing or increasing proportionally all d-c electrode potentials.**

2. **The amplification constants of a tube are unchanged by a proportional change in all its electrode potentials.**

3. **The plate current and screen current of a vacuum tube vary as the three-halves power of the screen voltage when all other electrode voltages are varied so as to remain proportional to the screen voltage.**

4. **The mutual conductance and internal plate resistance vary as the one-half and minus one-half powers, respectively, of the screen voltage when all other electrode voltages are varied proportionately.**

The first rule, as previously explained, specifies a desirable manner of changing the operating point of a vacuum tube from one recommended by the tube manufacturer. The proportional change in electrode voltages gives operating points close to the optimum and circuit values in accordance with good engineering practice. Rules 2, 3, and 4, are consistent with the three-halves power law as it is customarily stated, and they conform with the experimental facts sufficiently close for practical purposes. In spite of the exceptions, they are already in everyday use for the extrapolation of tube constants,[4] and whether the exponent is 1.5 or 1.7, as is sometimes suggested, really makes little practical difference. In the next following paragraphs the conversion equations are developed briefly.

The three-halves power law for the plate current in a screen grid tube usually is given in the following form:

$$I_p = k_1\left(E_c + \frac{E_s}{\mu_s} + \frac{E_p}{\mu_p}\right)^{3/2} \tag{16}$$

for $E_s \leqq E_p$

In this equation k_1 is a constant, E_c is the control-grid voltage, E_s/μ_s is the screen grid voltage referred to the grid plane, and E_p/μ_p is the plate voltage referred to the grid plane.

Equation 16 can be placed in the form:

$$I_p = k_2\left(\mu_s\frac{E_c}{E_s} + 1 + \frac{\mu_s}{\mu_p}\,\frac{E_p}{E_s}\right)^{3/2} E_s^{3/2} \tag{17}$$

For pentodes and tetrodes the plate amplification constant μ_p is usually an order of magnitude greater than the screen amplification constant μ_s. The d-c plate voltage is usually about equal to the screen voltage. It can be assumed, therefore, that

$$\frac{\mu_s}{\mu_p}\,\frac{E_p}{E_s} \ll \mu_s\frac{E_c}{E_s} + 1$$

or

$$I_p = k_2\left(\mu_s\frac{E_c}{E_s} + 1\right)^{3/2} E_s^{3/2} \tag{18}$$

This equation represents the flat portion of the plate-current–plate-voltage curve of tetrodes and pentodes, which for plate voltages greater than the screen voltage is independent of the plate voltage.

If, now, in accordance with rule 1, the tube is changed from one operating point to a second operating point by changing all electrode voltages by one and the same factor, the entire coefficient of $E_s^{3/2}$ in equation 18 is unchanged and we can write

$$I_p = \eta E_s^{3/2} \tag{19}$$

Similarly for the mutual conductance and plate resistance,

$$g_m \equiv \frac{\partial I_p}{\partial E_c} = k_m E_s^{1/2} \tag{20}$$

$$r_p \equiv \frac{\partial E_p}{\partial I_p} = k_r E_s^{-1/2} \tag{21}$$

The equations 19, 20, and 21 are the basis for the conversion rules 2 to 4 and they have been represented graphically on Figures 9, 11, and 12 in a form that is convenient for the extrapolation of known values of the tube constants. It is now necessary only to determine the factor by which the electrode voltages are to be changed.

In a practical problem, the plate supply voltage is given but the plate voltage is dependent upon the voltage drop in the resistor R_L, so that the situation is especially awkward if static characteristics are not available and conversion charts are to be used.

The difficulties of this everyday problem are greatly simplified by constructing

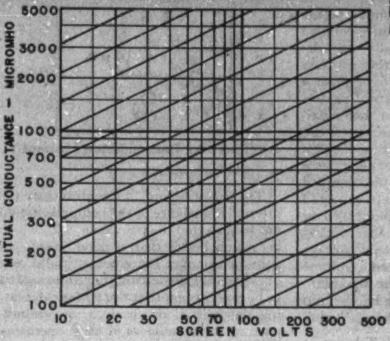

Figure 11 (left). Mutual-conductance conversion chart

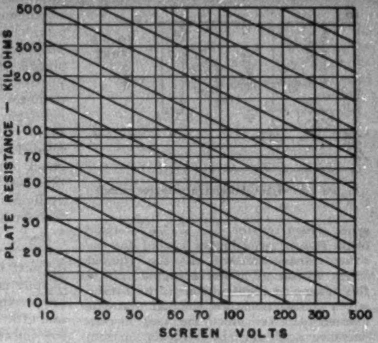

Figure 12 (right). Internal-plate-resistance conversion chart

a chart having the plate supply voltage and the plate voltage as variables. These are quantities in which the engineer is directly interested. The theory of this chart and its use now will be described.

The plate voltage is related to the plate supply voltage and the d-c drop in the plate resistor by the equation,

$$E_b = E_p + I_p R_L$$

But from equation 19 the d-c drop in the plate resistor is determined by the screen voltage,

$$I_p R_L = \eta R_L E_s^{3/2}$$

Hence,

$$(E_b - E_p) = \eta R_L E_s^{3/2} \qquad (22)$$

Equation 22 shows that two electrode voltages are related to the plate supply voltage by a single equation, and the designer is free to adjust the screen voltage relative to the plate. However, by assuming that $E_p = E_s$, equation 22 is easily solved, after which an excess of plate over screen voltage can be obtained, if desired, by a corresponding increase in the plate-voltage supply with all other supply voltages held constant.

On this assumption ($E_p = E_s$), equation 22 takes the form:

$$E_b = E_p + \eta R_L E_p^{3/2} \qquad (23)$$

The plate supply voltage E_b is given so that E_p can be found by reference to an E_p, E_b chart having $k = \eta R_L$ as a parameter. This chart is given in Figure 10.

Operating-Point Design

Before describing the use of Figure 15 we digress briefly to show that the screen grid types of tubes usually can be operated in resistance coupling with the screen voltage equal or nearly equal to that of the plate. With transformer coupling the screen grid types sometimes are operated with the screen voltage less than the plate voltage, because it is necessary to limit the plate dissipation. Tetrodes commonly are operated with reduced screen voltage to prevent distortion, but they rarely are used in resistance coupling.

When a vacuum tube is resistance-coupled, the designer usually is free of these considerations, and the screen voltage can be adjusted relative to the plate voltage so as to give a maximum gain or a maximum voltage output. However, for all practical purposes a pentode in resistance coupling gives both maximum gain and maximum voltage output when operated with the screen voltage equal or at least only slightly less than that of the plate. The restriction of designs to operation with equal plate and screen voltages is not an important practical limitation, and the design procedure is much simpler.

The procedure* for selecting a plate resistor when a given tube is specified depends on whether the screen voltage can be adjusted to a value required by the design or for some reason happens to be predetermined. If the screen voltage is not predetermined, so that the plate and screen electrode voltages can be adjusted to optimum values, then the plate resistor and the electrode voltages should be selected as follows:

1. From the plate current and screen voltages recommended for class-*A* operation of the given tube, find the η characteristic of the tube using Figure 9.

2. Refer to Figure 10 for which $E_s = E_p$ and

(*a*). Given the plate supply voltage, select k such that E_s is 20 or 25 per cent of E_b if maximum gain is required, or such that E_s is about 50 per cent of E_b if maximum voltage output is required.

(*b*). Given the plate resistor, use $k = \eta R_L$, and find the plate supply voltage required so that E_s and E_b are related as in (*a*).

(*c*). Given the plate resistor and the plate supply voltage, use $k = \eta R_L$ and find the required E_s.

3. Use as the screen voltage the value of E_s given by step 2. The plate and screen voltages are now equal, so that E_p is known. If an excess of plate voltage over screen voltage is required, then increase the voltage supplied to the plate resistor by a voltage equal to the required excess. If the screen voltage is to be obtained by the use of a

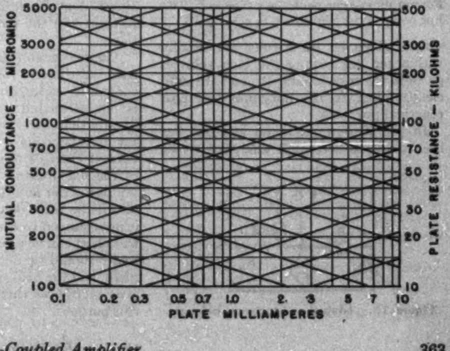

Figure 13. Conversion by plate-current chart

---

* In the procedure outlined it has been assumed that, once the plate resistor is determined, the grid resistor can be selected so that the maximum gain is not decreased seriously by too large a value of R_L/R_g. It is not usually advisable to permit the grid resistor R_g of the following tube to exceed a megohm, so that an upper limit is placed effectively on the value of the plate resistor. This happens only with tubes having a low plate current. In practical cases, the voltage gain and maximum voltage obtainable from the commercial tubes does not increase very much as the plate resistor is increased above 0.25 megohm so that a 1.0-megohm grid resistor does not really limit the applicability of Figure 10.

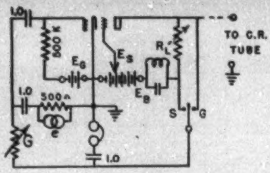

Figure 14. Transconductance-meter circuit

series screen resistor, find η characteristic of the screen, using Figure 9; and find the screen resistor that will give the required screen voltage using screen supply voltage this time on Figure 10 in place of E_b. If the screen voltage is known, the plate current, internal plate resistance, and mutual conductance are obtained by extrapolation from the values given in the tube handbook, using Figures 9, 11, and 12 as conversion charts.

For triodes the procedure is exactly the same as outlined above except that E_p is used any time either E_s or E_p is specified in the procedure just given.

If the screen voltage is specified (or if the screen supply voltage and screen resistor are given which in turn fix E_s), then the procedure for selecting the plate resistor and plate supply voltage is easily reversed. This case is not of sufficient importance to include details here. One point of importance, however, is that, if the screen supply voltage E_s and k are given, then the plate supply voltage required by Figure 10 is the lowest that can be used. If the available plate supply voltage is either appreciably greater or less than that given by Figure 10, then the specified screen voltage and k should be reconsidered.

Once the plate and screen voltages are determined, the grid bias of the tube, in conformity with rule 1, is to be reduced from the manufacturer's recommended value in proportion to the reduction in the screen voltage. On the other hand, and giving the same result, the following are very useful rules for setting the grid bias of a class-A vacuum tube:

For triodes: $E_c = -0.7E_p/\mu$
For amplifier-type pentodes: $E_c = -E_s/30$
For power-type pentodes: $E_c = -E_s/15$

Values given by these rules are usually within ten per cent of the bias voltages given in the tube handbooks and are sufficiently close to the optimum for most practical purposes.

In the present paper no attempt has been made to determine analytically the maximum voltage and maximum voltage gain obtainable in a resistance-coupled amplifier.[5] Amplifiers usually are designed either to produce the greatest possible gain per stage or to produce a definitely required voltage output so that rules for estimating the gain and maximum voltage that can be expected are needed for a starting point or as a rough check on measured values. For such purposes, a wide-band resistance-coupled audio-frequency amplifier can be expected to have a gain per stage of about 0.7μ or $^2/_3 g_m R_L$, whichever is the smaller. Correctly designed for a maximum voltage output, the rms "undistorted" voltage output is about one-seventh the plate supply voltage using high-mu triodes and one-fifth the plate supply voltage using low-mu triodes or pentodes.

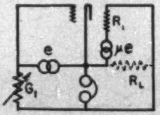

Figure 15. Mutual-conductance balance

Vacuum-Tube Conversion Charts

The conversion charts, Figures 9, 11, and 12, permit convenient extrapolation of dynamic constants when, and only when, there are proportional changes in all of the electrode voltages. Up to this point only proportional changes in the electrode voltages have been under consideration.

A conversion chart with the plate current as the independent variable can be used with care for some changes in the operating point not involving proportional changes in the electrode voltages.

With the dynamic constants given at one operating point, the constants can be found at *any* other operating point should it be safe to assume that the amplification "constants" in equation 16 are truly constant for arbitrarily chosen electrode voltages.

On this assumption the internal plate impedance and mutual conductance, as expressed in equations 20 and 21, can be made functions of the plate current alone by substituting E_s from equation 19. The conversion chart, Figure 13, represents these functions. To extrapolate g and r_p from one operating point to another, it is only necessary to know the plate current at both operating points. The chart is therefore useful when the plate current is specified or when the plate current can be measured in the circuit under consideration.

The conversion chart, Figure 13, can be used quite safely for extrapolating triode constants, especially if the plate current is not permitted to change by a factor greater than three or four. It can be used for extrapolating over reasonable plate-current changes the mutual conductance of the sharp cutoff pentodes if the plate voltage is not less than that of the screen and if the ratio of the electrode voltages is not changed too much. Whether or not this chart can be used for a particular tube really should be determined by measurement, and the bridge circuit described in a later section of this paper is suitable for this purpose.

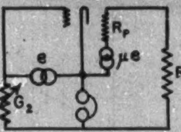

Figure 16. Transconductance balance

The use of Figure 13 to extrapolate the internal impedance of the pentodes should not be expected to give values of r_p which are much better than a good guess. In spite of this fact the chart is useful, unquestionably, for estimating values of r_p to be used in equation 1 or 24 for calculating the gain μ' or circuit transconductance s^* obtainable at a new operating point. As the actual gain of a pentode is relatively independent of its internal impedance, even for large variations in the latter, calculated values of the gain and circuit transconductance agree well enough with measured values to justify the use of the chart for this purpose. For example, in a set of 15 operating points for a 6K7-type tube where the plate current ranged from twice to one-fifth that given in the handbooks, the greatest difference between measured and calculated gains was 30 per cent, with an average difference of 12 per cent. Variations between tubes amount to as much or more, and the tube selected for this example is a "variable-mu" pentode, for which types the conversion chart is hardly applicable.

The methods outlined in the foregoing for selecting operating points of a tube with a resistor in its plate circuit certainly cannot be claimed to be universally applicable. Practical experience in the application of the charts and rules to a wide variety of problems has shown, however, that the methods usually give useful and reliable results. The conversion charts are convenient means for extrapolating the dynamic constants of tubes, but it is still to be regretted that the vacuum-tube manufacturers do not include some data in the handbooks for the lower-voltage applications.

A Vacuum-Tube Transconductance Bridge

The measurement of the dynamic constants of vacuum tubes requires for accurate results a carefully constructed bridge of a very specialized type. Good bridges are available for this purpose, but, because of the expense, they are not usually available to an engineer working on vacuum-tube amplifiers.

A transconductance meter which can be constructed easily is described in this section. With this instrument it is possible

---

[*] In this paper mutual conductance refers to the tube, whereas circuit transconductance or transconductance refers to the tube and plate resistor as defined in equation 24.

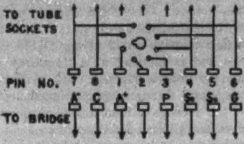

Figure 17. Socket connection plug

to make two independent transconductance measurements on a vacuum tube, from which the actual gain μ' and equivalent plate-circuit resistance R can be obtained and from which fairly accurate values of the three dynamic constants can be secured. Further, the circuit is conveniently arranged for making a rapid study of proposed operating points or of various tubes.

The transconductance-meter circuit is shown in detail in Figure 14. An alternating voltage is applied to the grid of the tube and through a variable resistor G to the headphones. The plate circuit of the tube connects through a two-position switch to the headphones. If the resistor G is adjusted to give a null in the headphones, the bridge measures (depending on the position of the switch) the mutual conductance of a tube, $g=\mu/r_p=\mu'/R$, and the circuit transconductance,

$$s=\frac{\mu}{r_p+R_L} \tag{24}$$

both with an external plate load resistor R_L in the plate circuit. For the mutual conductance balance the circuit reduces to that in Figure 15, and the mutual conductance of the tube is equal to the conductance G_1. For the circuit transconductance balance the transconductance s is equal to the conductance G_2 in Figure 16.

The actual amplification μ' of the tube with its plate resistor and the effective plate-circuit resistance R can be calculated very easily from the measured g and s by the following equations:

$$\mu'=sR_L \tag{25}$$

$$R=(s/g)R_L \tag{26}$$

The bridge is proposed principally for its usefulness in measuring μ' and R, but the amplification constant μ and the internal plate resistance r_p can be calculated as follows:

$$\mu=\frac{gR_L}{g/s-1} \tag{27}$$

$$r_p=\frac{R_L}{g/s-1} \tag{28}$$

As the ratio g/s approaches one in equations 27 and 28, the internal-impedance and amplification constant are very large and cannot be measured accurately. In this event an exact measurement of these constants is usually unimportant.

The bridge is a convenient circuit for making the usual amplifier-tube studies. By making R_L in Figure 14 a calibrated variable resistance, the plate resistor and the electrode potentials can be varied in order to find an operating point giving a maximum gain. By using a cathode-ray oscilloscope it is easy to observe the plate-circuit wave form and to locate an operating point suitable for a maximum voltage output.

The circuit in Figure 14 shows suitable values for the important elements. A 1,000-cycle oscillator (or high-frequency buzzer) can be used for the voltage e which for measurement of the dynamic constants should not exceed about 0.5 peak volt. The resistance G is best constructed and calibrated for direct reading as a conductance. The plate-circuit choke need only be large enough to prevent too serious shunting of the phones and may be replaced by a resistor, small compared to the plate load resistor. Capacitance to ground in the plate circuit should be kept at a minimum.

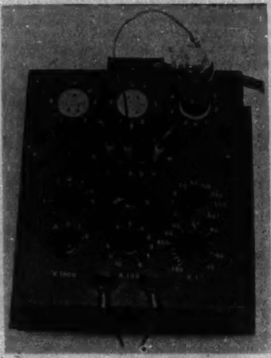

Figure 18. Transconductance meter

In constructing the bridge it is important to have a practical method for connecting different tubes into the test circuit. A convenient arrangement is to connect the tube socket to one side of a multiconductor power socket (Jones S400 series) and the bridge circuit and power supplies to the opposite side as shown in Figure 17. Then patch wires can be inserted to cross-connect the tube socket into the bridge circuit. Several different types of sockets, of course, can be connected in parallel to the same multiconductor plug.

Instruments and potentiometers for setting the electrode voltages complicate the construction and are hardly necessary. The electrode voltages can be obtained from tapped B and C batteries and measured, if necessary, with an external vacuum-tube voltmeter. A bridge of this type, which has proved to be of immense practical value, is shown in Figure 18. Obviously, it is simple enough to be used as an everyday laboratory instrument.

Summary

The routine problems of resistance-coupled amplifier design have been simplified and reduced to a set of graphs and convenient conversion charts.

In the first section it is shown that the coupling circuit (Figure 1) can be replaced by a pair of equivalent resistance–capacitance circuits (Figure 3) so that it is easy to calculate an amplifier's phase and amplitude-frequency characteristics. The design of a coupling circuit to give a specified band width and an acceptable loss has been simplified by the construction of curves of constant band width and peak-frequency loss (Figures 6, 7, 8).

In the second section a method and charts (Figures 9, 10) are presented for determining without the use of static characteristic curves a suitable operating point, electrode voltages, and plate or screen resistors for any vacuum tube operated class A. As the method given results in the tube being operated with proportionally reduced electrode voltages, its dynamic constants can be extrapolated from values furnished by the manufacturer. Charts facilitating the extrapolation are given (Figures 9, 11, 12, 13).

A simple transconductance meter for measuring the mutual conductance and circuit transconductance (equation 24) of a tube operated with an external plate resistor is described in the final section. The gain of the tube and the equivalent plate-circuit resistance can be calculated easily from these two measurements. The dynamic constants μ and r_p can be obtained also with an accuracy sufficient for most practical purposes.

The methods outlined in this paper were developed independently, and have proved to be thoroughly practical and reliable in work on a wide variety of resistance-coupled amplifiers.

References

1. A SIMPLIFIED GENERAL METHOD FOR RESISTANCE–CAPACITY-COUPLED AMPLIFIER DESIGN, D. G. C. Luck. *Proceedings* Institute of Radio Engineers, volume 20, August 1932, pages 1401–06.

2. DESIGN OF TUNED RESISTANCE–CAPACITY-COUPLED AMPLIFIERS, E. A. Johnson. *Physics*, volume 7, March 1936, pages 130–2.

3. AMPLIFICATION LOCI OF RESISTANCE–CAPACITANCE-COUPLED AMPLIFIERS, A. C. Seletzky. AIEE TRANSACTIONS, volume 55, 1936, December section, pages 1364–71; discussion and closure, volume 56, 1937, July section, pages 877–9.

4. RADIO CORPORATION OF AMERICA RECEIVING TUBE MANUAL *RC*-14, page 19.

5. CALCULATION AND DESIGN OF RESISTANCE-COUPLED AMPLIFIERS USING PENTODE TUBES, Frederick Emmons Terman, William Redington Hewlett, Charles Winslow Palmer, Wen-Yuan Pan. AIEE TRANSACTIONS, volume 59, 1940, pages 879–84.

Damping and Synchronizing Torques of Power Selsyns

C. CONCORDIA
MEMBER AIEE

GABRIEL KRON
ASSOCIATE AIEE

SELSYN systems are used very widely as power drives and as indicators when it is necessary to have the position of an element correspond synchronously with that of a controlling element which is remotely located. The receiver Selsyn is used either directly as the output driving motor or as an input to a following power-amplifying stage of a control system.* In the study of such Selsyn systems and of the control systems of which Selsyn systems form one of the links, it becomes necessary to determine the hunting-torque characteristics of these machines (that is, the damping and synchronizing torques for small oscillations) as affected by speed, load, oscillation frequency, and, of course, the various design factors. The direct calculation of these hunting-torque characteristics is difficult, but within the past few years methods have been developed whereby the machine performance may be represented by equivalent static electric circuits. The purposes of this paper are:

1. To show how these hunting-torque characteristics can be simply determined by measurements on equivalent electric circuits set up on an a-c network analyzer.
2. To present some of the results of studies made of specific Selsyn systems.

In addition to considerable information necessary for the proper design and application of Selsyns and for the calculation of the performance of the control systems of which the Selsyns may form a part, a principle of considerable generality has been found, by means of which the condition for stability of a power-Selsyn drive may be very simply stated. This condition is simply that the total effective short-circuit resistance must exceed the short-circuit reactance. The limitations of this statement will appear in the following discussion.

Single-Phase Selsyn System

The system studied consisted of two Selsyns with their two rotor windings connected together and their two stator windings connected together. Either the stator or the rotor pair is supplied with electric power. Both stator and rotor have balanced three-phase windings. The windings are assumed to be sinusoidally distributed, and saturation and possible variation of resistance with current are neglected. In an actual machine some additional effects may arise because of the space harmonics caused by the winding distribution. Also, at or very near the equilibrium point the rotor currents may in some cases be very small and the effective rotor resistance consequently somewhat larger than the nominal value because of the effect of brush drop.

The electric-power supply is either three phase or single phase; if it is single phase, the connections are as shown in Figure 1. In the method of analysis used the single-phase voltage is resolved into two polyphase-voltage systems of opposite phase rotation, so that the results for a polyphase supply are always obtained incidentally to the study of a single-phase case. The equivalent circuits for the Selsyn system of Figure 1 are shown in Figures 2 and 3; these circuits are derived and discussed in the appendix.

Table I. Two Selsyns—Receiver Hunting—Single-Phase Excitation

Value of r/x for Zero Damping—$h = 0.03$*

Case No.	r_{s1}	r_{s2}	r_r	δ	V	r/x
11	0.94		9.4	10°	0	1.00
12	0.94		9.4	10°	0	1.00
18	0.94		8.8	10°	0.2	0.95
19	6.0		5.0	10°	0.2	1.07
21	0		9.3	10°	0.2	0.90
25	0.94		9.2	10°	0	0.99
26	1.88		8.9	10°	0	1.05
28	5.4		5.4	10°	0	1.05
29	0.94		9.1	10°	0.1	0.98
31	0.94		8.4	8°	0	0.91
32	5.2		5.4	16°	0	1.03
34	0.94	9.1	5.4	10°	0	1.01
35	0.94	8.2	5.4	10°	0.2	0.97

* Except case 12 where $h = 0.06$.

Hunting

Figure 4 shows an example of the results obtained. The system consists of two identical Selsyns having resistances and reactances as shown in the figure, and with the stators excited by a single-phase source. One of the Selsyns, which may be considered as the receiver, has an average relative angle of lag of ten degrees and is hunting at a frequency of three per cent of normal. The synchronizing- and damping-torque coefficients and the average or load torque on the receiver are plotted as functions of rotor resistance. It is seen that load torque and synchronizing torque decrease continually with increasing resistance. On the other hand, the damping torque is negative for all values of rotor resistance less than 9.4 ohms and has both a minimum (at $r_r \leqq 3$) and a maximum (at $r_r \leqq 30$) value. At the point where damping becomes positive, the total resistance is $0.94 + 9.4 = 10.3$ ohms, while the total leakage reactance is also 10.3 ohms. (The total leakage reactance lies in this case between the two values of short-circuit reactance viewed from stator and rotor and is in any case a rather good approximation to the short-circuit reactance.)

Figure 5 shows the damping-torque coefficient for the same case as that of Figure 4 with both machines running at an average speed of 20 per cent of synchronous speed. The effect of speed is seen to be very small. Now the damping becomes positive at a rotor resistance of about 8.8 ohms, making the total circuit resistance $8.8 + 0.94 = 9.7$ ohms, instead of 10.3 ohms.

The effect of rotor speed is shown more directly by Figure 6. These data were obtained with a rotor resistance of 10.8 ohms, which is sufficiently large to give positive damping throughout the speed range. In this case the minimum damping occurs at zero speed. This is true, however, only if the circuit resistance is sufficiently great and is always true if damping is positive throughout the speed range. With a much smaller rotor resistance ($r_r = 0.94$), the characteristics are as shown in Figure 7. This figure is seen to resemble Figures 1, 2, and 3 of reference 1, which were found for a single polyphase Selsyn machine.

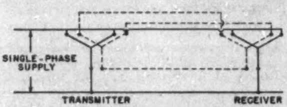

Figure 1. Two balanced Selsyns with single-phase supply

Solid line—Stator
Dashed line—Rotor

Figures 8 and 9 show the rather small effect of oscillation frequency on the damping- and synchronizing-torque coefficients, respectively, up to an oscillation frequency of 20 per cent. This indicates that the synchronizing torque should be very nearly equal to the slope of the steady-state torque–angle characteristic at the average load angle, and this has

---

Paper 45-22, recommended by the AIEE committee on electric machinery, for presentation at the AIEE winter technical meeting, New York, N. Y., January 22–26, 1945. Manuscript submitted October 30, 1944; made available for printing December 7, 1944.

C. CONCORDIA is in the analytical division, central-station engineering divisions, and GABRIEL KRON is consulting engineer, both with General Electric Company, Schenectady, N. Y.

* The case in which the receiver is rigidly coupled to the controlled output and in which the voltage differential is used as the indication of error is not considered here.

been found to be the case. Data at various load angles have been obtained but are omitted in order to shorten the paper.

Steady-State Torque-Angle Characteristics

Figures 10 and 11 show the steady-state torque-angle characteristics of two identical Selsyns for the system of Figure 1 at various rotor speeds. Figure 10 is for a rotor resistance (10.8 ohms) sufficiently large to insure positive damping, while Figure 11 is for a small rotor resistance as in Figure 7. It should be noted that cases in which the electrical damping is negative are still of interest since mechanical dampers may be added. It is seen further that the maximum torque is considerably greater when the circuit resistance is low.

Polyphase Selsyn System

As previously noted, the determination of the Selsyn characteristics with single-phase supply is obtained by the superposition of results for two polyphase-supply voltages, one of positive- and one of negative-phase sequence. Figure 12 shows, for example, the synchronizing, damping, and average torques for the two Selsyns of Figure 4 but now supplied only with the positive-sequence component of voltage. As the machines are at standstill and the load angle is small, the effects of polyphase voltage of either phase sequence are very nearly alike, and all the torques of Figure 12 are very nearly half of the corresponding torques of Figure 4.

Figure 13 shows the damping-torque coefficients as functions of rotor resistance for a rotor speed of 20 per cent and may be compared directly with Figure 5. The torque caused by both the positive- and the negative-phase-sequence voltages are shown. Since the load angle is small and its effect is also small, the two curves shown may also be considered to show directly the effect of the direction of rotation of the rotor. It will be noted that the two curves are similar to the damping-torque curve of Figure 12 (for $v = 0$) but shifted to the right and left. In fact, it may be shown for an idealized case that for polyphase excitation, the point at which the curve crosses the zero axis (that is, the resistance at which damping becomes positive) may be determined from the criterion that resistance must be greater than reactance if the reactance is again the short-circuit reactance or the sum of the leakage reactances and the resistance is the stator resistance plus the quotient of rotor resistance and slip, or

$$r = r_s + \frac{r_r}{s} \qquad x = 2x_l \tag{1}$$

where r_s and r_r are the total stator and rotor circuit resistances, respectively, and x_l is the total leakage reactance of stator or rotor. Equating r and x and solving for r_r, one obtains

$$r_r = s(x - r_s) \tag{2}$$

For $s = 0.8$, $r_r = 7.5$ ohms; for $s = 1.2$, $r_r = 11.2$ ohms.

The corresponding values read from the curves are $r_r = 6.8$ and $r_r = 10.7$.

The steady-state torque-angle characteristics at various rotor speeds and with polyphase excitation are shown in Figures 14 and 15 for the same two values of rotor resistance as in Figures 10 and 11.

Criterion of Stability

The criterion for stable operation of a Selsyn system previously suggested, that is, that the resistance must be greater than the reactance, applies exactly only to the case of infinite magnetizing reactance and zero oscillation frequency. In this case the damping-torque coefficient T_d may be shown to be given by the relation

$$T_d = \frac{k(k^2 - 1)}{x(k^2 + 1)^2} \tag{3}$$

where $k = r/x$, and the excitation voltage is unity. However, the results presented, as well as results obtained for many other cases studied, show that this criterion may be used for a wide range of conditions. It has been stated that for polyphase excitation the rotor resistance must be divided by the slip. On the other hand, for single-phase excitation the rotor resistance is used directly, regardless of speed. The reason for this is that there are in effect two slips, (s) and, $(2 - s)$, in the single-phase case, and this is a reasonable approximation, because these Selsyns

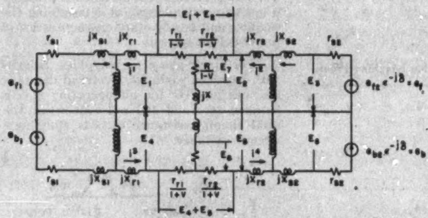

a) Steady-state network

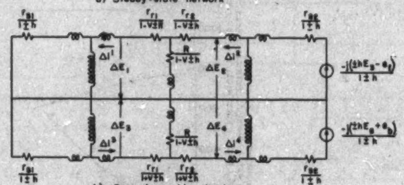

b) Second machine hunts

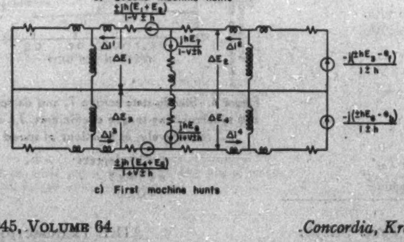

c) First machine hunts

Figure 2 (left). Two induction motors on unbalanced voltages

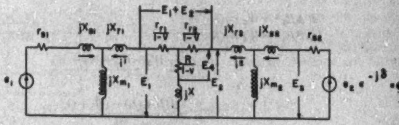

a) Steady-state network

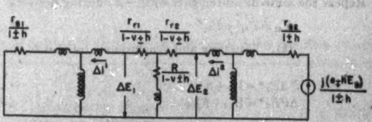

b) Second machine hunts

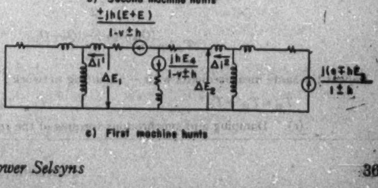

c) First machine hunts

Figure 3 (below). Two polyphase induction motors

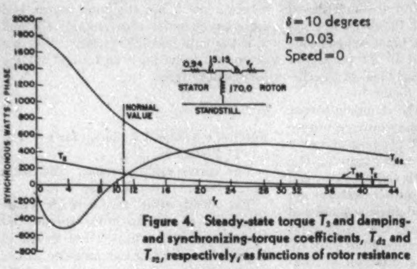

Figure 4. Steady-state torque T_2 and damping- and synchronizing-torque coefficients, T_{d2} and T_{s2}, respectively, as functions of rotor resistance

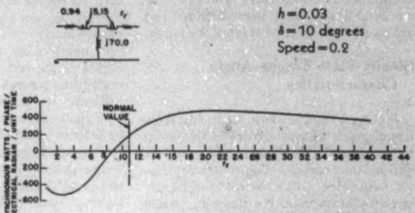

Figure 5. Damping-torque coefficient T_{d2} as a function of rotor resistance

Table II. Two Selsyns—Receiver Hunting—Polyphase Excitation

Value of r/x for Zero Damping

Case No.	r_s	r_r	δ	V	h	(r/x)*
1	0.42	4.75	30°	+0.10	0.03	1.04
2	1.44	7.2	30°	+0.40	0.03	0.97
3	0.94	10.8	−30°	−0.08	0.03	1.06
4	0.94	10.8	−10°	−1.6	0.03	1.00
5	0.94	10.8	−10°	−0.14	0.06	1.01
6	0.94	10.8	−10°	−0.08	0.01	1.06
7	0.94	5.4	+10°	+0.39	0.03	0.95
8	1.88	10.8	−10°	−0.32	0.03	0.98
11	0.94	9.3	+10°	0	0.03	1.00
12	0.94	9.0	+10°	0	0.06	0.97
18	0.94	10.6	−10°	−0.20	0.03	0.95
18	0.94	6.7	+10°	+0.20	0.03	0.91
19	4.4	4.9	+10°	+0.20	0.03	1.02
21	0	12.0	−10°	−0.20	0.03	0.97
21	0	8.1	+10°	+0.20	0.03	0.99
26	1.88	8.5	+10°	0	0.03	0.99
28	5.4	5.4	+10°	0	0.03	1.05
29	0.94	8.3	+10°	+0.10	0.03	0.97
39	0.94	0.94	+10°	+0.892	0.03	0.94
40	0.42	4.75	0°	+0.04	0.03	0.98

* Where $r=r_s+r_r/s$ and $s=1-V$.

Table III. Torque Formulas of Selsyns With Unbalanced Voltages if Either Machine Hunts

$$i^1E_1^*=W_1 \qquad i^2E_2^*=W_3$$
$$i^3E_3^*=W_2 \qquad i^4E_4^*=W_4$$
$$T_1=W_1+W_2$$
$$T_2=W_3+W_4$$

(*a*). Steady-state torques

$$i^1\Delta E_1^*=W_5+jQ_5 \qquad i^3\Delta E_3^*=W_7+jQ_7$$
$$\Delta i^1E_1^*=W_6+jQ_6 \qquad \Delta i^3E_3^*=W_8+jQ_8$$
$$T_{s1}'=\frac{W_5+W_6+W_7+W_8}{2}$$
$$T_{d1}'=\frac{(Q_6+Q_8)-(Q_5+Q_7)}{2h}$$

Repeat the same measurements with $-h$ hunting network

$$T_{s1}=T_{s1}'+T_{s1}'' \qquad T_{d1}=T_{d1}'+T_{d1}''$$

(*b*). Damping and synchronous torques of the *first* machine

$$i^2\Delta E_2^*=W_9+jQ_9 \qquad i^4\Delta E_4^*=W_{11}+jQ_{11}$$
$$\Delta i^2E_2^*=W_{10}+jQ_{10} \qquad \Delta i^4E_4^*=W_{12}+jQ_{12}$$
$$T_{s2}'=\frac{W_9+W_{10}+W_{11}+W_{12}}{2}$$
$$T_{d2}'=\frac{(Q_{10}+Q_{12})-(Q_9+Q_{11})}{2h}$$

Repeat the same measurements with $-h$ hunting network

$$T_{s2}=T_{s2}'+T_{s2}'' \qquad T_{d2}=T_{d2}'+T_{d2}''$$

(*c*). Damping and synchronous torques of the *second* machine

operate at speeds of less than about 30 per cent.

As a check upon the validity of the criterion, Tables I and II, for single-phase and polyphase excitation, respectively, have been included. These tables show the values of the effective resistance-to-reactance ratio at the point of zero damping for several cases as indicated. In no case does the ratio deviate by more than ten per cent, and in most cases it is much closer.

Conclusions

From the results presented here and from studies of additional cases, the following conclusions may be drawn:

1. The equivalent-circuit method provides a quick and simple way of determining the hunting and steady-state characteristics of power-Selsyn systems.
2. For single-phase or polyphase Selsyns with balanced windings, electrical damping becomes positive for all operating speeds between zero and 100 per cent when the total circuit resistance exceeds the short-circuit reactance.

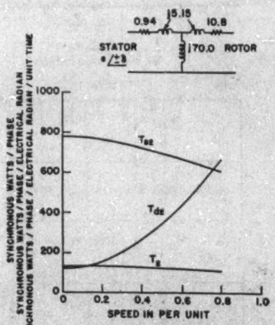

Figure 6. Steady-state torque T_2 and damping and synchronizing-torque coefficients, T_{d2} and T_{s2}, respectively, as functions of speed

δ=10 degrees
e=146.7
h=0.03

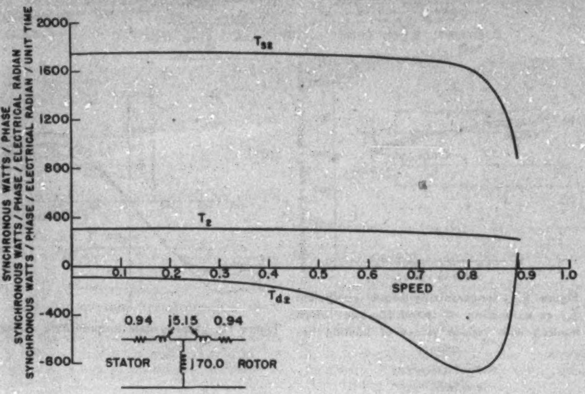

Figure 7. Steady-state torque T_2 and damping- and synchronizing-torque coefficients, T_{d2} and T_{s2}, respectively, as functions of speed

$h = 0.03$
$\delta = 10$ degrees

For polyphase Selsyns, the electrical damping may become negative at sufficiently high slips (that is, greater than 100 per cent) even if the criterion is satisfied. In this case the ratio of rotor resistance to slip should be substituted for the rotor resistance in the criterion.

3. The distribution of resistance between the stator and rotor, and the frequency of oscillation have little effect on either the damping- or synchronizing-torque coefficients.

4. Since synchronizing torque continually decreases with increasing resistance, the optimum resistance usually will be only slightly greater than that required for positive damping. Indeed, in many cases it may be advisable to use a smaller resistance and a mechanical damper.

5. When operation over the full-speed range is considered, the addition of rotor resistance rather than stator resistance to obtain stability is advisable, since this causes a smaller decrease in the pull-out torque.

Appendix. Derivation of the Equivalent Circuits

The Primitive System

The theory and equivalent circuits of two asymmetrical induction motors have been developed in reference 2. When the motors are symmetrical, the same theory and circuits still apply. However, now it is possible to remove the phase shifters from inside the circuits and shift instead the phase of the applied voltages, resulting thereby in simpler equivalent circuits. These latter may be derived from the fundamental equations of the induction motor without the introduction of advanced tensorial concepts as follows:

Let two polyphase-induction motors and a polyphase load $R+Lp$ be interconnected as shown in Figure 16. (When the load contains capacitors $1/Cp$, equations 4, 5, and 6 must be generalized in the manner shown in reference 3.) As a first step in their analysis, let all interconnections be removed, Figure 17. The $\mathbf{Z}$, $\mathbf{e}$, and $\mathbf{G}$ tensors of the primitive system are given in equations 4, 5, and 6.

$$\mathbf{Z} = \begin{array}{c|cc|cc|c} & s_1 & a_1 & s_2 & a_2 & l \\ \hline s_1 & r_{s1}+L_{s1}p & M_1p\epsilon^{j\theta_1} & & & \\ a_1 & M_1p\epsilon^{-j\theta_1} & r_{r1}+L_{r1}p & & & \\ \hline s_2 & & & r_{s2}+L_{s2}p & M_2p\epsilon^{j\theta_2} & \\ a_2 & & & M_2p\epsilon^{-j\theta_2} & r_{r2}+L_{r2}p & \\ \hline l & & & & & R+Lp \end{array} \qquad (4)$$

$$\mathbf{e} = \begin{array}{cc|cc|c} s_1 & a_1 & s_2 & a_2 & e \\ \hline e_1 & & e_2 & & \end{array} \qquad (5)$$

$$\mathbf{G}_1 = \begin{array}{c|cc|cc|c} & s_1 & a_1 & s_2 & a_2 & l \\ \hline s_1 & & & & & \\ a_1 & -jM_1\epsilon^{-j\theta_1} & -jL_{r1} & & & \\ \hline s_2 & & & & & \\ a_2 & & & & & \\ \hline l & & & & & \end{array}$$

$$\mathbf{G}_2 = \begin{array}{c|cc|cc|c} & s_1 & a_1 & s_2 & a_2 & l \\ \hline s_1 & & & & & \\ a_1 & & & & & \\ \hline s_2 & & & & & \\ a_2 & & & -jM_2\epsilon^{-j\theta_2} & -jL_{r2} & \\ \hline l & & & & & \end{array} \qquad (6)$$

The Successive Steps of Transformations

To establish equivalent circuits, five successive transformations have to be performed:

1. The two machines and the load are interconnected as shown in Figure 16 by equation 7.

$$\mathbf{C}_1 = \begin{array}{c|cccc} & s_1 & a & s_2 & l \\ \hline s_1 & 1 & & & \\ a_1 & & 1 & & \\ s_2 & & & 1 & \\ a_2 & & -1 & & -1 \\ l & & & & 1 \end{array} \qquad (7)$$

2. To get rid of the variable θ, the following reference frame has to be introduced:

(*a*). On the stator and rotor of the first machine and on the load, the axes are stationary in space.

(*b*). On the stator and rotor of the second machine, the axes rotate with slip speed $\nu_2-\nu_1$.

$$\mathbf{C}_2 = \begin{array}{c|cccc} & s_1' & a' & s_2' & l' \\ \hline s_1 & 1 & & & \\ a & & \epsilon^{-j\theta_1} & & \\ s_2 & & & \epsilon^{j(\theta_2-\theta_1)} & \\ l & & & & \epsilon^{-j\theta_1} \end{array} \qquad (8)$$

Equation 8 results where $\theta_2-\theta_1=\delta$. If the first machine is driven, then the second machine lags behind the first, θ_1 is larger than θ_2, and δ is negative. If $\mathbf{C}_1\cdot\mathbf{C}_2=\mathbf{C}$, the resultant transient tensors are found by equation 9.

$$\left.\begin{aligned} \mathbf{Z}' &= \mathbf{C}_t^*\cdot\mathbf{Z}\cdot\mathbf{C}+\mathbf{C}_t^*\cdot\mathbf{L}\cdot p\mathbf{C} \\ \mathbf{e}' &= \mathbf{C}_t^*\cdot\mathbf{e} \\ \mathbf{G}' &= \mathbf{C}_t^*\cdot\mathbf{G}\cdot\mathbf{C} \end{aligned}\right\} \qquad (9)$$

Table IV. Torque Formulas of Selsyns With Balanced Voltages if Either Machine Hunts

$i^1E_1^* = W_1$ $\qquad T_1 = W_1$ $\qquad i^2E_2^* = W_2$ $\qquad T_2 = W_2$

Steady-state torques

(*a*). Torques of first machine	(*b*). Torques of second machine
$i^1\Delta E_1^* = W_3+jQ_3$	$i^2\Delta E_2^* = W_5+jQ_5$
$\Delta i^1E_1^* = W_4+jQ_4$	$\Delta i^2E_2^* = W_6+jQ_6$
$T_{s1}' = (W_3+W_4)/2$	$T_{s2}' = (W_5+W_6)/2$
$T_{d1}' = (Q_4-Q_3)/2h$	$T_{d2}' = (Q_6-Q_5)/2h$
Repeat with $-h$ network	Repeat with $-h$ network
$T_{s1} = T_{s1}'+T_{s1}''$ $\quad T_{d1} = T_{d1}'+T_{d1}''$	$T_{s2} = T_{s2}'+T_{s2}''$ $\quad T_{d2} = T_{d2}'+T_{d2}''$

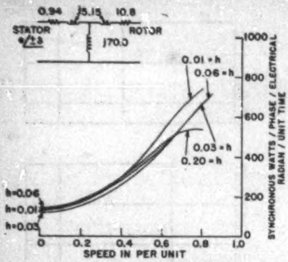

Figure 8. Damping-torque coefficient T_{d1} as a function of speed for one Selsyn hunting with various values of hunting frequency

$\delta = 10$ degrees
$e = 146.7$

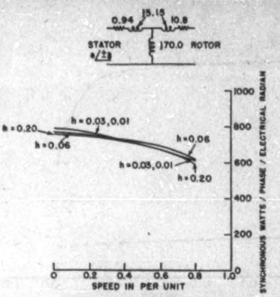

Figure 9. Synchronizing-torque coefficient T_{s1} as a function of speed for one Selsyn hunting with various values of hunting frequency

$\delta = 10$ degrees
$e = 146.7$

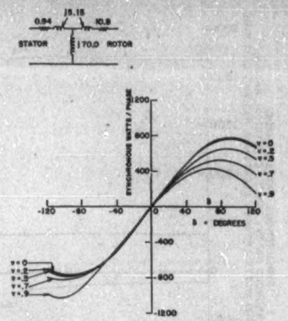

Figure 10. Steady-state torque–angle curves

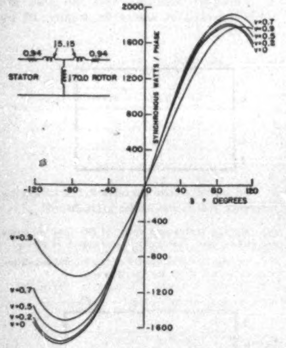

Figure 11. Steady-state torque–angle curves

Figure 12 (below). Steady-state torque T_2 and damping- and synchronizing-torque coefficients, T_{d2} and T_{s2}, respectively, as functions of rotor resistance for polyphase Selsyn

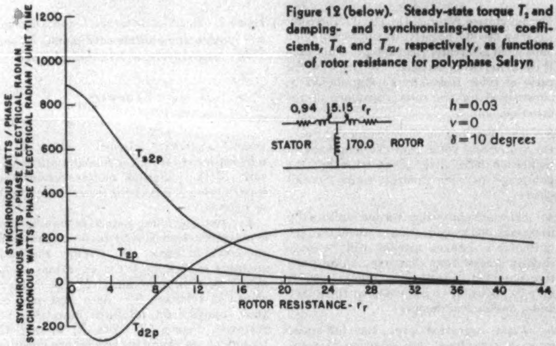

Figure 13 (below). Positive- and negative-sequence damping-torque coefficients, T_{d2p} and T_{d2n}, respectively, as functions of rotor resistance of polyphase Selsyn

$h = 0.03$
$\delta = 10$ degrees
$v = 0.2$

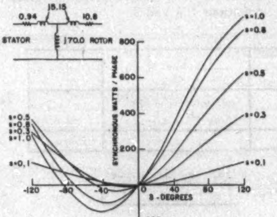

Figure 14 (left). Steady-state torque–angle curves for polyphase Selsyn

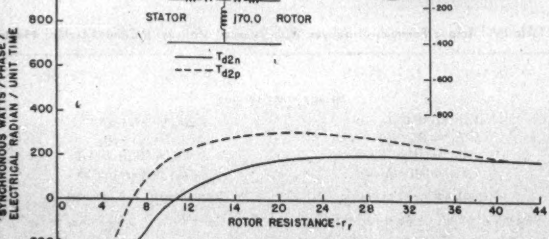

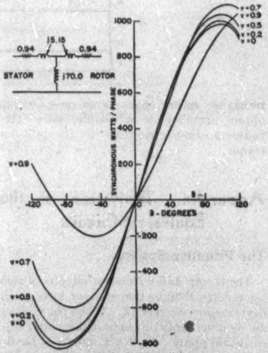

Figure 15. Steady-state torque–angle curves for polyphase Selsyn

3. The polyphase axes are replaced by real axes (at right angles in time) by replacing each component with a matrix as shown in equation 10.

$$\begin{array}{|c|}\multicolumn{1}{c}{s}\\ \hline e\\ \hline\end{array}=\begin{array}{|c|c|}\multicolumn{1}{c}{s_d} & \multicolumn{1}{c}{s_q}\\ \hline e_d & e_q\\ \hline\end{array}$$

$$s\begin{array}{|c|}\multicolumn{1}{c}{s}\\ \hline r+jx\\ \hline\end{array}=\begin{array}{c|c|c|}\multicolumn{1}{c}{} & \multicolumn{1}{c}{s_d} & \multicolumn{1}{c}{s_q}\\ \cline{2-3} s_d & r & -x\\ \cline{2-3} s_q & x & r\\ \cline{2-3}\end{array}\qquad(10)$$

4. Symmetrical components are introduced by equation 11,

$$C_1=\frac{1}{\sqrt{2}}\begin{array}{c|c|c|}\multicolumn{1}{c}{} & \multicolumn{1}{c}{s_f} & \multicolumn{1}{c}{s_b}\\ \cline{2-3} s_d & 1 & 1\\ \cline{2-3} s_q & -j & j\\ \cline{2-3}\end{array}\qquad(11)$$

using the laws of transformation of C (now $pC=0$).

5a. For the steady-state network, p is replaced by $j\omega$, Z by $n^{-1}\cdot Z$ and e by $n^{-1}\cdot e$ where n is a diagonal matrix, as shown in equation 12.

$$n=\begin{array}{c|c|c|c|c|c|c|c|c|}\multicolumn{1}{c}{} & \multicolumn{1}{c}{s_{1f}} & \multicolumn{1}{c}{s_{1b}} & \multicolumn{1}{c}{a_f} & \multicolumn{1}{c}{a_b} & \multicolumn{1}{c}{s_{2f}} & \multicolumn{1}{c}{s_{2b}} & \multicolumn{1}{c}{l_f} & \multicolumn{1}{c}{l_b}\\ \cline{2-9} s_{1f} & 1 & & & & & & & \\ \cline{2-9} s_{1b} & & 1 & & & & & & \\ \cline{2-9} a_f & & & 1-v & & & & & \\ \cline{2-9} a_b & & & & 1+v & & & & \\ \cline{2-9} s_{2f} & & & & & 1 & & & \\ \cline{2-9} s_{2b} & & & & & & 1 & & \\ \cline{2-9} l_f & & & & & & & 1-v & \\ \cline{2-9} l_b & & & & & & & & 1+v\\ \cline{2-9}\end{array}\qquad(12)$$

5b. For the hunting network, θ is replaced by $\theta+\Delta\theta$. Then:

(a). p is replaced by $j(1\pm h)\omega$

(b). The value of n' is the same as n above with $\pm h$

(c). The impressed voltage e is replaced by the value given in equation 13,

$$\Delta E^{(\alpha)}=(G^{(\alpha)}+V^{(\alpha)})\cdot ip-\frac{\partial e}{\partial\theta^{(\alpha)}}=E^{(\alpha)}p-\frac{\partial e}{\partial\theta^{(\alpha)}}\qquad(13)$$

where $E^{(\alpha)}$ is known for the steady-state network.

The Network Equations

When the final Z matrices with eight rows and columns are established, it is found that they subdivide automatically into two independent matrices, one for the forward, the other for the backward meshes, showing that the forward and backward equivalent circuits are not coupled together.

1. For the *forward* steady-state network, equations 14 and 15 hold.

$$Z_f=\begin{array}{c|c|c|c|c|}\multicolumn{1}{c}{} & \multicolumn{1}{c}{s_{1f}} & \multicolumn{1}{c}{a_f} & \multicolumn{1}{c}{s_{2f}} & \multicolumn{1}{c}{l_f}\\ \cline{2-5} s_{1f} & r_{s1}+jX_{s1} & jX_{m1} & & \\ \cline{2-5} a_f & jX_{m1} & \dfrac{r_{r1}+r_{r2}}{1-v}+j(X_{r1}+X_{r2}) & -jX_{m2} & \dfrac{r_{r2}}{1-v}+jX_{r2}\\ \cline{2-5} s_{2f} & & -jX_{m2} & r_{s2}+jX_{s2} & -jX_{m2}\\ \cline{2-5} l_f & & \dfrac{r_{r2}}{1-v}+jX_{r2} & -jX_{m2} & \dfrac{r_{r2}+R}{1-v}+j(X_{r2}+X)\\ \cline{2-5}\end{array}\qquad(14)$$

$$e_f=\begin{array}{|c|c|c|c|}\multicolumn{1}{c}{s_{1f}} & \multicolumn{1}{c}{a_f} & \multicolumn{1}{c}{s_{2f}} & \multicolumn{1}{c}{l_f}\\ \hline e_{f1} & & e_{f2}\epsilon^{-j\delta} & \\ \hline\end{array}\qquad(15)$$

The rotor fluxes are given in equations 16 and 17.

$$E_{1f}=\omega G_{1f}\cdot i_f=\begin{array}{|c|}\multicolumn{1}{c}{a_f}\\ \hline -(jX_{m1}i^{s1f}+jX_{r1}i^{af})\\ \hline\end{array}\qquad(16)$$

$$E_{2f}=\omega G_{2f}\cdot i_f=\begin{array}{|c|}\multicolumn{1}{c}{a_f}\\ \hline -jX_{r2}(i^{af}+i^{lf})+jX_{m2}i^{s2f}\\ \hline\end{array}\qquad(17)$$

2. For the *backward* steady-state network:

(a). Z_b is the same as Z_f except that $-v$ is replaced by $+v$.

(b). e_b is the same as e_f except that $-\delta$ is replaced by $+\delta$.

(c). The components of E_{1b} and E_{2b} have opposite signs to those of E_{1f} and E_{2f}.

3. For the two *forward* hunting networks (one with $+h$, the other with $-h$), equations 18 and 19 are valid.

$$Z_f=\begin{array}{c|c|c|c|c|}\multicolumn{1}{c}{} & \multicolumn{1}{c}{s_{1f}} & \multicolumn{1}{c}{a_f} & \multicolumn{1}{c}{s_{2f}} & \multicolumn{1}{c}{l_f}\\ \cline{2-5} s_{1f} & \dfrac{r_{s1}}{1\pm h}+jX_{s1} & jX_{m1} & & \\ \cline{2-5} a_f & jX_{m1} & \dfrac{r_{r1}+r_{r2}}{1-v\pm h}+jX_{r1}+X_{r2} & -jX_{m2} & \dfrac{r_{r2}}{1-v\pm h}+jX_{r2}\\ \cline{2-5} s_{2f} & & -jX_{m2} & \dfrac{r_{s2}}{1\pm h}+jX_{s2} & -jX_{m2}\\ \cline{2-5} l_f & & \dfrac{r_{r2}}{1-v\pm h}+jX_{r2} & -jX_{m2} & \dfrac{r_{r2}+R}{1-v\pm h}+j(X_{r2}+X)\\ \cline{2-5}\end{array}\qquad(18)$$

$$\Delta E_f^{\alpha}=\begin{array}{c|c|c|}\multicolumn{1}{c}{(\alpha)} & \multicolumn{1}{c}{(\Delta\theta_1)} & \multicolumn{1}{c}{(\Delta\theta_2)}\\ \cline{2-3} s_{1f} & & \\ \cline{2-3} a_f & \begin{array}{c}[X_{m1}i^{s1f}+(X_{r1}+X_{r2})i^{af}-X_{m2}i^{s2f}\\ +X_{r2}i^{lf}][\pm h/1-v\pm h]\end{array} & \\ \cline{2-3} s_{2f} & \begin{array}{c}[(-X_{m2}i^{af}+X_{s2}i^{s2f}-X_{m2}i^{lf})(\pm h)-\\ je_{s2f}\epsilon^{-j\delta}](1/1\pm h)\end{array} & \begin{array}{c}[(X_{m2}i^{af}-X_{s2}i^{s2f}+X_{m2}i^{lf})(\pm h)+\\ je_{s2f}\epsilon^{-j\delta}](1/1\pm h)\end{array}\\ \cline{2-3} l_f & \begin{array}{c}[X_{r2}i^{af}-X_{m2}i^{s2f}+\\ (X_{r2}+X)i^{lf}][\pm h/1-v\pm h]\end{array} & \\ \cline{2-3}\end{array}\qquad(19)$$

4. For the two *backward* hunting networks:

(a). Z_b is the same as Z_f except that $-v$ is replaced by $+v$.

(b). $\Delta E_b{}^{(\alpha)}$ has opposite signs to $\Delta E_f{}^{(\alpha)}$; also δ changes sign.

The equivalent circuits for the cases of unbalanced and balanced impressed voltages are given in Figures 2 and 3 and the formulas for the steady-state average and the hunting-frequency torques in Tables III and IV.

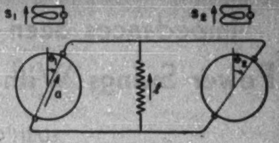

Figure 16. The interconnected system

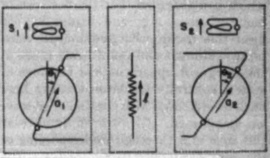

Figure 17. The primitive system

Selsyns Without Shunt Loads

When the shunt loads $R+Lp$ are absent,

1. In all matrices the last rows and columns of l are left out.

2. In the components of E and ΔE, all i^l becomes zero.

3. In the equivalent circuits the shunt loads are simply removed.

References

1. The Doubly Fed Machine, C. Concordia, S. B. Crary, Gabriel Kron. AIEE Transactions, volume 61, 1942, May section, pages 286–9.

2. Equivalent Circuits for Oscillating Systems and the Riemann-Christoffel Curvature Tensor, Gabriel Kron. AIEE Transactions, volume 62, 1943, January section, pages 25–31.

3. Steady-State and Hunting Equivalent Circuits of Long-Distance Transmission Systems, Gabriel Kron. *General Electric Review*, June 1943, pages 337–42.

Impedances Seen by Relays During Power Swings With and Without Faults

EDITH CLARKE
MEMBER AIEE

WE are at present in a period of power-system development during which it is essential that the best use be made of manpower and materials. To meet this requirement, equipment must be re-evaluated and refinements made in the design of apparatus and methods of system control. Loads on existing lines must be increased with continuity of service maintained. Of vital importance at this time is a thorough understanding of the operation of distance relays. The characteristics of the relays, and the system impedances "seen" by them, determine their performance. If it is known exactly what impedances are seen by a system of relays, their performance during power swings, with or without a fault on the system, can be predicted; and more important, relays having characteristics best suited for specific applications can be selected.

A valuable method of determining distance-relay performance is by means of an impedance chart with resistance and reactance as abscissa and ordinate, respectively. On this chart, the characteristic curve of the limit of operation of the relay and the system impedances seen by the relay under specified operating conditions are plotted to the same scale. If the system impedance seen by a relay falls within the boundary of the characteristic curve of the relay, the relay will operate; if it falls outside this boundary, the relay will not operate. This method of determining relay performance is given by J. H. Neher[1] in a paper on the performance of distance relays, in which he plots the characteristic curves of the boundary of operation of various types of relays in terms of resistance and reactance. The development of the general equations for distance relays, he credits to A. R. van C. Warrington. The paper provides equations from which *initial system impedances* seen by relays during faults of various types can be calculated and located on impedance diagrams for given relay systems. In his discussion of a paper by C. R. Mason,[2] presented at the same AIEE convention, Mr. Neher[3] points out that system impedances seen by distance relays during power swings can likewise be plotted on the same chart as the characteristic boundary curve of the relay. Following Mr. Neher's suggestion, Mr. Mason[4] gives a chart of the system impedances seen by a relay, during power swing under symmetrical system conditions, at any location in a single symmetrical three-phase linear circuit of negligible capacitance, with equal balanced generated voltages at its terminals. Later, Poage, Streifus, McGregor, and George in their excellent paper[5] extend the construction of system impedance charts, during power swings under symmetrical system conditions, by considering unequal balanced voltages at the terminals of a symmetrical three-phase linear circuit of appreciable capacitance, with relays located at its terminals. An outstanding contribution of their paper is the proof that the impedances seen by relays at the terminals of the circuit during power swings are circles for all constant ratios of the magnitudes of the voltages at these terminals, as the phase angle between the voltages varies from 0 to 360 degrees.

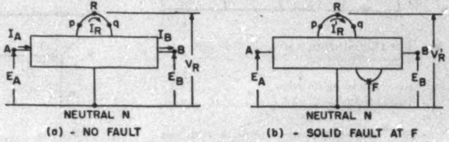

(a) - NO FAULT

(b) - SOLID FAULT AT F

In Figure 1b, the point of fault *F*, also shown outside the box, is short-circuited to neutral

Figure 1. Positive-sequence diagrams of a general symmetrical linear system between terminals *A*, *B*, and neutral *N*, represented as a box with section *pRq* of the circuit at *R* shown outside the box

The amount of effort necessary in a relay study, together with further work on this problem, has indicated that the relay application engineer should have a relatively simple means of determining the effect of power swings on distance relays, with or without a fault on the system. This paper is an attempt to provide such a means, by presenting in part I a simple method of constructing charts of the system impedances seen by distance relays during power swings, upon which their characteristic curves may be superposed. The method of constructing system impedance charts is applicable to any three-phase system which can be replaced during power swings by two equivalent synchronous machines with balanced generated voltages, connected by a three-phase linear network in which positive and negative impedances can be assumed equal. While the development of the method of constructing system impedance charts from equations in specified form given in part II and the derivation of these equations in part III are necessarily complex and somewhat lengthy, the net result presented in part I is a simple tool with which the behavior of a distance relay can be quickly determined by the use of tables and the adaptation of a general impedance chart.

The new features of the paper are:

1. The inclusion of generated voltages of unequal magnitudes at two equivalent power sources.

2. Systems in which there are one or more paths between the two power sources in addition to the path through the relays.

3. Power swings during all types of unsymmetrical faults as well as during symmetrical system conditions.

4. Proof that impedances seen by relays for constant phase angles between generated voltages of varying magnitudes are arcs of circles, two phase angles which differ by 180 degrees giving a complete circle.

5. A general impedance chart for determining the impedance seen by a relay during power swings, under various conditions of operation, without the necessity of constructing an entirely new chart for each new problem.

I. Construction of Impedance Charts From System Data

Notation

Vectors and complex numbers are represented by letters without distinguishing marks; scalar values of those quantities are enclosed in vertical bars. Thus, the vector voltage at point A is written V_A; the scalar of V_A is written $|V_A|$.

Assumptions

The method of constructing impedance charts given here applies to any three-phase system which can be replaced dur-

---

Paper 45-67, recommended by the AIEE committees on power transmission and distribution, and protective devices, and presented at the AIEE winter technical meeting, New York, N. Y., January 22-26, 1945. Manuscript submitted November 14, 1944; made available for printing December 27, 1944.

EDITH CLARKE is in the analytical division, central station engineering divisions, General Electric Company, Schenectady, N. Y.

The author acknowledges the assistance of L. F. Kennedy and A. J. McConnell in the development of the material in this paper; she wishes also to thank A. R. van C. Warrington and S. B. Crary for their helpful suggestions.

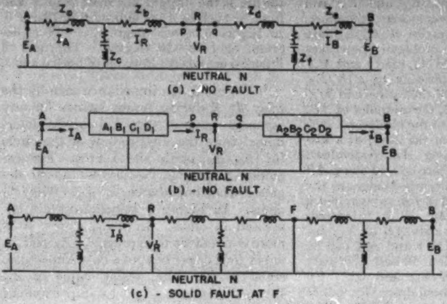

Figure 2. Positive-sequence diagrams of a symmetrical linear system with no connection between *A* and *B* except through the relays at *R*

Represented in (a) by two three-terminal networks, in (b) by two sets of general circuit constants, and in (c) by three three-terminal networks

ing power swings by two equivalent synchronous machines with balanced generated voltages E_A and E_B, connected by a symmetrical three-phase linear network having equal positive- and negative-sequence impedances, with the relays located at any point *R* in the network and a fault (if present) at any point *F*. It is assumed that phase distance relays are actuated by line-to-line voltages and the corresponding delta currents. In reducing a given system to one having two equivalent power sources, synchronous machines which can be represented by the same impedance in the direct and quadrature axes, and linear representation of loads, will be assumed. Initial transients, including d-c and natural-frequency components, and the effects of saliency in synchronous machines during power swing will be neglected. The voltages back of the internal impedances of the two equivalent machines will be assumed constant. Under these assumptions, there will be no harmonics because of saturation or other nonlinear effects, or from unequal impedances in the two axes of rotating machines. Initial transients will be of short duration in the usual transmission system because of the relatively high ratio of resistance to reactance. E_A and E_B will be constant sinusoidal voltages of fundamental frequency back of a single impedance in each of the two equivalent power sources. In the usual transient swings, transient impedance is assumed; but for swings which are long relative to the field time constants, an impedance higher than transient impedance may be a better representation.

System Diagrams

Under the stated assumptions, only the positive-sequence diagram is used in determining system impedance during symmetrical system conditions, or during line-to-line faults. In considering short circuits involving ground, Z_0, the zero-sequence impedance viewed from the fault, is required; and in the case of open conductors, z_0, the impedance offered to a series voltage inserted in the zero-sequence network at the opening, must be determined.

Positive-sequence diagrams of three types of symmetrical three-phase linear networks between E_A and E_B will be considered:

1. A general network.
2. A network in which there is no connection between E_A and E_B except through the relays at *R*.
3. A single circuit of negligible capacitance

In reducing the positive-sequence diagram of a given system to one having two equivalent power sources, the identity is retained of the point *R* at which the relays under consideration are located, and of the point *F* at which a fault is to be applied.

The positive-sequence diagram of a general symmetrical three-phase linear system with two power sources, or their equivalents, can be represented as a single-phase network having terminals *A* and *B* at which voltages to neutral E_A and E_B, respectively, are applied; when capacitance and constant-impedance loads are present, there will be one or more terminals connected to neutral *N*. Figure 1a shows the positive-sequence diagram of a general network between *A*, *B*, and *N* with no fault on the system. In Figure 1b a solid fault is indicated at *F*. In these diagrams, the general network is represented as a box with three terminals *A*, *B*, and *N* brought outside the box; a portion *pRq* of the circuit on which the relays are located is also shown outside the box. Points *p* and *q* are on opposite sides of the relays at *R* but at negligible distances from *R*. V_R is the voltage to neutral at *R*, and I_R is the line current at *R*, positive direction of current being from *p* to *q*, or from *A* to *B*. In Figure 1b, a portion of the circuit at the fault *F* is also shown outside the box.

Figure 2a is the positive-sequence diagram of a system without a fault which can be separated into two parts which have no connection with each other except through the relays at *R*. The portions of the positive-sequence network on each side of *R*, shown as three-terminal networks, may contain constant-impedance loads or line capacitance, or both. The impedance shunts Z_c and Z_f may be either inductive or capacitive; if there is neither capacitance nor constant-impedance loads, they become infinite. In Figure 2b, the positive-sequence diagram of Figure 2a is expressed in terms of two sets of general circuit constants. In Figure 2c, a solid fault is indicated at *F*. Figures 3a and 3b are special cases of Figure 2a in which capacitances and constant-impedance loads are negligible. In Figure 3a, the point *F* at which a fault will be applied is between *R* and E_B; in Figure 3b, *F* is between E_A and *R*.

Figures 4a and 4b are special cases of Figure 2a in which V_A and V_B are terminal voltages (not internal generated voltages) at *A* and *B*, the terminals of a symmetrical three-phase linear circuit of appreciable capacitance with relays located at *A* and *B*, respectively. In systems which cannot be replaced during power swings by two equivalent power sources, system impedance charts can be constructed from Figures 4a and 4b in terms of $|V_A/V_B|$ or $|V_B/V_A|$ and the phase angle δ by which V_A leads V_B; but some auxiliary means, such as an a-c network analyzer, will be required to determine the range of $|V_A/V_B|$ during power swings under given conditions of operation.

Procedure in the Construction of System Impedance Charts

Without a fault or with a symmetrical three-phase fault, the impedances seen by the relays in the three phases at *R* are identical; for this condition, only one chart is constructed. With unsymmetrical faults, the impedances seen by the relays in each phase at *R* will be different; for this condition, more than one chart will be required. The procedure in constructing system impedance charts for any system which can be replaced during power swings by two equivalent power sources, with or without an unsymmetrical fault, is as follows:

1. Draw the positive-sequence diagram of the given system, representing transmission circuits by equivalent *T*'s or π's, and constant impedance loads by impedance shunts to neutral. Reduce the network to its simplest form, preserving the identity of the point *R* at which the relays are located, and of the fault point *F* if power swings during faults are to be considered.
2. From the positive-sequence diagram of the system and the given type of fault (if a fault is specified), determine the constants required in the construction of the system impedance chart. These constants consist of three impedances Z_x, Z_z, and Z_y, related by the equation $Z_y = Z_x + Z_z$, and one complex ratio *K*. Written in polar form, $Z_y = |Z_y|\underline{/\theta_y}$ and $K = |K|\underline{/\theta_k}$, where $|K|$ may be unity or greater or less than unity and the angle θ_k may be positive or negative. With positive direction of current from *A* to *B*,

$-Z_x$ and Z_z locate the impedances seen by a relay at R when E_A and E_B, respectively, are zero. $|K|$ and θ_k are required in constructing or labeling the two sets of circles which make up the impedance chart. (See Figure 5.)

From the positive-sequence diagrams of the four types of networks shown in Figures 1–4, the constants Z_x, Z_z, Z_y, and K have been evaluated (in part III) for symmetrical system conditions and for various types of faults. They are tabulated in Table I for the condition of no fault on the system, and in Table II for a line-to-line fault in a single circuit of negligible capacitance. The quantities in Table I are expressed in terms of transfer and driving-point impedances, determined under specified conditions. Methods of determining the transfer and driving-point impedances used in Table I are explained below this table. In Table II, the required constants are given in terms of Z_A, Z_B, and Z_C, the impedances indicated in Figures 3a and 3b, where the total impedance between A and $B = Z_S = Z_A + Z_B + Z_C$.

3. From the calculated constants Z_x, Z_z, $Z_y = Z_x + Z_z = |Z_y|\underline{/\theta_y}$, and $K = |K|\underline{/\theta_k}$ construct the impedance chart. Two methods of constructing system impedance charts will be given:

Method A. Under this method, the entire chart is constructed for each new problem.

Method B. Under this method, only part of the chart is constructed, the remainder being obtained from the general impedance chart.

Method A—Construction of Complete Chart

1. On a sheet of rectangular cross-section paper, such as shown in Figure 5, locate the origin 0. As the chart gives the impedances seen by a relay at R, the origin represents R, the location of the relay. Selecting a convenient scale, with resistance and reactance as abscissa and ordinate, respectively, lay off $-Z_x$ and Z_z from the origin, locating points A and B, respectively. These points are shown in Figure 5. Point A corresponds to the impedance $-Z_x = Z_z - Z_y$ seen by the relay when $E_A = 0$; point B corresponds to the impedance $Z_z = -Z_x + Z_y$ seen by the relay when $E_B = 0$, positive direction of current being from A to B. Points A and B may be considered the terminals A and B at which the voltages E_A and E_B, referred to the relay, are applied.

2. Draw a straight line from A to B and determine its midpoint M. The line AB will have the length $|Z_y|$ and, in the direction $\overrightarrow{AB}$, the slope θ_y of $Z_y = |Z_y|\underline{/\theta_y}$. This is indicated in Figure 5. Extend the line AB in both directions. The line AB (extended) is the line of centers of the circles for constant values of the ratio $|E_A/E_B|$ or $E_B/E_A|$. Through M, the midpoint of AB, draw the line GMH perpendicular to AB. The line GMH is the line of centers of the arcs for constant values of δ, the angle by which E_A leads E_B.

3. For any assumed value of $|E_A/E_B|$ calculate $|E_AK/E_B|$. If E_A and E_B are internal generated voltages to neutral (or their equivalents) applied at A and B behind transient reactances, they can be calculated or estimated for a given system operating under normal specified conditions. Under the stated assumptions, $|E_A|$ and $|E_B|$ will not change during power swings; therefore, only a few circles for ratios of $|E_A/E_B|$ are required in a given problem—sometimes only one. From Table III, read r and MX in terms of $|Z_y|$ corresponding to $|E_AK/E_B|$ where r is the length of the radius and MX is the distance from M, the midpoint of AB, to X, the intersection of the circle with AB. Locate C, the center of the circle at a distance r from X along AB (extended). Positive values of MX are laid off along AB in the direction MB, negative values in the direction MA. C and X for any circle are on the *same* side of M. With C located, draw the circle which cuts AB at X. Instead of using Table III, r and MX can be calculated from equations 10 and 13 of part II in terms of $|E_AK/E_B|$ and $|Z_y|$. In Figure 5, circles have been drawn for values of $|E_AK/E_B|$ of 0.75, 1.00, and 1.50. The circles in Figure 5 are labeled in terms of $|E_A/E_B|$, $|E_B/E_A|$, and $|E_AK/E_B|$ for $|K| = 1.25$. When $|E_AK/E_B| = 1.0$, the circle becomes a straight line perpendicular to AB at M—this is the straight line GMH which is the line of centers of the arcs for constant values of δ.

4. For any assumed value of δ, calculate $\phi = \delta + \theta_k$, where θ_k may be positive or negative. The arcs for any two values of δ or ϕ which differ by 180 degrees have the same center C' but they intersect the line GMH at X' on opposite sides of M. The complete circle is divided into two arcs by points A and B which are common to all δ arcs. In Table IV, MC', the distance of the center of the arc C' from M, is given in terms of ϕ and $|Z_y|$, and the sign of MX' is indicated. For values of ϕ not included in Table IV, MC' can be calculated from equation 19, and the sign MX' determined from equation 18 of part II. Positive values of MC' and MX' are laid off along GMH in the direction MH, negative values in the direction of MG. As all arcs pass through A and B, the distance $C'A$ or $C'B$ on the chart gives the radius of the arc. In Figure 5 arcs are drawn for various values of ϕ between 0 and 360 degrees. For $\phi = 180$ degrees, the arc is the straight line from A to B; for $\phi = 0$, the arc is the straight line from B to ∞ and from ∞ back to A, as indicated in Figure 5. In Figure 5, $\theta_k = 20$ degrees, $\phi = \delta + 20$ degrees, or $\delta = \phi - 20$ degrees. The arcs of Figure 5 are labeled in terms of both ϕ and δ.

In Figure 5, the impedance seen by the relay at R during power swings for any assumed value of $|E_A/E_B|$ can be determined from the intersection of the circle for $|E_A/E_B|$ with the δ arcs. For example, if $|E_A/E_B| = 1.2$ and $\delta = 40$ degrees, the impedance is $Z_R = 65 + j\,4$ ohms. In Figure 5 impedances are expressed in ohms. In many cases, it is more convenient to express Z_x, Z_z, and Z_y in per unit or per cent of a base impedance equal to $|Z_y|$, the scalar value of Z_y. When this is done, $|Z_y| = 1.0$ in per unit of base ohms.

Method B—Use of General Impedance Chart

The general impedance chart suggested and first constructed by A. J. McConnell is shown in Figure 6. The line AB, equal in length to $|Z_y| = 1.0$ in per unit of base impedance, determines the scale. AB is shown in a vertical position. A horizontal line is perpendicular to AB at its midpoint. The line AB (extended) is the line of centers of the circles for constant values of $|E_A/E_B|$ or $|E_B/E_A|$. The horizontal line is the line of centers of the arcs for constant values of δ, the angle by which E_A leads E_B. The circles are labeled in terms of $|E_AK/E_B|$ and the arcs in terms of $\phi = \delta + \theta_k$. The origin and the coordinate axes are not indicated. To use the general impedance chart, the following procedure is suggested:

1. On a sheet of thin rectangular cross-section paper, locate the origin 0. Assume a base impedance equal to $|Z_y|$ and express Z_x, Z_z, and Z_y in per unit of this base imped-

Table I. Values of Z_x, Z_z, Z_y, and K, in Terms of Driving-Point* and Transfer Impedances in the Positive-Sequence Networks of Figures 1–4

No Fault

	Z_x	Z_z	Z_y	K
1. General network of Figure 1a	$Z_{RR}\dfrac{s_{BR}}{Z_{BR}}$	$Z_{RR}\dfrac{s_{AR}}{Z_{AR}}$	$Z_{RR}\left(\dfrac{s_{AR}}{Z_{AR}}+\dfrac{s_{BR}}{Z_{BR}}\right)$	$\dfrac{s_{BR}}{s_{AR}}$
2. Connection between A and B only through relay—Figure 2a	Z_{RR-A}	Z_{RR-B}	$Z_{RR-A}+Z_{RR-B}$	$\dfrac{Z_{RR-A}Z_{BR}}{Z_{AR}Z_{RR-B}}$
3. Same as 2 except negligible capacitance —Figure 3a. $Z_{RA} = Z_{RR-A}$; $Z_{RB} = Z_{RR-B}$	Z_{RR-A}	Z_{RR-B}	$Z_{RR-A}+Z_{RR-B}$	$1\underline{/0°}$
4. Relay located where E_A is measured—Figure 4a. $Z_{RR-A} = 0$; $Z_{RR-A}/Z_{AR} = 1$	0	Z_{RR-B}	Z_{RR-B}	$\dfrac{Z_{BR}}{Z_{RR-B}}$
5. Relay located where E_B is measured—Figure 4b. $Z_{RR-B} = 0$; $Z_{BR}/Z_{RR-B} = 1$	Z_{RR-A}	0	Z_{RR-A}	$\dfrac{Z_{RR-A}}{Z_{AR}}$

*All the impedances in Table I can be obtained from the positive-sequence diagrams of Figures 1–4 with A and B short-circuited to neutral and no fault on the system: With a voltage E_R applied between neutral and R, and A and B short-circuited to neutral, let I be the current entering the network at R and I_p and I_q the components of I at p and q, respectively, which are also the components of I at R flowing toward A and B, respectively; let I_A and I_B be the currents leaving the network at A and B, respectively. Then $Z_{RR} = E_R/I$; $Z_{RR-A} = E_R/I_p$; $Z_{RR-B} = E_R/I_q$; $Z_{AR} = Z_{RA} = E_R/I_A$; $Z_{BR} = Z_{RB} = E_R/I_B$. The impedances s_{AR} and s_{BR} are required only for the general network. With a series voltage e_R inserted at R in Figure 1a, and A and B short-circuited to neutral, let I_A and I_B be the currents at A and B, respectively. Then $s_{AR} = s_{RA} = e_R/I_A$; $s_{BR} = s_{RB} = e_R/I_B$.

ance. $|Z_y|=1.0$ in per unit of base impedance. Select a scale such that $|Z_y|=1.0=$ the length of AB in the general impedance chart of Figure 6. Plot $-Z_x=Z_s-Z_y$ and $Z_s=-Z_x+Z_y$ which locate points A and B, respectively.

2. Place the cross-section paper over the general impedance chart of Figure 6 so that points A and B coincide with A and B in Figure 6, and trace the various circles and arcs (or the significant portions thereof). The values given in Figure 6 correspond to $|E_A/E_B|$ and δ, if $|K|=1$ and $\theta_k=0$. If $|K|$ is not 1, the constant-voltage-ratio circles may be relabeled in terms of $|E_A/E_B|$ by dividing the values of $|E_AK/E_B|$ given in Figure 6 by $|K|$. If θ_k is not 0 degrees, the constant-angle arcs may be relabeled in terms of δ by subtracting θ_k from the value of ϕ given in Figure 6.

A practical example illustrating the use of methods A and B will now be given.

Problem. The given system can be represented as a single circuit of negligible capacitance between two equivalent generated voltages E_A and E_B with the relays located at R, as indicated in Figure 3a. A line-to-line fault between phases b and c occurs at F. The impedances Z_A, Z_B, and Z_C shown in Figure 3a are $Z_A=20\underline{/80^\circ}$ ohms; $Z_B=50\underline{/80^\circ}$ ohms; $Z_C=30\underline{/80^\circ}$ ohms; $Z_S=100\underline{/80^\circ}$ ohms. (It is not required that these impedance angles be equal; calculations are but slightly simplified by this assumption.) The impedances Z_{cb}, Z_{ac}, and Z_{ba} seen by the phase distance relays in the three phases at R will be different.

(*a*). Determine Z_{cb}, and construct charts for determining Z_{ac} and Z_{ba} during power swings.

(*b*). Assuming $|E_A/E_B|=1$, compare the impedances Z_{ac} and Z_{bc} determined under (*a*) with the impedances seen by the relays in the three phases at R during power swings when there is no fault on the system.

Solution of Problem. From Table II: $Z_{cb}=Z_B=50\underline{/80^\circ}$ ohms.

Chart for Z_{ac}. From Table II: $Z_x=Z_A=20\underline{/80^\circ}$ ohms.

$$K=1-j\frac{Z_S}{\sqrt{3}(Z_A+Z_B)}=1-j\frac{100}{70\sqrt{3}}$$
$$=1-j0.8248=1.296\underline{/-39.52^\circ}$$
$$=1.30\underline{/-40^\circ}\text{, approximately}$$
$$Z_y=\frac{Z_S}{K}\left(1-j\frac{1}{\sqrt{3}}\right)$$
$$=\frac{100\underline{/80^\circ}(1.155\underline{/-30^\circ})}{1.296\underline{/-39.52}}$$
$$=89.2\underline{/89.52^\circ}\text{ ohms}$$

The chart of the impedance Z_{ac} will be expressed in per unit of a base impedance equal to $|Z_y|=89.2$ ohms. In per unit of 89.2 ohms, $Z_y=1.00\underline{/89.52^\circ}=0.009+j1.00$; $Z_x=0.2244\underline{/80^\circ}=0.039+j0.221$, $Z_s=Z_y-Z_x=-0.030+j0.779$. K, being a complex ratio, remains unchanged. $|K|=1.30$ and $\theta_k=-40$ degrees. The chart of Z_{ac} given in Figure 7a was constructed in accordance with method A. To construct this chart, the origin 0 is located, and a convenient per-unit scale chosen. $-Z_x=-0.039-j0.221$ and $Z_s=-0.030+j0.779$ are plotted, locating points A and B, respectively. The line AB is drawn, its midpoint is determined; the perpendicular to AB at its midpoint is erected; and AB is extended in both directions.

Values of $|E_A/E_B|$ or $|E_B/E_A|$ covering the operating voltage range are selected and $|E_AK/E_B|=1.30\,|E_A/E_B|$ calculated. The lengths of the radii r and the distances MX from M, the midpoint of AB, to the intersections X of the circles for constant values $|E_AK/E_B|$ with the line AB are read from Table III. For example: if $|E_A/E_B|=1$, $|E_AK/E_B|=1.30$; and from Table III with $|Z_y|=1$, $r=1.884$ and $MX=0.065$. In Figure 7a the circle for $|E_B/E_A|=1$ is shown. The perpendicular bisector of AB which corresponds to $|E_AK/E_B|$ is the locus of $|E_A/E_B|=1/|K|=0.77$.

With $\theta_k=-40^\circ$, $\phi=\delta+\theta_k=\delta-40^\circ$: The distance MC' of the center of the arcs from the midpoint of AB for any constant values of δ can be read from Table IV corresponding to $\phi=\delta-40^\circ$. Thus: for $\delta=0^\circ$, $\phi=0-40^\circ=320^\circ$; for $\delta=60^\circ$, $\phi=20^\circ$. The line AB corresponding to $\phi=180^\circ$ is the arc for $\delta=\phi-\theta_k=220^\circ$; the line AB (extended) is the arc for $\delta=0-\theta_k=40^\circ$. The arcs for $\phi=90^\circ$ and 270° (circle with AB as diameter) are arcs for $\delta=130^\circ$ and 310°, respectively. These and other values of δ are indicated in Figure 7a.

Chart for Z_{ba}. From Table II:

$$Z_x=Z_A=20\underline{/80^\circ}$$
$$K=1+j\frac{Z_S}{\sqrt{3}(Z_A+Z_B)}=1+j0.8248$$
$$=1.296\underline{/39.52^\circ}$$

$|K|=1.30$ and $\theta_k=40^\circ$, approximately

$$Z_y=\frac{Z_S}{K}\left(1+j\frac{1}{\sqrt{3}}\right)=\frac{100\underline{/80^\circ}(1.155\underline{/30^\circ})}{1.296\underline{/39.52^\circ}}$$
$$=89.2\underline{/70.48^\circ}\text{ ohms}$$

Let base ohms $=89.2$ ohms. In per unit of base ohms, $Z_x=0.039+j0.221$; $Z_y=1.0\underline{/70.48^\circ}=0.334+j0.943$; $Z_s=Z_y-Z_x=0.295+j0.722$.

The chart for Z_{ba} will be constructed by using the general impedance chart of Figure 6. In Figure 7b, the origin 0 is located and a scale chosen so that $|Z_y|=1.0$ in per unit of base impedance $=$ the length AB of the general chart. $-Z_x=-0.039-j0.221$ and $Z_s=0.295+j0.722$ are plotted, locating points A and B, respectively. The chart of Figure 7b is then placed over Figure 6, with A and B on the two charts coinciding. The various circles and arcs of Figure 6 are then traced on the chart for Z_{ba}. (It is generally unnecessary to trace all circles and arcs completely. Usually the significant portions are obvious and only those portions need be traced.)

Since in this problem $|K|$ and θ_k are not 1 and 0, respectively, the various circles and arcs must be relabeled in values of $|E_A/E_B|$ and δ. For example, the constant $|E_AK/E_B|$ circle in Figure 6 labeled 1.3 when traced on Figure 7b corresponds to $|E_AK/E_B|=1.3$ or to $|E_A/E_B|=1.3+|K|=1.3/1.30=1.00$. Similarly, the constant ϕ arc in Figure 6 labeled 90 degrees, when traced on Figure 7b corresponds to $\phi=\delta+\theta_k=90$ degrees or to $\delta=\phi-\theta_k=90$ degrees -40 degrees $=50$ degrees.

Circles for $|E_A/E_B|=1$ from the charts of Figures 7a and 7b for Z_{ac} and Z_{ba}, respectively, are shown on the same chart in Figure 7c, and the intersections of these circles with various δ arcs are indicated. The point locating Z_{cb} is also shown. Base impedance in Figure 7c is 89.2 ohms.

Symmetrical System Conditions. From Table I, item 3, $Z_x=Z_{RR-A}=Z_A=20\underline{/80^\circ}$ ohms; $Z_s=Z_{RR-B}=Z_B+Z_C=80\underline{/80^\circ}$ ohms; $Z_y=Z_x+Z_y=100\underline{/80^\circ}$ ohms; $|K|=1$; and $\theta_k=0^\circ$. In per unit of 89.2 ohms (base ohms in Figure 7c), $Z_x=0.2244\underline{/80^\circ}=0.039+j0.221$; $Z_y=1.122\underline{/80^\circ}=0.195+j1.105$; $Z_s=Z_y-Z_x=0.156+j0.884$.

In Figure 7c, $-Z_x$ and Z_s are plotted locating points A and B, respectively. The line AB is drawn and its midpoint M

Table II. Values of Z_x, Z_s, Z_y, and K—Line-to-Line Fault Between Phases b and c at F in Figure 3a or 3b

Positive Direction of Current From *A* to *B*

Figure	Z_x	Z_s	$Z_y=Z_x+Z_s$	K
3a… $Z_{cb}=Z_B$				
Z_{ac}…………	Z_A	…$Z_B+\frac{Z_C}{K}$…	$Z_A+Z_B+\frac{Z_C}{K}=\frac{Z_S}{K}\left(1-j\frac{1}{\sqrt{3}}\right)$	…$1-j\frac{Z_S}{\sqrt{3}(Z_A+Z_B)}$
Z_{ba}…………	Z_A	…$Z_B+\frac{Z_C}{K}$…	$Z_A+Z_B+\frac{Z_C}{K}=\frac{Z_S}{K}\left(1+j\frac{1}{\sqrt{3}}\right)$	…$1+j\frac{Z_S}{\sqrt{3}(Z_A+Z_B)}$
3b… $Z_{cb}=-Z_B$				
Z_{ac}…………	KZ_A+Z_B…	Z_C	…$KZ_A+Z_B+Z_C=KZ_S\left(1-j\frac{1}{\sqrt{3}}\right)$	…$1/\left[1-j\frac{Z_S}{\sqrt{3}(Z_B+Z_C)}\right]$
Z_{ba}…………	KZ_A+Z_B…	Z_C	…$KZ_A+Z_B+Z_C=KZ_S\left(1+j\frac{1}{\sqrt{3}}\right)$	…$1/\left[1+j\frac{Z_S}{\sqrt{3}(Z_B+Z_C)}\right]$

determined. The line perpendicular to AB at M is drawn; this line corresponds to $|E_AK/E_B|=1.0$, and since $|K|=1$, it also corresponds to the desired value of $|E_A/E_B|=1$. The intersections of the δ arcs with the line for $|E_A/E_B|=1$ are indicated in Figure 7c for Z_R with no fault on the system.

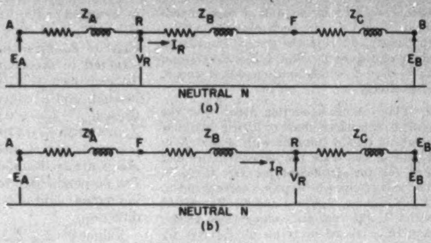

Figure 3. Positive-sequence diagrams of a single circuit of negligible capacitance between E_A and E_B

R and F are relay and fault locations, respectively

II. Construction of Impedance Charts From Equations in Specified Form

Assumptions

The assumptions in regard to the system are the same as those stated in part I, except that the three-phase linear network between E_A and E_B, when there is no unsymmetrical fault on the system, need not necessarily be symmetrical in the three phases. Under these assumptions, system voltages and currents during power swings are functions of E_A, E_B, and the characteristic impedances and admittances of the system. Any impedance Z which is defined as the ratio of a specified voltage V to a specified current I, with positive direction of current from A to B, may be written

$$Z=\frac{V}{I}=\frac{H_AE_A+H_BE_B}{G_AE_A-G_BE_B} \tag{1}$$

where H_A, H_B, G_A, and G_B, after initial transients have disappeared, are constant coefficients determined from the characteristic constants of the system under specified operating conditions.

Equation 1 may be expressed in terms of E_A/E_B or E_B/E_A, whichever is preferred.

$$Z=\frac{V}{I}=\frac{H_A}{G_A}-\frac{\left(\frac{H_A}{G_A}+\frac{H_B}{G_B}\right)}{1-\frac{E_A}{E_B}\left(\frac{G_A}{G_B}\right)}=-\frac{H_B}{G_B}+\frac{\left(\frac{H_A}{G_A}+\frac{H_B}{G_B}\right)}{1-\frac{E_B}{E_A}\left(\frac{G_B}{G_A}\right)} \tag{2}$$

The equations 2 are general. As given, they define an impedance. They may, however, be used to define the ratio of two currents or of two voltages, or any ratio which can be expressed in the general form of equation 1 with constant coefficients.

In equations 2, let $H_B/G_B=Z_x$; $H_A\div G_A=Z_z$; $(H_A/G_A+H_B/G_B)=Z_x+Z_z=Z_y$; and $K=G_A/G_B$. Then, replacing Z in equations 2 by Z_R, the impedance Z_R seen by a relay at R is

$$Z_R=Z_z-\frac{Z_y}{1-E_AK/E_B}=-Z_x+\frac{Z_y}{1-E_B/(E_AK)} \tag{3}$$

where Z_x, Z_z, and $Z_y=Z_x+Z_z$ are impedances, and K in the general case is a complex number. In special cases, Z_x or Z_z may be zero, or K may be unity.

If positive direction for current is from B to A, instead of from A to B, the signs of these equations for Z_R will be reversed.

In terms of magnitudes and angle, let $Z_x=|Z_x|\underline{/\theta_x}$; $Z_z=|Z_z|\underline{/\theta_z}$; $Z_y=|Z_y|\underline{/\theta_y}$; $K=|K|\underline{/\theta_k}$; $E_A/E_B=|E_A/E_B|\underline{/\delta}$; $E_B\div E_A=|E_B/E_A|\underline{/-\delta}$, where δ is the angle by which E_A leads E_B. With complex impedances and ratios in polar form, equation 3 becomes

$$Z_R=|Z_z|\underline{/\theta_z}-\frac{|Z_y|\underline{/\theta_y}}{1-\left|\frac{E_AK}{E_B}\right|\underline{/\delta+\theta_k}}=-|Z_x|\underline{/\theta_x}+\frac{|Z_y|\underline{/\theta_y}}{1-\left|\frac{E_B}{E_AK}\right|\underline{/-\delta-\theta_k}} \tag{4}$$

Equations 3 or 4 give Z_R in two different forms which are not independent of each other. Either form can be obtained from the other, since $Z_y=Z_x+Z_z$. Methods of determining Z_x, Z_z, $Z_y=Z_x+Z_z$, and K with and without faults are given in part III. With these constants known, two points on the impedance chart can be obtained by equating first E_A, and then E_B, to zero. From equation 3, with $E_A=0$,

$$Z_R=Z_z-Z_y=-Z_x \tag{5}$$

With $E_B=0$,

$$Z_R=Z_z=-Z_x+Z_y \tag{6}$$

In Figure 5, $-Z_x$ locates point A, corresponding to $E_A=0$; this point can also be located by Z_z-Z_y. Z_z locates point B, corresponding to $E_B=0$; this point can also be located by $-Z_x+Z_y$. The line AB connecting points A and B and measured from A to B has the magnitude and slope of $Z_y=|Z_y|\underline{/\theta_y}$.

In equation 4, let

$$\phi=\delta+\theta_k,\text{ or }\delta=\phi-\theta_k \tag{7}$$

Substitution of equation 7 in equation 4 gives

$$Z_R=Z_z\underline{/\theta_z}-\frac{|Z_y|\underline{/\theta_y}}{1-\left|\frac{E_AK}{E_B}\right|\underline{/\phi}}=-Z_x\underline{/\theta_x}+\frac{|Z_y|\underline{/\theta_y}}{1-\left|\frac{E_B}{E_AK}\right|\underline{/-\phi}} \tag{8}$$

A third point M in Figure 5 can be obtained from equation 8, if $|E_A/E_B|=1/|K|$ and $\phi=\delta+\theta_k=180$ degrees. Then the denominator of either fraction in equation 8 is two, and

$$Z_R=M=Z_z-\frac{Z_y}{2}=-Z_x+\frac{Z_y}{2} \tag{9}$$

Either of the impedance equations in equation 9 locates M at the midpoint of

Table III. Radii and Intersections With AB of Circles for Constant Values of $|E_A/E_B|$ in Terms of $|Z_y|=AB$ and $|E_AK/E_B|$

$\lvert E_AK/E_B\rvert$	$r^*/\lvert Z_y\rvert$	$MX^*/\lvert Z_y\rvert$	$\lvert E_AK/E_B\rvert$	$r^*/\lvert Z_y\rvert$	$MX^*/\lvert Z_y\rvert$	$\lvert E_AK/E_B\rvert$	$r^*/\lvert Z_y\rvert$	$MX^*/\lvert Z_y\rvert$
0	0	−0.5000	0.9	4.737	−0.0263	1.55	1.105	0.1078
0.1	0.101	−0.4091	0.95	9.744	−0.0128	1.6	1.026	0.1154
0.2	0.208	−0.3333	1.0	∞	0	1.65	0.958	0.1226
0.3	0.330	−0.2692	1.05	10.244	0.0122	1.7	0.899	0.1296
0.4	0.476	−0.2143	1.10	5.238	0.0238	1.75	0.848	0.1364
0.5	0.667	−0.1667	1.15	3.566	0.0349	1.8	0.804	0.1429
0.55	0.789	−0.1452	1.20	2.727	0.0455	1.85	0.764	0.1491
0.6	0.938	−0.1250	1.25	2.222	0.0556	1.9	0.728	0.1552
0.65	1.126	−0.1061	1.3	1.884	0.0652	1.95	0.696	0.1610
0.7	1.373	−0.0882	1.35	1.641	0.0745	2.0	0.667	0.1667
0.75	1.714	−0.0714	1.4	1.458	0.0833	2.5	0.476	0.2143
0.8	2.222	−0.0556	1.45	1.315	0.0918	5.0	0.208	0.3333
0.85	3.063	−0.0405	1.5	1.200	0.1000	10.0	0.101	0.4091
						∞	0	0.5000

*r is the radius of the circle; X is its intersection with AB. See Figure 5. MX is the distance from M the midpoint of AB to X in the positive direction MB. The center of the circle C is on AB (extended). MC has the sign of MX. $|MC|=r+|MX|$.

the line AB. This point is shown in Figure 5.

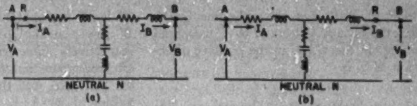

Relay location R at A

Relay location R at B

Figure 4. Positive-sequence diagrams of a symmetrical three-phase linear network between terminal voltages V_A and V_B

Circles for Constant Ratios of the Magnitudes of E_A and E_B

The first terms in the two equations 8 are constant impedances; the second terms involve E_A/E_B or E_B/E_A and other constants. In reference 5, it is shown that an impedance equation in the form of either of these second terms is the equation of a circle for any constant value of the ratio of the magnitudes of the two voltages when the phase angle between them varies from 0 to 360 degrees; and equations for the centers and radii of these circles are given. The addition of the constant first term shifts the centers of the circles but does not change their radii. If r is the length of the radius and C is the center of the circle referred to the origin, and Z_R is expressed in terms of E_A/E_B,

$$r=\frac{|Z_y|\left|\dfrac{E_AK}{E_B}\right|}{\left|\left|\dfrac{E_AK}{E_B}\right|^2-1\right|} \tag{10}$$

$$C=Z_s-\frac{Z_y}{1-\left|\dfrac{E_AK}{E_B}\right|^2}$$

$$=\left(Z_s-\frac{Z_y}{2}\right)+\frac{Z_y}{2}\,\frac{\left|\dfrac{E_AK}{E_B}\right|^2+1}{\left|\dfrac{E_AK}{E_B}\right|^2-1} \tag{11}$$

The line of centers of the circles for constant values of $|E_A/E_B|$ is given by equation 11. The term in parenthesis $(Z_s-Z_y/2)$ locates the midpoint of AB; the term following it locates C along the line AB, or AB extended. If MC is the distance from M to C measured along the line of centers AB (extended) in the direction MB,

$$MC=\frac{|Z_y|}{2}\,\frac{|E_AK/E_B|^2+1}{|E_AK/E_B|^2-1} \tag{12}$$

If $|E_AK/E_B|$ is greater than unity, MC in equation 12 will be positive and will be laid off in the direction MB. If MC is negative, it will be laid off in the direction MA.

In Figure 5, let X be the intersection of the circumference of any circle of radius r with AB, and MX the distance measured from M to X in the positive direction MB. If the outer bars enclosing the denominator in equation 10 are removed, and equation 10 then subtracted from equation 12, the distance MX is

$$MX=\left|\frac{Z_y}{2}\right|\frac{\left[\dfrac{E_AK}{E_B}-1\right]^2}{\left|\dfrac{E_AK}{E_B}\right|^2-1}=\left|\frac{Z_y}{2}\right|\frac{\left|\dfrac{E_AK}{E_B}\right|-1}{\left|\dfrac{E_AK}{E_B}\right|+1} \tag{13}$$

If $|E_AK/E_B|$ is greater than unity, MX is positive and will be laid off along AB in the direction MB. If $|E_AK/E_B|$ is less than unity, MX will be negative and will be laid off in the direction MA. This is shown in Figure 5 for $|E_AK/E_B|=1.50$ and 0.75, respectively. MX given by equation 13 and MC given by equation 12 will always be measured in the same direction from M. When radii are long relative to the length AB, instead of using equation 11 or 12 to locate C, a higher degree of precision can usually be secured (if one is not an expert draftsman) by laying off MX calculated from equation 13 and then adding r given by equation 10 to find the center C of the circuit which cuts AB at X.

In terms of E_B/E_A, the equations for r and MX are

$$r=\frac{|Z_y|\ |E_B/(E_AK)|}{\left|1-\left|\dfrac{E_B}{E_AK}\right|^2\right|} \tag{14}$$

$$MX=\left|\frac{Z_y}{2}\right|\frac{1-|E_B/(E_AK)|}{1+|E_B/(E_AK)|} \tag{15}$$

If $|E_B/(E_AK)|$ is less than unity, MX and $|MC|(=|MX|$ plus $r)$ will be laid off along AB (or AB extended) in the positive direction MB. If $|E_B/(E_AK)|$ is greater than unity, MX and MC will be laid off in the negative direction MA. As $|E_B/(E_AK)|$ is the reciprocal of $|E_AK\div E_B|$, circles for values of $|E_A/E_B|$ and $|E_B/E_A|$ which are reciprocals of each other will be identical. This is shown in Figure 5, where the circles are labeled in terms of both $|E_A/E_B|$ and $|E_B/E_A|$.

If $|E_A/E_B|=1/|K|$, $|E_AK/E_B|=|E_B\div(E_AK)|=1$; and from equations 10 or 14, $r=\infty$. From equation 12, $MC=\infty$. The circle, in this case, becomes a straight line perpendicular to AB. As MX from equation 13 or 15 is zero, the straight line passes through M and is the perpendicular bisector of the line AB. This straight line GMH is shown in Figure 5.

Arcs of Circles for Constant Angles δ Between E_A and E_B

The second term in either of the equations 4 can be equated to $1/D$ if numerator and denominator are divided by $|Z_y|\underline{/\theta_y}$; selecting the second equation, D is

$$D=\frac{1}{|Z_y|}\underline{/-\theta_y}-\left|\frac{E_B}{KE_AZ_y}\right|\underline{/-\delta-\theta_k-\theta_y} \tag{16}$$

where $|Z_y|$, θ_y, $|K|$, and θ_k are constants. For a constant value of δ but variable values of $|E_B/E_A|$, D in equation 16 is a straight line. This line passes through $|1/Z_y|\underline{/-\theta_y}$ and has a slope $180°-(\delta+\theta_k+\theta_y)$. It can be shown (any good analytic geometry) that if the equation of an admittance is a straight line extending to infinity in *both* directions, its reciprocal is the equation of a circle which passes through the origin. In the special case of a straight line which passes through the origin, the reciprocal is a circle of infinite radius, that is, a straight line. As $|E_B/E_A|$ is always positive, the straight line representing the admittance D for a constant value of δ extends to infinity in one direction only as $|E_B/E_A|$ varies from 0 to ∞. Its reciprocal $1/D$ is therefore the equation of an arc of a circle—not a complete circle. The addition of the first term in equations 4 shifts the center of the arc but does not change its radius. The equations 4, for any constant value of δ and ratios $|E_B/E_A|$ between 0 to ∞, are therefore the equations of arcs of circles.

It is shown in equations 5 and 6 that the impedance Z_R is $-Z_z=Z_s-Z_y$ when $E_A=0$, and $-Z_z+Z_y=Z_s$ when $E_B=0$. These impedances are indicated in Figure 5 by points A and B, respectively. As these two values of Z_R are independent of the angle δ by which E_A leads E_B, the arcs for all values of δ must pass through the points A and B. The centers of all arcs will therefore lie on the perpendicular bisector GMH of the line AB. The line GMH in Figure 5 is the curve for $|E_AK\div E_B|=|E_B/(E_AK)|=1$; it is also the line of centers of the constant δ arcs.

The intersection of the constant-δ arcs with their line of centers GMH can be obtained if $|E_B/(E_AK)|$ in equation 8 is replaced by unity. Let X' indicate the point of intersection; then X' referred to the origin is given by the following equation:

$$\left.\begin{aligned}X'&=-Z_z+\frac{Z_y}{1-\underline{/-\phi}}\\&=-Z_z+\frac{Z_y}{1-\cos\phi+j\sin\phi}\\&=-Z_z+\frac{Z_y(1-\cos\phi-j\sin\phi}{2(1-\cos\phi)}\\&=-Z_z+\frac{Z_y}{2}+\frac{|Z_y|\underline{/\theta y-90°}}{2\tan\dfrac{\phi}{2}}\end{aligned}\right\} \tag{17}$$

The first two terms in the last equation 17 locate M, the mid-point of AB. The third term gives the distance MX', measured from M to X' along a line perpendicular to Z_y at M, that is, along the line GMH. The distance MX' from M to X' measured along the line GMH in the positive direction MH, is

$$MX'=\frac{|Z_y|}{2\tan\frac{\phi}{2}}=|Z_y|\frac{\cot\frac{\phi}{2}}{2} \tag{18}$$

If cot ($\phi/2$) is positive, MX' is positive; if cot ($\phi/2$) is negative, MX' is negative. This is indicated in Figure 5 where MX' is positive for values of ϕ between 0 and 180 degrees, and negative for values of ϕ between 180 and 360 degrees. The intersections X' are shown for $\phi=60$ and 240 degrees.

From equation 18 and Figure 5, the angles $AX'M$ and $BX'M$ are each equal to $\phi/2$. If C' is the center of the arc, the angles $AC'M$ and $BC'M$ will each be equal to ϕ (an angle inscribed in a circle is one-half the angle at the center subtended by the same arc). The distance MC' is therefore

$$MC'=\frac{|Z_y|}{2\tan\phi}=\frac{|Z_y|}{2\tan(\delta+\theta_k)}=|Z_y|\frac{\cot\phi}{2} \tag{19}$$

If cot ϕ is positive, the center C' is in the direction MH; if cot ϕ is negative, C' is in the direction MG. Values of δ or of $\phi=\delta+\theta_k$ which differ by 180 degrees will have the same center C'; but from equation 18, their intersection X' with GMH will be on opposite sides of M. This is shown in Figure 5, where the arcs for $\phi=60$ degrees and $\phi=240$ degrees have the same center C' but their intersections X' with GMH are on opposite sides of M.

When the center C' has been located, the radius r' is equal to the distance from C' to A or B. The equation for the radius r' is

$$r'=C'A=C'B=\frac{|Z_y|}{2\sin\phi}=\frac{|Z_y|}{2\sin(\delta+\theta_k)} \tag{20}$$

To construct charts for constant values of $|E_B/E_A|$ or $|E_A/E_B|$ and δ, the assumed value of $|E_B/E_A|$ is divided by K to obtain $|E_B/(E_AK)|$, or the assumed value of $|E_A/E_B|$ is multiplied by $|K|$ to obtain $|E_AK/E_B|$, and the assumed value of δ is added to θ_k to obtain $\phi=\delta+\theta_k$. Circles for constant values of $|E_B\div(E_AK)|$ or $|E_AK/E_B|$ and arcs for constant values of ϕ are then constructed as explained above, but circles and arcs are graduated in terms of $|E_B/E_A|$ or $|E_A/E_B|$ and δ, respectively. This is illustrated in Figure 5, where circles and arcs are labeled in terms of $|E_A/E_B|$, $|E_B/E_A|$ and δ, as well as in terms of $|E_AK/E_B|$ and ϕ.

General Impedance Chart

A general chart for determining the system impedances seen by relays during power swings was first suggested and constructed by A. J. McConnell.

Referring to equations 10–15 and 18–20, it will be noted that when points A and B corresponding to $E_A=0$ and $E_B=0$, respectively, have been located, the set of circles for constant values of $|E_B/(KE_A)|$ or $|E_AK/E_B|$ and the arcs for constant values of $\phi=\delta+\theta_k$ can be determined from the length and slope of the line AB which represents the impedance $Z_y=|Z_y|\underline{/\theta_y}$. If line AB is taken as unity or 100 per cent, and a chart constructed with complete sets of circles and arcs of circles for constant values of $|E_B/(E_AK)|$ or $|E_AK/E_B|$ and $\phi=\delta+\theta_k$, respectively, this chart can be used for any system if impedances are expressed in per unit of a base impedance equal to $|Z_y|=AB$. The general chart is shown in Figure 6 with line AB in a vertical position. The length $AB=|Z_y|$ in this chart is five centimeters. Any convenient length may be selected. There are no co-ordinates on the chart. It consists of circles and arcs of circles and the straight lines AB (extended) and the perpendicular bisector of AB. The circles are graduated in terms of $|E_AK/E_B|$, the arcs in terms of $\phi=\delta+\theta_k$.

Illustrations of the use of the general impedance chart are given in part I. It may be preferable to use a template for the general impedance chart, in which case points A and B of the template would be placed over A and B of the rectangular co-ordinate paper, and the desired circles and arcs of circles drawn on the paper.

III. Equations for System Impedances Seen by Relays During Power Swings

Equations will be derived and expressed in the form of equation 3 of part II for the impedances seen by distance relays during power swings, with and without faults, based on the assumptions stated in part I. A brief discussion of three-phase linear systems containing unsymmetrical static circuits, with a suggested method of procedure, is given at the end of part III.

It has been shown[5] that a phase distance relay, using line-to-line voltage and the corresponding delta current, will see the same system impedance on three-phase, phase-to-phase, or two-phase-to-ground faults in a symmetrical three-phase linear system having equal positive- and negative-sequence impedances, provided the fault involves the phases to which the relay is connected. Accordingly, the three impedances at R are

$$Z_{cb}=\frac{V_{cb}}{I_b-I_c}=\frac{V_b-V_c}{I_b-I_c} \tag{21}$$

$$Z_{ac}=\frac{V_{ac}}{I_c-I_a}=\frac{V_c-V_a}{I_c-I_a} \tag{22}$$

$$Z_{ba}=\frac{V_{ba}}{I_a-I_b}=\frac{V_a-V_b}{I_a-I_b} \tag{23}$$

where V and I in the above equations are sinusoidal voltages to neutral and line currents, respectively, of fundamental frequency at R; and subscripts a, b, c refer to phases a, b, c, respectively.

Power Swings During Symmetrical System Conditions

This case covers symmetrical three-phase short circuits, and system conditions after a fault has been cleared and initial transients have disappeared. In a symmetrical three-phase system under balanced operation, there are only positive-sequence currents and voltages. $V_a=V_{a1}$ and $I_a=I_{a1}$. With phase order $a\ b\ c$: $V_b=a^2V_{a1}$; $V_c=aV_{a1}$; $I_b=a^2I_{a1}$; $I_c=aI_{a1}$. Substitution of these values in equations 21–23 gives $Z_{cb}=Z_{ac}=Z_{ba}=V_{a1}/I_{a1}=Z_R$.

The impedance Z_R seen by the relays in the three phases at any location R under symmetrical system conditions can be determined from the ratio of the positive-sequence line-to-neutral voltage at R to the positive-sequence line current at R. The problem is to express $Z_R=V_R/I_R$ by an equation in the form of equation 3 in terms of the positive-sequence system impedances, the ratio $|E_A/E_B|$ or $|E_B/E_A|$, and the angle δ; δ is the angle by which E_A leads E_B. With the equation in specified form, the three complex impedances

Table IV. Location of Centers of Arcs for Constant Values of δ in Terms of $|Z_y|=AB$ and $\phi=\delta+\theta_k$

$\phi^\circ=\delta+\theta_k$	*$MC'/\|Z_y\|$	$\phi^\circ=\delta+\theta_k$	*$MC'/\|Z_y\|$	$\theta^\circ=\delta+\theta_k$	*$MC'/\|Z_y\|$
0, 180	∞	60, 240	0.2887	120, 300	—0.2887
5, 185	5.715	65, 245	0.2332	125, 305	—0.3501
10, 190	2.836	70, 250	0.1820	130, 310	—0.4196
15, 195	1.866	75, 255	0.1340	135, 315	—0.5000
20, 200	1.374	80, 260	0.0882	140, 320	—0.596
25, 205	1.072	85, 265	0.0437	145, 325	—0.714
30, 210	0.866	90, 270	0	150, 330	—0.866
35, 215	0.714	95, 275	—0.0437	155, 335	—1.072
40, 220	0.596	100, 280	—0.0882	160, 340	—1.374
45, 225	0.500	105, 285	—0.1340	165, 345	—1.866
50, 230	0.4196	110, 290	—0.1820	170, 350	—2.836
55, 235	0.3501	115, 295	—0.2332	175, 355	—5.715

*MC' is the distance from M, the midpoint of AB, to C', the center of the arc on GMH. See Figure 5. MX' is the distance from M to X', the intersection of the arc with GMH in the positive direction MH. If ϕ is between 0 and 180 degrees MX' is positive; if ϕ is between 180 and 360 degrees, MX' is negative.

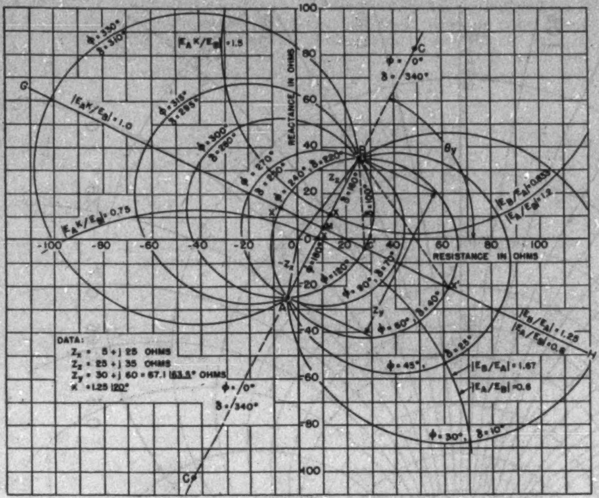

Figure 5. System impedance chart in ohms

Z_x, Z_z, $Z_y = Z_x + Z_z$, and the complex number K can be evaluated. Although Z_R is given in two forms by equation 3, except for a few illustrative examples, only one equation for Z_R will be given in the work which follows. Because of the relation $Z_y = Z_x + Z_z$, if Z_y and Z_z are known, Z_x can be determined by subtracting Z_z from Z_y: $Z_x = Z_y - Z_z$.

Positive-sequence diagrams are given in part I, Figures 1–4, for the types of systems which will be considered. There are two generally accepted methods of determining voltages to neutral and line currents in linear single-phase networks such as those shown in part I, Figures 1–4. One method is by means of driving-point and transfer impedances; the other is by the use of general circuit constants. Both methods will be used for the special systems of Figures 2 and 4, but only the former for the general system of Figure 1.

Driving-Point and Transfer Impedances. Referring to the positive-sequence diagrams of Figures 1a, 2a, 3a, 4a, and 4b, let

Z_{RR} = driving-point impedance between terminals R and N = ratio of the voltage to neutral applied at R to the total current entering the network at R when terminals A and B are short-circuited to neutral N

$\left.\begin{array}{c} Z_{RR-p}, Z_{RR-q} \\ \text{or} \\ (Z_{RR-A}, Z_{RR-B}) \end{array}\right\}$ = components of Z_{RR} in the directions p and q, respectively (or in the directions A and B when there is no ambiguity in regard to direction of current) = ratios of the voltage to neutral applied at R to the components of current entering the network at R and flowing through p and q, or toward A and B, respectively, when A and B are short-circuited to neutral

$Z_{AR} = Z_{RA}$ = transfer impedance between terminals A and N and terminals R and N = ratio of the voltage to neutral applied at A to the total current leaving the network at R when R and B are short-circuited to neutral = ratio of the voltage to neutral applied at R to the current leaving the network at A when A and B are short-circuited to neutral

$Z_{BR} = Z_{RB}$ = transfer impedance between terminals B and N and terminals R and N (Definition similar to that of $Z_{AR} = Z_{RA}$, with B and A interchanged)

$z_{AR} = z_{RA}$ = transfer impedance between terminals A and N and terminals p and q when p and q are short-circuited through R = ratio of the voltage to neutral applied at A to the line current at R when B is short-circuited to neutral and p and q are connected through R. (R is not short-circuited to neutral) = ratio of the series voltage inserted at R between p and q to the current at A when A and B are short-circuited to neutral

$z_{BR} = z_{RB}$ = transfer impedance between terminals B and N and terminals q and p when p and q are short-circuited through R. (Definition similar to that of $z_{AR} = z_{RA}$ with B and A interchanged)

From these definitions of Z_{RR-p} Z_{RR-q}, or (Z_{RR-A}, Z_{RR-B}) and Z_{RR}, it follows that

$$Z_{RR} = \frac{Z_{RR-p}Z_{RR-q}}{Z_{RR-p}+Z_{RR-q}} = \frac{Z_{RR-A}Z_{RR-B}}{Z_{RR-A}+Z_{RR-B}} \qquad (24)$$

General Network Between E_A and E_B. (See Figure 1a). With E_A and E_B applied at A and B, respectively, no current enters or leaves the network at R. Let V_R be the resultant voltage to neutral at R. Under the principle of superposition, R may be considered a network terminal at which a voltage to neutral V_R is applied through zero impedance so that the current sent into the network at R by V_R just equals the sum of the currents sent out of the network at R by E_A and E_B; V_R/Z_{RR} must equal the sum of E_A/Z_{AR} and $E_B \div Z_{BR}$ or

$$V_R = Z_{RR}\left(\frac{E_A}{Z_{AR}}+\frac{E_B}{Z_{BR}}\right) \qquad (25)$$

$$V_R = \frac{Z_{RR-A}Z_{RR-B}}{Z_{RR-A}+Z_{RR-B}}\left(\frac{E_A}{Z_{AR}}+\frac{E_B}{Z_{BR}}\right) \qquad (25a)$$

The line current I_R at R in the direction pRq may be determined by superposing the line currents resulting from E_A and E_B, separately applied. Thus,

$$I_R = \frac{E_A}{z_{AR}} - \frac{E_B}{z_{BR}} \qquad (26)$$

The impedance Z_R seen by the relay at R in the general network of Figure 1a is obtained by dividing V_R given by equation 25 by I_R given by equation 26:

$$Z_R = \frac{V_R}{I_R} = \frac{Z_{RR}z_{AR}z_{BR}}{Z_{AR}Z_{BR}}\left(\frac{E_AZ_{BR}+E_BZ_{AR}}{E_Az_{BR}-E_Bz_{AR}}\right)$$

Reference to equations 1, 2, and 3 shows that Z_R may be written in either of the forms given by equation 3.

$$Z_R = Z_{RR}\frac{z_{AR}}{Z_{AR}} - \frac{Z_{RR}\left(\frac{z_{AR}}{Z_{AR}}+\frac{z_{BR}}{Z_{BR}}\right)}{1-\frac{E_A}{E_B}\left(\frac{z_{BR}}{z_{AR}}\right)}$$

$$= -Z_{RR}\frac{z_{BR}}{Z_{BR}} + \frac{Z_{RR}\left(\frac{z_{AR}}{Z_{AR}}+\frac{z_{BR}}{Z_{BR}}\right)}{1-\frac{E_B}{E_A}\left(\frac{z_{AR}}{z_{BR}}\right)} \qquad (27)$$

Equation 27 can be replaced by equation 3 if $Z_x = Z_{RR}\frac{z_{BR}}{Z_{BR}}$; $Z_z = Z_{RR}\frac{z_{AR}}{Z_{AR}}$: $Z_y = Z_{RR}\left(\frac{z_{AR}}{Z_{AR}}+\frac{z_{BR}}{Z_{BR}}\right)$; $K = z_{BR}/z_{AR}$.

Special Network Between E_A and E_B. (See Figure 2a). When point R, the location of relays, divides the system into two parts which have no connection except through R, the impedance seen by the relays at R can be expressed in a form more convenient for calculation than that given by equation 27. Instead of using one driving point impedance and four transfer impedances to define V_R and I_R, two driving point impedances Z_{RR-A} and Z_{RR-B} and two transfer impedances Z_{RA} and Z_{RB} can be used if z_{AR} and z_{BA} are expressed in terms of these four impedances by the equations derived in the following paragraph.

In Figure 2a, with E_A applied between

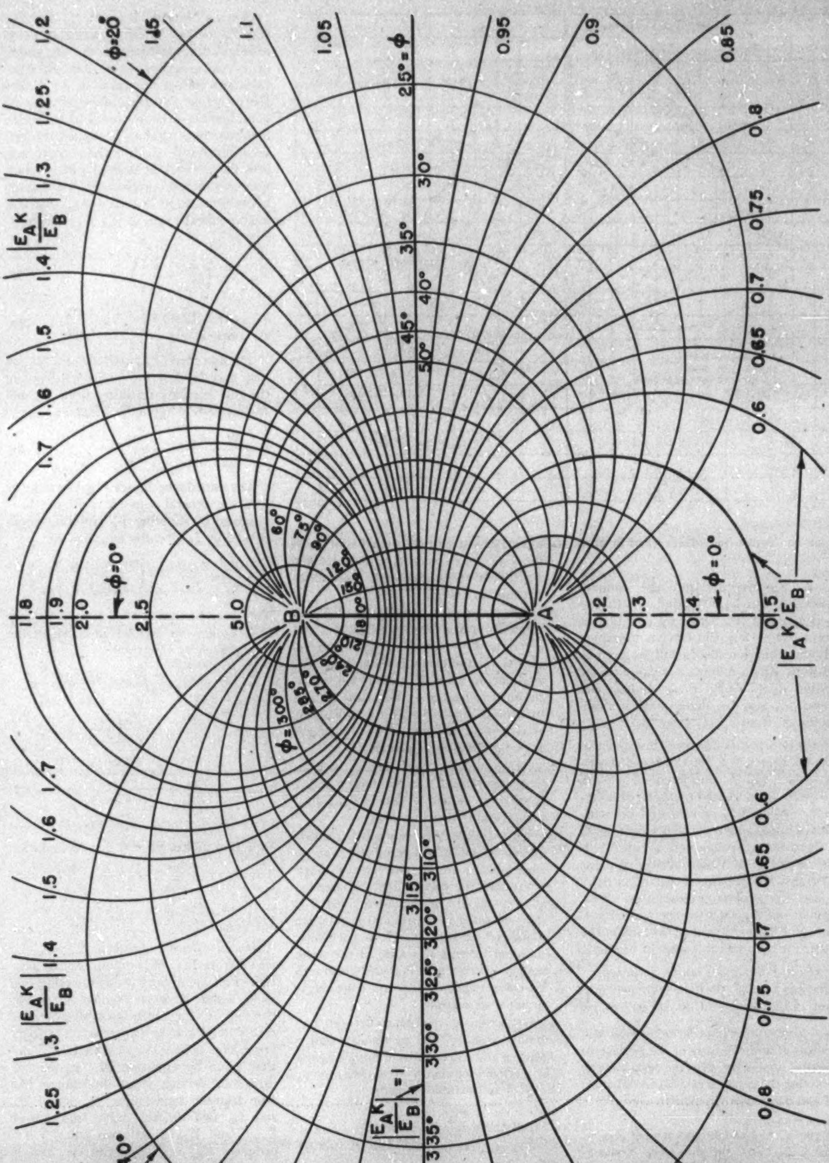

Figure 6. General impedance chart

neutral and A, and B short-circuited to neutral, let V_R be the line-to-neutral voltage at R and I_R the line current at R, positive direction of current being from A to B. Under this condition, by definition,

$$z_{AR}=\frac{E_A}{I_R} \tag{28}$$

By use of superposition, I_R is also given by the following equations when $E_B=0$:

$$I_R=\frac{E_A}{Z_{AR}}-\frac{V_R}{Z_{RR-A}}=\frac{V_R}{Z_{RR-B}} \tag{29}$$

Substitution of $V_R=I_RZ_{RR-B}$, from the second equation of (29) in the first, gives

$$\begin{aligned}\frac{E_A}{Z_{AR}}&=I_R\left(1+\frac{Z_{RR-B}}{Z_{RR-A}}\right)\\&=I_R\frac{Z_{RR-A}+Z_{RR-B}}{Z_{RR-A}}\left(\frac{Z_{RR-B}}{Z_{RR-B}}\right)\\&=I_R\frac{Z_{RR-B}}{Z_{RR}}\end{aligned}$$

$$\frac{E_A}{I_R}=\frac{Z_{AR}Z_{RR-B}}{Z_{RR}} \tag{30}$$

If E_A/I_R in equation 30 is replaced by z_{AR} from equation 28,

$$z_{AR}=Z_{AR}\frac{Z_{RR-B}}{Z_{RR}} \tag{31}$$

Similarly, it can be shown that

$$z_{BR}=Z_{BR}\frac{Z_{RR-A}}{Z_{RR}} \tag{32}$$

The voltage V_R at R is given by equation 25a. The current I_R at R, obtained by substitution of equations 31 and 32 in equation 26, is

$$\begin{aligned}I_R&=Z_{RR}\left(\frac{E_A}{Z_{AR}Z_{RR-B}}-\frac{E_B}{Z_{RB}Z_{RR-A}}\right)=\\&\frac{Z_{RR-A}Z_{RR-B}}{Z_{RR-A}+Z_{RR-B}}\left(\frac{E_A}{Z_{AR}Z_{RR-B}}-\frac{E_B}{Z_{BR}Z_{RR-A}}\right)\end{aligned} \tag{33}$$

Division of V_R from equation 25a by I_R from equation 33, or substitution of equations 31 and 32 in equation 27, gives

$$\begin{aligned}Z_R&=Z_{RR-B}-\frac{(Z_{RR-A}+Z_{RR-B})}{1-\frac{E_A}{Z_B}\left(\frac{Z_{RR-A}Z_{BR}}{Z_{AR}Z_{RR-B}}\right)}\\&=-Z_{RR-A}+\frac{(Z_{RR-A}+Z_{RR-B})}{1-\frac{E_B}{E_A}\left(\frac{Z_{AR}Z_{RR-B}}{Z_{RR-A}Z_{BR}}\right)}\end{aligned} \tag{34}$$

For use in equation 3:

$Z_x=Z_{RR-A};\ Z_z=Z_{RR-B};$

$$Z_y=Z_{RR-A}+Z_{RR-B};\ K=\frac{Z_{RR-A}Z_{BR}}{Z_{AR}Z_{RR-B}}$$

General Circuit Constants. The positive-sequence diagram of Figure 2a is given by Figure 2b in terms of two sets of general circuit constants A_1, B_1, C_1, D_1 and A_2, B_2, C_2, D_2. The transfer and driving point impedances which occur in equation 34, in terms of these general circuit constants, are $Z_{AR}=B_1$; $Z_{BR}=B_2$; $Z_{RR-A}=B_1/A_1$; $Z_{RR-B}=B_2/D_2$. Substitution of these equations in equation 34 gives

$$Z_R=\frac{B_2}{D_2}-\frac{\left(\frac{B_1}{A_1}+\frac{B_2}{D_2}\right)}{1-\frac{E_A}{E_B}\left(\frac{D_2}{A_1}\right)} \tag{34a}$$

For use in equation 3:

$Z_x=B_1/A_1;\ Z_z=B_2/D_2;$

$$Z_y=\frac{B_1}{A_1}+\frac{B_2}{D_2};\ K=D_2/A_1$$

Equation 34a will now be derived in terms of general circuit constants directly from Figure 2b of part I.

$E_A=V_RA_1+I_RB_1$ and $E_B=V_RD_2-I_RB_2$

Solution of these equations for V_R and I_R gives

$$V_R=\frac{E_AB_2+E_BB_1}{A_1B_2+D_2B_1}\text{ and }I_R=\frac{E_AD_2-E_BA_1}{A_1B_2+D_2B_1}$$

The impedance Z_R seen by a relay at R is

$$Z_R=\frac{V_R}{I_R}=\frac{E_AB_2+E_BB_1}{E_AD_2-E_BA_1}$$

This equation is in the form of equation 1; if expressed in the form of equation 2, it will be the same as equation 34a.

Single Circuit Between E_A and E_B of Negligible Capacitance. (See Figure 3a). If capacitance is negligible, the positive-sequence diagram of Figure 2a becomes that of Figure 3a in which the impedance between A and R is Z_A and that between R and B is Z_S-Z_A, where Z_S is the total impedance between A and B.

$$Z_{AR}=Z_{RR-A}=Z_A\quad Z_{BR}=Z_{RR-B}=Z_S-Z_A$$

Substitution of these equations in equations 25a and 33 for V_R and I_R, respectively, gives

$$\begin{aligned}V_R&=\frac{E_AZ_{RR-B}+E_BZ_{RR-A}}{Z_{RR-A}+Z_{RR-B}}\\&=\frac{E_A(Z_S-Z_A)+E_BZ_A}{Z_S}\end{aligned} \tag{35}$$

$$I_R=\frac{E_A-E_B}{Z_{RR-A}+Z_{RR-B}}=\frac{E_A-E_B}{Z_S} \tag{36}$$

Division of equation 35 by equation 36, or substitution of Z_{RR-A} for Z_{RA} and Z_{RR-B} for Z_{RB} in equation 34, gives

$$\begin{aligned}Z_R&=Z_{RR-B}-\frac{Z_{RR-A}+Z_{RR-B}}{1-\frac{E_A}{E_B}}\\&=-Z_{RR-A}+\frac{Z_{RR-A}+Z_{RR-B}}{1-\frac{E_B}{E_A}}\end{aligned} \tag{37}$$

For use in equation 3:

$Z_x=Z_{RR-A}=Z_A;\ Z_z=Z_{RR-B}=Z_S-Z_A;$
$Z_y=Z_{RR-A}+Z_{RR-B}=Z_S;\ K=1\underline{/0°}$

Relays at Terminals A and B. Let the relays be located at the terminals A and B of a general three-phase circuit, and let V_A and V_B be the positive-sequence *terminal* voltages to neutral at the relays. Let I_A and I_B be the positive-sequence line currents at A and B, respectively, positive direction of line current being from A to B. The positive-sequence diagram of this system is shown as a three-terminal network between A, B, and neutral N, in Figures 4a and 4b, with the relay location R at A in Figure 4a, and at B in Figure 4b.

Let R in Figure 4a approach A; then, in the limit, $Z_{AR}=Z_{RR-A}=0$; and $Z_{AR}/Z_{RR-A}=1$. Substitution of these values in equation 34, with E_A and E_B replaced by V_A and V_B, respectively, gives Z_R, the impedance seen by the relay at A:

$$\begin{aligned}Z_R&=Z_{RR-B}-\frac{Z_{RR-B}}{1-\frac{V_A}{V_B}\left(\frac{Z_{BR}}{Z_{RR-B}}\right)}\\&=\frac{Z_{RR-B}}{1-\frac{V_B}{V_A}\left(\frac{Z_{RR-B}}{Z_{BR}}\right)}\end{aligned} \tag{38}$$

For use in equation 3:

$Z_x=0,\ Z_z=Z_y=Z_{RR-B};\ K=Z_{BR}/Z_{RR-B}$

By analogy, the impedance Z_R seen by the relay at B in Figure 4b is

$$\begin{aligned}Z_R&=0-\frac{Z_{RR-A}}{1-\frac{V_A}{V_B}\left(\frac{Z_{RR-A}}{Z_{AR}}\right)}\\&=-Z_{RR-A}+\frac{Z_{RR-A}}{1-\frac{V_B}{V_A}\left(\frac{Z_{AR}}{Z_{RR-A}}\right)}\end{aligned} \tag{39}$$

For use in equation 3:

$Z_x=Z_y=Z_{RR-A};\ Z_z=0;\ K=Z_{RR-A}/Z_{AR}$

In terms of the general circuit constants A, B, C, and D, Z_{BR} (in equation 38) $=Z_{AR}$ (in equation 39) $=B$; Z_{RR-B} (in equation 38) $=B/D$; Z_{RR-A} (in equation 39) $=B/A$. If these equations are substituted in equations 38 and 39, the impedances Z_R seen by the relays at A and B, respectively, are

$$Z_R=\frac{B}{D}-\frac{\frac{B}{D}}{1-\frac{V_AD}{V_B}}=0+\frac{\frac{B}{D}}{1-\frac{V_B}{V_AD}} \tag{38a}$$

For use in equation 3:

$Z_x=0;\ Z_z=Z_y=B/D;\ K=D$

$$Z_R=0-\frac{\frac{B}{A}}{1-\frac{V_A}{V_BA}}=-\frac{B}{A}+\frac{\frac{B}{A}}{1-\frac{V_BA}{V_A}} \tag{39a}$$

For use in equation 3:

$Z_x=Z_y=B/A;\ Z_z=0;\ K=1/A$

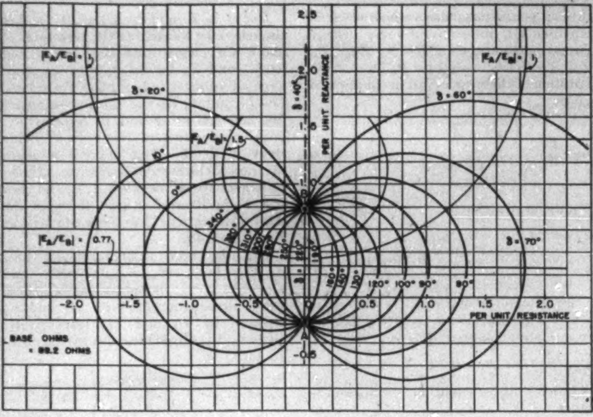

Figure 7a. Z_{ac} in per unit of 89.2 ohms

Figure 7b(below). Z_{ba} in per unit of 89.2 ohms

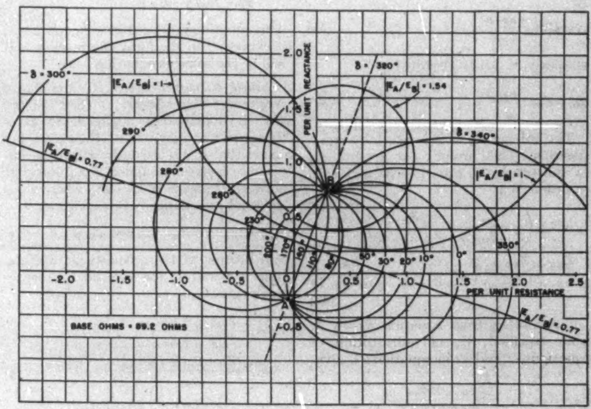

Equations 38a and 39a, in terms of general circuit constants, are given in slightly different form in reference 5.

Three-Phase Faults. The equations for V_R, given by equation 27 for the general network of Figure 1, can be applied to symmetrical three-phase faults if transfer and driving-point impedances are determined from Figure 1b with a solid fault at F. Impedances so determined will be designated by a prime (′) superscript, for example, Z'_{RR} Z'_{AR}. For the special case of no connection between B and R except at the fault F, $Z'_{BR} = \infty$, and the impedance Z_R seen by the relay at R is

$$Z_R = Z'_{RR-B} \tag{40a}$$

With no connection between R and A except at F, $Z'_{AR} = \infty$, and

$$Z_R = -Z'_{RR-A} \tag{40b}$$

For the special system of Figure 2, with a solid fault at F which separates the system into two parts at F, as indicated in Figure 2c, $Z'_{BR} = \infty$. From equations 25 and 33

$$V'_R = Z'_{RR} \frac{E_A}{Z'_{AR}} \tag{41a}$$

$$I_R = Z'_{RR} \frac{E_A}{Z'_{AR} Z'_{RR-B}} \tag{41b}$$

The impedance Z_R seen by the relay is given by equation 40a.

For a single circuit of negligible capacitance with a solid fault at F, as in Figure 3a, where the impedances between A and R, R and F, and F and B are Z_A, Z_B, and Z_C, respectively, V'_R and I'_R are

$$V'_R = \frac{E_A Z_B}{Z_A + Z_B} \tag{42a}$$

$$I'_R = \frac{E_A}{Z_A + Z_B} \tag{42b}$$

$$Z_R = \frac{V'_R}{I'_R} = Z_B \tag{42c}$$

Power Swings During Unsymmetrical Faults

The system impedances seen by the three relays at R during any condition of operation are given by equations 21–23 in terms of phase currents and voltages. When positive- and negative-sequence system impedances can be assumed equal, phase voltages and currents are conveniently expressed in terms α, β, and zero-sequence components,[7] or by positive-plus-negative, positive-minus-negative, and zero-sequence components.[8]

At any point R in a three-phase system, α components of line-to-neutral voltages and α components of line currents in phases b and c are equal; they are opposite in sign and of half the magnitude of those in phase a. There are no β components of voltage and current in phase a; in phases b and c, β components of line-to-neutral voltages and β components of line currents are equal in magnitude but of opposite signs. Zero-sequence components (indicated by the subscript 0) are equal in the three phases. The following equations satisfy these definitions:

$$\left.\begin{aligned}
V_a &= V_\alpha + V_0 \\
V_b &= -\frac{1}{2}V_\alpha + \frac{\sqrt{3}}{2}V_\beta + V_0 \\
V_c &= -\frac{1}{2}V_\alpha - \frac{\sqrt{3}}{2}V_\beta + V_0 \\
I_a &= I_\alpha + I_0 \\
I_b &= -\frac{1}{2}I_\alpha + \frac{\sqrt{3}}{2}I_\beta + I_0 \\
I_c &= -\frac{1}{2}I_\alpha - \frac{\sqrt{3}}{2}I_\beta + I_0
\end{aligned}\right\} \tag{43}$$

where the choice of the sign for β currents and voltages is arbitrary.[9]

Substitution of these equations in equations 21–23 gives the impedances seen by the relays in the three phases at R in terms of α and β components of current and voltage.

$$Z_{cb} = \frac{\sqrt{3}V_\beta}{\sqrt{3}I_\beta} = \frac{V_\beta}{I_\beta} \tag{44}$$

$$Z_{ac} = \frac{-\frac{3}{2}V_\alpha - \frac{\sqrt{3}}{2}V_\beta}{-\frac{3}{2}I_\alpha - \frac{\sqrt{3}}{2}I_\beta} = \frac{\sqrt{3}\,V_\alpha + V_\beta}{\sqrt{3}\,I_\alpha + I_\beta} \tag{45}$$

$$Z_{ba}=\frac{\frac{3}{2}V_\alpha-\frac{\sqrt{3}}{2}V_\beta}{\frac{3}{2}I_\alpha-\frac{\sqrt{3}}{2}I_\beta}=\frac{\sqrt{3}\,V_\alpha-V_\beta}{\sqrt{3}\,I_\alpha-I_\beta} \qquad (46)$$

where V_α, V_β, I_α, and I_β are α and β components of line-to-neutral voltage and line current at R, respectively. Zero-sequence components of voltage and current at R do not appear in the impedance equations; however, their presence will affect V_α and I_α.

α, β, and 0 one-line diagrams or component networks can be drawn for any three-phase system. Under the assumption of a symmetrical three-phase linear network, having equal positive- and negative-sequence impedance, α and β impedances are equal to positive-sequence impedances. With balanced generated voltages E_A and E_B applied at two system terminals A and B, respectively, generated α voltages will be the same as the positive-sequence generated voltages E_A and E_B; generated β voltages will be $-jE_A$ and $-jE_B$, the positive-sequence generated voltages E_A and E_B multiplied by $-j$. Before the fault occurs, the α network will be exactly the same as the positive-sequence network; the β network will differ from the positive-sequence network only in that the applied voltages at terminals A and B are multiplied by $-j$.

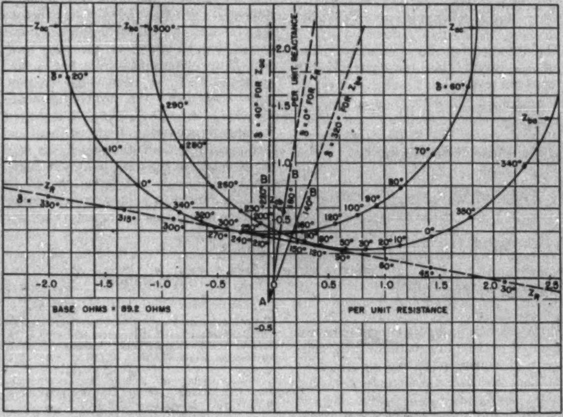

Figure 7c. Z_{cb}, Z_{ac}, Z_{ba} for line-to-line fault and Z_R with no fault in per unit of 89.2 ohms

$|E_A/E_B|=1$

Let the fault be at any system point F; and let the phases be designated so that line-to-line and double-line-to-ground short circuits involve phases b and c, while line-to-ground short circuits occur on phase a. In the case of one open conductor, let the opening occur at F in phase a; with two open conductors, let the openings occur at F in phases b and c.

Zero-Sequence Network. Let Z_0 be the zero-sequence impedance viewed from the fault at F. Let z_0 be the impedance offered to a *series voltage* inserted in the zero-sequence network at F. If F is on a single *ungrounded* circuit, Z_0 and z_0 will both be infinite; if the circuit is grounded at one terminal only, Z_0 will be finite but z_0 infinite. If F is on one of two parallel circuits, connected to bus bars at both ends, grounded or ungrounded, z_0 will be finite.

Under the assumption of a symmetrical three-phase linear network with equal positive- and negative-sequence impedances between E_A and E_B, there will be no connection between the α and β network even during unsymmetrical faults. This makes it possible to use the positive-sequence system diagrams of Figures 1–3, and the equations in terms of transfer and driving-point impedances already derived for V_R and I_R under balanced operation for V_α and I_α, or for jV_β and jI_β, *provided the transfer and driving-point impedances are defined and determined under the conditions imposed by the fault.* A system of notation is required to differentiate V_R and I_R and the transfer and driving-point impedances obtained from the positive-sequence network under seven different conditions. The following notation is suggested, where the phrase in parenthesis indicates the application of the stated condition:

1. No superscripts when F in the positive-sequence network is isolated from neutral. (α network—line-to-line fault; β network—line-to-ground fault or one open conductor.)
2. Prime (′) when F in the positive-sequence network is short-circuited directly to neutral. (β network—line-to-line or double-line-to-ground fault; positive-sequence network—three-phase fault.)
3. Double prime (″) when the positive-sequence network is open at F. (β network—two open conductors.)
4. One asterisk (*) when F in the positive-sequence network is short-circuited to neutral through $Z_0/2$. (α network—line-to-ground fault.)
5. Double asterisk (**) when F in the positive-sequence network is short-circuited to neutral through $2Z_0$. (α network—double-line-to-ground fault.)
6. One plus sign (⁺) where $2z_0$ is inserted in the positive-sequence network at F. (α network—one open conductor.)
7. Double plus sign (⁺⁺) where $z_0/2$ is inserted in the positive-sequence network at F. (α network—two open conductors.)

Under any one of the seven conditions given above, transfer and driving-point impedances are determined from the positive-sequence network and written with the designated superscript. V_R and I_R written with the same superscript, are then obtained from equations 25 and 26, respectively, for the general network, where impedances without subscripts are replaced by those with the designated superscript (except for condition 1, where no change is made). For the special case of a network with no connection between A and B except through R, equations 25a and 33 are used instead of equations 25 and 26; and for the single circuit of negligible capacitance between A and B, equations 35 and 36 are used. V_R and I_R, designated by the specified superscript (or no superscript) can be used directly for V_α and I_α; but they are multiplied by $-j$ to obtain V_β and I_β. V_α, I_α V_β, and I_β are then substituted in equations 44–46 to obtain the impedances seen by the three relays at R under the stated conditions. The following equations give V_α, I_α, V_β, and I_β in terms of V_R and I_R with specified subscripts for unsymmetrical faults:

(*a*). *Line-to-Line Short Circuit at F Between Phases b and c.* The α network is unaffected by fault; point F in the β network is short-circuited directly to neutral.

$$V_\alpha=V_R;\; I_\alpha=I_R;\; V_\beta=-jV_R';\; I_\beta=-jI_R'$$

(*b*). *Line-to-Ground Short Circuit at F on Phase a.* Point F in the α network is short-circuited to neutral through $Z_0/2$; the β network is unaffected.

$$V_\alpha=V_R^*;\; I_\alpha=I_R^*;\; V_\beta=-jV_R;\; I_\beta=-jI_R$$

(*c*). *Double-Line-to-Ground Short Circuit at F on Phases b and c.* Point F in the α network is short-circuited to neutral through $2Z_0$; point F in the β network is short-circuited directly to neutral.

$$V_\alpha = V_R^{**};\quad I_\alpha = I_R^{**};\quad V_\beta = -jV_R';\quad I_\beta = -jI_R'$$

(*d*). *Phase a Open at F.* The impedance $2z_0$ is inserted in the α network at F; the β network is unaffected.

$$V_\alpha = V_R^{+};\; I_\alpha = I_R^{+};\; V_\beta = -jV_R;\; I_\beta = -jI_R$$

(*e*). *Phases b and c Open at F.* The impedance $z_0/2$ is inserted in the α network at F; the β network is opened at F.

$$V_\alpha = V_R^{++};\quad I_\alpha = I_R^{++};\quad V_\beta = -jV_R'';\quad I_\beta = -jI_R''$$

After V_α, I_α, V_β, and I_β have been determined in terms of E_A, E_B, and the transfer and driving-point impedances of the positive-sequence network under the conditions imposed by the fault, they are substituted in equations 44–46. If these impedance equations are written in the form of equation 1, they can readily be expressed in the form of equation 3 and Z_x, Z_z, $Z_y = Z_x + Z_z$, and K determined. The general solution is as follows:

For any type of fault, with positive direction of current from A to B, let

$$\begin{aligned} &V_\alpha = aE_A + bE_B;\quad I_\alpha = cE_A - dE_B \\ &V_\beta = -j(eE_A + fE_B) \\ &I_\beta = -j(gE_A - hE_B) \end{aligned} \qquad (47)$$

where a, b, and so on, are constant coefficients.

Substitution of V_β and I_β in equation 44 gives

$$Z_{cb} = V_\beta / I_\beta = \frac{eE_A + fE_B}{gE_A - hE_B} \qquad 48)$$

Equation 48 is in the form of equation 1; to express it in the form of equation 3: $Z_x = f/h$; $Z_z = e/g$; $K = g/h$.

Substitution of V_α, I_α, V_β, and I_β in equation 45 gives

$$Z_{ac} = \frac{(\sqrt{3}\,a - je)E_A + (\sqrt{3}\,b - jf)E_B}{(\sqrt{3}c - jg)E_A - (\sqrt{3}\,d - jh)E_B} \qquad (49)$$

Equation 49 is in the form of equation 1; to express it in the form of equation 3:

$$\left.\begin{aligned} &Z_x = \frac{\sqrt{3}b - jf}{\sqrt{3}d - jh} \qquad Z_z = \frac{\sqrt{3}a - je}{\sqrt{3}c - jg} \\ &Z_y = Z_x + Z_z \qquad\quad K = \frac{\sqrt{3}c - jg}{\sqrt{3}d - jh} \end{aligned}\right\} \qquad (50)$$

The equation for Z_{ba} is similar to that for Z_{ac} except that the signs of all j terms are reversed. Equations for Z_{cb}, Z_{ac}, and Z_{ba} will be evaluated for a special case.

Line-to-Line Short Circuit Between Phases b and c in a Single Circuit of Negligible Capacitance. The given system is shown in Figures 3a and 3b, where $Z_A + Z_B + Z_C = Z_S$. In Figure 3a, the fault point F is between the relays at R and E_B; in Figure 3b, F is between E_A and R. For both cases, positive direction of current will be taken from A to B.

Fault Between Relays and E_B, as in Figure 3a. V_α and I_α are the same as V_R and I_R given by equations 35 and 36, and V_β and I_β are $-j$ times V_R' and I_R' given by equations 42a and 42b, respectively. If the coefficients in these equations are equated to those in equation 47, the constants in equations 48 and 49 are: $a = (Z_S - Z_A)/Z_S$; $b = Z_A/Z_S$; $c = d = 1/Z_S$; $e = Z_B/(Z_A + Z_B)$; $f = 0$; $g = 1 \div (Z_A + Z_B)$; $h = 0$. With $f = h = 0$ in equation 48,

$$Z_{cb} = \frac{e}{g} = Z_B \qquad (51)$$

Z_{ac}, given by equation 49, can be expressed in the form of equation 3 by evaluating Z_x, Z_z, Z_y, and K in equation 50:

$$\left.\begin{aligned} &Z_x = Z_A \qquad Z_z = Z_B + \frac{Z_C}{K} \\ &Z_y = Z_A + Z_B + \frac{Z_C}{K} = \frac{Z_S}{K}\left(1 - j\,\frac{1}{\sqrt{3}}\right) \\ &K = 1 - j\,\frac{Z_S}{\sqrt{3}(Z_A + Z_B)} \end{aligned}\right\} \qquad (52)$$

The equation for Z_{ba} is similar to that for Z_{ac} except that the signs of all j terms are reversed.

Fault Between E_A and Relays, as in Figure 3b.

$$V_\alpha = V_R = \frac{E_A Z_C + E_B(Z_A + Z_B)}{Z_S}$$

$$I_\alpha = I_R = \frac{E_A - E_B}{Z_S}$$

$$V_\beta = -jV_R' = -j\left(\frac{E_B Z_B}{Z_B + Z_C}\right)$$

$$I_\beta = -jI_R' = -j\left(\frac{-E_B}{Z_B + Z_C}\right)$$

If the coefficients in these equations are equated to those in equation 47, the constants in equations 48 and 49 are: $a = Z_C/Z_S$; $b = (Z_A + Z_B)/Z_S$; $c = d = 1/Z_S$; $e = 0$; $f = Z_B/(Z_B + Z_C)$; $g = 0$; $h = 1 \div (Z_B + Z_C)$. With $e = g = 0$ in equation 48,

$$Z_{cb} = f/(-h) = -Z_B \qquad (53)$$

Z_{ac}, given by equation 49, can be expressed in the form of equation 3 by evaluating Z_x, Z_z, Z_y, and K in equation 50:

$$\left.\begin{aligned} &Z_x = KZ_A + Z_B \qquad Z_z = Z_C \\ &Z_y = KZ_A + Z_B + Z_C = KZ_S\left(1 - j\,\frac{1}{\sqrt{3}}\right) \\ &K = 1 \Big/ \left[1 - j\,\frac{Z_S}{\sqrt{3}\,(Z_B + Z_C)}\right] \end{aligned}\right\} \qquad (54)$$

The equation for Z_{ba} is similar to that for Z_{ac} except that the signs of all j terms are reversed.

Systems With Unsymmetrical Static Circuits. The methods of constructing system impedance charts, given in part II, apply to three-phase linear systems with unsymmetrical static circuits, with or without an unsymmetrical fault on the system. The unsymmetrical circuit can be replaced by equivalent circuits in the α, β, and 0 networks. In the case of a general unsymmetrical circuit in an otherwise symmetrical system, the α, β, and 0 networks are mutually coupled. The procedure in determining the required constants Z_x, Z_z, Z_y, and K is too lengthy for discussion here. These constants, however, can be determined, and the work required is not excessive if an a-c network analyzer is available.

There are many unsymmetrical circuits which have equal impedances in two of the phases; if, in addition, the zero-sequence impedance of the circuit is infinite, as is the case with an open-delta transformer of two identical single-phase units, there will be no mutual coupling between the α, β, and 0 networks. For this special case, the procedure in determining Z_x, Z_z, Z_y, and K is similar to that for symmetrical three-phase systems except that V_α and I_α at the relay location R are determined from the α diagram and V_β and I_β from the β diagram, instead of using the positive-sequence diagram first for the α network and then for the β network. Even without an unsymmetrical fault, the impedance seen by the relays in the three phases at R will not be identical, and equations 44–46 will be required in all cases to determine the impedances seen by the relays.

References

1. A COMPREHENSIVE METHOD OF DETERMINING THE PERFORMANCE OF DISTANCE RELAYS, **J. H. Neher**. AIEE TRANSACTIONS, volume 56, 1937, July section, pages 833–44.

2. RELAY OPERATION DURING SYSTEM OSCILLATIONS, **C. R. Mason**. AIEE TRANSACTIONS, volume 56, 1937, July section, pages 823–32.

3. Discussion by **J. H. Neher** of reference 2. AIEE TRANSACTIONS, volume 56, 1937, pages 1513–14.

4. Closure by **C. R. Mason** of reference 2. AIEE TRANSACTIONS, volume 57, 1938, pages 111–14.

5. PERFORMANCE REQUIREMENTS FOR RELAYS ON UNUSUALLY LONG TRANSMISSION LINES, **F. C. Poage, C. A. Streifus, D. M. MacGregor, E. E. George**. AIEE TRANSACTIONS, volume 62, 1943, June section, pages 275–83.

6. FUNDAMENTAL BASIS FOR DISTANCE RELAYING ON THREE-PHASE SYSTEMS, **W. A. Lewis, L. S. Tippett**. ELECTRICAL ENGINEERING, volume 50, June 1931, pages 420–2.

7. CIRCUIT ANALYSIS OF A-C POWER SYSTEMS—SYMMETRICAL AND RELATED COMPONENTS (volume I), **Edith Clarke**. John Wiley and Sons, New York, N. Y., 1943. Chapter 10.

8. Chapter 5 of reference 7.

9. TWO-PHASE CO-ORDINATES OF A THREE-PHASE CIRCUIT, **Edward W. Kimbark**. AIEE TRANSACTIONS, volume 58, 1939, pages 894–904.

The Design of Bus-Bar Industrial Distribution Systems: an Epitomization of Available Data

THOMAS JAMES HIGGINS
ASSOCIATE AIEE

THE PURPOSE of this paper, evidenced in its title, is to acquaint the designer of bus-bar industrial distribution systems with the extent and whereabouts of the theoretical and experimental data available for design purposes. Attention is confined to those factors that essentially determine the operating characteristics of a bus-bar distribution system: voltage drop, temperature rise, and short-circuit capacity.

The extant literature apposite to these topics has been covered exhaustively. For in addition to examination of complete runs of the principal abstracting periodicals (*Engineering Record*, *Science Abstracts*, and *Elektrotechnische Berichte*) the writer scanned, volume by volume, the indexes of the important periodicals—American, British, French, German, and Italian—devoted to electrical engineering and to electrophysics. Further, textbooks pertinent to these two domains were covered as thoroughly. However, but limited mention of such will be found in this paper. For few contain relevant material, and what is to be found has been taken from periodical literature that is encompassed herein.

The excellent library facilities available in Chicago, several trips to the New York Public Library and to the Engineering Societies Library, the use of interloan library service, and the commercial literature sent in response to written appeal enabled the writer to read each of the items comprising the appended bibliography except references 151, and 576–83. Epitomization of the essential content of these items, subdivision of this material under appropriate headings, and integration of these grouped fragments to achieve a coherent whole comprise the present paper.

This paper* can be taken as a guide to most of the consequential literature on the design of bus-bar distribution systems, including many forgotten or little-known papers containing valuable material not to be found elsewhere. As to the practical usefulness of such a guide, it may be taken that the designer who acquaints himself with all of the information detailed in the writings mentioned will be enabled:

1. To better his own design procedures.
2. To improve on present bus designs.
3. To forestall costly experimentation undertaken to obtain data either extant—but unknown to those proposing experiment—or possible of calculation from existing theory.

General Considerations

Discussion of the general issues involved in the choice, layout, and broad design of industrial distribution systems** is to be found in papers by Stiebar,[1] McKeever,[2] Powel and Barnett,[3] Beeman and Kaufmann,[4] Parsons and Barnett,[5] Blacklock,[6] and others.[7] Discussion, both qualitative and quantitative, of the various general considerations that influence specific design of the bus proper is encompassed in the papers of Boyce;[8] McCauley;[9] Dwight;[10] Steidinger;[11] Adams, Fletcher, and Johnson;[11a] and others;[12,13] and in illustrated brochures[14–18] distributed by certain concerns active in the engineering of industrial distribution systems.

The different service requirements of electric welder, electric furnace, machine tool, general light and power, and other types of load have resulted in diversified bus design. Recently Deans[19] has argued the relative advantages of various conductor shapes and arrangements. The especial merits of busses comprised of coaxial tubular conductor have been advanced by Bogardus;[20] of parallel tubular conductor by Braley,[21] de Bellis,[22] and Eales and Hoeppner;[23] of square tubular conductor by Woodruff[24] and others;[25] of strap conductor by Michalke,[26] Gibson,[27] McCann,[27a] Housley,[28] Holthaus,[29] Bulen,[30] Hurley and Smith,[31] Tennant,[32] Fisher,[33] Morgan,[34] and others;[35–9] of channel conductor by Carpenter,[40] Papst and Bohn,[40a] Shannon,[41] Wilbraham and Bailey,[42] Specht,[43,44] Greer and Guess,[45] and others;[46,46a,46b] and of angle conductor by Schrager.[47]

Similar material on bus ways (enclosed prefabricated assemblies of strap conductor) is contained in papers by Wendelkin,[48] Hess,[49] Lloyd,[50] Schaal,[50a] Carlson,[51] Simmonds,[52] Lipps,[53] Siebert,[54] Craven and Collins,[54a] Ashmore,[55] and others.[56] A general report on bus ways, covering classification, terminology, and various points of design and operation, has been prepared by Fisher and Carlson for inclusion in an AIEE-sponsored publication on power distribution in industrial plants.[57]

The especial advantages accruing to particular metals—copper,[14–17] aluminum,[15,58–61,61a] and, less commonly, zinc[62] and sodium[63,64]—have been strongly represented.

Bus Impedance

Predetermination of the electrical performance of a bus—that is, its current rating and voltage regulation—requires accurate knowledge of the resistance and inductance parameters. It is common knowledge that:

1. The a-c values of these parameters differ from the d-c values.
2. These differences, though a consequence of the same electrodynamical principle (an excellent discussion of this principle is due to Rayleigh),[65] are commonly ascribed to the joint action of "skin" and "proximity" effects.
3. The resulting change in the magnitude of the resistance is described by the skin-effect factor $K_s (= R'/R_o$, the ratio of the a-c resistance R' of an isolated conductor to its d-c resistance R_o) and by the proximity-effect factor $K_p (= R/R'$, wherein R is the actual a-c resistance) through the equation $R = K_s K_p R_o$.
4. Like expressions hold for the inductance.

Paper 45-25, recommended by the AIEE committee on industrial power applications for presentation at the AIEE winter technical meeting, New York, N. Y., January 22–26, 1945. Manuscript submitted September 7, 1944; made available for printing December 9, 1944.

THOMAS JAMES HIGGINS is associate professor of electrical engineering, Illinois Institute of Technology, Chicago, Ill.

For copies of literature distributed by their concerns, for mention of several of the references utilized, and for various other kindnesses contributing to the preparation of this paper, the writer is indebted to R. E. Bassett, vice-president of manufacturing, American Brass Company; E. T. Carlson, manager, Norwood division, The Trumbull Electric Manufacturing Company; A. G. Darling, industrial engineering department, General Electric Company; W. Deans, chief engineer, I-T-E Circuit Breaker Company; H. B. Dwight, professor of electrical engineering, Massachusetts Institute of Technology; L. L. Fountain, switchgear engineering department, Westinghouse Electric and Manufacturing Company; L. E. Fisher, director of research, Bulldog Electric Products Company; L. F. Hickernell, chief engineer, Anaconda Wire and Cable Company; J. G. Jackson, director of engineering, Square D Company, S. C. Killian, chief engineer, Delta-Star Electric Company; R. W. Shoemaker, consulting engineer, Chase Brass and Copper Company; J. St. Peter, Aluminum Company of America; and H. L. Van Valkenburg, vice-president and chief engineer, Square D Company.

* Discussion of, roughly, one half of the items in the bibliography of this paper comprise the content of a paper, "Design of Direct-Current and Low-Frequency Bus Systems: a Guide to the Literature," presented at the 1943 Midwest Power Conference. Because of its length only the introductory remarks were printed in the *Proceedings* of the conference; interested readers were invited to write for photoprinted copies of the complete paper.

** To avoid redundance we understand, unless specific statement is made to the contrary, that all remarks refer to busses comprised of long linear nonmagnetic conductors of uniform cross section.

Items comprising a connected series of references are arranged in chronological order.

5. These factors are complicated mathematical functions of the bus geometry and frequency, of the conductor geometry, conductivity and permeability, and of yet other variables.

6. Actual determination of these factors is most difficult, having been effected to date for only a few conductor shapes and arrangements.

An inclusive account of the origins and developments of the concepts of skin and proximity effects has been given by Higgins.[66] Admirable qualitative discussions of various aspects of skin and proximity effects (as manifest in conductors of circular or tubular cross section) have been advanced by Miller,[67] Girault,[68] Northrup,[69] Schelkunoff,[70] and Bunet.[71]

The general mathematical theory has been developed from two points of view: that of partial differential equations, favored by the earlier writers—Maxwell,[72] Rayleigh,[73] Heaviside,[74] Kelvin,[75] Thomson[76]—and some of the recent writers—Carson[69] and Schelkunoff[77]; and that of integral equations—introduced by Manneback[78] and extended (not always correctly) in the papers of Noether,[79,80] Strutt[81–3]—especially, Rothe,[84,85] Lettowsky,[86] and Rytov.[87]

Whether couched in terms of partial-differential or of linear-integral equations, the solution of a particular skin- and proximity-effect problem is commonly effected by some approximate numerical procedure, usually one involving iterative solution of a set of linear algebraic equations. In this connection especial attention accrues to the recent work of Crout,[88] Hildebrand,[89,90] Magnusson,[91] Aitken,[92] Schmidt,[93] Freeman,[94] and Wright,[95] on procedures which bear directly on such methods of solution.

Despite, however, availability of this general theory, the mathematical difficulties pertinent to solution of the differential or integral equations have proved so formidable that exact formulas for K_s and K_p for actual busses have been effected directly for only a few arrangements of circular and tubular conductors. For other than these recourse has been to approximate analytic methods. In this instance certain theorems or "principles" have proved of much value. One such is Dwight's[96] "similitude principle": if of an isolated conductor or of a group of conductors comprising a circuit the linear dimensions of cross section are decreased (increased) N-fold and the frequency is increased (decreased) N^2-fold, the product K_sK_p remains unchanged. Slepian[96] has given a mathematical proof of the principle—Grieg[97] a recent nonmathematical discussion. Its validity has been amply verified by experiment: data easily taken at audio or radio frequencies on miniature conductors (hence its usefulness) when scaled to lower frequencies and larger conductors agree with corresponding values calculated from rigorous formulas or obtained by direct test.

Test data taken at radio frequencies on a miniature bus can be checked or supplemented by use of the "penetration" and "electrostatic" principles as a result of the joint efforts of Kelvin[75,98,99] and Rayleigh.[73,100] If the wave length corresponding to the frequency of impressed electromotive force is large compared to the dimensions of cross section of the bus; and if $(\sigma\mu f)$,$^{1/2}$ the square root of the product of the conductor conductivity σ, permeability μ, and frequency f is (1) large in comparison with the least radius of curvature of the perimeter of conductor cross section, and (2) not less than one-half the least distance to be measured between an arbitrary point in the perimeter and that point in the perimeter which is the intersection of the perimeter and the normal drawn inward at the arbitrary point, then:

1. The currents in the conductors (of arbitrary cross sections) can be considered as concentrated in thin surface strata of depth $[2\pi(\sigma\mu f)^{1/2}]^{-1}$, the current density varying around the perimeter but not through the depth.

2. The inductance coefficients and the distribution of current density around the perimeter approximate (become identical as $\sigma f \to \infty$) the elastance coefficients and the distribution of charge density in the corresponding electrostatic problem of the conductors maintained at the line potentials.

Known solutions of this latter problem furnish the desired values of the former, whence, both current density and penetration depth being known, the resistance can be calculated from a known formula involving simple line integrals taken around the perimeters of the cross sections of the conductors.

Kelvin's writings on these two principles are far from clear. Much better exposition, as well as certain extensions of one or the other of these principles, are to be found among the writings of Abraham,[101] Boucherot,[102] Carson,[103] Strutt[83,104–06]—particularly, Loebner,[107] Kaden,[108] Adams,[109] and Levasseur.[110] In using these principles precaution must be observed as to satisfaction of the necessary conditions previously stated. In more than one instance failure to do so has invalidated deductions stemming from use of the penetration formula.[111,112]

A guide to the whereabouts of tables of Bessel, Hankel, and allied functions occurring in the solution of particular problems by the methods outlined in this section is encompassed in the introduction to the monumental work on Bessel functions of complex argument recently published by the Work Projects Administration.[113] In addition to the 66 references cited we mention tables encompassed in the papers of Bisacre,[114] Wrinch,[115,116] Kessenich,[117] and Buchholz.[118] The general theory of these functions is to be found in the standard treatises by Watson[119] and Schafheitlin.[120]

CONDUCTOR RESISTANCE

Arnold[121–3] has epitomized the work of those whose study of skin and proximity effects in circular or tubular conductor precedes his. In three important papers he has reviewed, assessed, and summarized—directly or indirectly—the method, validity, accuracy, range of application, and relative merit of the analyses of many who achieve significant results: Maxwell,[72] Rayleigh,[73] Heaviside,[74] Stefan,[124] Kelvin,[75] Thomson,[76] Brylinski,[125] Sommerfeld,[126] Mie,[127] Nicholson,[128–30] Russell,[131,132] Larmor,[133] Howe,[134,135] Curtis,[136,137] Manneback,[78] Carson,[138] Butterworth,[139,140] Snow,[141] Mead,[142] Strutt,[82,83] Costello,[143] Dwight,[96,144–6] Försterling,[147] Wien,[148] Bisacre,[114] Bromwich,[149] and König.[150] Arnold's third paper, the most inclusive and the most important of the three, contains formulas and curves yielding for any frequency values of K_s and K_p for those single and three-phase arrangements of circular and tubular conductor in common use. Recent papers by Fischer,[151] Dwight[152] (on the three-phase concentric tubular bus), and Larrick and Race[153] complement Arnold's work.

Elsewhere[154] Arnold has discussed the more important of the approximate formulas for K_s of circular conductors advanced by Heaviside,[74] Brylinski,[155,156] Mascart,[157] Zenneck,[158] Pedersen,[159] Rushmore,[160] Spielrein,[161] Levasseur,[162] and others. Through comparison of values obtained from the rigorous and the approximate formulas he concludes that Levasseur's is the most accurate of those considered. Mathieu[163,164] has given slide rules and charts enabling rapid calculation with this formula. Also, it has been discussed (qualitatively) by Fromy[165] and Singh.[166] Singh's and Levasseur's own suggestion that it readily can be extended to other cross sections in the manner mentioned by them is incorrect: they have overlooked the variation in current density around the perimeter that occurs in conductors of other than circular or annular cross section.

Though, as mentioned, Arnold's work encompasses that of those previously named, the papers of several (especially those of Dwight,[96,144–6] Costello,[143] and Pedersen[159]) and yet others by Hospitalier,[167] Garnier,[168] Rosa and Grover,[169] Swyngedauw,[170] Miller,[67] Kennelly[171,172] and his associates, Butterworth,[173] Ewan,[174,175] Ursi,[176] Grünwald,[177] Heymann,[178,179] Maione,[180] Whinnery,[181] Wheeler,[182] and others[154,183] on skin effect, and by Dwight,[184] Carter,[185] Whitehead,[186] Buchholz,[187] Webb,[188] and Tschiassny[189] on proximity effect, contain formulas, curves, and tables, too varied to enumerate, that are of considerable aid in the solution of specific problems.

Test data taken for the purpose of confirming theoretical studies on skin and proximity effects in circular and tubular conductors are to be found in the writings of Kennelly[171,172] and his associates, Roberds,[190] Moullin,[191] Sterba and Feldman,[192] Hoyt and Mead,[193] Ochem,[194] Arnold,[121–3] and Larrick and Race.[153] The magnitude of these effects in actual practice is strikingly illustrated by Busch's[195,196] measurements of the radial variation, in phase and magnitude, of the current density in large isolated iron cylinders and of Wilson's[197] measurements of surface current density in one conductor of a three-phase circuit comprised of tubular conductor.

Of a circular conductor Broca,[198] Carson,[69] and Breitfeld[199] have calculated K_s for a total sinusoidal current comprised of conduction and displacement components, Brylinski[200] K_s for both a damped sinusoidal current and a current with several sinusoidal components of different frequencies, and Cocci and Sartori[201] K_s for an arbitrary current capable of representation by a Fourier series. Strutt[83] has calculated $K_p K_s$ at high frequency for two externally located parallel circular cylinders of unequal radii. Adams[100] and Schelkunoff[77] have obtained similar results for a circuit comprised of a circular conductor eccentrically located within a tubular conductor.

Skin-effect theory for bimetallic conductors—circular or tubular conductors coated with an annular layer of a different metal—has been effected by Harms,[202] Miller,[203] Försterling,[204] Pleijel,[205] Maione,[206] Fischer,[207,208] Strutt,[209] Ekelöf,[210] Kruse and Zinke,[211] Egloff,[212] Teare and Webb,[213] Proctor,[214] and Teare and Schatz.[215] The papers of Trautman,[216] Maione,[206] Ekelöf,[210] Steinhausen,[217] Teare and Webb[213] and Teare and Schatz[215] provide confirmation of much of this theory through comparison of values of K_s calculated from theory with values obtained from experiment. Pleijel[205] and Ekelöf[210] have indicated how their analyses could be expanded to include an indefinite number of coaxial layers; the actual theory has been effected by Schelkunoff.[77,218]

Studies on skin and proximity effects in large stranded conductors such as are used for electric-furnace circuits have been reported by Northrup and Thompson,[219] Randall,[220] Cook,[221] Middleton and Davis,[222] Dwight,[111] Dana,[223] Tweeddale,[224] and most accurately and completely in a paper by Arnold[225] and in a report[154]—partly prepared by Arnold—for the British Electrical and Allied Industries Research Association.

The recent shortage of critical metals has resulted in a considerable use of steel pipe and structural shapes for bus conductors.[225a] Inasmuch as the resistance of a ferromagnetic conductor is a function of the frequency and magnitude of the current carried, as well as of the conductivity, permeability, and geometry of the conductor itself, mathematical analysis is extremely complicated for even such simple shapes as those of circular and tubular cross section (a good résumé of the pertinent literature on such conductors is to be found in a paper by Maione[206]) and is quite out of the question for structural shapes. Accordingly, though some success has been attained in calculating the a-c resistance of conductors of circular and tubular cross section, the general practice is to resort to experiment for each different set of conditions and to present the data so obtained in tabular or graphic form.

The skin effect in various types of iron and steel pipe, full or slotted, has been the subject of experimental investigation by Dwight[226] (whose results invalidate certain conclusions by Wall[227]) and by Killian.[228] Similar work on structural steel shapes has been carried out by Killian and Alsaker.[229] Studies on steel rails, from which information about steel pipe and structural shapes can be inferred, have been reported by Wilson;[230] Villiers and Boucherot;[231] Kennelly, Achard, and Dana;[232] Benda;[233] Trueblood and Wascheck;[234] and Boice.[235]

Carlson[51] has stressed the ways in which skin and proximity effects affect the design and operation of modern industrial busses comprised of closely spaced strap conductors. In his discussion of this paper Schurig[51] has given the results of inclusive tests to determine the load characteristics (current rating, temperature rise, and a-c resistance and inductance) of typical single and three-phase busses comprised of strap conductor. These very illuminating data complement similar data on current density and distribution in multiconductor single and three-phase busses of strap conductor obtained earlier by Wagner,[236] Le Clair,[237] Stein,[238] Schwenkhagen,[239,240] Dannatt and Redfearn,[241] and Johann.[242] Very comprehensive data of a similar nature are indicated in Fisher and Frank's[243] (the writer is indebted to the senior author for a copy of the actual data) recent paper on the characteristics of the "paired-phase" bus.

Interestingly, the essential principle of this bus—partial neutralization at close spacing of the skin effect by the proximity effect--was investigated more than 25 years ago by Kennelly[171,172] and his associates in the course of their now classical investigations of the skin and proximity effects. Publication of their earlier data on this phenomenon led Dwight[244] to the derivation of the first formulas for the a-c resistance of a bus comprised of two closely spaced parallel strap conductors. From data contained in the same paper Dwight[245] evolved useful curves of K_s for strap conductor. Later Dwight,[96] and after him Carter,[246] advanced explicit formulas, confirmed by Kennelly's data, for K_s for thin strap conductor.

Certain current bus designs utilize rectangular conductor having rounded edges and a ratio of thickness to breadth such that it cannot be considered strap conductor. Cockroft,[247] invoking the "electrostatic" and "penetration" principles and his own solution[248] of the corresponding electrostatic problem, has derived formulas for K_s for such conductor, and by utilizing Kirchhoff's solution of yet another electrostatic problem has obtained some quantitative data on proximity effect in single-phase circuits of rectangular conductor. Cockroft's work has been confirmed experimentally by Jackson.[249]

The experimental work of Kennelly and his associates, the theoretical investigations of Cockroft and Dwight, Gorman and Forbes,[250,251] studies on miniature conductors at radio frequencies, and his own comprehensive experimental data taken at audio frequencies have been analyzed, compared, and correlated by Haefner.[252] The results of this study are presented in a valuable set of curves of K_s for rectangular conductor. This set of curves is complemented by that of Ursi.[176]

Several methods have been advanced for studying the variation of current density over the cross section of a rectangular conductor. Thus nearly two decades ago Reich and Fischer[253] determined by test the distribution of current density, in both magnitude and phase, over the cross section of an isolated strap conductor. Curves plotted from their data strikingly illustrate what Kennelly earlier termed the "edge effect," the concentration of current in the extremities of the breadth of a strap conductor.[254] Dannatt and Redfearn[241] have described a means of conjoining measured values of surface current density with Green's theorem whereby there are afforded for each of a group of rectangular conductors the current, power loss, and a-c resistance. Daley[255] has shown how, for an isolated conductor, Fourier analysis and measured surface current densities can be conjoined to yield these same quantities and, additionally, the current density over the cross section in both magnitude and phase. Though Daley's procedure can be extended to groups of conductors without appreciable difficulties, Schwenkhagen's[239,240] method of obtaining the same information through appropriate subdivision of the conductors and utilization of ordinary circuit theory is much better known—though, seemingly, little employed. Kohn,[256] comparing values calculated by Schwenkhagen's method with corresponding values taken from Gorman and Forbes' curves, has found the former to be in better agreement with values of K_s obtained experimentally at 60 cycles.

Much of the just mentioned experimental work on the determination of K_s for rectangular conductors has stemmed from the lack of a correct mathematical formula with which to calculate values of K_s. Subsequent to the recent successful efforts of Gross,[257] the mathematical difficulties of effecting a rigorous solution had proved intractable. Thus the solutions of Edwards,[258,259] Debye,[260] Press,[261] and Strutt[262] for rectangular conductors and those of Lampa[263] and Strutt[264] for elliptical cross section (undertaken in the expectation that values of K_s of suitably shaped elliptical conductors would approximate those of thin rectangular conductors) are invalid because of the erroneous assumed boundary conditions—as Noether[79,80] has pointed out regarding Strutt's solutions and Fischer[265] regarding the others. Though right in his assertion, Noether[79] was wrong in his reasoning, as Strutt[82] quickly made plain in the course of obtaining, through use of the "electrostatic" principle, the correct high-frequency formula for K_s for elliptical conductor. More recently, Lettowsky,[266,267] Gross,[257] and Fischer[268] have obtained formulas for K_s without restriction to frequency. For ratios of major axis to minor axis that are large an elliptical conductor approximates a strap conductor; for such conductor good approximations to K_s are afforded by the formulas of Strutt[82] (as has been verified by Jackson[249]), Lettowsky,[266,267] Gross,[257] and Fischer.[268]

Arnold[269] has combined theoretical analysis with experimental data to derive formulas for K_s and K_p for single- and three-phase circuits comprised of flat-spaced square tubular conductors. Curves of K_s for square tubular conductors, plotted from Arnold's formula, are contained in a paper by Dwight, Andrew, and Tileston.[270]

Arnold [271] has effected a formula, confirmed by experimental data, for calculation of K_s and K_p in single-phase busses comprised of channel conductors located back to back. Otherwise no studies on channel, angle, T-, or I-beam conductor (aside from those of Killian and Alsaker[229] on a few structural steel shapes) appear to have been published—though all are used, the first two shapes in considerable amount. The d-c resistances of standard sizes of channel and angle conductor, as well as of circular, tubular, strap, and square tubular conductor are to be found in the publications[14–17] of those marketing such conductor.

Studies of skin and proximity effects in a single-phase circuit comprised of two parallel infinite plates of equal thickness have been carried out by Cohn[272]; his results have been utilized, incorrectly, by Schumann[273] and by Niethammer.[112] Kelvin[99] and König[150] have studied skin and proximity effects in a single conductor comprised of a number of separated parallel infinite plates of equal thickness. Niethammer[274] has obtained K_s for a single infinite parallel plate carrying a current comprised of both displacement and conduction components.

JOINT RESISTANCE

If a bus contains a number of poorly bolted joints, the voltage drop due to joint contact resistance may be commensurate with that due to conductor resistance. The factors that affect contact resistance are diverse: the electrical and elastic properties of the conductors; the type and design of joint; its shape, area, smoothness, initial lubrication, and cleanness; the current degree of oxidation or corrosion; the operating temperature; and the mechanical pressure over the contact surfaces.

Early, purely qualitative discussions by Binder[275] and Harris[276] of the effects of some of these factors were followed, roughly a decade later, by the elaborate experimental researches of Melsom and Booth.[277] An important consequence of their work was experimental verification of the thesis that joint resistance could be considered as comprised of two components: contact resistance proper and resistance introduced by the "stream-line distortion" produced by the change in width of the current path at the joint. This latter effect has been studied mathematically by Wilmotte.[278] He found values calculated from his formulas to be in good agreement with the corresponding experiments of Melsom and Booth. Mathematical and experimental studies along a similar line have been carried out by Donati.[279] The papers of these men and those of Luke,[280] Enger,[281] Schälchlin,[282,283] Jones,[284] Contius,[285] Bern and Specht,[286] Wenner, Nusbaum and Cruickshanks,[287] Binder,[288] Paxton and Strang,[289] and Denault,[290] most of which detail additional experimental studies, encompass curves, formulas, tabulations of physical data, and other general information sufficient for the electrical design of bus joints.

Contact problems peculiar to magnesium bus bars are dealt with in a paper by Bulian.[291] Methods of lowering contact resistance in aluminum-to-copper joints have been mentioned by Schulze[292] and Warner.[293,294] The latter, Dallye,[59] Windred,[295] and Richter[296] have discussed the especial precautions to be observed in the preparation of aluminum bus bars for jointing. Richter's paper (a long and elaborate publication presenting the results and deductions of some 421 investigations on contact resistance between both bolted and brazed aluminum-to-aluminum or aluminum-to-other-metal joints) was followed some 18 years later by a paper by Richter and Schade,[297] wherein is reported the results of studies made to determine the time change of resistance of many of the joints used in Richter's original study. Especial attention is devoted to the effect of initial lubrication (or lack of it) on the long-time contact resistance of aluminum-to-aluminum and aluminum-to-copper joints.

Shand and Valentine,[298] Windred,[299] and Nefzger[300] have discussed the mechanical features of bolted joints. A considerable amount of physical data, recommended joint designs for specific conductor shapes and sizes, and other information of design value is contained in the publications[14–17] of concerns manufacturing bus conductor.

Metallurgical advances made in recent years and the attendant advantages of reduced resistance, possible diminished cost, and easier maintenance have resulted in an accelerating use of brazed, soldered, or welded joints. The relative merits of these and of bolted joints and various points concerning the technique involved in making such joints have been delineated by Martin,[301] Daniels,[302] Goeller,[303–07] Darner,[308] Windred,[299] Bessesen,[309] Schulze,[310] Woodruff,[24] Barton,[311] and others.[312–14]

An inclusive account of the problems involved in the design of electric contacts comprises a recent book by Windred.[315] This book, several classical papers by Holm[316,317] and a recent exhaustive paper by Windred[318,319] may profitably be consulted by those desiring knowledge of the modern theories of the physics of the phenomena of contact resistance or of references to the literature thereof.

INDUCTIVE REACTANCE

The voltage regulation of a bus is determined principally by the inductive voltage drop. In consequence, it follows that accurate predetermination of voltage regulation rests on accurate calculation of the inductance coefficients of the bus. A detailed account of the origins and development of the concept of inductance has been given by Higgins.[96] The texts* of Maxwell,[72] Webster,[320] Livens,[321] Smythe,[322] and Schelkunoff[77] on electromagnetic theory encompass excellent accounts of the general theory and of some of the mathematical techniques pertinent to calculation of inductance. Regarding these latter, O'Rahilly[323] has written a most illuminating paper on the flux-linkage (more properly, flux-current linkage) method of calculating inductance. It is quite the best exposition available of this method: which is both the one commonly advanced in technical texts and the one least applicable in actual practice.

The most useful method, that involving direct use of the vector potential, appears in the technical literature in the guise of Maxwell's method of geometric mean distances. Very understandable accounts of this method are contained in texts by Gray[324] and by Webster,[320] and, less clearly, in Maxwell's[72,325] writings. Formulas, tables, and curves, essential or helpful in calculation of the geometric mean distances relative to conductor sec-

---

* Specific mention of electrical-engineering texts is omitted because the treatment of inductance contained in most is incomplete—and not unoften actually incorrect.

tions and arrangements now in use, are embraced in the writings of Maxwell, Guye,[326,327] Orlich,[328,328a,329] Sumec,[330] Rosa and his associates,[169,331–3] Grover,[334,335] Yardley,[336] Tschiassny,[189] Woodruff,[337] Dwight,[338a] Carlson,[61] and Higgins.[339–42] Papers[341,342] of the last-named embrace geometric mean-distance formulas, not contained in the other references, that afford the inductance of conductors of structural shape, providing the conductor cross sections can be considered as comprised of line segments or of rectangular areas.

Calculation of geometric mean distances is facilitated by use of the 18 place tables of natural logarithms and of arctangents (with arguments in radian measure) lately published by the Work Projects Administration.[343] If the conductor sections are of such configuration that calculation of the required geometric mean distances is mathematically intractable, the graphical method outlined by Hak[344] is of value.

If the skin or proximity effects are of consequence the method of geometric mean distances cannot be used directly. For conductors of rectangular section Schwenkhagen[239,240] has sketched, illustrated by example, and confirmed by experiment a method whereby these effects can be encompassed through indefinite subdivision of conductors and subsequent utilization of the geometric mean distances of the resulting subareas.

Large, but somewhat dated collections of formulas for inductance, derived for various combinations of frequency, conductor section, and bus arrangements, are to be found in papers by Rosa and Grover.[169,334]

Maxwell[72] and Russell,[345–7] neglecting skin and proximity effects, have derived formulas for the inductance of various arrangements of circular and tubular conductor. Higgins[348,349] has studied single-phase circuits comprised of conductors of eccentric annular section. Various commercial publications[16,350,351] and papers by Darling,[352] Anderson and Vianey,[353] and Gussow[354] contain curves, tables, and nomograms for the reactance of standard sizes of circular and stranded copper conductor utilized in flat or triangularly spaced, single or multiple-circuit, three-phase busses.

With skin and proximity effects taken into account, formulas for the inductance of an isolated circular conductor have been derived by Maxwell,[72] Rayleigh,[73] Heaviside,[74] Kelvin,[75] Brylinski,[125,155] Garnier,[168] Pedersen,[159] Swyngedauw,[170] Spielrein,[161] Breitfeld[199] (whose treatment includes displacement as well as conduction current), Bromwich[140] and Cocci and Sartori;[201] of an isolated tube by Grünwald[177] and Heymann;[179] of a coaxial arrangement of circular and tubular conductors by Heaviside,[74] Thomson,[76] Russell,[131,132,345] Bisacre[114] (who extended Russell's work), and Larrick and Race;[153] of coaxial tubular conductors by Pleijel[205] and Schelkunoff;[77,218] of single-phase circuits of two externally located circular conductors by Mie,[127] Nicholson,[128–30] Curtis,[136] Carson,[138] and Mead;[142] of the three-phase circuit comprised of three coaxial tubular conductors by Dwight;[152] of a three-phase circuit of three triangularly spaced circular conductors by Curtis[137]; and for the self- and mutual inductances of two rectangularly spaced single-phase circuits comprised of circular conductor by Hoyt and Mead[193]—whose formulas are confirmed by experimental data. These papers include many useful curves, nomograms, and tables.

Stefan,[124] Rayleigh,[100] Russell,[355] Pidduck,[356] Strutt,[106] Maione,[180] Adams,[109] and König[180] have utilized the "electrostatic principle" to obtain the high-frequency inductance of single-phase circuits comprised of circular or tubular conductor. Silsbee,[357,358] summarizing experimental work undertaken to test the validity of application of this principle and to determine the relative magnitude of low-frequency skin and proximity effects in single-phase circuits comprised of tubular conductor, has given a formula for the a-c inductance of such a circuit wherein the magnitudes of skin and proximity effects are separately distinguishable. Yet other experimental data on the a-c inductance of single-phase circuits comprised of circular or tubular conductor have been obtained by Kennelly[171,172] and his associates and by Schurig.[61]

The a-c inductance of isolated bimetallic circular conductors has been studied by Miller,[203] Försterling,[204] Maione,[206] Fischer,[207,208] Ekelöf,[210] Kruse and Zinke,[211] Teare and Webb,[213] and Teare and Schatz.[215] The papers of Miller,[203] Maione,[206] Teare and Webb,[213] and Teare and Schatz[215] contain confirmatory experimental data and useful curves.

Kennelly, Achard and Dana,[232] Benda,[233] Trueblood and Wascheck,[234] and Boice[235] have studied experimentally the inductance of steel rails. From these studies they have derived formulas useful in the approximate calculation of the inductance of steel rails, pipes, and structural shapes.

Writings by Orlich,[328] Rogowski[359] (very comprehensive), Silsbee,[360] Dwight,[361,362] Yardley,[336] Hemmeter,[363] Grover,[335] Steidinger,[364] Bruderlink,[365] Papst,[366] Levy,[367] Schurig,[368] Herlitz,[369] Roth,[370] Bouse and Scarborough,[371] Darling[352] and others[7,14–17,351] encompass ormulas, curves, nomograms, illustrative examples, and other information (in some instances original, in others gathered from overlapping sources) required or useful for calculation of the inductance of the more commonly used arrangements of single- and three-phase circuits comprised of strap conductor. Yet another paper on single-phase circuits of strap conductor, and doubtless the most important, is that of Arnold[372] who has developed comparatively simple formulas that (as verified by cited experimental data) yield the inductance over a wide range of bus and conductor geometry. Additionally, he presents correction formulas for the end effect stemming from the finite length of conductors: seemingly, these should find considerable use in calculating the inductance of comparatively short rectangular loops such as are sometimes encountered in installations for electric furnaces.

A formula for the a-c inductance of a circuit of two very closely spaced strap conductors has been given by Dwight.[344] Experimental data on the a-c inductance of various single- and three-phase busses comprised of strap conductor has been advanced by Schurig[61] and by Fisher and Frank.[243]

Discussion, both qualitative and quantitative, of the especial problems encountered in the design of busses of strap conductor for electric furnaces and electrochemical plants is contained in the papers of Lindstrom,[373] Catani,[374] Yardley,[336] Levy,[367] Wejnarth,[375] Pan,[376] Andreae,[377] and Donati.[378]

Higgins[339,340,379] has advanced formulas for the inductance of single-phase busses constituted of two rectangular tubular conductors; Dwight and Wang[338] and Higgins[380] formulas for single and three-phase busses composed of flat-spaced square tubular conductors. Certain commercial publications[15–17,351] contain useful curves of reactance voltage drop in single and three-phase busses of flat-spaced square tubular conductors.

Recently Higgins[341,342] has advanced procedure and general formulas for calculating the inductance of any arrangement of conductors having cross sections comprised of combinations of parallel-sided rectangles. As well as strap and rectangular tubular conductors for which formulas are already available, specific formulas are given for single-phase circuit comprised of two channels back to back, two I beams, four channels forming two split (ventilated) rectangular tubular conductors; and for a three-phase circuit of three triangularly spaced rectangular tubular conductors. Where necessary, corrections for the effect of the rounded edges found on conductors of structural shape can be made by a formula developed by Dwight and Wang.[338] Higgins and Schwantz[381] have developed various convenient formulas for the inductance of single-phase conductors comprised of channels located back to back.

The a-c inductance of single-phase circuits made up of parallel infinite plates of definite thickness has been studied by Cohn;[272] his results have been utilized, incorrectly, by Schumann.[273] Niethammer[274] has determined the self-inductance of a single isolated infinite plate of definite thickness wherein the current comprises both conduction and displacement components. The high-frequency inductance of a single conductor constituted of a number of such plates in parallel has been given by König.[130]

Lettowsky[366,367] has determined formulas for the a-c inductance of an isolated elliptical conductor. The earlier solution of Strutt[123] is valid only for very high frequencies. A yet earlier solution by Strutt[364] and the work of Press[361] and Strutt[362] on the a-c inductance of isolated rectangular conductors is invalidated by their assumption of the erroneous boundary condition of constant current density over the perimeter of conductor cross section.

CAPACITIVE REACTANCE

Commonly, capacitance effects do not enter into the design of industrial busses. Occasionally, however, performance of certain calculations requires knowledge of the capacitive reactance: for example, in certain determinations of short-circuit currents. A considerable literature is available on the capacitance coefficients of groups of circular or tubular conductors. Approximate formulas, sufficiently correct except at very close spacings, are contained in most texts on transmission-line theory. Certain solutions of particular interest (the titles are self-explanatory) are contained in papers by Kennelly,[382] Russell,[383,384] Whipple,[385] Poritsky,[386] Adams,[100,387] and Dwight.[388]

Because of the intractable mathematics encountered in attempting solution, explicit formulas are not available for calculating the capacitance of even the simplest busses comprised of strap or structural conductor. Gabor[389] has approximated the capacitance of a single-phase circuit of strap conductor by replacing the rectangular cross section by appropriate elliptical cross sections. Alternatively, if the straps are sufficiently wide, the capacitance can be approximated by use of Kirchhoff's solution[248] for two semi-infinitely wide straps. But otherwise, if the capacitance is to be determined, recourse must be had to one of the many methods of analytic, graphic, or experimental field plotting.

Much of the literature (prior to 1932) pertinent to these methods has been epitomized by Hague.[390,391] We mention the more important or more interesting expositions of the methods available for plotting electric and magnetic fields: the applications of finite differences and of conformal mapping as delineated respectively by Muller[392] and by Weber;[393] the analytic-graphic procedures outlined by Deutsch[394] (who illustrates his analysis by calculation of the capacitance of a bus comprised of two strap conductors), Spielrein,[395] and Kraemer;[396] the use of conducting tanks or plates, various techniques being described by Smoot,[397] Cramp,[398] Simon and Kron,[399] Young,[400] McArthur,[401] and Godsey[402]; miscellaneous experimental methods outlined by Douglas,[403] Labus,[404,405,406a] and Weiller,[406] and Mueller;[406a] and graphical sketching as described in papers by Lehmann,[407,408] Richter,[409] Stauffer,[410] Cooper,[411] Stevenson,[412] Moore,[413] Wiesemann,[414] Johnson and Green,[415] Stevenson and Park,[416] Colvert and Harrison,[417] Wright and Tsang,[418] Leonard[419,420] and Poritsky,[421] and in Atwood's[422] book.

Current-Carrying Capacity and Temperature Rise

The current-carrying capacity of a bus is a function of diverse factors: among the more important are the nature and temperature of the ambient medium; the geometry, arrangement, and thermal characteristics of the conductors and enclosures; the state of the conductor and enclosure surfaces; the design of the conductor joints; and the circuit frequency.

Experimental investigations of the relative effects of various of these factors, both individually and in combination, have been carried out by Melsom and Booth,[423] Woll and Gable[424] (who have used their results to check the correctness of formulas advanced earlier by Luke[425]), Schurig and Frick,[426] Wilson,[427] Coe,[428] and Brügger.[429] Their papers, together with the writings of Frick[430] (extending the initial analysis of Schurig and Frick's[426] paper), of Papst[431] (who has given elsewhere a neat illustration of the use of his analysis[432]) and others[433] contain curves, formulas, nomograms, and tabulated geometrical, physical, and thermal data applicable to calculation of the current-carrying capacity of arrangements of circular and tubular conductor.

Similar material for various types of single- and three-phase busses of strap conductor is to be found in papers reporting experimental work by Melsom and Booth,[423] Garnier,[434] Le Clair,[287] Papst,[431] Bannister,[435] and others;[436,437] and in short qualitative articles by Freimark,[438] Billhimer,[439] Boyce,[8] Langrehr,[440] Beyaert,[441] Tennant,[442] Dannatt,[443] and others.[444,445] Writings by Papst,[431] Bohn and Papst,[40a,446] and others[447] contain data on ventilated rectangular tubular conductors comprised of strap, angle, channel, or drilled square tubular conductor.

Fugill[448] has reported on tests undertaken to determine the current-carrying capacity of single- and three-phase busses comprised of tubular or strap conductors housed in metal enclosures, and Childerhose and Turner[449] on tests to determine similar data for arrangements of strap conductor housed in ventilated (slotted) enclosures; and Von Normann[450] compared the relative ratings of strap conductors in air and in bus ways.

Dwight, Andrew, and Tileston[270] have advanced a procedure for determination of temperature rises in busses made up of circular, tubular, rectangular tubular, or structural conductor. They found calculated values of current-carrying capacities of several typical busses to be in good agreement with corresponding values obtained from test data or manufacturer's recommendations. Taylor[450a] has given formulas enabling correction for the end effects accompanying loading and temperature-rise tests on short samples of conductor.

The heavy conductor currents occurring during short circuit cause rapid rise in the temperatures of conductors and joints. If sustained too long, these overload temperatures result in melting of the conductors or of the alloy in brazed or soldered joints. Stauffacher[451] has given curves of ultimate time prior to melting for various standard sizes of copper circular conductor. These are also helpful in calculating joint temperatures. Similar curves for copper cables have been advanced by Coe.[452]

The temperature rise in conductors during short circuit is influenced by the change with temperature of the electrical resistivity, the thermal conductivity, and the temperature coefficient of linear expansion. Formulas and curves for temperature rise in circular conductors, wherein all three factors are taken into account, have been advanced by Avramescu;[453] the first two only, by Fabinger,[454] Edler,[455] and Guth and Grünberg;[456] the first only, by Biermann,[457] Binder,[458] and Prinz;[459] and none, by Holbrook.[460] Careful experimental studies of the change with temperature (up to 1,100 degrees centigrade) of the electrical resistivity and thermal conductivity of copper have been carried out by Avramescu.[461,461a] Scarpa[462–4] has carefully studied the change with temperature of the electrical resistivity of aluminum. A mathematical study of the temperature rise in circular conductor as influenced by the nonuniform distribution of circuit density due to skin effects during short circuit has been carried out by Strutt.[465] The relative effects on copper and aluminum strap conductor of localized hot spots produced by long-time short-circuit power arcs has been studied by Porter.[466] Retzoe[467] has described an investigation on the causes of damage to zinc bus bar due to short-circuit arcs.

Experimental studies and recommendations relative to the current-carrying capacity of steel and iron pipe have been reported by Dwight,[226] Wall,[227] and Killian;[228] and of various structural steel shapes by Killian and Alsaker.[229,468]

Power losses and temperature rise in structural steel paralleling, crossing, or enlooping bus conductors, and means of circumventing or minimizing these undesirable effects have been investigated by Schurig and Kuehni,[469] Unland and associates,[470,471] and quite recently by Killian.[472]

A method of equalizing current densities and temperatures in multiconductor single or polyphase busses by means of specially designed metal sleeves fitted around the conductors has been described by Egorov.[473] Installation of such sleeves on bus leads from generators with consequent increase in allowable generator output has been described recently by Boice.[473a]

Short-Circuit and Other Mechanical Forces

The mechanical forces encountered in bus design comprise three categories: the mutual forces exerted between the current-carrying conductors by virtue of electromagnetic attraction or repulsion; the forces thereby produced in the components of the supporting structures; miscellaneous forces originated by thermal expansion, extraneous vibrations, distortions due to conductor weight, and the like. Forces encompassed in the first two categories usually are of consequence only under short-circuit conditions.

In general, calculation of the electromagnetic forces on the conductors is effected through application of the general theory outlined in Maxwell's[72] treatise. Should ferromagnetic materials be involved, this theory requires elaboration. Such elaboration and illustrative important applications of the resulting analysis are contained in papers by Steinmetz,[474] Doherty and Park,[475] Karapetoff,[476] and Hague[477]—to mention several studies bearing directly on this topic. In routine design, though, resort to general electromagnetic theory is not often necessary: because of the absence (usually) of ferromagnetic materials, fewness of conductor shapes, and use of standardized conductor arrangements, formulas now in the literature suffice for most work.

Commonly, the bus can be considered a group of long-linear parallel nonmagnetic cylindrical conductors. If so, calculation of the electromagnetic force acting on a specific conductor revolves into successive determination of the mutual "shape factors" of the conductors, of the magnitudes and phase relationships of the currents in the conductors, and of the appropriate vector summation of these last. The shape factor of two circular or tubular conductors is unity; formulas for strap conductors have been derived by Dwight,[478] Duschek,[478a] and Higgins,[479] for rectangular tubular conductors and for conductors of structural shape by Higgins.[479–82]

Calculation of the actual short-circuit currents requires the use of symmetrical components. General procedures for short-circuit calculation in low-voltage a-c systems are encompassed in elaborate works by Hanna[483] and by Darling.[351,352] In an effort to lighten the numerical labor incident to use of this exact theory, methods of approximate procedure have been advanced by Seaword,[484] Moorhouse,[485] and Anderson.[486] The validity of their approximate procedures is attested by experimental data set forth in their papers. Illustratively, Schulze[487] has given a detailed numerical analysis of the short-circuit calculation of a typical distribution system. His paper and those of the other just named encompass various numerical data essential to calculation: electrical constants of conductors, of cables, of typical busses, and of the usual attached electrical apparatus.

Various other phases of the problem of calculation of the short-circuit currents and of the summation of the forces produced on one conductor by the other bus conductors have been discussed by Gross,[488] Leonard and Riker,[489] Robinson,[490] Stigant and Lacey,[491] Probst,[492] Beetz,[493] Beyaert,[494] Herlitz,[495] Papst,[496] McGraw,[497] Miller,[498] Tripp,[499] Bachert,[500] Schurig,[501] Killian,[502,503] and others.[504]

General techniques for calculating the forces on conductors in close proximity to ferromagnetic materials have been set out by Calvert,[505] Lehmann,[506] and Hague.[507] Morecroft and Turner[508] have studied the effects of enclosing conductors within iron pipes, Randall[509] the effect of galvanized sheets used in phase-isolating cellular structures, and Metz[510] yet other kinds of enclosure.

Occasionally it is necessary to calculate the electromagnetic forces or torques on the conductors in the neighborhood of bends or crossovers. Formulas due to Van Aspern,[511] Frick,[512] and Bayles and Donkin[513] suffice for most cases.

As well as on the electromagnetic forces exerted on the bus conductors, the mechanical forces produced on the components of the supporting structure depend on the elastic properties of this structure: its motional resistance, natural frequencies, and physical nature and arrangement. Seemingly, general attention was directed to the practical importance of these factors through publication of pertinent experimental data.[514] Thereafter, Schurig and Sayre,[515] Dahlgren,[516,517] Pilcher,[518] and Aebi[519] advanced analytic studies, substantiated by experimental data, of the individual and collective effects of these factors and of general methods of calculating the magnitudes involved. Whereas the work of the first named is frequently cited as a reference, that of the other three, seemingly, has attracted but little attention. Yet Pilcher's is an extension of the theory delineated by Schurig and Sayre, whereas Dahlgren's, an extended study of the important phenomena of mechanical resonance, complements both. Again, Aebi has effected the theory for the forces produced by transient direct current and by rectangular-pulse currents, whence extension to calculate the effects produced by any wave shape of current follows from well-known analysis. In short papers based on the work of Schurig and Sayre;[515] Schurig, Fricke, and Sayre;[520] Tanberg;[521] Specht;[522] Edson;[523] Josse;[524] Eigermann;[525] and others[526,527] have presented certain charts, nomograms, and short cuts that facilitate the numerical labor incident to actual computation.

Papst[528] and others[529] have discussed the use of springs or special clamps to minimize and dampen the force transferred through the insulator to the support.

Under short-circuit conditions the electromagnetic forces acting on disconnect switches (the mutual repulsive forces between the studs and the throwoff force on the movable blade) have been known to open unlatched or insufficiently latched switches, usually with disastrous results to some of the equipment on the line.[530] Accordingly, formulas for calculating these forces are of consequence. Torchi,[531] Garrand,[532] Louis and Sinclair,[533] Keel,[534] and Bresson[535] have advanced the results of tests to determine the magnitudes and effects of short-circuit forces on switches. Dwight[536,537] and Dunton[538,539] have advanced formulas for the throw-off force; they yield values in good agreement with experiment.[512,540,541,541a] The first named[542] has discussed the earlier incorrect work of Lobenstein[543] and Jolley;[544,545] the latter that of Kopec[546] (in turn, the truth of Dunton's [547] remarks on a general point of theory has been challenged by others[548–50]). Hak[551] has considered the general problem in some detail; Ferguson[552] has given curves for both stud and throw-off forces; Souben[553] and Kuntz[554] the effects of the changing position, mass, and frictional resistance of the switch blade on the transient magnitudes of the throw-off force; and Bayles and Donkin,[555] Churcher and Dannatt,[556] Wilson,[557] and Cleveland[558] have discussed yet other phases of calculation.

Samuels,[559] Keyes,[560] Bacon,[561] Hutter,[562] Beyaert,[563] Spruce,[564,565] Wall,[227] Sheering[566] and others[567] have prepared tables, curves, and nomograms useful in calculating conductor loading, deflection, and span length. Morton,[568] Anderson,[569] Eigermann,[525] and others[570–3] have concerned themselves with the stresses produced by thermal expansion; Kates[574] has studied the rupture by short-circuit forces of the reinforced concrete slabs used in cellular structures; and Schulze[575] has described load tests on porcelain supports to determine their cantilever strength under short-circuit forces.

References

1. 440-Volt Distribution Systems for Industrial Plants, T. E. Stiebar. *Electric Journal*, volume 35, 1938, pages 311–34.

2. A Distribution System for Wartime Plant Expansion, J. L. McKeever. AIEE Transactions, volume 60, 1941, September section, pages 862–5. Discussion, pages 1385–6.

3. Secondary Network to Serve Industrial Plants, C. A. Powel, H. G. Barnett. AIEE Transactions, volume 60, 1941, April section, pages 154–6.

4. The Fundamentals of Industrial Distribution Systems, D. L. Beeman, R. H. Kaufmann. AIEE Transactions, volume 61, 1942, May sec-

tion, pages 272–9. Discussion, page 480. *General Electric Review*, volume 45, 1942, pages 235–44.

5. Primary and Secondary Network Distribution Systems, **J. S. Parsons, H. G. Barnett.** Supplement to first edition of Electrical Transmission and Distribution Reference Book, Westinghouse Electric and Manufacturing Company, East Pittsburgh, Pa., 1943. Chapter 21.

6. The Technical and Economical Design of Electrical Distribution in a Large Factory, **J. S. Blacklock.** *Engineering* (London, England), volume 155, 1943, pages 65–6, 85–6.

7. Power Supply for Resistance-Welding Machines, AIEE subcommittee on power supply for welding operations. AIEE Transactions, parts I, II, volume 59, 1940, May section, pages 306–20; part III, volume 60, 1941, May section, pages 185–92. *Welding Journal*, volume 19, 1940, pages 350–5, 426–36; volume 20, 1941, pages 366–73.

8. Considerations That Influence Layout of Heavy Bus Structures in Industrial Plants, **H. Boyce.** *Industrial Engineer*, volume 85, 1927, pages 256–60.

9. Features of A-C and D-C Bus-Bar Design, **T. H. McCauley.** *Power Plant Engineering*, volume 33, 1929, pages 474–7.

10. Resistance Loss and Conductor Size, **H. B. Dwight.** *General Electric Review*, volume 41, 1938, pages 484–7.

11. Putting the Conductor Where the Current Is, **D. K. Steidinger.** *Allis-Chalmers Electrical Review*, September 1943, pages 9–13.

11a. The Design of Low-Voltage-Welding Power Distribution, **Comfort A. Adams, John R. Fletcher, Arthur C. Johnson.** AIEE Transactions, volume 63, 1944, pages 1180–90.

12. Bus-Bar Design and Construction. *Power Plant Engineering*, volume 35, 1931, pages 34–5.

13. Air-Insulated Bus Bars: Their Use in New and Renovated Factory Installations, Supervisor. *Electrician* (London, England), volume 126, 1941, pages 91–2.

14. Copper for Bus-Bar Purposes. Publication 22, London Copper Development Association (London, England), 1936.

15. Alcoa Aluminum Bus Conductors, Aluminum Company of America, Pittsburgh, Pa., 1940.

16. Chase Electrical Handbook, Chase Brass and Copper Company, Inc., Waterbury, Conn., 1941.

17. Anaconda Copper-Bus Conductors. Anaconda publication *C*-25 (third edition), The American Brass Company, Waterbury, Conn., 1942.

18. Electrical Busses and Bus Structures, **W. Deans.** Bulletin 4211, I-T-E Circuit Breaker Company, Philadelphia, Pa., 1942.

19. What Shape Conductors for Electrical Bus Bars?, **W. Deans.** *Power*, volume 87, 1943, pages 87–90.

20. Resistance Welder Feed Has Low Resistance Drop, **L. R. Bogardus.** *Electrical World*, volume 110, 1938, pages 702–04.

21. Modernizing New York's Waterside Station, **H. D. Braley.** *Electrical World*, volume 108, 1937, pages 1018–22.

22. Bus Design at Modernized Waterside Features Reliability, **A. M. DeBellis.** *Electrical World*, volume 108, 1937, pages 1185–8, 1260, 1263.

23. Maximum Availability Aim of Switchhouse Design—II, **H. W. Eales, H. L. Hoeppner.** *Electrical World*, volume 115, 1941, pages 802–05, 884.

24. Jointless Square-Tubular [Copper] Bus Bars Improve Distribution Efficiency, **R. B. Woodruff.** *Power*, volume 85, April 1941, pages 68–70.

25. Square Copper Tube Bus Bars. *Electrical Times* (London, England), volume 97, 1940, pages 502–03.

26. Hochstromleitungen und -Schalter für Wechselstrom, **D. Michalke.** *Elektrotechnik und Maschinenbau* (Vienna, Austria), volume 31, 1913, pages 637–9.

27. Interlacing Furnace Transformer Bus Bars, **C. B. Gibson.** *Electrical World*, volume 75, 1920, pages 991–3.

27a. Improved Design of Heavy-Duty 6,600-Volt Double Bus, **W. R. McCann.** *Electrical World*, volume 79, 1921, pages 1275–6.

28. 50,000-Ampere Aluminum Bus and Shunt, **J. E. Housley.** *Electrical World*, volume 95, 1930, page 889.

29. Aluminum Bus Bar for Plant Feeders, **C. Holthaus.** *Electrical World*, volume 102, 1933, pages 436–7.

30. Prebuilt Bus Goes in Quickly, **A. E. Bulen.** *Electrical West*, volume 80, 1938, pages 28–9.

31. Integrated Supply Improves Service to Welders, **W. B. Hurley, W. Smith.** *Electrical World*, volume 113, 1940, pages 1198–1200.

32. Interlaced Bus-Bar Design Solves Space Problem, **G. E. Tennant.** *Electrical World*, volume 114, 1940, pages 931–2, 1069.

33. Interleaved Phases for Welder Bus, **L. E. Fisher.** *Electrical World*, volume 116, 1941, page 1290.

34. New Circuits, Better Welds, **T. O. Morgan.** *Factory Management and Maintenance*, volume 99, September 1941, pages 92–3.

35. Interleaved Bus Solves Wiring Problem. *Electrical World*, volume 113, 1940, pages 2068–70.

36. Bus-Type Wiring Used for Electric Furnace. *Electrical World*, volume 116, 1941, page 1445.

37. Inclosure Guards Bus Against Water Leaks. *Electrical World*, volume 110, 1938, page 1740.

38. Bus Inclosure Arrangements (picture). *Electrical World*, volume 109, 1938, page 728.

39. Copper Saved to Make Magnesium: Bus-Bar and Feeder System for the Electrolytic Plant Located at Basic Magnesium, Inc. *Electrical West*, volume 89, October 1942, pages 48–50.

40. Channel Bus for Office-Building Risers, **C. A. Carpenter.** *Electrical World*, volume 100, 1932, pages 656–8.

40a. Structural-Shape Conductors Show Increased Efficiencies, **H. W. Papst, D. I. Bohn.** *Electrical World*, volume 98, 1931, pages 418–19.

41. Channel Shapes Solve Bus Problem, **C. W. Shannon.** *Electrical World*, volume 102, 1933, page 724.

42. Electrical Design Features of Richmond Station Unit, **R. W. Wilbraham, R. Bailey.** *Electrical World*, volume 105, 1935, pages 2113–15, 2153.

43. Concentric Bus for Resistance Welders, **W. Specht.** *Electrical World*, volume 114, 1940, page 558.

44. A Concentric Channel Bus for Resistance Welders, **W. Specht.** *Welding Engineer*, volume 26, June 1941, pages 31–2.

45. Suspended Busses Carry Heavy Current, **L. N. Greer, L. T. Guess.** *Electrical World*, volume 116, 1941, page 1889.

46. Increase Bus Capacity at South Meadow. *Electrical World*, volume 113, 1940, pages 1356–7.

46a. Aluminum Channels for Efficient Bus Bar. *Factory Management and Maintenance*, volume 92, 1934, pages 233–4.

46b. Copper Channel Bus Bars and Their Use at Boulder Dam. *Electrical Review* (London, England), volume 118, 1936, page 160.

47. Strength, Capacity in New Bus Design, **B. Schrager.** *Electrical World*, volume 112, 1939, page 1054.

48. Modern Distribution System Fills Rigid Requirements, **W. Wendelkin.** *Electric Journal*, volume 34, 1937, pages 499–501.

49. Bus Distribution Promotes Flexibilty, **G. A. Hess.** *Electrical World*, volume 110, 1938, page 186.

50. Flexible Distribution Aid to Aircraft-Plant Production, **A. G. Lloyd.** *Electrical World*, volume 110, 1938, pages 438–40.

50a. No Rewiring With Plug-in Power, **H. Schaal.** *Factory Management and Maintenance*, volume 98, 1940, pages 78–9.

51. Enclosed Bus-Bar Electrical Distribution Systems for Industrial Plants, **E. T. Carlson.** AIEE Transactions, volume 60, 1941, June section, pages 297–302. Discussion by **O. R. Schurig,** pages 700–01.

52. Modern Factory Distribution, **H. Simmonds.** *Electrical Review* (London, England), volume 128, 1941, pages 453–4. For correction see discussion of reference 497.

53. Welder Bus-Bar Distribution, **R. C. Lipps.** *Electrical Contracting*, volume 41, 1942, pages 20, 48.

54. Bus-Way Plant Distribution, **L. Siebert.** *Electrical West*, volume 89, December 1942, pages 64–5; volume 90, January 1943, pages 44–5.

54a. Factory Distribution: the Need for a Flexible Layout, **J. G. Craven, J. Collins.** *Electrical Review* (London, England), volume 133, 1943, pages 363–6.

55. The Rising Bus Bar, **J. Ashmore.** *Electrical Review* (London, England), volume 133, 1943, pages 767–9.

56. Overhead Bus-Bar System for Machine Shops. *Engineer* (London, England), volume 169, 1940, pages 541–2.

57. Electric Power Distribution for Industrial Plants, developed by AIEE committee on industrial power applications. AIEE, 1944.

58. L'Alluminio Nelle Centrali Elettriche, **M. Preiswerk.** *Alluminio* (Milan, Italy), volume 2, 1932, pages 209–15.

59. Aluminum Conductors for High-Capacity Electric Circuits, **F. R. Dallye.** *Power*, volume 75, 1932, pages 685–7.

60. Leichtmetallschweissung und -Loetung in der Elektrotechnik, **A. Winkel.** *Autogene Metallbearbeitung* (Halle, Germany), volume 35, 1940, 139–42.

61. Aluminum in der Installationstechnik. *Licht und Lampe* (Berlin, Germany), volume 30, 1941, pages 156–8.

61a. Aluminum Bus Bars on the SS *Aquatania*. *Engineering*, volume 158, 1944, page 195.

62. Zink und Zinklegierungen für Leitungszwecke, **C. Hasse, F. Pawlek.** *Zeitschrift für Metallkunde* (Berlin, Germany), volume 32, 1940, pages 327–35; discussion, pages 335–9.

63. 4000—A Sodium Conductor, **R. H. Boundy.** *Transactions*, American Electrochemical Society, volume 62, 1932, pages 151–60; discussion, page 160.

64. Sodium in Pipes Successful as Electrical Conductor, **R. H. Boundy.** *Electrical World*, volume 100, 1932, page 852.

65. The Reaction Upon the Driving Point of a System Executing Forced Harmonic Oscillations of Various Periods, With Applications to Electricity, **Lord Rayleigh.** *Philosophical Magazine* (London, England), [4], volume 21, 1886, pages 369–81; *Scientific Papers* (book), volume 2, pages 475–85.

66. The Origins and Developments of the Concepts of Inductance, Skin Effect, and Proximity Effect, **T. J. Higgins.** *American Journal of Physics*, volume 9, 1941, pages 237–46.

67. Skin Effect, **W. E. Miller.** *General Electric Review*, volume 12, 1909, pages 163–9; 221–8.

68. Sur la Comprehension de l'Effect de Peau, **P. Girault.** Société Française des Électriciens *Bulletin* (Paris, France) [3], volume 1, 1911, pages 543–54.

69. The Skin Effect and Alternating-Current Resistance, **E. F. Northrup.** (Mathematical treatment by John R. Carson.) *Journal* Franklin Institute, volume 177, 1914, pages 125–67.

70. A Skin-Effect Phenomena, **S. A. Schelkunoff.** Bell Laboratories *Record*, volume 11, 1932–33, pages 109–12.

71. Courants Parasites Avec Conducteurs Portant des Intensités Élevées et Notamment Dans les Installations de Fours Électriques, **P. Bunet.** Société Française des Électriciens *Bulletin* (Paris, France) [5], volume 5, 1935, pages 1104–31.

72. A Treatise on Electricity and Magnetism (3d edition), **J. C. Maxwell.** Clarendon Press, Oxford, England, 1892. Volume 2, pages 320–5.

73. On the Self-Inductance and Resistance of Straight Conductors, **Lord Rayleigh.** *Philo-*

sophical Magazine (London, England) [4], volume 21, 1886, pages 381–94.

74. Electrical Papers (book), **O. Heaviside.** Macmillan and Company, London, England, 1892, volume 2, pages 61–71; 97–101.

75. Ether, Electricity, and Ponderable Matter, **Lord Kelvin.** *Mathematical and Physical Papers* (book), volume 3, pages 484–515.

76. Recent Researches in Electricity and Magnetism (book), **J. J. Thomson.** Clarendon Press, Oxford, England, 1893. Chapters 4, 6.

77. Electromagnetic Waves (book), **S. A. Schelkunoff.** D. Van Nostrand Company, Inc., New York, N. Y., 1943. Pages 176–9, 260–6, 283–5.

78. An Integral Equation for Skin Effect in Parallel Conductors, **C. Manneback.** *Journal of Mathematics and Physics*, volume 1, 1921, pages 123–46.

79. Über Stromverdrängung in Zylindrischen Leitern von Allgemeiner Querschnittsform, **F. Noether.** *Annalen der Physik* (Leipzig, Germany), volume 84, 1927, pages 775–8. See correction in reference 87, page 787.

80. Bestimmung der Stromverteilung in Zylindrischen Leitern von Allgemeiner Querschnittsform, **F. Noether.** *Zeitschrift für Angewandte Mathematik und Mechanik* (Berlin, Germany), volume 7, 1927, pages 452–4.

81. Über der Berechnung Elektromagnetischer Felder, **M. J. O. Strutt.** *Zeitschrift für Physik* (Berlin, Germany), volume 45, 1927, pages 625–30.

82. Skineffekt in Zylindrischen Leitern, **M. J. O. Strutt.** *Annalen der Physik* (Leipzig, Germany) [4], volume 85, 1928, pages 781–93. See correction in reference 86.

83. Skineffekt, **M. J. O. Strutt.** *Annalen der Physik* (Leipzig, Germany) [5], volume 8, 1931, pages 777–93.

84. Zur Theorie des Skineffekts, **E. Rothe.** *Zeitschrift für Physik* (Berlin, Germany), volume 83, 1933, pages 184–6.

85. Über die Integral Gleichung des Skineffekts, **E. Rothe.** *Journal für die Reine und Angewandte Mathematik* (Berlin, Germany), volume 170, 1934, pages 218–30. See correction in reference 86.

86. Einige Kritische Betrachtungen Über die Integralgleichung des Skineffektes, **F. Lettowsky.** *Annalen der Physik* (Leipzig, Germany) [5], volume 33, 1938, pages 300–14.

87. Calcul du Skin-Effect par la Méthode des Perturbations, **S. M. Rytov.** *Journal of Physics* (Moscow, Soviet Union), volume 2, 1940, pages 233–42. For corrections see *Journal of Experimental and Theoretical Physics* (Leningrad, Soviet Union), volume 11, 1941, page 196.

88. An Application of Polynomial Approximation to the Solution of Integral Equations Arising in Physical Problems, **P. D. Crout.** *Journal of Mathematics and Physics*, volume 19, 1940, pages 34–92.

89. A Least Square Procedure for Solving Integral Equations by Polynomial Approximation, **F. B. Hildebranch, P. D. Crout.** *Journal of Mathematics and Physics*, volume 20, 1941, pages 310–35.

90. The Approximate Solution of Singular Integral Equations Arising in Engineering Practice, **F. B. Hildebrand.** *Proceedings* American Academy of Arts and Sciences, volume 74, 1941, pages 287–95.

91. A Numerical Method of Solving Integral Equations in Two Independent Variables, **P. C. Magnusson.** *Journal of Mathematics and Physics* volume 21, 1942, pages 250–63.

92. On the Evaluation of Determinants, the Formation of Their Adjugates, and the Practical Solution of Simultaneous Linear Equations, **A. C. Aitken.** *Proceedings* Edinburgh Mathematical Society (Edinburgh, Scotland) [2], volume 3, 1932–3, pages 207–19.

93. On the Numerical Solution of Linear Simultaneous Equations by an Iterative Method, **R. J. Schmidt.** *Philosophical Magazine* (London, England) [1], volume 32, 1941, pages 369–83.

94. On the Iterative Solution of Linear Simultaneous Equations, **G. F. Freeman.** *Philosophical Magazine* (London, England) [7], volume 34, 1943, pages 409–16.

95. The Solution of Simultaneous Linear Equations by an Approximation Method, **L. T. Wright.** Bulletin 31, Cornell University experimental station, April 1943.

96. Skin Effect in Tubular and Flat Conductors, **H. B. Dwight.** AIEE Transactions, volume 37, 1918, pages 1379–1400; discussion, pages 1401–03.

97. Skin Effect and Similitude. Nonmathematical Explanation—Experimental Design Data, **J. Greig.** *Electrician* (London, England), volume 126, 1941, pages 162–3.

98. On Alternate Currents in Parallel Conductors of Homogeneous or Heterogeneous Substance, **Lord Kelvin.** *Electrician* (London, England), volume 25, 1890, pages 510–12. *Mathematical and Physical Papers* (book), volume 5, pages 489–95.

99. On Antieffective Copper in Parallel Conductors or in Coiled Conductors for Alternate Currents, **Lord Kelvin.** *Electrician* (London, England), volume 25, 1890, pages 512–14. British Association *Report*, 1890, pages 736–40. *Mathematical and Physical Papers* (book), volume 5, pages 496–502.

100. On the Propagation of Electric Waves Along Cylindrical Conductors, **Lord Rayleigh.** *Philosophical Magazine* (London, England) [4], volume 44, 1897, pages 199–204. *Scientific Papers* (book), volume 4, pages 327–31.

101. Theorie der Elektrizität (2d edition), **M. Abraham, A. Föppl.** B. G. Teubner, Leipzig, Germany, 1904. Volume 1, pages 331–45.

102. Sur la Localisation Superficielle des Courants et Flux Variables, **P. Boucherot.** Société Française des Électriciens *Bulletin* (Paris, France) [2], volume 8, 1908, pages 663–74.

103. The Rigorous and Approximate Theories of Electrical Transmission Along Wires, **J. R. Carson.** Bell System *Technical Journal*, volume 7, 1928, pages 11–25.

104. Hydrodynamische Behandlung Hochfrequenze Electromagnetischer Aufgaben, **M. J. O. Strutt.** *Archiv für Elektrotechnik* (Berlin, Germany), volume 21, 1929, pages 525–8.

105. Die Ladungsverteilung auf Zwei Ungleichen Parallelen Kreiszylindrischen Leitern, **M. J. O. Strutt.** *Zeitschrift für Angewandte Mathematik und Mechanik* (Berlin, Germany), volume 9, 1929, pages 247–50.

106. Berechnung der Impedanz Zylindrischer Leiter von Beliebiger Querschnittsform, **M. J. O. Strutt.** *Elektrische Nachrichten-Technik* (Berlin, Germany), volume 8, 1931, pages 269–76.

107. Die Eindringtiefe von Hochfrequenzströmen und -Magnetflüssen in Starkstromleitern, **F. Loebner.** *Veröffentlichungen auf dem Gebiete der Nachrichtentechnik* (Berlin, Germany), volume 3, 1933, pages 253–62.

108. Über den Verlustwiderstand von Hochfrequenzleitern, **H. Kaden.** *Archiv für Elektrotechnik* (Berlin, Germany), volume 28, 1934, pages 818–25. *Veröffentlichungen auf dem Gebiete der Nachrichtentechnik* (Berlin, Germany), volume 4, 1933, pages 321–8.

109. The Resistance of Cylindrical Conductors at High Frequencies, **E. P. Adams.** *Proceedings* American Philosophical Society, volume 78, 1937, pages 271–85.

110. Coque Fictive Valable à Toutes les Fréquences et Application à l'Étude du Four à Induction Sans Noyau Magnetique, **A. Levasseur.** Société Française des Électriciens *Bulletin* (Paris, France) [5], volume 9, 1939, pages 450–4.

111. Bessel Functions for Calculating Skin Effect, **H. B. Dwight.** *Electrical World*, volume 79, 1922, page 964.

112. Zusätzliche Verluste Durch Stromverdrängung in Wechselstromdurchflossen Leitern, **F. Niethammer.** *Elektrotechnik und Maschinenbau* (Vienna, Austria), volume 35, 1917, pages 17–20, 32–7, 44–7.

113. Table of the Bessel Functions $J_0(s)$ and $J_1(s)$ for Complex Arguments (book), mathematical tables project, Work Projects Administration. Columbia University Press, New York, N. Y., 1943.

114. The Calculation of the Skin Effect in Electrical Conductors, **F. F. P. Bisacre.** *Philosophical Magazine* (London, England) [6], volume 45, 1923, pages 1026–49.

115. Tables of the Bessel Function $I_n(x)$, **H. E. H. Wrinch, D. Wrinch.** *Philosophical Magazine* (London, England) [6], volume 45, 1923, pages 846–9.

116. Tables of Bessel Functions, **H. E. H. Wrinch, D. Wrinch.** *Philosophical Magazine* (London, England) [6], volume 47, 1924, pages 62–5.

117. Eine Bemerkung Über die Angenäherte Berechnung des Ausdruckes $J_0(x)/xJ_0^1(x)$, **W. Kessenich.** *Annalen der Physik* (Leipzig, Germany) [5], volume 5, 1930, pages 606–10.

118. Approximation Formulae for a Well-Known Difference of Products, **H. Buchholz.** *Philosophical Magazine* (London, England) [7], volume 27, 1939, pages 407–20.

119. A Treatise on the Theory of Bessel Functions (2d edition), **G. N. Watson.** The Macmillan Company, New York, N. Y., 1943.

120. Die Theorie der Besselschen Funktionen (book), **P. Schafheitlin,** Leipzig, Germany, 1908.

121. The Alternating-Current Resistance of Parallel Conductors of Circular Cross Section, **A. H. M. Arnold.** Institution of Electrical Engineers (London, England) *Journal*, volume 77, 1935, pages 49–58; discussion, pages 571–3.

122. The Alternating-Current Resistance of Tubular Conductors, **A. H. M. Arnold.** Institution of Electrical Engineers (London, England) *Journal*, volume 78, 1936, pages 580–93; discussion, volume 79, 1937, pages 595–6.

123. Proximity Effect in Solid and Hollow Round Conductors, **A. H. M. Arnold.** Institution of Electrical Engineers (London, England) *Journal*, volume 88, 1941, pages 349–59.

124. Über Veränderliche Elektrische Ströme in Dicken Leitungsdrähten, **J. Stefan.** *Sitzungsberichte* der Mathematisch-Naturwissenschaftlichen Classe der Kaiserlichen Akademieder Wissenschaften (Vienna, Austria), volume 95, 1887, part II, pages 917–34.

125. Sur la Résistance des Conducteurs en Courant Variable, **E. Brylinski.** *L'Éclairage Électrique* (Paris, France), volume 12, 1897, pages 4–13, 97–107, 149–56, 200–04, 384.

126. Über die Fortpflanzung Elektrodynamischer Wellenlängs Eines Drahtes, **A. Sommerfeld.** *Annalen der Physik* (Leipzig, Germany), volume 67, 1899, pages 233–90.

127. Elektrische Wellen an Zwei Parallelen Drahten, **G. Mie.** *Annalen der Physik* (Leipzig, Germany) [4], volume 2, 1900, pages 201–49.

128. Self-Inductance of Parallel Wires, **J. W. Nicholson.** *Nature*, volume 77, 1908, page 295.

129. The Inductance of Two Parallel Wires, **J. W. Nicholson.** *Philosophical Magazine* (London, England) [6], volume 17, 1909, pages 255–75.

130. Inductance and Resistance in Telephone and Other Circuits, **J. W. Nicholson.** *Philosophical Magazine* (London, England) [6], volume 18, 1909, pages 417–32.

131. The Effective Resistance and Inductance of a Concentric Main, and Methods of Computing the Ber and Bei and Allied Functions, **A. Russell.** *Philosophical Magazine* (London, England) [6], volume 17, 1909, pages 524–51. *Proceedings* Physical Society of London (London, England), volume 21, 1907–09, pages 581–614.

132. Effective Resistance and Inductance of Concentric Mains at High Frequencies, **A. Russell.** *Electrician* (London, England), volume 62, 1909, pages 722–3.

133. On the Dynamics of Radiation, **J. Larmor.** *Proceedings* Fifth International Congress of Mathematicians (Cambridge, England), volume 1, 1912, pages 197–216.

134. The Application of Telephone-Transmission Formulae to Skin-Effect Problems, **G. W. O. Howe.** Institution of Electrical Engineers (London, England) *Journal*, volume 54, 1915–16, pages 473–80.

135. The High-Frequency Resistance of Wires and Coils, **G. W. O. Howe.** Institution of Electrical Engineers (London, England) *Journal*, volume 58, 1919–20, pages 152–62.

136. An Integration Method of Deriving the Alternating-Current Resistance and Inductance of Conductors, **H. L. Curtis.** United States Bureau of Standards *Scientific Papers*, volume 16, 1920, number 374, pages 93–124: Abstract, *Physical Review*, volume 15, 1920, pages 528–31.

137. Resistance and Inductance of Three-Phase Cables [of Circular Conductors] Including Proximity and Skin Effect, **H. L. Curtis.** *Physical Review*, volume 18, 1921, pages 156–7.

138. Wave Propagation Over Parallel Wires: Proximity Effect, **J. Carson.** *Philosophical Magazine* (London, England) [6], volume 41, 1921, pages 607–33.

139. Eddy-Current Losses in Cylindrical Conductors, With Special Applications to the Alternating-Current Resistances of Short Coils, **S. Butterworth.** *Philosophical Transaction* Royal Society of London (London, England), volume 222*A*, 1922, pages 57–100.

140. On the Alternating-Current Resistance of Solenoidal Coils, **S. Butterworth.** *Proceedings* Royal Society of London (London, England), volume 107*A*, 1925, pages 693–715.

141. Alternating-Current Distribution in Cylindrical Conductors, **C. Snow.** United States Bureau of Standards *Scientific Papers*, volume 20, 1925, number 509, pages 277–338. *Proceedings* International Mathematical Congress at Toronto (book), University of Toronto Press, Toronto, Ontario, Canada, 1924, volume 2, pages 157–218.

142. Wave Propagation Over Parallel Tubular Conductors, **S. P. Mead.** Bell System *Technical Journal*, volume 4, 1925, pages 327–38.

143. Proximity Effect: Single-Phase and Three-Phase Systems of Parallel Conductors, **J. C. Costello.** *Electrician* (London, England), volume 114, 1935, pages 240–1.

144. Skin Effect and Proximity Effect in Tubular Conductors, **H. B. Dwight.** AIEE Transactions, volume 41, 1922, pages 189–95; discussion, pages 195–8. AIEE Journal, volume 41, March 1922, pages 202–09.

145. A Precise Method of Calculation of Skin Effect in Isolated Tubes ,**H. B. Dwight.** AIEE Journal, volume 42, August 1923, pages 827–31.

146. Proximity Effect in Wires and Thin Tubes, **H. B. Dwight.** AIEE Transactions, volume 42, 1923, pages 850–9.

147. Hautwirkung in Röhren, **K. Försterling.** *Annalen der Physik* (Leipzig, Germany) [4], volume 74, 1924, pages 176–85.

148. Bemerkung zu der Vorstehenden Abhandlung von Hrn. Försterling "Über die Hautwirkung in Röhren," **M. Wien.** *Annalen der Physik* (Leipzig, Germany) [4], volume 74, 1924, pages 186–8.

149. Heaviside's Formula for Alternating Current in Cylindrical Wires, **T. J. I. A. Bromwich.** *Philosophical Magazine* (London, England) [7], volume 6, 1928, pages 842–54.

150. Anschauliche Ableitung Einiger Näherungsformeln Aus der Theorie der Stromverdrängung, **H. König.** *Helvetica Physica Acta* (Basel, Switzerland), volume 15, 1942, pages 433–44.

151. The Skin Effect in a Cylindrical Tube With Circular Cross Section, **J. Fischer.** *Hochfrequenztechnik und Elektroakustik* (Leipzig, Germany), volume 58, 1941, pages 17–24.

152. Reactance and Skin Effect of Concentric Tubular Conductors, **H. B. Dwight.** AIEE Transactions, volume 61, 1942, July section, pages 513–18. Discussion, pages 976–7.

153. High-Frequency Coaxial-Line Calculations, **C. V. Larrick, H. H. Race.** AIEE Transactions, volume 62, 1942, July section, pages 526–30.

154. Copper Losses in Large Cables at Power Frequencies, report (reference *F*/*T*55) of the British Electrical and Allied Industries Research Associations. Institution of Electrical Engineers (London, England) *Journal*, volume 76, 1935, pages 299–322; discussion, pages 707–08.

155. Sur la Force Électromotive Nécessaire Pour Produire en Courant d'Intensité Variable le Long d'un Conducteur Cylindrique, **E. Brylinski.** *L'Électricien* (Paris, France), volume 14, 1890, pages 97–110, 193–9. *Annales Télégraphiques* (Paris, France) [3], volume 22, 1895, pages 446–59.

156. Sur la Résistance des Conducteurs aux Courants Alternatifs, **E. Brylinski.** *L'Éclairage Électrique* (Paris, France), volume 7, 1896, pages 82–4.

157. Résistance des Conducteurs aux Courants Alternatifs, **E. Mascart.** Société Internationale des Électriciens *Bulletin* (Paris, France), volume 12, 1895, pages 435–9. See comments in reference 156.

158. Elektrischer und Magnetischer Widerstand bei Schwingungen, **J. Zenneck.** *Annalen der Physik* (Leipzig, Germany) [4], volume 11, 1903, pages 1135–44.

159. Wirbelstromverluste in und Effektiver Widerstand von Geraden, Runden Metallzylindern, **P. O. Pedersen.** *Jahrbuch der Drahtlosen Telegraphie und Telephonie* (Leipzig, Germany), volume 4, 1910–11, pages 501–15.

160. Frequency, **D. B. Rushmore.** AIEE Transactions, volume 31, 1912, pages 955–72; discussion, pages 973–83.

161. Sur l'Absorption des Ondes Electromagnetiques par un Conducteur Cylindrique (Effet Kelvin), **J. Spielrein.** *La Lumière Électrique* (Paris, France) [2], volume 25, 1914, pages 5–12.

162. Calcul Rapide de l'Effect Kelvin par une Nouvelle Formule, Valuable en Toutes Circonstances, **A. Levasseur.** *Revue Générale de l'Électricité* (Paris, France), volume 26, 1929, pages 963–7. Société Française des Électriciens *Bulletin* (Paris, France), [4], volume 10, 1930, pages 73–81. *Journal de Physique* (Paris, France), [7], volume 1, 1930, pages 93–8. Abstracted in Académie des Sciences (Paris, France) *Comptes Rendus*, volume 189, 1929, pages 529–30.

163. Règles à Calcul et Abaques Pour la Résolution de la Formule de M. Levasseur (Calcul de la Résistance des Conducteurs Pour Toutes les Fréquences du Courant), **M. Mathieu.** *Revue Générale de l'Électricité* (Paris, France), volume 27, 1930, pages 763–6.

164. Abaques Pour le Calcul des Résistances Chimiques à Toutes Fréquences, **M. Mathieu.** *L'Onde Électrique* (Paris, France), volume 9, 1930, pages 139–40.

165. La Formulation de l'Effect Kelvin, **E. Fromy.** *L'Onde Électrique* (Paris, France), volume 9, 1930, pages 69–74.

166. Resistance of a Conductor at High Frequencies, **K. Singh.** *Electrical Times* (London, England), volume 78, 1930, pages 227–8.

167. Calcul Practique et Rapide de la Résistance Effective des Conducteurs de Section Circulaire aux Courants Alternatifs, **E. Hospitalier.** *L'Industrie Électrique*, volume 2, 1893, pages 563–4.

168. L'Effect Kelvin, **A. R. Garnier.** *L'Industrie Électrique* (Paris, France), volume 19, 1930, pages 341–6, 396–8.

169. Formulas and Tables for the Calculation of Mutual and Self-Inductance—Revised and Extended, **E. B. Rosa, F. W. Grover.** United States Bureau of Standards *Bulletin*, volume 8, 1912, number 169, pages 1–237.

170. Sur l'Effect Kelvin, Distribution du Courant Alternatif Dans les Conducteurs Cylindriques, Dans les Lames et les Rails, **R. Swyngedauw.** *La Lumière Électrique* (Paris, France), volume 24, 1913, pages 40–4, 74–7, 103–06. Abstracted in Académie des Sciences (Paris, France) *Comptes Rendus*, volume 157, 1913, pages 397–400.

171. Experimental Researches on Skin Effect in Conductors, **A. E. Kennelly, F. A. Laws, P. H. Pierce.** AIEE Transactions, volume 34, 1915, pages 1953–2018; discussion, pages 2019–21.

172. Skin-Effect Resistance Measurements of Conductors at Radiofrequencies up to 100,000 Cycles Per Second, **A. E. Kennelly, H. A. Affel.** Institution of Radio Engineers *Proceedings*, volume 4, 1916, pages 523–74; discussion, pages 575–80.

173. Effective Resistance of Inductance Coils at Radiofrequencies, **S. Butterworth.** *Experimental Wireless and the Wireless Engineer*, volume 3, 1926, pages 203–10, 309–16.

174. A Set of Curves for Skin Effect in Isolated Tubular Conductors, **A. W. Ewan.** *General Electric Review*, volume 33, 1930, pages 249–51.

175. Kurven zur Berechnung des Skineffektes in Hohlleitern, **A. W. Ewan.** *Elektrotechnische Zeitschrift* (Berlin, Germany), volume 51, 1930, page 1338.

176. Rational Expressions of Electromagnetic Skin Effect by the Impedance Ratios, **R. Ursi.** Institution of Electrical Engineers of Japan *Journal* (Tokyo, Japan), number 509, 1930, pages 1303–18.

177. Zur Stromuerdrängung in Zylindrischen Rohrleitern, **E. Grünwald.** *Archiv für Elektrotechnik* (Berlin, Germany), volume 26, 1932, pages 513–17.

178. Über die Anwendung der Iterationsmethode zur Angenäherten Berechnung der Wirbelströme und des Werkwiderstandes, **O. Heymann.** *Archiv für Elektrotechnik* (Berlin, Germany), volume 28, 1938, pages 329–40. Dissertation, Danzig Technische Hochshule, 1934.

179. Über den Wirkwiderstand Eines Dünnwandigen Metallzylinders, **O. Heymann.** *Elektrische Nachrichten-Technik* (Berlin, Germany), volume 12, 1935, pages 175–80.

180. Impedanza Delle Conduttore Tubolari Formule Approssimate per le Alte Frequenze, **G. Malone.** *Elettrotecnia* (Milan, Italy), volume 23, 1936, pages 691–3.

181. Skin-Effect Formulas, **J. R. Whinnery.** *Electronics*, volume 15, 1942, pages 44–8, 94. Corrections on page 94.

182. Formulas for the Skin Effect, **H. A. Wheeler.** Institution of Radio Engineers *Proceedings*, volume 30, 1942, pages 412–24.

183. Resistance of Copper Wire. *Electronics*, volume 9, 1936, page 38.

184. Proximity Effects in Groups of Round Wires, **H. B. Dwight.** *General Electric Review*, volume 30, 1927, pages 531–6.

185. Eddy Currents in Thin Circular Cylinders, **F. W. Carter.** *Proceedings* Cambridge Philosophical Society (London, England), volume 23, 1927, pages 901–06.

186. Electromagnetic Reactions Between Conducting and Magnetic Material, **S. Whitehead.** *Philosophical Magazine* (London, England), volume 11, 1931, pages 897–914.

187. Schirmwirkung und Wirbelstromverluste Eines Hohlenkreiszylindrischen Leiters im Magnetischen Wechselfeld, **H. Buchholz.** *Archiv für Elektrotechnik* (Berlin, Germany), volume 29, 1929, pages 360–74.

188. Practical Value of the Proximity Loss in Parallel Go-and-Return Conductors, **J. K. Webb.** *Electrical Communications*, volume 10, 1931, pages 22–5.

189. Les Problèmes Magnétiques des Conducteurs Parallèles, Specialement des Cables à Courant Fort, **L. Tschiassny.** International Conference on Large High-Voltage Systems (CIGRE), *Compte Rendu des Travaux* (Paris, France), 1937, volume 2, pages 1–17.

190. Resistance of Copper Wires at Very High Frequencies, **W. M. Roberds.** *Physical Review* [2], volume 29, 1927, pages 165–73.

191. A Method of Measuring the Effective Resistance of a Condenser at Radio Frequencies, and of Measuring the Resistance of Long Straight Wires, **C. B. Moullin.** *Proceedings* Royal Society of London (London, England), volume 137*A*, 1932, pages 116–33.

192. Transmission Lines for Short-Wave Radio Systems, **E. J. Sterba, C. B. Feldman.** Bell System *Technical Journal*, volume 14, 1932, pages 44–50.

193. Mutual Impedances of Parallel Wires, **R. S. Hoyt, S. P. Mead.** Bell System *Technical Journal*, volume 14, 1935, pages 509–33.

194. Der Kopplungswiderstand Koaxialer Leitungen, **H. Ochem.** *Hochfrequenztechnik und Elektroakustik* (Leipzig, Germany), volume 48, 1936, pages 182–91.

195. Über Eine Direkte Messung der Stromverteilung Über den Querschnitt Eines Wechselstromdurchflossen Leiters, **H. Busch.** *Physikalische Zeitschrift* (Leipzig, Germany), volume 26, 1925, pages 509–14.

196. Ein Vorlesungsversuch zur Demonstration der Stromverdrängung (des Skin Effekts), **H. Busch.** *Physikalische Zeitschrift* (Leipzig, Germany), volume 26, 1925, pages 661–3.

197. Metal-Clad Switchgear, Automatic Protection, and Remote Control With Particular Reference to Developements During the Last Seven Years, **H. W. Clothier.** Institution of Electrical Engineers (London, England) *Journal*, volume 71, 1932, pages 285–330; discussion, pages 330–73. See discussion by **W. Wilson**, page 341.

198. Sur le Pouvoir Inducteur Spécifique des Métaux, **A. Broca.** Académie des Sciences (Paris, France) *Comptes Rendus*, volume 140, 1905, pages 1677–80. Corrections, volume 141, 1905, page 80.

199. Strom- und Feldverdrängung in Runden Leitern, **C. Breitfeld.** *Elektrotechnik und Maschinenbau* (Vienna, Austria), volume 38, 1920, pages 537–43.

200. Sur da Résistance des Conducteurs En-courant Variable, **E. Brylinski.** Société Internationale des Électriciens *Bulletin* (Paris, France) [2], volume 6, 1906, pages 255–300.

201. Expressione Operazione Dell'Effetto Pelle in un Conduttore Cilindrico, **G. Cocci, R. Sartori.** *Rendiconti* R. Istituto Lombardo di Scienze e Lettere (Milan, Italy) [2], volume 67, 1934, pages 879–89.

202. Elektromagnetische Wellen an Einem Draht mit Isolierender Zylindrischer Hülle, **F. Harms.** *Annalen der Physik* (Leipzig, Germany) [4], volume 23, 1907, pages 44–60.

203. Effective Resistance and Inductance of Iron and Bimetallic Wires, **J. M. Miller.** *Bulletin* Bureau of Standards, volume 12, 1915–16, pages 207–67.

204. Über die Fortpflanzung Elektrischer Wellen an Einem Geraden Metalldraht der mit Einem Leitenden Mantel Versehen Ist, **K. Försterling.** *Annalen der Physik* (Leipzig Germany) [4], volume 72, 1923, pages 30–57.

205. Electric and Magnetic Induction Disturbances in Parallel Conducting Systems: I—Formulas for the Resistance and Induction Coefficients for Concentric Metal Sheaths and for the Reductive Effect of the Sheaths Against Disturbances, **H. Pleijel.** *Ingeniörs Vetenskaps Akademiens* (Stockholm, Sweden), Handlingar *NR* 49, 1926, pages 1–46.

206. Sur la Disuniforme Distribuzione Delle Correnti Alternate Nelle Conditture Bimetalliche e Cave, **G. Maione.** *L'Elettrotecnica* (Milan, Italy), volume 33, 1929, pages 65–70, 91–100, 109–14.

207. Die Allseitige Feldverteilung in Zwei Kreiszylindrischen, Konaxial Geschichteten Stoffen bei Axialer Richtung des Wechselstrome, **J. Fischer.** *Hochfrequenztechnik und Elektroakustik* (Leipzig, Germany), volume 40, 1932, pages 207–14. See comment in reference 209, page 219.

208. Zur Elektrodynamik des Runddrahts mit Eisenmantel, **J. Fischer.** *Elektrische Nachrichten-Technik* (Berlin, Germany), volume 11, 1934, pages 140–52.

209. Skineffekt in Einem Geschichteten Kreiszylinder, **M. J. O. Strutt.** *Hochfrequenztechnik und Elektroakustik* (Leipzig, Germany), volume 41, 1933, pages 62–3, 219.

210. Über den Wechselstromwiderstand von Geraden Drähten mit Kreisförmigem Querschnitt die aus Mehreren Konzentrischen Schichten Bestehen, **S. Ekelöf.** *Elektrische Nachrichten-Technik* (Berlin, Germany), volume 10, 1933, pages 115–22.

211. Stromverdrängung in Geschichteten Zylindrischen Leitern, **H. Kruse, O. Zinke.** *Hochfrequenztechnik und Elektroakustik* (Leipzig, Germany), volume 44, 1934, pages 195–203. For comment see volume 45, 1935, page 140.

212. Zur Berechnung des Wechselstrom widerstandes Geschichteter Zylindrischer Leiter, **W. Egloff.** *Elektrische Nachrichten-Technik* (Berlin, Germany), volume 19, 1942, pages 191–6.

213. Skin Effect in Bimetallic Conductors, **B. R. Teare, J. R. Webb.** AIEE Transactions, volume 62, 1943, June section, pages 297–302.

214. High-Frequency Resistance of Plated Conductors, **R. F. Proctor.** *Wireless Engineer*, volume 20, 1943, pages 56–65.

215. Copper-Covered Steel Wire at Radio Frequencies, **B. R. Teare, E. R. Schatz.** Institute of Radio Engineers *Proceedings*, volume 32, 1944, pages 397–403.

216. Über den Hochfrequenzwiderstand von Geraden Drähten, die mit Leitenden Mänteln Versehen Sind, **F. Trautmann.** *Annalen der Physik* (Leipzig, Germany), volume 72, 1932, pages 1–29.

217. Ein Beitrag zum Hauteffekt bei Geschichteten Zylindrischen Leitern, **H. W. Von Steinhausen.** *Telefunken-Zeitung* (Berlin, Germany), volume 17, 1936, pages 45–57. Dissertation, Berlin Technische Hochschule, 1935.

218. The Electromagnetic Theory of Coaxial Transmission Lines and Cylindrical Shields, **S. A. Schelkunoff.** Bell System *Technical Journal*, volume 13, 1934, pages 532–79.

219. The Losses in Cables at High Frequencies, **E. F. Northrup, R. G. Thompson.** *Journal* Franklin Institute, volume 182, 1916, pages 1–17.

220. Heavy Alternating-Current Conductors, **K. C. Randall.** *Electric Journal*, volume 16, 1919, page 343.

221. Measurement of Relative Eddy-Current Losses in Stranded Cables, **James A. Cook.** AIEE Journal, volume 40, February 1921, pages 93–5.

222. Skin Effect in Large Stranded Conductors at Low Frequencies, **W. I. Middleton, E. W. Davis.** AIEE Journal, volume 40, September 1921, pages 757–63. See criticism in reference 111.

223. Discussion by **A. S. Dana** of Skin Effect and Proximity Effect in Tubular Conductor, AIEE Journal, volume 41, September 1922, pages 671–3.

224. Proximity Effect in Seven-Strand Cables, **J. E. L. Tweeddale.** Institution of Electrical Engineers (London, England) *Journal*, volume 47, 1928, pages 290–4.

225. Eddy-Current Losses in Single-Conductor Paper-Insulated Lead-Covered Unarmoured Cables of a Single-Phase System, **A. H. M. Arnold.** Institution of Electrical Engineers (London, England) *Journal*, Part 2, volume 89, 1942, pages 636–45.

225a. Wrought Iron Pipe Replaces Copper Bus, **J. A. Gerber.** *Engineering*, volume 157, 1944, page 127. *Welding Journal*, volume 23, 1944, page 73. *Metal Progress*, volume 46, 1944, page 297.

226. Alternating-Current Conductivity of Iron Pipe, **H. B. Dwight.** *Electric Journal*, volume 23, 1926, pages 295–7.

227. Selection of Tubular Bus Material, **J. W. Wall.** *Electrical World*, volume 89, 1926, pages 299–302. See comment in reference 226.

228. Evaluate Steel Pipe as A-C Conductor, **S. C. Killian.** *Electrical World*, volume 117, 1942, pages 1349–50, 2237–8. *Delta-Star Magazine*, May–June 1942.

229. Structural Steel Shapes as A-C Conductors, **S. C. Killian, A. A. Alsaker.** *Electrical World*, volume 118, 1942, pages 1773–5. *Delta-Star Magazine*, November–December 1942.

230. Self-Induction Effects in Steel Rails, **E. Wilson.** *Electrician* (London, England), volume 56, 1905–06, pages 757–9; volume 57, 1906, pages 453, 64.

231. Étude Expérimentale sur la Résistance des Rails D'Acier, en Courant Alternatif, **E. Villiers, P. Boucherot.** Société Française des Électriciens *Bulletin* (Paris, France) [3], volume 1, 1911, pages 529–42.

232. Experimental Researches on the Skin Effect in Steel Rails, **A. E. Kennelly, F. H. Achard, A. S. Dana.** *Journal* Franklin Institute, volume 182, 1916, pages 135–90. Abstracted in *Electrician* (London, England), volume 79, 1917, pages 692–5.

233. Beitrag zur Bestimmung des Innern Schweinwiderstandes Einer Eisenbahnschiene, **E. R. Benda.** *Wissenschaftliche Veroffentlichungen aus den Siemens-Werken* (Berliu, Germany), volume 10, 1931, pages 91–7.

234. Investigation of Rail Impedances, **H. M. Trueblood, G. Waschek.** AIEE Transactions, volume 53, 1934, pages 1770–80.

235. Voltage Drop in A-C Collector Systems for Cranes and Bridges, **W. K. Boice.** *Iron and Steel Engineer*, volume 20, October 1943, pages 46–53.

236. Current Distribution in Multiconductor Single-Phase Busses, **C. F. Wagner.** *Electrical World*, volume 79, 1922, pages 526–9.

237. Capacity of 60-Cycle Busses for Heavy Currents, **T. G. LeClair.** AIEE Transactions, volume 45, 1926, pages 203–10.

238. Untersuchung Unsymmetrischer Dreiphasen-Hochstromanlagen, **R. Stein.** *Siemens Zeitschrift* (Berlin, Germany), volume 6, 1926, pages 317–30.

239. Untersuchungen Über Stromverdrängung in Rechteckigen Querschitten, **H. Schwenkhagen.** *Archiv für Elektrotechnik* (Berlin, Germany), volume 17, 1926–27, pages 537–89. Dissertation, Berlin, 1927.

240. Bemerkungen zu der Arbeit des Herrn H. Schwenkhagen Untersuchungen Über "Stromverdrängung in Rechteckigen Querschnitten," **W. Geyger.** *Archiv für Elektrotechnik* (Berlin, Germany), volume 18, 1927, pages 369–73.

241. The Efficient Utilization of Conductor Material in Bus-Bar Sections, **G. Dannatt, S. W. Redfearn.** *World Power*, volume 14, 1930, pages 397–400, 492–6.

242. Anordung von Sammelschienen aus Aluminum für Hohe Stromstärken, **H. H. Johann.** Verband Deutscher Elektrotechniker *Fachberichte* (Berlin, Germany), 1935, pages 71–3; discussion, pages 73–4.

243. Paired-Phase Bus Bars for Large Polyphase Circuits, **Lawrence E. Fisher, Robert L. Frank.** AIEE Transactions, volume 62, 1943, February section, pages 71–7. Discussion, pages 417–18.

244. Skin Effect of a Return Circuit of Two Adjacent Strap Conductors, **H. B. Dwight.** *Electric Journal*, volume 13, 1916, pages 157–8.

245. Calculation of Skin Effect in Strap Conductors, **H. B. Dwight.** *Electrical World*, volume 67, 1916, pages 593–4.

246. Foucault Currents in Cylindrical Shells and Ribbons, **F. W. Carter.** *Proceedings* Cambridge Philosophical Society (London, England), volume 30, 1934, pages 341–6.

247. Skin Effect in Rectangular Conductors at High Frequencies, **J. D. Cockroft.** *Proceedings* Royal Society of London (London, England), volume 122*A*, 1929, pages 533–42.

248. The Effect of Curved Boundaries on the Distribution of Electrical Stress Round Conductors, **J. Cockroft.** Institution of Electrical Engineers (London, England) *Journal*, volume 66, 1927–28, pages 385–409, discussion, pages 900–01.

249. Skin Effect in Rectangular Conductors at High Frequencies, **W. Jackson.** *Philosophical Magazine* (London, England) [7], volume 18, 1934, pages 433–41.

250. Skin Effect in Rectangular Conductors, **L. J. Gorman, H. C. Forbes.** AIEE Transactions, volume 52, 1933, pages 516–19; discussion, pages 519–20. For comment see reference 251.

251. Skin Effect in Conductors of Given Shape (letter), **H. B. Dwight.** Electrical Engineering, volume 52, October 1933, pages 724–5. Re reference 250.

252. Alternating-Current Resistance of Rectangular Conductors, **S. J. Haefner.** Institute of Radio Engineers *Proceedings*, volume 25, 1937, pages 434–47.

253. Über die Stromverdrängung in Leitern mit Unrundem Querschnitt, **M. Reich, F. Fischer.** *Zeitschrift für Physik* (Berlin, Germany), volume 32, 1925, pages 327–32.

254. Edge Effect in Copper Bars. *Journal* Franklin Institute, volume 185, 1918, pages 417–19.

255. Current Distribution in a Rectangular Conductor, **John L. Daley.** AIEE Transactions, volume 58, 1939, pages 687–90.

256. Sur les Méthodes de Calcul des Pertes Supplémentaires Dans les Conducteurs non Magnétiques Parcourus par un Courant Alternatif Sinusoidal et Leur Application Dans la Pratique Courante du Constructeur de Machines Électriques, **S. Kohn.** Société Française des Électriciens *Bulletin* (Paris, France) [5], volume 9, 1939, pages 237–56.

257. Die Berechnung der Stromverteilung

in Zylindrischen Leitern mit Rechteckigem und Elliptischem Querschnitt, **H. G. Gross.** *Archiv für Elektrotechnik* (Berlin, Germany), volume 34, 1940, pages 241–68. Abstracted in *Elektrotechnische Zeitschrift* (Berlin, Germany), volume 61, 1940, pages 455–6.

258. The Distribution of Current and the Variation of Resistance in Linear Conductors of Square and Rectangular-Cross Section When Carrying Alternating Currents of High Frequency, **H. W. Edwards.** *Physical Review* [1], volume 33, 1911, pages 184–202.

259. Distribution of Current in Square and Rectangular Cross Sections, **H. W. Edwards.** *Electrician* (London, England), volume 68, 1912, pages 728–9.

260. Wirbelströme in Stäben von Rechteckigem Querschnitt, **P. Debye.** *Zeitschrift für Mathematik und Physik* (Leipzig, Germany), volume 54, 1907, pages 418–37.

261. Resistance and Reactance of Massed Rectangular Conductors, **A. Press.** *Physical Review* [2], volume 8, 1916, pages 417–22.

262. Stromverdrängung in Rechteckigen Leitern, **M. J. Strutt.** *Annalen der Physik* (Leipzig, Germany) [4], volume 83, 1927, pages 979–1000.

263. Über den Hauteffekt in Einem Draht von Elliptischem Querschnitt, **A. Lampa.** *Sitzungsberichte* der Mathematisch-Naturwissenschaftlichen Classe der Kaiserlichen Akademieder Wissenschaften (Vienna, Austria), volume 123, 1914, part 2*A*, pages 2313–20.

264. Wirbelströme in Elliptischen Zylinder, **M. J. O. Strutt.** *Annalen der Physik* (Leipzig, Germany) [4], volume 84, 1927, pages 485–506.

265. Zur Stromverdrängung in Zylindrischen Leitern, **F. Fischer.** *Zeitschrift für Physik* (Berlin, Germany), volume 33, 1925, pages 623–7.

266. Skineffekt in Zylindrischen Leitern mit Elliptischem Querschnitt, **F. Lettowsky.** *Archiv für Elektrotechnik* (Berlin, Germany), volume 29, 1935, pages 556–6.

267. Skineffekt in Zylindrischen Leitern mit Elliptischem Querschnitt bei Hohen Frequenzen, **F. Lettowsky.** *Archiv für Elektrotechnik* (Berlin, Germany), volume 35, 1941, pages 643–62.

268. Skineffekt in Zylindrischen Leitern, **J. Fischer.** *Physikalische Zeitschrift* (Leipzig, Germany), volume 42, 1941, pages 327–36, 419.

269. The Alternating-Current Resistance of Hollow Square Conductors, **A. H. M. Arnold.** Institution of Electrical Engineers (London, England) *Journal*, volume 82, 1938, pages 537–45.

270. Temperature Rise of Bus Bars, **H. B. Dwight, G. W. Andrew, H. W. Tileston.** *General Electric Review*, volume 43, 1940, pages 213–16.

271. The Transmission of Alternating-Current Power With Small-Eddy Current Losses, **A. H. M. Arnold.** Institution of Electrical Engineers (London, England) *Journal*, volume 80, 1937, pages 395–400.

272. Das Elektromagnetische Feld (book), **E. Cohn, S. Hirzel.** Leipzig, Germany, 1900. Pages 456–71.

273. Über die Verteilung des Wechselstromes in Unendlich Ausgedehnten Platten, **W. O. Schumann.** *Elektrotechnik und Maschinenbau* (Vienna, Austria), volume 39, 1913, pages 635–40, 659–65.

274. Flussverdrängung und Stromverdrängung, **F. Niethammer.** *Elektrotechnik und Maschinenbau* (Vienna, Austria), volume 38, 1920, pages 141–4.

275. Der Widerstand von Kontakten, **L. Binder.** *Elektrotechnik und Maschinenbau* (Vienna, Austria), volume 30, 1912, pages 781–8.

276. Electrical Contact Resistance, **F. W. Harris.** *Electric Journal*, volume 10, 1913, pages 637–44.

277. The Efficiency of Overlapping Joints in Copper and Aluminum Bus-Bar Conductors, **S. W. Melsom, H. C. Booth.** Institution of Electrical Engineers (London, England) *Journal*, volume 60, 1922, pages 889–99.

278. Theory of Overlapping Joints, **R. M. Wilmotte.** Institution of Electrical Engineers (London, England) *Journal*, volume 64, 1925–26, pages 1089–90.

279. Giunti a Sovrapprosizione per Circuiti di Forni Elettrici, **E. Donati.** *L'Energia Elettrica* (Milan, Italy), volume 12, 1935, pages 433–40.

280. The Resistance of Electrical Connections, **G. E. Luke.** *Electric Journal*, volume 21, 1924, pages 66–9.

281. The Contact Resistance of Large Conductors, **A. R. Enger.** *Electric Journal*, volume 21, 1924, pages 316–18.

282. Der Elektrische Uebergangswiderstand von Kontakter, **W. Schälchlin.** Schwiezerischer Electrotechnicher Verein *Bulletin* (Zurich, Switzerland), volume 15, 1924, pages 106–16.

283. Contact Resistance of Electric Switching Apparatus, **W. Schälchlin.** *Electric Journal*, volume 25, 1928, pages 386–91.

284. Contact Resistance, **B. W. Jones.** *General Electric Review*, volume 30, 1927, pages 85–6.

285. Einfluss der Grosse des Druckes und der Fläche auf den Kontaktwiderstand, **E. Contius.** Dissertation, Dresden, Germany, 1929.

286. Joints in Heavy Electrical Conductors, **E. G. Bern, W. Specht.** *General Electric Review*, volume 33, 1930, pages 389–93.

287. Note on the Electrical Resistance of Contacts Between Nuts and Bolts, **F. Wenner, G. W. Nusbaum, B. C. Cruickshanks.** Bureau of Standards *Journal of Research*, volume 5, 1930, pages 757–66.

288. Abhangigkeit des Berührungswiderstandes von der Zahl der Berührungspunkte, **L. Binder.** *Zeitschrift für Technische Physik* (Leipzig, Germany), volume 13, 1932, pages 442–3.

289. Designs of Current-Carrying Contacts in Modern Switchgear, **R. Paxton, H. E. Strang.** *General Electric Review*, volume 36, 1933, pages 524–8.

290. Electrical Contact of Bus-Bar Joints, **C. L. Denault.** *Electric Journal*, volume 30, 1933, pages 281–3.

291. Contact Problems in Connection With Use of Magnesium for Electric Conductors, **W. Bulian.** *Elektrotechnische Zeitschrift* (Berlin, Germany), volume 59, 1938, pages 879–81.

292. Anschlussteile fur Aluminum-Kuper-Stromübergänge, **R. Schulze.** Allgemeine Elektrizitäts Gesellschaft *Mitteilungen* (Berlin, Germany), 1938, page 672.

293. Joining Aluminum Bus Bars, **W. E. Warner.** *Power Plant Engineering*, volume 32, 1928, page 672.

294. Joints for Aluminum Bus Bars, **W. E. Warner.** *Electrical Review* (London, England), volume 106, 1930, page 159.

295. Jointing of Aluminum Bus Bars, **G. Windred.** *Electrical Power Engineer* (London, England), volume 6, 1938, pages 282–4.

296. Untersuchungen Über die Grösse und Beständigkeit von Kontaktverbindungen Unter Besonder Berücksichtigung des Aluminums, **R. Richter.** *Elektrotechnische Zeitschrift* (Berlin, Germany), volume 41, 1920, pages 345–7, 368–70, 386–92, 409–13, 433–4, 448–52.

297. Untersuchungen Über die Beständigkeit von Kontaktverbindungen Unter Besonderer Berücksichtigung von Aluminum, **R. Richter, G. Schade.** *Elektrotechnische Zeitschrift* (Berlin, Germany), volume 59, 1938, 1321–6.

298. Bolting of Bus-Bar Joints, **E. B. Shand, C. E. Valentine.** *Electric Journal*, volume 30, 1933, pages 377–80.

299. Joint in Electrical Conductors, **G. Windred.** *Beama Journal* (London, England), volume 42, 1938, pages 52–5.

300. Mittel zur Leitungsverlegung in Niederspannungsortsnetzen, **J. Nefzger.** *Elektrotechnische Zeitschrift* (Berlin, Germany), volume 62, 1941, pages 124–8.

301. Electric Resistance Brazing, **S. Martin.** AIEE Transactions, volume 50, 1931, pages 685–8; discussion, pages 688–90.

302. Welded Bus Offers Simple Structure, **H. C. Daniels.** *Electrical World*, volume 108, 1937, pages 1060, 1062.

303. Copper Brazing Lowers Bus Jointing Cost, **R. A. Goeller.** *Electrical World*, volume 108, 1937, pages 1530–2, 1588, 1590.

304. Silver Brazing Copper Bus Bars, **R. A. Goeller.** *Industry and Welding*, volume 10, 1937, December, page 44.

305. Brazing Bus Bars, **R. A. Goeller.** *Steel*, volume 102, February 1938, pages 50–1, 76.

306. Jointing Copper Bus Bars With Brazing Alloys, **R. A. Goeller.** *Welding Journal*, volume 17, February 1938, pages 26–31.

307. Brazing of Copper Bus Bars, **R. A. Goeller.** *Welding Engineer*, volume 22, December 1937, pages 34–5; volume 23, January 1938, pages 32–4.

308. We Brazed Our Bus-Bar Joints, **F. M. Darner.** *Factory Management and Maintenance*, volume 96, February 1938, pages 96–8.

309. Welding Copper Bus Bars, **B. B. Bessesen.** *Welding Journal*, volume 17, May 1938, page 21.

310. Unlösbare Verbindungen an Aluminum, Magnesium und Zink und Ihre Ausführung in der Elektrotechnik, **R. Schulze.** *Elektrotechnische Zeitschrift* (Berlin, Germany), volume 61, 1940, pages 1111–17.

311. Brazing Copper Bus Bars, **J. T. Barton.** *Welding Engineer*, volume 27, March 1942, pages 34–7.

312. Brazing Electrical Connections With Self-Fluxing Alloy. *Electrical Manufacturing*, 1938, number 9, pages 38–41.

313. Braze Tube Bus With Low-Melt Alloy. *Electrical World*, volume 112, 1939, page 1470.

314. Brazing Practice; Applications in the Electrical Industry. *Electrical Review* (London, England), volume 131, 1942, pages 513–16.

315. Electrical Contacts (book), **G. Windred.** Macmillan and Company, London, England; New York, N. Y.; 1940.

316. Über Metallische Kontaktwiderstände, **R. Holm.** *Wissenschaftliche Veroffentlichungen aus dem Siemens-Konzern* (Berlin, Germany), volume 7, 1929, pages 217–71.

317. Charakteristiken von Kontaktwiderständen, **E. Holm, R. Holm.** *Wissenschaftliche Veroffentlichungen aus dem Siemens-Konzern* (Berlin, Germany), volume 7, 1929, pages 272–304.

318. Electrical-Contact Resistance, a Review of Development, **G. Windred.** *Beama Journal* (London, England), volume 42, 1938, pages 122–5.

319. Electrical-Contact Resistance, **G. Windred.** *Journal* Franklin Institute, volume 231, 1941, pages 547–85.

320. Electricity and Magnetism (book), **A. G. Webster.** Macmillan and Company, New York, N. Y.; London, England; 1897.

321. The Theory of Electricity (book), **G. H. Livens.** Cambridge University Press, Cambridge, England, 1926.

322. Static and Dynamic Electricity (book), **W. R. Smythe.** McGraw-Hill Book Company, Inc., New York, N. Y.; London, England; 1939.

323. A Note on Self-Induction, **A. O'Rahilly.** Institution of Electrical Engineers (London, England) *Journal*, volume 86, 1940, pages 179–87; discussion, page 567.

324. Theory and Practice of Absolute Measurements in Electricity and Magnetism (book), **A. Gray.** London, England, 1888–93. Volume 2, part 1.

325. On the Geometrical Mean Distance of Two Figures in a Plane, **J. C. Maxwell.** *Transactions* Edinburgh Royal Society (Edinburgh, Scotland), volume 26, 1872, pages 729–33.

326. Coefficient Self-Induction des Fils Parallèles Égaux et Equidistants, Dont les Sections Sont Réparties sur une Circonférence, **C. E. Guye.** Académie des Sciences (Paris, France) *Comptes Rendus*, volume 119, 1894, pages 219–21.

327. Sur la Moyenne Distance Géométrique des Éléments d'un Ensemble de Surfaces et son Application Au Calcul des Coefficients D'Induction, **C. E. Guye.** Académie des Sciences (Paris, France) *Comptes Rendus*, volume 118, 1894, pages 1329–32.

328. Über Starkstrom Widerstände mit Kleiner Selbstinduktion, **E. Orlich.** *Zeitschrift für Instrumentenkunde* (Berlin, Germany), volume 29, 1909, pages 241–56.

328a. Über die Induktionswirkungen Parallelen Gestreckter Leiter, **E. Orlich.** *Elektrotechnische Zeitschrift* (Berlin, Germany), volume 29, 1908, pages 310–13.

329. Kapazitat und Induktivitat: Ihre Begriffs Bestimmung Berechnung, und Messung (book), **E. Orlich.** Brunswick, Germany, 1909.

330. Berechnung der Selbstinduktion Gerader Leiter und Rechteckiger Spulen, **J. K. Sumec.** *Elektrotechnische Zeitschrift* (Berlin, Germany), volume 27, 1906, pages 1175–9.

331. On the Geometrical Mean Distances of Rectangular Areas and the Calculation of Self-Inductance, **E. B. Rosa.** *Bulletin* Bureau of Standards, volume 3, 1907, pages 1–41.

332. The Self- and Mutual Inductances of Linear Conductors, **E. B. Rosa.** *Bulletin* Bureau of Standards, volume 4, 1907–08, pages 301–44.

333. Formulas and Tables for the Calculation of Mutual and Self-Inductance, **E. B. Rosa, L. Cohen.** *Bulletin* Bureau of Standards, volume 5, 1908–09, pages 1–132.

334. Additions to the Formulas for the Calculation of Mutual and Self-Inductance, **F. W. Grover.** *Bulletin* Bureau of Standards, volume 14, 1918–19, pages 537–70.

335. The Calculation of the Inductance of Single-Layer Coils and Spirals Wound With Wire of Large Cross Section, **F. W. Grover.** Institution of Radio Engineers *Proceedings*, volume 17, 1929, pages 2053–63.

336. Heavy Alternating-Current Busses for Furnaces and Synchronous Converters, **J. L. McK. Yardley.** *Blast Furnace and Steel Plant*, volume 11, 1923, pages 492–4, 624–32.

337. Principles of Electric Power Transmission (second edition), **L. F. Woodruff.** John Wiley and Sons, Inc., New York, N. Y.

338. Reactance of Square Tubular Bus Bars, **H. B. Dwight, T. K. Wang.** AIEE Transactions, volume 57, 1938, pages 762–5.

338a. Curves for the Geometric Mean Distance Between Identical Rectangles (master of science thesis), **C. E. Uluant** (Under the supervision of H. B. Dwight of Massachusetts Institute of Technology.)

339. Inductance of Hollow Rectangular Conductors, **T. J. Higgins.** *Journal* Franklin Institute, volume 230, 1940, pages 375–80.

340. Formulas for the Inductance of Rectangular Tubular Conductors, **Thomas James Higgins.** AIEE Transactions, volume 60, 1941, December section, pages 1046–50.

341. Formulas for the Calculation of the Inductance of Linear Conductors of Structural Shape, **Thomas James Higgins.** AIEE Transactions, volume 62, 1943, February section, pages 53–7.

342. Formulas for the Geometric Mean Distance of Rectangular Areas and of Line Segments, **T. J. Higgins.** *Journal of Applied Physics*, volume 14, 1943, pages 188–95.

343. Tables of Natural Logarithms; Tables of Arctangents (books), mathematical tables project, Work Projects Administration. Columbia University Press, New York, N. Y.

344. Graphische Bestimmung der Selbstinduktivität Gerarder Zylindrischer Leiter Beliebiger Querschnitts, **J. Hak.** *Zeitschrift für Angewandte Mathematik und Mechanik* (Berlin, Germany), volume 1, 1921, pages 227–30.

345. The Theory of Alternating Currents (2 volumes), **A. Russell.** Cambridge University Press, Cambridge, England, 1914. See volume 1.

346. Inaugural Address: Appendix, Inductance Coefficients of Cylindrical Conductors, **A. Russell.** Institution of Electrical Engineers (London, England) *Journal*, volume 62, 1923, pages 1–18.

347. Inductance Coefficients of a Part of a Circuit and Their Applications, **A. Russell.** Institution of Electrical Engineers (London, England) *Journal*, volume 69, 1931, pages 270–80.

348. The Inductance of Tubular Conductors of Eccentric-Annular Cross Section, **T. J. Higgins.** *Journal of Mathematics and Physics*, volume 21, 1942, pages 159–77.

349. The Vector Potential and Inductance of a Circuit Comprising Linear Conductors of Different Permeability, **T. J. Higgins.** *Journal of Applied Physics*, volume 13, 1942, pages 390–8.

350. Saving Copper, bulletin 4210, Delta-Star Electric Company, Chicago, Ill.

351. Short-Circuit Calculating Procedure for Low-Voltage A-C Systems. *General Electric Tract GET*-1009, 1941. Compiled by A. G. Darling.

352. Short-Circuit Calculating Procedure for Low-Voltage A-C Systems, **A. G. Darling.** AIEE Transactions, volume 60, 1941, pages 1121–35; discussion, pages 1294–5.

353. Self- and Mutual Induction Chart, **A. F. Anderson, L. R. Vianey.** *Electrical World*, volume 105, 1935, pages 2667, 2720, 2722.

354. Chart Computes Drop in Three-Phase Feeders, **L. H. Gussow.** *Electrical World*, volume 110, 1938, page 1480.

355. Electrical Theorems in Connection With Parallel Cylindrical Conductors, **A. Russell.** *Proceedings* Physical Society of London (London, England), volume 31, 1919, pages 111–30.

356. Note on the Calculation of High-Frequency Inductances, **F. B. Pidduck.** *Philosophical Magazine* (London, England) [6], volume 45, 1923, pages 783–6.

357. Inductance of Conductors at Close Spacings, **F. B. Silsbee.** *Electrician* (London, England), volume 77, 1916, pages 945–6.

358. Inductance of Conductors at Close Spacing, **F. B. Silsbee.** *Electrical World*, volume 68, 1916, pages 125–6.

359. Über die Induzierte Strömung und das Drehmoment die der Scheibl Eines Wechsel Strommotor Zählers, **W. Rogowski.** *Archiv für Elektrotechnik* (Berlin, Germany), volume 1, 1913, pages 205–32..

360. A Study of the Inductance of Four-Terminal Resistance Standards, **F. B. Silsbee.** *Bulletin* Bureau of Standards, volume 13, 1916–17, pages 375–422.

361. The Reactance of Strap Conductors, **H. B. Dwight.** *Electrical Review and Western Electrician*, volume 70, 1917, pages 1087–8.

362. Reactance Values for Rectangular Conductors, **H. B. Dwight.** *Electric Journal*, volume 16, 1919, pages 255–6.

363. Die Induktivität von Spulen, Ringen und Staben, **H. Hemmeler.** *Archiv für Elektrotechnik* (Berlin, Germany), volume 14, 1925, pages 153–63.

364. Induktivität Energie und Stromkraft von Sammelschienen, **W. Steidinger.** *Archiv für Elektrotechnik* (Berlin, Germany), volume 23, 1929–30, pages 153–62. See comment in reference 365.

365. Induktivität, Energie, und Stromkraft von Sammelschienen, **R. Brüderlink.** *Archiv für Elektrotechnik* (Berlin, Germany), volume 26, 1932, pages 121–2.

366. Current-Carrying Capacity of Hollow Conductors, **H. W. Papst.** *Electric Journal*, volume 28, 1931, pages 411–14.

367. Calculation of Inductance and Current Distribution in Low-Voltage Connections to Electric Furnaces, **C. C. Levy.** AIEE Transactions, volume 51, 1932, pages 903–13.

368. Engineering Calculation of Inductance and Reactance for Rectangular Bar Conductors, **O. R. Schurig.** *General Electric Review*, volume 36, 1933, pages 228–31.

369. Calculation of Reactance in Parallel Conductors of Rectangular Cross Section, **I. Herlitz.** Allmanna Svenska Elektriska Aktiebolaget (ASEA) *Journal* (Stockholm, Sweden), volume 11, 1934, pages 114–15.

370. Champ Magnétique et Inductance d'un Système des Barres Rectangulaires Parallèles, **E. Roth.** *Revue Générale de l'Électricité* (Paris, France), volume 41, 1938, pages 275–83.

371. Reactance Chart for Welder Bus Problems, **R. C. Bouse, J. D. Scarbrough.** *Electrical World*, volume 115, 1941, pages 832–3, 1014–15.

372. The Inductance of Linear Conductors of Rectangular Section, **A. H. M. Arnold.** Institution of Electrical Engineers (London, England) *Journal*, volume 70, 1931–32, pages 579–86.

373. Leads for Electric Furnaces, **A. Lindstrom.** *Metallurgy and Chemical Engineering*, volume 16, 1917, pages 683–7.

374. The Calculation of Electric-Furnace Circuits, **R. Catani.** *Transactions* Electrochemical Society, volume 52, 1927; pages 115–42; discussion, pages 142–55.

375. Electric-Arc and Arc-Resistance Furnaces and Their Power Factor, **A. Wejnarth.** *Transactions* Electrochemical Society, volume 63, 1933, pages 309–43; discussion, pages 344–8.

376. Bus Bars for Electrochemical Plants, **L. C. Pan.** *Transactions* Electrochemical Society, volume 66, 1934, pages 369–74.

377. The Reactance of Large Rectangular Three-Phase Electric Furnaces, **F. A. Andreae.** *Transactions* Electrochemical Society, volume 67, 1935, pages 151–67; discussion, pages 167–8.

378. Giunti a Sovrapposizioni per Circuiti di Forni Elettrici, **E. Donati.** *L'Energia Elettrica* (Milan, Italy), volume 12, 1935, pages 433–40.

379. Formulas for the Inductance of Rectangular Tubular Conductors, **T. J. Higgins.** *Journal of Applied Physics*, volume 13, 1942, pages 712–15.

380. New Formulas for the Inductance and Reactance of Square Tubular Conductors, **T. J. Higgins.** *Journal of Applied Physics*, volume 14, 1943, pages 185–7.

381. Formulas for the Inductance of Busses Comprised of Channels Located Back to Back, **W. Schwantz, T. J. Higgins.** Master of science thesis, Illinois Institute of Technology, 1944.

382. The Linear Resistance Between Parallel Conducting Cylinders in a Medium of Uniform Conductivity [and the Corresponding Capacitance Problem], **A. E. Kennelly.** *Proceedings* American Philosophical Society, volume 48, 1909, pages 142–65.

383. Electrical Theorems in Connection With Parallel Cylindrical Conductors, **A. Russell.** *Proceedings* Physical Society of London (London, England), volume 31, 1918–19, pages 111–30.

384. Problems in Connection With Two Parallel Electrified Cylindrical Conductors, **A. Russell.** Institution of Electrical Engineers (London, England) *Journal*, volume 64, 1925–26, pages 238–42.

385. Equal Parallel Cylindrical Conductors in Electrical Problems, **F. J. W. Whipple.** *Proceedings* Royal Society of London (London, England), volume 96*A*, 1919–20, pages 465–75.

386. The Field Due to Two Equally Charged Parallel Conducting Cylinders, **H. Poritsky.** *Journal of Mathematics and Physics*, volume 11, 1931–32, pages 213–17.

387. Electrical Distributions on Cylindrical Cylinders, **E. P. Adams.** *Proceedings* American Philosophical Society, volume 75, 1935, pages 11–70.

388. The Direct Method of Calculation of Capacitance of Conductors, **H. B. Dwight.** AIEE Transactions, volume 43, 1924, pages 958–65.

389. Berechnung der Kapazität von Sammelschienenanlagen, **D. Gabor.** *Archiv für Elektrotechnik* (Berlin, Germany), volume 14, 1925, pages 247–58.

390. Méthodes Analytiques, Graphiques, et Expérimentales Utilisées Pour l'Étude des Champs Magnétiques et Électriques Dans les Machines et Appareils Électriques, **B. Hague.** Congrès International d'Électricité, Paris, France, section 3. Report 7, 1932, 65 pages.

391. [Experimental Methods for] Determining the Distribution of Electric and Magnetic Fields, **B. Hague.** *Electrician* (London, England), volume 102, 1929, pages 185–7, 315–17.

392. Über Eine Neue Methode zur Zeichung der Feldbilder Magnetischer Kraftlinien, **A. O. Müller.** *Archiv für Elektrotechnik* (Berlin, Germany), volume 17, 1927, pages 501–10.

393. Mapping of Fields, **Ernst Weber.** AIEE Transactions, volume 53, 1934, December section, pages 1563–70. Contains a bibliography of 53 references on conformal mapping of fields.

394. Eine Graphische Methode der Kapazitätsberechnung Zylindrischer Gebilde, W.

Deutsch. *Archiv für Elektrotechnik* (Berlin, Germany), volume 2, 1913–14, pages 435–42.

395. Über die Angenähärte Bestimmung der Kapazität aus dem Kraftlinienbild Eines Parallelleben Elektrostatischen Feldes, **J. Spielrein.** *Archiv für Elektrotechnik* (Berlin, Germany), volume 10, 1922, pages 371–3.

396. Eines Verfahren zur Untersuchung des Magnetischen Feldes Stromdurchflossener Leitersysteme von Beliebiger Querschnittsform, **W. Kraemer.** *Elektrotechnische Zeitschrift* (Berlin, Germany), volume 53, 1931, pages 9–10.

397. An Experimental Determination of Air-Gap Reluctances, **C. H. Smoot.** Western Society of Engineers *Transactions*, volume 10, 1905, pages 500–08; discussion, pages 508–11.

398. The Measurement of Capacity by Analogy, **W. Cramp.** *World Power*, volume 2, 1924, pages 267–73.

399. A Quantitative Experimental Method of Mapping Equipotential Lines and Its Application to Electric Precipitator Problems, **A. W. Simon, L. C. Kron.** *Review of Scientific Instruments*, volume 1, 1930, pages 527–36.

400. On Plotting Electric Fields in Mixed Dielectrics, **J. F. T. Young.** *Proceedings and Transactions* Royal Society of Canada (Ottawa, Ontario) [3], volume 25, section 3, 1931, pages 185–9.

401. Determining Field Distribution by Electronic Methods, **E. D. McArthur.** *Electronics*, volume 4, 1932, pages 192–4.

402. Two Methods of Mapping Flux Lines, **F. W. Godsey, Jr.** AIEE Transactions, volume 54, 1935, October section, pages 1032–6.

403. Potential Gradient and Flux Density, Their Measurement by an Improved Method in Irregular Electrostatic and Magnetic Fields, **J. F. H. Douglas, E. W. Kane.** AIEE Transactions, volume 43, 1924, pages 982–8; discussion, page 989.

404. Einfache Experimentelle Bestimmung der Kapazitäten Beim Vorhandensein Beliebig Vieler Leiter, **J. Labus.** *Archiv für Elektrotechnik* (Berlin, Germany), volume 18, 1927, pages 40–8.

405. Experimental Solutions of Electrostatic Problems, **J. Labus.** *General Electric Review*, volume 32, 1929, pages 383–9, 548–51.

405a. Experimentelle Untersuchung Elektrostatischer Felder, **J. Labus.** *Archiv für Elektrotechnik* (Berlin, Germany), volume 25, 1931, pages 17–20.

406. The Fluxgraph, **P. G. Weiller.** *Electronics*, volume 15, May 1942, pages 52–3.

406a. Electro-Optical Field Mapping, **H. Mueller.** *Journal* Optical Society of America, volume 31, 1941, pages 286–91.

407. Graphische Methode zur Bestimmung des Kraft Linienverlaufes in der Luft, **T. Lehmann.** *Elektrotechnische Zeitschrift* (Berlin, Germany), volume 30, 1909, pages 995–8, 1019–22.

408. Détermination Graphique des Champs Magnétiques Laplaciens et Tourbillonnaires à Linges de Flux Planes, **T. Lehmann.** *Revue Générale de l'Électricité* (Paris, France), volume 11, 1923, pages 395–403.

409. Das Magnetische Feld in den Lufträumen Elektrischer Maschinen, **R. Richter.** *Archiv für Elektrotechnik* (Berlin, Germany), volume 11, 1922, pages 85–108.

410. Essai sur la Réfraction du Champ Électrique, **H. Stauffer.** *Revue Générale de l'Électricité* (Paris, France), volume 16, 1924, pages 1019–23.

411. The Graphical Estimation of Magnetic Field Surrounding a System of Conductors, **W. F. Cooper.** *World Power*, volume 3, 1925, pages 26–30.

412. Fundamental Theory of [Magnetic] Flux Plotting, **A. R. Stevenson.** *General Electric Review*, volume 29, 1926, pages 797–804.

413. Mapping Magnetic and Electrostatic Fields, **A. D. Moore.** *Electric Journal*, volume 23, 1926, pages 355–62.

414. Graphical Determination of Magnetic Fields Practical Applications to Salient-Pole Synchronous-Machine Design, **Robert W. Wieseman.** AIEE Transactions, volume 46, 1927, pages 141–54.

415. Graphical Determination of Magnetic Fields Comparison and Calculations and Tests, **E. E. Johnson, C. H. Green.** AIEE Transactions, volume 46, 1927, pages 136–40.

416. Graphical Determination of Magnetic Fields, **A. R. Stevenson, R. H. Park.** AIEE Transactions, volume 46, 1927, pages 112–35.

417. Graphical Flux Mapping, **J. F. Calvert, A. M. Harrison.** *Electric Journal*, volume 25, 1928, pages 147–50, 179–82, 246–9, 362–5, 399–401, 510–13.

418. An Accuracy Test for Flux-Plotting Methods, **R. B. Wright, N. F. Tsang.** *General Electric Review*, volume 32, 1929, pages 149–51.

419. Electrostatic-Field Analysis—A Graphical Method, **M. G. Leonard.** *Electric Journal*, volume 31, 1934, pages 471–4.

420. [Electric] Field Plotting in Nonuniform Media, **M. G. Leonard.** *Electric Journal*, volume 32, 1935, pages 31–3.

421. Graphical Field-Plotting Methods in Engineering, **Hillel Poritsky.** AIEE Transactions, volume 57, 1938, pages 727–32.

422. Electric and Magnetic Fields (second edition), **S. S. Attwood.** John Wiley and Sons, Inc., New York, N. Y., 1941.

423. The Current-Carrying Capacity of Solid Bare Copper and Aluminum Conductors, **S. W. Melsom, H. C. Booth.** Institution of Electrical Engineers (London, England) *Journal*, volume 62, 1923–24, pages 909–15. Discussion, volume 63, 1924–25, pages 203–06.

424. Current-Carrying Capacity of Bare Cables, **W. M. Woll, J. A. Gable.** *Electric Journal*, volume 23, 1926, pages 557–9.

425. Current-Carrying Capacity of Wires and Cables, **G. E. Luke.** *Electric Journal*, volume 20, 1923, pages 127–30.

426. Heating and Current-Carrying Capacity of Bare Conductors for Outdoor Service, **O. R. Schurig, C. W. Frick.** *General Electric Review*, volume 33, pages 141–57.

427. Emissivity of Heated Surfaces, **W. Wilson.** *Beama Journal* (London, England), volume 43, 1938, pages 91–5.

428. Effect of Bus-Bar Insulation on Heat Dissipation, **R. J. Coe.** *Electrical World*, volume 101, 1933, pages 223–4.

429. Vergleich der Erwärmung von Blanken und Isolierten Zylindrischen Leitern, **W. Brügger.** Association Suisse des Électriciens *Bulletin* (Zurich, Switzerland), volume 15, 1935, pages 412–17.

430. Current-Carrying Capacity of Bare Cylindrical Conductors for Indoor and Outdoor Service, **C. W. Frick.** *General Electric Review*, volume 34, 1931, pages 464–71.

431. Current-Carrying Capacity of Bus Bars, **H. W. Papst.** *Electrical World*, volume 94, 1929, pages 569–72.

432. Composite Tubular Bus Bars, **H. W. Papst.** *Electric Journal*, volume 31, 1934, page 338.

433. Bare Conductor for Bus Bars: Tubular and Laminated. *Electrical Times* (London, England), volume 100, 1941, pages 127–8.

434. Sur la Capacité des Barres Omnibus, **A. R. Garnier.** *L'Industrie Électrique* (Paris, France), volume 32, 1923, pages 266–70.

435. The Rating of Copper Conductors, **A. Bannister.** *Metropolitan-Vickers Gazette* (Manchester, England), volume 15, 1934, pages 57–60.

436. Report on Current-Carrying Capacity of Copper Bus Bars—60 Cycles. National Electric Light Association, Great Lakes Division, report of the electrical apparatus committee, 1927–28, appendix 3.

437. Current Capacities of Copper Bars. *Electrical World*, volume 92, 1928, pages 407–08. (Abstract of reference 436.)

438. Dimensions of Bus Bars, **M. Freimark.** *Electrical World and Engineering*, volume 44, 1904, pages 906–07.

439. Current Capacity of Copper Bus Bars, **F. M. Billhimer.** *Electric Journal*, volume 15, 1918, pages 94–6.

440. Calculations on High-Tension Plant, **H. Langrehr.** Allgemeine Elektrizitäts Gesellschaft *Progress* (Berlin, Germany), volume 4, 1928, pages 343–50.

441. Calcul et Détermination des Barres Omnibus, **R. Beyaert.** *Électricien* (Paris, France), volume 62, 1931, pages 434–8.

442. Interlaced Bus Design Solves Space Problem, **G. E. Tennant.** *Electrical World*, volume 114, 1940, pages 991–2, 1069.

443. "Electrical Conductors" Abstract, **C. Dannatt.** *Electrical Review* (London, England), volume 126, 1940, page 371.

444. Standard Bus-Bar Ratings Adopted, *Electrical World*, volume 81, 1923, pages 48–9.

445. Laminated Copper Connections, With Particular Reference to the Phase Grouping of Bars. *Electrical Times* (London, England), volume 94, 1938, pages 245–6.

446. Conductors for Heavy Alternating Currents, **D. I. Bohn, H. W. Papst.** *Power*, volume 74, 1931, pages 171–3. Also *Iron and Steel Engineer*, June 1931, page 253.

447. Current Ratings for Electrical Conductors. Physical Properties and Technical Data. Anaconda Wire and Cable Company, New York, N. Y., 1942. Anaconda publication *C*-51.

448. Carrying Capacities of Enclosed Busses, **A. P. Fugill.** *Electrical World*, volume 99, 1932, pages 539–40.

449. Cooler Busses With Vents, **E. A. Childerhose, H. P. Turner.** *Electrical World*, volume 109, 1938, pages 711, 791.

450. Bus-Bar Capacity Not Always the Same, **A. G. Von Normann.** *Electrical West*, volume 91, November 1944, pages 61–2.

450a. Temperature Correction for Short Conductors, **J. J. Taylor.** *Electrical World*, volume 122, November 25, 1944, page 98; December 23, 1944, page 104.

451. Short-Time Current-Carrying Capacity of Copper Wire, **E. R. Stauffacher.** *General Electric Review*, volume 31, 1928, pages 326–7.

452. Short-Time Fusing of Copper Cables. **R. J. Coe.** *Electrical World*, volume 101, 1933, pages 205–06.

453. Über die Berechnung der Kurzschlusser Wärmung, **A. Avramescu.** *Elektrotechnische Zeitschrift* (Berlin, Germany), volume 59, 1938, pages 985–8.

454. Zur Bestimmung der Erwarmung der Schutzdrosselspulen bei Kurzzeitiger Überlastung, **F. Fabinger.** *Elektrotechnik und Maschinenbau* (Vienna, Austria), volume 44, 1926, pages 149–57.

455. Belastungsstrom und Belastungszeit der Kupferleitungen bei Kurzschluss und bei Grosser Überlast, **R. Edler.** *Elektrotechnik und Maschinenbau* (Vienna, Austria), volume 43, 1925, pages 329–36.

456. Erwärmung von Leitern bei Kurzen Belastungszeiten und bei Kurzschlüssen, **G. Guth, L. M. Grünberg.** Schweizerischer Elektrotechnischer Verein *Bulletin* (Zurich, Switzerland), volume 18, 1927, pages 205–25.

457. Short-Circuit Risks on High-Tension Networks, **J. Biermann.** Allgemeine Elektrizitäts Gesellschaft *Progress* (Berlin, Germany), volume 4, 1928, pages 91–100.

458. Kurzschlüsserwärmung in Kraftwerken und Überlandnetzen, **L. Binder.** *Elektrotechnische Zeitschrift* (Berlin, Germany), volume 37, 1916, pages 589–90, 606–09.

459. Temperaturverlauf in Leitern bei Kurzzeitigen Strom- und Spannungsänderungen, **H. Prinz.** *Archiv für Elektrotechnik* (Berlin, Germany), volume 31, 1941, pages 682–4.

460. Temperature Stresses Under Short-Circuit Conditions, **H. S. Holbrook.** *Electrical Review* (London, England), volume 90, 1922, pages 512–13.

461. Temperaturabhängigkeit des Elektrischen Widerstandes von Kupfer und Aluminium bis zum Schmelzpunkt, **A. Avramescu.** *Zeitschrift für Technische Physik* (Leipzig, Germany), volume 20, 1939, pages 26–30.

461a. Temperaturabhängigkeit der Wahren Spezifischen Wärme X von Leitungskupfer und Leitungsaluminum bis zum Schmelzpunkt, **A. Avramescu.** *Zeitschrift für Technische Physik* (Leipzig, Germany), volume 20, 1939, pages 213–17.

462. Sul Coefficiente di Temperatura Dell. Alluminio **O. Scarpa.** *Alluminio* (Milan, Italy), volume 2, 1932, pages 317–22.

463. Sul Valore Medio de Assegnare al Coefficiente di Temperature Della Resistenza Elettrica dei Conduttori D'Alluminio, **O. Scarpa.** *Alluminio* (Milan, Italy), volume 4, 1935, pages 145–8.

464. L'Azione Della Dilatazione Termica Sulla Resistenza Elettrica dei Conduttori e la sua Influenza Sulle Misure dei Coefficienti di Temperatura Della Resistivita, **O. Scarpa.** *Alluminio* (Milan, Italy), volume 3, 1934, page 63.

465. The Distribution of Temperature in Alternating-Current Conductors, **M. J. O. Strutt.** *Philosophical Magazine* (London, England) [7], volume 5, 1928, pages 904–14.

466. Aluminum Bus Bars Resist Power Arcs, **J. D. Porter.** *Electrical World*, volume 98, 1931, pages 104–05.

467. Über Eine Zerstörung von Stromwandlerzufuhrungsschienen aus Zink, **U. Retzoe.** *Werkstattstechnik* (Berlin, Germany), volume 18, 1924, pages 257–60.

468. Devise Substitute for Tubular Bus. *Electrical World*, volume 118, 1942, pages 968, 970.

469. Temperature Rise and Losses in Solid Structural Steel Exposed to the Magnetic Fields From A-C Conductors, **O. R. Schurig, H. P. Kuehni.** AIEE Transactions, volume 45, 1926, pages 184–202; discussion, page 202.

470. A 7,000-Ampere Station Bus, **H. L. Unland, W. B. Morton, V. R. Bacon.** AIEE Transactions, volume 53, 1934, June section, pages 994–1004.

471. New Channel Bus Design Solves Station Limitations, **W. B. Morton, H. L. Unland.** *Electrical World*, volume 104, 1934, pages 18–21.

472. Temperature Rise in Steel Adjacent to A-C Conductors, **S. C. Killian.** *Delta-Star Magazine*, July–August 1941.

473. Equalizing Currents in Separate Lines of Complex Bus Bars, **V. G. Egorov.** *Elektrichestyo* (Moscow, Soviet Union), 1930, pages 244–5.

473a. Current-Balancing Reactors for Turbine Generators, **W. K. Boice.** *Power Plant Engineering*, volume 48, October 1944, pages 94, 120.

474. Mechanical Forces in Magnetic Fields, **C. P. Steinmetz.** AIEE Transactions, volume 30, 1911, pages 367–85; discussion, pages 392–3.

475. Mechanical Force Between Electric Circuits, **R. E. Doherty, R. H. Park.** AIEE Transactions, volume 45, 1926, pages 240–50; discussion, pages 250–2. AIEE Journal, volume 45, March 1926, pages 231–5.

476. Mechanical Forces Between Electric Fields and Saturated Magnetic Fields, **V. Karapetoff.** AIEE Transactions, volume 46, 1927, pages 563–9.

477. Electromagnetic Problems in Electrical Engineering (book), **B. Hague.** Oxford University Press, Oxford, England, 1929.

478. Repulsion Between Strap Conductors, **H. B. Dwight.** *Electrical World*, volume 70, 1917, pages 522–4.

478a. Stromkräfte Zwischen Parallelen Leitern von Rechteckigem Querschnitt, **A. Duschek.** *Archiv für Elektrotechnik* (Berlin, Germany), volume 37, 1943, pages 293–301.

479. Formulas for Calculating Short-Circuit Stresses in Bus Supports for Rectangular Tubular Conductors, **Thomas James Higgins.** AIEE Transactions, volume 61, 1942, August section, pages 578–80.

480. New Formulas for Calculating Short-Circuit Stresses in Bus Supports for Rectangular Tubular Conducto s, **T. J. Higgins.** *Journal of Applied Physics*, volume 14, 1943, pages 151–4.

481. Formulas for Calculating Short-Circuit Forces Between Conductors of S ructural Shape, **Thomas James Higgins.** AIEE Transactions, volume 62, 1943, October section, pages 659–63.

482. Formulas for Calculating Short-Circuit Forces Between Channels Located Back to Back, **Thomas James Higgins.** AIEE Transactions, volume 64, 1944, October section, pages 710–12.

483. Calculation of Short-Circuit Currents in A-C Networks, **W. M. Hanna.** *General Electric Review*, volume 40, 1937, pages 125–30, 189–96, 287–91, 383–8.

484. Short-Circuit Conditions on Large Industrial Low-Voltage Distribution Networks, **T. S. G. Seaword.** Institution of Electrical Engineers (London, England) *Journal*, volume 88, 1941, part 1, pages 113–19.

485. Short-Circuit Reductions, **C. E. Moorhouse.** Institution of Engineers of Australia *Journal* (Sydney, Australia), volume 14, 1942, pages 15–24.

486. Short-Circuit Currents: How Such Currents in Low-Voltage A-C Systems Can Be Reliably Calculated, **A. E. Anderson.** *General Electric Review*, volume 46, 1943, pages 316–19, 399–401.

487. Calculation of Fault Currents in Industrial Plants, **R. C. Schulze.** Electrical Engineering, volume 60, June 1941, pages 271–9.

488. Theoretical Investigation of Electric Transmission Systems Under Short-Circuit Conditions, **I. W. Gross.** AIEE Transactions, volume 34, 1915, pages 23–67; discussion, pages 68–84.

489. Repulsion Between Bus Bars, **S. G. Leonard, C. R. Riker.** *Electric Journal*, volume 14, 1917, pages 491–3.

490. Magnetomechanical Loads on Bus Supports, **L. N. Robinson.** AIEE Transactions, volume 42, 1923, pages 1020–4; discussion, pages 1025–8.

491. Unsymmetrical Sinusoidal Currents; Their Influence on Electromagnetic Forces, **S. A. S. Stigant, H. M. Lacey.** *Electrical Times* (London, England), volume 71, 1927, pages 574–5.

492. Die Gefahren der Anfangskurzschlusstrome bei Grösseren Kraftwerken, **D. Probst.** Allgemeine Elektrizitäts Gesellschaft (Berlin, Germany) special publication St. 1005a.

493. Die Stromkraft bei Parallelen und Konzentrischen Leitern, **W. Beetz.** *Elektrotechnik und Maschinenbau* (Vienna, Austria), volume 48, 1930, pages 761–3.

494. Calcul des Efforts Électrodynamiques Dans les Barres H. T. et B. T. des Centrales et Sous-Stations, **R. Beyaert.** *Électricien* (Paris, France), volume 62, 1931, pages 170–3.

495. Practical Methods of Calculating the Value and Effects of Short-Circuit Currents in Alternating-Current Networks, **I. Herlitz.** Allmanna Svenska Elektriska Aktiebolaget (ASEA) *Journal* (Stockholm, Sweden), volume 10, 1933, pages 2–9.

496. Fault Currents Low With Heavy Power Capacity, **H. W. Papst.** *Electrical World*, volume 102, 1933, pages 208–09.

497. Destructive Voltage Rises on Low-Tension Bus Bars, a Suggestion, **H. P. McGraw.** Institution of Electrical Engineers (London, England) *Journal*, volume 72, 1933, pages 402–12. Discussion, volume 73, 1933, page 318; volume 89, 1942, page 162. (See latter discussion for mention of error invalidating conclusions advanced in this paper.)

498. Mechanical Stresses under Short-Circuit Conditions—Some Practical Considerations, **W. H. Miller.** *Electrician* (London, England), volume 118, 1937, pages 578–81.

499. Forces on Conductors During Short Circuit, **W. A. Tripp.** *Electric Journal*, volume 34, 1927, pages 493–7.

500. Elektromagnetische Kraftwirkungen Grosser Ströme Im Innern von Stromleitern und Deren Berechnung, **P. Bachert.** *Elektrotechnische Zeitschrift* (Berlin, Germany), volume 61, 1940, pages 51–2; discussion, page 1204.

501. Fault Voltage Drop and Impedance at Short-Circuit Currents in Low-Voltage Circuits, **O. R. Schurig.** AIEE Transactions, volume 60, 1941, pages 479–86.

502. Mechanical Forces on Busses Due to Fault Currents, **S. C. Killian.** *Electrical World*, volume 118, 1942, pages 1938–40.

503. Forces Due to Short-Circuit Currents, **S. C. Killian.** *Delta-Star Magazine*, January–February, March–April, 1943.

504. The Switchgear Handbook, Volume 1—Apparatus, I. Pitman and Sons, London, England; New York, N. Y.; 1939. (See Chapter 1.)

505. Calculation of Electromagnetic Forces on a Conductor, **J. F. Calvert.** *Electric Journal*, volume 28, 1931, pages 108–10, 116.

506. The Calculation of Magnetic Attraction by the Aid of Magnetic Figures, **T. Lehmann.** AIEE Transactions, volume 45, 1926, pages 383–90; discussion, pages 390–4.

507. Forces Acting on Conductors Near Iron, **B. Hague.** *World Power*, volume 5, 1926, pages 124–30, 205–11.

508. Forces on Magnetically Shielded Conductors, **J. H. Morecroft, Alva Turner.** AIEE Journal, volume 48, January 1929, pages 25–7.

509. Mechanical Stresses Between Electrical Conductors, **D. C. Randall.** *Electric Journal*, volume 14, 1917, pages 283–7.

510. Electromagnetic Forces Set Up Between Current-Carrying Conductors During Short-Circuit, **G. L. E. Metz.** Institution of Electrical Engineers (London, England) *Journal*, volume 75, 1934, pages 527–41. Discussion, volume 76, 1935, pages 455–8.

511. Mechanical Forces on Bus Bars and Short-Circuit Conditions, **C. H. Van Aspern.** AIEE Transactions, volume 42, 1923, pages 1091–110.

512. Electromagnetic Forces on Conductors With Bends, Short Lengths, and Crossovers, **C. W. Frick.** *General Electric Review*, volume 36, 1933, pages 232–42.

513. Electromagnetic Forces on Conductors, **J. W. Bayles, A. Donkin.** *World Power*, volume 19, 1933, pages 216–18.

514. Short-Circuit Forces on Reactor Supports, **R. E. Doherty, F. H. Kierstead.** AIEE Transactions, volume 42, 1923, pages 552–61; discussion, pages 566–70. AIEE *Journal*, volume 42, August 1923, pages 832–41; discussion, August 1923, pages 842–4; December 1923, pages 1334–8.

515. Mechanical Stresses in Bus-Bar Support, **O. R. Schurig, M. F. Sayre.** AIEE Transactions, volume 44, 1925, pages 217–37.

516. Elektrodynamiska Krafter hos Strömförande Ställverksskenor, **F. Dahlgren.** *Teknisk Tidsskrift Elektroteknisk* (Copenhagen, Denmark) [7], volume 55, 1925, pages 117–21.

517. Electrodynamical Forces in Bus Bars, **F. Dahlgren.** *Electrical World*, volume 86, 1925, pages 473–4.

518. Short-Circuit Forces on Bus Bars and Their Supports in Cellular Switchgear Structures, **E. E. I. Pilcher.** *World Power*, volume 24, 1935, pages 118–23, 190–2, 231–4.

519. Übersuchungen Über Elektrodynamische Beanspruchung, **M. F. Aebi.** *Schweizer Archiv für Angewandte Wissenschaft und Technik* (Solothurn, Switzerland), volume 7, 1941, pages 185–95.

520. Practical Calculation of Short-Circuit Stresses in Supports for Straight Parallel-Bar Conductors, **O. R. Schurig, C. W. Frick, M. F. Sayre.** *General Electric Review*, volume 29, 1926, pages 534–44.

521. Stresses in Bus Supports, **R. Tanberg.** *Electric Journal*, volume 24, 1927, pages 517–25.

522. Short-Cut Methods of Calculating Stresses in Bus Structures, **W. Specht.** *General Electric Review*, volume 31, 1928, pages 413–18.

523. Short-Circuit Stress Charts, **W. M. Edson.** *Electrical World*, volume 94, 1929, page 1125.

524. Effects Électrodynamiques de Courts-Circuits sur les Porcelaines Supports de Barres des Postes de Transformation, **H. Josse.** International Conference on Large High-Voltage Systems (CIGRE), *Compte Rendu des Travaux* (Paris, France), 1931, volume 1, pages 735–69.

525. Calcul des Forces Intérieures Développées Dans des Systemes Mécaniques Soumis À des Efforts Électrodynamiques, **A. Eigermann.** *Revue Générale de l'Électricité* (Paris, France), volume 35, 1934, pages 677–88.

526. Report on Bus Stresses Under Short-

Circuit Conditions, National Electric Light Association, Great Lakes Division, electrical apparatus committee (engineering section) Report, 1927–28, appendix 4.

527. Bus Stresses Under Short Circuits. *Electrical World*, volume 92, 1928, pages 564–5. (Abstract of reference 526.)

528. Stresses in Busses During Short Circuit, **H. W. Papst.** *Electric Journal*, volume 31, 1934, pages 322–3.

529. Extension of Metal-Clad Units and Flexible Bus-Support Features of 1932 Switchgear. *Electric Journal*, volume 30, 1933, page 10.

530. Short Circuit Opens Knife Switch, **S. Ein.** *Electrical World*, volume 101, 1933, page 233.

531. High-Current Tests on High-Tension Switchgear, **Philip Torchi.** AIEE Transactions, volume 40, 1921, pages 61–86; discussion, pages 87–96. AIEE *Journal*, volume 40, February 1921, pages 120–31.

532. Mechanical and Electrical Effects of Large Currents on High-Tension Switchgear, **C. C. Garrand.** Institution of Electrical Engineers (London, England) *Journal*, volume 60, 1922, page 387.

533. The Effect of High Currents on Disconnecting Switches, **H. C. Louis, C. T. Sinclair.** AIEE Transactions, volume 41, 1922, pages 271–81; discussion, pages 282–7. AIEE *Journal*, volume 41, April 1922, pages 267–77.

534. Die Beschleunigung der Oelschaltertraverse Durch Elektrodynamische Druckkräfte, **K. Keel.** Association Suisse des Électriciens *Bulletin* (Zurich, Switzerland), volume 22, 1931, pages 295–8.

535. Phénomènes Électrodynamiques des aux Courants Intenses Dans L'Appareillage, **C. Bresson.** *Revue Générale de l'Électricité* (Paris, France), volume 29, 1931, pages 13–30.

536. The Force on Repulsion in Disconnecting Switches, **H. B. Dwight.** *Electrical Review and Western Electrician*, volume 71, 1917, pages 684–6.

537. Calculation of Magnetic Force on Disconnecting Switches, **H. B. Dwight.** AIEE Transactions, volume 39, 1920, pages 1337–50, discussion, pages 1351–5. Abstract, AIEE *Journal*, volume 39, June 1920, pages 550–2.

538. Electromagnetic Forces on Current-Carrying Conductors, **W. F. Dunton.** *Journal of Scientific Instruments*, volume 4, 1926–27, pages 440–6.

539. Electromagnetic Forces (letter), **W. F. Dunton.** *Electrical Review* (London, England), volume 103, 1928, pages 541–2.

540. Electromagnetic Induction: Correct Enunciation of the Law—Its Importance in Circuit-Breaker Design, **W. F. Dunton.** *Electrician* (London, England), volume 105, 1930, pages 681–2.

541. Two Cases of Calculation of Mechanical Forces in Electric Circuits, **H. B. Dwight.** AIEE Transactions, volume 46, 1927, pages 570–2; discussion, pages 573–4. AIEE *Journal*, volume 46, November 1927, pages 1238–40.

541a. Bridge Measurements of Electromagnetic Forces, **A. C. Seletzky, G. L. Priday.** AIEE Transactions, volume 54, 1935, November section, pages 1149–52.

542. Magnetic Force in Disconnecting Switches, **H. B. Dwight.** *Electrician* (London, England), volume 87, 1921, pages 290–1.

3. Forces Acting on Disconnecting Switches, **Loebenstein.** *Electrical World*, volume 69, 1917, ges 504–05.

4. Mathematical Analysis of the Mechanical Forces Acting on Switches and Blades, **L. B. W. Jolley.** *Electrician* (London, England), volume 85, 1920, pages 646–7, 676–7.

545. Forces Acting on Disconnecting Switches, **L. B. W. Jolley.** *Electrical World*, volume 75, 1920, page 381.

546. Dynamische Kräfte bei Hochspannungstrennschaltern und Ölschaltern, **L. Kopec.** *Elektrotechnik und Maschinenbau* (Vienna, Austria), volume 43, 1925, pages 658–60.

547. The True Law of Electromagentic Induction, **W. F. Dunton.** *World Power* (London, England), volume 17, 1932, pages 169–72.

548. Selbstinduktion bei Einer Verformung des Leiterkreises, **R. Rühle.** *Elektrotechnische Zeitschrift* (Berlin, Germany), volume 54, 1933, pages 796–8, 843–5.

549. Reconciliation of Flux-Cutting and Flux-Linkage Methods of Calculation, **W. H. Miller.** *Electrician* (London, England), volume 112, 1934, pages 662–3.

550. Controversies in Electromagnetism. I-Magnetic Force and Magnetic Induction; II Polarity and Permeability—the Law of Electro-Magnetic Induction—Physical Lines of Induction, **W. Cramp.** *Electrician* (London, England), volume 121, 1938, pages 122–3; 151–3.

551. Einige Bemerkungen zur Berechnung der auf Bewegliche Leiterteile Wirkenden Kräfte, **J. Hak.** *Elektrotechnik und Maschinenbau* (Vienna, Austria), volume 47, 1929, pages 149–54.

552. A General Survey of the High-Tension Switchgear Field, **S. Ferguson.** Institution of Electrical Engineers (London, England) *Journal*, volume 64, 1925–26, pages 49–82.

553. Étude sur les Efforts Électrodynamiques Qui Peuvent Provoquer l'Ouverture d'un Sectionneur, **G. Souben.** *Revue Générale de l'Électricité* (Paris, France), volume 22, 1927, pages 665–71.

554. Contribution à l'Étude des Efforts Électrodynamiques et Mécaniques Agissant sur l'Équipage Mobile d'un des Joncteur dans l'Huile à Haute Tension, **J. Kuntz.** *Revue Générale de l'Électricité* (Paris, France), volume 45, 1939, pages 17–25.

555. Electromagnetic Forces Set Up Between Current-Carrying Conductors During Short-Circuit, **J. W. Bayles, A. Donkin.** Institution of Electrical Engineers (London, England) *Journal*, volume 76, 1935, pages 455–8.

556. Measurement of Energy Losses in Large Oil Switches, **B. G. Churcher, C. Dannatt.** *World Power* (London, England), volume 4, 1925, pages 314–19.

557. The Design of Low-Tension Switchgear, **W. Wilson.** *World Power* (London, England), volume 12, 1929, pages 321–7.

558. Magnetic Forces in a Rectangular Circuit, **F. F. Cleveland.** *Philosophical Magazine* (London, England), volume 21, 1936, pages 416–25.

559. The Utilization of Pipe for Outdoor Bus Work, **M. M. Samuels.** *Electrical World*, volume 70, 1917, pages 1236–7.

560. Copper Wires and Cables, **J. J. Keyes.** *Electric Journal*, volume 14, 1917, pages 451–5.

561. Design of Tubular Copper Busses, **V. R. Bacon.** *Electrical World*, volume 88, 1926, pages 1066–8.

562. Design of Bus Bars and Connections, **H. E. Hutter.** *Electrical Review* (London, England), volume 106, 1930, pages 859–61; volume 107, 1930, pages 209–11.

563. Le Calcul des Barres Omnibus Tubulaires aux Points de Vue Mécanique et Électrique, **R. Beyaert.** *Électricien* (Paris, France), volume 62, 1931, pages 348–53.

564. Tubular Bus Bars: Their Deflection Characteristics When Applied to Outdoor Substations, **A. M. Spruce.** *Electrical Review* (London, England), volume 112, 1933, page 484.

565. Bus Bars for Outdoor Substations, **A. M. Spruce.** *Engineer* (London, England), volume 158, 1934, pages 563–4, 599–600, 612–13.

566. Determining Sag in Copper-Tube Busses—Standard Iron-Pipe Sizes, **W. S. Sheering.** *Electric Journal*, volume 33, 1936, page 468.

567. Outdoor Substation Design. National Electric Light Association publication 164, 1931, pages 21–5.

568. Rapid Solution for Bus-Expansion Problem, **W. B. Morton.** *Electrical World*, volume 102, 1933, page 825.

569. Avoiding Severe Stresses in Busses, **R. E. Anderson.** *Electrical World*, volume 103, 1934, pages 287–8.

570. Flexible Joints in Bus Bars; Methods of Relieving Strain in Rigid Connections. *Electrical Times* (London, England), volume 86, 1934, pages 297–8.

571. Avoiding Severe Stress in Busses. *Electrical World*, volume 103, 1934, pages 287–8.

572. Expansion of Rigid Conductors. *Electrical Times* (London, England), volume 92, 1937, pages 785–6.

573. Rigid Conductor Expansion; Quick Estimation by Means of a Nomogram. *Electrical Times* (London, England), volume 95, 1938, page 810.

574. Concrete Bus-Structure Tests, **W. A. Kates.** *Electrical World*, volume 91, 1928, pages 1379–82.

575. Indoor Bus-Support Tests, **R. C. R. Schulze.** *Electrical World*, volume 90, 1927, pages 311–3.

576. Bus Bars With Special Reference to the Use of Aluminum, **S. E. Van Dorg.** *Australasian Electrical and Radio Times* (Melbourne, Australia), volume 8, 1929, pages 35–39.

577. Berakning av Motstånd och Stålvinduktion hos Ledare, Omgivna med Metallmantal, **H. Pleijel.** Dissertation, Uppsala, Sweden, 1906.

578. The Resistance of Bimetallic Conductors and Tubes at High Frequency, **W. N. Kuleshow.** *Elektrotechnicky Svyas Ceskoslovensky* (Prague, Czechoslovakia), volume 5, 1941, pages 37–45.

579. Current Distribution in Stranded Conductors for Alternating Current, **E. Kluss.** *Archiv für Elektrotechnik* (Berlin, Germany), volume 35, 1941, pages 616–26.

580. Coppered-Steel Wire for Carrier-Frequency Overhead Lines, **F. Klein.** *Telegraphen-Fernsprech- Funk- und Fernseh- Technik* (Berlin, Germany), volume 31, 1942, pages 210–12.

581. Zur Stromverdrängung Beim Koaxialen Kabel, **W. Wiechowski.** *Hochfrequenztechnik und Elektroakustik* (Leipzig, Germany), volume 59, 1942. pages 174–9.

582. Indoor Bus Bars. *Power and Works Engineer* (London, England), volume 39, 1944, pages 133–4.

583. Elektromagnetische Wellen an Einem Draht mit Isolierender Dielektrischer Hulle, **F. Zaviska.** Ceska Společnost Nauk, *Vestnik* (Prague, Czechoslovakia), 1934, pages 1–16.

Field Tests and Performance of Heavy-Duty High-Speed 138-Kv Circuit Breakers—Oil and Air-Blast

PHILIP SPORN
FELLOW AIEE

HARRY P. ST. CLAIR
FELLOW AIEE

Synopsis: The heavy expansion brought about on the Central System of the American Gas and Electric Company in response to demands for power during the defense and war periods has produced a requirement for circuit-breaker rupturing duties close to 3,500 megavolt-amperes. In order to test the interrupting performance and reliability of two types of 138-kv 3,500-megavolt-ampere circuit breakers, the first an oil, the second an air-blast design, and also to explore faster reclosing cycles than now offered by the most improved oil circuit breakers, high-capacity field tests were carried out at the Philo Plant of The Ohio Power Company. In these tests, involving 20 interruptions on each breaker, there has been accomplished for the first time successful interruption of a full three-phase short circuit of 3,500 megavolt-amperes with three-cycle interruption and with 13-cycle reclosure. The results of these tests, it is believed, indicate that a goal of 5,000 megavolt-amperes with 12-cycle reclosure definitely is attainable.

THIS paper deals with the field tests of a 138-kv 800-ampere 3,500-megavolt-ampere three-cycle oil circuit breaker and a 138-kv 800-ampere 3,500-megavolt-ampere three-cycle air-blast circuit breaker. The development of these breakers was undertaken because of need for breakers of such high rupturing capacity on a number of interconnected power systems in the United States, included among which is the Central System of the American Gas and Electric Company. The search for higher opening (and, as will be brought out later, reclosing) speeds is part of a program undertaken close to ten years ago to improve high-voltage transmission-system performance by increasing speed of circuit opening and decreasing the time required for an ultra-rapid reclosing cycle.[1,2,3]

Only a comparatively short time ago there were described before the Institute the results of field tests and the performance of a 1,500-megavolt-ampere multi-break 138-kv oil circuit breaker and of a high-speed 1,500-megavolt-ampere air-blast circuit breaker.[4,5] These breakers, it is true, were tested at that time on a system having close to 2,000-megavolt-ampere rupturing-duty requirement. The fact that, under present conditions, rupturing duties of close to 3,500-megavolt-amperes are required would be surprising were it not for the fact that expansion at a much more than normal rate on this as well as on other systems, in response to demands for power during the defense and war periods, has taken place. But the important thing that this development has brought home is the fact that rupturing duties of a totally different order than any considered likely to be needed heretofore have been encountered on existing power systems. Furthermore, that trend does not seem to have run its course: there is reason to believe that further growth in short-circuit duty is bound to take place as long as transmission networks continue to be expanded in response to growth of system loads.

Specific and Broad Objectives of the Tests

The specific objective sought by the tests described herein was to test the interrupting-capacity performance and reliability of:

1. A 138-kv 800-ampere 3,500-megavolt-ampere, three-cycle opening 20-cycle reclosing oil circuit breaker.
2. A 138-kv 800-ampere 3,500-megavolt-ampere three-cycle opening 20-cycle reclosing air-blast circuit breaker.

Breakers of the stated rating, as has been pointed out, now are required on the Central System of the American Gas and Electric Company with which the authors are associated.

From a broader standpoint, corollary objectives were desired. Among these the most important are the following:

1. To explore the limits of improved oil-circuit-breaker design made possible by the further development of the principle of the self-generating pressure-type interrupter.
2. To test the ability of an air-blast design to meet the rupturing-duty performance of the highest development reached by the oil circuit breaker.
3. To explore the possibilities of a faster reclosing cycle on a 138-kv system than that offered by the oil circuit breaker even in its most improved form.

All these seemed natural and proper for the Central System of the American Gas and Electric Company in view of the needs outlined above and in view of the background of experience and of co-operation in the development of more reliable and improved high-voltage circuit-interrupting devices described previously, and going back almost two decades.[6,7]

System Setup During Tests

Between 1930 and 1938, and even as late as 1941, the short-circuit capacity available at Philo was not increased greatly even though comparatively substantial changes had been made on other parts of the system. In each of the three previous series of tests, therefore, 1930, 1938, and 1941, the short-circuit duties obtained lay in the range of from 1,500 to 2,000 megavolt-amperes. The general layout of the system as it was in 1938 is shown in Figure 4 of the paper[4] describing tests made at that time.

At the time of the present tests, however, a heavy program of expansion, some of it already under construction in 1941, had been completed, with the result that the short-circuit capacities available at Philo were far greater than for any of the previous tests. The extent of this expansion can be seen by comparing the system shown in Figure 4 of the 1938 paper[4] with Figure 1 of this paper which shows the present system facilities, most of which were available for the tests herein described. While the additional units at Philo, along with the third transmission circuit from Philo to Canton, contributed by far the greater part of the increased short-circuit duty, some increase also was obtained from other major additions as follows:

GENERATORS

Philo	2-94,445 kva
Cabin Creek	2-94,445 kva
Twin Branch	1-88,125 kva 1-94,445 kva
Windsor	1-66,667 kva
Glen Lyn	1-111,111 kva
Logan	1-50,000 kva

SYNCHRONOUS CONDENSERS

Canton	1-36,000 kva 2-20,000 kva
Muncie	1-20,000 kva
Lima	1-20,000 kva
Danville	1-20,000 kva

Short-circuit capacities on the system likewise are affected to some extent by corresponding growth in several neighboring systems which are tied in by interconnections at various points. Additional interconnections also have been established, notably, between Muncie, Indiana, and Trenton, Ohio, and be-

---

Paper 45-43, recommended by the AIEE committee on protective devices for presentation at the AIEE winter technical meeting, New York, N. Y., January 22–26, 1945. Manuscript submitted December 6, 1944; made available for printing January 3, 1945.

PHILIP SPORN is vice-president and chief engineer and HARRY P. ST. CLAIR is system planning engineer, both of the American Gas and Electric Service Corporation, New York, N. Y.

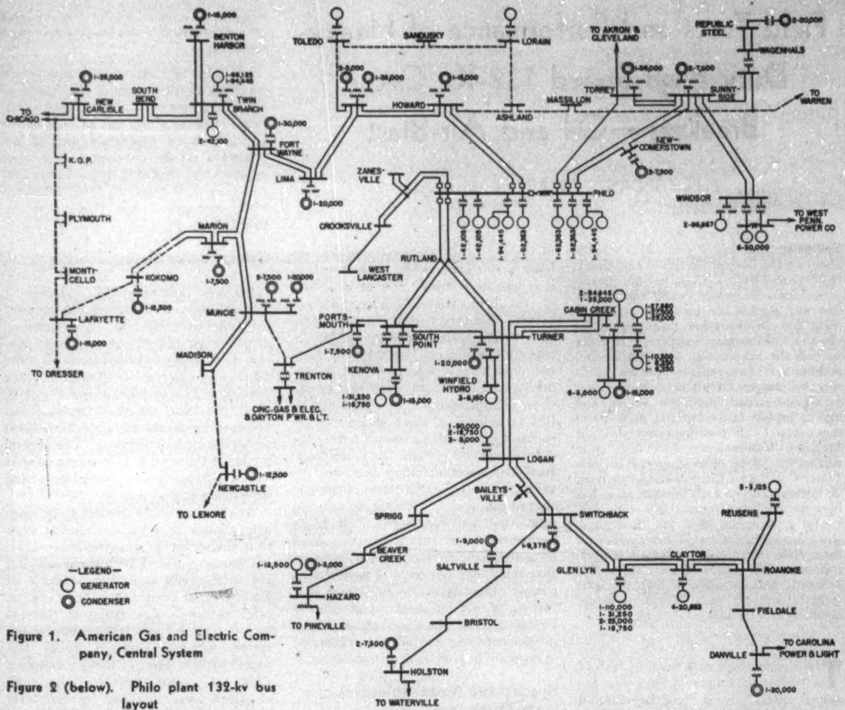
BENTON HARBOR
TOLEDO
SANDUSKY
LORAIN
TO AKRON & CLEVELAND
REPUBLIC STEEL
WAGENHALS
TO CHICAGO
NEW CARLISLE
SOUTH BEND
TWIN BRANCH
FORT WAYNE
HOWARD
ASHLAND
MASSILLON
TORREY
SUNNYSIDE
TO WARREN
NEWCOMERSTOWN
LIMA
ZANESVILLE
PHILO
K.O.P.
PLYMOUTH
CROOKSVILLE
WINDSOR
TO WEST PENN. POWER CO
MARION
RUTLAND
WEST LANCASTER
MONTICELLO
KOKOMO
MUNCIE
LAFAYETTE
PORTSMOUTH
SOUTH POINT
TURNER
CABIN CREEK
KENOVA
MADISON
TRENTON
WINFIELD HYDRO
TO DRESSER
CINC. GAS & ELEC. & DAYTON P'WR. & LT.
LOGAN
NEWCASTLE
TO LENORE
BAILEYSVILLE
REUSENS
SPRIGG
SWITCHBACK
BEAVER CREEK
SALTVILLE
GLEN LYN
CLAYTOR
ROANOKE
HAZARD
FIELDALE
TO PINEVILLE
BRISTOL
DANVILLE
TO CAROLINA POWER & LIGHT
HOLSTON
TO WATERVILLE
—LEGEND—
GENERATOR
CONDENSER

Figure 1. American Gas and Electric Company, Central System

Figure 2 (below). Philo plant 132-kv bus layout

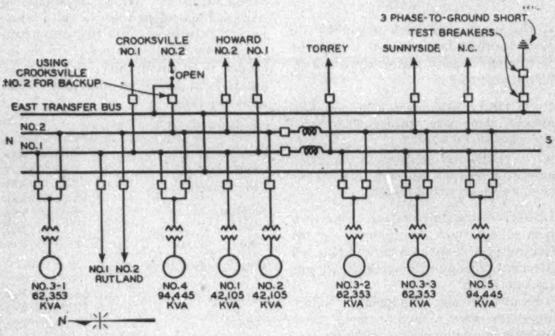
3 PHASE-TO-GROUND SHORT
TEST BREAKERS
CROOKSVILLE
NO.1
NO.2
HOWARD
NO.2
NO.1
TORREY
SUNNYSIDE
N.C.
USING CROOKSVILLE NO. 2 FOR BACKUP
OPEN
EAST TRANSFER BUS
NO. 2
NO. 1
N
S
NO.1
NO.2
RUTLAND
NO.3-1
62,353
KVA
NO.4
94,445
KVA
NO.1
42,105
KVA
NO.2
42,105
KVA
NO.3-2
62,353
KVA
NO.3-3
62,353
KVA
NO.5
94,445
KVA
N

tween Hazard, Kentucky, and the Tennessee Valley Authority system at Norris Dam.

As previously mentioned, Figure 1 represents the system as it is today and substantially as set up for the 1944 tests. While not appreciably affecting the short-circuit capacity at Philo, it should be pointed out that not quite all of the generating units indicated in Figure 1, particularly at points some distance from Philo, were in service at the time of the tests. Also, the Portsmouth–Trenton line, which would have contributed a slight increase at Philo, was not completed at the time of the tests.

As indicated in Figure 1, the 132-kv bus at Philo is divided into two sections separated by means of a 132-kv bus-tie reactor, the function of which is to limit the short-circuit duty on either bus section to values below 2,500 megavolt-amperes. With this reactor by-passed, the total short-circuit duty with all generators and lines in service would approach 4,000 megavolt-amperes. In the actual test setup, however, somewhat less than this maximum value was obtained since it was necessary to isolate one of the 42,100-kva generators to furnish an independent power supply to an important load area closely adjacent to Philo. In spite of this limitation, a maximum short-circuit value of 3,500 megavolt-amperes actually was obtained on one test, as shown in Table IV.

Switching and Physical Arrangements

While in Figure 1 the Philo 132-kv bus is shown divided into two sections separated by a single reactor, the actual layout, as shown in Figure 2, provides four main bus sections, two on the north and two on the south side of the reactor, with differential protection for each of the four

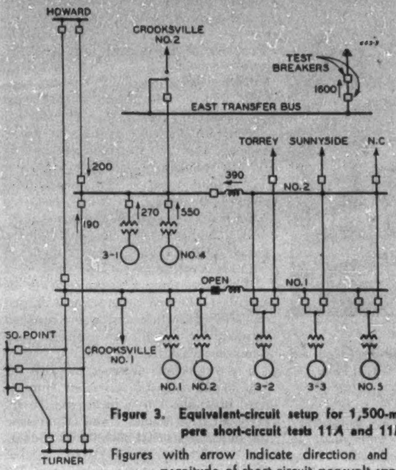
HOWARD
CROOKSVILLE NO.2
TEST BREAKERS
1600
EAST TRANSFER BUS
TORREY
SUNNYSIDE
N.C
200
390
NO.2
270
550
190
3-1
NO.4
OPEN
NO.1
SO. POINT
CROOKSVILLE NO.1
NO.1
NO.2
3-2
3-3
NO.5
TURNER

Figure 3. Equivalent-circuit setup for 1,500-megavolt-ampere short-circuit tests 11*A* and 11*B*

Figures with arrow indicate direction and approximate magnitude of short-circuit megavolt-amperes

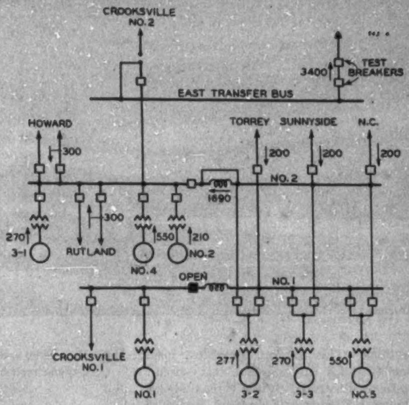
CROOKSVILLE NO.2
3400
TEST BREAKERS
EAST TRANSFER BUS
HOWARD
300
TORREY
SUNNYSIDE
N.C.
200
200
200
NO.2
1690
270
3-1
RUTLAND
300
NO.4
550
210
NO.2
OPEN
NO.1
CROOKSVILLE NO.1
NO.1
277
270
550
3-2
3-3
NO.5

Figure 4. Equivalent-circuit setup for maximum 3,500-megavolt-ampere short-circuit tests 13*A*, 13*B*, 14*A*, and 14*B*

Figures with arrow indicate direction and approximate magnitude of short-circuit megavolt-amperes

Table I. Philo Field Tests, 138-Kv Oil Circuit Breaker, Type FK-339-3500, July 22–23, 1944

Tests 1*B* Through 3*B* on July 22; Tests 4*B* Through 9*B* on July 23

		Current Amperes							Seismograph Readings, Inches				
		Maximum Loop											
Test	Duty	Peak	Rms	Initial in Arc, Rms	Equivalent Three-Phase Megavolt-Amperes	Short-Circuit Duration, Cycles	Arc Length, Cycles	Breaker Interrupting Time, Cycles	Up	Down	Fore	Aft	Remarks
1*B*	O	1,390	850	790	260	3.05	1.15	2.6					No disturbance
		2,200	1,340	1,070		3.1	1.30	2.75					
		1,920	1,120	910		2.7	0.75	2.20					
2*B*	O	8,700	5,300	4,700	1,100	2.85	1.15	2.55	0.04	0.11			No disturbance
		7,800	4,400	3,900		2.7	1.0	2.4					
		4,800	3,200	3,000		3.0	1.25	2.65					
3*B*	O	7,500	4,400	3,800	1,100	3.05	1.2	2.65	0.013	0.030			No disturbance
		8,000	4,700	4,300		2.95	1.25	2.7	0.023	0.053			
		8,800	5,300	4,600		2.8	1.05	2.5					
4*B*	O	15,200	9,000	7,400	1,800	2.75	1.05	2.5					Slight vapor out of vent on pole 1. No disturbance
		12,300	7,100	6,200		2.6	0.9	2.35					
		8,800	5,900	5,500		3.0	1.2	2.65					
5*B*	CO	14,800	8,700	7,300	1,800	2.7	1.0	2.45					Slight vapor out of either pole 2 or 3 but one pole only. No disturbance
		8,400	5,700	5,400		3.0	1.25	2.70					
		10,100	6,100	5,700		2.9	1.1	2.55	0.035	0.027			
6*B*	O	13,400	8,400	7,800	2,300	3.0	1.25	2.6					Slight vapor on pole 1. Slight jar. No undue disturbance
		20,000	11,800	9,500		2.95	1.15	2.5					
		20,000	11,800	9,400		2.7	0.95	2.3			0.015	0.022	
7*B*	CO	15,500	9,000	8,200	2,300	2.85	0.9	2.55	0.030	0.055			Slight vapor pole 3. Very slight jar.
		19,800	11,400	9,000		2.7	0.85	2.5	0.055	0.050			
		21,000	12,000	9,700		3.05	1.15	2.7					
	(15 second interval)												
	CO	17,000	9,800	8,900	2,300	2.9	1.0						Slight jar. Trip coil burned out at initiation of second fault
		19,200	11,100	8,900		3.0	1.3						
		20,000	11,600	9,600		3.0	1.05						
8*B*	O	22,000	12,900	10,900	2,900	2.65	0.9	2.25			0.15	0.125	Moderately heavy jar. No vapor observed from vents
		21,000	11,800	10,500		2.7	1.05	2.4					
		26,000	15,200	12,100		2.75	1.0	2.35					
9*B*	CO	26,000	14,900	11,700	2,800	2.7	1.1	2.5	0.073	0.055			Moderately heavy jar. No vapor observed from vents
		18,300	11,000	9,800		3.0	1.4	2.8	0.045	0.027			
		16,300	10,700	10,300		2.95	1.05	2.45					
	(15 second interval)												
	CO	27,000	15,500	12,200	2,900	2.7	1.1	2.6					Moderately heavy jar. No vapor observed from vents
		22,000	12,700	10,400		2.75	0.9	2.4					
		20,000	11,800	10,700		3.1	1.15	2.65					

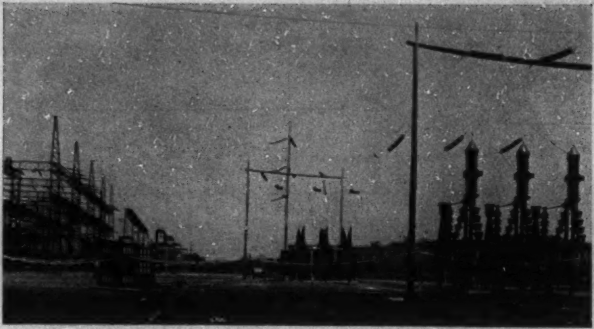

Figure 5. Setup and connections for oil- and air-blast-circuit-breaker tests at Philo

sections. This layout provides ideal flexibility for carrying out short-circuit tests, as illustrated by the typical setups shown in Figures 3 and 4. Figure 3 shows the circuit equivalent used to obtain approximately 1,500 megavolt-amperes, while Figure 4 shows the maximum setup with the reactor short-circuited.

Backup protection for tests at 3,500 megavolt-amperes, using existing 2,500-megavolt-ampere breakers, presented somewhat of a problem. Referring to Figure 4, this was solved by setting the bus-tie breaker relays to trip well in advance of the Crooksville number 2 line breaker, thereby reducing the duty on the latter breaker by approximately 1,700 megavolt-amperes. Furthermore, each test was conducted with the other test breaker acting as a backup for the breaker being tested, providing in effect double backup protection without exceeding the interrupting capacity of existing breakers.

The two test breakers, oil and air-blast, were mounted on temporary concrete foundations approximately 100 feet apart, as shown in Figure 5. Temporary 132-kv line connections were made to the south end of the east transfer bus, as shown on Figure 2, and the line conductors were arranged so that either breaker could be connected for "test" or "backup" as desired, and the changeover from one to the other could be made in 30 minutes or less. In this manner the tests on the two breakers were run concurrently, switching from one to the other for each system setup. Figures 6 and 7 show individual views of the oil and air breakers respectively, including details of the temporary high-voltage connections.

Two temporary buildings were provided, one for the magnetic oscillographs and darkroom, and another, of lightproof construction, to house a cathode-ray oscillograph placed directly under the high-tension leads between the transfer bus and the test breaker. A view showing the interior of the magnetic-oscillograph house is shown in Figure 8.

Program of Tests and Test Results

Tests were carried out on two week ends, first on July 22 and 23, and again on August 6. The first week end was devoted to nonreclosing tests at duties ranging from 250 megavolt-amperes up to the maximum available capacity. The second series of tests on August 6 covered high-speed reclosing tests on both breakers over the same range of duties, and, in addition, line-charging current-interrupting tests were made on both breakers.

With the physical arrangements as described, the test program was carried out fairly smoothly and was completed satisfactorily within the available time limits on each of the test days.

The test results obtained on both the July 23 and August 6 series, are summarized in Tables I to V inclusive. It will be noted from Tables I and II covering the July 23 tests that both the oil and air-blast breakers were subjected to a total of 11 tests, in each case ranging from 260 megavolt-amperes to 2,900 megavolt-amperes. In all of these 22 tests, it is worthy of note that breaker-interrupting time was consistently less than three cycles.

Oscillograms showing the interruption of 2,900 megavolt-amperes on the oil breaker, test 8*B*, Table I, and also 2,900 megavolt-amperes on the air-blast breaker, test 8*A*, Table II, are shown in Figures 9 and 10 respectively.

In order to determine what effect, if any, the interruption of heavy short circuits would have on the oil-circuit-breaker foundations, two independent methods of checking structural movement or shock on the breaker itself were employed. The first check consisted of placing a number of one-half-inch-diam-

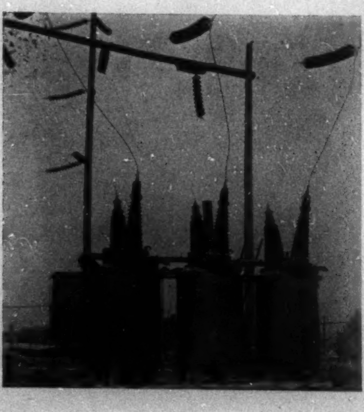

Figure 6 (left). 138-kv 800-ampere type-*FK*-339-3500 oil-circuit-breaker test at Philo

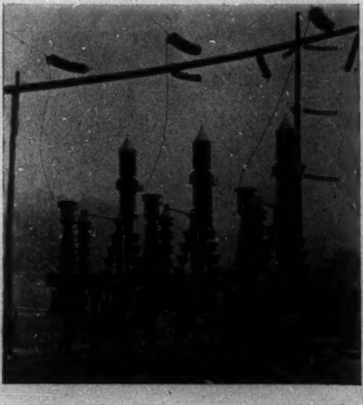

Figure 7 (right). 138-kv 800-ampere type-*AT*-138-3500 air-blast circuit-breaker test at Philo

Figure 8. Interior of magnetic - oscillograph house

Figure 11. One-half-inch-diameter pins mounted on oil circuit breaker for shock test

Figure 9 (below). Oscillogram for oil-circuit-breaker test 8B

Phase C, 12,100 amperes, 2,900-megavolt-ampere interruption

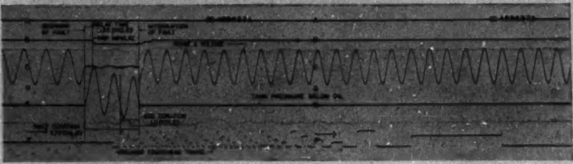

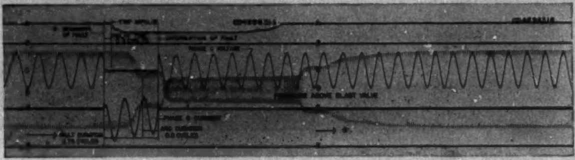

Figure 10. Oscillogram for air-blast-circuit-breaker test 8A

Phase C, 11,900 amperes, 2,900-megavolt-ampere interruption

eter round pins of varying lengths standing on end on a flat surface on top of one of the pole units, as shown in Figure 11. It was reasoned that any appreciable jar or movement would cause at least some of them to be toppled over. For the second check, giving an even more sensitive measurement, a seismograph was mounted on top of the same pole unit, as shown in Figure 12, to compare the vertical and horizontal displacement obtained during interruption with that obtained under no-load operation. Throughout both series of tests none of the pins described above were toppled over and the seismograph measurements, as shown on Tables I and III, indicated relatively small shock or movement. The actual movement of the structure was less than ten times the corresponding movement obtained with no-load operation, or approximately 0.1 inch. Both of these tests confirmed the visual impression of bystanders that the breaker showed no outward evidence of movement or noticeable shock to the foundations.

The contact parts of both breakers were removed for examination between the two series of tests. Figures 13, A and B, show the oil-breaker contacts, while the stationary contacts and moving contact arcing tips of the air-blast breaker are shown in Figure 14. While these contacts showed some burning, the actual amount of material wasted away was remarkably small and insufficient to require their replacement. Nevertheless, in view of the heavy duties contemplated for the next series of tests, it was believed advisable to go through with the original plan for replacing these contacts at this time.

The second series of tests, carried out on August 6, consisted chiefly of high-speed reclosing operations and short-circuit interrupting values ranging from 240 megavolt-amperes to 3,200 megavolt-amperes on the oil breaker, and from 260 megavolt-amperes to 3,500 megavolt-amperes on the air-blast breaker. Complete results for this series of tests are shown in Tables III and IV covering the oil and air-blast breakers respectively. The system short-circuit capacity was higher for this series by reason of the addition of one 42,100-kva generator which had been out for maintenance on July 23. This machine, of course, contributed to the increase from 2,900 megavolt-amperes to 3,500 megavolt-amperes obtained for the air-blast breaker in this series, but was insufficient to account for the entire increase. The remainder was due to a somewhat higher percentage offset in the current wave as well as to the usual random variation obtained in short-circuit current magnitudes.

Rates of rise of recovery voltage, as shown by cathode-ray oscillograms, ranged from values of the order of 250 to 300 volts per microsecond to a maximum value of 1,800 volts per microsecond. As to be expected, lower rates were obtained under the heavier short-circuit duties where a large number of transmission lines were connected to the test breaker. The highest rates, including the 1,800 volts per microsecond obtained on test 2*A*, were associated with interruptions of approximately 1,000 megavolt-amperes under a setup in which the entire short-circuit capacity was supplied to the test breaker direct from generators and from the system through one of the bus-tie reactors, so that no transmission lines were connected directly to the test bus.

Both breakers came through the entire series of tests, both on July 23 and August 6, without any visible evidence of distress. In the oil breaker, the occurrence

Figure 12. Seismograph mounted on oil circuit breaker for shock test

of an interrupting operation was evidenced only by wisps of smoke emerging from the separating chamber vents. Dielectric tests on the condition of the oil before the first series and after the second series of tests showed an over-all deterioration of only 30 kv to 26 kv. As compared with the oil breaker, the air-blast breaker, as to be expected, gives much greater outward evidence of interrupting performance, both from the high-velocity blast of air as well as from the clearly visible ejection of incandescent gases and smoke from the interrupter vents. Performance was consistent throughout, however, and there appeared to be no visible difference between the opening and close-opening tests in the first series, nor between the first and second shots of the high-speed reclosing tests. However, motion pictures taken at high speed on the heavy-duty reclosing tests, showed on the second interruption a considerably larger emission of gases and smoke than on the first. This would be expected as a result of the accumulation of some vaporized contact material remaining in the vicinity of the breaker contacts between the first and second shots.

As in the case of the nonreclosing tests, the air-blast breaker came through all of the reclosing tests with breaker-interrupting time of three cycles or under, whereas the oil breaker on one pole only went slightly higher on several tests, the maximum being 3$^1/_2$ cycles. The other two poles of the oil breaker showed consistent performance at three cycles or below on all tests except on the preliminary shot at less than ten per cent of rating.

Figures 15 and 16, covering tests 14*B* and 14*A* respectively, show the maximum duty reclosing test on the oil breaker at 3,100 megavolt-amperes and the maximum duty reclosing test on the air-blast breaker at 3,500 megavolt-amperes, which was also the maximum for either series of tests.

Throughout the entire series, both on July 23 and August 6, a total of 20 short-circuit interruptions were made on each breaker, ranging from 260 megavolt-amperes to 3,200 megavolt-amperes on the oil breaker and from 240 megavolt-amperes to 3,500 megavolt-amperes on the air-blast. On the oil breaker, with close to three-cycle interrupting time obtained throughout, there is indicated a consistent arcing time of approximately 1$^1/_2$ cycles for the entire range of currents. This performance is believed to be typical of the type of interrupter used in this breaker and also is consistent with laboratory tests described in a companion paper.[8]

Views showing the condition of the contacts on these breakers after the conclusion of the second series of tests, are shown in Figures 17 and 18 for the oil and air-blast breakers respectively. Here again, although there was some deterioration of the arc-resisting material with which the contacts are faced, it was evident that the same contacts could have been used for many more operations.

Reclosing tests in the second series showed a minimum of 15$^1/_2$ cycles reclosing time on the oil breaker, and down to 13 cycles on the air-blast breaker. While, as pointed out above, the principal objective in making the tests on these breakers was to obtain data on interrupting-capacity performance under conventional opening–closing combinations as well as under more or less standard high-speed reclosing duties, at the same time much faster reclosing speeds were hoped for and sought. From that standpoint the reclosing speed obtained was gratifying, particularly on the air-blast breaker at 13 to 13$^1/_2$ cycles. In the case of the oil breaker, although the decrease in time from 19 cycles to 15$^1/_2$ cycles for the last test in the series was obtained by means

Table II. Philo Field Tests, 138-Kv Air-Blast Circuit Breaker, Type AT-138-3500, July 22–23, 1944

Tests 1*A* Through 3*A* on July 22; Tests 4*A* Through 9*A* on July 23

		Current Amperes							
		Maximum Loop		Initial in Arc,	Equivalent Three-Phase Megavolt-	Short-Circuit Duration,		Breaker Interrupting	
Test	Duty	Peak	Rms	Rms	Amperes	Cycles	Arc Length, Cycles	Time, Cycles	Remarks
1*A*	O	2,300 1,650 1,220	1,410 950 730	1,090 810 730	260	2.75 3.0 2.95	0.90 1.1 1.15	2.4 2.6 2.65	No disturbance
2*A*	O	5,200 8,300 7,600	3,200 5,000 4,400	3,000 4,300 3,700	1,000	2.95 2.85 2.65	1.15 1.05 0.85	2.65 2.55 2.35	Some smoke from exhausts. No disturbance
3*A*	CO	8,400 6,900 6,600	5,000 4,100 3,800	4,100 3,500 3,200	990	2.9 2.65 2.95	0.95 1.2 1.0	2.45 2.7 2.5	Flash at disconnect on closing. A few sparks. No disturbance
4*A*	O	11,700 15,800 10,100	6,700 9,400 6,100	6,000 7,500 5,400	1,800	2.95 2.75 3.00	1.1 1.05 1.15	2.6 2.55 2.65	Some smoke out of interrupter exhausts. No flame. No undue disturbance
5*A*	CO	10,200 14,700 8,400	6,100 8,700 5,500	5,600 7,400 5,200	1,800	2.9 2.85 2.9	1.0 0.95 1.15	2.5 2.45 2.65	Moderate flash at disconnects on closing. No flame from interrupters on opening operation. No disturbance
6*A*	O	14,900 22,000 21,000	9,000 13,000 12,500	8,900 10,400 9,700	2,400	2.85 2.8 2.65	1.1 1.0 0.85	2.6 2.5 2.35	Smoke out of poles 2 and 3 interrupters. One foot of flame out of pole 1 interrupter. Slight discoloration on exhaust screen noted after test
7*A*	CO (15 second interval)	17,100 21,000 19,900	9,900 12,400 11,500	8,900 10,300 9,700	2,400	3.0 2.9 2.6	1.00 1.15 1.2	2.55 2.65 2.7	Bright flash one foot in diameter at disconnects on closing. One foot of flame out of interrupters on opening
	CO	14,400 18,600 18,600	9,500 10,700 10,800	8,200 9,500 9,300	2,300	2.9 2.55 2.65	0.9 1.35 1.1	2.5 2.95 2.7	Bright flash one foot in diameter at disconnects on closing. One foot of flame from pole 2 interrupter on opening
8*A*	O	23,000 16,500 25,000	13,400 10,600 14,600	11,200 10,200 11,900	2,900	2.75 2.95 2.75	0.85 1.05 0.8	2.35 2.55 2.45	One foot of flame from poles 2 and 3
9*A*	CO (15 second interval)	19,300 17,200 23,000	11,400 11,500 13,500	10,300 10,200 11,800	2,800	2.0 3.0 2.0	0.8 1.2 0.8	2.3 2.7 2.3	One foot of flame from poles 1 and 2. One foot diameter flash at disconnects on closing
	CO	19,700 24,000 16,200	11,600 14,000 10,600	10,500 11,700 10,000	2,800	2.9 2.9 2.95	0.7 0.95 1.1	2.55 2.55 2.7	One foot of flame from poles 1 and 2. One foot diameter flash at disconnects on closing

Figure 13A (above). External lower contacts of multibreak interrupters after July 23 tests

Figure 13B (left). Stationary and moving contacts of multibreak interrupter after July 23 tests

Figure 14 (below). Stationary and moving contacts of air-blast circuit breaker after July 23 tests

of certain adjustments that could be made in the field, it appears that this is about as far as it is feasible to go with the present design of the breaker and mechanism, and that any further marked reduction in time would require some redesign. In the case of the air-blast breaker, however, there appears to be no question but that 12-cycle reclosing definitely is attainable. This perhaps may represent one of its most attractive features, along with such other advantages as the stored-energy interrupting principle and the elimination of oil.

After the completion of the interrupting and reclosing tests on August 6, a special setup was made to check the performance of both breakers while interrupting the charging current of an 80-mile section of 132-kv line. This line was energized through the two test breakers in series and two line-opening tests were made on each breaker. The results of these tests, including actual current interrupted, breaker-interrupting time, restrike data, and so forth, are shown in Table V. The

Table III. Philo Field Tests, 138-Kv Oil Circuit Breaker, Type FK-339-3500, August 6, 1944

Test	Duty	Current Amperes: Maximum Loop: Peak	Current Amperes: Maximum Loop: Rms	Current Amperes: Initial in Arc, Rms	Equivalent Three-Phase Megavolt-Amperes	Short-Circuit Duration, Cycles	Arc Length, Cycles	Breaker Interrupting Time, Cycles	Reclosing Time, Cycles	Seismograph Readings, Inches: Up	Seismograph Readings, Inches: Down	Remarks
10B	O (Instantaneous)	1,400	830	770	260	3.4	1.35	2.95	19	0.020	0.008	No disturbance
		2,200	1,400	1,080		2.9	0.9	2.45				
		1,540	890	760		3.55	1.9	3.1				
	CO	1,870	1,100	870	240	3.6	1.6	3.1				
		1,330	790	710		3.4	1.35	2.9				
		1,980	1,200	980		3.8	1.8	3.3				
11B	O (Instantaneous)	10,000	5,800	5,700	1,800	2.95	1.25	2.65	19	0.082	0.078	Light jar. Slight vapor from vents on poles 1 and 2. No unusual disturbance
		14,700	8,800	7,300		2.8	1.05	2.5				
		12,600	7,200	6,200		2.65	0.95	2.4				
	CO	12,500	7,250	6,200	1,800	3.0	1.25	2.7				
		8,200	5,400	5,100		3.0	1.15	2.7				
		15,000	8,900	7,300		2.75	1.15	2.6				
12B	O (Instantaneous)	19,200	11,300	9,300	2,300	2.85	1.2	2.65	19.5	0.109	0.128	Moderate jar, slight vapor from poles 1 and 2. No disturbance
		21,000	12,400	9,500		2.7	1.05	2.5				
		18,800	10,900	9,200		2.65	0.9	2.3				
	CO	19,800	11,500	9,300	2,400	2.65	0.9	2.35				
		12,700	8,400	8,100		3.0	1.25	2.7				
		22,000	12,700	10,100		2.75	1.1	2.55				
13B	O	21,000	12,300	11,400	3,200	2.6	0.9	2.25		0.110	0.093	Moderately heavy jar. Slight vapor from vent on pole 2
		23,000	13,400	11,500		2.9	1.2	2.6				
		28,000	16,500	13,300		3.7	2.0	3.35				
14B	O (Instantaneous)	18,600	11,700	11,100	3,100	3.0	1.35	2.65	15.5	0.117	0.117	Moderately heavy jar. No vapor observed
		25,000	14,700	12,500		2.9	1.25	2.6				
		28,000	16,200	13,000		3.7	2.1	3.35				
	CO	18,000	11,300	10,700	2,600	3.0	1.1	2.6				
		20,000	12,000	10,800		3.0	1.4	2.8				
		20,000	12,200	11,000		3.55	1.75	3.25				

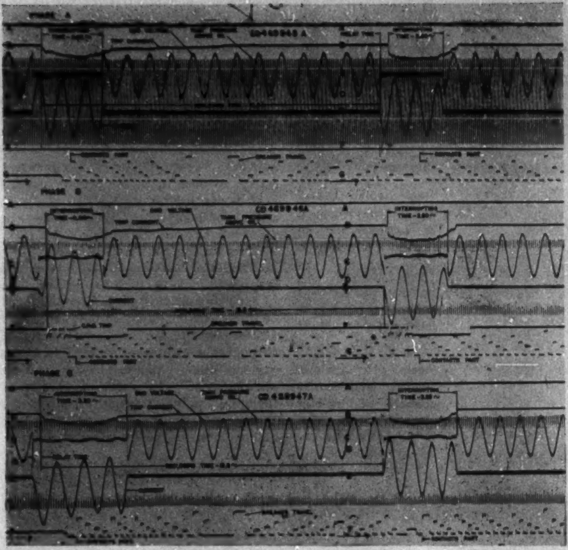

Figure 15 (above). Oscillograms for oil-circuit-breaker high-speed reclosing test 14*B* for all three phases

Maximum phase *C*, 13,000 amperes, 3,100-megavolt-ampere interruption

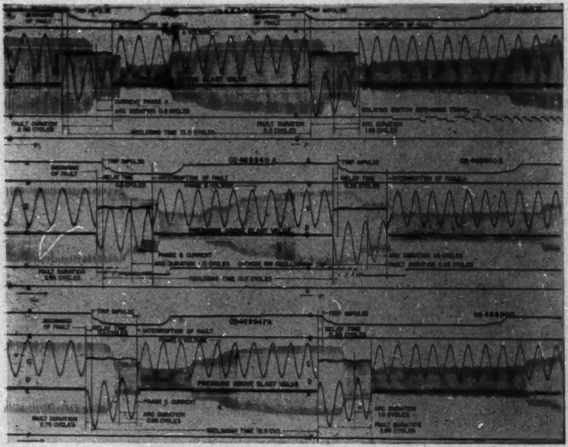

Figure 16 (below). Oscillograms for air-blast circuit-breaker high-speed reclosing test 14*A* for all three phases

Maximum phase *C*, 14,500 amperes, 3,500-megavolt-ampere interruption

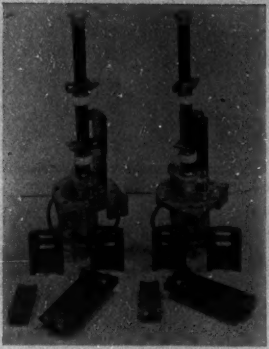

Figure 17. Stationary and moving contacts of multibreak interrupter after August 6 tests

interruption of capacitance current did not result in measurable overvoltages on either the oil or the air-blast breaker, even though restrike took place on one of the tests on the oil breaker at very small contact separation. Here the resistors used across the oil-breaker interrupters come into play to restrict the development of overvoltage, even though there is some restriking during the flow of the resistor current. The cathode-ray oscillograph for these line-opening tests was calibrated for substantial overvoltages which were expected but were not obtained. It is probable that if a larger number of line-interrupting tests had been made, some overvoltages would have resulted.

In addition to the line-opening tests at Philo, tests 17*A* and 18*A* were made to determine the effect of transient overvoltages on the air-blast breaker when connected to a transmission line being de-energized from the far end. In this case, the air-blast breaker was connected at Philo to the open end of the Philo–Howard line, the line being energized from Howard. The tests were made by de-energizing this line at Howard by means of a standard five-cycle oil circuit breaker. During these tests peak voltages of 250,000, 220,000, and 170,000 volts to ground were recorded, the maximum being 2.2 times normal.

From the standpoint of mechanical and electrical performance of the test breakers themselves, it is true beyond any doubt that this program of tests was accomplished with the least difficulties and with the highest degree of satisfactory performance of any series of tests yet carried out on the system with which the authors are associated. Likewise, from a system standpoint, the consistently high-speed performance on all tests undoubtedly was responsible for the almost complete absence of system-voltage complaints, notwithstanding the fact that many industries normally sensitive to voltage disturbances were in full operation during the tests. Furthermore, the entire test program produced no operating disturbances, such as faulty relay operations on the system, which often are disclosed under similar circumstances.

Table IV. Philo Field Tests, 138-Kv Air-Blast Circuit Breaker, Type AT-138-3500, August 6, 1944

Test	Duty	Current Amperes			Equivalent Three-Phase Megavolt-Amperes	Short-Circuit Duration, Cycles	Arc Length, Cycles	Breaker Interrupting Time, Cycles	Reclosing Time, Cycles	Remarks
		Maximum Loop		Initial in Arc, Rms						
		Peak	Rms							
10A	O	2,100	1,290	1,100	260	2.75	0.95	2.45		No disturbance
		1,650	930	750		3.0	1.05	2.55		
		2,100	1,230	990		2.85	1.0	2.5		
11A	O (Instantaneous)	8,600	5,600	5,500	1,700	3.0	1.2	2.7	13.5	No disturbance. Slight smoke from all interrupters
		14,500	8,700	7,200		2.85	1.05	2.55	13	
		12,000	7,100	6,100		2.6	0.85	2.35	13.5	
	CO	11,300	6,500	5,900	1,400	2.9	1.1	2.7		
		9,600	5,900	5,400		3.0	1.1	2.7		
		10,000	6,000	5,500		2.55	0.95	2.55		
12A	O (Instantaneous)	15,400	9,300	8,400	2,400	2.95	1.15	2.65	13.5	No undue disturbance. Two-foot flame from poles 1 and 2
		22,000	13,000	10,200		2.7	1.0	2.5	13	
		21,000	12,600	10,100		2.7	0.85	2.35	13	
	CO	19,500	11,100	10,000	2,500	2.1	0.85	2.45		
		22,000	13,100	10,500		2.75	0.8	2.4		
		15,400	9,800	8,800		3.0	1.0	2.6		
13A	O	22,000	13,000	11,500	3,200	2.6	0.8	2.3		No undue disturbance. One and one-half-foot flame from poles 2 and 3
		17,100	11,000	10,400		3.0	1.2	2.7		
		28,000	16,400	13,200		2.85	1.0	2.5		
14A	O (Instantaneous)	22,000	12,800	11,100	3,500	2.65	0.9	2.4	13	No undue disturbance. Two-foot flame from all three interrupters
		19,200	11,500	10,700		2.95	1.15	2.65	13	
		31,000	18,300	14,500		2.75	0.95	2.45	12.5	
	CO	23,000	13,000	11,400	3,200	2.6	1.35	2.95		
		22,000	12,900	11,600		2.95	1.1	2.7		
		28,000	16,100	13,400		2.95	1.0	2.6		

This may be due principally to the very high speeds obtained on all the tests, as has been pointed out, and it also may be due in part to greater perfection attained in the application and operation of relay schemes resulting from the constant vigil to improve and perfect relay operation. It always has been felt that one of the valuable by-products of staged system tests of this kind is the opportunity given to discover and correct imperfections in relay systems if and when they fail to accomplish the protective functions for which they are designed.

Table V. Summary of Line-Switching Tests, 138-Kv Oil Circuit Breaker, Type FK-339-3500 and Air-Blast Circuit Breaker, Type AT-138-3500, August 6, 1944

Breaker	Test	Initial in Arc Current, Amperes	*Trip Impulse to Interruption, Cycles	**Number of Restrikes	Maximum Instantaneous Peak Restrike Current, Amperes	Maximum Voltage to Ground
Oil	15B	33	1.45	1	56	Normal 60-cycle crest
		30	1.75	None		
		34	2.20	1	83	
Oil	16B	30	2.0	None		Normal 60-cycle crest
		30	1.85	None		
		34	1.65	None		
Air	15A	31	2.05	1	134	Normal 60-cycle crest
		35	2.15	None		
		33	2.0	None		
Air	16A	31	2,05	1	143	Normal 60-cycle crest
		30	2.2	None		
		35	2.0	None		
Air	17A 18A	Taken with air-blast breaker open and the line de-energized from the Howard end, with a conventional five-cycle oil circuit breaker. Peak voltages of 250,000, 220,000, and 170,000 volts to ground were recorded, the maximum being 2.2 times normal crest				

* This is measured to the beginning of resistor current or to interruption of restrike on the oil breaker; to final interruption on the air breaker.
**Does not include restrikes through resistors on oil breaker.

Conclusions

In these tests there has been accomplished for the first time the successful interruption of a full three-phase short-circuit of 3,500 megavolt-amperes with a speed of three cycles. In reviewing these tests and in comparing the performance of the two types of breakers, the following conclusions seem warranted:

1. The tests on the oil circuit breaker showed performance closely approaching 3,500 megavolt-amperes at a three-cycle interrupting time, even though the three-cycle time was slightly exceeded on one pole in some cases. The air-blast breaker, however, demonstrated unquestioned performance at 3,500 megavolt-amperes, and at three cycles or less on all of the tests.

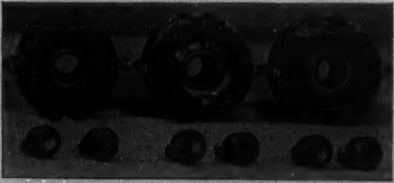

Figure 18. Stationary and moving contacts of air-blast circuit breaker after August 6 tests

2. Judging by the performance of both of these breakers in tests at or near 3,500 megavolt-amperes, it seems apparent that a goal of 5,000 megavolt-amperes is attainable with both oil and air-blast designs, and unquestionably with the latter.

3. It also has been demonstrated that 12-cycle reclosing is entirely feasible in the case of the air-blast breaker, even though not fully accomplished in the tests described. The deficiency is quite small, only one half to one cycle, and it is believed that this can be eliminated by relatively minor design changes.

4. It has been shown that field tests at short-circuit values as high as 3,500 megavolt-amperes can be conducted smoothly

and safely on a large and extensive interconnected power system without serious operating disturbances.

5. These tests have demonstrated again the value of full-capacity field tests to prove the adequacy of circuit-breaker designs. Such tests, made on a full three-phase basis, are most certain to disclose design weaknesses or even manufacturing irregularities in any part of the breaker. For example, it is quite apparent that single-pole tests on the oil breaker readily might have failed to disclose the excess over three-cycle timing which occurred on only one out of three poles. For the final over-all test on a completed circuit breaker, no other type of test can be as satisfactory and fully convincing.

6. It is interesting to point out that the carrying out of these tests, believed to be the first field tests ever made at values even approaching 3,500 megavolt-amperes, was accomplished without mishap, either to test breakers or system equipment, and without encountering serious delay necessitating any important departure from prearranged schedules. On each of the three days of test, the entire test program was completed successfully within the time available for testing, and substantially in accordance with the prearranged intervals of time.

Finally, the authors desire to acknowledge the fine co-operation and efficient organization which was achieved by the General Electric Company personnel and the personnel of The Ohio Power Company, which made the successful carrying through of these tests possible. While, if space permitted, a considerable number of names would be mentioned, it is perhaps even more important to note that the highly successful and gratifying results were obtained through the splendid teamwork and cooperation of all the participants.

References

1. Ultrahigh-Speed Reclosing of High-Voltage Transmission Lines, **Philip Sporn, D. C. Prince.** AIEE Transactions, volume 56, 1937, January section, pages 81–90.

2. Experience With Ultrahigh-Speed Reclosing of High-Voltage Transmission Lines, **Philip Sporn, C. A. Muller.** AIEE Transactions, volume 59, 1939, December section, pages 625–31.

3. Five Years' Experience With Ultrahigh-Speed Reclosing of High-Voltage Transmission Lines, **Philip Sporn, C. A. Muller.** AIEE Transactions, volume 60, 1941, May section, pages 241–6.

4. Tests on and Performance of a High-Speed Multibreak 138-Kv Oil Circuit Breaker, **Philip Sporn, H. P. St. Clair.** AIEE Transactions, volume 57, 1938, December section, pages 696–704.

5. Field Tests and Performance of a High-Speed 138-Kv Air-Blast Circuit Breaker, **Philip Sporn, H. E. Strang.** AIEE Transactions, volume 61, 1942, January section, pages 1–6.

6. High-Voltage Circuit-Breaker Tests, **Philip Sporn, H. P. St. Clair.** *Electrical World* volume 85, 1925, pages 970–3.

7. Tests on High- and Low-Voltage Oil Circuit Breakers, **Philip Sporn, H. P. St. Clair.** AIEE Transactions, volume 46, 1927, pages 289–314.

8. A High-Capacity High-Voltage Three-Cycle Oil Circuit Breaker, **H. L. Byrd, E. B. Rietz.** AIEE Transactions, volume 64, 1945, April section, pages 160–3.

9. A Three-Cycle 3,500-Mva Air-Blast Circuit Breaker for 138,000-Volt Service, **H. L. Byrd, B. S. Beall III.** AIEE Transactions, volume 64, 1945, May section, pages 229–32.

Evaluation of Electric Distribution Losses in Terms of Generating-Station-Capacity Investment

Discussion and author's closure of paper 45-4 by M. Mortara, presented at the AIEE winter technical meeting, New York, N. Y., January 22-26, 1945, and published in AIEE TRANSACTIONS, 1945, January section, pages 1-7.

M. J. Steinberg (Consolidated Edison Company of New York, Inc., New York, N. Y.): The author has reduced to mathematical terms the procedure normally followed in evaluating a reduction in peak power-distribution losses in terms of investment in generating-station capacity. By so doing, he has contributed materially to a better understanding of the fundamentals involved. One feature of the paper which should prove to be of value to planning engineers is the derivation of three empirical formulas, indicated in the paper as equations 9′, 13′, and 17′, since their use will simplify the calculations involved without the introduction of any appreciable error. This is obvious by a comparison of the results shown in Table III of the paper.

The writer independently has derived the equations in the paper and has found them to be correct within the assumptions made. Unfortunately, these assumptions are not indicated clearly in all instances. This is true particularly for equation 12 of the paper.

Referring to Figure 2 of the paper, and using the same notation indicated therein, if t is the time when a unit is required under the reference plan represented by line B, then $t+D''$ is the time when a unit would be required under the alternate plan represented by line B_2. At time t, log h_m or the tangent of the angle of slope of trend line B is represented by

$$\log h_m = \frac{\log (G+g) - \log G''}{D''}$$

or

$$D'' = \frac{1}{\log h_m} \log \frac{(G+g)}{(G)}$$

which is the correct expression for equation 12, making the deferment period at any time t_n

$$D_n'' = \frac{1}{\log h_m} \log \frac{G_0+nW+g}{G_0+nW}$$

and the correct expression for equation 13 as

$$D_n'' = \frac{1}{\log h_m} \log \frac{(2-k)p+n}{p+n}$$

It appears that equation 12 of the paper and the higher numbered dependent equations were derived on the basis that the vertical distance between lines B and B_2 is approximately the same at time $t+D''$ and time t. That this assumption introduces no appreciable error in the calculations is substantiated by a comparison of the values in column d of Table IV of the paper with those derived by the writer in Table I by the use of the exact expression for the deferment period.

Table I

Column d Corresponds to Column d in Table IV of the Paper

Unit No.	Column d	Correct Value
1	1.052	1.000
2	0.702	0.674
3	0.507	0.480
4	0.368	0.356
5	0.352	0.349
6	0.271	0.264
7	0.213	0.208
8	0.171	0.167
9	0.141	0.138
10	0.227	0.223
11	0.170	0.167
Summation	4.174	4.035

R. F. Hamilton (Foreign Economic Administration, Washington, D. C.): Doctor Mortara has presented an ingenious method for determining present worth of future distribution losses, presumably with the idea of justifying immediate and future investment in additional distribution-system copper. He is to be commended for his interesting and timely paper.

In actual practice, one adds generating units in a station to care for additional load, not additional losses, which, though important, are incidental and often supplied by the least efficient and oldest generating units in the station.

While agreeing in general with Doctor Mortara's conclusions, I am prompted to suggest a somewhat different approach to this type of problem, using data from the paper.

Refer to Figure 1 of this discussion; curve A is a typical utility-generation load curve, for which the load factor happens to be 0.64, the deviation factor 0.15, and, therefore, the loss factor 0.48.

The area between curves A and B is a measure of the variable system losses. The area between curves B and C is a measure of the fixed losses, curve C represents the metered load. Curve D shows the variable losses only.

Within a period of about 4½ hours, during which the peak load occurs, 13.3 per cent of the maximum power generated is required to supply the variable losses, and is useful for no other purpose. Note that the amount of capacity involved, when considered by itself, is operating on a load factor of 11 per cent only. At \$100 per kilowatt-installation cost and 13 per cent for fixed charges, these alone amount to 13½ mills per kilowatt-hour. Add 2½ mills for operation and the minimum cost assignable to the energy produced by the machines carrying the peak losses becomes 16 mills per kilowatt-hour. This energy represents 35 per cent of the total variable losses. If the balance is valued at three mills per kilowatt-hour, at least 7½ mills should be used in determining economic copper sizes.

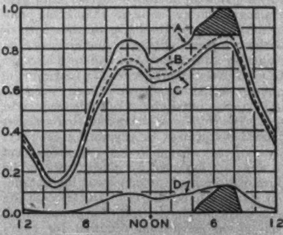

Figure 1. Utility load curve showing variable and constant distribution losses

Note that these quantities are related only to the shape of the load curve and the percentage of losses involved. If these remain substantially unchanged as the system grows, the cost per kilowatt-hour for energy lost in distribution will not vary. If these are expected to change in a known manner the effects are ascertained easily.

Assume that this capacity for variable losses is supplied by two equal machines fully loaded. What usually happens as the generation peak increases? For a time we may draw upon the spinning reserve or even upon spare capacity. A new unit is added eventually, but we are likely to be thinking in terms of load, present and future, and not losses, and the new unit probably will be larger and more efficient than those in use and go in as a base-load generator. If this machine is added at once, has the same capacity as the others, and is charged entirely to losses, the fixed charge per kilowatt-hour increases to 20¼ mills per kilowatt-hour and returns to 13½ mills only when the variable losses will have reached the capacity of the three machines. The average energy cost for all variable losses over this period of growth can be hardly less than ten mills, but the actual value can be determined from the shape of the growth curve.

I would be inclined to charge to distribution losses only that portion of generator capacity which is needed to supply them day by day, either at present or in the future. By integration of the losses over any given period the values may be determined, either in terms of kilowatt or kilowatt-hour, and reduced to present worth by assigning the proper costs and interest rates. Often too low a cost has been assigned to variable losses and most systems profitably can use more copper.

In addition to the symbols of the paper, let q be the ratio of the yearly rate of power growth to the yearly rate of money growth, or $q=h/(1+i)$. If s represents the yearly charge in dollars per kilowatt of capacity, then take

$$\Sigma_1 = \int_0^T sq^t dt = \frac{s}{\log_e q}[q^T-1]$$

$$= 0.43429 \frac{s}{\log_{10} q}[q^T-1] \qquad (1)$$

or

$$\Sigma_2 = \sum_{t=1}^{t=T} sq^t = s\left\{\frac{(q^T-1)}{(q-1)} - 1\right\} \qquad (2)$$

The Σ_1 of equation 1 gives the integral summation to determine present worth for continuous growth.

The Σ_2 of equation 2 gives a serial summation to determine present worth for growth calculated over equal recurring periods of time. There is little to choose between these two forms of Σ.

Annual charges per kilowatt would be given by

$$z=(Cr+8{,}760\ \Phi v) \tag{3}$$

Φ being the annual load factor for the capacity supplying the losses and v the kilowatt-hour operating cost in dollars.

Then Σ_1 or Σ_2 would give the present worth per kilowatt of original loss reduction for a period of T years, presuming that the percentage loss remains constant during this time. If the growth in losses is at a different rate than that of the total load, the rate for the losses would be used instead of h. The integral of equation 1 may be set up in a variety of ways to suit conditions.

As an example of the methods proposed, take

$T=10$ years
$C=\$100$ per kilowatt
$r=0.13$
$\Phi=0.11$
$h=1.08$
$i=0.06$
$v=\$0.003$ per kilowatt-hour

Then

$q=1.0189$
$Cr=\$13$ per kilowatt, yearly fixed charges
$8{,}760\ \Phi v=\$2.89$ per kilowatt operating costs
$z=\$15.89$ per kilowatt

and, to the nearest dollar

$\Sigma_1=\$175$ per kilowatt of original loss reduction
$\Sigma_2=\$176$ per kilowatt of original loss reduction

If the original and final capacities, or original and final losses, are given, T to use in these formulas would be found as in equation 6 of the paper, or specifically:

$$T=\frac{\log G_1/G_0}{\log h};\ \text{or}\ T=\frac{\log L_1/L_0}{\log h}$$

The figure of \$13 per kilowatt for fixed charges, compared to \$2.89 for operating costs, would seem to confirm the author's concluding statement to the effect that the worth of power losses (demand) may be appreciably above the corresponding energy losses.

Harold Goodwin, Jr. (consulting engineer, Wyncote, Pa.): It is good to see someone again taking up the economics of distribution and particularly distinguishing between power and energy losses.

The title refers to "distribution losses," but part of the text appears to refer to transmission. This should be clarified as there are some interesting distinctions between transmission and distribution losses.

In other points the phraseology might be clarified, as in the fifth paragraph: "economic *value* of peak power losses," might better read, "economic *cost* of peak power losses."

The load curve presented goes back 40 years. It is not necessary to divide it more or less arbitrarily, as is done in the paper, for there are certain logical divisions the adoption of which greatly clarifies thinking. This is shown and discussed in the *United States Geological Survey* and will not be repeated here.[1]

One might wonder how it is that so many electric systems are in successful operation if these fundamental costs had not been determined. One reason is that the curve of costs versus wire size is very flat so that the selection of the wrong size of conductor is not ruinous; in fact it is so flat that it is practically impossible to justify replacement of existing small conductor with larger till the current has grown heavy enough to anneal the copper.

The situation was summed up well by the late Professor Harris J. Ryan, AIEE Past President, who counseled choosing a wire large enough to satisfy the regulation requirements and then as much larger as finances would permit.

Apparently there have been no papers on this subject for many years. It would be very helpful, if the author has found such, to record them in a bibliography at the end of the paper, starting perhaps with the *Geological Survey* to which reference is made in this discussion.

Apparent criticism of some points is not intended to minimize the value of the paper, but rather to be constructively helpful, as there is still much to be done in the correct evaluation of distribution losses.

REFERENCE

1. A SUPERPOWER SYSTEM FOR THE REGION BETWEEN BOSTON AND WASHINGTON. *United States Geological Survey*, professional paper 123, 1921, page 145.

W. R. Bullard (Ebasco Services, Inc., New York, N. Y.): This paper presents a very comprehensive method of analyzing the effect of distribution losses on generating-station investment, but, unfortunately, there are implications as to the use of the results that are likely to lead to definite misapplication. Also, the examples chosen for illustration are of such type that practically the same results can be obtained in a much simpler manner.

In order to present in simple form a picture of the elements of the problem being considered, I submit Figure 2, in which straight-line load growth is assumed. Consider first only the two slanting straight lines. Assume that the lower of these two lines represents useful load and that the upper represents load plus a constant amount of losses. If it be assumed further that generating capacity is kept exactly in conformity with the total load (either with or without losses) by minute increments continuously added, then the two lines also can be used to represent generating capacity required (neglecting reserve capacity for simplification). Also, by a suitable change in scale, the lines may be made to represent capital investment in generating capacity. By a further change in scale, in proportion to any rate assumed for fixed charges, the lines may be made to represent instantaneous levels of fixed charges. In this case the area between the two lines (or annual fixed charges on generation required for losses times time in years) represents total fixed charges for generation required for losses during the period shown. It is clear under these hypothetical assumptions that the annual cost of generating investment to carry the losses equals fixed charges on an investment corresponding to an amount of generating capacity equal to the kilowatt demand of the losses.

Now consider the two stair-step lines representing the practical case where generating capacity is added in blocks. Total generation required, including losses, may be represented by the solid stair-step line, and the corresponding requirement without losses, by this line with the areas marked X removed, which brings the line down to the dotted lobes. As before, the two stair-step lines can be used to represent capital, and also levels of fixed charges, by the same changes in scales. The areas X represent individual savings in fixed charges by postponement of investment permitted by the removal of losses. Now it is significant that the sum of the areas X is equal to the area between the two slanting straight lines, provided the steps are equal in amount and there are enough of them (or the terminations of the curves are made correctly) to get a true comparison. This fact can be seen easily by inspection since it is evident that the total area under the solid step curve differs from the total area under the other step curve by the area included between the two slanting straight lines. (One is merely shifted that much with respect to the other.) The purpose of this discussion so far is to show that, under the simple and uniform conditions assumed, the total fixed charges representing annual demand cost of losses for a given long period, or the average annual value of these fixed charges, is the same whether the generating investment be increasing continuously or added in blocks. This is true regardless of the amount of the uniform rate of load growth, or the size of generating units, provided the period chosen is long enough to obtain a true long-period average.

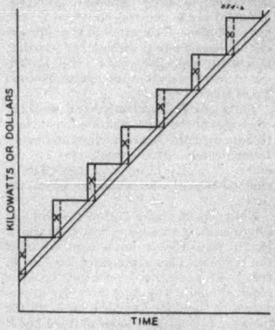

Figure 2

Now consider the more complicated load-growth assumptions of the paper. With a constant size of generating units added, and a constant unit investment per kilowatt, it would be expected that the summation of deferments of fixed charges over a long period of time would not differ greatly, under the exponential load-growth assumptions used, from those under a straight-line load-growth assumption as outlined in the foregoing. Such is found to be the case by examination of the examples of the paper. In example 1 of the paper the amount of losses increases continuously during the period considered, but, by integrating and averaging the loss curve, the average for the 50 years is found to be 29.6 megawatts. This times $100,000 per megawatt ($100 per kilowatt) gives an average capital investment of $2,960,000 for an equivalent amount of generating capacity. Fixed charges on this amount of capital for the 50-year period at 13 per cent are $19,250,000 total, which can be compared to the $18,700,000 total deferments obtained by the method of the paper.

In Doctor Mortara's example 2 the result of the calculations is given in terms of value of a fixed unit amount of loss, namely, one kilowatt. His use of present worth factors introduces a complication, but if these, represented by column *b* of Table IV of the paper, be eliminated from the resulting fixed charge deferments, represented by the middle column of Table III, the resulting summation of deferments for the 32-year period of the example is 4.25 *C* or $425. The result by the simple method of multiplying an annual fixed charge (13 per cent of $100) by the number of years (32) is $416 or a departure of approximately two per cent from the foregoing result obtained from the method given in the paper.

I come now to the chief point of my discussion, which is that the results obtained by present worth factors, as presented in example 2 for illustration, are misleading in that they easily may be applied improperly by the unwary engineer. Actually, all the 2.17 *C*, or $217, end result of example 2 means is that the periodic deferments of fixed charges on generating equipment caused by eliminating one kilowatt of loss can be represented by a present sum of $217 earning six-per-cent interest. The reason this sum differs widely from the capital investment of $100 per kilowatt of generating-station capacity is chiefly that the fixed charge deferments are calculated at an annual rate of 13 per cent whereas the present worth is figured at an interest rate of six per cent. Note that the ratio of 13 per cent divided by six per cent, or 2.167, is almost exactly the ratio between $100 and $217. This is closer correlation than might be expected in consideration of the relatively short period involved. Nevertheless, as an approximation, it is significant. The misapplication that may be made of the present-worth value is illustrated by the following example. Suppose that, by the purchase of a piece of distribution equipment costing $150 and requiring an annual fixed charge of 13 per cent, a constant saving of one kw of loss can be made, various other assumptions being as given in example 2 of the paper. The unwary engineer may make the calculations as indicated and may assume immediately that because he obtains a present worth of generating deferments equal to $217, the saving will be considerably greater than the cost represented by the distribution investment of $150. Actually, the $150 purchase will represent a loss because it carries a fixed charge of 13 per cent, not six per cent (energy component of cost of losses being ignored for simplification). To get a true comparison he should calculate the annual fixed charges at 13 per cent on $150 year by year for the 32 years (a fixed amount each year) and then make a summation of the present worths of each annual charge on a six-per-cent interest basis. A short-cut approximation (fully valid only for very long periods of time) merely is to multiply the $150 by the ratio of 13 to 6, which gives $325. This compared to the present worth of generating deferments of $217 indicates that the project is uneconomical insofar as the demand component of cost of losses is concerned. Of course, an even simpler method in this particular case is to compare the $100 generating investment with the $150 distribution investment, the ratio being the same as that of $325 to $217.

The foregoing misapplication might be prompted by casual interpretation of the meaning of the results based on the manner of presentation used in the paper. For example, the phrase in the title "In Terms of Generating-Station-Capacity Investment" may be construed easily as implying that the $217 is in direct terms of generating-station investment. This, of course, is not the case. As another example, note the following statement in the text under example 2.

> "It may be observed that all values of peak power losses calculated are greater than the capital cost *C* of new generating capacity, contrary to assumptions frequently made."

This, in general, would be interpreted as indicating, in consideration of the figures quoted, that the common practice of applying directly the capital cost of new generation in engineering problems, such as the foregoing, is greatly in error. Such is not the case, as this discussion discloses. The $217 present worth derived in example 2 is merely a convenient but intangible gauge for discontinuous fixed-charge deferments based on an arbitrary interest rate. It definitely is not the same as unit capital investment involved in generation required to carry the losses. The method presented in the paper, if properly applied, should be of considerable value in problems involving large departures from uniformity and large discontinuities in plans for expansion of generating facilities. It is to be hoped that misapplications, such as that outlined, will be avoided carefully by users of the method.

M. Mortara: With reference to Mr. Steinberg's discussion, it is recognized that the approximation on which was based the derivation of equation 12 of the paper should have been stated explicitly, although the error introduced by such approximation is small in most cases which can be considered in practice, as shown by the comparison presented by Mr. Steinberg. For values of (h_m-1) and $(1-k)$ smaller than 0.10, the ratio between the approximate and the correct expression of the individual terms under summation sign in equation 17′ is

$$\rho=\frac{p+n}{kp+n}$$

It is easy to see that this ratio equals $1/k$ for the first term $(n=0)$ and decreases rapidly for the successive terms, gradually approaching unity.

If, however, it is desired to use the correct value of D'', equation 17 and 17′ of the paper should be modified as follows:

$$s=\frac{1}{(1-k)p}\sum_{n=0}^{n=u-1}\frac{Cr}{(1+i)^{t_n}\log h_m}\times \log\frac{(2-k)p+n}{p+n} \qquad (17)$$

$$s=\sum_{n=0}^{n=u-1}\frac{Cr}{(1+i)^{t_n}(h_m-1)(p+n)} \qquad (17')$$

Nothing else is changed in the procedure illustrated by the paper, and, if the simplified form 17′ is chosen, as recommended, the nomogram Figure 5 of the paper still can be employed, provided the first scale to the left is labeled (p) instead of (kp) and the fifth scale, giving the final results, is labeled $[1/(h-1)(p+n)]$ instead of $[1/(h-1)\times(hp+n)]$. On the basis of the preceding expressions, the worth *s* calculated in example 2 of the paper is to be corrected from 2.17 *C* to 2.10 *C*.

The procedure suggested by Mr. Hamilton seems to include substantially the following steps: determine the amount of energy which is lost yearly during the daily periods of peak demand; assign to this energy a unit cost including charge on capital investment and operating cost; and, finally, calculate the totalized "present value" of such losses over a certain number of years. It is not thought that this method takes into account correctly the different way in which power losses and energy losses affect the economy of the system, as explained in the paper. Incidentally, it may be observed that, if Mr. Hamilton's conception of a separate generating capacity supplying the losses were accepted, the yearly load factor of this capacity, appearing in his equation 3, should be considerably smaller than its daily load factor, while in his discussion the same value is used for both.

Mr. Goodwin requests a clarification about transmission losses. That these should be considered as a separate problem is stated in the last paragraph of that section of the paper which outlines the procedure for evaluation applying to independent hydroelectric systems. The statement of Mr. Goodwin referring to annealing temperature of copper as the only practical justification for replacement of small-size conductors might be questioned.

Mr. Bullard's discussion shows that the significance and use of the worth of losses, designated in the paper by *s*, may be subject to misinterpretation and that a clarifying statement is necessary. This matter was briefly treated by the author in the oral presentation at the winter technical meeting and it was thought that no misunderstanding of the kind suggested by Mr. Bullard possibly could arise.

The value of *s* calculated by the paper's formula 9 (alternately 9′) is the totalized amount of savings on a limited series of carrying charges and the similar value calculated by formula 17 (alternately 17′) is the totalized "present value" of such savings. Therefore, it is clear that in neither case *s* can be interpreted as the equivalent of a capital investment, because it lacks the basic characteristic of such an investment, that is, to generate the burden of yearly charges on itself, which include return, amortization, taxes, and so forth. Consequently, a direct comparison between s and the capital expenditure required to produce one-kilowatt power-loss reduction would be erroneous. Furthermore, the worth of savings on energy losses, which are consequential to this reduction of power losses, is to be taken into account in such comparison.

The procedures suggested are as follows:

(*a*) *Case of two plans with different percentage of power losses* (*formulas 9 and 9′*). The savings s accumulated up to the ultimate development of the system, if invested at the interest rate i (in decimal) will yield an annual return $i\,s$. The yearly energy saved through one-kilowatt power-loss reduction is

$$w = 8{,}760\lambda$$

where λ is a loss factor which can be determined for each system on the basis of typical load curves. If the "incremental cost" of energy in dollars is e, the corresponding yearly economy will be $w\,e$.

The capital investment in the distribution system required to obtain one-kilowatt power-loss reduction being designated by I and the yearly rate of carrying charges (in decimal) applicable to that investment by r', the annual charge will be $r'I$. The investment I is justifiable, as long as

$$r'I \leq si + we$$

or

$$I \leq \frac{si + we}{r'} \qquad (1)$$

With the data of example 1 of the paper, and assuming

$$r' = r = 0.13 \quad i = 0.06 \quad \lambda = 0.30 \quad e = \$0.003$$

condition 1 becomes

$$I \leq \$[1.715C + 60.65] \qquad (2)$$

For $C = \$100$, the maximum justifiable investment per kilowatt of power-loss reduction would be approximately \$232. It should be noted that r' is not necessarily equal to r, because it applies to a different kind of capital investment.

(*b*) *Case of individual power-loss reduction* (*formulas 17 and 17′ of the paper*). In this case s is the "present value" of the future savings procured by one kilowatt of power-loss reduction, *at the time of outlay of the distribution investment I, required to obtain such a reduction*. Therefore, the conversion of s into an equivalent annual charge, for the purpose of comparison with the capital investment, should be made by determining the uniform annuity equivalent to s over the time interval necessary for the amortization of the aforesaid investment.

This annuity a_s can be derived from annuity tables, or calculated by the formula

$$a_s = s\frac{i(1+i)^N}{(1+i)^N - 1} \qquad (3)$$

where i is the rate of interest in decimal and N is the number of years over which the annuity is assumed to extend, that is, the interval required for the amortization of the investment I at the straight depreciation rate included in the carrying charges r'.

The worth of the consequent savings on energy losses is the same as indicated in the previous case, and therefore the condition of justifiability of investment I can be written

$$r'I \leq a_s + we$$

or

$$I \leq \frac{a_s + we}{r'} \qquad (4)$$

With the data of example 2 of the paper, corrected according to Mr. Steinberg's discussion, and assuming

$r' = r = 0.13$
$N = 30$ years
$i = 0.06$
$\lambda = 0.30$
$e = \$0.003$

condition 4 becomes

$$I \leq \$[1.17C + 60.65] \qquad (5)$$

For $C = \$100$, the maximum justifiable investment per kilowatt of power-loss reduction would be approximately \$178.

The general characteristics of the two examples being very similar, it appears that a greater investment is justified for a systematic reduction of the percentage of peak power losses than for an occasional such reduction, not followed by further attempt to maintain the lower loss percentage.

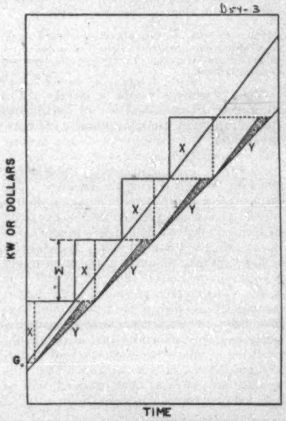

Figure 3. Figure 2 as it would appear assuming a condition of constant percentage of losses

The preceding clarification answers the closing paragraphs of Mr. Bullard's discussion and it is hoped it will be effective in preventing misapplications that Mr. Bullard feared might be prompted by unwarranted interpretation of the title of the paper, or of the sentence he quoted from the text. Mr. Bullard is to be thanked for calling attention to such possibility, but some of the propositions formulated in his discussion appear to be questionable.

To begin with, Mr. Bullard presents a diagram based on a very unusual hypothetical condition of *constant losses* and intended to prove that the total fixed charges on a number of generating units installed over a certain period are the same as the analogous charges which would result from a continuous gradual increase of the generating capacity. If the condition of *constant percentage of losses*, much more likely to occur, is assumed, Mr. Bullard's diagram will change as shown by Figure 3: the two lines representing load and generation are at an angle, instead of being parallel, and his geometric demonstration does not hold, because the area between those lines for each step of additional generating capacity exceeds the corresponding area X by the shaded triangular area Y. It can be proved that, for a number n of generating units of capacity W and using the various symbols adopted in the paper, the ratio of the area A enclosed between the two slanting lines and the two verticals at the origin and at the time of installation of the ($n+1$)*th* generating unit, to the area A' summation of the n areas X, is

$$\frac{A}{A'} = k\left(1 + \frac{1}{2p + n - 1}\right) \qquad (6)$$

For $p = 1$ and $n = 10$ this formula indicates an error variable from +9 per cent to −2 per cent as k varies from 0.99 to 0.90. With the data of example I of the paper, the error is practically zero, but this result cannot be generalized: it happens also, with those same data, that the weighted average of the loss reduction (29.6 megawatts) is almost identical to the mean value (29.5 megawatts) of its initial and ultimate amount. No one, however, would deduce from this particular case that the same is true in general.

Therefore, the statement of Mr. Bullard that his "simplified" method of calculation can be used, regardless of the assumptions on load growth and variation of losses, does not appear acceptable without qualifications. The procedure proposed in the paper, on the other hand, is not vitiated by any such systematic error and the use of formula 8 for the calculation of the total worth of losses is not more laborious than the process of "integrating and averaging the loss curve," suggested by Mr. Bullard.

A second question discussed by Mr. Bullard has reference to the "present value" of losses, calculated by formula 17 (or 17′). He observed that, if the "present value" were calculated on the basis of the rate of fixed charges rather than on the basis of the rate of interest, it would become equal to the unit cost of generating capacity C. Here again, an accidental result obtained using the data of example 2 is pointed out to confirm such contention, but there would be less close coincidence if the corrected present worth of 2.10 C were used.

It is well to emphasize that the definition of "present value" makes it inadmissible to use the rate of fixed charges as suggested, because these charges are applicable solely to generating-capacity investments and include: return on capital investment (which is not necessarily equal to the normal rate of interest), amortization, taxes, and other minor items. Furthermore, it is not clear what would be the significance of the "present value" being equal to the capital cost of generating capacity, since, later on, Mr. Bullard himself very rightly states that such worth of the losses should not be assumed as the equivalent of a capital investment.

Attention is called to a typographical error existing in Tables IV and V of the paper: the time of installation of unit number 11, shown in both tables as 26.5 years, should be corrected to 28.5 years.

Use of Dielectric-Absorption Tests in Drying Out Large Generators

Discussion and author's closure of paper 45-9 by H. C. Marcroft, presented at the AIEE winter technical meeting, New York, N. Y., January 22–26, 1945, and published in AIEE TRANSACTIONS, 1945, February section, pages 56–60.

J. S. Johnson (Westinghouse Electric and Manufacturing Company, East Pittsburgh, Pa.): There is a need for factual data relative to the insulation characteristics of large machines, such as is presented in this paper both on new machines and on machines during service life. As the author points out, dielectric-absorption or insulation resistance–time curves are of value in that they afford more definite information relative to the order of dryness of generator insulation. An expression describing the slope of the absorption curve for a given insulation as a function of dryness is advantageous in that it has the nature of a material constant and would be expected to be substantially independent of machine size.

As is stated in the paper, experimentation indicates that when a continuous voltage is applied to a solid insulating material the leakage current is characterized in general by three components.

1. The transient charging current resulting from the geometric capacitance of the insulation system, which is of very short duration.
2. The anomalous or absorptive charging current, which for most solid materials is proportional to the applied voltage and which decreases with time and finally disappears, obeys the superposition principle.
3. The normal leakage current which flows in the final steady state.

Moisture contamination in solid insulating materials results in an increase in both the steady-state leakage and in the absorptive current. For wet insulation the resistance–time curve becomes flat after very few minutes of electrification. From this it follows that under these conditions a relatively short time after electrification the steady-state leakage is large compared with the absorptive current. As insulation is subjected to drying treatment the insulation resistance–time curve flattens after increasingly longer times of electrification. As drying progresses the steady-state leakage therefore decreases faster than the absorptive current as measured at any given time after voltage application. For extremely dry conditions the insulation resistance–time curve on some insulations may continue to increase for days.

One fact that is significant is that, while the insulation resistivity as measured after any given time or at steady state increases to very high values with continued drying, the time rate of increase of resistance for a specific material is substantially constant on the portion of the resistance–time curve where the effects of the absorptive current predominate.

The slope factor as defined in the paper would be expected to increase from zero for wet insulation to some constant value after the insulation has become sufficiently dry so that up to ten minutes the absorptive current is still large compared with the steady-state leakage current. With further drying very little increase in slope factor would be expected. The slope factor therefore would appear to give a convenient means of determining a level of dryness in machine insulation.

As the author points out, it should be recognized that, whereas machines of varying size but with identical insulation would be expected to have the same order of maximum slope-factor, differences in insulating techniques and materials will affect the value of the maximum slope factor.

The value of maximum slope factor for a specific type of insulation is not a measure of the quality of the insulation but merely a convenient means of measuring the order of dryness.

In our insulation-resistance studies we use the ratio of the insulation resistance as measured after ten minutes and one minute of voltage application as a measure of the slope of the absorption curve. This is used because the insulation resistance–time curve approximates a straight line when plotted on log-log paper. This slope is equal to the logarithm of the ratio R_{10}/R_1. However, it can be shown that the slope factor as defined in the paper differs from this ratio by unity and that for practical purposes either is equally useful.

The author's data on temperature effects show that temperature–resistance characteristics of class-B insulation vary over rather wide limits. It would appear that the use of any general temperature-correction curve applicable to all machines is apt to result in rather large errors in some cases.

This paper is interesting and is a constructive contribution. The data given on the insulation-resistance characteristics of large generators as affected by drying treatment should be of value to the industry.

E. W. Whitmer (American Gas and Electric Service Corporation, New York, N. Y.): This paper deals with the interpretation of nondestructive tests of insulation that covers a very large area and therefore may not be of uniform quality throughout the entire winding of a large generator. In interpreting the results of such tests it is often helpful to segregate the windings into as many insulating paths as possible. When this is done a more comprehensive interpretation of the condition in the winding insulation may be obtained than is otherwise possible. In addition to this a comparison of the d-c tests to 60-cycle a-c test is of interest in determining the dryness of insulation.

Power-factor tests for indicating the dryness of insulation have been used quite widely for equipment such as transformer windings. For such purpose we have found the d-c insulation resistance may rise to a very high value prior to the time that dryness is indicated by a power-factor test. For instance, in a group of 25-kv oil-filled instrument current-transformer windings which were dried in air, the insulation resistance at oven temperature rose from about 30 to well over 2,000 megohms in approximately the first 20 per cent of total time required to dry out all of the insulation in the windings. These windings consisted mainly of a pad of varnished cambric in series with wooden blocks. It is probable that the wooden blocks dried out long before the varnished-cambric insulation, thus causing the d-c insulation resistance to increase to a very high value, while the remaining varnished-cambric insulation was still quite wet, as indicated by power-factor tests. It is not intended to compare this small transformer winding to that of a large generator, but the instance does serve to illustrate that there is a possibility that some part of a fabricated-winding insulation may become dry before other parts and therefore cause premature indication of dryness by d-c insulation-resistance tests. Whether or not such a condition occurs in drying large generator windings depends on tests and experience. Possibly the author of this paper has had some experience along this line that would be quite helpful.

E. H. Povey (Doble Engineering Company, Medford Hillside, Mass.): There has been a growing interest among operating companies in nondestructive d-c testing. Mr. Marcroft's excellent paper shows that definite progress is being made in this field.

There are two formulas being used to reduce the absorption characteristic to a single figure. The formula Mr. Marcroft uses, $(R_{10}-R_1/R_1,)$ called the slope factor, is the fractional increase in resistance over a nine-minute period. The other formula is simply R_{10}/R_1 and gives a value greater than the slope factor by a constant of plus one. In the interest of simplicity it is suggested that the latter formula be used in evaluating the absorption characteristics and that some descriptive term, such as "absorption index" be applied to the resulting value.

R. W. Wieseman (General Electric Company, Schenectady, N. Y.): Rotating-machine windings have many varieties of coils, insulations, and mechanical arrangements. Individual coil tests cannot be made on armature windings for practical reasons. A single reading of insulation resistance, therefore, does not give a good perspective of the winding insulation condition.

The rate at which insulation resistance increases after one minute of voltage application is an important feature of winding-insulation resistance. This rate of insulation-resistance increase known as dielectric absorption or polarization is a better insulation barometer than insulation resistance itself. The greater the observed polarization effect the lower is the moisture content of the insulation, and so we have a good indication when a dry-out run can be terminated.

Mr. Marcroft has demonstrated well the usefulness of the absorption characteristic as a moisture indicator of winding insulation. The paper also calls attention to an important item, namely, the necessity of having a constant direct voltage for the absorption test. True values of absorption coefficients cannot be obtained if the applied voltage has the slightest variation. The slope factor $(R_{10}-R_1)/R_1$ can be used to denote the degree of polarization. It is suggested that simply R_{10}/R_1 be used and that this term be called the polarization index. R_{10}/R_1 will vary from one to about seven for class-*B* insulation. A convenient method of judging the slope of the resistance curve is to plot the resistance on log-log paper with the resistance at one minute equal to unity. On this plot the polarization index is equal to the ordinate at ten minutes of voltage application. If a class-*B* winding is bone dry and if conducting paint has not been used on the end portion of the coils, the slope approaches 45 degrees.

Testing for insulation resistance at any temperature and then correcting for temperature should be avoided, because temperature coefficients are not necessarily the same for a given winding over a period of time. This is shown clearly in Figures 4 and 5 of the paper. Insulation-resistance testing, therefore, should be made at a temperature which can be reproduced in subsequent periodic tests. This and other variables encountered in insulation testing show the need for standardization. For comparison, values of insulation-resistance and polarization coefficients obviously must be on the same basis.

R. L. Webb (Consolidated Edison Company of New York, Inc., New York, N. Y.): Mr. Marcroft's paper adds materially to the information which has been published on insulation-resistance testing. His suggestions will be found valuable by users of generators and other rotating electric equipment generally.

The author indicated that comparison of test values taken at different voltages also are useful in detecting excessive moisture in insulation. We have used this method for several years by taking periodic dielectric-absorption curves on 13.8-kv generator stator windings at 1,000, 5,000, and 22,000 volts direct current. With the 1,000-volt five-minute megohm value used as 100 per cent, testing experience has shown that the five-minute values at 5,000 and 22,000 volts should be 75 per cent and 45 per cent or more respectively, if windings having class-*B* insulation are satisfactory so far as moisture content is concerned.

In addition to the use of slope factor to determine the degree of dryness in insulation the author might have added that certain minimum values of megohms also must be obtained. As a general rule, high insulation resistance will follow automatically with satisfactory slope factor, but its value should be taken into account in each case.

Slow drying of high-voltage stator windings at 75 degrees centigrade to 100 degrees centigrade is desirable. Any attempt to use higher temperatures and less drying time may cause damage to the insulation due to formation of steam pockets between layers of tape. Also fast drying may produce an increase in insulation resistance up to some minimum value in a short time, because only a portion of the winding is free of moisture. In such cases the coils in the lower part of the machine still may be too wet to permit application of normal voltage with safety. The drying time for a stator winding rarely is less than 72 hours and may be two to three times as long, depending on the amount of moisture present. Field windings of turbogenerators also require comparable periods of time for drying.

In Table II of the paper it is noted that generator *B* had a slope factor of 1.83 at 15 degrees centigrade before drying was started. Since generator *D* in Table IV had a lower slope factor when cold after dry-out, I would like to ask the author what it was that made him decide to dry the windings of generator *B*. Possibly the insulation-resistance value in megohms was considered too low for that machine.

H. C. Marcroft: The increasing use of dielectric-absorption testing for generator insulation is evident from the discussion on this subject. The use of absorption tests on insulation was described by R. W. Wieseman.[1] In using the Wieseman method, a numerical index for referring to absorption-curve slopes was desired, and, as none had been proposed previously, the term slope factor was used. This value was the difference between the ten-minute and one-minute values of resistance divided by the one-minute value. The minimum slope factor is then equal to zero for a completely wet machine.

However, as pointed out by Wieseman, Askey, Johnson, and Povey, the ratio of R_{10} to R_1 is simpler to use than the slope factor and is to be preferred. A completely wet machine would have a minimum value of R_{10}/R_1 of unity on this basis. Mr. Wieseman suggests the term "polarization index" for the R_{10}/R_1 ratio, and in the interest of standardization we agree to this as being a desirable term for the absorption characteristic. Polarization index is numerically equal to slope factor plus unity.

There has been some oral discussion on the difference in curve slopes to be obtained from the battery-power test equipment described in the paper, and other equipment. It is true that, if the instrument has high impedance in its output terminals, a variable voltage will be applied to the generator during a test, and this will result in a faulty curve and an erroneous polarization index. Ohmmeters with manually generated power usually have relatively low impedance and give values which agree well with battery tests.

Mr. Whitmer's comments on uneven drying are interesting. Some of the curves obtained on generators have shown evidences of this, as shown in the uneven resistance increment with time. Figure 3 of the paper shows this effect to some degree. The dielectric-absorption-curve method is a better indicator of the moisture content than the single one-minute-reading method and generally will show that drying should continue beyond the point that the short-time tests indicate dry insulation.

R. L. Webb has commented on a point along this same line, relative to the dry-out of generators *B* and *D* of Tables II and IV, respectively, of my paper. Generator *B* had been in steady service nine years when it was taken out of service for two months, during which time one quarter of the winding was replaced with new coils. The data of Table II are for the dry-out following this work. The dry-out was for the benefit of the new coils. Generator *D* of Table IV was a newly built machine (manufacturer *A*) at the time of the dry-out. Generator *B* is a good example of a machine with uneven drying, the point raised by Mr. Webb and Mr. Whitmer. In such a case the arbitrary limits must be raised to allow for the dry portion of the winding. In this case the dry-out could have ended at 72 hours, when the slope-factor rise became negligible, but other considerations allowed a continuation of the run until 108 hours. We have an arbitrary minimum standard of five megohms at one minute, regardless of temperature or size of generator, but the generator resistance generally exceeds many times this value.

REFERENCE

1. INSULATION RESISTANCE OF ARMATURE WINDINGS, R. W. Wieseman. AIEE TRANSACTIONS, volume 53, 1934, June section, pages 1010–21.

Frequency Changers—Characteristics, Applications, and Economics

Discussion of paper 45-34 by S. B. Crary and R. M. Easley, presented at the AIEE winter technical meeting, New York, N. Y., January 22–26, 1945, and published in AIEE TRANSACTIONS, 1945, June section, pages 351–8.

John G. Holm (Boston Port of Embarkation, Boston, Mass.): As the authors pointed out in their very interesting paper, the electronic load-regluating type of frequency changers has numerous advantages of its own and may be used more extensively when it is made economically competitive. It is realized with the authors that no economic comparison of a permanent nature could be made at this time between this type of frequency changers and those using the rotating equipment. However, in *F* of Figure 12 of the paper, it would be very desirable if the authors would give the cost of the 10,000-kw 60- and 25-cycle zigzag transformers of the voltages indicated, on the same comparative percentage basis as the cost of the two synchronous condensers. The cost of these transformers probably will remain more or less constant for quite some time to come. If, therefore, this cost is given, as requested, the rectifiers, inverters, their accessory operating equipment, and their foundations will remain the only equipment whose cost cannot be fixed at this time. It then will be possible to compare the total capital cost, of the electronic converters, with the cost of the synchronous-type induction-frequency converter. A comparison with the cost of the most expensive of the rotary frequency changers will give an indication of what should be the order of magnitude of the cost of the electronic converters, in order for the electronic load-regulating type of frequency changers to compete, on purely capital-cost basis, with the other types.

Harry P. St. Clair (American Gas and Electric Service Corporation, New York, N. Y.): The authors of this paper have presented a very interesting and useful summary of the various types of frequency changers available, along with comparative characteristics and costs. In the problem of power supply to main-line railroad electrification using 25 cycles, the cost of frequency conversion, especially for single-phase operation, becomes a major item. For this reason we have been greatly interested in developments and possibilities of electronic frequency conversion in the hope that such a radically new principle might give promise of ultimately reduced costs.

Although the authors, as pointed out, purposely have deleted the numerical cost comparisons on the electronic three-phase to three-phase frequency changer, from the other comparisons shown in Figure 12 of the paper, I recall that the over-all cost of this equipment including synchronous condensers, was of the order of 300 per cent compared with 100 per cent for the straight synchronous–synchronous outfit. Even if the 60-cycle condenser should not be needed, the comparison would not be improved greatly and would be made even worse for conversion to single phase, requiring additional synchronous equipment for balancing out the single-phase power pulsations.

For this reason, even though the electronic cost figures omitted by the authors are reduced substantially, there does not seem to be much promise in electronic-frequency conversion for single-phase main line railroad situations for a long time to come.

It is desirable, however, that electronic developments along these lines should continue, and to this end it is gratifying that a sufficient number of favorable factors were found in the case of the large installation at Pittsburgh to permit going ahead with a full-scale project of that nature.

Electrification and Signaling of the Canadian National Railways Terminal, Montreal, Canada

Discussion of paper 45-10 by R. G. Gage, presented at the AIEE winter technical meeting, New York, N. Y., January 22–26, 1945, and published in AIEE TRANSACTIONS, 1945, February section, pages 41–4.

C. C. Herskind (General Electric Company, Schenectady, N. Y.): This paper describes a rectifier application which differs from the usual practice in the United States in that it employs glass tubes instead of rectifiers of metal construction. American manufacturers never actively have sponsored large-size glass-tube mercury-arc rectifiers despite the wide acceptance and use of such rectifiers abroad. While the use of glass tubes has received serious consideration by American manufacturers, metal construction has been adopted in the sealed ignitron rectifiers for the following reasons:

1. *Strength.* The glass tube has definite size limitations arising from the thermal stresses and short-circuit forces applied to it. Metal tubes are easier to ship and handle than the corresponding glass-tube equipment.

2. *Manufacturing Methods.* Metal tubes are suited better to American manufacturing methods, requiring less highly skilled labor than do glass tubes. A simpler structural arrangement and more accurate assembly is possible by the use of metal tubes.

3. *Fault Protection.* The definite size limitations of glass tubes require the operation of a number of tubes in parallel where rectifier equipment of large capacity is desired. Parallel operation presents difficulties in the design and arrangement of equipment to protect the tubes from damage by high current obtained during arc-back. With metal construction, the number of anodes required for a rectifier equipment may be kept at a minimum consistent with the desired performance characteristics and the problem of fault protection is minimized.

4. *Cost Factors.* The choice of glass construction to such a large degree by European manufacturers, instead of metal construction, appears to be based on differences in material and labor costs. Skilled labor capable of manufacturing the glass designs is available in Europe at relatively lower costs than in the United States. Also, glass provides a lower-cost material than metal insofar as European manufacturers are concerned.

While metal construction of small rectifiers of from 10- to 500-kw capacity has been established firmly in American manufacture, the wide use of the glass rectifier abroad should be recognized, as it yet may compete with rectifiers of metal construction.

W. R. Bunting (nonmember; Northern Electric Company Ltd., Montreal, Quebec, Canada): I would like to make a few comments regarding the glass-bulb rectifiers installed at the Montreal Terminal.

The Hewittic Electric Company Ltd., the manufacturer of these rectifiers, was a manufacturer of glass-bulb rectifiers of moderate requirements before the first World War. After the war, they recognized the possibilities of rectifiers for large power applications, and were faced with the necessity of deciding whether they should pursue the use of glass or develop steel-enclosed rectifiers.

They decided in favor of the former, and today have many installations in successful operation and can cater to any current or voltage requirement within the limits of practical power distribution.

Glass is a very useful constructional material and, in fact, has ideal characteristics for this purpose. Think of the millions of lamps and vacuum tubes in existence today which could not possibly be produced without glass. The step to power bulbs is but a small one.

Insofar as the structural strength is concerned, the bombing of London has demonstrated the ability of the glass bulb successfully to withstand bomb concussion. Such bulbs as have been damaged have been injured by being struck by bomb fragments. Little consideration of the bulb is needed to realize that its shape is fundamentally strong.

The protection used on the Canadian National Railway rectifiers consisted of three elements:

1. An induction-type overcurrent relay.
2. A main d-c breaker arranged for high-speed tripping in the reverse direction.
3. Anode fuses.

The induction relays were supplied from current transformers in the main transformer tank and were arranged to cater to the normal overloads the rectifiers were expected to carry. In case of operation, the relays tripped the main d-c breaker, this operation being at normal speed. The main breakers were equipped also to trip at high speed in case of a feedback to the rectifier.

Fuses in the anode circuits provide a simple and effective protection against backfire. The incidence to backfire is so infrequent that this protection is ample.

I would like to add a thought about backfires although I do not claim to be a rectifier expert. Basically I think we can say that backfires are the result of anodes becoming too hot, whatever may be the actual cause of excess temperature. The glass-bulb rectifier for large powers uses a number of bulbs in parallel so that the current is divided into a number of, or even many, paths. The arc to an anode tends to go to a spot. So, if the anode is to carry much current, increasing the size does not help a great deal even though the heat-dissipating capacity is increased because the arc persists in going to a spot. This spot, becoming too hot, emits electrons and a backfire follows. The use of many paths eliminates much of the possibility for the anode to reach excessive temperatures.

The anode fuses are selected then to pass successfully normal overloads and, shall I say, normal short circuits, if a short circuit may be considered a normal thing. In the remote instance of a backfire, the fuses act rapidly, being in fact a current-limiting fuse, blowing more quickly than the rate of rise.

In addition, there are feeder breakers of the high-speed variety which clear track short circuits so quickly that other protective equipment is not called upon to function.

The main a-c breaker also is equipped with protective equipment similar to that which would be used for any radial feeder.

To put a rectifier in operation, it is only necessary to close the main a-c breaker when direct current is available immediately. The absence of pumps, either water or vacuum, and such auxiliaries, is so desirable that emphasis hardly need be expressed about it.

Grounding of Circuits on Self-Propelled Vehicles

Discussion of paper 45-11 by D. D. Ewing, presented at the AIEE winter technical meeting, New York, N. Y., January 22–26, 1945, and published in AIEE TRANSACTIONS, 1945, February section, pages 48–50.

W. S. H. Hamilton (New York Central System, New York, N. Y.): The comments presented here apply to vehicles running on steel rails only. While Professor Ewing's paper refers to self-propelled vehicles only, these comments also include vehicles on steel rails which are not self-propelled, such as main-line passenger cars, hauled by locomotives.

SELF-PROPELLED VEHICLES

The circuits on these may be classified as follows:

Circuits Connected to an External Power Supply (Third Rail or Trolley). These of necessity have one side grounded, and the practices in regard to them are so well known as to need no further comment here

Traction-Motor Circuits Not Directly Connected to an External Power Supply. Examples of these are transformer secondary circuits on a-c locomotives, and traction motor circuits on Diesel-electric locomotives.

It is my opinion that these should be of the metallic-return type with both sides of the circuit insulated from the frame of the vehicle but with a ground established through a ground relay. Professor Ewing has discussed the greater reliability of the complete metallic circuit, and I wish to stress the importance of having a definite ground on the circuit in order to limit the potential to ground to a known value and to indicate by the operation of the ground relay when an undesired ground occurs.

When the total voltage of the circuit is over 600 volts, and the circuit is such (as in the case of a transformer secondary winding) that the ground relay can be connected to the mid-point of the circuit, then that connection should be used. When the total voltage of the circuit is between 250 and 600 volts, the connection should be made either to the mid-point or to one side, and, when the voltage is 250 or less, the connection should be made to one side of the circuit.

A grounded mid-point in a circuit is sometimes a nuisance, which is the reason for the above recommendation for voltages between 250 and 600 volts. In some cases it may be better to connect the ground relay to one side of the circuit.

When the circuit is such that the ground relay cannot be connected to the mid-point, then it should be connected to one side of the circuit and a switch provided to disconnect the relay in case of a second ground, in order to permit the vehicle to be operated to a repair point under its own power but with the operator knowing that an undesired ground exists. Under normal conditions it always will be known that one side of the circuit is alive with respect to the frame of the vehicle, and proper precautions can be taken against accidental contact. These precautions cannot be taken so readily when a circuit is completely ungrounded (or supposed to be).

Control Circuits Which Control Motion of the Vehicle. It is my opinion that these should be of the metallic-return type but with one side grounded to the frame of the vehicle. This grounding should be through two or more ground connections in easily reached locations to insure continuity of the ground connection and yet permit it to be readily broken for testing.

Circuits of this type require somewhat greater maintenance than ungrounded circuits, but there is greater assurance against false operation due to short circuits, crosses, and undesired grounds. Such faults usually blow the control fuse and may render the vehicle temporarily inoperative until the fault can be located, but this is better than the possibility of false operation.

Such a connection also provides considerable assurance against the presence in the control circuits of higher voltages from the traction-motor circuits, due to either leakage or an accidental cross. This is a highly desirable feature.

On most modern vehicles such circuits will include a storage battery. Accidental grounds due to liquid leakage over the battery trays can be prevented by washing the batteries monthly when the vehicle is in for Interstate Commerce Commission inspection (if required) and by proper insulation of the trays.

Other Control and Auxiliary Circuits. When there are also circuits isolated from the traction motor and control circuits, it is my opinion that these also should have one side grounded in the same manner as the motion-control circuits. Professor Ewing has pointed out the desirability of grounding such circuits when fed from the secondary windings of transformers, and I concur with his statement.

NON-SELF-PROPELLED VEHICLES

Obviously there are no traction-motor circuits on such vehicles nor any circuits controlling motion. Such circuits as exist are used for lighting, air conditioning, and so forth and their associated control.

D-C Circuits, 0–110 Volts (Nominal). These in general include a battery, and, on account of the difficult conditions under which main-line cars operate, it generally has been considered that it was better not to ground such circuits. It is not feasible to give batteries on these vehicles the periodic washings at frequent intervals, which can be done with self-propelled vehicles, and, as accidental grounds cannot cause false motion, the practice of using ungrounded circuits seems to be justified.

D-C Circuits Over 110 Volts (Nominal). Such circuits have not yet been used, so far as I know, but, if they should be introduced, they should be grounded either on one side or at the mid-point, as circumstances may indicate to be most desirable.

A-C Circuits Not Connected to an External Supply. These may be either polyphase or single phase.

(*a*). *Polyphase Circuits.* These should be grounded at the mid-point in order to limit the voltage to ground at any point.

(*b*). *Single-Phase Circuits.* These should be grounded on one side as recommended by Professor Ewing in his conclusion 10. An exception might be made to this recommendation insofar as circuits supplying high-voltage fluorescent lamps are concerned. In such cases it may be preferable to ground the mid-point instead of one side.

A-C Circuits Connected to an External Supply. Under this category come the 220-volt three-phase circuits used for stand-by power supply for air conditioning, and other services on passenger cars. It is standard practice to ground the neutral of the power supply at the transformer (not on the car) and to carry a ground wire in the connecting cable up to the plug itself so as to protect persons handling the plugs from possible shocks.

On plugs used to service cars in electrified territory the two halves of the plug are insulated from each other to prevent any chance of carrying propulsion current through the ground wire. The portion of the plug which usually is handled still is connected to the ground wire.[1]

Single-phase circuits of this category should be grounded either at the mid-point or on one side.

GENERAL COMMENTS

The foregoing remarks all assume that care will be taken to ground the body of the vehicle effectively to the trucks (and to the rails) and all metal parts that might become charged with potential to the body. This is very important in the case of vehicles using external power for propulsion but also should be done on the other classes of vehicles mentioned, although the methods used for grounding need be for potential only and do not have to be arranged to carry the relatively heavy currents necessary when propulsion from external power is used.

The term "grounding" as used in this discussion is intended to indicate a metallic connection between the circuit involved and the frame of the vehicle and not a ground that is subject to interruption, as in the case where a circuit is grounded through a fuse.

Although I have recommended in several cases in the foregoing, grounding the mid-point of circuits, at the same time, I personally am not too enthusiastic about such an arrangement, when potentials of 600 volts and less are involved, and, when there is a choice, I would prefer to ground one side instead. The first locomotive of our fleet of combination third-rail engine battery locomotives, usually called three-power locomotives had a 218-cell battery grounded at the mid-point, but, as a result of experience with it, we changed it to a battery grounded on one side instead, and all later locomotives of this type were built with 240-cell batteries grounded on one side through a battery break up and disconnecting switch. With the switch open the battery is split electrically into two halves, neither of which is grounded, and maintenance on the battery is done under this condition. Operation in the last 15 years has indicated that this arrangement is entirely feasible.

The prize nightmare of all control circuits is one with the neutral grounded, on account of the faults that may occur due to accidental grounds. The next one to it is one that is not grounded at all, but which is at times connected to other circuits in which grounds can occur. I once worked in the field with some locomotives that had auxiliary generators which were used for control and also for supplying power for head-end train lighting on passenger cars. Grounds were often present on the batteries on these cars in varying degrees on either side of the circuit. As some of the switches used on the locomotives broke only one side of the circuit, we had some weird occurrences, such as lights staying lit when the switch was opened, although no actual harm was done. After that experience I swore "never again."

When ungrounded circuits are used, it is desirable that every switch break both sides of the circuit, and this is a nuisance in control work.

On the New York Central System we have 152 electric locomotives equipped with 32-volt control batteries which either are grounded solidly on one side or else grounded on one side when the battery switch is closed. We have experienced no particular difficulty in maintaining them.

When a battery is involved and the circuit permits, it is good practice to use a battery switch so arranged that when the switch is open the battery is disconnected from both sides of the circuit. This permits rapid isolation of any partial grounds in the battery itself, should they occur.

REFERENCE

1. MANUAL. Electrical section, mechanical division, Association of American Railroads. Section C, page 59.

Compressed-Air Circuit Breakers in A-C Railway Service

Discussion and authors' closure of paper 45-31 by H. M. Wilcox and D. C. Harker, presented at the AIEE winter technical meeting, New York, N. Y., January 22–26, 1945, and published in AIEE TRANSACTIONS, 1945, March section, pages 141–5.

W. F. Skeats and **E. W. Boehne** (General Electric Company, Philadelphia, Pa.): As the authors point out, the component parts of this circuit breaker have all been applied in one way or another in the past. Thus the creation of the circuit breaker as described in the paper involves primarily a co-ordination of these items. Though this is a less spectacular and usually much less time-consuming job than such a thing as the development of a new interrupter, for instance, it offers an opportunity for the exercise of considerable skill and the authors on the whole appear to have done a very good job.

With regard to the compressed-air system it should be noted that whereas the air entering the delivery system will have a moisture content substantially below saturation, a temperature drop of about 15 degrees Fahrenheit will bring it to the dew point, and any further drop will deposit moisture in the 150-pound system. As a drop substantially greater than this may be anticipated between afternoon and evening, care still must be exercised in the layout of the unheated portion of the system. It would be interesting to see what arrangement the authors propose at this point.

It is agreed that the latched-in type of mechanism is best adapted to a quick start of the moving contacts. However, it should be noted that the latch may be either mechanical with an electric trip coil, or magnetic. The magnetic latch, especially the flux-shifting type, has the advantage of operating on a short magnetic gap so that a relatively large change in flux can be produced with a small input of energy.

The flexibility of the magnetic latch is attested by its use on such widely divergent applications as railway circuit breakers for the duty discussed by the authors, the 287-kv 0.05-second impulse circuit breakers on the Boulder Dam line, and 138-kv 0.05-second tank-type oil circuit breakers.

In laboratory tests on such a circuit breaker as this, one is assured of a current zero very nearly 360 degrees after inception of short circuit, and, if the contacts are separated just a short time before this, the arc duration always will be relatively short and the current in the arc considerably below crest value. In the field, because of more rapid decay of the d-c component or gradual development of the fault, there may be deviations from this rule with consequent increases in arc duration and arc current. We should like to ask the authors whether the circuit breaker has been tested for its ability to perform satisfactorily under these conditions.

The lowest current at which the authors show tests on this circuit breaker is about 15,000 amperes. Have they investigated its ability to interrupt very light currents such as transformer magnetizing currents without producing overvoltages?

H. M. Wilcox and **D. C. Harker:** In pointing out the effects of a 15 degree Fahrenheit change in temperature between afternoon and evening, Mr. Skeats and Mr. Boehne refer to the unheated portion of the 150-pound system. Actually this portion consists only of the air line between the air-supply unit and the circuit-breaker unit. Since the volume of air contained in the pipe line is very small and since their discussion presupposes no air movement during the interval in which the temperature change takes place, the amount of moisture deposited in this line would be very small.

The authors therefore believe that Mr. Skeats and Mr. Boehne refer to the circuit-breaker reservoirs and that they are unaware that the reservoir compartment of the circuit breaker is heated. Thermostatically controlled heaters have been provided to insure that the reservoirs remain above ambient temperatures under all freezing conditions, and, hence, moisture may be expected to form only when the ambient temperature is 15 degrees Fahrenheit higher than the upper setting of the thermostat.

The conditions assumed by Mr. Skeats and Mr. Boehne further require that the circuit-breaker reservoirs shall have been charged largely during the period of high temperature and that little, if any, charging take place at low temperature. Consequently it appears to the authors that any appreciable condensation in the 150-pound system is very remote. A little further consideration indicates that the amount of condensation that possibly may accumulate even under the higher-temperature conditions just described, may be expected to be negligible. As described in the paper, the air is compressed to 250 pounds storage pressure and then cooled to ambient temperature. By doing this, approximately 94 per cent of the moisture content is precipitated in the storage reservoirs, where it is collected in suitable drains. The air then is expanded and delivered to the 150-pound system. If under the remotely possible conditions previously outlined the air should saturate in the heated circuit-breaker reservoirs, then, at most, it could precipitate only six per cent of the moisture content originally in the air. To take care of the little amount which possibly may accumulate over a period of time, drains have been provided both in the circuit-breaker reservoirs and in the 150-pound outlet of the air-supply unit, and it has been recommended that a slight slope be given the air line between the air-supply unit and the circuit-breaker unit.

Furthermore, in order to determine what effect moisture-laden air might have upon the circuit breaker's interrupting ability, a small portable compressor was connected directly to the circuit breaker during a considerable portion of the outdoor testing period at the high-power laboratory. Raw air—without benefit of aftercoolers, intervening tanks, or expansion down from 250 pounds—was fed directly into the circuit-breaker reservoirs. Under these conditions, which the authors believe are much worse than actual operating conditions, interrupting tests under a variety of weather conditions were taken over the entire current range, and no evidence of deterioration of insulation nor change in the circuit breaker's interrupting characteristics was observed.

In regard to Mr. Skeats and Mr. Boehne's question as to whether the circuit breaker was tested for its ability to perform satisfactorily under actual field conditions, as regards time of inception and growth of short-circuit, a considerable number of interrupting tests were taken at the high-power laboratory with the synchronous timer set to close the fault-initiating circuit breaker at ten-degree intervals over the full 360 degrees. Thus, faults were obtained, ranging consecutively all the way from nearly completely offset current with small first half cycle through symmetrical faults to offset current with large half-cycle. Oscillograms showed a wide variety of arc-duration times, ranging from a small fraction of a half cycle to slightly more than a half cycle. Since these tests were conducted over the entire current range and since a large number of close–open shots were taken, it is believed that all possible field conditions of arc duration and current were covered.

Low-current tests, about which Mr. Skeats and Mr. Boehne inquired, were made. This circuit breaker was tested by the authors down to 53 amperes at 11,000 volts. Other interrupting tests at lower current values were made at reduced voltages as necessitated by the test circuit. These low-current tests were made with an air-core reactor inserted in the circuit to give a more severe condition than might be expected in service. Reviewing these tests, as well as others made on a number of types of compressed-air circuit breakers over a period of years, has convinced the authors that such interruptions may be made without hazardous voltage conditions when the circuit interrupter is properly designed.

Mercury-Arc Rectifiers for Railroads

Discussion and author's closure of paper 45-17 by S. S. Watkins, presented at the AIEE winter technical meeting, New York, N. Y., January 22–26, 1945, and published in AIEE TRANSACTIONS, 1945, February section, pages 84–6.

Sidney Withington (The New York, New Haven, and Hartford Railroad Company, New Haven, Conn.): Mr. Watkins' paper presents a very interesting summary of rectifier operations recently developed.

Mention is made of the operation of unattended mercury-arc rectifier substations on the basis of remote or supervisory control. Consideration might be given in this connection to completely automatic substations, especially those near the end of long lines, to accomplish starting at low voltage and cutting off at low current values. This would eliminate the expense of the supervisory facilities.

Mr. Watkins suggests daily visits to each substation. This would seem to be more frequent attention than is necessary, at least under some circumstances. Mercury-arc substations installed as long ago as 1927, and even rotary-converter substations which are automatic, have been operated successfully with visits not more frequent than once a week. In at least one instance, a rotary substation maintained on this basis operated for 396 days without any trouble whatever, and there is no reason why mercury-arc substations should not have even better records.

Mr. Watkins refers somewhat indiscriminately to multitank and single-anode rectifiers. It would be advantageous to confine the designation to one or the other term.

It is suggested that, in connection with railroad operation of single-anode type for high-voltage service, "the degree of present development in that direction varies." It would be interesting to learn how many rectifier substations of this type for railroad service above 750 volts have been installed in the past 10 or 15 years.

Sealed tubes show such a great advantage over rectifiers with mercury pumps that serious consideration might be given to standardizing this form of installation. It is understood that industrial development is very largely on this basis, and this may be indicative of the trend.

Compounding characteristics are a decided advantage in railroad operation, as Mr. Watkins suggests, and he also might have included in his discussion the subject of regeneration, which is used to some extent, and which may develop worth-while advantages.

J. H. Cox (Westinghouse Electric and Manufacturing Company, East Pittsburgh, Pa.): By providing an up-to-date review of the various factors affecting the application of mercury-arc rectifiers for railroads, Mr. Watkins has provided a valuable reference for those contemplating an increase in d-c power supply for traction apparatus. I would like to supplement a few of the points.

With the earlier mercury-arc-rectifier installations it was quite natural that the operators would be conservative and provide ample maintenance. As time added experience, it was also natural that the amount of maintenance would be reduced, closer to the amount that was found actually to be needed. There is very little about a rectifier that requires maintenance and the frequency of maintenance probably is determined by the routine attention required by the switchboard devices. In normal surroundings, so far as the rectifier is concerned, the following should be adequate for routine maintenance; a visit to the station once per week; cleaning maintenance once per month; calibrating, checking, and overhaul of auxiliaries once per year; and water-pump and cooling-system maintenance as required. With sealed-tube rectifiers, the tubes should be replaced only as required by tube failure. With pumped rectifiers, the vacuum chambers should not be opened until required by actual troubles with vacuum or arc-backs. Experience indicates that this should not be required more often than once in five to ten or more years.

Single-anode tanks provide greater service reliability and flexibility in that any tank can be isolated from the vacuum and electrical systems and the unit continued in operation with slightly reduced capacity. Questions have been asked regarding the reliability of vacuum pumps on pumped rectifiers. Very little attention is required by modern vacuum apparatus. Furthermore, with modern rectifier manufacturing technique, tubes, even though built for continuous pumping, can be isolated from the vacuum pumps by closing the vacuum valves and maintain satisfactory operating vacuum for several days. This is true even through arc-backs.

In the past the usual practice on railroads has been to hold a rectifier unit out of service for one minute following an arc-back. There is no reason why a rectifier should not be returned to service as fast as the breakers can be reclosed. It has been established that an outage of ten cycles is adequate to restore the rectifier to satisfactory operating quality. Anode circuit breakers also have provided a possible improvement in operating reliability. It is entirely feasible to sequence the control so that only the pole to the arcing-back anode is opened and the remainder of the rectifier left in service. The pole which opened then can be reclosed without disturbing the others. In some circumstances, it appears attractive to depend entirely on the anode breakers and omit the usual cathode and a-c breakers, substituting fuses in the a-c circuit to provide for transformer faults.

The modern small-unit-type rectifier substation offers an attractive means of placing small units of power along a right-of-way where traffic is not too heavy, and obtaining better service than is possible with larger stations at less frequent intervals. By suitable choice of regulation characteristics and very simple voltage-control apparatus almost any desired load limitation at a station, or load division between station, can be obtained.

C. C. Herskind (General Electric Company, Schenectady, N. Y.): Attention is called to the fact that there is a definite trend toward the elimination of vacuum pumps on all size rectifiers. Evidence of this trend is the increasing use of sealed ignitron rectifiers of the smaller sizes in industrial and mining applications in this country, as reported in the paper, and the growing use of the pumpless multianode rectifiers abroad. While vacuum pumps have been developed to the point where they are thoroughly reliable and require very little maintenance, the simplification obtained by the elimination of vacuum pumps is obvious and desirable.

The overload rating of the rectifier and transformer combination, as given in the paper, reflects the service requirements for railway applications. Attention is called to the fact that these ratings do not match the capabilities of the rectifying elements under short-time loading. For example, in the rectifiers for heavy-duty main-line service having an overload rating of 300-per-cent load for five minutes, these are designed to meet this short-time loading and generally will be of such size that they could carry substantially more than 100-per-cent loading continuously. For some designs the ratio of the current capacity for one minute to the continuous capacity is approximately two to one. Data are being accumulated regarding the capacity of various rectifying elements as determined by arc-back and structural limitations, and it is hoped that they will be available to application engineers before too long to assist them in obtaining the best application.

H. D. Brown (General Electric Company, Schenectady, N. Y.): Mr. Watkins should be complimented for his fine summary on the performance and operation of multianode and single-tank mercury-arc rectifiers. It is gratifying to manufacturers to learn that their decision to develop and further perfect this type of apparatus is justified.

The question as to the ability of rectifiers to carry heavy-load swings is largely a function of insufficient vapor pressure and this, in turn, leads to starvation and oscillation of the arc, especially at the higher currents. In the older designs where long arc lengths between anode and cathode were encountered this condition was not infrequent.

In the newer designs this difficulty has been overcome by employing shorter arc lengths and applying a more accurate control of the vapor pressure. This is true especially of the ignitron single-tank rectifier in which the arc length is exceedingly short and the temperature control is very much more effective.

By employing added baffling, it is entirely possible to construct the ignitron type of rectifier for the higher voltages, say, 3,000. As a matter of fact, a frequency changer put into operation about a year ago employs ignitron tubes operating at approximately 20,000 volts direct current.

It is quite certain that up-to-date design and construction, together with more accurate means of determining vacuum tightness, will make available rectifiers which will give even improved operation in the future.

The fact that rectifiers have proved satisfactory as conversion apparatus leads one to expect confidently that many other applications will be found for this type of apparatus in the industrial and transportation fields.

A. Schmidt, Jr. (General Electric Company, Schenectady, N. Y.): We are gratified by the universal acceptance of rectifiers in the railway and electrochemical fields and their increasing recognition in other fields. We wonder if the gains of the last few years generally have been realized. Multitank ignitrons to the extent of over 2,000,000 kw have been installed since 1939. Development has kept pace with construction, and important gains in manufacturing technique and in performance have resulted. Progress has been so great that arc-back frequency is now usually less than one per year per rectifier. Improved gaskets have reduced maintenance; the opening of a tank is very rare indeed, and lost time for this purpose is negligible.

Recognition of rectifiers in the industrial field is evidenced by the installation of over 30,000 kw of industrial and mining units in the last year. The ease of installation of these package units is an especially attractive feature. The performance of these units has been outstanding. A noteworthy item in this connection is that operators generally have no previous knowledge of this type of equipment.

While there has been general acceptance of rectifiers in specific fields, other fields, such as d-c transmission, motor control, and electronic frequency changing, have been explored to lesser degrees. As industry learns how best to utilize developments in these fields, we may expect further progress, commensurate with the ultimate usefulness of specific applications.

R. G. Gage (nonmember; Canadian National Railways, Montreal, Quebec, Canada): Mr. Watkins' paper contains a graph of the estimated cost per kilowatt installed, showing the variation from about $55 to $65 for the 3,000-kw units and from $87 to $102 for the 1,000-kw units of the steel type. The glass-bulb rectifier station in Montreal with 3,000-kw installed normal-capacity, cost $38 per kilowatt. It should be borne in mind that this Canadian total cost includes duty from Great Britain and the Canadian sales tax.

S. S. Watkins: Completely automatic mercury-arc-rectifier substations, as suggested by Mr. Withington, should be considered for some applications. If supervision control is omitted, it would appear desirable to retain at least a single automatic alarm at a suitable attended location to signal the operator whenever a rectifier or a feeder circuit breaker automatically is locked out at the substation. No instance has come to my attention of a railroad installation of the single-anode-type rectifier above 750 volts. However, development by manufacturers has progressed to the point where the single-anode type can be furnished for railroad service at 1,500 or 3,000 volts.

Investigation of Hot-Spot Temperatures in Fractional-Horsepower Motors

(45-32)

Investigation of Hot-Spot Temperatures in Integral-Horsepower Motors

(45-33)

Discussion and authors' closure of paper 45-32 by L. H. Hirsch, R. F. Munier, M. L. Schmidt, L. W. Wightman, F. S. Himebrook, T. C. Lloyd, O. G. Coffman, and C. P. Potter, and paper 45-33 by L. E. Hildebrand, B. M. Cain, F. D. Phillips, W. R. Hough, J. G. Rosswog, and C. P. Potter, presented at the AIEE winter technical meeting, New York, N. Y., January 22–26, 1945, and published in AIEE TRANSACTIONS, 1945, March section, pages 128–36 and 124–8.

Cyril G. Veinott (Westinghouse Electric and Manufacturing Company, Lima, Ohio): Four methods of temperature measurement have been discussed by Mr. Hirsch and his associates:

1. Embedded detector.
2. Resistance.
3. Thermocouple.
4. Thermometer.

Comparison of results obtained by various methods has been the principal topic for their paper. While we normally do not install embedded detectors, we have, for many years, used the other three methods extensively. A study of more than 200 temperature tests on fractional-horsepower a-c motors shows that rise by thermocouple generally averages as high, or even higher, than rise by resistance. A part of these tests were reported in June 1940.[1] More of these tests, generally confirming previous results, were presented in a conference paper by E. M. Carville at the 1944 AIEE winter technical meeting. For these tests, the thermocouples were placed on the end windings in the "hottest location accessible to thermocouples"; in general, the installations were in accord with the surface-thermocouple method as defined in paragraph 7.34 of "AIEE Proposed Test Code for Single-Phase Motors, Number 502," dated November 1941.

As a result of these tests, the following conclusions, applying to fractional-horsepower a-c motors, were drawn:

1. The surface-thermocouple method, as defined in paragraph 7.34 of the "Single-Phase Test Code," should be an officially recognized method of temperature measurement.
2. Temperature limits assigned to the surface-thermocouple method of temperature measurement generally should agree with rise-by-resistance limits.
3. Temperature rise of enclosed motors should be 65 degrees centigrade either by resistance or by thermocouple.

Further experimental evidence presented by Mr. Hirsch and the others seems, in my opinion, to support the foregoing conclusions. However, it is not intended that these same conclusions necessarily be applied to integral-horsepower motors.

Thermocouples are used so widely and are so convenient that a more precise recognition of them should be given in AIEE Standards. Confusion has resulted from the practice of installing them in places "accessible to mercury thermometers" and using thermometer limits. This practice has penalized the fractional-horsepower motor industry, because thermometer limits then are applied to thermocouple temperatures. Automatic recording potentiometers for thermocouples, which are now available, have added considerably to the convenience of the thermocouple method.

Some additional results recently have been obtained on the correlation of thermocouple temperatures with resistance temperatures; these are of particular interest because the temperatures involved were all high—of the order of 180-degree-centigrade to 200-degree-centigrade total temperature. These tests were taken in connection with the application of thermoguards to a $^1/_{16}$-horsepower d-c aircraft motor. Thirteen locked-rotor tests were taken. Temperatures were measured by means of thermocouples soldered to the bare copper of the end windings. Temperatures also were measured by resistance. However, for these tests, resistance was measured by the voltmeter–ammeter method, while the armature was energized. (Voltage-drop leads were soldered to commutator bars in order to avoid errors due to brush contact drops.) In general, temperature rises by thermocouple averaged about six per cent higher than the rises by resistance; this amounted to nine degrees centigrade in the measured rises which were approximately 150 degrees centigrade.

Many of the tests presented give results obtained by use of embedded detectors located—it was hoped—at the hot spot. It may be well to point out, in this connection, that the magnetomotive force of the stator winding is not the same for all teeth. For example, in a full-pitch two-phase winding, the tooth between phase belts has 41 per cent more stator magnetomotive force than the tooth in the center of the belt. Even more variation than this may be found in irregular windings, which fall outside the familiar least-common-multiple arrangement.[2] One such winding is a three-phase six-pole 24-slot winding. Though these differences in magnetomotive force acting on stator teeth are largely damped out by the squirrel-cage rotor, there probably is a tendency for certain teeth and certain coils to get somewhat hotter as a result of this effect. This factor is but one of many variables involved in measuring the hot-spot temperature.

REFERENCES

1. Some Problems in the Standardization of Temperature Ratings of Fractional-Horsepower Motors, Cyril G. Veinott. AIEE Transactions, volume 59, 1940, pages 1055–61.

2. Irregular Windings in Wound-Rotor Induction Motors, R. E. Hellmund, C. G. Veinott. AIEE Transactions, volume 53, 1934, February section, pages 342–6.

H. Weichsel (Wagner Electric Corporation, St. Louis, Mo.): The industry as a whole should be grateful to Mr. Hirsch and his associates for their paper. It reveals a wealth of information regarding the distribution of temperatures in electric machines which was not up to the present readily available in such concise form. There is no doubt that the large amount of work spent on the necessary tests is well paid by the information obtained thereby.

In practically every one of the tests the authors used a large number of thermocouples, and in some cases thermometers, along the free ends of the stator winding. It is to be regretted that not all of these readings are recorded in the paper. They doubtlessly would give a very clear picture of the temperature variation along the free ends. Evidently the only readings recorded in this paper are the highest readings. The same reasoning holds true for the readings of the thermocouples mounted inside of the slot. If the complete information could be made available, it would assist the readers to predetermine in future tests with fair accuracy the position at which the thermocouple must be placed to obtain the highest temperatures.

It also is noticed that all temperature readings were taken while the motor was running. It is my experience that in cases where the free ends of the windings are subjected to a draft of cool air, the temperature readings taken on the surfaces of the free ends while the rotor is running are frequently considerably below the temperature readings indicated a few minutes after the machine has come to a standstill. Mr. Lloyd and Mr. Coffman refer to this phenomenon and explain it by the reflected heat from the rotor whose temperature is higher than that of the stator winding. Many cases are known to me where this phenomenon occurred, but the rotor did not have a temperature materially higher than the stator. It must, therefore, be reasoned that the heavy air draft over the stator coils while the machine was running extracted such a large amount of heat out of the free ends of the winding that a decided temperature drop existed between the inside of the winding and the outside of the winding. After the machine had come to a standstill, the hot parts inside of the winding gradually heated up the outside of the winding. It may be said the heat crept to the surface. It appears, therefore, more logical to consider, as the final temperature reading of the free ends, the highest reading found, no matter if this is obtained when the machine is running or shortly after the machine has come to a standstill.

Only a few of the authors state the method used for measuring the resistance. Particularly in the olden days, it was quite common practice to determine the resistance by sending direct current through the winding and measuring the volts and amperes required. The general tendency now seems to be to use the bridge method. The latter, according to my experience, is more reliable than the former. It is, however, essential that proper care is taken to eliminate the influence of the contact resistance. This, for instance, can be done by using a Kelvin bridge. The bridge method is further very advantageous for determining the resistance as a function of time, after the motor has come to a standstill. In recording the time-resistance curve, it would be very useful if a curve drawing bridge were available, similar to the well-known Micromax instrument which records the temperature as function of time.

Only one of the authors mentioned that for determining the cold resistance reading the motor was soaked in a room of constant temperature. Doubtlessly it is very important that this precaution be taken in every case.

From the data published in this paper, it follows that the temperatures derived from resistance readings, when taken properly, equal within a few per cent the hot-spot temperature of the machine. The temperature measurements by thermometers seemed to be by far the least reliable. The reason for this is to be found in the difficulty of locating the thermometers on the most desirable place and the difficulty of placing more than one thermometer on the winding. There also exists the danger that the binder used for joining the thermometer bulb to the winding cracks and thus leads to low temperature readings.

One of the authors stated that the motor under test was clamped to the metal bedplate of the dynamometer stand. It is fair to assume that during the reported test the heat flow from the motor frame to the bedplate of the dynamometer did not influence materially the distribution of the temperatures. On the other hand, it is essential to point out that the actual temperatures on small machines frequently are influenced seriously by mounting the motor frame directly on a heavy metal plate. Cases are known to me where the motor showed a considerably higher temperature rise when a sufficiently heavy layer of heat-insulating material, such as bakelite or wood, was placed between the feet of the motor and the heavy bedplate than it did when the motor was mounted directly in the bedplate. In any future standardizations, this should be taken into consideration.

Several instances are cited where certain parts, for instance parts of the free ends, of the machine were found to be hotter than other parts of the free ends. In the majority of cases, common sense tells us that such conditions must exist. It is self-evident that the free ends of the winding are hotter on that end of the machine which is opposite to the end on which a single ventilating fan is located, because the cooling air already is heated when it reaches the free ends opposite to the end where the blower is located. In another instance, the flow of the cooling air was such that not all parts of the free ends were contacted equally by the cooling air, and naturally the tests showed the highest temperature where the air flow was a minimum. This proves the importance of placing the thermocouple at those parts of the winding which, in accordance with common-sense reasoning and past experience, can be expected to give the highest reading.

Another result brought out by the tests, and this is in full agreement with common-sense reasoning, is that the temperature distribution is more uniform in totally enclosed motors than in well-ventilated motors.

Besides the information obtainable from these tests for arriving at the best methods and means for determining the temperature rise, there are other interesting facts brought out. For instance, in the majority of cases the treated windings gave somewhat lower temperatures than the untreated windings. This is in harmony with the general experience in motor and transformer work.

From the foregoing, it is concluded that, in preparing future standards for measuring temperature rises of machines, the following items should be considered:

1. The thermometer reading is the least reliable.
2. Thermocouple readings give fair agreement with the hot-spot readings, but it is advisable to use a number of thermocouples well distributed, and judgment is required to locate the thermocouples in places which are expected to show the highest temperatures.
3. The resistance readings give the nearest approach to hot-spot readings. It is advisable to standardize the method of measuring the resistance (Wheatstone bridge, Kelvin bridge, volt-ampere meter, or other means) and also to specify that resistance readings must be taken in a succession of time intervals immediately after the motor has come to a standstill. For determining the so-called cold temperature, the motor must be subjected to a soaking in a room in which the temperature is held reasonably constant and which is free from cold drafts.

The general statements made in my discussion of the paper by Mr. Hirsch and his associates are equally true for that of Mr. Hildebrand and his collaborators. There are a few additional items in the paper on integral-horsepower motors which deserve consideration.

In the report by Hildebrand and Cain an uncertainty exists in Table I. Two tests are given for plain enclosed motors, and two tests are given for fan-cooled motors. It is assumed that the two tests for a given type of machine are two runs on the same machine, as in the beginning it is stated that tests were made on a three-horsepower motor. It is thought advantageous to clarify this and to state definitely if these are two independent tests on the same motor or if they are tests on two different motors.

In the same paper, it is stated that "temperature resistance readings are obtained from a single hot resistance reading taken within 50 seconds after shutdown. Since cooling curves require more effort to obtain and interpret, their use does not appear to be justified." But immediately thereafter, it is stated that "The chief disadvantage is the uncertainty of relying on a single reading which must be taken with extreme care." It appears to me that said chief disadvantage can readily be avoided by not relying on a single reading but taking the cooling curve. In this connection, it should be brought out that the most important part in determining the temperature rise by resistance readings is the necessity of the correct cold temperature. If the cold temperature is not determined correctly, all other readings for determining the temperature rise are useless. It is self-evident that it is essential to have the thermocouples calibrated against the thermometer or other instrument that is used for measuring the ambient temperature.

In Table II by Mr. Phillips, an interesting feature is the fact that in several cases the temperature of the laminations is higher than either the temperature measured by thermocouples or the temperature measured by resistance but is lower than the temperature of the hot spot. This suggests that it may be wise in the standardization to consider that the highest temperature reading during the heat run, no matter if it is the winding temperature or the lamination temperature, is taken as the temperature nearest to the hot-spot temperature. This Table II discloses another interesting fact, which more or less is predictable, that the temperatures of the different parts of the machine are more uniform the less ventilation is used. In all cases the thermometer readings appear to be the least reliable.

The tests reported by Mr. Hough and Mr. Rosswog clearly bring out the importance in measuring the temperature rises not only during the running of the machine but also immediately after the machine is stopped. These readings again lead to the conclusion that that temperature should be considered as the one nearest to the hot-spot temperature, which is found to be the highest either during the running test or after stopping.

The tests reported by Mr. Potter verify the statement made previously in the discussion that the more ventilation a machine is subjected to, the larger the variation in the measuring of temperature rises and that thermometer readings are less reliable than thermocouple readings or resistance readings.

Summing up, we may say that the following features must be taken into consideration when preparing new standards.

1. Temperature readings taken by thermometer are the least desirable because it is difficult to place a therometer in such a position as to measure the actual temperature at the point at which the thermometer is placed. Further, in many cases the physical construction of the machine does not allow the placing of more than one thermometer on the windings, and in some cases it is impossible to use a thermometer at all.

2. Thermocouple readings are preferred to thermometer readings. A number of thermocouples must be used. The highest reading thus found approaches the hot-spot temperature. It is essential that great care be taken in selecting the positions of the thermocouples in accordance with best judgment and past experience to locate them at places which can be expected to be the hottest. It is desirable to take thermocouple readings not only while the machine is running but also somewhat after the

machine has stopped, and the highest reading should be considered the correct reading.

3. Temperature readings by resistance approach in most cases the hot-spot temperature more closely than any other readings. It is recommended, however, not to rely on a single resistance reading but to take a cooling curve and by extrapolation find the resistance at the moment of shutdown. So far no resistance readings have been found after shutdown which are higher than the resistance reading at shutdown. If later experience should show that this is not generally true, then the highest resistance reading, no matter if found at shutdown or after shutdown, should be considered as the reading nearest to the hot-spot temperature.

4. It is very essential that the machine be allowed to stand in a room with constant temperature for a sufficiently long time to soak it, that is to insure that all parts of the machine have the same temperature as the surrounding air. It is desirable to take ambient-temperature readings as well as thermocouple and resistance readings during the soaking period. It is extremely important that the thermocouples be calibrated against the instrument used for measuring the ambient temperature.

5. It is desirable to standardize the method to be used for measuring the resistance (Wheatstone bridge, Kelvin bridge, volt-ampere, or other methods).

6. It appears wise to consider that temperature as approaching nearest the hot temperature which is the hottest, no matter if this reading was obtained on the windings or on the laminations or if it was obtained during running or after the machine was stopped.

Table I. Results of Continuous Temperature Tests on 284-Frame Four-Pole 60-Cycle Three-Phase Induction Motor

				Temperature Rise						
				By Thermometer		By Thermocouple		By Resistance		
Enclosure	Volts	Horsepower	Type of Winding	Actual, Degrees Centigrade	Per Cent of Hot Spot	Actual, Degrees Centigrade	Per Cent of Hot Spot	Actual, Degrees Centigrade	Per Cent of Hot Spot	Hot Spot by Embedded Detector, Degrees Centigrade
Dripproof	220	7.5	Untreated	31.5	77	37	90	31.5	77	41.0
Dripproof	220	7.5	Treated	36.0	88	40	98	32.0	78	41.0
Plain enclosed	175	4.0	Untreated	59.0	92	64.0	99	62.5	97	64.5
Plain enclosed	175	4.0	Treated	61.5	92	65.5	98	61.0	91	67.0
Enclosed—fan-cooled	220	7.5	Untreated	55.5	90	60.0	98	55.0	90	61.5
Enclosed—fan-cooled	220	7.5	Treated	56.5	90	61.0	97	55.5	88	63.0

F. S. Himebrook (The Master Electric Company, Dayton, Ohio): Some of the data presented in the paper by Mr. Hildebrand and his associates indicate that, when the coil ends of open motors are ventilated by relatively high-velocity air, the rise by resistance is not a satisfactory method of arriving at hot-spot temperatures. In particular, tests on one motor (rated 150 horsepower when operated from a 60-cycle source) reported by Mr. Phillips, showed a resistance rise of 68 per cent of hot-spot value when the motor was run on 60-cycles, but, when the motor was run on 25-cycle power, the resistance rise jumped to 93 per cent of the hot-spot value. This suggested that perhaps the same characteristics might be observed in motors of smaller size when operated with single-end ventilation.

Description of Motor Tested

To determine whether or not this was the case, a Master Electric 284-frame four-pole 60-cycle three-phase motor rated $7^{1}/_{2}$ horsepower was built and tested. Tests were made as a

1. Standard open (dripproof) motor.
2. Totally enclosed nonventilated motor.
3. Totally enclosed fan-cooled motor.

The stator was wound as a standard one, except that it had a number of embedded detectors (thermocouples) inserted in the slots and coil ends. All the parts were those used in standard production.

When the motor tested was built as an open motor, the ventilating air was blown through the motor by a single fan. The direction of air flow was such that the air was exhausted at the lead end of the winding.

When a totally enclosed nonventilated motor was tested, totally enclosed end shields were used, and the single ventilating fan was replaced by two smaller fans mounted on the ends of the rotor.

Totally enclosed fan-cooled tests had the conventional external fan mounted on a shaft projection opposite the normal projection.

Location of Temperature Indicators

Embedded detectors (thermocouples) were placed adjacent to the conductors in the slots and end turns in both the upper and lower coil sides.

A surface thermocouple was tied to the winding at what was believed to be the most desirable point. This indicator was not on the winding at the time of impregnation.

A mercury thermometer was placed as near to the surface thermocouple as was possible without altering the motor construction or drilling special holes.

Results

Results of the tests are shown in Table I.

Discussion of Results

Hottest Spot. It was found that the hottest spot in the stator was in the upper coil side of the lead end (ventilating air exhausted here) in the coil-end extension. The actual hot spot was found to be nearer the end of the coil extension in the open motor and nearer the iron in the totally enclosed motor.

Hottest Normally Accessible Spot in Stator. An examination of the data reveals that a properly placed surface thermocouple gives a result, which for all totally enclosed and impregnated windings is close to the hot-spot temperature. In the case of the open motor the accuracy of this indicator was reduced.

Temperature Indicated by Mercury Thermometer. The temperature indicated by mercury thermometer is seen to provide fairly satisfactory data in the totally enclosed motors. However, for open motors, the accuracy is considerably reduced.

Temperature Indicated by Change in Stator Resistance. This method is also satisfactory for totally enclosed motors but is no better than the mercury thermometer for use on open motors. This result is brought about by the relatively high temperature gradient found in open motors. This high gradient is caused by the passage of high-velocity cool air over the coil extensions at one end while the opposite end of the motor (the coil extensions) is subjected to the air at exhaust temperature.

Temperature as Indicated by Surface Thermocouple. The temperatures indicated by a carefully placed surface thermocouple provide an accurate means of estimating the hot-spot temperature in an integral-horsepower single-end ventilated motor. In all cases the accuracy is considerably better than that obtained by any other method. The probable reason that the thermocouple is superior to the mercury thermometer in open motors is that the thermometer bulb is relatively large and the stem rigid and so cannot be placed in the most desirable position.

Conclusions

There is a considerable temperature gradient found in integral-horsepower open single-end ventilated polyphase induction motors. Because of this the change of resistance of the stator winding does not give a good indication of the maximum temperature. The most satisfactory method of finding the maximum temperature of such motors is by the use of a surface thermocouple.

In integral-horsepower totally enclosed motors any of the methods used will give a comparatively good indication of the internal temperature.

Scott Hancock (Westinghouse Electric and Manufacturing Company, East Pittsburgh, Pa.): Much discussion has taken place in the past on the subject of the relative desirability of various methods of taking temperature rise of induction motors and the differences in rise that can be expected between taking rise by resistance, by thermometer, and by embedded detector.

Any method selected must be practical in the case of the motor to be tested. To have any value results must be consistent.

The embedded-detector method never has been very practical for use in commercially taken engineering tests, in that it requires motors to be built specially for test. I see no probability in any change here.

Table II. Temperature Readings on 25-Horsepower Four-Pole 60-Cycle Open Squirrel-Cage Induction Motor

Test	1	2	3	4	5	6	7	8	9	10	Average of Ten Previous Tests	Maximum Deviation From Average	Average Deviation From Average
Date	8-11	9-6	9-8	9-8	9-11	9-10	9-7	9-18	9-19	9-20			
Amperes, 1	31.9	30.4	31.6	31.6	30.7	31.3	32.0	30.4	31.5	31.5			
Amperes, 2	31.5	30.2	30.6	30.5	30.8	31.0	30.8	30.1	30.5	30.8			
Amperes, 3	31.0	31.5	30.8	30.7	31.5	30.9	30.8	30.95	31.1	31.0			
Input—Watts	21,840	20,700	21,060	21,000	21,200	21,000	20,900	20,800	21,040	21,080			
Time—Hours	6	4	4	4	12	5	6	3	6	6			
Thermocouples													
1	39.0		39.0	40.5	38.7	34.0	29.7	41.0			37.4	+3.6 −7.7	3.2
2	42.5	36.0	39.3	39.5	39.5	30.0	31.9	42.5	40.5	39.0	38.1	+4.4 −8.1	3.3
3	41.0	36.0	38.3	37.0	37.7	28.5	31.0	40.0	40.0	39.0	36.9	+4.1 −8.4	2.99
4	40.0	36.0	38.0	35.5	37.7	27.5	30.5	38.0	39.0	36.7	35.9	+4.1 −8.4	2.83
5	41.5	37.0	40.0	35.5	40.3	28.0	32.4	38.0	41.0	39.2	37.3	+4.2 −9.3	3.25
6	39.5	37.0	38.3	36.5	37.5	27.0	31.3	38.0	40.0	37.5	36.3	+3.7 −9.3	2.82
7	40.0	36.0	40.0	37.0	39.7	27.0	31.6	37.0	40.5	38.2	36.7	+3.8 −9.7	3.1
8	39.5	37.0	39.5	35.5	38.7	26.5	30.7	37.0	40.5	38.2	36.3	+4.2 −9.8	3.25
9	40.5	37.0	39.8	36.0	40.3	27.0	31.1	37.5	40.5	38.2	36.8	+3.7 −9.8	3.25
10	41.0	37.0	39.7	37.0	40.3	27.0	31.2	37.5	41.0	39.0	37.1	+3.9 −10.1	3.21
11	40.0	37.0	40.5	37.0	39.7	27.0	30.0	37.0	40.5	39.0	36.8	+3.7 −9.8	3.29
12	39.5	37.0	39.3	36.5	40.0	26.5	29.5	37.0	40.0	38.4	36.4	+3.6 −9.9	3.33
13	37.5	31.0	34.7	34.0	35.1	26.0	24.5	35.0	35.5	32.5	32.6	+4.9 −8.1	3.25
14	34.5	29.0	33.3	33.0	34.3	25.5	21.5	35.5	33.0	29.5	30.9	+4.6 −9.4	3.63
15	34.5	29.0	31.7	32.0	22.0	24.5	20.5	33.0	33.0	29.0	28.9	+5.6 −8.4	3.96
16	34.5	29.0	34.1	34.0	23.9	25.5	20.5	34.0	31.0	29.5	29.6	+4.9 −9.1	3.92
17	36.0	30.0	35.0	34.0	39.4	26.5	23.0	35.0	34.0	31.0	32.4	+7.0 −9.4	3.81
18	35.5	28.0	34.5	33.0	33.6	26.0	21.3	34.0	30.0	31.0	27.7	+7.8 −6.4	4.61
19	34.5		33.7		34.5	26.0	21.3	34.0	33.0	30.0	30.9	+3.6 −9.6	3.82
20	34.5	31.0	33.7	33.0	34.4	26.0	21.3	34.0	32.5	31.0	31.1	+2.6 −9.8	3.06
21	36.0	33.0	27.8	33.0	39.7	32.0	30.5	29.0	34.5	32.7	32.8	+6.9 −5.0	2.42
22	29.7	25.0	26.7	34.0	29.7	26.0	22.5	23.0	29.0	36.5	28.2	+8.3 −5.7	3.57
23	27.5	25.0	26.5	26.5	30.1	25.0	24.5	22.0	27.0	25.0	25.9	+4.2 −3.9	1.61
24	31.7	30.5	26.7	27.0	35.4	30.0	30.5	29.0	33.5	33.0	30.7	+4.7 −4.0	2.13
25	35.0	30.0	28.3	25.0	37.1	33.0	28.5	31.0	40.5	33.5	32.2	+8.3 −7.2	3.63
26	34.5	30.0	27.7	24.0	28.0	31.0	25.0	29.0	34.0	35.5	29.9	+5.6 −5.9	3.13
27	35.3	29.0	27.3	25.0	38.3	31.0	29.5	29.0	35.0	39.5	31.9	+7.6 −6.9	4.11
28	38.0	32.0	29.0	26.5	39.1	33.0	26.7	33.5	38.0	34.5	33.0	+6.1 −6.5	3.59
29	36.7	31.0	29.3	25.0	38.4	33.0	29.7	31.0	36.5	36.0	33.7	+4.7 −8.7	3.33
30	36.7	31.0	28.7	27.0	38.4	33.0	30.5	31.5	36.5	36.0	32.9	+5.5 −5.9	3.19
31	38.3	32.0	29.7	26.0	40.3	33.0	30.5	33.0	37.5	34.0	33.4	+6.9 −7.4	3.27
32	38.5	32.0	29.8	26.0	40.3	34.0	30.5	32.0	37.5	34.5	33.5	+6.8 −7.5	3.45
33	31.5	31.0	27.3	27.0	40.3	33.0	28.3	31.0	36.0	33.4	31.9	+8.4 −4.9	3.04
34	33.0	32.0	26.1	27.0	37.9	29.5	27.3	28.5	35.0	32.5	30.9	+7.0 −4.8	3.2
35	34.5	32.0	26.7	27.0	37.7	29.5	28.3	29.5	36.0	33.8	31.5	+6.2 −4.8	3.3
36	35.3	32.0	26.7	28.0	39.4	30.0	29.0	30.0	36.0	33.9	32.0	+7.4 −5.3	3.09
Stator iron by thermometer	34.0	30.0	29.5	32.0	35.5	35.0	31.0	33.5	37.0	34.0	33.1	+3.9 −3.6	2.0
Stator copper by thermometer	34.0	31.0	26.5	30.5	35.5	30.5	28.0	27.0	33.0	30.5	30.6	+4.9 −4.1	2.2
Stator copper resistance	40.0	35.0	31.5	33.0	33.0	33.5	39.0	31.0	36.0	35.5	34.7	+5.3 −3.7	2.35
Rotor iron by thermometer	57.0	49.0	43.5	44.0	48.5	47.0	39.5	45.5	43.0	45.5	46.3		
Rotor aluminum by thermometer	47.0	38.0	45.0	45.0	48.0	49.0	46.0	47.5	48.0	40.5	46.4		
Room air	31.5	27.0	26.5	26.0	28.5	28.0	27.5	28.0	27.0	29.0	27.9		

The thermometer method has been very practical in the past, but with the continually growing use of more mechanical protection to motors there are fewer and fewer machines on which it can be used.

The resistance method always has been one that can be used practically on all induction motors. It appears to me that we are approaching the time when it will be the only practical method.

In previous discussions it has been assumed that the highest temperature shown on any embedded detector always accurately showed the hot-spot temperature of a motor. It has been claimed that the highest thermometer reading does not show the hottest surface temperature with any consistency. Questions have been raised as to the consistency of results obtained by the resistance method.

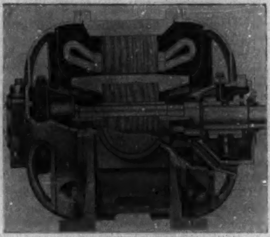

Figure 1

My experience has led me to believe that results obtained in commercial testing by the thermometer method are sufficiently consistent to avoid any serious difficulty. My experience in the use of rise by resistance was much more limited but left me feeling that the consistency of this method was open to grave doubts.

In order to satisfy myself as to the consistencies in rise that could be expected from these three methods when used commercially, I arranged to have a 25-horsepower four-pole 60-cycle open squirrel-cage induction motor built with many detectors embedded in the windings. I arranged to have ten different heat runs taken on this motor, reading each time the rise as shown by the embedded detectors, by thermometers, and by resistance. In each case the instructions to the test floor were to take the run at rated load and voltage. The thermometers were removed between runs. All runs were made by our regular test-floor men in the ordinary test manner. We were attempting to find what we ordinarily could expect to get on test, not what might possibly be gotten in a laboratory.

The motor used was of a construction as shown in Figure 1. The various detectors were located as shown in Figure 2. The test results obtained are shown in the ten numbered columns of Table II.

In the next column of Table II, I have shown the mathematically average rise for each item for the ten tests. In the next column I have shown the maximum any individual reading deviated from the average for that item. In the last column I have shown the average of the amount of deviation of individual readings from the average for the particular item.

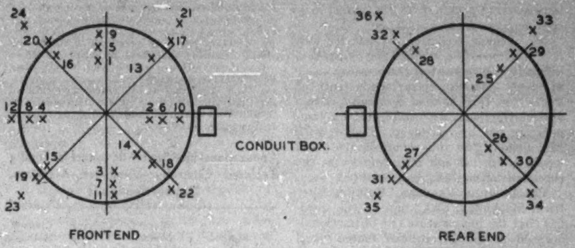

Figure 2

Thermoguard Number	Location	
1, 2, 3, 4	Center line of core in slot under top wedge	1 4+2 3
5, 6, 7, 8	Center line of core in slot under center wedge	5 8+6 7
9, 10, 11, 12	Center line of core in slot between side of slot cell and core	9 12+10 11
13, 14, 15, 16	On rotor side of coil extension on front and approximately two inches from stator core	16 13 × 15 14
17, 18, 19, 20	Between top and bottom coil extension on front end approximately two inches from stator core	20 17 × 19 18
21, 22, 23, 24	On bracket side of coil extension on front end approximately two inches from stator core	24 21 × 23 22
25, 26, 27, 28	On rotor side of coil extension on rear end approximately two inches from stator core	28 25 × 27 26
29, 30, 31, 32	Between top and bottom coil extension on rear end approximately two inches from stator core	32 29 × 31 30
33, 34, 35, 36	On bracket side of coil extension on rear end approximately two inches from stator core	36 33 × 35 34

In interpreting these tests I have assumed that the values obtained by averaging the ten tests were the values that we could hope to get. The variations from these represented our lack of consistency in our over-all test procedure.

It can be seen that the least consistent method of all is the embedded-detector method. The tests on thermocouple, the one that reads the hot test spot, have a total range of 13½ degrees or 35 per cent. This is representative.

The resistance method has a total range of nine degrees or 26 per cent.

The thermometer method is used for various readings with varying degrees of consistency. If that item is taken which is the hottest, that is rise of stator iron, the range is 7½ degrees or 22.6 per cent. The range on stator copper is 29 per cent.

The probable error in the rise of any individual run is of interest. I have assumed that the average of the ten runs represented the true rise. For each item, as rise of stator iron, I have found the degrees difference between the average rise for the ten runs and the rise for the particular run. The average of these differences then would show the probable error on any particular run. These averages are shown in the last column of Table II.

The greatest error to be expected again is found in the thermocouple readings. That thermocouple which shows the highest temperature has an average error of 3.3 degrees or 8.7 per cent. The rise by resistance has a probable error of 2.35 degrees or 6.8 per cent. The rise by thermometer on the iron has a probable error of two degrees, or six per cent.

My conclusion from these results is that there is no significant difference between the consistency of results that will be obtained on our test floor as between the resistance and the thermometer method.

I conclude that in the present case the hot spot should be taken as 38.1-degrees rise, the rise by resistance as 34.7 degrees or 91 per cent of the hot spot, and the rise by thermometer as 33.1 degrees or 87 per cent of the hot spot.

It may be of interest to note that the resistance readings were taken quickly after shutdown but were not corrected back to shutdown. The readings were made by means of a Kelvin bridge.

The embedded detectors used were thermocouples, and the readings of these were made by means of a potentiometer.

C. P. Potter: The additional test data submitted by Mr. Himebrook include information which will be useful in comparing the temperature rise of open, totally enclosed nonventilated, and totally enclosed fan-cooled motors. Mr. Himebrook has made a very pertinent observation when he states that thermometers and resistance methods are not so good as surface thermocouples for determining the temperature rise of single-end ventilated motors. This is a detail which should be given consideration when revising temperature standards.

Mr. Hancock has submitted data which were obtained from a different point of attack than those used by the authors and one observation which he has made deserves special attention. He states that "The resistance method has always been one that can be used practically on all induction motors. It appears to me that we are approaching the time when it will be the only practical method."

Mr. Weichsel calls attention to a great many details which must be given special attention in making temperature tests and also concludes that temperature rise by re sistance comes closest to the actual hot-spot temperature.

Mr. Veinott recommends that the surface thermocouple method be recognized officially as a method of temperature measurement. He also recommends that the limits for this method generally should agree with the limits established for temperature rise by resistance. I agree with Mr. Veinott that this should be done and would go further and recommend that the thermometer method be discouraged.

The American Standard, "Rotating Electrical Machinery, *C*50," dated 1943, specifies that the temperature rise of fractional-horsepower totally enclosed motors shall not exceed 55 degrees by thermometer and 65 degrees by resistance, while the same Standard specifies that the temperature rise of integral-horsepower totally enclosed motors shall not exceed 55 degrees by thermometer and 60 degrees by resistance. It will be noted that the Standard specifies the same temperature rise by thermometer for both fractional- and integral-horsepower motors, but allows a temperature rise by resistance five degrees higher for fractional-horsepower than it does for integral-horsepower totally enclosed motors.

The "Motor and Generator Standards" of the National Electrical Manufacturing Association publication 14-64 specifies that the temperature rise of either fractional- or integral-horsepower totally enclosed motors shall not exceed 55 degrees by thermometer and does not provide for the measurement of temperature rise by resistance. A proposal was made that the "Motor and Generator Standards" be changed to agree with the American Standard, *C*50, and this proposal resulted in a general discussion of the subject by the general engineering committee of the motor and generator section. It was pointed out in the meeting of the general engineering committee that certain integral-horsepower motors may be built using the same parts as fractional-horsepower motors, but their temperature rise must be five degrees less by resistance than that of fractional-horsepower motors. Furthermore, if a temperature rise of 65 degrees by resistance is permissible on fractional-horsepower totally enclosed motors, the difference between the hot-spot temperature and the temperature by resistance of these motors must be zero, otherwise the hot-spot temperature will exceed 105 degrees centigrade. The general engineering committee considered that there might be justification for allowing a temperature rise of 65 degrees by resistance on totally enclosed nonventilated motors, not because they were of fractional horsepower, but because these motors are not ventilated, and made the following suggestion.

"It is usually assumed that the temperatures of the various parts of the windings in an enclosed externally nonventilated machine are essentially the same. In these motors it is possible that the resistance method measures the actual hot-spot temperature. It might also be assumed that the temperatures of the various parts of the windings in an enclosed externally ventilated machine vary slightly due to the fact that one end of the windings may be cooled by the air which has just entered the enclosure and the other end is cooled by the air which is leaving the motor and is somewhat warmer than the entering air. In these motors it is possible that the temperature by the resistance method is less than the hot-spot temperature.

"If these assumptions are correct a temperature rise of 65 degrees by resistance might be permitted in totally enclosed externally nonventilated machines, while a temperature rise of only 60 degrees by resistance might be permitted in totally enclosed externally ventilated machines. If these values should be found to be correct, it would then be desirable to modify AIEE Standard 1 by changing Table III so that its title reads "Conventional Hot-Spot Allowances for Open, Dripproof and Splash-Proof Machines," and then prepare two new tables reading as follows:

Conventional Hot-Spot Allowances for Totally Enclosed Externally Ventilated Machines, Degrees Centigrade

Method	Class–O Material	Class–A Material	Class–B Material
Thermometer	10	10	15
Resistance or embedded detector	5	5	10

The second new table then would read:

Conventional Hot-Spot Allowances for Totally Enclosed Externally Nonventilated Machines, Degrees Centigrade

Method	Class–O Material	Class–A Material	Class–B Material
Thermometer	10	10	15
Resistance or embedded detector	0	0	5

Before making any changes in AIEE Standard 1 or in the "Motor and Generator Standards" of The National Electrical Manufacturers Association it seemed advisable to investigate the actual hot-spot temperature in fractional- and integral-horsepower motors, and various motor manufacturers agreed to make an investigation of this sort. The results of these investigations were presented at the June 1944 conference session of the AIEE in St. Louis, Mo., and summaries of these conference reports are now available in papers 45-32 and 45-33.

It seems that we now should consider American Standard, *C*50, and the recommendations of the "Motor and Generator Section" previously quoted to see whether the actual test results justify the *C*50 standards of the proposed changes in AIEE Standard 1. If the *C*50 standards covering the temperature rise of fractional-horsepower totally enclosed motors are consistent, the temperature of these motors by resistance should be exactly the same as the hot-spot temperature. The results shown in AIEE paper 45-32 show that the temperature by resistance of enclosed, nonventilated fractional-horsepower motors varies from 89 per cent to 106 per cent of the temperature taken by embedded detectors which have been located so as to obtain the hot-spot temperature. In other words, if the temperature rise by resistance is allowed to reach 65 degrees it would seem that the hot-spot temperature may go up as high as 73 degrees and with an ambient temperature of 40 degrees would give an actual winding temperature of 113 degrees, which exceeds the value ordinarily considered good practice. In the case of totally enclosed fan-cooled motors the results shown in AIEE paper 45-33 show that the temperature by resistances ranges from 85 per cent to 103 per cent of that bye mbedded detectors, and, therefore, if the temperature rise by resistance of totally enclosed fan-cooled motors is allowed to reach 60 degrees, the hot-spot temperature rise will be 71 degrees, which with an ambient temperature of 40 degrees gives a hot-spot temperature of 111 degrees.

Comparing temperature rise by thermometer with temperature rise by hot spot, we find that in the case of fractional-horsepower enclosed nonventilated motors the thermometer method gives results which are from 70 per cent to 97 per cent of the actual hot-spot temperature rise and in the case of totally enclosed fan-cooled integral-horsepower motors the thermometer ratings give from 70 per cent to 98 per cent of the actual hot-spot temperature rise. Since a rise by thermometer of 55 degrees is permitted by either *C*50 or NEMA rules, it would seem that the actual hot-spot temperature rise corresponding to 55 degrees by thermometer would be about 78 degrees which with an ambient temperature of 40 degrees gives a hot-spot temperature of 118 degrees.

This would indicate that actual hot-spot temperature in totally enclosed motors have always been somewhat higher than we suspected, and the question arises whether the temperature rise by thermometer should be reduced. It is believed that the life of totally enclosed motors operating in the field for many years has been perfectly satisfactory and that there should be no reduction in the temperature rise by thermometer. It is true, however, that the American and NEMA Standards should agree with each other, and the following recommendations are offered.

1. Table 14 of American Standard *C*50 should be modified by adding a note stating that the temperature rise of 65 degrees by resistance for totally enclosed motors refers only to nonventilated motors and that the temperature rise by resistance of totally enclosed fan-cooled motors should not exceed 60 degrees.

2. Table 13 of American Standard *C*50 should be modified by adding a note stating that the temperature rise of 60 degrees by resistance for totally enclosed motors refers only to fan-cooled motors and that the temperature rise by resistance of totally enclosed nonventilated motors should not exceed 65 degrees.

3. Paragraph 2.054 of American Standard *C*50 should be modified to read as follows: "This method consists in the determination of the temperature by thermocouples applied to the hottest part of the machine accessible to thermocouples." If this change is made the use of glass-tube thermometers would not be permitted. Though it is possible to obtain fairly accurate measurements of temperature by glass-tube thermometers in motors which are so constructed that a thermometer can be placed in the right location, many motors have mechanical features which prevent the satisfactory use of glass-tube thermometers without mutilating the motor. In such cases temperatures taken using a glass-tube thermometer are quite likely to be lower than the actual values.

It also is recommended that when American Standard *C*50 has been modified in accordance with these suggestions that the "Motor and Generator Standards" of NEMA should be changed to agree with them. In effect, this means recognizing the resistance method for measuring the temperature rise of enclosed motors and allowing a five-degree higher temperature rise by resistance on totally enclosed nonventilated motors than is permitted on totally enclosed fan-cooled motors.

Orthomagnetic Bushing Current Transformer for Metering

Discussion and authors' closure of paper 45-24 by A. Boyajian and G. Camilli, presented at the AIEE winter technical meeting, New York, N. Y., January 22–26, 1945, and published in AIEE TRANSACTIONS, 1945, March section, pages 137–40.

C. A. Woods, Jr. (Westinghouse Electric and Manufacturing Company, East Pittsburgh, Pa.): The characteristics of the bushing current transformers operating with superimposed triple-frequency magnetization indicate that the authors have been very successful in straightening out the excitation curve of the transformer. Many different schemes for rendering the normally nonlinear characteristics of magnetic materials linear have been worked out, but most of them have not proved too satisfactory in commercial application. One of the many difficulties has been the rather wide variation in magnetic quality of completed cores of the same design.

The method described in this paper for obtaining a high degree of accuracy on low-ratio bushing transformers requires a certain degree of sacrifice in the simplicity and ruggedness inherent in the bushing transformer. This results in an increase in first cost over the ordinary bushing current transformer but certainly leaves a favorable balance in the higher-voltage ratings when compared with the standard wound-type transformers. This saving then must be balanced against the increased maintenance required to insure that the auxiliary equipment and transformer windings are functioning properly and the cost of obtaining and operating the separate excitation source. Likewise, it is usually necessary to take more precautions with respect to the burden imposed on the transformer to insure that the adjustments of the auxiliaries are satisfactory for the service burden. It would be expected that each unit would have to be adjusted to suit the particular burden to be imposed on it.

It often has appeared to me that many metering requirements could be satisfactorily met with bushing current transformers in the lower range of ratios having high-quality cores such as the Hipernik which in many cases will give an accuracy meeting the American Standard Association 0.6 or 1.2 metering-accuracy classification. Such transformers have a higher first cost than standard bushing current transformers due to the cost of the core material but otherwise have characteristics, including good overcurrent performance, similar to the ordinary bushing current transformers. This is particularly true when they are used to energize indicating instruments having accuracies of one per cent of full-scale deflection.

The orthomagnetic bushing current transformer appears to be capable of providing a high degree of accuracy down to quite low primary-current ratings. However, it is complicated by the use of a separate three-phase power source and potential transcormers along with auxiliary windings on the fore for the superimposed excitation and auxiliary burden as well as auxiliary-current balance autotransformer and burden for compensation. Until a constant permeability-core material of suitable quality over the required density range is found, it will be necessary to use some artificial means of obtaining the equivalent, when manufacturing low-ratio bushing current transformers to meet extremely high metering-accuracy requirements.

F. B. Silsbee (United States Department of Commerce, Washington, D. C.): The orthomagnetic current transformer adds still another to the already long list of clever devices for improving performance of current transformers of the bushing type. It holds promise of great utility in those important metering installations where the cost and complexity of the auxiliary circuit for supplying triple-frequency current is justified by the value of accurate measurement.

It is interesting to note that Agnew, in his now classical paper on current transformers,[1] predicted that, if the loss exponent of the iron were two, the ratio of the current transformer would be independent of secondary current. Now, 33 years later, the present authors have succeeded in suppressing the bulk of the hysteresis and, with only the eddy-current loss remaining, have attained an exponent effectively close to two and thus have secured a nearly linear error curve which can be completely compensated.

It would add considerably to the interest of the presentation if they could give typical observed hysteresis loops for a single core to show just what sort of a figure eight the iron is carried through. The pattern of the loop doubtlessly will depend upon the relative magnitudes of the high- and low-frequency currents and also upon their relative phase. Examples showing the effects of variation in these conditions would be interesting.

REFERENCE

1. P. G. Agnew. *Bulletin*, Bureau of Standards, volume 7, 1911, *SP*164, page 423.

A. C. Schwager (Pacific Electric Manufacturing Corporation, San Francisco, Calif.): The problem of metering power at highest voltage by means of inexpensive bushing current transformers rather than by separately mounted wound-type transformers has been given considerable attention during the past 20 years. Attempts at obtaining the desirable accuracy of approximately 0.25-per-cent maximum ratio error and 25-minute maximum phase-angle error for the most commonly used ratios of from 200–5 to 400–5 and secondary burdens of not less than 15 volt-amperes were generally unsuccessful. The attempted solutions, which included the use of high-permeability nickel–iron steels, the application of the Brookes two-stage principle, and many others, did not produce sufficient accuracy.

The authors have to be congratulated for having developed a transformer which produces the high accuracy required. As in the case of the Iliovici-type transformer, a separate power supply is required. The simplicity inherent in the conventional current transformer not requiring an external power source and auxiliary connection disappears.

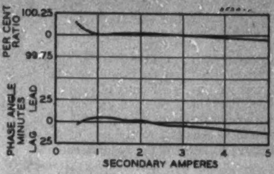

Figure 1. Ratio and phase-angle errors of 138-kv 200–5-ratio constant-permeability bushing-type current transformer

Secondary burden, 21 volt-amperes

As shown by the writer,[1] the linearity obtained by cross magnetization can be accomplished easily without the use of an external power supply. Transformers built on the constant-permeability principle have been in operation for many years and are metering power on a large number of systems with precision accuracy. Figure 1 of this discussion shows the characteristics of a 138-kv 200–5-ampere transformer with a secondary burden of 21 volt-amperes. These characteristics are suitable for precision metering and compare with those presented by the authors.

REFERENCE

1. SHAPING OF MAGNETIZATION CURVES AND THE ZERO-ERROR CURRENT TRANSFORMER, A. C. Schwager, V. A. Treat. AIEE TRANSACTIONS, volume 52, 1933, pages 45–52.

E. C. Wentz (Westinghouse Electric and Manufacturing Company, Sharon, Pa.): This paper is an excellent demonstration of a method by which a highly theoretical principle, which conceivably could be used to produce a nearly perfect current transformer, but only at prohibitive expense and complication with auxiliary equipment, is applied with practical and reasonably expensive auxiliary devices to produce a transformer which, although not entirely perfect, not only is much better than any unassisted transformer of equal size but also, with due regard to the limitations of application, is sufficiently perfect for any metering service. The errors are generally less than would be introduced by the meter itself. Mr. Boyajian and Mr. Camilli are to be complimented on the results obtained.

It will be in order to point out the only limitation in application; that is, the perfect transformation depends upon the burden being matched to the transformer by adjustment of the impedance Z and the tap on the autotransformer (Figure 3 of the paper). If the burden be changed, the impedance Z and the tap should be changed to suit. If this be done, the desired perfection can be obtained at any burden. This may be considered an advantage as well as a disadvantage. The performance of the transformer with high-frequency excitation is better than without it, even without any auxiliary impedance. The authors have not included the performance with impedance and autotransformer at X burden in Table II. The intent may be that the latter should be disconnected for any low value of burden, but the data would be of interest to one who wished to use the transformer as a guide to whether or not the impedance and autotransformer should be disconnected and at what burden.

It seems that the adjustment of the impedance and autotransformer must have been changed in going from Y to Z burden in Table II. It is difficult to account for the fact that the secondary current is higher with higher burden on any other basis. It would be essential for the user of the transformer to know if the adjustment must be changed, and how much, and a statement to clarify this would add to the value of the paper. It also would be of interest to know the performance at all three burdens with the same adjustment of Z and the tap on the transformer.

The performance at high currents no doubt will be better with the auxiliary excitation, but the two curves of Figure 5 should come together at values of 60-cycle flux density approaching saturation, and the performance would be little better with the high-frequency excitation. The authors may have additional data on this.

We have, for some years, built ring-type transformers with auxiliary excitation from the 60-cycle secondary current. The results of such excitation are not so good as those shown by 180 cycle, but the construction is very simple, and no auxiliary source is required. A place probably exists for both methods, and a place still may be found for transformers with still higher frequency excitation. The choice of method depends on striking a proper balance between cost of excitation and cost of additional core section, or higher-quality core material in the transformer.

Stuart D. Moreton (General Electric Company, Philadelphia, Pa.): With power being transmitted at higher and higher voltages there has developed an increasing need for a low-cost current transformer having metering accuracy. The bushing current transformer is most desirable from a cost standpoint, but its accuracy for low ratios is unsatisfactory. Many schemes of compensation have been used to overcome the limitation imposed by the one-turn primary winding and the exciting nuisance burden. These attempts have resulted in transformers that are critical with respect to burden, usually affected by the previous magnetic history of the iron, unsatisfactory for multiratio design, and exceedingly difficult to predict in performance. At best these transformers were limited to an accuracy class of 0.3 for 300:5-ampere ratios and 0.6 for 200:5-ampere ratios where the burden had to be limited to approximately 0.5 ohm (12.5 volt-amperes) to obtain these results. The author's disclosure makes available metering transformers having accuracies as good as 0.3 for 100:5-ampere ratio and 0.6 for 50:5-ampere ratio where the burden may be as large as two ohms (50 volt-amperes).

The primary results gained by the auxiliary excitation are twofold:

1. It reduces the magnitude of the nuisance burden, which means that less compensation is required through the use of auxiliary transformers and capacitors, thus resulting in less critical application and burden matching.
2. It linearizes the excitation curve, which means that the errors are constant and independent of primary current, thus permitting better accuracies at lower ratios.

This linearization greatly simplifies the compensation procedure. In fact the error is directly calculable as

$RCF/\underline{\beta}=1+Z_s/Z_e\underline{/\theta_s-\alpha_e}$

where $Z_s\underline{/\theta}$ is the burden impedance and $Z_e\underline{/\alpha_e}$ is the core impedance; $\mathbf{Z}_s$ and $\mathbf{Z}_e$ are both constants.

The secondary results gained are also twofold:

1. It makes possible the design of multiratio metering transformers, thus reducing application problems with expanding generation.
2. It automatically keeps the transformer demagnetized.

This latter point too often is ignored. The residual magnetism introduced by large fault currents upsets the accuracy characteristics of some previous designs to a troublesome degree. This can be particularly bad if the design is based on fixing the core impedance by means of auxiliary saturating parameters, the characteristics of which cannot respond proportionally to the residual magnetism.

There should be little concern over the requirements of the separate excitation, since there is always available single-phase power and often three-phase power for station lighting and battery charging. A three-phase source is desirable because of the resultant simplicity in the design of the harmonic generator. The power required from the external source is about 50 watts per transformer or 400 kilowatt-hours per year, which is a small price to pay for the improved performance.

A. Boyajian and **G. Camilli:** The current transformer to which Mr. Schwager's accuracy curves (Figure 1) apply had

(*a*). A burden less than one half of ours, 21 volt-amperes against 50 volt-amperes.

(*b*). A weight about twice as much.

(*c*). A primary current almost twice as favorable as ours.

The basis of (*c*) is the known fact that current-transformer errors are inversely proportional to the *square* of the primary ampere turns.[1] His linearization scheme is to connect a saturated shunt reactor across the secondary winding of the conventional bushing-type current transformer. Evidently, any linearization obtained in this manner is associated with greatly increased errors to be compensated by other means. This may make it clear why Mr. Schwager's scheme is applicable only under very favorable conditions such as those just mentioned.

Relative to the use of high-quality (high-cost) special magnetic alloys, referred to by Mr. Woods, these are useful in the borderline cases, but the improvement which they afford is not comparable with what is secured by the present scheme. With reference to our Table II, the use of these special alloys would cut down the errors shown under the "Plain Current Transformer" column by about one half, but even those reduced errors would be many times those given in the last two columns. Furthermore, the present scheme is not restricted to the use of silicon steel but is applicable to these other alloys also, thereby extending the field of application of the bushing-type current transformers to still smaller primary currents.

In connection with the hysteresis loop, on which Doctor Silsbee commented, a few observations were made, but, because of the present emphasis on postponing what is postponable, that was made a postwar project.

As Mr. Wentz commented, if a large change be made in the burden, naturally enough the impedor and autotransformer adjustments must be changed. These adjustments are made relatively easily, because the performance is linear, and therefore adjustments made at some intermediate current value, for example, three amperes, apply to the entire range. All operating companies having facilities for calibrating their metering equipment will have also a Silsbee set and can make these adjustments.

REFERENCE

1. A NEW HIGH-ACCURACY CURRENT TRANSFORMER, M. S. Wilson. AIEE TRANSACTIONS, volume 48, 1929, pages 783–8.

A Portable Instrument for Measuring Insulation Resistance at High Voltage

Discussion and authors' closure of paper 45-66 by F. W. Atkinson and Robert B. Taylor, presented at the AIEE winter technical meeting, New York, N. Y., January 22–26, 1945, and published in AIEE TRANSACTIONS, 1945, April section, pages 164–7.

L. J. Berberich (Westinghouse Research Laboratories, East Pittsburgh, Pa.): The instrument described by F. W. Atkinson and Robert B. Taylor should find an increasingly wider field of application. It already has demonstrated its usefulness in testing aircraft ignition cable. The unique simplicity brought about by the development of the point-to-plane rectifier tube is noteworthy. The drooping voltage-regulation curve shown in Figure 6 of the paper, while desirable from the standpoint of instrument protection, is not desirable when the instrument is used to determine dielectric-absorption curves, such as are shown in Figure 9 of the paper.

In obtaining dielectric-absorption curves, particularly on machines having relatively large capacitance, the voltage applied should be as near constant as possible. If the voltage changes, as a result of changing current or other causes, during the time the data for the curve are taken, there will be a charging current superimposed on the dielectric-absorption current which is equal to the magnitude of the capacitance times the rate of change of voltage with time. It is possible, in certain cases, when the rate of voltage change and capacitance are high, to have a charging current which is comparable to the sum of the dielectric-absorption and conduction currents. Thus, before this instrument is used on large machines, it should be demonstrated that no large error results from this cause. Undoubtedly something can be done to improve the instrument in this respect and in the meantime the instrument should not be applied where serious errors might result from this cause.

It appears, however, that this drooping current–voltage characteristic cannot be eliminated entirely because it is inherent in the gaseous electric discharge upon which the rectifying properties of the tubes depend.

J. S. Johnson and **J. S. Askey** (Westinghouse Electric and Manufacturing Company, East Pittsburgh, Pa.): F. W. Atkinson and Robert B. Taylor are to be congratulated on their description of an instrument which shows promise of being a very useful insulation-testing tool. We long have felt a need for a d-c insulation tester which has sufficient voltage range, capacity, and which is sufficiently portable to be useful generally. Kenotron sets, either stationary or mounted on trucks, have been available for some time, but their relatively greater size and bulk have limited their general usefulness.

Some comparative tests have been made with the TAKK tester at voltages in the range of 10 to 15 kv and with an electronic-type megohm bridge at 500 volts. Too few tests have been made to establish the relative value of testing at higher voltages or at 500 volts. There has been some evidence, however, that the higher voltages are useful in detecting mechanical or other defects which would not be detected at 500 volts. We are of the opinion that, particularly on large and important machines, it is reassuring to obtain such data at voltages in the neighborhood of machine operating voltage.

To be generally useful for obtaining dielectric-absorption data, a wider current range in which voltage regulation is good would be desirable. However, a number of tests were made and satisfactory results obtained on new large machines at room temperature where insulation resistance after one minute was a hundred megohms or more.

The cold-cathode tubes used in the power supply have characteristics well suited to this type of device in that the tubes are self protecting with respect to overloading.

While our use of the TAKK tester has been limited, we have found it a convenient and useful instrument. In addition to its light weight and portability, the use of illuminated instrument scales greatly enhances its practicability for shop and field use.

T. B. Whitson (James G. Biddle Company, Philadelphia, Pa.): I, too, wish to add my congratulations to the work which the TAKK Corporation has done in designing and developing this device. It is simple to operate. It is reasonably safe to use, although anyone handling high voltage should use proper precautions, and it is reasonably foolproof. One must, of course, recognize voltage characteristics in using any insulation-testing device, especially when making dielectric-absorption curves. It seems to me that the instrument supplements existing devices for insulation testing and has the advantage of extending the technique to higher voltages, beyond the customary 500, 1,000, and 2,500 volts.

The discussion here rather naturally involves generator windings, a subject in which this group is vitally interested. However, the authors point out the satisfactory use of the device for testing ignition equipment, including spark plugs. This suggests the possibility of the instrument being useful for other electric equipment, such as bushings and insulators.

I believe the industry has something to gain from further experiment with the use of this device.

R. L. Webb (Consolidated Edison Company of New York, Inc., New York, N. Y.): The high-voltage test instrument described by Mr. Atkinson should find practical application on many types of power equipment. It should provide another higher step in the voltage range of d-c portable testers. It was designed, primarily, for testing relatively small apparatus such as ignition cables. The data given in Figure 6 of the paper indicate insufficient current capacity for testing equipment such as main generator stator windings. The higher current capacity of ten milliamperes may serve satisfactorily for this purpose.

The new Takktron cold-cathode high-voltage rectifier tube appears to be well adapted to this sort of work because of its rugged construction and the simplification that comes from having no filaments to heat in the rectifier tubes.

We have used electronic rectifiers in different types of insulation-resistance test sets since about 1938. Their performance has been quite satisfactory, particularly on those jobs where long-time dielectric-absorption curves are to be taken. On tests of equipment having appreciable winding capacitance to ground, we find a magnetic-type voltage regulator, for the power input to the tester, is necessary to avoid fluctuations in the output of the instrument. For d-c testing of generator windings, electronic rectifiers are used on our system from 500 to 25,000 volts. Voltages above 5,000 are obtained from Kenotron test equipment.

The design of electronic rectifiers for insulation-resistance testing should avoid excessive voltage drop in series protective resistors. To obtain test data which are comparable with those taken on earlier or later tests we try to hold the test voltage across the insulation within 90 per cent to 100 per cent of the nominal value. Referring to Figure 6 of the paper, this limit would permit measurement of insulation resistance down to 13,500 volts (15,000 volts being nominal) where the current output is about 200 microamperes, or down to 67 megohms. Generator-winding insulation resistance is found below ten megohms occasionally. It may be found as high as 2,000 megohms which would take only $7^1/_2$ microamperes at 15,000 volts.

It is our practice to treat insulation testers, and the circuits being tested, the same as if they were conventional high-potential test equipments, above 1,000 volts. The omission of series protective resistors therefore is not objectionable from a safety viewpoint.

It is our custom, for example, to make periodic insulation-resistance tests on 13.8-kv generators at the following direct voltages, 1,000, 5,000, and 22,000. Comparison of the test results obtained in this way provides good supervision of dirt and moisture content on and in the insulation.

F. W. Atkinson and **Robert B. Taylor:** The authors wish to express their appreciation for the very constructive discussions of their paper. The instrument described has proved its usefulness for measuring insulation resistance of aircraft-ignition-system components, as well as dielectric absorption of equipment of limited capacitance, at voltages up to 15 kv. With the aid of these comments, the authors feel they are in a better position to design suitable portable equipment of this type for measuring dielectric absorption of larger machines and cables.

Measurement of the Subtransient Impedances of Synchronous Machines

Discussion and author's closure of paper 45-12 by Gordon F. Tracy and William F. Tice, presented at the AIEE winter technical meeting, New York, N. Y., January 22–26, 1945, and published in AIEE TRANSACTIONS, 1945, February section, pages 70–6.

F. K. Brainard (Allis-Chalmers Manufacturing Company, Milwaukee, Wis.): The authors have provided a new method of measuring subtransient reactances and, accordingly, also have provided a new definition, because, as pointed out by Concordia and Maginniss,[1] when a method of testing for a particular reactance is specified, any other definition has little practical significance. The question as to whether this method is superior to the others or not depends both upon the use to which it is to be put as well as possible errors and difficulties in making the test.

We have checked this method against method 3 of the AIEE Test Code, paragraph 1.846, for direct-axis subtransient reactance, and against the corresponding method for quadrature-axis subtransient reactance. In general, we find very good agreement, if the reactive component of the measured impedance is taken instead of the total impedance as specified in the above-mentioned rule. This rule should be changed as it is obviously incorrect.

However, it seems reasonable to assume that certain machines will show appreciably different results when tested by the two methods because of the differences in flux distribution during the two tests. In such cases, it would appear that the values obtained by the three-phase method given in this paper would be at least as good as the results of the single-phase test, because purely single-phase problems almost never arise. Even in the case of single-phase short circuits of power systems, there is usually a considerable initial three-phase load.

In order adequately to take account of saturation, it is desirable to make this test, as well as the single-phase test, at full voltage. This frequently is not practicable, however, on account of the rapid heating of many machines when full voltage is applied to the stator with the rotor blocked.

Also, there is another source of error in both the three-phase and single-phase methods because of the fact that the reactance of any machine with a rotor such as is furnished ordinarily is not entirely independent of the frequency. If there were no resistance in the rotor circuits, this would not be true, but since the rotor resistance is frequently quite large, the frequency at which the test is to be made should be specified in any standardization on the subject.

This problem provides an interesting application of the methods of tensor analysis. The following derivation checks the authors' equations 27 and 28 exactly. Also, expressions for Z_d'' and Z_q'' in terms of the phase quantities can be obtained as indicated, thus eliminating the necessity of determining the sequence components of current and voltage, since each is a vector quantity in the final equations as shown.

The authors are to be congratulated for developing this method which, as they say, avoids the necessity of placing the rotor accurately in a particular position for test. This feature is quite important for large machines and the method is well adapted for use, either on the manufacturer's test floor, or at the customer's plant after installation.

SUBTRANSIENT REACTANCES FROM THREE-PHASE BLOCKED-ROTOR TEST

Let

I_d and I_q = components of current when referred to the direct and quadrature axes of the rotor

V_d and V_q = components of voltage under same conditions

I_X and I_Y = components of same current when referred to the X and Y axes, which are at right angles, and where the X axis is the axis of phase A of the stator

β = the angle between the X axis and the direct axis of the rotor

V_X and V_Y = components of voltage when referred to the X and Y axes

I_1 and I_2 = positive and negative sequence components of current when the A phase is the reference

V_1 and V_2 = positive and negative sequence components of voltage under the same conditions

I_A, I_B, and I_C = currents in phases A, B, and C respectively

V_{BC} = voltage between lines B and C

V_{CA} = voltage between lines C and A

V_{AB} = voltage between lines A and B

V_{1a} and V_{2a} = positive and negative sequence components of V_{BC}, V_{CA}, and V_{AB} when V_{BC} is the reference

Then the transformation tensor transforming from the X-Y to the d-q axes is:

$$C_1 = \begin{array}{c|c|c|} & X & Y \\ \hline d & \cos\beta & \sin\beta \\ \hline q & -\sin\beta & \cos\beta \\ \hline \end{array}$$

since

$$I_d = I_X \cos\beta + I_Y \sin\beta$$
$$I_q = -I_X \sin\beta + I_Y \cos\beta$$
$$V_d = V_X \cos\beta + V_Y \sin\beta$$
$$V_q = -V_X \sin\beta + V_Y \cos\beta$$

To transform from sequence quantities to X-Y axis quantities

$$C_2 = \begin{array}{c|c|c|} & 1 & 2 \\ \hline X & 1 & 1 \\ \hline Y & -j & j \\ \hline \end{array}$$

since

$$I_X = I_1 + I_2$$
$$I_Y = -jI_1 + jI_2$$
$$V_X = V_1 + V_2$$
$$V_Y = -jV_1 + jV_2$$

Then

$$C_3 = C_1 \cdot C_2 = \begin{array}{c|c|c|} & X & Y \\ \hline d & \cos\beta & \sin\beta \\ \hline q & -\sin\beta & \cos\beta \\ \hline \end{array} \quad \begin{array}{c|c|c|} & 1 & 2 \\ \hline X & 1 & 1 \\ \hline Y & -j & j \\ \hline \end{array}$$

$$= \begin{array}{c|c|c|} & 1 & 2 \\ \hline d & \cos\beta - j\sin\beta & \cos\beta + j\sin\beta \\ \hline q & -\sin\beta - j\cos\beta & -\sin\beta + j\cos\beta \\ \hline \end{array}$$

$$= \begin{array}{c|c|c|} & 1 & 2 \\ \hline d & \epsilon^{-j\beta} & \epsilon^{j\beta} \\ \hline q & -j\epsilon^{-j\beta} & j\epsilon^{j\beta} \\ \hline \end{array}$$

Hence

$$I_d = \epsilon^{-j\beta} I_1 + \epsilon^{j\beta} I_2$$
$$I_q = -j\epsilon^{-j\beta} I_1 + j\epsilon^{j\beta} I_2$$
$$V_d = \epsilon^{-j\beta} V_1 + \epsilon^{j\beta} V_2$$
$$V_q = -j\epsilon^{-j\beta} V_1 + j\epsilon^{j\beta} V_2$$

But

$$Z_d'' = \frac{V_d}{I_d} \text{ and } Z_q'' = \frac{V_q}{I_q}$$

Hence

$$Z_d'' = \frac{V_1 + \epsilon^{j2\beta} V_2}{I_1 + \epsilon^{j2\beta} I_2}$$

and

$$Z_q'' = \frac{V_1 - \epsilon^{j2\beta} V_2}{I_1 - \epsilon^{j2\beta} I_2}$$

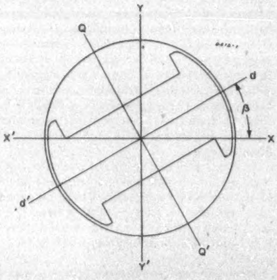

Figure 1

This agrees with the authors' equations 37 and 38.

To express Z_d'' and Z_q'' in terms of measured voltages and currents, proceeds as follows:

The transformation tensor transforming from the phase quantities A, B, and C to the sequence quantities when the A phase coincides with the X axis is:

$$C_4 = \frac{1}{3} \begin{array}{c|c|c|c|} & A & B & C \\ \hline 1 & 1 & a & a^2 \\ \hline 2 & 1 & a^2 & a \\ \hline \end{array}$$

since

$$I_1 = {}^1/_3(I_A + aI_B + a^2 I_C)$$

and

$$I_2 = {}^1/_3(I_A + a^2 I_B + aI_C)$$

Then

$$C_5 = C_3 \cdot C_4 =$$

$$\begin{array}{c|c|c|} & 1 & 2 \\ \hline d & \epsilon^{-j\beta} & \epsilon^{j\beta} \\ \hline q & -j\epsilon^{-j\beta} & j\epsilon^{j\beta} \\ \hline \end{array} \cdot \frac{1}{3} \begin{array}{c|c|c|c|} & A & B & C \\ \hline 1 & 1 & a & a^2 \\ \hline 2 & 1 & a^2 & a \\ \hline \end{array}$$

$$C_5 = \frac{1}{3} \begin{array}{c|c|c|c|} & A & B & C \\ \hline d & \epsilon^{-j\beta} + \epsilon^{j\beta} & a\epsilon^{-j\beta} + a^2\epsilon^{j\beta} & a^2\epsilon^{-j\beta} + a\epsilon^{j\beta} \\ \hline q & -j\epsilon^{-j\beta} + j\epsilon^{j\beta} & -ja\epsilon^{-j\beta} + ja^2\epsilon^{j\beta} & -ja^2\epsilon^{-j\beta} + ja\epsilon^{j\beta} \\ \hline \end{array}$$

This transforms line currents, or line-to-neutral voltages, to direct and quadrature currents or voltages; but since line-to-line voltages are measured, the direct and quadrature voltages must be expressed in terms of line-to-line voltages rather than line-to-neutral voltages.

If we take the reference phase as that which generates the voltage BC then the tensor to transform from line-to-line sequence voltages to line-to-neutral sequence voltages will be:

$$C_6 = \frac{1}{\sqrt{3}} \begin{array}{c|c|c|} & 1a & 2a \\ \hline 1 & -j & \\ \hline 2 & & j \\ \hline \end{array} \quad \text{since } V_1 = \frac{-j}{\sqrt{3}} V_{1a} \quad \text{and } V_2 = \frac{j}{\sqrt{3}} V_{2a}$$

To transform line-to-line voltages V_{BC}, V_{CA}, and V_{AB} to line-to-line sequence voltages V_{1a} and V_{2a}

$$C_7 = \frac{1}{3} \begin{array}{c|c|c|c|} & BC & CA & AB \\ \hline 1a & 1 & a & a^2 \\ \hline 2a & 1 & a^2 & a \\ \hline \end{array}$$

since $V_{1a} = {}^1/_3(V_{BC} + aV_{CA} + a^2 V_{AB})$

and $V_{2a} = {}^1/_3(V_{BC} + a^2 V_{CA} + aV_{AB})$

Then to transform line-to-line voltages to direct and quadrature voltages, the transformation tensor will be:

$$C_8 = C_3 \cdot C_6 \cdot C_7 = \begin{array}{c|c|c|} & 1 & 2 \\ \hline d & \epsilon^{-j\beta} & \epsilon^{j\beta} \\ \hline q & -j\epsilon^{-j\beta} & j\epsilon^{j\beta} \\ \hline \end{array} \cdot \times$$

$$\frac{1}{\sqrt{3}} \begin{array}{c|c|c|} & 1a & 2a \\ \hline 1 & -j & \\ \hline 2 & & j \\ \hline \end{array} \cdot \frac{1}{3} \begin{array}{c|c|c|c|} & BC & CA & AB \\ \hline 1a & 1 & a & a^2 \\ \hline 2a & 1 & a^2 & a \\ \hline \end{array}$$

$$C_8 = \frac{1}{3\sqrt{3}} \begin{array}{c|c|c|c|} & BC & CA & AB \\ \hline d & -j\epsilon^{-j\beta} + j\epsilon^{j\beta} & -ja\epsilon^{-j\beta} + ja^2\epsilon^{j\beta} & -ja^2\epsilon^{-j\beta} + ja\epsilon^{j} \\ \hline q & -\epsilon^{-j\beta} - \epsilon^{j\beta} & -a\epsilon^{-j\beta} - a^2\epsilon^{j\beta} & -a^2\epsilon^{-j\beta} - a\epsilon^{j\beta} \\ \hline \end{array}$$

From C_5 in the preceding

$$I_d = {}^1/_3[I_A(\epsilon^{-j\beta}+\epsilon^{j\beta})+I_B(a\epsilon^{-j\beta}+a^2\epsilon^{j\beta})+I_C(a^2\epsilon^{-j\beta}+a\epsilon^{j\beta})]$$

$$I_q = {}^1/_3[I_A(-j\epsilon^{-j\beta}+j\epsilon^{j\beta})+I_B(-ja\epsilon^{-j\beta}+ja^2\epsilon^{j\beta})+I_C(-ja^2\epsilon^{-j\beta}+ja\epsilon^{j\beta})]$$

and from C_6

$$V_d = \frac{1}{3\sqrt{3}}[V_{BC}(-j\epsilon^{-j\beta}+j\epsilon^{j\beta})+V_{CA}(-ja\epsilon^{-j\beta}+ja^2\epsilon^{j\beta})+V_{AB}(-ja^2\epsilon^{-j\beta}+ja\epsilon^{j\beta})]$$

$$V_q = \frac{1}{3\sqrt{3}}[V_{BC}(-\epsilon^{-j\beta}-\epsilon^{j\beta})-V_{CA}(a\epsilon^{-j\beta}+a^2\epsilon^{j\beta})+V_{AB}(-a^2\epsilon^{-j\beta}-a\epsilon^{j\beta})]$$

But

$$Z_d'' = \frac{V_d}{I_d} \text{ and } Z_q'' = \frac{V_q}{I_q}$$

This reduces to:

$$Z_d'' = \frac{1}{\sqrt{3}} \times \left[\frac{-V_{BC}\sin\beta + V_{CA}\cos(30^\circ-\beta) - V_{AB}\cos(30^\circ+\beta)}{I_A\cos\beta - I_B\cos(60^\circ+\beta) - I_C\cos(60^\circ-\beta)}\right] \text{ and}$$

$$Z_q = \frac{1}{\sqrt{3}}\left[\frac{-V_{BC}\cos\beta + V_{CA}\cos(60^\circ+\beta) + V_{AB}\cos(60^\circ-\beta)}{-I_A\sin\beta + I_B\cos(30^\circ-\beta) - I_C\cos(30^\circ+\beta)}\right]$$

REFERENCE

1. INHERENT ERRORS IN THE DETERMINATION OF SYNCHRONOUS-MACHINE REACTANCES BY TEST, C. Concordia, F. J. Maginniss. AIEE TRANSACTIONS, volume 64, 1945, June section, pages 288–94.

A. W. Rankin (General Electric Company, Schenectady, N. Y.): Mr. Tracy and Mr. Tice have presented an interesting suggestion for obtaining the subtransient impedances of synchronous machines. The suggested method has the commendable advantage of eliminating the oscillographic equipment needed in short-circuit testing, and does not require the accurate location of the rotor axes. Moreover, the values obtained would be close to the average of the three phases, and the interphase differences might be minimized thereby.

The value of the reactances so obtained seem to be questionable, however, when applied to short-circuit or similar subtransient analyses. The subtransient reactances of synchronous machines, particularly of the larger power-generation type, are influenced greatly by the saturation of the leakage paths. Because of this saturation, it is not unusual for the rated-current subtransient reactance of a turbine generator to be twice the rated-voltage value. It is recognized, of course, that this saturation effect is more pronounced on turbine generators with magnetic retaining rings than on salient-pole machines. To obtain an accurate value of the subtransient reactance of a turbine generator, the test procedure should duplicate, insofar as is practicable, the system condition in which the reactance will be operating. For these reasons, the test procedure suggested by the authors, in which rated stator current is caused to flow, might result in a test reactance more nearly approaching the rated-current value rather than the rated-voltage value needed for short-circuit analyses. It would be interesting if the authors would present a comparison of test data similar to that given in Figure 8 of the paper, but for larger machines with similar data obtained from rated-voltage short-circuit tests.

The suggested test would not give any information on the transient reactance, of course, this naturally being recognized by the authors, but if satisfactory values of the subtransient reactance could be obtained from this test, approximate values of the transient reactance could be obtained therefrom by experience factors.

Mr. Tracy and Mr. Tice are to be commended for presenting an interesting and provocative test procedure for the subtransient reactance since an easily applied test would be a major step in the accurate determination of one of the most intractable quantities in synchronous machines.

Gordon F. Tracy: Both F. K. Brainard and A. W. Rankin have pointed out the fact that the values of the subtransient impedances obtained by using rated current in test I of the paper will correspond to low saturation. Higher values of current could be used so as to approach a saturation corresponding to rated-voltage conditions. The machine would heat up rapidly, however, which would necessitate reading the instruments as quickly as possible. Further experimental work should be done in this connection.

It is interesting and gratifying to have equations 37 and 38 of our paper confirmed by F. K. Brainard in an alternative development that is quite different from that used in the paper. Brainard's alternative expressions for the subtransient impedances in terms of the vector values of the line-to-line voltages also are interesting. However, the amount of time required to calculate the values of the impedances using his expressions seems to be about the same as that required by using equations 37 and 38 directly. In either case, the vector values of the voltages and currents first must be calculated from the instrument readings; then it seems to be a matter of preference whether the sequence components of the voltages and currents are found next, from which the impedances follow, or the impedances are computed from Brainard's equations.

Standards and Insulation Characteristics of Oil-Insulated Transformers

Discussion and author's closure of paper 45-41 by F. J. Vogel, presented at the AIEE winter technical meeting, New York, N. Y., January 22–26, 1945, and published in AIEE TRANSACTIONS, 1945, April section, pages 167–71.

J. H. Hagenguth (General Electric Company, Pittsfield, Mass.): Mr. Vogel's discussion of the relative importance of the different types of insulation tests now in use for power transformers is timely. It is, however, my belief that he has covered only the surface of the problem.

Unfortunately, many of Mr. Vogel's statements are not supported by sufficient facts from which to draw the rather sweeping conclusions which he makes.

SWITCHING SURGES

> "Very few, if any, transformer failures attributed to switching surges ever have occurred. Even those transformers built before 1930 with low levels of impulse-voltage strength have had few, if any, switching-surge failures. Many of the transformers of the 138-kv class had levels of 500 kv and less, instead of the 750 kv now standard. This fact confirms that the voltage distribution of switching surges in windings is fairly uniform as inferred previously."

The service record of such transformers likewise proves that the voltage distribution due to impulse waves is uniform, because the facts are that a relatively small number of even the old transformers fail in service. Deductions of the kind used, therefore, can prove almost anything. Actually, it is extremely difficult in most cases to prove the cause of the failure because:

(*a*). Failures may be progressive and it may take many years of repeated application of overvoltage before the fault is of such nature that normal frequency current will follow through the fault and necessitate taking the transformer off the line. In many such cases it is impossible to state the cause or causes.

(*b*). Lightning disturbances and switching surges frequently occur at the same time. Unless instruments were installed at the time of fault, it would be impossible to say which of the two caused the failure.

(*c*). After a fault current is established in a transformer, the resulting destruction of the windings often makes it very difficult even to determine the original point of failure. In many cases, several of the windings are affected and the original fault may have occurred in either winding.

This situation is discouraging because transformer insulation could be applied

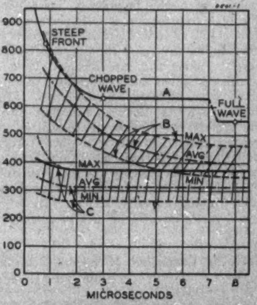

Figure 1. Comparison of ASA-NEMA impulse-test level for 115-kv class with voltages expected in the field when protected by a 20-inch rod gap and eight-unit station-type arrester

A—ASA-NEMA test levels for 115-kv voltage class

B—20-inch rod gap

C—eight-unit lightning-arrester and ground-wire protection

Table I. Impulse Ratio of Transformer Structures

Type of Spacing	Inch Spacing	Impulse Ratio	Type of Damage	Year	Reference
Barrier *C*	0.64	1.55–1.75	Corona	1938	1
		1.8	Breakdown	1938	1
Barrier *D*	2.5	2.3–2.5	Corona	1938	1
		2.6	Breakdown	1938	1
	0.056	1.6	Corona	1937	2
		2.87	Breakdown	1937	2
	0.125	1.83	Corona	1937	2
		2.85	Breakdown	1937	2
Core type		2.1	Breakdown	1933	3
Shell type		2.2	Breakdown	1933	3
Bare electrodes in oil	2	2.4–2.7	Breakdown	1939	Not published
	4	1.8–2.7	Breakdown		
	10	1.6–1.8	Breakdown		

more intelligently from an economical point of view, if the correct story behind the cause of failures always were known. Actually, of course, the voltage distribution in the transformer depends on the type of transformer, its natural period of oscillations, the type of switching surge, and whether its period of oscillation is in resonance with one of the transformer natural frequencies. Since the switching surges can reach amplitudes of the order of the present standard impulse test, their effect on the insulation co-ordination cannot be ignored.

Mr. Vogel, in his paper, attempts to show that more severe impulse tests are required to be more nearly equivalent to the relative stresses imposed by 60-cycle tests. The fact that so few of the older transformers with extremely low-impulse insulation failed in service seems to indicate that present standard impulse levels might be decreased rather than increased.

IMPULSE RATIO

Much of the author's argument in favor of a more severe impulse test than the present standard tests as compared to the 60-cycle tests is based on an impulse ratio of 2:1. When using impulse ratio, care must be taken whether breakdown or corona values are used. In order to insure long life of a transformer, it is important that test as well as service stresses in all parts of the winding are below the injurious corona level. Taking this into account, Table I of this discussion has been prepared to show data from different investigators. This table shows that there is no uniformity in the impulse-ratio factor. Particularly concerning corona, in all cases where corona values were reported, the corona impulse ratio varies between 1.6 and 2.5. In case of solid insulation, average values cannot be used to determine safety factors. The minimum values have to be met to be certain that, in every case, at least a certain safety factor is obtained. Using an impulse ratio of 1.6, instead of 2.1, the equivalent impulse-test levels would fall below the levels used at present.

The ratios of impulse test to 60-cycle test for the different voltage classes actually range between 2.7 for the 15-kv class to 1.87 for the 230-kv class. Test experience has shown that there is a good balance between present test levels at low frequency and impulse as far as the major insulation is concerned, although this seems to be contrary to the author's experience.

There is no disagreement with the author's statement that "ability to withstand 60-cycle test or 120-cycle induced test is no proof of a transformer's ability to withstand impulse tests," if that statement is confined to stresses along the windings. The impulse test is the only test that will detect weaknesses between coils and across larger portions of windings. Therefore, the suggestion to apply impulse tests to all transformers is in the right direction.

There are, however, several points which need considerable emphasis before such tests are placed on a general commercial basis.

1. It must be possible to detect all failures. While we have gone a long way toward that goal, there is, at present, no certainty of 100 per-cent detection.[5]

2. The cost of the impulse tests is considerably in excess of that for the low-frequency tests. Simplification of the present tests is needed to reduce the cost many times to make general impulse testing an economic proposition.[6]

3. The whole subject of impulse- and low-frequency-test levels should be reviewed to determine the most economical use of insulation for the service for which transformers are intended.

Mr. Vogel suggests that a three-microsecond or a one-microsecond or a steep-front impulse test might be substituted for the present applied or induced tests. I believe that the type of impulse test, as well as its amplitude, should be based on the type of protection used with the transformer, as well as the protection provided in the station and for the transmission lines. Mr. Vogel makes the statement:

> "Even if lightning arresters are mounted on the units and as close to the terminals as possible, some very high overvoltages can occur, but for very short times. If the arrester be 25 or 30 feet from the terminals and the wave front is steep, an appreciable voltage reflection may take place at the bushing terminals."

It is unfortunate that he does not give any figures as to the amplitude of such voltages. In our experience, the voltages at the transformer terminals, when protected by a modern arrester, were below the full-wave test level of the transformer, even though the lead between arrester and transformer was as long as 50 feet when wave fronts of 1,000 or more kv per microsecond were applied. The crest of such voltage peaks occurred at about 0.5 microsecond and rapidly was reduced to the normal *IR* drop of the arrester. The stresses produced in transformers by such waves would be of the order of 70 per cent of those caused by the chopped-wave test because the steep tail of the chopped wave does not occur.

Comparing arrester protection with the author's proposal of a steep-front test, the following applies:

1. A 1,050-kv wave chopped at one microsecond is more severe than the National Electrical Manufacturers' Association standard front-of-wave test of 960-kv crest.

2. In the region of one microsecond and less, the safety factors between present tests and lightning-arrester-protection levels are already unnecessarily high so that no increase is justified.

3. The rate of incidence of steep-front waves in transformer stations is so low compared to that of the slower and longer waves that the American Standards Association standard chopped-wave and full-wave tests more nearly represent service conditions than the steep-front test.

4. If, however, a transformer is not protected by arresters and ground wires are not used over the line conductors but protection is obtained by a gap, then a steep-front test is not only desirable but practically a necessity to establish that the transformer is capable of withstanding such stresses.

Figure 1 (of this discussion) shows the difference between gap protection and arrester protection as compared to the present standard impulse-test levels for a 115-kv system. The maximum and minimum curves shown for the rod gap represent the sparkover voltage variation of the gap due to changes in applied wave shape;[4] the range for lightning-arrester-protection levels represent accepted industry standards. These values of gap spacings and arrester units are actually in use. It is apparent that the transformer equipped with this gap for protection can be subjected in the field to excessively high short-time stresses. Therefore, in such cases, a steep-front test is fully justified. There is, however, no necessity for making this kind of test on transformers which are protected with modern lightning arresters.

The steep-front test is more complicated than the chopped-wave test, because frequently a different impulse generator setup is required for this test than for the full-wave test, while the chopped wave uses the same generator. It is, therefore, undesirable as a standard test because costs are increased further.

Table II. Comparison of Stresses Occurring Across Small Portions of a Winding of Type "Unshielded Transformer II"—138-Kv Class

Voltage Distribution Curve for Steep Front: Alpha = 20

		Voltages in Kilovolts Across Portion of Winding for			
Across Per-Cent Winding	Per-Cent Turns	2.5-Microsecond Front 750-Kv Crest	Tail of Chopped Wave 750-Kv Crest	1-µs Front Wave 1,050-Kv Crest	Lightning-Arrester Protection, Grounded Neutral 30-Foot Lead, 1,000-Kv per Microsecond Applied
98.2–96.2	2.0	143	412	347	259
96.2–92.6	3.6	230	430	420	285
81.9–78.3	3.6	174	275	347	220

Table II of this discussion shows a comparison of stresses in a winding called "unshielded transformer II" in Mr. Vogel's paper. This table compares the voltage stresses across various small portions of the winding for a chopped wave with 2.5-microsecond front up to time of chopping, the stresses due to the steep drop on the tail of the wave, as well as the stresses for a one-microsecond front 1,050-kv-crest test wave. The comparison shows that the chopped wave is capable of breaking down the insulation across such portions, if too weak, just as readily as the one-microsecond wave.

It is our experience that either the steep front or the chopped wave can produce failures of the same type, but detection of such failures often occurs only on the full wave.[5] Furthermore, the chopped wave produces coil-to-coil and other cross-winding stresses further into the winding than the steep-front test.

As stated, the whole subject requires considerable discussion by all those concerned with the problem to determine the best type of tests, as well as test methods, for power transformers. The subject should be considered, not only from the point of view of the transformer alone, but from the over-all conditions of system and station design. The latter determines to a large extent the amplitude and wave shape of surges which will be applied to transformers in the field.

References

1. Co-ordination of Power Transformers for Steep-Front Impulse Waves, **V. M. Montsinger.** AIEE Transactions, volume 57, 1938, April section, pages183–9.

2. Dielectric Strength of Transformer Insulation, **P. L. Bellaschi, W. L. Teague.** AIEE Transactions, volume 56, 1937, January section, pages 164–71.

3. Factors Influencing the Insulation Co-ordination of Transformers, **F. J. Vogel.** AIEE Transactions, volume 52, 1933, pages 411–16.

4. Volt–Time Areas of Impulse Sparkover, **J. H. Hagenguth.** AIEE Transactions, volume 60, 1941, July section, pages 803–10.

5. Progress in Impulse Testing of Transformers, **J. H. Hagenguth.** AIEE Transactions, volume 63, 1944, pages 999–1005.

F. J. Vogel: I appreciate Mr. Hagenguth's discussion of my paper very much; also, I feel that he takes too hopeless a view of the situation.

For example, in the case of switching surges, they exist primarily because of the capacity and reactance in the circuit. This has been studied quite thoroughly with respect to transient recovery voltages.[1] Also, Figure 7 in a paper by Bewley[2] is distinctly of interest. Since the surges originate in the inductance or the leakage reactance of the transformer, as well as other associated reactances, it is difficult to see how they would be distributed very badly within the windings. Further, I would like to point out that, to my knowledge, there have been no power-transformer failures in the field when they had been impulse tested. Although the reasoning is not rigorous or conclusive, it seems very likely that lightning impulse voltages will be more severe than switching surges. Indeed, reference to the book "Transformer Engineering" by some of Mr. Hagenguth's associates confirms this opinion.

With respect to the question of impulse ratio, all of the tests which I have seen have indicated a ratio of 2.1 or better when corona formed in the oil itself. Since we are attempting to avoid corona, even on 60-cycle tests, I still believe that a fair impulse ratio is 2.1. In the cases where lesser ratios are obtained, it is questionable if it is representative of good design. I have seen many models and test samples tested and have yet to see an impulse ratio less than this figure when corona values alone were considered. Impulse ratios of 1:6 have been found when 60-cycle and impulse ultimate strengths were obtained. In my opinion, this condition is not representative of good design and I fail to see why a manufacturer should be required to put extra material in to meet the 60-cycle test when it is not required to meet the impulse test. My position is, therefore, that if the impulse test can be reduced or lower levels are required, why insist on the 60-cycle test value, unless it will determine a greater degree of serviceability.

With respect to the problem of failure detection, it seems to me as though it is simpler than Mr. Hagenguth would have us believe. His position has been that, you may not only have trouble in finding failures, but also deterioration is caused by the test, since on repeated tests the actual strength is only eight tenths of the single-test value. I would like to point out that many observers have confirmed the fact that there is no deterioration providing the stress is lower than some critical value. Further, if the stress exceeds this critical value generally, failure will result on repeated shots within a number between 25 and 50. This does not say that sometimes one may occur after 60 or 70 shots, but the bulk of them will occur before 25 shots. I would like to suggest perhaps fewer cathode-ray oscillograms and less adherence to rigid rules as to wave shape and duration, and the application of enough surges to insure that the deterioration point is not reached. I believe that this is much safer than applying so few surges and accepting the possibility of undetected damage and injury. With such test procedures it may be that the surge test will be simpler and easier to provide than at present.

There is one interesting opinion in Mr. Hagenguth's discussion which I think to be incorrect. The steep-wave front is decidedly more severe than the steep drop on the tail of the wave for the chopped wave. From past experience I know that extra care is required to meet the steep-wave-front tests as compared to the ordinary chopped-wave test. Mr. Hagenguth would infer that any transformer which would withstand chopped waves would withstand the steep-wave-front tests. This definitely is not true.

References

1. Practical Calculation of Circuit Transient Recovery Voltages, **J. A. Adams, W. F. Skeats, R. C. Van Sickle, T. G. A. Sillers.** AIEE Transactions, volume 61, 1942, November section, pages 771–9.

2. Equivalent Circuits of Transformers and Reactors to Switching Surges, **L. V. Bewley.** AIEE Transactions, volume 58, 1937, pages 797–802.

Measurement of Stray-Load Loss in Induction Motors

Discussion and author's closure of paper 45-42 by D. H. Ware, presented at the AIEE winter technical meeting, New York, N. Y., January 22–26, 1945, and published in AIEE TRANSACTIONS, 1945, April section, pages 194–7.

M. M. Liwschitz (Polytechnic Institute of Brooklyn, Brooklyn, N. Y.): The stray-load losses of the induction motor consist of the following parts:

1. Eddy-current losses on the stator surface due to the step harmonics of the rotor.
2. Eddy-current losses on the rotor surface due to the step harmonics of the stator.
3. Eddy-current losses in the stator teeth (tooth-pulsation losses of the stator) due to the step harmonics of the rotor.
4. Eddy-current losses in the rotor teeth (tooth-pulsation losses of the rotor) due to the step harmonics of the stator.
5. Hysteresis losses.
6. Copper losses in the bars of the squirrel cage due to the flux pulsations in the rotor teeth.
7. Copper losses in the bars of the squirrel cage due to the stator harmonics of lower order. (5th, 7th, 11th....)

The losses under 3, 4, 5, and 6 depend upon the saturation of the stator and rotor teeth. Since the reverse-rotation test occurs under conditions which, with respect to saturation, are entirely different from the saturation conditions under load, larger differences between the dynamometer tests and reverse-rotation tests would be expected. The tests made by Mr. Ware are very promising. However, many more comparative tests on motors should be made before the reverse-rotation test, proposed by Professor Morgan, be included in the AIEE Test Code for Polyphase Induction Motors.

Theodore H. Morgan (United States Office of Education, Washington, D. C.): Mr. Ware's paper is a milestone in the measurement of stray-load loss in induction machines by a direct method, and judging from the test results obtained it is a milestone close to the end of the road.

In exploring any test method it is necessary to have a clear conception of all components included within a given measurement. The author has recognized this and has stated clearly and accurately all component losses in both the stator and rotor measurements of the reverse-rotation test. After determining the components involved, a study should be made of relative magnitudes. Possibly some are so small that they may be neglected. In devising the reverse-rotation method of measuring stray-load loss it was assumed that the stator component of this loss was negligible in comparison with the total loss, and thus could be considered zero and omitted. The test results of Table I of the author's paper indicate the validity of this assumption. If it were correct that the stator loss was of appreciable magnitude, the value of the stray-load loss finally determined would be too small by twice the amount of the stator-loss component. If the stray-load-loss values obtained by the reverse-rotation method be compared with those obtained by dynamometer measurement of output, it will be noted that in 7 of the 13 motors tested the reverse-rotation method gives a higher value of stray-load loss than the input–output method. It is a satisfaction to note that this result substantiates the original assumption that the stator component is of such small value that accuracy may be obtained when it is neglected in motors of this size.

When considering the results shown in Table I of the paper, we are confronted with the problem of what measurement to use as the standard of accuracy. The dynamometer method cannot be considered sufficiently accurate as a standard because of the large amount of power involved in both the input and output measurements. Separating the stray-load loss from such large measured values makes a high degree of accuracy impossible in the final determined loss. While all test results shown in this paper are excellent, the plotted points in Figure 1 indicate clearly that the dynamometer method cannot be justified as a standard of accuracy. Probably the most accurate value obtainable in Table I is the average of the loss value obtained by the two methods used. Taking this value as standard, it is interesting to note that in 6 out of the 13 cases the error resulting from use of the reverse-rotation method was within 0.1 per cent of the power output. In 12 of the cases, the error was within 0.5 per cent, and the remaining test showed an error of only slightly over 0.5 per cent. This high degree of accuracy justifies the author's conclusion that the reverse-rotation method should be included as a recognized method in the AIEE Test Code for Polyphase Induction Motors.

The author states that the stator loss should not be omitted in the case of large motors, but it is not entirely clear as to where the line should be drawn between a small and a large motor. In the test which he cites for a 500-horsepower motor the difference in values obtained by the two methods used is 300 watts. If the stator loss had been neglected, the final result by the reverse-rotation method would have been reduced 640 watts to 2,160 watts, making a difference of 340 watts between this value and that of the pump-back method. The difference in the error by the two methods would thus be 40 watts, which probably is not significant considering the size of the machine being tested. On the other hand, it clearly is evident that the assumption of zero stator loss in the case of the 1,750-horsepower motor leads to erroneous results. It would appear that further information regarding the magnitude of the stator component of the stray-load loss in large motors is needed and I hope that the author may be encouraged to continue his excellent work in this direction.

Mr. Ware is to be complimented for devising a method for the determination of the stator component of the stray-load loss in the case of large motors. It seems inevitable that any direct method for the measurement of this quantity at first would be open to question, as the validity of any proposed method can be established only by a large number of tests. Under actual operating conditions there are factors which are different from those used in the test proposed. The degree of saturation of the stator iron would be different, and the path and density of the stator leakage flux would be affected by the presence of the rotor iron. It is quite possible that compensating factors exist which result in negligible difference in the total quantity. This can be shown only by additional tests on large motors.

As methods of measuring stray-load loss have been developed, we have acquired a better understanding of the nature of the loss and the relative magnitude of the components involved. This is important, for it permits advance in the art and improvement in design. The author's determination that the stator component is of considerable magnitude in large motors presents an immediate challenge to designers of these machines.

In closing I desire to congratulate Mr. Ware on his excellent and valuable paper.

D. H. Ware: Professor Morgan has indicated that it is not clear what the division line should be between those motors in which stator-load loss at fundamental frequency should be considered and those motors in which stator-load loss should be neglected. The magnitude of the stator-load loss certainly must depend, not only on the size of the motor, but also on the design. Since the test for stator-load loss is simple and easy to perform and will not perceptibly affect results of a load-loss test if the test is made on a motor with low stator loss, it seems prudent to make the division line rather low, or to consider no division at all, and to make this additional test on all sizes. The test data presented would indicate that the division should be between 500 horsepower and 1,750 horsepower. However, two-pole motors smaller than 500 horsepower have been found to have an appreciable amount of stator-load loss. I would recommend that the division, if made, should be no higher than 100 horsepower.

Professor Morgan points out that the presence of the rotor iron should change the shape of the magnetic field which causes an error in the measurement of the fundamental frequency loss in the stator. Tests have been made to locate and control these losses, the results of which indicate that most of them occur in the end zone where the rotor iron would not be effective.

Mr. Liwschitz states that saturation conditions in the vicinity of the rotor and stator surface, teeth, and conductors, should change the stray losses as measured by the reverse-rotation test from those occurring under load. However, test data indicate that the difference in stray losses caused by the presence of the fundamental flux is a small part of the total. It would be a mistake to assume that the reverse-rotation test would give results which would be exactly correct. However, because of the practical difficulties of performing an input–output test, the reverse-rotation test may give results much nearer to the true value of stray-load loss unless unusual accuracy is realized.

In oral discussion of this paper, Mr. L. A. Kilgore suggested that it be required that all end bells, air deflectors, and other stationary parts be in place when the test for stray loss in the stator is made. This is a very constructive suggestion and I am in complete agreement.

In closing, I would like to express my appreciation for the encouraging discussion of this paper.

Analysis of Arc-Welding Reactors

Discussion and author's closure of paper 45-29 by Charles M. Wheeler, presented at the AIEE winter technical meeting, New York, N. Y., January 22–26, 1945, and published in AIEE TRANSACTIONS, 1945, March section, pages 87–90.

G. H. Fett (University of Illinois, Urbana, Ill.): The author states that the magnitude of the welding inductance of the arc-welding reactor is best determined from actual welding tests. The experimental points of Figure 5 of the paper, showing the relation between optimum inductance and arc current, indicate that there must be considerable variation in judgment of good welding, since the points given do not lie on a smooth curve. Furthermore the author apparently selects a value of current I' arbitrarily greater than any for which he has obtained data and specifies that the inductance must have the value obtained for the smaller current Iw'. It would seem that there are other factors which specify the optimum welding inductance.

If what constitutes satisfactory welding could be determined quantitatively and independently of operator technique, then the welding inductance for optimum performance could be determined. The use of the welding reactor has two objectives. First, it is to insure adequate voltage when the operator lifts the electrode from the work. When the generator is short-circuited the potential drop across the electrode-work junction is quite small. After the operator initiates the arc by lifting the electrode from the work, the potential drop across the circuit must rise to the value equal to the sum of the cathode and anode arc drops plus the product of the potential gradient in the arc and the arc length. Evidently operator technique will enter into consideration, for the speed with which the arc is lengthened will determine the voltage rise which the welding generator and the welding reactor must supply. The anode and cathode drops occur instantaneously with the initiation of the arc, within less than 10^{-4} second,[1] and these voltages also must be supplied by the circuit. The potential gradient will depend upon the electrode diameter, coating, and perhaps the actual length of the arc that is drawn. Since the cathode and anode drops do not exceed about 16 volts,[2] a value of welding inductance required to compensate for this voltage drop becomes $16\times10^{-4}+di$, where di is the largest current change which can be tolerated by the welding process. The actual value of the self inductance necessarily will be larger than this value to compensate for the gradient in the arc itself. When enough research work in this field is completed, it, too, may be susceptible to analysis.

Second, the welding reactor must act to supply or absorb voltage as the arc current tends to change momentarily during the process of welding. This smoothing action of the inductance must act swiftly to maintain approximately constant thermal conditions in the arc, if the value of thermal time constant of 0.001 second is accepted as being correct. The tendency for the current to change during welding again would depend, among other things, upon the operator technique.

It is evident that certain of the factors which govern the size of the reactor to be used can be evaluated. At present, however, it would seem that the largest possible inductance should be used, because avoidance of the annoyance as well as the loss in production which results when the arc goes out will counterbalance the slight additional cost. One factor, which is not brought out in the paper but which has a direct bearing on the problem, is the effect of the inductance upon the metallurgical results of the welding. Has the author any direct evidence of difference in the quality of the weld which can be attributed directly to a difference in the size of the reactor? Such data would be an important supplement to the data of Figure 5.

REFERENCES

1. Cathode Drop of an Arc, G. H. Fett. *Journal of Applied Physics*, volume 12, 1941, page 436.

2. Cathode Drop of an Arc, G. H. Fett. *Welding Journal Research Supplement*, volume 7, 1942, page 29.

Charles M. Wheeler: In his discussion of this paper, Professor Fett has made the very sound observation that the establishing of basic criteria for optimum welding performance would more clearly establish quantitatively optimum values for inductance.

The interdependence of inductance and transient-voltage characteristics with regard to their effect on arc stability makes the subject complex beyond the scope of the present paper. This can be appreciated, because the influence of inductance in welding is purely transient by its very nature and from a purely analytical approach must of necessity be evaluated in terms of the requirements of a particular source of power and a particular set of welding requirements.

The apparent anomalies of the experimental data represented in Figure 5 are due more to the different requirements of various types and sizes of electrodes than to the judgment of the welding operator. This has been demonstrated by repetitive tests with other operators.

As Professor Fett has suggested, there is, indeed, need for more complete analysis and fuller evaluation of the requirements of welding arcs for stability and quality of welds in terms of the characteristics of the power source. Although there is no known conclusive evidence available on the effects of increasing inductances above that required for stable-arc characteristics on the quality of welds, there is definite question as to whether the largest possible value of inductance would be desirable.

Power Supply for A-C Arc Welding

Discussion and authors' closure of paper 45-28 by A. U. Welch and R. F. Wyer, presented at the AIEE winter technical meeting, New York, N. Y., January 22-26, 1945, and published in AIEE TRANSACTIONS, 1945, March section, pages 116-20.

C. N. Clark (Duquesne Light Company, Pittsburgh, Pa.): Hundreds of a-c arc welders now are being supplied by the Duquesne Light Company. Some are in groups as large as 204 in one plant, and others are used singly or in small groups by many customers. From the reports received, the a-c arc welders are giving very satisfactory performance. In only a few cases have any troubles developed, and these were corrected by making relatively minor changes.

Because of its size and power factor it usually has not been practical to serve the welding load from the average lighting service supplied from overhead transformers and secondary wiring. The usual method employed has been to connect the welders to a new or existing three-phase power supply, distributing the welders over the three phases. In the smaller shops where no three-phase service was available, a limited number of welders has been connected to a separate single-phase supply of suitable voltage.

The voltage fluctuation on the 2,300- or 4,000-volt supply circuit has not been sufficient to cause complaints, but there are certain outlying areas where their use would result in objectionable lighting flicker near and beyond the location of the a-c arc welder. In general, our customers have separated the lighting and welder circuits within their plants in order to avoid this type of interference.

This paper has been discussed with some of our power salesmen and design engineers, all of whom showed considerable interest. Due to the lack of reliable information in the past on a-c arc welders, the estimates of customer demands have tended to be on the safe side, and in some cases the capacity provided has been somewhat larger than would have been required after making proper allowances for diversity between welders.

There seldom has been time available to contact the manufacturers of the equipment, and in many cases the customer had little or no performance data. On the Duquesne system these welders are being used both with and without capacitors. In certain plants the power factor of a group of welders is corrected by a single capacitor installation, and in others individual capacitors are applied at each welder.

In one plant 204 a-c arc welders of the transformer type are now in service. Two hundred of these are equipped with atomic hydrogen jets, and the remaining four are of the full automatic type.

The first transformer-type a-c arc welders were without capacitors. Others were added later with capacitors connected ahead of the welder switch. As a result of the capacitors, considerable trouble was encountered from high voltage during periods of light load. This was corrected by adding an electronic control to disconnect automatically the welder transformer and capacitors when not in use.

The four automatic a-c welders are provided with full electronic control, including the timing of the arc and disconnecting both the welder transformer and the capacitor from the line between successive welds.

At another plant 150 out of a total of 800 arc welders were of the a-c transformer type. In order to reduce the number of d-c welding machines required, the generator fields were reconnected in such a way as to give practically flat voltage characteristics, averaging about 65 volts. Each motor generator set supplied two sets of leads and electrodes through variable resistors in series with each arc. The total demand of the 800 welders, with cranes and shop lighting was 5,800 kva.

A. U. Welch and R. F. Wyer: The most important advantage obtained from the use of power-factor correcting capacitors on industrial welders is the considerable reduction in full-load input current resulting in large economies in primary wiring, switches, and fuses. As was shown in the paper, this amount of capacitance may be too high in cases where large numbers of a-c welders only, operating at light duty, are installed on a circuit. However, in more usual applications of a few welders on circuits supplying other loads this difficulty is not experienced, and the capacitors result in reduced over-all loading of the circuit.

The Power-Distribution Problem in Arc Welding

Discussion and authors' closures of paper 45-48 by H. W. Pierce and C. E. Smith, presented at the AIEE winter technical meeting, New York, N. Y., January 22-26, 1945, and published in AIEE TRANSACTIONS, 1945, April section, pages 178-84.

C. I. MacGuffie (General Electric Company, Schenectady, N. Y.): This paper covering the power-distribution problem involved in applying arc welders to a very heavily concentrated area supplies much factual data needed by welding engineers in many large shops. The authors are to be congratulated on this presentation of their solution to a major complex problem.

They mention the use of 2,000-ampere single-pole air circuit breakers in the feeders paralleling the shipways. This has not been general practice; many installations depend upon the breaker on the generator control panel for protection of the motor generator set, and it would be interesting to know if practice proved the desirability of these breakers.

Another point of considerable interest is the use of two tackers on a single panel without objectionable interference between operators. Were any attempts made to interlock the welding circuits so that one operator could not draw welding current while the other operator was using the panel?

R. F. Wyer (nonmember; General Electric Company, Schenectady, N. Y.): This paper should be most interesting to anyone involved in the problem of applying the proper arc-welding equipment to relatively large installations. It answers a number of questions which have come up from time to time in such application work.

In connection with the application of a-c arc welding, the authors make the statement that its use in ship work on the ways is debatable and point out that it is necessary to have moderately long lines from the machine to the work. This suggests that the a-c welding system is not adaptable to long leads, a very widespread impression. Tests made in the welding shop, however, indicate that with properly designed a-c welders, particularly in ratings of 300 amperes and below, no account need be taken of lead lengths up to 250 or 300 feet, except where both an electrode lead and a work lead are used, and they are spaced widely so that their reactance is high. Where the return current is carried through a steel deck or floor on which the electrode cable lies, long lengths of lead may be used because the reactance of the circuit including an iron-floor return is only slightly higher than the reactance of a circuit consisting of electrode and ground lead taped together.

Recognizing that on occasion conditions would be more severe, in that a good deal of iron could be included in the circuit loop in shipway work, we made some tests in shipyards under very severe conditions. With the standard return-current connection from the bottom of the hull to an a-c welder on the ground and with a 300-foot electrode lead carried over the steel side and deep into the hold, a welding current of 280 amperes or greater could be obtained from a standard 300-ampere a-c welder.

Other tests have indicated that leads up to 400 or 500 feet long can be used with standard a-c welders of good design under ordinary conditions of operation, where the electrode lead is carried down through hatches and bulkhead openings, while the a-c welder remains on the deck or on a staging platform. The one primary precaution is to avoid making a reactor by coiling the leads on an iron deck. Not only will this cut down the maximum obtainable current from the a-c welder, but also, as in the case of d-c welding, it results in overheating the cables due to reduced cooling radiation and convection.

It seems quite likely, in view of this flexibility with regard to lead lengths, that the advent of the high-quality all-position a-c electrode will result in its adoption for shipway work in the near future.

The authors' comments about the difficulties involved in using single-operator d-c sets in large numbers recall an installation where underground substations about 12 by 30 by 8 feet high were used to house 25 single-operator sets each. This necessitated running 25 individual 4/0 cables the full length of the way from each machine room. And it resulted in losses of 75 kw, even at no load, to be dissipated in an underground room a little over half the size of my basement.

H. W. Pierce: Mr. Wyer's remarks on a-c welding for the shipways serve to prove the statement that this topic has two sides, and that consistent improvement in both transformers and electrodes may lead shipbuilders to change their minds. Our experience with a-c in the turret shop, where moderately long leads and heavy masses of steel were involved, indicated a greater drop than Mr. Wyer claims. This is not in itself serious; the difficulty in this shop and for ship work lies in the change as the welder moves from one compartment or deck level to another. Although the work may be identical, as on a run of pipe, we feared the necessity of too frequent current readjustment. Coiling is almost impossible to avoid in the moves a ship welder makes and provides the best way of caring for excess cable when the job is near his outlet. Stretching out the full lengths to avoid reactive drop would penalize the operator and complicate the present difficult job of keeping passages and deck reasonably clear of hundreds of feet of cable. We have never noted evidence of overheating in the case of coiling d-c cables.

C. E. Smith: The use of 2,000-ampere single-pole air circuit breakers, protecting the main welding feeder circuits, has proved highly desirable and additional cost can be justified by the following conditions.

1. They afford protection for the individual feeder from fault and overload conditions. For example: with six 1,500-ampere welding machines operating in parallel on a common bus, supplying through four individual feeders, a group of 120 welders, only 25 per cent or 30 welders would be affected, because of the tripping of an air circuit breaker when fault or overload conditions arise, thereby saving 75 per cent of work stoppage.

2. The air circuit breakers become a means of disconnecting a circuit from the welding bus for shifting of welding outlet panels on a given circuit without a complete shutdown of the system.

While this could be accomplished at approximately half the cost by the use of large disconnecting switches, the load would have to be removed by shutting down all the individual resistor panels on the circuit, as a disconnecting switch could not be opened under load. Also it would require the survey of the entire circuit and involve considerable time and loss of production.

It has been found that the interlocking of welding circuits, due to the use of two tackers on a single panel, did not justify the expense involved as the duty cycle is so low that there is little interference between the two operators.

The Amplidyne Generator Applied to Speed-Controlled Electric Gun Turrets for Aircraft

Discussion and author's closure of paper 45-81 by L. A. Zahorsky, presented at the AIEE winter technical meeting, New York, N. Y., January 22–26, 1945, and published in AIEE TRANSACTIONS, 1945, May section, pages 221–5.

J. D. Thompson (General Electric Company, Schenectady, N. Y.): Mr. Zahorsky's suggested specification for turret Amplidyne performance is very worth while and fulfills a long-standing need for something of this sort. The surprising thing is that it has not been available before now. However, a great many not very well understood factors, often insignificant on commercial machines, enter importantly into the performance of these high-speed aircraft Amplidynes, and it has been difficult to correlate the sometimes erratic performance of the machines alone with the seemingly satisfactory performance of the motor and control combination. Ability to write such a specification at all represents a distinct advance. Note that even this specification still leaves the application engineer and circuit designer with quite a problem when the slope of the no-load saturation curve can vary two to one.

Item 2 in the section "Revised Limits and Their Purpose," seems somewhat misleading and does not agree with the thought of item 2 of the "Typical Specification." There is no occasion to check for zero voltage regulation under any condition, and it is believed that Mr. Zahorsky meant to specify a definite positive voltage regulation with constant or zero control-field current as shown in Figure 6. Does Mr. Zahorsky believe it feasible to take such a curve with zero control-field current?

R. D. Musselman (nonmember; Bendix Aviation Corporation, South Bend, Ind.): Mr. Zahorsky's paper interested me greatly and I most heartily agree with the text.

There is, nevertheless, one point that I believe should be covered, and that is the procedure for preparing the Amplidyne so that it can be properly compounded. This, I believe, is very essential to the successful performance of any Amplidyne.

L. A. Zahorsky: The comments in Mr. Thompson's discussion are quite appropriate and have a sound basis. He has pointed out that the slope of the no-load saturation curve can vary two to one. This has to do only with the slope of the saturation curve at lower voltages and does not refer to the height of the saturation curve. The limiting saturation curves approach each other near the maximum output voltage. The wide variation in the slope of the saturation curve is intended to take care of the limits of performance over the wide range of temperatures and loading the Amplidyne may receive.

Item 2 of the "Typical Specification" does not agree with item 2 of the "Revised Limits and Their Purpose" as Mr. Thompson pointed out. This is the one place where the practical limitations of testing limit the specification so that it cannot attain the ideal. It might have been better to write item 2 of the specification exactly like item 2, "Revised Limits," and specify in addition the test necessary to prove this condition. It is not feasible to take the curves shown in Figure 6 of the paper with zero-control field current due to the inherent instability in a unit with such rapidly rising characteristics.

Mr. Musselman's comments are very appropriate in the case where Amplidynes are applied to turrets for which specifications are the same as, or to tighter limits than, the specifications to which the Amplidynes were originally manufactured. Turret specifications can be made so that the Amplidyne, after being adjusted to the Amplidyne specification, can be used in the turret without readjustment, following a functional test which can be taken on a cold unit.

Anode-Circuit-Breaker Design and Performance Criteria

Discussion and authors' closure of paper 45-52 by E. W. Boehne and W. A. Atwood, presented at the AIEE winter technical meeting, New York, N. Y., January 22–26, 1945, and published in AIEE TRANSACTIONS, 1945, June section, pages 337–45.

R. C. Dickinson (Westinghouse Electric and Manufacturing Company, East Pittsburgh, Pa.): The authors of this paper show graphical illustrations of arc-back phenomena in mercury-arc rectifiers which are an aid in the visualization of the general nature of the complex events involved. However, in the writer's opinion, the exact quantitative statements should not be taken too literally as some of the factors are still subject to controversy among many competent members of the profession. For instance, the arc drop of the rectifier E_a is chosen to be one-tenth of the alternating voltage. This is, of course, mathematically convenient but conflicts with large masses of empirical and theoretical evidence to the effect that the voltage across an arc is a function of arc current and a number of other detailed factors having to do with the internal mechanism of the arc. For simplicity, an arc best can be visualized as a variable resistance. Evans and Maslin, in another paper,[1] show actual measured data on the relationship of arc drop and arc current up to 80,000 amperes.

The authors' statement to the effect that two breaker characteristics are indicated do not agree with later statements in describing the new breaker. For instance, it is said that, with the open-chute construction, blowout coils contribute little to the over-all performance. This feature, together with other simplifications and improvements pointed out by the authors, makes it appear that the previous breaker, presumably of the light-duty type, is inferior to the new breaker, both as to simplicity and performance. Therefore, why are two breakers indicated?

It is to be noted that both the previous breaker and the new breaker have open-type arc chutes, as the authors point out. It would appear that this type of arc chute would throw considerable flame and that the bare arc would extend considerably beyond the confines of the chute. It also seems that the flame would have considerable horizontal component. These factors make it necessary to use considerable care in the physical location of the breaker in relation to personnel, ground, and other circuits, to guard against injury and extraneous flashovers.

This new design of breaker seems to have an unnecessarily high current-interrupting capacity. This feeling is based on the following statement from the Seaman and Morton paper,[1] referring to the same company's previous anode breaker, "The advantage of this type of arc chute is, that having been designed for a specific voltage level, it has no current limitation." It thus would seem unnecessary to extend the interrupting ability even beyond an unlimited value.

The company with which the writer of this discussion is associated developed an anode breaker in 1941. It was tested extensively in the factory test plant having 6,000 kw of 750-volt d-c generating capacity

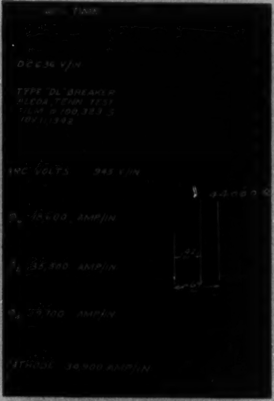

Figure 1. High-speed anode-breaker interruption of artificial arc-back on large electrochemical plant bus at transition from conducting to nonconducting condition of rectifier

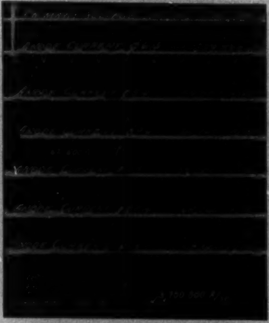

Figure 2 (above). Artificial arc-back test in laboratory, with anode breaker, 8,500-kva transformer, and 750-volt d-c output

Actual peak arc-back current, 62,500 amperes

Figure 3. Artificial arc-back test on anode breaker at 930-volt d-c output

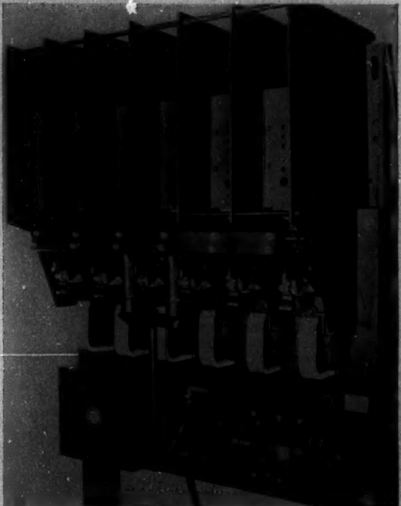

Figure 4. Complete six-pole anode breaker

Note that arc chutes completely enclose arc and project exhaust gases upward for parallel feed. It also was tested in a large aluminum plant on 30 artificial arc-backs made by short-circuiting a rectifier anode. Eleven 5,000-ampere rectifiers were on the d-c bus in addition to the one under test. These 30 tests were made with satisfactory performance, with and without the cathode reactor in the circuit. The breaker was left in trial service for about five months without reconditioning following the staged tests. Additional spontaneous arc-backs occurred during this period with good operation in every case. Figure 1 of this discussion shows a sample oscillogram made during the staged tests. The limitation time is 0.42 cycle and total time is 0.69 cycle.

Figure 2 is an illustration taken from the afore-mentioned paper by Evans and Maslin, showing the anode breaker opening an artificial backfire at 750 volts d-c output, with an actual peak current of 62,500 amperes, limited from 76,000 amperes without the anode breaker. Without the presence of a high-speed cathode breaker, both of these values would have been slightly higher.

Successful laboratory tests also have been made on this anode breaker at 940 volts d-c output. Figure 3 shows a typical operation at transition. It will be noted that the limitation time of 0.41 cycle is approximately the same as shown in Figure 1 at 650 volts d-c output.

Figure 4 shows our present design of anode breaker. The arc chute is a specialized form of the magnetic deion type,[2,3] which has met with considerable success in both the d-c breaker and a-c power-breaker fields. This interrupter confines the arc to the interrupting chamber and directs the arc products straight upward where they can do no harm. This breaker has six poles operated by a universal motor mechanism. It has such features as individual pole tripping and closing without opening the remaining poles. In addition to extensive d-c tests, this breaker has been tested on a straight a-c circuit capable of delivering 83,000 amperes crest at 1,500 volts rms on a single pole.

REFERENCES

1. A NEW MULTIPLE HIGH-SPEED AIR CIRCUIT BREAKER FOR MERCURY-ARC-RECTIFIER ANODE CIRCUITS AND ITS RELATION TO THE ARC-BACK PROBLEM, J. W. Seaman, L. W. Morton. AIEE TRANSACTIONS, volume 61, 1942, November section, pages 788–96.

2. MAGNETIC DEION AIR BREAKER FOR 2,500–5,000 VOLTS, L. R. Ludwig, R. H. Nau. AIEE TRANSACTIONS, volume 59, 1940, September section, pages 518–22.

3. A NEW AIR CIRCUIT BREAKER WITH 250,000-KVA INTERRUPTING CAPACITY, R. C. Dickinson, R. H. Nau. AIEE TRANSACTIONS, volume 60, 1941, May section, pages 197–201.

R. D. Evans (Westinghouse Electric and Manufacturing Company, East Pittsburgh, Pa.): Boehne and Atwood have carried out an interesting and, no doubt, useful study to determine for the anode breaker the most suitable characteristics of arc voltage as to the instant of application, the magnitude, and the wave shape. They state that the most favorable characteristics will not hold for circuits differing widely in the ratio $\omega L/R$, and that the higher values of this ratio are associated with circuits having the higher-interrupting-capacity requirements. The authors appear to attach considerable importance to the $\omega L/R$ ratio of the circuit. However, if the authors had treated rectifier arc drop as a part of the circuit resistance and included it in the circuit ratio of $\omega L/R$, lower rather than higher values of the ratio in some cases would have been obtained for circuits of the higher-interrupting-capacity requirements. For this reason, I am skeptical of the usefulness of the correlation which the authors indicate between the circuit $\omega L/R$ and the interrupting-capacity requirements. It would appear to me that practical, rather than theoretical, considerations were controlling in the development of the anode breaker for the higher-interrupting-capacity range.

The authors include in their paper two interesting oscillograms from arc-back tests. Their Figure 15 shows an arc-back on one phase which reached a crest value of 51,700 amperes. This arc-back was cleared promptly by an anode breaker but it gave rise to a sympathetic arc-back on another phase which reached a crest of 75,500 amperes. In connection with Figure 14, the authors state that this circuit is capable of delivering a crest current of 88,000 amperes, which figure appears to apply to an artificial arc-back simulated by a short-circuiting switch. It is of interest to compare these figures with those given in the paper* by A. J. Maslin and myself on the increase in current resulting from the use of a short-circuiting switch to simulate an artificial arc-back. In our paper this increase was from 81,500 to 95,000 amperes, an increase of 16 per cent. In connection with Figure 14 it may be pointed out that trace *F* shows a current limit of 26,000 amperes or less, which value may be compared with the data given in Figure 4 of our paper.

E. W. Boehne and **W. A. Atwood:** Mr. Dickinson and Mr. Evans, in their discussions, have presented quite widely diverging and interesting viewpoints. Mr. Dickinson suggests that, for simplicity, the arc of the rectifier best can be visualized as a variable, nonlinear resistance while Mr. Evans believes that the rectifier arc should be considered as part of the linear-circuit resistance and included in the $\omega L/R$ ratio of the circuit. Both seem to have overlooked the validity of the essential contribution of the paper, namely, that the effect of the arc drop of the rectifier, as well as that of the breaker, may be evaluated correctly and accurately by considering each voltage to act alone to produce its own current, the net circuit current being the algebraic addition of all components. This rigorous concept, a corollary of the superposition principle, recognizes the nonlinear nature of the arc, both in the rectifier and in the breaker, yet avoids the complexity of having to analyze quantitatively this resistance as a variable circuit parameter. After all, is this not the true simplicity which Mr. Dickinson seeks?

A demonstration of this simplicity is the fact that the rectifier arc resistance for each diagram and equation in the paper is the constant rectifier drop E_a divided by the actual reverse current. The rectifier resistance, therefore, automatically is assumed proportional to the reciprocal of the net circuit current. This nonlinearity is incorporated automatically in the analysis by the use of the simple linear equations developed, and fortunately does not specifically engage our consideration. This approach is more than justified as a practical engineering expedient since at present we are not studying the rectifier but, instead, its influence on the breaker duty.

Mr. Dickinson points out that a rectifier drop of only ten per cent of the alternating voltage is not representative of actual measurements. This is true. As stated in the paper, this choice of ten per cent is pessimistic and naturally will indicate a current slightly greater than expected. From a circuit-breaker-design viewpoint this is justified. The choice of ten per cent is no more mathematically convenient than the choice of 20 or 35 per cent. The rectifier-arc-drop data presented by Evans and Maslin as well as that presented by Herskind and Kellogg in their discussion of that paper, record the peak instantaneous value of a fluctuating rectifier arc drop. However, as adumbrated in our paper, the circuit current, and hence the anode breaker, is cognizant essentially of the volt–time area of the rectifier drop as a measure of the current-throttling property of the rectifier during arc-back (see Figure 4 of the paper). Hence the choice of a rectifier drop (constant d-c value) of ten per cent of the alternating voltage should be compared with the average value of a measured fluctuating arc drop and not with the measured peak instantaneous value. Because of this fact the value of ten per cent (60 volts on a 650 volt d-c rectifier system) is not as low as might be assumed.

To demonstrate the flexibility of the developed relations, Figure 1 of this discussion is presented which describes the variation in circuit current as a function of this assumed d-c value of rectifier arc drop, E_a. Also shown in this figure are the relative values of energy expended (during the flow of reverse current) by the breaker, the rectifier, and in the circuit resistance which is considered constant at one-eighth the equivalent circuit reactance ($R = 0.125\omega L$). Figure 2 of the paper forms one point on this diagram, namely for $E_a = 0.1E_{ac}$. Contemplate the complexity of arriving at the data given in this figure if it had been decided to throw the rectifier arc resistance (a nonlinear parameter) in with the normal linear circuit resistance as suggested by Mr. Evans.

It is interesting to note that the energies released within a rectifier during arc-back, on the basis of a flat top (d-c) rectifier drop (Figure 1 of this discussion) approach those liberated by the anode breaker when the d-c value of rectifier arc voltage approaches 0.375 of the alternating voltage, namely 220 volts on a 650-volt d-c application. It is interesting further to note that, for this value of rectifier arc drop, the initial peak of the arc-back current (no breaker opening) is reduced just 15 per cent from the value obtained with no rectifier present, that is, by using a short-circuiting switch to initiate the reverse current. This is the percentage change which Mr. Evans has found by test, described in his discussion, shown in his Table II, and generalized in his paper.[1] This is confirmed further by the arc-drop data given in his Figure 3, particularly for the first cycle of current in his reverse-connected ignitron, namely, voltages in the region of 220 volts. From these considerations it appears that the arc-drop data given in his Figure 3 might represent more of an average value of rectifier arc drop or indicate that the rectifier drop is essentially flat at the levels shown.

---

* See reference 1 of discussion by R. C. Dickinson.

Mr. Evans draws attention to the fact that the sympathetic arc-back shown in our Figure 15 reached a crest of only 75,500 in a circuit capable of delivering a crest of 88,000 amperes. From the ratio of these crests, namely 15 per-cent reduction, he suggests that the effect of this rectifier, in this circuit, reduced the available crest by 15 per cent. Actually, however, the sympathetic arc-back is invariably lower in current magnitude than the normal arc-back since the opening of the initial arc-back (trace *C*) has robbed the sympathetic arc-back (trace *F*) of one of its principal sources of a-c current. The effect of the initial interruption of the original arc-back (trace *C*) is evidenced clearly on the sympathetic arc-back current (trace *F*) by a distinct lowering of the slope of the rising sympathetic arc-back current at the instant of the initial interruption on trace *C*. Even if sympathetic arc-backs were of the same magnitude as the initial arc backs, a more representative measure of the effect of the rectifier drop in this study would be obtained by comparing the 75,500-ampere peak of the sympathetic arc-back of Figure 15 (trace *F*) with the 79,000-ampere peak in the same leg as shown in Figure 14 (trace *F*). Both currents were limited in magnitude by the same anode-breaker pole. This reduction in current is 4.5 per cent and not 15 per cent, which, from Figure 1 of this discussion, suggests an equivalent d-c rectifier arc drop in the neighborhood of ten per cent of the alternating voltage. The original arc-back in Figure 15 (trace *C*) rises only to 51,700 amperes due to the large initiating angle (β) of 75 degrees following conduction. (See equation 6.)

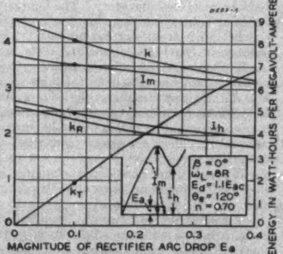

Figure 5. The effect of the magnitude of rectifier arc drop upon the relative current magnitudes and energies released during a single loop of reverse current associated with a normal arc-back.

Rectifier arc drop E_a is expressed in per unit of the nominal alternating voltage E_{ac}. The numerical cases shown in the paper assumed the rectifier drop, E_a, to be ten per cent of the alternating voltage, E_{ac}

k = arc energy released by the anode breaker in watt-hours per megavolt-ampere

k_T = arc energy released by the rectifier in watt-hours per megavolt-ampere

k_R = energy released by the circuit resistance ($R = 0.125\omega L$) in watt-hours per megavolt-ampere

The last sentence of Mr. Evans' comments probably refers to Figure 15 instead of Figure 14 to show that the forward current of trace *F* reached 26,000 amperes (13,000 amperes per anode) before the sympathetic arc-back occurred. It is interesting to note that, on the large rectifier installation where oscillograms of Figures 14, 15, and 16 were taken, a total of over 300 simulated arc-back tests gave rise to less than three-per-cent sympathetic arc-backs, although the nominal crest of the forward currents ranged from 12,000 to 15,000 amperes per anode. Figure 15 exhibits one such occurrence. At no time did sympathetic arc-backs occur on the other wye.

The size and design of an anode-breaker arc chute are governed more by the circuit voltage than by the current requirements. This was emphasized in the Seaman-Morton Paper (reference 1). The subject breaker, although designed to meet the heavy current requirements of a 650-volt (d-c) service will remain the smaller lower duty of the two breakers indicated. This is justified naturally by the simpler design. With the trend toward higher voltages a new anode breaker tested for 900-volt service, at available currents in excess of 100,000 amperes, and serviceable for the increase in duty of the 50-cycle over the 60-cycle system is available. This will become the larger of the two breakers indicated. Such breakers are being furnished to a large foreign customer. Both breakers exhaust their arc products above the breaker and only the normal procedure and precautions are recommended in locating the breaker with respect to personnel, ground, and other circuits. This is based upon test and the experience gained with several hundred anode breakers in regular service for over two years in this country.

With reference to Figure 1 of the discussion by Mr. Dickinson, the final current zero in this 650 test is so located with respect to the inverse voltage as to question the over-all time of 0.69 cycle. Using the 60-cycle timing wave shown on this film, a more competent measurement of the over-all time appears to be 0.75 cycle instead of 0.69 and a time to crest of 0.44 instead of 0.42. The rate of rise of current in this test is about 7,500,000 amperes per second. The initiating angle of the arc voltage of effectively 150 degrees may be compared with Figure 6 in the paper with respect to arc energy and initial recovery voltage. The actual energy released in this test is about 47 watt hours. Large typical 850-volt installations for 50-cycle operation will require an energy release in excess of 110 watt-hours per interruption. The corresponding breaker of General Electric manufacture has been tested in circuits whose voltages exceed the 900-volt d-c rectifier application, releasing energy in excess of 170 watt-hours per operation as compared to 85 watt-hours required on the largest 60-cycle 650-volt installation in this country.

Hence, the two breakers indicated, and available, are dictated principally on a voltage basis which, in turn, has defined the two kilovolt-ampere levels. The fact that high rates of rise of current and high values of $\omega L/R$ are associated with the higher kilovolt-ampere systems is not a controlling feature as suggested in Mr. Evans' discussion. They both contribute to the increased kilovolt-ampere requirements which, in turn, are a measure of the energy released. The voltage requirement is the basic controlling feature of the design. This is emphasized with the realization that, for all practical purposes, the maximum breaker duty at each voltage increases much faster than the first power of the ratio of the voltages.

The practicality of a theoretical analysis is not measured by our understanding of the theory, but rather by the degree to which it approximates faithfully the phenomena which we observe. Theoretical considerations, when extended beyond engineering requirements to include all the minor second-degree phenomena, will, in the limit, predict the observed phenomena in every detail. Ironically enough, when carried to this degree, such theoretical considerations often become impractical. Moreover, there is no road to a practical analysis by launching out with a basic misconception especially when a simpler, more exact, approach is at hand. A simple rigorous approach to the anode-circuit-breaker problem has been presented, which has not only produced qualitative and quantitative results which mirror the observed phenomena, but has afforded a clearer insight into the part played by each controllable element of the circuit. The concepts are applicable to numerous electronic circuits. In a fuller sense, the subject paper is an application of the principles outlined in an earlier paper referred to in reference 5 of the paper.

Arc-Backs in Rectifier Circuits—Artificial Arc-Back Tests

Discussion and authors' closure of paper 45-20 by R. D. Evans and A. J. Maslin, presented at the AIEE winter technical meeting, New York, N. Y., January 22–26, 1945, and published in AIEE TRANSACTIONS, 1945, June section, pages 303–11.

C. C. Herskind (General Electric Company, Schenectady, N. Y.): The artificial arc-back tests described in the Evans and Maslin paper contain much valuable data on rectifier operation during arc-back. The basic factors bearing on the problem of arc-back protection are discussed, and values are given for some of the factors for particular test conditions.

As the authors state, the values given in the paper apply to a particular rectifier. It is the purpose of this discussion to present data for similar equipment of different design.

With reference to the characteristics of the rectifying elements, the probability of arc-back at fault currents for a large pumped ignitron of size comparable to that referred to in the paper but of different design is shown on Figure 4 of reference 1. These data indicate a fault-current capacity at least 50 per cent greater than that shown by the curve in the paper. Although these data were obtained from current-limit tests made

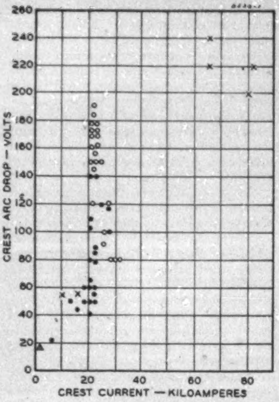

Figure 1. Arc-drop characteristic of pumped ignitron

Normal conduction—anode to cathode
△ Rated load
● First cycles of current-limit test—successful
○ First cycles of current-limit test—followed by arc-back
Reverse conduction—cathode to anode
× Natural arc-back

on a single ignitron in accordance with the method described in reference 1, experience indicates that the values are accurate.

In view of the similarity of the two designs and the fact that both are operating in the field under similar conditions with good results, the current values given in the paper appear to be low. Do the authors have any explanation for this difference?

The arc-drop characteristics for this same large pumped ignitron are shown on Figure 1. These data indicate a definite relationship between the crest value of the arc-drop voltage during normal conduction and the probability of arc-back on the succeeding inverse cycle. When the arc drop exceeds 100 or 120 volts, arc-back usually follows. This behavior is shown clearly by oscillographic records of current-limit tests taken at the same crest current. In test 30 the rectifier carried the fault current successfully, whereas in test 31 it arced back in the succeeding inverse period.

Current-limit tests on sealed ignitrons of approximately $^1/_4$ the diameter of the large pumped ignitron have shown a fault-current capacity nearly equalling that of the large ignitrons. Also, the sealed ignitrons have a somewhat lower arc drop than do the large pumped ignitrons.

In general, it is preferable to arrange rectifier circuits so that the fault current on the normal anodes during arc-back does not exceed the fault current capacity of the rectifying element, that is, the probability of sympathetic arc-backs is low. But this should not be considered essential to successful operation, as there are undoubtedly a number of successful installations in service where the fault-current capacity is exceeded. In such installations, provision must be made to limit the sympathetic arc-backs to the other anodes of the unit and prevent their extension to other rectifiers operating in parallel. For example, when anode breakers are used, the high-speed cathode breaker does not provide any added protection, except under conditions where sympathetic arc-backs are obtained. Under such conditions high-speed cathode breakers shorten the duration of the disturbance to the d-c system and reduce the probability of arc-back on parallel rectifiers.

When sympathetic arc-backs are obtained, it should be recognized that the duration of the fault and the duty on the equipment may be increased. It is particularly desirable to avoid sympathetic arc-backs on sealed-tube rectifiers, as the life of the tube may be affected. Fortunately, small sealed rectifiers of the pool type generally have a high fault-current capacity.

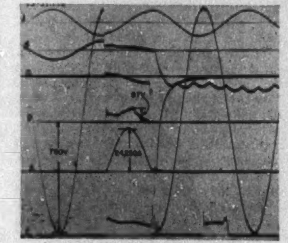

Figure 2A. Current-limit test 30

A—60-cycle timing wave
B—Grid-to-cathode voltage
C—Grid current
D—Anode-to-cathode voltage
E—Anode current
F—Ignitor-to-cathode voltage

The magnitude of the arc-back current is an important factor in the transformer design. In general, the maximum arc-back current exceeds the crest current which would be obtained on symmetrical short circuit. The ratio of maximum arc-back current to the crest current on symmetrical short circuit for any rectifier installation depends upon the speed of the protective switchgear and the reactance in circuit. The authors indicate ratios ranging from 1.56 to 1.83 for the equipments tested. These are quite usual values for equipment of the type described. However, other ratios may be employed successfully by proper co-ordination of rectifiers, transformers, and protective switchgear.

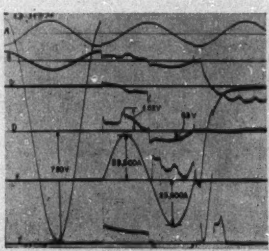

Figure 2B. Current-limit test 31

A—60-cycle timing wave
B—Grid-to-cathode voltage
C—Grid current
D—Anode-to-cathode voltage
E—Anode current
F—Ignitor-to-cathode voltage

The artificial arc-back test recorded on Figure 10 of the paper shows an unusually large feed from the anodes of the normal wye following the interruption of the d-c feed. Did the transformers used in these tests have the usual degree of interlacing?

Some transformer failures were experienced on early rectifier installations because of voltage surges. Voltage surges caused by arc extinction were eliminated successfully by the use of surge absorbers. Improvements in rectifier design have reduced the probability of surges produced by heavy currents. Numerous surge measurements on large rectifier installations during the past ten years confirm the results of the surge-voltage tests reported in the paper.

Reference

1. The Testing of Mercury-Arc Rectifiers, H. L. Kellogg, C. C. Herskind. AIEE Transactions, volume 62, 1943, December section, pages 765–73.

J. H. Cox (Westinghouse Electric and Manufacturing Company, East Pittsburgh, Pa.): In Figure 4 of the Evans and Maslin paper the authors have presented a fault-current limit curve based on their analysis of oscillograms taken in some 100 artificial arc-back tests in the laboratory. The figure also contains points resulting from five such tests on an ignitron in regular service. They point out that the laboratory tests were made on a new, and therefore unseasoned ignitron, and also that the facilities available did not permit the rectifier to be loaded at full load for a long enough time to bring it to what might be called normal operating condition. They also point out that the data from the field tests were too few to indicate much, when considered in connection with a curve based on the probability of arc-back.

Because of the surprisingly, and disturbingly, low current values indicated by the curve of Figure 4, particularly in the lower-percentage regions, a series of field tests were made on the same design of ignitron connected to a bus of ample capacity in regular service, to obtain data extensive enough to establish a more adequate curve for normal conditions. As expected, these data produced a curve having appreciably higher current values, particularly in the lower-percentage region. At the 90-per-cent point on this new curve the fault-current limit is approximately 26,000 amperes, and at the ten-per-cent point it is 20,000 amperes. Also, the curve does not meet the zero- and 100-per-cent lines at sharp points but tapers off, as would be expected of a probability curve.

From an application point of view, it is the lower portion of the curve that is most important. At least from a service-outage viewpoint, the region of the curve where a large percentage of the current applications result in arc-backs is not very important. This, of course, is particularly important for applications where use must be made of trip-free anode breakers which remove from service only those phases which arc-back. It is suggested that the ten-per-cent point be used in such considerations.

The field test also included short circuits made on the rectifier when cold. These produced data too erratic for plotting. They indicate that the fault-current limit of a rectifier tube when cold cannot be depended upon, even though the tube be thoroughly seasoned.

R. D. Evans and **A. J. Maslin:** C. C. Herskind and J. H. Cox have contributed valuable discussions, supplementing our paper in a number of respects. Mr. Herskind has inquired pertinently as to the reason for the differences between the current-limit test data on similar rectifiers as given in Figure 4 of our paper and by Figure 4 of his reference 1. We, also, were aware of these differences and discussed with Mr. Cox the desirability of field tests subsequently made and reported by Mr. Cox in his discussion. It is important to recognize the current values that practically are sure to result in an arc-back are closely the same for the three sets of tests; thus, Kellogg and Herskind give 25,000 amperes for 100-per-cent probability, our paper gives 24,000 amperes for 100-per-cent probability, and Mr. Cox gives 26,000 amperes for 90-per-cent probability. It is to be noted that the curve from the paper by Kellogg and Herskind shows zero probability for currents below 21,000 amperes, while the corresponding figure from our paper is 13,000 amperes, and a still lower figure was obtained by Mr. Cox. In our opinion the curve should be asymptotic to the *X* axis, and it occurs to us that the reason for the shape of the curve obtained by Kellogg and Herskind may have been the result of a limited number of tests in comparison with the hundreds of test points obtained in the other two series of tests. Another and probably an important difference may be anticipated as arising from the differences between seasoned units operating with normal-temperature conditions in the field and green units operating with subnormal temperatures in the laboratory. This difference between laboratory and normal field conditions was pointed out in our paper. Apparently these differences do not affect appreciably the current-limit value for a probability of 90 or 100 per cent, but they do increase importantly the probability of arc-back for lower currents.

Mr. Herskind asked whether the tests corresponding to Figure 10 of our paper were obtained on circuits supplied by transformers with closely coupled secondary windings. In reply we would say that the secondary windings were closely interlaced, giving an impedance diagram similar to that of Figure 2 of our paper.

We note with interest that Mr. Herskind states that the voltage-surge measurements made by him and his associates confirm the results of surge tests and conclusions presented in our paper that modern power rectifiers are unlikely to give rise to important overvoltages.

Rectifier Fault Currents

Discussion and author's closure of paper 45-51 by C. C. Herskind and H. L. Kellogg, presented at the AIEE winter technical meeting, New York, N. Y., January 22-26, 1945, and published in AIEE TRANSACTIONS, 1945, March section, pages 145-50.

R. D. Evans and **A. J. Maslin** (Westinghouse Electric and Manufacturing Company, East Pittsburgh, and Sharon, Pa.): The methods of calculating rectifier-circuit fault currents outlined in the paper by Herskind and Kellogg are an important addition to the published information on the subject. Three of the more important factors influencing the magnitude and duration of the transformer-secondary-circuit currents during sustained d-c short ircuits are:

1. The magnitude and disposition of reactances in the a-c circuit.
2. The magnitude of the inductance in the d-c circuit.
3. The method of firing the rectifier elements.

The duration is increased when the reactance is in the secondary circuit rather than in the primary circuit and by the presence of inductance in the d-c circuit. The duration is less for a controlled rectifier than for one continuously excited and not controlled. In practice the duration of the transformer secondary currents usually will exceed 180 degrees, a circumstance resulting chiefly from inductance in the d-c circuit. Rectifier short circuits, including consideration of primary reactance, are treated at length by W. Schilling[1] and by Prince and Vogdes.[2]

The principal parts of this paper by Herskind and Kellogg and the paper by Evans and Maslin[3] deal with arc-back phenomena from the circuit standpoint. It is pertinent, therefore, to compare the treatments presented. Evans and Maslin analyzed seven factors that influence arc-back currents and supplemented this by discussion as to arc drops for heavy currents, current limits for ignitron tubes, effects of saturation, and the characteristics of sympathetic arc-backs. Methods of making artificial arc-back tests are discussed and results of such tests made in the laboratory and in the field are given. Herskind and Kellogg present a mathematical analysis of the faults on a single wye together with a discussion of methods for extending the application to other rectifier circuits. They also present the results of some artificial arc-back tests and compare the results of tests and calculations. To a considerable extent, the papers supplement each other.

Herskind and Kellogg have introduced a logical analytical attack on the problem of calculating arc-back currents. Their method uses the conventional transient solutions for circuit changes caused by the beginning or end of conduction in each rectifier phase. We, independently, adopted the same mathematical approach, but carried it out in somewhat different fashion as we finally chose to represent arc drop as a resistance, instead of a counterelectromotive force as the authors have done. This difference should result in somewhat smaller arc-back currents, since arc-drop data given in Figure 3 of the Evans and Maslin paper are somewhat higher than the arc drops or rather counterelectromotive forces assumed by the authors. This should lead to somewhat closer checks with test results, since the data given by Herskind and Kellogg generally show test values lower than or equal to calculated values. It may be mentioned that the authors' method applied to test conditions described in the Evans and Maslin paper appears to give closer checks between tests and calculations than for some of the tests reported in their own paper. We have no explanation for this condition, unless the tests with low values were actually below the maximum that might be obtained for the circuit conditions.

The agreements between tests and calculations of arc-back currents are not all that could be desired. For example, the authors give in line 3 of Table I for an arc-back on a wye a calculated figure of 14,300 amperes and a test figure of 10,600 amperes. Again from lines 5, 6, and 7 of Table I for arc-backs with back feed from a d-c bus, the calculated figures are 62,000, 83,200, and 92,700 amperes but the test figures are 46,000, 54,200, and 79,400 amperes, respectively. In each of these cases the calculated figures are from 35 to 50 per cent greater than the test results. Actually the discrepancies are greater than these figures show, because, as the authors mention, the calculated values include the effect of arc drop resulting from arc-back currents in the phase subjected to arc-back, whereas the tests do not, since they were made with a short-circuiting switch. This would increase the discrepancies by about 16 per cent, a figure which was pointed out in our discussion of the paper by Boehne and Atwood[4] or which may be derived from data given in the Evans and Maslin paper.

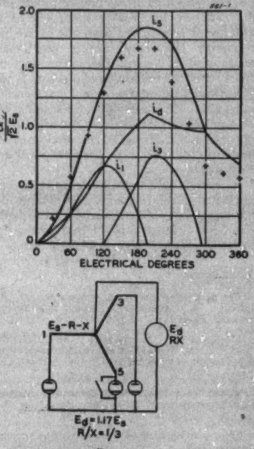

Figure 1

In their paper the authors give principal attention to the arc-back current during the first cycle. In our paper we have given considerable attention to the currents that would obtain after the back feed from the d-c bus has been removed and the feed through the interphase transformer from the other wye has reached a steady value. The currents contributed by the two anodes in the same wye group as the faulted anode is, of course, the determining factor in the total arc-back current. The contribution from the other wye, while smaller, is in many cases by no means negligible. This is shown clearly in oscillogams of Figures 10 and 11 of the Evans and Maslin paper. An equivalent circuit similar to Figure 9 of the authors' paper is closely representative of the actual circuit. The curves plotted on Figure 1 of this discussion were calculated for the circuit shown. The ratio $R/X = 1/3$ was calculated from the known characteristics of the circuit including a resistance equivalent for the arc obtained from Figure 3 of the Evans and Maslin paper. The plotted points are taken from the oscillogram shown in Figure 11 of that paper. The agreement between test and calculated values for the first third of a cycle is extremely good. At this time the opening of the high-speed cathode breaker manifests itself. When this breaker opens, the back-feed circuit is switched from the entire bus to merely the other wye of one transformer, and its contribution is therefore reduced. For the remaining two-thirds of the ycle, therefore, the test current is materially below the calculated value. These curves and test points indicate that the arguments supporting the simplified arc-back current shown in Figure 11 of the authors' paper are not justified.

In concluding it must be recognized that the task of calculating arc-back currents has only begun but that the authors have made an important contribution in publishing the solution for an arc-back on a single wye.

REFERENCES

1. DIE GLEICHRICHTERSCHALTUNGEN (book), W. Schilling. R. Oldenbourg, Munich and Berlin, Germany, 1938.

2. MERCURY-ARC RECTIFIERS AND CIRCUITS (book), Prince, Vogdes. McGraw-Hill Book Company, Inc., New York, N. Y.

3. ARC-BACKS IN RECTIFIER CIRCUITS—ARTIFICIAL ARC-BACK TESTS, R. D. Evans, A. J. Maslin. AIEE TRANSACTIONS, volume 64, 1945, June section, pages 303–11.

4. Discussion by R. D. Evans of ANODE-CIRCUIT-BREAKER DESIGN AND PERFORMANCE CRITERIA. AIEE TRANSACTIONS, volume 64, 1945, page 438.

C. C. Herskind: Mr. Evans and Mr. Maslin suggest that arc drop be represented as a resistance rather than a counterelectromotive force in the calculation of fault currents. Both methods have been employed by the authors. The choice of method is largely a matter of convenience, and it should be recognized that both are only approximations of the actual effect of rectifier arc drop.

Good agreement between test and calculated values is not always obtained for reasons which have been set forth in the paper. There are two general reasons for poor agreement, namely, either incomplete or inaccurate circuit data or inadequate analytical treatment. The means for correcting errors arising from the first cause are obvious. However, further analyses are needed particularly for

1. Arc-back in a wye, including the contribution of the other wye of a six-anode rectifier.
2. Arc-back with d-c feed, including the contribution of the normal anodes of the faulted wye.

It is hoped to treat these cases in future work.

Voltage and Current Relations for Controlled Rectification With Inductive and Generative Loads

Discussion and author's closure of paper 45-53 by K. P. Puchlowski, presented at the AIEE winter technical meeting, January 22–26, 1945, and published in AIEE TRANSACTIONS, 1945, May section, pages 255–60.

V. B. Baker (nonmember; Westinghouse Electric and Manufacturing Company, East Pittsburgh, Pa.): Mr. Puchlowski's paper is a worthy addition to the limited technical literature on the theory of controlled rectification. His analytical approach and straightforward derivation of certain fundamental expressions for controlled-rectifier voltages clearly emphasize the concept of "critical angle of firing" and the effect of load character on rectifier output voltage. Distinction between continuous and discontinuous current conduction is extremely important in many rectifier applications, and his treatment of the "critical angle of firing" which separates the two cases is particularly enlightening.

The average rectifier voltage as given by equation 18 would appear to be independent of the power factor of the rectifier load. However, for a given angle of ignition X_f, the angle of extinction X_s is dependent upon the load impedance. That is, the total period of anode conduction, being determined by X_f and X_s, is a function of load impedance, and, consequently, the average rectifier output voltage is very definitely dependent upon load character.

As an alternative to the method of gradual approximations used in the paper for calculating the angle of extinction, the following may, in certain cases, prove to be somewhat simpler. With reference to equation 12

$$\cos\theta \sin(X_s-\theta) - a + [a - \cos\theta \sin(X_f-\theta)]\epsilon^{-\frac{X_s-X_f}{\tan\theta}} = 0$$

From the chart, Figure 5 of the paper, the approximate angle of extinction, X_s, may be determined for the particular conditions in question. Using two values of X_s in the immediate vicinity of the angle of extinction obtained from Figure 5, calculate the absolute values given by the first part of equation 12, namely,

$$\cos\theta \sin(X_s-\theta) - a$$

Plot these values as ordinates against X_s as abscissa, and connect the two points so plotted with a straight line.

Repeat the above procedure using the same two values of X_s in the latter part of the equation 12, namely,

$$[a - \cos\theta \sin(X_f-\theta)]\epsilon^{-\frac{X_s-X}{\tan\theta}}$$

and plot these two points on the same graph. Where the two curves intersect defines the desired value of X_s.

This method assumes that the two parts of equation 12 are straight lines, but, if the two values of X_s chosen are close together and the point of intersection lies between or near these values of X_s, the assumption is reasonable, and the value of X_s obtained from the intersection is quite accurate.

K. P. Puchlowski: Mr. Baker's outline of a graphical method for the determination of the angle of extinction x_s is undoubtedly a valuable addition to the analytical method of gradual approximations given in the paper. The graphical method also may be used successfully in conjunction with the analytical method as a means for checking the results obtained analytically.

With reference to Mr. Baker's remark concerning equation 18 of the paper and the effect of load impedance angle on the rectifier output voltage represented by that equation, it must be pointed out that for discontinuous current the rectifier output voltage and the load terminal voltage are always a function of the impedance angle of the load. This is expressed clearly in equations 18 and 21, since, as Mr. Baker has remarked, the angle of extinction x_s appearing in these equations is a function of the impedance angle θ as represented by equation 12.

The importance of expression for the d-c load terminal voltage, equation 21, particularly should be emphasized. The significance of this equation lies in its general character and its validity for all the cases of controlled polyphase rectification with either discontinuous or continuous conduction, and for any combination of resistance, inductance, and counterelectromotive force in the load circuit.

Thus, in the case of continuous conduction the angle of extinction becomes

$$x_s = x_f + \frac{2\pi}{p}$$

and the load terminal voltage can be obtained directly from equation 21 by simple substitution

$$E_{dc}' = \frac{pE_s}{\sqrt{2}\pi}\left[\cos x_f - \cos\left(x_f + \frac{2\pi}{p}\right) - a_0\frac{2\pi}{p}\right] \tag{3A}$$

where $a_0 = \dfrac{E_0}{\sqrt{2}E_s}$

It should be noted that this is the equation 3A given in the paper, and here the load terminal voltage is independent of the load circuit constants and characteristics.

Further, if the arc voltage drop is neglected, a_0 becomes equal to zero. Then, by substitution in equation 3A

$$x_f = \frac{p\pi - 2\pi}{2p} + \varphi$$

where φ is the angle of the delay of ignition beyond the natural commutating point, we obtain the familiar form of the expression for the rectifier output voltage:

$$E_{dc} = E_{dc}' = \sqrt{2}E_s\frac{p}{\pi}\sin\frac{\pi}{p}\cos\varphi \tag{2A}$$

which is a particular case of the general equation 21.

Thus, the equations 2, 3A, and 18 in the paper and equation 2A can be derived directly from the paper's general equation 21.

Electrolytic Corrosion—Methods of Evaluating Insulating Materials Used in Tropical Service

Discussion and authors' closure of paper 45-73 by B. H. Thompson and K. N. Mathes, presented at the AIEE winter technical meeting, New York, N. Y., January 22–26, 1945, and published in AIEE TRANSACTIONS, 1945, June section, pages 295–9.

E. K. Cliver (Celanese Corporation of America, Newark, N. J.): The authors are to be commended on their ingenuity. The data presented in this paper will be of great value to the electrical industry and to to the armed services. Naturally, anything new, including a test method, brings up questions, arguments, and discussions, if it is of any interest. It is hoped that the following discussion will help to clarify some points mentioned in the subject paper.

Since all untreated fabrics produce essentially the same corrosion current at 100-per-cent relative humidity plus dew, this condition does not appear to be suited to evaluating insulating materials for use in a particular application. For, if a fabric is desirable for other reasons, it offers no way to choose which fabric shall be selected. In showing that there is little difference in the corrosion currents of cotton and cellulose-acetate fabrics, we feel sure that the authors did not mean to imply that, for tropical applications, one may use cotton fabric indiscriminately rather than cellulose-acetate fabric. As mentioned in the paper, fabrics generally are not used untreated. As also mentioned in the paper, treated fabrics in service are at some moisture condition below the atmospheric humidity to which the device is exposed. This, according to the Table I of the paper, means that treated insulation never reaches 100-per-cent relative humidity plus dew. Also, under conditions of a potential difference between the component and ground, the losses in the component would tend to raise the internal temperature above the dew point. With no voltage applied, any corrosion which occurred would be of a purely chemical nature and could be discovered in the laboratory without applying any voltage. At any humidity lower than 100 per cent plus dew, cellulose-acetate fabric offers distinct advantages over cotton or paper. It also gives a factor of safety at the exposed edge of a slit tape and in the case of cracks or abrasions in the treating material. In case of an actual soaking, cellulose acetate will rid itself of moisture much faster than cotton. There appears to be no evidence that any other fabric should be substituted for cellulose-acetate fabric.

Another point calling for discussion is the nature of the conducting film of moisture. We are not convinced that the corrosion current, for materials containing no known corrosive matter, is not entirely a function of the physical structure of the moisture film.

The fact that the curve for corrosion current versus the conductivity of the water extract passes through zero for fabrics and papers is not convincing as the current flows through a continuous water path in either case and the water, in each case, contains the same materials in solution. If the curve did not pass through zero, there would be more cause for investigation. It does not seem reasonable that cellulose-acetate fabric should show up so much better than cotton at all humidities below 100 per cent plus dew and then suddenly produce as much contamination as cotton. Figures for water alone, plotted on the same curve, would be interesting.

As for films, the fact that acetate and polystyrene films cause a water film to take the form of Figure 10A of the paper would indicate that there should be less current flow than caused by fabrics. A microscopic examination of the moisture on various films might correlate water-film structure directly with corrosion current. The fact that the curve for corrosion current versus conductivity of water extract for films does not pass quite through zero adds a straw to the weight of this evidence. However, the fact that it so nearly passes through zero lends considerable weight to the argument in favor of the corrosion-current method.

Certain tests, made at widely separate times, have shown inconsistencies in the corrosion-current test versus the visual test for cellulose-acetate films. Certain samples shown to be highly corrosive in the visual test were shown later to be noncorrosive according to the corrosion-current test. The reverse also was true. Further tests may show that materials being compared will have to be tested at the same time to give significant comparative data.

In going over the data presented, our curiosity was aroused by the apparent effect of thickness on the corrosion current in the case of cellulose-acetate films. In Table III of the paper as cellulose-acetate films *A*, *B*, and *C* increase in thickness, their corrosion currents increase and the increase in current is much more rapid than the increase in thickness. It appears possible that, if fairly thick films are used the thickness will have no effect on the corrosion current, but it also appears possible that thick films in general may show up much worse than thin films. No explanation was given in the paper as to why one plastic film about ten times the thickness of another should be more than 1,000 times as corrosive.

It is indicated in the paper that the current at the end of 15 seconds is a direct measure of corrosion resistance. However, much electric equipment would be under continuous d-c stress and, therefore, the ultimate conductivity or corrosion current would appear to be more indicative of corrosion resistance than the current after 15 seconds. This is borne out by the data given in Table II of the paper. It is shown that the first two materials have corrosion currents in the ratio of 4:3. From this it might be assumed that the time required for each to corrode would be in inverse ratio and of the same magnitude, but the data indicate that the time ratio is 1:7. The same thought applies to the rest of Table II and, instead of the ratio of times to corrode for the second and third items being a little over 1:4, the actual time ratio is 21:1.

In conclusion, we would like to express the opinion that the data mentioned in this paper are extremely interesting and bring up many important questions, but they would appear to be a little brief. We believe that much more work is necessary to strengthen or disprove the case for the corrosion-current test. It appears desirable to give further study to the nature of the moisture-film structure, to the behavior of treated fabrics, to the effect of the thickness of films, to the shape of the curves for corrosion current versus time, to the range of values for a single material, and to the coordination of the corrosion-current tests with the visual- and tensile-test methods since both of these, and especially the tensile test, are used more generally. It also would be desirable to study data on corrosion currents at humidities below 100 per cent plus dew as these lower humidities appear more nearly to represent actual insulation conditions in the tropics and elsewhere.

The concluding statement "Since so many factors may produce electrolytic corrosion, only actual test (of the finished component, we assume) can be the deciding factor" is most significant. It would lend much value to the corrosion-current method if it could be correlated with field data. Industries' preference for cellulose-acetate fabric and film apparently indicates that they have proved to be desirable materials in the field.

R. J. Oace (nonmember, Minnesota Mining and Manufacturing Company, St. Paul Minn.): The corrosion-current test, backed by such excellent data as presented in the report, should find ready acceptance by the electrical industry. However, based on our experience, it is misleading to call corrosion current a test for electrolytic corrosion. Although the correlation of these results to an actual corrosion test is close, I do not feel that the identical property is being tested in both cases. The property it does measure is very similar to that which is commonly referred to as "insulation resistance."

Some impurities, such as sulphur, tend to localize the corrosion. A given corrosion current concentrated at one point in a wire would cause failure much sooner than if the same corrosion current were distributed evenly along the wire. In a corrosion test, such points on a wire would be the portion of main interest. In the corrosion-current test, they would be averaged out and would not affect the final result.

Theoretically, materials such as glue, glycerin, and cellulose, undergo electrolysis during the process of electrolytic corrosion. This produces more ions, hence more current carriers, as the corrosion process proceeds. An instantaneous reading of corrosion current would miss this factor.

Figures 5 and 6 in the paper indicate that an appreciable amount of polarization occurs during continued application of current, tending to reduce the current. This effect is opposite to the previously mentioned effects, and might explain correlation of corrosion and corrosion current for some materials.

It is my hope that both electrolytic-corrosion and corrosion-current tests can be developed to high degrees of accuracy, and that the full meaning of each, with respect to practical application in the field, will be established.

B. H. Thompson and K. N. Mathes: We agree with Mr. Cliver in respect to the relative merits of cotton and cellulose-acetate fabrics. Values of corrosion current at a humidity of 96.5 per cent are given in Table I of this closure. The 1,000 to 1 superiority of cellulose-acetate is quite convincing.

It is our opinion that the conductivity of the film of moisture on fabrics and papers, Figure 9 of the paper, is due almost entirely to the ions absorbed by the moisture from the material. Since the curve passes through zero, the absorption of ionized material from the insulation must contribute predominantly to the corrosion current.

The apparent correlation between corrosion current and film thickness for cellulose acetate in Table III of the paper is accidental. The data given were selected to show the wide range of values for different types of cellulose acetate. For films which absorb little water, the corrosion current is independent of the thickness, as shown in Table II of this closure.

In general, we have had very good agreement between the results with visual tests and those with current tests, using the value 15 seconds after the application of voltage. Erroneous results occasionally have been obtained with films at a humidity of 100 per cent plus dew, which were caused by drops of water spreading and bridging between the electrodes. This happened more often with the visual test because of the longer time that the test specimens were exposed to the high humidity.

In reply to Mr. Oace, most investigators agree that, at the higher humidities (above 20 per cent), the conduction is almost completely ionic.[1] It may be looked at as either a conductor or a resistance. We have preferred the first when referring to corrosion, as an increase in one is accompanied by an increase in the other.

The results of a large number of tests indicate that materials which tend to produce pits in the copper of the visual test also give relatively high corrosion currents.

We never have observed an increase in corrosion current with time, although insulating materials containing glue, glycerin, and cellulose have been tested. This has been checked by repeated applications of voltage at sufficiently long time intervals to permit recovery from polarization.

Table I

	Corrosion Current, Microamperes, at 96.5-Per-Cent Humidity
Cotton fabric	12.9
Cellulose-acetate fabric	0.0104

Table II

	Thickness, Mils	Average Corrosion Current, Microamperes
Cellulose acetate	2.1	0.014
Cellulose acetate	5.0	0.0074
Cellulose acetate	5.5	0.0045
Cellulose acetate	20.0	0.048
Cellulose acetate	22.0	0.013

REFERENCE

1. INFLUENCE OF HUMIDITY UPON THE RESISTIVITY OF SOLID DIELECTRICS AND UPON THE DISSIPATION OF STATIC ELECTRICITY. United States Department of Interior information circular 7286, June 1944, page 30.

Preferred Practices for Electric Control Devices for Aircraft

Discussion and author's closure of paper 45-74 by F. W. Hottenroth, Jr., presented at the AIEE winter technical meeting, New York, N. Y., January 22–26, 1945, and published in AIEE TRANSACTIONS, 1945, April section, pages 197–200.

E. P. Barlow (nonmember; Glenn L. Martin Company, Baltimore, Md.): Mr. Hottenroth's proposal that the AIEE develop environmental and operating voltage standards for electric devices used on aircraft is concurred in most heartily. The need for a comprehensive standard, which will be recognized by all parties concerned, is most urgent. In the past it often has been necessary for each aircraft manufacturer to urge upon equipment manufacturers certain standards which we felt to be absolutely necessary but which the equipment manufacturers often believed to be unduly severe. This was true particularly of those cases where we, as aircraft manufacturers, felt that the requirements of existing Government specifications, covering similar equipment, were not sufficiently rigid to insure the satisfactory operation of the device under the operating conditions which have become progressively more severe during the recent rapid development of military aircraft. An adequate set of standards will save a great deal of time previously spent in negotiating these items as they affected each piece of equipment purchased. It is suggested strongly that, in preparing these specifications, the AIEE confer with the National Aircraft Standards Committee and with representatives of the United States Army and Navy.

It is recommended that the proposed standards be worked out to cover both high- and low-altitude conditions. Requirements for modern military aircraft indicate that we certainly must consider altitudes as high as 50,000 feet. However, there are other types of aircraft, including, I hope, a large volume of small commercial planes, for which such a requirement would be most unwarranted in that it would result in an article unnecessarily heavy and expensive.

It also is recommended that a similar breakdown be made in connection with the vibration requirements where the standard should recognize three different conditions:

1. Items mounted directly on the engine itself. Vibration characteristics of the various engine and propeller combinations should be obtained from all reliable sources: the engine and propeller manufacturers, together with the United States Army and Navy, will be the primary source for this information. Some aircraft manufacturers also will be able to contribute valuable data.

2. Items mounted on the engine bearer or any quickly removable portion of the engine installation, but isolated from the engine itself by the vibration absorbing engine mounts. The vibration in this area will be less severe but probably will exceed the requirements for area number 3.

3. Items mounted in any portion of the airplane other than the engine section.

With specific reference to Mr. Hottenroth's proposed "Standards for Electric Control Devices Used on Aircraft," the clause, "under any combination of these conditions," in paragraph *A*, is most important and should under no circumstances, be deleted. The references, in the paper, to vibration amplitude (paragraph *A*, item 3 and paragraph *B*, item 1) might be clarified by inserting the word "single" before "amplitude" in both places. In order to eliminate completely any possibility of misunderstanding, it is recommended also that the "total excursion" be given immediately following the single amplitude; namely, "(total excursion of 0.030 inch)" in paragraph *A*, item 3 and "(total excursion of 0.060 inch)" in paragraph *B*, item 1. With reference to paragraph *B*, item 2, it is recommended that temperature cycles in which the device is carried alternately from the highest to the lowest temperature be added to the proposed requirement. Many devices employing plastic material will function satisfactorily the *first* time at —70 degrees Fahrenheit but after prolonged exposure to 200 degrees Fahrenheit they lose their plasticizer and the next operation at reduced temperature —70 degrees Fahrenheit leads to failure. With reference to paragraph *C*, item 1, it is recommended that consideration be given to eliminating the fixed upper limit of coil temperature, namely, 325 degrees Fahrenheit, in favor of a statement to the effect that "Coil temperatures must be such that, with maximum volts and 200 degrees Fahrenheit, ambient temperature, and with the device mounted on aluminum plate in accordance with reasonable design practice, no significant deterioration of the insulation shall occur within a period of one hour." The intent of this change would be to allow scope for the use of the improved insulation materials now becoming available.

F. W. Hottenroth, Jr.: Mr. Barlow's fine discussion requires no rebuttal. We appreciate the good judgment shown by an aircraft manufacturer in realizing that standards which are more severe than necessary penalize the control by making it unduly heavy and thereby penalize the planes on which the controls are used. We think his suggestions should be incorporated in any standards issued by the AIEE.

Control manufacturers are not trying to hedge on standards in order to simplify their own problems. They want to build devices which will do their job well and will be as light as possible. A clear statement of requirements and environmental conditions by aircraft manufacturers and by the representative branches of our Armed Forces will eliminate many present misunderstandings.

There are some items in the proposed standards which definitely are controversial. Written discussion had been expected from interested individuals in the Bureau of Aeronautics and the Army Air Forces Electrical Equipment Laboratory. This applies particularly to the standards on vibration and clearances between parts of opposite polarity. Possibly such discussion may be forthcoming in time for a later issue.

Nine Years' Experience With Ultrahigh-Speed Reclosing of High-Voltage Transmission Lines

Discussion and authors' closure of paper 45-57 by Philip Sporn and C. A. Muller, presented at the AIEE winter technical meeting, January 22–26, 1945, and published in AIEE TRANSACTIONS, 1945, May section, pages 225–8.

David C. Prince (General Electric Company, Schenectady, N. Y.): It has been recognized for many years that the economic value of high-voltage transmission lines depends to a large extent upon the reliability of service that can be obtained from them. The greatest single threat to this continuity of service is lightning. Lightning strokes striking a line cause flashovers. These, until cleared in some manner, interrupt the transmission of power over the line.

The normal method of clearing such a flashover is to open circuit breakers on both sides of the fault. During the time, between the initiation of the fault and the reclosing of the circuit breakers, there is no force to hold the two ends of the line in synchronism, so that if this gap is long enough the two lines must be resynchronized before the circuit breakers can be closed. This produces a considerable interval during which the line is out of service and may reduce its economic value to a considerable extent.

Three solutions to this problem have been employed. One is a duplicate transmission line located far enough away so that the same lightning stroke may not cause flashovers of both lines. Another solution is the general installation of expulsion gaps. And the third solution is the use of Peterson coils. These solutions are quite expensive and therefore materially reduce the economic value of a single transmission line.

It was recognized several years ago that, if it would work, a much simpler and less expensive solution to the problem would be obtained if the circuit breakers could be tripped and reclosed in such a short time that no resynchronization would be required—and therefore, in effect, no practical discontinuity in the service would result. Exploration of the practical possibilities of this approach has required consistent work over a period of years.

At the start it was not known how quickly a circuit could be reclosed without reestablishing the arc responsible for the original outage. In the absence of this knowledge it was not possible to see whether or not high-speed-reclosing circuit breakers and relays, if developed, would accomplish any useful result. Therefore, an extended series of tests was initiated, first in the laboratory and then in the field, in which a fault was thrown on a circuit and cleared through one circuit breaker, while a second circuit breaker was used to close the circuit again and clear again if a second fault developed. In this way the dead time, that is, the time during which the line was deenergized, could be made as short as desired. The variation in necessary dead time with clearing time, current, various amounts of wind, and so forth, was investigated. It was found that with an eight-cycle breaker and 12 cycles of dead time the fault rarely would re-establish itself.

In that work we in the General Electric Company had the pleasure of co-operating with Mr. Sporn and his engineers of the American Gas and Electric Service Corporation, and I had the honor of participating as a joint author with Mr. Sporn in reporting this work to the AIEE in 1937.[1]

The combination of relays and high-speed-reclosing circuit breakers accordingly was set up on the above basis. It was realized that in the event of multiple lightning strokes the last stroke might restrike the arc just as the circuit was being reclosed. However, no method of predicting the frequency of such occurrences was apparent.

This dead period was found to be short enough so that the lines would not lose synchronism, and therefore the procedure appeared to take care of the service in all cases except those due to permanent line damage. From this point on it was a question of experience to determine whether the prevalence of multiple lightning strokes or any other unpredictable phenomena would affect seriously the economic value of high-speed reclosing. That question could be settled only by tests extended over a considerable geographical area and over a considerable period of time.

Mr. Sporn has had the courage to extend high-speed reclosing over a considerable area, and he and Mr. Muller are now able to report the result of this installation over a period of nine years—during which this courageous procedure has been amply justified.

While it probably should not be claimed that high-speed reclosing should supersede all other methods of improving continuity of service, it does provide a very powerful added tool, which can be used effectively not only in extending electric service provided by single transmission lines but also in improving the continuity of operation of existing lines with a minimum of cost. The value of this tool has been enhanced considerably during the period covered by the paper by the increase in relay speeds and both the opening and closing times of breakers.

This program has been a source of great satisfaction to all those concerned in it, and Mr. Sporn and Mr. Muller are to be complimented for the way in which the program has been carried on to such a successful outcome.

Reference

1. Ultrahigh-Speed Reclosing of High-Voltage Transmission Lines, Philip Sporn, David C. Prince. AIEE Transactions, volume 56, 1937, January section, pages 81–90, 100.

S. B. Crary (General Electric Company, Schenectady, N. Y.): The record of high-speed reclosing presented by Mr. Sporn and Mr. Muller represents an outstanding accomplishment. Particularly worthy of careful general consideration are the 65 reported unsuccessful reclosures, of which eight were attributed to permanent faults and others to nonsimultaneous relaying and out-of-step operation.

If we consider the possible reasons for unsuccessful reclosure, the following classification might be made:

1. Permanent faults.
2. Restriking of arc.
3. Irretrievable loss of synchronism.

Some methods of reducing the possibility of these three major reasons for unsuccessful reclosure also might be listed as follows:

1. Permanent faults.

(*a*). Reduction in mechanical failures by improved design and structure of line.

(*b*). Reduction in terminal-apparatus insulation failures by co-ordinated overvoltage protection, solid- or low-impedance system grounding, and circuit breakers having a minimum tendency for restriking.

2. Restriking of arc.

(*a*). Reduction of clearing time so as to allow for necessary deionization time.

(*b*). Application of carrier-current relaying so as to provide simultaneous clearing of breakers of faulted section.

3. Irretrievable loss of synchronism.

(*a*). Reduction in clearing time and use of lowest reclosing time which will permit deionization of arc.

(*b*). Co-ordination of system design for stability, such as use of high-voltage bussing and intermediate switching stations on parallel lines.

(*c*). Rational selection of type of reclosing, single phase or three phase, and corresponding reclosing times.

(*d*). Proper application and maintenance of modern control equipment, such as voltage regulators and governors.

There may be added other means for decreasing the unsuccessful reclosures, the importance and practicability of which will differ between systems and will depend upon relative cost and economics. As the above list illustrates, a good record with high-speed reclosure is more apt to be obtained from a system which has used other complimentary modern practices.

Still further improvement possibly may be obtained, depending upon future developments, by

1. Co-ordination of out-of-step relay blocking with preselected points of system separation for irretrievable loss of synchronism.

2. Relaying and switching which allows for maximum possible deionization time, as a function of fault severity and line electric loading.

It fully can be expected that in the future systems will be designed and operated with higher electric transmission-line loadings and that high-speed clearing and reclosing co-ordinated with system design, relaying, and control will play an important part in making this possible. It would seem, therefore, that the authors have every reason for their continued expectation for ever greater and improved performance by the use of three-cycle fault clearing breakers. This step logically can be expected, as the authors have believed unerringly from the beginning, to further the practicability and value of high-speed reclosing.

H. N. Muller, Jr. (Westinghouse Electric and Manufacturing Company, East Pittsburgh, Pa.): It is gratifying to all who have advocated the application of high-speed reclosing to transmission circuits to see the impressive figure of 89.6-per-cent successful reclosures given by the authors. This is particularly true of the paper by Mr.

Sporn and Mr. Muller, since the system under investigation is quite large and includes many transmission circuits in different locations and of different types of construction.

The discusser notes with interest the five unsuccessful reclosing operations experienced during 1943 and 1944 on the Saltville–North Bristol line. Mr. Sporn and Mr. Muller attribute these unsuccessful operations to loss of synchronism between connected synchronous sources during the fault and the de-energized period. Since instability is given as the cause for these operations and since the authors go on to explain that the faults were undoubtedly other than three phase in nature, the possibility of successful operation, had selective-pole relaying and reclosing been used, naturally presents itself. It would be interesting indeed to see the results of a stability analysis performed to indicate whether the higher transient stability limits obtainable with selective-pole switching would have presented a stable solution.

By way of brief explanation, the term selective-pole relaying and reclosing is used to designate the system of operation whereby only those phase conductors involved during a transmission-line fault are de-energized and reclosed. Thus, during all but three-phase faults, either one or two phase conductors are available for the transmission of synchronizing power, and an increase in transient power limits results. The term single-pole reclosing sometimes is used.

Of course, it is recognized by the discusser that this form of relaying and reclosing was not available in 1940, the time when the Saltville–North Bristol transmission line was equipped for ultrahigh-speed reclosing.

It also would be of interest to the industry, if some analysis could be made and data assembled indicating the prevalence of different types of faults which make up the total of 635 flashovers recorded by Mr. Sporn and Mr. Muller. Numerous investigators have estimated what percentage of transmission-line faults may be single line-to-ground in nature, double line-to-ground, phase-to-phase, or other types, but seldom is there such a large number of carefully recorded flashovers available for analysis. The discusser does not know whether such a compilation of data is possible, but, if it is, it should be of interest to many. This is particularly true since various types of construction are included in the large number of circuits involved.

The discusser expresses complete agreement with all five conclusions listed in the paper.

E. E. George (Southwest Power Pool, Little Rock, Ark.): This paper gives a valuable summary of operating experience with a development pioneered by the authors. Instantaneous reclosing of one end of a tie line and of feeders began in 1932, but simultaneous reclosing of both ends of tie lines was first used in the Fort Wayne area of the American Gas and Electric system in 1936.

This development was promoted by the operating company rather than by a manufacturer. The results have been so uniformly successful that henceforth the burden of proof should be on the operating engineer who fails to use high-speed reclosing on his tie lines. There is no other way of getting so much service improvement for so little money.

Philip Sporn and **C. A. Muller:** The analysis of the causes of unsuccessful performance is always an important step in improving apparatus, and Mr. Crary's list of possible causes of failures is quite comprehensive. Transmission-line and station design details must be reviewed in the light of experience with permanent faults, and improvements made when indicated. Co-ordination of insulation levels is important not only in connection with ultrahigh-speed reclosing but also in the more general problems of system operation. Solid system grounding is employed at all generating points except Reusens.

The general nature of the problems of successful reclosing of the Roanoke–Reusens lines was recognized at the time the installation was planned. It appeared impractical to redesign the existing station at Reusens to provide solid grounding, and it was expected that sufficient successful reclosures would be obtained to justify the high-speed-reclosing equipment. The record of $65^1/_3$ successful reclosures fully bears out this expectation.

Carrier-current relay protection is considered an essential to simultaneous opening of both ends of a line, and all lines except West Lancaster–Anchor Hocking are so equipped. This latter line has one-cycle pilot-wire relaying, and so far no operations have occurred. All breakers reclose 18 cycles after the trip coil is energized, and about ten per cent of them are eight-cycle tripping, the remainder being five cycles. Successful reclosures of the two types of breakers are in about the same proportion, indicating that ten cycles of de-energized time is sufficient for deionization. Progress can, therefore, be expected in avoiding loss of synchronism, as breakers with shorter tripping time and consequent shorter reclosing cycle are developed. Almost all of the generators are equipped with modern voltage regulators and governors, and this apparatus is given careful maintenance to insure its correct operation.

Mr. Prince has been associated with the development of ultrahigh-speed reclosing since its beginning, and his faith in its ultimate value to power transmission has contributed greatly to its successful development. His discussion presents the larger picture of the position which this tool has assumed in over-all system operation and outlines very well the alternatives which must be considered in deciding where it should be applied.

H. N. Muller's discussion suggests the possibility of improved performance on the Saltville–North Bristol line by the application of single-pole tripping and reclosing. It was thought in the beginning by the authors that in general the improvement in system stability which single-pole operation provided was not sufficiently great to justify the added complications in relaying which were necessary. As relaying and breakers are improved, it is recognized that it well may be in order to review this original opinion. It is also true that a general conclusion does not always apply to specific problems, and the absence of a stability study of this particular line makes any definite answer impossible at this time. Mr. Muller also suggests the value of further data on the types of faults which make up the total recorded. Unfortunately, this sort of classification has not been compiled, and the amount of statistical work involved in making it is prohibitive at this time. However, it is the opinion of the authors that such a classification would not differ materially from the figures which have been published previously by other investigators.

The authors feel that the case for ultrahigh-speed reclosing can be stated no better than has been done by E. E. George: "there is no other way of getting so much service improvement for so little money."

Graphical Method of Calculating Fault Currents on Rural Distribution Systems

Discussion and author's closure of paper 45-8 by F. W. Linder, presented at the AIEE winter technical meeting, New York, N. Y., January 22–26, 1945, and published in AIEE TRANSACTIONS, 1945, January section, pages 16–19.

Max W. Rothpletz (Rural Electrification Administration, St. Louis, Mo.): The author is to be complimented on his practical contribution to the methods of calculating short-circuit currents. This method produces a graphical record of the current magnitudes so that anyone who has become accustomed to its use can be quite sure that no mistakes have been made in calculations of line impedances.

An alternate method of calculating fault currents employing triangles is described briefly. As a matter of additional interest, we might mention that this method has been used extensively in preparing short-circuit studies for Rural Electrification Administration-financed systems. The original triangles for REA use were designed in the spring of 1941 by the late Lieutenant John Hey.

The reference to "two-phase lines" in the paper obviously is intended to describe a line comprising two phase wires and a neutral of a three-phase system. To distinguish this type of line from a true two-phase line, it is suggested respectfully that the Standards committee establish a more definite name for such a circuit. Possibly the term "V phase" would be appropriate.

While the observations made in the paper covering calculation of source impedance are correct when applied to relatively large power sources, we might add that many REA-financed rural systems are energized by small co-operatively or municipally owned generating plants. Under certain conditions, dependent upon the positive and negative sequence reactance, the line-to-line or line-to-ground fault currents supplied by these small plants may be greater than the three-phase fault current. Where such supply conditions exist, it will be necessary to calculate impedances for all probable types of faults. Regardless of the size of power source, fault currents under all probable conditions should be calculated for the load side and the equivalent current on the supply side of the substation so that co-ordination of load- and supply-side sectionalizing devices may be checked.

John G. Holm (Boston Port of Embarkation, Boston, Mass.): The author's method of calculating distribution-system fault currents is sufficiently straightforward and simple to expect that it will find applications for the purposes intended.

The part of the method on which, to a great extent, depends the accuracy of the results obtained is the correct location of the starting point. In determining the co-ordinates of this point, the magnitude of the short-circuit kilovolt-amperes on the transmission line at the location of the substation plays an important part, contributing perhaps as much as 25 per cent to the total accuracy. Since there are several methods in use in determining the short-circuit kilovolt-amperes at a certain point in the system, it is therefore quite appropriate that the author should indicate the method for their calculation which he considers necessary and sufficient in the application of his proposed graphical procedure: Should it be the method proposed by a subcommittee of the Institute committee on protective devices, or is it proposed that the decrement curves be used; is the load on the distribution system to be taken into account, and, if so, what assumptions are made in this connection? Admittedly, too much precision is not justified, since the author's graphical method involves other assumptions, such as in regard to the resistance and reactance components of the conductors, and the very significant fault resistance. Still, additional comments on the determination of the magnitude of the short-circuit kilovolt-amperes to be taken with the graphical method suggested are desirable, for they would place the method on more secure foundation and would contribute to its being more accurate and consistent.

J. M. Wallace (Westinghouse Electric and Manufacturing Company, East Pittsburgh, Pa.): The graphical method of fault-current calculation described by Mr. Linder answers a long needed requirement for a simple method which is readily understandable. Heretofore, the calculations of fault currents have required considerable work and a background in mathematics not always possessed by those wishing to make such calculations. This method will permit the accurate calculation of fault currents by one who is acquainted with the system being studied, but who may not have the requisite background for the methods previously available.

An outstanding advantage of this new method lies in the similarity of the completed diagrams to the system maps. This readily makes apparent the physical picture of what takes place in the system. Consequently, it is more readily understandable and in turn more usable. The actual location of protective devices can be shown on the charts and this should prove an aid in system planning.

The readiness with which changes in the system can be evaluated is another desirable attribute of this method. In the case where the system is to be extended, it is quite simple merely to add further extensions to the existing diagrams and thus it is easy to keep the diagrams up to date on an expanding system. It should be noted that the recalculation of the system upon changes in source capacity is easy, especially in view of the amount of labor involved in the methods heretofore available.

Mr. Linder is to be congratulated upon this new method described in his paper, as it is felt that he has devised a tool of great practical usefulness.

F. E. Andrews and **R. O. Askey** (Public Service Company of Northern Illinois, Chicago, Ill.): A number of simplified methods are in use by different engineers for making fault-current calculations on distribution circuits. The method proposed by Mr. Linder appears to be a valuable contribution to the subject of fault-current calculation. It is our observation that the utility of any given method depends upon the user's familiarity with it. Accordingly, where a certain method has been in use for some time, the most efficient procedure insofar as time saving is concerned is for the individual to continue the use of the method to which he is accustomed.

Suggestions to increase the value of and ease of using the method proposed by Mr. Linder are:

1. The author goes through a calculation to derive equivalent source ohms from source short-circuit kilovolt-amperes. A simpler method would be to start with source short-circuit amperes in terms of the reference voltage. A line would be drawn on the diagram at the slope corresponding to the source impedance angle used, that is, ratio of 0.98 to 0.2 in the author's example. The source short-circuit amperes would then be laid off directly on this line using the current scale of the diagram.

In case a more accurate starting point is desired than provided by an assumed standard source-impedance-line slope, it can be determined easily from the short-circuit ampere value expressed in complex quantity terminology.

2. To provide distribution-substation transformer-bank scales similar to the line mileage scales. The slope of these scales would be determined by the transformer impedance angles. The scales would be marked off in transformer sizes, one scale for each per cent impedance value required. If transformer impedance is standardized fairly well a single transformer scale probably would suffice, which might have the same slope as the source impedance line previously suggested, as in the case of the author's example.

3. If data are at hand on the short-circuit current available at the load side of the transformer bank, a further simplification can be effected by using this value as the starting point on the current diagram as described in item 1.

The statement is made in the paper that 40 ohms is a reasonable value to assume for fault resistance. It would be of considerable interest to know the basis for this assumption, and the corresponding value which might be assigned for circuits operating at 2,400 volts to ground.

M. A. Faucett (University of Illinois, Urbana, Ill.): Mr. Linder has presented a very interesting paper which should be helpful to those who are doing work and making calculations of a similar nature. Usually, calculations of this nature become uninteresting and routine and a different method of obtaining results will aid the distribution engineer.

One advantage to be obtained from this method would be the inclusion on one chart of the fault conditions for several different proposals for extensions from a substation using the different conductor sizes which might be under consideration. The co-ordination of fuses can be made from this chart, once the line characteristics have been determined and fault currents computed. Also, it is easier to get a better over-all picture of the various possibilities if all conditions can be placed on a single chart and the results compared to the same scale.

I am wondering why the author did not express his impedances on a per-cent or per-unit base. It would appear that the same ampere curves could be drawn with the resistance and reactance values in per cent at a kilovolt-ampere base and voltage base. Many distribution engineers and system-planning engineers do most of their calculations on a per-cent basis and hence might be somewhat reluctant to use ohmic values.

One suggestion might be made in regard to the contents of Table II of the paper. Because of the present emergency, many new men in the distribution departments of the power companies have been forced to do short-circuit calculations from formulas. These men, in many cases, do not know the reason for the relationships. For them, it would appear that an expansion of the material for this table might be of considerable benefit.

F. W. Linder: The author is pleased to note that Mr. Wallace, Mr. Faucett, and Mr. Rothpletz have observed several advantages which the graphical method of calculating fault currents has over other methods commonly used. All of the advantages mentioned, in addition to others stated in the paper, have been proved by several hundred fault-current studies which have been prepared by the graphical method of rural distribution systems financed by the Rural Electrification Administration. Mr. Wallace points out that it is very easy to revise a completed study when a revision is made necessary by system expansion or change in source capacity. It is believed that this advantage will become more important in the postwar period on systems where an appreciable increase in the load of existing consumers is expected and considerable system expansion is planned.

The author wishes to thank Mr. Andrews and Mr. Askey for the three valuable suggestions to improve the method. As explained in their discussion, scales for determining the source impedance calibrated in source short-circuit amperes or kilovolt-amperes and scales for determining the substation impedance calibrated in transformer kilovolt-amperes may be placed on the diagram along with the line mileage scales. Then the starting point on the diagrams in every case would be at zero ohms resistance and zero ohms reactance, and no mathematical impedance calculations would be necessary. For most applications sufficient accuracy could be obtained by using average values of source voltage and transformer per cent impedance in designing the source and transformer impedance scales which would reduce the number of required scales to a minimum. If there is not enough space on the diagrams to accommodate these scales, they may be drawn on a separate sheet which could be placed on the diagrams when they are needed.

The recommended value of 40 ohms for fault resistance is based on experience in the operation of sectionalizing devices installed on REA distribution systems, the majority of which are 7,200 volts line-to-neutral and 12,470 volts phase-to-phase multigrounded neutral systems. The calculated minimum fault current, based on a 40-ohm fault resistance, at the end of sections of line controlled by many sectionalizing devices (especially oil-circuit reclosers) installed on REA systems is approximately the same as the minimum tripping current of the sectionalizing device. Faults at these critical locations which do not cause enough current to flow to trip the sectionalizing device are very rare. Therefore, it is believed that 40 ohms is sufficient value of assumed fault resistance to give adequate protection. On some systems it would be impossible to obtain good sectionalizing with any one of the various types of sectionalizing devices available if a value larger than 40 ohms were assumed for the fault resistance in calculating minimum fault currents.

Mr. Faucett suggests expressing impedance on a per-cent or per-unit base, which was not done because the author is accustomed to using ohmic values. The impedances may be expressed on a per-cent or per-unit base by those who prefer to use the per-cent or per-unit system.

The problem of determining the short-circuit conditions on the transmission line at the supply side of the distribution substation was not considered because the subject is covered adequately in numerous papers and textbooks and generally is well known. It is believed that, in most cases, the accuracy by which the source impedance is determined is not as important as indicated in Mr. Holm's discussion. For example, on many REA systems supplied from transmission lines of 33 kv and higher voltages through substations up to and including a capacity of 1,000 kva, it has been found that the source impedance may be neglected. The source impedance in these cases, when referred to the distribution-system voltage, is so small compared with the substation impedance that the error caused from neglecting it is well within the limits of the accuracy necessary. Of course, the effect that the source impedance has on the final results increases as the capacity of the source becomes smaller and the capacity of the distribution substation and system becomes larger. Where the distribution system is supplied from a small generating plant or from a long low-voltage transmission line, the source impedance referred to the distribution-system voltage may be several times the distribution-substation impedance, and the accuracy of determining the source impedance is of considerable importance as Mr. Holm points out.

Mr. Rothpletz is correct in his comment that the reference to "two-phase lines" in the paper means two phase wires and a neutral of a three-phase system. Mr. Rothpletz indicates in his discussion that he obtained the impression that it is not necessary to calculate fault currents for all possible types of faults. The author agrees with Mr. Rothpletz that fault currents should be calculated for all probable types of faults. Line-to-ground, line-to-line, and three-phase faults generally are considered to be the probable types of faults, and each of these types is considered in the paper except in the illustrative example where only line-to-ground fault currents are calculated. As stated in the first paragraph of the illustrative example, only line-to-ground fault currents are calculated because the procedure for calculating each of the different types of faults is the same.

New Solenoid Mechanism for Magne-Blast Breaker

Discussion and authors' closure of paper 45-56 by B. W. Wyman and J. H. Keagy, presented at the AIEE winter technical meeting, New York, N. Y., January 22–26, 1945, and published in AIEE TRANSACTIONS, 1945, May section, pages 268–74.

R. C. Dickinson (Westinghouse Electric and Manufacturing Company, East Pittsburgh, Pa.): In this paper the authors have given a well-written report on a design problem of long standing among circuit-breaker engineers. For more than 20 years circuit breakers have been rated on the basis of a closing–opening operating cycle. Circuit breakers applied by the various manufacturers during that time have been presumed to be capable of performing a specified number of those operating cycles without undue damage. Consequently, the solution of this problem long has been a necessary part of good circuit-breaker design.

This is fundamentally a problem in co-ordination between the circuit breaker and the closing device. With few exceptions designers have made use of an interposed toggle linkage. The simple iron-clad solenoid inherently has a high pull toward the end of the closing stroke. Field and laboratory results over a long period of years show that it, in combination with a properly designed toggle linkage, can be and is being made to give satisfactory results.

It is to be pointed out that in respect to the static characteristic of the solenoid shown by the authors the pull in the latter part of the closing stroke may be increased only by making the area of the secondary gap considerably greater than the main-core area. If it is equal to the main-core area and if most of the magnetomotive force is consumed in the air gaps, the static pull for a given gap, coil, and control voltage may be about $^1/_2$ as great as that of a conventional solenoid of the same dimensions. If A is the main-core area, its pull will be proportional to B^2A. If the secondary gap area is equal to A, then the static pull of the flux-shifting solenoid will be approximately proportional to

$$\left(\frac{B}{2}\right)^2 \times 2A = \frac{B^2A}{2}$$

The factor $B/2$ appears, because air gap is double that of a conventional solenoid, except for the very end of the stroke.

The authors have made use of a principle which is recognized in the design of a-c operating magnets where the problem of obtaining adequate pull is considerably different from that of d-c magnets. In this case, because the magnetic circuit must be laminated, a T-shaped movable core commonly is used with the return air gap properly proportioned to shift flux to the additional gap at the proper point in travel for the device being operated, such as a contactor or a brake. This same principle also is applied in circular solid iron magnets for d-c brakes.

The practice of recommending instantaneous relays which are operated only during the closing stroke has not been common and has not been used by the company with which the writer is associated. Satisfactory results have been obtained without it, and it is an unnecessary complication of the relaying scheme. It appears that there would be no real advantage in using such a scheme. If selective relay action is required on a given application, it would be needed regardless of whether the circuit breaker is opening from the closed position or closes against the fault. Therefore, it would not appear to be advisable to eliminate the selective action on closing–opening operations by interlocking instantaneous relays with the closing circuit.

On the other hand, if the instantaneous relays to which the authors refer are not interlocked with the closing circuit and function only on heavy faults, they would not necessarily interfere with the selective relays on opening operations. Consequently, there would be no advantage whatever in interlocking such instantaneous relays with the closing circuit.

B. W. Wyman and **J. H. Keagy:** Mr. Dickinson points out that circuit breakers have been designed for many years on the basis of closing–opening operations at rated short-circuit currents. By definition this closing–opening cycle, when operating at full-rated interrupting capacity, makes instantaneous tripping a prerequisite. Many circuit breakers will function properly on this test which do not possess sufficient closing power to close and latch in the circuit breaker completely against a fault of the same magnitude. If instantaneous relays are not applied on those circuit breakers or if for any reason the instantaneous relays do not function properly, those circuit breakers may be in serious trouble.

As Mr. Dickinson points out, the problem is one of co-ordination between circuit breaker required input force and solenoid output force. With the shape of the conventional solenoid-output-force curve fixed, a complicated toggle linkage was the only tool the designer had to work with in his attempt to match these characteristics. We fail to see how Mr. Dickinson can imply that this is a satisfactory state of affairs, for, in the experience of the authors, such linkages all have the following very serious disadvantage. In increasing the mechanical advantage ratio, toggles necessarily decrease the travel ratio, which means that for a given solenoid speed, the corresponding circuit-breaker contact speed will be appreciably reduced. This is particularly undesirable for the operation of air circuit breakers, in which contact closing speed is as necessary as contact opening speed to keep arc erosion to a minimum. A much more desirable solution is the modification of the solenoid characteristics to give the desired force directly.

There was no intention in the paper of intimating that instantaneous tripping relays need be applied with this type of mechanism, which has sufficient force output to close and latch the circuit breaker positively without stalling even on its maximum momentary current rating. Extreme caution should be exercised, however, in the omission of instantaneous tripping relays on circuit breakers with conventional solenoid mechanisms which may stall when closing against high currents.

Variable-Unbalanced-Voltage Control

Discussion and author's closure of paper 45-27 by W. R. Wickerham, presented at the AIEE winter technical meeting, New York, N. Y., January 22–26, 1945, and published in AIEE TRANSACTIONS, 1945, March section, pages 98–102.

G. W. Heumann (General Electric Company, Schenectady, N. Y.): The author has described in his paper a new method to control the speed–torque characteristics of a wound-rotor induction motor which is subjected to overhauling loads, such as a crane hoist motor. The salient feature of the control system is the application of unbalanced voltages to the stator terminals with the amount of unbalance made a function of both the speed and the load. The author has made a noteworthy contribution by disclosing the control system and by presenting a qualitative analysis of its performance.

There are some points, however, which appear to require further clarification. The author has not presented a quantitative analysis, which makes it difficult, if not impossible, to check the curves presented in the paper. In order to evaluate properly the merits of this system of control and of its performance under actual operating conditions, it is believed necessary that many questions be answered.

In Figure 1 of the paper certain speed–torque curves are given for an induction motor with various fixed amounts of unbalanced voltage applied to the stator. The basic speed–torque curve of the motor is not given. From Figure 1A it appears that the motor in question has a maximum torque of approximately 275 per cent of normal, a slip of approximately 3.5 per cent at full load and that an external resistance of approximately 80 per cent in the secondary circuit. In Figure 3, speed–torque curves are given for the various points of the controller described. Are these curves calculated, or are they based on actual test data?

In Figure 2 a vector diagram is given which indicates how unbalanced voltages are obtained from a balanced system by introducing certain voltage-displacement vectors designated as $EX1$, and so forth. The text of the paper gives the magnitude of these vectors; however, no explanation is given as to how their phase angle is determined. In the legend of Figure 3, it is stated that the displacement vectors move along certain loci, as shown by dotted lines in Figure 2. It would be interesting to know how these loci have been determined. Is test data available to prove that the displacement vectors introduced between line terminal $L1$ and motor terminal $T1$ agree with the data given in Figure 2, both as to magnitude and phase angle?

The vector diagram of Figure 2 is drawn for the case where the stator windings are delta connected. Is it possible to apply the control system to motors with wye-connected stators?

In Figure 3 speed–torque curves are plotted which represent steady-state conditions. These curves are plotted up to a speed of 120 per cent. During acceleration or deceleration of a crane load being lowered, torques may occur on the motor shaft which are in excess of the steady-state load torque. Therefore, it is important to know the maximum torque or the stability limit of the motor. On the system as described, what maximum torque can the motor deliver for various degrees of unbalance in terms of its maximum torque under balanced operation? At what slip does maximum torque occur?

Both the magnitude and phase angle of the displacement vectors is affected by variations in load and in speed. When a heavy load is accelerated in the lowering direction to full speed, a good control system must respond promptly to limit the maximum lowering speed to a steady-state value and to prevent overshooting. Likewise, when lowering a heavy load at slow speeds, good control requires fast response to permit accurate spotting or inching. How fast do the saturable reactor and phase shifter and their associated controlling components respond to changes in speed and load?

In the past, one of the main objections raised against a-c control systems using unbalanced voltages on the stator was the fact that with such a system the heating of the stator windings is higher than with systems using balanced voltages. In Figure 8 it is shown that for torques above approximately 110 per cent the heating for unbalanced-voltage condition at slow speed is lower than for balanced-voltage condition. Offhand, this appears to be paradoxical. Any induction-motor torque under unbalanced-voltage condition can be regarded as the algebraic differences between the torque due to positive-sequence voltage and the torque due to negative-sequence voltage. Thus the net torque of the motor is the difference of two torques, which both contribute to the heating of the motor. Since the algebraic sum of the positive-sequence torque and the negative-sequence torque is larger than the net torque, it appears that the heating corresponding to a given net torque always should be higher with an unbalanced voltage condition. Perhaps the author could give a more detailed explanation of this phenomenon.

The curves in Figure 8 give current input and per cent average heating of the primary windings. Are the current and heating curves calculated or test data? Do the heating curves include the effect of difference in cooling at low and high speeds or are they based solely on per cent I^2R losses? In case the heating curves are calculated, how is the effect of unbalanced flux on iron losses taken into account?

With unbalanced voltage applied to the stator, the air-gap flux is unbalanced, and so is the rotor flux. When operating at high slip, the heating of the rotor may be affected, as compared with balanced voltage on the stator. Does the author have any information on the effect of the unbalanced voltage control on rotor heating?

The legend of Figure 8 states that the heating curves are average curves. It appears that the meaning of the term "average" should be explained. When operating under unbalanced conditions, the currents in the stator windings are not equal. Thus, in order to obtain a true picture of the heating it is necessary to know the heating effect on the winding which carries the highest current. Has the author information available which would show what the maximum heating would be in the winding carrying the highest load?

In the insert of Figure 8 the average heating obtained with the unbalanced-voltage scheme as described is compared with the average heating obtained with other control systems, especially with d-c excited stator, and with adjustable unbalanced alternating current on the stator. The latter two systems employ both control of the voltage impressed on the stator and variation in the resistance connected to the slip rings. The voltage condition on the stator determines essentially the maximum torque, whereas the amount of resistance in the rotor circuit determines essentially the slope of the speed–torque curves. In order to make the information given in the insert of Figure 8 conclusive, the exact conditions on which the comparison is based should be presented.

It is assumed that the connections of Figure 9 are intended to illustrate in a general manner one application of the control system described and are not intended to include all of the detailed circuits required in a hoist controller. For example, it is recognized practice to provide a contactor or relay for interrupting the brake coil circuit in the off position of the master controller, thereby insuring quick setting of the brake and more accurate jogging and spotting of loads.

Figure 10 shows a set of speed–torque curves which can be obtained with the control system described. These curves differ somewhat from the curves given in Figure 3. Are the curves of Figure 10 based on test data or on calculation and what factors cause them to differ from Figure 3?

C. B. Risler (Westinghouse Electric and Manufacturing Company, East Pittsburgh, Pa.): Mr. Wickerham's paper has described in detail the control system he is introducing and the apparatus it requires. To determine the value of this control system to the industrial user requires the study of the speed–torque curves of Figure 10 of the paper. The combination of these curves with standard wound-rotor motoring characteristics results in complete coverage of the four quadrants and meets the requirements of many drives.

This figure shows very clearly the manner in which this control system combined with a regenerative lowering point provides third and fourth quadrant characteristics essential to a successful crane-hoist drive. Slow lowering speeds, a good variety of speeds at all loads and slow, and high-speed lowering of a nonoverhauling light hook have featured the performance of cranes equipped with this system. Winch drives also can use these features to advantage.

The feature of subsynchronous motoring

speeds as shown in the first quadrant holds great possibility for reduced-speed light-load operation of a-c wound-rotor motors—a feature heretofore unavailable or at best available with extremely poor speed regulation or high currents. Slow speeds or inching operation of conveyors, crane bridge, and trolley drives and other machines formerly requiring armature-shunt d-c operation come to mind—also slow-speed hoisting of an empty crane hook and the slew or rotate drive of a hammerhead or portal crane. This slow-speed feature of the reactor system also has merit for a-c wire-drawing bench drive.

Aerial tramways characterized by inherent load shifts from motoring to overhauling are another field in which this control is being successfully applied.

Undoubtedly as the system is used new applications will come to light which will further enrich Mr. Wickerham's contribution to our art.

W. R. Wickerham: The discussions raise the general question as to whether the curves and data referred to in the paper are based on calculations or tests. Figures 1A, 2, 3, and 5 of the paper are based on test data as also are the current curves in Figure 8. So far we have not considered a complete qualitative analysis to be of sufficient importance to warrant the effort involved in making the same.

The data in the paper were compiled from tests taken on a ten-horsepower wound-rotor motor having a pull-out (maximum) torque of 290 per cent normal. The secondary resistor used for all the braking curves produced about 120 per cent normal torque at stall with balanced voltage applied. So long as this condition is met, the pull-out torque and other characteristics of the particular motor are inconsequential.

The vectors in Figure 2 were offered in explanation of what does happen and not as conditions that must be met to insure the successful performance of the system. The only requirements are that $EX2$ be approximately equal to $0.866\ E\ (\cos 60° \times E)$, and that $EX1$ be on the order of $0.25\ E$. The exact vector position of the voltages nor the path of the loci do not appreciably affect the performance. Delta vectors were used, because they more clearly demonstrate the problem. Actually the system performs identically, whether the motor is delta or wye wound.

The remarks in the discussion concerning the desirability of promptness of response in torque reactions are well taken. It is a function of the time constant of the main reactor, pilot reactor, and the natural period of oscillation of the motor and mechanical drive. There is a slight tendency to overshoot in magnitude of the decelerating torque for light loads, and thus momentarily decelerate to a lower speed than intended. Field experience on applications up to 150 horsepower has resulted in no complaint by operators. The maximum torque that the motor can deliver always is limited to something less than TQ-1 in Figure 1, hence the excess to the steady-state value is far within the limits of the machine.

The heat curves shown in Figure 8 are merely I^2R losses in the primary windings, associated with the braking curves. We agree that the unbalanced heating curves when compared to the balanced heating curves appear paradoxical; however, when it is remembered that the input current to the motor primary is always limited by the high secondary resistance and that the motor operates under essentially balanced conditions when handling heavy loads, the paradox fades out. Mr. Wohl's article[1] gives a discussion of the over-all heating of motors when operating under unbalanced applied voltage.

With reference to the connections for the magnetic brake, the diagram indicates the scheme employing a coil weakening resistor used for the majority of applications.

The diagram, Figure 9, does not include all detail features that might be included on a hoist controller, such as the brake relay mentioned where large brakes are concerned, certain variations of reactor control, and others. Where refined inching or spotting is of paramount importance in an application, auxiliary methods of reactor control are employed which eliminate the necessity for a high-speed brake.

The reactor control lends itself to many variations of performance. Certain of these that can be obtained are shown by the curves of Figure 10, in which it is illustrated that various degrees of negative-sequence torque at low speed may be associated with different controller points.

REFERENCE

1. R. F. Wohl. *Westinghouse Engineer*, May 1944, page 44.

A Comparison of the Amplitude-Modulation, Frequency-Modulation, and Single-Side-Band Systems for Power-Line Carrier Transmission

Discussion and author's closure of paper 45-68 by R. C. Cheek, presented at the AIEE winter technical meeting, New York, N. Y., January 22–26, 1945, and published in AIEE TRANSACTIONS, 1945, May section, pages 215–20.

E. W. Kenefake (General Electric Company, Schenectady, N. Y.): The author's paper is a good theoretical treatment of double-side-band and single-side-band amplitude modulation. The comparison of the two systems and frequency modulation as regards noise and band width is of interest in many areas, particularly where a number of carrier channels exist. The real problem is how to obtain more carrier channels in a given area, and that is basically a problem of interference between channels, which can be approached by a study of the noise-reducing features of various systems. Whether the system has half the band width or the same band width is merely a consideration in achieving that objective.

In a theoretical discussion it is quite generally true that certain assumptions must be made that do not hold precisely in practice. For example, the assumption that the band width in a frequency-modulation system must be $1^{1}/_{3}$ times twice the deviation cannot hold for all cases of modulation. As Hund points out, at the lower audio frequencies, where the deviation ratio is large, the band width approaches that of the deviation itself. For small deviation ratios, less than unity, the band width is established by the modulating frequency and not the deviation. Therefore, for voice modulation of a carrier, the band width will not exceed appreciably the actual deviation of the carrier in a unity-deviation ratio system due to the energy-versus-frequency characteristic of voice. In other words, it is the lower audio tones in voice that modulate the carrier to a large degree, and little contribution in modulation is made by the higher audio tones. This is true even when pre-emphasis is used with frequency modulation, since the degree of pre-emphasis is not so great as the decay in intensity of the energy of voice with increasing audio frequency.

In analyzing the amount of distortion which would be caused by the elimination of the higher side bands, the author also has neglected to take into account the full effect of the limiter in a receiver. Hans Roder in his paper[1] has shown that excessive distortion will not occur, if limiting occurs below the amplitude variations caused when a small percentage of the higher side bands are eliminated. When a 3,000-cycle tone modulates a carrier with a deviation of plus or minus three kilocycles, less than four per cent of the transmitted energy is contained in the side bands outside of a plus or minus three-kilocycle band width. Therefore, the curves shown in Figure 4 of the author's paper are not a true representation of the distortion in a frequency-modulation system.

Also, it is not necessary to restrict the deviation of frequency modulation to plus or minus two kilocycles when considering the noise reduction of the three systems. In actual practice it has been possible to realize the full plus or minus three-kilocycle deviation without increasing the channel spacing required for frequency modulation above that now needed for amplitude modulation.

In addition the author ignores pre-emphasis, which, to the best of my knowledge, is used in all frequency-modulation systems. The modulating characteristic of frequency modulation, which the author has described quite clearly in his paper, makes it uniquely suited to a pre-emphasis of the higher audio frequencies and a corresponding de-emphasis of these frequencies in a receiver. Actually, of these three systems, only in frequency modulation does pre-emphasis provide a larger contribution to noise reduction. From a theoretical approach, such as the author has made, the random noise reduction in decibels, on an equal-power-output basis, for frequency modulation and single-side-band amplitude modulation over double-side-band amplitude modulation is as given in Table I.

The author claims an additional six-decibel gain for single side band on the basis of efficiency modulation but neglects to point out that this is also applicable to frequency modulation because the frequency-modulation output circuit need not be linear, as is necessary for double-side-band and single-side-band amplitude modulation. That is, frequency modulation can run at full efficiency all the time. The comparison on that basis becomes that given by Table

Table I

	Frequency Modulation	Frequency Modulation Pre-emphasized	Single Side Band
Gain in average noise reduction	6	14	3
Gain in effective noise reduction	4.8	14	3

II. In either case frequency modulation can show an 11-decibel advantage over single side band.

As regards corona modulation, which is fundamentally an amplitude-modulation phenomena, the author states that single-side-band carrier-suppressed amplitude modulation offers an ideal solution. A theoretical treatment will show for single-side-band transmission a reduction in either average or effective noise of 4.76 decibels as contrasted with an infinite reduction by frequency modulation, whether pre-emphasized or not. In theory then, frequency modulation is the ideal solution, although in neither case would we expect in practice to realize the full theoretical value as was indicated in the data given in my AIEE paper on frequency-modulation carrier[2] and subsequent articles covering the Pacific Gas and Electric Company installation.

The advantages of single side band have many applications and are being used to advantage in the field where they can be realized. A large field has been multichannel service between two stations where line characteristics are not severe. The application of single-side-band carrier-suppressed amplitude modulation to power lines is not new, since several channels are now in operation. One installation is on the Pacific Gas and Electric Company system.

The characteristics of power lines at carrier frequencies are unique in many ways, particularly in regard to line loss. A carrier channel requires wide-range automatic-volume-control action to accommodate the changes in attenuation due to line switching and sleet. The introduction of automatic volume control a few years ago greatly aided the performance of double-side-band amplitude modulation. Since carrier-suppressed single-side-band modulation has no steady carrier for stable automatic-volume-control operation, it has been difficult to get a satisfactory automatic-volume-control scheme without a separate pilot channel.

The simultaneous reception in one receiver of telemetering signals from several different transmitters is described by the author as an important possibility of single side band, but he fails to describe how the level of these signals is controlled, when they may vary in magnitude with respect to one another or as a group with line attenuation changes.

Another common difficulty in single-side-band carrier-suppressed systems is keeping the local oscillator in the receiver in step with the oscillator in the distant transmitter.

It certainly would be of interest to everyone for the author to describe clearly how his system of carrier-suppressed single-side-band amplitude modulation overcomes these difficulties and why fundamentally it will be better than existing single-side-band installations. The author speaks of an efficiency-modulated type of transmitter, which, I assume, is simply grid or screen modulation.

Table II

	Frequency Modulation	Frequency Modulation Pre-emphasized	Single Side Band
Gain in average noise reduction	12	20	9
Gain in effective noise reduction	10.8	20	9

One of the important advantages of frequency modulation not treated by the author is its contribution to the channel-conservation problem without the loss of desirable features inherent in the double-side-band amplitude-modulation system. By the same means that frequency modulation discriminates against noise of all types better than double-side-band amplitude modulation, it also will discriminate against another carrier frequency on that channel better than double-side-band amplitude modulation.

It is now well known that frequency-modulation broadcast stations on the same frequency enjoy a much greater interference-free area than amplitude-modulation stations. Even with a unity-deviation ratio system, the amount of discrimination is appreciable, as can be seen from the previous noise considerations. A solution for the increase in the number of channels that can be provided by frequency modulation can be obtained for any given set of conditions. In general, however, this increase must be in proportion to the noise reduction of frequency modulation over amplitude modulation.

The question then arises as to the possibility of applying this logic to single side band. If so, only the three-decibel advantage, due to eliminating half of the noise by halving the band width, can contribute to channel saving, because the actual power levels of the carrier signals on a system do not affect the number of available channels in a given area. Could we not conclude likewise that pre-emphasized frequency modulation, which has a 14-decibel noise-reduction advantage over double-side-band amplitude modulation, will make a much greater contribution to channel conservation than single-side-band amplitude modulation?

In addition to the channel-conservation and noise-reduction features provided by frequency modulation, all of the desirable features of double side-band amplitude modulation not only are retained but also enhanced. This is exemplified by the fast and sensitive form of automatic volume control, due to the limiter in the receiver, and greater freedom from transmitter and receiver switching surges in single-frequency operation.

REFERENCES

1. EFFECTS OF TUNED CIRCUITS UPON A FREQUENCY-MODULATED SIGNAL, **Hans Roder.** *Proceedings* of Institute of Radio Engineers, December 1937.

2. FREQUENCY MODULATION FOR POWER-LINE CARRIER-CURRENT, **E. W. Kenefake.** AIEE TRANSACTIONS, volume 62, 1943, October section, pages 616-20.

R. C. Cheek: I disagree with Mr. Kenefake's fundamental premise that the increase in the number of channels provided by a given system of transmission must be proportional only to the noise-reducing features of that system. As a matter of fact, the exact opposite is true in the case of frequency modulation. If we followed Mr. Kenefake's logic, we naturally would assume that the ideal state of affairs would be to use as large a deviation ratio as possible at all stations on a power system, because the noise-reducing properties of frequency modulation are proportional to the deviation ratio employed. But, if at each station we used a deviation ratio large enough to fill up the entire carrier spectrum from 50 to 150 kilocycles with side-band components from that station alone, no station would be able to receive any signal except its own without strong interference, no matter how the center frequencies of the frequency-modulation signals were spaced in the spectrum. In other words, this logic leads us to the absurd requirement that the desired signal be appreciably stronger than all undesired signals, including those from local transmitters, at each receiving point.

A true measure of the number of channels provided by any given system is simply the amount of space in the carrier spectrum occupied by the signals from that system. Compromises, such as duplication of carrier frequencies and the requirement that desired signals be stronger than undesired signals, should be considered only as secondary means of placing more channels in a given frequency band. With the single side-band system, the signals occupy half the band width of those generated by the amplitude-modulation system. The selectivity of the receivers used to receive such signals can be increased to such a point that approximately twice the number of *individual* and *independent* channels are available with this system than with amplitude modulation, irrespective of the noise-reducing properties of the system.

Mr. Kenefake is incorrect in stating that I neglected to take into account the full effect of the limiter in analyzing the distortion introduced by eliminating the higher-order side-band components of a frequency-modulation signal. If he will read the appendix of my paper more carefully, he will note that amplitude variations introduced by eliminating these side-band components are neglected completely, that is, perfect limiting action is assumed, in the derivation of equation 3 of the appendix. This equation is an expression for the frequency variations only of the resultant signal. Mr. Kenefake correctly states that less than four per cent of the transmitted energy is contained in the side bands outside of a plus or minus three-kilocycle band width when a 3,000-cycle tone modulates a carrier with a deviation of plus or minus three kilocycles. He neglects to point out, however, that over 28 per cent of the energy is contained in these side bands when a tone of slightly over 1,500 cycles modulates the carrier with the same deviation. Hund's criterion for required band width of $1.5\times2\Delta F$ allows us to neglect, as Mr. Kenefake implies we may, the distortion introduced in the former case but not that introduced in the latter.

Audio pre-emphasis is essentially a distortion of the audio characteristics of a speech channel at the sending end with a corresponding distortion in the opposite direction at the receiving end. Inasmuch as pre-emphasis is purely a feature of the audio circuits of a channel and is not an inherent characteristic of any system, it was not considered in the paper. However, if pre-emphasis is to be considered, it is not fair to compare the systems on the basis of using pre-emphasis with frequency modulation and not using it with single side band, as Mr. Kenefake has done in claiming an 11-decibel advantage for frequency modulation. It is true, as Mr. Kenefake states, that a *given amount* of pre-emphasis provides a larger additional decibel gain for frequency modulation than for single side band. The amount of pre-emphasis that can be used with each system requires examination, however. In the second paragraph of his discussion Mr. Kenefake states that the amount of pre-emphasis used in frequency modulation must be limited to somewhat less than the decay in intensity of the energy of the voice with increasing frequency. This limitation, as he states, is imposed by the increase in band width required by the frequency-modulation system as the higher voice frequencies are brought up to a level comparable with that of the lower frequencies. No such limitation exists with the single-side-band system; so a larger amount of pre-emphasis can be used. Only first-order single-side-band components are produced, whatever the amount of pre-emphasis. If the speech is passed through a low-pass filter cutting off sharply at 3,000 cycles, the remaining high frequencies can be emphasized to full equality with the low frequencies, and gains comparable to those obtainable with frequency modulation can be obtained from pre-emphasis with single side band without exceeding a three-kilocycle band width.

Mr. Kenefake's figure of three decibels for the gain of single side band over amplitude modulation for average noise is incorrect. Average noise voltage is directly proportional to the band width accepted by an amplitude-modulation or single-side-band receiver, and effective noise voltage is proportional to the square root of the band width. The correct figure for single sideband is therefore six decibels, the same as the figure for frequency modulation. I used only effective values in the paper, even though comparison on this basis handicaps single side band by 1.8 decibels, because in my opinion the effective or integrated value is a better measure of the true interfering capability of noise. It is the value, for example, which would determine incorrect relay operation in telemetering service.

Aside from the theoretical considerations which have been discussed, a power-system operator is interested from a practical standpoint in the actual gains that he can obtain by converting amplitude-modulation equipment to single-side-band operation, as I have suggested in the paper. On this basis, I have included an additional six decibels in the total gain that can be realized when an amplitude-modulation transmitter of the line of equipment described in reference 5 of the paper is so converted. It is worth pointing out that the design of this equipment suits it peculiarly well to such conversion, and that this same additional six-decibel gain could not be obtained with all designs of amplitude-modulation transmitters upon conversion to either frequency modulation or single side band.

Mr. Kenefake states that corona modulation of a carrier is fundamentally an amplitude-modulation phenomenon and that frequency modulation offers an infinite reduction of the noise resulting from it. Proof of the falsity of these statements requires only a brief reference to fundamental transmission theory. The propagation constant of any line, usually denoted by γ, is defined as $\sqrt{(r+jx)(g+jb)}$, in which the terms have their usual meanings. The effect of corona on a line is to vary periodically the shunt-conductance term g. A variation in this term reflects itself in a variation of both the real and imaginary parts of the total expression, after the multiplication is performed, and the square root is extracted. The real part of the result is α, the attenuation constant, and the imaginary part is β, the phase-shift constant. Variations in α produce amplitude modulation of the carrier, to which an amplitude-modulation receiver will respond, and variations in β produce frequency modulation of the carrier, to which a frequency-modulation receiver will respond. It is not surprising, therefore, that Mr. Kenefake has not been able to realize in practice with frequency modulation an infinite reduction in the effect of corona modulation.

The effect of corona modulation upon the amplitude of a single-side-band signal deserves further discussion. Although the locally supplied carrier is not affected, the transmitted side-band component itself may be modulated by corona. The amount of modulation, however, will be a constant percentage of the amplitude of the signal, so that the loudness of the noise heard in the receiver will depend upon the loudness of the incoming signal, that is, upon the instantaneous volume of the speaker's voice or the amplitude of a telemetering tone. An analysis, based upon breaking the amplitude-modulated side-band component down into its original frequency plus two components of the original frequency, plus and minus the modulating frequency respectively, will show that the signal is always at least twice as great as the noise, that even when the loudest modulation is present a gain of three decibels over amplitude modulation is obtained, and that this gain goes up to infinity as the loudness of the intentional modulation goes down to zero. In other words, as the desired modulation becomes weaker, the noise modulation obligingly drops, always remaining below the signal. No such effect is obtainable with either amplitude modulation or frequency modulation, because the amount of noise is constant and, being fixed by the amplitude of the continuously transmitted carriers of these two systems, is independent of the amplitude of the modulating signal.

Mr. Kenefake has asked for details of the automatic-voltage-control system and the means used to keep the oscillators in step in the single-side-band system I am considering. Actually, it was not my purpose in the paper to consider any specific system. With the exception of the remarks regarding conversion from amplitude modulation to single side band, all the figures given, and in fact the entire discussion, are intended merely as a theoretical treatment of the characteristics of the signals transmitted in the various systems, regardless of the means used to produce the signals. The recent announcement of the commercial availability of a new single-side-band system no doubt prompted Mr. Kenefake to make this request. He may rest assured that all the details of the system of generating the single-side-band signals, the automatic-voltage-control system, and the means of keeping the oscillators in step will be disclosed shortly.

Tracer-Controlled Position Regulator for Propeller Milling Machine

Discussion and author's closure of paper 45-47 by C. R. Hanna, W. O. Osbon, and R. A. Hartley, presented at the AIEE winter technical meeting, New York, N. Y., January 22–26, 1945, and published in AIEE TRANSACTIONS, 1945, April section, pages 201–05.

G. A. Caldwell (Westinghouse Electric and Manufacturing Company, East Pittsburgh, Pa.): Mr. Osbon has stated that the tracer-controlled position regulator may be applied on other types of machines. The application which he describes is a large and rather complicated machine, and I believe it will be of interest to see how the equipment has been applied to a conventional machine tool of standard design.

Figure 1 shows schematically a vertical milling machine which is used for a wide variety of work and also is suitable for machining dies which must be made to exact contours. The tracer-controlled position regulator may be added to this machine to produce the desired contours automatically.

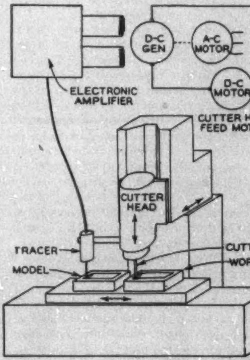

Figure 1

The work piece and the model are placed side by side on the table of the machine. This table can be moved forward or reverse in one plane, and the column of the machine carrying the milling cutter and the tracer mechanism can be moved in either direction in a plane at right angles to the movement of the table. The vertical movement of the cutter-head motor is controlled by the tracer mechanism mounted on the cutter head. The position of the tracer determined by the contour of the model gives the desired position of the cutting tool with respect to the work. As the table is moved horizontally by the operator, the tracer controls the cutter-feed motor, so that the tracer follows the contour of the model and thus causes the cutter to duplicate on the work piece the contour of the model.

The same type of adjustable voltage drive and regulating system as described by Mr. Osbon is used on this simpler application, and the only thing required on the machine to make use of this device is the mounting adapter for the tracer and the use of a shunt-wound d-c motor to drive the vertical feed of the cutter head.

W. O. Osbon: Mr. Caldwell has described briefly the application of a tracer-controlled position regulator to conventional machine tools for die-sinking work. The general principles and method of regulator design described in the paper apply also in this case. However, the system must be applicable to a variety of types of standard machine tools, and consequently the equipment must be of a more universal nature than that used on the highly specialized propeller milling machine. For this reason, a new tracer unit was designed for these applications. This tracer unit is a fixed-ratio unit in which the Silverstat is moved throughout its full range for a probe motion of ±0.004 inch. This motion may be either axial or in any direction perpendicular to the probe axis, making the unit truly universal in its action. It is also possible to modify the regulator circuit so as to provide a very wide-range speed control when tracer control is not required.

Application of Electric Equipment for Ship-Propeller Milling Machine

Discussion of paper 45-71 by H. Earl Morton and Oren G. Rutemiller, presented at the AIEE winter technical meeting, New York, N. Y., January 22–26, 1945, and published in AIEE TRANSACTIONS, 1945, April section, pages 205–08.

H. H. Gildner (nonmember; United States Navy Yard, Philadelphia, Pa.): The profiling machine described by this paper and paper 45-47 has been in service at the Philadelphia Navy Yard for about two years. The designers and builders of the machine are to be commended for the excellence of design and precision of performance.

My discussion will be limited to methods of checking the functioning of the machine and adjustments found necessary to produce the desired results.

Up to this time, the propellers machined have varied in weight from about five to more than 20 tons apiece. The amount of material removed by the milling operation has been a very substantial item and has released many man-hours for the important finishing operations. One of the large propellers is illustrated by Figure 1.

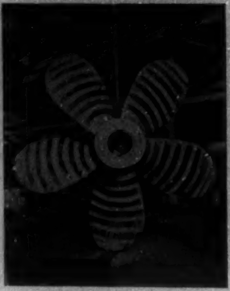

Figure 1

Working out the proper operating technique under a variety of manufacturing conditions has developed some interesting experiences, principally resulting from the geometrical principles involved and due to the great variations in the contours on each blade over which the milling cutters must travel. On each white strip painted on the blades of the propeller shown on Figure 1 are scribed lines representing the various cyclindrical section stations on which final measurements are made. When machining a propeller on the profiling machine, the milling cutter travels over a series of paths concentric with these cylindrical sections.

As mentioned in the paper by Hanna, Osbon, and Hartley,[1] the specifications under which the machine was designed and built required work to be performed within a tolerance of ±0.020 inch. During the early months of service, some erratic variations in machining were observed. On parts of some blades these tolerances would be met, whereas on other areas of the same blades the tolerances would be exceeded. On different propellers the results would vary for no obvious reason. A typical example is illustrated by Figure 2. The narrow grooves across the blades were chipped by hand to fit gauges made to the designed dimensions. These grooves were made for investigative purposes only and are not employed in the normal operation of the profiling machine. The small figures beside the grooves represent the amounts in thirty-seconds of an inch between the true dimensions and the actual milled surface. The manner in which the grooves are fitted to gauges is illustrated by Figure 3. The procedure employed at the Philadelphia Navy Yard for measuring propeller blades by the gauge method is described by L. H. Kenney.[2]

Figures 4, 5, and 6 show the first steps in an investigation carried out in consultation with Mr. Morton to determine the sources of variations in machining. With the machine running through a series of complete cycles, but without the cutters in operation, the movements of the cutter rams with respect to the tracer movements were found to be accurate and sensitive well within the required tolerances.

Further tests indicated that the accuracy

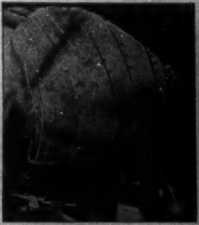

Figure 2

Figure 3 (right)

Figure 4

Figure 5

Figure 6

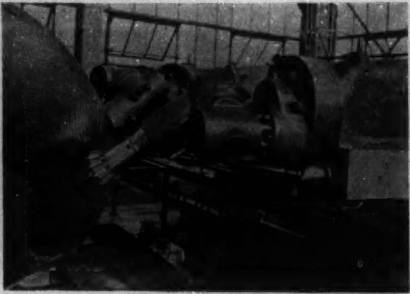

Figure 7

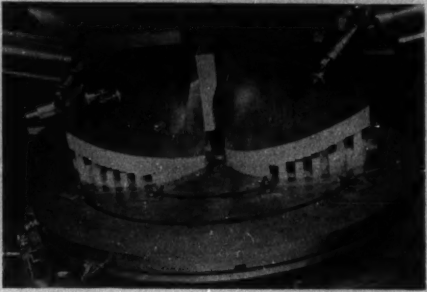

Figure 8

of the work performed was affected to a considerable degree by even slight errors not readily detected in settings of the cutter heads and tracer heads with respect to each other and relative to the propeller blade and master model respectively.

As mentioned by Mr. Morton and Mr. Rutemiller in their paper, the setting-up operation is a rather tedious process and too complex to permit full discussion here, but Figures 7 to 11 will illustrate some simple but effective devices provided to facilitate the work. As an example, when the machine is ready for operation, the cutter should be in exactly the same position relative to the ultimate finished surface of the blade as the tracer head (or probe) is located with respect to the model surface. On Figure 7, the pointer extension on the cutter spindle and a corresponding pointer on the tracer spindle (Figure 8) provide a quick and positive means for determining the positions of the cutter head and tracer head with respect to the propeller blade and the master model respectively. Figures 9 and 10 show fixtures employed to check the accuracy of angular settings prior to proceeding with the machining operation. The probe is operated along a straight edge on the tracer table as shown in Figure 9. Simultaneously through normal operation of the machine, the cutter head moves along the corresponding surface on the fixture shown in Figure 10. Actual movement of the cutter relative to the straight surface of the fixture is observed by means of the dial indicator (Figure 11). Adjustments are refined until the cutter follows parallel to the true surface on the arm of the fixture.

Some variations in machining arose, because adjustments of the relative angular settings of the cutter heads and tracer heads were away from their theoretically correct positions. These settings were made in order to avoid interferences which in some cases considerably limited the scope of the work or speed of operation. For example, after milling a blade from the tip inwards over about three fourths of the blade area, further cutting with this setting would be prevented by interference between the cutter head and a propeller blade or between the tracer head and the master-model surface. Such a condition becomes a tooling and operational problem. The original cutter head can be used with a considerable variety of conditions, but the Philadelphia Yard has developed another shape of head to broaden the scope of the work performed. In many cases it is advantageous to make a setting away from the true setting in order to remove a greater amount of metal without attempting to hold too close to the finished manufacturing tolerances.

The production of accurate master models which can be made quickly has received considerable attention in order to justify use of the profiling machine for relatively small lots of large propellers.

When the machine first was placed in operation, the master models were made at the David W. Taylor Model Basin. On account of the various production problems involved, however, it subsequently was considered preferable to manufacture the master models at the Philadelphia Navy Yard.

Various materials have been considered, but well-seasoned mahogany properly built up has appeared to be the most satisfactory and has been used on most of the models produced up to this time.

Finishing and accurately measuring the master-model surfaces involves very careful work. The magnification of movement in the ratios of 3:1, 4:1, and 5:1 between the

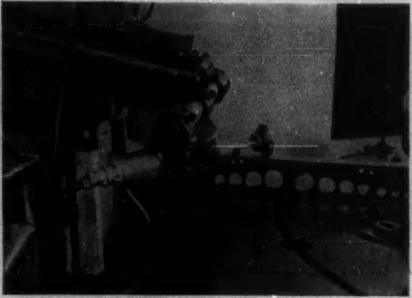

Figure 9

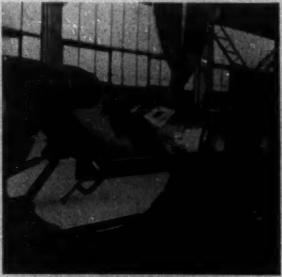

Figure 10

Figure 11

Figure 12 (below left)

Figure 13 (below right)

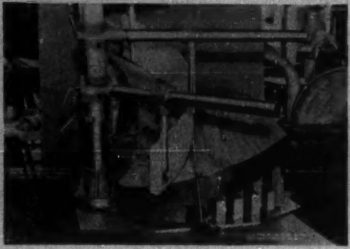

Figure 14

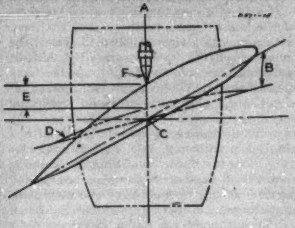

Figure 15

A—Hub B—Face pitch line
C—Center axis
D—Suction face at 0.95 *R*
E—Axial offset from 0.95 *R*
F—Point contactor

tracer head and cutter head requires the model surface to be held within tolerances on the order of $^1/_{100}$ of an inch or less, depending on the model ratio and the degree of accuracy desired of the milling cutter on the propeller blades.

Figures 12 and 13 show one method of measuring by gauges which has the merit of simplicity.

Another method of measurement by point offsets has been developed and now is used during manufacture of the model and for final checking of its accuracy. These point-offset measurements are the vertical distances between points on the model surface and a common reference plane normal to the shaft axis. The measurements are made with the model in position on the table of the profiling machine and using a pointer attached to the tracer ram. Figure 14 shows a model of a device to be used for manufacture of the propeller master model which incorporates the provision for making measurements of the model surface by the point-offset method.

Figure 16

Figure 15 indicates the variations in slope and curvature of typical blade cylindrical sections.

This discussion has not touched on the electrical features of the machine, but it is believed that a view of the control panel will be of interest (Figure 16).

The propeller milling machine has demonstrated in a very gratifying way both mechanically and electrically the care and thoroughness exercised in its design and construction.

References

1. Tracer-Controlled Position Regulator for Propeller Milling Machine, C. R. Hanna, W. O. Osbon, and R. A. Hartley. AIEE Transactions, volume 64, 1945, April section, pages 201–05.

2. L. H. Kenney. *Journal* of the American Society of Naval Engineers, volume 54, February 1942.

Ernest H. B. Anderson (nonmember; Parsons Marine Turbine Corporation, New York, N. Y.): This paper is of special value to marine engineers and I feel sure the authors will be interested to have the following particulars covering the *first* marine propellers which were machined on the driving faces by planing. An article in the *American Machinist*[1] described, with an illustration, the rig used, and I may say this work was carried out at the Bath (Maine) Iron Works. The article mentioned refers to three manganese bronze propellers with 60-inch diameters made and installed on the triple-screw Parsons Turbine steamship *Belfast* for the Eastern Steamship Company, built for passenger service between Boston, Mass., and Bangor, Maine.

In the following year, the same shipbuilders completed the scout cruiser USS *Chester* which had four propellers 72 inches in diameter with machined faces.[2]

In 1909 and 1910 the battleships *Michigan* and *South Carolina* were completed, and the twin propellers of both these ships were machined, and I quote the following paragraph:[3]

> "The driving faces of the blades were machined to a true screw by a machine specially designed for this purpose, the backing face being machined where possible and the balance of the surface ground and polished. Each propeller was accurately balanced."

The propellers of the USS *South Carolina* are described in reference 4.

These propellers were built up having three loose blades, about 17 feet zero inches in diameter.

The results obtained as regards elimination of vibration and uniform rpm of the machinery made the Bureau of Steam Engineering specify machined propellers for all Naval vessels.

References

1. Planing Propellers, J. C. Tourtillotte. *American Machinist*, January 17, 1907, page 83.

2. *Journal* of the American Society of Naval Engineers, volume 20, 1908, page 370.

3. *Journal* of the American Society of Naval Engineers, volume 21, 1909, page 941.

4. *Journal* of the American Society of Naval Engineers, volume 22, 1910, page 208.

W. O. Osbon (Westinghouse Electric and Manufacturing Company, East Pittsburgh, Pa.): Mr. Gildner's discussion of some of the problems encountered in the early operation of the propeller milling machine is very interesting to us, since it illustrates a point which frequently arises in regulator applications. Obtaining a certain specified regulator accuracy is purely a matter of design. A regulator may be designed to have a given accuracy just as readily as a generator may be designed to have a specified voltage droop. This is a fact which is not always recognized by those unfamiliar with regulator problems. It was only natural then that the regulators were suspected of inaccuracies when the discrepancies in machining mentioned by Mr. Gildner were first encountered. The thorough investigation conducted by Mr. Gildner and his associates proves, however, that, when the machine is set up correctly with due regard to the geometrical relationships between tracer and cutter axes, the accurate reproduction of the contour of the model in the propeller casting is assured. Thus it is demonstrated that the regulator performance fully meets the expectations of the designers and the requirements of the users in all respects.

Improving Stability by Rapid Closing of Bus-Tie Switches

Discussion and author's closure of paper 45-13 by Edward W. Kimbark, presented at the AIEE winter technical meeting, New York, N. Y., January 22–26, 1945, and published in AIEE TRANSACTIONS, 1945, February section, pages 61–4.

John G. Holm (Boston Port of Embarkation, Boston, Mass.): The method of improving stability by rapid closing of bus-tie switches proposed by Professor Kimbark has been discussed informally by engineers before. Professor Kimbark is the first to present the method in a concise form with accompanying engineering calculations.

The method is very logical and follows directly from the relationship between the fault action and the high-voltage bus. It is certainly true that rapid closing of bus-tie breakers at the time the line breakers open improves the system stability. This method however, will find only a limited application, the operational considerations and economic calculations being responsible for it.

In general the method is applicable to systems with two or more transmission-line circuits. In most cases such systems have double high-voltage busses and more than two generator units at the sending end. For these reasons operational considerations will require that the bus-tie breakers normally be closed when the system load exceeds the transmission capacity of one circuit. Bus-tie circuit breakers should be always ready for operation either way, open or closed, therefore the requirement that they normally be open restricts the system flexibility and impedes the facility and the economics of operation. System dependability may be impaired. The practice of mid-sectionalizing a two-circuit transmission line, with the involved cost of additional circuit breakers, accessories, and structure, is being followed, not only in order that the system stability be increased, but also that better operational facilities may be secured. The intermediate switching station in longer lines therefore hardly can be eliminated. The author points out the applicability of the proposed method to underground systems. But high-voltage a-c underground lines, for economic reasons, are always very short, and in short lines there simply is no stability problem.

From the stability viewpoint, the present bus-tie breakers do not require opening speeds below eight cycles, with rather slow initial closing speeds. The method of closing bus-tie breakers at the time of opening of line breakers requires breakers with very rapid initial closing time. The development of such breakers will result in the increase in the cost of standard bus-tie breakers. Additional wiring required also will contribute to increased costs, especially in the case of double busses.

The proposed method will find its most direct application, and will give an improvement in system stability, in existing systems with a rather slow opening time of the transmission-line circuit breakers and with lines not too heavily loaded, so as to permit the operation of bus-tie breakers as required by the method. Should the line have rapid-reclosing-type breakers, the proposed method also will be applicable, although with normal reclosing time of 35 cycles (on 60-cycle basis) of high-speed breakers of 115 kv and higher rated voltages, the improvement in stability obtained from the use of this method will be smaller than that given in the paper where breakers of 20-cycle reclosing time are assumed.

If a system uses ultrahigh-speed breakers of the latest design, be they oil or air-blast, with a reclosing time of 12 to 15 cycles, the improvement in system stability will be such that the contribution obtainable from closing the bus-tie breakers will appear insignificant. Single-pole rapid reclosing serves the purpose still better, for it not only increases stability, when compared with a three-pole reclosing, but, in addition, creates more favorable conditions for keeping motor loads in system and reduces switching surges. It may be had today at a very moderate increase in cost.

The author of the paper deserves credit for bringing the method of rapid closing of bus-tie breakers for discussion before the Institute.

E. L. Michelson (Commonwealth Edison Company, Chicago, Ill.): This paper by Mr. Kimbark is an excellent contribution to the literature on system stability. He has added a new idea to the various methods that have been proposed for improving system stability by controlling system connections.

I would like to point out the value of the ring bus as compared with the conventional type of bus with regard to improving system stability. In the conventional-type bus, a fault on the bus requires clearing all the circuits connected to it; with the ring bus, a bus fault limits the outage to one circuit. This improvement is obtained with the use of fewer breakers than the number required with the conventional-type bus. At the same time, the ring bus would be applicable to the type of operation suggested by Mr. Kimbark by properly selecting the breakers in the ring which normally would be closed and those which would be closed automatically when a fault occurred on the system.

S. B. Crary (General Electric Company, Schenectady, N. Y.): Professor Kimbark has made a very thorough analysis of the use of rapid-closing bus-tie switches for improving stability. He has shown the order of magnitude of advantages to be expected as well as the limitations. The advantages, as he points out, are small, particularly when high-speed clearing and relaying are used. The field of application for bus-tie reclosing, therefore, will depend considerably on the particular case. In general, the following factors will tend to limit the field of application or decrease the value of bus-tie breakers.

1. The necessity for using bus-tie reclosing breakers tends to be limited to systems where the power transferred is dependent upon the first-swing transient-stability limits as distinguished from the steady-state stability limit with the faulted section switched out. With modern switching and relaying this will be more likely to occur for the case of a hydroelectric station transferring power over long high-voltage lines. This was the case analyzed in the paper.

2. The generator inertia of such a hydroelectric station may be greater than the value assumed by the author. ($H = 3.0$.)

3. The number of lines may be greater than two, particularly for large hydroelectric developments.

4. Intermediate switching stations are evaluated, not only on the basis of improvement of first-swing transient stability, but also because of the increase in steady-state and emergency-power transfer, increased reliability for line maintenance and repair, and decrease in the amount of kilovars required for power transferred with a faulted section out.

5. Three-cycle fault-clearing circuit breakers are being made available.

6. Higher-interrupting-capacity breakers have been and will be made available as required.

7. Practically perfect synchronization will be difficult to realize except by special rapid bus-tie closing switches.

Edward W. Kimbark: I am glad that Mr. Michelson pointed out that the principle of switching proposed in the paper is applicable to the ring bus as well as to the conventional bus. When applied to a two-circuit transmission line, the ring bus requires two circuit breakers that can open rapidly and two switches that can close rapidly; or, for complete operating flexibility, it requires four circuit breakers that both can open rapidly and close rapidly. The conventional bus requires four circuit breakers that can open rapidly and one switch that can close rapidly.

The principle proposed in the paper is applicable to transmission systems of more than two lines, although the gain in power limit would be less than that obtained on systems of two lines. The switching stations for three or more lines could use the ring bus advantageously.

Both Mr. Crary and Mr. Holm call attention to the fact that intermediate switching stations are desirable for a number of reasons besides the improvement of transient stability. This fact is admitted. Nevertheless, the paper shows that the use of rapidly closed bus-tie switches at all switching stations on a double-circuit line raises the transient power limit by about the same percentage when there are intermediate switching stations as when there are switching stations at the terminals only.

Mr. Holm discounts the applicability of rapidly closed tie switches to cable systems by claiming that there is no stability problem on a cable system. This may be true of power systems consisting of cables only, but it is not necessarily true of mixed systems consisting partly of cables and partly of overhead lines. For example, there are in Chicago some 132-kv underground cables that are connected in series with, and operated as part of, 132-kv overhead lines extending outside of the city. If these overhead lines were connected to distant low-inertia hydroelectric generators, there would be a stability problem similar to that considered in the paper.

The rapid closing of bus-tie switches is not advocated as a cure-all for the problem of power-system stability. It is put forth merely as an additional method of improving stability, not previously described in the literature, and meriting consideration on some power systems. The calculated curves given in the paper show that, on the particular power system studied, the proposed method increased the transient power limit by a substantial amount, whereas alternative methods applied to the same system resulted in much smaller increases.

Circuit-breaker speeds were assumed that were available generally when the study was made; namely, five cycles and eight cycles. If three-cycle breakers are used, the gain in power limit because of rapid closing of bus ties is admittedly less than when five-cycle breakers are used. The extra cost of three-cycle breakers would have to be compared with the cost of achieving the desired increase of power limit by some other means in conjunction with slower, cheaper breakers.

Supervisory Control for New Chicago Subway

Discussion of paper 45-7 by W. A. Derr, C. J. Buck, and J. A. Stoos, presented at the AIEE winter technical meeting, New York, N. Y., January 22–26, 1945, and published in AIEE TRANSACTIONS, 1945, January section, pages 10–16.

J. J. Trainor (nonmember); and **C. E. Parks** (Public Service Company of Indiana, Inc., Indianapolis, Ind.): The authors have described well the very intricate control of a large and complicated electric system in their fine paper. The fact that it is possible to control so large a system from a central dispatching point speaks well for the place supervisory control occupies in the solution of present-day electric network problems. Without such means for co-ordinated operation, it is difficult to imagine the complexities that would present themselves to a system operator, if he were faced with the impossible job of performing all the duties involved by means of direct communication to each of the control points.

There are in operation at the present time on the system of the Public Service Company of Indiana, Inc., six pairs of control terminals using the Visicode system which the authors describe. Another pair of terminals is to be installed shortly. The control of breakers and air-break switches, the starting of rotary converters, and checking of synchronizing, voltage, and current are some of the uses to which this equipment is put.

One interesting pair of terminals on our system is located only some 500 feet apart. The decision to use supervisory control over so short a distance was prompted by comparison of costs between metallic control circuits and supervisory control coupled with the expected future development at the substations involved.

Our operating experience with the Visicode equipment has been very gratifying. Our maintenance department has experienced only minor trouble with the adjustment of the coding and control relays involved, after original adjustment was performed when the equipment was placed into operation. We have been using this type of supervisory control for almost eight years and during that time have experienced only minor difficulties with it. Experience has taught us that the least possible amount of maintenance performed on the relays involved is much the better method of assuring proper operation. This of course excepts the evident cases of trouble that needs to be taken care of immediately. Our original maintenance of the equipment was scheduled once every two or three months, at which time the relay contacts were burnished and adjusted. It was found that this method of maintenance produced much mis-operation in that the relays were unintentionally disturbed in their adjustment. It was found that this type of maintenance was entirely unnecessary, that the relay contacts were almost self-cleaning in their action, and that the slight burning of the contacts was not at all detrimental to the operation of the equipment. Our worst mistake was the effort, by the maintenance crew, to clean the contacts by passing a slip of paper between them. Such methods produced a deposit on the surface of the contact, making the contact resistance high and subsequently preventing proper operation of the equipment.

We have used both privately owned and leased pilot wires on our supervisory scheme and find that results obtained are good in both cases.

Organo-Silicon Compounds for Insulating Electric Machines

Discussion of paper 45-30 by T. A. Kauppi and G. L. Moses, presented at the AIEE winter technical meeting, New York, N. Y., January 22–26, 1945, and published in AIEE TRANSACTIONS, 1945, March section, pages 90–3.

L. J. Berberich (Westinghouse Research Laboratories, East Pittsburgh, Pa.): The recent introduction of silicones may be considered a historic event in the field of insulation as well as in the field of high polymer chemistry. They were developed by crossing organic and inorganic materials, and this resulted in a new breed of materials having thermal stabilities intermediate between the two parent stocks from which they were derived. Considering the short time they have been under development, the chemist has a surprising control over their synthesis and already these materials are available in the form of liquids, greases, and elastic and solid resins.

As Mr. Kauppi and Mr. Moses have pointed out, the basic chain structure of the silicones consists of alternate silicon and oxygen atoms. It is well known that the inorganic material quartz consists entirely of silicon and oxygen atoms and that this material has excellent electrical properties and thermal stability. Quartz, however, has the disadvantage of being a hard brittle material and having a melting point so high that it can be worked into a usable form only with great difficulty. The organic resins, on the other hand, have a basic chain structure consisting of carbon atoms, and their thermal stability is comparatively low because the carbon-to-carbon bonds are severed relatively easily by heat. While the silicon–oxygen chain is very stable thermally, hydrocarbon side groups must be attached to the silicon atoms in order to obtain the desirable mechanical properties observed in silicones. The chief function of these side groups along the chains is to keep the various silicon–oxygen chains far enough apart to make flexible or plasticize the material, thus getting away from the hard brittle character of quartz. The introduction of these hydrocarbon side groups, however, lowers the over-all thermal stability. This explains why the thermal stability of the silicones is intermediate between that of hydrocarbon resins and quartz. The nature of the product obtained, that is, whether liquid or solid, is controlled through choice of starting materials and the process for synthesis.

No one insulating material has universal application and this, of course, is true of the silicones. It is certain, however, that the chemist will exercise his ingenuity to the fullest to broaden the field of application of these materials. Some of the limitations that now exist gradually will be overcome. Even in the phenolics and alkyds introduced many years ago, improvements still are being made. Thus the ultimate in properties and range of application is to be expected only after a considerable number of years. The price of the silicones is rather high. Progress in this direction can be anticipated also, for chemical history is replete with price reductions. Thus, the silicones can be expected to go down in history as a marked advance in the field of electrical insulation, along with the phenolics introduced in 1907, the alkyds in the 1920's, and other synthetic materials of varying importance.

K. N. Mathes (General Electric Company, Schenectady, N. Y.): Our tests confirm that heat resistance of silicone varnishes is greater than for organic varnishes. Although there is considerable range in the properties of different silicones, in general the types available at present offer greatest promise in the range between 175 and 200 degrees centigrade.

Many people working with silicone films have encountered the fine cracks or crazing which develop after exposure to very high temperatures or to lower temperatures for considerable periods of time. Water penetrates these cracks very slowly because of its high contact angle against the silicone surface. It seems desirable, therefore, to make comparisons of moisture resistance such as shown in Figure 3 of the paper for longer periods of time (perhaps 24 hours). Presence of dirt or other contamination on the surface of the silicone may change the water contact angle and permit much more rapid entrance of water. A comparison of moisture resistance under these conditions more closely approximates actual service conditions and would be of interest.

Rating of High-Temperature Induction Motors

Discussion and authors' closure of paper 45-50 by P. L. Alger and H. A. Jones, presented at the AIEE winter technical meeting, New York, N. Y., January 22–26, 1945, and published in AIEE TRANSACTIONS, 1945, June section, pages 300–02.

John L. Fuller (Reliance Electric and Engineering Company, Cleveland, Ohio): The paper on the rating of high-temperature induction motors has served a very useful purpose in pointing out that high-temperature insulation is not a panacea for motor designers but that this very development has brought out other limitations such as bearings, overload capacity, and efficiency. These are certainly very real limitations in attempting to use the silicones with the primary purpose of reducing size and weight of motors.

However, it is hoped that the analysis will not dampen the ardor of those doing development work with these new materials. It appears entirely possible that the silicones may be as useful in the war on moisture as they are for high-temperature applications. Present indications are that greatly increased reliability can be obtained at class *B* temperatures through the use of silicone materials, particularly under adverse conditions exemplified by a heating–cooling cycle under high humidity, with the attendant condensation on the windings. Because of favorable results thus far, a new series of tests is being organized just now to explore further the value of the silicones in promoting reliability under class *B* temperatures and humid conditions.

The authors mentioned "hardened steel races of ball bearings gradually soften if kept at temperatures of 200 degrees centigrade or more." Information from ball bearing manufacturers has indicated that the danger point is of the order of 125 degrees centigrade for standard ball bearings. Special bearings with somewhat lower hardness and with variations from standard in their metallurgy have been made to withstand slightly higher temperatures without serious softening.

F. D. Phillips (General Electric Company, Schenectady, N. Y.): There has been much well-justified enthusiasm for the newer high-temperature insulating materials such as the silicones. Mr. Alger and Mr. Jones have discussed ably the economic as well as the engineering problems involved in their use, and have called attention to the factors, other than permissible temperature rise of the insulation, which govern the actual design of motors.

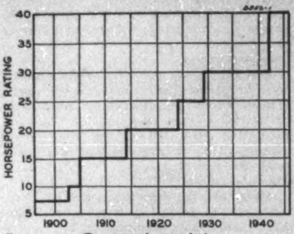

Figure 1. Output obtained from a given induction-motor frame

In the past 50 years there has been a continuous advance in the art, due, not to any one cause, but to successive improvements in the materials and processes involved in motor manufacture, as well as a widening knowledge, both theoretical and practical, of both design and manufacture. Figure 1 shows the progress in horsepower rating from the same amount of material from 1896 to the present date. Through this period, guaranteed temperature rise has remained 40 degrees centigrade, except for a very short time during which the guarantee was 50 degrees centigrade.

There is a very strong feeling among users against temperatures higher than 90 degrees centigrade. This is partly prejudice and partly with good reason, for example, the discomfort to men working near a higher temperature, the presence of dusts or lint, and the more rapid deterioration of lubricating oils and greases under increased temperature. The higher-temperature materials will have many uses in motors for special purposes and conditions, while in the near future the progress in general-purpose motors probably will continue more along present lines than toward radically higher temperatures. It would be difficult to convert the majority of motor users to a higher temperature rise than 50 degrees on the open motor with 15 per-cent service factor or 55 degrees on the enclosed motor with no service factor.

P. L. Alger and **H. A. Jones:** We have every confidence that the silicones and other synthetic insulating materials now becoming available will add greatly to the reliability and range of application of electric apparatus, for low- as well as high-temperature service. Many tests have shown that their moisture, as well as their temperature endurance, is outstanding, so that we heartily agree with Mr. Fuller's comments.

We welcome also Mr. Phillips' data, showing how markedly the size of motor for a given performance has decreased over the years, despite adherence to a 40-degree-centigrade rated-load temperature rise.

The studies presented in our paper were made in the course of a developmental program to find the best way of utilizing these new materials. A dispassionate review of all the factors involved in selecting the optimum temperature rise showed a surprising interdependence of the different aspects of motor design. The conclusion we draw, therefore, is that a balanced consideration of all factors in design and application is desirable, rather than that any particular temperature is best.

We are confident that, as time goes on, the problems of high-temperature lubrication will be solved, improvements in space factor of these new insulations will be made, and overload needs will be defined more closely; all of which will make high-temperature motors more reliable and useful.

One of our associates has advocated recently the use of 100-degree-centigrade temperature rise, measured by the resistance method, for control coils insulated with some of the newer synthetic materials of an organic nature. Even higher temperatures are being used successfully on aircraft and railway applications, with present class *B* materials. For naval and aircraft applications especially, where reliability is vital rather than very long life at full capacity, the silicones and other synthetic materials of high-temperature endurance certainly will play a vital part in future electric equipment.

Insulation Resistance and Dielectric-Absorption Characteristics of Large A-C Stator Windings

Discussion and author's closure of paper 45-49 by J. S. Askey and J. S. Johnson, presented at the AIEE winter technical meeting, New York, N. Y., January 22–26, 1945, and published in AIEE TRANSACTIONS, 1945, June section, pages 347–51.

R. L. Webb (Consolidated Edison Company of New York, Inc., New York, N. Y.): Mr. Askey and Mr. Johnson have done a commendable job in preparing a great mass of insulation-resistance test data on approximately 1,000 new machines rated 1,000 horsepower and above. The information supplied by the paper will assist the work of the AIEE insulation-resistance subcommittee, the work of which is now under way. It is hoped that the authors will find it possible to submit to the subcommittee the actual test data on these machines, giving the insulation-resistance values in megohms together with their associated machine ratings and the conditions for each test. These direct test data, if they can be made available, will permit other reviews and comparisons that will be of even greater assistance to the subcommittee in its present activities.

The suggested linear formula for minimum insulation resistance of large class-*B* insulated machines now is being considered, together with the Wieseman formula and other suggested formulas, by the subcommittee. It appears that much additional test data, taken under uniform conditions, will be required for review and analysis, before a final agreement can be reached on a standard set of formulas for minimum insulation resistance of rotating electric machines.

The authors might have added that the present AIEE formula, which is reproduced in the paper, is considered inadequate, since it does not take into account such items as

(*a*). Machine speed.
(*b*). Insulation class.
(*c*). Winding temperature.

All of these have large effects, as they vary, on the insulation-resistance values which reasonably may be expected for a particular machine. It is this situation that started the search for a more accurate formula some ten years ago. The search has been spurred along somewhat by the formation of the insulation-resistance subcommittee under the AIEE electric-machinery committee in 1941.

H. A. Eysenbach (James G. Biddle Company, Philadelphia, Pa.): The paper is a significant contribution to the information available on this important subject.

The measurement of insulation resistance is of practical importance not because we are interested in the magnitude of the insulation resistance, but rather because it may be an indication of the ability of the insulating materials to give adequate service. There are three principal applications of insulation-resistance measurements, namely:

1. Determination of quality (in new insulation before it is put into service).
2. Determination of trend in condition (in machines which are in normal service).
3. Determination of condition resulting from temporary effects (in machines subjected to the unusual effects of flood, live steam, excessive humidity, or periods of idleness).

This paper adds to the information available concerning the determination of quality in new machines of the types and sizes studied. It indicates clearly that there is work to be done before we shall have statistical information from which to judge the average magnitude of insulation resistance in acceptable new machines. Comparable studies of machines of other ratings and other designs as well as figures for machines in service also are needed. That these are being studied is indicated by the several other papers on related subjects presented at this meeting.

The authors are to be congratulated on their contribution.

H. C. Marcroft (Pennsylvania Water and Power Company, Baltimore, Md.): The additional data presented in this paper concerning electric-machine insulation have aided considerably the evaluation of resistance measurements on electric machinery in several respects:

First, wide variation in absolute resistance values was shown to exist for identical machines even when made at the same time of year. This suggests the authors' contention that simplification of the Wieseman formula could be made without impairing the over-all insulation standard for minimum allowable resistance. With the present state of the art, it appears possible to use the simpler formula for a working standard.

Resistance measurements were made in 1937 on 12 large water-wheel generators for comparison with the Wieseman formula. The generators were built between 1912 and 1925, had class-*B* insulation (except slot liners), and were well maintained. These generators were rated 10,000 to 15,000 kw, 13,000 volts, 100 rpm. The measured values of resistance at 75 degrees centigrade were between 5.7 and 28.8 times the minimum allowed by the Wieseman formula, using $K_s=0.10$. Machines of two large manufacturers were represented about equally in these measurements; the high and low values were fairly well divided between them.

Another group of six water-wheel generators, built since 1931, have insulation resistances of 8, 18, 35, 51, 55, and 62 megohms, measured at one-minute time and 75 degrees centigrade. The spread is believed to be caused by different coil-insulating techniques and materials, as these machines are all class *B* insulated with corona-preventive binding tape in the slot section. Machine rating is 31,100 kva, 13,200 volts, 109 rpm. For these machines, the Wieseman standard is 3.42 megohms at 75 degrees centigrade. The authors' proposed standard is 4.22 megohms. At 40 degrees centigrade, the measured resistance values are 125, 60, 120, 82, 82, and 82, respectively.

At room temperature, the resistance values are much higher, especially for the first two machines, which are much more sensitive to temperature. These data are taken from Figure 4 of the discusser's paper.[1]

These data confirm the findings of the authors concerning the large dispersion of resistance values. Of the machines tested, the region of lowest dispersion is at approximately 40 degrees centigrade, including machines of two manufacturers.

Secondly, the authors' contention that dielectric-absorption curves with time reflect the relative amount of moisture in the insulation with less dispersion than the absolute resistance values show agrees with our past experience on large water-wheel generators. We prefer to use dielectric absorption as a means of determining when large generators are dry. Our custom is to evaluate the absorption curve in terms of slope factor, which is defined as the ten-minute minus the one-minute resistance value divided by the one-minute value. The slope-factor values will be the same as the authors' value of R_{10}/R_1, if the latter value be decreased by unity. Figure 11 of their paper is interesting in showing a maximum value of R_{10}/R_1 between 4 and 5. This is confirmed in tests on operating generators in which top values of slope factor were in the range of three to four when dry, and at 60 degrees centigrade. The type of slot insulation influences this value. The authors show in Figures 8, 9, and 10 some very useful data for application to absorption testing. I should like to ask the authors, if the only difference between Figures 8 and 9 is that due to form-mica slot insulation in group 2 and wound mica tape in group 3, or are there also differences in varnish, coil size, winding dryness, temperature of insulation, and so forth? The answer to this should reveal if the R_{10}/R_1 ratio is sensitive to the mechanical assembly of the mica alone, while other factors remain unchanged.

Thirdly, the paper points out that simply designating insulation as class *A* or class *B*, though satisfactory as far as thermal considerations go, is not sufficient to fix resistivity values. More correlation of data relative to the effect of various binders and other reinforcing material on absorption characteristics is needed in order to fix narrower limits to resistance values of machine windings.

The authors' work in measurement of resistance values and analyzing the data has been a valuable contribution toward understanding insulation behavior.

REFERENCE

1. USE OF DIELECTRIC-ABSORPTION TESTS IN DRYING OUT LARGE GENERATORS, H. C. Marcroft. AIEE TRANSACTIONS, volume 64, 1945, February section, pages 56–60.

L. J. Berberich (Westinghouse Research Laboratories, East Pittsburgh, Pa.): The interpretation of insulation-resistance data taken on electric machines is difficult, because extremely large variations are possible even under the best conditions. The statistical analysis of the data on a relatively large number of machines made by Mr. Askey and Mr. Johnson brings some order out of the chaos.

Since, as is shown in the paper, variations as large as 20 to 1 are possible in identical machines, no great significance can be attached to any individual reading of insulation resistance. Any change in successive readings taken over a period of time may, however, be indicative of some change in the insulation.

Dielectric absorption is perhaps the least understood phenomenon in the whole field of insulation. Maxwell, many years ago, showed that a decreasing current with time in an insulating material can be attributed to inhomogeneity. He analyzed a two-layer dielectric and showed that, when the ratios of conductivity to dielectric constant of the materials in the two layers are not equal, dielectric absorption or a decreasing current with time is possible. This explanation appears to be correct for nonhomogeneous materials, such as generally are used for machine insulation. It is, however, questionable whether the Maxwell theory can be used to explain why dielectric absorption also takes place in relatively pure materials such as quartz. It appears that a molecular theory which goes beyond the Maxwell layer theory is necessary to explain all of the observed facts.

Dielectric-absorption tests, however, have proved to be very useful in detecting moisture and ionizable impurities in insulation. The charging current under direct current is made up of three components, namely:

(*a*). The current necessary to satisfy the instantaneous polarization of the dielectric, which has been called the geometric capacitance charging current.

(*b*). The current necessary to satisfy the polarizations requiring time to form, which has been called the reversible absorption current.

(*c*). The irreversible conduction current which is independent of time and is equal to the final constant current.

Moisture and ionizable impurities increase the conduction component and may, if sufficient ions be present, mask completely the absorption component. Thus, as moisture and ionic contaminants increase, not only is the level of the resistance–time lowered, but also the change of resistance with time becomes less. Leakage over the surface of the insulation caused by moisture or dirt will affect the resistance–time curve in a similar manner.

Attempts have been made to correlate insulation resistance with breakdown strength. There appears to be some degree of correlation in the case of very wet insulation. However, in moderately dry to very dry insulation there is no apparent relationship between insulation resistance and breakdown strength. Perhaps insulation-resistance tests made at higher voltages will provide more information regarding the condition of the insulation. Only a little work has been done at higher voltages, and much more must be done to determine the possibilities in that direction.

J. S. Johnson: The insulation-resistance measurements of all machines were expressed as a resistivity per inch megohm inch of insulation to put all machines studied on a comparable basis. This is necessary, since there are relatively few large machines of identical design. As indicated in the paper, however, groups 2 and 3 both represent data on a large number of identical machines. In answer to Mr. Marcroft's question, the treatment of both groups of machines was the same. Perhaps the significant difference between the two insulations, as far as the slope of the absorption curve is concerned, is the different mica reinforcing material.

The sheet-form mica wrappers used on machines of group 2 had a fibre-glass cloth-backing material, and the continuous mica tape on machines of group 3 had a cambric-backing material.

Usually insulation resistance–time curves on wound machines are not continued beyond 10 or 15 minutes, because, with the exception of extremely dry machines, the insulation-resistance curve is usually substantially flat after these times.

Another practical limitation is that, when the insulation resistance is very high and changes slowly with time, small fluctuations in line voltage affect the indication of available electronic instruments more than the resistance change in the insulation. Some long-time measurements have been made on insulation coils as shown in Figure 1 of the paper.

The Application of Silicone Resins to Insulation for Electric Machinery

Discussion and authors' closure of paper 45-23 by J. DeKiep, L. R. Hill, and G. L. Moses, presented at the AIEE winter technical meeting, New York, N. Y., January 22–26, 1945, and published in AIEE TRANSACTIONS, 1945, March section, pages 94–8.

Herman Halperin (Commonwealth Edison Company, Chicago, Ill.): It has been my good fortune to follow for a few years developments that led to the achievements accounted in these papers. When I first heard of a silicone resin, its cost was $75 a pound, or a few hundred times the cost of ordinary insulating varnishes or insulating oils. Now, I understand, the cost is down to about three dollars a pound.

With the present cost for silicones, it seems that the cost of a motor of a given output rating is considerably above the cost of a motor with class *A* insulation. It would, therefore, seem that the application of silicones to motors for factories and electric generating stations, for example, would be limited, because in almost all cases nowadays it is feasible to limit the ambient temperatures. There are some cases where the high "moisture-proofness" of a silicone-resin finish on the coil insulation may be of interest.

The use of silicones for some transformer applications may become very attractive, especially in those instances where a high ratio of emergency load rating to normal load rating (or to normal actual loading) is desired. One example of this situation would be some locations in an a-c network system.

Perhaps further reductions in cost of silicones will occur just as steadily occurred over the past decade for another synthetic material, namely, neoprene.

A. F. Lukens (General Electric Company, Lynn, Mass.): The authors have given some of the properties of this very interesting and useful new material, and detailed some of their experimental results. Investigation by the motor divisions of the General Electric Company has followed and is following along the same general lines. Silicones, as a class of material, possess the startling characteristic of a much greater heat endurance than any physically similar material previously used for insulation. The question is how best to use this new property.

Anything new first may be oversold or overapplied by the enthusiasts and then fail on some of its jobs, not because of any fault of the new thing, but because it was unsuited in the first place. However, during this shakedown stage, the whole project may receive such a "black eye" that it is delayed or discarded. Therefore, I would like to point out some pitfalls of high winding temperature, so that overenthusiasm may not harm this very useful program.

One of the first things that comes to mind when high temperature is mentioned is the chance to reduce total machine weight. However, higher temperature usually means lower efficiency and the extra cost of energy to care for the lower efficiency or the weight of the prime mover fuel, if it floats or flies, must be capitalized and considered in striking the final economic balance of the benefits gained by the higher temperature. As an example, to break even in total weight carried by a ship (fuel, generating equipment, and so forth) a continuously running motor must save seven pounds for every point of efficiency per horsepower dropped.

High temperature also means temperature creep. This may be defined, at least roughly, as a temperature rise on increased load that is much greater, and perhaps out of all proportion, to the increase in load. This means that a machine with an inherently high rise will have a much shorter life on overload as compared with a conventional-rise machine, provided each has the same life at nominal load. Motor engineers are accustomed to think of a 40-degree motor on 115-per-cent load as having about 50-degree rise or a 10-degree differential and about one-half the insulation life, since insulation life is halved for each 10-degree increase in temperature. On the same basis, a 135-degree-rise motor on 115-per-cent load will have a rise of 188 degrees or a difference of 50 degrees and a life of $^1/_{30}$ of the life on full load. Perhaps the comparison of $^1/_2$ and $^1/_{30}$ is too pessimistic, but the tendency is present.

Higher winding temperatures mean greater thermal expansions and, what is possibly more important, greater differential expansions during starting and coming up to temperature. Mechanical parts must have clearance enough to care for these increased expansions, or strength enough to withstand the stresses if the expansion is "locked in."

Bearing lubricants must keep pace with winding temperature if a practicable machine is to be built, since the bearing temperature of a small machine of conventional design is influenced to a great extent by winding temperature. In addition, it should be remembered that the permissible operating temperature of some conventional bearing materials is surprisingly close to the present operating temperatures. Tin-base babbit melts at approximately 240 degrees centigrade and ball bearings begin to anneal at about 150 degrees centigrade.

Although, as the sage has it, "all is not gold that glitters," gold does glitter and silicone insulation does have many possible profitable applications. Obvious examples are where space and weight are important and energy is cheap; where high ambient temperatures are encountered and proper precautions can be taken with the bearings; where a hot spot exists in a machine that is detrimental to insulation life, but is not large enough in extent to materially affect efficiency; and a myriad of others that will appear as experience is gained.

V. M. Montsinger (General Electric Company, Pittsfield, Mass.): While I am not a motor engineer, I would like to discuss the general subject of the use of the new high-temperature materials such as glass, asbestos, and so forth, impregnated either with phenolic or silicone varnishes for dry-type transformers, which have some problems in common with those of rotating machinery.

The authors have presented some interesting data on how these silicones compare with the high-temperature phenolic varnishes under aging tests, and have made what appears to be a reasonable suggestion of setting a temperature limit of 175 degrees centigrade for the silicones in motors which compares with 130-degree-centigrade limit for class-*B* insulation in AIEE Standard 1.

The authors' suggestion that high-temperature silicone material be restricted to a few specific applications lines up with the transformer situation. According to the best information available, it has not been possible to use silicone varnish in commercial dry-type transformers. For the time being, at least, the transformer industry must depend on the best high-temperature phenolic varnishes available.

Until positive proof is submitted to justify increasing the temperature limit above 130 degrees centigrade for high-temperature insulations impregnated with the best-known grades of phenolic resins, it seems quite certain that the transformer industry is not yet in a position to take full advantage of the new materials like glass tape and asbestos. It is from this standpoint that I wish to discuss the general question of high-temperature insulation and to present some additional aging data on phenolic varnish.

The authors give some interesting comparative data on the effect of 250 degrees centigrade on a good phenolic alkyd organic varnish and silicone varnish. They state that at 250 degrees centigrade the phenolic varnish was affected seriously after two hours, and completely deteriorated at the end of 20 hours, whereas the silicone had undergone no observable change. Also, at 200 degrees centigrade the phenolic organic varnish lasted about two hours before failure at 14-per-cent elongation. I assume that the phenolic varnish used for these tests was selected as being representative of a good type of high-temperature organic varnish for impregnating high-temperature insulating materials.

The results of some aging tests, made at Pittsfield over a period of approximately 15 months at 175 degrees centigrade, are shown in Table I.

These tests were made on strips of inorganic turn insulation material impregnated with one of the best phenolic organic varnishes; consequently, the deterioration (in tensile strength) was caused by the weakening of the varnish film and not by weakening of the structure of the base material. In fact, this was proved by aging some of the untreated material in parallel with the treated material.

Table I indicates that if such an insulation is expected to keep its film intact for 20 to 25, or 30 years, the temperature limit must be well below 175 degrees centigrade.

If we assume that 28 per cent of the initial strength (at the end of 15 months) represents the end of its useful life, then, by the ten-degree rule, the life at 130 degrees centigrade would be:

175 degrees centigrade—15 months
165 degrees centigrade—30 months
155 degrees centigrade—60 months
145 degrees centigrade—120 months
135 degrees centigrade—240 months (20 years)
130 degrees centigrade—approximately 30 years

All of the aforementioned tests at 250, 200, and 175 degrees centigrade indicate that the temperature limit for any kind of varnish other than silicone should not be radically different from the present AIEE value of 130 degrees centigrade continuous temperature.

Operating experience reported by W. W. Satterlee[1] where dry-type transformers operated successfully for limited periods of time at temperatures well above 130 degrees centigrade, indicated that a continuous limiting temperature might be supplemented by permitting higher temperatures for short-time loads similar to those used in transformers with class *A* insulation.

Table I. Aging of Insulation at 175 Degrees Centigrade

Date	Tensile Strength in Per Cent of Initial Strength
7/21/43	100 (start)
8/30/43	95.7
11/16/43	74.3
4/ 7/44	63.3
7/ 4/44	33.0
10/17/44	28.0

REFERENCE

1. DESIGN AND OPERATING CHARACTERISTICS OF MODERN DRY-TYPE AIR-COOLED TRANSFORMERS, W. W. Satterlee. AIEE TRANSACTIONS, volume 63, 1944, October section, pages 701–04.

John L. Fuller (Reliance Electric and Engineering Company, Cleveland, Ohio): The recommendation of the authors to establish at once a designation for silicone-type insulation and their selection of 175 degrees centigrade as a tentative limiting hot-spot temperature are endorsed. The temperature limit appears to be a sufficient increase over class *B* to be worthwhile to motor designers, and at the same time appears to be adequately conservative in the light of tests.

It is thought worthwhile to emphasize the excellent results obtained on the first motor tested which had silicone only in the form of the impregnant. This appears to be doubly important since considerable difficulty has been experienced in winding motors with glass wire bonded with silicone resin. Lack of abrasion resistance and presence of stickiness have been the primary causes. The excellent result with the silicone varnish only was corroborated by tests on a $1^1/_2$-horsepower motor similarly insulated. This motor was run 4,300 hours at 200 degrees centigrade as measured by resistance followed by 1,900 hours at 175 degrees centigrade, all on reversing service without noticeable deterioration of the insulation except for the bakelized canvas slot wedges. Insulation resistance and appearance, as well as coil tightness, showed no noticeable trends during this test, which was terminated by bearing failure and resultant stator destruction. These results make it worthwhile to consider the use of silicone varnishes on motors otherwise wound as class *B* motors in the interests of much greater protection than that afforded by the organic resins and less cost and complication than required for full silicone insulation. This might be considered a separate insulation class.

In addition to the afore-mentioned test, several other silicone-insulated motors have been put in service with no difficulties reported except for the one recorded here. A 30-horsepower 1,750-rpm motor was built in a 15-horsepower fan-cooled frame. This motor has run approximately 10,000 hours on a continuous-duty industrial job at about 175 degrees centigrade with no insulation or bearing troubles, bearing temperatures being kept below 105 degrees centigrade by the action of the fan. Lead balancing rivets were softened and thrown from the rotor and the connecting leads became short-circuited where they entered the motor; but with these repairs, the test is continuing satisfactorily. Silicone-rubber lead cable now gives the hope of a very practical solution to the lead-cable problem. It may be pointed out here, in connection with bearing troubles, that continuous running fan-cooled or open motors may have little or no difficulty with bearings while fully enclosed motors may have bearing temperatures approaching those of the windings, unless special precautions in design are taken. Where high winding temperatures are reached only infrequently, the bearing problem diminishes.

With regard to materials to be used, it is found that glass-base melamine laminate, though quite difficult to handle, appears to be a good match for silicone and, hence, useful as slot wedges. Thermosetting silicone varnishes have been much less satisfactory than the thermoplastic versions, and, consequently, the art has advanced more slowly on d-c than on a-c motors.

Two excellent applications for silicone-insulated motors should be pointed out. Excellent results can be obtained with a motor designed to be efficient and to run at class *A* or class *B* temperatures for normal operation, but where it is known that occasional severe overloads will be imposed for long enough periods to cause damage to class *B* insulation. Here silicone gives the reliability while retaining efficient operation at normal loads.

Where number of reversals obtainable with a given application is limited in large measure by the inertia of the rotor itself, silicone can be helpful by permitting the use of a smaller motor with lower inertia without lowering the over-all capacity of the motor within safe temperatures.

J. G. Noest (Consolidated Edison Company of New York, Inc., New York, N. Y.): At the outset I should like to point out that this discussion represents the viewpoint of an operating engineer who, for the last 20 years, has been connected intimately with the operation and maintenance of electric motors as used for auxiliary drives in large generating stations, and who, for the last few years, has been associated with the engineering groups responsible for the planning of central-station construction.

It is my belief that, had those in positions similar to mine simultaneously read the paper which I am discussing, the resulting whisper of relief could have been heard throughout the nation. Through this paper we are encouraged to look forward to a motor insulation, not only capable of withstanding considerably higher temperatures but, in addition, being capable of withstanding moisture. Not only are we promised a motor insulation that can withstand higher temperatures but, to go with it, a lubricant for the motor bearings which will retain suitable viscosity and resist sludging at the corresponding higher temperature.

Within the last few years a considerable number of utilities have installed topping turbogenerators supplied by large high-pressure boilers. In a good number of cases the auxiliary drives were electric. Most of these installations are operated as base-load plants, which means that the auxiliary drives operate at maximum loads practically continuously. Frequently, in spite of careful consideration beforehand, it turns out that the location of the driving motors gives ambient temperatures in excess of those anticipated, so that these auxiliary motors are operated in ambient temperatures of as high as 55 and 60 degrees centigrade. Moreover, the seasonal temperature variations do not, in general, penetrate into the plant, so that these high ambient temperatures are continuous throughout the year. Under these conditions of high load and high ambient temperature, checking of the insulating varnish, which is supposed to protect against moisture, takes place rapidly. During the last year one of these plants has experienced three cases of boiler-tube failure. In each case one of the 600-horsepower induced-draft fan motors failed within two minutes of the boiler-tube failure because of the absorption of water vapor condensed from the leaking steam. It was fortunate that the failure of one motor opened the load feeder, de-energizing the remaining motors in the affected area, since all motors in that area, shortly after the boiler-tube failure, were found to have very low insulation resistance.

Because of these experiences, and with the hope of reducing the cost of motor maintenance, we have swung recently to the use of totally enclosed fan-cooled motors wound with class *B* insulation for operation in 50-degree centigrade ambient air. Here we see a major application of silicone insulation with the hope that the differential in cost for the totally enclosed fan-cooled motor over the open or drip-proof frame motor will be reduced at the same time that reliability of such motors is increased. For the type of motor application with which we are concerned, increased reliability and freedom from trouble is of greater concern than first cost. To substantiate this last statement, let me point out that in some of these applications the loss of a motor represents a loss in station capacity of as much as 100,000 kw.

We also anticipate that the existing motor design of the totally enclosed fan-cooled enclosure type will be extended to the larger sizes of single-speed and multispeed motors for which this design is not available now. In these sizes the presently available enclosed forced ventilated motor and the enclosed motor with integral air–water heat exchanger is not a complete solution. The first design, for use in central stations, requires air filters, because of the coal-dust and fly-ash problem, with resulting high initial cost as well as constant high maintenance. The second involves high cost due to water piping and pumping facilities and, in addition, it presents the ever present possibility of water leaks within the motor enclosure.

Another point I should like to make is that the development of high-temperature silicone insulation undoubtedly will lead the manufacturing industry to survey their designs for the purpose of utilizing the capabilities of this insulation. This will present an opportunity to incorporate in the new designs other improvements for the purpose of reducing motor-maintenance costs. To illustrate the need for such improvements, I cite the result of a study of motor failures covering a period of five years. This survey covers only motors larger than 50 horsepower used as auxiliary drives in large power plants. This study divided the cause of motor failures into six responsibility groups:

1. *Design.* All failures where design features in the motors are a primary cause of failure. Number of failures.......................... 35

2. *Insulation.* All failures of motor-coil insulation to which no other major contributing cause could be found. Number of failures..... 50

3. *External Conditions.* All failures caused by factors external to the motor, such as flooding, salt-water exposure, or dust. Number of failures.................................... 35

4. *Workmanship.* Failures primarily attributable to poor workmanship of either the manufacturer or the agencies who have done major repairs at a previous date. Number of failures.................................... 22

5. *Maintenance.* All failures in which deficiencies in maintenance are a primary factor. Number of failures.......................... 22

6. *Unknown.* Those failures for which sufficient information is not available. Number of failures.................................... 24

188

It should be noted that, of the total number of 188 cases of motor failures investigated, 35 definitely were laid at the door of the motor manufacturer. In addition, an uncertain number of the 22 cases which are classed under "*Workmanship*" belong also at the manufacturers' doorsteps. A large contribution to this type of failure was insufficient mechanical strength built into the coil supports in the motor. A second large contributing factor was oil leakage from bearings into the motor windings.

Two other factors are of special interest: first, that the rate of motor failure increases with the size of the motor; and second, that the experience with antifriction bearings in motor sizes of over 50 horsepower and over 1,200 rpm generally has been disappointing. In regard to the first statement, it was found that in a group of 32-, 600-, and 1,000-horsepower motors, 26 failures that necessitated rewinding occurred within ten years. In these cases, overloading was not involved and high ambient temperature, while it existed, could not be held responsible. All failures were due to either of two causes: incorrect design, and abrasion of winding insulation by dust-laden atmosphere.

In regard to antifriction bearings, our experience in the larger motor sizes has been so bad that in sizes over 50 horsepower we avoid the use of that type of bearing whenever possible. The difficulty with antifriction bearings is twofold: oil or grease leaking into the motor windings, and the difficulty of replacing an antifriction bearing in the usual power plant atmosphere without contamination by coal dust and airborne grit.

It is my opinion that the manufacturers should prepare for the coming opportunity by having their contact men ask, not general, but pointed questions of the utility-plant operators to accumulate data for utilization in design improvements. Questionnaires are a nuisance to busy plant operators and are, therefore, not likely to produce the desired information. In closing, I should like to ask two questions:

(*a*). What is the abrasion resistance of silicone varnishes as compared to the best type of previously existing varnish?

(*b*). Are cured silicone varnishes soluble in silicone lubricants?

J. DeKiep, L. R. Hill, and G. L. Moses: It must be recognized that silicones are a broad class of materials and individual compounds in this class differ widely. The silicone resins referred to by the authors are Dow Corning number 990-*A* and number 993 varnishes. These resins were selected because of their relatively superior physical properties as compared to other silicone resins commonly available. When properly processed they possess suitable properties for shop use which is not true of some silicone resins. Their oil resistance and solvent resistance is acceptable for many applications, though they are not as good in this respect as certain organic resins. Varnish number 993 passes the American Society of Testing Materials' oil-resistance test. Heat stability of both number 990-*A* and number 993 varnishes is good, but not as high as some of the other silicone varnishes which have poorer mechanical properties and low resistance to oil and solvents.

Mr. Fuller's comments on poor abrasion resistance and presence of stickiness do not indicate which silicone resin was used nor the degree of processing. It has been found possible to overcome both these difficulties with number 990-*A* and number 993 silicone varnishes by proper processing.

The authors heartily concur with Mr. Lukens' comments that high-temperature insulation should not be "oversold." As indicated in the body of our paper, each application of silicone insulation should be analyzed and the advantages and possible disadvantages evaluated.

Mr. Noest suggests several possibilities which would justify the serious consideration of silicone insulation. Increased reliability of operation of an essential part of a complex system is, of course, difficult to evaluate, but in an emergency may be worth a great deal, as he indicates.

The test data on silicone materials and silicone machines presented in our paper are believed to represent reasonably good practice and to be valid as far as they go. The specific comments concerning materials and machines cannot be analyzed critically in the light of our present experience. As more silicone materials and machines are used we gradually will acquire experience which will answer some of the more critical points voiced by the various comments.

Field Tests and Performance of Heavy-Duty High-Speed 138-Kv Circuit Breakers—Oil and Air-Blast (45-43)

A Three-Cycle 3,500-Megavolt-Ampere Air-Blast Circuit Breaker for 138,000-Volt Service (45-44)

A High-Capacity High-Voltage Three-Cycle Oil Circuit Breaker (45-45)

The Next Step in Interrupting Capacity—5,000,000 Kva (45-46)

Discussion and authors' closures of papers presented at the AIEE winter technical meeting, New York, N. Y., January 22–26, 1945, and published as follows in AIEE TRANSACTIONS, 1945:

45-43 by Philip Sporn and Harry P. St. Clair, pages 401–10.

45-44 by H. L. Byrd and Ben S. Beall III, May section, pages 229–32.

45-45 by H. L. Byrd and E. B. Rietz, April section, pages 160–63.

45-46 by A. W. Hill and W. M. Leeds, June section, pages 317–23.

John G. Holm (Boston Port of Embarkation, Boston, Mass.): The very interesting paper by Mr. Sporn and Mr. St. Clair describes the performance of devices in the development of which the public-utility engineers and the manufacturer's development engineers participated, the latter probably to a greater extent. In this case it was the demand that determined the supply. And, since in the case of the high-voltage circuit breakers the tendency with each new development has been to ask for circuit breakers which are able to reclose in a shorter time and interrupt larger kilovolt-ampere magnitudes, it is natural to consider how far in these directions will go the demand which the manufacturers are expected to satisfy.

The speed of operation of a circuit breaker has to satisfy certain requirements which may be grouped as internal and external. To satisfy the internal requirements the circuit breaker will have to trip, open, and deionize in the minimum possible time. The higher the operating voltage, the more time has to be allotted for the deionization, so that the internal requirements will impose a certain minimum time. The tests have shown that for 138-kv circuit breakers the minimum time, at this stage of development, is about 12.5 cycles (on 60-cycle basis) for the air-blast type. Present indications are that it might be possible to shorten this time still further. The external requirements which the speed of the circuit breaker must satisfy are imposed by the condition of system stability and by the operational requirements of the load. The reclosing speed of 13 to 15 cycles is sufficient to prevent the machines from drifting dangerously apart from synchronism; it is satisfactory insofar as the operation of steel furnaces and radiobroadcasting are concerned, and it causes no insurmountable difficulties with certain synchronous-motor loads. From all these considerations, therefore, a 12.5-cycle circuit breaker is satisfactory, and there is little justification for requiring speeds much below the 12 cycles which have been practically attained.

On the subject of the circuit-breaker interrupting capacity there seems to be a general agreement that 5,000 megavolt-amperes are attainable, and some engineers think that, if necessary, this figure may be appreciably exceeded. If this is so, should here again the goal be for bigger and bigger units? The demand for larger interrupting capacities comes from two directions: from the integration of systems into more extensive units and from adding additional loads. Should these two tendencies be encouraged, or should they be resisted, and to what extent? The answer to this is of an economic nature. There unquestionably exists a size of any system, or of its particular parts, beyond which the expansion becomes uneconomical. It is to be regretted that it is seldom known where this limit is, for it is rarely, if ever, that studies of this type have been made for an interconnected system as a whole. The large size by itself is no solution. On the contrary, the size often has been the reason for the extinction of the species—from whatever domain one chooses to select examples for substantiation of this statement. Therefore the requirement for steadily increased interrupting capacity of circuit breakers should be determined by considerations of capacities that may be interrupted economically within a system of the most economical size, rather than be set by possibilities of developing larger and larger circuit breakers. This latter will lead ultimately to tremendous load concentrations and to systems expanded beyond their economic usefulness.

Whatever be said of the tendencies for defining desirable characteristics of circuit breakers, the tests have shown that the air-blast type is eminently more suitable for attaining shorter reclosing times and for interrupting larger kilovolt-ampere capacities. If we will adopt operating voltages of 345 kv in the United States, the statement in favor of air-blast circuit breakers will be more pronounced. Still one may say that, should the electric utilities require circuit breakers with interrupting capacities of the order of, let us say, 10,000 or 15,000 megavolt-amperes, it well may be that a start on the path of exploration of other, yet untried, methods of high-power circuit interruption is indicated. As the rockets in this war successfully have put an end to the development of heavier and heavier caliber guns, so also new types of circuit-opening devices may bring an all-around better solution to this problem. In the face of so many successful engineering developments, there is no reason to believe that this undertaking cannot be accomplished also.

What impresses most in this paper is the fact that the tests of the powerful circuit breakers were executed in actual operation on a large interconnected system and that they evidently came out without the slightest mishap or difficulty to the system. The preparation for these tests unquestionably involved a great deal of detailed planning, considerable load rearrangements, and a careful execution of the entire procedure. For this the authors of the paper and their colleagues deserve a great deal of praise and credit. The planning of the tests and the changes in the system load involved in it, so briefly described by the authors, well could form a subject for a separate valuable paper.

In connection with the test results shown by the air-blast circuit breaker, it perhaps might be of interest to refer to a meeting of one of the AIEE Sections held a couple of years prior to the beginning of the current war in Europe. At this meeting the speaker, a circuit-breaker development engineer, who just had returned from a European tour of electric-equipment manufacturing companies, made a statement that the Swiss never would have developed this, as he said, very much inferior air-blast type of circuit breaker, had they not been forced by the difficulties experienced in connection with importing special oils. The speaker made a prediction that, because of oil abundance in the United States and in view of the oil circuit breaker having all the advantages over the other type, the air-blast circuit breaker never would be accepted in the United States, and was not even worth a trial. This engineer is now in important charge on circuit-breaker developments with one of the leading companies.

What has been said on frequent occasions before seems again to be true, namely, that the majority of great engineering ideas originate in Europe; that they then are taken to the United States and developed to an extent undreamed of in Europe.

M. H. Hobbs (Westinghouse Electric and Manufacturing Company, East Pittsburgh, Pa.): Following presentation by Mr. Sporn and Mr. St. Clair of this excellent paper on field tests of high-voltage oil and air-blast circuit breakers, together with related papers, 45-44, 45-45, 45-46, which have been presented this year and others which have been presented in the past two or three years[1,2] (also reference 2 of B. P. Baker discussion), it seems desirable to pause and look ahead to see what the future trend appears to be.

It is absolutely essential that we as manufacturers do this, as it determines our future development program and its cost. Also, operating engineers may be somewhat confused about what to expect and would like to know what is to be available in the near future.

The papers have shown that it is possible to produce circuit breakers of either the oil or the air-blast type which will give high speed of arc interruption and high-speed reclosing, at least on a relatively limited number of tests.

On the other hand, the ability to produce a device does not mean that it is at present economically desirable to do so.

The total number of high-voltage outdoor circuit breakers which are manufactured and sold is somewhat limited, and it is questionable whether the development of parallel lines for the same application can be justified. So far, the design and development of the outdoor air-blast circuit breaker has been on an experimental basis as outlined by the Triple Joint Committee, comprising members from the operators' organizations (Edison Electric Institute and Association of Edison Illuminating Companies), the manufacturers (National Electrical Manufacturers Association), co-operating with the American Standards Association and the AIEE. The program was outlined early in 1941 as follows:

> "It is the judgment of the utility members of the Joint Committee that the time is not yet ripe for the commercial development of the lines of outdoor oilless or oil-poor circuit breakers. However, if the manufacturers feel that outdoor oilless or oil-poor circuit breakers show promise of being commercially attractive in the future, the Joint Committee is agreeable to a field trial of a limited number of ratings."

At that time a limited number of ratings were agreed upon, as a framework to guide the scope of the development. It is interesting to note that no higher than 2,500,000-kva ratings were included in this table. The program was laid out to cover all oilless breakers, including air-blast, oil-poor, and so on. Recent development has been limited largely to the air-blast type, which has seemed to offer the most promise, and several ratings including 34.5, 69, and 138 kv have been produced by several manufacturers.

The economic situation in regard to electric equipment undoubtedly will be more critical after the war than it has been in the past, and it will be essential that the manufacturers and operators co-operate to the fullest extent to prevent costs from rising. Several committees at the present time are working on standardization programs, including one set up by EEI on metal-clad switchgear. Results of value both to the users and manufacturers should be obtained.

Specifically, as to a comparison of the two circuit-breaker designs, oil and air-blast, in all designs so far proposed, including those which have been described before the AIEE, it is quite evident, even from a visual inspection, that the present air-blast designs will cost materially more than the dead-tank oil circuit breaker. There are several reasons for this, and the situation is quite different from that on the indoor air-blast circuit breakers. First is the insulation problem, involving as it does large porcelain columns and post insulators. Second is the relatively complicated mechanism required for the air-blast circuit breaker, particularly for quick reclosing, partly due to the operation of the isolating switch, whether this is internal or external. Third is the weatherproofing, which becomes a real problem on circuit breakers of this type. Fourth is the relative difficulty of providing for potential and current transformers. There is no thought here of saying that these problems are unsurmountable, but simply that we should be realistic and admit they have not been solved satisfactorily up to the present time in existing designs.

Present oil-circuit-breaker designs are entirely different from those produced only a few years ago. The new low-oil-content dead-tank oil circuit breaker has shown itself to be not only highly satisfactory from an operation standpoint, both as to interrupting and reclosing, but also to be relatively simple and convenient to manufacture and service in the field. It is suitable for either five- or three-cycle interruption and exceedingly fast reclosing, as we have seen from the oscillograms. The matter of oil handling in all except the most isolated locations should not prove to be a serious problem.

It is always hazardous to make long-range predictions in our industry, and no attempt is made here to do so. I am simply presuming to state the picture as it appears to us in January 1945. The development work which has been done now and the limited amount of field experience which has been obtained on air-blast circuit breakers have been very valuable to both manufacturers and users, and this should be continued, because it is only in this way that we learn. At the present time there seems no necessity for changing the program outlined by the Triple Joint Committee, which the committee has reaffirmed several times since it was set up in 1941, that commercial development and design work still should continue along the lines of the conventional dead-tank oil circuit breaker.

REFERENCES

1. A MULTIORIFICE INTERRUPTER FOR HIGH-VOLTAGE OIL CIRCUIT BREAKERS, L. R. Ludwig, W. M. Leeds. AIEE TRANSACTIONS, volume 62, 1943, March section, pages 119–25.

2. HIGH-VOLTAGE OIL CIRCUIT BREAKERS FOR RAPID-RECLOSING DUTY, A. W. Hill, W. M. Leeds. AIEE TRANSACTIONS, volume 63, 1944, March section, pages 113–18.

B. P. Baker (Westinghouse Electric and Manufacturing Company, East Pittsburgh, Pa.): When one reviews the work which has been done in the United States on outdoor high-voltage circuit breakers during the last four or five years, it is interesting and perhaps encouraging to note the general trend in design.

The oil circuit breakers discussed in the paper by Mr. Sporn and Mr. St. Clair and in papers 45-45 and 45-46 possess the same general features, give results which are comparable, and their conclusion regarding future possibilities are quite compatible.

When one compares this compressed-air circuit breaker with previous designs as shown in AIEE papers,[1,2,3] one must feel that some of our concepts and designs are pulling together. The elimination of fibrous insulation to ground in favor of all porcelain seems a good move, even though it has necessitated an awkward looking, propped-up structure. This propping-up idea is almost certain to become more important at higher voltages. The use of interrupting elements which approach the orifice construction seems to be an improvement over previous designs, at least it is consistent with results obtained in the Westinghouse laboratory, which were published in 1941.[1] Also, the shifting of the two interrupting elements to the same column and the use of a single isolating gap may prove to be more desirable. It is unfortunate that in practically every high-voltage compressed-air circuit-breaker design so far proposed the current transformers and potential devices have to be so costly, and, therefore, it is nice to see some structural use made of the current transformer in this design.

In spite of these improvements and the test results which appear to be quite remarkable, and in many respects are, I am sure the authors are inclined to regard this circuit breaker as still in the development stages. With this in mind, it seems pertinent to offer to the AIEE at least a review of additional available data.

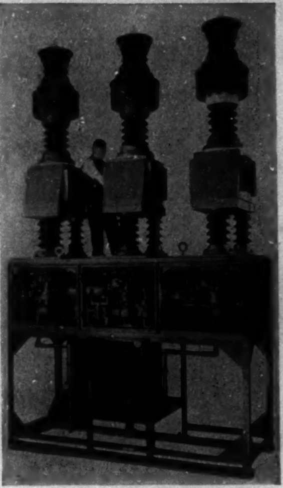

Figure 1. 34$^1/_2$-kv 1,000,000-kva compressed-air circuit breaker

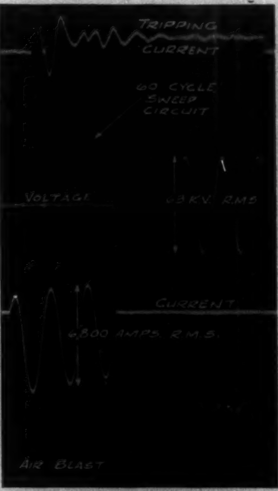

Figure 2. Oscillogram of 6,800 amperes being interrupted at 66 kv in 2.3 cycles

Figure 3 of reference 2 shows a 138-kv 1,500,000-kva compressed-air circuit breaker which has been in service on the West Penn Power Company system since August 1942. This circuit breaker has given a splendid account of itself electrically. However, there have been some mechanical troubles, and this circuit breaker may require some propping up. Before shipping this circuit breaker a single-pole unit was tested at 132-kv up to 6,600 amperes. Figure 3 of reference 1 is an oscillogram showing the interruption of 8,900 amperes at 132 kv on a circuit with a rate of rise of 2,970 volts per microsecond. This is the three-phase equivalent of 3,500,000 kva for 230-kv service.

Since then circuit breakers for 66- and $34^{1}/_{2}$-kv service have been developed, which are simplified considerably by utilizing an internal isolating switch. Figure 1 of this discussion shows a $34^{1}/_{2}$-kv compressed-air circuit breaker for 1,000,000-kva service. The interrupter consists of a single orifice located between the two upper porcelains. The moving contact first draws the arc through the orifice where interruption is obtained, after which it moves into the second porcelain where the isolating gap is formed.

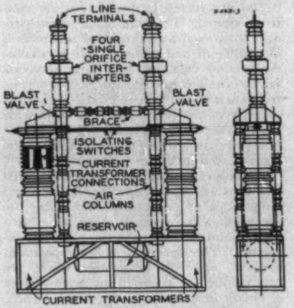

Figure 3. Single-pole unit of 3,500,000-kva 230-kv high-speed compressed-air circuit breaker

A single-pole unit of this circuit breaker has been tested successfully at 66 kv up to 13,400 amperes on a circuit with a recovery rate of 2,700 volts per microsecond, and at 44 kv up to 19,100 amperes at 1,800 volts per microsecond. The first test approaches 3,000,000 kva, three-phase equivalent for 138-kv service. The voltage is somewhat low; however, the circuit is exceptionally fast.

Considerable work has been done on the various elements for higher-voltage high-speed compressed-air circuit breakers. A high-speed blast valve was developed, which produced an 11-square-inch opening against 350-pounds-per-square-inch pressure in 1.1 cycles. This valve, in conjunction with a high-speed single-orifice interruption unit, was tested up to 6,800 amperes at 66 kv 300 pounds per square inch, 1,800 volts per microsecond, giving a circuit breaker time of 2.3 cycles. Figure 3 of this discussion shows the oscillogram of this operation. At 3,000 amperes 66 kv 2-cycle interruption was obtained.

A similar interrupting element, but with a slower-speed blast valve has interrupted 18,700 amperes at 66 kv 2,700 volts per microsecond giving a circuit breaker time of 3.8 cycles.

For 138 and 161 kv one of these units, consisting of two orifices and one blast valve, would be used. Double this, as shown in Figure 3 of this discussion, would be used for 230 kv. By allowing the difference between 4×66 kv and 230 kv for malvoltage division, three-phase power of 7,000,000 kva at 230 kv does not seem impossible even on a fast circuit. However, these test results do represent the high spots in interrupting performance obtained at our laboratory and are not meant to convey the impression that such quality results may be obtained consistently on the high rate of rise circuits.

The orifice or longitudinal-flow type of compressed-air interrupter is very sensitive to the combination of large current, high instantaneous values of restored voltage, and high rate of rise of restored voltage. These factors render such interrupters erratic and inconsistent. However, it has been demonstrated that, if the rate of rise is reduced from 3,200 volts per microsecond to 1,700 volts per microsecond at 132 kv, very consistent performance is obtained from 240 amperes to 7,500 amperes. Also, at 66 kv where the maximum rate of rise was reduced from 2,700 to 1,370, consistent operation was obtained from 500 amperes to 16,300 amperes.

In both sets of tests the maximum arcing time did not exceed 1.2 cycles.

One would, therefore, predict the excellent performance and uniform arcing time obtained on the field tests reported. In closing I would like to raise a question for consideration: Since the higher values of kilovolt-amperes are not generally obtainable on service circuits without a large connected network in which high recovery-voltage rates are not encountered, is it permissible when testing in a high-power laboratory to modify the circuit to obtain recovery-voltage rates equivalent to those which may be encountered in service?

References

1. A Vertical-Flow Outdoor Compressed-Air Breaker, L. R. Ludwig, B. P. Baker. AIEE Transactions, volume 60, 1941, May section, pages 217–22.

2. A Vertical-Flow Compressed-Air Circuit Breaker and Its Application on a 132-Kv Power System, H. A. P. Langstaff, B. P. Baker. AIEE Transactions, volume 62, 1943, April section, pages 188–92.

3. Field Tests and Performance of a High-Speed 138-Kv Air-Blast Circuit Breaker, H. E. Strang, Philip Sporn. AIEE Transactions, volume 6, 1942, January section, pages 1–6.

H. W. Haberl (Quebec Hydro-Electric Commission, Montreal, Quebec, Canada): The interrupting tests recorded by this paper at substantially higher values than heretofore reported are, of course, important and of general interest. There are, however, certain points which do not seem to be quite clear.

In paper 45-44 the authors state that the contacts part in approximately $1^{1}/_{2}$ cycles and reach the end of the restriction in approximtely $2^{1}/_{4}$ cycles and that interruption occurs at the subsequent current zero. Some of the tests, however, seem to show that the current was not interrupted at the "subsequent current zero" but continued until the second current zero. It is somewhat surprising that an air-blast circuit breaker of this importance would not have a shorter duration of arcing. The arcing time shown on the oscillograms appears to vary from 0.9 cycle to 1.35 cycles, in the latter case the interruption did not take place until the third current zero after parting of contacts. From an examination of Figures 2 and 3 of the paper it would appear that the parting of the contacts takes place at zero velocity of moving contact, which naturally would account for the relatively short time of contact parting and also for the relatively long duration of the arc.

Figures 3 and 4 also indicate a relatively indirect or tortuous path of the compressed air in reaching the contacts and the piston which moves the contacts; this applies especially to the upper contact, and it is rather surprising that the opening of the upper contact is shown as parting at the same time as the lower contact. Many tests on high-voltage circuit breakers in which there is a difference in the path of the air have shown that there is a substantial difference in the time of parting of the contacts.

In paper 45-44 the authors state: "More operating experience with high-voltage outdoor air-blast circuit breakers is needed." It must be assumed, of course, that the authors are referring to the particular design of circuit breaker used in these tests and not to air-blast circuit breakers of other designs.

The writer has been connected with the development and use of air-blast circuit breakers outdoors in Canada for more than ten years. In the early part of this period, experience showed many points which required modification, principally in connection with the maintenance of safe insulation outdoors. However, such troubles have been reduced to a practically satisfactory condition. From operating experience with a large number of 138-kv and 230-kv circuit breakers in late years, we have found that such outdoor air-blast circuit breakers do not require any greater amount of maintenance work than corresponding oil circuit breakers.

H. V. Nye (Allis-Chalmers Manufacturing Company, West Allis, Wis.): My interest in the circuit breaker described in paper 45-44 is very keen, as the interrupting performance of axial-blast compressed-air circuit breakers, both low-voltage and high-voltage has been so manifestly good that it seems only logical to turn to this type of interrupter where short arcing times and extremely fast reclosing cycles are required.

The design of the circuit breaker described in this paper seems to follow rather closely the European designs previously built for high-voltage air-blast circuit breakers, and I think this is a commendable and safe approach to the problem.

It would help if more information were given in the paper regarding the air system employed. I would appreciate knowing what operating pressure was used and whether a single-pressure or double-pressure system was employed. I also would like to inquire whether special precautions were taken to dry the intake air.

The description of an oil circuit breaker in paper 45-45 for three-phase interruption and fast reclosing is particularly interesting in view of paper 45-44 describing an air-blast circuit breaker for the same service and built by the same company. I feel that the experience gained with operating both of these breakers on the same system will go a long way toward clarifying the relative merits of the two types of circuit breaker.

The value of this paper would have been enhanced if some data had been given as to the circuit-breaker weights and over-all dimensions to give the reader a better basis of evaluating the relative merits of these designs.

The presentation of the test data to show that field tests substantiate the results indicated by laboratory tests at lower voltages should be very heartening to the users of these large-capacity circuit breakers where it is not feasible to test them at the factory under full-voltage full-capacity conditions.

The data presented on this circuit breaker show a very constant arcing time throughout the range of the circuit breaker, and for such a type of interrupter the assumptions made from the laboratory tests seem reasonably justified. This is particularly true when the low-voltage tests are carried up to a considerable margin above the circuit-breaker current rating. In this case Figure 7 shows the currents at low voltage were carried up nearly 50 per cent above the actual circuit-breaker rating.

It seems to me, however, that a word of caution should be sounded that such extrapolation of test results to prove a circuit-breaker rating can be relied on only when the tests are carefully co-ordinated to prove the performance of the interrupting element under all conditions and such interrupting element is shown to be consistent in its operating characteristics through the entire range of current interruption.

In paper 45-46 the authors have given a frank, interesting, and comprehensive survey of the possibility of the extension of the interrupting capacity of high-speed supervoltage oil circuit breakers. The paper also contains an excellent discussion of the value of data obtainable from a high-capacity test plant and the various methods of testing circuit breakers to prove their rating. Certainly, we all are agreed on the value of the data obtained from such testing equipment, and the increased reliability of the modern oil circuit breaker is directly attributable to such tests.

In the paper's discussion of "short-circuit tests above 3,500,000 kva" it seems rather hazardous to interpret a single-phase single-pole test as proof that the circuit breakers have a three-phase rating of three times the actual kilovolt-amperes interrupted on a single-pole unit. This might be justified if we could be sure that the circuit being interrupted always would be grounded through a ground of negligible resistance. This is, however, often not the case, and it would seem that some allowance must be made for this fact. The conservative construction of such a test is, of course, to take it as proof of a three-phase value of twice the kilovolt-amperes interrupted on the single pole. Once we reach the capacity of the test plant, of course, it is necessary to do a certain amount of extrapolation in proving the high capacity of circuit breakers. The answer to this would appear to be that such a test as just referred to can be taken only as proof of three times the single-phase kilovolt-amperes when it is supported by tests made at lower voltage and increased currents to prove the capacity of the interrupting device under arc-energy conditions equal to what may be anticipated at full rating. By a combination of such tests it seems reasonable to prove the capacity of the circuit breaker considerably beyond the actual kilovolt-ampere capacity of the test plant itself.

This is the method described in paper 45-45, and the results of the field tests on the circuit breakers therein described seemed to bear out the soundness of such test procedure.

D. M. Jones (General Electric Company, Schenectady, N. Y.): To anyone interested in the broader aspects of power systems, papers, 45-43, 45-44, 45-45, and 45-46, in which circuit-breaker designers are proposing with assurance interrupting capacities of 3,500,000 and 5,000,000 for medium- and high-voltage circuit breakers, are extremely welcome as representing a most acceptable change from earlier conditions, where the performance of available circuit breakers was often the limiting factor in system design.

From system experience and analysis, however, it is evident that such increases in circuit-breaker interrupting capacity as now are being discussed place renewed emphasis on the advisability of short circuit-breaker clearing time. Thus, it would appear that these higher-interrupting-capacity circuit breakers would be acceptable only on a three-cycle clearing basis.

Over-all reviews of power-system-design economics indicate that the proper ultimate interrupting requirements on high-voltage circuit breakers rise with voltage on essentially a constant interrupting-current basis. Thus, it is strongly suspected that 3,500,000- and 5,000,000-kva circuit breakers at 115 kv and 138 kv respectively may be beyond the economic limit from a system-design standpoint.

These new circuit-breaker ratings therefore will accentuate the need for the power-system engineer to approach his expanding power-system design problem, which fundamentally involves the proper timing of the necessary successive advances in the voltage level of the system backbone transmission on the basis of sound economics rather than simply waiting until the interrupting capacity of available circuit breakers forces him to move, a procedure often followed in the past. For with these new ratings he now easily may be able to delay such advances in layout beyond the advisable period for change.

Now that circuit breakers are lush with current-interrupting ability, it may be advantageous to make certain general comments on circuit-breaker testing. These new higher levels of interrupting capacity certainly should bring home to us the fact that it never will be economically feasible to provide testing equipment for the ultimate circuit-breaker capacities. Likewise, it should be evident that to meet the growing needs of the industry the available interrupting ratings of circuit breakers, at least at the higher end of the going voltage range, where of necessity no system yet will have developed the ultimate legitimate interrupting duty, always must appreciably exceed existing system requirements. Therefore there always will be many ratings in advance of any test facilities obtainable on existing systems, and such advanced ratings then will have to be based on a combination of synthetic test data and field testing plus extrapolation.

From a practical standpoint, short-circuit testing equipments always will be necessary to the designer as a basis for obtaining that broad background of experience and information necessary to circuit-breaker design. It is also perfectly apparent that as the interrupting duty of a circuit breaker on which test information is desired rises beyond the normal test capacity of the equipment, any sensible expedient should be resorted to which would enlarge the range of test data obtainable, and thus such procedures as pretripping of the test circuit breaker, testing single phase, testing to full current at reduced voltage, testing at full voltage and reduced current, and the like, long have been in common use.

The procedures in themselves are relatively simple. The translation of such results to an equivalent standard test basis is more difficult, and, although much valuable background data for such interpretations can be obtained from comparison of normal test data and synthetic test data (within the capacity of the test equipment to provide the normal tests), the real proof is obtained from full-scale tests on power systems to the highest interrupting levels obtainable.

The accuracy of the ultimate extrapolated data thus will depend upon the breadth and competence of the background data, the adequacy of the spot checking by system testing, and the ability of the engineers involved. The accuracy of extrapolation, however, also will be greater where the data throughout apply to the same variety of circuit-interrupting mechanism. Thus, we would approach the cross-blast type of interrupter, as applied to oil circuit breakers, with considerable confidence in terms of our long and favorable experience with it, and one cannot but note with interest that it now appears in its fundamentals in all the high-voltage oil circuit breakers discussed in these papers.

As a final comment, in view of the liberal advances in the high-voltage circuit-breaker ratings that have been presented and the associated movement to three-cycle interrupting time, it would seem most opportune to face now the *joint* question, often discussed, of the proper method of rating the interrupting capacity of circuit breakers and the corresponding appropriate method of calculating system short-circuit duty.

With the trend toward fast circuit breakers the artificiality of a higher apparent duty for faster circuit breakers should be recognized and eliminated. The concept of short-circuit duty being based on "rms current at contact parting" is an old one and a very approximate one. It reaches back to the days when a circuit breaker was expected only to clear a fault, whereas today it must close successfully as well as open and then reclose immediately. Some at least equally accurate approximation must be possible, which eliminates the contact-parting time variable and makes sounder application sense.

It now would appear timely to consider

changing the rating structure. One very simple solution would be to assign a nominal interrupting-current rating to a circuit breaker which would bear the same relationship to the circuit-breaker test requirements as the calculated system interrupting-current requirements (obtained by dividing system voltage by square root of three times the proper system reactance to the point of fault) would bear to the real interrupting duty on that system for the conditions and the location in question.

It then would be necessary only to compare the result of the above simple-system interrupting-current calculation with the nominal circuit-breaker interrupting rating reasonably to determine its proper application from an interrupting standpoint.

In addition the circuit-breaker rating then would be free from the slippery factor of contact parting time and also a present discrepancy between system calculation and circuit-breaker rating which is dependent upon the actual speed of the circuit breaker.

J. J. Trainor and **C. E. Parks** (Public Service Company of Indiana, Inc., Indianapolis, Ind.): As mentioned in paper 45-46, large concentrations of power due to system interconnections and greatly increased generating capacities have constituted a serious problem for utility operators in that these expansions within the last few years have caused them to be especially conscious of the increased interrupting duty of which their circuit-breakers must be capable. On the system of the Public Service Company of Indiana, Inc., we found that our rapidly expanded power facilities within the past five years necessitated a careful review of our circuit-breaker situation from an interrupting-capacity standpoint. Circuit breakers which possessed proper interrupting capacities for their particular location five years previously, were entirely inadequate. This prompted us to relocate, rebuild, or replace a large number of circuit breakers.

Although it is true that utility engineers are ever conscious of this problem when they plan new generating and transmission layouts and strive to arrange the system to reduce the duty to which their circuit breakers are subjected, certain economic and operating considerations often limit their ability to reduce their circuit-breaker duty figures to a low value.

Our system has yet to develop to the point where the presently manufactured 2,500,000-kva circuit breaker is not adequate. However, our planned expansion program, coupled with the fact that we make extensive use of high-speed single- and three-pole reclosing on our 66-kv and 132-kv system, makes it evident that the newly developed 5,000,000-kva circuit breaker possibly may be required at our major generating stations and substations in the near future.

The authors are certainly to be congratulated on the fine data which they have accumulated proving the operation of their circuit breaker to be all that is claimed for it. I was interested particularly in the successful double reclosing action as recorded in Figure 10 of their paper.

It would be appreciated if the authors would describe more fully the constructional differences between the grid used on this 5,000,000-kva circuit breaker as compared with that used on their present 2,500,000-kva circuit breaker. It also would be of interest to know whether or not this new grid will be available for use in the conversion of older-type circuit breakers and to what extent such conversion will affect the interrupting capacity as compared with conversion using the standard 2,500,000-kva grid.

H. A. Peterson and **C. A. Woodrow** (General Electric Company, Schenectady, N. Y.): The switching surge long has been recognized as a dangerous source of system overvoltage. In the past few years, both field tests and analytical studies have demonstrated that the phenomenon associated with capacitance-current interruption is an important—if not the most important—cause of switching-surge overvoltage. Roughly and briefly, if *delayed* restriking of the arc across the circuit-breaker contacts takes place, then there is a possibility of building up overvoltages which may be damaging if a succession of several such delayed restrikes takes place.

That this problem clearly is appreciated and that something is being done about it is made clearly evident in papers 45-43, 45-44, and 45-45. In the three-cycle oil-blast circuit breaker described in them, overvoltages are controlled by virtue of a shunting resistor of sufficiently low resistance (several thousand ohms) to drain momentarily the charge of the line back into the source, before final interruption is completed. On the other hand, the three-cycle air-blast circuit breaker requires no shunt resistor, because it does not permit the particular kind of delayed restrikes which otherwise could give rise to overvoltages. While the parting contacts are in the low-pressure throat, high-voltage restrikes are impossible. After this short initial parting interval dielectric strength between the opening contacts is regained so rapidly that the slow rate of voltage recovery associated with such a circuit interruption does not permit a restrike to occur. This characteristic is shown clearly in Figure 7 of the Byrd–Beall paper, and its effect on a capacitance-current interruption is illustrated in Figure 6 of the same paper.

Though the possibility of an oil-interrupter design with similar self-limiting characteristics cannot be denied, it must be remembered that the air-blast circuit breaker uses a definite, stored-energy interrupter, as does the FG-type oil impulse circuit breaker which has established such a successful high-voltage service record in the far West in the United States. Without the shunting resistor, it would appear that performance blind spots could develop much more readily with any interrupter, oil or air, which uses the current carried as a source of the necessary pressure for successful interruption.

From both an operating and system-design standpoint, it is comforting to realize that such overvoltages are being brought under control. Their elimination can benefit greatly the system overvoltage protective equipment. In many instances it has been demonstrated by field tests that arresters are required to operate very frequently on switching surges attending the interruption of capacitance currents. In the higher-voltage systems where cables or long overhead lines are switched, this has particular significance because in these systems the amount of energy associated with such surges may be greater than the discharge capacity of the arresters. It is therefore significant from the protective-equipment standpoint that such overvoltages now lend themselves to control *at the source*.

Philip Sporn (American Gas and Electric Service Corporation, New York, N. Y.): It is gratifying to learn from the paper 45-46 that definite progress has been made by the authors and their associates toward the development of higher-interrupting-capacity circuit breakers, with a view to reaching a goal of 5,000,000 kva. I am all the more pleased to see this further progress reported by the same authors who presented, just one year ago, a paper describing developments in high-capacity rapid-reclosing circuit breakers (reference 2 of M. H. Hobbs discussion), because at that time I expressed the opinion that they had not gone far enough, particularly with high-speed reclosing, to meet the present or impending requirements of modern systems. It thus is heartening to see that considerable further progress and enterprise has been shown in advancing these developments toward the goal which I then projected of a circuit breaker of 5,000,000-kva interrupting capacity, three-cycle operating speed, and capable of reclosing on a 12-cycle duty. Insofar as this further progress is reported in this paper, it is, I believe, a most timely and welcome contribution, and the authors, as well as the Westinghouse Company are to be congratulated.

It is, however, disappointing to note that to the various elements of this really commendable progress and enterprise there have been hitched loosely certain ideas about interrupter design and development, which the authors would like to have accepted as fact but which fall far short of factual achievement. Thus the idea that the credit for whatever progress has been made in circuit-breaker development should go entirely either to the high-power testing laboratory or to the development of the multiflow deion grid will not stand up to critical analysis. I am not minimizing the importance of factory testing in the development of the excellent arc-interrupting devices we have today, but I wish to point out that circuit-breaker developments went a long way before high-capacity laboratories were available. Again, while the present multiflow deion grid is undoubtedly very effective, it is after all only one effective form of the self-generating pressure type of arc interrupter, and both the broad principle and other forms of it have been known for a long time.

The authors agree to the proposition that final verification of a new design by field tests on an actual power system has advantages both to the manufacturer and the user. I always have contended that considering the importance of a circuit breaker's perfect functioning to the safety and performance of a power system, no reasonable measure should be left untaken to prove beyond doubt a circuit breaker's rating: the realistic duplication of short-circuit conditions on the system itself obviously provides the best and the only certain assurance of a circuit breaker's capability.

I would like to call attention also to a most significant finding by the authors that in the case of the multiflow deion grid circuit breaker and, presumably, in the case of all modern self-generating pressure type of circuit breakers "there is no inherent limitation in the rapidity with which a circuit breaker can be reclosed and interrupt a second fault." Mr. Byrd and Mr. Rietz bring out the same fact but do not comment on its significance. Our own repeated experiences through a succession of field tests, always making repeated shots as quickly as possible, have been that there is no reduction in interrupting capacity on the second shot of a fast reclosing cycle with a modern circuit breaker. It is obvious that Mr. Hill and Mr. Leeds have found the same thing to be true in their own tests. Yet, for reasons not quite clear to me, they negate their own findings and imply that such a reduction does take place. I submit that it is about time that we got down to modern facts on this matter and gave modern circuit interrupters credit for what they are really capable of doing. It is high time that modern circuit interrupters were unshackled and had their 25 per cent and 35 per cent derating-factor gyves struck off. The authors have shown the basis for it. Perhaps, if circuit-breaker users insist strongly enough, they can get it accomplished.

W. F. Skeats (General Electric Company, Philadelphia, Pa.): In order to get a definite determination of the motion of the circuit breaker in the tests described in paper 45-45, a seismograph was mounted on the mechanism box at the top of the first pole. Some of the records obtained in the heavier tests are shown in Figure 4, of this discussion. These are in accordance with the theory that the initial motion is downward and the upward motion in the nature of a rebound.

The maximum recorded motion in any test is approximately $^1/_8$-inch each way from the initial position. This is roughly ten times the motion on a no-load operation.

On the tests shown in Figure 4, numbers 11*B*, 12*B*, and 14*B* are reclosing operations, while 13*B* is a straight opening operation. It is interesting to note that the jar resulting from the second operation of a reclosing test is in all cases much less than that resulting from the first operation. This may be explained as the result of cushioning by the gas bubble produced by the first operation.

Mr. Hill and Mr. Leeds offer a review of testing procedures and enumerate several tests taken to indicate very high interrupting capacities.

In connection with their Figure 12, they indicate that constancy of arc length over a range of voltage shows suitability of the interrupter for extrapolation, and it is on this basis that they justify the interrupting abilities which they claim on three-phase ungrounded short circuits. This has been true to an ever increasing extent throughout the development of the whole family of oil-blast interrupters and is well exemplified by the tests plotted in Figure 6 and Figure 11 of paper 45-45. Here the arc lengths obtained in field tests at 138 kv three phase are shown to match arc lengths obtained at the same current in factory tests at voltages down to 22 kv single phase, or less.

A paper on the impulse circuit breaker presented by D. C. Prince in 1935 (see reference 1 of closure by Mr. Hill and Mr. Leeds) pointed out the applicability of tests on less than the full number of breaks with proper consideration of voltage distribution.

It is of interest to note that in discussing Mr. Prince's paper Mr. Leeds was kind enough to remark that using the aforementioned extrapolation procedure, the tests on a single break indicated an interrupting ability for the complete three-phase circuit breaker of 11,500,000 kva at a voltage somewhat higher than any yet employed in practice.

Philip Sporn and **Harry P. St. Clair:** Mr. Baker, in reviewing the performance of compressed-air circuit breakers under laboratory test conditions with relatively high rates of rise of recovery voltage in comparison with the performance of similar circuit breakers in field tests, where rates of rise under maximum concentrations of power are necessarily much lower, raised the question as to whether it would not be justifiable to reduce the recovery rates in testing laboratories to make them comparable with field tests.

At a voltage level of 138 kv it is, as far as we can see, impossible to encounter the maximum short-circuit duty on any practical system without having connected a certain number of transmission lines which inherently reduce recovery rates to relatively low values. The high recovery rates, comparable with those mentioned by Mr. Baker in laboratory testing, can be obtained only in the field at very substantially reduced interrupting capacities, and then only with rather unusual system conditions.

Though these statements would seem to answer Mr. Baker's question in the affirmative, the testing laboratory is really the tool used by the designers to develop and perfect their product, and the authors believe that Mr. Baker's suggested procedure is something that should be left entirely to the manufacturer's judgment of how far he wishes to go with the severity of his tests. If the laboratory is capable of providing the tests, it would seem to be good judgment on the part of the manufacturers to have at least some margin beyond what is normally to be expected in field service.

Mr. Hobbs has raised a question as to the economic justification for extensive development work at the present time on outdoor air-blast circuit breakers, particularly in view of the 1941 statement of the EEI-AEIC-NEMA Joint Committee on Preferred Ratings of Circuit Breakers. Further opinion is expressed that modern designs of conventional dead-tank oil circuit breakers will meet best the requirements of the industry for some time to come, and that development of air-blast circuit breakers should continue on the experimental basis suggested by the Triple Joint Committee.

The best answer to this point of view is given, we believe, in the discusser's own statement in his closing paragraph where he states that the development work and field experience on air-blast circuit breakers already have been very valuable and should be continued, because it is only in this way that we learn. The authors consistently have believed that progress in the art of circuit interruption could not and should not be discouraged from any quarter and that there was at least considerable question as to whether the Triple Joint Committee was itself on a sound basis when it attempted to dictate the course of developments in the art.

One or two of the air-blast circuit-breaker problems mentioned by Mr. Hobbs, we believe, should be clarified: first, it does not seem to be entirely true that the air-blast circuit-breaker mechanism is unduly complicated, particularly for quick reclosing. As a matter of fact, the simplicity of the reclosing operation, whereby the interrupting contact itself is the only thing that moves, would seem to be one of the advantages of the air-blast circuit breaker in this regard. Second, we do not believe that Mr. Hobbs intended to include potential transformers along with current transformers as one of the inherent difficulties of air-blast circuit breakers. Though it is true that some use is made of bushing potential devices on oil circuit breakers, in general, potential transformers are quite independent of circuit breakers.

Mr. Jones has made the interesting suggestion that, since the trend in high-voltage circuit breakers is toward three-cycle interrupting time with instantaneous reclosing requirements, it now would seem appropriate to rate the interrupting capacity of circuit breakers on the basis of the instantaneous symmetrical short-circuit current only, omitting factors of asymmetry and decrement entirely. Where the time is very short between the initiation of the short-circuit current and the parting of contacts, the proposed method of rating would give results differing by a relatively small amount from the present rule insofar as the a-c component is concerned. It would, however, eliminate the d-c component entirely so that the circuit breaker would get no credit for having interrupted anything higher than the symmetrical a-c component, even though a large d-c component were present. It always has been assumed by the manufac-

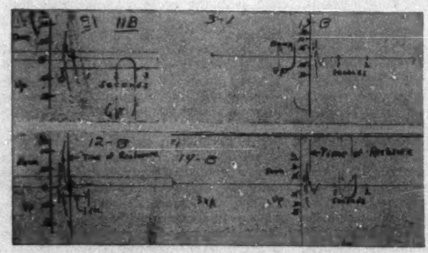

Figure 4. Seismograms taken on tests 11B, 12B, 13B, and 14B

turers in this country that the presence of a d-c component actually increased the duty on the circuit breaker, but just how much effect it has may never have been determined very scientifically. Whatever additional stress thus is produced would have to be taken care of, as Mr. Jones points out, by the necessary margin in the circuit-breaker design. This proposal would, of course, please our European friends, who consistently have maintained that circuit breakers should be rated on a symmetrical-current basis only.

As a general rule for rating circuit breakers, however, Mr. Jones's suggestion is likely to run into a great deal of protest among a large class of circuit-breaker users, particularly in the industrial field where high speed is not necessarily the rule and where, by taking advantage of a considerable amount of decrement, smaller circuit breakers can be used. To go all the way with Mr. Jones's suggestion would, therefore, seem to require two sets of ratings or rules for ratings; one for high-speed circuit breakers, and another for lower-speed breakers, where the a-c decrement is considerable.

As a compromise move, and speaking from the standpoint of circuit-breaker users, we see no reason to object to the elimination of the d-c component as a part of the rated interrupting duty on a circuit breaker, so long as it is understood that circuit breakers so rated are fully capable of handling whatever offset-current waves may be encountered in practice.

Mr. Jones also makes the interesting comment that 3,500,000- and 5,000,000-kva circuit breakers at 115 kv and 138 kv may be beyond the proper economic limit of power concentration for systems of these respective voltages. Although it is true that continued system growth resulting in increasing power concentrations does indicate the economic wisdom at the proper time for higher-voltage backbone transmission, particularly if distances are considerable, it is not necessarily obvious that the need for 5,000,000-kva circuit breakers at 138 kv is in itself evidence that good economic system-design principles have been violated. For example, even after a higher-voltage backbone has been superimposed upon a system, the low-voltage system, at least for a long time to come, must be of sufficient capacity to act as a backup for some of the important elements of the higher-voltage system. This in itself, along with the increase in generating capacity and transformation capacity between the two voltage systems, may require circuit breakers approaching 5,000,000 kva. Furthermore, the need for higher duties is bound to develop at generating stations as their size grows. Thus at the Philo Plant where the tests were made, the necessity for the use of large 138-kv reactors to keep short-circuit values within the 2,500,000 circuit-breaker ratings was not altogether a perfect solution to the problem. Though without these reactors the short-circuit duty would have been at least 4,000,000 kva, the loss of flexibility due to these reactors, particularly during maintenance outages of generating units, already has been felt. At such times sagging voltage may be experienced on one bus section, while there exists on the other section an excess of kilovar generating capacity which cannot be transferred through the reactors.

Mr. Holm raises a question as to whether 5,000,000-kva circuit breakers should be encouraged or whether the fact that circuit breakers of such size are needed should serve as some kind of a warning to power-system designers that perhaps some dangerous limits to size have been reached. It seems to the authors that the question is one of those moot theoretical questions, the asking of which would have been avoided by an examination of a few facts. Thus it is a fact that the present 3,500,000-kva oil circuit breaker is smaller in size, uses less oil, is more reliable, and is far safer than the 1,500,000 kva circuit breaker of 20 years ago. Why, therefore, take fright at 5,000,000 kva? Again, it is a fact that service on many modern systems calling for circuit breakers of from 2,000,000 to 3,500,000 kva is being delivered at higher quality, lower cost, and at greater distance from sources of generation than was dreamed possible two decades ago. Economical limits to size? Of course there are such limits. But they will be extended in the future, as they have been in the past, by technological advances. And they will be determined soon enough by closely watching such criteria as the above and not by the invocation of any examples from paleontological mists.

H. L. Byrd and Ben S. Beall III: The authors appreciate the comments of Mr. Peterson and Mr. Woodrow, stressing the value of controlling switching surges at their source by proper design of circuit breakers to prevent restriking during the switching of capacitors and long energized lines. In Figure 7 of our paper a number of capacitor switching tests are plotted. In every case in which a current zero appeared before the contacts were retracted from the restricted portion of the throats a restrike at very low voltage occurred. The restrike at a low voltage is due to the low dielectric strength of the gap between the stationary contact and the moving-contact tip. The contact tip acts somewhat like a valve while in the restricted portion of the throat and prevents high pressure from building up between the contacts. Figure 6 shows a characteristic restrike with the contacts in the restricted portion of the throat. The voltage in this case is limited to a low value. As the contact withdraws from the restricted portion of the throat the small volume between the stationary and movable contacts is charged immediately with high-pressure air. As a result the dielectric strength of the circuit breaker changes almost instantly from a relatively low value of approximately 100-kv crest breakdown to a condition which will theoretically withstand a value of 350-kv crest. The problem of capacitor switching was recognized early in the development of outdoor air-blast circuit breakers and has been treated as a very necessary requirement, a requirement which has been answered in a very straightforward and simple manner.

We are very interested in the comments submitted by Mr. Haberl in that he states certain points are now quite clear. In some respects Mr. Haberl has done an excellent job of analyzing certain points in the circuit breaker, but his conclusions are in some cases rather misleading. The dead time of the circuit breaker is approximately $1^1/_2$ cycles, 1.7 cycles to be exact, and the contacts reach the end of the restricted portions of the throats in approximately $2^1/_4$ cycles. The relationship is shown clearly in Figure 7 of the paper. In one respect the elapsed time from the parting of contacts to the withdrawal of the contacts from the restricted portion of the throat also may be considered as dead time in that the circuit breaker is not expected to interrupt fault currents until the contacts have reached this point in the interrupter. The end of the restriction is reached at approximately $2^1/_4$ cycles and is shown as the lower dotted line in Figures 5, 8, and 9 of the paper. All interruptions take place at the first current zero after passing this point in the stroke. When Mr. Haberl arrived at the conclusion that "some of the tests . . . continued until the second current zero" he must have overlooked the fact that the time interval between current zeros is not always one-half cycle. Due to the asymmetry of the current in several of the tests plotted in Figures 5, 8, and 9 of the paper the time interval between the current zeros is as much as 0.7 of a cycle during the last loop of current before interruption takes place. In several of these tests having asymmetrical currents the current zero previous to circuit interruption appeared almost simultaneously with the withdrawal of the contacts from the restricted portion of the throats. Because of this condition it was necessary for the circuit breaker to wait until the appearance of the next current zero, before interruption could be accomplished. Under these conditions the circuit was interrupted at 2.9 and 2.95 cycles after trip impulse. The two dotted horizontal lines show in Figures 5, 8, and 9 of the paper drawn at 2.25 and 2.95 form the theoretical boundaries between which all interruption takes place. The data show that the circuit breaker performed with remarkably little variation from these predetermined theoretical boundaries.

Mr. Haberl's next question arises from the fact that the upper and lower contacts of the interrupter begin to move at the same instant. Upon careful analysis of the interrupter, shown in Figure 3 of the paper, it will be seen that there are two separate and distinct interrupting chambers. These two interrupting chambers are charged with high-pressure air from a common header in the form of a vertical cylindrical passage. In order that the upper and lower contacts will start moving together and continue to move at the same velocity it is only necessary to charge the two interrupting chambers at the same rate. The rate of charging a given volume depends on

1. Supply pressure.
2. The volume to be charged.
3. The entrance and exhaust orifices.

These factors were considered along with certain other factors, such as the effect of gravity, during the design of the interrupter. A few modifications and adjustments during tests aligned the operations of the contacts almost perfectly. Not only do the upper and lower contacts of the same interrupter begin to move at the same time and move throughout their stroke at the same velocity, but the six interrupters of the triple-pole circuit breaker operate simultaneously.

In answer to Mr. Nye's question regarding the air-compressor equipment, we use a double-pressure system. The high-pressure side operates at 800 pounds per square inch and the low pressure at 350 pounds per square inch, the normal pressure maintained in the circuit-breaker air receiver. An absorption drying unit is an integral part of the system and eliminates all free moisture from the air. The experience of several winters with this factory's assembled equipment has shown this system to be more than adequate to perform satisfactorily during the most severe winters experienced in any part of the United States. Dew points of the air in the circuit-breaker receivers have been recorded over extended periods of time, below minus 50 degrees Fahrenheit.

H. L. Byrd and E. B. Rietz: We are in agreement with Mr. Nye's conclusions that the confirmation of laboratory tests demonstrated by these series of field tests should be encouraging to the large number of users of high-capacity oil circuit breakers. The same formulas used for the laboratory tests on this new interrupter have been used for a number of years to justify the expected performance of circuit breakers which could not be tested to rating. It is quite true that the performance of the more modern interrupters can be foretold with an increased degree of certainty because of the more consistent performance. But, nevertheless, the same general reasoning applies to the older designs. It is believed that the confirmation at interrupting duties never before approached will permit reasonable extrapolation of laboratory test results for the next higher rating. No one will contend with Mr. Nye's statement that extrapolation should not be carried to extremes.

The use of the seismograph which was described in more detail by Mr. Skeats proved to be an interesting venture. The need for holding down bolts actually was demonstrated, although for a number of years it has been evident to circuit-breaker designers that this upward thrust was in evidence as shown in many laboratory tests. Field tests also proved the mechanical design used for support of the oil tank. The individual tank supports are new and have found general acceptance because of the degree of accessibility that they provide. These tests proved the design of the tank supports.

Shunting resistors were developed and applied for the reason advanced by Mr. Peterson and Mr. Woodrow, that is, to prevent any performance blind spots on the interruption of capacitance currents from giving rise to dangerous overvoltages. It is known that these resistors are not required under certain favorable conditions, but for general application these conditions cannot be determined readily. Therefore, it seemed desirable to standardize the use of resistors for all 115- to 230-kv circuit breakers to control overvoltages at the source. The benefits of this practice to associated system apparatus is evident.

The section of Mr. Jones's discussion relating to circuit-breaker testing is very pertinent and agrees thoroughly with the authors' ideas of the future trend of circuit-breaker testing. With increased interrupting ratings it should be logical to expect that the rated circuit-breaker interrupting times will decrease. Interrupters which will give satisfactory performance at the higher ratings necessarily have to have excellent characteristics, and this means short arc durations. We are heartily in favor of considering that all higher rated circuit breakers should have a three-cycle rating.

The conclusion that Mr. Sporn reaches that very worthwhile advances in circuit-interrupting devices can be made with only limited test capacity is proved by the program on the multibreak interrupter which was started prior to 1937 and has culminated today with the design described by the authors. It is also true that the proof performance of this development is easier to believe with field-test confirmation. This assurance is valuable not only to the user but also to the circuit-breaker designer, who likes to have his theories checked by fact at regular intervals. We have no disagreement with Mr. Sporn's desire for an oil circuit breaker that has no inherent limitations in the rapidity with which it can be reclosed and interrupt a second fault. As pointed out in Mr. Skeats' discussion, there is an indication that the cushion of the gas bubble may aid the circuit breaker structurally on the second interruption. Additional experience will be required to be sure that any residual gas in the interrupter does not endanger prompt clearing on the second operation. The Philo, Ohio, station tests are extremely encouraging. With reduced reclosing times down to 12 cycles (because these are also practical) there might be an additional problem. But here too a satisfactory answer undoubtedly can be worked out.

A. W. Hill and W. M. Leeds: It is gratifying to have W. F. Skeats confirm the usefulness of the special testing procedures outlined in our paper by referring to earlier applications of one or more of these methods. Unfortunately, however, circuit-breaker rupturing capacity verification by tests on less than the full number of breaks described by D. C. Prince in 1935[1] was not carried to its logical conclusion. The 287-kv circuit breaker in question was equipped with eight breaks in series, voltage distribution tests showing that 44 kv appeared across the highest stressed break. The rating to be demonstrated was 5,000 amperes, and the data included a test with eight breaks in series interrupting 6,800 amperes at 44 kv. The verification would have been much more conclusive if this same test had been applied to a single break. The inference made at that time that a single-break test of 2,300 amperes at 110 kv in combination with an eight-break test of 9,300 amperes at 22 kv indicated the ability of one break to handle 110 kv and 9,300 amperes simultaneously still seems to us entirely unjustified.

In pointing out the similarity of the arc lengths obtained in the field tests reported by H. L. Byrd and E. B. Rietz at 138 kv three phase with those made in the high-power laboratory at voltages down to 14.5 kv single phase, Mr. Skeats gives the impression that there was no more duty on the circuit breaker when interrupting a given current at the high voltage than at the low voltage. The reason for the comparable arc lengths possibly may be found in circuit recovery rates of approximately the same magnitude, the low-voltage circuit in the laboratory having an undamped high natural frequency as compared with a damped low-frequency recovery voltage in the field.

J. J. Trainor and C. E. Parks have asked for more information concerning the constructional differences between the grids used for 5,000,000 kva and those for the present 2,500,000-kva circuit breakers. The general design and method of operation is identical for the two ratings, but the larger grid is built with a greater oil volume in the pressure chamber and a stronger mechanical construction obtained by larger diameter tie rods, heavier fiber plates, and a more substantial top casting. There is no reason why these high-strength grids might not be applied in revamping present circuit breakers, although the interrupting capacity assigned also would depend upon other factors, such as the age of the circuit breaker and the strength of the pole-unit levers and operating mechanism.

H. V. Nye questions the claim in our paper that single-phase testing at normal line-to-ground voltage can be used as a demonstration of interrupting capacity on three-phase ungrounded short-circuit duty. It is true that this apparent equivalence does not apply to all types of circuit interrupters, but the experimental evidence shows it to hold fairly well for modern interrupting devices which are not sensitive to relatively moderate changes in applied voltage. With regard to the test method advocated in our paper of interrupting rated short-circuit current with a subdivision of the test circuit breaker, across which rated voltage for that section of the circuit breaker is available, Mr. Nye seems to have confused this with the much less convincing method used by Mr. Byrd and Mr. Rietz, in which tests on the complete circuit breaker first at high voltage and low current and then at low voltage and high current are taken together to prove the circuit-breaker rating.

D. M. Jones believes that the highest circuit-breaker ratings always will exceed the capacity of either high-power laboratory-test facilities or short-circuit power obtainable on field tests. However, confirmation of laboratory-test methods by verification in the field means that considerable reliance can be placed upon those laboratory tests which seem to indicate the ability to handle higher powers than can be obtained on any existing systems.

We do not quite agree with Mr. Jones's statement that the only real proof is obtained from full-scale tests on power systems, as it is quite possible to put more severe tests on a circuit breaker in the laboratory, at least insofar as current, voltage, and rate of rise of recovery voltage is concerned for a single interrupting unit. The power-system test, however, does give the customer direct evidence of the performance which will be obtained on that particular system at the short-circuit power available.

The implication that the multiflow deiōn grid is one of the family of cross-blast circuit breakers is entirely without foundation. The multiorifice design consists of a multiplicity of oil streams converging radially on the arc with the flow passing longitudinally through orifices to the vents. This constitutes a distinct difference in operating principle, with corresponding advantages in interrupting effectiveness resulting from the centering effect produced by the oil flow on the arc stream.

We are in entire agreement with Mr. Jones's comments on the advantage of using first-cycle symmetrical current as the basis for rating circuit breakers; this proposal also has been discussed by R. C. Van Sickle.[2]

We cannot agree with Mr. Sporn's contention that there should be no reduction in interrupting capacity on the second test of a fast reclosing cycle using a modern circuit breaker. Our laboratory tests on oil circuit breakers as well as the motion pictures accompanying his paper on the recent compressed-air circuit-breaker tests at the Philo, Ohio, station definitely indicate more stress on the second test than the first. Until this condition changes, derating factors still should be applied.

REFERENCES

1. CIRCUIT BREAKERS FOR BOULDER DAM LINE, D. C. Prince. AIEE TRANSACTIONS, volume 54, 1935, April section, pages 366–72.

2. POWER-CIRCUIT-BREAKER RATINGS, R. C. Van Sickle. AIEE TRANSACTIONS, volume 60, 1941, September section, pages 882–4.

Impedances Seen by Relays During Power Swings With and Without Faults

Discussion of paper 45-67 by Edith Clarke, presented at the AIEE winter technical meeting, New York, N. Y., January 22–26, 1945, and published in AIEE TRANSACTIONS 1945, pages 372–84.

L. F. Kennedy (General Electric Company, Schenectady, N. Y.): The relay-application engineer is always appreciative of new or improved methods of determining system conditions which may affect relay operation. Now, in the field covered by Miss Clarke's paper, there has been a lack of fundamental information. In fact many of us held some definitely erroneous ideas of what the trends were. Mr. Mason and Mr. Neher were, I believe, the first ones to indicate the true nature of the phenomenon, but they did not give values. Mr. Poage, Mr. Streifus, Mr. MacGregor, and Mr. George improved the picture immensely. Now Miss Clarke has given us an inclusive paper showing how to evaluate the most common factors for any application. She has done more, however, in that we find a simple approach which gives the relay engineer a bench mark, which frequently may eliminate time-consuming detail studies.

The impedance seen at any point on a system without faults for an angular separation of 90 degrees between some two points is defined completely by a circle with sufficient accuracy for most purposes. If we take a circle and let a diameter represent to scale the impedance between two points, the circumference defines the possible impedances for a 90-degree angular separation of these points. This essentially is shown on Figure 6 of the paper where the circle is $\phi=270$ degrees and $\phi=90$ degrees and the diameter is AB. If we are at point A or B, the impedance varies from AB to zero. If we are at some intermediate point, which I shall call C, the impedance varies from AC to CB. If C is midway between AB, then the impedance is always a radius of the circle or $AB/2$. This concept assumes that all sections of impedance between A and B have the same impedance angle and that the effect of capacity is negligible. These assumptions are generally usable, at least to determine whether relay operation is probable or not. The most frequent use of this figure would be with points A and B representing the two terminals of a particular line or the system terminals back of the internal impedance of two equivalent terminal machines.

The circle represents the minimum impedance that can be seen for a 90-degree separation. Less than 90 degrees will give larger impedances outside the circle. If the characteristic of any proposed relay installation is superimposed to the same scale, a quick and reasonably accurate idea is obtained as to whether tripping on power swings is probable or not. In many cases the answer will be obvious—large separation between relay-tripping characteristics and the circle. In other cases more detailed study is necessary. We have achieved a simple method to solve some of our problems, leaving only the difficult ones to require extended study.

We can go a step further even without having Figure 8 of the paper. The 150-degree and 210-degree arcs of Figure 6 are those having a radius equal to AB. Hence, we always can easily draw the circle defining the 90-degree and 270-degree impedances and the arcs defining the 150-degree and 210-degree impedances. Each of these arcs has its center at the apex of one of the two equilateral triangles constructed on AB as a base.

With the smaller values of impedance which may be encountered along the 150-degree arc, errors introduced by neglecting capacity or variations in impedance angle may become more significant, and hence this second approximation must be used with greater consideration.

I wish to emphasize that a large part of the value to be obtained from Miss Clarke's contribution comes from the fact that, having analyzed all factors, we then can use approximations intelligently in order to obtain the desired answers with a minimum expenditure of time. I have not discussed the effects of unsymmetrical faults combined with a swing. However, even here the circle on diameter AB can be used by obtaining the new angular value δ to replace $\phi=90$ degrees, which will be a smaller or larger angle depending on fault location and the type of fault. However, evaluation of these results is beyond the scope of this discussion.

Miss Clarke is to be congratulated for making available to the relay-application engineer the tools for a complete analysis of any problem involving the performance of distance-type relays.

Edward W. Kimbark (Northwestern University, Evanston, Ill.): During the past year I had occasion to investigate the loci of impedances seen by relays during swings. I am therefore in position to appreciate what a thorough job the author has done in presenting the results in a form that is both general and usable.

Nevertheless, some relay engineers may be inhibited from using the results because of the somewhat formidable length of the paper and the number of equations and tables. This discussion aims, first, to show such engineers, if there be any, how extremely simple a task it is to find the loci for any condition. The second part of the discussion points out the similarity of the relay impedance chart to some charts used in other phases of electrical engineering.

The loci of impedance Z_R seen by any relay, connected in any manner, located anywhere on a two-machine power system, faulted or unfaulted, is given by the general impedance chart (Figure 6 of the paper), provided that this chart be altered in scale, orientation, location, and labeling of the circles. The data for these alterations are provided by measurement or calculation of the impedance seen by the relay under three conditions, as follows:

$-Z_x$, the impedance seen when $E_A=0$
Z_z, the impedance seen when $E_B=0$
Z_k, the impedance seen when $E_A=E_B$

The poles, A and B, of the chart are located at points $-Z_x$ and Z_z, respectively, in the Z_R plane. Thus the values of these two impedances fix the scale, orientation, and location of the chart with respect to the R and X axes. The circles of the chart may be drawn either by tracing Figure 6, in which case the scale must be that of Figure 6, or by constructing a similar figure to the desired scale from the information of Tables III and IV.

The circles of the general chart are labeled in terms of the magnitude and angle of the polar form of complex number KE_A/E_B. In order to change the labeling into terms of the magnitude and angle of E_A/E_B, it is necessary to divide by K. That is, the values of magnitude $|KE_A/E_B|$ on one set of circles of the general chart should be divided by $|K|$, and the values of angle on the other set of circles should have θ_k, the angle of K, subtracted from them.

The value of K is given by

$$K=\frac{Z_k+Z_x}{Z_k-Z_z}$$

(This relation may be verified from equation 3 of the paper by putting $E_A=E_B$, $Z_y=Z_x+Z_z$, $Z_R=Z_k$, and solving for K. This method of evaluating K from impedance Z_k is not given in the paper; it is a contribution of this discussion.)

That is really all there is to the construction of the impedance loci.

The three impedances, $-Z_x$, Z_z, and Z_k, may be determined by any desired method of network solution, either with or without a calculating board. Inasmuch as these impedances are defined in such manner that the network has only one impressed voltage for each, they may be found through use of a d-c calculating board, subject, of course, to the usual limitations of a d-c board; namely, that shunt capacitance and shunt loads must be neglected and all branches of the network must be assumed to have the same impedance angle. These assumptions give $Z_k=\infty$ and $K=1$ for an unfaulted network. A faulted network may be solved either by means of symmetrical components or by means of α, β, 0 components. The latter are recommended as simpler.

Two restrictions stipulated in the paper are actually unnecessary. The negative-sequence impedance need not equal the positive-sequence impedance, and the relays need not be supplied with delta voltage and delta current. The tables and equations for various special cases, though possibly convenient, are really superfluous, if the computer only grasps the idea of determining the impedance seen by the relay under the three stated conditions and if he understands the methods of solving three-phase networks under both balanced and unbalanced conditions.

The paper makes available a simple method for studying the performance of relays on the unfaulted phases, when swinging occurs and an unsymmetrical fault is present. The example given in the paper shows that there is more danger of false operation under these conditions than generally has been recognized.

To return to consideration of the form of the chart: The two orthogonal sets of circles which appear in the relay-impedance chart are called bipolar circles, and they have several other applications in electrical engineering. A map of the electric or magnetic field of two parallel cylindrical conductors consists of bipolar circles. The set of circles surrounding the conductors represents magnetic flux lines or electric equipotentials, while the circular arcs joining the conductors represent electric flux lines or magnetic equipotentials. The bipolar circles also occur in a widely used chart portraying the variation of input impedance of a transmission line with the length of line and the terminating impedance. The poles of this chart are at $\pm Z_0$, the characteristic impedance. The variation of impedance represented by a circle surrounding the poles is produced by change in the relative phase of the direct and reflected waves due to change of length of the transmission line, instead of by the change of phase due to mechanical swinging of two generators with respect to one another.

A. J. McConnell (General Electric Company, Schenectady, N. Y.): The purpose of this discussion is to illustrate further the use of the general impedance chart (method B of the subject paper) and also to provide substantiation by comparison with previous work. It is proposed, therefore, to construct an impedance diagram for the Omaha, Nebr.–Midian, Kans., line similar to the lower portion of Figure 11 of reference 1 of this discussion (impedance seen by a relay at Midian).

The resulting diagram, Figure 1 of this discussion, was obtained in the following manner in about one-half hour (the original was drawn freehand with pencil, before tracing in ink).

The constants of the Omaha–Midian line, including transformers, have been given[1] as $A=0.824\underline{/3.25^\circ}$, $B=282\underline{/77.3}$, $C=1{,}337\times 10^{-6}\underline{/90.9^\circ}$, and $D=0.77\underline{/3.6^\circ}$, the driving point impedance, viewed from Midian, being B/D.

Converting to the nomenclature used in the subject paper, assuming the Midian and Omaha terminals to be terminals A and B, respectively, the line constants are

$$Z_{BR}=B=282\underline{/77.3^\circ}\text{ ohms}$$

$$Z_{RR-B}=B/D=366\underline{/73.7^\circ}=102+j\,351\text{ ohms}$$

Since the curves of Figure 11 of reference 1 of this discussion are based upon line-terminal voltages, condition 4 of Table I of the subject paper applies or

$$Z_x=0$$
$$Z_y=Z_z=Z_{RR-B}=102+j\,351\text{ ohms}$$
$$K=|K|\underline{/\theta_K}=\frac{Z_{BR}}{Z_{RR-B}}=\frac{282\underline{/77.3^\circ}}{366\underline{/73.7^\circ}}=0.77\underline{/3.6^\circ}$$

With the magnitude of $Z_y=$unity

$$Z_z=Z_y=1\underline{/73.7^\circ}=0.28+j\,0.96$$

A thin piece of graph paper was chosen, so that five major divisions corresponded to the distance between points A and B of the general impedance chart, Figure 6 of the subject paper. Resistance and reactance axes were labeled, so that the distance between A and B corresponded to one per unit; point A was located at $R=0$, $X=0$ $(Z_z=0)$; and point B was plotted as Z_z, $R=0.28$, $X=0.96$.

The graph paper was placed on top of the general chart so that points A and B of the former coincided, respectively, with points A and B of the latter. The sheets were clipped together, and the significant portions of the general chart circles were traced freehand with a pencil.

The constant-voltage-ratio circles were labeled for E_A/E_B by dividing $|E_AK/E_B|$ given on the general chart by $|K|$, and the constant-angle arcs were labeled in terms of δ by subtracting θ_K from the values of ϕ given on the general chart.

In this instance, the curves were traced in ink for the purpose of this discussion. Ordinarily, if a record be desired, adequate reproductions may be made from the pencil tracing.

On the resulting diagram, Figure 1 of this discussion, four points from Figure 11 of reference 1 of this discussion have been plotted after reduction to per-unit values. It will be noted that there is close correspondence between these points and the results obtained from the general chart.

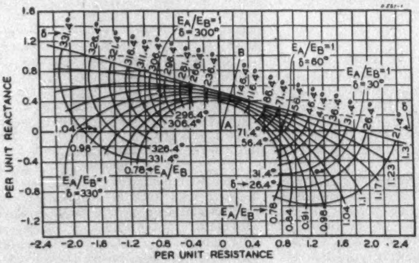

Figure 1. Impedance seen by a relay at Midian, Kans. (Omaha – Midian line)

Terminal A—Midian, Kans.
Terminal B—Omaha, Nebr.
Base ohms—366

REFERENCE

1. PERFORMANCE REQUIREMENTS FOR RELAYS ON UNUSUALLY LONG TRANSMISSION LINES, F. C. Poage, C. A. Streifus, D. M. MacGregor, E. E. George. AIEE TRANSACTIONS, volume 62, 1943, June section, pages 275–83.

Lightning Investigation on Transmission Lines—VIII

Discussion and authors' closure of paper 45-26 by W. W. Lewis and C. M. Foust, presented at the AIEE winter technical meeting, New York, N. Y., January 22–26, 1945, and published in AIEE TRANSACTIONS, 1945, March section, pages 107–15.

E. D. Sunde (Bell Telephone Laboratories, Inc., New York, N. Y.): I would like to make a few remarks regarding Figure 8 of the paper by Lewis and Foust, which shows the relation between the tower-footing surge resistance and the normal tower-footing resistance, as measured with low current. The telephone engineer is interested in the resistance of grounds to high surge currents in connection with the protection of the telephone plant against lightning. From the studies we have made, the curve shown in Figure 8 appears doubtful, unless the breakdown voltage of the soil is much lower than generally is assumed. To account for the decrease in surge resistance shown in Figure 8, the breakdown voltage of the soil would have to be in the order of 100 volts per centimeter, whereas the value derived from other experiments on the surge resistance of grounds, such as those by Bellaschi, indicate a value 20 to 100 times greater.

It is possible that the low ratio obtained may have been due to the soil formation along the line on which the experiments were made. If the soil consists of an upper layer of sand and a lower layer of good conducting material, the lightning current may channel through the sand to the good conducting soil, and the surge resistance then may be very much smaller than the normal tower-footing resistance. For a soil of fairly uniform conductivity, however, the reduction would be much smaller.

Another question in connection with the curve shown in Figure 8 is the validity of the method used to derive the surge resistance from the measured potential difference between the tower and a probe six feet to 12 feet away. In extrapolating from the measured potential difference to the potential which would be expected, if the probe were at a great distance, two assumptions were made. One is that the earth may be assumed to have a uniform resistivity, which is rather doubtful in the present case. The second assumption is that the same extrapolation method may be applied as in the case of low currents where breakdown of the soil does not take place. Assume for instance that breakdown of the soil occurred around the tower, so that a good conducting hemisphere extending out to the probe was formed in the ground. A negligible potential then would be measured between the tower and the probe, and, when this potential difference is multiplied by a factor of 2.5, as in reference 3 of the paper, a very small surge resistance would be obtained. The surge resistance, however, would in this case be that of a conducting hemisphere extending out to the probe, which would be about 60 per cent of the normal tower-footing resistance, when the probe is at a separation of six feet from the tower and the equivalent tower radius is assumed to be nine feet.

I would like to add that the data presented in this paper will be of considerable value in connection with studies of lightning damage to the telephone plant and that we are indebted to the authors for the paper.

J. H. Hagenguth (General Electric Company, Pittsfield, Mass.): The authors have obtained a great amount of data on the amplitude of lightning strokes to transmission lines. This knowledge has been used with great advantage in improvements of grounding conditions of transmission-line towers so that it appears possible to install lines which are practically lightningproof.[1]

Due to the scant oscillographic information of wave fronts of lightning surges near the point of origin, any attempt to measure the rate of rise by other means is highly commendable. Such information is very desirable for intelligent analysis of the type of impulse tests which need to be applied to apparatus installed in power-system stations.

The device used for these investigations easily is adapted for the purpose. It has, however, several limitations which must be kept in mind when analyzing the results.

1. It measures the maximum rate of rise. It is therefore not capable of accurately describing the wave front in its entirety. It is, however, the wave front as a whole which determines the stresses imposed on the apparatus. Figure 1 of this discussion shows two waves, both with the same maximum rate of rise. The difference in effect of the two waves as regards sparkover of insulation[2] and internal voltage distribution in transformers, for instance, is obvious.

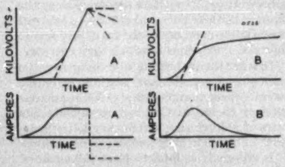

Figure 1. Response of wave-slope indicator

Wave-slope recorder indicates same rate of rise in both cases

A—Steep-front wave—high crest voltage

B—Slow-front wave—low crest voltage

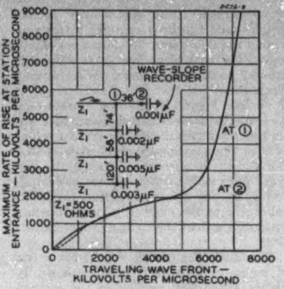

Figure 3. Relation between rate of rise of traveling wave and two points in the station

2. The device itself is a wave modifier, and this effect is beneficial, because the steepness of the incident traveling wave is reduced. In those cases where the coupling capacitor is of the order of 1,000 micromicrofarads, the steepest front permitted by the device on a line with insulation as described in the paper is of the order of 2,000 kv per microsecond. Incidentally, the same would be true for transformers, which have an impulse capacitance of about the same order. On phase wires not equipped with the device, much higher rates of rise can occur. Therefore, the highest rates of change measured are not necessarily the highest rates which can occur in a station, unless all phase wires are equipped with the same devices.

3. The fact that the capacitor is connected by means of some 30 or more feet of conductor between line conductor and ground introduces a considerable amount of inductance. The voltage across the capacitor in that case is, therefore, not a true reproduction of the voltage at the line conductor. Figure 2 of this discussion shows the voltage at the line conductor and across the capacitor proper at the entrance of a station with extended bus structure. The lead length was taken as 36 feet. It is obvious that the capacitor-voltage wave shape departs greatly from the actual voltage appearing at the conductor, particularly for the steepest applied waves.

4. However, this fact is mitigated in that in this particular example at least, the maximum rate of rise is about the same at the conductor and capacitor for 2,000 kv per microsecond and less as shown in Figure 3. Steeper fronts, however, cannot be measured.

5. In stations of the type investigated, where extended bus structures are used, the rate of voltage change at the station entrance is subjected to many large irregular reversals due to repeated reflections between points along the station bus where other circuits with their coupling capacitors or transformer capacitance are connected. With reversals of the order shown on Figure 2, it should be exceedingly difficult to arrive at the highest rate of change occurring at the point of measurement even when a unidirectional wave is applied. In practice, the steepest wave fronts applied to a given station will originate very close to the station and will consist of a steep rising front and a steep dropping tail. In this case, the voltage wave at the capacitor will appear as shown on Figure 4 neglecting the inductance of the lead. It seems impossible that the magnetic links are capable of evaluation for the maximum rate of change in such a case. Similarly, when successive waves of opposite polarity are applied between inspection periods, the evaluation of results should be extremely difficult.

6. The maximum wave-slope records obtained in stations during this investigation probably represent the average rate of rise of the station as a whole. In stations with extended bus structures, many connected circuits and relatively large capacitances (coupling capacitors and transformers), the rate of rise of voltage varies considerably from one end of the station to the other. At the far end the fronts are slower and the reversal is less pronounced than at the point where the traveling wave enters, and the resulting record will give a fairly true representation of the maximum rate of change at that point.

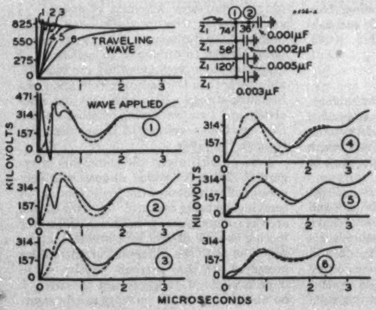

Figure 2. Difference between capacitor voltage and voltage to be measured

——— —Voltage at 1

– – – – —Voltage at 2

$Z_1 = 500$ ohms

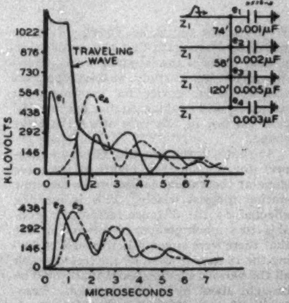

Figure 4. Effect of chopped wave on voltages in stations

$Z_1 = 500$ ohms

7. When using the wave-slope-indicator method, it would appear necessary to remove the links, at least after every storm, to minimize the possibility of overlapping records. This should result in a clearer picture of the true rates that existed during a minimum number of transients.

The authors mention that the voltage reaching the station will be limited to the reduced line insulation flashover or tube discharge voltage of the order of 680 to 850 kv. These values seem to be the critical flashover voltages. It is not clear why the crest voltages cannot reach values as given by the volt–time characteristics of the insulator string, which, for the reduced line insulation section, can be as high as 1,600 kv at the point of stroke contact. Of course, such waves will attenuate rapidly. However, in the paper by Gross and Lippert,[3] it has been shown that strokes contact the line wire either directly or by flashover from the tower structure or ground wire to the conductor within a few hundred feet of the station. Under such conditions, the crest as well as the rate of voltage rise of the traveling wave can be greatly in excess of the quoted values.

In Figure 7, it would be interesting to know whether the currents in towers plotted include all tower currents measured or only those through a stricken tower or the two towers nearest the stroke in case of a stroke to a ground wire in mid-span. These are really the important currents as far as evaluation of ground resistance and line insulation are concerned, and it would be worth while to have statistics on these currents separate from the remaining tower currents. The latter should be the greater number with amplitudes of 20,000 amperes or less and therefore should pull down the tower current-frequency curve considerably.

REFERENCES

1. AN EIGHT-YEAR INVESTIGATION OF LIGHTNING CURRENTS AND PREVENTIVE LIGHTNING PROTECTION ON A TRANSMISSION SYSTEM, E. Hansson, S. K. Waldorf. AIEE TRANSACTIONS, volume 63, 1944, May section, pages 251–8.

2. VOLT-TIME AREAS OF IMPULSE SPARK-OVER, J. H. Hagenguth. AIEE TRANSACTIONS, volume 60, 1941, July section, pages 803–10.

3. LIGHTNING INVESTIGATION ON 132-KV SYSTEM OF AMERICAN GAS AND ELECTRIC COMPANY, I. W. Gross, G. D. Lippert. AIEE TRANSACTIONS, volume 64, 1945, February section, pages 76–84.

W. W. Lewis and C. M. Foust: We agree with Mr. Hagenguth that the coupling capacitor modifies the incoming wave. However, in our 138-kv study, we used capacitors that were in service for carrier-current telephony and relaying, so that our installation did not in this case affect the wave shape.

As shown in the paper by Gross and Lippert (for example their Figure 8), the wave slope at the various indicators in the same station differed widely. This is possibly affected by the distance factor but probably to a much greater extent by the fact that there were apparently five strokes during the 16 days covered by the records, with all the various superpositions that would be brought about by so many strokes. Practically, the way things are, there isn't much that can be done about this situation. We only can take a mass of data, stand back, and look at it, and see if a trend can be discerned. The cathode-ray oscillograph would tell the story much better, providing the film could be shifted automatically after each surge and providing that several oscillographs were placed around the station.

For our Figure 7 one tower current only was selected for each stroke, and that was for the tower with the highest current, where several towers were involved in a stroke. For the stroke currents, Figure 6, the currents were added up for all the towers affected by the stroke, and the total was called the stroke current. This procedure was explained in the sixth paper of the series.[1]

Mr. Sunde has questioned the low ratios of surge to normal resistance shown in Figure 8 and the validity of the method used in arriving at these ratios. We have made two assumptions in our calculations: First, that the tower may be represented as a cylinder with a circular base which circumscribes the tower footings, and second, that the current from the tower footing to the earth is distributed uniformly in the earth. These assumptions are simple and obvious, although actually neither of them may be correct. Bellaschi, Armington, and Snowden,[2] check our low values for similar types of soil. Such values, however, may apply only to the high-resistance sandy soil encountered in this investigation. In other types of soil, especially low-resistance soil, the values of ratio of surge resistance to normal resistance may be and probably are higher.

REFERENCES

1. LIGHTNING INVESTIGATION ON TRANSMISSION LINES—VI, W. W. Lewis, C. M. Foust. AIEE TRANSACTIONS, volume 56, 1937, January section, pages 101–06, 189.

2. IMPULSE AND 60-CYCLE CHARACTERISTICS OF DRIVEN RODS—II, P. L. Bellaschi, R. E. Armington, A. E. Snowden. AIEE TRANSACTIONS, volume 61, 1942, pages 349–63.

Lightning Investigation on 132-Kv System of American Gas and Electric Company

Discussion and authors' closure of paper 45-18 by I. W. Gross and G. D. Lippert, presented at the AIEE winter technical meeting, New York, N. Y., January 22–26, 1945, and published in AIEE TRANSACTIONS, 1945, February section, pages 76–84.

F. J. Vogel (Illinois Institute of Technology, Chicago, Ill.): In order to use an economical amount of material in the design of a system, it is necessary to know the stresses which exist, and this paper adds to our store of knowledge in this respect.

One of the most prominent facts brought out in this paper is that the currents and voltages on the lines are quite low. I have heard it said that the basic insulation levels were too high. On the basis of the data in the paper, I wonder why a level of 550 kv might not be satisfactory for this system and perhaps generally for the operating voltage. If this method of attack were to be used generally, the system designer would need to know how to estimate the voltages and currents depending on the overhead protection and arrester characteristics, and I believe means are available for such estimates. I wonder if such estimates have been made and how well the results check.

On the other hand, I know of two cases where a transformer failure, or a relatively long air-gap flashover occurred, with arrester and overhead ground wire protection. From the results, I inferred, perhaps not correctly, that even with such protection, extremely high currents and voltages could be obtained. Whether they should be considered in apparatus design is another question. If so, perhaps transformers should be designed to withstand them. I believe that such rare overvoltages would be in the nature of steep-front surges, and that steep-front tests might be desirable. What do the authors think?

Figure 4 of the paper is of interest in indicating such extremely high rates of voltage rise for switching surges. Since they are probably low in magnitude, they must have had fronts of extremely short duration.

J. T. Lusignan, Jr. (Ohio Brass Company, Mansfield, Ohio): A worthwhile contribution to the lightning history of their 132-kv system has been given by Gross and Lippert. This history should prove very valuable to transmission-line designers in determining the proper steps for insuring lightning protection to their systems, particularly around the 132-kv range. The reports by Gross and Lippert show the steps taken by them and their associates to gain protection, and the successful goal they have attained, since the damage to their lines and station equipment is negligible even under the relatively severe lightning conditions in which they operate.

In addition to helping line designers, the data they have obtained are also valuable to equipment manufacturers. Of particular interest to me in this last report are the rates of voltage rise, which they have measured under lightning and surge conditions. It is especially helpful to have the authors' data vindicate the use of the present 1,000-kv-per-microsecond rate of rise for station apparatus, so that the manufacturers can continue to check their designs on laboratory life tests with that voltage application.

At the bottom of Table I of the paper, I would like to know what is meant by the phrase "discharge kilovolts of tubes." I am wondering whether the kilovolt figures represent the flashover of both the tube and series air gap to conductor in each case. I note that these voltage values are appreciably lower than the flashover voltages of the insulator strings with which they are associated, and I am wondering whether it takes that much less voltage to insure flashover through the tubes.

I am puzzled about the comments in regard to Table XI which discuss relatively greater effectiveness of the tower footings in carrying lightning currents. In other words, are the counterpoise, ground rod, and tower footing in each case of measurement, all in series, so that the different current values measured are due to their relative surge impedances? If they are not in series, I do not see how their currents can be compared. Perhaps the authors can refer me to a previous paper where the current paths involved have been diagrammed or more fully described.

J. H. Hagenguth (General Electric Company, Pittsfield, Mass.): The outstanding contribution of this investigation seems to be that it has been proved, over a five-year period, in stations equipped with lightning arresters and ground-wire protection over the line conductors that:

1. The bus voltage has not exceeded the full-wave voltage of 550 kv of the basic insulation level of the station equipment insulation.
2. Currents in lightning arresters were low.
3. No damage either to equipment or protection has occurred during the five-year period, although strokes to the lines occurred within a mile's distance from the station.

From the practical point of view, it therefore has been demonstrated that stations can be made lightningproof provided the proper protection is applied.

There are a few points brought out in this investigation which, at first glance, appear contradictory:

1. High line-conductor currents not associated with arrester operation.
2. Great difference of rate of voltage change in different parts of an extended station bus.

Transient theory permits calculations of all voltages and currents to a high degree of accuracy. It is impossible in this discussion to go into detail. Two types of stations investigated have been analyzed, and the results are shown on Figure 1 and Figure 2 of this discussion for stations of the type of Glen Lyn or Claytor and Reusens respectively.

As the applied wave, a slanted front has been chosen. The crest voltage is the maximum breakdown voltage of the line insulation for a straight rising front.[1] Attenuation is neglected. The resulting station voltages and currents represent, therefore, the maximum possible in case of a stroke very close to the station. After the wave reaches crest, it is assumed to decrease to zero rather rapidly.

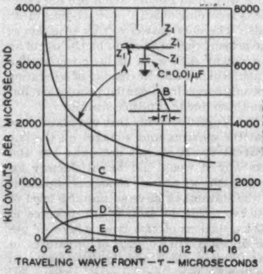

Figure 1. Transients in stations

A—Line currents
B—Traveling wave
C—Traveling-wave voltage and current
D—Station voltage and outgoing line current per line
E—Rate of change, station voltage
$Z_1 = 500$ ohms

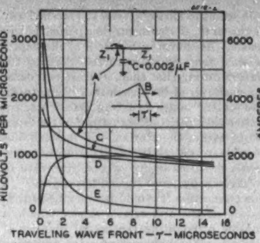

Figure 2. Transients in stations

A—Line current
B—Traveling wave
C—Traveling-wave voltage and current
D—Station voltage and outgoing line current per line
E—Rate of change, station voltage
$Z_1 = 500$ ohms

We find from Figure 1 of this discussion that the steepest waves will have the highest traveling-wave voltage, but the lowest resulting station voltage. For instance, a wave with 0.5-microsecond front, 1,590-kv crest, and 3,180-ampere traveling-wave current, will result in a line current of 6,150 amperes, but a station voltage of only 140 kv which, of course, is not sufficient to cause arrester operation. On the other hand, a front of four microseconds, with 1,140-kv crest, 2,280-ampere traveling-wave current, will result in a line current of 3,800 amperes and a station voltage of 410 kv, which is sufficient to cause arrester operation for the modern arresters for the 115-kv voltage class.

From Figure 2 of the discussion for a station with much smaller connected capacitance and fewer connected circuits, conditions are much less favorable, and arrester operation can occur for much lower values of traveling-wave voltage and current.

In the two examples, the wave was assumed to have arrived over one circuit only. Many of the lines of the system described are double-circuit lines on the same tower. In case of flashover to the same phase of both circuits, the station voltage and rate of voltage change will be doubled. For waves with longer tail, the station voltages will be of the same order, because, although the station voltage will be higher for equal traveling-wave crest voltage, the traveling-wave crest voltage will be much lower.[1]

Line current, as measured by the magnetic links, is the superposition of the traveling-wave current and the current wave reflected from the station impedance. As can be seen from Figure 1 and Figure 2 of this discussion, the line current is practically double the traveling-wave current for the steep waves. This is due to almost complete reflection from the station capacitance; for the longer wave fronts, the remaining connected circuits will act as the principal reflection agents.

This shows, therefore, that it is possible to have very high line currents without arrester operation.

In the examples, station impedance has been considered as lumped. Actually, some of the stations have very extensive bus work of the order of several hundred feet. The solution in this case has to take into account repeated reflections from all the reflection points. Calculations of this kind become very involved. It can, however, be proved that substitution of the equivalent inductances of the station bus conductors corresponding to the lengths of its sections will give the same results as calculations by means of repeated reflections. This method has been used to find voltages in the same station as on Figure 1, but with capacitances and connected circuits distributed as shown on Figure 3 of this discussion using the electric transient analyzer.[2] The traveling wave in this case was applied over one, as well as over two circuits.

The example shows the complex character of the waves, particularly at the station entrance. It is questionable that the wave-slope recorder is capable of identifying the proper high rate of voltage change occurring at that point. The rate of voltage change at the other end of the bus is, of course, much slower. It exhibits oscillations which are more regular and therefore more susceptible to interpretation by the wave-slope recorder. A station-voltage-distribution diagram of this kind, of course, proves the authors' conclusion that it is advisable to keep protective devices close to the equipment to be protected.

The method used to calculate the station voltages is accurate and very general in that any conceivable combination of station impedances connected by any number of bus wires can be investigated, including protective equipment. It is, therefore, possible in the laboratory to predict the expected transients in any station, including in many cases voltages transmitted to the low-voltage circuits, for any kind of traveling wave, provided the terminal impedances are known. The impedances of connected circuits can be calculated. Transformer impedance in high-voltage circuits is principally the surge capacitance to ground shunted by a rather high inductance, which can be neglected for short-time transients.

Finally, I would like to discuss briefly the high arrester-current record of 16,000 amperes. No details are mentioned other than that the stroke occurred within 400 feet of the station.

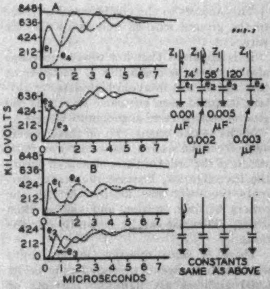

Figure 3. Transient voltages in stations with extended bus structure

A—Traveling wave on two circuits
B—Traveling wave on one circuit
$Z_1 = 500$ ohms

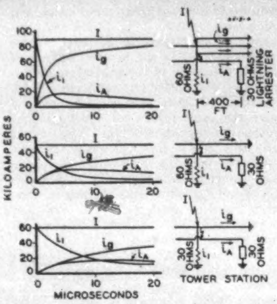

Figure 4. Currents in ground wires and lightning arresters for strokes close to the station

Similarly to substitution of surge impedance by inductance within the station, inductances can be used for longer lengths of lines.[3] If the stroke occurs within 400 feet, this probably means the first tower out. Neglecting, for convenience, the line side of the circuit, the equivalent diagram of Figure 4 of this discussion is obtained. For ease of calculation, a rectangular current wave was assumed. For lightning-arrester impedance, the lowest resistance occurring at the highest current crest was used. By means of the transient analyzer calculations can, of course, be made for different wave shapes and correct arrester impedance, including gap breakdown and also taking into account the line side of the system. The currents in the tower, ground wire, and arrester are shown for different conditions of ground-wire installation—single and three conductor—and tower resistance—60 ohms and 30 ohms.

From these calculations, it can be seen that:

1. Three ground wires from the first tower to the station are very effective in reducing the chance of high arrester currents, because a very high stroke current—90,000 amperes—is required to produce 17,000 amperes in the arrester.
2. Low ground resistance at the tower also increases the required stroke current amplitude.

This applies to the condition of a stroke to the ground wire as well as to the line wire.

It is apparent that low tower resistance also reduces the possibility of flashover at that tower, and to avoid high arrester current it would seem advisable to reduce the ground resistance to a minimum value.

If the stroke occurs two or three towers away from the station, the arrester currents will be of the order of those measured during the investigation, because the stroke currents then will flow mostly through the towers between station and the stricken tower. This also can be shown by calculations.

There is some question in my mind whether line currents measured at or below 3,000 amperes are lightning currents or system short-circuit currents. In a previous paper,[4] values of short-circuit currents of this order were mentioned. Since short-circuit currents follow the lightning flashover, it is likely that magnetization of the links at least will be greatly affected.

It seems to me impossible to correlate any of the data, if the inspection period is two weeks. As shown in Figure 8 of the paper, at least five strokes occurred close to the station during that time, at least two causing flashover of line insulation. Superposition of the many resulting transients, together with the complex nature of the transients within the station, will make it impossible to correlate any of the measurements as to damping effects, true rate of voltage change, and station impedance. In this connection it would be very helpful to install, at the arresters, a device which is capable of counting the actual number of discharges through the arrester occurring during an inspection period.

My opinion differs from the authors' opinion that the investigation has shown that the 1,000-kv-per-microsecond rate of rise for test specifications on apparatus seems reasonable, insofar as the amplitude of such tests are concerned. The investigation has shown that crest voltages were limited to 525 kv with a full-wave test level of 550 kv. The 1,000-kv-per-microsecond test requires a crest voltage of 800 kv. We then have the contradictory condition that for long waves with slow fronts, which are much more frequent, the margin between test voltage and arrester voltage is between 5 per cent and 37 per cent, while for the considerably less frequent 1,000-kv-per-microsecond waves, the margin is above 50 per cent. Perhaps consideration should be given to reducing the margin in the latter case to, say 20 per cent, which results in a crest voltage of the order of 630 kv or equivalent to the chopped-wave test. The investigation also has shown that flashover within the station did not occur, and consequently the steep voltage drop on the tail of steep front and chopped waves occurring during test is not realized in stations of the type discussed in the paper. It is this steep drop which is most dangerous for internal stresses in the transformer. By taking advantage of the excellent protection provided, the transformer insulation could be reduced, if tests equivalent to the stresses imposed in the field be applied, without impairing the effective strength of the transformer for the service intended.

References

1. Volt-Time Areas of Impulse Spark-Over, J. H. Hagenguth. AIEE Transactions, volume 60, 1941, July section, pages 803–10.

2. Oscillograph Electric Transient Analyzer, N. Rohats. *General Electric Review*, volume 39, 1936, pages 146–9.

3. Discussion by J. H. Hagenguth of Study of Driven Rods and Counterpoise Wires in High-Resistance Soil on Consumers Power Company 140-Kv System. AIEE Transactions, volume 61, 1942, pages 1001–02.

4. Protector-Tube Application and Performance on 132-Kv Transmission Lines—II, Philip Sporn, I. W. Gross. AIEE Transactions, volume 57, 1938, September section, pages 521–30.

I. W. Gross and G. D. Lippert: Mr. Hagenguth points out that our paper brings out the fact that stations can be made lightningproof provided the proper protection is applied. Our own experience over the past 15 years has borne this out quite emphatically. The few isolated cases of failure of equipment on our high-voltage system have been limited to very old equipment having questionable impulse characteristics. In this connection it may be of interest to note that shielding on our incoming lines had a protective angle of approximately 45 degrees, rather than the more recently proposed angle of 30 degrees, which some investigators seem to think necessary for best immunity from strokes to the conductors. Further, it should be pointed out that most of our 132-kv stations are protected by arresters rated 109 kv.

Mr. Hagenguth's discussion and theoretical analysis of the two points showing high line-conductor currents without arrester operation and large differences of rates of voltage change in different parts of the station are most interesting. He shows clearly what can be done by the use of a transient analyzer and theory in explaining some of the records which at first glance appear rather baffling.

His comments on the arrester-current record of 16,000 amperes mentioned in the paper assume that this current was the result of a stroke to the first structure from the station. This is correct. From his calculations it is indicated that a stroke of some 90,000 amperes would be required to produce such an arrester current. This is entirely possible. However, no instruments were in service on line conductors, ground wires, or towers in this particular case, so the actual stroke value is not definitely known.

The possibility of 60-cycle fault currents affecting the line-conductor current measurements has been considered carefully, and, while it is possible that some of our records may have been so affected, it is believed that cases of this sort are rare. The justification for believing that currents between 2,000 and 3,000 amperes were not due to 60-cycle fault currents is borne out by the fact that most of the currents in this range were not oscillatory, a feature which would have been shown up in the calibration by the two-link method of measurement.

Mr. Hagenguth mentions the difficulty in attempting to correlate simultaneously obtained data when the inspection period is as long as two weeks. This is one of the limitations in obtaining field data on lightning with instruments which are not capable of recording definite or short-time intervals. The only answer to this situation at the present time appears to be the use of an instrument such as a cathode-ray oscillograph, which would be capable of separating not only surges from one day to another, but also those due to multiple strokes.

Mr. Vogel mentions that our data show that the currents and voltages on the line adjacent to the station are quite low and asks why it would not be satisfactory for the system (we assume he means apparatus at the station) to have an impulse level of 550 kv. This, in fact, is our practice in 132-kv stations of this type, where we use the so-called 115-kv class of apparatus in transformers which are closely coupled to the 109-kv lightning arrester. This combination on paper, as well as in practice, gives an ample margin of impulse protection.

Mr. Vogel comments on the extremely high rates of voltage rise for switching surges and suggests that they were probably of low magnitude. It may be of interest to point out a record of a switching surge obtained during field research tests on the

Philo–Canton line of the Ohio Power Company in 1929.[1] This switching surge had a magnitude of 450 per cent of normal line-to-ground voltage—approximately 500-kv crest. Parts of the first cycle of this surge had an extremely high rate of voltage change as shown on the oscillogram. However, because the time scale is long duration, it possibly does not show up clearly as a high rate of change.

We believe that these rates of voltage change for switching surges reported in Figure 4 of our paper may have some considerable significance when studied in combination with the strength of insulation material as used in transformer design.[2,3]

The answer to Mr. Lusignan's question as to what is meant by "discharge kilovolts of tubes" at the bottom of Table I is that the phrase refers to the impulse voltage required to cause the protector tubes to go into action, or flashover internally and perform their function of discharging lightning from the line to ground. Since these tubes, when used, were mounted on the insulator assembly, they were designed to have a lower-impulse flashover than the insulator string, in just the same way as the lightning arrester, as applied, limits the voltage below the safe strength of the transformer or other equipment which it protects.

Mr. Lusignan commented on the relative effectiveness of tower footings, counterpoise, and ground rods in carrying lightning currents. These data in Table XI were obtained simultaneously on the three grounding elements, namely counterpoise, ground rod, and tower footing. In each case the counterpoise and ground rod were connected electrically directly to the tower footing. The relative currents in these three elements are compared on the basis of their magnitude in three parallel circuits. The ground rod was driven in line with two tower legs and midway between them. The buried counterpoise extended in a straight line directly underneath the transmission circuit.

The matter of steep-front surges has been mentioned by all three discussors. Mr. Lusignan seems quite satisfied that our data justify the continuance of the present 1,000-kv-per-microsecond rate of rise now generally accepted in the industry. Mr. Vogel, too, believes that steep-front tests are desirable on transformers at least. We heartily agree with him that such tests are just as important as, if not more than, the now generally accepted chopped-wave and full-wave tests on the transformers.

Mr. Hagenguth, however, does not seem to find anything in the data presented which justifies a 1,000 kv-per-microsecond rate of rise on test specifications for apparatus. The authors have shown the highest rate of rise recorded is 810 kv per microsecond, with two cases of approximately 650 kv per microsecond.

We are unable to understand Mr. Hagenguth's statement that "the 1,000 kv-per-microsecond test requires a crest voltage of 800 kv." This value is lower than we specify for test purposes on our 132-kv equipment. In fact, from the data presented in the paper it seems logical that a factor of safety of two well might be used, which would indicate a rate of voltage rise of two times 650 or two times 810, that is, in the order of 1,500 kv per microsecond rather than the present figure of 1,000 kv per microsecond.

The service supplied by large high-voltage power systems and equipment is too important, and the cost of failure and consequent disturbances too great, to push the margin of transformer strength down to the lowest possible limit. Many years of painstaking study and effort have been spent in building a needed insulation strength into equipment, and to let down the bars at this time by reducing test requirements on the limited amount of data, without fully evaluating the hazards involved, is decidedly questionable.

REFERENCES

1. AIEE LIGHTNING REFERENCE BOOK, 1918–35. Page 659.

2. BREAKDOWN CURVE FOR SOLID INSULATION, V. M. Montsinger. AIEE TRANSACTIONS, volume 54, 1935, December section, pages 1300–01.

3. PROTECTION OF POWER TRANSFORMERS AGAINST LIGHTNING SURGES, AIEE committee on electric machinery, transformer subcommittee. AIEE TRANSACTIONS, volume 60, 1941, pages 568–77.

The Dielectric Strength and Life of Impregnated-Paper Insulation—IV

Discussion and author's closure of paper 45-58, by J. B. Whitehead and J. M. Kopper, presented at the AIEE winter technical meeting, New York, N. Y., January 22–26, 1945, and published in AIEE TRANSACTIONS, 1945, April section, pages 171–7.

Herman Halperin (Commonwealth Edison Company, Chicago, Ill.): In investigations of condensers, coil insulation, and so forth, worth-while use might be made of the tool and method developed by Doctor Whitehead and associates to detect initial ionization and to follow ionization without failure of the dielectric. Their work has been on short samples representing impregnated-paper insulated cables, and there are many other electrical assemblies involving similar amounts of insulation.

I was connected actively with the initial development work of this kind which was done by E. B. Paine and his associates at the University of Illinois under the sponsorship of the Utilities Research Commission. They obtained encouraging test data in research on cable samples 10 or 20 feet long. We found, however, that the apparatus was not applicable to tests of long lengths of cable at the factory such as 500 feet, because apparently the indications of very high-frequency discharges were attenuated seriously by the time they reached the end of the length of cable.

Experience has shown in the ordinary ionization test, where the power factor usually is measured at 60 cycles at a high- and a low-voltage and the power factor at the lower voltage subtracted from the other power factor to get the so-called ionization factor, that the test results are confusing. This sometimes is especially true for insulation at elevated temperatures when the ionization factor is negative in value. The apparatus of the authors will give more direct and reliable data on ionization in such cases.

Regarding the authors' data on examinations of insulation made possible just before failure by use of their apparatus, I should like to call attention to data in a 1936 AIEE paper.[1] For those studies we had 60-cycle aging tests on cables stopped when the power factor started to rise abruptly, and then through dissection of the cables we found the nature of initial paths that were leading to failure. Most paths started at the conductor of the solid-type single-conductor 66-kv cable, but some started at the sheath, and some of these paths were helical in direction.

It is to be noted that the authors' investigations were of necessity at high stresses, for example three to five times the maximum operating stresses in oil-filled cable. Further work along such lines well might include some longer-time tests at stresses closer to operating stresses to disclose what changes in characteristics, if any, apply to such stresses.

REFERENCE

1. STUDIES OF STABILITY OF CABLE INSULATION, Herman Halperin, C. E. Betzer. AIEE TRANSACTIONS, volume 55, 1936, October section, pages 1074–82.

Wm. A. Del Mar (Phelps Dodge Copper Products Corporation, Yonkers, N. Y.): The authors have contributed a research tool of great value in their combination of Schering bridge, oscilloscope, and thyratron cutout which should prove of great value in the study of dielectric failure. One study that I should like to see made with it would be a check of Hoover's theory that, when breakdown is imminent, the maximum stress shifts outward from the surface of the conductor to a region in the depths of the insulation. Perhaps the data already obtained may throw some light on this, and I hope the authors will discuss this interesting point.

It is pleasing to note that the authors now confine their dictum about the superiority of low-density paper to cable of the oil-filled or completely impregnated type.

Manufacturers can accept this without any qualms, because oil-filled cable never has been designed for maximum 60-cycle dielectric strength but rather for maximum impulse strength which is attained by the use of high-density paper.

On the other hand high-density paper is used in the manufacture, of solid-type cable to obtain high dielectric strength at 60 cycles, as the wall thicknesses are ample to take care of impulses.

The authors deplore the lack of published data to prove the advantage of high-density paper in solid-type cable. The reason that such data are not available is that there is a considerable variation of dielectric strength in cables of that type because of their inherent irregularity. It is therefore impossible to differentiate between cables made with papers of moderately different densities except by averaging a large number of tests. This has been done, over and over again, and the high-density papers always average best. Moreover, if very low-density paper is used, the cables will not stand even the normal full-reel test voltage.

This difference in behavior of oil-filled and solid-type cable is no mystery, if one remembers that there are two basic factors to be considered in studying the dielectric strength of a cable, one, being its ability to resist the initiation of breakdown, and the other, its ability to resist the spread of breakdown once it has started.

In an oil-filled cable, such as represented by Doctor Whitehead's samples, initiation of breakdown requires the very high stress in the oil, which corresponds to the breakdown of oil into highly ionized gas. Paper of low dielectric constant, by throwing less stress on the oil for a given applied voltage, naturally raises the applied voltage at which breakdown of the oil occurs.

In a solid-type cable, initiation of breakdown occurs at the comparatively low stress required to ionize pre-existing voids, and the additional voltage test the cable will stand then depends on the ability of the insulation to resist ionic bombardment from the voids. The denser the paper, the greater its ability to accomplish this, and, therefore, the greater the dielectric strength of the cable.

This completely explains the apparent discrepancy between Doctor Whitehead's findings and those of the cable manufacturers.

However, there is one other factor that enters the picture. The effectiveness of high-density paper as a barrier to electronic streamers depends not only on its high density but also on the effective disposition of the tapes, that is, on the tape stagger or overlay. It is possible to lose completely the advantage of high-density paper in a solid-type cable by offering the electronic streamers a short cut around the paper tapes, through the use of too short an overlay. There is an optimum overlay for every paper density—that which gives equal dielectric strength through or around the tapes. Doctor Whitehead has used the same overlay for papers of all densities, a fact that should be remembered in evaluating his data. I called attention to the bearing of overlay on this question at the Williamsburg Insulation Conference of 1934, suggesting that Doctor Whitehead's overlays may have been too short to take full advantage of the greater dielectric strength of high-density paper. In other words, if he had repeated his tests using, however, less perfectly impregnated samples, he might have obtained results similar to those he has reported, but in that case the higher dielectric strength obtained with low-density paper would have been due, not to the merit of the paper, but to the use of an inappropriate overlay.

Finally I come to the matter of grading by the use of high-density paper near the conductor and lower-density paper over it. The authors' study applies, of course, only to oil-filled cable, and I have no experimental data to check their theory. Since the beginnings of oil-filled cable, however, it has been the practice to grade the paper of such cables in order to obtain the benefit of high impulse strength without sacrificing too much of the oil permeability of the insulation. It would, therefore, be gratifying to find that this construction adds to the 60-cycle dielectric strength. I am, however, very doubtful whether the authors' analysis is correct. Unfortunately their procedure for calculating stress in the oil channels is not given but appears to be based on the assumption that lines of force extend radially from conductor to sheath passing through whatever oil channels may be in the way and imposing a proportion of the total applied voltage on a channel at the conductor surface, which is determined by its capacitance and the capacitances of the several superimposed layers of paper of various densities and of oil channels all considered as capacitances in series. If so, their procedure entirely neglects the fact that the lines of force are diverted around each oil channel by the parallel paper paths by which they are surrounded. Moreover, the lines of force in a cable are very irregular due to the intrinsic irregularity of the paper. I therefore consider it a better approximation to use the formula for the stress in a cylinder of elliptical cross section given by E. B. Baker.[1] Using this formula and taking into account the over-all change in potential distribution resulting from grading, I obtain results widely different from the authors', indicating that no advantage in 60-cycle dielectric strength is obtained by grading oil-filled cable. Unfortunately I cannot check this by adequate experimental data, as no occasion has arisen which would justify the very expensive test setup that would be needed. Typical calculations using the Baker formula follow.

This formula for an elliptical cylinder, in a medium of different specific inductive capacity, is applicable, as a 5x75 mil oil channel with its fuzzy paper edges approximates a 5x75 ellipse as closely as the 5x75 rectangle, assumed by the authors. This formula is somewhat in error on the low side, because it neglects the proximity of the conductor, and, as Baker pointed out, the true factor may be greater; also, it will be greater for large values of K_p/K_o than for small values.

The formula is as follows:

$$G=\frac{1}{1-\dfrac{p(K_p-K_o)}{K_p(d+p)}}$$

where

G = ratio of stress in oil channel to that in impregnated paper
d = semiaxis in direction to field
p = semiaxis perpendicular to field
K_o = specific inductive capacity of cylinder
K_p = specific inductive capacity of medium

It will be noted, that if p is infinite, G becomes K_p/K_o which is correct for a continuous film of specific inductive capacity = K_o in series with a medium of specific inductive capacity = K_p. On the other hand, if d is infinite G becomes unity, so that the formula is correct at both limits.

Applying Baker's formula to the authors' *A* and *D* papers and assuming the specific inductive capacity of the oil to be 2.2, I obtain the following values of G using the following figures derived from the paper.

	A Paper	D Paper
d	2.5	2.5
$p=\frac{15\times 5}{2}$	37.5	37.5
K_p	3.78	4.9
K_o	2.20	2.20
G	1.64	2.08

Consider the case of two cables, number 1 graded, and number 2, made entirely of *A* paper, the dimensions being as follows:

		Cable 1, Graded	Cable 2, Not Graded
Radius of conductor, mils	a	264	264
Radius of outside of insulation	c	484	484
Radius of boundary between insulations	b	324	
Specific inductive capacity of the layers of insulation	K_{ab}	4.91	
	K_{bc}	3.78	
	K_{ac}		3.78

If we assume $V=50{,}000\,V$, the maximum stress in the impregnated paper will be as shown in the following tabulation calculated by well-known formulas.

Then using Baker's values of G, we find E_o, the stress in the oil, to be as follows, that is, the graded cable has a much higher oil stress than the ungraded.

	Cable 1, Graded	Cable 2, Not Graded
E_a (volts per mil)	260	312
G	2.08	1.64
E_o (volts per mil)	541	511

As pointed out, whatever error there may be in G will tend to make the 2.08 less in relation to the 1.64, and, therefore, the true E_o for cable is even greater in relation to that for cable 2, than indicated by the foregoing figures.

This puts a different aspect on the case, as with the authors' values of G for $n=4$, the graded cable would be favored as follows:

	Cable 1, Graded	Cable 2, Not Graded
E_a	260	313
G	1.70	1.46
E_o	443	456

However, the conclusions reached by the authors are not applicable to solid-type cables judging by test data we have obtained using the procedure given in sections 20 and 21 of the sixth edition of the Association of Edison Illuminating Companies "Specifications for Impregnated-Paper-Insulated Lead-Covered Cable, 'Solid' Type." These tests on new cable indicate no difference in 60-cycle dielectric strength whether the denser paper is placed inside or outside.

We prefer to place the high-density paper outside in solid-type cables, for reasons apart from initial dielectric strength. These reasons have to do with the ability of the cable to resist the combined action of high voltage and heat cycles, rather than high voltage alone, as described in another AIEE paper.[2]

REFERENCES

1. POTENTIAL AVAILABLE FOR GASEOUS DISCHARGE IN INSULATION VOIDS (letter), E. B. Baker.

Electrical Engineering, volume 53, February 1934, page 363.

2. A New Principle of Cable Design, Wm. A. Del Mar. AIEE Transactions, volume 60, 1941, May section, pages 206–10. Discussion, pages 705–17.

L. I. Komives (The Detroit Edison Company, Detroit, Mich.): Mr. Whitehead and Mr. Kopper state there is little or no published evidence in support of the view that the use of high-density paper in high-voltage cables increases dielectric strength "except perhaps as regards breakdown tests of the impulse type, and even in that case the picture is not clear."

In support of this statement they cite a paper by Mr. Foust and Mr. Scott published in July 1940.

I would like to call the authors' attention to a paper by Faucett and others.[1] In Table I of the paper average and maximum voltage gradients at breakdown are listed and the type of paper shown in each case. It should be noted that samples *A* and *C* having lower density papers near the copper broke down at a much lower voltage than samples *B* and *D*. Densities involved are 0.85 and 1 against 1.2.

There were a larger number of samples with higher-density paper which all tested high. This seems conclusive evidence that higher-density paper will produce higher impulse strength.

Reference

1. 120-Kv High-Pressure Gas-Filled Cable, I. T. Faucett, L. I. Komives, H. W. Collins, R. W. Atkinson. AIEE Transactions, volume 61, 1942, September section, pages 658–65.

J. B. Whitehead: In answering Mr. Del Mar there are two reasons why the Hoover analysis of breakdown is faulty as applying to impregnated paper-insulated cables; first, because it takes no account of the alternating character of the voltage and the fact that stress distribution is determined far more by the dielectric constant than by the conductivity; and second, the conductivity of impregnated paper is so low that the d-c volt–ampere curve on which the Hoover analysis is based cannot develop below stresses which are far above those at which, under alternating voltage, failure due to other causes occurs.

The Baker formula is a modified form of a number which have been presented (Maxwell, Lord Kelvin, and others) for the *uniform* field within a dielectric ellipse or sphere when placed in an originally *uniform* external field. The Baker formula is directed particularly to the determination of the stress in gas pockets within an insulating wall, making the somewhat questionable assumption that the gas pockets are elliptical in shape. The formula might be applied to an insulating wall in which similarly shaped, but isolated, oil pockets existed. Mr. Del Mar has made this assumption. It seems to me obviously wrong, for the oil in a channel is not in isolated drops, elliptical or other shape, but is a continuous ribbon filling the spiral of the oil channel. Our own approach at this point notes that the radial field is the same at all points along the oil ribbon and approximately uniform in its central region.

Moreover, formulas of this type give only the ratio of the internal to the original external field, and so the latter must be known if the former is sought. Mr. Del Mar assumes the original field to be the *average* field computed from the applied volts and the cable constants. This too is incorrect, for this value is not an original external field but contains the modifying influence of the field in the oil channels, the very quantity whose value is sought. In our analysis we have computed the field at the center of the oil channel in terms of the number of paper layers in radial series with the oil channel and the voltage over the characteristic number of layers, which, as determined by the overlay, repeats itself throughout the entire insulating wall.

The Baker formula takes no account of the number of paper layers in series with an oil gap (nor should it, for its particular application). By failing to take account of this fact Mr. Del Mar is led into the error of finding a higher value of *G* for the *D* paper (2.08) than for the *A* paper (1.64).

Mr. Del Mar again invokes his experiments on overlay reported at Williamsburg in 1941, but as yet unpublished. Naturally too small or too great an overlay may lead to short creepage paths along which failure might occur. But the failures reported in this series of papers for medium overlays, do not occur in that way, but originate in the oil channels themselves and are plainly due to radial stress.

The examples cited by Mr. Komives from the paper by Faucett and others, refer to gas-filled pressure cables. They, nevertheless, seem in large measure to agree with our own conclusions for oil-filled insulation, that is, cables *B* and *D* are graded cables with high-density paper inside, and they have higher breakdown values than cables *A* and *C*, both of lower-density paper throughout; no data are given for all-high-density paper.

The accumulated discussion of the four papers of this series has done much to clarify the open question as to the value of high-density paper for cable insulation. At first, our result showing the higher dielectric strength for lower-density paper was received with some skepticism. Cable manufacturers were using high-density paper with improved performance in solid-type cables, and several engineers seemed to find our results inconsistent with those of established practice. Now, however, it generally is recognized that our results were obtained on completely impregnated insulation of the oil-filled type and should not be invoked in the question of the influence of high-density paper in solid-type cables.

Further light is thrown on this question by noting the values of breakdown stress in our results. As pointed out by Mr. Halperin, these are from three to five times the operating stresses in oil-filled cables and consequently much higher still than those in solid cables. The absence of gas pockets in oil-filled insulation and their presence in solid-type insulation means that initial failure is due to different causes in the two cases; oil breakdown (and subsequent gas) in the one, and gaseous ionization in gas already present in the other, with the critical stress much higher in the former. Our results also indicate that, once gaseous ionization starts, the entire insulation wall is on the way to failure—sooner or later.

These things being so, it should be evident that the time element to complete failure in solid-type insulation may vary through wide limits, depending on the volume and distribution of gas present, on the chemical and structural stability of the paper and oil, and on the conditions of test. Thus, the use of high-density paper in one cable might result in higher dielectric strength owing to the higher resistance to chemical attack, whereas in another of the same type and the same paper a lower dielectric strength might result, owing to the greater volume and wider distribution of gas pockets and films and the consequent more rapid disintegration under gaseous ionization. The inability to control or foresee the distribution of gas spaces in solid insulation is a principal reason for the conflict of evidence and difference of opinion often arising in discussions of the behavior and properties of cable insulation in general.

One thing may be said definitely, however, about high-density paper; a graded cable, whether oil-filled or solid, with high-density paper on the inside, has a greater fraction of the total voltage thrown to the outer layers with a consequent reduction of stress values in the layers near the conductor. The extent of this lowering as dependent on dimensions and dielectric constant and its influence on the critical stress in the oil channels is mentioned briefly in our paper and will be discussed more extensively in a later paper.

Electrolysis and Corrosion of Underground Power-System Cables

Discussion and author's closure of paper 45-59 by L. J. Gorman, presented at the AIEE winter technical meeting, New York, N. Y., January 22–26, 1945, and published in AIEE TRANSACTIONS, 1945, June section, pages 329–36.

L. I. Komives (The Detroit Edison Company, Detroit, Mich.): The tabulation of types of corrosion in this paper is very readable and logical. Under type 5, "duct corrosion," what kind of a duct was the author referring to when he spoke of low duct resistance? Did he mean water entry through broken ducts or low-grade concrete?

In Mr. Gorman's paper, percentages of corrosion failures are given. What is the percentage of corrosion failure to all failures? The record of failures due to stray current is very good, much better than it used to be. Apparently co-ordinated efforts of all utilities concerned pays very well. This has been true in Detroit also during the last 20 years.

The author refers to a *special* cable grease. What is special about this grease? Is it the base, life, or inertness? In Detroit we use a lead-soap-base grease on all reconditioned cable. A thin layer of this grease is applied hot, about 280 degrees Fahrenheit, in the cable reconditioning plant, giving complete coverage to protect it against corrosion. In the field, additional amount of the same grease, which has sodium silicate incorporated, is applied as extra protection and to aid lubrication. We believe that inspection of the sheath and covering it with this grease has been a great help in combating corrosion.

In the summary and conclusion of the paper, it is mentioned that a small percentage of the total system area (one per cent) is responsible for a large percentage (30 per cent) of corrosion failures. Is there any significant explanation as to why such areas are more destructive than others? Is it filled-in ground or salting?

The author of this paper apparently is not in agreement with Sherer and Granbois with regard to the benefits of flushing ducts to eliminate alkaline or acid conditions. Mr. Gorman states that after flushing certain ducts an alkaline condition finally was corrected. Mr. Sherer and Mr. Granbois found that the resistance of the cable sheath to ground was reduced by flushing. If, as Mr. Gorman states, "the resistivity of the environment in immediate contact with the cable or pipe seems to be the principal factor in controlling cable sheath or pipe corrosion" would it not be better to let the alkaline condition remain and keep the higher resistance? Does Mr. Gorman have any corrosion rate data that would settle this point? We also wonder whether flushing ducts with hot cables and consequent change of temperature does not cause more harm than good? Perhaps this should be done only in winter time.

Herman Halperin (Commonwealth Edison Company, Chicago, Ill.): Mr. Gorman's paper has a wealth of background for his broad coverage of sheath-corrosion problems. I first learned of the method of pulling a short cable slug through a duct from the late Mr. Hippensteel of the Bell Telephone Laboratories. Our methods for both anodic and cathodic corrosion investigations are adaptations of his ideas and of information furnished a few years ago by Mr. Gorman. That sort of investigation has been very worthwhile in many cases.

My paper on cathodic corrosion of cable sheaths presented before the Electrochemical Society in 1943[1] may be of interest to one particularly involved in considering cathodic corrosion. As indicated in my paper, the use of various methods has prevented the number of service failures in Chicago due to cathodic corrosion, increasing from about 8 a year to maybe 25 a year. We found usually that no serious corrosion was occurring when the leakage current to the one-foot slug was one or two milliamperes or less, and the resistance was a few hundred ohms or more. Cathodic corrosion was found to occur even when the sheaths were only a fraction of a volt negative to earth, especially where much salt from electric street-railway-track switches had filtered into the ducts.

Mr. Gorman apparently has experienced no corrosion due to a-c electrolysis. Such corrosion has, however, occurred at Safe Harbor and in the utility systems in Chicago and Detroit. Frequently, conditions leading to a certain type of corrosion take time to develop and perhaps where unusually high alternating potentials exist on sheaths on single-conductor cables, some serious troubles may develop after 15 or 20 years. The development of such troubles, of course, is accentuated when there are local conditions tending to produce differential aeration, and so forth.

Regarding Mr. Gorman's discussion on protective coverings, we have tried a variety of materials in limited amounts. One construction that seemed quite interesting and attractive was Geon-treated tapes wrapped over the sheath.

Regarding corrosion where there are cinder fills, we have measured potentials approaching one volt between layers of clay and of cinders near conduits. In some cases, cinders have been replaced down to a level corresponding to the bottom of the conduit. In one case involving many hundreds of lengths of cable on a station property, a large system of cathodic protection was installed, especially because in a portion of a given section of conduit, the cable sheaths were positive to earth in many instances.

REFERENCE

1. CATHODIC CORROSION OF CABLE SHEATHS. **Herman Halperin.** *Transactions* of the Electrochemical Society, volume 87, 1945, page 132.

W. P. Monroe (Sargent and Lundy, Chicago, Ill.): The paper by Mr. Gorman is a very thorough presentation of the problem of electrolytic corrosion of lead-covered power cables and brings the power-transmission engineer up to date in the methods used for electrolysis tests and remedial measures.

In regard to the duct-survey method of testing, there is evidence that the relative position of the spare duct used for the lead-slug traverse among the other ducts may have an influence on the shape of the voltage and current curves obtained. If the spare duct used is at one side of the bank, will the direction of the current flow in the earth and the proximity of water pipes and other structures to one side of the duct run cause the curves to look different than if the survey were made in a duct on the opposite side of the bank? In the design of new duct runs for important cables might it not be worthwhile to locate spare ducts especially for the use of the electrolysis engineers in making duct surveys, in which case these test ducts could be located one on each side of the duct bank?

The voltmeter mentioned for use in electrolysis tests seems to have an exceptionally high resistance and I would like to know if this instrument is portable and rugged for the purpose. I understand that a so-called potentiometer voltmeter is available for such surveys which includes a battery and rheostat for balancing a battery voltage against the cable-sheath voltage so that the potential is measured without a current flow between the cable sheath and the test slug.

In Figure 1 of the paper, lead sheaths of cables are shown bonded together at each manhole. In cases where single-conductor cables are used, staggered bonding is sometimes the practice in order to minimize induced alternating voltages. This method would permit bonding the sheath only at certain manholes. In the other manholes the duct survey probably could be made by measuring the voltage to each sheath individually and taking an average instead of to all sheaths bonded together.

The data on variation of duct resistance and current leakage and their effects on the life of cable sheaths are a very valuable contribution since they evidently are based on the author's extensive experience on a very large system.

The relation between duct resistance and area of contact between cables and the walls of the ducts is applicable when the ducts are not submerged in water, but would they also be applicable for water-filled ducts?

The author has stated well the difficulty of draining stray currents from power cables which have their sheaths connected solidly to grounding systems of power stations and substations. It might be suggested that one way of making possible the draining of such cables without interfering with the protecting system would be to install spark gaps between the cable sheaths and the ground bus. These cable sheaths then would be isolated from the ground bus as far as stray current or galvanic potential is concerned, but the gaps would permit short-circuit current to flow to the ground bus. The gaps would have to be designed for very-low-voltage breakdown on account of providing for safety to maintainers, and should be very rugged for high-current capacity after breakdown.

In the last section of the paper the author mentions the use of zinc electrodes for cathodic protection. Metallic magnesium is also a possible electrode material with advantages for such applications, and magnesium should be available in quantities after the war. The use of zinc or magnesium for one pole of the galvanic cell for cathodic protection is of value where the galvanic voltage can be counteracted easily by such means and where there is no complication from stray currents of electric railways. Rectifiers might be used at locations requiring higher counteracting potentials.

R. C. Waldron (The Okonite Company, Passaic, N. J.): I would like to ask Mr. Gorman several questions regarding their use of protective coverings. He states that the covering consisting of two saturated canvas tapes has afforded adequate protection, but then refers to attempts to remove cable. Was this removed because of failures and, if so, were these failures due to corrosion or other causes?

We agree with Mr. Gorman regarding the advantages in pulling reinforced rubber-covered cables. We have an experimental cable which was installed in a local utility's ducts in November 1933 where unprotected cable originally failed because of corrosion. It has been pulled through a duct section six times at various intervals, the last time being in November 1944. While the outer fabric tape is now weak from rotting and some injuries have occurred, there has been no jamming in the ducts and no sticking. The cable pulls as easily now as when new, easier than most plain lead-covered cables.

Each time the cable was pulled from one duct section to the next it was examined as it passed through the intervening manhole. A sample also was cut from one end, the end having been in the duct, not in the manhole, and examined in the laboratory. The coverings of these samples were removed and the cables cleaned, but no evidence of corrosion has been found. A length installed at the same time with saturated canvas-tape coverings was removed in 1937 because of the deterioration of the covering and fear of jamming in the duct.

This sample also showed no corrosion when removed.

Laboratory tests on these two types of coverings made by applying ten volts direct current to the sheath while immersed in a three-per-cent salt solution, resulted in failure of the saturated canvas-tape covering in from three weeks to two months while the Okosheath protective covering (reinforced rubber-taped jacket) did not fail in six years. The cable sheath was maintained positive to the water and the sample was considered to have failed when the resistance of a six-foot length dropped below 50,000 ohms.

Mr. Gorman mentions that any imperfections in the coating will restrict the area of lead exposed and concentrate corrosion. This may be true for stray currents where there is sufficient voltage to force a certain amount of current from the sheath. If a definite current is restricted the corrosion will be concentrated, but is this the most common cause of failure? We believe the most troublesome types of corrosion are those listed by Mr. Gorman as types 4 through 7 which account for 88 per cent of his duct failures. Except for type 6, self-corrosion, which is eliminated by the protection afforded against scoring by the protective covering, these are caused by some type of electrolytic cell or voltage on the sheath. We cannot appreciate why this would result in concentration of the corrosion. We would expect the current to be proportional to the resistance from the sheath which should be dependent largely on the exposed area, resulting in the same current density independent of the exposed area.

R. M. Burns (nonmember; Bell Telephone Laboratories, Inc., New York, N. Y.): We are indebted to Mr. Gorman for this excellent presentation of the subject of corrosion of underground power cables and its control. He is to be congratulated on the reduction of failures of corrosion which it has been possible to bring about by understanding the nature of the corrosion problem and by application of suitable protective measures. The mechanism of corrosive attack is elucidated and much practical experience is cited to illustrate the types of sheath corrosion which occur in the underground plant. His classification of corrosion in eight different groups undoubtedly is convenient from an engineering standpoint in indicating the palliative measures which should be applied. From the standpoint of mechanism of corrosion, one would group his last five classes under electrolytic-cell action which differs from the first three classes principally in limitation of the size of potentials involved, that is, stray currents may involve higher potentials than can be developed in electrolytic cells. It is implied in class 6 that scoring or mechanical injuries set up local galvanic cells. While it is possible in the laboratory to develop areas of anodic potential on lead by mechanical injury, the tendency of lead to self-anneal at ordinary temperatures makes it unlikely to occur in the underground plant. It seems probable that corrosion resulting from mechanically injured areas is due to the operation of differential aeration cells, that is, the bottom of the trough or pit, being less accessible to oxygen, becomes anodic.

The author states that "in the usual-type soil and duct water, the natural formation of films does not appear to have any important influence on corrosion." In our experience we have come to recognize the importance of protective constituents in soil and duct waters. For example, cable sheathing is corroded rapidly in distilled water but very inert in most ground waters. Careful study has shown that the presence of silicates in concentrations of more than about ten parts per million of silicate ion tends to retard or prevent corrosive attack. Similarly, carbonates exert an important protective influence. These naturally formed silicate and carbonate films which are too thin to be visible are sufficient, in most instances, to prevent the corrosion of cable sheathing in the underground plant.

The discussion brought out the importance of cinders and cinder fills as corrosive agents. In order that there be no mystery as to how a cinder fill not in contact with a cable can contribute to its destruction, it may be pointed out that cinders, which usually contain some coal or coke, may function as a carbon electrode. When such fills are in contact with iron pipes or other metallic structures they function as cathodes in galvanic cells. As much as 0.8 volt may be measured between cinders and iron. Cables passing in the vicinity of such an iron structure may pick up current from the iron anode and lose it at another point in the vicinity of the cinder fill which, in contact with the iron structure, has formed the galvanic cell.

L. J. Gorman: In closing, the author will endeavor to answer the several questions which have been raised in the discussion of this paper.

The duct resistance questioned by Mr. Komives and referred to in my paper refers to the resistance measured in the duct survey as described in the paper. If this resistance is less than 250 ohms, it arbitrarily is considered low because experience shows that approximately 70 per cent of the corrosion cases occur in ducts in which the resistance is less than this value. Low duct resistance usually results from the low resistivity of the duct contents in ducts which are saturated with low-resistivity water, such as tidewater. Low duct resistance is not associated necessarily with broken ducts or low-grade concrete.

The grease used for cable protection is a heavy petroleum-base grease having a consistency somewhat similar to axle grease. This type of grease seems to stand up well under duct conditions. There is nothing special about the grease except its application. The special application is covered by a company specification and the particular grease specified is restricted in its use to corrosion prevention. Mr. Komives has called attention to a lead-soap-base grease which he uses on reconditioned cable and to the use of a sodium silicate incorporated in the grease for protection in cable ducts. The author feels that this combination should offer excellent possibilities.

As stated in the paper, a large percentage of the cable-sheath corrosion occurs in relatively small areas which have been identified through the corrosion surveys. For the most part, these areas occur in filled-in ground near the water front.

The statement made in the paper relative to flushing ducts to eliminate alkaline or acid conditions is based on the author's experience with numerous duct sections on the system. One case, in particular, involved a d-c substation from which approximately 40 lead-covered feeders were carried through concrete ducts encased in a large concrete envelope. In about 1938 there were a series of cable failures in these ducts due to corrosion. Investigation showed that the ducts were not well drained and that they contained an accumulation of alkaline water having a pH value of 11 or more. The ducts were flushed with fresh water and the pH reduced to nearly neutral. After three months, there was a recurrence of the alkaline condition and the ducts were flushed again. This process was repeated over a period of a year before the duct conditions appeared to be stabilized. No cable failures have been experienced since 1938. Similar results have been experienced in other duct sections where the accumulation of water in undrained portions of the duct contains a concentration of salt washed in from the earth and duct walls. In all cases, flushing has improved the conditions in these duct sections.

In answer to Mr. Halperin, the author appreciates the importance of cathodic corrosion and continued vigilance must be exercised to avoid this type of corrosion. It occurs where the cable sheaths are negative with respect to the duct walls and is associated more generally with stray current in sections where the current is "picked up" by the cable sheath.

In regard to a-c electrolysis, there have been no cases of corrosion on the single-conductor cross-bonded feeders of the Consolidated Edison Company which could be identified as a-c electrolysis. In all cases where corrosion has been experienced on these cables, there were d-c conditions present which readily would account for the corrosion. However, a-c electrolysis is regarded as a potential source of danger which may develop at higher alternating potentials or over longer periods of time.

In regard to the duct survey, referred to by Mr. Monroe, there may be a wide variation between ducts in the same duct section. For this reason, particular attention is given to the selection of the duct in which the survey is made. Whenever possible, the survey is made in the duct from which the cable is removed. If this is not possible, a vacant duct immediately adjacent to the occupied duct is selected. The author does not feel that spare ducts purposely provided for electrolysis testing would be of any great advantage.

The high-resistance voltmeter used in the duct survey is a standard Weston instrument. It is sufficiently portable and rugged for field use.

The cable sheaths are not bonded necessarily in all manholes. In the case of cross-bonded single-conductor feeders, the bonding and cross-bonding may be at intervals of a thousand feet or more. These bonds, however, are sufficient to equalize the potential differences between the sheaths. In any event, the potential differences between the cables are checked before the duct survey is undertaken and allowance is made for any discrepancies. In reference to cables in ducts which are submerged entirely in water, the life of the cable will be appreciably longer than that shown by the curves in Figure 4 of the paper for the respective values of duct resistance because of the greater contact area.

Discharge gaps between isolated sections of cable sheath and ground are used in a few cases. A discharge gap has been designed for this purpose which will break down at approximately 250 volts and carry fault current for sufficient time for the relays to clear the feeder. In other cases, insulating joints are inserted to break the continuity of the cable sheath and the insulator is shunted with a low resistor of 0.01 or 0.02 ohm. These resistors are constructed from iron grids and have sufficient capacity to carry the estimated fault current. At the low potentials involved in the flow of stray current on the cable sheath, these resistors have a very appreciable influence on the value of the current.

Doctor Burns calls attention to the classification of "self-corrosion" in the paper. "Self-corrosion" applies more particularly to steel pipe or other metal that is not self-annealing. However, in approximately ten per cent of the corrosion cases on our cable sheath, the corrosion is associated with scoring, duct rubs, or other mechanical injuries, whereas the undamaged portion of the sheath is in good condition. As pointed out by Doctor Burns, the lead is, to all practical purposes, self-annealing and the corrosion which is associated with the mechanical condition of the sheath is probably caused by differential-aeration cells rather than galvanic potentials set up by stresses in the metal. However, it seems desirable to include this particular type of corrosion in a separate classification to call attention to the effect of sheath damage on the corrosion problem.

In reference to Mr. Waldron's discussion of the removal of tape-protected cables, the removals are made usually because of cable or splice failures not caused by corrosion. In such cases, it usually is found that the fabric of the tape has become disintegrated, leaving a layer of compound on the sheath which appears to afford satisfactory protection. In the two or three cases where tape-protected cable was removed because of the corrosion, the tape had been improperly applied or damaged at the time of installation. In one case, the tape was applied half-lapped and severe corrosion was noted at the inner edge of the tape in contact with the lead. It was apparent that moisture had entered laterally through the tape or through the void left in the compound when the tape had disintegrated. For this reason, tapes should be applied in two layers with butt wrapping.

The statement made in the paper with reference to the concentration of corrosion at imperfections in the coating is based on the author's experience with coatings on both cables and pipes. Where such imperfections exist, the cable sheath or pipe is frequently penetrated in about half the time that would normally be expected on entirely bare pipe or cable. For example, in the case mentioned above, the failure occurred approximately five years after the cable had been installed. The normal life of unprotected cable in this particular duct section is from eight to ten years. The apparent concentration of corrosion is probably caused by the effects of differential-aeration.

Galvanic Corrosiveness of Soil Waters

Discussion and authors' closure of paper 45-60 by Howard S. Phelps and Frank Kahn, presented at the AIEE winter technical meeting, New York, N. Y., January 22–26, 1945, and published in AIEE TRANSACTIONS, 1945, April section, pages 156–9.

Edgar F. Wolf (Consolidated Gas Electric Light and Power Company, Baltimore, Md.): The authors of this paper have noted that there is a relationship between the static electrode potential of a lead electrode and the pH of the solution, when the pH is above a value of approximately ten. The basis for such a relationship can be shown by fundamental electrochemical equations. The reversible equilibrium potential of a lead electrode is determined by the lead-ion concentration in the liquid film surrounding the metal. At 25 degrees centigrade, this potential with respect to a standard hydrogen reference electrode is

$$E_{Pb}/_{Pb^{++}} = -0.126 + \frac{0.059}{2} \log [Pb^{++}]$$

where $[Pb^{++}]$ represents the lead-ion concentration. The lead-ion concentration at equilibrium will be governed by the concentration of negative ions present in the solution and the solubility product of the corresponding lead compound. Where the alkalinity of the solution is the factor which governs the lead-ion concentration, the foregoing equation may be converted to the following form by substitution of the values of lead hydroxide solubility product and ionization constant for water.

$$E = 0.249 - 0.059 \text{ pH}$$

This equation shows that, where the alkalinity is the governing factor, the lead electrode becomes 0.059 volt more negative for each increase of one unit of pH. The authors' measurements, when converted to the standard hydrogen scale, are approximately in accord with the theoretical values.

It should be pointed out, in connection with the discussion of electrode potential when current is flowing, that there are other factors than alkalinity of the water which affect the degree of polarization. In work published some years ago,[1] it was found that certain ions other than the hydroxyl ion very greatly affect polarization. In the presence of sulphate ions particularly, anodic polarization is very pronounced.

REFERENCE

1. FORMATION OF LEAD MONOXIDE AS A CABLE SHEATH CORROSION PRODUCT, **Edgar F. Wolf, Bonilla.** *Transactions* of the Electrochemical Society, volume 79, 1941, page 307.

Herman Halperin (Commonwealth Edison Company, Chicago, Ill.): Mr. Phelps and Mr. Kahn have greatly widened our scientific knowledge on soil waters. In our studies, analysis of soil waters has been helpful. Laboratory tests and field studies on alkaline waters have indicated that a pH value of 11.4 or more was a very serious hazard to the sheath; in fact, nowadays we try to keep the value down to 10.5 or less in particularly continuous-duct cable tunnels under rivers. Experience with calcium-hydroxide waters has indicated that the auxiliary information on the concentration of the alkaline was important; concentrations above 200 parts per million of calcium-hydroxide have been found serious.

This paper, along with the other two presented at the same time, present a needed combination picture and data on scientific and practical matters on corrosion of underground cable systems.

I should like to emphasize that there is no such thing as a dry duct in underground conduits. Moisture in the surrounding soil and conduit is necessary, so that the cables may carry some current safely, because otherwise the conduit and soil become wonderful heat insulators. Corrosion has been found when the ducts to all superficial appearances were dry; usually, such corrosion results in scattered though serious pitting.

R. M. Burns (nonmember; Bell Telephone Laboratories, Inc., New York, N. Y.): The authors have performed a useful service in showing that both the static potentials and the potentials with current flowing of lead, iron, and copper in soil waters are influenced by the composition of the water. The practical importance of this lies in the implication that the environment is of primary importance in determining the occurrence and course of corrosion. The potential relationships of certain pairs of common metals, lead and iron, for example, may be reversed when compared in different soil solutions. Furthermore, observations of marked polarization at low current densities provide assurance that rate of corrosion in such waters will be very low. Contrariwise, ground waters in which there is little evidence of polarization may permit more rapid corrosion. Thus, measurements of the type illustrated by the authors are useful in the exploration of the corrosiveness of underground waters. It is well to point out, however, that the validity of laboratory measurements depends upon reproduction of the conditions prevailing in the underground plant. Since oxygen concentration is the most influential factor affecting cathodic polarization and since it is usually low in underground waters, laboratory studies should include measurements under reduced oxygen pressures. It may be mentioned, also, that carbon dioxide pressures underground usually are markedly higher than in the outside air, and, since carbonates are anode polarizers, this factor should be considered in laboratory studies.

The authors have observed that the corrosion of lead, copper, and iron is more severe at low pH than at high pH. Since one may consider that corrosion of a single metal occurs by means of the operation of a metal-hydrogen galvanic cell in which the hydrogen electrode is the cathode and since the potential of this cathode becomes 59 millivolts more noble for each tenfold increase in hydrogen ion concentration (that is, for each pH decrease of one), it is evident that the potential of the metal-hydrogen cell may be increased similarly, if there is no corresponding change in the potential of the metal electrode. Under these circumstances the corroding current density will increase, if there is sufficient oxygen or other oxidants present to maintain depolarization of the more active cathode.

Howard S. Phelps and **Frank Kahn:** It is desired to emphasize that the paper under consideration represents the authors' idea of an initial approach to the problem of galvanic corrosion by soil waters. The tests were made under conditions which might, admittedly, differ considerably from those occurring in the field. For example, the tests were made on unagitated cells to improve reproducibility of results, although it had been observed previously that a different condition of stability occurred when there was movement of the electrolyte. On the other hand it is a point of interest that the results presented do appear to be valid over a considerable range of temperature.

In several of the electrolytes, chemical attack on one or more of the electrodes was evidenced by visible discolorations or deposits on the cleaned surfaces with no current flowing. The progress of this chemical action was reflected in the curve of static electrode potential versus time. Isolation of the galvanic effect was approximated in such cases and may not have been as clear cut as might be desired.

The authors undertook this presentation to encourage discussion and to stimulate independent development of techniques and investigations of other environmental factors such as those suggested in the discussion by Doctor Burns.

Study of A-C Sheath Currents and Their Effect on Lead-Cable-Sheath Corrosion

Discussion and author's closure of paper 45-61 by C. M. Sherer and K. J. Granbois, presented at the AIEE winter technical meeting, New York, N. Y., January 22–26, 1945, and published in AIEE TRANSACTIONS, 1945, May section, pages 264–8.

C. T. Hatcher (Consolidated Edison Company of New York, Inc., New York, N. Y.): I have read with interest the paper presented by Mr. Sherer and Mr. Granbois on the question of a-c electrolysis.

The theory of a-c electrolysis, as expounded, appears to have been checked by laboratory tests, and the conclusion reached that some rectification takes place on cables. Assuming that cables are subject to a-c electrolysis, the question that is important is, then, "When will the lead sheath deteriorate under the influence of constant a-c potential, especially if the cables are submerged?" Caution also should be taken in evaluating the destructive effect of alternating potentials when either, or both, galvanic potentials or chemical conditions are present.

If it is intended to infer that certain failures of cables in the field were caused by alternating current, it appears that Mr. Sherer and Mr. Granbois may have confused a-c electrolysis with galvanic potentials. Actual field experience is based on two failures and in these cases it is stated that conditions are suitable for galvanic potentials namely:

1. The installations consisted of single-conductor cables, the sheaths of which were bonded to a nearby copper ground bus.
2. A good electrolyte was provided by alkaline water in the duct bank.

From our rather extensive work on corrosion I would say that these conditions set up an ideal condition for straight galvanic potentials and that practically all of the sheath damage was due to this action.

We have given considerable study and have conducted investigations on the subject of a-c electrolysis resulting from the extensive use of large single-conductor cables on our system for the transmission of large blocks of power. In order to obtain maximum load out of large single-conductor cables installed in separate ducts, it is necessary to reduce sheath losses by the use of cross-bonding or bonding transformers. Approximately 15 or 20 years ago it became necessary for us to install the first insulating joints and cross bonding on some of our single-conductor 27-kv and 45-kv feeders and at this time we investigated the action of alternating potentials on lead.

At that time a four-month life test was made on pairs of lead electrodes immersed in tide water, having a resistivity of 150 ohms per cubic centimeter, with various a-c densities. The test showed distinct changes in the composition of the lead with high current densities and fairly little change at low current densities. These data indicate that the loss in weight of one-eighth-inch sheet lead due to a-c electrolysis on the exposed surface is about 0.024 per cent per year per milliampere per square inch.

Investigations were made to determine the actual leakage as a function of voltage between sheaths, and it was established that the leakage current density is a function of the voltage, other things being equal.

Our original lines were designed for operation at 20 volts between sheaths. It was estimated that current densities at this voltage with tidewater would result in 50-per-cent deterioration of the lead sheath in a cable when operated at 100-per-cent load factor, in approximately 30 years. Subsequent field measurements indicated that we were not reaching current densities of even 16 milliamperes per square inch. This conclusion appears to be justified by our cable-operating record. At the present time, we have approximately 930,000 feet of large single-conductor cable operating at 11 kv, 27 kv, 45 kv, and 132 kv. Measured voltages-to-ground range from 10 volts to 15 volts at full load. As stated heretofore, some of this cable has been in operation for over 15 years and no failures have occurred that could be attributed to a-c electrolysis. Examinations of numerous lengths of cable removed for other causes, including one in a very bad soil condition, have shown no signs of corrosion from this source.

Taking into consideration our test data and operating experience, we do not believe that a-c electrolysis is a serious consideration if the leakage current is restricted to small values. I would like to point out that the authors have referred to a value of 12 volts which has contributed to the destruction of the lead sheath of cables which have failed. I hope that this reference does not leave the impression that trouble will be encountered at this voltage as our experience indicates that, at voltages of this magnitude or higher, satisfactory operation is obtained.

Herman Halperin (Commonwealth Edison Company, Chicago, Ill.): The paper by Sherer and Granbois is important and instructive in showing that, under two sets of actual field conditions, serious corrosion did result from a-c shealth voltages. Some reports on laboratory tests and field experience are given in an article by Halperin and Miller.[1]

By laboraory tests, as well as field measurements, the authors determined that a rectification action occurs between copper and lead, or even between lead and lead, when unequally "seasoned." It would seem likely that, without a dissimilar metal such as copper present, rectification and corrosion could occur between the lead sheaths of cables having induced alternating voltages in any section of duct in which unequal conditions exist, such as unequal temperatures of adjacent cables, differential aeration, electrolyte concentration and resistance caused by sheath scoring, unequal sedimentation in ducts, partial coverage, or unequal wetting of a group of cables by water in vertical arrangement in ducts. Partial rectification of alternating current is likely to occur between any two electrodes dissimilar in any one or more important respects.

In Figure 7 of the paper, it is noted that several of the laboratory age-seasoning curves have reversed their trend in 10 to 50 days. This, together with the fact that field measurement of the Safe Harbor cables after three years showed some sheaths anodic, may indicate that "aging" may not remain permanent, or may reverse itself, particularly when complicated under actual field conditions with seasoned effects on temperature, chemical nature, amount of water in ducts, and so forth.

Figure 2 of the paper and the statement about sheaths becoming self-protecting with alternating current after aging, might lead the unwary to conclude that large a-c sheath voltages are more desirable than smaller ones. If this were true, and since a-c sheath potentials varied from zero at the solidly grounded end to maximum at the free end, then the most severe or excessive corrosion and failures in both field cases noted should have been at or near the grounded ends of sheaths. A definite statement of fact by the authors on this point would be most illuminating. Figure 6 of the paper shows that, when the lead is anodic, it becomes more so with increasing alternating current (*or* voltage).

It is unfortunate that control or blank cells (with plus and minus direct current only and one without any voltage at all) were not run to tabulate with cells *A*, *B*, and *C* of the corrosion study. Moreover, with electrode dimensions and weights not given, electrode areas and current densities cannot be estimated.

Despite the limited variety of electrolyte and number of field locations involved, the authors have given well-documented field results and ingenious laboratory tests which demonstrate beyond question that a-c corrosion does occur. Moreover, they have demonstrated one highly plausible mechanism of a-c corrosion and a practical method of dealing with it. In a subject as complicated as corrosion in which many types of action may be present simultaneously, in various degrees, it is probable that other types of a-c corrosion may occur.

Corrosion due to a-c electrolysis with alternating potentials of about 20 volts to ground has been experienced in Detroit and in Chicago. As indicated in my article presented before the Electrochemical Society in 1943,[2] sometimes corrosion conditions that will lead to sheath corrosion and cable failures may require 10 or 20 years to develop, and then may come an avalanche of troubles. One unfortunate fact about corrosion is that, once sheath pitting is started, the pitting develops at rates that may be much faster than the average loss of lead. Another unfortunate fact is that, even when the cause of the corrosion, such as positive direct potentials or excessive alternating potentials, is suitably modified, corrosion still will continue at a somewhat reduced rate. Therefore, an early sound analysis of a corrosion situation, and adoption of adequate methods and means to avoid serious corrosion in the 30 years or so of expected cable life, are essential.

REFERENCES

1. REDUCTION OF SHEATH LOSSES IN SINGLE-CONDUCTOR CABLES, **Herman Halperin, K. W. Miller.** AIEE TRANSACTIONS, volume 48, 1929, pages 399–414.

2. CATHODIC CORROSION OF CABLE SHEATHS, **Herman Halperin.** *Transactions* of the Electrochemical Society, volume 87, 1945, page 132.

R. M. Burns (nonmember; Bell Telephone Laboratories, Inc., New York, N. Y.): The authors have contributed to our knowledge of the corrosion of underground cables in showing that, in a location where corrosion occurred, the magnitude of direct current flowing from the cable to ground was influenced by the size of the load currents on the cable. This they attribute to rectification of these alternating currents in electrolytic cells in which the cable sheath is anode and a copper-ground-wire cathode. Laboratory studies appear to support this hypothesis.

As is well known, the electrical and chemical environment of the underground cable plant is exceedingly complex and usually contains factors which accelerate corrosion and other elements which tend to protect cable sheath against corrosion. Of the accelerating agents, oxygen, organic acids, and alkalies are most important; of the protective constituents, silicates, carbonates, and sulfates are most effective. When electric currents enter the picture, new products of electrolysis appear and may have significant effect, as in the case of alkalies liberated from neutral salts when the sheath is cathodic. The chemical components of the environment, whether originally present or produced by electrolysis, may react with the sheath producing more or less adherent films which may have rectifying properties. A similar situation may prevail at the copper electrode, further complicating the behavior. It is not surprising, therefore, that the authors observe a large variation in the amount of rectification or reversal of the polarity of the current.

In assessing the cause of failure of the two cables investigated by the authors, it seems desirable to bear in mind that 25-cycle alternating current alone is capable of destructive action and there also is involved a lead–copper galvanic couple which may account for anodic perforation of the sheath. Finally, higher temperatures, if these developed, have been observed to increase the corrosive action of alternating currents, as well as the rate of chemical reactions in general which may be involved in corrosion processes.

C. M. Sherer: Mr. Halperin suggests that, because of the higher a-c sheath voltage at the ungrounded end of a cable section, the degree of self-protection against corrosion should be greater at this end than at the grounded end where voltage is zero, hence corrosion should be more severe at the grounded end. This is true only after the lead has become seasoned and the rectified currents are in the cathodic direction. On new cable the opposite would be true, since the rectified currents make the lead anodic and increase the rate of corrosion. Actually, other variables are present which introduce complications, the uneven distribution of moisture in the duct being one of these. Of the two cable failures noted, one occurred 91 feet from the free end and 200 feet from the grounded end in a location which was definitely the wettest part of the duct; the other was 83 feet from the free end and 259 feet from the grounded end, also in a very wet location. These wet spots were favorable to the flow of galvanic currents, as well as rectified currents, both before and after polarity reversal.

Size of electrodes used in the laboratory test cells was $1^{1}/_{4}$ inches by 4 inches actually in contact with the electrolyte.

The observation of Mr. Burns that an increase in temperature has been observed to increase the corrosive action of alternating currents agrees with our laboratory tests in which an increase in temperature from 5 degrees to 50 degrees centigrade resulted in a ten per-cent increase in rectified current for a given value of applied 25-cycle current.

Mr. Hatcher's remarks indicate that he may have misinterpreted the authors' evaluation of a-c electrolysis in the cable failures. The claim is not made that a-c electrolysis alone produced the failures. The presence of galvanic corrosion is recognized and admitted, but corrosion was accelerated, when the cables were new, by the rectified a-c sheath currents which made the lead more anodic than the galvanic potentials alone, as determined by both field and laboratory tests. The tabulation given in the paper under "Field Observations" shows that, on the section of newly installed cable (number 4 section), galvanic current was present in the amount of 2.7 milliamperes, with the lead, of course, anodic. This value of d-c milliamperes increased to 12.0 milliamperes when a-c sheath potentials were introduced by passing load current through the cable. It is noted that the lead became over four times more anodic when the alternating sheath currents were present. Since laboratory tests show that lead–copper cells do rectify alternating current, it is concluded that the increased d-c sheath current observed in the field was the result of rectification of induced alternating currents.

On older cable, after the lead has become seasoned and effected a reversal of polarity of the rectified current, the action of galvanic corrosion is retarded because the galvanic currents then are opposed by the rectified current. This is illustrated by the graphic meter records in Figure 8 of the paper in which an increase in load current (or induced a-c sheath current) is shown to cause a *decrease* in the d-c sheath current to ground.

While Mr. Hatcher states that they never have had a cable failure which could be attributed to a-c corrosion, it is possible, in view of the absence of specific field tests to prove the contrary, that this type of corrosion may have been active on new cables concurrently with other forms of corrosion without being recognized.

Dodge Chicago Plant's Electric-Power-Distribution Scheme With Airplane-Engine-Testing Power Recovery

Discussion and author's closure of paper 45-21 by E. L. Bailey, presented at the AIEE winter technical meeting, New York, N. Y., January 22–26, 1945, and published in AIEE TRANSACTIONS, 1945, March section, pages 121–3.

L. A. Kilgore (Westinghouse Electric and Manufacturing Company, East Pittsburgh, Pa.): Mr. Bailey's paper covers some very interesting subject matter. One item on which more explanation might be helpful is the characteristics of the induction generators used in the production testing. These machines were essentially wound-rotor induction motors of 1,000-horsepower capacity designed to operate at high overspeed with corresponding high rotor frequency.

The ability of the induction motor to supply power when driven over synchronous speed is well known. With the wound-rotor-type motor it is possible to introduce resistance values into the secondary circuit to obtain a series of speed–torque curves such as the typical curves shown in the paper. Hence, with a sufficient number of resistance steps a value may be chosen which will load the engine to any desired torque and speed. By always working well below the pull-out point the operation is stable at all loads.

If machine losses be neglected, it can be seen that the ratio of primary-power output to mechanical-power input will be equal to the ratio of synchronous speed to operating speed. This suggests another interesting feature—the primary power is very nearly proportional to torque. The corrections for losses in a large machine of this type were found to be so small that corrections for normal voltage variations were unnecessary. Also the variations due to speed were so low that only three calibration curves of torque versus primary power were necessary to cover the complete range of speed.

These machines presented a number of interesting design problems. The periph-

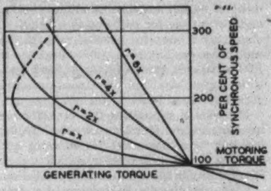

Figure 1. Typical speed–torque curves of a wound-rotor induction generator

eral speed was considerably higher than normally used, requiring careful design of banding and coil leads. Another unusual feature was the stranding of rotor conductors to reduce eddy currents at high slip frequencies.

W. L. Wright (General Electric Company, Schenectady, N. Y.): The author has given a very comprehensive outline of the electric equipment installed in one of the largest wartime plants. This plant is one of the largest in floor space as well as in the use of electric power.

Even though this plant was constructed during the war when material shortages were at the worst, all the electrical-engineering problems have been solved successfully, and it is safe to say that this plant encompasses modern engineering in every respect.

Metal-enclosed switchgear, high voltage, and low voltage, is used throughout the plant. Load-center distribution is used, and the scheme employed provides a high continuity of service. Liquid-filled transformers using a noncombustible liquid are used throughout the factory substations.

In line with conserving resources and materials power-recovery equipment was installed, which undoubtedly reduces the size of the main incoming service, thereby saving critical materials and by returning power to the system saves tons of coal daily in the nation's coal pile.

In this paper the author has revealed a number of interesting applications of electric apparatus. I am referring particularly to the induction-generator method of engine testing and the use of series capacitors as automatic voltage regulators to maintain constant bus voltages independent of widely varying loads. The author and his associates are to be congratulated on having the engineering fortitude to attempt these ventures in the face of more conventional methods that were at their disposal in the planning stage of this project.

The fact that the engine test cells now are delivering approximately 4,000,000 kilowatt-hours per month of by-product energy into the power system substantiates the sound economics of the power-recovery system employed in this plant. This means that not only are *B*-29 engines being turned out thoroughly tested and broken in, ready for the initial full power take-off under flight conditions, but the power salvaged from the gasoline consumed during this essential testing period represents almost a 20-per-cent return on the initial investment in testing equipment and incidentally reflects a saving of approximately $200,000 per year to the taxpayers, even though the full output of all test cells is not yet realized.

This same situation likewise is borne out by operating data from other aviation-engine plants employing power-recovery methods. One plant report shows that approximately 60 per cent of the entire plant load is supplied by the engine-testing equipment, which now exceeds 4,000,000 kilowatt-hours per month. Another plant recently reached a point where the monthly average of power generated actually balanced the average plant load for the same period, which totalled over 8,000,000 kilowatt-hours. It must be pointed out in this connection that the ratio of generated power to total plant load is not necessarily a significant comparison, as some plants do not manufacture all the parts required for their total engine production. It is, however, significant to know that power-recovery systems actually salvage as useful energy more than 50 per cent of the actual horsepower-hours generated by each engine during its testing cycle.

Production records of plants employing generator-loading methods reveal a consistently high unit production rate per cell installed. This is brought about by the fact that the cell usage factor is inherently high because of the comparatively short time required to move engines in and out, since all of the pretest harnessing is done outside the cell. In one plant the cell down time for changing engines is as low as 20 minutes. Because of this time saving in the testing cycle, it subsequently follows that fewer test cells of the recovery type are required for a given total engine output for a plant as compared with other types of test cells which require a longer down time to prepare the engines in the cells. Factual data indicate that this cell ratio might be as low as 9:10 and as high as 12:15, depending upon the type and size of engines involved.

I wish to point out that there is no obstacle in the design or construction of the induction-generator system that would limit its application in the load testing of the largest internal-combustion engines now contemplated, involving either single or contra-turning propellers.

Much credit must go to the automotive industry as a whole as well as to certain progressive aviation-engine manufacturers for their foresight in the adoption of power-recovery systems for production testing. This method of testing has contributed in no small way to the achievement of the high engine-production rates accredited to these plants.

When the enormous size of the plant, the critical times experienced during the installation period, and the urgency of getting the job completed, are considered, it is believed that this plant is outstanding in its use of modern industrial engineering practices.

J. Grotzinger (The Goodyear Tire and Rubber Company, Akron, Ohio): This discusser was interested especially in Mr. Bailey's method of determining the probable power demand of the Dodge engine plant. Well-established industries, in general, have a demand that is well known to the engineers of that industry. For instance, in the rubber industry we know that the energy requirements come to approximately 50 kilowatt-hours for every 100 pounds of compound and fabric in the finished product. The demand is approximately 1.1 kva for every 1,000 pounds produced in a month of 25 working days, or better expressed, 27.5 kva per 1,000 pounds of compound and fabric of daily production capacity. The load density runs approximately 13.5 watts per square foot for light and power.

When we deal with a new process, such as the production of synthetic rubber, or the case of an aircraft-engine plant, for which no precedent existed two years ago, the determination of the demand becomes a fascinating study, and it becomes the task of the electrical engineer to make the necessary analysis.

Table I of the paper evidently was the first approach in this case and resulted in an estimated demand of 61,000 kva and an over-all demand factor of 67 per cent. However, the author reached the conclusion that this figure was much too high and that 39,000 kw, or approximately 45,000 kva, was nearer the truth. He also recognized that it would take a good many months to put this large plant into full operation and that during this build-up period the demand would rise rather gradually, giving further opportunities for a final determination of the demand.

The load study presented in the paper should be of much interest to plant engineers, who are frequently called upon to make estimates of this type.

The presentation of the several methods available for testing aircraft engines and especially the last two, which are suitable for power recovery, is also of much interest. The author makes a good case for the variable-speed induction generator, which offers many attractive features. Among these I would stress the disposal of heat from rotor losses by means of forced-air-cooled resistors placed on the roof; the absence of slip couplings and magnetic couplings using liquid cooling; the convenience of obtaining the brake horsepower of the engines by direct readings from calibrated wattmeters.

From Figure 4 of the paper, it is evident that the engine is directly coupled to the generator. No gear reducer, single or multispeed, is used. It would appear then that the generator must operate a good part of the time at speeds far above synchronous speed, for which the percentage of power recovery is rather low.

Will the author please tell us what the synchronous speed of his induction generators is, and the approximate speed range to which they are subjected?

The use of series capacitors to reduce the voltage disturbances on the 12,000-volt bus when switching the variable-speed generators is another point of interest. Will the author please give us some details on the amount of improvement accomplished? Have readings been taken with and without the series capacitors, and what were the results?

E. L. Bailey: Mr. Grotzinger has surmised correctly that the demand of 61,000 kva was the first approach to determining our load. The apparently arbitrary reduction of value to 39,000 kw, 45,000 kva was made after partial operations had begun and it became evident that the over-all demand factor would probably be nearer 50 per cent than 67 per cent. The maximum demand to date has reached 35,700 kw, 46,000 kva.

In reply to the question regarding generator and engine speeds, the engine is equipped with a reduction gear in the head so that, when the engine is operating at 1,285 rpm, the propeller or output shaft is operating at 450 rpm. This was the first point on load required by the test engineers so that 450 rpm is the 60-cycle speed of the generator. The rotor resistance is zero for this speed, and on the engine power 100 per cent less losses is returned to the line. The top generator speed expected under load conditions is about 920 rpm, which is approximately double speed where work is 50 per cent rotor loss and 50 per cent returned to the power lines. The maximum kilowatts recovered also occurs at this speed, as this is the greatest engine output. A higher basic speed would be very desirable but, of course, not possible on account of the engine-load speed specifications.

In reference to the series capacitor tests were made to determine the effectiveness of this unit, and we found the following:

Without capacitor. Voltage on the 2,400-volt bus, which is fed through a 2,500-kva transformer, dropped to 2,260 volts for about three seconds and recovered to 2,380 volts within seven seconds, while the speed of another engine operating from the same bus changed from 2,400 rpm to 2,550 rpm, a condition which was not at all permissible.

With the series capacitor. With the series capacitor neither voltage nor engine-speed variation could be read. The application of the series capacitor gave 100-per-cent correction to the voltage desired, in spite of more than full load kilovolt-amperes at approximately 40-per-cent power-factor demand from the 2,400-volt bus.

The application of series capacitors, I am sure, is going to receive more attention in industrial plants in the future.

The author appreciates the very excellent and constructive discussion prepared by W. L. Wright and delivered by L. A. Umansky.

The Design of Bus-Bar Industrial Distribution Systems; An Epitomization of Available Data

Discussion and author's closure of paper 45-25 by Thomas James Higgins, presented at the AIEE winter technical meeting, New York, N. Y., January 22-26, 1945, and published in AIEE TRANSACTIONS, 1945, pages 385-400.

S. C. Killian (Delta-Star Electric Company, Chicago, Ill.): This paper, the result of a tremendous amount of tedious labor, is a very definite contribution to electrical-engineering literature and nicely proves the axiom that "in many cases the library can be used instead of the laboratory." Covering important subjects hardly touched upon by ordinary text books and heretofore available only by painstaking research through a library, Mr. Higgins has presented a bibliography that will return the hours he has spent manifold in time saving to engineers interested in bus design. Some phases of the subject cannot be analyzed mathematically and answers must be found in the laboratory. Making this type of information easily available will result in a great saving for those who would very likely run repeat tests to obtain data already extant.

The next logical step in making this material immediately available to the engineer is a book on the subject obviating the necessity of referring to almost 600 different texts. With this bibliography as a fine beginning, it would take a hardy soul to sift and correlate all this information, but a book unique in engineering literature and of inestimable value to the engineer would result.

L. F. Hickernell (Anaconda Wire and Cable Company, Hastings-on-Hudson, N. Y.): It seems incredible that anyone would have the patience to read 575 technical papers and prepare such a succinct digest! Having prepared some time ago a synoptical bibliography on power-system insulation in a much less comprehensive manner, I can, in a measure, appreciate the effort involved in this endeavor. The industry is indebted indeed to the author for this herculean task.

Although interested in this subject for many years, needless to say my own bibliography and library contains only a small portion of the author's collection. The only one I have *not* found recorded is:

WAYS TO CONTROL TEMPERATURES OF ELECTRICAL JOINTS, Emil G. Bern. *Electrical World*, **May 5, 1934, page 646.**

Upon different occasions, engineers have written to me regarding references number 436 and 526 of the paper. These reports were printed by the Great Lakes Division of the National Electric Light Association. Later the reports were presented to the electrical apparatus committee, engineering national section, National Electric Light Association, and were included as appendices to the minutes of its meeting at Virginia Beach, Va., May 19-20, 1930.

J. G. Jackson (Square D Company, Detroit, Mich.): This paper presents an enormous volume of material in reference form, a complete analysis of which would entail an amount of work comparable to that devoted to the subject by the author himself.

Some general observations may, however, be in order in addition to an expression of appreciation of the work done by Professor Higgins in compiling and classifying the references. Following the headings of the paper, the following comments are offered.

GENERAL CONSIDERATIONS

General considerations entering into the design of the types of enclosed busses now offered in "package" form by various manufacturers are, necessarily, cost and convenience of installation and use, plus freedom from hazards of various sorts, and low voltage drop and losses under load.

Busses for industrial installations tend to divide into those supplying closely spaced loads of small to relatively large size throughout the length of the bus run, and others intended to carry relatively large blocks of power to feed the first, or distribution, bus or to supply large individual loads.

The distribution bus ordinarily is provided with plug-in openings for the attachment of switch and fuse or circuit-breaker units up to ten for each ten-foot length of duct and is supplied commercially in bus capacities ranging from 250 amperes to 1,000 amperes, for two-, three-, and four-wire single-phase and three-phase systems at 600 volts and less.

Methods of supporting the bus structure by hangers and brackets attached to the building structure must be effective and convenient and preferably universal in their adaptability to the conditions of installation.

While the distribution (plug-in) bus may be fed at one end of a single run, or several similarly fed runs may extend along rows of equipment to be supplied, it is preferable to feed the longer runs at some mid-point or to divide the entire installation into a number of sections, each of which may be fed by a separate feeder-type bus extending from a central power source or from several suitably located banks of transformers with their individual controls.

This arrangement sometimes suggests the connection of the bus installation in network form, which, in turn, introduces problems peculiar to this arrangement, such as greater violence of possible short circuits and difficulty in localizing troubles and re-establishing service after outages.

A simple alternative to the solid network, which avoids these difficulties and hazards while providing full flexibility of service, lies in what may be called an open-network arrangement. In this arrangement sectionalizing points are provided in a loop or network installation which normally are locked open but with provision for the insertion of standard links for connecting an adjacent bus section which it may be desired to transfer from an affected area or feeder.

The usefulness of this arrangement for the localization of troubles and the quick transfer of sections of bus in emergency or for redistribution of load is evident. These advantages probably outweigh any slight gain in copper loss or drop which might seem possible when power sources are connected together solidly through the network.

BUS IMPEDANCE

While bus impedance (assuming normal cross section of conductors) is affected principally by spacing and configuration of the bus-bar assembly, the function of the distribution bus in providing accessibility for frequent connection of plug-in units necessitates bare bus bars with substantial spacing for electrical and mechanical clearance, so that reduction in inductive drop is not obtainable through close spacing of busses. This is not especially serious in the distribution-type bus because of the moderate and tapered loading, as well as the limitation of length of run obtainable by sectionalizing and suitable location of feeders.

In the feeder-type bus, however, in capacities from 1,000 amperes to 4,000 amperes, and fully loaded throughout the length, low impedance with consequent minimum voltage drop is extremely important. Fortunately, however, the lack of necessity for frequent access to the bus bars (except at joints), makes close spacing, with continuous insulation, feasible. For this purpose, in the capacities used, approximately the best results are obtainable with one-half-inch center spacing for copper bus bars of one-fourth-inch thickness.

While several arrangements of interleaving bars of subdivided phases have been employed, in pairs or groups of three for a three-phase system (thus giving six or nine interleaved bars), it has been found that the simple subdivision of one bar into two equal parts and the sandwiching between these half-busses of the remaining nonsubdivided phase bars results in a reduction in voltage drop for power factors in the 60-per-cent range and less of approximately one third, when compared with equally closely spaced busses not so arranged.

The reduced impedance is not only effective for a three-phase bus (thus provided with four bars, two being half capacity), but also in single phase, as for welder loads, with one bar sandwiched between two half bars. The elimination of necessity for transpositions of phases in this arrangement also is advantageous.

The factor of joint resistance is, in practice, held within close limits, usually as low as, or lower than, the resistance of an equal length of the solid bus, by the provision of silver-plated joint surfaces and strongly bolted connections.

It is important that the bolts be easily accessible for inspection and tightening after installation in case of necessity.

Current Rating and Temperature Rise

While conventional cross sections ordinarily are acceptable, current rating (or conversely, bus cross section) also is based on a limiting temperature rise which, for peace-time requirements, seems to be standardized effectively at 55 degrees centigrade above room temperature. (The wartime standard is 70 degrees centigrade.)

For this factor, the moderate capacities and distributed loading of the plug-in type of busses is helpful.

In the feeder busses, due to the relatively higher capacities, and in view of the possible continuous full loading throughout the length of the run, heating becomes a serious problem. A helpful factor, however, is found in the fact that, when closely spaced bus bars are insulated continuously with solid insulating material of high density strongly pressing against the copper bars, the heat is conducted so effectively to the exterior surfaces of the bus structure and dissipated, that the resulting temperature rise may be only one half or one third that existing in air-separated enclosed busses of equal cross section and loading.

Short-Circuit and Other Mechanical Forces

Obviously, short-circuit stresses and resulting bus movement are dependent upon the effective generator capacity connected to any section of bus, and increase with the multiplication of low-impedance sources tied together in a solid network. The open-network arrangement is helpful in limiting this factor. Obviously, also, the rigidity (or lack of it) of the bus bars themselves is an important factor in determining possible displacement and consequent probability of contact between adjacent bars or between a bus bar and an enclosing grounded-metal case when subjected to heavy current surges.

It is of interest that for busses of moderate capacity (the distribution type) the tubular (cylindrical) bar ordinarily is feasible, and is considerably more rigid than the flat, relatively thin, strap type.

For the larger busses (the feeder type) where substantial and continuous insulating separators are feasible, it is not only possible to increase the rigidity of the bus structure by supplemental clamping through the insulating separators, but, in addition, it is evident that the employment of continuous insulating separators between individual bus bars and between bars and grounded enclosure is an effective insurance against contact resulting from stresses exerted on the busses.

Other mechanical stresses and possible distortion of busses can arise from insufficient provision for expansion under load and during periods of high atmospheric temperature.

Rigidity of bus bars is helpful in preventing buckling of busses because of expansion caused by heating, but provision of frequent expansion joints also is important in avoiding forces of this nature.

R. W. Shoemaker (Chase Brass and Copper Company, Waterbury, Conn.): Professor Higgins has made a definite and valuable contribution to the field of bus-bar engineering by providing an exceedingly comprehensive bibliography on this subject. In the past, there has been considerable difficulty in locating information on the extremely varied range of problems that appear when attempting to make an efficient and authoritative design of bus-bar applications. By reference to the work of Professor Higgins, the time factor involved in locating necessary authoritative data, as may be applicable to any design problem, very materially can be improved. By reason of the very complete information tabulated, it also makes it possible to determine the performance of any proposed construction without physical tests.

I am sure copies of this paper will be found shortly in all designing-engineers' libraries.

Yale T. Chaney (The Trumbull Electric Manufacturing Company, Norwood, Ohio): Mr. T. J. Higgins has written a most comprehensive and valuable paper on a subject that is of great current interest and importance to the electrical industry.

The research necessary to compile so complete a bibliography on a subject that has appeared periodically in so many papers and scattered articles over the past hundred years should not be underestimated.

Arrangement of the bibliography and the authors coherent discussion of the major factors influencing the design of bus-bar distribution systems for industrial and commercial applications deserves additional mention.

It should be pointed out that this subject is by no means purely academic; manufacturers of enclosed bus-bar distribution systems have, in no small measure, assisted in increasing the production schedules necessary to meet the war demands by producing prefabricated distribution systems that in certain instances were installed and waiting for the machine and welder loads to be "plugged in."

In the paper a statement is made that the voltage regulation of a bus is determined principally by the inductive drop.

While this statement is generally true, it should be noted that rectangular nonmagnetic bar conductors when assembled on very close spacings (three-quarter-inch center lines or less) with the phases interlaced *ABCABC* and so forth produce reactances equal to or less than the a-c resistances.

This configuration of bus bars also produces a-c resistances that approach the d-c resistance of the bars (reference 270 of the paper). Hence, with impedance components reduced, a low-impedance feeder can be provided to meet present industrial demands for low-voltage systems with two- or three-per-cent regulations for power and with five-per-cent regulation for welder loads.

The presentation of this paper will provide electrical-distribution engineers and designers with a ready reference to all the important work that has been published to date. With such a valuable aid, bus-bar distribution systems should receive even greater acceptance in industry.

William Deans (I-T-E Circuit Breaker Company, Philadelphia, Pa.): To those of us who are concerned with investigations of electrical busses, Professor Higgins has done a service. The bibliography in his paper is to be admired in itself, but the text preceding it makes the bibliography so efficiently usable as to warrant applause.

It is hoped that authors of other bibliographies may use this idea. An essential in such procedure, however, is that the author carefully distinguish statements of opinion and of fact.

I would not take issue with the present author in any such case, except, perhaps, to soften his statement concerning the inadequacy of the flux-current linkage method of computing inductance of bus conductors. Analysis based upon that method often yields practically acceptable results when modified by the use of Maxwell's geometric-mean distances, both for the conductor under investigation, and for all others affecting it. Of course, vector potential is implicit in such use of geometric-mean distances, so perhaps these remarks essentially are academic. However, it also may be a manner of approach. I feel that what I have said is quite consistent with the author's remarks on the same point. Nevertheless, these remarks seem appropriate so that an investigator may not be frightened away from attacking his problem pending an opportunity for acquainting himself with vector potential.

Lawrence E. Fisher (BullDog Electric Products Company, Detroit, Mich.): The extensive bibliography presented in this paper is of considerable value to manufacturers of industrial distribution systems.

A slight revision of the sentence concerning the paired-phase theory, which reads as follows in the paper, would be desirable. "Interestingly, the essential principle of this bus, partial neutralization at close spacing of the skin effect by proximity effect, was investigated more than 25 years ago by Kennelly[171,172] and his associates in the course of their now classical investigations of the skin and proximity effects." This statement may have some meaning when referring to the usual method of bringing two bars close together to reduce the reactance, but it seems not to apply to the three-phase paired-phase arrangement of bus bars.

There is nothing in Kennelly, references 171 and 172 of the paper, that teaches how to design a three-phase bus arrangement such as the paired-phase arrangement, with the peculiar vectorial relationship between the three voltages and the currents in the six bus bars. It is believed that the paired-phase arrangement was disclosed for the first time publicly in the BullDog Electric Products Company's bulletin 412, in the paper, "Interleaved Phases for Welder Bus" (item 33 of the bibliography in Mr. Higgins paper) and in patents number 2,287,502 and 2,288,078.

I am not sure whether it is customary or not to include patents in bibliographies of technical papers, but the study of patents pertaining to any subject unquestionably would add materially to the knowledge of the subject. Two other patents on industrial distribution systems, patents number 2,116,676 and 2,211,109, refer to an enclosed distribution duct or busway with bare bus bars that will withstand power arcs without damage. These few patents are cited only as examples of a great number of patents on this subject.

Another source of information on this subject is the test-report files of industrial laboratories. As an example, in addition to the technical file in our research department which contains some of the technical papers listed in Mr. Higgins' bibliography, we have records covering a period of over ten years, consisting of about 38 books or volumes containing a total of about 7,000 pages of data and discussions of tests on plug-in ducts, paired-phase ducts, and "Trol-E-Ducts." Undoubtedly other industrial laboratories have considerable data on this subject and, although the information contained therein is not open to the public in general, nevertheless it is believed that most industrial laboratories would cooperate willingly with any engineer looking for some specific type of information.

A. G. Darling (General Electric Company, Schenectady, N. Y.): The investigator who can answer problems expeditiously either must have in his mind a working knowledge of the approach, or have at his finger tips sources of information well cataloged and cross referenced.

The recent trend toward the use of busses in manufacturing plants has revived much of the investigation work that had been done over a number of years. Improvements undoubtedly still can be made in bus design and a knowledge of bus characteristics is valuable. Those designers who more recently have come into the field will find much encouragement in the data which Mr. Higgins has accumulated with meticulous care and judgment. Others will save much time by using his summaries.

Believing that I am voicing the opinions of many, a sincere expression of thanks and compliments goes to Mr. Higgins for his very excellent work.

Thomas James Higgins: The author thanks each of the discussers for his kind remarks regarding the general usefulness of the paper under discussion.

The author is indebted to Mr. Hickernell for the additional reference cited and for corrections (by letter) of several typographical errors and for amplification of several of the references.

Mr. Jackson's comprehensive remarks comprise a useful, interesting summarization of certain factors important to the practical design of feeder and distribution busses.

The author someday would like to write the book mentioned by Mr. Killian. Publishing companies, however, are rather chary of publishing a book having a limited sale such as might accrue to this projected volume.

The author is pleased that Mr. Carlson has specified the exception to the statement that "the voltage regulation of a bus is determined principally by the inductive drop."

The author is somewhat at a loss as to Mr. Deans' remark, "That method [flux-current linkages] yields practically acceptable results when Maxwell's geometric-mean distances are used, both for the conductor under investigation, and all others affecting it." The flux-current linkage method of calculating inductance is distinct from the method of geometric-mean distances.[1]

Regarding Mr. Fisher's remarks, the author cannot do better than to quote from his recent letter to Mr. Fisher:

"Regarding my statement 'Interestingly, the essential principle of this bus, partial neutralization at close spacing of the skin effect by proximity effect, was investigated more than 25 years ago by Kennelly[171,172] and his associates in the course of their now classical investigations of the skin and proximity effects' I am now of the opinion after rereading your TRANSACTIONS paper that the phrase 'the essential principle' is too strong, as you maintain. For I see now that what really produces the approximate 180-degree phase shift between the currents in the pair is the conjunction of the paired phases and an allowable minimum spacing between adjacent pairs (the phase shift increasing toward 180 degrees as the inter-pair distance increases). Thus, by virtue of the close association of the conductors of the pair, flux densities at even small distances from the pair are weak whence the inductance, reactance, and voltage drop is minimized. Actually, the effect of neutralization of skin effect by proximity effect is more or less constrained to reduce the a-c resistance of the conductors; as is indicated in your curve showing reduction in a-c resistance as the conductors of a pair are brought closely together, the phenomenon noted by Kennelly. My idea of 'the essential principle' was that, inasmuch as this neutralization produces, as it does, essentially uniform current distribution over the conductor cross sections (indicated by the low ratio of a-c to d-c resistance) your analysis in the appendix (which is postulated on uniform current distribution, the assumption made in deriving *g.m.d.s*), is applicable; but if neutralization did not take place, the actual physical facts would be at variance with your theory, hence it is 'the essential principle.' But I guess that is carrying it too far. I am of the mind, therefore, that the phase 'the essential feature' should be changed to one of the following: 'an essential feature,' 'an important feature,' or 'a noteworthy feature.' How does one of these strike you?"

Additionally, the author agrees with Mr. Fisher that there is nothing in the articles by Kennelly that directly bears on the design of the paired-phase arrangement.

REFERENCE

1. A TREATISE ON ELECTRICITY AND MAGNETISM (third edition), J. C. Maxwell. Volume 2, pages 273, 314–18.

Modern Electric-Power-Distribution Ideas as Applied in a Large War Plant

Discussion and author's closure of paper 45-79 by R. H. Kaufmann and N. A. Kieb, presented at the AIEE winter technical meeting, New York, N. Y., January 22–26, 1945, and published in AIEE TRANSACTIONS, 1945, June section, pages 279–87.

L. C. Peterman (Ford, Bacon and Davis, Inc., New York, N. Y.): This paper describes an installation that has many commendable features. It shows how intelligent planning can promote speed of construction by making it possible to order electric equipment early in the planning stage, so that deliveries are made on time. Selection of a few sizes of standardized substations, changing spacing rather than changing size for different load densities, contributed greatly to this end. Combining the power and lighting substations simplified the installation and greatly reduced the cost as well as use of critical material.

It is noted that above 30,000 kva of load-center transformer capacity is installed, operating 50-per-cent to 100-per-cent load. If the average is 75 per cent, the total demand is 20,000 kva (possibly less if we allow for diversity) yet a total of 50,000 kva of transformer capacity has been installed in the main substation. Ten thousand kilovolt-amperes of this capacity is in a connection to a second utility company, yet apparently it is available as spare capacity. Even if we eliminate this 10,000 kva from consideration, we still have a full spare of 20,000 kva or, in other words, 40,000 kva of transformers carrying 20,000-kva load. Paralleling this excess transformer capacity, there is apparently about 70,000 kva in 13-kv cable capacity. Although the electric-system design in several respects stressed the saving of critical materials, this principle was not followed in planning the transformer and primary distribution installation. A use factor of 50 per cent for transformers and 30 per cent for cables seems pretty low. This, in the face of orders and directives from Government agencies that, in general, have prohibited the purchase and installation of spare equipment.

All the low-voltage circuit flexibility described would be obtainable from a single transformer of the type shown and the single transformer would be no more a bottleneck than the single incoming high-voltage line. Ordinarily we would say that service reliability of a single transformer is better than an average-grade open-wire transmission line. The second transformer, therefore, does not improve reliability of service, nor does it improve flexibility of the low-voltage circuits. Installing two transformers is apparently an admission by the manufacturer that the forced-oil air-pressure-cooled transformer is not as reliable as the more conventional machine, and that there is need for a full spare to equal the reliability of a single transmission line. There is certainly some reason to take this stand when we read the description of the auxiliary equipment of this transformer, here quoted in part:

> ". . . two pumps in parallel . . . oil-to-air heat exchanger with a multibank radiator and a multiplicity of cooling fans . . . operating power derived from control power transformers . . . ."

The word "multiplicity" from the foregoing quotation is quite significant. "Multiplicity" instead of "simplicity"; more auxiliaries to operate, look after, and maintain; and perhaps the corollary to this is less ruggedness, less reliability.

As to the grounding system, the 4/0 copper ground leads evidently are interconnected with the steel strand supporting the fluorescent lamps. If a heavy fault current flows from one 4/0 to another 4/0 through the steel strand, is there a possibility that the latter may burn off and drop the fluorescent lamps?

Closely spaced 480-volt open power feeders suggest possible future trouble from short circuits and grounds when painters, pipe fitters, steel workers, and other maintenance men not of the electric trades have to work among these wires. A shock from a poorly taped joint might throw one of these workers to the floor. As a wartime expedient, yes. But don't recommend that we do such things in the future, after the emergency is over.

Suspension of fluorescent units from an overhead messenger is represented as being an "ingenious innovation." True it is ingenious, but it is not an innovation, for this type of suspension has been in use ever since fluorescent lamps first were installed in industrial plants, and even before that incandescent lamps sometimes were suspended in this way.

But the matter deserving most careful consideration in this paper is the installation of 13-kv cables in wood troughs under the building roof, with this type of construction held up as a model for future work. Many reported advantages are claimed, but the disadvantages and the extreme hazard thereby introduced are ignored. Completely ignoring the National Electric Code and the simple tenets of safety and reliability as is done here is probably justified in time of national emergency but recommendation of this type of construction for the future indicates that the authors apparently have had no knowledge of, or experience with, the destructive effects of an arc in a 13-kv cable. Cables can and do fail, sometimes because of manufacturing defects, quite often from damage by workmen when not adequately protected, and I do not believe that anyone will claim that cables in a wood trough are protected adequately. Painters, roofers, and maintenance men, either when following their usual routine or when making changes in existing structures, are a source of possible injury to these cables. If a cable fault occurs, the wood trough will go up in flames, and it is not too remote a possibility to visualize the roof steel burned through with subsequent collapse of the affected structure. I do not believe that the authors would claim that cables never fail. In fact, such failure is specifically recognized as a possiblility where reference is made in the paper to quadrature arrangement of feeders and diverse routing of cables for the purpose of minimizing the effects of cable failure. It may be claimed that sensitive relaying will take out a cable before serious burning occurs. But do not forget that relay contacts sometimes stick, and sometimes control wiring becomes disconnected or broken with the trouble not discovered until a "blowup."

The authors of the paper claim that cables can be installed easily and repairs easily can be made. Granted. But utilities and many industrials install such cables the hard way, for bitter experience has taught the need for adequate protection to safeguard life and property. The authors' proposal to substitute a light metal trough for the wood trough for future construction also exhibits lack of experience with the effect of an arc on steel. An arc would burn through light steel work almost as quickly as through wood. Careful fireproofing of steel work in power stations and substations as currently practiced is recognition of the destructive effect of an arc on steel.

It should have been pointed out in the paper that this is a wartime installation and that the features described are not recommended necessarily for future use when the war emergency has passed.

R. H. Kaufmann: Mr. Peterman has viewed this project with a particularly critical eye which should be helpful in bringing out deficiencies and assist in making more expert applications of these principles in the future.

There are some remarks made by Mr. Peterman which are based on an erroneous premise and warrant reconsideration.

Mr. Peterman, in criticizing the incoming power substation capacity of 40,000 kva and the primary feeder capacity, has evaluated the sum total rated kilovolt-amperes of utilization substation capacity as 30,000 kva. Reference to Figure 1 of the paper will disclose that the main substation serves connected utilization substation capacity of 31,500 kva in the main-factory area, 1,600 kva in the office area, 15,000 kva in the test and dynamometer area, and 5,000 kva in the boiler-house area, aggregating 53,100 kva. This figure is about 75 per cent greater than that used by Mr. Peterman.

The apparent excess of aggregate primary-feeder-cable capacity is accounted for by diversity factors, the practical consideration of using relatively few different cable-conductor sizes, and, to some extent, a consideration of cable-circuit loading during emergency operation. While it is probable that some reduction in primary-feeder capacity could have been effected by additional study and planning, it is believed certain that the expenditure of the same additional effort in extending the study of low-voltage circuits would yield a greater return. Even with the short low-voltage feeders associated with this distributed-substation system, the investment in low-voltage circuits is about five times that of the 13.2-kv circuits.

Mr. Peterman contends that, since a transformer has a higher degree of reliability than an overhead line, the connection of a transformer in series with such a line does not detract from the over-all reliability. The number of outages on a series-connected system will be the sum of the outages in the several series-connected elements. Furthermore, the occurrence of a transformer failure would entail an extended outage period in contrast with the short time interval involved in restoring service on an overhead line. In many instances, the number of times that a transformer is de-energized voluntarily for purposes of inspection or maintenance will exceed greatly the number of forced outages. Certainly the ability to voluntarily de-energize a transformer is a valuable feature. The use of two transformers in the main substation in the manner indicated provides this improvement in reliability and, what is more important, it is accomplished at substantially no increase in investment of materials or cost.

While it would have been desirable to obtain the improved reliability of a double-circuit incoming high-voltage supply, its use would have entailed almost double the investment in materials and cost and was dismissed in view of the extremely critical material situation. Provision has been made in the main substation, however, for the acceptance of a duplicate incoming power line, should it become possible to allocate the necessary material at some future date.

The operating reliability of forced-oil air-pressure-cooled transformers is proving to be excellent. While the presence of moving parts is accepted as a disadvantage and may tend to restrict application to attended substations, this is far overshadowed by the advantages of reduced investment cost and physical size, together with reduced weight.

In regard to the grounding system, it is the multiplicity of interconnected members forming virtually a grid ground mesh which precludes danger of excessive temperature rise in any one member because of ground current flow. As a matter of fact, the lighting messenger cable normally would be grounded at each point of support, even though it was not used as the ground-return conductor for branch lighting circuits, and thus would be in no less danger of being overheated as a result of ground current flow.

Mr. Peterman's comments relative to the desirability of metal-clad low-voltage feeder circuits is endorsed heartily. The trend toward totally metal-clad electric circuits, all the way from the incoming-power substation to the utilization machine, will be again in evidence as soon as the war-time restrictions on the use of the necessary metal is lifted.

The point which has been raised relative to the use of wooden troughs for supporting the primary cables has been well taken. In postwar applications, the elimination of combustible material in the cable-supporting structure should be paramount, and, of course, should be executed in a manner approved by the National Electric Code and satisfactory to the Board of Fire Underwriters. On the other hand, we should not be hypercritical of this structure, merely because it happens to support electric-power cables. The potential fire hazard in such an overhead trough of wood construction should be substantially no different from that in an overhead catwalk of similar construction.

In general, there is a tendency to consider high-voltage feeder cables as being potentially more dangerous than low-voltage cables. Actually, the energy liberated at a fault will be proportional to the product of fault-current magnitude, arc voltage, and time. The arc voltage at a given fault-current magnitude will be of the same order for all operating voltages. Fault-current magnitudes are frequently highest on circuits of lower voltage. The speed with which the fault-current flow is interrupted plays a very important part in limiting the energy liberated at the fault. In the system here described, the use of grounded neutral operation, in combination with sensitive, fast-operating ground-current relays, goes far toward minimizing the damage at the point of failure. Upon the occurrence of a primary-feeder fault, the relaying system, in combination with the circuit breakers, will function to interrupt current flow in a small fraction of a second. Even though we admit that the feeder breaker becomes inoperative, the incoming line breakers to each 13.8-kv bus incorporate back-up ground relaying which would clear the fault current with no more than one-half-second additional duration.

I am in complete agreement with Mr. Peterman that the merits of the fundamental principles should not be confused with the details of execution. The critical war scarcity of metals has made necessary the use of some detail practices which should not be perpetuated in normal times.

Damping and Synchronizing Torques of Power Selsyns

Discussion and authors' closure of paper 45-22 by C. Concordia and Gabriel Kron, presented at the AIEE winter technical meeting, New York, N. Y., January 22–26, 1945, and published in AIEE TRANSACTIONS, 1945, pages 366–71.

Harold Chestnut (General Electric Company, Schenectady, N. Y.): The problem handled by Concordia and Kron is a worthwhile one in the field of power control and the information they have obtained should prove useful for designers of round-rotor Selsyns. An allied problem in Selsyn hunting is encountered with small salient-pole indicator Selsyns. Here two salient-pole rotors are excited in parallel with single-phase alternating current, and the stators of the two machines are connected in parallel, see Figure 1. The normal electric-machine design is such that inherent instability is produced in such a system. Mechanical dampers are used to obtain a highly damped system which does not run away during transients. Efforts were made using methods developed by the authors of this paper[1,2] to determine the modifications in electrical design necessary to produce a stable, highly damped system. Although some measure of success was achieved, calculations showed, and tests verified, that the damping performance to be obtained was not as satisfactory as could be produced with a mechanical damper.

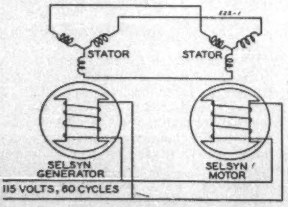

Figure 1. Schematic diagram of salient-pole Selsyn system

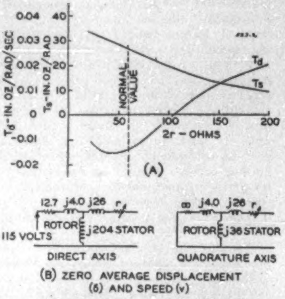

Figure 2. Damping and synchronizing torque coefficients for two identical salient-pole Selsyns as a function of sum of stator resistances of both machines

In brief, the study indicated that the stability could be improved by:

1. Increasing the resistance of the stator circuit. (See Figure 2.)

2. Installing a quadrature-axis winding on the rotor to form an "electrical damper." (See Figure 3.)

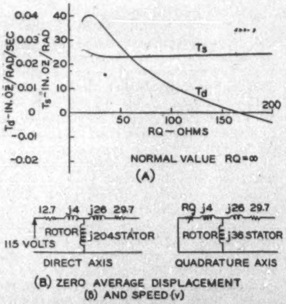

Figure 3. Damping and synchronizing torque coefficients for two identical salient-pole Selsyns as a function of quadrature-axis rotor resistance

Adding stator resistance confirms conclusion 5 of Concordia and Kron where they note that added resistance between machines was found beneficial. As Figure 2 shows, the improved damping characteristic is obtained at the expense of decreased synchronizing torque. For the salient-pole case, adding resistance in the excitation circuit is not effective in increasing stability. (Figure 4.)

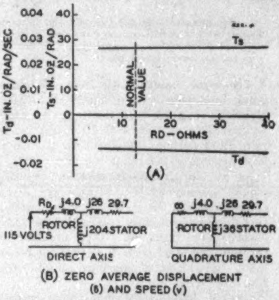

Figure 4. Damping and synchronizing torque coefficients for two identical salient-pole Selsyns as a function of direct-axis rotor resistance

However, if a winding is added in the quadrature axis and the rotor resistance of this circuit is decreased until it is comparable to the direct-axis rotor resistance, an increased degree of positive damping is obtained with but a slight decrease in synchronizing torque. (Figure 3.) Actual tests indicated that the maximum torque was decreased, although for an angular separation of less than 40–50 degrees from correspondence there was little decrease in torque caused by the presence of the added winding.

Small random oscillations in indicator Selsyns which occur at low values of constant speed are decreased somewhat by the introduction of the damper winding but are not eliminated entirely.

REFERENCES

1. EQUIVALENT CIRCUITS FOR THE HUNTING OF ELECTRICAL MACHINERY, Gabriel Kron. AIEE TRANSACTIONS, volume 61, 1942, May section, pages 290–6.

2. EQUIVALENT CIRCUITS FOR OSCILLATING SYSTEMS AND THE RIEMANN–CHRISTOFFEL CURVATURE TENSOR, Gabriel Kron. AIEE TRANSACTIONS, volume 62, 1943, January section, pages 25–32.

S. B. Crary (General Electric Company, Schenectady, N. Y.): The paper by Kron and Concordia has several features which are worthy of emphasis:

1. The expression of physical phenomena in terms of equivalent circuits provides a powerful method for the application of advanced mathematical methods, such as tensor analysis, to the solution of complex engineering problems. The elements of the circuit can be expressed in literal terms; a relatively simple circuit is substituted for a system of equations which are, in many cases, totally impossible of *practical* numerical solution. This is the network-analyzer method of solution of power-system problems carried forward, as one example, to the solution of rotating machinery.

2. The analysis of a complex problem by compara-

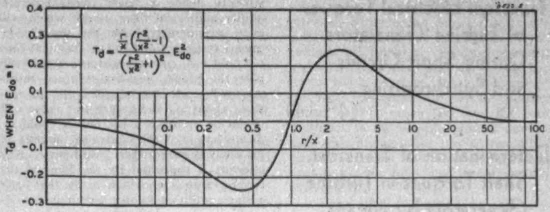

Figure 5

tively rigorous methods often results in a rather simple guiding principle or rule of thumb which may be used by all engineers working in the field, such as the authors' "R/X greater than one" criterion for stability. This is many times the reward for completing investigations in spite of the original complexity and is a direct refutation to those who deplore the complexity of applied mathematics in engineering.

3. The method of equivalent circuit representation provides a better physical interpretation for engineers of the phenomena than a set of equations and, therefore, is a powerful new mental tool for the engineer who must solve within the same life span increasingly more difficult problems than did his predecessors.

As a matter of interest, the following derivation shows that the simple approximate rule given by the authors is obtained from a consideration of a symmetric rotor machine with only one field winding having a zero-field time constant connected directly to an infinite bus through series line impedance. This corresponds to a simple $r+jx$ impedance tie between an infinite bus and a synchronous voltage which varies directly with speed. For this case, equation 64 of a paper by R. H. Park[1] for small angular deviations from an operating angle, may be used with the restrictions specified in the following equations 2.

$$\Delta T = \frac{\left(\begin{array}{l}[\psi_{do}+i_{do}x_q(p)]\{[e\sin\delta_o+\\ \quad\psi_{do}p]\,Z_d(p)+[e\cos\delta_o+\\ \quad\psi_{qo}p]x_d(p)\}+[\psi_{qo}+i_{qo}x_d\times\\ \quad(p)]\{[e\cos\delta_o+\psi_{qo}p]Z_q(p)-\\ \qquad[e\sin\delta_o+\psi_{do}(p)x_q(p)]\}\end{array}\right)}{Z_d(p)Z_q(p)+x_d(p)x_q(p)}\Delta\delta \quad (1)$$

where

$\psi_{do}=E_{do}-x_d i_{do}$
$\psi_{qo}=E_{qo}-x_q i_{qo}$
$e\sin\delta_o=-ri_{do}-\psi_{qo}$
$e\cos\delta_o=-ri_{qo}+\psi_{do}$

We have, for the case under consideration,

$$\left.\begin{array}{l}x_d(p)=x_q(p)=x\\ Z_d(p)=Z_q(p)=px+r\\ \quad\psi_{do}=E_{do}-xi_{do}\\ \quad\psi_{qo}=-xi_{qo}\end{array}\right. \quad (2)$$

$$\left.\begin{array}{l}e\sin\delta_o=-ri_{do}+xi_{qo}\\ e\cos\delta_o-E_{do}=-xi_{do}-ri_{qo}\end{array}\right. \quad (3)$$

Solving equations 3 for i_{do} and i_{qo}, we have

$$\left.\begin{array}{l}i_{do}=\dfrac{-re\sin\delta_o-xe\cos\delta_o+xE_{do}}{r^2+x^2}\\[2ex] i_{qo}=\dfrac{-re\cos\delta_o+rE_{do}+xe\sin\delta_o}{r^2+x^2}\end{array}\right\} \quad (4)$$

Substituting 2 and 4 in 1, we have

$$\Delta T = \frac{\left[\begin{array}{l}\{[e\sin\delta_o+\psi_{do}p][px+r]+\\ \qquad[e\cos\delta_o+\psi_{qo}p]x\}E_{do}\end{array}\right]}{(r+px)^2+x^2}[\Delta\delta] \quad (5)$$

In order to determine the damping torque for an assumed sinusoidal oscillation of $\Delta\delta=[\Delta\delta]\sin ht$. Let $\sin ht=1.0$ and $p=jh$, where h = oscillation frequency. Therefore equation 5 becomes

$$\Delta T = \frac{\left(\begin{array}{l}[e\sin\delta_o+\psi_{do}jh]\{r[r^2+x^2(1+\\ \quad h^2)]-jhx[r^2-x^2(1-h^2)]\}\times\\ \quad[e\cos\delta_o+\psi_{qo}jh]\{x[r^2+\\ \qquad x^2(1-h^2)]-j2hrx^2\}\end{array}\right)E_{do}}{r^4+2r^2x^2(1+h^4)+x^4(1-h^2)}[\Delta\delta] \quad (6)$$

Therefore the damping and synchronizing torque coefficients are

$$T_s = \frac{\left(\begin{array}{l}r[r^2+x^2(1+h^2)]e\sin\delta_o+\\ x[r^2+x^2(1-h^2)]e\cos\delta_o+\\ h^2x[r^2-x^2(1-h^2)]\psi_{do}+\\ \qquad 2h^2rx^2\psi_{qo}\end{array}\right)E_{do}}{r^4+2r^2x^2(1+h^4)+x^4(1-h^2)} \quad (7)$$

$$T_d = \frac{\left(\begin{array}{l}-x[r^2-x^2(1-h^2)]e\sin\delta_o-\\ \qquad 2rx^2e\cos\delta_o+\\ \quad r[r^2+x^2(1+h^2)]\psi_{do}+\\ \qquad x[r^2+x^2(1-h^2)]\psi_{qo}\end{array}\right)E_{do}}{r^4+2r^2x^2(1+h^4)+x^4(1-h^2)} \quad (8)$$

Equation 8 can be simplified by using equations 2 and 3 so that we obtain

$$T_d = \frac{[r^4+r^2x^2h^2-x^4(1-h^2)]rE^2_{do}}{[r^4+2r^2x^2(1+h^4)+x^4(1-h^2)][r^2+x^2]} \quad (9)$$

If the hunting frequency is small, equation 9 simplifies to equation 10

$$T_d = \frac{\frac{r}{x}\left[\frac{r^2}{x^2}-1\right]}{\left[\frac{r^2}{x^2}+1\right]^2 x}E^2_{do} \quad (10)$$

Figure 5 of this discussion is a plot of equation 10.

This illustrates that greatest negative damping is obtained for such a series impedance tie with constant terminal voltages when r/x is about 0.4 and becomes positive when r/x is greater than unity.

REFERENCE

1. TWO-REACTION THEORY OF SYNCHRONOUS MACHINES, PART I, R. H. Park. AIEE TRANSACTIONS, volume 48, 1929, pages 716–31.

C. Concordia and Gabriel Kron: Both Mr. Crary and Mr. Chestnut have made important contributions in their discussions which will help to complete and round out the theory. In connection with Mr. Crary's discussion, we should remark that it was he who first pointed out the simple criterion of stability as given in his equation 10. Mr. Chestnut's discussion brings out the fact that, in the case of a salient-pole machine (that is, a machine with different characteristics in the two rotor axes), the quadrature-axis characteristics determine the damping. Comparison of Figures 3, in which the quadrature-axis resistance is varied, and 4, in which the direct-axis resistance is varied, shows this, and Figure 2 shows that the stator resistance required for positive damping is very nearly equal to the quadrature-axis reactance. It is of interest to note that, in the case of synchronous machines with d-c field excitation, it is the direct rather than the quadrature-axis reactance that determines the limit of positive damping for the component of damping due to stator resistance, while on the other hand the quadrature axis is still the determining factor for the component due to rotor resistance when the stator resistance is negligible.

Since in the case of Selsyns the quadrature axis largely determines the damping-torque coefficient and the direct axis largely determines the synchronizing-torque coefficient, one has the opportunity, by a separate treatment of the two axes, to obtain positive damping without sacrificing a high synchronizing torque.

Inherent Errors in the Determination of Synchronous-Machine Reactances by Test

Discussion and authors' closure of paper 45-16 by C. Concordia and F. J. Maginniss, presented at the AIEE winter technical meeting, New York, N. Y., January 22–26, 1945, and published in AIEE TRANSACTIONS, 1945, June section, pages 288–94.

S. B. Crary (General Electric Company, Schenectady, N. Y.): System-design engineering requires the specification of apparatus-performance characteristics preferably in terms of a few definitive constants. These are the constants by which the system engineer is able to translate his requirements concisely to the designer or manufacturer. The reactances and time constants discussed in the paper by Concordia and Maginniss are some of the more important synchronous-machine quantities which originated from the fundamental work of investigators of the period in which Doherty and Nickle presented their five synchronous-machine papers (1926–1930).

These concepts and definitions have certain inaccuracies:

(a). Due to the idealization or assumptions made by these earlier investigators, such as constant flux linkages in all rotor circuits for subtransient reactance and constant flux linkages in the field winding for transient reactance.

(*b*). Introduced by the necessity of making a relatively simple definition, which does not allow for rigorous qualification.

In order to make the definitions practical and so they can be used in specifying performance, it is necessary to have a method or methods of testing. The test methods introduce additional inaccuracies such as

(*c*). Test variables not specified or controlled.
(*d*). Metering or measurement errors.

The paper by Concordia and Maginniss presents the result of a study of (*c*) and yields information in regard to (*a*) and (*b*). It could be expected, therefore, that their conclusions would show definite methods or suggestions for improvement of the test code for synchronous machines. Some of their suggestions confirm those previously made by other investigators and in this way are added confirmation of this other work. It would appear, as they have outlined, that it would be now advisable to suggest:

1. Elimination of method 2 of the test code for measuring reactances.
2. Reduction of sequential closing interval of the circuit breaker used for applying the test short circuit.
3. Recognition of the error introduced by the effect of the ratio of x_q'' to x_d''.

As the authors point out, the test methods in the AIEE test code are not in entire agreement with the corresponding definitions. This does not necessarily constitute a criticism. Actually, it is not feasible in many cases to have a practical test method which checks accurately the defined principle or concept. It well may be that they are more useful, if they are not required to be in rigorous agreement. It is possible, however, by a study such as that made by the authors, to understand more fully wherein these differences exist and to bring them into closer agreement without a sacrifice of practicability. This paper has done much to clear up reasons for some of the inaccuracies, particularly of the measurement of subtransient reactance, and also to provide practical suggestions for bringing into closer agreement the definition and the test for subtransient reactance.

C. Concordia and **F. J. Maginniss:** In connection with Mr. Crary's discussion, it should be noted that most of the differences discussed in this paper are not large, especially in comparison with the possible uncertainties of calculation and test. Also, the variation of reactance with saturation may be much greater than most of the variations we have discussed. This is especially true in the case of turbine generators, wherein the saturation effects are large and the subtransient saliency is slight. The principal significant variation shown in the paper is the large effect of sequential closing of the short-circuiting breaker in conjunction with the use of the asymmetrical component of short-circuit current in the determination of the subtransient reactance. It was not, however, our principal object to demonstrate such large and practically important effects, but rather to give a more or less rigorous discussion of the various fundamental relations among the definitions, methods of calculation, and test, a knowledge of which is necessary before much progress can be made in improving them.

Transient Electrical Torques of Turbine Generators During Short Circuits and Synchronizing

(45-14)

Determination of Transient Shaft Torques in Turbine Generators by Means of the Electrical–Mechanical Analogy

(45-15)

Discussion and author's closure of paper 45-14 by H. S. Kirschbaum and discussion of paper 45-15 by G. D. McCann, C. E. Warren, and H. E. Criner, presented at the AIEE winter technical meeting, New York, N. Y., January 22–26, 1945, and published in AIEE TRANSACTIONS, 1945, February section, pages 65–70 and pages 51–56.

A. W. Rankin (General Electric Company, Schenectady, N. Y.): Mr. Kirschbaum has made a valuable contribution to an important practical problem in his analysis of turbine-generator short-circuit torques. This problem is very complex, and in order to reduce it to a form amenable to analysis without the aid of mechanical devices, it is necessary to introduce several simplifications and assumptions.

The initial assumption given by the author is that this analysis is based on an ideal machine of the type defined and introduced by Park. The writer wishes to point out, however, that the subject analysis is based on a simplified version of Park's ideal machine, and one that would be more descriptively defined as a symmetric machine, since it assumes the quadrature axis to be a duplicate of the direct axis and to contain a definite field winding and field voltage which are both duplicates of the corresponding direct-axis quantities. Park's ideal machine makes no such assumption about the quadrature axis and, in general, is ideal only in the sense that saturation and armature-winding harmonics are neglected. The symmetric machine is employed usefully in system studies in which the system reactances tend to equalize the equivalent direct and quadrature axes but is not as applicable to direct short-circuit problems. Especially is it to be questioned if the symmetric machine is a satisfactory solution for turbine-generator short circuits in the transient period.

The author's statement concerning the impedance–frequency variation of the solid-rotor structure is applicable only when the surface permeability is constant. Test data indicate that this square-root relationship is not followed too closely in actual machines. The writer agrees with Mr. Kirschbaum that the negative-sequence resistance is not known very accurately for values of rotor-circuit current of the order of short-circuit currents.

Insofar as the writer knows, it is not possible to define a single constant-permeability additional rotor circuit which will even approximate both the negative-sequence resistance and the subtransient time constant. A circuit resistance which will give the proper negative-sequence resistance will result in a subtransient time constant about $^1/_{20}$ the known test value. It would be valuable if the author could indicate how well the equivalent circuits of his analysis satisfy these two limits. This question is suggested by the form of the torque expressions which imply that only a single additional rotor circuit is considered.

A more accurate value of electrical torque should be obtained if impedances are substituted for reactances in the torque expressions, since the negative-sequence resistance is comparatively large with respect to the reactances. This assumes, of course, that the test determinations of subtransient reactance actually measure reactance and not impedance.

The author's contributions to the subject of line-to-line-to-ground armature decrements are valuable, since these have not been analyzed, heretofore, so extensively as their importance justifies.

The foregoing discussion has tried to emphasize the complexity of the round-rotor machine under transient conditions, and to indicate some of the problems which are still to be solved. Mr. Kirschbaum is to be commended for his contribution to this torque problem, since his paper is a valuable step toward a complete solution.

M. D. Ross (Westinghouse Electric and Manufacturing Company, East Pittsburgh, Pa.): Just a few remarks in regard to the background of the Kirschbaum and the McCann, Warren, and Criner papers might be in order. Our consciousness of the problems connected with short-circuit torques has grown over the years. For instance the 1922 AIEE Standard says: "The Institute recognizes the self-destructibility, both mechanical and thermal, of certain sizes and types of machines when subjected to severe short circuits and recommends that ample protection be provided in such cases external to the machine if necessary." They recognized the problem at that time, but nothing was done to establish limiting conditions. At that time many machines were built with shafts and couplings proportioned on the basis of withstanding a certain number of times full-load torque, which figure had been arrived at more or less by experience.

About 1929 the subject was taken up actively by a number of investigators, and much of the ground work for the present papers was done in the early 30's. Tests on machines were made by Penney in 1929 and by Whitney and Criner in 1940 to confirm the theory in regard to short-circuit torques.

The first edition of the American Standards Association rules for synchronous machines in 1936 stated that the generator should be capable of withstanding a short circuit at no load with 110 per cent of rated voltage. The 1943 American Standards state that the generator shall be capable of withstanding a short circuit at rated load and power factor and 105 per cent of rated voltage and that the current is not to exceed the three-phase value under any condition of short circuit. This clause would seem to cover quite satisfactorily the worst short circuit that can be obtained in normal operation. As the single-phase line-to-line short circuit gives the highest value of short-circuit torque in line with the Standards, it has been emphasized throughout these papers.

As long as we were building 1,800-rpm generators with relatively low electrical torques, high inertias, and large shaft flexibilities, few problems were encountered in connection with shaft torques. With the advent (in recent years) of large 3,600-rpm generators with their lower reactances and relatively stiff mechanical coupling, it has become more important that we be able to calculate these torques with greater accuracy. We are now confident that this can be done using the methods outlined here with a minimum of work involved in the calculations.

Mr. Kirschbaum's paper covers a rather interesting feature—namely synchronizing out of phase. Many of us perhaps have seen the results of this in twisted shafts and sheared coupling keys. Generators designed to meet the ASA short-circuit clause would not necessarily withstand the most severe conditions of synchronizing out of phase.

The authors are to be congratulated on their valuable contributions to the subject of short-circuit torques.

H. S. Kirschbaum: I agree with Mr. Rankin when he points out that the assumptions which I made do not agree exactly with those which Park made and that the machine discussed might better be called a symmetric rotor machine. The discusser has questioned the use of a symmetric rotor machine as being equivalent to a turbine generator during the transient period of a short circuit. During this period, there will be harmonic torques introduced by the saliency of the turbine generator. However, these are usually very small and since the response of a mechanical system to high-frequency torques is usually negligible, they can be neglected. An unusual case might exist in which the mechanical system has resonant frequencies near the second, third, or fourth harmonics of fundamental frequency. In this case the more exact expressions derived by Nickle, Pierce, and Henderson must be used calculating the alternating components of torque.

Mr. Rankin also points out that the assumptions I have made regarding the variation of the rotor loss factor with frequency holds only for a constant permeability rotor. In actuality, permeability decreases with an increase in rotor current, permitting the rotor current to penetrate to a greater depth on the rotor surface. This, in effect, lowers the loss factor as the current increases, and we have found that assuming the square-root relationship to hold, the rotor loss varies as the 1.8 power rather than as the square of the current.

I did not, as the discusser implies, use an additional rotor circuit which was the same at all frequencies. The rotor circuit used had a resistance and reactance which varied as the square root of frequency. The decrement factor of the subtransient current in the rotor body is very small compared with the angular velocity (754 for a 60-cycle machine) of the second harmonic rotor currents. Therefore, the subtransient rotor currents will penetrate the rotor surface to a greater depth than will the second harmonic rotor currents. As a consequence the rotor resistance to the subtransient current will be much less than the rotor resistance to the second harmonic current, thus accounting for the discrepancy which results when the negative-sequence resistance is used to calculate the subtransient time constant.

In spite of the fact that the negative sequence resistance is comparatively large, it adds at right angles to the reactances involved, and the total impedance will not be increased very much. For example, the impedance of the positive and negative sequence networks for the machine of Table III in the paper, will be 0.1944 per unit. This is only 0.7 per cent larger than the reactance $(X_d'' + X_2)$ which was used in calculating the torque during a line-to-line short circuit. In very extreme cases this resistance may increase the total impedance five per cent, and the question of whether to include the negative-sequence resistance in the total impedance is at the discretion of the calculator.

I wish to thank the discussers for the interest which they have shown in the paper.

Power Geometry of General Transmission Systems

Discussion of paper 45-38 by Wm. Altar, presented at the AIEE winter technical meeting, New York, N. Y., January 22–26, 1945, and published in AIEE TRANSACTIONS, 1945, June section, pages 312–17.

Eric T. B. Gross (Cornell University, Ithaca, N. Y.): The application of simple geometrical methods to general-circuit and transmission-system analysis is a means to a better understanding of the relations involved. Graphical representations help enormously to visualize how voltage, current, power, and so forth, at one set of terminals depend upon each other and the constants of the circuit. It is of particular importance for the young engineer and for the student of electrical engineering to get a better knowledge of the subject by comparing the analytic and the geometric analysis. In many cases, the geometric approach is much easier to follow, mainly because one readily can see what each step means.

Doctor Altar's paper is a very valuable expansion of some methods used in the analysis of transmission networks. The mathematician who is specializing in the field of projective geometry will be pleased to see his science used in such a wide field of electrical-engineering practice. It is of interest to note that the new method also can be applied in the analysis of machinery problems, and the field of ultrahigh-frequency technique offers possibilities. The rigorous diagram of the induction motor can be derived amazingly simply (as shown in the lecture presentation of the paper), and it appears that a similar approach to more advanced topics, for example, various types of phase-advancer, or salient-pole synchronous-machine analysis might be simplified even more, compared with long analytical derivations.

Many a practising engineer should be interested to learn that the rigorous diagram of the induction motor can be drawn as easily as the mostly used simplified-circle diagram; it is hoped that the author may soon find the time to present a more detailed paper on this part of his investigation.

Formulas for Calculating Temperature Distribution in Transformer Cores and Other Electric Apparatus of Rectangular Cross Section

Discussion and author's closure of paper 45-39 by Thomas James Higgins, presented at the AIEE winter technical meeting, New York, N. Y., January 22–26, 1945, and published in AIEE TRANSACTIONS, 1945, April section, pages 190–94.

Max Jakob (nonmember; Armour Research Foundation and Illinois Institute of Technology, Chicago, Ill.; Purdue University, Lafayette, Ind.): The writer is pleased that his paper on steady-state temperature distribution in heat sources (reference 8 of the author's paper) has been taken up and extended so ably by Doctor Higgins: first in his earlier paper (reference 4 of author's paper) and now in the paper under discussion.

Mastering the mathematics involved with these problems, the author succeeds in solving the equation of temperature distribution in electric coils and transformer cores of rectangular cross section in a more general way than did the writer. Thus, though both the writer and the author earlier encompassed linear variation with temperature of the electric resistivity of the heat source, the author now extends the solution to cases of internal structure and boundary conditions of the heat source, which are not covered in the writer's paper.

Almost the only item which is not included in the author's papers is the variation with temperature of the thermal conductivity k of the material of the heat source. Now in a footnote in his previous paper (reference 4 of author's paper) the author mentions that in the linear one-dimensional problem variations of k are not covered by the equation,

$$d^2\theta/dx^2 = -q'''/k \qquad (1)$$

wherein θ is the temperature excess over surface temperature and q''' is the rate of heat developed in unit volume; but that, if k is variable, the correct equation is

$$\partial[k(\partial\theta/\partial x)]/\partial x = -q''' \qquad (2)$$

This statement is correct; however, it is known that equation 2 easily can be transformed into the form of equation 1, by a procedure used by Kirchhoff[1] as early as

1894. This procedure was extended to the three-dimensional case by van der Held[2] in 1936. It consists of introducing an auxiliary variable Θ and a *constant* k_m defined by

$$k(\partial\theta/\partial x)=k_m(\partial\Theta/\partial x) \qquad (3)$$

together with a boundary condition

$$\theta=\Theta \qquad (4)$$

which is to be satisfied for two values of x, for example, for $x=0$ and $x=s$.

Integration of equation 3 between these limits follows:

$$\int_{\theta=\theta_0}^{\theta=\theta_s} k d\theta=\int_{\Theta=\theta_0}^{\Theta=\theta_s} k_m d\Theta=k_m(\theta_s-\theta_0) \qquad (5)$$

Substituting from equation 3 in equation 2 gives

$$k_m(\partial^2\Theta/\partial x^2)=-q''' \qquad (6)$$

wherein k_m is given by equation 5.

Illustratively, let $k=k_0(1+\beta\theta)$ (7)

wherein k_0 and β are constants. Then from equation 5

$$k_m=(\theta_s-\theta_0)^{-1}\int_{\theta=\theta_0}^{\theta=\theta_s} k_0(1+\beta\theta)d\theta= k_0[1+\beta(\theta_0+\theta_s)/2] \qquad (8)$$

Thus we find that equation 1 can be used in the form of equation 6; that is, with constant thermal conductivity k_m given by equation 8 and a system of auxiliary temperatures Θ. These may be reconverted into ordinary temperatures θ in the following way. From equation 3

$$\int_{\theta_0}^{\theta} k d\theta=\int_{\theta_0}^{\Theta} k_m d\Theta=k_m(\Theta-\theta_0) \qquad (9)$$

Substituting from equation 7 in equation 9 gives

$$\int_{\theta_0}^{\theta} k_0(1+\beta\theta)d\theta=k_0[\theta-\theta_0+ \beta(\theta^2-\theta_0^2)/2]=k_m(\Theta-\theta_0) \qquad (10)$$

yielding θ as a function of Θ.

In discussing this procedure elsewhere the writer[3,4] has shown that it is not restricted to linear heat flow but can be employed as well for radial conduction in cylinders and spheres. In fact, it can be employed for any two- or three-dimensional configuration of heat source and for k expressed as any function of θ for which the boundary condition of the transformation can be satisfied. Owing to the small change in k over the temperature range occurring in an electric coil, the writer omitted in his previous paper (reference 8 of author's paper) consideration of change in k, hence discussion of this procedure, although it is applicable to the problems discussed therein.

However, application of this procedure is limited by the condition that two isothermal lines or surfaces must be used for the boundary condition on the transformation. Now regarding a given problem these must be the boundary surfaces of the heat source, but often this is not possible, since these latter are not isothermal surfaces. The writer suggests that the author give some thought to whether or not, and if so how, this procedure can be generalized so as to remove this limitation. If this could be done, his equations would cover a still greater range of problems than they now do.

REFERENCES

1. VORLESUNGEN ÜBER DIE THEORIE DER WAERME (book), **W. Kirchhoff.** 1894, page 13.

2. EINE IN VERGESSENHEIT GERATENE LÖSUNG DER DIFFERENTIALGLEICHUNG DER WAERMELEITUNG, **E. F. M. van der Held.** *Gesundheits-Ingenieur* (Berlin, Germany), volume 59, 1936, page 736.

3. DER CHEMIE-INGENIEUR (book), **A. Eucken, M. Jakob.** Akadem. Verlagsges, Leipzig, Germany, 1933; Edwards Brothers, Ann Arbor, Mich. (reprinted), 1943. Allgemeine Grundlagen der Waermeleitung, **M. Jakob.** Volume 1, part 1, pages 176–8.

4. A SURVEY OF THE SCIENCE OF HEAT TRANSMISSION, **M. Jakob.** *Engineering Bulletin*, Purdue University, volume 23, 1939, number 4a, page 41.

Thomas James Higgins: The author thanks Doctor Jakob for the kind remarks expressed at the beginning of his discussion. The footnote referred to by Doctor Jakob is one wherein the author points out the error in a remark made by one of the discussers of Doctor Jakob's paper (reference 8 of my paper): that in this paper a solution of the one-dimensional problem is given whereof linear temperature variations of both the electrical resistivity and the thermal conductivity are taken into account. This statement is incorrect as the differential equation solved encompasses only the linear variation in electrical resistivity. As Doctor Jakob brings out, however, the solution given for linear variation in electrical resistivity only can be utilized to obtain the solution for linear variation of both electrical resistivity and thermal conductivity through use of the procedure developed by Kirchhoff, van der Held, and no doubt others.

A serious limitation on this procedure is, as Doctor Jakob remarks, that the boundary points, lines, or surfaces (according as the problem is one, two, or three dimensional) must be an isothermal; that is, of constant temperature. Thus it would not apply to cases where the boundary condition is the general one considered in the present paper: equation 2 and others. In some instances, however, this boundary condition may be replaced by the desired one of constant temperatures (over a given boundary point, line, or surface) by use of a seemingly little-known artifice advanced by Fourier.[1]

REFERENCE

1. ANALYTIC THEORY OF HEAT (book), **J. Fourier.** Translated by A. Freeman. Cambridge University Press, Cambridge, England, 1878

Statistical Methods Applied to Insulator Development and Manufacture

J. J. TAYLOR
ASSOCIATE AIEE

Synopsis: The science of statistics is highly developed and applicable to a variety of engineering subjects. There remains the task of getting statistical methods out of books and into general use. Towards this end examples are given of problems that relate to high-voltage-insulator manufacture and for which statistical treatment seems desirable.

IN THE MANUFACTURE of high-voltage insulators almost every incentive for statistical analysis is present. The product is produced in large quantity and to meet an exacting service.. Product characteristics are determined by tests carried to destruction. Manufacturing control is difficult, because insulators are made in part from natural clays and are processed through incomplete chemical reactions. In service the finished product is exposed to all the vagaries of weather in almost every climate, and is expected to endure for a length of time far beyond a reasonable proof-test interval.

It is apparent, therefore, that the element of chance will be present at every stage of product use and manufacture. To deal effectively with the electrical and mechanical problems of the insulator industry the usual engineering conceptions shown in Figures 1A and 1B should be supplemented by an equivalent group of statistical tools and diagrams.

Statistical Distributions

Many product characteristics that are measured, studied, and specified show a relation between observed values and the frequency with which they occur. If observations are grouped as shown in Figure 2, the distribution is called "normal" and is defined by the value of the arithmetic mean, $\overline{X}$, and by the standard deviation. The standard deviation, σ, is a measure of variability and is the root-mean-square of all the deviations of the individual values from the mean value. It is analogous therefore to the rms value of alternating current.

To carry this analogy further, a sine wave is more often approximated than realized and so also is a "normal" curve. Where the departure is slight, an assumption of normality may introduce no intolerable error and permits the use of many published tables. Nonnormality in a product characteristic does not prove any deficiency in either the product or its control. In some instances, however, direct physical reasons for nonnormal distributions exist and can be ascertained.

In 1934 an excellent statistical manual published by American Society for Testing Materials[1] served as an incentive for the statistical study of a variety of suspension insulators. Frequency diagrams of ultimate-strength tests were plotted from data accumulated in the years preceding. Of the insulator types studied, two were found with distribution curves that proved later to be of particular interest. They are illustrated in Figure 3. A normal curve superimposed on distribution *A* indicates considerable flatness distortion or kurtosis. Distribution *B* is decidedly skewed, with less variability than would be expected in the upper range of observed values.

In both cases a direct physical cause was found for these abnormalities. The flatness of curve *A* resulted from a change in the firing cycle of the porcelain component. Figure 4[7] shows, in an exaggerated manner, how a shift in the average value of test groups produces a flat-top shape when all observations are plotted together.

The abnormality of Figure 3B was caused by a peculiarity of design and requires for its explanation a brief review of insulator construction. A suspension insulator has internal and external metal parts attached with Portland cement to a ceramic shape. In tests of ultimate strength the fracture occurs usually through the ceramic component—a not surprising result since ceramic materials fail at a unit deformation of about 0.1 per cent. The comparable figure for malleable cast iron is 200 times as great. In a design in which the metal sections and the cement matrix areas are liberal, the cement and metal respond under load in accordance with their respective elastic moduli. As a general rule, the elastic modulus of structural materials is exceptionally reliable and consistent; the ultimate strength is variable. One would expect to find, therefore, that the variability of an insulator assembly is determined largely by the variability in ultimate strength of its ceramic component, rather than by erratic performance of the metal parts or cement matrix. The skewness of Figure 3B was attributable to a cap section so thin that its yield point was reached in the upper range of observations. This yield prevented normal support of the ceramic section and development of the potential strength of the strongest ceramic components.

Similar nonnormal distributions to which a physical cause can be assigned are found in high-voltage measurements. Two of these are illustrated in Figure 5. In the parallel arrangement of insulator and sphere gap, a marked lack of symmetry is noticeable in the distribution of

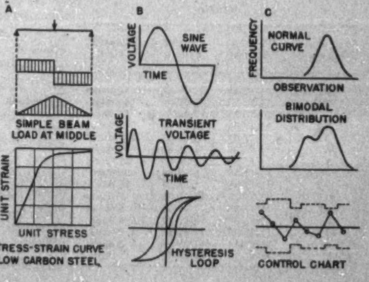

Figure 1. Diagrams of mechanical, electrical, and statistical performance

A. Mechanical
B. Electrical
C. Statistical

Paper 45-89, recommended by the AIEE subcommittee on applications of statistical methods of the Standards committee for publication in AIEE TRANSACTIONS. Manuscript submitted November 20, 1944; made available for printing March 8, 1945.

J. J. TAYLOR is chief engineer, insulator division, Ohio Brass Company, Barberton, Ohio.

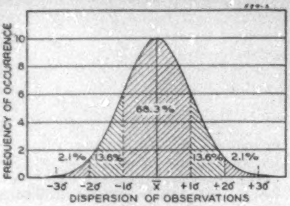

Figure 2. Significant areas and limits of a normal distribution

measurements. The consistent flashover value of the sphere gap cuts off the maximum end of the insulator-flashover distribution pattern.

The opposite type of skewness was observed in tests of imperfect spheres. A sharp projection on the grounded sphere introduced a discontinuity in the otherwise uniform electrostatic field. Flashover could occur from sphere to sphere or sphere to point. In the distribution shown conditions were such that the majority of the flashovers were between sphere and point.

Control of Product Quality

Since a great variety of insulator designs start from a common source of raw materials and go through essentially the same manufacturing process, a measure of quality control can be assured by observations on a few important types. The distribution for one such key insulator is shown in Figure 6. This type of insulator is manufactured in large quantity and, fortunately, has a frequency distribution approximately normal. The design was first produced in 1933. Control limits were not set up until 1937 and were then readily established by a study of accumulated test data.

Daily tests are made on units selected at random from current production and on factory rejects with imperfections that do not influence the characteristic being observed. As shown in Figure 7, the control limits are adjusted for variations in sample size. Sample averages falling beyond the control limits indicate an assignable cause of variation and are a signal for technical inquiry and corrective action.

Table I. Endurance Test of Suspension Insulators

Tested at 80 Per Cent of Average Ultimate Strength

Specimen Number	Placed on Test	Date of Failure	Elapsed Time
1	11-17-38	11-17-38	10 hours
2	11-17-38	3-12-39	115 days
3	11-17-38	1-14-39	58 days
4	11-17-38	11-22-38	5.1 days
5	11-17-38	8-23-39	279 days
6	11-17-38	11-18-38	1.1 days
7	11-17-38	12-8-38	21 days
8	11-17-38	2-13-39	88 days
9	11-17-38	12-3-38	16 days
10	11-17-38	11-17-38	7 hours
11	11-17-38	11-17-38	0.5 hours
12	11-17-38	3-17-42	1,216 days
13	11-17-38	11-21-38	4.2 days
14	11-17-38	11-25-38	8 days
15	11-17-38	11-28-38	11 days

Quality Control in Relation to Routine Tests

Ceramic parts may be inspected visually, sometimes with the aid of penetrating fluids, or aurally by "ringing-out" methods. Attention has been given also to X-ray examination and to nondestructive tests employing supersonic response. Many tests, however, are potentially destructive and would produce failure if increased sufficiently in severity. Dielectric soundness is checked by high frequency or 60-cycle flashover on ceramic parts and assembled units. For certain specialized types of insulators, impulse tests are routine procedure. Routine mechanical tests of assemblies are made at a load level about half the rated ultimate strength and are followed by a dielectric test.

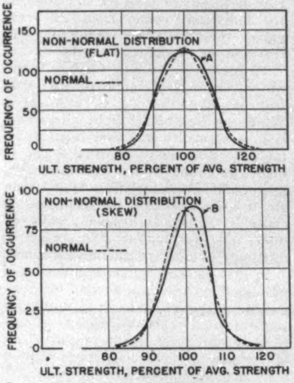

Figure 3. Nonnormal distributions of suspension-insulator strength

As routine tests for both dielectric and mechanical strength are potentially destructive, some compromise is necessary between tests too mild to eliminate defectives and those severe enough to damage an appreciable portion of specimens near the minimum end of the distribution pattern.

Mechanical tests at half the rated strength are not intended to cut off the minimum end of the distribution curve. They are used to give assurance against defectives with potential characteristics far below the minimum level of expectancy.

It cannot safely be assumed that high levels of routine test guarantee quality. Such tests may be particularly undesirable on a product manufactured with good factory control but with no great margin in average strength. In Figure 8 two distribution curves are shown that have the same probability of failure at or below the specified minimum level. If both groups of product are proof-tested to eliminate units lying below the minimum line and if the test is harmful to units only slightly stronger than the proof load, then it is likely that such testing will be detrimental to design (*a*) and beneficial to design (*b*). In the first case it damages more units than it eliminates and in the other case eliminates more units than it damages.

It is probable that no amount of proof testing, however drastic, can select from carelessly manufactured material a finished batch as dependable as one made in the first instance with good technical control and given routine tests at reasonable levels. This view implies, in specifications, emphasis on consistency of tested characteristics; a carefully drawn sampling plan; a cumulative record of test history so that past experience can be of real value in interpreting the results of samples under immediate review.

It should be noted also that some product characteristics cannot be given routine tests that will check them. Line and station insulators are designed and design-

Figure 4. The summation of two normal curves with different $\overline{X}$ values is nonnormal

Inset shows curves B and C with abscissa values plotted against a probability scale of ordinates. A normal curve so plotted gives a straight line

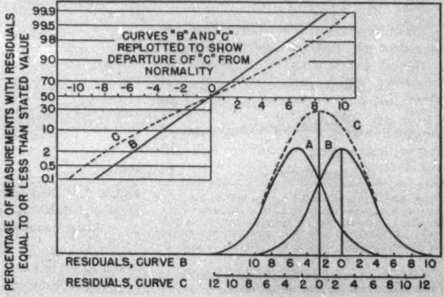

tested to withstand electrical surges of great severity, but so far it has not been practical to surge-test at these extreme levels in routine fashion. Even if it were possible, it might be proved an undesirable practice because of the damaging nature of the tests. In such instances reliance must be placed on methods of quality control which give high-probability assurance that the required characteristic is present.

Estimating and Predicting From Statistical Data

Specifications frequently require certain minimum or maximum characteristics in the product they cover. The best that a manufacturer can do, by conservative rating of his product and by technical control of process, is reduce the probability of a "defective" to some tolerable level. To choose a small sample from a large batch and in that small sample to focus attention on a single value, to the exclusion of other equally significant values and to the exclusion also of the supplier's over-all performance, is certainly uneconomical and may also be unfair. It is quite possible for a chance defective to appear in a product of good quality; and it is more than possible that poor quality will not be detected by looking for a single defective in a small sample. As product characteristics are by nature statistical, assurance of quality in purchasing standards logically might be obtained by stating limiting criteria for the frequency distribution of the quality characteristic in question. Consideration certainly should be given to the average, which is readily established from a small number of samples; to the shift in observed average from batch to batch; and, if additional assurance is needed and when the accumulation of data is adequate, to some measure of the dispersion of values about the average.

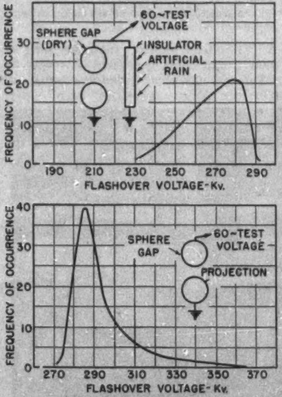

Figure 5. Assymetrical 60-cycle flashover distributions having an assignable cause

Figure 7. Suspension-insulator control chart

Control is exercised by limiting fluctuation of sample averages with respect to assumed grand average $\overline{X}$

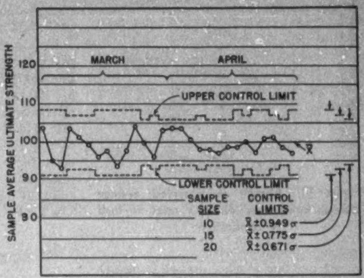

Although statistical methods cannot be expected to indicate such probabilities as one unit in a thousand being below minimum, they are nevertheless the most effective means for estimating limits beyond which not more than four or five units out of a thousand are likely to lie. Their use is indicated particularly in work on new designs for which test information is meager. Illustrative of the general problem of sampling are trials made from a batch of 1,000 specimens having a normal type of distribution and with the specimens divided into nine distribution "cells." The characteristics of the parent distribution were:

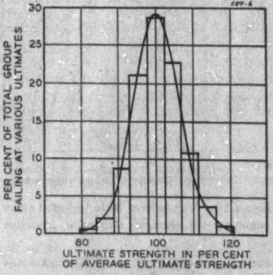

Figure 6. Nine-cell distribution of ultimate strength for a suspension insulator

Average—19,500 pounds
Maximum—23,100 pounds
Minimum—15,900 pounds
Standard deviation—1,245 pounds

As this was an artificially prepared batch, the actual minimum was known to be 15,900 pounds; yet samples of nine specimens each showed the appearance of a minimum unit in only ten per cent of the trials. Even with samples of 50 specimens each, an error of at least 1,000 pounds in observed minimum versus batch minimum occurred in 60 per cent of the trials. In 20 per cent of the trials the discrepancy between observed and batch minimum was more than 2,000 pounds. When the samples reported were analyzed statistically and the expected minimum calculated rather than observed, the error, even on the most misleading sample, was only 600 pounds. The most misleading sample was selected from 40 trials in each of which the sample size was 50 specimens.

Correlation of Product Characteristics

In some instances the determination of a product characteristic is inordinately time-consuming or expensive. If such a characteristic can be related intimately with one for which data are already available (or can be readily obtained) three advantages ensue:

1. The desired characteristic may be estimated.
2. Meager data about the desired characteristic may be expanded and confirmed.
3. Both characteristics may become more intelligible.

Since the characteristics sought are statistical distributions, correlation hardly can be expected between individual specimens. At least in tests that are of the destructive type the correlation must be between frequency-distribution diagrams or between terms defining these diagrams. An example of this approach is

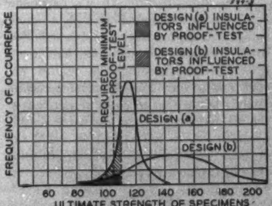

Figure 8. Proof testing in relation to strength distribution

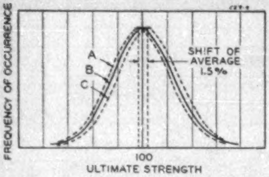

Figure 9. Change in observed average strength caused by different rates of load application

Increase in load per minute:

A—15 per cent of rated strength (minimum)

B—$22^{1}/_{2}$ per cent of rated strength

C—30 per cent of rated strength (maximum)

the relation between the ultimate strength of suspension insulators and their performance when endurance-tested, for extremely long intervals of time, by loads of varying severity.

In endurance or time–load testing, insulators are subjected to axial tension for a stated interval of time. In many specifications this is a "withstanding" test in which the failure of any unit is cause for rejection of the lot. To the design engineer, therefore, endurance tests carried to failure are a necessary part of his information about the product. A typical group of endurance-test results is shown in Table I.

It is obvious that interpretive effort has to be made if significant information is to be obtained from these test values. A clue is offered by the shift in strength observed when insulator groups are tension-tested at different rates of load application.

When insulators are tested for ultimate strength, the increase in load per minute may be from 15 to 30 per cent of the rated ultimate strength of the specimen.[2] At these limiting rates the distributions shown in Figure 9 were found. The shift in average strength was about 1.5 per cent.

There is an element of endurance testing in any ultimate-strength test, since the specimen responds to a combination of time and load. Some indication of this is given by Figure 9. The influence of time can be emphasized by rates of load increase that are exceedingly slow.

If the ultimate strength of a particular specimen is designated as 100 per cent, some contribution to the final destruction of the specimen is made by the load levels immediately preceding—99, 98, 97 per cent, and so on. For electrical porcelain loading history up to 85 or 90 per cent of the ultimate appears to make a negligible contribution to failure. This rapid decrease in sensitivity to load implies some type of exponential function. Moreover, since damage by the 99-per-cent, 98-per-cent, and preceding load levels has been assumed, it can be argued that, if it were possible to apply a 100-per-cent load instantaneously yet without shock, failure would not take place immediately.

By a series of tests[3] run at slow rates of load increase it was found that the interval to failure following application of a "100-per-cent" load was about equal to the time spent in going, at a uniform rate of load increase, from the 98-per-cent to the 100-per-cent level. Let us suppose, for example, that an insulator is tested at a 4,000 pounds per minute rate and that failure occurs at 20,000 pounds. The load change from the 98-per-cent to the 100-per-cent value is 400 pounds, and this change is effected in 0.1 minute. The expectation is, then, that, had a load of 20,000 pounds been applied instantaneously and without shock to this particular specimen, failure would have taken place in 0.1 minute.

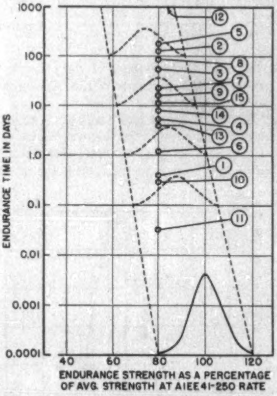

Figure 10. Values from Table I plotted on an endurance-test chart for suspension insulators

In Figure 9, a 100-per-cent change in the rate of load application produced a shift in the distribution pattern of only 1.5 per cent of the observed average ultimate strength. By changing the rates of load increase per minute according to some suitable exponential regression such as 1,000, 100, 10, 1, 0.1, and by testing at each chosen rate a liberal sample of specimens from the same batch of product, a series of distributions is obtained with a three-dimensional relation: observed strength, frequency of occurrence, and loading rate or equivalent endurance time. This expands Figure 9 into the developments shown in Figure 10. On Figure 10 the tabular values for 1938–42 appear rational and significant; they are part of a very much-extended frequency distribution, the plane of which is parallel to the time axis. The model illustrated in Figure 11 shows what might be expected of a complete batch of product if it were subjected to a fixed load and this load maintained without change until every unit had failed.

In concluding this effort at correlation it is interesting to compare original and final interpretations of the same set of data. Following a perfunctory study of the original endurance-test values, reasonable conclusions might be:

1. That the product was extremely erratic.
2. That with better endurance-test strength more consistent intervals to failure would be obtained.

After an analysis of Figures 9, 10, and 11, a very different set of conclusions is reached:

1. The endurance-test observations are consistent with the distribution pattern for ultimate tensile strength.
2. A product with perfect endurance-test resistance, subjected to a continuing load of a size between the limits of its quick-strength pattern would have
   (*a*). Immediate failures of minimum strength specimens.
   (*b*). Indefinite endurance of maximum-strength specimens.
3. Time–load sensitive materials such as lead would show consistent intervals to failure because of increased angularity be-

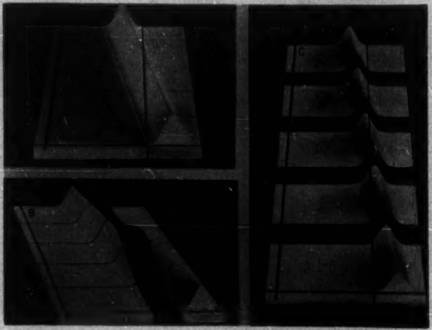

Figure 11. Model of Figure 10

Showing:

A—The three-dimensional nature of endurance strength

B—The elongated distribution parallel to the time axis associated with a specific value of test load

C—The influence of width of the distribution pattern in determining endurance time

Winding-Fault Detection and Location by Surge-Comparison Testing

G. L. MOSES
MEMBER AIEE

EARL F. HARTER
ASSOCIATE AIEE

Synopsis: Surge-comparison methods of testing insulation were investigated with the objective of locating as well as detecting faults. Experience of other investigators was confirmed and limitations of methods and equipment studied. Supplementary methods and equipment were devised to extend the field of usefulness of this basic type of tester, especially to the testing of very large machines with multiple-parallel windings. Apparatus studied included a-c motors from fractional-horsepower single-phase to very large three-phase types; a large variety of d-c armatures; and numerous armature, stator, and magnet coils. This surge-comparison tester has proved to be suitable for use by electrical manufacturers and by service and repair shops, as it can be used for testing most common types of electric windings.

SURGE-COMPARISON testing of electric windings is a new and very useful tool for detecting and locating insulation faults. Foust and Rohats[1] are to be commended for their great contribution to the art. The surge-comparison principle in combination with the cathode-ray oscilloscope opens the way to numerous possibilities for improving insulation testing equipment and technique. The application of a known and controlled voltage surge with visual comparison of the wave shape makes it possible to study insulation faults as well as to detect them.

The work reported by Foust and Rohats[1] was confined to testing of three-phase windings. The authors have extended the field of usefulness of the surge-comparison tester, applying it in its original form and with important modifications to numerous other types of apparatus. Other apparatus studied included d-c armatures, fractional-horsepower single-phase stators, and large three-phase stators. Means for fault location were developed to supplement the original scheme which included only fault detection. Voltage distribution was studied on several types of apparatus.

Description of Test Equipment

The surge-comparison tester is an electronic device designed for two functions:

1. To apply a voltage stress on turn-to-turn, phase-to-phase, and winding-to-ground insulation in coils and wound apparatus.
2. To detect grounded or short-circuited turns in the windings under test.

The turn and phase insulation is stressed by the application of a repetitive surge voltage to the winding terminals. The surge is produced by a charged capacitor, and a high rate of voltage rise is obtained. Because of this high rate of rise, a relatively high test voltage can be applied to most types of windings and coils. The detection of faults is accomplished by means of a cathode-ray oscilloscope on which is impressed the surge voltage across each part or half of the winding alternately. Two standing waves thus appear simultaneously on the oscillograph screen (screen persistence retains the traces between alternate cycles). A divergence or difference in these two waves reveals a dissymmetry in the winding which generally indicates the presence of a fault. The alternate appearance of the two waves is brought about by a synchronous reversing switch which interchanges the surge and ground connections repeatedly. The two detection voltages also may be obtained from exploring coils or other devices close to the winding under test. The applied surge voltage may be varied from zero to maximum as readily as the voltage of the ordinary 60-cycle test box. No other circuit constants can be conveniently changed.

Test Methods

The surge tester used by previous investigators was designed primarily for testing small three-phase induction motors. Three output terminals were provided for connection to the three terminals of the test motor. The surge and the oscilloscope could be connected to any combination of the three motor terminals by means of a manual transfer switch built into the tester as shown in the diagram of Figure 1A. Nearly all small three-phase motors can be tested for weak insulation and faults in the manner illustrated by this diagram.

Individual coils, single-phase motors, or other pieces having no inherent three-phase symmetry may be tested in pairs as shown in Figure 1B. Here one coil or winding of a type is used as a standard for comparison testing of other similar pieces. This method was applied to all coils and miscellaneous windings tested. A comparison method also was found useful in d-c armature testing. The surge was applied to the commutator at points one brush span apart with a third contact midway between to form the mid-point for the two-winding comparison scheme. Figure 1C illustrates this simple adaptation.

Variations from the connection arrangements of Figure 1A and 1B were made for certain tests and will be described in a discussion of the results. The surge test voltage used was generally made equal to the peak of the specified rms high-frequency test[2] voltage.

Cores or frames of all apparatus tested were always grounded during test for several reasons: to increase the operator's safety, to keep the voltage from conductors to iron at a known value, and to eliminate the effects of minor variations in capacitive couplings. The surge-tester frame also was always connected to a ground.

Results of Tests

The application of the surge tester and the results obtained will be described briefly for each type of apparatus tested.

ARMATURE AND STATOR COILS

Coils of various sizes from three-turn coils 16 inches long to ten-turn coils 36 inches long were tested as in Figure 1B. Faulty insulation and short-circuited turns were readily detectable in most coils. Examples are shown by the delineation, Figure 2A, of the oscilloscope-

---

Paper 45-94, recommended by the AIEE committee on electric machinery for publication in AIEE TRANSACTIONS. Manuscript submitted November 15, 1944; made available for printing March 12, 1945.

G. L. MOSES is section engineer, development insulation section, and EARL F. HARTER is insulation-development engineer, both of the transportation and generator division of Westinghouse Electric and Manufacturing Company, East Pittsburgh, Pa.

---

tween the central plane of the time–frequency–strength solid and the time axis.

4. Statistical methods aid in building a performance structure from which modest extrapolations can be made.

References

1. AMERICAN SOCIETY FOR TESTING MATERIALS MANUAL ON PRESENTATION OF DATA (latest printing, April 1943).

2. SPECIFICATION AIEE STANDARD 41, INSULATOR TESTS, September, 1944.

3. DURATION OF LOAD AND ITS INFLUENCE ON THE ULTIMATE STRENGTH OF SUSPENSION INSULATORS. J. J. Taylor.

4. INTERNATIONAL CONFERENCE ON LARGE HIGH-VOLTAGE SYSTEMS (CIGRE), Paris, France, 1939, report 228.

5. ECONOMIC CONTROL OF QUALITY OF MANUFACTURED PRODUCT (book), W. A. Shewhart. D. Van Nostrand Company, Inc., New York, N. Y. 1931.

6. THE APPLICATION OF STATISTICAL METHODS TO INDUSTRIAL STANDARDIZATION AND QUALITY CONTROL (book), E. S. Pearson. British Standards Institution, 1935.

7. TREATMENT OF EXPERIMENTAL DATA (book), Worthing, Geffner. John Wiley and Sons, Inc., New York, N. Y., 1943. Pages 177–81.

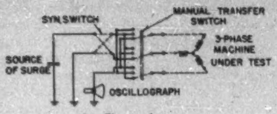

A. Three-phase test

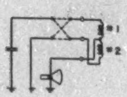

B. Two-coil comparison test

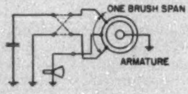

C. Armature comparison test

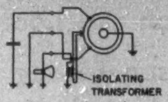

D. Armature bar-to-bar test

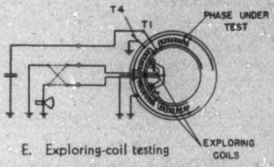

E. Exploring-coil testing

Figure 1. Circuits used in testing

voltage traces of two ten-turn synchronous-motor coils. Corona or arcing present in some coils could be detected readily and the voltage at which it started determined. Burning or heating of faults in coils usually was not great enough to facilitate exact location of the faults. This was due to the fact that the average power output of the surge generator is necessarily low because of the short duration of the impulses.

Field Coils

Many types of field coils were tested using the connection of Figure 1B. Excellent detection of one short-circuited turn was obtained with coils having either air or iron cores. Slightly better results were obtained with the types having the iron pole in place, but as shown by Figure 2B, detection of a short-circuited turn in a 477-turn air-core coil was very satisfactory.

Armature

Numerous types of railway and d-c generator armatures were tested. Dead grounds and short circuits were detected very satisfactorily using the comparison connection, Figure 1C. A typical example is Figure 3A which shows clearly the visual evidence of a dead short-circuited coil midway between the surge and oscillograph contacts on the commutator of Figure 1C. Armatures lying on the floor were tested by this method by use of a portable contact arm. Insulation could be tested completely by moving the contacts once around the commutator. Movement through one brush span served to detect faults as a preliminary test.

The comparison method was found inadequate for locating a short circuit or ground in cross-connected or wave-wound armatures. To overcome this difficulty, the bar-to-bar voltage-measuring circuit of Figure 1D was devised from equipment used with the high-frequency test.[3] With this arrangement, dead short-circuited or grounded coils were located exactly and quickly in any of the armature types tested. Arcing or intermittent short circuits were detected easily by either method, but too few examples of this type of fault were found to permit development of a satisfactory means of locating them.

Single-Phase Motors

The testing of fractional-horsepower single-phase motors was accomplished by

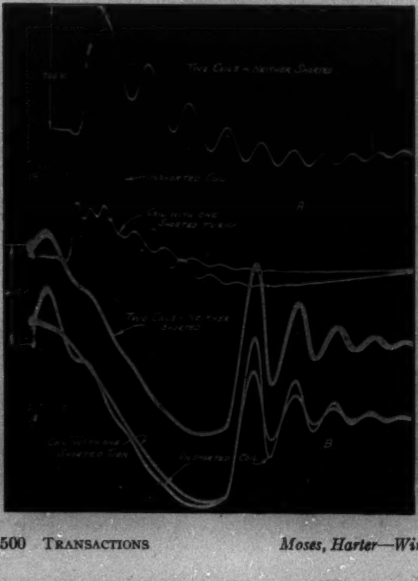

Figure 2. Short-circuited turn detection in stator and field coils

A. Ten-turn stator coils
B. 477-turn field coils. (No iron present)

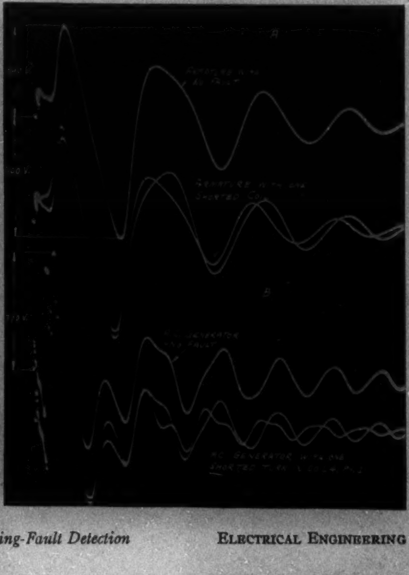

Figure 3. Short-circuited turn detection in a large d-c armature and in an a-c generator

A. Large d-c motor armature
B. Large a-c-generator

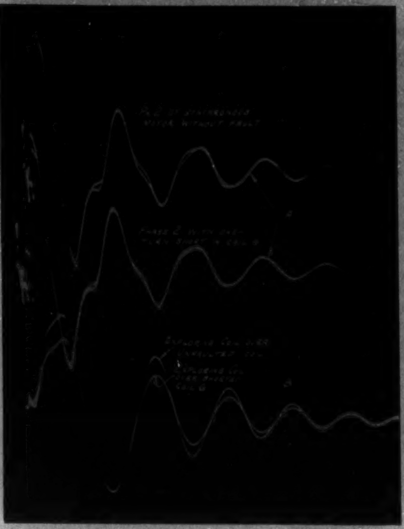

Figure 4. Tests on large synchronous motors

Comparison of detection of a single-turn short circuit in a winding having 12 parallel conductors per phase when tested by the two methods: simple phase comparison and exploring-coil comparison

A. Three-phase comparison test

B. Single-phase test using exploring coils

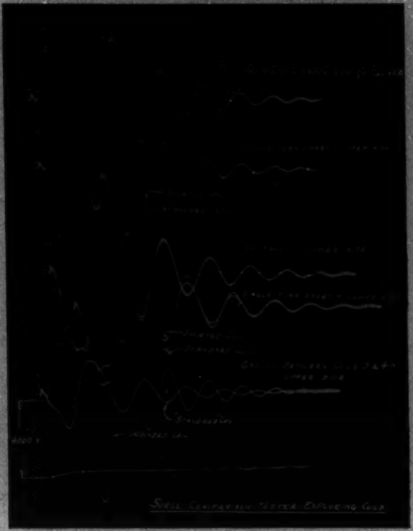

Figure 5. Exploring-coil voltage traces during test on large synchronous motor

One exploring coil over first the upper and then the lower side of a faulted coil in a winding with 12 parallel conductors

comparison either of two similar motors or of the two halves of a single winding. Both of these variations in the comparison technique yielded satisfactory results in the detection of short-circuited or grounded coils. One short-circuited turn in as many as 1,000 total turns was easily noticed.

THREE-PHASE MACHINES

Three-phase motors and generators of various sizes were tested with a surge-comparison tester. The simple phase-to-phase testing method, Figure 1A, permitted unmistakable detection of short-circuited or grounded coils in all windings of relatively few parallel circuits. Figure 3B illustrates the detection of a single-turn short-circuit in a large three-phase winding of 21 turns per phase. Detection of one-turn short circuits also was satisfactory in smaller motors having as many as 600 series turns per phase.

In windings with many parallel circuits, detection as well as location of a short-circuited turn or coil was found impossible with the simple conventional circuit of Figure 1A. This condition is illustrated by Figure 4A, which gives the result of a test on a very large synchronous motor which had 12 parallel circuits per phase, each consisting of eight ten-turn coils. Short-circuiting out one turn in phase *T*1-*T*4 of this winding made a nearly imperceptible difference in the voltage traces which actually made the winding look better than it did with no short circuit. Furthermore, inherent winding dissymmetries in these large motors caused oscillograph trace differences which added to the uncertainty. A close inspection of Figure 4A reveals the fact that the trace differences present in the unfaulted winding are greater than those caused by a short-circuited turn.

Because of these difficulties, the problem of detecting and locating faults in the windings of large three-phase machines with this tester was attacked first by using the simple comparison scheme of Figure 1B to compare the separate parallel circuits before connection to the paralleling rings. This method generally was satisfactory and made detection of a coil having a single short-circuited turn easily possible. Testing of the winding after completion also was desired, however, and the circuit and auxiliary equipment of Figure 1E ultimately were devised. With this method a unidirectional repeating surge voltage is applied to a terminal of one phase of the winding to stress the turn insulation and break down any weak places; the other terminal is grounded. While one phase at a time is thus placed under test, two identical exploring coils are moved by hand around one revolution in the bore of the machine. These coils are attached to the ends of an adjustable arm and so spaced as to be located over two winding coils that lie in identical electrical positions but in adjacent parallel circuits of the phase being tested. Since the two coils in the winding must react alike to the surge voltage if no fault is present, their emitted flux induces identical voltages in the two exploring coils. The induced voltages are compared by means of the oscillograph and synchronous reversing switch in a manner similar to that of the comparison connection of Figure 1B. A fault in either winding coil will cause a reduction in its flux, and hence a difference will appear in the oscillograph traces. By virtue of the complete revolution of the exploring coils, every coil in the phase will be compared with two other coils. The effect of a short-circuited turn in a winding coil under one of the exploring coils is illustrated by Figure 4B. The exploring coils used were wound on C-shaped iron cores. In Figure 5, a complete set of traces is shown for the exploring coils located over upper and lower sides of the faulted coil both with and without the fault of one short-circuited turn. The surge applied to the winding is included at the bottom of the page. This trace shows the extremely high rate of

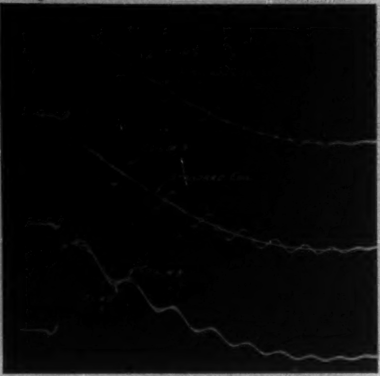

Figure 6. Oscillograms showing the possible effect of variations in varnish treatment on surge voltages

Railway-motor field coils. Coils 8 and 9 were varnish-impregnated; the standard coil was left untreated

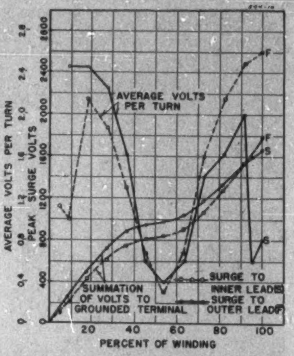

Figure 10. Average volts per turn in an autotransformer calculated from measurements obtained as in Figure 8

voltage rise across the winding (0.3 microsecond to crest).

Ground faults in any device could be detected unmistakably with the original tester circuit and equipment, but the location of grounds in large motors and generators required the use of the exploring coils and the new circuit in the manner just described. With the exploring coils, the location of a ground in any group of series coils could be narrowed down quickly to two adjacent coils. This location of the approximate position of the ground was based upon the fact that coils from the surge application terminal to the ground will induce voltages above normal, whereas those from the grounded coil to the grounded terminal will induce voltages far below normal. The exact coil then was found by opening the winding between the two coils in question and reapplying the surge and exploring coils. The connection opened always was one of the two which later would necessarily be broken to remove the grounded coil.

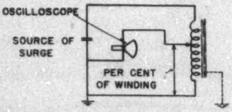

Figure 7. Method of measuring surge peaks

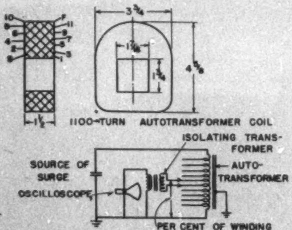

Figure 8. Circuit for determining volts per turn

MAGNET COILS

Tests were made on air-core magnet coils using the two-coil comparison connection, Figure 1B. One short-circuited turn in as many as 4,000 was readily detected. The maximum number of turns in which one short-circuited turn could be detected was not determined exactly, as it depends somewhat on the size and shape of the coil, but the limit appeared to be about 10,000 turns. Above 10,000 turns only a short circuit of several turns or more could be detected satisfactorily. The application of an appreciable turn-to-turn voltage stress was possible only in coils which had relatively few turns because of the practical limit to the available test voltage. Another and possibly more important obstacle to high turn-to-turn voltages in magnet coils is the fact that most coils are not provided with terminals and leads capable of withstanding the high total voltage which would be required.

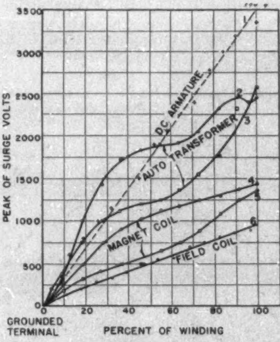

Figure 9. Surge-voltage distribution in four types of coils

Curve 1.	Large d-c armature
Curve 2.	1,100-turn autotransformer—surge to inner lead
Curve 3.	1,100-turn autotransformer—surge to outer lead
Curve 4.	35,000-turn magnet coil—surge to inner lead
Curve 5.	35,000-turn magnet coil—surge to outer lead

General Observations

Winding dissymmetries may cause differences in the voltage traces of two supposedly identical coils or windings even though no faults exist. This was observed often during tests on the apparatus described in this paper. Examples are the traces of Figures 2B and 4A. Many windings and coils seemingly have inherent dissymmetries caused by differences in their varnish treatment, amount of fill, moisture present in the winding, or unknown causes. An extreme example of this is illustrated by tests on three main field coils for a railway motor, Figure 6. Coils 8 and 9 both were impregnated in black solventless varnish and dipped in Thermoset varnish. The only difference in these two coils was in the resin treatment on the glass turn insulation. The standard coil was untreated and had mica-tape turn insulation. It may be seen that the voltage traces of the two treated coils have a superimposed oscillation caused by the presence of the resins (which increase the distributed capacity). The two treated coils, furthermore, are not identical owing to a difference either in the two resins or in the degrees of penetration into the coils. These effects of winding dissymmetries sometimes have caused uncertainty as to whether a fault was or was not present in the device under test. Nearly all examples of this uncertainty, however, were readily eliminated in a practical manner by placing the minimum possible fault, usually one short-circuited turn, in the winding and observing the effect. One short-circuited turn usually produced the greater and more unmistakable effect in most types of armature, field, and magnet coils, and in small machines with few parallel circuits. The inherent dissymmetries of large multiparallel windings, as previously discussed, rendered detection of short-circuited turns by the simple comparison scheme impossible.

Distribution of voltage magnitude across the winding turns of several representative pieces of apparatus was determined. This was first done by using the oscillograph in the tester simply to measure voltage from the grounded terminal of a winding to taps through the winding. Peak voltages only were recorded, and, as these occurred at nearly the same time after application of the surge, time differences were neglected. The method is illustrated by Figure 7. Data obtained in this manner yielded the curves of Figure 9. Additional measurements using a revised circuit, Figure 8, then were made on the autotransformer of curves 2 and 3 of Figure 9. The actual voltages between taps of the transformer were measured and the average volts per turn calculated. These data are plotted in Figure 10. Since this shell-type transformer had been chosen for its extremely nonuniformly distributed capacitance and inductance, its surge voltage distribution curves reveal approximately the worst condition that is likely to be present in any type of winding during this surge test. This uneven distribution, of course, could be improved by minor test-circuit revisions to reduce the steepness of the surge-voltage wave front.[6] The wave applied to this transformer had a time to crest of about 0.2 microsecond.

Figure 11. Comparison surge tester in use on large stator winding with many parallel circuits

The surge-comparison tester thus has been tried on numerous samples of all common types of coils and windings. In general, it was found to be a satisfactory test for many insulation-testing applications. The use of the cathode-ray oscilloscope for detection of faults permits accurate measurement of voltage when desired, gives the operator a view of the manner in which the winding is being tested, and, furthermore, reveals any arcing, corona, or other unusual phenomena occurring in the winding. The oscilloscope, however, does not provide a definite quantitative distinction between faulted or unfaulted windings. The interpretation of the oscilloscope evidence, however, could become easy and positive with experience on any particular application.

The problem of fault detection and location has been largely restricted in this paper to faults involving short-circuited turns or coils. Ground-fault detection was found easy and distinct in all windings so that no refined technique was necessary. In fact, any ground fault found in a winding during test had to be cleared up before other faults could be detected as its effect was to upset completely the symmetry of the winding. The location of grounds was attempted only on armatures and large three-phase machines, both of which have been discussed.

No circuit constants of this type of tester need be varied by the operator except the test voltage, which is set by turning a tap switch or a calibrated dial. The wave shape is fixed by the tester circuit components in conjunction with those of the winding on test. The connections for testing are simple and nearly the same for most types of apparatus.

Conclusions

The surge-comparison insulation tester is a highly versatile tool which, with further development, could be applied to many insulation testing problems. It possesses the following desirable or advantageous features:

1. The test voltage may be readily preset to any desired value which will not vary during the testing except with the line-voltage changes. The test voltage may not always be the same for different sizes of windings, however, because of the voltage drop in the protective resistor which becomes appreciable if the device under test has a relatively low surge impedance.

2. Control of the machine is simple and easy. Only the voltage requires setting by the operator, in addition to the usual control knobs for the oscilloscope.

3. Setting up for test usually is reduced to mere connection of three leads. No auxiliary equipment is needed for most testing, and testing instructions are simplified.

4. The surge tester is flexible; large generators or small magnet coils may be tested with no change in circuit constants or connections, except for the testing of windings with many parallel circuits.

5. The cathode-ray oscilloscope gives the operator a constant view of his test voltage and its effect on the winding. Arcing and corona can be detected along with steady-state faults. The oscilloscope also may be used to measure voltage to ground at any point.

6. The voltage stress applied to ground insulation is kept to a limited and known value, because cores and frames can be grounded. Personal safety also is increased by having all parts of a machine except conductors at ground potential.

7. The surge voltage applied has a wave front at least as steep as the wave fronts of most switching and lightning surges which are the sources of dangerous overpotentials in service.

8. The tester can be built as a relatively compact and lightweight unit which can be moved about easily for testing in numerous locations.

9. D-c armatures may be given an insulation and fault-detection test while lying on the floor or in winding frames and need not be placed in a special testing lathe as is now necessary with some conventional methods.

10. Photographic records may be easily made of any test to show unusual results obtained or for future comparison with other tests.

11. Grounded coils in large a-c machines can be located without the puncturing of insulation with probes or the unnecessary breaking of connections.

References

1. Insulation Testing of Electric Windings, C. M. Foust, N. Rohats. AIEE Transactions, volume 62, 1943, April section, pages 203–06.

2. A High-Frequency Voltage Test for Insulation of Rotating Electrical Apparatus, J. L. Rylander. AIEE Transactions, volume 45, 1926, pages 459–65.

3. Protecting Machines From Line Surges, J. F. Calvert. AIEE Transactions, volume 53, 1934, January section, pages 139–46.

4. Voltage Oscillations in Armature Windings Under Lightning Impulses—I, E. W. Boehne. AIEE Transactions, volume 49, 1930, pages 1587–1615.

5. Surge Protection for Rotating Electrical Machinery, J. F. Calvert, A. C. Monteith, E. Beck. *Electric Journal*, volume 30, 1933, page 91.

6. Calculation of Voltage Stresses Due to Traveling Waves With Special Reference to Choke Coils, E. W. Boehne. *General Electric Review*, December 1929.

7. Effects of Lightning Voltages on Rotating Machines and Methods of Protecting Against Them, F. D. Fielder, E. Beck. AIEE Transactions, volume 49, 1930, pages 1577–86.

Precision Testing of Electric Tachometers

M. A. PRINCI
MEMBER AIEE

Synopsis: The magnetic-drag electric tachometer which was developed especially for the measurement of aircraft-engine speed is inherently a more precise measuring device than those instruments which normally have been used as reference standards of speed measurement. This paper describes an electric-tachometer testing system which meets the requirements of high accuracy and is also suitable for large-quantity manufacture of tachometers. The system provides facilities for testing at 22 scale points in a range of speeds from 500 to 4,500 indicated rpm without referring to a standard instrument. The power to drive the tachometers being tested is supplied from tachometer generators which are driven by a d-c motor controlled by a precision tuning fork. The method of operation and the control system are explained.

AMONG the outstanding aircraft instruments developed to meet the urgent needs of the armed forces is the magnetic-drag electric tachometer.[1,2] This tachometer consists of an indicator, Figure 1A, and a three-phase synchronous generator, Figure 2. The indicator is mounted on the instrument panel, and the generator is coupled directly to the aircraft engine. The generator voltage, of frequency proportional to engine speed, operates a synchronous motor in the indicator. The disassembly view in Figure 1B shows the magnet assembly which is rotated by the motor. The magnet assembly is arranged so that an aluminum-alloy disk fastened to a shaft and pointer assembly and supported in independent bearings is displaced by electromagnetic torque against a spring-restoring torque. A pointer deflection thus is produced which is proportional to the speed of the rotating magnets or to the frequency of the generator output, and therefore to engine speed. As the indicator is a frequency-sensitive device, variations in magnitude of the generator output voltage do not influence the accuracy.

The inherent accuracy of the tachometer indicator and high-quantity production required that special test equipment for checking calibration be developed. Early methods of testing tachometer indicators were accomplished by manual control of the speed of a d-c motor driving the transmitting element of the tachometer being tested and by comparison with a reference standard. For each calibration point to be tested, the correct motor speed was adjusted manually according to the indication of the reference standard, and then the indication of the instrument being tested was observed. When a large number of scale points were to be checked, this procedure became lengthy and susceptible to the hazards of serious personal errors. Even more important, however, was the fact that the available standard tachometers, even those of the liquid type, were accurate to only ±0.2 per cent of full-scale calibration. These were not satisfactory for testing the aircraft tachometer, because the required accuracy of calibration as shown in Figure 1C is of the same order of magnitude.

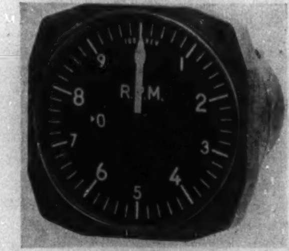

Figure 1A. The magnetic-drag electric tachometer indicator

When performed by the early methods of point-for-point comparison with a reference standard, testing is both slow and inaccurate. The well-known synchronizing-fork type of equipment, though accurate to ±0.1 per cent, is not adaptable to high-production testing. A tuning fork in this equipment provides means for manually synchronizing the speed of a d-c machine to which is coupled a tachometer generator through a step-ratio gear train providing a large number of test points.

The development of high-precision standards of frequency measurement[3,7] and automatic speed control has made the means available for vast improvement over old methods of tachometer testing. Described in this paper is a tachometer testing system which meets the requirements set by high-production rates and high accuracy.

Test Requirements

All of the testing operations require that voltage of a correct frequency corresponding to the desired scale point be applied to the indicator. These operations include: adjustment of bearings and adjustment of the full-scale point by reducing the magnetic strength of the rotating drag magnets. The entire calibration through 22 scale values then is checked both for increasing and decreasing frequency as well as for various angular positions of the instrument.

The most desirable method of performing the testing operations is to have available for immediate selection a series of voltage sources of the correct fre-

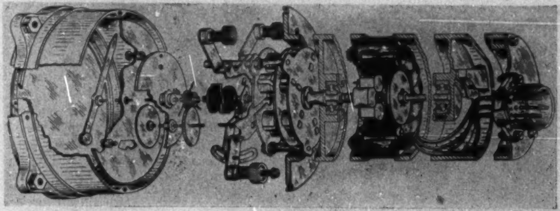

Figure 1B (above). Disassembly view of tachometer indicator

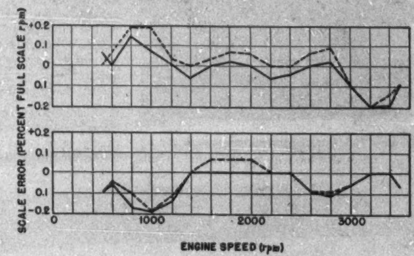

Figure 1C (right). Typical calibration curves

—— Engine speed increasing

- - - Engine speed decreasing

Paper 45-100, recommended by the AIEE committee on instruments and measurements for publication in AIEE TRANSACTIONS. Manuscript submitted December 7, 1944; made available for printing March 20, 1945.

M. A. PRINCI is assistant designing engineer, General Electric Company, West Lynn, Mass.

Figure 2. Tachometer generator which furnishes three-phase power to the indicator

quencies corresponding to the desired scale points. The indicator then can be correctly energized and the adjustments made without reference to a standard. The success of this method requires that each frequency corresponding to a scale point on the indicator be extremely accurate. An allowable error one-tenth that required of the tachometer-indicator calibration would be acceptable, although a higher accuracy, of course, is desirable.

Techniques of frequency measurement using piezoelectric crystals and precision tuning forks maintained at constant temperature have been developed to a high degree. It is now possible to measure frequency over a wide range to a precision of only one part in 10,000,000. By incorporating automatic control with the synchronizing-fork method of tachometer testing and utilizing these new techniques of frequency measurement, it has been possible to obtain testing equipment having an over-all precision of better than ±0.01 per cent.

Test Equipment

The line diagram, Figure 3A, shows the arrangement of the components in this equipment. The principal components are:

1. Test stand.
2. Gearbox and tachometer generators.
3. D-c motor.
4. Pilot generator.
5. Motor field control.
6. 60-cycle frequency standard.
7. Oscilloscope monitor.
8. 60-cycle laboratory standard of frequency using a piezoelectric crystal.

The gearbox, Figure 3B, drives a group of tachometer generators which supply voltage for testing at 22 different frequencies corresponding to the scale points on the tachometer indicator. Gearbox, d-c motor, and pilot generator all are connected to a common drive shaft through a two-to-one, one-half-to-one, one-to-one multiplier designated in the diagram as a gear shift. This unit extends the usefulness of the equipment to more than one instrument scale range. Speed of the drive shaft is maintained constant by control of motor field current by the field-control unit as determined by the deviation in frequency between the pilot-generator voltage and the reference signal from the tuning-fork standard. The pilot generator is a four-pole 60-cycle alternator, and the tuning-fork standard provides the 60-cycle reference signal. Continuous indication of the speed of the main drive shaft is obtained by comparing the frequency of the pilot-generator voltage with a voltage from the laboratory standard of frequency on a cathode-ray oscilloscope.

Terminating in a convenient test stand, Figure 4, are the voltage circuits from the group of tachometer generators. Through a series of interlocked push buttons, the tachometer being tested may be connected to the desired generator and thereby become energized at the precise frequency corresponding to the particular scale point. Reference to a standard tachometer is unnecessary as voltages for the scale range from 500 to 4,500 indicated rpm in the 22 specified steps are selected. The testing operation thus is so materially simplified that it can be accomplished in a few minutes by a relatively unskilled operator. When performed by a skilled operator, according to the early methods of testing, the operation required from 20 minutes to one-half hour. Moreover, the test stand is equipped with a knock-down coil necessary for the adjustment of the full-scale point. This coil is conveniently arranged so that the magnetic strength of the indicator drag magnets may readily be reduced while the instrument is mounted in the test stand.

The equipment was designed to provide for four of the test stands shown in Figure 4. Additional facilities were added by the use of three-phase power amplifiers.

Figure 3A. Line diagram of complete tachometer testing system

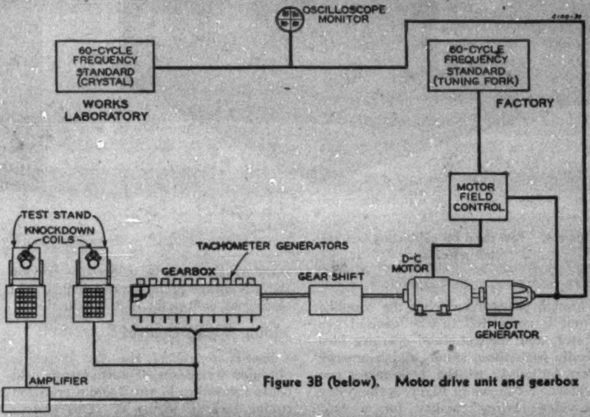

Figure 3B (below). Motor drive unit and gearbox

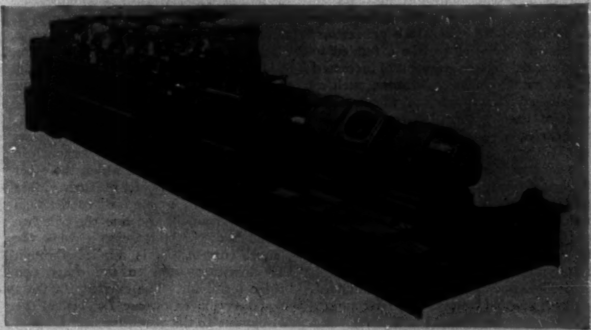

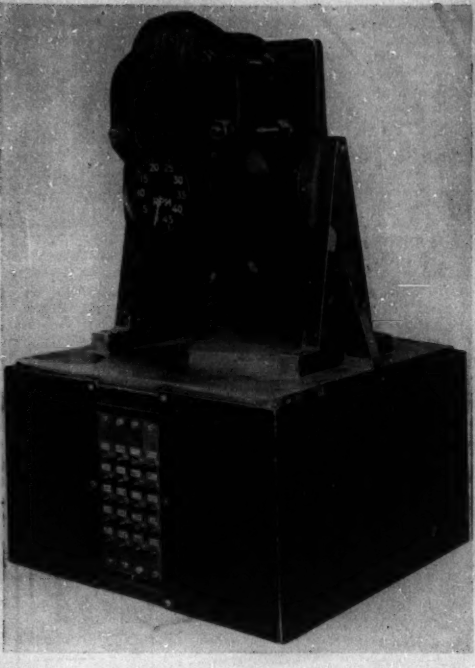

Figure 4. Test stand for calibrating tachometer indicators

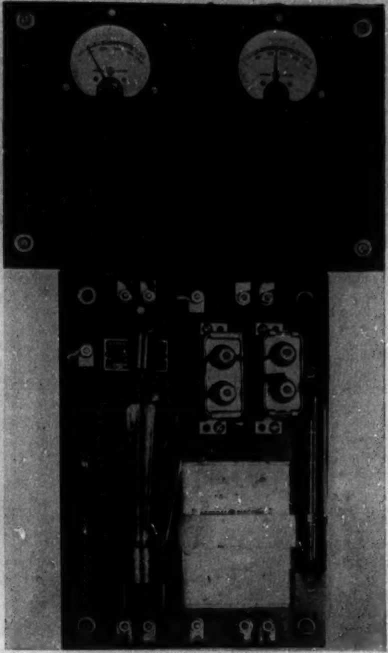

Figure 5. Field-current control panel

Through selector switches the amplifier input is connected to the desired generator, and the test stand operates identically with those stands which are connected directly to the tachometer generators. As shown in Figure 5, the system provides testing facility for a large number of testing stands to be operated simultaneously. Since the amplifiers draw no additional load from the generators, the testing facilities can be extended to meet any desired requirement of increased production. Smaller generators, such as magnetized gears or tone wheels, also may be used to furnish the range of frequencies desired if their output is supplied only to the amplifiers.

A modified testing system using small generators and one amplifier with the associated frequency standard and controlled-speed motor might be applicable in field testing of tachometer indicators. An even simpler arrangement for field testing might be developed by the use of an oscilloscope and frequency standard but with manual control of the d-c motor. The use of the tuning-fork frequency standard thus can be utilized to provide the advantage of high precision in field testing as well as in high production.

Motor Speed Control

Speed control of the d-c motor is obtained by means of a thyratron field control shown in Figure 5 and a precision tuning fork in Figure 6. This system of motor speed control was developed originally for turbine-governor application[8] where large power variations exist. As a precise tachometer testing system, it is subject to the same variables as well as variations in line voltage. But the magnitude of the variations is small and controllable.

The control circuit in Figure 7A shows the motor field windings connected in two arms of a bridge of which the other two arms are equal fixed resistors. Main field current I_f, is supplied to the field windings from the d-c line through two terminals of the bridge circuit, while the control current, I_c, is applied through the thyratron tube to the other two bridge terminals. The current, I_c, flows in a direction to oppose I_f; hence, the net current to the generator field is equal to I_f minus the average value of I_c. Any tendency for the motor to change speed is opposed by a restoring torque produced by a change in I_c, and consequently in the net field current.

The magnitude of I_c is controlled by the phase relation between the voltage E_g applied to the thyratron control grid and the plate voltage E. The voltage

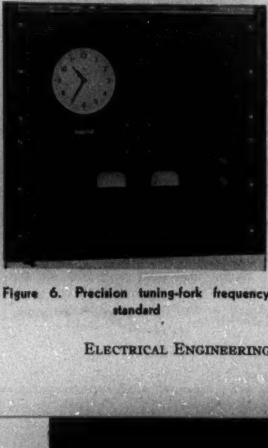

Figure 6. Precision tuning-fork frequency standard

E is obtained through transformer T_1 from the single-phase pilot generator which is connected directly to the d-c motor and gearbox drive shaft. The frequency of its voltage is proportional to the shaft speed. The voltage, E_g, is the vector sum of a standard voltage, E_f, obtained from a tuning-fork standard oscillator shown in Figure 6 and a voltage E_s from the pilot generator. Through the phasing network in Figure 7A, the voltage E_s from T_2 is brought in phase quadrature with the plate voltage E.

Plate- and grid-circuit relations are best described by referring to Figure 7B. As both E and E_s are supplied from the pilot generator, small changes in motor speed will not alter their phase relation. However, small changes in motor speed will be followed by a phase displacement between E and the tuning-fork voltage E_f. Thus, as the motor speed tends to increase, the resultant grid voltage becomes displaced in phase in the direction of the upper arrow in Figure 7B. A shift in phase in this direction causes a decrease in the average value of I_c. As I_c flows in a direction to oppose the main field current, I_f, a net increase in motor field strength results, and the tendency for the motor speed to increase is opposed. The opposite action takes place when the motor speed tends to decrease. The displacement of the grid voltage E_g is now indicated by the direction of the lower arrow in Figure 7B. The resulting increase in the average value of I_c causes the motor field strength to decrease, thus opposing the tendency of the motor speed to decrease.

Accuracy of Calibrating System

The factors which affect the performance of the speed control are:

1. Tuning-fork error.
2. Temperature variations.
3. Load variations.
4. Line-voltage variations.

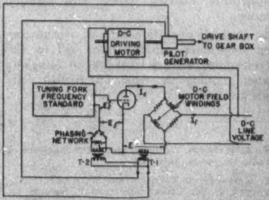

Figure 7A. Field-control circuit

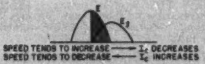
E
E_g
SPEED TENDS TO INCREASE ⟶ I_c DECREASES
SPEED TENDS TO DECREASE ⟶ I_c INCREASES

Figure 7B. Plate- and grid-voltage phase relation

The precision of the system is established principally by the magnitude of the frequency deviation of the tuning-fork oscillator.[3] The tuning fork in this unit is maintained at constant temperature, and its maximum frequency deviation does not exceed ±0.003 per cent.

Temperature, load, and line-voltage variations which operate to exceed the control range of the current I_c, Figure 7A, will cause the system to drop out of synchronism.[3] Figure 8A shows the range in control current for variations in line voltage while the load is constant. Figure 8B shows the control current range when the line voltage is held constant and the load varied. Only temperature variations caused by self-heating of the equipment cause the control range of I_c to be exceeded, and for this condition a compensating adjustment of I_f is made after stable thermal conditions have been established. Variations in load and line voltage which do not operate to exceed the control range of I_c contribute to the over-all error of the system by introducing hunting. This is kept to a negligible value, largely because the line voltage is obtained from an independent supply having good regulation; and the intermittent loading of the tachometer generators as tachometer indicators are alternately connected and disconnected is small.

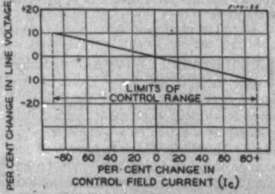

Figure 8A. Control-current range in terms of line-voltage variations for constant load

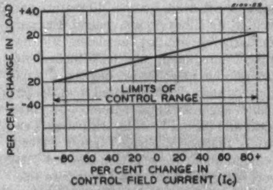

Figure 8B. Control-current range in terms of load variations for constant voltage

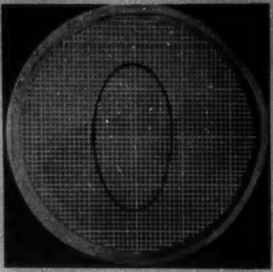

Figure 9. Lissajous figure on oscilloscope screen

A detailed study of the conditions influencing hunting is beyond the scope of this paper. It is evident, however, that the time constant of the control system is dependent almost entirely upon the inductance in the d-c motor field. Consequently, it is necessary that load and line-voltage variations be small. The curves in Figure 8A and 8B indicate acceptable limits of variations of these factors without causing appreciable hunting. By observing the precautions of small load changes and steady d-c line

Figure 10. Group of tachometer-indicator test stands installed in factory

voltage the over-all accuracy of the system is within ±0.01 per cent.

Continuous Reference to Primary Standard

Continuous check of the precision of the base speed and therefore to any one of the test points is obtained by reference to a standard signal from a piezoelectric crystal oscillator. A 60-kilocycle crystal and associated multivibrator stages are standardized daily with standard time signals from the Bureau of Standards radio station WWV. The precision of the 60-cycle output of the oscillator is better than ten parts in 1,000,000. This signal is wired to the factory testing system and connected to the vertical plates of a cathode-ray oscilloscope located prominently in the testing area. Connected to the horizontal plates of the same oscilloscope is the voltage output of the pilot generator in Figure 3A. Figure 9 shows the Lissajous figure formed by the two signals applied to the oscilloscope. The rate of displacement of an element of this figure is a measure of the deviation in frequency of the two applied signals. Displacement of one degree per second of a point on the image formed on the oscilloscope screen corresponds to the over-all error of 0.01 per cent and can be detected readily.

Conclusion

The convenience of operation and precision of the tachometer calibrating system as a factory testing device is apparent. Skill in accomplishing the tachometer calibrating operation is reduced to a minimum and an operator can be trained in a matter of hours. The testing time over early test methods has been reduced from one-half hour to a few minutes per instrument, thus making the large production requirements possible with a minimum of increase in personnel.

The use of such equipment because of its complexity and size is necessarily limited to use in high-production testing. Obviously, such a system is not adequate for field testing of electric tachometers. However, modifications in the applications of the oscilloscope, d-c motor with manual speed control, and the standard-frequency oscillator, can be adapted for small testing requirements. Such modification would retain the advantages of precision over the conventional types of standards for the testing of tachometer indicators.

References

1. The Magnetic-Drag Tachometer, R. G. Ballard. AIEE Transactions, volume 61, 1942, pages 366–9.

2. Recent Advances in Aircraft Tachometer Design, R. G. Ballard, C. P. Hall. AIEE Transactions, volume 63, 1944, September section, pages 646–8.

3. Standard Frequency Source, H. L. Clark, H. Johnston. *General Electric Review*, volume 47, May 1944, page 42.

4. Theory of Servo-Mechanisms, H. L. Hazen. *Journal* of the Franklin Institute, volume 218, number 3, September 1934, pages 279–331.

5. Stroboscopic Method of Speed and Frequency Measurement, G. E. Moore. *The Engineer*, February 1925.

6. United States patent 2,074,126, M. S. Mead, Jr.

7. A High-Precision Standard of Frequency, W. A. Marrison. *Proceedings* of the Institute of Radio Engineers, July 1929.

8. Calibrating Tachometers With the Oscilloscope, E. M. Glaser. *Instruments*, volume 14, October 1941.

9. Genaue Frequenz-Messung, G. Keinauth. *Archiv für Technisches Messen* (Munich, Germany), volume 23, May 1933.

10. Calibration of Frequency Meters, S. C. Richardson. *General Electric Review*, volume 39, October 1936.

11. A New Type of Precision Frequency Changer for Instrument Calibration, E. H. Greibach. *Electric Journal*, volume 26, March 1929.

A 400-Cycle Aircraft Motor

G. O. SCHWANDT
ASSOCIATE AIEE

Synopsis: The ever-present need for lighter-weight and more compact aircraft electric motors is evident as any reduction in weight or space provides increased fuel, bomb, or pay-load capacity. Reliable 400-cycle motors more compact and approximately 40-per-cent lighter than existing 24-volt d-c motors have been developed recently. Present trends indicate that these motors will be used extensively aboard the airplane of tomorrow. This paper describes some of the 400-cycle motors that have been developed and discusses their requirements with the view of disseminating information so that others may better understand the motors and the performance to be expected from them.

IN THE PAST FEW YEARS considerable thought has been given to proposed methods for reducing the weight of aircraft electric equipment below that possible from existing 24-volt electric systems. The value of high frequency as one avenue through which this could be accomplished was demonstrated by the 400-cycle electric system aboard the *B*-19 airplane built some time ago. This system functioned satisfactorily according to expectations, but the lack of a suitable constant-speed drive for the alternators prevented its adoption for general use, particularly on military airplanes, at that time. Subsequent months witnessed the inception of ideas for driving the alternators at nearly constant speed from the airplane engines. Practicability of these ideas and the need for electric power in excess of that possible from existing systems brought about the selection of a 208/120-volt 400-cycle three-phase four-wire electric system for several military airplanes under consideration.

Heretofore knowledge of the electric motors developed for use on these and other airplanes has been confined, generally, to the few intimately associated with their design. Much of the accumulated information pertaining to their design and application may be useful, particularly to aircraft electrical engineers or others who will apply the motors. Therefore, this paper was written, primarily from a design point of view, for the purpose of disseminating some of this information so that others may better understand the motors and the performance to be expected from them. It contains the following material:

1. A summary of the motor requirements.
2. The principles of operation compared briefly with those of 60-cycle commercial motors.
3. A comparison of characteristics with those of existing d-c aircraft motors.
4. The design factors involved.
5. A discussion of the motor characteristics related to loads encountered aboard aircraft
6. Illustrations and characteristic curves representative of a line of motors that has been developed.
7. Conclusions.

Requirements

The more important motor requirements mutually agreed upon by the United States Army, Navy, Air Force Command, interested motor manufacturers, and representatives of the aircraft industry are summarized as follows:

1. Dependable operation from −70 to +60 degrees centigrade according to National Aircraft Standards Committee charts at all altitudes to 40,000 feet and in all humidities existing within this altitude range.
2. Reliable operation without overheating on frequencies ranging from 380 to 420 cycles and voltages from 190 to 210 volts when running and from 180 to 210 volts when starting.

Paper 45-87, recommended by the AIEE committee on air transportation for publication in AIEE Transactions. Manuscript submitted November 22, 1944; made available for printing March 8, 1945.

G. O. Schwandt is electrical engineer, fractional-horsepower-motor engineering division, General Electric Company, Fort Wayne, Ind.

3. Ability to withstand shock and vibration encountered aboard airplanes.

4. High efficiency and power factor to permit minimum weight of associated electric equipment.

5. Small size and light weight consistent with other requirements.

6. A life of 500 hours without undue servicing on the specified duty cycle, preferably more.

7. Simplified construction arranged for easy servicing.

8. Intermittent-rated motors must operate on a duty cycle of one minute on and 20 minutes off. Their locked-rotor torque must be 300 per cent of the rated torque on normal voltage and frequency and at 25 degrees centigrade ambient temperature. The slip at rated torque must not exceed 15 per cent of the synchronous speed.

9. Continuous-rated motors must have 200-per-cent breakdown torque and 160-per-cent locked-rotor torque, both in terms of rated torque on normal voltage and frequency and at 25 degrees centigrade ambient temperature.

Comparison With Other Motors

These motors, most of which are three phase four wire, possess principles of operation similar to those applicable to 60-cycle motors of the same type. Generally the same fundamental laws and formulas applicable to 60-cycle alternating motors are usable although instances occur where it is necessary to modify or extend associated empirical data to embrace new conditions. They differ from the 60-cycle motors chiefly as follows:

1. Higher operating speed.

2. Smaller size and less weight for corresponding horsepower ratings.

3. Better material utilization—electrically, mechanically and thermally—to obtain lighter weight without sacrificing reliability.

4. Ability to operate over increased temperature, humidity, and altitude ranges.

Their characteristics compared with those of existing 24-volt d-c aircraft motors, segregated according to merit, are listed in the following paragraphs.

DESIRABLE CHARACTERISTICS

1. Lighter weight and smaller size for same output rating.

2. Higher efficiency, generally.

3. Simplicity of construction.

4. Absence of commutators and brushes which are difficult to maintain, particularly at high altitude, and which may permit erratic motor operation because of their susceptibility to external vibration.

5. Higher operating voltage and lower currents which permit a reduction in the weight of wiring and generating equipment.

6. Inherently longer life with less servicing.

7. Less speed variation over the normal load range, including that caused by normal voltage and frequency variations. This does not apply if the speed of the direct motor is controlled by a speed regulator.

8. Freedom from explosion-producing properties such as sparking at brushes.

9. Reduced voltage regeneration and hence less danger of damage to motor and system if direction of rotation is instantly reversed.

10. Inherent regenerative braking for overhauling loads.

11. Generally, a lower ratio of starting to running currents, a condition which makes it possible to simplify the design of associated equipment.

12. Easier to apply thermal overload protection.

13. Reduced rotor inertia—hence less braking required to stop motors in the same length of time.

14. Reduced danger of damage or faulty operation from corrosion of vital parts.

15. Moderate ratio of locked-rotor to running torque. D-c motors have locked-rotor torques up to about 1,000 per cent of their rated load torques. Continuous-rated a-c motors according to specifications have 160-per-cent locked-rotor torques. Intermittent-rated 400-cycle motors according to specifications have 300-per-cent locked-rotor torques.

16. Less filtering required to eliminate radio interference.

UNDESIRABLE CHARACTERISTICS

1. Locked-rotor and breakdown torque variations, caused by both voltage and frequency changes rather than voltage changes alone.

2. Lack of speed control.

Many engineers would list the moderate ratio of locked-rotor to running torque as an undesirable characteristic, as any increase in this torque is added assurance that the motors will start their loads. However, it must be remembered that generally increased locked-rotor torque is brought about by increased current which adds weight to the motor and associated equipment. Furthermore, there is never a need for additional assurance if the motor is correctly applied on the basis of starting as well as rated load conditions. It is better to use a larger motor to provide additional starting torque should a specific application require it rather than add a weight penalty to the entire system by building additional torque in all motors.

Basic Motor Constructions Involved

Open 400-cycle motors are most satisfactory for the majority of applications. Normally, they do not possess explosion-producing characteristics and can be ventilated with less complication and without excessive weight increases. Gasoline-pump motors will require an explosion-resisting construction. Some of these will operate submerged with their windings, bearings, and other vital parts directly exposed to the gasoline. A few totally enclosed intermittent motors may be required for engine nacelle or other locations saturated with oils or dirt.

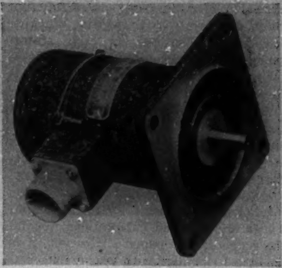

Figure 1. Aircraft motor; three-quarter horsepower, 10,800 rpm, 400 cycle, three phase

Synchronous speeds of 24,000, 12,000, 8,000, 6,000, 4,800, and 4,000 rpm are possible from 2-, 4-, 6-, 8-, 10-, and 12-pole windings, respectively. The four-pole motor will be used almost exclusively. Generally a lighter-weight power unit can be obtained by gearing down to the desired speed rather than increasing the number of poles. Nevertheless six- and eight-pole motors will have a limited use for driving loads such as centrifugal fans and gasoline pumps because of the noise and lubrication problems associated with gears. Lighter-weight motors could be obtained by using two-pole windings, but the lack of suitable bearings capable of withstanding speed approaching 24,000 rpm without freezing at low temperatures prevents using them at this time.

Design Considerations

In designing 400-cycle aircraft motors it is necessary to correlate functions of five different kinds of engineering: namely, electrical, mechanical, thermal, air-flow and lubrication. Individually, these functions are complicated by the high-speed operation, better material utilization, and varying conditions in which the motors must operate. Correlation is particularly difficult, as the interrelation is such that any one function may affect any or all of the others. Usually the electrical studies are given first consideration, followed by fitting the other engineering factors around the basic electrical design. This is desirable, not because of a position of greater importance, but rather because the other functions to a large extent are determined by the electric output and losses.

ELECTRICAL DESIGN

Usually, the electrical design can be determined best by calculating performance characteristics using several different rotor diameters, tooth widths, stacking lengths, and so on, for each stator-punching diameter contemplated. By so doing the less important factors such as different amounts of primary copper, reduced iron thickness, modified ratios of tooth to core section, which affect the characteristics appreciably, are given proper consideration. Also, this procedure permits making allowances for thermal-transfer surfaces and air-flow paths, both of which reduce the electric output. These are involved calculations beyond the scope of this paper. However, it is possible to predict with reasonable simplicity approximate characteristics to be expected by considering what happens when a 60-cycle motor is operated on 400 cycles. The flux should be held at the design value, and if so maintained the applied voltage must be increased in the ratio of the frequency change. This is demonstrated by the commonly used flux formula:

$$\phi=\frac{E\times 10^8}{2.22\times f\times W_k\times C_1}$$

where

ϕ = flux in lines per square inch
E = applied voltage per phase
f = applied frequency
W_k = the winding constant
C_1 = primary conductors per phase

Raising the frequency causes the motor reactances to increase in proportion to the frequency change but does not affect the resistance values. Iron loss increases by an amount dependent upon the magnetic material used and the density at which it operates. Available data indicate that the increase is 12.5 times for high-grade silicon iron at a density of 95,000 lines per square inch. Windage losses vary as the cube of the speed. So-called stray losses resulting from tooth pulsations and similar losses vary in different designs but usually are about five per cent of the calculated electric output. Friction losses are small and can be neglected without appreciably affecting the over-all results.

Table I, column 1, contains design data and calculated characteristics for a typical 200-volt 60-cycle three-phase motor. Column 2 contains similar data for 400-cycle operation of the same motor. Column 3 contains similar 400-cycle data for the same motor with increased secondary resistance to obtain 160-per-cent starting torque. For the considerations tabulated in columns 1 and 2 rated load is arbitrarily placed at 50 per cent of the breakdown torque. For column 3 rated load is established such that the slip at this point does not exceed ten per cent of the synchronous speed and such that the breakdown and starting torques are at least 200 and 160 per cent of the full-load torque, respectively. The slip would exceed ten per cent if rated load were placed at 50 per cent of the breakdown torque.

From these data it is noted that rated output increases 9.3-fold when the 60-cycle motor without modification is operated on 400 cycles. The locked-rotor torque decreases to 23.5 per cent of the full-load torque which is far too low for most applications.

Table I. Design Data and Calculated Characteristics for Typical 200-Volt Three-Phase Motors

	Column		
	1	2	3
Design Data			
Applied volts per phase	115.5	770	770
Applied frequency, cycles	60	400	400
Primary resistance per phase, ohms	1.3	1.3	1.3
Secondary resistance per phase, ohms	2.2	2.2	13.95
Primary leakage reactance per phase, ohms	2.7	18	18
Secondary leakage reactance per phase, ohms	2.7	18	18
Magnetizing leakage reactance per phase, ohms	90	600	600
Iron loss, three-phase, watts	30	375	375
Windage loss, three-phase, at 1,800 rpm, watts	5.0	5.0	5.0
Stray-loss factor	0.95	0.95	0.95
Calculated Characteristics			
Full-load output, watts	1,125	10,430	8,200
Full-load speed, rpm	1,645	11,880	10,850
Full-load slip, per cent of synchronous speed	8.6	1.0	10
Full-load efficiency, per cent	81.0	79.5	73.8
Full-load power factor, per cent	90		89.5
Full-load torque, ounce-feet	77	99	85.0
Full-load loss, watts	265	2,720	2,900
Full-load primary I^2R loss, watts	79	156	105
Full-load secondary I^2R loss, watts	97	119	780
Full-load iron loss, watts	30	375	375
Full-load windage loss, watts	4	1,450	1,110
Full-load stray loss, watts	57	620	410
Breakdown torque, per cent of full load	200	200	231
Locked-rotor torque, per cent of full load	161	23.5	161
Locked-rotor input, watts	3,495	5,210	17,185
Locked-rotor primary I^2R loss, watts	1,335	1,805	1,510
Locked-rotor secondary I^2R loss, watts	2,130	3,040	15,330
Locked-rotor iron loss, watts	30	375	375

The rated output increases 7.3 times when the secondary resistance and rated loads are adjusted simultaneously to obtain 160-per-cent starting torque without exceeding ten-per-cent slip at rated load. Standstill and rated load losses increase 5- and 11-fold, respectively. Rotor losses at standstill increase 7.2 times which means that the heating rate of the rotor also increases. Hence the ability of the rotor to withstand locked-rotor conditions is materially reduced, particularly if the resistance increase is obtained by changing the amount of secondary material but not the material itself.

The power required to establish air motion through rotation of the rotor and fans normally constitutes the windage losses. Considering that the rotor portion is usually small, it appears that sufficient cooling exists on 400-cycle operation to permit continuous-rated-load operation. Whether or not this is true depends upon the arrangement of thermal-transfer surfaces and the flow of a cooling medium across these surfaces.

THERMAL AND AIR-FLOW DESIGN

The designs of thermal-transfer surfaces and air-flow paths are coincidental. Two basic arrangements are possible, one for double-end ventilation, the other for through ventilation. Most intermittent-rated motors and continuous-rated motors having large diameters and thin magnetic structures can be cooled successfully by double-end ventilation. When used, cool air brought in through suitable openings is directed such that it impinges on the ends of the windings and magnetic structures at high velocity. Heat generated internally must transfer to the exposed surfaces by conduction for dissipation. Usually these exposed surfaces are not adequate to dissipate the heat of continuous-rated motors having stacking lengths which permit minimum compactness and weight. In these, adequate ventilation can be obtained by conducting air through special openings in the magnetic structure. Best results are obtained by placing these openings, which should be designed for maximum air velocity and heat-transfer surface, where most of the heat is generated. Excellent air paths are obtained by pressing the stator windings back into the slots. This permits air flow directly over the stator and rotor windings as well as sections of the stator and rotor teeth. All of these have good transfer surfaces and are parts in which much of the heat is generated. Also, holes punched in the stator and rotor core sections serve as good air-flow paths.

MECHANICAL CONSTRUCTION

Several equally satisfactory but distinctly different mechanical constructions are possible. Usually that used is deter-

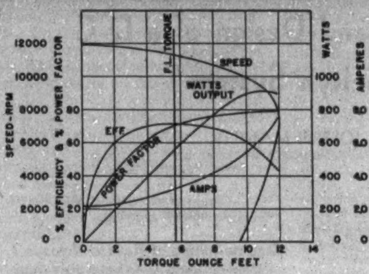

Figure 2. Characteristic curves for three-quarter-horsepower 10,800-rpm 400-cycle three-phase aircraft motor

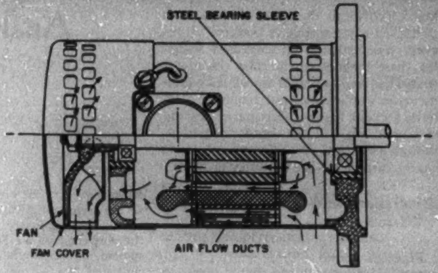

Figure 3. Section view of 400-cycle aircraft motor

mined by the basic requirements and other fundamentally extraneous considerations such as available manufacturing facilities, shop practices, and individual preferences. Such other considerations add to or detract from a design only to the extent of their influence on the making of individual parts or the assembly of these parts into the completed unit. Whether or not a design is satisfactory is determined wholly by weight considerations and ability to withstand burdens encountered over the range of operating conditions throughout its expected life, without destroying other essential characteristics. The most severe burdens are imposed by airplane vibrations. According to specifications vibrations up to 55 cycles per second with an excursion (double-amplitude) of $^{1}/_{16}$ inch may be expected.

The motor shells, end flanges, bearings, shafts, and a few other miscellaneous parts constitute the vital parts entering into the basic mechanical construction of most 400-cycle aircraft motors. Grease seals or other special features are required only for specific applications.

Comparable lightweight shells may be obtained either from low-specific-gravity materials such as aluminum or magnesium or from stronger high-specific-gravity materials such as steel but with the sections reduced. Steel shells with reduced sections permit a better over-all design, particularly in conventional constructions where accurate dimensions are necessary to maintain the radial location of stators slipped or pressed into the shells. These have the same coefficient of thermal expansion as that of the magnetic iron, and therefore the same accurate dimensions exist over the entire temperature range. Aluminum or magnesium shells have coefficients of thermal expansion greatly different from that of magnetic iron. Because of this, satisfactory dimensions at normal temperatures may not remain satisfactory and may cause failure through excessive stresses in the shells and magnetic structures when extreme temperatures below normal are approached.

Owing to limitations in manufacturing processes, the end flanges usually are made of low-specific-gravity materials. Internal rabbets should be used to eliminate failure from excessive stresses at low temperatures when the shells are made of steel.

At present, only ball bearings are satisfactory for the high-speed operation, but sleeve bearings with special lubrication may be used in the future. Bearings of the minimum size necessary for radial and thrust loads and the specified life should be used to prevent excessive torque for overcoming friction at low temperatures.

High-grade steel shafts with hardened extensions are required, particularly where pinions or splines are an integral part of the shaft extensions.

LUBRICATION

Suitable lubrication capable of withstanding high temperatures without freezing at low temperatures cannot be obtained. Those available lubricants capable of withstanding high temperatures freeze at about −30 degrees centigrade. Those satisfactory for low temperatures fail in a relatively few hours if operation is sustained at about 60 degrees centigrade or above. Lubricants do not remain frozen long after operation is started, and therefore they are objectionable only because of the added torque required to break the bearings loose. Generally, it is better to use the high-temperature lubricants and provide the additional torque required for starting.

Motor Characteristics

Specifications for the motor characteristics were established by considering many loads encountered aboard aircraft, together with anticipated variations caused by voltage and frequency fluctuations and changes in operating conditions. Both intermittent and continuous loads were scrutinized.

Intermittent motors are required principally to operate a variety of mechanisms such as wing flaps, cowl and oil cooler flaps, bomb-bay and turret doors, automatic temperature controls, and armament. However, some are required for driving hydraulic pumps, air compressors, or other miscellaneous applications. Fundamentally these are torque applications in which the power requirements vary almost continuously during the operating period.

Therefore the motors will be given a torque rating approximately equal to but not more than one third of the normal locked-rotor torque. In most of these applications peak torque requirements are considerably less than 200 per cent of the root-mean-square torque. The locked-rotor torques may decrease to about 200 per cent of their normal values under the most severe operating conditions which are brought about by a combination of minimum voltage, maximum frequency, and minimum temperature. Hence, 300-per-cent starting torque as established for the specifications is adequate for most applications. Usually there will be a surplus of torque as the factors entering into the most severe operating conditions do not occur simultaneously.

Continuous-rated motors are needed principally for driving fans, fuel pumps, hydraulic pumps, and air compressors, either directly or through gear reductions. Motorization of fans and fuel pumps of the centrifugal type, which are the devices "most used" usually, entails selecting ratings corresponding to the peak load requirements. Locked-rotor requirements are essentially those of the motor itself in the infrequent applications where gear reductions are used. Motorization of the other devices entails selecting ratings up to about ten times the normal or root-mean-square load if sufficient capacity for peak loads or starting is provided. The occasional or even frequent necessity of selecting ratings in excess of the normal load does not mean that the specifications should require greater breakdown and locked-rotor torques. Motor weights for these applications are the same, regardless of whether or not the ratings correspond to the normal or root-mean-square loads, providing the ratio of breakdown to locked-rotor torque is correct. However, standardizing on increased values for these torques would raise the motor weights as well as that of associated equipment for applications not requiring a reserve for peak loads or starting. The ratio of breakdown to locked-rotor torque, although not ideal for all applications, is nearly correct for the majority of them.

Illustrations and Characteristic Curves

Figure 1 shows a three-quarter-horsepower continuous 400-cycle 200-volt three-phase motor designed to operate in accordance with the requirements previously outlined. The weight of this motor is 3.4 pounds. It is about 40 per cent lighter than a d-c motor having the same horsepower and speed rating. Other 400-cycle and 24-volt d-c motors with corresponding ratings have about the same ratio of weight.

Figure 2 shows characteristic curves plotted from test data taken on the three-quarter-horsepower motor at normal voltage, frequency, altitude, and ambient temperature. Speeds, efficiencies, power factors, amperes, and watts output which are plotted against torques are included.

Figure 3 illustrates schematically the construction used for continuous-rated motors with outputs from one eighth to 25 horsepower. That used for intermittent-rated motors is similar except the ventilation ducts, overhung fans, and fan covers are omitted.

Major design features used in these motors are summarized as follows:

1. Magnetic structures fabricated from high-grade silicon steel with special anneal to permit high flux, good permeability, and low iron loss.

2. Insulation. Class-B material for insulating slots and for between-phase protection. Generally the stator windings are of heavy Formex-glass-covered wire to provide greater protection against heat shock. Stator core complete with windings impregnated with special moisture-resisting varnish.

3. Squirrel-cage-type rotors with brazed copper or brass windings. Protected with anticorrosion treatment.

4. Through ventilation in continuous-rated motors for minimum composition and weight. Double end-turn ventilation in intermittent-rated motors.

5. Shells made by expanding thin steel tubing to obtain light weight, rigid construction, and a temperature coefficient the same as that of the stator.

6. Magnesium or aluminum end shields for light weight.

7. Heat-treated alloy steel shafts for strength and dependability. Hardened shaft extensions with or without pinions or splines.

8. Double-shield-type permanently lubricated ball bearings housed in a steel insert in the end-shield castings to assure long life.

9. Protective finishes. Magnesium or aluminum castings treated against corrosion and primed with zinc chromate. Steel parts other than stator and rotor punchings cadmium- or zinc-plated. External parts except mounting surface have black wrinkle finish.

Conclusions

Present trends indicate an increasing demand for 400-cycle electric systems for both military and commercial airplanes. These trends are justified in part by the inherently light-weight rugged and dependable constructions possible in 400-cycle motors.

The information contained in the paper is that which seems most important. Many additional data have not been mentioned; however, it is hoped that the disclosures herein will assist in creating a better understanding of the motors and the performance to be expected from them.

Analysis and Design of a D-C Selsyn System

JOSEPH MANILDI
MEMBER AIEE

Synopsis: At the present time there are several remote-indicating systems in common usage in industry. These types include the conventional a-c Selsyn, a-c Magnesyn system, and the d-c Selsyn. The d-c Selsyn embodies two features which present a distinct advantage in aircraft systems.

1. The system does not require an a-c source of power.

2. The system requires only three wires between transmitter and receiver, whereas all other types of systems require at least five wires leading from the transmitter to the receiver.

To offset somewhat these advantages, all d-c Selsyn systems now in operation have a very slight natural error which, although not important in some applications, becomes very undesirable in applications where a high degree of accuracy is required. In this paper the author presents a rigorous analysis of a conventional d-c Selsyn remote-indicating system. The first part of the analysis shows that a natural error exists in the system, which has a 60-degree cycle and which reaches a maximum value of 1.1 degrees. The error is zero at each 30-degree point and reaches a maximum almost midway between the 30-degree points. The natural error of the Selsyn system arises from the fact that the transmitter resistance is a linear function of the transmitter angle θ. This natural error may be overcome by designing a transmitter resistance in a nonlinear manner. The equation is developed for the necessary variation of the transmitter resistance with the transmitter angle. Furthermore, the shape of the toroid on which this resistor should be wound to give this desired variation, is derived therefrom. The paper further presents optimum values of resistances for both transmitter and receiver, in order that the greatest amount of torque may be transmitted to the receiver for a given amount of power.

Determination of Natural Error in a Conventional D-C Selsyn System

THE INVESTIGATION of the d-c Selsyn embodies two separate questions.

1. If no frictional error is assumed, what are the magnitudes and characteristics of natural errors which may exist in the instrument, and how may they be corrected?

2. For a given amount of power consumption how should the instrument be constructed to give best follower properties from transmitter to receiver; that is, for a given amount of friction, how can the frictional error be reduced to a minimum?

In analyzing the first question, we consider the conventional d-c Selsyn shown in Figure 1. The receiver coils AB, BC, and CA are wound with their magnetic axes at 120 degrees to each other and connected in a delta connection. Points A, B, and C are connected to points A', B', C', respectively, located at 120-degree intervals on the transmitter winding. The battery contacts D' and E' are on a diameter and may be moved at will.

Ideally, the direction of the resultant field in the receiver should move in exact coincidence with the angle θ in the transmitter. There is no a priori reason for supposing that this situation will exist. Actually, as we shall see, if the resistances in the transmitter are linear with the angle θ, the ideal situation does not exist. The amount of natural error introduced is determined in the following analysis:

We obtain first the current distribution in coils AB, BC, and CA when the contacts D' and E' are rotated θ degrees from A' as shown. $0 \leqq \theta \leqq 60$ degrees. The transmitter is assumed to have a re-

---

Paper 45-101, recommended by the AIEE committee on instruments and measurements for publication in AIEE TRANSACTIONS. Manuscript submitted February 3, 1945; made available for printing March 21, 1945.

JOSEPH MANILDI is on the staff of the department of electrical engineering, California Institute of Technology, Pasadena, Calif.

sistance of R_1 ohms per degree, or 120 R_1 ohms per leg. The receiver is assumed to have a resistance of 120 R_2 ohms per leg. Each section of resistance in the circuit is numbered as shown in Figure 1, and the equivalent circuit is shown in Figure 2, with corresponding numbers and the value of each resistance shown. The points *C*, *A*, and *B* are marked, since we are interested in the voltages between these points.

To simplify the analysis we replace the delta sections 3-4-7 and 1-2-6 by their equivalent wye sections.

The transformation relationships which replace a delta system R_1-R_2-R_3 by a wye system r_1-r_2-r_3 are given by

$$\left.\begin{aligned} r_1 &= \frac{R_2R_3}{R_1+R_2+R_3} \\ r_2 &= \frac{R_1R_3}{R_1+R_2+R_3} \\ r_3 &= \frac{R_1R_2}{R_1+R_2+R_3} \end{aligned}\right\} \qquad (1)$$

The foregoing relationships leave the current and voltages at the three terminals unchanged.

Figure 3 shows the equivalent circuit after the transformation is made and the resistors 5 and 8 are combined. Values are shown. The resistance of the two parallel branches in Figure 3 are equal; hence half the total current flows in each branch. The system is further reduced in Figure 4, and we obtain for the total current

$$2i = \frac{60E(R_1+R_2)}{5{,}400R_1R_2+R_1^2(-\theta^2+60\theta+1{,}800)} \qquad (2)$$

The current in each branch is then

$$i = \frac{30E(R_1+R_2)}{5{,}400R_1R_2+R_1^2(-\theta^2+60\theta+1{,}800)} \qquad (3)$$

Referring to Figure 3, we have the following voltages:

$$E_{CA} = i\left(\frac{120R_1R_2}{R_1+R_2}\right) = \frac{3{,}600Er}{(-\theta^2+60\theta+1{,}800)+5{,}400r} \qquad (4)$$

$$E_{AB} = -i\left(\frac{R_1R_2(120-\theta)}{R_1+R_2}-\frac{\theta R_1R_2}{R_1+R_2}\right) = \frac{-30Er(120-2\theta)}{(-\theta^2+60\theta+1{,}800)+5{,}400r} \qquad (5)$$

$$E_{BC} = -i\left(\frac{R_1R_2(60+\theta)}{R_1+R_2}-\frac{R_1R_2(60-\theta)}{R_1+R_2}\right) = -\frac{60Er\theta}{(-\theta^2+60\theta+1{,}800)+5{,}400r} \qquad (6)$$

where $r=R_2/R_1$. The currents in the coils are then, from Figure 1,

$$I_{CA} = -\frac{30E}{R_1}\left[\frac{1}{(-\theta^2+60\theta+1{,}800)+5{,}400r}\right] = K\phi_{CA} \qquad (7)$$

$$I_{AB} = -\frac{E}{2R_1}\left[\frac{60-\theta}{(-\theta^2+60\theta+1{,}800)+5{,}400r}\right] = K\phi_{AB} \qquad (8)$$

$$I_{BC} = -\frac{E}{2R_1}\left[\frac{\theta}{(-\theta^2+60\theta+1{,}800)+5{,}400r}\right] = K\phi_{BC} \qquad (9)$$

For a fixed number of turns, the magnetic fields due to each of the coils are proportional to the currents. Figure 5 shows the relative orientation of these fields when the current in each branch is positive. We denote the direction of the resultant field, ϕ, with the *x* axis by the angle θ'. When $\theta=0$ we see from equations 7, 8, and 9 that ϕ_{CA} and ϕ_{AB} are equal in magnitude, and $\phi_{BC}=0$. ϕ_{CA} is positive, and ϕ_{AB} is negative. Hence when $\theta=0$, $\theta'=0$.

To obtain the value of θ' for any value of θ, we denote the *x* and *y* components of the resultant flux by ϕ_x and ϕ_y. From Figure 5 we see that

$$\phi_x = \frac{\sqrt{3}}{2}(\phi_{CA}-\phi_{AB}) \qquad (10)$$

$$\phi_y = -\phi_{BC}+{}^1/_2(\phi_{CA}+\phi_{AB}) \qquad (11)$$

and

$$\tan\theta' = \frac{\phi_y}{\phi_x} \qquad (12)$$

Using equations 7, 8, and 9 and noting that the proportionality constant between flux and current is the same in every case, in conjunction with equations 10, 11, and 12, we obtain

$$\tan\theta' = \sqrt{3}\frac{\theta}{120-\theta} \qquad (13$$

It is important to note that equation 13, which shows how the receiver angle θ' varies with the transmitter angle θ, is independent of the values of the resistances used in the Selsyn. Hence changing the values of the resistances can in no way compensate for natural error in the instrument.

Figure 6 shows a plot of θ' versus θ for 60 degrees. Conditions repeat themselves every 60 degrees, of course, since at 60-degree intervals one battery contact is in coincidence with a coil terminal. We see from the figure that the receiver gives an exact indication of the transmitter every 30 degrees. On one side of this point the receiver lags and on the other side it leads the transmitter.

If we denote by β the difference of the receiver angle and the transmitter angle, we have

$$\beta = \theta-\theta' = \theta-\tan^{-1}\left(\frac{\theta\sqrt{3}}{120-\theta}\right) \qquad (14)$$

It readily may be shown that this error angle is symmetrical in magnitude about the point θ = 30 degrees. Figure 7 shows a plot of β versus θ for $0 \leqq \theta \leqq 60$ degrees.

By differentiating equation 14 with respect to θ and setting the result equal

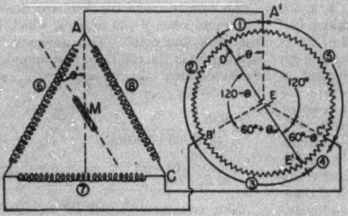

Figure 1 (left). D-c Selsyn transmitter and receiver

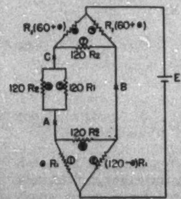

Figure 2 (lower left). Electric circuit of Figure 1

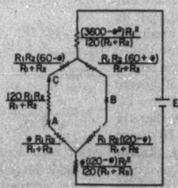

Figure 3 (center). Reduction of circuit in Figure 2

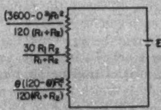

Figure 4 (below). Further reduction of circuit in Figure 2

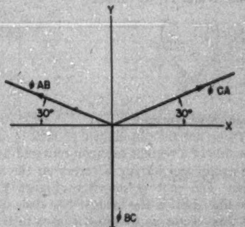

Figure 5. Space relationships of fluxes produced by receiver coils

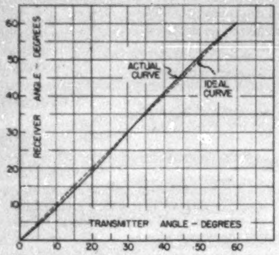

Figure 6. Variation of receiver angle with transmitter angle

to zero, we obtain the value of θ for which β is a maximum.* This gives values of $\theta = 13$ degrees 18 minutes and 46 degrees 42 minutes. The corresponding maximum values of β are 1 degree 6 minutes and -1 degree 6 minutes, respectively.

It is also of interest from a design standpoint to investigate the variation of the magnitude of the resultant field as θ is varied, since the friction error will depend on this magnitude. To do this we investigate first the case for $r \rightarrow \infty$, that is when the receiver resistance is many times larger than the transmitter resistance. Then $(-\theta^2+60\theta+1{,}800)$ is negligible compared to $5{,}400r$ in equations 7, 8, and 9. These equations become

$$I_{CA}=\frac{E}{180R_2} \qquad (7')$$

$$I_{AB}=\frac{-E(60-\theta)}{10{,}800R_2} \qquad (8')$$

$$I_{BC}=\frac{-E\theta}{10{,}800R_2} \qquad (9')$$

Figure 8 shows the current distribution in the coils for θ from 0 to 360 degrees. Equations 7, 8, and 9 are valid only from 0 to 60 degrees, but the rest of the cycle can readily be seen to be as shown. Substituting the foregoing values in equations 10 and 11, we obtain

$$\phi_x=K\left(2-\frac{\theta}{60}\right) \qquad (10')$$

$$\phi_y=K\sqrt{3}\,\frac{\theta}{60} \qquad (11')$$

where K = constant.

These are the parametric equations of one side of a regular hexagon centered at the origin and having a vertex on the x axis. The plot is shown in Figure 9. The line ABC is the locus of the ends of the flux vector as θ varies from 0 to 60 degrees.

To obtain the locus of the end of the flux vector for any value of r, we simply note that all the currents given by equations 7′, 8′, and 9′ will be equal to the currents given by equations 7, 8, and 9 when the former are multiplied by a factor proportional to $1/(-\theta^2+60\theta+1{,}800+5{,}400r)$. Hence, the vectors ending on the line ABC need only be multiplied by the afore-mentioned factor to give the locus for any value of r. It is to be noted that the angle the flux vector makes with the x axis is θ', not θ, and hence equations 10′ and 11′ multiplied by the foregoing factor should be used to determine the locus. The lines $AB'C$ and $AB''C$ show the locus for $r=1$ and $r=0$, respectively. For comparison purposes, the maximum values in each case have been made to coincide. The actual value of maximum flux depends on R_1 and R_2, but this is discussed in the second part of the report. Figure 10 shows the variation of current in each coil for $r=1$.

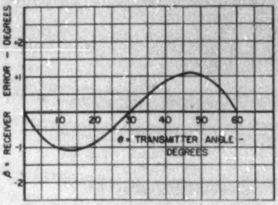

Figure 7. Natural error in Selsyn receiver

$$\beta=\tan^{-1}\left(\frac{\sqrt{3}\theta}{120-\theta}\right)-\theta$$

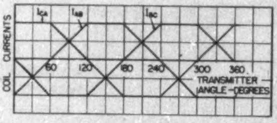

Figure 8. Current distribution in receiver coils, $r=R_2/R_1$

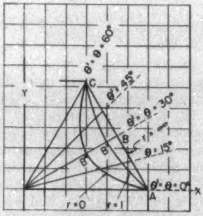

Figure 9. Loci of ends of flux vector for various resistance ratios

It may be seen from Figure 9 that the flux reaches a minimum every 60-degree interval of transmitter rotation. In the analysis which follows, design considerations will be based on making this minimum value of flux as large as possible for given power. As we shall see, this is not the same as making the maximum flux as large as possible.

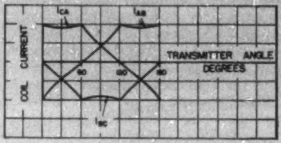

Figure 10. Current distribution in receiver, coils for $R_2/R_1=1$

Optimum Transmitter and Receiver Resistances

For a given amount of power, and a given amount of space in which to wind the receiver coil, it is possible to determine optimum resistances for both transmitter and receiver and hence the wire size to be used in the receiver. It is also possible to determine the best size of receiver coil, consistent with space limitations.

Let us assume that the coil is to have the dimensions shown in Figure 11.

l = length of one turn
a = cross-section area of coil
N = number turns on one coil
A = cross-section area of wire

We then have

$$120R_2=\text{total resistance of coil}=\frac{\rho lN}{A} \qquad (15)$$

$$NA=\alpha a$$

where α is a spacing factor. (16)

$$\alpha=0.91$$

We wish to make the resultant flux a maximum when $\theta=30$ degrees, which is the weak flux point. This amounts to making NI in the coil CA a maximum for $\theta=30$ degrees. Using equation 7, we have

$$NI=\frac{30E}{R_1}\,\frac{N}{2{,}700+5{,}400r}$$
$$=\frac{E}{90}\,\frac{N}{R_1+2R_2} \qquad (17)$$

Using equations 15 and 16, we eliminate N and obtain

$$NI=K\frac{R_2^{1/2}}{R_1+2R_2} \qquad (18)$$

where

$$K=\frac{E}{45}\sqrt{\frac{30\alpha a}{\rho l}}$$

It is evident from equation 18 that K is made large by increasing a, decreasing ρ, or decreasing l for a given supply

---

* See Appendix I.

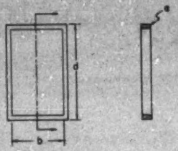

Figure 11. Coil dimensions

l = mean length
One turn
$= 2(d+b)$

voltage. It is not advisable to decrease l, since the enclosed area of the coil is proportional to torque for given NI. However, for best results, a should be made as large as possible and ρ as low as possible, that is, low-resistivity material should be used.

The maximum power consumed in the circuit is given by

$$P = \frac{E^2}{R_{\min}}$$

where $R_{\min}$ is the least value of resistance between battery terminals. From Figure 4 we see that

$$R_{\min} = \frac{30R_1}{R_1+R_2}(R_1+3R_2)$$

and since

$$P = \frac{E^2}{30}\,\frac{R_1+R_2}{R_1(R_1+3R_2)} \tag{19}$$

from which

$$R_2 = \frac{R_1\left(1-\frac{30P}{E^2}R_1\right)}{\left(\frac{90P}{E^2}\,R_1-1\right)} \tag{20}$$

Substituting value of R_2 from 20 in equation 18, we obtain

$$NI = K\frac{(-3K'^2R_1^2+4K'R_1-1)^{1/2}}{R_1^{1/2}(K'R_1+1)};\quad K' = \frac{30P}{E^2} \tag{21}$$

By differentiating expression 21 with respect to R_1 and equating result to zero, we obtain, for maximum NI*

$$R_1 = \frac{1+2\sqrt{2}}{7K'} = 0.547\frac{E^2}{30P} \tag{22}$$

$$120R_1 = \text{resistance per leg} = 2.19\frac{E^2}{P}$$

and from equation 20

$$R_2 = R_1\frac{(3-\sqrt{2})}{(3\sqrt{2}-2)} = \frac{1}{\sqrt{2}}R_1 \tag{23}$$

With the optimum values determined from equations 22 and 23, the size wire for the receiver may be calculated from equations 15 and 16.

Small variations of the receiver resistance from the optimum value will not affect the performance appreciably, although power consumption, of course, will change. This may be seen by writing equation 18 in the form:

$$NI = \frac{K}{R_1^{1/2}}\,\frac{r^{1/2}}{(1+2r)} \tag{18'}$$

Equation 18 is plotted in Figure 12 for both R_1 constant and R_2 constant. It may be seen that the variation of NI with R_2 is small, whereas the variation with R_1 is greater, in the region of $r = \frac{1}{\sqrt{2}}$.

Design equations based on making the flux a maximum in the strongest point, that is, when $\theta = 0$, lead to somewhat different equations. Analysis similar to the foregoing yields the following results:

$$120R = \text{resistance per leg} = 2.30\frac{E^2}{P} \tag{22'}$$

$$R_2 = \frac{R_1}{\sqrt{3}} \tag{23'}$$

For best performance, equations 22 and 23, not 22′ and 23′, should be used.

Correction of Natural Error in Selsyn System

In the first part of this report it was found that the error is zero in the receiver when the transmitter angle θ (see Figure 1) is 0, 30, 60 degrees, and so forth. Since one of the brushes is in contact with a terminal every 60 degrees, it is obvious that any nonlinear resistance must be symmetrical on either side of every 0, 60, 120 degrees, and so forth. Furthermore, since the natural error for a linear resistance is symmetrical and of opposite sign on either side of every 30-degree point, we may assume that the nonlinear resistance should be symmetrical on either side of 0, 30, 60 degrees, and so on.

The foregoing considerations reduce the problem to one of finding the deviation from linearity for the region from 0 to 30 degrees, making the deviation from 30 to 60 degrees symmetrical about the 30-degree point and of opposite sign, then repeating the cycle every 60 degrees.

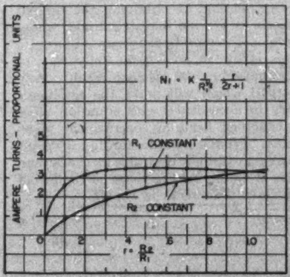

Figure 12. Variation of ampere turns with R_1 and R_2 constant power

Referring to Figure 1, we let the resistance of each transmitter leg be $120R_1$, and the resistance of each receiver leg $120R_2$, as before. For $\theta \leqslant 30$ degrees, let the resistance of that portion of the winding marked ① be equal to αR_1. The problem now resolves itself into one of finding α as a function of θ such that the error shall be zero for all values of θ from zero to 30 degrees.

Remembering the symmetry which we have noted, the values of the resistances ① to ⑤ of the transmitter then must be

① $= \alpha R_1$
② $= (120-\alpha)R_1$
③ $= (60+\alpha)R_1$
④ $= (60-\alpha)R_1$
⑤ $= 120R_1$

Referring to Figure 2, we see that the afore-mentioned resistances are exactly the same as those shown in Figure 2, with α substituted for θ. In our present situation, then, it is obvious that the receiver angle θ', will be given by equation 13, with α substituted for θ, or

$$\tan\theta' = \frac{\sqrt{3}\alpha}{120-\alpha} \tag{24}$$

In order to have zero error, $\theta = \theta'$, and $\tan\theta = \sqrt{3}\alpha/(120-\alpha)$.

Solving for α, we obtain

$$\alpha = \frac{120\tan\theta}{\sqrt{3}+\tan\theta} \tag{25}$$

This gives the necessary variation of α with θ for zero error and hence the variation of resistance with θ, since the resistance of segment ① is αR_1.

Figure 13 shows the variation of α with θ, along with the linear variation, so that the deviation may be noted.

It is to be especially noted that the variation of α with θ for zero error is independent of the receiver resistance and hence will work for all receivers or paralleled receivers.

To obtain the shape of the developed cylinder which will give a resistance in accordance with equation 25, we refer to Figure 14. $OABC$ represents 30 degrees

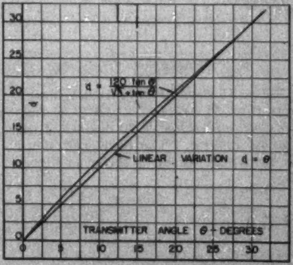

Figure 13. Variation of modification factor with transmitter angle θ

---

* See Appendix II.

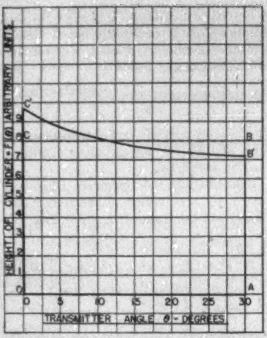

Figure 14. $F(\theta)$ **for 0 degrees** $\leqq \theta \leqq$ **30 degrees**

of the developed cylinder for a linear resistor. $OAB'C'$ represents the shape of 30 degrees of the developed cylinder for the nonlinear resistor.

Let us denote the equation of $C'B'$ as $F(\theta)$. For a particular value of θ, the ratio of the nonlinear resistance to the linear resistance will be equal to the ratio of the area beneath the curve $C'B'$ to the area beneath the curve CB. This ratio is obtained from the equations of the two curves in Figure 13. Hence we have

$$\frac{\int_0^\theta F(\theta)d\theta}{L\theta} = \frac{120\tan\theta}{\sqrt{3}+\tan\theta}\cdot\frac{\pi}{180\,\theta}$$

$$= \frac{2\pi}{3\theta}\,\frac{\tan\theta}{\sqrt{3}+\tan\theta}$$

where θ is expressed in radians, and $L = OC$ in Figure 15.

If we solve for the numerator in the lefthand side,

$$\int_0^\theta F(\theta)d\theta = \frac{2\pi L}{3}\,\frac{\tan\theta}{\sqrt{3}+\tan\theta} \tag{26}$$

If we differentiate both sides with respect to θ,

$$F(\theta) = \frac{2\pi L}{3}\,\frac{d}{d\theta}\left(\frac{\tan\theta}{\sqrt{3}+\tan\theta}\right)$$

$$= \frac{2\pi L}{3}\,\frac{1}{(\sqrt{3}\cos\theta+\sin\theta)^2} \tag{27}$$

Figure 15 shows $F(\theta)$ plotted against θ from 0 to 30 degrees. $OAB'C'$ is thus the developed shape of 30 degrees of the toroidal resistor. The developed shape for the whole resistor is shown in Figure 15.

Conclusions

In a d-c Selsyn a natural-error cycle exists which has a 60-degree period. The error is positive for 30 degrees and negative for 30 degrees, reaching a maximum of 1 degree 6 minutes at 13 degrees 18 minutes and 46 degrees 42 minutes on the transmitter.

Design equations to give maximum flux in receiver for a given voltage and power are given by

$$\text{Transmitter resistance} = 2.19\frac{E^2}{P}\text{ ohms per leg} = R_T \tag{22}$$

$$\text{Receiver resistance} = \frac{1}{\sqrt{2}}R_T\text{ ohms per leg} \tag{23}$$

Furthermore, the cross-sectional area of the receiver coil should be as large as is practical, and the resistivity of the receiver coil as low as possible.

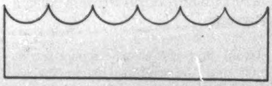

Figure 15. Developed shape of cylinder on which transmitter-resistor may be wound in order to produce zero error

The material and design dimensions of the transmitter coil are immaterial insofar as flux properties are concerned.

The natural error of a d-c Selsyn system may be eliminated completely by winding the transmitter resistance in a nonlinear manner.

The necessary variation of resistance with transmitter angle to give zero error is independent of receiver resistance. This correction for natural error may be attained for all possible loads on the transmitter.

One method of obtaining the desired resistor is to wind it on a cylinder whose developed shape is shown in Figure 16. This is by no means the only way of accomplishing the desired result. Any method which will make the resistance vary in accordance with equation 25 is satisfactory from an operational viewpoint. From a manufacturing viewpoint there may be more desirable methods than that of modifying the shape of the toroid on which the resistor is wound.

Appendix I. Maximum Natural Error in Selsyn

If we use equation 14, and express angles in radians, so that we may differentiate

$$\beta = \frac{\theta}{57.3} - \tan^{-1}\frac{\sqrt{3}\theta}{120-\theta}$$

$$\frac{d\beta}{d\theta} = \frac{1}{57.3} - \frac{1}{1+\left(\frac{\sqrt{3}\theta}{120-\theta}\right)^2}\times\frac{(120-\theta)\sqrt{3}+\sqrt{3}\theta}{(120-\theta)^2}$$

$$= \frac{1}{57.3} - \frac{120\sqrt{3}}{(120^2-240\theta+4\theta^2)} = 0$$

for maximum β

If we solve,

$$\left(\frac{\theta}{60}\right)^2 + \left(\frac{\theta}{60}\right) + 1 = \frac{57.3\sqrt{3}}{120} = 0.828$$

$$\left(\frac{\theta}{60}\right)^2 + \left(\frac{\theta}{60}\right) + 0.172 = 0;$$

$$\frac{\theta}{60} = \frac{1\pm\sqrt{1-0.69}}{2} = 0.778 \text{ or } 0.222$$

$$\theta = 13.3°,\ 46.7°$$

Appendix II. Conditions for Maximum *NI* in Receiver

If we use equation 21,

$$NI = K\frac{\Delta}{R_1^{1/2}(K'R_1+1)}$$

where

$$\Delta = [-3K'^2R_1^2+4K'R_1-1]^{1/2}$$

$$\frac{d(NI)}{dR_1} = 0$$

$$= K\left[\frac{R_1^{1/2}(K'R_1+1)\cdot{}^1/_2\Delta^{-1}\times(-6K'^2R_1+4K') - \Delta\{R_1^{1/2}K'+R_1^{-1/2}(K'R_1+1)\}}{R_1(K'R_1+1)^2}\right]$$

Setting numerator equal to zero, we have

$$R_1(K'R_1+1)(-6K'^2R_1+4K') = (-3K'^2R_1^2+4K'R_1-1)(R_1K'+K'R_1+1)$$

If we multiply and separate powers of R_1,

$$-7K'^2R_1^2+2K'R_1+1 = 0$$

$$R_1 = \frac{1}{K'}\,\frac{-2\pm\sqrt{4+28}}{14} = \frac{1}{K'}\,\frac{1\pm\sqrt{8}}{7}$$

If we discard negative values of R_1, as meaningless.

$$R_1 = \frac{1+2\sqrt{2}}{7K'} = \frac{0.547}{K'}$$

Dynamic Braking With Traction Motors

L. G. RILEY
MEMBER AIEE

G. M. WOODS
MEMBER AIEE

Synopsis: Retardation with traction motors, either independently or as an adjunct to mechanical braking, has been utilized in various forms on practically all types of electric vehicles from battery trucks to main-line locomotives. In some cases, it is used only to maintain uniform speeds on long grades and in others to make regular service stops. Although the general principles are nearly as old as the electric-traction industry itself, in recent years numerous refinements have greatly extended the usefulness of dynamic braking by affording improved performance, additional safety, and simplification of mechanical-braking systems. This paper discusses the various means by which favorable results have been accomplished, with a minimum amount of additional electric equipment.

The Origins of Dynamic Braking

FROM THE STANDPOINT of basic terminology, "dynamic braking" could cover any and all forms of retardation created by an electric motor acting as a generator. However, in traction parlance, the term is recognized as referring to a system of dissipating the generated energy in resistors carried on the vehicle, as distinguished from "regenerative braking" where the generated energy is returned to the power system, necessarily at line voltage.

In the early days when streetcar speeds and weights outgrew the hand brake, air brakes had not been developed for small equipments, and the need for some form of power-operated braking apparatus led to the application of several kinds of "magnetic" and "dynamic" brakes. The traction motors were used to generate on a closed resistor circuit, the dynamic current producing retardation in the motors themselves and also energizing magnetic track shoes and applying wheel brakes, both at the same time. For standing on grades, the magnetic shoes were energized by line current, becoming a direct "electric" brake.

It was known that a series motor, rotated backwards and short-circuited on itself, would generate current and "buck," as a result of building up circulating current from the residual field magnetism retained in the iron after operating with power. By reversing the field connections with reference to the armature, the motor would "buck" without changing the direction of rotation. Two motors permanently connected in parallel provide a loop circuit which permits both to build up as generators. This action is experienced when one is attempting to tow a four-motor car backwards without first opening the paralleling circuit between motors.

Conventional four-motor equipments can be stopped in emergency, without power, simply by reversing the motors. The result is a cumulative generating effect which builds up suddenly, after some delay, the current and voltage rising to excessive peaks. Before the car comes to a stop, frequently with a series of jerks, one motor usually will slip and start running backwards, being driven as a motor by the other machine, which continues to generate at a diminishing rate until the car slows down to a creeping speed.

In all of the early forms the traction motors were reversed in changing from power to brake operation and were operated all in parallel on a single load circuit consisting of brake magnet coils and variable resistors. A stabilizing connection was made, paralleling the motor fields to equalize the load on all armatures.

Later, additional stability was secured by cross-connecting pairs of armatures and fields, in effect producing separate excitation and better inherent equalizing of the load.

Typical forms of magnet-operated wheel and track brake shoes are illustrated in Figure 1. It is interesting to note that many of the operating advantages claimed for these equipments are as fully attractive today as they were when advocated 40 years ago. These may be summarized as follows:

1. Regulated braking independent of line power.
2. Safety in operation, with an additional powerful braking system.
3. Control of speed down long grades.
4. Use of braking energy for car heating.
5. Braking rates in excess of adhesion limits.
6. Prevention of skidding with locked wheels.

These pioneer systems were very effective and were used extensively abroad but fell into disuse in this country with the development of the simple "straight-air" brake equipment. Some of the limiting factors were the abuse of the electric apparatus, both motors and control, and the excessive weight and mechanical maintenance of magnetic-shoe devices. As a result, there was little advance in the art of "dynamic" braking over a period of several years.

Design and Performance of Motors Used as Series Generators

One of the major factors leading to the revival and extensive use of dynamic braking in recent years has been the improvement in commutating characteristics and overload capacities in the modern lines of traction motors. Normal proportioning of the operating characteristics found in passenger vehicles involve a balancing speed of at least twice the speed at which the motors have full voltage applied at full load. To produce a full-load braking rate in the balancing-speed zone, it is obvious that the generated voltage may be double the rated line voltage. Motors capable of satisfactory commutation under these conditions are in common use. To provide for braking at occasional excessive speeds, it is sometimes desirable to initiate the braking action with the fields shunted so as to limit the voltage to a safe maximum, accepting a reduced braking rate in the high-speed zone.

Inherent stability by inductance and also generous commutating and insulation factors are essential design characteristics.

In the case of four-motor equipments, the motors frequently are wound for half voltage and connected permanently two in series. In the limited space available, it is practicable to build low-voltage commutators and brush rigging with an increased margin for overvoltage operation, thus extending the speed range for full-load dynamic-brake operation.

Motor applications for dynamic braking must take into account grade conditions amounting to 20 pounds of retarding force per ton of total train weight for each one per cent of downgrade, in addition to the stored kinetic energy requiring approximately 100 pounds per ton of retarding force for each unit of miles per hour per second braking rate desired. The actual braking effort required of the motor is reduced by the friction and windage drag of the vehicle. Obviously, the total must be kept within the recognized adhesion limits of the motorized axles and the rated capacity of the motors.

The motor rating must be selected with sufficient margin to perform the combined duty of acceleration and braking. In the case of self-ventilated motors, the extra heating is minimized by the fact that it takes place mostly at high speeds where the ventilating system is most effective.

Where two motor circuits are available for interconnection, they will pick up generating voltage very quickly and give a prompt brake response over a wide range of speed. In the case of single-motor equipments, the response is not so prompt, and field flashing is desirable.

Paper 45-84, recommended by the AIEE committee on land transportation for publication in AIEE Transactions. Manuscript submitted November 22, 1944; made available for printing February 21, 1945.

L. G. Riley and G. M. Woods are both with Westinghouse Electric Corporation, East Pittsburgh, Pa.

The amount of exciting current normally is not more than ten per cent of full load, and it can be removed as soon as braking is initiated, so that the added power requirement is negligible.

The typical behavior of a motor in building up the braking load is illustrated by the oscillograph record shown in Figure 2.

Dynamic-Brake-Control Characteristics

Another factor in the rapid extension of the use of dynamic braking has been the development of simplified control systems for initiating and regulating the braking load.

By adopting a permanent connection for each pair of motors whereby in both power and brake the relations of armature and field are interchanged with reference to the line, the series and parallel connections for power and the parallel connection with cross-connected fields for braking can be obtained with a minimum of switching equipment. Furthermore, the transfer from power to brake can be made without operating the reversing devices, and practically all of the switching and resistor equipment required for acceleration also can be used in brake regulation. Figure 3 illustrates in simplified form the relative arrangement of motor and resistor circuits.

In addition to the accelerating resistor steps in each motor circuit which are kept balanced in value at all times, the brake circuit is completed through a common loop which carries the combined current from both motors and includes resistor steps of a value which essentially doubles the total effective resistance in each motor circuit. This total amount is determined by the excess voltage to be absorbed when applying the brake at maximum speed.

In order to secure prompt build-up of the brake without separate excitation, it is customary to close the brake loop circuit through a high resistance each time power is shut off. This recaptures the residual volts before the flux has collapsed and immediately circulates a braking current of low value, not enough to cause any appreciable retarding effect, but sufficient to keep the motors in a responsive state. Brake application then is uniformly prompt, depending on the rate at which resistance is reduced in the loop circuit. This is known as the "spotting" system.

The basic cross-connection of motors, whereby each becomes separately excited, not only produces inherent stability and load equalization, but also avoids skidding, because any tendency on the part of one motor to lower its speed immediately reduces the field of the other motor. This in turn reduces the voltage being applied to the motor which has attempted to slow down by creeping. There is no sudden or complete loss of retardation.

The regulation of braking rates may be controlled either manually or automatically. Locomotives with varying train weights and grade conditions normally would be manually operated and the brake used principally for holding a controlled speed on long grades. Where grade or slowdown brake requirements exceed the locomotive adhesion limits, dynamic braking must be supplemented by the train brakes, and some provision is desirable to prevent applying the air brakes on the locomotive as long as the dynamic brake is operating.

Passenger vehicles in frequent-stop service require uniform braking, sometimes at relatively high rates, all of which is best accomplished with automatic current regulation. The operator's attention then is concentrated on the selection of the desired braking rate, no particular skill being required to produce a smooth stop.

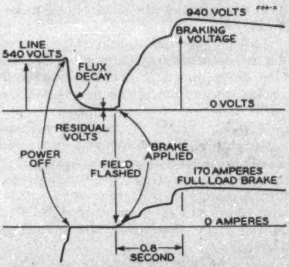

Figure 2. Motor voltage and current record of the transfer from power to brake operation

Figure 1. The Newell streetcar brake of the year 1900, comprising combined track and wheel-brake shoes, both energized with current generated by the traction motors

The minimum speed to which full-load braking can be maintained is determined by the internal resistance of the motor added to the resistance of the cables and switching equipment. For the average urban transit vehicle, this speed is two to three miles per hour, below which the brake fades out and disappears.

Selection of the total number of braking notches is governed by the same general factors as the selection of acceleration notches. Passenger comfort, slope of the motor saturation curve, maximum speed of application, bunching of slack in trains, adhesion limits, and minimum fade-out speed all require consideration. A study of Figure 4 shows that at high speeds the braking curves are very steep and can be spaced rather widely apart, whereas at low speeds they are relatively flat and require close spacing to hold the current increments within uniform acceptable limits. Obviously, the higher the braking rate, the greater the number of notches required.

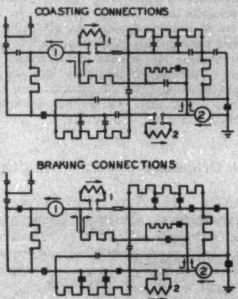

Figure 3. Standard motor circuit connections for power and brake operation, with pre-excitation by "spotting" in the coasting position

Many applications are based on an average braking load somewhat less than the full accelerating load and require the same number of notches for each, even though the speed range in braking may be twice the range over which the accelerating equipment is in operation. The apparatus required to control the braking, in excess of that used in acceleration, thus is held to a minimum.

Each application requires a careful study of the switching system and resistor-step values, if they are to be used to the best advantage in both power and brake operation.

Advantages and Economies in Operation

In making the fundamental decision as to whether or not dynamic braking should be included in any given application, the following benefits are to be considered:

1. Safety in operation, as provided by an effective brake system, in addition to the regular mechanical brakes.
2. The use of accelerating and braking resistor losses for heating the vehicle.
3. Simplification of the mechanical brake equipment.
4. A marked reduction in wear on brake shoes and wheel rims or brake drums, with less frequent adjustment and replacement.
5. Minimized skidding and side slipping under adverse rail or street conditions.
6. Better feeling of security on the part of operators.
7. Automatic regulation and graduation of the brake in making service stops.

Typical Applications and Results

THE PCC CAR

No dynamic-brake system has shown such phenomenal benefits as the equipment which is standard on all PCC streetcars, of which there are nearly 3,000 in operation and on order. Without such a system, the cushioned-wheel type of truck could not have been used because of the excessive heating and the massive brake rigging which would have been required to produce the high deceleration rates with mechanical brakes alone. Being independent of line power, this equipment is extremely reliable and makes possible the high schedule speeds for which the vehicle is designed.

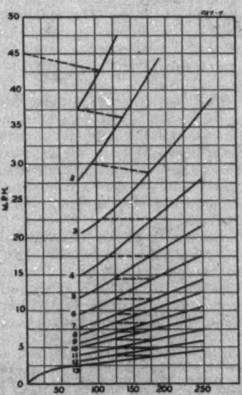

Figure 4. Typical dynamic-brake notching curves for service stops from maximum speed to three miles per hour

The converted energy of retardation, introduced into the ventilating system in the form of heat, provides adequate car heating without the use of supplemental heaters, in all except the most severe winter conditions.

A simple form of air brake and a magnet track brake supplement the dynamic brake. The latter normally is required only in emergency, and the light duty on the air-brake shoes has extended the life of brake shoes and the adjustment period to at least 15 times that for older types of streetcars.

The multinotch control developed for these cars produces exceedingly smooth brake performance, and deceleration rates as high as four miles per hour per second can be obtained with comfort. The "spotting" system of recapturing residual voltage for quick brake response is used to position the control in proportion to speed during coasting, so that the correct resistance value always is available for immediate full-brake application. The règulation is automatic with a wide selection of rates.

TROLLEY COACHES

With the prevailing tendencies toward high schedule speed, the necessary braking rates long since have exceeded the limitations of brake-drum and wheel-rim temperatures. Of the more than 3,500 trolley coaches in the United States, nearly half have included some form of dynamic or combined dynamic and regenerative braking. The results in operation compare favorably with those obtained on PCC cars, with an important increase in dependability and safety on slippery pavements. There has been a reduction in brake-block and brake-drum maintenance to about one fourth of that which existed when all braking is done mechanically.

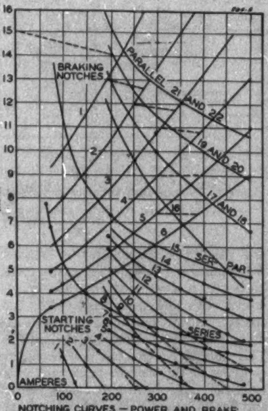

Figure 5. Complete locomotive starting and braking notching curves, with several brake-holding positions

HAULAGE LOCOMOTIVES

Braking conditions on material-handling systems, particularly in underground mining, are more severe than in any other branch of the traction industry. Grade and track conditions are extremely variable, and in many cases the cars have no power-brake equipment, all braking duty being concentrated on the locomotive itself. The advantages of a dynamic brake, supplementing the mechanical wheel-brake system, in safety and dependability have been demonstrated repeatedly. In open-pit mining, long grades frequently are encountered, and dynamic braking can be proportioned to absorb at least 50 per cent of the total braking effort required, with a corresponding increase in brake-shoe and wheel life on cars and locomotives.

Another notable application is the use of a dynamic holding brake on Diesel-electric main-line locomotives in high-speed mountain grade service.

Figure 5 shows the combined acceleration and braking performance curves for a haulage locomotive with several manually selected brake-holding notches.

RAPID TRANSIT

In this field dynamic braking has not yet found any general application. However, it is reasonable to anticipate that future extensions will follow the trend toward faster schedules and higher braking rates. The problems associated with brake-shoe dust, wheel wear, and skid flats will become increasingly critical, and dynamic braking will have definite advantages in this respect. Furthermore, uniform braking on all wheels in the train will be assured.

Summary

The many proved benefits to be realized in the use of dynamic-braking systems bear a most favorable proportion to the nominal amount of additional apparatus involved. They are applicable to practically all branches of the land-transportation industry.

Control of Electrical-Insulating Varnishes

D. L. GIBSON
ASSOCIATE AIEE

C. H. BRAITHWAITE
ASSOCIATE AIEE

Synopsis: Varnish treatment of electrical equipment is an important step in its manufacture. Varnish coatings protect apparatus from moisture and dirt and maintain the high electrical-insulating level required for insulation. The quality of the varnish film deposited depends upon the condition of the varnish in the processing tanks. Thickness of deposited varnish films varies with viscosity and body. Heavy films interfere with armature-coil sizes and make problems of heat transfer in field coils and magnet coils more difficult. Thin films give inadequate protection from moisture and dirt. Conducting contaminating materials are introduced into the tanks from rehabilitated apparatus and manufacturing atmosphere. These indicate that close control of tank varnish is necessary for consistently high quality of apparatus treated. Methods of control are discussed which include both laboratory tests of the varnish and physical tests which can be concluded at the tank. A system of daily inspection of tanks for proper quality and daily adjustments before use is described. Dielectric properties of the varnish film and the liquid varnish and periodic chemical analysis of samples from each tank reveal the condition of the varnish. A system of portable cold pressure filtering for removing much of the contamination present is described. It should be recognized by the electrical industry that insulating varnishes are complex chemical mixtures, and care should be maintained in their use. It is important that they be under the control and supervision of persons with the proper training and experience. Constant quality control is necessary for satisfactory results.

THE PROTECTIVE CAPACITY of varnish on electric equipment depends upon the quality of the varnish in which the apparatus is treated. Proper maintenance of varnish requires consideration of many factors. Modern synthetic varnishes are a complex combination of resins and solvents which must be properly controlled. The quality of the varnish film depends on many factors including the viscosity–body relationship, the degree of polymerization of the resins, chemical composition of the resin, and the purity of the film. There is a tendency for insulating varnish to become contaminated with various foreign materials in the course of its use. Contaminants seriously impair the insulation value of the varnish and lower the reliability of the electrical equipment treated.

Certain difficulties in manufacture may be overcome by proper control. For example, certain coils treated in varnish of excessive viscosity may result in oversize conditions due to deposition of heavy varnish films. Improper varnish treatments may cause unduly high temperature rises. Troublesome effects of poor varnish treatment may become apparent during factory tests or when the machine is in service.

Chemical Changes in Varnish

Body, viscosity, and specific gravity of varnishes are interdependent. Body is the per cent nonvolatile material (resin, drying oil, plasticizer) in the varnish. Deposition of the nonvolatile material from the solvent forms the varnish film.

Viscosity is a measure of the resistance of a fluid to flow. Viscosity is dependent upon the body of varnish and also upon the degree of polymerization—that is, the average chain length of varnish resin molecules. Polymerization in turn is a factor in the aging of varnish resins. Specific gravity is a measure of the amount of solid material in a given solvent. The amounts of solvent and solids, and the condition of resin may be interpreted by means of these tests.

For example, an increase in viscosity and specific gravity from a given standard usually means a loss in solvent. Adjustments of solvents are easily made. However, a continued increase in viscosity with the percentage solids and specific gravity remaining the same denotes a chemical change in the varnish. This indicates a gradual polymerization or aging of the varnish resin. In practice, the tank varnish becomes thicker and has to be cut back with solvents repeatedly to insure smooth coating. The percentage solids soon becomes low as a result of addition of solvents, and a thin varnish film with poor physical properties is deposited, which does not impart adequate insulation protection.

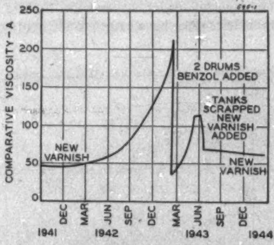

Figure 1. Comparative viscosity of synthetic varnish in toluol; viscosity versus time

Figure 1 gives comparative viscosity of a tank of synthetic varnish over a period of 29 months. Comparative viscosity is a method of comparing the viscosity of a varnish at a particular body to a viscosity at a reasonable standard reference body for the same varnish. Gradual rises in the curve with time show an increase in the degree of polymerization or aging of the resin. Eventually, the physical properties of the film deposited become so poor that the varnish must be scrapped. If one refers to the curve, 50 is the index for varnish in good condition. After nine months there is a steady rise in comparative viscosity to 130 (14 months after start). At this time the physical properties are definitely below standard.

If viscosity and specific gravity of tank varnish are allowed to increase owing to solvent losses without adjusting to a given standard, a thicker varnish coat is deposited. Thick coatings on armature coils result in difficulty in winding in slots because of their being oversize. Too heavy coats deposited on field coils and magnet coils decrease the rate of heat transfer and result in higher temperature rises. Table I gives the thermal conductivity of a magnet coil in degrees rise per watt after successive coats of varnish.

In general, film thickness is dependent upon viscosity, whether viscosity is adjusted by solvent or by heating the varnish. Figure 2 gives varnish build-up versus viscosity of a synthetic varnish (in toluol solvent) deposited on copper, paper, and fiber glass. Note that on glass a rise in viscosity from 35 seconds to 100 seconds deposits a film 30 per cent thicker.

It is apparent that a proper body–viscosity relationship must be maintained in the tanks to insure efficient treating results.

Contamination

In the usual electrical-manufacturing plant the varnish tank is open during use and is located in the center of the manufacturing activities, and the apparatus or coils to be coated are themselves not perfectly clean. Under such conditions a certain amount of contamination is unavoidable.

Previous work by the authors[1] indicates there are three mechanisms of contamination of the varnish. The contaminant may be washed from the piece while it is immersed in the varnish tank. This means the suspension of particles of a

---

Paper 45-95, recommended by the AIEE committee on electric machinery for publication in AIEE TRANSACTIONS. Manuscript submitted November 2, 1944; made available for printing March 12, 1945.

D. L. GIBSON and C. H. BRAITHWAITE are insulation development engineers, transportation and generator division, Westinghouse Electric and Manufacturing Company, East Pittsburgh, Pa.

The authors are indebted to T. J. Schrimser, L. R. Hill, M. W. Rider, P. B. Demmler, and associates, for advice on test methods and removal of contaminants.

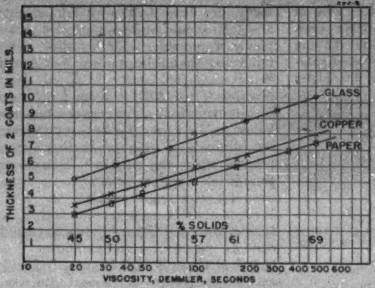

Figure 2 (left). Synthetic alkyd varnish, toluol thinner, build-up of film versus viscosity

All samples drained at 28 degrees centigrade

Figure 3 (right). Correction of viscosity to a base temperature of 25 degrees centigrade

Viscosity at temperature × viscosity factor = viscosity at 25 C

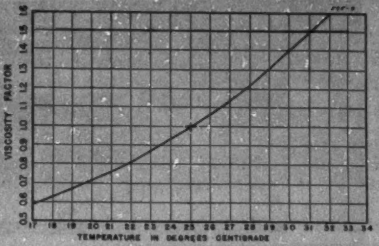

particularly troublesome nature in the varnish. For example, when rehabilitated armatures are being processed, some of the dust and dirt accumulated in field industrial use is washed into the varnish tanks on immersion of the apparatus.

A second means of contamination is through the air. Carbonaceous dust metal chips of small diameter, small droplets of paint from nearby spray booths, and other foreign material may enter the varnish when the tank lid is open. Each varnish-treating room is equipped with overhead cranes and lifts which are additional possible sources of contamination. Also material foreign to the varnish may be added by mistake. The addition of a varnish whose resin is only slightly soluble in the varnish and solvent in the tank is an example. Here the foreign resin would be precipitated out, possibly as troublesome colloidal particles.

Contaminants generally may be classified as conducting and nonconducting. Carbonaceous dust, lint, metal particles, and electrolytes are offenders as conducting contaminants. These often are introduced by apparatus being processed, but can be present due to the manufacturing atmosphere. Nonconducting particles are represented by wood chips and precipitated or polymerized resins, pieces of cotton, and asbestos and mica dust. This type of material comes from pieces of insulation washed off the coils and wound apparatus on immersion in the varnish bath.

Contamination may be classified into three types by use of wet and dry dielectric tests and heat-endurance tests Conducting particles lower wet and dry dielectric strength and generally impair the heat endurance of the varnish film. A second type is identified by a high dry dielectric strength, a low wet dielectric strength, and a low heat endurance. Contamination producing varnish gels or precipitated resins might not lower the dielectric strength but would lower the heat endurance or life of the varnish film.

Disruption of the varnish film by particles of foreign matter seriously impairs the properties of the insulation. On electrical equipment there is no need to mention the effect of conducting or ionizing particles on the dielectric breakdown value, particularly when they become imbedded in the insulation. In some cases, although the particles are not conducting, they cut into the insulation during processing, lowering the breakdown level of the material. In addition, the initial mechanical strength and life or endurance of the varnish film are reduced when foreign materials contaminate the varnish.

Thus, it is important to keep varnish for treating electrical equipment as clean from foreign material as possible. As a base or goal, the electrical properties and mechanical properties should be kept in the same order of magnitude as those of the new varnish.

Varnish Tests

To control the varnish adequate tests must be worked out which reflect the condition of the tank. Some of these are of a type which permit testing at the tank itself, whereas others require sampling of the varnish and testing in a chemical laboratory.

Those test methods which are practical to apply at the tank must be simple and require only a short time to perform. Viscosity and specific-gravity measurements fit easily into a daily inspection routine. Viscosity measurements may be made by one of several methods. The simplest of these involves the use of a cup with a calibrated orifice in the bottom which allows varnish to flow in or out at a definite rate. The time a definite volume of varnish fills or empties from this cup may be taken as a measurement of viscosity. Another method is to fill a convenient-length transparent tube with varnish. A small bubble is left at the top. When turned end for end the bubble rises slowly. The time required by the bubble to travel a certain distance is a measure of viscosity. However, a number of tubes with liquids of known viscosity may be used. The rate of rise of the bubble in the tube of tank varnish will be approximately the same as for one of the bubbles in a tank containing a liquid of known viscosity. The viscosity of the tank varnish is taken as the same as the liquid whose bubble rises at the same rate.

Viscosities with the cup or tube methods may be reported directly in seconds and will be comparable to other determinations made with the same apparatus. This is the most convenient arrangement.

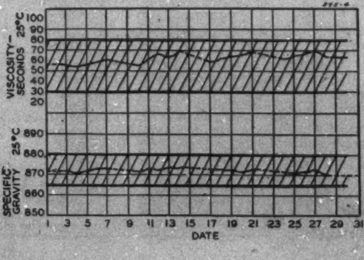

Figure 4. Daily varnish checks in tank of oleo resinous varnish, April 1 through April 30, 1944

Shaded area shows limit specified

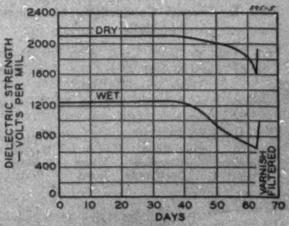

Figure 5. Wet and dry dielectric strength of heat-reactive varnish

Figure 6. View of the portable pressure filter showing the perforated stainless-steel filter plates

However, conversion to classical viscosity units may be made easily.

Specific gravity is taken easily with a hydrometer. Precautions should be taken to prevent bubbles in the varnish sample from contributing to erroneous results. Care should be exercised that the spindle be read at the surface of the liquid, not at the "high-tide" mark of the varnish.

Both specific gravity and viscosity are dependent upon temperature. Corrections to a standard base temperature are simple and should be made in all cases to provide a common basis of discussion. A value of 25 degrees centigrade is recommended as the standard base (refer to Figure 3 for a typical correction curve). The combination of viscosity and specific gravity, however, give many useful indications. Although samples for body may be taken at frequent intervals, this test requires an oven and despite its simplicity must be classified as a laboratory test.

Samples for laboratory tests should be taken at convenient and regular intervals. A number of tests have proved significant. Body of course is determined easily by evaporating the solvent and weighing the remaining resin. Body determination should be made more frequently than other laboratory tests since the information obtained is useful for correlation with the daily viscosity–specific-gravity determinations.

Table I. Thermal Conductivity of Magnet Coils

Tests Made on Same Coil, With No Outer Coat of Varnish, and With One, Two, and Three Varnish Coats

Each Test Is an Average of Three Temperature Runs

Varnish Treatment	Rise, Degrees Centigrade	Watts Input	Degrees Rise Per Watt
No outer coat	77.5	29.2	2.65
One dip coat	82.5	29.2	2.83
Two dip coats	85.5	29.3	2.92
Three dip coats	86.0	28.4	3.02

Other properties of varnish are not evaluated so easily. Wet and dry dielectric strengths of varnish films on copper panels, hardness of varnish cakes, heat endurance, oil resistance, and drying time all are important.[2] Many of these tests are affected by dust-laden atmospheres, by humidity conditions, and by temperature. They should be performed in a dust-free and moisture- and temperature-controlled room.

Dielectric strengths and heat endurance of varnish films have become important measures of the degree of varnish contamination. Heat endurance is determined by depositing varnish films 0.002 inch thick on copper strips 0.005 inch thick.[2] These are heated continuously at 150 degrees centigrade for accelerated tests, as suggested by Frost and Moses.[3] The time to produce failure of the film on bending about a one-eighth-inch mandrel is reported as the heat endurance of "flexing life." Dielectric tests consist of measuring the dielectric breakdown strength of a 0.002-mil-thick varnish film on each side of a 0.005-inch-thick copper sheet as received dry and after immersion in water for 24 hours.

Hardness measurements are made on varnish cakes at least one eighth inch thick with a Shore durometer *A*.[5] The measurements are taken after three hours bake at 135 degrees centigrade and again after six hours at 135 degrees centigrade. A further durometer measurement after 48 hours in oil at 110 degrees centigrade allows evaluation of the oil resistance of the varnish. These measurements are dependent upon temperature, and tests should be in a controlled atmosphere if possible. Drying time determinations should be made as per American Society for Testing Materials specifications (*D*115–39*T*).[2] A one-mil varnish film is deposited on a copper plate and baked at 110 degrees for baking varnishes. At intervals a strip of kraft paper is pressed upon the surface. The drying time is taken as that time when the paper does not stick to the panel.

From these data a representative picture of the condition of the tank varnish can be drawn. Contamination and chemical changes can be noted quickly and steps taken to compensate for these changes where necessary. Table II consists of a typical report on laboratory varnish tests.

Inspection System

An inspection system is essential to insure proper quality control of tank varnish. Inspectors should be assigned the responsibility of checking and adjusting varnish tanks and inspecting new varnish to be added to tanks. Each active tank should be checked for viscosity and specific gravity daily. It is not enough merely to inspect; tanks must be adjusted daily within definite limits by addition of solvent or new varnish. If tanks are not within the proper limits of viscosity and specific gravity, they should not be used until proper adjustments are made.

Limits of viscosity and specific gravity are set for each type of treatment and each type of varnish in the tank. Daily examinations should be made of the varnish for dirt, varnish skins, or gels. All varnish should come within specifications in all characteristics before addition to tanks. A single drum of overpolymerized varnish can initiate rapid polymerization throughout a large tank which may lead to scrapping. Daily records or curves may be kept of each tank with additions of solvent and new varnish indicated. At the end of each month a report on the condition of the varnish tanks should be made to interested parties. By the use of curves viscosity and specific-gravity trends can be followed and the necessity for adjustments readily seen.

Figure 4 is a record of the inspector's

Table II. Varnish Tests

Sample 58

Body	53.56 per cent
Specific gravity	0.985
Viscosity (Demmler 1) (25 C)	132 seconds
Drying time (ASTM at 110 C)	2 hours
Hardness varnish cake at 25 C (durometer *A*):	
3 hours bake at 135 C	2
6 hours bake at 135 C	24
48 hours in oil at 110 C	29
Flexing life (150 C)	60 hours
Wet dielectric	900 volts per mil
Dry dielectric	1,800 volts per mil

monthly report on specific gravity and viscosity of a tank of synthetic varnish. Note limits of viscosity and specific gravity for that particular tank.

In addition periodic chemical laboratory examinations should be made of every varnish tank to follow changes in electrical and mechanical properties. All of this is insurance against improper treatment of equipment. The benefits are apparent in the improved appearance of coils and wound apparatus and improved performance. Actual economies are hard to estimate.

Varnish and solvent added must be carefully mixed into the tank. Improperly mixed solvent will rise to the top in a separate phase, whereas the more viscous and dense varnish will tend to form a layer at the bottom of the tank. Either phenomenon results in stratified layers each with its own viscosity and body. Such a tank will not deposit consistently good protective films. This condition may be remedied by simple but thorough mixing of each drum into the tank as it is added.

Figure 8. Varnish inspector's test material

These include: stop watch, viscosity measurement cup, thermometer, hydrometer

Filtration

Careful control of the varnish requires an adequate filtration method.[1,4] The materials used in varnish manufacture are critical, and maintenance of the varnish in usable condition is essential. The particle sizes of contaminants range from large pieces of wood to colloidal carbon. Pieces of metal as small as 0.003 inch in diameter have been found. A study of the available methods suggested that the most efficient method of reclamation of the varnish and conservation of critical materials is by cold pressure filtration.

Figure 9. A Shore durometer for testing hardness of the varnish

Figure 7(below). Dielectric and heat-endurance panel

The dielectric panel has been slit to facilitate measuring thickness of the varnish film. Cracks in varnish film on heat-endurance strips indicate failure of the varnish

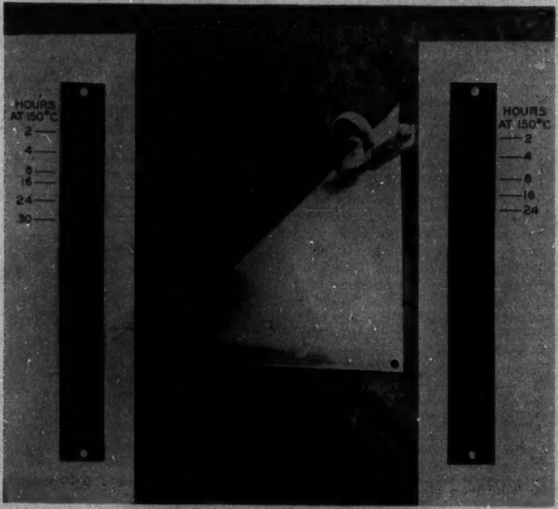

A portable-type pressure filter, consisting of a number of plates arranged vertically and enclosed in a shell, has been found to be satisfactory. Pressures of 15 to 28 pounds per square inch are used, with rates of flow varying from one to five gallons per minute depending upon the pressure, amount of cake, and viscosity of filtrate.

Filtration is carried out using a diatomaceous earth as a filter aid. This is particularly necessary as some of the contaminating material filtered out is a gel and quickly fills up the pores of the filter medium. The addition of filter aid allows a porous cake to build up which is not so easily clogged as the filter medium alone. In order to avoid addition of the filter aid to the large varnish tanks small portable tanks may be set up in which the diatomaceous earth may be mixed continuously with the incoming varnish stream. Varnish is pumped from here through the filters and into a clean tank in the system.

The efficiency of the filtering treatment is judged by a series of chemical and physical tests on samples taken before and after filtration. Percentage of body, viscosity, and specific gravity show whether or not there is a loss of solvent or varnish resin during the filtering operation. The results of the heat-endurance tests and dielectric tests before and after the operation show whether or not harmful foreign materials were present and have been removed.

Improvements in dielectric properties produced by filtering the varnish are remarkable. A typical increase in dry dielectric strength in the order of 30 per cent and in the wet dielectric strength in the order of 70 per cent was found (see Figure 5). Heat endurance and the mechanical properties of the varnish improved from 10 to 20 per cent upon filtering. In one case a badly contaminated sample was filtered with a resulting improvement in heat endurance of over 100 per cent. Plastic asphalt-type varnish improved in this characteristic over 40 per cent after filtering. An increase in heat endurance indicates that particles of colloidal matter which damage the varnish film have been removed. It is apparent that the type of contaminant depends upon the material treated in the tank. The length of time between filtering operations depends upon the use or activity of the tank.

Filtration in itself would be of no avail if the filtered varnish is pumped back to become recontaminated by dirty tanks. Tanks should be cleaned periodically; frequent filtrations provide an opportune time for cleaning.

Conclusions

Thus a system of varnish control which includes testing and inspection of varnish and methods of maintenance is essential in sustaining the quality of insulating varnishes. Such a system will reduce the number of possible sources of electrical failures in shop testing and in the field. In addition it will eliminate certain manufacturing problems. The economies resulting from longer use of the varnish are difficult to estimate. This control and filtration system is a step forward in the conservation of critical varnish materials. It should be recognized by the electrical industry that insulating varnishes are complex chemical mixtures, and care should be exercised in their use. Persons of the proper training and experience are required for their supervision. Constant quality control is necessary for satisfactory use of insulating varnishes.

References

1. MAINTENANCE OF QUALITY IN INSULATING VARNISHES CONSERVES CRITICAL MATERIALS, D. L. Gibson, C. H. Braithwaite. *Chemical Industries*, volume 55, number 1, July 1944, pages 70–2.

2. American Society for Testing Materials STANDARDS ON ELECTRICAL-INSULATING MATERIALS, American Society for Testing Materials committee *D*-9, February 1944.

3. SYNTHETIC-RESIN VARNISH—ADVANTAGES FOR COIL INSULATION, L. E. Frost, G. L. Moses. *Product Engineering*, March 1942, pages 144–6.

4. THE CONTROL, SPECIALIZED TESTING, AND USE OF SOME MODERN INSULATING MATERIALS, A. R. Dunton. *Journal* Institution of Electrical Engineers (London, England), volume 90, part 1, November 1943, pages 463–70.

5. SYMPOSIUM ON RUBBER, American Society for Testing Materials, March 9, 1932, pages 93–102.

6. VARNISH MAKING, Oil and Color Chemists Association (papers presented at London convention 1939). Chemical Publishing Company, 1940.

Statistical Tools for Controlling Quality

JOSEPH MANUELE
MEMBER AIEE

CASPER GOFFMAN
NONMEMBER AIEE

THE MANUFACTURER is always faced with the problem of getting the maximum output from his available equipment, material, and man power. This means operating with a minimum amount of scrap production or producing a minimum amount of products which fall outside of specification limits and which will require reworking. But since tools of production are subject to wear, and since materials vary in quality or characteristics, the manufacturer must have a means of predicting the probable quality of products he is likely to get sometime in the future.

Having satisfied himself that his quality is satisfactory now, he wants to be able to control or maintain that quality indefinitely, or as long as that particular product is made. This prediction must be clear and definite enough to serve as the basis for action to remove assignable causes which if not removed will result in the production of parts outside of specification limits.

Furthermore, in modern mass production where several tools perform the same operation, as with multicavity molds and gang cutters, the manufacturer wishes to know if there is any significant difference in the quality of products coming from different cavities in the same mold or from different cutters in the same setup involving a number of cutters on the same machine.

The Frequency Distribution

In a manufacturing process, it is desirable to know, as soon as possible after production is started, what the quality of the product is likely to be. The "frequency distribution" is a simple way of obtaining this information. By measuring the quality characteristic in question on a number of pieces produced at the start of a run, a simple computation can be made to show the range within which measurements are most likely to fall for the subsequent production. Comparison of these limits with the tolerance limits shows whether the process should be allowed to continue or if a change in the setup is required. The data obtained from the screw-machine part, shown in Figure 1, illustrate the frequency distribution.

A sample of 50 pieces was taken and each piece was measured for over-all length, which was required to be 4.450 inches ± 0.010 inch. The measurements obtained are shown in Table I.

The data in Table I do not give much information in their present form. However, the data can be reorganized as shown in Table II so as to become very enlightening. A survey of the data shows that exactly 16 pieces were 4.450 inches long, eight pieces were 4.451 inches long, nine pieces were 4.449 inches long, and so on.

Such a table is called a *frequency distribution*. It indicates the number, or frequency of occurrence, of measurements in each size. In practice, the pieces may be tallied as they are measured, as is shown in Figure 2. This gives visual meaning to the frequency distribution. It will be noted that the distribution is bell-shaped and symmetrical about the center, high in the center, and falls off sharply at both ends. The envelope curve of the tallied marks is known as the *frequency curve*. For best-quality production the frequency curve must lie totally within the specification limits.

Figure 3 shows the frequency curve, for this part, in relation to the specification limits. It is evident, in this case, that the process is capable of producing good pieces and will continue to do so provided nothing happens to change the shape or location of the frequency distribution. A periodic check of five pieces per hour on this item, suffices to show whether the frequency distribution remains unchanged. If the distribution does remain unchanged the entire production is considered to be within toler-

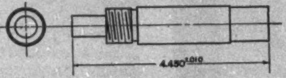

Figure 1. Screw-machine part

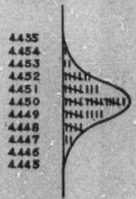

Figure 2. Frequency curve of 50 measurements on screw-machine part shown in Figure 1

Paper 45-99, recommended by the AIEE subcommittee on applications of statistical methods of the Standards committee for publication in AIEE TRANSACTIONS. Manuscript submitted December 15, 1944; made available for printing March 20, 1945.

JOSEPH MANUELE and CASPER GOFFMAN are both with Westinghouse Electric and Manufacturing Company, East Pittsburgh, Pa.

Table I. Fifty Measurements on Screw-Machine Part Shown in Figure 1 (Inches)

1.	4.450	14.	4.451	27.	4.450	40.	4.450
2.	4.449	15.	4.448	28.	4.450	41.	4.449
3.	4.449	16.	4.450	29.	4.448	42.	4.447
4.	4.450	17.	4.451	30.	4.450	43.	4.448
5.	4.452	18.	4.451	31.	4.450	44.	4.449
6.	4.452	19.	4.452	32.	4.450	45.	4.449
7.	4.451	20.	4.454	33.	4.448	46.	4.450
8.	4.452	21.	4.453	34.	4.449	47.	4.451
9.	4.451	22.	4.450	35	4.450	48.	4.450
10.	4.451	23.	4.450	36.	4.450	49.	4.448
11.	4.452	24	4.453	37.	4.452	50.	4.449
12.	4.452	25	4.449	38.	4.450		
13.	4.451	26.	4.447	39.	4.449		

Table II. Frequency Distribution of 50 Measurements on Screw-Machine Part Shown in Figure 1

Length of Piece (Inches)	No. of Pieces
4.455	0
4.454	1
4.453	2
4.452	7
4.451	8
4.450	16
4.449	9
4.448	5
4.447	2
4.446	0
4.445	0

ance limits, and final inspection may be dispensed with. The central location of the frequency distribution with respect to the specification limits and its narrowness compared to the tolerance range guarantee that the product is of high quality.

The shape and position of a frequency curve with respect to the specification limits are indicative of assignable causes which must be corrected if products being produced are to be kept within specification limits. Two types of curves most frequently encountered are shown in Figure 4A and Figure 4B.

Figure 4A is an example of a process for which the band spread, or the variation from part to part, is narrow enough to produce a good product, but the machine is not properly adjusted. In other words, the frequency distribution is not centralized with respect to tolerance limits. As a matter of fact, this distribution was obtained, at an earlier stage of the process when the machine was being set up to produce the part, the distribution of which is shown in Figure 3.

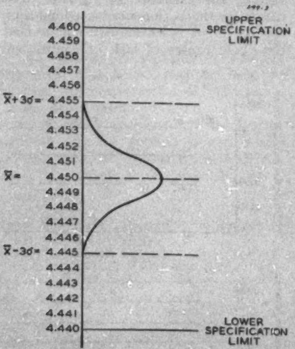

Figure 3. Relative position of frequency curve of the process relative to the specification limits shows good statistical control

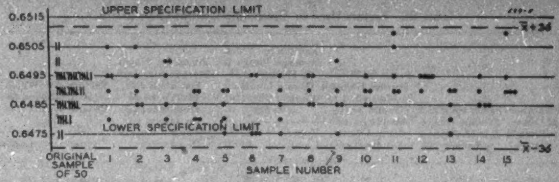

Figure 5. Typical control chart for samples of five pieces, showing individual observations

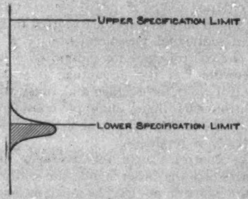

A. Process not centralized

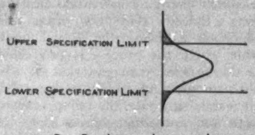

B. Band spread too wide

Figure 4. Typical frequency curves showing assignable causes

Figure 4B illustrates a frequency distribution which has a wider band spread than the tolerance range. Such a situation may be easily remedied. A few assignable causes indicated by a wide band spread are worn bearings in the machine, flimsy and unstable fixtures, and excessive variation in hardness of stock.

It should be apparent from the foregoing discussion that a frequency distribution has two characteristics which are of practical importance, the "central tendency" and the "amount of band spread" or degree of dispersion. These characteristics may be represented numerically by the mean, $\bar{X}$, and standard deviation, σ. The standard deviation is merely the root-mean-square value of the deviations. Another characteristic of a frequency distribution is its skewness, or amount of deviation from symmetry, but we are not particularly interested in this at present. A normal process will have a distribution which is nearly symmetrical. Statistical tests exist for symmetry, but one is often able to judge by sight whether or not a given frequency distribution is sufficiently symmetrical for purposes of controlling quality.

The Control Chart

After control of quality has been achieved by means of the frequency distribution, and production is under way, it is necessary to maintain this control in order to avoid the production of defective parts. The control chart is the tool used for maintaining this control; it is a take-off from the frequency distribution. It is necessary to calculate the mean, $\bar{X}$, and standard deviation, σ, from the frequency distribution in order to establish limits for the control chart. In many cases a rough approximation of the control limits may be obtained from an inspection of the frequency distribution.

After it has been established that $\bar{X}$ and σ are satisfactory for the process, and a control chart has been constructed, a periodic check of, say, five pieces is sufficient to detect tendencies toward loss of control. The time interval between samples may be an hour or a day, or a sample might represent a batch of material. The choice of samples is governed by such factors as tool wear, skill of operator, closeness of specification limits, and rate of production. Practically all measurements made on samples should fall within a distance of 3σ from $\bar{X}$, or within the "control limits." If any measurements fall more than 3σ from $\bar{X}$, this is a strong indication that a change has occurred in the process at those points which has changed the frequency distribution.

As an illustration, consider the data of Figure 5, which were obtained from a dimension on the breech block of an antiaircraft gun. The dimension is 0.6495 inch ± 0.002 inch. As shown in the figure, a frequency distribution of 50 measurements was obtained and $\bar{X}$ and σ computed. The results of this computation are $\bar{X}=0.6491$ inch and $\sigma=0.0007$

Table III. Factors Used in Computing Control-Chart Limits

Number of Observations in Sample	Factor by Which Average Range $\overline{R}$ Is Multiplied to Obtain 3σ	Factor by Which Average Range $\overline{R}$ Is Multiplied to Obtain $3\sigma/\sqrt{n}$ for Limits on Control Chart for Average	Factors by Which Average Range $\overline{R}$ Is Multiplied to Obtain Limits on Control Chart for Range		Factor by Which Average Standard Deviation σ Is Multiplied to Obtain $3\sigma/\sqrt{n}$ for Limits on Control Chart for Average	Factors by Which σ Is Multiplied to Obtain Limits for σ Chart	
			Upper Limit	Lower Limit		Upper	Lower
3	1.77	1.02	2.57	0	2.39	2.60	0
4	1.46	0.73	2.28	0	1.88	2.33	0
5	1.29	0.58	2.11	0	1.60	2.13	0
6	1.18	0.48	2.00	0	1.41	2.00	0
7	1.11	0.42	1.92	0.08	1.28	1.90	0.10
8	1.06	0.37	1.86	0.14	1.18	1.83	0.17
9	1.01	0.34	1.82	0.18	1.09	1.77	0.23
10	0.97	0.31	1.78	0.22	1.03	1.72	0.27

Table IV. Turbine-Blade-Edge Thickness Above Nominal (Inch)

	Cutter 1	Cutter 2	Cutter 3	Cutter 4
Cam 1	0.004	0.004	0.009	0.016
Cam 2	0.008	0.010	0.015	0.022
Cam 3	0.007	0.008	0.010	0.015
Cam 4	0.009	0.009	0.012	0.018
Cam 5	0.009	0.011	0.022	0.027
Cam 6	0.004	0.007	0.013	0.017

inch. Thus $\overline{X}-3\sigma=0.6470$ inch, and $\overline{X}+3\sigma=0.6512$ inch. Dotted lines are drawn at $\overline{X}-3\sigma$ and $\overline{X}+3\sigma$. These are called "control-chart limits." In this example 15 samples each containing five measurements were then obtained—a sample a day for 15 consecutive days. As is apparent from the chart, all 75 measurements fall within the control-chart limits. The process accordingly is considered to be "in control."

In this particular example, the control-chart limit falls below the lower specification limit by 0.0005 inch. Hence, although the process is consistent—therefore, in control—it is not quite centralized and has a slightly too wide band spread. Accordingly, the process will produce some defective pieces, and adjustments should be made to assure that all pieces are within specification limits. This emphasizes the fact that there are three statistical requisites of a process—control, centralization, and small band spread.

Figure 6. Control chart for "average" and "range"

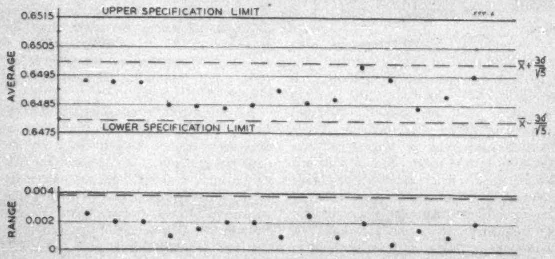

It should be noted that every measurement of the five pieces in each sample actually is plotted on the chart. This is in contrast to the standard control chart on which only averages are plotted rather than individual measurements.

The control chart for individual measurements has the advantage over the control chart for average and range that control-chart limits may be considered to be the limits within which the process actually is producing.

In control charts for averages and ranges, on the other hand, the control-chart limits do not have so much meaning to the man in the shop as they have in the control charts for individual measurements. Indeed, they are often misunderstood as being the actual limits within which the process is producing. For this reason we suggest that at least until a program of statistical control is well established in the shop control charts for individual observations be used.

In a control chart for averages, charts are run simultaneously for "average" and for "range" or "standard deviation." "Range" is simpler to calculate than "standard deviation" and will be used here. In Figure 6 we have such a control chart for the data of Figure 5. The average was computed for each of the 15 groups of five measurements, and the results are plotted on the "average" chart. The ranges are plotted on the "range" chart.

Table V. Showing Calculation of Between-Column Variance and the Ratio of Between-Column Variance to Within-Column Variance (Inch)

	Cutter 1	Cutter 2	Cutter 3	Cutter 4
Cam 1	0.004	0.004	0.009	0.016
Cam 2	0.008	0.010	0.015	0.022
Cam 3	0.007	0.008	0.010	0.015
Cam 4	0.009	0.009	0.012	0.018
Cam 5	0.009	0.011	0.022	0.027
Cam 6	0.004	0.007	0.013	0.017
Totals	0.041	0.049	0.081	0.115
$\overline{X}_{cu}$	0.0068	0.0082	0.0135	0.0192

$$\overline{\overline{X}}_{cu}=\frac{\sum_{1}^{4}\overline{X}_{cu}}{4}=0.0119$$

The between-column variance is

$$\frac{6\Sigma(\overline{X}_{cu}-\overline{\overline{X}}_{cu})^2}{(4-1)}=0.0001911 \text{ inch}$$

The within-column variance is 00001350 inch.

$$\frac{\text{Between-column variance}}{\text{Within-column variance}}=\frac{0.0001911}{0.0000135}=14.1$$

Obviously, averages of five measurements obtained from a process will not deviate from each other by as much as will the individual measurements themselves. The control-chart limits for averages accordingly must be drawn much closer together than for individual measurements. For averages of five, the factor of shrinkage is $\sqrt{5}$. The control-chart limits for averages are therefore $\overline{X}-(3\sigma/\sqrt{5})$ and $\overline{X}+(3\sigma/\sqrt{5})$. If the values $\overline{X}=0.6489$ inch and $3\sigma=0.0023$ inch are substituted, the control-chart limits become 0.6479 inch and 0.6499 inch. Factors for computing these limits and limits for the range chart are given in Table III.

It should be stated that the control chart frequently is used in such a way as actually to tell the source of trouble as well as the existence of trouble. The reason for this is that most machine-shop operations are essentially so simple that the likely causes of lack of control are

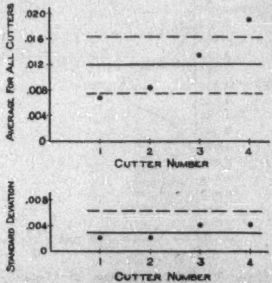

Figure 7. Control chart for between-cutters variance

few in number and are known beforehand, and it is easy to discern which will manifest itself as a lack of control of ranges and which as a lack of control of averages.

For example, we mention briefly a grinding operation on bars of rectangular stock which were running off as much as 0.004 inch. This was considerably excessive. The operation was performed by placing about 50 bars on a magnetic chuck and grinding with a circular motion. Two most likely causes of variation were dirt on the chuck and a variation in the distance to which the grinder was run down each time. A control chart for average and range was kept on the operation by taking groups of five bars at random from the 50 ground at each grinding. The first cause of variation obviously would show "range" out of control on the chart, and the second cause would show "average" out of control. The control chart showed both average and range out of control. By proper cleaning of the chuck, range was brought into control. Average was brought within control when steps were taken to assure that the grinder ran down to the same position each time. With a control chart on the operation to show that the right practice is being continued, the dimension is now held to 0.001 inch.

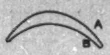

Figure 8. Sectional view of turbine blade

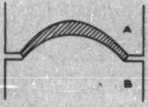

Figure 9. Showing method of gauging edge thickness of turbine blade

The Analysis of Variance

The analysis of variance is another statistical tool which may be used to uncover the existence of assignable causes of variation in a product. The type of shop problem to which this method may be applied is one where several tools or machines perform the same operation. For example, in a multicavity molding operation it may be that, due to differences between cavities, there is a variation in the product significantly greater than that which would exist if all the cavities were alike. It is true that tools which are supposedly alike do not always perform similarly.

Table VI. Data Collected After Regrinding Cutters

Compare With Table IV

Cutter 1 (Inch)	Cutter 2 (Inch)	Cutter 3 (Inch)	Cutter 4 (Inch)
0.002	0.003	0.002	0.008
0.003	0.010	0.004	0.004
0.008	0.006	0.002	0.004
0.003	0.006	0.003	0.003
0.008	0.010	0.010	0.018
0.003	0.007	0.001	0.006

One method of analyzing such a problem is by making a control chart, as shown in Figure 7. The standard deviation is computed for each tool, or cavity, and for the whole process. The control chart shows the average for the process and for each tool. Another statistical method which lends itself to this type of problem is the analysis of variance. We shall now illustrate this method, giving the calculation in detail.

An example of this type of problem is a drum-mill operation on turbine blades. The drum mill consists of a circular drum with six rows of pockets equally spaced around the circumference. Each row contains four pockets, making a total of 24 pockets, each holding a blade; there are six cams, one for each row, and four cutters, each of which cuts six blades, one from each row, as the drum rotates. Variations in the product can be caused by differences between cutters, between cams, or between the pockets themselves.

Figure 8 shows a cross-sectional view of the blade. The drum-mill operation considered consists of forming the surface *A*. This is called the "convex" of the blade. The surface *B*, called the "concave" of the blade, is formed on a previous operation.

Figure 9 shows the method used to measure the form of the blade. A feeler gauge inserted between the sections *A* and *B* of the gauge showed how much stock had to be removed by grinding and polishing. Statistical evidence that this could be controlled showed that the grinding operation was unnecessary. As a result of action taken on the basis of statistical data on this operation, this grinding operation was ultimately eliminated.

The data shown in Table IV were obtained for a single revolution of the drum. To learn whether a significant difference exists between cutters, the data are arranged as shown in Table V. The variance between columns and the variance within columns are then computed.

To Obtain Variance Between Columns

1. Obtain the average of each column. In this example the averages are $\bar{X}_1=0.0068$, $\bar{X}_2=0.0082$, $\bar{X}_3=0.0135$, and $\bar{X}_4=0.0192$, respectively, for the four cutters.

2. Obtain the grand average $\bar{\bar{X}}$ of all the measurements. In this example, $\bar{\bar{X}}=0.0119$.

3. Subtract the respective column averages obtained in item 1 from the grand average in item 2. In this example,

$\bar{\bar{X}}-\bar{X}_1=0.0119-0.0068=0.0051$
$\bar{\bar{X}}-\bar{X}_2=0.0119-0.0082=0.0037$
$\bar{\bar{X}}-\bar{X}_3=0.0119-0.0135=0.0016$
$\bar{\bar{X}}-\bar{X}_4=0.0119-0.0192=0.0073$

4. Square the results of item 3. In this example,

$(\bar{\bar{X}}-\bar{X}\ )^2=(0.0051)^2=0.00002601$
$(\bar{\bar{X}}-\bar{X}_2)^2=(0.0037)^2=0.00001369$
$(\bar{\bar{X}}-\bar{X}_3)^2=(0.0016)^2=0.00000256$
$(\bar{\bar{X}}-\bar{X}_4)^2=(0.0073)^2=0.00005329$
0.00009555

5. Add the results of item 4. In this example, the total is 0.00009555.

6. Multiply the result of item 5 by the number of measurements in each column. In this example, there are six measurements in each column.
Therefore, we have $6\times0.00009555=0.00057330$.

7. Divide the result of item 6 by the total number of columns minus 1 (the degrees of freedom $=4-1=3$). In this example, there are four columns. Hence, we divide the result of item 6 by 3 to obtain $0.00057330\div3=0.00019110$. This last figure is the between columns variance.

To Obtain Variance Within Columns

1. Subtract each measurement from the average of the column in which it appears. In this example, the results are:

$0.0068-0.004=0.0028$
$0.0068-0.008=0.0012$
$0.0068-0.007=0.0002$
$0.0068-0.009=0.0022$
$0.0068-0.009=0.0022$
$0.0068-0.004=0.0028$

$0.0082-0.004=0.0042$
$0.0082-0.010=0.0018$
$0.0082-0.008=0.0002$
$0.0082-0.009=0.0008$
$0.0082-0.011=0.0028$
$0.0082-0.007=0.0012$

$0.0135-0.009=0.0045$
$0.0135-0.015=0.0015$
$0.0135-0.010=0.0035$
$0.0135-0.012=0.0015$
$0.0135-0.022=0.0085$
$0.0135-0.013=0.0005$

$0.0192-0.016=0.0032$
$0.0192-0.022=0.0028$
$0.0192-0.015=0.0042$
$0.0192-0.018=0.0012$
$0.0192-0.027=0.0078$
$0.0192-0.017=0.0022$

2. Square the results in item 1. In this example, the results are:

$(0.0028)^2=0.00000785$
$(0.0012)^2=0.00000144$
$(0.0002)^2=0.00000004$
$(0.0022)^2=0.00000484$
$(0.0022)^2=0.00000484$
$(0.0028)^2=0.00000784$
0.00002685

$(0.0042)^2 = 0.00001764$
$(0.0018)^2 = 0.00000324$
$(0.0002)^2 = 0.00000004$
$(0.0008)^2 = 0.00000064$
$(0.0028)^2 = 0.00000784$
$(0.0012)^2 = 0.00000144$

0.00003084

$(0.0045)^2 = 0.00002025$
$(0.0015)^2 = 0.00000225$
$(0.0035)^2 = 0.00001225$
$(0.0015)^2 = 0.00000225$
$(0.0085)^2 = 0.00007225$
$(0.0005)^2 = 0.00000025$

0.00010950

$(0.0032)^2 = 0.00001024$
$(0.0028)^2 = 0.00000784$
$(0.0042)^2 = 0.00001764$
$(0.0012)^2 = 0.00000144$
$(0.0078)^2 = 0.00006084$
$(0.0022)^2 = 0.00000484$

0.00010284

3. Adding the column totals in item 2, we get a grand total of 0.00027003.

4. Divide the result of item 3 by the total number of measurements minus the total number of columns. In this example, there are 24 measurements and four columns. Hence, we divide 0.00027003 by 20. The answer, 0.00001350, is the within-column variance.

Use of Figure 10 to Determine Whether Difference Is Significant

1. Divide the between-column variance by the within-column variance. In this example, the result is 0.00019110÷0.00001350 = 14.16.

2. The between-column degrees of freedom is the number of columns minus one. The within-column degrees of freedom is the total number of measurements minus the number of columns. In this example, the between-column degrees of freedom is 3 and the within-column degrees of freedom is 20.

3. Using the between-column degrees of freedom as ordinate and the within-column degrees of freedom as abscissa, locate the curve on Figure 10, passing through their intersection. In this case the point of intersection is almost at 5, and we shall call it 5.

4. If the answer obtained in item 1 exceeds the value on this curve, then a significant difference exists. In this example, the cutters produce significantly different parts, since 14.16 is greater than 5 (14.16 > 5).

Hence it is necessary to regrind the cutters before running the operation. The cutters were reground and the data on Table VII were obtained. For these data, the between-column variance is 0.0000144 and the within-column variance is 0.0000129. Reference to Figure 10 shows that significant difference between cutters is unlikely. The blades obtained from these cutters were sufficiently uniform to eliminate the grinding operation.

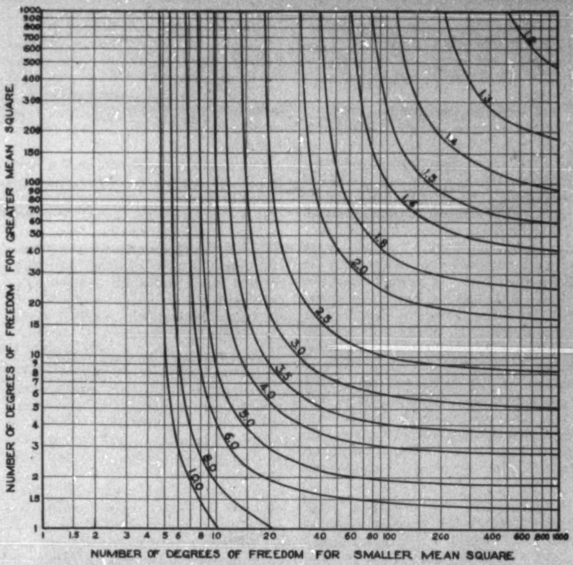

Figure 10. Analysis of variance chart—one-per-cent probability levels

References

1. ASTM Manual on Presentation of Data. The American Society for Testing Materials, August 1940.

2. American War Standards Z1.1 and Z1.2, Guide for Quality Control and Control-Chart Method of Analyzing Data. American Standards Association, 1941.

3. American War Standard Z1.3 Control-Chart Method of Controlling Quality During Production, American Standards Association, 1942.

4. Economic Control of Quality of Manufactured Product, Walter A. Shewhart. D. Van Nostrand Company, Inc., New York, N. Y., 1931.

5. Statistical Methods, George W. Snedecor. Iowa State College Press, Ames, Iowa.

Basic Concepts of Moving-Magnet-Instrument Rotors

LEWIS I. MENDELSOHN
ASSOCIATE AIEE

DURING RECENT YEARS the progress made in the development of permanent-magnet materials has brought about a considerable increase in the use of permanent-magnet rotors in d-c instruments. One such application is in the d-c Selsyn position indicator,[1] another in a newly developed electric instrument,[2] and a third in a new ratio-type instrument.[3] The space limitations in these designs predicated small actuating elements which were obtained by using permanent-magnet moving systems.

In view of these developments and the increasing number of permanent-magnet materials now available, it is appropriate to analyze the basic concepts on which the design of permanent-magnet rotors should be based. Although it is not possible to cover all rotor shapes, the elliptic spheroid, which can be shown to have uniform internal magnetization, lends itself to complete analytical treatment. A general analysis of this shape made in terms of its major and minor axes can be used as a good approximation for many rotor shapes and gives a clear physical insight into the behavior of permanent-magnet rotors.

The demagnetization portion of the hysteresis loops for several permanent-magnet materials are shown in Figure 1A, with their more important properties listed in Table I. These data are based on tests made on ring samples or the equivalent and without the demagnetizing effects of air paths in the magnetic circuit. All practical permanent-magnet applications, however, involve such air paths, and the designer is faced with the problem of applying these ring-sample data to designs subject to the demagnetizing effects of air paths.

The objects of this paper are:

1. To provide the instrument designer with a method for determining from ring-sample data and appropriate demagnetizing factors the intrinsic induction and the magnetic moment of a given rotor design.

2. To show how the value of the minimum field strength necessary to magnetize the rotor fully follows logically from the analysis.

3. To present a graphical method for determining the effect of an externally impressed field on a magnetized rotor.

4. To outline a scientific approach to the selection of materials for such applications.

Demagnetizing Factor of a Ring and Air Gap

The conventional analysis of permanent magnets usually deals with the case of a simple ring and air gap as shown in Figure 2B. The concept of a demagnetizing factor is not introduced as such, although it actually occurs in the relation which is established between the intrinsic induction and the magnetizing force. It is worthwhile, therefore, to re-examine the conventional analysis to identify this factor which is essential to the analysis of the magnetized rotor of elliptic-spheroid shape.

In the conventional analysis,[5] Ampere's law, $\oint H \cdot dl = 0$, is applied to the case of the ring and air gap to obtain the expression:

$$H_m l_m + B_g d = 0 \qquad (1)$$

where H_m is the magnetizing force in the material in oersteds, B_g is the flux density of the gap in gausses, l_m is the mean length of the magnetic material in centimeters, and d is the air-gap length in centimeters.

The assumption is then made that the leakage flux is negligible so that the flux density in the material,

$$B_m = B_g \qquad (2)$$

Equation 1 then becomes

$$\frac{B_m}{H_m} = -\frac{l_m}{d} \qquad (3)$$

But in the electromagnetic system of units, which is used throughout this paper

$$B_m = B_{im} + H_m \qquad (4)$$

where B_{im} is the intrinsic induction in the material for a given value of H_m as determined experimentally by a ring-sample test. Thus

$$B_{im} = f(H_m) \qquad (5)$$

where $f(H_m)$ is the demagnetizing portion of the major hysteresis loop for the continuous ring of the material as shown in Figure 2A.

Equations 3 and 4 then are combined to obtain

$$B_{im} = -\left(\frac{l_m + d}{d}\right) H_m = -\frac{1}{\left(\dfrac{d}{l_m + d}\right)} H_m \qquad (6)$$

As indicated in Figure 2C, the equations 5 and 6 can be solved graphically for the values of B_{im} and H_m needed to provide an approximation of the air-gap flux density available from the permanent-magnet circuit shown in Figure 2B. It should be emphasized that the analysis is based on the assumption that the leakage flux is negligible and that the resulting value of flux density is in error to the extent that this assumption varies from actual conditions.

In the graphical solution of equations 5 and 6, the slope of the line OQ, which represents equation 6, is given by the coefficient of H_m. The value of $\dfrac{d}{l_m + d}$ may be defined as the *demagnetizing factor*, K, for this magnetic circuit as it determines the amount by which the intrinsic induction, B_{im}, is reduced from its residual value, OS, to its value, OR, in the magnetic circuit as a result of the demagnetizing effect of the air gap. An increase in the value of K reduces the value of OR.

Demagnetizing Factor of a Permanent-Magnet Rotor

The concept of the demagnetizing factor which has been identified for the relatively simple analysis of ring and air-gap magnets, greatly facilitates the more complex analysis of permanent-magnet rotors. It permits engineers to translate the results of the analysis of a difficult field problem into terms of magnetic-circuit theory which is more widely understood.

In the general case, a permanent-magnet rotor of any shape will not be uniformly magnetized when it is immersed in a uniform magnetic field. For example, the intrinsic induction in a rectangular bar magnet varies from a maximum at its center to a minimum close to its ends. Thus internally the intrinsic induction must be represented as a space function of some selected co-ordinate system. Under such conditions, the concept of a single demagnetizing factor is not valid. This factor becomes a demagnetizing function, to be specified from point to point within the rotor, and the mathematics required to evaluate it is lengthy, difficult, and beyond the scope of this paper.

If, however, a shape is chosen in which the intrinsic induction is uniform, a straightforward analysis using a single demagnetizing factor is possible. Such a shape is an elliptic spheroid, the surface of which is generated by rotating an ellipse about either its major or minor axis to develop the prolate or oblate forms of it

---

Paper 45-90, recommended by the AIEE committee on instruments and measurements for publication in AIEE TRANSACTIONS. Manuscript submitted November 21, 1944; made available for printing March 9, 1945.

LEWIS I. MENDELSOHN is meter-development engineer, General Electric Company, West Lynn, Mass.

The author expresses his appreciation for the interest and encouragement of many of his associates during the preparation of this paper. Particular credit is due H. C. Dickinson and H. T. Faus for their contributions.

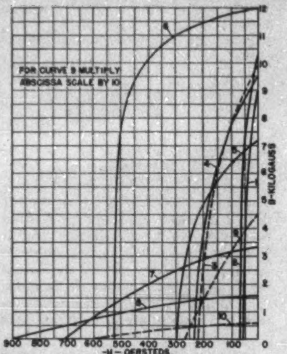

A. Curves for materials numbered 1 through 10 in Table I in terms of flux density, *B*, and demagnetizing force, *H*

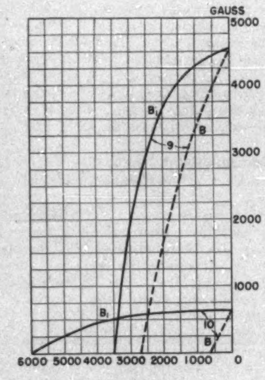

B. Curves for cobalt-platinum- and silver-aluminum-manganese alloys in terms of *B* and *H* and also in terms of intrinsic induction, B_i, and demagnetizing force, *H*

Figure 1. Demagnetizing curves for permanent-magnet materials

shown in Figures 3A and 3B, respectively. Uniform intrinsic induction has been proved to occur in magnets of this shape if they are magnetized either along the generating axis or normal to it.[4] This shape has been used successfully as an approximation of many permanent-magnet-rotor designs. In doing so, the designer must distinguish clearly between the generating axis of the elliptic spheroid and the axis about which the rotor turns in the instrument. These axes may either coincide or be normal to one another. In addition, it should be noted that the direction of magnetization is always normal to the axis of rotation in the instrument.

The problem of determining the demagnetizing factor for the elliptic spheroid necessitates solving Laplace's equation $\Delta^2 F = 0$ for the magnetomotive force distribution of the rotor and the applied uniform field. In addition, the basic physical relations[5] must hold at the boundary surface. With the magnetomotive-force distribution determined, the flux paths are found and then the demagnetizing factor. Another method of approach[4] recognizes the solution of Laplace's equation required for uniform magnetization by analogy with the gravitational potential theory, and from this solution the demagnetizing factor for the elliptic spheroid is found. In any case the simple use of Ampere's law as outlined for the ring and air gap cannot be used until the flux paths are determined.

In Appendix I equations are given for the demagnetizing factors for the two forms of the elliptic spheroid, each magnetized either along the generating axis or normal to it. From these equations curves of the demagnetizing factors for values of the ratio of the generating axis to the axis normal to it are shown in Figure 4A. Figure 4B illustrates the elliptic-spheroid approximation of a short cylinder and also of a thin disk. The relationship among the three mutually orthogonal axes, the appropriate axis ratio c/a, and the demagnetizing factor *K* are indicated in each case.

Determination of the Intrinsic Induction and Magnetizing Force

The demagnetizing factors given by the curves in Figure 4A can be used to determine the intrinsic induction and magnetizing force for elliptic-spheroid rotors of any dimensions. In Figure 3A such a rotor is introduced into a uniform field of magnetizing force H_A. The source of this magnetizing force is assumed sufficiently large so that the presence of the rotor in the field has negligible effect on it. The rotor causes a redistribution of this original field outside the rotor which may be attributed to a distribution of poles on the surface as shown. The pole distribution which is associated with the intrinsic induction exerts a demagnetizing effect on the original field H_A within the rotor, and the final magnetizing force H_x in the material, while still uniform, is reduced to a smaller value than H_A. The reduction in internal magnetizing force is proportional to the intrinsic induction. The constant necessary to determine this proportion is the demagnetizing factor *K*. Thus

$$H_x = H_A - KB_{ix} \tag{7}$$

where H_x is the resultant magnetizing force in the material in oersteds, B_{ix} is the intrinsic induction in the direction *x* in gausses, and *K* is the demagnetizing factor which depends on the ratio of the length of axis *c* to that of axis *a*.

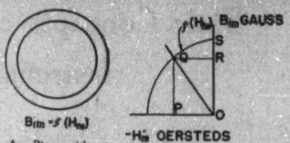

A. Ring without air gap for determining fundamental data of Figures 1 and 2

C. Graphical construction for determining operating point Q of ring and air-gap magnet

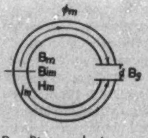

B. Ring and air-gap magnet

Figure 2. Conventional ring-shaped magnet

In equation 7 H_A is known, and *K* can be determined from Figure 4A. Two unknowns B_{ix} and H_x remain to be found. Hysteresis loops for the material based on ring-sample tests represented graphically or in symbols as $B_{ix} = f(H_x)$ furnish the other relationship needed to obtain numerical results. With equation 7 transposed, the problem may be formulated as follows:

$$\left.\begin{array}{l} B_{ix} = (1/K)(H_A - H_x) \\ B_{ix} = f(H_x) \end{array}\right\} \tag{8}$$

These equations can best be solved graphically to obtain numerical results. In Figure 5 *OM* is laid off equal to the magnetizing force H_A. The line *MP* is of

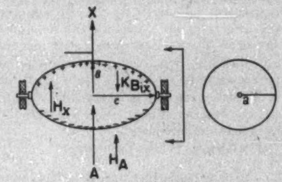

A. Prolate form

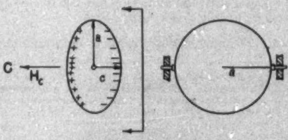

B. Oblate form

Figure 3. Elliptic spheroid

The intrinsic induction is always normal to the axis of rotation

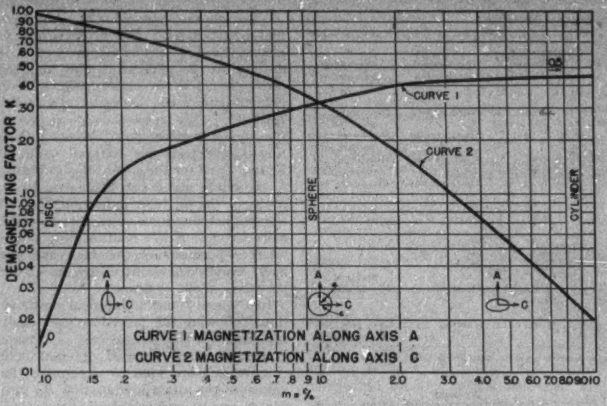

Figure 4

A (above). Curves giving values of the demagnetization for elliptic-spheroid rotors in terms of the axis ratio c/a

B (right). Elliptic-spheroid approximation of a short cylinder and of a thin disk

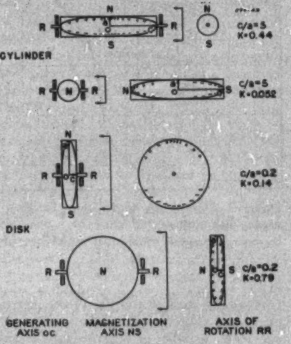

such slope that PN read on the ordinate scale divided by NM read on the abscissa scale equals $1/K$. As the major hysteresis loop is a multivalued function, there are three solutions P, Q, R, for this particular value of H_A, depending on how the magnetization takes place.

When the rotor is saturated by a large value of H_A which is then reduced to zero, its magnetic characteristics are represented by the point P_1, the ordinate and abscissa of which are the values of the intrinsic induction (B_{ix}) and the demagnetizing force ($-H_x$) for the permanent-magnet rotor. The point P_1 is found by the intersection of a line from the origin having slope $1/K$ and the demagnetizing portion of the hysteresis loop.

The magnetizing force H_A' needed to saturate the rotor can be obtained from the value H_s of this force required to saturate the ring sample. H_A' is determined by the intersection of a line drawn from S having slope $1/K$ and the abscissa. H_A' is larger than H_s because of the self-demagnetizing effect of the rotor shape. Thus the value needed to saturate a thin disk magnetized across its thickness is usually many times that required for the ring sample, and that for a long axially magnetized cylinder is nearly equal to it.

The foregoing analyses have been based on ring-sample hysteresis loops in terms of the intrinsic induction (B_{ix}) and the magnetizing force (H_x) rather than the more usual terms of flux density (B_x) and magnetizing force (H_x). When only the latter are available, B_{ix}–H_x curves are readily obtainable as $B_{ix}=B_x-H_x$. The B_{ix}–H_x relation is preferred for permanent-magnet-rotor analyses, as the intrinsic induction is equal to the magnetic moment per unit volume from which the mechanical torque provided by the rotor for instrument indication can be calculated.

Effect of External Fields on Magnetized Rotors

A properly magnetized rotor of course must be immersed in an external field with which it reacts in order to produce mechanical torque. This external field, however, tends to alter the intrinsic induction of the rotor along minor hysteresis loops. For example, a rotor having an intrinsic induction B_{ix}, corresponding to point S_1 on the major hysteresis loop in Figure 6A is immersed in an external field H_u. The relative directions of B_{ix} and H_u may vary from alignment to opposition as indicated by Figures 6B and 6C. In Figure 6B the magnetizing force is increased and the material performance follows the minor loop S_1S_2, returning to S_1 if H_u is reduced to zero. When, as in Figure 6C H_u opposes B_{ix}, the path follows the major loop from S_1 to S_4, but, if H_u is reduced to zero, the path now becomes S_4S_5. Thus the intrinsic induction is permanently reduced to a value corresponding to S_5, and further demagnetization will not occur unless the rotor is exposed to an external field greater than H_u and in opposition to the intrinsic induction. It also has been shown experimentally that, if the rotor has been demagnetized to S_5 as in Figure 6C, no further reduction will occur in the condition shown by Figure 6D. If the minor hysteresis loops which determine points such as S_3 and S_5 are not available from ring-sample tests, they can be closely approximated for high-coercive-force materials by drawing lines parallel to the tangent to the major loop at the point of residual induction (B_r).

Calculation of Mechanical Torque of a Rotor

The intrinsic induction, B_{ix}, determined by the foregoing analyses for an elliptic-spheroid rotor, is by definition the magnetic moment per unit volume, M.[5] The mechanical torque of the rotor can be calculated from this moment, M. In practical designs the value of B_{ix} used for this purpose should be the minimum expected in service as determined by the relation of it to the field H_u, where H_u produces the strongest demagnetization effects as in Figure 6C.

With this value of B_{ix} selected, the magnetic moment in maxwell-centimeters is

$$M=B_{ix}\times(4/3)\pi a^2c \tag{9}$$

where $(4/3)\pi a^2c$ is the volume of the elliptic spheroid. The mechanical torque for the general case of the elliptic spheroid is therefore

$$T=\frac{M}{4\pi}\times H_u \tag{10}$$

where T is the torque in dyne-centimeters, M is the magnetic moment in maxwell-centimeters, and H_u is the operating-field intensity in oersteds. In most practical applications motion is so restricted that only coplanar components of vectors M and H_u can produce motion. A discus-

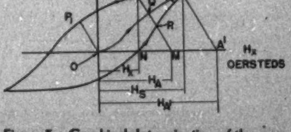

Figure 5. Graphical determination of the magnetizing force in an elliptic-spheroid rotor from the major hysteresis loop

Table I. Permanent-Magnet Materials

Number	Alloy Designation	Coercive Force, Oersteds	Residual Induction, Gausses	Density, Grams Per Cubic Centimeter	Mechanical Properties	Method of Fabrication
1	Chrome steel	63	9,000	8.20	Hard, strong	Hot forge, cast, machine
2	Tungsten steel	70	10,300	8.18	Hard, strong	Hot forge, cast, machine
3	Comol	220	10,000	8.15	Hard, strong	Hot forge, machine, cast
4	Cobalt steel	240	9,500	8.16	Hard, strong	Hot forge, machine, cast
5	Copper–nickel–iron	300	7,200	8.62	Ductile	Cold roll, machine punch
6	Alnico V	525	12,500	7.30	Hard, brittle	Cast grind
7	Copper–nickel–cobalt	710	3,400	8.30	Ductile	Cast, cold roll, machine
8	Sintered oxide	900	1,800	2.76	Hard, brittle	Mold, sinter
9	Cobalt platinum	2,700	4,500	18.0		
10	Silver–aluminum–manganese	6,000*	550	9.00	Ductile	Cold roll, machine punch

* Demagnetizing force required to reduce the intrinsic induction to zero, usually denoted by jH_c

sion of this departure from the electromagnetic system of units is found in Appendix II. Thus equation 10 can be simplified to the following scalar form:

$$T = \frac{M}{4\pi} H_u \sin\theta \qquad (11)$$

where M is the magnitude of the magnetic moment determined from equation 9 and is directed along the magnetization axis, H_u is the magnitude of the operating-field component normal to the axis of rotation, T is the torque in dyne-centimeters about this axis, θ is the angle between the directions of $\boldsymbol{M}$ and $\boldsymbol{H_u}$.

Practical Rotor Designs

The application of the analysis of the elliptic-spheroid rotor to practical instrument-rotor designs serves to explain the use of this method of approach in selecting the proper permanent-magnet material.

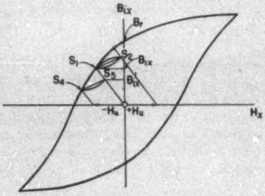

A. Graphical construction for determining the effect of the operating field on a magnetizing rotor

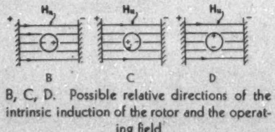

B, C, D. Possible relative directions of the intrinsic induction of the rotor and the operating field

Figure 6

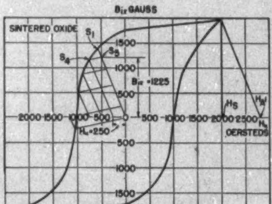

Figure 7. Graphical construction for determining the intrinsic induction of a one-half-by-one-centimeter cylindrical sintered-oxide rotor

In a specific design, the size of the instrument and therefore the permanent-magnet rotor usually is determined by the space limitations of the instrument application. Cylindrical rotors one centimeter long and one-half centimeter in diameter, magnetized diametrically and pivoted on the cylinder axis, may therefore be used in considering designs made of two materials, sintered oxide and silver–aluminum–manganese, which are well adapted to instrument rotors.

The elliptic spheroid which approximates this shape is the prolate form in which the direction of magnetization is normal to the generating axis and the ratio of major to minor axis, $c/a = 2$. From Figure 4 the demagnetizing factor $\boldsymbol{K} = 0.41$. This factor then is applied to the hysteresis-loop data obtained from ring-sample tests for sintered oxide in Figure 7 and for the silver alloy in Figure 8. It will be noted that these data are in terms of the intrinsic induction, B_i, and the magnetizing force, H, rather than the more usual B–H relationships. The relative positions of the B–H and the B_i–H curves are shown in Figure 1B for the silver alloy.

In Figures 7 and 8 graphical constructions following the procedure previously explained for the general case of a rotor immersed in an opposed external field (Figure 6C) are used to determine the values of the intrinsic induction B_{iz} corresponding to various values of the external field H_u. In Figure 7, S_1, S_4, S_5 correspond to the same points in the general analysis of Figure 6A. The condition of this field in opposition to the intrinsic induction of the rotor is used, since it is assumed that the rotor is allowed to turn to the position at which this condition can occur.

From the values of B_{iz} thus obtained for sintered oxide and the silver alloy, the corresponding values of magnetic moment M then are calculated from

$$M = B_{iz} \times (2\pi a^2 c) \qquad (12)$$

where $2\pi a^2 c$ is the volume of the cylindrical rotor or in terms of the dimensions chosen,

$$M(\text{maxwell-centimeters}) = \frac{\pi}{16} B_{iz} \qquad (13)$$

These values of M for sintered oxide and the silver alloy are plotted in Figures 9 and 10 for values of the external field H_u. From equations 11 and 13, the mechanical torque for the rotor position at which $\theta = 90$ degrees is

$$T_{\theta=90°}\ (\text{dyne-centimeters}) = \frac{B_{iz}}{64} H_u \qquad (14)$$

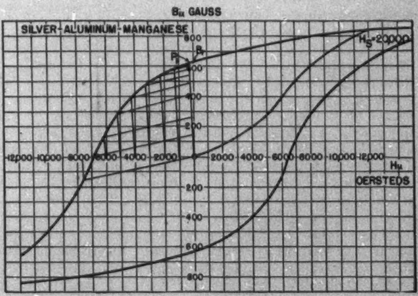

Figure 8. Graphical construction for determining the intrinsic induction of a one-half-by-one-centimeter silver–aluminum–manganese rotor

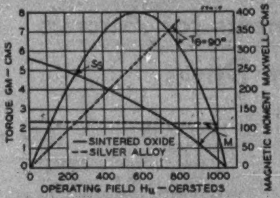

Figure 9. Magnetic moment and 90-degree torque available from a sintered-oxide rotor, and a silver–aluminum–manganese rotor of the same shape operated in field strengths to 1,050 oersteds

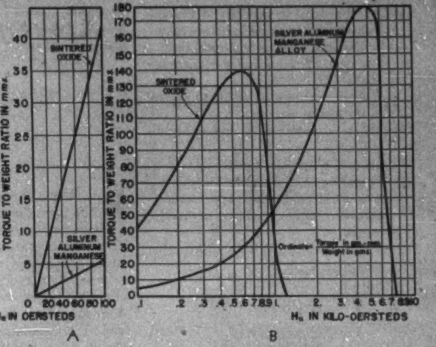

Figure 11. The performance of one-half-by-one-centimeter cylindrical rotors of sintered-oxide and silver – aluminum–manganese materials compared on the basis of torque-to-weight ratio for operating fields of 0 to 100 oersteds in A and 100 to 7,500 oersteds in B

$$T_{\theta=90°} \text{ (gram-centimeters)} = \frac{B_{tr}H_u}{64\times 980} \quad (15)$$

The torque values calculated from equation 15 also are plotted in Figures 9 and 10.

The comparison of the torque values for the two materials in Figure 9 shows that higher torques are available from sintered oxide for external fields below 770 oersteds, and for stronger fields the silver alloy is superior. As instrument designers are more often concerned with the torque per unit weight of the rotor rather than its absolute value, Figure 11 is given to compare the materials on this basis and further emphasizes the advantages of sintered oxide for field intensities below about 800 oersteds.

It is also interesting to note that, for field strengths between 3,000 and 6,000 oersteds, the silver-alloy rotor develops even higher torque per unit weight than the sintered oxide used with its most favorable field of 600 oersteds.

The instrument designer also will note that the values of torque to weight are considerably higher than those obtained in moving-coil designs. This is no doubt one of the chief reasons for the increasing popularity of moving-magnet instruments for applications in which sufficient operating field strength can be provided by stationary coils or other means.

In the preceding comparison of sintered-oxide and silver-alloy rotors, the operating field in which the rotor is immersed to produce torque has been assumed to be equal to the maximum field to which the rotor will ever be exposed. If, however, this operating field is exceeded because of overload currents in the coils producing it or other temporary conditions, the rotor will be further demagnetized. To take an extreme case, assume that the silver-alloy rotor while operating normally in a 500-oersted field may be subject to a momentary field of 5,000 oersteds in a direction to oppose the intrinsic induction of the rotor. Once the rotor has been demagnetized by this 5,000-oersted field, subsequent applications of it will cause no further demagnetization. The rotor magnetization therefore can be made permanent for all fields up to this value by subjecting it to an initial equivalent demagnetization. This, however, is accompanied by a reduction in the magnetic moment and torque from the values corresponding to the 500-oersted field. From Figure 10 the magnetic moment would be 77 maxwell-centimeters instead of 119, but a rotor having this reduced moment and operating normally in a 500-oersted field still has a 90-degree torque of 3.1 gram-centimeters. As this corresponds to a torque-to-weight ratio of about 17 millimeters, the rotor demagnetized to stand the momentary 5,000-oersted field should be satisfactory for most applications. This result exemplifies the value of the silver alloy in applications where a permanent magnet must withstand excessive demagnetizing fields.

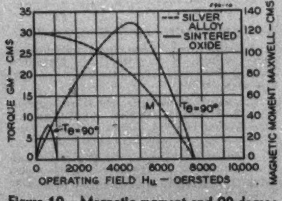

Figure 10. Magnetic moment and 90-degree torque available from the silver-alloy rotor operated in field strengths to 7,500 oersteds

Conclusions

The analyses presented are of value in determining the performance of permanent-magnet rotors for instruments. The assumptions made to simplify the treatment and particularly the use of the elliptic spheroid to approximate cylinders or other actual rotor shapes should be understood clearly by the designer applying the analyses to specific designs. He must continue to exercise sound judgment, especially in the selection of the elliptic spheroid which provides the closest approach to the magnetic conditions existing in the actual rotor under consideration. The writer has used the analyses presented for numerous instrument-rotor designs. The results obtained have agreed with experimental tests of samples of these designs within the accuracy limits of the tests and of the ring-sample data on which the calculations were based.

Materials other than the sintered oxide and the silver alloy already considered can be used for rotors and are preferable under certain conditions. Although economic as well as technical considerations should determine the final choice, the foregoing analyses can be of great assistance in making the selection, as the performance of a given rotor shape made of several different materials can be determined rapidly without recourse to building and testing samples of each. They may also serve as a basis for comparing moving-coil- and moving-magnet-instrument designs and for evaluating various rotor shapes. As the methods of calculation developed are based on well-established electromagnetic theory, it should be feasible to provide similar procedures for other permanent-magnet applications which will continue to increase both within and outside of the field of instruments and measurements.

List of Symbols

B_g—Air-gap flux density in gausses.

B_m—Flux density in the magnetic material in gausses.

H_m—Magnetizing force in the magnetic material in oersteds.

B_{tm}—Intrinsic induction in the magnetic material in gausses.

l_m—Length along an assumed flux line in centimeters.

d—Air-gap length in centimeters.

H_x—Magnetizing force acting in the uniformly magnetized material in the direction x.

H_A—The intensity in oersteds of the uniform magnetizing field, before an unmagnetized rotor is immersed in it.
K—The demagnetizing factor (dimensionless).
B_{ix}—Uniform intrinsic induction in gausses in the direction x.
M—Magnetic moment in maxwell-centimeters.
T—Torque in dyne-centimeters.
H_u—Operating-field intensity in oersteds into which a saturated permanent-magnet rotor is introduced to produce torque.
c, a—Semiaxes of an elliptic spheroid in centimeters.
m—Ratio c/a (dimensionless).

Appendix I

For a prolate elliptic spheroid magnetized along the c and a axes, respectively, in Figure 3A, the demagnetization factors are:[4]

$$K_c = \frac{1}{(m^2-1)} \times \left[\left\{ \frac{m}{\sqrt{m^2-1}} \log_e \left(m + \sqrt{m^2-1} \right) \right\} - 1 \right]$$

$$K_a = \frac{m^2}{2(m^2-1)} \left[1 - \frac{1}{m\sqrt{m^2-1}} \times \log_e \left(m + \sqrt{m^2-1} \right) \right]$$

$$m = c/a$$

For an oblate elliptic spheroid magnetized along the C and A axes, respectively, in Figure 3B, the demagnetization factors are:[4]

$$K_c = \frac{1}{(1-m^2)} \left[1 - \frac{m}{\sqrt{1-m^2}} \sin^{-1} \sqrt{1-m^2} \right]$$

$$K_a = \frac{m}{2(1-m^2)} \left[\left(\frac{1}{\sqrt{1-m^2}} \sin^{-1} \sqrt{1-m^2} \right) - m \right]$$

$$m = c/a$$

Appendix II

If $\boldsymbol{M'}$ is the magnetic moment in electromagnetic units (poles times centimeters), and $\boldsymbol{H}$ is the field intensity in oersteds, $\boldsymbol{T} = \boldsymbol{M'} \times \boldsymbol{H}$ gives torque in dyne-centimeters. Now M' has the dimensions unit poles times centimeters, and, since 4π maxwells of flux emanate from a unit pole, the following equality may be written:

$$\boldsymbol{M'} \text{ unit poles} \times \text{centimeters} = \boldsymbol{M} \text{ maxwells} \times \text{centimeters} \times \frac{1 \text{ unit pole}}{4\pi \text{ maxwells}}$$

whence

$$\boldsymbol{M'} = \frac{\boldsymbol{M}}{4\pi}$$

Thus $\boldsymbol{T} = \frac{\boldsymbol{M}}{4\pi} \times \boldsymbol{H}$ will give the torque in dyne-centimeters if $\boldsymbol{M}$ is in maxwell-centimeters, and $\boldsymbol{H}$ is in oersteds. Permeameter values of B_i are measured in gausses or maxwells per square centimeter. But this B_i value is identical to maxwell times centimeters per cubic centimeter, or the magnetic moment in maxwell-centimeters per unit volume. Thus for uniformly magnetized rotors it is convenient to modify the electromagnetic units as given in equations 10 and 11.

References

1. A D-C TELEMETER OR D-C SELSYN FOR AIRCRAFT, R. G. Jewell, H. T. Faus. AIEE TRANSACTIONS, volume 61, 1942, June section, pages 314–17.

2. A NEW MOVING-MAGNET INSTRUMENT FOR DIRECT CURRENT, H. T. Faus, J. R. Macintyre. AIEE TRANSACTIONS, volume 61, 1942, August section, pages 586–8.

3. A UNIQUE MOVING-MAGNET RATIO INSTRUMENT, F. R. Sias, D. B. Fisk. AIEE TRANSACTIONS, volume 63, 1944, September section, pages 634–6.

4. ABSOLUTE MEASUREMENTS IN ELECTRICITY AND MAGNETISM (book), Andrew Gray. The Macmillan Company, New York, N. Y., 1893. Volume 2, part 1, pages 54–5.

5. ELECTRIC AND MAGNETIC FIELDS (second edition), Stephen S. Attwood. John Wiley and Sons, Inc., New York, N. Y., 1941. Chapter 14, pages 343–50, 201.

Governor Requirements for Aircraft Alternator Drives

W. K. BOICE
MEMBER AIEE

L. G. LEVOY, JR.
MEMBER AIEE

RECENTLY much engineering thought has been directed toward the use of a-c power systems in very large aircraft.[1,2] To permit operation at substantially constant frequency, when generators are driven by accessory drive shafts of main aircraft engines, variable-ratio transmissions have been designed. The ratio of such a transmission may be varied by means of a governor which maintains generator speed within a narrow range while the aircraft engine speed varies over a wide range. The engine speed range in typical cases may be three to one or greater. The frequency of a typical a-c system as now designed for large military aircraft must be held within about five per cent of normal, except during unusual transient conditions, when somewhat greater variations are permissible. When alternators are to be operated in parallel, differences in engine speeds should not be permitted to cause loss of synchronism of the generators.

The requirements for governing the variable-ratio transmissions differ in several ways from governor requirements for ordinary prime movers for industrial and central-station generators. In the aircraft systems considered, the prime mover is the main airplane engine which drives the propeller. This may be 100 times as powerful as the generator and will vary in speed over a wide range independently of the generator's requirements. Rapid changes in engine speed may be encountered. These conditions indicated that analysis of governor requirements for aircraft alternator drives would involve special study.

As a part of the development program for certain military aircraft, a study was undertaken to establish performance specifications for governors for variable-ratio transmissions. Some of the results of this study are presented in this paper.

The action of the governors should be sufficiently rapid so that the transmission ratios will follow changes in engine speeds closely enough to prevent loss of synchronism or undue variations of frequency. The rates of acceleration or deceleration of the engines determine the response which a governor must have to operate successfully. The effect of sudden acceleration of one engine was investigated for a variety of operating conditions. Accelerations are considered to affect performance more adversely than decelerations, because under transient conditions acceleration of a generator tends to increase its electrical load, whereas deceleration tends to reduce this load. Also, when one generator of a group of paralleled generators is decelerated, its effect on frequency and synchronism is minimized by use of a free-wheeling device in its drive. That is, when an engine is decelerated, decelerating torques are not imposed on the generator by its transmission. As a result of these considerations the study reported in this paper is devoted to the effects of acceleration rather than decelerations of main aircraft engines. The major part of the paper concerns parallel operation, but certain information concerning nonparallel operation is also given.

The results and discussion included may help to give a clear conception of system performance during periods of engine speed changes.

Paper 45-85, recommended by the AIEE committee on air transportation for publication in AIEE TRANSACTIONS. Manuscript submitted November 21, 1944; made available for printing March 7, 1945.

W. K. BOICE and L. G. LEVOY, JR., are electrical engineers in the industrial engineering division, General Electric Company, Schenectady, N. Y.

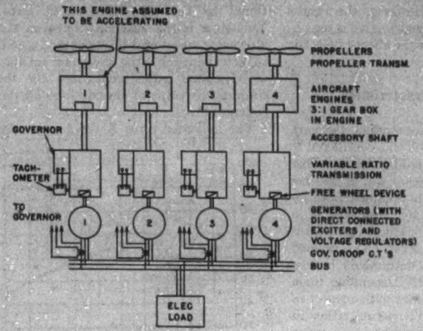
THIS ENGINE ASSUMED TO BE ACCELERATING
PROPELLERS
PROPELLER TRANSM.
1
2
3
4
AIRCRAFT ENGINES 3:1 GEAR BOX IN ENGINE
GOVERNOR
ACCESSORY SHAFT
TACH-OMETER
VARIABLE RATIO TRANSMISSION
FREE WHEEL DEVICE
TO GOVERNOR
GENERATORS (WITH DIRECT CONNECTED EXCITERS AND VOLTAGE REGULATORS)
GOV. DROOP C.T'S
BUS
ELEC LOAD

Figure 1. Schematic diagram of a-c power-supply system for airplane

System Arrangement

Figure 1 is a schematic diagram illustrating the arrangement proposed for operating four 40-kva 30-kw 6,000-rpm a-c generators in parallel for supplying 208-wye/120-volt three-phase 400-cycle power for use on an airplane. Each alternator is driven by a variable-ratio transmission, which in turn is driven from the main airplane engine.

Such a transmission may take any of a number of forms. One form consists of an oil pump with continuously variable stroke and a hydraulic motor driven by the variable oil flow. The stroke of the pump is varied by a servomechanism controlled by the governor. Each transmission is driven from an accessory drive shaft of a main aircraft engine. The engine rating is, of course, many times the rating of the alternator and transmission. Each transmission is controlled by its governor which operates to maintain alternator speed in spite of variations in engine speed. A free-wheeling device is included in the output shaft of each transmission. Each governor operates from the speed indication of a tachometer connected to the driving end of the free-wheeling device. An electric power-measuring circuit using a current transformer and a potential connection in each alternator output circuit is connected to the governor in such a way as to cause the generator speed to be reduced somewhat (droop) as the output is increased. Generators are controlled by individual voltage regulators. These regulators are connected to hold constant voltage and to divide reactive kilovolt-amperes properly among generators operating in parallel. Switching equipment in the electric-power circuits is not shown on the diagram.

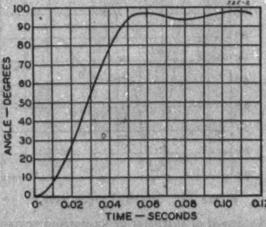

Figure 2. Angle between generators, case 1

Angle shown is the electrical angle between the alternator of the accelerated engine and the other three alternators

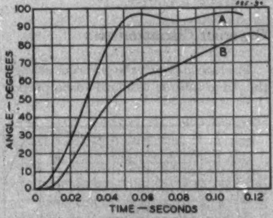

Figure 3. Effect of slip in drive

Angle shown is the electrical angle between the alternator of the accelerated engine and the other three alternators

A—Case 1; no slip in drive

B—Case 2; one-per-cent slip at full load

Engine Acceleration

If the engine speed changes very quickly, the governors cannot be expected to maintain absolutely constant speed on the alternators; instead, the alternator speed will change somewhat until the governors can restore normal frequency. If one engine (say number 1, Figure 1) accelerates while the speed of the other engines remains constant, the accelerated alternator will tend to pull away from the other alternators and may pull out of step. The governor should act sufficiently quickly to prevent the accelerated alternator from pulling out of step.

In all cases studied, one engine was accelerated at a rate of 2,150 rpm per second which was assumed to be the maximum possible. This value was determined by applying rated engine torque to the propeller inertia of a typical engine-propeller combination for a large airplane. The corresponding accessory-drive-shaft acceleration is 6,450 rpm per second. This value is probably much higher than any acceleration which will be encountered in normal operation. The engine acceleration was assumed to appear instantly. In practice the maximum acceleration probably will not appear instantly; the assumption made tends to make the results conservative.

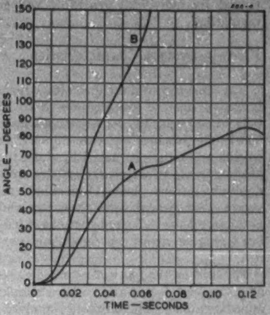

Figure 4. Effect of increasing applied acceleration

Angle shown is the electrical angle between the alternator of the accelerated engine and the other three alternators

A—Case 2; 6,450 rpm per second applied to alternator

B—Case 3; 14,300 rpm per second applied to alternator

The acceleration is considered to be sustained throughout the short time intervals investigated. It was necessary to study only the first few tenths of a second after the sudden appearance of acceleration, since synchronism was either lost or definitely established during this time.

In practice, the accelerations will not last indefinitely, and so the calculations are conservative in this regard.

Operating Conditions

A variety of initial operating conditions was investigated as outlined in the list of cases, Table I. Thus the effect of various factors, such as engine input speed, electric load, parallel versus nonparallel operation, governor action, drive slip, was investigated.

Each drive is considered to be controlled by an individual governor with an individual droop circuit for division of load. The load on paralleled generators was assumed to be balanced prior to the disturbances studied.

The voltage was considered to be controlled by individual generator voltage regulators.

Electric-System Characteristics

The time required for the voltage regulators to operate was considered to be 0.02 second, which is conservatively long. The exciter response was determined from calculated exciter characteristics, and the alternator electrical characteristics were determined from calculated machine constants. Subsequent tests on exciter and alternator have indicated that the calculated characteristics are reasonably correct.

The load on the bus was assumed to be at 0.75 power factor and to be a simple impedance load. The actual airplane electric load will consist of a mixture of motors and static loads. However, the results obtained are considered to give a reasonably accurate idea of the effect of electric load.

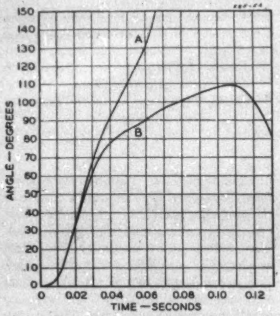

Figure 5A. Effect of governor action

Angle shown is the electrical angle between the alternator of the accelerated engine and the other three alternators

A—Case 3; no governor

B—Case 4; governor operating

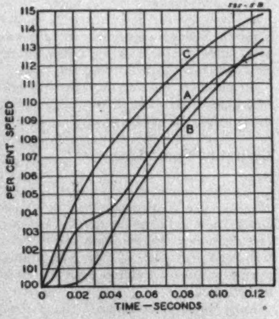

Figure 5B. Speed changes, case 4

A—Speed of alternator of accelerated engine

B—Speed of other three alternators

C—Speed A + drive slip = input speed × no-load ratio

Transmission Characteristics

In most of the cases studied, the variable-ratio transmission was considered to have a slip proportional to load such that full-load output causes a slip of one per cent. This value was obtained from information supplied by designers of a typical transmission. The drive ratio is varied by moving a lever. The no-load ratio of the drive is determined by the position of this lever. Depending upon the position of this lever with respect to neutral, the drive will operate either in underdrive (output speed less than input speed) or in overdrive.

Governor Characteristics

The rate at which the governor changes the drive ratio is assumed to be proportional to the alternator speed error. This error is the difference between the alternator speed and the reference speed, as determined by the governor setting, droop circuit adjustment, and the instantaneous value of electric load on the governor.

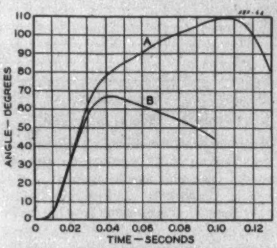

Figure 6A. Effect of increasing governor response

Angle shown is the electrical angle between the alternator of the accelerated engine and the other three alternators

A—Case 4; governor response = 0.0025 (ratio change per second) per rpm error

B—Case 5; governor response = 0.005 (ratio change per second) per rpm error

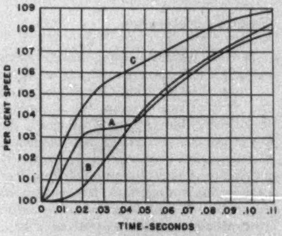

Figure 6B. Speed changes, case 5

A—Speed of alternator of accelerated engine

B—Speed of other three alternators

C—Speed A + drive slip = input speed × no-load ratio

The indicated error is the sum of the

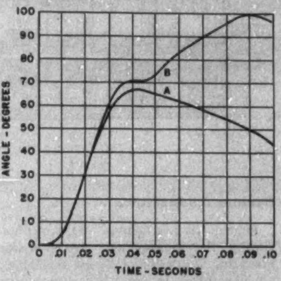

Figure 7A. Effect of electric load

Angle shown is the electrical angle between the alternator of the accelerated engine and the other three alternators

A—Case 5; no electric load

B—Case 6; electric load = 67 per cent per generator

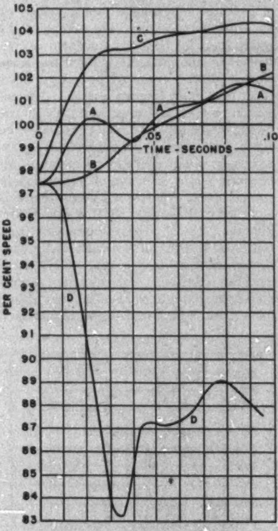

Figure 7B. Speed changes, case 6

A—Speed of alternator of accelerated engine

B—Speed of other three alternators

C—Speed A + drive slip = input speed × no-load ratio

D—Speed called for by governor droop circuit

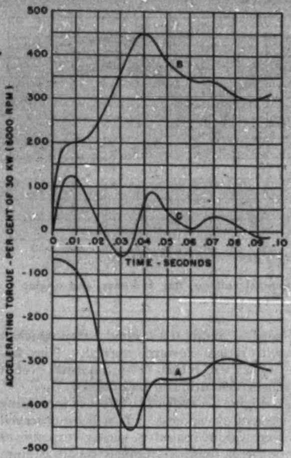

Figure 7C. Torques on generator, case 6

A—Electrical torque on generator of accelerated engine

B—Mechanical torque on shaft of same generator

C—Net torque on same generator

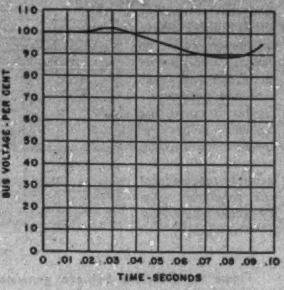

Figure 7D. Bus voltage, case 6

actual error indicated by the tachometer circuit and the apparent error indicated by the droop circuit. Such an apparent error occurs whenever the alternator power output increases (or decreases) as a result of transient conditions. Thus, an overload due to acceleration of an alternator causes the droop circuit to call for a lower speed and thus increases the signal to the governor in the direction of restoring correct speed. The correct speed in each case is considered to be the proper speed for the particular electric load under balanced steady conditions, as determined by the governor setting and droop-circuit adjustment.

In practice, there probably will be a maximum rate at which the governor can change the drive ratio, but it is assumed that the governor is so designed that this is reached only for speed errors outside the range encountered in the cases studied.

In each case, the governor is assumed to have a definite constant value of response in (drive-ratio change per second) per rpm of indicated error. The value selected is not the same in every case, and so the effect of changes in this value can be ascertained.

The drive ratio is the output speed divided by the input speed.

For the cases studied, there is a three-to-one gear ratio between engine shaft and accessory drive shaft. At an engine rpm of 900 the input speed is 2,700 rpm, so that for an output speed of 6,000 the ratio is 2.22. For this condition a rate of ratio change of 0.005 per second corresponds to a rate of alternator speed change of 13.5 rpm per second.

The governor is assumed to have no time lags in attaining the assumed response values. Actually there will be some time delay between the appearance of a speed error and the start of movement of the transmission ratio-control lever by the governor. Some idea of the effect of delays can be obtained by comparison of cases involving no delay and those including no governor action. These indicate that some delay is permissible and indicate approximately its allowable magnitude.

Cases Studied

The cases studied are outlined in Table I. A review of the results of the calculations for these cases form the basis of the conclusions given in this report.

The constants selected for the calculations are typical of a system for a large airplane using a-c power distribution. These constants are listed in Appendix III. Table II illustrates the manner in which the conclusions were obtained by comparing various results listed in Table I.

Sufficient cases have not been studied to be sure that the most severe conditions have been investigated; however, number 6 is considered to be fairly representative of a very severe case. This is the case of accelerating one engine at the maximum rate when operating at low speed, connected to a loaded alternator which is in parallel with three other loaded alternators.

Analysis of Results

The results of the cases studied have been plotted on Figures 2 to 8. These results may be analyzed by comparing various cases as outlined in Table II.

On several of the figures (Figure 2 for example) the electrical angle between generators is plotted. When the machines are operating at equal loads and excitations, as would be the case for normal operation, this angle is zero. That is, the rotors of the machines rotate at exactly the same speed and pass by a given point in each generator stator at exactly the same instant. If one generator is accelerated, its poles will pass any given point in the stator ahead of the corresponding poles in the other generators, so that the angle between the accelerated machine and the other machines is said to be increased from zero to a positive value. As this angle increases, the accelerated alternator delivers more load and may even furnish power to the other generators. The power transferred between generators tends to slow down the alternator of the accelerated engine and to speed up the other alternators, and thus resists the increase in angle.

Since the power transferred is only a very small fraction of the rating of the airplane engines, it will have practically no effect on the speed of the engines. However, it will cause changes in the slip in the transmissions, and it will cause the governor droop circuits to function in a

Table I. List of Cases

	Figure Numbers			Intial Conditions				Governor Characteristics			Results	
Case	Showing Angle	Showing Speed	Showing Other Quantities	No. of Generators in Parallel	Load Per Generator (Per Cent)	Engine Rpm	Slip in Drive at Full Load (Per Cent)	Full-Load Droop (Per Cent)	Response* (Ratio Per Sec) Per Rpm	Engine Acceleration Rpm Per Sec	Max Angle Between Generators (Degrees)	Max Speed Change (Per Cent)
1	2, 3			4	0	2,000	0		0	2,150	98	
2	3, 4			4	0	2,000	1		0	2,150	86	
3	4, 5A			4	0	900	1		0	2,150	Pulls out	
4	5A, 6A	5B		4	0	900	1	3.75	0.0025	2,150	109	16
5	6A, 7A	6B		4	0	900	1	3.75	0.005	2,150	68	9
6	7A	7B	7C, 7D	4	67	900	1	3.75	0.005	2,150	100	4.2
7		8		Nonparallel	0	900	1		0.005	2,150		12.2

* Governor response is measured in (drive-ratio change per second) per rpm of indicated alternator-speed error.

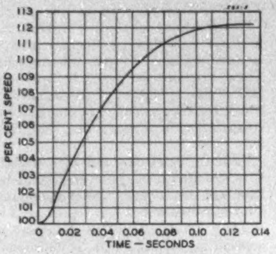

Figure 8. Generator speed, case 7

Speed returns to normal even if engine acceleration is sustained

One generator pulling ahead of three others. Impedance load on system, 0.75 power factor, 2.5 times rating of one generator

Figures on curves are per-unit values of armature flux linkages behind direct-axis transient reactance of one generator, value for other generators being unity

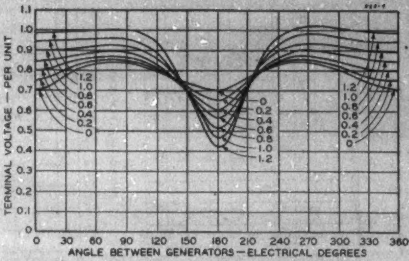

Figure 9. Relations between generator terminal voltage, flux linkages, and angles

direction to help maintain synchronism. The synchronizing torques also may cause the slower alternators to free-wheel at a speed above their drive output speed, thus tending to minimize alternator speed difference and keep the angle between generators within safe limits. Hence, the synchronizing torques between generators are very helpful in preventing loss of synchronism.

The electrical characteristics of the generators under transient conditions are such that the synchronizing torque increases with angle until an angle of about 130 degrees is reached. At this angle, the torque is several times normal. Beyond this angle the torque falls off rapidly, so that the machine is very likely to pull out of step if the angle exceeds 130 electrical degrees.

The angle for maximum transient torque is greater than 90 degrees because of the effect of flux trapped by the field winding. Typical transient torque–angle characteristics are given by Figure 10.

Table II. Schedule of Comparative Results

For Effect of	Compare	With
Slip in drive	Case 1 (no slip)	Case 2 (1% slip)
Applied acceleration	Case 2 (6,450 rpm per second acceleration applied to alternator)	Case 3 (14,300 rpm per second acceleration applied to alternator)
Governor action	Case 3 (no governor)	Case 4 (with governor)
Governor response	Case 4 (governor response—0.0025 per second per rpm error)	Case 5 (governor response—0.005 per second per rpm error)
Bus load	Case 5 (no load)	Case 6 (67% load per generator)
Nonparallel operation	Case 5 (parallel operation)	Case 7 (nonparallel)

In Figure 2 (case 1) the angle between machines does not exceed 100 degrees and returns toward zero after about 0.10 second. Hence synchronism is maintained. Since there is no governor in this case, the frequency, of course, continues to increase as long as the engine accelerates. Free wheeling permits the other three generators to be accelerated by electric power from the alternator of the accelerated engine.

Figure 3 shows the effect of slip in the drive. On curve *B* (case 2) the angle does not increase so rapidly nor reach so high a value as for curve *A* (case 1), so that there is less tendency to pull out and more time for governor action in this case than in the previous case. This shows that slip in the drive is helpful. See Table II.

Figure 4 shows the effect of increasing the acceleration applied to the alternator. On curve *B* (case 3) the angle increases rapidly beyond 130 degrees so that the generator can be seen to be pulling out of step as a result of the acceleration of the engine. It may be noted (Table I) that the engine acceleration is the same as for the previous case (curve *A*), but the drive ratio is higher, resulting in a higher acceleration of the alternator. In case 3 (curve *B*), the free wheeling and drive slip are unable to prevent pull-out.

In Figure 5A (case 4) the angle does not exceed 110 degrees and returns toward zero, so that the action of the governor, which was not present in the previous case, may be seen to be responsible for maintaining synchronism. (Table I shows that the initial conditions for this and the previous case are the same.)

In Figure 5B is shown the speed changes for case 4. The speed of all machines is increased, the other three machines being accelerated (free wheeling) by the electrical synchronizing torque. The effect of the slip in the drive may be observed by comparing curves *A* and *C* of this figure. The frequency may be seen to be approaching a maximum of about 116 per cent at about 0.2 second, after which it will return toward normal. The frequency will return toward normal even if the acceleration is maintained.

Figure 6A shows the effect of increasing governor response. It will be observed that the increased governor response of curve *B* (case 5) reduces the maximum angle reached.

It is evident that, when accelerations are less than the maximum possible, there will be more time for the governor to make corrections, so that a governor may have appreciable time lag and less than the maximum required response, if the acceleration does not attain its maximum value immediately. It is expected that in practice accelerations will not reach their maximum values instantly, so that the calculations may be conservative even though an actual governor will not attain its maximum response instantly. More complete data must be obtained before the net effect of delays in attaining maximum acceleration response and maximum governor response can be determined.

Figure 6B shows the speed changes for case 5. By comparison of this figure with Figure 5B (case 4) it will be seen that the greater governor response of case 5 reduces the change in frequency resulting from the engine acceleration. The frequency will return to normal sooner than in case 4.

Figure 7A shows the effect of electric load. This figure shows that the maximum angle is increased by the addition of electric load to the system. On curve *B* (case 6) the alternator does not pull out of step. However, the maximum angle reached in this case is quite large, (100 degrees), so that the generator probably would pull out if the governor response were appreciably less. Hence the response for this case (0.005 per second per rpm error) is just about sufficient to maintain synchronism in this severe case.

Figure 7B shows the speed changes for this case. The effect of the governor droop circuit is clearly shown by curve *D*, which shows the speed called for by this circuit as a result of the electric overload on the generator during the disturbance.

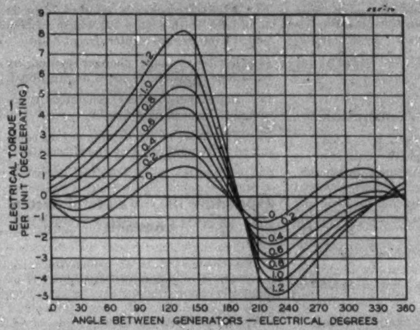

Figure 10. Relations between generator angles and flux linkages and the electrical torque on one generator

One generator pulling ahead of three others

Impedance load on system, 0.75 power factor, 2.5 times rating of one generator

Torque values are for generator which is being pulled away from others

Figures on curves are per-unit values of armature flux linkages behind direct-axis transient reactance of one generator, value for the other generators being unity

Torque values given on curves do not include torques due to amortisseur windings

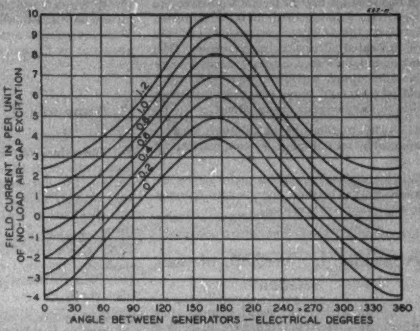

Figure 11. Relations between generator angles and flux linkages and the field current of one generator

One generator pulling ahead of three others

Impedance, load on system, 0.75 power factor, 2.5 times rating of one generator. Field-current values are for generator which is being pulled away from others

Figures on curves are per-unit values of armature flux linkages behind direct-axis transient reactance of one generator, value for the other generators being unity

The signal to the governor introduced by this circuit is seen to be greater than the actual speed change of the generator. The selected per-cent droop (3.75 per cent) is less than the value (five per cent) specified by the Army, so that droop circuit actually used may be even more effective if time delays do not hamper its action seriously. The initial speed is 97.5 per cent, because the initial load on the generators causes the droop circuit to establish a speed lower than the no-load speed, which was taken as 100 per cent.

The maximum speed change is less in case 6 (Figure 7B) than in the previous case, because the electric load tends to prevent overspeeding.

Figure 7C shows the torques acting on the alternator of the accelerated engine. The electrical torque (curve *A*) is seen to reach a value of over four times normal due to the angular displacement. This opposes the mechanical torque (curve *B*) exerted by the drive, so that the net accelerating torque (curve *C*) is relatively small and results in only a relatively small frequency error.

Figure 7D shows the bus voltage for this same case (case 6). It will be noted that, when four generators are operating in parallel, one generator may undergo a severe disturbance without causing more than about a ten-per-cent dip in the system voltage.

Figure 8 illustrates the performance during nonparallel operation, when the engine acceleration and governor characteristics are the same as for the preceding two cases. It will be noted that the maximum speed error is greater with nonparallel operation, because there is no synchronizing torque from other generators to minimize overspeeding. The frequency increases to about 112 per cent, after which it returns toward normal.

Conclusions

1. A free-wheeling device in the output shaft of each variable-ratio transmission is very helpful for maintaining parallel operation during periods of engine acceleration. Under favorable conditions such devices permit synchronism to be maintained without any governor action whatever.

As most accelerations are expected to be moderate and of short duration, they normally will produce only momentary unbalances in load division among generators, which will be corrected by governor action and by the cessation of the accelerations.

When free wheeling is employed, the generators usually will resynchronize themselves following a disturbance which causes pullout to occur.

2. Even a small amount of slip (say one per cent at full load) in the transmission is helpful for maintaining sychronism, during transients due to engine acceleration.

3. If the acceleration which appears at the alternator is increased, it becomes more difficult to maintain synchronism. For a given amount of engine acceleration, the alternator acceleration is greatest when the transmission is at maximum overdrive ratio.

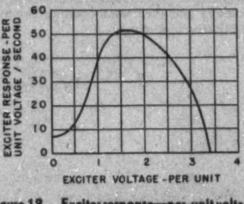

Figure 12. Exciter response—per-unit voltage per second

Exciter voltage is expressed in per unit of the value required for no-load air-gap rated-voltage excitation of the alternator

4. For the maximum accelerations considered, the effects of free wheeling and drive slip are not sufficient to maintain synchronism, so that reliance on governor action is necessary.

5. The effect of electric load on the bus is to increase the required governor response to maintain synchronism during periods of engine acceleration. This is true, because the load reduces the transient electrical synchronizing torque between generators.

6. Parallel operation tends to cause the frequency to be maintained within closer limits when one engine is accelerated, than would be the case for the same acceleration and governor response with nonparallel operation.

7. The rate of increase of acceleration is important in establishing governor requirements, as well as the maximum value of acceleration.

8. Time lag in attaining governor response should be kept to a minimum.

9. The governor droop circuit (which causes the alternator speed to droop with increased load) has a very beneficial effect in maintaining synchronism.

10. For the most severe case studied (case 6) the governor should attain its maximum required rate of ratio change in about 0.03 second to maintain synchronism. This maximum rate of ratio change is 5.3 per second for the assumed maximum engine acceleration of 2,150 rpm per second. The calculations indicate that to attain this rate

of ratio change in 0.03 second would require a governor response of about 0.005 expressed in (drive-ratio change per second) per rpm of indicated alternator-speed error. The maximum indicated alternator-speed error includes about three per cent (180 rpm) actual error, and 14 per cent apparent error, due to the governor droop circuit.

11. The method of calculation used is adaptable to studying a wide variety of cases.

When test data on system performance are available, the method may be used to assist in analyzing test results.

Appendix I. Method of Calculation

The calculations of electrical angle and other quantities versus time were made by a step-by-step process. At each value of time the rates of change of angles, speeds, generator flux linkages, transmission ratios, and exciter voltages were determined. These rates of change were assumed to remain constant for a short interval of time and the increments in these various quantities thus determined. By adding these increments to the original values, the angles, speeds, generator flux linkages, transmission ratios, and exciter voltages after the time interval were calculated. By making use of these new values and the constants of the system, rates of change for the next interval of time were determined. The process was repeated continuously, beginning with the time of first appearance of engine acceleration and continuing until the behavior of the system was ascertained.

In determining the rates of change of the quantities mentioned, certain other quantities, such as terminal voltage and torques, were calculated and plotted. The rates of change were determined using the constants given by Appendix III. The calculations for these rates were made on the basis of the assumptions listed in Appendix II.

The time intervals employed in making calculations in all cases were only 0.005 second or less. The interval used was determined by repeating calculations for one case with successively smaller intervals until further reduction in the interval produced substantially no difference in the result obtained.

It was found convenient to plot the calculated relations between terminal voltage, electrical angle, electrical torques (except amortisseur torque), generator flux linkages, and generator field currents, prior to making the step-by-step calculations, as these relations were independent of time. The calculations for these relations were aided by use of the a-c network analyzer. Typical results are given by Figures 9, 10, and 11.

Appendix II. Assumptions

1. The effect of magnetic saturation is neglected. This is considered justifiable, because the flux-linkage changes involved are relatively small. Methods for including this effect are available for cases requiring them.

2. The effect of amortisseur windings on generator armature currents is neglected. Preliminary calculations showed this effect to be small.

3. Torque due to amortisseur windings is assumed to vary directly with the rate of change of electrical angle with respect to terminal voltage, to be unaffected by rotor angular position, and to vary directly as the square of terminal voltage. Preliminary calculations indicated that this assumption is reasonably correct for the range of speed differences involved.

4. Voltages due to rates of change of direct- and quadrature-axis armature flux linkages are neglected. This assumption is justifiable, because these voltages are small compared to those resulting from rotation.

5. Generator friction, windage, core loss, and exciter torque are neglected.

6. Deviations in speed up to about ten per cent are assumed to have no effect on machine reactances or the ratio between power and torque. The effect of speed variations on terminal voltage is considered, however.

7. Alternators, voltage regulators, and governors are assumed to be identical so that several machines operating in parallel may be lumped into one, provided their engine speeds do not differ.

8. The rate at which the governor changes the drive ratio is assumed to be proportional to the alternator-speed error, within the range of speed changes involved.

9. Voltage-regulator action for small voltage errors (up to three per cent) is neglected. For greater voltage disturbances, the regulators are assumed to act, but to delay exciter response for 0.02 second. The effect of reactive cross-current compensation is neglected. This effect will be small if the regulators and their compensating circuits are adjusted properly.

10. Exciter response is assumed to be in accordance with Figure 12, which was obtained from typical exciter design data.

11. Exciter voltage changes caused by variations in generator speed are neglected.

12. Impedance between generators is assumed to be negligibly small.

13. The speed of the driving engine is assumed to be unaffected by the alternator.

Appendix III. Values of System Constants

The selected values of system constants used for the examples studied were as follows:

Engine Characteristics

Speed range	900–2,700 rpm
Accessory-shaft gear ratio	3:1
Accessory-shaft speed range	2,700–8,100 rpm

Alternator Constants

Rating:
40 kva, 30 kw, 6,000 rpm, 208 wye/120 volts, three phase, 400 cycles

Open-circuit field time constant	0.10 second
Amortisseur damping coefficient	7.0 (per-unit torque) ÷ (per-unit slip)
Inertia constant, H	0.21 second
Transient reactance, x_d'	0.16 per unit
Synchronous reactance, x_d	1.04 per unit
Quadrature reactance, x_q	0.58 per unit
Armature resistance	0.03 per unit

Exciter Characteristics

Response	Figure 12

Transmission Constants

Slip (when present)	0.010 per unit at 45-horsepower mechanical torque (6,000 rpm)
Input speed range	2,700–8,100 rpm
Output speed rating	6,000 rpm

Governor Characteristics

Speed droop (when present)	0.0375 per unit at 30 kw electrical torque (6,000 rpm)
Response	Up to 0.005 drive-ratio change per second per rpm error

References

1. Basic Considerations in Selection of Electric Systems for Large Aircraft, W. K. Boice, L. G. Levoy, Jr. AIEE Transactions, volume 63, 1944, June section, pages 279–87.

2. Why Tomorrow's Planes Will Have A-C Electrical Systems, T. B. Holliday. *Electrical Manufacturing*, July 1943.

3. Parallel Operation of Airplane Alternators. D. W. Exner. AIEE Transactions, volume 62, 1943, December section, pages 755–60.

A Current-Limiting Fuse for Aircraft Applications

A. H. POWELL
ASSOCIATE AIEE

Synopsis: Although many fuses are available for aircraft applications, it has become increasingly evident that the trend to large aircraft electric systems necessitates a review of existing fuse devices, particularly with regard to their interrupting ability. Such a survey indicates many applications for an improved interrupting device. A new current-limiting fuse has been designed to meet the requirements. This paper describes the device and presents test data to indicate its suitability.

MUCH has been said about electric systems in aircraft including the history af their growth—voltage, available current, frequency, design, protection—as well as predictions of systems to come.[1,2] Articles, discussions, and lectures have indicated a trend that will require improved protective devices, particularly fuses. The fuse is a very widely used overcurrent protective device in aircraft electric systems today, because it provides maximum benefits for a minimum weight, space, and cost. Fuses which have proved satisfactory for present-day aircraft, however, should not be considered suitable for larger aircraft of the future. The definite trend to larger aircraft has resulted in three fundamental changes in the electric system:

1. There is an increasing number of operations being performed electrically, requiring larger amounts of available generated power.
2. Short circuits caused by battle damage in military airplanes or normal failures of connected equipment must be removed rapidly and satisfactorily to prevent system disturbances.
3. The circuits have become more complicated, requiring accurate, consistent, and correct fuse or protective-device operation.

The following general specifications for the required fuse and support are therefore proposed:

1. Adequate interrupting capacity.
2. Accurate and consistent time-current characteristics.
3. One-half cycle or less of arcing time.
4. Uniform contact resistance.
5. Vibration and shock resistance.
6. The foregoing characteristics to be affected only slightly by altitude up to 40,000 feet or ambient temperatures of −70 to +60 degrees centigrade.
7. Small size, compactness, light weight, and easy replacement.

Admittedly, a lot is required of a relatively simple device. Nevertheless, to meet these specifications, a new current-limiting fuse has been designed particularly for aircraft use. This paper discusses this fuse and presents information regarding applications.

Construction and Operation

For several years there has been available for central-station and industrial users a current-limiting power fuse.[3] This fuse, consisting essentially of a pure silver-wire element in an interrupting medium in the form of granular quartz, is unique in the way it operates on short circuits. The fuse limits the magnitude of the short-circuit current, under most conditions, to a value below that which would be produced in a direct short circuit. This action is summarized by the curves in Figure 2.

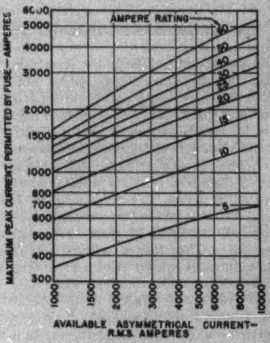

Figure 1. Current-limiting characteristics

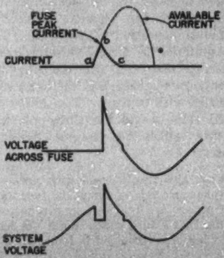

Figure 2. Wave forms of typical oscillogram of current-limiting fuse operation on a 60-cycle circuit

Short circuit starts at a, fuse melts at b, and arcing and interrupting complete at c

It was decided that this current-limiting action would be extremely desirable in aircraft electric systems, and therefore a fuse was designed, using this basic principle, which would meet the other specifications, particularly as to size, operating conditions, and vibration. The results are shown in Figure 3 and Figure 4.

The device is built at present in two frame sizes, one for a fuse of 30-ampere maximum rating and the other for a fuse of 60-ampere maximum rating. This division of ratings was arrived at after

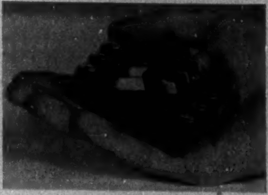

Figure 3. The new current-limiting fuse for aircraft applications

Thirty amperes, 208 wye/120 volts, 400 cycles. Fuse unit partially removed from holder

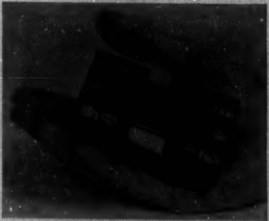

A. Fuse unit and latching bar are in place

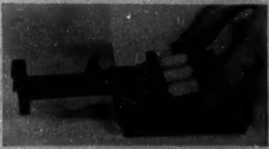

B. Latch bar open and fuse being removed

Figure 4. The new current-limiting fuse for aircraft applications

Sixty amperes, 208 wye/120 volts, 400 cycles

Paper 45-88, recommended by the AIEE committee on air transportation for publication in AIEE TRANSACTIONS. Manuscript submitted November 8, 1944; made available for printing March 8, 1945.

A. H. POWELL is designing engineer, device division, switchgear department, General Electric Company, Philadelphia, Pa.

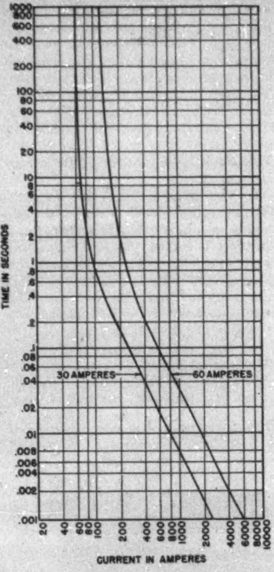

Figure 5. Melting-time–current curves for new current-limiting aircraft fuse

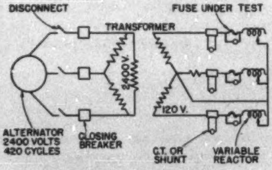

Figure 6. Test-circuit diagram

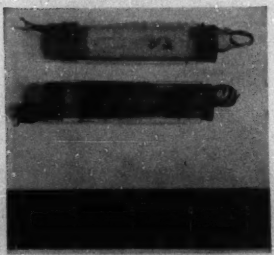

Figure 7. First sample fuses for preliminary tests, following interruption

Upper unit, silver wire, quartz filler. Lower unit, copper wire, air filler

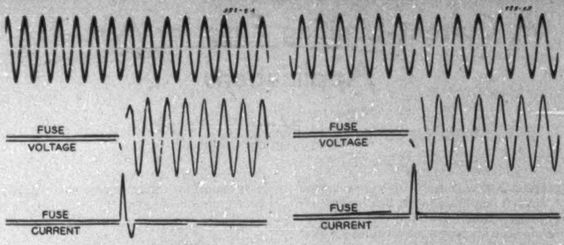

A. Copper wire, air filler

Available current, 3,000 amperes; melting time, 0.00119 second; arcing time, 0.00059 second (Test 2, Table II)

B. Silver wire, quartz filler

Available current, 4,500 amperes; melting time, 0.00059 second; arcing time, 0.00030 second (Test 6, Table II)

Figure 8. Oscillograms for test samples shown in Figure 7

Tests made at 120 volts, 420 cycles

careful consideration of probable load requirements and design limitations of the maximum continuous current which could be carried safely by the terminals, contacts, and the fuse unit itself.

Fuse Units

The two fuse units are similar in construction, each consisting of two molded end pieces with three blade inserts for the contacts, three Pyrex glass tubes, silver-wire elements, and the special granular-quartz filler. The molded parts are made of a compound that will withstand vibration, shock, and the expected extremes of temperature. The blades which mate with contacts in the supports are silver-plated. The Pyrex tubes fit into counterbores in the molded pieces and are cemented in place during assembly. The fusible elements pass through small holes in the blades and are soldered to them with a lead–silver alloy which will not be affected by the operating temperature of the fuse. A brightly colored paint is applied to the inside of the glass tubes on the side towards the top of the fuse. The paint will be changed in color by the heat from the melting of the fuse element to indicate the blown condition of the fuse. The filler material is added through small holes in the fuse ends, after the tubes and elements are in place, and the holes then are sealed with cement. The design described thus provides a three-pole fuse assembly which has several desirable features:

1. When this fuse is used with proposed three-phase electric systems, the fuse units in all phases are replaced simultaneously, assuring that a fuse which might not have melted but was damaged is replaced.

2. There is no chance of one phase being accidently left open.

3. The phases are in separate isolated compartments, entirely preventing phase-to-phase short circuits within the device during the interruption.

The fuse element is made of pure silver wire with a reduced center section to limit the length which melts during interruption. There are, of course, many materials which could be used for the element, but silver was selected as the most suitable after careful investigation. Silver has a low specific resistance; thus a minimum cross section of wire will carry a given current, and there is a minimum amount of material to be dissipated during interruption. Furthermore, its melting and vaporizing action has proved more satisfactory in fuse operation than that of copper, which was also considered. Resistance to oxidation and corrosion are other characteristics in which silver is superior.

In the fuses for aircraft applications which are being considered in this paper, it is essential that ambient temperature have very little effect on the fuse time–current characteristics, for fuses which must co-ordinate may be in locations where ambient temperatures differ by 100 degrees centigrade. Thus, this is another reason why a high-melting-point element is superior to a low-temperature material such as zinc.

Many factors in the application of a

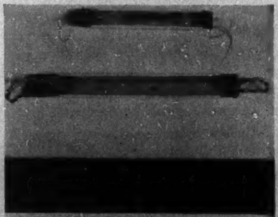

Figure 9. Sample fuses for second set of preliminary tests, after interruption

Upper unit rated 30 amperes; lower unit rated 60 amperes fuse dictate that it normally should be employed only as a short circuit rather than an overload protective device. This is discussed more fully later in the paper, but to meet this condition a fuse with "fast" characteristics is desirable, and this condition is obtained with the current-limiting fuse using a silver-wire element. Figure 5 shows typical time–current curves for 30- and 60-ampere aircraft fuse units.

Fuse Supports

The fuse supports shown in Figures 3 and 4 are similar in that two molded end pieces are fastened to an insulated base to form the support for the terminals and contacts. Beryllium–copper spring contacts, silver-plated, are used in the 30-ampere holder in order to provide uniform contact resistance. The fuse unit is latched into the fuse support, to prevent loosening from vibration, by having the blades on one end of the fuse unit assembled under a pin at one end of the support, while a spring backed catch at the opposite end of the fuse support locks over a projection on the other end of the fuse unit. Thus the fuse unit operates similar to the blade of a disconnecting switch and may be readily removed from the support when in the "open" position. The catch must be released before the fuse unit can be moved to the "open" position.

The 60-ampere support differs from the 30-ampere design, in that silver-plated copper contacts, backed by steel compression springs, are used. Furthermore, a hinged latching bar is arranged to swing into closed position after the fuse is inserted. The closing of the latching bar puts added pressure on the contacts, thus assuring uniform contact resistance, and holds the fuse in place against vibration and acceleration. The latching bar is held in place by a catch which is operated in the same manner as the catch described for the 30-ampere holder.

The over-all dimensions and weights of the fuse units and holders, given in Table I, indicate that the device is small and lightweight.

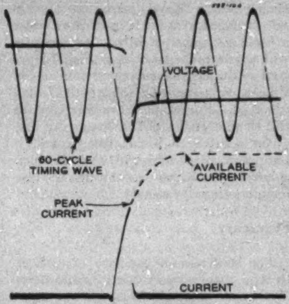

A. Thirty-ampere fuse

Available current, 3,149 amperes; peak current, 1,640 amperes; melting time, 0.0067 second; arcing time, 0.0015 second (Test 5, Table III)

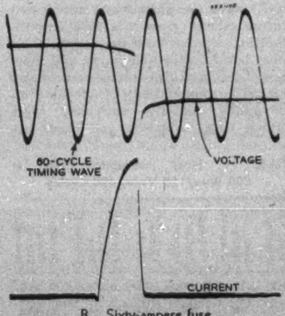

B. Sixty-ampere fuse

Available current, 3,149 amperes; peak current, 2,640 amperes; melting time, 0.013 second; arcing time, 0.0023 second (Test 6, Table III)

Figure 10. Oscillograms of d-c short-circuit tests made at 135 volts

Tests

The current-limiting aircraft fuse was developed primarily for use on relatively high-voltage a-c electric systems. Specifically, the anticipated application was on a 208-wye/120-volt three-phase 400-cycle system. Therefore, the majority of the tests were made using this type of circuit. To check for operation of the fuses under other conditions, short-circuit tests also were made on 135-volt d-c circuits, and 120-volt 60-cycle a-c circuits.

Approximately 350 short-circuit tests were made during the development of the new fuse. Except for final check tests with a three-phase circuit, all tests were made with a single-phase 120-volt circuit, arranged as indicated in Figure 6, with a frequency of 420 cycles, which was the nearest available to 400 cycles. The initial series of tests was made using crude sample fuses to determine length of element, filler material, and other design limitations. Two of these samples after interruption are shown in Figure 7, and oscillograms for the two tests, Figure 8, indicate clearly the short arcing time obtained by using a suitable filler material. Table IIA lists the results of some of the preliminary tests made for the purpose of comparing the interrupting characteristics of silver and copper element in air and in quartz filler. Table IIB lists results of tests which demonstrate the current-limiting action of the fuses. Note that tests were made at currents up to 5,600 amperes and 40,000 feet altitude using a suitable pressure chamber. The arcing time was generally long and erratic with the air filler, but consistently short with the quartz filler. Thus the current-limiting fuse will meet the specifications for adequate interrupting capacity and short arcing time.

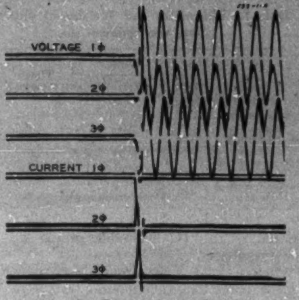

A. Twenty-ampere fuse

Available current, 3,100 amperes; melting time, 0.00071 second; arcing time, 0.0003 second (Test 2, Table IV)

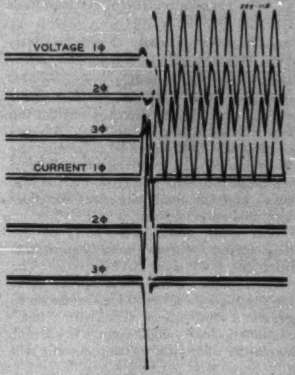

B. Fifty-ampere fuse

Available current, 3,100 amperes; melting time, 0.0019 second; arcing time, 0.0003 second (Test 4, Table IV)

Figure 11. Oscillograms of final three-phase interrupting tests at 208 wye/120 volts, 420 cycles

Following the preliminary tests, a second series was made using samples with smaller-diameter tubes and elements designed in accordance with the results of the first series of tests. Typical samples for these tests are shown in Figure 9. The results were similar to the first series of tests and confirmed the suitability of the design. Tests also were made using the second set of samples, Figure 9, on a 135-volt d-c circuit. The results were very satisfactory. Figure 10 shows typical oscillograms of the tests, and again the very short duration of arcing should be

Table I. Dimensions and Weights of Fuse Units and Holders

Device	Inches: Length	Inches: Width	Inches: Height	Weight (Ounces)
30-ampere support	$2\frac{3}{4}$	$1\frac{11}{16}$	$1\frac{1}{4}$	1.9
5–30-ampere fuse unit	For 30-ampere support			1.1
60-ampere support	$3\frac{1}{2}$	$2\frac{1}{4}$	$1\frac{9}{16}$	3.9
40–60-ampere fuse unit	For 60-ampere support			1.6

noted. Table III lists some of the d-c test results.

Before final short-circuit tests were made, many long-time melting tests were required in order to determine the exact size of fusible-element wire to obtain the required continuous-current ratings. Two factors govern this determination:

1. The temperature rise of the fuse while carrying the full current.
2. The melting current at some relatively long time, five minutes for example.

It was found that satisfactory results were obtained when the five-minute melting current was about twice the normal full load-current rating of the fuse. A series of tests was then made to determine the five-minute melting current of a range of wire sizes (both one and two wires per fuse tube) and the final wire sizes were determined and checked.

The lower ends (short-time) of the time–current curves were determined from the final short-circuit tests. The various points were combined to form the completed curves which, as shown in Figure 5, indicate a fuse with "fast" characteristics (a slight change in current above the minimum melting current will produce very rapid melting). The lower end of the curve is a straight line with a two-to-one slope.[4] Results of some of the final tests are listed in Table IV, and typical oscillograms are shown in Figure 11.

Vibration tests show conclusively that the particular filler material used has no detrimental effects on the elements. After 50 hours of vibration with a frequency of 10 to 55 cycles per second, no reduction in cross section of the element was observed. This may well be due to two factors in the design:

1. The special size and shape of the grains of the filler material.
2. The fact that the filler material is tightly packed in the fuse tubes.

Application

The subject of application of fuses in aircraft electric systems is too broad to be covered in this paper. However, a few suggestions as to the fundamental points are in order.

Good fusing practice dictates that a fuse should be used for short-circuit protection, not overload protection. There are other devices, such as automatic motor protectors[5] and temperature relays, which provide satisfactory overload protection. However, in aircraft systems it is essential that the circuits remain operable at all times, except when they are damaged, in which case the fuse must operate to disconnect that part of the system. The current-limiting fuse which has been described is ideally suited for circuit protection, for its current-carrying ability and time–current characteristics are similar to those of the conductor and are not appreciably affected by differences in ambient temperatures.

Table III. Short-Circuit Tests at 135 Volts Direct Current

‡ Test Number	Fuse Rating (Amperes)	Available Current (Amperes)	* Peak Current (Amperes)	Melting Time (Seconds)	Arcing Time (Seconds)
1	10	480	296	0.003	0.0007
2	40	480	480	0.042	0.0022
3	20	1,675	870	0.0055	0.0009
4	50	1,675	1,580	0.022	0.0022
5	30	3,149	1,640	0.0067	0.0015
6	60	3,149	2,640	0.013	0.0023

‡ All tests made at 500 feet altitude.

* Actual maximum peak current permitted by fuse.

Table II. Preliminary Interruption Tests at 120 Volts, 420 Cycles, Single-Phase

A. To Compare Effect of Filler Materials

Test Number	Fuse Rating	Element Material	Filler	*Available Current	Altitude (Feet)	Melting Time (Second)	Arcing Time (Second)
1	20	Copper	Air	3,400	1,000	0.00089	0.00040
2	20	Copper	Air	3,000	40,000	0.00119	0.00059
3	22	Silver	Quartz	4,500	1,000	0.00059	0.00030
4	20	Copper	Quartz	3,400	40,000	0.00062	0.00030
5	20	Silver	Quartz	172	40,000	0.128	0.00035

B. To Indicate Current-Limiting Action. Silver Wire, Quartz Filler

Test Number	Fuse Rating	**Available Current	‡Peak Current	Closing Angle (Degrees)	Altitude (Feet)	Melting Time (Second)	Arcing Time (Second)
6	22	6,380	4,000	30	1,000	0.00059	0.00030
7	20	5,940	4,100	70	40,000	0.00050	0.00030
8	22	4,250	2,780	75	1,000	0.00094	0.00035
9	25	8,180	4,800	30	40,000	0.00055	0.00030

* Available current is maximum rms current which the circuit can produce in the absence of the fuse, calculated from the rms symmetrical current available and corrected for the actual closing angle.

** Available current is maximum peak current which the circuit can produce in the absence of the fuse, calculated from the rms symmetrical current available and corrected for the actual closing angle.

‡ Peak current is the maximum instantaneous current permitted by the fuse.

Thermal damage to a fuse element also must be considered when one is applying a fuse. Sufficient tests have been made to indicate that a change takes place in any element material when it is heated nearly to its melting temperature and then cooled. To make sure that a fuse is not damaged, it is a safe practice to select a fuse for a given circuit so that the fuse will not have to pass more than 75 per cent of the melting current shown on the time–current curve for the length of time involved. For example, in reference to the characteristics of the 30-ampere fuse given in Figure 5, if the circuit carries a temporary overload of 70 amperes, such a current should not pass through the fuse for more than 0.9 second.

Summary

The short-circuit capacity of aircraft electric systems is increasing constantly so that many available fuses are not satisfactory for the duty imposed on them. Furthermore, higher voltages are being used in order to transmit more power with smaller conductors. A fuse is an excellent short-circuit protecting device, but it must be properly built and correctly applied.

To meet the present and anticipated future circuit growth, a new current-limiting fuse has been developed. This fuse, based on the well-known and time-tested design of high-voltage power fuses, meets the requirements of adequate interrupting capacity, extremely short arcing time, vibration and shock re-

Table IV. Final Interruption Tests at 208 Wye/120 Volts, 420 Cycles

Test Number	Fuse Rating (Amperes)	* 3-Phase Available Current	Altitude (Feet)	‡ Average Melting Time (Second)	Average Arcing Time (Second)
1	10	3,100	1,000	0.0003	0.0003
2	20	3,100	1,000	0.00071	0.0003
3	40	3,100	1,000	0.0012	0.0003
4	50	3,100	1,000	0.0019	0.0003
5	60	4,580	1,000	0.0018	0.0003
6	60	2,990	1,000	0.0038	0.0004

* Available current is the rms symmetrical current (average three phases) which the circuit can produce in the absence of the fuse.

‡ Melting time is average of three phases. The variation in time was caused by the closing angle of the three phases.

sistances, high altitude and wide-range temperature operation, and small size and weight.

Tests demonstrated that the new fuse will interrupt dependably more than 4,000 amperes at 120 volts, 400 cycles, single-phase alternating current or at 120 volts direct current, with an arcing time of less than one-quarter cycle on the a-c circuit.

To obtain satisfactory operation of aircraft fuses, they should be used for short-circuit protection, not overload protection, and selected so that they will not be damaged by overloads.

References

1. Basic Considerations in Selection of Electric Systems for Large Aircraft, W. K. Boice, L. G. Levoy, Jr. AIEE Transactions, volume 63, 1944, June section, pages 279–87.

2. Why Tomorrow's Planes Will Have A-C Electrical Systems, T. B. Holliday. *Electrical Manufacturing*, July 1943.

3. The Current-Limiting Power Fuse, D. C. Prince, E. A. Williams, Jr. AIEE Transactions, volume 58, 1939, January section, pages 11–18.

4. Time-Current Curves for Outdoor High-Voltage Fuses, E. A. Williams, Jr. *Electrical World*, January 1937.

5. Principles of Aircraft Electric-Motor Protection, V. G. Vaughan. AIEE Transactions, volume 69, 1943, December section, pages 760–5.

Measurement of Railway-Motor Temperatures in Service

J. W. TEKER
ASSOCIATE AIEE

THE EVER-INCREASING application of Diesel-electric locomotives to the many diversified traffic requirements of the railway systems over the nation is an acknowledgment of the versatility and effectiveness of this type of motive power. It brings to the steam road the high availability of the Diesel engine, the practical adaptation of which to railway-traction requirements is made possible through the electric transmission. The electric generator coupled to the Diesel engine enables the essentially constant torque and speed output of the prime mover to be converted to the widely variable range of torque and speed required for traction by means of electric motors geared to the locomotive drivers. This same transmission is used again when electric braking is applied to reduce or hold train speed.

The application of the Diesel-electric locomotive is then actually based on the speed-tractive-effort or braking characteristics of the transmission, the size of which for a given duty is dictated by economic considerations and the greater over-all advantages of utilizing to full extent an optimum standardized equipment of given continuous rating. However, tractive effort far in excess of continuous rating can be exerted by the smoothly applied motor torque to drivers with all the locomotive weight available for adhesion, and this capacity for overload is limited only by the heating of the windings.

Temperature of windings therefore is a prime consideration in the application of Diesel motive power wherever loads exceeding the continuous rating are encountered to see that the maximum permissible limits are not exceeded or maintained over a period of time to shorten unduly the insulation life. To this end, the silent movement of an ammeter needle over its scale is, psychologically to the man trained in steam operation, a poor exchange for the attention-compelling blast of a laboring steam-locomotive exhaust as an indication of exerted effort. There is an unquestioned finality when a steam locomotive stalls with its load that finds no adequate equivalent in the electric drive. The steady unemphasized beat of the Diesel exhaust continues, irrespective of the overload coupled to the locomotive which it moves with an apparent effortless ease with no sensible external impression of the winding's rising temperature or its proximity to the limit, until smoke and smell of burning insulation announce the damage to equipment.

The Diesel-electric locomotive does not know when to quit; nevertheless its ability to handle overloads is dependent upon the thermal capacity of the electric apparatus so that the duration, for which a given overload may be maintained with safety, is determined by the temperature of the windings preceding its application. Where ruling grades or speed of operation limit train weights, the load is generally below the continuous rating of the equipment, so that low winding temperatures provide a useful margin of overload capacity. This is an advantageous attribute of the electric drive in railway operation when it is correctly utilized.

It is essential to know motor temperatures just before a given overload to be able to determine the permissible duration for such duty. Temperature measurements taken in the intended service will be a check on the assumptions made during application study. It is often difficult to make proper assumptions of variables when making such studies for a difficult service. When steam helpers are required to move heavy trains over long grades, it is necessary at times to reduce Diesel-engine speed and power input to the motors in order to accommodate differences between the speed–tractive-effort characteristics of the steam and Diesel locomotives. If traction-motor blowers are belt-driven, the volume of ventilating air then is decreased, so that even operation at the continuous rating may be questioned. Temperature measurements are useful to obtain data and checks on such operation.

The use of cut-and-try overload application methods in service on narrow margins without knowledge of apparatus temperature is an uncertain undertaking the inadequacy of which may not be immediately evident, but will show up in time by increased maintenance cost and frequent motor or generator failures. Severe overheating in a single instance may be sufficient to shrink wedges and relax bands, without causing immediate failure, but subsequent movement of the winding under influence of vibration will cause the insulation to wear through and fail by short circuit or ground even before complete deterioration of insulation is achieved.

Various means have been developed in the past to give a continual indication of motor temperature, but none have been favored by general use. Until such time as temperature-indicating instruments are developed for railway use reliable enough to warrant general application, the measure of motor temperatures by the resistance method is the most reliable and accurate means available today. It is a recognized and familiar means of temperature determination by electric-apparatus manufacturers and is common on their test floors where the personnel is trained and skilled in its use.

This same method has been developed for the railway field by a series of evolutionary experiences until the technique and required skill have been reduced to a point where measurements can be made under these adverse conditions by an operator and the help of men unskilled in laboratory or test-floor methods. The results equal and sometimes surpass in speed, accuracy, and uniformity those obtained under more favorable conditions on the test floor, and it becomes a practical tool for general field use where questions pertaining to motor temperatures have a bearing on railway operation.

Method

The method selected for determination of average motor winding temperature is dependent upon the known change in electrical resistance of a copper conductor with temperature and is expressed by the

---

Paper 45-83, recommended by the AIEE committee on land transportation for publication in AIEE Transactions. Manuscript submitted November 24, 1944; made available for printing February 21, 1945.

J. W. Teker is in the transportation engineering department of General Electric Company, Erie, Pa.

relation $T=(R/r)(234.5+t)-234.5$. The initial or cold resistance, r, of each component winding in question is measured after the motors have stood without power long enough to allow all motor parts to cool to a uniform ambient temperature, t, which is measured directly with mercury thermometers placed upon the motor parts and checked with each other and surrounding ambient temperature. The hot winding resistance, R, is measured at prearranged stops on the main line with the train and at the point where the temperature of the motors in the actual service is questioned. The temperature, T, is then readily evaluated from the corresponding cold resistance, r, at temperature, t.

It is necessary to remove power from the motors and bring the train to a stop before these resistances can be measured. During this interval the motors are cooling, and the temperature of the winding as determined is for the instant of time when the resistance is obtained. This temperature is lower than the actual temperature of the winding at the instant when power was removed by the amount of cooling taking place during this elapsed time. However, by continuing to measure the resistance of the winding, as it cools with respect to a time started at the instant of power removal, it is possible to plot these values and draw a cooling curve through the related points. By extending this curve back to zero time, the most probable actual temperature of each winding is determined at the instant of power off and is well within the limits of accuracy for all practical purposes.[1]

Figure 1. Instruments and special equipment required for measurement of railway-motor temperatures in service

Used to obtain operating data

A—Thermocouple selector switch
B—Hand tachometer
C—Hand pyrometer
D—Motor-field-resistance selector switches opened and closed
E—Padlocks
F—U-tube manometer
G—Static pressure tube
H—Armature-resistance contact yoke with flexible cable
I—Signal bell
J—Thermocouples
K—Flashlight
L—Thermocouple potentiometer
M—Special vibration-proof self-balancing double bridge
N—One-thousand-volt voltmeter
O—Special vibration-proof recording-chart ammeter and voltmeter
P—Millivoltmeter
Q—One-thousand-ampere shunt
R—Millivolt leads calibrated with shunt and meter
S—Centigrade mercury thermometer
T—Stop watch
U—Clip board

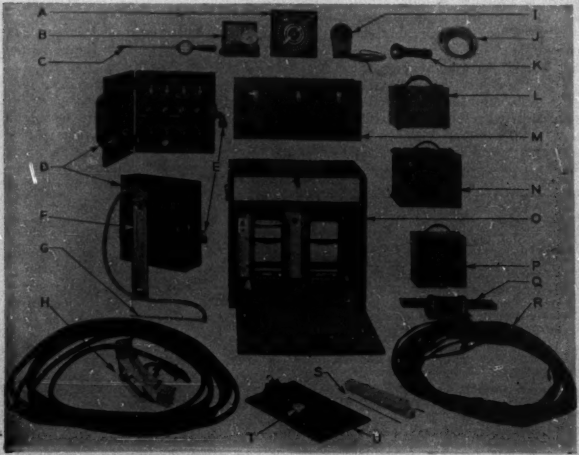

Although temperature is the primary consideration determining motor life, it is expedient to plot the data in terms of temperature rise so that performance can be compared between successive tests under different conditions. Measurements, therefore, must be made of the ambient temperature during the test of the traction-motor ventilating air, as well as of the air surrounding the locomotive. The volume of ventilating air delivered to each motor being tested also must be determined, as well as the power input to the motors, so that rms current values can be calculated for the train tonnages hauled.

The success of the method outlined is dependent upon practical means for making the necessary measurements and upon a test crew organized and equipped to make these measurements without causing serious loss of time to the scheduled run of the train.

Instruments

The instruments and their connections are shown in Figures 1 and 2.

The Resistance Bridge

The traction motors in common use with Diesel-electric road locomotives are of the series type having armature, commutating, and series exciting fields of low resistance. The Kelvin double-resistance bridge circuit is ideal for the measurement of these low-resistance values. A vibration-proof galvanometer or its equivalent is required to obtain a balance on the bridge. This element of vibration requires careful attention in the selection and preparation of the instrument, as it is advantageous to keep the locomotive Diesel power plant running at idling speed during the stop for resistance measurement so that a quick train start can be made at the conclusion of measurements, and to keep the air compressors in operation to recharge the air-brake system after bringing the train to a stop. Even though the one power plant close to the instrument is shut down, enough vibration will come through from the remaining engines, through the couplers between units, to cause erratic behavior of the standard galvanometer when one is attempting to obtain a balance of the bridge.

A vibration-proof self-balancing portable instrument was constructed for this special purpose by the Erie works laboratory of the General Electric Company for the engineering department to be used in checking railway-motor application and has demonstrated ability in actual service to obtain data with speed, uniformity, and accuracy surpassing that obtained by previously used methods.

Connections to Motor Fields

The motor field windings are connected to the instrument with temporary wiring and suitable switches, so that resistance measurements can be made quickly. The instrument station should be located in the cab as close to the motors as possible so as to hold the interconnecting leads to a minimum. A pair of leads, a current and a voltage lead, is run to each terminal point of the winding and should be securely connected or soldered. The series field winding and one end of the commutating winding can be connected to the end of the motor cable in the junction box where they are joined with the locomotive power cable. They must connect to the motor end of the terminal to avoid the terminal contact resistance. The connection of the other end of the commutating winding can be made in-

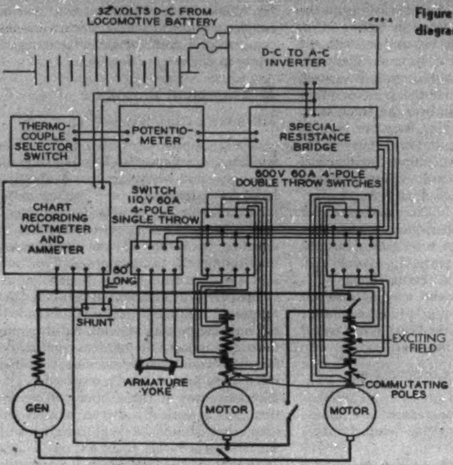
32 VOLTS D-C FROM LOCOMOTIVE BATTERY
D-C TO A-C INVERTER
THERMO-COUPLE SELECTOR SWITCH
POTENTIO-METER
SPECIAL RESISTANCE BRIDGE
600V 60A 4-POLE DOUBLE THROW SWITCHES
SWITCH 110V 60A 4-POLE SINGLE THROW
CHART RECORDING VOLTMETER AND AMMETER
60' LONG
SHUNT
EXCITING FIELD
ARMATURE YOKE
COMMUTATING POLES
GEN
MOTOR
MOTOR

Figure 2. Connection diagram for measurement equipment

side the motor where it joins the brush holder. These two instrument leads should be brought out of the frame without interfering with the motor inspection cover as it will have to be removed for armature-resistance readings and then quickly replaced. A hole may be drilled through a noncritical section of the frame to let these leads through, to be closed at the conclusion of the test. These leads should be run and secured alongside one of the main motor cable, as far as the junction box under the locomotive floor, where it can join the bundle of leads coming off the terminals and going to the instrument station. This bundle of instrument leads should have additional protection where it passes through and bends over structural members to avoid damage to the insulation.

Connections to Motor Armature

The armature resistance is obtained by selecting a span of the armature winding to which connection is made by contacts spaced apart by the desired number of commutator segments and held in fixed relationship by a special yoke applied by hand pressure to the commutator through the motor inspection opening.

This yoke has a locating lip to engage the undercut mica space between two adjacent commutator segments to align the contact points correctly on the segment at each end of the selected span of bars and prevent their coming in between two segments to cause erratic measurements. The number of segments included in the span should be as large as the space between brush holders permits without cramping the yoke, so as to obtain a maximum value of resistance for measurement. The contacts are individually spring-loaded and slide in parallel ways to accommodate slight inequalities in the hand pressure applied to the yoke.

Connection between contacts of the yoke and the instrument station is made through a multiple-wire flexible cable long enough to reach through a cab window down to the motors in the locomotive truck. This equipment is coiled and carried in the cab between stopping points for measurements.

Resistance Selector Switches

The switches are 600-volt four-pole double throw, with flexible jumpers connected around the hinge point of the blade. They should be completely enclosed with provision for padlocking the switch in the open-circuit position. This is a safety precaution, as the instrument leads are connected with the high-voltage power circuit when the locomotive is in operation, and will serve to isolate the instruments and personnel from harm. It also permits wiring to be installed during layovers between runs, thereby keeping the locomotive available for service while preparation for the test is being made. It also permits removal of instruments after a test run until results are checked. The switches should be located within reach of the instrument table so that the bridge can be switched from one connection to another in prearranged sequence.

Communication System

A signal system is necessary between the man at the instrument station and the men in position at the motors when measurements are in progress because of their remote location and the magnitude of noise level with Diesel engines idling. A push button fixed at the instrument station and a simple electric bell properly protected against injury during handling are used for this purpose, interconnected with flexible leads long enough so that they can be lowered from the cab to a man on the road bed. The signal code used is as follows:

One bell—make contact with yoke on armature.

Two bells—hold contact; measurement is in progress.

Three bells—remove contact.

An ammeter placed in the battery circuit of the bridge indicates the instant a circuit is established through the armature and informs the resistance bridge operator to proceed with measurement, while the man making the contact is informed to hold it by signaling two bells. A failure to establish contact with all four points on the commutator simultaneously is evidenced by failure of the ammeter to indicate if the current circuit is open or by an off-scale swing of the bridge if the voltage or drop circuit is open. In this case, the operator continues to call for contact by repeating the one-bell signal.

Arrangement for Power-Input Measurement

The power input to the motors is measured with a voltmeter and ammeter with respect to time, the interval of which is dependent upon the profile of the railroad and the operation being studied. This is a laborious and tedious procedure which may be eliminated by installing chart-recording instruments to keep a graphic record of the test. Recording instruments should be equipped with special marker pens, energized periodically by means of a Telechron-driven contact-making switch to put a reference mark on each graph. A push button also should be provided to enable operating the marker pens at will for special purposes, such as the passage of significant locations. In addition, the chart must be clearly marked with notes to aid analysis after these tests are completed.

The recording instruments must be shockproof-mounted to obtain a smooth graphic record. The indicating voltmeter and ammeter should be retained for a periodic calibration check of the recording instrument. All instruments must be secured to the cab structure to prevent displacement when curves at high speed are being negotiated.

The ammeter shunt must be connected to the motor power circuit on the low-voltage or grounded side of the circuit to minimize hazard to personnel. The leads between the indicating ammeter and shunt must be calibrated together with the shunt and recording instrument before being installed in the locomotive. One side of the voltmeter always will be on the high side of the power circuit and must be safeguarded.

---

1. With fuses small enough to prevent fire in case of accidental short circuit.

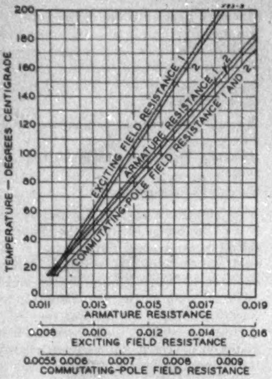

Figure 3. Typical temperature–resistance curves for motors 1 and 2

Resistance at 25 Degrees Centigrade

	Number 1	Number 2
Armature	0.01175	0.01190
Exciting field	0.00875	0.00890
Commutating pole	0.00605	0.00605

2. With a cutout switch in the event it is necessary to remove or make adjustments to the voltmeters.

A small rotary inverter operating on 32 volts direct current provides alternating current at 110 volts, 60 cycles, from 16 cells of the locomotive storage battery to operate the self-balancing bridge, the recording instrument, and the Telechron timer for the marker pens. The circuit between the storage battery and the inverter should be protected with fuses.

INSTALLATION OF THERMOCOUPLES

Thermocouples made up from copper and copnic wire serve to measure the temperatures at remote locations inaccessible while under way, such as the roof and road-bed ambient temperature, traction-motor-armature and axle-bearing, frame, and air-out temperatures. Thermocouples are connected to a selector switch which becomes the cold junction and should be equipped with a thermometer so that the measuring potentiometer connected with it can be corrected for variations in temperature of the selector switch which may fluctuate with cab temperature.

The potentiometer may be set up in shockproof mountings so that the galvanometer can be balanced, or it may be connected with the balancing element of the special resistance bridge which is unaffected by vibration. This is feasible as thermocouple readings usually are taken while under way in between test stops.

The roof-air-temperature thermocouple fastened to a length of spring wire should project above the boundary layer, but care must be taken that it stay within the clearance diagram when operating in an electrified zone to avoid contact with the high-voltage overhead system. The road-bed-temperature thermocouple is secured to a step bracket on the pilot or other structure entering air near the track level. Thermocouples reading frame or bearing temperatures must be kept out of the wind stream by protecting the junction end from its influence. They must be secured in tight contact with the member to be measured. Thermocouples for roller-bearing temperatures should be clamped between the outer race of bearing cap if opportunity permits; otherwise, a spring wire with the thermocouple junction soldered to its end may be inserted through the grease pipe to make contact with the bearing or the bearing cap metal in contact with the bearing.

MEASUREMENT OF COMMUTATOR TEMPERATURES

Commutator temperatures are measured with a contact-type hand pyrometer. This is an open-junction thermocouple instrument with inherent ambient compensated millivoltmeter reading directly in degrees centigrade.

Measurement Procedure

MEASURING COLD RESISTANCE

The cold-resistance value of the motor windings is a first consideration after instruments and wiring are installed as it is basis for subsequent temperature determination. To permit all windings to cool off to a uniform temperature and to equalize with that of the entire motor may require 12 to 24 hours and will present a real problem unless the layover between runs is of sufficient duration for this purpose. Arrangement should be made to cut out the motors selected for measurement and to keep the blowers running before the train arrives at the terminal, when they are no longer required. This may gain two or three hours of cooling time. If electrically driven blowers are used, they should be kept running with the motors or power plant cut out.

As soon as the locomotive is spotted in a final position for servicing, mercury thermometers can be applied to the frames, field coils, pole tips, armature core, and commutator risers. It is well to caution against the application of putty directly on the brush surface of the commutator, as it may present some difficulty in cleaning without at the same time destroying the commutating film, thereby altering conditions for subsequent tests. Comparative ambient temperature may be obtained by placing a thermometer on the track rail head with putty over the bulb, or by placing a thermometer in a small can filled with oil so as to stabilize fluctuation in air temperature when large doors are opened in the locomotive service shop or roundhouse, or

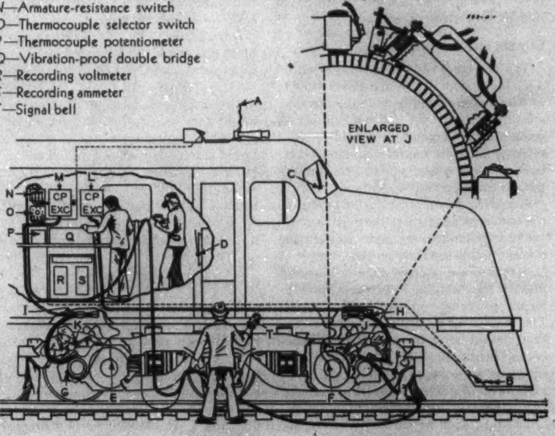

Figure 4. Position of personnel when taking temperature measurements

A—Roof-air-temperature thermocouple
B—Road-bed-air-temperature thermocouple
C—Windshield air thermometer
D—Traction-motor blower air-in thermometer
E—Pinion-end armature-bearing-temperature thermocouple
F—Commutator-end armature-bearing-temperature thermocouple
G—Axle-bearing-temperature thermocouple
H—Number-1-motor field-resistance leads
I—Number-2-motor field-resistance leads
J—Armature-resistance yoke
K—Commutator-temperature pyrometer
L—Number-1-motor field-resistance selector switch
M—Number-2-motor field-resistance selector switch
N—Armature-resistance switch
O—Thermocouple selector switch
P—Thermocouple potentiometer
Q—Vibration-proof double bridge
R—Recording voltmeter
S—Recording ammeter
T—Signal bell

when the wind is variable when the locomotive is standing in a railroad yard. Cold-resistance measurements can be started as soon as comparative observations of thermometers show reasonable agreement. Record the date, time, temperatures, with resistance values, and check at intervals.

When armature cold resistance is being measured, the armature yoke should be applied on several alternative segment positions available, and, after the armature thermometers are removed, the locomotive may be moved sufficiently to present different sections of the commutator, the measurements on which should check reasonably with one another. If a wide variation is detected, the reason for it should be ascertained and corrected. The section showing disagreement may be explored by making bar-to-bar measurements to see if a high-resistance fault exists in the armature windings or its connection to the commutator risers. Motors will operate without any visible sign of distress on the commutator and yet may have appreciable variation in bar-to-bar resistance; although this is permissible for operation, it would not be acceptable for a temperature test, as the data obtained may be erratic if the train happens to stop with this fault in the accessible section of the commutator for the temperature measurement. It may prove a wise precaution to bar-to-bar-test the armatures of the motors before selecting them for temperature tests, as a visual inspection will only detect faults which have progressed to an advanced stage.

Cold-resistance readings again should be measured at the conclusion of all testing and checked with the initial readings to ascertain that no changes had occurred during the testing period. For this purpose, resistance values should be evaluated at 25 degrees centigrade as a common basic temperature for comparison.

TEMPERATURE–RESISTANCE CURVES

The work of reading temperatures will be facilitated greatly by drawing temperature–resistance curves for each winding in each motor being tested (Figure 3). Since this curve is a straight line within the range of temperatures under consideration, it is only required to plot the cold-resistance values at their measured temperature and calculate the value of resistance for 200 degrees centigrade as being the extreme value when hot. A straight line is drawn through these two points, and any intermediate value can be read directly from the curve.

DETERMINATION OF COOLING-AIR VOLUME

The air delivered to the motors by the blower is best measured by drilling the commutator inspection cover to admit a static pressure tube into the commutator chamber, and then reading the air pressure in inches of water on a manometer. The readings should be taken at idling, one-half and full speed of the blower, and at the same time the speed of the engine should be measured. When tests are concluded, engine and blower speed again should be measured to see that conditions remained the same during the testing period. Record date, time, speed, temperature of air at blower intake, and barometric pressure, if the data are to be used for comparative reference.

A similar procedure for electrically driven blowers should be followed, except that speed would be dependent upon blower voltage instead of engine speed as with the belt-driven blower.

The volume of air to the motors is determined from a pressure–volume curve usually available for the type of motor being tested. If one is not available, it can be prepared by blowing a similar motor through a calibrated pipe to determine the volume delivered for corresponding pressures in the commutator chamber as outlined by blower manufacturer's testing code.

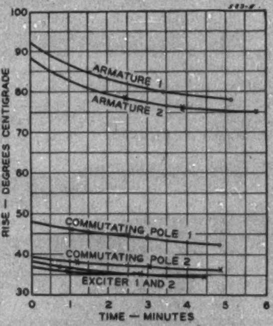

Figure 5. Typical cooling curves

Total train weight 1,224 tons (13 cars + locomotive) rms current 449 emperes for 67 minutes or total distance of 81 miles

O = motor 1 X = motor 2

Rises Based on 42 Degrees Centigrade

	Number 1		Number 2	
	Temperature	Rise	Temperature	Rise
Armature	135	93	131	89
Commutating field	89.5	47.5	81.5	39.5
Exciting field	80.0	38.0	79.0	37.0
Commutator	110	68	105	63

MAKING THE SERVICE TEMPERATURE MEASUREMENTS

Before the test run is made the locomotive should be moved from over the service pit onto a section of track similar to the main-line road bed. Assign the test crew to their stations, and outline the testing procedure and the duties for each station. The entire sequence of the test should next be rehearsed, including the making of measurements, and the entire operation timed from start to finish. This practice will prove invaluable to the men by relieving tension and instilling confidence and teamwork in preparation for the actual measurements on the main line.

The following program of events is performed in sequence (Figure 4):

1. Just before the arrival at the designated stop for heating measurements, a prearranged signal from the head end is given when power is no longer required to make the stopping point. Padlocks are removed from the switches, and all equipment is made ready.

2. As soon as power is shut off at the head end and the engines come to idling speed, a stop watch is started at the instrument station, and the electric-driven blower or the Diesel engine belted to the blower, as the case may be, is shut down completely.

3. As soon as the train comes to a stop, it is made safe (removal of reverser handle or other means to lock power off) by a man at the head end who then leaves the cab and takes a position on the road bed at the truck while two other men, one for each motor, climb under the locomotive and remove the motor inspection covers.

4. While step 3 is taking place, the two men at the instrument station unwind cables and pass the armature yoke, signal bell, and pyrometer down to the man on the road bed adjacent to the truck, who retains the bell and gives the resistance yoke to one man at the motors and the pyrometer to the other.

5. Resistance measurements are made in the following order by two men at the instrument station:

(a). Motor 1 commutating field, then exciting field, followed by the field measurements on motor 2.

Figure 6 (below). Average armature-cooling curves obtained from heat-run data

	Amperes	Rpm	
A	650	1,300	Continuous
B	675	778	Continuous
C	1,000	450	30 minutes
D	1,130	374	13 minutes

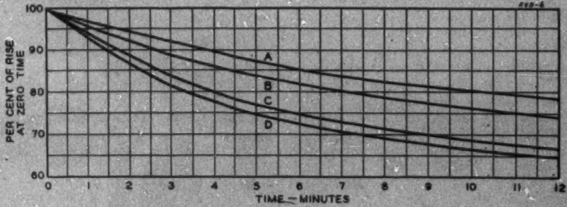

(*b*). Signal for armature contact to be made and held on armature 1 while commutator 2 temperature is measured. Signal as soon as resistance is obtained, and the man on the road bed will pass the yoke from motor 1 to motor 2 and the pyrometer from motor 2 to motor 1 and make a record of commutator temperature. As soon as contact is established on armature 2, the instrument station will acknowledge by signal to hold contact while resistance is measured, after which the concluding signal is given. Meanwhile record is made of commutator 1 temperature.

(*c*). The fields of motors 1 and 2 again are measured while the yoke and pyrometer are exchanged by the man on the track in readiness for repeating armature and commutator temperatures. At least three readings on fields and armatures of each motor should be obtained in six minutes time from the instant the power is off, which may be broken down into an average of two minutes to make the stop and get the first armature contact and four minutes for all subsequent measurements. As each resistance value is called off by the instrument operator, the other man notes the time and enters the value on a prepared data sheet.

6. As soon as measurements are concluded, the cables are pulled into the cab, motor covers are replaced, and both men climb from under the locomotive; when all is clear the shutdown engine or blower is started and the run is resumed.

7. The commutator temperatures which were recorded by the men on the track are transferred to the data sheet at the time values corresponding with the opposite motor's armature-resistance values.

8. During the run, and especially for a period of time preceding a stop for winding-temperature measurements, readings are taken and recorded in the log of air temperature on the roof and road bed, and at traction-motor blower intake. Readings also are made periodically of motor-frame, air-out, and bearing temperatures. The chart-recording instruments are inspected to see if they are inking, and calibration is checked with readings on the indicating instruments. At the head end of the locomotive, windshield temperature, speed, location on the railroad, and controller notch position are recorded with respect to time so that they may be related to the readings in the test log.

For the purpose of obtaining these readings, the test crew is reassigned to secondary duties, so that there is a division of labor, but co-ordination of all data at one point is insured. The make-up of the train in tons and number of cars for each test run should be recorded with the train identification and direction of travel.

Determination of Operating Temperature

The Cooling Curve

The resistance value can be read off directly as temperature from the resistance–temperature curve and by subtracting the motor-blower air-in temperature the rise of the winding is obtained, corresponding with the time of measurement. These values of rise are plotted with respect to time, and a smooth exponential curve is drawn through related points to zero time, and the intercept with the temperature axis is the most probable temperature rise of the corresponding winding at the instant of power removal (Figure 5). The importance of getting the first readings as soon as possible after power off becomes evident for it minimizes the extent of extrapolation of the curve.

The cooling-curve technique also is applied to the hand-pyrometer commutator-temperature readings to arrive at the probable rise just before power off.

The Use of Average Cooling Curves

Occasionally, circumstances will prevent immediate measurement of armature resistance and a prolonged cooling period will result before the first reading is obtained. The extrapolation of these delayed data to zero time is aided by the use of average armature-cooling curves (Figure 6). These curves are prepared from factory test data on the same type of motor for several different conditions of power input and are expressed in terms of per-cent temperature rise with respect to time. Generally, heavy loads of short duration have steeper cooling-curve shapes than continuous runs. This is caused by the steep temperature gradient between the copper and the iron core which lags behind during the short heating-up period, whereas during a continuous run their temperature becomes more nearly equalized.

The proper cooling shape is selected by evaluating the power input for the period preceding the shutdown in service and identifying it with a corresponding curve shape, or by interpolating between the two curves coming closest. From this curve is read, for the elapsed cooling time at which the first service reading was taken, the percentage value of the actual measured temperature rise, from which is prorated the 100 per cent value at zero time.

Determination of Rms Current

The rms current value is obtained from the chart made by the recording ammeter by dividing the graph into intervals of time, and the average current value for each interval is squared and multiplied by that time interval. The sum of these products is divided by the total time, to get the average current squared for the run. The square root of this value is the rms current value for the test.

Adaptation of Method to Varying Conditions

It is not always practical to obtain the full desired train tonnage without delaying the test, or during the test run it may be desired to check performance with one power plant hypothetically broken down. These situations can be approximated by purposely reducing the locomotive power by multiples of the number of motors until the desired prorated train tons per motor is obtained. The temperature measurements then are made under this artificial condition. For example, if two out of eight motors are cut out of a locomotive in an 18-car test train having a combined weight of 1,680 tons, the load per motor will be increased from 210 to 280 tons. The heating of the motors then would be equivalent to that of a 25-car train of 2,240 tons total weight.

The method, procedure, and equipment also are applicable to measurements of generator temperature which can be made in a multiple-unit locomotive by shutting down the one power plant for a few minutes to obtain measurements without the necessity of stopping the train.

The recording-chart instrument with calibrated instruments affords data on engine horse-power output by reference to a generator characteristic for the generator efficiency values over the operating range from which the horsepower input to the generator can be calculated.

Conclusion

Temperature of locomotive electric apparatus is more than a question for academic consideration; it is an active economic factor, never at rest and continually exerting its influence with time on the life of the equipment. The penalties of rash application or abusive operation are inescapable.

The effect of elevated temperatures on organic insulation materials follows the approximate rule of half the life for each 8–12-degree-centigrade increase in temperature.[2] The indisputable and direct approach to correct utilization or application of motive power is with a full knowledge of electric-apparatus temperature. The testing facilities and method outlined provide these necessary data for railroad operating and motive-power departments, as well as engineering information of application and design value. It is a means whereby a railroad can take the measure of its tough spots and with which the engineer can correct his shots.

References

1. American Standard *C* 35.1, Rotating Electrical Machinery on Railway Locomotives and Rail Cars and Trolley, Gasoline-Electric, and Oil-Electric Coaches, AIEE Standard 11, March 1943. Sections 156, 158–9.

2. Report on General Principles for Rating of Electrical Apparatus for Short-Time, Intermittent, or Varying Duty, AIEE Standard 1*A*, September 1941.

A 208Y/120-Volt 120-Ampere Three-Pole 400-Cycle Electrically Operated Aircraft Circuit Breaker

C. H. TITUS
ASSOCIATE AIEE

P. J. REIFSCHNEIDER
ASSOCIATE AIEE

Synopsis: With the selection of the 208Y/120-volt three-phase 400-cycle a-c system by the Army Air Forces for large aircraft, there has arisen the need for appropriate switchgear. In order to be applicable to the electric systems of such planes, switchgear must be able to perform its normal and emergency functions under the encountered conditions of temperature, pressure, humidity, vibration, and acceleration. This paper describes a 120-ampere remotely controlled electrically operated air circuit breaker designed for use as a bus sectionalizing, ring tie, or generator breaker on the 400-cycle grounded-neutral system. The interrupting rating of this breaker is 3,800 amperes at all pressures from sea level to 50,000 feet altitude. The closing solenoid and shunt trip coils have been designed to operate over a wide range of ambient temperature and control voltage. Weight and size, being primary considerations in aircraft equipment, have been held to a minimum.

To MEET the demands of increased electric loads in aircraft, the Army Air Forces has selected the 208Y/120-volt three-phase 400-cycle grounded-neutral a-c system as applicable to large aircraft.[1] Supplementing this system will be found a 24-volt d-c source for control power and some small loads. There are many reasons why an a-c system of this voltage and frequency has been selected for large aircraft. However, it is beyond the scope of this paper to treat them. A complete study of the factors entering into the selection of electric systems for aircraft has been presented in another paper.[2]

Heretofore, only small amounts of 400-cycle power, by comparison, have been used on aircraft. Equipment for the generation, distribution, and utilization of large amounts of 400-cycle power has been recently developed or may be still undergoing development. The weight and size of this equipment, it is specified, must be held to a minimum. Circuit breakers must be able to perform their normal and emergency functions under these conditions:

1. Altitude—from sea level to 50,000 feet, or a pressure range of from 14.7 to 1.68 pounds per square inch.
2. Temperature — ambient - temperature range from 60 to −70 degrees centigrade at sea level and from −40 to −65 degrees centigrade at 50,000 feet altitude.
3. Humidity—a relative humidity of from 0.5 to 100 per cent.
4. Vibration and acceleration—an amplitude of 0.030 inch at all frequencies from 10 to 50 cycles per second.

An air circuit breaker, custom built for aircraft to operate under these conditions, has been developed for the 400-cycle system. Figure 1 shows several views of this breaker designed for use as a bus sectionalizing, ring tie, or generator breaker. The weight of this breaker is five pounds and the over-all size is $7^1/_4$ inches high, $4^1/_8$ inches wide, and $4^{17}/_{32}$ inches deep. All parts are enclosed within a dust-resisting molded phenolic case on the back of which are the line, load, auxiliary-switch, and control-circuit terminals. The breaker may be mounted with these terminals either toward or away from the panel. In either position, the terminals are covered with insulating barriers.

Throughout the breaker, parts have been plated in accordance with accepted aircraft standards to prevent corrosion. Precautions have been taken to prevent moisture absorption and fungus growth by applying protective finishes to nonmetallic parts.

In the development of a circuit breaker, it is the requirements of the interrupter in terms of pressure, wipe, separation, and acceleration of the contact tips which determine the design of the operating mechanism and in turn the design of any closing and tripping devices. The interrupter, therefore, will be described first.

The Interrupter

It is required that the interrupter and contacts of this breaker be able to do the following:

1. Withstand vibration and acceleration as specified without physical damage or excessive heating.
2. Close and interrupt maximum available short-circuit current in the 208Y/120-volt three-phase grounded-neutral 400-cycle system at any altitude from sea level to 50,000 feet.
3. Carry 120 amperes continuously, 165 amperes for five minutes, and 245 amperes for five seconds without excessive temperature rise.

Before the interrupter and contact structure for a circuit breaker can be designed there are two dependent variables to be evaluated, namely, the type of contact material and the arc-quencher construction to be used.

Table I. Data for Representative Three-Phase Interrupting Tests Made at 230Y/133 Volts, 420 Cycles

Breaker Current, Rms Amperes	Maximum Arc Duration in Milliseconds at Pressures Equivalent to the Indicated Altitudes		
	1,000 Ft	20,000 Ft	50,000 Ft
80	3.7	2.5	1.2
120	2.5	1.2	1.2
250	3.7	2.5	1.2
310	5.0	2.5	3.7
750	2.5	2.5	2.5
1,700	2.5	2.5	2.5
2,800	3.7	3.7	3.7
3,800	6.2	5.0	5.0

Contact Material

The contact material has a direct bearing on arc duration and the operating temperature, welding current, and deterioration of the contacts. The influence of the contact material on arc duration is determined by:

1. Melting temperature of contact material.
2. Ionization potentials of the metal vapors derived from contact-material decomposition.

Paper 45-96, recommended by the AIEE committee on air transportation for publication in AIEE Transactions. Manuscript submitted December 4, 1944; made available for printing March 13, 1945.

C. H. Titus and P. J. Reifschneider are with the General Electric Company, Philadelphia, Pa.

The authors acknowledge the assistance of R. M. Bennett and other associates in assembling and preparing the material for this paper.

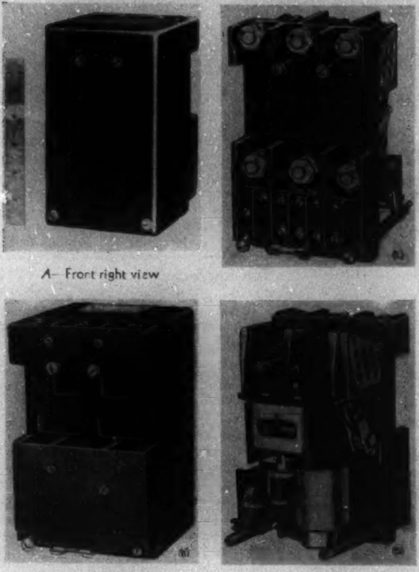

A— Front right view

B—Rear left view

C—Rear left view without covers showing load, line, and control-circuit terminals

D—Front right view without covers

Figure 1. A 208Y/120-volt 120-ampere three-pole 400-cycle electrically operated aircraft circuit breaker

3. Instantaneous temperature of contacts at time of parting.

The following factors determine the contact operating temperature:

1. Operating temperature of the member to which the contact itself is attached.
2. Resistivity of the contact material.
3. Resistance of the point of contact of the movable and stationary members. This is a function of the contact pressure and the formation of chemical compounds on the surface of the contacts.
4. Composition and mass of material surrounding the contact structure. It is this material which determines the amount of heat energy removable from the contacts at any given operating temperature.

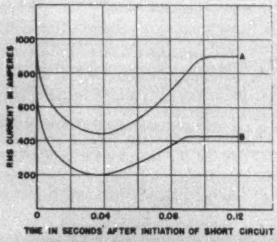

Figure 2. Short-circuit characteristics of 40-kva 208Y/120-volt three-phase 400-cycle aircraft alternator

Curves represent envelope of 400-cycle symmetrical current. First peaks may be increased because of offset. Voltage regulator operating in exciter field

A—Line-to-ground short circuit
B—Three-phase short circuit

The instantaneous value of current at which a given set of contacts will weld is determined by:

1. Physical properties of contact material, namely, composition, melting temperature, thermal conductivity, and hardness.
2. Contact temperature, that is the transient temperature attained for any given value of current.
3. The instantaneous pressure present for any given operating current.

The following determine the deterioration of the contacts when interrupting both normal and short-circuit currents:

1. Magnitudes of the arc current.
2. Arc duration.
3. Melting temperature of contact material.
4. Hardness of the contact material.
5. Presence of gas-producing substances included in contact composition.

In order to determine the type of contact material which best meets the requirements of low operating temperature, high welding current, short arc duration, and minimum contact deterioration, approximately 1,100 tests were made using 14 types of contact material. These tests were made at ten per cent above the rated voltage and at pressures equivalent to altitudes ranging from 1,000 to 50,000 feet using 16 different types of arc quenchers. The type of contact material selected as best fulfilling these requirements is a sintered mixture of silver and tungsten.

ARC-QUENCHER DESIGN

The design of the arc quencher has a direct bearing upon the magnitude of voltage and current which can be successfully interrupted, the arc duration for any combination of voltage and current, and the atmospheric conditions of humidity, temperature, and pressure under which the interrupter will function satisfactorily. The type of mechanism needed to operate the contacts and the size and weight of the arc quencher are dependent upon its design.

Since the neutral of the 208Y/120-volt three-phase 400-cycle system is solidly grounded, it is unlikely that a sustained voltage of more than ten per cent in excess of 120 volts will appear across a given breaker pole. Consequently, 132 volts will be considered the rms operating voltage of each arc quencher.

The system is supplied by four 40-kva 0.75-power-factor 400-cycle alternators. The short-circuit characteristics of the alternator, exciter, and voltage regulator combined are shown in Figure 2. Inspection of Figures 2 and 3 shows that the maximum fault current results from a single-phase line-to-ground fault. From Figure 3, it is evident that with any possible location of such a fault, the maximum short-circuit current which a single pole of any breaker may be called upon to interrupt is that contributed by three generators and the connected motors. Studies of the proposed system,

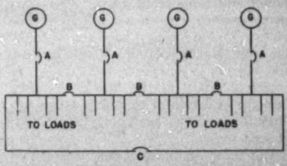

Figure 3. Proposed power circuit for 400-cycle aircraft system, using remotely controlled electrically operated circuit breakers

G—208Y/120-volt 40-kva 0.75-power-factor 400-cycle alternator
A—Generator breaker
B—Bus-sectionalizing breaker
C—Ring-tie breaker

which take into account circuit impedances, indicate that the interrupting rating of the breaker, 3,800 amperes, will not be exceeded.

A test circuit was set up as shown in Figure 4 for determining, at first, the best type of arc quencher, and later, the overall performance of the complete breaker under single-phase and three-phase fault conditions. Test currents ranging from 3 amperes to 4,000 amperes for both single- and three-phase operation were obtainable on a 230Y/133-volt 420-cycle system with a system power factor of approximately 15 per cent. All interrupting tests were made in a chamber capable of being evacuated to an equivalent pressure less than that encountered at 50,000 feet altitude.

Because the arcing time of most conventional 120-volt air circuit breakers increases materially at the decreased atmospheric pressures encountered at high altitude, it seemed necessary at first to use a compression-type interrupter. An interrupter of this type is capable of generating its own internal pressure. However, interrupting tests indicated that over the operating range of currents and pressures of this breaker, a converging-slot-type arc quencher performs as well as the compression-type interrupter. The advantages of the lightweight, mechanically simple, converging-slot-type arc quencher over the heavier, more complex, compression-type interrupter made it ideally suited to this type of aircraft application.

Two views of this converging-slot-type arc quencher with the lower portion of one side removed are shown in Figure 5. A front right view of the breaker is shown in Figure 6 with the cover, one phase barrier, and half of the right-pole arc quencher removed. The movable and stationary contact members together with the magnet frame are so arranged that the arc stream and its terminals are driven toward the top of the breaker as it is shown in Figure 6. The contour of the inside of the arc quencher has been made such that unnecessary extension of the arc is avoided to obtain a maximum amount of cooling in a minimum amount of time. The deterioration of the arc quencher and the contacts is thereby minimized during interruption.

Table I is a tabulation of data of representative three-phase interrupting tests made at 230Y/133 volts, 420 cycles, and pressures equivalent to altitudes from 1,000 to 50,000 feet. The maximum arc duration in milliseconds is shown for various currents and altitudes. Oscillograms showing typical breaker operation when interrupting three-phase 420-cycle short-circuit currents of approximately 2,900 amperes and 3,600 amperes at corresponding pressures equivalent to 50,000 feet and 20,000 feet altitude are shown in Figures 7 and 8. Continuous-current-carrying tests made at 120 amperes and short-time overload tests made at 165 amperes and 245 amperes indicate that the thermal capacity of the breaker is adequate for use on this system.

Operating Mechanism

A latching-type solenoid-operated toggle mechanism is used to close the hinged contacts against a heavy opening spring. The contacts are opened by energizing the shunt trip coil, the plunger of which releases the latch and permits the opening spring to pull the contacts rapidly to the open position. It is necessary that the contacts be parted as quickly as possible to minimize the over-all interrupting time.

No means have been provided for closing or opening the breaker manually, nor have any overload tripping devices been incorporated in the breaker.

In Figure 9 is shown the relative size of the subassembly of the shunt trip device and the closing solenoid. Because of the design of these two devices and the fact that the coils have only a short-time rating, the work output per unit of weight is high for both of them. The ratio of the

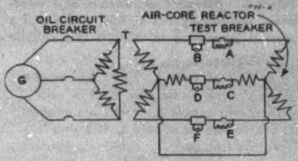

Figure 4. Test circuit used for interrupting tests

Letters *A–F* indicate magnetic oscillograph vibrators:

A—Voltage across pole 1
B—Current, pole 1
C—Voltage across pole 2
D—Current, pole 2
E—Voltage across pole 3
F—Current, pole 3
G—Alternator, 3,000 kva, 2,400 volts, three phase, 420 cycles
T—Transformer, 600 kva, 2,400 delta–208Y volts (60-cycle rating)

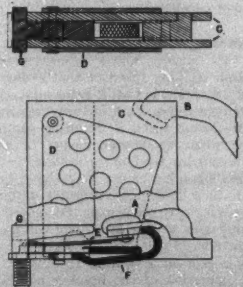

Figure 5. Top and side views of converging-slot-type arc quencher for 208Y/120-volt 120-ampere three-pole 400-cycle aircraft circuit breaker

Lower portion of one side removed

A—Stationary contact
B—Movable contact
C—Arc chute
D—Magnet frame
E—Leaf spring
F—Flexible braid
G—Shield

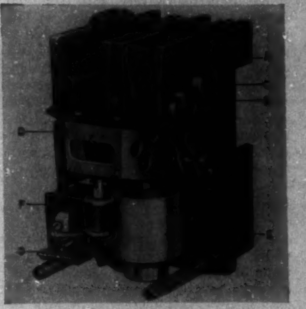

Figure 6. Front right view of breaker

One phase barrier and half of right-pole arc quencher removed showing the contact and arc-quencher construction

A—Arc quencher
B—Movable contact
C—Stationary contact
D—Mechanism
E—Closing solenoid
F—Shunt trip
G—Cutoff switch for closing solenoid

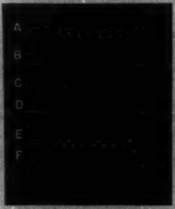

Figure 7. Magnetic oscillogram of a three-phase interrupting test at 420 cycles and a pressure equivalent to 50,000 feet altitude

A—Voltage across pole 1, 133 volts
B—Current, pole 1, 2,860 rms amperes
C—Voltage across pole 2, 133 volts
D—Current, pole 2, 3,230 rms amperes
E—Voltage across pole 3, 133 volts
F—Current, pole 3, 2,750 rms amperes

product of the force at the beginning of the stroke and the length of the stroke to the weight is 3.1 inch-pounds per pound for the closing solenoid and 3.3 inch-pounds per pound for the shunt trip device. This same ratio for a continuously rated commercial solenoid is 0.34 inch-pounds per pound. Weighing only 19 ounces, the closing solenoid develops more than 45 pounds at the point near the end of its stroke where the overtravel of the plunger begins. The shunt trip device weighs four ounces.

The pull curve of the closing solenoid has been so shaped that even at as low a voltage as 18 volts, measured at the terminals of the battery, with 0.25 ohm in series with the coil to represent line resistance, the breaker closing time is 0.027 second. Higher closing speed could be obtained at this low closing voltage only at the expense of increased weight of the closing solenoid. The minimum tripping voltage is 12 volts measured at the terminals of the battery with 0.25 ohm resistance in series with the shunt trip coil.

Control Circuit

A cutoff switch connected in series with the coil of the closing solenoid prevents it from overheating after the closing impulse has been delivered to the mechanism. This switch is actuated by the solenoid plunger in the overtravel portion of its stroke after the mechanism has been fully closed. As long as the closing circuit is energized after the breaker has been closed, the cutoff switch, shown in Figure 10, is maintained in the open position by a holding coil. As this holding coil is continuously rated, it is possible to use either a momentary- or a maintaining-contact switch to control the closing of the breaker. When using the latter type of switch, the closing circuit must be de-energized after tripping and before reclosing the breaker. With this control scheme, it is impossible for the breaker to pump should it be closed against a fault with the closing circuit energized.

Included as an integral part of the breaker is a four-stage auxiliary switch. Each stage or set of contacts of this switch is a small snap-action vibration-proof contact mechanism. One stage is used as the auxiliary contact in series with the shunt trip to open its coil circuit the instant the breaker primary contacts open. The other three sets of contacts may be arranged individually to be either normally open or normally closed and used with external relays for breaker control. The terminals of these contacts are brought out to the back of the breaker with the close, trip, and ground terminals as shown in Figure 1C.

The three control-circuit coils have a tropical treatment. Polyvinyl-chloride-insulated wire is used for all internal control-circuit connections to guard against corrosion.

Figure 8. Magnetic oscillogram of a three-phase interrupting test at 420 cycles and a pressure equivalent to 20,000 feet altitude

A—Voltage across pole 1, 133 volts
B—Current, pole 1, 3,510 rms amperes
C—Voltage across pole 2, 133 volts
D—Current, pole 2, 3,940 rms amperes
E—Voltage across pole 3, 133 volts
F—Current, pole 3, 3,420 rms amperes

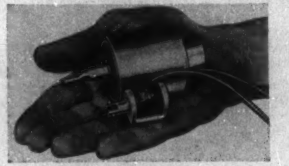

Figure 9. Shunt-trip and closing-solenoid subassembly

Operating Characteristics

High tripping speed of the breaker is very important in that it helps materially to reduce the over-all interrupting time. High closing speed is desirable particularly when automatic means of synchronizing are used on the system.

Oscillographic timing tests have been made in a 25-degree-centigrade ambient temperature to determine the speed of closing over a range of control voltage of from 18 to 28 volts and the speed of tripping over a range of from 12 to 28 volts. The operation of the breaker has been found to be satisfactory over these same voltage ranges while being subjected to vibration with an amplitude of 0.030 inch at all frequencies from 10 to 50 cycles per second. For all operation tests, both closing and tripping, a 0.25-ohm resistor was connected in series with the ground terminal of the breaker control circuit to simulate line resistance in the plane.

Although the resistance of the coils increases somewhat when the breaker is placed in an ambient temperature of 60 degrees centigrade, the breaker closes satisfactorily at 18 volts and trips at 12 volts, both voltages being the open-circuit control voltage.

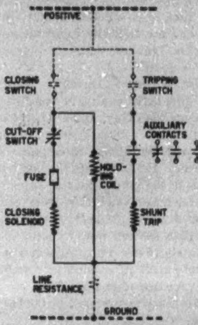

Figure 10. Control-circuit diagram, 208Y/120-volt 120-ampere three-pole 400-cycle electrically operated aircraft circuit breaker

Nominal d-c control voltage 24 volts

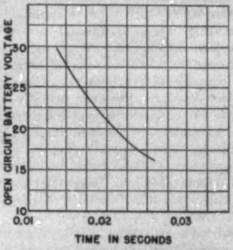

Figure 11. Closing characteristic, 208Y/120-volt 120-ampere three-pole 400-cycle electrically operated aircraft circuit breaker

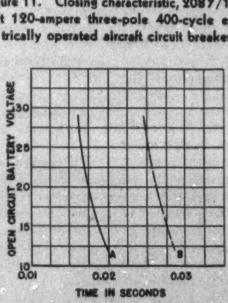

Figure 12. Opening characteristics, 208Y/120-volt 120-ampere three-pole 400-cycle electrically operated aircraft circuit breaker

A—Breaker primary contacts part
B—Breaker primary contacts fully open

The closing characteristics, time from the instant the closing circuit is energized until the breaker primary contacts meet versus the open-circuit control voltage,

Oil Stresses in Impregnated-Paper Insulation

J. B. WHITEHEAD
FELLOW AIEE

RECENT EXPERIMENT on fully impregnated cable-type paper insulation, has shown that under certain conditions use of a paper of low density results in a higher dielectric strength than does the use of a paper of higher density.[1] It has also been shown that failure of such insulation usually begins in the oil channels between successive turns of paper tape.

The former result is in apparent conflict with general experience that the denser a given substance or medium, the higher the dielectric strength. But the conflict is apparent only, for impregnated paper is not a homogeneous substance, and failure begins first in its weaker constituent, namely, the oil. High-density paper with its higher dielectric constant throws a higher stress into the oil channels and the critical or breakdown stress is reached at a lower applied voltage than when low-density paper of lower dielectric constant is used.

The following approximate analysis indicates that under certain conditions in a single-conductor cable of circular cross section, the use of high-density paper next the conductor and low-density paper outside should result in a higher over-all dielectric strength than that of the same cable insulated throughout with either low- or high-density paper. The higher specific inductive capacity of the high-density paper shifts a greater proportion of the over-all voltage to the outer less dense paper thereby reducing the stress at the conductor surface. This reduction under certain conditions may cause the critical oil-channel stress to fall below that for the same cable insulated throughout with low-density or high-density paper.

Over-All Average Stress at Conductor Surface

Let a, b, and c be the radii of the conductor and of the outer surfaces of the denser and less dense papers respectively; K_{ab} and K_{bc} the measured dielectric constants of the two impregnated papers when assembled separately as cable insulation, and V_{ab} and V_{bc} the division of the total voltage, V_o, between them. Then we have:

$$V_{ab}+V_{bc}=V_o \qquad (1)$$

$$\frac{V_{ab}}{V_{bc}}=\frac{K_{bc}}{K_{ab}}\cdot\frac{\log (b/a)}{\log (c/b)} \qquad (2)$$

$$V_{ab}=\frac{K_{bc}}{K_{ab}}\cdot\frac{\log (b/a)}{\log (c/b)}\,(V_o-V_{ab}) \qquad (3)$$

$$=\frac{A}{1+A}\cdot V_o;\quad A=\frac{K_{bc}\log (b/a)}{K_{ab}\log (c/b)} \qquad (4)$$

Also, let E_a and E_b be the mean values of the radial stresses at the surface of the conductor, and at the outer surface of the inner denser paper respectively; then we have

$$\left.\begin{aligned} E_a&=\frac{V_{ab}}{a\log (b/a)}\\ E_b&=\frac{V_{bc}}{b\log (c/b)}\end{aligned}\right\} \qquad (5)$$

and from equation 2

$$\frac{E_a}{E_b}=\frac{V_{ab}}{V_{bc}}\cdot\frac{b}{a}\cdot\frac{\log (c/b)}{\log (b/a)} \qquad (6)$$

$$=\frac{K_{bc}}{K_{ab}}\cdot\frac{b}{a} \qquad (7)$$

Also

$$E_a=\frac{V_o\cdot A}{(1+A)a\log (b/a)}$$

$$E_a=\frac{V_o}{a\left[\dfrac{K_{ab}}{K_{bc}}\cdot\log (c/b)+\log (b/a)\right]} \qquad (8)$$

In equation 8 E_a is a mean or average value of the electric stress at the conductor surface. Its value is readily determined from measured values of V_o and of the dimensions a, b, and c, and of the specific inductive capacity of each of the papers when assembled separately as cable-type insulation. For an insight as to how the value of E_a varies as the proportion of dense to lighter papers varies, we may consider two papers each five mils thick; paper A (specific gravity 0.74; K = 3.78) and paper D (specific gravity 1.18; K = 4.91). Also in order to limit the number of variables, let us consider the particular case in which the total thickness of insulation is equal to the diameter $2a$ of the central conductor: thus $c = 3a$; in Figure 1 the curve E_a shows how E_a varies for all values of b. We note that for $b = a$ (all A paper) and for $b = 3a$ (all D paper), the values of E_a are the same and at their greatest. Introduction of any small amount of D paper inside of

---

Paper 45-103, recommended by the AIEE committee on power transmission and distribution for publication in AIEE TRANSACTIONS. Manuscript submitted February 3, 1945; made available for printing May 3, 1945.

J. B. WHITEHEAD is professor of electrical engineering in the school of engineering, The Johns Hopkins University, Baltimore, Md.

---

are shown graphically in Figure 11. At the nominal control voltage, 24 volts, the closing time is 0.02 second.

The opening characteristics, time from the instant the shunt trip is energized until the breaker primary contacts part and until they are fully open versus the open-circuit control voltage, are shown in Figure 12. The time from the parting of the contacts until they reach the fully open position, 8.5 milliseconds, is independent of the control voltage. The arcing time at pressures equivalent to altitudes up to 50,000 feet and currents up to 3,800 amperes rms, from Table I, never exceeds 6.2 milliseconds. The right-hand curve of Figure 12, contacts fully open, shows the interrupting time of the breaker versus control voltage at 50,000 feet altitude and rated interrupting current.

Conclusions

Designed primarily for the 208Y/120-volt 400-cycle a-c system selected by the Army Air Forces for large aircraft, this breaker in its application is the counterpart of industrial air circuit breakers.

The outstanding features of this breaker are:

1. Satisfactory and reliable operation under extreme conditions of temperature, pressure, humidity, vibration, and acceleration normal to aircraft.
2. Adequate interrupting capacity for the proposed 400-cycle aircraft system.
3. Short closing and tripping times over a wide range of control voltage.
4. Light weight and small space requirements.
5. Protection of parts against fungus growth and corrosion.

Future increases in aircraft electric loads will undoubtedly call for more extensive systems using breakers of higher continuous and short-circuit ratings. The experience gained in the design of this breaker indicates that these demands can be met without sacrificing any of the present features.

References

1. WHY TOMORROW'S PLANES WILL HAVE A-C SYSTEMS, T. B. Holliday. *Electrical Manufacturing*, volume 32, July 1943, page 88.

2. BASIC CONSIDERATIONS IN SELECTION OF ELECTRIC SYSTEMS FOR LARGE AIRCRAFT, W. K. Boice, L. G. Levoy, Jr. AIEE TRANSACTIONS, volume 63, 1944, June section, pages 279–87.

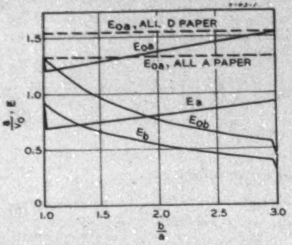

Figure 1. Stresses in a graded cable, denser paper inside, range of b/a from 1 to 3

Paper *D*, inside, specific gravity 1.18
Paper *A*, outside, specific gravity 0.74
25 per cent overlay, $n=4$
E_a—Average stress at conductor surface
E_{oa}—Stress in oil channel of paper *D* at conductor surface
E_{ob}—Stress in oil channel of inside layer of paper *A*
E_b—Average stress at surface of separation of the two papers

A paper, that is, for values of b slightly above a, E_a is sharply reduced and then increases approximately linearly to its maximum at $b = c = 3a$.

Similarly, the average stress at the surface of separation of the two papers (equation 7) is plotted as curve E_b. Its maximum value occurs at $b = a$ (all *A* paper) and is the same as the maximum value of E_a.

Figure 2 shows similar variations of the several stresses for values of b/a of from 1 to 2, that is for insulation wall thickness equal to the radius of the conductor.

Stress in Oil Channels

So far E_a and E_b are independent of the thickness and overlay of the paper tapes, except as these affect the measured values of K_{ab} and K_{bc}.

But we have taken the stress in an oil channel at the conductor as a measure of dielectric strength, and so it remains to determine the value of this stress, E_{oa}, in terms of some measurable quantity, for example, E_a. Efforts to derive the completely accurate value for E_{oa} lead to difficult and cumbersome expressions. We can proceed however, much more easily and with perhaps equal accuracy if we make two assumptions:

(*a*). That the pattern of overlay of tapes repeats itself regularly through the insulation wall.

(*b*). That the electric stress in the central region of the oil channel and immediately overlaying paper tapes is radial and uniform.

Under the first assumption the insulation wall may be considered as made up of a number of coaxial cylindrical capacitors, each having the same radial thickness, the same number of paper layers, the same overlay of tapes, and the same width of oil channel; also, for any one type of paper the dielectric of each elementary capacitor will have the same value of specific inductive capacity; or in other words K_{ab} and K_{bc} in the respective papers would have the same value if measured over any one or more of the characteristic elementary capacitors.

Assumption b is warranted by the fact that the oil channel is usually from 10 to 20 times as wide as it is thick (0.005 inch). We fix our attention on the central part of the channel where the stress is very nearly uniform and at its maximum value.

With all dimensions of the single-conductor cable and the applied voltage given, these assumptions enable us to compute, to a close approximation the value of the voltage, V, across the innermost characteristic capacitor, and further to derive the value of the stress in the innermost critical oil channel in terms of the average surface stress E_a of equation 8, as follows:

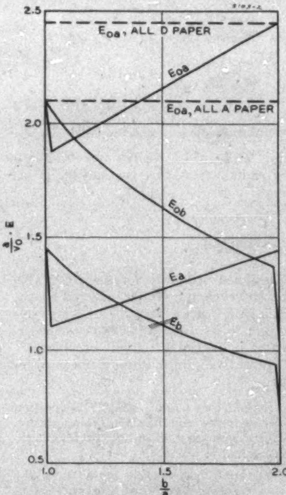

Figure 2. Stresses in a graded cable, denser paper inside, range of b/a from 1 to 2

See subcaption of Figure 1

The characteristic capacitor will have a number of layers, n, depending on the overlay, and any oil channel adjacent to the conductor will be in series radially with $n-1$ paper tapes. Let us consider only that elementary portion of the innermost capacitor for which an oil channel is next to the surface of the conductor. Then, if we make the not too violent assumption that the stress in the central region of the channel is radial, we may compute the stress in the oil channel from the relations in a cylindrical capacitor with an inside layer of oil, and above it $n-1$ layers of impregnated paper.

If a is the radius of the conductor, and $a_1, a_2 \ldots a_n$ the radii of the successive paper layers, and V is the voltage over the innermost capacitor, and K_o and K_p the dielectric constants of oil and impregnated papers respectively, then remembering the assumption b and formula 4, we find V_{oa}, the voltage over the oil channel,

$$V_{oa}=\frac{BV}{B+1}$$

where

$$B=\frac{K_p \log (a_1/a)}{K_o \log (a_n/a_1)} \tag{9}$$

and the stress E_{oa}, in the oil channel and at the surface of the conductor,

$$E_{oa}=\frac{V_{oa}}{a \log (a_1/a)}$$

$$=\frac{V}{a\left[\log (a_1/a)+\frac{K_o}{K_p}\log (a_n/a_1)\right]} \tag{10}$$

Also since the innermost capacitor in each paper is typical of all:

$$E_a=\frac{V}{a \log (a_n/a)}=\frac{V}{a \log\left(\frac{a+nt}{a}\right)} \tag{11}$$

where t is the thickness of the paper tape. Whence

$$E_{oa}=\frac{E_a \log\left(\frac{a+nt}{a}\right)}{\log (a_1/a)+\frac{K_o}{K_p}\log (a_n/a_1)}=GE_a \tag{12}$$

$$G\equiv\frac{\log\left(\frac{a+nt}{a}\right)}{\log (a_1/a)+\frac{K_o}{K_p}\log (a_n/a_1)} \tag{13}$$

the stress in an oil channel at the surface of the conductor.

For a given conductor, paper, and overlay in assembly G is a constant; when two papers are used, G has two values, one for each paper as determined by the two values of K_p, the specific inductive capacity of the impregnated paper. The values of G will always be greater than the average stress E_a at the conductor surface, if as is commonly the case K_p is greater than K_o.

In Table I values of G are given for several values of a and n, within the range of cable practice, and for each of the papers *A* and *D*. As will be seen, the values of G are practically independent of the conductor radius within the range 0.125 inch to 0.500 inch but increase with increase in n, the numbers of layers of paper in the "characteristic capacitor" or pattern of assembly. The greatest

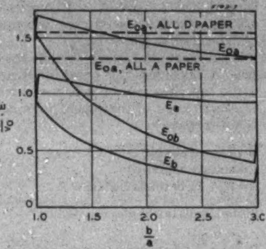

Figure 3. Stresses in a graded cable, denser paper outside, range of b/a from 1 to 3

Paper *A* inside, paper *D* outside; see subcaption of Figure 1

value of *G*, within the range examined, is 1.70, *D* paper with $n = 4$ (25 per cent overlay), and the smallest 1.26, *A* paper with $n = 2$ (50 per cent overlay). These then are the factors by which the values of E_a and E_b plotted in Figure 1 are to be multiplied to give the stresses in the oil channels of the innermost layers of the inside denser paper and the outside less dense paper respectively. The resulting curves E_{oa} and E_{ob} have been plotted in Figure 1; also, in horizontal dotted lines, for the purposes of comparison, the values of the stresses in the oil channels at the conductor surface when the insulation is entirely of *D* paper and of *A* paper respectively.

We note from Figure 1 that in the special case there considered ($n = 4$, $b/a = 1$ to 3), for $b/a = 1$ (all *A* paper) and for $b/a = 3$ (all *D* paper) the average stress E_a has the same value as is well understood. However, in both cases the maximum oil stress is higher than E_a—the average maximum stress, 1.7 times for the denser paper *D* and 1.46 times for the less dense paper *A* (see Table I); the resulting difference is indicated by the horizontal dotted lines at the top of the figure.

This confirms qualitatively, and in terms of simple physical principles, the experimental result found by the author that in cable-type fully impregnated paper insulation a denser paper has a lower dielectric strength than a less dense paper.

When both types of paper are used in the same insulation wall, and, as we have assumed, the denser paper is on the inside, we see at once that for values of b/a between 1 and 1.75 the maximum oil stress E_{oa} in the denser paper is lower than the maximum oil stress in the case when the entire wall consists of the less dense paper. Thus properly proportioned graded insulation may have a lower maximum oil stress and a higher dielectric strength than either of its constituents when used singly for the same wall thickness of insulation.

Table I. Values of G for papers of two values of density (*D* and *A*)

Radius of Conductor, a, Inch	n=2		n=3		n=4	
	D	A	D	A	D	A
0.126	1.37	1.26	1.65	1.37	1.68	1.45
0.25	1.37	1.26	1.66	1.37	1.70	1.46
0.375	1.40	1.29	1.62	1.41	1.67	1.43
0.500	1.38	1.28	1.61	1.37	1.70	1.45

The stress E_{ob} in the inside oil channels of the outer less dense paper is always less than that in the inside channels of either paper used alone. However, in the graded case we note from Figure 1 that for values of b/a between 1 and 1.12, E_{ob} rises above E_{oa}, that is to say, breakdown is more likely to occur in the inside layers of the outer less dense paper.

Figure 2 shows that similar relations with only small variations in values occur when the total insulation wall thickness is one-half the diameter of the conductor, that is, the range of b/a is from 1 to 2.

It is of interest to note the relations which arise when in the graded cable the positions of the two grades of paper are reversed, that is, when the low-density paper is placed on the inside, adjacent to the conductor. These relations are shown in Figure 3 for a variation of b/a from 1 to 3, and so may be compared with those of Figure 1. As seen, for all values of b/a, that is, for any radial depth of the less dense paper, the stress in the oil channels next to the conductor is higher than if the low-density paper were used alone; up to $b/a = 1.55$ the stress is higher than if the high-density paper were used alone. The higher dielectric constant of the outer high-density paper shifts such a large fraction of the total voltage to the low-density paper that the lower oil-paper stress ratio of the latter is surpassed over the entire range.

The methods used in the foregoing analysis are approximate at several points, and several conditions obtaining in cable insulation as manufactured have not been introduced, as for example the stranding of the central conductor, the spiral course of the oil channels, and space-charge action in the oil channels. It is believed, however, that the bearing of these elements will be much the same relatively in each of the several cases compared, and that their influence would appear only in a possible attempt at a quantitative derivation of stress values.

The experiments referred to in the opening paragraph were conducted at 60 cycles, on thoroughly impregnated insulation in which there was at no time any evidence of internal gas pockets. Discussion has suggested, therefore, that the clear evidence of a higher dielectric strength of a lower density over a higher density paper should be restricted to thoroughly impregnated insulation of the oil-filled or other similar type, and not be extended to so called solid-type insulation, in which it is generally admitted that following load cycles, or due to other cause, gas pockets or layers are present, and that the range of breakdown stress values is substantially lower than those encountered in the author's tests. It is also suggested that a different result might be found even in insulation of the oil-filled type in breakdown tests of impulse type.

Some comment on this type of discussion will be found in the paper by Whitehead and Kopper.[1] It is not, however, within the purpose of this paper to continue that discussion, but rather to show in terms of simple physical principles and of the experiments referred to, that the use of high-density paper in cable insulation should result in a higher dielectric strength if used in combination with lower density paper in suitably proportioned graded insulation, than would result in the use of either grade of paper alone.

It is also fair to emphasize that the principles utilized herein, depending as they do only on variations of dielectric constant, must apply to all types of cable insulation, oil-filled, solid, gas-filled, or other, insofar as the values and distribution of dielectric stress are concerned. Whether or not complete breakdown is a function of maximum dielectric stress only, is another question, discussion of which also falls outside the scope of this paper.

The results of this study are offered as a possible explanation of the recent conflict of opinion as to the influence of high-density paper in cable insulation.

Conclusions

1. In cable-type impregnated-paper insulation the use of all high-density paper results in a higher maximum stress in the oil channels than does a low-density paper.

2. The use of both high- and low-density paper, with the former inside, as in a graded cable, may result in a lower maximum oil stress, and so a higher dielectric strength, than if all low-density paper or all high-density paper is used.

Reference

1. THE DIELECTRIC STRENGTH AND LIFE OF IMPREGNATED PAPER—IV, **J. B. Whitehead, J. M. Kopper.** AIEE TRANSACTIONS, volume 64, 1945, April section, pages 171–7.

The Role of Frequency in Industrial Dielectric Heating

G. W. SCOTT, JR.
MEMBER AIEE

A TENDENCY has developed to look upon frequency as a variable in dielectric heating which may be increased at will in order to increase the rate of heating quite independently of other factors. No doubt this tendency has been fostered by the acceptance without knowledge of its derivation of the equation for rate of dissipation of high-frequency energy in a dielectric, wherein the frequency term appears to the first power and in the numerator. The purpose of this paper is to analyze more carefully the role of frequency in industrial dielectric heating. The expression for the rate of heating will be critically examined, particularly with reference to the direct influence of frequency and its indirect influence through certain of the other variables of the heating equation that are not independent of frequency. In the light of this and other known effects of frequency, an attempt will be made to determine the practical upper limit of frequency for large-scale industrial dielectric-heating installations. It is hoped that, as a result of this discussion, there will result in the future a more precise use of the term frequency as related to dielectric heating. It should be pointed out that, in order to express the effect of frequency quantitatively, it has been necessary either to assume the ideal condition of pure L and C or to assume reasonable values of capacitance to ground and of distributed L and C. For this reason it has been possible in certain instances only to establish limits.

It is apparent from the analysis to follow that:

1. None of the variables in the heating equation is completely independent of frequency or its effects.
2. As frequency is increased, load capacitance must be decreased to allow tuning and to avoid short-circuiting the generator.
3. At higher frequencies load length must be kept at a minimum to eliminate the possibility of standing waves.
4. Increased frequency accentuates the load-shunting effect of stray capacitance and seriously reduces the over-all efficiency of the dielectric heating.

Therefore, it appears likely that the frequency band from 10 to 30 megacycles will prove best adapted for large-scale industrial dielectric heating, that is for load capacitances up to 500 micromicrofarads and for output power as high as 100 kw.

Equations for Development of Dielectric Heat

An expression for the heat developed in a dielectric by the application of an alternating voltage may be derived readily from the theory of the imperfect capacitor, represented schematically in Figure 1. Whenever there is an imperfectly insulating material to be heated between the plates of a capacitor, the latter may be considered as a capacitance with either a resistance R_s in series or a resistance R_p in parallel. These resistances are defined as

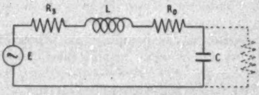

Figure 1. Equivalent circuit of dielectric heating load

E—Oscillator
C—Capacitance
R_s—Effective series resistance
R_p—Effective parallel resistance
L—Residual inductance
R_o—Residual resistance

$$R_s = \frac{\cos\theta}{\omega C} \qquad (1)$$

$$R_p = \frac{1}{\omega C \cos\theta} \qquad (2)$$

where

$\cos\theta$ = power factor of material heated and $\cos\theta \leqq 0.1 = \sin\delta = \tan\delta$
C = capacitance of load
$\omega = 2\pi$ (frequency)
E = alternating voltage

In addition there is associated with the capacitor a certain residual inductance L and resistance R_o. As, for simplicity in this analysis, the effect of leads will be ignored, the L term may be neglected and R_o reduces to the effective resistance of the capacitor plates.

If the concept of effective series resistance is employed, the power dissipated in the capacitor may be determined from an examination of the phase diagram of Figure 2 where

I = current flowing
E = voltage impressed
$R = R_s + R_o$, or total resistance

From Ohm's law it may be stated:

$$\text{Power} = \frac{E^2}{R} = \text{heat per unit time} = H$$

Therefore, the heat developed in the resistance R may be expressed:

$$H_R = \frac{E_R{}^2}{R} = \frac{E^2\cos^2\theta}{\dfrac{1}{\omega C\tan\theta}} = \omega C E^2 \cos\theta\sin\theta \qquad (3)$$

where

$$\theta = \tan^{-1}\left(\frac{1}{\omega C R}\right)$$

$\cos\theta$ = power factor of capacitor

Equation 3 is the general equation governing the development of heat in an imperfect capacitor. If desired, $\sin\theta$ may be replaced by $\sqrt{1-\cos^2\theta}$.

If the effective resistance of the capacitor plates may be neglected, an expression for the purely dielectric heat developed within the plates may be derived as follows:

$$H = \frac{E_R{}^2}{R_s} = \frac{E^2\cos^2\theta}{\dfrac{\cos\theta}{\omega C}} = \omega C E^2 \cos\theta \qquad (4)$$

where

$\cos\theta$ = power factor of material heated ($\leqq 0.1$)

Equation 4 may be verified by considering the effective parallel resistance R_p as the dissipative element.

For plane parallel electrodes and negligible effective resistance equation 3 takes the form:

$$W = \frac{5}{9} k \cos\theta f \left(\frac{E}{d}\right)^2 \times 10^{-12} \qquad (5)$$

where

W = heat in watts per cubic centimeter
k = dielectric constant of material heated
$\cos\theta$ = power factor of material heated ($\leqq 0.1$)

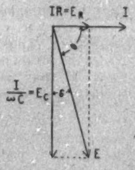

Figure 2. Phase diagram for dielectric-heating load

Paper 45-106, recommended by the AIEE committee on industrial power applications for publication in AIEE TRANSACTIONS. Manuscript submitted February 24, 1945; made available for printing May 5, 1945.

G. W. SCOTT, JR., is assistant chief physicist, Armstrong Cork Company, Lancaster, Pa.

Credit is due to I. J. Barsey for assistance in certain of the calculations and to G. E. Gard and K. D. Lawson for advice on the practical aspects of frequency in dielectric heating.

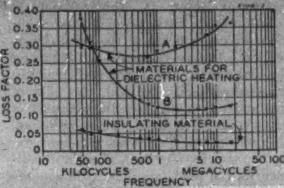

Figure 3. Variation of loss factor with frequency for typical materials to be heated (*A* and *B*), and a typical insulator

f = frequency in cycles per second

$\frac{E}{d}$ = voltage gradient in volts per centimeter

Equation 3 may be evaluated for any electrode configuration whose capacitance may be expressed although the heating will be uniform only in those instances where the electric field is uniform.

Examination of equations 4 and 5 shows that the magnitude of the heat generated is determined collectively by

(*a*). The geometry of the load.

(*b*). Its electrical properties.

(*c*). The characteristics of the source of high-frequency power.

The appearance of C in equation 4 clearly establishes the dependency of the heating upon load geometry. Equation 5 for plane parallel electrodes, perhaps the most frequent situation in industrial dielectric heating, includes dielectric constant and power factor which are, of course, inherent electrical properties of the material being heated. Furthermore, both equations contain frequency and voltage terms, which are determined not altogether independently by the oscillator and the coupling to the load circuit.

From a cursory analysis of equation 5, it is reasoned that increased frequency will allow somewhat decreased voltage to accomplish equivalent heating or linearly decreased time of heating if the voltage is maintained constant. As a result considerable emphasis has been placed on higher frequency for industrial dielectric heating to gain these advantages. This emphasis in many instances, has been misplaced since

1. The acquirement of greater skill has allowed high-frequency voltages up to 25 kv to be insulated.
2. The remaining terms in the heat equation are not independent of frequency.
3. Increased frequency causes serious limitations in itself.

Variables in Heat Equation not Independent of Frequency

In equations 3, 4, and 5 no terms are independent of frequency except the numerical constants, although certain quantities are more directly a function of frequency than others. Both dielectric constant, k, and power factor, $\cos\theta$, are direct functions of frequency and incidentally of temperature as well. The product of these two quantities is known as the loss factor of the material in question, and it has been plotted versus frequency in Figure 3 for two materials suitable for industrial dielectric heating, *A* and *B*, and for one material suitable as a high-freqnency insulator. Although attention has been called by some to frequencies at which maxima and minima occur in the loss-factor curve, this fact is not of great value in shortening heating cycles because, even in approaching such points, a given percentage change in frequency normally results in a much smaller percentage change in loss factor. In general, it may be said that relatively good high-frequency insulators exhibit a loss-factor characteristic that slowly diminishes as frequency increases, whereas materials suitable for high-frequency heating may either increase, decrease, or go through maxima and minima as frequency increases. Although variations of loss factor in a given material seldom warrant choice of a particular frequency to increase the heating rate, large variations between different materials may require higher frequencies to heat the better insulators.

When a parallel resonant circuit containing an imperfect capacitor, as is the case in a dielectric-heating load circuit, is tuned to resonance, it presents to the oscillator an approximate resistive impedance:

$$Z_R = 10^6/(2\pi f C \cos\theta) \text{ ohms} \qquad (6)$$

where

f = frequency in megacycles

C = capacitance in micromicrofarads between electrodes

$\cos\theta$ = power factor of dielectric

This is true because at resonance the parallel circuit offers infinite impedance, but shunted with the effective parallel resistance of the dielectric, R_p. Consequently, the impedance, Z_R, in equation 6 is merely R_p, since the latter is much less than infinity for conditions that allow the development of appreciable dielectric heat.

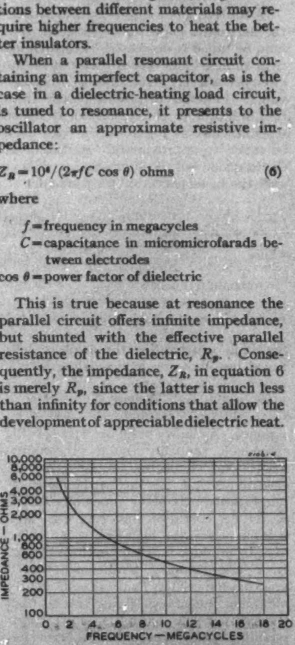

Figure 4. Variation with frequency of impedance for a dielectric-heating load (material *A*, Figure 3) tuned to parallel resonance

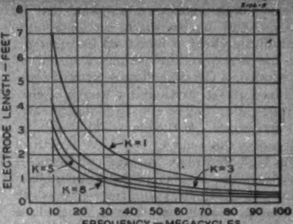

Figure 5. Maximum tolerable electrode length allowing ten-per-cent voltage variation as a function of frequency

K = dielectric constant

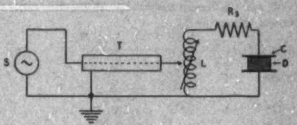

Figure 6. Tuned load circuit for dielectric heating

S—Oscillator

T—Coaxial transmission line

L—Tuning inductance

R_s—Effective series resistance

C—Electrodes

D—Material to be heated

In Figure 4 Z_R has been plotted as a function of frequency for a 36-by-36-by-3-inch (100-pound) load of material, *A*, presented in Figure 3. For this load the capacitance varies from 388 to 330 micromicrofarads over the frequency range considered. The impedance across the load is seen to diminish markedly with frequency.

The power transfer to and voltage drop across a load necessary for heating depend upon the impedance match between the output of the oscillator and the load circuit. As an increase in frequency will reduce load impedance, a reduced voltage will exist across the load, thereby minimizing power transfer, other factors remaining the same and the load capacitance having been tuned to the new frequency. Consequently, voltage may not be maintained constant across a load to shorten a heating cycle as frequency is increased unless adjustments are made to maintain the impedance match. If the oscillator is assumed to have an output impedance of 300 ohms and the load to be tuned with a high Q parallel resonant circuit, Figure 4 shows that the impedances would be matched for the load in question at 15.5 megacycles if the terminals of the oscillator were connected directly across the load. At much higher frequencies some sort of impedance-matching network would be required. There are, of course, practical limits beyond which impedance matching may be of no avail in overcoming the load short-circuiting effect of increased frequency.

Furthermore, the geometrical factors included in the capacitance term of equations 3 and 4, particularly length of electrodes, may not be chosen independently of frequency. If the electrode length approaches one-quarter the wave length of the high-frequency voltage employed, it will act as an open-ended transmission line upon which a quarter-wave-length standing wave is maintained. In the case of longer electrodes, half- or full-wave-length standing waves may exist or any multiples thereof. This, of course, will result in nonuniform generation of dielectric heat.

In the case of such a standing wave the voltage varies sinusoidally along the electrode, that is:

$$V = \sin \omega t \tag{8}$$

where

$\omega = 2\pi f$
t = time

For an electrode the voltage at any point may be expressed:

$$V = V_{max} \cos 2\pi f t$$

where

$$t = \frac{x\sqrt{k}}{c}$$

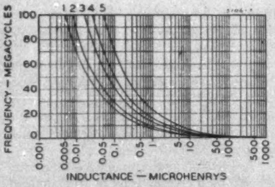

Figure 7. Ideal tuning inductances required as a function of frequency for loads of specified capacitance

1—C = 500 micromicrofarads
2—C = 300 micromicrofarads
3—C = 150 micromicrofarads
4—C = 100 micromicrofarads
5—C = 50 micromicrofarads

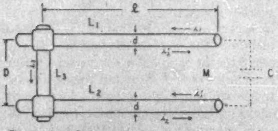

Figure 8. Schematic drawing of tuning stub

L_1, L_2—Parallel conductors
L_3—Movable short-circuiting bar
i_1, i_2, i_3—Primary currents
i_1', i_2'—Induced currents
C—Distributed capacitance

so that

$$V = V_{max} \cos 2\pi f \left(\frac{x\sqrt{k}}{c} \right) \tag{9}$$

in which

V_{max} = maximum voltage
x = distance from point of maximum voltage
k = dielectric constant of medium between electrodes
c = velocity of light
f = frequency

If it is assumed that a ten-per-cent voltage variation may be tolerated along the greater dimension of a rectangular electrode, it is possible to calculate from equation 9 the maximum permissible electrode length as a function of frequency. These lengths are plotted in Figure 5 and are seen to be considerably reduced as frequency is increased, particularly for media with high dielectric constant. For the data of Figure 5 the generator is assumed to be connected to the mid-point of the shorter edge of the rectangular electrode.

Limitations of Increased Frequency

As the frequency employed is increased, the maximum capacitance, or load, that may be tuned is decreased, because practical tuning inductances may not be devised below a certain minimum inductance value. In order to absorb energy from the oscillator in the arrangement shown schematically in Figure 6, the load must be tuned to approximately resonance at the frequency of the source in accordance with the basic condition for resonance:

$$f = \frac{1}{2\pi} \frac{1}{\sqrt{LC}} \tag{10}$$

where

f = resonant frequency
C = capacitance of load
L = inductance of tuning element

Speaking practically, the load is best tuned just above resonance on the capacitative side as operation at this point is more stable and efficient than either at resonance or on the inductive side of resonance. As shown in Figure 6 for parallel resonance, probably the most common load-circuit connection in industrial dielectric heating, this means the load presents nearly maximum impedance to the source, a condition favoring the high voltage across the load electrodes necessary to produce inphase heating current. In a series-resonant arrangement tuned near resonance, the load presents nearly minimum impedance giving rise to high transmission-line currents and corresponding losses. This undesirable feature, together with the fact that in a series arrangement the voltage across the capacitor is greater than the impressed voltage by a factor, Q, which frequently causes voltage breakdown, has led to the more widespread use of the parallel connection. However, equation 10 holds for the series case; and, if the voltage across the electrodes is identical, the facts of this analysis apply to either parallel or series connection unless otherwise stated.

Equation 10 defines the resonant frequency strictly for the case of zero resistance in the load circuit. Although the residual resistance of such a parallel circuit reasonably may be neglected, the effective series resistance, R_s, of the dielectric should be considered, leading to a shifted resonant frequency defined:

$$f_r = \frac{1}{2\pi} \frac{1}{\sqrt{(L - CR_s^2)C}} \tag{11}$$

However, for the materials whose dielectric properties are shown in Figure 3 (that is, $\cos \theta \leq 0.1$) this correction is negligible. If C is assumed constant the change in frequency may be defined as

$$\frac{f_r}{f} = \sqrt{1 + \cos^2 \theta} \tag{12}$$

where

f_r = resonant frequency with resistance
f = resonant frequency with zero resistance
$\cos \theta$ = power factor of material

More important is the fact that the term CR_s^2 in equation 11 diminishes as the temperature of the dielectric is increased owing presumably to changes in k and $\cos \theta$ with temperature. Because of incomplete information regarding the effect of temperature on these dielectric properties, it can only be said that, as the temperature of the load is increased, less tuning inductance is required.

It is evident, from equation 10 that, as the load capacitance is fixed, at least at the beginning of the heating cycle, it is necessary to reduce the inductance of the tuning element in order to resonate the fixed load at higher frequencies. In Figure 7 are plotted, from equation 10

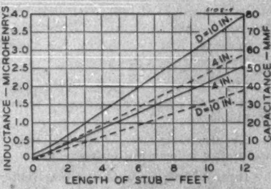

Figure 9. Calculated *L* and C characteristics of tuning stub of Figure 8 as a function of conductor length and separation

D = conductor separation
Conductor diameter—$1^3/_8$ inches
Solid line—Inductance
Dashed line—Capacitance

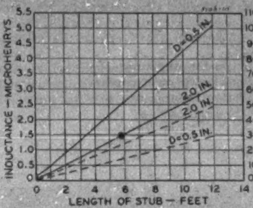

Figure 10. Calculated *L* and *C* characteristic of tuning stub of Figure 8 as a function of conductor length and diameter

D = conductor diameter
Conductor separation—8 inches
Solid line—Inductance
Dashed line—Capacitance

for pure L and C, the inductances required to tune loads of 50 to 500 micromicrofarads over a frequency range from 10 to 100 megacycles. Although it is recognized that these frequencies are shifted by the effective series resistance of the dielectric and the latter's rise in temperature during the heating cycle, they are sufficiently accurate for illustrative purposes. So far as temperature rise of dielectric is concerned, the inductances presented are maximum required values for a particular load geometry. The 500-micromicrofarad capacitance corresponds approximately to a 2.25-cubic foot 108-pound load of material A in Figure 3 at room temperature. Although ideally inductances of the order of magnitude of those indicated would be possible, there exists, however, a practical lower limit for an inductance suitable to tune a load dissipating a large amount of high-frequency power.

Such loads have been successfully resonated by means of a so-called tuning stub, that is, two parallel copper pipes connected with a sliding cross piece or short-circuiting bar, as is illustrated in the schematic drawing of Figure 8. In Figure 9 are plotted the L and C characteristics for tuning stubs from 0 to 12 feet in length, separated four and ten inches, respectively, and made from $1^3/_8$-inch-outside-diameter copper pipe. Variation of L and C as a function of conductor diameter is shown in Figure 10. The calculations, for which the details are presented in the appendix are ideal to the extent that zero capacitance to ground has been assumed for the stub. It is apparent, from an examination of Figures 9 and 10, that 0.1 to 0.15 microhenry is the minimum calculated inductance that may be expected from such an arrangement. Furthermore, the tuning stub does not act as an inductance under all circumstances, an additional limitation on the maximum capacitance that may be tuned at a specified frequency. As there is always capacitance associated with the inductance of a stub, the latter has a natural or resonant frequency. When the frequency of the voltage applied to the stub is in excess of the natural frequency, the stub presents a capacitative impedance and is no longer useful as a load-tuning element. At intermediate frequencies the effective inductance of the stub may be computed from the approximate formula:

$$L_{eff} = \frac{L}{1-\gamma^2} \qquad (13)$$

where

L = calculated inductance
γ = ratio of actual to resonant frequency (accurate for $\gamma < 0.8$)

In Figure 11 has been plotted the resonant frequency of the stub in question with a conductor spacing of ten inches. The frequencies corresponding to each length are the maximum frequency at which the stub presents an inductive impedance. Of course, if some capacitance to ground had been assumed, these maximum frequencies would be reduced.

The data of Figures 9 and 11 and experience have led to the conclusion that a straight piece of tubing one foot long may be taken to represent the practical minimum inductance that may be employed as a load-tuning element. The calculated inductance of such a length of tubing $1^3/_8$ inches outside diameter is 0.149 microhenry. In practice there arises the necessity of shielding such an element to avoid interfering radiation. A cylindrical grounded shield of eight-inch radius introduces a capacitance to ground of 6.91 micromicrofarads, from which information the effective inductance may be computed as a function of frequency. From equation 10 the maximum effective capacitance that can be tuned can be calculated. If an inherent inductance of 0.00006 microhenry per micromicrofarad is assumed in the load of Figure 1, its geometrical capacitance may be computed from the relation:

$$C = \frac{C_{eff}}{1+4\pi^2 f^2 C_{eff}} \qquad (14)$$

Based on these assumptions, the maximum geometric capacitance that may be tuned by conventional methods has been plotted as a function of frequency in the curve labeled "practical" in Figure 12. These maxima are to be compared with those of the curve designated "ideal" in Figure 12 computed for the case of pure L and C. It is apparent that, if the 500-micromicrofarad 2.25-cubic foot 108-pound load already referred to is to be tuned by ordinary means, the frequency should not exceed approximately 20 megacycles.

There are means by which the maximum tunable capacitance may be increased, but such means are not feasible in all cases. The capacitance of a load may be halved by connecting a similar capacitance in series; but if the additional capacitance is air-insulated it robs part of the available voltage from the load, and if it is a duplicate load the power requirements are doubled, which may prove uneconomical. Bierwirth and Hoyler[1,2] have ingeniously tuned a 700-micromicrofarad load at 45 megacycles by means of multiple-tuning stubs each of minimum inductance, which incidentally tune out the standing waves that would otherwise appear on the load electrodes. However, such a scheme is of limited application.

It should be emphasized that the impedance across a capacitative load is diminished as the frequency is increased. Quantitatively, this impedance is expressed for the general case:

$$Z_C = \frac{1}{2\pi f C}\sqrt{\cos^2\theta + 1} \qquad (15)$$

where

f = the frequency employed
C = capacitance
$\cos\theta$ = power factor of medium

Relatively small stray capacitances to ground frequently exist in a practical dielectric-heating load. As the medium is usually air ($\cos\theta = 0$), for low frequency

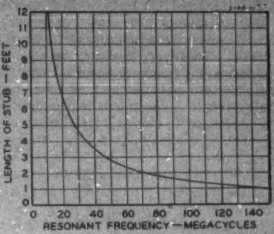

Figure 11. Resonant frequency of tuning stub of Figure 8 as a function of conductor length

Conductor separation—10 inches
Conductor diameter—$1^3/_8$ inches

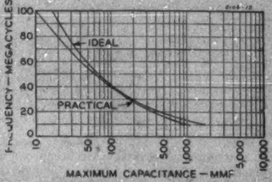

Figure 12. Maximum tunable load capacitance as a function of frequency, if 0.149-microhenry minimum practical tuning inductance is assumed

Ideal—Pure L and C
Practical—Residual parameters

Z_C is large and may be ignored. However, as f is increased Z_C decreases, which effectively adds to the capacitative load to be tuned. Therefore, not only is there a maximum C that may be tuned but also a minimum capacitative load that practically may be presented in an effort to compensate for increased frequency.

Finally the over-all efficiency of an arrangement of circuits as shown in Figure 6 for dielectric heating is seriously reduced as the frequency is increased; and this is an important consideration in so expensive a mode of heating. The efficiency should be kept between 50 and 60 per cent for economic operation. Not only are there resistive and radiation losses throughout the circuits, but an inherent limitation is the efficiency of the oscillator power tubes. The plate efficiency of available power tubes is reduced as the frequency of the input is increased largely on account of

1. Dielectric losses in glass walls and elsewhere.
2. Increased grid dissipation because of higher circulating currents due to lower grid impedance and because of long electron transit times.
3. Increased plate dissipation because of a phase shift between grid voltage and plate voltage due to long electron transit time.

Although plate efficiency data are not available, rated reduction in power input for several oscillator tubes that may be used for industrial dielectric heating with output power up to 100 kw has been plotted versus frequency in Figure 13. A conventional triode will function with 60-70-per-cent plate efficiency up to 20 megacycles. Above this frequency losses increase until at approximately 100 megacycles losses equal input power and the tube ceases to oscillate. It is apparent that, if higher frequency is required for shorter heating cycles, limited power output must be anticipated but not necessarily with reduced input power.

Choice of Frequency

In conclusion it must be emphasized that in reality the choice of frequency for a dielectric-heating application is a compromise among

1. The geometry of the load.
2. The electrical characteristics of the material constituting the load.
3. The oscillator tubes available.

Frequency must be selected with these factors clearly in mind, as well as the desire for minimum duration of heating cycle.

Broadly speaking, as high a frequency as is practical, available, and economical should be used. In particular, highest frequency is suited to very small loads, thin sections not capable of insulating high voltages, and materials with low loss factor. There is a limit to the extent that frequency may be increased to accommodate thin sections because, as thickness diminishes, load capacitance increases, presenting a serious tuning problem. Emphasis on high frequency to obtain short heating cycles may frequently be misplaced because

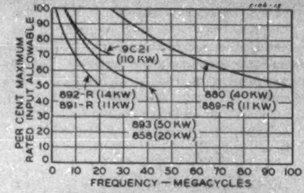

Figure 13. Allowable percentage of maximum rated input as a function of frequency for certain power tubes suited to dielectric heating

1. Extraneous circumstances often set a practical lower time limit to acceptable heating cycles.
2. Too rapid heating may have a deleterious effect on the material.
3. Increased production rate may not be economical unless accompanied by increased volume of production.

This analysis of the role of frequency in industrial dielectric heating indicates that at least for several years to come the range of frequency from 10 to 30 megacycles only will be utilized for large-scale dielectric heating, that is, for powers up to 100 kw. Changes in dielectric properties with elevated temperature will make close frequency control difficult unless means of automatic tuning are devised. Therefore, users and suppliers should coordinate their research and development activities with these facts in mind.

Appendix. Calculation of *L* and C for Tuning Stub

The total inductance L_T of the tuning stub shown schematically in Figure 8 may be calculated from the relation:

$$L_T = L_1 + L_2 + L_3 - 2M \qquad (16)$$

where

L_1 = self-inductance of first conductor
L_2 = self-inductance of second conductor
L_3 = self-inductance of short-circuiting bar
M = mutual inductance between first and second conductors

It is apparent that the relatively small mutual inductance between the short-circuiting bar and the other conductors has been neglected. The mutual-inductance term has been subtracted since, as may be seen from the currents indicated in Figure 8, the induced currents i_2', i_1' oppose the existing ones i_1, i_2.

The self-inductance in microhenrys of a tubular conductor of length l centimeters and diameter d centimeters may be expressed by the equation:[3]

$$L = 0.002l\left(2.303 \log_{10}\frac{4l}{d} + \frac{d}{2l} - 1 + \mu\delta\right) \qquad (17)$$

where $\delta \approx 0$ for copper tubing employed at frequencies above one megacycle. The mutual inductance in microhenrys of two parallel conductors of length l centimeters separated by a distance D centimeters from center to center as in Figure 8 may be computed from the relation:[3]

$$M = 0.002\left(2.303l \log_{10}\frac{l+\sqrt{l^2+D^2}}{D^2} - \sqrt{l^2+D^2} + D\right) \qquad (18)$$

When equations 17 and 18 are substituted in equation 16, the total inductance L_T of the tuning stub may be simplified to the form:

$$L_T = 0.004l\left(2.303 \log_{10}\frac{4lD}{d(l+\sqrt{l^2+D^2})} + \frac{d+2\sqrt{l^2+D^2}-2D}{2l} - 1\right) + L_3 \qquad (19)$$

Where L_3 is the self-inductance of the short-circuiting bar, which may be computed from the relation:

$$L_3 = 0.002D\left(2.303 \log_{10}\frac{4D}{d} + \frac{d}{2D} - 1\right) \qquad (20)$$

The values of tuning-stub inductance plotted in the curves of Figures 9 and 10 were computed from equations 19 and 20.

The tuning stub in question is, of course, not pure inductance but has a certain distributed capacitance between the parallel conductors that has been represented in the schematic drawing of Figure 8. If the effect of the short-circuiting bar is neglected and the conductors are assumed to be infinitely removed from ground, this capacitance in micromicrofarads may be computed from the relation:

$$C = \frac{0.1208l}{\log_{10}\dfrac{2D}{d}} \qquad (21)$$

where l is length of conductors in centimeters and D is their separation in centimeters, center to center. The values of capacitance for the tuning stub plotted in Figures 9 and 10 were computed from equation 21.

References

1. Radio-Frequency Heating Applied to Wood Gluing, R. A. Bierwirth, C. N. Hoyler. *Proceedings* Institute of Radio Engineers, volume 31, 1943, pages 529–37.

2. United States patent 2,308,043, 1943.

3. Radio Instruments and Measurements, circular 74, United States Bureau of Standards, 1924, pages 235–86.

Rewinding Commutator-Type Traction Armatures

N. J. GREENE
MEMBER AIEE

D. E. STAFFORD
ASSOCIATE AIEE

C. GENTILINI
ASSOCIATE AIEE

THE AMERICAN RAILROADS achieved more than twice as many passenger-miles and hauled twice as many ton-miles of freight in 1943 as in the corresponding period of 1918. Incomplete reports indicate increases for 1944. This enormous job is being done with smoothness and dependability and with far less congestion than was possible with the equipment and personnel of World War I.

Locomotives with electric transmissions, which include straight electric, Diesel-electric, and gasoline motorcars, and their attendant electric equipment, have played an important part in this accomplishment. With the increased number of electric locomotives in use, the longer hours of operation, and the heavier loads, old maintenance problems have been accentuated; new ones have arisen. Down the long list of these problems is one entitled "Armature Rewinding."

The object of this paper is to review for those experienced in the art of armature rewinding and to cite for the newcomer some of the important and frequently overlooked factors which must be considered to restore a damaged armature to its original condition and to modernize and improve, consistent with current practices. The factors will be discussed under the following headings:

1. Analysis of failure.
2. Cleaning.
3. Magnetic inspection.
4. Commutator.
5. Rewinding materials.
6. Armature windings.
7. Banding.
8. Impregnating.
9. Balancing.

Railway armatures present an interesting though difficult problem as they must withstand the severe strains imposed upon them by varying loads at varying speeds,[1] plus the several combinations of vibration and strains resulting from train motion and roadbed shock, and often with rapidly changing ambient temperatures.

Analysis of Failures

Traction motors are of necessity rugged in design because of inherently severe duty requirements. The kind of service is such that road failures must be kept at a minimum, not only because of the direct cost but because of the consequent expense incurred when traffic movement is obstructed. In most industrial plants a replacement motor or part can be installed in a comparatively short time. With motive power, however, the point of operation is not fixed and failures may occur many miles from the nearest repair or exchange facility.

In spite of equipment design and operating precautions taken to prevent failures, they will happen. To minimize these failures, an analysis of the cause of each must be made and steps taken to lessen the possibility of a recurrence.

Figure 1. View of vapor cleaning tank

Powerful cleaning action is effected by hot vapors condensing on the object to be cleaned by virtue of:

1. Strong solvency of cleaning fluid
2. Distilled vapor is full strength, undiluted by dissolved grease
3. 188 degrees Fahrenheit temperature helps to clean and to cook off paints and varnishes

Causes of armature failure can be divided into two classes:

1. Those which can be attributed to faulty operating conditions.
2. Those originating within the motor due to mechanical or electrical defects.

Causes of armature failures may be numerous and varied; however, some of the major and frequently occurring troubles are discussed in the following paragraphs. The armature winding may be completely roasted because of a mechanical fault causing excessive overload; it may be roasted because of heat resulting from friction generated when worn-out bearings or journals allow the armature to rub the pole pieces. The armature winding or commutator may be grounded, short-circuited, or open-circuited; bands may fail owing to overspeeding, but in all cases the cause can be assigned to either the category of faulty operation or to that of a defect in the motor proper.

Most failures traceable to a motor defect originate first as a mechanical failure. Improperly seasoned armature insulation caused by incorrect baking and hot banding procedure may permit relative movement of wires or coils which will cause actual mechanical destruction of the insulation and result in an electrical failure. Faulty commutator seasoning on high-speed traction motors, weak brush-holder spring tension, and short or binding brushes are only a few additional things to consider when analyzing armature failures. The advantage of a thorough investigation to determine the cause of each failure cannot be stressed too strongly.

Cleaning and Preparation of Core

The proper cleaning of cores to be rewound goes beyond removing the old coils and scraping out the slots. Grease must be removed, old paint stripped, vent ducts cleared, and the outer surfaces of laminations cleaned. One of the most effective methods of accomplishing these aims is by the use of hot vapor cleaning—a process termed by the sheet-metal industry "degreasing." The equipment consists of a heated tank with a few inches depth on the bottom of the liquid cleaning solution (normally trichlorethylene) and a water-cooled condensing coil around the tank about halfway up the side wall.[2]

In operation, an armature to be cleaned, with its old winding intact, is lowered into the gaseous medium existing between the boiling pan and the condensing coils. As the vaporized cleaning solution is kept at a temperature of 188 degrees Fahrenheit, much higher than the object being cleaned, the vapor condenses upon the object, attacking grease, dirt, and varnish. Condensation is so rapid that the fluid flows from the work in a steady stream, carrying with it dissolved materials. Upon first seeing this action, one would think that liquid was being fed onto the object from an invisible pipe line.

When the entire armature is placed in the tank, not only is the grease and dirt removed but the insulating and bonding varnishes are softened, facilitating the removal of the old winding. This procedure minimizes the hazard of lamination damage when extremely tight coils must be stripped from the slots.

After the temperature of the work has reached that of the vapor, condensation ceases and the cleaning process stops. The

---

Paper 45-91, recommended by the AIEE committee on land transportation for publication in AIEE TRANSACTIONS. Manuscript submitted December 8, 1944; made available for printing March 12, 1945.

N. J. GREENE is chief engineer, D. E. STAFFORD, assistant chief engineer, and C. GENTILINI, design engineer, all of National Electric Coil Company, Columbus, Ohio.

Figure 2. Clearing surface-fused laminations

armature may be withdrawn from the cleaning tank, and a few strokes with a wire brush removes loose residue and flakes of varnish. If the slots have been dirty, it may be necessary, after removing the coils, to return the stripped core to the cleaning tank for another treatment, but a second cleaning is only occasionally required.

The solvents normally used in this type of apparatus have little or no dissolving effect upon some types of coating materials such as shellac and certain synthetic enamels. The vapors have no effect on water glass (silicate of soda) or other standard lamination-insulating varnishes. Tests reveal that, after these lamination-insulating materials have been suspended in the degreasing vapors for ten minutes, neither their surface smoothness nor adherence to the metal has been affected. A mica commutator segment and cone ring given the same treatment were found to have a very small increase in weight, which was caused by the shellac softening under heat and allowing some vapor to collect. This increase in weight was lost after cooling took place, with no damage to the mica splittings or the shellac bond.

Over a period, repeated dips and bakes build multiple layers of baking varnish on the laminations, in the radial vents, and in the longitudinal core ducts. This insulating coating retards heat transfer and restricts air flow. The removal of this varnish in the "degreaser" will restore original ventilating efficiency to the armature. The elimination of grease from commutator, mica, and cone rings provides a clean surface to which insulating and protective coatings may be applied.

Core laminations of armatures which have failed frequently are found to have been damaged by arcing in slots between conductors and core. Also, the outer surface of core may have been defaced by pieces of conductors or bands being caught between armature and pole faces. Where any of the damage is severe, new core stacking may be necessary. However, after most armature failures, core stacking will not be required.

A very effective method of removing the fused surfaces in the core slots is to grind them out with a high-speed portable tool as shown in Figure 2. Sufficient grinding should be done to clean up all short circuits between laminations. Otherwise, hot spots may be expected to occur in operation, their severity depending principally upon the amount of fusion, the relative location, the magnitude of the armature current, and the frequency.

On older-type armatures having core bands it is often desirable to true up the banding grooves before rewinding. They are often burred over by the tangled mass of banding wire and copper that sometimes gets between the armature surface and the pole piece. An often used practice for accomplishing this is to drive a hard maple block into each slot, filling to the bottom of the band groove, and then, with the armature turning in a lathe, true up burred-over laminations at edges of band groove, taking light cuts with a high-speed tool-post grinder.

Magnetic Inspection

Magnetic inspection is the term applied to the process of examining ferrous metal pieces for flaws by magnetizing the piece and dusting fine iron particles or flowing over the piece a solution with iron particles in suspension. Since different magnetic poles are formed at the cracks, a concentration of the magnetic particles will collect so that the defects can be found by visual inspection.[3]

Magnetic inspection, although not new, has come into common use only since the great forward developments of aircraft, which must, of necessity, use materials efficiently to achieve lightness and safety. Railway equipment, although not limited to the same extent as that of aircraft, is subjected to repeated stresses that may cause costly failures. Armature shafts continuously are subjected to twisting torques while rotating. Improved alloy steels are used for these shafts; however, a metal that is fatigue-proof is not available. Shafts, before complete failure, will develop fatigue cracks. The application of magnetic inspection to traction armature shafts is comparatively recent, and only a limited amount of data are available. The available data indicate that many factors must be evaluated, such as shaft design, the load or torque on the shaft, and frequency of application of loads. The users of traction-motor equipment must compile data on the fatigue of shafts in order that shafts which have reasonable possibility of fatigue cracks may be tested by magnetic inspection.

The general practice in the magnetic inspection of traction armature shafts is to apply the test to exposed surfaces without pressing the shaft from the armature core. One class-1 western railroad has found that most fatigue cracks are detected on the tapered pinion fit adjacent to the bearing fit. This finding has resulted in the following handling procedure for all armatures that are removed from the motor frame for any reason:

1. Remove the pinion and antifriction bearings.
2. Clean all exposed shaft surfaces, removing all grease and dirt.
3. Magnetic-test and inspect for fatigue cracks, fractures, and defects.
4. Check for shaft trueness and alignment.
5. Renew defective shafts.

Fatigue cracks in armature shafts are not limited to the zone between the bearing and pinion fit. If a complete check is wanted, the shaft must be removed and tested over its full length.

Various types of equipment are available for performing magnetic inspection. Some use alternating current, some direct current from storage batteries, and others rectified alternating current for excitation of the magnetic structure.[4] Any type excitation is generally suitable for inspecting traction-motor armature shafts for fatigue cracks. The equipment for checking consists essentially of a magnetic yoke assembly with adjustable pole pieces for contacting the ends of the shaft and an excitation coil with control for allowing current to flow in the coil for comparatively short intervals (0.00001 to 3 seconds), similar to that shown in Figure 3. Magnetic particles in liquid suspension are easier to use, as the solution may be pumped or flowed over the shaft.

Magnetic testing of the wheels, axles, and locomotive crank pins of rolling stock has been used by many railroads for a

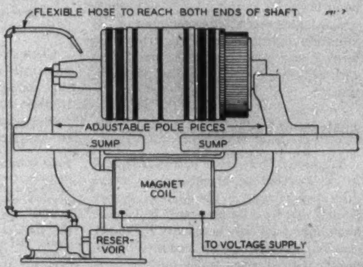

Figure 3. Traction armature in position for magnetic inspection of shaft

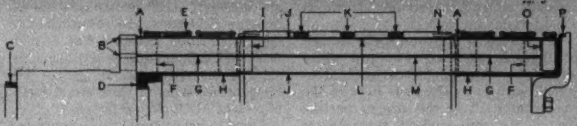

Figure 4. Guide for armature-rewinding materials

See Table III

A—Insulation under bands
B—Commutator-neck fillers
C—Commutator V ring
D—Mica seal
E—Band wire and clips
F—Insulation between coil-end turns
G—Insulation between layers
H—Coil-rest insulation
I—Formed U slot-end insulation
J—Slot insulation
K—Core bands and insulation
L—Strip filler
M—Slot-insulation strip separator
N—Slot stick
O—Coil-connection insulation
P—End-shield insulation

number of years. Some railroads are effectively using the same equipment for testing armature shafts.

Commutators

The condition of a commutator may indicate a real story to the experienced operator. A close examination is, therefore, of prime consideration so that corrective measures can be taken if necessary.

National Electrical Manufacturers Association Standard *RP*4-20 specifies that the Brinell hardness shall be 75 for bars of 0.125 inch and less at the thick edge, 70 for thickness of 0.125 inch to 0.250 inch, and 65 for bars over 0.250 inch. When a commutator shows evidence of having been very hot, it is good practice to test the hardness of the bars and to replace those which are too soft. It is also important on commutator of high peripheral speed that the amount of bar stock depthwise be checked so that there will be no danger of the bar bowing outward because of centrifugal forces. When there is doubt as to the depth of the bar remaining, a check with the commutator manufacturer is warranted. If the depth is less than a safe value, the commutator must be renewed.

After the winding is removed from the armature, the commutator slots are cleaned for the new coil leads, all burrs and fins are removed, and the commutator is given a ground test with the proper test voltage as specified by AIEE Standards. The authors have been unable to find a published Standard for a bar-to-bar test but have used very successfully a value of 220 volts alternating current, 60 cycles.

If the *V* rings are loose or have been disturbed, the commutator should be seasoned before the armature again is placed in service. Many different practices are followed in the seasoning of commutators, and most of them have good points. The object of seasoning is to obtain a tight commutator that will not develop high and low bars after being placed in service. To accomplish this objective we must apply the same elements that produce distortion in service, namely, heat and centrifugal force. The commutator assembly may be rotated in a heating rig and the bolts uniformly tightened at intervals. For the required uniformity in tightening the clamping bolts, it is recommended that a torque wrench be used.

As little copper as possible is removed from the commutator in turning and truing. The point of the tool should be rounded so that a smooth surface results. Final surfacing can be done with a stationary stone mounted in the tool post with the armature running at a high speed. A final polish may be given with a hand stone or very fine sandpaper. The commutator should be true within 0.001 inch for any high-speed motor. Where greater precision is wanted, the commutator may be ground with a carborundum wheel while the armature is rotated at full speed in its own bearings in a special grinding rig.[5]

Undercutting of commutator mica segments first came into use over 35 years ago, and, though at first it was not accepted, there is today little occasion to doubt its merits. However, expert care must be exercised in the operation, or the merits of undercutting are lost. It is very important that all mica fins be removed, as they are frequently the source of unsatisfactory operation. After undercutting, the rough corners of the copper bars must be removed.

After the commutator has been finished, it should be cleaned thoroughly and the armature blown out to remove all the copper chips and dust. It should be inspected carefully and then given a ground test according to AIEE Standards.

Table I. Banding Tension

Brown and Sharpe Gauge	Diameter (Inches)	Grade-C Steel and 18-8 Stainless Steel *Tension (Pounds)	Phosphor Bronze *Tension (Pounds)
8	0.128	850	600
10	0.102	600	400
12	0.081	400	250
14	0.064	250	160
16	0.051	160	100

* When double-deck bands are used, reduce the tension values by ten per cent for the top band.

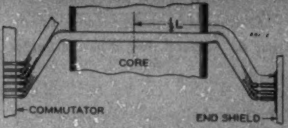

Figure 5. Increase in length of armature-coil bars from copper expansion

One-half length at 20 degrees centigrade = 17.000 inches

One-half length at 125 degrees centigrade = 17.036 inches

One-half length at 200 degrees centigrade = 17.058 inches

The protection of the outside surface of the *V*-ring mica that projects beyond the commutator can be accomplished readily by applying a coat of shellac, running over this a single layer of Fiberglas braid, and coating repeatedly with red enamel, sandpapering between coats. This will result in a very smooth surface which will minimize the collection of dust and oil.

Rewinding Materials

An often overlooked important element of armature rewinding is engineering planning of the rewinding materials. Rewinding materials include all insulation, solder, band wire, and like material, exclusive of the coils. Figure 4 gives the location of various items of rewinding material, and the table therewith will serve as a general guide to good practice in the use of material with AIEE class-*A* and class-*B* windings. Precision armature rewinding necessitates complete drawings of the armature assembly with detailed instructions on the method of application of each item of rewinding material. Information gathered from the analysis of failures is a part of the engineering data required for preparation of these rewinding specifications. Each item of rewinding material must be engineered for its job.

Too often certain items of insulation are applied to an armature, because it has been customary to use insulation in that particular spot on similar equipment. Frequently overlooked in applying rewinding insulation are:

1. Formation of pockets for trapping carbon dust and other foreign material.
2. Obstruction of ventilation.
3. Formation of dead air pockets.
4. Use of materials that are heat insulators.

These factors weigh heavily in the selection of proper rewinding materials. As an example, the material under the bands is preferably of a cushioning nature such as

Figure 6. Sectional view of band at anchor clip

varnished asbestos cloth or paper, in order that the material will not chafe and disintegrate with winding movements resulting from expansion, contraction, acceleration, and deceleration.

Economical rewinding requires that many items of the insulation be precut and fabricated. Volume production permits the use of tools and dies for shaping the rewinding material to greater accuracy than is possible by hand cutting and shaping. Better-quality workmanship may be expected by the use of packaged precut rewinding material, along with complete instructions for its use.

Armature Windings

The most important factors to be considered in the design, fabrication, and installation of armature and equalizer coils are copper fatigue and insulation deterioration. The number of turns, span, connections, copper size, and arrangement, and minimum dielectric requirement of windings are factors fixed for a given set of electrical characteristics. Changed operating requirements or need for modernization may necessitate the altering of one or more of these factors. When such is the case, it is an electrical-design problem, and complete design analysis should be made.

Copper fatigue and the resultant wire breakage in armature windings can be attributed to many causes, and there are equally as many devices for countering the supposed causes. There are, however, some fundamentals that must be followed to minimize copper failures.

The basic copper must be of the highest quality and the most fatigue-resistant available. Several premium coppers having superior properties are obtainable under various trade names. Soft annealed copper is generally accepted as desirable; any severe strains set up in the copper grain structure by edge bending, swaging, and similar cold working should be relieved by annealing. Surface scratching and nicking the copper must be avoided, as well as excessive pounding while forming the coils.

Table II. Acceptable Limits of Unbalance

Maximum Speed (Rpm)	Amplitude Unbalance at Bearings (Inch)		
	Fair	Good	Very Smooth
600	0.004	0.0025	0.0013
900	0.003	0.0016	0.001
1,200	0.002	0.0015	0.0007
1,500	0.0016	0.001	0.0006
1,800	0.0013	0.0008	0.0005
2,400	0.0009	0.00051	0.0003
3,000	0.0006	0.0004	0.0002
3,600	0.0005	0.0003	0.0002

The foregoing is particularly true at positions in armature windings where vibration and bending forces are concentrated, such as at the leads back of the commutator, at the coil corners near the end of the core, and at the clips or knuckles. Prominent among the several causes of bending forces is the linear expansion and contraction of the copper wire.

Figure 5 shows the amount of increase in length of an armature-coil bar from expansion caused by increased temperature. The dotted loop at the end of the slot portion illustrates coil distortion at a position where a large portion of this increased metal length is relatively free to be relieved. After the armature body has absorbed some heat, the increased copper length relative to the core is then a function of the difference in coefficients of expansion of the copper and the steel of the armature. It is not so much the difference between the coefficients of expansion of the two metals that causes the trouble but rather the wide difference in their temperature. The increase in copper length from expansion relative to the core is greatest when heavy starting currents flow through a cold armature; however, there is a continual variation in coil length during operation, caused by the variable-type load on traction motors.

This changing of coil length and resultant bowing of the coil at the end of the slot section not only contributes to copper fatigue but also disturbs the coil insulation; and the same heat that causes the expansion and contraction accelerates thermal aging of the insulation. In time, flexible coil insulations will be destroyed by heat and movement.

All modern traction armature windings are fabricated with class-*B* insulation, having an AIEE (Standard 11) temperature rating of continuous operation at 120 degrees centigrade above ambient. Often, higher temperatures are reached in operation, and the best of insulating materials are strained to their limit.

Class-*B* insulation covers a wide variety of combinations of inorganic substances in conjunction with organic bonds and backing materials. Some maintain their flexibility after being subjected to prolonged high temperatures, whereas others become brittle and lose their ability to withstand movement. The backing materials normally used are organic papers and fabrics; however, in some instances inorganic paper and cloth are used. There are applications where each of the different backings may have advantages. In recent years Fiberglas cloths, some as thin as 0.00175 inch and 0.002 inch, have proved highly successful for class-*B* backing materials. Along with the step-up in inorganic content of class-*B* material, we now have a new heat-stable organosiliconoxide polymer in the form of varnishes and binders.[6] Although too early for exhaustive field tests, the performance to date on traction armature coils is most favorable, and an entirely new line of insulating materials has resulted. The temperature limits of these are in excess of present AIEE class-*B* ratings.

Equal in importance to the copper and insulation consideration is the proper installation and physical fit of the armature windings. The size of the slot portions must be held to a very close tolerance and must be correct for a tight drive fit without the necessity of adding filler materials. However, rather than have coils loose in the slot, it is preferable to use even organic fillers, though mica is the normally accepted material. A tight-fitting coil may be driven into the slots with less hazard of damage by painting with an insulating varnish just prior to installation. The wet varnish serves as a lubricant and, after it sets, provides a bond between the coils and the core.

The coils must be shaped so that when they are installed the preformed copper will lie in its normal position without setting up strains and binding points.

The point at which the coil slot section leaves the core lamination is hazardous in any winding and is even more so on railway-type armatures. The distortion from expansion shown in Figure 5 and the forces caused by vibration and by inertia of the end windings concentrate combined motion and pressure between the coil and the ends of the core lamination. The slots of many armatures are recessed at their ends to accommodate a U-shaped piece of heavy paper or fabric, thus affording a cushion and method of distributing the strain. Where recesses in the core may not have been provided, another effective method of minimizing strain concentration is to taper the core slot from $^{1}/_{32}$ to zero inches for about one-half inch back into the core, rounding off the outer edges.

The placement of the various insulations should be executed in accordance with carefully prepared drawings especially for the armature under consideration and made along the lines as shown in Figure 4.

Banding

A properly cleaned and insulated armature core and the correct use of insulating materials and coils must be complemented by carefully considered banding procedure. The quality of the finished armature may be lowered, unless the same careful planning is given to the banding method, as has been followed in the other steps of armature rewinding.

To calculate the load which the bands must carry, the usual procedure is to consider as separate problems the stresses in each of three sections of the winding, that is, the pinion end, the core section, and the commutator end section. The stresses in each of these sections can be calculated by the empirical formula:[7]

$$S=3.25\times\left(\frac{\text{rpm}}{1{,}000}\right)^2 WD$$

where

S = stress on the bands in pounds
W = weight of coils, including insulation and band wire in the particular section under consideration
D = armature diameter in inches

(For core bands use a constant of 2.8 instead of 3.25.)

After the value of S has been determined for each end and for the core section (except when slot wedges are used), a suitable-size wire is selected. The allowable tension per wire for the wire size chosen is given in Table I. Divide this value into the stress to get the number of wires required in each band. On coil ends use double-deck bands, if necessary, to accommodate the required number of wires.

Steel wire having a tensile strength of 240,000 to 270,000 pounds per square inch generally is used for banding armatures. However, to reduce commutation voltage and band losses, a nonmagnetic band wire is desirable on higher-speed traction armatures. Nonmagnetic stainless-steel wire is used in preference to phosphor bronze because of its greater tensile strength, 225,000 to 256,000 pounds per square inch, as compared to 130,000 to 150,000 pounds per square inch for phosphor bronze. The band wire must be of such quality and toughness that it can be bent 180 degrees on itself without breaking.

The anchoring of the ends of the band wire is most important, and it should be such that it will hold even after the solder may have melted and thrown off.[8] A frequently used method satisfying this requirement of fastening the band-wire ends is shown in Figures 6 and 7, which are, respectively, a section and a plan view. This method is applicable principally to bands on the end windings, because core-band grooves normally do not have sufficient space for the double folded-over clip. A good method for applying core bands is, first, to insulate each band groove with a layer of saturated 0.010-inch asbestos paper, over which is placed a strip of 0.015-inch tinned copper. Apply the band on the tinned-copper strip, using standard folded-over band clips, and solder to form a solid mass of band wire, copper strip, and clips.

The intermediate band clips normally are made from tinned copper and are usually spaced five or six inches apart, except at the beginning and ending of the band, at which point the clips are placed closer together. The number of clips must be an odd number that is not a multiple of any whole number divisor of the number of poles in the machine or closer than ten per cent (more or less) of the number of poles.[9]

Temporary "hot banding" is necessary on traction armatures to insure against lack of solidity that may lead to premature failure. Hot banding is accomplished by heating the armature to 250 degrees Fahrenheit before soldering the leads into the commutator and before brazing coil-connection clips where they may be used. A temporary band is run over the hot armature from the commutator riser to the pinion end of the windings. The end windings are protected with a cushioning pressboard strip under the band, and a filler strip of metal, fiber, or hard wood is placed in each slot projecting above the slot.

In the case of a wedged armature, install band clips so that the core portion of the temporary band can be removed for wedging with the end bands in place. After the slot wedges are in and before removing the temporary end bands, solder and braze the windings as required and then dip and bake the armature according to established standards. After the armature has cooled to room temperature, remove the temporary bands and apply the band insulation and permanent bands.

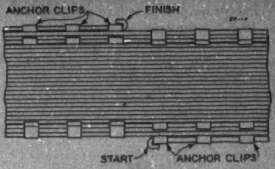

Figure 7. Plan view of beginning and ending of band wire showing method of anchoring

It is very important that the tension be uniformly applied. There are a number of tension devices on the market which control and uniformly apply any prescribed tension, the amount of which should not be a matter of guess. The values in Table I have proved satisfactory.

Table III. Guide for Armature Rewinding Materials

See Figure 4

Type	Position	Use With AIEE Class-A Coils	Use With AIEE Class-B Coils
Core	Coil rests	Pressboard or tapings of varnish cloth and cotton tape	Flexible mica, oiled asbestos paper or 0.030-inch varnished glass cloth, tapings of glass tape, molded mica rings
	Coil shield	Rope paper and varnished cloth	Flexible mica and 0.030-inch varnished glass cloth, molded mica rings
Slot	Troughs or cells	Fish paper or high-density rag paper	Preferably none—use uncut mica if filler is needed
	U end pieces	Rag pressboard	Treated asbestos tape
	Bottom fillers	Pressboard, fish paper, or high-density rag paper	Sheet bakelite, oiled asbestos paper, or molding mica
	Coil separators	Pressboard, fish paper, or high-density rag paper	Sheet bakelite, oiled asbestos paper, or molding mica
End	Between layers	Treated duck or rag pressboard	Oiled asbestos paper
	Between leads and knuckles	Treated duck or high-density rag paper	Flexible mica or 0.030-inch varnished glass cloth or Mica-Glas combination
	Between knuckles or rear coil connections	Treated duck or high-density rag paper	Flexible mica or 0.030-inch varnished glass cloth or Mica-Glas combination
	Between coil end turns	Treated duck or high-density rag paper	Glass, asbestos, or canvas-base bakelite, molding mica
Wedges or sticks	Coil retainer or protective strip	Canvas-base bakelite	Asbestos-base bakelite, glass-base bakelite, or canvas-base bakelite
Band	On core	Fish paper, rag paper, or rag pressboard	Uncut mica or varnished asbestos paper
	On coils	Treated duck, fish paper, or high-density rag paper	Flexible mica and oiled asbestos paper or varnished asbestos cloth
Miscellaneous	Commutator seal	1/16-inch flax cord painted with Red Commutator Enamel	1/16-inch glass braid painted with Red Commutator Enamel
	Band wire	Tinned steel, grade C-1, or tinned 18–8 stainless steel	Tinned steel grade C-1 or tinned 18–8 stainless steel
	Band clip	Tinned steel or tinned copper	Tinned steel or tinned copper
	Solder	50 per cent tin—50 per cent lead or Alloys upward to 100 per cent tin	100 per cent tin, 95 per cent tin—5 per cent antimony, or high-temperature alloy
	Flux	Nonacid rosin flux	Nonacid rosin flux
	Dipping varnish	Synthetic black baking	Synthetic black baking
	Spray varnish	Black oilproof air-dry	Black oilproof air-dry

Except on phosphor-bronze band wire, a high-temperature soldering alloy or high-tin-content solder should be used when possible. Care must be exercised to prevent annealing of the band wire during the soldering process, and the wire should not be heated to values exceeding those below:

Phosphor bronze—450 degrees Fahrenheit

Plain steel—600 degrees Fahrenheit

Nonmagnetic steel—1,000 degrees Fahrenheit

Solders having a liquefaction point higher than 450 degrees Fahrenheit should not be used on phosphor-bronze band wire.

Impregnation

The proper varnish treatment ranks close to the top of the list of those things that may be done to improve the quality of a winding, and yet it is one of the least expensive to execute. Consequently, it would be imprudent to use anything but the highest-grade insulating varnish and the best method for treating and baking.

Most of the varnish manufacturers have a top-grade varnish; and although there may be many formulas for producing such a material, the generally preferred properties are:

1. Long life at elevated temperatures.
2. Deep-drying ability.
3. Only slight resoftening under heat.
4. Toughness.
5. Resistance to oil, moisture, and chemical attack.
6. Good wet and dry dielectric strength.
7. Satisfactory viscosity for proper draining and build-up.
8. Reasonably safe flash point.

Vacuum-pressure impregnation usually is accepted as the best method of application for the initial treatment followed by one or two dips. The impregnating cycle may require 10 to 12 hours elapsed time, 1 hour preheat, 3 hours vacuum, 3 hours pressure, and 3 hours draining. During this treatment, the innermost parts of the winding become saturated and coated, even though more than half the varnish forced in may drain or "bleed" out during baking. The additional varnish dips fill surface cracks and voids, providing a protective film over the entire winding.

A good impregnation and dip treatment bonds and solidifies the entire winding, resulting in:

1. Increased heat conduction.
2. Sealing out dirt, oil, and other foreign materials.
3. Improved and prolonged life of insulation.
4. Less damage from mechanical shock.
5. Moisture resistance.

The armature should be baked after impregnation and after each dip in a well-ventilated, preferably recirculating-air-type, oven at from 250 to 275 degrees Fahrenheit. The time, of course, depends upon the drying properties of the varnish, characteristics of the oven, and the physical size of the armature. A typical baking cycle for a 400-horsepower high-speed traction armature with 18-inch-diameter by 16-inch-long core, using a high-grade synthetic varnish of the afore-mentioned general properties is as follows:

1. Preheat in oven one hour at 250 degrees Fahrenheit.
2. Allow to cool to 90 degrees Fahrenheit before placing in vacuum tank.
3. Bake 12 hours at 275 degrees Fahrenheit after impregnation.
4. Bake 12 hours at 275 degrees Fahrenheit after first dip.
5. Bake 18 hours at 275 degrees Fahrenheit after second dip.

It is usually desirable to permit the armature to cool to approximately 100 degrees Fahrenheit before each dip. This procedure gives a heavier film build-up and minimizes polymerization of the heat-reactive varnish in tank.

Dynamic Balancing

Traction drives are using higher-speed motors to obtain better efficiency and lighter weight as is evidenced by the increase in peripheral speeds from 8,000 to 12,000 feet per minute during the past 25 years. Motors operating at these speeds must have precision-built dynamically balanced rotating members. An unbalanced armature may destroy antifriction bearings, break armature-coil leads, damage gearing, and cause bad commutation, and, in addition may have undesirable physiological effect.

Modern-designed rotating elements usually have provisions for fastening the dynamic-balancing weights, though the methods may vary widely. Some units have grooves on both the pinion and commutator ends into which the counterbalancing weights are electrically welded. Others require the fastening of the weight by bolts secured against loosening by lock plates. Practically all traction-motor armatures are dynamically balanced by their maker after assembly of the spider, laminated core, and commutator, and before the application of the windings. This minimizes the amount of balancing weights required after the armature is wound and finished. Various types and designs of machines are available for dynamic-balancing operations.

Figure 8 illustrates a traction-type armature mounted in a balancing machine for dynamic balancing.

Experience of the operator is a large factor in the quality and cost of the operation, irrespective of the machine. The tolerances to which the armatures are dynamically balanced affect the cost. The various balancing machines do not have indicators measuring in the same units such as ounce-inches or thousandths-of-inch amplitude. Table II gives limits of unbalance that have proved acceptable.[10] The values in this table are in thousandths-of-an-inch amplitude as measured at the motor bearings. (Amplitude is the extent of the vibratory movement measured from one extreme to the oppo-

Figure 8 (left). Traction armature in dynamic-balancing machine

Figure 9 (right). Traction motor being checked for unbalance with vibrometer

Per-Unit Impedances of Synchronous Machines

A. W. RANKIN
ASSOCIATE AIEE

THE ANALYSIS of synchronous machinery is dependent upon a correct and complete knowledge of the machine impedances. The progress of synchronous-machine analysis has been characterized by the recognition of an increasing number of rotor circuits and by an accompanying need for accurate numerical data on the impedances of these additional rotor circuits. The modern equivalent-circuit method of analysis demands an almost limitless array of impedances involving not only mutual reactances but mutual resistances as well. As the application engineer, confronted by more complex application problems, has created more complete equivalent circuits, he has demanded of the design engineer accurate numerical data on the impedances of additional rotor circuits previously ignored. The design engineer himself has been confronted with more complex design problems which have made him directly cognizant of the need for more complete impedance data.

It is the purpose of this paper to present generalized formulas by means of which the per-unit impedances of the new additional rotor circuits may be calculated directly from the physical impedances (in ohms and henrys), and by means of which these new per-unit impedances can be made consonant with the per-unit impedances of rotor circuits previously analyzed.

The technical literature contains several articles which give design formulas for many machine impedances, but these articles are all characterized by the desire to present the impedance formulas in a per-unit form immediately applicable to routine design calculations. This practice is commendable to some degree, since correct numerical impedances usually are obtainable from these published formulas, but in a broader sense is to be deplored. The published per-unit formulas not only tend to obscure the physical characteristics of the various impedances, but they also imply that all per-unit impedances are unique and single-valued when expressed "in per unit of the machine kilovolt-amperes and voltage." This paper will show, however, that, if those impedances which are measurable from the machine terminals are neglected, all machine impedances are multivalued when expressed only in per unit of the machine kilovolt-amperes and voltage, and all these multiple values may be correct when defined properly in terms of rotor-current bases.

It is general practice at the present time to derive the per-unit impedances of the various circuit elements in an individual and detached sense. For instance, an impedance measurable from the stator is converted to per unit by dividing the physical value by the selected unit value of stator ohms X_{ao} (universally taken as phase voltage divided by phase current); the per-unit impedances of the various elements in the multiple rotor circuits are obtained by transferring the corresponding physical impedances to the stator by some effective stator-rotor turn ratio, and dividing the transferred values by X_{ao}. The various rotor-circuit impedances published by any one investigator usually are consistent among themselves when studied as a detached group, but the per-unit impedances published by different investigators do not always agree when placed in apposition, because the different investigators do not necessarily select the same effective turn ratio.

Such ambiguity could be predicted by noting that the turn ratio of a synchronous machine is an elusive quantity, as there is no unique value which could be called "the" turn ratio. For instance, one turn ratio could be defined as the ratio of the series turns per stator phase to the rotor turns per pole; a second turn ratio could use the effective series turns per stator phase including the K_pK_d factor; still another ratio could use the mathematical turns per pole in the fundamental components of the stator- and rotor-excited flux waves; and there are still other turn ratios, all of which have strong physical characteristics arguing for their use. It is not surprising, therefore, that published formulas for rotor-circuit impedances are not in strict accord

---

Paper 45-92, recommended by the AIEE committee on electric machinery for publication in AIEE TRANSACTIONS. Manuscript submitted October 20, 1944; made available for printing March 12, 1945.

A. W. RANKIN is in the turbine-generator engineering division of General Electric Company, Schenectady, N. Y.

The author acknowledges the co-operation of his associates in the General Electric Company in the preparation of this paper. In particular, thanks are extended to S. B. Crary for his constructive criticism and suggestions and to C. Concordia for his several discussions of per-unit systems.

---

site.) The values indicated are applicable when the armature is revolving at maximum rated speed in its own bearings.

Checks on the amplitude of unbalance may be made with a simple vibrometer of the type shown in Figure 9, which consists of a dial indicator mounted in a heavy base. The heavy base provides high inertia allowing the dial-indicator case to remain substantially stationary in space while the indicator plunger is free to follow the linear motion of the bearing. Other types of simple portable indicators are available for these measurements.

Conclusions

Restoring damaged armatures to their original condition and making improvements where needed involves many factors and combinations of many arts. Some of the considerations are peculiar to the armature repairing trade, requiring the application of engineering techniques of comparable order to those used in the building of new armatures if new-armature efficiency is to be maintained.

By their omission it is not the intention to minimize the importance of other equally essential, though better publicized, factors as: Process and final testing, soldering and brazing, and record keeping.

The methods and desired results discussed are not all new, but it is hoped this paper has correlated some of the older methods and injected some new ones that will result in better armature repairing.

References

1. SINGLE PHASE A-C ELECTRIC LOCOMOTIVES ON THE PENNSYLVANIA RAILROAD—PROTECTION AND TONNAGE RATING, **H. C. Griffith.** AIEE TRANSACTIONS, volume 60, 1942, April Section, pages 224-8.

2. VAPOR CLEANING OF MOTORS, **N. J. Greene, R. W. Shoup.** *Railway Mechanical Engineer*, volume 118, March 1944, pages 138-9.

3. THEORY AND PRACTICE OF MAGNAFLUX TESTING. Bureau of Aeronautics, Navy Department, August 2, 1938, serial 38.

4. MAGNAFLUXING PROCEDURES, **Doane, Mages.** *Iron Age*, March 12, 1942, and March 19, 1942.

5. CARE OF COMMUTATORS. *Railway Electrical Engineer*, volume 33, May 1942, pages 106-09.

6. SILICONES—HIGH POLYMERIC SUBSTANCES, **S. L. Bass, J. F. Hude, E. C. Britton, R. R. McGregor.** *Modern Plastics*, volume 22, November 1944, pages 124-26, 212-14.

7. BANDING OF ARMATURES, **R. E. Ferris.** *Electric Journal*, volume 35, 1938, pages 145-8.

8. KEEP THEM ROLLING, **J. W. Teker.** AIEE TRANSACTIONS, volume 62, 1943, March Section, pages 107-12.

9. TO BEAT THE BAND, **W. F. King.** *Allis-Chalmers Electric Review*, volume 5, March 1940, pages 8-11.

10. VIBRATION TOLERANCE, **T. C. Rathbone.** *Power Plant Engineering*, volume 43, November 1939, pages 721-24.

Table I

e_a, e_b, e_c	in per unit of	e_{ao}
ψ_d, ψ_q	in per unit of	ψ_{ao}
i_d, i_q	in per unit of	i_{ao}
Ψ_{fd}, Ψ_{fq}	in per unit of	Ψ_{fdo}
Ψ_{nd}, Ψ_{nq}	in per unit of	Ψ_{xdo}
I_{fd}, I_{fq}	in per unit of	I_{fdo}
I_{nd}, I_{nq}	in per unit of	I_{xdo}

since these formulas of necessity employ some turn ratio. The question then arises as to which of these ratios is correct, or, if there is no unique correct value, which turn ratio should be used to obtain the per-unit impedances for synchronous-machine analysis; and to what degree are these various impedances affected by the turn-ratio selection.

The importance of the role played by the selected turn ratio in the magnitude of the per-unit impedances is physically self-evident, but the equal importance of the rotor-circuit current selected as unity is not so evident. By means of X_{afd}, however, it can be proved as follows that the selection of the turn ratio is tantamount to the selection of unit rotor-circuit current. X_{afd} is defined as the voltage induced in each stator phase per ampere field current, and X_{afd} is the corresponding per-unit value. As normal stator voltage is universally taken as unity, however, the product $X_{afd}I_{fd}$ must be unity at normal open-circuit air-gap-line stator voltage which shows that the unity field current I_{fdo} is not submissive to free selection after the turn ratio has been selected.

The relation which exists between the turn ratio and the unit field current suggests that these are equivalent and that rather than selecting a turn ratio it should be just as practicable to select a unit field current and have the turn ratio be derived therefrom. This is proved in the analysis of this article, not only for the field-winding circuit but for any of the rotor circuits, and, as unit rotor-circuit currents are visualized more easily than turn ratios, they are employed in the generalized impedance formula which are presented in this article.

The foregoing discussion has not answered the question as to which turn ratio should be used in the per-unit impedance formulas, but the emergence of the rotor-circuit unit currents shows that the per-unit impedances and the unit currents must be obtained simultaneously. The per-unit impedance formulas must be obtained in terms of the ampere-inch impedances and the selected unit currents. To obtain these results it is ineluctable that the synchronous-machine equations be derived first in the physical ampere-inch system and converted as a group into per-unit equations. The per-unit impedance formulas thereby obtained will then show which of the limitless series of unit currents should be used.

The method previously outlined is presented in this paper. The per-unit impedance formulas thereby obtained are given in the following section, and are in terms of the selected unit currents. The flexibility and generality of these expressions are discussed in the subsequent section, "Conclusions."

Results

Formulas for the per-unit impedances of a three-phase synchronous machine are given in the following in terms of the "ampere-inch" impedances and the "base-current ratios." The ampere-inch impedances are defined as the circuit impedances in physical units such as amperes, inches, seconds, as contrasted to the per-unit impedances which are pure numerics. The base-current ratios are defined as the ratio of the rotor-circuit currents selected as bases to $^3/_2$ the peak value of rated stator-phase currents. As previously discussed, the selection of base-current ratios is equivalent to the selection of stator-rotor turn ratios. The degree to which each impedance is dependent upon the base-current ratios is apparent from the following expressions. A consistent per-unit system with reciprocal per-unit mutual impedances will be obtained from these formulas. All terms are defined in the nomenclature.

$$x_d=\frac{L_d}{L_{ao}} \tag{1a}$$

$$x_{ad}=\frac{L_{ad}}{L_{ao}} \tag{1b}$$

$$X_{afd}=X_{fad}=\frac{3}{2}\frac{L_{afd}}{L_{ao}}\left(\frac{I_{fdo}}{\frac{3}{2}i_{ao}}\right) \tag{2a}$$

$$X_{and}=X_{nad}=\frac{3}{2}\frac{L_{and}}{L_{ao}}\left(\frac{I_{xdo}}{\frac{3}{2}i_{ao}}\right) \tag{2b}$$

$$X_{ffd}=\frac{3}{2}\frac{L_{ffd}}{L_{ao}}\left(\frac{I_{fdo}}{\frac{3}{2}i_{ao}}\right)^2 \tag{3a}$$

$$X_{nnd}=\frac{3}{2}\frac{L_{nnd}}{L_{ao}}\left(\frac{I_{xdo}}{\frac{3}{2}i_{ao}}\right)^2 \tag{3b}$$

$$X_{nfd}=X_{fnd}=\frac{3}{2}\frac{L_{nfd}}{L_{ao}}\left(\frac{I_{fdo}\,I_{xdo}}{\frac{9}{4}i_{ao}^2}\right) \tag{3c}$$

$$X_{nmd}=X_{mnd}=\frac{3}{2}\frac{L_{nmd}}{L_{ao}}\left(\frac{I_{xdo}}{\frac{3}{2}i_{ao}}\right)^2 \tag{3d}$$

$$r=\frac{r}{X_{ao}} \tag{4}$$

$$R_{ffd}=\frac{3}{2}\frac{R_{ffd}}{X_{ao}}\left(\frac{I_{fdo}}{\frac{3}{2}i_{ao}}\right)^2 \tag{5a}$$

$$R_{nnd}=\frac{3}{2}\frac{R_{nnd}}{X_{ao}}\left(\frac{I_{xdo}}{\frac{3}{2}i_{ao}}\right)^2 \tag{5b}$$

$$R_{nfd}=R_{fnd}=\frac{3}{2}\frac{R_{nfd}}{X_{ao}}\left(\frac{I_{fdo}\,I_{xdo}}{\frac{9}{4}i_{ao}^2}\right) \tag{5c}$$

$$R_{nmd}=R_{mnd}=\frac{3}{2}\frac{R_{nmd}}{X_{ao}}\left(\frac{I_{xdo}}{\frac{3}{2}i_{ao}}\right)^2 \tag{5d}$$

The per-unit values of the rotor-circuit voltages are given by the following formulas:

$$E_{fd}=\frac{E_{fd}}{e_{ao}}\left(\frac{I_{fdo}}{\frac{3}{2}i_{ao}}\right) \tag{6a}$$

$$E_{nd}=\frac{E_{nd}}{e_{ao}}\left(\frac{I_{xdo}}{\frac{3}{2}i_{ao}}\right) \tag{6b}$$

$$p=\frac{1}{\omega}p \tag{6c}$$

The direct-axis field-winding current as obtained in any per-unit system defined by the foregoing formulas will be in per unit of the selected base current I_{fdo}, but the currents of all the additional rotor circuits are expressed in per unit of the base current of the xth direct-axis additional rotor circuit, with the xth circuit submissive to free selection. When advantages are obtainable by the introduction of individual base currents for any or all of the additional rotor circuits, these new bases may be introduced by the methods originating in this article. It is evident from the foregoing formulas, however, that a change in the base currents will result in a change in the per-unit impedances.

Only the direct-axis impedances are given explicitly in the preceding formulas. The quadrature-axis impedances can be obtained from the direct-axis expressions previously given by merely replacing the d subscripts by q; this will express all the quadrature-axis currents in terms of the selected quadrature-axis base currents. It is often advantageous, however, to express the quadrature-axis currents in terms of the direct-axis bases since the latter are more easily determined: in this case, the quadrature-axis per-unit impedances are obtained from the direct-axis formulas previously given by first replacing all the d subscripts by q, and then placing the quadrature-axis current bases equal to the direct-axis bases.

Conclusions

Given in the foregoing are conversion formulas for converting ampere-inch impedances into per-unit impedances. These expressions were obtained by converting a *system* of ampere-inch equations into a *system* of per-unit equations, rather than by deriving the per-unit impedance of each circuit element as a detached independent entity. The only condition imposed during the derivation of the conversion formulas, and it is important to note that in a per-unit system this is an externally imposed condition, was that the per-unit mutual impedances must be reciprocal.

The most important result given by the foregoing formulas is the proof that no unique value of base-current ratio is demanded by the general per-unit system. The base rotor-circuit currents are entirely submissive to free selection, conditioned only by the restriction that when any value of rotor-circuit current has been selected as a base it must be used in the calculation of the machine impedances in the consistent method defined by the foregoing formulas.

The preceding expressions definitely prove, however, that the numerical values of many of the per-unit impedances are dependent upon the value of the rotor-circuit current which has been selected as a base. It is not surprising, therefore, that different numerical values may be published for the same machine impedance, as the base currents are not necessarily equal in the various publications. Before the results of different investigations are compared, the impedances must be reduced to a common current base. This can be done by reducing the impedance expressions to forms analogous to those already given as the base-current ratios will then be identifiable.

Not all the per-unit impedances are dependent upon the base-current ratios as is shown by equations 1a, b, and 4. If the stator base is defined as rated kilovolt-amperes and rated voltage, the impedances 1a, 1b, and 4 are invariant. That these are all measurable from the stator terminals is suggestive that all such impedances measurable from the stator terminals (the definitive impedances) are similarly invariant. This is proved in Appendix I wherein the $x_d(p)$ function[1,3] —the operational machine impedance viewed from the stator—is given in terms of the foregoing conversion formulas. It is there shown that the base-current ratios may be canceled out leaving $x_d(p)$ and $x_q(p)$ as invariant impedances. Hence, all impedances measurable from the stator terminals, such as x_d, x_d', x_2, r, are independent of the values of rotor-circuit currents selected as bases. The impedances which are not invariant are those internal impedances which cannot be measured from the machine terminals.

The invariance of the definitive impedances is of great importance in system studies, and so forth, wherein only the machine terminal phenomena are desired, but, in those more general problems for whose solution the internal organization of the machine is indispensable, all the machine impedances are employed, and the base rotor-circuit currents used in the calculation of the machine impedances must be known, and the corresponding base-current ratios must be employed in the impedance calculations in the consistent method defined by the foregoing formulas.

The second and concluding part of this paper presents a review of the base-current ratios which have been used, generally implicitly, in contemporaneous technical literature and suggests the adoption of a standard or preferred rotor-circuit current as a base value so as to make various published results consonant with each other.

Derivation of Generalized Per-Unit Impedance Formulas

Ampere-Inch Linkage Equations

Using the inductance coefficients defined in the nomenclature, the stator-phase linkages due to the rotor-circuit currents in the direct and quadrature axes can be written directly as in equations 7a, b, respectively.

$$10^{-8}\psi_{a1}=+(L_{afd}I_{fd}+L_{a1d}I_{1d}+L_{a2d}I_{2d}+\ldots)\cos\theta_a \quad (7a)$$

$$10^{-8}\psi_{a2}=-(L_{afq}I_{fq}+L_{a1q}I_{1q}+L_{a2q}I_{2q}+\ldots)\sin\theta_a \quad (7b)$$

The corresponding linkages in the *b* phase and *c* phase may be written from equations 7a, b by replacing θ_a by θ_b and θ_c, respectively.

The stator phase linkages due to the stator currents can be written as in equation 7c. This ampere-inch expression can be derived in a manner analogous to the per-unit expression of Park.[3]

$$10^{-8}\psi_{a3}=-\frac{2}{3}\left(\frac{L_d+L_q}{2}\right)\left(i_a-\frac{i_b+i_c}{2}\right)-\frac{1}{3}L_0(i_a+i_b+i_c)-\frac{2}{3}\left(\frac{L_d-L_q}{2}\right)\times(i_a\cos 2\theta_a+i_b\cos 2\theta_c+i_c\cos 2\theta_b) \quad (7c)$$

The corresponding linkages in the *b* phase and *c* phase may be obtained from equation 7c by cyclic rotation of the phase currents and phase angles.

The linkages in the direct-axis field winding due to the rotor currents in the direct-axis may be written as in equation 8a by means of the self- and mutual-inductance coefficients defined in the nomenclature.

$$10^{-8}\psi_{fd1}=L_{ffd}I_{fd}+L_{f1d}I_{1d}+L_{f2d}I_{2d}+\ldots \quad (8a)$$

The corresponding equations for the linkages in the direct-axis additional rotor circuits can be written from equation 8a by analogy. The linkage equations for the quadrature-axis circuits can be written from equation 8a by substituting *q* for *d*.

In the physical ampere-inch system, all the mutual-inductance coefficients must be reciprocal. The linkages in the direct-axis and quadrature-axis field windings due to the stator currents thus may be written as in equations 8b, c directly from equations 7a, b, respectively.

$$10^{-8}\psi_{fd2}=-L_{fad}(i_a\cos\theta_a+i_b\cos\theta_b+i_c\cos\theta_c) \quad (8b)$$

$$10^{-8}\psi_{fq2}=+L_{faq}(i_a\sin\theta_a+i_b\sin\theta_b+i_c\sin\theta_c) \quad (8c)$$

The linkages in the additional rotor circuits can be written from equations 8b, c by analogy.

The complete stator and rotor linkages will be simplified considerably if the direct-axis and quadrature-axis linkages, defined as in equations 9a, b, are first introduced.

$$\psi_d=+\frac{2}{3}(\psi_a\cos\theta_a+\psi_b\cos\theta_b+\psi_c\cos\theta_c) \quad (9a)$$

$$\psi_q=-\frac{2}{3}(\psi_a\sin\theta_a+\psi_b\sin\theta_b+\psi_c\sin\theta_c) \quad (9b)$$

The i_d and i_q equations can be obtained from equations 9a, b by substituting i for ψ everywhere.

Introducing equations 9a, b into the preceding equations gives the complete direct-axis linkages of equations 10a, b.

$$10^{-8}\psi_d=L_{afd}I_{fd}+L_{a1d}I_{1d}+L_{a2d}I_{2d}+\ldots-L_di_d \quad (10a)$$

$$10^{-8}\psi_{fd}=L_{ffd}I_{fd}+L_{f1d}I_{1d}+L_{f2d}I_{2d}+\ldots-\frac{3}{2}L_{fad}i_d \quad (10b)$$

The linkage equations of the direct-axis additional rotor circuits can be written from equation 10b by analogy. The complete quadrature-axis linkages can be obtained from the direct-axis linkages by substituting *q* for *d*.

Note that the mutual-inductance coefficients between the rotor and stator as obtained in equations 10a, b are no longer reciprocal because of the presence of the factor $^3/_2$. This nonreciprocity has been introduced by the definitions 9a, b, since with these definitions unit stator-phase current will give only two-thirds units of i_d or i_q.

Per-Unit Linkage Equations

A per-unit system consistent in both per-unit impedances and per-unit linkages and currents will be obtained by converting the system of ampere-inch equations represented by equation 10a, b into a corresponding per-unit system. The various quantities will be expressed in terms of the base values given in Table I.

This paper expresses all the rotor quantities in per unit of the base values of the field winding and the *x*th additional rotor circuit.

Only the first three base quantities in Table I are thus far specified, since these are to be taken as the values corresponding to rated stator kilovolt-amperes and voltage. The base rotor quantities can be specified by introducing the following relations between the various base currents and linkages:

$$\boldsymbol{k}_{1f}\boldsymbol{\psi}_{ao}=10^8\boldsymbol{L}_{afd}\boldsymbol{I}_{fdo} \tag{11a}$$

$$\boldsymbol{k}_{2f}\boldsymbol{\Psi}_{fdo}=10^8\boldsymbol{L}_{ffd}\boldsymbol{I}_{fdo} \tag{11b}$$

$$\boldsymbol{k}_{1d}\boldsymbol{\psi}_{ao}=10^8\boldsymbol{L}_{axd}\boldsymbol{I}_{xdo} \tag{11c}$$

$$\boldsymbol{k}_{2d}\boldsymbol{\Psi}_{xdo}=10^8\boldsymbol{L}_{xxd}\boldsymbol{I}_{xdo} \tag{11d}$$

Dividing the linkage equations $\boldsymbol{\psi}_d$, $\boldsymbol{\Psi}_{fd}$, $\boldsymbol{\Psi}_{1d}$, $\boldsymbol{\Psi}_{2d}$, and so forth, by equations 11a, b, c, d, respectively, gives the per-unit equations of 12a, b, c, d.

$$\psi_d=k_{1f}I_{fd}+k_{1d}\frac{\boldsymbol{L}_{a1d}}{\boldsymbol{L}_{axd}}I_{1d}+ k_{1d}\frac{\boldsymbol{L}_{a2d}}{\boldsymbol{L}_{axd}}I_{2d}+\ldots-\frac{10^8\boldsymbol{L}_d\boldsymbol{i}_{ao}}{\boldsymbol{\psi}_{ao}}i_d \tag{12a}$$

$$\Psi_{fd}=k_{2f}I_{fd}+k_{2f}\frac{\boldsymbol{L}_{f1d}\boldsymbol{I}_{xdo}}{\boldsymbol{L}_{ffd}\boldsymbol{I}_{fdo}}I_{1d}+ k_{2f}\frac{\boldsymbol{L}_{f2d}\boldsymbol{I}_{xdo}}{\boldsymbol{L}_{ffd}\boldsymbol{I}_{fdo}}I_{2d}+\ldots-\frac{1.5\times10^8\boldsymbol{L}_{afd}\,\boldsymbol{i}_{ao}}{\boldsymbol{\Psi}_{fdo}}i_d \tag{12b}$$

$$\Psi_{1d}=k_{2d}\frac{\boldsymbol{L}_{1fd}\boldsymbol{I}_{fdo}}{\boldsymbol{L}_{xxd}\boldsymbol{I}_{xdo}}I_{fd}+k_{2d}I_{1d}+ k_{2d}\frac{\boldsymbol{L}_{12d}}{\boldsymbol{L}_{xxd}}I_{2d}+\ldots-\frac{1.5\times10^8\boldsymbol{L}_{a1d}\,\boldsymbol{i}_{ao}}{\boldsymbol{\Psi}_{xdo}}i_d \tag{12c}$$

$$\Psi_{2d}=k_{2d}\frac{\boldsymbol{L}_{2fd}\boldsymbol{I}_{fdo}}{\boldsymbol{L}_{xxd}\boldsymbol{I}_{xdo}}I_{fd}+k_{2d}\frac{\boldsymbol{L}_{21d}}{\boldsymbol{L}_{xxd}}I_{1d}+ k_{2d}\frac{\boldsymbol{L}_{22d}}{\boldsymbol{L}_{xxd}}I_{2d}+\ldots-\frac{1.5\times10^8\boldsymbol{L}_{a2d}\,\boldsymbol{i}_{ao}}{\boldsymbol{\Psi}_{xdo}}i_d \tag{12d}$$

In order that the per-unit equations should retain the physical features of the ampere-inch system and not degenerate into an array of mathematical expressions, the per-unit mutual-inductance coefficients must be made reciprocal. Note that this is an applied condition which removes the nonreciprocity introduced by the definitions 9a, b. The *k* quantities accordingly must satisfy the relations given by equations 13a, b, c.

$$k_{1f}=\frac{1.5\times10^8\boldsymbol{L}_{afd}\,\boldsymbol{i}_{ao}}{\boldsymbol{\Psi}_{fdo}} \tag{13a}$$

$$k_{1d}=\frac{1.5\times10^8\boldsymbol{L}_{axd}\,\boldsymbol{i}_{ao}}{\boldsymbol{\Psi}_{xdo}} \tag{13b}$$

$$k_{2f}\frac{\boldsymbol{L}_{f1d}\boldsymbol{I}_{xdo}}{\boldsymbol{L}_{ffd}\boldsymbol{I}_{fdo}}=k_{2d}\frac{\boldsymbol{L}_{1fd}\boldsymbol{I}_{fdo}}{\boldsymbol{L}_{xxd}\boldsymbol{I}_{xdo}} \tag{13c}$$

Eliminating between equations 11a, b, c, d and 13a, b, c, d results in the following explicit expressions for the *k* quantities:

$$k_{1f}=\frac{3}{2}\frac{\boldsymbol{L}_{afd}}{\boldsymbol{L}_{ao}}\left(\frac{\boldsymbol{I}_{fdo}}{\frac{3}{2}\boldsymbol{i}_{ao}}\right) \tag{14a}$$

$$k_{1d}=\frac{3}{2}\frac{\boldsymbol{L}_{axd}}{\boldsymbol{L}_{ao}}\left(\frac{\boldsymbol{I}_{xdo}}{\frac{3}{2}\boldsymbol{i}_{ao}}\right) \tag{14b}$$

$$k_{2f}=\frac{3}{2}\frac{\boldsymbol{L}_{ffd}}{\boldsymbol{L}_{ao}}\left(\frac{\boldsymbol{I}_{fdo}}{\frac{3}{2}\boldsymbol{i}_{ao}}\right)^2 \tag{14c}$$

$$k_{2d}=\frac{3}{2}\frac{\boldsymbol{L}_{xxd}}{\boldsymbol{L}_{ao}}\left(\frac{\boldsymbol{I}_{xdo}}{\frac{3}{2}\boldsymbol{i}_{ao}}\right)^2 \tag{14d}$$

$$\frac{\boldsymbol{\psi}_{ao}}{\boldsymbol{\Psi}_{fdo}}=\frac{\boldsymbol{I}_{fdo}}{\frac{3}{2}\boldsymbol{i}_{ao}} \tag{15a}$$

$$\frac{\boldsymbol{\psi}_{ao}}{\boldsymbol{\Psi}_{xdo}}=\frac{\boldsymbol{I}_{xdo}}{\frac{3}{2}\boldsymbol{i}_{ao}} \tag{15b}$$

Substituting equations 14a, b, c, d into equations 12a, b, c, d results in the system of per-unit equations of 16a, b, c, d with the per-unit impedances given by the generalized formulas of 1a, b, 2a, b, and 3a, b, c, d. The impedances also may be written in terms of base linkages rather than base currents by means of equations 15a, b.

$$\psi_d=X_{afd}I_{fd}+X_{a1d}I_{1d}+X_{a2d}I_{2d}+\ldots-x_di_d \tag{16a}$$

$$\Psi_{fd}=X_{ffd}I_{fd}+X_{f1d}I_{1d}+X_{f2d}I_{2d}+\ldots-X_{fad}i_d \tag{16b}$$

$$\Psi_{1d}=X_{1fd}I_{fd}+X_{11d}I_{1d}+X_{12d}I_{2d}+\ldots-X_{1ad}i_d \tag{16c}$$

$$\Psi_{2d}=X_{2fd}I_{fd}+X_{21d}I_{1d}+X_{22d}I_{2d}+\ldots-X_{2ad}i_d \tag{16d}$$

The quadrature-axis equations can be obtained from equations 16a, b, c, d by substituting *q* for *d*. The foregoing equations may be reduced to those of Park[1] by the methods of reference 4.

Ampere-Inch Rotor-Circuit Voltage Equations

Conversion formulas for the rotor-circuit resistances and voltages are obtained from the rotor-circuit voltage equations. These are given in the ampere-inch system by equation 17 and are converted to per-unit in the following section.

$$\boldsymbol{E}_{fd}=10^{-8}\boldsymbol{p}\boldsymbol{\Psi}_{fd}+\boldsymbol{R}_{ffd}\boldsymbol{I}_{fd}+\boldsymbol{R}_{f1d}\boldsymbol{I}_{1d}+\boldsymbol{R}_{f2d}\boldsymbol{I}_{2d}+\ldots \tag{17}$$

The equations for $\boldsymbol{E}_{1d}$, $\boldsymbol{E}_{2d}$, and so forth, can be written from equation 17 by analogy. The quadrature-axis equations can be obtained from equation 17 by substituting *q* for *d*.

Per-Unit Rotor-Circuit Voltage Equations

The rotor-circuit voltage equations are converted to per-unit equations by dividing the equation for $\boldsymbol{E}_{fd}$ by $\boldsymbol{\Psi}_{fdo}$, and by dividing the analogous equations for $\boldsymbol{E}_{1d}$, $\boldsymbol{E}_{2d}$, and so forth, by $\boldsymbol{\Psi}_{xdo}$. The system of per-unit equations thereby obtained is given by equations 18a, b, c.

$$\frac{\boldsymbol{E}_{fd}}{\boldsymbol{\Psi}_{fdo}}=10^{-8}\boldsymbol{p}\Psi_{fd}+\frac{\boldsymbol{R}_{ffd}\boldsymbol{I}_{fdo}}{\boldsymbol{\Psi}_{fdo}}I_{fd}+\frac{\boldsymbol{R}_{f1d}\boldsymbol{I}_{xdo}}{\boldsymbol{\Psi}_{fdo}}I_{1d}+\frac{\boldsymbol{R}_{f2d}\boldsymbol{I}_{xdo}}{\boldsymbol{\Psi}_{fdo}}I_{2d}+\ldots \tag{18a}$$

$$\frac{\boldsymbol{E}_{1d}}{\boldsymbol{\Psi}_{xdo}}=10^{-8}\boldsymbol{p}\Psi_{1d}+\frac{\boldsymbol{R}_{1fd}\boldsymbol{I}_{fdo}}{\boldsymbol{\Psi}_{xdo}}I_{fd}+\frac{\boldsymbol{R}_{11d}\boldsymbol{I}_{xdo}}{\boldsymbol{\Psi}_{xdo}}I_{1d}+\frac{\boldsymbol{R}_{12d}\boldsymbol{I}_{xdo}}{\boldsymbol{\Psi}_{xdo}}I_{2d}+\ldots \tag{18b}$$

$$\frac{\boldsymbol{E}_{2d}}{\boldsymbol{\Psi}_{xdo}}=10^{-8}\boldsymbol{p}\Psi_{2d}+\frac{\boldsymbol{R}_{2fd}\boldsymbol{I}_{fdo}}{\boldsymbol{\Psi}_{xdo}}I_{fd}+\frac{\boldsymbol{R}_{21d}\boldsymbol{I}_{xdo}}{\boldsymbol{\Psi}_{xdo}}I_{1d}+\frac{\boldsymbol{R}_{22d}\boldsymbol{I}_{xdo}}{\boldsymbol{\Psi}_{xdo}}I_{2d}+\ldots \tag{18c}$$

Introducing equations 15a, b into equations 18a, b, c will give the per-unit equations 19a, b, c with the per-unit resistances defined by the generalized formulas of 5a, b, c, d, and with the per-unit rotor-circuit voltages given by the generalized formulas 6a, b. The per-unit differential operator is given by equation 20.

$$E_{fd}=p\Psi_{fd}+R_{ffd}I_{fd}+R_{f1d}I_{1d}+R_{f2d}I_{2d}+\ldots \tag{19a}$$

$$E_{1d}=p\Psi_{1d}+R_{1fd}I_{fd}+R_{11d}I_{1d}+R_{12d}I_{2d}+\ldots \tag{19b}$$

$$E_{2d}=p\Psi_{2d}+R_{2fd}I_{fd}+R_{21d}I_{1d}+R_{22d}I_{2d}+\ldots \tag{19c}$$

$$p=\frac{1}{\omega}\boldsymbol{p}=\frac{1}{\omega}\frac{d}{dt}=\frac{d}{d(\omega t)} \tag{20}$$

Nomenclature

The quantities given in the following are per-unit values (unless in bold-face type) in a consistent per-unit system with reciprocal mutual impedances. The bold-face characters used throughout the text are defined as given in the following but are in the "ampere-inch" system.

The ampere-inch system is defined as the system in which all quantities are expressed in their physical dimensions, such as amperes, inches, seconds. Impedances such as *R* and *L* must be calculated initially in the ampere-inch system before a per-unit value can be obtained.

The rotor circuits are separated into the main field-winding circuits and the "additional" rotor circuits. The additional rotor circuits comprise all the rotor circuits except the main field winding.

Subscript Notation

The subscript notation is as follows:

a, b, c = armature phases
f = field-winding circuit
m, n, x = additional rotor circuits
d, q, 0 = direct, quadrature, and "zero" axes
o = base quantities

The quantities *L*, *R*, and *X* use a triple subscript notation in which the first two subscripts refer to the circuits in which these impedances act, and the third subscript locates the (*d* or *q*) axis.

e_a, e_b, e_c = stator-phase voltages, peak values
e_{ao} = peak value of rated stator-phase voltage
E_{fd} = field-winding circuit voltage
E_{nd} = voltage in *n*th additional rotor circuit
i_a, i_b, i_c = stator line currents, peak values
i_{ao} = peak value of rated stator line current
i_d, i_q, i_O = stator current in *d*, *q*, and *O* axes, respectively
I_{fd}, I_{fq} = current in field-winding circuits
I_{fdo} = base value of field current
I_{nd}, I_{nq} = current in *n*th additional rotor circuits
I_{xdo} = base value of current in additional rotor circuits
L = mutual inductance between the circuits specified by the first two subscripts

L_{ao} = base (stator) inductance = $\dfrac{10^{-8}\psi_{ao}}{i_{ao}} = \dfrac{X_{ao}}{\omega}$
L_{ad}, L_{aq} = inductance of armature reaction with the stator magnetomotive force in the direct and quadrature axes, respectively
L_d, L_q, L_O = synchronous inductance; direct, quadrature and zero axes, respectively
p, p = differential operator $\dfrac{d}{dt}, \dfrac{d}{d(\omega t)}$ respectively
r = stator resistance per phase
R = mutual resistance between the circuits specified by the first two subscripts
X = mutual reactance between the circuits specified by the first two subscripts
X_{ao} = base reactance = ωL_{ao}
x_{ad}, x_{aq} = reactance of armature reaction
x_d, x_q = synchronous reactance
x_2 = negative-sequence reactance
$x_d(p)$ = operational impedance viewed from stator terminals
$\theta_a, \theta_b, \theta_c$ = angle between center-line of direct-axis (main pole) and center line of stator phase indicated by subscript
ψ_a, ψ_b, ψ_c = stator phase flux linkages, peak values
ψ_{ao} = peak value of rated stator-phase linkages
ψ_d, ψ_q = stator linkages in *d* and *q* axes, respectively
Ψ_{fd}, Ψ_{fq} = linkages in field-winding circuits
Ψ_{nd}, Ψ_{nq} = linkages in *n*th additional rotor circuits
$\omega = 2\pi$ times frequency

Appendix. The $x_d(p)$ and $x_q(p)$ Functions

The $x_d(p)$ function is defined as the operational impedance as viewed from the stator terminals. In a general per-unit system, the $x_d(p)$ of a machine with only one additional rotor circuit in the direct axis is as given by equation 21a.[2]

$$x_d(p) = x_d - \frac{\left[p^2(X_{11d}X_{afd}^2 - 2X_{f1d}X_{a1d}X_{afd} + X_{ffd}X_{a1d}^2) + p(X_{afd}^2R_{11d} + X_{a1d}^2R_{ffd})\right]}{\left[p^2(X_{11d}X_{ffd} - X_{f1d}^2) + R_{11d}R_{ffd} + p(X_{11d}R_{ffd} + X_{ffd}R_{11d})\right]} \tag{21a}$$

Substituting the per-unit formulas given under "Results" into equation 21a gives $x_d(p)$ in terms of the ampere-inch impedances as in equation 21b.

$$x_d(p) = \frac{L_d}{L_{ao}} - \frac{1.5}{L_{ao}} \times \frac{\left[p^2(L_{11d}L_{afd}^2 - 2L_{1fd}L_{a1d}L_{afd} + L_{ffd}L_{a1d}^2) + p(L_{afd}^2R_{11d} + L_{a1d}^2R_{ffd})\right]}{\left[p^2(L_{11d}L_{ffd} - L_{1fd}^2) + R_{11d}R_{ffd} + p(L_{11d}R_{ffd} + L_{ffd}R_{11d})\right]} \tag{21b}$$

Since equation 21b is independent of any base-current ratios $x_d(p)$, is invariant when expressed in per unit of the machine kilovolt-amperes and voltage, and is independent of the base rotor-circuit currents; $x_q(p)$ is similarly invariant. The foregoing proof can be extended to include any number of additional rotor circuits.

References

1. Two-Reaction Theory of Synchronous Machines, R. H. Park. AIEE Transactions, volume 48, 1929, page 716.

2. Operational Impedances of a Synchronous Machine, M. L. Waring, S. B. Crary. *General Electric Review*, volume 35, 1932, page 578.

3. Definition of an Ideal Synchronous Machine, R. H. Park. *General Electric Review*, volume 31, 1928, page 332.

4. Equations of the Idealized Synchronous Machine, A. W. Rankin. *General Electric Review*, volume 47, June 1944.

Application of Quality Control to Resistance Welding

L. S. HOBSON
MEMBER AIEE

R. S. INGLIS
NONMEMBER AIEE

R. P. McCANTS
NONMEMBER AIEE

Synopsis: This paper describes a system of quality control of resistance welding that has been used successfully for the past few years in manufacturing switchgear cubicles and equipment. Standard samples of material identical with production parts are periodically inserted in the welding machine and welded without disturbing the settings and then tested to destruction in a torsion device. The diameter, torque, and angle of twist at failure all are measured and combined into a single figure indicative of weld quality. This number is plotted on control charts, and corrective action is taken whenever the control limits are exceeded. By setting these limits well within allowable values the quality of production parts is assured.

QUALITY CONTROL of resistance welding, in shops handling a large variety of work, has been simply and effectively accomplished. The methods of testing and control give assurance of uniform weld quality on a process where visual inspection leaves considerable to be desired, making possible the use of resistance welding on assemblies where high quality must be maintained at all times.

Standardization of the welding procedure is essential to the statistical control of the process. Suitable tables, giving the proper settings of the welding-machine controls, must be available to operators so that adjustments can be made to secure the best possible results for the conditions of each job. These settings are too important to be determined by any approximate methods. It is, likewise, essential that the equipment itself and its controls be adequately maintained to insure that, at a given setting, welds of uniform quality are produced. An adequate supply of electric power is necessary to insure consistent performance.

The quality-control procedure described in this article was developed over a considerable period of time. This report will give a brief picture of the method and its application. The mathematical details involved in the development of the quality index and statistical-control limits are not intended to be within the scope of this paper.

The structural stability of assemblies which are made with the use of resistance welding depends chiefly upon:

1. The quality of the parts used.
2. The quality of the welded section.

The quality of the parts used is controlled easily by usual methods of inspection and quality control. Attention, therefore, is directed entirely to the quality of the welded joints. Primarily, we are interested in the strength and ductility of the welds—the two things which are most difficult to determine without destruction of the fabricated parts. We also are interested in the appearance of the weld, the proper dimensions of the welded assemblies, and the change in dimensions caused

---

Paper 45-98, recommended by the AIEE subcommittee on applications of statistical methods of the Standards committee for publication in AIEE Transactions. Manuscript submitted November 24, 1944; made available for printing March 16, 1945.

L. S. Hobson is assistant works superintendent, R. S. Inglis is superintendent of quality control and inspection, and R. P. McCants is welding engineer in the works laboratory, all with General Electric Company, Philadelphia, Pa.

by the welding. These can be determined easily by visual inspection and measurement.

In determining the best method for testing the strength and ductility of resistance welds where it is not practical to test to destruction, we have chosen to make test specimens of material identical in quality and thickness to the regular production parts but of a suitable size for testing. These samples are made with the machine settings identical to those under which the production work is being done. These samples are made at frequent intervals to insure that the quality of the welds made by the machine is maintained at the required quality level. From the results of the tests, a quality-control index is determined, and the average value is charted to give a continuous record of performance.

On highly repetitive jobs it is only necessary to establish the proper welding procedure once and then continue on that basis for the duration of the job. However, when the welding conditions are variable, as in the case of fabrication of switchgear equipment, it is necessary to have a specific procedure for each combination of materials. Figure 1 is an example of a cubicle frame showing the many combinations of materials that may be encountered in this type of structure.

In the absence of basic fundamental data for such conditions, it was necessary to undertake an extensive program to determine the effects of the several variables, such as: material type and thickness; welding current, pressure, and time; proximity of adjacent welds; and overlap.

Many thousands of tests were made on weld specimens in which these factors were independently varied. From this study it was possible to establish the proper welding procedures and the physical properties of the welds. This information was given to both the engineering and the manufacturing sections and is prominently posted on each welding machine.

With a standardized welding procedure, it is obviously necessary to have properly calibrated reliable welding machines. Our machines are equipped with thyratron synchronous controls to assure that, once the machine has been set for a definite procedure, all of the welds made will be consistent. Figure 2 shows a typical machine. Note that the adjusters for the thyratron control panel, the current regulator, the sequence panel, and the air circuit breaker, as well as the pointer stop ammeter and pressure gauge, are conveniently located on the front of the machine, readily accessible to the operator.

By means of plug-in jacks, the calibrations of the machines are checked at regular intervals; thus, it is necessary only for the operator to set the controls, using the applicable welding procedure.

Once the machine has been adjusted, good consistent welds should be obtained. However, it is necessary to check the results periodically to guard against carelessness on the part of the operator, improper functioning of the welding machine, or inconsistencies in the parts.

The quality of a resistance weld is dependent largely upon three factors: appearance, strength, and ductility; and it is these factors which the quality-control system must control. The necessity for maintaining the appearance of the welds is obvious. This factor is controlled by measuring the tip indentation on spot welds and by comparing with visual

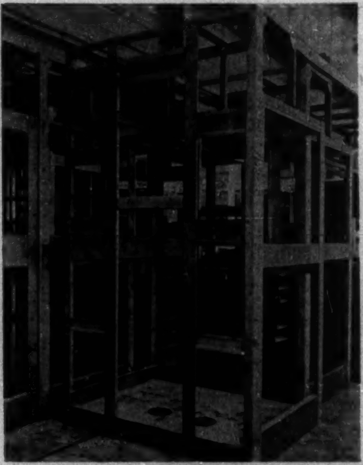

Figure 1 (left). Switchgear cubicle fabricated by spot welding—rear view

Figure 2 (below left). Control apparatus for resistance-welding machine

Figure 3 (below right). Resistance-spot-welded test specimen being placed in testing machine

standards. The strength of the weld is essential as the design of the structure is based on the established minimum weld strength. The ductility of a weld is essential as it is an indication of the resistance to shock and fatigue strength.

At the present time no method has been found to determine the ultimate strength and ductility of a weld except by a destructive test.

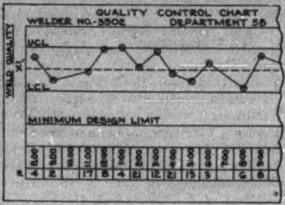

Figure 4. Control chart

In the investigation undertaken to determine the optimum welding procedures, it was found that the most satisfactory method of test for spot welds on heavy steels (one-eighth inch thick and over) was torsional testing. A special machine for this purpose was designed and built in the Philadelphia works laboratory of the General Electric Company. This machine subjects the weld to torsional shear about the center of the weld, and the ultimate torque and angle of twist at the ultimate torque are measured. Figure 3 shows one of the torsional testing machines now being used by the inspection and quality-control division. This torsional testing gives a simple and accurate means of determining the weld strength and ductility, since the strength is proportional to the ultimate torque and the weld diameter (which is easily measured). The ductility is proportional to the angle of twist.

These factors are combined to give a quality-control number which is an index of the quality of the weld. By the use of this comparative index in statistical control, it is possible to show the changes in process performance.

Because of limitations in the skill and ability of the control operators available for this work and the necessity of limiting the time required for testing, a simple, quick, and effective control method is essential to the success of this program.

The control-chart method of controlling quality as covered by the American Standards Association publications Z1.1, Z1.2, and Z1.3 was adopted for this work using a chart for averages ($\overline{X}$) with a modified range (R) chart. After a few weeks of trial testing, during which the process was checked for control by a study of the frequency-distribution charts on data collected, it was found that a sample lot of three would be adequate for control of this process. Control limits were established for the grades of steels in common use. Control-chart scales were developed for each grade of steel so that one set of control limits would be common for all combinations of materials. This simplified the control chart and made possible a form of report which is a composite picture of the quality level being maintained in an operating division on all spot welding, regardless of how diversified the work.

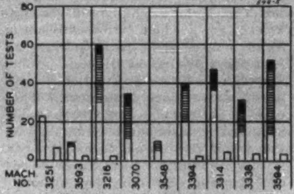

Figure 5. Weekly machine performance

The control-chart scales are so proportioned that all limit lines coincide with common lines on the chart, with the distance from the central line to the upper and lower limits divided into a suitable number of equal divisions. The scale distance from the lower control line to the minimum design-limit line and the distance from the upper control line to the upper limit of the chart are similarly divided. Averages below ten are plotted as zero and averages above 60 are plotted as 60. Distribution diagrams for the various grades of steels thus will be shown in proper relationship to the limit lines on the chart, and the composite diagram will be an indication of the over-all control of the process.

The weld test specimens are made from drop-off pieces of materials currently being used in the shop. A supply of these samples is kept in suitable containers in the welding areas. A test is taken on each welder in operation once each hour. Three samples of the same combination of materials and thicknesses are welded under the same conditions of machine control setting being used on the production work at the time of test. No adjustment of the machine is permitted at the time of test, as control is based upon machine performance under production conditions.

Control charts shown in Figure 4 are placed on each machine, and the results of tests are posted after each test. A record sheet is filled in by the control operator and becomes a permanent record of performance in the welding sections. The machine chart is forwarded to the foreman's office the following morning, and the record sheet is forwarded to the central control office for analysis.

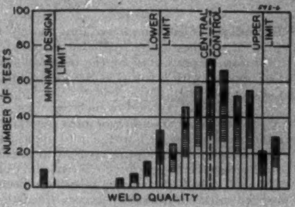

Figure 6. Weekly weld-quality distribution

The daily records are posted on a weekly record sheet in convenient form to show the frequency-distribution totals for all welding combinations based on machine and process performance. When completed, this record sheet contains complete information for the weekly report which is distributed to the department heads, manufacturing superintendents, welding engineers, quality-control specialists, and inspection supervisors.

The weekly report gives a complete analysis of weld quality control by showing the relative performance for each machine in the section, Figure 5, and frequency-distribution diagrams, Figure 6, showing the relative effect of materials and welding methods on the over-all level of weld quality.

This method of controlling weld quality has given excellent results. Proof tests on welded structures made under controlled conditions have proved the effectiveness of the control. Special test structures have been made and subjected to severe shock conditions without any weld failures. Resistance welding, properly controlled, becomes a safe dependable fabrication process. Quality control of this process can insure strong dependable welds of uniformly high quality.

Treatment of High-Altitude Brushes by Application of Metallic Halides

HOWARD M. ELSEY
MEMBER AIEE

Synopsis: It has been found that the rapid wear of brushes under high-altitude conditions can be prevented by the treatment of the brushes with a suitable metallic halide. Carbon, electrographitic, and metal-graphite brush grades all respond to such treatments. A great many nondeliquescent metallic iodides, bromides, chlorides, and fluorides have been tested and found to prevent brush dusting on the heavy-duty electric units of aircraft. These treatments also have been applied with considerable success to earth-surface machines operating under severe commutating conditions. A mechanism by which this class of chemical compound may react to maintain a satisfactory low-friction film on a commutator is proposed.

IT IS BELIEVED that the manufacturers and operators of commutating electric machines and the producers of brushes for them are in complete agreement on only two points:

1. They agree that a film on the commutator is essential for long brush life.
2. The film on a commutator should be as uniform as possible on the entire commutator surface if optimum commutation is desired.

The precise chemical nature of this essential film is still a subject of discussion. The mechanism of its formation is also not certain. The film is extremely thin, and its weight per unit area is so small that an accurate chemical analysis is difficult. Recently Van Brunt and Savage[1] reported a typical film to consist largely of cuprous oxide and carbon (with a number of minor ingredients totaling only 12 per cent). They calculated the film thickness as 5.4×10^{-6} centimeters of which 2.1×10^{-6} centimeters was copper oxide. These workers and many others stress the complex composition of commutator films. It is the thesis of the present paper that an *ideal* commutator film is composed substantially of cuprous oxide (the oxide of monovalent copper) and that all other substances which are present in *actual* films are either nonessential or are definitely harmful.

The color of the track produced on a copper commutator by a given brush grade is a measure of the thickness of the commutator film. This thin protective nonmetallic layer holds the brushes from direct contact with the metal and thus prevents rapid wear. This film should develop to a uniform thickness under all brushes if they are all alike and if the operating conditions are the same for all brushes. Experience has shown that a high uniformity in the color of all of the brush tracks on a commutator goes with an excellent machine performance. Uniformly colored brush paths indicate uniform current division between brushes. Streaking and threading within a single brush track (which again reveal differences in film thickness) may be diagnosed as caused by nonuniform current distribution within the brushes themselves. On an *ideal* commutator there will be no bar-edge burning; streaking and threading will be absent; and the color of all commutator bars will be exactly the same.

An *actual* commutator never meets these desired standards of uniformity. The brush tracks are never exactly alike in color, and a critical eye can always detect some evidence of streaking, no matter how slight. Though an electrographitic brush is expected to develop a rich satiny chocolate-brown polish on the copper, there is wide disagreement as to the depth or shade of color which is most desirable.

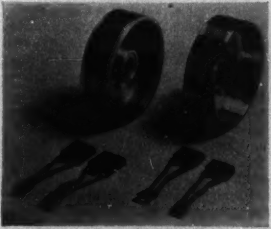

Figure 1. Copper slip rings and brushes after test in high-altitude test chamber

Early in World War II it was reported that brushes wore rapidly at times on certain airplane equipment when they were operated at altitudes above 20,000 feet. Apparently the commutator film, normally maintained at low altitudes, might disappear quite suddenly at high altitudes, and rapid brush wear, or brush dusting, then would follow through abrasion.

A discussion of this failure of commutator films under the abnormal atmospheric conditions prevailing at high altitudes is best prefaced by a consideration of the mechanism by which these films may normally be formed and maintained.

Clean metallic copper cannot be exposed to air without acquiring a tarnish film. At room temperature this film gradually increases in thickness, although the rate of growth is so slow that the film remains transparent and practically colorless for a long time. (Vernon[2] has found that the film on copper heated in air for one hour at only 130 degrees Fahrenheit has a thickness of 1.05×10^{-7} centimeters.)

The commutator is "turned to size" as one of the final steps in the manufacture of an armature. During this turning operation the copper is heated by the work done upon it. As copper is oxidized more rapidly at higher temperatures, each spot of the metal, as it emerges from under the turning tool, acquires a thicker film than it would get if it had been exposed at room temperature. In addition this initial film is further thickened during the seating of the brushes. The coefficient of friction between unseated brushes and a copper commutator is normally high. As the brushes are worn to a seat under light electric loads, their faces become polished. At the same time the film upon the commutator increases in thickness as its surface is burnished by the mechanically loaded brushes under which it moves. If the brushes have been properly chosen, if the machine is well designed, and if the running-in conditions are correct, the film will gradually increase in color, thickness, and polish, and the friction between brushes and commutator will gradually decrease.

However, the formation of a commutator film by electrically loaded brushes is a relatively complex dynamic process and is by no means so simple as the description in the preceding paragraph might indicate. The heat appearing at the brush-commutator interface is generated not only by friction but also by the electric energy dissipated at this interface. (The coefficient of friction between a high-grade well-seated electrographitic brush and the burnished copper-oxide commutator film is often two tenths or higher. The double contact drop for this same type of brush will range from $1^1/_2$ to 3 volts. The actual value for each of these properties will vary with the electric load, the brush grade, and the condition of the commutator.) At any given instant the electron transfer between the commutator and a brush takes place only at a few highly localized areas on the brush face. When the electric load is

---

Paper 45-108, recommended by the AIEE committee on air transportation for publication in AIEE TRANSACTIONS. Manuscript submitted November 24, 1944; made available for printing May 12, 1945.

HOWARD M. ELSEY is in the research laboratories of Westinghouse Electric Corporation, East Pittsburgh, Pa.

The author acknowledges the assistance of L. E. Moberly of the research laboratories, Westinghouse Electric Corporation, and the co-operation of J. V. Dobson, Stackpole Carbon Company.

added to the already present mechanical load these spots become very hot. These overheated active areas of the brush being in close contact with the commutator will react chemically with the copper-oxide film to form metallic copper and carbon monoxide. Thus the electron transfer areas on a brush face become chemically reducing agents and defilming rather than filming agents.

When one of the minute areas of freshly reduced metallic copper emerges out from under the brush and contacts the air, it immediately is reoxidized. But as this same area soon passes under another brush, it may perhaps be reduced again before the oxide film has been re-established to normal thickness. However, under normal operating conditions at any given instant the active electron transfer area is small; thence a freshly oxidized spot may pass under several brushes without again being reduced, thus allowing the film to be built up to equilibrium thickness during the repeated periods of air exposure. Nevertheless, with continued operation, an area on a commutator is frequently reduced and again reoxidized. Therefore the oxide film should be regarded as dynamic rather than static.

The character of the cuprous-oxide film on a commutator will depend on many variables: the properties of the brushes, the shape of their faces, the angle at which they contact the commutator, the spring loading placed upon them, the area of the commutator covered by them, their operating temperature, the temperature of the commutator, and the purity of the ventilating air all play essential roles in controlling the thickness and quality of the film which is developed. The film, as previously explained, is a dynamic, alterable structure. It is possible that a slight change in operating conditions will alter it drastically overnight. A seemingly insignificant change in the surroundings may affect it; for example, a shift in the wind direction may bring a trace of hydrogen sulphide into the room. A leaking gas tunnel has also been responsible for the malperformance of a group of machines in a steel mill. The edges of the commutator in such contaminated atmospheres became covered with a continuous gray film of copper sulphide, and the brush tracks were blotched with irregular patches of this compound scattered in between the normal cuprous-oxide areas. Copper sulphide may completely replace cuprous oxide as a commutator film, if the hydrogen sulphide in the air reaches the concentrations sometimes found in a kraft paper mill. Brush wear is always excessive under such conditions. Generally it can be said that anything will impair the performance of a machine and affect brush wear which alters the ability of the air to oxidize copper and thus maintain a continuous well-polished cuprous-oxide film on its commutator.

It is well known that the surface of a piece of copper, which initially had a high polish, will be roughened by exposing it to repeated oxidation and reduction. However, continued operation of a commutator under ideal operating conditions increases rather than diminishes the finish of the surface. It is believed that a properly chosen brush polishes the oxide film as it is formed and prevents the roughening which otherwise would follow as a result of the repeated oxidation and reduction. Thus the *ideal* brush is an excellent burnishing tool: it "flows" rather than abrades the commutator film. *Actual* brushes, however, to a greater or lesser degree, fail to maintain a burnished continuous layer of cuprous oxide which is substantially free of other materials. Frequently the film becomes very rough in service and so nonuniform in its composition and properties that cleaner brushes are added to remove this undesirable film. Or, as a last resort, the commutator may be "re-turned" and the development of a new film attempted, probably with the aid of another brush grade.

Figure 2. A simple high-altitude test chamber for testing slip rings

In view of the foregoing discussion it can be easily understood why the heavy-duty airplane generators present such a difficult problem to the designer. As these generators must be as light as possible, their commutators and brushes have to be loaded to the limit. Heavily loaded commutators retain an oxide film only with difficulty even in ground service or in low-altitude flying. If the bombers are flown to an altitude of 33,000 feet, where the oxygen content of the air is approximately one fourth of that on the earth's surface, the commutator film naturally will not be maintained.

Lack of the active oxidizing agent, however, is not the only cause for the loss of the essential cuprous-oxide film in high-altitude flying. The water content of the rarefied air, is only one-thousandth that normally fed to electric machines. The extreme dryness of the ventilating air is a major cause of the disappearance of the film. The beneficial effects of water vapor usually are ascribed to lubrication of the brush-commutator interface by water vapor adsorbed in the film or brush. Possibly the true role of the water is that not of a lubricant but of a catalytic agent promoting the oxidation of copper by the oxygen of the air. As soon as the film on the commutator disappears, the brushes and copper grind one another away in a very short time.

Figure 1 shows two copper slip rings and brushes tested in our laboratory high-altitude tester. Both sets of brushes were seated on the rings while these were running in normal laboratory air. At the end of the seating period, the air was changed to simulate the pressure and dryness of the atmosphere at an altitude of 40,000 feet. After 15 minutes of operation, under electric load, one pair of brushes wore out. The faces of the brushes and their path on the copper ring were badly roughened. The second pair of brushes, tested under the same conditions for a testing time of seven hours, showed no measurable wear. The polish of the brush faces and of the brush track was unchanged. The first pair of brushes were of high-quality electrographitic material which has given excellent performance on electric machines under normal service. The second pair of brushes were from the same stock but had been treated for high-altitude operating conditions.

Epidemics of rapid brush wear occur frequently on ground-operated machines also. Such epidemics often, if not always, are associated with an unusually low water concentration in the air. The trouble often is avoided by feeding steam into the air of a generator room during extremely cold weather. However, if high-speed exciter brushes suddenly disappear in a central station, although repercussions may be heard in the front office, a standby unit usually can be thrown on the line. Or, if the brushes chatter and disintegrate on the motors of a 90-mile-an-hour locomotive during subzeor weather, while the passengers may miss engagements, they still stay alive. But if the brushes on the fully loaded generators of a fighting bomber wear out, and the turrets cannot revolve and a dozen other units fail to function, the crew on that bomber may not survive.

When rapid brush wear was shown to be a real hazard to high-altitude flying, means to combat it were sought in many places. To study brushes under simulated high-altitude conditions it was necessary to design suitable testing equipment. A simple slip-ring tester is pictured in Figure 2 and diagrammed in Figure 3. Several of these "testing chambers" have been in constant use for several years in testing hundreds of

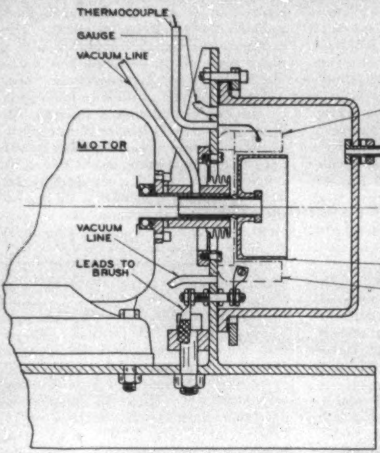

Figure 3. Cross section of test chamber shown in Figure 2

brushes. The tester consists of a copper slip ring $3^{1}/_{4}$ inches in diameter which is mounted on the shaft extension of a 3,500-rpm motor. This shaft enters the glass chamber through a close-fitting carbon tube. This tube is separately evacuated to a pressure low enough to prevent room air entering the chamber along the shaft. The pressure in the testing chamber is maintained at the desired "test altitude" while dry air is passed through to sweep out the impurities. With this tester the brushes can be operated under any mechanical or electric load throughout a wide range: the angle of the brushes can be changed, and the positive and negative brushes can run on the same or separate paths. The temperatures of the brushes and the double contact drop are recorded continuously. This tester has proved extremely useful and very reliable: it has the added advantage over most laboratory dusting testers that it gives results on the pessimistic rather than on the optimistic side.

This tester aided greatly in the search for a brush grade which would maintain a film on the commutator under all service conditions. It soon was found that for each brush grade there was a correlation between the "test altitude," the electric load, and the dusting tendency. A certain brush grade was giving long life in actual flight test. It was possible to predict on the basis of the evidence in Figure 4 that a moderate increase in the electric load in flight would cause this brush to fail. This prediction soon was verified when further flights proved that a load of 50 amperes or more would wear out in three hours the same brushes which promised a life of several hundred hours when the load was limited to 35 amperes or less.

Tests of a large number of untreated brushes failed to find any existing grade which would not dust in the laboratory tester. Therefore as the next step attention was turned to brushes impregnated with various organic compounds as lubricants. The use of paraffin and other waxes in brushes to lower their friction against copper is well known. Unfortunately, all of the organic treatments, which seem to behave as lubricants, were ineffective for this purpose as they are too volatile to stay in the brushes for more than a few hours when subjected to heavy loading.

After organic lubricants had failed to solve this problem, it was suggested by L. W. Chubb that an inorganic lubricant, molybdenum sulphide, be tried. This compound is stable, has a low vapor pressure at moderately high temperatures, and has been applied successfully as a solid lubricant in a number of specialized fields. It resembles graphite and certain other solids in having crystals of layer lattice structure.

Brushes treated with molybdenum sulphide failed to develop a characteristic dark cuprous-oxide film but transferred a thin film of a sulphide itself to the commutator. This acted as a protective lubricating film which was held tenaciously by the copper, and generators equipped with molybdenum-sulphide-treated brushes have shown low brush wear on high-altitude flights. However, sooner or later the sparking which is always present under the face of a brush, even when commutation is apparently black, must convert some of the molybdenum sulphide to molybdenum carbide. The latter is very hard and causes severe grooving of the commutator.

We arrived at the conclusion that a solid film having lubricating properties would be helpful. In accordance with this theory much thought was given to providing these solid lubricating films on commutators. It occurred to us to try lead iodide. This experiment yielded wholly unexpected and gratifying results. From previous experience it was expected that this soft yellow solid would behave like molybdenum sulphide by coating the copper with an adhering lubricating film. However, much to our surprise this did not happen. Instead the lead-iodide-treated brushes developed a characteristic dark satiny film that seemed identical with the normal cuprous-oxide film. This film then became burnished as it passed successively under the brushes and stayed on the surface even in air of low oxygen and water-vapor content. It was found that lead-iodide-treated brushes are able to maintain a perfect film even in the most adverse conditions. This we presume is made possible by the formation of an intermediate compound, cuprous iodide, which being extremely unstable is readily oxidized to cuprous oxide even in an atmosphere where the normal oxidation of copper would not take place.

If this explanation is correct, the rate at which a copper commutator can be oxidized has been increased greatly, even in air of low oxygen content and with almost no water-vapor content. After the favorable results obtained with lead iodide, it seemed reasonable to suppose that other iodides which do not have layer-lattice structure and which are not solid lubricants also should aid in the maintenance of an oxide film and thus prevent brush dusting. Actually many iodides have been tested in the laboratory and have been found to be effective.

An even more convincing evidence for the effectiveness of iodine compounds is the prevention of dusting by only a trace of iodine vapor. Under simulated-high-altitude conditions, untreated brushes, which dusted in the absence of iodine, showed low wear and developed an oxide film on a copper ring when iodine vapor was introduced.

As bromine vapor also prevents brush dusting, studies were extended to cover all metallic halides as a class. Tests were made of typical iodides, bromides, chlorides, and fluorides, and all were found effective. It is believed that each of them thermally decomposes at the brush-commutator interface to form the corresponding metal and free halogen. The latter may recombine, either with its original metallic partner, or with the carbon of the brush, or with a bare copper spot on the commutator.

However, the copper halides differ greatly in their thermal stability, the iodide being the least stable and the fluoride the most stable compound. The comparatively high stability of copper fluoride should slow down the rate at which it is oxidized. Under operating

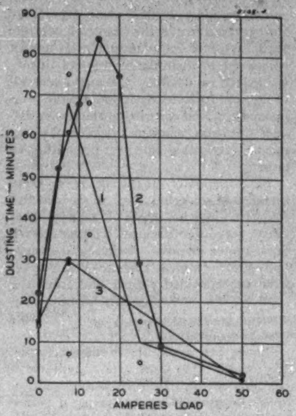

Figure 4. Amperes of load versus dusting time for an untreated hard carbon brush

Curve 1 at pressure equivalent to 30,000 feet; curve 2 at 35,000 feet; curve 3 at 40,000 feet. This brush does not dust at 25,000 feet

conditions this might lead to the existence of a film that contains substantial amounts of both the oxide and the fluoride of copper. It is therefore preferable to choose a treatment that, under the given operating conditions, develops a film substantially free of any compound other than cuprous oxide.

All of the metallic halides which have been tested as brush treatments are capable of limiting brush dusting under simulated-high-altitude conditions. Those selected for actual flight test have effectively limited brush wear. However, there are many practical difficulties in the use of many of these compounds. For example, certain halides, which are water soluble, but not deliquescent, and which contain no water of crystallization, can be put in the brushes from a water solution. However, these water-soluble halides accidentally could be leeched out of the brushes when the ventilating air duct connected to the generator happens to direct water onto the commutator and brushes. That is the reason why the easily soluble halides are less desirable as treating agents.

Difficulties also arise in the case of halides which are thermally unstable to such a degree that dissociation of the compound takes place, not only at the brush-commutator interface, but throughout the brush itself. The ideal halide should be thermally stable to temperatures up to those attained in the face of the brush. Another major objection to a great many halides is the fact that they adsorb water and dissolve in it. Or, one or more of the thermal-decomposition products may deliquesce in air or react so as to leave an undesirable residue in the brush or on the commutator.

The lead formed by the thermal decomposition of lead iodide may remain in the brush either as lead or as lead oxide. Some of it may be mechanically transferred and enter as an impurity into the copper-oxide film on the commutator. In any case, the physical and chemical properties of the solid residues are such that they are not detrimental to commutation. A number of the other metallic halides that were tested gave nonuniform films and high contact drops even though they did prevent actual brush dusting.

The war needs necessitated the early adoption of a treated brush. Lead iodide was chosen in preference to others as the most promising halide treatment for the first large-scale application. Most of the *P*-1 generators now in service have been equipped with Stackpole brushes containing this treatment. Nevertheless, tests with other halides have continued both here and elsewhere, and it is believed that at the present time all heavy-duty generators placed on high-altitude bombers are fitted with brushes containing one of the metal halides as an antidusting agent.

A number of practical problems had to be solved in the initial application of the lead-iodide treatment. The temperatures at which electrographitic brushes are fired are so high that the iodide must be placed in the plate after manufacture. This may be done either by immersing the brushes in the fused salt or by carrying out metathetic reactions in the plate by successive immersion in the proper chemical solutions. The latter operation must be done with great care, as trace amounts of excess reagents or products of reaction often affect brush performance disastrously, and the leeching out of small concentrations of such compounds is very laborious.

Many of the halides can be incorporated into metal-graphite brush grades at the time of molding. Some halides are so unstable that they react with the copper in the brushes at all practical molding temperatures. While lead iodide can be molded successfully into metal-graphite grades, care must be taken in the curing of the brushes; otherwise undesirable reactions take place between the copper and the iodide.

Brush treatments which are capable of maintaining an oxide film on a heavily loaded commutator operating under the adverse conditions encountered in the upper air certainly warrant a trial in difficult brush applications at more normal levels. Man power and material limitations have severely handicapped the execution of such tests. However, in such severe service as is imposed on the brushes of high-speed electric locomotives halide treatments definitely have improved commutator conditions and increased brush life. Recently a group of test brushes was removed from a locomotive after 85,000 miles of high-speed service. The brushes are in excellent condition, and the wear has averaged only ten mils per thousand miles of service.

Exploratory applications have been made in other fields where commutating conditions are unusually difficult. Each application presents a new problem. In all cases, the brush grade and the type and the amount of treatment must be properly matched to the machine and to the operating conditions. Though progress necessarily has been slow, experience has now been accumulated to prove that this new purely chemical approach to the old problem of forming and maintaining a satisfactory copper-oxide film on commutators and slip rings will prove as effective in many ground applications as it was in its initial one, namely, the solution of the high-altitude brush problem.

References

1. Carbon-Brush Contact Films, C. Van Brunt, R. H. Savage. *General Electric Review*, volume 47, July 1944, pages 16–19.

2. The Formation of Protecting Oxide Films on Copper and Brass by Exposure to Air at Various Temperatures. W. H. J. Vernon. *Journal* Chemical Society (London, England) 1926, pages 2273–82.

Chemical Contamination as Causes of Electrical-Insulation Failure

C. H. BRAITHWAITE, JR.
ASSOCIATE AIEE

G. L. MOSES
MEMBER AIEE

Synopsis: Electrical-insulation failures were investigated and found to be due to chemical contamination with ionizable materials. Examples of such contamination are certain types of hand creams, soldering fluxes, and germicides in lubricating oils. Contamination mechanisms often involve operations which are otherwise insignificant in manufacturing processes. The effect of these materials on the electrical characteristics of the insulation is reported. The need for close correlation of industrial-hygiene manufacturing processes, insulation design, and quality control is emphasized.

ELECTRICAL-INSULATION troubles sometimes occur which baffle the observers. Frequently the failure is attributed to some entirely innocent cause. Several such failures when carefully studied were found to be caused by the presence of ionizable substances which when dry were not harmful but when exposed to humidity were a constant hazard in the presence of a voltage differential. The insidious behavior of such materials in insulation may allow apparatus to pass a high-potential test and subsequently cause failure during a less severe test or in service. Furthermore, the presence of ionizable materials near a damaged spot in insulation increases the hazard manyfold. As insulation ages and the protective varnish coating deteriorates, these contaminants become a more active hazard to insulation. Harmless-appearing substances such as hand creams and soldering fluxes may be sources of chemical contaminants which cause inestimable damage.

As a consequence, investigations of such failures must be thorough and include each component material down to and including the glass, mica, cotton, and other material which make up the insulation. Careful attention should be paid to recent changes in methods or technique and even to safety and hygiene campaigns. The examples which follow illustrate only a few mechanisms of chemical contaminations.

Soldering Fluxes

Several years ago trouble was experienced with a number of cases of short-circuited commutators as a result of unauthorized use of zinc-chloride soldering flux. One commutator in particular for an experimental motor was an outstanding example. After several short circuits occurred, the bar-to-bar insulation resistance was checked. Seventy bars out of 300 had far below normal insulation resistance, which were about 0.1 megohm instead of above ten megohms. Upon application of a 60-cycle dielectric test it was found that bars with low insulation resistance stood a 200-volt test but generally broke down at 400 volts. Bars with normal insulation resistance withstood a 600-volt test and failed at not less than 800 volts.

Mica segments were removed from the spots having low insulation resistance for chemical tests in comparison with uncontaminated mica segments. A 15-gram sample of each mica segment was boiled with 15 milliliter of distilled water and the conductivity of the solution determined as shown in Table I.

This test clearly indicated the presence of ionizable contaminants in the low-resistance mica segments which increased the conductivity of the extracted solution by a factor of more than ten to one as compared to a similar extract of uncontaminated insulation. Chemical analysis of the solutions clearly indicated the presence of zinc and chlorine in the low-resistance solutions, whereas the control specimens had less than one part per million of either.

Erikson[1] points out the effects of a combination of soldering flux and moisture on fine-wire magnet coils. Failures were due to corrosion of copper by fluxes which caused open circuits. Failures to ground and short circuits due to electrolytes from the corroded copper and from the soldering fluxes themselves forming conducting paths are also possible in this type of application.

Fluxes are available in many forms. The acid type, zinc and ammonium chloride, are available in water solution or in the form of a paste using a petrolatum or other grease vehicle. Milder fluxes include rosin and alcohol solutions and rosin–petrolatum pastes. An example of a zinc-chloride water solution on mica V rings has been discussed previously. Zinc chloride, the electrolyte on these V rings, was deposited from water solution throughout the insulation. Under humid conditions these electrolytes formed a conducting path which leads to the burning of the mica as seen in Figure 1. Zinc- and ammonium-chloride fluxes in water contribute to corrosion of copper.

The effect of zinc chloride on insulation under moist conditions is summarized in Table II. These results were determined on sample coils similar to those shown in Figure 2 and on mica by a jig similar to that shown in Figure 3. Sample coils had been immersed in zinc-chloride solution and others in distilled water for two days and then allowed to stand in air for

Figure 1. Typical failures of commutator mica V rings due to acid flux on segments

---

Paper 45-97, recommended by the AIEE committee on electric machinery for publication in AIEE TRANSACTIONS. Manuscript submitted October 28, 1944; made available for printing March 14, 1945.

C. H. BRAITHWAITE, JR., is engineer and G. L. MOSES is section manager, development insulation section, a-c engineering department, Westinghouse Electric and Manufacturing Company, East Pittsburgh, Pa.

The authors are grateful for the contributions and criticisms of D. L. Gibson, R. A. Lubker, R. L. Ferguson, and P. W. Hernick, all of Westinghouse Electric and Manufacturing Company, East Pittsburgh, Pa.

Table I

Segment Identification	Resistance (Ohms)
2	600
13	1,000
20	1,200
21	950
23	950
24	1,210
35	590
Uncontaminated control segment	13,600
Uncontaminated control segment	16,000
Fresh distilled water	35,000

Table II. Insulation Resistance in Megohms

Wire Insulation Used	Soaked in Flux for 48 Hours, Stood in Air 7 Days	Soaked in Distilled Water for 48 Hours, Stood in Air 7 Days
Asbestos	0.15–43	4,000
Glass	15 –29	1,800
Glass (sliver)	3.8 –18	3,000
Double cotton	16 –39	72
Mica*	0.25– 0.30	30–75

Fluxed samples were soaked in the following solution for 48 hours:

Zinc chloride	1 pound
Ammonium chloride	2 ounces
Water	3.3 gallons

These together with the distilled-water-soaked samples were allowed to stand one week in the air before testing.

* Aged one week at 100-per-cent relative humidity.

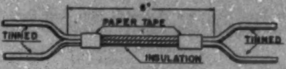

Figure 2. Coil for testing soldering fluxes on insulation

seven days. Insulation resistances of the coils then were taken and are reported in Table II.

Insulation resistance of cotton-covered wire was poor after this treatment in distilled water but was even lower after the acid flux treatment. The asbestos-insulated wire after treatment in flux had an insulation resistance of 0.5 per cent of that treated in distilled water. Mica behaved in a manner similar to the wire insulation.

Zinc chloride or ammonium chloride may be mixed into a petrolatum vehicle as a paste. In this form corrosion and electrical failures due to use of acid fluxes may be apparently reduced. The dangerous electrolytes still are introduced into the insulation; their effects are merely postponed. Under humid conditions, particularly after the petrolatum vehicle has disappeared, the zinc and ammonium chlorides become conductors. They lower insulation resistance and decrease breakdown strengths of insulation. This leads to failures in service rather than failures in tests during manufacturing the latter which might occur if water solutions of these fluxes were used.

Rosin and alcohol, another type of soldering flux, are relatively safe for use near insulation. No electrolytes are deposited, and the corrosion problem is greatly reduced. This flux has been in use many years without causing failure epidemics.

Each worker should be informed thoroughly as to the proper flux for his application. Acid-type fluxes may be used on parts which are not insulated if the flux deposits are washed carefully from the metal after completion of the operations. No form of soldering flux which contains zinc chloride, ammonium chloride, or other electrolytes should be tolerated for use near insulation. Rosin in alcohol solutions, or other organic nonelectrolytic types of flux, should be used in all doubtful cases. The security in using an electrolyte in grease mixture as a flux is false. It should be remembered that these electrolytes will ionize and become conducting under humid conditions, and, in addition, many of these substances are hygroscopic and thus will become conducting in only moderate humidity conditions.

Hand Creams

The use of hand creams in shop practice was suspected as a cause of insulation failures. Protective-hand-cream use was being encouraged in varnish-treating rooms, in coil-insulating, and wire-insulating departments as insurance against dermatitis. Such creams are effective in prevention of irritation due to varnish solvents and adhesives. However, investigation proved many creams contained conducting materials which are corrosive to copper or harmful to insulation.

Schwartz[2,3] points out that ointments fall into a number of classes:

1. Simple vanishing-cream types which fill the pores with soap and facilitate removal of soil when washing after work.

2. A type which leaves a thin film of resin or wax on the skin and thus prevents the irritant from direct contact with the skin.

3. A third type which fills pores and covers the skin with a harmless fat that repels water-soluble irritants and prevents entrance of petroleum oils, greases, and coal-tar derivatives.

4. A fourth type which contains nonirritant chemicals intended to detoxify the irritants.

5. Another form which causes inert powders to adhere to the skin, forming a physical barrier against skin irritants.

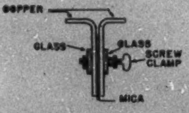

Figure 3. Device for testing soldering fluxes on mica

A series of determinations was made to discover the conducting properties of the various hand creams in use in the shops and the effect of ointments and humidity on ointment-contaminated insulation. Six-mil filter paper was wrapped around five-eighths-inch-diameter glass tubes. Various creams were rubbed into the paper, and the insulation resistance was determined between two electrodes $1^1/_2$ inches apart. These tests were conducted at 20-, 50-, and 97-per-cent relative humidity. Test bars also were prepared of asbestos-insulated wire onto which various creams had been applied. These wires were tested for insulation resistance between strands and for dielectric breakdown.

It was found that those creams which had soap bases and were therefore alkaline in reaction became conducting at higher humidities and lowered insulation resistances. This is reflected by the lower insulation resistances of certain hand creams upon the porous paper tubes (Table III). Hand creams lowered the insulation resistance and dielectric breakdowns when test bars of asbestos-insulated wire were subjected to hand creams and humidity (Table IV). These humidity conditions approximate summer weather conditions. The hand creams which proved most troublesome

Table III. Effect of Hand Creams on Insulation Resistance in a Humid Atmosphere

	At 20–30-Per-Cent Relative Humidity (Megohms)	At 50-Per-Cent Relative Humidity (Megohms)	At 97-Per-Cent Relative Humidity (Megohms)
A	950	17	0.095
B	Over 1,000,000	22,000	1.3
C	200,000	200	0.06
D	Above 200,000	8,000	2.5
E	Above 200,000	6,500	4.6
F	Above 200,000	20,000	7.7
G	Very high	150,000	12

Conductance in water solution was measured in a cell with platinum electrodes by an a-c conductivity bridge at 20 degrees centigrade after suspending the creams in 20 parts of water

	Resistance in Ohms
Distilled water	156,000
A	975
B	2,600
C	750
D	4,370
E	19,300
F	4,500

A = alkaline soap base
B = neutral grease
C = alkaline soap base
D = neutral grease
E = lanolin and olive oil
F = alkaline soap base
G = blank paper

A contains Bentonite clay.

C is a clear solution in water when hot, setting to a gel on cooling, like soap. Both these contain water and are mildly alkaline.

C has a tendency to turn copper green.

B contains grease and no water, with a mineral filler. It is neutral in reaction.

D and *E* are neutral greases.

F is alkaline in reaction. These do not contain water.

Table IV. Insulation Resistance and Dielectric Breakdown on Asbestos Wire Test Bars

	(Megohms) Insulation Resistance		Dielectric Breakdown In Volts (Failed at)	
Cream Used	At Room Condition	After Conditioning at 70-Per-Cent Relative Humidity	At Room Condition	After Conditioning at 70-Per-Cent Relative Humidity
A	500– 1,400	8 and 14	1,500	2,000
B	11,000–13,000	120 and 130	2,000	2,500
C	1,800– 2,000	0.08 and 0.08	2,000	800–800
D	13,000–13,000	5 and 4.6	2,000	2,500
No cream	1,400– 2,300	10 and 8.5	2,500–2,000	2,000–2,500

A = alkaline soap base *B* = neutral grease *C* = alkaline soap base *D* = neutral grease

Test conditions:

Strands rubbed with protective hand creams, formed into straight-side test bars, and hot pressed.

All tests made between two conductors at room conditions (20–30-per-cent relative humidity), and after conditioning 48 hours at 70-per-cent relative humidity, and 25 degrees centigrade.

Test bars were allowed to stand one week before testing.

were of the alkaline soap-base vanishing-cream type.

One of these soap-base hand creams was applied to copper panels which were dipped into varnish. The cream tended to dissolve in the varnish, thus contaminating it, and to melt and run during the baking operation. As a consequence a very poor film resulted which suffered a 75-per-cent decrease in dry dielectric strength over a control panel prepared clean and free of hand cream.

On the basis of these data, the hand creams used in manufacturing were limited to the types which leave a thin film of resin or wax on the hands but which are neutral in reaction. The use of these hand creams is not detrimental to insulation if moderation is practiced. However, each hand cream used should be investigated thoroughly by the engineers and industrial-hygiene department before its use is authorized.

Germicide Additions to Lubrication Oils

An excellent example of the type of failures produced by contamination of insulation with ionizing materials is shown in Figure 4. This was found to be due to the addition of a very small percentage (0.4 per cent) of germicide to the compound used for lubricating the blocks for pressing armature coils to size. Tests showed that the addition of one per cent of the lubricating compound to the germicide raised the conductivity of distilled water by a factor of ten, and the addition of one per cent of the germicide raised the conductivity of distilled water by a factor of 200. Chemical analysis of the coil-insulation and winding material adjacent to this failure disclosed no inorganic salts (sodium zinc, chloride, or sulphates). The germicide used was of the phenolic type. A phenol coefficient of at least 18 (Federal Druggists Association method) was specified. This is not, however, a measure of the compound's conducting properties. However, phenolic-type compounds are acidic and hence conductors; organic germicides of this type are chemical relatives of carbolic acid. Insulating materials pressed in molds lubricated with the compound having germicide were found to have high conductivity when humidified. The evidence appeared to be conclusive that this was the cause of the creepage failure shown in Figure 2.

Motors Operating in Chemical Plants

A more obvious type of failure due to chemical contamination occurred in service. A large motor with class-*A* insulation was installed in a magnesium plant. After eight months service this motor was found to have three grounded field coils. Scrapings from the windings were analyzed by microchemical methods. The material was found to be chiefly magnesium chloride and other hygroscopic salts. This contaminant did not deteriorate the varnish film but formed a conducting path through cracks in the film and around the leads into the coil. Magnesium chloride also will decompose cotton insulation.

Adhesives Used in Asbestos Wire Insulation

The adhesive used to bond asbestos insulation to wire was found to be the cause of certain failures. A casein-type glue in water solution had been used. A change in formulation by the manufacturer had introduced inorganic salts These, sodium carbonate and sodium phosphate, are electrolytes and in humid conditions corroded the copper. The insulation turned green, and failures resulted during standard proof tests. Inadequate drying of the glue contributed to the corrosion and allowed ionization to take place which led to early test failure of many of these coils. This situation was corrected by use of an organic-type synthetic adhesive which contained no inorganic salts.

Figure 4. Creepage failure of armature coil due to conducting germicide in press lubricant

Carbon-Dioxide-Type Fire Extinguishers

Proper construction of varnish tank systems should include some fire-control device. Frequently fire extinguishers are so arranged that they will release automatically in case of fire. In some cases, the extinguishers accidentally will set off and spray the surface of the varnish with the extinguisher's contents. Foamite-type extinguishers often are used which consist of a small container of an inorganic acid and a larger one of sodium carbonate. When mixed, carbon-dioxide gas will be formed which propels the mixture from the extinguisher and sprays the varnish with a mixture of electrolytes: unreacted acid, unreacted sodium carbonate, carbon dioxide, water, and the sodium salt of the inorganic acid. This contaminates the varnish with electrolytes and water, thus lowering its insulation qualities. Filtration methods[4] will not remove this type of contaminant. The use of this contaminated varnish would introduce electrolytes into the insulation which would prove as detrimental to the machine as the other types of ionizable chemical contaminants already discussed.

Conclusions

Causes of insulation failures which may seem obscure or mysterious may be due to chemical contaminations. Chemicals introduced into the insulation in manufacture, repair, or service may be of the electrolytic type and reduce the insulation resistance and dielectric breakdown of the insulation. They may be of a type which

A New Outdoor Air Switch and the Principles Involved in Its Design

H. W. GRAYBILL
MEMBER AIEE

J. S. FERGUSON
ASSOCIATE AIEE

THE OUTDOOR air switch is a universally used device which through the years has evolved into a few well-known types. Increasing preference has been shown for the rotating-insulator vertical-break switch, which has become almost a standard for outdoor service. A new switch of this type is described, and a discussion of the problems associated with its design is presented.

It may seem, at first glance, that the design of air switches should have been reduced to a few simple calculations and a few hours' work on the drawing board. As a matter of fact, their correct design requires a long period of development, including many calculations and laboratory tests. It is a comparatively simple task to design a switch that fulfills the essential requirements when new, but it is much more difficult to design an economically practical switch that will retain its characteristics after years of use outdoors where sun, wind, ice, and dust prevail and where corrosion is always at work. In the course of development of a new outdoor switch, a thorough study was made of the basic problems involved without regard to existing opinions on the subject. A complete review and analysis of past and present-day switch designs followed to determine the relative merits and defects of each. This study led to new approaches to some of the problems including the use of recently developed materials.

Design Problems

Reduced to its essentials a switch consists of two terminals, a blade hinged on one terminal to open and close the circuit between the terminals, a suitable base for mounting, and insulation between the terminals and ground. Past experience with air switches indicates that the contacts between the blade and the terminals are likely to be the chief source of trouble. For this reason, the subject of contacts must be given first consideration in the design of any switch. That there is a wide divergence of opinion on the subject is shown by the fact that almost every known type of contact can be found on present-day switches.

The blade mechanism—that is, the means for converting rotation of the insulator into the desired blade motion—is the second consideration. The type of blade mechanism selected is the determining factor in the ability of the switch to operate with ease under both normal and adverse conditions. The choice of a mechanism for performing this operation is influenced by the type of contacts adopted, since certain types of contacts require a more elaborate mechanism than others, if the switch is to operate easily and reliably.

Fortunately, the insulation no longer presents a problem to the outdoor-switch designer. As a result of excellent work of standardization committees, electrical and mechanical properties of outdoor air switch and bus insulators, as well as minimum spacings for switch insulators, all have been standardized. The resulting advantages to user and manufacturer are obvious.

Contacts

There are only two major requirements of air-switch contacts:

1. They must carry their rated current without reaching injurious temperatures, not only when new, but also after many years of service.
2. They must carry without injury the maximum short-circuit current of the system to which they are applied, until this current is interrupted by a circuit breaker. This ability also must be maintained for the life of the switch.

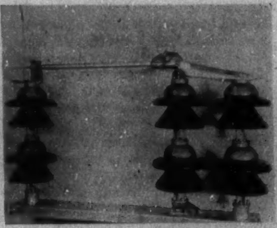

Figure 1. The new disconnecting switch, 69-kv 600-ampere rating

Low contact resistance is necessary to meet both of these requirements. As early as 1892[1] the importance of the total pressure in regard to its effect on contact resistance was realized. In 1913 F. W. Harris[2] showed that the contact resistance varies inversely with the total pressure and is substantially independent of the

---

Paper 45-112, recommended by the AIEE committee on protective devices for publication in AIEE TRANSACTIONS. Manuscript submitted November 18, 1944; made available for printing May 14, 1945.

H. W. GRAYBILL and J. S. FERGUSON are design engineers in the switchgear and control engineering department, Westinghouse Electric Corporation, East Pittsburgh, Pa.

---

is harmless when dry and at room temperatures, but which will become conducting under high humidity conditions, particularly when hot. The contaminant may cause metallic corrosion which produces electrolytes, and this tends to accelerate failure. Failures due to contaminations may occur in epidemics in factory testing or may not occur until the machine is in field service.

Close co-operation between the manufacturing, hygiene, and engineering departments is necessary to control this problem. Each worker should be educated in the importance of his operation on the final product and the ever-present danger that he may introduce dangerous chemicals into insulation from apparently harmless sources. All precautions should be taken, particularly in the use of new materials, to see that toxicity and irritation are eliminated, but not at the expense of insulation quality. Hygiene campaigns should be co-ordinated with insulation engineering to protect both the workers and the apparatus quality.

Both materials in everyday use and those which are new material should be investigated thoroughly as possible sources of contaminations. Use of chemicals even for insignificant-appearing jobs should be reviewed. Review of soldering fluxes, for instance, is essential.

Changes in manufacturing technique should be considered carefully. A small change may cause more damage than more obvious changes. Possible sources of chemical introductions into insulation should be investigated thoroughly, and the harmful effects of this type of contamination should be kept ever in mind.

References

1. CORROSION LOSSES AND REMEDIES IN FINE-WIRE MAGNET COILS, B. W. Erikson. *Product Engineering*, 1944, pages 158–60.

2. INDUSTRIAL DERMATITIS, SYMPTOMS AND CAUSES, AND HOW TO PREVENT IT, Louis Schwartz. *Industrial Medicine*, volume 1.

3. SYMPOSIUM ON INDUSTRIAL HYGIENE. *Industrial and Engineering Chemistry*, news edition, July 10, 1943.

4. FILTRATION SAVES CRITICAL VARNISH MATERIALS, D. L. Gibson, C. H. Braithwaite, Jr. *Chemical Industries*, July 1944, pages 70–2.

area. This was confirmed some years later by A. R. Enger,[3] who found experimentally that the temperature rise of switch contacts was not increased appreciably by slight misalignment of the blade in the switch jaw, since this decreased the contact area but increased the unit pressure. In 1928 a mathematical relation between the contact resistance and the total pressure was developed by W. Schaelchlin.[4] He showed that

$$R = cP^{-k}$$

where R is the contact resistance, c a constant depending on the material and shape of the contact, P the total pressure, and k a constant which may have any value from 0.5 (if the number of contact points remains constant as the pressure increases) to 1.0 (if the number of contact points increases linearly with the pressure).

The shape of contacts is important, inasmuch as it affects unit pressure and the amount of material immediately adjacent to the contact. There are three general shapes of contacts: plane or surface contact, as between two planes; point contact, as between a sphere and a plane; and line contact, as between a cylinder and a plane.

The surface contact when new and clean is entirely adequate for both rated and fault current. However, because of low unit pressure it is extremely susceptible to corrosion. While formerly widely used on outdoor air switches, the surface contact now is used chiefly for low-current indoor knife switches.

The point contact, used to some extent in air switches,[5] meets the requirements of high unit pressure and low contact resistance and is completely adequate for carrying rated current. However, under fault conditions the small amount of metal adjacent to the contact limits the rate at which heat is conducted away and thereby limits the short-circuit current that can be carried without damage.

The line contact has found increasing use in recent years and has proved very satisfactory. B. W. Jones[6] determined experimentally that, with copper contacts and pressures between 10 and 500 pounds, one inch of line contact has only one half to one third the resistance of a surface contact one inch square. This results in excellent characteristics under normal load currents. The amount of material adjacent to a line contact available for heat conduction is inherently greater than that adjacent to a point contact and is, therefore, able to carry the heat away from the contact more rapidly with the result that much higher fault currents can be carried without damage. This principle is used widely in the high-pressure single-line switch contact and the modern medium-pressure, multiple-line contact.[7]

The material for contacts must be selected on the basis of its resistivity, chemical activity, hardness, and annealing temperature. The initial contact resistance varies directly with the resistivity of the contact material.[3] However, this resistance tends to increase with age, due to the formation of surface films. The base metals, such as copper and its alloys, form a high-resistance oxide film when exposed to air, the rate of oxidation being comparatively low at room temperature, but becoming more rapid at elevated temperatures. The noble metals do not oxidize in air, but silver, which is a widely used contact material, does react with sulphur in the atmosphere to form silver sulphide. However, this film has comparatively low electric resistance, is thin, and is easily rubbed off. The high electric and thermal conductivity of silver make it an ideal material for indoor or enclosed locations where a medium-pressure contact is satisfactory.

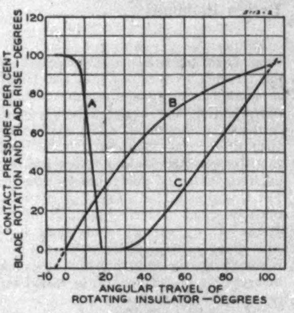

Figure 2. Curve showing relative motion of moving parts

A—Contact pressure in per cent
B—Blade rotation in degrees
C—Blade rise in degrees

Contacts exposed to the weather must meet additional requirements, since dirt, dust, and corrosion accumulate more rapidly and since there is likelihood of ice formation. Here the contact must have sufficient pressure to break through coatings of ice, dirt, and corrosive films. Even in enclosed locations, rubbing action, desirable on silver, is essential on copper and its alloys in order to remove corrosion from the surface. In high-pressure rubbing contacts soft metals, such as silver and copper, are subject to excessive wear and galling, and harder alloys must be used. These alloys must not anneal when heated to temperatures of several hundred degrees centigrade, which may be reached under short-circuit conditions.

Both flexible shunts and contacts are used on the hinge end of outdoor switches at the present time. Shunts are subject to oxidation and corrosion, particularly in sulphurous industrial atmospheres, and the combination of corrosion and flexing may break the fine wires until eventually the shunt breaks completely. The same conditions that cause rapid deterioration of shunts also cause rapid deterioration of exposed contacts. At the break jaw contacts necessarily must be left exposed. At the hinge connection, however, it is not necessary to use either a shunt or an exposed contact, since the contacts can be completely enclosed, protecting them from the elements and, to a great extent, from corrosive atmospheres.

Blade Mechanisms

There are two chief requirements of blade-operating mechanisms:

1. They must permit easy operation of the switch, even after a number of years in service with infrequent operation.
2. They must permit operation of the switch when it is covered with ice.

The effort necessary to operate switches is due entirely to friction, except in the opening operation on small switches where the weight of the blade is not counterbalanced. The only essential friction is that produced by the rubbing motion in contacting the switch. This motion should be separated from the blade-elevating motion and accomplished with maximum mechanical advantage. All other friction is incidental to switch operation and should be reduced to a minimum. For this reason, the number of pins and bearing points should be as small as possible. In normal service wear on a disconnecting switch can be neglected and, without maintenance, its life depends on freedom from corrosion of bearings and contact surfaces. Even though bearings must be made of materials that are corrosion resistant, they still should be designed with ample clearances so that corrosion will not cause seizing.

The earliest rotating-insulator vertical-break switches were merely hook-stick-operated switches with the hook-stick eye omitted and with a third rotating insulator added. A crank at the top of the rotating insulator raised and lowered the blade. In 1924 Koppitz conceived the earliest of the modern dual-motion switches. These switches utilize a second motion, usually a continuation of the first (blade-closing) motion to apply contact pressure during or after entry of the blade into the break jaw. This contacting motion makes use of a much greater mechanical advantage than is available for the blade-closing motion. The dual-motion switch made possible the high-pressure switch contact as known today.

Contact pressure can be applied in a number of ways. In some switches the blade is pushed forward into the break contact. In others contact tips are expanded by two blade members to engage the break jaw. Still others use a flat blade tip which is rotated in a resilient break jaw to establish contact pressure. Though each of these has its advantages, it must be kept in mind that each additional bearing is one more point to corrode and stick; each additional link or lever is one more part which may break or become frozen in ice. The mechanism should, therefore, be as simple and contain just as few moving parts as possible.

Description of Switch

The switches designed as a result of these studies are unique in their simplicity with only three moving parts and one exposed contact. The 69-kv 600-ampere pole unit shown in Figure 1 is typical of the line of switches, which are of the rotating-blade type. The rotating-blade motion was chosen because it permits application and release of contact pressure at the break jaw with a single blade member and with maximum mechanical advantage. It obviates the necessity for a number of parallel links at the hinge end, and it eliminates the possibility of cantilever stress on the jaw insulator due to switch operation. It further permits large deflections of the break-jaw insulator stack due to stresses from connecting lines or busses without affecting operation of the switch.

As the switch is opened, the blade is rotated until the contact pressure is fully released, then with the contact completely free the blade is elevated to the open position. In closing the reverse sequence is followed. The contacting motion is accomplished with high mechanical advantage to overcome the high frictional forces. After contact pressure is released, these forces are no longer present, and the blade is raised easily. This complete release of contact pressure before vertical movement of the blade is essential for easy operation. The relations between insulator rotation, blade rotation, and blade rise are shown in Figure 2. This ideal sequence of blade motions has been accomplished by the use of independent means for performing the two functions.

The mechanism for obtaining this sequence of motions is shown in Figure 3. An operating arm, bolted to the top of the rotating insulator stack and pivoted in the hinge support, engages two separate parts to give the independent motions. The blade-elevating motion is obtained through the action of the roller at the end of the operating arm in a slot on the inside surface of the mechanism housing. This slot is designed so that the portion corresponding to the first 27.5 degrees of insulator rotation lies on the circle traversed by the roller in revolving about the center line of the insulator stack. The housing and axis of the blade therefore remain stationary, while the roller rolls in this portion of the slot, rotating the blade only on its own axis. The next portion of the slot is inclined so that the blade is accelerated uniformly to its final velocity, which is maintained to the full open position by uniform rotation of the insulator.

The contacting motion is accomplished through a forked crank rigidly fastened to the hinge end of the tubular blade, engaging the operating arm in such a way that rotation of the arm results in rotation of the blade. The physical relation of the arm and the fork is such that one degree of movement of the rotating insulator twists the blade approximately two degrees when the blade is within the jaws. The rapid initial twisting of the blade permits complete disengagement of the contacts before the elevating movement of the blade begins. Figure 4 clearly shows the sequence of these motions.

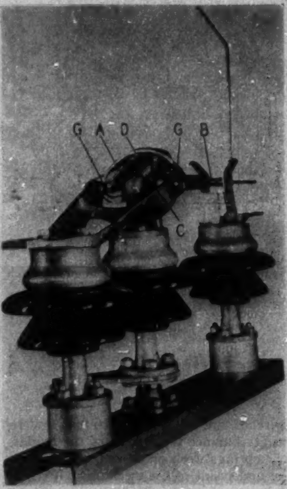

Figure 3. Early model of the new switch with special cutaway housing, which shows the mechanism for operating the blade (hinge contact not shown)

The tubular blade *B* is mounted in the mechanism housing *A*, free to rotate on its own axis. The fork *D* is part of the blade and rotates with it. The housing *A* rotates about the horizontal axis formed by the hinge bearings *GG*. The operating arm *C* extends through the fork *D*, and a roller at its outer end rolls in a groove in the inner surface of the housing *A*. To operate the switch the center insulator is rotated by turning the lever near the base. This rotates the operating arm *C*, which is bolted to the top of the rotating insulator. During the first 27.5 degrees of rotation of the operating arm, the arm engages the fork and rotates the blade to release the contact pressure on the jaw at the far end of the switch. Then the roller strikes the inclined portion of the groove, and, since the roller is constrained to revolve in a horizontal plane, the housing is rotated until the blade reaches a vertical position

Figure 5 is a top view of the center portion of the switch indicating the current path and showing the general arrangement of the hinge contacts. One end of the internal contact member bears against the heavy hinge stud to form a self-aligning annular-line contact. The other end bears against a machined surface on the fork to form a straight-line contact, which is also self-aligning. Contact pressure is supplied by a compression spring with adequate deflection so that the loss of contact pressure would be negligible even under the most severe conditions of contact wear. The hinge stud is threaded in the tie casting and locked against turning by a special locking washer and lock nut, which maintain intimate high-pressure contact at this point.

The mechanism housing completely encloses the hinge contacts and protects the moving parts from ice formation, so that the switch can be operated readily under heavy ice and sleet conditions. Furthermore, because the parts are protected from sun, rain, dust, and harmful atmospheric gasses, corrosion is very greatly reduced inside the enclosure, and lubrication is unnecessary.

Troubles due to annealing of work-hardened nonferrous materials, such as hard copper and phosphor bronze, have been eliminated by the use of precipitation-hardened (heat-treatable) alloys at the break contact. The jaw is beryllium cobalt copper, a comparatively new but already well-known and proved material. Under short-circuit conditions beryllium cobalt copper will not be affected at temperatures which would completely anneal work-hardened copper or phosphor bronze. This guarantees that the hardness of 90 Rockwell *B* and tensile strength of 90,000 pounds per square inch will be maintained for the life of the switch. As the physical characteristics of the material will be unchanged throughout the life of the switch, the jaw itself is used as the spring member as well as the current-carrying part.

The formed contact over the flattened end of the blade is chromium copper. This alloy, developed within the past decade, is similar to beryllium cobalt copper in that it is also precipitation-hardened. Though its strength and hardness are not so great, it has an electric conductivity 80 per cent that of copper, as compared with 45 per cent for beryllium cobalt copper. Hence, it is an ideal material for contacts in which extremes of hardness and deflection are not required.

Figure 4. Three views of the switch of Figure 3 showing the blade in various positions

The beryllium–cobalt–copper jaw and chromium–copper contact tip permit high-pressure rubbing line contact capable of breaking up and wiping away coatings of dirt or oxide. The break jaw has adequate deflection to shatter ice formations. The dissimilarity in the contact materials assures a minimum of wear and eliminates the possibility of galling. These factors, together with the non-annealing characteristics of the alloys, assure that the break contact characteristics will remain unchanged after years of severe service even under extreme climatic or atmospheric conditions.

Ease of operation has been considered essential in the design of these switches. The enclosed blade mechanism just described provides high mechanical advantage during the contacting operation where friction is greatest. Friction has been reduced elsewhere by the use of a minimum number of moving parts and bearings. The rotating insulator columns of switches above 15 kv are equipped with either dry-type ball bearings or with roller bearings having pressure fittings for easy lubrication. In the higher-voltage and higher-current ratings, the switches are provided with springs to counterbalance the weight of the blades. The springs work on an arm attached to the under side of the mechanism housing and are mounted within the hinge support for complete protection from the weather.

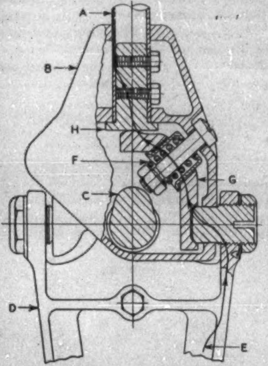

Figure 5. Partial top view of the switch showing construction of hinge contacts

A—Blade
B—Mechanism housing
C—Operating arm
D—Hinge support
E—Current path
F—Spring
G—Internal contact member
H—Fork

Tests

In the development of this switch numerous models were built and subjected to tests to check their performance under normal and extreme operating conditions. Temperature-rise tests were made on all ratings to insure that the switches would carry their rated current with a temperature rise of less than 30 degrees centigrade. Pole units were operated as many as 10,000 times to check wear on contacts, bearings, and operating mechanism parts. Short-circuit tests were made on all ratings to insure that the switch would carry its rated short-circuit current without mechanical injury and without damage to the contacts. To check their ability to operate properly under ice and sleet conditions, various ratings of switches were operated when covered with over a half inch of ice. Tests have been made to verify the effectiveness of the smooth contours in reducing corona and radio interference. Though flashover and withstand tests are considered insulator characteristics, 60-cycle wet and dry tests and impulse tests have been made to check over-all switch characteristics.

Summary

The new outdoor air switch strikes a new note in simplicity, as it has only three moving parts. All parts are simple and rugged with stresses kept to safe values for the materials employed. Hinge contacts and live parts with relative motion are protected from rain, dust, corrosion, and ice by a housing having smooth contours to minimize corona losses and radio interference. Critical adjustments and alignments have been eliminated. The sole exposed contact, at the break end, utilizes new materials which can withstand severe overcurrents and years of weathering without damage. Because of these features the new switch offers improved ease of operation and maximum reliability under all conditions.

References

1. Gesammelte Werke (book), H. R. Hertz. Leipzig, Germany, 1892. Volume 1, pages 155, 183.

2. Electrical Contact Resistance, F. W. Harris. *Electric Journal*, volume 10, 1913, pages 637–44.

3. Contact Resistance of Large Conductors, A. R. Enger. *Electric Journal*, volume 21, July 1924, pages 316–18.

4. Contact Resistance of Electric Switching Apparatus, W. Schaelchlin. *Electric Journal*, volume 25, 1928, pages 386–91.

5. Point Contacts for Heavy Currents, W. H. Lindae. *Electrical World*, volume 108, July 31, 1937, page 414.

9. Contact Resistance, B. W. Jones. *General Electric Review*, volume 30, 1927, pages 85–6.

7. 60-Line Contacts Aid Switch Operation. *Electrical World*, volume 112, October 7, 1939, page 1052.

8. 287-Kv Boulder Dam Disconnecting Switches, A. J. Bowie, C. P. Garman. AIEE Transactions, volume 55, 1936, June section, pages 582–9.

9. Electrical Contacts (book), G. Windred. D. Van Nostrand Company, Inc., New York, N. Y., 1940.

10. A Bibliography on Electrical Contacts. American Society for Testing Materials, Philadelphia, Pa., 1944.

Design of Induction-Heating Coils for Cylindrical Nonmagnetic Loads

J. T. VAUGHAN
ASSOCIATE AIEE

J. W. WILLIAMSON
ASSOCIATE AIEE

EQUATIONS are presented for the calculation of the required number of coil turns to match a given power source for solenoidal coils with coaxial cylindrical loads of nonmagnetic materials in electromagnetic induction circuits. The equations apply to both solid and hollow loads. A correction factor is established for coil shortness providing the coil length is equal to or greater than the coil diameter. Also given are equations for power distribution and impedance values. The accuracy of the calculations is substantiated by experimental results.

At the present time induction heating of nonmagnetic materials is used in annealing, forging, brazing, melting, heating for shrink-fitting, and other purposes.

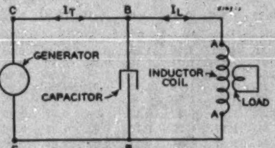

Figure 1. Conventional induction heating circuit using motor generator set

In any application a proper match must be obtained between the heating circuit and power source. In the case of multiturn coils connected directly to the output of a constant-frequency generating device, if the coil has too few turns, the output voltage is low at the rated output current of the generator. Consequently rated power output from the generator cannot be realized without employing some other matching device (transformer or series reactor). If the coil has too many turns, at rated generator output voltage, the current is low. To obtain the desired match to a given power source with a direct connected inductor, a specific number of coil turns must be used for any given physical dimensions. In the past determining the proper number of turns has been a cut-and-try process with many users of induction-heating equipment.

Baker[1] has presented equations for calculating the electrical characteristics of solenoidal coils with coaxial cylindrical loads of nonmagnetic conductors. The equations apply with accuracy to solid loads where the axial length of the coil is large relative to its inside diameter.

He also gives an equation for the power input to hollow cylinders where "the depth of current penetration" is several times the wall thickness. The purpose of the present paper is as follows:

1. To extend the range of equations applying to solid cylinders, so that accurate results may be obtained when the coil has an inside diameter of the same order of magnitude as its axial length.

2. To extend the range of equations applying to hollow cylinders so that accurate results may be obtained regardless of the cylinder wall thickness.

3. To present the equations in a form such that the required number of coil turns may be found to match a given power source.

4. To present tabulated values of experimental and calculated results over the proposed application range of these equations.

Definition of Symbols

Symbols used in appendixes are defined therein.

A = coil resistance divided by N^2, from equation 6
a_o = outside diameter of load, inches
a_m = average diameter of load, inches, = $a_o - t_2$
B = load resistance divided by N^2 from equations 9, 11, and 13
b_1 = inside diameter of inductor coil, inches
C = internal reactance of coil divided by N^2, from equation 7
D = internal reactance of load divided by N^2, from equations 10, 12, and 14
d_1 = reference depth for inductor, measure of current penetration, inches, from equation 15
d_2 = reference depth for load, measure of current penetration, inches, from equation 16
E = air-gap reactance divided by N^2, from equation 8
E_c = voltage across capacitor terminals BB, volts, from equation 23
E_L = voltage across inductor coil terminals AA, volts
E_T = voltage across generator terminals CC, volts
E_R = voltage rating of capacitor, volts
f = frequency cycles per second
h = radial thickness of inductor coil, inches
I_L = current through inductor coil, amperès, from equation 22
I_T = generator output current, amperes
K_1 = coil shortness correction factor, from equation 17
K_2 = resistance coefficient for thick wall and solid rods from Figure 5
K_3 = resistance coefficient for thin-wall rods from Table I
K_4 = reactance coefficient for thin-wall rods from Table II
K_5 = Nagaoka's constant[2] from Figure 4
L = axial length of inductor coil, inches
N = total turns in inductor
n = efficiency of power conversion through inductor to load, from equation 20
P_A = power dissipated in transmission line resistance R_A in watts, from equation 24
P_L = power input to inductor coil and load in watts
P_2 = power dissipated in load in watts, from equation 19
P_T = total power input at capacitor terminals in watts, from equation 25
ρ_1 = resistivity of conductor material in inductor, ohms inches
ρ_2 = resistivity of load material, ohms, inches
s = space factor of inductor coil
t_1 = wall thickness of conductor in coil in inches
t_2 = wall thickness of load in inches
R_A = resistance of transmission line from capacitor terminals BB to coil terminals AA in ohms
R_p = resistance of inductor coil itself in ohms, from equation 1
R_2 = resistance of load as reflected in inductor coil in ohms, from equation 2
W = axial width of conductor in inductor coil in inches
X_A = reactance of transmission line from capacitor terminals BB to coil terminals AA in ohms
X_o = reactance due to flux in air gap between coil and load in ohms, from equation 5
X_p = reactance due to flux between inside and outside radius of inductor coil in ohms, from equation 3
X_2 = reactance due to flux within the load as reflected in inductor coil in ohms, from equation 4

Circuit Description

The conventional induction-heating circuit used with rotating generators is shown in Figure 1. The purpose of the capacitor is to adjust the power factor of the generator load as viewed from terminals CC to approximately unity. The power factor as viewed from terminals AA may be considerably in the lag. Adjusting the capacitor to a value such that load power factor as viewed from the generator terminals is unity, results in a higher current I_L flowing through the coil circuit than the generator

---

Paper 45-107, recommended by the AIEE committee on industrial power applications and the subcommittee on induction and dielectric heating for publication in AIEE TRANSACTIONS. Manuscript submitted March 14, 1945; made available for printing May 7, 1945.

J. T. VAUGHAN and J. W. WILLIAMSON are development engineers with Tocco division, Ohio Crankshaft Company, Cleveland, Ohio.

output current I_T, allowing a given load power dissipation at minimum generator output current for a given generator terminal voltage.

The circuit from capacitor terminals through load is resolved as shown in Figure 2 when the intercircuit capacitance is negligible, as it generally is for induction-heating circuits of 15,000 cycles or below. The power accomplishing the load heating is dissipated in R_e. The power dissipated in R_A, the transmission-line resistance, and R_p, the inductor-coil resistance, should be kept as low as possible for most efficient heating. The power dissipated in the capacitor is generally negligible.

The physical detail of an induction-heating circuit consisting of a solenoidal coil and coaxial cylindrical load is shown in Figure 3. The inductor is shown as a single-layer solenoid wound with a tubular conductor of rectangular shape. A multilayer coil could be used but would result in less efficient power transfer to the load. The conductor is made tubular to permit the flow of a coolant to carry away the heat dissipated in the coil. A round conductor could be used but generally results in a somewhat less efficient heating circuit.

In the inductor-coil circuit, the values R_p, X_p, X_e, X_s, and R_s determine the power dissipated for a given value of E_L. For given coil and load dimensions these values may be adjusted to obtain the desired power by changing the number of turns in the inductor.

Circuit Equations and Their Limitations

EQUATIONS

For derivations of the equations which follow see references 1 or 5 for the impedance values of solid cylinders, Appendix I for the impedance of hollow loads, and Appendix II for coil shortness correction factor.

Impedance values in coil circuit in ohms are

$$R_p = N^2 A \tag{1}$$

$$R_s = N^2 B \tag{2}$$

$$X_p = N^2 C \tag{3}$$

$$X_s = N^2 D \tag{4}$$

$$X_e = N^2 E \tag{5}$$

where

$$A = \frac{3.14 \rho_1 b_1}{sL} \left[\frac{1}{d_1} + \frac{1}{b_1} \right] \tag{6}$$

$$C = \frac{3.14 \rho_1 b_1}{sLd_1} \tag{7}$$

$$E = \frac{15.7 f (b_1^2 - a_0^2) K_1 10^{-8}}{L} \tag{8}$$

Equations 9 and 10 are used to determine B and D for solid rods. For hollow rods the equations used to determine B and D

Table I. Resistance Coefficient, K_3

For Hollow Rods Where Ratio of Wall Thickness to Reference Dimension $\frac{t_2}{d_2} < 2.0$ and $\geqq 0.5$

t_2/a_0 \ t_2/d_2	0.500	0.522	0.545	0.569	0.595	0.621	0.648	0.677	0.707	0.74	0.77	0.805	0.88	1.00	1.19	1.41	2.00
0	2	1.93	1.86	1.78	1.70	1.64	1.58	1.51	1.45	1.39	1.34	1.29	1.20	1.08	0.97	0.92	0.94
0.025	1.96	1.89	1.83	1.76	1.70	1.64	1.58	1.51	1.45	1.39	1.34	1.29	1.21	1.10	0.99	0.93	0.95
0.0500	1.77	1.75	1.72	1.68	1.64	1.58	1.54	1.49	1.44	1.39	1.34	1.30	1.23	1.11	1.04	0.95	0.96
0.0648	1.60	1.60	1.59	1.58	1.56	1.53	1.50	1.46	1.42	1.37	1.33	1.29	1.23	1.12	1.04	0.95	0.96
0.077	$\underline{1.45}$	1.47	1.48	1.48	1.48	1.47	1.45	1.43	1.39	1.36	1.32	1.29	1.23	1.13	1.04	0.96	0.96
0.084	1.35	$\underline{1.38}$	1.40	1.42	1.44	1.43	1.42	1.40	1.37	1.34	1.32	1.28	1.22	1.13	1.04	0.97	0.96
0.092	1.24	1.29	$\underline{1.32}$	1.35	1.37	1.38	1.38	1.36	1.35	1.33	1.31	1.27	1.21	1.13	1.04	0.97	0.96
0.100	1.14	1.19	1.23	$\underline{1.27}$	1.30	1.32	1.34	1.34	1.34	1.32	1.30	1.27	1.21	1.13	1.04	0.98	0.97
0.109	1.03	1.08	1.13	1.17	$\underline{1.21}$	1.24	1.26	1.27	1.28	1.27	1.27	1.25	1.20	1.13	1.05	0.98	0.97
0.119	0.91	0.97	1.03	1.08	1.14	$\underline{1.17}$	1.20	1.22	1.24	1.24	1.24	1.23	1.19	1.13	1.05	0.99	0.97
0.130	0.80	0.86	0.92	0.98	1.03	1.08	$\underline{1.12}$	1.16	1.18	1.19	1.20	1.20	1.18	1.13	1.06	0.99	0.97
0.141	0.68	0.75	0.82	0.88	0.94	0.99	1.04	$\underline{1.08}$	1.12	1.14	1.16	1.17	1.17	1.13	1.06	1.00	0.98
0.154	0.57	0.62	0.68	0.75	0.83	0.89	0.94	1.00	$\underline{1.04}$	1.08	1.11	1.13	1.16	1.13	1.07	1.01	0.98
0.168	0.46	0.53	0.58	0.63	0.72	0.79	0.86	0.92	0.97	$\underline{1.02}$	1.06	1.09	1.14	1.13	1.08	1.01	0.99
0.183	0.38	0.43	0.48	0.54	0.60	0.66	0.73	0.81	0.88	0.94	$\underline{1.00}$	1.04	1.09	1.13	1.09	1.02	0.99
0.200	0.28	0.33	0.38	0.43	0.49	0.56	0.62	0.70	0.77	0.83	0.91	0.97	1.06	1.12	1.10	1.03	1.00

Note: Values below heavy lines not checked experimentally.

Table II. Reactance Coefficient, K_4

For Hollow Rods Where Ratio of Wall Thickness to Reference Dimension $\frac{t_2}{d_2} < 2.0$ and $\geqq 0.5$

t_2/a_0 \ t_2/d_2	0.500	0.545	0.595	0.648	0.707	0.77	0.84	0.92	1.00	1.09	1.19	1.30	1.41	1.54	1.68	2.00
0	0.33	0.36	0.39	0.43	0.47	0.51	0.55	0.60	0.65	0.70	0.75	0.80	0.86	0.91	0.95	0.99
0.0063	0.43	0.44	0.45	0.48	0.51	0.54	0.57	0.61	0.66	0.71	0.75	0.80	0.86	0.91	0.95	0.99
0.0088	0.47	0.46	0.47	0.49	0.52	0.55	0.58	0.62	0.67	0.71	0.76	0.81	0.86	0.91	0.95	0.99
0.0125	0.53	0.51	0.51	0.52	0.54	0.56	0.59	0.63	0.67	0.72	0.77	0.82	0.86	0.91	0.95	0.99
0.0177	0.61	0.57	0.56	0.56	0.57	0.59	0.61	0.64	0.69	0.73	0.77	0.82	0.87	0.91	0.95	1.00
0.0210	0.67	0.62	0.59	0.59	0.59	0.60	0.62	0.65	0.69	0.74	0.78	0.83	0.87	0.91	0.95	1.00
0.0250	0.73	0.68	0.63	0.62	0.61	0.62	0.63	0.66	0.70	0.74	0.78	0.83	0.87	0.91	0.95	1.00
0.0297	0.80	0.72	0.68	0.66	0.64	0.64	0.65	0.69	0.71	0.75	0.78	0.84	0.87	0.91	0.95	1.00
0.0354	0.89	0.79	0.74	0.70	0.67	0.67	0.67	0.70	0.72	0.76	0.79	0.84	0.88	0.92	0.95	1.00
0.0420	0.99	0.89	0.80	0.75	0.72	0.70	0.70	0.72	0.74	0.77	0.80	0.84	0.88	0.92	0.95	1.00
0.0500	1.09	0.98	0.88	0.82	0.76	0.74	0.73	0.74	0.75	0.78	0.81	0.85	0.89	0.92	0.95	1.00
0.0595	1.20	1.07	0.97	0.88	0.82	0.78	0.76	0.76	0.78	0.80	0.83	0.86	0.89	0.93	0.96	1.00
0.0707	$\underline{1.31}$	1.18	1.07	0.96	0.89	0.84	0.81	0.80	0.80	0.82	0.84	0.88	0.90	0.93	0.96	1.00
0.084	1.40	$\underline{1.30}$	1.19	1.07	0.97	0.90	0.86	0.84	0.84	0.84	0.86	0.89	0.91	0.93	0.96	1.00
0.100	1.46	1.38	$\underline{1.28}$	1.18	1.07	0.99	0.93	0.89	0.87	0.88	0.88	0.90	0.92	0.94	0.96	0.99
0.119	1.49	1.46	1.37	$\underline{1.27}$	1.17	1.08	1.01	0.96	0.92	0.91	0.90	0.92	0.93	0.95	0.97	0.99
0.141	1.44	1.46	1.43	1.36	$\underline{1.28}$	1.20	1.11	1.04	0.99	0.96	0.94	0.94	0.95	0.96	0.97	0.99
0.168	1.36	1.42	1.44	1.42	1.38	$\underline{1.30}$	1.22	1.14	1.07	1.02	0.98	0.97	0.97	0.97	0.98	0.99
0.200	1.23	1.34	1.40	1.44	1.44	1.41	1.34	1.26	1.17	1.10	1.04	1.01	0.99	0.99	0.98	0.99

Note: Values below heavy lines not checked experimentally.

depend on the relation t_2/d_2 and are as follows:

For hollow rods where $t_2/d_2 \geqq 2.0$ and for solid rods

$$B=\frac{3.14\rho_2 a_o K_2 K_1^2}{Ld_2} \tag{9}$$

$$D=\frac{3.14\rho_2 a_o K_1^2}{Ld_2} \tag{10}$$

For hollow rods where $0.5 \leqq t_2/d_2 < 2.0$

$$B=\frac{3.14\rho_2 a_m K_1^2 K_3}{Ld_2} \tag{11}$$

$$D=\frac{3.14\rho_2 a_o K_1^2 K_4}{Ld_2} \tag{12}$$

For hollow rods where $t_2/d_2 < 0.5$

$$B=\frac{15.7fa_m^2K_1^2 10^{-8}}{L}\times\frac{\dfrac{2d_2^3}{a_m t_2}}{1+\dfrac{4d_2^4}{a_m^2t_2^2}} \tag{13}$$

$$D=\frac{15.7fa_m^2K_1^2 10^{-8}}{L}\left[\frac{a_o^2}{a_m^2}-\frac{1}{1+\dfrac{4d_2^4}{a_m^2t_2^2}}\right] \tag{14}$$

The following equations are for determining values for use with the proceeding equations:

$$d_1=3{,}160\sqrt{\frac{\rho_1}{sf}} \tag{15}$$

$$d_2=3{,}160\sqrt{\frac{\rho_2}{f}} \tag{16}$$

$$K_1=K_5\left(1-\frac{a_o^2}{b_1^2}\right)+\frac{a_o^2}{b_1^2} \tag{17}$$

The required number of coil turns to obtain given power P_L at given voltage E_L are

$$N=E_L\sqrt{\frac{A+B}{P_L[(A+B)^2+(C+D+E)^2]}} \tag{18}$$

Power dissipated in load, P_s in watts, is

$$P_s=P_L\left[\frac{B}{A+B}\right] \tag{19}$$

Efficiency of power conversion through inductor to load is

$$n=\frac{B}{A+B} \tag{20}$$

Capacitor rating for unity power factor at capacitor-terminal input is

$$\text{kva}_{\text{rated}}=\frac{(P_L+P_A)E_B^2}{1{,}000E_c^2}\times\frac{(C+D+E)N^2+X_A}{(A+B)N^2+R_A} \tag{21}$$

Current through inductor coil, I_L, amperes is

$$I_L=\frac{E_L}{N^2\sqrt{(A+B)^2+(C+D+E)^2}} \tag{22}$$

Capacitor voltage, E_c, volts is

$$E_c=I_L\sqrt{[N^2(A+B)+R_A]^2+[N^2(C+D+E)+X_A]^2} \tag{23}$$

Power dissipated in transmission line, P_A in watts is

$$P_A=I_L^2R_A \tag{24}$$

Total power input at capacitor terminals (neglecting power loss in capacitor), P_T in watts, is

$$P_T=P_L+P_A \tag{25}$$

Limitations

For an accuracy of ± ten per cent the foregoing equations will apply in the range of the following limitations:

1. **Single-layer solenoidal coil wound with rectangular conductor.**
2. **Cylindrical load telescoped in coil, coaxial with coil.**
3. **Length of load equal to or greater than length of coil with ends of load flush with ends of coil or extending out of ends of coil.**
4. **Ratio of inside diameter of coil to length $b_1/L \leqq 1.0$.**
5. **Ratio of coil thickness to length $h/L \leqq 0.07$.**
6. **Ratio of conductor wall thickness to inductor reference dimension $t_1/d_1 \geqq 1.35$.**
7. **Inductor-coil space factor $\geqq 0.70$.**
8. **Permeability of coil and load material relative to a vacuum = 1.0.**
9. **Ratio of inside diameter of coil to reference dimension of coil $b_1/d_1 \geqq 3.5$.**
10. **Ratio of outside diameter of load to reference dimension of load $a_o/d_2 \geqq 2.0$.**
11. **Intercircuit capacitance negligible.**

Coil Design and Use of Equations

Physical Dimensions

The length and diameter of the inductor coil are determined by the dimensions of the piece to be heated, the heat pattern desired, and the allowable clearance between inside of coil and outside of load. For a heating operation in which the piece or pieces of metal to be heated are fed continuously through the inductor, the length of the coil is determined by whether surface heating or through heating is desired and the amount of power utilized. For surface heating the coil is made short to realize high power densities, whereas for through heating a relatively long coil gives more satisfactory results. To minimize coil I^2R loss and required kilovolt-amperes of condenser, the inside diameter of the coil should be kept as small as possible. However, in the case of multiturn coils with a substantial potential difference between one end of the coil and the other, sufficient space must be allowed for an insulation coating between conductor and load piece, in addition to the necessary mechanical clearance. Also allowance must be made for expansion of the load when heated. The diameter of the load used in calculation should correspond to that at the particular load-material temperature used for load-resistivity determination.

The conductor wall thickness t_1 should be equal to or greater than 1.35 d_1 (d_1 is measure of current penetration) for effi-

Table III. Calculated Impedance Values Versus Experimental Results for Solenoidal Coils With Coaxial Cylindrical Loads of Nonmagnetic Materials at 10,000 Cycles Per Second*

			Case 1	2	3	4	5	6	7	8	9	10
Inductor, copper	Resistivity, ρ_1, microhm, inches		0.73	0.73	0.71	0.73	0.73	0.76	0.76	0.76	0.76	0.76
	Total turns, N		10	10	10	10	10	20	20	20	20	20
	Inside diameter, b_1, inches		3.010	3.010	3.010	3.010	3.010	1.127	1.127	1.127	1.127	1.127
	Length over turns, L, inches		3.0	3.0	3.0	3.0	3.0	5.95	5.95	5.95	5.95	5.95
	Conductor	Width, W, inches	0.252	0.252	0.252	0.252	0.252	0.248	0.248	0.248	0.248	0.248
		Height, h, inches	0.252	0.252	0.252	0.252	0.252	0.248	0.248	0.248	0.248	0.248
		Wall, t_1, inches	0.042	0.042	0.042	0.042	0.042	0.044	0.044	0.044	0.044	0.044
Load	Material		Copper	Brass	18-8	18-8	18-8	18-8	18-8	18-8	18-8	18-8
	Resistivity, ρ_2, microhm, inches		0.75	2.68	31.2	29.9	28.7	28.9	28.0	29.3	28.5	30.2
	Outside diameter, a_o, inches		2.500	2.500	2.500	1.005	1.001	1.005	1.001	1.000	0.625	0.375
	Wall, t_2, inches		0.131	0.034	0.133	0.135	0.061	0.135	0.061	Solid	Solid	Solid
Impedance values, ohms	Coil resistance, R_p	Calculated	0.0094	0.0094	0.0093	0.0094	0.0094	0.0074	0.0074	0.0074	0.0074	0.0074
		Measured	0.0091	0.0090	0.0090	0.0095	0.0098	0.0073	0.0073	0.0073	0.0073	0.0073
	Load resistance, R_s	Calculated	0.0057	0.0169	0.0485	0.0099	0.0122	0.0372	0.045	0.0290	0.0137	0.0032
		Measured	0.0056	0.0162	0.0465	0.0102	0.0121	0.0360	0.045	0.0280	0.0132	0.0029
	Total reactance, $X_p+X_s+X_a$	Calculated	0.148	0.148	0.170	0.328	0.333	0.071	0.090	0.0702	0.115	0.130
		Measured	0.144	0.143	0.165	0.316	0.326	0.0756	0.095	0.0755	0.119	0.138
Load reference dimension, d_2			0.0274	0.0518	0.177	0.173	0.170	0.170	0.167	0.171	0.169	0.174
Ratio, t_2/d_2			4.78	0.657	0.75	0.78	0.359	0.795	0.365			

* For further details see text.

cient heating. Generally, if the wall thickness is made less than 1.35 d_1, the coil losses will be increased.

LOAD RESISTIVITY ρ_2

The resistivity of load material may vary considerably during the heat cycle. If the heat operation is of the continuous type, the required turns may be based on average values of load resistivity and outside diameter. If the load remains fixed in the coil during heating, separate calculations should be made for maximum and minimum temperature conditions. When the generator is to be loaded to its rated power output, then the greatest number of turns obtained should be used. This allows rated generator output at one end of the heat cycle without exceeding the generator rating at the other end of the heat cycle.

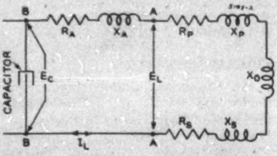

Figure 2. Equivalent electric circuit from capacitor through load

CONDUCTOR RESISTIVITY ρ_1 AND COIL SPACE FACTOR

The coil resistivity used in calculation should correspond to that at the actual operating temperature of the coil conductor. In determining the required turns it is necessary to assume some value of space factor. After the turns are calculated, a check should be made to find if the assumed space factor can be realized with available tubing. If not, a new calculation should be made on the basis of the obtainable space factor. Over the range of the prescribed limitations, greatest efficiency is obtained by making the space factor as close to unity as possible. In the case of multiturn coils with sufficient insulation for terminal voltages of 800 volts or less at 15,000 cycles or below, it is generally possible to realize a space factor of 0.80.

SELECTION OF FREQUENCY AND POWER REQUIREMENT

When the required power input to the load piece (based on past experience or a complete thermal calculation) is known, the necessary power input to the coil to produce this load power is found by dividing load power by efficiency of power conversion. This efficiency is given as follows when the appropriate expressions for A and B are substituted in equation 20:

$$n=\frac{1}{1+\frac{1}{sK_1^2}\frac{\rho_1}{\rho_2}\frac{b_1}{a_o}\frac{d_2}{d_1'}\frac{1}{K_2}}\qquad\left(\text{solid loads or }\frac{t_2}{d_2}\geqq 2.0\right)\tag{26}$$

$$n=\frac{1}{1+\frac{1}{sK_1^2}\frac{\rho_1}{\rho_2}\frac{b_1}{a_m}\frac{d_2}{d_1'}\frac{1}{K_3}}\qquad\left(\text{hollow loads }0.5\leqq\frac{t_2}{d_2}<2.0\right)\tag{27}$$

$$n=\frac{1}{1+\frac{1}{sK_1^2}\frac{\rho_1}{\rho_2}\frac{b_1}{a_m}\frac{d_2}{d_1'}\left[\frac{t_2}{d_2}+\frac{4d_2^3}{a_m^2t_2}\right]}\qquad\left(\text{hollow loads }\frac{t_2}{d_2}<0.5\right)\tag{28}$$

where

$$d_1'=\frac{d_1}{1+d_1/b_1}$$

For most applications of induction heating the reference depth of the coil d_1 is small compared to the coil diameter b_1. Therefore d_1', is approximately equal to d_1, and for this condition the ratio of d_2/d_1' is nearly constant as frequency is varied. The only quantities which change appreciably with frequency in equations 26, 27, and 28, are K_2, K_3, and the expression in brackets respectively. Inspection and comparison of these equations will show:

(*a*). Where equation 26 applies power conversion efficiency increases with K_2 and therefore frequency (see Figure 5). In an analysis of efficiency and kilovolt-ampere requirements Stansel has advocated the use of frequencies at least sufficient to make[3]

$$\frac{a_o}{d_2}=3.54\tag{29}$$

He points out, however, that there is no objection to higher frequencies, if economic factors warrant their use.

(*b*). Where equation 27 applies, power-conversion efficiency increases with K_3.

(*c*). Where equation 28 applies, power-conversion efficiency increases as the bracket expression decreases.

(*d*). Comparison of equations 26 and 27 and reference to Table I will show that for hollow loads with wall thicknesses less than 0.13 of the outside diameter greatest electric efficiency is realized by selecting a frequency to make K_3 maximum or to make the bracket expression of equation 28 minimum. This frequency is given approximately by

$$f=\frac{34.6\times10^6\rho_2}{a_mt_2}\tag{30}$$

This is the frequency for minimum value of the bracket expression in equation 28 and corresponds very closely to the frequency for maximum K_3.

COIL VOLTAGE E_L

The transmission-line impedance between capacitors and coil terminals should be kept relatively small for efficient power transmission. The effect of this impedance is to reduce the voltage E_L across coil terminals with respect to capacitor voltage E_c. In the solution of the foregoing equation for coil turns, E_L may be assumed to be equal to 0.9 E_c; then it usually will be economically feasible to design a transmission line to meet or better this condition.

Calculated Impedance Values Versus Experimental Results

In Table III a portion of the experimental results obtained is compared to calculated values in order to substantiate the use of equations 1 through 25 over the proposed range of limitations. All data given in Table III were obtained at 10,000 cycles per second (±0.5 per cent) with sinusoidal voltages and currents. All loads used in obtaining the data in this table were 18 inches long, located coaxial with the inductor, and extended through the inductor, so that ends of load were either flush with ends of coil or extending out of ends of coil. With the load extending out of both ends of the coil and then moved axially through the coil no change in impedance values was obtained up to the point where one end of the load was flush with the end of the coil. However, with further axial movement, such that the load did not extend fully through the coil, the impedance values changed. This condition of the load not extending fully through the coil represents a separate problem and is not considered in this paper.

Experimental impedance values were arrived at from voltage and current measurements made with thermocouple-type instruments. For this purpose the primary of the current transformer was

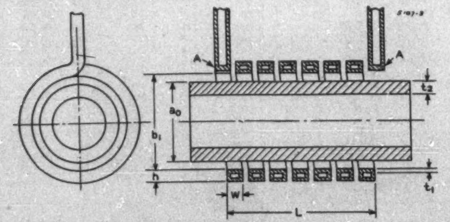

Figure 3. Inductor coil and load

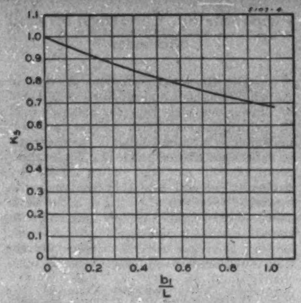

Figure 4. Nagaoka's constant $K5$

connected in series with the inductor coil (Figure 1), and the voltmeter was connected across AA. The total generator output was measured by a wattmeter connected at CC. This wattmeter was calibrated against thermocouple instruments for unity power-factor loads. The capacitor BB was adjusted so that the reactive volt-amperes measured at CC were negligible. The input to the coil was obtained by subtracting power losses in condenser and connectors from the generator output. These losses never exceeded 10 per cent of the output of the generator.

Where hollow loads were used, primary and secondary resistances were measured calorimetrically. Cooling water was circulated through the load and coil. Power dissipation was obtained by flow temperature-rise methods. Measured generator output less capacitor and connector losses was found to agree within ±3 per cent with measured power to the cooling water. In making resistance measurements where solid loads were used it was observed that:

1. Such loads could not be held at a constant low temperature, unless a surrounding water jacket were provided. This would make it impossible to separate coil and load losses where the air gap was small.

2. Direct calorimetric methods were therefore impracticable. However, the accuracy of the electrically determined input to the coil had been substantiated by experiments with hollow loads.

3. For the particular coil used in cases 6 to 10 (Table III) experiments with hollow loads had demonstrated that the nature of the load had little effect upon the resistance of the coil. Therefore, the total resistance of the coil with load inserted, R_p+R_s, was obtained from the electrically measured watts to the coil. R_s then was found by subtracting the value of R_p measured for hollow loads.

The operating temperature of the load was determined by averaging thermocouple measurements over the conducting volume. The resistivity at this temperature was measured with a Kelvin bridge. The test sample was an open ring cut from a cylindrical section of the load. The ring was heated to the desired temperature in an oven.

Conclusions

1. The proposed equations apply over the given range of limitations with sufficient accuracy for calculating inductor coils for induction heating of nonmagnetic cylinders.

2. For hollow cylindrical loads with wall thicknesses less than 0.13 of outside diameter a definite frequency exists at which maximum power-conversion efficiency is obtained (see equation 30).

3. It is important to remember that the voltage across the coil is not necessarily equal to the generator output voltage due to the effect of transmission lines.

Appendix I. Expressions for Impedance—Hollow Loads

Units

Identical definitions apply to quantities previously defined, except that units in Appendix I are in the absolute or centimeter-gram-second electromagnetic system.

Consider a long solenoidal coil AA (Figure 1) wound closely about its load. The flux density on the outside of the load or in the air gap is

$$H=4\pi\frac{N}{L}I_L \tag{31}$$

Load With Wall Thickness Small Relative to Reference Depth

At any given time current density in the load may be assumed constant. Therefore, concentrated circuit theory applies.

Let

R_2 = resistance of load

$=\frac{\pi a_m}{Lt_2}\rho_2$ abohms

X_2 = reactance of load

$=2\pi f\left(\frac{4\pi}{L}\right)\left(\frac{\pi}{4}a_m^2\right)$ abohms

X_M = mutual reactance between load and coil

$=NX_2$ abohms

d_2 = reference depth

$=\frac{1}{2\pi}\sqrt{\frac{\rho_2}{f}}$ centimeters

The primary impedance associated with secondary current flux is:

$$\frac{X_M^2}{R_2+jX_2}=\frac{2\pi^3a_m^2N^2f}{L}\times\frac{1}{\frac{R_2}{X_2}+j}$$

The primary impedance associated with primary current flux inside the load is:

$$j\,\frac{2\pi^3a_o^2N^2f}{L}$$

Adding, the total primary impedance due to flux inside the load gives:

$$R_s+jX_s=\frac{2\pi^3a_m^2N^2f}{L}\left[\frac{\frac{R_2}{X_2}-j}{\frac{R_2^2}{X_2^2}+1}+j\frac{a_o^2}{a_m^2}\right] \tag{32}$$

where

$$\frac{R_2}{X_2}=\frac{\rho_2}{2\pi^2a_mft_2}=\frac{2d_2^2}{a_mt_2} \tag{33}$$

When one converts this to the ohm-inch system and separates into real and imaginary parts, equations 2 and 4 are obtained, B and D being given by equations 13 and 14. (Under the assumptions of Appendix I, K_1 is unity.)

Loads of Intermediate Wall Thickness

The current density in the load is neither constant at any given time nor the same as for a solid load, at the same depth beneath the surface. Let

i = rms current density in abamperes per cm²

Φ = rms flux in maxwells

H = flux density in lines per cm²

r = distance from axis of load in centimeters

$k=2\pi\sqrt{2f/\rho_2}$

$x=\sqrt{jkr}$

o and I refer to outside and inside of load (except where subscript 0 denotes a Bessel function of zero order)

$r_m={}^1/_2(r_1+r_o)$ centimeters

Consider an element of inside radius r, outside radius $r+dr$, and unit length, and apply Ohm's law. Then

$$2\pi\rho_2ri+j2\pi f\Phi=0 \tag{35}$$

The rate at which flux density changes with radius is

$$\frac{dH}{dr}=-4\pi i \tag{36}$$

By definition

$$\Phi=2\pi\int_0^r rHdr \tag{37}$$

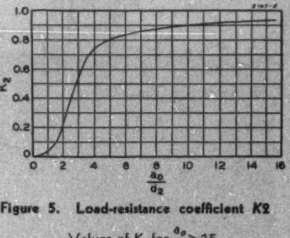

Figure 5. Load-resistance coefficient $K2$

Values of K_2 for $\frac{a_o}{d_2}>15$

$\frac{a_o}{d_2}$	K_2
30	0.97
100	0.99
∞	1.0

Differentiating equation 35 with respect to r and making use of equations 36 and 37 gives

$$\frac{d^2H}{dr^2}+\frac{1}{r}\frac{dH}{dr}-jk^2H=0 \tag{38}$$

Equation 38 is a standard form of Bessel's equation of zero order.[4] The general solution is

$$H=C_1I_{0(\chi)}+C_2K_{0(\chi)} \tag{39}$$

Where $I_{0(\chi)}$ and $K_{0(\chi)}$ are modified Bessel functions of zero order, of the first and second kinds. Substituting the boundary conditions for the inside radius into equation 35 and making use of equation 36

$$\psi_{(\chi_I)}C_1+\phi_{(\chi_I)}C_2=0 \tag{40}$$

where

$$\left.\begin{aligned}\psi_{(\chi)}&=-\frac{\rho_2\chi}{2}I_0{}'_{(\chi)}+j2\pi^2fr^2I_{0(\chi)}\\ \phi_{(\chi)}&=-\frac{\rho_2\chi}{2}K_0{}'_{(\chi)}+j2\pi^2fr^2K_{0(\chi)}\end{aligned}\right\} \tag{41}$$

Inserting the boundary conditions for the outside radius into equation 39 gives

$$H_o=I_{0(\chi_0)}C_1+K_{0(\chi_0)}C_2 \tag{42}$$

Solving equations 40 and 42 for C_1 and C_2 and substituting into equation 39 gives

$$H=\frac{1}{1-m}\left[\frac{I_{0(\chi)}}{I_{0(\chi_0)}}-m\frac{K_{0(\chi)}}{K_{0(\chi_0)}}\right]H_o \tag{43}$$

where

$$m=\frac{\psi_{(\chi_I)}K_{0(\chi_0)}}{\phi_{(\chi_I)}I_{0(\chi_0)}} \tag{44}$$

The total flux inside the rod is

$$\Phi_o=\pi r_I^2H_I+2\pi\int_I^{r_0}rHdr \tag{45}$$

Integrating $I_{0(\chi)}$ and $K_{0(\chi)}$

$$\int rI_{0(\chi)}dr=\frac{r^2}{\chi}I_0{}'_{(\chi)}\quad \int rK_{0(\chi)}dr=\frac{r^2}{\chi}K_0{}'_{(\chi)}$$

Therefore, from equations 43 and 45

$$\begin{aligned}\Phi_o=\frac{1}{1-m}\pi r_I^2H_o&\left[\frac{I_{0(\chi_I)}}{I_{0(\chi_0)}}\left(1-\frac{2}{\chi_I}\cdot\frac{I_0{}'_{(\chi_I)}}{I_{0(\chi_I)}}\right)-\right.\\ &\left.m\frac{K_{0(\chi_I)}}{K_{0(\chi_0)}}\left(1-\frac{2}{\chi_I}\cdot\frac{K_0{}'_{(\chi_I)}}{K_{0(\chi_0)}}\right)\right]+\\ &\frac{1}{1-m}\cdot\frac{2\pi r_0^2}{\chi_0}H_o\left[\frac{I_0{}'_{(\chi_0)}}{I_{0(\chi_0)}}-m\frac{K_0{}'_{(\chi_0)}}{K_{0(\chi_0)}}\right]\end{aligned} \tag{46}$$

From equations 41 and 44

$$m=\frac{K_{0(\chi_0)}}{I_{0(\chi_0)}}\cdot\frac{I_{0(\chi_I)}-\frac{2}{\chi_I}I_0{}'_{(\chi_I)}}{K_{0(\chi_I)}-\frac{2}{\chi_I}K_0{}'_{(\chi_I)}} \tag{47}$$

Therefore the first expression in brackets in equation 46 vanishes, leaving

$$\Phi_o=\frac{2\pi r_o^2H_o}{\chi_0}\cdot\frac{1}{1-m}\left[\frac{I_0{}'_{(\chi_0)}}{I_{0(\chi_0)}}-m\frac{K_0{}'_{(\chi_0)}}{K_{0(\chi_0)}}\right] \tag{48}$$

The flux density at the outside of the load with unit current in the coil is $4\pi N/L$. The impedance of the coil associated with flux inside the load is $j2\pi fN$ times the corresponding Φ_o, or

$$R_s+jX_s=j\frac{16\pi^3fN^2r_o^2}{L\chi_0}\cdot\frac{1}{1-m}\times\left[\frac{I_0{}'_{(\chi_0)}}{I_{0(\chi_0)}}-m\frac{K_0{}'_{(\chi_0)}}{K_{0(\chi_0)}}\right] \tag{49}$$

For sufficiently high values of χ the following approximations may be made:

$$I_{0(\chi)}=\frac{1}{\sqrt{2\pi}}\cdot\frac{e^{\chi}}{\sqrt{\chi}}\qquad K_{0(\chi)}=\sqrt{\frac{\pi}{2}}\cdot\frac{e^{-\chi}}{\sqrt{\chi}} \tag{50}$$

Therefore:

$$\left.\begin{aligned}\frac{I_0{}'_{(\chi)}}{I_{0(\chi)}}&=1-\frac{1}{2\chi}\approx1\\ \frac{K_0{}'_{(\chi)}}{K_{0(\chi)}}&=-1-\frac{1}{2\chi}\approx-1\end{aligned}\right\} \tag{51}$$

Also, from equation 47

$$m\approx e^{-2(\chi_0-\chi_I)}\left(1-\frac{4}{\chi_I}\right) \tag{52}$$

Substituting equations 51 and 52 into equation 49 and dropping terms in $1/\chi_I$ in the numerator gives

$$R_s+jX_s=j\frac{16\pi^3fN^2r_o^2}{L\chi_0}\times\frac{1+e^{-2(\chi_0-\chi_I)}}{1-e^{-2(\chi_0-\chi_I)}\left(1-\frac{4}{\chi_I}\right)} \tag{53}$$

For loads with thin walls, equation 53 should agree with equation 32. Due to the approximations introduced by equations 51 and 52, this condition is more nearly satisfied if $4/\chi_I$ in the denominator is replaced by $4/\chi_0+4t/r_0$. An improvement in accuracy also results from the use of a correction factor r_m/r_0 for R_s. After these changes are made, equation 53 may be expressed

$$R_s=\frac{\pi a_m\rho_2N^2}{Ld_2}K_3\qquad X_s=\frac{\pi a_o\rho_2N^2}{Ld_2}K_4 \tag{54}$$

where K_3 and K_4 are, respectively, the real and imaginary parts of

$$(1+j)\frac{1+e^{(1+j)\frac{2t_2}{d_2}}}{e^{(1+j)\frac{2t_2}{d_2}}-1+\frac{8t_2}{a_o}\left(\frac{1-j}{2}\cdot\frac{d_2}{t_2}+1\right)} \tag{55}$$

Appendix II. Correction for Coil Shortness

1. The theoretical relations derived in Appendix I assume an inductor coil and load of dimensions such that the reluctance of the return magnetic path outside the coil is negligible in relation to that of the magnetic path between the coil and load. Under these conditions it can be shown easily by Ampere's integral law that the magnetic intensity, H, within the air gap is the same as would exist in an infinitely long coil with the same number of ampere turns per unit length. Therefore, no coil-shortness correction is required if the air-gap area is sufficiently small.

2. If the air-gap area amounts to practically the entire area inside the coil (that is, if the space taken up by the load is negligible) the air-gap reactance is:

$$X_o=K_sX_o'$$

where X_o' is the air-gap reactance which would be calculated by neglecting the reduction in flux density due to coil shortness, and K_s is Nagaoka's constant.[3]

3. The correction introduced in case 2 involves a reduction of $(1-K_s)$ of X_o'. The correction required in case 1 is zero. In intermediate cases it appears reasonable to subtract (air-gap area ÷ total area of coil) $(1-K_s)$ of X_o'. This gives

$$\begin{aligned}X_o&=X_o'\left[1-\left(1-\frac{a_o^2}{b_1^2}\right)(1-K_s)\right]\\ &=K_1X_o'\end{aligned}$$

where K_1 is defined by equation 17.

While X_o is directly proportional to the air-gap flux density, H_o, the I^2R loss and time rate of change of magnetic energy in the load are proportional to H_o^2. Therefore, a coil-shortness correction of K_1^2 is required for R_s and X_s.

References

1. Heating of Nonmagnetic Electric Conductors by Magnetic Induction—Longitudinal Flux, R. M. Baker. AIEE Transactions, volume 63, 1944, June section, pages 273–8.

2. Radio Instruments and Measurements. United States National Bureau of Standards. Circular C74, 1937, Table 10, page 283.

3. Induction Heating—Selection of Frequency, N. R. Stansel. AIEE Transactions, volume 63, 1944, October section, pages 755–9.

4. Bessel Functions for Engineers (book), McLachlan. Oxford (England) University Press, 1934. Pages 119–48, 157–72.

5. Theory of Eddy-Current Heating (book), Burch, Davis. Ernest Benn, Ltd., London, England, 1928. Pages 30–2.

A Tachometer—Accelerometer—Vibrometer for Instrument-Gyroscope Testing

R. M. LAURENSON
NONMEMBER AIEE

T. H. LONG
MEMBER AIEE

Synopsis: This paper gives an account of the development, operating principles, and use of a possibly unique instrument that has been and is of considerable value on instrument-gyroscope manufacturing and repair production lines. It is used to indicate gyroscope-rotor speed when the rotor is brought up to 1,000 rpm for bearing adjustment. Then, by the turn of a switch, the instrument indicates the rate of deceleration as the bearing is adjusted, thus permitting accurate adjustment of bearing pressures. A third position of the same selector switch gives tachometer operation up to 15,000 rpm for vibration tests. Excessive vibration is indicated visibly and audibly through another amplifier, independently of the selector-switch position.

In the manufacture of gyroscopic instruments for aircraft it has in the past been the practice to adjust the contact pressure of the ball bearings on which the rotor turns to a satisfactory working value by a coast test. At the point in assembly procedure at which this adjustment is to be made, the rotor is enclosed in a housing (in the case of the horizon gyroscope) as shown in Figure 1. The coast test was made by running the gyroscope up to substantially normal revolutions per minute as indicated by applied air pressure (occasionally checked by Strobotac), turning the air off, and measuring the coast time. This coast time was required to be between 8.5 and 13.5 minutes. This seems like a rather wide tolerance and in fact it was, but in spite of this it sometimes required several trials to get a proper adjustment.

A further objection to setting the bearings by clocking the coast times was the fact that rejections from the operation frequently ran as high as 50 per cent. As there were a number of other operations in the manufacture of gyroscopes that resulted in 50 per cent rejections this one did not seem outstandingly bad. Since some of the rejections were definitely caused by the burning or battering of the bearing surfaces by running at full speed with the rotor too tight or too loose, it seemed possible to improve the process by making the coast test from a lower speed.

At lower speeds (as determined by operating air pressure) coast time was not a reliable measure of bearing pressure, evidently because the starting speed was not determined accurately. It was proposed that equipment be developed to measure the speed of the coasting rotor by determining the frequency of the tone generated by the buckets after the air supply had been shut off; two such measurements a minute apart would give an accurate measure of bearing pressure and save a great deal of time in making adjustments. This development resulted in a workable device, but it was subject to the disadvantages of a low sound level at low speeds and standing waves at high speeds.

A workable photoelectric system was also produced, using a photoelectric tube, amplifier, synchronous motor, and tachometer; a stroboscopic pattern on the rotor was visible through holes in the end of the casing (see Figure 1). There were objections to any method which required that the rotor of the horizon gyroscope be exposed. In the completed instrument the holes in the rotor housing were covered by a cap secured to the housing by four screws. Some manufacturers made bearing adjustments with a ring assembled to the housing in an attempt to reproduce any distortion of the case that would be caused by the final assembly with the cap, and thus eliminate the effect of this distortion on bearing adjustment.

Another possible solution to the problem was suggested by a hole in the rotor housing, intended eventually for the caging screw (filled during the coast test with a plug) through which a probe could readily be brought up close to the rotor buckets. By energizing this probe with several hundred volts of direct current through about two megohms resistance, the variation in electrostatic capacitance between the probe and the buckets as the rotor turned would cause a variation in the potential of the probe that could be impressed on the grid of an amplifier tube. This voltage variation was amplified, divided down in frequency[1] to the range of the synchronous motor and amplified further to run the motor; a tachometer driven by this motor was, in effect, geared to the gyroscope rotor.

First Acceleration-Measuring Model

Because it was the rate of change of rotor speed that was to be measured, and as there are a number of electric devices which are by their very nature such that they give a time differential, it seemed logical to measure this differential directly instead of measuring the speed at the beginning and end of a time interval.

It seemed desirable to start the coast at about 1,000 rpm, which would correspond to 60 cycles or 1,800 rpm for the synchronous motor to be used, and would allow over one minute of adjusting time before the speed dropped 50 per cent. The operation of the synchronous motor with the previously developed amplifier circuit was not reliable below 30 cycles. With a voltage change of two volts per minute from a standard tachometer magneto and with appropriate meters (which were not available), a meter–capacitor circuit would have given adequate results but there would have been something of a problem of adequately protecting the meter from severe overcurrents due to rapid speed changes.

Some 0–500 microammeters were available so an amplifier circuit was designed around these meters, and arranged to give a more expanded coast-time scale than would have been available with the direct-measurement system.

Figure 1. Bottom view of gyroscope-rotor assembly cut away to show rotor buckets and electrostatic probe

---

Paper 45-105, recommended by the AIEE committee on instruments and measurements for publication in AIEE Transactions. Manuscript submitted December 4, 1944; made available for printing May 3, 1945.

R. M. Laurenson, formerly with C. G. Conn Ltd., Elkhart, Ind., is now with Union Switch and Signal Company, Swissvale, Pa.; T. H. Long is in the research department, C. G. Conn Ltd.

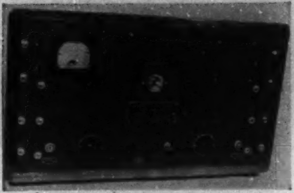

Figure 2. Front view of gyroscope test unit

This instrument is a combination tachometer, accelerometer, and vibrometer

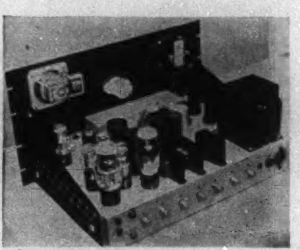

Figure 3. Chassis of gyroscope test unit showing calibration adjustments and test jacks

Figure 5. View of completion of bearing adjustment by coast test

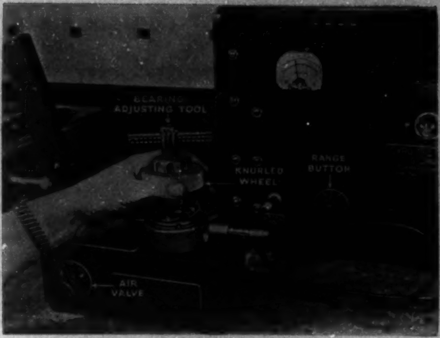

This apparatus was developed and tested quite thoroughly. It was found practicable to set the coast time to within 0.5 minute of any desired value, and in the case of the horizon gyroscope this could be done in an over-all time of less than two minutes per instrument. Since the gyroscope was not run above 1,000 rpm until the bearings were properly adjusted it seemed reasonable to believe that the only rejections from such an operation would be those due to defective bearings. As nearly as it could be determined, the maximum error in deceleration measurements with this equipment was about 1.5 per cent. There was no error between the gyroscope and the synchronous motor, and the principle subsequent error was due to the voltage change on the regulated side of a constant-voltage transformer. See appendix for details of test method.

These results were so encouraging that it seemed certainly worthwhile to make some additional units, but it was found that certain items required a year for delivery. It was, therefore, decided to continue the development in order to eliminate the scarce items and reduce the size of the apparatus.

Final Model, Tachometer, Accelerometer, Vibrometer

It was found possible to obtain a pulsating unidirectional voltage having an average value that was linearly related to the speed of gyro rotor from an appropriate vacuum-tube circuit. Most of the pulsation was smoothed out in a resistance–capacitance filter, and the differentiating accomplished in the same way as when the direct current was supplied from a magneto. It was necessary to use substantially more circuit damping than in the earlier equipment, and in consequence the readings lagged behind the adjustment by an appreciable time, roughly two seconds. Other differences worth noticing were that the equipment was noiseless after the moving machinery had been eliminated, was less than half as large since it was also possible to eliminate several frequency-divider circuits, and the error in measuring decelerations was approximately twice as great as in the earlier model, but still of no consequence (at least in this application). Figure 2 shows a front view of this instrument, Figure 3 a view of the chassis.

Figure 4. Schematic circuit diagram of tachometer–accelerometer circuits

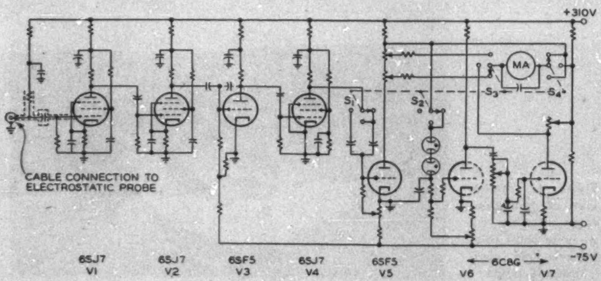

Circuit Details

As there are some elements of novelty in the circuit used, it will be described in some detail. The tachometer–accelerometer part of the circuit is shown in Figure 4, in which S_1, S_2, S_3, and S_4 constitute a four-pole three-position range switch, shown in the 1,000-rpm tachometer position. The central position is for coast test and the third position provides a 15,000-rpm tachometer.

There is a transient of perhaps 15 seconds duration associated with any abrupt change in the grid voltage of *V*6. Since *V*6 is concerned only with the coast test and the coast test is always preceded by use as a 1,000-rpm tachometer it is possible to eliminate this abrupt change, and with it most of the starting transient, by tying together the first and second positions of S_2 as shown.

Tubes *V*1 and *V*2 constitute a voltage amplifier with a gain of about 10,000. This permits satisfactory operation with the probe as much as 0.015 inch from the rotor. Tube *V*3 is a limiter and tube *V*4 is a clipper whose plate voltage is a square wave of bucket frequency, say 400 cycles per second at 1,000 rpm if the rotor has 24 buckets. The principal use of *V*3 is to keep the meter quiet when there is no input on the rotation channel. The capacitor from plate to grid of *V*3 (shown dotted) furthered this purpose. This

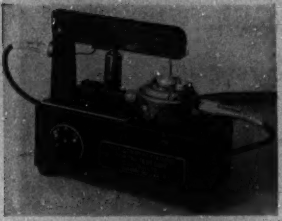

Figure 6. Horizon-gyroscope test fixture with vibration pickup in operating position

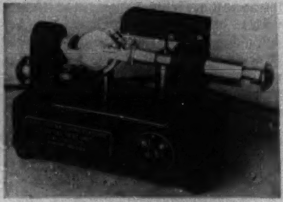

Figure 7. Test fixture for directional gyroscope

capacitor was very small and it has been found expedient to eliminate it by rearranging some of the wires.

Tube $V5$ is biased to cut off and coupled to $V4$ through a capacitance–resistance arrangement so that each stoppage of plate current of $V4$ causes a pulse of plate current in $V5$. This pulse of plate current in $V5$ is of such short duration that the average plate current of $V5$ is directly proportional to the speed of the gyroscope (over a wide range) and is read on a meter calibrated directly in revolutions per minute. Because the average plate current of $V5$ is proportional to the gyro rotor speed, the average voltage at the $V5$ plate will increase as the speed decreases, and speed versus average voltage will be linear. This average is an assumed average over a few cycles.

It is desirable at this point to be able to couple directly to the grid of the next stage and at the same time to reduce the magnitude of the voltage pulsation involved without losing any of the change in the average voltage. A glow-discharge device operating at low currents is essentially a constant-potential-drop device and furnishes a satisfactory coupling.[2] A capacitor in the grid circuit of $V6$ is a satisfactory first-averaging device.

Tube $V6$ is used in measuring deceleration as a voltage amplifier to magnify the change in average voltage and incidentally to reverse the direction of the change. A differentiating circuit is connected to the plate of $V6$ and the output of this differentiating circuit goes through a resistance–capacitance filter to the grid of tube $V7$. The plate current of tube $V7$ is then an inverse measure of the deceleration, so that longer coast times are indicated by higher deflections of the meter.

Advantage is taken of the curvature of the grid-voltage–plate-current characteristic of $V6$ to obtain a constant coast-time reading from the normally slightly decreasing deceleration. Since the plate voltage of $V5$ increases with decreasing rotor speed, the grid of $V6$ will accordingly become more positive. As the grid of $V6$ becomes more positive (within the normal operating region) the amplification factor increases. Therefore the normal gradual decrease in de/dt at the plate of $V5$ is considerably compensated for by a gradual increase in the amplification applied to the small changes in average voltage by $V6$. This results in de/dt at the plate of $V6$ being substantially constant during the useful part of the coast period (1,000 to 500 rpm).

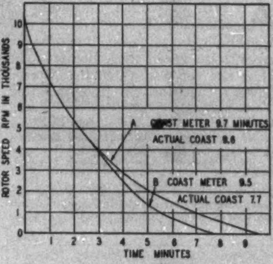

Figure 8. Coast curves of two directional-gyroscope rotors

Curve *A* is typical, and curve *B* exceptional on account of the shape at the lower end

The vibration circuit has not been shown as it consists only of a conventional audio amplifier and loudspeaker, with a $G10$ neon lamp that can be set to glow at any predetermined vibration level. The power supply has not been described because it is also entirely conventional.

Method of Use

In the actual operation of the equipment, for instance with a horizon gyroscope, the rotor assembly is placed in position so that air can be supplied to the inlet provided, and the cord is attached to the electrostatic probe that is already in place. The air valve is turned on with the range switch of the tachometer-accelerometer-vibrometer unit in the low position, and the speed is brought up to 1,000 rpm or slightly higher. Air is cut off and the range switch is turned to the coast position. The meter will swing off scale to the right and then come back to the appropriate coast reading in about five seconds. This reading will usually be too high or too low and it is necessary to loosen the bearing locknut, adjust the bearing, and reset the locknut before reading again. The meter will settle down on a new reading within a couple seconds after the locknut is reset. Figure 5 shows a picture taken after satisfactory adjustment. An experienced operator will usually have the proper bearing adjustment made by the time the rotor has slowed to 800 rpm and will then observe the constancy of the coast time reading for another 20 or 30 seconds. A slow random variation over a range of one minute or less is to be expected. A downward drift of as much as one minute is a definite indication of a defective bearing as will be explained later.

After the bearing tension is properly adjusted, the gyroscope may be safely operated at normal speed for vibration and bearing-noise test. For these tests a crystal pickup with a hardwood needle is dropped into position and lowered by a dash pot (Figure 6). Any vibrations are amplified by a conventional audio amplifier and reproduced by a loudspeaker. A neon lamp in the audio circuit can be set to glow when the vibration level is too high, thus making the test objective. The lamp adjustment is independent of the audio gain for the loudspeaker; the latter is controlled by a volume control on the front of the instrument.

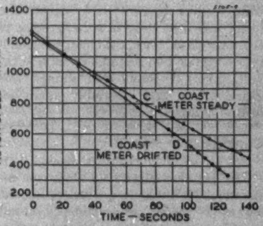

Figure 9. Low-speed coast curves for two gyroscopes

Curve *C* is normal, and curve *D* is abnormal, being convex upward. This is indicated on test by a pronounced downward drift in the coast reading

The use of the equipment in adjusting directional gyroscopes is to a considerable extent the same as that described above for horizon gyroscopes, but the holding fixture is different, as shown in Figure 7. In this case, both rotor bearings are adjustable so the rotor is held horizontally so that both are accessible.

The bearing tension is adjusted as before, and then the gyroscope is checked for possible misalignment of rotor bearings by running the speed up to 2,000 or 3,000 rpm with the pickup in place. Misalignment to the extent usually encountered gives a recognizable rumble or beat in the loudspeaker and can nearly always be corrected by simultaneously adjusting both bearings to the right or left. After this correction it is necessary to readjust the bearing tension to the proper coast-time reading. After misalignment has been corrected, the vibration check at normal speed is made.

PERFORMANCE IRREGULARITIES

In Figure 8 are shown coast curves of two directional gyroscope rotors. Curve *A* is typical of nearly all rotors, and shows the agreement between coast-meter reading and coast time that is usual. Curve *B* shows the performance of a (probably) defective assembly. The coast-meter readings were nearly the same and properly so since they were taken below 1,000 rpm where the curves are nearly parallel. It seems obvious that in such a case, the reading of the coast meter is a better measure of bearing pressure than the actual coast time.

Curve *C* of Figure 9 is in effect an enlargement of the low speed end of curve *A*, and shows normal performance in that the curve is convex downward. This corresponds to a slowly decreasing rate of deceleration. The circuit of the coast meter is so arranged as to compensate for this curvature and give a constant coast-time reading. Curve *D* is abnormal in being convex upward; this causes the meter indicated coast time to decrease as the rotor slows down, the change amounting to one or two minutes or more. Investigations of rotors that showed this characteristic have invariably shown defective bearings.

Conclusion

The practicability of an electronic instrument for measuring accelerations as low as 0.7 radian per second per second with instrument errors limited to a few per cent has been convincingly demonstrated by numerous installations, both in factory production lines and in field repair depots. There is no apparent reason why even smaller accelerations cannot be measured with greater accuracy if the need should arise, and by the present method. The instrument described has been entirely adequate for the present job.

Appendix. Deceleration Measurements by Coast Curves

As a check on apparent irregularities in coast-meter readings it was necessary to provide an independent method of measuring deceleration. This was accomplished by measuring time with a synchronous clock having a one revolution-per-second sweep, and measuring rotor bucket frequency with the Conn chromatic stroboscope.[3,4] The chromatic stroboscope is an instrument for measuring frequencies from 32 to 4,067 cycles per second by a stroboscopic method with a precision of ±0.05 per cent. This frequency range is in effect distributed logarithmically over a scale about 336 inches long. The error in reading a slowly varying frequency in the range of interest here is around 0.1 per cent since a stroboscopic pattern must be held stationary by slowly adjusting a variable-frequency tuning fork. The combined error in time and frequency measurements over a ten-second period is around two per cent but over a period of 100 seconds should be below 0.25 per cent.

Calibration

The factory calibration procedure is quite straight forward. The grid bias of *V5* is set at an appropriate value (about −8 volts) after a five-minute warm-up. Then the lower *V5* plate potentiometer is set so that on the 1,000-rpm range the meter reads 1,000 rpm with 400 cycles per second (five millivolts or more) input. The upper *V5* plate potentiometer is then set so that on the 15,000-rpm range the meter reads 10,000 rpm at 4,000-cycles per second (50 millivolts or more) input. This completes the speed calibration.

The coast calibration is made by adjusting the *V7* plate rheostat until the meter reads at a reference line (about 90 per cent of full scale) with no signal input. Then the *V6* grid bias is set to give −0.5 volt on the grid at 200 cycles per second input and checked for appropriate change at 400 cycles per second. Then the grid potentiometer of *V7* is set so that coast-time readings correspond to actual coast times for a number of gyroscopes.

References

1. THE USE OF COUNTER CIRCUITS IN FREQUENCY DIVIDERS, **E. L. Kent.** *Journal* of the Acoustical Society of America, volume 14, January 1943, pages 175–8.

2. SENSITIVE D-C AMPLIFIERS WITH A-C OPERATION, **Stewart E. Miller.** *Electronics*, November 1941, page 27.

3. THEORY OF THE CHROMATIC STROBOSCOPE, **Robert W. Young, Allen Loomis.** *Journal* of the Acoustical Society of America, volume 10, October 1938, pages 112–18.

4. AN ADJUSTABLE TUNING-FORK FREQUENCY STANDARD, **O. Hugo Schuck.** *Journal* of the Acoustical Society of America, volume 10, October 1938, pages 119–27.

Selenium Power Rectifiers for A-C Aircraft Systems

ALVIN L. EMBRY
ASSOCIATE AIEE

Synopsis: Increasing electric-power requirements for large aircraft have brought about the introduction of a-c power systems. Two major systems have been developed. In the first power is generated at variable frequency and converted to direct current; in the second power is generated at substantially constant frequency, and both a-c and d-c power are used. In both systems selenium rectifiers can be used as converters. Rectifier units developed to supply 28.5-volt regulated d-c power, which include step-down transformers and voltage-regulating equipment, are described in this paper. Ratings vary from 100 to 800 amperes.

AS THE SIZE and complexity of modern aircraft have increased, the demand for electric power to operate accessories has grown tremendously. The larger size also means that the distance between engine-driven generators and their load has increased. When the 28.5-volt d-c power system is used, large heavy conductors are necessary to keep voltage drops within operating limits. To reduce conductor weight to a practical value and provide a more flexible power system, many of the still larger aircraft of the future will use power generated at higher voltage as alternating current.[1] The Army Air Forces have standardized on a three-phase 208-volt 400-cycle system, where constant frequency is used. Variable-frequency systems also are being considered for some applications.

Generation of power at 208 volts reduces the weight of conductors to a fraction of that required for 28.5-volt power.[1] Alternators are lighter and simpler than d-c generators of the same kilowatt output. With a-c generators brush problems are reduced, and, where simple induction motors can be used, motor brush troubles are eliminated.

Even with the constant-frequency system, where the fullest economical use can be made of alternating current directly, there is a definite need for appreciable amounts of d-c power. If batteries are used, they must be charged. Many in-

---

Paper 45-86, recommended by the AIEE committee on air transportation for publication in AIEE TRANSACTIONS. Manuscript submitted November 17, 1944; made available for printing March 7, 1945.

ALVIN L. EMBRY is design engineer, Tungar and metallic rectifier section, lighting engineering division, General Electric Company, West Lynn, Mass.

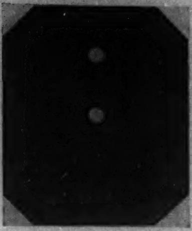

Figure 1. Selenium-rectifier cell for aircraft use

Weight 1.75 ounces. Over-all size: 6 by $7^5/_{16}$ inches

struments now are designed to operate on direct current; with 28.5-volt d-c power available present designs of such instruments may be used, saving the time and man power required to develop new types.

If 28.5-volt control power is used, present low-voltage control switches can be used on crowded instrument panels. Some apparatus, although it can be designed to operate on alternating current, may be lighter or have more satisfactory operating characteristics if operated on direct current, for example, contactor coils.[2] In such cases the weight and efficiency of the apparatus required for both a-c and d-c operation must be determined. Then, before it is decided whether to use alternating or direct current, the cruising range of the airplane, the required duty cycle, and the amount of d-c power required for other applications must be taken into account.

To provide the required d-c power from the a-c system the selenium rectifier offers outstanding advantages. It does not have the high voltage drop of an electronic tube nor the moving parts and brushes of a rotating machine. It is simple, reliable, and easy to maintain. For three-phase power input a selenium rectifier can be designed for 85-per-cent efficiency. The weight of a complete unit including transformer and voltage-regulating equipment compares favorably with that of a motor generator set of the same rating.

Selenium rectifiers can be used with transformers to obtain any desired output voltage. Input may be single phase or polyphase. The widest present application is for 28.5-volt d-c units with three-phase input.

Selenium-Rectifier Cells

A selenium-rectifier cell is made by applying a thin layer of selenium to a base plate which is usually iron or aluminum. After heat treatment a low-melting-point alloy known as the "counterelectrode" is sprayed over the selenium surface. The resultant cell will permit current to flow freely from the selenium to the counterelectrode and block almost entirely the flow from counterelectrode to selenium. Characteristics of selenium-rectifier cells have been discussed thoroughly elsewhere.[3] Although special cells have been developed for aircraft use, they are manufactured in the same way and have the same general characteristics as commercial cells now on the market.

The weight of any apparatus for aircraft use is important. Since the heaviest part of the selenium cell is the base plate, this plate should be as light as possible. The size of the cell affects the over-all weight; a large size will reduce the dead weight of inactive areas and the necessary connecting hardware. Large cells also have lower leakage current per unit area. Size is limited by manufacturing facilities and mechanical considerations. Figure 1 shows a cell developed to meet aircraft requirements. This cell has 36 square inches of active rectifying area, the base plate is aluminum alloy 0.020 inch thick, and the finished cell weighs 1.75 ounces.

Current density in a selenium rectifier normally is limited by temperature rise and permissible aging when cooled by natural convection. With forced-air cooling, however, efficiency and voltage drop impose practical limits. As operating life for aircraft applications generally is 1,000 hours or less, aging is relatively unimportant. Tests have shown that to maintain a constant d-c output voltage of 30 volts, it is necessary to raise the a-c input voltage to the rectifier from an initial value of 26.8 volts to 27.5 volts after 1,200 hours of operation, an increase of 2.6 per cent.

Rated current of the cell shown in Figure 1 is 50 amperes d-c output from a three-phase bridge circuit for each cell in parallel per leg. This current density is considerably higher than that used for commercial rectifiers and is based on an adequate flow of cooling air. The voltage rating of a three-phase bridge rectifier is 15 volts per cell in series. Higher-voltage rated cells have been produced but are difficult to manufacture, aging characteristics are less desirable, and ability to withstand overvoltage is not so good.

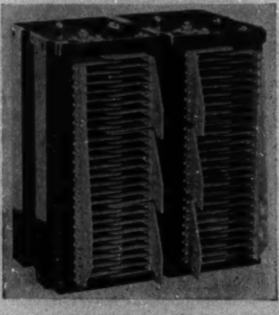

Figure 2. Selenium-rectifier stack assembly, rated 800 amperes 30 volts d-c output. Weight 35 pounds

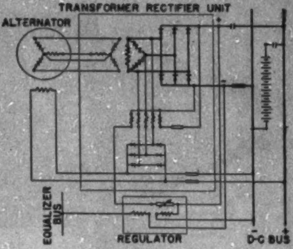

Figure 3. Diagram of variable-frequency power-supply system, showing alternator, transformer, main rectifier, field rectifier, saturable reactor, and voltage regulator

Selenium-Rectifier Stacks

Single rectifier cells act as "check valves" or half-wave rectifiers. For high efficiency a number of cells are connected in one of several possible circuits.[3] The three-phase bridge circuit is used most widely on three-phase power systems. It is simple to build mechanically, and only three connections are made to the a-c supply. If properly designed, a simple arrangement of connecting hardware can be used, and weight can be reduced to a minimum.

Figure 2 shows the three-phase selenium-rectifier stack assembly built for a unit rated 800 amperes 30 volts d-c output. In this assembly 192 cells are used, weighing 21 pounds or 0.87 pound per kilowatt. The complete stack assembly with all connecting and mounting hardware weighs 35 pounds or 1.46 pounds per kilowatt. Cells and connectors are assembled on insulated studs and held under pressure by nuts external to the end brackets. Elements are spaced to obtain maximum cooling effect with minimum air flow.

Cooling

The maximum design temperature of rectifier cells should not exceed 80 degrees centigrade. As Air Corps specifications call for operation in an ambient temperature of 60 degrees centigrade at sea level, sufficient air must be provided, either from the slip stream or a self-contained fan, to limit temperature rise to 20 degrees. Because of this low permissible rise, maximum volume of cooling air is required under sea-level conditions.

As the maximum operating temperatures of reactors, transformers, and fan motors are much higher than that of the

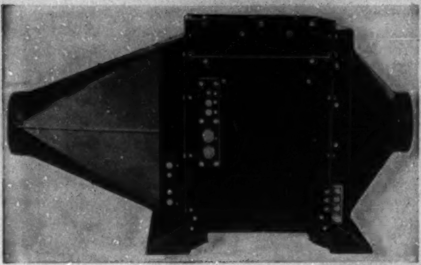

Figure 4. Complete rectifier unit used in variable - frequency system rated 800 amperes 30 volts d-c output

Figure 5 (below). Internal arrangement of rectifier stacks and transformer in rectifier unit of Figure 4

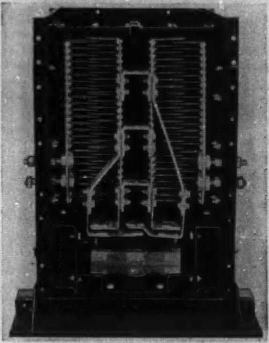

rectifier, the initial permissible rise is greater, and more cooling air generally will be required at high altitudes. Adequate air must be supplied to these auxiliaries to insure safe operation at the highest altitude for which the equipment is intended. With a constant volume of air through a fan-cooled rectifier the load on the fan motor decreases with altitude, so that requirements are less severe than those for a constant-load motor. For a given volume of air forced through the motor, however, a limiting altitude is reached beyond which it will overheat.

Selenium rectifiers have a negative temperature coefficient of resistance, and as the temperature falls the resistance increases.[3] The decrease in resistance of copper wiring and transformer windings partially compensates for this increase.[4] Operating temperature of the rectifier can be raised and resistance lowered under extreme low-temperature conditions by restricting the flow of cooling air. For large rectifiers to be used on high-altitude airplanes sufficient gain in efficiency may be made to justify the inclusion of automatic air-regulating devices.

Units with self-contained cooling fans are more satisfactory for operation within pressurized areas as blast-cooled units would require pressure-tight ducts and casings. There is some danger of damaging blast-cooled units by operating them on the ground with no cooling air available, unless air-flow protection is provided. Fan-cooled units with the fan motor connected directly to the input terminals eliminate this danger, as the motor will be energized at the same time as the rectifier. The major advantages of blast-cooled rectifiers are their lighter weight and the elimination of all moving parts.

Transformers and Reactors

In voltage-regulated power-rectifier equipments for aircraft transformers are used to provide the proper input voltage. Saturable core reactors connected in series with rectifiers and controlled by voltage regulators are used for voltage control. Both transformers and reactors for these applications use special core materials, and high-flux densities are permissible. They may be of the high-temperature type, with operating temperatures of over 200 degrees centigrade.[5] Copper conductors are cadmium-plated to prevent oxidation at high temperatures. Joints are silver-soldered. Glass fiber and glass tapes are used for insulation and impregnated with a special high-temperature resin. Forced-air cooling makes high-current densities possible.

Design of the reactor and transformer must be co-ordinated carefully with that of the rectifier and voltage regulator. Output-voltage variations are caused by changes in load, input voltage, frequency, and temperature. The saturable reactor must have sufficient range in reactance to permit the voltage regulator to hold constant voltage for extreme operating variation of the foregoing factors.

Rectifiers for Variable-Frequency Systems

If alternators are direct-connected to main engines, system frequency varies with engine speed. As the range of speed variation is usually more than two to one, direct application of a-c power is difficult.[6] Parallel operation of alternators is out of the question.

By furnishing a rectifier for each alternator and using direct current, all generating units can be made to feed power to the same bus. As far as distribution is concerned, this is a d-c system similar to those used at present. However, power is generated with alternators whose weight is a fraction of that of d-c generators of the same kilowatt output and is transmitted to the rectifiers, which may be located near the load center, at alternator voltage, reducing low-voltage wiring and bus work to a minimum.

Figure 3 is the diagram of a variable-frequency system in which all of the alternator output is rectified. All rectification, transformation, and voltage-regulating equipment except the voltage regulator proper are included in the casing shown in Figure 4. This includes step-down transformer, main power rectifier, saturable reactor for controlling alternator field current, and a field rectifier. Rated d-c output is 800 amperes 30 volts; input is three phase, 350 to 1,000 cycles, with maximum alternating voltage 250 volts. Combined efficiency of the transformer and main rectifier is 81 per cent at full load. Weight of the complete rectifier unit is 135 pounds, and the 32-kva alternator developed for this system weighs 50 pounds, a total weight for the system of 185 pounds or 7.7 pounds per kilowatt. This compares with a weight for engine-mounted d-c generators of 5.2 pounds per kilowatt. Obviously the alternator-rectifier system cannot be justified on the basis of weight of equipment alone. However, it should be noted that the alternator can be mounted directly on the engine, whereas a d-c machine of the same rating would be separately mounted, requiring additional weight for support. In addition, the saving in weight of conductors from generator to load center will be appreciable. With further development it is probable that the weight of the rectifier unit can be reduced considerably.

The voltage-regulating system is similar to that of a self-excited d-c machine in that field power is taken from the alternator output. As alternator field current is of the order of 50 amperes, it cannot be handled directly by a standard aircraft-type voltage regulator, and some type of

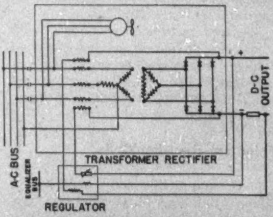

Figure 6. Diagram of rectifier unit used in constant-frequency system, showing saturable reactor, transformer, fan, rectifier, and voltage regulator

d-c current amplifier must be used. In this case the amplifier consists of a three-phase saturable core reactor in series with a three-phase bridge-connected selenium rectifier. Alternating current is supplied to the reactor input from the low-voltage side of the main transformer. The impedance of the saturable reactor varies with the current in its saturating coil which is controlled by a standard-type regulator. The output current of the saturable reactor is rectified and supplied to the alternator field. With this arrangement the voltage regulator controls currents up to ten times the current it can control directly. To make operation more stable a d-c damping winding is connected across the main rectifier output. An equalizing winding is provided on the regulator so that rectifiers may be paralleled, using the same scheme as that used with d-c generators.[7]

Under low-temperature conditions with the engine running at minimum speed, residual voltage may not be sufficient to cause the alternator to build up. This is due largely to the increased rectifier resistance at low temperatures, added to the field resistance and the impedance of the saturable reactor. To provide for positive build-up the field is connected across the main bus through current-limiting resistors. With the bus energized by a battery or other d-c source, sufficient field current will flow to initiate the build-up cycle. When the voltage of the field-supply rectifier reaches normal, current flow through these resistors is reduced to a negligible value.

The arrangement of transformers and main rectifier inside the casing is shown in Figure 5. To keep the center of gravity low, the transformer is mounted near the base. Cooling air flows in parallel paths through the transformer and rectifier. Automatic shutters regulate the flow of air through the rectifier stack; they are adjusted to begin to open when the temperature of the exit air from the rectifier reaches 50 degrees centigrade. At low temperatures, the gain in rectifier efficiency is considerable; by raising the operating temperature from 0 to 50 degrees centigrade, the efficiency is increased by six per cent. Air flow through the transformer is unrestricted. Cooling air is supplied from the slip stream and a pressure of six inches of water must be maintained at the air inlet.

Rectifiers for Constant-Frequency Systems

By maintaining a reasonably constant system frequency most of the generated power can be utilized as alternating current. If alternators are driven from the main engines a constant-speed coupling must be provided which will maintain proper alternator speed regardless of engine speed. Alternators may be paralleled.[8]

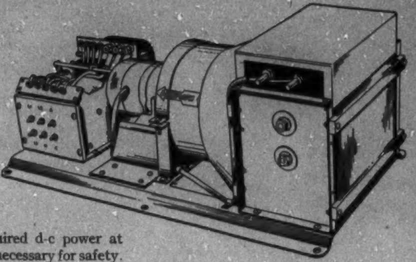

Figure 7. Aircraft rectifier unit for constant-frequency system, rated 200 amperes 30 volts d-c output

Note open construction; only rectifier and fan blade are enclosed

To furnish the required d-c power at least two rectifiers are necessary for safety. The number and ratings of rectifiers should be chosen so that all vital equipment taking power from the d-c bus can be operated with the largest unit out of service.

Figure 6 is the diagram of a unit designed for operation with the constant-frequency system. A saturable core reactor, transformer, rectifier, voltage regulator, and fan are included. For blast-cooled units the fan is omitted. Output voltage is controlled by a standard aircraft-type voltage regulator and a saturable reactor. In general, the regulating system is the same as that of the 800-ampere unit, but in this case the entire rectifier output is controlled instead of alternator field current. An equalizer winding is provided on the regulator to permit parallel operation of rectifiers. The voltage regulator is separately mounted and can be located at any convenient point.

In Figure 7 is shown a transformer rectifier unit rated 200 amperes 30 volts d-c output designed to take three-phase power from a 208-volt 400-cycle system. Cooling air is supplied by a magnesium-alloy fan mounted on the shaft of a 7,600-rpm induction motor. This unit will operate under all conditions encountered from a 60-degree-centigrade ambient temperature at sea level to an altitude of 40,000 feet. To save weight no enclosing case is used. The fan is located inside the air duct extending from the rectifier stack and discharges air over its driving motor to the transformer and reactor. Weight complete is 47 pounds.

Figure 8. Aircraft rectifier unit for constant-frequency system rated 100 amperes 30 volts d-c output

Cooling air supplied from external source

Another unit developed for the constant-frequency system is shown in Figure 8. It is rated 100 amperes 30 volts d-c output, is blast-cooled, and requires an air pressure of three inches of water at the inlet. All parts except the voltage regulator are mounted inside the casing; the compact arrangement of parts is shown in Figure 9. Over-all dimensions are $6^{1}/_{8}$ by $6^{5}/_{8}$ by 26 inches, and weight is 28 pounds.

Operation

Operating characteristics of these saturable-reactor-controlled rectifier units are similar to those of a d-c generator. They have a drooping volt–ampere characteristic due to the regulation inherent in the reactors, transformers, and rectifiers. As load increases, the voltage regulator keeps output voltage constant by increasing saturating current in the reactor. After the saturating current has reached its maximum value, further increase in load will reduce output voltage. This, in turn, reduces saturating current, lowering still further the output voltage. The result is that a critical point is reached beyond which operation becomes unstable and the voltage breaks down. In the case of the variable-frequency system, short-circuit currents are low, as the a-c supply voltage also breaks down. Constant-frequency units, on the other hand, have short-circuit currents of the order of 150-per-cent load current if a-c input voltage is maintained. Current in this latter case is

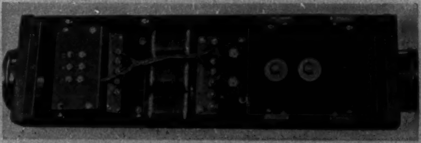

Figure 9. Aircraft rectifier unit, same as Figure 8

Cover removed, showing compact arrangement of parts

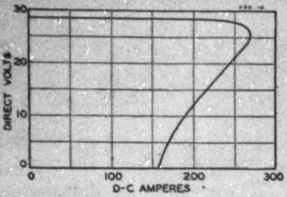

Figure 10. Volt-ampere characteristic curve of aircraft rectifier unit shown in Figure 8

limited primarily by the maximum reactance of the saturable reactor.

Figure 10 shows the volt-ampere characteristic of the 100-ampere unit of Figure 8, with the voltage regulator set to hold 28.5 volts. Input voltage and frequency are held at normal values. Short-circuit current under these conditions is 160 per cent and maximum current 270 per cent of rated value. The effect of a short circuit applied with the same rectifier carrying rated load current and the regulator set to hold 30 volts is shown in the oscillogram of Figure 11. Instantaneous peak current was 411 per cent which decayed to a steady-state value of 165 per cent in $^{1}/_{60}$ of a second. Instantaneous peaks as high as 600 per cent have been noted under no-load initial conditions. The values of peak and steady-state currents depend on alternating voltage, frequency, load, and regulator setting.

Maximum load and short-circuit currents are increased if a separate source of reactor-saturating current is provided. The volt-ampere characteristic then resembles that of a separately excited d-c generator. For the constant-frequency system this source of current may be a small "exciter" rectifier.

A "compounding" series winding may be added to the saturable reactor through which all or part of the output current flows. By proper design any degree of compounding may be obtained. Compounding reduces the required resistance range of the voltage regulator but adds to the weight of the reactor and complicates the wiring.

Division of load between units, even those of different ratings, is satisfactory. Figure 12 shows the load division between the 100-ampere and 200-ampere units of Figures 7 and 8 under conditions of normal voltage and frequency. The division will vary somewhat, depending on regulator settings and input voltage and frequency.

All of the units described can be overloaded for a short time. With maximum ambient temperature for which the apparatus is designed they are rated at 150-per cent normal current for three minutes. At lower ambient temperatures this overload rating can be increased. All overloads should be applied with caution as the thermal capacity of the rectifier is low. These units never should be operated at higher than rated voltage, or the cells may be damaged permanently.

All data so far obtained on these rectifiers are the results of extensive ground tests, including tests in altitude chambers. No flight-test data are as yet available, but it is expected that thorough flight tests will be made in the near future.

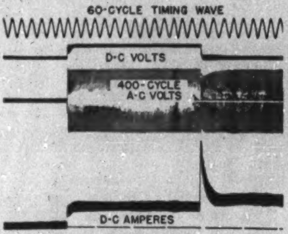

Figure 11. Oscillogram of short circuit applied to rectifier unit shown in Figure 8

Regulator set to hold 30 volts. Rectifier was carrying rated load when short circuit was applied

Applications of Unregulated Rectifiers

For some applications where the d-c load is substantially constant it may be practical to use selenium rectifiers without voltage regulation. Such rectifiers may be designed to operate directly from the a-c line or with suitable transformer to provide any desired direct voltage. Variations in direct voltage will be only slightly greater than those of the system alternating voltage.

In all the regulated units described the transformer weighs more than the rectifier stack, so that the use of rectifiers operated directly from the a-c lines offers attractive weight-saving possibilities. This scheme has one serious drawback; only three direct voltages are available, 220, 170, and 100 volts. These are obtained by the use of a three-phase bridge-connected rectifier, a single-phase bridge connected line to line, and a single-phase bridge connected line to neutral, respectively. Some saving in transformer weight can be made by the use of autotransformers. In either case the d-c circuit is electrically connected to the a-c lines, and neither d-c terminal can be grounded if the a-c system is grounded at any point.

In any case where the rectifier supplies a fixed load no d-c switch is necessary. The rectifier may be connected permanently to its load and all switches, contactors, and protective devices located in the a-c line.

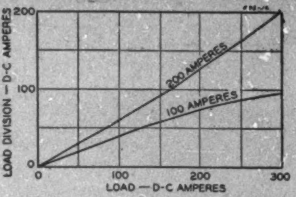

Figure 12. Distribution of load between rectifier units shown in Figures 7 and 8

Rectifiers paralleled through 0.5-volt dropping resistors. Regulators set for 30 volts

Conclusion

It must be kept in mind that the selection of an electric-power system is an individual problem for each airplane. The size of the airplane, its ceiling, its maximum cruising range, and its purpose all must be considered. Power requirements for a cargo airplane, a passenger airplane, and a bomber will differ widely even when all are the same size and general design. Larger airplanes of all classes are being considered for the future, and many of them will have auxiliary power generated as alternating current. In most cases considerable amounts of d-c power still will be required, and in supplying this power the selenium rectifier will find a wide field of application.

References

1. Why Tomorrow's Planes Will Have A-C Electrical Systems, T. B. Holliday. *Electrical Manufacturing*, July 1943, page 88.

2. A-C Contactors for Aircraft, F. J. Russell, A. P. Charbonneau. AIEE Transactions, volume 63, 1944, September section, pages 613-16.

3. Characteristics and Applications of Selenium-Rectifier Cells, E. A. Harty. AIEE Transactions, volume 62, 1943, October section, pages 624-9.

4. Aircraft Electric-Power-Supply System, J. E. Yarmack. AIEE Transactions, volume 62, 1943, October section, pages 655-8.

5. Aircraft Transformers—Small and Light, O. Kiltie. AIEE Transactions, volume 62, 1943, pages 899-902; also published in Electrical Engineering, volume 63, March 1944, pages 84-8.

6. Basic Considerations in Selection of Electric Systems for Large Aircraft, W. K. Boice, L. G. Levoy, Jr. AIEE Transactions, volume 63, 1944, June section, pages 279-87.

7. Present D-C Aircraft Electric-Supply Systems, H. C. Anderson, S. B. Crary, N. R. Schultz. AIEE Transactions, volume 63, 1944, June section, pages 265-72.

8. Parallel Operation of Airplane Alternators, D. W. Exner. AIEE Transactions, volume 62, 1943, December section, pages 755-66.

Static Voltage Regulator for Rototrol Exciter

E. L. HARDER
MEMBER AIEE

C. E. VALENTINE
MEMBER AIEE

THE CONCEPT of a generator voltage regulator as an amplifier which produces a large correction in field current for a small departure from normal voltage is quite well known.[1] In the conventional regulator, such as a direct-acting type, this amplification is secured partly in the regulator and partly in the exciter. A rotating amplifier-type regulator provides the amplification almost entirely in the rotating machines. Exciters may be used to obtain two or more stages of amplification, or a single machine having high amplification such as a Rototrol exciter may be used. An example of two-stage excitation is a system with the regulator working in a pilot exciter field.

With high amplification available in the excitation system, voltage regulation can be secured by arranging the control field of the exciter or Rototrol[2] to raise or lower in response to any deviation of generated voltage from the standard of reference.

The particular Rototrol referred to in this paper is a d-c generator operated on the linear part of its saturation characteristic and completely self-excited by shunt and series fields. As such, it will support itself at any voltage from zero up to the point of saturation. It has one or more control fields which run it up or down in voltage as required and keep it operating stably at any desired point.

The present development was undertaken on the basis that a battery could not be used for the standard of reference and that the voltage reference must be inherent in the circuit. Also vacuum tubes could not be used; there must be no moving parts except for the rotating machines, and these should have air gaps approximately as large as in conventional d-c generators.

The choice of voltage reference was narrowed down to "intersecting impedance characteristics." This is the general name given to circuits that detect and respond to voltage level in the following manner. At normal voltage two impedances are adjusted to draw equal or proportional currents; at least one impedance is nonlinear. At higher voltage one impedance draws more current than the other, and the difference current is in a direction indicating voltage above normal. It can be used for control. At lower voltage the same impedance draws less current than the other and the difference thus is reversed, indicating voltage below normal. The currents are rectified before comparison.

Static Voltage-Regulating Circuits

A static type of circuit for the purpose of regulating the voltage of an a-c generator has been used previously,[3] a three-core saturable reactor being employed for amplification as part of the static circuit. Similar circuits using Rototrols for the amplification are illustrated in Figure 1.

The voltage-measuring circuit of Figure 1A consists of a resistor path I_R and a saturating-reactor path I_X, with the current in each path rectified and fed into the control fields of the Rototrol. This illustrates a circuit using a Rototrol pilot exciter, an exciter of conventional design, and an a-c generator. The Rototrol control fields are connected to be equal and opposite magnetically, when the a-c generator voltage is normal at the regulated value. Under this condition the Rototrol output voltage is maintained at the required value by its self-energizing shunt and series fields. If the alternating voltage rises or falls, the control fields adjust the Rototrol as needed to restore normal voltage.

Figure 1B shows the intersecting impedance characteristics, *R* for the resistor circuit, and *X* for the reactor circuit. In regulating circuits of this kind means are provided for raising or lowering the point of intersection or "normal" voltage, to allow adjustment of the value which the regulator is set to maintain. Figure 1C shows the same static regulator except used with a Rototrol exciter, thus eliminating the pilot machine. The Rototrol exciter is designed to have relatively high amplification, so that the required output to the field of the a-c generator may be controlled by a small amount of energy in the control field.

Other static circuits are shown in Figure 2. The generator terminal voltage is balanced against a reference voltage, and the differential which appears when the generator voltage deviates from normal is applied to the Rototrol field or fields. For the reference voltage a separate source either direct or alternating current may be used, or, if none is available, a constant potential device may be employed, energized by the voltage of the generator with which the regulator is used. This device is designed to provide essentially constant alternating voltage on its output terminals in spite of relatively large changes in its input voltage.

Figure 2A shows a static regulator controlling a Rototrol exciter which has two control fields. These are connected to have equal and opposite magnetic effect when the a-c generator voltage is at the desired normal value. Should load be added to the generator, thus causing drop in the terminal voltage, the "raise" field predominates and raises the Rototrol armature voltage thus restoring the alternating voltage to normal. The Rototrol control fields again reach a balance.

Figure 2B shows a balanced-voltage circuit arranged to feed a single control field. In this case the control field normally has no current flowing through

Table I. Sample Calculation of E_f/E_R versus E_x/E_R

Refer to Figure 6

These Calculations Are for the Case, $R' = 0.2R$ and $R_f = 0.3R$

$E = 1.00$, $E_{eq} = \frac{R_f}{R+R_f} = 0.2308$

$R_{eq} = \frac{RR_f}{R+R_f} = 0.2308R$, $\frac{R_{eq}}{R'+R_{eq}} = 0.534$

1 θ	2 $E_x = \sin\theta$	3 $E_d = \cos\theta$	4 $E_R = E_d + E_{eq} = E_d + 0.2308$	5 E_x/E_R	6 $E_f = \frac{R_{eq}E_R - E_{eq}}{R' + R_{eq}} = 0.534E_R - E_{eq}$	7 E_f/E_R
0	0	1.0000	1.2308	0	0.428	0.347
10	0.1736	0.9848	1.2156	0.143	0.419	0.347
20	0.3420	0.9397	1.1705	0.292	0.395	0.337
30	0.5000	0.8660	1.0968	0.456	0.355	0.324
40	0.6428	0.7660	0.9968	0.645	0.302	0.303
50	0.7660	0.6428	0.8736	0.878	0.235	0.269
60	0.8660	0.5000	0.7308	1.186	0.160	0.219
70	0.9397	0.3420	0.5728	1.640	0.0752	0.131
80	0.9848	0.1736	0.4044	2.432	−0.0148	−0.0366
90	1.0000	0	0.2308	4.333	−0.1076	−0.466

Paper 45-111, recommended by the AIEE committee on electric machinery for publication in AIEE TRANSACTIONS. Manuscript submitted November 15, 1945; made available for printing May 12, 1945.

E. L. HARDER is central-station engineer, industry engineering department, and C. E. VALENTINE is section engineer, switchgear and control engineering division, both with Westinghouse Electric Corporation, East Pittsburgh, Pa.

The authors acknowledge the assistance of H. M. Rustebakke in carrying out the development work in the laboratory and of H. S. Kirschbaum in making the calculations for several of the curves in the paper.

it. By reason of this, it is evident that there are no losses and no heating in this field so long as the a-c generator voltage remains at the normal regulated value. This permits using a minimum of material in the frame of the Rototrol, as winding space and winding losses are less than in the case where continuously energized equal and opposite control fields are employed.

Requirements of New Regulating Circuit

In the development described in this paper, generators having ratings exceeding 1,000 kva at 1,200 rpm were to be controlled, and conventional exciter air gaps were desirable for mechanical reasons. This fixed the control-field energy requirements. Previous designs of static regulators such as described hereinbefore would have been excessive in size and losses, had they been designed to provide adequate control power. It became necessary to make a thorough analysis of the design of such devices to secure optimum energy output for a given voltage departure from normal.

Average three-phase (or positive-sequence) voltage response was required. This further increased the energy requirements, as the positive-sequence network size must be adequate to carry the larger power of the measuring circuit. This problem was solved by deducting negative-sequence voltage from line voltage rather than filtering positive-sequence voltage directly in the conventional manner.

Considerable error in regulated voltage due to frequency was tolerated on earlier static regulators. In the new development it was desired to regulate closely for the same voltage level over a plus- or minus-five-per-cent departure from normal frequency.

To meet these requirements a static regulator of high efficiency was devised. Figure 3 shows a regulator of this type. The following paragraphs describe this regulating network and give its theory and performance.

Circulating-Current-Type Static Network—Theory

One arrangement of the circulating-current type of static-regulating network is shown in Figure 4A. A saturating reactor and resistor are used for the nonlinear and linear branches, respectively. The voltage gradient may be viewed as shown in Figure 5. At normal voltage the voltage drops in the resistor, *KR*, and reactor, *X*, are equal and the control-field voltage is zero, as in Figure 5B. As the input voltage is raised or lowered, the saturating-reactor voltage remains nearly constant and the control-field voltage becomes positive or negative, respectively. This is shown in Figures 5A and 5C.

Performance Calculation

Calculations were made to determine the most efficient design of this type of network. First it was necessary to develop a method of calculating the power output from the network as a function of the parameters *X*, *R*, *R'*, and R_f of the network and connected control field of Figure 6. Also, a method was developed for the calculation of the direct voltage on the rectifiers to determine whether *R'* and $(1-k)$ *R* were large enough to keep both rectifier voltages positive over the necessary range of operation (usually for a plus- or minus-ten-per-cent departure from normal line voltage).

Calculations then were made using these methods to determine the relative values of the parameters *X*, *R*, *R'*, and R_f which would produce optimum control-field input power as a function of line-voltage departure from normal, with minimum energy consumed in the network itself.

This method of calculation assumes pure sine-wave currents and voltages in the a-c circuits and smooth direct current in the d-c circuits. It is recognized that the actual wave shapes are considerably distorted and that an empirical factor determined from test must be used to allow for this difference. This factor was found to be of the order of 0.5 in field current. The analytical method used with this empirical factor serves as a very satisfactory basis of direct design. The method also affords valuable insight into the operation of the network and a close approach to optimum efficiency which then can be further refined by experimental work.

Method of Calculation

The problem may be stated as follows:

Given the saturation curve of the reactor *X*, such as Figure 7, and the values of *R*, *R'*, and R_f.

Required to determine field voltage, E_f, as a function of the applied line voltage.

The network of Figure 6A contains a-c and d-c circuits and a nonlinear element, and hence, cannot be solved by conventional methods of analysis.

The saturating reactor can best be treated by assuming a value of current, reading the corresponding voltage from the saturation curve, and then calculating the currents and voltages throughout the balance of the network.

As the alternating voltages being dealt with are about to be rectified in single-phase full-wave rectifiers, it is convenient to use their average rather than their rms magnitudes. Then no factor need be applied when passing from alternating to direct current through the rectifier.

Figure 6C shows a vector diagram

Table II. Sample Calculation of Field Power From Static Regulating Network

Refer to Figure 6A

The Subscript *n* Denotes the Value of a Quantity at the Normal Regulated Voltage Condition. Calculation Based on: $R'=0.2R$ and $R_f=0.3R$

Let $E_{xn}=1.000$ $I_{xn}=1.000$ $X_n=1.000$

$$E_n=E_{xn}/\cos\sin^{-1}\frac{R'}{R}=E_{xn}/0.98=1.02$$

$R=E_n/I_{xn}=1.02,\ R'=0.204,\ R_f=0.306$

$$P_n=E_nI_{xn}=\frac{R'+R}{R}=1.02\times1.00\times1.20=1.224$$

$$R_{eq}=\frac{R_f}{1+R_f/R}=\frac{0.306}{1.300}=0.2354$$

$R'+R_{eq}=0.4394$

$$E=\frac{R}{R'+R_{eq}}E_R-\frac{R}{R_{eq}}E_f=2.320E_R-4.33E_f$$

1 E_x	2 I_x (Figure 7)	3 $E_R=I_x(R'+R_{eq})=0.4393I_x$	4 E_x/E_R	5 E_f/E_R (Figure 8)	6 $E_f=(3)\times(5)$	7 $E=2.320E_R-4.33E_f$	8 E/E_n P.U. Line Voltage	9 $P_f=E_f^2/R_f=E_f^2/0.306$	10 $\frac{100P_f}{P_n}$ Per Cent Field Power	11 $\frac{100}{(10)}\left[\frac{1-(8)}{0.1}\right]^2$	12 $\frac{E_f}{E_n}$
0.890	0.467	0.2054	4.33	−0.466	−0.0958	0.890	0.872	0.0299	2.440		0.0937
0.915	0.555	0.2440	3.75	−0.334	−0.0815	0.920	0.902	0.0217	1.770	54.3	0.0800
0.950	0.707	0.3110	3.06	−0.178	−0.0554	0.961	0.942	0.0100	0.820		0.0538
1.000	1.000	0.4394	2.28	0	0	1.020	1.000	0	0		0
1.025	1.189	0.5225	1.960	+0.064	0.0334	1.069	1.048	0.00365	0.298		0.0328
1.050	1.414	0.621	1.690	+0.119	0.0739	1.121	1.100	0.01785	1.458		0.0725
1.075	1.682	0.739	1.455	+0.160	0.1180	1.188	1.163	0.0455	3.72		0.1160

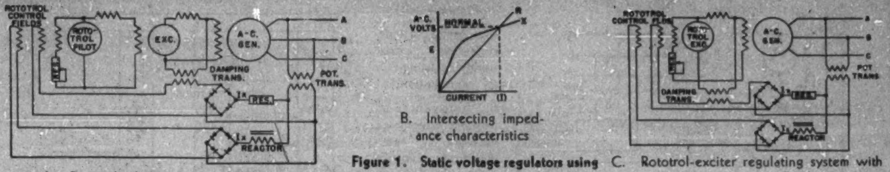

A. Rototrol-pilot-exciter regulating system

B. Intersecting impedance characteristics

Figure 1. Static voltage regulators using intersecting impedance characteristics

C. Rototrol-exciter regulating system with opposed control fields

which is a convenient representation of the complete circuit. To understand it, note first that Figure 6A can be simplified to Figure 6B using Thevenin's theorem.[4] The values of $\boldsymbol{E}_{eq}$ and R_{eq}, in terms of $\boldsymbol{E}$, R, and R_f are shown by the equations in Figure 6. Note that in the d-c circuit of Figure 6B, the voltage drop across R' and R_{eq} in series is the numerical sum of $\boldsymbol{E}_d$ and $\boldsymbol{E}_{eq}$. Also note that $\boldsymbol{E}_d$ is obtained from $\boldsymbol{E}$ by subtracting the I_xX drop vectorially from $\boldsymbol{E}$. The current I_x must be in phase with $\boldsymbol{E}_d$ as the circuit below $\boldsymbol{E}_d$ in Figure 6B appears as pure resistance or in phase. Hence, the drop I_xX must be at right angles to $\boldsymbol{E}_d$, and this fixes the form of the vector diagram Figure 6C. Note that the relationships in the d-c part of the circuit all are treated as though in phase.

If we start with the current I_x, the voltage $\boldsymbol{E}_x$ is readily determined from the saturation curve, Figure 7. $\boldsymbol{E}_R$ is obtained by multiplying I_x by $(R' + R_{eq})$. $\boldsymbol{E}$ is known and $\boldsymbol{E}_{eq}$ determined from the equation in Figure 6. It remains to find the field voltage, $\boldsymbol{E}_f$. This can be done most easily by letting θ vary and calculating $\boldsymbol{E}_x/\boldsymbol{E}_R$ and $\boldsymbol{E}_f/\boldsymbol{E}_R$ for various values of θ, and plotting $\boldsymbol{E}_f/\boldsymbol{E}_R$ as a function of $\boldsymbol{E}_x/\boldsymbol{E}_R$ as shown in Figure 8. From these curves the value $\boldsymbol{E}_f/\boldsymbol{E}_R$ and then $\boldsymbol{E}_f$ readily can be determined. A derivation and sample calculation of these curves for $R' = 0.2R$ and $R_f = 0.3R$ is given in Appendix I. Figure 8 gives curves for $R' = 0.2R$ for various values of R_f.

A derivation and sample calculation also is given in Appendix II for field input voltage and power as a function of the departure of line voltage from normal. Figure 9A shows field power and voltage as a function of line-voltage deviation from normal, for the range of operation in which the rectifier voltages are above zero. Figure 9B shows the field power over an extended range of line voltage drop. Another curve, Figure 10, has been drawn for various values of R_f and R', giving watts input to the network per watt input to the field, for a ten-per-cent a-c line voltage drop. This curve is based on several calculations similar to Table II of Appendix II. It indicates that the best performance is obtained with $R' = 0.2R$ and $R_f = 0.3R$. However, the field resistance, R_f, may be varied 40 per cent from this value without reducing the control-field input, at ten-per-cent voltage drop, more than 20 per cent.

A capacitor or a linear inductance may be substituted for the resistor to form the linear branch. The capacitor has the advantage of minimum power loss and correction of power factor, which reduces the required size of potential transformers and compensators.

The foregoing analysis applies equally well whether the impedance kR consists of a resistor, capacitor, or linear reactor having the same ohmic value. With the assumption of smooth direct current, phase relationships are not reflected through the d-c circuit. If the branch, kR, is a capacitor or a reactor, the curves of Figure 10 should be interpreted as giving the summation of volt-amperes (arithmetic sum) in branches, R', $(1-k)R$, and kR, per watt in the control field.

It may be more significant in this case to give the *total* network volt-amperes (arithmetic sum of volt-amperes in each part) per watt in the control field. This can be done by substituting the total volt-amperes for P_n in Table II. The summation of network volt-amperes is given by

$$P_n' = \boldsymbol{E}_n I_{xn} \frac{R'+R}{R} + 1$$

For the example worked out in Table II, P_n' would be 2.224 and the network volt-ampere scale would be 2.224/1.224 times the network watt scale of Figure 10.

The summation volt-amperes as used in the foregoing are of significance chiefly in providing a measure of size of the network. The volt-amperes drawn from the source also are important in determining the design of the potential transformer, sequence network, compensator, and so forth, through which this burden is drawn. The input volt-amperes may be obtained by vector addition of the volt-amperes of parts. Use of a capacitor for the linear branch then largely offsets the saturating-

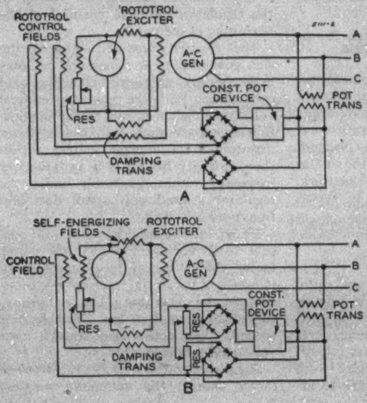

Figure 2 (left). Static voltage regulators using fixed reference potential

A. Opposed control fields

B. Balanced-voltage network and single control field

Figure 3 (right). Static-Voltage-Regulator units

A—Potential and compensator unit

B—Voltage-regulator unit

C—Voltage-adjusting rheostat

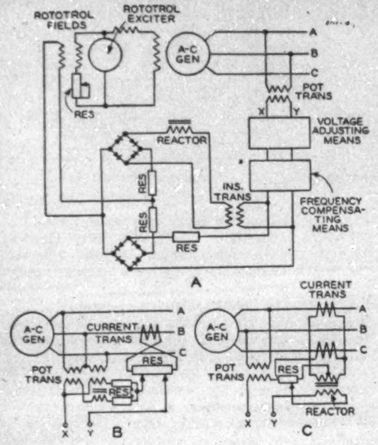

Figure 4 (left)

A. Static voltage-regulating system using circulating-current network

B. Conventional positive-sequence network and reactive-droop compensator

C. Current-energized sequence network including reactive-droop compensation

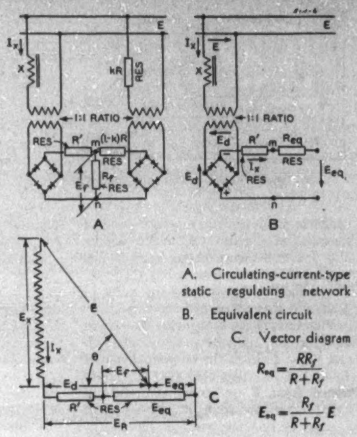

A. Circulating-current-type static regulating network

B. Equivalent circuit

C. Vector diagram

$$R_{eq} = \frac{RR_f}{R+R_f}$$

$$E_{eq} = \frac{R_f}{R+R_f}E$$

Figure 6 (right)

reactor volt-amperes at the normal regulated voltage and minimizes the input volt-amperes to the measuring circuit.

Positive-Sequence Response

The static-regulator volt-ampere parts are determined by the power requirements of the control field as outlined in the foregoing section. In the present development this burden proved to be much larger than the normal burden of a conventional regulator element. In order to provide positive-sequence response the regulator current in the past has been drawn through a positive-sequence network or filter.[5] However, this device increases in size directly with the burden supplied through it; consequently, some other plan for obtaining positive-sequence response was needed.

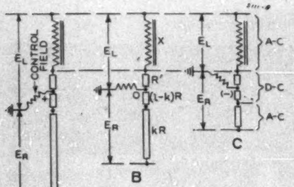

Figure 5. Approximate voltage gradient in circulating-current-type static regulating network

A—Overvoltage—control-field voltage positive

B—Normal voltage—control-field voltage zero

C—Undervoltage—control-field voltage negative

The positive-sequence voltage can be derived by subtracting the negative-sequence voltage from line voltage. This is accomplished by passing the secondary currents of the current transformers through a network proportional to the negative-sequence impedance of the generator. The derived negative-sequence voltage then is deducted from the line voltage. The previously used voltage filter and the new current filter are indicated in Figures 4B and C, respectively. The remainder of the regulating circuit is the same in either case and is as shown in part A. The current-energized sequence filter required about $^1/_{50}$ of the volt-amperes of parts as compared with the voltage-type sequence network of Figure 4B. Tests showed it to be accurate and reliable. One potential and two current transformers are used in place of two potential transformers and one current transformer.

Reactive-Droop Compensation

With the single potential transformer and current-energized sequence network shown in Figure 4C, the reactive-droop compensator for parallel operation becomes a resistor in the phase-*C* current and thus can be combined with the similar resistance of the sequence network. Thus, the resistor in Figure 4C serves this double purpose.

Frequency Compensation

As the frequency is varied the static measuring circuit can be kept in balance only by varying the voltage applied thereto in a predetermined fashion. As it is desired to regulate for the same generator voltage with some departure from normal frequency, it is necessary to introduce between the potential transformer and the measuring circuit an impedance which will produce the necessary voltage variation with frequency on the measuring circuit. Network synthesis studies developed the proper combination of inductances and capacitances for this purpose. As the inductance required was a series device, it was obtained simply by proportioning the sequence network to have this value of inductance as viewed from the output terminals.

Conclusions and Test Results

A static regulator was designed and built using the methods outlined in the paper. This regulator, whose circuit is shown in Figures 4A and C was designed for use with a Rototrol exciter and 1,500-kva generator. Tests have demonstrated it to be a highly satisfactory solution to the regulating problem outlined at the beginning of the paper.

The sensitivity was well within the design goal of plus or minus one per cent under steady or slowly changing load conditions. With the generator terminal voltages unbalanced due to the application of a single-phase load, the regulator maintained the average voltage within the sensitivity limits. For variations of frequency within reasonable limits, the regulator showed only small deviation from normal voltage.

Under sudden application of a 50 per cent rated current load, at low power factor, the voltage dip[8] was only slightly in excess of the initial transient-reactance drop in the generator. The voltage returned to normal in less than one-half second. The action was smooth with very good damping.

Parallel-operation tests at rated power factor showed the automatic wattless load division to be within six per cent of rated generator current up to full rating. This excellent paralleling was obtained with reactive-droop compensation of 5.5 per cent at full-load zero power factor, which is 3.3 per cent at full-load 0.8 power factor.

Appendix I. Curve of E_f/E_R Versus E_x/E_R

With reference to Figure 6C, a curve of E_f/E_R versus E_x/E_R can be calculated, using θ as a parameter. E can be taken as 1, since ratios of voltages are to be determined and the actual values are immaterial. The steps in the computation are as follows:

1. Values of θ are taken from 0 to 90 degrees as the parameter.
2. Then E_x is equal to $E \sin\theta = \sin\theta$, and
3. E_d is equal to $E \cos\theta = \cos\theta$
4. The resistor branch is represented by an equivalent voltage, E_{eq}, and an equivalent internal resistance, R_{eq}, where

$$E_{eq} = \frac{R_f}{R+R_f}\,E = \frac{R_f}{R+R_f}$$

and

$$R_{eq} = \frac{RR_f}{R+R_f}$$

The total voltage across R_{eq} and R' is

$$E_R = E_d + E_{eq}$$

5. The ratio of E_x/E_R is then computed.
6. The field voltage, E_f, is a potentiometer fraction of E_R, minus E_{eq}. That is:

$$E_f = \frac{R_{eq}}{R'+R_{eq}}\,E_R - E_{eq}$$

7. The ratio E_f/E_R is then computed and plotted as a function of E_x/E_R.

Note that $\theta = 90$ degrees is the limit of performance, according to this theory, because, as shown in Figure 6C, the rectifier voltage, E_d, becomes zero at $\theta = 90$ degrees.

A sample calculation follows; the results are plotted in Figure 8 for the ratio $R_f/R = 0.3$.

Appendix II. Circulating-Current-Type Static-Network Field Input Power and Rectifier Voltages

With reference to Figure 6, and saturation curve, Figure 7, the steps in a power computation are as follows:

The field power P_f and voltage E_f are to be computed for a given departure of line voltage from normal, and a given set of proportions R', R_f, and R. This calculation cannot be made directly. It is necessary to start with a given reactor voltage E_x, and calculate the field power and line voltage corresponding. After repeating for several values of E_x, curves of line voltage and field power can be drawn from which the field power can be read for the desired line voltage.

It is assumed that the network is so proportioned that the field voltage and power are zero at normal line voltage.
This requires that at balance:

$R = \sqrt{(R')^2 + X^2}$, that is, equal impedances in the two branches up to the point of field connection. Thus, at balance the reactor voltage is slightly less than the line voltage. It is

$$E_{xn} = E_n \cos \sin^{-1} (R'/R)$$

where the subscript, n, denotes the value of a quantity at the normal balanced condition or

$$E_n = E_{xn}/\cos \sin^{-1} (R'/R)$$

In other words, if the reactor voltage is taken as unity at the balance point, the normal line voltage, E_n, is slightly over unity as given by the foregoing equation.

Procedure

The steps of procedure are then as follows:

The basis is stated; that is, R' and R_f in terms of R from which

$$R_{eq} = \frac{RR_f}{R+R_f},\ \text{and}\ (R'+R_{eq})$$

are determined. The coefficients in the equation for E in terms of E_R and E_f are then determined.

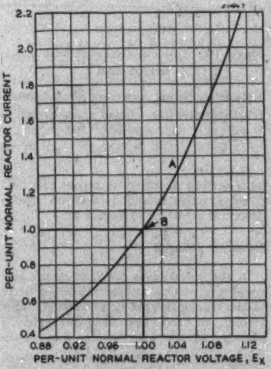

Figure 7. Typical saturation curve of saturating reactor

$$I_x = 2^{\left(\frac{E_x - 1.0}{0.10}\right)}$$

A—Current doubles for every ten-per-cent increase in voltage

B—Balance point or normal operating point

$$E = E_R\,\frac{R}{(R_{eq}+R')} - E_f\,\frac{R}{R_{eq}}$$

The normal line voltage is calculated from the normal reactor operating point voltage as follows:

$$E_n = E_{xn}/\cos \sin (R^1/R)$$

where $E_{xn} = 1.0$.

And finally the normal network power is calculated from

$$P_n = E_n I_{xn}\,\frac{R'+R}{R},\ \text{where}\ I_{xn} = 1.0$$

The steps in the calculations are as follows, item numbers being the same as the column numbers in the example, Table II.

1. A value of E_x is selected.
2. The corresponding current, I_x, is determined from the saturation curve (see Figure 7).
3. This current flows through the resistance $(R'+R_{eq})$ in series and produces the voltage drop E_R, where, $E_R = I_x(R'+R_{eq})$.
4. From this value of E_R, the ratio E_x/E_R is calculated.
5. The ratio E_f/E_R is determined from a curve obtained as described in Appendix I and shown in Figure 8.
6. The field voltage then can be calculated as follows:

$$E_f = E_R(E_f/E_R) = \text{Item } 3 \times \text{item } 5$$

7. E is then calculated as follows: From Figure 6, it can be seen that E_{eq} equals the voltage on R_{eq} minus E_f.

Since

$$E_{eq} = \frac{R_f}{(R+R_f)}\,E$$

this may be written

$$\frac{R_f}{(R+R_f)}\,E = \frac{R_{eq}}{(R'+R_{eq})}\,E_R - E_f$$

but since

$$\frac{R_f}{R+R_f} = \frac{R_{eq}}{R}$$

$$E = \frac{R}{(R'+R_{eq})}\,E_R - \frac{R}{R_{eq}}\,E_f$$

8. The per-unit line voltage is then calculated, E/E_n.

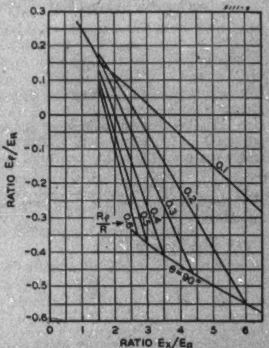

Figure 8. Curves of E_f/E_R versus E_x/E_R for use in computing power output of static regulating network

$R' = 0.20R$

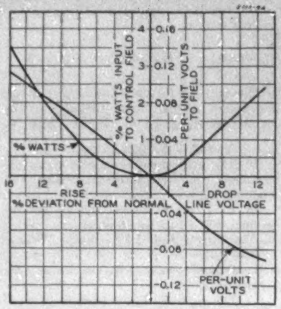

A. Normal range

$R' = 0.20R$

$R_f = 0.30R$

Per-cent watts are based on network watts at normal voltage

Per-unit field volts are based on average normal line volts

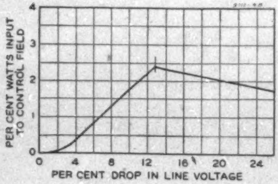

B. Extended range

$R' = 0.20R$

$R_f = 0.30R$

Per-cent watts are based on network watts at normal line voltage

Figure 9. Calculated static regulating circuit performance—control field

Input power versus line-voltage deviation from normal

9. The power consumed by the field is E_f^2/R_f.

10. The per-cent field power then can be calculated as $100P_f/P_n$. This is also the field watts per 100 watts drawn from the line by the network.

11. Or the network watts per field watt at ten-per-cent line voltage drop may be calculated,

$$\frac{100}{\text{Item 10}}\left[\frac{1-(\text{Item 8})}{0.1}\right]^2$$

This calculation should be made for the line voltage (column 8) corresponding most nearly to ten-per-cent voltage drop.

12. The field voltage in per unit of the average value of normal line voltage is given by E_f/E_n.

Table II gives a sample calculation by this method, the results of which are plotted in Figure 9A.

For drops in line voltage beyond the point at which the reactor rectifier goes to zero, the field power and voltage can be calculated setting E_d equal to zero. The field power for this extended range of voltage deviation is plotted in Figure 9B.

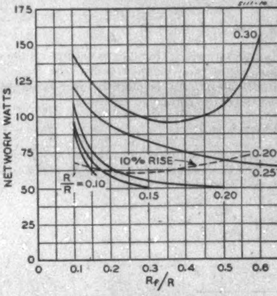

Figure 10. Calculated static-network power requirements

Network watts per watt input to control field at ten-per-cent line voltage drop (except as noted)

Rectifier Voltages

In the calculations for field power and voltage, of which a sample is given in Table II, the reactor current I_x is obtained. This current, rectified, also flows through R'. Thus the equations for rectifier voltages are

Reactor Rectifier—Refer to Figure 6C.

$$E_d = E_f + I_x R'$$

Resistor Rectifier

$$E_d' = -E_f + (I_x - I_f)(1-k)R$$

At line voltage ± ten per cent from normal the rectifier voltages should be checked since the performance as calculated only holds true if the rectifier voltages are positive up to these limits, (or to whatever limits of operation the network is designed).

For example, if we refer to Table II, for $R' = 0.2R = 0.204$, and $R_f = 0.3R = 0.306$ at 90-per-cent line voltage, which is the point at which E_d is lowest, the reactor rectifier voltage is

$$E_d = E_f + I_x R'$$
$$= -0.0816 + 0.555 \times 0.306$$
$$= -0.0816 + 0.1698 = +0.0882$$

This indicates that R' is sufficiently large and could be reduced somewhat. It must be remembered that harmonics have been neglected and that these calculations therefore must be used with considerable margin.

If it is desired only to ascertain that the reactor rectifier voltage is positive for a particular line voltage drop, no calculations are needed beyond those illustrated in Tables I and II. As long as the E_x/E_R value used in Table II corresponds to θ less than 90 per cent in Table I, the reactor rectifier voltage is positive, as explained previously. Thus it is convenient to stop the curves of Figure 6, prepared from calculations like Table I, at the boundary $\theta = 90$ degrees. They cannot then be used beyond the proper operating limit.

The resistor rectifier voltage decreases as the line voltage drop increases to ten per cent. At ten-per-cent high (a point available in Table II) if the resistor rectifier voltage is just zero, then

$$E_d' = -E_f + (I_x - I_f)(1-k)R$$

$$0 = -0.0739 + \left(1.414 - \frac{0.0739}{0.036}\right)(1-k)1.02$$

or

$$(1-k) = \frac{0.0739}{1.173 \times 1.02} = 0.0617$$

that is, $(1-k)$ must be about 6.2 per cent in order that the resistor rectifier voltage remains positive up to ten-per-cent voltage increase.

References

1. Recent Developments in Generator Voltage Regulation, C. R. Hanna, K. A. Oplinger, C. E. Valentine. AIEE Transactions, volume 58, 1939, page 838.

2. Rototrol—A Versatile Electrical Regulator, W. H. Formhals. *Westinghouse Engineer*, May 1942, page 51.

3. A Generator Voltage Regulator Without Moving Parts, C. P. West, I. D. Applegate. *Electric Journal*, April 1936.

4. Thevenin's Theorem, E. L. Harder. *Electric Journal*, volume 35, October 1938, page 397.

5. Typical Sequence Segregating Networks, Transmission and Distribution Reference Book. Westinghouse Electric and Manufacturing Company. Chapter 10, pages 248-9, Figure 25.

6. Regulation of A-C Generators With Suddenly Applied Loads, E. L. Harder, R. C. Cheek. AIEE Transactions, volume 63, 1944, June section, page 310.

Statistics as an Aid to Engineering Judgment in the Manufacture of Lightning-Arrester Blocks

CASPER GOFFMAN
NONMEMBER AIEE

IN THIS PAPER we show how modern statistical methods may be used as an aid to engineering judgment in determining the causes of variability in a complex manufacturing process.

Assistant Secretary of War for Air Lovett has said that "a statistician is a man who can lead you directly from a preconceived idea to a foregone conclusion." If properly interpreted, this statement contains an element of truth. But it is not the kind of statement which should be made under oath. For while it is the truth and nothing but the truth, it certainly is not the whole truth. The whole truth might be phrased in similar language as follows: "Among a given class of preconceived ideas, the statistician can tell, with a definite degree of certainty, which subclass constitutes foregone conclusions."

In our particular example on lightning-arrester blocks, the set of preconceived ideas are the variables in the process of manufacturing blocks which were thought to affect the electrical characteristics of blocks. The foregone conclusions are those among these variables which actually do affect significantly the electrical characteristics of the blocks. The term "significantly" is used here in an engineering sense—not a statistical sense.

Production Procedure

A brief description will be given of the production and testing of blocks.

The blocks consist of silicon carbide and a binder. The electrical characteristics of the silicon carbide are the determining factor of fitness for use.

The silicon carbide and binder are mixed in suitable proportions. After proper mixing, the material is screened and stored and is ready for molding into blocks.

The amount of material to be molded per block is weighed, by machine, directly into the mold with the bottom punch in place. The top punch then is inserted and the block pressed. The blocks then are subjected to a 24-hour baking cycle.

The ends of the blocks are sprayed with copper, and the lateral surfaces are coated with an insulating compound.

Figure 1 shows a lightning-arrester block cut through the middle.

Testing Procedure

The blocks are subjected to a life test and a volt-ampere characteristic test. We are here interested in the latter only. The functioning of a lightning-arrester block depends upon the fact that its resistance does not vary linearly. It has high resistance for low currents and low resistance for high currents. Figure 2 shows the volt-ampere characteristics of a lightning-arrester block taken by a cathode-ray oscillograph. The block is subjected to a surge whose crest value is 1,500 amperes. The time of the surge is ten microseconds from zero current to maximum and 20 microseconds to half value. The volt-ampere characteristic is read on a cathode-ray oscillograph. The maximum voltage attained across the block is called the "maximum rise" of the block.

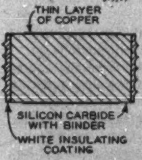

Figure 1. Lightning-arrester block

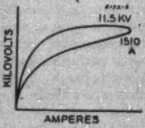

Figure 2. Volt-ampere characteristic curve of lightning-arrester block

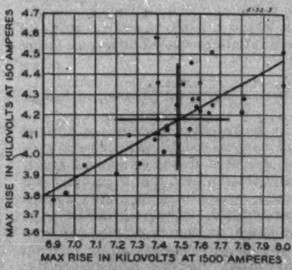

Figure 3. Correlation between maximum rise at 150 amperes and 1,500 amperes

Variables

Among the known factors which could cause electrical variations are such things as weight, length, and density of blocks; variations in the manufacturing techniques, and the character of the raw silicon carbide; and variations in the testing equipment.

Correlation Between Two Tests

As the voltages across the block at both high and low currents are important in the functioning of the blocks, it is of value to know the degree of correlation between these voltages.

Accordingly, for a set of 30 blocks, maximum rise was obtained for a 150-ampere surge and for a 1,500-ampere surge. The data were plotted on a scatter diagram as shown in Figure 3. The regression of Y on X is given by the equation $Y = 0.5X$. The calculation given in Table I shows that the regression is highly significant.

The 0.01 probability level for F with 1 and 28 degrees of freedom is about 8.0. Hence the regression is highly significant.

It may be of interest to note that the dependence of Y on X may be inferred from the fact that only two of the 30 points in Figure 3 fall in the second and fourth quadrants. The chance that this will happen for uncorrelated data is one in 2,000,000. For that reason, plus the fact that the variance from the regression line is small, the test for a 150-ampere surge was eliminated.

Effect of Molding Technique on Electrical Characteristics

To determine the effect of variations in molding technique on electrical characteristics of blocks, a batch of material was mixed and divided into four portions

---

Paper 45-132, recommended by the AIEE subcommittee on applications to statistical methods of the Standards committee for publication in AIEE TRANSACTIONS. Manuscript submitted April 30, 1945; made available for printing May 15, 1945.

CASPER GOFFMAN is staff assistant, quality-control department, Westinghouse Electric Corporation, East Pittsburgh, Pa.

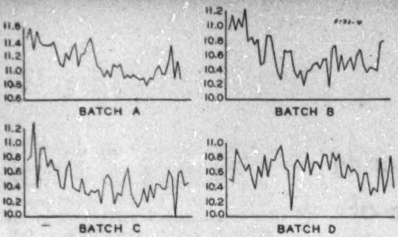

	Batch *A*	Batch *B*	Batch *C*	Batch *D*
$n\sigma^2=$	2.0113	3.0102	3.3774	1.8208
$(n-1)\delta^2=$	1.1691	2.3625	2.3576	3.1626
$\delta^2/\sigma^2=$	0.585	0.787	0.693	1.738

Figure 4 (left). Trends shown by data obtained in experiment on molding technique

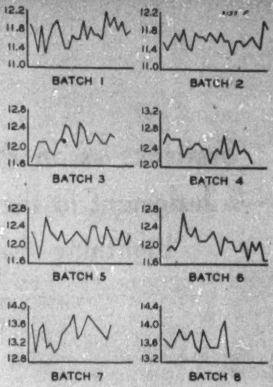

Figure 5 (right). Effect of aging on stabilizing electrical characteristics of blocks

	Batch 1	Batch 2	Batch 3	Batch 4	Batch 5	Batch 6	Batch 7	Batch 8
$n\sigma^2=$	1.53	0.75	0.99	0.65	0.88	1.38	1.16	0.77
$(n-1)\delta^2=$	2.59	1.47	1.10	1.08	1.52	1.68	1.56	1.52
$\delta^2/\sigma^2=$	1.69	1.96	1.11	1.67	1.73	1.22	1.34	1.98

from each of which 50 blocks were molded under different conditions. These will be called batches *A*, *B*, *C*, and *D*.

Batch *A* was molded in the laboratory under controlled conditions. Batches *B*, *C*, and *D* were molded in the shop. For *B* the attempt was made to control the variables. For *C* no attempt at control was made, but the operator was under observation. Batch *D* was molded without letting the operator know that it was a special batch.

Incidentally, since batches *A*, *B*, and *C* were molded immediately after mixing, and batch *D* was molded several days later, this experiment shows the effect of aging on maximum rise. Thus a trend definitely exists for batches *A*, *B*, and *C*, although it is not so evident for batch *D*. See Figure 4. The statistic δ^2/σ^2 has values of 0.585, 0.787, 0.693, and 1.738 for batches *A*, *B*, *C*, and *D*, respectively. The 0.01 and 0.05 probability values for this statistic for 50 observations are 1.40 and 1.58, respectively.

The following application of the χ^2 test was made to see whether significant differences exist between the variances of the afore-mentioned four batches.

Table I

	Sum of Squares	Degrees of Freedom
Total	1.0099	29
Regression	0.6881	1
Error	0.3218	28

$$F=0.6881+\frac{0.3218}{28}=60$$

Table II

Before Aging	After Aging
0.585	1.69
0.787	1.96
0.693	1.11
	1.67
	1.73
	1.22
	1.34
	1.98
$\overline{X}=0.69$	$\overline{Y}=1.59$

$$\chi^2\cong\frac{2.3026}{C}\left(n\log S'^2-\Sigma n_i\log S_i'^2\right)$$

with $K-1$ degrees of freedom, where $S_i'^2$ is the estimated *i*th variance with *n* degrees of freedom and S'^2 is the estimated total variance with *n* degrees of freedom.

$$C=1+\frac{1}{3(k-1)}\sum\left(\frac{1}{n_i}-\frac{1}{n}\right)$$

In this case,

$$\chi^2\cong\frac{2.3026}{1.01}(196\log 0.0462-49\log 0.00000349)$$
$$=2.3\,(-261.73+267.40)$$
$$=13.04$$

But the 0.01 probability level for χ^2 with three degrees of freedom is 11.34.

The conclusion drawn from these data is that the variables of the shop molding practice actually do affect the volt-ampere characteristics of blocks. Further attempts to determine these factors have not been made at this time, primarily because a control chart showed that within-batch variations were small compared to between-batch variations. Maximum effort accordingly was devoted to eliminating causes of between-batch variations. As the effect of variations in molding technique will most likely manifest itself within a batch, a critical study of these variations was left until some future date.

Effect of Aging on Maximum Rise

In the preceding section it was found that material molded without being aged first exhibited trends in maximum rise. The indication was that if material was aged for a suitable length of time no such trends existed. Of course standard practice based on long experience and engineering knowledge was to age the material before using. However, statistical analysis brings a definiteness into the picture which otherwise seems to be lacking and sometimes refutes accepted practice. For this reason, the data shown in Figure 5 were obtained for eight batches aged for what was considered to be a sufficiently long period of time. The data are for every eighth block in order of production. The values of δ^2/σ^2 for the eight batches were respectively 1.69, 1.96, 1.11, 1.67, 1.73, 1.22, 1.34, and 1.98. That trends exist even after aging is evident from the fact that all eight values obtained are less than two, which is the expected value of this statistic if there are no trends. However, the trend obtained after aging is significantly less than that obtained before aging as shown by the *t* test in Table II.

$$t=\frac{\overline{Y}-\overline{X}}{\sqrt{\left(\frac{1}{n_1}+\frac{1}{n_2}\right)\frac{\Sigma(\overline{X}-X)^2+\Sigma(\overline{Y}-Y)^2}{n_1+n_2-2}}}$$
$$=\frac{90}{\sqrt{(1/3+1/8)\frac{(0.02+0.7550)}{9}}}$$
$$=\frac{0.90}{0.198}=\underline{4.54},\ 9\text{ degrees of freedom}$$

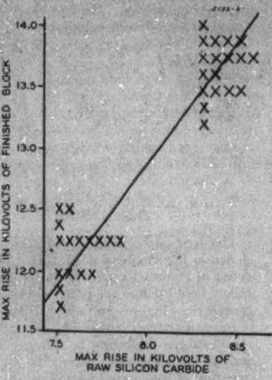

Figure 6. Effect of maximum rise of raw silicon carbide on maximum rise of finished blocks

The 0.01 probability level with nine degrees of freedom is 3.25. Hence the difference is significant.

Effect of Baking Temperature on Blocks

Sixteen blocks were taken from the same batch. Eight of the blocks selected at random were baked in an oven at the standard temperature. The other eight blocks were subjected to a baking cycle whose maximum temperature was 75 degrees centigrade lower. The data are shown in Table III. A value of t = 1.89 was obtained. This falls between the 0.05 and 0.10 probability level of the t distribution. A retest was made with 16 more blocks. A value of t = 3.63 was obtained. This value is higher than the 0.01 probability level, which shows that oven temperature should not be allowed to deviate by as much as 75 degrees centigrade.

Table III

Hot Oven	Cool Oven
First Test	
12.94	13.92
13.17	13.67
13.14	12.64
12.64	12.83
12.81	13.36
13.42	13.57
12.90	13.14
12.67	13.22
$\overline{X} = 12.96$	$\overline{Y} = 13.29$

$$t = \frac{13.29 - 12.96}{\sqrt{\frac{1/4(1.6809)}{14}}} = \frac{0.33}{17} = 1.94$$

Hot Oven	Cool Oven
Retest	
12.53	12.53
12.37	13.22
12.48	13.01
12.77	12.97
12.52	12.96
12.81	13.03
12.76	12.82
12.52	13.43
$\overline{X} = 12.60$	$\overline{Y} = 13.00$

$$t = \frac{13.00 - 12.60}{\sqrt{\frac{1/4(0.6697)}{14}}} = \frac{0.40}{0.11} = 3.63$$

Table IV

Position								
	1	2	3	4	5	6	7	8
	12.3	12.6	12.3	12.3	12.4	12.4	12.3	12.3
	12.1	12.3	12.0	12.2	12.4	12.2	12.0	12.4
	12.2	12.2	12.1	12.1	12.2	12.2	12.2	12.3
	11.7	12.1	12.2	12.2	12.0	12.0	12.3	12.1
Average	12.075	12.3	12.15	12.2	12.25	12.2	12.2	12.275

$\overline{X} = 12.20$

Total sum of squares $= 0.86$ — 31 degrees of freedom

Between positions $= 4(0.03625) = 0.145$ — 7 degrees of freedom

Error $= 0.715$ — 24 degrees of freedom

$$F = \frac{0.145/7}{0.715/24} = 0.696$$

To determine whether or not significant differences in electrical characteristics exist between blocks baked in various positions in the oven, 32 blocks were randomized and placed in groups of four in eight positions in the oven. The data are shown in Table IV. An analysis of variance performed with these data yields a value of F = 0.696 with seven degrees of freedom for the between-position variance and 16 degrees of freedom for the error term (within-position variance). This test indicates strongly that significant differences do not exist between positions in oven as far as electrical characteristics are concerned.

Effect of Clearance Between Mold and Punch on Electrical Characteristics of Blocks

There had been some indication in the shop that blocks molded with large clearance between mold and punch had different electrical characteristics from blocks molded with small clearance. Although there was no apparent reason for this difference, a test was made to determine whether or not such a difference actually exists.

Fourteen blocks taken from the same batch of material were molded as special blocks; every other block was molded with a certain large clearance between molds and punches. The remaining blocks were molded with a certain small clearance between molds and punches. The results are shown in Table V. A value of t = 10.1 was obtained. This shows significant difference. That a significant difference exists also may be seen from the fact that every block molded with large clearance had a higher maximum rise than every block molded with small clearance.

Characteristics of Raw Silicon Carbide

The electrical characteristics of raw silicon carbide are obtained by getting the volt-ampere curve for a sample of the raw material. It would be of value to verify the degree of correlation between the maximum rise of raw material and finished product although theoretically the two should be proportional. However, at the time the test was run only two varieties were available. One had a maximum rise of 7.5 kv, the other 8.2 kv. The data are plotted in Figure 6 and show that the maximum rise of finished blocks is roughly proportional to the maximum rise of raw silicon carbide. The test should be repeated with batches of silicon carbide whose electrical characteristics vary along the scale to determine the regression lines.

Table V

Large Clearance	Small Clearance
12.6	12.1
12.6	11.9
12.8	12.0
13.2	11.9
13.0	11.9
12.6	11.8
13.0	11.9
$\overline{X} = 12.825$	$\overline{Y} = 11.9375$

$$t = \frac{0.8875}{\sqrt{\frac{0.43(1/4)}{14}}} = 10.1$$

Conclusion

As applied to lightning-arrester blocks, statistics helped engineering judgment by verifying that some of the variables which had been thought to affect electrical characteristics actually did so. This led to emphasis of control of these factors at the expense of others which had been thought to affect maximum rise but were found, by statistical analysis, to have a less significant effect. As a consequence of this study a more uniform product is

New Transmission-Line Diagrams

A. C. SCHWAGER
FELLOW AIEE

P. Y. WANG
ASSOCIATE AIEE

IN THE DESIGN and operation of transmission lines the following quantities are of primary importance: sending-end power, receiving-end power, sending-end voltage, receiving-end voltage, power angle between sending-end and receiving-end voltage. Numerous diagrams have been developed for the solution of transmission-line problems, graphically illustrating relations between some of the afore-mentioned quantities. Among these, the modified Evans and Sels charts, based on the general circuit constants *ABCD*, have found wide acceptance.[1,2,3] In these charts the determination of the power at one end with the power given at the other end requires a transfer of points from one chart to another. It is one of the purposes of this paper to supplement the modified Evans and Sels diagrams in such a manner that this transfer of points can be eliminated. This can be accomplished by relating power at one end to power at the other end directly, without intermediate quantities such as voltage ratio and power angle. The diagrams developed are essentially admittance-circle diagrams, relating admittance at one end to admittance at the other end.

It is a further purpose of this paper to develop corresponding circle diagrams for the impedances, directly relating the impedance at one end to the impedance at the other. These diagrams might be useful in conjunction with impedance-relaying problems where a transfer through voltage ratio and power angle is not essential.

The modified Evans and Sels charts apply to fixed circuit constants. For each new set of values *ABCD*, a new chart must be prepared. Numerous charts have been developed to eliminate this shortcoming, resulting in universal transmission-line charts. These charts permit the determination of the performance of any line with arbitrary constants. In many of these charts it is necessary, however, to execute certain constructions to arrive at solutions. It is a further purpose of this paper to develop a universal transmission-line chart based on general circuit constants from which all the desired values can be read directly.

The following equations and notations will be used:

$$E_S=AE_B+BI_R \tag{1}$$

$$I_S=CE_R+DI_R \tag{2}$$

$$AD-BC=1$$

$$\frac{E_R}{E_S}=\left|\frac{E_R}{E_S}\right|\underline{/-\delta}$$

where bars enclosing a quantity indicate magnitude.

δ = angle that E_S leads E_R = power angle

Vector power usually is defined by its components *P*, *Q*. In order to simplify the following formulas a single symbol denoting vector power representing a complex quantity is introduced:

$$p=P+jQ=\text{power vector}$$

$$\frac{p_S}{|E_S|^2}=Y_S=G_S+jB_S=\text{sending-end (input) admittance}$$

$$\frac{p_R}{|E_R|^2}=Y_R=G_R+jB_R=\text{receiving-end (load) admittance}$$

$$\frac{p_S}{|E_R|^2}=Y_{RS};\qquad \frac{p_R}{|E_S|^2}=Y_{SR}$$

Circle Diagram for the Calculation of Power at One End From Power at the Other End

The modified Evans and Sels charts are essentially admittance diagrams. For practical purposes, however, they are labeled in terms of power divided by the square of voltages. As the use of admittances produces more compact equations, admittance quantities will be employed freely, the results later being interpreted in power quantities. The four charts are based on the following equations:

$$\frac{p_S}{|E_S|^2}=Y_S=\frac{D}{B}-\frac{1}{B}\left|\frac{E_R}{E_S}\right|\underline{/-\delta} \tag{3}$$

$$\frac{p_R}{|E_R|^2}=Y_R=-\frac{A}{B}+\frac{1}{B}\left|\frac{E_S}{E_R}\right|\underline{/\delta} \tag{4}$$

$$\frac{p_S}{|E_R|^2}=Y_{RS}=\frac{D}{B}\left|\frac{E_S}{E_R}\right|^2-\frac{1}{B}\left|\frac{E_S}{E_R}\right|\underline{/-\delta} \tag{5}$$

$$\frac{p_R}{|E_S|^2}=Y_{SR}=-\frac{A}{B}\left|\frac{E_R}{E_S}\right|^2+\frac{1}{B}\left|\frac{E_R}{E_S}\right|\underline{/\delta} \tag{6}$$

The four corresponding diagrams are shown in Figures 1A, 1B, 1C, 1D. Diagrams of Figures 1A and 1B are the most widely used because the power circles are concentric. Figures 1C and 1D consist of eccentric circles, which limits their use considerably. Referring to Figures 1A and 1B, these diagrams permit the determination of the power and voltage quantities at one end from the power and voltage quantities at the other end. For instance, if it is desired to determine P_S+jQ_S for a given P_R+jQ_R and a known receiving-end voltage E_R, $P_R/|E_R|^2$ and $Q_R/|E_R|^2$ are computed, locating a point in the receiver-end chart, Figure 1B. This point determines the value of $|E_S/E_R|$ and δ. The corresponding point with identical $|E_S/E_R|$ and δ next is located in the sending-end diagram, Figure 1A whereupon the values $P_S/|E_S|^2$ and $Q_S+|E_S|^2$ can be read, and P_S, Q_S, and E_S can be computed. The necessity of transfer of points is common to all these modified diagrams since, essentially, they relate an admittance to the voltage ratio and power angle. It can be eliminated only if sending-end admittance and receiving-end admittance are brought in direct relation, as follows:

$$\left.\begin{aligned}Y_S&=\frac{I_S}{E_S}=\frac{CE_R+DI_R}{AE_R+BI_R}=\frac{C+DY_R}{A+BY_R}\\ Y_S&=\frac{D}{B}-\frac{1}{B^2\left(Y_R+\dfrac{A}{B}\right)}\end{aligned}\right\} \tag{7}$$

or, in vector-power form:

$$\frac{p_S}{|E_S|^2}=\frac{P_S+jQ_S}{|E_S|^2}=\frac{D}{B}-\frac{1}{B^2\left(\dfrac{P_R+jQ_R}{|E_R|^2}+\dfrac{A}{B}\right)} \tag{7a}$$

Paper 45-126, recommended by the AIEE committee on power transmission and distribution for publication in AIEE TRANSACTIONS. Manuscript submitted April 30, 1945; made available for printing May 15, 1945.

A. C. SCHWAGER is vice-president in charge of engineering, Pacific Electric Manufacturing Corporation, San Francisco, Calif., and P. Y. WANG is electrical engineer, National Resources Commission of China, New York, N. Y.

The authors acknowledge the encouragement given them by Frank Poage, who, by repeatedly pointing out the demand for additional charts, initiated the efforts leading to the diagrams developed in this paper.

---

being made, and an appreciable reduction in the scrap loss during manufacturing has resulted.

Statistical methods now are being further applied to determine superior designs. The main tool being used for this purpose is the designed experiment.

References

1. STATISTICAL METHODS, **George W. Snedecor.** Collegiate Press, Inc., Ames, Iowa, 1938.

2. STATISTICAL METHODS FOR RESEARCH WORKERS, **R. A. Fisher.** Oliver and Boyd, London, England, 1934.

3. AN INTRODUCTION TO MODERN STATISTICAL METHODS, **Paul R. Rider.** John Wiley and Sons, Inc., New York, N. Y., 1939.

4. ECONOMIC CONTROL OF QUALITY OF MANUFACTURED PRODUCT, **W. A. Shewhart.** D. Van Nostrand Company, New York, N. Y., 1931.

5. MATHEMATICAL STATISTICS, **S. S. Wilks.** Princeton University Press, Princton, N. J., 1941.

6. DISTRIBUTION OF THE RATIO OF THE MEAN-SQUARE SUCCESSIVE DIFFERENCE TO THE VARIANCE, **John von Neumann.** *Annals of Mathematical Statistics*, volume 12, 1941, pages 367–95.

In equation 7, Y_S is represented as an analytic complex function of the independent variable Y_R. Analytic functions have interesting properties which are particularly useful in the analysis of electric-circuit diagrams and which are described in detail in mathematical texts.[4,5,6] Analytic functions map the plane of the independent variable into the plane of the dependent variable in such a manner that corresponding infinitely small configurations are similar. Such mappings are called conformal mappings. Conformal mapping retains the angle between corresponding intersecting lines, in particular, an orthogonal system of lines in one plane transforms into another orthogonal system in the other plane.

Y_S is called a linear fractional transformation of Y_R. Since the mappings produced by this function have been discussed in detail before,[4] it will be sufficient to indicate the steps leading to the final $Y_s=f(Y_R)$ diagram. Analyzing the expression $1/(Y_R+A/B)$, the Y_R plane with origin OY_R and axis G and B is drawn (Figure 2). Addition of A/B produces the Y_R+A/B plane with origin O. In this plane, lines B_1=constant and G_1=constant are drawn. It is well known that the expression $1/(Y_R+A/B)$ can be obtained by a process of complex inversion. Inversion transforms circles into circles. Specifically, the straight lines B_1=constant and G_1=constant are transformed into the circles B_1=constant and G_1=constant respectively, as shown. Additional lines G=constant and B=constant all intersect at O and produce an orthogonal system of circles. Centers of the G=constant circles are located on the real axis, centers of the B=constant circles on the imaginary axis. The diameter of the circles is the reciprocal of the shortest distance of the straight lines from the origin and readily can be computed as shown in Figure 2. The final expression of Y_S requires multiplication of $1/(Y_R+A/B)$ by $-1/B^2$ and addition of D/B, resulting in Figure 3, which lists in detail the steps necessary to arrive at the circles $G=P_R/|E_R|^2$=constant and $B=Q_R\div|E_R|^2$=constant in the $P_S/|E_S|^2+jQ_S\div|E_S|^2$ plane. If numerous circles representing varying $P_R/|E_R|^2$ and $Q_R/|E_R|^2$ values are drawn, $P_S/|E_S|^2+jQ_S/|E_S|^2$ can be determined readily as co-ordinates of the intersection point of circles representing $P_R/|E_R|^2$ and $Q_R/|E_R|^2$ values applying to the particular problem. If Figure 3 is used as a separate chart, the additional use of the modified Evans and Sels chart, Figure 1B, is required to determine the voltage ratio necessary for the calculation of the sending-end power and for the determination of the power angle. It is apparent that the separate use of the chart of Figure 3 has no advantages over previous charts. However, if this chart is superimposed upon the modified Evans and Sels sending-end power chart, Figure 1A, what appears to be a useful new chart is produced.

This superposition is executed in Figure 4, using data and nomenclature of a previously published chart for easy comparison.[8] As can be seen, all receiving-end power circles intersect in the center of the $|E_R/E_S|$=constant circles. Since all circles P_R=constant, Q_R=constant intersect at right angles, the intersecting points are determined accurately. The chart is therefore more convenient to use than the synchronous-machine charts which it resembles.

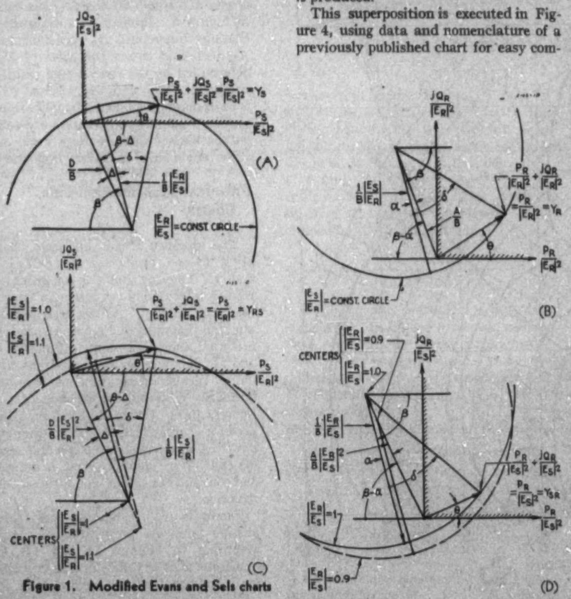

$\frac{jQ_S}{|E_S|^2}$
$\frac{P_S}{|E_S|^2}+\frac{jQ_S}{|E_S|^2}=\frac{P_S}{|E_S|^2}=Y_S$
$\frac{P_S}{|E_S|^2}$
θ
β-Δ
δ
$\frac{D}{B}$
Δ
$\frac{1}{B}\left|\frac{E_R}{E_S}\right|$
β
$\left|\frac{E_R}{E_S}\right|$=CONST CIRCLE
(A)
$\frac{jQ_R}{|E_R|^2}$
$\frac{P_R}{|E_R|^2}+\frac{jQ_R}{|E_R|^2}$
$=\frac{P_R}{|E_R|^2}=Y_R$
$\frac{1}{B}\left|\frac{E_S}{E_R}\right|$
α
β
δ
$\frac{A}{B}$
β-α
θ
$\frac{P_R}{|E_R|^2}$
$\left|\frac{E_S}{E_R}\right|$=CONST. CIRCLE
(B)
$\frac{jQ_S}{|E_R|^2}$
$\left|\frac{E_S}{E_R}\right|$=1.0
$\left|\frac{E_S}{E_R}\right|$=1.1
$\frac{P_S}{|E_R|^2}+\frac{jQ_S}{|E_R|^2}=\frac{P_S}{|E_R|^2}=Y_{RS}$
θ
$\frac{P_S}{|E_R|^2}$
β-Δ
δ
$\frac{D}{B}\left|\frac{E_S}{E_R}\right|^2$
Δ
$\frac{1}{B}\left|\frac{E_S}{E_R}\right|$
β
CENTERS
$\left|\frac{E_S}{E_R}\right|$=1
$\left|\frac{E_S}{E_R}\right|$=1.1
(C)
CENTERS
$\left|\frac{E_R}{E_S}\right|$=0.9
$\left|\frac{E_R}{E_S}\right|$=1.0
$\frac{jQ_R}{|E_S|^2}$
$\frac{1}{B}\left|\frac{E_R}{E_S}\right|$
$\frac{A}{B}\left|\frac{E_R}{E_S}\right|^2$
β
α
δ
β-α
θ
$\frac{P_R}{|E_S|^2}+\frac{jQ_R}{|E_S|^2}$
$=\frac{P_R}{|E_S|^2}=Y_{SR}$
$\frac{P_R}{|E_S|^2}$
$\left|\frac{E_R}{E_S}\right|$=1
$\left|\frac{E_R}{E_S}\right|$=0.9
(D)

Figure 1. Modified Evans and Sels charts

The chart is equally useful in determining receiving-end quantities with sending-end quantities known, the steps being reverse of those indicated in the preceding problem. Essentially, the advantages of the Figure 4 chart are that power and voltage at either end can be determined from power and voltage at the other end by the use of a single chart, eliminating the transfer of points required on previous charts.

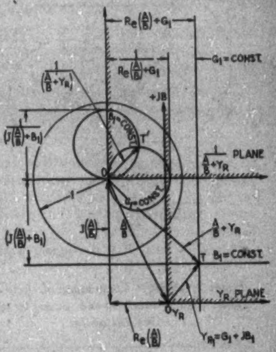

$Re\left(\frac{A}{B}\right)+G_1$
G_1=CONST
$\frac{1}{\left(\frac{A}{B}+Y_R\right)}$
$Re\left(\frac{A}{B}\right)+G_1$
+JB
$\frac{1}{J\left(\frac{A}{B}\right)+B_1}$
B_1=CONST
T'
$\frac{1}{\frac{A}{B}+Y_R}$ PLANE
O
G_1=CONST
1
$J\left(\frac{A}{B}\right)$
$\frac{A}{B}$
$\frac{A}{B}+Y_R$
$J\left(\frac{A}{B}\right)+B_1$
T
B_1=CONST
Y_R PLANE
OY_R
$Re\left(\frac{A}{B}\right)$
$Y_{R_1}=G_1+JB_1$

Figure 2. Complex inversion of Y_R+A/B

In a similar manner Y_R can be expressed as a function of Y_S:

$$Y_R=\frac{p_R}{|E_R|^2}=\frac{P_R+jQ_R}{|E_R|^2}=-\frac{A}{B}-\frac{1}{B^2\left(\frac{p_S}{|E_S|^2}-\frac{D}{B}\right)} \quad (8)$$

A diagram similar to Figure 4 results, mapping the sending-end plane upon the receiver plane. Corresponding to the Evans and Sels diagrams, Figures 1C and 1D, two additional diagrams exist for the transformation of the $P_S/|E_R|^2=Y_{RS}$ plane into $P_R/|E_S|^2=Y_{SR}$ plane and vice versa. It will be sufficient to list the formulas for one of these transformations,

$$Y_{RS}=f(Y_{SR})$$

$$\frac{P_S+jQ_S}{|E_R|^2}=\frac{D}{B}\left|\frac{E_S}{E_R}\right|^2-\frac{1}{B^2\left(\frac{P_R+jQ_R}{|E_S|^2}+\frac{A}{B}\left|\frac{E_R}{E_S}\right|^2\right)} \quad (9)$$

The resultant diagrams are still circle diagrams, however, the circles do not intersect in one point. They have similar practical limitations as do the diagrams of Figures 1C and 1D.

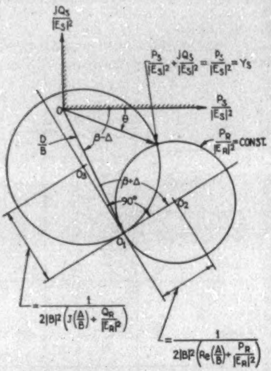
$\frac{jQ_S}{|E_S|^2}$
$\frac{P_S}{|E_S|^2}+\frac{jQ_S}{|E_S|^2}=\frac{P_S}{|E_S|^2}=Y_S$
$\frac{P_S}{|E_S|^2}$
0
θ
$\frac{D}{B}$
β−Δ
$\frac{P_R}{|E_R|^2}$=CONST.
O_S
β+Δ
90°
O_2
O_1
$=\frac{1}{2|B|^2\left(J\left(\frac{A}{B}\right)+\frac{Q_R}{|E_R|^2}\right)}$
$=\frac{1}{2|B|^2\left(Re\left(\frac{A}{B}\right)+\frac{P_R}{|E_R|^2}\right)}$

Figure 3. (above) Construction of circle diagrams relating receiving-end power to sending-end power

Circle Diagram for the Calculation of the Impedance at One End From the Impedance at the Other End

In conjunction with protection problems involving impedance relays with phase-angle control, circle diagrams relating impedances to $|E_R/E_S|$ and δ have found wide application.[7] These diagrams follow readily from equations 3, 4, 5, and 6. It will be sufficient to analyze but one specific case.

$$Z_S=\frac{1}{Y_S}=-\frac{B}{\left(\left|\frac{E_R}{E_S}\right|\underline{/-\delta}-D\right)} \tag{10}$$

Since Z_S is a linear fractional transformation of the independent complex variable $|E_R/E_S|\underline{/-\delta}$, straight lines and circles in the plane of the independent variable transform into circles in the Z_S plane. In particular, the circles $|E_R/E_S|$ = constant and the lines δ = constant transform into circles. Since the lines $|E_R/E_S|$ = constant and δ = constant are orthogonal, they will produce an orthogonal system of lines in the Z_S plane.[8] A similar diagram can be developed for the impedance Z_R. If it is required to determine the value of Z_S for a given value of Z_R, it is necessary to determine the values of $|E_R/E_S|$ and δ from the Z_R diagram and transfer the point to the Z_S diagram. This procedure is analogous to that required in the Evans and Sels diagrams.

In the following, circle diagrams will be developed for the direct determination of one impedance from the other, without transfer through the intermediate variables $|E_R/E_S|$ and δ. Since these diagrams closely resemble the admittance diagrams developed previously, it will be sufficient to consider one specific case, for instance, the mapping of Z_R into Z_S. Referring to equations 1 and 2, it follows:

$$Z_S=\frac{E_S}{I_S}=\frac{AE_R+BI_R}{CE_R+DI_R}=\frac{AZ_R+B}{CZ_R+D}$$

$$=\frac{A}{C}-\frac{1}{C^2\left(Z_R+\frac{D}{C}\right)}$$

and with $Z_R=R_R+jX_R$:

$$Z_S=\frac{A}{C}-\frac{1}{C^2\left(R_R+jX_R+\frac{D}{C}\right)} \tag{11}$$

As in the admittance diagrams where B = constant and G = constant lines mapped into circles, the foregoing equation transforms lines R_R = constant and X_R = constant into circles which intersect at one point. A particularly simple diagram results when the phase of the circuit constant C equals 90 degrees, as is shown in Figure 5. From such a diagram including numerous R_R = constant and X_R = constant circles the value of Z_S is determined as the intersecting point of appropriate R_R and X_R circles. This type of diagram might find application in conjunction with special impedance-relaying problems where voltage ratio and power angle are of secondary importance.

Universal Transmission-Line Charts

The modified Evans and Sels charts apply to one specific set of $ABCD$ constants. They are simple to construct and furnish information concerning a specific line very quickly. As has been pointed out, the diagrams of Figures 1A and 1B are used most commonly. Figures 1C and 1D diagrams are used rarely as they do not furnish information conveniently, ordinarily requiring construction of particular δ lines. There is, therefore, still a need for charts which furnish sending-end power from receiving-end power and sending-end voltage, and vice versa, in a direct and convenient manner, and without construction.

Furthermore, in planning new transmission lines, the preparation of charts according to Figures 1A and 1B for numerous $ABCD$ values is time consuming. Universal charts, giving data for

Figure 4. Chart relating receiving-end power to sending-end power, voltage ratio, and power angle

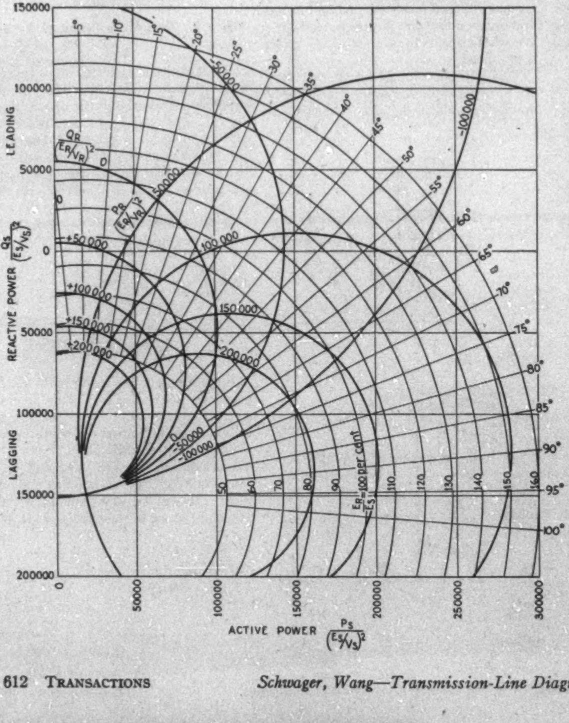

any line of arbitrary *ABCD* constants, are preferred. Most of the existing charts, however, again require constructions to arrive at solutions. In the following, four charts similar to the Evans and Sels charts will be developed which will permit the quick calculation of power and voltage quantities for any *ABCD* constants without construction and with a minimum of computation. These charts also will eliminate the shortcomings inherent to the charts shown in Figures 1C and 1D.

The principal handicap against the modified Evans and Sels charts being suitable for universal charts is the fact that each new value of *B* and *D* introduces a new distance and, more particularly, produces a change in angular relations. Different diagrams result even if $|D|$ and $|B|$ do not change, but Δ and β only. This suggests that the method used in Figure 1, representing the angular relations, should be modified, and that more emphasis should be placed on the angular co-ordinates. For instance, it seems indicated to identify sending-end power, not by $P_S=P_S+jQ_S$, but by $|p_S|$ and the power-factor angle θ_S. Furthermore, the power-factor angle θ_S is not as suitable as the angle ϕ_S to which it is related by $\phi_S=\beta-\Delta+\theta_S$. ϕ_S will be given preference in the following. In Figure 6A, the chart Figure 1A is reproduced with emphasis on these angular quantities. p_S is represented by $|p_S|=$ constant circles (only one shown) and $\phi_S=$constant lines (only one shown). As can be seen, each set of values δ and $|E_R/E_S|$ determines a corresponding set of values for $|p_S|$ and ϕ_S.

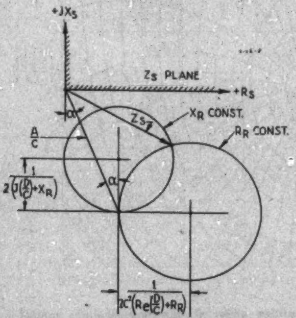
+JX$_S$
Z$_S$ PLANE
+R$_S$
X$_R$ CONST.
R$_R$ CONST.
Z$_S$
α
α
$\frac{A}{C}$
$\frac{1}{2\left(J\left(\frac{D}{C}\right)+X_R\right)}$
$\frac{1}{2C^2\left(Re\left(\frac{D}{C}\right)+R_R\right)}$

Figure 5. Diagram relating receiving-end impedance to sending-end impedance

In the following chart, Figure 6B, a new orthogonal co-ordinate system for δ and $|E_R/E_S|$ is introduced with δ as abscissa and $|E_R/E_S|$ as ordinate. If the values of $|p_S|$ and ϕ_S corresponding to various values of δ and $|E_R/E_S|$ are determined from Figure 6A and entered in Figure 6B, a useful chart results if the $|p_S|=$constant and $\phi_S=$constant lines are indicated. In this manner $|P_S|$ and ϕ_S can be determined for any given values of δ and $|E_R/E_S|$ and conversely. In order to arrive at a universal diagram, equation 3, representing Figure 6A, is divided by $|D/B|$, resulting in

$$p_S\left|\frac{B}{E_S^2D}\right|=-\left(\left|\frac{E_R}{E_SD}\right|\underline{/-\delta}-1\underline{/\Delta}\right)\underline{/-\beta}$$

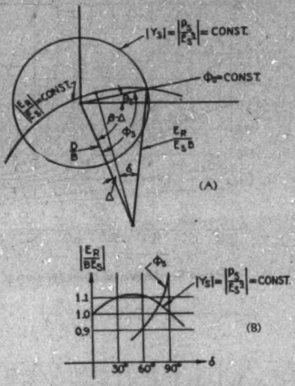
$|Y_S|=\left|\frac{p_S}{E_S^2}\right|=$ CONST.
Φ$_S$=CONST.
$\left|\frac{E_R}{E_S}\right|$=CONST.
p_S
β-Δ
Φ$_S$
$\frac{D}{B}$
$\frac{E_R}{E_SB}$
δ
Δ
(A)
$\left|\frac{E_R}{BE_S}\right|$
Φ$_S$
$|Y_S|=\left|\frac{p_S}{E_S^2}\right|=$CONST.
1.1
1.0
0.9
30°
60°
90°
δ
(B)

Figure 6. Transformation of conventional power diagram into E_R/E_S, δ diagram

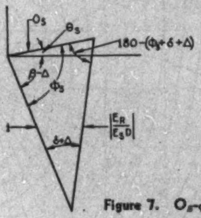

Figure 7. O_S-ϕ_S diagram

Denoting the real quantity $|p_SB\div E_S^2D|=O_S$, the Figure 7 diagram results, from which the following trigonometric relations can be established for the determination of the lines $O_S=$constant and $\phi_S=$constant in the $|E_SD/E_R|$, δ co-ordinate system:

$$\cos(\delta+\Delta)=\frac{1+\left|\frac{E_R}{E_SD}\right|^2-O_S^2}{2\left|\frac{E_R}{E_SD}\right|} \tag{12}$$

$$\left|\frac{E_SD}{E_R}\right|=\frac{\sin(\phi_S+\delta+\Delta)}{\sin\phi_S} \tag{12a}$$

Figure 8 shows the resulting plot covering a wide range of values. This chart represents conditions at the sending end and corresponds to the modified Evans and Sels chart, Figure 1A. For the receiving-end chart corresponding to Figure 2A the following formulas can be derived when $|p_RB/E_R^2A|=O_R$, $\phi_R=\beta-\alpha+\theta_R$.

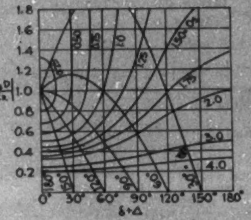

Figure 8. Universal transmission-line chart in E_R/E_S, δ co-ordinates

E_S and E_R in kilovolts

$\delta=$power angle between E_S and E_R

$\phi_S=\beta-\Delta+\theta_S$, $\theta_S=$power-factor angle

$O_S=(\text{kva})_S\times|B/E_S^2D|$

$$\cos(\delta-\alpha)=\frac{1+\left|\frac{E_S}{E_RA}\right|^2-O_R^2}{2\left|\frac{E_S}{E_RA}\right|} \tag{13}$$

$$\left|\frac{E_RA}{E_S}\right|=\frac{\sin(\phi_R-\delta-\alpha)}{\sin\phi_R} \tag{13a}$$

Comparison of equations 13 and 13a with equations 12 and 12a brings out the fact that identical plots are produced in slightly different co-ordinate systems. Figure 8 therefore could be used readily as receiving-end chart as well, with $|E_RA/E_S|$ as ordinate and $(\delta-\alpha)$ as abscissa. This feature brings out the inherent symmetry in the choice of the co-ordinates. In order to avoid confusion it appears advisable, however, to physically separate the two charts. Figure 9 shows one possible method suitable for practical use. The left-hand side of this chart is marked for receiving, the right-hand side for sending-end quantities. Figure 10 shows a section of chart of Figure 9 which covers the range of most common operating conditions. The use of these charts is illustrated best in conjunction with a practical example.

Given a transmission line with the following constants,

$A=0.917\underline{/1.06°}=D$

$B=153\underline{/78.56°}$

$C=0.00106\underline{/90°}$

Determine sending-end power, power factor, and voltage if 75 megawatts at 99-per-cent power-factor leading is delivered at the receiving end at 154 kv.

Solution:

$(\text{kva})_R\cos\theta_R=(\text{kva})_R\times0.99=75$ megawatts; $(\text{kva})_R=75.75$ megavolt-amperes, $\theta_R=8.1°$

$O_R = \frac{(\text{kva})_R|B|}{154^2|A|} = 0.533, \quad \phi_R = 8.1° + 78.56°$
$-1.06° = 85.6°$

With the foregoing values, the operating point is located in the left-hand side of Figure 10, giving

$|E_RA/E_S| = 0.856$
$\delta - \alpha = 27.2°$

from which

$$|E_S| = \frac{0.917}{0.856} \times 154 = 165 \text{ kv}$$

$$\delta = 27.2° + 1.06° = 28.26°$$

Next, computation of $|E_SD/E_R| = 165 \times 0.917/154 = 0.983$ and $\delta + \Delta = 29.32$ furnishes the operating point for the right-hand side of the Figure 10 chart, which corresponds to

$$O_S = 0.51 = \left|\frac{(\text{kva})_S B}{E_S^2 A}\right|$$

giving

$(\text{kva})_S = 83.1$ megavolt-amperes
$\phi_S = 77.7 = \beta - \Delta + \theta_S$

giving

$\theta_S = -0.4°, \cos\theta_S \approx 1$

From the foregoing example it can be seen that this universal chart furnishes the desired information quickly and with a minimum of calculations.

Whereas the charts in the first two sections of this paper were obtained as mappings of analytic complex functions, the universal charts are obtained by a purely geometrical process and do not represent such mappings. The orthogonal system of O_S = constant and ϕ_S = constant lines of Figure 7 does not map into an orthogonal system, as can be seen by inspection of Figure 9. An orthogonal system could be obtained if Figure 7 were mapped according to the function $1_g|E_R/E_SD|\underline{/\delta+\Delta}$; however, this would produce a logarithmic scale for the ordinate which is less practical than the linear scale employed in Figure 9.

Charts of Figures 9 and 10 are applicable for the solution of problems where power and voltage at one end of the transmission line are given. Similar universal charts can be developed with power given at one end and voltage at the other. Since the derivation of the charts is similar to that of the preceding ones, it will be sufficient to list the relations corresponding to equations 12 and 13. The following notations and abbreviations are used in deriving them:

$\phi_R = \beta - \alpha + \theta_R$

$O_{RS} = (\text{kva})_S\left|\frac{DB}{E_R^2}\right|$

$O_{SR} = (\text{kva})_R\left|\frac{AB}{E_S^2}\right|$

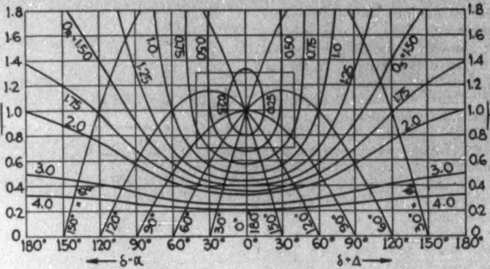

Figure 9. Universal chart for power and voltage given at one end of line

$\phi_R = \beta - \alpha + \theta_R, \; O_R = (\text{kva})_R\left|\frac{B}{E_R^2A}\right| \qquad \phi_S = \beta - \Delta + \theta_S, \; O_S = (\text{kva})_S\left|\frac{B}{E_S^2D}\right|$

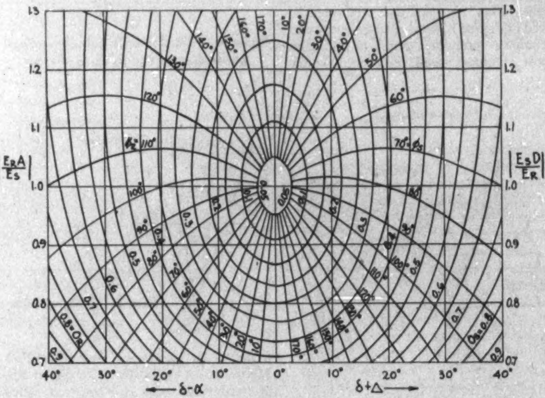

Figure 10. Universal chart for power and voltage given at one end of line, normal operating range

$\phi_R = \beta - \alpha + \theta, \; O_R = (\text{kva})_R\left|\frac{B}{E_R^2A}\right| \qquad \phi_S = \beta - \Delta + \theta, \; O_S = (\text{kva})_S\left|\frac{B}{E_S^2D}\right|$

resulting in

$$\cos(\delta+\Delta) = \frac{\left|\frac{DE_S}{E_R}\right|^2 + \left|\frac{DE_S}{E_R}\right|^4 - O_{RS}^2}{2\left|\frac{DE_S}{E_R}\right|^3} \tag{14}$$

$$\left|\frac{E_SD}{E_R}\right| = \frac{\sin(\phi_S+\delta+\Delta)}{\sin\phi_S} \tag{14a}$$

$$\cos(\delta-\alpha) = \frac{\left|\frac{AE_R}{E_S}\right|^2 + \left|\frac{AE_R}{E_S}\right|^4 - O_{SR}^2}{2\left|\frac{AE_R}{E_S}\right|^3} \tag{15}$$

$$\left|\frac{E_RA}{E_S}\right| = \frac{\sin(\phi_R-\delta+\alpha)}{\sin\phi_R} \tag{15a}$$

The resulting charts are shown in Figure 11, covering a wide range of values, and in Figure 12, applying to the normal operating range. Since appearance and use of the charts is similar to the previous ones, it will be sufficient to compute one example.

Referring to the afore-mentioned transmission line it is required to determine the receiving-end voltage and sending-end power when 50 megavolt-amperes at 96-per-cent power-factor lagging is delivered at the receiving end with the sending-end voltage maintained at 160 kv.

Solution:
As given,

$\cos\theta_R = 0.96$

therefore

$\theta_R = -16.3°$
$\phi_R = \beta - \alpha + \theta_R = 78.56° - 1.06° + (-16.3°) = 61.2°$

$$O_{SR}=(\text{kva})_R\left|\frac{BA}{E_S^2}\right|=\frac{51.2\times153.16\times0.917}{160^2}$$

$$=0.286$$

Referring to the left-hand side of chart Figure 12, the intersection of $\phi_R=61.2$ and $O_{SR}=0.286$ furnishes

$$|E_RA/E_S|=0.77$$

from which

$$|E_R|=\frac{0.77\times160}{0.917}=134.2 \text{ kv}$$

$$\delta-\alpha=19°$$

from which

$$\delta=19°+1.06°=20.06°$$

To find the sending-end power, compute

$$|E_SD/E_R|=\frac{160\times0.917}{134.2}=1.09$$

$$\delta+\Delta=1.06°+20.06°=21.12°$$

Referring now to the right-hand side of Figure 12

$$\phi_S=66.3° \quad O_{RS}=0.43$$

giving

$$(\text{kva})_S=\frac{0.43\times134.2}{153.16\times0.917}$$
$$=55 \text{ megavolt-amperes}$$

$$\theta_S=66.3°-78.56°+1.06°$$
$$=-11.2°, \cos\theta=0.981 \text{ lagging}$$

Sending-end power $55\times0.981=54$ megawatts.

From the foregoing example it can be seen that the desired information can be obtained quickly. It is particularly interesting to note that in this universal type of diagram none of the difficulties inherent in the modified charts of Figures 1C and 1D are encountered.

Additional data follow readily from these charts. The dotted line in Figure 10 indicates the optimum-power-limit line, corresponding to the envelope of the nonconcentric circles in the conventional diagram. This line corresponds to the line $O=1$ in Figure 10 and therefore can be constructed readily.

The power-limit parabola which is the locus of the maximum power transmitted at regulated potentials in the conventional diagram coincides with the constant-power-angle line where $\delta=\beta$.

Power-angle curves can be developed quickly from these charts.

Conclusions

1. A circle diagram is developed, relating power at one end to power at the other end

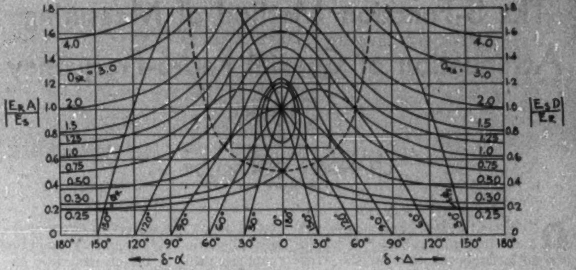

Figure 11. Universal chart for power given at one end and voltage at other end

$\phi_R=\beta-\alpha+\theta_R,\ O_{SR}=(\text{kva})_R\left|\frac{BA}{E_S^2}\right|$ $\phi_S=\beta-\Delta+\theta_S,\ O_{RS}=(\text{kva})_S\left|\frac{BD}{E_R^2}\right|$

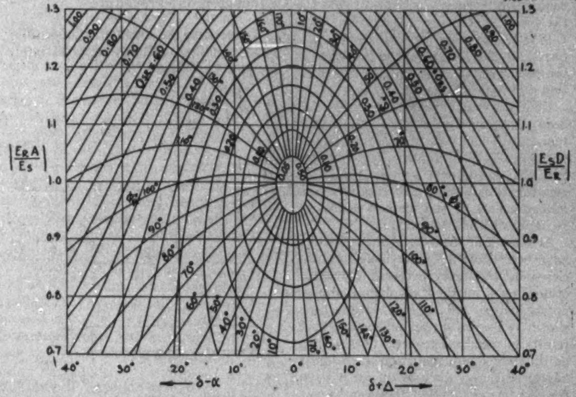

Figure 12. Universal chart for power given at one end and voltage at other end, normal operating range

$\phi_R=\beta-\alpha+\theta,\ O_{SR}=(\text{kva})_R\left|\frac{BA}{E_S^2}\right|$ $\phi_S=\beta-\Delta+\theta,\ O_{RS}=(\text{kva})_S\left|\frac{BD}{E_R^2}\right|$

2. A circle diagram is developed, relating impedance at one end to that at the other.

3. Universal transmission-line charts are developed based on a new co-ordinate system from which the essential data pertaining to any line readily can be computed. The difficulty enountered in the conventional charts with power and voltage given at different ends is eliminated by this type of chart.

References

1. Circle Diagrams for Transmission Systems, R. D. Evans, H. K. Sels. *Electric Journal*, 1922, page 550.

2. The Circle Diagram of a Transmission Network, F. E. Terman. AIEE Transactions, volume 45, 1926, pages 1081–92.

3. Electric Circuits (book), O. G. C. Dahl. Page 296.

4. Electric Circuits (book), electrical engineering staff, Massachusetts Institute of Technology, Cambridge, Mass. Chapter IX.

5. The Complex Variable, Sidney Frankel. *Communications*, September 1943, page 62.

6. Some Graphical Solutions of A-C Circuits, F. W. Lee. AIEE Transactions, volume 45, 1926, pages 948–54.

7. Performance Requirements for Relays on Unusually Long Transmission Lines, F. C. Poage, C. A. Streifus, D. M. MacGregor, E. E. George. AIEE Transactions, volume 62, 1943, June section, pages 275–83.

8. Impedances Seen by Relays During Power Swings, Edith Clarke. AIEE Transactions, volume 64, 1945, pages 372–84.

The S-Function Method of Measuring Attenuation of Coaxial Radio-Frequency Cable

CHANDLER STEWART, JR.
NONMEMBER AIEE

DURING the last few years coaxial radio-frequency cable has been purchased in large quantities by the Army and the Navy for use in aircraft and surface vessels as radio and video transmission lines. Inspection of this cable has been carried out at the factories in accordance with the requirements of the applicable specifications, the latest of which is the Joint Army–Navy Specification *JAN-C*-17. These specifications require frequent measurements, at the factories, of the characteristic impedance and attenuation during production.

Characteristic impedance generally has been determined from results of capacitance and velocity of propagation tests on samples of cable approximately five feet long, by means of a formula similar to equation 32 of this paper. Accuracy of measurements by this method easily can be kept to within one per cent.

Attenuation measurements generally have been made at one or more frequencies such as 100 megacycles or 400 megacycles, by a method involving samples approximately 100 feet long. It has been shown by a series of comparison tests that results of measurements by this method on different equipments and at different laboratories may vary by as much as 20 per cent on one sample. This can be partially attributed to the use of nonstandard equipment and to the highly skilled technique required in making the measurements.

A new method of measuring attenuation, known as the *S*-function method, is here proposed. This method has been found to be simpler, faster, and more convenient than any other in general use. Also, it required samples which are shorter and the lengths of which are less critical than do other methods so far proposed. For example, the best length of radio-frequency cable *RG-8/U* for a 100-megacycle test is 11 inches. Although a knowledge of the characteristic impedance is required, an error in its value generally will not affect adversely the attenuation results, which is in contrast to some methods using resonant lengths of cable, which are subject to errors in direct proportion to the relative error in the supplied value of the characteristic impedance. This method, however, is limited by the design of presently available equipment to frequencies from about 1 to 100 megacycles.

Measurement Procedure

To measure the attenuation of a cable, cut a sample of total length approximately equal to (see Figure 1A)

$$d_0=\frac{144V}{f_{mc}}\text{ feet} \tag{26}$$

where

V = relative velocity of propagation of cable
f_{mc} = test frequency in megacycles

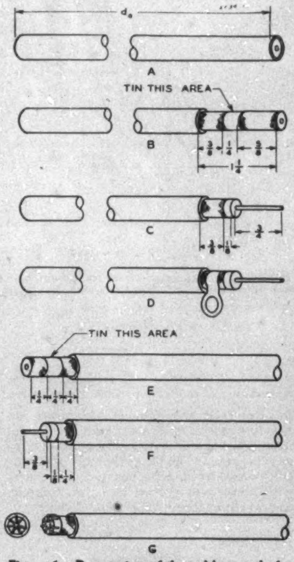

Figure 1. Preparation of the cable sample for measurement

Strip back outer covering for about $1^1/_4$ inches from one end and apply solder to the outside of the braid in a circular band as shown in Figure 1B. Cut through the braid and insulation to the inner conductor at about three-quarters inch from the end (Figure 1C), exercising care not to cut into the inner conductor. Solder a lug to the braid (Figures 1D and 3), making certain that a large part of the lug surface makes contact with the braid and that the entire region around the lug is well soaked in solder. An iron with about 200 watts capacity should be used. Strip back the covering at the other end of the sample for about three-quarters inch (Figure 1E), and soak solder into the braid in a circular band. Cut through the braid and insulation as shown in Figure 1F, and bend back the central strands radially and solder to the braid (Figures 1G and 3). It is important that each strand and this entire end of the braid be well soaked in solder to insure a low-resistance connection. It has been found that making only "spot" contacts has the effect of raising the values obtained for attenuation, *N*, by as much as ten per cent.

The prepared sample is connected to the *Q* meter (Figures 2, 5A, and 5B), which is operated in the usual manner for testing coils, and values of *f*, *Q*, and *C* recorded. These are applied to the solid curve of Figure 6 to obtain the value of *S*, which is inserted in the following formula for attenuation:

$$N=\frac{S}{Qd}\text{ decibels per 100 feet} \tag{20}$$

As a guide in subsequent sample cutting, the dashed line of Figure 6 gives the ratio of preferred sample length (d_0) to the actual sample length (d).

At the lower frequencies it may become necessary to employ auxiliary capacitors. These should be of the silver mica type, and are connected to the "Cond" terminals of the *Q* meter. The amount of external capacitance required is determined easily from the fact that the total capacitance in micromicrofarads required to resonate a cable sample of length d_0 will be

$$C_{\mu\mu f}=\frac{120{,}000}{f_{mc}Z_0} \tag{29}$$

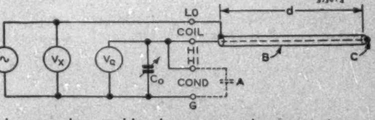

Figure 2. Schematic diagram of the measuring circuit

Standard *Q* meter such as Boonton type 160*A* or 170*A*
A—Auxiliary silver-mica capacitor as required
B—Cable sample under test
C—Inner conductor soldered to outer conductor at end

Paper 45-134, recommended by the AIEE committee on communication for publication in AIEE TRANSACTIONS. Manuscript submitted September 25, 1944; made available for printing May 18, 1945.

CHANDLER STEWART, JR., is attached to headquarters, Army Air Technical Service Command, Wright Field, Dayton, Ohio.

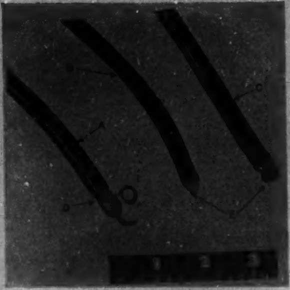

Figure 3. Prepared ends of cable samples for attenuation measurement

A. Radio-frequency cable *RG-8/U*
B. Radio-frequency cable *RG-7/U*
C. Radio-frequency cable *RG-8/U*
D. Connection to *Q* meter
E. Short-circuited ends of cable samples (should be well soldered in this fashion to insure minimum resistance and inductance)

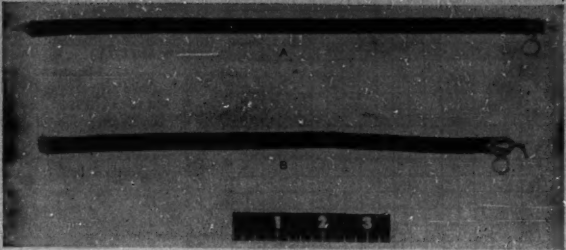

Figure 4. Cable samples prepared for attenuation measurement at 100 megacycles

A. Radio-frequency cable *RG-7/U* B. Radio-frequency cable *RG-8/U*

where

f_{mc} = test frequency in megacycles
Z_0 = characteristic impedance of the cable in ohms

From equation 30 it may be noted that the lowest frequency at which 50-ohm cable can be tested on a type-160*A* Q meter without external capacitance is six megacycles.

Following is a typical example of data obtained in making an attenuation measurement on a sample of radio-frequency cable *RG-8/U:*

d = 3.0 feet
Z_0 = 52 ohms
f_{mc} = 30 megacycles
Q = 89
$C_{\mu\mu f}$ = 82 micromicrofarads
S = 274
N = 1.03 decibels per 100 feet

Appraisal of the Method

A typical sample of coaxial cable, about 200 feet long, was tested at several government and commercial laboratories by various methods at 100 megacycles. The results are listed in Table I. It will be seen that the result obtained by the *S*-function method agrees closely with the average of the results of the other methods.

In Figure 7 results obtained on a sample of radio-frequency cable *RG-7/U* at frequencies from 1 to 100 megacycles by the *S*-function method have been plotted and compared with nominal values listed in the Joint Army–Navy Specification *JAN-C*-17. The measurement results lie almost in a straight line on "log–log" paper.

By use of equations 18 and 33 it can be shown that if the sample length, d, is held to within ten per cent of the length d_0, prescribed by equation 26, a ten-per-cent error in Z_0 will cause less than a two-per-cent error in attenuation, N, and likewise a 20-per-cent error in Z_0 will cause less than a six-per-cent error in N.

Tests were attempted at 200 megacycles, but in each case the results were from 10 to 15 per cent higher than values obtained from other methods or by extrapolation from lower frequencies. This is probably due to losses in the *Q* meter and its terminals, and possibly to some radiation. At frequencies below one megacycle, for most types of cable now in use, the *Q* values are too low to be read accurately. Consequently, it is recommended that for presently available equipment this method be limited to frequencies from 1 to 100 megacycles.

Definitions of Terms

α = attenuation constant of the cable sample in nepers per foot
β = wave-length constant of cable sample in radians per foot
$\gamma = \alpha + j\beta$
c = velocity of light in vacuum in feet per second = $983.57 \cdot 10^6$
C = distributed capacitance of cable in farads per foot
C_0 = capacitance required to resonate cable at test frequency in farads
d = length of cable sample in feet
d_0 = preferred length of cable test specimen in feet
ϵ = base of naperian logarithms
f = test frequency in cycles per second
G = distributed conductance of cable in mhos per foot
$j = \sqrt{-1}$
L = distributed inductance of cable in henrys per foot
$M = Z_0/X_{sc}$, introduced for convenience
M_0 = value of M for least error in N caused by an error in Z_0
N = attenuation of cable in decibels per 100 feet
P = power factor of the cable dielectric

Figure 5A. Connection of cable samples to Boonton type 160*A* Q meter for attenuation measurement by the *S*-function method at frequencies from 1 to 35 megacycles

1. Care must be taken that outer braid clears all metal except *LO* terminal by at least one-eighth inch
2. *LO* terminal
3. Connect silver-mica auxiliary capacitor to these terminals if required (usually unnecessary above six megacycles)

Figure 5B. Connection of cable sample to Boonton type-170*A* Q meter for attenuation measurement by the *S*-function method at frequencies from 35 to 100 megacycles

1. Care must be taken that outer braid clears all metal except *LO* terminal by at least one-eighth inch
2. *LO* terminal

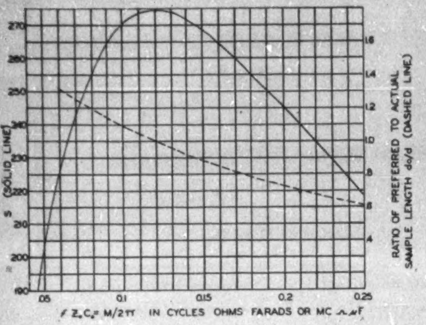

Figure 6. Plot of $S = \dfrac{2{,}000 \log_{10}\epsilon}{M+1/M+1/\text{arccot } M}$ (solid line), and $d_0/d = 0.923 \div \text{arccot } M$ = ratio of preferred to actual sample length (dashed line)

$Q = X_{sc}/R_{sc}$

R = cable-conductor resistance in ohms per foot

R_{sc} = input resistance of short-circuited cable sample in ohms

S = function of M defined in equation 18 and plotted in Figure 6

V = ratio of velocity of radio-frequency potential in cable to velocity of light

ω = angular velocity of test voltage in radians per second

X_{sc} = input reactance of short-circuited cable sample in ohms

Z_0 = absolute magnitude of cable characteristic impedance

$\underset{\cdot}{Z}_0$ = complex cable characteristic impedance in ohms

$\underset{\cdot}{Z}_{sc}$ = input impedance of short-circuited cable sample, in ohms $= R_{sc} + jX_{sc}$

Derivation of Formulas

From fundamental transmission-line theory is obtained the following group of formulas[3]:

$$\alpha = {}^1/_2(G\sqrt{L/C} + R\sqrt{C/L}) \tag{1}$$

$$\beta = \omega\sqrt{LC} \tag{2}$$

$$\underset{\cdot}{Z}_0 = \sqrt{L/C}\,\underline{/{}^1/_2(G/\omega C - R/\omega L)} \tag{3}$$

From basic capacitor theory[4]

$$G = P\omega C \tag{4}$$

$$P = G/\omega C \tag{4a}$$

If we divide equation 1 by equation 2,

$$\alpha/\beta = {}^1/_2(G/\omega C + R/\omega L) \tag{5}$$

Subtracting equation 5 from equation 4a yields

$$P - \alpha/\beta = {}^1/_2(G/\omega C - R/\omega L) \tag{6}$$

Combining equation 3 and equation 6 produces

$$\underset{\cdot}{Z}_0 = \sqrt{L/C}\,\underline{/P - \alpha/\beta} \tag{7}$$

which, by definition, becomes

$$\underset{\cdot}{Z}_0 = Z_0\underline{/P - \alpha/\beta} \tag{7a}$$

In practice $P \ll 1$ and $\alpha/\beta \ll 1$, so that the following approximation is accurate:

$$\underset{\cdot}{Z}_0 \cong Z_0[1 - j(P - \alpha/\beta)] \tag{7b}$$

From transmission-line theory:[5]

$$Z_{sc} = \underset{\cdot}{Z}_0 \tanh \gamma d \tag{8}$$

Substituting equation 7b in equation 8 yields

$$Z_{sc} = Z_0[1 - j(P - \alpha/\beta)](\sinh 2\alpha d + j \sin 2\beta d)/2(\cosh^2 \alpha d - \sin^2 \beta d) \tag{9}$$

As these tests are made on short lengths of cable such that $\alpha d \ll 1$, the following approximation of equation 9 is justified:

$$Z_{sc} = Z_0[2\alpha d - (P - \alpha/\beta)\sin 2\beta d - j \sin 2\beta d]/2 \cos^2 \beta d \tag{9a}$$

By definition and from equation 9a,

$$Q = X_{sc}/R_{sc} = \sin 2\beta d/[2\alpha d - (P - \alpha/\beta) \sin 2\beta d] \tag{10}$$

$$1/Q = (2\alpha d/\sin 2\beta d) - (P - \alpha/\beta) \tag{10a}$$

$$X_{sc} = Z_0 \sin 2\beta d/2 \cos^2 \beta d = Z_0 \tan \beta d \tag{11}$$

By definition and from equation 11,

$$M = Z_0/X_{sc} = \cot \beta d \tag{12}$$

$$\beta = (\text{arccot})\ M/d \tag{12a}$$

$$1/\sin 2\beta d = {}^1/_2\sqrt{2 + \tan^2 \beta d + \cot^2 \beta d} \tag{13}$$

If we combine equations 10a, 12, and 13,

$$1/Q = \alpha d\sqrt{2 + M^2 + 1/M^2} - (P - \alpha/\beta) \tag{14}$$

From equations 14 and 12a we obtain

$$\alpha = (1/Q + P)/d(M + 1/M + 1/\text{arccot } M) \tag{15}$$

$$N = (2{,}000 \log_{10}\epsilon)\alpha \tag{16}$$

so that

$$N = (1/Q + P)2{,}000 \log_{10}\epsilon/d(M + 1/M + 1/\text{arccot } M) \tag{17}$$

Let

$$S = 2{,}000(\log_{10}\epsilon)/(M + 1/M + 1/\text{arccot } M) \tag{18}$$

This is plotted in Figure 6. Then

$$N = S(1/Q + P)/d \tag{19}$$

American Society for Testing Materials specifications require polyethylene to have a power factor of less than 0.005 at 1 megacycle and at 100 megacycles. Measurements made on various samples of radio-frequency cable *RG-8/U* with Q meters showed power factors of the order of 0.0002 at 10 megacyles and of 0.0003 at 100 megacycles. Consequently, for most work involving cables with this insulation, the assumption $P \ll 1/Q$ is justified, in which case equation 19 becomes

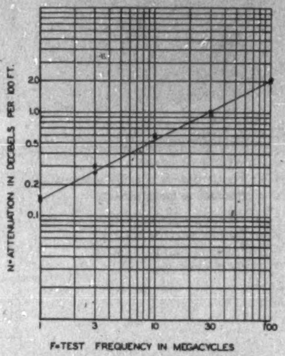

Figure 7. Results of attenuation measurements on radio-frequency cable *RG-7/U* by the S-function method (⊙) compared with engineering data listed in Joint Army–Navy Specification *JAN-C-17*, paragraph E-3 (X)

⊙ Results of S-function test on typical sample
× Engineering data listed in joint Army–Navy specifications

$$N = S/Qd \tag{20}$$

This assumption introduces an error in opposition to the effect of losses in the Q meter and cable-sample terminals, so that even in cases where P is as great as two or three per cent of $1/Q$, equation 20 in practice may yield results as accurate as does equation 19.

From equation 18 is obtained

$$1/S = (M + 1/M + 1/\text{arccot } M)/2{,}000 \log_{10}\epsilon \tag{21}$$

From inspection of equations 12, 19, and 21, it is seen that the value of d resulting in the least possible error in N introduced by a given error in Z_0 would result from the condition:

$$d(1/s)/dM = 0 \tag{22}$$

Solving equations 21 and 22 for M_0 yields

$$M_0 = \cot(M/\sqrt{1 - M})^4 \cong 0.7567 \tag{23}$$

From equations 23 and 12a, the length of cable which would give least error in N by an error in Z_0 is

$$d_0=(\text{arccot } M_0)/\beta=0.923/\beta \qquad (24)$$

From fundamental theory,[6]

$$\beta=2\pi f/Vc \qquad (25)$$

so that equation 24 becomes

$$d_0=Vc(\text{arccot } M_0)/2\pi f=144.5\cdot 10^6 V/f \qquad (26)$$

In the case of a cable with $V\cong 0.65$, such as those with polyethylene or polyisobutylene dielectrics, this becomes about

$$d_0=94\cdot 10^6/f \qquad (26a)$$

For cables with air dielectrics, $V=1.0$, in which case

$$d_0=144\cdot 10^6/f \qquad (26b)$$

If the measurement of X_{sc} is made on a Q meter,

$$X_{sc}=1/\omega C_0 \qquad (27)$$

from which, with equation 12,

$$M=Z_0\omega C_0=2\pi f Z_0 C_0 \qquad (28)$$

and the setting obtained for the preferred length of cable will be, from equations 23 and 28,

$$C_0=M_0/\omega Z_0\cong 0.12/fZ_0 \qquad (29)$$

For 50-ohm cables, such as radio-frequency cable *RG-8/U*,

$$C_0=2{,}400\cdot 10^{-6}/f \qquad (29a)$$

Table I

Method		Laboratory	Decibels Per 100 Ft
Diode voltmeters at ends of long terminated sample[1]		*E*	1.65
		S	2.32
Tuned circuit-coupled-oscillator and diode voltmeter (most commonly employed at radio-frequency cable factories)		*E*	2.01
		T	2.13
		B	2.0
Short resonant lengths[2]	($d=19$ in.)	*S*	2.14
	($d=38$ in.)	*S*	2.17
	($d=59$ in.)	*S*	2.14
The *S*-function method	($d=11$ in.)	*S*	2.13

It will be found in practice that the lowest frequency at which tests by this method can be made on the type 160A Q meter without auxiliary capacitors is limited by the size of the tuning capacitor, whose highest usable capacitance is approximately 400 micromicrofarads. This frequency is given by equation 28, and for a 50-ohm cable would be

$$f=2400\cdot 10^{-6}/400\cdot 10^{-12}=6\cdot 10^6 \text{ cycles per second}=6 \text{ megacycles per second} \qquad (30)$$

Obviously, the frequency range can be extended downward by connecting low-loss fixed capacitors to the capacitor terminals of the Q meter, so that the total capacitance at the center of the dial range will be approximately that given by equation 29.

From equation 7 and by definition of Z_0,

$$Z_0=\sqrt{L/C} \qquad (31)$$

which, with equations 2 and 25, yields

$$Z_0=1/VcC \qquad (32)$$

From equations 12a and 24,

$$d_0/d=(\text{arccot } M_0)/\text{arccot } M\cong 0.923/\text{arccot } M \qquad (33)$$

This has been plotted as a dashed line in Figure 6.

References

1. Coaxial-Cable-Attenuation Measurements at 300 Megacycles, H. H. Race, C. V. Larrick. *General Electric Review*, volume 44, September 1941, pages 507–10.
2. A Method of Measuring Attenuation of Short Lengths of Coaxial Cable, Chandler Stewart, Jr. *Proceedings* of the Instititute of Radio Engineers, volume 33, January 1945, pages 46–8.
3. Communication Engineering (second edition), W. L. Everitt. 1937. Page 118.
4. The Radio Engineers' Handbook (first edition), F. E. Terman. 1943. Page 110.
5. Reference 3, page 145.
6. Reference 3, page 108, equation 23.

Line Drop Produced by Resistance Welders

R. L. LONGINI
NONMEMBER AIEE

Synopsis: Resistance-welding machines normally form a very reactive pulsating load on a power system which sometimes produces undesirable line regulation. The regulation can be calculated, and, if it is too high, it can be reduced by operation directly on 2,300 volts or by power-factor-correction means. From a line-regulation point of view, the system of 2,300-volt operation is usually the most satisfactory. The effect of electronic controls on line drop is also discussed.

LARGE CURRENTS flowing across the junction between two metals evolve heat because of the contact and material resistance. Both the resistance and current are controlled in a resistance-welding machine so that the heat will be just right to produce a fusion weld. The contact resistance is controlled by proper surface cleaning and control of the contact forces by the welding machine. Current is controlled as to duration and magnitude by timing, heat-control circuits, and welding-transformer taps. The currents involved are very large, being between a few hundred and a few hundred thousand amperes, depending on the welding operation.

It is often necessary for mechanical reasons to have long arms on the welding-transformer secondary. This structure will have an inductance of the order of one microhenry. This inductance, although small, will be the main impedance to the welding current. In order to pass 10,000 amperes through this inductance at 60 cycles the transformer secondary must produce about four volts. The transformer will thus involve 40 kva just for this relatively small welding current.

Welding currents are normally of

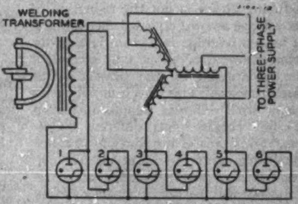

Figure 1a. Power circuit of three-phase to single-phase low-frequency converter

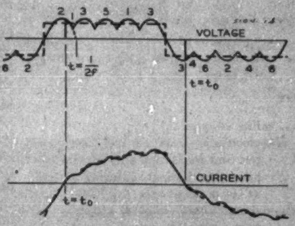

Figure 1b. Voltage and current waves

The solid lines are the actual voltage and current. The dashed lines are the values assumed in the mathematical analysis in the appendix. Numerals indicate which ignitrons are conducting

---

Paper 45-104, recommended by the AIEE committee on electric welding for publication in AIEE Transactions. Manuscript submitted December 19, 1944; made available for printing May 8, 1945.

R. L. Longini is with the Westinghouse Electric Corporation, East Pittsburgh, Pa.

short duration. In production there ordinarily will be several pulses of current per second. This large, pulsating, low-power-factor (usually 0.25 to 0.4) single-phase load frequently requires a power system designed from a regulation point of view entirely without regard for thermal characteristics.

Line-Drop Calculations on Uncorrected Systems

The most common complaint occasioned by line regulation concerns light flicker. The eye is extremely sensitive to flicker if it occurs 2 to 12 times per second, less than one-per-cent voltage fluctuation being objectionable. The voltage drop producing flicker is not the reduction in rms voltage as read on a voltmeter but is the largest average reduction lasting for a time interval of about 0.02 second, a time determined by the physiology of visual response. This time interval varies greatly with different people and even with one person under different conditions. Some welder installations produce enough regulation to upset control circuits. It is desirable to know what the regulation will be for a system before installing a welder.

Regulation can be calculated by the relationship (developed in Appendix I):

$$\text{Per cent line drop} = 100\frac{\Delta E_{line}}{E_{line}}$$

$$= \frac{H^2 \cdot P}{100(kva)_{sc}}(\cos\theta_2 + \sin\theta_2 \tan\theta_1) \quad (1)$$

where

E_{line} = line voltage

H = electronic heat control setting = per cent maximum rms current

P = kilowatts dissipated during a weld at 100 per cent heat

$(kva)_{sc}$ = short-circuit kilovolt-amperes of power-supply system

θ_1 = phase angle of total circuit impedance

θ_2 = phase angle of power system impedance

A given welding operation will require a certain value of the kilowatts, P, dissipated during the weld. It is of interest, however, to see how the other parameters enter into the line drop. The power factors or impedance phase angles enter into the line drop critically. The phase angle of the power system, θ_2, is normally between 60 and 85 degrees so that the term $\sin\theta_2 \tan\theta_1$ is of primary importance in this factor. The total impedance of the circuit is largely that of the load so that θ_1 is almost entirely determined by the load power factor. The phase angle θ_1 is usually greater than 65 degrees, thus a slight improvement in power factor may reduce the line drop very greatly as the tangent varies rapidly in this region. Since low-load power factor is largely due to the inductance of the secondary loop, the loop should be designed with as low an inductance as is compatible with other considerations.

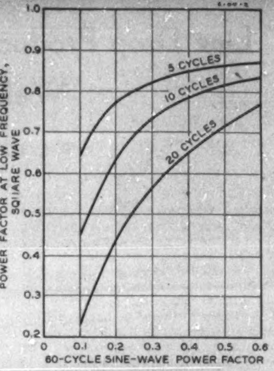

Figure 2. Comparison of the power factor at 60-cycle operation with the power factor of the same machines at low-frequency square-wave operation

It is apparent from the formula that it is desirable to have the short-circuit kilovolt-amperes of the power system, as seen from the welder, as large as possible. On low-voltage power systems the short-circuit characteristics are determined largely by the step-down transformers which limit the short-circuit current greatly. This limitation is avoided and the short-circuit kilovolt-amperes greatly increased by working directly from the high-voltage distribution lines. Welder controls for direct operation on 2,300-volt distribution systems are now available. Operation from these may be direct or may be through a transformer used for the individual welder only in which case the step-down transformer should be considered to be a part of the welding system. Line drop for 2,300-volt operation may be as little as ten per cent of its value for low-voltage operation. Though 2,300-volt operation is usually desirable it is not always possible. Some power-factor-correction means therefore may be required.

Low-Frequency Systems

Certain electronic frequency-changing circuits draw almost balanced three-phase power from the line and have a low-frequency single-phase output. Because power factor is increased when the load is operated at low frequency a double advantage can be had from such an electronic circuit. There are a number of circuits, all fundamentally alike, designed to produce single-phase low-frequency power from a polyphase system. By a system of rectifiers, current is first passed through the load in one direction, then, after one-half cycle of low frequency, the current is passed through the load in the opposite direction.

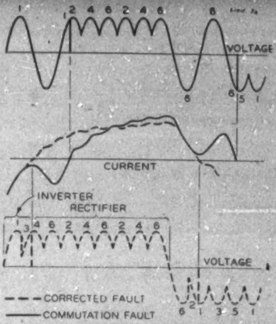

Figure 3a. Current and voltage waves for corrected and uncorrected commutation faults

Numerals indicate which ignitrons of Figure 1a are conducting

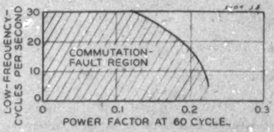

Figure 3b. Region of commutation fault

Figure 1 shows a circuit for three-phase to single-phase conversion with resultant voltage and current waves. The low-frequency voltage wave can be approximated very closely by a square wave plus some high harmonics. The current wave will have these harmonics but only to a very slight degree due to relatively high reactive impedance to these high frequencies. The power factor and other properties of the secondary loop resulting from low-frequency operation can be calculated. (See Appendix II.) The power factor of the entire welder depends on the type of rectifier and the regulation of the transformer involved. Figure 2 shows power-factor curves for a low-frequency welding system having good transformer regulation, being used at full heat. Heat control, which involves delaying the ignition of the rectifier ignitrons, reduces the power factor greatly.

Voltage and Current Reversal

Each ignitron carries current until another ignitron with properly applied voltage takes over this task or until the load current becomes zero. When it is desired to reverse the voltage no subsequent ignitron is fired to which the current can

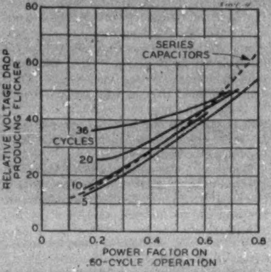

Figure 4. Light flicker for low-frequency and series-capacitor systems compared with 60-cycle uncorrected systems (equal 100 on voltage scale)

The voltage drop producing light flicker depends on the physiology of the eye

commutate so that the last ignitron fired in each voltage pulse carries current until the current ceases.

Before the last ignitron extinguishes, the voltage of the corresponding rectifier-transformer secondary winding reverses. The current is then flowing against the applied voltage and is quickly reduced in magnitude, but continues to flow against the applied voltage because of the reactive nature of the load. When the current finally reaches zero the ignitron extinguishes. The operation can best be seen by referring to Figure 1b. Tube 3 is the last tube to be fired in the upper portion of the voltage wave shown. It continues to carry the current until time t_0, at which instant the current is zero. At that time, or very shortly thereafter, tube 4 is ignited. This tube applies the voltage to the loop in such a way as to reverse the direction of the current. The subsequent firing order is shown in the figure.

If the load is so reactive that $t_0 > {}^1/_{120}$ second, the rectifier transformer voltage again reverses and the current will be built up again instead of being reduced to zero. Therefore the ignitron will continue to conduct. This condition, known as a commutation fault, is shown in Figure 3a. The boundary of the commutation-fault region (calculated in Appendix II) is shown in Figure 3b.

Commutation Fault and Limitations and Correction

Commutation fault introduces drawbacks to the use of low-frequency systems. During one or more cycles (on supply-frequency basis) the entire load is single phase, resulting in a momentarily increased voltage drop of two lines. Though this momentary drop will have a very small value when read on an rms meter it may cause objectionable light flicker. The drop that must be considered is the drop on the loaded phase lines.

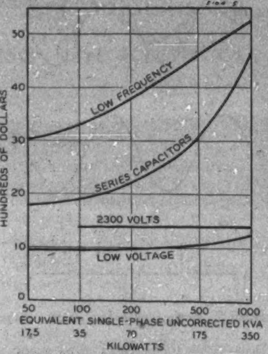

Figure 5. Cost of controls for various systems having a resistance-to-inductance ratio giving 35-per-cent power factor at 60 cycles

It is possible to avoid commutation fault by a different method of operation. Refer again to Figure 3a. The dashed curve shows a system corrected for commutation fault. At the time tube 3 (left of the corrected-voltage-wave, lower part of the figure) is fired, its anode is more positive than that of tube 1 so that the current can commutate to it readily. Very shortly after the commutation is completed, however, the applied anode voltage of tube 3 goes negative, thus the current continued to be opposed. This process is repeated until the current reaches zero. The operation described is that of an inverter. Power from the reactive energy of the electrode loop has thus been fed back into the power-distribution system. After the current reaches zero, the system is again operated as a rectifier. This inverter–rectifier operation eliminates any single-phase operation such as occurs during a commutation fault. The power-factor-correction curves of Figure 2 are based on this inverter–rectifier system.

Series-Capacitor Systems

The power factor of a welder can be corrected by inserting capacitors in series with its primary winding. The capacitance is of such a value that it tunes to resonance, or close to it, with the inductance of the welding transformer. Thus the capacitor and welding transformer in series have no 60-cycle reactive component. The current is limited entirely by the reflected resistance of the welding-transformer secondary winding.

At full heat a series-capacitor-corrected welder operates on unity power factor. When reduction of current by electronic heat control is used, the ignitrons are fired later in the cycle than at 100 per cent heat. This makes the 60-cycle component of current lag behind the line voltage, therefore making the load appear reactive. Because the current is large at 90 per cent heat and is lagging behind the line-voltage the regulation is actually greater than at 100 per cent heat. As the heat is reduced below 90 per cent the regulation improves.

The inductance of the system may be altered by adjusting the secondary loop for different welding operations, or, very slightly, by varying the amount of iron in the secondary loop. Any large inductance changes require readjustment of the capacitor bank if perfect power-factor correction is desired.

Light-Flicker Comparisons

Figure 4 compares the light flicker produced by series-capacitor and low-frequency systems with the flicker resulting from uncorrected-power-factor systems. The curves are based on a power line with 0.3 power factor. Series capacitors correct the power factor completely at 100 per cent heat, but when the ignition is delayed harmonics are introduced which destroy this perfect correction. As a result, maximum line drop occurs at about 90 per cent heat, for which the series-capacitor curve is shown. The drop produced by the low-frequency system was on the basis of full heat. At reduced heat the system utilization is poor and rectifier power factor differs very appreciably from unity so that the greatest drop will be at reduced heat. The drop produced by low-frequency operation will, of course, pulsate at a low frequency to which the eye is very sensitive.

Metallurgical Considerations in Power Factor Correction Problems

Power-factor correction alters one metallurgical factor, the heat generated at the weld being dependent in a different way on work resistance. A slight change in resistance at the weld on uncorrected systems has only a very slight effect on the current as the current is largely inductively limited. In the low-frequency system the current is almost entirely resistance limited. In series-capacitor circuits the welding transformer gets its voltage by virtue of a resonant condition, the primary voltage on the welding transformer being, as a result, approximately inversely proportional to secondary resistance. The secondary current is thus dependent on secondary resistance as it is in low-frequency systems.

The resistance of the work depends on surface conditions, electrode pressure, and materials being welded. The power delivered to the spot, I^2R, will vary with the work resistance depending on how the current varies with resistance. In low-power-factor uncorrected systems, where the weld current is independent of resistance, the power dissipated at the weld is directly proportional to the weld resistance. In corrected systems the heating is inversely proportional to the secondary resistance. The quality of the weld is determined to a large extent by the power dissipation at the spot and therefore on the power factor of the welding machine.

Cost

Both the low-frequency systems and the series-capacitor systems are expensive. The cost depends on many factors, among them: duration of "on" and "off" periods, power factor before correction, type of control, and power required. Figure 5 shows how the cost of the controls varies. The cost is dependent on the power factor before correction and on the power demand. To put the systems on a comparative basis, the power demand is plotted as that for an equivalent uncorrected system.

Conclusions

The line drop of a system can be readily calculated for a given welder. If the line drop turns out to be too great there are several alternatives possible to reduce it, the most satisfactory and least expensive usually being operation on 2,300 volts.

Not only power line but also welding properties must be considered in determining the desirability of using a power-factor-correction system. The dependence of power dissipated at the weld on the power factor is pronounced. No general statement can be made as to the most desirable power factor but it should be pointed out that power-factor correction may be, on some jobs, very undesirable from a welding point of view. Depending on the welding job it might be desirable or undesirable to use power-factor-correction systems.

Series-capacitor systems are less expensive than low-frequency systems for the same improvement in light flicker and kilovolt-ampere demand, though they are still single phase. If the welding loop is to be varied appreciably in any dimension there must also be adjustments of the series capacitors if perfect power-factor correction is to be maintained. Low-frequency systems do not require readjustment with change of the welding loop, but may be subject to commutation fault.

Appendix I. Voltage Drop for Single-Phase Uncorrected-Power-Factor Electronically Controlled Welder

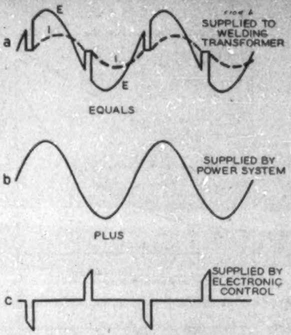
a
E
I
I
E
SUPPLIED TO WELDING TRANSFORMER
EQUALS
b
SUPPLIED BY POWER SYSTEM
PLUS
c
SUPPLIED BY ELECTRONIC CONTROL

Figure 6. Analysis of applied welder voltage

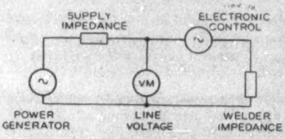

Figure 7a. Schematic circuit with assumption of linear elements

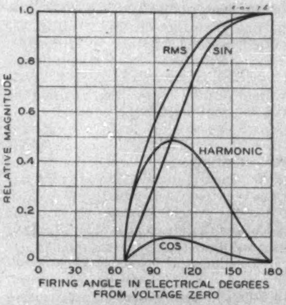

Figure 7b. Typical output of electronic generator

Supply voltage = −1.0

An oscillogram of the voltage and current waves of a heat-controlled wave appear as shown in Figure 6a. The inductive nature of the load causes the current to continue to flow even after the voltage has reversed in direction. It will be noted, on examination of the voltage wave, that it is the sum of the two voltages shown in b and c of Figure 6. Figure 6b is the voltage supplied by the power system and Figure 6c is the voltage generated by the electronic controls. By this division of the electromotive force it is possible to treat the circuit as though it were composed entirely of linear impedance elements. The circuit then has two voltage sources, the power system and the electronic-control system, as shown in Figure 7a.

The voltage generated by the electronic-control system, though very rich in harmonics, has a considerable line-frequency component. Figure 7b shows an analysis of the voltage generated by the electronic-control system as a function of the phase of firing. To determine the total applied fundamental-frequency voltage the two voltages must be added vectorially. The harmonic voltages have as their sole source the electronic-control system. They, therefore, tend to increase the rms line voltage. Their contribution to the rms voltage turns out to be negligible, however, as their contribution is less than one tenth of one per cent. In these calculations, therefore, they have been neglected entirely.

Equation 1 was derived on this basis. It is interesting to note that the line drop is the same for input cut down by electronic heat control as for reduction of P by tap adjustment.

Appendix II. Calculation of Three-Phase to Single-Phase Low-Frequency Welder Characteristics

Calculations of power factor on the basis of a perfect square-wave generator. Actual power factors may be only 60 per cent of F_f.

$$F_f = \text{kw}/\text{kva} = 1{,}000P/VI_{rms} \tag{2}$$

where

F_f = power factor at low frequency, f
P = kilowatts
V = square-wave voltage
I_{rms} = low-frequency rms current

$$I_{rms}^2 = \frac{1{,}000P}{R_f} \tag{3}$$

where

R_f = resistive component of low-frequency impedance

$$F_f = \frac{I_{rms}R_f}{V} \tag{4}$$

The current resulting from the square voltage wave will have an exponential form for each half cycle given by

$$i = \frac{V}{R_f}\left[1 - \frac{2\epsilon^{-at}}{1+\epsilon^{-a/2f}}\right] \tag{5}$$

Where f is the square-wave frequency, a is the R/L ratio of the secondary loop and is given by

$$a = 377\left(\frac{1}{F_{60}^2} - 1\right)^{-1/2}$$

where F_{60} is the power factor for the given R/L ratio when operated on a 60-cycle sine-wave voltage. The time t is measured from the instant of voltage reversal.

From the definition of I_{rms}

$$I_{rms}^2 = \frac{2fV^2}{R_f^2}\int_0^{\frac{1}{2f}}\left[1 - \frac{4\epsilon^{-at}}{1+\epsilon^{-a/2f}} + \frac{4\epsilon^{-2at}}{(1+\epsilon^{-a/2f})^2}\right]dt \tag{6}$$

Evaluation of the integrals gives

$$I_{rms}^2 = \frac{2fV^2}{R_f^2}\left[\frac{1}{2f} - \frac{4}{a}\,\frac{1-\epsilon^{-a/2f}}{1+\epsilon^{-a/2f}} + \frac{2}{a}\,\frac{1-\epsilon^{-a/f}}{(1+\epsilon^{-a/2f})^2}\right] \tag{7}$$

Coincidence-Factor Relationships of Electric-Service-Load Characteristics

CONSTANTINE BARY
MEMBER AIEE

Synopsis: This paper contains a demonstration of the existence in practice of relationships between group coincidence factors and number of consumers, and between group coincidence factors and consumers' load factors. Empirical relationships developed from test observations are analyzed from theoretical considerations, formulated in a general manner, and qualified as to the significance of the quantitative values.

THE STUDY of electric-service loads may be divided into two major parts; one dealing with the gradual ebb and flow of loads which are integrated over specified intervals of time measured in terms of minutes, and the second dealing with momentary surges of load which last for short intervals of time measured in terms of seconds. The load characteristics of each of these parts in turn may be subdivided into four distinct components; one taken as at the terminals of the individual appliances and applications, the second one as at the service entrance of individual consumers of electric service, the third one for the diversified conditions of groups of consumers or groups of specified appliances and applications, and the fourth for all classes of consumers or for all classes of appliances and applications, which results in what may be called the "system" conditions.

This paper will be confined to a discussion of the interrelation of some of the factors of the first part of the subject. It will outline two fundamental relationships which have been found in practice to exist between the probable behavior of coincidence factors of individual consumers' loads and

1. A change in the number of consumers.
2. A change in their individual load factors.

These basic relationships were selected for this paper because they have the greatest significance in the engineering and economic features of central-station supply and because comparatively little is known of their probable behavior.

Diversity factor, which is a measure of the degree of diversity present between maximum loads of individual parts of a system, is defined by the AIEE as "the ratio of the sum of the maximum power demands of the subdivision of the system or part of the system to the maximum demand of the whole system or part of the system under consideration measured at the point of supply." For purposes of this discussion, however, it will be easier to visualize and deal with the reciprocal of this relation, that is, with the coincidence in maximum power demands. Its measure is expressed as a "coincidence factor" and will be defined as the ratio of the maximum coincident total power demand of a group of consumers to the sum of the maximum power demands of the individual consumers comprising the group, both taken at the same point of supply and for the same period of time.

While the diversity factor can never be *lower* than unity, the coincidence factor can never be *greater* than unity and, therefore, in dealing with the coincidence factor, we deal in values between zero and unity, while in the case of diversity factor we deal in values between unity and infinity. Since a large part of the facilities required to render electric service depends upon the coincident or diversified maximum demands of groups of consumers, it is evident from the foregoing definition that the higher the coincidence factor, the larger becomes the amount of facilities required per kilowatt of the noncoincident maximum demands of individual consumers, and the lower the coincidence factor, the smaller it becomes.

Major Factors Affecting the Coincidence in the Use of Service

The manner in which electric service is used by individual consumers or groups of consumers, and thus the degree of coincidence in this use, is determined by many factors. Among the more important ones may be mentioned population habits, community and business practices, weather and other climatic conditions, design of utilization equipment, and methods employed in the control of use of the service rendered. The significance of these factors may become clearer from the following discussion.

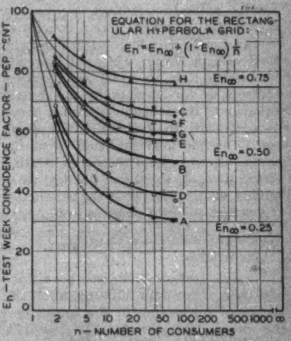

Figure 1. Probable trend in relation between group coincidence factor and number of consumers in group

Based on one-half-hour integrated demands in December reflecting 1938 and 1939 test data, and for a range in average of consumers' monthly load factors, as follows:

Domestic, without electric ranges:
A—12-per-cent load factor
B—23-per-cent load factor
C—31-per-cent load factor

Domestic, with electric ranges:
D—10-per-cent load factor
E—16-per-cent load factor

Retail light and power, industrial:
F—17-per-cent load factor

Retail light and power, commercial:
G—18-per-cent load factor
H—28-per-cent load factor

Paper 45-116, recommended by the AIEE committee on domestic and commercial applications for publication in AIEE TRANSACTIONS. Manuscript submitted April 27, 1945; made available for printing May 21, 1945.

CONSTANTINE BARY is rate research engineer, Philadelphia Electric Company, Philadelphia, Pa.

The author acknowledges the valuable suggestions received from N. E. Funk, I. L. Craig, and F. J. Berger of the Philadelphia Electric Company on the original manuscript of this paper, and the assistance of A. Abramovitz and Miss Helen Hughes of that company in preparing the material contained therein.

---

but

$$\frac{1-\epsilon^{a-/f}}{(1+\epsilon^{-a/2f})^2}=\frac{1-\epsilon^{-a/2f}}{1+\epsilon^{-a/2f}}=\frac{\epsilon^{a/4f}-\epsilon^{a/4f}}{\epsilon^{a/4f}+\epsilon^{-a/4f}}$$

$$=\tanh\frac{a}{4f}$$

Therefore, by equations 4 and 7

$$F_f^2=1-\frac{4f}{a}\tanh\frac{a}{4f} \qquad (8)$$

Calculation of Commutation Fault

A commutation fault occurs if t_0, the time for the current to reach zero after voltage reversal, is greater than $^1/_{120}$ second.

From equation 5

$$i=0=\frac{V}{R_f}\left[1-\frac{2\epsilon^{-at_0}}{1+\epsilon^{-a/2f}}\right] \qquad (9)$$

For $t_0 > {}^1/_{120}$ second, the condition of commutation fault,

$$\epsilon^{a/120}(1+\epsilon^{-a/2f})<2 \qquad (10)$$

or

$$a<84 \qquad F_{60}<0.22$$

A fault occurs if inequality 10 holds.

POPULATION HABITS AND COMMUNITY AND BUSINESS PRACTICES

Population habits and community and business practices exert a powerful influence upon the degree of coincidence in the consumers' use of electric service. The difference in the time when people get up; when they go to bed; how, when, and what they eat; where they live; the holidays they observe; where, when, and at what they work; the amount of leisure they have; and, generally speaking, how they live, work, and play on different days of the week and in different seasons of the year; all of this is reflected in the degree of coincidence of consumers' use of electric service. These conditions are not subject to precise mathematical formulations, and their resultant effect will be different for different communities and different climatic, social, and political conditions. But for any given community, operating under a given set of social and political conditions, the resultant effects of population habits and community and business practices upon the manner of use of electric service usually fall into some general pattern and thus result in some determinable values of the degree of coincidence of individual consumer's use of service. These forces are generally too strong to be subject to control by individuals, although major policies of service-supply may have some minor influences upon them. They are, however, very susceptible to social and political controls, as, for example, by the general behavior of the community during a war as contrasted to its behavior in peacetime; by the artificial changes in the setting of clocks from the normal setting on sun time; by social and political revolutions and by the lack or the presence of regimentation of the people's lives.

WEATHER AND OTHER CLIMATIC CONDITIONS

Weather and other climatic conditions also exert a powerful influence upon the degree of coincidence in the consumers' use of electric service. For example, the advent of severe darkness because of an oncoming storm during otherwise daylight hours may create a full coincidence of the power and lighting loads, wiping out the normal diversity between their individual maximum demands and thus increasing the coincidence factor. A severe cold spell causing the almost continuous operation of individual heating plants increases the extent of coincidence in the use of electric service in connection with such plants. A severe hot spell, causing an almost continuous operation of individual air-conditioning plants and other forms of cooling and ventilating equipment, increases the extent of coincidence in the use of electric service in connection with these appliances. These forces are beyond the control of individuals. They are not subject to exact mathematical determinations. But they are susceptible, in general, to appraisals from available weather records for average, maximum, and minimum conditions.

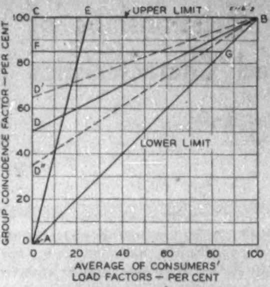

Figure 2. Illustration of the significance of certain lines on chart of coincidence factors versus consumers' load factors

DESIGN OF UTILIZATION EQUIPMENT

The design of utilization equipment has a considerable influence upon the degree of coincidence of consumers' use of electric service. For example, generally speaking, to perform a given task through expenditure of a given amount of energy, devices which are "overcapacitied" may have lower coincidence factors than devices which are "undercapacitied," although the coincident maximum demand of the former may be higher than the coincident maximum demand of the latter. Devices designed for full automatic operation under intermittent cycles may have lower coincidence factors than those designed to accomplish the same purpose under manual operation. These design features are well within the control of design engineers, although it should be realized that the effects of different designs cannot be ascertained from laboratory tests, but must be obtained from extensive research and tests of sample applications in actual use.

METHODS OF CONTROL

Methods for artificial control in the use of service also have important influences upon the degree of coincidence of consumers' demands. Generally speaking, a group of identical devices operating without any restrictive control will experience a smaller coincidence in their individual maximum demands than the same group of devices operating under a predetermined control cycle, even though the group of uncontrolled devices may possess features which are undesirable from other considerations affecting the system while the controlled devices may not have such undesirable features.

Notwithstanding the complexity of forces which affect the degree of coincidence in the use of electric service, experience has demonstrated the existence of two general phenomena relative to the behavior of group coincidence factors. One is the relationship between group coincidence factors and the number of consumers in a group, and the other, which only recently has received closer attention, is the probable relationship between group coincidence factors and average load factors of individual consumers of a group. These constitute the two basic coincidence-factor relationships of electric-service-load characteristics and are of fundamental significance in central-station service supply. They find applications in engineering and economic studies dealing with load forecasting for system planning, design of distribution systems, provision of service facilities, development of utilization appliances and applications, determination of cost to serve for widely different characteristics of service requirements, design of rates, and determination of service-sales-promotion policies for best economic results.

Coincidence Factor Versus Number of Consumers

In a general way the coincidence-factor-versus-number-of-consumers relationship may be formulated as follows:

For consumers of equal size, with no artificial restrictions placed in the way of their service use, and with all other things equal, the degree of coincidence of the maximum power requirements of a group of consumers decreases along a path resembling that of a rectangular hyperbola from unity for one consumer in a group to values approaching the asymptote of the rectangular hyperbola for an infinite number of consumers in a group.

Figure 1 depicts a mathematical grid of the simplest equation for a rectangular hyperbola and demonstrates that the results of actual test observations for various types of consumers of the domestic, commercial, and industrial classifications in general follow the mathematical relationships of the assumed empirical equation reasonably well. It also illustrates two very important conditions present in this relationship in practice: first, that the convergence of the relationship toward the asymptote is comparatively rapid for all values of $E_{n\infty}$ indicating that beyond 100 consumers in a group the change in coincidence factors is relatively small, and, secondly, that the convergence to the asymptote is more rapid for the higher values of $E_{n\infty}$ than for the lower ones.

The practical significance of these conditions is found in the fact that statistically stable results, as to diversified-load characteristics, may be expected in the practical range of $E_{n\infty}$ when as few as 100 consumers are involved in any one group, and results of sufficient engineering stability can be obtained even from groups of only 30 to 50 consumers for values of E_{a_m} of 20 per cent and higher.

Coincidence Factor Versus Load Factor

The subject of the probable behavior of coincidence factors of groups of consumers with a change in their individual load factors only recently received closer attention throughout the electric-utility industry. In the past there existed a feeling among students of this problem that, in a general way, the extent of coincidence in time of the load requirements of a group of consumers of electric service ordinarily increases as the load factors of the individual consumers of a group increase. But, in general, the practical nature of the relationship was not known. It was in 1937 that the author first demonstrated the existence of a probable relationship between coincidence factors and individual load factors of groups of consumers over the complete load-factor range.[1] Subsequently it has been studied, in a thorough manner, by a subcommittee (E. M. Terry, chairman)[2] and H. E. Eisenmenger rationalized and verified the shape of the author's original empirical curve, in a classical manner, from mathematical considerations.[3] The following discussion will elaborate upon some of the more important theoretical aspects of this subject and will expand upon the author's original findings in the light of new and additional information secured since the original demonstration of the relationship.

Theoretical Considerations

It is obvious that a group of consumers, each having a 100-per-cent load factor, has a coincidence factor equal to unity. Furthermore, it may be demonstrated that a group of many consumers, each having a load factor approaching zero, and being unrestricted in the manner of operation throughout the entire period under consideration, will have a coincidence factor which will approach the value of one divided by the number of consumers, and which will approach zero for small demand intervals and for a very large number of consumers in a group. Thus, with the two extreme values known, it may be expected that, for a large number of consumers and under natural conditions of load behavior, there will exist some probable relation which will connect these two points.

It also may be demonstrated that under no condition can the value of the coincidence factor of a group of consumers, each having the same load factor, drop below the load factor, nor can it, by definition, exceed the value of unity. With these limits set, the probable relations should lie between these limits marked *AB* and *CB* in Figure 2. Theoretically, of course, for any given value of consumers' load factors, the group coincidence factor can have any value between these limits.

From theoretical considerations of an equal probability in the influence of the two limits upon the coincidence factor of a group of consumers with a given load factor, one may expect to find the path of the probable relationship to follow the line *BD* whose points for a given load-factor value will be equidistant from the limits of the possible relationships depicted by lines *AB* and *CB*. Straight lines emanating from *B* above or below line *BD*, for example, line *BD′* or *BD″*, produce relationships with unequal weights in the probability of the influence of the upper and lower limits upon a given group coincidence factor, the line above the line *BD* giving greater weight to the influence of the upper limit, and the lines below giving greater weight to the influence of the lower limit.

Actual experience has demonstrated, however, that the most probable relationships between group coincidence factors and individual consumers' load factors do not follow the straight lines depicting certain predetermined and constant relative weighing of the values of the upper and lower limits over the entire range of

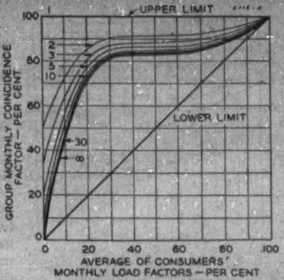

Figure 4. Empirical trend in the relation between coincidence factor and load factor for different numbers of consumers in group

Based on one-half-hour integrated demands in December

Numbers affixed to curves indicate number of consumers in group

Figure 3. Empirical trend in the relation between coincidence factor and load factor

Based on one-half-hour integrated demands in December for groups of 30 consumers

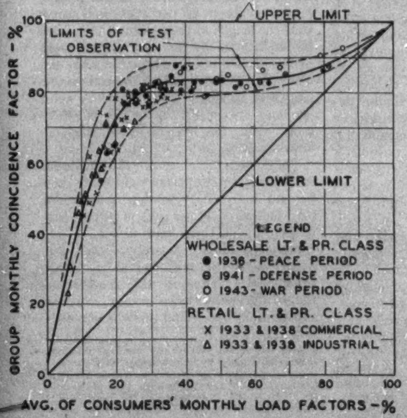

Figure 5. Comparison of empirical trends in the relations between coincidence factors and load factors of different classes of consumers

Based on one-half-hour integrated demands in December for groups of 30 consumers reflecting 1936 test data for the wholesale light and power consumers and 1939 test data for domestic consumers

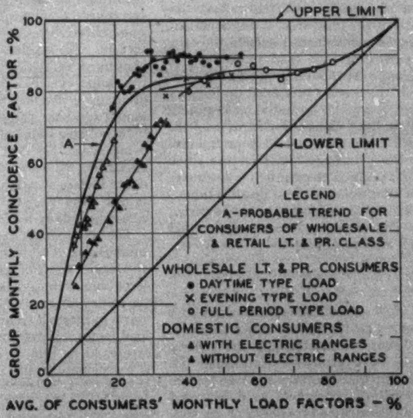

load factors. *The existence of the probable relationships can be obtained only from a large number of test observations of the actual behavior of loads of different classes of consumers.*

At this point it may be well to pause to consider the theoretical significance of certain lines and slopes depicted in Figure 2. It may be demonstrated that any straight line, such as *AE*, from the origin upward and above the lower limit line *AB*, represents the path of the coincidence-factor-versus-load-factor relationship for the theoretical conditions when the predominant and, therefore, the maximum use of service for a large group of consumers is confined to a certain portion of the entire period under consideration, and when all the changes in the consumers' load factors are accomplished through changes in energy use in that period. Hereinafter it will be referred to as the period of high load probability. The shorter this period, the steeper the slope of the straight line, so that, for example, line *AC* represents the shortest period or the full coincidence of maximum demands of all consumers in a group. Line *AB*, however, depicting the lower limit of the relationship or, as it may be called, the "best possible line," represents the longest period of high load probability as it applies to conditions when the loads of all consumers have the same probability of occurring throughout the entire period under consideration. The measure of the length of this period of high load probability in relation to the total period under consideration is obtained by projecting upon the abscissa the point of intersection of such a line as *AE* with the upper limit of the possible relationship indicated by line *CB*.

A horizontal line such as *FG* drawn from the ordinate or from any line such as *AE* toward the "best possible line" will be the path of the coincidence-factor-versus-load-factor relation when the change in the individual consumers' load factors is accomplished outside the original period of high load probability of the group. It should be noted, however, that as this period gets filled up with increased energy use of individual consumers, it in itself causes an extension of the original period of high-load probability until the consumers' load factors reach values at which their group coincidence factor intersects the "best possible limit," line *AB*, at which point the entire period under consideration becomes the period of high load probability.

EMPIRICAL RELATIONSHIP FROM TEST DATA

Figure 3 presents the results of research conducted by the author over a period of many years in establishing the general features of a probable relationship between coincidence factors and load factors of groups of consumers as determined from the service loads of one large electric-utility system operating in metropolitan, suburban, and rural territories in the eastern part of the United States.

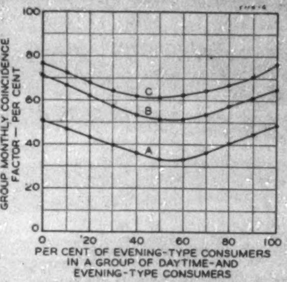

Figure 6. Illustration of effects of different mixtures of load types, for groups of 30 consumers, upon group coincidence factors of the retail light and power class reflecting 1938 test data

A—Consumers with 10-per-cent monthly load factors

B—Consumers with 20-per-cent monthly load factors

C—Consumers with 30-per-cent monthly load factors

The test observations were obtained generally for the month of December over a period of several years from integrated half-hourly load records and from a large number of consumers of several classes of the general service. They include test data for almost a decade before World War II, data during the defense period of this country and, finally, data at the height of this country's war-production activities. The procedure of analysis was uniform throughout. Consumers studied were arranged into groups, each falling into specified rather narrow load-factor limits. Each group consisted of 30 consumers, a sufficient number to produce representative results of the coincidence factors. The maximum load values of all consumers in each group were placed on the same relative-size basis either by grouping consumers with maximum demands of about the same magnitude, or by expressing each half-hour demand of a consumer in per cent of the consumer's maximum half-hour demand. Coincidence factors shown in Figure 3 were obtained from an analysis of individual consumer's daily load curves.

The relationship for the industrial and commercial consumers of the wholesale and retail classes of service, for which observations were available for practically the entire range of monthly load factors, starts out from a value close to zero* at a load factor approaching zero, rapidly increases along almost a straight line to a coincidence-factor value of about 75 per cent at 20-per-cent load factor, thereafter bends sharply to the right and rises slowly to 84 per cent at 40-per-cent load factor and then remains substantially fixed at that level of coincidence factor until reaching a load factor in excess of 70 per cent beyond which it turns up sharply and approaches the "best possible line" in the ultrahigh load-factor range.

Thus, from the foregoing theoretical considerations, the broad generalized behavior of the coincidence-factor-versus-load-factor relationship in practice appears to follow three distinct phases, although, as may be expected, the conditions obtained toward the end of the first phase merge with the conditions obtained at the beginning of the second phase, and the conditions obtained at the end of the second phase merge with the conditions obtained at the beginning of the third phase.

Phase one, obtained in the low-load-factor range, appears to indicate that, for a given classification of consumers, the high probability for the occurrence of the consumer's predominant energy use is confined to a certain well-defined portion of the entire period under consideration, and the predominant changes in the individual-consumer's-load factors are accomplished through changes in the extent of energy use almost entirely in that period.** Thus, in this load-factor region, the coincidence factor rises rapidly and almost in direct proportion to the rise in individual-consumer's-load factors. This phase of coincidence-factor-versus-load-factor behavior approximates that depicted by the theoretical line *AE* in Figure 2. Projecting upwards the portion of the empirical line which approaches a straight line from zero, we find it intersects the upper limit of the possible relationship at a point which corresponds to an individual consumer's monthly load factor of about 22 per cent, indicating that the length of the period of high-load probability is 22 per cent of the total period under consideration. Since the entire period is the month of December, the length of the high load probability thus becomes about 164 hours, or slightly more than four weeks of 40 working hours each.

Phase two, obtained in the medium-load-factor range appears to indicate that beyond individual consumers' monthly load factors of 30 per cent, a further improvement in their load factors is accomplished almost entirely *outside* the period of the group's original high load probability. Thus in this load-factor range the coincidence factor remains substantially fixed, and its behavior with respect to load factor approximates that depicted by the theoretical line *FG* in Figure 2. This phase of the relationship was of utmost significance in appraising the combined load requirements of industrial consumers during this war as a result of substantial changes in the industrial-consumers' load factors through the addition of the second and third shifts and through the extension of the working periods into Saturdays, Sundays, and holidays. Actual experience through this war period, and as indicated by the test points in Figure 3, substantiate the fundamental nature of the empirical relationship developed from actual test observations before the war.

---

* For 30 consumers in a group used in this study, the starting point at load factor approaching zero is actually 1+30=0.0333.

** Actually, minor changes must be occurring outside of this period because the empirical relationship as determined by test observations in the low-load-factor range is not strictly a straight line, but is a curve sloping toward the lower limit of the possible relationship, thus indicating the presence of a small horizontal component, in addition to a major upward one.

Phase three, obtained in the ultrahigh-load-factor range, appears to indicate that beyond an 80-per-cent monthly load factor the entire period under consideration becomes the period of high load probability for the occurrence of the consumers' predominant use of service so that further improvement in consumers' load factors are accomplished at random throughout this entire period. Thus in this ultrahigh-load-factor region the coincidence-factor-versus-load-factor relationship approaches the lower limit of the possible relationship or what may be called the "best possible line."

Present indications point to the fact that this general relationship is basic and fundamental over the entire range of load-factor values, but the numerical values obtained in practice will be different, not only for different classes of consumers, or different appliances and applications, but also for the same types of consumers and appliances in different communities.

The slope of the line in the low-load-factor range depends upon the relationship between the length of period of high load probability of the classification to the total length of the entire period under consideration. That relationship is determined largely by factors mentioned at the beginning of the paper such as population habits, community and business practices, weather and other climatic conditions, and, in addition, also depends upon the relative composition of the types of load represented by a given classification.

Based on the foregoing discussion it is now possible to formulate qualitatively the coincidence-factor-versus-load-factor relationship as follows:

> For a large number of consumers, of equal size, with no artificial restrictions placed in the way of their service use, and with all other things equal, the degree of coincidence of the maximum power requirements of individual consumers in a group changes with the change in their individual load factors. In the low-load-factor range the coincidence factor increases rapidly with the increase in the individual consumers' load factors. Its rate of change is substantially constant and is inversely proportional to the relative length of the high load probability of the class. In the medium range of load factors the magnitude of the group coincidence factor remains substantially fixed, until very high-load-factor values are reached, when the relation between load factor and coincidence factor approaches the lower limit of the possible relationship.

Care should be exercised in the interpretation and the use of this relationship and the following qualifications must be borne in mind:

1. It is an empirical relation and is based on the conditions and experience of one utility system supplying a given community. Other communities with different population habits, different definition as to what constitutes a class of service, different weather and other climatic conditions, may differ in the actual magnitudes of the coincidence factors shown throughout the entire load-factor range.
2. The relation is confined to consumers of substantially the same size, taking the same class of service, operating at the same load factors, and always taken in sufficient numbers for each type, size, and load factor to produce representative results on a coincidence factor of the group. It is obvious that, unless these qualifications are observed fully, different coincidence factors may be obtained.
3. The coincidence factors obtained from Figure 3 are those for individual consumers within a group applied to monthly conditions. There will be additional coincidence factors between different groups of any one class of service, for longer periods than a month, and between different classes of service of a system.

It should be noted also that the foregoing empirical relationship depicted the coincidence factors which, when applied to the consumers' individual maximum monthly demands, would, by definition, produce the coincident maximum demand of the group without indicating its time occurrence. Additional information is required for translating these coincident maximum group demands to load values for different hours of the day or for different days of the month. Such information can be secured only through extensive study of load-curve shapes of individual groups or classes of consumers.

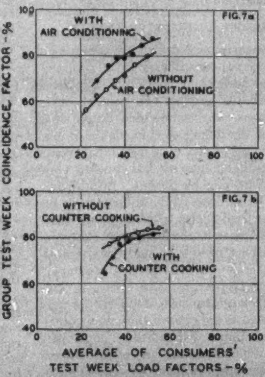

Figure 7. Illustration of the effect of the addition of certain appliances upon the coincidence factors of consumers of the commercial class reflecting 1940–1941 test data

Effect of Number of Consumers on the Coincidence-Factor-Versus-Load-Factor Relationship

The results of practical observations reflected in Figure 3 are based upon 30 consumers in a group. Obviously, for one single consumer in a group, by definition the coincidence factor is unity no matter what the load factors, and for an infinite number of consumers, from Figure 1, the coincidence factor may be expected to be lower than for groups of 30 consumers, throughout the entire load-factor range.

Referring to Figure 1, it is possible to construct a set of curves depicting the coincidence-factor-versus-load-factor relationships for various numbers of consumers in a group ranging from one to infinity. These relationships are shown in Figure 4, employing the equation of Figure 1 and the coincidence-factor-versus-load-factor relationship of the commercial and industrial classification shown in Figure 3. It should be noted that these relationships too, insofar as numerical values are concerned, are subject to the same qualifications as the relationship depicted in Figure 3.

The Influence of Different Classes of Consumers, or of Consumers With Different Types of Loads, Upon the Coincidence-Factor-Versus-Load-Factor Relationship

Figure 5 shows the coincidence-factor-versus-load-factor relationship for domestic consumers without electric ranges, and for domestic consumers with electric ranges, in comparison with the relationship for consumers of the commercial and industrial classification shown in Figure 3.

It will be noted that the relationships for the domestic consumers follow the general trend of the commercial and industrial consumers in the lower-load-factor range, although at a lower level. No test observations were available for these classes of consumers in the medium- and high-load-factor ranges, although it is believed that the extended relationship beyond the available test observations will merge with the horizontal portion of the relationship for the commercial and industrial consumers and thereafter follow it to the lower limiting value. The slope of the relationship for the domestic-service class without ranges is lower than that for the commercial–industrial classification. This would indicate that the period of high load probability for the domestic consumers is relatively longer than for the commercial and industrial ones, since the use period of domestic consumers without electric ranges can extend easily to twice the number of hours per week than that of consumers of the commercial and industrial classes whose individual load factors correspond to those of the domestic consumers, especially since Saturdays, Sundays, and holidays are days of fairly high domestic activity insofar as the use of electric service is concerned. For some of the appliances, the electric refrigerator for example, the entire period under consideration becomes the period of high load probability. However, the difference in the coincidence factors of the domestic and commercial classes of service practically disappears with the introduction of the electric range load in the domestic class because the period of high load probability of the range, with its predominant load requirements, is confined to much shorter periods during the day.

Figure 5 also shows the individual coincidence-factor-versus-load-factor relationship for three major types of consumers in the wholesale light and power classification, in comparison with the general relationship for the commercial and industrial consumers. For purpose of this comparison a classification depending upon the period of maximum average use of energy was employed. The daytime-type consumer was defined as one having maximum average use between 9 a.m. and 4 p.m.; the evening type as having the maximum average use between 4 p.m. and 9 p.m.; and the full-time type as having about an equal use in each of these periods with a resulting high load factor. This classification of load types caused the industrial consumers to fall principally into the daytime and full-time groups, whereas the commercial consumers fell principally into the evening group.

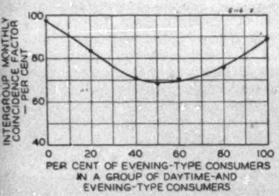

Figure 8. Illustration of the effect of different mixtures of load types upon the intergroup coincidence factor of the retail light and power class reflecting 1938 test data

It will be noted that the coincidence-factor-versus-load-factor relationships for individual types of consumer loads of a given classification follow the general trends of the formulated relationship, but the numerical values of the coincidence factors of the individual types are generally higher than those of the entire class.

Figure 6 illustrates the effect on group coincidence factors of a different mixture of load types for given consumers' load factors. The curves on this chart show the variation in group coincidence factors of a mixed group of thirty consumers with variation in the degree of mixture of daytime and evening load types, averaging 10-per-cent, 20-per-cent and 30-per-cent load factors. They bring out the fact that higher coincidence factors are obtained for groups of consumers homogeneous as to load type than for heterogeneous groups, and the greatest deviation between homogeneous and nonhomogeneous groups is found at the lower load factors.

Figure 7 shows the coincidence-factor-versus-load-factor relationships for two special types of commercial consumers. From Figure 7a it will be observed that the coincidence-factor-versus-load-factor relationship for commercial consumers *with* air conditioning is higher than for the same consumers *without* air conditioning. The difference is substantial in the range of consumers' load factors commonly encountered in practice (between 20 per cent and 40 per cent).

From Figure 7b it will be observed that the coincidence-factor-versus-load-factor relationship for commercial consumers *with* electric counter cooking equipment is lower than for the same consumers *without* the counter cooking equipment, indicating the beneficial effects of this load upon consumers' load characteristics. It should be noted, however, that one of the reasons for this is due to the fact that, for the consumers tested, the relative size of the connected electric counter cooking load did not exceed three times their other connected load.

INTERGROUP COINCIDENCE FACTORS

It is apparent that with any grouping of consumers there will exist, in all probability, an additional factor of coincidence between the groups. In general, when consumers are subdivided into small groups, the degree of coincidence in consumers' use of service of individual groups will be greater than when they all are combined into one big group. In addition, when, as a result of the difference in the average load factor of each group, there is a difference in the load-curve shapes of the various groups, an additional coincidence factor between groups becomes a practical certainty.

The intergroup coincidence factor may be defined as the ratio of the actual coincident maximum demand of all consumers of a given class to the sum of the diversified demands obtained by the application of the coincidence-factor-versus-load-factor relationship to the individual consumers' load characteristics.

The intergroup coincidence factors for consumers homogeneous as to load type may be expected to be higher than for the entire group of consumers of diverse types of load. Figure 8 illustrates the trend in the intergroup coincidence factors for various combinations of daytime- and evening-loading-type consumers, bringing out the point that higher intergroup coincidence factors will be obtained for groups with highly homogeneous-type loads, than for groups with comparatively high heterogeneous load types.

From the indicated curves of Figures 3, 4, and 5, and actual test-load-curve data, the intergroup coincidence factors were found to vary from between 93 per cent and 100 per cent for the commercial and industrial classes of consumers, and from 92 per cent to 95 per cent for consumers of the domestic classification with and without electric ranges.

Conclusion

From the foregoing discussion, it is possible to make the following significant observations:

1. The degree of coincidence in the use of electric service depends upon many factors. Among the more important ones are population habits, community and business practices, weather and other climatic conditions, design of utilization equipment, and methods used in the control of service.

2. Numerical values of coincidence factors will differ for different load applications, different classes of consumers, and different composition of load types in a given classification. They can be obtained with any degree of certainty only from actual test observations, and must be checked periodically to detect the effects of changing conditions. In view of the complexity of forces influencing group load characteristics, it is obvious that no single mathematical formula with a given set of constants can be right for all conditions. Mathematical considerations can serve only as a means for rationalizing the results of practical observations.

3. In general, the degree of coincidence in the maximum requirements of electric service of a group of consumers homogeneous as to some controlling characteristic decreases along a path resembling that of a rectangular hyperbola from a value of unity for one consumer in a group to values approaching the horizontal asymptote of the rectangular hyperbola for an infinite number of consumers in a group. The convergence of the relationship toward this asymptote is comparatively rapid for all asymptotic values of coincidence factors, and is more rapid for the higher values than for the lower ones.

Statistically stable results in coincidence factors may be expected in the practical range of load factors for as few as 100 consumers in a group and results of sufficient engineering stability even can be obtained from groups of 30 to 50 consumers.

4. In general, the degree of coincidence in the maximum requirements of electric service of groups of consumers changes with the change in their individual load factors.

Synchronous Starting of Generator and Motor

C. CONCORDIA
MEMBER AIEE

S. B. CRARY
MEMBER AIEE

C. E. KILBOURNE
MEMBER AIEE

C. N. WEYGANDT, JR.
ASSOCIATE AIEE

A SYNCHRONOUS motor, generator, or condenser can be started from rest, by means of shaft torque, induction-motor (amortisseur winding) torque, or synchronizing torque. This paper presents data on the last method of starting. The system studied consists of a prime mover driving a synchronous generator, and a synchronous machine driven electrically by the generator. The whole system is started from rest by means of torque applied to the generator shaft, the motor being accelerated to normal speed by the synchronous torque developed. The performance of such a system was determined both by tests on several machines and by calculations with the aid of the differential analyzer at the University of Pennsylvania, and limiting conditions and criteria for successful starting were found in terms of the various pertinent system parameters. In a few cases a system consisting of a generator and two motors was studied.

Synchronous motors and condensers ordinarily are started by means of the induction-motor torque developed by their amortisseur windings. In some cases, however, for example when a generator is used as a condenser, it becomes necessary to start the machine in some other way. A salient-pole generator may have no amortisseur winding or one of insufficient torque and thermal capacity. A turbine generator will, in general, develop a large starting torque but will have insufficient thermal capacity. In many such cases the machine has been started by electrically connecting the motor and generator with both machines at rest and excited, then starting the generator by applied turbine torque and pulling up the motor by the synchronous torque developed at very low speeds. This method has been used for many years in the field testing of water-wheel generators and in miscellaneous shop tests. In case of extremely large motors with high starting torques, it may be convenient to arrange the electric-system connections so that a generator may be assigned the job of starting the motor on its synchronizing torque, thus permitting a reduction in the required capacity of the amortisseur winding.

The conditions required for successful starting in this manner have been studied in an approximate way by several investigators[1,2] and certain rules have been developed. However, it is believed that the problem is sufficiently complex and of sufficient general interest to justify the presentation of a more exact treatment, particularly since this more exact treatment has been found necessary to predict starting performance correctly in the range studied.

The problem is very similar to that of synchronizing or pulling-into-step of synchronous motors at normal speed[3,4] except that now the performance of two or three machines must be considered simultaneously, and the speed range is relatively very much greater.

Conclusions

From the results of the tests and calculations discussed in this paper, the following conclusions can be drawn regarding starting performance in the range covered:

1. The optimum ratio of motor excitation to generator excitation is such that the ratio of the normal speed, open circuit voltages is about 0.8. That is, at this ratio the maximum motor friction torque can be started (Figure 1). In general, the gener-

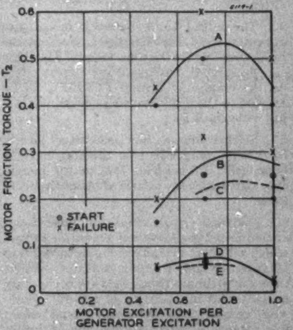

Figure 1. Motor and generator starting from standstill with applied generator shaft torque

Maximum motor friction torque, T_2 which can be started, as function of excitation ratio E_2/E_1. $H_2=2.53$, $E_1=1.3$

Curve	r	x	H_1
A	0.01	1.0	5.05
B	0.025	1.0	5.05
C	0.025	1.0	1.26
D	0.05	1.0	5.05
E	0.05	0.5	5.05

Paper 45-119, recommended by the AIEE committee on electric machinery for publication in AIEE TRANSACTIONS. Manuscript submitted March 23, 1945; made available for printing May 21, 1945.

C. CONCORDIA and S. B. CRARY are in the central station engineering division and C. E. KILBOURNE is in the motor and generator engineering division, all of the General Electric Company, Schenectady, N. Y. C. N. WEYGANDT, JR., is with the Moore School of Electrical Engineering, University of Pennsylvania, Philadelphia, Pa.

The authors wish to acknowledge the assistance of S. B. Farnham, W. K. Boice, H. A. Peterson, and I. A. Terry of the General Electric Company, and of S. Hare, formerly of the University of Pennsylvania.

In the low load-factor range the coincidence factor increases rapidly with the increase in the individual consumers' load factors. In the medium range of load factors its magnitude remains substantially fixed at a level of around 84 per cent until very high load-factor values are reached when it approaches the lower limit of the possible relationship.

5. The general level in the degree of coincidence in the maximum requirements of electric service are higher for groups of consumers homogeneous as to load type than for heterogeneous groups, and large deviations between homogeneous and nonhomogeneous groups are found at the lower load factors than at the higher ones.

6. Intergroup coincidence factors for homogeneous-type loads may be expected to be higher than those for diverse types of load.

References

1. ECONOMIC SIGNIFIANCE OF LOAD CHARACTERISTICS AS APPLIED TO MODERN ELECTRIC SERVICE, Constantine Bary. *Proceedings*, 53rd Annual Meeting of the Association of Edison Illuminating Companies, 1937 volume (not published).

2. Reports of Subcommittee on Coincidence Factors of the Special Committee on Load Studies of the Association of Edison Illuminating Companies. *Proceedings*, 55th and 56th Annual Meeting of the Association of Edison Illuminating Companies, 1939 and 1940 volumes (not published).

3. STUDY OF THE THEORETICAL RELATIONSHIP BETWEEN LOAD FACTOR AND DIVERSITY FACTOR, H. E. Eisenmenger. *Proceedings*, 55th Annual Meeting of the Association of Edison Illuminating Companies, 1939 volume (not published).

4. ECONOMIC AND SALES PROBLEMS OF ELECTRIC UTILITY SERVICE IN THE SMALL COMMERCIAL MARKET, J. F. Gaskill, Constantine Bary. *Proceedings*, World Power Conference, Vienna, Austria, 1938.

5. FACTORS AFFECTING GENERATING CAPACITY, N. E. Funk. *Edison Electric Institute Bulletin*, volume 7, 1939.

6. CHARACTERISTICS OF COMMERCIAL LIGHTING LOAD, R. R. Herrmann. *Journal of Land and Public Utility Economics*, February 1937.

7. Discussion by Constantine Bary of SUMMATION OF LOAD CURVES, R. F. Hamilton. AIEE TRANSACTIONS, volume 63, 1944, pages 1361–3.

8. SYNTHETIC OR EQUIVALENT LOAD CURVES, R. F. Hamilton. AIEE TRANSACTIONS, volume 61, 1942, pages 369–81.

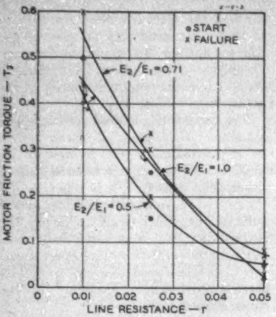

Figure 2. Motor and generator starting from standstill with applied generator shaft torque

Maximum motor friction torque T_2 which can be started, as function of circuit resistance r. $H_1=5.05$, $H_2=2.53$, $x=1.0$

ator excitation should be as great as possible.

2. Considerable motor torque can be developed by synchronous starting when the total armature-circuit resistance is low, but high resistance reduces the maximum allowable motor friction torque (T_2) very much. With line resistances greater than five per cent, T_2 becomes less than seven per cent (Figure 2).

3. With small line resistance r ($r=0.01$) the maximum motor friction torque T_2 which can be started is practically inversely proportional to line reactance x, while with high r ($r=0.05$) T_2 is nearly independent of x (Figure 3).

4. The initial angle between motor and generator field axes has little effect on the maximum motor friction torque T_2 which can be started, but has a very great effect on the maximum torque T_1 which can be applied to the generator for successful starting with small T_2.

5. Neither motor nor generator inertia have very much effect on the starting performance. In general, low motor inertia and high generator inertia are slightly beneficial.

6. For each circuit condition there is an optimum value of applied generator torque which will start the maximum motor friction (Figures 3 and 4). For torques smaller than the optimum value, T_2 is approximately proportional to T_1; it is, in general, somewhat greater than the proportional value. For torques T_1 greater than the optimum value, T_2 decreases rapidly to zero, and if T_1 is too large the generator will run away leaving the motor oscillating about zero speed.

7. It is desirable to have a fairly low-resistance amortisseur winding on both motor and generator if they are not of solid-pole-face construction.

8. When motor and generator are directly connected electrically, turbomachines should, in general, be easier to start than salient-pole machines.

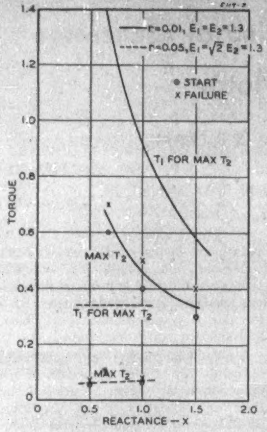

Figure 3. Motor and generator starting from standstill with applied generator shaft torque

Maximum motor friction torque T_2 which can be started, as function of circuit reactance X. $H_1=5.0$, $H_2=2.55$

Analysis

The systems considered are shown in Figure 5. In order to reduce the performance equations of these systems to practically soluble forms, it was assumed that:

1. All machines have symmetric rotors.

2. The effective machine excitations and reactances are constant during the starting period. This may be interpreted as meaning that the rotor flux is constant or that some average value is taken as representative.

3. Amortisseur effects are negligible.

The system equations for the case of two machines, in an integral form suitable for solution on the differential analyzer, are then (see appendix)

$$\left.\begin{aligned}
xi_\alpha &= +E_1\cos\theta_1 - E_2\cos\theta_2 - \int ri_\alpha dt\\
xi_\beta &= +E_1\sin\theta_1 - E_2\sin\theta_2 - \int ri_\beta dt\\
M_1p\theta_1 &= -E_1\int \cos\theta_1 d\int i_\beta dt + E_1\times\\
&\qquad \int \sin\theta_1 d\int i_\alpha dt - \int T_1 dt\\
M_2p\theta_2 &= +E_2\int \cos\theta_2 d\int i_\beta dt - E_2\times\\
&\qquad \int \sin\theta_2 d\int i_\alpha dt - \int T_2 dt
\end{aligned}\right\}\quad(1)$$

where

t = per-unit time
x = per-unit armature-circuit reactance
r = per-unit armature-circuit resistance
E = per-unit excitation
θ = rotor angle
M = per-unit rotor inertia
$M=4\pi fH$, where H is the inertia constant as conventionally defined in stability studies

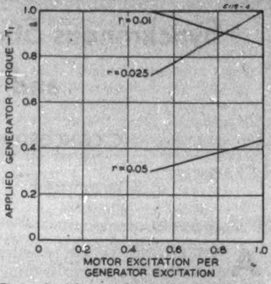

Figure 4. Motor and generator starting from standstill

Required generator shaft torque T_1 to obtain maximum motor friction torque T_2, as function of excitation ratio E_2/E_1
$H_1=5.05$, $H_2=2.53$, $x=1.0$, $E_1=1.3$

$$H=\frac{0.231\times WR^2\times(\text{rpm})^2}{10^6\ \text{kva (base)}}$$

f = rated circuit frequency in cycles per second ($f=60$ in all numerical examples)
i_α, i_β = per-unit equivalent two-phase armature currents of machine one
T = per-unit load torque

Subscripts 1 and 2 refer to generator and motor, respectively. A schematic diagram of the required analyzer connections is shown in Figure 6.

With the motor (machine two) at standstill θ_2 is constant and the performance is determined by the first three parts of equation 1. The motor torque is

$$\text{torque} = i_\beta E_2\cos\theta_2 - i_\alpha E_2\sin\theta_2 \qquad (2)$$

so the motor may be started (that is, the fourth equation may be connected in the circuit) when its torque becomes equal to the friction torque selected.

The procedure followed on the differential analyzer was as follows. For each value of resistance, reactance, motor inertia, generator inertia, motor excitation, generator excitation, and applied generator torque, the motions of the two machines were determined up to a point where it was decided that the motor could or could not be started successfully. This was done for several values of motor friction and initial motor–generator angle until the maximum friction torque which could be started at any angle was found. Occasionally this procedure was varied in detail by finding the limiting generator torque for a given motor torque. Figure 7 shows a typical limiting curve and illustrates the fact that the allowable motor friction torque increases to a maximum and then decreases to zero as the applied (constant) generator torque is increased.

In most of the work done, the motor

friction torque was maintained at its static breakaway value throughout the starting period. The friction torque actually will decrease somewhat, but, for generators with large numbers of poles, the total mechanical angle through which the motor has turned by the time it either definitely has pulled in or failed to pull in is very small, since the total electrical angle is only two or three revolutions. For machines with two or four poles the results may be somewhat pessimistic in the sense that the calculations may indicate a failure to start when a start actually might be accomplished. An investigation of this point in a particular case showed about a 40-per-cent increase in the allowable motor static friction, if it were dropped to zero at the instant of motor starting.

The generator excitation E_1 was 1.3 in nearly all cases. This was considered to correspond to about the highest value of field flux which could be maintained in a normal machine without exceeding the capacity of the field winding. The motor excitation E_2 was varied from 1.3 down to 0.65 since one of the principal objects of the study was to determine the optimum excitation ratio as a function of the other system parameters. In order to interpret the results in terms of other generator excitations, and, in general, to obtain the maximum amount of information from the results, one may note that the system behavior may be expressed in terms of the six groups:

$$\frac{xM_1}{E_1^2},\ \frac{xM_2}{E_1^2},\ \frac{xT_1}{E_1^2},\ \frac{xT_2}{E_1^2},\ \frac{r}{x},\ \frac{E_2}{E_1}$$

The attempt to start was taken as successful if the motor speed exceeded the generator speed at least twice. That is, in a successful start the motor usually would start up and oscillate about the generator. Since all rotor damping was neglected it sometimes was observed that these oscillations tended to increase in magnitude. A calculation for the condition of small oscillations about a constant average speed shows that in the speed range considered the system treated here is damped negatively. At very low speeds the damping is positive, but at between one per cent and two per cent speed the damping becomes negative, reaching a negative maximum at about two per cent speed and remaining negative but becoming continually smaller in magnitude thereafter. Calculations have shown that an amortisseur winding of normal design on both motor and generator is adequate to keep the damping positive at all speeds. Moreover, even if damping is negative over a certain speed range, the machines may not drop out of step unless the period of operation in the range is sufficiently long.

Calculations were made to find the effects of line resistance and reactance, excitation ratio, motor–generator initial electrical angle, inertias of motor and generator, and applied torque on the starting characteristics, that is, on the permissible motor starting friction. The total reactance was taken as 1.0 per unit, which should correspond approximately to the total transient reactance of the usual two-machine system. This reactance was varied in a few cases between 0.5 and 1.5. The total line resistance was varied from 0.01, which could correspond to that for two machines tied directly together, to 0.05, which allows for some tie-line resistance.

Depending on the initial displacement angle, the motor starts either forward or backward and may or may not synchronize if it is a border-line case. The worst initial angle of the motor relative to the generator was usually between −90 degrees and −180 degrees. In most cases only 90-degree intervals were checked, but in a few cases 45-degree intervals were considered. The effect of angle was not sufficiently great to make it necessary to consider smaller intervals.

Test Checks

In order to check the validity of the simplified equations used to represent the system, several tests were made. A 9,000-horsepower 18-pole vertical synchronous motor having a static friction of 17 per cent was started from a 20-pole horizontal machine of about equal size. The prime mover was a d-c motor and the system was started by closing the motor

Figure 6. Motor and generator starting from standstill with applied generator shaft torque

Differential-analyzer connection diagram

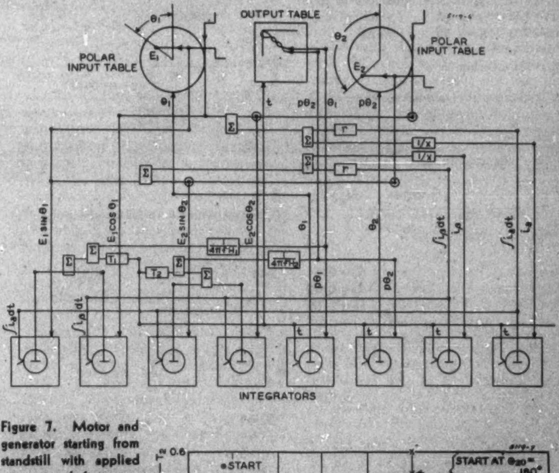

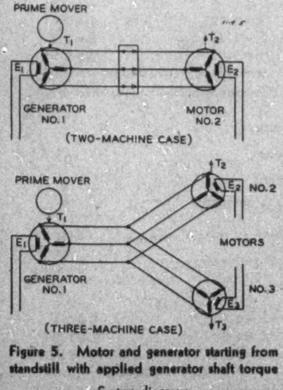

Figure 5. Motor and generator starting from standstill with applied generator shaft torque

System diagrams

Figure 7. Motor and generator starting from standstill with applied generator shaft torque

Motor friction torque T_2 which can be started, as function of generator applied torque T_1

$H_1=5.0$, $H_2=2.55$, $r=0.01$, $x=1.0$, $E_1=E_2=1.3$

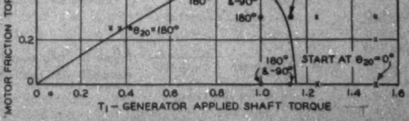

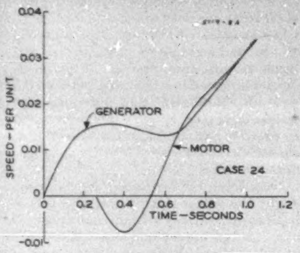

(A)

$T_1=1.0$ $T_2=0.41$ (Reduced to zero
$E_1=1.3$ $E_2=0.65$ when motor
$H_1=5.0$ $H_2=2.55$ starts)
$x=1.0$ $r=0.015$
$\theta_{20}=180$ degrees

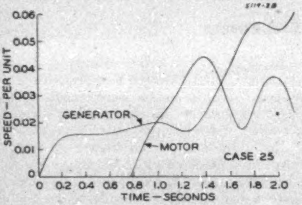

(B)

$T_1=1.0$ $T_2=0.648$ (Reduced to zero
$E_1=1.3$ $E_2=0.65$ when motor
$H_1=5.0$ $H_2=2.55$ starts)
$x=1.0$ $r=0.015$
$\theta_{20}=180$ degrees

(Compare with Figure 8A for effect of T_2)

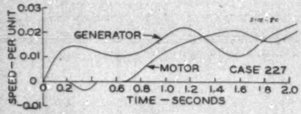

(C)

$T_1=1.0$ $T_2=0.5$
$E_1=1.3$ $E_2=0.92$
$H_1=5.0$ $H_2=2.53$
$x=1.0$ $\theta_{20}=180$ degrees $r=0.01$

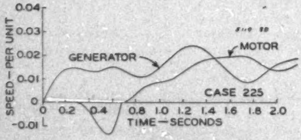

(D)

$T_1=1.0$ $T_2=0.5$
$E_1=1.3$ $E_2=0.92$
$H_1=5.0$ $H_2=2.53$
$x=1.0$ $\theta_{20}=-90$ degrees $r=0.01$

(Compare with Figure 8C for effect of θ_{20})

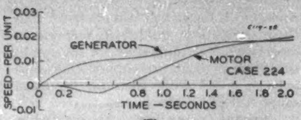

(E)

$T_1=0.375$ $T_2=0.0667$
$E_1=1.3$ $E_2=0.92$
$H_1=5.0$ $H_2=2.53$
$x=1.0$ $\theta_{20}=180$ degrees $r=0.05$

(Compare with Figure 8C for effect of r, and with Figure 8F for effect of θ_{20})

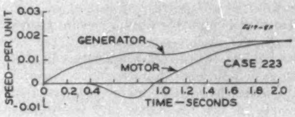

(F)

$T_1=0.375$ $T_2=0.0667$
$E_1=1.3$ $E_2=0.92$
$H_1=5.0$ $H_2=2.53$
$x=1.0$ $\theta_{20}=-90$ degrees $r=0.05$

(Compare with Figure 8E for effect of θ_{20}, and with Figure 8D for effect of r)

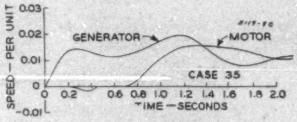

(G)

$T_1=1.0$ $T_2=0.4$
$E_1=1.3$ $E_2=0.65$
$H_1=5.0$ $H_2=2.55$
$x=1.0$ $\theta_{20}=180$ degrees $r=0.01$

(Compare with Figure 8K for effect of E_2/E_1)

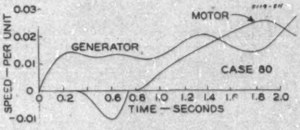

(H)

$T_1=1.0$ $T_2=0.4$
$E_1=1.3$ $E_2=0.65$
$H_1=5.0$ $H_2=2.55$
$x=1.0$ $\theta_{20}=-90$ degrees $r=0.01$

(Compare with Figure 8G for effect of θ_{20})

Figure 8. Motor and generator starting from standstill with applied generator shaft torque

Curves of speed versus time

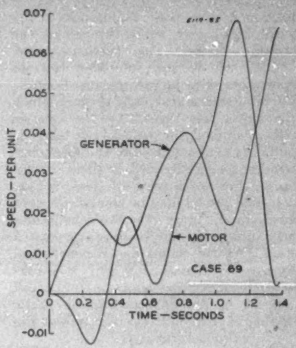

(I)

$T_1=1.125$ $T_2=0$
$E_1=1.3$ $E_2=1.3$
$H_1=5.0$ $H_2=2.55$
$x=1.0$ $\theta_{20}=180$ degrees $r=0.01$

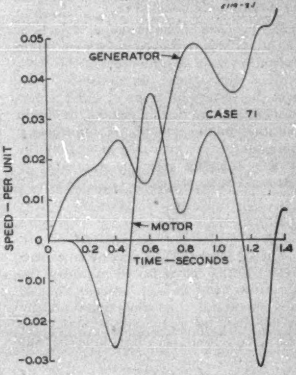

(J)

$T_1=1.125$ $T_2=0$
$E_1=1.3$ $E_2=1.3$
$H_1=5.0$ $H_2=2.55$
$x=1.0$ $\theta_{20}=-90$ degrees $r=0.01$

(Compare with Figure 8I for effect of θ_{20})

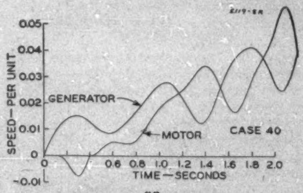

(K)

$T_1=1.0$ $T_2=0.4$
$E_1=1.3$ $E_2=1.3$
$H_1=5.0$ $H_2=2.55$
$x=1.0$ $\theta_{20}=180$ degrees $r=0.01$

(Compare with Figure 8G for effect of E_2/E_1)

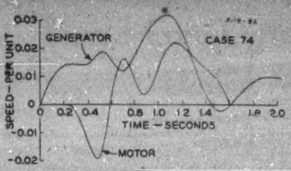

(L)

$T_1=1.0$ $T_2=0.4$
$E_1=1.3$ $E_2=1.3$
$H_1=5.0$ $H_2=2.55$
$x=1.0$ $r=0.01$
$\theta_{20}=-90$ degrees

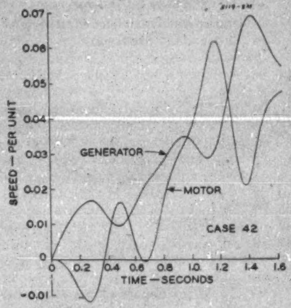

(M)

$T_1=1.0$ $T_2=0$
$E_1=1.3$ $E_2=1.3$
$H_1=5.0$ $H_2=2.55$
$x=1.0$ $r=0.01$
$\theta_{20}=180$ degrees
(Compare with Figure 8K for effect of T_2)

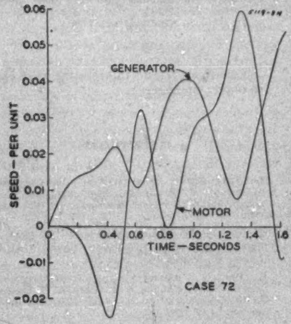

(N)

$T_1=1.0$ $T_2=0$
$E_1=1.3$ $E_2=1.3$
$H_1=5.0$ $H_2=2.55$
$x=1.0$ $r=0.01$
$\theta_{20}=-90$ degrees
(Compare with Figure 8L for effect of T_2)

armature switch with field already applied. The torque thus was built up very rapidly and decayed slowly as the d-c motor accelerated. With excitation ratios of from 0.5 to 1.0 the lowest generator excitation (about 65 per cent) at which the a-c motor could be started was found.

The critical excitations for this system then were calculated on the differential analyzer and checked very closely. (See Table I.) There were, however, some differences between the test and analyzer conditions which are enumerated in the following.

In the calculation the motor friction torque was reduced to zero as soon as the motor started, while the friction of the test motor may be presumed to require some little time to fall to a completely negligible value. This indicates that the calculation may be really pessimistic since the consideration of an additional motor friction would have increased the critical excitations obtained. An increase of about five to ten per cent in excitation would be expected.

On the other hand, an armature resistance of $r=0.015$ was used in some of the calculations, while the test d-c resistance was closer to $r=0.01$. This indicates a somewhat optimistic calculation. The resultant decrease in critical excitation is shown by Figure 2 to be not more than about five per cent (torque varies as the square of excitation). Thus the two differences between calculation and test offset each other to a considerable degree. Moreover, the calculations at $E_2/E_1=0.5$ were made with $r=0.01$ and showed little deviation.

Other factors which should be considered are that the test machines had rather small field time constants, which would indicate that the calculations would be more pessimistic for larger machines, and rather effective amortisseurs, which would indicate that the calculations might be somewhat optimistic for machines with little or no amortisseur effect. The machines were represented by their transient reactances in the calculations.

Results and Discussion

The results obtained directly from the differential analyzer are in the form of curves of motor and generator speeds, and of the two components of armature current. The motor and generator angles also were determined in most cases. Figure 8 shows a few typical curves of motor and generator speed.

The information taken from these curves is summarized in Figures 1–4. Figure 1 shows the effect of excitation ratio and of line resistance. It is seen that regardless of line resistance the optimum excitation ratio is about 0.8, and that for the highest resistance ($r=0.05$) the permissible motor friction at a ratio of 1.0 is relatively much lower. For this high-resistance case an optimum ratio of 0.7 might apply, since it is possible to draw the curve in several ways through the check points.

Figure 2 is a replot of some of the curves of Figure 1 to show the effect of line resistance more directly. This curve brings out very clearly the importance of a low tie-line resistance if this method of starting is to be used on a motor having any very large breakaway torque, and also shows that if the tie resistance is kept down considerable torque may be developed.

Figures 3 and 4 show the generator torque T_1 which should be applied in order to start the maximum possible motor torque. These T_1 curves are only approximate, as the optimum value of T_1 is not very critical (see Figure 7). From Figure 7 it is seen that the optimum T_1 should not be greatly exceeded. Each point of the summary curves (Figures 1–4) was determined from curves similar to Figure 7, and each point of Figure 7 was, in turn, determined from curves similar to those of Figure 8.

Figure 9 shows the results of a calculation for the case of one generator starting two motors simultaneously, each of half the generator rating. One motor is at an initial angle of 90 degrees, the other at 180 degrees. If both motors are initially at 180 degrees, they may be considered as one. The starting performance is then the same as that of the two-machine case of Figure 10A, which is slightly worse than that of Figure 9. In general, it would seem that the two-machine case, with the motor at the worst angle, adequately should represent also the worst three-machine case. The case of Figure 10B differs only slightly from that of Figure 10A. It was worked out on the differential analyzer as an approximate check of the step-by-step calculations required for Figures 9 and 10A.

Appendix

In this appendix the performance equations for three electrically connected symmetric rotor machines will be derived first, since they may be of interest, not only to study, for example, the case of a single generator starting two motors simultaneously or of two generators starting a single motor, but also as an indication of the phenomena to be expected when several machines are so connected together. The equations for two machines studied in detail in this paper then will be derived as a special case.

Table I

E_2/E_1	E_1 (Calculated)	E_1 (Test)
0.5	0.65	0.64
0.67	0.64	0.63
1.0	0.60	0.58

The voltage equations for machine one are[6]

$$\begin{aligned} e_{\alpha 1} &= p\psi_{\alpha 1} - r_1 i_{\alpha 1} \\ e_{\beta 1} &= p\psi_{\beta 1} - r_1 i_{\beta 1} \end{aligned} \qquad (3)$$

Under the assumptions, the flux linkages are[5]

$$\begin{aligned} \psi_{d1} &= E_1 - x_1 i_{d1} \\ \psi_{q1} &= -x_1 i_{q1} \end{aligned} \qquad (4)$$

The d-, q-axis quantities are related to the α-, β-axis quantities by the relations[6]

$$\left.\begin{aligned} i_d &= i_\alpha \cos\theta + i_\beta \sin\theta \\ i_q &= -i_\alpha \sin\theta + i_\beta \cos\theta \end{aligned}\right\} \qquad (5)$$

with similar relations for ψ and e. Substituting equations 5 in equations 4, yields

$$\left.\begin{aligned} \psi_{\alpha 1} &= E_1 \cos\theta_1 - x_1 i_{\alpha 1} \\ \psi_{\beta 1} &= E_1 \sin\theta_1 - x_1 i_{\beta 1} \end{aligned}\right\} \qquad (6)$$

Now by substituting equation 6 in equation 3, the voltage equations become

$$\left.\begin{aligned} e_{\alpha 1} &= E_1 p \cos\theta_1 - (px_1 + r_1) i_{\alpha 1} \\ e_{\beta 1} &= E_1 p \sin\theta_1 - (px_1 + r_1) i_{\beta 1} \end{aligned}\right\} \qquad (7)$$

Similarly, for machines two and three

$$\left.\begin{aligned} e_{\alpha 2} &= E_2 p \cos\theta_2 - (px_2 + r_2) i_{\alpha 2} \\ e_{\beta 2} &= E_2 p \sin\theta_2 - (px_2 + r_2) i_{\beta 2} \end{aligned}\right\} \qquad (8)$$

$$\left.\begin{aligned} e_{\alpha 3} &= E_3 p \cos\theta_3 - (px_3 + r_3) i_{\alpha 3} \\ e_{\beta 3} &= E_3 p \sin\theta_3 - (px_3 + r_3) i_{\beta 3} \end{aligned}\right\} \qquad (9)$$

To connect the three machines together, one puts

$$\left.\begin{aligned} e_{\alpha 1} &= e_{\alpha 2} = e_{\alpha 3} \\ e_{\beta 1} &= e_{\beta 2} = e_{\beta 3} \\ i_{\alpha 3} &= -i_{\alpha 1} - i_{\alpha 2} \\ i_{\beta 3} &= -i_{\beta 1} - i_{\beta 2} \end{aligned}\right\} \qquad (10)$$

whence equations 7, 8, and 9 become

$$\left.\begin{aligned} (Ap^2+Bp+C)i_{\alpha 1} &= [(x_3+x_2)p+ \\ &\quad (r_3+r_2)]pE_1\cos\theta_1 - (x_3p+r_3)\times \\ &\quad pE_2\cos\theta_2 - (x_2p+r_2)pE_3\cos\theta_3 \\ (Ap^2+Bp+C)i_{\beta 1} &= [(x_3+x_2)p+ \\ &\quad (r_3+r_2)]pE_1\sin\theta_1 - (x_3p+r_3)\times \\ &\quad pE_2\sin\theta_2 - (x_2p+r_2)pE_3\sin\theta_3 \\ (Ap^2+Bp+C)i_{\alpha 2} &= [(x_3+x_1)p+ \\ &\quad (r_3+r_1)]pE_2\cos\theta_2 - (x_3p+r_3)\times \\ &\quad pE_1\cos\theta_1 - (x_1p+r_1)pE_3\cos\theta_3 \\ (Ap^2+Bp+C)i_{\beta 2} &= [(x_3+x_1)p+ \\ &\quad (r_3+r_1)]pE_2\sin\theta_2 - (x_3p+r_3)\times \\ &\quad pE_1\sin\theta_1 - (x_1p+r_1)pE_3\sin\theta_3 \end{aligned}\right\} \qquad (11)$$

where

$$\left.\begin{aligned} A &= x_1x_2 + x_2x_3 + x_3x_1 \\ B &= r_1(x_2+x_3) + r_2(x_3+x_1) + r_3(x_1+x_2) \\ C &= r_1r_2 + r_2r_3 + r_3r_1 \end{aligned}\right\} \qquad (12)$$

The torque equation of each machine is of the form

$$Mp^2\theta + Ei_q + T = 0 \qquad (13)$$

where T is the load torque. From equations 5 and 10, the three torque equations are

$$\left.\begin{aligned} &M_1p^2\theta_1 + E_1(i_{\beta 1}\cos\theta_1 - \\ &\qquad i_{\alpha 1}\sin\theta_1) + T_1 = 0 \\ &M_2p^2\theta_2 + E_2(i_{\beta 2}\cos\theta_2 - \\ &\qquad i_{\alpha 2}\sin\theta_2) + T_2 = 0 \\ &M_3p^2\theta_3 + E_3[(i_{\alpha 1}+i_{\alpha 2})\sin\theta_3 - \\ &\qquad (i_{\beta 1}+i_{\beta 2})\cos\theta_3] + T_3 = 0 \end{aligned}\right\} \qquad (14)$$

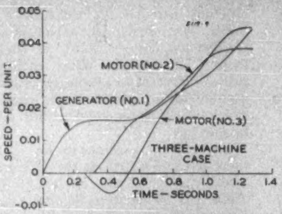

Figure 9. Two motors and generator starting from standstill with applied generator shaft torque

Speed versus time

$T_1 = 0.985$ $\quad$ $T_2 = T_3 = 0.20$*
$E_1 = 1.3$ $\quad$ $E_2 = E_3 = 0.65$
$H_1 = 5.0$ $\quad$ $H_2 = H_3 = 1.65$
$x_1 = 0.5$ $\quad$ $x_2 = x_3 = 1.0$
$r_1 = 0.008$ $\quad$ $r_2 = r_3 = 0.016$
$\theta_{10} = 0$ degrees, $\theta_{20} = 90$ degrees, $\theta_{30} = 180$ degrees

*T_2 and T_3 reduced to 0.008 when motors start

(Compare with Figure 10A for effect of combining the motors)

Although equations 11 and 14 may be put directly in an integral form for solution on the differential analyzer, the number of integrations required is large. They may be simplified with little loss in generality by making the ratios of resistance to reactance the same in all three machines. If

$$\frac{r_1}{x_1} = \frac{r_2}{x_2} = \frac{r_3}{x_3} = \rho \qquad (15)$$

then

$B = 2\rho A$ and $C = \rho^2 A$

and

$Ap^2 + Bp + C = A(p+\rho)^2$

The current equations 11 are reduced to

$$\left.\begin{aligned} A(p+\rho)i_{\alpha 1} &= (x_3+x_2)pE_1\cos\theta_1 - \\ &\quad x_3pE_2\cos\theta_2 - x_2pE_3\cos\theta_3 \\ A(p+\rho)i_{\beta 1} &= (x_3+x_2)pE_1\sin\theta_1 - \\ &\quad x_3pE_2\sin\theta_2 - x_2pE_3\sin\theta_3 \\ A(p+\rho)i_{\alpha 2} &= (x_3+x_1)pE_2\cos\theta_2 - \\ &\quad x_3pE_1\cos\theta_1 - x_1pE_3\cos\theta_3 \\ A(p+\rho)i_{\beta 2} &= (x_3+x_1)pE_2\sin\theta_2 - \\ &\quad x_3pE_1\sin\theta_1 - x_1pE_3\sin\theta_3 \end{aligned}\right\} \qquad (16)$$

Machine number three may be eliminated by letting $x_3 = \infty$, $i_{\alpha 1} = -i_{\alpha 2} = i_\alpha$, and $i_{\beta 1} = -i_{\beta 2} = i_\beta$. The first and last pair of equations 16 become identical and are represented by

$$\left.\begin{aligned} (xp+r)i_\alpha &= p(E_1\cos\theta_1 - E_2\cos\theta_2) \\ (xp+r)i_\beta &= p(E_1\sin\theta_1 - E_2\sin\theta_2) \end{aligned}\right\} \qquad (17)$$

where

$x = x_1 + x_2$ and $r = r_1 + r_2$

The torque equations 14 become

$$\left.\begin{aligned} &M_1p^2\theta_1 + E_1(i_\beta\cos\theta_1 - \\ &\qquad i_\alpha\sin\theta_1) + T_1 = 0 \\ &M_2p^2\theta_2 + E_2(i_\alpha\sin\theta_2 - \\ &\qquad i_\beta\cos\theta_2) + T_2 = 0 \end{aligned}\right\} \qquad (18)$$

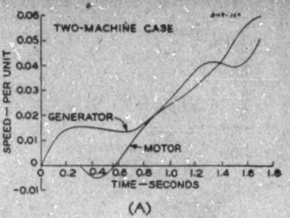

(A)

$T_1 = 0.985$ $\quad$ $T_2 = 0.4$*
$E_1 = 1.3$ $\quad$ $E_2 = 0.65$
$H_1 = 5.0$ $\quad$ $H_2 = 3.3$
$x = 1.0$ $\quad$ $r = 0.016$
$\theta_{20} = 180$ degrees

*T_2 reduced to 0.015 when motor starts

(Compare with Figure 9 for effect of two half-size motors)

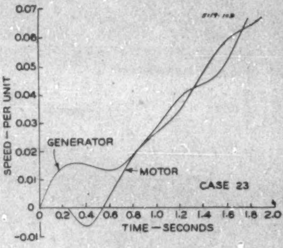

(B)

$T_1 = 1.0$ $\quad$ $T_2 = 0.409$ (Reduced to zero when motor starts)
$E_1 = 1.3$ $\quad$ $E_2 = 0.65$
$H_1 = 5.0$ $\quad$ $H_2 = 3.4$
$x = 1.0$ $\quad$ $r = 0.015$
$\theta_{20} = 180$ degrees

Figure 10. Motor and generator starting from standstill with applied generator shaft torque

Speed versus time

Equations 17 and 18 are integrated once to obtain equations 1.

References

1. FREQUENCY STARTING OF SYNCHRONOUS MACHINES, R. Bruderlin. *Electrotechnische Zeitschrift* (Berlin, Germany), November 13, 1924, page 1239.

2. MAKING TURBINE-GENERATORS DO DOUBLE DUTY, S. Nakazawa, T. Tokuda. *Electric Journal*, volume 28, August 1931, page 469.

3. PULL-IN CHARACTERISTICS OF SYNCHRONOUS MOTORS, D. R. Shoults, S. B. Crary, A. H. Lauder. AIEE TRANSACTIONS, volume 54, 1935, December section, pages 1385–95.

4. "ANGLE SWITCHING" of SYNCHRONOUS MOTORS, C. C. Shutt, J. W. Dawson. AIEE TRANSACTIONS, volume 54, 1935, November section, pages 1191–5.

5. TWO-REACTION THEORY OF SYNCHRONOUS MACHINES—PART I, R. H. Park. AIEE TRANSACTIONS, volume 48, 1929, pages 716–27.

6. RELATIONS AMONG TRANSFORMATIONS USED IN ENGINEERING PROBLEMS, C. Concordia. *General Electric Review*, volume 41, July 1938, page 323.

Biased-Core-Current-Transformer Design Method

THEODORE SPECHT
ASSOCIATE AIEE

THAT peculiar improvement in performance often occurred when a current-transformer core was divided into two parallel magnetic circuits, with different turns on each, has been well known for years, and the reasons for it have been understood in a general way. The calculation of performance of the transformer, however, has been a most baffling problem—one that could be worked out only on a tedious trial-and-error basis. The lack of a practical and straightforward method has been a serious handicap to full use of the method of construction, despite strong evidence that this method of construction, which is both practical and simple, would produce real improvement in performance.

The difficulty of calculation lies in the fact that the flux densities in the cores are different by an amount depending on the ratio and phase angle between the primary and secondary currents and that the ratio and phase angle depend in turn on the two flux densities.

Solution depends on the conception of series magnetizing impedances for the two magnetic circuits, representing the impedance curve functions in such a way that simultaneous solution is not tedious. The principal purpose of the paper is to develop a method of calculation which is sufficiently simple, yet sufficiently accurate, to be used in engineering design.

The conventional current-transformer core operates at a relatively low flux density (less than 1,000 gausses), because only in this way can the ampere turns required to circulate the flux in the core be kept to a sufficiently low value for high accuracy of current transformation. Unfortunately, however, magnetic materials generally have a low permeability at small values of flux; thus, if the flux could be greater, the permeability would be higher. The idea of supplying auxiliary biasing ampere turns from an independent source to raise the total flux density to a value where the core would have good permeability was conceived long ago, but has been little used in practice, partly because of the complications involved in supplying the bias, but mostly because it is by no means clear that the effective permeability will be raised to any easily determined value.

A method invented by Wilson[1] in 1929 supplies bias to a very small element of the core simply by passing the secondary conductor through a hole in the core. The improvement in performance is difficult to calculate with any degree of exactness, and is not so great as that obtained when the whole core can be biased. A method described by Boyajian and Camilli[2] has the disadvantage of requiring auxiliary apparatus for excitation.

The general method to be described in this paper is illustrated by Figure 1. The core is divided into two separate magnetic circuits. The primary winding links both, but (for the general case) the secondary main windings and the secondary biasing windings are wound separately on each core. Then the main windings on the two cores are connected series aiding and the biasing windings series opposing—an arrangement that will give the minimum of coupling between the total main secondary winding and the total biasing winding. This can be seen more clearly from Figure 1.

It is not obvious that the biasing winding can produce a flux density corresponding to maximum permeability; nor is it obvious that this maximum permeability would be the effective permeability which would govern the performance of the transformer; nor is it clear how the bias can be practically obtained. These difficulties have prevented wide practical application of the idea, although many patents have been issued on various schemes for using the idea.

A practical and almost obvious method for using the biasing idea shown generally in Figure 1 is the double core with a single secondary winding shown in Figure 2, in which the bias is obtained by bringing the secondary conductor through between cores. The biasing ampere turns are then proportional to the secondary current. This construction is obviously practical, but the calculation of flux density in the two cores, the effective permeabilities, and the resulting performance of the current transformer, present a most tedious problem. The calculation process is not fundamentally obscure, but, like any problem in parallel magnetic circuits, solution by conventional methods is a cut-and-try procedure, is incredibly tedious, and is not practical from an engineering design standpoint. Thus, although a structure has been devised which is practical, economical, and promises real improvements in performance, it has been impossible to apply it to advantage, because no method of calculation has existed whereby performance could be calculated. It has been impossible to determine analytically the proper proportions of the cores and the best degree of bias.

This paper will develop the theory of a method for calculating performance. Since the arrangements of Figure 1 with the main and biasing windings in series, and of Figure 2 and Figure 4, to be used later for the actual development of theory, are all identical fundamentally, the theory will be equally applicable to any one of them.

Theory of Operation

On closer examination of Figure 1, the following facts are evident, which will assist analysis of the operation. The

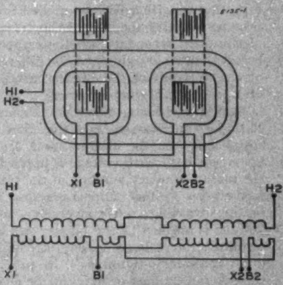

Figure 1. General construction of a biased-core current transformer

The primary winding $H1-H2$ links both the cores. The main secondary windings are connected series aiding and are labeled $X1-X2$. The biasing secondary windings are connected series bucking and are labeled $B1-B2$

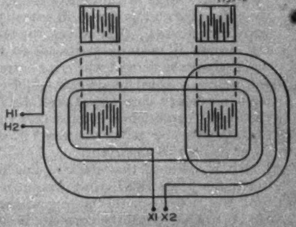

Figure 2. Practical construction of biased-core current transformer

Bias is secured from secondary current by having a few additional secondary turns around one core

---

Paper 45-135, recommended by the AIEE committees on instruments and measurements, and protective devices for publication in AIEE TRANSACTIONS. Manuscript submitted April 10, 1945; made available for printing May 14, 1945.

THEODORE SPECHT is electrical design engineer, Westinghouse Electric Corporation, Sharon, Pa.

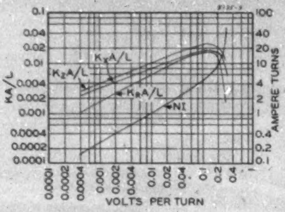

Figure 3. Nominal 60-cycle characteristic curves for the cores used in the tests and calculations

The ampere turns and the coefficients for the formulas for the resistance, reactance, and impedance of the equivalent series circuit for the core are plotted as functions of the volts per turn

main secondary windings in Figure 1 are connected in series aiding, and the secondary biasing windings are in series bucking; that is, with a voltage applied to the primary winding the sum of the voltages of the main secondary windings appears across the two in series, and the difference of the voltages of the biasing windings appears across the two in series.

At first it will be assumed that the main secondary turns on each of the cores are equal and that the biasing turns are so arranged that, when voltage is applied to the main secondary winding of the transformer, no voltage appears across the biasing winding; or conversely, when voltage is applied to the biasing-winding terminals, no voltage appears across the main secondary terminals. In practice this restriction may or may not be necessary, depending on the source for the biasing winding. If the coupling between the main and biasing windings is not zero, an error current will flow in the main secondary windings proportional to the current in the biasing winding. This error current can be used to compensate the transformer. If the biasing current does not vary with the main secondary current, this error current will become an increasingly large percentage of the main secondary current as the main secondary current decreases. If, however, the biasing current is made proportional to the main secondary current, the error current will remain a constant percentage of the main secondary current. Therefore, for the former condition it is important that the coupling be zero, whereas for the latter it is not so important.

If it is assumed that the coupling between the main and biasing windings is zero, the current in the biasing winding can be adjusted until the cores are biased at their point of maximum permeability without affecting the main secondary current. Various methods of supplying the biasing winding are possible, but the most usual one is simply to put it in series with the main secondary winding. This puts an additional burden on the main secondary winding, but for a small current transformer this will be less than five volt-amperes. Inasmuch as this burden is largely reactive, it usually will reduce the phase angle of the current transformer.

In an actual transformer, the windings will be arranged in a different manner from that just described. The two cores are put end to end with a spacer between them. The larger portion of the winding is wound about both cores, and then a few additional turns are wound about one core only. See Figure 2. This arrangement then can, by properly proportioning the turns, be made exactly equivalent to the arrangement in Figure 1.

The Derivation of the Mathematical Theory

The double-core current transformer is difficult to analyze, because simultaneous solution of the flux densities in the two cores must be made, and, unless a simple mathematical expression for the exciting current in terms of the induction is available, the equations cannot be solved. Any number of trial-and-error methods have been devised, all of which have been found to be impractical on account of the amount of numerical work involved. The method given in the following analysis is based on the equivalent circuit of Figure 4 (see Table I for explanation of the symbols). The arrangement of the windings in Figure 4 is fundamentally the same as in Figure 2, since the turns linking each of the cores are the same in the two figures. With the arrangement shown in Figure 4 the equivalent circuit for the transformer is much more apparent, as Figure 4 is essentially two current transformers in series. In the equivalent circuit the primary as well as the secondary windings are connected in series. The exciting impedance for each core is shown external to its transformer. In this analysis it was found more convenient to use an equivalent series circuit consisting of a resistance and reactance to represent the exciting-current branch. The fundamental procedure based on Figure 4 is as follows:

(*a*). Estimate the approximate value of the volts per turn per square inch in the core as the sum of the zero-burden biasing volts per turn per square inch (obtained from the biasing ampere turns per inch and a curve) plus the volts per turn per square inch required for the burden.

(*b*). Determine the resistance and reactance of the equivalent circuit for the cores from a curve, and, assuming the resistance and reactance to be constant, recalculate the volts per turn per square inch in each core. The use of a curve is the key to a rapid solution of the problem.

(*c*). Continue recalculating until the volts per turn per square inch calculated is that first assumed. This then represents the actual operating condition of the transformer. Usually the second calculation is sufficiently accurate.

(*d*). Calculate the transformer ratio and phase angle at the final values of volts per turn per square inch.

The principal reason this method has merit is that an initial value quite close to the actual value of volts per turn per square inch can be determined and that the resistance and reactance of the equivalent circuit for the core do not change too rapidly with changes in volts per turn per square inch. Usually the second estimate is sufficiently close to the final value.

An equivalent series circuit for the core was found to be the most convenient for this analysis. To obtain the curve we must secure a general expression for the resistance, reactance, and impedance of the equivalent series circuit for the core in terms of the volts per turn per square inch at 60 cycles as follows.

The flux density in the core is given by

$$B = \frac{E}{NA} \cdot \frac{1}{4.44 f \, 10^{-8}}$$

and, if $f = 60$ cycles,

$$B = 3.75 \times 10^5 \left(\frac{E}{NA} \right) \text{ lines per square inch} \tag{1}$$

The watts, volt-amperes reactive, and volt-amperes necessary for the core are

$$W = \left(\frac{W}{\#} \right) \delta l A \tag{2}$$

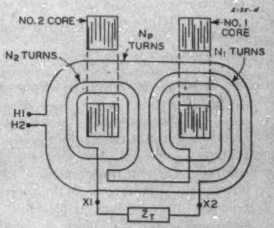

ACTUAL TRANSFORMER

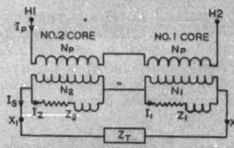

EQUIVALENT CIRCUIT

Figure 4. Arrangement of double-core current transformers used for development of the theory of calculation

The transformers are considered ideal, and the exciting branches, Z_1 and Z_2, are placed across the secondary windings of the transformers

$$VAR=\left(\frac{VAR}{\#}\right)\delta lA \tag{3}$$

$$VA=\left(\frac{VA}{\#}\right)\delta lA \tag{4}$$

The impedance of the equivalent circuit for the core is

$$Z=\frac{E^2}{(VA)}=\frac{E^2}{\left(\frac{VA}{\#}\right)\delta lA}\cdot\frac{N^2A}{N^2A}$$

$$Z=\frac{N^2A}{l}\left[\frac{\left(\frac{E}{NA}\right)^2}{\left(\frac{VA}{\#}\right)_\delta}\right]\text{ohms} \tag{5}$$

The resistance component of this impedance is

$$R=Z\frac{W}{VA}$$

Substituting in this the values for Z, W, and VA from equations 5, 2, and 4, we find

$$R=\frac{N^2A}{l}\left[\frac{\left(\frac{E}{NA}\right)^2}{\left(\frac{VA}{\#}\right)_\delta}\right]\left[\frac{\left(\frac{W}{\#}\right)}{\left(\frac{VA}{\#}\right)}\right]$$

$$=\frac{N^2A}{l}\cdot\left[\frac{\left(\frac{E}{NA}\right)^2\left(\frac{W}{\#}\right)}{\left(\frac{VA}{\#}\right)^2_\delta}\right] \tag{6}$$

The equation for the reactance component of Z can be developed in a similar manner and is

$$X=\frac{N^2A}{l}\cdot\left[\frac{\left(\frac{E}{NA}\right)^2\frac{VAR}{\#}}{\left(\frac{VA}{\#}\right)^2_\delta}\right] \tag{7}$$

The quantities in the brackets in equations 5, 6, and 7 are only functions of the flux density in the core. For convenience they will be called K_Z, K_R, and K_X as follows:

$$K_R=\frac{\left(\frac{E}{NA}\right)^2\left(\frac{W}{\#}\right)}{\left(\frac{VA}{\#}\right)^2_\delta} \tag{8}$$

$$K_X=\frac{\left(\frac{E}{NA}\right)^2\left(\frac{VAR}{\#}\right)}{\left(\frac{VA}{\#}\right)^2_\delta} \tag{9}$$

$$K_Z=\frac{\left(\frac{E}{NA}\right)^2}{\left(\frac{VA}{\#}\right)_\delta} \tag{10}$$

These constants, K_R, K_X, and K_Z then can be plotted in curve form. The equation for the impedance can be written

$$Z=\frac{N^2A}{l}\quad K_Z=\frac{N^2A}{l}\,(K_R+jK_X) \tag{11}$$

$$K_Z=K_R+jK_X \tag{12}$$

It will also be necessary to know the volts per turn per square inch induced as a function of the ampere turns per inch. This is developed as follows.

The exciting current for the core is

$$I=\frac{VA}{E}=\frac{\left(\frac{VA}{\#}\right)\delta lA}{E}$$

Solving equation 10 for $VA/\#$, substituting it in the above equation, and rearranging the terms gives

$$\frac{E}{NA}=K_Z\left(\frac{NI}{l}\right) \tag{13}$$

It is also possible then to plot as a function of E/NA, the value of NI/l which, as will be explained, leads to solution of the problem.

In the equivalent circuit of the double-core current transformer as shown in Figure 4, it is assumed that the mean lengths of flux paths are equal. N_1 is greater than or equal to N_2, but A_1 can be greater than, equal to, or less than A_2. The transformers also are assumed to be ideal and their exciting impedances represented by shunt impedances external to the transformers. It is desired first to develop three sets of equations:

(*a*). For calculating the volts per turn per square inch in each core for values of K_Z corresponding to estimated values of volts per turn per square inch.

(*b*). For estimating the approximate values of volts per turn per square inch in each core for the first try in (*a*).

(*c*). For calculating the ratio and phase angle when the actual values of volts per turn per square inch have been determined.

From Figure 4, the following equations may be written

$$N_1(I_S+I_1)=N_2(I_S+I_2) \tag{14}$$

Table I. 200-to-5-Ampere Current Transformer, Biased-Core Through-Type Construction

Burden: 2.5 *VA*, 90 Per-Cent Power Factor
Frequency: 60 Cycles

Data	Per-Cent Current	Per-Cent Ratio	Phase Angle, Minutes
*	100	100.17	+ 3
*	10	100.34	+13
**	100	100.06	+ 3
**	10	100.23	+13
†	100	100.07	− 1
†	10	100.17	+16
††	100	100.22	+ 9
††	10	100.45	+26

* Calculated values from nominal core data using method of this paper.

** Calculated values corrected for ratio instability, −0.11 per cent, due to cores with different characteristics.

† Test values of actual transformer as a biased current transformer.

†† Test values of actual transformer as an unbiased current transformer.

$$I_SZ_T=I_1Z_1+I_2Z_2 \tag{15}$$

Solving equations 14 and 15 simultaneously for I_1 and I_2 yields

$$I_1=I_S\frac{N_2Z_T-(N_1-N_2)Z_2}{N_1Z_2+N_2Z_1} \tag{16}$$

$$I_2=I_S\frac{N_1Z_T+(N_1-N_2)Z_1}{N_1Z_2+N_2Z_1} \tag{17}$$

$E_1=I_1Z_1$. Substituting in this equation the value of I_1 from equation 16 and the values of Z_1 and Z_2 from equation 11, yields

$$\frac{E_1}{N_1A_1}=\frac{I_SK_{Z1}}{l}\left[\frac{lZ_T-(N_1-N_2)N_2A_2K_{Z2}}{N_2A_2K_{Z2}+N_1A_1K_{Z1}}\right] \tag{18}$$

Similarly,

$$\frac{E_2}{N_2A_2}=\frac{I_SK_{Z2}}{l}\left[\frac{lZ_T+(N_1-N_2)N_1A_1K_{Z1}}{N_2A_2K_{Z2}+N_1A_1K_{Z1}}\right] \tag{19}$$

With equations 18 and 19, if the values of K_{Z1} and K_{Z2} for the cores are known, the values of volts per turn per square inch can be calculated. It is necessary to know initially an approximate value for the volts per turn per square inch in each core so as to have some place from which to start. Equations 18 and 19 now will be modified, so that approximate values can be calculated.

If equations 18 and 19 now are rewritten, assuming that $K_{Z1}=K_{Z2}=K_Z$,

$$\frac{E_1}{N_1A_1}=\frac{I_SZ_T}{N_2A_2+N_1A_1}-\left[\frac{I_S(N_1-N_2)N_2A_2}{l(N_2A_2+N_1A_1)}\right]K_Z \tag{20}$$

$$\frac{E_2}{N_2A_2}=\frac{I_SZ_T}{N_2A_2+N_1A_1}+\left[\frac{I_S(N_1-N_2)N_1A_1}{l(N_2A_2+N_1A_1)}\right]K_Z \tag{21}$$

The first terms in each equation may be calculated now, but the last terms still contain K_Z. The last term in each equation is a function of the secondary current and the difference in turns between the two cores; or in other words, it is proportional to the biasing ampere turns. This can be shown as follows: rewriting equations 16 and 17, substituting in the values of Z_1 and Z_2 from equation 11, letting $K_{Z1}=K_{Z2}$, and multiplying the equations respectively by N_1/l and N_2/l gives:

$$\frac{N_1I_1}{l}=\frac{I_SZ_T}{(N_2A_2+N_1A_1)K_Z}-\left[\frac{I_S(N_1-N_2)N_2A_2}{l(N_2A_2+N_1A_1)}\right] \tag{22}$$

$$\frac{N_2I_2}{l}=\frac{I_SZ_T}{(N_2A_2+N_1A_1)K_Z}+\left[\frac{I_S(N_1-N_2)N_1A_1}{l(N_2A_2+N_1A_1)}\right] \tag{23}$$

If equations 22 and 23 are multiplied through by K_Z, they are identical to equations 20 and 21. That the left-hand terms also should be equal was shown by equation 13. The last terms of equations 22 and 23 then represent the approximate biasing ampere turns per inch for each of the cores. From equation 13 it is seen that the last terms of equations 20 and 21 then can be read from the curve where the volts per turn per square inch are a function of the ampere turns per inch. Equations 20 and 21 then may be rewritten in functional notation where the last term of each equation is read from the curve as a function of the ampere turns per inch.

$$\frac{E_1}{N_1A_1}=\frac{I_SZ_T}{N_2A_2+N_1A_1}-f\left[\frac{I_S(N_1-N_2)N_2A_2}{l(N_2A_2+N_1A_1)}\right] \quad (24)$$

$$\frac{E_2}{N_2A_2}=\frac{I_SZ_T}{N_2A_2+N_1A_1}+f\left[\frac{I_S(N_1-N_2)N_1A_1}{l(N_2A_2+N_1A_1)}\right] \quad (25)$$

For the first approximation it is sufficiently accurate if only the arithmetic sum of the two terms is taken.

With the values of E/NA, calculated by equations 24 and 25, the values of K_z may be read from the curve and new values of voltage determined from equations 18 and 19. Sufficient calculations are made until no further significant changes in the voltages result. Usually only two calculations are required.

The actual transformer ratio then can be calculated when the correct values of voltage have been determined. The reversed primary current then is

$$N_pI_p=N_2(I_S+I_2) \quad (26)$$

Substituting in the value of I_2 from equation 17 and using the values for Z_1 and Z_2 from equation 11 yields

$$N_pI_p=I_S\left[N_2+\left(\frac{lZ_T+(N_1-N_2)N_1A_1K_{z1}}{N_2A_2K_{z2}+N_1A_1K_{z1}}\right)\right] \quad (27)$$

This equation will reduce to the form:

$$N_pI_p=I_S(N_2+a+jb) \quad (28)$$

where a is the real part of the last term of equation 27, and b is the imaginary part. Both a and b are usually small compared to N_2. If the name-plate ratio is npR, the transformer ratio is approximately

$$\text{per cent } R=\frac{N_2+a}{(npR)N_p}\times 100 \quad (29)$$

and the transformer phase angle is

$$\text{phase angle}=-\frac{b}{N_2+a}\,3{,}438 \text{ minutes} \quad (30)$$

The negative sign is introduced by virtue of the definition of phase angle. That is, the transformer phase angle is positive if the secondary current leads the reversed primary current.

The nominal per-cent ratio at zero burden and cores of equal characteristics is a useful equation for estimating the ratio. In equation 27 let $Z_T=0$ and $K_{z1}=K_{z2}$

$$N_pI_p=I_S\left[N_2+\frac{(N_1-N_2)N_1A_1}{N_2A_2+N_1A_1}\right] \quad (31)$$

Hence, the nominal per-cent ratio is

$$\frac{N_2+\dfrac{(N_1-N_2)N_1A_1}{N_2A_2+N_1A_1}}{(npR)N_p}100 \quad (32)$$

If the two cores in the transformer are better or worse than they are supposed to be nominally, they have a considerable effect on the ratio and produce a phenomenon we might call "ratio instability." With reference to equation 27 the per-cent ratio is

$$\text{per cent } R=\frac{100}{N_p(npR)}\times\left[N_2+\frac{lZ_T}{N_2A_2K_{z2}+N_1A_1K_{z1}}+\frac{(N_1-N_2)N_1A_1K_{z1}}{N_2A_2K_{z2}+N_1A_1K_{z1}}\right]$$

The total derivative with respect to K_{z1} and K_{z2} is

$$\Delta \text{ per-cent } R=\frac{100}{N_p(npR)}\left[-\frac{lZ_T(N_2A_2\Delta K_{z2}+N_1A_1\Delta K_{z1})}{(N_2A_2K_{z2}+N_1A_1K_{z1})^2}+\frac{(N_1-N_2)N_1N_2A_1A_2(K_{z2}\Delta K_{z1}-K_{z1}\Delta K_{z2})}{(N_2A_2K_{z2}+N_1A_1K_{z1})^2}\right]$$

The only case considered will be that in which the first quantity in the brackets is small, which is so if either the burden Z_T or $N_2A_2\Delta K_{z2}+N_1A_1\Delta K_{z1}$ is small. Simplifying the last term of the foregoing expression by letting N_1, N_2, $N_p(npR)$ be about equal to each other, and K_{z1} and K_{z2} about equal to each other:

$$\Delta \text{ per cent } R=\frac{N_1-N_2}{N_1\left(2+\dfrac{A_1}{A_2}+\dfrac{A_2}{A_1}\right)}\times\left[\frac{\Delta K_{z1}}{K_{z1}}-\frac{\Delta K_{z2}}{K_{z2}}\right]100 \quad (33)$$

From equation 10 at constant induction

$$\frac{\Delta K_z}{K_z}=-\frac{\Delta\left(\dfrac{VA}{\#}\right)}{\left(\dfrac{VA}{\#}\right)}$$

$$\Delta \text{ per cent } R=\frac{N_1-N_2}{N_1\left(2+\dfrac{A_1}{A_2}+\dfrac{A_2}{A_1}\right)}\times\left[\frac{\Delta\left(\dfrac{VA}{\#}\right)_2}{\left(\dfrac{VA}{\#}\right)_2}-\frac{\Delta\left(\dfrac{VA}{\#}\right)_1}{\left(\dfrac{VA}{\#}\right)_1}\right]100 \quad (34)$$

$\Delta\left(\frac{VA}{\#}\right)$ is the difference between the actual and the nominal volt-amperes per pound at some average point. $\Delta\left(\frac{VA}{\#}\right)\div\left(\frac{VA}{\#}\right)$ is not constant at all inductions. Equation 34 is not an exact equation but is meant only as a guide to how accurately the cores must be matched. It is also valid only for low secondary burdens or where $\Delta\left(\frac{VA}{\#}\right)/\left(\frac{VA}{\#}\right)$ for the two cores vary in opposite directions.

Another difficulty is immediately perceived; that is, as the diameter of the transformer is increased, N_1-N_2 must increase in order to keep the biasing flux density constant. This means that the nominal no-load ratio becomes even more erratic. The possibility of adjusting this no-load ratio by means of short-circuited turns of resistance wire on one core is entirely practical; and, if the unit is a bushing-type current transformer competing with a wound-type high-voltage current transformer, the expense in adjustment can be justified.

It has been postulated previously that, if the effective coupling between the main secondary winding and the biasing winding be zero, the biasing winding will act as an additional burden in series with the total secondary burden.[*] If the following values are substituted in equation 27, they will fulfill the requirement for zero coupling:

$$N_1=N+n;\quad N_2=N-n;\quad K_{z1}=K_{z2}=K_z;\quad A_1=A_2=A$$

where N is the main secondary turns per core and n the biasing turns per core. Figure 1 shows the arrangement assumed for this. The biasing winding is in series with the secondary.

$$N_pI_p=I_SN\left[1+\frac{Z_T+\dfrac{2n^2AK_z}{l}}{\dfrac{2N^2AK_z}{l}}\right] \quad (35)$$

From equation 11 it is seen that n^2AK_z/l would be the impedance of one of the biasing windings and twice that would be the impedance of the two in series. It is

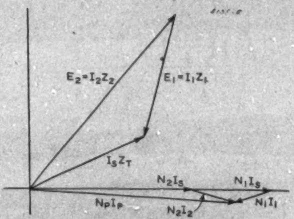

Figure 5. Vector diagram for double-core current transformer whose equivalent circuit is shown in Figure 3

E_1 and E_2 are the induced voltages of the current transformer secondary windings

Figure 6. Type *FW* current transformer, 200-to-5-amperes ratio with double-core construction

This transformer has an accuracy class of 0.3 at a *B*-0.1 burden

to be noted that this impedance appears in equation 35 in series with the total secondary burden, Z_T. Also from equation 11, N^2AK_Z/l would be the impedance of one of the secondary main windings and twice that would be the impedance of the two in series.

For an ordinary current transformer with a series burden of Z_T' ohms, and a shunt exciting impedance of Z_X ohms, the ratio is

$$1+\frac{Z_T'}{Z_X} \qquad (36)$$

If equation 35 is compared with equation 36, it is seen that the numerator of the last term of equation 35 corresponds to Z_T' of equation 36, the total series burden, and the denominator corresponds to Z_X, the shunt exciting impedance. It becomes apparent that the full permeability of the core at the point of bias is utilized, for K_Z is calculated on the basis of the a-c permeability at the point of actual operation. Also, it is apparent that the least variation in errors with secondary load or current will occur if K_Z is a maximum, or if the transformer is biased at the point of maximum permeability. Of course, instability of the nominal ratio according to equation 34 may be a factor in determining whether it is desirable to bias the transformer at so high an induction.

A vector diagram of the equivalent circuit of Figure 4 is shown in Figure 5. In general E_1 and E_2 are both large and about 180 degrees out of phase, the vector sum of the two voltages being equal to the voltage of the total burden. For high-power-factor burdens, the reversed primary current usually lags the secondary current, whereas for low-power-factor burdens it will lead.

In Figure 6 is a typical low-voltage through-type current transformer using the biased-core type of construction. This type of transformer has found much application in metering boxes where the through-type construction is convenient for the three-wire metering connection and makes possible changing transformer ratio by taking the primary conductor through the opening a number of times.

Experimental and Calculated Results

The following data are for the sample transformer used:

npR: 40 to 1; 200 to 5 amperes
$N_1=41$ turns
$N_2=39$ turns
$A_1=A_2=A$
$\Delta(VA/\#)_2/(VA/\#)_2=-0.18$
$\Delta(VA/\#)_1/(VA/\#)_1=-0.09$
Secondary resistance = 0.035 ohm

Figure 3 is the nominal curves for both cores. For this problem, the curves are plotted as follows:

Ampere turns as a function of volts per turn
$\frac{KA}{l}$ as a function of volts per turn

To use these curves, the equations are modified as follows:

Equation 13: $$\frac{E}{N}=\left(\frac{K_ZA}{l}\right)(NI) \qquad (37)$$

If this equation is transposed, its significance is more apparent:

$$\frac{K_ZA}{l}=\frac{E}{IN^2}$$

which means that K_ZA/l is the exciting impedance measured at the terminals of N turns divided by the turns squared. K_RA/l is K_ZA/l multiplied by the power factor and K_XA/l is K_ZA/l multiplied by the reactive factor. This shows how KA/l can be obtained from measurements on an actual winding on one core.

Equation 18: $$\frac{E_1}{N_1}=I_s\left(\frac{K_{Z1}A}{l}\right)\times\left[\frac{Z_T-(N_1-N_2)N_2\left(\frac{K_{Z2}A}{l}\right)}{N_2\left(\frac{K_{Z2}A}{l}\right)+N_1\left(\frac{K_{Z1}A}{l}\right)}\right] \qquad (38)$$

Equation 19: $$\frac{E_2}{N_2}=I_s\left(\frac{K_{Z2}A}{l}\right)\times\left[\frac{Z_T+(N_1-N_2)N_1\left(\frac{K_{Z1}A}{l}\right)}{N_2\left(\frac{K_{Z2}A}{l}\right)+N_1\left(\frac{K_{Z1}A}{l}\right)}\right] \qquad (39)$$

Equation 20: $$\frac{E_1}{N_1}=\frac{I_sZ_T}{N_2+N_1}-\left[\frac{I_s(N_1-N_2)N_2}{N_2+N_1}\right]\left(\frac{K_ZA}{l}\right) \qquad (40)$$

Equation 21: $$\frac{E_2}{N_2}=\frac{I_sZ_T}{N_2+N_1}+\left[\frac{I_s(N_1-N_2)N_1}{N_2+N_1}\right]\left(\frac{K_ZA}{l}\right) \qquad (41)$$

Equation 27: $$N_pI_p=I_s\left[N_2+\frac{Z_T+(N_1-N_2)N_1\left(\frac{K_{Z1}A_1}{l}\right)}{N_2\left(\frac{K_{Z2}A_2}{l}\right)+N_1\left(\frac{K_{Z1}A_1}{l}\right)}\right] \qquad (42)$$

Equations 40 and 41 are the equations for the first estimation of the volts per turn in each core. The bracketed term of each of these equations is the biasing ampere turns for each of the cores. From equation 37 it is seen that when this is multiplied by K_ZA/l the result is the biasing volts per turn. This quantity may be read directly from Figure 3, where the ampere turns are plotted as a function of the volts per turn. The actual values of the volts per turn are found by repeated substitution in equations 38 and 39 and then the true primary ampere turns from equation 42. The per-cent ratio and the phase angle then may be determined by equations 28, 29, and 30. The results of these calculations are shown in the first two lines of Table I. The ratio must be corrected though, for the difference in the core characteristics according to equation 34. This correction is −0.11 per cent and the corrected values are shown in lines 3 and 4 of the table. The actual test values on the biased transformer also are given as well as tests as a straight unbiased transformer. For this latter condition, 40 turns linked each core.

Conclusions

A method of calculation for the double-core current transformer has been developed that is practical and has sufficient accuracy that the designer can determine the proper proportions of core and the best degree of bias to get the best possible performance, as well as the performance obtainable. It shows that much can be gained in reducing transformer ratio errors and in correcting phase-angle errors in bushing-type current transformers by using the double-core construction. This method of calculation also makes it possible to determine how closely the cores must be matched, and whether adjustment by test will be necessary. This will make possible the construction of high-accuracy bushing-type current transformers to smaller dimensions and lower primary-current ratings than was heretofore possible.

List of Symbols

Subscripts 1 and 2 refer to values for cores 1 and 2.

B—Induction in lines per square inch
E—Voltage across a given winding, volts

Impulse-Failure-Detection Methods as Applied to Distribution Transformers

H. C. STEWART
MEMBER AIEE

J. E. HOLCOMB
ASSOCIATE AIEE

Synopsis: Investigation of several methods for the detection of impulse failures in distribution transformers has strengthened our belief in the inadequacy of the methods described in American Standard *C*57.2. All of the methods are discussed in detail, and the most hopeful one is compared with the present method of analyzing the voltage wave and making the physical observations as outlined in the Standards. Data are presented on transformers utilizing present and proposed methods.

DEMONSTRATION of the ability of electric apparatus to withstand impulse tests is of little value unless adequate failure-detection methods are used. Everyone who has had occasion to do impulse testing at one time or another has experienced some uneasiness concerning the certainty of detecting small failures when utilizing present testing technique as covered in the Standards. Many transformers have received impulse tests as a condition of specification and purchase to demonstrate the ability of their windings to withstand such tests. Examination of the windings after testing has disclosed failures which had not been suspected from any known failure indications. Since such a procedure is impractical and often impossible because of economics, it becomes necessary to revise impulse-testing technique relative to failure detection so as to acquire an accurate knowledge of the true condition of windings after impulse voltages have been applied.

Present Impulse-Failure-Detection Methods

For many years now it has been the practice to follow the testing procedure covered in American Standard *C*57.2, 10.122. This reference is quoted here for convenience.

> "*Detection of Failure During Impulse Test.* Because of the nature of impulse-test failures, one of the most important matters is the detection of failure. There are a number of indications of insulation failure. Some of these are: noise within the transformer; presence of smoke; excessive current or drop in voltage in the excitation circuit as indicated by the magnetic oscillograph; failure of the gap or bushing to flash over, although the oscillogram indicates a chopped wave; presence of oscillations or other variations from the expected wave shape as indicated by cathode-ray oscillograms."

It may be seen that certain electrical observations are required, such as the wave shapes of the applied impulse by means of cathode-ray oscillograph by comparison between reduced-full-wave and full-wave oscillograms, and also inspection of the normal-frequency disturbance occasioned by normal-frequency follow current which may be initiated by an impulse failure. In addition to this there are such physical observations to be made as the notation of unusual sound and the presence of smoke or bubbles occasioned by arcing within the apparatus.

Experience With Present Impulse-Failure-Detection Methods

The experience cited here is the result of the test and examination of a great many small distribution transformers which were tested to destruction with impulse voltages. With smaller transformers, the ratio of capacitive impedance to inductive impedance is much smaller than is the case with larger power transformers. Therefore, the problems involved in impulse-failure detection are different. Superimposed high-frequency oscillations[1] rarely occur on the crest of the applied voltage wave as they do in the case of power transformers, so that meticulous examination of the voltage wave near its front is of little help in failure detection in small transformers. Likewise, the examination of the applied voltage wave on its tail yields unpredictable results, in some cases actually showing a shortening of the tail due to a layer failure, while in other instances revealing a considerable portion of the coil to be short-circuited out in the failure

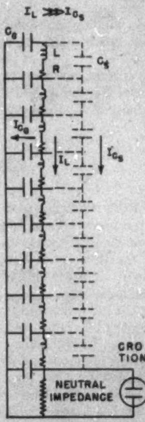

Figure 1. Equivalent circuit of idealized power-transformer winding

Paper 45-129, recommended by the AIEE committee on electric machinery for publication in AIEE TRANSACTIONS. Manuscript submitted April 16, 1945; made available for printing May 21, 1945.

H. C. STEWART is electrical engineer, distribution-transformer engineering division, and J. E. HOLCOMB is engineer, works laboratory, both with General Electric Company, Pittsfield, Mass.

N_p—Primary turns
N—Secondary turn in a given winding
A—Cross sectional area of a given core, square inches
W—Watts, core loss
VAR—Volt-amperes reactive, core loss
VA—Volt-amperes, core loss
δ—Density of core, pounds per cubic inch
l—Mean length of flux path, inches
R—Equivalent series resistance of core, ohms
X—Equivalent series reactance of core, ohms
Z—Equivalent series impedance of core, ohms
$W/\#$—Watts per pound core loss
$(VAR)/\#$—Volt-amperes reactive per pound core loss
$(VA)/\#$—Volt-amperes per pound core loss
K_R—See equation 8
K_X—See equation 9
K_Z—See equation 10
I—Exciting current in a given winding, amperes
I_s—Secondary current of current transformer, amperes
I_p—Primary current of current transformer, amperes
Z_T—Total secondary burden of current transformer winding resistance plus external burden ohms
npR—Transformer name-plate ratio
Per-cent R—Transformer per-cent ratio

References

1. A NEW HIGH-ACCURACY CURRENT TRANSFORMER, M. S. Wilson. AIEE TRANSACTIONS, volume 48, 1929, pages 783–9.

2. ORTHOMAGNETIC BUSHING CURRENT TRANSFORMER FOR METERING, A. Boyajian, G. Camilli. AIEE TRANSACTIONS, volume 64, 1945, March section, pages 137–40.

3. IRON BIASED BY ALTERNATING CURRENT, G. Stein. *The Electrician* (London, England), March 23, 1934, pages 391–3.

4. INSTRUMENT TRANSFORMERS (book), B. Hague. Sir Isaac Pitman and Sons. Pages 95–103.

5. A. Iliovici. *Elektrotechnik und Maschinenbau* (Vienna, Austria), volume 41, 1923, page 725.

6. DIE NEUESTE ENTWICKLUNG IM STROMWANDLERBAU, J. Goldstein. *Elektrotechnische Zeitschrift* (Berlin, Germany), volume 54, 1932, pages 377, 428, 503.

without the tail of the voltage wave being altered.

Smoke and bubbles cannot always get out of buried layers with sufficient velocity to be noticeable to the observer and therefore are not a dependable failure-detection method. The presence of normal-frequency excitation confuses the oscillography with disturbances caused by arcing of isolating gaps and should not be considered as a dependable indicator of failure, since many transformers known to have failed on impulse have successfully withstood normal voltage.

The usual sequence of evidence secured during tests deliberately increased in kilovolts until failure occurs, with the present American Standards Association methods, is as follows:

1. Failure may occur without any of the indicators showing the occurrence of failure.
2. Failure is shown by slight changes in wave shape of the applied wave without bubbles, or
3. Bubbles become noticeable.
4. Normal-frequency current will follow through the impulse path as the applied impulse voltage is increased above normal test levels.

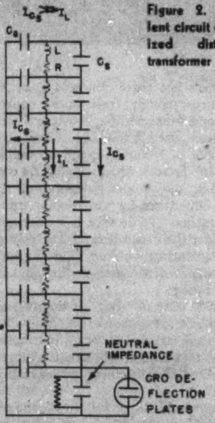

Figure 2. Equivalent circuit of idealized distribution-transformer winding

As a result of this experience, it is known that these methods of failure detection often will not show turn or layer failures or even the failure of major insulation to ground.

In view of such experience, we believe that the present procedures for fault detection are not satisfactory.

Table I. Description of Test Method

	Record Impulse Voltage Wave					Record Impulse Current Wave in Neutral Impedance Consisting of		
Method	Applied Wave C_1	Applied Wave C_2	Core	On Winding Tap	Low-Voltage Winding	Resistance	Capacitance	Shunt Capacitance and Resistance
1	x							
2		x						
3			x					
4				x				
5					x			
6						x		
7							x	
8								x

C_1 Impulse-generator capacitance—0.025 microfarad.

C_2 Impulse-generator capacitance—0.006 microfarad.

Table II

Efficiency of Testing—Method								Rating of Test Piece		
1	2	3	4	5	6	7	8	Kva	Kv	Per Cent of Winding Failed
U	*F*	*E*	*P*	*E*	*F*	*E*	*E*	1.5	7.2	4.0
			P					1.5	7.2	8.0
G	*E*	*G*	*E*	*G*	*E*	*E*	*E*	5.0	2.4	12.0
			E					5.0	2.4	17.5
P	*E*	*F*	*G*	*F*	*E*	*E*	*E*	5.0	7.2	7.0
U	*P*	*F*	*G*	*P*	*F*	*E*	*E*	10.0	13.8	1.0
								10.0	13.8	3.0
E	*E*	*E*	*E*	*E*	*E*	*E*	*E*	25.0	2.4	10.0

Definition of method efficiency:
E—Excellent *G*—Good *F*—Fair *P*—Poor *U*—Unsatisfactory

Investigation of Impulse-Failure-Detection Methods

In an effort to improve this situation, several impulse-failure-detection methods were investigated as applying to distribution transformers, with the aid of the electric transient analyzer, and the most promising were checked with the usual design of impulse generator. The work done with the transient analyzer is described in methods 1 to 8 inclusive, Table I, and the relative efficiency of the methods is tabulated in Table II. Methods 1, 2, 3, 4, and 5 consist of measurement of a voltage wave at some point in the transformer structure, whereas methods 6, 7, and 8 constitute current-wave measurements in the transformer neutral.

METHODS 1 AND 2

Methods 1 and 2 consist of the observation of the applied voltage wave which is the present recommended procedure, except for the omission of normal-frequency voltage, for the determination of the electrical condition of a winding when subjected to impulse voltages. Method 2 employs a loosely coupled impulse generator; that is, a generator of small capacitance so as to have an inherently high regulation (voltage drop) as a result of a change in the impedance of the test piece brought about by the failure of its windings.

It was found that anything less than a generator capacitance of 0.006 microfarad was impractical, because it could not deliver a $1^1/_2$ x 40 microsecond wave to low-impedance high-voltage windings. When the results of method 2 are compared with the results of method 1 (in Table II), in which the generator capacitance of 0.025 microfarad more nearly represents present testing practice, the advantage as far as failure detection is concerned lies with the low-capacitance generator (method 2).

METHOD 3

Oscillations within the winding of a transformer can be recorded to some extent by measuring the voltage produced on its core. In general, this voltage is due to its capacitive coupling with the winding and is a reproduction of the applied wave plus some high-frequency oscillations. The magnitude of this voltage is a function of capacitance coupling and may be sufficiently high to stress unduly the insulation between core and coil. Although the method works very well in some cases, it should not be considered as a universal method of failure detection, because the utilization of this method involves the isolation of the core from ground which in itself produces voltage stresses unnatural to those experienced in conventional circuits.

METHOD 4

A modification of method 1 consists of the observation of the voltage at some other point in the same winding than that to which the wave is applied. This can be done where taps have been provided in the winding. The impulse voltage from tap to ground, when measured on the tap nearest the ground end of the

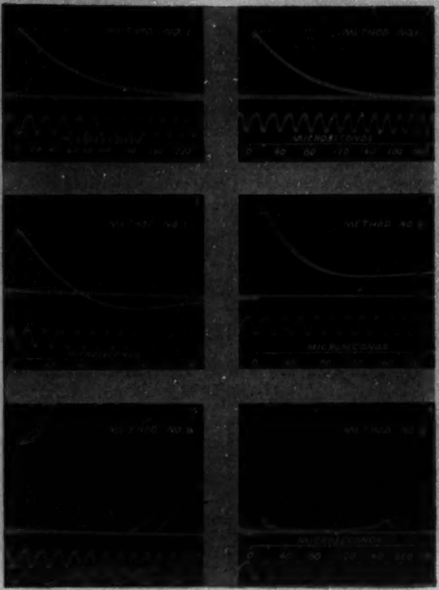

Figure 3 (left). 10-kva 2,400-volt transformer

Applied voltage wave

1. No failure
2. Failure of one turn (0.1 per cent)
3. Failure of ten per cent of winding

Impulse current

4. No failure
5. Failure of one turn (0.1 per cent)
6. Failure of ten per cent of winding

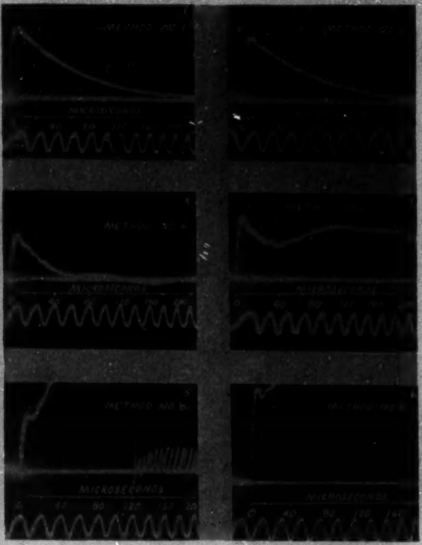

Figure 4 (right). 1½-kva 7,200-volt transformer

1. Applied voltage wave—no failure
2. Applied voltage wave—failure of $13^1/_3$ per cent of winding (ground end)
3. Impulse current—no failure
4. Impulse current—failure of 0.02 per cent of winding (one turn)
5. Impulse current—failure of $13^1/_3$ per cent of winding (ground end)
6. Impulse current—$4^1/_2$ per cent of coil short-circuited through 300.0 ohms

winding, in many cases changes substantially in both wave shape and magnitude at the occurrence of a failure. The utilization of this method is contingent on the presence of suitable taps within a given winding and the problem of bringing out of the tank an additional bushing not provided for in the design.

METHOD 5

This method involves the observation of voltage on a winding other than the one under test. This is equivalent to loose coupling in the impulse generator in that observation is made on a winding which is loosely coupled both electrostatically and magnetically with the winding to which the impulse is applied. In many cases, a layer failure in the high-voltage coil will change substantially the shape of the wave which is reflected in the low-voltage coil. Since one end of the low-voltage coil may be conveniently grounded during test, this method can be more readily adapted to impulse-failure detection than methods 3 and 4.

Measurement of Neutral-Impedance Current

METHODS 6, 7, AND 8

The dielectric condition of a winding during impulse testing can be determined by the measurement of the impulse current[1] as measured in a neutral impedance connected outside the transformer. Changes in the impedance of the transformer winding due to impulse failure will bring about a change in the impulse current.

The use of a neutral impedance during impulse testing results in a circuit not encountered in actual transmission service. However, it should be stated that such a procedure does not alter perceptibly the impulse-voltage distribution within the transformer windings.

As there are three different types of impedance, namely, resistance, capacitance, and combination resistance and capacitance, used in the circuits described in methods 6, 7, and 8, it will be well to review the factors which should be considered in the proper selection of the neutral impedance for a particular transformer rating. To do this, it is necessary to consider the controlling characteristics of the transformer winding. This depends upon the size of the transformer and its voltage rating.

Impulse current that flows through a distribution-transformer winding during the time interval in which it is desirable to detect failures will have a changed distribution from that of power transformers.

In the case of the power transformers,[1] the equivalent circuit is represented by Figure 1, where a major part of the impulse current flows through the inductance–resistance circuit, as indicated by the bold lines of the circuit. Although no dividing lines can be drawn, distribution transformers in general would be represented more nearly by the equivalent circuit of Figure 2, where a major part of the impulse current flows through the capacitance circuit, as indicated by the bold lines of the figure.

As the measurement of impulse neutral current is accomplished by measuring the voltage drop across a neutral impedance which is placed in series with the transformer under test, and as this circuit is a voltage-divider arrangement, it is ad-

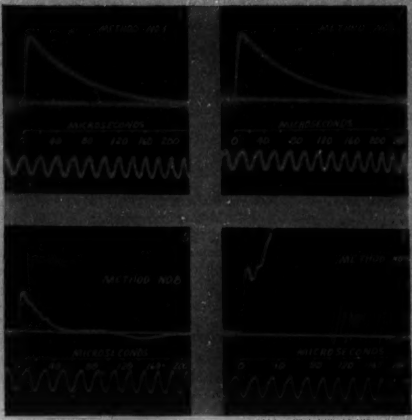

Figure 5. 1½-kva 7,200-volt transformer

Applied voltage wave
1. No failure
2. Failure of 2.0 per cent of winding

Impulse current
3. No failure
4. Failure of 2.0 per cent of winding

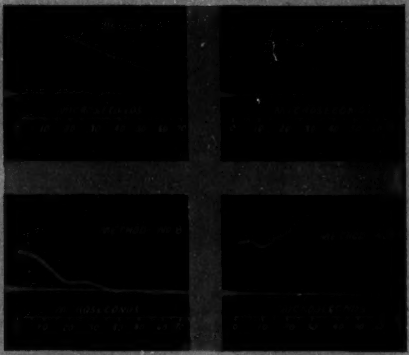

Figure 6 (upper right). 3-kva 7,200-volt transformer

Applied voltage wave
1. No failure
2. Failure of 50 per cent of winding (ground end)

Impulse current
3. No failure
4. Same failure as in oscillogram 2

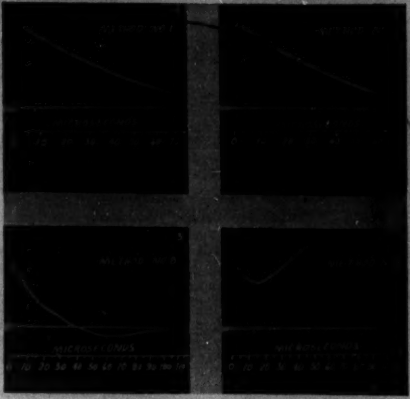

Figure 7 (right). 37½-kva 13,200-volt transformer

Applied voltage wave
1. No failure
2. Failure of 33⅓ per cent of winding (line end)

Impulse current
3. No failure
4. Same failure as in oscillogram 2

vantageous to match the neutral impedance with the controlling impedance of the transformer network. In other words, the desirable neutral impedance consists of a resistance[1] or an inductance in the case of large transformers, Figure 1, and a capacitor in the case of small distribution transformers, Figure 2. When a capacitor is used for a neutral impedance, the charge increases as long as current flows, and there is a tendency to increase the amplitude of the trace on the oscillogram. The use of a resistor in shunt with the capacitor helps to drain off the charge, thereby improving the oscillography and at the same time providing a discharge circuit for the capacitor.

Method 6 evaluates this current by measuring the voltage across an impedance consisting of a resistor placed in the transformer-winding neutral.[1] As most of the current is charging current, a pure resistance shunt will give a very large initial deflection. This peak current is of little value in failure detection, and so some means such as gaps has to be devised to protect the oscillographic equipment.

Method 7 utilizes a capacitor as the neutral impedance. This gives a very sensitive failure-detection method. An impedance change, caused by the short-circuiting of one layer (seven per cent) of a high-voltage coil, caused the impulse current to increase 3,300 per cent. A disadvantage of this method is that the capacitor charge continues to increase for a considerable time, particularly if isolating gaps are used between the test piece and the testing circuit. If isolating gaps are used, the capacitor cannot discharge except by leakage.

In method 8 it was found that a resistor could be used in shunt with the capacitor without appreciably reducing the sensitivity of the scheme. This method is an improvement of methods 6 and 7, and in the work done, a *time constant* of this capacitor–resistor combination of 100 microseconds or less was found to be satisfactory.

Experience in the Application of Methods 1 and 8

Tests on Transformers With Controlled Faults

In order to study impulse-failure detection where turn and layer failures are involved, it was necessary to provide full-scale transformers with a single turn and some portion of the layers brought out so that turn or layer failures could be arranged at will; otherwise a great many transformers might have to be tested to get the type of failure desired.

The data presented on these transformers were obtained using the present ASA method 1, and the best of the methods, as outlined in Table II, method 8. Circuit diagrams for these methods are shown in Figures 8 and 9. The oscillograms shown in Figures 3, 4, and 5 were taken on transformers having such con-

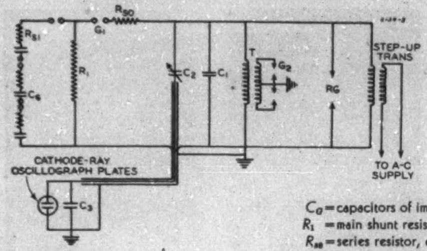

Figure 8. Conventional impulse test circuit for distribution transformers

C_g = capacitors of impulse generator
R_1 = main shunt resistor
R_{s0} = series resistor, external to generator
R_{s1} = series resistor, internal to generator
C_1 = auxiliary capacitor to control wave shape
C_2 = main capacitor of voltage divider
C_3 = auxiliary capacitor of voltage divider
G_1 = protecting gaps (high-vacuum)
T = transformer under test
G_2 = gaps to protect low-voltage winding
RG = test gap (rod gap)

trolled points of failure while using a conventional impulse generator of ASA recommended voltage level for the particular transformer voltage class. It was necessary to omit normal-frequency voltage because of the controlled faults.

10-Kva 2,400-Volt Transformer, Figure 3. When testing with method 1 turn failures could not be detected, but a layer failure is indicated by a shortening of the tail of the wave. The impulse current, method 8, readily detects both the turn and layer failures. In this instance, it was necessary to protect the oscillograph equipment by means of gaps. It would have served the same purpose to reduce the resistivity of the current-measuring impedance.

$1^{1}/_{2}$-Kva 7,200-Volt Transformer, Figures 4 and 5. Because of its higher voltage rating, this transformer has a considerably larger number of turns and layers than the ten-kilovolt-ampere 2,400-volt transformer shown in Figure 3. Oscillograms 1 and 2 in Figures 4 and 5 show that method 1 will not detect failures involving either 2 or $13^{1}/_{2}$ per cent of the winding by observing the applied voltage wave. The impulse-current detection, method 8, readily detects either defect, as shown in Figures 4 and 5. It is also to be observed in this case that this method shows a one-turn failure very effectively (see Figure 4, oscillogram 4). As the detection of failure using the impulse-current method is contingent on being able to observe current changes due to impedance changes of the circuit brought about by failures within the winding, it is important to demonstrate that this method will detect failures even though this current is relatively small. To do this, a $4^{1}/_{2}$-per-cent winding fault was closed through a 300.0-ohm resistance (see Figure 4, oscillogram 6).

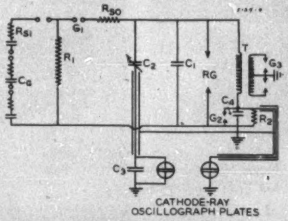

Figure 9. Recommended impulse test circuit for distribution transformers

C_g = capacitors of impulse generator
R_1 = main shunt resistor
R_{s0} = series resistor, external to generator
R_{s1} = series resistor, internal to generator
C_1 = auxiliary capacitor to control wave shape
C_2 = main capacitor of voltage divider
C_3 = auxiliary capacitor of voltage divider
G_1 = protecting gaps (high-vacuum)
RG = test gap (rod gap)
C_4 = capacitor of impulse-current-measuring shunt
R_2 = auxiliary resistor of impulse-current-measuring shunt
G_2 = gap to protect oscillograph
T = transformer under test
G_3 = low-voltage protective gap

TESTS ON TRANSFORMERS IN WHICH THE FAULTS DEVELOPED DURING TESTING

Oscillograms shown in Figures 6 and 7 are actual breakdown tests on developmental transformers built for that purpose. In these cases, the transformers were excited at normal-frequency voltage. However, the voltage wave shapes recorded on oscillograms 1 and 2 of Figures 6 and 7 are tests made in addition to the ASA method with normal-frequency voltage purposely omitted to avoid confusing the oscillography by the arcing of isolating gaps.[1]

3-Kva 7,200-Volt Transformer, Figure 6. In this case, a failure of 50 per cent of the winding occurred at the ground end of the high-voltage winding. Oscillogram 4 definitely indicates a failure by the neutral-current method. Oscillogram 2 does not indicate a failure although this oscillogram was recorded after the winding had failed, as shown in oscillogram 4. This was a consistent failure, and this condition was observed on many repeat tests.

$37^{1}/_{2}$-Kva 13,200-Volt Transformer, Figure 7. In this case, a failure of $33^{1}/_{3}$ per cent of the winding occurred at the line end of the transformer. Here again, the current method, film 4, shows the failure, but oscillogram 2 for the potential method 1 cannot be interpreted to indicate a failure, although this test followed the current test. Here also, many checks were made to verify this finding.

Conclusions

1. The observation of changes in the impulse-voltage wave cannot be depended upon to indicate a fault in transformers.

2. The use of normal-frequency excitation in conjunction with impulse testing as a means of fault detection cannot be justified, on the basis of either the data submitted here or experience obtained in the past.

3. Smoke or bubbles are difficult to detect in small transformers with compact and buried layers and therefore cannot be depended upon to indicate impulse failure.

4. The utilization of the present ASA methods of fault detection will not detect a very large percentage of failures.

5. The observation of voltage across a neutral impedance in which impulse neutral current flows in a relatively simple and effective method of impulse-failure detection and therefore is recommended for inclusion in the test code.

Reference

1. PROGRESS IN IMPULSE TESTING OF TRANSFORMERS, J. H. Hagenguth. AIEE TRANSACTIONS, volume 63, 1944, pages 999–1005.

When the Welding Load Outgrows the Distribution Power Supply

C. N. CLARK
ASSOCIATE AIEE

C. M. STEARNS
NONMEMBER AIEE

Synopsis: The ability of a 2,300–4,000-volt distribution system to supply single-phase a-c welders is limited not only by current-carrying capacity, but also by voltage regulation. The voltage limitations are reviewed and methods suggested for increasing the limits by changes in the power system and the customers' installations. Three types of subtransmission connections are described for use when the welding load outgrows the distribution power supply.

SINCE THE BEGINNING of World War II there has been a very rapid increase in both the size and number of electric welders in operation. Not only are they used in large numbers and in many sizes for large-scale production in industrial plants, but individual units and small groups of welders are being used for light manufacturing and for repair work in the smaller shops. A large portion of these welders are of the single-phase a-c resistance or arc types. The power factors are relatively low, and the loads are highly fluctuating in character.

In specifying the type of power supply for these welders, the power-company engineers have encountered certain system limitations which would not apply in serving an equivalent steady three-phase load. Service to single-phase welding loads from the usual 2,300–4,000-volt distribution system can be permitted only under favorable combinations of locations, welder sizes, and operating sequences.

The expense of a connection from a subtransmission system frequently may be avoided by modifications to the existing distribution supply or the customer's installation. In other cases, the size, characteristics, and location of the welder load are such that it is necessary to make a connection from the subtransmission system.

This paper will review some of the more commonly encountered limitations of the 2,300–4,000-volt distribution system and modifications of existing power systems and customer installations to permit serving welding loads and will describe some of the more common types of higher-voltage power supply for the larger welding loads.

Limitations of the Existing 2,300–4,000-Volt Distribution System

The two principal system limitations are those due to

A. Lighting flicker at adjacent customers caused by the fluctuating characteristics of welding loads.

B. Delivery of sufficient voltage at the welder to permit satisfactory operations.

Both of these limitations are due to the inherent impedances of the power system, including the customers wiring for each location. Attention is called to the fact that all references in this paper to the power-system impedance include the entire electric system to the welder input terminals.

The annoyance from lighting flicker is dependent upon both the magnitude of the voltage fluctuation and the frequency with which it occurs, or at which the welding load is applied. The most critical frequency is of the order of six times per second, and the annoyance is progressively less for slower operations. The Duquesne Light Company uses the following limits for voltage fluctuation where lighting service is affected, based upon tests and operating experience over a number of years.

Frequency of Load Application	Volts (115-Volt Terms)	Per Cent
Over 1 per second	0.50	0.44
1 per second to 15 per minute	1.00	0.87
15 per minute to 3 per hour	2.00	1.74

The foregoing three frequency classifications correspond approximately to the frequencies of load and voltage fluctuations commonly encountered in electric welding. For example, seam and pulsation welders operate in the first frequency band. The second group includes many spot welders used for regular production work. The lower-frequency classification usually is applied to manually controlled welders, such as spot and a-c arc welders used for repair work or for very limited production. In order to insure the proper frequency classification, the customer is asked to furnish an estimate showing the proposed frequency of operation and welding load for each new installation.

In determining what voltage will be delivered at the welder, account must be taken of the total impedance from the welder to the sources of power. For the smaller welders, under 20 kva, the regulation of the substation, transmission, and power stations ahead of the local 2,300- or 4,000-volt circuit usually can be ignored.

Representative values of voltage regulation in 230-volt terms are shown in Figure 1 for typical 2,300-volt single-phase circuits, and also for several combinations of transformer and secondary wire sizes. The transformer regulation is based upon impedances of 2.6 per cent to 3 per cent for the sizes shown. The assumed spacing of conductors is 16 inches for 2,300-volt circuits and eight inches for 230-volt circuits. In this chart, a welding load of 50 amperes at 60-per-cent power factor has been assumed at the 220-volt welder input terminals. For practical purposes the voltage drops for other small low-power-factor welding loads would be approximately proportional to the currents assumed.

Primary and secondary distances are shown in feet, and the voltage drops for the primary circuit must be added to that for the transformer and secondary circuit to obtain the approximate voltage drop at the customer's service. An additional small allowance may be made, if desired, for the regulation ahead of the primary circuit and in the customer's wiring. Figure 1 is particularly useful in determining the power supply for small welders. The calculation time is reduced by the early elimination of high regulation methods.

In selecting a suitable power supply for the larger single-phase a-c resistance and arc-type welders, the usual approach is to calculate the voltage regulation at the welder for a number of supply methods. This procedure is simplified and the calculation time reduced through the use of the curves in Figure 2 to obtain the allowable power-system impedance for the proposed welder load.

These curves assume 200 volts at the welder input terminals with the welder in operation and 220, 230, and 240 volts at the welder input terminals with the welder out of service; 200 volts is the approximate lower limit of voltage usually supplied for 220-volt power service and is within the plus and minus ten-per-cent voltage range usually tolerated by the manufacturers.

The impedance values used in the curves are expressed in volts drop per ampere at 60-per-cent power factor in 230-volt terms. The impedance value from the curve then is compared with corresponding values, calculated by simple addition from tables or curves, for each supply method being considered. All high regulation methods can be

---

Paper 45-118, recommended by the AIEE committee on electric welding for publication in AIEE Transactions. Manuscript submitted April 2, 1945; made available for printing May 25, 1945.

C. N. Clark is distribution section engineer and C. M. Stearns is transmission and plant subsection engineer, both of the planning and development department, Duquesne Light Company, Pittsburgh, Pa.

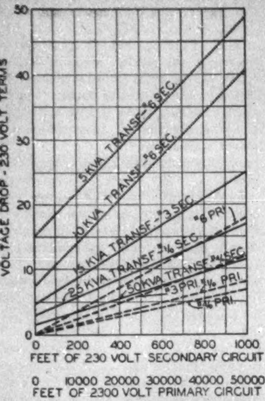

Figure 1. Voltage regulation due to supplying a load of 50 amperes at 60-per-cent power factor from a 230-volt single-phase service

eliminated easily in the early stages, and full attention can be concentrated on the low regulation methods. Separate calculations are necessary to determine if lighting flicker will result.

In working out welder problems, it is helpful to consider the welder as a load of variable impedance which can be adjusted within the limitation of the equipment design to draw a required kilovolt-ampere load from the line under a rather wide range of voltages. The relation between voltage at the welder and the impedance of the power system for a constant kilovolt-ampere load is illustrated in reference 3.

Corrective Methods to Permit Service From the Local 2,300–4,000-Volt Distribution Circuit

When a preliminary investigation shows that a given welder with specified duty cannot be tolerated at a proposed location due to excessive lighting flicker, or would not make satisfactory welds due to abnormal voltage regulation at the welder terminals, there are a number of changes which can be made either to the electric-supply system or to the customer's installation which often will eliminate the necessity for bringing in a service from a higher-voltage source. Some of these methods are described here.

SUBSTITUTE 4,000–230-VOLT TRANSFORMER FOR 2,300–230-VOLT TRANSFORMER AND CONNECT BETWEEN PHASES

On the 2,300–4,000-volt system, a change in the welder supply from 2,300 volts to 4,000 volts doubles the substation impedance but does not increase the impedance of the primary circuit. For locations near the substation, the allowable load fluctuation is increased by only 50 per cent. At the end of long primary circuits, the substation impedance becomes negligible, and the allowable load fluctuation is increased by nearly 200 per cent.

SUBSTITUTE A THREE-PHASE STAR–DELTA TRANSFORMER BANK FOR A SINGLE-PHASE 2,300–230-VOLT TRANSFORMER

When a star–delta bank with a floating primary neutral is used, two thirds of the load is supplied from one phase of the primary circuit, and the drop in the neutral conductor has been eliminated. This again reduces the regulation to the distribution transformer. The allowable load fluctuation is increased by 50 per cent near the substation and by 200 per cent at the end of a long primary circuit. To obtain the same distribution-transformer regulation, 1–75-kva transformer would be replaced with 1–50-kva and 2–25-kva transformers, as two thirds of the load is supplied by one transformer.

REPLACE PRIMARY CONDUCTORS

The replacement of conductors with those of larger size generally will be found more expensive than other methods, and the possible improvement is rather small due to the small change in regulation for low-power-factor loads. This method is seldom recommended to eliminate lighting flicker.

REPLACE OR RELOCATE DISTRIBUTION TRANSFORMERS

A considerable improvement in regulation often can be obtained by replacing the distribution transformer with a larger size, also by relocation of the distribution transformer to reduce the length of the 230-volt secondary winding.

INSTALL INDEPENDENT PRIMARY CIRCUITS

In those cases where the principal problem is lighting flicker, this may be reduced considerably by installing independent primary conductors from the industrial plant back to some point on the electric supply system where the voltage fluctuation will be within the required limits.

INSTALL SERIES CAPACITOR

A limited improvement may be obtained by installing a series capacitor in the primary circuit to compensate for part or all of the increase in primary-circuit regulation due to the welder load, but the protective equipment is expensive, and the space for mounting on poles in urban areas usually is limited. Improvement also can be obtained through the use of welders equipped with suitable series capacitors to reduce the kilovolt-ampere input for a given weld.

INSTALL A TRANSLATOR AND NECESSARY COPPER

Under certain conditions the translator described by R. O. Askey and E. R. Hendrickson,[4] is a very economical method of eliminating lighting flicker for other customers supplied from the same distribution circuit. The authors claim that 100-per-cent voltage correction results from the use of this device.

DISTRIBUTE THE WELDERS OVER THE THREE PHASES

The regulation of the primary circuit due to the operation of a single welder is the same as described for the star–delta bank. With a number of welders balanced between phases and operating at the same time, the primary-circuit regulation near the substation would be one third of that obtained when the same total load is served from one phase. At the end of a long primary circuit the regulation for the balanced welding load would be only one sixth of the single-phase value, due to division of load between phases and elimination of the neutral drop.

The transformer regulation due to a given single-phase welder supplied from a three-phase bank is greater than when it is served from a single-phase transformer of the same total capacity. With only one third of the welders connected to each phase, less advantage can be taken of diversity between welders than when all are supplied from one phase. Therefore, the three-phase service to a few welders may require more transformer capacity than the single-phase service. The size of transformers to supply a large number of welders usually is determined by the equivalent thermal loading.

USE THREE-PHASE WELDERS

A few installations of three-phase resistance-type welders have been made. This development should be watched carefully, since the three-phase balanced load which can be supplied from a three-phase power system is much larger than the single-phase value from the same system for the same frequency of load fluctuations. If it should operate in the cyclic flicker range, however, the permissible kilovolt-ampere demand might be less than for many of the conventional types of welders.

USE STORAGE-TYPE WELDERS

The instantaneous kilovolt-amperes drawn from the line are much less for the storage-type welders than for the conventional resistance welder. It is particularly applicable for certain types of welding, but to date the storage type has been costlier for many operations.

INSTALL A THREE-PHASE MOTOR-GENERATOR SET

The voltage fluctuations on the supply circuit can be reduced greatly by supplying single-phase welding loads through a three-phase motor-generator set. The regulation of the generator and the cost of the added equipment limit the applications of this method.

Higher-Voltage Supply for the Larger Welding Loads

When it is necessary to serve a large number of small welders, or a small number of large welders, the possibilities for stretching the local 2,300–4,000-volt system often are exhausted. When this occurs it is necessary to provide some other system possessing greater capacity and a lower impedance in terms of the service voltage. Since the higher-voltage circuits are not found on nearly every street like the 2,300–4,000-volt distribution circuits, the connection from the higher-voltage circuit usually involves quite large expenditures.

The relatively low load factor of many welding loads makes it imperative that the most economical use be made of existing facilities. In this connection, there is a quite general feeling that welders should pay a fair share of the costs involved in serving them, but that they should not be penalized by requiring a more expensive installation than is necessary to protect the service to other customers.

A description follows of some typical 11-kv and 22-kv connections for welder loads which are beyond the modified 2,300–4,000-volt distribution-circuit limits.

Exclusive 2.3-Kv Circuit From Distant 22–2.3-Kv Station

There are two of these cases and both are supplied by single-phase circuits. In general if a three-phase exclusive distribution circuit is required for load or voltage reasons, then it might be as well to consider a single-phase transmission extension instead.

The first installation utilizes the spare 667-kva 22,000-to-2,300-volt transformer at one of the distribution substations, a 5,700-foot extension of two number-three wires, and a 75-kva 2,300–460-volt transformer adjacent to the customer's plant. This load was supplied initially over a regular circuit from the distribution substation, but changes in the customer's process resulted in complaints of lighting flicker. These were eliminated by connections as just described.

This method of correction is a wartime expedient and would not be utilized for a new installation in peacetime. Due to very large voltage regulation on this supply circuit, it is necessary to connect the electronic controls for the 200-kva welder to the lighting circuit, which is separate from the welding circuit.

The second installation consists of one 100-kva 22,000–2,300-volt transformer adjacent to a through transmission line, a 3,200-foot extension of two number-three wires, and one 100-kva 2,300–230-volt transformer adjacent to the customer's plant.

The main objection to this type of installation is the fact that it does not lend itself very well to growth. In general the impedance of the two transformers in series is a very large part of the total, and, if regulation is a problem, and it usually is, then this is not a satisfactory solution.

One analysis made prior to an expected change in welders resulted in the following comparison of voltage drops for four methods of reinforcement:

(*a*). 2,300-volt, single-phase—doubling the size of one transformer, 82 per cent drop as compared with present.

(*b*). 2,300-volt, single-phase—doubling the size of both transformers, 68.3 per cent drop as compared with present.

(*c*). 4,000-volt, single-phase—doubling the size of both transformers, 54.5 per cent drop as compared with present.

(*d*). 22,000-volt, single-phase—doubling the size of one transformer, 21.3 per cent as compared with present.

22-Kv or 11-Kv Customer's Substations for Welders Only

Six installations of this type are served from the 11,000- or 22,000-volt cable or overhead transmission system. These installations in general are single phase but may be three phase. Service is provided by a tap to the transmission system, using either cable or overhead wire, depending upon the district, and an air-break switch, fuses, transformer, and metering in the customer's substation.

This type of installation is very satisfactory and lends itself very nicely to growth merely by changing the size of the transformer and possibly replacing the fuses and metering current transformers with larger ones.

22-Kv or 11-Kv Customer's Substation for Power and Welders

These installations are three-phase by definition, since they involve three-phase power loads as well as single-phase welders. They may or may not require the same voltage for the welders and for power.

One installation consists of a three-phase cable tap and an air-break switch, fuses, 11,000–440–220-volt transformer bank and metering for both 440- and 220-volt services. Welders are supplied at 440 volts and motor load is supplied at 220 volts.

Another installation is similar except that fortunately the welders and power load are of the same voltage. Separate feeders are operated by the customer in his plant for service to the various power and welding loads.

Conclusions

The use of electric welding has been greatly accelerated during World War II. More general use of present types of welders and new developments in welding equipment and applications in the post-war period may necessitate changes in power-system design.

With the concentration of greater numbers of larger welders with automatic controls for high-speed production in individual plants, the voltage variation at the welder input terminals becomes very important. The regulation must be kept within small limits in order that the rejections will be small and that a uniformly high quality can be maintained in the finished product.

The increasing use of electronic controls and pulsation welding will require greater ingenuity by power-system engineers in the prevention of objectionable flicker at adjacent lighting customers. The annoyance from lighting flicker is dependent upon both the magnitude and frequency of the voltage fluctuations.

The important key to providing adequate voltage at the welder and prevention of lighting flicker is the design of the electric-supply system for relatively low impedance. The regulation at the welder is affected by the design of the power system and customer's wiring to the welder, but the lighting flicker is affected only by the design of that portion of the power system which is common to both the welding and lighting loads.

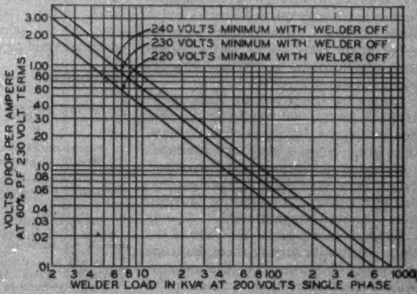

Figure 2. Limiting volts drop per ampere of power system to deliver 200 volts minimum to various 60-per-cent power-factor welder loads

Much calculation time can be saved in the solution of both general and specific welder problems through the use of charts similar to those shown in Figures 1 and 2. High regulation methods can be eliminated in the early stages, and attention then can be given to a choice between adequate supply methods.

Larger and faster welding loads can be supplied from 2,300–4,000-volt distribution circuits by making certain modifications in the power system and customer's equipment, as outlined in this paper. When these possibilities have been exhausted, a connection must be provided from a higher-voltage circuit.

Welders should pay a fair share of the costs involved in serving them, but they should not be burdened with a more expensive installation than is necessary to insure satisfactory operations and to avoid complaints from lighting flicker. In choosing between several methods of power supply, consideration should be given to the over-all cost of welding equipment and power-system facilities.

References

1. Lessons Learned in Serving Electric Welders, C. N. Clark. *Electrical World*, May 2, 1942.

2. Precautions in Welder Service, C. N. Clark. *Electrical World*, October 2, 1943.

3. Good Weld Voltage Demands Low Supply Impedance, C. N. Clark. *Electrical World*, February 19, 1944.

4. Voltage Translator Scheme Cuts Light Flicker Due to Welders, R. O. Askey. *Electrical World*, January 6, 1945.

5. Power Supply for A-C Arc Welding, A. U. Welch, R. F. Wyer. AIEE Transactions, volume 64, 1945, March section, pages 116–20.

An Interval and Dwell Tester for Bomb-Release Interval Controls

T. H. LONG
MEMBER AIEE

Synopsis: The device described is essentially a frequency meter with a scale proportional to the logarithm of 1/frequency, and a dwell meter suitable for use on inductively loaded contacts in d-c circuits. It has been found useful in several jobs in military aviation, one of which is described in some detail. An appendix gives a simple analysis of the shape of the frequency scale distribution obtained.

IN MILITARY AVIATION the device that originates the release impulses when a train (or series) of bombs is to be dropped is known as a bomb-release interval control. This bomb-release interval control (or interval control) receives its starting impulse either manually or automatically from the bomb-sight mechanism.

The usual interval control is adjustable as to speed at which the bombs are to be dropped; that is, the interval between the dropping of the bombs is preset on a dial graduated in feet of interval, opposite a ground speed scale graduated in miles per hour (or knots). The number of bombs to be dropped is preset on another dial, and after that the procedure can be automatic.

The interval range usually covered is from 7.3 to 147 feet at 100 miles per hour, corresponding to 1 to 20 release impulses per second. In the high-speed part of the range the duration of the release impulses becomes quite important, as each impulse must last long enough to operate the bomb-release mechanism, and the space between impulses must be long enough to permit a switching operation that automatically sends the next release impulse to the next bomb release.

This situation results in rather narrow tolerances on the operation of the interval control at short intervals, and, even though these tolerances are met at the factory, there has been no positive assurance that they still would be met when the device went into service. There has been still less assurance that they would be met after several months of service. In fact the effectiveness of bombing missions was being reduced by failure of bomb-release interval controls, mainly because there was no practicable method available for preflight tests.

Requirements for Instrument for Preflight Tests

It was believed that an instrument for adequate preflight testing should include an indicator that would give a direct reading of the interval between bombs, and another indicator that would give direct information as to the duration of contact and the "off time" between contacts. For short-interval operation the impulses from certain interval controls are originated alternately by two relays; so it is necessary to measure not only the average contact duration and spacing but also the average performance of each of two series of alternating contacts; that is, the average of the even-numbered impulses must be measured independently of the average of the odd-numbered impulses.

As the interval calibration must extend over a range of approximately 25/1 and should be reliable within at least five per cent throughout, it was essential that the scale be at least approximately logarithmic; and the divisions should correspond to the interval dial of the bomb-release interval control. Other requirements were that the instrument must be portable, small enough to be used in restricted space, durable, and essentially independent of ambient temperature.

As the performance of interval controls is influenced by applied voltage and by the nature of the load, it was necessary to include a voltmeter and an internal dummy load closely approximating the usual bomb release and average wiring.

It was expected that the instrument frequently would be used while the bomb racks of the airplanes were being loaded, and so it must be impossible under any circumstances for impulses from an interval control under test to reach the bomb releases.

A further requirement was that the equipment should operate with either 100-microfarad electrolytic or 1-microfarad paper snubbing capacitor across the load contacts of the interval control.

Interval and Dwell Tester

The basic design of the instrument to be described was developed as a direct-reading frequency and dwell meter in 1942 and demonstrated at Wright Field early in 1943. ("Dwell" as used here is the contact duration expressed as a per cent of the contact period.) The final instrument was almost identical to the original with the addition of a sorting circuit to make possible independent dwell measurements on the even- and odd-numbered impulses. The complete instrument is shown in Figure 1 in actual operation as a bench testing device, testing the 50-foot interval setting of the interval control in the foreground. Figures 2 and 3 are sketches illustrating the use of the interval and dwell tester to test an interval control mounted in a bombing plane.

The compartments shown on either side of the instrument panel hold the connection cords and spare fuses.

Interval Circuit

With reference to the circuit diagram of Figure 4, the interval circuit includes a small 45-volt radio *B* battery, low-temperature-coefficient resistors R_1, R_3, and R_6, damping capacitor C_1, and interval relay *I*, arranged alternately to charge and

---

Paper 45-127, recommended by the AIEE committee on air transportation for publication in AIEE Transactions. Manuscript submitted December 4, 1944; made available for printing May 23, 1945.

T. H. Long is senior research engineer with C. G. Conn, Ltd., Elkhart, Ind.

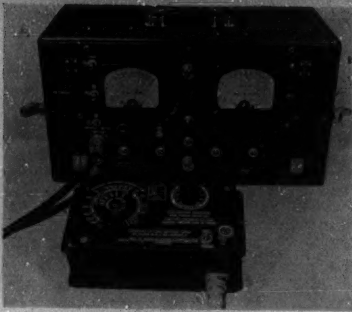

Figure 1. Interval and dwell tester in use as bench-instrument testing bomb-release interval control in foreground at 50-foot interval setting

discharge metering capacitors C_2 and C_3. The dummy load is connected between the lower point of S_1 and ground, with provision for the alternative use of an external load. Relay 1 is in parallel with either load so that each impulse takes capacitors C_2 and C_3 through a charge and discharge cycle. The dummy load is a five-ohm 200-watt resistance in series with an inductance. The inductance is a single-layer winding on a three-eighths-inch-diameter soft-iron rod ten inches long.

It is obvious that if C_1 is large enough that the cyclic variations in its voltage are negligible when relay I is operating, the discharge current i through metering capacitors C_2 and C_3 will be equal to fCe where

f = the impulse frequency
$C = C_2 + C_3$ in farads
e = voltage across C_1

If we ignore for the moment the current through the microammeter circuit which is in fact quite small, and assume that e is a small part of the battery voltage, then i will be approximately constant as it is limited by R_1. Then $e = i/fC$ and the scale is reciprocal with frequency, as the instrument deflection is proportional to e.

A reciprocal frequency scale is a linear-interval scale, and the lower part of the interval scale is substantially linear. For increasing intervals the scale becomes more condensed and is in fact a good approximation of a logarithmic scale, since i is reduced and e is increased until at full scale e is roughly 40 per cent of battery voltage. A more detailed analysis is given in the appendix.

Field calibration of the interval circuit is made by adjusting the instrument zero adjuster to a zero calibration mark, turning power on (S_2), opening calibrate switch (S_3), and setting the interval meter by an adjuster under the instrument (this is the potentiometer across the instrument) to a full-scale calibration mark. Switch S_3 then is released, the pointer swings off scale to the right, and the instrument is in calibration. This calibration eliminates any influence on interval readings that otherwise would result from changes in battery voltage or from the temperature coefficients of the instrument winding and its shunted potentiometer.

Temperature will affect the accuracy of the interval circuit by its effect on R_1, R_2, R_6, C_2, and C_3. A one-per-cent increase in capacitance or in resistance will reduce the interval reading by one per cent. The variation of capacitance within the operating-temperature range is somewhat irregular but on the order of one per cent. The temperature change in the resistance is of course below one per cent.

DWELL CIRCUIT

The dwell circuit comprises an input potentiometer, a resistance-loaded selenium rectifier, an averaging circuit, and a microammeter calibrated in per-cent dwell. Switch S_4 and an external resistance make it convenient to use this instrument to check battery voltage so the instrument is also calibrated in volts.

At the usual operating voltage of 27 volts the input to the dwell circuit measures on the order of 500 ohms resistance so that it will have a negligible damping effect on the inductive kick from the six-ohm load circuit. This inductive kick is blocked out of the instrument circuit by the two disk rectifier. Dwell full-scale calibration is made by setting the input potentiometer for full-scale reading when a continuous forward voltage is applied from the interval-control power supply through switch S_4. The instrument then will read in proportion the average forward voltage of a series of impulses which is by definition the dwell in per cent. Of course, if the nature of the load were such that current interruption caused oscillations that become appreciably positive, this method of measuring dwell would be subject to some error, but the usual bomb release is definitely not of this type.

Under operating conditions the maximum reverse voltage that appears across the rectifier output is from 0.3 per cent to 4 per cent of the impressed reverse volt-

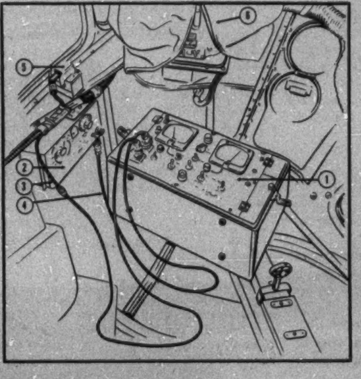

Figure 2 (left). Interval and dwell tester connected inside bomber

1—Tester
2—Interval control
3—Connection to power cable
4—Connection to interval control
5—Bomb-release switch
6—Bomb sight

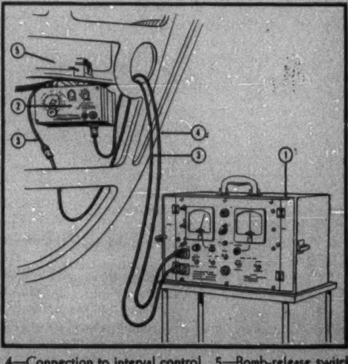

Figure 3 (right). Interval and dwell tester connected outside of bomber

1—Tester
2—Interval control
3—Connection to power cable
4—Connection to interval control
5—Bomb-release switch

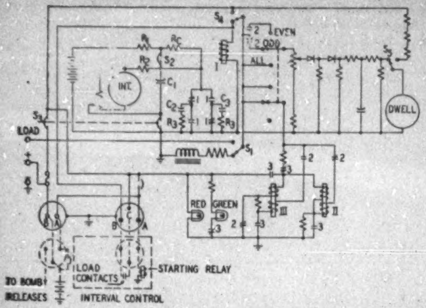

Figure 4. Circuit diagram of interval and dwell tester

The circuits associated with the interval and dwell tester are shown in broken lines

The impulse selector is shown in position to measure the dwell of odd-numbered impulses

age. With the internal load in use the error introduced by the rectifier is negligible, but if a 15-ampere solenoid is used there may be an error of about one per cent attributable to the rectifier.

As the dwell circuit only makes a comparison measurement it has no temperature error.

The dwell full scale must be recalibrated whenever the interval-control voltage changes. This is particularly important at short intervals since a one-volt increase can cause the dwell to change from 50 per cent to 53 per cent. If the dwell circuit is not recalibrated the dwell reading would change from 50 per cent to 55 per cent.

The sorting circuit alternately connects and disconnects the dwell circuit and the load in the idle time between impulses. This makes it possible to measure the dwell of even-numbered and odd-numbered impulses independently. This is accomplished by relays II and III in a modification of a conventional circuit in which the operation of relay III during an impulse changes the circuit to reduce the operating time of relay II at the end of that impulse. Then the operation of relay II sets up the circuit to reduce the release time of relay III at the beginning of the next impulse, and so on. When ordinary telephone-type relays are used, this circuit operates reliably at 30 impulses per second in parallel with the dummy load and 100-microfarad capacitor. It is required to follow 20 impulses per second with any dwell from 35 per cent to 65 per cent at 27 volts supply.

As the operation of the sorting circuit keeps half of the impulses out of the dwell circuit, the effective impulse period is doubled and the actual dwell reading halved. This simply means that the individual readings must be multiplied by two, or that the two readings must be added together.

The impulse selector switch energizes the sorting circuit only in the "odd" and "even" positions. If a train containing an odd number of impulses is run off, the sorting circuit will be left with both relays energized, and unless the circuit is "cleared" by momentarily operating S_4 (the dwell calibrate switch) the odd impulses in the next train will be read at the "even" switch position, and vice versa. Necessity for clearing is indicated when the green "clearance-for-sorting" light is out.

The impulse selector switch is of the short-circuiting type so that it is possible to switch back and forth from "odd" to "even" during a series of impulses without losing step.

Discussion

It has been found possible to keep the interval meters within three per cent of a printed scale calibration throughout the range in spite of instrument variations. This is done by setting the instrument zero adjuster and the potentiometer adjustment so the calibration is exact at intervals of 7.5 feet and 150 feet. Then two or three points in the middle of the scale are checked. Occasionally one will be more than three per cent low. To correct this the resistance of either R_1 or R_2 is reduced about 15 per cent by shunting with another resistor, and the process of line-up is repeated. This 15-per-cent reduction in resistance increases the mid-scale readings about four per cent when the ends are lined up, so that the new mid-scale readings will be within the three-per-cent limit. After checking this the full-scale and zero calibration points are established and marked. The assembly is then completed and a deviation card run on the interval circuit in two positions (panel vertical and horizontal) and the dwell and sorting circuits are tested. The deviation card is shipped with the instrument.

In wet climates the internal load makes it simple to dry out the interior of the device. It is only necessary to connect to a 20-volt storage battery, turn the power switch on, and tie down the "dwell-calibrate" switch (S_4).

Other uses of a similar nature are being found for this equipment. A specific example of this is in the measurement of the performance of the "peck" relay in the *C-1* pilot.

It should be understood in connection with possible other uses that the intervalmeter circuit is restricted to a maximum frequency on the order of 30 cycles unless vacuum tubes are to be used. The present dwell circuit is not limited as to frequency, but for some applications a vacuum-tube circuit would eliminate frequent adjustments and errors caused by oscillations.

Appendix

In the following notation capacitors and resistors are identified by the same subscripts used in Figure 4:

f = contacts per second of any one contact of relay *I*

S = interval in feet at 100 miles per hour ground speed $= 146.7/f$

C = capacitance of $C_2 + C_3$ in farads

E = battery electromotive force, volts

e = volts across C_1

e_0 = volts across C_1 during calibration ($f = 0$)

i = average current to $C_2 + C_3$

i_1 = average current through R_1

i_2 = average current through R_2

R_1 includes battery resistance

R_2 includes instrument and shunt resistance

C_1 is assumed large in comparison to $C_2 + C_3$

$$i = fCe \tag{1}$$

$$E = e + R_1 i_1 = e + R_1(fCe + e/R_2) \tag{2}$$

$$\begin{aligned} E/e &= 1 + R_1(fC + 1/R_2) \\ &= \{R_2 + R_1(fCR_2 + 1)\}/R_2 \end{aligned} \tag{3}$$

$$e/E = R_2/(R_1 + R_2 + fCR_1R_2) \tag{4}$$

$$e_0/E = R_2/(R_1 + R_2 + R_e) \tag{5}$$

$$\begin{aligned} e/e_0 &= (R_1 + R_2 + R_e)/(R_1 + R_2 + fCR_1R_2) \\ &= (R_1 + R_2 + R_e)/(R_1 + R_2 + \\ &\qquad 146.7CR_1R_2/S) \end{aligned} \tag{6}$$

if $R_1 = R_2$ ($= R$)

$$e/e_0 = (2 + R_e/R)/(2 + 146.7CR/S) \tag{7}$$

The voltage variation across C_1 that is ignored in equation 1 introduces an error in the calculated scale distribution of equation 7 that amounts to about one per cent of full-scale deflection at mid-scale; this is for a practical case where $R_1 = R_2 = R = 139{,}000$ ohms, $C_1 = 31.5$ microfarads, $C_2 = C_3 = 2.16$ microfarads, $R_e = 560$ ohms, and $f = 1$ to 30 cycles per second.

Voltage versus time for C_1 can be assumed linear while increasing and approximately, rate of change

$$= \frac{E/2 - e}{(C_1 + C/2)R/2} = fe/n \text{ volts per second} \tag{8}$$

if $C_1 + C/2 = nC$. The balance of a half period may be called the partial-discharge time T, and during this period voltage versus time is exponential. This exponential begins when C_2 or C_3 is connected to C_1 and may be assumed to continue until the rate of voltage

Symmetrical Components as Applied to the Single-Phase Induction Motor

F. W. SUHR
ASSOCIATE AIEE

THIS PAPER is intended to show in detail the application of the method of symmetrical components to the solution of single-phase-induction-motor performance characteristics. By the use of this method single-phase-motor theory follows very closely the simpler case of the balanced polyphase-motor theory. The author of this paper is of the opinion that a clearer concept of the physical theory can be obtained as contrasted to other methods—either from the revolving-field or the cross-field concepts.

In their AIEE paper of May 1936, Lyon and Kingsley[1] ably presented this subject in a more general manner and also with particular emphasis on the motor having main and start phases not in space quadrature. Their work and the work of Mr. Morrill[2,3] form the basis of the thesis now to be considered.

Assumptions

1. The motor is magnetically symmetrical:

(*a*). Sinusoidal distribution of conductors in the stator slots.

(*b*). Uniform air gap.

(*c*). Uniform iron permeance.

2. Sinusoidal voltage applied.

3. Linear constants—saturation of the iron flux paths is negligible.

4. Friction and windage, iron loss,[5] and load losses are subtractive from the rotor output.

5. Main and start phases are in space quadrature (90 electrical degrees between axes of these windings).

General Considerations

The solution of power or current flow in polyphase circuits when the applied voltages are not balanced, or when the load impedances are not equal can be accomplished best by the application of the method of symmetrical components. We will show presently that the case of the single-phase motor is a special case of an unbalanced two-phase motor.

Let us assume the general two-phase circuit with phase voltages (V_M and V_S) unequal in magnitude and not in time quadrature. It has been shown[4] that two balanced systems can be formed: one system, called the "positive sequence" (+) consists of components of V_M and V_S which are equal in magnitude and in time quadrature, and have positive (+) phase rotation or the same rotation as the V_M and V_S system; the other system, called the "negative sequence" (−) consists of other components of V_M and V_S equal in magnitude and in time quadrature, *but* phase rotation is opposite that of the positive-sequence components. No "uniphase" or "zero-sequence" components exist.

Part I

By definition we then have

$$V_M = V_M^+ + V_M^- \tag{1}$$

$$V_S = V_S^+ + V_S^- \tag{2}$$

$$V_S^+ = V_M^+ \underline{|90^\circ} = +jV_M^+ \tag{3}$$

$$V_S^- = V_M^- \underline{|\overline{90^\circ}} = -jV_M^- \tag{4}$$

Phase *S* leads phase *M* in time angle. From equations 2, 3, and 4 we then have

$$V_S = j(V_M^+ - V_M^-) \tag{2a}$$

which defines V_S in terms of the components of V_M. When the magnitude and time phase of V_M and V_S are each known, the symmetrical components of each can be calculated by adding equation 1 and $-j$ times equation 2a and clearing

$$V_M^+ = \frac{V_M - jV_S}{2} \tag{5}$$

By subtracting $-j$ times equation 2a from equation 1 and clearing we have

$$V_M^- = \frac{V_M + jV_S}{2} \tag{6}$$

All the foregoing quantities are vectors representing rms magnitude and time phase voltages.

By the same procedure we arrive at current values:

$$I_M = I_M^+ + I_M^- \tag{7}$$

and

$$I_S = I_S^+ + I_S^- \tag{8}$$

$$I_S^+ = jI_M^+ \tag{9}$$

$$I_S^- = -jI_M^- \tag{10}$$

$$I_M^+ = \frac{I_M - jI_S}{2} \tag{11}$$

and

$$I_M^- = \frac{I_M + jI_S}{2} \tag{12}$$

In a general two-phase system as shown in Figure 1, Z_M and Z_S are the load impedances of phases *M* and *S*, respectively. Now applying Ohm's law, we have

$$V_M = I_M Z_M \tag{13}$$

and

$$V_S = I_S Z_S \tag{14}$$

Then from equations 13, 7, and 1,

$$V_M^+ + V_M^- = (I_M^+ + I_M^-) Z_M \tag{15}$$

and from equations 14, 8, and 2,

$$V_S^+ + V_S^- = (I_S^+ + I_S^-) Z_S \tag{16}$$

or from equations 3 and 4 equation 16 becomes

$$jV_M^+ - jV_M^- = (+jI_M^+ - jI_M^-) Z_S \tag{16a}$$

or

$$V_M^+ - V_M^- = (I_M^+ - I_M^-) Z_S \tag{16b}$$

Adding equations 15 and 16b we have

$$V_M^+ = {}^1/_2[I_M^+(Z_M + Z_S) + I_M^-(Z_M - Z_S)] \tag{17}$$

Subtracting equation 16b from equation 15 and clearing, we have

$$V_M^- = {}^1/_2[I_M^+(Z_M - Z_S) + I_M^-(Z_M + Z_S)] \tag{18}$$

Paper 45-102, recommended by the AIEE committee on electric machinery for publication in AIEE TRANSACTIONS. Manuscript submitted October 31, 1944; made available for printing May 3, 1945.

F. W. SUHR is design group leader, fractional-horsepower-motor engineering division, General Electric Company, Fort Wayne, Ind.

The author acknowledges the criticisms and helpful suggestions made by P. L. Alger during the preparation of this paper.

---

drop across C_1 (ignoring currents through R_1 and R_2) $= fe/n$.
Then

$$T = (R_2C/2) \log_e (1/fR_2C) \tag{9}$$

This varies from 0.0073 to 0.0032 second for *f* from 1 to 30 cycles per second. This makes the magnitude e_v of the voltage variation across C_1

$$e_v = (1 - 2fT)e/2n \tag{10}$$

Then from equation 1

$$i = fC(e + e_v/2) \tag{11}$$

and a more correct value of

$$e/e_0 = \frac{2 + R_c/R}{2 + 146.7CR[1 + (1 - 2fT)/4n]/S} \tag{12}$$

This reduced the one-per-cent error in scale distribution to about 0.25 per cent. The error was determined by establishing 13 frequencies to ±0.05 per cent by a tuning fork method and measuring the average current in the microammeter circuit by a resistance and potentiometer.

It will be seen that the interval-meter deflection is independent of the dwell, provided that the minimum duration of contact is greater than about $2T$.

In the case of a transformer or single-phase motor where there are not the same turns in each of the windings or phases then,

$$|I_S^+| = \frac{M}{S}\,|I_M^+| = \frac{|I_M^+|}{a} \tag{19}$$

and

$$|I_S^-| = \frac{|I_M^-|}{a} \tag{20}$$

$$V_S^+ = \frac{S}{M}|V_M^+| = a|V_M^+| \tag{21}$$

and

$$V_S^- = a|V_M^-| \tag{22}$$

where

M = effective conductors of the M phase
S = effective conductors of the S phase
$a = S/M$

We can now write

$$V_S^+ = jaV_M^+ \tag{3a}$$

$$V_S^- = -jaV_M^- \tag{4a}$$

$$V_S = ja(V_M^+ - V_M^-) \tag{2b}$$

similarly

$$I_S = j/a(I_M^+ - I_M^-) \tag{8a}$$

In a single-phase motor it is obvious that

$$V_S \equiv V_M \tag{23}$$

Now equation 2b becomes

$$V_M = ja(V_M^+ - V_M^-) \tag{2c}$$

Furthermore, we will find that the impedance to positive-sequence currents is not the same as for negative-sequence currents in rotating apparatus.

Let

$\mathbf{Z}_M^+$ = impedance to I_M^+
$\mathbf{Z}_M^-$ = impedance to I_M^-
$\mathbf{Z}_S^+$ = impedance to I_S^+
$\mathbf{Z}_S^-$ = impedance to I_S^-

Multiplying equation 2c by $-j/a$ and adding to equation 1, we obtain

$$V_M^+ = \frac{V_M}{2}(1 - j/a) \tag{24}$$

or by subtraction we obtain

$$V_M^- = \frac{V_M}{2}(1 + j/a) \tag{25}$$

From equations 3a and 24 we have

$$V_S^+ = \frac{V_M}{2}(1 + ja) \tag{26}$$

and from equations 4a and 25 we have

$$V_S^- = \frac{V_M}{2}(1 - ja) \tag{27}$$

Equations 13 and 14 now can be reconsidered together with equations 9, 10, 8a, and 23 and at the same time the sequence impedances $\mathbf{Z}_M^+$, $\mathbf{Z}_M^-$, $\mathbf{Z}_S^+$ and $\mathbf{Z}_S^-$ can be included.

$$V_M = I_M^+\mathbf{Z}_M^+ + I_M^-\mathbf{Z}_M^- \tag{13a}$$

$$V_M = j/a(I_M^+\mathbf{Z}_S^+ - I_M^-\mathbf{Z}_S^-) \tag{14a}$$

To solve for I_M^- multiply equation 13a by $\mathbf{Z}_S^+/a^2$ and equation 14a by $-j/a\mathbf{Z}_M^+$

$$V_M\,\frac{\mathbf{Z}_S^+}{a^2} = I_M^+\mathbf{Z}_M^+\,\frac{\mathbf{Z}_S^+}{a^2} + I_M^-\mathbf{Z}_M^-\,\frac{\mathbf{Z}_S^+}{a^2} \tag{13b}$$

$$-jV_M\,\frac{\mathbf{Z}_M^+}{a} = I_M^+\,\frac{\mathbf{Z}_S^+}{a^2}\mathbf{Z}_M^+ - I_M^-\mathbf{Z}_M^+\,\frac{\mathbf{Z}_S^-}{a^2} \tag{14b}$$

If we subtract equation 14b from equation 13b

$$V_M\left(\frac{\mathbf{Z}_S^+}{a^2} + j\,\frac{\mathbf{Z}_M^+}{a}\right) = I_M^- \times \left(\frac{\mathbf{Z}_M^-\mathbf{Z}_S^+}{a^2} + \frac{\mathbf{Z}_M^+\mathbf{Z}_S^-}{a^2}\right)$$

or

$$I_M^- = V_M\left[\frac{\mathbf{Z}_S^+ + ja\mathbf{Z}_M^+}{\mathbf{Z}_M^+\mathbf{Z}_S^- + \mathbf{Z}_M^-\mathbf{Z}_S^+}\right] \tag{28}$$

By applying equations 10 and 20

$$I_S^- = V_M\left[\frac{\mathbf{Z}_M^+ - j\dfrac{\mathbf{Z}_S^+}{a}}{\mathbf{Z}_M^+\mathbf{Z}_S^- + \mathbf{Z}_M^-\mathbf{Z}_S^+}\right] \tag{29}$$

To solve for I_M^+ multiply equation 13a by $\mathbf{Z}_S^-/a^2$ and equation 14a by $j/a\mathbf{Z}_M^-$.

$$V_M\,\frac{\mathbf{Z}_S^-}{a^2} = I_M^+\mathbf{Z}_M^+\,\frac{\mathbf{Z}_S^-}{a^2} + I_M^-\mathbf{Z}_M^-\,\frac{\mathbf{Z}_S^-}{a^2} \tag{13c}$$

$$jV_M\,\frac{\mathbf{Z}_M^-}{a} = -I_M^+\mathbf{Z}_S^+\,\frac{\mathbf{Z}_M^-}{a^2} + I_M^-\mathbf{Z}_S^-\,\frac{\mathbf{Z}_M^-}{a^2} \tag{14c}$$

If we subtract equation 14c from equation 13c,

$$V_M\left(\frac{\mathbf{Z}_S^-}{a^2} - j\frac{\mathbf{Z}_M^-}{a}\right) = I_M^+ \times \left(\mathbf{Z}_M^+\,\frac{\mathbf{Z}_S^-}{a^2} + \mathbf{Z}_M^-\,\frac{\mathbf{Z}_S^+}{a^2}\right)$$

or

$$I_M^+ = V_M\left(\frac{\mathbf{Z}_S^- - ja\mathbf{Z}_M^-}{\mathbf{Z}_M^+\mathbf{Z}_S^- + \mathbf{Z}_M^-\mathbf{Z}_S^+}\right) \tag{30}$$

By applying equations 9 and 19

$$I_S^+ = V_M\left[\frac{\mathbf{Z}_M^- + j\dfrac{\mathbf{Z}_S^-}{a}}{\mathbf{Z}_M^+\mathbf{Z}_S^- + \mathbf{Z}_M^-\mathbf{Z}_S^+}\right] \tag{31}$$

From equations 7, 28, and 30 we then obtain the general equation:

$$I_M = V_M\left[\frac{(\mathbf{Z}_S^+ + \mathbf{Z}_S^-) + ja(\mathbf{Z}_M^+ - \mathbf{Z}_M^-)}{\mathbf{Z}_M^+\mathbf{Z}_S^- + \mathbf{Z}_M^-\mathbf{Z}_S^+}\right] \tag{32}$$

and from equations 8, 29 and 31

$$I_S = V_M\left[\frac{(\mathbf{Z}_M^+ + \mathbf{Z}_M^-) - j/a(\mathbf{Z}_S^+ - \mathbf{Z}_S^-)}{\mathbf{Z}_M^+\mathbf{Z}_S^- + \mathbf{Z}_M^-\mathbf{Z}_S^+}\right] \tag{33}$$

The line current is the combined current of main and start phases.

$$I_L = I_M + I_S \doteq V_M\left[\frac{(\mathbf{Z}_M^+ + \mathbf{Z}_M^- + \mathbf{Z}_S^+ + \mathbf{Z}_S^-) + j\left({}^{+} - a\mathbf{Z}_M^- + \dfrac{\mathbf{Z}_S^-}{a} - \dfrac{\mathbf{Z}_S^+}{a}\right)}{\mathbf{Z}_M^+\mathbf{Z}_S^- + \mathbf{Z}_M^-\mathbf{Z}_S^+}\right] \tag{34}$$

Part II

These general equations will now be applied specifically to the single-phase motor.

The equivalent circuits of the M phase are shown in Figure 2. (See end of paper for definition of symbols.)

$$\mathbf{Z}_{2M}^+ = \frac{R_2}{S} + jX_2 \tag{35}$$

secondary impedance to positive-sequence current.

By combining the magnetizing impedance jX_ϕ with the secondary impedance $\mathbf{Z}_{2M}^+$ the "apparent secondary impedance" can be written

$$\mathbf{Z}_2^{+\prime} = \frac{1}{\dfrac{1}{R_2/S + jX_2} + \dfrac{1}{jX_\phi}} = \frac{X_\phi^2 R_2/S}{(R_2/s)^2 + (X_\phi + X_2)^2} + j\,\frac{X_\phi\left(\dfrac{R_2}{S}\right)^2 + X_\phi X_2(X_\phi + X_2)}{(R_2/s)^2 + (X_\phi + X_2)^2} \tag{36}$$

or

$$\mathbf{Z}_2^{+\prime} = R_2^{+\prime} + jX_2^{+\prime} \tag{36a}$$

where $R_2^{+\prime}$ and $jX_2^{+\prime}$ are apparent secondary positive-sequence resistance and apparent secondary positive-sequence reactance, respectively.

Similarly,

$$\mathbf{Z}_{2M}^- = \frac{R_2}{2-S} + jX_2 \tag{37}$$

secondary impedance to negative-sequence current and

$$\mathbf{Z}_2^{-\prime} = \frac{X_\phi^2\dfrac{R_2}{2-S}}{\left(\dfrac{R_2}{2-S}\right)^2 + (X_\phi + X_2)^2} + j\,\frac{X_\phi\left(\dfrac{R_2}{2-S}\right)^2 + X_\phi X_2(X_\phi + X_2)}{\left(\dfrac{R_2}{2-S}\right)^2 + (X_\phi + X_2)^2} \tag{38}$$

$$\mathbf{Z}_2^{-\prime} = R_2^{-\prime} + jX_2^{-\prime} \tag{38a}$$

where $R_2^{-\prime}$ and $X_2^{-\prime}$ are apparent secondary negative-sequence resistance and apparent secondary negative-sequence reactance, respectively.

The primary impedance of the M phase is

$$\mathbf{Z}_{1M}^+ = \mathbf{Z}_{1M}^- = R_{1M} + jX_{1M} \tag{39}$$

and of the S phase is

$$Z_{1S}^{+}=Z_{1S}^{-}=(R_{1S}+R_C)+j(X_{1S}-X_C) \qquad (40)$$

in the case of a capacitor motor or

$$Z_{1S}^{+}=Z_{1S}^{-}=(R_{1S}+R_C)+jX_{1S} \qquad (40a)$$

in the case of a resistance-split-phase motor having external resistance R_C.

The generalized impedances of the single-phase motor can now be written:

$$Z_M^{+}=(R_{1M}+R_2^{+\prime})+j(X_{1M}+X_2^{+\prime}) \qquad (41)$$

$$Z_M^{-}=(R_{1M}+R_2^{-\prime})+j(X_{1M}+X_2^{-\prime}) \qquad (42)$$

$$Z_S^{+}=(R_{1S}+R_C+a^2R_2^{+\prime})+j(X_{1S}-X_C+a^2X_2^{+\prime}) \qquad (43)$$

$$Z_S^{-}=(R_{1S}+R_C+a^2R_2^{-\prime})+j(X_{1S}-X_C+a^2X_2^{-\prime}) \qquad (44)$$

If we combine equation 30 with equations 41, 42, 43, 44,

$$I_M^{+}=V_M\times\left[\frac{(R_{1S}+R_C+a^2R_2^{-\prime})+j(X_{1S}-X_C+a^2X_2^{-\prime})-ja(R_{1M}+R_2^{-\prime})+a(X_{1M}+X_2^{-\prime})}{\{(R_{1M}R_2^{+\prime})+j(X_{1M}+X_2^{+\prime})\}\{(R_{1S}+R_C+a^2R_2^{-\prime})+j(X_{1S}-X_C+a^2X_2^{-\prime})\}+\{(R_{1M}+R_2^{-\prime})+j(X_{1M}+X_2^{-\prime})\}\{(R_{1S}+R_C+a^2R_2^{+\prime})+j(X_{1S}-X_C+a^2X_2^{+\prime})\}}\right] \qquad (45)$$

$$=V_M\times\left[\frac{\{(R_{1S}+R_C+a^2R_2^{-\prime})+a(X_{1M}+X_2^{-\prime})\}+j\{(X_{1S}-X_C+a^2X_2^{-\prime})-a(R_{1M}+R_2^{+\prime})\}}{\{\text{denominator of equation 45}\}}\right]$$

Likewise from equation 28,

$$I_M^{-}=V_M\times\left[\frac{\{(R_{1S}+R_C+a^2R_2^{+\prime})-a(X_{1M}+X_2^{+\prime})\}+j\{(X_{1S}-X_C+a^2X_2^{+\prime})+a(R_{M}+R_2^{+\prime})\}}{\{\text{denominator of equation 45}\}}\right] \qquad (46)$$

and from equation 32,

$$I_M=V_M\times\left[\frac{\{2R_{1S}+2R_C+a^2(R_2^{+\prime}+R_2^{-\prime})\}+j\{2X_{1S}-2X_C+a^2(X_2^{+\prime}+X_2^{-\prime})\}+ja\{(R_2^{+\prime}-R_2^{-\prime})+j(X_2^{+\prime}-X_2^{-\prime})\}}{\{\text{denominator of equation 45}\}}\right] \qquad (47)$$

From equation 31,

$$I_S^{+}=V_M\times\left[\frac{\left\{(R_{1M}+R_2^{-\prime})-\frac{1}{a}(X_{1S}-X_C+a^2X_2^{-\prime})\right\}+j\left\{(X_{1M}+X_2^{-\prime})+\frac{1}{a}(R_{1S}+R_C+a^2R_2^{-\prime})\right\}}{\{\text{denominator of equation 45}\}}\right] \qquad (48)$$

From equation 29,

$$I_S^{-}=V_M\times\left[\frac{\left\{(R_{1M}+R_2^{+\prime})+\frac{1}{a}(X_{1S}-X_C+a^2X_2^{+\prime})\right\}+j\left\{(X_{1M}+X_2^{+\prime})-\frac{1}{a}(R_{1S}+R_C+a^2R_2^{+\prime})\right\}}{\{\text{denominator of equation 45}\}}\right] \qquad (49)$$

From equation 33,

$$I_S=V_M\times\left[\frac{\{(2R_{1M}+R_2^{+\prime}+R_2^{-\prime})+j(2X_{1M}+X_2^{+\prime}+X_2^{-\prime})\}-\frac{j}{a}\{a^2(R_2^{+\prime}-R_2^{-\prime})+ja^2(X_2^{+\prime}-X_2^{-\prime})\}}{\{\text{denominator of equation 45}\}}\right] \qquad (50)$$

Output and Torque

In the case of a balanced two-phase motor, the *gross* rotor output is

$$WO_{2\phi}=2|I_2|^2\frac{R_2}{S}(1-S)\text{ watts} \qquad (51)$$

Here only positive-sequence currents exist. The net rotor output is the gross output less friction and windage, iron loss, and load loss.

The motor torque in ounce feet is

$$T_{2\phi}=WO_{\text{net}}\times\frac{16\times33{,}000}{2\pi\times\text{rpm}\times746}$$

$$=\frac{112.7}{\text{rpm}}\times WO_{\text{net}} \qquad (52)$$

The positive-sequence currents in the secondary winding produce torque in the direction of the phase rotation of these currents. When negative-sequence currents exist they produce a counter torque. As we are dealing with two balanced systems of two-phase currents we may consider the torques they produce as positive sequence and negative sequence.

Since

$$I_{2M}^{+}=\frac{jX_\phi}{R_{2/S}+j(X_\phi+X_2)}I_M^{+} \qquad (53)$$

or

$$I_{2M}^{+}=\frac{X_\phi(X_\phi+X_2)+jX_\phi\frac{R_2}{S}}{(R_{2/S})^2+(X_\phi+X_2)^2}I_M^{+} \qquad (53a)$$

and

$$I_{2M}^{-}=\frac{jX_\phi}{\frac{R_2}{2-S}+j(X_\phi+X_2)}I_M^{-} \qquad (54)$$

or

$$I_{2M}^{-}=\frac{X_\phi(X_\phi+X_2)+jX_\phi\frac{R_2}{2-S}}{(R_{2/2-S})^2+(X_\phi+X_2)^2}I_M^{-} \qquad (54a)$$

We now can write the gross power output in terms of the component secondary currents.

$$WO_{\text{gross}}=\left[|I_{2M}^{+}|^2\left(\frac{R_2}{S}\right)+|I_{2S}^{+}|^2\left(a^2\frac{R_2}{S}\right)-|I_{2M}^{-}|^2\left(\frac{R_2}{2-S}\right)-|I_{2S}^{-}|^2\left(a^2\frac{R_2}{2-S}\right)\right](1-S) \qquad (55)$$

From equations 9 and 10,

$$|I_{2S}^{+}|=\frac{|I_{2M}^{+}|}{a}\quad\text{and}\quad|I_{2S}^{-}|=\frac{|I_{2M}^{-}|}{a}$$

Substituting these in equation 55, we have

$$WO_{\text{gross}}=2\left[|I_{2M}^{+}|^2\frac{R_2}{S}-|I_{2M}^{-}|^2\frac{R_2}{2-S}\right]\times(1-S)\text{ watts} \qquad (55a)$$

Now observe that from equations 53a, 36, and 36a

$$|I_{2M}^{+}|^2\frac{R_2}{S}=\frac{X_\phi^2\frac{R_2}{S}}{(R_{2/S})^2+(X_\phi+X_2)^2}|I_M^{+}|^2$$

$$=R_2^{+1}|I_M^{+}|^2 \qquad (56)$$

and from equations 54a, 38, and 38a,

$$|I_{2M}^{-}|^2\frac{R_2}{2-S}=\frac{X_\phi^2\frac{R_2}{2-S}}{\left(\frac{R_2}{2-S}\right)^2+(X_\phi+X_2)^2}|I_M^{-}|^2 \qquad (57)$$

$$=R_2^{-\prime}|I_M^{-}|^2$$

so that equation 55a reduces to the more convenient form:

$$WO_{\text{gross}}=2[|I_M^{+}|^2R_2^{+\prime}-|I_M^{-}|^2R_2^{-\prime}](1-S)\text{ watts} \qquad (55b)$$

Efficiency and Power Factor

By adding I_M (equation 47) and I_S (equation 50) the line current I_L can be obtained.

The "inphase" component of I_L multiplied by the line voltage (V_M) gives us the watts input, while $I_L \times V_M$ gives us the volt-ampere input.

$$\text{Power factor}=\frac{\text{watts input}}{\text{volt-amperes input}} \qquad (58)$$

After subtracting the rotational losses (friction and windage, iron loss and load loss) from equation 55b, we have the net output watts, *WO* net

$$\text{Efficiency}=\frac{WO\text{ net}}{\text{watts input}} \qquad (59)$$

Part III. Some Cases of Particular Interest

Exact Two-phase Motor Performance

A single-phase motor can be made to have phase balance and perform as a two-phase motor if the negative-sequence components of current can be made to vanish. From equations 46 and 49 we can write

$$O=\{(R_{1S}+R_C+a^2R_2^{+\prime})-a(X_{1M}+X_2^{+\prime})\}+j\{(X_{1S}-X_C+a^2X_2^{+\prime})+a(R_{1M}+R_2^{+\prime})\} \qquad (46a)$$

$$O=\left\{(R_{1M}+R_2^{+\prime})+\frac{1}{a}(X_{1S}-X_C+a^2X_2^{+\prime})\right\}+j\left\{(X_{1M}+X_2^{+\prime})-\frac{1}{a}(R_{1S}+R_C+a^2R_2^{+\prime})\right\} \qquad (49a)$$

By equating the real and imaginary components to zero separately, in each case

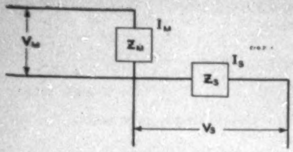

Figure 1

we can write the required condition for balance,

$$\begin{cases} R_C = a(X_{1M}+X_2^{+\prime}) - (R_{1S}+a^2R_2^{+\prime}) & (60) \\ X_C = a(R_{1M}+R_2^{+\prime}) + (X_{1S}+a^2X_2^{+\prime}) & (61) \end{cases}$$

This relationship holds for a particular value of speed as $X_2^{+\prime}$ and $R_2^{+\prime}$ are functions of slip. The condition cannot always be met as $(R_{1S} + a^2R_2^{+\prime})$ may be greater than $a(X_{1M} + X_2^{+\prime})$ which would require R_C to be negative. Completely eliminating the negative-sequence currents does not necessarily mean higher efficiency as additional losses may be incurred if R_C must be much greater than a small percentage of R_{1S}.

START PHASE DISCONNECTED

In the usual capacitor-start or resistance-split-phase motor the start phase is disconnected by centrifugal switch or relay action at one half to eight tenths of synchronous rpm. Of course, I_S becomes zero, but its symmetrical components still exist.

We can consider

$$R_C \xrightarrow{\lim} \infty$$

If ∞ is substituted for R_C in equations 45 and 46, they will take the indeterminate form ∞/∞. By differentiating numerators and denominators with respect to R_C and again substituting ∞ for R_C we have in the limit,

$$I_M^+ = V_M \frac{1}{\{(R_{1M}+R_2^{+\prime})+j(X_{1M}+X_2^{+\prime})\}+\{(R_{1M}+R_2^{-\prime})+j(X_{1M}+X_2^{-\prime})\}} \qquad (62)$$

$$= V_M \frac{1}{(2R_{1M}+R_2^{+\prime}+R_2^{-\prime})+j(2X_{1M}+X_2^{+\prime}+X_2^{-\prime})}$$

and

$$I_M^- = V_M \frac{1}{(2R_{1M}+R_2^{+\prime}+R_2^{-\prime})+j(2X_{1M}+X_2^{+\prime}+X_2^{-\prime})} \qquad (63)$$

Note that $I_M^+ \equiv I_M^-$

so that

$$I_M = I_M^+ + I_M^- \qquad (7)$$

or

$I_M = 2I_M^+ = 2I_M^-$ for this case

or

$$I_M^+ = \frac{I_M}{2} = I_M^- \qquad (64)$$

Therefore,

$$I_M = \frac{V_M}{\left(R_{1M}+\frac{R_2^{+\prime}+R_2^{-\prime}}{2}\right)+j\left(X_{1M}+\frac{X_2^{+\prime}+X_2^{-\prime}}{2}\right)} \qquad (65)$$

or

$$I_M = V_M \frac{\left(R_{1M}+\frac{R_2^{+\prime}+R_2^{-\prime}}{2}\right) - j\left(X_{1M}+\frac{X_2^{+\prime}+X_2^{-\prime}}{2}\right)}{\left(R_{1M}+\frac{R_2^{+\prime}+R_2^{-\prime}}{2}\right)^2 + \left(X_{1M}+\frac{X_2^{+\prime}+X_2^{-\prime}}{2}\right)^2} \qquad (65a)$$

From equations 64 and 55b we can now obtain the output for this condition

$$\begin{aligned} WO_{\text{gross}} &= 2\left[\left|\frac{I_M}{2}\right|^2 R_2^{+\prime} - \left|\frac{I_M}{2}\right|^2 R_2^{-\prime}\right](1-S) \\ &= |I_M|^2\left(\frac{R_2^{+\prime}-R_2^{-\prime}}{2}\right)(1-S) \text{ watts} \end{aligned} \qquad (66)$$

At standstill $(S=1)$ $R_2^{+\prime} = R_2^{-\prime} = R_2''$ since

$$\frac{R_2}{S} = \frac{R_2}{2-S}$$

Equation 66 shows that the output is zero in actual as well as synchronous watts. As the synchronous-watts output is zero there naturally can be no torque.

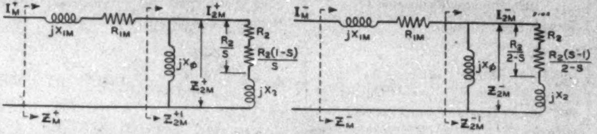

Figure 2

The standstill current input becomes

$$_{SS}I_M = \frac{V_M}{(R_{1M}+R_2'')+j(X_{1M}+X_2'')} \qquad (67)$$

At synchronous speed $(S=0)$

Examining equation 36 we find that $Z_2^{+\prime}$ takes the indeterminate form $\infty/\infty + j\infty/\infty$. When numerators and denominators are differentiated with respect to R_2/S and ∞ is again substituted for R_2/S, the equation becomes:

$$_{S=0}Z_2^{+\prime} = jX_\phi \quad _{S=0}R_2^{+\prime} = 0 \quad _{S=0}X_2^{+\prime} = jX_\phi \qquad (68)$$

while

$$_{S=0}Z_2^{-\prime} = \frac{X_\phi^2\frac{R_2}{2}}{\frac{R_2^2}{4}+(X_\phi+X_2)^2} + j\frac{X_\phi\frac{R_2^2}{4}+X_\phi X_2(X_\phi+X_2)}{\frac{R_2^2}{4}+(X_\phi+X_2)^2} \qquad (69)$$

From equation 65a we derive

$$I_M = V_M \frac{\left\{R_{1M}+\frac{X_\phi^2\frac{R_2}{4}}{R_2^2/4+(X_\phi+X_2)^2}\right\} -}{\left\{R_{1M}+\frac{X_\phi^2R_2^2/4}{R_2^2/4+(X_\phi+X_2)^2}\right\}^2 +} \frac{j\left\{X_{1M}+\frac{X_\phi}{2}\left[1+\frac{R_2^2/4+X_2(X_\phi+X_2)}{R_2^2/4+(X_\phi+X_2)^2}\right]\right\}}{\left\{X_{1M}+\frac{X_\phi}{2}\left[1+\frac{R_2^2/4+X_\phi(X_\phi+X_2)}{R_2^2/4+(X_\phi+X_2)^2}\right]\right\}} \qquad (70)$$

VOLTAGE ACROSS START PHASE

Frequently there is need of knowing the voltage across the starting winding proper to make control applications either on the motor or for auxiliary apparatus.

Case of Capacitor Motor

$$V_{\phi S} = V_M - E_C \qquad (71)$$

where

$$E_C = I_S(R_C - jX_C) \qquad (72)$$

I_S is calculated from equation 50.

Case of Capacitor-Start or Resistance-Split-Phase Motor After the Starting Switch Opens the Start Phase

If

$$R_C \xrightarrow{\lim} \infty$$

equations 48and 49 take the indeterminate form ∞/∞, but by differentiation it will be found that

$$I_S^+ = V_M \frac{j/a}{(R_{1M}+R_2^{+\prime})+j(X_{1M}+X_2^{+\prime})+(R_{1M}+R_2^{-\prime})+j(X_{1M}+X_2^{-\prime})} \qquad (73)$$

$$I_S^+ = V_M \frac{j/a}{\{(2R_{1M}+R_2^{+\prime}+R_2^{-\prime})+j(2X_{1M}+X_2^{+\prime}+X_2^{-\prime}} \qquad (73a)$$

and

$$I_S^- = V_M \frac{-j/a}{(2R_{1M}+R_2^{+\prime}+R_2^{-\prime})+j(2X_{1M}+X_2^{+\prime}+X_2^{-\prime})} \qquad (74)$$

Note that $I_S^+ = -I_S^-$ and $I_S = I_S^+ + I_S^- = 0$

$$V_{S\phi}^+ = I_S^+a^2Z_2^{+\prime} \qquad (75)$$

$$V_{S\phi}^- = I_S^-a^2Z_2^{-\prime} = -I_S^+a^2Z_2^{-\prime} \qquad (76)$$

If we add

$$\begin{aligned} V_{S\phi} &= V_{S\phi}^+ + V_{S\phi}^- = I_S^+a^2(Z_2^{+\prime}-Z_2^{-\prime}) \\ &= V_M\frac{j/a\{a^2(R_2^{+\prime}-R_2^{-\prime})+ja^2\times(X_2^{+\prime}-X_2^{-\prime})\}}{\{(2R_{1M}+R_2^{+\prime}+R_2^{-\prime})+j(2X_{1M}+X_2^{+\prime}+X_2^{-\prime})\}} \end{aligned} \qquad (77)$$

$$V_{S\phi}=V_M a\frac{-(X_2^{+\prime}-X_2^{-\prime})+j(R_2^{+\prime}-R_2^{-\prime})}{(2R_{1M}+R_2^{+\prime}+R_2^{-\prime})+j(2X_{1M}+X_2^{+\prime}+X_2^{-\prime})} \quad (77a)$$

Observe that at standstill, when

$X_2^{+\prime}=X_2^{-\prime}=X_2''$ and $R_2^{+\prime}=R_2^{-\prime}=R_2''$

$V_{S\phi}$ becomes zero

STARTING TORQUE

In routine design work the calculation of starting torque, together with the capacitor voltage or starting current, is of particular importance as the running performance can often be proportioned accurately from existing similar tested designs.

$$\text{Let } I_M=A+jB=\frac{V_M}{Z_M} \quad (78)$$

$$\text{Let } I_S=C+jD=\frac{V_M}{Z_S} \quad (79)$$

Since

$R_2^{+\prime}=R_2^{-\prime}=R_2''$ and $X_2^{+\prime}=X_2^{-\prime}=X_2''$
$Z_S^+=Z_S^-=Z_S$ and $Z_M^+=Z_M^-=Z_M$

Equation 30 becomes

$$I_M^+=V_M\frac{Z_S-jaZ_M}{2Z_SZ_M}=\frac{V_M}{2Z_M}-ja\frac{V_M}{2Z_S} \quad (80)$$

or

$$I_M=\frac{I_M}{2}-ja\frac{I_S}{2} \quad (80a)$$

and equation 28 becomes

$$I_M^-=V_M\frac{Z_S+jaZ_M}{2Z_MZ_S}=\frac{V_M}{2Z_M}+ja\frac{V_M}{2Z_S} \quad (81)$$

or

$$I_M^-=\frac{I_M}{2}+ja\frac{I_S}{2} \quad (81a)$$

Now if we use equations 78 and 79 in equation 80a,

$$I_M^+=\left(\frac{A}{2}+j\frac{B}{2}\right)-ja\left(\frac{C}{2}+j\frac{D}{2}\right)$$
$$=\left(\frac{A}{2}+a\frac{D}{2}\right)+j\left(\frac{B}{2}-a\frac{C}{2}\right) \quad (82)$$

$$|I_M^+|^2=\frac{(A+aD)^2}{4}+\frac{(B-aC)^2}{4} \quad (83)$$

Similarly if we use equations 78 and 79 in equation 81a,

$$I_M^-=\left(\frac{A}{2}+j\frac{B}{2}\right)+ja\left(\frac{C}{2}+j\frac{D}{2}\right)$$
$$=\left(\frac{A}{2}-a\frac{D}{2}\right)+j\left(\frac{B}{2}+a\frac{C}{2}\right) \quad (84)$$

$$|I_M^-|^2=\frac{(A-aD)^2}{4}+\frac{(B+aC)^2}{4} \quad (85)$$

and

$$|I_M^+|^2-|I_M^-|^2=a(AD-BC) \quad (86)$$

to obtain the theoretical torque we will combine equations 52, 55b, and 85 and

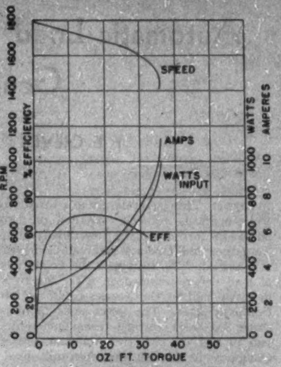

Figure 3. Calculated one-quarter-horsepower-motor performance data

at the same time eliminate the motor speed by the following relationship

rpm = (1 − S) synchronous rpm

so that

$$T=\frac{112.7}{(1-S)\text{synchronous}}\times 2R_2''a(AD-BC)(1-S) \quad (87)$$

This is an indeterminate of the form 0/0 for S = 1, but

$$\lim_{S\to 1}\frac{1-S}{1-S}=1$$

$$T=\frac{225.4}{\text{synchronous}}R_2''a(AD-BC)\text{ ounce-feet} \quad (87a)$$

For the usual capacitor motor:

A is positive.
B is negative.
C is positive.
D is positive.

For the usual resistance-split-phase motor:

A is positive.
B is negative.
C is positive.
D is negative.

This theoretical value of standstill torque must be modified by an empirical factor to take account of friction, iron loss, and tooth-locking effects in a practical design.

Conclusions

The author has endeavored to demonstrate the versatility of the symmetrical-component method in the solution of single-phase induction motors. The theory is "continuous" mathematically in that special cases are set up simply by allowing some parameter to be zero or infinity to fit the physical aspects of the problem.

The derivations are general enough so that, if R_2 is not the same for the low-frequency positive-sequence rotor currents as it is for the higher-frequency negative-sequence rotor currents, allowances can be made in the calculations.

Nomenclature

V_M = main-phase rms volts
V_S = start-phase rms volts
V_M^+ = positive-sequence component of V_M
V_M^- = negative-sequence component of V_M
V_S^+ = positive-sequence component of V_S
V_S^- = negative-sequence component of V_S
I_M = main-phase rms amperes
I_S = start-phase rms amperes
I_M^+ = positive-sequence component of I_M
I_M^- = negative-sequence component of I_M
I_S^+ = positive-sequence component of I_S
I_S^- = negative-sequence component of I_S
$a=\frac{\text{effective conductors of } S \text{ phase}}{\text{effective conductors of } M \text{ phase}}$
s = per-unit slip
I_{2M}^+ = positive-sequence component of M-phase secondary current referred to primary current
I_{2M}^- = negative-sequence component of M-phase secondary current referred to primary current
I_{2S}^+ = positive-sequence component of S-phase secondary current referred to primary current
I_{2S}^- = negative-sequence component of S-phase secondary current referred to primary current
Z_M^+ = total positive-sequence impedance of M phase
Z_M^- = total negative-sequence impedance of M phase
Z_S^+ = total positive-sequence impedance of S phase
Z_S^- = total negative-sequence impedance of S phase
X_{1M} = reactance of M-phase primary winding
R_{1M} = resistance of M-phase primary winding
R_2 = equivalent M-phase secondary resistance referred to primary winding
X_2 = equivalent M-phase secondary reactance referred to primary winding
X_ϕ = equivalent M-phase mutual or magnetizing reactance
$Z_2^+=\frac{R_2}{S}+jX_2$ = positive-sequence secondary impedance of M phase referred to primary winding
$Z_2^-=\frac{R_2}{2-S}+jX_2$ = negative-sequence secondary impedance of M phase referred to primary winding
$R_2^{+\prime}$ = apparent positive-sequence M-phase secondary resistance
$=\frac{X_\phi^2R_{2/s}}{(R_{2/s})^2+(X_\phi+X_2)^2}$
$R_2^{-\prime}$ = apparent negative-sequence M-phase secondary resistance

$$=\frac{X_\phi^2\frac{R_2}{2-S}}{\left(\frac{R_2}{2-S}\right)^2+(X_\phi+X_2)^2}$$

$X_2^{+\prime}$ = apparent positive-sequence M-phase secondary reactance

$$=\frac{X_\phi(R_2/s)^2+X_\phi X_2(X_\phi+X_2)}{(R_2/s)^2+(X_\phi+X_2)^2}$$

$X_2^{-\prime}$ = apparent negative-sequence M-phase secondary reactance

$$=\frac{X_\phi(R_2/(2-S))^2+X_\phi X_2(X_\phi+X_2)}{(R_2/(2-S))^2+(X_\phi+X_2)^2}$$

$\mathbf{Z}_2^{+\prime}=R_2^{+\prime}+jX_2^{+\prime}$ $\mathbf{Z}_2''$ = standstill apparent secondary impedance

$\mathbf{Z}_2^{-\prime}=R_2^{-\prime}+jX_2^{-\prime}$ R_2'' = standstill apparent secondary resistance

X_2'' = standstill apparent secondary reactance

$\mathbf{Z}_{1M}^{+}=\mathbf{Z}_{1M}^{-}=R_{1M}+jX_{1M}$ = primary impedance

R_{1S} = resistance of S-phase primary winding

X_{1S} = reactance of S-phase primary winding

X_C = capacitor reactance

R_C = capacitor resistance or other external resistance in S phase

$T_{2\phi}$ = two-phase-motor torque, ounce-feet

Synch = synchronous rpm

WO = gross watts output of rotor

T = single-phase-motor torque, ounce-feet

E_C = capacitor voltage

$V_{S\phi}$ = voltage across S-phase winding

Sample Calculation

One-quarter horsepower, four pole, 110 volts 60 cycle; capacitor-start motor

Constants

$R_2=2.48$ (25 degrees centigrade)

$R_1=1.63$ (25 degrees centigrade)

$X_1=2.47,\ X_2=2.44,\ X_\phi=67.28$

Friction loss $=W_f=16.5$ watts

Iron loss $=W_i=23.5$ watts

$S=0.038$

Rpm $=(1-0.038)\ 1{,}800=1{,}732$

$R_{2/S}=65.25 \quad R_{2/1-S}=1.264$

$$R_2^{+\prime}=\frac{67.28^2\times65.25}{65.25^2+(67.28+2.44)^2}=32.40$$

$$R_2^{-\prime}=\frac{67.28^2\times1.264}{1.264^2+(67.28+2.44)^2}=1.177$$

$$X_2^{+\prime}=\frac{67.28\times65.25^2+67.28\times2.44(67.28+2.44)}{65.25^2+(67.28+2.44)^2}$$

$$=32.70$$

$$X_2^{-\prime}=\frac{67.28\times1.264^2+67.28\times2.44(67.28+2.44)}{1.264^2+(67.28+2.44)^2}$$

$$=2.375$$

$$I_M=110\left[\frac{\left(1.63+\dfrac{32.40+1.18}{2}\right)-j\left(2.47+\dfrac{32.70+2.38}{2}\right)}{\left(1.63+\dfrac{32.40+1.18}{2}\right)^2+\left(2.47+\dfrac{32.70+2.38}{2}\right)^2}\right]$$

$$=110\left[\frac{18.42-j20.01}{339.5+441}\right]$$

$$=2.595-j2.962 \quad |I_M|=3.94$$

$$|I_M|^2=15.51$$

$$WO_{\text{gross}}=15.51(1-0.038)\left(\frac{32.40-1.18}{2}\right)$$

$$=15.51\times0.962\times15.61=233.2 \text{ watts}$$

$$WO_{\text{net}}=233.2-16.5-23.5=193.2$$

Torque $=(112.7/1732)\times193.2=12.55$ ounce-feet

Watts input $=110\times2.595=285.5$

Eff $=193.2/285.5=0.695$

References

1. ANALYSIS OF UNSYMMETRICAL MACHINES, W. V. Lyon, Charles Kingsley, Jr. AIEE TRANSACTIONS, volume 55, 1936, May section, pages 471–6.

2. THE REVOLVING-FIELD THEORY OF THE CAPACITOR MOTOR, W. J. Morrill. AIEE TRANSACTIONS, volume 48, 1929, pages 614–32.

3. THE APPARENT-IMPEDANCE METHOD OF CALCULATING SINGLE-PHASE-MOTOR PERFORMANCE, W. J. Morrill. AIEE TRANSACTIONS, volume 60, 1941, December section, pages 1037–41.

4. ELECTRIC CIRCUITS—THEORY AND APPLICATION (first edition), O. G. C. Dahl. Pages 80–9, 138–44.

5. INDUCTION-MOTOR CORE LOSSES, P. L. Alger, R. Ekergian. AIEE JOURNAL, volume 39, October 1920, pages 906–20.

Automatic Load Control for Turbine Generators

F. E. CREVER
ASSOCIATE AIEE

R. L. JACKSON
NONMEMBER AIEE

Synopsis: This paper describes a load-control apparatus recently installed on two 20,000-kw turbines at the power plant of the Tennessee Coal Iron and Railroad Company at Fairfield, Ala., to reduce the magnitude of load swings imposed on a tie line by a hot-strip mill in the Tennessee Coal Iron Company plant. The power plant contains three 20,000-kw turbine-driven generators and is tied in with the Alabama Power Company to furnish the steel-mill load. Previous to the installation of the equipment herein described, the three 20,000-kw turbine generators have carried load under control of their speed governors and the variations in strip-mill load which are about 20,000 kw were imposed upon the Alabama Power Company tie line causing objectionable disturbances on the connecting power system. It was desired to develop a means of imposing all or part of the strip-mill load on the Tennessee Coal Iron and Railroad Company turbine generators to reduce these disturbances. Several methods were considered, and the one selected was based upon a static watt-measuring circuit, the output of which is an Amplidyne generator. The Amplidyne in turn operates the pilot motor of an hydraulic (oil) relay at the turbine to control the steam admission valves.

GIVEN a base load and a variable load and a variable supply of steam for either one of two prime movers, the regulator is to cause the prime movers to take

(*a*). A base load, adjustable from $^1/_{20}$th rated load to rated load.

(*b*). In addition to condition *a* any desired percentage of the variable load from 0 to 100 per cent.

(*c*). Both the base load and the variable load are to be reduced automatically as the steam pressure falls below a nominal pressure.

(*d*). The variable load is to be divided in any desired ratio between the two prime movers by simple adjustment.

(*e*). The variable load may have instantaneous rates of change as high as 5,000 kw per second with average rates of approximately 2,000 kw per second during load increase and decrease. The variable load peaks are approximately 20,000 kw in magnitude of 20 to 100 seconds duration with intervals of light load of about the same duration. It is desired to minimize the variation of load on the tie line insofar as practical.

In addition, the governing system is desired to have the following features:

(*a*). A definite limit on turbine speed must at all times be in opeation.

(*b*). It must be possible for operating either or both turbines on their speed governors.

(*c*). It must be possible to change easily from power to speed governing and vice versa.

(*d*). The power-governing system must be fast in response and be stable in operation.

Fundamentals of Electric-Power-Measuring Circuit

As balanced three-phase loads are to be governed a single-phase power-measuring circuit suffices to control the operation. Also, as the machines operate at constant voltage it is sufficient to control the unity power factor or kilowatt component of generator current.

The essentials of the power-measuring circuit are shown in Figure 1.

The Amplidyne generator has been described adequately elsewhere.[1–4] For pres-

---

Paper 45-114, recommended by the AIEE committees on automatic stations and power generation for publication in AIEE TRANSACTIONS. Manuscript submitted April 11, 1945; made available for printing May 14, 1945.

F. E. CREVER and R. L. JACKSON are both with General Electric Company, Schenectady, N. Y.

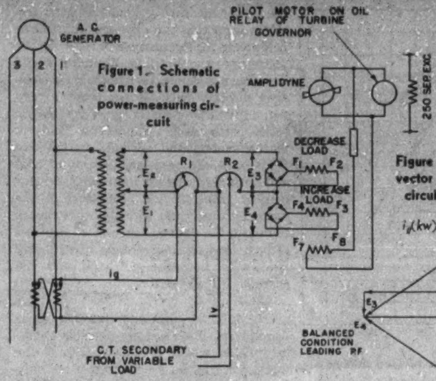
A.C. GENERATOR
3
2
1
PILOT MOTOR ON OIL RELAY OF TURBINE GOVERNOR
AMPLIDYNE
250 SEP EXC
DECREASE LOAD
INCREASE LOAD
R1
R2
E2
E1
E3
E4
F1
F2
F4
F3
F7
F8
Ig
Iv
C.T. SECONDARY FROM VARIABLE LOAD

Figure 1. Schematic connections of power-measuring circuit

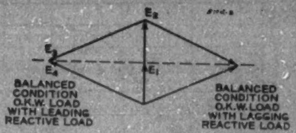
E2
E3
E4
E1
BALANCED CONDITION O.K.W. LOAD WITH LEADING REACTIVE LOAD
BALANCED CONDITION O.K.W. LOAD WITH LAGGING REACTIVE LOAD

Figure 2 (right). Voltage vector diagram of measuring circuit at zero load setting

Figure 3 (below). Voltage vector diagram of measuring circuit at fixed load setting

$$i_g(kw)R_1 = \frac{E_1+E_2}{2} - E_2 = \frac{E_1-E_2}{2}$$

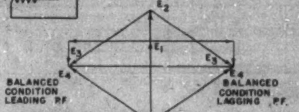
E2
E1
E3
E3
E4
E4
BALANCED CONDITION LEADING PF
BALANCED CONDITION LAGGING PF

ent purposes it is sufficient to say that the Amplidyne output voltage is extremely sensitive to a difference between the ampere turns of the fields F_1F_2 and F_3F_4 which are excited in opposite directions (so as to oppose each other) from selenium rectifiers as shown. The Amplidyne output voltage will be zero, and the motor which operates the hydraulic governing mechanism will be at rest only when the currents in these two fields are equal and opposite. As the two fields have the same number of turns and the same resistance this balance occurs only when the alternating voltages at the rectifier inputs are equal in magnitude. Assume for the moment that the adjustable voltage tap is set so that $E_1=E_2$ and that $i_v=0$ in Figure 1. Then $|E_3|=|E_4|$ only when the kilowatts or unity-power-factor component of current i_g is zero regardless of the reactive component of current i_g. Figure 2 illustrates this.

If the adjustable tap is set so that E_1 is greater than E_2 while the sum of E_1 and E_2 remains constant, the balanced condition when $|E_3|=|E_4|$ will occur only when the kilowatt load on the turbine generator is constant so that the inphase component of $i_g \times R_1 = (E_1-E_2)/2$.

Figure 3 illustrates this condition at various power factors on the generator.

From the foregoing it is evident that for a fixed value of R_1 and with R_2 set at zero the load on the turbine when the Amplidyne output voltage is zero is proportional to the voltage between the midtap of the potential-transformer secondary winding and the position of the adjustable tap. The adjustable tap then is used as the base-load setting of the generator.

If R_2 is not zero the load on the turbine when $|E_3|=|E_4|$ will be such that

$$i_g \times R_1 = \frac{E_1-E_2}{2} + i_v \times R_2$$

where

i_g = unity-power-factor component of generator current

i_v = unity-power-factor component of variable load current

By setting the adjustable voltage tap the base load of the turbine is fixed at any desired value and by setting the value of R_2 any desired percentage of the variable load up to 100 per cent may be carried.

In order to decrease both the base-load setting and the percentage of the variable load taken by the turbine the value of R_1 is increased automatically as the steam pressure decreases below a set value.

In Figure 1 field F_7F_8 of the Amplidyne is connected as an inverse feedback of the Amplidyne output into its input. This results in a more linear relationship between the Amplidyne input and output than would be the case without this connection and gives a means of adjusting rate of operation of the governing mechanism as a function of the deviation between the load on the turbine and the load setting of the regulator

Electrical Connections

A schematic diagram of the electric-system connections and of the power regulators is shown in Figure 4. In order to make the kilowatt component of turbogenerator current in phase with the voltage to the regulator circuit it was necessary to add the currents of phases 1 and 2 when using potential 1–2. This was done with current transformers in the secondary circuits of existing current transformers. Owing to existence of a wye–delta transformer bank between the generator and the strip-mill circuit a single current transformer in phase 1 gave the required phase relationship of strip-mill current with respect to the regulator voltage. This latter current is transmitted approximately 4,000 feet to the control room of the power plant. As it was desired to shift the variable load between the two power-regulated generators without disturbing the percentage of strip-mill load carried an adjustable-ratio current transformer was used to divide the strip-mill current between the two regulators in any ratio so that the sum of the currents to the two regulators remains in constant ratio to the strip-mill current. A "variac" was used as a means of adjusting the relationship of voltages E_1 and E_2, and its setting determined the base load. The transformers used between

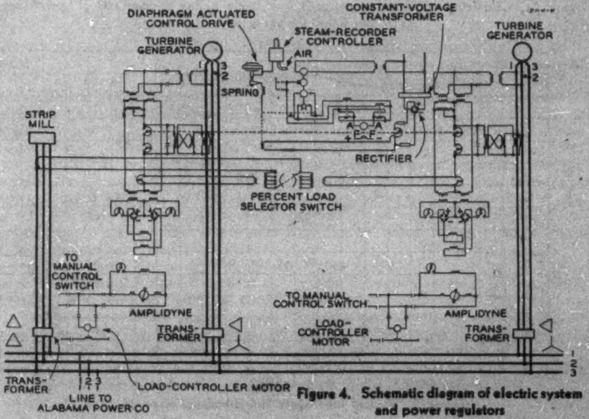
DIAPHRAGM ACTUATED CONTROL DRIVE
CONSTANT-VOLTAGE TRANSFORMER
STEAM-RECORDER CONTROLLER
TURBINE GENERATOR
TURBINE GENERATOR
AIR
SPRING
STRIP MILL
RECTIFIER
PER CENT LOAD SELECTOR SWITCH
TO MANUAL CONTROL SWITCH
TO MANUAL CONTROL SWITCH
AMPLIDYNE
AMPLIDYNE
TRANS-FORMER
TRANS-FORMER
LOAD-CONTROLLER MOTOR
TRANS-FORMER
LINE TO ALABAMA POWER CO
LOAD-CONTROLLER MOTOR
1
2
3

Figure 4. Schematic diagram of electric system and power regulators

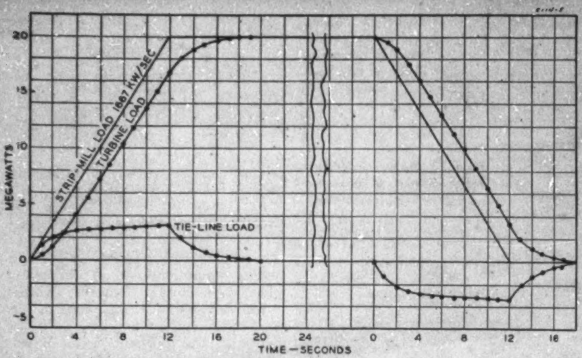

Figure 5. Calculated response to assumed load cycle having constant rate of load change of 1,667 kw per second

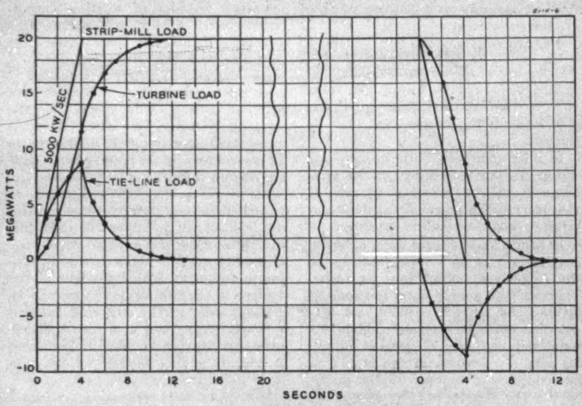

Figure 6. Calculated response to assumed load cycle having constant rate of load change of 5,000 kw per second

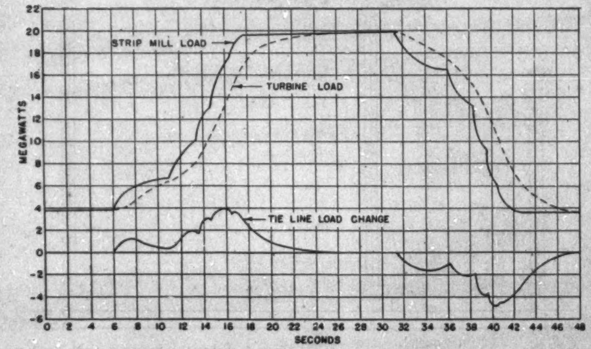

Figure 7. Actual load cycle and calculated response

the power-measuring circuit and the rectifiers supplying the opposing Amplidyne fields were for the purpose of reducing the voltages to the rectifiers, though it would have been possible to rectify these voltages directly without the transformers. An adjustable resistor is connected in series with each Amplidyne field to match exactly the currents to the two fields with the base-load setting at zero and with zero current from the generator current transformers. Resistors in the current-transformer circuits were chosen to obtain the desired range of adjustment of base load and percentage of strip-mill load, with both the potential and the current transformer ratios taken into account.

Owing to the high amplification of the Amplidyne, it was easily possible to obtain fields which would withstand the highest currents to which they are subjected (which vary with power factor) and at the same time to obtain more than adequate sensitivity to power variation.

Sensitivity

The Amplidyne voltage output per kilowatt difference between regulator setting and turbogenerator load may be adjusted by means of the variable resistor in series with field F_7F_8 of the Amplidyne. Without this feedback it requires approximately 2,000 kw deviation between regulator setting and generator load to run the pilot motor through full travel in four seconds. In practice it was necessary to adjust the feedback to obtain stable operation so that the deviation required to cause the generator to increase its load at a rate of 5,000 kw per second was approximately 6,500 kw. Final adjustment with which the operation data were taken was with 10,000 kw deviation required to give a rate of 5,000 kw per second. With this adjustment the kilowatt deviation to cause the Amplidyne voltage necessary just to rotate the pilot motor against friction was approximately 200 kw, so that with a setting of 20,000 kw the power is held within plus or minus one per cent during steady state.

Response

All of the regulating elements are relatively fast in response in comparison with the time required to operate the pilot motor of the governing mechanism. This time together with the kilowatts deviation required to obtain a given pilot-motor speed determines the response of the system. Also, it will be shown that these factors, together with the rate of change of the variable load and the percentage of the variable load carried by the Tennessee Coal Iron and Railroad Company turbines, determine the effectiveness of the regulating system

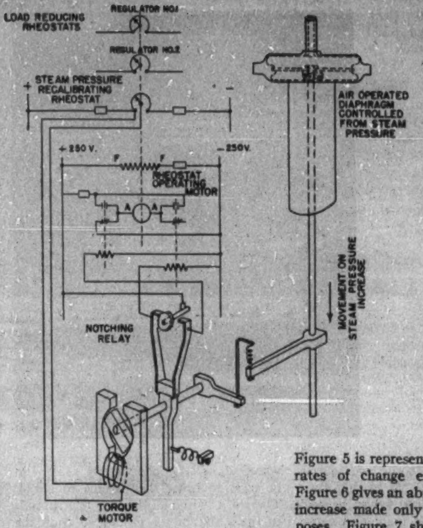
LOAD REDUCING RHEOSTATS
REGULATOR NO.1
REGULATOR NO.2
STEAM PRESSURE RECALIBRATING RHEOSTAT
+
−
+250 V.
−250V.
F
F
RHEOSTAT OPERATING MOTOR
A
A
NOTCHING RELAY
TORQUE MOTOR
AIR OPERATED DIAPHRAGM CONTROLLED FROM STEAM PRESSURE
MOVEMENT ON STEAM PRESSURE INCREASE

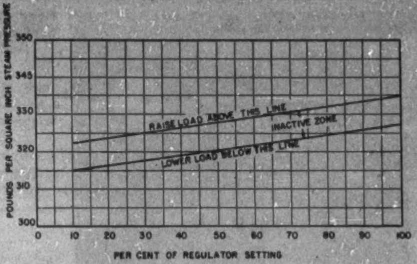

Figure 9 (above). Characteristics of steam-pressure regulator

Figure 8 (left). Schematic diagram of steam-pressure-regulating system

in minimizing the variation in tie-line load.

Let

Tkw = kilowatt load on turbine generator
Lkw = kilowatt setting of load regulator
$P = \frac{d}{dt}$
K = proportionality constant between rate of change of turbine load and deviation of load from regulator setting

Then

$$KP\ Tkw = (Lkw - Tkw)$$

$$Tkw = \frac{Lkw}{KP+1}$$

With

Tkw = 5,000 kw per second
Lkw − *Tkw* = 10,000 kw
K = 2

The solution for unit change of *Lkw* (caused by a change of strip-mill load) is

$$Tkw = Lkw(1 - \epsilon^{-\frac{1}{2}t})$$

If now *Lkw* is varying at a constant rate *R* it can be shown by the superposition theorem that (if we assume *Lkw* = 0 when *T* = 0)

$$Tkw = R(t - 2 + 2\epsilon^{-\frac{1}{2}t})$$

With an assumed load cycle as in Figure 5 the response and the variation in tie-line load were calculated as shown in this same figure from this formula and the preceding one. A similar curve is shown in Figure 6 for a rate of strip-mill-load increase of 5,000 kw per second. Figure 5 is representative of the average rates of change encountered, whereas Figure 6 gives an abnormally high rate of increase made only for comparison purposes. Figure 7 shows an actual strip-mill-load peak taken from a load chart. The calculated turbine load based upon 100-per-cent pickup of strip-mill load and the load on the tie line are calculated and shown in this same figure.

Means of Reducing Loads Upon Decrease in Steam Pressure

The means of reducing both the base load and the variable load in equal percentages upon reduction in steam pressure was to increase resistance R_1, Figure 1. A Bailey Meter Company pilot valve was used to give a definite motion of a spring opposing the action of a torque motor to control a motor-operated rheostat to vary the value of R_1. Figure 8 shows a schematic diagram of this equipment.

For full normal steam pressure or above the torque-motor notching system is balanced with the rheostat all cut out. For any steam pressure within a range of 30 pounds per square inch, that is, from 340 pounds per square inch to 310 pounds per square inch the rheostat is notched until the value of load is decreased to a point where the torque motor is balanced. The notching contacts have adjustable dead band, and the action is to notch to the center of the dead band so that the load will be reduced to hold an average steam pressure. Figure 9 shows the characteristics of the steam-pressure regulator. This steam-pressure regulator is intended primarily as a means of reducing the loads to keep the steam pressure above a certain minimum. It can operate continuously in range to regulate steam pressure. Normally, however, it was intended that the load settings would be such that full steam pressure could be maintained, with the steam pressure above the range of the pressure regulator. Figure 10 shows the control panels for the two turbine generators. The panel at the left is for one generator. The middle panel contains the variable-ratio current transformer by means of which the strip-mill load may be divided between the two machines. The third panel from the left duplicates the first panel for the other turbine. On the extreme right is the steam-pressure controller. The base-load adjustment, regulator on-and-off switch, and the percentage of strip-mill load all are operated from the front of these panels.

Turbine Valve Control

The schematic arrangement of the turbine control is shown on Figure 11. The load-control relay unit and the initial pressure regulator were added to the original governor unit and connected with a telescope joint in the governor connection so that, while the load control is used, the speed governor can be run to its full-load position and act as a pre-emergency governor. In this condition the telescope joint is pulled open and the the load-control piston rod controls the main pilot valve through connection *F* and *E*. The initial pressure-regulator piston rod can pick up through connection *D*. These three connections (*F*, *D*, and *E*) will transmit motion only in one direction, so that any one of them may close the control valves regardless of the setting of the others. This allows the speed governor to close the valves in case of loss of load and the pressure regulator to close the valves in case of loss of pressure.

The load-control unit has a shunt-wound d-c motor with constant excitation from a 250-volt source. The armature current comes from the Amplidyne generator. The motor operates a lead screw raising and lowering the relay pilot valve and so raises and lowers the relay piston. A friction clutch is provided in the drive so that no limit

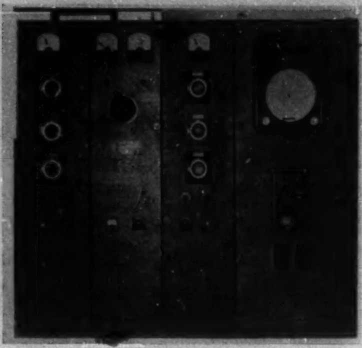

Figure 10 (left). Load-control panel installation

Figure 12 (right). Load-control unit of turbine-valve control

switches are necessary and limit-switch dead band is eliminated. An oil spray lubricates the clutch to prevent wear in case the motor runs long periods of time at the end of the travel. Motion of the relay piston is transmitted to the main pilot valve and so to the main hydraulic piston, opening and closing the control valves through the rack and pinion and the cams.

The pressure regulator consists of a spring-loaded bellows which operates a relay pilot valve and controls an oil piston. The spring plug may be adjusted by handwheel *C* so that the regulator will close the valves at pressures from 275 to 350 pounds per square inch. A stop is provided on both the load control and the pressure regulator so that they cannot close the turbine valves beyond the no-load steam-flow point and cause overheating of the turbine by motoring. The speed governor always can close the valves completely on a rise in speed to the pre-emergency setting. However, an adjustment is provided on the load-control piston rod so that when the turbine is shut down the control valves can be closed completely, and then handwheel *A* on the pilot-motor shaft can be used to bring the turbine to speed. There is a switch on the load-control unit to open the motor circuit so that the handwheel can be used without danger of the motor starting up. The load-control and initial pressure regulator are enclosed in a small case mounted on the turbine base adjacent to the front pedestal. Figure 12 is a view of the installation.

The rates of load change imposed by this regulator will exceed what normally is considered good practice from the standpoint of economy and maintenance, but the 20,000-kw turbines at Tennessee Coal Iron and Railroad Company are low pressure and temperature and of a rugged design with a relatively short span between bearings; they should be able to withstand the quick load changes without undue distress. There most likely will be some increased maintenance necessary on machines subjected to continuous quick load changes, especially on the control mechanism, valves, cams, rack, and pinion, and so on.

The actual performance of the load-control unit was as good as anticipated. Load changes were made quickly, positively, and without hunting.

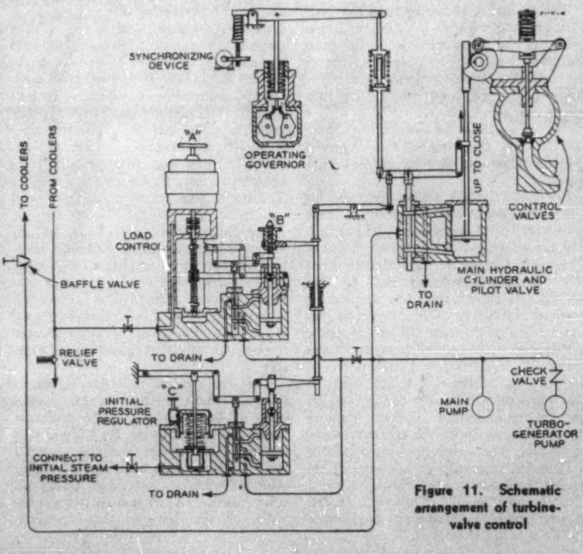

Figure 11. Schematic arrangement of turbine-valve control

References

1. INDUSTRIAL APPLICATIONS OF AMPLIDYNE GENERATORS, D. R. Shoults, M. A. Edwards, F. E. Crever. *General Electric Review*, volume 43, 1940.

2. THE AMPLIDYNE GENERATOR—A DYNAMOELECTRIC AMPLIFIER FOR POWER CONTROL, E. F. W. Alexanderson, M. A. Edwards, K. K. Bowman. *General Electric Review*, volume 43, 1940.

3. DESIGN CHARACTERISTICS OF AMPLIDYNE GENERATORS, A. Fisher. *General Electric Review*, volume 43, 1940.

4. STEADY-STATE THEORY OF THE AMPLIDYNE GENERATOR, T. D. Graybeal. AIEE TRANSACTIONS, volume 61, 1942, October section, pages 750–6.

Tapered-Thickness Bimetal

WILLIAM B. ELMER
ASSOCIATE AIEE

Synopsis: The most important properties of thermostatic bimetal strips of uniformly tapered width or thickness or both have been analyzed mathematically, and the findings are described in this paper. A tapered-thickness form is found to be the best practical one from the standpoint of economy of material. Conveniently usable charts are included which are applicable in the form of correction coefficients to the standard formulas for thermostatic deflection and mechanical deflection of strips of uniform thickness and width. The dual-tapered form is especially useful in reducing vibration troubles in slow-acting thermostats, and formulas are given for determining the fundamental frequency of single- or dual-tapered strips of any taper ratio.

THERMOSTATIC BIMETALS of the "low-temperature" or brass–Invar type have been used for many years in the construction of innumerable thermostatic-control devices. The substitution of stronger and more active metals for the brass component by Spencer and others during the '20's led to an impressive extension of the use of bimetals. The announcement of the manganese–Invar bimetal in 1942 gave the industry a further remarkable fundamental improvement.

Bimetals now are used almost universally in sheet form, and extensive work has been done in development of various outlines and bent shapes for which well-known simplified deflection and force formulas are available. In addition, a limited amount of progress has been made toward the useful development of bimetal rods, cones, and tapered-thickness sheets. The last-mentioned form gives promise of a substantially increased effectiveness in utilization of the material, and this, coupled with discoveries of inexpensive fabrication methods, has led to the present exploration of its characteristics. The results of these studies have been interpreted into suitable form for convenient engineering use.

Although it is well-known that unloaded bimetal strips deflect into circular curvatures in response to temperature changes, the temperature-deflection formulas and constants in common use are based upon the assumption of parabolic curvatures. Such an approximation is reasonably acceptable, as the errors are very small for the short arcs involved and the parabolic formulas are vastly simpler than the circular ones. The assumption of parabolic curvatures will be retained throughout the present studies.

Deflection Characteristics

The deflection characteristic of an initially flat bimetal strip of uniform thickness, supported at one end and subject to uniform temperature variations, is given approximately by the parabolic expression:

$$\delta = \frac{K\Delta l^2}{t_0} \tag{1}$$

where

K = deflection constant governed by composition of strip
l = distance along strip from support
t_0 = thickness of strip
Δ = temperature change of strip
δ = deflection of strip at distance l from support, due to temperature change Δ

If we differentiate equation 1, the slope of the strip at any point is

$$\frac{d\delta}{dl} = \frac{2K\Delta l}{t_0} \tag{2}$$

and if we differentiate again the rate of change of slope is

$$\frac{d^2\delta}{dl^2} = \frac{2K\Delta}{t_0} \tag{3}$$

If we consider now a bimetal strip of variable thickness t, the rate of change of slope will be

$$\frac{d^2\delta}{dl^2} = \frac{2K\Delta}{t} \tag{4}$$

If the strip tapers uniformly, it will appear as shown in Figure 1, where

L = length of strip
t_0 = thickness of strip at base or support
t_1 = thickness of strip at free end
t = thickness of strip at any point
l = distance along strip from t_0 to t_1
b = width
R_t = taper ratio = $\frac{t_1}{t_0}$

It will be seen from Figure 1 that

$$\frac{t_0 - t_1}{L} = \frac{t - t_1}{L - l}$$

and

$$t = t_0\left[1 - \left(\frac{1-R_t}{L}\right)l\right] \tag{5}$$

If we substitute equation 5 in equation 4, the rate of change of slope of the tapered strip of Figure 1 is

$$\frac{d^2\delta}{dl^2} = \frac{2K\Delta}{t_0\left[1 - \left(\frac{1-R_t}{L}\right)l\right]} \tag{6}$$

If we integrate twice, the deflection characteristic of a uniformly tapering bimetal strip is found to be

$$\delta = \frac{K\Delta l^2}{t_0}\cdot\frac{2L}{l(1-R_t)}\times \left\{\left[1 - \frac{L}{l(1-R_t)}\right]\ln\frac{1}{1 - \frac{(1-R_t)l}{L}} + 1\right\} \tag{7}$$

The deflection of the free end ($l = L$) is

$$\delta = \frac{K\Delta L^2}{t_0}\cdot\frac{2}{(1-R_t)}\left\{1 - \frac{R_t}{1-R_t}\ln\frac{1}{R_t}\right\} \tag{8}$$

With reference to equation 1, the ratio of deflection of a tapered-thickness strip to that of a uniform strip of identical thickness at the support is expressible in terms of the taper ratio alone, as follows:

$$\frac{\delta \text{ tapered strip}}{\delta \text{ uniform strip}} = \frac{2}{(1-R_t)}\left\{1 - \frac{R_t}{1-R_t}\ln\frac{1}{R_t}\right\} \tag{9}$$

and this expression may be treated as a correction to be applied to the conven-

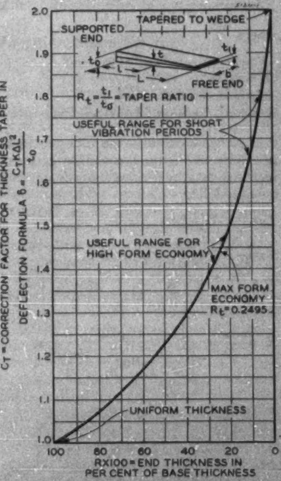

Figure 1. Deflection characteristics of flat bimetal strips having uniformly tapered thickness

Supported rigidly at thick end

Paper 45-120, recommended by the AIEE committee on electric machinery for publication in AIEE TRANSACTIONS. Manuscript submitted March 22, 1945; made available for printing May 21, 1945.

WILLIAM B. ELMER is section engineer, engineering department, lighting division, Westinghouse Electric Corporation, Cleveland, Ohio.

tional formula for bimetal deflections when the deflection of any tapered-thickness bimetal strip is to be found. This correction will be designated C_T and may be conveniently represented graphically, as in Figure 1. The conventional formula for the deflection of a bimetal strip may now be generalized as follows:

$$\delta = \frac{C_T K \Delta L^2}{t_0} \tag{10}$$

where C_T is a form factor for the strip and is obtainable directly from Figure 1. From this figure it is found that the deflection of any flat bimetal strip is exactly doubled if the strip is uniformly tapered to zero thickness at the free end. The width evidently does not enter into this relation.

Force Characteristics

Consider the general case of a flat bimetal strip rigidly supported at one end, of a negligible weight, and loaded as a cantilever beam, at the free end by a concentrated load. If the strip is nontapered as well as flat and of uniform width, the following conventional formulas are readily available from handbooks.

Uniform-Thickness Strips:

$$\text{Deflection} = \delta = \frac{4FL^3}{Eb_0t_0^3} = \frac{FL^3}{K^1b_0t_0^3} \tag{11}$$

$$\text{Force} = F = \frac{Eb_0t_0^3\delta}{4L^3} = \frac{K^1b_0t_0^3\delta}{L^3} \tag{12}$$

$$\text{Stiffness} = \frac{F}{\delta} = \frac{Eb_0t_0^3}{4L^3} = \frac{K^1b_0t_0^3}{L^3} \tag{13}$$

where

F = concentrated load at free end
b_0 = width
E = modulus of elasticity
K^1 = force constant for bimetal composition

If we now consider the tapered-thickness strip of Figure 1, a similar group of formulas may be derived by ordinary calculus as follows:

Tapered-Thickness Strips:

$$\delta = \frac{FL^3}{K^1b_0t_0^3} \cdot \frac{3}{(1-R_t)^2} \times \left[\frac{1}{(1-R_t)} \ln \frac{1}{R_t} - \frac{(3-R_t)}{2}\right] \tag{14}$$

$$F = \frac{K^1b_0t_0^3\delta}{L^3} \cdot \frac{(1-R_t)^2}{3\left[\frac{1}{(1-R_t)} \ln \frac{1}{R_t} - \frac{(3-R_t)}{2}\right]} \tag{15}$$

$$\frac{F}{\delta} = \frac{K^1b_0t_0^3}{L^3} \cdot \frac{(1-R_t)^2}{3\left[\frac{1}{(1-R_t)} \ln \frac{1}{R_t} - \frac{(3-R_t)}{2}\right]} \tag{16}$$

Here again the effect of tapering the thickness of the strip can be expressed as a correction C_{Ft} expressed in terms of R_t, which may be applied to equations 14, 15, and 16, resulting in generalized equations as follows:

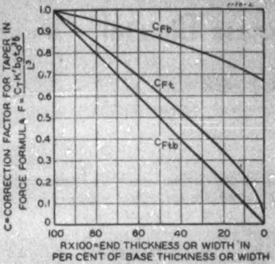

Figure 2. Force characteristics of flat bimetal strips having uniformly tapered dimensions and supported rigidly at thick end: cantilever load on free end

C_{Ft}—Thickness taper
C_{Fb}—Width taper
C_{Ftb}—Equal thickness and width taper combined

$$\delta = \frac{FL^3}{C_{Ft}K^1b_0t_0^3} \tag{17}$$

$$F = \frac{C_{Ft}K^1b_0t_0^3\delta}{L^3} \tag{18}$$

$$\frac{F}{\delta} = \frac{C_{Ft}K^1b_0t_0^3}{L^3} \tag{19}$$

where

$$C_{Ft} = \frac{(1-R_t)^2}{3\left[\frac{1}{(1-R_t)} \ln \frac{1}{R_t} - \frac{(3-R_t)}{2}\right]} \tag{20}$$

Specific values of C_{Ft} for any taper ratio may be obtained conveniently from a plot of this expression as given in Figure 2. The conventional bimetal force formulas therefore may be used for tapered bimetals provided the appropriate correction factors from Figure 2 are applied to the values.

For comparative purposes, similar expressions and curves have been derived for the cases of width-tapered bimetal strips of uniform thickness, and bimetal strips tapering in both width and thickness.

C_{Fb}(width tapered only)

$$= \frac{(1-R_b)^2}{3\left[\frac{R_b^2}{(1-R_b)} \ln \frac{1}{R_b} - \frac{3R_b-1}{2}\right]} \tag{21}$$

$$C_{Ftb}(\text{equal dual taper}) = R_t = R_b \tag{22}$$

where

R_b = width–taper ratio $= \frac{b_1}{b_0}$
b_1 = width of strip at free end

Economy

In judging the relative merits of different tapered forms of thermostatic bimetal members, it will be useful to determine the amount of work performed per unit weight of each taper form under comparable conditions. From such values a criterion will be established and called the "form-economy" characteristic of the shape. This criterion will be defined as the ratio of the work obtainable from a bimetal piece of a specified form to the work obtainable from a piece of flat bimetal of uniform cross section and of equal total weight.

Form economy will be indicated by the symbol ϵ, and for the flat reference standard under this definition ϵ is taken as unity and may be expressed more formally as follows:

$\epsilon = 1.00 =$ constant × work required to restore free end of flat strip of uniform section to original position after deflection due to unit temperature change ÷ weight of bimetal strip

= (constant × $^1/_2$ × unloaded thermostatic deflection × force to restore bimetal end by amount of thermostatic deflection) ÷ (volume of bimetal × density of bimetal)

$$= \frac{k_f \times {}^1/_2 \times \frac{K\Delta L^2}{t_0} \times \frac{K^1b_0t_0^3\delta}{L^3}}{b_0t_0L \times W} \tag{23}$$

Since by equation 1,

$$\delta = \frac{K\Delta L^2}{t_0}$$

$$\epsilon = 1.00 = \frac{k_f \times {}^1/_2 \times \left(\frac{K\Delta L^2}{t_0}\right)^2 \times \frac{K^1b_0t_0^3}{L^3}}{b_0t_0L \times W} \tag{24}$$

$$= \frac{k_f K^2 K^1 \Delta^2}{2w} \tag{24a}$$

and

$$k_f = \frac{2w}{K^2K^1\Delta^2} \tag{25}$$

For a tapered bimetal, the form economy will be

$$\epsilon = \frac{\frac{2w}{K^2K^1\Delta^2} \times {}^1/_2 \times \left(\frac{C_T K \Delta L^2}{t_0}\right)^2 \times \frac{C_F K^1 b_0 t_0^3}{L^3}}{\text{volume} \times W} \tag{26}$$

or

$$\epsilon = \frac{C_T^2 C_F L b_0 t_0}{\text{volume}} \tag{26a}$$

But volume can be expressed in terms of b_0, t_0, and L, and the taper ratio R, for example:

Volume (tapered thickness, parallel edges)

$$= b_0t_0L\left(\frac{1+R_t}{2}\right) \tag{27}$$

Volume (uniform thickness, tapered edges),

$$= b_0t_0L\left(\frac{1+R_b}{2}\right) \tag{28}$$

Volume (tapered thickness, tapered edges $[R_b = R_t = R_{tb}]$)

$$= b_0t_0L\left(\frac{1+R_{bt}+R_{bt}^2}{3}\right) \tag{29}$$

Consequently, from equation 26a,

ϵ_t(tapered thickness, parallel edges)

$$= \frac{2C_T^3C_{Ft}}{(1+R_t)} \qquad (30)$$

ϵ_b(uniform thickness, tapered edges)

$$= \frac{2C_{Fb}}{(1+R_b)} \qquad (31)$$

ϵ_{tb}(tapered thickness, tapered edges $[R_b = R_t]$)

$$= \frac{3C_T^3}{1+R_{bt}+\dfrac{1}{R_{bt}}} \qquad (32)$$

The form economy of the foregoing shapes has been evaluated for various values of taper ratio and the results plotted in Figure 3. Maximum values of form economy and corresponding taper ratios were determined by calculus. These maxima occur as given in Table I. From an inspection of these values, it is evident that for flat bimetal strips of the taper forms studied, the most economical in point of work performed per unit weight is the conventional bimetal sheet of uniform thickness, and having the side edges tapering to a point at the free end. Unfortunately, however, this form seldom can be utilized in any practical thermostatic construction, as it is always necessary to make the free end of the bimetal strip physically wide enough to carry an electric contact or to actuate a co-operating working member. For any value of width-taper ratio of more than 0.1, which generally is below a usable minimum, the form economy is seen to have fallen off to approximately less than that for the thickness-tapered bimetal, and the latter form would take preference.

Maximum form economies for the thickness-tapered bimetals appear in the taper-ratio region between $R = 0.2$ to 0.3. In this region the metal will perform approximately one-third more work than it would if shaped as a conventional uniformly thick strip. If the bimetal can be produced at costs appreciably less than 130 per cent of the cost of flat bimetal stock, then the tapered-thickness bimetal construction becomes the most economical form for general flat-strip applications. Actual costs of the tapering process are said to be negligible compared to the gain in performance.

Fortunately, a thickness-tapered bimetal strip of maximum form economy will have a free-end thickness lying between one fourth to one fifth of the base thickness, which usually will be quite adequate mechanically for mounting of electric contacts. This form, therefore, can be recognized as a new and very useful embodiment of the bimetallic thermostatic strip.

Table I. Maximum Form Economy and Taper Ratio for Several Taper Forms

Form	ϵ_{Max}	Taper Ratio for ϵ_{Max}
Tapered thickness Uniform width	1.304	0.2495
Uniform thickness Tapered width	1.333	0.000
Tapered thickness Tapered width ($R_t = R_b$)	1.206	0.435

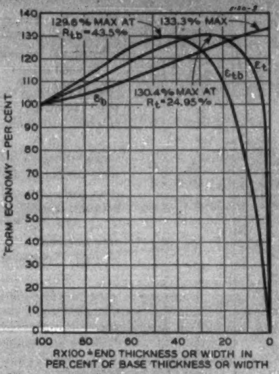

Figure 3. Form economy of flat bimetal strips of various taper forms

ϵ_t—Thickness taper

ϵ_b—Width taper

ϵ_{tb}—Equal thickness and width taper combined

It will be noticed that the dual-tapered form yields a form economy nearly equal to that for the tapered-thickness strip if a taper ratio of somewhat less than 0.5 is used for the former. This form is rendered uneconomical, however, by the practical consideration that cutting of width-tapered strips from thickness-tapered stock would produce an appreciable quantity of scrap, rendering the high economy unrealizable.

In order to visualize better the manner in which the tapered-thickness form improves the form economy of the bimetal, Figure 4 has been prepared. In this figure, a flat bimetal strip has been subjected to a progressive alteration of form consisting in a shift of the angle between faces over the range from parallelism to wedge form. The total quantity of metal, as well as all other factors, has been held constant during this metamorphosis in order to show precisely how the properties of the strip are modified by the change. Figure 4 reveals that the deflection decreases during the transformation until a taper ratio of 22.35 per cent is reached, at which point the deflection is 89.65 per cent that of the original flat strip. Beyond this point the deflection again increases until the full original value is regained at the point where the strip reaches wedge form. The base thickness evidently is doubled at this time. During this transformation the stiffness of the member increased much more rapidly, however, reaching 161.7 per cent of the stiffness of the flat strip at $R = 23.92$ per cent. The net result is an increase in form economy to a maximum of 130.4 per cent at $R = 24.95$ per cent, which confirms this finding from Figure 3.

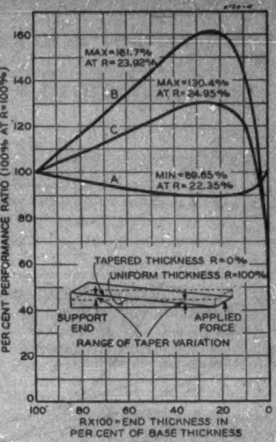

Figure 4. Variation in bimetal-strip characteristics with change in thickness taper

Volume, width, and length held constant

A—Deflection

B—Stiffness

C—Form economy

Vibration Characteristics

In slow-acting bimetal thermostatic controls considerable trouble may be encountered at the moment of make or break of the electric control circuit, especially if the rate of temperature change is very slow, because of vibrations of the bimetal strip. Such vibrations produce chattering of the contacts and consequent disturbances in the controlled system. It has been found that such disturbances can be prevented if the bimetal member be so designed that its natural frequency is higher than that of the components of the controlled system. Single or dual tapers of the bimetal strip have been found sufficient in some instances to eliminate completely such vibration troubles and to render the slow-acting thermostat construction entirely satisfactory for the stable control of relays. Small telephone-type relays which formerly chattered severely when controlled by conventional flat-strip thermostats with heavy silver contacts, were found to close slowly and remain closed when the bimetal strip was tapered in width and thickness and the contact reduced in weight. Elimination of thickness taper only restored the chattering condition.

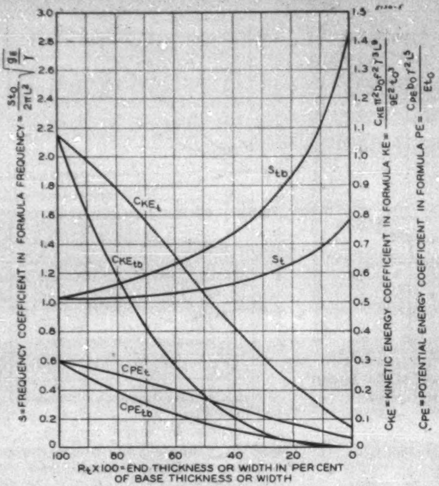

Figure 5. Energy and frequency characteristics of tapered bimetal strips

C_{KE_t} = kinetic-energy coefficient for tapered-thickness strip

$C_{KE_{tb}}$ = kinetic-energy coefficient for strip of tapered thickness and width

C_{PE_t} = potential-energy coefficient for tapered-thickness strip

$C_{PE_{tb}}$ = potential-energy coefficient for strip of tapered thickness and width

S_t = frequency coefficient for tapered thickness strip

S_{tb} = frequency coefficient for strip of tapered thickness and width

An analysis of the natural frequencies of tapered bimetal strips has been made, to determine the vibration characteristics as a function of form. The frequencies (fundamental only) were calculated for plain flat strips of various tapers, with rigid support at the base assumed and zero mass carried by the free vibrating end. If the contact actually carried by the end of such a tapered strip in practice is light in weight compared to the weight of the strip, the contact weight will have slight effect on the frequency of the strip, and the results of the present analysis will be applicable. If the contact is made large and heavy, its weight will predominate in the determination of frequency, and tapering of the supporting strip will be defeated.

The frequencies were here determined by the method of Rayleigh in which the potential and kinetic energies of the vibrating strip are equated. The results are believed accurate to within 0.5 to 1.5 per cent. An exact mathematical determination would be difficult and very laborious and will not be attempted as the accuracy of the present method is entirely adequate.

The steps in computation of the natural frequencies are given in Table II for three flat-strip forms; the conventional strip of uniform thickness, the thickness-tapered wedge and the pyramidal or dual taper.

Expressions similar to those given in Table II also were derived for the more general case of bimetal strips of taper R_t or R_{tb}. These expressions yield the values given in Table II, columns 1 and 2, when values of R_t = 100 per cent and R_t = 0 per cent, respectively, are substituted. The complete expressions are given in Appendix I. The coefficients for the expressions for natural frequency for all ratios are plotted in Figure 5.

The curves of frequency-versus-taper ratio show the wedge form to vibrate about 50 per cent faster than a strip of uniform thickness. For a usable and economical strip of taper ratio 0.25, the increase in frequency over that of a flat strip is only about 20 per cent. Consequently, where high frequency of the strip is the predominant design consideration, thickness tapering alone is only slightly effective.

Figure 5 similarly shows the dual wedge or pyramid to have a theoretical maximum increase in frequency to over $2\tfrac{1}{2}$ times the value for strips of uniform thickness and width. For practically usable strips, increases to 200 to 220 per-cent frequency probably cannot be exceeded. In those cases, however, in which suppression of vibration troubles is of much greater importance than economy of material, the dual taper is of considerable practical value.

It is interesting to note that thermostatic deflection and period of vibration are governed by the same dimensional parameters, L^2/t_0. Because of this fact, short vibration periods cannot be obtained by modifying the physical proportions of any type of strip when a specified thermostatic deflection is required. Change of shape appears to be the most convenient means of obtaining independent frequency adjustment of the thermostatic strip.

Appendix I

Frequency of Tapered-Thickness Strips

$$\text{Thickness } t=t_0\left[(1-R_t)\frac{(L-l)}{L}+R_t\right] \quad (33)$$

$$\text{Bending moment}=\frac{\gamma b_0t_0}{2}(L-l)^2\times\left[\frac{(1-R_t)(L-l)}{3L}+R_t\right] \quad (34)$$

Table II. Natural Frequencies of Flat Bimetal Strips

Fundamentals Only

Form	Uniform Thickness	Wedge	Pyramid
Moment of inertia	$\frac{b_0t_0^3}{12}$	$\frac{b_0t_0^3(L-l)^3}{12L^3}$	$\frac{b_0t_0^3(L-l)^4}{12L^4}$
Bending moment	$\frac{\gamma b_0t_0(L-l)^2}{2}$	$\frac{\gamma b_0t_0(L-l)^3}{6L}$	$\frac{\gamma b_0t_0(L-l)^4}{12L^2}$
Deflection of strip under its own weight	$\frac{6\gamma}{Et_0^2}\left(\frac{L^2l^2}{2}-\frac{Ll^3}{3}+\frac{l^4}{12}\right)$	$\frac{\gamma L^2l^2}{Et_0^2}$	$\frac{\gamma L^2l^2}{2Et_0^2}$
Maximum velocity at any point if free end is released from rest under its own weight	$\frac{12\pi f\gamma}{Et_0^2}\left(\frac{L^2l^2}{2}-\frac{Ll^3}{3}+\frac{l^4}{12}\right)$	$\frac{2\pi f\gamma L^2l^2}{Et_0^2}$	$\frac{\pi f\gamma L^2l^2}{Et_0^2}$
Kinetic energy under maximum velocity	$\frac{1.1556\pi^2b_0f^2\gamma^3L^9}{gE^2t_0^3}$	$\frac{0.0666\pi^2b_0f^2\gamma^3L^9}{gE^2t_0^3}$	$\frac{0.00476\pi^2b_0f^2\gamma^3L^9}{gE^2t_0^3}$
Potential-energy change	$\frac{0.3b_0\gamma^2L^5}{Et_0}$	$\frac{0.04166b_0\gamma^2L^5}{Et_0}$	$\frac{0.00833b_0\gamma^2L^5}{Et_0}$
Frequency from $KE=PE$	$\frac{1.02t_0}{2\pi L^2}\sqrt{\frac{gE}{\gamma}}$	$\frac{1.58t_0}{2\pi L^2}\sqrt{\frac{gE}{\gamma}}$	$\frac{2.646t_0}{2\pi L^2}\sqrt{\frac{gE}{\gamma}}$

where

γ = density of material
f = natural frequency of strip
g = acceleration of gravity

Moment of inertia

$$=\frac{b_0t_0^3}{12}\left[(1-R_t)\frac{(L-1)}{L}+R_t\right]^3 \qquad (35)$$

Deflection of strip under its own weight

$$=\frac{2\gamma L^4}{Et_0^2}\left[\frac{l^2}{2(1-R_t)^2}+\frac{LR_t^2(3-R_t)l}{(1-R_t)^3}+\frac{3L^2R_t^2}{(1-R_t)^4}\ln\frac{L-(1-R_t)l}{L}+\frac{L^2R_t^2l}{(1-R_t)^3[L-(1-R_t)l]}\right] \qquad (36)$$

Kinetic energy

$$=\frac{\pi^2b_0f^2\gamma^2L^9}{gE^2t_0^3(1-R_t)^9}\left[(16R^8-96R^7+98R^6-16R^5+12R^4)\ln\frac{1}{R_t}-36R_t^6\left(\ln\frac{1}{R_t}\right)^2-2R_t^{10}+22.66R_t^9-86.266R_t^8+124.8R_t^7-67.5R_t^6+18.933R_t^5-13R_t^4+4.266R_t^3-1.966R_t^2+0.0666\right] \qquad (37)$$

Potential-energy change

$$=\frac{b_0\gamma^2L^5}{Et_0(1-R_t)^6}\left[\frac{3}{2}R_t^4\ln\frac{1}{R_t}-\frac{R_t^6}{3}+2R_t^5-\frac{15}{8}R_t^4+\frac{2}{3}R_t^3-\frac{R_t^2}{2}+\frac{1}{24}\right] \qquad (38)$$

Frequency was found for values of R_t by equating kinetic and potential energies.

Frequency of Dual-Tapered Strips

$$\text{Thickness}=t_0\left[(1-R_{bt})\frac{(L-l)}{L}+R_{bt}\right] \qquad (39)$$

$$\text{Width}=b_0\left[(1-R_{bt})\frac{(L-l)}{L}+R_{bt}\right] \qquad (40)$$

Bending moment

$$=\frac{\gamma b_0t_0L^2}{12(1-R_{bt})^2}\left\{\left[(1-R_{bt})\frac{(L-l)}{L}+R_{bt}\right]^4-R_{bt}^3\left[\frac{4(1-R_{bt})(L-l)}{L}+R_{bt}\right]\right\} \qquad (41)$$

Moment of inertia

$$=\frac{b_0t_0^3}{12}\left[(1-R_{bt})\frac{(L-l)}{L}+R_{bt}\right]^4 \qquad (42)$$

Deflection of strip under its own weight

$$=\frac{\gamma L^4}{Et_0(1-R_{bt})^4}\left[\frac{u^2}{2}-\frac{2R_{bt}^3}{u}+\frac{R_{bt}^4}{2u^2}-(1+2R_{bt}^3-R_{bt}^4)u+\frac{1}{2}+4R_{bt}^3-\frac{3R_{bt}^4}{2}\right] \qquad (43)$$

where

$$u=1-(1-R_{bt})\frac{1}{L}$$

Kinetic energy

$$=\frac{\pi^2b_0f^2\gamma^2L^9}{gE^2t_0^3(1-R_{bt})^9}\left[4R_{bt}^7\ln R_{bt}-\frac{2R_{bt}^{13}}{5}+\frac{31R_{bt}^{12}}{10}-\frac{101R_{bt}^{11}}{10}+\frac{52R_{bt}^{10}}{3}-\frac{224R_{bt}^9}{15}+\frac{7R_{bt}^8}{10}+\frac{204R_{bt}^7}{35}-\frac{12R_{bt}^6}{5}+\frac{2R_{bt}^5}{5}+\frac{23R_{bt}^4}{30}-\frac{3R_{bt}^3}{10}+\frac{1}{210}\right] \qquad (44)$$

Potential-energy change

$$=\frac{b_0\gamma^2L^5}{Et_0(1-R_{bt})^6}\left[-\frac{R_{bt}^8}{8}+\frac{R_{bt}^7}{2}-\frac{2R_{bt}^6}{3}+\frac{R_{bt}^5}{5}+\frac{R_{bt}^4}{4}-\frac{R_{bt}^3}{6}+\frac{1}{120}\right] \qquad (45)$$

Frequency was similarly determined from the energy expressions.

In all cases the foregoing general equations are reducible to the specific cases for $R=0$ and $R=1$ as given in Table II in the body of this paper. In order to accomplish such reductions it is usually necessary to apply L'Hopital's theorem for the evaluation of indeterminate forms. In the case of the expressions for kinetic energy it was necessary to perform nine successive differentiations.

Response Time and Lag of a Thermometer Element Mounted in a Protecting Case

W. N. GOODWIN, JR.
FELLOW AIEE

Synopsis: In this paper equations are derived and applied for determining the response time and temperature lag, in general, of a body which exchanges heat with a medium indirectly through a second body. Application is made to a thermometer element mounted in a protecting case, with specific reference to a resistance-type thermometer such as is used for aircraft and marine purposes. The temperature distribution along the stem and the errors resulting when the head of the bulb and medium differ in temperature also are derived.

IN THE DESIGN of many forms of thermometers it is frequently customary and often necessary to mount the active element within a protecting case. This is particularly true in the case of resistance and bimetal types and often true with the thermocouple and ordinary mercury types.

When protecting cases are used, the active element is not in direct contact with the surrounding medium, the temperature of which is to be measured, but its exchange of heat, in acquiring the temperature of the medium, must take place through the protecting case and through the thermal contact between the element and case.

Under the conditions referred to, there is an additional time lag in the indications of the thermometer element over that which would result if the element were in direct contact with the medium, when the temperature of the latter differs from it or changes with time.

The object of this analysis is to determine the equations of the cooling and heating curves of an element contained in a protecting case, from which design data and operating characteristics can be determined for specified conditions. Part of this analysis was done in 1921 and completed and applied practically during recent years.

Application to a Resistance-Type Thermometer

To make the analysis of this problem of more practical use, we will direct our attention to a specific device by considering a resistance-type thermometer bulb developed by an associate of the author, K. M. Lederer. This is illustrated in Figure 1, cut away to show the construction. The analysis, however, is perfectly general and applies to any object exchanging heat with a surrounding medium indirectly, through another body in direct contact with the medium.

In this part of the paper the final equations and their applications are given. The complete derivations, however, are given in the appendixes.

The thermometer element m in Figure 1 consists of a wire resistor wound on a thin-walled tube and electrically insulated from it. This tube is contained in a protecting tube M and is in good thermal contact with it.

The protecting tube containing the resistor element is secured to the head B through which the connections to the resistor element pass to the indicating instrument.

In the derivation of the equations the following quantities appear, MS/h_1, $ms+h_2$, and ms/h_1; in which M and m are the masses, S and s the specific heats of the protecting tube and thermometer element, respectively, and h_1 and h_2 the rates of heat transfer per degree difference in temperature, from the protecting tube to the surrounding medium, and from the thermometer element to the protecting tube, respectively, all corresponding to the heat-exchange area. The definitions of these and other symbols are given in the list of symbols. These

---

Paper 45-133, recommended by the AIEE committee on instruments and measurements for publication in AIEE TRANSACTIONS. Manuscript submitted April 9, 1945; made available for printing May 16, 1945.

W. N. GOODWIN, JR., is vice-president in charge of research and engineering, Weston Electrical Instrument Corporation, Newark, N. J.

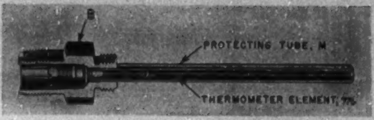

Figure 1. Resistance-type-thermometer bulb, cut away to show internal construction

have the dimensions of time, which we will designate as t_1, t_2 and t_m, respectively, where $t_1 = MS/h_1$ is the time constant of the protecting tube relative to the surrounding medium, $t_2 = ms/h_2$ is the time constant of the resistor element relative to the protecting tube, and t_m is the mutual time constant ms/h_1 of the resistance element relative to the surrounding medium acting through the protecting case. That is, it is the time constant the inner tube would have if its heat were exchanged with the surrounding medium from the surface of the protecting tube.

Physically considered, the time constant is the time required for the body to change one degree in temperature, for the specified rate of heat exchange, if the temperature difference is maintained at one degree.

Thermometer Transferred From a Hotter to a Cooler Medium

If the thermometer bulb, having its resistor element and protecting tube both initially at the temperature θ_0 is suddenly immersed in the cooling medium at a temperature T_c, then the ratio of the temperature elevation $(\theta - T_c)$ of the element above that of the cooling medium at any time t, to the initial elevation $(\theta_0 - T_c)$, is, as shown in Appendix I,

$$\frac{\theta - T_c}{\theta_0 - T_c} = \frac{1}{P} e^{-\left[\left(\frac{t}{t_0}\right)\sqrt{P^2+1}\right]} \times \sinh\left[P\left(\frac{t}{t_0}\right) + \sinh^{-1} P\right] \quad (1)$$

where

$$P = \sqrt{\frac{(t_1 + t_2 + t_m)^2}{4t_0^2} - 1}$$

and

$$t_0 = \sqrt{t_1 t_2}$$

Thermometer Transferred From a Cooler to a Hotter Medium

If the initial temperature θ_0 of the thermometer element is lower than that of the surrounding medium T_c, then the resulting heating curve is exactly similar to the cooling curve previously given, except that it is reversed as shown in Figure 3 in accordance with the following equation, as shown in Appendix II,

$$\frac{\theta - \theta_0}{T_c - \theta_0} = 1 - \frac{1}{P} e^{-\left[\left(\frac{t}{t_0}\right)\sqrt{P^2+1}\right]} \times \sinh\left[P\left(\frac{t}{t_0}\right) + \sinh^{-1} P\right] \quad (2)$$

To apply these equations to a practical device, let us consider the resistance-thermometer bulb cooled in various media for which the constants given in Table I have been determined experimentally. As the inner and protecting tubes are actually in contact in this case, it is convenient to use values for M, m, h_1, and h_2 per square centimeter of contact area.

Cooling curves derived from this equation for the tabulated values for P and t_0 are shown in Figure 2. As an example, assume that a bulb is heated to 100 degrees centigrade and suddenly plunged into ice water at zero degrees centigrade, it will fall to ten degrees centigrade in 8.3 seconds.

The curves in Figure 2 are based upon the time t as the independent variable. If t/t_0 is made the independent variable, the curves become more general and will apply to devices of any time constant, consistent with the value of P. Such a family of curves is shown in Figure 3, which for the resistance-type thermometer, range from water to still-air cooling.

Mechanical Analogy

The temperature equations previously given have the same form as that for an aperiodic mechanical motion derived by the author in about the year 1908, namely:

$$\frac{\theta}{\phi} = \frac{1}{\sqrt{n^2-1}} e^{-2\pi n\left(\frac{t}{T_0}\right)} \times \sinh\left[2\pi\sqrt{n^2-1}\left(\frac{t}{T_0}\right) + \sinh^{-1}\sqrt{n^2-1}\right] \quad (3)$$

in which, when applied to a spring-controlled damped instrument, for example, ϕ is the initial deflection, θ the deflection after a time t given in terms of a time constant T_0 which is the undamped period, and n the ratio of the actual to the critical damping coefficient, designated by the author as the specific damping coefficient.

When the constants in equations 1 and 2 are equated to those given in equation 3, it will be found that n corresponds to $\sqrt{P^2+1}$, and T_0 to $2\pi t_0$.

If, therefore, a permanent-magnet movable-coil-type instrument has an undamped period of $T_0 = 2\pi t_0$ seconds and is damped to an amount such that $n = \sqrt{P^2+1}$, then the motion of the pointer toward zero, as a function of time, will follow the same curve as the thermal system having the constants t_0 and P.

Temperature Lag

When a thermometer is used to measure the temperature of a medium, which is changing in temperature, the indication of the thermometer lags behind the temperature of the medium as a result of the heat capacity of the thermometer and the thermal resistance to the exchange of heat between the medium and the thermometer element. An example of this condition occurs when measurements are made of the surrounding air from an airplane which is changing its altitude. Assume that a thermometer has initially the same temperature as the surrounding medium. Then let the temperature of the medium change at a constant rate of r degrees per second. The indication of the thermometer will start to follow, relatively slowly at first, but, as the difference in temperature or lag increases, the change in indication of the thermometer increases its rate until finally it approaches the same rate r as that of the change in temperature of the medium. This final difference in temperature then is maintained and is the maximum value of the lag.

The value of the lag in indication for a thermometer element in a protecting case, for an increasing temperature, relative to the final lag, at any time t after the initial change, as shown in Appendix III, is

$$\frac{T_a - \theta}{L} = 1 - \frac{1}{2P\sqrt{P^2+1}} e^{-\left[\left(\frac{t}{t_0}\right)\sqrt{P^2+1}\right]} \times \sinh\left[P\left(\frac{t}{t_0}\right) + \sinh^{-1} 2P\sqrt{P^2+1}\right] \quad (4)$$

where L is the final and maximum value of the lag, and is

$$L = 2rt_0\sqrt{P^2+1} = r(t_1 + t_2 + t_m) \text{ degrees} \quad (5)$$

and r is the rate of change in temperature in degrees per second, which is positive for increasing and negative for decreasing temperatures.

This shows that the lag is a simple function of the three time constants of the thermometer bulb or other device.

For a falling temperature, the lag equation is the same as equation 4 except that r becomes negative and therefore L is negative, and the left-hand member becomes $(\theta - T_a)/L$, whereas the right-hand member is unchanged.

Figure 4 gives curves showing the increase of lag with time, for various values of time constants as represented by P, in terms of time as a function of the time constant t_0 of the thermometer bulb or other device.

The ranges in values of P illustrated are perfectly general, but as applied to a resistance-type thermometer they cover ambient media from water to still air.

As a specific example, let us determine the temperature lag of the resistance thermometer previously referred to, for which $P = 0.780$, and $t_0 = 3.32$ seconds when immersed in air moving at a speed of 50 miles per hour. Assume, for example, that the air is changing in temperature at a rate of five degrees centigrade per minute = (1/12) degree per second; then the maximum lag is, from equation 5,

$$L = 2\times(1/12)\times 3.32\times\sqrt{(0.780)^2+1}$$
$$= 0.702 \text{ degree centigrade}$$

The time for the lag to attain any fractional part of its final value can be determined from the curves in Figure 4 derived from equation 4. By interpolating between curves for $P=0.5$ and $P=1$, for $P=0.780$, we find that the time for the lag to reach, for example 90 per cent of its maximum value, is approximately $5.2\times t_0 = 5.2\times 3.32 = 17.3$ seconds.

The same curves may be used for both increasing and decreasing temperatures.

Errors Resulting If Head of Bulb and Stem Differ in Temperature, Under Static Conditions

Let us assume that the bulb is screwed into the walls of a tank containing a material the temperature of which is to be measured and that the tank and therefore the head of the bulb have a temperature differing from that of the material. We shall determine the temperature at any point along the stem and also determine the error by computing the average deviation of the stem temperature from that of the material contained in the tank.

In Figure 5 the sketch in solid lines shows the bulb screwed into the walls of a tank. Assume that the head of the bulb is at a temperature T_h, and that of the material in the tank T_c. The dotted-line portion is referred to later.

In a previous paper[1] by the author, equations are given for the temperature distribution along a conductor connected at its ends to terminals, as a function of the terminal temperatures, the ambient temperature, and the heat generated in the conductor.

If the two terminals have the same temperature, then the conductor and its terminals are symmetrical with respect to the center of the conductor. The stem of the thermometer bulb, therefore, can be considered as one half of a symmetrical conductor with terminals, the other half being shown in dotted lines in Figure 5. From symmetry it is obvious that the two halves may be considered as entirely independent, as no heat passes the mid-point of the conductor, and exactly similar but opposite heat flows and temperature distribution occur in the two sides.

Table I. Thermal Constants of a Resistance-Type Thermometer

Object	Quantity*	Medium: Water	Medium: Still Air	Medium: Air at 50 Miles Per Hour
Protecting Case				
$M=0.295$	h_1	0.109	0.00151	0.0306
$S=0.529$	t_1	1.432	100.0	5.10
Thermometer Element	h_2	0.0164	0.0164	0.0164
$M=0.0384$	t_2	2.16	2.16	2.16
$s=0.916$	t_m	0.326	22.5	1.16
Derived	P	0.491	4.12	0.780
Constants	t_0	1.76	14.7	3.32

* h_1, h_2, watts per square centimeter per degree centigrade; t_1, t_2, t_0, t_m, seconds; M, m, grams per square centimeter; S, s, joules per gram per degree centigrade; P, numeric.

Therefore, the same equations apply to the half conductor that would apply if the conductor were completed by its image shown dotted.

After modifying the general equation given in the paper referred to, to meet the conditions of the present problem, assuming that no heat is generated in the bulb itself, we have, from the reference paper:

$$\frac{\theta_x - T_c}{T_h - T_c} = \frac{\sinh\,(2l-x)\sqrt{\frac{cp}{ak}} + \sinh x\sqrt{\frac{cp}{ak}}}{\sinh 2l\sqrt{\frac{cp}{ak}}} \tag{6}$$

where

T_h, T_c, and θ_x = temperatures of the head, of the surrounding medium, and of the stem at any point x, respectively

cp = heat loss per second per unit length of stem per one degree difference in temperature between stem and medium

a = cross-sectional area of tube

k = thermal conductivity of tube material

l = the length of the stem

Expanding the numerator, simplifying, and for ease in handling the equation express x in terms of l, letting $x = yl$, and we have

$$\frac{\theta_y - T_c}{T_h - T_c} = \frac{\cosh\left[(1-y)l\sqrt{\frac{cp}{ak}}\right]}{\cosh l\sqrt{\frac{cp}{ak}}} \tag{7}$$

This gives the temperature at any point along the stem above that of the surrounding medium relative to the corresponding elevation in temperature of the head of the bulb above the temperature of the medium.

At the end of the tube, where $y=1$, this reduces to

$$\frac{\theta_y - T_c}{T_h - T_c} = \frac{1}{\cosh\left[l\sqrt{\frac{cp}{ak}}\right]} \tag{8}$$

In a resistance-thermometer bulb, for example, the constants, experimentally determined are as follows:

The convection rate in watts per centimeter length of tube per one degree centigrade, for still air, $cp=0.0032$; for air moving at 50 miles per hour $cp=0.0612$; and for water $cp=0.218$.

Then, $l\sqrt{cp/ak}$ for still air is 5.45; for air moving at 50 miles per hour, 16.75; and for water, 44.7; in which $a=0.0706$ square centimeter; $k=0.2$ watt per centimeter cube per degree centigrade, $l=11.4$ centimeters, and diameter of tube = 0.635 centimeter.

If we substitute these constants in equation 7, and give y various values from 0 to 1, temperature-distribution curves for the resistance-type thermometer are obtained which are shown in Figure 6.

For the more general problem of any thermometer having a stem of uniform cross section, a family of curves is shown in Figure 7, giving the distribution of temperature along the stem, for various values of $l\sqrt{cp/ak}$, when the head of the thermometer and the medium differ in temperature. Values should be considered posi-

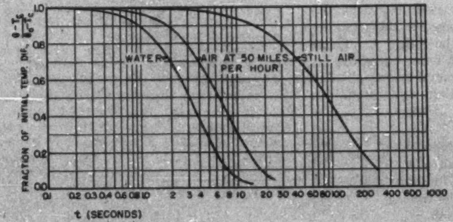

Figure 2. Cooling curves for resistance-type-thermometer bulb cooled in water, still air, and in air moving at 50 miles per hour

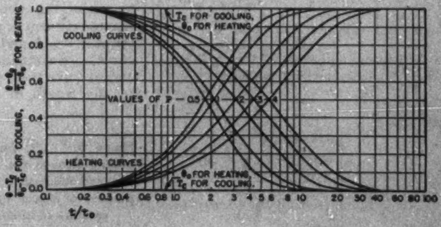

Figure 3. General cooling curves for a thermometer element in a protecting case in terms of its time constants

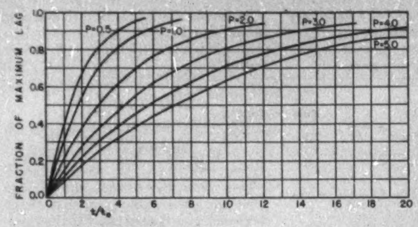

Figure 4. Temperature lag at any time, as a fraction of its maximum lag, of a thermometer in a protecting case, immersed in a medium changing in temperature at a constant rate, in terms of its time constants

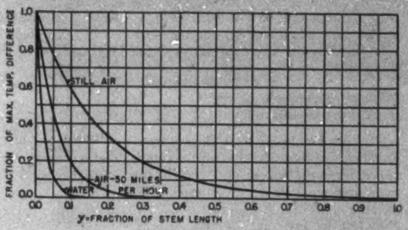

Figure 6. Distribution of temperature along a resistance-type-thermometer stem extending into a medium, as, for example, a thermometer inserted into a tank, when the head of the thermometer and the medium differ in temperature

Values are given as fractions of this difference in temperature

tive when the thermometer temperatures are higher than that of the medium, and negative when they are lower than that of the medium.

Errors

When the temperature of the head of the thermometer bulb differs from that of the medium being measured, then an error results. If a linear relationship between temperature and electrical resistance of the thermometer element throughout its length in the protecting tube is assumed, then the resistance change at any part of the tube is proportional to the change in temperature at that part of the tube. The total effect or error then, in terms of the difference in temperature (T_h-T_c) between the head and the medium, is the ratio of the average deviation in temperature throughout the active part of the stem from that of the medium, to the maximum temperature difference (T_h-T_c). Equation 7 gives the temperature at any point y, relative to the maximum temperature difference (T_h-T_c). Assume that the resistance element extends from the end of the stem to a point y. The average temperature then can be computed by dividing the area under the curve of temperature distribution for the active part of the stem by the length of this part of the stem as a function of y, that is by $(1-y)$. The average value is then

$$\left[\frac{\theta_y-T_c}{T_h-T_c}\right]_{\text{average}}=\frac{1}{1-y}\int_y^1\left(\frac{\theta_y-T_c}{T_h-T_c}\right)dy \qquad (9)$$

Substituting equation 7 for $(\theta_y-T_c)\div(T_h-T_c)$ in equation 9 we have

$$\left[\frac{\theta_y-T_c}{T_h-T_c}\right]_{\text{average}}=\frac{1}{1-y}\int_y^1\frac{\left[\cosh (1-y)l\sqrt{\frac{cp}{ak}}\right]dy}{\cosh l\sqrt{\frac{cp}{ak}}} \qquad (10)$$

Integrating this between the limits 1 and y and simplifying, we have

$$\left[\frac{\theta_y-T_c}{T_h-T_c}\right]_{\text{average}}=\frac{\sinh\left[(1-y)l\sqrt{\frac{cp}{ak}}\right]}{(1-y)l\sqrt{\frac{cp}{ak}}\cosh l\sqrt{\frac{cp}{ak}}} \qquad (11)$$

For example we shall use this equation to determine the errors in the resistance-thermometer bulb in which the resistance element extends from $y=0.17$ to $y=1$, and for which constants are already given.

For still air, by substituting $l\sqrt{op/ak}=5.45$ in equation 11, we have

$$\left[\frac{\theta_y-T_c}{T_h-T_c}\right]_{\text{average}}=\frac{\sinh[(1-0.17)\times 5.45]}{(1-0.17\times 5.45)\times\cosh 5.45}=0.0878$$

Then the error in degrees is $0.0878\times(T_h-T_c)$.

For air moving at 50 miles per hour, for which $l\sqrt{cp/ak}=16.75$ we find

$$\left[\frac{\theta_y-T_c}{T_h-T_c}\right]_{\text{average}}=\frac{\sinh[(1-0.17)\times 16.75]}{(1-0.17)\times 16.75\times\cosh 16.75}=0.00418$$

Then the error in degrees is $0.00418\times(T_h-T_c)$.

For water immersion the error is negligible as is evident by inspection of Figure 6.

Figure 8 shows a family of curves giving errors as a fraction of the difference in temperature (T_h-T_c) between the head of the bulb and the medium, for any length of resistor element relative to the length of the stem, assuming that the resistor element is placed in the stem between its end and the point y. These curves are computed from equation 11, and to make them general and applicable to any length or other dimensional or thermal constants they are given as a function of $l\sqrt{cp/ak}$.

List of Symbols

M = mass of the part of the protecting case which transfers heat from the thermometer element to the outside medium, grams

m = mass of thermometer element, grams

S = specific heat of material of protecting tube, watt-seconds per gram per degree centigrade

s = specific heat of material of thermometer element, watt-seconds per gram per degree centigrade

h_1 = rate of heat exchange of protecting case with outside medium, watts per degree centigrade

h_2 = rate of heat exchange of thermometer element with protecting case, watts per degree centigrade

$t_1 = MS/h_1$ = time constant of protecting case relative to outside medium, seconds

$t_2 = ms/h_2$ = time constant of thermometer element relative to protecting case, seconds

$t_m = ms/h_1$ = mutual time constant, seconds, the thermometer element would have if its exchange of heat with the external medium were effected from the surface of the protecting case

t = time, independent variable

P = for brevity $=\sqrt{\frac{(t_1+t_2+t_m)^2}{4t_0^2}-1}$, a numeric

$t_0=\sqrt{t_1t_2}$ seconds

θ = temperature of the thermometer element at any time t

Figure 5. A thermometer passing through the wall of a tank and attached to it, for the purpose of measuring the temperature of its contents

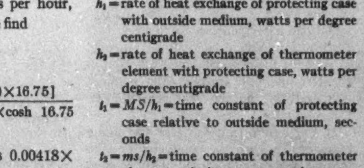

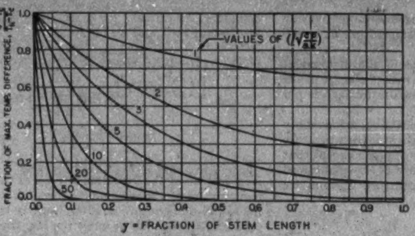

Figure 7. Temperature distribution along any thermometer stem of uniform cross section, immersed in a medium, when the temperature T_h of the thermometer head is higher than that of the medium T_c, given as a function of $l\sqrt{cp/ak}$

When T_h is lower than T_c, values are negative

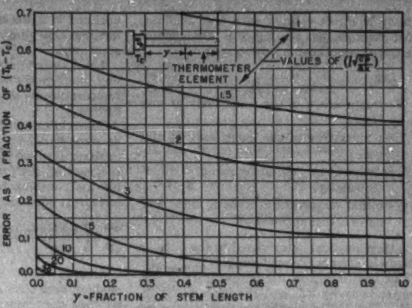

Figure 8. Errors of a resistance-type thermometer, with head at a temperature T_h and stem immersed in a medium at temperature T_c, when the resistance element extends inside the stem from its end to any position y, for various values of $l\sqrt{cp/ak}$, given as a function of y

θ_0 = initial temperature of the thermometer element and protecting tube

T = temperature of the protecting case at any time t

T_c = temperature of the surrounding medium when constant

T_a = temperature of the surrounding medium at any time t, when changing

θ_x = temperature of the thermometer stem above that of medium at any distance x from head

l = length of stem of thermometer, centimeters

a = cross-sectional area of thermometer stem, square centimeters

k = thermal conductivity in watts per centimeter cube per degree centigrade

cp = heat convection from tube to surrounding medium per second per unit length of tube, watts per degree centigrade

e = base of natural logarithms

Appendix I

This analysis considers the problem of the cooling of a body indirectly by a lower constant-temperature medium through a second body in direct contact with that medium, as for example, the cooling of a thermometer element contained in a protecting case.

With reference to Figure 2, and the list of symbols, the values M and m refer in general to the masses of the outer and inner bodies, respectively, and h_1 and h_2 to the rates of heat exchanges per degree difference in temperature between the outer body and the medium, and the corresponding values between the inner and outer bodies, respectively. When the specific case of a thermometer element in a protecting case is being considered, it is convenient to consider these values per square centimeter of contact area between the element and protecting tube, since the two are practically in direct contact.

The rate at which heat is dissipated from the outer body to the cooling medium is made up of the heat loss in this body together with that lost by the inner body. In the time dt, the outer body drops dT and the inner body drops $d\theta$, in temperature. Then in the time dt

$$(T-T_c)h_1dt=-(MSdT+msd\theta) \tag{12}$$

where $MSdT$ and $msd\theta$ are the heat losses per dT and $d\theta$ for the outer and inner bodies, respectively, having masses of M and m, and specific heats of S and s, respectively.

The transmission of heat from the inner body to the outer body is equal to that lost by the inner body, and, therefore, in time dt,

$$(\theta-T)h_2dt=-msd\theta \tag{13}$$

The negative signs are used as these are decreasing functions with time.

From equation 13

$$T=\theta+\frac{ms}{h_2}\frac{d\theta}{dt}$$

Differentiating this equation for T with respect to time and substituting in equation 12 for T and dT/dt, we have after collecting terms

$$\left(\frac{MSms}{h_1h_2}\right)\frac{d^2\theta}{dt^2}+\left(\frac{MS}{h_1}+\frac{ms}{h_2}+\frac{ms}{h_1}\right)\frac{d\theta}{dt}+(\theta-T_c)=0 \tag{14}$$

Now MS/h_1, ms/h_2 and ms/h_1 have the dimensions of time, and so for brevity let them be t_1, t_2, and t_m, respectively, as the time constants of the thermometer. Substituting these time constants in equation 14 there results,

$$\frac{d^2\theta}{dt^2}+\left(\frac{t_1+t_2+t_m}{t_1t_2}\right)\frac{d\theta}{dt}+\frac{\theta-T_c}{t_1t_2}=0 \tag{15}$$

Integrating this in the usual manner by letting

$$(\theta-T_c)=e^{vt} \tag{16}$$

and substituting this in equation 15 and solving for v, we have

$$v=-\alpha\pm\sqrt{\alpha^2-\beta^2} \tag{17}$$

where for brevity

$$\alpha=\frac{1}{2}\left(\frac{t_1+t_2+t_m}{t_1t_2}\right)$$

and

$$\beta=\frac{1}{\sqrt{t_1t_2}}$$

Substituting the value for v in equation 16 we have

$$(\theta-T_c)=e^{-\alpha t}\left[ae^{t\sqrt{\alpha^2-\beta^2}}+be^{-t\sqrt{\alpha^2-\beta^2}}\right] \tag{18}$$

where a and b are constants of integration. Let $a=(^1/_2)(A+B)$, and $b=(^1/_2)(A-B)$, where A and B are constants to be determined. Then, substituting these values in equation 18, multiplying, and dividing by $\sqrt{B^2-A^2}$, expanding, and collecting terms, we have,

$$(\theta-T_c)=(\sqrt{B^2-A^2})e^{-\alpha t}\times \sinh\left[t\sqrt{\alpha^2-\beta^2}+\sinh^{-1}\frac{A}{\sqrt{B^2-A^2}}\right] \tag{19}$$

The constants A and B are determined by applying the known boundary conditions, $\theta=\theta_0$, and $d\theta/dt=0$, at $t=0$, which, when introduced into equation 19, there results,

$$\frac{\theta-T_c}{\theta_0-T_c}=\sqrt{\frac{\beta^2}{\alpha^2-\beta^2}}e^{-\alpha t}\times \sinh\left[t\sqrt{\alpha^2-\beta^2}+\sinh^{-1}\sqrt{\frac{\alpha^2-\beta^2}{\beta^2}}\right] \tag{20}$$

Substitute in this equation the values of α and β in terms of t_1, t_2, and t_m, and for brevity let

$$P=\sqrt{\frac{\alpha^2-\beta^2}{\beta^2}}=\sqrt{\frac{(t_1+t_2+t_m)^2}{4t_0^2}-1}$$

where $t_0=\sqrt{t_1t_2}$, and we have

$$\frac{\theta-T_c}{\theta_0-T_c}=\frac{1}{P}e^{-\left[\left(\frac{t}{t_0}\right)\sqrt{P^2+1}\right]}\times \sinh\left[P\left(\frac{t}{t_0}\right)+\sinh^{-1}P\right] \tag{21}$$

which is equation 1 used in the descriptive part of this paper.

Appendix II

This analysis considers the problem of heating of a body indirectly, by a higher constant-temperature medium through a second body in direct contact with that medium; for example, the heating of a thermometer element contained in a protecting case.

Let

θ = temperature of the inner body at any time t

T = temperature of the outer body at any time t

T_e = temperature of surrounding medium (constant)

θ_0 = initial temperature of both inner and outer bodies at time $t=0$

Then the heat transmitted to the outside body in dt from the medium is $(T_e-T)\,h_1dt$. This heat increases the temperature of the outer body by dT, and the inner body by $d\theta$. The heat absorbed by these bodies in dt is then $MSdT+msd\theta$.

Therefore

$$(T_e-T)h_1dt=MSdT+msd\theta \qquad (22)$$

The heat transmitted from the outside body to the inside body in dt is $(T-\theta)h_2dt$, and this equals the heat absorbed by the inner body, $msd\theta$.

Therefore

$$(T-\theta)h_2dt=msd\theta \qquad (23)$$

It will be noted that these are the same equations as those found in the problem of the cooling bodies, namely, equations 12 and 13, and the same final equation follows:

$$\frac{d^2\theta}{dt^2}+\left(\frac{t_1+t_2+t_m}{t_1t_2}\right)\frac{d\theta}{dt}+\frac{\theta-T_e}{t_1t_2}=0 \qquad (24)$$

This reduces in form, therefore, to the same equation as for the cooling problem, namely:

$$\frac{\theta-T_e}{\theta_0-T_e}=\frac{1}{P}e^{-\left[\left(\frac{t}{t_0}\right)\sqrt{P^2+1}\right]}\times \sinh\left[P\left(\frac{t}{t_0}\right)+\sinh^{-1}P\right] \qquad (25)$$

However, in this heating problem, what we wish to know is the elevation at any time t of the temperature θ of the inside body above the initial temperature θ_0; that is $(\theta-\theta_0)$, and not $(\theta-T_e)$ as given in equation 25.

Now if we subtract unity from each side of this equation, and multiply both sides by -1, we get

$$\frac{\theta-\theta_0}{T_e-\theta_0}=1-\frac{1}{P}e^{-\left[\left(\frac{t}{t_0}\right)\sqrt{P^2+1}\right]}\times \sinh\left[P\left(\frac{t}{t_0}\right)+\sinh^{-1}P\right] \qquad (26)$$

which is in the form desired for the problem of the heating body.

Appendix III

The following analysis considers the time-temperature lag in a thermometer element enclosed in a protecting case immersed in a medium changing in temperature at a constant rate.

Let T_a = temperature of the medium at any time t, and r = the rate of change in the temperature of the medium in degrees per second.

Then the same differential equations apply as were found for a constant-temperature medium as given in Appendix I except that the varying temperature T_a is substituted for the constant temperature T_e, and we have from equation 15, Appendix I,

$$\frac{d^2\theta}{dt^2}+\left(\frac{t_1+t_2+t_m}{t_0^2}\right)\frac{d\theta}{dt}+\frac{\theta-T_a}{t_0^2}=0 \qquad (27)$$

Assume that the thermometer and medium both start at the same temperature θ_0; then the temperature of the medium at any time t will be

$$T_a=\theta_0+rt \qquad (28)$$

The rate r will be positive for increasing temperatures and negative for decreasing temperatures.

Substituting equation 28 in equation 27 we obtain,

$$\frac{d^2x}{dt^2}+\frac{a}{b}\frac{dx}{dt}+\frac{x}{b}=\frac{rt}{b}=\frac{f(t)}{b} \qquad (29)$$

where for brevity, $a/b=(t_1+t_2+t_m)/t_0^2$, $b=t_0^2$, and $x=(\theta-\theta_0)$. The integral of an equation of the form of equation 29 in general, as given in any book on differential equations, is

$$x=\frac{1}{\sqrt{a^2-4b}}\left[e^{-\frac{t}{T_1}}\int e^{\frac{t}{T_1}}f(t)dt-e^{-\frac{t}{T_2}}\int e^{\frac{t}{T_2}}f(t)dt\right]+c_1e^{-\frac{t}{T_1}}+c_2e^{-\frac{t}{T_2}} \qquad (30)$$

where c_1 and c_2 are constants to be determined, and

$$T_1=\frac{2b}{a-\sqrt{a^2-4b}}=\frac{t_0}{\sqrt{P^2+1}-P}, \text{ and}$$

$$T_2=\frac{2b}{a+\sqrt{a^2-4b}}=\frac{t_0}{\sqrt{P^2+1}+P}$$

In this problem $f(t)=rt$. Substituting the thermal constants corresponding to a and b, and rt for $f(t)$, we have

$$(\theta-\theta_0)=\frac{1}{2t_0P}\left[e^{-\frac{t}{T_1}}\int rte^{\frac{t}{T_1}}dt-e^{-\frac{t}{T_2}}\int rte^{\frac{t}{T_2}}dt\right]+c_1e^{-\frac{t}{T_1}}+c_2e^{-\frac{t}{T_2}} \qquad (31)$$

Integrating, collecting terms, and substituting values of T_1 and T_2, we have

$$(\theta-\theta_0)=r\left[t-2t_0\sqrt{P^2+1}\right]+c_1e^{-\frac{t}{T_1}}+c_2e^{-\frac{t}{T_2}} \qquad (32)$$

To determine the constants of integration, substitute for T_1 and T_2 and apply the boundary conditions, $\theta=\theta_0$ at $t=0$, and $d\theta/dt=0$ at $t=0$, and we obtain

$$(\theta-\theta_0)=r\left[t-2t_0\sqrt{P^2+1}\right]+\frac{rt_0}{P}e^{-\left[\left(\frac{t}{t_0}\right)\sqrt{P^2+1}\right]}\times\sinh\left[P\left(\frac{t}{t_0}\right)+\sinh^{-1}2P\sqrt{P^2+1}\right] \qquad (33)$$

Now instead of the deviation $(\theta-\theta_0)$, of the temperature of the element at time t from the initial temperature as given directly by equation 33, we wish to know the lag, that is $(T_a-\theta)$. We know from equation 28 that $T_a=\theta_0+rt$, and if we substitute in equation 33 the value of θ_0 in terms of T_a and r we obtain the lag at any time,

$$(T_a-\theta)=2rt_0\sqrt{P^2+1}-\frac{rt_0}{P}e^{-\left[\left(\frac{t}{t_0}\right)\sqrt{P^2+1}\right]}\times\sinh\left[P\left(\frac{t}{t_0}\right)+\sinh^{-1}2P\sqrt{P^2+1}\right] \qquad (34)$$

The maximum lag results when $t=\infty$, and by substituting this value in equation 34 and evaluating we find that the maximum lag is

$$L=[T_a-\theta]_{\max}=2rt_0\sqrt{P^2+1}=r(t_1+t_2+t_m) \qquad (35)$$

Dividing equation 34 through by $L=2rt_0\sqrt{P^2+1}$, we have for the equation for increasing temperatures,

$$\frac{T_a-\theta}{L}=1-\frac{1}{2P\sqrt{P^2+1}}e^{-\left[\left(\frac{t}{t_0}\right)\sqrt{P^2+1}\right]}\times\sinh\left[P\left(\frac{t}{t_0}\right)+\sinh^{-1}2P\sqrt{P^2+1}\right] \qquad (36)$$

For decreasing temperatures, r becomes negative, and the resulting equation is the same as equation 36 except that $(T_a-\theta)/L$ becomes $(\theta-T_a)/L$. Since r does not appear in the right-hand member of the equations, the form of the lag curve with time is independent of the rate of change in temperature.

The maximum lag can be determined directly from the fundamental differential equation 27, by remembering that at $t=\infty$, $d^2\theta/dt^2$ becomes zero, and $d\theta/dt$ becomes r. Then

$$\left(\frac{t_1+t_2+t_m}{t_0^2}\right)r=\frac{[T_a-\theta]}{t_0^2}\max$$

which results in the same equation 35 as found by the complete analysis, namely:

$$L=[T_a-\theta]_{\max}=(t_1+t_2+t_m)r$$

Reference

1. The Compensated Thermocouple Ammeter, W. N. Goodwin, Jr. AIEE Transactions, volume 55, 1936, January section, pages 23–33.

Ferroinductance as a Variable Electric-Circuit Element

J. D. RYDER
ASSOCIATE AIEE

IT HAS LONG been known that the inductance of iron-cored coils is not a constant, but varies with the value of current flowing, and that this is not a linear relation, owing to the shape of the magnetization curve of the iron used.

Mathematical analysis of such circuits leads to differential equations with variable coefficients which are very difficult to solve. To obtain usable results the engineer is accustomed to assume the inductance of the iron-cored reactor as constant, thereby obtaining equations with constant coefficients and an easy mathematical solution for the circuit.

However, for this analysis, in terms of complex algebra or differential equations, it is assumed that the value of the inductance is not a function of current or time. In many present-day problems this assumption cannot be supported, and a new method of analysis is needed.

Definitions

Inductance is the proportionality factor between instantaneous induced voltage and the rate of change of current in an electric circuit. That is

$$L = \frac{-e}{\frac{di}{dt}} \qquad (1)$$

is the basic defining relation for inductance.

If it is remembered that equation 1 is a relationship between instantaneous quantities, then equation 1 becomes fundamental, and other definitions such as summarized by Raner and Litscher[1] become only special cases, based on weighted averages.

Ferroinductance or ferroreactance are terms used to designate the special properties of an inductance when iron is introduced into the magnetic circuit. Defining equation 1 still holds, but the value of L, the proportionality factor, is no longer a constant but is a function of i, the current.

Historical Background

Since the time the first magnetization curve was measured for a steel, there have been attempts to develop equations to fit the curve. These attempts have followed mathematical or physical paths, but it cannot be said that either method has been more successful than the other.

One of the oldest, and certainly the most famous, of the equations developed for the purpose is Frölich's equation: $B = H/(a + bH)$, which gives a satisfactory fit up to approximately the knee of the curve. Zenneck,[6] in his 1920 paper on the analysis of magnetic frequency doublers, used the relation: $B = sH - s'H^3$. It should be noted that this equation cannot be used much beyond the knee of the magnetization curve because of the negative cubic term. Zenneck succeeded in obtaining an expression for ferroinductance in terms of current, but did not carry the matter further and submitted no experimental proof.

Ryan,[7] also for the analysis of magnetic frequency doublers, used the relation: $B = A \tan^{-1} ax + Cx$, which is related to that of Zenneck through the arc tangent series. Keller[11] also used a similar series. Boyajian,[14] in order to simplify the mathematics, used an approximation to the magnetization curve consisting of two straight lines, one for use below the knee, the other above. The results, while easily obtained, are not too satisfactory for a design basis.

In 1926, Gokhale,[5] using physical methods, developed an exponential form which fitted well above saturation, leaving much to be desired below the knee. Rader and Litscher[1] have used the equation: $H = K'B + K''B^{10}$, and while this fits the magnetization curves fairly well, it is impossible for use for circuit analysis, as will be discussed in the next section.

One of the earliest applications of the nonlinear voltage-current characteristics of ferroinductors was made by Zenneck[12] in 1899. This involved the use of transformers, with d-c excitation to accentuate the nonlinearity, connected to produce frequency doubling. The first report of the phenomena present in *R-L-C* series circuits, in which the L was ferroinductive, was made by Martienssen[8] in 1910. This is the type of circuit which we now call ferroresonant. Martienssen, while obtaining what appear to be correct qualitative results, invalidated them for quantitative use by a serious mathematical error.

More recent investigators ordinarily have used the graphic approach for a solution, but this involves the construction of a reactor before the design of the other components of the ferroresonant circuit can be completed.

A New Equation for the Magnetization Curve

The shape of the magnetization curve is obviously the cause of the phenomena observed in ferroinductive circuits. If an empirical equation for the magnetization curve is to be useful in the analysis of a-c circuits it must be a function which behaves in every way exactly as the true magnetization curve. Since actual magnetization curves are "odd" functions, and display equal and opposite effects for positive and negative currents, then the function chosen to represent the magnetization curve must likewise be an "odd" function.

The magnetization curve affects our

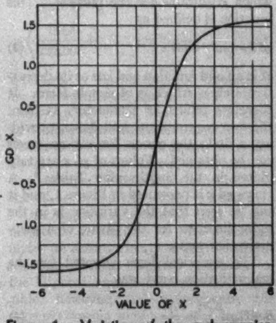

Figure 1. Variation of the gudermannian

Paper 45-121, recommended by the AIEE committee on basic sciences for publication in AIEE TRANSACTIONS. Manuscript submitted September 16, 1944; made available for printing May 17, 1945.

J. D. RYDER is professor of electrical engineering, Iowa State College, Ames, Iowa.

The material presented in this paper is abstracted from a dissertation presented for the doctor-of-philosophy degree at Iowa State College. The complete dissertation is on file at the Iowa State College Library, Ames, Iowa.

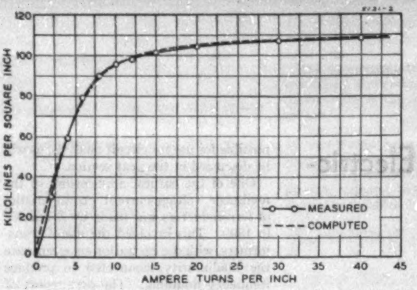

Figure 2. Measured and calculated magnetization curves for Hipersil steel

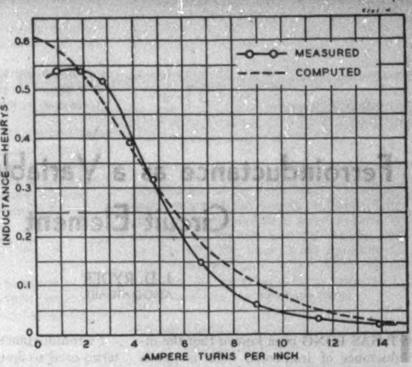

Figure 4. Measured and calculated inductance of a 156-turn reactor on Hipersil core

electric circuits indirectly, through the phenomena of flux-linkage changes or inductance. Since inductance is one of our basic circuit parameters, it is obvious that, for convenience alone, the equation chosen to represent the magnetization curve should lead to a simple expression for inductance.

Another equation for inductance, derived from equation 1 is

$$L=N\frac{d\phi}{di}\times 10^{-8} \tag{2}$$

Thus, inductance is proportional to the slope of the magnetization curve.

It is then possible to set up two criteria which a function, to be useful as an approximation for the magnetization curve of a steel, must fulfill:

1. The function must be "odd."
2. The current derivative or slope of the function must be mathematically simple.

By applying this test to the functions used by other investigators it is found that none of the empirical relationships considered are entirely suitable for the analysis of a-c circuits. However, there exists a function, the "gudermannian",[2] which is suitable for the purpose. This function is defined as

$$gd\ x=\tan^{-1}\sinh x \tag{3}$$

It is an odd function and has as its derivative sech x, which is of simple form. It therefore fulfills, in satisfactory fashion, the two requirements laid down, providing a fit to the curves for various steels can be obtained. Values of $gd\ x$ are tabulated in the Smithsonian Tables.[3] A curve $gd\ x$ is presented in Figure 1, and it can be seen that the variation is in the right direction for the fitting of a magnetization curve.

The empirical form adopted for the magnetization curve was

$$B=B_m gd\frac{aNi}{l}+\frac{cNi}{l} \tag{4}$$

This equation, being a transcendental relation, does not lend itself to direct solution for the values of the constants B_m, a, and c. The method developed was that of a trial process for a, after which B_m and c were obtained directly, as outlined in Appendix III.

Results for Typical Steels

As an indication of the ability of equation 4 to approximate the magnetization curves for various commercial steels, two types were selected. The first, Hipersil, was selected as typical of modern transformer steel. As no magnetization curves were obtainable from the manufacturer, the curve was measured in the laboratory. The second steel was Nicaloi (Allegheny 4750), a high permeability alloy. The curve was available from manufacturer's data.

Using English units, the equations determined for these steels were

Hipersil:

$$B=65{,}000gd\left(0.273\frac{Ni}{l}\right)+180\frac{Ni}{l} \tag{5}$$

Nicaloi:

$$B=36{,}600gd\left(4.58\frac{Ni}{l}\right)+6{,}200\frac{Ni}{l} \tag{6}$$

Curves of equation 5 compared with the measured data are shown in Figure 2, with excellent agreement indicated. Equally good results have been secured for many steels other than the two described.

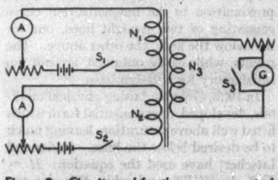

Figure 3. Circuit used for the measurement of ferroinductance

Applications of the Equation

In most modern magnetic steels the hysteresis-loop area has been much reduced and has been here neglected to simplify the mathematics. It was assumed that magnetization of the steel throughout an a-c cycle took place along the normal magnetization curve, rather than around the hysteresis loop. Leakage flux also has been neglected as it was small for the core structures used.

Normal permeability is the term obtained from the relation

$$\mu=K\frac{B}{H} \tag{7}$$

and setting $K = 0.3125$ for English units, normal permeability can be calculated from equation 4 giving

$$\mu=0.3125\left[\frac{B_m gd\frac{aNi}{l}}{\frac{Ni}{l}}+c\right] \tag{8}$$

Equation 8 has been used to calculate the permeability of Hipersil and other steels with accurate results.

Differential permeability is defined as the slope of the magnetization curve, or the permeability to small changes of magnetizing force. That is

$$\mu_d=K\frac{dB}{dH} \tag{9}$$

and, setting $K = 0.3125$ for English units,

$$\mu_d=0.3125\left[aB_m\ \text{sech}\ \frac{aNi}{l}+c\right] \tag{10}$$

Calculations for various steels using equation 10 yield results which closely check values of permeability obtained from the slopes of the magnetization curves.

Since

$$\phi = AB_n \text{gd}\frac{aNi}{l} + \frac{cANi}{l} \quad (11)$$

$$\frac{d\phi}{di} = \frac{aAB_nN}{l} \operatorname{sech} \frac{aNi}{l} + \frac{cAN}{l} \quad (12)$$

Then, from equation 2

$$L = \frac{aAB_nN^2}{10^8 l} \operatorname{sech} \frac{aNi}{l} + \frac{cAN^2}{10^8 l} \quad (13)$$

Equation 13 gives the value, in henrys of the inductance of a ferroinductor with any value of current flowing. The first term on the right is the contribution resulting from the presence of iron, the second term is the value if the iron is removed, leaving an air core.

As the maximum value of sech x is unity and occurs for x zero, then the inductance is maximum at zero current. Actually, because of the small reverse curvature of the magnetization curve near zero, the measured inductance maximum occurs, not at, but near zero. By noting that sech ∞ equals zero, the value of inductance is seen never less than cAN^2/l. High values of current can reduce the effectiveness of the iron but never can reduce the inductance below that of the coil on an air core.

Equation 13 is a simple expression for the calculation of ferroinductance. By its use an inductor can be designed in advance of construction, to have a given inductance at a given value of current, the only data required being the constants B_n, a, and c of the steel.

Measurement of Ferroinductance

Ordinary a-c bridge methods of inductance measurement are not satisfactory. The voltage applied to the inductor varies as the bridge is balanced, changing the inductance, and a sliding balance results. If balance is obtained, knowledge of the actual current flowing through the reactor is not obtainable, and the value of inductance means nothing.

A bridge especially designed for this,[4] and including means for measuring alternating and direct currents still overlooks a fundamental point. It may give information on the inductance under the particular operating conditions, but it gives no clue to a means for determining the inductance under different conditions.

It has been necessary to develop a new method by which ferroinductance can be measured at any value of current or ampere turns. This new method is based on the relation

$$L = N\frac{d\phi}{di} \times 10^{-8} \quad (14)$$

From equation 14, it can be seen that an inductance can be measured at any value of steady current, if a differential change in current be made, the resulting differential change in flux measured, and the ratio taken and multiplied by the number of turns in the coil.

The method is based on the fact that, after demagnetization, an iron core is magnetized along the normal curve, and if the differential change is made additive, then the iron is taken further along the normal curve and the effect of a hysteresis loop is eliminated.

For accurate measurement of the differential current change it is most convenient to use a three-coil arrangement, as shown in Figure 3. The steady d-c ampere turns are applied in N_1, the differential-current change is made by closing the circuit of N_2 whose inductance is to be measured, and N_3 is for the ballistic measurement of the flux change with the galvanometer. The ampere turns of the first and second coils must be connected to aid.

The size of the differential change can be made too small for the sensitivity of the apparatus used. Values of the change used were as low as 0.001-ampere turns per inch, but it was found that values of 0.1- to 0.5-ampere turns per inch gave satisfactory results. The values of inductance so obtained were checked independently by calculations made from values of permeability obtained at the operating points. Measurements made with the Hipersil core having an area of 1.87 square inches, length of 13.2 inches, and a coil of 156 turns, are shown in Figure 4, compared with the dashed-line curve secured by computation from equation 13.

Close agreement between measured and computed values is secured over most of the range, resulting in a check of the theory and measuring method developed.

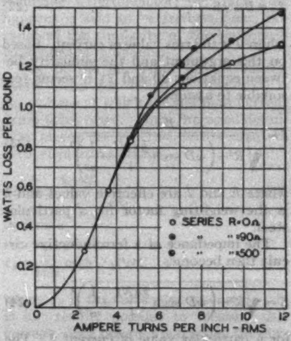

Figure 5. Wattage iron loss as a function of effective current

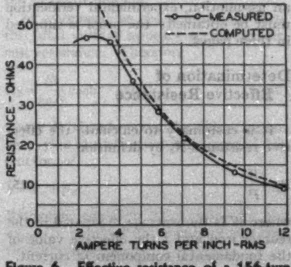

Figure 6. Effective resistance of a 156-turn reactor on Hipersil core

Value of Inductance for Applied Sine Electromotive Force

Consider a ferroreactor with sinusoidal electromotive force applied, neglecting the resistance of the circuit. As shown in Appendix I, an expression for the inductance as a function of time can be obtained

$$L = \frac{aAB_nN^2}{10^8 l}[J_0(G) + 2J_2(G)\cos 2\omega t +$$
$$2J_4(G)\cos 4\omega t + 2J_6(G)\cos 6\omega t + \ldots\ldots] \quad (15)$$

where

$$G = \frac{E_m 10^8}{\omega a B_n N} \quad (16)$$

This shows that, for a sine voltage, the inductance of a ferroinductor consists of a constant term plus sinusoidally varying terms in even harmonics of the applied frequency. This provides an explanation of the source of the harmonic components appearing in the current that flows through a ferroreactor.

Likewise, an expression for the current flowing can be secured in terms of the harmonic components (Appendix II)

$$i = \frac{l}{aN}\left[\left(G + \frac{G^3}{8} + \frac{5G^5}{192} + \frac{2{,}135G^7}{322{,}000} + \ldots\ldots\right)\times\right.$$
$$\sin\omega t - \left(\frac{G^3}{24} + \frac{5G^5}{384} + \frac{1{,}280G^7}{322{,}000} + \ldots\ldots\right)\times$$
$$\sin 3\omega t + \left(\frac{G^5}{384} + \frac{427G^7}{322{,}000} + \ldots\ldots\right)\sin 5\omega t -$$
$$\left.\left(\frac{61G^7}{322{,}000} + \ldots\ldots\right)\sin 7\omega t + \ldots\ldots\right] \quad (17)$$

Equation 17 shows that the frequencies are odd harmonics, and alternate in algebraic sign, as is well known for this case. In Table I is presented an analysis, made with a General Radio Company wave analyzer, of an input-current wave form for sine voltage. For comparison also presented is an analysis using equation 17.

One important source of error is represented. Equation 17 was developed under an assumption of negligible circuit resistance. The effective resistance of the Hipersil core reactor was not negligible, however, and consequently the currents flowing were somewhat less than had been predicted.

Impedance of a Circuit Containing a Ferroinductor

For a series circuit of resistance, ferroinductance, and capacity, the circuit-differential equation is

$$D \operatorname{sech} \frac{aNi}{l} \frac{di}{dt} + Ri + \frac{\int i dt}{c} = e \tag{18}$$

where

$$D = \frac{aAB_nN^2}{10^8 l} \tag{19}$$

This so far has been insoluble for sinusoidal electromotive force, but if $i = I_m \times \sin \omega t$ is assumed, then the equation becomes

$$RI_m \sin \omega t + I_m\left(\omega D \operatorname{sech} \frac{aNI_m \sin \omega t}{l} - \frac{1}{\omega c}\right) \cos \omega t = e \tag{20}$$

For equation 20 to be fulfilled, e must be nonsinusoidal. The equation is so similar in form to the conventional circuit equation

$$RI + jI\left(\omega L - \frac{1}{\omega c}\right) = E \tag{21}$$

involving rms values of current and voltage, that it should be possible in some manner to bridge the gap between the instantaneous quantities of equation 20 and the rms quantities of equation 21.

Inductance as determined by the ferroinductance equation 13 is an instantaneous quantity, dependent on the instantaneous value of a varying current. Over a cycle of current variation the inductance changes through a considerable range of values. Its effect in the circuit will be some sort of a weighted average of the values taken during the current cycle, or a weighted function of the current or ampere turns.

The magnitude of the weighting factor will depend on the manner in which the inductance varies with the current and this is fixed by the magnetization curve. The factor in the inductance relation which reflects the shape of the magnetization curve is sech (aNi/l). Consequently, if a weighting factor is present, it will appear in the angle of the hyperbolic secant as some factor k. The effective value of inductance L_e then may be written as

$$L_e = D \operatorname{sech} \frac{kaNI}{l} \tag{22}$$

where I is the rms value of current. Based on this argument and the similarity between equations 20 and 21 it seems reasonable to assume

$$I = \frac{E}{\sqrt{R^2 + \left(\omega D \operatorname{sech} \frac{kaNI}{l} - \frac{1}{\omega c}\right)^2}} \tag{23}$$

where E and I are effective values and k is the weighting factor for a particular steel.

The impedance of a ferroinductive circuit then becomes

$$Z = \sqrt{R^2 + \left(\omega D \operatorname{sech} \frac{kaNI}{l} - \frac{1}{\omega c}\right)^2} \tag{24}$$

for a particular value of current I. The resistance R includes the effective resistance of the reactor as well as other circuit resistance. Since equation 23 is an assumption, experimental verification must be obtained; the proof is supplied in these pages.

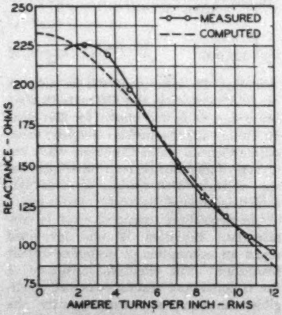

Figure 7. Measured and calculated reactance of the 156-turn reactor on Hipersil core

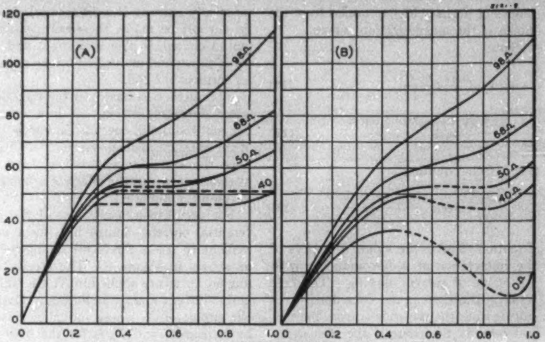

Figure 8. Voltage across a ferroresonant circuit, for various values of circuit resistance exclusive of the effective resistance

A—Measured
B—Calculated

Determination of Effective Resistance

It is customary to calculate the effective resistance R_e by definition

$$R_e = \frac{W}{I^2} \tag{25}$$

where W is the wattage dissipated in the reactor iron and I the effective value of the fundamental component of current.

When a ferroinductor is in series with another impedance across a sinusoidal voltage, neither the current nor the voltage of the ferroinductor is sinusoidal, in general. Therefore the flux is not sinusoidal but is made up of harmonic frequencies. The total iron losses vary as some power of the frequency and are also a function of peak flux density. For convenience of measurement, the rms current, voltage, and power most readily are obtained. Consequently the relation between rms current, or ampere turns, and watts loss for such distorted wave forms would be interesting as it would reflect, not only the variation of iron losses with wave form, but also the variation of the losses with peak flux.

Data have been taken showing that the variation of losses with wave form is as much a function of rms current as of peak flux density. Evidently the change of the losses with frequency is somewhat compensated for by the accompanying change in peak factor of the current.

Figure 5 shows the losses of a reactor on Hipersil steel for various wave forms induced by the use of resistance in series with the reactor. The curves of Figure 5 can be approximated to a fair degree of accuracy by a power series of the form

$$W/\text{lb} = K_1 \frac{NI}{l} + K_2\left(\frac{NI}{l}\right)^2 + \ldots\ldots \tag{26}$$

which then gives as an expression for R_e, by use of equation 25, the following equation, in which I is in rms amperes

$$R_e/\text{lb} = \frac{K_1N}{lI} + \frac{K_2N^2}{l^2} + \ldots\ldots \tag{27}$$

An experimental check of equation 27 was obtained by measuring the iron losses of the 156-turn coil on Hipersil core, com-

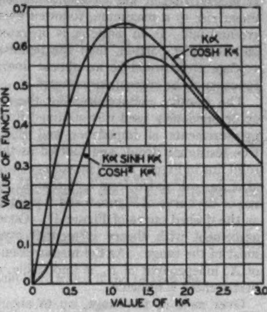

Figure 9. Values of the functions

$$\frac{k\alpha \sinh k\alpha}{\cosh^2 k\alpha} \text{ and } \frac{k\alpha}{\cosh^2 k\alpha}$$

puting the effective resistance by equation 25 and plotting as the solid curve of Figure 6. The dashed curve was computed from equation 27 using the weight of 6.9 pounds and $K_1 = 0.213$ and $K_2 = -0.00784$. The accuracy is good except over the unimportant low portion of the current values.

Calculation of Reactance

A discussion of reactance and of the design of units to give a specified value really hinges on the proof of existence of the weighting factor k of equation 22. The reactance then would be

$$X = \omega D \operatorname{sech} \frac{k\alpha NI}{l} \qquad (28)$$

The reactance can be obtained by measurement of impedance and effective resistance and using

$$X = \sqrt{Z^2 - R_e^2} \qquad (29)$$

Such measurements were made on the reactor previously used and are plotted as the solid curve of Figure 7.

From Figure 7, k now can be calculated. Arbitrarily choose a point well out on the reactance curve, say at ten ampere turns per inch, at which point the reactance is 112 ohms. If a value k exists, then this point, and all other values on the curve, should be predicted by equation 28. Solving for k, a value of $k = 0.5$, is obtained. By using this value of k the calculated curve of Figure 7 was obtained, showing good agreement with the measured value. Similar good agreement has been obtained using other reactors and a wide range of steels, with values of k ranging from 0.3 to 0.5.

Table I. Harmonic Analysis of Input Current to a Reactor

	Voltage Applied = 60 Rms		Voltage Applied = 83 Rms	
	Measured	Calculated	Measured	Calculated
Total I rms	0.27	0.31	0.40	0.53
Fundamental (per cent)	100.0	100.0	100.0	100.0
Third harmonic (per cent)	7.8	7.5	20.4	17.5
Fifth harmonic (percent)	1.8	0.7	6.7	2.7
Seventh harmonic (per cent)	0.4	0.4	3.1	2.1

The experimental evidence definitely seems to establish that a factor k does exist as a weighting factor. It fully substantiates the assumptions of equation 28, and permits its use to calculate the reactance of a coil for any value of current, or to design a coil to have a particular reactance at a definite effective current value.

The Ferroresonant Circuit

Referring to equation 23, the possibility exists that the second term under the radical may go to zero at some value of I. At this point the denominator is small and the current rises. A circuit, including a ferroreactor, in which this happens is said to be ferroresonant, because of the similarity of the properties to frequency resonance.

One of the important circuit values, useful either for design or operation, is the voltage at which the resonant current jump takes place. Since the usual definition places the reactive terms equal to zero, then at resonance

$$\omega D \operatorname{sech} \frac{k\alpha NI}{l} = \frac{1}{\omega C} \qquad (30)$$

and then

$$I_R = \frac{l}{k\alpha N} \cosh^{-1} \omega^2 DC \qquad (31)$$

where I_R is the current at resonance. It is not readily possible to measure this current, since before it is reached the current rises to a higher value. The voltage is, however, practically constant through this range and can be measured as E_R, the resonant voltage.

At resonance, as the reactance is zero, the total voltage appears across the circuit resistance. Therefore

$$E_R = \frac{Rl}{k\alpha N} \cosh^{-1} \omega^2 DC \qquad (32)$$

where R is made up of the circuit resistance plus the effective resistance of the reactor, or

$$R = R_c + R_e \qquad (33)$$

Reversing equation 32 a value for the capacity required for resonance at a particular voltage E_R is

$$C = \frac{1}{\omega^2 D} \cosh \frac{k\alpha N E_R}{Rl} \text{ farads} \qquad (34)$$

Table II presents data taken to check equation 32.

Assume a series circuit using the reactor with Hipersil core and 156 turns, a capacity C of 25 microfarads, and external resistance R_x variable. Figure 8 is a plot of the voltage across the circuit, computed from equation 23, for various values of external circuit resistance R_x. The dashed portions of the curves having a negative slope cannot be realized experimentally, as the current jumps directly across. Apparently this jump starts at the point at which the negative rate of change of impedance exceeds the rate of change of current.

Measured values of voltage for various values of R_x also are plotted in Figure 8. There is a very marked agreement, especially in values of voltage at which the current jumps occur, between the measured and totally calculated values.

For values of small R_x, the jump does not occur at the same value of voltage for decreasing as for increasing voltage. The current in this region is multivalued. The amount of resistance which just permits resonance without multivalued current,

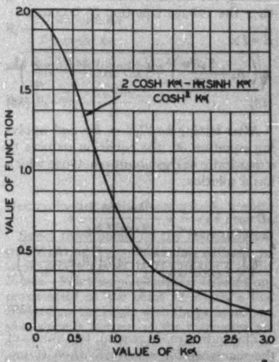

Figure 10. Value of the function

$$\frac{2 \cosh k\alpha - k\alpha \sinh k\alpha}{\cosh^2 k\alpha}$$

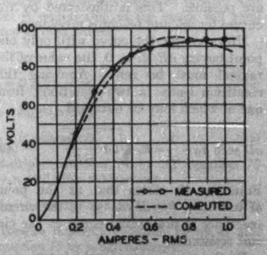

Figure 11. Variation of voltage across a pure reactance, measured and calculated

or the value producing the curve with a single point having a tangent of zero slope, is called the critical resistance R_k of the circuit. For many control applications the possibility of two current values is undesirable, so that the value of the critical resistance is of importance.

The value of R_k can be determined (see Appendix II). Briefly, the voltage can be expressed as

$$E=I\sqrt{R^2+\left(\omega D\operatorname{sech}\frac{kaNI}{l}-\frac{1}{\omega C}\right)^2} \qquad (35)$$

and the point of zero slope will have

$$\frac{dE}{dI}=0 \qquad (36)$$

Before taking the derivative it is necessary to write R as a function of I, as R includes the effective resistance. From equation 27 the effective resistance may be written, and adding R_x and the copper resistance of the reactor, with w signifying the weight in pounds,

$$R=R_c+R_x+\frac{K_1Nw}{lI}+\frac{K_2N^2w}{l^2} \qquad (37)$$

Taking the three constant terms as R_0, then the voltage equation 35 becomes

$$E=I\times\sqrt{\left(R_0+\frac{K_1Nw}{lI}\right)^2+\left(\omega D\operatorname{sech}\frac{kaNI}{l}-\frac{1}{\omega C}\right)^2} \qquad (38)$$

After letting $kaNI/l = k\alpha$ and applying equation 36, the equation reduces to a quadratic in the circuit reactance which has a solution,

$$\omega D\operatorname{sech}k\alpha-\frac{1}{\omega C}=\frac{\omega Dk\alpha\sinh k\alpha}{2\cosh^2 k\alpha}\pm\frac{\sqrt{\left(\frac{\omega Dk\alpha\sinh k\alpha}{\cosh^2 k\alpha}\right)^2-4R_0\left(R_0+\frac{K_1Nw}{lI}\right)}}{2} \qquad (39)$$

This indicates, in general, two values of the reactance for which $dE/dI = 0$, unless the radical is zero. The curves of Figure 8 support this. For large R_0 the value of the radical is imaginary, hence no real values of reactance for $dE/dI = 0$ are possible. This is illustrated by the curves for 98- and 68-ohms resistance.

However, for the curve with only one point having $dE/dI = 0$, the value of the radical must be zero. Applying this condition leads to two equations, from one of which may be obtained

$$\omega D\operatorname{sech}k\alpha-\frac{1}{\omega C}=R_0\sqrt{1+\frac{K_1Nw}{lIR_0}} \qquad (40)$$

Equation 40 states that at the point of inflection for $dE/dI = 0$, the circuit reactance is practically equal to the circuit resistance.

Table II. Resonant Voltage in a Ferroresonant Circuit

C, μf	Total R, Ohms	E_R Measured, Volts	E_R Computed, Volts
16.7	78	43	45
25.0	66	54	57
41.7	53	68	64
50.0	47	70	66

By the use of curves for the functions of $k\alpha$ involved, the value of the current at the inflection point may be found, and with further use of Figures 9 and 10 values may be obtained for substitution in

$$R_0=\frac{\omega D}{2}\,\frac{k\alpha\sinh k\alpha}{\cosh^2 k\alpha} \qquad (41)$$

and

$$R_x=R_0-R_c-\frac{K_2N^2w}{l^2} \qquad (42)$$

Values larger than this must be placed in the circuit to insure single-valued current at all times.

The value of R_k has been calculated for the circuit used for the curves of Figure 8. This results in a value of 52 ohms, which, by consideration of both measured and computed curves, is a satisfactory check.

Variation of Ferroreactive Voltage Drop

As mentioned, it has been customary for many years to assume ferroinductance a circuit constant, and the ferroreactive-voltage drop in a-c circuits as proportional to the current, as in

$$E_m\sin(\omega t+\theta)=\omega LI_m\sin\omega t \qquad (43)$$

This is an obvious impossibility if L is considered a variable with either time or current, as actually occurs in an a-c circuit. It is now possible to determine just why and to what extent the assumption can be supported.

If

$$X=\omega D\operatorname{sech}k\alpha \qquad (44)$$

then the ferroreactive voltage drop may be written as

$$E_L=\frac{\omega AB_mN}{10^8k}\,\frac{k\alpha}{\cosh k\alpha} \qquad (45)$$

The ferroreactive voltage drop is seen to be a function of $k\alpha/\cosh k\alpha$. This function is plotted against $k\alpha$ in Figure 9.

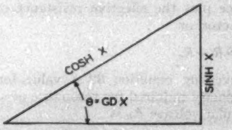

Figure 12. Property of the gudermannian

It is seen that it has an approximately linear rise to a maximum, followed by a gradual fall. If an inductor is operated on the rising portion, then the reactive voltage drop would be an almost linear function of the current, as assumed.

The reactive voltage drop for the reactor previously used was obtained from measurements of impedance and effective resistance drops, and plotted as the solid line in Figure 11. The voltage drop also was calculated from equation 45 by use of the curve of Figure 9 and is plotted as the dashed curve of Figure 11. Good agreement with theory is secured over most of the range. As the measurement of X, independent of R_e, is impossible, a better check is difficult.

Over most of the range, up to about five ampere turns per inch, the assumption of linear reactive drop is not difficult to support. This means that the linear region extends almost to the point at which the peak of the ampere-turns wave reaches the knee of the magnetization curve (see Figure 2).

Summary

This investigation was instituted in an attempt to develop methods which would make ferroinductive circuits as susceptible to analysis as circuits with constant parameters.

The work has led to the development of an accurate empirical equation for the magnetization curve of a steel. This equation has been applied in predicting the inductance of a ferroinductor at any value of current, and methods have been developed for measuring this inductance, which check the theory closely.

The equation for ferroinductance has been generalized into a relation for effective ferroreactance by an assumption, and experimental evidence has been obtained to support the validity of the assumption. Methods also were developed for calculating the effective resistance of an iron-cored reactor. Application then was made of both of these developments in calculating the impedance of circuits containing ferroreactors, and the results were again well supported by experiment.

Another application of the theory was made to the ferroresonant circuit, and simple relations for resonant voltage, capacity required, and the value of the critical resistance secured. All were checked satisfactorily by experiment.

Appendix I

Value of Inductance for Applied Sine Electromotive Force

With $e=E_m\cos\omega t$ and neglecting the resistance of the circuit, an equation for the flux present in the iron can be written

$$\phi=\frac{10^8}{N}\int e\,dt=\frac{E_m10^8}{\omega N}\sin\omega t \qquad (46)$$

By the expression for the magnetization curve

$$\phi = AB_n gd\,\frac{aNi}{l} + \frac{cANi}{l} \qquad (47)$$

and ordinarily the last term on the right can be neglected as very small. Then

$$gd\frac{aNi}{l} = \frac{\phi}{AB_n} \qquad (48)$$

From the properties of the gudermannian[3] a right triangle can be drawn (Figure 12) where

$$\theta = gd\,\frac{aNi}{l} = \frac{\phi}{AB_n} \qquad (49)$$

and from which it can be seen that

$$\text{sech}\,\frac{aNi}{l} = \cos\frac{\phi}{AB_n} \qquad (50)$$

Substituting equation 46 into 50

$$\text{sech}\,\frac{aNi}{l} = \cos\left(\frac{E_m 10^8}{\omega AB_n N}\sin\omega t\right) = \cos\,(G\sin\omega t) \qquad (51)$$

Then equation 13 for ferroinductance, neglecting the term containing c as small, becomes

$$L = \frac{aAB_nN^2}{10^8 l}\cos\,(G\sin\omega t) \qquad (52)$$

Now it is known that

$$\cos\,(x\sin r) = J_0(x) + 2J_2(x)\cos 2r + 2J_4(x)\cos 4r + \ldots\ldots \qquad (53)$$

where $J_0(x)$, $J_2(x)$, $J_4(x)$ ..... are Bessel-function coefficients which can be evaluated from tables of the function. Consequently the expression for inductance becomes

$$L = \frac{aAB_nN^2}{10^8 l}\,[J_0(G) + 2J_2(G)\cos 2\omega t + 2J_4(G)\cos 4\omega t + 2J_6(G)\cos 6\omega t + \ldots\ldots] \qquad (54)$$

Current Through a Ferroinductor, Sine Electromotive Force Applied

From equations 46 and 48 the following can be written

$$gd\frac{aNi}{l} = \frac{E_m 10^8}{\omega AB_n N}\sin\omega t \qquad (55)$$

and then

$$i = \frac{l}{aN}gd^{-1}\left(\frac{E_m 10^8}{\omega AB_n N}\sin\omega t\right) = \frac{l}{aN}\,gd^{-1}(G\sin\omega t) \qquad (56)$$

The series expression for the antigudermannian is

$$gd^{-1}\mu = \mu + \frac{\mu^3}{6} + \frac{\mu^5}{24} + \frac{61\mu^7}{5{,}040} + \ldots\ldots \qquad (57)$$

and equation 56 becomes

$$i = \frac{l}{aN}\left[G\sin\omega t + \frac{G^3}{6}\sin^3\omega t + \frac{G^5}{24}\sin^5\omega t + \ldots\ldots\right] \qquad (58)$$

By substituting for the trigonometric relations their identities in terms of multiple angles and collecting terms,

$$i = \frac{l}{aN}\left[\left(G + \frac{G^3}{8} + \frac{5G^5}{192} + \frac{2{,}135G^7}{322{,}000} + \ldots\ldots\right)\times \sin\omega t - \left(\frac{G^3}{24} + \frac{5G^5}{384} + \frac{1{,}280G^7}{322{,}000} + \ldots\ldots\right)\times \sin 3\omega t + \left(\frac{G^5}{384} + \frac{427G^7}{322{,}000} + \ldots\ldots\right)\sin 5\omega t - \left(\frac{61G^7}{322{,}000} + \ldots\ldots\right)\sin 7\omega t + \ldots\ldots\right] \qquad (59)$$

Appendix II

The Value of the Critical Resistance R_x

The circuit voltage, after inserting the resistance as a function of current, and setting $kaNI/l$ equal to $k\alpha$, is

$$E = I\sqrt{\left(R_0 + \frac{K_1Nw}{lI}\right)^2 + \left(\omega D\,\text{sech}\,k\alpha - \frac{1}{\omega c}\right)^2} \qquad (60)$$

Then applying the condition of equation 36 and collecting terms

$$0 = \frac{dE}{dI} = \left(\omega D\,\text{sech}\,k\alpha - \frac{1}{\omega c}\right)^2 - \omega D\frac{k\alpha\sinh k\alpha}{\cosh^2 k\alpha}\left(\omega D\,\text{sech}\,k\alpha - \frac{1}{\omega c}\right) + \left(R_0 + \frac{K_1Nw}{lI}\right)^2 - I\left(\frac{R_0K_1Nw}{lI^2} + \frac{K_1^2N^2w^2}{l^2I^3}\right) \qquad (61)$$

The last two terms reduce to

$$R_0\left(R_0 + \frac{K_1Nw}{lI}\right) \qquad (62)$$

and equation 61 is seen to be a quadratic in the net circuit reactance and has a solution,

$$\left(\omega D\,\text{sech}\,k\alpha - \frac{1}{\omega c}\right) = \frac{\dfrac{\omega Dk\alpha\sinh k\alpha}{\cosh^2 k\alpha} \pm \sqrt{\left(\dfrac{\omega Dk\alpha\sinh k\alpha}{\cosh^2 k\alpha}\right)^2 - 4R_0\left(R_0 + \dfrac{K_1Nw}{lI}\right)}}{2} \qquad (63)$$

For the curve for the critical resistance only one value of reactance is possible, so that the radical is zero, leading to

$$\frac{\omega Dk\alpha\sinh k\alpha}{\cosh^2 k\alpha} = 2R_0\sqrt{1 + \frac{K_1Nw}{lIR_0}} \qquad (64)$$

$$\omega D\,\text{sech}\,k\alpha - \frac{1}{\omega c} = \frac{\omega D}{2}\,\frac{k\alpha\sinh k\alpha}{\cosh^2 k\alpha} \qquad (65)$$

Substitute equation 64 into 65:

$$\omega D\,\text{sech}\,k\alpha - \frac{1}{\omega c} = R_0\sqrt{1 + \frac{K_1Nw}{lIR_0}} \qquad (66)$$

Return to equation 65 and rewrite it as

$$\frac{2}{\omega^2DC} = \frac{2\cosh k\alpha - k\alpha\sinh k\alpha}{\cosh^2 k\alpha} \qquad (67)$$

The left-hand side of this equation is calculable from circuit constants. Figure 10 is a plot of the right-hand side against values of $k\alpha$. By computing the left side of equation 67, entering the curve at the value obtained for the right side, the value of $k\alpha$ may be read from the curve.

The value of I may be secured from

$$I = \frac{(k\alpha)l}{aNk} \qquad (68)$$

and from equation 64 may be written

$$R_0^2 + \frac{K_1NwR_0}{lI} - \left(\frac{\omega Dk\alpha\sinh k\alpha}{2\cosh^2 k\alpha}\right)^2 = 0 \qquad (69)$$

and this may be solved as a quadratic,

$$R_0 = -\frac{K_1Nw}{2lI} \pm \frac{\sqrt{\left(\dfrac{K_1Nw}{lI}\right)^2 + \left(\dfrac{\omega Dk\alpha\sinh k\alpha}{\cosh^2 k\alpha}\right)^2}}{2} \qquad (70)$$

Figure 9 is a plot of the function,

$$\frac{k\alpha\sinh k\alpha}{\cosh^2 k\alpha} \qquad (71)$$

against $k\alpha$. From the value of $k\alpha$ obtained in the foregoing, and the value of I from equation 68, the value of R_0 may be determined. However, for most practical conditions, equation 70 reduces to

$$R_0 = \frac{\omega D}{2}\,\frac{k\alpha\sinh k\alpha}{\cosh^2 k\alpha} \qquad (72)$$

and then R_x is found from

$$R_x = R_0 - R_c - \frac{K_2N^2w}{l^2} \qquad (73)$$

Appendix III

Determination of the Constants B_n, a, and c

Select three points on the magnetization curve having co-ordinates x_1, y_1; x_2, y_2; x_3, y_3; where x is on the H axis and y on the B axis. Point x_1, y_1, should be selected approximately at the point at which a line drawn from the origin with the greatest possible slope is tangent to the magnetization curve. Point x_2, y_2 should be chosen near or above the middle of the curved portion of the knee, and point x_3, y_3, at a position above the knee and having x_3 equal to $2x_2$ or greater.

It is possible, if x_2 or x_3 are chosen too low, to have c become a negative number and this is undesirable as the curve will then drop at high values.

Then

$$y_1 = B_n gdax_1 + cx_1 \qquad (74)$$

$$y_2 = B_n gdax_2 + cx_2 \qquad (75)$$

$$y_3 = B_n gdax_3 + cx_3 \qquad (76)$$

Multiply equation 74 by x_2, equation 75 by x_1 and after subtracting

$$x_2y_1 - x_1y_2 = B_n[x_2gdax_1 - x_1gdax_2] \qquad (77)$$

Likewise multiply equation 75 by x_3 and equation 76 by x_2 and subtract

$$x_3y_2 - x_2y_3 = B_n[x_3gdax_2 - x_2gdax_3] \qquad (78)$$

Heat-Flow Effects in a Resistance-Type Thermometer

N. P. MILLAR
ASSOCIATE AIEE

IT IS a well-established fact that temperature can be measured by observing the change in resistance of a given material whose resistivity is a function of temperature. This principle of temperature detection is utilized in present-day resistance-type thermometers which commonly are called "aircraft thermometer bulbs." When used in conjunction with the proper indicating instrument, the resistance-type thermometer provides an accurate system for furnishing information to the instrument panel on temperatures at remote points in an aircraft. This information is transmitted in the form of changes in electric current that are caused by variations in the electrical resistance of the temperature-sensitive element.

There are several kinds of resistance-type thermometers in use today. Probably the most common is the two-lead type used in aircraft for the measurement of engine-oil, engine-coolant, cabin-air, and free-air temperature. Figure 1 shows this type of thermometer. For these applications, the specified accuracy requirement is a resistance change of approximately 0.5 per cent throughout the temperature range of −70 degrees centigrade to +150 degrees centigrade. Although this accuracy generally is tabulated for several conditions of temperature in terms of resistance limits, it will be convenient to use per-cent accuracy or per-cent error, as the case may be, in terms of temperature change in degrees centigrade for the purpose of the discussion in this paper.

In addition to the accuracy requirement of temperature detection, this type of thermometer must have a fast response to temperature change. For a change of temperature from 100 degrees centigrade to 0 degrees centigrade in water, the thermometer must reach the 10 degree-centigrade point within eight seconds.

Since specifications for the resistance-type thermometer for aircraft applications are necessarily severe with respect to accuracy and response, a theoretical investigation of some of the factors affecting the accuracy and time of response will be of value from the viewpoint of both test and design. Although there are several factors involved in an analysis of this sort, the discussion in this paper will be limited to the effects of variations in the speed of agitation of the medium being measured on:

1. The accuracy of temperature detection for several conditions of ambient temperature affecting the screw-base head.
2. The response of the temperature-sensitive element independent of head effects.

An analysis of the first condition will be useful from a test and calibration viewpoint as it is proposed to show how errors may be introduced when ambient-temperature conditions are not controlled adequately. In the second condition, the factors affecting response as analyzed will be of interest primarily to the designer. The equations derived for response aside from emphasizing the importance of controlled conditions in test should serve as an example of a method of attack in the solution of response problems.

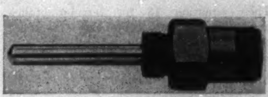

Figure 1. Typical resistance-type temperature transmitter

The fundamental equations for heat conduction between bulb and head and resulting temperature gradient expressions are completely general and may be used where two cylinders or bars of different cross sections are joined. The response expression is sufficiently general in character that it can be applied with slight modifications to other makes of re-

---

Paper 45-110, recommended by the AIEE committee on instruments and measurements for publication in AIEE Transactions. Manuscript submitted October 27, 1944; made available for printing May 11, 1945.

N. P. Millar is design engineer, West Lynn Works, General Electric Company, Lynn, Mass.

Divide equation 77 by equation 78 and after clearing

$$(x_3y_1-x_1y_3)gdax_2=(x_2y_1-x_1y_2)gdax_3+(x_3y_2-x_2y_3)gdax_1 \quad (79)$$

The coefficients of each term in equation 79 can be evaluated and the equation divided by the coefficient of the left-hand term, giving

$$gdax_2=F_1gdax_3+F_2gdax_1 \quad (80)$$

Values of a then are assumed and inserted in equation 80 until the equation is satisfied, thereby fixing a for the steel used. After determining a, B_n may be found from either equation 77 or 78, and c from either equation 74, 75, or 76.

Special Symbols

a = constant of a steel
A = area
B_n = constant of a steel
c = constant of a steel
$D = aAB_nN^2/10^8l$
$G = E_m10^8/aB_nN$
k = weighting constant
K_1 = iron-loss constant
K_2 = iron-loss constant
R_e = effective resistance
R_k = critical resistance
R_0 = constant circuit resistance
R_c = reactor copper resistance
R_x = resistance outside reactor
w = weight
W = watts
$\alpha = ani/l$ or anI/l

References

1. SOME ASPECTS OF INDUCTANCE WHEN IRON IS PRESENT, L. T. Rader, E. C. Litscher. AIEE TRANSACTIONS, volume 63, 1944, March section, pages 133–9.

2. ELEMENTS OF THE DIFFERENTIAL AND INTEGRAL CALCULUS (revised edition), W. A. Granville, P. F. Smith, W. R. Longley. Ginn and Company, New York, N. Y., 1941. Page 435.

3. SMITHSONIAN MATHEMATICAL TABLES, HYPERBOLIC FUNCTIONS, G. F. Becker, C. E. Van Orstrand. Smithsonian Institution, Washington, D. C., 1931.

4. INDUCTANCE OF COILS WITH SUPERIMPOSED D-C CURRENT, W. T. Wilhelm. *Bell Laboratories Record*, volume 14, 1935, pages 131–5.

5. LAW OF MAGNETIZATION, S. L. Gokhale. AIEE TRANSACTIONS, volume 45, 1926, pages 1013–31.

6. CONTRIBUTION TO THE THEORY OF MAGNETIC FREQUENCY DOUBLERS, J. Zenneck. *Proceedings* of the Institute of Radio Engineers, volume 8, 1920, pages 468–92.

7. STATUS OF FREQUENCY DOUBLERS IN RADIO PRACTICE, F. C. Ryan. *Proceedings* of the Institute of Radio Engineers, volume 8, 1920, pages 509–24.

8. UBER NEUE RESONANZERSCHEINUNGEN IN WECHSELSTROMKREISEN, O. Martienssen. *Physikalische Zeitschrift* (Leipzig, Germany), volume 11, 1910, pages 448–60.

9. CRITICAL CONDITIONS IN FERRORESONANCE, P. D. Odessy, Ernst Weber. AIEE TRANSACTIONS, volume 57, 1938, August section, pages 444–52.

10. STUDIES IN NONLINEAR CIRCUITS, C. G. Suits. AIEE TRANSACTIONS, volume 50, 1931, pages 724–36.

11. RESONANCE THEORY OF SERIES NONLINEAR CIRCUITS, E. G. Keller. *Journal* of the Franklin Institute, volume 225, 1938, pages 561–77.

12. SIMILITUDE OF CRITICAL CONDITIONS IN FERRORESONANT CIRCUITS, W. T. Thomson. AIEE TRANSACTIONS, volume 58, 1939, March section, pages 127–30.

13. DIE TRANSFORMATION EINES WECHSELSTROMS AUF DOPPELTE WECHSELZAHL MIT HÜLFE EINES RUHENDEN TRANSFORMATORS, J. Zenneck. *Annalen der Physik und Chemie*, volume 69, 1899, pages 858–60.

14. MATHEMATICAL ANALYSIS OF NONLINEAR CIRCUITS, A. Boyajian. *General Electric Review*, 1931, pages 531–7, 745–51.

sistance-type thermometers whose construction is similar to that shown in Figures 1 and 2.

The specific problems to which these equations are applied in this paper were encountered primarily in the development of the bulb which is illustrated. The constants used in the calculations refer to developmental samples of this type of temperature bulb.

Longitudinal Temperature Distribution of Bulb and Average Temperature Error

CONDITION WHERE BASE TEMPERATURE IS CONSTANT

In the application of the bulb to a normal measurement problem, the heat flow between the threads of the screw-base head and the wall into which the head is screwed is likely to be large enough to maintain the head at substantially the temperature of the wall. For this condition the temperature gradients that exist in the outer portion of the head become unimportant with respect to the temperature distribution in the bulb. In order that the temperature distribution of the bulb for the above condition may be obtained, it becomes necessary to make the following assumptions:

1. The temperature of the head is constant.
2. The bulb cross-sectional area is constant throughout its length.
3. The temperature at any one cross section of the bulb is constant, and the flow of heat through the lead supports inside the bulb is negligible.
4. At steady state the temperature distribution in the element inside the bulb is essentially that of the bulb.
5. The heat lost from the tip can be accounted for by imagining the length of the bulb extended to such a distance that the additional surface area is equivalent to the area of the tip. For this condition no heat is lost from the end; hence, the temperature gradient becomes zero.
6. The agitated medium (gas or liquid) flows uniformly at right angles to the bulb.

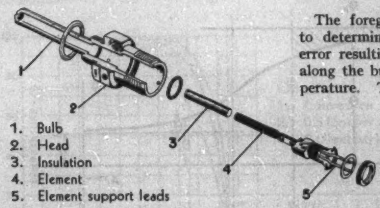

Figure 2. Exploded view of a typical resistance-type temperature transmitter

Assumption 5 can be explained best by referring to Figure 3, which is a schematic sketch of the bulb and extended length and a representative temperature-distribution curve. From Figure 3 (refer to Appendix I for list of symbols employed) let

$$\theta = T_l \pm \theta_x \tag{1}$$

In the foregoing expression θ_x is positive if θ_0 is a rise above T_l and negative if θ_0 is a drop from T_l.

From assumption 5

$$\frac{\pi D_0^2}{4} = \pi D_0 \delta$$

or solving for δ

$$\delta = D_0/4 \tag{2}$$

Therefore, the effective bulb length is

$$L' = L + D_0/4 \tag{3}$$

As the solution of this type of heat-conduction problem has been worked out completely elsewhere,[1] the derivation will not be repeated here. The temperature distribution along the bulb becomes

$$\theta_x = \theta_0 \frac{\cosh (x-L')N}{\cosh L'N} \tag{4}$$

If we assume that in equation 1 θ_x is positive, as shown in Figure 3, the temperature rise then becomes

$$\theta = T_l + \theta_0 \frac{\cosh (x-L')N}{\cosh L'N} \tag{5}$$

Once the expression for the temperature distribution is determined, it becomes useful in evaluating the average temperature error of the detector element. Referring again to Figure 3, the cross-hatched area under the curve represents the temperature error of the element because of the conduction of heat along the length of the bulb. An evaluation of this error can be determined from the average obtained by integrating equation 5.

The average temperature over the effective length of the element inside the bulb becomes

$$\theta_{av} = T_l + \frac{\theta_0 \sinh b'N}{b'N \cosh L'N} \tag{6}$$

Finally, the per-cent error is

$$\text{Per-cent error} = 100(\theta_{av} - T_l)/\theta_0 \tag{7}$$

The foregoing equation enables one to determine the average temperature error resulting from conduction of heat along the bulb for a constant base temperature. The accuracy of results depends on how accurately the base temperature and ambient temperature of the medium are known. In practice very little error will be experienced, since the base temperature generally will be very near the value of the medium temperature.

CONDITION WHERE TEMPERATURE GRADIENTS EXIST IN THE SCREW-BASE HEAD

In the previous section the expression for the average temperature of the bulb is sufficient for evaluating the error for most applications, when it can be assumed reasonably that the temperature of the screw-base head is constant. However, for isolated cases where temperature gradients exist in the head, the foregoing equation will not be adequate. This condition can be realized to some extent when the bulb is supported by a material which is a relatively poor conductor of heat. It then can be assumed that negligible heat is conducted from the threads of the screw-base head into the supporting member and that the average temperature of the head is not constant. For the sake of completeness, it is proposed to record in this section the equations that may be used for evaluating the error of the bulb when ambient-temperature conditions control the average temperature of the screw-base head. No attempt will be made to derive these equations as the solution to this type of problem is described in the literature.[2]

Figure 4 shows a sketch of the bulb-head combination in which we have assumed that the head can be represented as having an average uniform cross section throughout its length. If we apply assumption 5 to the head, then

$$l' = l + D_1/4 \tag{8}$$

For the condition assumed in Figure 4

$$\theta = T_l - \theta_x \tag{9}$$

for the bulb, and

$$\theta_1 = T_a + \theta_x' \tag{10}$$

for the head.

Once the expression for the temperature rise of the bulb (θ_x) and the head (θ_x') have been derived, equations 9 and 10 can be integrated to obtain the average temperature of the bulb and head respectively. For the bulb the average temperature becomes

$$\theta_{av} = T_l - \frac{(T_l - T_a)}{b'N}\left[\frac{1}{Z\dfrac{\tanh L'N}{\tanh l'N_1}+1}\right] \times \frac{\sinh b'N}{\cosh L'N} \tag{11}$$

Similarly for the head

$$\theta_{av}' = T_a + \frac{(T_l - T_a)}{l'N_1}\left[\frac{1}{1+\dfrac{\tanh l'N_1}{Z \tanh L'N}}\right] \times \frac{\sinh l'N_1}{\cosh l'N_1} \tag{12}$$

Finally, using the average temperature of the bulb (equation 11), the per-cent error becomes

$$\text{Per-cent error} = 100(T_1-\theta_{av})/(T_1-T_a) \quad (13)$$

Heat-Transfer Coefficients

At this point it might be well to consider a few expressions for the heat-transfer coefficient of gases and liquids. An expression for the heat-transfer coefficient between a solid and a gas or a solid and a liquid is extremely complicated and does not lend itself readily to rigorous mathematical treatment. However, empirical relations have been worked out for bodies of simple geometry. The equations herein listed are for liquids or gases flowing at right angles to single cylinders[3].

COEFFICIENT FOR LIQUIDS OR GASES FLOWING AT RIGHT ANGLES TO SINGLE CYLINDERS (FORCED CONVECTION)

$$h=0.86k_f/D_o(D_oV\rho_f/\mu_f)^{0.43}(c_p\mu_f/k_f)^{0.3} \quad (14)$$

$$h=k_f/D_o[0.35+0.47(D_oV\rho_f/\mu_f)^{0.52}](c_p\mu_f/k_f)^{0.3} \quad (15)$$

For gases use equation 14 where $(D_oV\rho_f/\mu_f)$ varies between 0.1 and 1,000.

For liquids use equation 14 when $(D_oV\rho_f/\mu_f)$ lies between 0.1 and 200 and equation 15 above 200.

COEFFICIENT FOR HEAT TRANSFER BY NATURAL CONVECTION (SINGLE CYLINDERS)

$$h_c=0.53k_f/D_o\left[\left(\frac{D_o^3\rho_f^2\beta g\,\Delta t}{\mu_f^2}\right)\left(\frac{c_p\mu_f}{k_f}\right)\right]^{0.25} \quad (16)$$

This expression assumes that the cylinder is placed horizontally in the liquid or gas. The writer has been unable to find a relation for vertical single cylinders. However, it is felt that for short cylinders there would be very little difference in the coefficient for the two conditions, and therefore for approximations of the coefficient equation 16 can be used for either liquids or gases. Although in some cases radiation effects may be of the same order of magnitude as convection effects, radiation will not be considered in this article.

Any consistent set of units may be used for equations 14, 15, and 16. However, in the illustrative example of computations in Appendix III, English units were used in these expressions, as these are the generally preferred units. Consequently, the heat-transfer coefficients are in English units and a conversion factor must be applied to use these coefficients in the foregoing equations for average temperature. For conversion factors refer to Appendix II and for symbols used in equations 14, 15, and 16 see Appendix I.

Effect of Agitation Velocity on Average Temperature Distribution

In the preceding paragraphs for the heat-transfer coefficient we can see that among other variables the velocity of agitation is one that might considerably affect the value of the heat-transfer coefficient. Also, the error which a change in the velocity of agitation may cause in temperature detection certainly will be to a large extent dependent upon the ambient-temperature conditions affecting the head. For example, the head may be held in an ice bath or in air and cooled by natural convection, or again in air and cooled or heated by forced convection. To show the magnitude of these effects we will assume several test conditions where we arbitrarily have selected constants from a given design for illustrative purposes only.

CONSTANT HEAD TEMPERATURE

Suppose it is required to compare the temperature measured by the resistance bulb with some other means of an oil bath where the oil-bath temperature T_1 = 100 degrees centigrade and the head temperature is controlled by an ice bath where T_a = 0 degrees centigrade. It also will be assumed that the container for the ice surrounding the head is insulated sufficiently from the oil bath that the head temperature is essentially constant at 0 degree centigrade. This condition corresponds to the required specification for test of thermal conductivity or the effect the head has on the accuracy of temperature detection. Figure 5 shows three separate plots of equation 5 of 0.5, and 2.0 feet per second, and for natural convection.

Referring again to Figure 5, the cross-hatched section represents the average temperature error over the limits of x = 0 to $x = b'$ where b' is the effective length of the detector element and for this particular case is equal to 4.25 centimeters. For the several conditions of agitation assumed, the errors represented by the cross-hatch sections using equations 6 and 7 are

(a). Natural convection per-cent error = −7.10 per cent

(b). V = 0.5 foot per second per-cent error = −1.39 per cent

(c). V = 2.0 feet per second per-cent error = −0.55 per cent

In the following table are a few average temperature errors taken from experiment on early sample production bulbs where the head has been packed in ice, the bulb inserted in oil at 100 degrees centigrade, and the oil agitation approximately 2.0 to 2.5 feet per second:

Bulb	Per-Cent Error
Number 1	−0.281
Number 2	−0.384
Number 3	−0.247
Number 4	−0.262
Number 5	−0.372
Number 6	−0.315

These errors are in good agreement with the calculated value of −0.55 per cent for an agitation of 2.0 feet per second on the same design bulb.

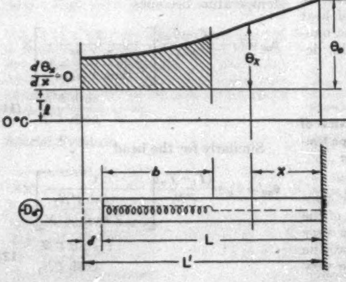

Figure 3 (left). Sketch of temperature distribution of bulb for constant base temperature

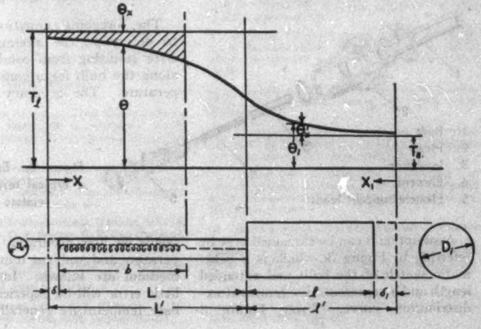

Figure 4 (right). Sketch of temperature distribution for bulb–head combination

VARIABLE AMBIENT TEMPERATURE CONTROLLING HEAD TEMPERATURE

In the previous section we have shown how the velocity of liquid agitation of the medium being measured affected the accuracy of temperature detection for constant head temperature. In this section we shall reverse the process and hold the bath conditions constant and determine the errors resulting from variable ambient-temperature head conditions.

Assume that the bath is oil at constant temperature T_1 = 100 degrees centigrade and the velocity of agitation is also constant at V = 0.5 foot per second. For the temperature of the air, T_a = 25 degrees centigrade. Figure 6 shows a plot of the temperature distribution where the head is in air and cooled by natural convection and again by air flowing at right angles at a velocity of 15 feet per second. The errors as represented by the cross-hatched section for b' = 4.25 centimeters using equation 13 are

(*a*). Natural convection per-cent error = 1.09

(*b*). Velocity of air = 15 feet per second per-cent error = 1.82

From this analysis it is seen how variable ambient-temperature conditions controlling both the bulb and the head temperature distributions can affect materially the accuracy of temperature measurement. In an actual measurement problem in practice the ambient temperature generally will be closer to the temperature of the medium measured; hence, any errors because of conduction will tend to be negligible. However, for test purposes, in order to obtain measurable errors, the ambient temperatures often are held at extremes, and for this setup the importance of maintaining constant ambient-temperature conditions such as velocity of bath agitation, temperature, and so forth, cannot be overemphasized.

Equation for Response Time of Element

In the resistance-type temperature bulb, the time of response of the detector element is an important factor in the bulb's performance. It is desirable that the detector reach a steady-state condition in the shortest time possible. The ideal performance would be instantaneous response, but this is practically impossible to obtain as component parts of the bulb structure have certain heat capacities that introduce lagging-time characteristics. It is the designer's aim to reduce this time lag to a minimum. Consequently, from a design point of view, it would be helpful to have an expression for the response time of a typical temperature bulb that ties together all the variables of dimension and heat constants of material. Considerable testing time could be saved in the development of a design by using such an expression, as the engineer would be able to predict what would happen to the response time if changes in the variables of dimension or material were made.

Most temperature bulbs exhibit comparable component parts as viewed cross sectionally from the detector support to the outside casing. Figure 7 shows the essential components in cross section of the bulb pictured in Figure 2.

Before an analysis can be made, the following assumptions will be necessary:

1. For temperature bulbs of circular cross section, heat flow is radial to or from the detector.
2. Heat flowing along the bulb casing has negligible effect on the response time. It is recognized here that this is not a valid assumption but is made to simplify the problem. It is felt that in a properly designed bulb envelope this effect would be minimized.
3. Negligible heat flows along element support to the head.

The component parts of Figure 7 can be grouped to form bodies having definite heat capacities and resistances which impede the flow of heat. Schematically, these groups can be represented as a series-parallel circuit as shown in Figure 8. This is analogous to an electric circuit with capacitance and resistance.

The differential equation for the series-parallel heat diagram as shown in Figure 8 is

$$\{ss_1R_1R_hD^2+[s_1R_h+s(R_1+R_h)]D+1\}\theta_y = (R_1+R_h)q+T_1=\theta_p \quad (17)$$

The solution to the differential equation 17 becomes

$$\theta_y=\frac{\theta_1-\theta_p}{m_2-m_1}[m_2e^{m_1t}-m_1e^{m_2t}]+\theta_p \quad (18)$$

(Refer to Appendix IV for the derivation of equation 17 and solution 18 where m_1 and m_2 also are defined.)

Effect of Agitation Velocity on the Response Time

Referring to the expression for θ_p in equation 17 we see that θ_p is a sum of two temperatures, T_1 which is the temperature of the medium being measured, and $(R_1+R_h)q$, which possibly could be called the temperature of the detector element due to self-heat when current flows through it. In good designs the effect of self-heat is made very small, and if this is done the term $(R_1+R_h)q$ can be neglected for all practical purposes. Should it ever become necessary to conduct response-time tests where it is felt the self-heat of the element is a contributing factor, then the complete expression of equation 17 should be used.

In the representative response curves of Figure 9 this self-heat term has been omitted from the calculations. These curves show the response of the element for various velocities of bath agitation. The solid lines are calculated curves assuming essentially the same arbitrary constants as previously used in the analysis of the effect of conduction, and the dotted curve is taken from experiment. The curves represent a test condition where the bulb has been heated to 100 degrees centigrade in a water bath and then suddenly immersed into a zero-degree-centi-

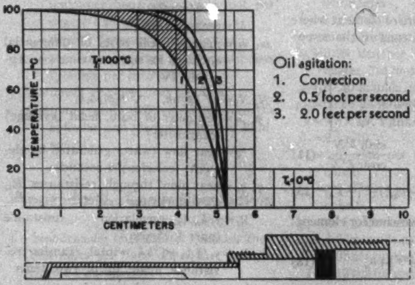

Figure 5 (left). Temperature distribution of bulb, head temperature constant

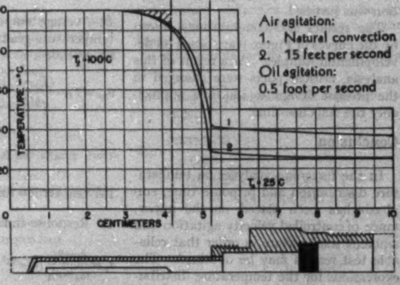

Figure 6 (right). Temperature distribution of bulb and head, bulb ambient controlled

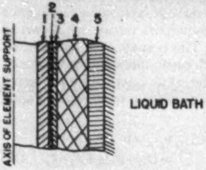

Figure 7. Sectional view of component parts for temperature bulb

1. Element support
2. Wire-wound temperature detector
3. Binder
4. Insulation
5. Wall of outside casing

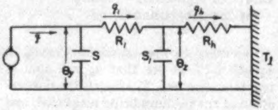

Figure 8. Diagram of grouped components for series-parallel heat flow

grade water bath. Equation 18 was used where

$\theta_i = 100$ degrees centigrade

and

$T_l = \theta_p = 0$ degrees centigrade

Again, it is seen how a change in the velocity of agitation affects the response time. The error in reponse readily can be visualized by noticing the differences in time at any particular temperature level; for example, the ten-degree-centigrade level.

The experimental curve tends to approach the zero-degree-centigrade level slower than the calculated curves. This is possibly due to the effect of the screw-base head cooling down slower than the element. It will be recalled that the effect of the head was neglected in the calculations, but the good agreement between experimental and calculated effects would seem to indicate that the assumption was justified.

The results and computations shown by the curves of Figure 9 are based on developmental samples. As a result of this analysis, critical parts were changed in the present design to improve appreciably the response time.

Conclusion

In the foregoing analyses on temperature distribution and response time, emphasis has been placed on the importance of controlled velocity agitation and ambient temperature in order that reliable test results may be obtained. The expressions for the temperature distribution of the bulb-head combination are general and can be applied to any similar problem where two bars or cylinders of different cross sections and materials are joined. Generality cannot be assigned to the response-time expression, as it must be modified and adapted to each make of temperature bulb. It was included in the discussion as an example of a method of attack in the solution of a particular response problem. The use of the response expression is limited in its accuracy when it is required to determine time-lag errors under ten per cent of the initial temperature difference. Above ten per cent of the initial temperature difference, the expression is entirely satisfactory. The condition that exists as the indicated temperature approaches more closely the final temperature is discussed extensively in an article by Noyes.[4]

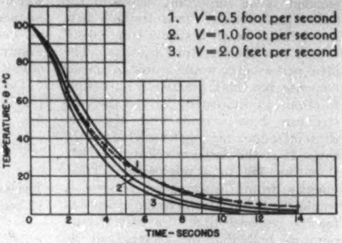

Figure 9. Response time of bulb

Response for temperature from 100 to 0 degrees centigrade in water

Solid line—Calculated
Dashed line—Experimental (V=0.75 foot per second approximately)

For reference convenience the equations applicable to the temperature sensitive element are grouped and listed again as follows:

A. Average temperature of element for constant base temperature:

$$\theta_{av} = T_l + \theta_0 \frac{\sinh b'N}{b'N \cosh L'N} \qquad (6)$$

$$\text{Per-cent error} = 100(\theta_{av} - T_l)/\theta_0 \qquad (7)$$

B. Average temperature of element where temperature gradients exist in the screw-base head:

$$\theta_{av} = T_l - \frac{(T_l - T_a)}{b'N} \left[\frac{1}{Z \dfrac{\tanh L'N}{\tanh l'N_1} + 1} \right] \times \frac{\sinh b'N}{\cosh L'N} \qquad (11)$$

$$\text{Per-cent error} = 100(T_l - \theta_{av})/(T_l - T_a) \qquad (13)$$

C. Response-time expression for element:

$$\theta_y = \frac{\theta_i - \theta_p}{m_2 - m_1} [m_2 e^{m_1 t} - m_1 e^{m_2 t}] + \theta_p \qquad (18)$$

Appendix I. Symbols Used for Conduction and Response Expressions

A_0 = outside surface area of bulb casing (square centimeters)
A_i = inside surface area of bulb casing (square centimeters)
A_e = outside surface area of element (square centimeters)
$A_m = \frac{A_i + A_e}{2}$ = mean surface area of insulation (part 4, Figure 7) (square centimeters)
A_s = mean surface area of bulb casing normal to radial flow of heat (square centimeters)
a, a_1 = average area of cross section of bulb casing, head (square centimeters)
b = length of element (centimeter)
$b' = (b + \delta)$ = effective length of element (centimeter)
c_p = thermal capacity; numerically equal to specific heat (calories per gram per degree centigrade)
D_0, D_1 = average outside diameter of bulb casing, head (centimeter)
δ, δ_1 = additional length required to make the extended surface area equal to the area at the end of the bulb, head (centimeter)
h, h_1 = heat-transfer coefficient (forced convection) between medium and bulb, head (calories per second per square centimeter per degree centigrade)
h_c, h_{c1} = heat-transfer coefficient (natural convection) between medium and bulb, head (calories per second per square centimeter per degree centigrade)
k, k_1 = thermal conductivity of bulb, head (calories per second per square centimeter per degree centigrade per centimeter)
k_m = thermal conductivity of insulation (part 4, Figure 7) (calories per second per square centimeter per degree centigrade per centimeter)
L = normal length of bulb (centimeter)
$L' = (L + \delta)$ = effective length of bulb (centimeter)
l = normal length of head (centimeter)
$l' = (l + \delta_1)$ = effective length of head (centimeter)
M = mass (grams)
m_1, m_2 = negative real roots of differential equation for response time (see Appendix IV)
$N, N_1 = \sqrt{hp/ak}, \quad \sqrt{h_1 p_1/a_1 k_1}$
p, p_1 = perimeter of bulb, head (average) (centimeter)
q = heat flow (watts generated by element) (calories per second)
q_1, q_h = heat flow through resistances R_1, R_h (calories per second)
$R_1 = y/k_m A_m$—insulation resistance (part 4, Figure 7)
$R_h = y_1/kA_s + 1/hA_0$ = total transfer resistance made up of two items

y_1/kA_b = the resistance of bulb casing to normal flow of heat

$1/hA_0$ = the transfer resistance to heat flow between bulb and medium

s, s_1 = total heat capacities of components (calories per degree centigrade)

$= \sum_1^n (Mc_p)_i$ (see Appendix IV)

T_a = ambient temperature around head above 0 degrees centigrade (degrees centigrade)

T_l = ambient temperature around bulb above 0 degrees centigrade (degrees centigrade)

t = time (seconds)

θ, θ_1 = temperature above 0 degrees centigrade reference for any value x, x_1 for the bulb, head (degrees centigrade)

θ_x, θ_x' = temperature change for any value x, x_1 for the bulb, head (degrees centigrade)

θ_i = initial temperature of bulb at $t=0$ (degrees centigrade)

θ_o = temperature at junction of bulb and head above medium temperature (degrees centigrade)

$\theta_p = (R_1+R_h)q+T_l$

θ_v = temperature of detector at time t (degrees centigrade)

θ_s = temperature of grouped component s_1 (degrees centigrade)

x, x_1 = distance along bulb, head (centimeter)

y = width of space occupied by insulation (centimeter)

y_1 = thickness of bulb wall (centimeter)

$Z = akN/a_1k_1N_1$

Symbols used in heat-transfer coefficient expressions, equations 14, 15, and 16

β = coefficient of expansion

c_p = thermal capacity at constant pressure (British thermal units per pound per degree Fahrenheit)

D_0 = outside diameter of cylinder (feet)

g = acceleration due to gravity $= 4.17\times 10^8$ (feet per square hour)

h, h_c = coefficient of heat transfer, forced and natural convection respectively (British thermal units per hour per square foot per degree Fahrenheit)

k_f = thermal conductivity (British thermal units per hour per square foot per degree Fahrenheit per foot)

ρ_f = density (pounds per cubic foot)

μ_f = absolute viscosity; $2.42\times$ centipoises (pounds per hour per foot)

V = linear velocity (feet per hour)

Δt = temperature differential between the cylinder and medium (degrees Fahrenheit)

Appendix II. Conversion Factors[5]

h = heat-transfer coefficient; (British thermal units per hour per square foot per degree Fahrenheit)

Divide h by

7,373 to get calories per second per square centimeter per degree centigrade
0.2048 to get kilogram calories per hour per square meter per degree centigrade
1,763 to get watts per square centimeter per degree centigrade

k = thermal conductivity; (British thermal units per hour per square foot per degree Fahrenheit per inch)

Divide k by

12.0 to get British thermal units per hour per square foot per degree Fahrenheit per foot
8.064 to get kilogram calories per hour per square meter per degree centigrade per meter
694.0 to get watts per square centimeter per degree centigrade per centimeter
2,903.0 to get calories per second per square centimeter per degree centigrade per centimeter

Appendix III. Example of Computations

For the purpose of illustrating how the conduction equations can be applied, one example of the computations will be given. The per-cent error will be computed from constants of a given design for one condition of medium agitation. For this condition it will be assumed that the head is placed in water at 0 degrees centigrade and that heat is transferred from the head to the water by natural convection only. The temperature of the medium being measured will be held constant at 100 degree centigrade and the medium will be a light grade of machine oil.

Constants (see Appendix I for list of symbols)

T_l = 100 degrees centigrade

T_a = 0 degrees centigrade

D_0 = 0.711 centimeter = 0.0233 foot

D_1 = 1.53 centimeter = 0.0502 foot

a = 0.139 square centimeter

a_1 = 1.84 square centimeters

p = 2.24 centimeters

p_1 = 4.81 centimeters

k = 0.036 calorie per second per square centimeter per degree centigrade per centimeter

k_1 = 0.160 calorie per second per square centimeter per degree centigrade per centimeter

$k_f = 5.68\times 10^{-2}$ Btu per hour per square foot per degree Fahrenheit per foot

k_{f1} = 0.29 Btu per hour per square foot per degree Fahrenheit per foot

ρ_f = 57.40 pounds per cubic foot

ρ_{f1} = 62.40 pounds per cubic foot

$\beta = 9.5\times 10^{-4}$

$\beta_1 = 2.1\times 10^{-4}$

c_p = 0.51 Btu per pound per degree Fahrenheit

c_{p1} = 1.0087 Btu per pound per degree Fahrenheit

μ_f = 43.5 pounds per hour per foot

μ_{f1} = 4.33 pounds per hour per foot

L = 5.08 centimeters

l = 4.13 centimeters

Let V = one foot per second (velocity of agitated oil bath)

From equations 3 and 8

L' = 5.26 centimeters

l' = 4.51 centimeters

In determining which equation to use for the heat-transfer coefficient for the agitated oil bath, we must evaluate the expression $(D_0V\rho_f/\mu_f)$, remembering that all the variables in all the expressions for the heat-transfer coefficients are in English units and V is in feet per hour.

$$\left(\frac{D_0V\rho_f}{\mu_f}\right)=\frac{0.0233\times 3{,}600\times 1\times 57.40}{43.5}=111$$

This is less than 200; therefore, we must use equation 14.

$$h=\frac{0.86k_f}{D_0}\left(\frac{D_0V\rho_f}{\mu_f}\right)^{0.43}(c_p\mu_f/k_f)^{0.3} \tag{14}$$

$$h=\frac{0.86\times 5.68\times 10^{-2}}{2.33\times 10^{-2}}\times \left(\frac{0.0233\times 3{,}600\times 57.40}{43.5}\right)^{0.43}\left(\frac{0.51\times 43.5}{5.68\times 10^{-2}}\right)^{0.3}$$

$h = 2.1(111)^{0.43}(390)^{0.3} = 95$ Btu per hour per square foot per degree Fahrenheit or in the metric system (see Appendix II for conversion factors)

$h=\dfrac{95}{7{,}373}=0.013$ calorie per second per square centimeter per degree centigrade

Now

$$N=\sqrt{\frac{hp}{ak}}=\sqrt{\frac{0.013\times 2.24}{0.139\times 0.036}}=2.41$$

$$L'N=5.26\times 2.41=12.68$$

Before we can proceed any further with calculations on the bulb, we now will have to evaluate the heat-transfer coefficient for the head. For this determination we must use equation 16 for natural convection as the water bath was assumed unagitated.

$$h_{c1}=\frac{0.53k_{f1}}{D_1}\left[\left(\frac{D_1^3\rho_{f1}^2\beta_1 g\,\Delta t}{\mu_{f1}^2}\right)\left(\frac{c_{p1}\mu_{f1}}{k_{f1}}\right)\right]^{0.25} \tag{16}$$

It will be noticed that this expression involves the term Δt which is the temperature difference between the water and the head. Therefore, it becomes necessary by trial and error to assign values to Δt until the value assigned is approximately equal to the temperature difference between the ice water and the average temperature of the head.

Let us assume for the first approximation that

Δt = 4 degrees centigrade = 7.2 degrees Fahrenheit

$$h_{c1}=\frac{0.53\times 0.29}{0.0502}\times\left[\left(\frac{\overline{0.0502}^3\times\overline{62.4}^2\times 2.1\times 10^{-4}\times 4.17\times 10^8\times 7.2}{\overline{4.33}^2}\right)\times\left(\frac{1.0087\times 4.33}{0.29}\right)\right]^{0.25}$$

$$h_{cl}=3.07[(16.5\times10^{3})(15.05)]^{0.25}$$
$$=3.07\times22.3=68.5 \text{ Btu per hour per square foot per degree Fahrenheit}$$

or

$$h_{cl}=\frac{68.5}{7{,}373}=0.0093 \text{ calorie per second per square centimeter per degree centigrade}$$

Now

$$N_1=\sqrt{\frac{h_{cl}p_1}{a_1k_1}}=\sqrt{\frac{0.0093\times4.81}{1.84\times0.160}}=0.389$$

and

$$l'N_1=4.51\times0.389=1.76$$

$$Z=\frac{akN}{a_1k_1N_1}=\frac{0.139\times0.036\times2.41}{1.84\times0.160\times0.389}$$
$$=10.54\times10^{-2}$$

We can now calculate the average temperature of the head from equation 12.

$$\theta_{av}'=T_a+\frac{(T_l-T_a)}{l'N_1}\times\left[\frac{1}{1+\dfrac{\tanh l'N_1}{Z\tanh L'N}}\right]\frac{\sinh l'N_1}{\cosh l'N_1} \quad (12)$$

$\tanh L'N=1$
$\tanh l'N_1=0.943$
$\sinh l'N_1=2.820$
$\cosh l'N_1=2.992$

Therefore

$$\theta_{av}'=\frac{100}{1.76}\left[\frac{1}{1+\dfrac{0.943}{10.54\times10^{-2}}}\right]\frac{2.820}{2.992}$$

$$\theta_{av}'=56.8\left(\frac{1}{9.95}\right)\times0.943=5.4 \text{ degrees centigrade}$$

Now, since $T_a=0$ degree centigrade, this value represents the temperature change between the ice water and the head. Comparing this value of 5.4 degrees centigrade with the originally assumed value of $\Delta t=4$ degrees centigrade, we see that we must assume another value and go through the same procedure as previously outlined until the two values check within reasonable limits. The value of Δt obtained after two more trials is

$\Delta t=4.9$ degrees centigrade

If we use this value, then

$h_{cl}=0.00979$ calorie per second per square centimeter per degree centigrade
$N_1=0.399$
$l'N_1=1.80$
$Z'=10.28\times10^{-2}$

Having once found the above variables for the correct Δt, we now can proceed with the calculation of the average temperature of the bulb and the consequent error.

From equation 11 we have

$$\theta_{av}=T_l-\frac{(T_l-T_a)}{b'N}\times\left[\frac{1}{\dfrac{Z\tanh L'N}{\tanh l'N_1}+1}\right]\frac{\sinh b'N}{\cosh L'N} \quad (11)$$

which is the expression for the average temperature distribution between the limits $x=0$, $x=b'$ for the element inside the bulb. (Refer to Figure 4)

$b'=4.25$ centimeters
$b'N=4.25\times2.41=10.25$

$\tanh L'N=1$
$\tanh l'N_1=0.947$
$\sinh b'N={}^1/_2e^{b'N}=1.41\times10^4$
$\cosh L'N={}^1/_2e^{L'N}=15.9\times10^4$

For $(L'N)$ or any other value of the hyperbolic radian > 6.0,

$$\sinh L'N=\cosh L'N={}^1/_2e^{L'N}$$

Therefore,

$$\theta_{av}=100-\frac{(100-0)}{10.25}\times\left[\frac{1}{\dfrac{10.28\times10^{-2}}{0.947}+1}\right]\times\frac{1.41\times10^4}{15.9\times10^4}$$

$$\theta_{av}=100-9.75\left(\frac{1}{1.109}\right)\times0.0887=100-0.78$$

$\theta_{av}=99.22$ degrees centigrade

Finally from equation 13

$$\text{Per-cent error}=\frac{(T_l-\theta_{av})}{T_l-T_a}\times100 \quad (13)$$

$$\text{Per-cent error}=\frac{(100-99.22)}{100}\times100=0.78$$

Appendix IV. Derivation of Equation for Response Time

Referring to Figure 7, the summation of the heat capacities of parts 1, 2, 3, and one half of part 4 can be expressed mathematically as follows:

$$s=(Mc_p)_1+(Mc_p)_2+(Mc_p)_3+{}^1/_2(Mc_p)_4 \quad (19)$$

where, for example, $(Mc_p)_1$ is the heat capacity of part 1 or its mass M times its specific heat c_p.

Similarly

$$s_1={}^1/_2(Mc_p)_4+(Mc_p)_5 \quad (20)$$

Now referring to Figure 8, the heat gained in calories per second by the body having a heat capacity s is

$$s\frac{d\theta_y}{dt}=q-q_1$$

or, solving for $\frac{d\theta_y}{dt}$,

$$\frac{d\theta_y}{dt}=\frac{q-q_1}{s} \quad (21)$$

Similarly

$$\frac{d\theta_z}{dt}=\frac{q_1-q_h}{s_1} \quad (22)$$

Now the flow of heat from one body to another is equal to the difference in temperature of the two bodies divided by the resistance of the path; therefore

$$q_1=\frac{(\theta_y-\theta_z)}{R_1} \quad (23)$$

and

$$q_h=\frac{(\theta_z-T_l)}{R_h} \quad (24)$$

Substituting equations 23 and 24 in 21 and 22 and simplifying

$$\frac{d\theta_y}{dt}=1/sR_1[qR_1-(\theta_y-\theta_z)] \quad (25)$$

and

$$\frac{d\theta_z}{dt}=1/s_1R_1R_h[R_h\theta_y-(R_1+R_h)\theta_z+R_1T_l] \quad (26)$$

Making use of the differential operator $D=\frac{d}{dt}$ equations 25 and 26 can be written

$$(D+1/sR_1)\theta_y-\theta_z/sR_1-q/s=0 \quad (27)$$

$$[D+(R_1+R_h)/s_1R_1R_h]\theta_z-\theta_y/s_1R_1-T_l/s_1R_h=0 \quad (28)$$

If equation 28 is solved for θ_z and substituted in equation 27 and remembering that $Dq=0$, that is, for any one condition the flow of heat is constant, thus making the rate of change of heat flow equal to zero, one obtains after simplifying, the differential equation for the response time

$$\{ss_1R_1R_hD^2+[s_1R_h+s(R_1+R_h)]D+1\}\theta_y=(R_1+R_h)q+T_l=\theta_p \quad (17)$$

Now the solution of the differential equation

$$(\alpha D^2+\eta D+1)\theta_y=0 \quad (29)$$

will be of the form

$$\theta_y=c_1e^{m_1t}+c_2e^{m_2t} \quad (30)$$

where c_1 and c_2 are constants to be evaluated for the boundary conditions and m_1 and m_2 are roots of the auxiliary equation

$$\alpha m^2+\eta m+1=0 \quad (31)$$

Also

$$\alpha=ss_1R_1R_h \quad (32)$$

$$\eta=s_1R_h+s(R_1+R_h) \quad (33)$$

The auxiliary equation yields two negative real roots,

$$m_1=\frac{-\eta+\sqrt{\eta^2-4\alpha}}{2\alpha} \quad (34)$$

and

$$m_2=\frac{-\eta-\sqrt{\eta^2-4\alpha}}{2\alpha} \quad (35)$$

By actual substitution for the quantities under the radical sign it can be shown that m_1 and m_2 are negative real roots.

A particular solution of the differential equation 17 will be

$$\theta_y=(R_1+R_h)q+T_l \quad (36)$$

or

$$\theta_y=\theta_p \quad (37)$$

Sag and Tension Calculations for Cable and Wire Spans Using Catenary Formulas

JOHN F. NASH
MEMBER AIEE

JOHN F. NASH, JR.
NONMEMBER AIEE

IT IS generally agreed that, in order to obtain accurate solutions of sag and tension problems involved in stringing electric power line conductors, it is necessary to use catenary formulas. The basic formulas are, of course, well known In order to utilize them, however, a great amount of laborious calculating is required. Certain short cuts in these calculations have been evolved, notably by James S. Martin whose published tables and method have proved of great help to engineers in simplifying sag calculations.

In connection with the design and construction of transmission lines in the mountainous Appalachian region the writers have evolved a method of making mathematically exact sag and tension calculations based on catenary formulas which is quite different from the Martin method, and which eliminates the trial-and-error assumptions involved in a portion of the Martin method. The working formulas used by the writers require only simple arithmetical calculations which can be handled by clerical personnel usually available in the engineering office. The calculations are not laborious, and can be easily checked.

The writers' method not only develops the sags, tensions, and conductor lengths for the various final and initial conditions of the design span (basic or ruling span), but also similar data for span lengths other than the ruling span.

The procedure outlined is applicable to any cable or wire whose modulus of elasticity and coefficient of expansion are uniform throughout the cross section, such as is the case with copper, copper-coated-steel, or steel cables. Sag and tension problems for composite cables such as aluminum cables steel reinforced, are usually solved by graphic methods based on stress–strain curves developed from laboratory tests on the particular cable under consideration.

The writers' method does, however, develop previously unpublished relationships between sags, tensions, and cable lengths which are applicable not only to copper, copper-coated-steel, and steel cables, but also to problems involving composite cables, which information cannot be secured by graphic methods alone.

The following text gives the basic catenary formulas, the derivations thereof, and an explanation of the procedure followed in actual sag calculations.

The basic formulas of the catenary are shown on Figure 1. The nomenclature used in this figure is as follows:

X and Y = Cartesian co-ordinates of any point in the catenary curve, designated point B
Z = length of catenary from the vertex A to point B
S = the deflection of the vertex A below any point B which may be under consideration
V = vertical distance from the axis of abscissas of the catenary to the vertex A
A = vertex of the catenary curve
ϵ = base of the Naperian or natural system of logarithms equals 2.71828

These formulas are well known and need no proof of derivation. Formula A determines the shape of the catenary curve which shape depends on the V function. Formula B determines the length of the curve which depends on the same V function. It will be shown later that the value of V depends on the cable tension at the span vertex, and the value of Y depends on the total tension in the cable. The sag is $Y-V$ (formula C) which can be expressed in terms of the V value and span length (formula D).

Referring to Figure 1 note that point B is a cable support, X the horizontal distance from the vertex (low point of sag) to support, and Z the cable length from vertex to support. S is the sag of the cable below its support, or the span sag in problems with equal elevation supports.

Unit Values of Catenary Functions

In catenary spans the values of V, Y, S, and Z bear definite relationships to each other expressed by the basic formulas, A, B, and C. When these formulas are divided by X, unit value formulas result as follows:

$Y/X = V/X \cosh X/V$
$Z/X = V/X \sinh X/V$
$S/X = (Y/X)-(V/X)$

Related unit values of V/X, Y/X, S/X, and Z/X are tabulated in Table I, which values can be applied to any length span, or any type cable. When V, Y, Z, or S is known for any span the other values are quickly determined by interpolation. These table values are derived from ten-place hyperbolic sine and cosine tables and these values have the same accuracy as the sinh and cosh tables. Table I values

---

Paper 45-144, recommended by the AIEE committee on power transmission and distribution for publication in AIEE TRANSACTIONS. Manuscript submitted February 23, 1945; made available for printing July 11, 1945.

JOHN F. NASH is electrical engineer with the Appalachian Electric Power Company, Bluefield, W. Va.; JOHN F. NASH, JR., is a student at Carnegie Institute of Technology, Pittsburgh, Pa.

The authors acknowledge the assistance of T. H. Worman and H. H. Rodee.

---

where

$$\theta_p=(R_1+R_h)q+T_i \tag{38}$$

therefore the general solution to equation 17 is

$$\theta_y=c_1e^{m_1t}+c_2e^{+m_2t}+\theta_p \tag{39}$$

The boundary conditions that must be satisfied are

$\theta_y=\theta_i$

and

$\frac{d\theta_y}{dt}=0$

when $t=0$,

and

$\theta_y=\theta_p$

when $t=\infty$.

If these boundary conditions are substituted in equation 39, the value of c_1 and c_2 can be determined

$$c_1=(\theta_i-\theta_p)m_2/(m_2-m_1) \tag{40}$$

$$c_2=-(\theta_i-\theta_p)m_1/(m_2-m_1) \tag{41}$$

Finally putting c_1 and c_2 back into equation 39 the solution to the differential equation 17 becomes

$$\theta_y=\frac{\theta_i-\theta_p}{m_2-m_1}[m_2e^{m_1t}-m_1e^{m_2t}]+\theta_p \tag{18}$$

References

1. MATHEMATICAL EQUATIONS FOR HEAT CONDUCTION IN THE FINS OF AIR-COOLED ENGINES, D. R. Harper, W. B. Brown. National Advisory Committee for Aeronautics Report 158, 1922.

2. HEAT FLOW IN TURBINE-GENERATOR ROTORS, C. E. Peck. AIEE TRANSACTIONS, volume 53, 1934, October section, pages 1359–65.

3. HEAT TRANSMISSION (second edition), W. H. McAdams. McGraw-Hill Book Company, New York, N. Y., 1942. Pages 220–44.

4. STEM LAG OF INDUSTRIAL THERMOMETERS, Bradford Noyes. *Instruments*, volume 15, November 1942, pages 449–52, 454, and so forth.

5. THE BASIC LAWS AND DATA OF HEAT TRANSMISSION, W. J. King. *Mechanical Engineering*, April–May issues, 1932.

eliminate laborious calculations and provide speed and accuracy in solving sag and tension problems.

Additional Formulas and Nomenclature

The following text explains the additional formulas, derived from the basic catenary characteristics, which are used in this procedure.

Let the following nomenclature be used:

l = horizontal span length between supports
L = catenary arc length of the span
T = tension (total) in cable
F = horizontal longitudinal component of tension in cable. It will be seen from formulas given hereinafter that F equals T at the span vertex
H = horizontal loading per foot of cable due to wind pressure on cable (cable only or cable with ice loading)
W = vertical loading per foot of cable due to weight of cable (cable only or cable with ice loading)
R = resultant loading per foot of cable due to horizontal and vertical loading
ZE = elongation of Z (not permanent stretch) due to loading
ZT = change in length of Z due to temperature change
a = cross-section area of cable
M = modulus of elasticity of cable
C = coefficient of linear expansion per degree temperature change
d = temperature change in degrees
ku = unit permanent set of cable due to loading
kt = total permanent set of cable due to loading

The additional formulas are set out and explained in the following:

$l=2X$ (when both supports are at the same elevation) (E)

Refer to appendix for the relationship of l to x where span supports are at unequal elevations.

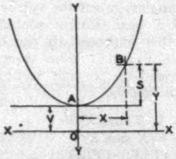

Figure 1. The catenary and its basic formulas

$$Y=(V/2)(\epsilon^{X/V}+\epsilon^{-X/V}) \qquad \text{(AA)}$$

$$Y=V\cosh X/V \qquad \text{(A)}$$

$$Z=(V/2)(\epsilon^{X/V}-\epsilon^{-X/V}) \qquad \text{(BB)}$$

$$Z=V\sinh X/V \qquad \text{(B)}$$

$$S=Y-V \qquad \text{(C)}$$

$$S=V(\cosh X/V-1) \qquad \text{(D)}$$

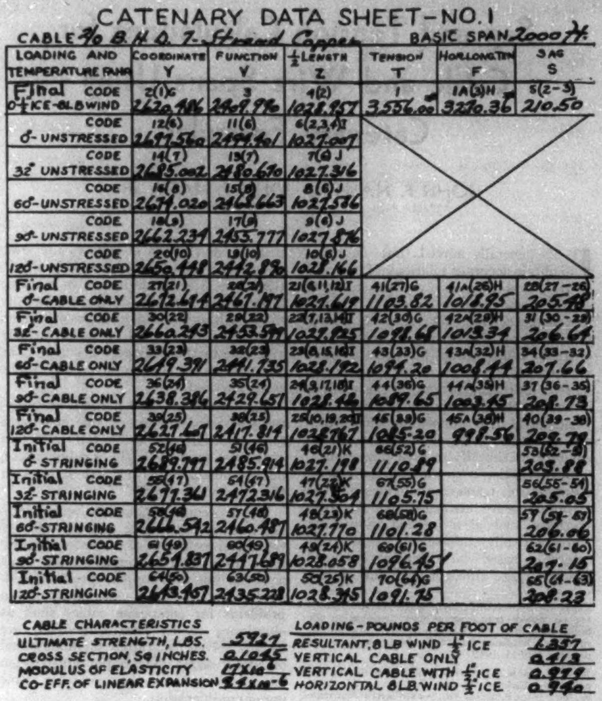

CATENARY DATA SHEET—NO. 1

CABLE 2/0 B.H.D. 7-Strand Copper BASIC SPAN 2000 ft.

LOADING AND TEMPERATURE FAHR	COORDINATE Y	FUNCTION V	½ LENGTH Z	TENSION T	HOR.LONG.TEN. F	SAG S
Final CODE 0°-½" ICE-8LB WIND	2(1)G 2620.486	3 2409.996	4(2) 1028.957	1 3556.00	1A(3)H 3270.36	5(2-3) 210.50
CODE 0°-UNSTRESSED	12(6) 2697.560	11(6) 2494.401	6(2,3,4)I 1027.007			
CODE 32° UNSTRESSED	14(7) 2685.002	13(7) 2480.670	7(6)J 1027.316			
CODE 60°-UNSTRESSED	16(8) 2674.020	15(8) 2468.663	8(6)J 1027.586			
CODE 90°-UNSTRESSED	18(9) 2662.234	17(9) 2455.777	9(6)J 1027.876			
CODE 120°-UNSTRESSED	20(10) 2650.448	19(10) 2442.890	10(6)J 1028.166			
Final CODE 0°-CABLE ONLY	27(21) 2672.694	26(21) 2467.197	21(6,11,12)I 1027.619	41(27)G 1103.82	41A(26)H 1018.95	28(27-26) 205.50
Final CODE 32°-CABLE ONLY	30(22) 2660.243	29(22) 2453.599	22(7,13,14)I 1027.925	42(30)G 1098.68	42A(29)H 1013.34	31(30-29) 206.64
Final CODE 60°-CABLE ONLY	33(23) 2649.391	32(23) 2441.735	23(8,15,16)I 1028.192	43(33)G 1094.20	43A(32)H 1008.44	34(33-32) 207.66
Final CODE 90°-CABLE ONLY	36(24) 2638.386	35(24) 2429.651	24(9,17,18)I 1028.446	44(36)G 1089.65	44A(35)H 1003.45	37(36-35) 208.73
Final CODE 120°-CABLE ONLY	39(25) 2627.607	38(25) 2417.814	25(10,19,20)I 1028.767	45(39)G 1085.20	45A(38)H 998.56	40(39-38) 209.79
Initial CODE 0°-STRINGING	52(46) 2689.797	51(46) 2485.914	46(21)K 1027.198	66(52)G 1110.89		53(52-51) 203.88
Initial CODE 32°-STRINGING	55(47) 2677.361	54(47) 2472.316	47(22)K 1027.504	67(55)G 1105.75		56(55-54) 205.05
Initial CODE 60°-STRINGING	58(48) 2666.542	57(48) 2460.487	48(23)K 1027.770	68(58)G 1101.28		59(58-57) 206.06
Initial CODE 90°-STRINGING	61(49) 2654.837	60(49) 2447.689	49(24)K 1028.058	69(61)G 1096.45		62(61-60) 207.15
Initial CODE 120°-STRINGING	64(50) 2643.467	63(50) 2435.228	50(25)K 1028.345	70(64)G 1091.75		65(64-63) 208.23

CABLE CHARACTERISTICS	
ULTIMATE STRENGTH, LBS.	5927
CROSS SECTION, SQ INCHES.	0.1045
MODULUS OF ELASTICITY	17×10^6
CO-EFF. OF LINEAR EXPANSION	9.4×10^{-6}

LOADING—POUNDS PER FOOT OF CABLE	
RESULTANT, 8LB WIND ½" ICE	1.357
VERTICAL CABLE ONLY	0.413
VERTICAL CABLE WITH ½" ICE	0.979
HORIZONTAL 8LB WIND ½" ICE	0.940

Figure 2

$L=2Z$ (supports at the same elevation) (F)

Refer to appendix for relationship of L to Z where span supports are at unequal elevations.

$T=YR$ (G)

The tension in a cable at any point is equal to the Y co-ordinate at that point times the per foot loading of the cable. In problems without wind pressure, $T=VW$.

This formula is due to a certain peculiarity of the catenary. The tension in a cable at any point in a span is equal to the loading on a piece of cable of the length of the function Y at that point in the span. If the cable, assumed to be perfectly flexible, were hung in a frictionless pulley at any point in the span with a length of cable hanging down just sufficient to reach the axis of the Y co-ordinate, the curve of the catenary would be undisturbed. (Reference: Martin's tables.)

The formula shows that the Y function used in the catenary formulas is proportional to the total tension in the cable.

At the low point of sag (vertex) $Y=V$ (refer to formula A) and $T=F$ so that substitutions in formula just given produces the one which follows.

$F=VR$ (H)

The horizontal longitudinal component of tension in a cable is equal to the V function times the per-foot cable loading. In problems without wind pressure, $F=VW$.

This formula shows that the V function used in the catenary function is proportional to the tension at the cable vertex.

Since $Y=V+S$ (from formula C) formula G may be written:

$T=(V+S)R$

Therefore:

$T=F+SR$

This indicates that the tension in a cable at a support is equal to the horizontal longitudinal component of tension plus the product of the sag times the per foot cable loading. This relationship holds with spans which have supports at the same or at unequal elevations provided S is taken as the deflection of the vertex below the support in question. This formula provides a quick determination of tension increase at sup-

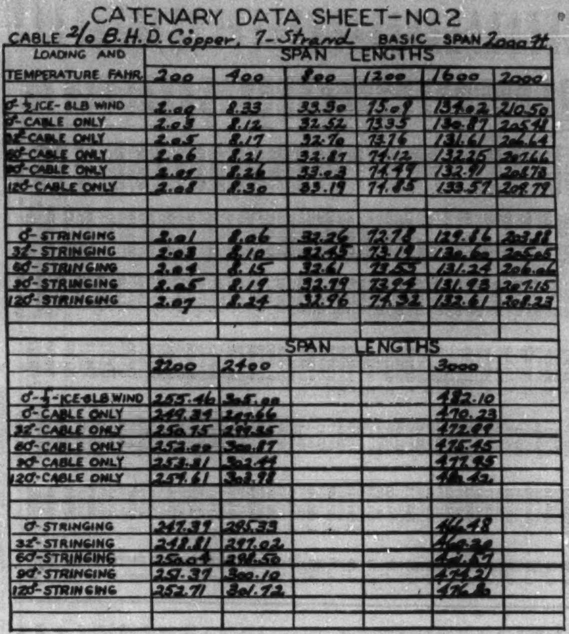

CATENARY DATA SHEET-NO.2

CABLE 2/0 B.H.D. Copper, 7-Strand BASIC SPAN 2000 ft.

LOADING AND TEMPERATURE FAHR.	SPAN LENGTHS 200	400	800	1200	1600	2000
0°-½-ICE-8LB WIND	2.09	8.33	33.30	75.09	134.02	210.50
0°-CABLE ONLY	2.03	8.12	32.52	73.35	130.87	205.48
32°-CABLE ONLY	2.05	8.17	32.70	73.76	131.61	206.64
60°-CABLE ONLY	2.06	8.21	32.87	74.12	132.25	207.66
90°-CABLE ONLY	2.07	8.26	33.03	74.49	132.91	208.73
120°-CABLE ONLY	2.08	8.30	33.19	74.85	133.57	209.79
0°-STRINGING	2.01	8.06	32.26	72.78	129.86	203.88
32°-STRINGING	2.03	8.10	32.45	73.19	130.60	205.05
60°-STRINGING	2.04	8.15	32.61	73.55	131.24	206.06
90°-STRINGING	2.05	8.19	32.79	73.94	131.93	207.15
120°-STRINGING	2.07	8.24	32.96	74.32	132.61	208.23

	SPAN LENGTHS 2200	2400			3000	
0°-½-ICE-8LB WIND	255.46	305.00			482.10	
0°-CABLE ONLY	249.34	299.66			470.23	
32°-CABLE ONLY	250.75	299.55			472.99	
60°-CABLE ONLY	252.00	300.87			475.45	
90°-CABLE ONLY	253.81	302.44			477.95	
120°-CABLE ONLY	254.61	303.98			[illegible]	
0°-STRINGING	247.39	295.33			466.48	
32°-STRINGING	248.81	297.02			[illegible]	
60°-STRINGING	250.04	298.50			[illegible]	
90°-STRINGING	251.37	300.10			[illegible]	
120°-STRINGING	252.71	301.72			[illegible]	

Figure 3

Solve for sag by using Table I, remembering that the V in V/X is the same V value occurring for the basic span under similar loading conditions. The related S/X value multiplied by one-half the span produces the sag value

ports over tension at the vertex. In long-span construction this increase is an appreciable item.

Effect in Change of Loading

Elongation of Z (not permanent stretch) due to cable loading is determined by formula I.

$$ZE = (R/2aM)(XV + YZ) \qquad \text{(I)}$$

This formula is ably developed in the Martin method of sag and tension calculations Under conditions of no wind W replaced R in this formula.

Note the following variations in formula I.

$$ZE = (RVX + RYZ)/2aM$$

Therefore:

$$ZE = (FX + TZ)/2aM \qquad \text{(I-1)}$$

Effect of Temperature Change

Changes in cable length due to temperature changes are found by using formula J.

$$Z1 = CdZ \qquad \text{(J)}$$

The change in conductor length due to variation in temperature depends on the original length, the coefficient of expansion, and the degrees temperature variation.

Determination of Permanent Stretch

The following procedure is suggested for securing the permanent set (in Z) due to loading previously unstressed cables.

First determine loaded stress in cable as follows:

Stress (at support) = T/a

Stress (at vertex) = F/a

Stress (span average) = $(T+F)/2a$

This value is a close value to use with permanent-set charts for the cable under consideration From the chart determine the unit permanent set, ku, caused by design loading, $(T+F)/2a$, and the unit permanent set, ku, for the probable stringing stress. The difference between these k values will be the net unit permanent set to be used in calculating stringing sags and tensions.

$$KT = KuZ \qquad \text{(K)}$$

Problem Solution Procedure

The authors recently designed and built an 88-kv transmission line located in mountain country. The sag and tension design data for this line are contained in data sheets 1 and 2 as shown in Figures 2 and 3, and it is suggested that these be studied to determine the solution procedure of this paper. These data sheets are coded to show the sequence of calculations. The left-hand number gives the calculation sequence, the numbers in parentheses the previous values used to derive the present value, and the right-hand key letter the formula used. Where no key letter is shown the value is obtained by using Table I. S values result from subtracting V from Y.

Data sheet number 1, shown in Figure 2, covers calculations for the basic (ruling) span where X is constant. Data sheet number 2, shown in Figure 3, covers calculations for other length spans related to the basic span where X varies with the span length, but the V value for each final or initial condition remains constant throughout varying span lengths.

While the data sheets are largely self-explanatory the steps in problem solution are further explained in the following paragraphs

1. Tabulate the cable characteristics, the per-foot cable loading values, the basic design span, and design final tension, item 1.

2. Calculate Y, item 2, for design load conditions using formula G. Use Table I to secure related values of V, item 3, and Z, item 4. Design sag item 5 is simply $Y-V$. Horizontal longitudinal component of tension F (item 1A) is secured by formula H. The calculating steps just outlined are based on the tension at support in the basic design span. If the design is to be based on a desired F value for the basic span first tabulate item 1A and calculate V, item 3, using formula H. Use Table I to secure related design values of Y, item 2, and Z, item 4. Sag is $Y-V$, and total tension, item 1, is solved by using formula G.

3. Solve for unstressed Z, item 6, all loads removed, but with the cable still at design temperature, using formula I.

4. Solve for unstressed Z at other temperatures, items 7, 8, 9, and 10, using the item 6 value of Z and formula J.

5. Determine related V and Y values for each unstressed Z value from Table I.

6. Calculate Z (cable only) at various temperatures, items 21 to 25 inclusive, using formula I.

7. Determine related V and Y values for each cable only load condition from Table I. Sags for each condition are $Y-V$.

8. Solve for Z values (initial conditions, not prestretched) at various temperatures, items 46 to 50 inclusive by the use of for-

Table I. Unit Values of *V*, *Y*, *Z*, and *S*, Catenary Functions

Function X/V	Function V/X	Difference in X/V	Function Y/X	Difference in Y/X	Function S/X	Difference in S/X	Function Z/X	Difference in Z/X
0.00	Infinity	Infinity	Infinity	Infinity	Infinity	Infinity	0.0000000	1.0000167
0.01	100.00000	50.000000	100.00500	49.995000	.00500000	.00500000	1.0000167	.0000500
0.02	50.000000	16.666667	50.01000	16.661667	.01000000	.00500000	1.0000667	.0000833
0.03	33.333333	8.333333	33.34833	8.328330	.01500000	.00500300	1.0001500	.0001167
0.04	25.000000	5.000000	25.020003	4.994997	.02000300	.00500300	1.0002667	.0001500
0.05	20.000000	3.333333	20.025006	3.328331	.02500600	.00500200	1.0004167	.0001834
0.06	16.666667	2.380953	16.696675	2.375947	.03000800	.00500600	1.0006001	.0002168
0.07	14.285714	1.785714	14.320728	1.780707	.03501400	.00500700	1.0008169	.0002501
0.08	12.500000	1.388889	12.540021	1.383880	.04002100	.00500900	1.0010670	.0002835
0.09	11.111111	1.111111	11.156141	1.106099	.04503000	.00501200	1.0013505	.0003170
0.10	10.000000	.909091	10.050042	.904078	.05004200	.00501300	1.0016675	.0003504
0.11	9.090909	.757576	9.145964	.752559	.05505500	.00501700	1.0020179	.0003838
0.12	8.333333	.641025	8.393405	.636005	.06007200	.00502000	1.0024017	.0004174
0.13	7.692308	.549451	7.757400	.544429	.06509200	.00502200	1.0028191	.0004507
0.14	7.142857	.476190	7.212971	.471163	.07011400	.00502700	1.0032698	.0004845
0.15	6.666667	.416667	6.741808	.411637	.07514100	.00503000	1.0037543	.0005178
0.16	6.250000	.367647	6.330171	.362613	.08017100	.00503400	1.0042721	.0005516
0.17	5.882353	.326797	5.967558	.321759	.08520500	.00503800	1.0048237	.0005852
0.18	5.555556	.292398	5.645799	.287355	.09024300	.00504300	1.0054080	.0006186
0.19	5.263158	.263158	5.358444	.258110	.09528600	.00504800	1.0060275	.0006525
0.20	5.000000	.238095	5.100334	.233042	.10033400	.00505300	1.0066800	.0006863
0.21	4.761905	.216450	4.867292	.211392	.10538700	.00505800	1.0073663	.0007200
0.22	4.545455	.197629	4.655900	.192567	.11044500	.00506200	1.0080863	.0007537
0.23	4.347826	.181159	4.463333	.176089	.11550700	.00507000	1.0088400	.0007878
0.24	4.166667	.166667	4.287244	.161592	.12057700	.00507500	1.0096278	.0008215
0.25	4.000000	.153846	4.125652	.148764	.12565200	.00508200	1.0104493	.0008555
0.26	3.846154	.142450	3.976888	.137362	.13073400	.00508800	1.0113048	.0008897
0.27	3.703704	.132275	3.839526	.127180	.13582200	.00509500	1.0121945	.0009236
0.28	3.571429	.123153	3.712346	.118051	.14091700	.00510200	1.0131181	.0009577
0.29	3.448276	.114943	3.594295	.109834	.14601900	.00510900	1.0140758	.0009917
0.30	3.333333	.107527	3.484461	.102410	.15112800	.00511700	1.0150675	.0010262
0.31	3.225806	.100806	3.382051	.095681	.15624500	.00512500	1.0160937	.0010606
0.32	3.125000	.094697	3.286370	.089564	.16137000	.00513300	1.0171543	.0010948
0.33	3.030303	.089126	3.196806	.083985	.16650300	.00514100	1.0182491	.0011294
0.34	2.941177	.084034	3.112821	.078884	.17164400	.00515000	1.0193785	.0011636
0.35	2.857143	.079365	3.033937	.074206	.17679400	.00515900	1.0205421	.0011984
0.36	2.777778	.075075	2.959731	.069908	.18195300	.00516700	1.0217405	.0012330
0.37	2.702703	.071124	2.889823	.065947	.18712000	.00517700	1.0229735	.0012675

Function X/V	Function V/X	Difference in V/X	Function Y/X	Difference in Y/X	Function S/X	Difference in S/X	Function Z/X	Difference in Z/X
0.38	2.631579	.067476	2.823876	.062289	.19229700	.00518700	1.0242410	.0013027
0.39	2.564103	.064103	2.761587	.058906	.19748400	.00519700	1.0255437	.0013371
0.40	2.500000	.060976	2.702681	.055769	.20268100	.00520700	1.0268808	.0013722
0.41	2.439024	.058072	2.646912	.052855	.20788800	.00521700	1.0282530	.0014073
0.42	2.380952	.055371	2.594057	.050143	.21310500	.00522800	1.0296603	.0014423
0.43	2.325581	.052854	2.543914	.047615	.21833300	.00523900	1.0311026	.0014777
0.44	2.272727	.050505	2.496299	.045254	.22357200	.00525100	1.0325803	.0015130
0.45	2.222222	.048309	2.451045	.043048	.22882300	.00526100	1.0340933	.0015484
0.46	2.173913	.046253	2.407997	.040979	.23408400	.00527400	1.0356417	.0015840
0.47	2.127660	.044327	2.367018	.039041	.23935800	.00528600	1.0372257	.0016189
0.48	2.083333	.042517	2.327977	.037220	.24464400	.00529700	1.0388446	.0016550
0.49	2.040816	.040816	2.290757	.035505	.24994100	.00531100	1.0404996	.0016910
0.50	2.000000	.039216	2.255252	.033893	.25525200	.00532300	1.0421906	.0017265
0.51	1.960784	.037707	2.221359	.032370	.26057500	.00533700	1.0439171	.0017628
0.52	1.923077	.036285	2.188989	.030936	.26591200	.00534900	1.0456799	.0017985
0.53	1.886792	.034940	2.158053	.029576	.27126100	.00536400	1.0474784	.0018352
0.54	1.851852	.033671	2.128477	.028294	.27662500	.00537700	1.0493136	.0018707
0.55	1.818181	.032467	2.100183	.027075	.28200200	.00539200	1.0511843	.0019079
0.56	1.785714	.031328	2.073108	.025922	.28739400	.00540600	1.0530922	.0019443
0.57	1.754386	.030248	2.047186	.024827	.29280000	.00542100	1.0550365	.0019808
0.58	1.724138	.029223	2.022359	.023787	.29822100	.00543600	1.0570173	.0020174
0.59	1.694915	.028248	1.998572	.022796	.30365700	.00545200	1.0590347	.0020548
0.60	1.666667	.027323	1.975776	.021856	.30910900	.00546700	1.0610895	.0020911
0.61	1.639344	.026441	1.953920	.020959	.31457600	.00548200	1.0631806	.0021286
0.62	1.612903	.025601	1.932961	.020101	.32005800	.00550000	1.0653092	.0021663
0.63	1.587302	.024802	1.912860	.019287	.32555800	.00551500	1.0674755	.0022030
0.64	1.562500	.024038	1.893573	.018506	.33107300	.00553200	1.0696785	.0022411
0.65	1.538462	.023310	1.875067	.017761	.33660500	.00555000	1.0719196	.0022785
0.66	1.515152	.022615	1.857306	.017048	.34215500	.00556600	1.0741981	.0023157
0.67	1.492537	.021949	1.840258	.016365	.34772100	.00558400	1.0765138	.0023542
0.68	1.470588	.021313	1.823893	.015711	.35330500	.00560200	1.0788680	.0023922
0.69	1.449275	.020704	1.808182	.015084	.35890700	.00562000	1.0812602	.0024305
0.70	1.428571	.020120	1.793098	.014482	.36452700	.00563800	1.0836907	.0024694
0.71	1.408451	.019562	1.778616	.013904	.37016500	.005658	1.0861601	.0025073
0.72	1.388880	.019026	1.764712	.013349	.37582300	.00567700	1.0886674	.0025460
0.73	1.369863	.018512	1.751363	.012817	.38150000	.00569500	1.0912134	.0025847
0.74	1.351351	.018018	1.738546	.012302	.38719500	.00571600	1.0937981	.0026239
0.75	1.333333	.017543	1.726244	.011807	.39291100	.00573600	1.0964220	.0026638

Table I. Unit Values of *V*, *Y*, *Z*, and *S* Catenary Functions (continued)

Function X/V	Function V/X	Difference in V/X	Function Y/X	Difference in Y/X	Function S/X	Difference in S/X	Function Z/X	Difference in Z/X
0.76	1.315790	.017089	1.714437	.011334	.39864700	.00575500	1.0990858	.0027017
0.77	1.298701	.016650	1.703103	.010874	.40440200	.00577600	1.1017875	.0027419
0.78	1.282051	.016228	1.692229	.010430	.41017800	.00579800	1.1045294	.0027820
0.79	1.265823	.015823	1.681799	.010005	.41597600	.00581800	1.1073114	.0028211
0.80	1.250000	.015432	1.671794	.009593	.42179400	.00583900	1.1101325	.0028614
0.81	1.234568	.015056	1.662201	.009194	.42763300	.00586200	1.1129939	.0029012
0.82	1.219512	.014693	1.653007	.008810	.43349500	.00588300	1.1158951	.0029417
0.83	1.204819	.014343	1.644197	.008437	.43937800	.00590600	1.1188368	.0029823
0.84	1.190476	.014005	1.635760	.008076	.44528400	.00592900	1.1218191	.0030236
0.85	1.176471	.013680	1.627684	.007728	.45121300	.00595200	1.1248427	.0030638
0.86	1.162791	.013366	1.619956	.007392	.45716500	.00597400	1.1279065	.0031043
0.87	1.149425	.013061	1.612564	.007062	.46313900	.00599900	1.1310108	.0031468
0.88	1.136364	.012768	1.605502	.006745	.46913800	.00602300	1.1341576	.0031877
0.89	1.123596	.012485	1.598757	.006439	.47516100	.00604600	1.1373453	.0032287
0.90	1.111111	.012210	1.592318	.006139	.48120700	.00607100	1.1405740	.0032712
0.91	1.098901	.011944	1.586179	.005847	.48727800	.00609700	1.1438452	.0033137
0.92	1.086957	.011688	1.580332	.005567	.49337500	.00612100	1.1471589	.0033550
0.93	1.075269	.011439	1.574765	.005292	.49949600	.00614700	1.1505139	.0033978
0.94	1.063830	.011198	1.569473	.005025	.50564300	.00617300	1.1539117	.0034407
0.95	1.052632	.010965	1.564448	.004766	.51181600	.00619900	1.1573524	.0034832
0.96	1.041667	.010739	1.559682	.004513	.51801500	.00622600	1.1608356	.0035261
0.97	1.030928	.010520	1.555169	.004268	.52424100	.00625200	1.1643617	.0035693
0.98	1.020408	.010307	1.550901	.004027	.53049300	.00628000	1.1679310	.0036133
0.99	1.010101	.010101	1.546874	.003793	.53677300	.00630800	1.1715443	.0036569
1.00	1.000000	.009901	1.543081	.003566	.54308100	.00633500	1.1752012	.0037008
1.01	.990099	.009707	1.539515	.003344	.54941600	.00636300	1.1789020	.0037448
1.02	.980392	.009518	1.536171	.003126	.55577900	.00639200	1.1826468	.0037898
1.03	.970874	.009336	1.533045	.002915	.56217100	.00642100	1.1864366	.0038332
1.04	.961538	.009157	1.530130	.002707	.56859200	.00645000	1.1902698	.0038795
1.05	.952381	.008984	1.527423	.002505	.57504200	.00648000	1.1941493	.0039236
1.06	.943396	.008817	1.524918	.002308	.58152200	.00650900	1.1980729	.0039691
1.07	.934579	.008653	1.522610	.002112	.58803100	.00654100	1.2020420	.0040155
1.08	.925926	.008495	1.520498	.001925	.59457200	.00657000	1.2060575	.0040604
1.09	.917431	.008341	1.518573	.001738	.60114200	.00660200	1.2101179	.0041072

Function X/V	Function V/X	Difference in V/X	Function Y/X	Difference in Y/X	Function S/X	Difference in S/X	Function Z/X	Difference in Z/X
1.10	.909091	.008190	1.516835	.001557	.60774400	.00663300	1.2142251	.0041531
1.11	.900901	.008044	1.515278	.001379	.61437700	.00666500	1.2183782	.0041995
1.12	.892857	.007901	1.513899	.001204	.62104200	.00669700	1.2225777	.0042471
1.13	.884956	.007763	1.512695	.001034	.62773900	.00672900	1.2268248	.0042934
1.14	.877193	.007628	1.511661	.000866	.63446800	.00676200	1.2311182	.0043407
1.15	.869565	.007496	1.510795	.000700	.64123000	.00679600	1.2354589	.0043890
1.16	.862069	.007368	1.510095	.000539	.64802600	.00682900	1.2398479	.0044368
1.17	.854701	.007243	1.509556	.000380	.65485500	.00686300	1.2442847	.0044852
1.18	.847458	.007122	1.509176	.000226	.66171800	.00689600	1.2487699	.0045324
1.19	.840336	.007003	1.508950	.000071	.66861400	.00693200	1.2533023	.0045817
1.20	.833333	.006887	1.508879	.000080	.67554600	.00696700	1.2578840	.0046310
1.21	.826446	.006774	1.508959	.000228	.68251300	.00700200	1.2625150	.0046805
1.22	.819672	.006664	1.509187	.000375	.68951500	.00703900	1.2671955	.0047299
1.23	.813008	.006556	1.509562	.000518	.69655400	.00707400	1.2719254	.0047805
1.24	.806452	.006452	1.510080	.000659	.70362800	.00711100	1.2767059	.0048294
1.25	.800000	.006349	1.510739	.000799	.71073900	.00714800	1.2815353	.0048807
1.26	.793651	.006249	1.511538	.000937	.71788700	.00718600	1.2864160	.0049315
1.27	.787402	.006152	1.512475	.001071	.72507300	.00722300	1.2913475	.0049816
1.28	.781250	.006056	1.513546	.001205	.73229600	.00726100	1.2963291	.0050340
1.29	.775194	.005963	1.514751	.001337	.73955700	.00730000	1.3013631	.0050853
1.30	.769231	.005872	1.516088	.001467	.74685700	.00733900	1.3064484	.0051373
1.31	.763359	.005783	1.517555	.001596	.75419600	.00737900	1.3115857	.0051897
1.32	.757576	.005696	1.519151	.001722	.76157500	.00741800	1.3167754	.0052425
1.33	.751880	.005611	1.520873	.001848	.76899300	.00745900	1.3220179	.0052953
1.34	.746269	.005528	1.522721	.001971	.77645200	.00749900	1.3273132	.0053485
1.35	.740741	.005447	1.524692	.002092	.78395100	.00753900	1.3326617	.0054015
1.36	.735294	.005367	1.526784	.002215	.79149000	.00758900	1.3380632	.0054564
1.37	.729927	.005289	1.528999	.002335	.79907200	.00762400	1.3435196	.0055111
1.38	.724638	.005214	1.531334	.002451	.80669600	.00766500	1.3490307	.0055637
1.39	.719424	.005138	1.533785	.002572	.81436100	.00771000	1.3545944	.0056215
1.40	.714286	.005066	1.536357	.002685	.82207100	.00775100	1.3602159	.0056759
1.41	.709220	.004995	1.539042	.002800	.82982200	.00779500	1.3658918	.0057295
1.42	.704225	.004924	1.541842	.002924	.83761700	.00784800	1.3716213	.0057887
1.43	.699301	.004857	1.544766	.003019	.84546500	.00787600	1.3774100	.0058419
1.44	.694444		1.547785		.85334100		1.3832519	

In a given span *V*, *Y*, *S*, and *Z* bear definite interrelationships expressed by the formulas, $Y = V \cosh (X/V)$, $Z = V \sinh (X/V)$, and $S = Y - V$. When these formulas are divided by *X*, unit values, $(Y/X) = (V/X) \cosh (X/V)$, $(Z/X) = (V/X) \sinh (X/V)$, and $(S/X) = (Y/X) - (V/X)$ result which apply to any length span.

Related unit values are tabulated in Table I. If *V*, *Y*, *Z*, or *S* is known for any span the other values can be quickly determined by the use of this table.

Differences for interpolations speed these calculations.

These tables also will supply cosh and sinh values for use in the formulas $Y = V \cosh (X/V)$ and $Z = V \sinh (X/V)$. The *Y/X* value of the table when multiplied by *X/V* becomes the cosh (X/V) of *X/V*, and *Z/X* value when multiplied by *X/V* becomes the sinh (X/V) of *X/V*.

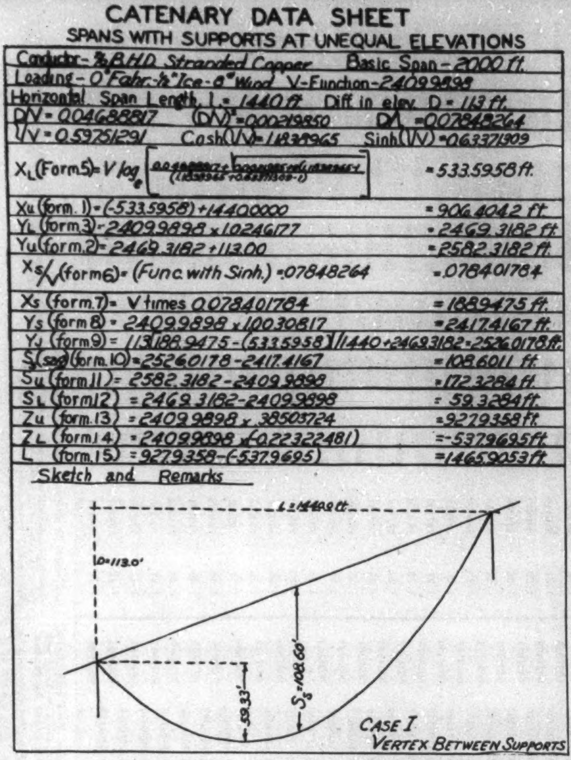

CATENARY DATA SHEET
SPANS WITH SUPPORTS AT UNEQUAL ELEVATIONS

Conductor - ⅜ B.H.D. Stranded Copper   Basic Span - 2000 ft.
Loading - 0° Fahr. - ½" Ice - 8# Wind   V-Function - 24099898
Horizontal Span Length, l = 1440 ft   Diff in elev. D = 113 ft.
D/V = 0.04688817   (D/V)² = 0.00219850   D/l = 0.07848264
l/V = 0.59751291   Cosh(l/V) = 11838965   Sinh(l/V) = 0.63371909
X_L (Form 5) = V log_e [[illegible]]   = 533.5958 ft.
Xu (form. 1) = (-533.5958) + 1440.0000   = 906.4042 ft.
Y_L (form 3) = 2409.9898 × 1.0246177   = 2469.3182 ft.
Yu (form. 2) = 2469.3182 + 113.00   = 2582.3182 ft.
Xs/V (form 6) = (Func. with Sinh.) = .07848264   = .078401784
Xs (form. 7) = V times 0.078401784   = 188.9475 ft.
Ys (form 8) = 2409.9898 × 1.0030817   = 2417.4167 ft.
Y_J (form 9) = 113[188.9475 - (533.5958)]/1440 + 2469.3182 = 2526.0178 ft.
S_s (sag) (form. 10) = 2526.0178 - 2417.4167   = 108.6011 ft.
Su (form 11) = 2582.3182 - 2409.9898   = 172.3284 ft.
S_L (form 12) = 2469.3182 - 2409.9898   = 59.3284 ft.
Zu (form. 13) = 2409.9898 × .38503724   = 927.9358 ft.
Z_L (form 14) = 2409.9898 × (-0.22322481)   = -537.9695 ft.
L (form. 15) = 927.9358 - (-537.9695)   = 1465.9053 ft.

Sketch and Remarks

Figure 4

mula K. For this problem the following *Ku* values were used:

Ku—design loading	=	0.00049
Ku—stringing	=	0.00008
Ku (for formula K)	=	0.00041

The stress–strain chart from which these values were secured is reproduced in Figure 4. It should be noted that the *Ku* values for stringing (initial) conditions varies very little over the range of stringing stresses encountered. This indicates that even with a variation between assumed stringing tensions used to secure *Ku* (stringing) and the final determined stringing tension, close stringing sag and tension values are secured. Stringing temperature variations have practically no effect on the *Ku* value taken from the stress–strain chart.

9. Determine related V and Y values (initial) from Table I. Solve for stringing sags, $Y-V$.

10. Solve for T and F (if desired) under various conditions. The cable loading per foot, and the Y and V values for each condition give the T and F values.

11. Solve for sags under various final and initial conditions for other span lengths. Remembering that the V value for a given final or initial condition is the same for all span lengths (related to the design span), use these V values and Table I to secure these sags. Tabulate these sags on data sheet number 2 (Figure 3). F values for the related spans are the same as the value for the design span under like final or initial conditions. If desired, the T value can be quickly determined for any related span by means of Table I and formula G.

The procedure outlined here gives full sag and tension data for final and initial conditions, not only for the design span, but also for similar conditions in other related span lengths.

The calculation procedure can be reversed, if it is desired to base the calculations on other conditions such as final, cable only at 60 degrees Fahrenheit.

Hillside Span Calculations

Several approximate methods of determining sags in hillside spans are in use. One of the best of these methods is published in Martin's tables. Martin has also developed another method of calculating hillside spans which has an extremely high degree of mathematical accuracy.

The appendix outlines a mathematically exact method, developed by the writers and their associates, for determining sag, deflection of vertex below supports, and horizontal distances from the vertex to supports in hillside spans. This method is recommended where precision results are desired.

Appendix. Hillside Span Calculations

This paper outlines a mathematically accurate method, developed by the authors, of determining sag, deflection of vertex below supports, and distance (horizontally) from the vertex to supports in spans with supports at unequal elevations. Its use is recommended whenever precision results are necessary, such as with certain span designs crossing railroads, highways, or other lines.

The method is based on maintaining the same horizontal longitudinal component of tension, and therefore the same V value, as in the ruling span to which the hillside span is related.

The procedure outlined is applicable to any type cable such as copper, copper-coated steel, steel, or aluminium cable steel reinforced, where the ruling span sag (for a level span) is known.

There are two general types of spans with supports at unequal elevations:

Case I. Catenary vertex located between supports.
Case II. Catenary vertex located below the lower support.

Figure 5 illustrates these two conditions.

Nomenclature (Refer to Figure 5)

D = difference in elevation of cable supports
l = span length (horizontally)
X_u, Y_u = co-ordinates of upper support
X_L, Y_L = co-ordinates of lower support
S_s = sag of cable, which is the maximum deflection of the cable from the straight (slope) line between supports
X_s, Y_s = co-ordinates of catenary curve at the point of maximum deflection, S_s
Y_J = Y co-ordinate of a point on the slope line (between supports) directly above Y_s
S_u = deflection of vertex below upper support
S_L = deflection of vertex below lower support
Z_u = catenary length from vertex to upper support
Z_L = catenary length from vertex to lower support
L = catenary length of span (hillside span)

V = the ruling (basic) span V value for the cable under the assumed loading conditions

If this V value is not known, it may be quickly determined as follows:

Divide ruling span sag (level span) by X (1/2 span), to secure S/X. From Table I determine by interpolation the corresponding V/X value. This multiplied by X (1/2 span), gives the required V value.

This procedure may be used with any type cable.

The various formulas and their derivation are given in the following. In developing these formulas the writers have assumed that the upper support is to the right of the lower support. Under case I conditions the lower-support X and Z values should be set in the formulas as minus quantities since they are to the left-hand (minus) side of the vertex.

$$l = X_u - X_L \qquad (1)$$

or

$$X_u = X_L + l$$

Case II—As X_u and X_L are on the same side of the vertex, both represent positive values.

Case I—As X_u and X_L are on opposite sides of the vertex, X_L is taken as a negative value.

$$Y_u = Y_L + D \qquad (2)$$

$$Y_u = V \cosh (X_u/V)$$

$$Y_u = V \cosh \left(\frac{X_L + l}{V}\right)$$

$$Y_L = V \cosh (X_L/V) \qquad (3)$$

$$D = Y_u - Y_L$$

Therefore:

$$D/V = \cosh\left(\frac{X_L+l}{V}\right) - \cosh\left(\frac{X_L}{V}\right)$$

$$\frac{D}{V} = \frac{\epsilon^{\left(\frac{X_L+l}{V}\right)} + \epsilon^{-\left(\frac{X_L+l}{V}\right)}}{2} - \frac{\epsilon^{(X_L/V)} + \epsilon^{-(X_L/V)}}{2}$$

Transpose and rearrange:

$$\frac{2D}{V} = \epsilon^{(X_L/V)}[\epsilon^{(l/V)} - 1] + \epsilon^{-(X_L/V)}[\epsilon^{-(l/V)} - 1]$$

Multiply by $\epsilon^{(X_L/V)}$:

$$\frac{2D\epsilon^{(X_L/V)}}{V} = [\epsilon^{(X_L/V)}]^2[\epsilon^{(l/V)} - 1] + [\epsilon^{-(l/V)} - 1]$$

Transpose:

$$[\epsilon^{(X_L/V)}]^2[\epsilon^{(l/V)} - 1] - \frac{2D}{V}\epsilon^{(X_L/V)} = -\epsilon^{-(l/V)} - 1]$$

Multiply by $[\epsilon^{(l/V)} - 1]$ and add $(D/V)^2$:

$$[\epsilon^{(X_L/V)}]^2[\epsilon^{(l/V)} - 1]^2 - \frac{2D}{V}\epsilon^{(X_L/V)}[\epsilon^{(l/V)} - 1] + \left(\frac{D}{V}\right)^2 = \epsilon^{(l/V)} + \epsilon^{-(l/V)} - 2 + \left(\frac{D}{V}\right)^2$$

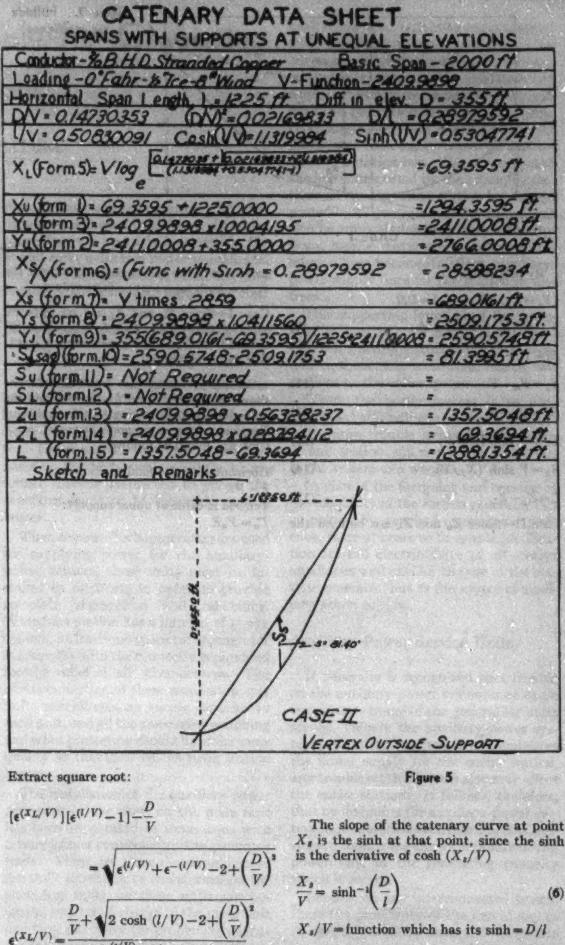

CATENARY DATA SHEET
SPANS WITH SUPPORTS AT UNEQUAL ELEVATIONS

Conductor - 9/0 B.H.D. Stranded Copper Basic Span - 2000 ft
Loading - 0° Fahr - ½" Ice - 8# Wind V-Function - 2409.9898
Horizontal Span Length, l = 1225 ft Diff. in elev. D = 355 ft.
D/V = 0.14730353 $(D/V)^2$ = 0.02169833 D/l = 0.28979592
l/V = 0.50830091 Cosh(l/V) = 1.1319984 Sinh(l/V) = 0.53047741
X_L (Form 5) = V $\log_e\left[\frac{0.14730353 + \sqrt{0.02169833 + 2(1.1319984 - 1)}}{(1.1319984 + 0.53047741 - 1)}\right]$ = 69.3595 ft
Xu (form 1) = 69.3595 + 1225.0000 = 1294.3595 ft.
Y_L (form 3) = 2409.9898 x 1.0004195 = 2411.0008 ft.
Yu (form 2) = 2411.0008 + 355.0000 = 2766.0008 ft.
Xs/V (form 6) = (Func with Sinh = 0.28979592 = 28588234
Xs (form 7) = V times .2859 = 689.0161 ft.
Ys (form 8) = 2409.9898 x 1.0411560 = 2509.1753 ft.
Y_J (form 9) = 355(689.0161 - 69.3595)/1225 + 2411.0008 = 2590.5748 ft.
Ss (sag) (form. 10) = 2590.5748 - 2509.1753 = 81.3995 ft.
Su (form. 11) = Not Required =
S_L (form. 12) = Not Required =
Zu (form. 13) = 2409.9898 x 0.56328237 = 1357.5048 ft.
Z_L (form. 14) = 2409.9898 x 0.28784112 = 69.3694 ft.
L (form. 15) = 1357.5048 - 69.3694 = 1288.1354 ft.

Sketch and Remarks

Figure 5

Extract square root:

$$[\epsilon^{(X_L/V)}][\epsilon^{(l/V)} - 1] - \frac{D}{V} = \sqrt{\epsilon^{(l/V)} + \epsilon^{-(l/V)} - 2 + \left(\frac{D}{V}\right)^2}$$

$$\epsilon^{(X_L/V)} = \frac{\frac{D}{V} + \sqrt{2\cosh(l/V) - 2 + \left(\frac{D}{V}\right)^2}}{[\epsilon^{(l/V)} - 1]}$$

$$\epsilon^{(X_L/V)} = \frac{\frac{D}{V} + \sqrt{\left(\frac{D}{V}\right)^2 + 2\,[\cosh (l/)V - 1]}}{[\cosh (l/V) + \sinh (l/V) - 1]} \qquad (4)$$

$$X_L = V \times \log_e\left[\frac{\frac{D}{V} + \sqrt{\left(\frac{D}{V}\right)^2 + 2[\cosh (l/V) - 1]}}{\cosh (l/V) + \sinh (l/V) - 1}\right] \qquad (5)$$

After X_L is determined, Y_L is found by equation 3.

$$\frac{D}{l} = \sinh\left(\frac{X_s}{V}\right)$$

The slope of the catenary curve at point X_s is the sinh at that point, since the sinh is the derivative of cosh (X_s/V)

$$\frac{X_s}{V} = \sinh^{-1}\left(\frac{D}{l}\right) \qquad (6)$$

X_s/V = function which has its sinh = D/l

X_s = formula 6 value multiplied by V (7)

$$Y_s = V \cosh (X_s/V) \qquad (8)$$

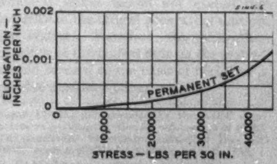

Figure 6. Stress–strain chart

Seven-strand hard-drawn copper cable

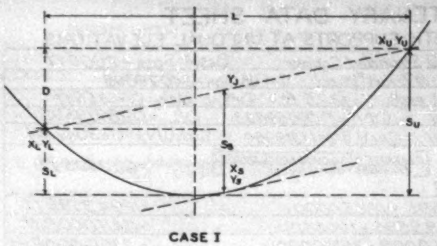

CASE I

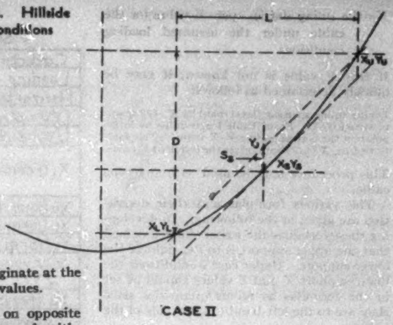

CASE II

Figure 7. Hillside sag conditions

By proportion:

$$(Y_J - Y_L)/(X_s - X_L) = D/l$$

$$Y_J = D(X_s - X_L)/l + Y_L \tag{9}$$

$$S_s = Y_J - Y_s \tag{10}$$

$$S_u = Y_u - V \tag{11}$$

$$S_L = Y_L - V \tag{12}$$

$$Z_u = V \sinh (X_u/V) \tag{13}$$

$$Z_L = V \sinh (X_L/V) \tag{14}$$

$$L = Z_u - Z_L \tag{15}$$

Case II—Since Z_u and Z_L are both on the same side of the vertex, and originate at the vertex, both represent positive values.

Case I—Since Z_u and Z_L are on opposite sides of the vertex, and L is equal arithmetically to $Z_u + Z_L$, Z_L represents a negative value (algebraic).

Sample problems, case I and case II, are shown in Figures 6 and 7 which explain the procedure used in solving hillside problems. Tension values at supports in case-I problems are found as follows:

Horizontal longitudinal component:
$F = VR$

Tension in cable at upper support:
$T_u = Y_u R$

Tension in cable at lower support:
$T_L = Y_L R$

References

1. Sag Calculations by the Use of Martin's Tables (book), James S. Martin. 1931.

2. Mechanical Characteristics of Transmission Lines (book), L. E. Imlay. 1928.

Auxiliary-Power Supply for Generating Stations

V. E. McCALLUM
MEMBER AIEE

Synopsis: Industry, in general, has been adopting the electric motor drive and its control to all types of machines. In the central station, where sequential and correlated operation is a necessity, the use of electric-motor-driven auxiliaries also has shown a marked increase. All recent stations have been built with a major portion of their auxiliaries driven by electric motors. The author suggests the use of the station generator bus as the most reliable source of auxiliary-power supply in electric stations of a closely interconnected system similar to that in the Chicago area. Separate auxiliary service units, not exceeding in size the requirements of the largest turbogenerator unit, also are recommended.

THE PRESENT ELECTRIC generating station is dependent at all times on the integrity of the auxiliary-power system. Therefore, this system must be designed for maximum reliability. Other desirable characteristics of the auxiliary-power system are: safety of personnel, flexibility, simplicity of operation, ease of maintenance, and reasonable cost.

The auxiliaries of the modern electric station consume approximately five per cent to seven per cent of the gross output. Therefore, when designing an auxiliary-power system, the engineer should bear in mind that he is designing the equivalent of approximately 1/20th of the entire conversion and distribution system fed from the station. He also should bear in mind that on the integrity of this 1/20th rests to a large degree the usefulness of the remaining 19/20ths.

An ideal auxiliary-power-supply system, regardless of its size, always should remain a simple system. The tendency to cross-connect and interconnect should be strongly curbed. Dependency should be placed on sturdy, rugged, and well-insulated equipment rather than on complicated switching and relay arrangements designed to remedy faulted conditions.

Trend to Electric Drive

In electric stations on a closely interconnected system similar to that in the Chicago area there has been a steady trend from individual steam drive to electric drive for all station auxiliaries.

The modern induction motor has become the simplest and most reliable of rotating machines, and it is being adopted by the industry as a universal drive. New insulations have been developed to withstand boiler-room temperature with continuous operation. In those applications where variable speed is a necessity, the wound-rotor induction motor is available, but with some sacrifice of reliability and simplicity and somewhat higher first cost.

Early Sources of Auxiliary-Power Supply

Several sources of electric power have been used to provide service for the auxiliary motors. The most common was the turbine connected to an auxiliary generator. Other sources were the shaft alternator on the main turbine and the transformer directly connected to either the generator leads or to the main station busses.

When separate turbogenerators are used for supplying power for the auxiliary-power centers, these units must be installed in duplicate in order to provide complete segregation and reliability. Where the station has a number of power centers, at least one spare turbogenerator is necessary with the connections provided for the relief of all other centers. The cross-connecting of these auxiliary-power units necessitates an excess capacity in each unit, and all the associated switching and relay protection should be of the same quality as that used on the main station busses.

The installation of the auxiliary-power generator on the shaft on the main unit has been supplanted in some cases with a transformer connected to the generator leads. There are some disadvantages of the shaft alternator or transformer on the generator leads, as these units are potential sources of outage of the main unit and they introduce the problem of changing the power source for the auxiliaries in the starting and stopping periods. If the auxiliary-power transformer is disconnected from the generator leads and reconnected to the main bus to which the unit itself is connected, the principle has not been changed, but there is greater flexibility, and there is no need for switching operations during the starting and stopping periods.

Station Bus as the Source of Auxiliary-Power Supply

The main bus of a station to which the generators are connected is the simplest type of electrical equipment, and it lends itself readily to a high order of mechanical and electrical protection. When the busses are divided into sections with each section in a separate bus chamber and equipped with either balanced relays or fault bus protection, it is difficult to conceive any major fault which would shut down more than one or two adjacent sections of a station bus. As each section of the bus is supported by the adjoining sections and as the entire station bus is supported by all generators in the station and also by transmission lines from other stations, during disturbances, these transmission lines become, in effect, auxiliary-power-supply lines for the station in distress.

This supporting function of the transmission lines makes it unnecessary to provide self-starting auxiliary-power generation equipment in more than one or two stations on the entire system.

Where the power system is so constructed that it will sectionalize automatically during trouble, a complete shutdown of any section will not prove disastrous to the system as a whole.

In view of the foregoing and because of the reliability of the station generator bus as proved by years of operating experience, there appears to be ample justification for full electric drive of all station auxiliaries and also for the use of the station generator bus as the source of auxiliary-power supply.

Auxiliary-Power Service Units

It generally is recognized that trouble on the auxiliary-power system may cause temporary outage of the generating units served. Where the auxiliary-power system is so interconnected that it embraces the power supply for the entire station, any trouble on this system also may affect the entire station. It follows, therefore, that by designing the auxiliary-power system in noninterconnected units, it is possible to confine the effects of failure of any power unit to the generating capacity which it serves.

Because on any interconnected system there is a possibility of the loss of any of the larger generating units and the system is so set up as to sustain such loss without undue disturbance, it follows that the size of the auxiliary-power service unit should be such that the generating capacity which it serves should not exceed the capacity of the largest generating unit on the system. Therefore, the generating capacity of the largest unit on the system should be used as the basis of design of a reliable auxiliary-power supply.

Paper 45-152, recommended by the AIEE committee on power generation for publication in AIEE TRANSACTIONS. Manuscript submitted June 22, 1945; made available for printing July 30, 1945.

V. E. McCALLUM is assistant station design engineer, Commonwealth Edison Company, Chicago, Ill.

The author acknowledges the assistance given in preparing this paper by H. A. Louret.

In spite of the inherently high reliability of power lines and transformers, two supply lines are still considered necessary for each auxiliary-power unit. These auxiliary-power supply lines should be equal in reliability and capacity so that either can be considered as a reserve for the other, and each should be capable of carrying the entire auxiliary service unit.

This principle is illustrated in Figure 1. Here the station busses are shown in their simplest form consisting of two bus sections connected by a tie circuit breaker. One of the auxiliary-power supply lines is connected to the bus supported by the generating capacity served by the auxiliary-power unit, and the other supply line is connected to a bus supported by a transmission line. It will be noted that each auxiliary-power center bus is fed from two transformers, one on each of the auxiliary-power supply lines. Section circuit breakers in these busses can be used for automatic power restoration in case of loss of either of the supply lines or to divide the busses for maintenance purposes.

To secure the maximum utilization of the equipment employed and to take advantage of its short-time overload capacity, the transformers supplying each bus could be selected to have a definite overload during the outage of the opposite transformer or of the power line which feeds it. When both transformers are in service, the total load of each bus will be divided between the two transformers, allowing a safe loading margin for this type of equipment.

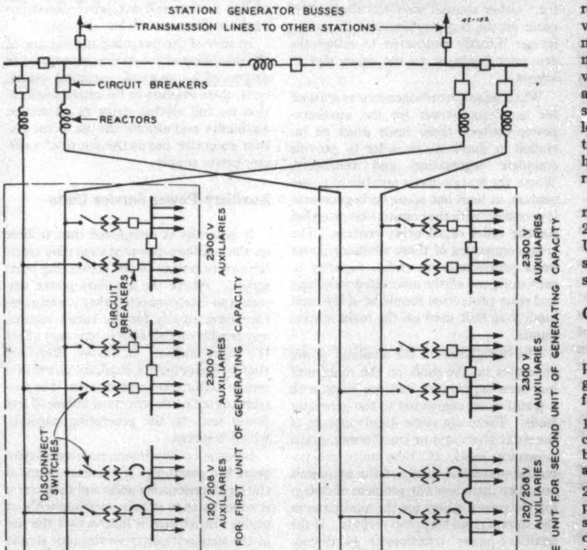

Figure 1. Auxiliary-power system for a generating station

Auxiliary-Power Centers

In designing the auxiliary-power center primary consideration must be given to features having a direct bearing on the reliability, ease of maintenance, and equipment life. Auxiliary-power centers should be located as near the load center as possible, and particular attention should be paid to the protection from external hazards such as water, smoke, and so forth. The room should be ventilated with filtered air and all auxiliary power switching equipment, relays, and associated control apparatus should be treated as any other vital station equipment. The switchgear should be of the draw-out type and easily interchangeable. The manufacturers are ready to furnish such equipment completely assembled which can be compactly and easily installed.

Separate auxiliary-power centers serving auxiliaries common to the entire station such as crib house and coal-handling equipment may be connected to the first pair of auxiliary-power lines to be installed to the station. These centers should be housed in the individual rooms with the same precautions taken as with the larger centers.

Auxiliary-Power Voltages

In the interest of simplification and the reduction of kinds of equipment and voltages, it appears desirable to limit the number of voltages on two For large motors, that is, above 100 horsepower, the voltage of 2,300 is universally used, and, as the manufacturers are now ready to supply motors at this voltage in sizes as low as 60 horsepower, it would be difficult to justify the change of this voltage to a higher or lower value. Therefore, it is recommended as a standard voltage.

On the other hand, for the smaller motors and lighting requirements the 120–208-volt system has many advantages. Unless there are some other special reasons, this voltage should be used as the second standard voltage.

Conclusions

The essential characteristics of the power supply to the auxiliary motors of a generating station may be summarized as follows:

1. In an electric power station on an interconnected system the station generator busses should be used as the source of auxiliary-power supply.
2. A separate and independent auxiliary-power service unit should be provided to serve the maximum amount of generating capacity, the loss of which could be sustained by the system without undue disturbance.
3. Each auxiliary-power center should be supplied by two lines operated in parallel, one line connected to the bus supported by the generator and one line to the bus supported by a transmission line.
4. There can be as many auxiliary-power center busses connected to the supply lines through transformers as are required by the design of the station and by the limitations of the switching equipment involved.
5. All contactors, circuit breakers, relays, and control apparatus should be installed in separate well-ventilated rooms.

Industrial Control: Heating of Shunt-Motor Starting Resistors

G. F. LELAND
MEMBER AIEE

L. T. RADER
MEMBER AIEE

THE USUAL METHOD of starting a shunt motor from a constant-potential source is to insert one or more steps of armature resistance which are short-circuited by contactors operated after a definite time. The required capacity of a resistor for this type of duty is directly related to load conditions and time setting of relays as well as duty-cycle requirements. If time settings are made arbitrarily without some co-ordination with the kind of load, the energy dissipated in the resistor may be unduly high, because the load may be up to speed in a time much less than the setting. On the other hand if the load has a high inertia, the definite time may be too short, causing excessively high peaks on switching points after the first one. Although d-c motors have been used extensively in this way, equations governing such operation do not appear to have been published.

In many industrial applications load data have not been well known to the electric-system designer. He has had to depend upon a systematic grouping into a single classification of various loads, based only on initial inrush current and duty cycle. Such a classification in one case includes conveyors, line shafting, boring mills, punch presses, ball mills, and coal crushers. A better approach to starting-resistor design requires more information on load characteristics as well as the effect of these characteristics on starting-resistor capacity.

Scope of Paper

This paper presents an analysis of conditions which exist when a d-c shunt motor with constant applied field is started by inserting one step of armature resistance. Two cases are treated:

(*a*). Constant-load torque.

(*b*). Load torque varying directly as the speed.

It is the purpose of this work to obtain theoretical expressions for the total energy dissipated in a resistor as a function of load inertia, torque, final speed, initial inrush current, and accelerating time. Relations existing between speed, current, and second current peak as a function of time and circuit parameters are examined.

Assumptions

1. The starting resistor is assumed to hold constant resistance independent of temperature.

2. Armature reaction is neglected. This is a fairly good assumption for currents of 200 per cent or less.

3. In this paper all curves are plotted for a motor internal resistance of ten per cent. In practice this internal resistance may vary from 12 per cent at five horsepower to 4.5 per cent at 150 horsepower.

Results

The co-ordinates of all curves shown are in dimensionless form, so that the data are applicable to any size motor or load.

Time Constant. The developed equation of speed for both torque cases is similar to the equation for current build-up in a *RL* circuit, which allows the concept of time constant to be used. For the constant-torque case the term $\Omega J/T_o$ is the time constant of the system, and for the variable-torque case the equivalent term is $\Omega J/(T_o + \Omega k)$. At one time constant the speed is 63.2 per cent of its ultimate speed, and after two-time constants the speed is 86.5 per cent of the final. All results obtained in this paper are presented as a function of the number of time constants rather than time in seconds. In general two time constants has been selected as a good switching time, and most curves are presented for this value.

Speed and Current Curves. The curves in Figures 4a, 4b, 5a, and 5b show the current and angular velocity during the accelerating time for various ratios of load torque to full-load torque. The parameter, *a*, in Figures 4a and 4b is the ratio of load torque to full-load torque and, *g*, in Figures 5a and 5b is the ratio of the load torque at the no-load angular velocity Ω, to the full-load torque.

Resistor Watt-Seconds. The curves in Figure 6 show the factor by which the $J\Omega^2$ of the system can be multiplied to give the watt-seconds generated per start in the starting resistor. They are plotted for the case where the resistor is short-circuited after two time constants. These curves show clearly that the energy dissipated in the resistor is decreased as the initial inrush is increased. For example for a fully loaded motor the watt-seconds decrease in the ratio 1.37 to 0.83 as the initial current is raised from 125 per cent to 200 per cent.

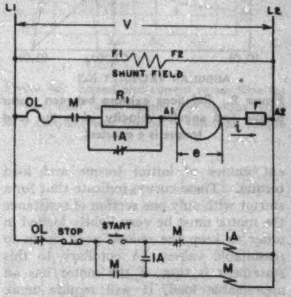

Figure 1. Elementary wiring diagram showing typical definite-time starting circuit

M = line contactor
IA = time accelerating contactor
OL = overload relay
R = total circuit resistance = $R_1 + r$
V = line voltage
e = counterelectromotive force
i = armature current
R_1 = external resistance
r = internal resistance

Figure 7 represents the same data as Figure 6 for the case where the load torque varies directly as the speed.

Although the curves in Figure 7 show that the watt-seconds in the resistor decrease as the load is increased, it should be noted that the switching speed also has decreased because of a decrease in $d = T_o/(T_o + \Omega k)$, and $t_1 = 2\Omega J/(T_o + \Omega k)$ as Ωk is increased.

Second Current Peak. Figure 8 shows how the second current peak varies in terms of the first current peak for differ-

---

Paper 45-125, recommended by the AIEE committee on electric machinery for publication in AIEE TRANSACTIONS. Manuscript submitted February 19, 1945; made available for printing May 21, 1945.

G. F. LELAND is electrical engineer, industrial-control engineering department, General Electric Company, Schenectady, N. Y., and L. T. RADER is director of the department of electrical engineering, Illinois Institute of Technology, Chicago, Ill.

---

6. For simplicity it is recommended that only two voltages be employed for the auxiliaries and that the service to all motors be uniform and have the same method of operation.

7. The entire auxiliary-power system for any unit should be so protected by relays that in case of a fault on any part of the auxiliary service unit the faulted equipment would be automatically disconnected.

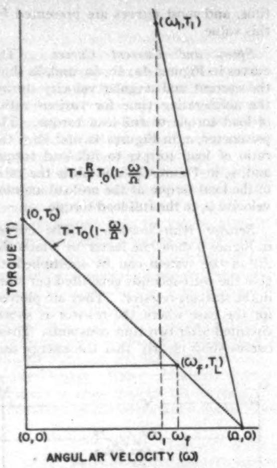

Figure 2. Relations existing between motor torque and angular velocity when the load torque is a constant

ent values of initial torque and load torque. These curves indicate that for a starter with only one section of resistance the motor must be very lightly loaded in order to keep the second peak down to reasonable values. A corollary to this statement is that, if the motor has an appreciable load, it will require more than one resistance step for good commutation.

Switching Time. Figure 9 shows how the watt-seconds generated in the resistor vary with the time allowed for acceleration. These curves indicate that, if a motor has an appreciable load (over 25-per-cent full load), it is important to short-circuit out the resistor as soon as possible consistent with a safe second current peak. For a switching time longer than two time constants Figure 9 shows how the heating severity on the resistor increases with only a slight gain in angular velocity. For example, if $a = T_L/T_{FL} = 0.75$ and $T_o = 2.0\ T_{FL}$ and switching occurs at two time constants, the speed is 86.5 per cent, $\omega_f = 62.5$ per cent Ω, and M is equal to 0.7. If switching occurs at three time constants, the speed is 95 per cent ω_f, and $M = 0.87$. This shows an increase of 24.3 per cent in watt-seconds in the resistor for a gain of only 9.8 per cent in speed. If the load is full load, then $a = 1.0$, and there is an increase of 31 per cent in watt-seconds for the same 9.8 per cent gain in speed.

Circuit Diagram

Figure 1 shows a typical definite time-starter connection diagram. When the start button is pressed the coil of the accelerating contactor 1*A* is energized, thus opening its normally closed power contact and closing its normally open control contact. When the control contact on 1*A* closes, it energizes the line contactor coil *M* which seals itself in through its own interlock. The closing of contactor *M* connects the motor armature to the line through the resistor R_1 and allows the initial current I_o to flow. Simultaneously, the coil of 1*A* is de-energized, so that after a definite time 1*A* drops out short-circuiting the resistor R_1 and allowing the second current peak I_1 to flow.

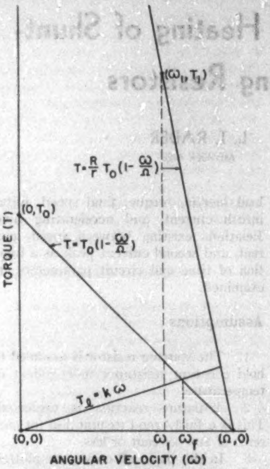

Figure 3. Relations existing between motor torque and angular velocity when the load torque varies directly as the speed

Speed–Torque Diagram

Figures 2 and 3 show relations between torque and angular velocity for the constant- and variable-torque case respectively. The developed motor torque is given by equation 8 and is shown as a straight line going through the points (O, T_o) and (Ω, O). The point of intersection of this line, with the load torque line determines the steady-state operating speed (ω_f) when resistance is in the armature circuit. The point ω_1 represents the speed at switching. The torque after switching rises to T_1 which is on the line given by equation 8a for a motor with internal resistance of r.

Analysis

For nomenclature used in this analysis see the appendix.

In a d-c motor the well-known equations for torque and back electromotive force are

$$T = \frac{c\phi i}{2\pi 10^8} \tag{1}$$

and

$$e = \frac{c\phi\omega}{2\pi 10^8} \tag{2}$$

Since $V = e + iR$, then

$$i = \frac{V - e}{R} = \frac{V}{R} - \frac{c\phi\omega}{R 2\pi 10^8} \tag{3}$$

Putting equation 3 into equation 1 gives

$$T = \frac{c\phi V}{2\pi 10^8 R} - \left[\frac{c\phi}{2\pi 10^8}\right]^2 \frac{\omega}{R} = \frac{c\phi}{2\pi 10^8} \frac{V}{R}\left[1 - \frac{c\phi\omega}{2\pi 10^8 V}\right] \tag{4}$$

With no load on the machine e becomes V, and $\omega = \Omega$, so that equation 2 resolves to

$$V = \frac{c\phi\Omega}{2\pi 10^8} \text{ and}$$

$$\Omega = \frac{2\pi 10^8 V}{c\phi} \tag{5}$$

Substituting equation 5 into equation 4 gives

$$T = \frac{c\phi}{2\pi 10^8} \frac{V}{R}\left[1 - \frac{\omega}{\Omega}\right] \tag{6}$$

At $t = 0$, $\omega = 0$, and

$$T = T_o = \frac{c\phi}{2\pi 10^8} \frac{V}{R} = \frac{c\phi}{2\pi 10^8} I_o \tag{7}$$

Then equation 6 may be written

$$T = T_o\left(1 - \frac{\omega}{\Omega}\right) \tag{8}$$

The torque equation for internal resistance r is

$$T = T_o \frac{R}{r}\left(1 - \frac{\omega}{\Omega}\right) \tag{8a}$$

as initial torque is inversely proportional to circuit resistance. Dividing equation 7 by equation 5 gives the useful relationship,

$$\frac{T_o}{V} = \frac{V}{R\Omega} = \frac{I_o}{\Omega} \tag{9}$$

so that equating 6 and equation 1 gives the following equation for current

$$i = \frac{V}{R\Omega}(\Omega - \omega) = \frac{T_o}{V}(\Omega - \omega) = I_o\left(1 - \frac{\omega}{\Omega}\right) \tag{10}$$

Case 1: Constant-Torque Load

The graphical representation for this case is shown in Figure 2.

The difference between generated motor torque, T, and load torque, T_L, causes acceleration, so that

$$T - T_L = \frac{Jd\omega}{dt} \tag{11}$$

Substituting for T from equation 8 gives

$$\frac{Jd\omega}{dt}+T_o\frac{\omega}{\Omega}=T_o-T_L \tag{12}$$

whose solution is

$$\omega=\left(\frac{T_o-T_L}{T_o}\right)\Omega+A_e{}^{-\frac{T_ot}{\Omega J}} \tag{13}$$

At $t=0, \omega=0$, so that

$$A=-\frac{(T_o-T_L)}{T_o}\Omega$$

and equation 13 becomes

$$\omega=\left(\frac{T_o-T_L}{T_o}\right)\Omega\left[1-e^{-\frac{T_ot}{\Omega J}}\right] \tag{14}$$

At $t=\infty$,

$$\omega=\omega_f=\left(\frac{T_o-T_L}{T_o}\right)\Omega \tag{15}$$

so that

$$\omega=\omega_f\left[1-e^{-\frac{T_ot}{\Omega J}}\right] \tag{16}$$

Putting the expression for ω from equation 14 into equation 10 yields

$$i=I_o\left[\frac{T_L}{T_o}+\left(\frac{T_o-T_L}{T_o}\right)e^{-\frac{T_ot}{\Omega J}}\right] \tag{17}$$

Let

$$\left(\frac{T_o-T_L}{T_o}\right)=b, \text{ so that } \frac{T_L}{T_o}=1-b$$

and the equation for current becomes

$$i=I_o\left[(1-b)+be^{-\frac{T_ot}{\Omega J}}\right] \tag{18}$$

The energy dissipated in the resistor in time t_1 is

$$E=\int_0^{t_1}i^2R_1dt=I_o{}^2R_1\times \int_0^{t_1}\left(1-b+be^{-\frac{T_ot}{\Omega J}}\right)^2dt \tag{19}$$

$$=I_o{}^2R_1\left[(1-b)^2t_1+2b(1-b)\frac{\Omega J}{T_o}\times \left(1-e^{-\frac{T_ot_1}{\Omega J}}\right)+\frac{b^2\Omega J}{2T_o}\times\left(1-e^{-\frac{2T_ot_1}{\Omega J}}\right)\right] \tag{20}$$

Let $t_1=\dfrac{2\Omega J}{T_o}$ so that equation 20 reduces to

$$E=\frac{I_o{}^2R_1\Omega J}{T_o}[2-2.27b+0.761b^2] \tag{21}$$

When the value for I_o from equation 9 is put in, equation 21 reduces to

$$E=J\Omega^2\left[\frac{R_1}{R}\right][2-2.27b+0.761b^2] \tag{22a}$$

or

$$E=J\Omega^2\left[\frac{R_1}{R}\right]\left[0.491+0.748\frac{T_L}{T_o}+0.761\left(\frac{T_L}{T_o}\right)^2\right] \tag{22b}$$

At $t_1=\dfrac{2\Omega J}{T_o}$ equation 14 becomes

$$\omega_1=\omega_f(1-e^{-2})=0.865\omega_f \tag{23}$$

Second Current Peak, I_1

At $t=t_1$ the timing relay $1A$ (Figure 1) drops out short-circuiting out the external resistance R_1, so that the resistance of the circuit changes from R to r.

Just before switching

$$i=I_o\left(1-\frac{\omega_1}{\Omega}\right) \text{ and } e_1=\frac{c\phi\omega_1}{2\pi 10^8}$$

Now

$$\frac{e_1}{V}=\frac{\omega_1}{\Omega}=\frac{0.865\omega_f}{\Omega} \tag{24}$$

The new current peak is given by

$$I_1=\frac{V-e_1}{r}=\frac{V}{r}\left[1-\frac{0.865\omega_f}{\Omega}\right] \tag{25}$$

The same relationship can be obtained by considering similar triangles in Figure 2. Equation 25 also can be written using the relationship of equation 15.

$$I_1=\frac{V}{r}\left[1-0.865\,\frac{T_o-T_L}{T_o}\right] \tag{26a}$$

$$=\frac{V}{r}\left[0.135+0.865\frac{T_L}{T_o}\right] \tag{26b}$$

$$=\frac{V}{r}\left[0.135+0.865\frac{I_L}{I_o}\right] \tag{26c}$$

since $\dfrac{T_L}{T_o}=\dfrac{I_L}{I_o}$ from equation 1.

If switching takes place at $t=\infty$ so that

$$i=I_o\left(1-\frac{\omega_f}{\Omega}\right)$$

then from equation 15 and equation 1

$$I_1=\frac{V}{r}\left[1-\left(1-\frac{I_L}{I_o}\right)\right]=\frac{V}{r}\frac{I_L}{I_o} \tag{27}$$

CASE 2: LOAD TORQUE DIRECTLY PROPORTIONAL TO SPEED

Let

$$T_l=k\omega \tag{28}$$

and

$$T_\Omega=k\Omega$$

As before

$$T=T_o\left(1-\frac{\omega}{\Omega}\right)$$

These relationships are shown in Figure 3. Then

$$T-T_l=J\frac{d\omega}{dt}$$

so that

$$J\frac{d\omega}{dt}+\omega\left(\frac{T_o+k\Omega}{\Omega}\right)=T_o \tag{29}$$

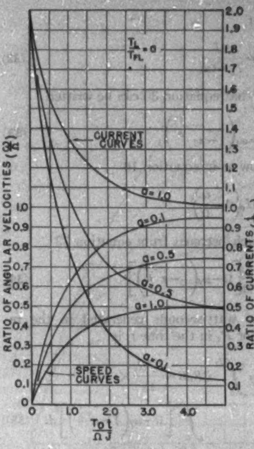

Figure 4a. Speed and current versus time for 200-per-cent initial torque and various ratios of a constant-load torque to full-load torque

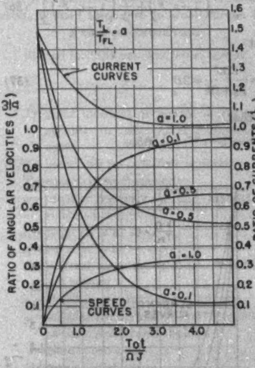

Figure 4b. Speed and current versus time for 150-per-cent initial torque and various ratios of a constant-load torque to full-load torque

and

$$\omega=\frac{T_o\Omega}{T_o+\Omega k}+Ce^{-\left(\frac{T_o+\Omega k}{\Omega J}\right)t}$$

At $t=0$, $\omega=0$, so that C is determined and

$$\omega=\frac{T_o\Omega}{T_o+\Omega k}\left[1-e^{-\left(\frac{T_o+\Omega k}{\Omega J}\right)t}\right] \tag{30}$$

At

$$T=\infty,\ \omega=\omega_f=\frac{T_o\Omega}{T_o+\Omega k} \tag{31}$$

Let

$$B=\frac{\Omega J}{T_o+\Omega k} \tag{32}$$

so that equation 30 can be written

$$\omega=\omega_f\left(1-e^{-\frac{t}{B}}\right) \tag{33}$$

Now as in equation 10

$$i=I_o\left(1-\frac{\omega}{\Omega}\right)$$

which becomes from equation 33

$$i=\frac{I_o}{\Omega}\left[\Omega-\omega_f\left(1-e^{-\frac{t}{B}}\right)\right] \tag{34}$$

The watt-seconds generated in the resistor R_1 in the time t_1 is

$$E=\int_0^{t_1} i^2R_1dt=\frac{I_o^2R_1}{\Omega_2}\times \int_0^{t_1}\left[\Omega-\omega_f\left(1-e^{-\frac{t}{B}}\right)\right]^2dt \tag{35}$$

which becomes

$$E=\frac{I_o^2R_1}{\Omega^2}\left[(\Omega-\omega_f)^2t_1+B(2\omega_f)(\Omega-\omega_f)\times \left(1-e^{-\frac{t_1}{B}}\right)+\frac{\omega_f^2}{2}\left(1-e^{-\frac{2t_1}{B}}\right)\right] \tag{36}$$

Let

$$t_1=\frac{2\Omega J}{T_o+\Omega k}=2B \tag{37}$$

so that

$$\omega_1=\omega_f(1-e^{-2})=0.865\omega_f$$

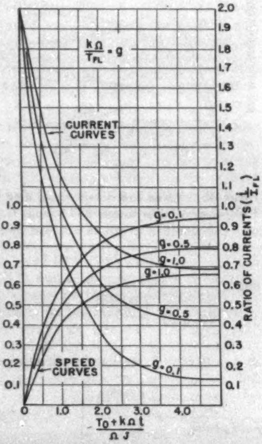

Figure 5a. Speed and current versus time for 200-per-cent initial torque and various ratios of load torque to full-load torque when the load torque varies directly as the speed

Let

$$d=\frac{\omega_f}{\Omega} \tag{38}$$

so that from equation 31

$$\frac{\omega_f}{\Omega}=d=\frac{T_o}{T_o+\Omega k} \tag{39}$$

Then from equation 37

$$B=\frac{\Omega J}{T_o+\Omega k}=\frac{d\Omega J}{T_o} \tag{40}$$

Substituting equation 38 and equation 40 into equation 36 gives

$$E=I_o^2R_1[2(1-d)^2+2d(1-d)(0.865)+0.491d^2]\frac{d\Omega J}{T_o}$$

which, using equation 9, reduces to

$$E=J\Omega^2\frac{R_1}{R}\,[2-2.27d+0.761d^2]d \tag{41}$$

Example 1

A centrifugal casting machine used for spinning molten metal to desired shapes is driven by a five-horsepower 230-volt 1,200-rpm d-c shunt motor with a full-load current of 20 amperes. The inertia referred to the motor shaft is 20 pounds feet squared. The load during acceleration is practically all friction and is ten per cent of rated full-load torque. A two-point starter with one section of starting resistance is to be used. In order to make the accelerating time short 200-per-cent starting torque is indicated.

The accelerating time setting for the timing relay and the watt-seconds lost per start in the starting resistor are required.

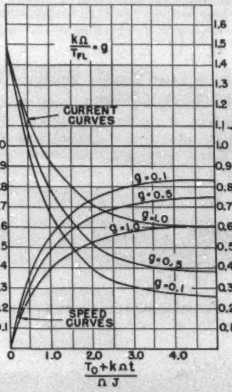

Figure 5b. Speed and current versus time for 150-per-cent initial torque and various ratios of load torque to full-load torque when the load torque varies directly with the speed

The rated full-load torque is 5(5,250) ÷ 1,200 = 21.9 foot-pounds, so that the initial torque and load torque are 43.8 and 2.19 foot-pounds respectively. Since the rated motor speed is 1,200 rpm, and the speed regulation or internal resistance drop is assumed to be ten per cent, the no-load speed is 1,333 rpm. From Figure 4a where $T_L = 0.1\ T_{FL}$ the switching speed is 0.82 × 1,333 or 1,093 rpm, and the steady-state speed, ω_f is 1,266 rpm. The time constant $\Omega J/T_o$, in the practical system, is given by the relation $(WR^2N) \div (307.8T_o)$ where WR^2 is in pounds foot squared, N is no-load revolutions per minute, and T_o is initial torque in foot-pounds. Inserting the values WR^2, N, and T_o given in this example gives the time constant of the system as 2.0 seconds. In a time of 1, 2, 3, and 4 time constants the speed will be 63.2, 86.5, 95, and 98 per cent of ω_f and the watt-seconds lost in the resistor will be 5,920, 6,950, 7,160, and 7,220.

If switching occurs at two time constants, the second current peak is given by equation 25 or can be obtained graphically from a construction similar to Figure 2. This current peak equals

$$I_1=\frac{V}{r}\left[1-0.865\ \frac{\omega_f}{\Omega}\right]$$

$$=\frac{230}{1.15}\left[1-0.865\left(\frac{1,266}{1,333}\right)\right]=36.0 \text{ amperes}$$

This inrush is allowable, being less than 200-per-cent full-load current, so that

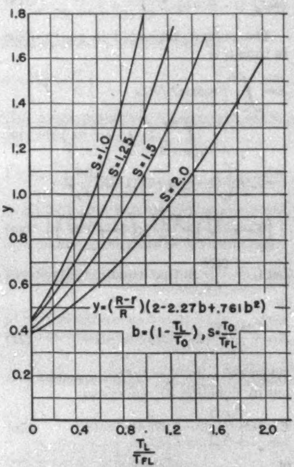

Figure 6. Multiplying factors for $J\Omega^2$ to obtain watt-seconds dissipated in resistor per start for various ratios of initial torque to full-load torque when the load torque is constant and switching occurs at a time equal to two time constants

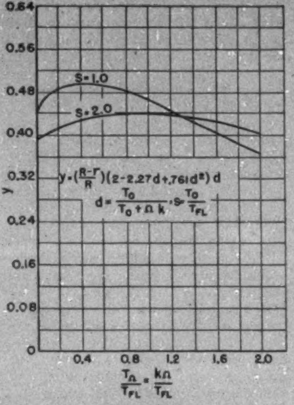

Figure 7. Multiplying factor for $J\Omega^2$ to obtain watt-seconds dissipated in resistor per start for various ratios of initial torque to full-load torque, when the load torque varies directly with the speed and switching occurs at a time equal to two time constants

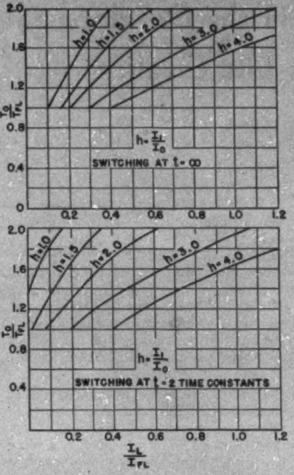

Figure 8. Curves showing the relation between first and second current peaks as a function of load torque, initial torque, and switching time

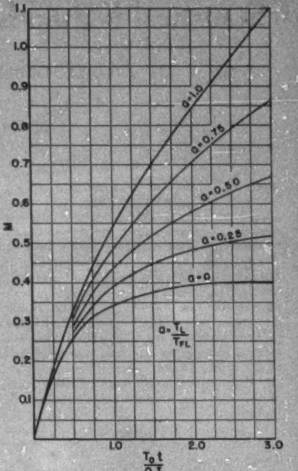

Figure 9. Multiplying factor for $J\Omega^2$ to obtain watt-seconds dissipated in resistor per start as a function of switching time for various ratios of load torque to full-load torque for a constant-torque load

Plotted for 200-per-cent initial torque

switching at two time constants or four seconds is satisfactory.

Example 2

A five-horsepower planer motor rated 500 rpm, 230 volts with a full-load current of 20 amperes drives a friction load of 25-per-cent full-load torque. If a two-point starter is used, the switching time and watt-seconds in the starting resistor are to be determined.

The WR^2 of the system referred to the motor shaft is ten pounds feet squared. The full-load torque is 52.5 foot-pounds. If 200-per-cent starting torque is allowed T_o = 105 pounds. The no-load speed is 556 rpm. Then the time constant becomes $\frac{10\ (556)}{307.8\ (105)} = 0.172$ second.

The $J\Omega^2$ of the system is

$$\frac{4.62(WR^2)(N^2)}{10^4} = \frac{4.62(10)(556)^2}{10^4}$$
$$= 1{,}430 \text{ watt-seconds}$$

At two time constants the second current peak from equation 26 is

$$I_1 = \frac{230}{1.15}\left[0.135 + 0.865\left(\frac{0.25}{2}\right)\right]$$
$$= 48.6 \text{ amperes}$$

The multiplying factor for $J\Omega^2$ obtained from Figure 6 is 0.475. Then the watt-seconds become 0.475 × 1,430 = 685 watt-seconds.

It should be noted that this value is approximately ten per cent of the value found for the motor of example one, which has the same applied voltage, horsepower, internal resistance, and inrush current.

The watt-seconds per start are not much different for two, three, or four time constant because of the low-load torque. If a high-load torque is present, a two-point starter is not satisfactory because of the high resultant second peak.

Appendix. Nomenclature and Units

e = counter electromotive force at any instant
e_1 = value of e at time t_1
V = line voltage
i = armature current at any instant
I_o = armature current at $t=0$
I_1 = armature current after switching time $t=t_1$
I_L = current corresponding to torque T_L
R = total resistance in armature circuit
R_1 = external (starting) resistance
r = internal resistance of motor
T = torque developed by motor in watt-seconds
T_o = value of T at $t=0$
T_L = constant load torque in watt-seconds
T_l = variable load torque at any speed in watt-seconds
T_Ω = value of T_l at speed of Ω
KE = kinetic energy of rotating system in centimeter-gram-second units
J = polar moment of inertia of rotating system in centimeter-gram-second units
WR^2 = inertia in pounds feet squared
E = energy in watt-seconds
ω = angular velocity at any instant in radians per second
ω_1 = value of ω at $t=t_1$
ω_f = value of ω at $t=\infty$
Ω = no-load angular velocity in radians per second
N = speed in revolutions per minute
α = angular acceleration at any instant in radians per second squared
t = time in seconds
t_1 = value at t at $\omega=\omega_1$
ϕ = useful flux per pole crossing the air gap
k = constant
A, C = constants of integration
$b = (T_o - T_L)/T_o$
$d = T_o/(T_o + \Omega k) = \omega_f/\Omega$

In order to change from metric units to the practical system the following factors can be used.

$$\frac{WR^2}{32.2} \times 1.358 = J \text{ watt-second}^2$$

$$4.62\,WR^2N^2 10^{-4} = J\Omega^2 \text{ watt-seconds}$$

$$\frac{2\pi N}{60} = \Omega \text{ radians per second}$$

Statistical Methods in the Development of Apparatus Life Quality

ENOCH B. FERRELL
NONMEMBER AIEE

Synopsis: Life tests on a new design of relay were so planned that the methods of statistical quality control could be used to separate assignable causes for variation from random causes for variation during life.

The relays were inspected frequently at the beginning of the test and less frequently later. The results of these inspections were plotted in the form of control charts. From a study of points outside control limits, improvements were made in the design, the method of manufacture, and the method of test. From a study of the control limits and the number of points within them, predictions were made as to the useful life to be expected.

Simplified methods used in recording and analyzing the data and in establishing trends are described.

DEVELOPMENT PEOPLE, manufacturers, even consumers, make a great many life tests. A common way of making these life tests is something like this: Go to the end of the assembly line, get a number of whatever kind of gadget is being made, put them in a life-test station, and run them to destruction. Results: A nice table of numbers and a lot of dead gadgets. Nothing more.

Now, what is the purpose of a life test? The consumer wants to know: How often will I have to replace this piece of equipment? The manufacturer or his development man wants to know: How long a life can we guarantee to our customer?

The very nature of these questions shows that they are not at all interested in how long a particular gadget that was made last month did run before failure. They are interested only in predictions about how long many gadgets that will be made next month will run before failure. To restate the questions to be answered: First, can reliable predictions be made about the life of the gadget? Second, if predictions can be made, what are the expected average and dispersion of the life, or, if reliable predictions cannot be made, why not, and what can be done about it?

There is another question: Can a design change be made that will increase the life or reduce the cost? That question was given little consideration in setting up the tests to be described, because we had a design that we intended to produce in the existing form to meet certain uses. We wanted to know whether this same design might be useful elsewhere. We did, of course, learn things from the investigations that led us to both design improvement and process improvement. If they had been our main objectives, we would have made little, if any, change in our method of study. But our original objective was simply an evaluation of a design.

Consider the first question, reliability. One of the fundamental requirements for reliable predictions of this type is that they be based on measurements of representative samples from a uniform product. In the tests to be described here the product to be studied was a new type of relay which was in the midst of development and preparation for manufacture. We had made a good many small lots. We had studied the more important characteristics of these by the control-chart technique.[1,2] We had some confidence in a process standard that had been based on our control limits. We were getting a good many outages in our manufacturing process. That is, we were getting a good many points outside our control limits. But we were identifying and eliminating the troubles. Another way to say this is that we were making a good many relays that were not what we intended, but we knew what we wanted to make, and we knew a process that would do it.

For the life test we took samples from those lots which were in statistical control. We believed our samples were representative of the stable manufacturing process that would exist after we had eliminated the troubles. And we knew what the characteristics of the relays made by that process would be, knew that they would be useful to our customers.

We believed that, if we were to put much faith in an ultimate life figure, it must be arrived at by a more or less continuous and understandable process. That is, we were not satisfied merely to let these relays die; we wanted to know how they aged and what was the nature of their final failure. We arranged to operate and release each relay in a work circuit 60 times per second in an effort to wear it out. At stated intervals we would remove it from this work circuit and inspect it. This inspection would consist of accurate measurements of its two principal characteristics: the current at which it would operate or pull up, and the current at which it would release or drop out. We would plot a control chart for each relay. We wanted several points on each control chart before its relay failed.

We arranged to make about 20 inspections during the first ten days. If the relays failed in less than ten days and we had not enough data, we could start over without too much loss. But to continue two inspections per day was too expensive. Moreover, it would give us more data than we had time to study. So, after an initial period, we would inspect the relays whenever their age had increased about ten per cent. Table I shows the inspection schedule. It will be noticed that, if we plot control charts using subgroups of two or four, the time intervals within a subgroup show some uniformity. Beyond the schedule shown, the ten-per-cent rule was applied. Throughout there was some adjustment to fit convenient working hours.

In measuring the operate and release current at the inspections, we have used a measuring set that minimizes the influence of the operator or the surroundings. The relay is connected to the measuring set, and the operating switch is thrown. The measuring set automatically increases the current in the relay slowly until it operates and then displays the value of the operate current on a meter for several seconds. The operator merely throws the switch, reads the meter, and writes down the reading. The meter has a six-inch scale and is read to one or two parts in 1,500.

Table II shows the method of recording the data. This is one half of a double page. Release current is recorded on the other half. There is a separate double page for each relay. At each inspection four observations of operate current are made and recorded on one line. After them are recorded the range and midrange of these four repetitive observations. They may be called repetition range and repetition midrange. When two inspections have been made, the two

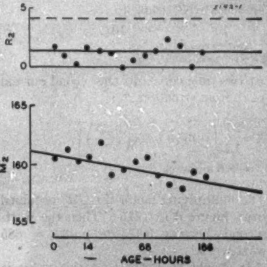

Figure 1. Operate current: relay 740

Paper 45-142, recommended by the AIEE subcommittee on applications to statistical methods for publication in AIEE TRANSACTIONS. Manuscript submitted May 22, 1945; made available for printing July 10, 1945.

ENOCH B. FERRELL is with Bell Telephone Laboratories, Inc., New York, N. Y.

repetition midranges are treated as new data, and the range and midrange are computed for the group of two.

In this work and in most of our work we have used ranges and midranges in preference to standard deviations and averages. The ranges and midranges are easier to compute, and the method of computing them is exactly the same in all details, whether the sample size is two or six. This simplifies the instructions to the technical assistants and speeds up their work. As these statistics depend on only the extreme observations, they may be a little more useful in detecting trouble. Control chart coefficients are published for ranges. For a sample size of two, the midrange and average are, of course, the same. For small samples, in general, it may be that the midranges and the averages, with their statistical fluctuations, are enough alike to permit their interchange in an analysis of this type. We have assumed this to be so, and up to sample sizes of six, we have used the midrange with the published control-chart coefficients for the average.

Repetition ranges represent variations in the relay, and also variations due to meter reading, building vibration, and the like. We would expect this dispersion to be constant, both within and among the relays. The average repetition range and control limits based on it were computed by lumping together several inspections on several relays. They are shown at the bottom of Table II. The repetition ranges here are badly out of control. This was at the beginning of the tests. We convinced ourselves that the trouble was due to operator inexperience and was not seriously affecting the experiment. The repetition ranges later did come into fairly good control.

The group ranges represent the aforementioned variations plus the variations caused by handling the relays, drifts in the measuring set and the like, plus any variation due to real aging in the relay. They show, on the whole, very good control. They indicate that the effect of aging between inspections is small as compared with what we might call the effect of handling.

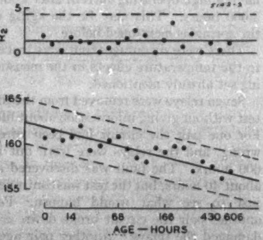

Figure 2. Operate current: relay 740

We do not expect the repetition midranges to stay within limits based on repetition ranges, because an additional cause for variation, the handling, is interposed between inspections.

We might have expected the group midranges to be in control within limits based on group ranges. They were not. They showed definite trends. Here was a real indication of aging. This aging trend was evaluated in the following manner.

After some 14 group midranges had been plotted for a relay, a median line was drawn as in Figure 1. It was a sloping median line. It was placed at such a height that half the points were above it and half below. It was placed at such a slope that the number of runs, above and below, was a maximum.

The use of this line and the method of placing it may need some explanation. If we believed that there existed some functional relation between operate current and age, we could compute the current for each age on the basis of that functional relation, subtract the computed current from the observed current, and get a set of remainders. These remainders would represent the departure of our experience from the assumed functional relation. We could study these remainders statistically. If we found, in the remainders, evidence of cycles or trends, then we would say there are functional relations other than that already considered. If we found what the statistician calls "no evidence of lack of control," then we would think there is no functional relation between the remainders and the age. Our confidence in this belief would depend on the thoroughness of our search for lack of control.

We have done just this, but have done it graphically. We have used, in effect, a graphical transformation of co-ordinates. The functional relation that we have used is defined by the time scale, the position, the slope, and the straightness of the line. Because we have an unusual time scale, we are testing an unusual functional relation. There may be a better or more logical functional relation. The best of statistical control in the remainders would not prove that this functional relation is "the right one" but merely that empirically it is a good approximation in the region studied.

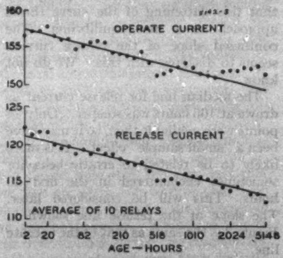

Figure 3. Operate and release currents: average of ten relays

Table I. Life-Test Inspection Schedule

Number of Inspection	Age in Hours	Added Age	Number of Days	Number of Groups (2)	Number of Groups (4)
1*	0				
2**	0	0		1	
3	1	1			
4	2	1	1	2	1
5	5	3			
6	8	3	2	3	
7	11	3			
8	14	3	3	4	2
9	17	3			
10	20	3	4	5	
11	23	3			
12	26	3	5	6	3
13	33	7			
14	40	7	6	7	
15	47	7			
16	54	7	7	8	4
17	61	7			
18	68	7	8	9	
19	75	7			
20	82	7	9	10	5
21	89	7			
22	103	14	10	11	
23	110	7			
24	124	14	11	12	6
25	131	7			
26	145	14	12	13	
27	152	7			
28	166	14	13	14	7
29	188	22	14		
30	210	22	15	15	
31	232	22	16		
32	254	22	17	16	8
33	276	22	18		
34	298	22	19	17	
35	320	22	20		
36	342	22	21	18	9

*At completion of manufacture.
**At start of life test.

In our case the time scale and straightness of the line were purely matters of convenience. They fixed the form of a two-parameter function whose two parameters, the height and slope of the line, could be easily chosen. The choice of height rests on our desire to have the central value of the remainders after transformation equal to zero. It is somewhat easier to use the median as the measure of central value than some of the others. So, we placed the line with half the points above and half below.

We have chosen the slope of the line in an effort to make one of the simplest tests for control show no assignable causes. This test is the study of runs[3] above and below the median. A run is a sequence of consecutive points on the same side of the line. The expected number of runs is roughly half the number of points, actually $(n+2)/2$. This makes the expected average length of run about two. The presence of longer and fewer runs tends to indicate the presence of trends. We would like to include any such trends in our functional relation, and that would eliminate those long runs. The presence of shorter and more numerous runs, which

Table II. Life-Test Data

NI_{op} Switch 740

Date	Age	Observations				Repetition		Group	
						R_4	M_4	R_1	M_1
713	0	159.8	160.1	159.9	160.1	0.3	160.0		
806	0	160.3	160.2	163.8	160.0	3.8	161.9	1.9	160.9
	1	162.0	161.9	162.0	162.0	0.1	162.0		
807	2	161.9	160.2	161.8	160.0	1.9	161.0	1.0	161.5
	5	160.1	160.0	160.8	160.1	0.8	160.4		
	8	160.4	159.8	160.5	159.9	0.7	160.2	0.2	160.3
809	11	160.2	159.7	160.2	159.8	0.5	160.0		
	14	162.0	161.7	162.0	161.9	0.3	161.9	1.9	160.9
810	17	161.9	161.0	161.9	161.5	0.9	161.5		
	20	162.5	162.4	163.1	162.4	0.7	162.7	1.2	162.1
811	23	159.9	160.0	159.9	159.8	0.2	159.8		
	26	158.3	159.0	158.8	159.0	0.7	158.7	1.1	159.2
812	33	158.0	160.0	160.5	160.0	1.5	159.8		
813	40	159.8	159.9	159.8	159.9	0.1	159.8	0.0	159.8
	47	160.0	160.0	160.0	160.0	0.0	160.0		
814	54	161.0	160.2	161.0	160.2	0.8	160.6	0.6	160.3
816	61	160.0	160.2	160.5	160.5	0.5	160.3		
	68	161.0	161.8	161.5	161.5	0.8	161.4	1.1	160.8
817	75	160.5	159.8	161.0	159.9	1.2	160.4		
818	82	158.5	158.5	159.0	158.5	0.5	158.7	1.7	159.6
Process standard	Average					0.24		1.33	
	Limits					0 0.55		0 4.35	

means many runs of length one, indicates a cyclic variation with a period of two. That would not affect our choice of slope to represent a long trend. So, we have used that slope which gave the greatest number of runs.

These ideas explain, whether or not they justify, our method of drawing this line, which because of its characteristics we call a median line. Because this is an extension of the original concept of the median of a lumped or unordered distribution to the concept of a median of an ordered array, we have qualified it and called it a sloping median. Perhaps trend median would be a better name.

These sloping median lines were drawn for eight relays with encouraging results. The number of runs was fairly close to the expected number. The slopes were in good agreement. To show this we measured and averaged these slopes and redrew the plotted medians, so that all had this average slope. Since the manufacturing variations among relays is greater than any of the variations discussed here, each line was drawn at a height to make it the median for that one relay.

To study further the singleness of this assignable cause for variation, control limits were placed above and below these median lines at spacings derived in the usual manner from the average group range. Figure 2 shows the complete control chart for group range and midrange.

Note that this chart goes up to 600 hours age. The determination of slopes and control limits was made on eight relays at an age of 166 hours. The control chart is holding good through an extrapolation by a factor of nearly four in age.

Figure 3 shows the aging trend up to 5,000 hours. The upper curve is for operate current, the lower for release current. Each point is the average for ten relays. It represents four repetitive readings, at each of two inspections of each of ten relays—a total of 80 observations, averaged in each point. The slope of the median line for operate current is the same as that determined at an age of 166 hours. The last few points are significantly above the line. It may be that the whole aging trend is caused by change in a repeatedly overstressed spring and that this flattening of the curve shows approach to a new equilibrium. The continued slope of the release current seems to disagree with this. We do not know.

Table III. Summary of Outages

Number of Relays	Identification	Action
All	General trend	New spring
9	Initial	Preage product
10	Measuring set	Repair set
14	Spring stabilization	New spring
6	Temperature	Redesign measuring set
7	Faulty test	Start over
	Faulty manufacture	Modify process
3	Heavy load	Study load circuits
10*	Unexplained	No action

*Number of individual points outside control limits

The median line for release current as drawn at 166 hours was steeper. Only 14 points were available then, so it may have been a "small sample" effect. It is more likely to be related to erratic behavior sometimes encountered in the first 20 hours. This will be considered later. The slope of the release line shown in Figure 3 is the same as that of the operate line.

Control limits have not been drawn on the ten relay average curves of Figure 3. If they were, they would be spaced less than a third as far apart as in Figure 2, and we would observe many outages. We think the explanation is this: In addition to the dispersion due to what we called "handling," there is an effect of temperature on the measuring set. This is less than the "handling" effect, and, in single relays, is concealed by it. When we average ten relays, the dispersion due to handling is reduced. But, because the relays were started into their tests in a few groups and measured together later as a group on a cold day or a hot day, averaging does not reduce the temperature effect. This now shows up to give outages on limits set by the "handling" dispersion. This also will be mentioned again. This same temperature effect probably accounts for some of the long runs observed in the individual curves.

At the beginning of this discussion two questions were asked: What prediction? How reliable? A prediction has been obtained: A life of over 5,000 hours with an aging in that life of nine parts in 150. For reliability it is necessary to return to our control charts.

Table III is a summary of outages observed in tests on 28 relays. At the time of preparing this summary, some had been run to destruction, others had been run a few hundred hours without failure, and others a few thousand hours.

Nine relays showed outages in the first 20 hours, mainly high values. The time scale used was that of the schedule of Table I. If the chart is replotted on other time scales, some of these outages disappear, and others appear. We do not know what time scale should be used. It may not be important. We think these early outages indicate a real trouble and contributed to our bad guess on the aging rate for release current at 166 hours. There is still more to be said about this.

Ten relays showed outages all at about the same time when the measuring set went bad. That trouble was corrected. It was found that the calibration of the set had been in error by about two per cent. In the plotting of these charts, the early points have been corrected by that amount.

Fourteen relays showed outages by having high operating current after about 2,000 hours. This may be the aging of the spring as mentioned before.

There were six outages that were traced to the temperature effects in the measuring set already mentioned.

Seven relays were removed from the life test without giving information about life. For one pair the circuit had been wired wrong, and the relays were worn out in 600 hours. The fault was discovered at about 40 hours, but the test was continued just to see what would happen. For another pair the circuit broke down and damaged the relays. Another pair aged very rapidly and was found to have been

Selsyn Design and Application

T. C. JOHNSON
MEMBER AIEE

IN the last few years, new developments of Selsyn principles and new applications of modified designs have opened a vast field of use, the emphasis of which is on the system, within which the Selsyns exert control. The many advantages of these new uses are not yet fully realized. Therefore an explanation of the fundamentals of design and application of Selsyns will give a firmer basis for present applications and increase the future usefulness of this highly versatile means of control.

In certain forms Selsyns have had a reasonably long and distinguished service in industry in the past in such applications as remote indication of water level, controller position, and so forth. Many improvements have been made, and much has been learned about the possibilities and limitations of such systems. This paper presents a discussion of design and application fundamentals as distinguished from the mathematical analysis.

What Is a Selsyn

Selsyns, as discussed in this paper, are electric machines used as control devices which in systems involving two or more units can indicate the relative position of their shafts to a high degree of accuracy, even though a considerable distance may intervene between the units (the name is a contraction of self-synchronous). A servo mechanism, or servo system, is an arrangement of power and power-control units within which the Selsyn system operates to guide the action of the power units.

The different kinds of Selsyns can be classified roughly by size and accuracy as:

1. Power Selsyns.
2. Instrument Selsyns.
3. Indicator and control Selsyns.

Power Selsyns are similar in construction to wound-rotor induction motors and have an equivalent size. They might be used, for example, to maintain synchronism of the ends of a lift bridge. Instrument Selsyns are usually extremely small and light and used only to carry a lightweight pointer to indicate position, for example, of the trim tabs or wheels in an airplane. Extreme accuracy is not required of either of the foregoing kinds of Selsyns. Indicator and control Selsyns are midway in size and have errors counted only in tenths of degrees. Because of their high accuracy as control devices they enjoy a much wider field of use than either of the other two types.

Basic Selsyn Systems

An explanation of elementary Selsyn systems is needed as a basis for design specifications. Selsyn systems may be divided into two basic groups, depending on whether their principle of operation is

1. Torque transmission

or

2. Voltage indication.

Each type of system has its own unique advantages, depending on the needs of

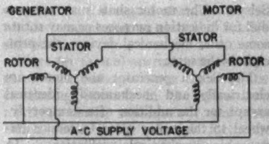

Figure 1. Selsyn generator and motor connection diagram

Paper 45-123, recommended by the AIEE committee on electric machinery for publication in AIEE TRANSACTIONS. Manuscript submitted November 10, 1944; made available for printing May 25, 1945.

T. C. JOHNSON is electrical engineer in the aeronautics and marine-engineering division of the General Electric Company, Schenectady, N. Y.

---

improperly made. The seventh failed suddenly at 2,690 hours and was found to have a foreign particle in it that had worked into the hinge. This also was faulty manufacture. These seven told us nothing about normal relays.

Three relays operated at heavier loads have failed. The ten relays used to plot the average aging curve were worked into loads of 20 watts or less. One of these three relays was worked at 200 watts. It shows a normal aging curve but failed at 2,645 hours. The other two were worked at 300 watts. They showed abnormal aging and failed at 490 hours. There was some question as to the manufacture of these two as they were taken from a lot with a large number of known defectives. From this meager information we are tempted to guess that at these heavy loads the dependable life is about 500 hours.

In addition to these outages for which causes have been assigned, there were ten outages in over 2,000 points for which the cause is unknown. With three sigma limits, the expected number of outages is six, and the sampling fluctuations might take this up to 13. It is possible that these ten outages are really due to random fluctuations.

From these tests we have two sets of conclusions to draw. For the consumer, we can promise a useful life of over 5,000 hours at 60 operations per second with a load of 20 watts or less in a properly designed circuit. At 200 or 300 watts, we have some indication of a life of a few hundred hours. This applies to relays made by the standard process as it existed at the time of the test.

For the development man we have several conclusions. First, we need a measuring set that is easier to operate and free from temperature effects. We are now building a set that we think will be better. Second, something should be done about the initial aging. We now think this is caused by a combination of chemical action and impact polishing. It seems to stabilize after a few hours. We have introduced a stabilization aging run as part of the manufacturing procedure. Third, the aging trend, though small as relay aging usually goes, is undesirable. We should note that the very fact that we had to draw our control charts on sloping medians indicates the presence of an assignable cause. We traced this to the over-stressed spring; we changed the spring material, and new tests indicate that we have almost eliminated this slope. Fourth, the relays were damaged by heavy loads in the circuit used. This may be because of the load and hence an inherent limitation, or it may be because of the circuit which is now being studied.

This report may be summarized this way: The life tests were so designed that random causes and assignable causes could be separated. From the data related to the random causes we have made predictions about the useful life of our standard product in which we have much confidence. From the data related to the assignable causes we have been led to improvements in our design, our manufacturing process, and our testing process, and we may be led to improvements in our method of use.

References

1. MANUAL ON PRESENTATION OF DATA. American Society for Testing Materials.

2. CONTROL-CHART METHOD OF CONTROLLING QUALITY DURING PRODUCTION. American Standards, Z 1.3, 1942.

3. CONTRIBUTIONS OF STATISTICS TO THE SCIENCE OF ENGINEERING, W. A. Shewhart. University of Pennsylvania Bicentennial Conference. Volume on Fluid Mechanics and Statistics, 1941, pages 97–124.

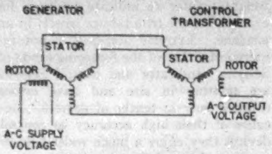

Figure 2. Selsyn generator and control-transformer connection diagram

the application. In some cases a group of interconnected Selsyns forms a system of its own, but more generally it is only part of a larger servo system which it controls.

SELSYN GENERATOR AND MOTOR SYSTEM (TORQUE TRANSMISSION)

The first basic type of system comprises two Selsyns between which torque is transmitted electrically to rotate the shaft of the motor, or receiver Selsyn, in synchronous correspondence with the shaft of the generator, or transmitter Selsyn. The motor shaft may carry a dial for indication purposes or may rotate some other mechanical device; the principle is the same.

The Selsyn generator and motor are electrically and mechanically identical except for the addition of a damper flywheel to the motor rotor to reduce undesirable mechanical oscillations. In each excitation power is applied to a single-phase primary (usually rotor) winding which induces voltages by transformer action in the three secondary (usually stator) windings which are connected in the conventional Y with 120-degree mechanical spacing.

When the stator windings are interconnected as in Figure 1, any lack of correspondence between generator and motor rotors causes the voltages in the stator windings to become unequal, thus circulating currents through the windings and producing restoring torques to bring the motor into correspondence with the generator. When both rotors are in correspondence, the stator voltages are equal, and no current flows.

The voltages induced in the stator windings are all in time phase, since only single-phase power is applied to the rotor and the Selsyn revolves only slowly. The magnitudes of the various voltages depend on the relative postion of stator and rotor windings, and thus a unique set of voltages is produced in the stator for each position of the rotor. The fact that these sets of voltages are a very accurate measure of rotor position is responsible for the widespread use of Selsyn systems.

SELSYN-GENERATOR AND CONTROL-TRANSFORMER SYSTEM (VOLTAGE INDICATION)

The second basic type of system comprises two Selsyns connected electrically, in the second of which (the control transformer) a voltage is induced whose polarity and magnitude are functions of the relative direction and amount of displacement between the shafts of the two units. This voltage can be used for indication purposes but generally acts as control voltage for a servo system.

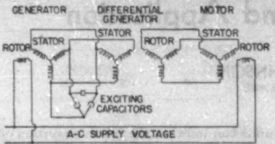

Figure 3. Selsyn-system connection diagram including differential Selsyn and exciting capacitors

The Selsyn generator of this system is identical in all respects to that of the first basic system described. The Selsyn control transformer is similar to the generator, except that it has a high-impedance winding on the stator and the rotor winding is not connected to the power supply.

When stator windings of generator and control transformer are interconnected as in Figure 2, the currents in the control-transformer winding are proportional to the voltages in the generator windings, thus producing a magnetic field in the control transformer corresponding to that in the generator. The voltage induced in the single-phase winding of the control transformer is thus a sine function of the relative displacement of the rotors.

MODIFICATION OF BASIC SYSTEMS

A differential Selsyn may be included in either basic system. It functions either as a differential generator to transmit a set of Selsyn voltages, while modifying them by adding or subtracting the amount of rotation of its shaft, or as a differential motor to receive voltages from two generators and rotate the sum or difference of their rotations. The voltages applied to the three-phase primary (usually stator) windings of a differential generator from the Selsyn generator induce a new set of voltages in the secondary three-phase windings, which appear as if the generator has been turned additionally by the amount of shaft rotation of the differential. An exciting capacity in parallel with the primary winding of a differential Selsyn often is used to reduce the heating of the rest of the system. Figure 3 illustrates a typical connection diagram for a Selsyn system, including a differential generator.

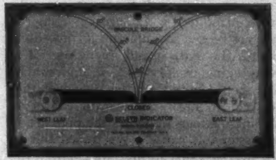

Figure 4. View of indicator panel for bascule bridge showing Selsyn-operated indicators

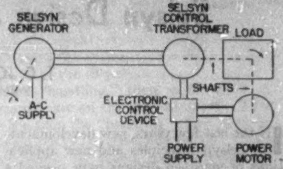

Figure 5. Connection diagram for typical servo system

Typical Selsyn Applications

To illustrate the basic systems just described, some typical applications of Selsyn systems are helpful.

SELSYN GENERATOR–MOTOR SYSTEM AS POSITION INDICATOR

The leaves of a bascule bridge must be kept closely synchronized in position to insure correct operation. Automatic equipment is provided to accomplish this, but Selsyn systems often are used to provide visual proof to the operator that all is well.[1] A Selsyn generator is geared to each leaf of the bridge, and the shafts of corresponding Selsyn motors are attached to pointers on a dial to represent the bridge. The pointers correspond accurately to the position of the leaves and thus quickly check operations. Figure 4 shows the dial of such an installation. Figure 1 shows the connection diagram for the installation.

Similar applications of Selsyn systems were made as early as 1914 to show the position of lock gates, safety chains, and water levels in the Panama Canal.[2]

SELSYN GENERATOR–MOTOR SYSTEM USED FOR TRANSMITTING TORQUE

Continued rotation of a Selsyn generator will cause rotation of the connected Selsyn motor, whose shaft will rotate any attached load up to the limit of the allowable transmitted torque. This flexible-shaft operation of Selsyns is similar in all respects to the previous example, except that an average angular difference between generator and motor is required to supply load torque.

This use of Selsyns is obviously very convenient in many cases but has definite limitations in the amount of torque that can be transmitted without overheating the system and in the mechanical oscillations that may occur with changes in load. A better system is described in the following paragraphs.

SELSYN-GENERATOR–CONTROL-TRANSFORMER SYSTEM CONTROLLING TYPICAL SERVO SYSTEM

Torque amplification, or the control of a large or high-power object by means of a small or low-power one is often necessary in industry (for example, in the machine-tool trade). Many new developments, and therefore the greatest possibilities, are in a system utilizing the high accuracy of control of a servo system possible with a Selsyn-generator–control-transformer system. A typical servo system is diagrammed in Figure 5.

The output voltage of the control transformer (which is proportional to the relative position of generator and control transformer) is fed to an electronic control device, which controls the flow of power to the driving motor. The driving motor turns the load (and control transformer) until the output voltage of the control transformer becomes zero. Any motion of the generator results in a corresponding motion of the load with an accuracy independent of the size of the load, as the driving motor is chosen accordingly. This is a new type of application for Selsyns and bids fair to eclipse all others in versatility of usefulness. A great amount of development has been done designing electronic control devices for maximum performance for each application. Their design is highly important to successful system operation but is outside the scope of this paper.

Characteristics, Design, and Construction of Selsyns

The use specifies the operating characteristics of a machine, and these in turn determine the design and method of construction. Selsyn systems of the first basic type have been in operation for some time, although the use of both types has been rapidly broadening in the last few years. Consequently, many present standard types of construction and methods of design have evolved from other machines such as small a-c synchronous motors. From a study of the requirements of each kind of Selsyn the most suitable design may be evolved.

SELSYN GENERATOR

For a generator used in either of the basic Selsyn systems, the general specifications are about the same.

1. Secondary voltages are such functions of rotor position that a highly accurate indication of position can be obtained when operated with a complementary Selsyn.

2. Sufficient torque developed when coupled with a suitable Selsyn motor, so that motor friction, or the resistance of a specified connected load, may be overcome sufficiently for required accuracy.

3. Minimum drain of current and power from supply lines when operated at rated voltage and frequency.

Table I. Torque Gradients

Values Are for 60 Cycles

Model*	Inch-Ounces Per Degree	Model	Inch-Ounces Per Degree
1	0.07	2	0.16
3	0.45	4	0.40
5	1.2	6	1.75
7	3.4		

* See Figure 9 for relative sizes of units.

4. Adequately large torque capacity and low-voltage regulation to give proper performance of the rated number of connected Selsyns in specified systems.

5. A temperature rise under operating conditions adequate to insure satisfactory life.

6. Bearing design and lubrication suitable for high position accuracy and adequate life at specified rotation speeds and temperatures. Allowance must be made for possible limitations in available torque from the driving device.

7. Construction must include convenient means of mounting and resistance to normal hazards of operation such as vibration, shock, moisture, dust, fungus, and so forth.

The design of a Selsyn generator is like that of any small a-c machine, and the construction is often similar. A standard type of construction of stator and rotor for a generator is shown at the left in Figure 6. All circuit quantities and methods necessary to make standard analyses of Selsyns and their circuits are contained in the usual analysis of synchronous a-c machines.[4] Unfortunately, since Selsyn errors are caused by deviations from the approximate theory commonly used, there is as yet no precise method of predicting error or designing for a given controlled amount of it. The usual design formulas for larger synchronous machines can be used for excitation and torque calculations on all types of Selsyns, if correction is made for the changes in relative dimensions. Ordinary precautions regarding distribution of the coils of the winding, number and skew of slots, and so forth must be taken, but special precautions are needed on machining tolerances, if accuracy is to be high.

Most Selsyns have a sinusoidal variation of stator line voltage with rotor position. Figure 7 shows the variation of the magnitude of the three line voltages. All voltages are in time phase. It has been shown that any space harmonics in the flux distribution, caused by the location of coils or dissymmetry of the magnetic structure, and time-phase differences between current in the various windings, caused by any circuit unbalance, can produce errors in the Selsyn system. The collector rings and brushes must be of durable materials with low stable voltage drop to avoid erratic errors. Gold or silver alloys are commonly used.

The torque developed by a pair of Selsyns (except control transformers) when their rotors are out of correspondence varies with the sine of the relative angular difference as shown in Figure 8. The amount of this torque for a given design may be calculated in terms of the usual electric-machine-circuit constants.[3] Representative generators develop torque gradients with electrically identical motors as shown in Table I.

The models 1, 3, 5, 7 generally are used for position indication only, whereas models 2, 4, 6 are used alternatively for torque transmission as electrical flexible shafts.

Since for normal operation Selsyns are at or near correspondence position, the circulating currents in the stator are relatively small; consequently, the excitation power is the principle factor in determining heating. A stiffer torque gradient therefore can be built into Selsyns which are intended for position-indication use only, resulting in increased torque to overcome bearing and brush friction and provide better accuracy.

Recommended system loadings of various sized generators are given in the next section. Accuracy and heating are the limiting factors.

SELSYN MOTOR

A motor is used only in the first of the basic systems—that utilizing torque transmission. As previously mentioned there are two possible uses of that system;[5] the motor shaft may carry a lightweight dial

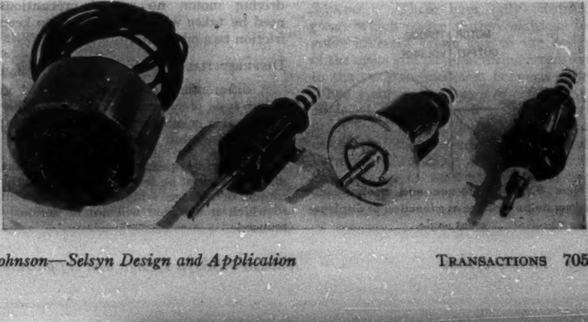

Figure 6. Standard Selsyn construction showing stator, generator rotor, motor rotor with damper, and differential generator rotor

which, once set properly, records the position of the generator shaft very accurately, or the motor shaft may drive some device or load in synchronism with the generator shaft. The requirements are the same as for generators, but, in addition

1. The motor must come quickly into synchronism with the generator and not oscillate unduly when power is applied.
2. Bearing and brush friction must be kept low to insure a high accuracy of correspondence with the generator.

The design of all motor parts is identical with that of the generator in order to satisfy the general requirements of torque and accuracy, but in addition a damper is required. Oscillation of the motor is reduced by a mechanical inertia-friction damper fastened to the shaft, as shown in the middle rotor in Figure 6.

Special precautions must be taken with bearings for indicator Selsyns to insure low friction and high accuracy. All parts are cleaned carefully and aligned, and in critical cases special bearings are used. On the other hand Selsyns for torque transmission are inherently less accurate and in some cases may be built entirely from standard small induction-motor parts without special design.

SELSYN CONTROL TRANSFORMER

A control transformer is used only in the second of the two basic systems—that using voltage indication. Its special requirements are:

1. The output voltage should be an accurate measure of the relative angle between generator and control transformer, and the power available should be sufficient to operate specified electronic devices.

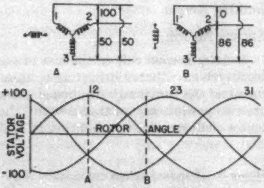

Figure 7. Selsyn-stator line voltages as a function of rotor angle

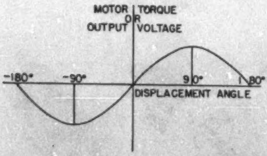

Figure 8. Motor-torque and control-transformer output voltage as a function of displacement angle

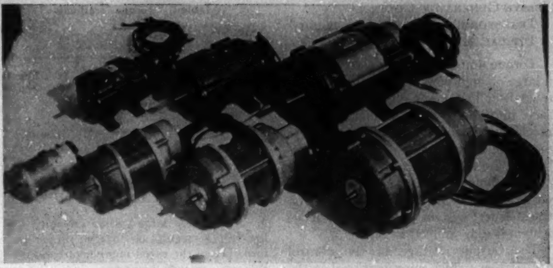

Figure 9. Standard Selsyn sizes

Left to right, front row: models 1, 3, 5, 7; back row: models 2, 4, 6

2. The excitation power and current must be a minimum, as they must flow through the generator and therefore limit the number of control transformers that can be connected.
3. The reaction of a control transformer on the generator must not affect seriously the accuracy of transmission of position information to other control transformers that may be connected to the generator.

The mechanical design of a control transformer is similar to that of a generator. The variation of the output voltage with rotor position is sinusoidal as shown in Figure 8. To minimize the reaction of the control transformer on the generator the magnetic circuit is kept symmetrical by carefully shaping the rotor as shown in Figure 10 and using a three-phase stator winding similar to that on the generator but of much higher impedance. Thus only an equalized three-phase load is presented, the generator signal is not unbalanced, and the excitation power required is kept low.

The volt-ampere burden of electronic devices operated by the control transformer is commonly low, making easy the fulfillment of the requirements. However, if the load consists of peaking transformers for operating thyratron circuits, the volt-ampere burden is high, and a compromise is necessary with the requirement for low power drain from the generator, or excessive voltage regulation will be present.

Because the control transformer produces practically no torque and its shaft always will be positioned by some external driving motor, no special precautions need be taken with the bearings to keep friction to a minimum.

DIFFERENTIAL SELSYN

A differential Selsyn may be used in either type of system and may be either a generator or motor with similar general requirements, but in addition

1. The series impedance introduced by the differential must be low enough, so that the torque or voltage stiffness of the system to which it is added will not be seriously reduced.
2. The excitation power and current requirements must be a minimum to reduce the heating of the generator.

The foregoing requirements require a compromise for best design. Usually a low-impedance design is aimed at, and then exciting capacity is placed in shunt with the primary winding to reduce the current drain load from the generator. The rotor at the right in Figure 6 is that for a Selsyn differential generator. The corresponding stator winding is practically identical with that of a generator.

Design Modification for Special Applications

The standard Selsyn designs just described can be built in all the variations of mounting, voltage, frequency, number of phases, and so forth of equivalent-sized standard induction motors. The fundamental Selsyn principle, however, can be applied in two special designs which are worthy of note here because of the flexibility of Selsyn application which they indicate.

Extremely small size may be obtained by a radical change in design to a Gramme ring type as shown in Figure 11. Here the stator winding is in the form of a toroid, while the rotor is of salient-pole design. This design lends itself to automatic machine winding in core and wire sizes impractical with conventional slotted stators. The principal disadvantages are that the impedance is inherently high and the design of a differential is quite awkward. The accuracy possible is quite comparable to that for larger standard units of the generator and control-transformer varieties.

For applications of limited rotation (±30 degrees), very high accuracy is sometimes made possible by winding the stators with only one phase, thus utilizing the winding volume and distribution to best advantage. The physical appearance of such Selsyns may be identical with those previously shown, or stator and rotor may be mounted independently to occupy minimum space. The circuit in Figure 12 illustrates such an application.

The single-phase Selsyn units are identical and are operated as generators. The secondary voltages are connected opposing (for like rotation), and the difference voltage operates a servo system with one unit rotated by the sending mechanism and the other turned into synchronism by the servo-system power drive. Note the differences between Figures 12 and 5.

Possible Selsyn and Servo Systems

Selsyn systems of generators and motors for remote indication or generators and control transformers for controlling servo systems may consist of from 2 to 40 Selsyns or more. The problems of such systems are largely those of heating limitations in the generators and differential generators, since the accuracy is determined readily and the stability of the system is controlled by proper design of the electronic control device. Table II shows the number of motors and control transformers that can be handled by different sizes of generators without overheating. The model numbers refer to standard sizes and are not proportional to dimensions.

In general each proposed Selsyn system must be checked for heating experimentally as this method is much simpler and less fallible than usual calculations for small machines.

Accurate control of large amounts of power by simple and low-power means is the object of the design of a servo system.[6] A vast fund of knowledge has been acquired on the design of these systems during the last few years, and much of this data is yet to be applied industrially. An understanding of the principles of Selsyn control should hasten such applications. Servo systems controlled by Selsyns have been developed in a range from $^1/_{200}$ horsepower to 65 horsepower (there is no apparent upper limit).

Table II. Motor and Control Transformers Handled by Generators

Values Are for 60-Cycle Machines

Generator Model Number	Number of Motors Model 1	Number of Motors Model 3	Number Current Transformers Model 1 or 3	
			No Cap.*	With Cap.*
1	1	0	0	1
3	4	2	2	12
5	18	9	6	24
7	36	18	10	40

* Cap. refers to the exciting capacity needed for power-factor correction to reduce current drain.

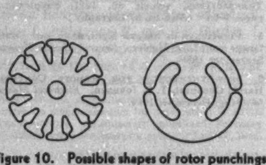

Figure 10. Possible shapes of rotor punchings for control transformer

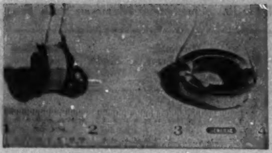

Figure 11. Miniature Selsyn using Gramme ring construction

The typical servo system of Figure 5 described previously used Selsyn generator and control transformers whose output controlled a power motor with the aid of an electronic device such as an amplifier. This is the most accurate Selsyn system and allows plenty of latitude in the choice of power control equipment. Any size of load motor can be controlled equally accurately by simple changes in the amplifier design.

Selsyn motors also may be used to control servo systems, however. If a suitable contact-making arrangement is fastened to its shaft, a Selsyn motor can control a split-series d-c motor which drives the load and at the same time repositions the stator of the Selsyn motor (ball-bearing mounted and called a control motor), until a null position is reached by the contacts. Figure 13 shows the circuit arrangement for such a servo system. Figure 14 shows a control motor disassembled. The cage in the upper part of the figure carries the stator on ball bearings, so that it may be turned by means of a gear (not shown). Alternatively, a Selsyn system similar to the foregoing might be connected to a pilot valve in a hydraulic pump and motor system thus obtaining delicate and accurate control over large forces.

All applications of Selsyn systems which use Selsyn motors as the control element suffer from the vagaries of friction in the Selsyn and the load it drives.

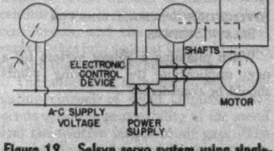

Figure 12. Selsyn servo system using single-phase Selsyns for limited-rotation application

Possible instability is thereby increased, and many manufacturing difficulties may crop up. It is best where possible to drive the shafts of Selsyns positively and employ the excellent and predictable accuracy possible with the generator–control-transformer system.

Selsyn Errors

Errors in Selsyn systems are caused by friction or electrical discrepancies such as impedance unbalance. The reasons for the various errors and the probable magnitudes will be discussed.

Selsyn Systems Involving Selsyn Motors. These always have friction in the motor bearings and sometimes friction in the load to contend with. There is also some electrical error of the magnetic field, but usually the error due to friction is larger. Representative values of guaranteed maximum static error for pairs of like units used as indicators are given in Table III.

The insertion of another Selsyn, such as a differential, or the presence of appreciable line impedance reduces the torque that can be developed by the Selsyn motor, and therefore increases its error. For example, a Selsyn generator and motor system of model-3 series has a guaranteed static error of not more than ±0.6 degree maximum; the insertion of a differential generator of the same size increases the system static error by from 50 per cent to 75 per cent. The effect of line impedance on torque can be seen in Figure 15. Error presumably will change inversely with torque. The addition of several Selsyn motors in parallel will reduce the available torque per motor and therefore increase the error of each.

Selsyn motors have dampers to reduce unwanted oscillations, but during changing conditions or continual motion a certain amount of oscillation is likely to be present. These dynamic errors vary considerably, but it is easily possible to have errors twice or three times those for static conditions. It is important to note that this oscillation is inherent in generator–motor systems and is almost impossible to remove. Variations in torque caused by line-impedance unbalance will of course accentuate this trouble.

Selsyn-Generator–Control-Transformer Systems. These have only electrical errors which under static conditions involve inherent errors due to the design of the units and manufacturing errors due to the various tolerances between parts. When a curve was drawn of error versus angle of rotation from some reference point for a certain design, the inherent error was found to be principally a sixth harmonic of rotation, whereas the manufacturing errors tend to be second harmonics. Reduction of the second harmonic may be possible by better control of manufacture; the reduction of the

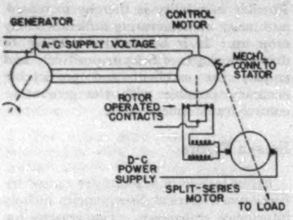

Figure 13. Selsyn-generator and control-motor contact follow-up system

sixth harmonic is possible only through a change in design.

The maximum error of a reasonably good generator–control transformer is not more than ±0.3 degree. Insertion of a differential Selsyn will increase this maximum error about 75 per cent. It will be noted that among other advantages the generator–control-transformer system has approximately one half the error of a generator–motor system. Improved design will better these figures.

One of the sources of errors in Selsyn systems is unbalance of the line impedances. It has been found necessary to keep the sections of the exciting capacity used for differential Selsyns balanced within 1 per cent. In the case of one control transformer it was found that a 1 per cent unbalance in resistance in the stator windings caused nearly a ten percent increase in maximum error. Balanced loads may be connected safely, but unbalanced loads change impedance and cause time-phase differences between the currents of the various circuits, resulting in an extraneous voltage or error appearing.

Each Selsyn generator–control-transformer system has an inherent limit of accuracy, as the output-voltage signal of the control transformer becomes too small for convenient use at very small angles from correspondence. By paralleling the original Selsyn system with another geared up by 16–1 to 36–1 it is possible to multiply the accuracy of any given system and obtain very much smaller system errors. The two systems can be synchronized automatically electrically, so that the low-speed system prevents the high-speed system from pulling-in on a false zero point.

One operational error in generator–control-transformers system is worthy of note. Rotation of the system produces generated voltages in the control-transformer output in addition to those induced by transformer action. The magnitude of this effect is dependent on the Selsyn impedances and usually may be compensated for at a given speed only. For 60-cycle units the control transformer will lag the generator by 0.5 degree to one degree when rotating at 200 rpm.

Table III. Guaranteed Maximum Static Error

Model Number	Maximum Static Error, Degrees	Model Number	Maximum Static Error, Degrees
1	1.5	2	1
3	0.6	4	1
		6	1

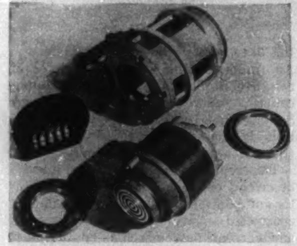

Figure 14. Selsyn generator with ball-bearing-mounted stator showing stator support and brush rigging

Selsyn Application Suggestions

Selsyns are high-grade accurate instruments and should be treated as such. Ordinary tests in the field can check only the continuity of the wiring and do not give any indication of the accuracy of a unit. Selsyns are built to withstand all reasonable conditions of operation, but careful handling is a requisite during installation. Manufacturer's suggestions on mounting should be followed if the best use is to be made of them.

ZEROING

In order to provide a reference position from which to measure rotation, for each Selsyn type there has been arbitrarily designated a combination of stator and rotor voltages and corresponding relative positions known as zero positions. The procedure of locating these positions is known as zeroing. Standard instructions are available.

APPLICATION SPECIFICATIONS FOR SELSYN SYSTEMS

When planning a Selsyn system for a new application the following points should be considered.

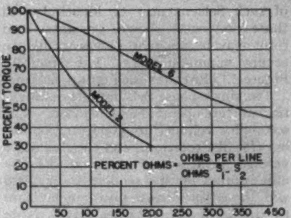

Figure 15. Variation of motor torque with line impedance for models 2 and 6

1. Is a generator-motor or a generator–control-transformer system indicated?
2. Check supply voltage and frequency. Determine allowable drain in watts and amperes and regulation of supply.
3. What are requirements of load in torque, speed of rotation, duty cycle, accuracy? Will any tendency of a generator-motor system to oscillate be objectionable?
4. Determine limiting conditions at application location: temperature, humidity, dirt, vibration, shock, and so forth.
5. Does the generator have a stiff driving mechanism, or is the friction of bearings and brush rigging important? If a generator-motor system is used, can the driving mechanism handle the friction of both machines as well as the load?
6. Are the line impedances balanced, including any exciting capacities?
7. Are the method of mounting, the gearing, and so forth accurate enough to make the best use of the Selsyn system?

An understanding of the general principles of Selsyn system operation is the best guide to satisfactory applications; with it the possibilities for greatly increased use of Selsyn-controlled systems will come into use rapidly in industry.

References

1. CONTROLS FOR MOVABLE BRIDGES, C. P. Hamilton, G. W. Newman. *Engineering News Record*, May 4, 1944.

2. LOCK CONTROL BOARDS AND INTERLOCKING SYSTEMS FOR PANAMA CANAL, C. H. Hill, C. T. Hentschel. *General Electric Review*, January 1914.

3. SELSYN INSTRUMENTS FOR POSITION SYSTEMS, T. M. Linville, J. S. Woodward. AIEE TRANSACTIONS, volume 53, 1934, June section, pages 953–60.

4. FUNDAMENTAL CONCEPTS OF SYNCHRONOUS MACHINE REACTANCES, B. R. Prentice. AIEE TRANSACTIONS, volume 56, 1937, Supplement, pages 1–26. (Also see bibliography.)

5. PRINCIPLES OF SELSYN EQUIPMENT AND THEIR OPERATION, L. F. Holder. *General Electric Review*, September 1930.

6. SELF-SYNCHRONIZE FOR REMOTE CONTROL, Harold Chestnut, T. C. Johnson. *Electrical Manufacturing*, December 1944.

Optimum Air Gap for Various Magnetic Materials in Cores of Coils Subject to Superposed Direct Current

V. E. LEGG
MEMBER AIEE

Synopsis: A method is developed for calculating optimum air gap and core size for choke coils whose windings must carry direct current in addition to alternating current. It is employed with data on typical magnetic materials to give curves from which design dimensions can be obtained readily to fulfill specified requirements for inductance, resistance, and d-c burden.

THE PROBLEM of proper proportioning of air-gap and metallic-path length of the magnetic core of choke coils and transformers frequently arises in the design of coils whose windings must carry direct current along with the desired alternating current. This problem has been approached in the past along lines laid down by Hanna.[1] This involved calculations based on known characteristics of the magnetic materials and taking into account the effects of air gaps of various lengths inserted in the magnetic circuit. Taking an estimatedly correct core volume, V, the optimum value of applied field then was computed, from which the number of turns in the coil was obtained. The resulting coil resistance then was calculated to see if it was satisfactory. If not, a new core volume was assumed, and the calculations were repeated until the desired winding resistance was attained.

It has seemed that a more direct approach to optimum dimensions could be devised, which would give an immediate answer as to the suitability of any given core material for a specified inductance, resistance, and d-c burden. An analysis of the problem has been made, and curves have been plotted for several important magnetic materials from which design dimensions can be readily obtained.

General Problem: L, R, and I Specified

The general method is based on the known fact that prerequisites of inductance L, resistance R, and d-c burden I, can be met by proper expansion or contraction of the size of a core, leaving the ratios of dimensions fixed. Thus, for example, all dimensions can be expressed as fixed multiples of the metallic core length. The essential equations then can be set up and solved for minimum core length. This gives relationships between the (μ, B) curve, (μ_r, B) curve, and the specified L, R, and I of the coil, which must be met for the optimum conditions. The necessary metallic path length, air-gap percentage, and number of turns in the coil follow directly.

Considerable study has been given by others to determine the ratios of dimensions in various types of coils to apportion space properly to windings and magnetic materials. The present analysis assumes that technically or commercially approved dimension ratios are known for whatever coil and core configuration may be considered and confines itself to determination of core and air-gap relationships. If the metallic-path length is l, the average length of a turn of wire in the winding will be ul, the area available for copper winding will be vl^2, and the cross-sectional area of the magnetic core will be wl^2, where u, v, and w are known constants. The length of the air gap is similarly αl, where the factor α is to be adjusted to make l as small as possible. Air gaps will be initially assumed so short as to avoid fringing, so that the flux density in the air is as great as that in the metal. Necessary adjustments to take account of fringing with longer air gaps will be described.

With these assumptions the specified resistance R, inductance L, and d-c burden I enter into the equations as follows.

The resistance of the copper winding will be proportional to the total length of wire ($N \times$ average turn length, ul) and inversely proportional to the cross-sectional area per turn, vl^2/N, or

$$R = \frac{\rho N u l}{v l^2/N} = \frac{u \rho N^2}{v l} \text{ ohm} \tag{1}$$

where N is the number of turns, l is in centimeters, ρ is the resistivity in ohm-centimeters, and the copper area constant v takes into account the packing factor and insulation of the winding.

The inductance, as measured with alternating current of small amplitude, depends upon the permeability of the metal and the relative length of air gap. The permeability to be used is the a-c permeability at the value of superposed field set up by the direct current in the winding. For simplicity only the reversible permeability μ_r will be considered. The results for values of alternating current differing from zero will approximate quite closely those obtained for zero current, namely, μ_r. This follows from the fact that the a-c permeability changes less with changing current in the presence of superposed field than without The inductance is derived from the basic equation

$$L = \frac{N\Phi_m}{i_m} \times 10^{-8} \text{ henry}$$

where Φ_m is the peak flux in maxwells corresponding to the a-c peak i_m, in amperes. The flux can be written as the ratio of magnetomotive force, $0.4\pi N i_m$, to the reluctance, $l/wl^2\mu_r + \alpha l/wl^2$, whence

$$L = \frac{4\pi N^2 wl}{l+\mu_r+\alpha} \times 10^{-9} = 4\pi N^2 \mu_e wl \times 10^{-9} \tag{2}$$

where μ_e is the effective permeability, that is, the permeability of a uniform core material occupying the same space as the

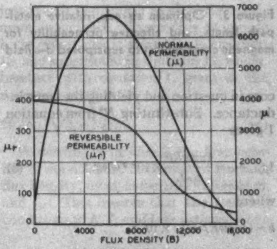

Figure 1. Normal and reversible permeability of four-per-cent silicon iron

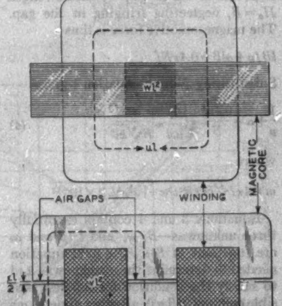

Figure 2. Typical shell-type core with relative dimensions indicated

---

Paper 45-149, recommended by the AIEE committee on communication for publication in AIEE TRANSACTIONS. Manuscript submitted February 23, 1945; made available for printing July 27, 1945.

V. E. LEGG is in the apparatus development department, Bell Telephone Laboratories, Inc., New York, N. Y.

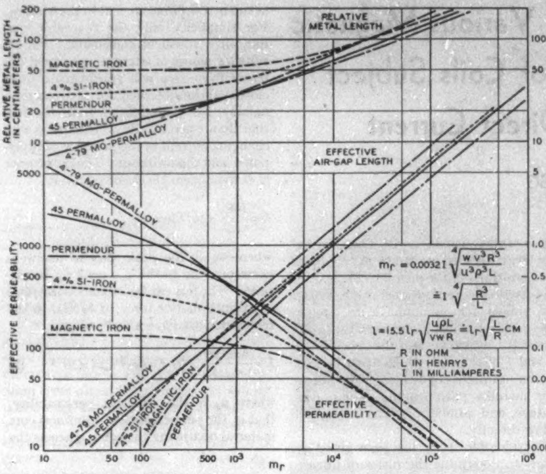

Figure 3. Optimum air gap, relative metal-path length, and effective permeability for magnetic cores subject to superposed d-c field

core in question and yielding the same inductance. Substituting N^2 from equation 1 gives

$$1/\mu_r+\alpha=\frac{4\pi vwRl^2}{u\rho L}\times 10^{-9}=kl^2 \tag{3}$$

where

$$k=(4\pi vwR/u\rho L)\times 10^{-9}$$

The magnetomotive force due to direct current in the winding is distributed between the magnetic core and the air gap so as to maintain the steady flux density B in the core by means of field strength $H=B/\mu$, and in the air gap by field strength $H_a=B$, neglecting fringing in the gap. The magnetomotive force is thus

$$lB/\mu+\alpha lB=0.4\pi NI$$

Substituting N from equation 1 gives

$$\frac{1}{\mu}+\alpha=\frac{0.4\pi I}{B}\sqrt{\frac{Rv}{u\rho l}}=\frac{m}{B\sqrt[4]{kl^2}} \tag{4}$$

where

$$m=4\pi I\sqrt[4]{(4\pi R^3v^3w\div[u^3\rho^3L])\times 10^{-12}}$$

Equations 3 and 4 contain essentially three unknowns—B, α, and l (μ and μ_r are functions of B). The final equation needed to determine these unknowns and to satisfy the condition for smallest possible coil is $dl/dB=0$, all other dimensions having been assumed proportional to powers of l. Eliminating α between equations 3 and 4 gives

$$B\sqrt[4]{kl^2}(1/\mu-1/\mu_r+kl^2)=m \tag{5}$$

Differentiating with respect to B and setting $dl/dB=0$ gives

$$kl^2=\frac{1}{\mu_r}-\frac{1}{\mu}+B\left[\frac{1}{\mu^2}\frac{d\mu}{dB}-\frac{1}{\mu_r^2}\frac{d\mu_r}{dB}\right]=\frac{1}{\mu_r}-\frac{1}{\mu}+B\Delta \tag{6}$$

where

$$\Delta=\left[\frac{1}{\mu^2}\frac{d\mu}{dB}-\frac{1}{\mu_r^2}\frac{d\mu_r}{dB}\right]$$

Substituting this value of kl^2 back into equation 5 gives

$$B^2\Delta\sqrt[4]{B\Delta+1/\mu_r-1/\mu}=m \tag{7}$$

This equation gives the optimum value of B for the desired value of m, but it also implies selection of corresponding values of μ, μ_r, $d\mu/dB$, and $d\mu_r/dB$, to satisfy the equation. These functions must be determined from (μ, B) and (μ_r, B) curves such as shown in Figure 1 for four per cent silicon iron. On account of the involved nature of the data, equation 7 is handled most readily in reverse direction, by inserting known values of B, μ, μ_r, and so forth, from the magnetic data and solving for the constant m. Such calculations from the curves of Figure 1 are given in Table I.

The value of the air-gap ratio is obtained from equations 3 and 6 as

$$\alpha=B\Delta-1/\mu \tag{8}$$

The metallic-path length from equation 6 is

$$l=\sqrt{(B\Delta+1/\mu_r-1/\mu)/k} \tag{9}$$

A function which reveals the influence of the air gap is the effective permeability, μ_e. Thus, from equations 2 and 8

$$\mu_e=\frac{1}{1/\mu_r+\alpha}=\frac{1}{B\Delta+1/\mu_r-1/\mu} \tag{10}$$

The necessary number of turns in the winding follows from equations 1 and 9.

It is now feasible to plot pertinent data of air-gap and metal length for any desired magnetic material against values of m. From such curves essential dimensions of any coil can be read off immediately when m has been computed. For practical purposes it is convenient to use values for m corresponding to typically proportioned cores. The parameters in the foregoing equations are

$$m=4\pi I\times 10^{-6}\sqrt[4]{4\pi R^3v^3w/(10u^3\rho^3L)} \text{ and}$$

$$k=4\pi vwR\times 10^{-9}\div(u\rho L)$$

where I is in milliamperes, R in ohms, ρ in ohm-centimeters, L in henrys, and l is in centimeters. The constants u, v, and w will have various values, depending on the shape of the core, whether annular, shell type, or otherwise. Under the assumption that shell-type cores as illustrated in Figure 2 are most common for use with air gaps, typical cores have been measured for values of the dimension ratios. Thus $u=1.8$, $v=0.02$, and $w=0.04$, approximately. Inserting these values in the above equations gives

$$\left.\begin{aligned}&m=4.17\times 10^{-3}IR\div\sqrt[4]{RL}\\&\text{and}\\&k=3\times 10^{-6}R/L\end{aligned}\right\} \tag{11}$$

For cores having such typical dimension ratios, it is convenient to express results in terms of

$$m_r=IR\div\sqrt[4]{RL}=m\div(4.17\times 10^{-3})$$

Table I. Data and Computations for Four-Per-Cent Silicon Iron

B(gauss)	2,000	4,000	6,000	8,000	10,000	12,000	15,000
μ	4,520	6,150	6,740	5,950	4,550	2,600	430
$d\mu/dB$	1.03	0.45	0	−0.56	−0.85	−1.00	−0.42
μ_r	386	369	343	294	188	95	20
$d\mu_r/dB$	−0.007	−0.010	−0.017	−0.034	−0.068	−0.031	−0.008
$\Delta\times 10^9$	98	85	144	377	1,889	3,292	17,720
$kl^2\times 10^3$	2.56	2.89	3.63	6.25	24.0	49.5	313.5
m	0.0882	0.315	1.27	6.77	74.2	2,230	29,900
m_r	21.15	75.6	305	1,625	17,800	535,000	7,170,000
α (per cent)		0.018	0.072	0.285	1.87	3.90	26.3
l_r	29.2	31.0	34.7	45.6	89.5	128.5	
μ_e	386	346	276	160	41.6	20.2	3.2
LI^2/V	0.478	5.09	59.4	740	11,780	3,120,000	
$(N/l)\sqrt{V/L}$	451	479	536	704	1,383	1,985	
$NI/l\times 10^{-3}$	0.312	1.082	4.13	19.18	150.0	3,760	

Values of m_r have been computed as given in Table I for four per cent silicon iron. They have been used as abscissas in Figure 3, for plotting optimum air gap and effective permeability of four per cent silicon iron. Computations similar to those in Table I based on published magnetic data[3] have been made for magnetic iron, Permendur, 45 Permalloy, and 4–79 molybdenum-Permalloy, and the results plotted in Figure 3.

An additional family of curves is shown in Figure 3, labeled relative metal length, l_r. The necessary metal length from equation 9 involves k, for which an expression is given in equations 11 for typical core dimension ratios. If the ratio R/L is taken as unity, the typical value of k is 3×10^{-4}. With this value "relative metal-path lengths" have been computed from equation 9. The actual core length in any given case then would be $l_r\sqrt{L/R}$.

If other values of u, v, and w are to be used than the assumed typical values the curves of Figure 3 apply if the abscissas are calculated from the equation

$$m_r=(4/4.17)\pi I\times10^{-8}\sqrt[4]{4\pi R^3v^2w/(10u^3\rho^3L)} \tag{12}$$

Similarly the correct metal length l will be obtained from equation 9 in terms of the relative length l_r given in the curves by the equation

$$l=l_r\sqrt{3{,}000u\rho L/4\pi vwR} \tag{13}$$

Special Case I. L, I, and l (or V) Specified

The problem thus far has assumed complete freedom in the choice of dimensions. Frequently, however, the problem may begin with a certain size of core and inquire after the optimum air-gap length to provide a specified inductance in the presence of a given amount of direct current. In this case it will be necessary to adjust the coil resistance along with the air-gap length to satisfy the optimum conditions. The problem becomes that of ascertaining the values of l_r and m which correspond to the optimum conditions as defined by the above equations and which yield the specified inductance and metallic-path length for the specified current.

The metallic-path length l is known in this case, but l_r and R in equation 13 are not known. Substituting the value of R from equation 13 in equation 12 gives

$$\frac{26.6m_r^2}{l_r^3}=\frac{LI^2}{wl^3}=\frac{LI^2}{V} \tag{14}$$

where V is the volume of the core. This resembles the fundamental equation derived by Hanna,[1] but it has the advantage that m_r and l_r can be computed for any given flux density and material by the methods here described. If the first member of equation 14 is computed using associated values of m_r and l_r which already satisfy the optimum conditions, it yields the necessary parameter to insure that the corresponding l_r and α are optimum under the specified conditions of L, I, and l.

With optimum values of l_r and α, the required number of turns in the winding from equations 1 and 13 becomes

$$N=l_r\sqrt{\frac{3{,}000L}{4\pi lw}}=ll_r\sqrt{\frac{3{,}000L}{4\pi V}} \tag{15}$$

The resistance in the winding then follows from equation 1.

The data used for Figure 3 have been analyzed further to find the values of LI^2/V which correspond to the optimum values of m_r, l_r, and α. The results have been plotted in Figure 4, showing values of

$$l_r\sqrt{3{,}000/4\pi}=(N/l)\sqrt{V/L}$$

and α against LI^2/V.

Figure 4. Optimum air gap and number of turns for a coil having specified inductance, core size, and d-c burden

L in henrys
l in centimeters
I in milliamperes

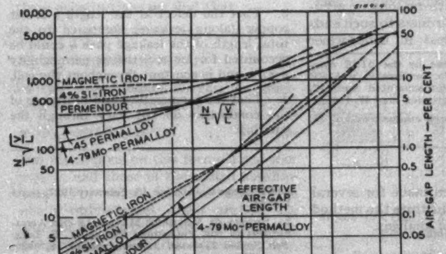

Case II. L, N, (or R), and l (or V) Specified

If inductance is specified, and it is desired to know the percentage air gap required to permit the use of the largest possible direct current in the winding of a coil which is already constructed, the curves in Figure 4 can again be used. All of the factors required to compute $N\div l\sqrt{V/L}$ now are specified. It remains only to locate the indicated point on the $N\div l\sqrt{V/L}$ curve for the material of which the core is constructed, and read the corresponding value of LI^2/V. From the latter value can be calculated the maximum current which can be employed without understepping the specified inductance.

The necessary air-gap length can be read off directly from Figure 4.

Case III. N (or R), I, and l (or V) Specified

If the d-c burden is specified, and the coil is already constructed (that is, l and N or R are fixed) it may be desired to adjust the air-gap length to yield the maximum inductance. Proceeding as in case I, the inductance is solved for in equation 13, and substituted in equation 12, which, together with equation 1, gives as the necessary relation

$$79.6m_r/\sqrt{l_r}=NI/l \tag{16}$$

Proceeding as in case I, the first member of equation 16 is computed for each flux density, using associated values of m_r and l_r. This insures that the specified conditions of N, I, and l are satisfied when

Figure 5. Optimum air gap and permeability for a coil having specified inductance, core size, and d-c burden

L in henrys
l in centimeters
I in milliamperes

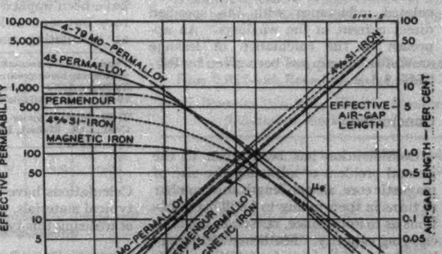

the optimum conditions of l_r and α are employed. Curves in Figure 5 give the effective permeability and air gap plotted against NI/l. The inductance attained with the values of μ_e and α so chosen will be the maximum possible. The inductance in henrys is computed from equation 2.

Case IV. N (or R), L, and l (or V) Specified

If the inductance is specified and the coil is already constructed, the curves of Figure 5 can be read backwards to find the allowable direct current and the necessary air gap.

Case V. N (or R), l (or V), and α Specified

If a finished coil is at hand, the question may arise as to the direct current which should be used to employ the core and coil most efficiently. Curves on Figure 5 may be used in this case to locate the value of NI/l which corresponds to the specified value of α. With this value of NI/l, optimum current is computed. Similarly the corresponding effective permeability is read from the curves, from which the optimum inductance is found.

The Air Gap

The foregoing analysis has been concerned with determining the optimum air-gap length to satisfy certain conditions. When the practical question arises as to the number of millimeters spacing to insert, still further analysis is required, on account of magnetic fringing at the gap. In general a longer physical gap must be inserted into the magnetic circuit than indicated by the optimum percentage. The correction is less for very short gap lengths, or if the total amount of gap is divided into two or more short sections with interspersed core material. The correct gap length can be found empirically by building the coil as designed and then adjusting the air gap to give the calculated inductance with the specified direct current in the windings. An approach to the calculation of leakage around an air gap has been given by Partridge.[3]

Conclusion

Consideration has been given to the general problem of adjusting the size of magnetic core, air-gap length, and number of turns in the winding to fulfill specifications as to inductance, resistance, and d-c carrying capacity. Mathematical means have been worked out for fulfilling specified conditions with a minimum quantity of core materials whose permeability and reversible permeability curves are given. Calculations have been made for several typical materials, to illustrate the method of utilizing this type of analysis.

References

1. Design of Reactances and Transformers Which Carry Direct Current, C. R. Hanna. AIEE Journal, volume 46, February 1927, pages 128–31.

2. Survey of Magnetic Materials and Applications in the Telephone System, V. E. Legg. *Bell System Technical Journal*, volume 18, 1939, page 438.

3. The Inductance of Iron Cored Coils Having an Air Gap, G. F. Partridge. *Philosophical Magazine* series 7, volume 22, 1936, page 665.

Eddy-Current Resistance of Multilayer Coils

T. H. LONG
MEMBER AIEE

Synopsis: Most of the earlier studies of eddy-current resistance have been made by those interested primarily in the effect of compromise transpositions on the losses of rotating equipment. Their results have included formulas for the eddy-current resistance for perfect transpositions, but these have gotten into handbooks in difficult form or have been ignored entirely. Such formulas are presented here in more usable form, with more information on their limitations, and further formulas are derived for minimum losses for a number of different cases. Included is a set of curves showing eddy-current resistance as a function of the number of layers and conductor thickness. Formulas also are included that take into account the differing lengths of conductor in successive layers and that approximate the end losses in a spiral coil on account of radial flux.

THE CUSTOMARY approach to the problem of eddy-current-loss calculations for multilayer coils has been to assume a coil side surrounded on three sides by a medium of infinite permeability and no loss and the use of rectangular conductors. There has been one exception to this that is discussed later.

The principal aim of most of these investigations has been to arrive at a loss factor that might be applied to the d-c resistance of slot windings of various types to find the effective or a-c resistance. This has included evaluating the loss factor for the individual layers, which is all that needs to be applied if the layers are in series or if a perfect transposition system is used, and a different loss factor that includes the circulating current caused by compromise transpositions in certain practical windings.

Formulas so derived for slot windings have been applied with reasonable accuracy but some awkwardness to such ends as calculating the loss in transformer coils. It is the purpose of the present work to derive a formula that can be modified readily to account for the difference in layer lengths, and that will lead to simple and general approximate formulas that can be used for a very rapid survey of design possibilities in many cases.

A paper by Butterworth[7] considers an inductance without the usual partial iron circuit and wound with round conductors. It is shown that the ratio of reactance to resistance is a maximum for a coil so proportioned that the ratio of diameter to length is from 2.5 for low frequencies to 3.2 for high frequencies, the distinction between low and high frequencies being made according to the degree to which skin effect is evident in an isolated conductor. At high frequencies the reactance-to-resistance ratio is improved by a spaced winding. Formulas are derived for losses in such coils and shown to correspond to measured results. It also is shown that for the coils in question the losses are almost entirely due to the radial component of flux rather than the axial component. As these results are limited in their application to single-circuit systems (also end-to-end coupling) of rather limited proportions, they are not considered further here.

Returning to the more usual analysis of eddy-current problems, it has been customary to assume further that:

1. The conductors could be represented by rectangular bars of the type shown in Figure 1A, so disposed that two of their flat surfaces are parallel to the general direction of the leakage flux.

2. That component of leakage flux parallel to the other two flat surfaces could be neglected.

3. That the defect in the length l of net copper (along leakage) compared to the total length of the leakage path l_1 could be accounted for by a fictitious permeability $\mu = l/l_1$ and is constant throughout the coil.

4. That the temperature and resistance of the conductors do not vary through the winding.

Paper 45-137, recommended by the AIEE committee on basic sciences for publication in AIEE Transactions. Manuscript submitted April 17, 1944; made available for printing May 17, 1945.

T. H. Long is senior research engineer with C. G. Conn, Ltd., Elkhart, Ind.

Coil Loss and Effective Resistance

In the derivation outlined in the appendix additional assumptions have been made to the effect that the eddy-current losses in question are due only to the current in the coil being examined and that this current is in phase through all of the layers comprising the coil. Appropriate modifications for other cases are reasonably obvious and have been given by Lyon, among others.

It is shown in equation 33 that the loss in the nth layer is, in watts

$$wA = B_\Delta^2 C_1 A[(2n^2-2n+1)F_1+F_2] \qquad (1)$$

n which

B_Δ = increment in leakage-flux density through layer in lines per square inch
$C_1 = 1.935 m\rho 10^{-8}/\mu^2$
A = area in square inches of one surface of conductor parallel to leakage flux
$x = 1.01 r_1\sqrt{\mu f/\rho}$ (r_1 is in inches, see Figure 1B)
f = frequency in cycles per second
$F_1 \approx x^3/48 - x^7/18{,}660$
$F_2 \approx 2/x - 14x^3/1{,}440$
$\mu = l/l_1$
$m = 0.505\sqrt{\mu f/\rho}$
ρ = microhms per centimeter cube
w = watts loss per square inch of A

Precise definitions of F_1 and F_2 are given in the appendix.

From this result it follows that the sum of these losses from $n = 1$ to $n = N$ is, in watts

$$B_N^2 C_1 A\{(2N^2+1)F_1/3+F_2\}/N \qquad (2)$$

where B_N is the highest flux density associated with the Nth layer under the original assumptions. For comparison it is shown in equation 41 that the loss neglecting eddy current is $2B_N^2C_1A/Nx$. Therefore it follows that

$$R_{ac}/R_{dc} = (x/2)\{(2N^2+1)F_1/3+F_2\} \qquad (3)$$

When $x < 2$ the error involved in approximating F_1 and F_2 by writing their series to the first terms in x with positive exponents amounts to +4.5 per cent and −0.4 per cent, respectively. Making these substitutions we find that

$$W = B_N^2 C_1 A\{x^3(5N^2-1)/360+2/x\}/N \qquad (4)$$

$$R_{ac}/R_{dc} = x^4(5N^2-1)/720+1 \qquad (5)$$

So the proportionate increase in resistance due to eddy current is

$$R_e/R_{dc} = x^4(5N^2-1)/720 \qquad (6)$$

The restrictions on this formula are that $x < 2$, and those of the stated assumptions. For most practical designs in which eddy-current losses are on the order of ten per cent, this approximation gives results of slide-rule accuracy.

Accounting for differences in layer circumferences, it is shown in equation 38 that if a_0 and a_1 are, respectively, the radii (or circumferences) of the layers at zero and maximum leakage-flux densities, the loss for the coil is

$$W = (B_N^2 C_1 A/N)\left\{F_1\left[\frac{2N^2+1}{3} - \frac{3N^2+N+1}{6}\,\frac{a_0-a_1}{a_0}\right] + F_2\frac{(a_0+a_1)}{2a_0}\right\} \qquad (7)$$

From this and from equation 41 it follows that, for $x < 2$,

$$R_e/R_{dc} \approx \frac{x^4}{720}\left\{5N^2-1-\frac{15N^2+5N+5}{4}\,\frac{a_0-a_1}{a_0}\right\}\frac{2a_0}{a_0+a_1} \qquad (8)$$

Derivations for Minimum Loss

The minimum practicable loss in an a-c coil is usually desirable, and in order to investigate the relation between parameters for this condition it will be convenient to use equation 4. This may be treated as a variable in either N or x and the condition for minimum loss determined by setting the appropriate differential equal to zero.

This shows that when N is variable the losses are a minimum when $N \approx 12/x^2$, and that when x is variable the condition for minimum loss is that $x = \sqrt[4]{240/(5N^2-1)}$.

Substituting these relations successively in equation 5, we find that if N is variable minimum loss corresponds to $R_e/R_{dc} = 1$, and that if x is the variable minimum loss corresponds to $R_e/R_{dc} = 0.33$. This may seem a little surprising at first glance, but the first relation simply represents a less efficient use of conductor. It is necessary that the relationships be different in order that they be valid. For any particular frequency either relation can be shown to be a condition for a maximum in the ratio of reactance to resistance.

These two cases are of more academic than practical interest at standard frequencies except in the case of air-core reactors, since they assume that economy is unimportant as applied to conducting material and space. At radio frequencies, and even at lower frequencies, economy of conducting material and space is not important as very little of either can be used from considerations of energy economy.

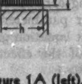

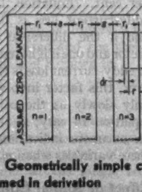

Figure 1A (left). Geometrically simple coil side assumed in derivation

Coil is surrounded on three sides by iron

Figure 1B (right). Enlarged view of one corner of Figure 1A

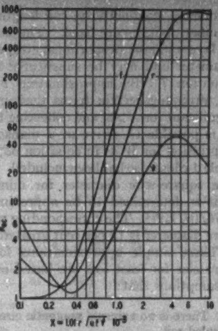

Figure 2. Effective resistance of 100-layer coil plotted against x

Three cases are shown to illustrate the effect of varying f, r_1, and γ independently

Equation 4 can be rewritten as a function of ρ by writing out the various terms included in C_1 and x. Then by setting the differential with respect to ρ equal to zero it can be shown that the losses are a minimum when ρ is such that $N \approx 12/x^2$. This is the same as the condition for minimum losses with N variable.

It can be shown that where both direct and alternating currents are present in a coil the total loss is

$$W = (2B_N^2 C_1 A/N)\{x^3(5N^2-1)/720+k_s/x\} \qquad (9)$$

where $k_s = 1 + 2I_{dc}/I_{ac}$ in which the ratio is taken for the peak value of the a-c wave, and B_N refers only to the alternating component of flux. From this it can be shown that if x is taken as the variable the losses are a minimum when

$$x = \sqrt[4]{240k_s/(5N^2-1)} \qquad (10)$$

A somewhat more practical case is for square or round wire and for which the

Table I. Data on Two Small Coils Wound From 0.022-Inch Round Enameled Wire

Inside Diameter ¹³/₁₆ Inch, Outside Diameter 1⁵/₁₆ Inches, Eight Layers

	Long Coil	Short Coil
Turns	686	332
Length, inches	2	1
D-c resistance, ohms	3.88	1.93
Axial space factor for equivalent rectangular wire	0.83	0.83
Nagaoka's constant	0.828	0.703
Millihenrys at 1,000 cycles per second	3.97	1.93
μ	0.687	0.583
$x/f^{1/2}$	0.01273	0.01173

frequency, conductivity, coil length, and number of turns are fixed. The number of layers is now proportional to the wire diameter and may be substituted for in equation 7. By approximating F_1 and F_2, dropping certain terms that are not significant for $N>3$, and collecting terms, it is possible to arrive at a manageable expression for W as in equation 53; possible d-c loss also has been included. Then the square-wire diameter for minimum loss is determined to be approximately $2.76/(tf/l_3)^{1/3}$. The corresponding round-wire diameter is 12 per cent greater.

These simple approximations for the wire size for least loss are based on the assumptions that:

1. There is no external magnetic circuit or coupled coil.
2. There is no unidirectional component of current.
3. Coil length ≈ effective coil diameter and $a_0 \approx 2a_1$.

If these conditions are not all fulfilled a more exact solution for the wire diameter for minimum loss from equation 56 should be used. Any one of the foregoing items readily can influence the wire diameter by one gauge number (12 per cent).

Figure 7 shows the relation between frequency, turns per inch of coil length, and round-wire diameter for minimum loss based on the approximations in equation 57 outlined in the foregoing.

For comparison with the minimum-loss, cases in which N, X, or ρ are independent variables, the value of x from equation 55 can be substituted in equation 6, assuming that $k_5=1$ and that $a_0=a_1$ so that $k_4=0.5$. Then $R_e/R_{dc}=0.5$.

In this last case for least loss it has been assumed tacitly that in the absence of an external magnetic circuit (see Figure 1) the radial field could be ignored. Some justification is given for this later.

A situation that is more frequently of practical importance is the case in which dimension h of Figure 1A, that is, the radial thickness of the coil, is fixed, and the insulation required between laminations is of fixed thickness. Ordinarily extra insulation will be required between conductors, and still more extra insulation between coil sides, but these extras may be lumped together as a constant before determining h. In this case N is a function of x, or $N = 2mh/(x + 2m\delta)$; this value for N can be substituted in equation 7, and, after approximations that are reasonably good for $N > 3$, the value of r_1 for minimum loss can be found from

$$r_1q/\delta = \sqrt[3]{\frac{9}{2\delta^2h^2m^4}\,\frac{2k_4}{3k_4-1}} \qquad (11)$$

where $k_4 = (a_0 + a_1)/2a_0$, and $q = \{(1 + 3\delta/2r_1)/(1 + \delta/r_1)^2\}^{1/3}$; r_1/δ may be plotted as a function of r_1q/δ and then this may be used as a step in determining r_1. As an approximation when $r_1/\delta > 1$, and to slide-rule accuracy when $r_1/\delta > 3$,

$$r_1 = \delta\left(0.17 + \sqrt[3]{\frac{9}{2\delta^2h^2m^4}\,\frac{2k_4}{3k_4-1}}\right) \qquad (12)$$

An instructive approximation can be made from equation 12 when $r_1/\delta > 4$, and if the influence of k_4 is neglected, the value of r_1 for minimum losses becomes

$$r_1 \approx \sqrt[3]{\frac{9\delta}{2h^2m^4}} \qquad (13)$$

This can be substituted back into equation 6 along with the definition of N in terms of r_1, and the eddy-current loss for that value of r_1 that makes the total loss the least can be determined as

$$R_e/R_{dc} \approx (1/36)(m^4h^2\delta^2)^{1/3}(1-\delta/r_1)^2 \qquad (14)$$

To take a numerical example assume that at 60 cycles

$m=2$
$h=6$ inches
$\delta=0.01$ inch

Then, for minimum-loss equation 12 determines r_1 to be 0.0444 inch and N to be 110 layers, and as $x = 0.1776$ equation 6 evaluates the eddy-current loss at 8.35 per cent. Equation 14 states that the eddy-current loss is 0.117 $(1 - \delta/r_1)^2$, and if the difference between this last factor and one is ignored the determination of eddy-current loss is rather rough. However, this factor involving δ/r_1 will vary only slowly as the other parameters of equation 14 vary, so that equation gives an accurate indication of the effect of these variables when $r_1/\delta > 4$.

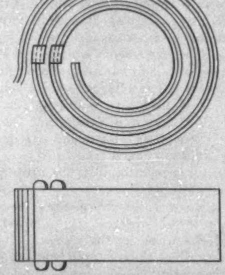

Figure 3. Three-turn spiral with three parallels showing simple method of transposing

Effect of Radial Component of Field

The work up to this point has assumed that the winding is surrounded on three sides by a medium of infinite permeability and no loss so that the loss for rectangular conductors could be determined quite precisely under the assumption of no radial component of field. If the external circuit be removed the situation becomes quite different, whether the conductors are round or rectangular.

By measurement on an eight-layer coil (described later) in which the length was about equal to the diameter, the field strength along the axis of the coil varied about 50 per cent from the center to the ends, and the radial component at the ends was not much less than the axial component at the ends. It would seem that in such a case, as far as losses are concerned, the presence of the radial field would just about make up for the deficit in the axial field. Experiment shows this to be the case, and, when the ratio of coil-length to diameter is greater than one, eddy-current losses can be approximated reasonably by using equation 6 with r_1 determined as the diameter of a square wire having the same cross section as the actual round wire. In this case μ should be determined as the space factor of the assumed square wire in the axial direction multiplied by a factor giving the ratio between the actual inductance and the inductance calculated from the long-coil formula. Such a factor can be approximated from Nagaoka's constant by using for coil diameter the actual diameter plus two thirds of the radial depth.

When $l_2/D>0.3$, Nagaoka's constant can be approximated to within two per cent by $1.02-1/(1+2l_2/D)$ in which l_2 is the axial length of the coil and D is the effective diameter of the coil.

It should be pointed out that, if the radial thickness of a winding is less than about one quarter of the effective coil diameter and also less than one quarter of the coil length, the eddy-current loss may be mainly the result of the radial component of field, and the formulas derived here cannot be used correctly.

These formulas are intended for concentrically coupled coils having equal and opposed ampere turns, and for other coils in which the coil geometry indicates that most of the eddy-current losses are due to the axial field. For concentrically coupled coils, the effective diameter can be taken as the radial distance between coils plus one third of the sum of their radial thicknesses.

In the case of coils wound with rectangular conductor with the flat of the conductor parallel to the principal magnetic field, the situation is not so clear, as a given radial field can produce much higher losses on account of having a wider conductor to work on.

It is quite apparent that the losses will be reduced by any steps that will reduce the radial component of field, and this dictates the use of coils that are long as compared to their diameter, and what amounts to the same thing, the close coupling of load coils either inside or outside the coil being studied.

As a one-turn-per-layer coil has no radial field except at the ends when energized by alternating current the use of such a coil may represent a step in the right direction when a considerable conductor area per turn is required. From a practical point of view such a coil has the additional recommendation that voltage stresses from steep-wave-front transients are distributed rather equally between turns, because the turn-to-turn capacity is large and quite uniform, and all except the first and last turns are quite well shielded from ground. Figure 3 is an illustration of such a coil, and it also shows a transposition system that can be used when the number of turns must be less than the number of layers.

It should be noted that if other conditions are appropriate the end losses for a one-turn-per-layer coil will be the same as for a two-turn-per-layer coil formed by assembling two spirals each half as long and suitably connecting them in series. It would seem that spiral coils would represent the most efficient construction possible since they have radial field losses only at the ends; a possible exception would be those cases in which conductors can be used for which the x measurement, determined for the radial field, can be less than one or two. This follows as otherwise the losses at the ends will be about the same in any case, and the spiral construction eliminates radial field losses through the rest of the coil.

In practical constructions the conductor width of such spirals will be limited to perhaps five inches or less by considerations of heat transfer, but a number of such spirals can be assembled end to end and connected in parallel to make up any desired conductor width, with spaces between the spirals for coolant circulation.

The end losses of such a spiral coil can be approximated from equation 1 for both ends as

$$\frac{R_a}{R_{dc}} \approx \left(\frac{B_a}{B_N}\right)^2 \frac{\mu^{1/2}}{(\mu')^{1/2}} \frac{2\pi a_0|a_0-a_1|}{A} Nx \qquad (15)$$

in which B_a is the radial component of field strength and μ' is the radial space factor. This is not a particularly satisfactory approximation as it assumes the radial field to be constant over the end of the coil, but it at least will indicate the magnitude of the end loss to be expected.

Experimental Measurements

Round-Wire Coils

In order to test the application of formulas derived for rectangular conductors and a partial magnetic circuit to coils from round wire and surrounded by air, two small coils were wound from 0.022-inch round enameled wire, each coil having an inside diameter of 0.81 inch, an outside diameter of 1.19 inches, and eight layers. Other information is given in Table I.

Table II. Observations on 60-Turn Spiral Coil of Electrolytic-Copper Ribbon

One Inch Wide by 0.0035 Inch Thick

a_0, inches radius	0.97
a_1, inches radius	0.437
D-c resistance, ohms	0.0715
Effective ribbon thickness, inches	0.0025
μ	0.642
μ'	0.281
$m/f^{1/2}$	0.3075
Millihenrys at 10,380 cycles per second	0.0706

Table III

x	0.157	0.174	0.206	0.226
R_a/R_{dc}	2.83	2.95	3.43	3.87
R_a/R_{dc} corrected	2.45	2.82	3.43	3.87
B_a/B_N calculated	0.71	0.724	0.731	0.743

The effective resistance was measured by providing a mica decade capacitor for parallel resonance and driving from the 5,000-ohm tap of an oscillator through a 33,000-ohm decoupling resistance that was noninductive. The voltage across the parallel-resonant circuit was measured by a vacuum-tube voltmeter, and then a decade resistance was substituted for the parallel circuit and so adjusted that the voltage across the resistance was the same as that which had appeared across the parallel circuit. If the capacitor loss is charged to the inductance the effective series resistance of the inductance is given by the formula: inductance ÷ (capacitance times substitution resistance).

This method is not precise but for frequencies such that $x < 2$ the change in inductance with frequency will be very small and the method is reasonably satisfactory. The reactance–resistance ratio of the coils used was roughly from 10 to 30 for frequencies from 2,500 cycles to 20,000 cycles. At the upper limit of frequency the method begins to introduce appreciable inaccuracies on account of the inductance in the resistance decade, but a check by using a carbonized resistance indicated that the error was only two or three per cent.

The results are shown in Figure 6 as two sets of points plotted and the theoretical curve of equation 8 drawn in.

Equation 56

Another test of the same nature, but intended specifically as a check on equation 56, was made on a series of five 2,000-turn coils and at the single frequency of 10,000 cycles. These coils were each one inch long, they were layer wound but not layer insulated, and they were wound on wooden bobbins of 0.75-inch diameter.

A series resonance and substitution method was used to determine the effective resistance, using either 0.003 or 0.004 microfarad of a mica decade plus a variable air capacitor.

The following observations were made at 10,000 cycles:

Nominal wire diameter, mils	8.9	10.0	11.8	12.6	15.9
Outside coil diameter, inches	1.12	1.19	1.39	1.52	1.92
D-c resistance, ohms	65.5	54.1	44.8	39.3	29.2
R_{ac} by equation 8, ohms	71.6	63.9	59.8	63.8	93.0
R_{ac} measured, ohms	74.5	66.5	64.3	68.0	91.0

The measured value of R_{ac} includes a capacitor resistance correction arbitrarily figured for 0.001 power factor. This amounts to five ohms for the first three columns and seven ohms for the last two columns. Correction is necessary since the reactance/resistance ratio of some of the coils was above 60.

The round-wire diameter for minimum loss as determined from equation 56 is 0.0107 inch which is confirmed by the foregoing experimental result of 0.0110 inch.

Effect of Small Radial Depth of Winding

By way of emphasizing the inherent defects of the approximations used, in the absence of an external magnetic circuit and for the case in which the radial depth of the winding is small in comparison to the effective diameter of the coil, three coils of 2.375 inch inside diameter were wound from 0.010 round wire.

Data on the coils and measurements at 10,000 cycles follow:

Total turns	600	1,000	1,250
Number of layers	12	8	5
Coil length, inches	0.58	1.45	2.00
Radial thickness, inches	0.180	0.12	0.075
D-c resistance, ohms	41.8	69.0	84.7
R_{ac} by equation 8, ohms	42.4	70.2	85.2
R_{ac} measured, ohms	49.2	92.0	155

The same correction for capacitor power factor was made in the foregoing case as was made for the set of five coils.

It is obvious from the geometry of these coils that most of their eddy-current loss will result from the radial field when there is no external magnetic circuit, and so any method based on axial field losses only must be seriously in error.

End Loss in Spirals

Experimental work on small-scale spiral coils is complicated by the low impedances involved, and the following account is not presented as being particularly conclusive, but rather as being the only experimental evidence available relative to equation 15.

A 60-turn spiral coil of electrolytic-copper ribbon 1 inch wide by 0.0035 inch thick was wound and the observations listed in Table II were made.

Measurements were made with parallel capacitances from 0.768 to 3.33 microfarads corresponding to frequencies from 10,380 to 21,660 cycles and substitution resistances from 89 to 203 ohms. The circuit was driven from the 125-ohm tap of the oscillator through a 500-ohm resistance. Results were calculated as shown in Table III.

The corrected values were arrived at by plotting on logarithm paper and drawing the best possible straight line to fit the points. Values of B_a/B_N were calculated from equation 15 as the curves of Figure 4 indicate that the maximum value of eddy-current loss would be about six per cent; these values substituted into equation 15 give the corrected end-loss factors. The value of B_a/B_N was measured with a 20-turn one-quarter-inch-diameter search coil, and the maximum that could be measured at 10,000 cycles was just under 40 per cent. This makes it seem questionable as to whether the actual value could have been as large as the 70-per-cent tabulated indication. The measuring method would be expected to give results that are substantially too small, and the corrected end-loss factor is too large as it includes both the axial-field loss and the capacitor loss.

Comparison With Literature

Equation 1 is equivalent to equation 12 of Field's[1] paper and to equation 27 of Bennett and Larson's.[4]

Equation 6 is a refinement of an equation given in the appendix of Summers' paper[5] and is equivalent to Taylor's[2] equation 3.

Equation 3 is exactly equivalent to an expression given by Lyon[3] for the loss factor in a one-coil-side-per-slot winding of N layers. To demonstrate this it is necessary only to expand the hyperbolic functions of complex arguments given there into the corresponding combination of hyperbolic and circular functions of real arguments. The latter form seems to be much easier to look up in tables, but the functions of complex arguments in this case are much easier to expand into series if the series is to be carried beyond the first positive exponent with a real coefficient.

Conclusions

The formulas presented here to measure the eddy-current resistance of coils with partial magnetic circuits (but excluding the losses in the iron) are equivalent to earlier formulas that have been reasonably well tested by a number of years' experience.

The extension of these formulas to coils wound from round wire and without an external magnetic circuit by the device of correcting for the end effect with a fictitious permeability and for the wire shape by using an equivalent square section seems to give results of usable accuracy, at least up to frequencies for which the eddy-current resistance is 50 per cent of the d-c resistance. This may be subject to a further limitation that the coil length should be at least as great as half the diameter. It will take more experimental work to establish such limitations definitely.

The extension of the original formulas to coils from ribbon conductors wound spirally to give a net effect of one or two turns per layer seems to be justified by the addition of another formula to calculate the end-effect loss as a separate item. While the end-effect formula cannot be regarded as satisfactory, in most practical constructions it will be possible to keep the end losses quite low simply by keeping B_a/B_N low, and it seems reasonable to expect that the end losses will be substantially smaller than the axial-field loss.

Another generally practicable method of keeping down the loss due to radial field is the construction shown in Figure 1; as long as the iron does not saturate, the

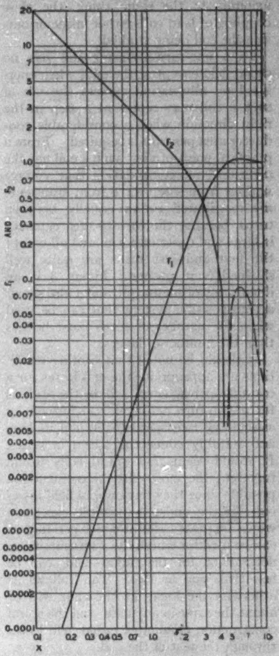

Figure 5. F_1 and F_2 plotted against x

Broken line indicates negative values

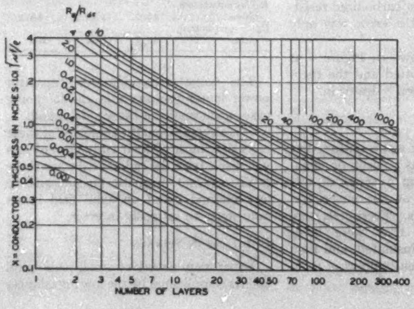

Figure 4. R_e/R_{dc} as a function of x and N, for the case that neglects the difference in length of layers and assumes arrangement of Figure 1A

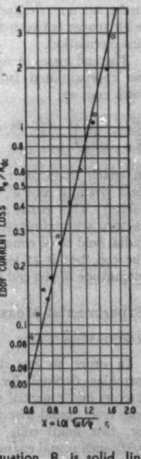

Figure 6. Eddy-current resistances plotted against x for round-wire coils

Circles are for long coil; dots are for short coil. Theoretical curve of equation 8 is solid line

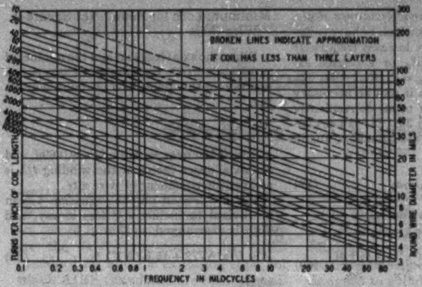

Figure 7. Relation of frequency, turns per inch of coil length, and round-wire diameter for minimum loss

Taken from equation 57 with $\rho = 1.8$

radial field will approach zero as l_1 approaches l.

Certain formulas have been derived for determining conditions for minimum losses, and as these have been arrived at by conventional mathematical methods they seem certainly valid. The end losses of spiral coils have been ignored in these derivations, because the end losses are determined for the most part by coil proportions and not by layer thickness. These formulas are presented, not as requirements of logical design, but as a formulation of simple standards against which logical designs can be measured, and as exploring tools.

It should be noted that when the layer thickness of spiral coils is selected for minimum loss the total loss varies as $N^{-1/2}$. This relation is quite precise for $N>4$, and for $N=1$ the theoretical minimum of loss occurs for $x=3.14$ and is about eight per cent less than that determined by $N^{-1/2}$.

As a speculative item, the possibility is indicated of increasing the output of such equipment as transformers, while decreasing the amount of active material and increasing the efficiency, by the simple expedient of increasing the winding section in a direction perpendicular to the principal leakage flux. There will be of course cases in which such improvement is difficult or impossible.

Appendix

Practical units and inch dimensions are used throughout this paper except that ρ is in microhms per centimeter cube, and γ is in mhos per centimeter cube to correspond to customary usage in tables.

Notation is defined where first used, but for convenience those terms used more than once are defined below;

a_0 = radius of turn at zero leakage-flux density

a_1 = radius of turn at maximum leakage-flux density

A = area of layer at zero flux density, measured parallel to leakage

B = flux density at plane of dr in nth layer in lines per square inch

B_N = highest flux density associated with Nth layer in lines per square inch

B_Δ = increase in flux density per layer in lines per square inch

$C_1 = 1.935m\rho10^{-8}/\mu^2$

e = resistance drop per inch of periphery at plane of dr

f = frequency in cycles per second

$$F_1 = \left\{\sinh x + \sin x - 2\left(\cosh\frac{x}{2}\sin\frac{x}{2} + \sinh\frac{x}{2}\cos\frac{x}{2}\right)\right\}/(\cosh x - \cos x)$$

$$F_2 = 2\left(\cosh\frac{x}{2}\sin\frac{x}{2} + \sinh\frac{x}{2}\cos\frac{x}{2}\right) \div (\cosh x - \cos x)$$

i = current density in amperes per square inch at dr

$k_1 = (n-1)/n$

$k_2 = (a_0-a_1)/(N-1)a_0$

$k_3 = (a_0-a_1)/2a_0$

$k_4 = (a_0+a_1)/2a_0$

l = net conductor dimension in inches measured along leakage flux

l_1 = length of leakage-flux path in inches

l_2 = axial coil length in inches

$m = 0.505\,(\mu f/\rho)^{1/2}$

n = layer number counting from zero leakage-flux density

N = total number of layers in winding being studied

r = distance of plane of dr from high flux-density side of layer in inches

r_1 = thickness of layer in inches as measured across leakage flux

w = total loss in watts for one square inch of the flat surface of layer n

W = total loss in watts for N layers

$x = 2mr_1$

γ = conductivity in mhos per centimeter cube

δ = insulation thickness in inches

ρ = resistivity in microhms per centimeter cube

μ = fictitious permeability l/l_1 or lL/l_2L_1

R = resistance as denoted by subscripts; R_a/R_{dc} is proportionate increase in resistance due to end loss in both ends of spiral

L = actual inductance

L_1 = inductance calculated by long-coil formula (that is, without correction for end effect)

Derivation for Loss in Layer n

This part of the derivation is not new and so is presented in outline only. The method is simular to that of Bennett and Larson, in that the differential equation is set up for the flux density. This permits a direct substitution for the boundary conditions and a differentiation to determine current density.

It will be assumed that one side of a spiral coil is shown in section in Figure 1, and that the conditions are as set forth in the introduction. It will be convenient to take as the differential element of the conductor a piece one inch by one inch in the directions of current flow and leakage flux, with a thickness of dr inches measured across the leakage flux.

Let the voltage impressed on any particular layer of this spiral coil be E volts per inch of periphery, and let the induced voltage be e' per inch at the position of dr, a thin section parallel to the flat of the conductor and located r inches from that side of the conductor that is at the highest flux density. Then, if e is the resistance drop in volts per inch,

$$E + e' = e \tag{16}$$

If γ is the conductivity in mhos per centimeter cube, and i is the current density in amperes per square inch of conductor cross section,

$$2.54e\gamma = i \tag{17}$$

Due to idr, there is, in lines per square inch,

$$dB = 0.4\pi 2.54^2 e\gamma\mu dr = 8.1e\gamma\mu dr \tag{18}$$

in which μ is the ratio of the leakage path to the net conductor along that path. If the difference in e' on the two sides of dr per inch of periphery is called de', then

$$de' = -j2\pi fBdr10^{-8} = de \tag{19}$$

and from equation 18,

$$\frac{d^2B}{dr^2} = 8.1\gamma\mu\frac{de}{dr} \tag{20}$$

If we substitute from equation 19,

$$\frac{d^2B}{dr} = -j50.8f\gamma\mu B10^{-8} = -2jm^2B \tag{21}$$

A solution of equation 21 is

$$B = A_1\epsilon^{(1-j)mr} + A_2\epsilon^{-(1-j)mr} \tag{22}$$

If n is the layer number counting from the region of zero leakage flux, the boundary conditions can be stated thus: when $r=0$, $B=B_n$; when $r=r_1$, $B=B_{n-1}$;

$$B_{n-1} = [(n-1)/n]B_n = k_1B_n \tag{23}$$

If we eliminate A_1 and A_2:

$$B = B_n\frac{\left\{\begin{matrix}k_1(\epsilon^{(1-j)mr} - \epsilon^{-(1-j)mr}) + \\ \epsilon^{(1-j)m(r_1-r)} - \epsilon^{-(1-j)m(r_1-r)}\end{matrix}\right\}}{\epsilon^{(1-j)mr_1} - \epsilon^{-(1-j)mr_1}} \tag{24}$$

$$\frac{dB}{dr} = \frac{B_n(1-j)m\left\{\begin{matrix}k_1\cosh mr\cos mr - \\ \quad\cosh m(r_1-r)\cos m(r_1-r) \\ -j[k_1\sinh mr\sin mr - \\ \quad\sinh m(r_1-r)\sin m(r_1-r)]\end{matrix}\right\}}{\sinh mr_1\cos mr_1 - j\cosh mr_1\sin mr_1} \tag{25}$$

The rate of power loss per cubic inch of conductor in watts is

$$2.54e^2\gamma/2 \tag{26}$$

If the conductor is measured on one of its flat sides (parallel to principal flux) the loss per square inch of conductor is in watts:

$$\int_0^{r_1}\frac{2.54e^2\gamma}{2}dr=\int_0^{r_1}\left|\frac{dB}{dr}\right|^2\frac{dr}{51.6\gamma\mu^2}=w \tag{27}$$

Let

$$C_1=m/51.6\gamma\mu^2 \tag{28}$$

$$w=\frac{2mB_n^2C_1\times\displaystyle\int_0^{r_1}\left\{\begin{matrix}k_1^2(\cosh 2mr+\cos 2mr)+\\ \cosh 2m(r_1-r)+\\ \cos 2m(r_1-r)\\ -2k_1[\cosh mr_1\times\\ \cos m(r_1-2r)+\\ \cosh m(r_1-2r)\cos mr_1]\end{matrix}\right\}dr}{\cosh 2mr_1-\cos 2mr_1} \tag{29}$$

$$=\frac{B_n^2C_1\left\{\begin{matrix}(k_1^2+1)(\sinh 2mr_1+\sin 2mr_1)-\\ 4k_1(\cosh mr_1\sin mr_1+\\ \sinh mr_1\cos mr_1)\end{matrix}\right\}}{\cosh 2mr_1-\cos 2mr_1} \tag{30}$$

$$=B_n^2C_1\{(k_1^2+1)F_1+F_2/n^2\} \tag{31}$$

in which F_1 and F_2 have the meanings defined under notation.

Now let the increment of flux density per layer

$$B_n/n=B_\Delta \tag{32}$$

$$wA=B_\Delta^2C_1A\{(2n^2-2n+1)F_1+F_2\} \tag{33}$$

Total Loss for N Layers

$$\Sigma wA=W$$

$$=B_\Delta^2C_1A\{F_1\sum_1^N(2n^2-2n+1)+NF_2\} \tag{34}$$

$$W=B_N^2C_1A\{F_1(2N^2+1)/3+F_2\}/N \tag{35}$$

It will be found that for $x<2$ the foregoing expression can be closely approximated by writing the series expansions for F_1 and F_2 to include the first term in x with a positive exponent. If we make this substitution,

$$W=B_N^2C_1A\{x^3(5N^2-1)/360+2/x\}/N \tag{36}$$

Correction for Differences in Layer Lengths. In the foregoing two equations no account has been taken of the difference in periphery of the various layers of a spiral coil. As the area of the layer at zero leakage-flux density has been taken as A, the area of any other layer will be $A\ \{1-(n-1)k_2\}$, where $k_2=(a_0-a_1)/(N-1)a_0$; a_0 is the length of the layer at zero flux density, and a_1 is the length of the layer at maximum flux density. Then:

$$W=B_\Delta^2C_1A\{F_1\sum_1^N(2n^2-2n+1)\times$$

$$[1-(n-1)k_2]+F_2\sum_1^N[1-(n-1)k_2]\} \tag{37}$$

$$=\{B_N^2C_1A/N\}\left\{F_1\left(\frac{2N^2+1}{3}-\frac{3N^2+N+1}{6}\frac{a_0-a_1}{a_0}\right)+F_2\frac{(a_0+a_1)}{2a_0}\right\} \tag{38}$$

Effective Resistance and Resistance Ratio. The most useful form in which to have information on eddy-current losses is frequently an expression for R_{ac}/R_{dc} or a related expression $(R_{ac}-R_{dc})/R_{dc}=R_e/R_{dc}$. To obtain such an expression it will be necessary to state the d-c loss in terms conveniently comparable to equation 36. If l is net conductor width measured along leakage flux in inches,

$$R_{dc}=NA(a_0+a_1)/5.08r_1l^2\gamma a_0 \tag{39}$$

$$\text{D-c loss}=\frac{B_N^2A}{25.8\gamma\mu^2Nr_1}\frac{a_0+a_1}{2a_0}$$

$$=\frac{4B_N^2C_1A}{Nx}\frac{a_0+a_1}{2a_0} \tag{40}$$

Since for a given value of B_N and ignoring eddy-current losses the a-c loss will be one half of the d-c loss, this a-c loss may be called W' and then $R_{ac}/R_{dc}=W/W'$. If layer length differences are neglected,

$$W'=2B_N^2C_1A/Nx \tag{41}$$

$$R_{ac}/R_{dc}=x^4(5N^2-1)/720+1 \tag{42}$$

Determination for Minimum Loss With Dimension h Restricted

To determine the layer thickness for minimum loss when dimension h is restricted, it is expedient to make the usual series approximations for F_1 and F_2 in equation 38 that are quite accurate for $x<2$, and to assume that $N>3$, so that the loss equation becomes

$$W\approx B_N^2C_1A\left\{\frac{x^3N}{72}\left(1-\frac{3}{2}k_3\right)+\frac{2}{Nx}(1-k_3)\right\} \tag{43}$$

Since

$$N=2mh/(x+2m\delta)$$

$$W\approx B_N^2C_1A\left\{\frac{hm}{36}\left(1-\frac{3}{2}k_3\right)\left(x^2-2mx\delta+4m^2\delta^2-\frac{8m^3\delta^3}{x+2m\delta}\right)+\left(\frac{1}{mh}+\frac{2\delta}{hx}\right)(1-k_3)\right\} \tag{44}$$

$$\frac{dW}{dx}=B_N^2C_1A\left\{\frac{hm}{36}\left(1-\frac{3}{2}k_3\right)\left(2x-2m\delta+\frac{8m^3\delta^3}{(x+2m\delta)^2}\right)-\frac{2\delta}{hx^2}(1-k_3)\right\}=0 \tag{45}$$

$$\frac{1-\frac{3}{2}k_3}{1-k_3}\ \frac{h^2mx^4}{18}\ \frac{x+3m\delta}{(x+2m\delta)^2}=2\delta \tag{46}$$

$$\frac{3k_4-1}{2k_4}\ h^2m^4r_1^3\ \frac{(1+3\delta/2r_1)}{(1+\delta/r_1)^2}=\frac{9\delta}{2} \tag{47}$$

$$\frac{r_1^3}{\delta^3}\ \frac{1+3\delta/2r_1}{(1+\delta/r_1)^2}=\frac{9}{2\delta^2h^2m^4}\ \frac{2k_4}{3k_4-1} \tag{48}$$

$$\frac{r_1}{\delta}q=\sqrt[3]{\frac{9}{2\delta^2h^2m^4}\ \frac{2k_4}{3k_4-1}} \tag{49}$$

$$r_1\approx\delta\left(0.17+\sqrt[3]{\frac{9}{2\delta^2h^2m^4}\ \frac{2k_4}{3k_4-1}}\right) \tag{50}$$

when $r_1/\delta>1$

Minimum Loss for Round- (or Square-) Wire Coils

When the axial length l_h and the number of turns t are fixed, the number of layers is a function of the diameter d of round wire, so that

$$N=tr_1/l=tx/2ml \tag{51}$$

in which the only variable is $r_1=0.89d$, and the axial space factor of the winding l/l_h is assumed independent of wire size.

For the present purpose equation 43 can be revised to include d-c loss if any, and slightly rearranged, so that

$$W\approx U(x^3N/72+4k_5k_6/NX) \tag{52}$$

where

$$k_6=1-2a_1/(a_0+3a_1)$$

and

$$U=B_N^2C_1A(1-3k_3/2)$$

Substituting from equation 51

$$W\approx U(x^4t/144ml+8k_5k_6ml/tx^2) \tag{53}$$

$$dW/dx=U(x^3t/36ml-16k_5k_6ml/tx^3)=0 \tag{54}$$

$$x=2.88(k_5k_6)^{1/6}(ml/t^{1/3} \tag{55}$$

$$r_1=1.44(k_5k_6)^{1/6}(l/m^2t)^{1/3}$$
$$=2.27(k_5k_6/K^2)^{1/6}(\rho l_h/ft)^{1/3} \tag{56}$$

since

$$m^2=0.254fKl/l_h\rho$$

in which K = Nagaoka's constant.

If there is no d-c loss $k_5=1$; $(k_6/K^2)^{1/6}$ usually will exceed unity by not more than a few per cent. Then if $\rho=1.8$ for copper,

$$d=r_1/0.89=3.11/(ft/l_h)^{1/3} \tag{57}$$

In this equation d is the round-wire diameter for minimum loss, and r_1 is the square-wire diameter for minimum loss, provided that $N>3$. The approximation is fair for $N=2$.

It is interesting to note that the wire diameter for minimum loss is independent of the axial space factor (assumed constant) except as this influences K and k_6.

References

1. Eddy Currents in Large Slot-Wound Conductors, A. B. Field. AIEE Transactions, volume 24, 1905, pages 659–86.

2. Eddy Currents in Stator Windings, H. W. Taylor. *Journal* Institution of Electrical Engineers (London, England), volume 58, 1920, pages 279–300.

3. Heat Losses in Conductors of A-C Machines, Waldo V. Lyon. AIEE Transactions, volume 40, 1921, pages 1361–95.

4. Heat Losses in Stranded Armature Conductors, Waldo V. Lyon. AIEE Transactions, volume 41, 1922, pages 199–214.

5. Reduction of Armature Copper Losses, Ivan H. Summers. AIEE Transactions, volume 46, 1927, pages 101–11.

6. Effective Resistance to Alternating Currents of Multilayer Windings. Edward Bennett, Sidney Larson. AIEE Transactions, volume 59, 1940, pages 1010–17.

7. Eddy-Current Losses in Cylindrical Conductors, S. Butterworth. *Philosophical Transactions* Royal Society (London, England), series *A*, 222, 1921–22, pages 57–100.

Lightning Arresters for Distribution Apparatus

EDWARD BECK
MEMBER AIEE

A. D. FORBES
MEMBER AIEE

THERE are today two general types of lightning arresters in use for the protection of distribution apparatus. They are the valve type covered by AIEE Standard 28, and the expulsion type, for which AIEE Standards are being formulated. Both have been used widely for many years. Typical specimens are illustrated in Figure 1. The valve type is the older. The first distribution-valve arrester was an Autovalve produced in 1922. The first expulsion-type distribution arrester was the deion arrester (United States Patent, 2,050,397) used on surge-protected distribution transformers in 1931. By far the largest number of expulsion-type arresters manufactured have been applied as part of completely self-protected transformers. Many of these have used a somewhat different physical construction and mounting as shown in Figure 2 than that used for the arresters installed separately from the transformers. There exist today several variations of both the expulsion and valve types.

With so many years of service behind the two types, the question arises why both still persist. Why has not the industry decided that one is better and discarded the other? Why do some manufacturers make both types, and some only one? Affiliated with a company that manufactures both types, the authors frequently are asked, not only by users but also by associates in the company, why the company does not eliminate one of them and concentrate on the other. From a manufacturing standpoint this would be a highly desirable simplification, but the reason why both are made is that there are demands for both. Apparently the industry is not ready to accept only one in lieu of both.

A brief review of the history that stimulated the two types is of passing interest. There were two major reasons for the development of the expulsion type to parallel the valve type. These were radio broadcasting and the growth of rural electrification.

Valve-type arresters in the 1920's were contemporary with the growth of radio broadcasting into a public service. In those days the valve arresters were frequent causes of radio interference as a result of moisture collecting inside of them. Methods of testing for radio interference were not developed, and arresters were not designed to avoid it as it was not a known requirement. It soon became evident, however, that it was a very important requirement. Many engineers believed that it was impossible to seal an arrester against moisture entrance and that an arrester should be thoroughly ventilated. The expulsion arrester is such a device, and this was then greatly in its favor. At the present time radio interference is hardly a worry in either valve or expulsion arresters since methods of sealing and testing valve arresters have been devised that effectively prevent moisture collection. Autovalve arresters manufactured since 1932 have been signally free from moisture or radio interference.

Most expulsion-type arresters, because of the requirement of clearing appreciable power-follow currents, inherently possess a high degree of ability to discharge severe lightning current without damage to themselves. In this respect they surpass the early valve types. The importance of surge capacity became more apparent as rural electrification proceeded. It might be said that the appearance and the successful operation of the expulsion-type arrester threw a challenge to the valve type which resulted in a general increase in quality of both types of arresters. This is a healthy condition, consequently, it is well that the industry has not yet settled on one type to the exclusion of the other.

The Functions of Lightning Arresters

Fundamentally lightning arresters, regardless of type, must perform the same function, to provide by-passes around insulation. When lightning strikes a circuit, transient currents flow in the system. With these currents are associated potentials that are functions of the current and the impedance to the current flow. If the flow of lightning current is not obstructed by impedance or insulation, the voltages between points that are electrically adjacent in the circuit are small, but, if the flow is obstructed, very high voltages may appear, because the lightning current puts forth all its effort to flow. If the obstruction consists of insulation, the voltage developed across it may be sufficient to puncture or flash around it, thereby giving the current a means of continuing by way of damage or outage. A lightning arrester provides an easy path for the lightning current to get around the insulation so that high voltages will not develop. The by-pass, however, must be such that it does not interfere with the supply of power to users. This means that, when operating conditions are normal with no surges on the system, the arrester must be an insulator, so that it prevents flow of power current. When a transient voltage appears which might exceed the insulation strength of the apparatus to be protected, the arrester must become as quickly as possible a good by-pass for lightning current. After the release of this current, the by-pass must transform itself back to its insulation condition so quickly that no circuit breakers or fuses in the circuits are called upon to open in order to interrupt flow of system current through the arrester.

A lightning arrester may be looked upon as a very fast circuit breaker connected from line to ground, normally open, but

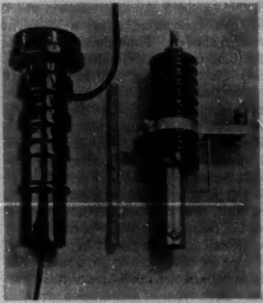

Figure 1. Typical distribution lightning arresters of the valve and expulsion types

Rating, nine kilovolts

Figure 2. Completely self-protected distribution transformer with internally mounted expulsion-type arresters

---

Paper 45-147, recommended by the AIEE committee on protective devices for publication in AIEE TRANSACTIONS. Manuscript submitted April 13, 1945; made available for printing July 23, 1945.

EDWARD BECK is section engineer, switchgear division, Westinghouse Electric Corporation, East Pittsburgh, Pa., and A. D. FORBES is section engineer in the transformer division of the company at Sharon, Pa.

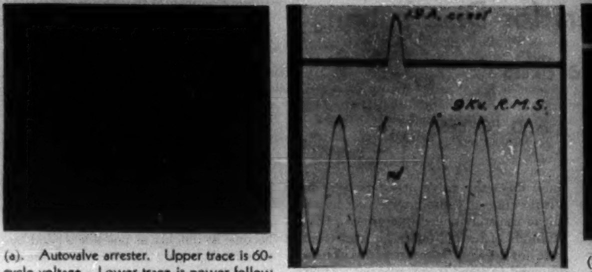

(a). Autovalve arrester. Upper trace is 60-cycle voltage. Lower trace is power-follow current. Crest of follow current is 36 amperes. Current limited by valve element only as apparent from uniformity of voltage wave

(b). Deion arrester. Lower trace is 60-cycle voltage. Upper trace is follow current limited by circuit

(c). Deion arrester. Follow current higher than in b. Short-circuit current of test circuit was 10,000 amperes rms. Arrester limits follow current

Figure 3. Typical oscillograms of power-follow currents and their interruption for valve and expulsion arresters

Arrester ratings, nine kilovolts
Power voltage used in tests, nine kilovolts rms

one which closes immediately at a predetermined voltage and reopens quickly after the disturbances have passed. The closing mechanism in the lightning arrester is a spark gap of some form which becomes conducting when a transient voltage appears. Thus, the circuit for the lightning current is established, but this circuit is then also a path to ground for system fault current. Arresters therefore must incorporate a contrivance that will open this power current path or aid the spark gap to reopen it. Simple gaps, such as rod gaps, are not classed as arresters, because, although they will provide more or less effective by-passes for lightning currents, they are unable to interrupt the path. Their power-follow currents must be cleared from the circuit by the operation of a circuit breaker or a fuse. The lightning arrester takes care of this by itself. Both types of distribution arresters accomplish the closing and reopening of the relief circuit in essentially the same fashion. The differences lie principally in the process involved in re-establishing the insulation of the arrester and in the magnitudes of the impulse voltages that appear across the terminals of the devices.

The simplest analogy to the expulsion type of arrester is that it is like a fuse with the fuse link omitted. It consists essentially of a tube, usually of fiber, with electrodes in each end. In series with this is a spark gap. When a high voltage occurs, the series gap and the gap in the tube spark. By this process a circuit is made through the tube just as if a fuse link had been present. The arrester thus becomes a path of low impedance, and the surge voltage across the terminals drops to a low voltage after spark-over. This voltage drop consists only of the arc drop in the extinction chamber. Therefore, as far as power-follow current is concerned, the device may become nearly a short circuit. However, like the fuse, it interrupts the system fault current when its current wave passes through zero because of the gas evolved by the heat of the arc from the walls to the extinction chamber. Unlike the fuse, it does not have to be refilled, because it has no fuse link. The expulsion-type arrester operates repeatedly without attention. The devices are so designed that their spark-over is sufficiently low to provide protection for the apparatus or insulation they are intended to protect. In some recent constructions for use on distribution circuits, there are incorporated features that produce appreciable arc voltage while power current flows, so that the power current follow is determined partly by the device and partly by the system characteristics. This arc voltage may be an appreciable part of the normal circuit voltage, but compared to the spark-over voltage it is small.

The expulsion arrester thus performs the cycle required of a lightning arrester. It is normally an insulator, it becomes a conductor of low impedance when necessary to prevent high voltage, and it interrupts the system current quickly and reverts to an insulator. Its operation does not interfere with the flow of power in the system.

A familiar analogy for the valve type of arrester is not so easily found, unless it be likened to an automatic valve that opens and closes as circumstances require. The valve arrester, too, has a spark gap which normally provides insulation and operates as a switch to close by sparking when a surge voltage appears. Unlike the expulsion arrester, the series gap in the valve arrester also must reopen the circuit after the necessity for limiting the voltage has passed. Simple air gaps are not capable of interrupting high currents such as might be involved in system faults. Gaps such as are used in valve arresters can interrupt reasonably high alternating currents, of 50 to 100 amperes, but not much more. Therefore, to insure successful operation of the device, the power-follow current that flows after the lightning discharge must be limited to a magnitude that the gap can interrupt. This can be accomplished by series resistance. However, if this is the common type of constant resistance and of such a magnitude that it will limit the power-follow current to the afore-mentioned value when system voltage only is impressed across its terminals, then when high lightning currents flow the *IR* drop will be large. This would impress high voltage on the insulation supposedly protected. An example, would be a nine-kilovolt arrester with a constant series resistance that will limit the current at nine kilovolts to 100 amperes. If a surge current of 2,000 amperes flows through it, it will develop 20 times normal voltage or 180 kv. Such a device would be inadequate for purposes of lightning protection. For this reason the series impedance used in valve arresters is of a special kind that has a high effective resistance at low voltage and a low effective resistance when high currents flow. It is for this reason that they are called valve elements. The impedance or the valve opening regulates itself to the flow of current and limits the voltage. The regulation in most valve elements is a property of the electrical contacts between the particles of which it consists. If we choose to think of the valve element as a resistor, then in a 3,000-volt valve-type arrester its apparent resistance at 3,000 volts may be 100 or more ohms, whereas when it is passing 50,000 amperes of surge current its apparent resistance may be less than half an ohm.

By the co-operative functioning of the series gap and the valve element, the valve type also performs the functions expected of an arrester. It is normally an insulator, it becomes a path of relatively low impedance, and it re-establishes itself as an insulator after the lightning discharge has passed. It does not interfere with the flow of power in the system.

The principal difference in the operation of the two types of arresters is in the way in which they dispose of the system follow current. In the valve arrester the follow current is limited by the device itself regardless of system capacity. Valve arresters, therefore, are rated only on the basis of voltage. The rating defines the maximum voltage applied across the arrester terminals against which the arrester can return itself to an insulator subsequent to a surge discharge. In the expulsion arrester the follow current may be determined principally by the system and these devices generally are rated in both voltage and current somewhat like fuses. As far as service is concerned, the difference between the two is not significant because either device, as shown by Figure 3, operates without causing what is generally termed a fault.

Protective Characteristics

The most important quality that an arrester should possess is the ability to protect insulation against high voltage. The magnitudes to which it limits surge voltages are related in various ways to the power voltage which the arrester is able to clear.

Valve and expulsion arresters both provide surge protection for distribution apparatus. This can be seen by comparison of the impulse characteristics of the arresters with the standard impulse levels of the equipment. The major use of distribution lightning arresters is to protect distribution transformers against damage to their insulation or flashover with consequent outage. A ready means of comparison is found in the relation of the lightning-arrester characteristics to the impulse withstand tests required of transformers. The transformer manufacturers have, in the National Electrical Manufacturers Association Transformer Standards stated certain impulse voltages which the transformers covered by these standards are able to withstand without damage. The test voltages are described and coordinated with the insulation class designations of the transformers as in Table I. They provide a definition of the impulse strength of transformers and thus a means of relating the lightning protection to them directly. Present AIEE Standards for valve arresters specify a number of tests which are complete and possibly more voluminous than necessary to furnish the industry with adequate information of the characteristics of these protective devices. The tests described in lightning-arrester standards are not related directly to the withstand impulse-voltage tests specified for transformers, although their relation can be determined by reference to curves. A simple and complete comparison between transformer-insulation strengths and the degree of protection provided by arresters can be made by applying to the arrester the withstand test voltages specified for those transformers with which the arresters may be used. If the arrester, when subjected to this test voltage, prevents voltages of the magnitude and character of the withstand voltages from developing, it is obvious that the transformer is protected by the arrester. The relation between transformer strength and arrester performance for a typical application is shown by the oscillograms of Figure 4. The 15-kv insulation class transformer and the nine-kilovolt arresters, a common combination, are illustrated. In order to show both the arrester impulse spark-over characteristics and the effect of voltage drop while the arrester carries current, two sets of oscillograms are shown with different time scales.

Impulse Spark-Over Voltages

Figures 4a and b show the arrester spark-over characteristics in relation to the transformer withstand voltages. In Figure 4a the trace marked 96 kv is the 1.5x40 wave which the transformer withstands if it meets NEMA Standards. If a nine-kilovolt expulsion arrester of the type illustrated in Figure 1 is connected in the test circuit and the transformer withstand voltage applied, spark-over of the arrester occurs at 69 kv. The nine-kilovolt valve arrester shown in Figure 1 sparks at 52.5 kv. Both of these are well below the full-wave voltage that the transformer will withstand.

The response of arresters to the chopped wave used for transformer testing is practically the same as in the case of the full wave. Therefore, it has not been shown. Of interest, however, would be the arrester behavior on a front of wave test for the transformer, because this would have an appreciably faster rate of voltage rise. Such front of wave tests have not been standardized for distribution transformers. An approximate value, which might in the authors' opinion be used, is shown in Figure 4b by the broken-line trace marked 165 kv. Such a test wave applied to a nine-kilovolt deion arrester causes spark-over at 113 kv and on the nine-kilovolt Autovalve arrester at 57 kv. Again, both of these values are well below the impulse voltage that can be impressed on a transformer without damage. It should be

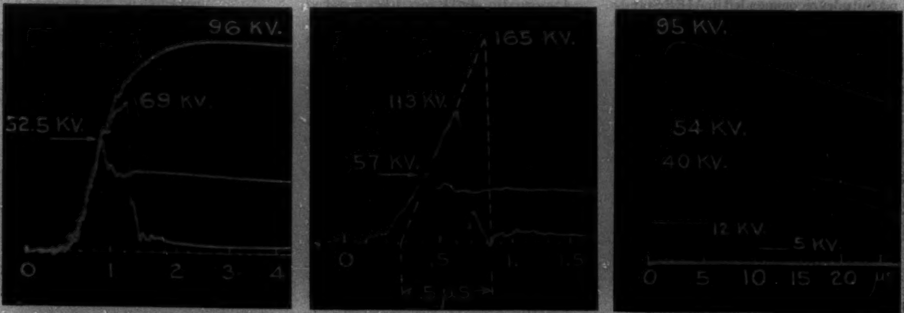

Figure 4. Relation between transformer impulse withstand voltage (see Table I) and arrester voltages

Transformer insulation class, 15 kv
Arrester ratings, nine kilovolts

(a). Transformer full wave, 96 kv. Deion arrester spark-over, 69 kv. Autovalve spark-over, 52.5 kv

(b). Transformer assumed front of wave test, 165 kv. Deion arrester spark-over, 113 kv. Autovalve spark-over, 57 kv

(c). Transformer full wave, 95 kv. Voltage across arresters during discharge of specified surge currents:

Deion arrester, 20,000 amperes, 12–5 kv
Autovalve arrester, 5,000 amperes, 40 kv, 20,000 amperes, 54 kv

These oscillograms do not show the spark-over voltages. They are shown in Figures 4a and b noted from the comparison of Figures 4a and b that the transformer will withstand a higher voltage, if applied for only a short time, than the full 1.5x40 wave test voltage.

Figure 4 indicates that the impulse spark-over voltage of the expulsion arrester is higher than that of the valve arrester. In the expulsion arrester, spark-over takes place over two air gaps, the series gap, and the gap in the extinction chamber. The gap in the extinction chamber is relatively long to insure clearing of the power-follow current, and the time lag curves of spark-over, Figure 5, indicate that the spark-over voltage increases with decreasing time to spark-over. This is not serious since insulation time-lag curves have somewhat the same shape. Although the spark-over characteristics can be modified by means such as the electrostatic shielding used in the arrester shown in Figure 1, the foregoing factors in general fix the order of impulse spark-over voltage.

The gap in the valve arrester is not called upon to interrupt high power-follow currents, as their magnitude is limited by the valve element. Therefore, it can be made with low spark-over voltage and with time-lag characteristics that resemble those of sphere gaps which are more or less flat and begin to turn up only at very short times to spark-over as illustrated in Figure 5. Although there is this difference between the spark-over voltages of the valve and expulsion types, Figure 4 shows that there is ample margin between the transformer impulse strength and the impulse spark-over of either arrester.

Voltage During Discharge

More than the impulse spark-over should be taken into account in the correlation between transformer strength and protective characteristics of the arrester, because, while the arrester is discharging surge current, some voltage exists across its terminals as the result of arc or impedance drops. In Figure 4c are shown these voltage characteristics of both types of arresters for several discharge currents of magnitudes recommended in AIEE Standards. These again are related to the transformer full-wave withstand voltage shown again in Figure 4c by the trace marked 95 kv. The spark-over voltages of the arresters are not apparent in Figure 4c because of the larger time scale. The spark-over voltages are shown in Figures 4a and b.

Consider the valve arrester characteristics. The trace marked 54 kv is the voltage developed across the arrester during discharge of a 20,000-ampere test surge. The trace marked 40 kv is the voltage across the arrester with a test current of 5,000-amperes crest. It should be noted that the voltage across the valve arrester drops from the crest reached after a few microseconds. It is sometimes thought that the voltage drop of the valve arrester persists at its crest magnitude for the duration of the discharge. This is not the case, especially when high currents are involved.

The voltage that exists across the expulsion arrester while discharging 20,000 amperes is shown by the lowest trace in Figure 4c. Immediately after discharge, the voltage collapses to 12 kv and then drops further, until after several microseconds it has decayed to five kilovolts. For the expulsion arrester, the voltage for a 5,000-ampere discharge is not shown. It is less than that for 20,000 amperes. It is apparent that the discharge voltages of the expulsion arrester are appreciably lower than those for the valve arresters. However, in either case, there is considerable margin between the withstand voltage of the transformer and the voltages developed across either arrester during the discharge of surge current. These differences are thus not of practical importance, although they sometimes arouse controversy. The valve arrester becomes conducting on steep impulse voltages at lower values than the expulsion type. One might say that this is an advantage. On the other hand, the voltage across the expulsion arrester collapses to a lower value once discharge has begun. This is an advantage in favor of the expulsion arrester.

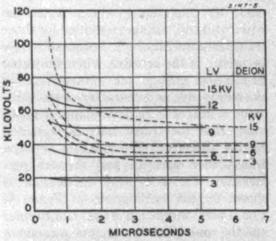

Figure 5. Impulse spark-over time-lag characteristics of distribution arresters of the valve and expulsion types

Full lines—Autovalve arresters
Broken lines—Deion arresters
Numbers on curves indicate voltage rating

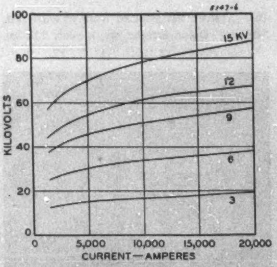

Figure 6. Relation between crest of 10x20-microsecond discharge current and crest of voltage developed by the current for Autovalve arresters

Numbers on curves are arrester ratings

The important impulse characteristics of both arresters are shown in curve form in Figures 5 and 6. As far as transformers manufactured during the last decade or so are concerned, either device is adequate. This is particularly true on completely self-protected transformers where the manufacturer has a known insulation strength with which it is relatively easy to co-ordinate the arresters. On very old transformers the impulse strength may be lower, as they were not built to meet present standards. For the protection of such transformers, the valve arrester may be preferable because of its lower sparking voltage. It is true that with very heavy current discharges the voltage developed across the valve arrester during the discharge may exceed the impulse strength of the old transformer, so that the transformer will not be protected under these conditions. For example, when discharging a surge current with a crest of 65,000 amperes, the peak voltage across a nine-kilovolt valve arrester may be 70 kv. Though this is well below the full-wave strength of a recent transformer that meets Table I, it may well exceed the strength of a very old transformer. However, the occurrence of such heavy currents is rare. Field measurements of the surge currents discharged by arresters in rural service indicate that 50 per cent of the operations involve currents of less than 1,500-amperes crest and 96 to 98 per cent less than 20,000 amperes. By and large, therefore, valve arresters should give better protection to the old transformers being considered. On the other hand it is probably desirable that transformers with such low-impulse strengths be replaced by modern ones.

Surge-Current Capacity and Life

An arrester fundamentally is intended to prevent service outages during thunder storms. Therefore, it should not only prevent insulation failures as far as possible but also should be rugged to prevent damage to itself. Electrical damage may result from very severe lightning—after all a distribution arrester is a device of only modest size—or it may result from a temporary system voltage condition in excess of the arrester rating or because of a defect in the arrester. Any of these is possible. Considering the effects of lightning, it is desirable that the arrester have surge discharge capacity sufficient to

Table I. Impulse Insulation Withstand Tests for Distribution Transformers (Oil Immersed)

Insulation Class, Kilovolt Rms	Transformer* Voltage Rating	Chopped Wave		Full-Wave Voltage, Kilovolt Crest	Arrester** Voltage Rating, Rms
		Voltage, Kilovolt Crest	Minimum Time to Flashover, Microseconds		
2.5		54	1.25	45	
5.0	2,400	60	1.5	60	3,000
8.66	4,800	88	1.6	75	6,000
15.0	7,200	110	1.8	95	9,000
15.0	13,200	110	1.8	95	15,000

*These are usual standard ratings and usually fall into the insulation classes shown. The insulation class indicates the insulation strength.

**These are the arrester ratings usually used with the transformers listed in column 2. In some cases because of circuit conditions, other arrester ratings may be used with a given transformer rating.

Test voltage wave shape is 1.5x40 microseconds (1.5 microseconds from 0 to crest, 40 microseconds to half of crest).

Full-wave test is an application of the full unmodified 1.5x40 wave to the test specimen. (See Figure 4a.) In the chopped-wave test, a 1.5x40 wave shape is applied, but the test voltage is removed or chopped by flashover of a properly set parallel gap in the time specified in the table.

In front of wave tests, the voltage applied to the test specimen is removed or chopped by a gap in a specified time, but while the test voltage is still rising. (See Figure 4b.) Front of wave tests for distribution transformers have not yet been determined.

This table is based on Table V of NEMA Transformer standards, publication 42-73. For more complete data, refer to those standards.

Table II. Comparison of Deion and Autovalve Lightning Arresters for Distribution Apparatus

Characteristic	Type of Arrester	
	Deion	Autovalve
Impulse spark-over, 0.5 microsecond		Lower
Voltage during discharge	Lower	
Power-follow current		Less
Surge-current capacity:		
65,000 amperes	Same	Same
Long low currents	Better	
Service life	Comparable	Comparable
Construction	Open	Sealed
Series gap	Integral part of arrester	
Is series gap setting critical	No	Sealed
Is application affected by system recovery voltage	No*	No*
Is application limited by system fault currents	No**	No
Is co-ordination of feeder relaying or fusing and arrester required	Usually not	
Does operation depend on expenditure of material	Refer to text	
Does system frequency affect arrester application	***	****
Is arrester applicable to delta systems	Yes	Yes
Radio interference	No	No
Line lockouts	No	No

*Theoretically yes, practically no. Experience shows that either type operates satisfactorily on existing distribution circuits.

**Holds for the arrester described in text.

***Ratings are based on 60 cycles.

****Ratings are based on 25–60 cycles.

minimize the chances of arrester damage by lightning in the field. Experience has developed a basis of test for the distribution arrester. This is the 65,000-ampere test recommended in the AIEE Standards. Years of experience with arresters of various surge current capacities indicate that capacities of less than 65,000 amperes will engender unsatisfactory rates of failure from lightning in the field. The 65,000-ampere test is thus a reasonable index to the ability of arresters to weather severe storms. Both of the arresters shown in Figure 1 meet this criterion, and field experience with both has been excellent.

The dangers of system overvoltage are well known. A valve arrester is sensitive to the system voltage impressed on its terminals during the clearing period. In fact excessive system voltage may be called its chief enemy. It is not in general sensitive to rate of system recovery voltage, because it itself determines the rate of recovery voltage across its series gap as a result of the effective resistance of the valve element. However, if the system voltage exceeds the arrester rating, the gap may not be able to clear and the arrester may be damaged.

The ability of the expulsion arrester to interrupt depends on several factors besides voltage, such as the rate of recovery voltage, overshoot of recovery voltage, current to be interrupted, and on the power factor of the circuit. When any of these conditions are not as severe as those for which the arrester is designed, an additional margin in interrupting ability results. It is not recommended, however, that a lower voltage arrester be used because of any margin of this type. The voltage rating should be considered a maximum rating.

A very live question to which a direct answer is difficult involves the life of an arrester. How long should it last, and how long may the various types be expected to last? Laboratory tests and records of discharges through arresters in actual service give clues on the basis of which estimates may be made, but the best indication is experience. This may appear unfair to the user, because he is the one that has to acquire the experience. Fortunately, the art is now in a phase where considerable experience has been accumulated.

Discharges of appreciable magnitude combined with the arrester's normal power follow will have little effect on the ability of the valve arrester to function for many operations. The impulse protective characteristics of the valve arresters of Figure 1 are not affected by high discharge currents. Repeated discharges of currents of 20,000 amperes or more exert some effect on the valve material which ultimately will cause it to puncture. With the 65,000-ampere surge-capacity test, a few repeated discharges may damage the arrester. The test current that will destroy a distribution arrester with the first shot may be considerably higher. The duration of the discharges also has a bearing on life. There is no doubt a relation between crest magnitude of current and shape and duration of wave tail on the one hand and the number of discharges an arrester will withstand on the other. This relation is not well known. Something is known of the high-crest short-duration effects and something is known of the low-current long-duration effect as shown by the 1/2 to several cycles of normal power follow current that the arrester may withstand. Between these is a range that is not determined because of the tedious labor and the expense that would be involved in establishing it. The lack of this information is not serious as indicated by the low rate of damage in the field to modern distribution arresters of either type.

The expulsion arrester wears. Expenditure of material is the principle upon which it operates to interrupt power-follow current. The wear caused by surge current is on the whole small. An excessively high surge current may burst the device or crack it, but this is the exception. The principal cause of wear in an expulsion arrester is the follow current that it must interrupt. The degree of erosion is a function of the magnitude and the duration of the follow current, and this again depends to some degree on the system characteristics and the relation of the timing of the surge discharge with respect to the phase of the system voltage. The factors that affect erosion are so variable that it is difficult to evaluate wear in terms of years of service. The expulsion arrester has been in use for some 13 years as part of the *SP* and *CSP* transformers. Neglecting causes of damage other than lightning, the life, measured in annual percentage of arresters damaged, obtained from the deion arresters used on those transformers as well as from deion arresters used as separately mounted devices actually has been better than secured from the comparable Autovalve arrester. This would indicate that the erosion effect of power-follow current, which can be accentuated by specific test conditions, is not the complete determinant of service in years. There is further corroboration of this by the fact that lightning field studies have indicated that a lightning arrester on any given distribution transformer in rural service discharges on an average of about once a year, but that over a period of years the number of discharges in any year may vary between zero and eight. Further, as already mentioned, power follow in expulsion arresters depends on how the surge and the 60-cycle power voltage overlap. In many cases there will be no power follow at all, and it is found in laboratory testing that the conditions of timing must be controlled carefully to obtain the worst power-follow conditions. Moreover, heavy discharge currents in themselves often cause the evolution of sufficient gas from the walls of the extinction chamber to prevent power follow. Although tests can be made which will show a longer life, in number of operations for valve arresters than for expulsion arresters and vice versa, it is logical to expect that both arresters will give comparable years of satisfactory service. Experience appears to bear this out. It may be that within certain ranges of lightning-discharge wave shape and magnitude the effect of the surge alone is less marked on the expulsion arrester than it is on the valve type.

Some weight should be given to the consideration that practically all makers of self-protecting distribution transformers employ expulsion arresters for protection. They have had excellent experience with their choice. On the other hand for separately mounted arresters the activity on valve-type distribution arresters exceeds that of expulsion arresters

Physical Differences

As the operation of the expulsion arrester generates gas which must be vented, it must be more or less open in construction. This has advantages in the eyes of many users and designers and is something not readily feasible in valve arresters.

Most valve arresters do not generate gas, nor do they have to handle high power-follow currents. Therefore, total enclosure is feasible, thereby protecting the parts from the weather and avoiding any exposed line or ground terminals or leads. This in turn is regarded as an advantage by many users, and it is something not readily done with expulsion arresters.

Effect on Operation of Primary Fuses

Recently some statements have been made that the collapsing voltage of the expulsion arrester has a distinct advantage in that it will permit fewer primary fuse operations. In brief, the reason given for this is that the expulsion arrester, because of this voltage collapse, exposes the transformer to less voltage for the duration of the discharge than the valve type, and, therefore, there is less tendency for lightning current to penetrate through the transformer winding and the fuse. There is clearly a difference in these voltages; however, if all of the factors that enter into the problems of fuse operation are considered, so broad a statement hardly is warranted. The subject is complex and beyond the scope of this paper. It should be explored further. If fuse operations can be decreased by the use of a certain type of lightning arrester, that is important, and it is to be hoped that experience of operating engineers in this connection may be presented to the Institute.

Special Application

There is one application in which there exists a definite preference. It is an application which requires both types of arresters to supplement each other and is, therefore, a good case. It is the protection of rotating machines. This subject is covered elsewhere.[1] In this application arresters must be used at the terminals of the machine and arresters also must be used at some point on the line removed from the machine terminals. The arresters at the machine terminals definitely must be of the valve type, because they spark at low voltages and because the voltage does not collapse after spark-over. For the arresters on the line, however, the expulsion type is to be preferred for the reason that its voltage does collapse and thereby aids the functioning of the capacitors and arresters at the machine.

Conclusion

This paper describes the operating characteristics of the two types of lightning arresters and discusses their advantages and disadvantages. A generalized comparison is shown by Table II. If there were conclusive evidence as to the superiority of one type over another, only one type would be in demand and only one type manufactured. Manufacturers who build both do so, because they believe that superiority of one type over the other cannot be demonstrated clearly and that operating engineers will insist that both be available. It is the authors' opinion that both devices serve the purpose for which lightning arresters are intended. There are certain advantages that can be cited for either one. Probably the selection of one or the other is influenced largely by the weight given by the user to those points in which the expulsion and valve arresters for distribution service differ.

Reference

1. LIGHTNING PROTECTION FOR ROTATING MACHINES, G. D. McCann, E. Beck, L. A. Finzi. AIEE TRANSACTIONS, volume 63, 1944, pages 319–33.

Resistance and Capacitance Relations Between Short Cylindrical Conductors

F. L. REQUA
MEMBER AIEE

THE CONVENTIONAL FORMULA for computing capacitance or conductance between parallel cylindrical conductors is derived on the assumption that the electrostatic or current flux between conductor surfaces is confined to paths lying in planes perpendicular to the axes of the conductors.

Actually this condition obtains only at the mid-point between the ends of the conductors. At all other points along the length the lines of flux curve outwardly toward the ends. However, for conductors of length which is very great compared to the distance of separation the flux paths are nearly planar except near the ends. Hence the conventional formula, which indicates direct proportionality between capacitance or conductance and length of the conductors, gives values which approach more and more closely to the true value as the length of the conductors increases.

For relatively short conductors however the effect just mentioned becomes of increasing importance. The true capacitance or conductance is not even approximately proportional to length of conductors and the values given by the conventional formula are no longer satisfactory.

In this paper formulas are developed in which the end effect is taken into account. This leads to an indicated integration which can be closely approximated by the summation of a small number of terms but is inconvenient for engineering computation. It is found that the func-

---

Paper 45-138, recommended by the AIEE committee on basic sciences for publication in AIEE TRANSACTIONS. Manuscript submitted August 17, 1943; made available for printing May 17, 1945.

F. L. REQUA is electrical engineer, Public Utilities Commission, City and County of San Francisco, Calif.

tion to be integrated may be approximated by a parabolic function and by this empirical substitution simplified formulas are derived which give results of satisfactory precision for the requirements of engineering design and may be expressed in simple functional form. Tabulated values of this function are given in the paper.

Experimentally determined values obtained from tests on a large three-phase water rheostat at Bonneville are compared with the same quantities computed by the formulas derived in this paper, and the agreement is found to be satisfactory.

Relationship Between Formulas for Capacitance and Conductance

The electrical capacitance C between any two conductors, spatially related in a specified manner and immersed in a dielectric medium of permittivity p, bears a simple relation to the conductance G between the same conductors immersed in a medium of conductivity γ. It is

$$C/p \propto G/\gamma \tag{1}$$

The constant of proportionality will depend upon the system of units adopted. In this paper all derivations are based upon the meter–kilogram–second system, modified so that the unit of length is inches instead of meters. Hereby the unit of capacitance is the farad, of conductance the mho, of resistance R the ohm, of conductivity the mho per inch cube, of resistivity ρ the ohm per inch cube and

$$C/p = G/4\pi\gamma = \rho/4\pi R \tag{2}$$

The absolute permittivity p in equation 2 is the permittivity p_0 of free space multiplied by the dielectric constant k of the medium. In the system of units used herein p_0 has the value 2.8262×10^{-12}.

All formulas in this paper are derived initially for the capacitance between parallel cylindrical conductors of equal diameter. Corresponding formulas for resistance between the conductors then are obtained by use of the relations 2.

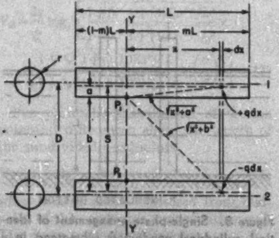

Figure 1. Space relation between elements of equivalent linear charges and surface potential points on two parallel cylindrical conductors

Derivation of Conventional Formula for Capacitance

The conventional formula for capacitance between two parallel cylindrical conductors 1 and 2 of length L, radius r, and distance D between centers, is derived on the assumption that L is so large compared to D that, for a given difference of potential between the conductors, the charge per unit of axial length may be considered to be the same at all points along the length of each conductor.

The surface charge per unit length so transferred can be shown to be the electrostatic equivalent, for points lying outside the conductor surfaces, of the same charge per unit length concentrated along a line inside each conductor in the plane of and parallel to the axes of the two conductors.

When L is very large compared to D the distance S between these two lines of charge is related to D and r by the expression:[1]

$$S = \sqrt{D^2 - 4r^2} \tag{3}$$

The shortest distance a from the line of charge inside conductor 1 to the surface of conductor 1 is readily deduced from equation 3 to be

$$a = \frac{\sqrt{D^2 - 4r^2} - (D - 2r)}{2} \tag{4}$$

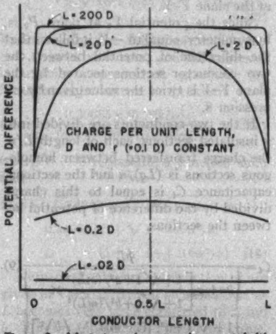

Figure 2. Variation of sectional potential difference with length along parallel cylindrical conductors with uniform linear charge

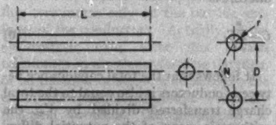

Figure 3. Three-phase arrangement of identical cylindrical conductors, equilaterally spaced in a homogeneous medium of infinite extent

Use formula 20 for capacitance

Use formula 23 for resistance

Similarly, the shortest distance b from the line of charge inside conductor 2 to the surface of conductor 1 is

$$b = \frac{\sqrt{D^2 - 4r^2} + (D - 2r)}{2} \tag{5}$$

From equations 4 and 5 it follows that

$$\frac{b}{a} = \frac{D + \sqrt{D^2 - 4r^2}}{2r} \tag{6}$$

When L is very small compared to both D and r, the relations 3, 4, and 5 are shown in the appendix to change to

$$S = D - \frac{2r^2}{D^2} \tag{3'}$$

$$a = \frac{D^2 - r^2}{D^2} \cdot r \tag{4'}$$

$$b = D - \frac{D^2 + r^2}{D^2} \cdot r \tag{5'}$$

If a linear charge of $+q$ per unit length is assumed within one conductor and $-q$ per unit length within the other, the potential at a point on the surface of each conductor midway between the ends can be computed. The magnitude of the total charge transferred, qL, divided by the computed difference of potential between the mid-points of the two conductors gives the familiar formula[3] for capacitance:

$$C = \frac{0.30685 \times 10^{-12} kL}{\log_{10}\left(\frac{b}{a}\right)}$$

$$= \frac{0.30685 \times 10^{-12} kL}{\log_{10}\left(\frac{D + \sqrt{D^2 - 4r^2}}{2r}\right)} \tag{7}$$

and thence its approximate equivalent,

$$C = \frac{0.30685 \times 10^{-12} kL}{\log_{10}\left(\frac{D}{r} - \frac{r}{D}\right)} \tag{7'}$$

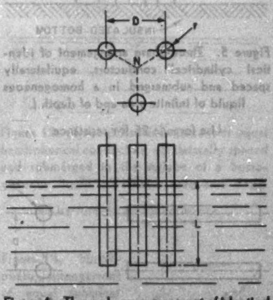

Figure 4. Three-phase arrangement of identical cylindrical conductors, equilaterally spaced and submerged in the surface of a homogeneous liquid of infinite area and depth

Use formula 23 for resistance

The approximate values obtained by use of formula 7′ differ by less than one eighth of one per cent from those of formula 7 for all cases where r does not exceed 20 per cent of D.

Formulas 7 and 7′ and corresponding expressions for resistance derived therefrom are applicable when the flux between conductors follows planes perpendicular to the conductor axes. This condition obtains

1. Approximately, when the length L of the conductors is very great compared to the distance of separation D.

2. Exactly, in the case of electric-current flow, when the conducting liquid of finite depth L is confined in a tank of infinite area with an insulated floor and the conductors are immersed vertically to the full depth of the liquid.

Derivation of More General Formula for Capacitance

Figure 1 represents two parallel tubular conductors of length L and radius r separated by a distance D between axes. It is postulated that each conductor is subdivided into a very large number of short tubular sections formed by cutting through the original conductors with a corresponding number of insulating planes of negligible thickness, each normal to the axes of the conductors. Hereby the necessity of assuming the same potential at all points along the length of the conductor is eliminated.

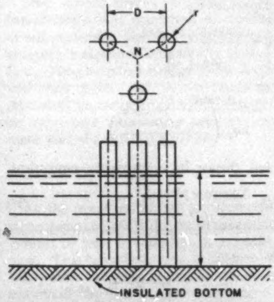

Figure 5. Three-phase arrangement of identical cylindrical conductors, equilaterally spaced and submerged in a homogeneous liquid of infinite area and of depth L

Use formula 25 for resistance

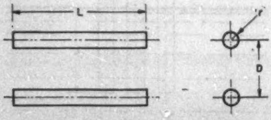

Figure 6. Single-phase arrangement of identical cylindrical conductors in a homogeneous medium of infinite extent

Use formula 18 for capacitance
Use formula 24 for resistance

It is assumed that a charge of q per unit length has been transferred from conductor 2 to conductor 1 and that the resulting deficit and surplus, respectively, of charge are located along two symmetrically disposed lines inside the conductors, separated by the distance S.

If the point P_1 is located at a distance mL from one end of the conductor, where m is a numeric equal to or less than unity, then the potential V_1 at this point is

$$V_1=\frac{q}{p}\left[\int_0^{mL}\frac{dx}{\sqrt{x^2+a^2}}+\int_0^{(1-m)L}\frac{dx}{\sqrt{x^2+a^2}}-\int_0^{mL}\frac{dx}{\sqrt{x^2+b^2}}-\int_0^{(1-m)L}\frac{dx}{\sqrt{x^2+b^2}}\right]$$

$$=\frac{q}{p}\log_e\left[\frac{1+\sqrt{1+a^2/(mL)^2}}{1+\sqrt{1+b^2/(mL)^2}}\times\frac{1+\sqrt{1+a^2/[(1-m)L]^2}}{1+\sqrt{1+b^2/[(1-m)L]^2}}\times\left(\frac{b}{a}\right)^2\right] \quad (8)$$

This is also the potential at all other points on the periphery of the short cylindrical section of conductor 1 located at the plane $Y-Y$.

Since the potential V_2 at point P_2 is, by symmetry, equal to $-V_1$ it follows that the difference of potential between the two conductor sections located by the plane $Y-Y$ is twice the value given by expression 8.

If the two conductors are divided into n insulated sections, each of length L/n, the charge transferred between homologous sections is $(Lq)/n$ and the sectional capacitance C_t is equal to this charge divided by the difference of potential between the sections,

$$C_t=\frac{pL}{\left\{2n\log_e\left[\frac{1+\sqrt{1+a^2/(mL)^2}}{1+\sqrt{1+b^2/(mL)^2}}\times\frac{1+\sqrt{1+a^2/[(1-m)L]^2}}{1+\sqrt{1+b^2/[(1-m)L]^2}}\times\left(\frac{b}{a}\right)^2\right]\right\}} \quad (9)$$

and the total capacitance between conductors is

$$C=\sum_{t=1}^{n}C_t \quad (10)$$

It follows that the total capacitance between conductors is also equal to the total charge transferred divided by V_m, the arithmetic mean of the potential differences between all pairs of homologous sections. If we refer to Figure 2, which shows sectional difference of potential along the length of pairs of conductors of given r and D but differing length L, it will be noted that for relatively long conductors the mean sectional difference of potential is very nearly the same as the difference of potential at the mid-point. However for shorter conductors this is not true.

A satisfactory approximation for engineering purposes to the mean difference of potential can be obtained by computing the difference of potential at the mid-point of the sectionalized conductor and at two points near to and equidistant from the ends, passing a parabolic curve through these three points and computing the mean difference of potential therefrom. It is found that, if the two end points arbitrarily are taken at nine tenths of the distance from mid-point to end, the approximate value will not differ by more than one half of one per cent from that obtained by subdividing the conductors into 20 sections and using equation 8 as the basis for computation.

The potential at the mid-point and that near either end of one of the sub-

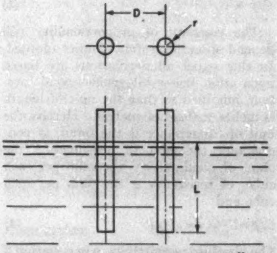

Figure 7. Single-phase arrangement of identical cylindrical conductors submerged in the surface of a homogeneous liquid of infinite area and depth

Use formula 24 for resistance

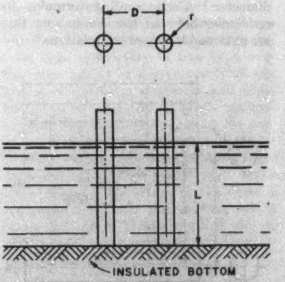

Figure 8. Single-phase arrangement of identical cylindrical conductors submerged in a homogeneous liquid of infinite area and of depth L

Use formula 26 for resistance

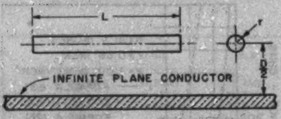

Figure 9. Single-phase arrangement of a cylindrical and a plane conductor in a homogeneous medium of infinite extent

Use formula 20 for capacitance
Use formula 23 for resistance

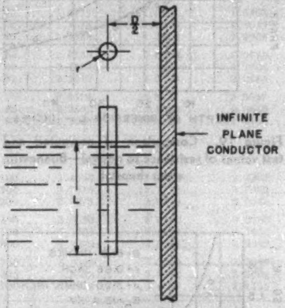

Figure 10. Single-phase arrangement of a cylindrical and a plane conductor submerged in the surface of a homogeneous liquid of infinite area and depth

Use formula 23 for resistance

divided conductors can be determined from equation 8, taking $m = 0.5$ and $m = 0.05$ in turn. The values so obtained, multiplied by two, will give the difference of potential between homologous sections at each of these two locations. If we call the difference of potential at the midpoint V_C and that near the ends V_E,

$$V_C=\frac{4q}{p}\log_e\left[\frac{1+\sqrt{1+(4a^2)/L^2}}{1+\sqrt{1+(4b^2)/L^2}}\times\frac{b}{a}\right] \tag{11}$$

$$V_E=\frac{2q}{p}\log_e\left[\frac{1+\sqrt{1+(400a^2)/L^2}}{1+\sqrt{1+(400b^2)/L^2}}\times\frac{1+\sqrt{1+(1.108a^2)/L^2}}{1+\sqrt{1+(1.108b^2)/L^2}}\times\left(\frac{b}{a}\right)^2\right] \tag{12}$$

For parabolic distribution of section potential differences along the length of the subdivided conductors,

$$V_z=A+Bz^2 \tag{13}$$

where z is distance measured from midpoint of the conductor toward either end. The mean potential difference,

$$V_M=\frac{\int_0^{0.5L}V_z dz}{0.5L}=A+\frac{BL^2}{12} \tag{14}$$

If we evaluate the constants A and B from $V_z = V_C$ at $z = 0$ and $V_z = V_E$ at $z = 0.45L$ and substitute into equation 14,

$$V_M=\frac{143V_C+100V_E}{243} \tag{15}$$

If we insert the values of V_C and V_E from equations 11 and 12 into equation 15, the expression for the capacitance between two cylindrical conductors becomes

$$C=\frac{243pL}{\left\{572\log_e\left[\frac{1+\sqrt{1+4a^2/L^2}}{1+\sqrt{1+4b^2/L^2}}\times\frac{b}{a}\right]+200\log_e\left[\frac{1+\sqrt{1+400a^2/L^2}}{1+\sqrt{1+400b^2/L^2}}\times\frac{1+\sqrt{1+1.108a^2/L^2}}{1+\sqrt{1+1.108b^2/L^2}}\times\left(\frac{b}{a}\right)^2\right]\right\}} \tag{16}$$

If we replace p by its value $2.8262 \times 10^{-12}\,k$ and convert the logarithms to base ten,

$$C=\frac{0.52142\times10^{-12}kL}{\left\{\log_{10}\left[\frac{1+\sqrt{1+4a^2/L^2}}{1+\sqrt{1+4b^2/L^2}}\times\frac{b}{a}\right]+0.34965\log_{10}\left[\frac{1+\sqrt{1+400a^2/L^2}}{1+\sqrt{1+400b^2/L^2}}\times\frac{1+\sqrt{1+1.108a^2/L^2}}{1+\sqrt{1+1.108b^2/L^2}}\times\left(\frac{b}{a}\right)^2\right]\right\}} \tag{17}$$

By expressing the denominator of equation 17 in terms of sums and differences of logarithms, appropriately grouped, the formula can be written in the form:

$$C=\frac{0.30685\times10^{-12}kL}{\log_{10}(b/a)-[F(b/L)-F(a/L)]} \tag{18}$$

where F (—) represents a function such that

$$F(u)=0.58848\left[\log_{10}(1+\sqrt{1+4u^2})+0.34965\{(1+\sqrt{1+400u^2})\times(1+\sqrt{1+1.108u^2})\}\right] \tag{19}$$

Numerical values of the function 19 are given in Table I. It will be noted that as L becomes very large compared to a and b, $F(b/L)$ approaches $F(a/L)$ in value, and thus formula 18 approaches the conventional formula 7 as a limit.

All of the foregoing derivations are based on an implicit assumption that the flux terminates only on the outside surfaces of the conductors. Actually, in the electrostatic case, some flux always terminates on the planes forming the ends, or on the interior surfaces adjacent to the ends if the conductor is tubular. In many practical problems the proportion so terminating is small enough so that it may be neglected without introducing appreciable error. In any event the capacitance given by the formulas will be less than the true value in the ratio of peripheral to total flux.

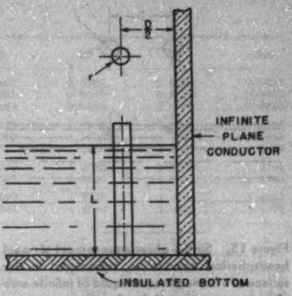

Figure 11. Single-phase arrangement of a cylindrical and a plane conductor submerged in a homogeneous liquid of infinite area and of depth L

Use formula 25 for resistance

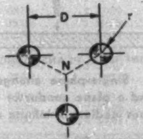

Figure 12. Three-phase arrangement of equal spherical conductors, equilaterally spaced in a homogeneous medium of infinite extent

Use formula 22 for capacitance
Use formula 27 for resistance

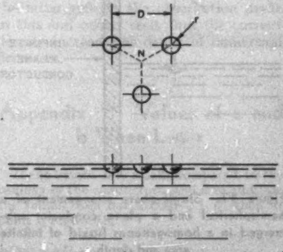

Figure 13. Three-phase arrangement of equal hemispherical conductors, equilaterally spaced and submerged in the surface of a homogeneous liquid of infinite area and depth

Use formula 28 for resistance

Figure 14. Single-phase arrangement of equal spherical conductors in a homogeneous medium of infinite extent

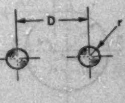

Use formula 21 for capacitance
Use formula 28 for resistance

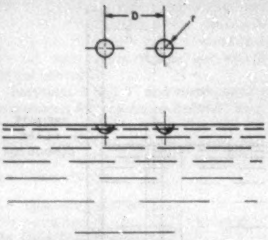

Figure 15. Single-phase arrangement of equal hemispherical conductors, submerged in the surface of a homogeneous liquid of infinite area and depth

Use formula 29 for resistance

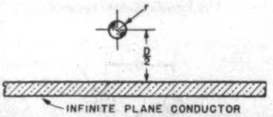

Figure 16. Single-phase arrangement of a spherical and a plane conductor in a homogeneous medium of infinite extent

Use formula 22 for capacitance
Use formula 27 for resistance

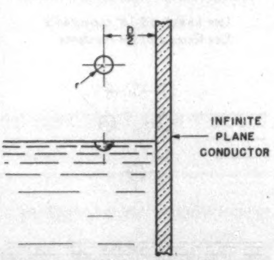

Figure 17. Single-phase arrangement of a hemispherical and a plane conductor submerged in a homogeneous liquid of infinite area and depth

Use formula 28 for resistance

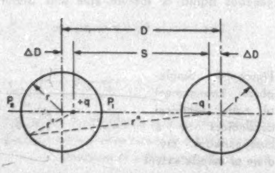

Figure 18. Position of equivalent internal charge in short cylindrical conductors

In the resistance case, it is possible for the plane ends of the conductors to be of insulating material, and in this event the fact accords with the assumption. Otherwise, the same comment applies as for the electrostatic case, except that the error is in the opposite sense so that the resistance given by the formulas will be greater than the true value in the ratio of total to peripheral flux.

Formulas for Capacitance and Resistance

In the following formulas, all linear dimensions are in inches, k is the dielectric constant of the medium (unity for air), and ρ is the resistivity of the medium in ohms per inch cube. C, the capacitance in farads and R, the resistance in ohms, are from line to line for single-phase circuits and from line to neutral for three-phase circuits. F (—) is the function of which tabulated values are given in Table I.

In addition to formulas based on the derivations given in this paper, approximation formulas for capacitance and resistance between spheres are included for convenience. The accuracy of these latter increases as D/r increases, capacitance formulas 21 and 22 giving values lower than actual, resistance formulas 27, 28, and 29 giving values higher than actual, by the percentages indicated in Table II.[3]

For $L \gg D$,

$$a=\frac{\sqrt{D^2-4r^2}}{2}-\frac{D-2r}{2} \tag{4}$$

$$b=\frac{\sqrt{D^2-4r^2}}{2}+\frac{D-2r}{2} \tag{5}$$

$$\frac{b}{a}=\frac{D+\sqrt{D^2-4r^2}}{2r} \tag{6}$$

For $L \ll D$,

$$a=\left[1-\left(\frac{r}{D}\right)^2\right]\times r \tag{4'}$$

$$b=D-\left[1+\left(\frac{r}{D}\right)^2\right]\times r \tag{5'}$$

CAPACITANCE FORMULAS

Figure 6:

$$C=\frac{0.3068\,kL\times10^{-12}}{\log_{10}(b/a)-[F(b/L)-F(a/L)]} \tag{18}$$

Figures 3, 9:

$$C=\frac{0.6137\,kL\times10^{-12}}{\log_{10}(b/a)-[F(b/L)-F(a/L)]} \tag{20}$$

Figure 14:

$$C=\frac{1.411\,kDr\times10^{-12}}{D-r} \tag{21}$$

Figures 12, 16:

$$C=\frac{2.822\,kDr\times10^{-12}}{D-r} \tag{22}$$

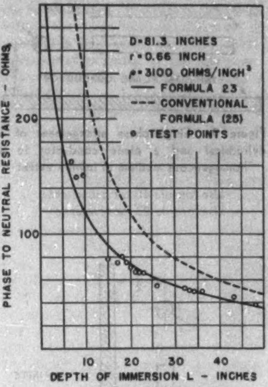

Figure 19. Comparison of computed and test values of resistance to neutral—Bonneville water rheostat

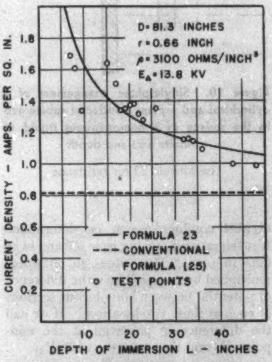

Figure 20. Comparison of computed and test values of electrode-surface current density—Bonneville water rheostat

RESISTANCE FORMULAS

Figures 3, 4, 9, 10:

$$R=0.3665\,\frac{\log_{10}(b/a)-[F(b/L)-F(a/L)]}{L}\,\rho \tag{23}$$

Figures 6, 7:

$$R=0.7330\,\frac{\log_{10}(b/a)-[F(b/L)-F(a/L)]}{L}\,\rho \tag{24}$$

Figures 5, 11:

$$R=0.3665\,\frac{\log_{10}(b/a)}{L}\,\rho \tag{25}$$

Table I. Values of the Function *F*(*u*)

u	0.0	0.1	0.2	0.3	0.4	0.5	0.6	0.7	0.8	0.9
0.0	0.3010	0.3468	0.3957	0.4366	0.4733	0.5075	0.5397	0.5701	0.5990	0.6264
1.0	0.6524	0.6779	0.7019	0.7246	0.7461	0.7666	0.7861	0.8049	0.8229	0.8402
2.0	0.8569	0.8730	0.8886	0.9037	0.9184	0.9326	0.9464	0.9599	0.9730	0.9858
3.0	0.9983	1.0100	1.0214	1.0327	1.0437	1.0545	1.0651	1.0756	1.0857	1.0957
4.0	1.1055	1.1151	1.1244	1.1335	1.1425	1.1512	1.1597	1.1680	1.1761	1.1840
5.0	1.1917	1.1994	1.2069	1.2144	1.2217	1.2290	1.2361	1.2432	1.2501	1.2570
6.0	1.2637	1.2703	1.2769	1.2833	1.2896	1.2959	1.3020	1.3080	1.3140	1.3198
7.0	1.3255	1.3312	1.3368	1.3423	1.3478	1.3533	1.3587	1.3640	1.3692	1.3744
8.0	1.3796	1.3847	1.3897	1.3947	1.3996	1.4044	1.4092	1.4140	1.4186	1.4232
9.0	1.4278	1.4323	1.4368	1.4413	1.4457	1.4501	1.4544	1.4586	1.4628	1.4670
u	0	1	2	3	4	5	6	7	8	9
10	1.4711	1.5103	1.5463	1.5796	1.6106	1.6396	1.6668	1.6924	1.7166	1.7395
20	1.7613	1.7820	1.8019	1.8208	1.8369	1.8563	1.8730	1.8890	1.9045	1.9194
30	1.9338	1.9473	1.9606	1.9736	1.9863	1.9988	2.0110	2.0229	2.0345	2.0459
40	2.0569	2.0678	2.0783	2.0886	2.0986	2.1083	2.1177	2.1269	2.1358	2.1443
50	2.1527	2.1611	2.1694	2.1775	2.1856	2.1935	2.2012	2.2089	2.2165	2.2239
60	2.2312	2.2384	2.2454	2.2524	2.2592	2.2659	2.2725	2.2790	2.2853	2.2915
70	2.2976	2.3037	2.3097	2.3156	2.3214	2.3272	2.3330	2.3386	2.3442	2.3498
80	2.3552	2.3606	2.3659	2.3712	2.3764	2.3815	2.3865	2.3915	2.3965	2.4013
90	2.4061	2.4109	2.4156	2.4203	2.4250	2.4295	2.4340	2.4385	2.4429	2.4473
u	0	10	20	30	40	50	60	70	80	90
100	2.4516	2.4926	2.5302	2.5648	2.5969	2.6268	2.6548	2.6811	2.7059	2.7294
200	2.7516	2.7728	2.7930	2.8123	2.8307	2.8485	2.8655	2.8818	2.8975	2.9128
300	2.9273	2.9410	2.9545	2.9676	2.9805	2.9931	3.0055	3.0175	3.0293	3.0408
400	3.0520	3.0630	3.0736	3.0840	3.0941	3.1039	3.1134	3.1227	3.1317	3.1404
500	3.1489	3.1573	3.1656	3.1738	3.1819	3.1899	3.1977	2.2054	3.2130	3.2205
600	3.2279	3.2351	3.2422	3.2492	3.2561	3.2629	3.2695	3.2760	3.2824	3.2887
700	3.2948	3.3009	3.3069	3.3129	3.3188	3.3247	3.3304	3.3361	3.3418	3.3473
800	3.3528	3.3582	3.3636	3.3689	3.3741	3.3792	3.3843	3.3893	3.3942	3.3991
900	3.4039	3.4087	3.4135	3.4182	3.4228	3.4274	3.4320	3.4365	3.4409	3.4453

Figure 8:

$$R=0.7330\,\frac{\log_{10}(b/a)}{L}\,\rho \tag{26}$$

Figures 12, 16:

$$R=0.7970\,\frac{D-r}{Dr}\,\rho \tag{27}$$

Figures 13, 14, 17:

$$R=0.1594\,\frac{D-r}{Dr}\,\rho \tag{28}$$

Figure 15:

$$R=0.3188\,\frac{D-r}{Dr}\,\rho \tag{29}$$

Comparison Between Test Values and Those Computed by Formula

At the time acceptance tests were to be made on the generators at Bonneville power plant the need arose for a conveniently adjustable artificial load. Accordingly, a preliminary experimental water rheostat was constructed and tested by R. L. Earnheart of the Corps of Engineers, United States Army.[4] Mr. Earnheart is now on foreign duty with the Army and it is through the courtesy of F. M. Lewis, senior engineer, War Department, Portland, Oregon, District, that data from the original field notes have been made available to the author.

The tests were made on a three-phase rheostat immersed in the water of the tailrace. It consisted of three one-inch standard iron pipes parallel to one another and equilaterally spaced 81.3 inches between centers, Figure 4. Readings of current were taken at recorded line-to-line potentials between 12 and 14 kv and at immersion depths varying from 7 to 48 inches. The depth of tailrace water was 50 to 56 feet during the tests.

Table II. Error in Formulas 21, 22, 27, 28, and 29

$\frac{D}{r}$	Per-Cent Error
2.1	20.8
2.2	14.8
2.5	6.25
3.0	2.28
3.5	1.14
4	0.60
5	0.24
6	0.17

In the reference article it is stated that the resistivity ρ of Columbia River water is 3,620 ohms per inch cube at 45 degrees Fahrenheit and 2,200 ohms per inch cube at 80 degrees Fahrenheit. Water temperature during tests, which would be expected to vary somewhat with load, was not given. An intermediate value of 3,100 ohms per inch cube, which seems to approximate the data best, therefore has been used for computations.

Computed values are compared graphically with test values in Figures 19 and 20. Figure 20, in particular, emphasizes the basic difference between the conventional formula 25 and that developed in this paper, 23, for relatively small depth of immersion. The former indicates no change in electrode-surface current density with depth of immersion; the latter reflects the observation made in this and other[5] tests that the current density increases as depth of immersion decreases.

Appendix I. Values of a and b When $L \ll r$

If the length L is small, compared to the radius r of the conductors, and if in addition the radius does not exceed 0.1 D, then at point 1, Figure 18,

$$r_1'=r-\Delta D$$
$$r_1''=D-\Delta D-r$$

and V_1 is proportional to

$$\frac{1}{r_1'}-\frac{1}{r_1''}=\frac{1}{r-\Delta D}-\frac{1}{D-\Delta D-r}\approx$$

$$\frac{1}{r}\left(1+\frac{\Delta D}{r}\right)-\frac{1}{D}\left(1+\frac{\Delta D}{D}+\frac{r}{D}\right)\approx$$

$$\frac{1}{r}+\frac{\Delta D}{r^2}-\frac{1}{D}-\frac{\Delta D}{D^2}-\frac{r}{D^2}$$

Similarly, at point 2,

$$r_2'=r+\Delta D$$
$$r_2''=D-\Delta D+r$$

Automatic Temperature Control for Aircraft

R. A. GUND
ASSOCIATE AIEE

AUTOMATIC temperature control for aircraft long has been neglected, and it is only during the war that adequate attention has been given to this important subject. The increased duties imposed upon flight personnel by the requirements of modern military aircraft, together with the necessity for reducing air drag to the minimum consistent with required cooling, have prompted aircraft designers to give consideration to automatic operation of cowl flaps, oil and coolant flaps, and intercooler doors. Automatic flap operation can be appreciated fully when it is considered that engine cowl flaps fully opened might represent an air drag as high as 40 miles per hour on a 400-mile-per-hour airplane.

A primitive form of automatic temperature control was used initially on oil or coolant and employed the by-pass valve principle. This method directed the oil or coolant through or around the cooling surface in response to its temperature. Serious problems of oil congealing were introduced. As this type of control provides no control of the air through the cooler, the drag on the airplane is dictated by the amount of air required to provide the necessary cooling under the most adverse conditions of heat release, cooling air temperature, air density, and air speed. Much has been done to reduce congealing difficulties, but many authorities believe that fast-acting controls, operating to modulate the cooling air supply, offer the most direct approach to the problem.

Since most cooling flaps or doors are subjected to air loads of considerable magnitude, an electric motor or hydraulic servo mechanism is used as the load actuating device. The operating characteristics of the load actuating device are allied closely to the over-all operation of the system and must be considered as a component part of the system. The control of engine-head, oil or coolant, and carburetor-air temperature requires the same fundamental equipment, and further discussions will be confined to engine-head control as a representative system.

Types of System

Before any detailed discussion of automatic temperature control is attempted, it is desirable to establish complete understanding of the various types of systems together with a clear appreciation of the limitations and advantages offered by each. The more common classifications are described briefly under the headings by which they are generally known. Only electric types of thermosensitive elements are considered, although it is understood that the same fundamentals apply if the thermosensitive element is

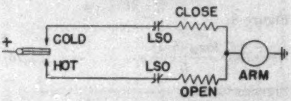

Figure 1. Schematic diagram of on–off system of temperature control

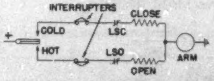

Figure 2a. Schematic diagram of point-modulating system of temperature control showing use of periodic interrupters

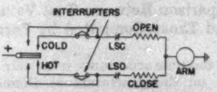

Figure 2b. Schematic diagram of point-modulating system of temperature control showing by-pass principle

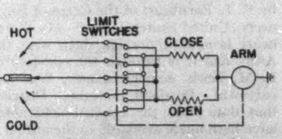

Figure 3. Schematic diagram of multipoint system of temperature control

---

Paper 45-109, recommended by the AIEE committee on air transportation for publication in AIEE TRANSACTIONS. Manuscript submitted May 2, 1945; made available for printing May 29, 1945.

R. A. GUND is in the industrial-control engineering division, General Electric Company, Schenectady, N. Y.

---

and V_2 is proportional to

$$\frac{1}{r_2'}-\frac{1}{r_2''}=\frac{1}{r+\Delta D}-\frac{1}{D-\Delta D+r}\approx$$

$$\frac{1}{r}\left(1-\frac{\Delta D}{r}\right)-\frac{1}{D}\left(1+\frac{\Delta D}{D}-\frac{r}{D}\right)\approx$$

$$\frac{1}{r}-\frac{\Delta D}{r^2}-\frac{1}{D}-\frac{\Delta D}{D^2}+\frac{r}{D^2}$$

In order that V_1 shall equal V_2

$$\frac{1}{r}+\frac{\Delta D}{r^2}-\frac{1}{D}-\frac{\Delta D}{D^2}-\frac{r}{D^2}$$

$$=\frac{1}{r}-\frac{\Delta D}{r^2}-\frac{1}{D}-\frac{\Delta D}{D^2}+\frac{r}{D_2}$$

from which $\Delta D=r^3/D^2$ and

$$S=\frac{D^3-2r^3}{D^2}$$

$$a=\frac{D^2-r^2}{D^2}\times r$$

$$b=D-\frac{D^2+r^2}{D^2}\times r$$

Appendix II. List of Symbols

A = constant, equation 13
B = constant, equation 13
C = capacitance, farads
D = conductor spacing, inches
$F(u)$ = a function of the numeric u (see Table I)
G = conductance, mhos
L = conductor length, inches
R = resistance, ohms
S = hypothetical charge spacing, inches
V = potential, volts
a = shortest distance from hypothetical line of charge to surface of the same conductor, inches
b = shortest distance from hypothetical line of charge to surface of the opposite conductor, inches
k = dielectric constant of the medium
m = distance from a point to the end of the conductor, in terms of L
n = number of hypothetical insulated sections into which the conductor is assumed to be divided
p_0 = permittivity of free space, 2.870×10^{-13} in the dimensional system used in this paper
p = permittivity of the medium, kp_0
q = charge, coulombs
r = radius of conductors, inches
γ = conductivity, mho per inch cube
ρ = resistivity, ohms per inch cube

References

1. ELECTRIC CIRCUITS (book), electrical engineering staff, Massachusetts Institute of Technology, Cambridge, Mass., 1940. Pages 41–50.

2. STANDARD HANDBOOK FOR ELECTRICAL ENGINEERS (seventh edition), page 66.

3. THE MATHEMATICAL THEORY OF ELECTRICITY AND MAGNETISM (fifth edition), J. H. Jeans. Page 199.

4. WATER RHEOSTAT IS TEST LOAD FOR BONNEVILLE, R. L. Barnheart. *Electrical West*, volume 81, number 3, September 1938.

5. TRANSMISSION RELAYING PROBLEMS ON THE FORT PECK PROJECT, Erik Floor, H. N. Muller, Jr., S. L. Goldsborough. AIEE TRANSACTIONS, volume 63, 1944, May section, pages 209–14.

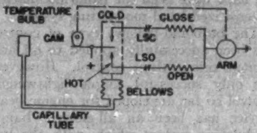

Figure 4a. Schematic diagram of the bulb-and-bellows type of band-modulating temperature-contol system

used to actuate hydraulic or pneumatic valves instead of electric contacts.

ON–OFF SYSTEM

The on–off system is the simplest of all temperature-control methods. It is well exemplified by the conventional household heating system. In this system a thermostat is calibrated to open or close contacts at some predetermined temperature. When the temperature is below this value, circuits are completed to start the heat-generating equipment. When the temperature rises to the calibrated value, the supply of heat is discontinued.

The on–off system is shown schematically in Figure 1. When the engine-head temperature reaches a predetermined value, the hot contact is closed, which energizes the flap motor in the open direction. When the temperature falls to a predetermined value, the cold contact is energized, and the flaps are closed. This system might tend to hold engine-head temperatures within narrow limits, but the resulting duty cycle would be quite impractical from the standpoint of the life of the equipment. Flying characteristics also would be affected violently, as the flaps suddenly would go wide open or completely closed.

POINT-MODULATING SYSTEM

In an attempt to overcome the deficiencies of the on–off system, the point-modulating system was developed. This system must have the speed of flap opening or flap closing slow enough to permit stabilization before reaching the limits of travel. Various methods have been employed to reduce the speed of flap operation. One such method is shown in Figure 2a, where interrupters are interposed between the thermostat and the motor to permit opening and closing in a series of increments. This gives the cowl flaps more positions and permits the temperature of the engine to stabilize, which allows the thermostat to assume a neutral position. Modifications of this general idea range from thermal time relays to interrupters operated by centrifugal action from the flap motor. Another modification of this system is that shown in Figure 2b, wherein the interrupter is by-passed when the temperature is at wide variance but becomes operative as the temperature approaches the balance point.

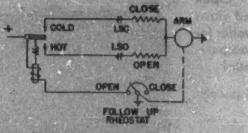

Figure 4b. Schematic diagram of an electric type of band-modulating temperature-control system

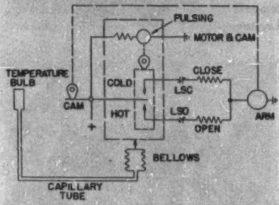

Figure 5. Schematic diagram of the sensitized band-modulating system of temperature control

This system introduces the element of time, and it is almost impossible to balance the time of flap operation with the time constant of the heating or cooling system. For instance the engine-head time constant varies over a wide range with the power output of the engine.

In many industrial applications where only a single variable exists, the point-modulation system has been successfully applied. However, in aircraft work where the cooling air temperature, air density, air speed, and heat release represent the variables, any attempt to fit the time of flap operation to the wide range of conditions encountered becomes an extremely difficult problem.

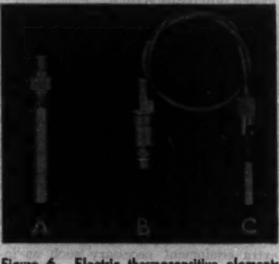

Figure 6. Electric thermosensitive elements

A—Oil or coolant service
B—Carburetor-air service
C—Engine-head service
Respective weights: 0.167 pound, 0.088 pound, 0.093 pound

MULTIPOINT SYSTEM

In this system the thermostat becomes a multicontact device with each contact representing a definite flap position as shown in Figure 3. As the temperature of the controlled medium varies, the flaps assume corrective positions until a balance is reached where the cooling supply approaches the cooling demand. To be successful this system requires a reasonable number of steps or points on the thermostat. If the thermostat has many points, then a large number of conductors between the thermostat and motor or limit switch assembly are required. If a small number of points are used, continuous hunting may result between the two steps nearest the required flap opening. This type of thermosensitive element is large and bulky and is very difficult to apply.

BAND-MODULATING SYSTEM

Band-modulating temperature control may be defined as a control which recalibrates the temperature-sensing element as the flaps assume successive positions. As its name implies, the band-modulating system operates over a temperature range. The temperature range or band width is determined by two factors: system sensitivity, that is, the temperature change required to make the control operate and the number of flap positions required by the airplane's cooling system in order to obtain stable operation. Figure 4a is a typical aircraft control system of this type where the thermosensitive element is the bulb of a bulb-and-bellows assembly, and where the follow-up or

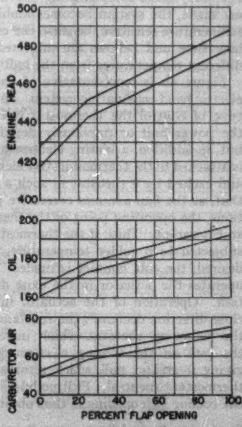

Figure 7. Temperature–resistance curves for engine-head, oil, and carburetor-air thermosensitive elements

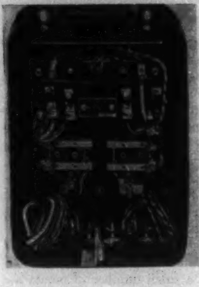

Figure 8. Open and enclosed views of the controller for automatic temperature control

Weight, 3.5 pounds

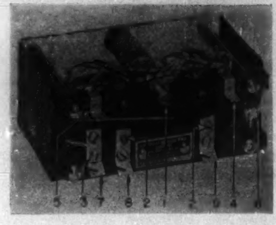

Figure 9 (below). Terminal identification of the polarized relay used in the automatic temperature-control system

recalibrating action is obtained by cam motion in the power unit. In this system one element of the contact mechanism is moved by the pressure in the bellows, while the recalibrating action is obtained through the cam which returns the other element of the contact mechanism to neutral. Many modifications of this system have been employed, differing chiefly in the type of follow-up mechanism used.

One of the difficulties of this system is in the relatively large size and low response rate of the bulb. In order to obtain the degree of sensitivity required, the amount of liquid in the bulb must be relatively large, and, since the ratio of surface to volume is low, the response rate is correspondingly low. In order to overcome this difficulty some systems employ multiple bulbs connected to a common bellows, thus giving a lower ratio of volume to surface. This, of course, takes more space. Another difficulty encountered in this system is the use of a capillary tube. If a long run is necessary, it becomes vulnerable to damage, and, unless compensating provisions are made, the system becomes ambient-temperature sensitive, because the capillary tube and bellows are subjected to different temperatures from the bulb.

Figure 4b is representative of an all-electric band-modulating system. In this type of control the thermostat controls the power unit as previously described, but, in addition, a biasing electromagnet is attached to the thermosensitive element and excited by a rheostat in such a way that, as the flap assumes corrective positions, the operating point of the thermostat is varied. Thus, if the thermostat is subjected to a colder temperature than desired, the cold contact is made. This operates the actuator in the close direction. Operation of the actuator in the close direction decreases the resistance of the follow-up rheostat which increases the pull on the biasing electromagnet, giving it greater pull which returns the thermostat to neutral. Full modulation of the cooling flap opening is thus obtained.

SENSITIZED BAND-MODULATING SYSTEM

In an effort to obtain higher system sensitivity and, therefore, narrower band widths several schemes, all basically alike, have been devised. A mechanical pulse is imposed on the system such that in its neutral position the control almost operates in either direction; a slight change in temperature will cause a small correction to be made in the flap position. Figure 5 represents such a system. A small motor continuously operates a cam, which in turn moves the contacts up and down so that they almost make contact. If the bellows either expands or contracts slightly, a momentary contact is made, and the flap motor is jogged in the proper direction. If a large change should take place, the pulsing action will not break the contact until the flap is almost in position, at which time the flap will be jogged into position.

Very sensitive systems can be made in this manner, but the more sensitive the system becomes the greater the duty cycle of the flap actuator becomes. Also the pulsing motor must be a continuously rated motor with exceptionally long life.

Since the advent of the resistance-bulb temperature indicators, several electronic temperature control systems have been designed. Narrow band widths can be obtained because of the great amplification obtained with electronic tubes. However, an electronic system has a great weight disadvantage because of the extra equipment necessary such as inverters, transformers, and so forth.

An Electric System

The only systems which have had any success in controlling engine-head cooling flaps have been the band-modulating or sensitized-band-modulating systems.

The bulb-and-bellows type of control has been successfully applied to oil and coolant temperature control. However, the only successful simple lightweight control so far developed for engine-head service has been an all-electric band-modulating system which, with the use of different thermosensitive elements, also will control oil carburetor-air, or coolant temperatures.

Components of the System

The system consists of a thermosensitive element, an actuator, which may be either an electric motor or hydraulic servo mechanism, and a follow-up rheostat to recalibrate the system. The necessary cockpit switch and limit switches also must be included.

The thermosensitive element, see Figure 6 for illustrations, consists of a material which has a high negative temperature coefficient of resistance. Figure 7 shows the resistance temperature curves for three types of elements: engine head, oil, and carburetor air. The constants of the circuit are such that the thermosensitive element always has approximately constant wattage input over the systems operating band. This heat input is such that the thermosensitive elements themselves are always at a higher temperature than the body being cooled.

The controller, Figure 8, consists of a very sensitive polarized relay and power relays. The power relays control the operation of the flap motor; they are of conventional design.

The polarized relay works in conjunction with the thermosensitive element and the follow-up rheostat and controls the power relays. The relay, Figure 9, is a flux-balancing relay. It consists of a permanent magnet for polarization, two coils, and a balanced armature. Each

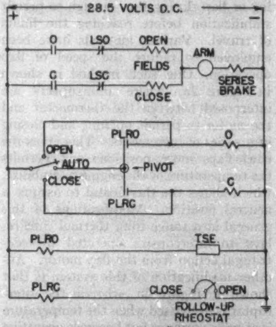

Figure 10. Elementary diagram of an automatic temperature-control circuit

coil has an inside winding, connected in series and to terminals 4 and 5, and an outside winding, connected in series and to terminals 4 and 6. The inside windings have twice as many turns as the outside, but both windings have equal resistance. The armature has a common connection at terminal 7 which may contact either terminal 8 or terminal 9.

Figure 10 is an elementary diagram of the basic circuit. The high-turn windings of the polarized relay are coil *PLRO* and the low-turn windings, coil *PLRC*. In order to balance the relay equal flux must be produced by each coil, therefore, the current through coil *PLRC* must be twice as great as the current through coil *PLRO*. This condition can be met only if the thermosensitive-element (*TSE*) resistance is equal to the resistance of coil *PLRC* plus twice the resistance of the follow-up rheostat.

Inasmuch as the thermosensitive element controls the position of the flap, the excitation of coil *PLRO* always is changed first. When the flap position is changed, it moves the follow-up rheostat until the relay is rebalanced. Figure 11 is a graphical representation of the operation of the polarized relay. Note that it takes a greater change in the flux produced by coil *PLRO* to reverse direction. This is done in order to prevent overshooting or hunting. Coil *PLRO* is energized only 0.8 of a milliwatt greater or less than its balancing excitation in order to operate the relay.

Figures 12 and 13 are typical examples of follow-up units. Figure 12 is a geared actuator with the follow-up unit mounted at the left on the assembly; Fig. 13 is a separately mounted follow-up unit which can be connected by a cable to any part of the flap actuating mechanism which has relatively straight line motion. Both of these units incorporate a rheostat and limit switches. The resistance of the rheostat controls the width of the temperature band as previously described.

Since a given flap change near the flap-closed position produces more cooling effect than the same flap change near the flap-open position, the follow-up rheostat must compensate for this condition by being tapered.

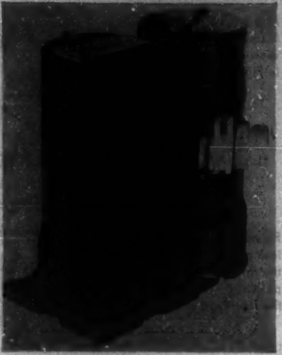

The rheostat in the gear-driven follow-up unit has a tapered winding. The taper is produced by the cam in the separately mounted follow-up unit. Both tapers are shown in Figure 14.

Any conventional actuator, either electric or hydraulic, can be used with this system, so long as it can be stopped quickly.

System Operation

In the diagram, in Figure 10, when the medium to be cooled is at a low temperature, the flaps are closed. The follow-up rheostat then has full resistance in coil *PLRC* circuit. As the medium rises in temperature the temperature-sensing element (*TSE*) decreases in resistance until the excitation of coil *PLRO* is greater than that of coil *PLRC*. This causes contact *PLRO* to close, exciting coil *O*. When coil *O* is energized, it closes contact *O* which energizes the motor in the open direction. As the flaps are opened, the follow-up rheostat decreases in resistance until coil *PLRC* is energized the same amount as coil *PLRO*. This causes contact *PLRO* to open, de-energizing

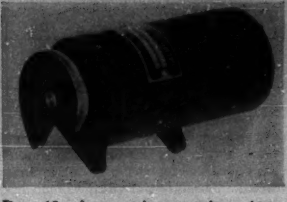

Figure 13. A separately mounted cam-driven follow-up unit

Weight, 1.32 pounds

Figure 12 (left). Electric actuator with follow-up unit forming a complete unit assembly

Weight of follow-up unit, 1.2 pounds

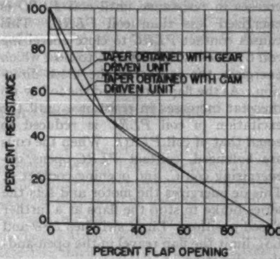

Figure 14. Typical per-cent resistance versus per-cent flap opening curves for follow-up units

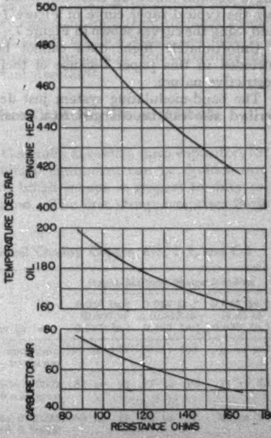

Figure 15. Calculated envelopes of temperature versus per-cent flap opening for engine-head, oil, and carburetor-air service

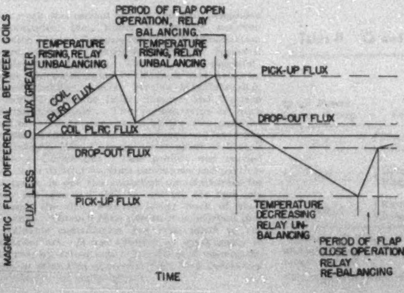

Figure 11. Graphical representation of the polarized-relay operating principle

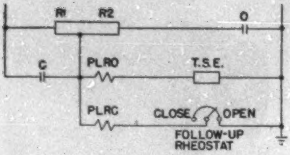

Figure 16 (left). Elementary diagram showing how circuit in Figure 10 can be sensitized

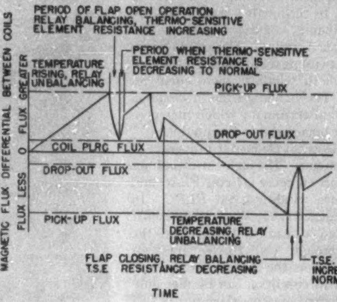

Figure 17. Graphical presentation of the operation of the polarized relay in the sensitized circuit

coil *O*, and opening contact *O*. This de-energizes the motor and sets the series brake, thus stopping the flaps at an open position. If the medium to be cooled is not yet receiving enough cooling air, the same procedure is followed. The flaps will stabilize at a point where the cooling air equals the heat release of the medium.

If the medium drops in temperature, then the temperature-sensing element increases in resistance until coil *PLRO* is energized less than coil *PLRC*. This causes contact *PLRC* to close energizing coil *C* and causing contact *C* to close which energizes the motor in the close direction. As the flaps are closed the follow-up rheostat increases in resistance until the excitation of coil *PLRC* is reduced to equal that of coil *PLRO*. When the coils are balanced, contact *PLRC* opens, de-energizing coil *C*, and opening contact *C*. This de-energizes the motor and sets the series brake to stop the flaps at a further closed position. Limit switches *LSO* and *LSC* limit the flap travel in the open-and-close direction.

Figure 15 shows the various envelopes of temperature versus flap opening for the engine-head, oil, and carburetor-air service. These curves are plotted assuming a 32-ohm follow-up rheostat, following the typical taper curve of Figure 14 and using the curves shown in Figure 7.

Unfortunately flight data cannot be included in this paper because of their restrictive nature.

The band-modulating system just described also can be changed to a sensitized band-modulating system. It must be remembered that the thermosensitive elements dissipate about two watts which causes them to be at a higher temperature than the medium being cooled. If it is possible to introduce less heat to the element when the flaps are opening or more heat to the element when the flaps are closing (preheating and precooling), the system can be sensitized. This is done by varying the voltage across the polarized relay coil circuits as shown in Figure 16.

In the balanced condition the voltage drop across *R*1 is the drop due to the current flowing through the polarized relay coils, the thermosensitive element, and the follow-up rheostat. When the flaps are driven in the open direction, contact *O* closes, which causes an additional voltage drop through *R*1 due to the current drawn through *R*2. Thus the power input to the thermosensitive element is decreased by reducing the voltage across it, which causes the resistance of the element to increase. This causes the polarized relay to rebalance sooner than it normally would.

When the flap is driven in the close direction, contact *C* closes, throwing the sensitive circuit across the line. This increases the power to the thermosensitive element by increasing the voltage across it, which causes the element to decrease in resistance. Again the polarized-relay rebalances sooner than it normally would. Figure 17 presents graphically the operation of the polarized relay under sensitized conditions. Note that a small amount of time is necessary for the relay to build up its flux differential after rebalancing. This prevents relay chatter which is present in every other type of sensitizing scheme so far devised for this system.

Conclusions

Automatic temperature control of cooling flaps increases the performance of the airplane, because it protects against destructive operating temperatures. It insures maximum efficiency and minimum drag by eliminating the human element.

Electric controls are more flexible than mechanical controls and are therefore easier to apply, especially in fighter aircraft where space in certain parts of the air frame is at a premium.

Judging Mica Quality Electrically

K. G. COUTLEE
NONMEMBER AIEE

MICA CAPACITORS by the millions have been used in radio, radar, and other important electronic equipment for our Armed Forces. The unprecedented demand has strained all our resources, and much time and money have been spent in efforts to solve the mica supply problem. One of these was a research project conducted by Bell Telephone Laboratories for the War Production Board. It was concerned with the development of electrical test methods to predetermine the quality of raw mica in terms of end-use requirements in various grades of capacitors. After over two years of work covering development, design, laboratory trial and an extensive commercial trial of two types of test instruments, this project has been brought to a successful conclusion. As the electrical method of classification makes possible the use of mica available in large quantities, but previously considered unsuitable for capacitors, the mica supply for capacitors is greatly increased. An estimated saving up to 60 per cent of the total amount of higher-quality mica used in capacitors is indicated.

Mica possesses many useful properties that make it particularly attractive as a capacitor dielectric. In general, these are high dielectric strength, high dielectric constant, low dielectric loss, chemical inertness, low-temperature coefficient of expansion, and good resistance to heat. The important feature that makes it possible to utilize these properties in a capacitor is that mica can be readily split into very thin films of uniform thickness.

India is the chief source of supply of capacitor mica due to its extensive resources of high-quality mica, low labor cost, and a long established business in supplying world-wide markets. Other less developed sources are South America, the United States, and Canada. With the advent of war, the sharp increase in demand for mica, coupled with wartime shipping hazards, created a scarcity. The Government immediately took steps to insure that the supply from established sources would be increased, to find new sources, and to encourage the development and use of mica substitutes.

Visual Quality Classification of Mica

The Indian visual system of classifying natural ruby mica incorporated in American Society for Testing Materials method *D*351 lists seven different qualities (see Table I). It had become more or less standard practice with capacitor manufacturers to consider all qualities below fourth quality (ruby good stained) as unsuitable for capacitor use, and a great many preferred not to go beyond third-best quality (ruby fair stained). Under no conditions was mica used that contained black spots or stains. Capacitor manufacturers had found from experience that by employing these better qualities of ruby muscovite mica a satisfactory product would be obtained. Unfortunately, the better qualities constitute a relatively small portion of total mica production, and the expected wartime demand far exceeded the supply. There was no satisfactory evidence however, that some and perhaps much of the lower-quality ruby and other types of mica might not also have been suitable for capacitor use.

Table I. India* Visual System for Classifying Quality of Natural Mica

Clear
Clear and slightly stained
Fair stained
Good stained
Stained
Heavy stained
Black stained and spotted

*See reference 1.

More Positive Test Needed

The War Production Board sought the assistance of Bell Telephone Laboratories in the fall of 1942 to devise electrical test methods that could be used to select mica for capacitor use. Such tests, or methods of classification, while assuring that no defective mica could be put into finished capacitors, were also to insure that no good mica of any type was rejected. The problem was not only to select mica from new sources where appearance was a questionable guide, but, of perhaps even greater importance, to salvage satisfactory capacitor mica from the large available stocks of mica which had been rejected as unsuitable for capacitors by visual standards.

Mica-Capacitor Requirements

Generally speaking, mica capacitors for military equipment can be divided into two broad groups in respect to duty required. The first group comprises those

Table II. Q and Power-Factor Values for Electrical Quality Groups, *E*-1, *E*-2, and *E*-3

Q or Power-Factor Group	Form	Q Value	Power Factor	Rapid-Method Meter Reading 0.010 In.† (0.007 to 0.015 In.)	0.020 In.† (0.015 to 0.025 In.)	0.030 In.† (0.25 to 0.035 In.)
E-1	Block mica	2,500 minimum	0.0004 maximum	95 to 100	95 to 100	95 to 100
	Films*	2,500 minimum	0.0004 maximum			
E-2	Block mica	350 to 2,500	0.00285 to 0.0004	87 to 95	77 to 95	71 to 95
	Films*	1,500 minimum	0.00066 maximum			
E-3	Block mica	50 to 350	0.02 to 0.00285	50 to 87	32 to 77	24 to 71
	Films*	200 to 1,500	0.005 to 0.00066			

*Probable *Q* values of molded-type 1,000-micromicrofarad (American War Standard *C*75.3) stacked-foil and silvered capacitors. These will apply when all factors that would adversely influence the *Q* value are under control.

†Thickness of block mica or mica films stacked to this thickness.

Paper 45-155, recommended by the AIEE committee on communication for publication in AIEE TRANSACTIONS. Manuscript submitted June 5, 1945; made available for printing August 1, 1945.

K. G. COUTLEE is with the Bell Telephone Laboratories, Inc., New York, N. Y.

This work was carried out by the Bell Telephone Laboratories, Inc., under a contract between Western Electric Company and the War Production Board under the supervision of the National Academy of Sciences. The capacitor manufacturers that participated in the tests were Aerovox, Cornell-Dubilier, Electro Motive Manufacturing, Micamold, Sangamo, Solar, Sprague, and Western Electric Companies. The various types of mica used in the tests were chosen by the mica-graphite division of the War Production Board and furnished by Colonial Mica Corporation as agent of Metals Reserve Corporation. This project was carried out under difficult wartime conditions, and particular credit is due the capacitor manufacturers for their patience and skill in steering the test lots through the shop without losing track of their identity. Through their efforts, it is believed that a valuable contribution has been made to the capacitor art. It has afforded an opportunity to observe, by actual tests, the effects of various defects in mica that generally have been considered undesirable for capacitor use.

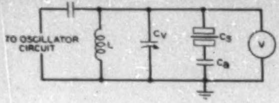

Figure 1 (left). Simplified circuit indicating the method of testing for Q or power factor

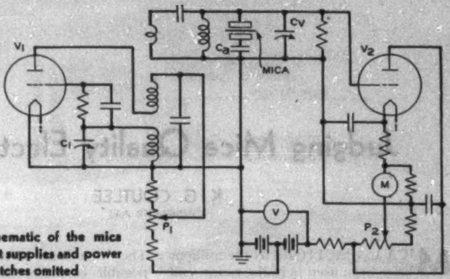

Figure 2. Circuit schematic of the mica Q test set with filament supplies and power and voltage switches omitted

used principally in high-stability tuned circuits, some of which must carry appreciable amounts of radio-frequency current. The second group embraces those used in less critical circuits for coupling, blocking, and by-pass purposes. Of equal importance to both groups is dielectric strength and long life; hence, all capacitor mica must be free of cracks, tears, pinholes and conducting foreign inclusions, which might adversely influence such properties. Mica for the first group must have low dielectric loss, and its characteristics must be such that wide temperature changes will cause only minor capacitance changes, and these always must repeat themselves. It is also preferable that mica be free of excessive waviness and air inclusions.

In the case of capacitors in the second group, the requirements are such that they can be met easily even with low-quality mica; a number of other materials, such as oil-impregnated paper, resin-treated paper, and resin-treated clay, also proved suitable. There also are certain other materials such as fused silica, titanium-dioxide mixtures, steatite, and glass, with characteristics that permit their use in some capacitors of the first group. However, the inferiority to mica in either dielectric strength or dielectric constant generally limited their use to smaller capacitance types.

Mica Properties Needing Control

As the dielectric constant of mica was found to show relatively little variation for different types and qualities from world-wide sources, no control of this property seemed necessary. Efforts were directed accordingly toward developing suitable test methods to determine the other important electrical properties of mica for capacitors: namely, dielectric loss and dielectric strength. As it seemed considerable testing might be carried out at mine locations, standard[7] power-factor methods for mica obviously were too cumbersome and slow. The ideal would be a rapid power-factor test method in a portable test-set form. Several methods were tried, and finally one was found that appeared suitable for quickly classifying the power factor of raw "block" mica (0.007 to 0.030 inch thick) as it appears in commerce.

Rapid Power-Factor Test Method

This method gives a reliable numerical indication of power factor or its approximate reciprocal equivalent *Q* as a single reading of a meter. Essentially it comprises a resonant circuit in conjunction with adjustable two-inch circular flat test electrodes mounted in a heavy metal frame. The choice of two-inch electrodes was based on the optimum size of block mica used for capacitors, and permitted the testing of mica somewhat smaller than the electrodes up to five inches in width. Forming an integral part of the moving upper electrode and connected to the grounded side of the test circuit is a fixed air capacitor of 20 micromicrofarads (20×10^{-12} farads). A schematic of the test circuit is shown in Figure 1, and in diagrammatic form in Figure 2. A vacuum-tube oscillator is capacitively coupled and tuned to the test circuit. Resonance is indicated by a vacuum-tube voltmeter connected in parallel with the tuned circuit. The inductive portion of the tuned circuit is a coil having a *Q* of approximately 300 at one megacycle. A test frequency of one megacycle was used at the request of the War Production Board, as the greatest number of capacitors were operating in the radio-frequency range. During initial adjustment, the test electrodes are closed, which connects the 20-micromicrofarads fixed capacitor in parallel with the coil. Oscillator input and tuning adjustments are made to bring the reading of the voltmeter to full-scale deflection. The electrodes then are opened by turning the knob that raises the upper fixed-capacitor electrode, and a test sample is clamped between electrodes. Only one adjustment is necessary to re-establish resonance. This is accomplished by adding to the circuit the small amount of capacitance that is lost when the relatively high-capacitance block-mica sample (150 to 450 micromicrofarads) is placed in series with the 20-micromicrofarad fixed capacitor. This additional capacitance is furnished by a 10-micro-

Table III. Electrical, Physical, and Visual Quality Requirements of Natural Block Mica and Mica Films for Use in Capacitors

		Class C-1	Class C-2	Class C-3
Electrical Properties				
Conductivity		None	None	None
Q value or power factor at 1 megacycle		*E*-1	*E*-2	*E*-3
Dielectric strength, volts per mil at 60 cycles per second	average	1,000	1,000	1,000
	single	850	850	850
Dielectric constant		*	*	*
Physical Properties				
Weight loss on heating (5 min at 600 C), maximum, per cent		0.2	0.2	
Thickness uniformity (mica films)		Best	Best	Intermediate
Temperature coefficient of capacitance and retrace		†	†	†
Visual Qualities				
Air inclusions	*A*	None to slight	None to slight	None to slight
	B	Medium	Medium	Medium
	C	Medium to heavy	Medium to heavy	Medium to heavy
Waves	*A*	Flat to slight	Flat to slight	Flat to slight
	B	Medium	Medium	Medium
	C	Medium to heavy	Medium to heavy	Medium to heavy
Cracks		None	None	None
Tears		None	None	None
Pinholes		None	None	None
Stones		None	None	None
Buckles		None	None	None
Ridges		None	None	None

*As the dielectric constant of natural block mica suitable for use in capacitors is fairly uniform, no specified requirement is needed.

†It has been found that the temperature coefficient of capacitance and retrace of capacitors made with classes *C*-1, *C*-2, and *C*-3 mica are more dependent on such factors as electrical and mechanical design and manufacturing technique than any differences that may be attributed to the mica itself.

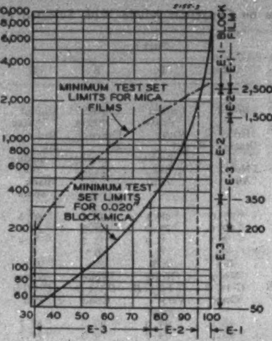

Figure 3 (left). Typical calibration curves for mica Q test set

Figure 4 (right). Meter scale of the mica Q test set

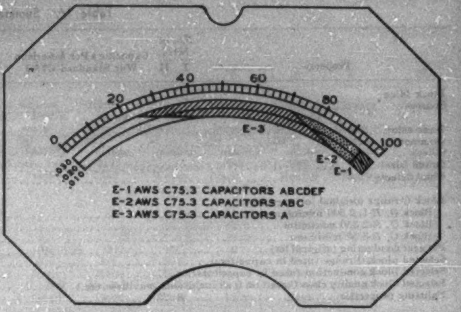
0
20
40
60
80
100
E-3
E-2
E-1
.030
.020
.010
E-1 AWS C75.3 CAPACITORS ABCDEF
E-2 AWS C75.3 CAPACITORS ABC
E-3 AWS C75.3 CAPACITORS A

microfarad vernier capacitor connected in parallel with the coil.

In following such a procedure the initial frequency of the circuit is duplicated each time a sample is tested. In other words, once the initial setting is made, all that is necessary to make a series of tests is to clamp the test specimen between the electrodes each time, make one simple adjustment of the vernier capacitor to obtain maximum deflection of the meter and read the meter scale corresponding to the thickness of the specimen as indicated by a scale on the clamping dial. It was possible to test up to 15 samples per minute, compared with about 15 minutes per sample.

If the *Q* of the test specimen of mica is of the order of 10,000 (power factor 0.0001), the needle of the meter will return to the initial full-scale deflection. If the *Q* is lower, the meter will read less than full scale, depending upon its magnitude.

The *Q* of block mica of any basic color or visual quality (based on minimum values) is shown in terms of rapid method *Q* test-set readings in Figure 3. The minimum equivalent *Q* of films split from such block mica (in the form of molded silver-electrode 1,000-micromicrofarad capacitors) also is plotted in terms of *Q* test-set readings originally obtained for the block. These data indicate that the *Q* at one megacycle of films (in capacitors) split from high *Q* block may not attain so high a value as the block. Probable reasons for this are dielectric loss in the molded capacitor housing, impregnants and moisture residuals, as well as series resistance in leads and electrodes. In the case of films split from low *Q* block such films most always show a higher *Q* at one megacycle than the block. Generally, this is believed to be due to the release of moisture during splitting, since the *Q* reading of a bundle of splits usually is higher than that of the block. However, in some cases this apparently is not so, and no improvement in *Q* is accomplished, even after baking at temperatures as high as 1,000 degrees Fahrenheit. Such behavior does not seem to be specifically confined to any particular type of mica or to any peculiar variety of foreign inclusions. Persistently low *Q* mica may be:

1. Clear with no visible foreign inclusions.
2. Clear with numerous small air inclusions.
3. Clear with minute black specks in the form of a gray cloudy haze.
4. Black spotted and stained mica.

It seems evident, based on *Q*-frequency behavior, wherein the *Q* drops to abnormally low values at low frequency, that such low *Q* as cases 1 and 2 is due to entrapped moisture that is not readily released. In cases 3 and 4 low *Q* apparently arises from dielectric loss in the spots and stains.

In setting limits for *Q*, it appeared reasonable to establish three ranges based on *Q* actually obtainable with mica rather than on *Q* requirements imposed by circuits. The upper range would cover the highest *Q* obtainable for any block mica, the middle range a very high order of *Q* but somewhat less than the best obtain-

Table IV. Experimental Laboratory Trial of Mica Test Sets

		Block					Capacitors Made With Films From Electrical Selected Block						
				Electrical Quality			Average† Q	Dielectric Strength‡	Insulation Resistance‡	Corona Voltage§	Life Test§		Aging¶
Lot	Source	Visual Quality	Color	Conducting Inclusions	1 Mc Q Range	Meter Reading	(1 Mc)	(Per Cent Correct)	(Per Cent Correct)	(Volts 60 Cps)	(Tested)	(Failed)	(Per Cent Change in Capacitance)
India	India	Fair stained	Ruby	No	*E*-1	99	5,000	100	100	244 average	8	0	0.077 average
A	S. D.	Clear	Ruby	No	*E*-1	99	3,900	100	100	269 average			0.195 average
A	S. D.	Stained	Ruby	No	*E*-2	93	3,100	100	100	253 average	6	2	0.211 average
B	N. C.	Clear	Ruby	No	*E*-1	99	4,900	100	100	270 average			0.100 average
B	N. C.	Stained	Ruby	No	*E*-2	94	3,800	100	100	261 average	6	1	0.177 average
C	N. M.	Clear	Green	No	*E*-2	93	2,800	100	100	256 average			0.077 average
C	N. M.	Stained	Green	Yes	Below *E*-3	*	140	100	100	268 average	6	0	0.319 average
D	N. C.	Clear	Green	No	*E*-1	96	3,500	100	100	265 average			0.212 average
D	N. C.	Stained	Green	No	*E*-2	93	2,800	100	100	243 average	6	0	0.161 average
E	N. H.	Clear	Ruby	No	*E*-1	97	4,100	100	100	266 average			0.260 average
E	N. H.	Stained	Ruby	No	*E*-1	96	3,800	100	100	245 average	6	0	0.169 average
F	Conn.	Clear	Ruby	No	*E*-2	93	3,500	100	100	260 average			0.216 average
F	Conn.	Stained	Ruby	No	*E*-2	89	2,400	100	100	246 average	6	0	0.264 average
G	N. C.	Stained	Green	Yes	*E*-2	80	1,700	100	100		4	0	

* Satisfactory readings could not be obtained in most cases.

† 1,000-micromicrofarad silver-molded capacitors.

‡ 1,000-micromicrofarad silver and 4,000-micromicrofarad foil-molded capacitors.

§ 4,000-micromicrofarad foil-molded capacitors.

¶ 5 cycles, +72 F to −40 F to +72 F to +185 F. 1,000-micromicrofarad silver-molded capacitors.

Table V. Summary of Manufacturers' Data on Capacitors Made With Selected *E*-1,

Property	No. of Mfrs. I	No. of Mfrs. II	Capacitors Per American War Standard C75.3		Part I A	Part I B	Part I D	Part I E	Part I F
Block Mica									
Source					India	Brazil	United States	United States	United States
Basic color					Ruby	Ruby	Ruby	Green	Ruby
Commercial quality					Stained	Stained *B*	2d quality	2d quality	2d quality
Grade (size)					No. 4	No. 4	2x2	2x3	2x2
Chief defects					*Air	Air	Air		Black spots
Block *Q* range (original lot), per cent									
Block *Q*, *E*-1, 2,500 minimum					94.0	77.0	68.1	64.3	80.5
Block *Q*, *E*-2 350 minimum					6.0	20.6	31.0	34.5	19.1
Block *Q*, *E*-3 50 minimum					0.0	2.4	0.9	1.2	0.4
Per cent conducting (original lot)					0	0	0	0	5
Selected block *Q* range (used in capacitors)					*E*-1	*E*-1	*E*-1	*E*-1	*E*-1
Selected block conduction (used in capacitors)					None	None	None	None	None
Selected block quality class (based on *Q* air inclusions, waviness, etc.)					**C*-1*BB*	*C*-1*CB*	*C*-1*C*+*B*	*C*-1*AB*	*C*-1*BB*
Splitting properties	8	2			Fair	Good	Very good	Good	Fair
Films, 1 to 4 mils (per cent yield)	9	2		Average	75.0	93.0	94.0	90.5	87.7
				Minimum	75.0	93.0	94.0	79.0	77.7
Laminations (per cent yield)	7	2		Average	35.5	37.1	34.8	39.3	35.4
				Minimum	22.8	28.9	27.3	31.2	21.3
Silvered laminations (per cent yield)	5	1		Average	89.9	86.8	81.7	90.3	88.5
				Minimum	82.5	82.0	70.7	84.6	79.3
Capacitors									
Capacitor *Q* (statistical distribution)	5	1	*CM*30—1,000-μμf, silver	Per cent>2,500	98.8	93.7	90.1	97.1	99.1
				Per cent 1,500-2,500	1.1	5.7	9.0	2.8	0.9
				Per cent 200–1,500	0.1	0.6	3.7	0.1	0.0
	6		*CM*30—1,000-μμf, foil	Per cent>2,500	94.5	95.6	97.2	94.7	96.8
				Per cent 1,500–2,500	5.4	4.1	2.4	5.2	2.2
				Per cent 200–1,500	0.1	0.3	0.4	0.1	1.0
	3	1	*CM*55—1,000-μμf, foil	Per cent>2,500	99.8	95.0	96.6	99.1	98.8
				Per cent 1,500–2,500	0.2	2.7	2.1	0.7	1.0
				Per cent 200–1,500	0.0	2.3	1.3	0.2	0.2
	3	1	*CM*70—510-μμf, foil	Per cent>2,500	76.5	87.0	51.3	86.0	78.1
				Per cent 1,500–2,500	18.5	13.0	44.2	7.0	21.9
				Per cent 200–1,500	5.0	0.0	4.5	7.0	0.0
American War Standard dielectric strength (per cent meeting requirement)	7	1	*CM*30—1,000-μμf, silver		95.5	98.1	98.7	97.0	96.7
	8		*CM*30—1,000-μμf, foil		95.5	95.6	96.8	96.6	96.7
	3	1	*CM*55—1,000-μμf, foil		95.9	98.2	95.8	96.5	96.1
	2	1	*CM*35—6,200-μμf, foil		92.2	94.8	99.3	96.8	99.7
	2	1	*CM*60—6,200-μμf, foil		96.1	99.5	98.9	93.2	91.0
	4	1	*CM*70—510-μμf, foil		100.0	100.0	100.0	100.0	100.0
American War Standard insulation resistance (per cent meeting requirement)	7	1	*CM*30—1,000-μμf, silver		99.9	99.6	99.7	99.8	99.6
	8		*CM*30—1,000-μμf, foil		99.8	99.1	99.3	99.8	99.4
	3	1	*CM*55—1,000-μμf, foil		99.7	99.7	99.9	99.9	99.9
	2	1	*CM*35—6,200-μμf, foil		98.4	99.2	99.2	96.0	99.3
	2	1	*CM*60—6,200-μμf, foil		100.0	100.0	100.0	100.0	100.0
	4	1	*CM*70—510-μμf, foil		100.0	100.0	100.0	100.0	100.0
American War Standard radio-frequency heating (per cent meeting requirement)	4	1	*CM*70—510-μμf, foil		100.0	100.0	100.0	100.0	100.0
Corona starting voltage—60 cycles per second—(no American War Standard requirement)	1		*CM*70—510-μμf, foil	(5 sections)	1,900	2,200	2,700	2,300	2,000
	1		*CM*70—510-μμf, foil	(8 sections)	3,600	3,500	3,600	3,600	3,400
	1		*CM*70—510-μμf, foil	(9 sections)	4,300	4,100	4,000	4,000	4,600
					†1 2 3	1 2 3	1 2 3	1 2 3	1 2 3
American War Standard temperature-coefficient and drift (American War Standard characteristic)	5	1	*CM*30—1,000-μμf, silver		*E D B*	*D C B*	*D C B*	*E D B*	*E D C*
	6		*CM*30—1,000-μμf, foil		*C B B*	*B B B*	*B B B*	*B B B*	*C B B*
	3		*CM*55—1,000-μμf, foil		*B B B*	*B B B*	*B B B*	*C B B*	*C B B*
	2	1	*CM*70—510-μμf, foil		*D D D*	*D D D*	*D C B*	*D D C*	*D D D*
‡ American War Standard capacitor life (per cent meeting requirement)	5	1	*CM*30—1,000-μμf, silver		93.7	100.0	100.0	97.9	100.0
	5		*CM*30—1,000-μμf, foil		100.0	100.0	98.2	98.2	100.0
	3	1	*CM*55—1,000-μμf, foil		100.0	92.7	100.0	100.0	98.3
	2	1	*CM*35—6,200-μμf, foil		100.0	96.0	96.0	100.0	100.0
	1	1	*CM*60—6,200-μμf, foil		92.0	88.0	96.0	96.0	96.0
	3	1	*CM*70—510-μμf, foil		100.0	100.0	100.0	100.0	100.0
Grand Averages									
American War Standard dielectric strength (per cent meeting requirement)			All types and sizes of above capacitors		95.8	97.7	98.2	96.6	96.7
American War Standard capacitor life (per cent meeting requirement)			All types and sizes of above capacitors		97.6	96.1	98.4	98.7	99.1

able, and a third range of somewhat lower order of *Q*, but high as compared with other types of insulating materials in general. The top *Q* range simulated that normally assumed for mica and presumably used in capacitors in the past. While it became evident that such high *Q* actually is only needed in a relatively small percentage of capacitors, of the previously mentioned first group, it affords a margin of safety to which capacitor manufacturers apparently are accustomed. The middle range probably is high enough for all but the most critical types of capacitors of the first group, and the third *Q* range is suitable for by-pass, blocking, and coupling types of capacitors of the second group. These three ranges are designated *E*-1, *E*-2, and *E*-3, respectively, and the minimum *Q* limits assigned to each range are shown in Table II as well as equivalent test-set readings. This table also shows minimum *Q* limits for mica films split from the block. The actual calibration of the scale of the meter is shown in Figure 4.

Spark-Test Set

It was observed in studies of various types of block mica that the *Q* of "black stained and spotted" samples, in some cases, was just as high as that observed

E-2, and E-3 Block Mica Showing Over-All Performance From Block to Capacitors

H	I	J	L	M	N-1	N-2	N-3	N-4	N-5	O	P	Q	R
Part I (Continued)					Part II								
United States	United States	United States	Canada	India	United States	United States	United States	United States	United States	United States	United States	Canada	Canada
Ruby	Green	Ruby	Green	Ruby	Ruby	Ruby	Ruby	Ruby	Ruby	Green	Green	Green	Green
2d quality	2d quality	2d quality	2d quality	Good stained	3d quality	3d quality	3d qualify	3d quality	3d quality	3d quality	3d quality	2d quality	3d quality
2x3	2x2	2x3	2x3	No. 4	Mixed sizes, 1x1½ to 2x3					2x3	2x3	2x3	2x3
Waves	Black spots	Waves		Air	Black spots	Reeves	Smoke	Clay	Waves	Black spots	Reeves	Smoke	Spots
79.0	67.8	91.2	45.6	96.6						35.0	92.0	41.5	18.1
20.5	27.7	8.4	34.8	3.1						42.0	8.0	30.8	18.0
0.5	3.6	0.4	19.6	0.3						23.0	0.0	27.7	63.9
0	5	0	0	0	0	0	0	0	0	0	0	0	50
E-1	*E*-1	*E*-1	*E*-1	*E*-1	*E*-1	*E*-1	*E*-1	*E*-1	*E*-1	*E*-1	*E*-1	*E*-1	*E*-3
None	None	None	None	None	None	None	None	None	None	None	None	None	Slight
C-1BC	*C-1BC*	*C-1AB*	*C-1AA*	*C-1BB*	*C-1AB*	*C-1BC*	*C-1BB*	*C-1BB*	*C-1BC*	*C-1BB*	*C-1BC+*	*C-2AB*	*C-3AB*
Good	Fair	Good	Good	Very good	Very good	Poor	Good	Good	Poor	Fair	Poor	Good	Good
87.9	90.4	90.8	90.3	93.7	95.2	90.9	95.4	93.7	94.0	83.4	66.0	84.3	83.4
78.0	83.0	82.0	86.0	92.0									
36.8	35.7	35.7	38.6	38.5	42.3	42.6	41.6	43.4	43.1	34.2	26.8	36.1	38.6
23.5	22.6	27.0	28.2	21.8									
82.9	87.5	85.3	90.0	85.8						97.2	91.1	90.2	86.6
68.2	80.6	69.3	81.6	75.8									
99.5	94.9	98.8	95.0	98.2						87.1	98.5	79.2	16.2
0.3	4.7	1.1	3.0	1.4						11.6	1.5	17.9	37.3
0.2	0.4	0.1	2.0	0.4						1.3	0.0	2.9	46.5
95.3	92.1	97.9	92.0	96.2									
4.0	5.6	2.0	4.5	3.7									
0.7	2.3	0.1	3.5	0.1									
99.0	92.8	99.7	96.0	98.6						91.7	98.0	59.0	3.4
0.8	6.1	0.3	1.2	1.0						6.7	0.5	20.0	13.6
0.2	1.1	0.0	2.9	0.4						1.6	1.5	21.0	83.0
95.2	82.0	89.3	46.1	91.9	100.0	80.0	90.0	100.0	100.0				
4.8	10.2	8.3	47.7	8.1	0.0	10.0	10.0	0.0	0.0				
0.0	7.8	2.4	6.2	0.0	0.0	10.0	0.0	0.0	0.0				
97.7	96.1	96.7	97.9	99.0						95.9	98.8	98.8	98.3
96.6	95.2	97.5	97.4	96.3									
94.4	93.5	97.9	98.6	98.5						92.3	98.7	98.1	95.1
95.7	99.2	96.2	94.0	97.7						86.9	99.2	97.7	95.7
93.7	94.0	99.1	97.9	96.1						89.4	79.1	95.5	93.1
100.0	100.0	100.0	100.0	100.0	100.0	100.0	100.0	100.0	100.0				
99.9	99.5	99.4	98.4	99.7						100.0	100.0	100.0	100.0
99.6	99.8	99.7	99.8	99.7									
98.9	99.9	99.8	99.7	98.1						100.0	100.0	100.0	100.0
99.6	96.1	100.0	99.6	97.7						100.0	100.0	100.0	100.0
100.0	100.0	100.0	100.0	100.0						100.0	100.0	100.0	100.0
100.0	100.0	100.0	100.0	100.0	100.0	100.0	100.0	100.0	100.0				
100.0	100.0	100.0	100.0	100.0	100.0	100.0	100.0	100.0	100.0				
2,000	2,500	1,900	1,900	2,400									
3,500	3,800	3,500	3,800	3,600									
3,900	4,200	4,200	3,400	4,100									
1 2 3	1 2 3	1 2 3	1 2 3	1 2 3	1 2 3	1 2 3	1 2 3	1 2 3	1 2 3	1 2 3	1 2 3	1 2 3	1 2 3
E D C	*E D B*	*D C B*	*E D B*	*E D C*						*F — D*	*F — D*	*F — D*	*F — D*
C B B	*C B B*	*C B B*	*C B B*	*C B B*									
B B B	*C B B*	*B B B*	*C B B*	*C B B*									
D D D	*D C B*	*D D D*	*E D D*	*D D D*	*D — B*	*E — D*	*E — B*	*D — B*	*D — B*				
100.0	97.9	100.0	100.0	100.0						100.0	100.0	100.0	100.0
100.0	96.6	100.0	100.0	98.2									
98.0	95.5	100.0	96.9	97.9						100.0	100.0	100.0	100.0
91.0	91.0	96.0	91.0	100.0						100.0	100.0	100.0	92.0
92.0	96.0	96.0	88.0	96.0						96.0	91.0	92.0	75.0
100.0	100.0	100.0	100.0	100.0	100.0	100.0	100.0	100.0	100.0				
96.3	96.3	97.9	97.6	97.9	100.0	100.0	100.0	100.0	100.0	91.1	93.9	97.5	95.5
96.8	96.2	98.7	96.0	98.7	100.0	100.0	100.0	100.0	100.0	99.0	97.7	98.0	91.7

* Quality designation per ASTM 748. † 1 = average–averages. 2 = average–minimums. 3 = minimums

‡ Excluding breakdowns due to causes other than mica puncture.

for any of the samples including the clear ones, whereas other "black stained and spotted" samples had very low *Q* values. It was found that low *Q* in "black stained and spotted" samples usually occurred when the stains were semiconducting in nature. Such conductivity, when present, could be detected by a high-voltage spark furnished by a vibrator-type induction coil, connected to a probe electrode, when the probe was used to explore the surface of the mica. Conducting spots and stains are revealed by sparkling and glowing at or near the probe but not by puncture by the spark. Mechanical faults, such as pinholes, tears, and cracks also can be located with this test; such defects are revealed by puncture of the mica by the spark. A schematic of this test circuit is shown in Figure 5.

Laboratory Trial of Test Sets

First, an experimental laboratory trial of the two types of test instruments was conducted in which "clear" to "black stained and spotted," green and ruby block mica from seven domestic mines was classified for *Q* at one megacycle with the rapid-method *Q* test set and tested for conducting inclusions with the spark test set. This electrically selected block was split and punched into capacitor laminations 1.2 to 1.6 mils thick using standard commercial methods. These laminations were used indiscriminately, regardless of any visual inclusions and only were discarded if found to be mechanically unsound. Both 1,000-micromicrofarad and 4,000-micromicrofarad molded-silvered and foil "postage-stamp"-type capacitors were made by the Western Electric Company with this mica.

Thorough performance tests were made on these capacitors, and they satisfactorily met *Q*, insulation-resistance, dielectric-strength, corona-voltage and life requirements (see Table IV). As a result of these tests, it was concluded that block mica could be selected dependably for use in capacitors, some for the better grades and the rest for less critical types, and that the test methods appeared entirely adequate for the electric control of capacitor mica. Even the two lots of capacitors made with block mica in which conducting inclusions were detected by the spark test and low *Q* by the block-mica *Q* test gave excellent dielectric strength and life performance. It therefore appeared evident that such mica of *E*-2 and *E*-3 electrical quality might be used for less critical grades of capacitors with better over-all characteristics than can be obtained with some of the available alternate materials. However, as a precautionary measure, the use of mica with conducting inclusions was ruled out, in view of the apparent plentiful supply of types not possessing this defect.

Over-All Quality Specification

A specification[8] was developed containing over-all requirements for block mica for use in capacitors incorporating the two electrical test methods as well as other electrical, visual, and physical requirements. The electrical requirements covered *Q*, dielectric strength, and absence of conducting inclusions. The physical requirements covered splitting quality and weight loss on heating. Visual requirements covered air inclusions, waves, buckles, ridges, cracks, tears, pinholes, and stains. Three quality classes were set up for block mica suitable for use in capacitors, designated *C*-1, *C*-2, and *C*-3. Class *C*-1 is considered adequate for any and all of the various grades of capacitors in American War Standard *C*75.3. Classes *C*-2 and *C*-3 are considered usable for the less exacting grades. *C* classifications cover both electrical and physical properties and *E* classifications electrical properties only. Class *C*-1 covers *E*-1 mica with best electrical and physical properties, *C*-2 covers *E*-2 mica with intermediate electrical and physical properties and *C*-3 covers *E*-3 mica with fair electrical and physical properties. The stipulation is made, however, that mica shall meet all requirements of its respective class.

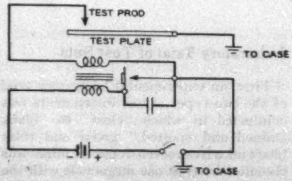

Figure 5. Circuit schematic of the spark-test set

Commercial Trial of Test Sets

The next step was to try out the proposed system on a commercial scale, using the testing equipment that had been developed. A commercial design of the block-mica *Q* test set which is portable and contains its own batteries is shown in Figure 5. The spark-coil conductivity test set, which also is battery-operated and portable, is shown in Figure 6.

The commercial trial covered the electrical classification of over 3,000 pounds of block mica of 22 different types from the United States, India, Canada, and Brazil, previously classified by visual standards as stained, stained *B*, United States second and United States third quality. All such classifications were previously considered unsuitable for capacitor use. After being split, gauged, and punched, this mica was used, regardless of visible inclusions, providing it did not contain cuts, tears, or other visible mechanical imperfections, in the manufacture of over 47,000 capacitors of the following types and sizes per American War Standard *C*75.3: molded *CM*30 and 55, 1,000-micromicrofarad silvered and stacked-foil; and *CM*35 and 60, 6,200-micromicrofarad stacked-foil capacitors; as well as potted *CM*70; 510-micromicrofarad transmitter-type capacitors. A total of eight capacitor manufacturers participated in the commercial trial, and the number that made specific types of capacitors and tests in each case is shown in Table V. This table contains a grand summary of test results and manufacturing experience in connection with the processing of electrically selected block mica into finished capacitors. It shows the number of capacitors that passed test requirements specified in American War Standard *C*75.3 and gives the results of other special tests.

Conclusions

Based on satisfactory *Q*, dielectric strength, insulation resistance, temperature coefficient, capacitance stability, radio-frequency heating, corona voltage, and life tests on these capacitors obtained by eight participating manufacturers, it is concluded that electrically selected *E*-1, nonconducting block mica is suitable for use in the manufacture of all types and sizes of fixed mica-dielectric capacitors per American War Standard *C*75.3 up to and including *CM*70. However, nothing has been revealed by these studies which would indicate that such mica would not be equally as satisfactory for use in all sizes and types of capacitors, per American War Standard *C*75.3. Likewise, based on somewhat less extensive tests on electrically selected *E*-2 and *E*-3 nonconducting block mica, such mica within the limits specified for class *C*-2 and *C*-3 mica, per ASTM *D*-748-45*T*, is suitable for use in the manufacture of all types and sizes of capacitors up to and including *CM*60 per American War Standard *C*75.3.

Figure 6. The mica Q test set developed by Bell Telephone Laboratories

Figure 7. The spark test locates conducting regions in block mica and permits defective material to be rejected before the application of the Q classification test

The splitting quality and yield of satisfactory splittings and punchings of all lots of selected *E*-1 nonconducting mica of part 1 of the commercial trial, considered as a group, is estimated to be 10 to 20 per cent poorer than that reported for the lot-*M*

India (good stained) sample. The poorest splitting quality and film yield was reported for selected *E*-1 nonconducting lot-*P* (heavy-reeved and ribbed) light-green mica of part II. This lot did not conform to the physical requirements of class *C*-3 mica per ASTM *D*-748–45*T*, but was included in the tests to study the performance of such mica. It is important to note, however, that the electrical performance of capacitors made with mechanically sound punchings from lot *P* electrically selected mica approached that obtained for the control sample. The poorest capacitor life performance was experienced with lot *R*, *E*-3 mica which did not pass the spark-test requirement but was included to check the *E*-3 range of the *Q* test set.

The proposed system of classifying block-mica quality based on a combination of dielectric and physical properties has been shown to be commercially reliable and practicable. This system differs radically from past practices, and previous concepts of mica quality considered suitable for use in capacitors. It does not discriminate against the presence of spots and stains in even first-quality electrically selected block mica, providing the mica conforms to specific electrical and physical requirements. Air inclusions and waviness also are permitted in the lower-quality classes, providing the mica meets specific electrical and physical requirements. Mica capable of meeting specific electrical and physical requirements also may be of any basic color.

The experimental work in connection with part I and II of the commercial trial on all lots of mica confirms that Bell Telephone Laboratories block-mica *Q*-test and spark-test sets or commercial equivalents* are satisfactory for classifying block mica in accordance with ASTM specification *D*-748–45*T*. Furthermore, the requirements for all classes of block mica, per this specification, have been found to be conservatively set, thereby providing a good factor of safety.

As the electrical system of classification qualifies mica previously considered unsuitable for capacitors, the mica supply for such use is greatly increased owing to the much more plentiful supply of lower visual-quality types of mica. An estimated saving up to 60 per cent of the total amount of good stained or better mica now used in capacitors is indicated.

References

1. MICA FOR WAR PURPOSES, F. J. Given. Bell Laboratories *Record*, October 1943.

2. ALTERNATIVES FOR MICA CAPACITORS, F. E. Hanson. *Electronics*, May 1944.

3. EQUIPMENT AND METHOD OF MEASUREMENT OF POWER FACTOR OF MICA, E. L. Hall. Institute of Radio Engineers *Proceedings*, July 1944.

4. MICA IN WAR, R. G. Wayland. *Mining Technology*, July 1944.

5. THE WARTIME PROBLEM OF MICA SUPPLY, M. H. Billings, S. A. Montague. *Engineering and Mining Journal*, August 1944.

6. SAVING MICA BY TESTING, K. G. Coutlee. Bell Laboratories *Record*, September 1944.

7. AMERICAN SOCIETY FOR TESTING MATERIALS SPECIFICATIONS *D*351 AND *D*150.

8. AMERICAN SOCIETY FOR TESTING MATERIALS *D*-748–45*T*.

---

*Boonton Radio Corporation instruments.

Electric Drives for Steam-Electric Generating-Station Auxiliaries

WM. R. BROWNLEE
MEMBER AIEE

J. A. ELZI
MEMBER AIEE

Synopsis: For several years there has been an increasing trend toward all-electric drives for steam-station auxiliaries on account of the recognized advantages in flexibility, convenience, low operating cost, and comparable investment cost. Substantial economies in first cost also have been obtained along with further improvements in flexibility through the use of transformers as the sole means of station power supply. Gratifying reliability of performance has been achieved by co-ordinating design, backed by extensive tests, including momentary interruptions of station power supply, and has been incorporated in approximately 500,000 kw of modern plants of the 850-pound 900-degrees-Fahrenheit powdered-fuel-fired unit type. Operating experience has demonstrated the over-all reliability and economy of all-electric drives for station auxiliaries and of the use of transformers as the sole source of station power supply.

THE INCREASING RELIABILITY of modern steam-electric generating stations has been an important factor in the dependable supply of electric power in the face of decreasing reserves and promises future economies in system investment. One of the vital elements of this reliability is the treatment of station auxiliaries and station power-supply equipment.

Before the advent of the extraction turbine, the need of steam for feed water heating strongly favored small steam turbines as drives for most of the station auxiliaries. Multistage bleeding brought about a critical examination of operating costs of turbine-driven auxiliaries, and resulted in the application of electric motors to many of them, certain steam-turbine drives being retained either to obtain convenient variable-speed operation or with the objective of securing greater reliability for critical drives.[1] The advent of modern steam pressures such as 850 pounds and above has resulted in even lower efficiencies for small turbines, unless they are made so complex that their reliability is seriously reduced.

Many factors have contributed to the improved reliability of electrically driven auxiliaries.[1] Modern motors are highly reliable, and variable-speed couplings provide flexible and efficient operation where required. The growing interconnection of both stations and systems makes it feasible to secure emergency electric power for auxiliaries not only from several points within a station but from remote sources as well. Several years' experience has demonstrated that the proper co-ordination of driven equipment, motors, control, and power source insure an extremely high degree of reliability. Many stations now operate with all auxiliaries electrically driven, with the minor exception in some cases of the turbine-bearing oil pump, which is furnished by the manufacturer as a part of the turbine.

Basic Requirements of Auxiliary Drives

The requirement of reliability for many auxiliary drives is most important. Especially with powdered-fuel-fired boilers, the interruption for even a few seconds of certain critical drives may result in flame extinction, and the resulting necessity of purging the furnace system and relighting may cause a serious (though temporary) loss of capacity. Thus the over-all system must be made relatively immune to short-time disturbances, but without sacrificing the simplicity and flexibility which are so essential to successful operation. Adequate safety interlocking is required but must be scrutinized for possible hazards to reliability.

For some of the drives variable-speed operation or its equivalent is necessary. Where storage capacity can be secured readily, the automatic intermittent running of constant-speed motors provides convenient, flexible, and low-cost performance. For other auxiliaries the use of constant-speed motors with variable-speed couplings can provide the desired solution.

Paper 45-151, recommended by the AIEE committee on power generation for publication in AIEE TRANSACTIONS. Manuscript submitted June 28, 1945; made available for printing July 30, 1945.

WM. R. BROWNLEE and J. A. ELZI are both with the Commonwealth and Southern Corporation, Jackson, Mich.

Though consideration of cost is secondary to that of reliability, a careful consideration of all factors will facilitate low-first-cost design without any measurable sacrifice in reliability. The low operating cost of electric-driven auxiliaries is inherent when compared with steam-driven auxiliaries.

Figure 1. Typical power supply and motor connections for station auxiliaries

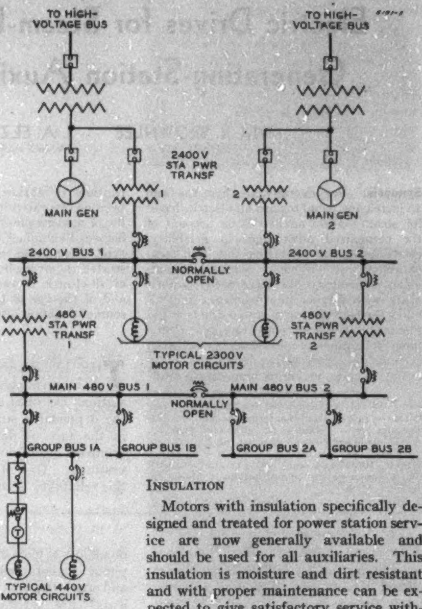

Motor Application

By far the largest portion of motors used for station auxiliary drives are three-phase squirrel-cage induction motors conforming to National Electrical Manufacturers Association standards regarding starting current, starting torque, and maximum torque. In spite of the requirements of high reliability, only a very few motors and auxiliaries, such as boiler feed pumps, pulverizers, and circulating water pumps, are installed in duplicate. For this reason particular attention is paid to the mechanical and electrical construction of the motors purchased. This does not mean that the motors need to be of special design or construction.

VOLTAGE RATING AND STARTING CHARACTERISTICS

A few of the small motors are rated 220 volts, but most drives use either 440- or 2,300-volt motors. An economic survey taking into consideration the cost of motors, control equipment, and the station distribution system has resulted in a decision to place the dividing line between the use of 440-volt and 2,300-volt motors at approximately 100 horsepower.

Full-voltage starting is used for both 440- and 2,300-volt motors. This permits the use of a low-cost control scheme which is simple and direct in its operation and lends itself to quick automatic transfer from one power source to another in an emergency. It also provides full starting and pull-in torque for normal voltage conditions. It may, however, be necessary at times to start an essential auxiliary when the voltage at the motor terminals is below normal as the result, for example, of the loss of a sizable amount of generation from the system. The speed-torque requirements of all auxiliaries are given careful consideration, and motors having adequate speed-torque characteristics at the minimum operating voltage are selected.

For some applications, such as certain types of pulverizers, the starting torque is the critical value, and, if a motor is selected having adequate torque to start the pulverizer during low-voltage conditions, no difficulty will be experienced in bringing the pulverizer up to speed. In other applications, such as boiler feed pumps the starting duty is relatively light, but the torque curve of the pump may rise very rapidly with speed, and in this case it is necessary to check the speed-torque curve of the motor under minimum-voltage conditions to make sure that it remains above the pump characteristic at all speeds.

Motors having normal starting current usually are provided, as light flicker due to motor starting is not usually a problem when transformers are used for station power supply. Co-ordinated unit design results in satisfactory operation from the standpoint of disturbances resulting from starting the largest motor or the transferring of a group of running motors from one bus to another.

MECHANICAL CONSTRUCTION

In order to assure reliable continuous operation, careful consideration is given to mechanical construction. The motor windings and rotor bars must be braced to withstand the stresses due to full-voltage starting and must be thermally adequate for the current associated with it. Insofar as practicable the construction should be such as to provide ease in making periodic inspections and checks. This means, for example, that it should be easy to check the oil level in the bearings and to make sure that the oil rings are performing properly. Provision should be made for checking bearing temperatures, and suitable openings for checking air gaps are essential. Proper end play is important, especially in 3,600-rpm motors, and the motor should be so constructed that this can be checked readily.

INSULATION

Motors with insulation specifically designed and treated for power station service are now generally available and should be used for all auxiliaries. This insulation is moisture and dirt resistant and with proper maintenance can be expected to give satisfactory service without the necessity of using splashproof or totally enclosed motors. Dripproof motors are provided where there is a possibility of water dripping on the motor.

Both class-*A* and class-*B* insulation are used. In general it is easier to obtain satisfactory class-*A* insulation for power-station service, and class-*B* insulation is specified only for motors operating in ambients above 40 degrees centigrade, such as draft fan motors.

SPEED CONTROL

For most station auxiliary applications constant-speed drives are used. The induced- and forced-draft fans are an exception to this. The power requirements of these fans are substantial, and their speed adjustment is controlled automatically by the combustion-control equipment.

In many of the earlier plants the motors for these drives were of the wound-rotor variable-speed type. However, equal efficiency and better control can be provided with constant-speed motors and variable-speed couplings of the hydraulic or magnetic type.[3] These are in most cases used to provide the entire range of speed control and have proved quite satisfactory, responding very well to the combustion-control equipment. In some instances two separate motors are provided with different constant-speed ratings, with dampers to provide intermediate control.

Power-Supply Systems

The choice of a system for supplying power to electrically driven auxiliaries is a vital one. The primary objective of adequate reliability must be obtained, but this does not mean that the most elaborate and expensive scheme is necessary or even desirable. One of the important advantages of electric drive for station auxiliaries in an interconnected transmission system is that power may be secured from a large number of sources and transferred instantly from a central location. The extension and improved performance of interconnected power stations and systems have increased the popularity of the unit system of plant design; that is, one boiler, one turbine, and one step-up transformer operating as a unit, with electric connections with other units made at the high-voltage bus only. The interconnected system can compensate for the loss of any one unit, and accordingly the statement has been made that the over-all reliability of the station auxiliaries need be no greater than that of the main units. This is true with certain minor exceptions. In the case of an emergency outage of a main generator for a temporary cause, it may be necessary to provide emergency service within a short time to the boiler feed pump. If the interruption to the main unit is long enough for the turbine to stop turning, then the availability of emergency power for the auxiliary turbine-turning motor will save a delay of two or three hours in restoring the unit to service.

HOUSE TURBINE, SHAFT GENERATOR, TRANSFORMER

In early applications of electric drive to include essential auxiliaries, it was sometimes thought necessary to provide an entirely separate house turbogenerator, supplemented with an auxiliary generator on the shaft of the main unit and a transformer source. Such an installation was so expensive as to offset in part the $1^1/_2$ per cent to $2^1/_2$ per cent reduction in operating costs achieved with electric drive. Experience soon showed that the costly house turbogenerator was unnecessary and added very little to reliability. The upward trend in steam pressures and co-ordinated bleeding cycles was also a factor in the gradual abandonment of the house turbine.

The less costly auxiliary generator driven on the shaft of the main unit is still much more expensive than a transformer. The principal advantage of the shaft generator is that the auxiliary bus supplied from it is not exposed to voltage disturbances originating on the transmission system. On the other hand the line starting of large induction motors from a shaft generator may involve serious voltage disturbances of several seconds' duration which are not encountered with transformer supply.

Careful analysis of fundamental requirements has shown that the proper co-ordination of the characteristics of motors and control with those of the driven equipment provides adequate reliability using transformers for the sole supply of auxiliary power. Some of the factors contributing to the improved reliability of systems using transformers are:

1. Co-ordination of control methods to avoid unnecessary interruptions.

2. The more rapid clearing of transmission-system faults.

3. The use of squirrel-cage induction motors with full-voltage starting.

4. The choice of power sources to provide a natural cushion against external power-system faults.

Special tests were made to check the over-all operation of the systems and subsequent experience provided further confirmation

TRANSFER SCHEME WITH UNIT SYSTEM

Figure 1 illustrates a typical scheme of connections with the station power transformers connected to their respective main units at generator voltage and with the latter grouped in pairs for emergency operation of both sets of auxiliaries from either main generator. Transfer of an entire group of auxiliaries may be made from the control center and normally is accomplished automatically in case a station power transformer separates by differential relay. This automatic transfer also may be initiated by operation of the relays protecting the main transformer bank. Reliability suitable for a unit system is obtained with single busses which are well protected electrically and mechanically. In the case of the 480-volt system, the relatively large number of motors makes it desirable to divide them among group busses as shown so as to limit the total exposure on the main 480-volt busses. Experience to date has not shown the desirability of providing voltage-chasing schemes.

INFLUENCE OF VOLTAGE DIPS DURING EXTERNAL FAULTS

The main step-up transformer of a unit installation provides a natural cushion for the station auxiliary bus against transmission faults. Figure 2 shows the positive sequence voltage on the station power busses as a function of the type of fault and its duration for short circuits immediately adjacent to the high-voltage bus. The initial voltage drop does not lower the pull-out torque of standard squirrel-cage induction motors below the normal full-load torque in case of these most pessimistic phase-to-ground or phase-to-phase faults. Even during three-phase faults adjacent to the bus the motors develop appreciable torque. With control properly co-ordinated the motors and

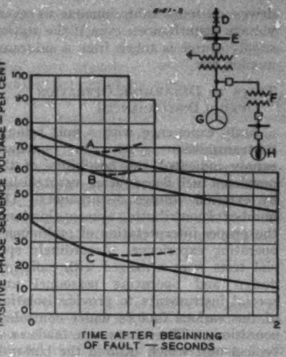

Figure 2. Influence of transmission faults on auxiliary-motor voltage

---------Effect of voltage regulator
A—Single phase to ground
B—Single phase to phase
C—Three phase
D—Fault
E—High-voltage bus
F—Station power transformer
G—Main generator
H—Motor

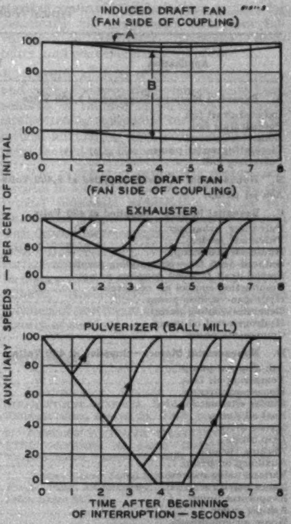

Figure 3. Speed variations caused by power interruptions

A—Power restored at 2.3 seconds
B—Power restored at 3.7 seconds

drives are remarkably immune to severe voltage disturbances, even if the station supply source is taken from a subtransmission bus.

TESTS TO DETERMINE OPERATION DURING DISTURBANCES

Early experience with a unit using a subtransmission system for auxiliary supply indicated the possibility of the powdered-fuel flame being extinguished by external voltage disturbances. The number of contributing elements hindered the proper interpretation of preliminary operating experience. Accordingly special tests were arranged with sufficient design and operating personnel and special instruments to provide isolation of the various factors under controlled conditions. These tests were made on a typical unit which utilized the ball-mill type of unit pulverizers (two per boiler) to determine the influence of surges on the boiler operation. With one pulverizer (and two burners) operating at its maximum output, the entire group of boiler auxiliaries was intentionally interrupted for varying periods of time, checking the speed reduction of the different drives with oscillographs and recording indications of the boiler draft gauges with a moving picture camera.

At first the automatic transfer scheme was used to provide an interruption of some 18 cycles to the boiler auxiliaries. There was no observable difference in the flame performance and the speed changes were imperceptible. Fluctuations in the induced draft, forced draft, mill pressure, and mill differential could not be distinguished from those experienced for normal operation. The power interruption period was extended on subsequent tests to as much as six seconds. Figure 3 illustrates the speed reduction and return to normal of the various drives for the different lengths of power interruption. In no case did the disturbances themselves extinguish the flame, but after some five seconds the pulverizer exhauster slowed down sufficiently that the pressure responsive safety devices operated to close the emergency dampers and thus shut down the boiler. The inertia of most of the drives carried them through the interruption. The ball mill pulverizer running at slow speed slows down rapidly and comes to a complete stop in $3^1/_2$ to 4 seconds. However, the coal carried in suspension provides the necessary carry-over and subsequent restarting of the motor and mill is rapid.

Figure 4 illustrates the ratio of the total inrush current to the total normal load current of the auxiliaries and the duration of this inrush current as a function of the length of the interruption. It is seen that this automatic transfer of the auxiliaries involves no difficulties with inrush current or voltage reduction.

Table I. Steam-Plant Auxiliaries— Two Units

Typical Motor Classification

Application	Horsepower	Revolutions Per Minute	Number of Motors
A. Essential Motors—Supplied at 2,400 Volts			
Induced-draft fan	700	900	2
Forced-draft fan	350	1,200	2
Boiler feed pump	800	3,600	3
Circulating water pump	200	400	4
Pulverizer mill	250	360	4
B. Nonessential Motors—Supplied at 2,400 Volts			
Ash jet pump	100	1,800	2
C. Essential Motors—Supplied at 480 Volts			
Pulverizer exhauster	75	1,200	4
Pulverize feeder	1	1,200	4
House-service pump	50	1,800	3
Induced-draft fan—oil coupling pump	$^3/_4$	1,200	2
Forced-draft fan—oil coupling pump	$^3/_4$	1,200	2
Combustion-control air compressor	$7^1/_2$	1,800	2
Hydrogen-vacuum pump	2	360	2
Generator-cooling pump	10	1,800	2
Hydrogen-seal oil pump	$7^1/_2$	438	2
Condensate pump	60	1,200	4
D. Nonessential Motors—Supplied at 480 Volts			
Ash-disposal pump	60	600	2
Tempering-air fans	$7^1/_2$	1,800	2
House sump pump	10	1,800	2
Cinder eliminator	20	1,200	4
Fuel-oil pump	$^3/_4$	1,200	2
Screen drive	3	1,200	2
Drip pump	1	1,800	2
Turbine turning	$7^1/_2$	1,200	2
Auxiliary oil pump	3	1,200	2
Various valve motors	$2–7^1/_2$		12
Vapor extractor	$^1/_2$	1,800	2
Evaporator pump	3	3,600	2
Ash-pit sump	2	1,800	1
House air compressor	60	1,200	1
Pure-oil pump	5	1,800	1
Oil purifier	1	1,800	1
High-level tank pump	10	3,600	1
Battery-charging motor generator set	$7^1/_2$	1,800	1
Vacuum cleaner	20	3,600	1
Elevator	25		1

Control and Switching Schemes

As shown in Figure 1, 2,300-volt motors are connected to the bus through circuit breakers which provide automatic protection against faults in the motor or circuit (and in some instances thermal protection) and also serve as motor starters. Either air or oil circuit breakers of adequate interrupting ability are used, but the trend is toward the use of air circuit breakers because of their superior performance for starting duty. Air circuit breakers also have an advantage from the standpoint of inspection and maintenance of contacts. This is of considerable importance in view of the fact that these circuit breakers are operated much more frequently than circuit breakers on distribution circuits.

For 440-volt motors the control for many of the individual motors consists of a small air circuit breaker with instantaneous trip attachment for fault protection and a magnetic contactor for starting duty. For nonessential motors standard industrial control equipment is satisfactory. For some applications, however, latched-in contactors or air circuit breakers suitable for motor-starting service are required.

In a powdered-fuel plant it is necessary for safety and operating reasons that the sequence of starting and stopping certain motors be carefully interlocked. For example, the induced-draft fan is started first. This is followed in sequence by the starting of the forced-draft fan, the exhauster, the pulverizer, and the feeder. In order to avoid clogging of the fuel-supply system and to avoid a possible explosion if any piece of equipment in the afore-mentioned group is stopped, provision is made to stop automatically all of the motors ahead of it. In the above group, if the exhauster stops for any reason, its circuit breaker or contactor is opened, and an auxiliary switch trips the pulverizer, which in turn trips the feeder. It is essential that the device which initiates the tripping sequence respond to failure of the driven quantity and not simply to undervoltage, because stoppage may be the result of a sheared pin, a broken shaft, or some cause other than failure of power supply to the motor. In the example taken, the emergency dampers are tripped by the differential-pressure relay, damped to give a slight time delay. This in turn trips the exhauster motor and the remaining motors in the sequence.

Though undervoltage protection is not required for full-voltage starting motors, the use of standard magnetic starters for 440-volt motors would provide unintentional low-voltage protection. Most of these starters will drop out at around 50 per cent of normal voltage and remain open, unless a latched-in type of auxiliary relay is used. This is not serious for automatic-start intermittent running equipment with storage capacity such as the feeder, house-service pump, combustion-control air compressor, and condensate pump, provided they are not included in any interlocking scheme. Standard starters even with latched-in auxiliary relays are not suitable for motors in an interlocked scheme, because the auxiliary switch on the contactor would start the tripping sequence of the other motors and emergency safety devices in the series. For such motors either latched-in contactors or circuit breakers suitable for starting duty are used.

Latched-in contactors or circuit breakers also are provided for highly essential motors, even though they may not be part of an interlocked sequence. This will permit utilization of all available power, even at voltages below 50 per cent of normal.

Protection of Motors and Circuits

Reasonably adequate devices of the relay type are available for the protection of 2,300-volt motors and circuits. However, for smaller 440-volt motors, it has been customary to employ devices designed for industrial use. These are usually of the thermal variety, based on extra protection to the motor, allowing for wide manufacturing tolerances in inexpensive equipment, different ambient conditions at the motor and the controller, unusual operating conditions, and so forth. This is not a suitable basis for central-station practice where conditions are materially different from the typical industrial installation. Proper co-ordination with driven equipment and mechanical protection of the motors and circuits is inherent in central-station design. Operators are able to devote more careful attention to the motors and drives, and maintenance is usually on a program basis. Conditions most likely to result in motor overloading usually will be detected through operating results.

ESSENTIAL VERSUS NONESSENTIAL MOTORS

An essential motor is classed as one which, if interrupted, would cause a serious loss of unit output within a relatively short time. Induced-draft fans, forced-draft fans, boiler feed pumps, circulating water pumps, and pulverizer mills are examples of the larger essential drives. Some of the smaller units are just as essential, such as pulverizer exhausters and condensate pumps and to a lesser extent such drives as pulverizer feeders, combustion control air compressors, and even small 3/4 horsepower motors used to pump oil into the hydraulic couplings for the forced draft and induced-draft fans. Typical nonessential motors are ash-jet pumps, cinder eliminators, fuel-oil pumps, screen drives, evaporator pumps, house air compressors, and so forth. A typical list of essential and nonessential motors is given in Table I.

TYPES OF PROTECTION

Conditions found in central-station practice, together with improved reliability of properly applied motors, have led to the use of less protection for the motors with emphasis on eliminating unnecessary interruptions. For both essential and nonessential motors, instantaneous overcurrent protection is provided which will cover the entire circuit but will be safely above locked-rotor current. For essential motors this is the only automatic protection used, but thermal devices are provided to light warning lamps, so that the operator can take necessary steps to shut down the motor after making alternate provision for its drive. In the case of nonessential motors thermal devices are provided which will disconnect the motor but at values of current somewhat higher than found in industrial practice.

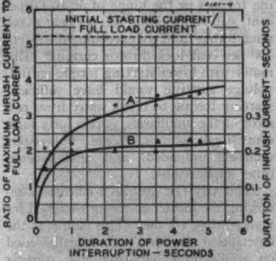

Figure 4. Effect of power interruptions on auxiliary-motor inrush current and its duration

A—Inrush current

B—Duration of inrush current

It is seldom practicable to provide positive locked-rotor protection for motors without risking unnecessary shutdown during normal starting. This is because under locked-rotor conditions, the motor does not have the inherent air cooling experienced in normal starting. Proper precautions will minimize the probability of locked-rotor conditions and alert operators usually can guard against the remaining ones.

There is a definite need for improved devices, especially for the protection of motors of the 440-volt class. Typical industrial devices are not sufficiently reliable, are subject to unsatisfactory tolerances, and are influenced by too many factors for the most reliable operation. There is also a need for a simple but positive method of locked-rotor protection.

Conclusions

1. Experience over a number of years, including that with 500,000 kw of modern 850-pound 900-degree steam plants, has demonstrated the reliability and economy (both first cost and operation) of a station power system supplied from transformers rather than from house turbines or shaft generators.

2. In the unit system of plant arrangement, it is advantageous to connect station power transformers at generator voltage, so as to provide a natural cushion against transmission-system faults. However, this is not so necessary, if faults on the transmission system are cleared with modern relay and circuit-breaker speeds and the control system is properly co-ordinated.

3. The use of intermittent-running automatic-starting constant-speed motors for certain applications and variable-speed couplings for others results in the use of line-starting squirrel-cage induction motors for practically all drives with important advantages in reliability, simplicity, flexibility, and convenience in operation.

4. Careful analysis of drive characteristics and comprehensive performance tests have resulted in the use of inexpensive control and switching equipment for the many noncritical auxiliaries, with more costly equipment limited to a few essential applications.

5. The problem of protecting motors and circuits in a central station differs from the typical industrial application, as in the former the proper co-ordination of motors with drive characteristics, maintenance on a program basis, and close surveillance by station operators of equipment and its performance eliminates many causes of motor failures. Accordingly, in central stations schemes of protection should emphasize continuity of service.

References

1. Electrically Driven Auxiliaries for Steam Power Stations, Lyle W. Smith. AIEE Transactions, volume 51, 1932, pages 337–41.

2. Progress in Power Generation—1933–39, AIEE committee on power generation. AIEE Transactions, volume 59, 1940, pages 1277–87.

3. Power Plant Auxiliaries, George C. Daniels. *Power Plant Engineering*, volume 43, September 1939, pages 615–16.

Central-Station Auxiliary-Drive Motors for Constant and Adjustable Speed

HAL GIBSON
ASSOCIATE AIEE

IN SELECTING MOTORS for central-station auxiliary drives it might be of interest to note that the range of motor sizes for any particular voltage from the standpoint of reliable operation is much wider than the range when considered from the standpoint of a distribution system and the over-all economic situation including transformers, distribution system, switchgear, and motors.

Table I indicates what would be considered good practice, for the central-station auxiliary drives, from the standpoint of *motor design only*. Completely satisfactory motors can be built, with a maximum reliability for central-station drives, through the range of horsepower indicated at the commonly accepted voltage levels used in central-station auxiliary drive systems, as indicated in the table. Motor manufacturers build motors for the various voltages over a wider range than indicated. However, the table shows roughly the essentials of what might be called good central-station auxiliary practice.

Type of Motors

The great majority of motors used in central-station auxiliary drives, in new modern power-plant practice, are the induction type, although recently in smaller power plants with the advent of adjustable-speed couplings synchronous motors have been used to some extent. The use of d-c motors, in the large modern stations, is at present practically extinct.

The induction motors which are used for central-station drives can be divided readily into three classifications, the most widely used being the normal starting-torque motor. This type of induction motor is used and recommended, for nearly all of the major auxiliary drives, such as draft fans, boiler-feed pumps, condensate pumps, most pulverizers, and service and miscellaneous pumping applications throughout the station. Usually the motor will have a locked-rotor full-voltage inrush current of approximately 600 to 700 per cent of normal full-load motor rating. This design is commensurate with high efficiency, and power factor, adequate starting, and maximum torque. It is well suited for accelerating loads involving high inertias, which frequently arise in central-station practice on the induced-draft fans whose wheels are built very heavy to resist erosion. With the values of inrush current indicated, and with normal WK^2 or inertias, this motor usually is built with a starting torque in the range of 100 to 125 per cent. However, in the case requiring the motor to accelerate exceedingly high WK^2 requiring long accelerating periods, these motors may be designed with lower starting torques in the range of 50 to 60 per cent, still maintaining 200 per cent maximum torque, and not exceeding the 600 to 700 per cent locked-rotor current. This motor with lower starting torque on full-voltage starting would have sufficient starting torque to break away from rest most of the auxiliaries, particularly fans, centrifugal pumps, some pulverizers (starting unloaded) and miscellaneous other applications.

Relatively few are the applications requiring the induction motor designed for high starting torque. This motor, as the description implies, is normally used on applications requiring high starting torque, such as compressors starting loaded, or on some types of pulverizers, such as a ball-bearing type, which requires a very high starting torque, owing to the large bearings and massive construction. Other applications might be small air compressors, used for station service. It might be well to point out that the high-starting-torque motor should be checked carefully for high-inertia drives before being used, inasmuch as it might have very low-heat storage capacity in the rotor, which might make it unsatisfactory for this type of drive. High starting torque is sometimes confused with the ability to accelerate the inertia rapidly, reducing the starting time, and thus not requiring a motor which could accelerate the high inertia over a long accelerating period. The high-starting-torque induction motor could be used on some types of stoker drives which also require high starting torque but have low effective inertia.

The wound-rotor induction motor is used for adjustable-speed drives and constant or adjustable drives with especially difficult starting duties, which might require the starting of inertia beyond the ability of the normal-starting-torque induction motor, or loads which require a high starting torque beyond the ability of high-starting-torque induction motor.

The usual application of the wound-rotor motor, in central-station auxiliary drives, is for adjustable-speed drives on draft fans and boiler-feed pumps.

As previously indicated, synchronous motors are not used very extensively, with the exception of the drive for large low-speed air compressors, requiring compressor-shaft-mounted motors, wherein the low-speed synchronous motor, without base, bearing, or shaft, becomes the most economical drive for the machine. Synchronous motors have been used on a few occasions for driving special types of pulverizers, and at other times for driving large low-speed constant-speed condensate pumps In recent years, the most frequent application of synchronous motors has been found in the smaller power plants, for driving draft fans through variable-speed couplings of either the hydraulic or the electric type.

Usually, the small advantages, such as better power factor and possibly better efficiency, would not offset the disadvantages of increased costs and more complicated control.

In the future, with the increased size and pressure of central stations, larger and higher-speed boiler-feed pumps may come into use. If such is the case, the large two-pole synchronous motor, similar

Figure 1. Drip-proof sleeve-bearing normal - starting - torque squirrel-cage induction motor coupled to forced-draft [redacted] fan

---

Paper 45-153, recommended by the AIEE committee on power generation for publication in AIEE Transactions. Manuscript submitted June 1, 1945; made available for printing July 30, 1945.

Hal Gibson is in the industrial engineering division of General Electric Company, Schenectady, N. Y.

Figure 2. Splashproof sleeve-bearing normal-starting-torque squirrel-cage induction motor coupled to centrifugal circulating-water pump at end of steam condenser

Figure 3 (below). Base-ventilated high-speed sleeve-bearing induction motor

Longitudinal semisection showing typical construction

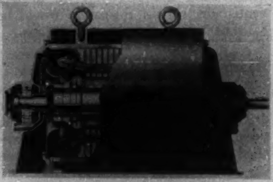

in construction to the turbine generator, may find application in central stations in the range of 2,000 horsepower and above. In this range and at 3,600 rpm, synchronous motors are less expensive than the induction motors of similar size and speed and should be equal in reliability at least to wound-rotor motors.

All the motors mentioned, both of the induction and synchronous types, are suitable for full-voltage starting. The inrush currents drawn, during the starting period are not excessive, particularly in view of the closeness of the motors to the source of generated power. The motor is satisfactory for withstanding the higher electric and mechanical shocks which occur on full-voltage starting even if they are repeated frequently. The motor shafts are liberally designed to have low tensile stress. The end turns are strongly supported by means of steel supporting rings, tie blocks, and binding. By this method the end turns are prevented from chafing and bending, which could cause mechanical failure of the insulation. Similarly by the proper use of insulation and slot wedges, the coils are prevented from making large movements in the slots, which might eventually cause failure owing to stresses encountered under starting conditions

Modern central-station auxiliary practice is to use full-voltage starting in nearly 100 per cent of the cases.

High-Speed Motors and Gears

For high-speed drives, particularly above 1,800 rpm, lower-speed motors with speed-increasing gears are occasionally used.

This is sometimes an economical solution to the question of what type of motor to use for high-speed drives, since a two-pole motor of the synchronous, induction, or wound-rotor type is more expensive than a lower-speed motor at its highest speed. It may be found that the two-pole motor costs about 50 per cent more in smaller sizes encountered in a central-station auxiliary drive and up to 100 per cent more in the larger sizes. In some cases, it is possible to purchase a gear for less than the difference between the cost of the two-pole motor and the most economical speed motor.

A drive consisting of a motor and a gear is entirely reliable, particularly for application to fans and pumps of the centrifugal type, which do not have any pulsating or reverse-torque loads, and which are infrequently started. If a high-precision-type gear is used under the foregoing circumstances, long life and high reliability usually result. The high-precision-type gear is mentioned in contrast to the usual industrial-type gear so frequently found in many industrial applications where reliability is not so important as in a central-station auxiliary drive. High-precision-type gears are the type used by the United States Navy for marine-propulsion applications.

Enclosures

For most of the applications encountered in a modern clean central station, it has been found that the dripproof motor, so constructed or protected that its successful operation is not interfered with when it is subjected to falling moisture or dirt, is entirely satisfactory and reliable. This is especially true for the auxiliaries, such as the draft fan, boiler-feed pumps, pulverizers, and most service and miscellaneous drives. Such a motor is illustrated in Figure 1 which shows a dripproof (open) motor, driving a forced-draft fan. This motor is protected against falling water. The dripproof construction also shields against accidental contacts with windings or rotating parts, and thus the motor is protected against accidental damage. This type of motor is furnished with split-sleeve-bearing end shields on both ends from 125 to 2,000 horsepower at 1,800 rpm. This construction greatly facilitates the maintenance of the motor by making it very easy to inspect or to change a bearing without removing the motor rotor from the stator, or without the necessity of pressing off the motor half of the coupling.

Other types of motors, such as splashproof, totally enclosed fan-cooled, base-ventilated, and totally enclosed motors with surface air coolers should be used if the ambient conditions justify the additional expense.

For application to auxiliaries, subject to continually splashing water (such as those which might be located in the lower part of the station), or in the case of auxiliaries located where it is necessary quite frequently to hose down the surrounding area, splashproof motors should be used instead of dripproof. A splashproof motor is shown in Figure 2 driving a circulating pump, and it can be seen that the major difference between it and the dripproof motor, is a different type of end shield, which is more protected from splashing water than is the dripproof motor.

Totally enclosed fan-cooled motors are not frequently used for central-station auxiliary drives, with the possible exception of motors used for coal-handling equipment. A motor of the open type exposed to coal dust will require frequent cleaning in order to prevent the coal dust from blocking the ventilating paths in and around the windings. Obviously, if these paths become blocked, the motor will overheat and eventually fail.

Similarly, where particularly dirty conditions are encountered, requiring too frequent cleaning of an open or dripproof motor (and in sizes too large for totally enclosed fan-cooled motors), base-ventilated motors, as shown in Figure 3, may be used if access is available to clean air below the motor. If not, a forced-ventilated motor, by means of duct work from a clean area, may be used; or in some cases totally enclosed motors with surface air coolers may justify the additional expense, particularly if the heat picked up in the motor can be returned to the system heat balance.

It is well to bear in mind that any large high-speed motor, particularly a 3,600-rpm, probably will have a long stator and rotor stacking. Where such motors are required, it is necessary to consider the additional cost of totally enclosed forced-ventilated motors, or totally enclosed motors with surface air coolers, as well as the fact that the ventilating passages are more numerous and more difficult to clean than is the case when lower-speed large motors are used, which are more open, and consequently have ventilating passages more easy to clean. However, the probable longer life of the totally enclosed motor may offset its higher costs.

Explosion-proof motors seldom are required, as hazardous atmospheric conditions are not present in most stations. The possible exception is a coal-dust condition which might require a totally enclosed "dust- and explosion-proof" class-II group-*F* motor.

Insulation

In general, for central-station auxiliary drives, class-*A* motors, rated 40 degrees centigrade rise have given satisfactory service. For low voltages, 440 volts or below, motors are given an extra insulation treatment for boiler-room applications. For voltages 2,300 volts and above, the high-voltage insulation is usually adequate.

Ambient temperatures should be checked to determine if the temperature will be above the standard of 40 degrees centigrade. In some cases, even in new well-ventilated central stations, the ambient may exceed 40 degrees centigrade; for example, in case the motors driving the fans are installed directly over boilers, the ambient might reach 125 degrees Fahrenheit or over 50 degrees centigrade. In case dripproof motors are to be recommended or used, class-*A* insulation would not be satisfactory for the normal rated motor. In this case, a larger motor with lower resulting temperature rise could be used with class-*A* insulation, as long as the maximum total temperature did not exceed 90 degrees centigrade; or a motor of normal rating corresponding to the load requirements, could be used with class-*B* insulation, which would allow a higher rise with the maximum total temperature not exceeding 110 degrees centigrade.

Before one concludes that a larger-size motor, or a motor with class-*B* insulation is required, the ambient temperature should be weighted over the entire operating year.

Of course, if for other reasons, it is necessary to use forced ventilation or motors with surface air coolers, such that the air entering the motor is held at a temperature not exceeding 40 degrees centigrade, class-*A* insulation would be satisfactory even for these conditions.

Bearings

The great majority of motors used for driving central-station auxiliaries are the sleeve-bearing type. When properly applied and serviced, sleeve bearings have an excellent operating record and are highly reliable. They are available in motors ranging from the maximum to the minimum horsepower requirements. Rolling-contact bearings, on the other hand, are available only in a limited range of sizes and speeds.

Figure 4 shows cross sections of large high-speed pedestal bearings, used on high-speed motors driving boiler-feed pumps. This particular drawing is for a forced-feed lubricated bearing, and it will be noted that two oil rings are provided to lubricate the bearing initially when it is being started up, before the oil pump begins to deliver oil (in case the oil pump is directly connected to the motor shaft), and also to give some lubrication in case of forced-feed-system failure. The bearing is of the spherical type, and the double metal baffles of the labyrinth-type construction which prevent leakage of oil vapor along the motor shaft, can be seen. Sleeve bearings for lower-speed motors of the end-shield type of construction are similar to these, except that they are not of the spherical type and are not forced-lubricated. Spiral oil grooving, in the lower half of the bearing, is used instead of the rectangular oil grooves shown in Figure 4.

The oil deflectors machined in the shaft as noted in the axial cross section also serve to take a small amount of thrust for intermittent conditions. It will be noted that the babbitt or bearing material is "turned up" on the ends to furnish a rubbing surface for the small thrust collars. It is well to bear in mind that these thrust collars are for intermittent loading only, and have a very small thrust capacity, somewhere in the range of 200 to 300 pounds, for the larger motors. This point is often overlooked,

Figure 4. Sleeve bearing and pedestal for high-speed polyphase induction motor

Two vertical sections along and across shaft

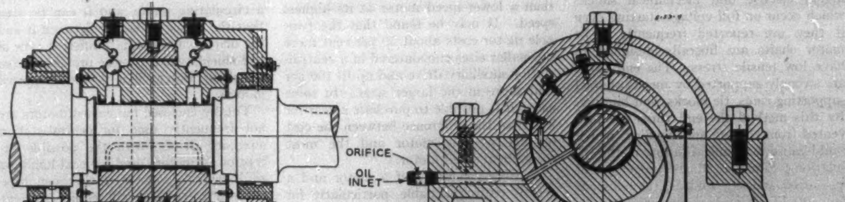

particularly in applying couplings between the motor and the driven auxiliaries. As is known, nearly all types of couplings, even the so-called "gear" type, can and do transmit thrust under certain conditions of loading. Quite frequently the thrust which can be transmitted by the coupling, or which actually may be generated in the coupling, because of the transmission of torque, will exceed the allowable thrust capacity of the thrust collars. Another misconception often associated with this same problem is the amount of axial magnetic pull developed by the motor under normal full-voltage operating conditions. Obviously, when the motor is moved off the magnetic center an axial force is generated which tends to bring the motor rotor back to the magnetic center. However, this force is zero when the rotor is on magnetic center, and it increases as the rotor is displaced from magnetic center to some maximum value. For practical purposes, the maximum value which will be produced is very small, usually not exceeding 200 or 300 pounds, even on large induction motors. This maximum value often will occur at a displacement which may be of little use in preventing the wiping of a thrust collar when the motor is subjected to axial thrust.

Motors with rolling-contact bearings are available at 250 horsepower at 3,600 rpm and 400 horsepower at 1,800 rpm. Certain applications will require the motor to carry a high axial thrust, which necessitates the use of a rolling-contact bearing. Such an application might be a vertical pump motor in smaller sizes.

In general the use of sleeve-bearing motors is recommended for central-station auxiliary drives where thrust is not involved.

Adjustable-Speed Drives

For adjustable-speed drives for auxiliaries, there are available multispeed motors, wound-rotor induction motors with secondary control, constant-speed motors with adjustable-speed hydraulic or magnetic couplings, brush-shifting a-c motors, and d-c motors, utilizing adjustable variable-voltage Ward Leonard control, or adjustable variable voltage by electronic means.

At the present time, the wound-rotor motor with secondary control is by far the most widely used of any of the types of drives previously mentioned. In particular, the wound-rotor motor has been applied to the boiler-feed pumps and the draft fans.

Table I. Range of Horsepower for Motors at Commonly Accepted Voltage Levels Used in Central-Station Auxiliary-Drive Systems

Volts	Motor Rating (Horsepower)
220	Minimum requirements to 500
440	1/3 to 1,000
2,300	100 at 60 cycles, and up
4,000	250 at 60 cycles, and up

When boiler feed pumps are driven by wound-rotor motors, they are usually arranged for a nominal speed reduction of 20 to 30 per cent. This relatively small speed reduction is satisfactory to give the necessary control of feed water over a wide range of load conditions. When the boiler-feed-pump system involves one constant-speed and one adjustable-speed pump, the required adjustable speed range may be greater than indicated.

For draft fans, when driven by wound-rotor motors, the speed reduction usually has not exceeded 50 per cent of rated speed. Where wider speed ranges are required, wound-rotor motors can be furnished for speed ranges of at least 5 to 1.

It is believed, based on experience and observation, that the wound-rotor motor with secondary control is as stable and as reliable as any other type of adjustable-speed drive, and much more reliable than some of the available types. There is only one piece of rotating equipment required, and it is of standard construction, with no particular mechanical difficulties to overcome. The controlling equipment is of the nonrotating type and highly reliable.

Secondary control of either the metallic-resistor secondary and multipoint switch or the liquid regulator with an infinite number of steps can be furnished. Recent developments have reduced the size and increased the speed of liquid rheostats.

For motors of all sizes up to 1,000 amperes at 1,000 volts 20-point cam switches are available for secondary control. For motors 500 horsepower and below, secondary-speed-control switches up to 40 or 50 points can be furnished.

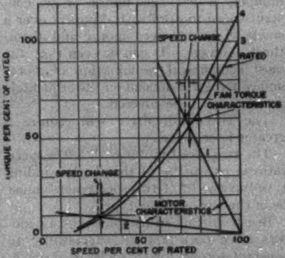

Figure 5. Speed regulation of wound-rotor induction motor driving a draft fan with change in fan load

1—Motor-torque characteristic, 75 per cent speed

2—Motor-torque characteristic, 30 per cent speed

3—Fan-torque characteristic, rated load

4—Fan-torque characteristic, 13.5 per cent overload

There has been some misconception in the past in regard to the stability of a wound-rotor motor, particularly at speeds below 50 per cent of rated speed, when it is operating with a fan or pump, whose torque curve decreases as the square of the speed. The wound-rotor motor is inherently stable, if by the definition of stability is meant that there is no tendency for hunting in the motor-torque characteristic, or there is no tendency for hunting when both the motor-torque characteristic and the torque characteristic of the load are considered. The wound-rotor induction motor has positive damping characteristics at low speed, as well as at high speed. It is true that the magnitude of this positive damping is lower at the low speeds, or, in other words, the drive inherently has more speed regulation at low speed than it does at high speed. This should not be confused with stability. Therefore, if the load torque does not change, there will be little or no cause for change of system speeds.

Table II was prepared to show the resultant system speed change, in per cent of running speed, which might be caused by certain changing conditions in the system of a draft fan. The conditions considered are:

1. A voltage change.
2. An arbitrary positive increment in fan-torque characteristic (the increment being equal at all speeds).
3. A change in the duct system resistance, such as change in the position of the dampers.
4. A change in the temperature of the flue gas.
5. Changes in secondary-resistor temperature.

For each of the conditions listed, two values of secondary ohms are shown, one value for approximately 75 per cent speed and the other for a 25 to 30 per cent speed, based on a fan or centrifugal-pump curve, with the torque varying as the square of the speed, and the load being equal to full load at rated speed. Also indicated is the change in fan- and motor-torque characteristics and the resultant change in system speed.

Figure 5 shows two fan-torque and two motor-torque characteristic curves. To analyze how Table II was derived, consider the intersection of curve 1 and curve 3. Curve 1 is the motor-torque characteristic curve with sufficient secondary resistance to result in 75 per cent of rated speed with the rated fan-torque characteristic. Similarly the intersection of curves 2 and 3 indicates that the motor operating with a value of secondary resistance results in a speed of 30 per cent with the rated fan-torque characteristic.

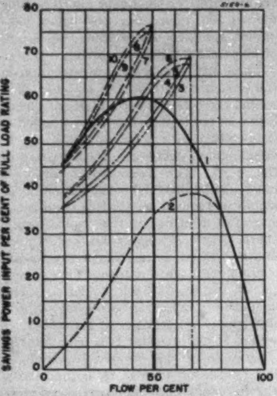

Figure 6. Input power savings of various types of driving motors and air-flow control over a constant-speed motor and throttling dampers

1—Wound-rotor motor
2—Constant-speed motor, inlet vanes
3—Two-speed motor, throttling dampers
4—Two motors, throttling dampers
5—Two-speed motor, inlet vanes
6—Two motors, inlet vanes
Curves 7, 8, 9, 10 are same as 3, 4, 5, 6, except that low speed is one half of rated speed instead of two thirds of rated speed

If the dampers are opened the fan-torque characteristic will be raised as shown by curve 4. If the same two values of secondary resistance are considered, the change in speed is evaluated from the intersection of curves 1 and 2 with curve 4, and this change in speed is expressed as a percentage of the speed resulting from the curves 1, 2, and 3, the values of the last column in the table will be found.

As will be noted, Figure 5 is for condition 3 for a 25-per-cent change in system resistance.

In all cases, the change in system speed is not considered a detriment. In the case of the 25-per-cent rise in stack temperature, the resultant speed increase will tend to offset some necessary manual or automatic speed change to compensate for the reduced weight flow, which will result at constant speed, but will increase gas temperature. For a fixed firing rate, the flow by weight probably should be held constant, even if changes do occur in the temperature of the stack gases entering the induced-draft fan owing to changes in position of superheater by-pass dampers, and so on.

Table II. Resultant System Speed Change Which Might Be Caused by Certain Changing Conditions in System of a Draft Fan

Changed Condition	Secondary Ohms for	Torque Characteristic Change, Per Cent		System Speed Change, Per Cent of Running Speed
		Fan	Motor	
−5 per cent voltage	30 per cent speed	None	—10	—6
	75 per cent speed	None	—10	—1
Constant torque increase (drag)	30 per cent speed	+5	None	—2
	75 per cent speed	+5	None	—1.0
25 per cent system resistance	30 per cent speed	+13.5	None	—5.5
	75 per cent speed	+13.5	None	—2
25 per cent rise, stack temperature at 300 degrees Fahrenheit	30 per cent speed	—9	None	+3.6
	75 per cent speed	—9	None	+2.6
25 per cent rise, stack temperature at 500 degrees Fahrenheit	30 per cent speed	—13	None	+5.7
	75 per cent speed	—13	None	+3
200 degrees rise, secondary resistance	30 per cent speed	None	—1 to —2	—0.5 to —1.5
	75 per cent speed	None	—5	—0.5 to —1.5

Multispeed variable-torque motors are sometimes used for driving draft fans. In other cases two separate motors of suitable rating are used, one for maximum speed, the other for some reduced speed. The choice between a two-speed motor and two motors should be made on the basis of reliability, operating cost, first cost, and space requirements.

In the larger sizes, if one considers switchgear or control as well as the motors, first cost is about equal with the two motors showing a little lower first cost, especially if the two-speed motor is of the two-winding type, and the smaller of the two motors (considering the two-motor drive) is small enough to operate on low voltage while the larger must operate on the 2,300-volt or higher bus.

The separate two-motor drive might be considered to be more reliable, as the failure of one bearing or one winding would still allow the other motor to operate with damper control.

Figure 6 indicates approximate values of power savings using an adjustable varying-speed wound-rotor motor and no dampers, a two-speed motor, or two constant-speed motors with dampers over a single constant-speed motor and throttling dampers. It can be seen that the most economical combination of motor and control will depend on the adjustable speed range to be covered.

The two-motor drive will require a greater floor space.

The two-speed motor with a 2/1 speed ratio is or can be of the single winding type but the 1.5/1 two-speed motor must be of the two-winding type.

Brush-shifting adjustable-speed a-c motors have been applied successfully to constant-torque loads, such as positive-displacement fuel-oil pumps in oil-fired stations.

About the only place that an adjustable-voltage d-c drive is used in central stations at present is in the handling of the coal, such as in coal towers or skip hoists. The flexibility of the adjustable-voltage d-c control and the high accelerating torque of the d-c motors will provide more capacity per horsepower of motor in a coal tower than can be obtained with wound-rotor motor drive. This type of system results in low coal-handling-equipment maintenance, owing to the smooth accelerating and decelerating characteristics of the adjustable-voltage d-c drive, which eliminates all sudden increments of torque and consequently is much easier on the mechanical parts of the coal-handling system.

An adjustable-voltage d-c system can be designed in the case of coal-hoisting equipment, for future increase in coal tonnage, by increasing the hoisting speed.

Also, some figures are available to indicate that the adjustable-voltage d-c system takes less power from the distribution system than would an adjustable-speed a-c drive.

Recently some demand has been shown by manufacturers of both pulverizers and operating companies for an adjustable-voltage d-c drive for coal feeders, to operate from an adjustable-voltage system. Such a system takes power from three-phase or single-phase a-c power supply and rectifies the alternating current to direct current, and also of controlling the voltage by means of grid control on the thyratron rectifiers.

Such coal feeders probably would be associated with pulverizers which have little or no storage capacity in the pulverizers themselves, but which pulverize the coal at a rate depending upon the rate of feeding coal into the pulverizers.

Similarly, the same type of adjustable-voltage d-c drive has been quoted for small stokers to operate in conjunction with combustion systems.

Such applications have not been made in central stations in sufficient number and for a sufficient length of time to give any comments in regard to the success and maintenance record of such drives, although the record is excellent in other industries.

Automatic Regulation of Turbine Generators to Relieve Power-Supply Systems of Steel-Mill Load Swings

W. W. EBERHARDT
MEMBER AIEE

C. W. HARRISON
NONMEMBER AIEE

E. J. KOHN
NONMEMBER AIEE

A. G. DARLING
MEMBER AIEE

Synopsis: Certain steel-mill loads are fast, cyclic, and of considerable magnitude. Given a set of conditions involving such a load, a relatively small steel mill, speed-controlled generating capacity all connected to a large power-supply system, much of the swings in the steel-mill load will be taken by the large supply system. Of itself, this result may not assume special importance. When transmissions in the large power-supply system, well-loaded under steady-state conditions, are involved, and speed governing of the system is at the remote end of the transmissions, the cyclic loads tend to reappear in the transmissions. These circuits may, according to their finite transmitting abilities and the swing peaks imposed on them, be unable to carry the peaks without undesirable voltage depressions or cause undesirable frequency variations on the system. Generation of power from by-product fuels in a steel mill is generally economical but is dependent on the continuity and quality of the nonstorable fuel as well as on the steaming and generating capacity installed. Relief to a large power-supply system from the cyclic load swings normally carried by that supply system has been made possible by a new static load control and hydraulic servomotor to cause the steel-mill turbine generators to respond to the regulator. The combination has been applied successfully to two 20,000-kw turbine generators, causing one or both to take a base load, a percentage of the variable load, and to modify their total loads according to available steam pressure. The turbine-generator response can be as high as 5,000 kw per second on each unit. High-speed charts show the loads on the various circuits with and without the load control in operation.

The Basic Problem as Seen From the Standpoint of Power Systems Interconnected by Circuits of Finite Transmitting Capacities[*]

SUPPLYING POWER to large hot-strip continuous-rolling mills such as are now used so extensively in steel mills to produce wide thin-gauge metal strip has presented a new problem to the electric-power industry. The power drawn by a large continuous hot reduction mill is characteristically cyclic and, starting with the introduction of the slab, may build up to 25,000 kw in a period of ten seconds, stay nearly constant at peak value for a period of 40 to 60 seconds during the sojourn of the metal in all of the rolls, and then fall off to nearly zero in another ten-second period as the strip moves out of the rolls. This is followed by an idle period approximately equal to the rolling period while the succeeding slab is being oriented. The cycle then repeats itself, usually at the rate of 25 or more times per hour, depending on the size of the slabs.

A heavy cycling load of this kind, if not absorbed before it gets into the connected utility system, will produce: (1) wide frequency variations on an isolated system or (2) wide load swings on the tie lines of interconnected utility systems.

This problem is exemplified by the effect on the system of the Alabama Power Company of a 48-inch six-stand continuous hot-strip mill operated by the Tennessee Coal, Iron, and Railroad Company at their Fairfield plant near Birmingham, Ala. The steel company purchases power from the Alabama Power Company to supply its load requirements over and above the output of its own steam-generating plants which are fired principally with blast-furnace gas. As the availability of blast-furnace gas bears little relationship to the variable power-load requirements of the steel mill, the power taken from the Alabama Power Company system, consequently, is extremely variable. The cyclic nature of this load as recorded on the high-voltage side of the 70,000-kva 110/44/6.6-kv supply bank with the strip mill in operation is shown in Figure 1. It will be noted from this load chart that, when the hot-strip mill is shut down, the balance of the steel-mill load is comparatively free of rapid cyclic load swings, indicating that the loads of the other steel-mill production processes are not only well diversified, but also of smaller magnitude and less violent than the hot-strip-mill load cycle.

If the Alabama Power Company system were operated isolated from other utility systems, the effect of these load swings would be to produce wide frequency variations, probably of the order of plus or minus two tenths of a cycle, and the control problem would be primarily one of frequency control, as no tie lines would be involved. Isolated operation, however, is distinctly an abnormal condition, because the economics of interconnected operation between power systems, achieved through the minimization of generating reserves, the utilization of load diversity, and the interchange of economy energy between systems, long ago dictated the closure of tie lines as a normal operating condition between neighboring power companies in the Southeast and adjacent areas. As interconnections are extended between utility systems, thereby bringing more rotating equipment into parallel operation, the system flywheel effect is increased, and frequency variations from load changes become less pronounced, but wide load swings appear on the interconnecting tie lines, and the control problem then becomes predominately one of tie-line load control on the local systems. This is demonstrated very clearly in Figure 2 where frequency and tie-line loading are shown for both isolated and interconnected operation under identical load conditions.

As the Alabama Power Company's load-control problem is affected by the extent of its interconnections with other systems, a brief description of these interconnections will be in order. The Alabama Power Company together with the Georgia Power Company, South Carolina Power Company, Mississippi Power Company, and Gulf Power Company constitute the completely integrated Southern Group of systems of the Commonwealth and Southern Corporation, having a combined diversified peak load in excess of 1,250,000 kw, of which over 40 per cent is in Alabama. This Commonwealth and Southern composite system is normally interconnected through several ties with power systems in Florida on the South, and through three tie lines with the system of the Tennessee Valley Authority on the North. The Tennessee Valley Authority system, in turn, is normally tied in at Memphis, Tenn., with the interconnected group of power systems in the Southwest, and with the interconnected power systems in the northcentral area at Louisville, Ky.

This combined group of power systems, located in 24 states, normally is operated interconnected and has an estimated peak load of approximately 16,000,000 kw, not including the loads of large industries

---

[*] Prepared by W. W. Eberhardt.

Paper 45-113, recommended by the AIEE committees on automatic stations and power generation for publication in AIEE TRANSACTIONS. Manuscript submitted April 11, 1945; made available for printing May 14, 1945.

W. W. EBERHARDT is supervisor of system operations, Alabama Power Company, Birmingham, Ala. C. W. HARRISON and E. J. KOHN are both with the Tennessee Coal, Iron, and Railroad Company, Mr. Harrison as chief electrical engineer at Fairfield, Ala., and Mr. Kohn as chief of the bureau of steam engineering at Ensley, Ala. A. G. DARLING is application engineer, industrial engineering division, General Electric Company, Schenectady, N. Y.

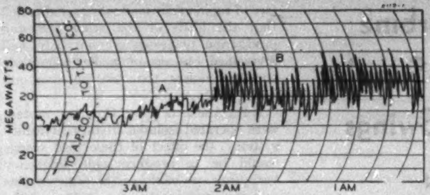

Figure 1 (above). Typical wattmeter chart of power supply to Tennessee Coal, Iron, and Railroad Company by Alabama Power Company

A—Hot-strip mill shut down
B—Hot-strip mill in operation

Figure 2 (right). Alabama Power Company system frequency chart and Commonwealth and Southern–Tennessee Valley Authority tie-line wattmeter chart for open and closed operation of tie line

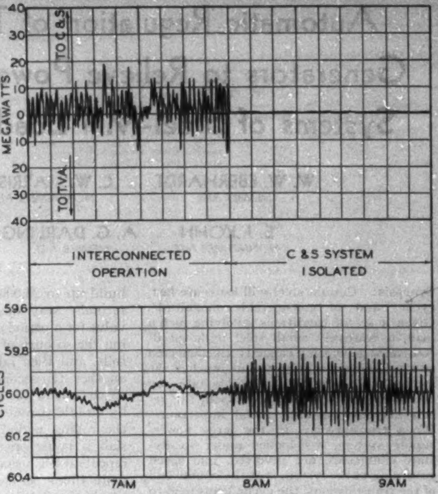

carried on their own plants operating in parallel with the public utilities. While the torque-versus-frequency characteristics of this system as a whole have not been determined, a fairly close estimate can be made from tests and observations taken on the major portion of the system. In 1937 a series of tests was carried out on the portion of the interconnected system east of the Mississippi River extending from the Great Lakes to the Gulf of Mexico, during which speed was quickly varied 0.1 to 0.2 cycle by the regulating plant with all generator and tie-line regulating devices out of service, and the change in kilowatt output noted. For either increases or decreases, the change in kilowatt output was about one per cent per one-tenth-cycle variation in frequency. Different results may be obtained as the interconnection is extended and may vary over a period of years, if the ratio of motor load to noninductive load changes. The reason for this is that a noninductive lighting or heating load does not vary with frequency, provided constant voltage is maintained, whereas a motor load does. The load on the interconnected system has grown considerably during the past eight years and especially so during the last four years with the addition of war industries with heavy motor loads. It reasonably may be assumed, therefore, that the load variation per one-tenth cycle of frequency variation still represents a change of at least one per cent, if not more.

On the basis of the one-per-cent figure, a 25,000-kw load swing in the 16,000,000-kw system total load would vary the frequency 0.0156 cycle. This variation hardly would be noticeable on the interconnected-system frequency, as it would not ordinarily be outside of the normal-frequency band width. Variations in loading of the close-in tie lines, due to such a load swing, however, are very pronounced and have created a difficult regulating problem when the swing is more rapid than the response time of the tie-line regulator.

When interconnections first were made about 15 years ago, joint regulation of frequency was attempted, but the results were unsatisfactory, because of tie-line tripouts due to overloads. This was due to the fact that load swings were shared in the various areas regardless of where the swings originated. The resultant load transfers over the tie lines were such that no definite value of tie-line loading, in the form of either load or capacity, could be scheduled and maintained. Based on experience and operating results over the years, it has become the accepted practice normally to assign the frequency regulation to a selected plant or system located near the interconnected load center and require all other systems normally to hold their tie-line loads on predetermined schedules towards that area. The frequency-regulating plant and the various tie-line-regulating plants complement each other in that close frequency regulation makes possible equally close adherence to tie-line schedules, and, conversely, if all tie lines are held on schedule, each system, by necessity, has to absorb its own load swings and thereby assist the frequency-regulating plant to the fullest extent in the control of frequency. In addition to assisting the frequency regulation, close tie-line regulation is also essential in obtaining maximum tie-line loading without risk of tripouts due to overload swings when large blocks of energy are being moved. This is a very important consideration, because tie lines, by necessity, are of finite transmitting capacity, depending on the economic considerations involved in the interconnection, and usually have a capacity rating less than ten per cent of the generating capacity of either of the participating systems.

Since the frequency regulation for the interconnected system ordinarily is assumed by plants in the northcentral area, the regulating problem of the Commonwealth and Southern group, therefore, becomes that of regulating the tie lines between it and the system immediately on the north, which is the system of the Tennessee Valley Authority.

The load south of the Commonwealth and Southern–TVA tie lines is approximately 1,600,000 kw including the Florida system, or approximately ten per cent of the whole interconnected-system load. On this basis 90 per cent of any instantaneous unbalance between load and generation in the Southeast is reflected north through the Commonwealth and Southern–TVA tie lines and ten per cent of any unbalance in northern and southwest areas is reflected south through the same ties. This apportionment of load swings applies only before governors and load controllers have had time to function. It is evident, therefore, that 90 per cent of rapid load swings in the Southeast, such as the type caused by continuous strip-mill operation, which are faster than the response time of tie-line regulators, will be reflected through the ties unless the tie-line load controller is nearly instantaneous in action.

Fast tie-line regulation is only possible in the ideal case where only a single tie

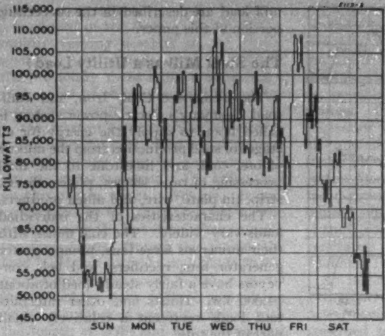

Figure 3. Typical hourly power demands of the Tennessee Company

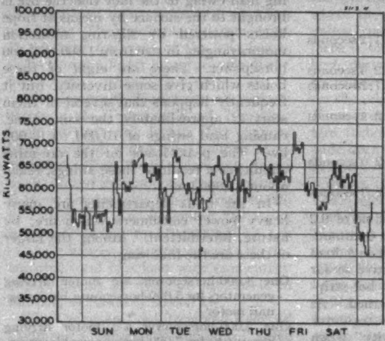

Figure 4. Typical hourly generation of electric power by the Tennessee Coal, Iron, and Railroad Company

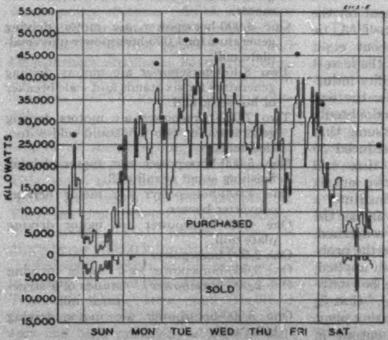

Figure 5. Typical unregulated hourly demands of the Tennessee Coal, Iron, and Railroad Company upon the Alabama Power Company (circles indicate maximum 15-minute daily demands)

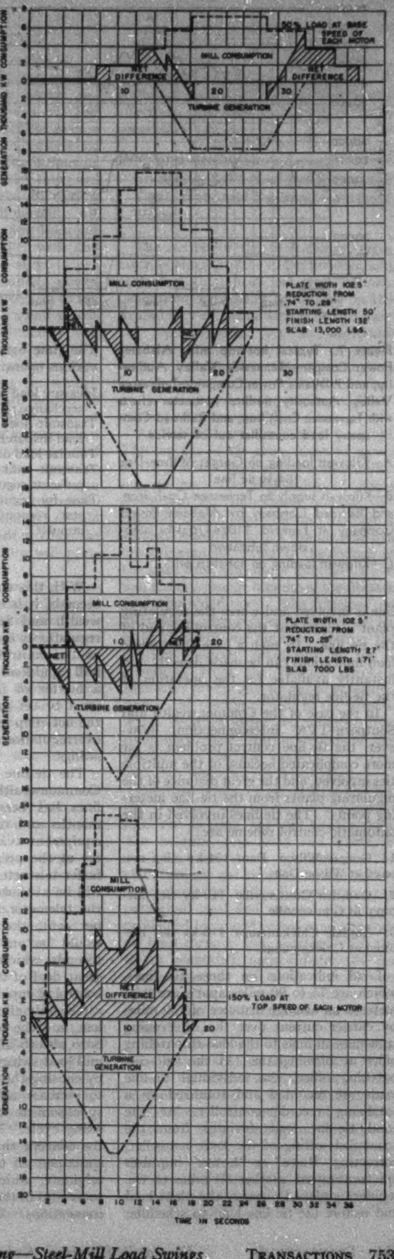

Figure 6 (right). Probable effect of an "anticipator" operating a conventional synchronizing motor of a turbine generator having a response of 2,000 kw per second (time lags in relaying neglected)

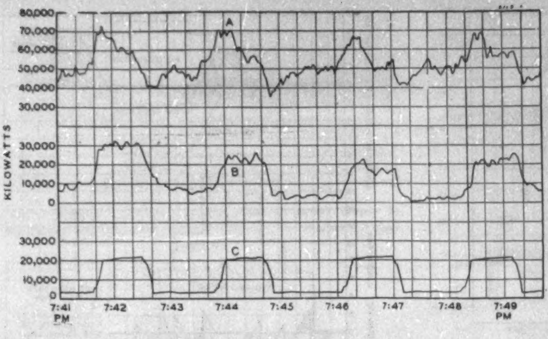

Figure 7. Typical hot-strip mill, Alabama Power Company–Tennessee Valley Authority, and Alabama Power Company–Tennessee Valley Authority tie-line wattmeter charts with Tennessee Coal, Iron, and Railroad Company load controller out of service

A—Kilowatt loading on Gorgas–Wilson Dam 154-kv tie line

B—Kilowatt supply to Tennessee Coal, Iron, and Railroad Company by Alabama Power Company at Fairfield 110/44/6.6-kv step-down substation

C—Kilowatt loading on hot-strip mill

line is involved and where the regulating plant is located at the controlling end of the tie line. In such a case the tie-line load indications can be made directly and instantly available for the operation of the tie-line regulator.

In the case of the Commonwealth and Southern–TVA interconnection, however, the tie-line control problem is far more complicated because of the multiple ties involved, and the great distance of the regulating plants from the tie-line metering points. The tie lines involved in the automatic-control scheme are:

1. Gorgas–Wilson Dam 154-kv tie, metered at Wilson Dam.
2. Gadsden–Guntersville 110-kv tie, metered at Guntersville.
3. Lindale–Chickamauga 110-kv tie, metered at Chickamauga.

Load indications on these tie lines, which are 75 to 90 miles apart, are telemetered an average distance of 150 miles by carrier current over the intervening transmission lines to the load-dispatching office at Birmingham. At the load-dispatching office, the individual tie-line loads are recorded and totalized on a totalizing recorder–controller. As the total tie-line load deviates from the scheduled setting of the load controller, correcting "Raise" or "Lower" impulses are transmitted another 80 miles to the regulating plant to change the plant load and restore the tie-line load to schedule. The time consumed in completing these various operations is as follows:

Measure load on tie line at interchange point	1.2 seconds
Transmit load indication to load-dispatching office	2.4 seconds
Totalize load on three tie lines	1.2 seconds
Transmit load correcting impulses to regulating plant	2.4 seconds
Time for regulating plant to start responding to control impulse	2.0 seconds
	9.2 seconds

With this over-all response time of 9.2 seconds, it is obvious that the Commonwealth and Southern–TVA tie-line load regulator is completely ineffective so far as the control of continuous hot-strip-mill rapid load swings are concerned. As a matter of fact, the tie-line regulator must be set on "Low sensitivity" when the hot-strip mill is in operation to avoid overregulation or magnification of load swings.

The tie-line control equipment on the Commonwealth and Southern–TVA tie lines has been in service about eight months and represents about the fastest equipment available to the utility industry at the present time. After the war faster telemetering schemes undoubtedly will be available, but, if we assume that the telemeter time could be reduced 50 per cent, the total response time still would be on the order of five or six seconds which would not constitute a great deal of improvement so far as the control of rapid load swings is concerned.

The only effective solution to the problem, and the one that has been applied, is to absorb all or part of the hot-strip-mill load swings at their source: that is, by causing the steel-mill generating plant to increase and decrease its output in synchronism with the strip-mill load-swing cycle. This, in principle, satisfies the concept that disturbances should be contained on the system on which they originate, which concept has proved so successful in the operation of utility interconnections. The elements of the steel-mill load are described in the succeeding portion of this paper.

The Steel Mill as a Utility Load†

The Tennessee Coal, Iron, and Railroad Company's electric-power system is called upon to supply the energy for all stages of steel production from the mining of ore, coal, and limestone to the final processing of rails, shapes, plates, sheets, strip, tin plate, wire, and allied products.

The characteristics of the individual loads vary widely. The coal mines with their numerous large fans, pumps, motor generator sets, rectifiers, and belt conveyors have a fairly steady load of about 14,000 kw. Hoists and other intermittent loads represent a relatively small part of the total.

The ore mines have a widely fluctuating load owing to the fact that the ore is brought to the surface by means of slope hoists powered by slip-ring induction motors ranging in size from 1,800 to 3,500 horsepower. There are eight of these hoists which give some diversity, but it frequently happens that several of them start at approximately the same time, causing load swings of 10,000 to 14,000 kw. The peak loads on the ore-mine circuit, as a result of these swings, reach about 35,000 kw.

In the mills departments are many heavy power consumers which are, by nature, intermittent. Among the larger of these are the following:

One 4,000-horsepower a-c motor driving generators for 5,600-horsepower blooming-mill motor.
One 5,000-horsepower a-c motor driving generators for 7,000-horsepower blooming-mill motor.
One 6,000-horsepower a-c motor driving generators for 7,000-horsepower plate-mill motor.
One 4,900-horsepower a-c motor driving generators for 4,000-horsepower universal-plate mill.
Two 8,400-horsepower a-c motors driving generators for six stands and scale breaker of hot-strip mill.
Two 7,050-horsepower a-c motors driving generators for two five-stand cold-reduction mills.
One 5,000-horsepower a-c motor driving finishing stand of rail mill.
One 4,000-horsepower a-c motor driving converter blower.
One 4,000-horsepower a-c motor driving plate mill.
One 2,500-horsepower } a-c motor driving stands of a structural mill.
One 3,000-horsepower }
One 2,000-horsepower }
One 5,000-horsepower a-c motor driving billet mill.

The mill rolling schedules are worked out to have as few as possible of the heavy power consumers operating during the same shifts. However, there are not enough idle shifts for the several mills to prevent most of them operating together a good part of the time. The result is a rapidly varying demand on the power system. As the steel enters any one of the previously listed mills, a momentary peak equal to or greater than the motor rating may result.

---

† Prepared by C. W. Harrison.

The greatest concentration of power is in the hot-strip mill. The peaks here are not only higher than for any other mill but are more consistent. The idling load on this mill is about 3,000 kw. It normally takes from 10 to 12 seconds for the steel to reach the last stand after entering the first stand. During this period, the load builds up to peaks as high as 25,000 kw for heavy slabs and 15,000 or 18,000 kw for lighter slabs. These peaks hang on for a number of seconds, varying with the length of slab, and fall off at about the same rate that they came on. When rolling a large order of the same size slabs, the load swings come with clocklike precision. The number varies from about 25 per hour for some of the long heavy slabs to over 100 per hour for some of the short ones.

The composite load from all departments of the Tennessee Coal, Iron, and Railroad Company is one that changes from day to day and from hour to hour. Figure 3 shows hourly demands for a week, picked at random. It will be seen that on Sunday this ranged from 49,000 to 75,000 kw. On weekdays, the range was from 64,000 to 110,000 kw. Each of these hourly figures represents the integrated total of a load with momentary swings having at times an amplitude in the neighborhood of 40,000 kw.

The Tennessee Coal, Iron, and Railroad Company's generators consist of three 20,000-kw units at the main power station of the Fairfield Steel Works and five units totaling 18,500 kw at the Ensley Steel Works power stations. As blast-furnace gas, which fluctuates both in volume and Btu content, is the primary fuel, and blast-furnace auxiliaries have first claim, the steam available for electric generation is not sufficient to maintain a steady output.

Figure 4 shows the total hourly generation of all the foregoing generators for the same week as was covered by Figure 3. This shows a variation from 50,000 to 72,000 kw which is not exceptional. There are times when the hourly generation exceeds 75,000 kilowatt-hours or drops below 40,000 kilowatt-hours.

Obviously another source of power is necessary to meet the demands of the Tennessee Coal, Iron, and Railroad Company system. If additional generators had been provided, additional boilers using fuel, other than blast-furnace gas, would have been necessary. The alternative was to purchase the additional power from the Alabama Power Company. To date, it has been found economical to purchase, rather than generate this power.

The procedure has been to operate two of the 20,000-kw machines, speed-governed, at or near their full capacity with the third 20,000-kw unit governed by pressure and allowed to generate as much as possible from whatever steam remained. Under such conditions the generation of this third machine swings up and down following variations in steam pressure rather than variations in system load. The small Ensley units are speed-governed and generate all that a limited supply of steam will permit. All of the Tennessee Coal, Iron, and Railroad generators operate in parallel with the Alabama Power Company system.

As might be expected, sudden power swings have been largely passed on to the power-company system. A small speed-governed power system inherently will not rush in and grab a large part of a sudden load from a large power system where the two are operating in parallel, unless special provisions are added to force it to do so. The small system, at best, normally will take little more than its pro-rata share of the new load based on the relative sizes of the two systems. If, as previously outlined, the small-system turbines already are running nearly wide open under speed regulation or held in check by pressure regulation when the upswing of load occurs, they will practically ignore the swing.

Figure 5 covering the same period as Figures 3 and 4 shows the interchange of power between the two systems. This chart, like Figures 3 and 4, shows the one-hour demands. Momentary peaks and valleys are, of course, much higher and lower than the values shown. The circles show the maximum 15-minute demand for each day. It is interesting to note that, during some hours over the weekend, the power flow was in both directions.

The contract between the power company and the Tennessee Coal, Iron, and Railroad Company has some special features to cover local conditions but basically consists of an energy charge for kilowatt-hours purchased and a demand charge. At present the demand charge is based on 50,000 kw and is a fixed amount so long as the 15-minute demand does not exceed 50,000 kw. In the event of an overrun, the new demand becomes the billing demand for that and the 11 succeeding months, provided another overrun does not occur during that 11-month period. A schedule is worked out for taking off the Tennessee Coal, Iron, and Railroad Company turbines for repairs during periods of the year when water power is most plentiful. At such times, a definite additional or seasonal demand is permitted over and above the 50,000-kw firm demand previously mentioned. A fixed charge is made for this seasonal demand.

Such in brief were the load conditions, the generators available, and the power-contract features which existed at the time the load control was installed.

The succeeding portion of the paper states the nature and sources of energy available in the Tennessee Coal, Iron, and Railroad Company plant as well as the effect the new load control has on these sources.

Fuel and Steam Facilities and Effect on Steam System of the Tennessee Coal, Iron, and Railroad Company Plant‡

The action of the peak-control regulator, operation of the steam turbines, and the resultant effect on electric-power generation are wholly contingent on the availability of steam with which to meet the cyclic peaks. As no additional steam-generating equipment or accessories were added when the regulator was installed, the method used and the effect on the existing steam-generating and consuming units are worthy of comment.

At Fairfield are three blast furnaces. The top gas of the three furnaces serves as the primary fuel for the steam-generating station. The availability of gas is contingent on the number of blast furnaces in operation. Not only is there a seasonal variation in gas volume and Btu heating content, owing to the change in the coke rate, but also a fluctuating and momentary change because of the furnace operating conditions. The furnaces are alternately checked each half-hour for approximately one minute. During the checking periods, practically no gas is generated from the furnace checked. Likewise, practically no gas is generated during the casting periods of the furnace which requires about ten minutes, four times each day. During periods of furnace delays, such as changes of tuyères and blow pipes, no gas is generated.

Approximately 14 per cent of the top gas is utilized at practically a constant rate for heating the hot-blast stoves. The balance, less leaks and waste, is available for steam generation. The blast-furnace gas supplied to the boilers is supplemented with a limited amount of pulverized coal and natural gas during prolonged high-load periods and intervals of blast-furnace gas shortage. Of the steam generated, approximately 34 per cent is used by the three turboblowers and miscellaneous users, leaving 66 per cent of the steam available for electric generation.

The turboblowers and miscellaneous users have first claim on the steam. The balance of steam available for electric current is subject to wide variations and fluctuations. The mill and mine electric loads also vary but bear no relations to the steam availability for electric generation.

Prior to the operation of the new load control and to utilize the widely varying and fluctuating volume of blast-furnace gas to full advantage, a steam-pressure regulator had been used which, in effect, maintained a constant steam pressure on the entire system by loading or unloading the turbogenerators in steps of 500 kw. When the new load control went in service, the old steam-control regulator was limited to the number 3 20,000-kw turbogenerator. To meet the peak demands for electric power, the steam, when required by the turbogenerators, must be available for instantaneous use. A gas holder, for the storage of blast-furnace gas, even if practicable, would not be of help in meeting the peak load, as the time element needed to generate steam in response to the peak load is too great for the existing boilers to carry all peak as well as a portion of the base load. An isolated boiler would be impractical as steam would only be utilized during the intervals of mill peak loads. During the off-peak loads, the steam would be lost at the relief valves of the boilers. Firing the boiler as required to meet the peak demand is impractical owing to the time element involved in generating the varying rate of steam and the time lag in the control equipment. An ample steam receiver, if practical, would be of advantage in meeting the peaks. The pipe lines serve, in part, as such a receiver. Supplementing the limited receiver capacity of the piping system, the boilers act as a heat flywheel and generate steam by flashing of the water stored in the boiler, due to the lowering of the steam pressure.

---

‡ Prepared by E. J. Kohn.

Normally the boiler steam pressure is maintained at 335 pounds per square inch by the steam-pressure regulator previously mentioned. With the new load control in service, the boiler steam pressure is pulled down to a new level, and a quantity of water in the boilers is flashed into steam. This added steam supplies the requirements for meeting the peak demand imposed on the generators. The magnitude and duration of the permissible peak demand determine the added steam requirements. The extent of generation by the Tennessee Coal, Iron and Railroad Company of the peak is determined largely by the permissible drop in steam pressure and the duration of no-peak load. The latter enables the boilers to recover full steam pressure in anticipation of rolling the next slab. The number, type, and size of the boilers, or in other words, the steam-releasing space and water storage in the boiler for flashing determine the permissible drop and ability to recover steam pressure. The type of control valve supplying the feed water to the boilers further influences the steam-releasing space in the boiler.

The steam-generating equipment consists of eight Babcock and Wilcox boilers of the four-drum type with integral two-drum economizer. Five of the boilers each have three 42-inch steam drums and one 48-inch mud drum with a heating surface of 14,607 square feet and a normal output of 134,000 pounds steam per hour with blast-furnace gas as fuel. Three of the boilers each have three steam drums 36 inches, 48 inches, and 42 inches in diameter and one 48-inch mud drum with a heating surface of 19,800 square feet and a normal output of 170,000 pounds per hour with blast-furnace gas as fuel. All eight boilers are equipped with superheaters. Normally only seven boilers are in service. With one of the larger boilers out of service the effect on steam generation and the ability to meet the peak demand is noticeable and accordingly reduced.

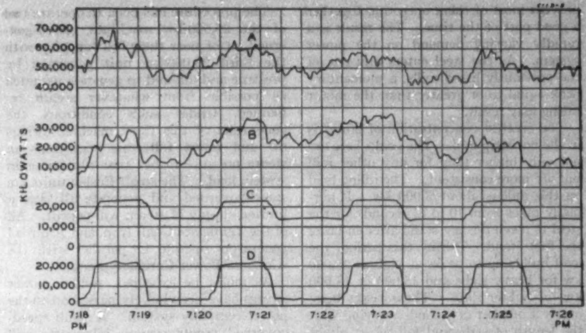

Figure 8. Typical hot-strip-mill regulating generator, Alabama Power Company–Tennessee Coal, Iron, and Railroad Company and Alabama Power Company–Tennessee Valley Authority tie-line wattmeter charts with Tennessee Coal, Iron, and Railroad Company load controller in service

A—Kilowatt loading on Gorgas–Wilson Dam 154-kv tie line

B—Kilowatt supply to Tennessee Coal, Iron, and Railroad Company by Alabama Power Company at Fairfield 110/44/6.6-kv step-down substation

C—Kilowatt loading on Tennessee Coal, Iron, and Railroad Company regulating generator

D—Kilowatt loading on hot-strip mill

The numbers 1 and 2 generators since the regulator was put in service are each set to carry a base load of approximately 15,000 kw. The number 3 generator, with the constant-steam-pressure regulator in operation, is loaded or unloaded in steps of 500 kw in accordance with the steam available to maintain the normal operating steam pressure of 335 pounds per square inch. This pressure control is not so sensitive as the new load control and in a measure acts to permit some of the steam to go to the load-controlled turbine generators. For instance, when the load controller functions to supply the additional steam for the numbers 1 and 2 generators, the steam pressure drops and the number-3-generator output, in accordance with the constant-steam-pressure control is reduced in steps of 500 kw to meet the new low steam pressure.

Maintaining the load controller in continuous service resolves itself into the problem of determining the drop in steam pressure permissible during the peak load period to permit the boilers to recover fully their initial steam pressure during the off-peak period of the mill.

A study of the test curves made December 9, 1944, with 13,000-pound slabs through the hot-strip mill, shows time of rolling is one minute with a peak of 19,000 kw and the time between slabs to mill is also one minute.

Number 1 generator only was under the control of the load controller during the test. The generator load was increased from base load of 14,000 kw with steam rate of 163,000 pounds per hour to peak of 23,000 kw with steam rate of 260,000 pounds per hour or an increase of 9,000 kw requiring additional steam at the rate of 97,000 pounds per hour. For one-minute duration 16,160 pounds of steam were supplied from the line storage and the flashing of water in the boilers. The steam pressure dropped from the normal of 335 pounds per square inch to the predetermined low level of 315 pounds per square inch or 20 pounds per square inch drop. Only once during the test of over two hours duration, and then when the last slab was being rolled, did the steam pressure drop below the predetermined low limit. The pressure bias control acted automatically to transfer that portion of the peak which the boilers could not supply to the Alabama Power Company's system.

Two alternate operations present themselves: to operate as per test with an occasional peak thrown on the Alabama Power Company's system, or to operate at a lower peak generation. The latter recourse has been followed, because the fluctuating demands on the boilers are reduced with less resultant disturbance to the equipment. The control now is set to pick up 6,000 kw generation to meet the mill peaks. This peak, requiring steam at rate of about 64,000 pounds per hour, is divided between the two turbogenerators, numbers 1 and 2. No difficulty has been experienced even when rolling smaller slabs with a shorter cycle of operation.

From the viewpoint of reducing the peak electric demands, the control functions as intended. The favorable results obtained are due in part to the fact that excess electric-generating capacity is available. The electric generators are operated at less than full output, owing to the limited boiler capacity and the limited blast-furnace gas available as fuel.

The control equipment and the generators are adequate to extend further the favorable results obtained, but, as emphasized in the foregoing, the limiting factor is the steam available for the peak electric generation. Further limiting factors and of prime concern to the plant operators are the effects of the modified operations on the steam-generating and consuming units.

With the peak control inactive, one of the noticeable features of the plant is the generally uniform water and steam conditions.

Had the generating plant of the Tennessee Coal, Iron, and Railroad Company been designed to carry the mill load under isolated operation, adequate provisions would have been made both in the steam-generating and consuming units. Of primary consideration would have been steam generators with larger steam drums and provisions for continuous fuel supply. Not designed for such requirements, the generating-plant equipment therefore has to be operated within its capabilities. Of chief concern to the operators is the possibility of water carry-over from the boilers to the steam users which, more than the ability of the boilers to recover steam pressure, is the limiting factor in determining the peak electric generation possible. This condition is aggravated owing to the varying blast-furnace fuel supply. During the periods of diminished blast-furnace gas there is a cooling of the boiler firebox with resultant effect on the boiler conditions. When this condition occurs concurrently with the increased cycle demand of steam, the effect is a widely varying boiler water level with increased possibility of carry-over in the steam. Greater demands are made on turbine valves and control equipment, and additional stresses are imposed on the turbine wheels, condenser tubes, boilers and their control equipment under peak load regulation. It is to be expected that repair and maintenance costs will be increased over the corresponding costs incurred under speed governing of local turbines in parallel with a large power system.

Various alternative methods of imposing peak loads on speed-governed prime movers operating in parallel with large power systems are discussed in the succeeding portion of this paper.

Various Means of Effecting Load Control of Turbine Generators*

A study of the conditions previously stated led to the formulation of the following specifications which a load control should meet in order to relieve the external power-supply system from peak loads of the hot-strip mill:

1. Given a variable supply of steam for the turbine generators operating in parallel with a large power system, one or each of two turbine generators should be so controlled that:

(*a*). A constant base load (10 to 100 per cent of generator rating) can be carried.

(*b*). A percentage (0 to 100 per cent of generator rating) of the variable load in the strip-mill circuit can be added to the base load.

(*c*). The base load is to be divided in any desired ratio between the two prime movers or all put on one.

(*d*). The percentage of variable load assigned to the prime movers is to be divided between the two prime movers in any desired proportions or all put on one prime mover.

(*e*). The base and variable loads placed on the prime movers are to be reduced from their maximums at maximum predetermined steam pressure as the pressure is reduced below maximum until both such loads are reduced to zero at a predetermined minimum operating pressure.

2. The variable load may have maximum conditions of:

Total load	20,000 kw
Rate of change—average over period of change	5,000 kw per second
Duration of peak	100 seconds

Various approaches to a set of conditions like these have been suggested. Some of these are discussed to bring out their features.

Scheduling of loads tends to reduce a tendency toward a cumulative demand and is quite effective in reducing demands which otherwise would extend over appreciable time periods. It requires suitable instruments, meters and communication or remote-control systems, and an operator to supply the necessary intelligence from a given set of facts or a control system to accomplish the same result automatically. From the standpoint of correcting instantaneous changes of load, it is an ineffective method as the procedure is too slow.

Numerous types of *anticipators* have been suggested, usually to be applied to an existing prime mover and its control. Normally the rate of response from the correcting element is excessively slow compared to the rate of load change under consideration. The initiating signals suggested include photoelectric cells, mechanical triggers, limit switches, and characteristics of certain initial steps of load changes.

Incomplete consideration of such anticipators sometimes indicates a relatively inexpensive arrangement with the thought projected that it could be put together in a repair shop. The suggestion, generally made, is that the anticipator operate the synchronizing motor of the prime mover.

Synchronizing-motor controls of turbine-generators usually have a rate of response of full load in about 30 seconds. To offset load changes of the type under discussion, one or more prime movers of at least a total size equal to the load change should be used. Therefore, the anticipator is expected to compensate for, say, 20,000-kw load changes which pass from minimum to maximum or vice versa at rates of 1,500 to 7,000 kw per second. Contrasted with the actual rate of load change, the anticipator and its auxiliaries can only count on a rate of response from the prime mover corresponding to its rating divided by 30 seconds, which, if it were a 20,000-kw unit, would respond at 667 kw per second excluding delays due to relaying and acceleration.

In many instances the incremental rates of load change when a slab or billet enters a stand are much faster than the average rates suggested.

Some mills use a scale breaker as the first stand in a mill. The scale breaker requires a relatively small amount of power, but sufficient when a slab enters it to cause a change in the series field current of the motor. Such a change might be used as a signal to trigger the operation of the synchronizing motor on the turbine generator. Several charts, showing in Figure 6 what might be accomplished if no time lags in the operation of the relaying were considered, illustrate the effect of

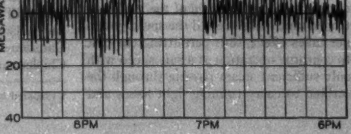

Figure 9. Gorgas-Wilson Dam 154-kv tie-line wattmeter chart showing the effect of the Tennessee Coal, Iron, and Railroad Company load controller on tie-line load swings

A—Load controller set on zero-load pickup

B—Load controller set on 50-per-cent-load pickup such an anticipator working on a turbine generator having a rate of response by synchronizing motor of approximately 2,000 kw per second. It will be observed from the several charts that:

---

*Prepared by A. G. Darling.

1. The turbine generator never follows the load changes.
2. There are as many peaks created on the system when the regulator is in operation as the mill creates plus two more in some instances.
3. There is an opportunity for actual power reversal in the interconnecting line between the mill and the power supply system.

Lastly, it also will be observed that, for each schedule of the mill, a change must be made in the timing elements introduced in the response element to correspond with the time and load increments created by the mill load. The mill operator is the best source of information for presetting such an anticipator, but, as his job is to get out production, it is likely that the responsibility for prescheduling will be placed on the prime-mover operator who is at a disadvantage from lack of first-hand information.

Fixed-value modifications to local prime-mover loadings also have been suggested which modifications would follow a preset schedule, depending upon the type of product to be rolled. An initiating signal of some type is required, and a set of timing devices which can be modified readily are also necessary. This method involves the same disadvantages as the anticipator method and, in addition, is not sensitive to what actually occurs in the mill.

By the time all the relays, control cable, and safety devices are considered, the cost of the anticipator and the accomplishment of fixed-value modifications is likely to approach that of a good load controller.

The type of control which was furnished and is described in detail in another Institute paper[1] meets the specifications, responds to the power in the circuit or circuits to be measured from which the variable loads emanate, and reinterprets not only the rates of change but also the value of the loads as they occur to an hydraulic servomotor capable of modifying the load on the turbine at the rate of 25 per cent of turbine rating per second. The electric circuits and servomotor arrangements are such that, when the load control is in operation, the speed governor is made inactive in its "preemergency" speed setting, that is, slightly above the speed at which the power system normally operates. In the event of loss of connection of the controlled generator from the electric system, the speed of the load-controlled unit will rise until the speed governor takes effect, thus permitting the unit to continue operation at a safe speed with only sufficient steam passing through the turbine to carry running light losses and keep the turbine at a reasonable temperature. The load controller holds the desired base load on the turbine generator and compares the measured consumption of the strip mill with the excess output of the generator over base load. If any difference occurs in these values, the load controller operates the turbine valves through a servomotor to rebalance the equation. Steam-pressure variations work through pressure-control elements to apportion the total generator output to the pressure variations between preset limits. Electric circuits are used to interpret the conditions in the strip-mill and generator circuits to the pilot motor of the hydraulic servomotor. Steam-pressure modifications are accomplished mechanically since the rates of change are slow. The connection from the servomotor cylinder to the turbine steam valves is the same as used for speed governor and is a chain of mechanical linkages, rack, pinions and cams.

Means of transferring the prime movers from speed governing to automatic load control as well as full adjustment of the base and percentage of the variable load to be assigned to the prime movers and adjustment of the pressure regulator are incorporated in the load-controller panel, so placing facilities and responsibility on one power-station control-board operator. The details of design and construction of the regulator are given in the companion paper.[1]

The effect of the regulator on the tie lines of the external power system is discussed in the last portion of this paper.

Effect of Load Regulation of Local Prime Movers on the Power System†

In order to check the over-all effect of the load control, an operating test of the controller action was made while the hot-strip mill was rolling a series of 56 13,000-pound slabs in quick succession at the rate of about 25 slabs per hour. The load controller was set to pick up 50 per cent of the load swing which, in the case of these slabs, amounted to approximately 10,000 kw. During this test the controller was cut in and out of service at 30-minute intervals in order to evaluate the effectiveness of the regulator by making a direct comparison of the two operating conditions.

Synchronized wattmeter charts, traveling three inches per minute, were obtained for the hot-strip-mill load, the steel-mill generator output, the Alabama Power Company's energy supply to the steel-mill load, and the load on the Gorgas–Wilson Dam 154-kv tie line. The Gadsden–Guntersville and Lindale–Chickamauga tie lines were open during the test to permit direct recording of the total tie-line load on a single chart. Representative load-test curves, replotted to a common kilowatt scale on rectangular co-ordinate paper, are shown in Figure 7 for the nonregulated condition, and in Figure 8 for the regulated condition. The effectiveness of the controller in suppressing the strip-mill load swings is clearly evident from a comparison of the two charts. The over-all effect as recorded on the tie-line wattmeter chart, traveling at the normal chart speed of three inches per hour, is shown in Figure 9, which indicates a considerable reduction in band width.

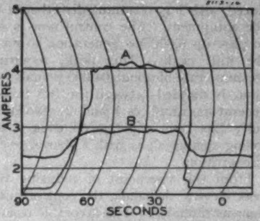

Figure 10. Timing chart of regulating generator and hot-strip-mill a-c secondary amperes

A—Hot-strip-mill current
B—Regulating generator current

As the effectiveness of the controller in offsetting fast load swings is dependent on close synchronism between the response variations in generator output and the strip-mill load-swing cycle, a further check was made to determine the over-all response time of the generator by feeding the strip-mill and generator a-c amperes directly into two high-speed ammeters having their charts driven from a common drive shaft. The results of this test are shown in Figure 10 and indicate an over-all response time of approximately two seconds.

In conclusion, it can be said that the controller performs as it was intended to function, with quick response, good stability, and negligible overshoot. Judging from the performance of the load controller when set for a 50-per-cent load pickup, it may be concluded safely that if the steam-plant boiler conditions would permit operation with a 100-per-cent pickup setting, the hot-strip-mill load swings would be completely eliminated from the Commonwealth and Southern–TVA tie lines.

Reference

1. AUTOMATIC LOAD CONTROL FOR TURBINE GENERATORS, F. E. Crever, R. L. Jackson. AIEE TRANSACTIONS, volume 64, 1945, September section, pages 656–60.

---

† Prepared by W. W. Eberhardt.

Dielectric Strength and Protection of Modern Dry-Type Air-Cooled Transformers

P. L. BELLASCHI
FELLOW AIEE

EDWARD BECK
MEMBER AIEE

TODAY there are in service over 1,000,000 kva of large dry-type air-cooled transformers, some in ratings as high as 4,000 kva and including the 15-kv voltage class. This wide acceptance in industry of the modern dry-type transformer and its continual growth, naturally has increased interest in its application and standardization. In a prior AIEE paper[1] the design characteristics, particularly with regard to thermal performance, have been discussed. The purpose of this paper is to review the development of the modern dry-type transformer, specifically with reference to its dielectric strength, and to present recommendations on impulse levels and methods of protection for applications which may be affected by lightning surges.

Application to Circuits Unexposed to Lightning

The development of the modern dry-type transformer was initiated in 1936, and at that time it was intended primarily for application to indoor and unexposed circuits where surge overvoltages are of internal origin. Until recently this has been the principal application for this type of apparatus. In this field of application surge overvoltages seldom will exceed three and one-half times the line-to-neutral crest voltage. Furthermore, the character of these surges is relatively slow compared to the abrupt effects resulting from impulse voltages. Figure 1, reproduced from reference 2, presents surge overvoltages that have been recorded in an extensive investigation on a 12-kv grounded-neutral system. A comprehensive survey of the subject is provided by the bibliography of reference 3. The data are typical of conditions encountered in these applications. On some ungrounded-neutral systems possibilities may exist of higher-surge overvoltages.

The low-frequency dielectric tests specified for dry-type transformers in American Standard *C*57.1, correspond to four or greater than four times the line-to-neutral operating voltage, and therefore in relation to the character of service the test has a practical significance. This and other requirements were taken fully into consideration in the design of dry-type transformers. In circuits unexposed to lightning no surge protection was deemed necessary, and none has been recommended. The experience with some 2,000 transformers in service amply bears out the adequacy of the design and the soundness of the practice recommended for these applications.

Impulse Insulation Levels

Though the greater part of the dry-type transformers built since 1936 has been applied to unexposed circuits, as in industrial services, it was recognized that even circuits otherwise unexposed may be subject to surges transferred through the medium of transformers from circuits exposed to lightning.[4] For this reason attention was given from the beginning to a balanced insulation design. Even more compelling have been the specific applications where practical considerations and economy dictated connecting dry-type transformers directly to incoming overhead lines exposed to lightning. Also, it will be well to note that the possibility of developing the dry-type transformer for application generally to distribution systems—exposed and unexposed—definitely has been in the foreground.

Let us consider the insulation design and construction of modern dry-type air-cooled transformers. The core and coil assembly is the conventional core form of construction as shown in Figure 2. For operating voltages up to 5,000 a cylindrical winding commonly is used, and above 5,000 and up to and including 15,000 the winding consists of a column of disk-type coils. The winding conductors are insulated with glass. The high- and low-voltage windings are arranged symmetrically about the core with the low-voltage cylindrical winding on the inside. Both the high- and low-voltage coils are wound and assembled separately on insulating barriers. First, the individual windings and then the assembled core and coils are treated with a high-temperature thermosetting varnish to add strength, to bond the conductor and coil insulation in place, and to give the assembly a smooth tough glossy finish which makes it highly resistant to moisture and dirt. The high-voltage coil column is supported at the top and bottom by large porcelain spacers. Porcelain spacers separate the high-voltage coils and space the coils from the high-voltage insulating barriers. Porcelain spacers also separate the low-voltage coils from the core assembly. The high- and low-voltage windings are centered and supported, so that an unimpeded air duct separates them and forms the major insulation of the transformer. The transformer leads, taps and terminals, and other live parts are supported on porcelain insulators.

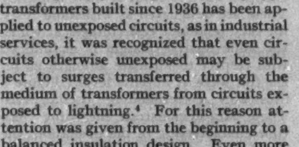

Figure 1. Surge voltages on 12-kv system[2]

Sphere-gap data 1932–38

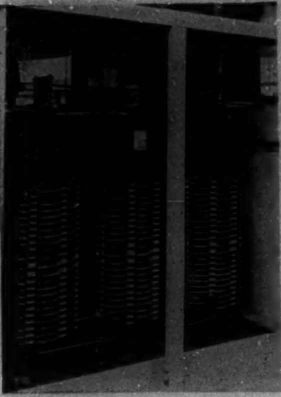

Figure 2. View of core and coil assembly of dry-type air-cooled transformer

The problem of securing a balanced insulation design in dry-type transformers fundamentally does not differ from the corresponding problem in other transformer apparatus. Figure 3 gives a typical impulse-voltage distribution, and Figure 4 illustrates a detailed study of the stresses developed throughout the high-voltage winding of a dry-type transformer. It is from these studies and the strength of the insulation parts that the design is

---

Paper 45-156, recommended by the AIEE committee on electric machinery for publication in AIEE TRANSACTIONS. Manuscript submitted June 21, 1945; made available for printing August 3, 1945.

P. L. BELLASCHI is section engineer with the Westinghouse Electric Corporation, Sharon, Pa. EDWARD BECK is section engineer in the switchgear engineering department of the corporation in East Pittsburgh, Pa.

The authors acknowledge the assistance of their associates in securing the test data presented.

Table I. Typical Withstand Impulse Tests Applied to High-Voltage Terminals of Dry-Type Transformers

Transformer Rating	Impulse Wave*	Voltage, Kilovolts	Remarks
600 kva 13,800–480 volts Three phase, 60 cycles	$1^1/_2$x40-μs wave	50	With power-voltage excitation
500 kva 13,800–480 volts Three phase, 60 cycles	$1^1/_2$x40-μs wave	52	With power-voltage excitation
350 kva 13,800–480 volts Three phase, 60 cycle	$1^1/_2$x40-μs wave	51	With power-voltage excitation
	Steep-front wave, 0.30 μs	86	No power-voltage excitation
1,000 kva 12,000–480 volts Three phase, 60 cycles	$1^1/_2$x40-μs wave	54	No power-voltage excitation
	Chopped wave, two μs	62	No power-voltage excitation
200 kva 2,400–480 volts Three phase, 60 cycles	$1^1/_2$x40-μs wave	25	With and without power-voltage excitation

*Impulse wave of positive polarity applied in all tests.

established. Modern dry-type transformers are of balanced-insulation design; that is, the coil, turn, and the other minor insulation are balanced with the major insulation so that the transformer can withstand an impulse wave of the voltage specified.

The impulse strength of transformers designed with balanced insulation is the product of the 60-cycle strength and the impulse ratio of the insulation. The dry-type transformer depends for its dielectric strength on air which has an impulse ratio of 1.1 to 1.3, depending upon the construction. Based on these fundamental considerations and the verification of designs from actual impulse tests as shown in Table I, the impulse levels in Table II have been established, and these have been proposed for standardization.

The impulse levels in Table II correspond to the $1^1/_2$x40-microsecond full wave. For purposes of standardization, in addition to the full wave, two chopped waves have been suggested to conform with present American Standards Association methods of testing. The chopped-wave voltage may well be 115 per cent of the full wave. Waves of positive polarity generally are more effective for testing dry-type apparatus and therefore are recommended.

Table II. Impulse Insulation Levels of Dry-Type Transformers

Insulation Class, Kilovolts	Low-Frequency, Dielectric Tests, Kilovolts Rms	Impulse Levels $1^1/_2$x40-μs Wave, Kilovolts Crest
1.2	4	10
2.5	10	20
5.0	12	25
8.66	19	35
15.0	31	50

Table I illustrates typical tests that have been applied to dry-type transformers, ranging from full-wave to chopped-wave to front-of-wave impulses. These are designated as withstand tests, for they represent test voltages at which the same relative margin is maintained with respect to ultimate strength as for the full wave at impulse level. Figure 5 illustrates corresponding oscillograms. These data demonstrate the rising volt-time characteristic of the insulation, the significance of which will become more apparent under the discussion of protection. A second point of practical interest to note is the ability of these modern dry-type transformers to withstand repeated impulses without any sign of deterioration, even when carried to the point of flashover. For instance, in a series of tests applied to 13,800-volt windings of the 350-kva transformer referred to in Table I, this transformer was subjected to a combined total of 100 impulses divided between full wave, chopped wave, and front of wave. Some of these tests were carried to the point of flashover of the insulation without causing any ill effect to the transformer. In the impulse tests to failure, flashover usually occurred across porcelain insulators supporting the leads or from lead terminals to ground, not affecting the more vital parts of the transformer.

Protection Against Lightning Surges

When dry-type transformers are applied to circuits exposed to lightning surges, the impulse characteristics of the apparatus in relation to the protective devices available and to the degree of protection expected need to be considered. In such cases only lightning arresters having a low protective ratio are recommended, and for effective protection they should be connected at the terminals of the transformer as shown in Figure 6. These arresters are the types that have been developed for the protection of rotating machines and applied to motors and generators for many years. They are available in station and line types. In the application to dry-type transformers, only the line type is justified economically in most cases. This arrester is known as the type *RM*, indicating its application to rotating machinery. The characteristics of the arresters are given in Table III, which summarizes data from recent tests on commercial arresters.

Verification tests have been conducted on these lightning arresters in combination with transformers. In a series of tests the complete transformer assembly plus the arrester were excited at normal power voltage from a 2,000-kva power supply, much in the manner the installation would operate in service. The impulses applied were synchronized to the crest of the 60-cycle voltage as in the standard impulse tests. For instance, the oscillograms *A* and *B* in Figure 7 demonstrate the impulse voltages at the 13,800-

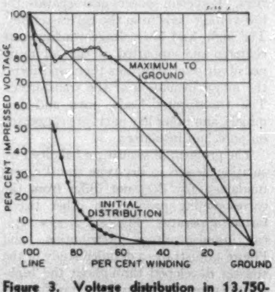

Figure 3. Voltage distribution in 13,750-volt winding, 1.6x37-microsecond wave applied

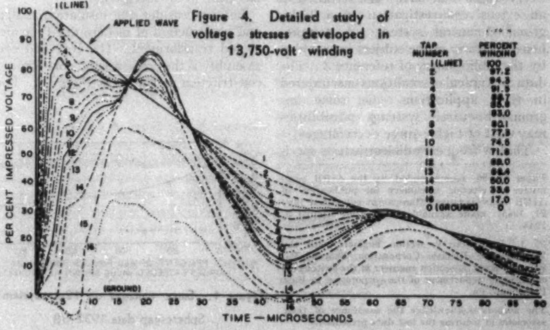

Figure 4. Detailed study of voltage stresses developed in 13,750-volt winding

Table III. Performance Characteristics of Type-RM Arresters*

Arrester Rating, Kilovolts Rms	Phase-to-Phase Circuit Voltage Rating		60-Cycle Gap Breakdown, Kilovolts Rms	Impulse Breakdown in Kilovolts Crest		Discharge-Voltage Kilovolt Crest on 10x20-μs Currents	
	Ungrounded Neutral System	Solidly Grounded Neutral System		Front of Wave**	1½×40-μs Wave	1,500 Amperes	3,000 Amperes
3	2,400	4,160	6	13	9	9	10
6	4,800	7,200	12	24	18	18	20
9	7,200	11,500	18	32	27	27	30
12		13,800	24	40	36	36	40
15	13,800		30	48	45	45	50

*These arresters are special and should not be used interchangeably with standard distribution arresters.

**Test wave as recommended in AIEE Standard 28 for standard valve-type arresters.

volt terminal of a 350-kva transformer without protection and with a 15-kv *RM* arrester connected from terminal to case respectively. In another series of tests the voltage generated and applied was increased to several times the full-wave insulation level of the terminal. For instance, oscillogram *C* of Figure 7 is the generated voltage applied on repeated tests (ten) to one of the 13,800-volt terminals of the 350-kva transformer with a 15-kv *RM* arrester connected from the terminal to case. In effect this test corresponds to an incoming surge on a well-insulated overhead line having a surge impedance of 450 ohms, since the series resistance in the impulse generator was of this amount. As shown by oscillogram *D*, the voltage at the transformer is limited by the arrester. In this particular test lengths of leads included in the protective circuit produced an additional momentary voltage above the arrester characteristic, as shown by the initial instantaneous peak of 79 kv. In no instance during these tests was any ill effect whatsoever observed on the transformer insulation so that the conclusion definitely is drawn that even under these severe lightning surge conditions a good degree of protection can be provided to dry-type transformers with *RM* arresters, provided they are properly applied.

The rating of a lightning arrester for a particular installation is determined by the maximum dynamic voltage from line to ground. With solidly grounded-neutral systems the arrester rating can be less than line-to-line circuit voltage. Usually the next lower rating may be applied. For instance, on a 13.8-kv system with solidly grounded neutral, a 12-kv arrester may be applied with the advantage of an additional 20-per-cent increase in the margin of protection and at lower cost. Likewise, the availability of *RM* arresters at intermediate ratings as 4.5 kv and 7.5 kv should contribute to better protection in applications at the lower voltages.

Classes of Application and Protective Methods

In all problems of protection the question is to determine first, the extent apparatus may be endangered, and, second, whether the relative risk incurred, weighed against the importance of the installation and the cost of damage, warrants protective equipment. Where protection is required, the method should be effective and in keeping with economy. Let us consider the various possible applications and protective methods for modern dry-type transformers.

The extent dry-type transformers may be subject to lightning surges depends entirely upon the degree of exposure of the circuits to which they connect. For convenience, these are classified as follows:

1. Unexposed.
2. Quasiexposed.
3. Exposed.
4. Highly exposed.

The protective methods recommended for these various applications are outlined schematically in Figure 8.

The unexposed circuit is one on which lightning surges practically are nonexistent. That is, the circuit is either disassociated from lightning surges or only remotely coupled electrically to their source. Most industrial applications indoors, applications in mines and to underground cable systems, and many others come within this classification. As stated previously, system overvoltages on distribution and network circuits as commonly operated in this country seldom exceed three to four times line-to-ground normal crest voltage. On systems with the neutral isolated, conditions may develop resulting in somewhat higher-surge overvoltages. Considering that the strength of dry-type transformers to these surges is comparable to the impulse strength (Table II), system overvoltages five to six times, and higher for the lower classes, are permissible. Several years' experience from many transformer installations on various systems has indicated no instance of difficulty from system overvoltages. In general, no protection is required for these applications (Figure 8A).

The quasiexposed circuit would be one in which there is an intervening bank of oil-immersed transformers between the dry-type transformer and the exposed or highly exposed circuit, as shown in B of Figure 8. When a dry-type transformer is connected in the manner indicated, it is in general not necessary to use lightning-arrester protection at the transformer, provided the intervening transformers are protected properly on the exposed side.

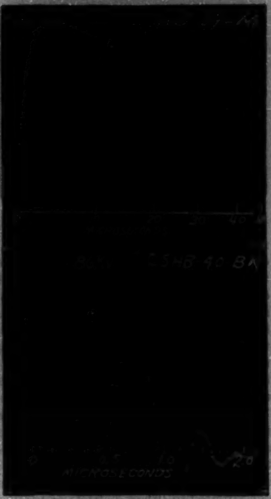

Figure 5. Typical full-wave and front-of-wave impulse voltages applied to dry-type air-cooled transformers, 15-kv insulation class

Oscillograms from tests on a 350-kva 13,800–480-volt three-phase 60-cycle transformer

Figure 6. Built-in lightning-arrester protection in dry-type air-cooled transformer

Figure 7. Impulse tests on transformer provided with lightning-arrester protection

350-kva 13,800–480-volt three-phase 60-cycle transformer and 15-kv *RM* arrester

It is assumed that the secondary circuit from the intervening transformers is unexposed; for instance, that it extends to the supply centers as a cable system or it enters directly into an industrial establishment. Should the dry-type transformer be connected closely adjacent to the secondary terminals of the intervening transformer and it alone become the entire load, lightning protection of the dry-type transformer would be necessary.[4]

Exposed and highly exposed circuits are treated here as one. They differ in degree as to the frequency of occurrence and intensity of lightning surges to which each are subject. The exposed circuit would be one situated in urban districts or located such that there is some shielding from surrounding buildings or objects. It may have an impulse level of the order of 100 to 150 kv. The highly exposed circuit is one which is insulated with wood construction throughout, that is, wood poles, wood crossarms, wood braces, and so forth, and located in a territory which has a high lightning occurrence and intensity. Such a line would have an impulse level of 300 kv or greater and impulse voltages of this order actually may build up on it. In either case the incoming line connects directly to the dry-type transformers.

In these applications standard expulsion or valve-type distribution arresters are recommended on the incoming lines, in addition to the low-ratio arresters at the terminals of the transformer, preferably 500 to 1,000 feet from the transformer, as shown in C of Figure 8. The addition of the protective device on the line contributes to the over-all scheme of protection in that it takes the brunt of incoming high-current surges and permits the arrester at the transformer to function within its rating and provide a higher degree of protection to the transformer. Capacitors such as specified for rotating machines are not required. On urban circuits where "shielding" of the circuit is known to reduce the frequency and intensity of surges to a fractional part of the amount encountered in rural exposed circuits, the protective device on the line may be omitted. On highly exposed circuits some risk of direct strokes to the 500- or 1,000-foot section of line between the line arrester and the transformer may be present. This probability must be recognized, although it is fairly small. In general an overhead ground wire to shield the 500- to 1,000-foot end section of the line would not be justified. It is recognized that the special station-type arrester used for rotating-machine protection provides a somewhat greater margin of safety, because in the rare event of a stroke to the section of line adjacent to the transformer the station arrester gives added protection because of its greater current-discharge capacity and somewhat better protective level. For certain large and important installations its use may be justified, but for the general application the type *RM* arrester is the most practical.

Up to the present specific applications of dry-type transformers to exposed circuits have been almost entirely as shown schematically in D of Figure 8. The principal reason for this arrangement is that it lends itself quite conveniently to the entire installation. This commonly consists of the incoming distribution line, usually of wood construction, terminating outside the industrial establishment or adjacent to the site of power supply, the circuit continuing to the transformer proper as a cable section up to several hundred feet long. This arrangement has inherent merits also from a protection standpoint. As indicated, *RM* line-type arresters at the transformer combined with standard expulsion or valve-type distribution arresters applied to the cable pothead at the line end will provide a high degree of protection in this type of installation. At the line end the arrester ground terminals should connect directly to the cable sheath and to ground through a ground wire. The arresters at the transformer preferably should be built in, as shown in Figure 6, thus securing minimum length of arrester leads from the terminals to case and therefore the best over-all protection; this combination has other constructional and safety advantages. On distribution circuits which operate under conditions of low exposure, the arrester at the line end of the cable may be dispensed with.

The foregoing recommendations are based on fundamental engineering considerations. In addition they have been corroborated by test. For instance, tests were conducted on a test setup corresponding to the arrangement of Figure 8D, with a lead-sheath cable 250 feet in length. One end of the cable was connected to the high-voltage terminal (high-voltage insulation of 15-kv class) of a 1,000-kva air-cooled dry-type transformer, the other end to the impulse generator. In these tests a 15-kv *RM* line-type arrester was applied at the transformer, backed up by a line-type 15-kv arrester at the line-end of the cable, in the manner recommended for highly exposed circuits. The series resistance of the generator was approximately 450 ohms for generated voltages above 200 kv and considerably less for other voltages. The term "generated voltage" as used here simply means the voltage that the impulse generator would have developed with no connection made to the cable. It represents, so to speak, the impulse applied to the line terminal of the cable, modified and limited, of course, by the circuit and the arresters. The front of the generated voltage in these tests was close to one microsecond. The duration of the wave to half-crest value as

Figure 8. Classes of application and protective methods

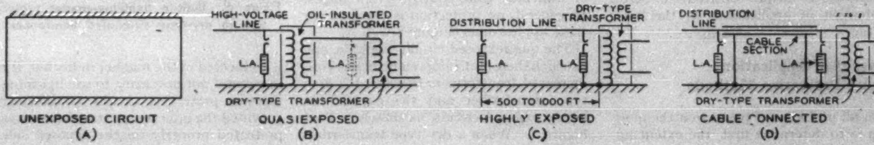

recorded from the arrester oscillograms is in the order of 30 microseconds. The results of the tests may be summarized as follows.

The voltage generated and applied to the line-end of the cable was raised starting from below the *RM*-arrester operating voltage in steps to 100 kv, then to 186 kv and 300 kv, finally to 600-kv generated voltage. Many tests were applied. Protection was effective throughout the tests. To illustrate one of the tests: At 186-kv generated voltage the voltage developed at the transformer was limited to 51 kv at the crest of arrester spark-over and to 45 kv during arrester discharge. In this test the voltage at the line-end of the cable was held under 60 kv. The corresponding currents discharged at the line and transformer arresters were approximately 2,500 and 1,500 amperes.

In conclusion these are the general recommendations on methods of protection and protective schemes applicable to modern air-cooled dry-type transformers. In specific cases practical considerations may demand modifications or additions to fit the protection effectively and economically to the particular case.

References

1. Design and Operating Characteristics of Modern Dry-Type Air-Cooled Transformers, W. W. Satterlee. AIEE Transactions, volume 63, 1944, October section, pages 701–04.

2. Surges on Chicago 12-Kv System, F. O. Wollaston, H. J. Plumley. AIEE Transactions, volume 60, 1941, June section, pages 260–65.

3. Correlation of System Overvoltages and System-Grounding Impedances, AIEE committee on protective devices. AIEE Transactions, volume 62, 1943, January section, pages 17–24.

4. Lightning Surges Transferred From One Circuit to Another Through Transformers, P. L. Bellaschi. AIEE Transactions, volume 62, 1943, December section, pages 731–8.

Constant-Speed Drives for Aircraft Alternators

C. J. BREITWIESER
MEMBER AIEE

IN LARGE MILITARY AIRCRAFT the demand upon the electric system has been increasing exponentially. At the start of the war, 50-ampere generators were considered ample; this rating soon jumped to 100, and now 200-ampere generators on our four-engine bombers are inadequate. As the limits of power output are reached, the necessity for satisfactory parallel operation and equality of division of the load becomes extremely important.

During ground operations, the main engines operate at low speed, and the battery is called upon to supply essential loads since at low speeds the generators are not supplying power. Before a flight, the crew frequently check the operation of turrets and other equipment and quickly discharge the low-capacity storage batteries of the airplane.

In this is seen the shaping of a demand for a more constant-speed type of drive for generators for airplanes. The problem of paralleling generators and obtaining equality of load distribution is greatly reduced if the generators can all be driven at a constant speed, and also power for ground operation or low engine speed would be provided automatically.

As the demands for more electric power and transmission distances have increased, it has become apparent that the present 30-volt d-c system is no longer adequate. In a current design of a large airplane, the conductor weight for a 30-volt system would be in excess of a ton and a half; whereas, if the voltage were increased to 250 volts, the weight would be reduced to approximately 250 pounds.

Contrary to a popular misconception, weight is just as important, if not more so, in large airplanes as in small. There is a tendency, in large airplanes, for designers to be more extravagant with weight and size; and, if this tendency is not curtailed and an effort made to use the most advanced metallurgy and efficient structural design, progress will be at a standstill, for advancement cannot be made by aerodynamic efficiency alone.

The demand for increased range also has emphasized the importance of weight in aircraft. It is not at all unusual to find present-day airplanes carrying once again their own weight in fuel and oil.

In other words, every pound that could be saved on the airplane represents two pounds' reduction in the gross weight of a long-range airplane.

Every ounce on an airplane must pay for itself. In military aircraft an increase in weight must provide either an important operational or tactical function, structural advantage, increased reliability, or decreased vulnerability. In commercial operation, extra pounds mean reduced pay-load and revenue. The cost of extra pounds has been evaluated quite accurately in dollars and cents by the commercial lines. Estimations range from $500 to $1,500 a pound. If dollars and cents talk, this should be a mighty strong talking point for the reduction in weight.

Constant-Frequency A-C System for Large Aircraft

Weight saving cannot be made, however, at the sacrifice of reliability. The "in-the-air" reliability of aircraft components must be very high. High-altitude flying conditions place additional burdens on equipment. The wide ranges of ambient temperatures encountered with military aircraft also add to the difficulties.

After careful study of the particular problems of some large-size long-range airplane designs, it was concluded that a high-voltage high-frequency three-phase a-c system would result in improved altitude performance and a weight saving. A voltage of around 200 volts permits a large reduction in conductor weight, and the reliability of a three-phase induction motor is unsurpassed by any other type of motor. Other factors such as circuit-breaker and switch design, and ease of voltage transformation, also influenced the choice of alternating current.

A variable-frequency variable-voltage system was ruled out because of the demands of many existing accessories which have been designed for constant-voltage supply. Because of the favorable speed ranges, light motor and transformer weights, and the possibility of direct application to many existing pieces of equipment, a frequency of 400 cycles was chosen.

This question then presented itself: How would the alternator be driven? A small auxiliary power plant was an obvious solution. However, upon more careful consideration, it is apparent that the installation would involve an excessive amount of weight. The auxiliary power plant must be pressurized for high-altitude operation, heated for the extreme cold of the upper atmosphere, and cooled for ground operation. The specific fuel consumption of the auxiliary power plant is greater than that of the main engines, and also prime mover capacity is, in effect, duplicated, resulting in a weight increase. A study on a large airplane indicated that on a long-range mission the use of an auxiliary power plant would add 1,500 pounds to the gross weight of the airplane. It was, therefore, apparent that the main engines should be used as a source of prime power for the electric system.

Requirements for a Constant-Speed Drive

With a decision to use the main engines as a source of driving power for the alter-

---

Paper 45-163, recommended by the AIEE committee on air transportation for publication in AIEE Transactions. Manuscript submitted July 23, 1945; made available for printing August 17, 1945.

C. J. Breitwieser is design engineer in charge of radio electrical engineering, Consolidated Vultee Aircaft Corporation, San Diego, Calif.

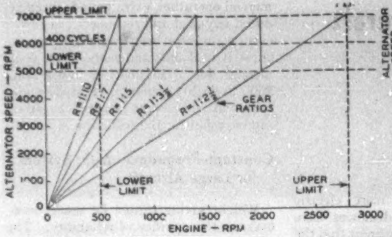

Figure 1. Alternator speed versus engine speed for a five-speed gearbox

Gear ratios chosen to provide an alternator speed 6,000 ± 1,000 rpm throughout operating range of the engine

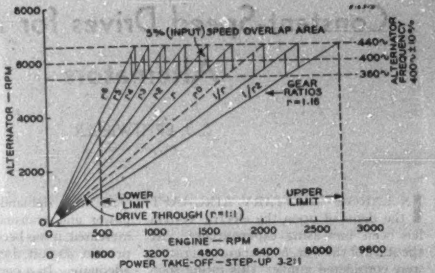

Figure 2. Alternator speed versus engine speed for a multiple staging of constant-ratio gear sets to provide a frequency regulation of ±10 per cent with a 5-per-cent speed overlap for clutching

nators, the necessity for some form of a variable-ratio coupling becomes apparent. An aircraft engine may vary from 500 rpm at idling to 3,000 rpm at military power. For a fixed-frequency system, the alternator requires a constant driving speed at all times. Since the power output of an induction motor is inversely proportional to the square of the frequency, it is desirable to maintain essentially constant frequency. If the system frequency is 400 cycles and an eight-pole alternator is used, the variable-ratio drive would be required to supply a constant 6,000-rpm output for input speeds ranging from 500 to 3,000 rpm. This is a ratio variation of 12:1 at low speed, to 2:1 at high speed.

The auxiliary power requirements of some of the new heavy bombers are upwards of 50 horsepower. Ordinarily an alternator must be capable of supplying a 100-per-cent overload for short-time periods. The variable-ratio drive, therefore, must be capable of supplying 50 horsepower continuously and 100 horsepower for short intervals.

This must be accomplished for a minimum of weight and mechanical complexity. If the device becomes too heavy and complex, it would lose its advantage over a direct-driven auxiliary power plant.

Finite-Ratio Versus Infinite-Ratio Drive

A selective fixed-ratio device could be used to maintain the alternator within a certain specific speed range. For example, a multiple-stage gearbox which would provide selective ratios of 10, 7, 5, $3^1/_2$, and $2^1/_2$ to 1 would maintain the alternator at speeds which would vary roughly 1,000 rpm above and below the required 6,000 rpm as the engine speed changed from 500 to 3,000 rpm (Figure 1). The speed variation would not be too objectionable so far as most of the motor applications were concerned, but a variation of plus or minus 1,000 rpm would result in a torque variation (assuming the voltage was held constant) of approximately 2:1 which would be objectionable.

Another disadvantage of a finite ratio is the difficulty which would be encountered in the parallel operation of alternators. Unless some auxiliary flexible coupling were used, it would not be possible to maintain parallel operation of the alternators.

This flexible coupling would have to provide for a speed differential of approximately 1,000 rpm if the afore-mentioned ratios were used in the fixed-ratio drive. A certain amount of droop would be desirable. These characteristics could be provided by a fluid coupling, but would add weight to the drive and reduce efficiency.

A planetary gear set can be switched from one ratio to another by means of electrically actuated clutches without too much difficulty. The clutches may be energized by suitable contacts on the governor. Overlap of the ratio-change contacts must be provided to eliminate chattering or hunting when the speed is in the vicinity of the ratio-change values.

The design and operation of an automatic ratio selector may be simplified considerably by using a constant ratio between successive gear sets. The ratios already indicated are not related by any common ratio. A separate gear set would have to be used for each ratio which has no common factor. A factorial relationship between gear sets permits various combinations of gear groups to be used to produce the desired over-all ratios.

Chrysler Corporation photo

Figure 3. An infinite-ratio mechanical-drive coupled to an experimental 37.5-kva aircraft alternator

The chart in Figure 2 shows the variation of alternator speed over the range in engine speed. The multispeed gearbox is connected to an engine-power take-off which has a step-up ratio of 3.2:1. The multistage gearing consists of two step-down ratios of $1/r$ and $1/r^2$, a drive-through or 1:1 ratio, and six step-up ratios of r, r^2, r^3, r^4, r^5, r^6. By the use of this common ratio, r, considerable simplification in the multistage gear can be accomplished by using various combinations of the factorially related gear sets to obtain the desired over-all ratios.

The arrangement shown in Figure 2 will provide an alternator speed range such that the frequency will vary only ± 10 per cent from the desired 400 cycles.

An overlap of five per cent of the input speed is provided to eliminate sporadic operation of the automatic ratio selector. This selector may be coupled to either the input or output shaft. The fixed percentage of input speed for overlap and sequential operation of the gear sets can probably best be provided for by a control governor attached to the input shaft. An overspeed protective governor would preferably be attached to the alternator shaft.

Infinite-Ratio Coupling

For parallel operation of alternators, the multistage gearbox would not be suitable unless some auxiliary flexible coupling, capable of adjusting the speed over a range of ten per cent, were used. This would not be entirely satisfactory, for there may be times when the main engines are operating in the same speed range. This coupling also would have to be capable of acting very rapidly, for, during the intervals of gear-set changes, large differential in output speeds would arise.

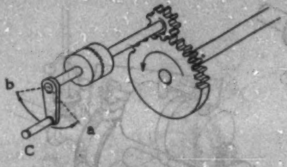

Figure 4. A spur gear driven by an oscillating small pinion gear

The pinion is connected by means of a freewheeling unit to a crank *C* which rocks from *a* to *b*

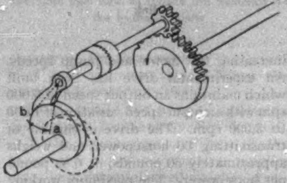

Figure 5. A cam and follower have been substituted for the crank

The same oscillating motion is provided

A more satisfactory drive would be one in which the ratio could be varied infinitely and rapidly. A fluid coupling of the hydraulic clutch would function, but its efficiency is so low over the required speed range that it is impractical to use.

The same criticism applies to any other type of drive which utilizes a slipping element for speed change, be it hydraulic, mechanical, or electrical. Slip, regardless of the type of element is manifest in energy loss and is wasteful of power.

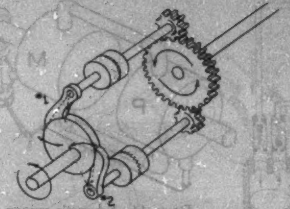

Figure 6. An additional pinion, freewheeling unit, and cam follower have been added to double the number of impulses from the rotating cam

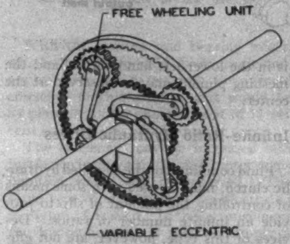

Figure 7. A four-pinion assembly with freewheeling units integral with the pinion gears and a variable eccentric cam on the input shaft

In an airplane, efficiency is important from two standpoints:

(*a*). The amount of fuel which must be carried to furnish the auxiliary power.

(*b*). Cooling provisions which must be provided for the drive.

Added fuel increases the gross weight, and cooling provisions usually add to both weight and drag.

Two infinite-ratio coupling systems have been developed, which embody positive translations. One system is strictly mechanical, and the other is hydraulic. Because these systems do not depend upon slip, their efficiency is high. In general, it is easier to govern a slip device than a variable positive-translation device. This has been found to be true in the case of these devices. The governing has proved a problem, and it has been difficult to attain the desired rapidity of ratio change necessary to maintain constant-output speed throughout the range of speeds and accelerations of the engines.

Infinite-Ratio Mechanical Drive

A unique and efficient mechanical system has been developed by the Chrysler Corporation for providing continuously variable-ratio coupling (A drive attached to a 37.5-kva alternator is shown in Figure 3).

The device operates in the following manner:

In Figure 4 the output shaft is driven by means of the small pinion and spur gear. Oscillation of crank *C* from positions *a* to *b* transmits, through the freewheeling ratchet, intermittent rotation of the pinion gear in a clockwise direction. The pinion gear drives the output spur gear, revolving the output shaft in a counterclockwise direction.

In Figure 5 the crank has been replaced by a shoe riding on a cam. The cam is attached to the input shaft, and, as the input shaft revolves, the shoe will oscillate from *a* to *b*, driving the pinion and spur gear in a manner similar to the oscillating crank arrangement of Figure 4.

The output shaft will receive an impulse of acceleration each time the shoe is displaced from *a* to *b*. An additional impulse may be added by arranging another shoe and freewheeling pinion gear diametrically opposite shoe 1, as indicated in Figure 6.

Additional impulses likewise may be given the output spur gear by the additional shoe and pinion gear assemblies. The magnitude of the impulse is determined by the angular acceleration and displacement of the shoe, which is dependent

Figure 8. Components of a pinion gear and freewheeling assembly from the infinite-ratio mechanical drive

Chrysler Corporation photo

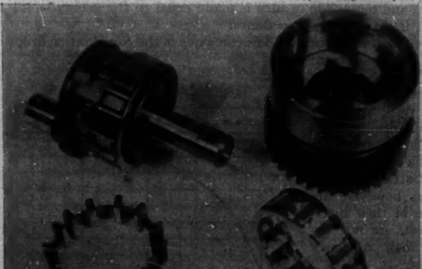

Figure 9. Assembly showing the pinion gears and one of the cam followers

Chrysler Corporation photo

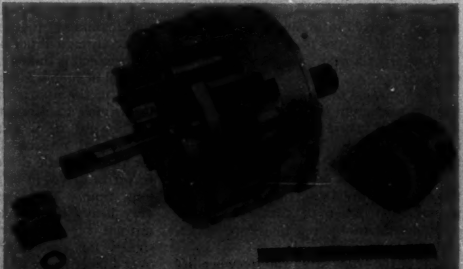

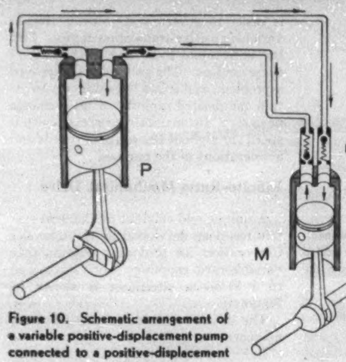

Figure 10. Schematic arrangement of a variable positive-displacement pump connected to a positive-displacement hydraulic motor

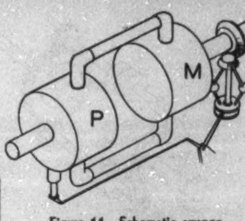

Figure 11. Schematic arrangement of a hydraulic-pump and motor combination with a governor controlling the pump displacement attached to the output shaft

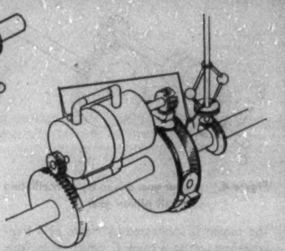

Figure 12. Schematic arrangement of a pump and motor combination utilizing a differential gear to limit the demands upon the hydraulic link

upon the speed and eccentricity of the cam.

In Figure 7 an arrangement is shown with four pinion units with concentric freewheeling units coupled by means of connecting rods to shoes which slide on the driving cam. In this arrangement the pinions are planets in a planetary gear system. As the cam revolves, these planet pinions impart driving impulses to the driven spur gear in the same manner as in Figure 6.

The ring gear is coupled by means of reduction gearing (not shown in the figure) to the drive shaft and drives the output shaft directly, since the planet pinions are locked effectively by the ratchet action of the freewheeling elements.

Since the ring gear is geared down from the drive shaft, the cam will revolve faster than the ring gear and will impart accelerating impulses to the planet pinions proportionate to the amount of eccentricity, which will add to the speed of the driven spur.

The acceleration impulses are proportional to the eccentricity of the cam. The additive speed differential may be varied by changing the amount of eccentricity. Therefore, the ratio of the drive can be changed from the fixed ratio of the ring gear to the fixed ratio plus the additional speed added by the planet pinions when the cam is in a position of maximum eccentricity.

The variation of cam eccentricity from zero to maximum may be perfectly continuous and, therefore, will provide an infinite number of ratios between the aforementioned limits.

This illustrates in principle the drive shown in Figures 3, 8, and 9; however, actual construction details of the drive differ considerably from the simplified arrangement of Figure 7.

One of the crank arms and freewheeling assembly is shown in Figure 8.

In Figure 9, one of the shoes is shown attached to the crank arm. A single shoe is in the lower left-hand corner, and the meshing pinions may be observed at the center.

Infinite-Ratio Hydraulic Drives

Fluid couplings, or the so-called hydraulic clutch, may be used with some means of controlling the amount of slip to provide an infinite number of ratios. Devices of this type, however, are not efficient over a very wide range in speed.

Drives have been developed which embody essentially the same basic principle as the previously described mechanical system and are quite efficient throughout a wide speed range. These drives are direct-coupled and depend upon a controllable positive displacement.

For example, Figure 10 shows a simplified arrangement of this type of drive. The unit consists of positive displacement motor *M*, coupled to a positive displacement pump *P*, in which the displacement may be controlled.

By varying the eccentricity of the drive cam, the volume of the fluid which is pumped each stroke is changed, and accordingly the ratio between the input shaft and output is changed. The ratio is infinitely variable over a large range of speeds.

Usually both the pump and motor are multicylinder. Figure 11 indicates schematically a governor placed on the output shaft which is linked to the displacement control in such a manner that the output speed of the unit is maintained constant for driving an alternator.

The use of a variable-displacement pump and positive-displacement motor for variable-ratio drives has been applied to turret drives in large battleships for a long time. These units, however, are very heavy and, because of their intermittent type of operation, are not designed for particularly high efficiency over a large range of ratios.

The weight of this type of drive may be reduced by two methods: by increasing the working hydraulic pressures, and by increasing the motor and pump speeds. An experimental drive has been built which maintains an output speed of 6,000 rpm with an input-speed variation of 1,000 to 3,000 rpm. The drive is capable of transmitting 60 horsepower and weighs approximately 50 pounds, or 0.83 pound per horsepower. The maximum working pressure is 4,500 pounds per square inch, and the motor pump speeds are on the order of 18,000 rpm. Even though the unit is extremely light and of high speed, the efficiency is surprisingly good, varying from about 70 per cent at the worst condition to 83 per cent at maximum.

Methods For Improving Efficiency

A method for improving the efficiency of a variable-ratio drive of this type is shown in Figure 12. The method is based upon the fact that the efficiency of a variable-displacement pump and constant positive-displacement pump is a maximum for one particular flow. This is a condition in which the reflected mechanical impedance of the motor load most nearly matches the effective internal impedance of the pump and the associated hydraulic circuit. This is analogous to the conditions for transferring maximum power in an electric circuit when the load impedance is made equal to the generator impedance.

The efficiency of the combination drops

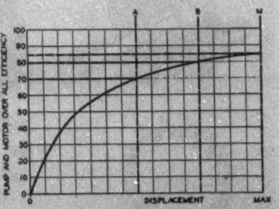

Figure 13. Efficiency of a hydraulic pump and motor combination versus displacement

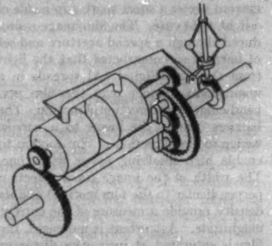

Figure 14. Schematic arrangement for improving the efficiency of a drive by the use of an epicyclic gear train to reduce the demands on the hydraulic units

slightly as the displacement is changed from this optimum value. When the pump and motor are of equal size, this point is usually the point of maximum displacement for the pump. See Figure 10.

In the arrangement of Figure 12, the pump and motor combination supplies only the differential speed which is necessary to bring the output shaft up to the desired constant speed. For example, if the drive-shaft speed varies from 2,000 to 6,000 rpm, and it is desired to maintain 6,000 rpm on the alternator, it will be necessary for the hydraulic unit to supply, through the differential gear, an additional 4,000 rpm to the alternator when the input is 2,000.

This would be the point of maximum demand on the hydraulic unit and would require the maximum displacement of the pump which occurs at maximum efficiency.

As the driver speed increases, the demands on the hydraulic units become less and less until an end point is reached when the driver is revolving at 6,000 rpm and there is zero demand from the differential gear. The efficiency falls off as zero is approached (see Figure 13), but, as the unit is supplying proportionately less power (the major portion of the power being supplied directly through the differential gear), the net over-all efficiency will remain high since it is a combination of the mechanical and hydraulic efficiency.

For purposes of rough comparison, assume a median efficiency of 70 per cent for a straight hydraulically coupled system, as indicated in Figure 13, and compare it with the foregoing. If one neglects the bearing and gear efficiency, it may be assumed roughly that the power demands will be divided between the hydraulic and mechanical sections proportional to the speed requirements.

With the driver varying from 2,000 to 6,000 rpm, the driver median speed is 4,000 rpm, and the speed demand on the hydraulic unit is 2,000 rpm. If one assumes the same median over-all hydraulic efficiency as above 70 per cent, the over-all efficiency of this arrangement is then 90 per cent.

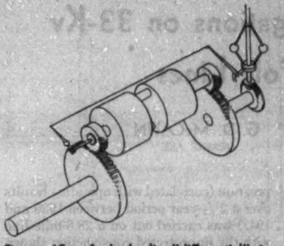

Figure 15. A hydraulic "differential" in which the pump and motor units revolve as a unit forming part of the gear set

With the gearing and bearing losses, which had previously been neglected, approximated as 10 per cent, the over-all efficiency of this arrangement would be 81 per cent, or an improvement of 11 per cent over the straight hydraulic drive.

The efficiency may be increased still further by using a pump and motor combination which can be reversed. The same type of arrangement, as illustrated in Figure 12, is used. In this arrangement the hydraulic unit is used to supply a differential speed above and below a median speed of the driver.

If the drive shaft had the same speed range as before (2,000 to 6,000 rpm), an epicyclic differential-gear set could be substituted for the conventional differential shown in Figure 14. The epicyclic gear set would incorporate a step-up to the output shaft of $1^1/_2$:1 such that the speed range of the output shaft would be 3,000 to 9,000 rpm if no differential-speed increment was supplied through the hydraulic unit.

At the median speed of the driver, 4,000 rpm, there would be no differential-speed demand as the output shaft would be revolving at the required 6,000 rpm. For input speed below this value, (2,000 to 4,000 rpm), the hydraulic unit would act as an overdrive and supply the necessary differential speed to bring the output up to 6,000 rpm (2,000 to 0 times the $1^1/_2$:1 ratio of the epicyclic gear). For the driver speed range of 4,000 to 6,000, the hydraulic unit would act as an underdrive, supplying the necessary negative differential to bring the speed down to the required 6,000 rpm.

The absolute speed range of the hydraulic unit, in this manner, is limited to 0 to 2,000 rpm, rather than the range of 0 to 4,000 rpm which was required in the previous case.

If one considers a hydraulic unit similar to the previous one, the efficiency at the median speed will be of the order as indicated by the dashed line *B* on Figure 13, or 80 per cent, which is a 10-per-cent improvement over the other arrangement. If the efficiency is calculated on the same basis as before, the over-all efficiency of the unit, with gearing and bearing losses neglected, would be approximately 96.6 per cent and, if a 10-per-cent loss in these two items were assumed, the total over-all efficiency would be 87 per cent, or a 6-per-cent improvement over the previous arrangement and a 17-per-cent improvement over the direct-coupled hydraulic arrangement shown in Figure 11.

The same results could be accomplished if the gear ratio of the power take-off were increased so as to provide a 3,000-to-9,000-rpm range of the driven shaft and a conventional differential gear were used instead of the epicyclic set.

Another arrangement which utilizes the same principle of overdrive and underdrive for increasing efficiency by limiting the speed range of the hydraulic units is shown in Figure 15. This arrangement does not use a differential gear, but the differential speed is supplied in a similar manner by the hydraulic unit.

For this method, the hydraulic pump and motor must be capable of rotating as a unit (zero displacement of hydraulic fluid) and also rotating in either direction relative to each other.

The pump is likewise a variable-displacement unit; and the motor, a con-

Sundstrund Machine Tool Company

Figure 16. A hydraulic infinite-ratio drive for a 40-kva aircraft alternator

Army standard spline and pad for 208/110-volt 400-cycle alternators

Sundstrund Machine Tool Company

Figure 17. Hydraulic infinite-ratio drive showing pad for connection of drive shaft to airplane main engine

Lightning Investigations on 33-Kv Wood-Pole Lines

F. E. ANDREWS
MEMBER AIEE

G. D. McCANN
MEMBER AIEE

IN RECENT YEARS the importance of providing reliable service over lines in the transmission class of 22 to 44 kv has greatly increased. However, little fundamental data have been obtained on the severity of lightning duty on such lines or upon the detailed lightning performance of various types of line design and lightning protection. Most of such information has been gathered on the higher-voltage steel-tower lines. A comprehensive lightning investigation of this type has been undertaken jointly by the Public Service Company of Northern Illinois and the Westinghouse Electric Corporation on several types of 33-kv wood-pole circuits.

The study has consisted of four principal parts. A detailed climbing inspection program (correlated with operating results over a 2½-year period between 1939 and 1942) was carried out on a 28.8-mile line with the unprotected construction shown in Figure 1. This represents about the optimum amount of line insulation generally feasible for an unprotected line of this voltage class.[1] The inspections have provided valuable fundamental and correlating data on the nature of insulator flashover markings and on the distribution of lightning flashover and cases of sustained power follow between the different types of poles. At the beginning of the 1942 lightning season, two types of recording installations were put in service. One type is for the purpose of determining the character of line flashovers on unprotected lines. Sections of line were chosen where recorders could be placed on poles one-half to one mile apart whose insulation was comparable to a guyed pole, and with fully insulated tangent poles intervening. The line construction for these sections is also that of Figure 1. Photographic surge-current recorders and surge-crest-ammeter links were placed in the grounding circuit. The photographic surge-current recorder, which has been described in detail elsewhere,[2] employs the principle of photographing the luminosity produced by the flow of the surge current across a short spark gap inside of a light-tight case. The film image is produced through a special aperture and set of barriers so constructed that the light from the gap (Figure 5A) spreads in a nonuniform manner over the film perpendicular to its direction of motion. The barriers confine the image to a narrow wedge in the direction of film motion to enable high resolving power with time. The width of the image (in a direction perpendicular to the film motion) and its density provide a measure of the current magnitude. As current is increased, the film is saturated at increasing distances from the center axis. However, at a point just beyond this region, the film density can be measured to determine the approximate current magnitude. Current can be measured to an accuracy of about two to one but over the very great range of 0.1 to 150,000 amperes with a time-resolving power of 600 microseconds. Initially, there were 20 of these installations on three different line sections. However, the recorded prevalence of multiple flashovers extending over a mile or more made it advisable to select a single longer section of line. At present 14 poles on a ten-mile section of the line where the climbing inspection was made are equipped with recorders as shown in Figure 2. Two additional recorders have been placed at each pole to measure both the lightning and power-follow flashover currents from each side phase to a neutral point and from neutral to ground. Thus, it is possible to record for each of these paths the multiple character, duration, and approximate magnitude of the lightning-flashover currents together with the duration and approximate magnitude of the power-follow currents. A longer cross arm has

Paper 45-115, recommended by the AIEE committee on power transmission and distribution for publication in AIEE TRANSACTIONS. Manuscript submitted May 4, 1945; made available for printing May 16, 1945.

F. E. ANDREWS is engineer, transmission and distribution design, Public Service Company of Illinois, Chicago, Ill., and G. D. McCANN is transmission engineer, industry engineering department, Westinghouse Electric Corporation, East Pittsburgh, Pa.

The authors acknowledge the assistance of W. H. Johnson, A. M. Shefveland, and L. J. Davis, of the Public Service Company of Northern Illinois for their assistance in obtaining the fundamental field data of this investigation.

---

stant-displacement unit. When the push-pull rod which controls the amount of displacement is in the middle position, there is no flow of hydraulic fluid and the pump–motor combination is hydraulically locked together and drives as a unit. The losses at zero differential speed are essentially mechanical—gear and bearings.

By varying the control rod on the pump, the flow is increased. The pump is capable of pumping in either direction, and, therefore, the rotation of the motor will be in one direction or the other, so that its speed will either add to, or subtract from, the speed of the hydraulic pump.

This type of drive has the same advantages of gain in efficiencies as the type previously described and, because of the effective overdrive and underdrive arrangement, is capable of operating over a large speed range.

An advantage of this design is that the speed of the pump and motor combination may be very easily stepped up so that the transmitted torque is low and the unit may be of very light weight.

A unit of this type has been built for less than one pound per horsepower and with an efficiency of 92 to 83 per cent over the speed range.

The sketches in Figures 16 and 17 are of a unit of this design built by the Sundstrand Machine Tool Company. Figure 16 shows the alternator-coupling flange and spline, and Figure 17 is the pad for connecting to the main engine.

Conclusion

The problem of providing a constant drive speed with a variable-speed prime mover is by no means new. There have been many solutions to this problem—electrical, mechanical, and hydraulic. Unfortunately, however, for an aircraft application they have all been too heavy or inefficient. In aircraft design, inefficiency is tantamount to weight for inefficient operation means more fuel is used, which means more weight is carried.

Many forms of constant-speed drives have been suggested and worked upon. It was not within the scope of this report to describe them all, many of which show considerable promise. The ones described in this report have all been at least in experimental production and have given us sufficient background information for us to draw a reasonable picture of the type of constant-speed drive which will soon be making its appearance in large aircraft.

The production units may be expected to have efficiencies of 85 to 95 per cent, a weight of less than one pound per transmitted kilowatt, will hold a preset output speed to within ±1 per cent total variation over an input-speed range of from 500 to 3,000 rpm, and will fit within a space of 50 cubic inches per kilowatt of rating.

The large airplanes of today with a-c systems will have drives of this type. It is probable that with continued development the efficiency will be increased and the size and weight reduced to a point where it may be practical to use a constant-speed drive for d-c generators and other pieces of auxiliary equipment.

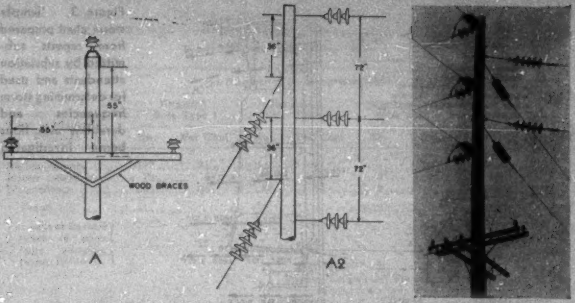

Figures 1A (left) and B (right). Types of line construction on unprotected line used for detailed climbing inspection and photographic-surge-current-recorder study

A. Type 1, unguyed
When guyed, guy attached 30 inches below crossarm, and insulated with three 5$^3/_4$-inch suspension units
A2. Type-2 corner pole

been installed lower down on the pole to provide the normal wood insulation path between the insulators and the recorder circuit.

For the second type of recorder installations, surge-crest-ammeter links have been placed in the ground leads of protected lines having the types-4 and 5 overhead-ground-wire construction of Figure 9, lines of type-3 construction (Figure 9) having deion protector tubes on the top conductor only and a line of type-6 construction (Figure 10) having protector tubes on each phase but on only one phase per pole and rotated between phases. The pole-ground-lead current records obtained in this way provide data on the frequency of direct strokes, the crest-stroke currents, and the division of current between ground leads as correlated with line performance. The magnetic links are placed so as to record crest currents ranging from a minimum of about 600 amperes to about 55,000 amperes. The presence of only a single straight conductor for each pole ground enables a more accurate recording of the pole currents than is possible on steel-tower lines where there is a multiplicity of paths down the tower and where only one tower-leg current is usually recorded. In addition magnetic links have been installed on a number of isolated protector-tube installations to correlate the difference in protector-tube duty under the two operating conditions.

In the fourth phase of the investigation a detailed record of the frequency and extent of lightning storms passing over the region occupied by the lines under investigation has been obtained. This was started at the beginning of the 1943 lightning season, and the manner in which it is accomplished is illustrated in Figure 3. Observers at the numbered substations submit a report on the apparent storm centers as illustrated by the samples at the bottom of the chart for every individual storm that they can observe. Each of their observations as to the location and direction of travel (at the time they are first able to observe it, when it passes closest to their observation station, and when they last observe it) and the time of the observation, are plotted, as shown, by an arrow. From these, the storm path, storm extent, and duration over each line can be determined. Such data provide a valuable correlation between the number of annual storm-days, number of storms, total annual storm duration, the frequency of strokes to the various lines, and the number of line tripouts.

Results of Climbing Inspection—Insulator Markings

In the course of the climbing inspection previously mentioned, 8.6 miles of line were inspected after about 1$^1/_2$ years of operation of the line. The remaining 16.8 miles were inspected after about 2.5 years of operation. A total of 180 of the pin-type insulators that had flashover markings were removed from the pole for a more detailed inspection. Typical markings are illustrated by Figure 4. When flashover is first produced by lightning, the path of lowest dielectric strength is along the surface of the porcelain, so that breakdown occurs there first. Thus, for most lightning flashovers, heating of the porcelain glaze is more or less uniform along this flashover surface and results in the "lightning-only" markings illustrated by Figures 4A, B, C. Lightning markings are characterized by roughening of the insulator glaze (with a texture resembling fine sandpaper) over a path closely following the insulator contours. This frequently includes the underside of the top skirt. It may vary in width from a narrow line (Figure 4A) to a wide path extending several inches circumferentially around the insulator (Figure 4B). The length of the lightning markings varies greatly. In some cases there may be only a short narrow mark somewhere on the upper side of the top skirt. For others, the insulator surface may be marked almost continuously from tie wire to the lower edge of the inner skirt. In many cases a multiplicity of lightning paths is found on one insulator (Figures 4A and C). These can be formed by entirely separate lightning strokes or by different components of the same stroke.

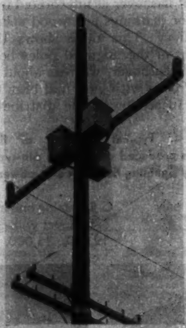

Figure 2. Installation of flashover recording equipment on line construction of Figure 1

Photographic surge-current recorders in both crossarm flashover paths and ground path. Crest-ammeter links in ground path

In case of power follow, the long-duration arc will tend to move away from the porcelain surface and maintain contact only at its terminals. This results in broad splashes of burned porcelain glaze at these points, often with considerable conductor and tie-wire pitting. The power-follow markings usually are localized in spots on the top and bottom of the insulator where the glaze has been burned through to the porcelain and frequently has a blistered appearance (Figure 4D). In less severe cases the glaze may be only partially burned through and is left with a color lighter than that of the normal surrounding glaze. Then the burned spot may have a crackled rather than blistered appearance. Sometimes the power-follow arc appears to strike from the conductor to the insulator pin, and the principal burn on the top of the insulator is at the edge of the top skirt under the conductor. In other cases, when the arc strikes from the tie wire, burns are found on the upper surface close to the tie wire. A power arc between line conductors usually will leave pits and beads or points of metal, often uniformly spaced out along the conductor from where the flashover started. These are the result of the arc traveling along the line, one melted spot occurring with each half cycle of current. The interpretation

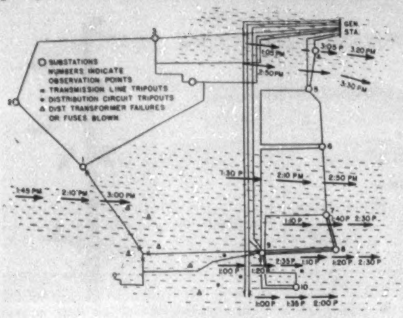

Figure 3. Sample storm chart prepared from reports submitted by substation attendants and used for determining storm frequencies and durations over lines being investigated

Sample Thunderstorm Reports

Observation Station	First Observation			When Over or Nearest Station			Last Observation		
	Time	Direction	Distance	Time	Direction	Distance	Time	Direction	Distance
1	1:45 p.m.	Southwest	7 mi	2:10 p.m.	South	2 mi	3:00 p.m.	East	6 mi
4	1:35 p.m.	Northwest	4 mi	3:05 p.m.	Over		3:20 p.m.	North	2 mi

No storm visible from stations 2 and 3

1—Lightning, thunder, no rain. Seemed to come from southwest, stay two miles south of station, then go east
4—Heavy rain at 3 p.m.

of evidence, as previously described, may not always be infallible, as some lightning strokes probably can have sufficient duration to produce effects resembling those attributed to power follow. Neither are so-called power-follow markings always evidence of sustained power follow causing circuit interruptions, as the 60-cycle arc may be extinguished before a circuit-breaker relay operation. These cases, however, are thought to be infrequent, as is borne out by correlation of similar inspection data with actual flashover-current records that subsequently will be discussed.

Distribution of Line Flashovers

A length of 3.4 miles of the line inspected in detail parallels and is shielded by a 132-kv tower line, with overhead ground wire. The normal heights of the towers and poles above ground are 92.5 feet and 38 feet, respectively. The horizontal distance between tower-line ground wire and ridge-pin conductor on the pole line varies from 88 feet to 99 feet. No evidence of line flashover was found on the inspections. However, one stroke occurred to this section in 1943 as evidenced by a splintered pole. Thus, in $5^{1}/_{2}$ years the section has been struck once.

The remaining 25.4 miles of unshielded line on which the climbing inspections were made has 453 poles with an average span of 293 feet. A total of 411 poles are type 1 (Figure 1) unguyed with 108 having a distribution circuit below the high-voltage circuit, 12 poles are guyed type-2 vertical corner poles, and 30 are guyed type-1 poles. Thus about ten per cent of the poles are guyed. Table I presents a summary of the distribution of the two types of flashover as interpreted from the insulator markings and wood splintering inspection. This table shows that 36 per cent of the unguyed poles bore evidence of flashover, whereas about 80 per cent of poles with guys had been flashed over. Inspection of the distribution of flashed poles showed that unguyed poles tend to be protected by guyed poles several spans away. The trend in the case of power-follow arcs is more significant. Only 13 per cent of the tangent unguyed poles that flashed over had evidence of power follow, whereas the percentage for the guyed type-1 poles was 42 and for the vertical corner poles (with still lower insulation to ground) 90. As far as can be determined, the presence of distribution circuits or transformers (distribution arm five feet below transmission arm) has little bearing on the effects of lightning on the transmission line, 34 per cent of poles with distribution having flashover evidence. This particular analysis cannot determine accurately the actual number of individual cases of each type of flashover. However, it provides very significant evidence on the nature of the flashover of such lines which can be discussed more clearly when correlated with the additional data obtained from the photographic-recorder measurements.

Character of Flashovers on Unprotected Line

The section of line equipped with the photographic recorders is inspected after each storm, the photographic recorders and magnetic links being checked for flashover-current records together with a visual inspection for additional flashover evidence. Where necessary, a climbing inspection is made as frequently as possible to determine the location and type of insulator markings and other evidence not visible from the ground. This is for the purpose of detecting flashover on intervening poles not equipped with recorders and to provide correlating information with the flashover currents at the recorder poles. During the three-year period 49 cases of line flashover have occurred on the sections under investigation for which it could be determined whether or not a sustained power follow or a line tripout was produced. For 35 cases a detailed record was obtained of the number of poles flashed over, together with the type of lightning flashover and sustained power follow (if occurring) at each pole. It is recognized that the mechanism of arc restriking and dielectric recovery is quite

Figure 4. Typical example of flashover markings produced on 34.5-kv pin-type insulators by lightning flashover and power follow

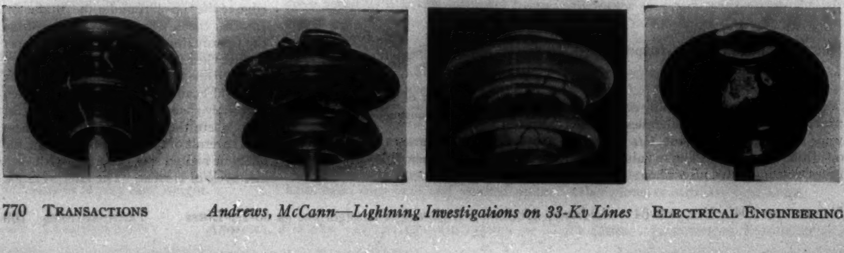

A. Lightning only, seven paths

B. Lightning only

C. Lightning only after four recorded cases of flashover with crest currents of 12,500, 12,000, 35,000, and 22,000 amperes

D. Two power-follow markings and lightning track complex, being a function of a large number of factors that cannot be evaluated adequately from the data so far obtained. However, there are certain important facts that have been ascertained which are described here briefly.

One of these is the prevalent occurrence of simultaneous flashover produced over an extended section of line by a single stroke. It was found that a stroke occurring between recorder stations usually flashes over several of the unguyed poles in the vicinity of the stroke in addition to one or more of the recorder poles having the lower insulation to ground. This is illustrated by the records of Figures 5A and B. Figure 5A is typical of several obtained showing simultaneous flashover for each component of a multiple stroke. It is the usual case that, if an appreciable duration of the lightning current is indicated for any one stroke component, it frequently occurs only at one pole, the same pole having power follow when present. Figure 5B is another record showing simultaneous flashover produced over about 1.5 miles of line. For this case, although lightning flashover occurred between all three phases and ground at pole 280 power follow occurred only between the top and one side conductor. Evidence of similar multiple-flashover characteristics on 220-kv wood-pole lines has been presented elsewhere.[3]

Table I. Summary of Lightning and Power-Follow Inspection on 33-Kv Unprotected Wood-Pole Line—25.4-Mile Line—453 Poles—Average Span 285 Feet—Line Put in Service 1939, Last Inspection 1941

Type of Flashover Evidence	Number of Poles on Which Evidence Was Found							
	Unguyed Pole Type 1		Insulated Guys Type 1		Vertical Corner Pole Type 2		Total Poles	
	No.	Per Cent	No.	Per Cent	No.	Per Cent	No.	Per Cent
Lightning only	127	31	14	47	1	8	142	31
Power follow also	19	5	10	33	9	75	38	8
No evidence	265	64	6	20	2	17	273	61
Totals	411		30		12		453	
Per cent of flashed poles of each type showing power follow		13		42		90		

	Positive Critical Dry Flashover Values in Kilovolts		
	Unguyed Type 1	Guyed Type 1	Vertical Corner Type 2
Top conductor to lower conductor	1,100	1,100	935
Top conductor to ground	(3,000–4,000)	1,000	950

Character of Voltages Produced by Direct Strokes to Unprotected Lines

The data presented by the foregoing two types of study provide definite substantiation of the nature of the voltage produced by direct strokes as visualized from our present knowledge of stroke mechanism.[4] This is illustrated by Figure 6. Strokes to open ground or to relatively low structures such as transmission lines are initiated by streamers propagating from cloud to ground (Figure 6A) which lower charge at a relatively slow rate onto the stroke channel being formed. During this period the electric field at the ground is being increased at an accelerating rate. During the initial stages of this process charge of opposite polarity to that on the stroke channel can flow along the conductor into the region below the stroke channel neutralizing this effect and holding the conductors at ground potential. However, at some instant before stroke contact, the rate of change of field produced by the stroke exceeds the rate at which charge can be drawn in on the conductors, and the conductor potentials start to rise (Figure 6B). It is indicated[4] that such induced voltages may start to be appreciable from 50 to 250 microseconds before actual stroke contact and reach magnitudes ranging from 100 to at least 1,000 kv. Just before the start of the "return-streamer" process (Figure 6A), short upward streamers may occur from the conductor, tending to modify the voltage to varying degrees. However, the general character of the voltage is one of an accelerated rate of rise which would become greatest after stroke contact (at the instant of maximum rate of current rise on the front of the discharge-current wave) if flashover did not occur first.

For such lines as being considered here, the voltage easily can reach the insulation strength to ground of a guyed pole in the initial period before actual stroke contact. Being of a slow rate of rise, it will cause flashover at the lowest insulation point, even though it be several miles distant. After stroke contact, the much higher rate of rise also may produce flashover at or near the point of contact. Further, the initial breakdown of wood insulation usually is just inside the surface, resulting in very high arc drops that frequently permit the simultaneous flashover of a number or adjacent unguyed poles (sometimes ten of more). Thus strokes to such lines should set up several simultaneous discharges as shown by the climbing inspection and photographic-recorder data. Parallel arc paths are very unstable, and one will tend to rob the others of the arc. This should be the path with lowest rate of dielectric recovery as characterized by the length and type of flashover medium and the magnitude and duration of current it has conducted. It would be expected that any sustained arcs would tend to concentrate at the guyed poles with flashover paths producing the lowest arc impedance and rate of dielectric recovery. As shown by Table I, 50 per cent of the poles showing power-follow evidence were guyed poles that constituted only ten per cent of the total poles. If the number of individual cases of power follow could have been counted accurately, the percentage probably would have been still higher. As previously mentioned, the unstable character of simultaneous arcs usually results in the concentration not only of the power follow but also the long-duration portion of each stroke component at

Table II. Lightning Exposure and Performance of Unprotected 33-Kv Wood-Pole Lines

Line No.	Predominate Construction	Length, Miles	Number of Storm-Days			No. of Separate Storms			Total Storm-Hours		Tripouts Per 100 Miles Per Year		
			1942	1943	1944	1942	1943	1944	1943	1944	1942	1943	1944
A	Types 1, 2	23.8	27	20	25	29	27	31	31.5	40.5	80	38	13
B	Types 1, 2	10.2	16	19	18	17	24	21	25	25	49	29	39
C	Types 1, 2, 7*	58.9	22	27	36	32	32	42	42.5	78	78	61	73
D	Type 7*	27.1	17	31	28	20	35	35	43	43	44	44	15
E	Types 1, 2	10.6	18	21	42	21	28	47	33	21	38	66	21

* Type-7 lines with flat configuration, ten-foot crossarms, steel braces, and no guy insulation.[1] Critical breakdown voltages at tangent poles = 590 kv line-to-line, 3,000–4,000 line-to-ground. At guyed crossarm poles 325 kv line-to-ground, at vertical corner poles 600 kv line-to-line and 350 kv line-to-ground. For 4,099 mile-years (1929–32) average tripouts per 100 miles per year = 38.

Lines of types 1 and 2 construction (see Figure 1 and Table I). For 571 mile-years (1938–44) average tripouts per 100 miles per year = 31.

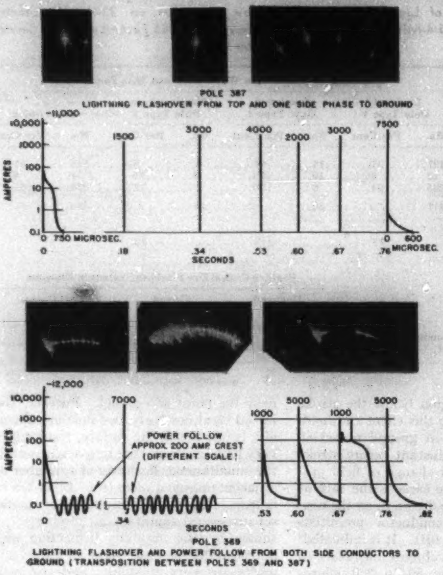

Figure 5A. Photographic surge-current record of multiple-lightning flashovers produced simultaneously at two recorder stations with power follow at one

Three tangent poles adjacent to pole 387 had lightning-flashover evidence. Photographic recorders were installed only in ground path. Distance between recorders is one mile. First component started power follow at pole 369 that apparently extinguished itself, second component started power follow extinguished by breakers. Additional components occurred after circuit was interrupted

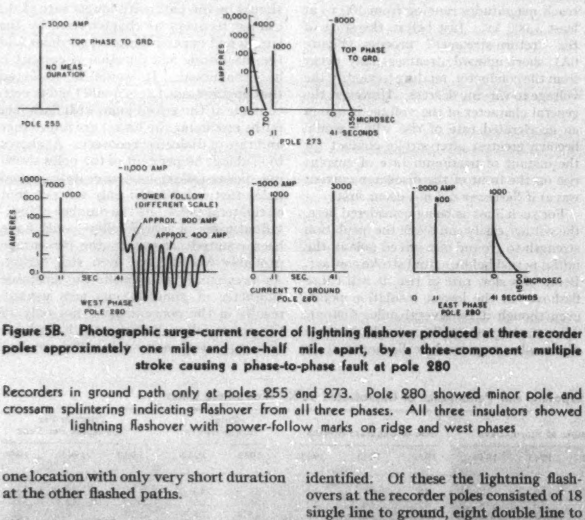

Figure 5B. Photographic surge-current record of lightning flashover produced at three recorder poles approximately one mile and one-half mile apart, by a three-component multiple stroke causing a phase-to-phase fault at pole 280

Recorders in ground path only at poles 255 and 273. Pole 280 showed minor pole and crossarm splintering indicating flashover from all three phases. All three insulators showed lightning flashover with power-follow marks on ridge and west phases

one location with only very short duration at the other flashed paths.

Character of Recorded Flashovers

For the total of 49 recorded cases of flashover 21 or 43 per cent caused a sustained power follow. For 35 of these the type of flashover at each pole could be identified. Of these the lightning flashovers at the recorder poles consisted of 18 single line to ground, eight double line to ground, and nine involving all three phases and ground. However, all but five involved lightning flashover between more than one phase at some point along the line. Fifteen or 40 per cent of the 35 caused a sustained power follow. All but three of these occurred at the guyed poles. Eight of the power follow cases were single line to ground, six double line to ground, and one line to line. Thus, although 30 out of 35 cases caused multiphase lightning flashovers, only seven or 20 per cent caused a sustained multiphase fault. In addition to the 15 out of 35 recorded cases of sustained power follow, one case of $3^{1}/_{2}$ cycles of power follow and one of one cycle of power follow were recorded (apparently self-extinguishing) together with a case in which sustained power follow was initiated after the third component discharge at one recording station while the same three-stroke components produced one, two, and one-half cycle, respectively, of power follow at an adjacent station.

It is of interest that the insulator inspection records of flashover at each recorder pole correlated quite well with the flashover-current records. In every case where only lightning-flashover currents were recorded, the insulator markings were interpreted as "lightning only." The same correlation was obtained for the cases of power follow except that no marked distinction could be made between the cases of sustained power follow, requiring operation of the eight-cycle breakers, and the power follow cases that lasted from 1 to $3^{1}/_{2}$ cycles. Also in one case power-follow evidence was not discernible at one of the two insulators shown by the recorders to have been involved in a sustained arc.

Storm Frequencies and Durations

Tables II and III list the data obtained on the number of storms, storm days, and total storm hours per year recorded over each of the unprotected and protected lines being investigated. These data were obtained from the storm charts prepared as illustrated in Figure 3. Correlated with the data are the number of tripouts per 100 miles of line per year and the number of strokes to the protected lines continuously equipped with magnetic links. It is of interest that although the ratio between storm-days, storms, and storm-hours varies considerably as does also the magnitude of each of these quantities from year to year and between different lines, the order of magnitude of all three is the same. No one of the above three indexes of storm activity appears to bear a closer relation to the frequency of direct strokes or line tripouts than the others. This indicates that the intensity of the electric storm or the density of direct strokes to ground is a variable of at least as great importance as the others.

Crest Stroke Currents

Before discussing in more detail the relation between the frequency of storms, direct strokes, and line tripouts, it would be best to examine the magnetic-link rec-

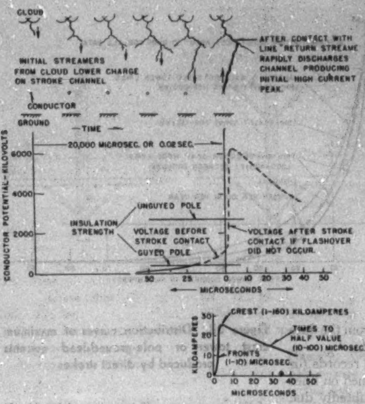
CLOUD
INITIAL STREAMERS FROM CLOUD LOWER CHARGE ON STROKE CHANNEL
AFTER CONTACT WITH LINE "RETURN STREAMER" RAPIDLY DISCHARGES CHANNEL PRODUCING INITIAL HIGH CURRENT PEAK.
CONDUCTOR
GROUND
TIME
20,000 MICROSEC. OR 0.02 SEC.
CONDUCTOR POTENTIAL–KILOVOLTS
6000
4000
2000
0
UNGUYED POLE
INSULATION STRENGTH
VOLTAGE BEFORE STROKE CONTACT
GUYED POLE
VOLTAGE AFTER STROKE CONTACT IF FLASHOVER DID NOT OCCUR.
50
25
0
10
20
30
40
50
MICROSECONDS
KILOAMPERES
CREST (1–160) KILOAMPERES
TIMES TO HALF VALUE (10–100) MICROSEC.
FRONTS (1–10) MICROSEC.
MICROSECONDS

Figure 6. Mechanism of the direct-stroke discharge by which relatively high voltage of slow rate of rise can be induced upon conductors of unprotected transmission lines before actual stroke contact

A (left). Voltage produced by direct stroke to conductor of unprotected 33-kv wood-pole line

B (below). Assumed stroke current and principal ranges of variation[5]

ords of pole-ground-lead currents upon which the stroke-frequency data are based. It is first necessary to consider the possible sources of surge currents that might produce a record. These are somewhat different for lines having an overhead ground wire than for lines equipped with protector tubes. As has been pointed out previously,[5] not only direct strokes but indirect strokes striking nearby can induce smaller magnitude currents in the ground leads. At least 90 per cent of all strokes to ground are negative which will induce positive currents in the ground leads. It was estimated[5] that for spans of 800–1,000 feet, induced currents as high as 5,000 amperes might be produced in a single tower of an overhead-ground-wire line. Similar estimates indicate possible induced currents as high as 1,500 amperes for spacings between ground leads of the order of 300 to 400 feet. For lines equipped with protector tubes higher currents can be produced, because such an indirect stroke will flash over a relatively few tubes and thus provide a limited number of paths to ground. Another important source for ground-lead-current records on lines equipped with tubes is the simultaneous flashover of a tube of lower breakdown voltage some distance away from the point of stroke contact due to the previously mentioned initial slow rate of voltage rise. Thus, an appreciable number of isolated pole-ground-lead-current records can be produced simultaneously with those close to the point of stroke contact. For the afore-mentioned reasons it is important to consider the crest-ammeter records carefully.

Such factors have been recognized to some extent in previous magnetic-link investigations on higher-voltage lines[6,7,8] and some sort of arbitrary method set up for throwing out certain records and not identifying them with direct strokes. However, in plotting the results of such previous studies it has been customary to plot percentage distribution curves showing the per cent of records exceeding a given magnitude. When this is done the character of the resulting curve depends to a great extent upon the accuracy of the judgment used and the number of records eliminated. A more fundamental way to approach this problem is to plot the total number of records (or the number per 100 miles of line per year) that exceeds each magnitude. The resulting curve will eliminate the afore-mentioned judgment factor except for the lower range in which other sources can produce records. This is important, as it is the higher-magnitude currents that are most likely to cause a flashover. Curves plotted in this way from this investigation are shown in Figure 7A together with a similar analysis of the Hansson and Waldorf data[6] in which all records thought by them to be direct strokes were used. Figure 7B presents a comparison of the more generally used percentage distribution curves from this and other investigations. The curve of Figure 7A for 33-kv lines with an overhead ground wire shows more high-current records than either the 33-kv protector-tube-line data or the steel-tower-line data. This same trend is shown for the individual maximum crest pole-ground-lead currents associated with each stroke. It was not found that any significantly greater number of grounds on the overhead-ground-wire lines tended to carry current than for the protector-tube lines. This indicates that more of the higher-current strokes actually were recorded on the ground-wire lines. This curve is based upon only 66 records, and for this reason a definite conclusion cannot be reached. However, it is of interest that an analysis of the data obtained by Hansson and Waldorf[6] from different lines indicates curves agreeing quite closely as long as about 100 records were available for each curve.

The factors which might affect such curves may be summarized briefly as follows: Because of the traveling-wave effect the sum of the crest tower currents should be greater than the actual crest stroke current. The difference will be greater the shorter the wave front and the longer the span. Further the sum of the crest tower currents is the sum of the respective maximum components as produced by several component discharges (in the case of multiple strokes) which

Figure 7A. Probability curves showing the number of recorded stroke currents per 100 miles of line per year exceeding a given crest magnitude

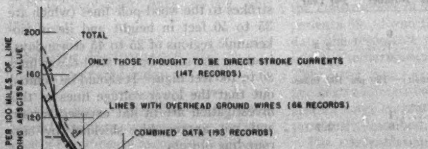

Figure 7B. Percentage distribution curves of direct-stroke crest currents

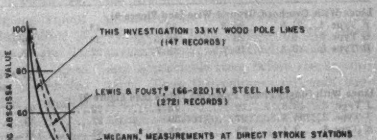

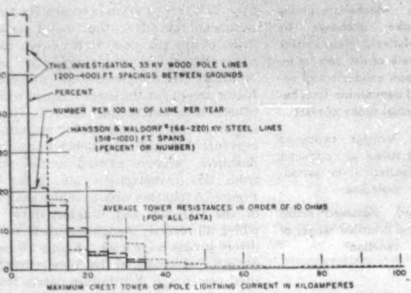

Figure 8A. Distribution curves of maximum crest tower or pole-ground-lead currents produced by direct strokes

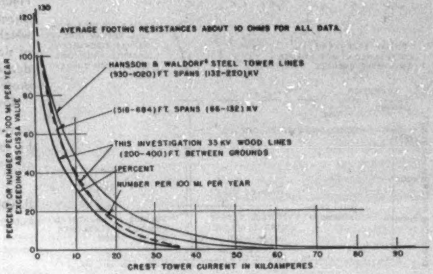

Figure 8B. Distribution curves of maximum crest tower or pole-ground-lead currents produced by direct strokes

might not bear the same proportionate relation to each other and cause the data to be high. Further, the effect of several strokes in some cases may be considered as one. On the other hand, magnetic-link measurements on steel-tower lines will indicate less than the total tower current, as no account usually is taken of the cross-brace currents.[5] There is one more very important effect that might account for the higher stroke currents on the 33-kv line with ground wires as compared to the 33-kv protector-tube-line data. The availability of the charge from ground that must combine with the stroke charge can be appreciably greater for a line with overhead ground wires. Then, there is a large number of paths provided by each ground lead, whereas for the tube line the only paths are those provided by the tubes that flash over. The possibility of more rapid combinations of the charges for the former case might result in a prevalence of higher crest currents. Although this effect cannot yet be definitely verified from the data so far obtained, it is indicated.

The higher number of total records (or low-magnitude records) obtained on lines with protector tubes is undoubtedly due to the two factors mentioned previously, induced surges, and simultaneous flashover. For instance, of 127 records to the tube lines, 57 were isolated surges involving only a single pole ground Fifty per cent of these were positive. Of the 66 records from the ground-wire lines only eight (75 per cent positive) were of this nature. This latter would be expected, as they should be caused predominantly by indirect strokes. In order to form a basis for eliminating all but those records thought to be caused by direct strokes, all isolated tower-current records (involving only one pole) below 1,500 amperes for overhead-ground-wire lines and below 5,000 amperes for protector-tube lines were arbitrarily removed from the data. This produced the lower solid curve in Figure 7A.

Frequency of Direct Strokes

The curve obtained in this way gives an average of 130 direct strokes per 100 miles of line per year. Hansson and Waldorf[4] estimate a general average of 100 strokes per year from their studies on steel lines. However, as shown by the curve of Figure 7A their data represent the number exceeding about 2,500 amperes (the lower limit of their recorders). This point lies very close to the corresponding point on the combined curve of this investigation, which indicates that they also would have measured more actual direct strokes if conditions had permitted the recording of lower-magnitude direct strokes. On the other hand, when comparing the percentage distribution curve obtained by the foregoing method of removing certain records with the curve obtained in the Westinghouse direct-stroke investigation (Figure 7B) it is seen that a higher percentage of lower-magnitude records is still present in the data of this investigation The direct-stroke study shows that about ten per cent of all direct strokes are below 2,000 amperes and 16 per cent are below 5,000 amperes, whereas the curve of this study shows corresponding percentages of 15 and 30. Adjustment of the data of this study to fit the direct-stroke data in this range would produce a curve in Figure 7A that would indicate about 95 direct strokes per 100 miles of line per year. It appears evident that, with a possible range of from 95 to 130, the frequency of strokes to the wood-pole lines (which are 35 to 50 feet in height and lie in isokeraunic regions of 25 to 45 storm-days) is about the same as for steel-tower lines 80 to 100 feet high. It should be pointed out that the lower-voltage lines of this investigation are in flat exposed terrain and not appreciably shielded by surrounding objects.

Stroke Polarity

Of the 147 records considered as caused by direct strokes, 134 or 91 per cent were of negative polarity. The highest-magnitude recorded positive stroke had a

Table III. Lightning Exposure of Protected 33-Kv Wood-Pole Lines

							Normal Tripouts From Lightning	
Line	Mile-Years	Storm-Days Per Year	Storms Per Year	Storm-Hours Per Year	Total Direct Strokes	Total Tripouts	Number	Number Per 100 Miles Per Year
Lines With Overhead Ground Wire (see Figure 9)								
F Type 4	21.9	25.3	30	43	21	0	0	
G Type 4	9	23	28.5	33	19	1	1	2.3
H Type 5	13.5	19.7	28.7	22	13	0	0	
					53	Average density—120 per 100 miles per year		
Lines With Single-Phase Protector Tubes (see Figure 9)								
I Type 3	13.8	19.7	28.7	22	24	2*	1	
J Type 3	36.3	27	39	27	49	0	0	3.7
K Type 3	3.4	23	25.3	33	11	1	1	
					84	Average density—136 per 100 miles per year		
Lines With Flat Construction, Three-Phase Tubes, Staggered Every Third Pole Per Phase (see Figure 10)								
L Type 6	8.5	23	25.3	33	10	2	2	43

Average number of strokes per 100 miles of line per year $= \frac{147}{112.7} = 130.$

*One occurred at end of line where it connects to an unprotected line. Pole ground resistances range from 3 to 20 ohms with an average for each line of approximately 10 ohms.

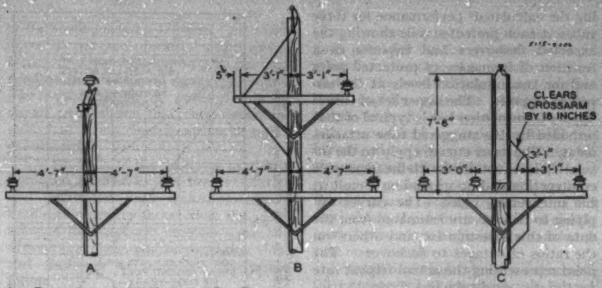

A. Type 3 with single-phase tubes
BIL 725 kv
370-foot average spacings between grounds
Average spans 185 feet

B. Type 4
BIL 725 kv
250-foot average spacings and spans

C. Type 5
BIL 600 kv
320-foot spacings and spans

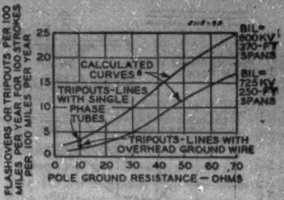

D.

Figure 9. Comparison of actual and calculated performance of three types of 33-kv protected line construction employing an overhead ground wire or deion protector tubes on a top phase

crest current of 90,000 amperes and the highest negative stroke 113,000 amperes.

Pole-Ground-Lead Currents

Figure 8 presents the data on the maximum pole-ground-lead currents for each record identified as a direct stroke and compared with similar data of Hansson and Waldorf.[6,7] In these figures the data are plotted in two ways showing both the per cent and the number of tower currents per 100 miles of line per year corresponding to the given values. Since the average recorded direct strokes for the Hansson and Waldorf data is 100 per 100 miles per year, their curves for the two ordinate systems coincide. These curves show the benefit of short spacings between spans in reducing the maximum tower current. The highest-pole ground lead current recorded for the 33-kv lines of this investigation is 36,000 amperes as compared to a maximum of 95,000 amperes for the steel-tower lines with longer spans.[6] As shown by Figure 8B the maximum pole-ground-lead current produced by five per cent of the strokes to the wood-pole lines with the shorter spans is 26,000 amperes whereas the corresponding value for the 500–700-foot-span steel lines is 38,000 amperes and for the 900–1,000-foot-span lines 49,000 amperes.

Flashover Performance of Unprotected Lines

At the bottom of Table II is listed a general summary of the tripout performance of two types of unprotected line construction. The first type consists of flat construction using ten-foot crossarms and steel braces typical of installations prior to 1929.[1] The second type of construction is that of Figure 1 with the insulation levels listed in Table I. For both types of construction the average frequency of guyed poles is about once every half to one mile with spans of 150 to 300 feet. As shown in Table II, the flat construction experienced an average of 38 tripouts per 100 miles per year as compared to only 31 for the construction of types 1 and 2 (Figure 1). It is indicated that this improvement in performance is due partly to a reduction of lightning flashovers because of the higher insulation level but that a greater effect is the improvement of the dielectric-recovery characteristics of the line with greater wood insulation.

It has been recognized for some time that a path over wood has a greater "arc-quenching" action than through air or over insulators alone. Studies of the performance of higher-voltage steel-tower lines[8,9] show that about 85 per cent of the flashovers of lines 100 miles in length or less result in a tripout. Calculations from present direct-stroke data[2,7] (including the crest-stroke-current curve (Figure 7A) of this investigation) indicate that lines of the earlier flat construction should experience about 91 lightning flashovers per 100 miles per year, whereas the construction of Figure 1 should experience 88. From the foregoing tripout data the respective percentage ratios of tripouts to flashovers are thus 42 and 35. This latter figure compares with 40–43 per cent as determined from the photographic-surge-current-recorded studies previously described.

The concentration of cases of power follow at guyed poles suggests the possibility of materially reducing the outages on lines of Figure-1 construction by installing deion protector tubes either at or adjacent to all guyed poles. An investigation program of this type is planned. For best protection tubes should be installed on all three phases since, as shown by the special flashover study, most strokes to such lines result in multiphase lightning flashovers, even though the ridge-pin conductor shields the other two.

Performance of Continuously Protected Lines

Table III summarizes the lightning performance of the protected lines being studied in detail. Only one tripout and case of flashover evidence has occurred for an estimated 53 direct strokes to the lines with an overhead ground wire. The type-3 (Figure 9) construction with single-phase protector tubes has experienced three tripouts for 84 direct strokes. However, Line 1 (Table II) is connected to an unprotected line section, and one of the flashovers occurred at the end pole of the protected section which is also a transposition point. This, therefore, was not attributed to the protected construction. Both of the other two tripouts were associated with tube failures. Thus, the ground-wire lines averaged one tripout per 53 strokes as compared to one per 42 strokes for the single-phase tube construction.

Figure 9 gives the actual number of tripouts per 100 miles of line per year for the combined lines of the two aforementioned general types as compared to calculated performance[8,9] using the stroke-current wave-shape data of direct-stroke studies[2] and the crest-stroke-current frequency curve of Figure 7A. The character of the lightning voltages on an overhead ground wire or a conductor equipped with protector tubes is quite different from that appearing on an unprotected phase conductor.[9] The multiple grounds provided continually for the grounded wire and after a relatively low voltage has been reached by the tubes prevent any significant voltages occurring any appreciable time before stroke contact. Thus the voltages on such conductors are determined primarily by the stroke discharge current. Surprisingly close agreement is shown by the calculated and actual data of Figure 9, indicating that when the actual frequency of direct strokes is known our present knowledge of the characteristics of lightning-stroke currents[2,6,9] provides a reliable basis for determining line perform-

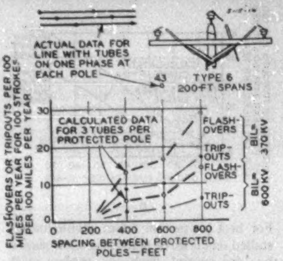

Figure 10. Calculated lightning performance of 33-kv line equipped with protector tubes on all three phases showing effect of spacing between protected poles and insulation at unprotected poles

Also comparison is made with operating performance of line with one tube per pole rotated between phases

ance. As shown in Figure 9, the somewhat higher outage rate for the tube construction is due to its lower insulation level and longer spans as compared to the ground-wire lines. By separating the pole ground lead from the pole,[9] it is quite practical to reduce the flashover rate for this type of construction by about one half. It should be pointed out that the calculated curves apply to flashovers whereas the operating records are tripouts. However, a detailed line-inspection program has been carried out on these lines which so far has detected no flashovers other than those resulting in the tripouts. These inspections are made periodically at all locations shown by the magnetic-link records to have received a direct stroke. That the application of protector tubes only on the ridge conductor of lines such as that of type 1 (Figure 1) provides both an effective and economical method of protection had been shown by previous experience.[10]

The second type of protector-tube application studied in detail is that shown in Figure 10 with a single tube at each pole but the tubes rotated between phases. As shown by the operating data for this construction (Table III) the performance has not been so good as for the other protected lines. For only ten direct strokes there have been two tripouts. One of these flashovers occurred at a switch pole near one end of the line section. The poorer performance is due primarily to the lower insulation level that results from the tube grounds at each pole. This is illustrated by Figure 10. The performance of such construction should be comparable to that with all three tubes installed at every third pole and the same phase-to-phase insulation level at the unprotected poles as provided by the staggered construction at each pole. In Figure 10 are curves showing the calculated[9] performance for three tubes at each protected pole showing the expected flashovers and tripouts as a function of frequency of protected poles and for two insulation levels at the unprotected poles. The upper set of curves applies to insulation levels typical of that provided by the staggered tube arrangement. The lower curves apply to the insulation level obtained with the given pole construction and no grounding circuit at the intervening poles. The curves applying to tripouts are estimated from the data of this investigation and others[9] on the ratios of outages to flashovers. The point representing the actual tripout rate for the staggered tube line shows 43 tripouts per 100 miles of line per year as compared to an estimated 17 flashovers and 12 tripouts, whereas, if the tubes actually had been placed three to a pole every third pole, the estimated flashover rate would have been only seven with four tripouts per 100 miles of line per year.

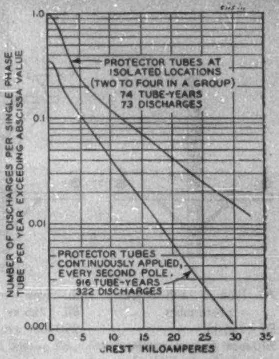

Figure 11. Surge-crest-ammeter records of the discharge duty on deion protector tubes installed on 33-kv wood-pole transmission lines

Duty on Deion Protector Tubes

The records of the lightning surge currents discharged by deion protector tubes are summarized in Figure 11. Two general types of application were studied. One consists of tubes applied continuously on the lines of Table III for which the bottom curve of Figure 11 applies. For the other type of application isolated groups of two to four poles adjacent to a vertical corner pole are equipped with one tube on the ridge-pin conductor. For both curves of Figure 11 all recorded surges are considered, although several tubes might be involved in one disturbance. The much greater tube duty for isolated applications is shown. Each protector tube at the infrequent installations discharged about once per year as compared to a frequency of 0.35 discharge per tube on the continuously protected lines. The tube duty should be considered from two viewpoints, one the duty imposed by high lightning currents and the other by the interruption of fault current. As shown by Figure 11 the tubes at isolated locations discharged about 12 times as many of the higher lightning currents. The actual duty from interrupting fault current depends upon the number of tubes involved for each disturbance. This is not known. In most cases it should be only one. Upon the assumption that one tube interrupts a fault current for every case of flashover, the average number of cases of fault-current interruptions is 0.7 per tube per year for the isolated installations and only 0.17 for the continuously applied tubes; a ratio of about four to one. These differences should be even more marked if cases of single isolated tube-equipped poles were considered. The foregoing data show the material benefit of closely spaced tubes in reducing the individual tube duty and maintenance. After 916 tube-years of experience with lines continuously protected by about 320 tubes, there have been three tube failures.

Conclusions

An analysis of the electric fields produced by the "initial streamers" of direct strokes to an unprotected transmission line indicates that surge voltages of appreciable magnitude can be induced on a conductor as much as 50 to 250 microseconds before actual stroke contact. These may reach potentials ranging from 100 to over 1,000 kv before the stroke actually discharges into the line. This is confirmed by a detailed climbing inspection of an unprotected 33-kv wood-pole line and by 49 recorded cases of flashover on sections of unprotected line equipped with photographic surge-current recorders. Having relatively slow rates of voltage rise, these "initial streamers" can flash over points of lower insulation several miles from the stroke, after which higher insulation close to the stroke also may be flashed over by the much higher rates of rise following actual stroke contact.

In the special flashover studies simultaneous multiple flashovers were recorded that extended over as much as two miles of line. In some cases they were caused by multiple strokes, and each component of the multiple discharge was recorded at several of the flashover points. In these cases one path usually (but not always) robs the others of the long-duration portion of each stroke component so that the flashovers at the other points along the line are of very short duration with no evidence of power follow except at the one location.

About 40 per cent of the recorded cases

of flashover caused a tripout. Although about 85 per cent produced a multiphase flashover at some point, only 20 per cent resulted in a sustained multiphase fault. The concentration of power follow at guyed poles shows that they determine to a great extent the tripout performance of such lines.

Examination of the flashover markings produced on 34.5-kv pin-type insulators and correlated with measurements of flashover currents shows that the character of the markings provides a method of detecting flashover from lightning alone and flashover accompanied by power follow.

Magnetic-link studies on continuously protected 33-kv wood-pole lines 35 to 50 feet high show that the direct-stroke frequency is of the order of 95 to 130 per hundred miles of line per year or the same order of frequency as higher-voltage steel-tower lines 80 to 100 feet high lying in regions of about the same lightning severity. Storm observations at substations provide a method of plotting storm maps for each lightning storm over the area covered by the lines being studied. Detailed records of storm frequencies and durations show a wide fluctuation in the number of storm-days, storms, and total annual storm durations both from year to year and between different lines only a few miles apart. As shown by the storm maps, this is caused by large local variations in the extent and paths of the storms. No one of the three indexes bears a close relation to the frequency of direct strokes to the line. This is probably due to the importance of an additional factor, the density of strokes emanating from each storm.

It was found that a more accurate and fundamental method of plotting crest stroke currents and tower currents is in terms of the number per unit length of line per year rather than the per cent that exceed a given value. Because of the uncertainty of the lower-magnitude surges the latter method can produce considerable error in the frequency of the more important higher-current records. There is an indicated prevalence of higher-magnitude strokes to lines equipped with overhead ground wire. A possible explanation for this is the better conducting path provided by the greater number of grounds in the case of a ground-wire line, so that the earth charges may combine more rapidly with the charge on the stroke channel. Comparison of the crest-pole ground lead currents recorded in this investigation (where average spacings between grounds range from 250 to 400 feet) with similar data from high-voltage lines (having spans ranging from 500 to 1,000 feet) shows the definite benefit of closely spaced grounds in reducing the maximum pole or tower currents.

Comparison of lightning-tripout records for unprotected 33-kv wood-pole lines of limited insulation and lines with about the optimum insulation for this voltage class (see Table II and Figure 1) shows an average rate of 38 tripouts per 100 miles of line per year for the former as compared to 31 for the latter.

Detailed data have been obtained on the lightning performance of 33-kv wood-pole lines continuously protected both by overhead ground wires and by protector tubes. Although only a relatively few mile-years of experience have been gained on each type of construction, the detailed nature of the records showing actual stroke frequencies together with line tripouts have established the degree of performance of the various types of construction. Lines equipped with an overhead ground wire and having insulation levels of 600 to 725 kv with spacings between grounds ranging from 250 to 320 feet (Figure 9) experience only about two tripouts per 100 miles of line per year when an average ground resistance of ten ohms is provided. The same degree of protection is shown to be provided by lines with one protector tube on the ridge-pole conductor of every other pole of lines with average spans of about 200 feet (Figure 10) if the same insulation level is provided. The performance record of a line with flat construction (Figure 10) having one tube per pole on alternate phases shows the importance of obtaining a reasonably high insulation level for unprotected phases at each pole. This line shows an outage rate of 43 tripouts per 100 miles of line per year, whereas the use of three tubes per pole on every third pole should result in only about four tripouts per 100 miles of line per year when the full insulation level of the unprotected poles is maintained.

Data have been obtained on the surge discharge duty of deion protector tubes installed continuously on protected lines and at isolated points on lines. For the former case the discharge rate for lightning surges is about 0.35 per individual tube per year, while the frequency of power-fault interruptions is only about 0.17 per individual tube per year. The corresponding rates of discharge are much higher for isolated tube installations. Likewise, the crest magnitudes of the surges that must be discharged at isolated installations are much greater.

References

1. Transmission Research and Design With the Field as a Laboratory, F. E. Andrews, C. L. Stroup. AIEE Transactions, volume 49, 1930, pages 959–69.

2. The Measurement of Lightning Currents in Direct Strokes, G. D. McCann. AIEE Transactions, volume 63, 1944, pages 1157–64.

3. Wood-Pole Line Protection Without Ground Wires, H. L. Rorden. *Electrical World*, December 8, 1944, page 94.

4. Induced Voltages on Transmission Lines, C. F. Wagner, G. D. McCann. AIEE Transactions, volume 61, 1942, pages 916–30.

Field Disturbances Produced by Lightning, G. D. McCann, D. E. Morgan. AIEE Transactions, volume 62, 1943, pages 345–57.

5. Lightning Phenomena, C. F. Wagner, G. D. McCann. Electrical Transmission and Distribution Reference Book, Westinghouse Electric Corporation, East Pittsburgh, Pa., chapter 12, page 312.

6. An Eight-Year Investigation of Lightning Currents and Preventive Lightning Protection on a Transmission System, E. Hansson, S. K. Waldorf. AIEE Transactions, volume 63, 1944, May section, pages 251–8.

7. Discussion by C. F. Wagner and G. D. McCann. AIEE Transactions, volume 60, 1941, page 702.

8. Lightning Investigations on Transmission Lines—VIII, W. W. Lewis, C. M. Foust. AIEE Transactions, volume 64, 1945, March section, pages 107–15.

9. Fundamental Characteristics of Lightning Surges and Their Effect on the Comparative Performance of Transmission Lines, G. D. McCann. *Electric Light and Power*, May 1945.

10. Lightning Protection for Transmission Lines, A. W. Gothberg, A. S. Brookes. AIEE Transactions, volume 56, 1937, January section, pages 13–16.

Control of Load, Frequency, and Time of Interconnected Systems

C. K. DUFF
MEMBER AIEE

Synopsis: The general problem is stated and typical solutions indicated. Characteristics of governors and of frequency- and load-control devices are briefly explained, and effects on generator and tie-line loads are summarized. Illustrating the principles enunciated, interconnected systems in southern Ontario and adjacent portions of Quebec totaling 1,650,000-kw generating capacity are described, also operating experience with automatic frequency control, and automatic load control of two ties, one of which is a 45,000-kw frequency-changer set interconnecting systems of relatively large capacity.

THIS IS the era of superpower. Two or three decades ago, engineers envisioned the day when the power resources of whole countries or even continents would be interconnected by vast networks of high-voltage transmission lines distributing electric power to all parts of the country. Today their dreams are approaching realization in large areas of the United States, in Britain,[6] and to a lesser degree in Canada and other countries.

On this continent these power networks or power pools as they are sometimes called, have grown up piecemeal by progressive interconnections within local areas, and finally by ties to more distant areas, which in turn may be connected to other areas beyond them. One of the earliest problems encountered in the operation of interconnected systems was the regulation of the transfer of power between one system and another, and closely related thereto, the regulation of frequency. A by-product of frequency control is time control, which demands precise *average* frequency, so that synchronous electric clocks may keep pace with the slow but inexorable advance of Father Time. These related problems are dealt with in this paper.

Purposes of Interconnection

At the outset, let us consider briefly the questions—why interconnection? and why control? Interconnections may be made for one or more of the following reasons:

1. Transfer of power from systems having a surplus to areas of shortage.
2. Diversity of loads on different systems.
3. Diversity of stream flow and storage facilities, affecting hydroelectric generation available in different areas.
4. Pooling of reserve generating facilities, with large savings in capital cost of stand-by generating capacity.
5. Greater reliability of service, and resources for emergencies.
6. Convenience in arranging outages of equipment for maintenance.

For example, water which would otherwise be spilled over the dam at some run-of-river plant might be used to permit storage of water at some other plant where storage facilities are available, which in effect transfers useable energy in the form of ponded water from one river to another which may be many miles distant; or alternatively, that water may be used to save expensive coal at some distant steam plant; or conversely, steam generation may be used to help out water-power areas in dry seasons. Diversity of loads and pooling of reserve capacity by interconnection make it possible to carry a greater total firm load on the combined systems than they could carry separately.

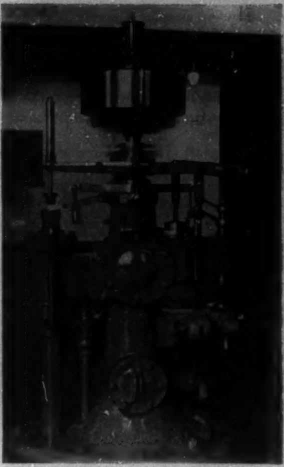

Figure 1. Governor of older type in use at Queenston plant

Control of some kind is necessary in order that the power transferred from one system to another over the interconnecting tie lines may conform to plans based on economic or contractual considerations. Tie-line load control is bound up with the control of frequency and time, since no one of the three may be changed without affecting the other two. Apart from their relation to load control, frequency and time demand close regulation on their own account; frequency, because many modern industrial processes with electric motor drives are dependent upon steady and accurate frequency; and time, because of the millions of electric clocks which time the movements of modern society to an accuracy measured in seconds. Some industries wish frequency to be controlled to a tolerance of plus or minus one quarter of one per cent on one-minute average values. This is not always attainable, but on the Southern Ontario system of the Hydro-Electric Power Commission of Ontario, that precision is attained for more than 98 per cent of the average day's run, using automatic frequency control. For the sake of electric clocks, the average frequency must be maintained even more precisely, since an error as small as 1/100 of one per cent will in 24 hours create a time deviation of eight seconds on electric clocks. Time on the Commission's Southern Ontario system is usually controlled more precisely than this, but emergency conditions and heavy war-time demands occasionally cause temporary time deviations up to five seconds and sometimes more. These errors are automatically corrected over a period of time after the emergency or overload condition has passed.

On interconnected systems, automatic frequency control is now almost universal, and automatic tie-line load control is becoming more and more extensively used. Where tie-line capacity or stability limits

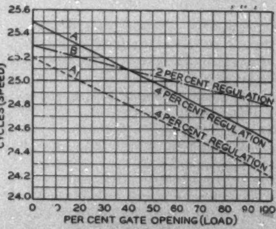

Figure 2. Characteristic curves of turbine governors, showing the relation between gate opening and speed

---

Paper 45-139, recommended by the AIEE committee on power generation for publication in AIEE TRANSACTIONS. Manuscript submitted December 1, 1944; made available for printing July 6, 1945.

C. K. DUFF is a meter engineer in the operating department, Hydro-Electric Power Commission of Ontario, Toronto, Ontario, Canada.

The author extends acknowledgments to the Hydro-Electric Power Commission for the use of illustrative material and to the editor of *Hydro News* for the use of photographs for Figures 11 and 15; also to the Gatineau Power Company for permission to publish information and to use photographs of equipment on their system.

are critical factors, automatic tie-line load control is essential for the maximum utilization of line capacity.

A recent article[13] describes an interesting example of interconnected systems in the northwestern states, where 11 important power systems in five states have a total of $3^1/_2$ million kw generating capacity with 13,000 miles of major transmission lines ranging from 40 to 220 kv. This interconnection takes advantage of diversity of loads in two time zones and diversity of river flow in several watersheds on both sides of the Rocky Mountains, the resulting economies being equivalent to 100,000 kw of added generating capacity.

In this power pool we have examples of the two types of interconnection which are commonly met:

1. Systems connected like links of a chain, which may have side branches but no loops.
2. Multiple interconnections, forming loops.

One particularly complicated situation was solved by the unique method of phase-angle control,[8] but the usual problems were met by conventional methods of automatic frequency control and tie-line load control referred to later in the present paper.

Governor Characteristics

Regulation of frequency and tie-line load involves the regulation of the output of generators connected to the systems, and this requires regulation of the power input to their turbines. In a typical hydroelectric plant, the working fluid, water, is conducted from the forebay through the penstock to the turbine, and is discharged through the draft tube to the tail race. The discharge is controlled by the gates, consisting of a set of overlapping vanes arranged in a circle in the turbine casing at the point where the water enters the wheel. The gate stems pass through the upper wall of the turbine casing and all are connected to a gate ring, which is moved by servo-motor pistons under control of the governor.

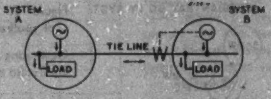

1	2	3	4	5	6	7	8	9	10
LOAD CHANGE	FREQ.	T.L.L. (1)	F.F.C. A	T.L.L. (2)	F.T.L. B	T.L.B. B	SELEC. FREQ. A	SELEC. FREQ. B	T.L.L. (3)
+A	LOW	←	R	0	L(R)	L-R	R	—	0
+B	LOW	→	R	→	R	R	—	R	0
−A	HIGH	→	L	0	R(L)	R-L	L	—	0
−B	HIGH	←	L	←	L	L	—	L	0

T.L.L.=TIE-LINE LOAD. F.T.L.=FLAT TIE-LINE LOAD CONTROL
F.F.C.=FLAT FREQUENCY CONTROL. T.L.B.=TIE-LINE BIAS CONTROL
S.F. (COL. 8, 9)=SELECTIVE FREQUENCY CONTROL.
R=RAISING; L=LOWERING (ADJUSTMENT TO GOVERNORS).

Figure 4. Schematic diagram of two systems interconnected by a single tie line

Tabulation shows effect of load change on frequency and tie-line load due to governor droop characteristics only (columns 1, 2, and 3), followed by the effect of flat frequency control only on system *A* (columns 4 and 5); same plus flat tie-line control on *B* (column 6), or tie-line bias control on *B* (column 7); or selective frequency control on *A* and *B* (columns 8 and 9)

Figure 1 shows one of the governors of the Queenston plant—not of the most modern make, but well adapted to an explanation of its operation, because its principal parts are large and exposed to view. The flyballs are on a vertical shaft, belted to the main generator shaft. The balls fly outward with increasing speed of the unit, and in so doing they raise a collar to which the center of the floating lever is coupled by a sliding shoe. The left end of the floating lever is connected to the pilot valve, which controls the turbine gates through the medium of the servo motor. The right end of the floating lever is positioned by a rod coming back from the gates. This mechanical construction determines a fixed relation between the steady-state speed and gate opening, which is called the speed-droop characteristic of the governor.

One other feature which should be noticed is the handwheel at the lower right and near it a small motor, called the synchronizing motor, which is geared to the handwheel. The synchronizing motor is used by the operator when starting the unit to adjust the generator to the proper speed for synchronizing to the bus, and after synchronizing, the same motor is used for adjusting load on the unit, or for regulating frequency of the system.

Automatic load or frequency regulators act through the medium of governor synchronizing motors. A change in the governor speed setting by means of this motor has the same effect as lengthening or shortening the gate return rod, causing a change in the speed associated with a given gate opening.

The relation between speed and gate opening is shown graphically in Figure 2 by the speed-droop curves of a governor. The base line is actually gate opening, starting from the no-load gate opening as zero, but it can also represent output or load on the unit, assuming that output is directly proportional to gate opening. This is not usually the case, but it will simplify our explanations to assume that it is true, and that our base represents per cent of full gate or per cent of full load.

As applied to a single isolated generator, curve *A* means that at no load, the frequency will be 25.5 cycles per second (hereinafter usually abbreviated to "cycles"). As load increases, the governor holds a lower frequency, which at

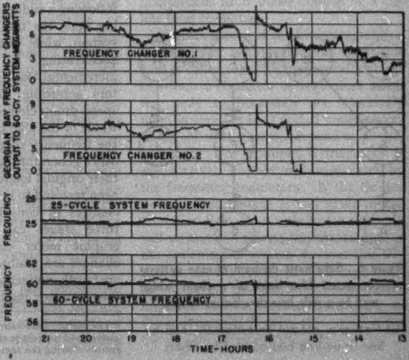

Figure 5. Fluctuating load on two frequency-changer sets in parallel constituting the tie between the Georgian Bay 60-cycle system and Niagara 25-cycle system

Frequency was manually controlled on the Niagara system and the frequency-changer load was unregulated

Figure 3. Frequency, and load of two Queenston generators, one (number 10) controlled by a frequency regulator and the other (number 3) on free governor control

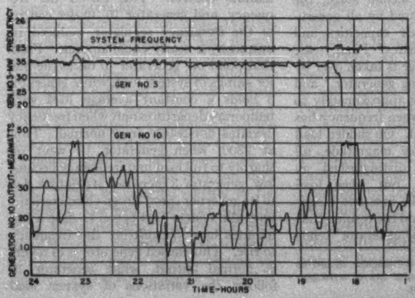

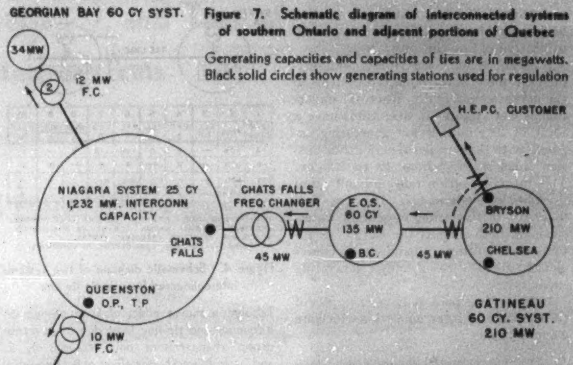

Figure 7. Schematic diagram of interconnected systems of southern Ontario and adjacent portions of Quebec

Generating capacities and capacities of ties are in megawatts. Black solid circles show generating stations used for regulation

half load will be 25 cycles. Further increase in load causes further reduction in speed, till at full load the frequency is 24.5 cycles—a total droop from no load to full load of one cycle on 25, or four-per-cent regulation.

When generators are operating in parallel, as on interconnected systems, frequency is the same for all generators, no matter whether they are side by side in the same generating station, or miles apart in different stations. Hence this speed-droop characteristic provides a basis for load sharing among generators operating in parallel, for example, two generators having speed-droop curves like *A* and *B* in Figure 2. All may not have the same per-cent regulation or the same full-load capacity, and these factors will affect the amount of any system load change which will be taken by each generator; but the main point is that generators in parallel tend to share all changes in system load due to their governor speed-droop characteristics, provided that no changes are made to the governor speed settings.

Effects of Frequency Control

In the early days of electric power, when frequency was not so important as it is now, the governor speed-droop characteristic was satisfactory, both for its main purpose as a basis of stable load sharing, and also for a crude sort of frequency control. Now, when frequency must be precisely controlled, the governors must be adjusted from time to time to compensate for changes in system load. Instead of making simultaneous equal adjustments to governors of all generators on the system, it is more convenient to adjust one or a few large generators, which are called the frequency-regulating generators of the system.

The effect of making an adjustment to the speed setting of a governor by means of the synchronizing motor shown in Figure 1 is to raise or lower the speed-droop curve parallel to itself. For example, curve *A* may be lowered to A_1, which would reduce the output of generator *A* and lower the frequency of the system. If frequency of the system is being regulated by adjustments to generator *A*, with no adjustments to generator *B*, then generator *A* will be compelled to take care of all load changes of the system, because when frequency is restored to 25 cycles, generator *B* will always be at the 60-per-cent load point. In other words, frequency control has the effect of counteracting the speed droop of generators to which it is applied—not eliminating the drooping characteristic, but shifting it to a new level after each load change.

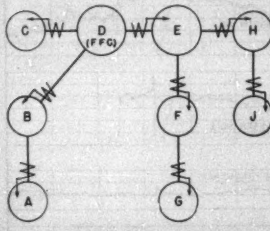

Figure 6. Schematic diagram of nine systems interconnected like links of a chain which may have side branches but no loops

Flat frequency control on system *D*. Flat tie-line or tie-line bias control on others

When load change occurs suddenly, there are three stages in the restoration of normal frequency. In the first stage, inertia of the generator and of other rotating machinery connected to the system is the governing factor, and so the frequency falls for the first few seconds following a sudden increase of load, drawing upon the total kinetic energy of the system, while water in the penstocks is accelerating. In the second stage, the incremental load is shared by all generators according to their capacities and speed-droop characteristics. Finally, the whole of the load change is taken over by the frequency-regulating generator,* and other generators return approximately to their original loading when frequency has been restored to normal. On sudden load changes of considerable magnitude, all three stages can be distinguished on graphic meter charts, but when load changes are gradual, the first two stages are hardly noticeable, and the result is that the frequency-regulating generator* tends to vary its output with all changes in system load, while other generators maintain approximately constant output.

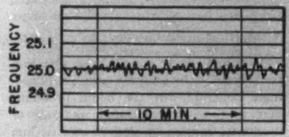

Figure 8. Uncontrollable fluctuations of Niagara system frequency (1936) showing irregular swings with a period averaging about 25 seconds

This is illustrated in Figure 3.

Time runs from right to left. The lower curve shows the fluctuating load on generator 10 at Queenston when it was being used as a frequency-regulating generator for the Niagara system, with automatic frequency control. A little before 1800, a sharp increase in system load depressed the frequency temporarily and caused the output to increase to full load, in response to raising impulses from the frequency regulator. The frequency was slightly low for 20 minutes until 1815 when generator 3 was loaded to about 85 per cent of its maximum capacity by manual control. This raised the frequency, and generator 10, under control of the frequency regulator, reduced its output by a nearly equal amount. From that point on, generator 10 takes the major swings of system load, while generator 3 holds a constant average load with temporary departures only when frequency deviates noticeably from normal. Thus at 2300, when generator 10 went up sharply to full load and frequency became low, generator 3 increased its output due to its governor speed-droop characteristic, until the system load began to drop a few minutes later, permitting the frequency to rise. This caused generator 3 to revert to normal output, while generator 10 follows the variations of system load

---

* The word "generator" in the singular should be understood to include the case of two or more generators sharing the regulation.

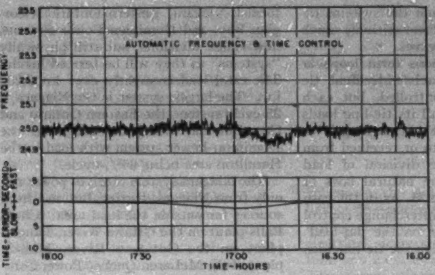

Figure 9. Automatically regulated frequency and time error of Niagara system (interconnected as in Figure 7)

Low frequency between 1640 and 1700 is due to regulating generators being at full load. Time lost owing to low frequency is later regained by automatic bias holding frequency slightly high from 1700 to 1725

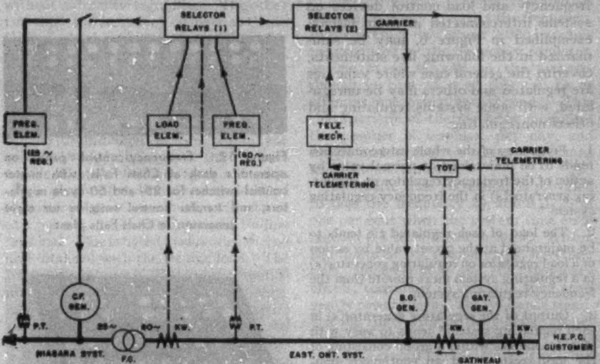

Figure 10. Schematic diagram of frequency- and load-control system centered at Chats Falls

Power circuits are in heavy lines, governor control circuits in light full lines, and metering circuits in broken lines

under control of the frequency regulator. The cause of the load increase on generator 10 at 2300 was reduction of generation at a base load plant elsewhere on the system. This has the same effect as increase of system load.

Figure 4 represents two power systems with an interconnecting tie line, numerous generators and numerous loads being reduced to a single equivalent generator and equivalent load for each system. Circuit breakers, transformers, and other details are omitted. This differs from the case of two generators in parallel feeding a common load only in the separation of the generators and loads into two divisions. With no external control of the governors, the two generators will still share all incremental load of the combined systems, according to their speed-droop characteristics and generating capacities. Power flow in the tie will depend upon these two factors and also upon the origin of the load change—whether the change occurred in area *A* or in area *B*. For example, if load increases in system *A*, frequency will become low, and tie-line load will deviate in the direction *B* to *A*.

In a consideration of regulation of frequency of these systems, it is usual to make one system responsible for the regulation of frequency and time. This will usually be the larger system, or the one having greater generating reserves, or ability to handle load swings more efficiently. Let us choose system *A* as the frequency-regulating system. In accordance with the principles already explained, all changes in total load of both systems will appear as changes in the load of generator *A*, while the load of generator *B* will remain substantially constant. Therefore, if load change occurs in system *A*, it will not permanently affect the tie-line load, but all load changes occurring in *B* will appear as changes in the tie-line loading, because the changes are being absorbed by the frequency-regulating generator *A*.

Under the conditions just considered, unregulated tie-line loads tend to vary with all fluctuations in load of systems remote from the frequency-regulating system. This is illustrated in Figure 5, which shows load fluctuations on an unregulated tie consisting of two frequency changers in parallel, interconnecting two systems of the Hydro-Electric Power Commission in southern Ontario, the Niagara 25-cycle system, and the Georgian Bay 60-cycle system. The power flow is all in one direction, toward the 60-cycle system, which was deficient in stream flow and was receiving assistance from the Niagara system. One machine alone was on at first, and then two in parallel. At 1615, when the load on the frequency-changers was high, a sudden loss of load on the Niagara system caused the frequency to rise suddenly, and forced extra power through the frequency-changers to accelerate the 60-cycle system. This tripped off the already heavily loaded machines and the systems separated, Niagara frequency rising due to the loss of load, and Georgian Bay frequency dropping due to the loss of supply from Niagara. The drop of 60-cycle frequency was great because most of the generators on the Georgian Bay system were blocked and could not increase their output until the operators raised the blocks. The systems were paralleled again a few minutes later. The frequency here was manually controlled, which accounts for sustained deviations up to 0.3 cycle on 25 cycles.

Tie-Line Load Control

In many cases it is necessary to regulate the interchange of power through a tie line, holding the tie-line load substantially constant at a predetermined value. Referring again to Figure 4, when system *A* is regulating frequency, tie-line load may be regulated by control of generation in system *B*. A regulator sensitive only to tie-line load exerts what is called "flat tie-line load control." This tends to make each system "mind its own business," the generators in system *A* taking care of load fluctuations in that system under control of the frequency regulator, and generators in system *B* taking care of load fluctuations in *B* under control of a tie-line load regulator.

Another means of combining regulation of frequency with regulation of tie-line load is called selective frequency control,[9] in which a regulator or regulators sensitive only to frequency act selectively upon generators in *A* and *B* under supervision of watt relays, responsive to tie-line load. For example, if frequency is low, a raising impulse will be initiated by the frequency regulators. If the tie-line load at that instant is too great in the direction *B* to *A*, the tie-line watt relay will permit the raising impulse to pass to the governors of system *A*, since this will tend to correct the tie-line loading as well as to correct the frequency, but raising impulses will be blocked from going to the governors of *B*, since this would make the tie-line deviation greater.

When systems are connected like links of a chain, which may have side branches, but no loops, it is usual to assign frequency control to one large central system such as D in Figure 6, and have other systems regulate load in the tie leading toward the frequency-regulating system. This is simply an extension of the principle of load control on a tie line between two systems as already explained. If any system such as F is unable for any reason to regulate load in the tie between F and E, the tie F–E will become an unregulated tie, and system E will automatically assume the regulation for the two systems E and F, holding load on tie E–D up to the limit of the available generating capacity in system E. An overload on system E would make it impossible further to control the load in tie E–D, and would throw additional burden on the frequency-regulating system D.

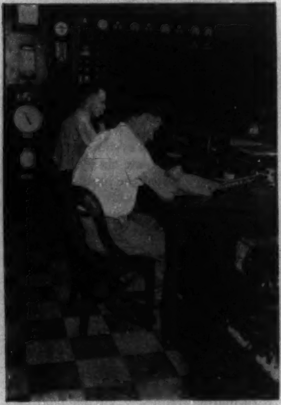

Figure 11. View in Chats Falls control room showing frequency-control supervisory panel switches on operator's desk

Round dial at left indicates total 60-cycle delivery from Gatineau Power Company, with load-setting controls in upper part of indicator case

On large interconnections it is usually desirable to provide for automatic assistance to the frequency-regulating system on the occurrence of unexpected overloads or emergency conditions. For this purpose it is customary to use tie-line load regulators in which the load setting is automatically biased by deviations in frequency, and perhaps also by time error.[7] This is known as "tie-line load control biased by frequency," abbreviated to "tie-line bias control." This system of mutual aid enables interconnections of vast magnitude to operate successfully, meeting demands which the systems individually could not meet without much greater generating reserves.

When interconnections form loops or networks, load on each individual tie cannot readily be controlled, but each system may totalize all its tie-line loads and regulate the "net interchange" or total power supplied to or received from the pool, leaving the division of load among the ties to the natural laws of power flow in networks.[13] As in the case of single tie lines, net-interchange control may be applied either on the flat-load-control principle, or with the tie-line-bias modification.

The characteristic effects of automatic frequency- and load-control devices on systems interconnected in chain fashion exemplified in Figure 6, may be summarized in the following five statements, covering the general case where some ties are regulated and others may be unregulated, with some systems regulating and others nonregulating.

1. Frequency of the whole interconnection tends to be maintained at normal value by action of the frequency regulator on regulating generator(s) in the frequency-regulating system.*

2. The load of each regulated tie tends to be maintained at the preset value by action of a load regulator on regulating generator(s) in a regulating system more remote from the frequency-regulating system.

3. Output of the regulating generator(s) in each regulating system* tends to vary with all load changes within a group consisting of the local system and all contiguous nonregulating systems as far as the nearest regulated ties.

4. Load of each unregulated tie tends to vary with all load changes of contiguous nonregulating systems of the group (as defined in 3) on the side of the tie remote from the regulating system of the group.

5. The output of generators other than regulating generators tends to remain approximately constant.

Interconnections in Ontario and Quebec

In Canada, the largest interconnection of power systems is in the province of Quebec, where three large systems operate with interconnected generating capacity of about 2,000,000 kw (1942). Frequency is regulated automatically by either of two of these systems, but automatic tie-line control is not used because of the long distances between load metering points and the generating stations, making installations difficult and expensive.[11]

Next in magnitude is the Southern Ontario system of the Hydro-Electric Power Commission of Ontario which is the product of the amalgamation of the former Niagara, Eastern Ontario, Georgian Bay, and Dominion Power systems, now called divisions, but still physically "systems" as they will be termed herein. The total load is slightly over 1,500,000 kw. The largest system is the Niagara, a 25-cycle system, the Eastern Ontario and Georgian Bay being 60-cycle, and the Dominion Power system with load in the Hamilton area being $66^2/_3$-cycle.

The Niagara system receives power not only from Niagara district, but also from sources far outside the load area: Chats Falls plant on the Ottawa River, Paugan plant on the Gatineau River, Masson plant of the McLaren-Quebec Power Company on the Lievre River, and Beauharnois on the St. Lawrence.[5,6] Each of the other systems is connected to the Niagara system through one or two frequency-changer sets. The single frequency-changer set for the $66^2/_3$-cycle system is located at Niagara Falls; for the Georgian Bay system, two sets at Hanover, at the end of a 110-kv 25-cycle line from Kitchener; and for the Eastern Ontario system, one set at Chats Falls plant. Generation on the Eastern Ontario system is supplemented by power from High Falls plant on the Lievre River, and from the Gatineau Power Company's 60-cycle system, both in the Province of Quebec. Tie lines interconnecting the Eastern Ontario system and Gatineau 60-cycle system cross the Ottawa River at a point just above the city of Ottawa.

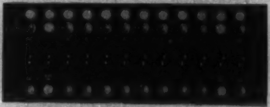

Figure 12. Frequency-control panel on operator's desk at Chats Falls, with master control switches for 25- and 60-cycle regulators, and transfer control switches for eight generators in Chats Falls plant

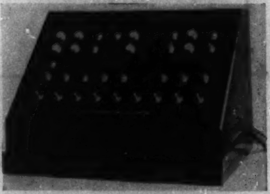

Figure 13. Load-control supervisory cabinet on operator's desk at Chats Falls, with switches and lamp indications for all load-control functions

These four systems of the Commission

---

* "Regulating system" is a general term which includes "frequency-regulating system" as a special case.

and the Gatineau 60-cycle system operate normally interconnected, with total connected generating capacity of about 1,650,000 kw.

Figure 7 shows schematically the five interconnected systems with the generating capacity in each system and the capacity of the ties indicated in megawatts. The normal direction of power flow is shown by the arrows. Flat frequency control with automatic time-error correction is maintained on the Niagara system by regulation at one of two points, Queenston plant on the Niagara River, or Chats Falls plant on the Ottawa River. The Georgian Bay and Dominion Power system frequency-changer ties are floating without automatic regulation. The other two ties—the frequency changer at Chats Falls and the Gatineau tie line—are equipped for automatic regulation, the first because of limited capacity of the frequency-changer set, and the second because of contractual obligations. The Gatineau Power Company delivers power to the Commission at two points, the principal supply being over the tie lines to the Eastern Ontario system, and a minor portion fed directly to an isolated customer of the Commission and metered at a point about 45 miles from the tie-line terminal. The isolated load is telemetered and totalized with the tie-line load. The totalized quantity is again telemetered 30 miles to Chats Falls where the load-regulating equipment is located. Control therefore may be applied to the totalized quantity rather than to the tie line only. Telephone-line carrier is used for telemetering and control.

Frequency-Regulator Characteristics

The type of frequency-regulating equipment in use at Queenston and Chats Falls was designed at the School of Engineering Research of the University of Toronto, under the supervision of H. W. Price, and all regulators were built in the Commission's shops. The initial installation at Queenston has been in service since 1934, and two regulators—one 25-cycle and one 60-cycle—have been in service at Chats Falls since 1942.

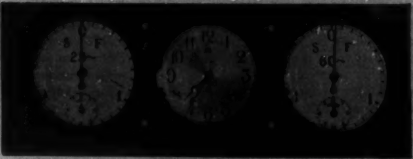

Figure 14. Time-error dials (25- and 60-cycle) and station clock in control room at Chats Falls

In a preliminary study of Niagara system frequency and governor characteristics, it was observed as shown in Figure 8 that frequency of a large system is continually fluctuating with an irregular period averaging about 25 seconds, even when the system load is relatively steady. These swings are too rapid to be controlled, and too small to be of vital consequence when they are of short duration. Therefore, the frequency regulator was designed to disregard these minor fluctuations, but to be very sensitive to deviations in average frequency. The regulator maintains a close comparison between total integrated cycles of system frequency and the nominal cycles corresponding to rated frequency of the system. Whenever the difference changes by one half cycle—not one half cycle per second, but one half cycle in phase position, or 180 electrical degrees—on the 25-cycle system, or 1.2 cycles on the 60-cycle system, a frequency-corrective impulse is sent out to the governors. This is repeated as often as necessary to correct the frequency. In the average day, about 2,000 impulses are produced by the frequency regulator, or one in 45 seconds on the average, though in time of need this can be as often as one every two seconds. This characteristic of the regulator minimizes the number of impulses per day, and avoids undue wear on relays, governors, and gate mechanisms.

Automatic time correction is provided to bias the frequency by about 1/20 of one per cent when the system time error reaches 0.4 second fast or slow. Within the limits of 0.4 second error, a vernier bias, imperceptible on the frequency charts, continues to urge the time error gently toward zero. The reference standard for time error is the station master clock, which may develop errors of its own with regard to radio time signals, but is usually not more than five seconds out.

Figure 9 shows the uncontrollable frequency fluctuation at a slower chart speed. It also shows a frequency dip resulting from overload on the regulating unit, and the resulting time error; then after relief from overload, the automatic frequency bias, just perceptible as a change in the average level of the frequency line, and finally restoration of normal average frequency when the time error is less than 0.4 second.

Scheme of Frequency and Load Control

Figure 10 is a schematic diagram showing the essential elements of the scheme of combined frequency and load control from the 60-cycle control equipment centered at Chats Falls. Corrective impulses may be initiated either by the frequency-sensitive element, supplied from 60-cycle potential, or from the load-sensitive element, responsive to load measured on the 60-cycle side of the frequency-changer set. These impulses, from both sources, are sorted by the first set of selector relays, raising impulses being sent to 25-cycle generators in Chats Falls plant and lowering impulses toward 60-cycle generators, or vice-versa, depending upon the direction of the existing deviation of frequency-changer load from the scheduled value as set on a watt relay. Impulses which are directed toward 60-cycle generators must now pass a second set of selector relays, which determine on the basis of the total Gatineau delivery, totalized and telemetered back to Chats Falls, whether raising impulses should be permitted to go to Gatineau plants and lowering impulses to Barrett Chute, or vice-versa.

Figure 15. Telephone-line carrier transmitting and receiving equipment for telemetering and remote control at Chats Falls

Figure 16. Telemetering and load-control panel in control room at Bryson plant of Gatineau Power Company

The principle of this control system is a combination of selective frequency control and flat tie-line load control. The frequency-sensitive element, initiating impulses on the basis of frequency deviation only, and the selector relays, distributing these impulses on the basis of deviations in the tie-line loads, embody the principles of selective frequency control. This control alone is prompt in regulation of frequency, and also has a tie-line load-regulating effect, but is rather slow in shifting load after a change in setting of the watt relay, because impulses are initiated only by random swings of frequency. Selective frequency control is therefore supplemented by load-regulating impulses initiated by the load-sensitive element, regardless of frequency. All the impulses from the load element go to 60-cycle generators, either Barrett Chute or Gatineau. Impulses from the load element are sent at either of two rates, once every $6^2/_3$ seconds for deviations exceeding 5,000 kw or once every 20 seconds for smaller deviations. The combination of a 20-second time interval with a suitable dead band on the watt relay gives the regulating generators time to respond to each impulse, and gives stable operation. The watt relay is designed to be insensitive to the rapid swings of synchronizing power which are typical of tie-line loads, but to be sensitive to sustained deviations in either direction.

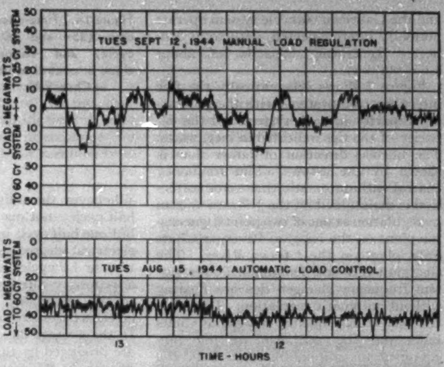

Figure 17. Comparison of load on Chats Falls frequency-changer set with and without automatic control

Figure 11 is a view of part of Chats Falls control room showing the large dial on which the Gatineau 60-cycle delivery is indicated. Adjustable contacts in this instrument are used to set any desired delivery. In front of the farther operator is the control panel for supervision of the 25- and 60-cycle frequency regulators, and for the eight generating units in this plant. At his left and hidden from view is a control cabinet for supervision of the load regulator.

Chats Falls frequency regulator and generator control panel is shown in Figure 12. Master control keys for the two frequency regulators are at the extreme ends of this panel, 25-cycle at the right and 60-cycle at the left. The 60-cycle regulator is always in use, and the 25-cycle regulator is also required when the systems are separated. With the systems separated, Chats Falls generators may be transferred to the 25-cycle regulator as suggested in Figure 10. Next to each master key is the frequency bias key for automatic time correction. This key is "on" except when Queenston is regulating frequency and time. The other eight keys are for placing the eight Chats Falls units on automatic control, from the 60-cycle regulator if the keys are up, or from the 25-cycle regulator if the keys are down. Lamps indicate the position of the keys, and other lamps (upper row) indicate when the units are approaching full gate, which is their limit of control. Limit switches on the governor prevent the automatic control from raising the units above 90 per cent gate or lowering below 50 per cent, in order to keep them in a fairly efficient operating range.

Figure 13 shows Chats Falls load control supervisory cabinet. This cabinet, located on the operator's desk, is for control and supervision of the 60-cycle frequency and load regulation centered at Chats Falls. Indicating lamps show where each impulse goes—to Chats Falls generators, to Barrett Chute, or to Gatineau generators—and whether it is a raising or a lowering impulse. Lamps also indicate whether the tie-line loads are above or below the scheduled setting, and a special red lamp and intermittent buzzer signal draw the operator's attention when the frequency-changer load deviates more than 5,000 kw from schedule. The switches may be used to set up the control for abnormal operating conditions. For instance, when the frequency changer is out of service for maintenance, thus separating the 25- and 60-cycle systems, Chats Falls units are taken off the 60-cycle control, and the 60-cycle regulator is then used for regulation of 60-cycle generators only. This change in control setup also takes place automatically when the frequency changer trips off for any reason, and the change is indicated by a red lamp signal. Other lamps are for supervision of the three carrier sets, two transmitters and one receiver, which may be seen in Figure 15.

The clock case shown in Figure 14 is mounted above the switchboard in front of the operator's desk in Chats Falls control room. The two outer dials are time error indicators, 25- and 60-cycle respectively, and the center one is a time clock operated electrically by impulses at half-minute intervals from the station master clock which is checked daily by radio time signals. The large time-error dial covers a range of $1^1/_2$ seconds fast or slow, and a smaller inset dial goes to 12 seconds fast or slow. These indicators operate by position-type telemeter system, from the time-error element of the frequency regulators. When the systems are interconnected both dials read alike, and normally not more than one half second fast or slow. Time-error recorders give a graphic record on a chart with range of 25 seconds fast or slow, which is rarely overrun even in times of serious trouble. The ordinary range of time deviations during present conditions is from five seconds fast to five seconds slow, which is due to shortage of spinning reserve because of war loads. The reference standard, as already stated, is the station master clock.

Figure 15 shows telemetering and load-control carrier terminal equipment at Chats Falls. This consists of two carrier transmitters on the nearest panel, one transmitting to Barrett Chute and one to Gatineau plants, and one receiver on the lower part of the second rack, receiving telemetering signals representing Gatineau total 60-cycle delivery. This equipment is located at the terminals of the open-wire telephone circuits on which the carrier is superimposed on audio-frequency voice communication.

The telemetering transmitter and load control panel at Bryson is shown in Figure 16. A carrier receiver, connected to the telephone line, brings in load-regulating impulses to the relays on this panel, and these in turn operate on the governors. At the same time, the telemetering transmitter, measuring the local delivery to the Commission, is sending out telemetering signals on the same telephone line at a different frequency. Indicating lamps and buzzer give all necessary indications and warnings. The instrument at the top of the panel is a frequency relay which is intended to block the incoming control signals from Chats Falls in case of a separation between the Eastern Ontario and Gatineau systems. If such a separation should occur the Gatineau frequency would rise, closing a high-frequency contact of the frequency relay and locking out the automatic control until reset by the operator. Except for the telemeter transmitter, this equipment is typical of the installations at each of the three remote generating stations.

Operating Performance

Figure 17 shows the comparison between automatic and manual control of frequency-changer load at Chats Falls. The noon hour was picked as the time when load changes occur at the greatest rates on both 25- and 60-cycle systems and when load swings are likely to be severe. Manual control was considered permissible only because the desired transfer was about zero, and swings would not likely overload the set, if watched. An operator was assigned to watch the load

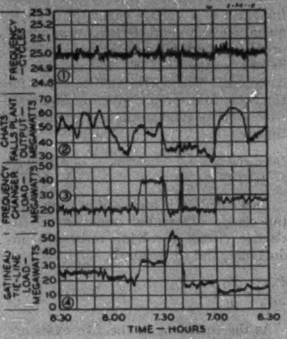

Figure 18. Charts showing results of automatic frequency and load control during trouble conditions on Eastern Ontario system

throughout this period and to telephone for correction of 60-cycle generation when required. With automatic control, the set carries as much as 40,000 kw average load at any time it is required with little or no attention on the part of the operator and rarely a telephone call for load correction. The chart shows a change in the load setting from 40,000 kw to 35,000 kw at 1225, an operation which is quickly and easily performed by a setting on the watt relay. The load responds promptly to this.

The capacity of this frequency-changer set is 45,000 kw which is about 13 per cent of the connected generating capacity of the 60-cycle systems. During two years of interconnected operation it has tripped off and separated the systems 13 times, ten of these separations being due to severe disturbances on one or both systems, and the other three due to overload occasioned by lack of experience in interconnected operation during the first year. The set has withstood surprisingly large disturbances without tripping, but on these occasions the initial load on the set happened to be small, or was in such a direction that the disturbance reduced or reversed the direction of the power flow.

Figure 18 illustrates the behavior of the control system and the interconnected generators during trouble. Generators at High Falls supplying 35,000 kw to the Eastern Ontario system suddenly tripped off. The meter charts shown are:

1. Twenty-five-cycle system frequency.

2. Output of Chats Falls plant, which was being used as the regulating station for the Niagara system.

3. Chats Falls frequency-changer load, which was being regulated by the automatic load regulator, acting on Gatineau 60-cycle generators.

4. Gatineau tie-line load, which was not being regulated at the time because Barrett Chute plant was shut down and was therefore not available for regulation.

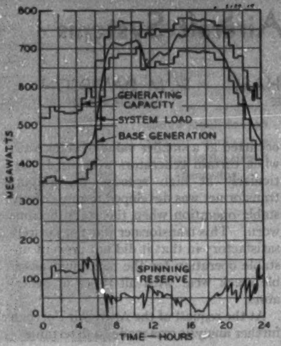

Figure 19. Daily load curve for a portion of the Niagara system, showing total connected generating capacity, base load generation, and spinning reserve, based on half-hourly readings

Thursday November 6, 1941

Under these conditions it is to be expected that the Gatineau tie-line load will fluctuate with all changes in load or generation in the Eastern Ontario system, since the only 60-cycle generators available for regulation were in the Gatineau system.

At 7:19 p.m., when the 60-cycle generators at High Falls tripped off, depriving the Eastern Ontario system of their 35,000 kw generation, the frequency suddenly dropped to 24.8 cycles on the 25-cycle system, and by a corresponding amount on the 60-cycle systems, but quickly recovered to 24.95 cycles approximately, and finally to 25 cycles in about three minutes. It is apparent that the sudden change in load was carried initially by the kinetic energy of the system while frequency was dropping during the first few seconds, then was shared by both 25- and 60-cycle generators because of their speed-droop characteristics, and finally was absorbed by the regulating generator of the 60-cycle systems. The swing of 25,000 kw in the frequency-changer load is the share of the load change which was contributed temporarily by the 25-cycle system, a small part (5,000 kw) coming from Chats Falls generators, and the balance, or 20,000 kw, from other generators, at Queenston and elsewhere. The other 10,000 kw came from the Gatineau generators, as shown by the initial rise in the lower curve. The automatic regulator immediately began to send raising impulses to Gatineau generators, in an effort to raise the low frequency and also to correct the deviation in the frequency-changer load. This was accomplished in three minutes, when the frequency-changer chart shows its load was back to schedule at 7:22, and the whole of the 35,000 kw lost generation was made up by the Gatineau generators. Notice that Chats Falls output returned to its original value. This shows how sudden load change is shared initially by all generators having any spinning reserve, but is absorbed ultimately by regulating generators in the system or group where the disturbance originated.

Although the automatic load control had successfully performed its function in relation to the frequency-changer load, the effect was to increase the Gatineau 60-cycle delivery above the contract amount. Since Chats Falls generators had spinning reserve capacity available, the load setting on the frequency changer was manually changed at 7:27 from 20,000 kw to 40,000 kw toward the Eastern Ontario system. This increased Chats Falls output by 20,000 kw and reduced Gatineau output by a similar amount by 7:30 p.m. Finally, at 7:45, High Falls generators came back on load, and all conditions were restored to normal.

Automatic Controls and the Human Element

Although much can be said for automatic controls, it must be recognized that they have definite limitations. Automatic regulators do a job which human operators either cannot successfully perform, or can perform only by constant attention to an exacting and never-ending task. Nevertheless it should not be inferred that a system equipped with a few control devices at strategic points practically runs itself. Regulators can function only within the limits of capacity of the generators under their control, and this may be in the order of five to ten per cent of the total generating capacity of the system or group of systems for which these generators are regulating. The remaining generation, on base load, must be adjusted up or down from hour to hour to conform to the general trend of the system daily load curve as estimated by the power supervisor, so as to keep the regulating generators within their regulating range. This is illustrated by Figure 19 showing a 24-hour curve of connected capacity, load, and base load generation for a portion of the Niagara system. Load assignments are made partly by prearranged schedule, but the supervisor must be prepared at any moment to meet unforeseen conditions with such power resources as are available. For this purpose, automatic controls must be supplemented by adequate communication facilities, and by telemetering of critical quantities such as forebay levels, loads on ties, and loads on generating stations, especially those that are under control of automatic regulators.

In conclusion, it is interesting to note that interconnection has developed a high degree of co-operation without which its fullest benefits would be unattainable. Operating staffs and managements of interconnected systems have learned that what is best for the whole is usually best for each. Best results are attained when all systems are prepared to contribute according to their ability, to meet the need of any—a principle which works well in all human relationships.

References

1. Hydraulic Turbine Governors and Frequency Control. National Electric Light Association report 13, December 1930, 32 pages.

2. Remote Metering and Automatic Load Control, J. T. Logan. AIEE Transactions, volume 55, 1936, January section, pages 40–7. Discussion, pages 891–3.

3. Phase-Angle Control of System Interconnections, R. E. Pierce, B. W. Hamilton. AIEE Transactions, volume 58, 1939, March section, pages 83–91.

4. Regulation of System Load and Frequency, Herbert Estrada, H. A. Dryar. American Society of Mechanical Engineers *Transactions*, volume 62, April 1940, pages 221–35.

5. Experiences in System Speed Regulation, Otto Holden. American Society of Mechanical Engineers *Transactions*, volume 62, April 1940, pages 237–40.

6. A Method of Measuring and Recording the Frequency Error of Alternating-Current Power Supplies, F. O. Morrell, G. R. Oman, and discussion thereon by J. S. Forrest. Institution of Electrical Engineers *Journal* (London, England), volume 87, November 1940, pages 507–20.

7. Methods of System Control in a Large Interconnection, Earle Wild. AIEE Transactions, volume 60, 1941, May section, pages 232–6. Discussion, pages 737–9.

8. Prime-Mover Speed Governors for Interconnected Systems, R. J. Caughey, J. B. McClure. AIEE Transactions, volume 60, 1941, April section, pages 147–51. Discussion, pages 728–31.

9. The 220,000-Volt System of the Hydro-Electric Power Commission of Ontario–II, A. H. Frampton, E. M. Wood. AIEE Transactions, volume 60, 1941, pages 1215–21.

10. Supplementary Control of Prime-Mover Speed Governors, S. B. Crary, J. B. McClure. AIEE Transactions, volume 61, 1942, April section, pages 209–14. Discussion, pages 395–400.

11. Power-System Interconnection in Quebec, W. R. Way. AIEE Transactions, volume 61, 1942, December section, pages 841–7.

12. Power Pool Operating Problems. *Electrical West*, volume 91, November 1943, pages 52–7.

13. Kilowatt-Hours Pooled for War in the Pacific Northwest, W. C. Heston. *Electrical West*, volume 92, March 1944, pages 51–63.

Instability in D-C Aircraft Systems

H. B. BUNCE
ASSOCIATE AIEE

J. C. CUNNINGHAM
ASSOCIATE AIEE

W. M. DAVIDSON
ASSOCIATE AIEE

Synopsis: A laboratory and theoretical study was made to determine the causes and methods of combating an unstable oscillatory voltage condition which has been encountered in aircraft d-c electric systems, using types *P*-1, *P*-2, and *R*-1 generators with carbon-pile voltage regulators.

The generator characteristics were found to be such that oscillatory instability would not occur without the presence of a voltage regulator which was out of adjustment and which had inadequate damping.

A method is given for determining the amount of damping required for stable operation in terms of the generator field time constant and certain regulator characteristics.

INSTABILITY has been encountered in aircraft electric systems employing 28.5-volt generators, 24-volt batteries, and carbon-pile voltage regulators. In systems in which the regulators were out of adjustment, sudden application or removal of load has initiated sustained oscillations in load current and system voltage. The frequency of these oscillations has been between 10 and 60 cycles per second with amplitudes as large as the maximum value of load current.

In an analysis by the Army Air Forces it was determined that this type of system instability was associated with wear of the regulator stack and could be corrected by readjustment of the regulators. The analysis also disclosed that instability occurred at a smaller value of stack wear when certain generators were used, particularly at high speeds. A damping transformer was developed to prevent unstable operation when the stack became worn. This transformer was not entirely satisfactory in that it did not prevent unstable operation for the maximum possible stack wear with all types of generators.

At the request of the Army Air Forces a further analysis was made to determine

1. The causes and nature of the unstable condition.

2. A means of evaluating the generator and regulator characteristics to determine whether they tend to be unstable.

3. A means of preventing instability.

Generator Stability Analysis

The first approach was to determine whether a generator without a regulator could sustain an oscillation initiated by a switching transient.

Equivalent Circuit for Generator and Load

From the mathematical analysis given in Appendix II, it is possible to determine the relation of the electrical quantities and characteristics of the generator and load circuits which would be necessary to produce oscillatory instability without the effect of a voltage regulator. These quantities and characteristics were measured on a particular generator and used in the evaluation of the operational equations. The operational equation for the equivalent circuit, given in Figure 1, which relates generator load current with time is

$(p^2+\alpha p+\beta)i_1 = C$ (equation 11 of Appendix II)*

This equation is identical in form with the classic differential equation of the electric circuit involving resistance, inductance, and capacitance,

$$\frac{d^2i_1}{dt^2}+\alpha\frac{di_1}{dt}+\beta i_1=C$$

As the equations in the two cases are identical, there must, of course, be found in the solution of the former the same oscillations and transients as are contained in the well-known solution to the latter.

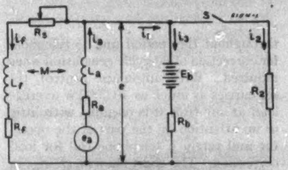

Figure 1. Equivalent circuit of generator with battery and resistance load

In Figure 1, although there is no condenser capacity involved and therefore no electrostatic energy, there are nevertheless two different magnetic circuits in which energy can be stored. During an oscillation all of the energy stored in the generator field cannot be transferred to the armature circuit. Most of it is dissipated as i^2r. One of the objects of this investigation is to determine whether the characteristics are such as to transfer enough energy between the field and armature circuits that oscillations may be produced. Such oscillations, although small and highly damped, might be amplified by the voltage regulator so as to produce subsequent oscillations.

Generator Characteristics

The generator characteristics necessary to evaluate the above operational equation were measured for *P*-1, *P*-2, and *R*-1 generators, with the test equipment shown in Figure 2. Values of r_f, L_f, L_a

---

Paper 45-154, recommended by the AIEE committee on air transportation for publication in AIEE Transactions. Manuscript submitted June 14, 1945; made available for printing August 1, 1945.

H. B. Bunce, J. C. Cunningham, and W. M. Davidson are in the aviation section, industry engineering department of the Westinghouse Electric Corporation, East Pittsburgh, Pa.

* For explanation of symbols see Appendix I.

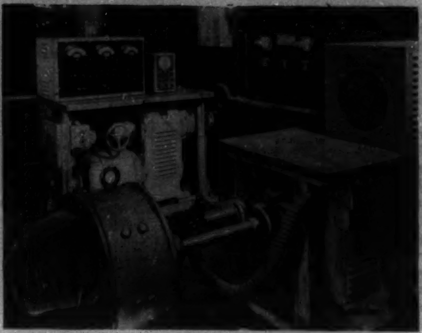

Figure 2. General view of test equipment showing in left foreground special d-c drive motor used to obtain minimum speed regulation on sudden application of load to the aircraft generator

and field time constant for all types of generators are given in Table I.

OSCILLATORY INSTABILITY

In the solution of equation 11 it is found that the condition for no oscillation in the circuit containing generator, battery, and load is that existing when $\beta < \alpha^2/4$. With the characteristics of the *P*-1 generator of manufacturer *A* from Table I and the following:

Generator	Load
$M = -0.16$ millihenry	$E_b = 27.6$ volts
$R_a = 0.03$ ohm	$R_b = 0.028$ ohm
$r_f = 14.76$ ohms	$R_1 = 0.57$ ohm
$Kk_a = 0.031$ volt per ampere	
$Kk_f = 12.0$ volts per ampere	
$e_0 = 5.18$ volts	

it may be shown that the circuit is nonoscillatory. There is no value of Kk_a which can make the circuit oscillatory with the other parameters remaining the same as given above. However, with the initial value of Kk_a and a value of $M = -0.8$ millihenry, it can be shown by calculation that a damped oscillation of about six cycles per second theoretically could be produced. This value of M is five times the measured value for this generator. The brushes as set to give maximum output were about 1/4 bar behind neutral. It is possible that a similar generator with a larger brush shift might have a greater M, but it is not likely that it will approach 0.8 millihenry. Mutual inductance in a generator is a very difficult quantity to measure with accuracy.

Inasmuch as the *P*-1 generator of manufacturer *A* has shown the greatest tendency for unstable operation and its measured parameters were so far short of the values necessary to produce instability without a regulator, these equations were not evaluated for any other generator.

It is interesting to note that in all cases where oscillations may be produced it is necessary to have cumulative compounding (this does not imply overcompounding) with armature current; that is, a positive value for Kk_a. Practically, this will be obtained only with generators having series, interpole, or compensating windings and with brushes shifted against rotation, the cumulative compounding direction. Generators without interpole or compensating windings normally have their brushes shifted in the direction of rotation, because they do not commutate satisfactorily with brushes shifted against rotation. In the laboratory rising volt-ampere characteristics were obtained at maximum rated speed for *P*-1 generators of manufacturer *A*, which have interpole and compensating windings. In all cases it was necessary to have

1. Brushes set for maximum output.
2. Well-polished and well-seated brushes.
3. A black carbon film deposited on the commutator.

For generators without interpole or compensating windings volt-ampere output was increased by application of a film, thus indicating a cumulative effect. *P*-2 and *R*-1 generators exhibited the same compounding characteristics as the *P*-1 generator of manufacturer *A*, except that the film was more difficult to maintain at the maximum speed of 10,000 rpm.

A theoretical calculation and laboratory test were made to determine load current as a function of time for the generator of manufacturer *A* running at 4,500 rpm in parallel with a *G*-1 battery while switching a 50-ampere load. The circuit arrangement is shown in Figure 1. The generator and load characteristics are given in the foregoing table.

The calculated transient value of load current after switching load R_1 in parallel with the battery (battery previously floating on line) is

$$i_1 = -63.06\epsilon^{-8.39t} + 2.96\epsilon^{-179.1t} + 64 \text{ amperes}$$

At $t = 0.66$ second the load R_1 is switched off, and the calculated expression for load current becomes

$$i_1' = 62.9\epsilon^{-8.63t} - 2.8\epsilon^{-180t} + 3.9 \text{ amperes}$$

These expressions are plotted as a function of time in Figure 3. A comparison with data from an actual test oscillogram for the same generator and the same circuit conditions also is shown in Figure 3. Discrepancy between the test and calculated values is caused by variations in generator and load circuit parameters under operating conditions and by unavoidable inaccuracies in measurement of parameters. In the expression for load current it should be noted that there are no oscillatory terms.

It can be seen from the test curve that, although no oscillations were present, load current reversed, and the system became unstable. There was actually a reversal of polarity of the residual field in the generator each time this unstable operation occurred. This reversal of polarity probably is caused by the resultant armature, interpole, and compen-

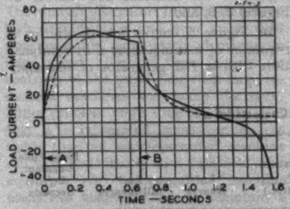

Figure 3. Comparison of calculated and test curves of load current as a function of time for switching a resistance load in parallel with a battery (*P*-1 generator, manufacturer *A*)

- - - - Calculated
——— Test oscillogram
A—Switch *S* closed
B—Switch *S* opened

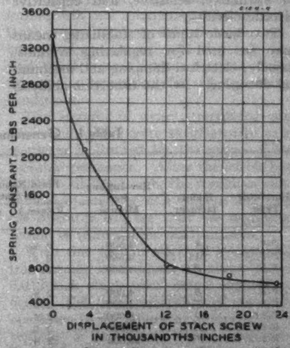

Figure 4. Spring constant versus stack displacement (regulator manufacturer *C*)

sating-winding flux overcoming the main-field-winding flux, as in a series motor with brush shift against rotation.

Although this latter phenomenon constitutes a form of instability, its action is sufficiently slow that a voltage regulator easily can prevent the voltage collapse. As all of the instability troubles recorded in service were oscillatory in nature, the analysis of this phenomenon was not pursued further.

Regulator Stability Analysis

Once it was found that the generator of manufacturer *A* without a regulator would not sustain an oscillation, the next approach was to determine what characteristics of carbon-pile regulators would produce instability in combination with generator characteristics.

A voltage regulator in any system behaves in a manner similar to an amplifier. Small deviations in the regulated voltage are made to produce relatively large changes in the generated voltage of the final machine to offset the internal voltage drop caused by variations in load. Such devices as vibrating contacts, motor-operated rheostats, and carbon-pile rheostats have been used to produce the large changes in excitation for small errors in the regulated voltage, and, although in some cases their action is intermittent, the net result produced has been amplification.

The chief difficulty in stabilizing all regulating systems is the presence of time delays. These may be analyzed in terms of the time constants of the various inductive circuits, such as the fields of rotating machines and also the time constants of the regulator itself. The latter may be electrical, mechanical, or both. Such a system may be idealized by showing the amplifier or regulator without delay but with an extra exciter to represent its delay, so that all the constants can be represented by simple inductive and resistive, or inductive, resistive, and capacitive electric circuits.

Two basic types of stabilizing means may be used for regulating systems, namely, electrical damping and mechanical damping. At the time this analysis was made no mechanical damper had been devised for aircraft carbon-pile regulators because of the difficulty of obtaining sufficient damping with the extremely small armature travel.

In this analysis a damping transformer was assumed to be the most satisfactory method of electrical damping. The problem then resolved into finding the correct size damping transformer to provide stable operation with all combinations of generators and regulators which would be used.

In Appendix III a mathematical analysis of the problem is given which includes all the characteristics of the system that have a major effect upon stability. Some of the constants for this system are difficult to measure, and a few assumptions are necessary, but from this analysis one can determine the approximate size damping transformer necessary for stable operation. Once the approximate amount of damping necessary is known, the optimum size damping transformer can be determined quickly from laboratory tests.

It had been shown in service and laboratory tests that wear or maladjustment of the carbon stack was the initiating cause of oscillatory instability. Decrease of the spring constant with increasing stack displacement, which is shown for a particular regulator in Figure 4, appears as an increase in the value of C_m in equation 30, Appendix III. This equation also shows that the value t_d $(=M/R_p)$ is the determining factor in the design of the damping transformer. Additional factors in the design of a damping transformer are discussed in another AIEE paper.[1]

Results of Calculations and Regulator Tests

Curves of stack displacement versus the value of M/R_p necessary to maintain stable operation for several generator and regulator combinations are shown in Figures 5, 6, and 7.

In Figure 5 curves are shown for a regulator of manufacturer *C* in combination with a *P*-1 generator of manufacturer *C*. This regulator was the earlier model containing no antihunt resistor. The test curve is plotted from points where stability was just maintained with the regulator at operating temperature. The calculated curve shows the value for critical* damping using the following constants in equation 30, Appendix III:

$R_c = 30$ ohms
$L_c = 0.0875$ henry
$R_m = 0$ and 0.1 pound-inch per second
$1/C_m =$ value obtained from Figure 4
$AR_c = 200$

The curves shown in Figure 6 are for the same regulator, manufacturer *C*, with a *P*-1 generator of manufacturer *A*.

The curves shown in Figure 7 are test curves taken with a regulator of manufacturer *B* in combination with a *P*-1 generator of manufacturer *A*. This regulator contained an antihunt resistor, and curves were taken with and without this resistor to illustrate its effect.

There can be noted a discrepancy of about two to one in the calculated and

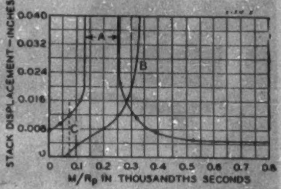

Figure 5. Distance stack screw can be moved out before instability occurs versus M/R_p of damping transformer (regulator manufacturer *C*, *P*-1 generator manufacturer *C*)

A—Test
B—Calculated (mechanical damping = 0)
C—Present transformer

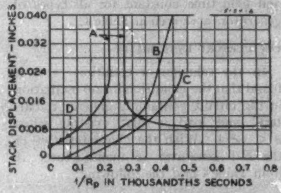

Figure 6. Distance stack screw can be moved out before instability occurs versus M/R_p of damping transformer (regulator manufacturer *C*, *P*-1 generator manufacturer *A*)

A—Test
B—Calculated (mechanical damping = 0.1 pound-inch per second)
C—Calculated (mechanical damping = 0)
D—Present transformer

Table I. Generator Characteristics

Generator Type	Manufacturer	Revolutions Per Minute	Field Resistance in Ohms R_f(gen.)	Field Resistance in Ohms r_f(tot.)	L_f,* Henrys	L_a,* Millihenrys	Field Time Constant, L_f/r_f, Seconds
P-1	*A*	4,500	2.3	14.0	0.28	0.14	0.020
P-1	*A*	4,500	2.4	15.3	0.20	0.14	0.013
P-1	*B*	4,500	2.8	20.0	0.36 (calc. 0.28)	0.22	0.018
P-1	*B*	4,500	2.8	18.6	0.33	0.22	0.018
P-1	*C*	4,500	2.9	16.5	0.51	0.19	0.031
P-2	*D*	8,000	2.7	14.0	0.22	0.10	0.016
R-1	*E*	10,000	2.6	20.0	0.27	0.08	0.013
R-1	*F*	10,000	2.8	20.0	0.43	0.07	0.021
M-2	*G*	2,500	3.6	20.0	0.53		0.026

* Inductance values obtained from oscillographic measurements.

---

* For definition see Appendix III.

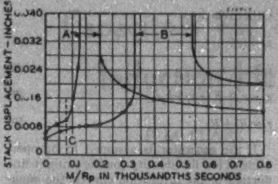

Figure 7. Distance stack screw can be moved out before instability occurs versus M/R_p of damping transformer (regulator manufacturer *B*, *P*-1 generator manufacturer *A*)

A—500 damping resistor
B—No damping resistor
C—Present transformer

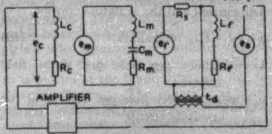

Figure 8. Representation of system with three time delays and one damping transformer

test values for the amount of damping required for a given stack displacement. This can be attributed to several factors. The measurement of the spring constant of the regulator was a tedious procedure, requiring observations of armature displacement in the order of 1/10,000 inch where a small error would be greatly magnified. Also the values of M/R_p for the test curve might be in small error because of interpolation from the inductance curves. The value of mechanical damping of 0.1 pound-inch per second was obtained from equation 30, Appendix III, using the spring constant for the stack position from the observed critical damping of the regulator with no damping transformer or antihunt resistor. The mechanical damping may be greater than this, which would make the calculated and test curves in closer agreement. There is no direct method of measuring the mechanical damping of this type regulator. It is also likely that the assumed amplification of 200 is higher than the actual value.

Test curves show that for a given transformer there is an upper limit to the value of M/R (obtained by decreasing R_p) which will provide stable operation. Although the feedback voltage (proportional to M/R_p) can be further increased by reducing R_p, the self-inductance in the primary winding (neglected in Appendix III) becomes appreciable and causes the feedback correction to lag the error voltage, so that the resultant damping is reduced. A lower limit for the value of R_p to give maximum feedback for effective damping with a given transformer, generator, and regulator combination could be obtained by solving a fifth-order equation. The practical way to obtain this limiting value is from test curves.

Conclusions

FACTORS AFFECTING STABILITY

Mutual Coupling in Generator. It is theoretically possible for an oscillatory condition to occur following a switching transient in a system composed of a generator (without voltage regulator), a battery, and a resistance load. The condition necessary to produce oscillation is large mutual coupling between the armature and shunt field windings. This coupling must be in the direction to produce cumulative compounding.

Cumulative Compounding in Generator. Generators having compensating and interpole windings and having the brushes shifted against rotation (in order to give maximum output) most nearly approach this condition. However, the measured constants of present *P*-1, *P*-2, and *R*-1 generators fall so far short of the values necessary to produce oscillatory instability (without a regulator) that the compounding tendency was concluded to be a secondary factor in the creation of an oscillatory condition.

Generators having rising volt-ampere characteristics may become unstable when operating with other generators or a battery. This is a nonoscillatory type of instability. This phenomenon was reproduced in the laboratory with a *P*-1 generator having compensating windings and a film on the commutator such as to give maximum compounding. However, this transient was so slow that the addition of a voltage regulator prevented occurrence of the phenomenon. This characteristic may tend to make the task of the voltage regulator more difficult but is again a secondary factor in the creation of system oscillations.

Time Constant of Generator Shunt Field. The aircraft generators investigated have high amplification and very small field time constants, particularly at maximum rated speed. Both of these factors are contrary to the usual case with large industrial machines and make the regulating problem more difficult. The fact that a compensated generator is less stable than an uncompensated machine can be linked directly with their field time constants. A compensated machine needs less main-pole flux to maintain a given voltage and for the same field current requirements will have a weaker shunt field winding with less inductance. This difference in inductance between machines is greater than the difference in total field resistance of the machines for no-load and light-load operating conditions, so that the compensated machine will have a smaller field time constant. The test and calculated curves in Figures 4 and 5 bear out this relationship. Both curves were made with the same regulator, but in Figure 5 the *P*-1 generator having the largest field time constant was used, whereas in Figure 6 the generator having the smallest field time constant was used. The use of interpole or series windings will have a similar effect.

Regulator Mechanical Construction and Assembly. The original assembly and adjustment of the regulator has a bearing on the amount of wear necessary to cause system instability. No two springs are identical, but the differences in individual springs should be maintained as small as possible by checking before assembly. This spring discrepancy and a noncritical final adjustment of the regulator can affect the amount of allowable stack wear by a thousandth of an inch or more. This is illustrated by comparison of the test curve in Figure 6 and the test curve without the antihunt resistor in Figure 7 at $M/R_p = 0$.

REGULATOR ANTIHUNT RESISTOR

The effect of the antihunt resistor is shown in Figure 7. This resistance allows an additional wear of about 0.0015 inch without any damping transformer and about 0.002 inch with the present Westinghouse damping transformer. Although this antihunt resistor has a damping effect, its full benefit will not always be obtained, because part of the additional wear may be lost in the final adjustment and the regulator still satisfy all regulation and stability requirements.

From the above it can be seen that, if any electrical damping is to be used on this type regulator, the total damping should be in the form of a transformer which can be inserted after final stack and core adjustments have been made.

OPTIMUM DAMPING TRANSFORMER

It can be seen from the curves of stack wear versus amount of feedback necessary for stability that one damping transformer will not compensate for infinite stack wear for all combinations of regulators and generators. Allowance for infinite stack wear is not necessary to maintain stable operation for all operating conditions.

The amount of wear a regulator can allow and still operate satisfactorily as a regulator is limited by the range of its variable resistance. After the stack has worn about 0.012 inch, the regulator cannot be adjusted for 28.5 volts or less, and the operator will see that the regulator should be returned for readjustment.

With this fact in mind, if a damping transformer is designed to allow about 0.012-inch stack wear before instability occurs, the only possibility of unstable operation is the failure of an operator to replace a regulator which obviously should be replaced. A regulator set for 28.5 volts on a 28-volt system still may share load because of its equalizing coil, but the operator can see that it needs replacing from its no-load voltage.

To obtain the correct value of damping transformer, curves similar to the ones shown in Figures 5, 6, and 7 are necessary for each combination of generator and regulator. From these curves it can be seen that an M/R_p of about 0.0003 second would allow a maximum stack wear of 0.013 inch or greater with all combinations shown in these figures. If the regulators of manufacturer *B* without antihunt resistor, Figure 7, were omitted from this analysis (none of this type is in use) an M/R_p of 0.00022 second would allow a maximum stack wear of 0.0245 inch or greater with the other combinations.

A well-designed transformer with the foregoing amounts of damping could be made weighing five ounces or less. Present carbon-pile regulators are 2.5 pounds.

RATE OF RESPONSE

Damping transformers reduce overshoot but do not materially reduce the speed of response.

PARALLEL OPERATION

In laboratory tests covered in a previous report to the Army Air Forces it was shown that, if one regulator is poorly adjusted and does not have a damping transformer, this regulator will affect the whole system and cause instability. Damping transformers on the other regulators in the system have little effect upon the poorly adjusted regulator. Therefore, for stable system operation, each individual regulator must have a damping transformer, and, if each regulator is stable in itself, the system will be stable.

Appendix I. Symbols

Generator:

R_f = resistance of shunt field

R_s = control or stack resistance in series with shunt field

r_f = total resistance of shunt field circuit (R_f+R_s)

R_a = resistance of armature, interpole, and compensating windings

L_f = self-inductance of shunt field

L_a = self-inductance of armature, interpole, and compensating windings

M = mutual inductance between shunt field and armature circuit windings, including mutual inductance of any demagnetizing or magnetizing armature, interpole, or compensating turns

$T_f = (=L_f/r_f)$ time constant of shunt field circuit

e_a = generated armature voltage

Kk_f = volts generated in the armature per ampere in the shunt field. Determined from the no-load saturation curve at maximum rated generator revolutions per minute, Kk_f is the slope of a line tangent to the saturation curve at the operating voltage

e_0 = fictitious residual voltage determined by intersection of straight line assumed for Kk_f with voltage axis at zero field current; e_0 includes brush drop

Kk_a = volts generated in the armature per ampere in the armature. Kk_a includes any cumulative or differential effect of brush shift or interpole and compensating windings

Load:

R_2 = resistance of load

R_b = internal resistance of battery

E_b = open-circuit battery voltage

Regulator:

R_c = resistance of regulator coil

L_c = inductance of regulator coil

$T_c = (=L_c/R_c)$ time constant of regulator coil

R_m = mechanical damping of regulator in dyne centimeters per second

$1/C_m = S$, spring constant of regulator in dynes per centimeter. This includes the combination of both spring and carbon stack and is assumed to be a constant for small deviations from a given position

L_m = mass of moving portion of regulator in grams. (Value taken equal to weight of armature plus one third of carbon stack)

$t_d = M/R_p$ feed-back ratio of transformer which has the dimensions of a time constant (= transformer mutual inductance/primary resistance)

A = amplification factor of regulator. (The total amplification of the system can be expressed as AR_c which is in the order of 200 for this system)

Appendix II. Operational Equations for Generator and Load Circuits

Figure 4 shows the arrangement of the system analyzed to determine the effect of generator characteristics on the oscillatory instability condition which had been observed in service. From preliminary tests and field reports it was observed that instability occurred in a system composed of a single generator and resistance load just as readily as in more complicated systems. For this reason it was not considered necessary to analyze the more general (and more complicated) system with inductive or overhauling loads and more than one generator. Lead resistance between the generator and battery was ignored for the sake of simplicity.

The operational equations for the voltage in the different circuits are as follows:

Load circuits

$$e = E_b + i_2R_b \tag{1}$$

$$e = i_2R_2 \tag{2}$$

Generator shunt field circuit

$$e = (R_s+R_f+L_fp)i_f + Mpi_a \tag{3}$$

Generator armature circuit

$$e = e_a - (R_a+L_ap)i_a - Mpi_f \tag{4}$$

Other relations

$$i_a = i_f + i_1 \tag{5}$$

$$i_1 = i_2 + i_3 \tag{6}$$

$$e_a = e_0 + K(k_fi_f + k_ai_a) \tag{7}$$

$$r_f = R_s + R_f \tag{8}$$

If the generator is assumed to be operating at low flux density (on the straight-line portion of the saturation curve), the equation for the generated voltage is

$$e_a = e_0 + K\phi \tag{9}$$

where

ϕ = flux per pole (megalines)

K = total generated armature volts per megaline of flux per pole

The flux, ϕ, is a function of both the shunt field current and the armature current.

$$\phi = k_fi_f + k_ai_a \text{ (megalines)} \tag{10}$$

k_f = megalines per pole per shunt field ampere

k_a = megalines per pole per ampere in the armature circuit

If the foregoing simultaneous equations are solved for the relationship between i_1 and t, the following well-known operational equation is obtained:

$$(p^2+\alpha p+\beta)i_1 = C \text{ (amperes per second}^2\text{)} \tag{11}$$

where

$$\alpha = \frac{(R_2+R_b)[(L_f+M)(Kk_a-R_a) - r_fL_a - (Kk_f+Kk_a-R_a)M] - R_bR_2(2M+L_a+L_f)}{(R_2+R_b)(M^2-L_fL_a)} \tag{12}$$

$$\beta = \frac{(R_2+R_b)(Kk_a-R_a)r_f + R_bR_2(Kk_f+Kk_a-r_f-R_a)}{(R_2+R_b)(M^2-L_fL_a)} \tag{13}$$

and

$$C = \frac{-e\delta(R_2+R_b)r_f - E_bR_2(Kk_f+Kk_a-r_f-R_a)}{(R_2+R_b)(M^2-L_fL_a)} \tag{14}$$

Equation 11 is a second-order linear operational equation whose solution is

$$i_1 = \epsilon^{-\alpha/2\,t}[c_1\epsilon^{\gamma t} + c_2\epsilon^{-\gamma t}] + i_0 \tag{15}$$

where

$$\gamma = \sqrt{\alpha^2/4-\beta} \tag{16}$$

and

$$i_0 = C/\beta$$

The integration constants c_1 and c_2 can be determined as follows from the boundary conditions of switch *S* having been opened previously and then closed at $t=0$:

$$c_1 + c_2 + i_{20} = i_0 \tag{17}$$

where

$$i_0 = \frac{C}{\beta},\ R_2 = \infty \text{ initial condition} \tag{18}$$

Capacitors for High-Frequency Induction-Heating Circuits

F. M. CLARK
ASSOCIATE AIEE

M. E. SCOVILLE
MEMBER AIEE

Synopsis: Increased military production has accelerated the application of high-frequency heating where accurate control of temperature for short intervals is fundamentally important. The heating of metals by induction has been widely applied. The present paper describes the development of a new type of dielectric liquid called Lectronol. Capacitors containing this liquid are particularly well adapted for use in the tank circuit of electronic heaters used in induction heating. The capacitor is water-cooled and is housed in a hermetically sealed completely filled nonmagnetic container so constructed as to provide sufficient flexibility to take care of the liquid expansion due to thermal changes. The capacitor is noteworthy because of the absence of cellulose sheet insulation, satisfactory operation being entirely dependent on the superior insulating properties of the Lectronol. Capacitors containing this liquid are characterized by low dielectric loss and high dielectric strength over the frequency range utilized in power oscillators. The capacity per unit volume is approximately twice that obtained with mineral oil. The electrical characteristics of the capacitor are stable under severe conditions of use.

The Need for a New Capacitor

HIGH-FREQUENCY ELECTRIC power has been applied to practical industrial uses for more than 20 years. The use of high-frequency generating equipment has increased steadily during that time. Not only has such equipment been familiar to many in the communication, radio, medical, and scientific-investigation fields, but in recent years it has come to be recognized as an economic industrial machine. Particularly since the start of industrial production for military use, there has been a tremendous increase in the application of powerful high-frequency generators for concentrated heating applications. The use of high-frequency currents and voltage industrially is largely for heating where speed in attaining a localized temperature for a very short interval is fundamentally important. The heating of metals by induction and heating of nonconductive materials by dielectric absorption has been widely described in recent technical literature.[1-6]

The generation of high-frequency current, whether by rotating generators, by spark gaps, or by electronic-tube oscillators, involves tuned circuits of inductance and capacitance. Since large amounts of heat energy are most readily transferred from the power source to the part heated by the use of high voltage, high current, or both combined, we must deal with coils and capacitors as well as other components of the oscillating circuit which will stand the high-voltage stresses and carry large currents. Such a circuit is commonly referred to as a "tank" circuit because of its energy-storage properties.

Capacitors for tuning such circuits are a fundamental part of the high-frequency generating set, in fact, representing up to one third of the cost of a complete equipment in some representative designs in use. In the past, capacitors used in tank circuits operating at frequencies above 15,000 cycles have been mostly mica-di-

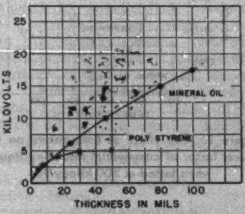

Figure 1. The dielectric-strength–thickness relation for mineral insulating oil and polystyrene films

Test temperature—25 degrees centigrade
Test frequency—500 kilocycles

Paper 45-157, recommended by the AIEE subcommittee on induction and dielectric heating for publication in AIEE TRANSACTIONS. Manuscript submitted April 12, 1945; made available for printing August 4, 1945.

F. M. CLARK is assistant engineer of the laboratory, and M. E. SCOVILLE is engineer in the capacitor engineering division, both with General Electric Company, Pittsfield, Mass.

The authors acknowledge the assistance given them by their associates, J. F. Byrne and G. L. Viles.

$$i_{ss}=\frac{C}{\beta},\ R_2=R_2 \text{ final condition} \tag{19}$$

$$c_1=\frac{(i_0-i_{ss})(\gamma+\alpha/2)}{2\gamma} \tag{20}$$

$$c_2=\frac{(i_0-i_{ss})(\gamma-\alpha/2)}{2\gamma} \tag{21}$$

Appendix III. Application of Damping Transformer

The present system is idealized in Figure 8.[2] The regulator is represented by two time constants, one electrical and one mechanical which is shown by an electrical equivalent. The circuit equations for voltage changes can be written as follows:

$$e_c=(R_c+L_cp)i_c=(1+T_c)i_cR_c \tag{22}$$

$$R_ci_c=e_m=(R_m+1/C_mp+L_mp)i_m \tag{23}$$

This circuit represents the mechanical part of the regulator, where the resistance is dependent upon the spring position for any one condition or, in electrical terms, the voltage output of the regulator is equal to the voltage across the condenser times the amplification of the regulator. In this analysis the amplification of the regulator is represented by a separate amplifier.

$$i_m/C_mp=e_f=(r_f+L_fp)i_f=(1+T_fp)i_fr_f \tag{24}$$

$$i_fr_f=e_a \tag{25}$$

$$e_c=-A[e_a+t_dp(e_f-i_fR_s)] \tag{26}$$

(The negative sign is used because corrections must be opposite to deviations.)

From equations 22, 23, and 24

$$e_c=(1+T_cp)(1/C_m+R_mp+L_mp^2)(1+T_fp)C_me_a \tag{27}$$

From equations 24 and 25

$$e_f=(1+T_fp)e_a \tag{28}$$

Substituting 25 and 28 into 26 gives

$$e_c=A[1+t_dp(1-R_s/r_f+T_fp)]e_a \tag{29}$$

Combining equations 27 and 29 yields

$$e_a=\frac{-Ae_a/C_m[1+t_dp(R_s/r_f+T_fp)]}{(1+T_cp)(1+T_fp)(1/C_m+R_mp+L_mp^2)} \tag{30}$$

Upon using the constants for any particular regulator and generator combination in equation 30, a value of t_d can be obtained to give critical damping. The value necessary for critical damping can be obtained by the use of Routh's criterion without the labor of solving a fourth-order equation.

For a fourth-order equation, such as

$$ap^4+bp^3+cp^2+dp+e=0$$

the necessary condition for critical damping is that

$$bcd\geq b^2e+d^2a$$

where critical damping is defined that the system will be stable and nonoscillatory in the steady state.

References

1. DESIGN OF REACTANCES AND TRANSFORMERS WHICH CARRY DIRECT CURRENT, C. R. Hanna. AIEE TRANSACTIONS, volume 46, 1927, pages 155–60.

2. RECENT DEVELOPMENTS IN GENERATOR VOLTAGE REGULATION, C. R. Hanna, K. A. Oplinger, C. E. Valentine. AIEE TRANSACTIONS, volume 58, 1939, pages 838–44.

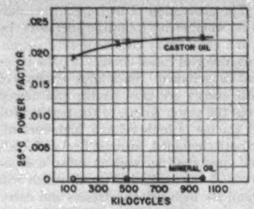

Figure 2. The comparative power-factor characteristics of mineral insulating oil and castor oil

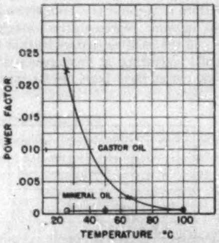

Figure 3. The effect of temperature on the power factor of commercial insulating liquids when tested at 500 kilocycles

electric types. However, the tremendous requirements for mica capacitors by the military services for communication and radar applications, along with difficulty in importing the higher grades of mica, was expected to restrict its use to those applications for which another dielectric could not be readily used. Fortunately other dielectric materials have been found possessing both better operating characteristics and economic advantages for use in induction-heating tank circuits.

What Are the Requirements of a Suitable Capacitor?

Basically, the characteristics required of capacitors for use in industrial high-frequency heaters are not widely different from those required for the familiar use in broadcast transmitters. However, the following requirements should be noted:

1. The current and voltage rating must be high to allow handling more energy. Thus it becomes desirable and economical to build higher kilovolt-ampere (kilovolts × amperes) ratings into single units to avoid a multiplicity of series and parallel connections of smaller ratings.

2. Dissipation of capacitor losses with the continuous operation necessary to meet high-production requirements in industrial plants requires adequate consideration. Although capacitor losses may be very small as compared to the total losses in a complete heater equipment, the effective dissipation of these losses with low-temperature rise is essential. Since cooling water is necessary for quenching of the heated parts, for load coils, spark gaps, vacuum tubes, or other circuit components, water-cooled capacitors are also practical. Forced-air cooling is a practical solution for the lower range of kilowatt ratings where water-cooling is undesirable.

3. Variation in operating frequency is not so critical as for radio transmitters. Therefore, the allowable variation of capacitance with temperature is not so critical in capacitors for induction heaters. This makes it possible to use a number of different dielectric materials.

4. Industrial usage requires much longer periods of operation without shutdown for maintenance or repair than has been accepted as satisfactory for earlier high-frequency radio and laboratory equipment. Reliability is, therefore, an important consideration.

5. The physical size, mounting features, means for both electric and water connections to other circuit components, and accessibility must be suitable for industrial use.

Since electronic heaters use circuits developed first for radio transmitters, the natural course was to use the same circuit components. However, as new development will permit, circuit components more adapted for industrial heating are to be desired. For example, most manufacturers recognize that economics dictates a policy of building equipment for industrial use having operating features and factors of safety which allow operation for very long periods without maintenance or inspection by technical personnel. Such has not often been true with radio equipment or laboratory equipment where constant technical supervision and frequent replacement of parts have been the practice.

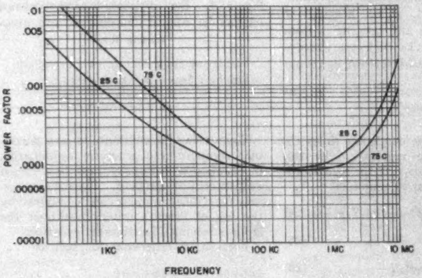

Figure 4. Power-factor versus frequency characteristics for Lectronol measured on standard concentric test cell with low-voltage oscillator

The Capacitor Dielectric Material

A rather exhaustive search of the entire field of dielectric materials suitable for high-frequency operation has been made.

Liquid dielectrics have been traditionally accepted as adaptable for high-voltage use only when used in conjunction with a solid insulation. In capacitors and cables, the solid used has invariably been paper sheets or tapes. These alone have not been satisfactory for high-voltage use because of their low-dielectric-strength value. When carefully dried and impregnated with a liquid dielectric, however, the replacement of the air normally present in the fibrous structure of the cellulose sheet by the liquid dielectric has produced a combination which has proved to be highly efficient as a dielectric for high-voltage use. In the low-frequency-capacitor application, a noninflammable synthetic liquid is particularly well adapted because of its high dielectric constant.

With the advent of the power oscillator, however, the traditional interdependency

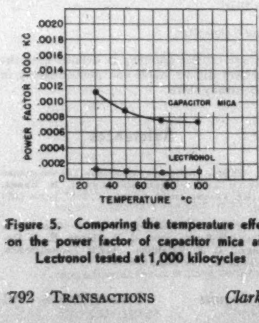

Figure 5. Comparing the temperature effect on the power factor of capacitor mica and Lectronol tested at 1,000 kilocycles

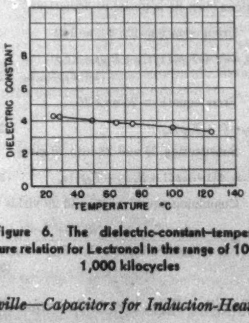

Figure 6. The dielectric-constant–temperature relation for Lectronol in the range of 100–1,000 kilocycles

of the liquid and solid insulation for high-voltage use has been subjected to critical review. The presence of the cellulose sheet insulation in capacitors operating at high voltage in the range of frequencies above 100 kilocycles has not been found to be entirely practicable. The result has been the development of a capacitor which is noteworthy because of the entire absence of cellulose sheet insulation between the electrode plates. The satisfactory operation of the capacitor is entirely dependent on the insulating liquid used. Such capacitors have been designated as "liquid-filled high-frequency parallel-plate capacitors" or more simple "class-*HFP* capacitors."

The Effect of Frequency on the Dielectric Strength

Montsinger[7] has suggested that the dielectric strength of solid insulation varies with frequency and the duration of voltage application in accordance with the relation:

$$E=1.225+\frac{0.525}{\sqrt[4]{T}}\times f^{-0.137}$$

where

E = dielectric strength (volts)
T = duration of voltage application (seconds)
f = frequency of test voltage (cycles per second)

Although the effect of frequency on the breakdown of solid insulation is dependent to some extent on the thickness of insulation tested, the relationship suggested by Montsinger for frequencies up to 90 kilocycles has been found to be approximately true at frequencies in the range of 100 to 1,000 kilocycles. Thus, Montsinger's relation would predict that the dielectric strength of solid insulation at 500 kilocycles would equal 30 per cent of the corresponding 60-cycle value. By actual test using dielectric pads made up of styrene films, a material of good dielectric properties at both low and high frequencies, the dielectric strength at 500 kilocycles averages 21 per cent of the 60-cycle breakdown value.

In contrast with this severe loss in dielectric strength which is exhibited by solid insulation, liquid dielectrics show marked stability. When tested at 60-cycle voltages the dielectric strength of insulating liquids in good condition averages about 30 kv, using one-inch-diameter square-edge brass electrodes, in accordance with the procedures prescribed by the American Society for Testing Materials.[8] The dielectric strength tested under the same conditions at a frequency of 500 kilocycles average about 60 per cent of the 60-cycle value. The greater dielectric-stability characteristic of insulating liquids when tested at the higher frequencies renders this type of dielectric well suited for application in high-frequency high-voltage capacitors. This is illustrated in Figure 1, which compares the dielectric strength of polystyrene and mineral oil tested at 500 kilocycles 25 degrees centigrade. It is only for the lower dielectric thickness that the solid dielectrics are possessed of dielectric strengths comparable to the liquids. It is in this manner that they have heretofore been widely used. For high-voltage use at high frequency, the liquid dielectrics have marked superiority.

Table I

Voltage	Microfarad	Microhenrys	Megacycles Resonant Frequency
2,000	0.034	0.075	3.5
2,000	0.025	0.085	3.0
6,000	0.010	0.12	4.5
6,600	0.009	0.10	5.3
9,000	0.0056	0.13	5.8
9,000	0.0029	0.12	9.0

Commercial Dielectric Liquids

Mineral transformer oil and castor oil heretofore have been considered to possess characteristics suitable for use under high-frequency voltage. In the range from 100 to 1,000 kilocycles, mineral transformer oil has low electrical loss. As illustrated in Figure 2, the power factor is less than 0.0005 at 30 degrees centigrade. Castor oil, however, has excessively high losses at room temperature. A capacitor using castor oil as a dielectric therefore would be expected to operate at temperatures well above room temperature. As illustrated in Figure 3, an increase in temperature results in a continuously decreasing electrical loss. At 100 degrees centigrade, the electrical losses in castor oil are reduced to values equally as low as those characteristic of mineral oil.

In high-frequency-capacitor use, neither of these insulating liquids is satisfactory. Mineral transformer oil, although possessing excellent high-frequency loss values, has a dielectric constant of such low value (2.18) that capacitors using this liquid possess large physical volume per microfarad. Castor oil possesses a suitably high dielectric constant (4.2 at 30 degrees centigrade). Its high electrical losses, however, coupled with its recognized chemical instability at elevated temperature, greatly restrict its application in high-frequency electric capacitors.

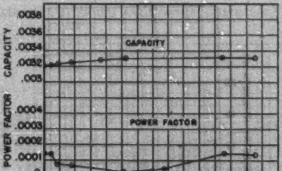

Figure 7. Illustrating the electrical stability of high-frequency parallel-plate capacitors filled with Lectronol heated at 70 degrees centigrade in contact with air

Test frequency—500 kilocycles
Temperature of electrical measurement—25 degrees centigrade

Electrical and Chemical Requirements

A liquid dielectric suitable for use in high-frequency plate capacitors must meet exacting electrical and chemical requirements. It must possess low electrical losses over the whole range of possible operating temperatures and frequencies. It must possess high dielectric strength. It must be chemically stable under high-voltage stress at the electrical frequencies to which it will be subjected. If subject to oxidation, the products formed must be of a type which do not affect its electrical losses, dielectric strength, or other properties which would prevent its continued successful operation under high-frequency electrical stresses. Lectronol is such a liquid. This synthetic oil is a thin, colorless, mobile, synthetic, organic liquid possessing the following characteristics:

Flash point—180 degrees centigrade
Reaction—Neutral
Pour point—−8 degrees centigrade
Dielectric constant (25 degrees centigrade)—4.4
Dielectric strength (25 degrees centigrade)—40 kv (average for 0.1-inch gap)

Power Factor or Losses

Over the frequency range utilized in power oscillators the synthetic oil described is characterized by low dielectric loss, as shown in Figure 4. As illustrated in Figure 5, the losses are even lower than those obtained with mica over the tem-

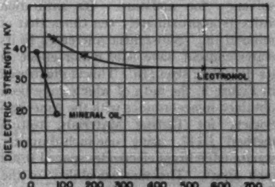

Figure 8. The dielectric strength of Lectronol is maintained at a high value even in the presence of moisture of sufficient amount to produce a marked drop in the dielectric strength of mineral oil

Test temperature—25 degrees centigrade
Test frequency—60 cycles
Test gap—100 mils

perature range from 30 to 100 degrees centigrade.

Most liquids characterized by low dielectric loss at high frequency are also characterized by a low dielectric constant. Lectronol is an exception. Although having a loss even lower than that of mica, its dielectric constant is approximately twice that of mineral oil. In Figure 6 is illustrated the dielectric constant as affected by temperature over the range from 25 to 125 degrees centigrade. The dielectric constant falls in a linear relation to the increase in temperature.

A liquid to be satisfactory for capacitor use must not only possess a suitably low dielectric loss but also be able to maintain this favorable characteristic under the most adverse operating conditions. Parallel-plate capacitors having Lectronol as the sole high-frequency dielectric show substantially no electrical deterioration even when heated for 200 days at 70 degrees centigrade (Figure 7).

Repeated studies with Lectronol substantiate its remarkable suitability for use in high-frequency capacitors. Those factors which normally would be expected to result in increased power factor have been found to have but little effect. Oxidation produces neither sludge nor dielectric deterioration. Neither power factor nor dielectric strength are affected measurably by arcing a hundred or more times when the current in the arc is of low value and not many cycles duration. Accidental arcing between capacitor plates through the liquid does not cause measurable deterioration, if the arc currents are limited to low values of a few amperes which avoids melting of the plates.

DIELECTRIC STRENGTH

Lectronol is characterized by a high and stable dielectric strength. Most insulating liquids, such as mineral oil, show a rapid drop in dielectric strength with increasing water content. Such liquids have but little capacity for holding water in solution. This insulating liquid, on the other hand, has substantially greater solvency for moisture. Its saturation value is approximately ten times that of mineral oil. Substantial increases in its water content have only minor effect on its dielectric strength. This is illustrated in Figure 8, the data of which have been obtained in accordance with the American Society for Testing Materials, testing method *D*117, using one-inch-diameter square-edge brass electrodes spaced 0.100 inch apart. The marked ability of the liquid to resist the deteriorating effects of contaminants, such as moisture, is reflected in its excellent dielectric strength on high-frequency voltage under conditions of practical use.

In Figure 9 are illustrated the comparative dielectric-strength values of dry liquid-filled class-*HFP* capacitors, plotted as a function of the gap distance under 550-kilocycle voltage. Even under the condition of low water content, most favorably adapted to produce the highest dielectric-strength values for mineral oil, it shows no superiority to the synthetic insulating liquid under high-frequency voltage. The excellent dielectric strength of the latter is not materially affected by temperature increase from 25 to 100 degrees centigrade (Figure 10).

Capacitor Construction

After the selection of the liquid with suitable characteristics, the plate assembly, insulators, supports, and terminal bushings are next important. The two sets of parallel plates must be spaced accurately and permanently, for which heavy-gauge aluminum stock is most desirable. The two plate assemblies must be rigidly supported and yet allow for thermal expansion, which is accomplished with Mycalex plates. This insulating material has very good high-frequency voltage strength as well as low loss under high-frequency stress and also high mechanical strength. More than ample voltage-creepage surfaces are obtained readily with the large sheet used.

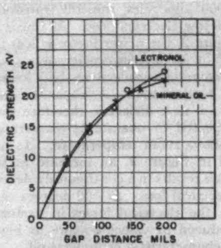

Figure 9. A comparison of the dielectric-strength characteristics of high-frequency parallel-plate capacitors filled with dry mineral oil and Lectronol measured at 25 degrees centigrade under 500-kilocycle test voltages

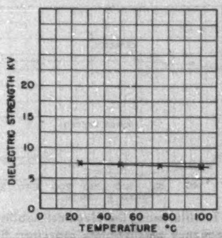

Figure 10. The effect of temperature on the dielectric strength of high-frequency parallel-plate capacitors filled with Lectronol

Test frequency—500 kilocycles
Gap distance—36 mils

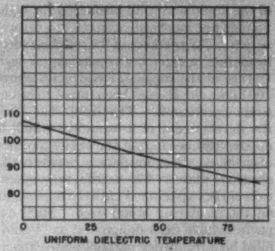

Figure 11. Variation of capacitance with temperature in degrees centigrade measured at 60 cycles

Very effective water cooling of the assembly is obtained by connecting the cooling coil to the grounded set of plates, thus giving direct heat flow from the plates through the connectors into the tubing and into the water. Also the water tubing serves as a current conductor, making possible small-size high-current connections going directly to the load transformer or tank coil. Current-carrying connections between series or parallel connected units may be combined with cooling water tubing connections.

The container is nonmagnetic of double-lock seam construction, providing sufficient flexibility in side walls to take care of liquid expansion due to thermal changes. The case is completely filled with liquid and hermetically sealed. Removable footed-type mounting brackets are provided for supporting the capacitor in any desired position, protecting the ends from damage and yet not interfering with flexibility of the capacitor sides.

Terminal bushings require particular design consideration to obtain sufficiently low-voltage stress distribution to avoid dielectric heating in the insulating material and yet have high current-carrying capacity. When a hollow shell type of ceramic bushing is used and the interior is filled with the low-loss, high-strength liquid, the dielectric loss in the bushing assembly is held to a minimum, and liquid cooling about the current-carrying parts is effective in dissipating losses. Two or more such bushings, connected in parallel to split the current and having water-cooling tube connections at the top, allow high-current operation of a single capacitor. For voltage ratings of six kilovolts and above, corona shields added at the base of the bushing are an advantage, making it possible to use a smaller bushing and less creepage surface and at the same time providing a definite flashover voltage value at a point away from the ceramic surface.

Electrical Characteristics

It is comparatively easy to maintain a close tolerance in capacitance of ± 5

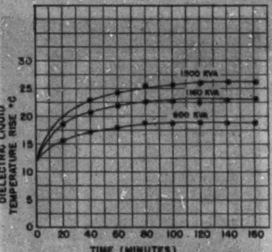

Figure 12. Typical dielectric-liquid temperature rise in degrees centigrade above outlet water temperature variation with time in operation for high-frequency parallel-plate capacitor rated 0.0056 microfarad, 500 kilocycles, and one-half-gallon-per-minute water flow

per cent in production of such capacitors, as capacitance variation between units is almost entirely a result of variation in physical dimensions.

Change in capacitance with temperature is dependent on both change in dielectric constant of liquid temperature and change in physical spacing of plates with linear metallic expansion. Capacitance variation with temperature is between one fourth and one third of 1 per cent per degree centigrade as shown by Figure 11. This change in capacity is recognized as being too great for use where the frequency of the tank circuit must be held within narrow limits, such as for radiobroadcasting. However, a slight change in frequency of three to four per cent which is typical of changes from no-load to full-load operating temperature is not objectionable for induction heating. The use of cooling water aids appreciably in holding a constant operating temperature in capacitors, as the full-load continuous temperature rise is held to a reasonably low value.

The internal inductance of such capacitors is low with only a small variation due to change in physical dimensions such as height of terminal bushings above the case. Since internal inductance varies only between 0.075 and 0.13 microhenrys, the resonant frequency varies with the microfarad rating as shown by Table I.

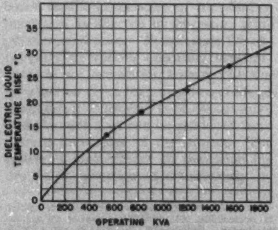

Figure 13. Typical dielectric-liquid temperature rise in degrees centigrade above outlet water-temperature variation with operating kilovolt-amperes for capacitor rated 0.0056 microfarad, nine kilovolts, 540 kilocycles with one-half-gallon-per-minute water flow

Though individual capacitors with minimum length of bus connections are suitable for operation at several megacycles, particular consideration must be given to keeping the length of the tank circuit and loop area of the circuit connections at a minimum, if the higher-frequency range of the capacitors is to be utilized.

An outstanding characteristic is the low loss of these capacitors at high frequency. Losses are a combination of I^2R or metallic-conductor loss and the dielectric loss in the liquid. Metallic losses are low, because design features include parallel-current paths, good electric conductors, and well-made joints between conductors. In fact in the practical application losses in the tank coil and the two capacitor terminals are a much larger factor than the internal losses of the capacitor. For example, a capacitor rated 0.0056 microfarad operating at 540 kilocycles, 9,000 volts rms, and 171 amperes, on continuous operation will show 3.3 degrees rise in cooling water with a flow rate of one-half gallon per minute. Using the constant of 31.6 watts per pound of water per minute per degree centigrade, we calculate a total loss of 448 watts.

Thus, the calculated power factor with full-load operation at 1,539 kva is 0.00029. With reference to Figure 5, the liquid dielectric power factor is 0.0001, leaving a power factor of 0.00019 assignable to I^2R or metallic losses.

Some designers prefer the use of Q factor for comparison of circuit component losses. As the Q factor of a capacitor is equal to the reciprocal of the per cent power factor times 100, we get a factor of approximately 3,450 for this rating and operating load.

The use of water cooling tends to stabilize operating temperatures with constant temperature rise reached in about $1^1/_2$ hours continuous operation.

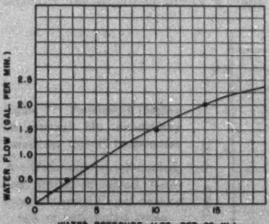

Figure 14. Water-flow variation with pressure applied to cooling coil of high-frequency parallel-plate capacitors

Typical temperature-rise curves are shown in Figure 12. The outlet water temperature controls the operating temperature of the capacitor. In order that the temperature of the dielectric liquid does not exceed 68 degree centigrade, the outlet water temperature is limited to 35 degrees centigrade at 1,500 kva and above. With a limit on operating temperature of liquid, it is reasonable that outlet temperature may be higher when kilovolt-ampere loading is lower, as shown by Figure 13. For economy in use of cooling water, several capacitors may be connected in series for water flow, depending on the pressure available. Figure 14 shows the pressure drop per capacitor for a range of different water-flow rates. The temperature rise in the cooling water is low and dependent on the operating kilovolt-amperes as shown by Figure 15.

Basis of Rating

The voltage rating is fixed by two factors:

1. The maximum peak transient voltage which the capacitor is expected to withstand.
2. The continuous rms operating voltage which contributes to the temperature rise or heating load on a capacitor.

Consistent with dielectric strength of the liquid and plate spacing, all capacitors are designed for operation with transient voltage peaks not to exceed 200 per cent of the rms high-frequency rating.

The usual practice of listing test-voltage ratings on mica capacitors in place of maximum continuous rms rating has not proved to be satisfactory for industrial application. Having only the ultimate short-time voltage strength listed as a rating makes it necessary for each designer of equipment in which mica capacitors are used to decide for himself the factor of safety to be allowed on operating voltage as against test voltage. In too many cases the pressure of space requirements and economics, along with inex-

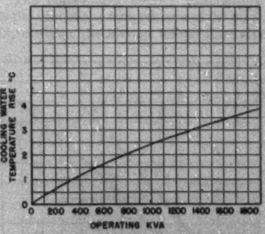

Figure 15. Variation in cooling-water temperature rise in degrees centigrade with operating kilovolt-amperes for high-frequency parallel-plate capacitor rated 0.0056 microfarad, nine kilovolts, 540 kilocycles

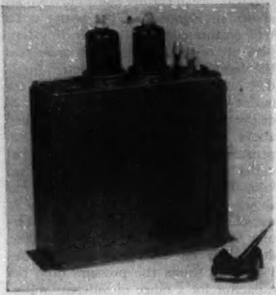

Figure 16. General Electric high-frequency parallel-plate capacitor unit for electronic-heater resonant-circuit applications

High-frequency, parallel-plate, water-cooled, rated 0.0056 microfarad, 9,000 volts, 171 amperes, at 540 kilocycles

perience on life statistics if at all available, all lead to the result that mica capacitors are used with insufficient factor of safety for continuous operation.

It is essential that adequate consideration be given to the effective dissipation of losses for continuous operation of all capacitors and that operation is in accordance with predetermined ratings under which the capacitor is designed to operate. For a safe economical industrial installation, a capacitor designer must establish the operating rating.

For class-*HFP* capacitors both voltage and current ratings are based on a frequency of 540 kilocycles which has been selected as being in the most popular range for electronic induction-heater operation. As the capacitor is rated for a maximum voltage at 540 kilocycles, the current rating at lower frequencies must be reduced in direct proportion to the frequency change, while the voltage rating remains unchanged. For frequencies above 540 kilocycles, the current rating can be increased to limits allowed by operating temperatures of the dielectric liquid and terminal conductors. Water cooling of terminal conductors has been found practical because of much higher current rating allowed. For example, a typical pair of terminals as shown by Figure 16 will carry 95 amperes at 540 kilocycles with 45 degrees rise when connected with conductors having natural air cooling but will carry 171 amperes when connected to water-cooled tubing with approximately the same rise.

Conclusions

1. A much improved and more economical high-voltage high-current tank circuit capacitor has been developed for induction-heating and dielectric-heating oscillators.

2. A new high-dielectric-strength liquid with high dielectric constant and very low loss over a wide frequency range has been applied in a practical fixed-plate capacitor design. Having the container, including terminal bushings, completely filled with liquid and hermetically sealed insures that the capacitor will keep its original electrical characteristics.

3. Installation of capacitors with larger sizes required for electronic heaters has been simplified. Maintenance cost has been reduced because of larger factor of safety from overheating on continuous operation in high ambient temperatures.

4. Large amounts of mica previously used for capacitors in electronic heating oscillators have been saved for military radio and radar applications requiring capacitors with minimum change in capacitance with temperature and requiring physical dimensions interchangeable with standard mica capacitor sizes previously available.

References

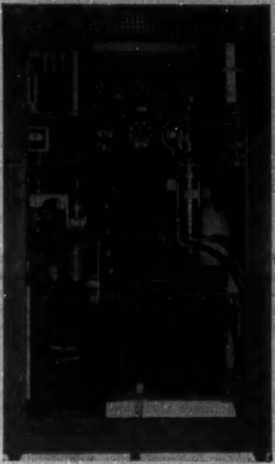

Figure 17. Rear view of electronic heater, 15 kw, type *F*-15, model *4F15E1*, without rear door

1. INDUCTION HEATING—SELECTION OF FREQUENCY, N. R. Stansel. AIEE TRANSACTIONS, volume 63, 1944, October section, pages 755–9.

2. HEATING OF NONMAGNETIC ELECTRIC CONDUCTORS BY MAGNETIC INDUCTION—LONGITUDINAL FLUX, R. M. Baker. AIEE TRANSACTIONS, volume 63, 1944, June section, pages 273–8.

3. SURFACE HEATING BY INDUCTION, Herbert F. Storm. AIEE TRANSACTIONS, volume 63, 1944, October section, pages 749–55.

4. THE THEORY AND PRACTICE OF INDUSTRIAL ELECTRONIC HEATING, J. P. Jordan. *General Electric Review*, December 1943.

APPLICATION OF VACUUM-TUBE OSCILLATORS TO INDUCTIVE AND DIELECTRIC HEATING IN INDUSTRY, J. P. Jordan. AIEE TRANSACTIONS, volume 61, 1942, November section, pages 831–4.

5. DEHYDRATION OF FOOD BY RADIO-FREQUENCY ENERGY, THIN CASE HARDENING WITH RADIO-FREQUENCY ENERGY, V. W. Sherman. *Electric Communication*, volume 21, number 2, 1943.

6. HEATING WOOD WITH RADIO-FREQUENCY POWER, J. P. Taylor. American Society of Mechanical Engineers *Transactions*, April 1943.

7. EFFECTS OF TIME AND FREQUENCY ON INSULATION TESTING OF TRANSFORMERS, V. M. Montsinger. AIEE TRANSACTIONS, volume 43, 1924, pages 337–47.

8. AMERICAN SOCIETY FOR TESTING MATERIALS STANDARDS 1942 (book), part 3, *D*117-42, page 350.

Guides for Operation of Transformers, Regulators, and Reactors

AIEE TRANSFORMER SUBCOMMITTEE

Guide for Loading Oil-Immersed Distribution and Power Transformers

SCOPE

THIS guide covers general recommendations for loading all types of oil-immersed transformers with class-*A* insulation except water-cooled transformers built before 1929, self-cooled transformers rated at 200 kva or less, and transformers having a rated full-load current less than ten amperes. They include transformers immersed in synthetic or noninflammable liquids.

The manufacturer should be asked for recommendations relating to water-cooled transformers built before 1929 and for more specific recommendations for large and important transformers if required.

CAUTION

It must be recognized that loads above rating should not be applied without a thorough study of the various limitations involved. Among these limitations are oil expansion, pressure in sealed-type units, bushings, leads, soldered connections, tap changers, and the thermal capability of associated equipment such as cables, reactors, circuit breakers, disconnecting switches and current transformers. These may constitute the practical limit in load-carrying ability.

Before loading apparatus above rating to the full extent covered in these guides, it is recommended that load capabilities be checked with the manufacturer.

GENERAL

Recommendations in this guide are based on life expectancy of transformer insulation as affected by operating temperature and time. Transformer life expectancy at various operating temperatures is not accurately known, but the information given regarding loss of life of insulation is considered to be conservative and the best that can be produced from present knowledge of the subject. The effects of temperature on insulation life are being investigated continuously by the transformer subcommittee, and new findings may affect future revision of the guides. The word "conservative" is used in the sense that the expected loss of insulation life for a single recommended overload will not be greater than the amount stated.

The rated kilovolt-ampere output of a transformer is that load which it can deliver continuously at rated secondary voltage without exceeding a given temperature rise measured under prescribed test conditions. The temperature rise on which the rating is based takes into consideration the experience of the industry regarding

1. Insulation life as affected by operating temperature.

2. The ambient temperatures assumed to exist throughout the life of the transformer.

The actual output which a transformer can deliver at any time in service without undue deterioration of the insulation may be more or less than the rated output, depending upon the ambient temperature and other attendant operating conditions.

Practically all of the data in reference to the aging of insulation at different temperatures has been obtained in laboratory tests in which the decrease in mechanical strength has been measured. The relation between the life expectancy of insulation as indicated by laboratory tests and the actual life of a transformer is largely theoretical, so that loading based on such information must be tempered by sound judgment based on experience.

As the evaluation of the cumulative effects of temperature and time in causing deterioration of transformer insulation is not thoroughly established, it is not possible to predict with any great degree of accuracy the length of life of a transformer even under constant or closely controlled conditions, much less under widely varying service conditions.

The change in rate of deterioration with change in temperature has received much study, but the actual values for different operating temperatures are not completely agreed on. An average value which has been used for a number of years is that the rate of deterioration doubles with each eight degrees centigrade that the temperature of the insulation increases. This value is not accurate for all temperatures nor for all points in the life of a transformer. It is given here to show the importance of controlling ambient temperatures in indoor installations by means of ventilation, thus controlling the insulation temperature and life.

Owing to the many variables mentioned and particularly to the many varying conditions of load and ambient to which a transformer can be subjected in service, it is not possible to give definite rules for the loading of transformers. It is only possible to give suggested loadings under specified conditions and look to the user to make the best use of this information for his particular problem.

AMBIENT TEMPERATURES AND LOADING FOR NORMAL LIFE EXPECTANCY

The basic loading condition of a transformer for normal life expectancy is continuous loading at rated kilovolt-amperes and rated delivered voltage with the temperature of the cooling air at no time exceeding 40 degrees centigrade and with the average temperature of the cooling air during any 24-hour period equal to 30 degrees centigrade. For water-cooled transformers comparable temperatures are 30 and 25 degrees centigrade, the five-degree-centigrade lower average temperature of the cooling medium being to allow for possible less efficient cooling due to coils that are not clean. (It is assumed that operation under the foregoing conditions is equivalent to operation at a continuous ambient temperature of 30 degrees centigrade for cooling air and 25 degrees centigrade for cooling water.)

The hottest-spot copper temperature is the sum of the temperature of the cooling medium, the average temperature rise

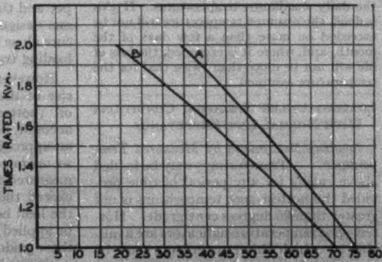

Figure 1. Permissible loading for normal life expectancy based on top-oil temperature

A—Water-cooled, self-cooled, and forced-air-cooled transformers rated 133 per cent or less of self-cooled rating

B—Forced-oil-cooled transformers or forced-air-cooled transformers rated over 133 per cent of self-cooled rating

---

Paper 45-130, recommended by the AIEE committee on electric machinery for publication in AIEE TRANSACTIONS. Manuscript submitted February 26, 1945; made available for printing May 23, 1945.

This paper is a complete revision of AMERICAN RECOMMENDED PRACTICE—GUIDES FOR OPERATION OF TRANSFORMERS AND REGULATORS, American Standard C57.3—1942. It will be presented to the American Standards Association sectional committee on transformers C57 for inclusion in proposed revision of transformer Standards.

of the copper and the hottest-spot allowance. For oil-immersed transformers operating continuously under the foregoing conditions with normal life expectancy this temperature has been assumed to be 95 degrees centigrade.

Other usual service conditions, as given in American Standard C57.1, section 2.000, must be complied with.

Years of experience have indicated that a transformer rated in accordance with the Standard and operated under the foregoing conditions will have a reasonably long life.

Ambient Temperatures

Ambient temperature is an important factor in determining the load capability of a transformer. Whenever the actual ambient temperature can be determined from readings taken at the time of the load being considered, such temperatures should be used.

It is often necessary to predict the load that a transformer can carry safely at some future time when the actual ambient temperature is unknown. A method of approximating the ambient temperature for the month in which the expected load is anticipated is as follows (Temperatures referred to are contained in reports prepared by the Weather Bureau of the United States Department of Commerce and are available for various sections of the country):

1. For loads with normal life expectancy:

Use the average temperature over a period of years for the month involved. Some believe that this temperature should be increased by as much as five degrees centigrade because

(*a*). The average temperature for a given month may be above the average temperature of the same month for a period of years.

(*b*). Increased aging at higher than average temperature is not offset by decreased aging at lower than average.

2. For short-time loads with moderate sacrifice of life expectancy:

Use the average of the daily maximum temperatures for the month involved averaged with similar values for the same month over a period of years.

During any one day there is an even chance that the maximum temperature will exceed this value. Some feel that five degrees centigrade should be added to the average of the daily maximum temperatures. If this is done, the assumed temperature will not be exceeded on more than a few days of the month, and, where it is exceeded, the loss of life will not be more than twice that for the temperature assumed.

Loading Under Specified Conditions With Normal Life Expectancy

Loading Determined by Measured Temperature. Transformers may be loaded above rating for any period of time provided the hottest-spot temperature is not greater than 95 degrees centigrade. Hottest-spot temperature indicators are available by which this temperature may be measured.

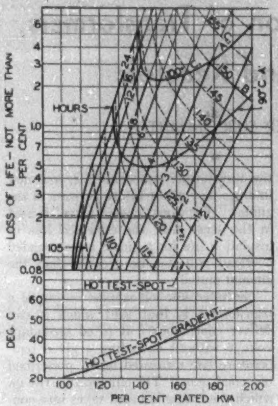

Figure 2. Short-time loading with moderate sacrifice of life expectancy, self-cooled and water-cooled transformers

Following 50 per cent or less of rated kilovolt-amperes or top-oil temperature rise of 25 degrees centigrade

Ambient temperature 30 degrees centigrade for air, 25 degrees centigrade for water

Subtract hottest-spot gradient from hottest-spot temperature to obtain top-oil temperature

A—Assumed temperature limitation for top oil (protected)

A'—Assumed temperature limitation for top oil (unprotected)

B—Assumed temperature limitation for hottest-spot copper

Time, Hours	Times Rated Kilovolt-Amperes to Use not More Then Following Life (Per Cent) 0.1	0.25	0.50	1.0
1/2	2.00	2.00	2.00	2.00
1	1.76	1.91	2.00	2.00
2	1.50	1.62	1.72	1.82
4	1.27	1.38	1.46	1.53
8	1.13	1.21	1.30	1.37
24	1.05	1.10	1.15	1.23

For explanation of degree of accuracy, see Appendix II.

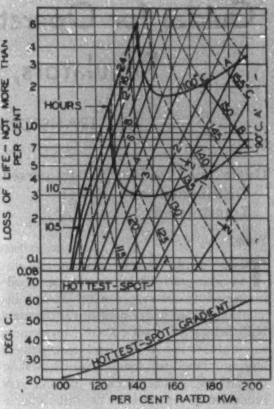

Figure 3. Short-time loading with moderate sacrifice of life expectancy, self-cooled and water-cooled transformers

Following 100 per cent of rated kilovolt-amperes or top-oil temperature rise of 45 degrees centigrade

Ambient temperature 30 degrees centigrade for air, 25 degrees centigrade for water

Subtract hottest-spot gradient from hottest-spot temperature to obtain top-oil temperature

A—Assumed temperature limitation for top oil (protected)

A'—Assumed temperature limitation for top oil (unprotected)

B—Assumed temperature limitation for hottest-spot copper

Time, Hours	Times Rated Kilovolt-Amperes to Use not More Than Following Life (Per Cent) 0.1	0.25	0.50	1.0
1/2	1.75	1.92	2.00	2.00
1	1.54	1.69	1.81	1.92
2	1.35	1.48	1.58	1.68
4	1.20	1.32	1.40	1.48
8	1.11	1.20	1.28	1.35
24	1.05	1.09	1.15	1.23

For explanation of degree of accuracy, see Appendix II.

On account of large variations in the difference between the hottest-spot copper and the top-oil temperatures of various designs under full load, oil temperature alone should not be used as a guide in loading transformers.

However, by taking the temperature rise of the hottest-spot copper over top oil (hottest-spot copper gradient) into account, oil temperatures may be used as an approximate guide in loading. When so operated for any period of time, the measured top-oil temperature should not exceed the values given in Figure 1 for the load being carried. These loads can be applied to any transformer covered by these guides as they are conservative.

Oil temperatures may be used as a more accurate guide, by using the hottest-spot copper gradient of any particular transformer for the load it is carrying at the time. If the hottest-spot copper gradient at full load is known, the gradient at other loads may be determined easily by using Figure 10 in Appendix II. The limiting oil temperature for normal life expectancy for any load, regardless of the time carried, can be determined by subtracting the hottest-spot copper gradient for that load from 95 degrees centigrade.

Loading on Basis of Test Temperature Rise. For each degree centigrade in excess of two degrees that the test temperature rise is below the standard temperature rise specified in the Standard, the transformer load may be increased above rated kilovolt-amperes by the percentages shown in second column of Table I. Making use of this factor gives the kilovolt-amperes that the transformer can deliver with 55 degrees centigrade temperature rise. The leeway of two degrees is to provide for a negative tolerance in the measurement of temperature rise.

Some transformers are designed to have the difference between hottest-spot and average copper temperatures greater than the nominal allowance of ten degrees centigrade. This will result in a temperature rise for average copper of less than 55 degrees centigrade, but the hottest-spot copper temperature rise may be at the limiting value of 65 degrees centigrade.

Such transformers should not be loaded above rating as outlined under this heading. The manufacturer should be consulted to give information as to design hottest-spot allowances.

Loading on Basis of Ambient Temperature. For each degree centigrade that the average temperature of the cooling medium is above or below 30 degrees centigrade for air or 25 degrees centigrade for water, a transformer may be loaded for any period of time below or above its kilovolt-ampere rating as specified in Table I. Average temperature should be for periods of time not exceeding 24 hours with maximum temperatures not more than ten degrees centigrade greater than average temperatures for air and five degrees centigrade for water. On the basis used in this guide for calculating loss of life, life expectancy will be approximately the same as if it had been operated at rated kilovolt-amperes and standard ambient temperatures over that period.

The use of transformers in cooling air above 50 degrees centigrade, or below 0 degrees centigrade, or with cooling water above 35 degrees centigrade is not covered by Table I and should be taken up with the manufacturer.

Loading on Basis of Load Factor. When the load factor for a period of time not exceeding 24 hours is below 100 per cent, the maximum loading of a transformer during that period may be increased above rated kilovolt-amperes by the percentages shown in Table II for each per cent that the load factor is below 100 per cent. On the basis used in this guide for calculating loss of life, life expectancy will be approximately the same as if it had been operated at rated kilovolt-amperes during that period.

Loading on Basis of Short-Time Loads Above Rating. When short-time loads above rating occur not more than once in any 24-hour period, the maximum loading of a transformer during that period may be increased conservatively above rated kilovolt-amperes, as given in Table III. On the basis used in this guide for calculating loss of life, life expectancy will be approximately the same as if it had been operated at rated kilovolt-amperes during that period.

Effect of Various Factors Existing at One Time. When two or more of the following factors affecting loading for normal life expectancy exist at one time, the effects are cumulative and the increase in loads due to each may be added to secure the maximum suggested load (each increase must be based on rated kilovolt-amperes):

1. Loading on basis of test temperature rise.

2. Loading on basis of ambient temperature.

3. Either loading on basis of load factor or loading on basis of short-time overloads. Do not use both.

SHORT-TIME LOADING WITH MODERATE SACRIFICE OF LIFE EXPECTANCY

To be able to give an idea of the relative loss of life due to loads above rating under various conditions, we have assumed a conservative aging rate of insulation based on tests and operating experience. The information is not intended to furnish a basis for calculating the normal life expectancy of transformer insulation.

Transformers may be loaded above rated kilovolt-amperes following various

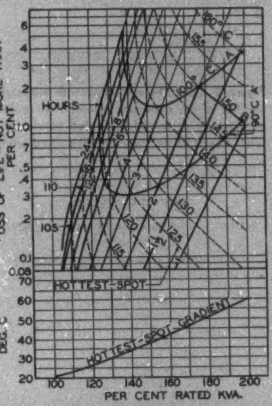

Figure 4. Short-time loading with moderate sacrifice of life expectancy, forced-air-cooled transformers rated 133 per cent or less of self-cooled rating

Following 50 per cent or less of rated kilovolt-amperes or top-oil temperature rise of 25 degrees centigrade

Ambient temperature 30 degrees centigrade for air

Subtract hottest-spot gradient from hottest-spot temperature to obtain top-oil temperature

A—Assumed temperature limitation for top oil (protected)

A'—Assumed temperature limitation for top oil (unprotected)

B—Assumed temperature limitation for hottest-spot copper

Time, Hours	Times Rated Kilovolt-Amperes to Use not More Than Following Life (Per Cent) 0.1	0.25	0.50	1.0
½	1.97	2.00	2.00	2.00
1	1.66	1.79	1.90	2.00
2	1.39	1.51	1.59	1.68
4	1.21	1.31	1.38	1.45
8	1.11	1.19	1.26	1.33
24	1.05	1.09	1.15	1.22

For explanation of degree of accuracy, see Appendix II.

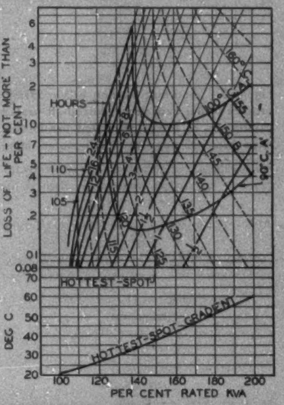

Figure 5. Short-time loading with moderate sacrifice of life expectancy, forced-air-cooled transformers rated 133 per cent or less of self-cooled rating

Following 100 per cent of rated kilovolt-amperes or top-oil temperature rise of 45 degrees centigrade

Ambient temperature 30 degrees centigrade for air

Subtract hottest-spot gradient from hottest-spot temperature to obtain top-oil temperature

A—Assumed temperature limitation for top oil (protected)

A'—Assumed temperature limitation for top oil (unprotected)

B—Assumed temperature limitation for hottest-spot copper

Time, Hours	Times Rated Kilovolt-Amperes to Use not More Than Following Life (Per Cent) 0.1	0.25	0.50	1.0
½	1.67	1.82	1.94	2.00
1	1.47	1.60	1.71	1.81
2	1.29	1.41	1.50	1.58
4	1.18	1.28	1.35	1.43
8	1.10	1.18	1.26	1.33
24	1.05	1.09	1.15	1.21

For explanation of degree of accuracy, see Appendix II.

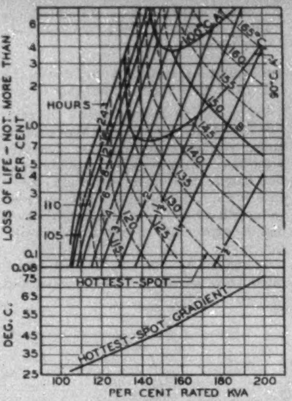

Figure 6. Short-time loading with moderate sacrifice of life expectancy, forced-oil-cooled transformers or forced-air-cooled transformers rated over 133 per cent of self-cooled rating

Following 50 per cent or less of rated kilovolt-amperes or top-oil temperature rise of 22 degrees centigrade

Ambient temperature 30 degrees centigrade for air

Subtract hottest-spot gradient from hottest-spot temperature to obtain top-oil temperature

A—Assumed temperature limitation for top oil (protected)

A'—Assumed temperature limitation for top oil (unprotected)

B—Assumed temperature limitation for hottest-spot copper

Time, Hours	Times Rated Kilovolt-Amperes to Use not More Than Following Life (Per Cent) 0.1	0.25	0.50	1.0
1/2	1.78	1.92	2.00	2.00
1	1.53	1.64	1.73	1.82
2	1.32	1.42	1.49	1.57
4	1.18	1.26	1.33	1.40
8	1.10	1.17	1.24	1.31
24	1.05	1.08	1.14	1.20

For explanation of degree of accuracy, see Appendix II.

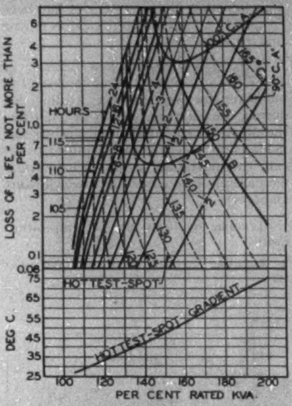

Figure 7. Short-time loading with moderate sacrifice of life expectancy, forced-oil-cooled transformers or forced-air-cooled transformers rated over 133 per cent of self-cooled rating

Following 100 per cent of rated kilovolt-amperes or top-oil temperature rise of 40 degrees centigrade

Ambient temperature 30 degrees centigrade for air

Subtract hottest-spot gradient from hottest-spot temperature to obtain top-oil temperature

A—Assumed temperature limitation for top oil (protected)

A'—Assumed temperature limitation for top oil (unprotected)

B—Assumed temperature limitation for hottest-spot copper

Time, Hours	Times Rated Kilovolt-Amperes to Use not More Than Following Life (Per Cent) 0.1	0.25	0.50	1.0
1/2	1.56	1.70	1.80	1.90
1	1.39	1.50	1.59	1.69
2	1.26	1.36	1.43	1.51
4	1.16	1.25	1.32	1.39
8	1.10	1.18	1.24	1.31
24	1.05	1.09	1.14	1.20

For explanation of degree of accuracy, see Appendix II.

loads by various amounts for various times, and the approximate relative loss of life may be estimated.

The load capability of transformers varies widely and is affected by the following characteristics:

1. Top-oil rise over ambient temperature.
2. Hottest-spot rise over top-oil temperature (hottest-spot copper gradient).
3. Ratio of load losses to no-load loss.
4. Time constant.*
5. Ambient temperature.

It is not possible to give a single set of loads which will apply to all transformers for a given set of operating conditions. Therefore, such values are given for a transformer having specified characteristics, and these characteristics have been selected so that allowable loads for practically all other combinations of characteristics will be at least as great as those given.

As the operating conditions under which transformers may be loaded are so extremely variable, particularly with regard to frequency of load, data are given so that the approximate relative loss of insulation life for various loads for various times may be determined. The user can then determine the allowable load for his conditions by taking into account the probable number of such loads during the life of the transformer and the approximate percentage of life which he is willing to sacrifice.

Appendix I gives a method by which the user can produce similar data for transformers having other characteristics, and the loads for a given hottest-spot temperature may be somewhat greater than those given hereafter.

In the curves and tables that follow, the following limitations have been used:

Maximum oil temperature (unprotected)* .... 90 degrees centigrade‡
Maximum oil temperature (protected)*.... .... 100 degrees centigrade‡
Maximum hottest-spot copper temperature .... 150 degrees centigrade
Maximum short-time loading (one-half hour or more)..200 per cent**

Short-Time Loads Above Rating for Transformer With Specified Characteristics

Assumed Transformer Characteristics. (See Table IV.) By the use of the data in the Table V the user may determine hottest-spot copper temperature for various loads and times following 50-per-cent load or less and 100-per-cent load and from this determine the approximate loss of life for such loading. Or he may determine loading for any selected loss of life. The user can select loadings and losses of life most suitable to his conditions. An average loss of life of one per cent per year incurred during emergency operations is considered reasonable.

Top-oil temperature, when known, is a better criterion of conditions at the start of a given load than the previous conditions of load, because the oil may not have reached its ultimate temperature for the previous load.

On each of the afore-mentioned figures ultimate top-oil temperature rise for the preceding load is given. This value may be used to determine the curve to use and as a guide in interpolation.

Hottest-spot copper temperatures versus loss of life assumed in making up figures are given in Figure 11.

Additional Short-Time Loading Available. In addition to the short-time loads outlined, the transformer may be loaded above or below kilovolt-ampere rating in accordance with directions given under "Loading for Normal Life Expectancy." (Each increase must be based on rated kilovolt-amperes.)

1. Loading on basis of test temperature rise.

---

*See Appendix II for explanation.

†Oil is considered to be protected, or unprotected, depending on whether the transformer is or is not equipped with conservator or inert gas above the oil.

‡At high oil temperatures precautionary measures, such as draining oil, may be necessary to prevent overflow or excessive pressures.

**Current-carrying parts, other than windings, may impose a lower limit.

2. Loading on basis of ambient temperature.

THERMAL RELAYS

Thermal relays designed for application to individual transformers are available. They make use of hottest-spot temperature in their operation and automatically take into account ambient temperature and previous conditions of loading, since the actuating element is influenced by the hottest oil and the load current. Higher loads are permitted for short times than are permitted for long times. These relays can be designed, at the option of the user, to permit loads which will produce practically no sacrifice of life expectancy or some predetermined moderate sacrifice of such expectancy. Contacts may be wired to cause sounding an alarm, starting of fans, or disconnecting of the transformer. Application of such relays should be discussed with the manufacturer.

SUPPLEMENTAL COOLING OF EXISTING SELF-COOLED TRANSFORMERS

The load that can be carried on existing self-cooled transformers can be increased by as much as 66 per cent by adding auxiliary cooling equipment such as fans, external forced-oil coolers, or water-spray equipment. The amount of additional loading varies widely, depending on:

(*a*). Design characteristics of the transformer.

(*b*). Type of cooling equipment.

(*c*). Permissible increase in voltage regulation.

(*d*). Limitations of associated equipment.

No general guides can be given for such supplemental cooling, and each transformer should be considered individually.

Table I. Loading on Basis of Ambient Temperature

	Per Cent of Rated Kva	
Type of Cooling	Decrease Load for Higher Temp	Increase Load for Lower Temp
Self-cooled	1.5	1.0
Water-cooled	1.5	1.0
Forced-air-cooled	1.0	0.75
Forced-oil-cooled	1.0	0.75

Guide for Loading Pole-Type Constant-Current Transformers

INCREASED PERIODS OF OPERATION OF POLE-TYPE CONSTANT-CURRENT TRANSFORMERS FOR AMBIENT TEMPERATURES LOWER THAN NORMAL

Since pole-type constant-current transformers operate outdoors at night when the ambient temperature is comparatively low, it is often desirable to take advantage of the longer period of operation within the limiting temperature rise which is made possible by an ambient temperature lower than normal. The time of operation of a pole-type constant-current transformer may be increased as the average ambient temperature decreases, as shown in Table VI.

Guide for Loading Step-Voltage and Induction-Voltage Regulators

A voltage regulator has a short-time load capability greater than the nameplate rating, the magnitude depending on the initial load and ambient temperature, as in the case of a transformer. However, there are some additional factors that must be considered in this type of equipment. The fact that the induction machine has a winding in slots on a rotating member mounted in bearings necessitates a limit to the load to prevent excessive hottest-spot temperatures and undue vibration. Also, a regulator must be capable of operating or holding against the torque produced by load. In the case of a step-voltage regulator, the burning of contacts is the limiting feature.

Table II. Loading on Basis of Load Factor

Type of Cooling	Increase in Per Cent of Rated Kva	Maximum Per Cent Increase*
Self-cooled	0.5	25
Water-cooled	0.5	25
Forced-air-cooled	0.4	20
Forced-oil-cooled	0.4	20

* Corresponds to 50 per cent load factor.

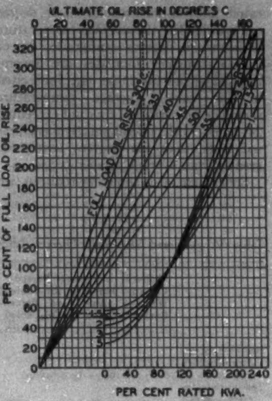

Figure 8. Ultimate top-oil temperature rise

A working group of the AIEE transformer subcommittee is now reviewing the loading of regulators to determine if the loads given here can be increased safely.

SHORT-TIME LOADS ABOVE RATING FOR OIL-IMMERSED SELF-COOLED REGULATORS

Short-time loads above rated kilovolt-amperes may be applied to oil-immersed self-cooled regulators with daily average cooling air at 30 degrees centigrade in accordance with the limits given in Table VII.

Loads with normal life expectancy may be carried once every 24 hours, whereas those with moderate sacrifice of life expectancy should be carried infrequently.

With cooling-air temperatures other than 30 degrees centigrade the short-time loads may be increased by one per cent of

Table III. Loading on Basis of Short-Time Loads Above Rating

	Times Rated Kilovolt-Amperes								
Time, Hours	Self-Cooled and Water-Cooled Transformers			Forced-Air-Cooled Transformers Rated 133 Per Cent or Less of Self-Cooled Rating			Forced-Air-Cooled Transformers Rated More than 133 Per Cent of Self-Cooled Rating and All Forced-Oil-Cooled		
*Initial Load (per cent)	90	70	50	90	70	50	90	70	50
1/2	1.59	1.77	1.89	1.45	1.58	1.68	1.36	1.47	1.50
1	1.40	1.54	1.60	1.31	1.38	1.50	1.24	1.31	1.34
2	1.24	1.33	1.37	1.19	1.23	1.26	1.14	1.18	1.21
4	1.12	1.17	1.19	1.11	1.13	1.15	1.09	1.10	1.10
8	1.06	1.08	1.08	1.06	1.07	1.07	1.05	1.06	1.06

*Percentages fix the load which is assumed to exist before the short-time load is applied. Use either average load for two hours previous to load above rating or average load for 24 hours (less overload period), whichever is greater.

Ambient temperature assumed for this table is 30 degrees centigrade for air and 25 degrees centigrade for water.

As the loads may be applied once every 24 hours, and as there is some evidence that the rate of insulation deterioration at about 100 degrees centigrade doubles with less than 8 degrees centigrade increase in insulation temperature the values have been based on 4 degrees centigrade rather than on 8 degrees centigrade.

rated kilovolt-amperes for each degree centigrade that the average temperature is below 30 degrees centigrade, except that no further increases are recommended beyond the 25-per-cent limit cited in the table. Average temperature should be for periods of time not exceeding 24 hours with maximum temperatures not more than ten degrees centigrade greater than average temperatures.

Short-time loads should be reduced two per cent of the continuous self-cooled rating below the recommended load for each degree centigrade that the daily average temperature of the cooling air exceeds 30 degrees centigrade.

Table IV. Assumed Transformer Characteristics

	Self-Cooled Water-Cooled	Forced-Air-Cooled*	Forced-Air-Cooled† or Forced-Oil-Cooled
Hottest-spot rise (degrees centigrade)	65	65	65
Top-oil rise (degrees centigrade)	45	45	40
Time constant at full load (hours)	3.0	2.0	1.5
Ratio of copper to iron losses	2.5 to 1	3.5 to 1	5 to 1
Ambient temperature (degrees centigrade)	30	30	30

*Forced-air-cooled rating is 133 per cent or less of self-cooled rating.

†Forced-air-cooled rating is over 133 per cent of self-cooled rating.

Table V. Reference to Figures

	Self-Cooled Water-Cooled	Forced-Air-Cooled*	Forced Air-Cooled† or Forced-Oil-Cooled
Following 50-per-cent load or less	Figure 2	Figure 4	Figure 6
Following 100-per-cent load	Figure 3	Figure 5	Figure 7

Values between 50 and 100-per-cent load may be interpolated with sufficient accuracy.

*Forced-air-cooled rating is 133 per cent or less of self-cooled rating.

†Forced-air-cooled rating is over 133 per cent of self-cooled rating.

Guide for Loading Current-Limiting Reactors

See Interim Report on Overloading Current-Limiting Reactors, by transformer subcommittee of the AIEE committee on electric machinery.[1]

Application at Altitudes Greater Than 3,300 Feet (1,000 Meters)

OPERATION AT LESS THAN STANDARD AMBIENT TEMPERATURES

It is recognized as good practice to use apparatus of standard temperature rise at rated kilovolt-amperes at altitudes greater than 3,300 feet (1,000 meters), provided the temperature of the cooling air does not exceed the values for the respective altitudes given in Table VIII. Standard temperature limits will not be exceeded.

Table VI. Loading Pole-Type Constant-Current Transformers

Average Ambient Temperature, Degrees Centigrade	Period of Operation, Hours
30	8
25	10
20	12
15	14
10	16

Table VII. Loading Regulators

Starting at an Oil Temperature Corresponding to Continuous Operation at	Normal Life Expectancy, Per Cent		Moderate Sacrifice of Life Expectancy, Per Cent	
	1 Hr	2 Hr	1 Hr	2 Hr
Full load	0	0	35	30
$^3/_4$ load	20	14	50*	45
$^1/_2$ load	25*	17	50*	50*

*This load is the maximum that can be allowed, owing to hottest-spot temperature, vibration, torque, or contact-burning considerations on this class of equipment.

Table VIII. Application at Altitudes Greater Than 3,300 Feet (1,000 Meters)

Method of Cooling Apparatus	Maximum Allowable Average Temperature of Cooling Air for Carrying Rated Kilovolt-Amperes, Degrees Centigrade			
	3,300 Ft (1,000 M)	6,600 Ft (2,000 M)	9,900 Ft (3,000 M)	13,200 Ft (4,000 M)
Oil-immersed self-cooled	30*	28	25	23
Oil-immersed forced-air-cooled	30*	26	23	20
Oil-immersed forced-oil-cooled with oil to air cooler	30*	26	23	20
Dry-type self-cooled				
Class-*A* insulation	30	27	24	21
Class-*B* insulation	30	26	22	18
Dry-type forced-air-cooled				
Class-*A* insulation	30	24	19	14
Class-*B* insulation	30	22	14	6

*See section 2.000 of American Standard *C*57.1 for explanation of average ambient temperature.

Obviously when advantage is taken of lower ambient temperatures at the higher altitudes to offset the increased temperature rise caused by decreased air density, the output cannot be increased to the full extent covered under "Loading on Basis of Ambient Temperature." For such loading the temperature base should be in accordance with Table VIII.

OPERATION AT STANDARD AMBIENT TEMPERATURES

It is recognized as good practice to use apparatus of standard temperature rise at altitudes greater than 3,300 feet (1,000 meters), provided the load to be carried is reduced below rating by the percentages given in Table IX for each 330 feet (100 meters) that the altitude is above 3,300 feet (1,000 meters). Standard temperature rise will not be exceeded.

INSULATION

The dielectric strength of equipment which depends upon air for its insulation decreases as the altitude increases. The dielectric strength at 3,300 feet or less for a given insulation class should be multiplied by the proper altitude correction factor to obtain the dielectric strength at the required altitude (see Table X).

Appendix I. Calculations of Temperature and Loss of Life for Short-Time Loading of Transformers

Short-time loads above rating that use up different amounts of life expectancy for transformers having definite characteristics have been given in Figures 2 through 7. Generally, transformers included in these guides which have other characteristics will have greater load capabilities. This appendix gives information by which similar curves may be derived for such transformers.

In explaining the use of Figures 8 and 9 through 11, a self-cooled transformer having the same characteristics as those selected in the main portion of the guides, and having a load of 160 per cent for two hours following 50 per-cent load, is used as an example. The figures also apply to forced-air-cooled and forced-oil-cooled transformers.

Characteristics at Rated Kilovolt-Amperes Required to Be Known	Example
1. Hottest-spot rise	65 C
2. Top-oil rise	45 C
3. Time constant at full load	3.0 hr
4. Ratio of copper to iron losses	2.5 to 1
5. Ambient temperature	30 C

Top-Oil Rise

1. Determine ultimate top-oil rise for initial load (50 per cent). On Figure 8 start at per cent for initial load (50) and go up to curve for ratio of losses (R=2.5). Go to left to line for full-load oil rise (45 degrees

centigrade). Go vertically and read ultimate oil rise (25 degrees centigrade).

2. Determine ultimate top-oil rise for short-time load in question. Repeat procedure in paragraph 1, starting at per-cent load in question (160) and read ultimate oil rise (82 degrees centigrade).

3. On Figure 9 set a straightedge at the initial oil temperature rise on the left scale (25 degrees centigrade) and at the ultimate oil temperature rise on the right scale (82 degrees centigrade). At the intersection of the line so determined and the vertical line through the intersection of lines for the desired time (two hours) and time constant (three hours), determine the oil temperature rise (52 degrees centigrade) at the end of the assumed time (two hours).

Hottest-Spot Copper Rise Over Top-Oil Temperature (Copper Gradient)

On Figure 10 start at per-cent load (160) on horizontal scale and go up to the curve for full-load hottest-spot rise (20 degrees centigrade). Go to left and read copper gradient (42 degrees centigrade) for the per-cent load in question (160).

Hottest-Spot Copper Temperature

Obtain hottest-spot copper temperature by adding ambient temperature (30 degrees centigrade), top-oil rise (52 degrees centigrade), and hottest-spot rise (42 degrees centigrade), giving 124 degrees centigrade.

Per Cent Loss of Life

From Figure 11 obtain the loss of life (0.2 per cent) for the hottest-spot copper temperature (125 degrees centigrade) and the duration of the load (two hours). In calculating these curves it has been assumed that hottest-spot temperature is constant at its final value during the overload period. When this assumption is made, the elevated temperature during the cooling period need not be considered.

Table XI is suggested as a convenient method of tabulating values obtained by the foregoing procedure and covers values for the example assumed.

Appendix II. Formulas for Calculating Transient Heating of Oil-Immersed Transformers

List of Symbols

θ_a = ambient temperature (degrees centigrade)

θ_g = hottest-spot rise over top-oil temperature (degrees centigrade)

$\theta_{g(fl)}$ = hottest-spot rise over top-oil temperature at full load

θ_{hs} = hottest-spot temperature (degrees centigrade)

θ_o = top-oil rise over ambient temperature (degrees centigrade)

θ_{fl} = full-load top-oil rise (degrees centigrade)

θ_i = initial oil rise for $t=0$ (degrees centigrade)

θ_u = ultimate oil rise for load P (degrees centigrade)

Table IX. Application at Altitudes Greater Than 3,300 Feet (1,000 Meters)

Types of Cooling	Correction Factor, Per Cent
Oil-immersed self-cooled apparatus	0.4
Oil-immersed water-cooled apparatus	0.0
Oil-immersed forced-air-cooled apparatus	0.5
Oil-immersed forced-oil-cooled apparatus with oil to air cooler	0.5
Oil-immersed forced-oil-cooled apparatus with oil to water cooler	0.0
Dry-type self-cooled apparatus	0.3
Dry-type forced-air-cooled apparatus	0.5

P = ratio of load to full load

P_i = ratio of equivalent initial load to full load (load which results in an ultimate rise of θ_i)

R = ratio of load loss to no-load loss

e = 2.71828

t = time load is applied in hours

B = thermal time constant of transformer for any load or any ratio of initial to ultimate oil temperature (hours)

B_r = time constant for full load beginning with initial temperature rise of 0 degrees (hours)

W_{fl} = total loss at full load (watts)

C = thermal capacity of transformer (watt-hours per pound per degree centigrade)

Hottest-Spot Temperature

The hottest-spot temperature

$$\theta_{hs}=\theta_a+\theta_o+\theta_g \tag{1}$$

Transient heating and cooling equation for top-oil rise over ambient temperature

$$\theta_o=(\theta_u-\theta_i)(1-e^{-\frac{t}{B}})+\theta_i \tag{2}$$

Ultimate top-oil rise for load P

$$\theta_u=\theta_{fl}[(P^2R+1)/(R+1)]^{0.8} \tag{3}$$

Hottest-spot rise over top oil

$$\theta_g=\theta_{g(fl)}P^{1.6} \tag{4}$$

$$\theta_{g(fl)}=\frac{\text{average copper rise over top oil*}+\text{10 degrees centigrade}}{\text{Time constant at rated kilovolt-amperes}} \tag{5}$$

Figure 9. Top-oil temperature rise at end of specified load period

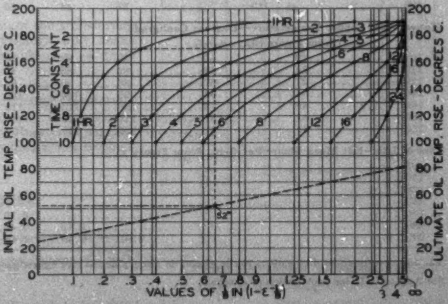

Table X. Application at Altitudes Greater Than 3,300 Feet (1,000 Meters)

Altitude	Altitude Correction Factor A for Insulation Class
3,300 feet (1,000 meters)	1.00
4,000 feet (1,200 meters)	0.98
5,000 feet (1,500 meters)	0.95
6,000 feet (1,800 meters)	0.92
7,000 feet (2,100 meters)	0.89
8,000 feet (2,400 meters)	0.86
9,000 feet (2,700 meters)	0.83
10,000 feet (3,000 meters)	0.80
12,000 feet (3,600 meters)	0.75
14,000 feet (4,200 meters)	0.70
15,000 feet (4,500 meters)	0.67

Altitude of 15,000 feet is considered a maximum for standard apparatus.

$$B_r=\frac{C\theta_{fl}}{W_{fl}} \tag{6}$$

C = 0.06 (weight of core and coils) + 0.04 (weight of tank) + 1.33 (gallons of oil)

Theoretical Corrections for Preceding Formulas

Theoretically several corrections should be made in the foregoing formulas when one is calculating transient oil rises, such as corrections for change in:

1. Time constant for loads above rating.
2. Ultimate copper loss at end of load period.
3. Oil viscosity.

Practical Application of Formulas for Calculation of Oil Rises

In making general calculations based on assumptions of transformer characteristics and maximum hot-spot temperatures which generally have a large factor of safety, results close enough for all practical purposes are obtained if all of these corrections are omitted and the simpler formulas are used.

The overload values given in Figures 2 to 7 were calculated by the formulas without corrections.

1. *Time Constant.* The time constant is the length of time which would be required for the temperature of the oil to change from the initial value to the ultimate value if the initial rate of change were continued until the ultimate temperature was reached.

*At rated kilovolt-amperes from manufacturer's test.

The time constant is usually the length of time required for a specified percentage of

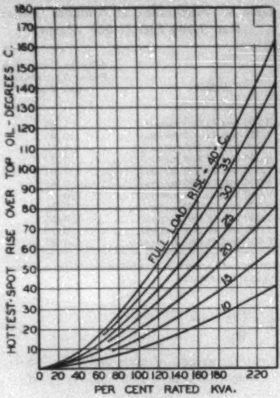

Figure 10. Hottest-spot copper rise over top-oil temperature

the change in temperature from initial value to ultimate value to take place.

If n* equals unity, 63 per cent of the temperature change occurs in a length of time equal to the time constant, regardless of the relationship of initial temperature and ultimate temperature. If n is not unity, the percentage varies and is a function of both initial temperature rise and ultimate temperature rise. In particular, if n equals 0.8, the percentage is 67 if the initial temperature rise is zero.

If the initial temperature rise is greater than zero, the percentage is lower than 67 and decreases as the initial temperature rise increases for a given ultimate temperature rise. If the initial temperature is approximately equal to the final temperature, whether just above or just below it, the percentage is approximately 63. If the initial temperature is greater than the ultimate temperature, the percentage is less than 63.

Since evaluation of the exact percentage for cases where n is not unity and the initial temperature rise is not zero becomes very laborious, it is frequently advisable to use the value of 63 per cent as an approximation. In the more frequently encountered cases where n is approximately 0.8, the error resulting from this procedure is not large compared to the expected error in transient thermal calculations.

If $n=1.0$, equation 6 is correct for any load and any starting temperature. If n is less than 1.0, equation 6 holds only for full-rating starting cold. If $n=0.8$, the time constant for any load and for any starting temperature for either a heating cycle or cooling cycle is given by equations 7 and 8.

$$B=B_r\left[\frac{\dfrac{\theta_u}{\theta_{fl}}-\dfrac{\theta_i}{\theta_{fl}}}{\left(\dfrac{\theta_u}{\theta_{fl}}\right)^{1.25}-\left(\dfrac{\theta_i}{\theta_{fl}}\right)^{1.25}}\right] \tag{7}$$

If starting cold ($\theta_i=0$) equation 7 reduces to

$$B=B_r\left(\frac{\theta_{fl}}{\theta_u}\right)^{0.25} \tag{8}$$

2. Copper Loss. As the resistance of the copper for ultimate conditions is greater when the temperature is greater for loads above rating than for rated load conditions, a resistance correction factor should be added to equations 3 and 4.

3. Viscosity of Oil. The ultimate temperature rise of oil for a constant loss decreases slightly as the temperature of the oil increases, owing to a decrease in the viscosity of the oil. For hot-spot rise over oil the viscosity correction tends to offset the effect of increased resistance.

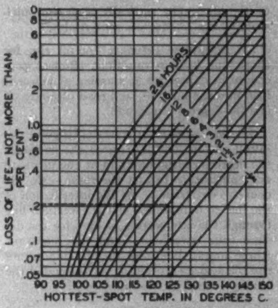

Figure 11. Hottest-spot copper temperature versus loss of life

Time, Hours	Temperatures in Degrees Centigrade to Use not More Than Following Life (Per Cent) 0.1	0.25	0.50	1.0
½	132	142	150	
1	124	134	142	150
2	117	126	134	142
4	111	119	126	134
8	105	112	119	126
24	99	104	109	115

For explanation of degree of accuracy, see Appendix II.

---

*Exponential power of temperature rise versus loss.

Explanation of Degree of Accuracy of Figures 2 to 7 and Figure 11

The percentage loss-of-life values which will not be exceeded, shown on these figures, of necessity have been made quite conservative, as they depend on the rate of insulation

Table XI. Summary of Values Used in Plotting Figure 2

Per Cent Rated Kva	Ultimate Oil Rise		Hours Duration 0.5	1.0	1.5	2.0	3.0	4.0	6.0	8.0	12.0	16.0	24.0
Top Oil Rise—Degrees Centigrade (θ_o), From Figure 9													
105	48		28	31	34	36	39	42	45	47	47	48	48
110	51		28	32	35	37	41	44	47	49	50	51	51
120	56		29	33	37	40	44	48	52	54	55	56	56
140	68		31	36	42	46	52	57	62	65	68	69	69
160	82		34	41	47	52	61	67	74	78	81	82	82
180	97		36	45	53	60	71	78	87	92	96	97	97
200	113		37	48	59	66	80	80	101	107			
Hottest-Spot Copper Temperature—Degrees Centigrade													
	θ_g (From Figure 10)	$\theta_g+\theta_a$						$\theta_{hs}=\theta_o+\theta_g+\theta_a$					
105	22	52	80	83	86	88	91	94	97	99	99	100	100
110	24	54	82	86	89	91	95	98	101	103	104	105	105
120	27	57	86	90	94	97	101	105	109	111	112	113	113
140	34	64	95	100	106	110	116	121	126	129	132	133	133
160	42	72	106	113	119	124	133	139	146	150	153	154	154
180	51	81	117	126	134	141	152	159					
200	61	91	128	139	150	157							
Loss of Life—Not More Than—Per Cent, From Figure 11													
105											0.05	0.07	0.11
110										0.06	0.13	0.18	0.27
120									0.12	0.21	0.38	0.53	0.80
140							0.14	0.30	0.76	1.43	2.49	3.60	5.40
160					0.10	0.22	0.74	1.65	4.70	8.40			
180				0.13	0.40	0.96	3.65	9.50					
200			0.07	0.40	1.46	3.90							

The above values contain numbers to the second decimal place to give figures used in plotting curves. No such high degree of accuracy in actual life loss is implied.

See Appendix II for explanation of symbols.

The Self-Inductance of a Toroidal Coil Without Iron

H. B. DWIGHT
FELLOW AIEE

IF A NONMAGNETIC BAR is bent into the shape of a ring and a single layer of wire is wound around the bar, the self-inductance of the "toroidal coil" formed in this way is given by well-known short expressions.

If the cross section of the nonmagnetic bar, that is, the cross section of the toroidal coil, is rectangular, the self-inductance is

$$L=2hN^2 \operatorname{logn}\frac{r_2}{r_1} \text{ abhenrys} \qquad (1)$$

where

h = axial length of the coil
r_1 = radius to inner face of the coil, centimeters
r_2 = maximum radius of the coil, centimeters
N = number of turns in the coil
logn denotes natural logarithm

If the cross section of the toroidal coil is round, that is, if each turn is a circle, the self-inductance is

$$L=4\pi N^2\left(R-\sqrt{R^2-a^2}\right) \text{ abhenrys} \qquad (2)$$

where

R = mean radius of the complete ring
a = radius of a single turn, centimeters[1]

It was suggested to the writer by R. F. Field of the engineering department of the General Radio Company that a computation for inductance of a toroidal coil with a rectangular section and a comparatively thick winding would be useful. In this paper is derived a formula for such a coil.

If, when the current in the wire is taken to be one abampere, the number of lines in each portion of magnetic flux is multiplied by the number of turns which it surrounds or links, the sum of such products or linkages is equal to the self-inductance of the coil in abhenrys.

Let the thickness of the winding on the inner side of the coil be t_1 (see Figure 1). Then

$$r_3=r_1-t_1$$

$$\text{Length of element } dx=h+(h_1-h)\frac{(r_1-x)}{t_1} = h+(h_1-h)\frac{r_1}{t_1}-(h_1-h)\frac{x}{t_1}$$

Let it be assumed that the wire follows along dx and has a sharp corner when it goes to the right, instead of a rounded corner.

Let the density of turns per square centimeter be n, a constant depending on the size of wire and the amount of insulation.

$$n=\frac{N}{\pi(r_1^2-r_3^2)} \qquad (3)$$

Also

$$t_2=\frac{N}{2\pi r_1 n} \qquad (4)$$

since the wires cross the axial line t_2 practically at right angles. Similarly,

$$t_3=\frac{N}{2\pi r_2 n} \qquad (5)$$

The dimension h_1, Figure 1, is found by drawing a straight line through the ends of t_2 and t_3.

$$h_1=h+2\left\{t_3+\frac{(w+t_1)(t_2-t_3)}{w}\right\} \qquad (6)$$

Turns linking element dx are

$$T_{(x)}=\pi n(x^2-r_3^2)$$

$$\text{Flux density at } dx=\frac{4\pi T_{(x)}}{2\pi x}=\frac{2T_{(x)}}{x}$$

Linkages for flux in element dx are

$$\text{Flux density}\times T_{(x)}\times\left\{h+(h_1-h)\frac{r_1}{t_1}-(h_1-h)\frac{x}{t_1}\right\}dx$$

$$=\frac{2\pi^2n^2}{x}(x^4-2x^2r_3^2+r_3^4)(h+pr_1-px)dx$$

$$=\frac{2\pi^2n^2}{x}\left\{-px^5+(h+pr_1)x^4+2pr_3^2x^3-2(h+pr_1)r_3^2x^2-pr_3^4x+(h+pr_1)r_3^4\right\}dx$$

where

$$p=\frac{h_1-h}{t_1} \qquad (7)$$

Integrate from $x=r_3$ to r_1.
Linkages due to flux in the inner trapezoid of base h_1 (Figure 1) are

$$2\pi^2n^2\left[-\frac{px^5}{5}+(h+pr_1)\frac{x^4}{4}+2pr_3^2\frac{x^3}{3}-(h+pr_1)r_3^2x^2-pr_3^4x+(h+pr_1)r_3^4 \operatorname{logn} x\right]_{x=r}^{r_1} \qquad (8)$$

The triangle ABC, Figure 1, is filled with wires that are nearly horizontal. The linkages of the magnetic flux in ABC are about one per cent of the total for the coil in the example given. To simplify the computation of this part, the triangle ABC can be replaced by the triangle ADC. These triangles have the same

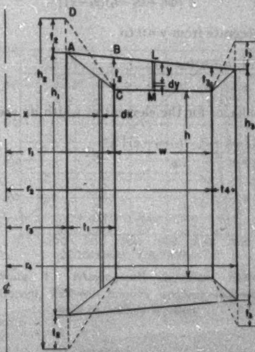

Figure 1. Section of toroidal coil

Paper 45-159, recommended by the AIEE committee on basic sciences for publication in AIEE TRANSACTIONS. Manuscript submitted July 24, 1945; made available for printing August 27, 1945.

H. B. DWIGHT is professor of electric machinery, Massachusetts Institute of Technology, Cambridge, Mass.

---

deterioration occuring at various temperatures.

Transformer life expectancy with continuous operation at 95 degrees centigrade is not known, but past experience indicates that the life is satisfactory. As a basis for these tables, operation at 115 degrees centigrade for 24 hours has been assumed to give not over one-per-cent loss of insulation life, as determined by tensile strength.

Information given is considered to be the best that can be produced from the present knowledge of the subject. In spite of its approximate nature, it is believed that it will be of much value to the industry as a guide.

The subject of insulation life is receiving the continuous attention of the transformer subcommittee. New findings may make future revision and modification of these guides necessary.

The transformer subcommittee does not recommend that any particular transformer life expectancy be assumed. It specifically points out that more than approximate accuracy in loss of life values is not implied.

Reference

1. INTERIM REPORT ON OVERLOADING CURRENT-LIMITING REACTORS, AIEE transformer subcommittee. AIEE TRANSACTIONS, volume 62, 1943, October section, pages 611–12.

area, as they have the same height t_1, and equal bases $AD=BC=t_2$. In both triangles the flux density is 0 along the side AD or AB and increases toward the vertex C and so the triangle ADC, treated as an extension of the trapezoid of base h_1, gives a close approximation to the linkages of triangle ABC.

Therefore, instead of computing equations 7 and 8, take

$$h_2=h_1+2t_2 \tag{9}$$

$$q=\frac{h_2-h}{t_1} \tag{10}$$

and linkages due to flux in the enlarged trapezoid of base h_2 are

$$2\pi^2n^2\left[-\frac{qx^5}{5}+(h+qr_1)\frac{x^4}{4}+\frac{2}{3}qr_3^2x^3-\right.$$
$$\left.(h+qr_1)r_3^2x^2-qr_3^4x+(h+qr_1)r_3^4\operatorname{logn}x\right]_{x=r_3}^{r_1}$$
$$=2\pi^2n^2\left[(h+qr_1)\left(r_3^4\operatorname{logn}\frac{r_1}{r_3}-r_3^3t_1+\right.\right.$$
$$\left.\frac{1}{2}r_3^2t_1^2+r_3t_1^3+\frac{1}{4}t_1^4\right)-qt_1^3\left(\frac{4}{3}r_3^2+\right.$$
$$\left.\left.r_3t_1+\frac{1}{5}t_1^2\right)\right] \tag{11}$$

since $r_1=r_3+t_1$.

Consider a vertical elementary strip LM of width dx, at a distance x from the axis.

$$LM=t_3+(t_2-t_3)\frac{(r_2-x)}{w}=\frac{wt_3+(t_2-t_3)(r_2-x)}{w}$$

The turns which link the flux in $dxdy$ are

$$T=\frac{y}{LM}N=\frac{wyN}{wt_3+(t_2-t_3)(r_2-x)}$$

Flux density at $dxdy=\dfrac{2T}{x}$

Linkages of the flux in $dxdy$ are

$$\frac{2T^2}{x}\,dxdy=\frac{2}{x}\,\frac{w^2y^2N^2}{\{wt_3+(t_2-t_3)(r_2-x)\}^2}\,dxdy$$

Integrate from $y=0$ to

$$\frac{wt_3+(t_2-t_3)(r_2-x)}{w}$$

Linkages for the element of width dx are

$$\frac{2}{3x}\,\frac{\{wt_3+(t_2-t_3)(r_2-x)\}N^2}{w}\,dx$$

Integrate from $x=r_1$ to r_2 and multiply by 2.

Linkages for the trapezoids at the ends of the coil

$$=\frac{4N^2}{3w}\left[\{wt_3+r_2(t_2-t_3)\}\times\right.$$
$$\left.\operatorname{logn}x-x(t_2-t_3)\right]_{x=r_1}^{r_2}$$

$$=\frac{4N^2}{3}\left[\left\{t_3+\frac{r_2(t_2-t_3)}{r_2-r_1}\right\}\operatorname{logn}\frac{r_2}{r_1}-(t_2-t_3)\right] \tag{12}$$

For the outer trapezoid of the coil section, Figure 1,

$$n=\frac{N}{\pi(r_4^2-r_2^2)} \tag{13}$$

from which r_4 and t_4 may be found.

Note that measured values of t_2, t_3, and t_4 may be used instead of values computed on the basis of constant density of turns.

The length of a vertical element at radius x in the outer trapezoid is

$$h+\frac{x-r_2}{t_4}(h_3-h)=h-(h_3-h)\frac{r_2}{t_4}\,(h_3-h)\,\frac{x}{t_4}$$

where

$$h_3=h+2\left\{t_3-\frac{t_4}{w}\,(t_2-t_3)\right\} \tag{14}$$

Turns linking the element at radius x are

$$T_{(x)}=\pi n(r_4^2-x^2)$$

Flux density at $dx=\dfrac{2T_{(x)}}{x}$

Linkages for flux in element of width dx are

$$\text{Flux density}\times T_{(x)}\times\left\{h-(h_3-h)\frac{r_2}{t_4}+\right.$$
$$\left.(h_3-h)\frac{x}{t_4}\right\}dx$$
$$=\frac{2\pi^2n^2}{x}(x^4-2x^2r_4^2+r_4^4)(h-p_1r_2+p_1x)dx$$
$$=\frac{2\pi^2n^2}{x}\{p_1x^5+(h-p_1r_2)x^4-2p_1r_4^2x^3-$$
$$2(h-p_1r_2)r_4^2x^2+p_1r_4^4x+(h-p_1r_2)r_4^4\}dx$$

where

$$p_1=\frac{h_3-h}{t_4}$$

Integrate from $x=r_2$ to r_4. Linkages for flux in trapezoid of base h_3 are

$$2\pi^2n^2\left[\frac{p_1x^5}{5}+(h-p_1r_2)\frac{x^4}{4}-\frac{2}{3}\,p_1r_4^2x^3-(h-\right.$$
$$\left.p_1r_2)r_4^2x^2+p_1r_4^4x+(h-p_1r_2)r_4^4\operatorname{logn}x\right]_{x=r_2}^{r_4}$$

In order to include the effect of the two outer triangles, change h_3 to

$$h_4=h_3+2t_3 \tag{15}$$

Then

$$q_1=\frac{h_4-h}{t_4} \tag{16}$$

Linkages for flux in the enlarged trapezoid of base h_4 are

$$2\pi^2n^2\left[(h-q_1r_2)\left(\frac{4}{3}\,r_4t_4^3+\frac{1}{5}\frac{t_4^5}{r_4}+\frac{1}{6}\frac{t_4^6}{r_4^2}+\ldots\right)+\right.$$
$$\left.q_1t_4^3\left(\frac{4}{3}\,r_4^2-r_4t_4+\frac{1}{5}\,t_4^2\right)\right] \tag{17}$$

since $r_2=r_4-t_4$, and t_4 is small compared with r_4.

The self-inductance of the coil in abhenrys is given by the sum of formulas 1, 11, 12, and 17.

Example. The following coil was constructed and measured by R. F. Field. If centimeter dimensions are used,

$r_1=2.54$, $r_2=7.62$, $r_3=0.698$
$r_4=8.23$, $t_2=1.173$, $t_3=0.635$
$h=12.7$, $N=1{,}680$

According to these dimensions, the density of the turns in the inner and outer parts is different.

$w=r_2-r_1=5.08$
$t_1=r_1-r_3=1.842$
$h_1=15.44$, $h_2=17.78$, $q=2.76$, $h+qr_1=19.71$
Linkages for the rectangle $wh=78.8\times10^6$
Linkages for enlarged inner trapezoid of Figure $1=17.0\times10^6$
Linkages for the two end trapezoids $=3.9\times10^6$
Linkages for enlarged outer trapezoid $=2.0\times10^6$
Inductance of coil $=(78.8+17.1+3.9+2.0)10^6$ abhenrys $=0.1018$ henry

The measured value agreed with this within less than one per cent.

Reference

1. **Theory of Alternating Currents, Alexander Russell. Edition of 1914, page 74.**

Resonant-Circuit Constant-Current Regulators

G. M. KEVERN
ASSOCIATE AIEE

Synopsis: Airport-approach and runway-marker light circuits are quite similar to the usual street-lighting circuits, except that the important additional feature of brightness control is required. Standard moving-coil regulators were found to be unsatisfactory for this purpose, and so the development of resonant-circuit constant-current regulators with built-in brightness control was fostered by the Army Air Forces. Four years of service have proved regulators of this type to be entirely satisfactory, and they have been adopted as standard by the Army, Navy, and Civil Aeronautics Administration.

Resonant-circuit regulators have no moving parts and operate at high efficiencies and power factors, even at light loads. Detailed performance data, together with a comparison of resonant-circuit and moving-coil regulators, are presented in this paper.

ALTHOUGH the theoretical aspects of resonant-circuit constant-current regulators were published by Steinmetz as early as 1900, the lack of satisfactory capacitors prevented their use until comparatively recently.[1] Moving-coil regulators were universally adopted for street-lighting circuits and were found so satisfactory that only a very few experimental resonant regulators were built prior to 1940, even though satisfactory capacitors were then available.

In 1940, the Army Air Forces were confronted with the problem of providing brightness control for airport-approach and runway lighting circuits, for the following reasons:

1. The high-candle-power lamp assemblies being installed in an attempt to permit landings under adverse weather conditions were sometimes blinding under clear weather conditions.
2. Black-out operations necessitated a great reduction in candle power in addition to providing hoods for the lamp assemblies.

The brightnesses found to be necessary, together with the average currents which most nearly produce those brightnesses on all the lamp assemblies used, are as enumerated in Table I.

Runway and approach lighting circuits in use in 1940 were nearly identical with conventional street-lighting circuits, except, of course, that a different type of lamp assembly was used. The circuit consisted of a moving-coil regulator, together with a series circuit from two to six miles in length. A series–multiple or series–series transformer frequently was provided for each lamp assembly in order to isolate the assembly from the high-voltage circuit, and to prevent service interruptions in the event that a lamp assembly was damaged by an airplane or other vehicle.

Moving-Coil Regulators

The first method of brightness control considered was the installation of a tapped autotransformer in the output circuit of a moving-coil regulator. Although the desired current values were obtained in this manner, the scheme was found to be unsatisfactory for the following reasons:

1. When connected to a rated lamp load, the regulator operates at only 20.5 per cent of its rated kilowatt output, when the one-per-cent brightness tap is selected.
2. Conventional moving-coil regulators overheat when operated at less than 50 per cent load. This permits only intermittent use of the ten-, three-, and one-per-cent brightness taps.
3. On the one-per-cent brightness tap, primary power factor and efficiency are excessively low, being only 22 per cent and 66 per cent, respectively, for the three-kilowatt combination tested.
4. Voltage encountered on open circuit is increased by approximately the same ratio as the current was decreased.

For comparison with resonant-regulator performance, curves showing results of tests conducted upon a conventional three-kilowatt 220-volt-input 6.6-ampere-output moving-coil regulator connected to a variable lamp load are included in Figure 1. Within the region of short circuit to rated load, it can be seen that the input current is approximately constant, and the primary power factor is nearly proportional to the load.

Resonant-Regulator Development

The first experimental resonant-circuit regulator was received by the Army Air Forces and installed in the early part of 1941. Test results and service experience proved satisfactory, and so it was decided to use resonant regulators for all future installations. The first regulator to be produced in quantity was an oil-immersed self-cooled five-kilovolt-ampere 230/115-volt 6.6-ampere unit which included five brightness-selector relays, four runway-selector relays, a power-supply relay, and an open-circuit protector relay. The brightness- and runway-selector relays were interlocked with the power relay in such a manner as to insure that the regulator would be de-energized when they were operated. This regulator was adopted as standard by the Army Air Forces (type *A*-1, specification 32360), and later standardized by the Army, Navy, and Civil Aeronautics Administration (specification *AN-R-3a*). A monocyclic square, and later a resonant *T* circuit, were used to obtain the constant-potential–constant-current transformation in this regulator.

In 1943 a 7.5-kw 2,300-volt regulator was developed in order to meet increased power demands, and to fit into the complete airport lighting system then being standardized. This regulator (specification *AN-R*-17) is the present Army,

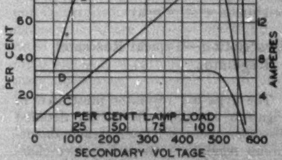

Figure 1. Moving-coil regulator, three-kilowatt, 220-volt primary winding, 6.6-ampere secondary winding

A—Primary current
B—Efficiency
C—Primary power factor
D—Secondary current

Paper 45-165, recommended by the AIEE committees on air transportation and electric machinery for publication in AIEE TRANSACTIONS. Manuscript submitted August 1, 1945; made available for printing August 17, 1945.

G. M. KEVERN is chief of the lighting unit, equipment laboratory, Air Technical Service Command, Wright Field, Dayton, Ohio.

Figure 2 (left). Resonant-circuit regulator, 7.5 kw, 2,300 volts, 6.6/5.5/-4.8/4.2/3.8 amperes, remote brightness control

Figure 3. Resonant-circuit regulator, type-*B*-1, six kilowatts, 230 volts, 6.6/5.5/4.8/4.2/3.8 amperes, manual brightness control

Navy, and Civil Aeronautics Administration standard, and several hundred have been procured from two separate sources. It is illustrated in Figure 2. The 7.5-kw regulator is oil-immersed, self-cooled, weighs approximately 1,000 pounds, and includes five brightness-selector relays and one open-circuit protective relay. It is designed for use with a separate remote-controlled oil switch, and a control panel (specification *AN-P*-59) which is installed in the airport control tower.

Shortly afterwards, a requirement arose for a 230-volt manually controlled regulator for overseas installations of high-intensity runway and approach lights. This resulted in the development of the six-kilowatt regulator known as the type-*B*-1 (Army Air Forces specification 32470) which is illustrated in Figure 3. This type of regulator is similar to the 7.5-kw unit, except for the lower primary voltage, and the use of a manually operated brightness tap changer in lieu of the brightness-selector relays.

Description—Typical Resonant Regulator

The type-*B*-1 regulator illustrated in Figure 3 has been selected for detailed discussion, because it is a typical resonant-circuit regulator with performance characteristics similar to the majority of units tested. This regulator consisted of the major items shown on the wiring diagram of Figure 4, inclosed in or mounted on the front of a sheet-steel tank containing 28 gallons of oil. The complete assembly weighs 965 pounds and is approximately 24 by 29 by 31 inches high.

The essential portion of the regulator is the resonant circuit, sometimes called "monocyclic square," which consists of two five-microfarad, 1,400-volt mineral-oil capacitors (items *F*, Figure 4), and two 530-ohm 60-cycle reactors (items *E*, Figure 4). The constant-potential–constant-current transformation is performed by this circuit. It has been demonstrated mathematically that the following relation exists, assuming that there are no losses, and that all four reactances are equal in magnitude:[1]

$$I_s = \frac{jE_p}{X}$$

where

I_s = output current

E_p = input voltage

X = reactance of one side of square

j = operator denoting 90 degrees counterclockwise rotation

Inspection of this relation reveals that output current is independent of the load, but that it is directly proportional to and 90 degrees out of phase with the input voltage. Experience with actual regulators indicates that the relation may be used with negligible error over the normal operating range. Losses in well-designed reactors and capacitors have little effect on the output current, but the reactances should be held within one per cent of the desired value (or compensated for by means of factory adjustment taps on the input or output transformer).

The functions of the two coil 200-210-220-230/1,900-1,580-1,380-1,210-1,090-volt 6.5-kw-input transformer (item *C*) are to provide the correct voltage for the monocyclic square and to isolate the high-voltage from the low-voltage-input circuit. The tap changer (item *D*) is used to compensate for sustained variations in voltage impressed upon the monocyclic square; the five values of lamp brightness are easily obtained by means of the brightness tap changer (item *B*) which may be operated without de-energizing the regulator.

The manually operated 35-ampere circuit breaker (item *A*) provides on–off control, and open-circuit protection by means of the shunt trip which is energized through the normally closed contacts of the series relay (item *H*) when open circuit occurs. The resistor (item *J*) provides a slight time delay, thereby preventing undesirable tripping during switching.

The purpose of the two-coil 3.5/6.6-ampere, six-kilowatt-output transformer (item *G*) is to limit the open-circuit voltage. Theoretically the open-circuit output voltage of the monocyclic square would be infinite; in an actual regulator (without output transformer), it would rise dangerously high, and might cause immediate

Table I

Brightness in Per Cent	Current in Amperes
100	6.6
30	5.5
10	4.8
3	4.2
1	3.8

failure of the capacitors. When the secondary winding of the regulator under discussion is opened, the monocyclic square maintains the current in the primary winding of the output transformer, the core becomes saturated, and the output voltage is limited to approximately 175 per cent of the full-load voltage.

Performance Data—Typical Resonant Regulator

The regulator illustrated in Figure 3 was subjected to extensive laboratory tests, and the results obtained are shown in Figures 5 to 9, inclusive.

The data shown in Figures 5, 6, and 7 were taken by operating the regulator on a 230-volt 60-cycle power supply with a variable lamp load, and making direct measurements of input and output current, voltage, and power. The current-regulation curves for all five brightness taps, shown in Figure 5, indicate a maximum drop in current of 3.5 per cent from short circuit to full load. Figure 6, when compared with Figure 1, illustrates the basic difference in performance between resonant and conventional moving-coil regulators. The moving-coil unit has a constant input current and a power factor which is nearly proportional to the load, while the resonant circuit unit has an input current which is nearly proportional to the load, and a power factor of unity from 25-per-cent load to full load. Figure 7 shows that the resonant regulator has excellent power factors and efficiencies even at the lowest brightness tap (3.8 amperes) whereas the moving-coil regulator would have a power factor of less than 25 per cent lagging.

The data shown in Figure 8 were taken with two regulators placed in a large cold room, connected to a 230-volt 60-cycle power supply and to a six-kilowatt lamp load. Meters were placed outside the cold room, with provision made for switching from one regulator to another. Test runs were made at several temperatures, with each temperature held constant during the test and for at least 24 hours before the test run was started. Readings were taken immediately after energizing the regulator, and the time required for the output current to reach normal room-temperature values was recorded. The two regulators, although made by different manufacturers, were quite similar in performance at room temperature. The curves of Figure 8 show very plainly that chlorinated-diphenyl capacitors are not satisfactory, unless the regulator is to be installed in a heated room.

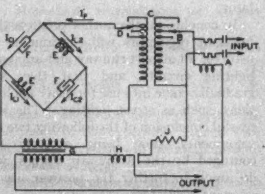

Figure 4. Wiring diagram, type-*B*-1 resonant-circuit regulator

A—Manual circuit breaker with shunt trip
B—Brightness tap changer
C—Input transformer
D—Primary-voltage tap changer
E—Reactor
F—Capacitor
G—Output transformer
H—Series relay
J—Resistor

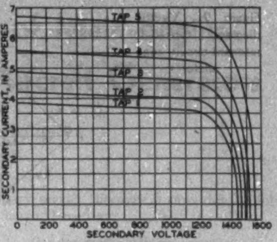

Figure 5. Current-regulation, type-*B*-1 resonant-circuit regulator

The vector diagrams shown in Figure 9 were plotted from data taken with the regulator connected to a 60-cycle power supply held constant at 230 volts and a lamp load which was varied from short circuit to open circuit. The two diagrams are oriented so that the correct relation between corresponding currents and voltages exists. The values of currents and voltages existing in the monocyclic square under rated load conditions are shown by the solid lines, while the dotted lines show the loci of the corners of the diagrams, so that the vector diagrams for any load may be visualized. The change in voltage applied to the square due to voltage drop in the input transformer as the load is increased from short circuit to rated load is too small to be shown, but the increase in voltage due to the large leading current flowing in the input transformer at overloads is illustrated.

Resonant-Regulator Characteristics

The current regulation of the resonant-circuit regulator depends primarily upon the accuracy of tuning of the resonant circuit, and upon the regulation of the input and output transformers. Since the output current of existing regulators varies in proportion to variations in a supply voltage, it has been considered uneconomical to specify better than four-percent regulation (±2 per cent of the specified current), although it could be obtained without difficulty. The importance of current regulation is minimized by the fact that, after installation, the normal load current may be corrected by means of taps on the regulator input transformer, and/or adjustment of the supply voltage.

Efficiency of a resonant regulator is determined by the losses in reactors, capacitors, and transformers, and is maintained at a comparatively high value, even at light loads. Power consumed by built-in relays ordinarily is included in the regulator losses, unless supplied from separate control circuits.

Except at extremely light loads, a properly designed resonant regulator has a primary power factor which is approximately equal in magnitude but opposite in sign to the secondary power factor. For example, the input power factor of a regulator feeding a 90-per-cent-lagging series load would be approximately 90 per cent leading. The actual input power factor is determined by the following factors:

1. Manufacturing tolerance in monocyclic square.
2. Exciting current of input transformer.
3. Exciting current of output transformer.
4. Series coil of protector relay.
5. Inductive reactance of series load.

Factors 3, 4, and 5 cause leading power factors, factor 2 has a lagging effect, and the first factor may have either a lagging or leading effect.

The effect of frequency variations upon resonant-circuit regulators is much less than one would expect at first thought. The regulator illustrated in Figure 3 has been used satisfactorily on 50-cycle power supplies without modification. The output current at full load is approximately three per cent less on 50 cycles than it is on 60 cycles.

Oscillographic studies indicate that the output current from a resonant regulator operating near full load has no switching surges. This is in direct contrast to the effective value of the output current from a moving-coil regulator, which surges to a high value and then oscillates about the steady-state value, immediately after the unit is energized. Observations made on a monocyclic square regulator operating at rated lamp load also indicate that the input and output current waves approximate sine waves. Although time limitations have prevented a complete study of harmonics under all load conditions, no trouble due to harmonics has been reported during four years operating experience with loads consisting of lamps, and lamps connected to well-designed isolating transformers.

Summary

The satisfactory service obtained from over 1,500 resonant regulators procured

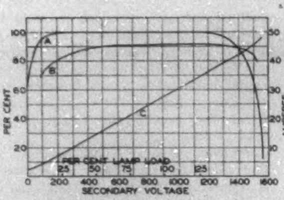

Figure 6. Performance data, brightness tap 5, type-*B*-1 resonant-circuit regulator

A—Primary power factor
B—Efficiency
C—Primary current

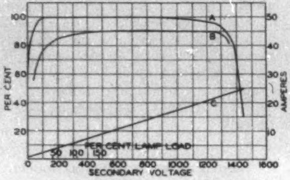

Figure 7. Performance data, brightness tap 1, type-*B*-1 resonant-circuit regulator

A—Primary power factor
B—Efficiency
C—Primary current

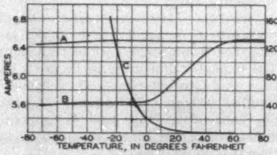

Figure 8. Low-temperature performance, resonant-circuit regulators

A—Initial output current, resonant regulator with mineral-oil capacitors
B—Initial output current, resonant regulator with chlorinated-diphenyl capacitors
C—Time required for output current of regulator with chlorinated-diphenyl capacitors to reach rated value

Figure 9. Vector diagram, type-*B*-1 resonant-circuit regulator

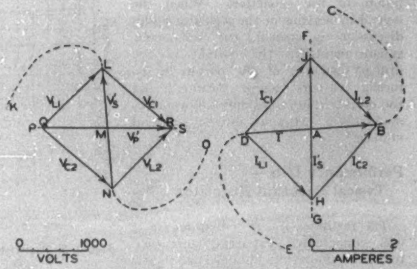

Voltages:	Currents:
As load is increased from short circuit to rated load:	As load is increased from short circuit to rated load:
Point *L* moves from *M* to *L*	Point *B* moves from *A* to *B*
Point *N* moves from *M* to *N*	Point *D* moves from *A* to *D*
As load is increased from rated load to open circuit:	As load is increased from rated load to open circuit:
Point *L* moves from *L* to *K*	Point *B* moves from *B* to *C*
Point *N* moves from *N* to *O*	Point *D* moves from *D* to *E*
Point *R* moves from *R* to *S*	Point *J* moves from *J* to *F*
Point *Q* moves from *Q* to *P*	Point *H* moves from *H* to *G*

since 1940 is evidence that this type of regulator has moved out of the experimental category. Resonant regulators are the most satisfactory means of providing power for airport runway and approach lighting circuits, which must be operated at reduced intensities on clear nights, and they have been standardized by the Army, Navy, and Civil Aeronautics Administration. Moving-coil regulators still are used for applications where operation at reduced intensities is not required, such as street lighting and airport boundary lighting.

Existing resonant-circuit regulators have the following definite advantages and disadvantages:

A. Advantages:

1. No moving parts (except relays).

2. Unity power factor with resistance loads, leading power factor with inductive loads.

3. High power factor and efficiency maintained with loads as low as 20 per cent. This permits satisfactory operation of lighting circuits at one-per-cent brightness.

4. Brightness control easily obtained by varying input voltage to resonant circuit.

5. No switching surges of sufficient duration to affect lamp life.

B. Disadvantages:

1. Output current varies with input voltage.

2. Not familiar to most operating and maintenance personnel.

In contrast to the foregoing, moving-coil regulators have the following characteristics:

A. Advantages:

1. Output current constant regardless of primary voltage.

2. Conventional equipment, familiar to most electrical personnel.

B. Disadvantages:

1. Moving parts which require accurate adjustment.

2. Power factors of 75 to 85 per cent lagging at full load, unless supplied with capacitors for power-factor correction.

3. May not be used at less than 50-per-cent load, owing to overheating.

4. Unsatisfactory for brightness control, owing to overheating, and extremely low power factors and efficiencies at low brightnesses.

5. Current surges immediately after energizing shorten lamp life, especially for airport use where frequent switching may be required.

Sufficient data for an accurate cost comparison of the two types of regulators are not available, owing to the fact that all resonant regulators procured to date included an input transformer and brightness tap-changing equipment. Elimination of these items, however, should make the cost of a resonant regulator equal to or less than the cost of a moving-coil regulator.

In conclusion, the author predicts that resonant regulators will continue to be used for all airport runway and approach lighting circuits, and that they will gradually come into use for other applications, such as street lighting. The successful conclusion of the following two developments, now being actively encouraged by the Army Air Forces, will do much to further the postwar use of resonant regulators:

1. A lightweight air-cooled design.

2. A method of compensating for primary-voltage variations.

Reference

1. Theory and Calculation of Alternating-Current Phenomena (fourth edition), Charles Proteus Steinmetz. McGraw Publishing Company, 1908. Pages 78–129.

Parallel Operation of Main-Engine-Driven 400-Cycle Aircraft Generators

L. G. LEVOY, JR.
MEMBER AIEE

Synopsis: This paper reports progress in the development of variable-ratio drives and governors for parallel operation of aircraft alternators driven from the main engines. Preliminary tests have been made demonstrating successful parallel operation of such drives under various conditions of acceleration and loading. The general system of operation and results of some of the first tests are described in this paper.

POTENTIAL military requirements may create a demand for very large aircraft. Four-hundred-cycle three-phase 208Y–120-volt a-c power appears to be quite suitable for most of the electrically operated devices. The electrical manufacturers in this country have been asked by the Army Air Forces to develop an electric system to generate, distribute, and utilize this power to perform various required functions on such aircraft.

For reasons of space, weight, economy, and reliability, it was decided to drive these generators from the main engines. Several other means of driving such generators were considered, but because of the very limited time available for the development this method was selected, as it appeared to hold most promise for a quick solution. Among the other means considered were:

1. Auxiliary engines or gas turbines.
2. Exhaust-gas turbines.
3. Waste-heat boilers and steam turbines.
4. Hydraulic torque converters.
5. Mechanical transmissions of various types.
6. Rotating electric machines in various combinations.
7. Electronic means.

Some of these now are being perfected, and much of the experience gained with the present system will be applicable to these other systems.

Parallel operation of the generators on a multiengine airplane is desired for military service, because it provides the following benefits:[1]

1. Greater motor-starting capacity.
2. Reduction of time and magnitude of voltage disturbance from fault, motor starting, or loss of generation.
3. More effective use of spare capacity, so that smaller or fewer generators can be used without excessive load-transfer switching.
4. Greater ability to withstand fault without disruption of service and greater ability to burn faults clear.
5. Continued operation of load equipment following engine or generator failure; does not require any automatic-transfer equipment nor any immediate attention from the operator.

Statement of the Problem

The aircraft engines are relatively large compared with the generators, as they are used for main-propulsion power. Consequently, their rating may be from 50 to 100 times the rating of the generators which are used for auxiliary electric power on the airplane. In addition the main-engine speed may vary over a wide range (three to one or more), depending upon the conditions of flight. Furthermore, all engines are not always operated at equal speeds at all times. These factors presented several new problems to the electrical industry.

Parallel operation of a-c generators is common in industrial or central-station practice. However, usually most of the following conditions prevail for constant-frequency a-c systems with generators operated in parallel:

1. The prime mover is comparable in rating with the generator.
2. The prime mover usually is operated at constant speed.
3. The prime mover is governed to operate in accordance with the requirements of the generator.
4. All prime movers on the system are operated at a speed exactly proportional to the system frequency.
5. Transient speed changes of the prime movers are relatively small.

In contrast with this, in the proposed aircraft system:

1. The prime mover is large, frequently being 50 to 100 times the rating of the generator.
2. The prime movers are operated over a wide speed range to meet changing conditions of flight.
3. The prime mover is governed to operate in accordance with the propeller and propulsion requirements of the airplane.
4. Different engines on the same airplane may be operated at different speeds at the same time.
5. Transient speed changes of the prime movers may be very rapid.

The problem is, with this combination of conditions, to provide a means of driving the alternators from the main engines, maintaining frequency and voltage at all times, and keeping all the machines operating in synchronism and sharing the load. Of course, in addition to these fundamental requirements the system must be suitable for use in aircraft, which conditions bring in a host of additional requirements which have been listed elsewhere.[1]

The alternators now in use have eight poles and operate at 6,000 rpm to deliver 400 cycles. This means that one mechanical degree is equivalent to four electrical degrees. Thus to maintain synchronism it is necessary that the mechanical displacement among generators does not exceed about 20 mechanical degrees, and to divide load properly they should be within one or two mechanical degrees of each other. This close relationship should be maintained, even though the individual engine speeds vary widely and are subject to high rates of acceleration. To the uninitiated, it looks like an impossible job, except with some type of slip device such as a fluid coupling. A slip device is out of the

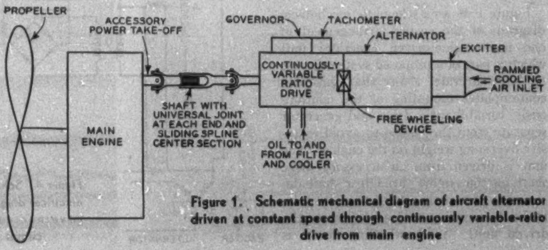
PROPELLER
ACCESSORY POWER TAKE-OFF
GOVERNOR
TACHOMETER
ALTERNATOR
EXCITER
CONTINUOUSLY VARIABLE RATIO DRIVE
RAMMED COOLING AIR INLET
SHAFT WITH UNIVERSAL JOINT AT EACH END AND SLIDING SPLINE CENTER SECTION
FREE WHEELING DEVICE
MAIN ENGINE
OIL TO AND FROM FILTER AND COOLER

Figure 1. Schematic mechanical diagram of aircraft alternator driven at constant speed through continuously variable-ratio drive from main engine

---

Paper 45-158, recommended by the AIEE committee on air transportation for publication in AIEE TRANSACTIONS. Manuscript submitted July 3, 1945; made available for printing August 9, 1945.

L. G. LEVOY, JR., is in the industrial engineering division of the General Electric Company, Schenectady, N. Y.

The author wishes to express his appreciation to colleagues in his own organization for their cooperation in carrying on these experiments and to the engineers of the Sundstrund Machine and Tool Company for providing the variable-ratio drive units.

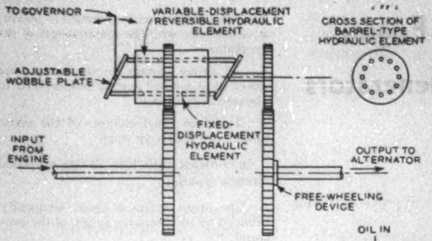
TO GOVERNOR
VARIABLE-DISPLACEMENT REVERSIBLE HYDRAULIC ELEMENT
CROSS SECTION OF BARREL-TYPE HYDRAULIC ELEMENT
ADJUSTABLE WOBBLE PLATE
FIXED-DISPLACEMENT HYDRAULIC ELEMENT
INPUT FROM ENGINE
OUTPUT TO ALTERNATOR
FREE-WHEELING DEVICE

Figure 2. Schematic mechanical diagram of one form of continuously variable-ratio-drive unit

Figure 3 (below). Schematic mechanical diagram of governor and servo mechanism

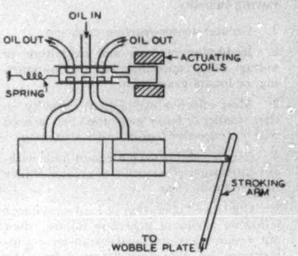

question, however, because of the wide speed range involved, which makes it too inefficient to be applicable. The use of a positive-displacement type of drive to improve efficiency requires the development of a high-speed governor.

For constant frequency to be obtained from conventional generators the latter must be operated at constant speed. This means that, if the prime mover has a variable speed, some type of variable ratio transmission must be interposed between the prime mover and the generator and governed to provide the desired result.

Procedure

An analytical approach[3] provided specifications for governor design and indicated that the characteristics required for parallel operation were well within practical design values and that parallel operation could be achieved.

It was necessary to overcome many obstacles, and some are yet to be mastered. Nevertheless, the fundamental principles of accomplishing this job have been established and demonstrated.

Because the solution of this problem required the development of a governing system with a very high speed of response, it was thought that many engineers would be interested in a description of the general method of accomplishing this result. The purpose of this paper is to give a brief description of the governor and what is believed to be the first 400-cycle a-c system of this type which has been successfully demonstrated.

Description of the System

Figure 1 shows a schematic mechanical diagram of the system arrangement of one main-engine-driven generator unit which is part of a proposed system for use on large aircraft. Note that this plan contemplates mounting of the continuously variable-ratio drive and generator separate from the engine to avoid excessive overhung weight on the engine. The unit is driven from an accessory drive shaft on the engine through a shaft designed to permit the engine to move in its resilient mounting without injury to the driven unit. A free-wheeling device is located between the variable-ratio drive and alternator, which permits driving the alternator but never permits the alternator to try to drive the engine. The governor adjusts the ratio of the variable-ratio drive to maintain frequency and load division, as explained later, in spite of variations in engine speed.

The setup used in test differs from Figure 1 in that the driving power was taken from the main output shaft of the engine through a suitable gear box, as the accessory drive shafts on these engines were not large enough to provide the required power.

Figure 2 is a schematic mechanical diagram of one form of continuously variable-ratio drive unit. This unit is a differential type of hydraulic drive using oil as the working medium. A simple valve arrangement (not shown) is located between the pump and motor end of the unit, providing a properly valved path for the flow of the working fluid between the pump and motor.

The input end of the unit has a variable stroke. This stroke is varied by the angle of the wobble plate, which in turn is positioned by the governor. The output end of the unit has a fixed stroke. Thus the angle of the adjustable wobble plate on the input end of the unit establishes the relative speed of the fixed stroke element with respect to the variable displacement element. When the stroke of the latter is zero, both elements are locked hydraulically and rotate as a unit. This is the straight-through drive ratio. At this ratio hydraulic losses in the unit are at a minimum. The variable-ratio drive unit should be designed to have maximum efficiency at engine speeds corresponding to the cruising speed of the airplane.

Figure 3 is a schematic mechanical diagram of the governor and servo mechanism which operates to position the wobble plate and thereby adjusts the drive ratio to provide the desired output speed.

Oil at a moderate pressure is supplied to an electromagnetically operated pilot valve, which is balanced against a spring. A valve movement of a few thousandths of an inch permits oil to enter one side of the piston and leave from the other side, thus causing the piston to move. The piston is linked mechanically to the wobble plate of the variable-ratio drive. As a result of the very small valve movement required, and by proper design of the ports, a very high speed of response is achieved. The pilot valve position is governed by the electrical signal introduced into its actuating coil. The governor uses a constant-current balanced-valve system. The pilot valve always returns to its neutral position after the speed correction is made. The transient position of the valve is determined by the change in signal above or below the balance-position signal.

Figure 4 is a schematic electrical diagram of the governor control circuit showing the principle of operation. For

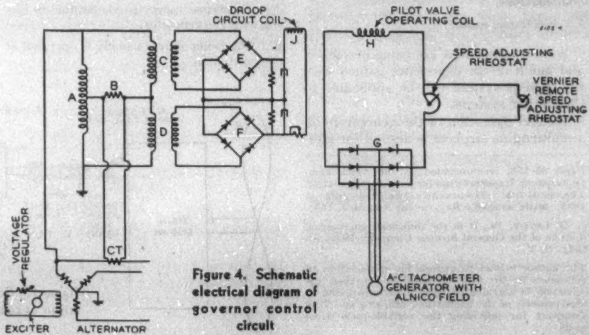
DROOP CIRCUIT COIL
J
C
E
B
A
D
F
PILOT VALVE OPERATING COIL
H
SPEED ADJUSTING RHEOSTAT
VERNIER REMOTE SPEED ADJUSTING RHEOSTAT
G
VOLTAGE REGULATOR
CT
EXCITER
ALTERNATOR
A-C TACHOMETER GENERATOR WITH ALNICO FIELD

Figure 4. Schematic electrical diagram of governor control circuit

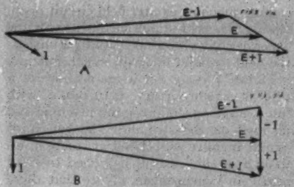

Figure 5. Vector relations in load-frequency droop circuit

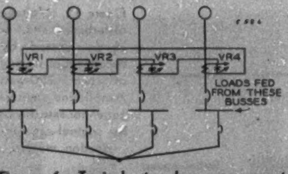

Figure 6. Typical star bus arrangement showing current-transformer connections for differential cross-current compensation for division of reactive load among generators

simplicity certain other circuits including stabilizing and emergency overspeed circuits are not shown.

The operation is as follows: A small a-c tachometer generator using a permanent-magnet field is driven from the output of the variable-ratio drive. The output of this tachometer is rectified by rectifier *G* and applies a signal, which is directly proportional to speed on the operating coil *H*.

Another signal, which is proportional to load, is placed on droop-circuit coil *J*, which is wound on the same core as *H*. This provides a five-per-cent frequency droop at full load. This load-frequency droop causes the generators to share the kilowatt load when operating in parallel.

The load–frequency-droop signal is derived from a circuit which is sensitive to the inphase component of current. This provides a signal approximately proportional to power load on the alternator and is accomplished in the following manner. Terminal voltage of the alternator is fed into a midtapped autotransformer *A*. Another signal, which is proportional to current, is obtained from a current transformer and fed into the resistor at *B*. This latter signal is added and subtracted vectorially from the voltage signal, the results of the addition and substraction appearing in transformers *C* and *D* respectively. The outputs of these transformers are rectified by full-wave dry-type rectifiers *E* and *F*. The resulting two d-c signals are subtracted, and their difference placed on the droop-circuit coil *J*.

Figure 5 shows the vector relations involved in the load–frequency-droop circuit.

Figure 5a shows the condition with a lagging power-factor load. Note that there is a substantial difference between the voltage vectors $\mathbf{E} + \mathbf{I}$ and $\mathbf{E} - \mathbf{I}$, which provides a signal to the droop coil.

Figure 5b shows the condition with a zero power-factor load. Here $\mathbf{E} + \mathbf{I}$ and $\mathbf{E} - \mathbf{I}$ are equal, hence their difference is zero, and no signal is introduced into the droop coil.

The droop circuit is responsive to real power and not to reactive power.

The division of reactive kilovolt-amperes among several generators connected in parallel can be achieved by means of differential cross-current compensation in the voltage-regulator circuits. This provides for reactive division without voltage droop. Schematically this connection is shown in Figure 6. A normally closed interlock is provided on each generator circuit breaker to short-circuit its reactive division current transformer when the circuit breaker is open and the generator is taken out of service.

This differential reactive-division circuit is ideal for parallel operation, providing the units are to operate in parallel at

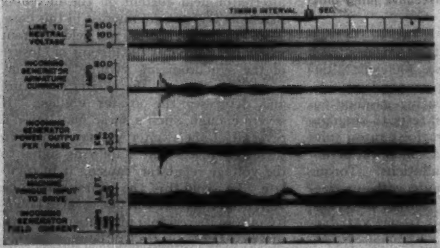

Figure 7. Synchronizing disturbance with incoming machine at full voltage with no load on system

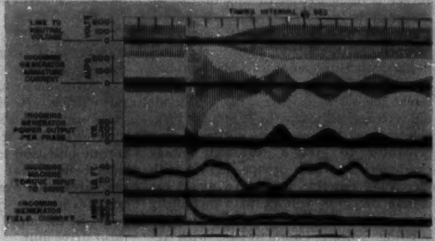

Figure 9. Synchronizing disturbance with incoming machine at full voltage and both incoming and running machines carrying load

Incoming machine purposely synchronized 180 electrical degrees out of phase with running machine

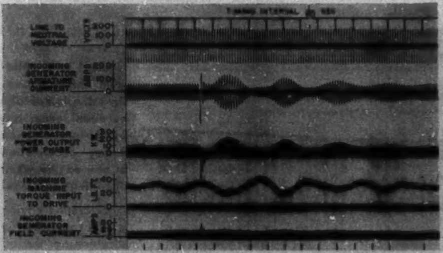

Figure 8. Synchronizing disturbance with incoming machine at full voltage and both incoming and running machines carrying load

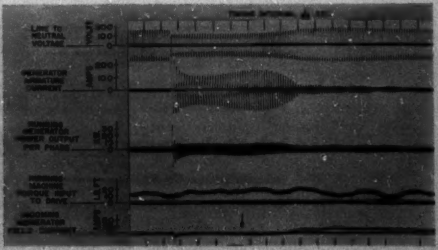

Figure 10 (below). Synchronizing disturbance with incoming machine running unexcited

Arrow indicates time of closure of exciter field switch

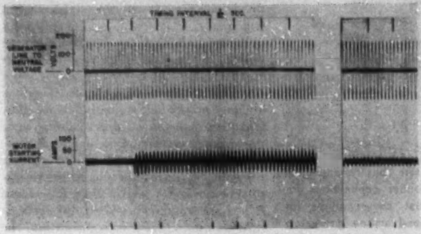

Figure 11. Voltage disturbance and recovery caused by simultaneous starting of two 750-watt Amplidyne motor-generator sets driven by squirrel-cage induction motor.

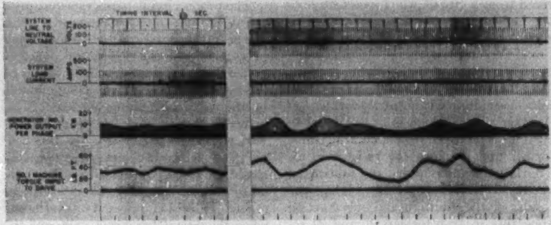

Figure 12. First section of oscillogram shows normal parallel operation with smooth engine, and second section shows effect of making engine rough by short-circuiting spark plugs on two cylinders in consecutive firing order

all times. If, however, nonparallel operation is desired, or operation with the system split into various combinations other than all machines operating in parallel, a rather complicated switching of the reactive-division control circuits is involved. To avoid this, individual cross-current compensation can be used. For this method there is no interconnection between reactive-division circuits for different generators. Instead, each individual voltage regulator is biased by reactive current output of its corresponding generator to give a regulated-voltage characteristic which droops slightly with increasing reactive load. To avoid excessive droop of voltage with increasing load, compensation can be added to give a rising voltage characteristic with resistive load and the combination designed to hold substantially flat voltage at the average load power factor.

Operating Experience

Tests have been made with a laboratory setup using two 450-horsepower air-cooled radial aircraft type engines, each driving a 30-kw 40-kva 400-cycle alternator through a step-up gear and variable-ratio drive. Reciprocating gasoline engines were selected for tests to simulate appropriately acceleration rates and torque pulsation effects which will be obtained in actual installations. Torque measurements were made with an electric-strain-gauge-type torque meter located in the input shaft to one variable-ratio drive unit.

The presence of the free-wheeling between the alternator and drive was found to make synchronization very easy even with purely random synchronization. The machines have been synchronized at random at full voltage with and without load at widely different speeds. They also have been synchronized with the incoming-machine exciter field circuit open, closing the field simultaneously with the generator circuit breaker and permitting the field to build up while synchronizing.

Figure 7 is an oscillogram showing a typical synchronizing disturbance with full voltage on the incoming machine and no load on the system. The generator circuit breaker was closed at random, although in this case it happened to close nearly in synchronism. Note that there is very little disturbance to the system voltage. With automatic speed matching and synchronizing equipment, equal or better performance could be achieved consistently.

Figure 8 is an oscillogram showing a synchronizing disturbance similar to Figure 7, except that both machines had an initial load on them prior to synchronization.

Figure 9 is an oscillogram showing a synchronizing disturbance on the two generator system with each generator carrying load at normal voltage, and with the synchronizing switch purposely closed when the generators are 180 electrical degrees out of phase. At the instant of closure this corresponds to a three-phase short circuit on both machines with correspondingly high armature currents. The machines pull into step, and system voltage has recovered in 0.1 second.

The lower trace on Figure 9, showing alternator field current on the incoming machine, is of special interest in this case. Note the high transient field current which is induced at the instant of closure of the synchronizing switch. This current flows through the exciter armature and depresses the exciter voltage. If severe enough, such a surge may cause a reversal of the exciter voltage, which in turn may reverse the stabilizing signal to the voltage regulator, causing it to oscillate. To avoid this, the exciter should be designed so that it will not reverse polarity or lose its residual magnetism on such surges. These surges will be more severe on a system with more generators and with running loads.

The power trace indicates that the generator is free-wheeling for a short interval as the machine is pulling into step. The drive input torque does not go negative, however, as the generator is free-wheeling and the drive losses are supplied

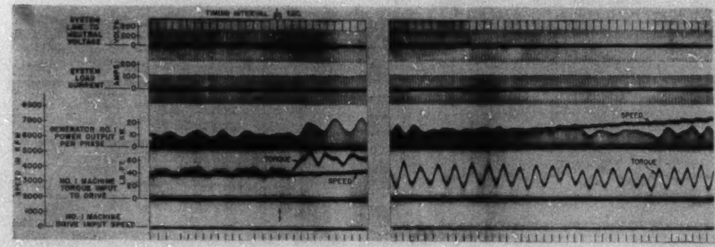

Figure 13. Oscillogram showing transient division of load between generators by governor action during acceleration of one engine when operating in parallel

Accelerating engine is very rough during accelerating period

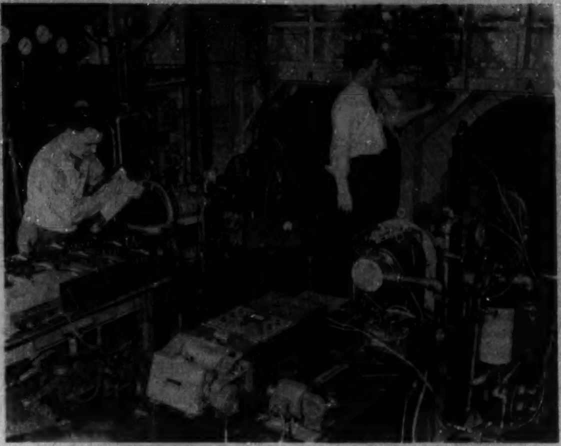

Figure 14 (above). General view of test setup

Driving engines are located behind wall

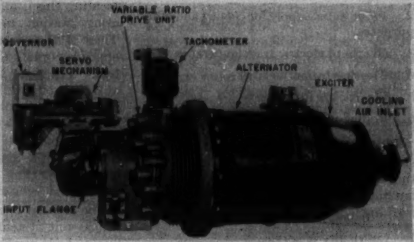

Figure 15. Side view of combined variable-ratio drive and alternator used in tests

by the input shaft. The power and torque curves pulsate for a few cycles as the generators oscillate about their equilibrium position, but no destructively large torques appear during the synchronization in this case.

Figure 10 is an oscillogram showing the disturbance resulting from bringing the incoming machine on the bus running at approximately full speed but unexcited. In this case the exciter field switch was closed slightly later than the alternator armature switch at the time indicated by the arrow. There was no load on the system in this case. When the incoming generator switch is closed, the incoming machine operates as an induction motor running light, taking magnetizing current from the line, but practically no power. (See power trace.) When the exciter field switch is closed, the exciter of the incoming machine builds up, pulling the machine into step and furnishing its own excitation so that the circulating current drops to practically zero. The bus-voltage disturbance would be substantially less with more generators on the system.

Figure 11 is an oscillogram showing voltage disturbance and recovery from a suddenly applied load. In this case two generators were running in parallel at no load, and two squirrel-cage induction motors, each driving a 750-watt Amplidyne generator were started simultaneously. There is a momentary voltage dip of about four per cent and the voltage is restored to normal in about 0.05 second. The induction-motor Amplidyne sets accelerated to full speed in about 0.7 second, and, as the Amplidynes were unloaded, the induction-motor current dropped to exciting current only. The oscillogram was shortened for reproduction purposes, and the portion between the two parts shown represents a time interval of 0.6 second.

This oscillogram gives some idea of the nature of voltage disturbances resulting from switching loads an the system. With more generators on the system, the disturbance would be less for a given load increment.

Figure 12 is an oscillogram showing two machines operating in parallel. The first part of the oscillogram shows normal operation with a normal engine. The second part of the oscillogram shows the effect of purposely making one engine rough by short-circuiting spark plugs on two cylinders in consecutive firing order. Note that the power division between generators pulsates but that, even in this severe case, the generator does not free-wheel. The system load current and voltage are influenced only slightly. In a four-engine set the influence on the system would, of course, be less.

Figure 13 is an oscillogram showing transient division of load during an acceleration of one engine, when the machines are operating in parallel. The accelerated engine was very rough during the accelerating interval in this case. Acceleration begins at the time indicated by the double-headed arrow. The oscillogram was shortened for reproduction purposes, and the portion between the two parts shown represents a time interval of 1.4 seconds. The rate of acceleration is about 1,700 rpm per second at the input to the accelerated drive. Note that the machines remain in step and that, though the accelerated machine picks up load initially, the governor reduces the load even before the acceleration is completed.

The oscillograms presented here are typical of more than 100 oscillograms which have been taken under a great variety of conditions in exploring the effect of various factors and combinations of conditions.

Figure 14 is a general view of the test setup. The engines are behind the wall and are coupled directly to the gear boxes which in turn are coupled to the variable-ratio drives which drive the alternators.

Figure 15 is a side view of an early design of one of the variable-ratio drive units and alternators used for these tests. This particular unit is rated 50 horsepower continuous and has an input speed range of 2,700 to 7,000 rpm. The over-all length of the combined unit is 29 inches, and the weights are as follows: alternator and exciter, 78 pounds; variable-ratio drive, 55 pounds; governor and servo mechanism, nine pounds; tachometer, 2.9 pounds.

Final designs have not been completed, and efficiency and life tests have not been run. However, these tests are planned for the near future. It is expected that these new variable-ratio drive units will weigh about 70 pounds and have a maximum efficiency of about 85 per cent. The new units will cover a wider speed range and be rated to correspond with the continuous and overload ratings of the generator.

This test program should contribute much data which will help to evaluate the a-c system for aircraft.

Conclusions

The operation of 400-cycle a-c alternators for the supply of auxiliary power in large aircraft, driven from the main engines through variable ratio drives, is feasible, and parallel operation of these alternators is practical. No elaborate synchronizing equipment is required. Thus, the use of higher-voltage alternating current now can be considered as another form of electric power supply for large aircraft, and we can begin to evaluate its properties in a realistic manner.

References

1. Basic Considerations in Selection of Electric Systems for Large Aircraft, W. K. Boice, L. G. Levoy, Jr. AIEE Transactions, volume 63, 1944, June section, pages 279–87.

2. Governor Requirements for Aircraft Alternator Drives, W. K. Boice, L. G. Levoy, Jr. AIEE Transactions, volume 64, 1945, July section, pages 534–40.

Electric Power in a Steel Plant

R. W. GRAHAM
MEMBER AIEE

If all the applications of electricity were listed, it would be found that this servant of man is used more extensively and in a greater variety of applications in the manufacture of steel than in any other industry. From the tiny photoelectric cell to the giant slow-speed reversing rolling-mill motor delivering torques of 2,000,000 pounds at one-foot radius, the application of electric power with its ease of control in the manipulation of steel is amazing as well as fascinating to anyone.

The use of electric power to replace hand labor and other less efficient methods of power supply has been most pronounced in the following applications in a steel plant:

1. Material handling, as coal and ore unloading.
2. Plant water supply for cooling and other purposes.
3. Overhead electric traveling cranes.
4. Transportation facilities.
5. Electric arc furnaces.
6. Rolling-mill drives.

Electric-power requirements in the steel industry are more demanding than those in many other industries. The two outstanding requirements to be considered are:

1. Continuity of service.
2. Methods and equipment to eliminate interruptions.

It is well known, that, when large tonnages of steel are in the process of pouring or rolling, an interruption of minutes and even seconds may in some instances make it necessary to scrap the entire mass of steel which is being processed. Because of the rapid drop in the working temperature of the steel there is always the question, after the restoration of a short power interruption, whether to attempt to roll the steel then in the mills or to take the loss in tonnage, as the bar of steel is then too long to be reheated in the soaking pits.

For adequate protection against power interruptions there are generally two or more sources of current supply. The Bethlehem Steel Company plant in Lackawanna has two outdoor substations with a combined capacity of 70,000 kva receiving 60,000-volt 25-cycle power over two transmission lines from the Niagara system, which is located approximately eight miles from the plant. Supplementing this is an auxiliary steam-generating station of 20,000-kw capacity. These stations feed into a tie network on opposite corners of a rectangular loop system. The steam station generates energy at 6,600 volts while the power purchased from the public utility system is stepped down from 60,000 to 6,600 volts, which gives a complete 6,600-volt distributing system for the main power supply to the larger consuming units and to the departmental substations.

The normal operation of the Niagara 60,000-volt system is for both incoming lines to be in service with oil circuit breakers at both ends of the line and a tie circuit breaker between them. These lines are tee-taped to the 20,000-kva transformer station which feeds the strip and bar mills through selective switching, permitting either line to feed the mills.

Because of the large number of synchronous motors on the Ward-Leonard-control motor generator sets and the synchronous motors on large mill drives, a leading power factor easily can be obtained on the system.

The Bethlehem Company has 2,250-horsepower synchronous motors on motor generator sets starting directly across the line (6,600 volts) with an inrush of 9,500 kva and with a voltage drop no more noticeable than starting through reactors of the 8,500-horsepower synchronous motors, which drive 6,000-kw motor generator sets. It also has a 1,000-horsepower squirrel-cage induction motor on a mill-scale-breaker drive, starting directly across the line at 6,600 volts. These machines have special bracing to withstand the heavy inrush of across-the-line starting. Elimination of reduced voltage starters simplifies the switchgear required for these units.

The amount of energy back of this system together with the synchronous machines operating in the plant, confined in such a congested area, allow short circuits of a high magnitude. These short-circuit currents require oil circuit breakers of 500,000-kva rupturing capacity to clear faults when they occur.

The outdoor substation transformers originally were water-cooled, but, on account of the excessive cost of filtered water, they have been changed to air-cooling and provided with blowers. This eliminates the danger of failure due to freezing or leakage in the water system, which might contaminate the transformer oil. The larger transformer installations comprise three single-phase units in delta. In case of trouble in any unit, operation can be continued on open delta at reduced capacity until such time as the transformer giving trouble has been repaired.

In addition to the split-up in the main Niagara power supply to the larger consuming units, which probably represents 75 per cent of the load, the steam-generated power supply has been split into two branches, the regular load bus, *B*, and the emergency bus load, *A*. In case of Niagara power failure or trouble within the plant, the load bus *B* is dropped immediately by relaying, and bus *A* is kept alive from the steam-station source.

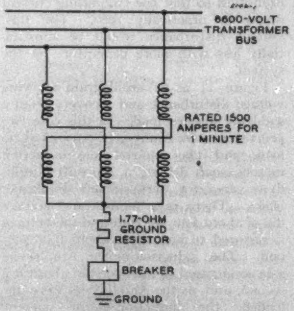

Figure 1. Three-phase zigzag grounding transformer

Paper 45-140, recommended by the AIEE committee on industrial power applications for publication. Manuscript submitted May 14, 1945; made available for printing July 6, 1945.

R. W. Graham is electrical superintendent, Bethlehem Steel Company, Lackawanna, N. Y.

This emergency bus *A* furnishes power to steam-plant auxiliaries such as boiler induced-draft fans, forced-draft fans, and powdered-fuel drives.

The steam station normally is supplied with surplus gas from the blast furnaces, fed to the boilers as fuel. This is supplemented with an auxiliary powdered-coal and fuel-oil supply. The emergency bus *A* also takes care of boiler-room auxiliary drives, exciters, and plant water supply.

The water supply in a steel plant is particularly important. It must be maintained constantly for cooling purposes, in the blast-furnace hearths, in the charging doors and valves of the open-hearth furnaces, in the gas scrubbers, and in many other applications where high temperatures are encountered.

The emergency bus *A* also supplies power to a few motor generator sets which furnish d-c power to open hearths and coke ovens. This d-c power must be a dependable supply, as the open-hearth cranes may be handling hot molten metal, and the coke oven machinery may be pushing hot coke, which cannot be interrupted without damage to the large pusher rams.

An industrial plant with its large integrated power system is quite similar to a public utility, except that the distances between consumers are very short.

In general the transmission system consists of several three-phase 500,000-circular-mil or 1,000,000-circular-mil copper cables supported on steel towers with wide spacing to prevent the conductors from whipping together under unfavorable wind and sleet conditions. Wide spacing is permissible with the heavy conductors, as both the supporting steel spans and the distances between the various mills are short, and with 25-cycle current line reactances are not objectionable.

ϕ—Phase-to-phase-fault protection
GR—Ground-fault protection
HCB—Westinghouse type *HCB* pilot-wire relay
IAC—General Electric Company induction overcurrent relay
CO—Westinghouse induction overcurrent relay
IBC—General Electric Company directional overcurrent relay
CR—Westinghouse directional overcurrent relay
IJD—General Electric Company pilot-wire relay
ICC—General Electric Company current polarized ground directional relay
CWC—Westinghouse current polarized ground directional relay

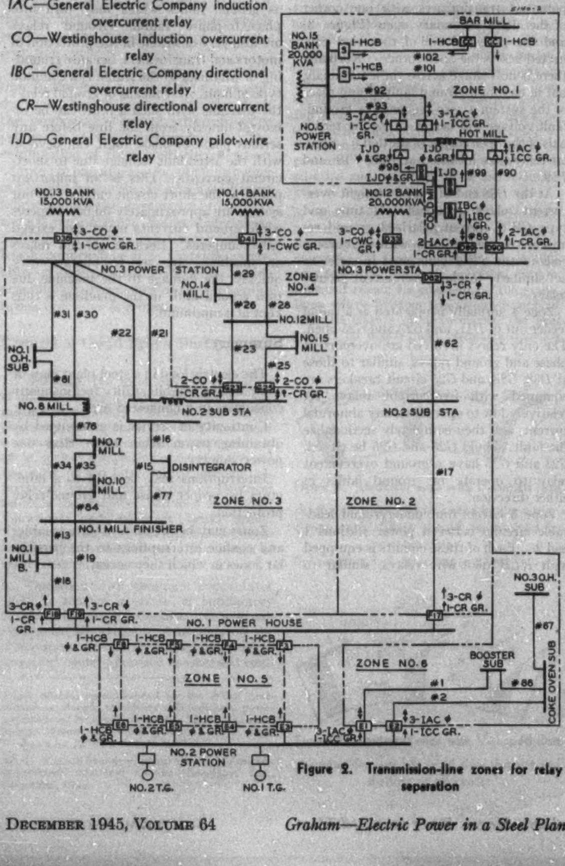

BAR MILL
NO.15 BANK 20,000 KVA
1-HCB
#102
#101
ZONE NO.1
#92
#93
3-IAC ϕ 1-ICC GR.
NO.5 POWER STATION
HOT MILL
IJD ϕ&GR.
#98
#99
#90
IAC ϕ ICC GR.
COLD MILL
IBC ϕ IBC GR.
#89
2-IAC ϕ 1-CR GR.
NO.13 BANK 15,000 KVA
NO.14 BANK 15,000 KVA
NO.12 BANK 20,000 KVA
3-CO ϕ 1-CWC GR.
D36
D41
D35
D89
D90
NO.3 POWER STATION
NO.3 POWER STA.
D62
3-CR ϕ 1-CR GR.
ZONE NO.4
NO.14 MILL
#29
#26
#28
NO.12 MILL
NO.15 MILL
#23
#25
#31
#30
#22
#21
NO.1 O.H. SUB
#81
2-CO ϕ 1-CR GR.
NO.8 MILL
NO.2 SUB STA
#62
#76
NO.7 MILL
#16
#34
#35
#15
DISINTEGRATOR
NO.10 MILL
#77
#17
#84
ZONE NO.3
ZONE NO.2
NO.1 MILL FINISHER
#13
#19
NO.1 MILL B.
#18
NO.3 O.H. SUB
3-CR ϕ 1-CR GR.
F16
F19
F17
#67
NO.1 POWER HOUSE
1-HCB ϕ&GR.
F8
F5
F4
F3
ZONE NO.5
ZONE NO.6
BOOSTER SUB
#1
#2
#86
COKE OVEN SUB
E6
E5
E4
E3
E1
E2
3-IAC ϕ 1-ICC GR.
NO.2 POWER STATION
NO.2 T.G.
NO.1 T.G.

Figure 2. Transmission-line zones for relay separation

Due to the proximity of the various mills and substations, it is rather difficult to set up any relaying scheme with the time elements necessary to give much selection in clearing the various lines in the system. Recent relay developments have been applied from time to time, but it is hard to keep up with advancements made in relay protection.

Relays

The original relay installation in our plant for line protection made use of *CZ* impedance-distance relays. These did not prove satisfactory, due to the relatively short lines and high currents involved, and they have been replaced with various other types, the purpose of which is to sectionalize the plant by clearing a section of the power system rather than an individual line. This is a simpler scheme and does not involve the coordination of as large a number of relays, and yet outages due to line troubles are kept relatively low.

In order to provide still better protection for the equipment, grounding transformers have been installed, as shown in Figure 1, to establish a definite ground neutral and provide adequate ground current for ground relaying. The relaying system thus is divided into two parts:

1. **Phase-to-phase fault relaying.**
2. **Phase-to-ground fault relaying.**

With the normal power system setup, the system is sectionalized into zones by means of relays, as shown in Figure 2. In case of a fault in zone 1 it is separated from zone 2 by means of overcurrent phase relays, type *IAC*, and directional overcurrent ground relays, type *CR*, at *D*89 and *D*90. Within zone 1 further separation on lines 89 and 90 is obtained by means of directional overcurrent relays, type *IBC*, and directional ground relays, type *ICC*, at *BB*89 and *A*90. Lines 98 and 99 between the hot-mill and the cold-mill busses are protected by type *IJD* pilot-wire relays, which function on either a phase or ground fault between the ends of the line while being inoperative on a through fault beyond the ends of the lines.

Pilot-wire, type *HCB*, relays are installed on lines 101 and 102 to the bar mill. The *HCB* relay takes the current in each end of the line and passes it through a positive- and zero-sequence network in each relay. The voltages across these networks are compared and are equal and opposite for any through fault beyond the line terminals. For either a phase or a ground fault between line terminals, these voltages are not equal and opposite but add up to operate

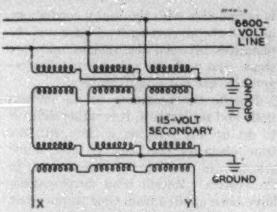

Figure 3. Potential connections for *CR* directional ground relays

relays at both ends of the line, thus clearing the faulted section.

In the original installation the 6,600-volt strip-mill substation consisted of one solid line of 24 metal-clad oil circuit breakers. After a failure of an oil switch which ruptured its tank and started a fire which destroyed several units, the bus was split into three sections, with a reactor placed between two sections and a third section relocated closer to the apparatus which it served.

All the 6,600-volt machines operating in this section of the plant are of recent design, with neutrals brought out with a double set of current transformers arranged for differential-relay protection as well as for protection from overload, phase failure, or undervoltage.

Surge protection equipment consisting of capacitors and Thyrite arresters is located in pockets in machine foundations as close as possible to the machine leads.

When the station was rebuilt, a reactor of three-per-cent reactance on 10,000-kva base was installed to reduce the asymmetrical amperes on a short circuit from 81,000 to 63,600 amperes under the worst conditions. Cross-differential protection was installed on both sections of the two hot-mill busses, and differential protection was installed on the cold-mill bus at the time of this change-over.

*A*92 and *A*93 circuit breakers are operated by straight overcurrent relays, type *IAC* on phase faults, and by ground directional relays, type *ICC*, for ground faults. This is a current-polarized relay obtaining its directional characteristic from a second current winding which is energized by the ground current flowing in the neutral of grounding transformer 30 at power station 5. The same type of relay is used for ground protection at *A*90. These ground relays operate to clear faults away from the bus.

Zones 2 and 3 separate from the rest of the system by means of directional overcurrent relays, acting as phase relays and ground relays and operating when the fault is within the zone. A typical case would be at *F*17 where there are three type-*CR* phase relays and a low-energy *CR* ground relay for protection. These relays consist of a directional element operated from phase current and voltage and an overcurrent element. The relays operate only:

1. When the direction of the current is proper.

2. When the amount of current exceeds the setting.

The ground relay is similar, but the potential for the directional element is supplied from a set of star–delta-connected potential transformers with one corner of the delta secondary open (Figure 3) and the potential coil of the relay connected across the open corner. Normally there is no voltage across these terminals, but in case of a ground fault at any place of the system a zero-sequence or ground-fault voltage will occur across the terminals of the open corner of the delta. Similar relays are installed at *D*62, *F*18, and *F*19.

At the *D*38 end of zone 3 straight overcurrent relays with sufficient time and type *CWC* current-polarized ground relays are depended upon, with the current coils of the *CWC* connected in series to act similarly to plain overcurrent ground relays.

Zone 4 normally is operated as a radial feeder out of *D*41, and *G*23 and *G*25 open. The only relays involved are overcurrent phase and ground relays, similar to those at *D*38, *G*23, and *G*25 circuit breakers are equipped with overcurrent relays set relatively low to operate on any abnormal current, and they completely sectionalize the fault, should *G*23 and *G*25 be closed. *G*23 and *G*25 have a ground overcurrent relay to operate on ground faults in either direction.

Zone 5 covers four underground lead-cable circuits between power stations 1 and 2. Each of these circuits is equipped with *HCB* pilot-wire relays, similar to the relays on lines 101 and 102 to the bar mill previously described. These relays have operated on two occasions to clear cable faults, performing satisfactorily without disturbing the rest of the system.

Zone 6 is treated as a radial feeder out of power station 2 with *IAC* phase relays. At present there are no ground relays in this section, but it is planned to install *ICC* current-polarized directional ground relays, with the direction of operation away from power station 2.

All transformer banks and 6,600-volt motors are protected with either differential relays or phase and ground relays, the ground relays being set to operate almost instantaneously in order to clear any faulty machine from the line at once.

A general over-all picture of our ground relaying scheme is shown in Figure 2. Not all lines but only the circuits controlled by the ground relays on lines are shown on this sketch. Ground relaying is particularly desirable, as the greater portion of all faults usually develop first as ground faults which may turn into phase-to-phase faults. Ground relays are also very desirable in the protection of motors and transformers, because grounding of windings to the frame is a common type of fault. By means of ground relays the machine with such a fault can be removed quickly from the line before any serious phase-to-phase fault can develop with the attendant damage due to short-circuit currents. This is an important point, as the short-circuit currents on our system are approximately 50,000 amperes while ground currents never can exceed 5,000 amperes. Because ground relays on machines are set to operate very quickly, the damage to the machine due to a ground fault in the machine is thus kept at a minimum.

Summary

The electric load in a steel plant may be compared to a public utility feeding many consumers in a congested area.

Continuity of service is guaranteed by obtaining power from more than one power supply.

Interruptions may be held to a minimum by proper phase and ground-relay protection.

Zones may be set up to isolate troubles and confine interruptions to the particular zones in which they occur.

Maintenance of Good Brush Performance

W. C. KALB
FELLOW AIEE

BRUSHES used on electric equipment have three distinct functions to perform. First, they must carry the load current into and away from the rotating element of the machine. Second, they must function as bearings on the surface of the commutator or slip ring, preferably without any applied lubrication, and at surface speeds sometimes in excess of 100 miles per hour. Third, on commutating machines, the brushes must control within safe limits the short-circuit current resulting from uncompensated voltages in the armature coils undergoing commutation and must resist the destructive action of the very high local current densities which are frequently characteristic of the commutation cycle.

This is quite an assignment. In addition to the need for good electrical conductivity, heavy demands are placed on the lubricating, thermal, and refractory properties of the brush material. The combination of these characteristics best adapted to one application obviously may not be best for another in which a different relationship of the three major brush functions is encountered. Before undertaking a discussion of the maintenance of good brush performance it is therefore advisable to consider the criteria by which acceptable performance of these essential brush functions is judged.

Criteria of Good Brush Performance

1. Sparking, the most obvious indication of unsatisfactory brush performance, may result from a variety of causes. Among the numerous causes may be mentioned poor commutator surface; faulty commutation cycle, such as completion of current reversal too early or too late; faulty machine adjustment; various mechanical or electrical faults in the machine; bad load conditions; vibration; and incorrect brush grade. Freedom from sparking of injurious intensity may well be considered the first criterion of good brush performance.

2. Operation with minimum commutator wear is another measure of satisfactory brush performance. Commutator wear accompanied by evidence of burning on the commutator surface is usually traceable to imperfect contact between brushes and commutator. This, in turn, may be due to low spring pressure, tight brush holders, excessive vibration, high or feather-edge mica, or brush chattering. A bright surface on the worn commutator indicates actual abrasion, either from foreign material in the brush face, or from the use of an abrasive brush grade.

3. The nature of the surface film on the commutator is being given increasing recognition as a gauge of brush performance. Satisfactory operation requires that a smooth surface film of uniform character be maintained. This subject will be discussed in greater detail later.

4. Brush performance is also judged on the basis of associated losses or, conversely, machine efficiency. Energy losses from short-circuit currents during commutation, from the resistance of a glazed commutator surface to the passage of load current, from the unbalancing effects of selective action, and from brush friction may at times be enough to affect seriously the efficiency or the satisfactory performance of a motor or generator. However, with proper brush selection and operation, these losses can be kept to a small value.

5. Quietness of operation is dependent, primarily, on the maintenance of uninterrupted contact between brushes and commutator. On some applications an audible tone from the brushes in operation may be sufficient reason for condemning the grade. Even where freedom from noise is not an essential feature of performance, the firm contact on which quiet operation depends has an important influence on satisfactory performance in other respects.

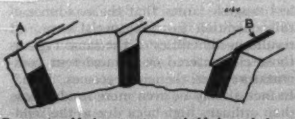

Figure 1. Undercut mica with U-shaped slots

A—Rough edges may be raised by the undercutting tool. These should be removed by beveling

B—Slotting off center leaves mica fins

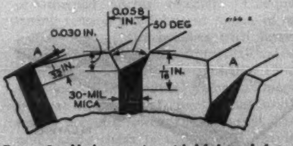

Figure 2. Undercut mica with V-shaped slots

A—Mica fins are left in V slots that are too shallow or off center

6. Brush life is often given undue weight in judging brush performance. While long brush life is desirable, its attainment at the sacrifice of good performance in some other respects may prove far from economical. When satisfactory brush performance in respect to the criteria previously cited is achieved, reasonable brush life may well be expected to follow as a natural result.

Good Commutator Surface Essential to Good Brush Performance

Economical maintenance and satisfactory operation of electric equipment is dependent to a large degree upon the care used in preparing the surface of the commutator or slip rings and the attention given thereafter to keeping the surface in good condition. Systematic inspection and immediate correction of incipient faults greatly reduce liability to shutdown, as well as the cost of repairs incurred when faults such as bar burning, high mica, and flat spots are allowed to develop to a serious stage.

SURFACING

The best way to produce a true cylindrical surface on a commutator or slip ring is by turning or grinding. Before undertaking this operation on a commutator it should be carefully examined to make sure that all segments are firmly clamped by the V rings and, if necessary, it should be retightened. On large machines the grinding or turning operation is usually performed with the armature in the machine but on small machines it is usually transferred to a lathe. In either case, rigid mounting of the turning tool or grinding equipment is essential to good results. Windings should be shielded from copper clips and dust during this operation. A diamond-shaped tool and fine-pitch feed are usually preferred for turning, finishing with a very light cut to minimize "threading." Some manufacturers use an actual diamond tool on small high-speed commutators where a high degree of precision is essential. Mounting the armature and its bearings on V blocks, rather than on lathe centers, is also recommended practice for lathe finishing. Grinding fixtures are available carrying a revolving abrasive wheel and there are also other types using a stationary stone held in a manner similar to a lathe tool.

The commutator stone is definitely superior to sandpaper for hand surfacing of commutator and rings. Such stones, of suitable grit and bond and with handles attached, are readily available. The stone should be formed or worn to the same curvature as the surface being finished and should have a span in the direction of rotation greater than the broadest flat spot to be removed. Presenting a rigid surface, the hand stone, properly applied,

---

Paper 45-164, recommended by the AIEE committees on electric machinery and industrial power applications for publication in AIEE TRANSACTIONS. Manuscript submitted May 2, 1945; made available for printing August 8, 1945.

W. C. KALB is manager, brush service engineering department, National Carbon Company, Inc., Cleveland, Ohio.

will remove high mica, flat spots, burned bar edges and other surface defects without disturbing the cylindrical contour. By the use of a hand stone when such faults first appear, the need for turning or grinding can be postponed or entirely avoided. A hand stone should also be used after turning to remove all traces of the thread-like ridges left by the lathe tool. The stone should be pressed firmly against the commutator or ring and moved very slowly from side to side to avoid diagonal scratches.

Sandpapering is an acceptable method of removing deposit from a commutator surface, correcting roughness, or reducing high mica, provided the accurate contour of the surface has not been seriously disturbed. However, sandpaper cannot be depended on to remove flat spots. Because the paper is flexible it tends to broaden, rather than remove, the flat spot. The rigid face of the commutator stone, on the other hand, will cut down the high areas and remove the spot by restoration of a true cylindrical surface. Best results with sandpaper are obtained by attaching it to a wooden block formed to the radius of the commutator or ring. Paper of relatively fine grain is usually preferable.

UNDERCUTTING

The practice of undercutting the mica of commutators has now attained such general approval that there is no need to argue its merits. There are relatively few applications on which flush mica commutators have any advantage over undercut. The tools used for undercutting range from the hacksaw blade and triangular file for hand operation to a great variety of motor-driven tools, most of which use revolving disk-shaped cutters. Shape of slot is largely a matter of individual preference. The square bottom or U-shaped slot shown in Figure 1 has the advantage of being effective until the commutator is worn down the full depth of the undercut. Accumulated dust, however, is not thrown out from the U-shaped slot as readily as it is from the V-shaped slot, Figure 2. Depth of U-shaped slots is generally made about 1/32 inch to 3/64 inch. Cutters for V-shaped slots are made with different angles between the cutting edges. Forty-degree cutters are generally preferred for thin mica, 50-degree for medium mica, and 60-degree for thick mica. The depth of cut should be sufficient to leave approximately 1/32 inch of mica-free copper at each side of the slot. Before undercutting a commutator, it should be turned, ground, or stoned depending on its previous condition, so that all surface faults, such as grooves, ridges, and flat spots, are eliminated. After undercutting, the commutator surface should be lightly polished with a fine-grain commutator stone or sandpaper to remove the small burrs raised at the edges of the slots by the undercutting tool. It is also good practice to burnish the commutator surface with hardwood blocks applied under heavy pressure. Hard maple is an excellent wood for this purpose and should be applied with the end grain against the commutator. This produces a well polished surface and, since considerable heat is developed, tends to form an oxide film on the segments which has a favorable influence on brush performance.

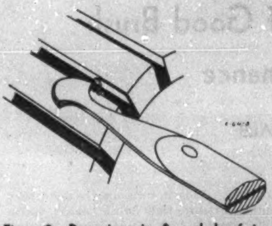

Figure 3. Removing mica fin and chamfering edge of commutator bar with home-made tool

Dimensions of slots exaggerated for clarity

MICA FINS

A frequent source of trouble on undercut commutators is variously described as "feather-edge mica," "side mica," or "mica fins." These terms refer to the thin edges of mica often left along the sides of the slots through failure to center the cutter accurately on the mica, deviation from a straight line parallel to the commutator segments, or insufficient depth of V-shaped slots. Commutator wear may also reach mica fins not in evidence immediately after undercutting. Troubles traceable to feather-edge mica are encountered with such frequency on commutating equipment, and the cause is so often overlooked in the search for less tangible faults, that the avoidance of this condition justifies special care. It results in difficulties of the same type as those encountered on nonundercut commutators when the mica becomes "high." In fact, it may be even more troublesome than ordinary high mica due to the tendency for small particles of mica to break loose and become embedded in the brush faces. Sparking, bar burning, picking up of copper by the brush faces, and noisy operation are among the operating difficulties often traced to this fault. After undercutting the commutator, or whenever faulty operation indicates the possible presence of feather-edge mica, every slot on the commutator should be inspected carefully. If mica fins are detected they should be removed with a knife blade or other suitable tool. An effective tool for this purpose can be made by grinding a hook-shaped cutting edge at the end of a hacksaw blade and attaching a suitable handle. This type of tool can be drawn through the slot, as illustrated in Figure 3, cutting at the root of the side mica on one side and slightly chamfering the opposite edge of the slot at the same time. Of course, frequent resharpening will be necessary to insure complete removal of the mica. After completing this operation the slots and armature windings should be blown out thoroughly to remove all loose particles of mica and copper.

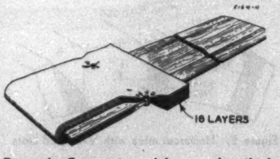

Figure 4. Canvas wiper of the type described in text

CANVAS WIPER

Another home-made device which has proved effective in maintaining good brush performance is the canvas wiper, Figure 4. Several layers of six- or eight-ounce hard-woven canvas or duck are folded over the end of a strip of strong pliable wood of suitable dimensions and secured by rivets. Countersinking the strip at the points where the rivets are inserted reduces the danger of the rivet heads making contact with the commutator. The canvas is held against the commutator under heavy pressure and rubbed slowly back and forth. This removes oil, grease and smudge from the commutator surface without hazard of the hand coming in contact with live parts of the machine. Applied with sufficient frequency, it removes the oxidation at bar edges caused by sparking and may forestall the development of serious bar burning. However, it does not destroy the desirable oxide or electrographitic surface film on which good brush performance is largely dependent. Maintenance departments which have adopted the use of the canvas wiper as regular practice have found commutator maintenance greatly reduced. Frequency of application depends on the tendency for surface deposit to accumulate. With moderate accumulation, daily application is recommended while more severe conditions may require application at shorter intervals. This has proved a very effective method of establishing and maintaining a good commutator surface with a minimum of major resurfacing operations.

Installation and Setting of Brushes

Users of electric equipment seldom have any choice in regard to the type of brush holders supplied on motors and generators but are not thereby relieved of the responsibility of keeping brush holders in good condition, free from any accumu-

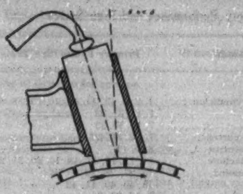

Figure 5. Brush held in trailing position

lation which might interfere with normal movement of the brushes, accurately located and firmly secured, and correctly adjusted in respect to spring pressure.

BRUSH ANGLE

The angle at which the brush is held against the commutator is a subject which might be discussed at great length. For the present, however, it is probably sufficient to make the following general recommendations. The radial position is usually preferred for reversing motors although there are numerous examples of successful operation with the brushes inclined at a substantial angle from the radial. For trailing operation, that is, with the commutator revolving toward the wider of the two angles at the brush face, as in Figure 5, an inclination of 15 degrees from the radial is representative of general practice. A certain amount of wedging action may be encountered when brushes having a relatively high coefficient of friction are operated at larger trailing angles. With leading operation, where the commutator revolves toward the acute angle at the brush face, as in Figure 6, an inclination of from 30 to $37^{1}/_{2}$ degrees is preferred. This insures a reactive force against the leading side of the brush holder which gives stability to the brush position. The critical angle for leading operation is in the neighborhood of 20 degrees. At this and smaller angles, disturbances to brush friction are liable to induce chattering of the brushes. In practice it is customary to bevel the top or free end of brushes operated at a leading angle, as indicated by dotted line in Figure 6, thus giving increased stability to the brush position.

STAGGERING

Most brushes now used have very mild abrasive properties, or none at all, so that the need for staggering the position of the brushes around the commutator to prevent the brushes wearing deep grooves no longer exists. However, the practice is continued for the sake of uniformity in commutator-surface appearance. A rule which should be observed when setting the brush holders in staggered relation is to make this arrangement in positive and negative pairs, as shown in Figure 7. A brush of one polarity should be followed, in the same path, by one of the opposite polarity. The next pair, in a circumferential direction, should then be shifted in an axial direction from the first pair. The character of the surface film developed under the positive brushes differs from that under the negative brushes, but when the brushes are staggered in pairs as described, no part of the commutator is contacted by brushes of one polarity more than by those of the other.

SYMMETRY

Lack of symmetry, either electrical or mechanical, results in inequalities of voltage between different pairs of brush-holder studs and may be the source of heavy circulating currents in the armature. Overheating of armature windings and more severe sparking on some brush studs than on others are operating faults often traceable to lack of electrical or mechanical symmetry. When such indications are noted, check the spacing of the brushes from toe to toe, the alignment of brushes on each stud with the commutator segments, the spacing of field poles, the length of air gaps, and the security of cross connections. Any inequalities found should be corrected.

SANDING FACES

New brushes, when first installed, should be carefully sanded to the contour of the commutator. A coarse grade of sandpaper is suitable for removing most of the carbon, but the final surface should be formed with paper of fine grain or with a brush-seating stone. The latter is a fine-grain free-wearing stone of special composition sold by various manufacturers of commutator-maintenance equipment. Sandpaper should be drawn only toward that side of the brush holder against which the brush rests when in operation and the brush should be lifted to return the sandpaper strip for succeeding strokes. This avoids forming a double face on the brush. The time required for facing in the brushes will be reduced by using considerably heavier pressure than that used in operation. Keep the sandpaper in contact with the commutator during the cutting stroke to prevent rounding the edges of the face.

SPRING PRESSURE

Careful attention should be given to the adjustment of spring pressure on the brushes. Many instances of faulty brush operation have been traced to improper or unequal spring tension. Unequal spring tension is a frequent source of selective action, the brushes with heavy tension tending to take a proportionately larger share of the load current than those with less. The resulting higher temperature at the faces of the brushes under heavy pressure lowers their contact drop and causes them to take a still heavier share of the load. It can readily be seen that this effect is cumulative and may result in excessive overloading of individual brushes. Pressure on all brushes on a machine should, therefore, be kept as nearly equal as the adjustment provided on the brush holders will permit. For any grade of brush and type of service there is a certain range of pressure within which best performance is obtained. At higher pressures friction losses and brush wear are increased, while at lower pressures the brushes are not kept in intimate contact with the commutator. Sparking, injury to the commutator surface, and rapid brush wear are likely to result from operating brushes at too low a pressure. One pound below the optimum range of pressure will usually result in more rapid brush wear than one pound above the optimum range. In other words, the disintegration of the brush face from electrical causes at low pressure is greater than the increased mechanical abrasion produced by pressure correspondingly higher than the normal range. That is why more brush complaints originate from low pressure than from high pressure. The relationship of brush pressure to rate of wear for a typical electrographitic grade is shown in Figure 8. Brush pressures are recommended by the manufacturer in terms of pounds per square inch. To determine this value, divide the pressure in pounds parallel to the length of the brush by its cross sectional area in square inches. As a rule no correction is made for the increased area of face resulting from a face bevel. Manufacturers' specific recommendations should be followed, but the following figures, in pounds per square inch, are indicative of representative practice.

Industrial service:	
Electrographitic grades	2–3
Carbon and carbon-graphite grades	$1^{3}/_{4}$–$2^{1}/_{2}$
Soft graphite grades	$1^{1}/_{2}$–2
Metal-graphite grades (slip rings)	$2^{1}/_{2}$–$3^{1}/_{2}$
Fractional-horsepower motors	4–5
Traction service	5–7

NEUTRAL POSITION

The fact is generally understood that brush position has a pronounced influence on commutation. On noninterpole machines the neutral position, that is, the

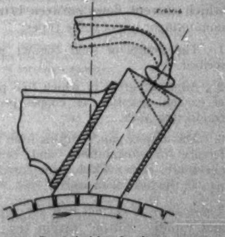

Figure 6. Brush held in leading position

position giving best commutation, shifts with the load. A permanent setting of brush position must, therefore, be a compromise between no-load and heavy-load conditions and can only be determined by a consideration of load characteristics. Interpole machines, on the other hand, have a fixed neutral point, theoretically unaffected by change in load. There is accordingly one best brush position for all load conditions. Time will not be taken for a discussion of the several methods in use for locating the neutral point on interpole machines. It should be mentioned however, that there is little latitude in neutral position on most machines of interpole design. If the brushes are shifted appreciably from the correct position a compounding effect from the interpole field flux is introduced.

Table I. Indications of Unsatisfactory Performance and Their Source

Indications	Immediate Causes	Primary Faults (See Table II)
Appearing at brushes		
Sparking	Commutator surface condition	1, 2, 3, 43, 44, 45, 46, 49, 58, 59
	Overcommutation	7, 12, 31, 33
	Undercommutation	7, 12, 30, 32
	Too rapid reversal of current	7, 12, 30, 32
	Faulty machine adjustment	8, 9, 11
	Mechanical fault in machine	14, 15, 16, 17, 18, 19, 20, 21, 22
	Electrical fault in machine	25, 27, 28, 29
	Bad load condition	38, 39, 40, 41, 42
	Poorly equalized parallel operation	7, 13, 23, 34
	Vibration	50, 51
	Chattering of brushes	See "Chattering or noisy brushes"
	Wrong brush grade	54, 56, 58
Etched or burned bands on brush face	Over commutation	7, 12, 31, 33
	Undercommutation	7, 12, 30, 32
	Too rapid reversal of current	7, 12, 30, 32
Pitting of brush face	Glowing	See "Glowing at brush face"
	Embedded copper	See "Copper in brush face"
Rapid brush wear	Commutator surface condition	See specific surface fault in evidence
	Severe sparking	See "Sparking"
	Imperfect contact with commutator	11, 14, 15, 16, 50, 51
	Wrong brush grade	53, 57
Glowing at brush face	Embedded copper	See "Copper in brush face"
	Faulty machine adjustment	7, 12
	Severe load condition	38, 39, 41, 42
	Bad service condition	46, 47
	Wrong brush grade	56, 60, 61
Copper in brush face	Commutator-surface condition	2, 3
	Bad service condition	43, 46, 47, 48, 49
	Wrong brush grade	58, 60
Flashover at brushes	Machine condition	14, 35
	Bad load condition	38, 39, 41, 52
	Lack of attention	5, 11
Chattering or noisy brushes	Commutator surface condition	See specific surface fault in evidence
	Looseness in machine	15, 16, 17
	Faulty machine adjustment	10, 11
	High friction	43, 45, 49, 51, 57, 58
	Wrong brush grade	54, 57, 58
Brush chipping or breakage	Commutator surface condition	See specific surface fault in evidence
	Looseness in machine	15, 16, 17
	Vibration	51
	Chattering	See "Chattering or noisy brushes"
	Sluggish brush movement	14

Nature of Brush Contact and Commutator Surface Film

It is now widely recognized that brush performance is influenced to a pronounced degree by the interface conditions between the brush and the commutator on which it bears. A great deal of study has been and is still being given to this subject. The commutator surface and the brush face, regardless of the high polish acquired, do not present to each other surfaces of exactly identical curvature or profile. The play of the brush in its holder and the yielding of supporting members under stress may give the brush face a slightly longer radius of curvature than the commutator. The effective area of contact for a particular brush at a given instant may represent, therefore, a relatively short span of the brush face in the direction of rotation. Furthermore, within this area, actual contact between brush and commutator is limited to a few points, or very small areas, carrying the load current at an extremely high current density. Rotation of the commutator, mechanical abrasion, and the disintegrating effects of the high localized current densities cause constant shifting of these areas of contact so that contact at any given point of either brush face or commutator is probably of extremely short duration, except for firmly embedded points which protrude to a substantial degree from the surrounding areas. The paths through which current flows between brush and commutator are of three types:

1. The points of solid contact just described.
2. Adjacent areas in which free particles of carbon, graphite, or copper provide a conducting path.
3. The minute gap, resulting from the difference in commutator and brush-face curvature, across which some current may pass in the form of an arc.

These areas of current flow are constantly and rapidly shifting within the boundaries of the brush face and in a very short space of time, possibly comparable to one full revolution of the commutator, current flow will have occurred through every portion of the brush face, giving it an appearance indicating complete and uniform contact.

Surface Film

Increased recognition is also being given to the influence of the commutator surface film on brush performance. Emphasis has been placed on the importance of this surface film by experiences encountered on military aircraft at altitudes of 25,000 feet and higher. Ordinary grades of brushes which perform in an entirely satisfactory manner at normal altitudes, wearing at a rate of one inch in several thousand hours, may wear out completely in the course of one flight at high altitude. This failure has been shown to be due to the failure of the commutator surface film under the atmospheric conditions existing thousands of feet above the earth's surface. This brings us to a consideration of the character of this surface film. It appears to be of complex structure, including in its make-up a thin layer of copper oxide on the surface of the commutator bars and a thin deposition of graphite over this oxide. On this solid layer of protective film an adsorbed layer of oxygen and water vapor is formed under normal atmospheric conditions. This adsorbed water vapor and oxygen film, although probably of submicroscopic thickness, provides boundary lubrication between the brush face and the graphite–copper-oxide film beneath. Wear of the latter film is thereby reduced and oxygen released by electrolysis of the water vapor tends to maintain the copper-oxide film. The graphite film, of course, is deposited by the brushes. At high altitude there is much less oxygen in the atmosphere and practically no water vapor, so that the boundary film disappears and the brushes come into such close contact with the commutator that atomic cohesive forces become effective. The protective graphitic and copper-oxide film is then quickly stripped off and rapid brush and commutator wear follow. A similar effect has been observed on the slip rings of rotary converters and on some commutating equipment during winter periods of extremely low humidity. Dusting and rapid brush wear has been stopped in such instances by humidifying the atmosphere of the substation or by adding some lubricating agent to the brush to take the place of the missing film of adsorbed water vapor. Such means of correction not being applicable to aircraft equipment,

Table I. Indications of Unsatisfactory Performance and Their Source (Continued)

Indications	Immediate Causes	Primary Faults (See Table II)
Appearing at commutator surface		
Rough or uneven surface		1, 2, 3, 4, 17
Dull or dirty surface		5, 44, 59
Eccentric surface		1, 19, 22, 51
High commutator bar		17
Low commutator bar	Sparking	2, 25
Streaking or threading of surface	Sparking	43, 44, 45, 46, 49, 58
	Copper or foreign material in brush face	2, 3, 46, 47, 48, 60
	Glowing	See "Glowing at brush face"
Bar etching or burning	Sparking	2, 3, 7, 12, 30, 31, 32, 33
	Flashover	5, 11, 14, 35, 38, 39, 41, 52
Bar marking at pole-pitch spacing	Sparking	25, 37
Bar marking at slot-pitch spacing	Sparking	7, 12, 30, 56, 59
Flat spot	Sparking	19, 23, 25, 41, 42, 52
	Flashover	5, 11, 14, 35, 38, 39, 41, 52
	Lack of attention	1, 5, 11
Discoloration of surface	High temperature	See "Heating—at commutator"
	Atmospheric condition	44, 46
	Wrong brush grade	59
Raw-copper surface	Embedded copper	See "Copper in brush face"
	Bad service condition	43, 45, 47, 49
	Wrong brush grade	58, 60
Rapid commutator wear with blackened surface	Burning	2, 3, 11, 14
	Severe sparking	See "Sparking"
Rapid commutator wear with bright surface	Foreign material in brush face	43, 45, 47, 40
	Wrong brush grade	60
Appearing as heating		
Heating in windings	Severe load condition	38, 41, 42, 52
	Unbalanced magnetic field	18, 19, 20, 21, 27, 28, 29
	Unbalanced armature currents	8, 19, 22, 25, 27, 28, 29, 37
	Poorly equalized parallel operation	7, 13, 23, 34
	Lack of ventilation	6
Heating at commutator	Severe load condition	38, 41, 42
	Severe sparking	7, 8, 9, 12, 20, 33, 45, 56
	High friction	10, 11, 36, 43, 45, 49, 57, 58
	Poor commutator surface	See specific surface fault in evidence
	Depreciation	24
	High contact resistance	55
Heating at brushes	Severe load condition	38, 41, 42
	Faulty machine adjustment	7, 10, 11, 12, 26
	Severe sparking	See "Sparking"
	Raw streaks on commutator surface	See "Streaking or threading of surface"
	Embedded copper	See "Copper in brush face"
	Wrong brush grade	56, 57, 58, 60, 61

Table II. Primary Sources of Unsatisfactory Brush Performance

Preparation and care of machine

1. Poor preparation of commutator surface.
2. High mica.
3. Feather-edge mica.
4. Bar edges not chamfered after undercutting.
5. Need for periodic cleaning.
6. Clogged ventilating ducts.

Machine adjustment

7. Brushes in wrong position.
8. Unequal brush spacing.
9. Poor alignment of brush holders.
10. Incorrect brush angle.
11. Incorrect spring tension.
12. Interpoles improperly adjusted.
13. Series field improperly adjusted.

Mechanical fault in machine

14. Brushes tight in holders.
15. Brushes too loose in holders.
16. Brush holders loose at mounting.
17. Commutator loose.
18. Loose pole pieces or pole-face shoes.
19. Loose or worn bearings.
20. Unequal air gaps.
21. Unequal pole spacing.
22. Dynamic unbalance.
23. Variable angular velocity.
24. Commutator too small.

Electrical fault in machine

25. Open or high-resistance connection at commutator.
26. Poor connection at shunt terminal.
27. Short circuit in field or armature winding.
28. Ground in field or armature winding.
29. Reversed polarity on main pole or interpole.

Machine design

30. Commutating zone too narrow.
31. Commutating zone too wide.
32. Brushes too thin.
33. Brushes too thick
34. Magnetic saturation of interpoles.
35. High bar-to-bar voltage.
36. High ratio of brush contact to commutator surface area.
37. Insufficient cross connection of armature coils.

Load or service condition

38. Overload.
39. Rapid change of load.
40. Reversing operation of noninterpole machine.
41. Plugging.
42. Dynamic braking.
43. Low average current density in brushes.
44. Contaminated atmosphere.
45. "Contact poisons."
46. Oil on commutator or oil mist in air.
47. Abrasive dust in air.
48. Humidity too high.
49. Humidity too low.

Disturbing external condition

50. Loose or unstable foundation.
51. External source of vibration.
52. External short circuit or very heavy load surge.

Wrong brush grade

53. "Commutation factor" too high.
54. "Commutation factor" too low.
55. Contact drop of brushes too high.
56. Contact drop of brushes too low.
57. Coefficient of friction too high.
58. Lack of film forming properties in brush.
59. Lack of polishing action in brush.
60. Brushes too abrasive.
61. Lack of carrying capacity.

---

special grades of brushes have been developed containing an ingredient which produces and maintains a protective film on the commutator or ring surface under the adverse atmospheric conditions of extreme altitudes. It is too early to say to what extent these or similar grades will find application under normal altitude conditions, but investigations are being conducted along this line on various types of power, traction, and industrial equipment.

The thin layer of copper oxide normally developed on the commutator surface is very beneficial to brush performance, aiding commutation and reducing brush friction. Certain forms of atmospheric contamination, particularly those of a reducing character, tend to destroy the oxide film and interfere with good operation. These contaminants injurious to the commutator surface have been termed "contact poisons." Some of the most active materials of this type are carbon tetrachloride, alcohol, acetone, turpentine, chlorine, smoke, acid, and other corrosive fumes.

Electrographitic Surface Film

Electrographitic brushes possess, to greater or less degree, the property of depositing an electrographitic surface film on the commutator which is a highly effective aid to good brush performance. It not only has its own inherent value in reducing friction and maintaining intimacy of contact between brushes and commutator, but it also provides protection to the underlying layer of oxide on the commutator surface which apparently is a factor in the maintenance of normal contact drop and commutation. To some extent this deposition occurs through the graphite of the brush being rubbed into the minute crevices of the commutator surface. There is evidence, however, that a substantial portion of this deposition results from electrolytic action and is influenced both by the characteristics of the brush and by the current density in the brush faces. A series of brush grades commercially available provides a good illustration of this point. The regular grades of this series have normal film-forming properties. They will develop and maintain a good electrographitic surface film under average load conditions on heavy-duty power equipment.

However, on applications where the average load is under 40 amperes per square inch, film may not be deposited as rapidly as it is being worn away. Spots and streaks of raw copper sometimes appear on the commutator surface, often followed by the deposition of copper particles in the brush faces and serious threading or grooving of the commutator. The rate of film deposition is doubtless a function of the combined load and short-circuit currents at the brush face since it has been observed that a machine on which the brushes are slightly off neutral may maintain a good electrographitic surface film at a lower load-current density than a similar machine in perfect adjustment. In general, 40 amperes per square inch may be considered the minimum safe current density for the regular grades of this series. The foregoing figure assumes a clean atmosphere, free from oil vapor or contaminating gases which tend to produce a film or deposit on the commutator surface. In the presence of such contamination these grades may be able to maintain the surface film at an average current density as low as 30 amperes per square inch.

A corresponding series of grades with increased film forming properties has been developed for applications where the average load current density is consistently under 40 amperes per square inch. These brushes will maintain a good surface film at current densities as low as 30 amperes in a clean atmosphere or 20 amperes where oil vapor or other atmospheric contamination tends to accelerate film formation.

In the presence of some types of contaminating atmosphere or excessive oil vapor, a surface film of such high resistance may develop that brush performance is impaired rather than improved. For such conditions there is a third group of grades which have a mild polishing action. These grades tend to remove excess film deposition and have also proved advantageous in overcoming a moderate tendency toward edge burning or marking of the commutator bars from over oxidation, such as that produced by very high current peaks in the commutation cycle. The minimum safe current density for grades of this class is usually about 50 amperes per square inch under clean atmospheric conditions or 40 amperes in the presence of a contaminated atmosphere.

INTIMACY OF CONTACT

The trend of design toward higher angular velocities and higher surface speeds for commutators and slip rings has given prominence to the importance of intimate contact being maintained between the brush and the moving surface. Interruption of contact resulting from very slight irregularities of the commutator or ring surface may be sufficient to cause sparking and injury to the surface. Such a condition tends to become cumulative and may interfere seriously with machine performance. The nature of the surface film on a commutator, atmospheric conditions, frictional properties of the brushes, brush pressure, and angle of inclination all have an influence on the intimacy of contact at the brush face. Another factor, possibly more important than any of the foregoing, is related to the elastic property of the brush. This property is subject to accurate quantitative determination and, because of its direct influence on commutating performance, has been termed the "commutation factor." The commutation factor is an index of the capacity of the brush to absorb the shocks resulting from slight irregularities on the revolving surface. Experience with applications under widely varied conditions of service has demonstrated the importance of this property in respect to brush operation. By selecting a brush of suitable commutation factor, intimate contact between brushes and commutator can be maintained, with good commutation and quiet operation, in the face of disturbing conditions that could not readily be overcome in any other manner.

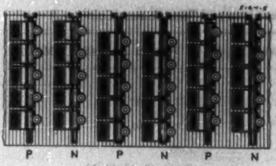

Figure 7. Correct method of staggering brushes

P—Positive N—Negative

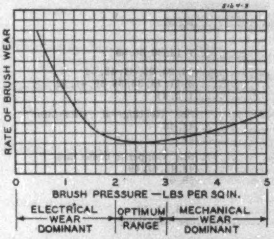

Figure 8. Relationship between brush pressure and rate of brush wear for typical electrographitic grade

Correction of Unsatisfactory Performance

Maintenance of good brush performance is facilitated by seeking the primary source of trouble as soon as the first indication of unsatisfactory operation is observed. Immediate correction of the primary fault will avoid interruption of service and the necessity for more expensive repairs at a later date. There are numerous indications of unsatisfactory performance and a great many primary faults from which they may result. Most of these primary sources of poor performance can be grouped under the following headings:

1. Poor preparation and care of the machine.
2. Faulty machine adjustment.
3. Mechanical fault in machine.
4. Electrical fault in machine.
5. Machine design.
6. Load or service conditions.
7. Disturbing external conditions.
8. Wrong brush grade.

The problem of determining the primary source of trouble in a specific case can be simplified to some extent by a systematic analysis of symptoms. A plan for making such an analysis, together with lists of the more common indications of unsatisfactory performance and the primary faults from which they may result, is given in the appendix to this paper.

Summary

It is difficult to say what is the most important characteristic of a carbon brush. The property which makes a brush grade the ideal selection for one application may be of secondary importance on another. For heavy duty service it seems preferable that those characteristics which aid or permit the maintenance of a uniform surface film on the commutator should be given first consideration. Particular attention should be given to the ability of the brush to maintain close contact with the commutator or ring surface. In addition to care in the selection of brush grade, equal attention should be given to the initial preparation of the commutator or ring surface, avoidance of high or feather-edge mica, accurate machine adjustment, careful brush installation, maintenance of correct and uniform spring pressure, and periodic use of the canvas wiper. Such routine care costs little but aids greatly in maintaining good brush performance at minimum expense. Finally, at the first indication of unsatisfactory performance, an effort should be made to determine the primary fault and to correct it in time to prevent serious disturbance of operation.

Appendix

The accompanying tables have been prepared as a guide to systematic analysis of unsatisfactory brush performance with a view to determining the primary fault.

Phase-Comparison Carrier-Current Relaying

A. J. McCONNELL
ASSOCIATE AIEE

T. A. CRAMER
ASSOCIATE AIEE

H. T. SEELEY
ASSOCIATE AIEE

DIFFERENTIAL PROTECTION is recognized as the ideal means of quickly isolating faulty electric equipment. The carrier-current relaying system described herein is a differential system comparing the phase angles, via a carrier-current channel, of the currents entering and leaving a transmission-line section, and is known as phase-comparison carrier-current relaying.

Functional Summary of Relay System

The equipment operates when fault currents are above predetermined limits, and simultaneously energizes the trip coils of the circuit breakers at both ends of a faulty line section when the fault-current magnitudes are large enough at both terminals. On all unbalanced faults, that is, other than three-phase faults, the sensitivity is such that operation is obtained with fault currents of less than full-load magnitude. For three-phase faults, the current magnitude for operation must be greater than full load. Since the system operates in response to current alone, no potential supply is necessary.

On all unbalanced faults, the carrier-current blocking signal is sent automatically, that is, independently of the operation of the contacts of any mechanical relay.

The relay operating time is, on the average, less than 2.5 cycles, and sensitivity is obtained with unusually low burden.

Only one carrier-current frequency is required and the channel is available, except during faults, for other uses such as telemetering and supervisory control. The equipment can be used on a two-frequency duplex channel if other services make such an arrangement desirable.

Carrier-Current Channel Requirement

The ideal relaying system should require only one carrier frequency in order to conserve channel space. This eliminates any system requiring simultaneous transmission from the two terminals. Comparison of more than one quantity requires either tone modulation for each quantity or a separate carrier frequency for each quantity, either of which exceeds the single-channel goal. Consequently, a single quantity is derived from the phase currents and this single quantity is used in such a way that transmission in both directions over one carrier-current channel is possible.

The means of accomplishing two-way transmission over a single carrier-current channel and the method of obtaining a single quantity for comparison are discussed hereinafter.

Fundamental Operating Principle

Fundamentally, the operating principle of this equipment is exactly the same as the first carrier-current relaying system,[1] but in the present application, the use of modern methods has eliminated the limitations of certain components of the earlier equipment. Since the fundamental principle has been explained before,[1,2] it should suffice here to review the explanation only briefly.

At each line terminal, the local single quantity derived from the polyphase currents has two functions, namely:

1. During one half cycle it causes a blocking signal to be transmitted, via the carrier-current channel, to the remote line terminal.
2. During the alternate half cycle, it causes tripping if no blocking signal is received from the remote terminal.

Since blocking requires that a signal must be received from the remote terminal in the half cycle assigned to tripping at the local terminal, the two terminals must alternate in transmitting blocking impulses during successive half cycles. The current transformers are connected so that this action occurs on external faults.

During internal faults, there is a relative current reversal of approximately 180 degrees and the two line terminals transmit blocking signals during one half cycle, leaving both terminals free to trip during the other half cycle. Since lack of a signal from the remote terminal permits tripping, tripping at one terminal (but not at both terminals) is obtained for an internal fault fed from that end only.

Derivation of Single Quantity for Comparison

In order to determine the best method of combining the three individual phase currents into a single quantity for comparison, it is helpful to examine the currents present during each type of fault in terms of symmetrical components as follows:

Single-phase-to-ground fault	I_1..I_2..I_0
Two-phase-to-ground fault	I_1..I_2..I_0
Phase-to-phase fault	I_1..I_2
Three-phase fault	I_1
Normal load current (no fault)	I_1

POSITIVE-PHASE-SEQUENCE CURRENT

Since positive-phase-sequence current (I_1) is present during all types of faults, it immediately appears to be the logical choice for the single quantity for comparison. However, except during three-phase faults, the use of I_1 has serious objections. These are the following:

1. While I_1 is present on all types of faults, it is also present during normal load conditions. Thus, a fault can be recognized only if the magnitude of I_1 is greater than full-load current. For different types of faults at the same location, the magnitude of I_1 varies, being a maximum on three-phase faults and a minimum on single-phase-to-ground faults. Hence, if the three-phase short-circuit current is just sufficient for pickup, operation would not be obtained on any unbalanced fault. As an example, on a phase-to-phase fault, I_1 is approximately one half of its value during a three-phase fault at the same location (Appendix I).

Paper 45-148, recommended by the AIEE committee on protective devices for publication in AIEE TRANSACTIONS. Manuscript submitted June 21, 1945; made available for printing July 27, 1945.

A. J. McCONNELL and T. A. CRAMER are in the central station engineering divisions of the General Electric Company, Schenectady, N. Y. H. T. SEELEY is relay application engineer in the switchgear engineering department of the company in Philadelphia, Pa.

In Table I are listed some of the more common indications of unsatisfactory performance together with the immediate cause and primary faults from which these conditions most frequently arise. The primary faults are indicated in Table I by numbers which refer to corresponding items in Table II.

There may be several primary faults from which the same indication of unsatisfactory performance can result. This is one reason it is often very difficult to determine the exact cause of poor brush operation. On the other hand, there is usually more than one indication of a faulty condition. If the primary faults usually responsible for each of these indications are noted, and those selected which are common to all observed indications, the number of probable sources of trouble will be considerably reduced and isolation of the existing fault thereby simplified.

It is not practicable to include in these tables all indications of unsatisfactory brush performance nor all primary sources of trouble. These lists are representative of the difficulties more commonly encountered and, supplemented by other items from the experience of the observer, offer a systematic plan for diagnosing faulty brush performance and determining what corrective measures should be applied.

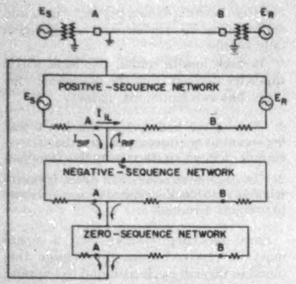

Figure 1. Symmetrical-component currents during a single-phase-to-ground fault

This means that three-phase fault current must be twice the pickup value in order to obtain sufficient I_1 for operation on a phase-to-phase fault.

2. The I_1 component is influenced by load conditions for all types of internal faults except three-phase faults. This is illustrated in Figure 1 for an internal single-phase-to-ground fault and in Appendix I, equations 7 and 8, for a phase-to-phase fault. In the positive-phase-sequence network, there are two components of each line-terminal current, a fault component which enters the faulted line at each terminal, and a through-current component. The through-current component may adversely affect the relaying system in two ways:

1. Decrease the I_1 sensitivity.
2. Cause incorrect blocking.

To summarize, the use of I_1, necessarily operating only above the maximum load value, does not provide the desired sensitivity for faults involving only one or two phases.

NEGATIVE-PHASE-SEQUENCE CURRENT

Since negative-phase-sequence current (I_2) is present during all except three-phase faults, its use should be considered; two of its advantages being the following:

1. Under balanced load conditions there is no I_2 component, and on most transmission lines the load normally will be practically balanced.
2. The I_2 component under fault conditions is substantially unaffected by load conditions (Figure 1 and Appendix I, equations 9 and 10).

These advantages show that the use of I_2 would permit attainment of the desired sensitivity on phase-to-phase faults, and perhaps on ground faults as well, without interference from load current.

ZERO-PHASE-SEQUENCE CURRENT

The presence of zero-phase-sequence current is, of course, the best evidence of a ground fault. For ground faults, I_0 has the same advantages as I_2, that is, the desired sensitivity can be obtained without interference from load current.

Phase-Sequence Currents Used in This Equipment

Since the use of negative-phase-sequence current appears desirable for all types of faults except the three-phase fault, this equipment uses a negative-phase-sequence network with provision for developing a network output on three-phase faults. This provision consists of three phase-overcurrent relays, operation of all three shifting the network so as to introduce a positive-phase-sequence component into the network output. Thus, the equipment functions on three-phase faults at a current magnitude above full load, but for unbalanced faults, phase currents of less than full-load magnitude will cause operation.

Any relaying system for the general application must provide high sensitivity during ground-fault conditions. Because of possible unbalanced load, it is not considered practical to attempt to attain the necessary high sensitivity by means of the use of negative-phase-sequence current alone. For that reason, it is possible to use zero-phase-sequence current should the available minimum negative-phase-sequence current be too low to assure relay operation. Since the phase-to-phase fault still requires the use of negative-phase-sequence current, a combination of negative-phase-sequence and zero-phase-sequence currents is then used for unbalanced faults, the network output being of the form $(I_2 + KI_0)$.

When two different phase-sequence components are added without taking account of their relative magnitudes, it may be possible to obtain an internal ground-fault condition wherein one of the phase-sequence quantities has control at one terminal with the other phase-sequence quantity having control at the other terminal. Such a condition might easily result in a "blind spot" (failure to trip at any terminal).

Therefore, when zero-phase-sequence current is used, it is essential that the zero-phase-sequence current outweigh (by adjustment of K) the negative-phase-sequence current at both terminals under all internal-ground-fault conditions. The determination of the value of K should be as simple as possible, and here again there is a further advantage in the use of negative-phase-sequence current. Since the flow of negative-phase-sequence current is practically independent of load current, the determination that the system is free of blind spots is relatively simple. This is discussed more fully in Appendix VII.

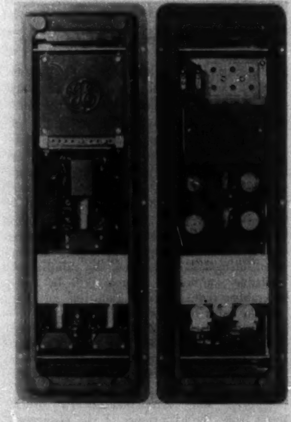

Figure 2. Network unit (left) and tripping unit (right) in draw-out cases for semiflush mounting

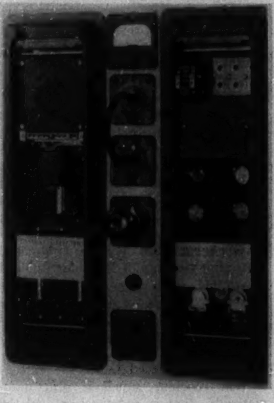

Figure 3. Network and tripping units mounted with a-c and d-c test equipment on a panel section

Description of Relaying Equipment

The physical embodiment of the operating principles developed and outlined in the foregoing is shown in Figure 2 which illustrates all the relay elements mounted in drawout cases for convenience in adjustment and maintenance. Figure 3 shows these cases assembled with test equipment on a panel. The relations of the various elements are shown in the block diagram, Figure 4, and Figure 5 is a simplified elementary diagram of the circuit.

All of the tubes are type *25B6G* like those used in the associated carrier-current transmitter–receiver. All of the auxiliary relays except the seal-in relay are of the telephone type, operating at their normal contact pressures, thus insuring reliability proved by long experience.

Phase-Sequence Network

With reference to Figures 2 and 5, the network is housed in the left-hand case, and consists of transformers *T*1 and *T*2, resistors *R*1, *R*2, and *R*3, and capacitor *C*1. *T*1 and *T*2 are fed from phases *a* and *c*, respectively, and *R*3 and *C*1 provide a 60-degree phase shift of the output of *T*1 so that, with balanced load, the voltage across *C*1 is in phase with the output of *T*2, which is then adjusted to equal magnitude by *R*2 so that the vector difference is zero. Zero-phase-sequence current is neutralized by ground-current windings, one of which has taps for adjustment of *K*. Equation 18, Appendix II, shows that the output of such a network is proportional to negative-sequence and zero-sequence currents only, and independent of positive-sequence current. On a phase-to-phase fault, such a network gives the same magnitude of output voltage regardless of which pair of phases is involved.

In order to provide for a three-phase fault, overcurrent relays in the three phases (*O*, Figure 5) are so connected that if all three pick up, they change the setting of *R*1 so as to unbalance the network and thus introduce a positive-sequence component into the output (equation 18*a*, Appendix II).

Amplifier

The amplifier allows the use of a low-burden network by permitting it to operate into a high impedance, and provides energy to drive the carrier-current transmitter as explained later. Also, the amplifier output controls the fault detector and provides the comparer with a local voltage for comparison with the incoming carrier-current signal. These elements are described in the following sections.

The amplifier consists of two tubes operating in push-pull through an output transformer which provides a match with the load resistance consisting principally of the transmitter screen grids.

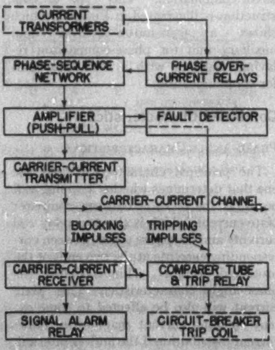

Figure 4. Block diagram showing relations between elements of the protective system

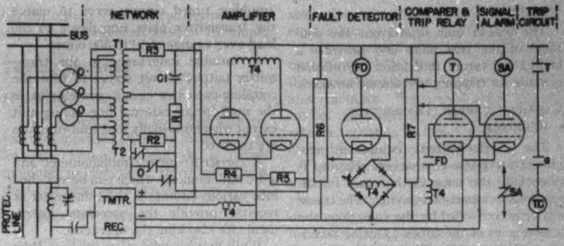

Figure 5. Schematic elementary diagram of the protective system

C—Capacitor
FD—Fault detector
O—Phase overcurrent relay
R—Resistor
REC.—Carrier-current receiver
SA—Signal-alarm relay
T—Trip relay
TC—Circuit-breaker trip coil
*T*1, *T*2, *T*4—Transformers
TMTR.—Carrier-current transmitter

Fault Detector

The fault detector is controlled by the amplifier, rather than by the network output directly, in order to take advantage of its voltage amplification.

This element is necessary to insure (on an external fault) that the network output is sufficient to drive the transmitter and produce an adequate blocking signal at the remote terminal, before permitting any attempt to trip. If the same carrier channel is used for communication, the fault detector also serves to transfer control of the channel temporarily from communication to relaying for the duration of a fault.

The fault detector, Figure 5, consists of a voltage-divider resistor, a full-wave rectifier, a tube, and an auxiliary relay for its plate circuit. The rectifier is supplied from a separate winding on the amplifier output transformer. The use of a fault-detector tube permits compensation, by proper biasing, for the reduction of amplifier output voltage with d-c supply voltage, thus providing a fault-detector pickup which is substantially constant over an adequate range of d-c supply voltage.

Comparer and Trip Relay

All of the elements described in the foregoing, together with the carrier-current transmitter and receiver, are subsidiary to the comparer. They gather and deliver to the comparer the information necessary to determine the fault location. The comparer makes the decision in accordance with the previous discussion under "Fundamental Operating Principle."

The comparer consists of a tube, a voltage-divider resistor to adjust its plate voltage, and the trip relay in its plate circuit. The tube is mounted on the relay auxiliary unit in the carrier cabinet to minimize the pickup in the lead from the carrier receiver to the comparer control grid. The other elements are mounted in the tripping relay case, Figure 2.

A winding of the amplifier output transformer *T*4, Figure 5, energizes the screen grid of the comparer tube, positive relative to the cathode, during one half cycle, and negative during the other half cycle. During the positive half cycle, the comparer tube will conduct and cause the trip relay to operate if no incoming carrier-current signal is received during that half cycle. On the other hand, reception of a carrier-current signal during that half cycle causes a negative voltage (rectified carrier signal) to be applied to the control grid, thereby blocking tube conduction, and consequently, operation of the trip relay. Figure 6 shows oscillograms of the carrier-frequency voltage during internal and external faults, and the d-c blocking impulses on the comparer control grid during an external fault.

Signal Alarm

The signal alarm provides a means for calling a person to the carrier telephone (simplex) and for indicating the failure of the d-c supply or opening of the heater of any tube (since all five heaters are in series).

This element consists of a tube, a voltage-divider resistor to adjust its screen-grid voltage, and an auxiliary relay in the plate circuit. The tube is mounted in the carrier cabinet with the comparer tube to minimize pickup, the other elements being mounted in the tripping relay case, Figure 2.

The screen-grid voltage is adjusted so that the signal-alarm tube normally carries enough current to pick up the signal-alarm relay. When carrier current is received, the same negative voltage that served as blocking voltage in the comparer is applied to the control grid, reducing the signal-alarm plate current, thereby causing the auxiliary relay to drop out and close the external alarm circuit.

Seal-in Unit

The seal-in unit shunts out the contacts of the trip relay and provides a hand-reset target indication. Provision is made for tripping two circuit breakers.

Carrier-Current Transmitter-Receiver

The carrier-current equipment employed for phase-comparison relaying is essentially the same as that used for directional-comparison relaying. The transmitter is controlled by the voltage on the screen grids of the tubes. During standby conditions, this voltage is zero and no carrier is transmitted.

When the 60-cycle excitation voltage from the network amplifier is applied to the screen-grid circuit, the transmitter sends a signal on the positive half cycle and is definitely blocked during the negative half cycle of the excitation wave. The transmitter cannot lock in and transmit continuously.

The carrier-current receiver rectifies and filters the incoming carrier wave and thus provides a pulsating d-c blocking voltage which is applied to the control grid of the comparer tube. A twin-diode tube is used in the receiver; one of the diodes is used for the relaying function while the other is used to drive an audio amplifier for telephone or other services employing audio modulation. These diodes operate on opposite half waves of the carrier-frequency cycle to obtain a balanced load on the receiver circuit and to reduce interaction between the two circuits.

The transmitter consists of a single-tube master oscillator driving a four-tube power amplifier. The operating frequency range is 50 to 150 kilocycles, and the temperature stability is better than 0.005 per cent per degree centigrade. Variable permeability tuning is used in all tuned circuits. Taps on the power-amplifier tuned circuit serve to match the transmitter plate impedance to the load over a range of 50 to 500 ohms.

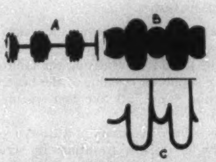

Figure 6. Oscillograms of voltages

A—At terminals of carrier-current set during internal fault. Ripples are due to heterodyne between simultaneous signals of local and remote transmitters. (Length of trace—three cycles at 60 cycles per second)

B—At terminals of carrier-current set, during external fault. Large amplitude is local signal; small amplitude, remote signal

C—At control grid of comparer tube, during external fault, 2.5×pickup current. This pulsating d-c blocking signal results from rectification of the carrier-frequency voltage of B. Zero axis added at top

A variable inductance in the transmitter output circuit serves to tune the coupling-capacitor circuit and eliminates the need for an external line-tuning unit except where unusually long lead-in cables are required.

A carrier-frequency milliammeter and a d-c milliammeter which can be switched into various circuits in the transmitter or receiver provide the necessary instruments for checking the operation.

While many carrier relay sets have been installed outdoors, the present trend is for indoor installation. The connection between the carrier set and the coupling capacitor is made with low-loss concentric cable which may be run in ordinary conduits or ducts, or buried in the ground.

Other Functions

Like other carrier relaying installations where the carrier is controlled by a fault detector, the carrier channel is available for other functions such as telephone, remote control, telemeter readings, and supervisory control. The operation of the fault detector cuts off the auxiliary services and gives the relaying function full use of the carrier channel during a fault.

Construction

The carrier-current equipment is built on chassis units having standardized unit dimensions. Many standard units, such as audio oscillators, modulators, and receivers, are available to make up any desired combination. This type of construction is illustrated in Figure 7 which shows a transmitter–receiver and auxiliary unit for phase-comparison relaying, together with a modulator unit for communication.

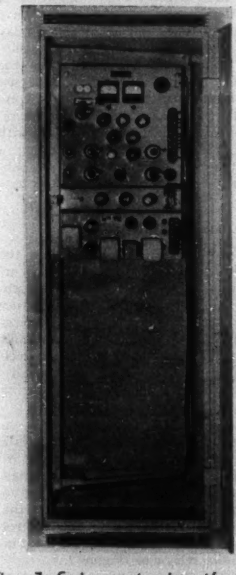

Figure 7. Carrier-current equipment for phase-comparison relaying

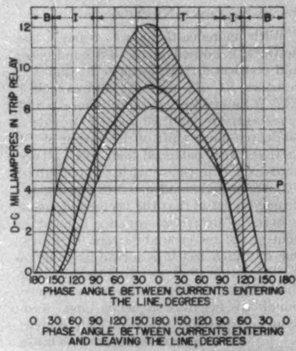

Figure 8. Phase-angle characteristic of one of a pair of production units

Heavy line is for:
1.5×pickup current
ten-decibel line loss
129 volts direct current at each station
Shaded band covers the range from
1.5×pickup current in each terminal
five-decibel line loss
110 volts direct current
to
20×pickup current in each terminal
15-decibel line loss
140 volts direct current

B—Blocking zone
I—Indeterminate zone, where tripping depends on the afore-mentioned variables
P—Range of pickup of tripping relay
T—Tripping zone
(On external faults, the through current is at the same phase angle so that only a narrow band is required for blocking)

Combined Characteristics

Phase-Angle Characteristic

The principal characteristic, and the one that determines whether tripping will occur, is the relation between comparer plate current (which is also trip-relay coil current) and the phase angle between corresponding currents at the two ends of the protected section This is called the phase-angle characteristic. This plate current will also be affected to some extent by fault-current magnitude, fault-current distribution if the fault is internal, carrier-frequency line losses, d-c source voltage at the local terminal, and d-c source voltage at the remote terminal.

This phase-angle characteristic indicates the margin available for blocking on an external fault, and for tripping on an internal fault. Since no single value of fault current or line losses can be considered as normal, the choice of standard conditions is arbitrary; these have been chosen as 1.5 times fault-detector pickup, ten-decibel line loss, and 129 volts, direct current. The solid line of Figure 8 is typical of the average comparer plate (trip relay) current of one unit as a function of phase displacement between the two terminals. This curve is for normal conditions of control voltage, line loss, and fault-current magnitude. The shaded area shows the cumulative effect, on that characteristic, of the most adverse combination of all variables.

Figure 9 shows separately the effects of each variable on the phase angle at which tripping occurs, with all the other variables at standard value.

Fault-Detector Pickup

Figure 10 shows the dependence of fault-detector pickup and drop-out on d-c source voltage.

Operating Time

Figure 11 shows the dependence of operating time on current magnitude. These are typical values, not necessarily maximum for any unit.

Burden

The maximum burden on any one current transformer for any fault not involving ground is 0.2 ohm. The maximum burden on any current transformer for a single-phase-to-ground fault is 1.1 ohms.

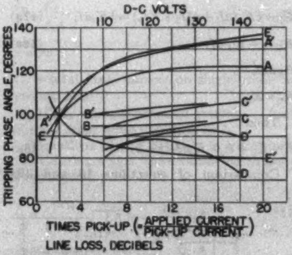

Figure 9. Variations in tripping phase angle due to changing one variable at a time

A to *E* are with one terminal leading, and *A'* to *E'* are with the other terminal leading

A, *A'*—Equal current in both terminals, 1.1 to 20×pickup current

B, *B'*—Line loss, 5 to 15 decibels

C, *C'*—D-c control voltage at local station 110 to 140 volts direct current

D, *D'*—D-c control voltage at local station dropped to 100 volts for two seconds after being at 110 to 140 volts for two minutes

E, *E'*—Current at local station 1.5×pickup, current at remote station 1.1 to 20×pickup

Testing Facilities

D-C Test Equipment

The tripping unit is provided with six jacks for measuring the five plate currents and the heater current, on a panel-mounted milliammeter provided with a cord and plug, as shown in Figure 3.

A-C Test Equipment

A five-position switch (shown in Figure 3) and an artificial-load resistor are provided to cut the relays out of service and make an over-all check of both pairs of relays and the carrier apparatus. If the switches are turned in like directions, the test currents applied to the relays simulate an internal fault, and the tripping impulse which should result lights a lamp but is blocked from the trip coil by a switch contact. If the switches are turned in opposite directions, the test currents simulate an external fault, and failure to again light the indicating lamp proves successful blocking. The test current is purposely chosen about ten per cent above the pickup value, and failure to trip or to block at this current indicates that maintenance is required.

Application

Since the equipment described here is based upon current magnitude, it is essential that currents in excess of the relay pickup (with a margin) be available. If simultaneous operation is required, pickup current must be present at each terminal upon the inception of the fault. On the other hand, sequential tripping can be obtained with initial current below pickup at one terminal, if the redistribution of current, upon the operation of the first circuit breaker, is such as to provide pickup current for operation of the second relay.

The amount of margin of calculated fault current above pickup is a matter of personal opinion. However, it is believed that a margin of 50 per cent above pickup is acceptable. This margin can reasonably be reduced at one terminal if a margin of 50 per cent above pickup is available after the other terminal circuit breaker has opened.

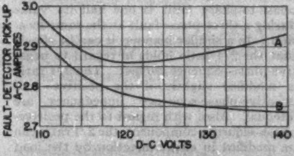

Figure 10. Fault-detector pickup

A—At 110 to 140 volts direct current

B—After operating at 100 volts for two seconds preceded by operation at 110 to 140 volts

It is conservative to assume that the currents which actuate the relay will be those corresponding to transient generator reactance. Since most short-circuit studies are based upon subtransient reactance, currents so based should be decreased by an estimated factor.

The application of any relaying system usually passes through two distinct phases. First, it is necessary to determine, with minimum effort, that a particular system is applicable in a given situation. Later, the application is studied in greater detail to determine the actual settings, operating margins, and other items.

Regarding the relaying system described herein, the first phase, the determination of its applicability, is discussed in the following section. The second phase is outlined in Appendix VII.

Three-Phase Faults

In order for the equipment to trip for an internal three-phase fault, the secondary current must be above the three-phase pickup of the relay, eight amperes.

Ground Faults (Using Negative-Phase-Sequence Current Only)

For ground-fault operation, sufficient negative-phase-sequence current will be available if the total current in the fault is approximately the same for three-phase and single-phase-to-ground faults. More precisely, negative-phase-sequence current alone may be used if the ratio of the *total* three-phase fault current to the *total* single-phase-to-ground fault current ($I_{3\phi}'/I_G'$) is between 0.8 and 1.5 for an internal fault at either terminal (Appendix IV).

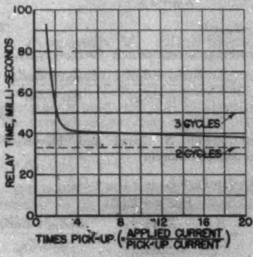

Figure 11. Operating time

Ground Faults (Using Zero-Phase-Sequence Current)

If the ratio ($I_{3\phi}'/I_G'$) is outside of the limits 0.8–1.5, it may be necessary to add ground-current excitation. For zero-phase-sequence excitation to predominate, one of the following conditions must be met:

If $(I_{3\phi}'/I_G')$ is less than 1, then C_1/C_0 must be less than 8.5 (equation 45, Appendix V). If $(I_{3\phi}'/I_G')$ is greater than 1, then

$$\frac{C_1}{C_0}\left[3\,\frac{(I_{3\phi}')}{(I_G')}-2\right]$$

must be less than 8.5 (equation 46, Appendix V), where

$C_1=I_{3\phi}/I_{3\phi}'$
$C_0=I_G/I_G'$
$I_{3\phi}$ = portion of $I_{3\phi}'$ at terminal in question
I_G = portion of I_G' at terminal in question

In order for the equipment to trip for internal ground faults when ground-current excitation is used, the secondary ground current must be above the following:

Single-end feed—0.5 ampere*
Double-end feed—1.65 amperes (maximum)*

Appendix I. Effect of Load Current

To determine the effect of load current on positive-phase-sequence and negative-phase-sequence currents during a phase-to-phase fault and to determine the relative magnitudes of those currents during three-phase and phase-to-phase faults, refer to Figure 12 and assume that the positive-phase-sequence and negative-phase-sequence impedances are equal.**

Before fault (before closing switch S)

$$I_{S1}=-I_{R1}=\frac{E_S-E_R}{Z_{S1}+Z_{R1}} \tag{1}$$

$$I_{S2}=I_{R2}=0 \tag{2}$$

E = voltage across switch $S=E_S-I_{S1}Z_{S1}$

$$=E_S-\frac{E_SZ_{S1}-E_RZ_{S1}}{Z_{S1}+Z_{R1}}=\frac{E_SZ_{R1}+E_RZ_{S1}}{Z_{S1}+Z_{R1}} \tag{3}$$

With switch S closed and $E_S=E_R=0$ (Thévenin's theorem)

$$I_1=-I_2=I_{S1}+I_{R1}=-(I_{S2}+I_{R2})$$

$$=\frac{E}{2Z_1}=\frac{\dfrac{E_SZ_{R1}+E_RZ_{S1}}{Z_{S1}+Z_{R1}}}{\dfrac{2Z_{S1}Z_{R1}}{Z_{S1}+Z_{R1}}}=\frac{E_SZ_{R1}+E_RZ_{S1}}{2Z_{S1}Z_{R1}}$$

$$=\frac{E_S}{2Z_{S1}}+\frac{E_R}{2Z_{R1}} \tag{4}$$

$$I_{S1}=-I_{S2}=\left(\frac{E_S}{2Z_{S1}}+\frac{E_R}{2Z_{R1}}\right)\frac{Z_{R1}}{Z_{S1}+Z_{R1}}$$

$$=\frac{E_SZ_{R1}+E_RZ_{S1}}{2Z_{S1}(Z_{S1}+Z_{R1})} \tag{5}$$

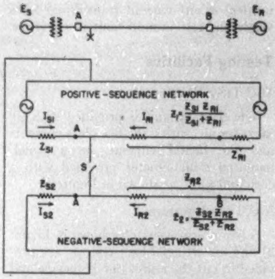

E_S
A
B
E_R
X
POSITIVE-SEQUENCE NETWORK
I_{S1}
I_{R1}
$Z_1=\frac{Z_{S1}Z_{R1}}{Z_{S1}+Z_{R1}}$
A
Z_{S1}
Z_{R1}
S
Z_{S2}
Z_{R2}
A
B
I_{S2}
I_{R2}
$Z_2=\frac{Z_{S2}Z_{R2}}{Z_{S2}+Z_{R2}}$
NEGATIVE-SEQUENCE NETWORK

Figure 12. Symmetrical-component currents during a phase-to-phase fault (for Appendix I)

$$I_{R1}=-I_{R2}=\left(\frac{E_S}{2Z_{S1}}+\frac{E_R}{2Z_{R1}}\right)\frac{Z_{S1}}{Z_{S1}+Z_{R1}}$$

$$=\frac{E_SZ_{R1}+E_RZ_{S1}}{2Z_{R1}(Z_{S1}+Z_{R1})} \tag{6}$$

Total Current

From equations 1 and 5

$$I_{S1}=\frac{E_S-E_R}{Z_{S1}+Z_{R1}}+\frac{E_SZ_{R1}+E_RZ_{S1}}{2Z_{S1}(Z_{S1}+Z_{R1})} \tag{7}$$

From equations 1 and 6

$$I_{R1}=-\frac{E_S-E_R}{Z_{S1}+Z_{R1}}+\frac{E_SZ_{R1}+E_RZ_{S1}}{2Z_{R1}(Z_{S1}+Z_{R1})} \tag{8}$$

From equations 2 and 5

$$I_{S2}=-\frac{E_SZ_{R1}+E_RZ_{S1}}{2Z_{S1}(Z_{S1}+Z_{R1})} \tag{9}$$

From equations 2 and 6

$$I_{R2}=-\frac{E_SZ_{R1}+E_RZ_{S1}}{2Z_{R1}(Z_{S1}+Z_{R1})} \tag{10}$$

Comparison of the magnitude of I_{S1}, equation 7, with the three-phase short-circuit current (E_S/Z_{S1}) is obscured by the two different voltages E_S and E_R.

If $E_S=E_R$, equation 7 becomes:

$$I_{S1}=\frac{E_S}{2Z_{S1}} \tag{7a}$$

This same result may be obtained more easily by considering only the left-hand portion of Figure 12, from which equation 7a is obtained directly.

From equation 7a, it is seen that the positive-phase-sequence current during the phase-to-phase fault is one half its value during a three-phase fault at the same location. In a similar manner, it can be shown that the 2/1 ratio holds in regard to negative-phase-sequence current. The 2/1 ratio is modified slightly if the positive- and negative-phase-sequence impedances are unequal. Also, with regard to the positive-phase-sequence component, the 2/1 ratio can be modified in either direction by the load component, the first term of equation 7.

Comparison of equations 7 and 8 shows that the fault components have the same sign, indicating an internal fault, whereas the load components have different signs, indicating a through-current condition.

Appendix II. Network Output

Referring to Figure 13, windings N have one-third the number of turns of windings A and C, and tapped winding KN has K times the number of turns of winding N. For an unbalanced fault (that is, a fault not operating all three overcurrent relays, O),

$$E_c=K_c[I_c+\frac{(K-1)}{3}I_G]=K_c[I_c+(K-1)I_0] \tag{11}$$

$$E_a=K_a[I_a-(I_G/3)]=K_a(I_a-I_0) \tag{12}$$

where K_c and K_a are constants of proportionality.

By adjustment of $R3$, E_C lags E_a by 60 degrees.

$$E_C\alpha-aE_a \tag{13}$$

where a is the vector operator which rotates a vector 120 degrees in the positive direction.

$$I_a=(I_1+I_2+I_0) \tag{14}$$

$$I_c=(aI_1+a^2I_2+I_0) \tag{15}$$

where I_1, I_2, and I_0 are positive-, negative-, and zero-phase-sequence components of I_a.

From equations 12, 13, and 14

$$E_C=K_a'(-aI_1-aI_2) \tag{16}$$

From equations 11 and 15

$$E_c=K_c(aI_1+a^2I_2+KI_0) \tag{17}$$

By design, and adjustment of $R2$, $K_c=K_a'$, and the network output voltage

$$E=E_C+E_c=K_c[(a^2-a)I_2+KI_0]\cdot$$
$$=K_c[-j\sqrt{3}I_2+KI_0] \tag{18}$$

With a balanced three-phase fault $I_2=I_0=0$, and the operation of overcurrent relays O changes to another tap on $R2$, which is adjusted to reduce E_c by a factor k, or

$$E_c=kK_c(aI_1+a^2I_2+KI_0)=kK_caI_1 \tag{17a}$$

$$E_C=-K_a'aI_1 \tag{16a}$$

Again,

$$K_c=K_a'$$

Then

$$E=E_C+E_c=K_caI_1(k-1) \tag{18a}$$

Comparison of equations 18 and 18a

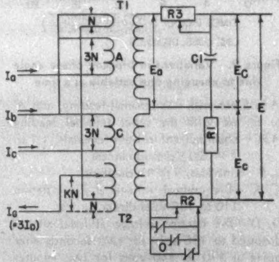

Figure 13. Connections and symbols (for Appendix II)

---

* On two-phase-to-ground faults, ground current may be calculated by means of equation 36, Appendix III.

** Negative-phase-sequence machine reactance is nearly equal to transient and subtransient reactance and hence is nearly equal to positive-phase-sequence reactance during the first few cycles after a fault.

shows that the network output voltage is less as a function of I_1 during three-phase faults than it is as a function of I_2 during unbalanced faults. Consequently, the network is more sensitive to unbalanced faults than it is to three-phase faults.

Appendix III. Negative- and Zero-Phase-Sequence Currents

Negative-phase-sequence and zero-phase-sequence currents and their ratio during single- and two-phase-to-ground faults in terms of three-phase and single-phase-to-ground short-circuit currents now will be determined.

General Relations

Refer to Figure 14 for the negative-phase-sequence network, and if $Z_1=Z_2$,

$$\frac{I_2}{I_2'}=\frac{I_{3\phi}}{I_{3\phi}'} \tag{19}$$

Where $I_{3\phi}'$ = total three-phase short-circuit current; $I_{3\phi}=C_1I_{3\phi}'$ = three-phase short-circuit current from same direction as I_2.

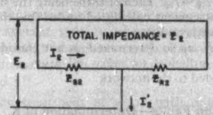

Figure 14. Negative-phase-sequence network (for Appendix III)

Referring to Figure 15 for the zero-phase-sequence network,

$$\frac{I_0}{I_0'}=\frac{I_G}{I_G'} \tag{20}$$

where

I_G' = total fault current on single-phase-to-ground fault

$I_G=C_0I_G'$ = single-phase-to-ground fault current from same direction as I_0

Equations 19 and 20 apply to any type of fault during which those values are present. From equation 19

$$I_2=I_2'\frac{I_{3\phi}}{I_{3\phi}'} \tag{21}$$

From equation 20

$$I_0=I_0'\frac{I_G}{I_G'} \tag{22}$$

From equations 21 and 22

$$\frac{I_2}{I_0}=\frac{I_2'}{I_0'}\left(\frac{I_{3\phi}I_G'}{I_{3\phi}'I_G}\right) \tag{23}$$

Single-Phase-to-Ground Fault

$I_0'=I_2'$

From equation 21

$$I_2=I_2'\frac{I_{3\phi}}{I_{3\phi}'}=I_0'\frac{I_{3\phi}}{I_{3\phi}'}\doteq\frac{I_{3\phi}}{I_{3\phi}'}\,\frac{I_G'}{3}=\frac{C_1I_G'}{3} \tag{24}$$

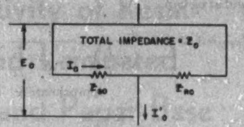

Figure 15. Zero-phase-sequence network (for Appendix III)

From equation 23

$$\frac{I_2}{I_0}=\frac{I_2'}{I_0'}\left(\frac{I_{3\phi}I_G'}{I_{3\phi}'I_G}\right)=\frac{I_{3\phi}I_G'}{I_{3\phi}'I_G}=\frac{C_1}{C_0} \tag{25}$$

Two-Phase-to-Ground Fault

$$\frac{I_2'}{I_0'}=\frac{Z_0}{Z_1}=\frac{Z_0}{Z_1}+2-2=\frac{Z_0+2Z_1}{Z_1}-2 \tag{26}$$

But $Z_0+2Z_1=E/I_0'$ for single-phase-to-ground fault.

$$Z_0+2Z_1=\frac{3E'}{I_G{}^*} \tag{27}$$

From equations 26 and 27

$$\frac{I_2'}{I_0'}=\frac{3E}{Z_1I_G'}-2=3\left(\frac{I_{3\phi}'}{I_G'}\right)-2=R \tag{28}$$

From equations 23 and 28

$$\frac{I_2}{I_0}=\frac{I_2'}{I_0'}\left(\frac{I_{3\phi}I_G'}{I_{3\phi}'I_G}\right)=R\left(\frac{I_{3\phi}I_G'}{I_{3\phi}'I_G}\right)=R\frac{C_1}{C_0} \tag{29}$$

$$I_1=\frac{E(Z_1+Z_0)}{Z_1(Z_1+2Z_0)}$$

$$E_2=E-I_1Z_1=E-\frac{E(Z_1+Z_0)}{Z_1+2Z_0}$$

$$E_2=\frac{EZ_0}{Z_1+2Z_0}=\frac{E}{(Z_1/Z_0)+2} \tag{30}$$

From equations 26 and 28

$$\frac{Z_1}{Z_0}=\frac{1}{R} \tag{31}$$

From equations 30 and 31

$$E_2=\frac{E}{(1/R)+2} \tag{32}$$

$$I_2'=-\frac{E_2}{Z_1}=-\frac{E}{Z_1}\left(\frac{R}{1+2R}\right)=-I_{3\phi}'\left(\frac{R}{1+2R}\right) \tag{33}$$

From equations 19 and 33

$$I_2=-I_{3\phi}\left(\frac{R}{1+2R}\right)=-C_1I_{3\phi}'\left(\frac{R}{1+2R}\right) \tag{34}$$

From equations 29 and 34

$$I_0=\frac{I_2}{R}\,\frac{C_0}{C_1}=-C_0I_{3\phi}'\left(\frac{1}{1+2R}\right) \tag{35}$$

$$\text{Ground current}=3I_0-3C_0I_{3\phi}'\left(\frac{1}{1+2R}\right)=-\frac{3I_{3\phi}'I_G}{I_G'}\left(\frac{1}{1+2R}\right) \tag{36}$$

Appendix IV. Operation During Ground Faults

Conditions during which sufficient negative-phase-sequence current is available for relay operation during ground faults will now be determined.

Single-Phase-to-Ground Fault

From equation 24, Appendix III,

$$I_2=\frac{C_1I_G'}{3}=\frac{I_{3\phi}}{3}\,\frac{1}{(I_{3\phi}'/I_G')} \tag{37}$$

When $I_{3\phi}$ is just equal to the three-phase relay pickup (eight amperes), the magnitude of I_2 must be equal to or greater than the negative-phase-sequence pickup ($\sqrt{3}$ amperes) or

$$I_2=\frac{8}{3}\,\frac{1}{(I_{3\phi}'/I_G')}\gtreqqless\sqrt{3}$$

$$\frac{I_{3\phi}'}{I_G'}\lesseqgtr\frac{8}{3\sqrt{3}}=1.5\text{ (approximately)} \tag{38}$$

Two-Phase-to-Ground Fault

From equation 34, Appendix III,

$$I_2=I_{3\phi}\left(\frac{R}{1+2R}\right)=I_{3\phi}\left[\frac{3(I_{3\phi}'/I_G')-2}{6(I_{3\phi}'/I_G')-3}\right] \tag{39}$$

Again, I_2 in equation 39 must be equal to or greater than $\sqrt{3}$ when $I_{3\phi}=8$ amperes.

$$8\left[\frac{3(I_{3\phi}'/I_G')-2}{6(I_{3\phi}'/I_G')-3}\right]\gtreqqless\sqrt{3}$$

$$24(I_{3\phi}'/I_G')-16\gtreqqless6\sqrt{3}(I_{3\phi}'/I_G')-3\sqrt{3}$$

$$13.6\ (I_{3\phi}'/I_G')\gtreqqless10.8$$

$$\frac{I_{3\phi}'}{I_G'}\gtreqqless0.8\text{ (approximately)} \tag{40}$$

Appendix V. Blind Spots

Conditions necessary to avoid blind spots during ground faults (when ground-current excitation is used) will now be determined. The network output from equation 18, Appendix II, is

$$E=K_c(-j\sqrt{3}I_2+KI_0) \tag{18}$$

If it is assumed that I_2 can be at any angle relative to I_0, KI_0 will overcome $\sqrt{3}I_2$ when

$$KI_0>\sqrt{3}I_2$$

or when

$$K>\sqrt{3}\left(\frac{I_2}{I_0}\right) \tag{42}$$

If (as an additional safeguard against failure to trip due to excessive phase displacement between the network outputs at the two terminals) it is specified that $(-j\sqrt{3}I_2+KI_0)$ shall not be in excess of 45 degrees from I_0, at either terminal, KI_0 must be larger than $\sqrt{3}(I_2/I_0)$ by an additional multiplier, $\frac{1}{\sin 45°}=\sqrt{2}$

$$KI_0>\sqrt{2}\sqrt{3}I_2;\quad K>2.45\left(\frac{I_2}{I_0}\right) \tag{43}$$

---

*I_G' previously defined as applying to a single-phase-to-ground fault *only*.

With the maximum available value of K as 21,

$$21 > 2.45\left(\frac{I_2}{I_0}\right)$$

or

$$\frac{I_2}{I_0} < 8.5 \text{ (approximately)} \tag{44}$$

But from equation 25, Appendix III, $I_2/I_0 = C_1/C_0$ or

$$\frac{C_1}{C_0} < 8.5 \text{ for a single-phase-to-ground fault} \tag{45}$$

From equation 29, Appendix III, $I_2/I_0 = (RC_1/C_0)$ or

$$\frac{C_1}{C_0}\left[3\left(\frac{I_{3\phi}'}{I_G'}\right)-2\right] < 8.5 \quad \text{for two-phase-to-ground fault} \tag{46}$$

Thus, if $I_{3\phi}'/I_G'$ is less than 1, equation 45 gives the limiting condition, whereas if $I_{3\phi}'/I_G'$ is greater than 1, equation 46 gives the limiting condition.

Appendix VI. Relay Pickup

Relay pickup in terms of ground current (when ground-current excitation is used) is determined as follows. From equation 18, Appendix II, the network output is

$$E = K_c(-j\sqrt{3}I_2 + KI_0) \tag{18}$$

For any condition for which I_2 and I_0 are known at pickup, E/K_c can be found. Knowing E/K_c, pickup in terms of I_G can be determined knowing only I_2/I_0.

The single-phase-to-ground single-end-feed pickup values given in Appendix VII are for a fault on the phase giving the highest pickup, that is, the phase for which I_2 and I_0 are most nearly in opposition. For a fault on phase b, I_2 (phase a being the reference phase) lags I_0 by 120 degrees. The quantity $-jI_2$ lags I_0 by 210 degrees ($I_2 = -ja^2I_0$), or 30 degrees from complete opposition. In magnitude, $I_2 = I_0$. By choosing any combination of K and ground current at pickup (for example, $K = 21$, $I_G = 0.5$), and by substitution in equation 18b,

$$E = K_c(-ja^2\sqrt{3}I_0 + KI_0)$$

$$-\frac{K_cI_G}{}[(K-\sqrt{3}\cos 30)^2 + (\sqrt{3}\sin 30)^2]$$

$$= \frac{K_c 0.5}{3}[(21-1.5)^2 + (\sqrt{3}/2)^2]$$

$$E/K_c = 3.25$$

With double-end-feed, and with the assumption that I_2 and I_0 can be in complete opposition,

$$E/K_c = -\sqrt{3}\,I_2 + KI_0 = \frac{I_G}{3}\left(K - \sqrt{3}\frac{I_2}{I_0}\right)$$

$$I_G = \frac{E}{K_c}\frac{3}{\left(K-\sqrt{3}\dfrac{I_2}{I_0}\right)}$$

and at pickup

$$I_{GPU} = 3.25\frac{3}{\left(K-\sqrt{3}\dfrac{I_2}{I_0}\right)} = \frac{10}{K-\sqrt{3}\dfrac{I_2}{I_0}} \quad \text{approximately} \tag{41}$$

Appendix VII. Detailed Application of Relay System

The application of the relay system can be reduced to the following steps:

1. Determination of margin above pickup during three-phase faults with minimum generating conditions.
2. Determination of margin of the negative-phase-sequence current, above pickup, during single-phase-to-ground and two-phase-to-ground faults.
3. The determination of K (the proportion of added excitation from I_0) to avoid blind spots if sufficient negative-phase-sequence current is not available in 2.
4. If I_0 is used, the determination of relay pickup in terms of ground current, to check the margin of fault current above pickup.

Three-Phase Faults

Under minimum generating conditions, determine the current in the relay at A (Figure 16) for a fault at 2. Repeat for the relay at B for a fault at 1. The three-phase pickup of the relay is eight amperes. If in either instance one of the currents is insufficient to operate the relay, assume sequential operation and determine the current at the questionable terminal with the opposite circuit breaker open. Hereafter, this note is not repeated but is assumed.

Phase-to-Phase Faults

It is not necessary to consider this type of fault, unless the incidence of three-phase faults is assumed negligible, since the relay system is more sensitive to phase-to-phase faults than to three-phase faults. The relay pickup for this condition is three amperes ($\sqrt{3}$ amperes negative-phase-sequence).

Ground Faults—Determination of I_2

In the determination of the available negative-phase-sequence current, it is necessary to know only the three-phase and single-phase-to-ground short-circuit currents which must be known in any overcurrent relay application.

For a single-phase-to-ground fault (equation 24, Appendix III):

$$I_2 = \frac{I_{3\phi}}{I_{3\phi}'}\frac{I_G'}{3} \tag{24}$$

where

I_G' = total ground amperes in single-phase-to-ground fault

I_G (used in equation 25 in this appendix) = portion of I_G' from terminal in question

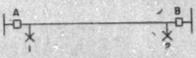

Figure 16. Fault locations (for Appendix VII)

$I_{3\phi}'$ = total phase amperes in three-phase fault

$I_{3\phi}$ = portion of $I_{3\phi}'$ from terminal in question

With a single-phase-to-ground fault at 2 (Figure 16), determine the negative-phase-sequence current I_2 at terminal A from equation 24. Repeat for terminal B for a fault at 1.

For a two-phase-to-ground fault, repeat the determination of I_2 with this type of fault using equation 34 (from Appendix III).

$$I_2 = I_{3\phi}\left(\frac{R}{1+2R}\right) \tag{34}$$

where

$$R = \frac{3I_{3\phi}' - 2I_G'}{I_G'}$$

If there is sufficient negative-phase-sequence current available during all of these conditions, no further calculation is necessary (that is, it is not necessary to consider the introduction of I_0 into the network). If I_2 is to be checked after the opening of the first breaker, the same formulas can be used with $I_{3\phi} = I_{3\phi}'$, each of these being the short-circuit current calculated under this single-end-feed condition.

If I_2, as so determined, is not considered to be sufficient for relay operation, I_0 must be added to the network.

Ground Faults—Determination of K

With a single-phase-to-ground fault at 2 (Figure 16), determine the ratio I_2/I_0 at terminal A from equation 25 as given here (from Appendix III):

$$\frac{I_2}{I_0} = \frac{I_G'I_{3\phi}}{I_GI_{3\phi}'} \tag{25}$$

Repeat for terminal B with a fault at 1.

Repeat for two-phase-to-ground faults using equation 29 from Appendix III.

$$\frac{I_2}{I_0} = \left(\frac{I_G'I_{3\phi}}{I_GI_{3\phi}'}\right)R \tag{29}$$

By use of the highest of the four values of I_2/I_0 found, choose an available value of K (6, 8, 11, 15, or 21) so that

$$K > 2.45\,\frac{(I_2)}{(I_0)} \text{ (from Appendix V)} \tag{43}$$

It is noted from equation 43 that if it is necessary to introduce I_0 into the network, ground current must be available from both terminals. The relay system is not applicable if an internal fault will, under any circumstances, draw I_0 from one direction only and I_2 from the other direction, unless negative-phase-sequence currents alone are sufficient for at least sequential relay operation.

Ground Faults—Determination of Pickup in Terms of Ground Current

If it is assumed that the negative-phase-sequence current can be at any phase angle relative to the zero-phase-sequence current, the resultant pickup in terms of ground cur-

The Electrical Resistivity of Resin-Treated Wood and Laminated Hydrolyzed-Wood and Paper-Base Plastics

RICHARD C. WEATHERWAX
NONMEMBER AIEE

ALFRED J. STAMM
NONMEMBER AIEE

WOOD in the dry state is an excellent dielectric, having a volume resistivity in the range of 3×10^{17} to 3×10^{18} ohm-centimeters.[2] The resistivity decreases rapidly, however, with an increase in moisture content, reaching values of 10^5 to 10^6 ohm-centimeters at the fiber-saturation point (30-per-cent moisture content on the basis of the dry weight of the wood).[3] This tremendous change in the electrical resistance of wood with changes in moisture content, which so overshadows the variations due to varying species and specific gravity and ash content of the wood,[4,5] furnishes an excellent means of measuring the moisture content of wood.[6,12]

The treatment of wood with aqueous phenol-formaldehyde resin-forming solutions according to the methods developed at the United States Forest Products Laboratory[7–11] has been shown to reduce greatly the moisture adsorption and swelling even under equilibrium conditions. Because of the reduced moisture content of resin-treated wood (*impreg*[10]) and the corresponding resin-treated compressed wood (*compreg*[11]) in equilibrium with any relative humidity, the electrical resistivity should be correspondingly increased. The data given in this report show that this is the case and that wood, hydrolyzed-wood sheet, and paper properly treated with resins are suitable for various dielectric uses even under relatively high-humidity conditions.

The electrical resistivity of normal wood and *impreg* and *compreg* of ten different species was determined on single sheets of veneer after kiln drying and in equilibrium with four different relative humidities. The changes in resistivity resulting from variations in resin content, degree of compression, and the presence of glue lines in laminated material were determined. The extent of surface resistivity was investigated for the resin-treated wood. The volume resistivities of a limited number of hydrolyzed-wood sheet specimens containing both aniline-furfural and phenol-formaldehyde resins, and laminated Mitscherlich sulphite paper treated with both water- and alcohol-soluble phenolic resins were also determined.

Electrical Measurements

D-c resistivity measurements were made with a sensitive galvanometer used as an ammeter in an ammeter-voltmeter circuit as shown in the circuit diagram of Figure 1. The galvanometer had a sensitivity with the scale at four meters of 7.60×10^{-10} amperes per centimeter scale deflection. High potentials ranging from 20 to 300 volts were obtained with a d-c motor generator set. Low potentials, from 15 to 0.01 volts, were obtained from dry cells with the use of potential dividers. The apparatus was thus capable of measuring any resistance from 30 ohms to 4×10^{13} ohms.

All the switches were coated with ceresin wax, which has a high-surface resistivity, to minimize current leakage. Switches S_3, S_4, and S_7 were shielded by wrapping bare copper wires about the bases in three directions and connecting these to the circuit at α, thus leading any stray current around the galvanometer. To avoid confusion, these leads are not shown in Figure 1. In spite of these precautions, stray currents were found to be excessive in damp weather. Hence the apparatus was set up in a constant relative-humidity room held at 30-per-cent relative humidity and 80 degrees Fahrenheit. With these precautions the volume leakage of the system was reduced to the point that the conductivity was only about 5×10^{-13} ohms, which was insufficient to affect the results seriously.

The electrodes consisted of two rectangular brass plates, each with a surface area of 35.0 square centimeters and a brass guard rim one centimeter wide that fitted around the perimeter of one of the electrode plates with a 0.5-centimeter gap between the guard rim and the electrode. This, together with the other shield wires, was connected at α in Figure 1, so that any current flowing along the surface of the sample was led around the galvanometer.

The electrode plates were held against the sample by a screw clamp with hard rubber jaws. The clamp had a resistance of 2×10^{12} ohms, which was about ten times that of the highest resistance measured and from 100 to 1,000 times the usual resistance measured.

It was found that the resistance of a specimen varied inversely with the pressure applied to the electrodes at lower pressures, but above a pressure of 23 pounds per square inch the resistance change became negligible. The clamp was tightened to exceed this pressure for all the measurements.

The surface resistivity was measured with six bar electrodes ten centimeters long and one centimeter wide. Three parallel electrodes on each surface were paired opposite each other on the two faces of a specimen and bolted through holes in the specimens slightly larger than the bolts. The two outer bars on both surfaces were electrically coupled so that a flow of current occurred from the cen-

---

Paper 45-161, recommended by the AIEE committee on air transportation for publication in AIEE TRANSACTIONS. Manuscript submitted June 4, 1945; made available for printing August 13, 1945.

RICHARD C. WEATHERWAX and ALFRED J. STAMM are with the forest products laboratory, forest service, United States Department of Agriculture. The laboratory is maintained at Madison, Wis., in cooperation with the University of Wisconsin.

---

rent ($3I_0$) may be increased if I_2 opposes I_0. The resultant pickup may be as high as 3.25 (Appendix VI) times the single-end-feed ground-fault pick-up values ($3I_0 = 2.2$, 1.55, 1.05, 0.75, or 0.5 amperes corresponding respectively to the values of K just given).

The ground-fault currents ($3I_0$) are the following:

Single-phase-to-ground $= I_G$ (one of the known currents)

$$\text{Two-phase-to-ground} = \frac{3I_{\phi\phi}'I_G}{I_G'}\left(\frac{1}{1+2R}\right) \quad \text{(from Appendix III)} \qquad (36)$$

If the available ground currents calculated are less than 3.25 times the single-end-feed pickup, the actual pickup in terms of ground current (I_{GPU}) can be calculated by means of equation 41, Appendix VI.

$$I_{GPU} = \frac{10}{K - \sqrt{3}\left(\frac{I_2}{I_0}\right)} \qquad (41)$$

If the available ground current is not sufficient to operate the relay (pickup calculated from equation 41), the value of K may be increased. K should not be increased unnecessarily, since a higher value of K means higher burden on the current transformers.

References

1. A CARRIER-CURRENT PILOT SYSTEM OF TRANSMISSION LINE PROTECTION, A. S. Fitzgerald. AIEE TRANSACTIONS, volume 47, 1928, pages 22–9.

2. A NEW CARRIER RELAYING SYSTEM, T. R. Halman, S. L. Goldsborough, H. W. Lensner, A. F. Drompp. AIEE TRANSACTIONS, volume 63, 1944, August section, pages 568–72.

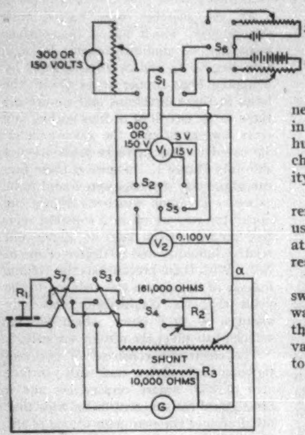

Figure 1. Wiring diagram of resistivity equipment

tral to the two outer bars on both faces across a 0.10-centimeter gap. The surface resistivity r_s was calculated from the equation $r_s = 4R_s \frac{l}{d}$ where R_s is the measured surface resistance, l is the bar length, and d is the distance between the bars.

The wood specimens were cut from $^{1}/_{16}$-inch rotary-cut veneer (0.16 centimeter). The *compreg* specimens were one third to one half as thick, as a result of compression. The hydrolyzed-wood sheet and laminated-paper plastic specimens varied from 0.06 to 0.15 centimeter in thickness.

The specimens were kiln dried or conditioned in humidifiers containing saturated salt solutions. At 30 degrees centigrade the barium chloride, sodium chloride, manganese chloride, and magnesium chloride used gave 90.8-, 75.8-, 53.9-, and 32.7-per-cent relative humidity, respectively.

The specimens were moved from the lower to the higher relative-humidity conditions. The resistivity–moisture content curves to follow are hence all adsorption curves.

Resistivity measurements made after different times of humidification indicated that moisture equilibrium was obtained in all cases in 20 days or less. The measurements recorded in the following figures were all made after 30 days' humidification to insure definitely the attainment of equilibrium conditions.

All the volume-resistivity measurements were made in the 30-per-cent relative-humidity room as rapidly as possible after the specimens were removed from the humidifiers, which required about three minutes. During this time the moisture-content change for all the resin-treated specimens was practically negligible. Even in the untreated wood in equilibrium with 90-per-cent relative humidity, for which the moisture-content change is most rapid, the volume-resistivity change was only five to ten per cent.

Three methods of measuring the current flowing through the samples were used. They gave widely varying results at low humidities, but closely checking results at high humidities (Figure 3).

Method 1 observed the maximum swing of the galvanometer as the switch was closed and current surged through the sample. This method gave the lowest values for the resistivity. It was subject to the objection that the electrode plates acted as a capacitor and so contributed to the magnitude of the swing.

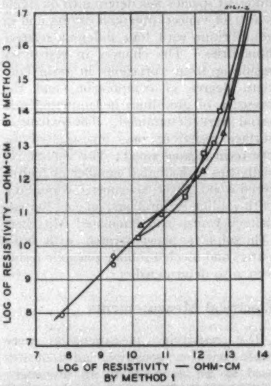

Figure 2. Logarithm of average volume resistivity of ten species of wood (basswood, yellow birch, cottonwood, Douglas fir, white fir, sweetgum, Western hemlock, yellow poplar, redwood, and Sitka spruce), and of *impreg* and *compreg* made therefrom determined by method 3 versus the corresponding values determined by method 1

○ Untreated wood
△ *Impreg*
□ *Compreg*

Method 2 observed the first steady deflection of the galvanometer after the switch was closed. The polarity of the electrodes was changed by means of the reversing switch S_7 (Figure 1), and the average of the readings for the flow of current in the two directions was used. The value of the resistivity obtained by this second method probably approximated most nearly the true value of the resistivity. The chief difficulty was that some samples polarized so rapidly that no steady deflection could be observed.

Method 3 was that used by the American Society for Testing Materials,[1] namely, that of reading the galvanometer deflection after the current had been flowing through the sample for one minute. This, however, gave a value of the resistivity which had been considerably increased by polarization.

By plotting corresponding values of the resistivity obtained by methods 1 and 3 against each other and extrapolating the curve, it was possible to determine method-3 resistivities from method-1 resistivities that were too high to measure directly but which were still within the range of the apparatus for method 1 (Figure 2). This procedure was used to obtain method-3 resistivities for the kiln-dried samples before they were exposed to the 32.7-per-cent relative humidity. The kiln-dried samples contained from 0.5 to 2-per-cent moisture and had method-3 resistivities of the order of 10^{16} ohm-centimeters.

Volume Resistivity of Wood

Volume-resistivity measurements were made on matched specimens of the ten

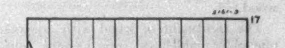

Figure 3. Logarithm of the average volume resistivity of *impreg* and *compreg* made from ten species of wood (basswood, yellow birch, cottonwood, Douglas fir, white fir, sweetgum, Western hemlock, yellow poplar, redwood, and Sitka spruce), determined by three methods versus the equilibrium relative humidity

□ Method 1
△ Method 2
○ Method 3

species of wood, listed in Figure 2, in the untreated form and made up into *impreg* and *compreg* by previously described methods[9-11] using Bakelite Corporation resinoid *BR*5995. Both the *impreg* and the *compreg* were cured in a hydraulic press for 45 minutes at 300 degrees Fahrenheit, *impreg* under a negligible pressure and *compreg* under 1,250 pounds per square inch. The resin contents of the different specimens varied from 31 to 57 per cent on the basis of the weight of the dry untreated wood. It will be shown later (Figure 7) that within this range the volume resistivity changes but slightly with variations in resin content. Because of this and the fact that the variation in volume resistivity with species was practically within the range of experimental error, average values for all the species are plotted in Figures 2 through 5.

Figure 3 gives a comparison between the average volume resistivities of *impreg* and *compreg* determined by the three different methods plotted against the equilibrium relative humidity. Variations between the values obtained by the three methods are appreciable only for low relative humidities at which the resistivities are relatively high. The resistivities given in the following figures were all determined by method 3, that recommended by the American Society for Testing Materials.[1]

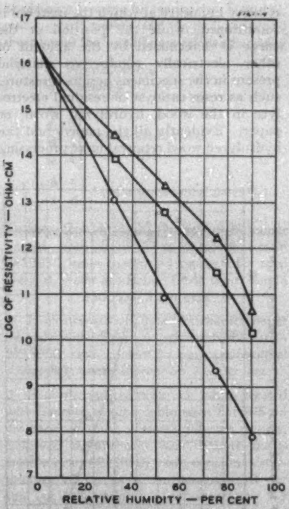

Figure 4. Logarithm of the average volume resistivity (method 3) of ten species of wood (basswood, yellow birch, cottonwood, Douglas fir, white fir, sweetgum, Western hemlock, yellow poplar, redwood, and Sitka spruce), and of *impreg* and *compreg* made therefrom versus the equilibrium relative humidity

○ Untreated wood
△ *Impreg*
□ *Compreg*

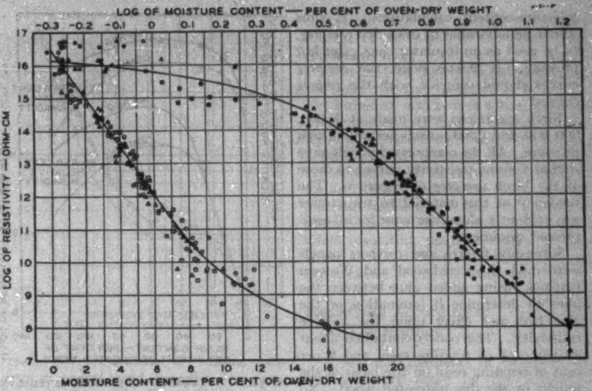

Figure 5. Logarithm of the average volume resistivity (method 3) of ten species of wood (basswood, yellow birch, cottonwood, Douglas fir, white fir, sweetgum, Western hemlock, yellow poplar, redwood, and Sitka spruce), and of *impreg* and *compreg* made therefrom versus the moisture content

Per cent moisture content:
○ Untreated wood
△ *Impreg*
□ *Compreg*
Log per cent moisture content:
● Untreated wood
▲ *Impreg*
■ *Compreg*

Figure 4 gives the logarithm of the average resistivity for untreated wood, *impreg*, and *compreg*, made from ten different species, plotted against the equilibrium relative humidity. The resistivity of *impreg* is slightly higher than that of *compreg* and considerably higher than that of normal wood under the same relative-humidity conditions. The three curves, when extrapolated to zero relative humidity, give practically identical resistivities. The reason for this is shown in Figure 5, in which the same resistivity data are plotted against the moisture content. On this basis, the values for the three materials fall on a single curve, indicating that the resistivity depends primarily upon the moisture content. Differences between the curves of Figure 4 merely show differences in hygroscopicity (or apparent hygroscopicity, as will be shown later) of the three materials.

Figure 6 gives the volume resistivity of birch *impreg* and *compreg*. The values are very similar to the average values for the ten species given in Figures 4 and 5.

Figure 7 shows the effect of the resin content of both *impreg* and *compreg*, made from two different species, upon the volume resistivity at two different relative humidities. The resistivity increases rapidly with an increase in resin content up to about 30-per-cent resin content on the basis of the dry weight of the wood, and then remains relatively constant, but again decreases with very high resin content. The original increase is due to the decrease in hygroscopicity with increasing resin content.[7] On the other hand, electrolyte introduced with the resin will decrease the resistivity as the proportion of resin to wood increases. This decrease in resistivity is evidently small, compared to the increase in resistivity due to decreased hygroscopicity up to about 30-per-cent resin content. Above this resin content the decrease in hygroscopicity is small.[7] Between this resin content and one of 70 per cent the two effects evidently neutralize each other, whereas above 70-per-cent resin content the effect of the electrolyte predominates.

The rapid decrease in the hygroscopicity in both the *impreg* and the *compreg* with increasing resin content up to about 30 per cent, followed by a smaller decrease in hygroscopicity with a further increase in resin content, is clearly shown in Figure 8 for the specimens of Figure 7.

Figures 4 through 8 all show that *impreg* has a higher resistivity than *compreg* for the same relative humidity, although it is the same for the same moisture content. This difference between the two materials makes it appear that *compreg* is more hygroscopic than *impreg*. This explanation does not seem so probable as the possible entrapping of water within the resin of the *compreg* which was not lost in the curing or in the kiln drying of these samples prior to humidification, but which is lost during the final oven drying to determine the dry weight for moisture-content calculations. It thus would be advisable to oven-dry *compreg*, to be used as an insulator, just after hot pressing. If this is done, the *compreg* curves should coincide with the *impreg* curves.

Birch specimens were made at 0, 300, 600, 900, and 1,200 pounds per square inch pressure. All the compressed panels gave similar volume-resistivity curves to those of the birch *compreg* of Figure 6. The tendency of the material to trap water was evidently about the same for all compressed specimens.

Seven-ply *impreg* and *compreg* panels were made from redwood and Western hemlock, using added glue between the plies to determine if lamination or the glue had any effect upon the volume resistivity. The panels contained about 40 per cent of treating resin and 9 per cent of bonding resin on the basis of the weight of the dry untreated wood. No significant differences in the volume resistivity between these specimens and the single-ply specimens were observed.

Surface Resistivity of Wood

Figure 9 shows the relationship between the surface resistivity and the relative humidity to which oven-dry samples of *impreg* and *compreg* were exposed for 15 minutes. The relative humidity of the chamber in which the measurements were made was controlled by blowing air over different concentrations of sulphuric acid. Relative humidities corresponding to different concentrations were taken from tables given by Wilson.[13] Fifteen minutes' exposure was adequate to allow the surface film to come to approximate equilibrium without causing the volume resistivity to decrease to the point where it would affect the results appreciably. During this period two to three check readings were made, using the first steady galvanometer deflection. The specimens were freshly dried before exposure to the next higher relative humidity. No difference between *impreg* and *compreg* was observed; hence a single curve was plotted for both. Below a relative humidity of 40 per cent the surface resistivity is so small that it becomes of the same order as the volume resistivity, so that an appreciable part of the current flow is through the specimens. The curve shows that volume resistivity measurements made in a 30-per-cent relative-humidity room are inappreciably affected by the surface conductivity. Listray[3] similarly found that the surface resistivity of several different dielectrics became constant below a relative humidity of about 40 per cent.

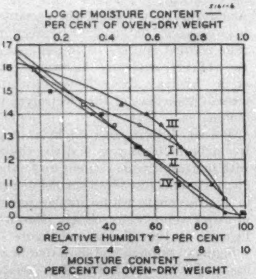

Figure 6. Logarithm of the volume resistivity (method 3) of yellow birch *impreg* and *compreg* versus the equilibrium relative humidity and the moisture content

Resistivity of birch *impreg* and *compreg*

I	○	*Impreg*	relative humidity
II	●	*Compreg*	
III	△	*Impreg*	log of moisture content
	▲	*Compreg*	
IV	□	*Impreg*	moisture content
	■	*Compreg*	

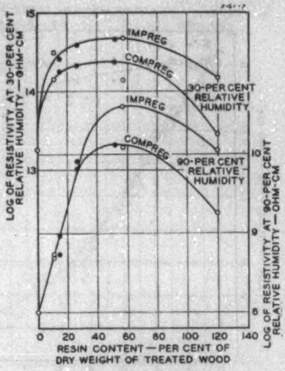

Figure 7. Logarithm of the volume resistivity (method 3) of white fir and yellow birch *impreg* and *compreg* at two different relative humidities versus the resin content

○ White fir
⊕ Yellow birch

Volume Resistivity of Paper and Hydrolyzed-Wood Laminates

The volume resistivities of resin-treated paper and hydrolyzed-wood sheets are given in Figures 10 and 11, together with the average values for normal wood and *compreg*. When plotted against the relative humidity (Figure 10) all the values fall between those for normal wood and for *compreg*. When plotted against the moisture content (Figure 11), most of the values fall on a single curve below the composite curve for wood, *impreg*, and *compreg*. It appears that the position of a point on one of the curves of Figure 11 is determined by the hygroscopicity and the relative humidity at which the material is conditioned, while the position of the curve is determined by the amount of other electrically conductive material present in the specimens besides moisture, such as resin catalyst or residual electrolyte in the wood, hydrolyzed wood, or paper. Evidently all the papers and the hydrolyzed wood retained more processing

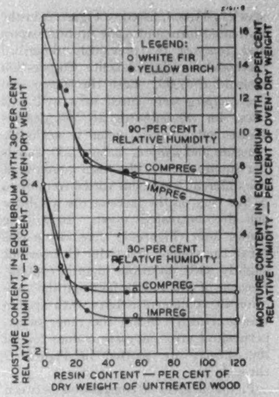

Figure 8. Equilibrium moisture content of white fir and yellow birch *impreg* and *compreg* at two different relative humidities versus the resin content

○ White fir
⊕ Yellow birch

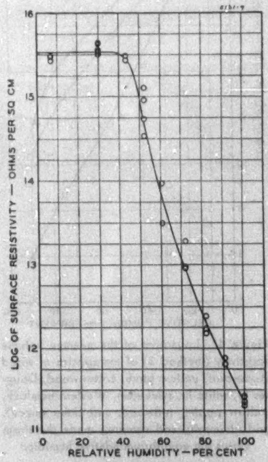

Figure 9. Logarithm of the surface resistivity of several species of *compreg* versus the atmospheric relative humidity

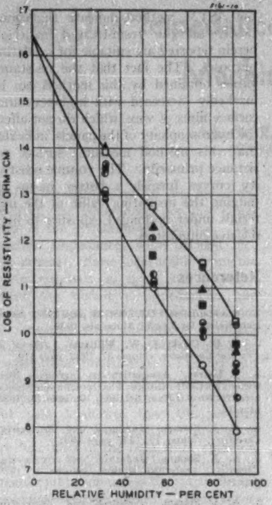

Figure 10. Logarithm of the volume resistivity of *compreg* (average for ten species, Figure 4), resin-treated paper, and hydrolyzed-wood sheet versus the equilibrium relative humidity

○ Normal wood
□ *Compreg*
▲ 1 } Resin-treated paper
◐ 2
■ 3
⊖ 4
● 5 } Hydrolyzed-wood sheet
⊗ 6

1—Soft (low-strength) Mitscherlich paper treated with Bakelite spirit-soluble resin *BR*13850, resin content 44 per cent (of total weight), water absorption (*AAF* specification 15065) 1.5 per cent

2—High-strength modified Mitscherlich paper treated with Bakelite spirit-soluble resin *BR*13850, resin content 34 per cent (of total weight), water absorption 7.5 per cent

3—High-strength Mitscherlich paper treated with Bakelite water-soluble resin *BR*5995 on the paper machine with no diffusion period, followed by treatment with Bakelite spirit-soluble resin *BR*13850; resin content, water-soluble, 20 per cent; spirit-soluble 13 per cent (of total weight), water absorption 1.3 per cent

4—High-strength Mitscherlich paper (same as 3) treated only with Bakelite water-soluble resin with no diffusion period; resin content 35 per cent (of total weight)

5—Hydrolyzed-wood sheet containing 15 per cent (of total weight) of aniline–furfural

6—Hydrolyzed-wood sheet containing 15 per cent (of total weight) of Bakelite water-soluble resin *BR*5995

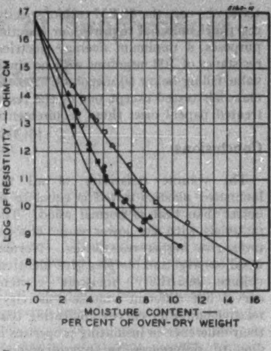

Figure 11. Logarithm of volume resistivity of normal wood, *impreg* and *compreg* (average of ten species, Figure 4), resin-treated paper and hydrolyzed-wood sheet, versus the moisture content. For key to specimens see Figure 10

○ Normal wood
△ *Impreg*
□ *Compreg*
▲ 1 } Resin-treated paper
◐ 2
□ 3
⊖ 4
● 5 } Hydrolyzed-wood sheet
⊗ 6

electrolyte than the normal electrolyte content of the wood, or the resins used contained more electrolyte. It is of interest that all the curves extrapolate to the same volume resistivity at zero relative humidity and zero moisture content. This might be expected, as the conductivity of any contained electrolyte is largely dependent upon moisture being present. Hydrolyzed-wood sheet 5 with an aniline–furfural plasticizer is the only treated material tested which does not contain a phenolic resin. Its definitely poorer electrical insulating properties may be due either to the difference in resins used or the presence of more electrolyte.

Resistivity According to ASTM Method

A few measurements of electrical resistance were made by the American Society for Testing Materials method.[1] This test determines the resistance between adjacent binding posts that are bolted through panel specimens. Three binding posts were bolted through $2^1/_2$-by-4-inch specimens, of thicknesses shown in Table I, one at the center and two at $1^1/_4$ inches (center to center) from the central binding post in the length direction of the specimen and equally distant from each of the edges. Brass washers 9/16 inch in outside diameter were used on both surfaces of the bolted-in binding posts, giving a distance between adjacent washers on the surfaces of the specimens

Table I. Electrical Resistance According to the ASTM Method

Material	Resin*	Resin† Content, Per Cent	Thickness, Inch	Cycle	Electrical Resistance, Megohms
Birch *impreg*	*BR*5995	28.7	0.060	1 2	5,605 6,490
Cottonwood *compreg*	*BR*15100	21.8	0.252	1	146
Cottonwood *compreg*	*BR*15100	21.8	0.074	1 2 3	317 439 412
Hydrolyzed-wood sheet	*BR*5995	15.0	0.043	1	13,300
Hydrolyzed-wood sheet	*BR*5995	15.0	0.065	1 2	1,890 1,020
Hydrolyzed-wood sheet	Aniline–furfural	15.0	0.059	1	550
Soft (low-strength) Mitscherlich paper	*BR*13850	44.0	0.034	1	2,035
High-strength Mitscherlich paper	*BV*16303	36.9	0.145	1 2	5 5
High-strength Mitscherlich paper (waxed surfaces)‡	*BV*16303	36.9	0.142	1 2	3,560 7,120
High-strength Mitscherlich paper	*BV*16526	36.0	0.256	1 2 3	100 110 95
High-strength Mitscherlich paper	*BV*16526	36.5	0.132	1 2	82 100
High-strength Mitscherlich paper (waxed surfaces)‡	*BV*16526	36.5	0.130	1 2	279,000 39,800

* All resins but aniline–furfural are Bakelite Corporation resins.

† Resin content is on the basis of total weight of product. The resin content of the *impreg* and the *compreg*, on the basis of the dry weight of the untreated wood, on which basis they are normally expressed, are 48.3 and 28.0 per cent, respectively.

‡ The waxed specimens were coated with a thin film of wax by dipping the heated panels in cooler molten wax. The films were so thin that they were barely perceptible to the eye.

of 11/16 inch. The specimens were dried for seven hours at 160 degrees Fahrenheit according to the ASTM specifications and then exposed to a relative humidity of 90.5 ± 0.5 per cent for 96 hours at 80 degrees Fahrenheit (specified 87 degrees Fahrenheit ± 2 degrees Fahrenheit). Resistance measurements were made using the previously described apparatus. The results are shown in Table I. The insulation resistances are the averages of values obtained between adjacent pairs of binding posts. Most of the specimens were heated a second time for seven hours at 160 degrees Fahrenheit and again humidified for 96 hours to give second-cycle measurements. In some cases third-cycle tests were made. The agreement between the values for the different cycles was quite good for all materials tested except when waxed specimens were used. The *impreg* and the hydrolyzed-wood sheet plasticized with phenolic resin gave the highest electrical resistance values of the unwaxed specimens. The soft readily penetrated paper (number 1, Figure 10) gave the highest values of the treated but not waxed papers. The high-strength paper plastic made with *BV*16303 resin gave the lowest values while the high-strength paper plastic made with *BV*16526 gave intermediate values. The low values obtained with the *BV*16303 resin are probably due to the electrolyte content of the resin. The *compreg* values are not so high as they might have been if the material had contained more resin, as is evident in Figure 7. The waxed specimens gave high but not so consistent results. Differences are probably due to slight imperfections of the surface films. Although considerable wax drained off the specimens while heating prior to the second-cycle measurements, the electrical resistances were still high on the second measurement.

A large manufacturer of electrical material who uses the ASTM test for specifying panel material requires, for exacting purposes, a minimum average electrical resistance of 100 megohms with no single value falling below 60 megohms. All the materials tested except one of the resin-treated papers meet these requirements.

Conclusions

The volume resistivity of all the laminated plastics tested is equal to or better than that of normal wood. The materials with the lower water absorptions give higher resistivities. Normal wood, *impreg*, and *compreg* give identical volume - resistivity – moisture - content curves but different volume-resistivity–relative-humidity curves, indicating that their difference in insulating properties is due to differences in hygroscopicity. *Impreg* and *compreg* have volume resistivities about ten times that of normal wood at 30-per-cent relative humidity and about 100 to 1,000 times that of normal wood at 90-per-cent relative humidity, the *impreg* values tending to be somewhat greater than the *compreg* values. Resin contents in the range of 35 to 70 per cent have a negligible effect in changing the volume resistivity of *impreg* and *compreg*.

The surface resistivity at relative humidities below about 40 per cent is sufficiently small to be ineffective in controlling the insulating properties. The insulating properties of dry material exposed to higher relative humidities are largely determined by surface conductivity effects.

The volume resistivities of the laminated-paper plastics and hydrolyzed-wood plastics tested are somewhat lower than the values for *impreg* and *compreg*. This is, in part, due to greater hygroscopicity, but it also appears to be due to a somewhat greater electrolyte content.

Electrical-resistance measurements by the ASTM method indicate that practically all the resin-treated materials herein reported are suitable for insulating purposes. The fact that the resistance values obtained by this method can be markedly increased with high-resistance surface films of wax, which do not affect the hygroscopicity of the panels, indicates that this method measures surface resistance primarily. The volume-resistivity curves furnish a better means of judging the insulating value of the materials under prolonged exposure to high relative humidities.

References

1. Standards, part III, *D257-38*, page 299. American Society for Testing Materials, 1939.

2. **J. D. Clark, J. W. Williams.** *Journal of Physical Chemistry*, volume 37, 1933, page 119.

3. **J. Listray.** Association des Ingénieurs Électriciens Sortis de l'Institut Électrotechnique Montefiore *Bulletin* (Liége, Belgium), volume 13, 1935, page 13.

4. **A. J. Stamm.** *Industrial and Engineering Chemistry*, volume 19, 1927, page 1021.

5. **A. J. Stamm.** *Industrial and Engineering Chemistry*, analytical edition, volume 1, 1929, page 94.

6. **A. J. Stamm.** *Industrial and Engineering Chemistry*, analytical edition, volume 2, 1930, page 240.

7. **A. J. Stamm, R. M. Seborg.** *Industrial and Engineering Chemistry*, volume 28, 1936, page 1164.

8. **A. J. Stamm, R. M. Seborg.** *Industrial and Engineering Chemistry*, volume 31, 1939, page 897.

9. **A. J. Stamm, R. M. Seborg.** *Transactions* of American Institute of Chemical Engineers, volume 37, 1941, page 385.

10. Forest Products Laboratory Resin-Treated Wood (*Impreg*), **A. J. Stamm, R. M. Seborg.** Forest Products Laboratory Mimeo 1380 (restricted), November 1941.

11. Forest Products Laboratory Resin-Treated Laminated Compressed Wood (*Compreg*), **A. J. Stamm, R. M. Seborg.** Forest Products Laboratory Mimeo 1381 (restricted), January 1942.

12. **C. G. Suits, M. E. Dunlap.** *General Electric Review*, volume 34, 1931, page 706.

13. **R. E. Wilson.** *Industrial and Engineering Chemistry*, volume 13, 1921, page 326.

Per-Unit Impedances of Synchronous Machines—II

A. W. RANKIN
MEMBER AIEE

THE preceding part[1] of this paper derived the generalized per-unit equations of the synchronous machine. The machine impedances were divided into two groups: those measurable from the stator terminals (x_d, x_d', r, and so forth), called the definitive impedances, and those internal impedances which cannot be measured from the stator terminals (X_{afd}, X_{ffd}, R_{ffd}, and so forth), called the nondefinitive impedances. The per-unit values of the definitive impedances are independent of the base rotor currents, but part I showed that the per-unit values of the nondefinitive impedances are functions of the base rotor currents, and accordingly are subject to misuse and misinterpretation unless the rotor-current bases are explicitly defined. These rotor-current bases and their corresponding base-current ratios are the fundamental quantities in any per-unit system, and this concluding part II is devoted to a fuller exposition of the base-current ratios of the more important per-unit systems.

To a considerable extent, the subject of base-current ratios is of primary interest only to the design engineers directly responsible for the calculation of the per-unit impedances. They must continuously guard against any inadvertent change of base during the analysis of new rotor circuits, since this would result in an impedance not in accord with the other rotor circuits. However, the application engineer also is directly interested in base-current ratios, because:

1. Such knowledge is necessary in order that he may be assured that all the per-unit impedances are in accord.

2. In many applications it is of advantage to introduce new bases or to use impedances calculated on some other base.

One specific base-current ratio is defined and evaluated in this paper, and its adoption or use as a preferred base in the calculation of per-unit impedances is suggested. Such standardization is essential in order that published values of per-unit impedances may be properly interpreted and used. Many advantages will accrue to the general use of a preferred base rotor current. The chief of these is that, if all impedances are calculated on the preferred base, they then become immediately available for use in general analysis or general equivalent circuits without fear of misapplication, and without the trouble and possible errors involved in determining the base current on which they were calculated and in converting this to a preferred base. As another example of the advantages of a preferred base rotor current, it should be noted that without recourse to a preferred base it is not possible when studying two per-unit impedance formulas to separate an improvement in the quality of the underlying analysis from a mere change in the rotor-current base.

It is obvious that the adoption of some preferred rotor-current base will have no effect upon vector diagrams as seen from the machine terminals. The base field current for such diagrams will continue to be that corresponding to normal open-circuit air-gap-line voltage, although the preferred base rotor currents will be used in calculating the impedance values.

This paper also brings together and evaluates the several base-current ratios which are found in contemporary literature; this evaluation is necessary in order to harmonize the various published per-unit impedance formulas. The method of converting all per-unit impedances to preferred-base impedances is evident from the expressions given in "Results", part I.

Suggested Preferred Bases

It is unnecessary to discuss the stator bases since by universal practice these are taken as the name-plate values (e_{ao}, i_{ao}, L_{ao}, x_{ao}). No corresponding universal practice exists in the selection of the rotor base quantities, and the adoption of some base-current ratio as a preferred standard for use in the calculation of machine impedances would be of advantage.

The base field current which in the author's experience offers the most advantages is that field current which will induce in each stator phase a voltage equal to $x_{ad}i_{ao}$. This will hereinafter be termed the "x_{ad}" base. Because of the advantages of this base itemized in the following, it is suggested that this x_{ad} base be adopted as a preferred standard:

(*a*). It makes X_{afd} numerically equal to x_{ad}, and at once makes unnecessary any further differentiation between these quantities.

(*b*). It makes the stator leakage reactance (x_d-X_{afd}) identical with the more familiar "leakage" reactance (x_d-x_{ad}). With a similar definition of the base current in the fictitious quadrature-axis field circuit, the stator leakage reactance is the same for both axes.

(*c*). It is in more common use at present than any other base (although implicitly only), and many of the present impedance formulas are based on it.

The base-current ratio for this field current is given by equation 1c. This expression is derived in the following section under definition 1.

$$\frac{I_{fdo}}{(3/2)i_{ao}}=\frac{4}{\pi}\frac{A_{d1}}{F_{d1}}\frac{N}{K_pK_dP_1}\frac{1}{N_{fd}} \tag{1c}$$

The foregoing definition of base current is also suggested for the additional rotor circuits of machines with one additional rotor circuit in each axis. The advantages are the same as those given for the base field current. The base-current ratio for the additional rotor circuits is then as given by equation 1d. This expression is also derived in the following section under definition 1.

$$\frac{I_{xdo}}{(3/2)i_{ao}}=\frac{4}{\pi}\frac{A_{d1}}{D_{d1x}}\frac{N}{K_pK_dP_1}\frac{1}{N_{xd}} \tag{1d}$$

Synchronous machines with more than one additional rotor circuit in each axis require an involved analysis in which it is often advantageous to use specialized base quantities. For that reason it does not appear advisable to adopt preferred bases for multiple rotor circuits.

Specific Base-Current Ratios

The more important base-current ratios with practical advantages are given by the following four definitions. These definitions are summarized in Table I.

Definition 1: Let base field current I_{fdo} be that current which will induce in each stator phase a voltage equal to $x_{ad}i_{ao}$; let base rotor-circuit current I_{xdo} be similarly defined. These are the base currents presented in the preceding section. These bases are hereinafter termed the x_{ad} bases.

With three-phase currents of magnitude i_{ao} in the stator, and with the rotor cir-

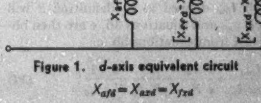

Figure 1. *d*-axis equivalent circuit

$X_{afd}=X_{axd}=X_{fxd}$

Paper 45-143, recommended by the AIEE committee on electric machinery for publication in AIEE TRANSACTIONS. Manuscript submitted April 11, 1945; made available for printing July 10, 1945.

A. W. RANKIN is in the turbine-generator engineering division of General Electric Company, Schenectady, N. Y.

The author acknowledges the co-operation of his associates in the General Electric Company in the preparation of this paper. In particular, thanks are extended to S. B. Crary for his constructive criticisms and valuable suggestions and to C. E. Kilbourne for the use of several of his unpublished reports on machine reactances.

cuits open, the maximum of the fundamental-component flux density is as given by equation 1a.

$$B_{ga}(\max)=0.4\pi\frac{4}{\pi}\frac{1.5i_{ao}N}{K_pK_dP_1}\frac{2.54}{g}A_{d1} \qquad \text{(1a)}$$

The corresponding phase voltage is $x_{ad}i_{ao}$. By definition 1, I_{fdo} is the field current which will give a fundamental-component density equal to equation 1a. The maximum of the fundamental component due to I_{fdo} is as given by equation 1b.

$$B_{gf}(\max)=0.4\pi N_{fd}I_{fdo}\frac{2.54}{g}F_{d1} \qquad \text{(1b)}$$

The base-current ratios of definition 1 are thus as given in equations 1c, d.

$$\frac{I_{fdo}}{(3/2)i_{ao}}=\frac{4}{\pi}\frac{A_{d1}}{F_{d1}}\frac{N}{K_pK_dP_1}\frac{1}{N_{fd}} \qquad \text{(1c)}$$

$$\frac{I_{xdo}}{(3/2)i_{ao}}=\frac{4}{\pi}\frac{A_{d1}}{D_{d1x}}\frac{N}{K_pK_dP_1}\frac{1}{N_{xd}} \qquad \text{(1d)}$$

It is evident from definition 1 that these x_{ad} bases make X_{afd} and X_{axd} numerically equal to x_{ad}.

Definition 2: Let base field current I_{fdo} be that current which will give a magnetomotive force per pole equal to the flat-topped armature reaction at normal stator current; let base current I_{xdo} be similarly defined. These bases are hereinafter termed the magnetomotive-force bases.

The base-current ratios can be written directly as in equations 2a, b.

$$\frac{I_{fdo}}{(3/2)i_{ao}}=\frac{N}{K_pK_dP_1}\frac{1}{N_{fd}} \qquad \text{(2a)}$$

$$\frac{I_{xdo}}{(3/2)i_{ao}}=\frac{N}{K_pK_dP_1}\frac{1}{N_{xd}} \qquad \text{(2b)}$$

Note that the base currents of these magnetomotive-force bases are easily evaluated since equations 2a, b do not contain pole-shape coefficients such as A_{d1}, F_{d1}, D_{d1x}, etc.

Definition 3: Let base field current I_{fdo} be the field current required to produce normal, open-circuit, air-gap-line stator voltage; let base current I_{xdo} be similarly defined. These bases are hereinafter termed the unit-voltage bases.

$$\psi_{ao}=10^8L_{afd}I_{fdo}=10^8L_{ao}i_{ao} \qquad \text{(3a)}$$

Therefore

$$\frac{I_{fdo}}{(3/2)i_{ao}}=\frac{L_{ao}}{(3/2)L_{afd}} \qquad \text{(3b)}$$

$$\frac{I_{xdo}}{(3/2)i_{ao}}=\frac{L_{ao}}{(3/2)L_{axd}} \qquad \text{(3c)}$$

Dividing equation 1a by equation 1b with I_{fdo} defined as in definition 3 will give x_{ad}, and equations 3d, e are then obtained from equations 3b, c.

$$\frac{I_{fdc}}{(3/2)i_{ao}}=\frac{4}{\pi}\frac{A_{d1}}{F_{d1}}\frac{N}{K_pK_dP_1}\frac{1}{N_{fd}}\frac{1}{x_{ad}} \qquad \text{(3d)}$$

$$\frac{I_{xdo}}{(3/2)i_{ao}}=\frac{4}{\pi}\frac{A_{d1}}{D_{d1x}}\frac{N}{K_pK_dP_1}\frac{1}{N_{xd}}\frac{1}{x_{ad}} \qquad \text{(3e)}$$

The major advantage of the unit-voltage bases is that the stator–rotor mutual coupling coefficients are unity for the field circuit and the base additional rotor circuit.

Definition 4: Let the base rotor currents be defined so that the mutual impedances (X_{afd}, X_{axd}, X_{fxd}) for a machine with one additional rotor circuit are all equal. These bases are hereinafter termed the equal-mutuals bases.

$$X_{afd}=X_{axd}=X_{fxd} \qquad \text{(4a)}$$

Equating 2a, 2b, and 3c of part I gives the base-current ratios in terms of the mutual inductances corresponding to equation 4a. These are evaluated in terms of design dimensions in equations 4b, c, d, and the base-current ratios of equations 4e, f thereby obtained.

$$L_{afd}=3.19\times10^{-8}\frac{4Rl}{P_1g}\frac{N}{K_pK_d}N_{fd}F_{d1} \qquad \text{(4b)}$$

$$L_{axd}=3.19\times10^{-8}\frac{4Rl}{P_1g}\frac{N}{K_pK_d}N_{xd}D_{d1x} \qquad \text{(4c)}$$

$$L_{fxd}=3.19\times10^{-8}\frac{4Rl}{g}N_{fd}N_{xd}D_{dox}y_{xd} \qquad \text{(4d)}$$

$$\frac{I_{fdo}}{(3/2)i_{ao}}=\frac{N}{K_pK_dP_1}\frac{1}{N_{fd}}\frac{D_{d1x}}{D_{dox}y_{xd}} \qquad \text{(4e)}$$

$$\frac{I_{xdo}}{(3/2)i_{ao}}=\frac{N}{K_pK_dP_1}\frac{1}{N_{xd}}\frac{F_{d1}}{D_{dox}y_{xd}} \qquad \text{(4f)}$$

The equal-mutuals bases are of particular importance with machines having only one additional rotor circuit in each axis, as they result in the simple equivalent circuit of x_{la} in series with the parallel combination of X_{afd}, X_{lfd}, and X_{lxd}. It should be noted, however, that it is not now possible to replace X_{afd} by the more common x_{ad}, as these quantities are no longer equal. This fact seems to have been overlooked in the application of this simplified circuit.

Rotor Bases in Current Use

From the preceding analysis, it is evident that impedance formulas are subject to misuse unless the base-current ratios are known. A compendium of the base-current ratios of the present technical literature is needed in order to harmonize the various published results. This section offers the first step toward such a general compendium.

It is not necessary to study those publications which considered only the definitive impedances, since these are independent of the rotor bases. Examples of the papers which presented formulas for the rotor impedances as well as the stator quantities are Doherty and Shirley,[2] Linville,[3] and Kilgore.[4] The papers of Doherty and Nickle,[5] Park and Robertson,[4] Park,[7] and Waring and Crary[8] are illustrative of the papers on the operational machine equations. It is obvious that these two groups fail to include many important publications, but those listed are adequate to illustrate the need for a more complete survey.

Table I. Base Rotor Currents Used in the Calculation of Per-Unit Machine Impedances

Definition Characteristic	Base Field Current and Base Additional Rotor-Circuit Current Will
1. . x_{ad}	Induce in each stator phase a peak voltage equal to $x_{ad}i_{ao}$
2. . Magnetomotive force	Give in their respective windings a magnetomotive force equal to the flat-topped armature reaction at normal stator current
3. . Unit voltage	Induce in each phase normal open-circuit air-gap-line stator voltage
4. . Equal mutuals	Result in equal mutual impedances ($X_{afd}=X_{axd}=X_{fxd}$) for a machine with one additional rotor circuit

The base field current used by Doherty and Shirley may be derived from their expression for the increase in field magnetomotive force* due to the short-circuit current. It is the field current which will produce a magnetomotive force equal to $1/K_\phi$ times the flat-topped armature reaction, and differs only by the factor K_ϕ from the base field current of the magnetomotive-force base (definition 2). The corresponding base-current ratio is given by equation 5.

$$\frac{I_{fdo}}{(3/2)i_{ao}}=\frac{N}{K_pK_dP_1}\frac{1}{N_{fd}}\frac{1}{K_\phi} \qquad \text{(5)}$$

Doherty and Shirley did not discuss any additional rotor circuits.

The base rotor currents used by Linville are explicitly defined as those which will produce in their respective windings a magnetomotive force equal to the flat-topped armature reaction. These are the base currents of the magnetomotive-force bases (definition 2), and the corresponding base-current ratios are evaluated in equations 2a, b.

Kilgore uses "effective" rotor leakage reactances defined as the quantities which when added to (x_d-x_{ad}) will give x_d' and x_d''. The base rotor currents are then such as to make the base stator–rotor mutual inductances numerically equal to x_{ad}. These are the base currents of the x_{ad} base (definition 1), and the corresponding base-current ratios are evaluated in equations 1c, d.

Doherty and Nickle specified as base field current that current which would produce normal open-circuit air-gap-line stator voltage. For a per-unit system with reciprocal mutual impedances, this is the base field current of the unit-voltage base (definition 3), and the corresponding base-current ratio is evaluated in equation 3a.

---

* Equation 2, page 1259, reference 2.

A relatively large amount of machine analysis is based on the simplified circuit of Figure 1 although x_{ad} is commonly used in place of X_{afd}. The base currents which result in this circuit are the equal-mutuals bases of equations 4e, f (definition 4). Note that x_{ad} should not be used in place of X_{afd} as these two are equal only for the conditions of definition 1, the x_{ad} bases.

The base field current used by Park and Robertson was that which would give normal open-circuit air-gap-line stator voltage, but nonreciprocal mutual-impedance relations were used which resulted in the following expression for x_d'.

$$x_d' = x_d - \frac{X_{afd}}{X_{ffd}}\,^{*} \tag{6a}$$

If equation 6a is compared with equation 6b which is the more general expression for x_d',

$$x_d' = x_d - \frac{X^2_{afd}}{X_{ffd}}\,^{**} \tag{6b}$$

it is evident that satisfactory values of x_d' can be obtained only if X_{afd} is calculated on a base which recognizes the nonreciprocal mutual impedances.

The base current of Park is that of definition 3, but nonreciprocal mutual impedances are used which for all practical purposes restrict the application to machines with no additional rotor circuits.

The equations of Waring and Crary are general and dimensionally correct, and are not restricted to any specific base current. The base quantities are set by the design engineer in the calculation of the impedances. If it is desired to use the restricted operational equations of references 5 and 6 on machines with multiple rotor circuits, the necessary nonreciprocal mutual impedances can be best obtained by modifying the corresponding reciprocal mutual impedances of Waring and Crary as recently published by the author.[9]

To illustrate quantitatively the effect which the foregoing multiplicity of bases has upon the machine impedances, consider a machine with the design constants given by equation 7.

$$\left.\begin{array}{lll} K_\phi = 0.98 & \dfrac{4}{\pi}\dfrac{A_{d1}}{F_{d1}} = 1.10 & x_{ad} = 1.20 \\ D_{d1x} = 0.84 & D_{dox}y_{xd} = 0.73 & \end{array}\right\} \tag{7}$$

Assume that x_d, X_{fd}, X_{ffd} are calculated by formulas using the base-current ratios of the x_{ad} bases (definition 1). If these same quantities are calculated for the same machine but by formulas based on the other ratios given in the foregoing review, the numerical values so obtained will be as shown in Table II. The values in this table are in per cent of the values calculated by formulas based on the x_{ad} bases.

Table II. Calculated Numerical Values for x_d, X_{afd}, and X_{ffd}

	x_d	X_{afd}	X_{ffd}
By the x_{ad} bases (definition 1)	100	100	100
By the magnetomotive force bases (definition 2)	100	91	83
By the unit-voltage bases (definition 3)	100	83	69
By the equal-mutuals bases (definition 4)	100	105	110
By equation 5	100	93	86

The magnitude of the possible error due to the misapplication of a per-unit impedance which has been calculated on a rotor-current base not explicitly defined is evident from Table II. The nonreciprocal relations of references 6 and 7 are not included in this table as their application is relatively rare. It is self-evident that this example is applicable only to the machine with the constants given by equation 7. The variations for other machines may be much greater or much less than those illustrated, depending on the design data.

Nomenclature

The nomenclature consists of the quantities given in the following plus the nomenclature of part I. All dimensions are in inches. As in part I, all quantities are in per unit except those in bold-face type which are in the physical ampere-inch system (ohms, henrys, and so forth). Quantities such as N, P_1, K_p, etc., for which it is obviously unnecessary to distinguish the ampere-inch values by a special script are in standard type only.

ar = flat-topped armature reaction at base current $= \dfrac{1.5Ni_{ao}}{K_pK_dP_1}$ ampere turns per pole

A_{d1}† = factor by which the maximum flux density is multiplied to obtain the maximum of the fundamental component of flux density; machine excited by a sine-wave armature magnetomotive force in direct axis

$\frac{2}{\pi}D_{dox}$ = factor by which the maximum flux density is multiplied to obtain the average density within the damper circuit of span $2y_{xd}$; machine excited by the damper circuit of span $2y_{xd}$ in the direct axis

D_{d1x} = same as A_{d1}, but with machine excited by the magnetomotive force of the xth additional rotor circuit in the direct-axis

F_{d1}‡ = same as A_{d1}, but with machine excited by the magnetomotive force of the direct-axis field winding

g = effective air gap

K_p, K_d = pitch and distribution factors, respectively (greater than 1.0)

K_ϕ# = ratio of total flux per pole to the total fundamental flux per pole, at no load; machine excited by the magnetomotive force of the direct-axis field winding

l = machine stacked length, inches

N = stator series turns per phase

N_{fd} = turns per pole of field-winding circuit

N_{xd} = turns per pole of xth additional rotor circuit

P_1 = number of poles

R = stator bore radius, inches

x_d', x_d'' = transient and subtransient reactances, respectively

x_{la}, X_{lfd}, X_{lxd} = leakage reactances; armature, field, and xth additional rotor circuits; for use with equal-mutuals bases only

$2y_{xd}$ = span of xth additional rotor circuit, direct axis, in per unit of half pole pitch

References

1. Per-Unit Impedances of Synchronous Machines, A. W. Rankin. AIEE Transactions, volume 64, 1945, August section, pages 569–73.

2. Reactance of Synchronous Machines, R. E. Doherty, O. E. Shirley. AIEE Transactions, volume 37, 1918, pages 1209–97.

3. Starting Performance of Salient-Pole Synchronous Motors, T. M. Linville. AIEE Transactions, volume 49, 1930, pages 531–47.

4. Calculations of Synchronous Machine Constants, L. A. Kilgore. AIEE Transactions, volume 50, 1931, pages 1201–13.

5. Synchronous Machines—I, II, R. E. Doherty, C. A. Nickle. AIEE Transactions, volume 45, 1926, pages 912–42.

6. The Reactances of Synchronous Machines, R. H. Park, B. L. Robertson. AIEE Transactions, volume 47, 1928, pages 514–35.

7. Two-Reaction Theory of Synchronous Machines, R. H. Park. AIEE Transactions, volume 48, 1929, pages 716–27.

8. Operational Impedances of a Synchronous Machine, M. L. Waring, S. B. Crary. *General Electric Review*, volume 35, 1932, page 578.

9. Equations of the Idealized Synchronous Machine, A. W. Rankin. *General Electric Review*, volume 47, June 1944.

10. Graphical Determination of Magnetic Fields, R. W. Wieseman. AIEE Transactions, volume 46, 1927, pages 141–48.

---

* Equation 20, reference 6.

** Equation 20, reference 8.

† See Figure 13, reference 10.

‡ This is the A_1 factor given by Figure 8, reference 10.

See Figure 10, reference 10.

Wound- and Dummy-Rotor Methods of Quality Control and Trouble Shooting of Induction-Motor Windings and Cores

P. H. TRICKEY
MEMBER AIEE

ONE OF THE FUNDAMENTAL principles in the solution of problems is the division of the large problem into several smaller ones. This principle is used throughout electric-motor engineering. One of the most common examples is the use of design constants or parameters. For instance, the complete characteristics of an induction motor are fixed and performance is determined if six constants are known.

r_1 = primary resistance
r_2 = secondary resistance
X = short-circuit reactance
X_0 = open-circuit reactance
F_e = iron loss
$F+W$ = friction plus windage

If quality-control methods are used in the factory to prevent the values of these constants from straying beyond desired limits for a given design, then final assembly and test will not be plagued with rejections of defective motors.

It is the function of this paper to discuss means of controlling the variation of F_e iron loss and X_0 open-circuit reactance. The open-circuit reactance is also a measure of the ampere turns necessary to set up the magnetic flux and a measure of the final magnetizing current and no-load amperes.

Because most induction motors have permanently short-circuited secondary windings in the form of squirrel-cage rotors, it has become customary to measure X_0 and F_e by running the motors at synchronous speed. Under this condition, there is no current in the rotor of a polyphase motor, and a condition equivalent to open-circuited secondary winding exists. Actually, except for very small motors, satisfactory results are obtained at no-load speeds slightly under synchronism.

While the measurement of X_0 and F_e on completed motors is necessary and desirable in quality control and trouble shooting, its obvious objection is that defective parts have not been eliminated at the source, but have continued through all the expensive and time-consuming manufacturing operations. Another very serious disadvantage is that small variations in the iron loss and ampere turns of the magnetic circuit are obscured and confused by ordinary variations in friction and air gap.

The stator is the most frequent source of troublesome variation, and one method of overcoming the difficulties mentioned is to test all stators in a fixture with rotor on bearings and duplicating normal operating conditions. The main objections to this method are its practical difficulties of construction, cost, and the necessity of applying it to a completely machined and ground stator.

Since the purpose is to duplicate the condition of open-circuited secondary winding, why not abandon the substitute method of running at synchronous speed and go directly to the open-circuited rotor? If only a single motor were involved, of course, there would be the expense of making a special rotor without squirrel cage. When hundreds or thousands of motors are in quantity production, however, the cost of a special "dummy" rotor for testing is negligible.

Dummy Rotors

Dummy test rotors are constructed exactly like the regular rotors, except without squirrel cage, and ground to the finished diameter of the regular rotor to obtain the regular air gap when testing finished stators. If it is necessary to provide means for holding the lamination in place, such means must not be conducting if it includes the magnetic circuit. The slots usually are left in to keep flux distribution as near normal as possible. Regular shafts are not necessary, because they do not rotate, but usually some sort of unfinished shaft is used to provide a convenient handle.

If polyphase power is applied to a polyphase stator and dummy rotor, the magnetic conditions differ somewhat from the open-circuit conditions in the regular motor. The first difference is that the high-frequency pulsation and surface losses caused by motor teeth and slot openings passing each other are not present. Partly offseting these, the rotor iron loss is at line frequency instead of slip frequency. The second difference is that the helpful effect of rotor currents in improving the sinusoidal flux distribution are not present. The nearer the stator winding is to having a sinusoidal distribution itself, the less will be this difference.

However, for quality control and trouble shooting, relative values and difference between good and bad stators are much more important than the actual value.

One of the difficulties in both no-load and dummy rotor tests with polyphase stators is the low power factor. This gives the difference of two large values when reading input by the two-wattmeter method. Since relative values are desired, and not actual, dummy-rotor test investigations very often are made with only single phase on the stator. This excites one phase only and gives about half the polyphase iron loss.

In general for comparative purposes, it is necessary to deduct only the primary copper loss before comparing readings; however a more accurate measure of the percentage variation is obtained when the constant-rotor iron loss also is deducted. The main difficulty in this is a means to measure it. Since it is usually small, a calculation from iron-loss curves may be

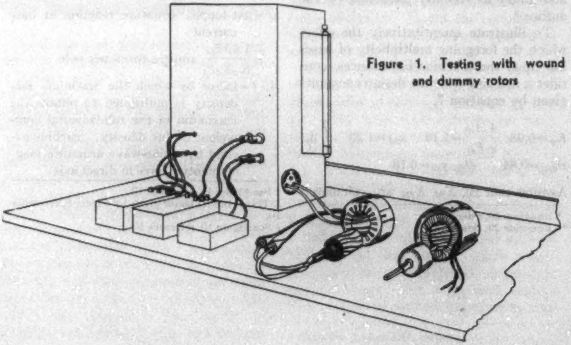

Figure 1. Testing with wound and dummy rotors

Paper 45-166, recommended by the AIEE committee on electric machinery for publication in AIEE TRANSACTIONS. Manuscript submitted April 17, 1945; made available for printing August 20, 1945.

P. H. TRICKEY is chief engineer of the Diehl Manufacturing Company, Somerville, N. J.

Table I. Regular Test of Stator Cores

Volts = 91

	Stator Number					
	1		2		3	
	Max	Min	Max	Min	Max	Min
Amperes	2.13	1.82	2.08	1.82	2.13	1.92
Watts	24.0	22.0	25.5	24.5	23.0	22.0
Resistance after test	1.410		1.410		1.410	
I^2R	6.4	4.7	6.1	4.7	6.4	5.2
Total iron loss	17.6	17.3	19.4	19.8	16.6	16.8
Total iron loss from item 1	5.5	5.5	5.5	5.5	5.5	5.5
Stator iron loss	12.1	11.8	13.9	14.3	11.1	11.3

sufficiently accurate. If a test value is desired, it may be necessary to put a temporary winding on the rotor and test with an oversize dummy stator as described later.

For quality control of polyphase wound-rotor motors or single-phase repulsion motors, readings may be taken on every new design with the brushes lifted, thus providing a dummy-rotor reading for comparison in case of future trouble. In case of regular squirrel-cage motors, the special dummy rotor must be provided. It is not necessary that a separate rotor be provided for every core stack. One rotor longer than any expected size is usually sufficient. In fact, it is better to have the rotor longer than the stator to eliminate the necessity for special care on axial location in testing.

The dummy-rotor method provides one of the most accurate tests of a wound stator that there is. Its accuracy may be increased even further for iron-loss or short-circuit investigation by using higher frequencies such as 500 or 1,000 cycles. Of course, any comparison to actual value disappears, and the tests become relative only.

Very often, the high-frequency test will provide a high-potential test between turns as a by-product.

Wound Rotors

We have mentioned the advantage of the dummy rotor over the running test in eliminating confusion due to variation in friction. However, the dummy-rotor test does require a winding in the stator with the possibility that expensive winding and machining operations may be completed before it is found that the stator cores have excessive iron loss. Under certain conditions it is difficult to distinguish between excessive iron loss and stator short circuits of one turn only. Also small variations in the number of stator turns may be confused with excess iron loss.

To overcome these disadvantages, the "wound-rotor" method may be used. This method consists of providing a winding on the test rotor and exciting from the rotor instead of the stator. Tests may then be made on bare cores without any windings, housing, or any machining whatsoever, thus eliminating any question of defective windings when iron loss is being investigated or controlled. Also progressive tests may be made after each winding and machining operations to see if any harm has been done to the magnetic structure and increased the iron loss.

The same differences occur between the condition of actual operation and the condition of wound-rotor test as occur with the dummy rotor. That is, the flux in the rotor is at line frequency instead of slip frequency, and the flux distribution may be less sinusoidal than in the actual machine with squirrel-cage rotor. If the wound rotor is designed for this purpose, it can have sinusoidally distributed windings which will keep this difference fairly small. The main difference in the flux distribution of the wound rotor is that the excitation comes from the rotor. This means that the gradual loss of leakage flux from the useful flux progresses from rotor to stator instead of from stator to rotor. To be specific, in the regular case the air-gap flux is less than the stator flux by the leakage but in the wound-rotor test, the air-gap flux must be kept greater than the stator flux by the leakage in order to give the same stator flux; actually the matter can be easily taken care of by adjusting the turns of the rotor, and except for extremely high densities the difference in flux distribution does no harm.

Wound rotors are usually made single phase to eliminate the error of two large wattmeter readings which occurs on the two-wattmeter method with three phase.

It is usually necessary to deduct the rotor copper loss when comparing iron-loss readings, particularly if some of the stator cores are ground to finished diameter and some are as punched. In order to obtain a better representation of percentage differences, the rotor iron loss also may be deducted. The value may be obtained by calculation or by test with a special oversize dummy stator, bored to size, but having no slots and a diameter much bigger than the regular stator. The densities in this will be very small, and even a rough calculation is sufficient to determine the iron loss. To be more specific, a test is made of the wound rotor in the dummy stator. The rotor copper loss and calculated stator iron loss are subtracted from the input. The remainder is used as the rotor iron loss for all further testing with the wound rotor.

For some work it is desirable to keep all conditions of the wound-rotor tests as near like actual conditions as possible. In these cases, the same number of poles are used as in the motor windings. However, many times the readings are magnified and more useful when two-pole rotors are used.

As in the case of the dummy rotors, high frequency may be used to make the tests more sensitive.

It is often necessary to turn the wound rotor in the stator being tested and take maximum and minimum readings. The effect of the grain of rolling the steel, and the effect of rivet and bolt holes are often quite pronounced.

Very often the need of a wound rotor for test analysis or trouble shooting occurs without warning, and there is no time to design and build a special rotor. Sometimes in these cases, a d-c or repulsion-motor armature may be obtained and leads soldered to opposite commutator bars for connections. Even if the air gap is larger than desirable or unusual test voltage and frequency necessary, comparative readings usually can be obtained which are usable in separating good and bad stator cores.

If wound rotors are used continuously, the windings and core structure are apt to become damaged. Protective coatings of varnish or other material should be used. Sometimes it is desirable to have a master standard kept in the laboratory for calibrating new or rewound rotors.

Wound rotors may be used as turn counters for stator windings by reading the induced voltage in the maximum position. If the test is a routine one comparing production stators with a master or sample stator, a direct reading is sufficient. If turns of an unknown winding are desired, it is necessary to apply voltage and read induced voltage on both rotor and stator. In this case

$$K = \frac{\text{effective turns of stator}}{\text{effective turns of rotor}}$$

$$= \sqrt{\frac{E_s\ \text{read}}{E_r\ \text{applied}} \times \frac{E_s\ \text{applied}}{E_r\ \text{read}}}$$

Very often stator short circuits can be distinguished from excessive iron loss by turning the wound rotor. Usually stator short circuits are of a single-phase nature such as one turn or one coil short-circuited. In this case, the maximum reading shows up the short circuit very prominently, and the minimum reading shows no effect at all.

A typical example of the use of wound and dummy rotors occurred some years ago. The first indication of trouble was an excessive number of rejects on final motor test. After a number of the

Power Systems for Auxiliary Drives in Steam-Electric Stations

J. B. McCLURE
ASSOCIATE AIEE

S. I. WHITTLESEY
ASSOCIATE AIEE

A STEAM-ELECTRIC power station in general consists not only of such major items as boiler equipment, steam-turbine-generator units and condensers, but also of many auxiliaries. These auxiliaries now have come to be almost exclusively a-c-motor-driven, although steam-driven auxiliaries are used occasionally in some topping installations where their use improves the heat cycle and in other cases for stand-by service. Since the reliability of a station can be no better than the reliability of its auxiliaries, the power-supply system for these auxiliaries, as well as the associated motors and control, become important items in the design of a steam-electric-power station.

These considerations in conjunction with the recent rapid rise in the quality and acceptance of factory-assembled switchgear, control, and transformer equipments make it now opportune to consider the design of the power system for these auxiliaries, taking full advantage of factory-assembled equipments. It is hoped that this discussion will not only direct proper attention to this over-all problem, but also indicate how a new level of reliability, economy, simplicity both in installation and operation, and safety to personnel can be obtained readily on power systems for auxiliaries by proper design approach based on such factory-assembled equipments.

As a result of discussions with several operating groups and after studying various types of auxiliary-power systems, together with the existing methods of obtaining auxiliary power, the following general conclusions have been reached. These conclusions should serve as a guide in planning power systems for auxiliaries.

Conclusions

1. A separate auxiliary-power system should be considered for each boiler.

2. Power supply from the main-generator leads is being increasingly used.

3. The preferred voltages are 460 and 2,400 volts.

4. It is economical to use a single-voltage 460-volt system, where the required transformer capacity per boiler does not exceed 1,000 kva.

5. A dual-voltage system comprising 2,400 and 460 volts should be considered where the required transformer capacity per boiler is 1,500 kva or greater.

6. In a dual-voltage system motors up to at least 250 horsepower can be economically applied at 460 volts.

Power Requirement of the Auxiliaries

The over-all auxiliary-power requirements for any given new steam-turbine-generator capacity can never be determined precisely until the plant is placed in operation. However, it can be reasonably estimated if proper attention is given to such details as the number and type of boilers, the pressure and maximum flow of steam, the nature of the feed-water piping, and the type and treatment of fuel. This last item is particularly significant, as it is evident that pulverized-coal-fired boilers will require more auxiliary power than boilers using other types of fuel, because of the pulverizers and exhauster fans.

Figure 1 gives the approximate total auxiliary power in per cent of the maximum output of a turbine-generator set. In addition, the probable individual power requirements for the major auxiliaries are indicated. The auxiliary-power requirement should be based upon the actual maximum output of the turbine-generator set. In a specific case this output may be any value between the nominal rated and the maximum permissible from the set, depending upon the capacity of the boiler plant. Thus, since the boiler capacity is selected normally with a margin to cover adverse conditions of fuel, draft, and boiler maintenance, it is evident that the boiler-plant capacity really determines the auxiliary-power requirements, through its effect on the actual maximum output of the set.

The total auxiliary power, of course, is the difference between the gross and net output of the turbine-generator set. The total auxiliary transformer capacity can be approximated by assuming a power factor of 0.8 to 0.85 for the power requirements obtained from Figure 1. In the final design, however, transformer capacities should be determined conservatively by totalizing the coincidental loads with due regard for power factor. In addition, provision must be made for general station power facilities such as lighting, machine shop, and coal-handling equipment. These general station power requirements are very often associated with the auxiliary-power supply for the first one or two units in a station.

The size of the individual motors for the major auxiliaries is determined largely by the rating of the individual boilers and

---

Paper 45-150, recommended by the AIEE committee on power generation for publication in AIEE TRANSACTIONS. Manuscript submitted June 21, 1945; made available for printing July 30, 1945.

J. B. McCLURE and S. I. WHITTLESEY are both in the central-station engineering division of General Electric Company, Schenectady, N. Y.

The authors express their appreciation to the representatives of the operating companies who contributed during the discussions on this subject, and acknowledge the helpful suggestions of A. H. Fish, D. M. Jones, and J. C. Page, in the preparation of this paper, and the assistance of F. S. Li in making the economic studies summarized herein.

---

good and bad motors were tested by the dummy-rotor method, it became certain that the trouble was in the stator and was due either to short circuits or excessive iron loss. Resistances and torques indicated that the number of turns were probably correct.

After the good and bad stators were tested by the wound-rotor method, it was found that the bad stators were bad in both maximum and minimum positions. This created considerable suspicion of short circuits in the stator windings. This point was settled when the stators were stripped. The good stators remained good, and the bad stators remained bad, with the readings the same as before the windings were removed.

This was considerable relief to the winding department which had previously been rewinding so called "defective" stators.

The next step was to institute a 100-per-cent wound-rotor test on all stator cores before winding. This immediately removed the rejects.

Upon further investigation of the good and bad cores as they came from the core building department, the trouble was found to be due to a lack of insulating iron-oxide scale which was the only insulation between individual laminations. Once this condition was corrected, and proper insulation provided between laminations, the rejects of defective cores prior to winding dropped to practically zero and the 100-per-cent core test was taken off.

Appendix. Typical Test and Analysis

1. Wound rotor tested with dummy stator to determine rotor iron loss:

Volts = 91
Amperes = 0.64
Watts = 8.30
Resistance after test = 1.406
$I^2R = 0.58$
Total iron loss = 7.72
Calculated stator iron loss = 2.22
Rotor iron loss = 5.50

2. The regular test of stator cores is shown in Table I.

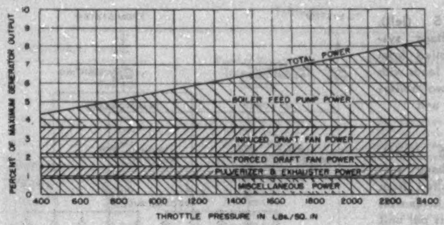

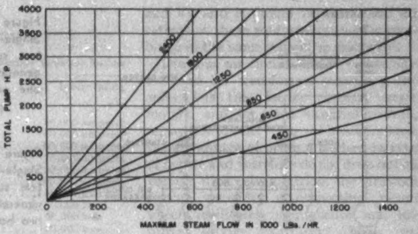

Figure 1 (left). Approximate total auxiliary power in per cent of maximum generator output in kilowatts and approximate division of power between major auxiliaries

Figure 2 (right). Boiler-feed-pump power for various pressures and maximum steam flows

does not necessarily bear any direct relation to the size of the turbine-generator set or the total auxiliary power associated with that set. As an aid in estimating the probable boiler arrangement for any contemplated installation, present boiler practice may be broadly summarized as follows:

Steam-turbine-generator units up to approximately 30,000 kw maximum rating generally have a single boiler; units between 30,000 kw and 60,000 kw maximum rating may have either one or two boilers, and practice is about equally divided in this region; units above 60,000 kw maximum rating generally have two boilers, although single boilers are now available and occasionally used up to a capacity of 1,000,000 pounds of steam per hour.

Boilers are usually rated in pounds of steam per hour, and a reasonable average steam rate for modern turbine-generator sets is nine pounds of steam per kilowatt-hour. Thus, it is evident that a 1,000,000-pound boiler would supply steam for a set output of at least 110,000 kw.

Figure 2 shows the estimated boiler feed-pump power for various pressures and flows, including liberal allowance for head loss in piping. In the smaller plants it is the usual practice to have a minimum of two pumps, each large enough to deliver maximum flow. This results in at least 100-per-cent spare pump capacity. In the larger plants two pumps often are required to provide maximum flow, and a third serves to provide 50-per-cent spare capacity. In some of the larger plants, boiler feed-water supply is provided by a combination of tank and booster pumps in series. In such arrangements, the booster pump is usually variable speed and of sufficient capacity to give the required outlet pressure range for the particular plant conditions and at the same time offset the rising pressure characteristic of the constant-speed pump at the lower flows. The capacity of such a combination may vary from 50 to 100 per cent of the total boiler requirements.

The actual motor ratings, in most cases, will be slightly greater than the values derived from Figure 2.

Figures 3 and 4 show approximate motor ratings for induced-draft and forced-draft fans, respectively. These curves are based on average values obtained by plotting actual motor ratings for several boiler ratings. The discontinuity between 200,000 pounds and 300,000 pounds flow results from a change in boiler construction in this region. It will be noted that induced-draft fans require more power than forced-draft fans. Thus, in practice, as the size of a boiler increases, two induced-draft fans often will be used with one forced-draft fan. Finally, in the largest boilers, both induced- and forced-draft fans may be split into two groups.

Power System Application Guides

A power-supply system for auxiliary drives in a steam-electric station is unique in many respects, for example:

1. There are a few large motors.
2. There are many small motors.
3. The cable runs are short.
4. The load is relatively constant
5. Voltage regulation is very seldom a problem.

In planning a system the following principles and practices which have demonstrated their soundness in service should be recognized:

(*a*). An adequate source of power must be available for starting up the plant.

(*b*). The entire system should be considered essential, since the essential motors are both large and small and are not confined to any one location in the plant.

(*c*). In cases where two voltages are used, it simplifies operation and switching arrangements to bring all the power to the higher-voltage bus.

(*d*). The reliability of metal-clad, insulated five-kilovolt busses and metal-enclosed 600-volt busses justifies a single-bus system.

(*e*). The reliability of power transformers justifies the use of a conventional radial system.

(*f*). High short-circuit currents should be avoided.

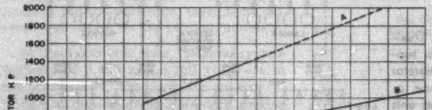

Figure 3 (left). Induced-draft-fan power

A—One fan per boiler or total power
B—Two fans per boiler—power per fan

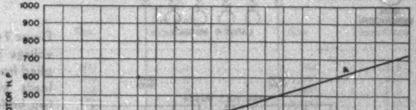

Figure 4 (right). Forced-draft-fan power

A—One fan per boiler or total power
B—Two fans per boiler—power per fan

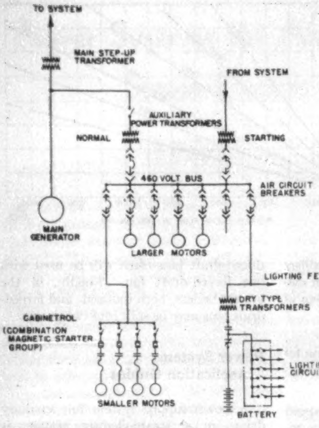
TO SYSTEM
MAIN STEP-UP TRANSFORMER
FROM SYSTEM
AUXILIARY POWER TRANSFORMERS
NORMAL
STARTING
460 VOLT BUS
AIR CIRCUIT BREAKERS
MAIN GENERATOR
LARGER MOTORS
LIGHTING FEEDER
DRY TYPE TRANSFORMERS
CABINETROL (COMBINATION MAGNETIC STARTER GROUP)
LIGHTING CIRCUITS
SMALLER MOTORS
BATTERY

Figure 5 (left). Single-voltage system supplied from generator leads with one or two boilers per unit

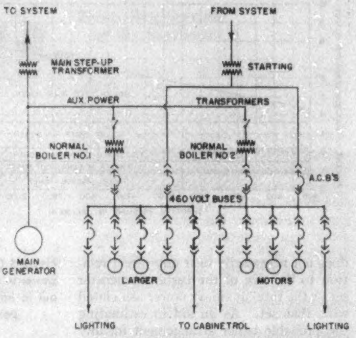
TO SYSTEM
FROM SYSTEM
MAIN STEP-UP TRANSFORMER
STARTING
AUX POWER
TRANSFORMERS
NORMAL BOILER NO.1
NORMAL BOILER NO 2
A.C.B'S
460 VOLT BUSES
MAIN GENERATOR
LARGER
MOTORS
LIGHTING
TO CABINETROL
LIGHTING

Figure 6 (right). Single-voltage system supplied from generator leads with two boilers per unit

The Auxiliary Power Source

Auxiliary power may be obtained from any of the following sources:

(*a*). Main-generator leads.
(*b*). Generator bus.
(*c*). House turbine-generator set.
(*d*). Direct-driven shaft generator.

The choice among the afore-mentioned sources of power is frequently based upon opinion which may in turn be founded upon some annoying experience. When a shaft generator or house turbine-generator set is used, the performance of the auxiliary-power system is not affected by disturbances on the main system. So far as efficiency is concerned, the house turbine-generator set is at a disadvantage because of the inherent lower efficiency of the smaller turbines. In cases where either type of auxiliary generator is used, there are the disadvantages of the resultant added cost and complexity.

In addition there are such detailed difficulties as starting large motors from a relatively small generator, and the possible troubles with paralleling main and auxiliary generators and transferring from the starting power source to the separate generator. Auxiliary generators used in these applications are usually of the high-speed turbine-generator type, and, when equipped with an automatic voltage regulator, a motor with a rating up to one-third that of the generator generally can be started acceptably. A more severe voltage condition may occur after the transfer of a large group of motors from a starting source to an auxiliary generator, resulting from the increased reactive motor currents at the reduced motor speeds.

Auxiliary Power From Generator Leads

There seems to be, however, an increasing trend toward the unit system and with it an increased tendency to obtain power directly from the leads of the main generator. So far as cost and simplicity are concerned, this method has definite advantages. This provides auxiliary power at the efficiency of the main set and permits the unit to go back into service immediately after having been tripped off as a result of a system disturbance. Practice indicates that the short length of cable plus the auxiliary transformer connected to the leads of the main generator very seldom is responsible for an outage of the unit. Of course, a starting source of power is required, but one such source

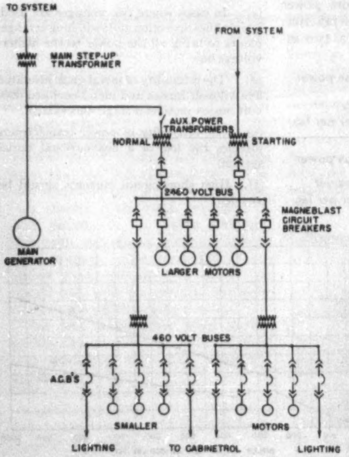
TO SYSTEM
FROM SYSTEM
MAIN STEP-UP TRANSFORMER
AUX POWER TRANSFORMERS
NORMAL
STARTING
2400 VOLT BUS
MAGNEBLAST CIRCUIT BREAKERS
MAIN GENERATOR
LARGER MOTORS
460 VOLT BUSES
A.C.B'S
SMALLER
MOTORS
LIGHTING
TO CABINETROL
LIGHTING

Figure 7 (left). Dual-voltage system supplied from generator leads with one or two boilers per unit

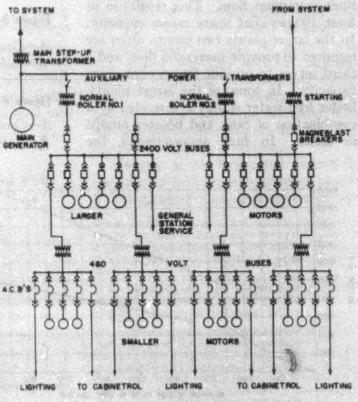
TO SYSTEM
FROM SYSTEM
MAIN STEP-UP TRANSFORMER
AUXILIARY
POWER
TRANSFORMERS
NORMAL BOILER NO.1
NORMAL BOILER NO.2
STARTING
MAIN GENERATOR
MAGNEBLAST BREAKERS
2400 VOLT BUSES
LARGER
MOTORS
GENERAL STATION SERVICE
460
VOLT
BUSES
A.C.B'S
SMALLER
MOTORS
LIGHTING
TO CABINETROL
LIGHTING
TO CABINETROL
LIGHTING

Figure 8 (right). Dual-voltage system supplied from generator leads with two boilers per unit

Table I

Transformer Rating		Feeder Breaker Interrupting Rating	Transformer-Secondary Breaker Rating	
Kva	Secondary Voltage		Current	Interrupting
300	480	15,000 amperes	800 amperes	50,000 amperes
500	480	25,000 amperes	800 amperes	50,000 amperes
750	480	25,000 amperes	1,600 amperes	50,000 amperes
1,000	480	50,000 amperes	2,000 amperes	75,000 amperes
1,000*	480	25,000 amperes	1,600 amperes	50,000 amperes
1,500	480	50,000 amperes	4,000 amperes	100,000 amperes
1,500	2,400	50,000 kva	600 amperes	50,000 kva
2,000	2,400	50,000 kva	600 amperes	50,000 kva
2,500	2,400	50,000 kva	600 amperes	50,000 kva
3,000	2,400	100,000 kva	1,200 amperes	100,000 kva
3,750	2,400	100,000 kva	1,200 amperes	100,000 kva
5,000	2,400	100,000 kva	1,200 amperes	100,000 kva

* It will be noted that one transformer rating, 1,000 kva at 480 volts, has an impedance higher than the generally accepted standard. This permits the use of feeder breakers having a lower-than-normal interrupting rating for this transformer size and results in a more economical installation in spite of the special transformer. It will be found that attempting to use special impedance values for smaller transformer ratings at 480 volts will result in only a minor saving in equipment cost and a small reduction in fault currents which are already considered acceptable. In the case of larger transformers at 480 volts, the high impedance required to permit the use of lower breaker ratings results in both impractical transformer design and excessive voltage regulation.

will suffice for several unit busses. When the supply is through a transformer, the voltage dip incident to motor starting is seldom a problem.

The Auxiliary-Power Voltage

In laying out an auxiliary-power-supply system, there are two voltage classes of equipment to be considered, namely, 600 volt and 5,000 volt. The cost of cable and control equipment in any voltage class is dependent largely upon its current rating. Thus, unless there are other offsetting factors, equipment and apparatus should be used at as high a voltage rating in its class as is practical.

In the 600-volt class, nominal system voltages of 115, 230, 460, and 575 volts have been used. In this discussion 460 volts is considered throughout as the preferred level in the 600-volt class for the following reasons:

1. The 460-volt system is considered to be the conservatively high voltage in this class.
2. Motors and control at this voltage are widely used and therefore readily available.
3. At 440 volts practical motor ratings are large enough to overlap the lower practical motor ratings for both 2,300 volts and 4,000 volts.
4. At 440 volts practical motor ratings include those down to one-half horsepower and thus overlap the higher practical ratings of single-phase 120-volt motors.
5. Since motor prices are the same for all levels in the 600-volt class, there is no disadvantage in cost for the 440-volt motors.

In the 5,000-volt class, nominal system voltages of 2,400 and 4,160 volts are in use. However, the increase in cost of 4,000-volt motors over 2,300-volt motors makes it desirable to use 2,400-volt systems, except in special cases, which will be discussed later.

Thus, in this discussion 440, 2,300, and 4,000 volts are recognized as the standard motor voltages, with corresponding nominal bus voltages of 460, 2,400 and 4,160 volts, respectively. To insure 460 volts at the bus a transformer secondary voltage of 480 is normally used. At the two higher voltages transformer secondary voltages are usually the same as the bus voltages, in view of the short cable runs encountered.

600-Volt Equipments

There are various types of control for low-voltage a-c motors, all of which include means for starting and stopping the motors, and also for providing any combination of motor overload and short-circuit protection. These types may be grouped as follows:

(*a*). Combination magnetic starters, using thermal air circuit breakers for short-circuit protection. These are available in sizes up to and including size-V starters.

(*b*). Combination magnetic starters, using fusible disconnects for short-circuit protection. These are available in sizes up to and including size-III starters.

(*c*). Drawout electrically operated air circuit breakers, which are available in all ratings of the breakers.

The specific ratings of the foregoing equipments are shown later in Tables V and VI, and it should be noted that all ratings of these equipments may be combined in the same respective assembly.

Drawout air circuit breakers generally are used for transformer secondary circuits, bus ties, feeder circuits, larger motors, and for most essential motors, regardless of size. The air breakers have the advantage of being a latched-in type of device and therefore do not drop out on voltage dips. In addition, the drawout feature provides disconnecting means which facilitates maintenance and improves service continuity. Their use, however, should be confined to applications where the required number of operations is not excessive.

Combination magnetic starters are used customarily for the smaller motors and also on applications where repetitive starting conditions are encountered. They can be furnished in factory-assembled, metal-enclosed groups, known as Cabinetrols. In general, it also will be found that drawout air circuit breakers will be less expensive than size-IV or larger combination starters, whereas combination starters will be less expensive up to and including size III.

Electrically operated drawout air circuit breakers for this type of service are furnished in metal-enclosed groups and referred to as drawout-air-circuit-breaker equipments.

5,000-Volt Equipments

There are two arrangements available for controlling high-voltage a-c motors, both of which provide combination short-circuit and overload protection:

(*a*). Metal-enclosed high-voltage contactors with current-limiting fuses.

(*b*). Vertical-lift metal-clad switchgear, with Magneblast circuit breakers.

The complete ratings of these equipments are given later in tables.

The fused starters are available for motors up to 700 horsepower at 2,300 volts. Fuses will, in general, clear a short-circuit more rapidly than the breaker. The contactors have long mechanical life and are best applied where a large number of operations will be encountered. From

Table II

2,400–480 Volts		13,200–480 Volts		13,200–2,400 Volts	
Kva	Per Cent Impedance	Kva	Per Cent Impedance	Kva	Per Cent Impedance
200	5.0	200	5.0	750	5.5
300	5.0	300	5.0	1,000	5.5
500	5.0	500	5.0	1,500	5.5
750	5.5	750	5.5	2,000	5.5
1,000*	5.5	1,000*	5.5	2,500	5.5
				3,000	5.5
1,500	5.5	1,500	5.5	3,750	5.5
				5,000	5.5
				6,000	5.5
				7,500	5.5

* In some cases it will be advantageous to specify 8.0 per cent impedance for these ratings. See Table I for their application.

a cost standpoint 50,000-kva metal-clad switchgear and fused starters are about equal, while for the higher interrupting ratings the first cost of fused starters is less.

On the other hand, when fuses are applied, there is always the possibility of single-phase motor operation due to the blowing of one fuse. Also, most large motors for station auxiliary drives do not require frequent starting and stopping. Further, most installations of this size will have one or more motors larger than 700 horsepower. It has thus been general practice to use circuit breakers for controlling the larger motors, and in the transformer, bus tie, and feeder circuits.

Transformers

Three-phase transformers are used almost exclusively in both the single- and dual-voltage auxiliary-power systems. Oil-filled or Pyranol-filled transformers for outdoor use and Pyranol-filled or dry-type transformers for indoor use are available. Transformers having ratings and characteristics as indicated in Table II may be obtained and are regularly provided with manually adjustable taps.

Unit Substations

The metal-clad switchgear equipments, using vertical-lift Magneblast breakers, and their transformers are available in unit equipments as shown in Figure 10 and are known as master unit substations.

The metal-enclosed drawout-air-circuit-breaker equipments and their transformers are generally furnished in unit equipments as shown in Figure 11 and are known as load-center unit substations. Cabinetrol equipments and transformers also can be furnished in unit equipments known as Cabinetrol unit substations.

Power-System Arrangements

Figures 5 to 9 suggest several auxiliary-power-system arrangements, and there are obviously many more which could be shown. Most of these arrangements show the auxiliary power coming from the main-generator leads primarily because of its increased use.

Figure 5 applies to a plant with one or two boilers, where all the auxiliary power may be properly supplied at 460 volts. Individual feeder positions control the larger motors, and others supply one or more lighting circuits, as well as one or more groups of magnetic starters which control the smaller individual motors. Transformer secondary breakers are used so that transfer from the starting to running supply may be readily made. Interrupter switches, where shown, permit isolating the transformers for maintenance purposes.

Table III

Interrupting Rating in Kva	Ampere Rating
50,000	600 1,200
100,000	600 1,200 2,000
150,000	600 1,200 2,000

Figure 6 applies particularly for a small unit having two boilers in which the auxiliary power is split into a supply for each boiler. This arrangement reduces the short-circuit duty on the low-voltage busses and prevents outages on one boiler system from involving the other boiler's system. One transformer is shown as a starting supply for either bus, but a separate starting transformer for each bus will give complete reserve capacity.

Figure 7 applies to plants using either one or two boilers, where the amount of auxiliary power is sufficient to justify the use of two voltages. The high-voltage transformer-interrupter switches and secondary breakers at 2,400 volts serve functions similar to those indicated on Figure 5. The larger motors are supplied at 2,400 volts, and one or more 2,400-volt feeder positions supply transformers which step down a portion of the total power to 460 volts. Bus ties are not shown between the 460-volt busses, and thus transformer secondary breakers are not required at 460 volts. When reserve transformer capacity to the 460-volt busses is considered desirable, transformer-secondary and bus-tie breakers may be added. In order to keep within the interrupting rating of the 600-volt air circuit breakers it is sometimes advantageous to supply two or more transformers from one 2,400-volt feeder. If bus-tie breakers are used in this arrangement, they should be used between 460-volt busses which are fed from different 2,400-volt feeders.

Table IV

Voltage	Interrupting Rating—Kva	Horsepower Rating
2,400	150,000	50–700
4,160	250,000	50–1,250

Figure 8 applies particularly for the larger units having two boilers. Dividing the power into a supply for each boiler reduces short-circuit duties and prevents outages on one boiler system from involving the other boiler's system. One transformer is shown as a starting supply for either 2,400-volt bus, but one for each bus would give 100 per cent reserve capacity.

Figure 9 shows how a power supply for auxiliaries can be taken directly from the low-voltage station bus when such a bus is available.

Table V

Interrupting Amperes	Continuous Ampere Rating	Maximum Motor Horsepower at 440 Volts	Maximum* Setting of Instantaneous Trip—Amperes
15,000	15–225	150	3,375
25,000	15–225	150	3,375
25,000	250–400	275	6,000
25,000	450–600	400	9,000
50,000	100–225	150	3,375
50,000	250–600	400	9,000
50,000	800–1,200	800	18,000
50,000	1,600		24,000
75,000	2,000–2,500		30,000
75,000	3,000		36,000
100,000	4,000		48,000

* The maximum setting of the nonadjustable instantaneous short-circuit trip on the air circuit breakers is important in determining the rating of the transformer-secondary breaker, so that it will not trip for feeder faults.

For the larger stations, it may be desirable to establish a separate centrally located bus from which the general station service power is distributed. The so-called starting transformer can then be used to bring power from the system to this bus which in turn can also be arranged to provide starting power for the individual unit busses.

Single-Voltage Systems

Studies show that, so far as investment is concerned, on the basis of the typical number of feeder positions usually required by the smaller turbine-generator units, the straight 460-volt system and the 2,400–460 dual-voltage system are practically equal when the normal power supply demands a 1,500-kva transformer. Below this rating there is a definite cost advantage in favor of the straight 460-volt system. In fact, if the auxiliary power supply can be held within the capacity of a 1,000-kva transformer, the short-circuit duty on such a 460-volt auxiliary system will be limited accordingly, and the 440-volt motors and control for the larger auxiliaries associated with this amount of total auxiliary power, will not result in an impractical solution.

Dual-Voltage Systems

As previously indicated, studies show that a dual-voltage system should be considered when the auxiliary-power supply requires a 1,500-kva or larger transformer. In most of these applications, 2,400 volts will be more economical than 4,160 volts. Actually transformer capacities up to and including 5,000 kva at 2,400 volts may be used with economical and practical switch gear having an interrupting rating of 100,000 kva.

A 5,000-kva transformer will supply power to a boiler having a flow of approximately 600,000 pounds per hour. Boilers larger than this are most always provided with split auxiliaries such as two induced-

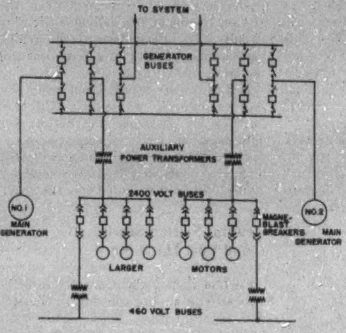

Figure 9. Dual-voltage system supplied from generator bus

draft fans, two forced-draft fans, and two or more boiler-feed pumps. So far as auxiliaries are concerned, such a boiler has the advantages of a two boiler installation, and the 2,400-volt auxiliary power may be divided as shown in Figure 8. Thus, by using divided auxiliaries and two auxiliary-power transformers rated either 3,750 or 5,000 kva, the power for most of the largest boilers may economically be supplied at 2,400 volts.

For the larger installations, where individual transformer ratings greater than 5,000 kva may be required, the use of 4,160 volts should be considered. Systems using 4,160 volts have the advantage of lower-current ratings and lower short-circuit currents but may not necessarily show an advantage in cost owing to the higher cost of 4,160-volt motors. Whatever the relative economics of the motors and control are, it should be recognized that raising the voltage always reduces the short-circuit amperes, and thus at 4,160 volts the kilovolt-ampere capacity of the supply transformer can be larger than at 2,300 volts.

In the case of 2,400–460 dual-voltage systems, studies indicate that, by evaluation of such cost items as difference in control equipment, cable, motors, and additional transformer capacity including evaluation of losses, it is economical for the short runs normally encountered in a steam station to include motors up to 250 horsepower in the 460-volt class. Similarly, in the case of 4,160–460 dual-voltage systems, it is generally economical to include motors up to 350 horsepower in the 460-volt class.

It will be seen from Figure 1 that in the normal auxiliary-power system the few motors associated with the larger auxiliaries account for two thirds to three quarters of the total auxiliary power. Thus, when a complete list of the motors and their ratings is available, there should be little difficulty in selecting not only the motors which are to be supplied at 460 volts but also the total transformer capacity required to serve these motors.

In plants where medium-size boilers are used, this one third of the total kilovolt-ampere is often stepped down from 2,400 volts to 460 volts through one transformer on a radial basis. Where larger boilers are employed, two or more transformers may be used on a radial basis to step down power from the 2,400-volt bus. This has the advantage of permitting the use of control equipment of lower interrupting rating and of allowing the control to be located nearer individual groups of motors.

When a strictly radial system is not considered adequate, the first departure will consist usually of adding a tie breaker between 460-volt busses. In order to take full advantage of this feature, excess transformer capacity must be provided. The magnitude of this excess capacity admittedly is a matter of judgment, however, and 50-per-cent excess capacity should be sufficient in most cases. Provision should be made to prevent closing the bus-tie breaker between any pair of busses unless one of the two source breakers is open, or at least will be opened promptly after the bus-tie breaker is closed.

In a plant with two boilers per generating unit, with a separate auxiliary-power supply for each boiler, it will simplify operation to adhere strictly to the unit-system concept in the auxiliary-power supply and thus avoid such complications as providing bus ties between 460-volt busses which normally supply auxiliaries for different boilers.

Relaying Selectivity

For essential types of service such as power-station auxiliary drives, selective operation of feeder breakers and transformer-secondary breakers is desirable during fault conditions on the feeders. When a transformer-secondary, bus-tie, or group feeder breaker is to be selective with the feeder breakers it must not trip instantaneously. In this way the feeder breaker is given an opportunity to trip and clear the fault, and therefore it must have an interrupting capacity at least equal to the available fault. Low-voltage air circuit breakers are all equipped with instantaneous trips, and thus any of these breakers in backup positions must be of sufficient rating so that their instantaneous trips will not cause breaker operation on feeder faults.

Power circuit breakers on motor circuits usually are equipped with instantaneous over-current relays for fault protection; thus, the breakers in backup positions may be timed to be selective with respect to motor breakers and other feeder breakers.

Table I summarizes the present breaker ratings which can be used with the transformer ratings listed in Table II and can be expected to give selective operation of 600-volt air circuit breakers during short-circuit conditions. The maximum setting of the nonadjustable instantaneous short-circuit trip on low-voltage air breakers is given in Table V. For convenience the ratings of 5,000-volt breakers for larger transformers also are included in Table I. The higher system short-circuit duties, encountered in this type of service, have been used in selecting these ratings.

Cabinetrol equipments as normally applied are not selective with the group feeder breakers over a wide range of ratings. This will not be serious if all essential motors, regardless of how small they may be, are supplied from their individual 600-volt air circuit breakers. In some cases, small essential motors will require contactors because of the frequency of operation of their control. If such auxiliaries are in duplicate, they may be supplied from two different Cabinetrol groups and in this way still meet the service reliability requirements.

Selectivity of Cabinetrol as normally applied may be expected with certain com-

Table VI

NEMA Size	Interrupting Element	Interrupting Rating—Amperes	Maximum Horsepower at 440 Volts
1	Fuse*	50,000	7½
2	Fuse*	50,000	25
3	Fuse*	50,000	50
1	Thermal air circuit breakers†	15,000	7½
2		15,000	25
3		15,000	50
4		15,000	100
5	Air circuit breaker	25,000	200

*The fusible-combination magnetic starters, when equipped with nonrenewable nonindicating National Electric Code fuses, are adequate for installing in circuits where the available symmetrical short-circuit current at the incoming-line terminals of the starter does not exceed 50,000 amperes and the short-circuit is at or beyond the load terminals of the starter.

† Where these combination magnetic starters with thermal air circuit breakers are supplied through a 25,000-ampere 460-volt air circuit breaker, the starters may be applied on a bus having an available short-circuit duty of 25,000 amperes.

bination ratings. Fused Cabinetrol equipment at 460 volts up to and including size II will, in general, be selective with a 25,000-ampere group feeder breaker. For larger-fused Cabinetrol units and for all Cabinetrol units using thermal air breakers, a 25,000-ampere group feeder breaker can be expected to trip during a short-circuit.

However, when selectivity of Cabinetrol in a wider range of ratings is desirable, it may be obtained either by choosing a group feeder breaker with a sufficiently high instantaneous setting or by using a series feeder reactor. Either of these approaches increases the spread between the available short-circuit current and the maximum instantaneous trip setting for the feeder breaker.

Protective Features

Instantaneous short-circuit protection is provided on all types of control equipment. Combination magnetic starters are equipped with either fuses or thermal air circuit breakers, and low-voltage air circuit breakers are equipped with instantaneous trips. Instantaneous overcurrent relays are also used on the Magneblast air breakers.

Inverse time-delay short-circuit protection should be normally provided as backup protection on transformer-secondary, bus-tie, and transformer-feeder circuit breakers. When these breakers are of the 600-volt type, this feature preferably should be obtained by using separate relays with current transformers. On Magneblast breakers separate relays must be used.

Thermal devices are available in all the types of equipments discussed, and their function is to provide inexpensive overcurrent protection for motors against stalled rotor and single-phase operation or prolonged overloads. They may be arranged either to trip the motor circuit or to sound an alarm, and the opinions of operators are not uniform on this subject.

When the thermal device is arranged for tripping, it opens the coil circuit on magnetic starters; it acts directly on the trip element of low-voltage air circuit breakers and on the larger breakers is used in conjunction with current transformers to energize the breaker shunt trip coil. In applications where a special thermal characteristic must be met, a separate thermal relay, energized from current transformers can be used to provide the trip function on any of the equipments.

When alarm features only are desired, the thermal devices in all the equipments discussed can be arranged to sound an alarm instead of opening the motor circuit. Since an alarm is of no use except where there is time to profit by it, this feature is of advantage only during overloads and not during stalled rotor conditions and probably may be tolerable only on the smaller inexpensive motors.

A combination feature which gives alarm on overload and which trips on stalled rotor conditions is available. This consists of a thermal relay, energized from current transformers, and an overcurrent relay, which transfers the thermal relay from the alarm to the trip circuit upon the occurrence of excess current.

Undervoltage time-delay protective features are sometimes desirable. A voltage dip which drops out contactors and does not return to the required pickup value in a few seconds may damage the a-c operating coils of contactors equipped with undervoltage release, and protection against such a voltage dip may be arranged to trip any of the feeder circuits having devices of this type.

Differential protection of the main generator should be extended to include the normal auxiliary-power transformer. Generally, the ratios are not sufficient to allow the main differential relaying to detect faults in the auxiliary transformer; therefore an additional relay system should be provided for the auxiliary transformer to trip the generator breaker, field breaker, auxiliary-transformer-secondary breaker, and, in some cases, the turbine stop valve. In addition, automatic throwover may be provided to energize the auxiliary bus from the starting supply whenever differential relays trip off the main source. This allows the boiler to be brought down under full control of its auxiliaries.

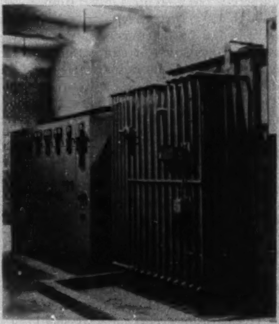
Figure 10. Typical master unit substation

It is common practice to operate 460-volt and 2,400-volt auxiliary-power systems ungrounded but with ground indication facilities.

Lighting

Station lighting can be economically taken from the 460-volt busses through one or more three-phase feeder positions. Single-phase dry-type transformers, of proper rating and number to balance the feeder load, may be located about the station to supply the individual lighting circuits. By interspersing these circuits, the loss of one feeder for a short time will not be serious.

It is customary to provide an emergency source of lights from a battery. This may be done by arranging the battery for automatic throwover to a fraction of the circuits which are again interspersed or by having an entirely separate emergency lighting circuit distributed over the area.

General Station Service and Coal Handling

Certain items, which are not directly associated with any one unit in the station, require power. These include coal-handling equipment, yard floodlighting, service water, machine shop, and cranes, and the amount of power required will vary widely for different plants. This power may be supplied from the auxiliary bus for the first unit in the plant, in which case provision should be made for an alternate source when additional units are added, or for the larger stations from a separate centrally located bus. It will be advantageous to supply this power from the higher auxiliary voltage since long cable runs are often involved.

Calculation of Short-Circuit Currents

In preparing the tabulated application guides, conventional methods of calculating short-circuit kilovoltamperes and currents were used.

The interrupting rating of Magneblast air circuit breakers is customarily given in kilovoltamperes at a certain voltage. The relay and interrupting times for these breakers are such that induction-motor contributions and offset currents may be neglected. Thus, the short-circuit kilovoltampere is determined directly from transformer reactance and system reactance beyond. In these applications the ratio of transformer reactance to system reactance is such that the system may as well be considered infinite. The momentary duty in these cases is obtained by multiplying the short-circuit kilovoltamperes by 1.4 and also adding the induction-motor contribution.

The interrupting rating of low-voltage air circuit breakers is the rms current averaged for the three phases and determined at the first half cycle, which is the time at which contacts part. This average value is determined by applying the multiplying factor of 1.25 to the symmetrical contribution through the transformer and then adding the contribution of induction- and synchronous-motor loads. The motor contribution is customarily taken into account by adding five times the connected motor load, which, in these applications, will be approximately

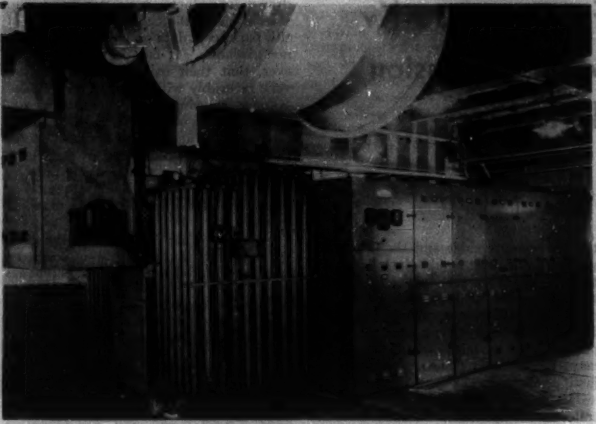

Figure 11. Typical load-center unit substation

five times the transformer rating. The momentary duty for this class of breaker is considered to be equal to the interrupting duty.

The interrupting rating of 600-volt fusible-combination magnetic starters is given in amperes based on the available symmetrical short-circuit amperes. This value may be obtained in a similar manner to that for low-voltage air circuit breakers, except omitting the 1.25 factor.

Location of Equipment

In steam-electric stations the major part of the power is used at or near the boiler. There is usually space available in the bay between the boiler plant and the turbine room where the auxiliary-power-system equipment can be advantageously located. This location should result in short power and control cable runs.

In the smaller plant where the power is supplied entirely at 460 volts, the complete switchgear and associated stepdown transformer may well be at one centralized location. The Cabinetrol may be at a remote location near a group of small motors which it serves.

In the larger plant where a dual-voltage system is used, the 2,400-volt switchgear logically should be at a central location in the plant. The 460-volt load-center units and Cabinetrol panels may be at remote locations near the load they serve. If the normal starting transformer is of moderate rating, consideration should be given to placing it at the centralized location, where it can be combined readily with the 2,400-volt switchgear into a unit substation. When the normal transformer is in the larger ratings, it will be located outdoors in most cases. Similarly, the starting transformer will be located outdoors, since it generally will be energized from the high-voltage bus, and in this way long high-voltage cable runs may be avoided.

Appendix

Transformer Ratings

Table II lists the standard transformer ratings which will be used normally for this type of service.

5,000-Volt Switchgear Equipments

Metal-clad switchgear, with electrically operated removable oilless circuit breakers, is available in the ratings shown in Table III.

Combination High-Voltage Fused Contactors

Metal-enclosed contactors with high-interrupting-current limiting fuses and with air or oil-filled contactors are available in the ratings shown in Table IV.

600-Volt Switchgear Equipments

Metal-enclosed low-voltage switchgear, with electrically operated drawout air circuit breakers have the ratings shown in Table V.

Combination 600-Volt Magnetic Starters

Combination magnetic starters with either fusible disconnects or thermal air circuit breakers are available for use as low-voltage motor starters. These starters are available in the ratings shown in Table VI.

References

1. Advanced Design—Original Features Embodied in New 160,000-Kw Oswego Steam Station. **N. R. Gibson, H. M. Cushing.** *Transactions* of the American Society of Mechanical Engineers, August 1942, pages 541–65.

2. Chesterfield "Satisfies" Demand for Power in a Most Unconventional Way. **R. S. Reed, L. J. Tracy, C. C. Dodge.** *Electric Light and Power*, April 1944, pages 74–80.

3. Electrical-Driven Auxiliaries for Steam-Generating Stations, a report by the electrical apparatus committee, engineering national section of the National Electric Light Association, April 1930.

4. Auxiliary Drive for Steam-Power Stations (symposium). AIEE Transactions, volume 51, 1932, pages 329–52.

5. Frank R. Phillips Station, Simple, Flexible Ingenious. **F. S. Brown, R. B. Horner, W. H. Jones.** *Electrical World*, October 16, 1943.

6. Burlington Station Adds 100,000-Kw Condensing Unit. **H. Weisburg.** *Power*, July 1941.

7. Avon, Martinez, Oleum—Achievement in Co-operation. *Power*, August 1941.

Study of Costs of 69- to 230-Kv Underground Power-Transmission Systems and Tie Lines

JOHN G. HOLM
MEMBER AIEE

Synopsis: This is a study of high-voltage underground-cable systems, consisting of the cable line and the terminal equipment at each of its ends. The study undertaken indicates the economic zone of application of cables and attempts to find an economic relationship between the voltage and the block of power transmitted over distances up to 15 miles. Thirty transmission lines have been designed using both the solid and the oil-filled cables. The lines can be considered as either transmission links with a unidirectional power flow or as tie lines between large metropolitan steam-power stations. The prices of underground cable and terminal equipment were obtained from manufacturers, and refer to the 12-month period immediately preceding World War II. The costs of various system parts, as installed on foundations, were obtained from the study of actual construction projects in different parts of the country and reduced to the 12-month period. The system capital cost and its annual cost are analyzed separately. The quantities of major equipment items in each system are given, and costs of major equipment groups, or of major items, are represented on a percentage basis. Such a representation permits the estimating of the cost of an underground line, or of the entire transmission project, when copper prices and the cost of equipment differ from those taken in the study.

THE RECORDS of engineering thought and development as reflected in the technical literature show that some 20 years ago there was displayed in the United States a great interest in the newly developed oil-filled cable. At that time 138-kv oil-filled cable was being installed in the United States and abroad. Since then extensive installations of this cable have been made, and the art has taken several steps forward—not only by developing an oil-filled cable for 230 kv but by evolving the gas-pressure cable and the Oilostatic system. The most notable installation of the 230-kv cable took place in France around the year 1936 when the intra-Paris cable 11.6 miles long was installed.[1-3] Cables of the newer type have also been placed in a few initial installations and may be considered as having amply justified their development.

The economic phase of underground transmission systems, however, did not receive during these years the attention given to the technical end of this problem. The only outstanding record in the literature is the study made by Roper[4] in 1931. In view of this, therefore, it seems that an economic study of this problem may be in order.

This study covers underground power-transmission and tie lines using impregnated-paper-insulated cables of the so-called solid and oil-filled types. Cables of other designs, such as the Oilostatic system in which the cables are installed in a pipe and maintained under a 200-lb.-per-square-inch oil pressure, or the high-pressure gas cables installed in a pipe or drawn into ducts, have not been considered, as at the time of preparation of this paper cost data on both systems were not available. It has been stated, however, that their over-all costs compare very favorably with those of an oil-filled system, showing costs in some cases smaller and in other cases slightly higher than those of an oil-filled system. It appears, therefore, that when a study is to be made of the cost of a projected underground power-transmission system consideration also must be given to these systems.

No attempt has been made to compare the economics of the underground and the overhead lines of equal length and equal

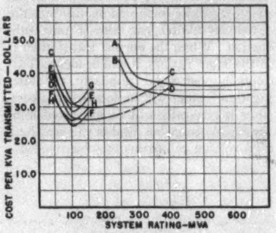

Figure 1. Capital cost of the entire system, including terminal substations, per kilovolt-ampere transmitted

A . . . 15 . . 230 . . . Oil-filled cable
B . . . 10 . . 230 . . . Oil-filled cable
C . . . 15 . . 138 . . . Oil-filled cable
D . . . 10 . . 138 . . . Oil-filled cable
E . . . 15 . . 69 . . . Oil-filled cable
F . . . 10 . . 69 . . . Oil-filled cable
G . . . 15 . . 69 . . . . Solid cable
H . . . 10 . . 69 . . . . Solid cable

The first figure represents transmission distance in miles; the second, kilovolts of transmission voltage

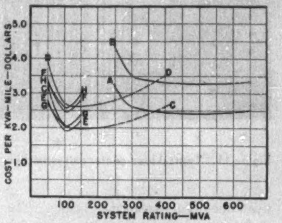

Figure 2. Capital cost of the entire system, including terminal substations, per kilovolt-ampere-mile

For explanation of identification letters, see Figure 1

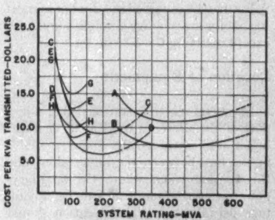

Figure 3. Capital cost of the transmission line per kilovolt-ampere transmitted

For explanation of identification letters, see Figure 1

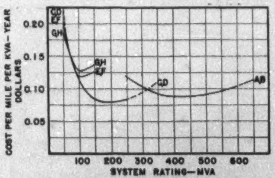

Figure 4. Capital cost of the transmission line per kilovolt-ampere-mile

For explanation of identification letters, see Figure 1

Paper 45-160, recommended by the AIEE committee on power transmission and distribution for publication in AIEE TRANSACTIONS. Manuscript submitted November 10, 1944; made available for printing August 11, 1945.

JOHN G. HOLM is electrical engineer of Isolantite, Inc., Belleville, N. J.

To the engineers of the General Electric Company, the Westinghouse Electric Corporation, the General Cable Corporation, the Okonite Company, the Simplex Wire and Cable Company, and to several electrical-public-utility and consulting engineers the author expresses appreciation for valuable data and advice.

block of power transmitted. The systems differ from those studied by Roper in that in all cases they have terminal substations at both ends; they are studied and analyzed, however, both as complete systems with terminal equipment included, and as underground cable lines alone. The indirect expenses, which seem to have been purposely left out of Roper's study, are included in this paper. The general structure of the present study is similar to that used by the writer in his study of the costs of overhead power-transmission systems.[5] Therefore only an outline of the approach to the problem will be given here, and for a detailed method of analysis the reader is referred to similar parts of the other paper.

The underground systems investigated in this paper have no definite geographic location. The prices taken are those prevailing in the years preceding World War II. The prices of equipment are obtained from the manufacturers, and the cost of land, structures, substation secondary equipment, labor, and installation on foundation were obtained from various public-utility companies and from the literature. All these data were reduced to the common one-year period, with appropriate labor indexes being used. Irrespective of the variations in costs of particular items, the relationship between the costs of individual systems will remain basically unchanged. The study of the transmission of various blocks of power at two different voltages permits one to obtain the relationship of the voltage, the transmission distance, and the most economical block of power transmitted. It shows the general trend of high-voltage underground-system costs and defines the economic zone of application of the various cables studied.

The system capital and annual costs are calculated and analyzed separately.

System Description

The study covers 30 systems rated at 50,000 to 600,000 kva and transmitting power over one to four circuits of underground lines 10 and 15 miles long, at voltages of 69, 138 and 230 kv, at 60-cycle frequency. The systems are lines in metropolitan areas transmitting from steam-power stations, or lines tying in two great metropolitan load centers and permitting power to be transmitted in both directions. The transformer kilovolt-ampere capacity is assumed to be slightly greater at the sending end of the system.

The 69-kv cables are of both solid and oil-filled type, and all the 138-kv and 230-kv cables are oil filled, all cables being single-conductor cables. The underground lines are connected to high-voltage busses at both ends, and at no intermediate point are they connected to overhead transmission lines. Since the lines pass through metropolitan areas, there is no right-of-way problem, the assumption being made that permission to dig the trenches will be obtained from the municipalities.

The system and cable data are given in Table I.

The systems as taken in this study include the underground line, completed with all accessories, and the sending and the receiving substations. All systems have high-voltage busses and high-voltage circuit breakers at both ends of the system. All single-circuit systems have a single nonsplit high-voltage bus. The 149,700-kva-rated systems, with two circuits, have a single bus, split in two. For systems rated from 247,500 to 600,000 kva, double busses are provided; these busses are split into as many sections as there are circuits in the system. The load assumed on the system for the purpose of calculating the circuit-breaker interrupting capacity is at both system ends. The total load is the function of the block of power transmitted,[6] 60 per cent of the total being placed at the system receiving end, and the remaining 40 per cent at its sending end.

The underground lines have standard relay protection. Lines with solid cable

Table I. List of Systems Designed—Type and Size of Cables

System Identification Number	System Data			Cable Data					
	System Rating, Kva	Transmission Distance, Miles	Transmission Voltage, Kv	Type of Cable	Cross Section, Thousand Circular Mils	Number of Circuits in System	Cable Insulation Thickness, Inch	Thickness of Lead Sheath, Inch	Outside Diameter of Cable Over Lead Sheath, Inches
U-33a	54,200	10	69	Solid	600	1	0.656	0.125	2.452
U-331a	52,800	10	69	Oil-filled	350	1	0.315	0.125	1.790
U-34a	65,200	10	138	Oil-filled	168	1	0.560	0.141	2.165
U-35a	54,200	15	69	Solid	600	1	0.656	0.125	2.452
U-351a	52,800	15	69	Oil-filled	350	1	0.315	0.125	1.790
U-36a	65,200	15	138	Oil-filled	168	1	0.560	0.141	2.165
U-361a	75,300	10	69	Solid	1,000	1	0.656	0.125	2.872
U-362a	75,300	15	69	Solid	1,000	1	0.656	0.125	2.872
U-363a	76,900	10	69	Oil-filled	700	1	0.315	0.125	2.014
U-364a	76,900	15	69	Oil-filled	700	1	0.315	0.125	2.014
U-37a	103,600	10	69	Solid	1,750	1	0.656	0.125	3.482
U-371a	106,000	10	69	Oil-filled	1,250	1	0.315	0.125	2.300
U-38a	103,600	10	138	Oil-filled	400	1	0.560	0.141	2.342
U-39a	103,600	15	69	Solid	1,750	1	0.656	0.125	3.482
U-391a	106,000	15	69	Oil-filled	1,250	1	0.315	0.125	2.300
U-40a	103,600	15	138	Oil-filled	400	1	0.560	0.141	2.342
U-401a	149,700	10	69	Solid	1,250	2	0.656	0.125	3.052
U-402a	149,700	15	69	Solid	1,250	2	0.656	0.125	3.052
U-403a	149,700	10	69	Oil-filled	800	2	0.315	0.125	2.070
U-404a	149,700	15	69	Oil-filled	800	2	0.315	0.125	2.070
U-405a	160,000	10	138	Oil-filled	900	1	0.560	0.141	2.646
U-406a	160,000	15	138	Oil-filled	900	1	0.560	0.141	2.646
U-41a	255,000	10	138	Oil-filled	750	2	0.560	0.141	2.562
U-42a	247,500	10	230	Oil-filled	400	2	0.925	0.156	3.234
U-43a	255,000	15	138	Oil-filled	750	2	0.560	0.141	2.562
U-44a	247,500	15	230	Oil-filled	400	2	0.925	0.156	3.234
U-441a	378,000	10	230	Oil-filled	1,000	2	0.925	0.156	3.556
U-442a	378,000	15	230	Oil-filled	1,000	2	0.925	0.156	3.556
U-45a	600,000	10	230	Oil-filled	600	4*	0.925	0.156	3.352
U-46a	600,000	15	230	Oil-filled	600	4*	0.925	0.156	3.352

The system identification number is kept throughout the entire study.

The 69-kv and 138-kv oil-filled cables have an 0.500-inch hollow core, and the 230-kv cables have an 0.690-inch core.

*Systems *U-45a* and *U-46a* have two duct banks, two circuits per duct bank.

Table II. System Major Equipment Items

System Identification Number	Sending-End Transformers—Total System Kva	Receiving-End Transformers—Total System Kva	High-Voltage Oil Circuit Breakers—Number of Breakers in System and Their Interrupting Capacity*	High-Voltage Air-Break Disconnectors—Total Number in System and Their Ampere Rating†
U-33*a*	67,900	65,800	6–500	12–600
U-331*a*	66,733	64,050	6–500	12–600
U-34*a*	81,200	78,400	6–750	12–600
U-35*a*	68,367	65,800	6–500	12–600
U-351*a*	67,550	64,050	6–500	12–600
U-36*a*	81,783	78,400	6–750	12–600
U-361*a*	94,033	91,233	6–1,000	12–600
U-362*a*	94,617	91,233	6–1,000	12–600
U-363*a*	96,600	93,217	6–1,000	12–600
U-364*a*	97,417	93,217	6–1,000	12–600
U-37*a*	129,150	125,533	6–1,000	12–600
U-371*a*	132,533	128,333	6–1,000	12–600
U-38*a*	127,983	124,250	6–1,500	12–600
U-39*a*	129,733	125,533	6–1,000	12–600
U-391*a*	133,350	128,333	6–1,000	12–600
U-40*a*	128,683	124,250	6–1,500	12–600
U-401*a*	200,000	194,500	14–1,500	28–600
U-402*a*	200,875	194,500	14–1,500	28–600
U-403*a*	201,125	194,500	14–1,500	28–600
U-404*a*	202,500	194,500	14–1,500	28–600
U-405*a*	211,125	205,625	10–1,500	20–600
U-406*a*	211,750	205,625	10–1,500	20–600
U-41*a*	336,500	327,750	20–2,500; 4–1,500	48–600
U-42*a*	321,375	314,500	24–2,500	48–1,200
U-43*a*	337,625	327,750	20–2,500; 4–1,500	48–600
U-44*a*	322,375	314,500	24–2,500	48–1,200
U-441*a*	392,700	384,500	20–3,500; 4–2,500	48–1,200
U-442*a*	393,400	384,500	20–3,500; 4–2,500	48–1,200
U-45*a*	624,000	611,000	24–5,000; 12–3,500	72–1,200
U-46*a*	625,500	611,000	24–5,000; 12–3,500	72–1,200

Sending-end and receiving-end transformer kilovolt-amperes include spare transformer capacity as follows: Systems *U*-33*a* to *U*-40*a*, inclusive, have one single-phase spare unit; systems *U*-401*a* to *U*-44*a*, inclusive, have a spare three-phase bank. Systems *U*-441*a* to *U*-46*a*, inclusive, have no spare kilovolt-ampere capacity, their transformers permitting a 25-per-cent overload for two hours (Overload accounted for in system cost).

*First figure indicates number of three-phase oil circuit breakers; second figure indicates breaker interrupting capacity in megavolt-amperes.

†First figure indicates number of three-phase air-break disconnectors; second figure indicates disconnector current rating.

are provided with a relay cable (pilot wire), and the oil-filled-cable lines have an oil-signal cable for each power-cable circuit. Two wires of the relay and the oil-signal cables are used for communication purposes.

The system major equipment items are given in Table II.

General Principles of System Design

Since the systems studied are parts of existing metropolitan systems, the position is taken that no other transmission systems in the vicinity depend on them for continuity of operation, but rather the reverse is the case. Therefore the underground lines are designed to have as many circuits as are necessary for the transmission of the specified block of power, no provision being made for spare circuits or spare single cables.

Voltages at which transmission is being effected are those which appear suitable for the particular block of power transmitted. No attempt is being made to secure the economical loading of cables for a certain cyclic load. However, the accepted annual load factor, loss factor relationship,[6,7] is used throughout the study. The selection of the cable copper cross section is made from temperature considerations, calculations being based on the cable summer rating. No credit is given for the charging current of cables.

A study of underground transmission systems shows that stability is no problem in these systems, neither steady-state nor transient stability. Therefore round-rotor machines of standard design are applicable, no stability-improving devices are required, and standard breakers are used of eight-cycle opening time. For this reason, as well as for voltage regulation purposes, no synchronous condensers are placed at the receiving end of the system. Voltage drop in an underground line being very small, voltage is assumed to be controlled by adjustment of the reactive power of the receiving-end steam-station generators, supplementing the plus–minus-ten-per-cent load-ratio control of the receiving transformers.

System rating is expressed in kilovolt-amperes and is equal to the rating of all cable circuits. The rating of terminal equipment installed is obtained by adding to the system rating all the losses in all parts of the power-transmission system, at appropriate power factors.

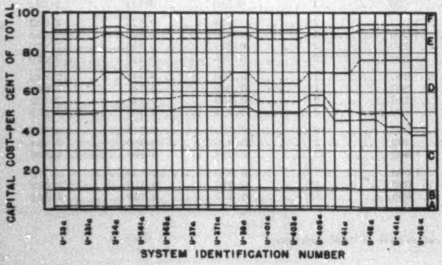

Figure 5. Division of capital costs of sending and receiving substations into their major component parts, in transmission systems ten miles long

A—Land
B—Structures
C—Power transformers
D—High-voltage switching and protective equipment
E—Low-voltage switching, protective and control equipment
F—Auxiliary substation equipment

Dash-and-dot lines represent those parts of the receiving-end substation which differ substantially from the sending-end percentages (*C* and *E*)

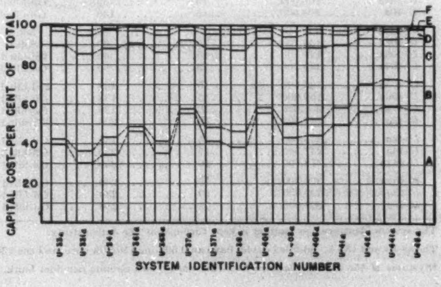

Figure 6. Division of capital cost of the transmission line into its component parts, in transmission systems ten miles long

A—Cables
B—Cable accessories
C—Duct banks
D—Manholes
E—Bonding
F—Equipment for communication and relaying

Underground-Line Design Data

In choosing the size of the underground cable required for the transmission of a certain block of power, the maximum allowable temperature of cable insulation is taken as the determining factor. This temperature is taken at 60 degrees centigrade for the solid cables, and at 70 degrees centigrade for the oil-filled cables, with the base temperature of the earth at 20 degrees centigrade. Losses and voltage drops are taken as obtained for these current-temperature conditions.

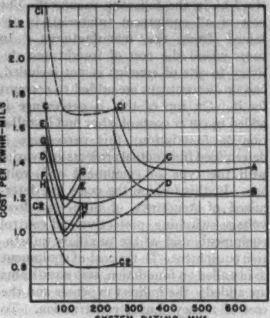

Figure 7. Cost of the entire system, including terminal substations, per kilowatt-hour

For explanation of identification letters, see Figure 1. All costs at 50 per cent annual load factor except as follows:

C1 . . . 15 . . 138 at 35 per cent
C2 . . . 15 . . 138 at 75 per cent
annual load factor

The selection of the 69-kv solid cables is made on the basis of the Insulated Power Cable Engineers' Association tables,[8] for cables laid in ducts, for 100-per-cent daily load factor. The kilovolt-ampere rating of these cables is taken for current-carrying capacities as given in these tables. The selection of the 69-kv, 138-kv, and 230-kv oil-filled cables is made from data obtainable in literature[9, 10] and from tables supplied by the cable manufacturers. In every case tables were used for cables laid in ducts, and where the cable winter rating is given the ratio of summer to winter rating was taken at 0.85. There being no standards for the current-carrying capacity of the oil-filled cables generally accepted by the industry, in the same sense as are accepted the IPCEA tables for solid cables, the current rating of these cables is taken as obtained by calculation for each case; and the kilovolt-ampere rating of the oil-filled cables is based on the permissible current calculated.

For the calculation of permissible current-carrying capacities, the insulation thickness, thickness of lead sheath, and the dielectric power factor of cables were taken as recommended by the Association of Edison Illuminating Companies[11] and as given by the manufacturers. The calculation of the cable outside diameter, of its geometric factor, of the thermal resistance to I^2R loss and to dielectric loss between conductor and base, the calculation of current rating and of the cable three-phase dielectric loss were made as recommended by Simmons.[12, 13]

All cables have special bonding.[14] Sheath voltage per length of cable between manholes was calculated, and wherever this voltage at rated current loading exceeds 11 volts the series impedance bonding is used. Bonding transformers are installed in the manholes for the joints. The percentage residual sheath losses allowed after special bonding is 5 in 69-kv cables, ten in 138-kv and 20 in 230-kv cables.

In determining the number of normal joints and stop joints, the practice recommended by cable manufacturers and given in the literature[15] was followed. The length of a section for oil-filled cables is taken at one mile; lines are assumed to be of a substantially level profile. The distance between manholes for solid cables is 754 feet, and for oil-filled cables 660 feet. The pilot-wire and oil-signal cables are placed in separate ducts, so

Table III. Ducts, Manholes, and Cable Accessories

System Identification Number	Joints, Number in System		Ducts		Manholes, Number in System			Reservoirs—Type, Capacity, and Number in System*		
	Normal Joints	Stop Joints	Conduit Size, Inches	Number of Ducts in a Bank	For Normal Joints	For Stop-Joints	For Reservoirs	CC—Feeder or Gravity Type	AC—Gas-in-Cell Type	DC—Oil-in-Cell Type
U-33*a*	207		3.5	4	69					
U-331*a*	210	33	3.5	4	70	11	9	6–9	6–9	48–9
U-34*a*	210	33	3.5	4	70	11	9	6–15	6–14	48–15
U-35*a*	312		3.5	4	104					
U-351*a*	315	48	3.5	4	105	16	14	6–9	6–9	78–9
U-36*a*	315	48	3.5	4	105	16	14	6–15	6–14	78–15
U-361*a*	207		3.5	4	69					
U-362*a*	312		3.5	4	104					
U-363*a*	210	33	3.5	4	70	11	9	6–12	6–12	48–12
U-364*a*	315	48	3.5	4	105	16	14	6–12	6–12	78–12
U-37*a*	207		4.5	4	69					
U-371*a*	210	33	3.5	4	70	11	9	6–15	6–14	48–15
U-38*a*	210	33	3.5	4	70	11	9	6–18	6–14	48–15
U-39*a*	312		4.5	4	104					
U-391*a*	315	48	3.5	4	105	16	14	6–15	6–14	78–15
U-40*a*	315	48	3.5	4	105	16	14	6–18	6–14	78–15
U-401*a*	414		4.5	7	69					
U-402*a*	624		4.5	7	104					
U-403*a*	420	66	3.5	7	70	11	9	12–12	12–12	96–12
U-404*a*	630	96	3.5	7	105	16	14	12–12	12–12	156–12
U-405*a*	210	33	3.5	4	70	11	9	6–19	12–9	48–18
U-406*a*	315	48	3.5	4	105	16	14	6–19	12–9	78–18
U-41*a*	420	66	3.5	7	70	11	9	12–19	24–9	96–18
U-42*a*	420	66	4.5	7	70	11	9	24–18	36–12	192–15
U-43*a*	630	96	3.5	7	105	16	14	12–19	24–9	156–18
U-44*a*	630	96	4.5	7	105	16	14	24–18	36–12	312–15
U-441*a*	420	66	4.5	7	70	11	9	24–19	36–12	192–18
U-442*a*	630	96	4.5	7	105	16	14	24–19	36–12	312–18
U-45*a*	840	132	4.5	7	140	22	18	48–18	72–12	384–18
U-46*a*	1,260	192	4.5	7	210	32	28	48–18	72–12	624–18

Number of normal joints in 69-kv solid cables is seven per mile. In all the oil-filled cables seven normal joints and one stop joint per mile are used.

All manholes are of straight type, made of concrete. All manholes and duct banks paved with eight-inch concrete.

*First figure indicates number of reservoirs in system; second, the reservoir unit capacity in gallons.

that in each system a duct bank has one more duct than there are single-conductor cables. Separate manholes are provided for normal joints, for stop joints, and for the reservoirs. Three types of reservoirs are used—the *CC*, *AC*, and *DC* types.

The detailed data on ducts, manholes, and cable accessories are given in Table III.

Method of Estimating System Capital Cost

For the purpose of estimating the capital cost, the system is divided into the following three groups:

1. The sending-end substation.
2. The underground line.
3. The receiving-end substation.

The subdivisions of the groups are shown in Table IV, which gives a typical calculation of system capital cost.

The capital cost of each group is arrived at in the following manner:[5] The cost of all equipment (material) is obtained from the manufacturers. In cases where the cost of freight and delivery to site of erection is not included, certain percentages are added to account for it. On top of this, a percentage is added to cover costs of labor and installation on foundation; this percentage is determined from actual projects and varies with the type of equipment and voltage. In this fashion the costs are determined of structures, of high- and low-voltage switching, protective and control equipment, and of the auxiliary substation equipment. To the cost of equipment as installed on foundation, two more items are added: the indirect expenses and the cost of money during construction. To cover the indirect expenses, 22.5 per cent is added. The cost of money is taken at six per cent for one-half the length of the construction period, which is taken at six months for all the systems under study.

Table IV. Typical Calculation of Total System Capital Cost—System *U*-41*a*

In Dollars

	Cost of Item as Delivered (Material)	Cost of Item as Installed (on Foundation Where Needed) Including Labor Cost	Group Cost
1. Sending substation			
1.1 Land	33,700	33,700	
1.2 Structures		206,500	
1.3 Power transformers	629,000	754,800	
1.4 High-voltage switching equipment			
1.41 oil circuit breakers	271,600	325,900	
1.42 air-break disconnectors	61,200	73,450	
1.43 busses and supports		115,400	
1.5 Low-voltage switching, protective, and control equipment		500,000	
1.6 Auxiliary substation equipment		154,000	
		2,163,750	
Indirect expenses		486,850	
Cost of money during construction		39,800	2,690,400
2. Line			
2.1 Underground cables*	669,000	669,000	
2.2 Cable accessories*			
2.21 terminals	4,550	4,550	
2.22 joints	64,100	64,100	
2.23 reservoirs	48,150	48,150	
2.24 oil	900	900	
2.3 Duct banks*		421,300	
2.4 Manholes*		68,400	
2.5 Bonding		32,400	
2.6 Equipment for communication and relaying	24,700	29,600	
		1,338,400	
Indirect expenses		301,150	
Cost of money during construction		24,550	1,664,100
3. Receiving substation			
3.1 Land	33,700	33,700	
3.2 Structures		206,500	
3.3 Power transformers	727,000	872,400	
3.4 High-voltage switching equipment			
3.41 oil circuit breakers	271,600	325,900	
3.42 air-break disconnectors	61,200	73,450	
3.43 busses and supports		115,400	
3.5 Low-voltage switching, protective, and control equipment		432,500	
3.6 Auxiliary substation equipment		154,000	
		2,213,850	
Indirect expenses		498,100	
Cost of money during construction		40,650	2,752,600
Total system capital cost			7,107,100

System *U*-41*a* is rated at 255,000 kva. Power is transmitted over a distance of 10 miles, at a voltage of 138 kv, over two circuits of a 750,000-circular-mil oil-filled cable.

Construction period taken at six months. Cost of money during construction taken at six per cent for one-half construction period.

*Cost of duct banks includes the cost of laying cable and affixing terminals. Cost of manholes includes affixing joints and placing reservoirs.

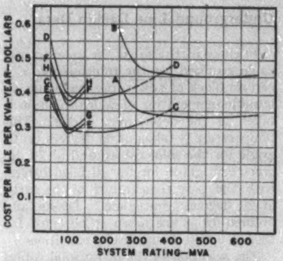

Figure 8. Cost of the entire system, including terminal substations, per mile per kilovolt-ampere-year at 50 per cent annual load factor

For explanation of identification letters, see Figure 1. Costs per mile per kilovolt-ampere-year at 35 and 75 per cent annual load factors differ very little from the cost at 50 per cent annual load factor

All prices are based on a cost of copper of $10^1/_8$ cents per pound of ingot copper, and on a cost of lead of 4.6 cents per pound, fob, New York. Cost of fabricated steel of shapes involved in substation structures is taken at $102 per ton, fob, Pittsburgh.

The kilovolt-ampere rating of power transformers at both ends of the system having been increased to cover appropriate losses in system parts, the losses thus become capitalized.

Discussion of System Capital Cost

Capital cost of the systems under study is calculated per kilovolt-ampere transmitted and per kilovolt-ampere-mile for the system as a whole, including terminal substations, and for the underground line alone. The total capital cost figures are given in Table V. The capital cost of the entire system is represented in Figures 1 and 2, and that of the transmission line in Figures 3 and 4. The costs of major subdivisions of the costs of the substations and of the transmission line, in per cent of their total costs, are represented in Figures 5 and 6.

The results obtained show that there is a definite relationship between the block of power transmitted (system rating) and the transmission voltage. As the block of power transmitted increases, the cost of the entire system and of the transmission line per kilovolt-ampere and per kilovolt-ampere-mile at first decreases; then, having reached a certain minimum, it increases again. The most economical block of power, therefore, is not the largest that may be transmitted with a certain type of cable at a certain voltage.

At a rating under 65,000 kva the 69-kv solid cable is unquestionably the most economical. As the system rating increases, the 69-kv oil-filled cable comes

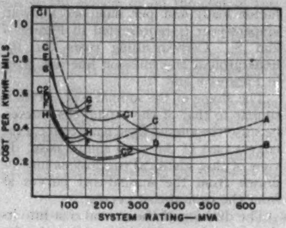

Figure 9. Cost of the transmission line per kilowatt-hour

For explanation of identification letters, see Figure 1. All costs at 50 per cent annual load factor except as follows:

C1...15..138 at 35 per cent
C2...15..138 at 75 per cent
annual load factor

definitely into the picture. The over-all cost of the entire system, and of the underground line alone, for this cable is the lowest when somewhat over 100,000 kva is transmitted. With system ratings above 65,000 kva and up to almost 100,000 kva there is very little difference in the cost of the underground line alone whether a 69-kv oil-filled or a 138-kv cable is used; with still higher system ratings, a 138-kv oil-filled cable is very much more economical. When, however, the system as a whole is considered, the lower cost of the 69-kv terminal equipment extends the application of the 69-kv oil-filled cable up to ratings as high as 125,000 kva. For the 138-kv oil-filled cable the over-all cost of the entire system is the lowest when about 150,000 kva is transmitted; for the cable line alone the lowest cost is obtained with a transmission of about 200,000 kva. The different economical power limits in the two cases, when the costs of the entire system and of the transmission line alone are considered, is due to the high cost of the terminal substations compared with the cost of the underground line in systems of this voltage. The 138-kv oil-filled cable may be economically applied for transmission up to somewhat over 300,000 kva when the underground line alone is considered; and it may be used up to 375,000 kva when the entire system is evaluated, including the terminal substations. When still larger blocks of power are transmitted, then either a 230-kv oil-filled cable may be used, or the block of power should be split into a greater number of 138-kv oil-filled-cable circuits. Within the economical range of power quantities investigated, the cost of transmission with the 230-kv cable changes rather little. It is quite likely, however, that as the block of power exceeds 600,000 kva, the transmission costs will rise again, and either a different type of cable will have to be selected or an increased number of circuits will have to be used. The differences in the cost of transmission, as affected by the magnitude of the block of power, on the one hand, and the type and voltage of cable, on the other hand, are so great that a thorough study of any project is certainly warranted.

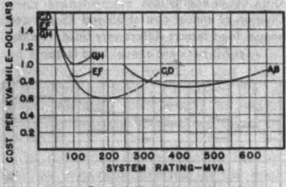

Figure 10. Cost of the transmission line per mile per kilovolt-ampere-year at 50 per cent annual load factor

For explanation of identification letters, see Figure 1. Costs per mile per kilovolt-ampere-year at 35 and 75 per cent annual load factors differ very little from the cost at 50 per cent annual load factor

The division of the system capital cost into its three component groups, given in Table V, shows that in the great majority of cases the underground line is the largest cost item in the total cost, the percentage cost depending on the relationship between the total cost of the line and the cost of the terminal equipment required for the transmission of the block of power involved. The analysis of the costs of the substations, given in Figure 5, shows that the power transformers constitute the largest cost item of both the sending and the receiving substations in all the systems except the two rated at 600,000 kva, where the circuit-breaker interrupting capacity is so high that the cost of the high-voltage switching equipment exceeds that of the power transformers. The percentage division of the capital cost of the transmission line into its main component parts, given in Figure 6, indicates that in the systems rated at 106,000 kva and more the cost of the underground cables forms the largest item of the cost of the line. Only in systems of smaller rating the cost of the duct banks represents the largest of all items; this is due to the high proportion of labor costs in the duct banks. The cost of cable accessories in the 230-kv oil-filled cable lines is very much higher than that in the 69- and 138-kv cable systems.

The percentage division of the capital cost into its component parts makes it possible to evaluate the effect of changes in the cost of system parts or in the cost of basic materials, when it is desired to consider costs different from those employed in the paper. By multiplying the percentage change in the cost of a particular item, or, for example, in the price of copper, by the corresponding percentage given for that item in the figures, the de-

Table V. Capital and Annual System Cost

In Thousands of Dollars

System Identification Number	Capital Cost				Total Annual System Cost at 50-Per-Cent Annual Load Factor
	Entire System	Sending Substation	Receiving Substation	Transmission Line	
U-33a	1,759	496	511	752	251
U-331a	1,725	489	504	732	255
U-34a	2,221	717	735	769	320
U-35a	2,138	498	513	1,127	301
U-351a	2,093	493	505	1,095	309
U-36a	2,613	721	736	1,156	364
U-361a	2,140	634	658	848	311
U-362a	2,567	638	659	1,270	367
U-363a	2,113	646	670	797	315
U-364a	2,516	650	673	1,193	373
U-37a	2,679	810	835	1,034	390
U-371a	2,584	827	852	905	388
U-38a	2,744	915	952	877	402
U-39a	3,195	812	836	1,547	457
U-391a	3,037	828	853	1,356	453
U-40a	3,185	919	954	1,312	463
U-401a	4,472	1,399	1,451	1,622	640
U-402a	5,307	1,404	1,453	2,450	748
U-403a	4,232	1,399	1,451	1,382	626
U-404a	4,928	1,406	1,454	2,068	708
U-405a	4,330	1,632	1,700	998	628
U-406a	4,827	1,634	1,701	1,492	697
U-41a	7,107	2,690	2,753	1,664	1,026
U-42a	10,805	4,164	4,197	2,444	1,457
U-43a	7,938	2,694	2,754	2,490	1,130
U-44a	12,052	4,189	4,207	3,656	1,613
U-441a	12,663	4,854	5,000	2,809	1,750
U-442a	14,096	4,878	5,013	4,205	1,928
U-45a	19,810	7,272	7,412	5,126	2,722
U-46a	22,379	7,287	7,418	7,674	3,046

The total annual system cost at 35- and 75-per-cent annual load factors closely approximates the cost at the 50-per-cent factor.

Table VI. Annual Fixed Charges and Annual Expenses for Maintenance and Operation on System Parts

In Per Cent of Their Capital Cost

Item	Annual Fixed Charges					Annual Expenses for Maintenance and Operation
	Taxes	Insurance	Depreciation and Obsolescence	Interest on Money Invested	Total	
Sending substation	2.0	0.5	1.823	6.0	10.323	2.0
Transmission line	2.0		1.823	6.0	9.823	1.3
Receiving substation	2.0	0.5	1.823	6.0	10.323	2.0

Charges for depreciation and obsolescence calculated by the sinking-fund method, at six per cent per annum money cost, for a 25-year life span of all system parts.

sired changes may be evaluated[5] and applied, on a percentage basis, to the calculated costs per kilovolt-ampere or kilovolt-ampere-mile. Changes in the system design, in the accepted permissible current rating for particular cables, or in the amount of equipment used, changes in the percentage allotted to cover the indirect expenses, or in the cost of money during construction, may be similarly introduced.

Method of Estimating System Annual Cost

The system annual cost is taken as the sum of the annual fixed charges and the annual operating expenses and is calculated for annual load factors of 35, 50, and 75 per cent. Both the annual fixed charges and the annual expenses for maintenance and operation are calculated as percentages of the capital cost separately for each of the three major groups into which the capital cost structure is divided. These are given in Table VI. The cost-of-energy loss, forming a separate part of the annual operating expenses, is taken equal to the sum of the cost of generation and the cost of transmission.

The capital cost of the steam-power station is taken at $100 per kilowatt for all systems designed. The annual fixed charges of the power plant are taken at the same rate as for the substations of the system, that is 10.323 per cent. The cost of maintenance and operation of the power plant consists of three parts: fixed operating costs, taken at $1.25 per kilowatt per year; variable maintenance costs, which at the annual load factors of 35, 50, and 75 per cent are taken correspondingly at $0.875, $1.25, and $1.85 per kilowatt; and operating supplies (labor) taken at 0.25 mills per kilowatt-hour. The cost of fuel at the annual load factors of 35, 50, and 75 per cent is taken correspondingly at 1.897, 1.795, and 1.70 mills per kilowatt-hour.

The losses in various system parts are given in Table VII. For simplification purposes, losses in the underground-cable line have been taken as fully dependent on load, although, strictly speaking, this is not entirely correct, especially in the 230-kv cables. It will be observed from the table that losses in the cable line represent the largest single item of the system losses. A careful design of the cable line is therefore exceedingly important.

The cost of energy loss per kilowatt-hour for the entire system is given in Table VIII. It is calculated for an 85-per-cent power-factor load.

Discussion of System Annual Cost

The total annual system cost at 50-per-cent annual load factor is given in Table V. The cost of the entire system per kilowatt-hour (at 85-per-cent power-factor load) and per mile per kilovolt-ampere-year is represented in Figures 7 and 8. Corresponding costs for the underground transmission line are given in Figures 9 and 10.

The shape of the annual-cost curves is similar to that of the capital-cost curves, because the annual fixed charges form the largest part of the total annual cost. In view of this, identical conclusions may be drawn from the annual-cost curves as from the capital-cost curves.

The division of the annual cost into its three major component parts at the 50-per-cent annual load factor is given in Figure 11 for the entire system and in Figure 12 for the underground line alone. The fixed charges form by far the largest percentage of the total annual cost. Any changes which may take place in the capital cost may be introduced into the annual cost through the percentages which the fixed charges form of the total annual cost. Similarly, the effect of changes which it may be desired to make in the rate of taxes, in the insurance, in the rate of depreciation and obsolescence, or in the interest on money invested may be estimated easily.[5] When the maintenance and operation costs, the cost of the energy loss, or the cost of generation are other than those taken in the study, their effect on the annual cost of the entire system, or on the cost of the underground line alone, may be evaluated in like fashion.

Effect of Design Conditions and Economic Factors on System Cost

Within the scope of this paper it is impossible to estimate the effect which the modification of the various design conditions adopted and of the economic factors assumed in the study would have on the

Figure 11. Division of annual cost of the entire system, including terminal substations, at 50 per cent annual load factor, in transmission systems ten miles long

A—Fixed charges
B—Expenses for maintenance and operation
C—Cost of energy loss

Division of annual cost at 35 and 75 per cent annual load factors differs very little from that at 50 per cent annual load factor

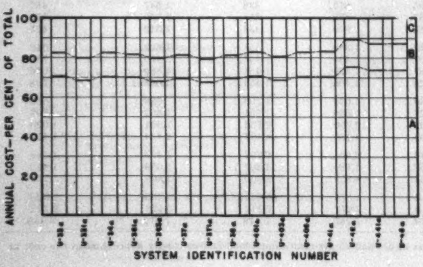

Figure 12. Division of annual cost of the transmission line at 50 per cent annual load factor, in transmission lines ten miles long

A—Fixed charges
B—Expenses for maintenance and operation
C—Cost of energy loss

Division of annual cost at 35 and 75 per cent annual load factors differs very little from that at 50 per cent annual load factor

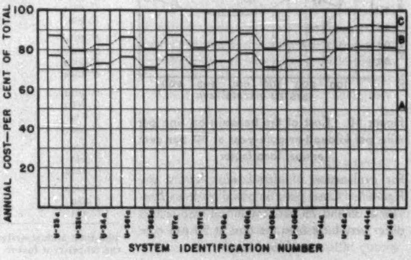

cost of the system or on the cost of the transmission line.

Among the design conditions affecting the cost is the condition of service reliability. This could have been modified either by installing an extra single-conductor cable, or by requiring that systems carry full load with a loss of one circuit. The length of the oil-filled cable section and the number of joints and manholes assumed per mile could be changed in either direction. The power factor of the load could be taken other than the assumed 85-per-cent lagging power factor, with its consequent effect on kilowatt-hour cost. Self- instead of water-cooled power transformers could be used, and their spare capacity could be modified. Finally, the system of high-voltage busses and their sectionalization, the number of high-voltage circuit breakers and their interrupting capacity, calculated for a certain assumed load, could be made somewhat different from those taken in the study.

Table VII. System Losses in Kilowatts

System Identification Number	Losses Independent of Load: Sending-End Transformers	Losses Independent of Load: Receiving-End Transformers	Losses Independent of Load: Total Losses	Losses Dependent on Load: Line	Losses Dependent on Load: Sending-End Transformers	Losses Dependent on Load: Receiving-End Transformers	Losses Dependent on Load: Total Losses*
U-33*a*	194	177	371	723	291	264	1,378
U-331*a*	196	176	372	1,206	281	263	1,850
U-34*a*	230	215	445	1,040	344	322	1,836
U-35*a*	195	177	372	1,081	293	264	1,738
U-351*a*	193	176	369	1,810	289	263	2,462
U-36*a*	231	215	446	1,560	347	322	2,359
U-361*a*	269	251	520	871	402	376	1,799
U-362*a*	270	251	521	1,306	405	376	2,237
U-363*a*	275	255	530	1,292	413	384	2,239
U-364*a*	278	255	533	1,938	417	384	2,889
U-37*a*	358	345	703	955	536	517	2,208
U-371*a*	367	353	720	1,433	549	529	2,711
U-38*a*	361	341	702	1,115	541	512	2,368
U-39*a*	359	345	704	1,433	537	517	2,687
U-391*a*	368	353	721	2,150	552	529	3,431
U-40*a*	363	341	704	1,673	546	512	2,931
U-401*a*	533	498	1,031	1,384	799	747	3,230
U-402*a*	535	498	1,033	2,076	803	747	3,926
U-403*a*	536	498	1,034	2,176	804	747	4,027
U-404*a*	539	498	1,037	3,265	809	747	4,121
U-405*a*	546	527	1,073	1,215	818	791	3,144
U-406*a*	548	527	1,075	1,822	822	791	3,755
U-41*a*	845	840	1,685	1,884	1,373	1,260	5,017
U-42*a*	732	705	1,437	1,464	1,100	1,059	4,123
U-43*a*	888	840	1,728	2,827	1,336	1,260	5,923
U-44*a*	734	705	1,439	2,211	1,103	1,059	4,873
U-441*a*	1,270	1,076	2,346	1,476	1,900	1,614	5,740
U-442*a*	1,274	1,076	2,350	2,214	1,906	1,614	6,484
U-45*a*	1,780	1,710	3,490	2,954	2,665	2,565	9,384
U-46*a*	1,785	1,710	3,495	4,431	2,675	2,565	10,871

Line losses are the sum of copper losses and dielectric losses in cables.

*These include losses in the current-limiting reactors.

The method of cost estimating has by itself an important bearing on the final cost. For example, had the winter rating been used for the cables instead of the summer rating, or had credit been allowed for the charging current of the underground cables, the total costs could have been appreciably lowered. The various economic factors, such as the price of copper and lead; cost of the terminal equipment, of the underground cable, of labor, and installation on foundation; financial methods of cost estimates; annual fixed charges; and the cost of maintenance and operation, may also vary from those taken in the study and may affect the system cost.

In estimating the magnitude of error in the final cost figures of this study, it may be said that the error in the design is very likely less than ten per cent. Of the same order is the error in the cost figures obtained from various manufacturers. The error in estimating costs of labor and installation, and other miscellaneous costs is around 15 per cent.

Summary and Conclusions

Results of design and cost estimates of cable-transmission systems and tie lines may be summarized as follows:

1. The type and voltage of the underground cable selected for a certain transmission line or tie line depend on the magnitude of the block of power to be transmitted. It is shown in the paper that, as the block of power increases beyond certain values, it becomes more economical to use a cable of higher voltage—or of a different type—rather than to employ a cable of the type and voltage which are more suitable for a smaller block of power. In particular this is evident when the 69-kv solid and oil-filled cables are being compared with the 138-kv oil-filled cable.

2. The most economical block of power is neither the smallest nor the largest that may be transmitted at a particular voltage. When properly selected, however, it will lower considerably the cost per kilovolt-ampere-mile, as well as the annual cost.

3. At prices for the 230-kv oil-filled cable and its accessories as taken in this study, this cable can compete with the 138-kv oil-filled cable only as a tie line between two 230-kv systems with available 230-kv terminal equipment. If an underground cable line requires installation of new terminal equipment, it will be very much less expensive to employ a 138-kv oil-filled cable. Otherwise a 230-kv cable tie line alone, without terminal equipment, is not much more expensive than a 138-kv cable line when a block of power of optimum value is transmitted, and at some system ratings it is the more economical.

4. The cost of the 230-kv oil-filled cable accessories as taken in this study appears to represent a very high percentage of the cost of the cable tie line. It is the cost of these accessories that limits the application of the 230-kv cable, and the lowering of it will extend considerably the region of the economical application of this cable. On the other hand, it might perhaps be possible to use sections of greater length and to place the normal joints farther apart than would follow from present-day practice.

5. Since cables in this country, as a general rule, use greater insulation for a certain voltage and operate at higher temperatures than is the practice in some European countries, the thought is expressed that it perhaps would lead to useful economic results, should a broad study be made of the relationships of the cable insulation for a certain voltage, the maximum operating temperature, the cable current-carrying capacity, and the cost of the cable. The relationship between the insulation and the current rating at the operating temperature must not be more favorable than that which would result in a satisfactory cable of a minimum cost. Such a study probably would involve an analysis of the various parts of the cable structure, such as the diameter of the hollow core and the thickness of the lead sheath. Even if such studies are being made by some companies, indications are that more extensive studies carried on by the industry as a whole, as a co-operative effort between the producers and the consumers, would bring gratifying results both to the cable manufacturers and the public utilities.

6. Figures are given showing the division on a percentage basis of the system capital and annual costs into their major component parts. Tables show the

Table VIII. Cost of Energy Loss Per Kilowatt-Hour

In Mills

System Identification Number	Annual Load Factor 35 Per Cent	 50 Per Cent	 75 Per Cent
U-33a	7.67	6.00	4.98
U-331a	7.67	6.01	4.98
U-34a	7.76	6.07	4.73
U-35a	7.97	6.20	4.82
U-351a	7.98	6.23	4.82
U-36a	7.95	6.20	4.82
U-361a	7.48	5.88	4.60
U-362a	7.73	6.05	4.72
U-363a	7.45	5.85	4.59
U-364a	7.67	6.01	4.98
U-37a	7.38	5.80	4.55
U-371a	7.32	5.76	4.52
U-38a	7.42	5.82	4.57
U-39a	7.59	5.94	4.65
U-391a	7.49	5.88	4.61
U-40a	7.60	5.95	4.64
U-401a	7.57	5.93	4.64
U-402a	7.80	6.09	4.75
U-403a	7.49	5.88	4.60
U-404a	7.69	6.02	4.69
U-405a	7.45	5.84	4.59
U-406a	7.58	5.94	4.64
U-41a	7.48	5.88	4.60
U-42a	8.23	6.39	4.94
U-43a	7.63	5.98	4.67
U-44a	8.45	6.53	5.04
U-441a	7.75	6.06	4.72
U-442a	7.92	6.17	4.80
U-45a	7.72	6.04	4.71
U-46a	7.90	6.17	4.80

Cost of steam generation is taken at 6.20 mills per kilowatt-hour at 35-per-cent annual load factor, 4.97 mills at 50-per-cent annual load factor, and 3.99 mills at 75-per-cent annual load factor.

Cost of transmission is calculated from the sum of the annual fixed charges and annual expenses for maintenance and operation, both taken for the entire system, terminal substations including.

amount of various equipment used in the system. Through their use, changes in the system cost may be evaluated when costs other than those used in this study are taken for the cable and its accessories, for the system equipment, for labor and installation, or for the duct banks; when prices of basic materials change; or when some of the financial factors affecting the capital or annual cost structure are modified. Similarly, the data may be used for estimating the cost when the design of some system parts, or the amount of terminal equipment, is modified; when it is desired to modify the current-carrying capacity of the cable line; when the duct banks or the number of cable accessories is changed, while at the same time the costs and economic assumptions made in the study are retained. The tables and figures may be used either for complete systems, including terminal equipment, or for the underground cable line alone, whether it be a straight transmission line, a tie line, or a cable termination of an overhead transmission line approaching the power station. The cost curves given may be interpolated within the range of values investigated.

7. This paper is an indication of the general trend of costs of underground power-transmission and tie lines. For an exact determination of the capital or annual costs of a projected system, or of an underground cable line, the costs must be calculated in detail. In some cases, with certain combinations of the various factors involved, costs lower or higher than those given in this study may be obtained. The relative costs and the effect of various factors, however, will remain as presented.

References

1. Les Câbles à 220 Kv de la Région Parisienne, **M. Laborde.** International Conference on Large High-Voltage Systems (CIGRE), Paris, France, 1937, volume 2, report 214.

2. Le Résrau et les Postes d'Interconnection à 220 Kv de la Région Parisienne, **M. Laborde, H. Josse.** *Revue Générale d'Électricite* (Paris, France), volume 39, 1936, pages 827–45; 863–76.

3. La Prima Granda Linea in Cavo a 220 Kv. *L'Elettrotecnica*, volume 24, 1937, pages 404–07.

4. Economics of High-Voltage Cable, **D. W. Roper.** AIEE Transactions, volume 50, 1931, pages 1399–1411.

5. Costs Study of 69- to 345-Kv Overhead Power-Transmission Systems, **John G. Holm.** AIEE Transactions, volume 63, 1944, pages 406–22.

6. Load Factor—Equivalent Hours Compared, **F. H. Buller, H. R. Woodrow.** *Electrical World*, volume 92, 1928, pages 59–60.

7. Economic Choice of Electrical Plant, **D. J. Bolton.** *World Power*, volume 17, 1932, pages 12–16.

8. Current-Carrying Capacity of Impregnated-Paper, Rubber and Varnished-Cambric-Insulated Cables, Insulated Power Cable Engineers Association publication, 1943.

9. Carrying Capacity of Cables, **T. F. Peterson.** *Electrical World*, volume 94, 1929, pages 1132–5.

10. The Lower-Voltage Sections of the British Grid System, **C. W. Marshall.** *Journal* of the Institution of Electrical Engineers (London, England), volume 74, 1934, pages 105–30.

11. Specifications for Impregnated-Paper-Insulated Lead-Covered Cables, Association of Edison Illuminating Companies.

12. Cable Geometry and the Calculation of Current-Carrying Capacity, **D. M. Simmons.** AIEE Transactions, volume 42, 1923, pages 525–39.

13. Calculation of the Electrical Problems of Underground Cables, **D. M. Simmons.** *Electric Journal*, 1932.

14. Reduction of Sheath Losses in Single Conductor Cables, **H. Halperin, K. W. Miller.** AIEE Transactions, volume 48, 1929, page 399.

15. Symposium on 132,000-Volt Single-Conductor Lead-Covered Cable, **P. Torchio, L. Emanueli, W. S. Clark, A. H. Kehoe, C. H. Shaw, J. B. Noe, D. W. Roper.** AIEE Transactions, volume 47, 1928, pages 186–210; discussion, pages 210–216.

The Direct- and Quadrature-Axis Equivalent Circuits of the Synchronous Machine

A. W. RANKIN
ASSOCIATE AIEE

THE EQUIVALENT-CIRCUIT method of analysis is a tool of unquestioned competence in the solution of machine and system problems involving a number of simultaneous equations. Its efficacy in obtaining practical results has been demonstrated in many diverse applications. In particular, the complete equivalent circuit of the synchronous machine—complete in the sense that the field-winding circuit and the multiple damper-winding circuits are individually included—is used whenever a detailed knowledge is needed of the operation of all the rotor circuits. Specific examples of its use are in the design of the damper-winding circuits, in problems involving single-phase and asynchronous operation, in the determination of damping and synchronizing torque, and in the determination of the transient and subtransient impedances; these few by no means exhaust the list.

When we consider the many practical applications of the complete equivalent circuit of the synchronous machine, it is somewhat surprising to note that it has been analyzed only somewhat superficially in the technical literature and has been the subject of very few technical papers, the most important of these being the papers of Linville[1] and Liwschitz.[2] Linville presented an equivalent circuit which was complete within the limits of certain well-defined approximations and also derived formulas for all the machine impedances. Liwschitz recognized that there were many applications in which the complexity of Linville's equivalent circuit would not be warranted and accordingly presented simplified equivalent circuits which were easier to use. The simplified circuits of Liwschitz give satisfactory results in many important problems, but in those applications which require a knowledge of the details of damper-winding operation the complete equivalent circuits are indispensable.

Because these complete equivalent circuits of the synchronous machine are becoming of ever-increasing importance, especially in these times with systems and machines being subjected to higher and higher specific loadings, it is the purpose of this paper to derive more complete and more exact equivalent circuits than heretofore have been available. These circuits are developed primarily for use on a-c network analyzers, since the modern analysis of problems of the type discussed in this paper tends more and more toward the use of such mechanical aids.

This paper also presents formulas for all the impedances needed by the equivalent circuits. An assemblage of the impedance formulas such as is here given is necessary when presenting an equivalent circuit in order to be certain that all the impedances are in accord and calculated on the same base. It will be found that the per-unit impedance formulas presented in this paper differ from those of Linville in that, in addition to improved permeance coefficients, the rotor current base is the x_{ad} base[7] which is more familiar to designers than the magnetomotive-force base of Linville. These impedance formulas are presented in this paper in a direct systematized form which considerably simplifies the determination of the per-unit values, and which is not subject to the misinterpretation which sometimes causes errors in the determination of the per-unit impedances of the multiple rotor circuits.

The permeance coefficients which are an integral part of the reactance formulas are determined in this paper by means of a gap-reluctance expression whose accuracy is proved by comparison with similar coefficients evaluated from flux plots. These permeance coefficients are evaluated numerically for a typical pole configuration and presented in tabular form. The specific results and a discussion of their superiority over presently available data are given in the following section.

Results and Discussion

The complete direct-axis equivalent circuit of the synchronous machine is given by Figure 1. The quadrature-axis equivalent circuit is obtained from Figure 1 merely by substituting q for d. This circuit is an improvement over previous equivalent circuits in the following particulars:

(*a*). The impedances are given in their most general form and are all present, although some can be eliminated by a suitable choice of base-current ratio in the calculation of the per-unit impedances. For instance, this paper uses a base-current ratio which makes $X_{gnnd}=X_{fnd}$, and, accordingly, if the end-ring impedances can be neglected, the coupling transformers of Figure 1 are unnecessary.

(*b*). The end-ring impedance is correctly represented, and is separated from the field-winding circuit by means of 1/1 coupling transformers.

(*c*). The component impedances are given directly in terms of resistance and capacitive reactance, so that the circuit can be set up on an a-c network analyzer without introducing the resistance errors of inductive reactance. The circuit impedance $\hat{x}_d(j\omega)$ is obtained by direct measurement of the terminal voltage and current.

The equivalent circuit of Figure 1 is developed directly from the operational equations of the synchronous machine by noting the physical relations which exist between the various impedances. This development is given in the section, "Development of Equivalent Circuits."

The per-unit impedances for use in the equivalent circuit of Figure 1 are developed in the sections, "Impedances of Direct-Axis Circuits" and "Impedances of Quadrature-Axis Circuits." Because of the large number of formulas so obtained, it is not practical to collect and present them in this section. The origin of most of the difficulties in the determination of these multitudinous impedances is in the stator–rotor turn ratio of the short-pitched damper-winding circuits. In order to maintain a consistent stator–rotor turn ratio and thereby obtain an harmonious system of per-unit impedances, the latter are evaluated herein by first determining the physical ampere-inch-second impedances, and converting these to per unit by the direct conversion factors previously published by the author.[3] In the author's judgment, this method is superior to any other method presently available, since the physical concept of the impedance is maintained up to the last step at which point the per-unit impedances are obtained merely by introducing the conversion factor. In addition, the stator–

Paper 45-167, recommended by the AIEE committee on electric machinery for publication in AIEE TRANSACTIONS. Manuscript submitted June 11, 1945; made available for printing August 29, 1945.

A. W. RANKIN is in the turbine-generator engineering division of General Electric Company, Schenectady, N. Y.

The author acknowledges the co-operation and contributions of his associates in the General Electric Company in the study presented in this paper: S. B. Crary, who first brought to the author's attention the practical importance of a satisfactory and general solution of this problem and who contributed valuable suggestions and constructive criticism throughout the entire study; C. E. Kilbourne for his encouragement and for placing at the author's disposal several of his unpublished reports on machine impedances; C. Concordia for his suggestions regarding the equivalent circuit and for his contribution to the analytical work; and Gabriel Kron who developed the equivalent circuit. The gap-reluctance expressions on which the permeance integrals are based were developed by M. B. Siedd on the basis of a suggestion by C. E. Kilbourne. C. Gosney and M. Grems conducted the numerical integrations on which Tables I and II are based.

rotor turn ratio is used systematically without possibility of error.

The rotor-current base selected for the per-unit impedances of this paper is the so-called x_{ad} base which is the base which makes X_{afd} numerically equal to x_{ad}. This base has been selected, because it is the base in most common use among designers, and most design formulas are based on it. If desired, however, the per-unit impedances can be converted to any other base by the consistent expressions previously published.[3]

The permeance coefficients necessary for the reactance formulas of the multiple damper-winding circuits are evaluated in Appendixes I and II by numerical integration of definite integrals based on a reluctance expression developed from a study of the work of Doherty and Nickle.[4] These coefficients are evaluated for a typical pole configuration, and the resulting numerical values are given in Table I. Design experience has indicated that these permeance coefficients are more accurate than any previously published, especially in the quadrature axis. A direct indication of their accuracy is given by comparison with the work of Wieseman[5] who evaluated similar quantities for the field-winding circuit from actual flux plots. The correspondence with the work of Wieseman is given in Table II.

The definite-integral expressions for the pole-shape coefficients as derived in this paper are not intended to compete with any future evaluation by flux plotting but instead are offered as an acceptable and satisfactory solution until more accurate values can be obtained from flux plots and design experience. The author believes, however, and the correspondence with the work of Wieseman substantiates this belief, that these integrals are sufficiently accurate that future investigations can be directed at complementary correction factors for strategic points rather than at complete new integrals or tabular values.

Numbering of Damper-Bar Circuits

Particular attention is called to the numbering of the damper-bar circuits. This numbering system is shown on Figure 2. The numbering of the physical bars proceeds outward from the polar axis. If a single bar lies directly on the polar axis, it should be hypothetically divided at its center line with the two halves thus becoming bar 1 on each side of the polar axis.

The numbering of the direct-axis circuits is identical with the numbering of the physical bars, and proceeds outward from the direct or polar axis. In contradistinction to the direct-axis circuits, the numbering of the quadrature-axis circuits proceeds outward from the quadrature or interpolar axis. The advantage of this method is that all the logic and equivalent circuits developed for one axis are immediately applicable to the other axis with only a change of subscript from d to q or vice versa. The disadvantage is that the term n, upon superficial examination, seems somewhat ambiguous since the same bar has one number in the direct axis and another in the quadrature axis. This superficial ambiguity is eliminated by noting that the subscript n followed by d specifies the nth circuit numbered from the direct axis, the subscript n followed by q specifies the nth circuit numbered from the quadrature axis, and the subscript n without either d or q following specifies the nth physical bar numbered from the polar axis.

Analysis

DEVELOPMENT OF EQUIVALENT CIRCUITS

The generalized per-unit equations 1a, b, ... and 2a, b, ... were derived in a recent publication by the author.[3]

$$\psi_d = X_{afd}I_{fd} + X_{a1d}I_{1d} + X_{a2d}I_{2d} + \ldots - x_d i_d \quad (1a)$$

$$\Psi_{fd} = X_{ffd}I_{fd} + X_{f1d}I_{1d} + X_{f2d}I_{2d} + \ldots - X_{fad} i_d \quad (1b)$$

$$\Psi_{1d} = X_{1fd}I_{fd} + X_{11d}I_{1d} + X_{12d}I_{2d} + \ldots - X_{1ad} i_d \quad (1c)$$

$$\Psi_{2d} = X_{2fd}I_{fd} + X_{21d}I_{1d} + X_{22d}I_{2d} + \ldots - X_{2ad} i_d \quad (1d)$$

$$E_{fd} = p\Psi_{fd} + R_{ffd}I_{fd} + R_{f1d}I_{1d} + R_{f2d}I_{2d} + \ldots \quad (2a)$$

$$E_{1d} = p\Psi_{1d} + R_{1fd}I_{fd} + R_{11d}I_{1d} + R_{12d}I_{2d} + \ldots \quad (2b)$$

$$E_{2d} = p\Psi_{2d} + R_{2fd}I_{fd} + R_{21d}I_{1d} + R_{22d}I_{2d} + \ldots \quad (2c)$$

The corresponding equations in the quadrature axis can be written from equations 1a, b, ... and 2a, b, ... by substituting q for d.

If all the rotor-circuit voltages are zero, the foregoing equations reduced to equations 3a, b, ...

$$\psi_d = X_{afd}I_{fd} + X_{a1d}I_{1d} + X_{a2d}I_{2d} + \ldots - x_d i_d \quad (3a)$$

$$0 = \left(X_{ffd} + \frac{R_{ffd}}{p}\right)I_{fd} + \left(X_{f1d} + \frac{R_{f1d}}{p}\right)I_{1d} + \left(X_{f2d} + \frac{R_{f2d}}{p}\right)I_{2d} + \ldots - X_{fad} i_d \quad (3b)$$

$$0 = \left(X_{1fd} + \frac{R_{1fd}}{p}\right)I_{fd} + \left(X_{11d} + \frac{R_{11d}}{p}\right)I_{1d} + \left(X_{12d} + \frac{R_{12d}}{p}\right)I_{2d} + \ldots - X_{1ad} i_d \quad (3c)$$

$$0 = \left(X_{2fd} + \frac{R_{2fd}}{p}\right)I_{fd} + \left(X_{21d} + \frac{R_{21d}}{p}\right)I_{1d} + \left(X_{22d} + \frac{R_{22d}}{p}\right)I_{2d} + \ldots - X_{2ad} i_d \quad (3d)$$

It is evident from equations 3a, b, ... that Ψ_d and all the rotor currents are

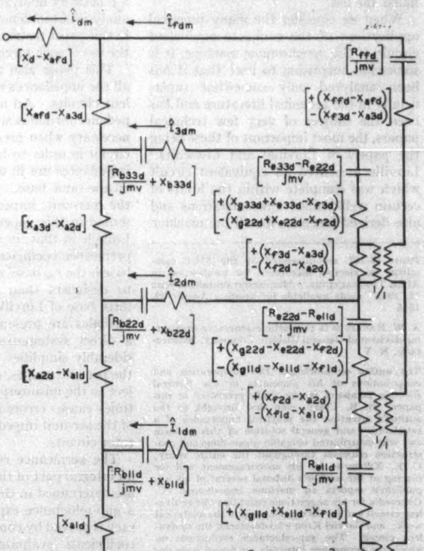

$\hat{i}_{dm}$
$\hat{I}_{fdm}$
$[x_d - X_{afd}]$
$\left[\frac{R_{ffd}}{jmv}\right]$
$\left[\begin{matrix}+(X_{ffd} - X_{afd})\\ -(X_{f3d} - X_{a3d})\end{matrix}\right]$
$[X_{afd} - X_{a3d}]$
$\hat{I}_{3dm}$
$\left[\frac{R_{b33d}}{jmv} + X_{b33d}\right]$
$\left[\frac{R_{e33d} - R_{e22d}}{jmv}\right]$
$\left[\begin{matrix}+(X_{g33d} + X_{e33d} - X_{f3d})\\ -(X_{g22d} + X_{e22d} - X_{f2d})\end{matrix}\right]$
$[X_{a3d} - X_{a2d}]$
$\left[\begin{matrix}+(X_{f3d} - X_{a3d})\\ -(X_{f2d} - X_{a2d})\end{matrix}\right]$
1/1
$\hat{I}_{2dm}$
$\left[\frac{R_{b22d}}{jmv} + X_{b22d}\right]$
$\left[\frac{R_{e22d} - R_{e11d}}{jmv}\right]$
$\left[\begin{matrix}+(X_{g22d} - X_{e22d} - X_{f2d})\\ -(X_{g11d} - X_{e11d} - X_{f1d})\end{matrix}\right]$
$[X_{a2d} - X_{a1d}]$
$\left[\begin{matrix}+(X_{f2d} - X_{a2d})\\ -(X_{f1d} - X_{a1d})\end{matrix}\right]$
1/1
$\hat{I}_{1dm}$
$\left[\frac{R_{b11d}}{jmv} + X_{b11d}\right]$
$\left[\frac{R_{e11d}}{jmv}\right]$
$[+(X_{g11d} + X_{e11d} - X_{f1d})]$
$[X_{a1d}]$
$[+(X_{f1d} - X_{a1d})]$
1/1

Figure 1. Direct-axis complete equivalent circuit for five or six bars per pole, $\hat{x}_d(jmv)$

$\frac{R}{jmv}$ = capacitive reactance

x = resistance

The quadrature-axis complete equivalent circuit is obtained from this circuit by substituting q for d

Table 1. Pole-Shape Coefficients Evaluated for a Typical Pole Configuration

$\rho = 1.50 \quad \alpha = 0.70 \quad p_p^{-1}g = 0.03$

y_{nd}, y_{nq}	$D_{d0n}y_{nd}$	$D_{q0n}y_{nq}$	D_{d1n}	D_{q1n}
0	0	0	0	0
0.1	0.157	0.0316	0.198	0.0394
0.2	0.310	0.0690	0.388	0.0858
0.3	0.457	0.123	0.562	0.148
0.4	0.598	0.210	0.713	0.243
0.5	0.726	0.329	0.839	0.348
0.6	0.845	0.460	0.938	0.466
0.7	0.933	0.598	0.996	0.558
0.8	0.986	0.747	1.022	0.630
0.9	1.024	0.900	1.034	0.676
1.0	1.056	1.056	1.037	0.692

linear operational functions of i_d. If i_d is assumed to have the vectorial form, equation 4, then ψ_d and the rotor currents must have the vector forms, equations 5a, b, c. The *mv* notation of equations 4 and 5a, b, c is used, because it is adaptable to different machine operating conditions. The *m* specifies the order of the harmonic when any are present, and the *v* is a generalized rotor-velocity term. For asynchronous operation at constant slip *s* and with only fundamental currents flowing, *v* is replaced by *s*, and *m* equals unity only and may be dropped. For asynchronous single-phase operation, harmonics are present, and *m* is needed to define the particular harmonic being studied, and *v* becomes equal to the rotor velocity.

$$i_d = \hat{I}_{dm}\epsilon^{+jmvt} \qquad (4)$$

$$\psi_d = \hat{\psi}_{dm}\epsilon^{+jmvt};\; I_{fd} = \hat{I}_{fdm}\epsilon^{+jmvt};\; I_{nd} = \hat{I}_{ndm}\epsilon^{+jmvt} \qquad (5a, b, c)$$

Substituting equations 4 and 5a, b, c into equations 3a, b, ..., using only the steady-state solution of the operational equations, and canceling the exponentials gives equations 6a, b, ...

$$\hat{\psi}_{dm} = X_{afd}\hat{I}_{fdm} + X_{a1d}\hat{I}_{1dm} + X_{a2d}\hat{I}_{2dm} + \ldots - x_d\hat{I}_{dm} \qquad (6a)$$

$$0 = \left(X_{ffd} + \frac{R_{ffd}}{jmv}\right)\hat{I}_{fdm} + \left(X_{f1d} + \frac{R_{f1d}}{jmv}\right)\hat{I}_{1dm} + \left(X_{f2d} + \frac{R_{f2d}}{jmv}\right)\hat{I}_{2dm} + \ldots - X_{fad}\hat{I}_{dm} \qquad (6b)$$

$$0 = \left(X_{1fd} + \frac{R_{1fd}}{jmv}\right)\hat{I}_{fdm} + \left(X_{11d} + \frac{R_{11d}}{jmv}\right)\hat{I}_{1dm} + \left(X_{12d} + \frac{R_{12d}}{jmv}\right)\hat{I}_{2dm} + \ldots - X_{1ad}\hat{I}_{dm} \qquad (6c)$$

$$0 = \left(X_{2fd} + \frac{R_{2fd}}{jmv}\right)\hat{I}_{fdm} + \left(X_{21d} + \frac{R_{21d}}{jmv}\right)\hat{I}_{1dm} + \left(X_{22d} + \frac{R_{22d}}{jmv}\right)\hat{I}_{2dm} + \ldots - X_{2ad}\hat{I}_{dm} \qquad (6d)$$

Equations 6a, b, ... can be applied to the subject problem by recognizing the physical relations which exist between the self- and mutual impedances of the various rotor circuits. These relations are introduced in the following paragraphs. They are the foundation for the direct- and quadrature-axis equivalent circuits.

Consider the *n*th additional rotor circuit in the direct axis. The reactance X_{nnd} is the sum of the reactance due to the air-gap flux within the bars which form the *n*th additional rotor circuit, the reactance due to the leakage flux in the bar slots, and the reactance due to the end-ring flux.

$$X_{nnd} = X_{gnnd} + X_{bnnd} + X_{ennd} \qquad (7a)$$

The mutual reactance X_{nkd} between the *n*th additional rotor circuit and any outer additional rotor circuit *k* is the sum of the reactance due to the air-gap flux and the reactance due to the end-ring flux; the bar-slot flux is pure leakage.

$$X_{nkd} = X_{gnnd} + X_{ennd}\ (k > n) \qquad (7b)$$

The mutual reactance between the *n*th additional rotor circuit and any inner additional rotor circuit is obtainable from the inner-circuit reactances. This important relation is a direct result of the reciprocal per-unit mutual impedances to which attention was directed in previous publications.[3,6]

The mutual reactance between the *n*th additional rotor circuit and the field-winding circuit depends upon only the air-gap flux of the *n*th additional rotor circuit, since the bar-slot flux and the end-ring flux are not mutual with the field winding. These mutual reactances are reciprocal because of the reasons stated in the preceding paragraph.

Concerning the resistance components, the resistance of the *n*th additional rotor circuit is the sum of the bar and end-ring resistances of that circuit.

$$R_{nnd} = R_{bnnd} + R_{ennd} \qquad (7c)$$

The mutual resistance between the *n*th additional rotor circuit and any outer additional rotor circuit *k* is the end-ring resistance of the *n*th circuit, since the bar resistance is not mutual with the *k*th circuit.

$$R_{nkd} = R_{ennd}\ (k > n) \qquad (7d)$$

The mutual resistance between the *n*th circuit and any inner circuit is obtained from the inner-circuit resistances as these mutual impedances are reciprocal.

There are no mutual resistances between the additional rotor circuits and the field-winding circuits since these circuits are coupled only magnetically.

The impedances of the quadrature-axis circuits can be written directly from the preceding expressions by substituting *q* for *d*.

When the physical relations of the preceding paragraphs are introduced into equations 6a, b, ... the equations obtained can be electrically duplicated by the a-c circuit of Figure 1 with $\hat{\psi}_{dm}$ the alternating voltage across the terminals. Figure 1 is therefore the equivalent circuit of the direct-axis equations of a synchronous machine.

In regard to equations 3a, b, ..., the relation between ψ_d and i_d may be written operationally as in equation 8a.

$$\psi_d = -x_d(p)i_d \qquad (8a)$$

Substituting equations 4 and 5a, b, c and taking only the steady-state solution reduces equation 8a to equation 8b.

$$\hat{x}_d(jmv) = -\frac{\hat{\psi}_{dm}}{\hat{I}_{dm}} \qquad (8b)$$

Reversing the direction of $\hat{I}_{dm}$ in Figure 1 permits $\hat{x}_d(jmv)$ to be defined as the a-c impedance of the direct-axis equivalent circuit since $\hat{\psi}_{dm}$ is the voltage across the circuit and $-\hat{I}_{dm}$ is the current into it. $\hat{x}_q(jmv)$ can be obtained in an analogous manner from the quadrature-axis equivalent circuit.

The current moduli $\hat{U}_{ndm}$ are defined as the rotor-circuit currents obtained when the terminal current $\hat{I}_{dm}$ is equal to $1.00\underline{/0}$. $\hat{U}_{nqm}$ is analogously defined.

$$\hat{U}_{ndm} = \hat{I}_{ndm} \text{ for } \hat{I}_{dm} = 1.00\underline{/0} \qquad (9a)$$

The rotor-circuit currents $\hat{I}_{ndm}$ and $\hat{I}_{nqm}$ are obtained from the product of the actual terminal current $\hat{I}_{dm}$ and the corresponding modulus as shown in equation 9b, c. The terminal currents $\hat{I}_{dm}$ and $\hat{I}_{qm}$ are determined by the machine operating conditions.

$$\hat{I}_{ndm} = \hat{U}_{ndm}\hat{I}_{dm};\; \hat{I}_{nqm} = \hat{U}_{nqm}\hat{I}_{qm} \qquad (9b, c)$$

The actual currents in the physical damper bars (as distinguished from the sub-*d* and sub-*q* currents in the hypothetical direct- and quadrature-axis circuits which are introduced only to simplify the mathematics) are given by equations 9d, e. It is evident from these expressions that, in general, there is unequal loading of the bars in the leading and trailing pole halves. The degree of this inequality depends upon the pole saliency and lack of symmetry between the direct- and quadrature-axis circuits. Equal loading of the trailing and leading pole halves exists only when $\hat{I}_{nd}$ and $\hat{I}_{nq}$ are in time quadrature.

Bars on trailing pole halves:

$$\hat{I}_{nm} = +\hat{I}_{ndm} + \hat{I}_{nqm} \qquad (9d)$$

Bars on leading pole halves:

$$\hat{I}_{nm} = -\hat{I}_{ndm} + \hat{I}_{nqm} \qquad (9e)$$

Due consideration must be given to the numbering system previously described by which the direct-axis circuits are numbered from the direct axis, and the quadrature-axis circuits are numbered from the quadrature axis. For instance, the third bar from the direct axis in Figure 2 is the second bar from the quadrature axis, and the total current in this bar (in the trailing half) is as given by equation 9f.

$$\hat{I}_{3m} = \hat{I}_{3dm} + \hat{I}_{2qm} \qquad (9f)$$

IMPEDANCES OF DIRECT-AXIS CIRCUITS

Experience in the use of these equivalent circuits has shown that the safest and shortest method of calculating the per-unit impedances is first to determine the ampere-inch-second values and convert these to per-unit values by the conversion factors previously published.* This method is followed in this paper.

Unit field current as used hereinafter is that field current which will induce in each stator phase a voltage of $x_{ad}i_{ao}$. Let this current be I_{fdo}. The corresponding base-current ratio is given by equation 10a. This base current has the advantage that it makes X_{afd} numerically equal to x_{ad} and at once eliminates the necessity for differentiating between these two quantities. In a previous paper[7] the author has suggested the universal adoption of this current as a preferred base.

$$\frac{I_{fdo}}{(3/2i)_{ao}}=\frac{4}{\pi}\frac{A_{d1}}{F_{d1}}\frac{N}{K_pK_dP_1}\frac{1}{N_{fd}} \tag{10a}$$

The unit current for the additional rotor circuits as used hereinafter will be that current which when flowing in the additional rotor circuit of 100-per-cent pitch will induce in each stator phase a voltage $x_{ad}i_{ao}$. Let this current be I_{xdo}. The corresponding base-current ratio is given by equation 10b. A 100-per-cent-pitch circuit is not usually present in modern synchronous machines, but it is convenient to use it as a base circuit since it has maximum effectiveness.

$$\frac{I_{xdo}}{(3/2i)_{ao}}=\frac{4}{\pi}\frac{A_{d1}}{D_{d1x}}\frac{N}{K_pK_dP_1} \tag{10b}$$

Base stator inductance L_{ao} and fundamental flux per pole at rated voltage will be needed for the evaluation of the per-unit impedances. These quantities are expressed in the following in terms of machine dimensions.

$$\beta'_{\max}=3.19\frac{F_g}{g} \quad \beta'_{\text{fund}}=3.19\frac{F_g}{g}F_{d1} \tag{11a, b}$$

$$\phi_f=12.76\frac{Rl}{P_1g}F_gF_{d1} \tag{11c}$$

$$\frac{1}{L_{ao}}=10^8\frac{i_{ao}}{\psi_{ao}}=\frac{10^8}{1.5P_1}\left(\frac{K_pK_dP_1}{N}\right)^2\frac{A}{\phi_f} \tag{11d}$$

$$\frac{1}{L_{ao}}=\frac{10^8}{19.14}\frac{A}{F_gF_{d1}}\frac{g}{Rl}\left(\frac{K_pK_dP_1}{N}\right)^2 \tag{11e}$$

$$\begin{aligned}19.14&=1.5\times12.76=1.5\times4\times3.19\\&=1.5\times4\times0.4\pi\times2.54\end{aligned} \tag{11f}$$

Stator Synchronous Reactance, x_d. The stator synchronous reactance x_d can be obtained most easily by arbitrarily separating it into the components x_{ad} and (x_d-x_{ad}). The former is the reactance of armature reactance, and the latter, somewhat unfortunately, has been termed the "leakage" reactance.

Assume the stator windings sinusoidally distributed with three-phase currents i_{ao} flowing therein. At the instant when the resulting sine wave of armature magnetomotive force is in the direct axis, the fundamental flux per pole will be as given by equation 12a. The corresponding per-unit generated voltage is given by equation 12b; this is x_{ad} by definition.

Fundamental flux per pole =

$$\frac{3.19}{g}\frac{4}{\pi}\frac{1.5Ni_{ao}}{K_pK_dP_1}A_{d1}\frac{2}{\pi}\frac{2\pi Rl}{P_1} \tag{12a}$$

$$x_{ad}=\frac{4}{\pi}\frac{A_{d1}}{F_{d1}}\frac{A}{F_g}=k_{ad}\frac{A}{F_g} \tag{12b}$$

The quantity (x_d-x_{ad}) has been evaluated several times in the technical literature. The most accurate published expressions are probably equation 37 of Alger[8] and equation 4a of Kilgore,[9] and the reader is referred to these references. In both cases, this quantity has been termed the armature "leakage" reactance.

Field-Winding Reactance, X_{ffd}. With a current of one ampere flowing in the field winding, the flux per pole due to air-gap flux is given by equation 14a. The corresponding inductance in henrys for the entire field-winding circuit of P_1 poles is given by equation 14b.

$$\text{Flux per pole}=3.19\frac{N_{fd}}{g}\frac{2}{\pi}F_{do}\frac{2\pi Rl}{P_1} \tag{14a}$$

$$L_{ffd1}=12.76\times10^{-8}\frac{Rl}{g}N_{fd}^2F_{do} \tag{14b}$$

Let Ψ_b and Ψ_t be the effective permeance† of the pole-body and pole-tip "leakage" paths per axial inch of machine length per pole, respectively. The inductance in henrys of the field-winding circuit of P_1 poles due to the pole-tip and pole-body flux is given by equation 14c.

$$L_{ffd2}=3.19\times10^{-8}N_{fd}^2lP_1(\Psi_b+\Psi_t) \tag{14c}$$

The total inductance in henrys of the field-winding circuit is given by equations 14d, e. Introducing equation 10a gives the per-unit value of the field-winding reactance, equation 14f.

$$L_{ffd}=3.19\times10^{-8}N_{fd}^2P_1l\left[\frac{4RF_{do}}{P_1g}+(\Psi_b+\Psi_t)\right] \tag{14d}$$

$$L_{ffd}=10^{-8}N_{fd}^2P_1l\left[\frac{K_\phi\phi_f}{F_gl}+3.19(\Psi_b+\Psi_t)\right] \tag{14e}$$

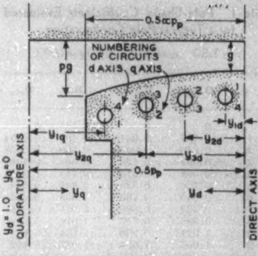

Figure 2. Pole and damper-bar dimensions and numbering of damper-winding circuits

y_d and y_q are measured in per unit of half the pole pitch ($0.5p_p$). y_{nd} and y_{nq} are the values of y_d and y_q, respectively, to circuit n, measured from and numbered from the corresponding (d or q) axis

$$X_{ffd}=k_{ad}K_\phi x_{ad}+3.19k_{ad}^2\frac{Al}{\phi_f}(\Psi_b+\Psi_t) \tag{14f}$$

Mutual Reactance Between Stator and Field Winding, X_{afd}. The fundamental flux per pole per ampere field-winding current is given by equation 15a. If sinusoidal distribution of the armature winding is assumed, the corresponding mutual inductance in henrys is given by equation 15b. Introducing equation 10a into equation 15b gives X_{afd} as shown in equation 15c.

Fundamental flux per pole

$$=3.19\frac{N_{fd}}{g}\frac{2}{\pi}F_{d1}\frac{2\pi Rl}{P_1} \tag{15a}$$

$$L_{afd}=3.19\times10^{-8}\frac{N_{fd}}{g}F_{d1}\frac{4R_1}{P_1}\frac{N}{K_pK_d} \tag{15b}$$

$$X_{afd}=\frac{4}{\pi}\frac{A_{d1}}{F_{d1}}\frac{A}{F_g}=k_{ad}\frac{A}{F_g}=x_{ad} \tag{15c}$$

Equation 15c illustrates a major advantage of the selected base-current ratio: X_{afd} and x_{ad} are numerically equal. .

nth Additional-Rotor-Circuit Reactance, X_{nnd}. With one ampere in the nth additional rotor circuit, the average flux density in the air gap within the bars which bound the nth circuit is given by equation 16a. The corresponding inductance in henrys for the entire circuit of P_1 poles is given by equation 16b.

$$B_{\text{avg}}=\frac{3.19}{g}\frac{2}{\pi}D_{don} \tag{16a}$$

$$L_{gnnd}=12.76\times10^{-8}\frac{Rl}{g}D_{don}y_{nd} \tag{16b}$$

The inductance due to the bar-slot leakage flux is given by equation 16c. This expression neglects the small amount of leakage flux around the bars where they emerge from the pole body. Equa-

---

* See "Results", reference 3.

†The permeance factor $(\Psi_b+\Psi_t)$ is difficult to evaluate and depends considerably upon the characteristics of the machine type being studied. Its complete derivation would be too long to be included in this paper. Satisfactory expressions have been given by Kilgore and Linville, and the permeance factor previously given is related to the corresponding quantities of Kilgore and Linville as follows:

$$3.19(\Psi_b+\Psi_t)=\lambda_{Ps}+\lambda_{Pe}=L_b+L_t$$

wherein λ_{Ps} and λ_{Pe} are evaluated in equations 15a and 16a of Kilgore, and L_b and L_t are evaluated in equation 14a of Linville.

tion 16c assumes that the slots are in open round slots as shown in the nomenclature; for rectangular slots, the factor 0.625 within the bracket should be replaced by ($0.333\, d_{sr}/w_{sr}$); for closed slots, the bracketed expression should be replaced by test or estimated values of the slot permeance.

$$L_{bnnd}=6.38\times10^{-8}P_1l\left(\frac{d_r}{w_r}+0.625\right) \qquad (16c)$$

The inductance due to the end-ring leakage flux can be approximated by considering the end rings as two wires of a single-phase transmission line with a distance between centers of D_e and an (effective) cross-sectional radius of r_e. This inductance is given by equation 16d.

$$L_{ennd}=0.508\times10^{-8}P_1l_{end}\left(9.2\log_{10}\frac{D_e}{r_e}+1\right) \qquad (16d)$$

The per-unit values of equations 16b, c, d, based upon the base-current ratio 10b, are given by equations 16e, f, g respectively.

$$X_{gnnd}=\left(\frac{4}{\pi}\frac{A_{d1}}{D_{d1x}}\right)^2\frac{A}{F_g}\frac{D_{don}}{F_{d1}}y_{nd} \qquad (16e)$$

$$X_{bnnd}=0.5\left(\frac{4}{\pi}\frac{A_{d1}}{D_{d1x}}\right)^2\frac{A}{F_g}\frac{P_1g}{F_{d1}R}\left(\frac{d_r}{w_r}+0.625\right) \qquad (16f)$$

$$X_{ennd}=0.04\left(\frac{4}{\pi}\frac{A_{d1}}{D_{d1x}}\right)^2\frac{A}{F_g}\frac{P_1g}{F_{d1}R}\frac{l_{end}}{l}\times\left(9.2\log_{10}\frac{D_e}{r_e}+1\right) \qquad (16g)$$

The per-unit reactance of the nth additional rotor circuit is given by equation 16h.

$$X_{nnd}=X_{gnnd}+X_{bnnd}+X_{ennd} \qquad (16h)$$

Mutual Reactance Between Stator and nth Additional Rotor Circuit, X_{nad}. With one ampere flowing in the nth additional rotor circuit, the maximum value of the fundamental component of flux density is given by equation 17a, and the mutual inductance in henrys between the stator and the nth additional rotor circuit is given by equation 17b.

$$\beta_{fund}=\frac{3.19}{g}D_{d1n} \qquad (17a)$$

$$L_{nad}=12.76\times10^{-8}\,\frac{Rl}{P_1g}\frac{N}{K_pK_d}D_{d1n} \qquad (17b)$$

If the base-current ratio 10b is used, the per-unit mutual reactance corresponding to equation 17b is given by equation 17c.

$$X_{nad}=\left(\frac{4}{\pi}\frac{A_{d1}}{D_{d1x}}\right)\frac{A}{F_g}\frac{D_{d1n}}{F_{d1}}=\frac{D_{d1n}}{D_{d1x}}x'_{ad} \qquad (17c)$$

Note that with the base-current ratio 10b, the mutual reactance X_{nad} becomes numerically equal to x_{ad} for the xth additional rotor circuit.

Mutual Reactance Between Additional Rotor Circuits, X_{nkd} ($k>n$). The mutual inductance L_{nkd} between the nth additional rotor circuit and any outer rotor circuit k is equal to the sum of L_{gnnd} and L_{ennd} since the fluxes which define the latter inductances are mutual with the outer circuit. L_{nkd} is therefore as given by equation 18a. The per-unit mutual reactance X_{nkd} of equation 18b is based on the base-current ratio 10b. X_{gnnd} and X_{ennd} are given by equations 16e and 16f, respectively. The mutual reactance between the nth additional rotor circuit and any inner circuit can be obtained from the impedances of the inner circuit, since all mutual impedances in this article are reciprocal.

$$L_{nkd}=L_{gnnd}+L_{ennd} \qquad (18a)$$

$$X_{nkd}=X_{gnnd}+X_{ennd}\quad(k>n) \qquad (18b)$$

Mutual Reactance Between Field-Winding Circuit and nth Additional Rotor Circuit, X_{nfd}. The mutual inductance L_{nfd} between the field-winding circuit and the nth additional rotor circuit is $N_{fd}L_{gnnd}$, since the flux which defines the latter inductance is mutual with the field-winding circuit. L_{nfd} is given by equation 19a, and the corresponding per-unit value, based on the base-current ratios equations 10a and 10b is given by equation 19b.

$$L_{nfd}=N_{fd}L_{gnnd}=12.76\times10^{-8}\frac{Rl}{g}D_{don}y_{nd}N_{fd} \qquad (19a)$$

$$X_{nfd}=\left(\frac{4}{\pi}\frac{A_{d1}}{F_{d1}}\right)\frac{D_{don}}{D_{d1x}}y_{nd}x_{ad} \qquad (19b)$$

Stator Resistance, r_a. The stator resistance is a definitive impedance, and its per-unit value is given by equation 20a.

$$r_a=\frac{r_a}{x_{ao}} \qquad (20a)$$

Field-Winding Circuit Resistance, R_{ffd}. R_{ffd} is easily obtained from the design or name-plate data. The corresponding per-unit value, based on the base-current ratio 10a, is given by equation 21a.

$$R_{ffd}=\frac{10^8}{\omega P_1}\left(\frac{4}{\pi}\frac{A_{d1}}{F_{d1}}\right)^2\frac{1}{N_{fd}^2}\frac{A}{\phi_f}R_{ffd}$$

(no external resistance) (21a)

Table II. Comparison of Pole-Shape Coefficients Obtained in This Paper by Numerical Integration With Corresponding Values Obtained by Wieseman

$\rho=1.50 \quad \alpha=0.70 \quad p_p^{-1}g=0.03$

	A_{d1}	A_{q1}	F_{d1}	K_ϕ
1	0.874	0.472	1.037	1.020
2	0.876	0.481	1.062	1.010

1 = values obtained in this paper by numerical integration.

2 = values obtained by Wieseman[3] from flux plots.

Resistance of nth Additional Rotor Circuit, R_{nnd}. The resistance of the two bars which form the nth additional rotor circuit in each pole is given by equation 22a. The resistance of the corresponding end-ring section is given by equation 22b. The resistance of the entire nth additional rotor circuit of P_1 poles is given by equation 22c, and the corresponding per-unit value is given byequation 22d.

$$R_{bnnd}=1.67\times10^{-6}\frac{l_{bn}}{a_{bn}}P_1 \qquad (22a)$$

$$R_{ennd}=3.33\times10^{-6}\frac{l_{end}}{a_{end}}P_1 \qquad (22b)$$

$$R_{nnd}=1.67\times10^{-6}P_1\left(\frac{l_{bn}}{a_{bn}}+2\frac{l_{end}}{a_{end}}\right) \qquad (22c)$$

$$R_{nnd}=\frac{10^8}{\omega P_1}\left(\frac{4}{\pi}\frac{A_{d1}}{D_{d1x}}\right)^2\frac{A}{\phi_f}R_{nnd} \qquad (22d)^*$$

Mutual Resistance Between Additional Rotor Circuits, R_{nkd} ($k>n$). The mutual resistance between the nth additional rotor circuit and any outer rotor circuit k is the end-ring resistance of the nth additional rotor circuit. R_{nkd} is given by equation 23a, and the corresponding per-unit value by equation 23b. The mutual resistance between the nth additional rotor circuit and any inner rotor circuit is obtained from the latter, since in this article all the mutual impedances are reciprocal.

$$R_{nkd}=R_{ennd}=3.33\times10^{-6}\frac{l_{end}}{a_{end}}P_1 \qquad (23a)$$

$$R_{nkd}=\frac{10^8}{\omega P_1}\left(\frac{4}{\pi}\frac{A_{d1}}{D_{d1x}}\right)^2\frac{A}{\phi_f}R_{nkd} \qquad (23b)^*$$

IMPEDANCES OF QUADRATURE-AXIS CIRCUITS

The currents in the additional rotor circuits in the quadrature axis are expressed in per unit of I_{xdo} which is the base current of the direct-axis additional rotor circuits. This base is adopted so that the per-unit currents in the direct- and quadrature-axis additional rotor circuits may be added directly.

The concept of a field winding in the quadrature axis appears academic, but it is convenient to assume such a winding (but of infinite resistance), with a base current defined analogously to I_{fdo}. By this concept the stator flux which is leakage with respect to all the rotor circuits is (x_d-x_{ad}) for both the direct and quadrature axis. In addition, the assumption of the existence of a quadrature-axis field winding is convenient, since it maintains symmetry between the direct- and quadrature-axis equations.

The equations of the quadrature-axis circuits, including the quadrature-axis field winding, are identical with the direct-axis equations with the d replaced by q. It would appear therefore that the formulas for the quadrature-axis impedances could be obtained from the corresponding direct-axis formula by merely substituting q for d. This is actually true for the ampere-inch-second values (ohms and henrys), but is not true for the per-unit values because I_{zdo} is the base current for the additional rotor circuits in both axes. The per-unit quadrature-axis impedances are obtained by substituting q for d in the corresponding direct-axis ampere-inch-second impedance formula, and converting the result into a per-unit value based on the base-current ratio 10b.

---

*Equations 22d and 23b are evaluated for copper at 75 degrees centigrade. For any other material at/or any other temperature, these equations should be multiplied by the material resistivity in per unit of the resistivity of copper at 75 degrees centigrade.

Stator Synchronous Reactance, x_q. x_q is evaluated by separating it into the two components x_{aq} and (x_q-x_{aq}) analogously to the method used in the evaluation of x_d. x_{aq} is given by equation 24a. (x_q-x_{aq}) is independent of the rotor position and is equal to (x_d-x_{ad}).

$$x_{aq}=\frac{4}{\pi}\frac{A_{q1}}{F_{d1}}\frac{A}{F_g}=\frac{A_{q1}}{A_{d1}}x_{ad} \qquad (24a)$$

$$x_q-x_{aq}=x_d-x_{ad} \qquad (24b)$$

nth Additional-Rotor-Circuit Reactance, X_{nnq}. The components of L_{nnq} can be obtained from the corresponding components of L_{nnd} by substituting q for d. If the base-current ratio 10b is used, the corresponding per-unit values are given by equations 25a, b, c. The total reactance X_{nnq} is given by equation 25d.

$$X_{gnnq}=\left(\frac{4}{\pi}\frac{A_{d1}}{D_{d1x}}\right)^2\frac{A}{F_g}\frac{D_{qon}}{F_{d1}}y_{nq} \qquad (25a)$$

$$X_{bnnq}=0.5\left(\frac{4}{\pi}\frac{A_{d1}}{D_{d1x}}\right)^2\frac{A}{F_g}\frac{P_1g}{F_{d1}R}\left(\frac{d_r}{w_r}+0.625\right) \qquad (25b)$$

$$X_{ennq}=0.04\left(\frac{4}{\pi}\frac{A_{d1}}{D_{d1x}}\right)^2\frac{A}{F_g}\frac{P_1g}{F_{d1}R}\frac{l_{enq}}{l}\times\left(9.2\log_{10}\frac{D_e}{r_e}+1\right) \qquad (25c)$$

$$X_{nnq}=X_{gnnq}+X_{bnnq}+X_{ennq} \qquad (25d)$$

Mutual Reactance Between Stator and nth Additional Rotor Circuit, X_{naq}. L_{naq} can be obtained from equation 17b by substituting q for d. The corresponding per-unit value, based on the base-current ratio 10b, is given by equation 26a.

$$X_{naq}=\left(\frac{4}{\pi}\frac{A_{d1}}{D_{d1x}}\right)\frac{A}{F_g}\frac{D_{qn}}{F_{d1}}=\frac{D_{q1n}}{D_{d1x}}x_{ad} \qquad (26a)$$

Mutual Reactance Between Additional Rotor Circuits, X_{nkq} $(k>n)$. In a manner similar to that used in the derivation of X_{nkd} it can be shown that X_{nkq} is given by equation 27a.

$$X_{nkq}=X_{gnnq}+X_{ennq} \quad (k>n) \qquad (27a)$$

Resistance of nth Additional Rotor Circuit, R_{nnq}. R_{nnq} as given by equation 28a is obtained from equation 22c by substituting q for d. The corresponding per-unit value, based on the base-current ratio 10b, is given by equation 28b.

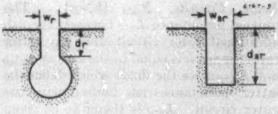

Figure 3. Rotor slots

$$R_{nnq}=1.67\times10^{-6}P_1\left(\frac{l_{bn}}{a_{bn}}+2\frac{l_{enq}}{a_{enq}}\right) \qquad (28a)$$

$$R_{nnq}=\frac{10^8}{\omega P_1}\left(\frac{4}{\pi}\frac{A_{d1}}{D_{d1x}}\right)^2\frac{A}{\phi_f}R_{nnq} \qquad (28b)^*$$

Mutual Resistance Between Additional Rotor Circuits, R_{nkq} $(k>n)$. R_{nkq} as given by equation 29a is obtained from equation 23a by substituting q for d. The corresponding per-unit value, based on the base-current ratio 10b, is given by equation 29b.

$$R_{nkq}=R_{ennq}=3.33\times10^{-6}\frac{l_{enq}}{a_{enq}}P_1 \qquad (29a)$$

$$R_{nkq}=\frac{10^8}{\omega P_1}\left(\frac{4}{\pi}\frac{A_{d1}}{D_{d1x}}\right)^2\frac{A}{\phi_f}R_{nkq} \quad (k>n) \qquad (29b)^*$$

Appendix I. Evaluation of Pole-Shape Coefficients

The pole-shape coefficients D_{don}, D_{qon}, D_{d1n}, and D_{q1n} must be evaluated by flux plots if extreme accuracy is desired since the actual magnetic gap obviously cannot be represented exactly by any known mathematical expression. However, the flux-plotting method is too time-consuming to be used in the majority of actual problems. A more practical method is to obtain, by any means, whatsoever, a satisfactory mathematical expression for the gap permeance, and by means of numerical integration then evaluate the pole-shape coefficients. Such a method is used in this appendix.

The gap-reluctance expression by which satisfactory values of the pole-shape coefficients are obtained in this paper is given by equations 30a, b, ...h; these expressions give the gap length in per unit of the minimum gap g.

$$g_y=g_d \text{ in the region } 0<y_d<\alpha_\eta \qquad (30a)$$

$$g_y=g_q \text{ in the region } \alpha_\eta<y_d<1 \qquad (30b)$$

$$g_d=1+(\rho-1)\left(\frac{y_d}{\alpha}\right)^2 \qquad (30c)$$

$$g_q=g_\eta+\beta g_\eta\sin^2\left(\frac{y_d-\alpha_\eta}{1-\alpha_\eta}\right)\frac{\pi}{2} \qquad (30d)$$

$$g_\eta=1+(\rho-1)\left(\frac{\alpha_\eta}{\alpha}\right)^2 \qquad (30e)$$

$$\beta=-1+\sqrt{1+\frac{1}{4}\left(\frac{1-\alpha}{p_p^{-1}gg_\eta}\right)^2} \qquad (30f)$$

$$\alpha_\eta=\alpha-3.5\rho p_p^{-1}g \qquad (30g)$$

$$y_d+y_q=1.0 \qquad (30h)$$

D_{don}, D_{qon}, D_{d1n}, and D_{q1n} are defined in the following subsections, and definite-integral expressions for each are derived in terms of the reluctance expression 30a, b, ...h. Numerical values obtained from these definite-integral expressions are given in Table I for a typical pole configuration.

Evaluation of D_{don}

$(2/\pi)D_{don}$ is defined as the factor by which the maximum gap density must be multiplied to obtain the average density within the damper circuit of span $2y_{nd}$ with the machine excited by the damper circuit of span $2y_{nd}$ in the direct axis. Expressing the corresponding flux per pole in the two ways shown by equation 31a leads directly to the evaluation of $D_{don}y_{nd}$ as given by equation 31b.

$$\phi=2\int_0^{y_{nd}}\frac{3.19}{gg_y}dy_d=2\frac{3.19}{g}\frac{2}{\pi}D_{don}y_{nd} \qquad (31a)$$

$$D_{don}y_{nd}=\frac{\pi}{2}\int_0^{y_{nd}}g_y^{-1}dy_d \qquad (31b)$$

Evaluation of D_{qon}

$(2/\pi)D_{qon}$ is analogous to $(2/\pi)D_{don}$, but in the quadrature axis. Its value as given by equation 32a is obtained by the same derivation as was used for D_{don}. The integral value given by equation 32b is obtained from equation 32a by changing the origin of integration by means of equation 30h.

$$D_{qon}y_{nq}=\frac{\pi}{2}\int_0^{y_{nq}}g_y^{-1}dy_q=\frac{\pi}{2}\int_{1-y_{nq}}^{1}g_y^{-1}dy_d \qquad (32a, b)$$

Evaluation of D_{d1n}

D_{d1n} is defined as the factor by which the maximum flux density must be multiplied to obtain the maximum of the fundamental component of flux density with the machine excited by the nth additional rotor circuit in the direct axis. The flux density per ampere turn at any point along the gap can be written as in equation 33a; the maximum value of the fundamental component is then given by equation 33b. By the definition of D_{d1n}, the maximum value of the fundamental component can also be written as in equation 33c, and D_{d1n} can be evaluated as in equation 33d by equating expressions 33b and 33c.

$$\beta_y=\frac{3.19}{gg_y} \qquad (33a)$$

$$\beta_{y\,\text{fund}}=2\int_0^{y_{nd}}\frac{3.19}{gg_y}\cos\frac{\pi}{2}y_d\,dy_d \qquad (33b)$$

$$\beta_{y\,\text{fund}}=\frac{3.19}{g}D_{d1n} \qquad (33c)$$

$$D_{d1n}=2\int_0^{y_{nd}}g_y^{-1}\cos\frac{\pi}{2}y_d\,dy_d \qquad (33d)$$

---

*Equations 28b and 29b are evaluated for copper at 75 degrees centigrade. For any other material at/or any other temperature, these equations should be multiplied by the material resistivity in per unit of the resistivity of copper at 75 degrees centigrade.

Evaluation of D_{q1n}

D_{q1n} is analogous to D_{d1n}, but in the quadrature axis. Its value as given by equation 34a is obtained by the same derivation as was used for D_{d1n}. The integral value given by equation 34b is obtained from equation 34a by changing the origin of integration by means of equation 30h.

$$D_{q1n}=2\int_0^{y_{nq}} g_y^{-1}\cos\frac{\pi}{2}y_q dy_q \qquad (34a)$$

$$D_{q1n}=2\int_{1-y_{nq}}^{1} g_y^{-1}\sin\frac{\pi}{2}y_d dy_d \qquad (34b)$$

Appendix II. Accuracy of the Derived Pole-Shape Coefficients

It is obviously not possible at present to obtain complete checks on the accuracy of the foregoing integral expressions, because the necessary experimental information is lacking. If such information were available, the reluctance expression 30a, b, ...h would be unnecessary, since the pole-shape coefficients could be obtained directly from the experimental data. It is possible, however, to use the work of Wieseman as follows to check the accuracy of the limiting points $y_{nd}=1.00$, $y_{nq}=1.00$, and thereby obtain a qualitative estimate of the over-all accuracy.

Wieseman presented curves, based on actual flux plots, for the quantities A_{d1}, A_{q1}, F_{d1}, and K_ϕ. A check on the reluctance expression 30a, b, ...h, can be obtained by evaluating these same expressions by numerical integration based on equation 30a, b, ...h, and comparing these derived values with the corresponding quantities calculated by Wieseman. A_{d1}, A_{q1}, F_{d1}, and K_ϕ are defined in the following subsections, and definite-integral expressions for each are derived in terms of the gap-reluctance expression 30a, b, ...h. Numerical values as obtained from these definite integrals are given in Table II for a typical pole configuration and are there compared with the corresponding values obtained by Wieseman from flux plots. The agreement with Wieseman's results is sufficiently close as to warrant fully the use of the integral expressions for the pole-shape coefficients D_{don}, D_{qon}, D_{d1n}, and D_{q1n} until absolutely accurate values can be obtained from actual flux plots.

Evaluation of A_{d1}

A_{d1} is defined as the factor by which the maximum flux density must be multiplied to obtain the maximum of the fundamental component of flux density with the machine excited by a sine-wave armature magnetomotive force in the direct axis. Assuming a sine-wave magnetomotive force of one ampere turn peak value in the direct axis, the flux density at any point in the gap is given by equation 35a, and the maximum value of the corresponding fundamental component of flux density is given by equation 35b. Based on the definition of A_{d1}, the maximum value of the fundamental component can also be written as in equation 35c, and A_{d1} can be evaluated as in equation 35d by equating expressions 35b and 35c.

$$\beta_y=\frac{3.19}{gg_y}\cos\frac{\pi}{2}y_d \qquad (35a)$$

$$\beta_{y\,\text{fund}}=2\int_0^1\frac{3.19}{gg_y}\cos^2\frac{\pi}{2}y_d dy_d \qquad (35b)$$

$$\beta_{y\,\text{fund}}=\frac{3.19}{g}A_{d1} \qquad (35c)$$

$$A_{d1}=2\int_0^1 g_y^{-1}\cos^2\frac{\pi}{2}y_d dy_d \qquad (35d)$$

Evaluation of A_{q1}

A_{q1} is analogous to A_{d1} but in the quadrature axis. Its value as given in equation 36a is obtained by the same derivation as was used for A_{d1}. An alternative expression for A_{q1} in terms of y_d measured from the polar axis is given by equation 36b; this was obtained by substituting equation 30h into equation 36a.

$$A_{q1}=2\int_0^1 g_y^{-1}\cos^2\frac{\pi}{2}y_q dy_q \qquad (36a)$$

$$A_{q1}=2\int_0^1 g_y^{-1}\sin^2\frac{\pi}{2}y_d dy_d \qquad (36b)$$

Evaluation of F_{d1}*

F_{d1} is defined as the factor by which the maximum flux density must be multiplied to obtain the maximum of the fundamental component of flux density with the machine excited by the direct-axis field winding.

The field winding links only the flux which enters the pole, and its effective span or pitch is accordingly somewhat less than 100 per cent. However, the effective span is greater than the physical-pole arc, because the field winding links the flux which enters the side of the pole tip. Hence, the effective span of the field winding approaches but remains slightly less than the full 100-per-cent value. A study of Table I, however, shows that D_{d1n} is relatively constant (for given values of ρ, α, and $p_p^{-1}g$) for values of y_{nd} in the neighborhood of 1.00. Relatively little error is introduced therefore by assuming that F_{d1} is given by D_{d1n} for $y_{nd}=1.00$. Wieseman's values of F_{d1} thus may be compared directly with D_{d1n} for $y_{nd}=1.0$ as obtained in this paper by numerical integration.

Evaluation of K_ϕ

K_ϕ is defined as the factor by which the total fundamental flux per pole must be multiplied to obtain the total flux per pole, with the machine excited by the direct-axis field winding. By means of the previously justified assumption that the field-winding circuit is equivalent to a damper-winding circuit of 100-per-cent pitch (with negligible error), K_ϕ can be evaluated in terms of D_{don} and D_{d1n}, for $y_{nd}=1.00$, as shown in the following.

By the definition of D_{don} and D_{d1n}, the total flux per pole and the total fundamental flux per pole are given by equations 37a, b, respectively, with y_{nd} taken as unity. The ratio of equation 37a to equation 37b then gives K_ϕ as in equation 37c, by definition.

$$\text{Total flux per pole}=\frac{3.19}{g}\frac{2}{\pi}D_{don} \qquad (37a)$$

$$\text{Fundamental flux per pole}=\frac{3.19}{g}\frac{2}{\pi}D_{d1n} \qquad (37b)$$

$$K_\phi=\left.\frac{D_{don}}{D_{d1n}}\right|_{y_{nd}=1.0} \qquad (37c)$$

Nomenclature

The quantities given below are per-unit values unless in bold-face type in which case they are in the physical ampere-inch-second system (amperes, ohms, henrys, and so forth). Quantities such as N, P_1, R, l, for which it is obviously unnecessary to distinguish the ampere-inch-second values by a special script are in standard type only. Vector values are indicated by a circumflex (ˆ) over the symbol.

All dimensions are in inches.

The subscript notation is as follows.

a, b, c = armature phases
f = field-winding circuit
n, k, x = damper-winding circuits. n is the general term; k refers to a damper-winding circuit external to $n (k>n)$; and x refers to the 100-per-cent-pitch (most external) circuit which is used as a base
$d, q, 0$ = direct, quadrature, and "zero" axes
o = base quantities
m = order of harmonic

Only the direct-axis quantities are defined in the following, as the quadrature-axis quantities are obtained from these by merely substituting q for d.

a_{bn} = cross-sectional area of bar n
a_{end} = average cross-sectional area of end ring for bar n
A = flat-topped armature reaction at base stator current
$A=\dfrac{1.5i_{ao}N}{K_pK_dP_1}$
A_{d1} = defined in Appendix II
D_{don}, D_{d1n} = defined in Appendix I
D_e = axial distance between end rings minus axial length of pole, or twice the distance between one end ring and side of pole
e_{ao} = peak value of rated stator phase voltage
E_{fd}, E_{nd} = rotor-circuit applied voltages
$F_{do}=D_{don}$ for $y_{nd}=1.0$
F_{d1} = defined in $B3$
F_g = field-winding ampere turns for rated air-gap-line stator voltage
g = minimum gap, effective
g_y = gap length at any point y_d, in per unit of g
i_{ao} = peak value of rated stator line current
I_{fdo}, I_{xdo} = base-current; field winding, and xth additional rotor circuit, respectively
i_d, I_{fd}, I_{nd} = direct-axis currents; stator, field winding; and nth additional rotor circuit, respectively
I_n = total current in nth physical bar
$k_{ad}=\dfrac{4}{\pi}\dfrac{A_{d1}}{F_{d1}}$
K_p, K_d = pitch and distribution factors, respectively (greater than 1.0)

---

*Wieseman called this quantity A_1.

K_ϕ = defined in Appendix II

l = machine stacked length

l_{bn} = length of bar n

l_{end} = circumferential length of end ring measured from direct axis to center of bar n

L = ampere-inch-second inductance corresponding to per-unit reactance x

L_{ao} = base stator inductance

$$L_{ao}=\frac{10^{-8}\psi_{ao}}{i_{ao}}=\frac{x_{ao}}{\omega}$$

N = stator series turns per phase

N_{fd} = turns per pole of field winding

p = differential operator $=\dfrac{d}{d(\omega t)}$

p_p = pole pitch $=\dfrac{2\pi R}{P_1}$

P_1 = number of poles

r_a = stator resistance per phase

r_e = effective radius of end-ring cross section; $\pi r_e^2=a_{end}$

R_{bnnd}, R_{ennd} = resistances of nth additional rotor circuit; bar and end ring, respectively

R_{ffd}, R_{nnd} = resistance of field-winding and nth additional rotor circuits, respectively

R_{nfd}, R_{nkd} = mutual resistances, nth additional rotor circuit to field winding and kth circuit, respectively

s = slip in per unit

$\hat{U}_{ndm}$ = current modulus defined in equation 9a

v = general rotor-velocity term of equation 4

x_{ao} = base stator ohms

$$x_{ao}=\frac{e_{ao}}{i_{ao}}=\omega L_{ao}$$

x_{ad} = reactance of armature reaction

x_d, X_{ffd}, X_{nnd} = direct-axis reactances; stator, field winding, and nth additional rotor circuit, respectively

X_{afd}, X_{and}, X_{nfd}, X_{nkd} = mutual reactances; stator field, stator–nth rotor circuit, nth rotor circuit to field winding, and nth rotor circuit to kth rotor circuit

X_{bnnd}, X_{ennd}, X_{gnnd} = reactance components of nth rotor circuit; due to bar-slot flux, end-ring flux, and air-gap flux, respectively

$x_d(p)$ = operational stator impedance as viewed from stator terminals

y_d, y_q = peripheral distances on pole face measured in per unit of half the pole pitch; see Figure 2

α = ratio of pole arc to pole pitch

β'_{max} β'_{fund} = maximum flux density and maximum value of the fundamental component of flux density at normal voltage no load

ρ = ratio of maximum gap to minimum gap; see Figure 2

ϕ_f = fundamental flux per pole at normal voltage no load

ψ_{ao} = peak value of rated stator phase linkages; $e_{ao}=10^{-8}\omega\psi_{ao}$

ψ_d, Ψ_{fd}, Ψ_{nd} = direct-axis linkages; stator, field-winding, and nth additional rotor circuits, respectively

Ψ_b, Ψ_t = effective permeance of the pole-body and pole-tip leakage paths per axial inch of machine length per pole

References

1. Starting Performance of Salient-Pole Synchronous Motors, T. M. Linville. AIEE Transactions, volume 49, 1930, pages 531–47.

2. Starting Performance of Salient-Pole Synchronous Motors, M. M. Liwschitz. AIEE Transactions, volume 59, 1940, pages 913–19.

3. Per-Unit Impedances of Synchronous Machines, A. W. Rankin. AIEE Transactions, volume 64, 1945, August section, pages 569–73.

4. Synchronous Machines—I, R. E. Doherty, C. A. Nickle. AIEE Transactions, volume 45, 1926, pages 912–26.

5. Graphical Determination of Magnetic Fields, R. W. Wieseman. AIEE Transactions, volume 46, 1927, pages 141–54.

6. Equations of the Idealized Synchronous Machine, A. W. Rankin. *General Electric Review*, volume 47, June 1944.

7. Per-Unit Impedances of Synchronous Machines—II, A. W. Rankin. AIEE Transactions, volume 64, November section, pages 839–41.

8. Calculation of Armature Reactance of Synchronous Machines, P. L. Alger. AIEE Transactions, volume 47, 1928, pages 493–513.

9. Calculation of Synchronous-Machine Constants, L. A. Kilgore. AIEE Transactions, volume 50, 1931, pages 1201–14.

Modern Practice in Power-Plant Auxiliary Equipment and Systems

H. N. MULLER, JR.
MEMBER AIEE

THIS DISCUSSION of central-station auxiliary equipment and systems cannot cover the entire field of practice, but must touch only selected high spots. The particular points selected were chosen to include those items where the user may exercise judgment in choosing alternate arrangements of supply or items of apparatus, or where his specifications may influence apparatus design by emphasis on particular requirements.

The discussion is timely, because power-plant auxiliary equipment has undergone important development in the past several years, and because the interruption in normal construction of new facilities, necessitated by war activities, provides an opportune moment for analysis of what is available and how to apply it.

Supply systems for auxiliaries have received extensive study with the result that loop and network systems now find application along with the more conventional radial distribution system. The change in equipment is keynoted by the swing to air circuit breakers and the currently marked trend toward the use of air-cooled transformers. Both motors used for central-station auxiliary service and the associated motor starters have been given close attention with the general result that more economical reliable drives will be available to meet rigid requirements. One fact is ever apparent: the central-station operator demands maximum reliability. Nowhere else on the entire power system is the requirement of reliability so great compared to the investment in equipment involved.

There follows, thus, a discussion of particular design features of motors, desirable arrangements of switchgear and control, and data on distribution systems that may be helpful when selection of the method of supply is under consideration.

Motor Design

As in the past, the squirrel-cage induction motor for across-the-line starting is the best selection for an auxiliary drive wherever constant-speed operation is desired. The simplicity, reliability, and low cost all enter to make it the number-one choice. Its control is simple as well. The higher power factor and efficiency of synchronous drives is offset by the increased complication of synchronizing control and a source of excitation. Also, since the cost of both real and reactive power is a minimum at the generator bus, higher efficiency and power factor is not a large incentive.

ROTOR DESIGN

Draft fans and some pulverizers have high inertia, and motors for these loads are best designed to limit the temperatures and expansion of the rotors to safe values. The WR^2 of each drive of this nature should be supplied to the motor designer for an analysis of the particular application. Certain types of pulverizers are subject to jamming, and it is known from experience that operators may try several times to start them. Motors for these pulverizers require an extra margin in rotor thermal capacity. An ample air gap is especially desirable for motors on

---

Paper 45-168, recommended by the AIEE committee on power generation for publication in AIEE Transactions. Manuscript submitted June 1, 1945; made available for printing September 5, 1945.

H. N. Muller, Jr., is central-station engineer with Westinghouse Electric Corporation, East Pittsburgh, Pa.

The author expresses his appreciation to members of the design and application department of Westinghouse Electric Corporation for assistance in selection of subjects and the digesting of material included in this paper.

these two types of loads because of rotor expansion and should not be discouraged by unnecessary emphasis on high power factor. Similarly, adequate thermal capacity with ample starting torque may require higher starting current than might be obtained with a less reliable design, and unnecessary restrictions in this respect should not be imposed. Motors for high-inertia loads also should be designed to withstand the high transient torque which occurs when the motor is energized.

Another consideration which affects reliability but does not appear on the performance sheet is magnetic stability. This requires a satisfactory relation between the stiffness of the shaft and the unbalanced magnetic pull which occurs when the rotor is displaced radially with respect to the stator. Such displacement may be either deflection of the shaft and other structural parts caused by vibration or an initial displacement caused by machining tolerances. Here again an ample air gap is required for a reliable motor.

Insulation of Windings

The insulation of motor windings for central-station auxiliary service should be highly resistant to moisture, coal dust, and fly ash. Although the atmospheric conditions are no more severe than in many industrial plants, the extreme importance of reliability of the auxiliaries requires the best possible insulation job. The smaller motors should be given ample varnish dips and bakes with carefully controlled viscosity and temperature, and the larger motors should be impregnated by the vacuum-pressure method. Mica insulation is to be used where practicable. The insulation between turns should be tested by a high-frequency testing set in addition to the conventional high-potential tests between the winding and ground.

Insulating materials good for higher temperatures and adverse moisture conditions have been written about widely during the last year. These are silicone varnishes that are now available in forms similar to the usual varnishes used by the electrical industry. They have been used with mica, glass, and asbestos to produce high-temperature insulations. The improved thermal endurance can be utilized in a number of important ways in the design of electric equipment, such as reduction in size and weight, increased service life for conventional size and weight, and operation in ambient temperatures beyond the limits permissible for usual types of insulation. A few cases of power-plant operation may justify trial of silicone insulations. One likely application is for motors driving induced-draft fans subject to high ambient temperatures.

At the present time quantities of silicone products are limited, and their cost is high compared to good insulating varnishes. Much is still to be learned about processes of handling and manufacturing that will have to be studied before application to motor equipment becomes general.

Motor Bearings

Both antifriction and sleeve-type bearings are furnished today. Each type has its advantages and consequently is to be preferred for certain applications. The sleeve bearing has advantages for many general applications. It requires less precision work both in manufacture and maintenance, it inherently is suitable for operation in locations where coal dust and fly ash are present, and it can be operated at higher peripheral speeds. The antifriction bearing may find preference because of smaller space requirements, because of its ability to take thrust loads, or because of the low starting friction inherent to its design. This last point refers particularly to vertical pump motors where heavy thrust is encountered. Prelubricated ball bearings are now used on some small motors. This practice stands to become more popular since field experience with it has been excellent. These bearings have shown unusual freedom from trouble.

Boiler-feed-pump motors generally are connected to the load through flexible couplings. Certain of these couplings have a natural tendency to lock into a fixed running position while transmitting torque, thus preventing the motor and pump from moving axially with respect to each other. Because of shaft expansion which results from high-temperature operation of the pump in handling feed water, heavy thrust can be imposed upon the motor bearings. Failure of these bearings may result, since this thrust is beyond the capacity of simple sleeve-bearing shoulders. Occurrence of such phenomena can be prevented if the "limited end-float" type of coupling and a motor having shaft end play more than the end play of the coupling is specified.

Noise Level of Motors

Although the noise level in different power plants may vary somewhat, an average figure can be taken to be about 100 decibels in the general vicinity of the turbine and principal auxiliaries. If the noise level of motors is to be kept to a value that will not contribute seriously to powerhouse noise, it is logical to assume that no motors should have a level as high as 100 decibels.

The greatest source of noise in large high-speed motors is windage and the siren effect resulting from jets of air from the rotor vent ducts. A system of axial-flow surface cooling of the rotor is used today that effectively reduces noise level on the very large two-pole motors. Figure 1 illustrates the construction of a large 3,600-rpm motor employing this type of design. Careful selection of slot combinations in the stator and rotor will reduce noise in addition to keeping stray loss and parasitic torques to a minimum.

Adjustable-Speed Drives

There are several auxiliaries which require adjustable-speed drives. Cranes, coal bridges, and similar material-handling equipment can be driven best by wound-rotor induction motors. The most suitable electric drive for stokers is a series variable-voltage a-c–d-c drive. Boiler-feed pumps are usually driven at constant speed, but when speed adjustment is desired a wound-rotor induction motor with a multipoint drum furnishes adequate control.

Adjustable speed is very desirable for draft-fan drives in order to reduce losses and erosion. Two speeds can be obtained with a pole-changing squirrel-cage motor, and this combination is used frequently with inlet-vane control. Thirteen or 20 speed steps can be obtained with a wound-rotor motor and drum, but this still requires the use of dampers or vanes for continuous control of gas flow. A squirrel-cage motor with a hydraulic coupling gives continuous speed control over about a four-to-one range. The coupling requires cooling water and involves extra bearings. Electric couplings do not require cooling water and give ten-to-one speed range but involve extra bearings,

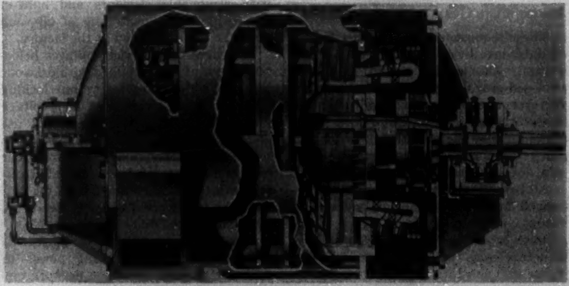

Figure 1. Cutaway view of 3,600-rpm squirrel-cage induction motor

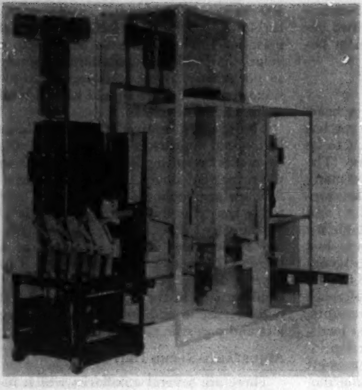

Figure 2 (left). Cell and air breaker for 2,300-volt auxiliary feed (five-kilovolt insulation, 150,000-kva interrupting capacity)

Figure 3 (right). Cell and air breaker for 600 volts or below; breaker shown is 800-ampere unit

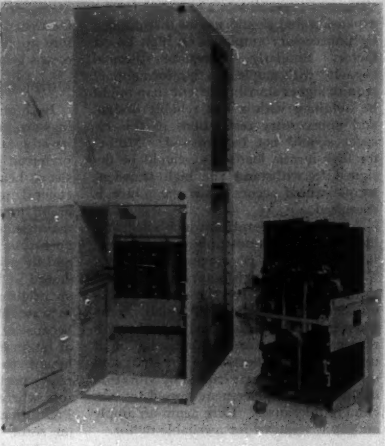

an excitation system, and relatively high operating temperatures. A wound-rotor motor with a new type of liquid rheostat for secondary control has been used recently for large draft fans. This combination provides three-to-one speed range. It requires cooling water and an electrolyte, but eliminates extra bearings and rotating apparatus. The liquid rheostat appears to offer an attractive solution for future application.

The cost and efficiency of all of the afore-mentioned drives are comparable, so that the choice of drive should be made primarily to give maximum reliability with the particular operating conditions which will be encountered.

Switchgear and Control

As pointed out in the introduction, reliability is the outstanding qualification for all central-station auxiliary devices, and switchgear is no exception. Safety of operation, ease of installation, ease of maintenance, and so forth, are all important qualifications desirable here, just as in other classes of service, but dependability is paramount. Circuit breakers, contactors, fuses, and assemblies of these component parts all stress this virtue.

METAL-CLAD GEAR

These requirements all are met by up-to-date metal-clad gear in its various forms. The service record of metal-enclosed gear is enviable, and the manufacturers continue to make improvements in the breakers, housings, and other parts. Purchasers of metal-enclosed switchgear can rely on receiving the benefits of all new developments promptly.

All breaker and auxiliary units are arranged for line assembly. They can be throat-connected to liquid-cooled transformers or supplied as part of an integral structure with air-cooled transformers. These unit substation arrangements form a most satisfactory assembly of transforming and distributing apparatus. Switchgear structures, or the switchgear portion of unit substations, can be shipped fully assembled or in groups as large as the purchaser's handling equipment can accommodate. This usually saves considerable installation cost. Factory connections on control wiring are not disturbed, so that tests need not be repeated.

The reliability of metal-clad switchgear is now so well recognized that double-breaker arrangements for load circuits seldom are considered necessary, and even auxiliary or transfer busses are not common. Special circuits may have double feeds, usually from different breaker groups, but duplication of breakers beyond this is not often justified. Where motors may require frequent starting, air breakers in metal-clad gear are well suited for this service. Duplicate power supply or normal and alternate power supply to auxiliary busses with automatic transfer is frequently provided. Relays for this function and for other normal protective functions are mounted on the gear. Relays are preferably of the Flexitest type with removable elements and built-in test switches. Functioning of all such control circuits is tested at the factory.

Switchgear for service voltages below 600 is now usually supplied with drawout breakers which have safety interlocking features similar to those in high-voltage metal-clad switchgear. Increased use and improved manufacturing methods have brought the prices of drawout gear so close to the equivalent enclosed breakers with fixed mountings that the advantages of the removable breaker types easily justify the difference.

Low-voltage metal-clad switchgear is well suited for distributing power in radial, loop, or low-voltage network circuits. Standard units are available which contain the limiters and loop-circuit disconnecting switches when the switchgear is part of a network system. The flexibility with which the various units can be grouped permits arranging the limiter sections and supply circuits wherever they best tie in with the plant distribution system. The network breakers which are used in network systems may be mounted on the transformers or in a unit of the switchgear assembly.

Unit substations and power centers, usually with air-cooled transformers, form the most modern arrangement for supplying low-voltage power. These assemblies also may include high-voltage gear if the plant distribution system makes this arrangement desirable. The transformers used in network distribution arrangements also can be provided as parts of unit substations or power centers. A co-ordinated housing is provided which gives good uniform over-all appearance and full accessibility to the transformers and switchgear.

AIR CIRCUIT BREAKERS

Air circuit breakers virtually have replaced oil for power-plant auxiliary work. The switchgear for central-station auxiliary service is built around air breakers, in practically all ratings up through the 15,000-volt class. Various forms of high-voltage air breakers have been used since 1929, and all have given satisfactory operation. Their reliability has been definitely proved. The many advantages of air interruption, particularly for this service, are well recognized, and consequently they are usually included today in the purchaser's specifications.

Figure 2 shows a typical five-kilovolt removable unit, 150,000-kva interrupting capacity, equipped with its own wheels for movement outside the steel cell. Units of five-kilovolt insulation class (for 2,300-volt auxiliary service) with 60-cycle test of 25 kv and impulse test of 60 kv are supplied in interrupting ratings up to 150,000 kva and in current ratings up to 2,000 amperes. These ratings adequately cover the larger central-station auxiliary field.

The low-voltage breakers are available in all ratings to cover the necessary application to central-station auxiliary drives. Interrupting ratings at 600 volts go as high as 100,000 amperes, and current ratings as high as 6,000 amperes at this highest interrupting rating. Figure 3 shows an electrically operated 800-ampere removable breaker and cells for 600-volt application.

Low-voltage breakers often are applied on the cascade principle, an arrangement which permits the lower breakers in the series to open fault currents in excess of their interrupting rating. This is permitted on the basis that the main or group breakers shall be free to open instantaneously to assist the smaller breakers in the interruption. It is obvious that such an arrangement does not provide selective tripping and that feeder circuits other than the one in trouble may be deenergized.

The standard duty cycle is not possible with breakers applied in cascade arrangements, and it is necessary that they be inspected before being reclosed if they have opened currents above their interrupting ability. This is indicated by the breaker next higher in the cascade having opened to assist in clearing the fault.

Because of the limited selectivity which exists in cascaded circuits, the application of this arrangement in central-station auxiliary service seldom will be found satisfactory. It usually will be necessary to make breaker applications in the same way that they are made with high-voltage circuits, with all interrupters of adequate capacity for the faults to which they will be subjected. This will frequently mean that the cost of breakers for a given installation will be somewhat more, but it is the only way in which the essential full selective tripping on faults can be obtained. On nonessential auxiliaries, cascaded arrangements might be considered, but in general their application in central-station auxiliary installations requires careful scrutiny.

Table I. High-Interrupting-Capacity Contactors

Air Break, 600 Volts and Below

Normal Eight-Hour Rating, Amperes	Interrupting Capacity, Rms Amperes	Maximum Horsepower Ratings	
		220 Volts	440–550 Volts
150	15,000	50	100
300	25,000	100	200
600	40,000	200	400

Currently, consideration is being given to mechanical timing as a means of co-ordinating breakers in series to avoid unnecessary tripping of circuits other than the faulted one, since breakers with means for instantaneous tripping will frequently go out simultaneously under heavy currents. Such co-ordinated timing is not permissible with cascaded breakers. All breakers in a time-co-ordinated scheme must have fully adequate interrupting capacity.

CONTACTORS, STARTERS, AND FUSES

There has been considerable discussion of the use of interrupters other than circuit breakers for protecting load circuits during high fault currents. High-interrupting-capacity contactors at 600 volts and below, of the air-break variety, are now available. Typical ratings are shown in Table I.

The contactors listed in Table I are designed and rated in accordance with National Electrical Manufacturers Association Standards. They are furnished with overload relays which provide thermal time-delay characteristics suitable for motor starting and protection in combination with instantaneous trip to take care of short-circuit conditions. The overload relays can be connected for alarm only on essential auxiliaries.

Still another idea has been receiving consideration to provide a motor starter which has a high interrupting capacity at a moderate cost. This is the combination of an oil-immersed contactor with overload relays and a current-limiting power fuse.

These starters may be applied safely to 2,300-volt circuits having a short-circuit capacity of 150,000 kva and to 4,600-volt circuits having a short-circuit capacity of 250,000 kva. They are available with either 100- or 200-ampere contactors. When determining the size of fuse to be used with a motor of a given rating it is necessary to give consideration to the locked-rotor current as well as the full-load current of the motor so that a co-ordinated design will result and the fuses will furnish the necessary short-circuit protection without blowing under ordinary motor starting conditions.

For essential circuits, such as most power-plant auxiliaries, it is believed that interrupting means that can be electrically or manually closed after fault clearing should be used. If an interrupter must be replaced after each short circuit, valuable time is lost that in the extreme case could be disastrous. For a few of the less essential auxiliary circuits, and particularly where short circuits are least likely to occur, the suggested combination starter can provide a very economical installation.

A blanket recommendation of this starter-and-fuse combination is impossible. Each case must stand on its own merits, or be discarded in favor of an air circuit breaker. If rapid restoration of service is of value in any given case, air breakers are dictated. If the available ratings of current-limiting fuses do not completely satisfy the individual requirements, breakers are again the answer. Central-station auxiliary service can be considered as the application requiring the utmost of dependability. As such, engineering and economics require very careful balancing before a decision to use the fuse and starter is reached.

Power-Distribution System

The radial system of power supply, studied carefully in many alternate forms, for decades has provided satisfactory service. It is characteristic of a radial system that the degree of reliability is somewhat proportional to its cost, and a high-performance system or a very skimpy system can be designed, depending upon just how far the engineer will go in sacrificing economics. The author believes that the more popular and time-proved forms of the radial system are well known to central-station operating men and that detailed description has no justified place in this discussion. Figure 4 pictures a typical radial system of supply to auxiliaries.

THE SECONDARY NETWORK FOR POWERHOUSE SUPPLY

The application of a secondary network to auxiliary supply is rather novel, and detailed description, at least of the salient principles of application, will be included. The fact that central-station engineers have had a long-time knowledge of secondary networks for urban distribution has misled many when power-plant application is under consideration. The different forms that an auxiliary system network may take frequently are overlooked, since the engineer pictures only the city network and hence does not consider flexible arrangements applicable particularly to central-station auxiliary supply. Factors pertinent to the selection of a network system for auxiliary supply will be discussed.

The a-c secondary network system has

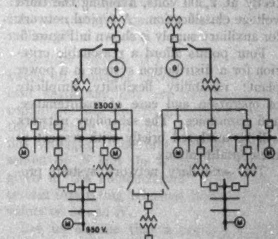

Figure 4. Radial distribution system for central-station auxiliary supply

been used for almost a quarter of a century in the commercial areas of some cities. Today there are 167 cities in the United States whose business districts are served by a-c secondary network systems, and this type of system is now recognized as the standard for serving heavy-load-density areas where the highest grade of service is required. During the last three or four years the advantages of the secondary network system have begun to be recognized in the industrial field, and the system has been installed in about 50 industrial plants. To date, however, the system has been used very little for supplying generating-station auxiliaries. One installation operating at 120/208 volts was made in a small station about eight years ago. Four installations operating at 460 volts have been made during the last four years. The performance of these five a-c secondary networks supplying generating-station auxiliaries has been up to expectations.

Each generating station is a separate problem requiring individual study. The network system for a plant may take the form of a grid, a loop, one or more spot network busses, or a combination of these. It is dangerous to generalize, but detailed studies on 12 stations ranging in size from 10 to 100 megavolt-amperes, indicate several things that are general enough to be of assistance in laying out a network for a particular power station.

First, in more than 50 per cent of the cases, a network grid will be more economical than a secondary loop or spot busses. Small stations are the exception to this rule. Next, a 460-volt grid is cheaper than a 208-volt network, except in very small stations. And also, unless maximum motor size exceeds 600 horsepower, all auxiliaries should be supplied from a 460-volt network. Motors above 600 horsepower should be supplied directly at 2,300 volts, or from a grid or spot networks at this voltage. The same primary windings are used for both the 2,300- and 460-volt networks. If 208 volts should prove economical in a small station, then all motors larger than about 50 or 75 horsepower should be served directly at 2,300 volts, avoiding the third voltage classification. A typical network for auxiliary supply is shown in Figure 5.

Four points afford a reasonable criterion for a distribution system in a power plant: reliability, flexibility, simplicity of operation and ease of maintenance, and economics. The secondary network will be analyzed briefly with respect to these qualifications.

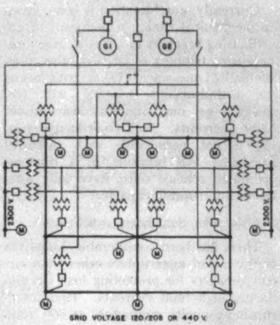

Figure 5. Secondary-network distribution system for central-station auxiliary supply

The secondary network system provides maximum reliability and flexibility. The many years of experience with city network systems indicates that they are substantially as reliable as their source of supply and that they can be readily and economically expanded to take care of load growth. The network system is at least as simple as any type of system which will give somewhere near the same degree of reliability. The fact that any primary feeder together with its associated transformers can be removed from service without any interruption to service facilitates the operation, maintenance, and expansion of the system. Based on a number of careful economic studies, the investment cost of the network system has been found to vary from about 15 per cent more to about 14 per cent less than the cost of a radial system. In about 75 per cent of these studies the network system showed a saving of from 6 to 14 per cent. The result of any cost comparison will depend upon the form of network system used and the form of radial system with which it is compared. If lesser reliability is accepted, a radial system always can be designed that is the cheapest usable scheme. The foregoing figures refer to radial systems currently used and considered adequate.

The matter of short-circuit current on a secondary network is something that must be watched in designing the system; otherwise the fault currents may run considerably higher than on a radial system, and the cost of the load circuit breakers will become excessive. The following are methods of keeping the interrupting duty on the load circuit breakers down.

1. Limit the amount of load on any one secondary grid or loop to a maximum of around 5,000 or 6,000 kva. This usually means a separate secondary grid or loop for each 100,000 kva of generating capacity or thereabouts, and less if small generators are involved and all load is supplied at low voltage.

2. Where necessary, two or more separate secondary grids or loops can be supplied from the same group of primary feeders. The secondary networks preferably should be supplied over three or four primary feeders to keep the amount of spare-network transformer capacity to a small value.

3. The network transformers should have an inherent impedance of around ten per cent. This high impedance has the additional advantage of improving load division between the transformers supplying a network, and of minimizing circulating currents between primary feeders whose voltages may be slightly different in magnitude and phase angle.

4. If a spot network system is employed instead of a grid or loop form, the amount of load per spot bus should be kept down to 1,500 to 2,500 kva.

If the foregoing points are kept in mind as guides when a network system is being designed for supplying power to generating-station auxiliaries, the advantages of reliability, flexibility, and simplicity of this type of system usually can be obtained at less cost than those forms of radial system which will give somewhere near comparable reliability.

As stated, each generating station requires individual study. If the best system for a particular station is to be chosen, such study should be started early, before physical details of station design place limiting factors on the application of one type of system or the other. Whether new generation involves a new plant or simply additions to existing plant, of course affects the choice, although this fact is not necessarily limiting in itself.

Conclusion

In conclusion the author wishes to repeat that the foregoing paragraphs were selected as high lights, not as a general coverage on the subject of auxiliary apparatus and distribution systems. The selection of items and the discussion of them prove that central-station auxiliary performance will be improved through better supply-system layout and more reliable individual motors and control. It is sincerely hoped that the discussion may prove of help to central-station engineers when auxiliary apparatus specifications and auxiliary power-supply problems are under consideration.

Fundamentals of the Amplidyne Generator

J. L. BOWER
MEMBER AIEE

THE PRIMARY PURPOSE of this paper is to provide for the system designer a logical basis for the understanding and use of Amplidyne generators. Because of the point of view adopted, much interesting material on Amplidyne design has been omitted. No attention has been given to the solution of equations representing specific applications of the Amplidyne generator, since it is the purpose of this paper to furnish only the basis for such analyses.

Introduction

Discussion

Commutation. The characteristics of an Amplidyne are greatly dependent upon commutation effects, particularly in the quadrature axis. Since this is a point frequently neglected, a brief explanation will be devoted to it.

Looking at the equations which describe the forms of the quadrature regulation, total saturation, and total regulation curves, and the quadrature time constant, we find that all are affected to a large degree by variations in R_q'. As given in the nomenclature, R_q' includes a term, N_{qq}, which is controlled by the location, relative to mechanical neutral, of the effective quadrature commutating zone. Brush position, of course, and the strength of the quadrature commutating field determine this location. Brush resistance across the face of the brush, the circumferential dimension of the brush, and surface contact resistance also are factors since they affect the short-circuit currents in the armature conductors undergoing commutation, which, in turn, contribute magnetomotive force in the direct axis.

The processes involved are, in simple terms, about as follows: a change in brush position (or one of the other factors previously enumerated) alters the magnetomotive force in the direct axis for a given quadrature current. This affects the generated voltage in the quadrature circuit. Since this voltage increment is proportional to the quadrature current, an increment of quadrature resistance, R_q' has been introduced. The change in R_q' then increases or decreases the quadrature time constant and the slopes of saturation and regulation curves as mentioned. An effect which necessarily accompanies the change in R_q' is the alteration of M_{fq}, the coefficient of inductive coupling between control and quadrature circuits.

To the extent that the foregoing commutation effects permit the existence of linear relations between generated voltages and circuit currents, they are included directly in the analysis in this paper. The effects of nonlinearities often can be found by the study of incremental effects, using the linear-system equations. Effects of speed on steady-state currents and voltages can be found from the analysis without approximation. For example, the reason can be seen why terminal voltage of an Amplidyne does not, in every machine, rise as the square of speed. Using equation 46 and neglecting N_{df}, we have

$$\frac{\partial V_d'}{\partial i_f} = \frac{N_{df}N_{dq}'}{R_q+R_s+N_{qq}+N_{qs}}$$

If the quadrature commutating zone were adjusted so as to make N_{qq} zero, and if the quadrature series field produced no direct-axis flux, the voltage V' would rise as the square of speed (all N's being proportional to speed). Such conditions do not always exist; hence, N_{qq} and N_{qs} are not always absent, and the voltage–speed relation is some power between first and second.

It might be mentioned here that although there are many factors—commutating-pole strength, brush material, brush position, and so forth—which affect commutation, only brush position is mentioned in the sections on characteristics, since it is generally the only factor which can be controlled once the machine is installed. As a matter of practical experience, the "resistance" method of setting brushes is much more accurate than the "inductive" method. Because of the simplicity of the latter, however, it is sometimes useful. Unless a machine is equipped with quadrature commutating poles, the quadrature brushes ordinarily are set off neutral in the direction of rotation. Practically all machines have direct-axis commutating poles, however, and can be set on direct-axis neutral. In any case, it is wise to follow the advice of the designer if it becomes necessary to adjust brushes.

Hysteresis and Saturation. As mentioned in the assumptions, no consideration is given to hysteresis and saturation effects. This, of course, does not mean that they are of no importance. A good approximation of the effect of hysteresis is an additional phase lag which is independent of frequency in the low-frequency range, and, therefore, cannot be represented in terms of a time constant. Amplidyne designers have reduced hysteresis effects to a great extent by good design, so that they can often be neglected.

Saturation, of course, is one of the limiting factors in the design of the Amplidyne. It comes into play in a rather interesting way in determining the shape of the total saturation curve. Since the direct and quadrature fluxes share the same paths in part, saturation produced by the relatively high quadrature flux affects any further increase of direct flux from the control circuit, and so on. Saturation also can enter into the determination of the total regulation curves at high load currents when the distribution of compensating magnetomotive force is not perfect. A detailed discussion of this effect is, however, beyond the scope of this paper.

Eddy Currents. To reduce effects of eddy currents to a minimum, all magnetic circuits of an Amplidyne are laminated, except in a few cases where the maximum of performance is not required. To include the effects of eddy currents in the analyses presented here would require that each of the K's, N's, L's, and M's be multiplied by an operational expression to represent the time lag between the application of a current and the appearance of flux. Although the effect is distributed throughout the magnetic circuits, a fair approximation is given by using $1/(1 + T_e p)$ as the operational multiplier. This is equivalent to assuming a short-circuited electric circuit around each flux path. Depending greatly upon the care taken to insulate the laminations, the value of T_e may vary from a negligible quantity up to a few milliseconds.

Relation Between M's and N's. Between an armature circuit and an adjacent stationary one are two types of coupling: that due to speed voltage in the armature, and that due to mutual flux linkages. The first type is represented by N and the second by M, as given in the nomenclature. There are certain interesting relations between the values of M and N.

Let us assume that a current i the stationary coil produces a flux ϕ linking the n turns of an armature coil moving with an angular velocity ω and having an instantaneous angular position α. Then

---

Paper 45-162, recommended by the AIEE committee on electric machinery for publication in AIEE TRANSACTIONS. Manuscript submitted May 26, 1945; made available for printing September 4, 1945.

J. L. BOWER is with the Control Instrument Company, Brooklyn, N. Y. At the time this paper was written he was in the aeronautic and marine engineering division of General Electric Company, Schenectady, N. Y.

The author is indebted to C. C. Lawry, Jr., for suggestions, especially on testing procedure. M. A. Baker, Alec Fisher, and B. H. Caldwell contributed greatly to the "Discussion" section of this paper through their valuable suggestions.

by the usual definitions, the mutual inductance is

$$M_1 = \frac{n}{i}\phi$$

if we use the subscript 1 to indicate constants of one coil. At the same time by definition of N in this paper,

$$N_1 = \frac{n}{i} \cdot \frac{d\phi}{dt}$$

$$= \frac{n}{i} \cdot \omega \frac{d\phi}{d\alpha}$$

From the foregoing relations:

$$N_1 = \omega \frac{dM}{d\alpha}$$

Since N and M for the entire armature are the sums, respectively, of the N_1's and M_1's of the individual coils, the preceding relation applies exactly to the entire armature circuit for any instantaneous connection to the brushes.

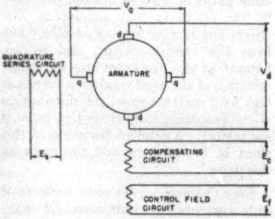

Figure 1. Circuits of the Amplidyne

Under certain conditions the value of $dM/d\alpha$ at one position is equal to the value of M 90 degrees away. For example, when the direction of the field is the same throughout the armature, M varies sinusoidally with α. If such a field is set up by the control winding for example, the relation between N_{qf} and M_{df} is given by

$$N_{qf} = M_{df} \cdot \omega$$

However, the field set up by the control circuit is not usually unidirectional, and so this relation does not apply exactly.

Typical Amplidyne Time Constants. Time constants of typical Amplidyne generators designed for high-performance control circuits are as follows:

Control, L_f/R_f: 0.13 to 0.17 sec.
Quadrature, L_q/R_q': 0.02 to 0.07 sec.
Direct, L_d'/R_d': 0.008 to 0.028 sec.

The machines selected range between 1.5 and 25 kw. They all operate at 3,500 rpm for two poles and at corresponding speeds for machines with larger numbers of poles. The time constants bear no regular relation to capacity for these examples.

ASSUMPTIONS AND APPROXIMATIONS

1. Mutual resistance coupling between quadrature and direct armature circuits is neglected because of its small magnitude.
2. Hysteresis effects are neglected.
3. Eddy currents in the material comprising the magnetic circuits are neglected.
4. Commutation is assumed to be perfect and to take place at one fixed point under the brush.
5. Saturation is not considered in the mathematical analysis.

The presence of hysteresis and saturation does not invalidate the equations derived in this paper, provided they are applied only to incremental effects. Any use of the relations where hysteresis and saturation effects are being considered should be done in such a way as to make the coefficients, L, M, N, and K suitable functions of the currents.

NOMENCLATURE

The following symbols are used throughout this paper:

L = self-inductance in henrys
M = mutual inductance in henrys
R = resistance in ohms
N = coefficient of direct coupling in generated volts per ampere
K = coefficient relating flux in maxwells along a magnetic axis to amperes in some circuit
B = coefficient relating generated volts in a circuit to maxwells through the proper magnetic axis, such that $N = BK$, with appropriate subscripts (B does not take a subscript)
i = current in amperes
ϕ = flux in maxwells
V = load voltage in volts
E = applied voltage in volts
ψ = flux linkages in henry-amperes
p = differential operator to indicate a first derivative with respect to time
t = time in seconds
f = subscript indicating the control circuit
q = subscript indicating the quadrature armature circuit
s = subscript indicating the quadrature series circuit
d = subscript indicating the direct armature circuit
c = subscript indicating the compensating circuit

Where a double subscript is used, the first refers to the circuit or axis in which the effect appears, and the second refers to the circuit in which the cause (usually a current) exists.

Certain relations between the foregoing quantities are in the nature of definitions, and will be stated here for convenience:

$$\left.\begin{array}{l} N_{qf} = BK_{df} \\ N_{df} = BK_{qf} \end{array}\right\}$$

$$\left.\begin{array}{l} N_{qq} = BK_{dq} \\ N_{dq} = BK_{qq} \end{array}\right\}$$

$$\left.\begin{array}{l} N_{qs} = BK_{ds} \\ N_{ds} = BK_{qs} \end{array}\right\}$$

$$\left.\begin{array}{l} N_{qd} = BK_{dd} \\ N_{dd} = BK_{qd} \end{array}\right\}$$

$$\left.\begin{array}{l} N_{qc} = BK_{dc} \\ N_{dc} = BK_{qc} \end{array}\right\}$$

$$\left.\begin{array}{l} V_q' = V_q - E_s \\ V_d' = V_d - E_c \end{array}\right\}$$

$$\left.\begin{array}{l} M_{fq}' = M_{fq} + M_{fs} \\ M_{qf}' = M_{qf} + M_{sf} \end{array}\right\}$$

$$\left.\begin{array}{l} M_{fd}' = M_{fd} - M_{fc} \\ M_{df}' = M_{df} - M_{cf} \end{array}\right\}$$

$$\left.\begin{array}{l} M_{qd}' = M_{qd} - M_{qc} + M_{sd} - M_{sc} \\ M_{dq}' = M_{dq} - M_{cq} - M_{ds} - M_{cs} \end{array}\right\}$$

$$\left.\begin{array}{l} L_q' = L_q + L_s + M_{qs} + M_{sq} \\ L_d' = L_d + L_c - M_{dc} - M_{cd} \end{array}\right\}$$

$$\left.\begin{array}{l} R_q' = R_q + R_s + N_{qq} + N_{qs} \\ R_d' = R_d + R_c + N_{dd} + N_{dc} \end{array}\right\}$$

$$\left.\begin{array}{l} N_{qd}' = N_{qd} - N_{qc} \\ N_{dq}' = N_{dq} + N_{ds} \end{array}\right\}$$

Signs of N's and K's are inherently positive for an Amplidyne whose direct and quadrature brushes are set off neutral in the direction of rotation.

It will be noted that mutual inductances are given with two different orders of the same subscripts. Obviously such pairs of inductances as M_{dq} and M_{qd} must be equal in value. In order to show the direction of effects, the two orders of subscripts are used, since it results in no additional complication.

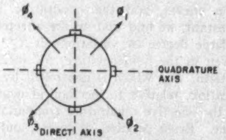

Figure 2. Quadrature and direct fluxes

CIRCUITS

In the machine to be analyzed here the principal circuits (see Figure 1) are:

1. The control-field circuit, to which is applied the voltage E_f.
2. The quadrature armature circuit, from which is taken the voltage V_q.
3. The quadrature series circuit, to which is applied the voltage E_s.
4. The direct armature circuit from which is taken the voltage V_d.
5. The compensating circuit (including commutation windings) to which is applied the voltage E_c.

QUADRATURE- AND DIRECT-AXIS FLUXES

The "direct axis" may be defined as that surface which passes radially through the centers of the zones on the armature

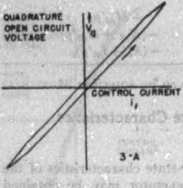

Figure 3a. Quadrature-control saturation curve

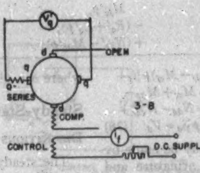

Figure 3b. Circuit for obtaining Figure 3a

surface under which the conductors are undergoing commutation by the "direct" or "load" brushes (see Figure 2).

The "quadrature axis" may be similarly defined with respect to the quadrature brushes.

In Figure 2 ϕ_1, ϕ_2, ϕ_3, and ϕ_4 are the fluxes issuing from the four segments into which the armature is divided by the two axes. The quadrature flux is:

$$\phi_q=\phi_1+\phi_2 \tag{1}$$

It is this flux which generates direct-axis voltage. Also since

$$\phi_1+\phi_2+\phi_3+\phi_4=0 \tag{2}$$

$$\phi_q=-(\phi_3+\phi_4) \tag{3}$$

Similarly

$$\phi_d=\phi_1+\phi_4=-(\phi_2+\phi_3) \tag{4}$$

Now, the direct and quadrature fluxes are functions of the currents flowing in all the circuits of the Amplidyne. According to our assumptions, the relation must be linear, in the absence of saturation. Then,

$$\phi_q=-K_{qf}i_f+K_{qq}i_q+K_{qs}i_s-K_{qd}i_d+K_{qc}i_c \tag{5}$$

and

$$\phi_d=-K_{df}i_f+K_{dq}i_q+K_{ds}i_s+K_{dd}i_d-K_{dc}i_c \tag{6}$$

Generated Voltages

The generated voltage between either pair of brushes is proportional to the flux crossing the corresponding axis, the rotational speed, and the number of armature conductors. Since the last two factors are the same for the direct as for the quadrature flux axis, we may use the one ratio of proportionality between generated voltages and flux. This ratio will be called B.

Flux Linkages

Let us now define the flux linkages of all circuits. It should be noted here that the flux linked by the quadrature- and direct-armature circuits need not be ϕ_q and ϕ_d, respectively.

Field linkages:

$$\psi_f=L_fi_f-M_{fq}i_q-M_{fs}i_s-M_{fd}i_d+M_{fc}i_c \tag{7}$$

Quadrature armature linkages:

$$\psi_q=-M_{qf}i_f+L_qi_q+M_{qs}i_s+M_{qd}i_d-M_{qc}i_c \tag{8}$$

Quadrature series linkages:

$$\psi_s=-M_{sf}i_f+M_{sq}i_q+L_si_s+M_{sd}i_d-M_{sc}i_c \tag{9}$$

Direct armature linkages:

$$\psi_d=-M_{df}i_f+M_{dq}i_q+M_{ds}i_s+L_di_d-M_{dc}i_c \tag{10}$$

Compensating linkages:

$$\psi_c=M_{cf}i_f-M_{cq}i_q-M_{cs}i_s-M_{cd}i_d+L_ci_c \tag{11}$$

Basic Circuit Equations

We are now prepared to write the circuit equations for the Amplidyne. External voltages will be designated in the case of applied voltages by E, and in the case of load voltages by V.

Then, for the field circuit:

$$E_f-p\psi_f-R_fi_f=0 \tag{12}$$

for the quadrature armature circuit:

$$-B\phi_d-p\psi_q-R_qi_q-V_q=0 \tag{13}$$

for the quadrature series circuit:

$$E_s-p\psi_s-R_si_s=0 \tag{14}$$

for the direct armature circuit:

$$B\phi_q-p\psi_d-R_di_d-V_d=0 \tag{15}$$

and for the compensating circuit:

$$E_c-p\psi_c-R_ci_c=0 \tag{16}$$

These equations may be rewritten, making use of definitions of fluxes and flux linkages from equations 5 through 11, as follows:

From equation 12,

$$-(R_f+L_fp)i_f+M_{fq}pi_q+M_{fs}pi_s+M_{fd}pi_d-M_{fc}pi_c=-E_f \tag{17}$$

From equation 13,

$$(BK_{df}+M_{qf}p)i_f-(R_q+BK_{dq}+L_qp)i_q-(BK_{ds}+M_{qs}p)i_s-(BK_{dd}+M_{qd}p)i_d+(BK_{dc}+M_{qc}p)i_c=V_q \tag{18}$$

From equation 14,

$$M_{sf}pi_f-M_{sq}pi_q-(R_s+L_sp)i_s-M_{sd}pi_d+M_{sc}pi_c=-E_s \tag{19}$$

From equation 15,

$$-(BK_{qf}-M_{df}p)i_f+(BK_{qq}-M_{dq}p)i_q+(BK_{qs}-M_{ds}p)i_s-(R_d+BK_{qd}+L_dp)i_d+(BK_{qc}+M_{dc}p)i_c=V_d \tag{20}$$

From equation 16,

$$-M_{cf}pi_f+M_{cq}pi_q+M_{cs}pi_s+M_{cd}pi_d-(R_c+L_cp)i_c=-E_c \tag{21}$$

Coefficients of Direct Coupling

In the foregoing equations, the coefficients containing B relate generated voltage in quadrature and direct armature circuits to currents in the same or other circuits. These may be referred to as coefficients of direct coupling. In the case of BK_{dq} and BK_{qd}, the coefficients are the same in form and effect as quadrature and direct resistances. For simplicity in analysis, it is convenient to use coefficients with subscripts as shown below:

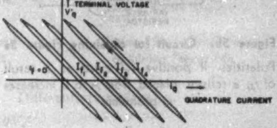

Figure 4a (above). Quadrature regulation curve

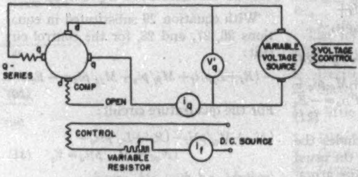

Figure 4b. Circuit for obtaining Figure 4a

Let us substitute:

$$\left.\begin{aligned}
BK_{df}&=N_{qf}\\
BK_{qf}&=N_{df}\\
BK_{dq}&=N_{qq}\\
BK_{qq}&=N_{dq}\\
BK_{ds}&=N_{qs}\\
BK_{qs}&=N_{ds}\\
BK_{dd}&=N_{qd}\\
BK_{qd}&=N_{dd}\\
BK_{dc}&=N_{qc}\\
BK_{qc}&=N_{dc}
\end{aligned}\right\} \tag{22}$$

With these substitutions the equations 10 through 14 become:

Control field: $-(R_f+L_fp)i_f+M_{fq}pi_q+M_{fs}pi_s+M_{fd}pi_d-M_{fc}pi_c=-E_f$ (17)

Quadrature armature: $(N_{qf}+M_{qf}p)i_f-(R_q+N_{qq}+L_qp)i_q-(N_{qs}+M_{qs}p)i_s-(N_{qd}+M_{qdp})i_d+(N_{qc}+M_{qc}p)i_c=V_q$ (23)

Quadrature series: $M_{sf}pi_f-M_{sq}pi_q-(R_s+L_sp)i_s-M_{sd}pi_d+M_{sc}pi_c=-E_s$ (19)

$$\Delta = \begin{vmatrix} -(R_f+L_fp), & M_{fq}'p, & +M_{fd}'p, \\ (N_{qf}+M_{qf}'p), & -(R_q'+L_q'p), & -(N_{qd}'+M_{qd}'p), \\ -(N_{df}-M_{df}'p), & +(N_{dq}'-M_{dq}'p), & -(R_d'+L_d'p), \end{vmatrix} \quad (34)$$

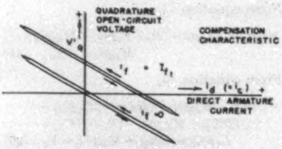

Figure 5a. Compensation characteristic curve

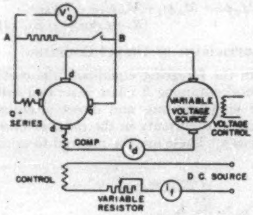

Figure 5b. Circuit for obtaining Figure 5a

Polarities—If positive V_q' exists as a result of i_f, a resistor placed from *A* to *B* increases i_d positively

Direct armature: $-(N_{df}-M_{df}p)i_f+(N_{dq}-M_{dq}p)i_q+(N_{ds}-M_{ds}p)i_s-(R_d+N_{dd}+L_dp)i_d+(N_{dc}+M_{dc}p)i_c=V_d \quad (24)$

Direct compensating: $-M_{cf}pi_f+M_{cq}pi_q+M_{cs}pi_s+M_{cd}pi_d-(R_c+L_cP)i_c=-E_c \quad (21)$

In the Amplidyne which includes the five circuits mentioned thus far, the usual connection is with the quadrature armature and quadrature series circuits connected in series, and a similar connection between direct armature and compensating circuits. The resulting currents and voltages are such that

$$\left.\begin{matrix} V_q-E_s=V_q' & \qquad V_d-E_c=V_d' \\ i_s=i_q & \qquad i_c=i_d \end{matrix}\right\} \quad (25)$$

If we substitute these relations in equations 23 through 27:

Control circuit: $-(R_f+L_fp)i_f+(M_{fq}+M_{fs})pi_q+(M_{fd}-M_{fc})pi_d=-E_f \quad (26)$

Quadrature circuit: $+[N_{qf}+(M_{qf}+M_{sf})p]i_f-[(R_q+R_s+N_{qq}+N_{qs})+(L_q+L_s+M_{qs}+M_{sq})p]i_q-[(N_{qd}-N_{qc})+(M_{qd}-M_{qc}+M_{sd}-M_{sc})p]i_d=V_q' \quad (27)$

Direct circuit: $-[N_{df}-(M_{df}-M_{cf})p]i_f+[(N_{dq}+N_{ds})-(M_{dq}-M_{cq}+M_{ds}-M_{cs})p]i_q-[(R_d+R_c+N_{dd}-N_{dc})+(L_d+L_c-M_{dc}-M_{cd})p]i_d=V_d' \quad (28)$

A great simplification may be made by lumping with quadrature armature and direct armature resistances, inductances, and coefficients of direct coupling, similar coefficients of quadrature series and direct compensating circuits. To do this, the following substitutions are made:

$$\left.\begin{matrix} M_{fq}+M_{fs}=M_{fq}' \\ M_{fd}-M_{fc}=M_{fd}' \\ M_{qf}+M_{sf}=M_{qf}' \\ L_q+L_s+M_{qs}+M_{sq}=L_q' \\ M_{qd}-M_{qc}+M_{sd}-M_{sc}=M_{qd}' \\ M_{df}-M_{cf}=M_{df}' \\ M_{dq}-M_{cq}+M_{ds}-M_{cs}=M_{dq}' \\ L_d+L_c-M_{dc}-M_{cd}=L_d' \\ R_q+R_s+N_{qq}+N_{qs}=R_q' \\ N_{qd}-N_{qc}=N_{qd}' \\ N_{dq}+N_{ds}=N_{dq}' \\ R_d+R_c+N_{dd}-N_{dc}=R_d' \end{matrix}\right\} \quad (29)$$

Simplified Amplidyne Equations

With equation 29 substituted in equations 26, 27, and 28, for the control circuit:

$$-(R_f+L_fp)i_f+M_{fq}'pi_q+M_{fd}'pi_d=-E_f \quad (30)$$

For the quadrature circuit:

$$(N_{qf}+M_{qf}'p)i_f-(R_q'+L_q'p)i_q-(N_{qd}'+M_{qd}'p)i_d=V_q' \quad (31)$$

And for the direct circuit:

$$-(N_{df}-M_{df}'p)i_f+(N_{dq}'-M_{dq}'p)i_q-(R_d'+L_d'p)i_d=V_d' \quad (32)$$

Solving for the terminal voltage, we have

$$V_d'=E_f\frac{(N_{qf}+M_{qf}'p)(N_{dq}'-M_{dq}'p)-(R_q'+L_q'p)(N_{df}-M_{df}'p)}{(R_f+L_fp)(R_q'+L_q'p)-M_{fq}'p(N_{qf}+M_{qf}'p)}+$$
$$i_d\frac{\Delta}{(R_f+L_fp)(R_q'+L_qp)-M_{fq}'p(N_{qf}+M_{qf}'p)}+$$
$$V_q'\frac{-(R_f+L_fp)(N_{dq}'-M_{dq}'p)+M_{fq}'p(N_{df}-M_{df}'p)}{(R_f+L_fp)(R_q'+L_q'p)-M_{qf}'p(N_{qf}+M_{qf}'p)} \quad (33)$$

where Δ is given by equation 34.

Steady-State Characteristics

DEFINITIONS

The steady-state characteristics of the Amplidyne generator may be obtained from several curves. In the order in which they will be discussed, they are:

1. Quadrature-control saturation.
2. Quadrature regulation.
3. Compensation characteristic.
4. Direct-quadrature saturation.
5. Direct-control saturation.
6. Total saturation.
7. Direct regulation.
8. Total regulation.

It will be assumed that the Amplidyne is being tested with compensating and quadrature series fields connected.

QUADRATURE - CONTROL SATURATION CURVE

The quadrature-control saturation curve shows the relation between open-circuit generated voltage in the quadrature armature circuit and control-field current. Its slope is $\partial V_q'/\partial i_f$ obtained from equation 31 by setting equal to zero p and all currents except i_f. There remains

$$N_{qf}i_f=V_q' \quad (35)$$

or, if we differentiate

$$\frac{\partial V_q'}{\partial i_f}=N_{qf} \quad (36)$$

The general shape of this curve may be seen in Figure 3 for an Amplidyne generator.

The form of the quadrature-control saturation curve is dependent (for a given machine) upon speed. It is little affected, if at all, by

1. Direct-axis brush settings.
2. Quadrature-axis brush settings.
3. The degree of compensation.
4. Resistance of windings (temperature).

QUADRATURE REGULATION CURVES

The quadrature regulation curve shows for a fixed control excitation the variation

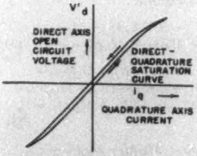

Figure 6a. Direct-quadrature saturation curve

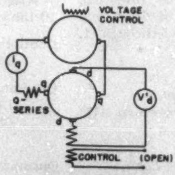

Figure 6b. Circuit for obtaining Figure 6a

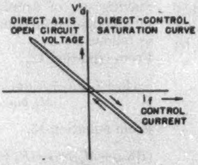

Figure 7a. Direct-control saturation curve

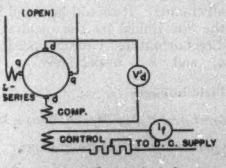

Figure 7b. Circuit for obtaining Figure 7a

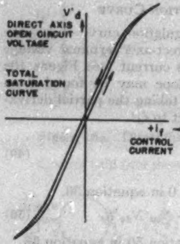

Figure 8a. Total saturation curve

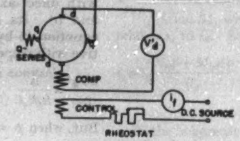
q
d
Q-SERIES
V'd
COMP
CONTROL
i_f
D.C. SOURCE
RHEOSTAT

Figure 8b. Circuit for obtaining Figure 8a

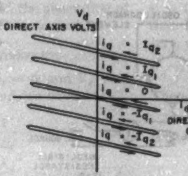

Figure 9a. Direct regulation curve

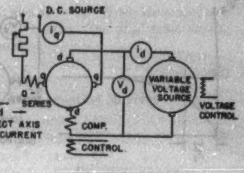
D.C. SOURCE
i_q
d
q
Q-SERIES
V_d
i_d
VARIABLE VOLTAGE SOURCE
VOLTAGE CONTROL
COMP.
CONTROL

Figure 9b. Circuit for obtaining Figure 9a

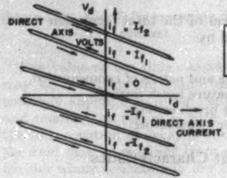

Figure 10a. Total regulation curve

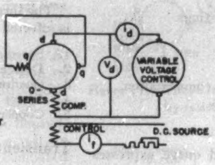
i_d
q
d
V_d
VARIABLE VOLTAGE CONTROL
Q-SERIES
COMP.
CONTROL
i_f
D.C. SOURCE

Figure 10b. Circuit for obtaining Figure 10a

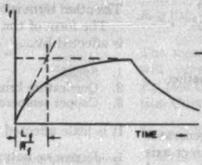

Figure 12a. Control-field time constant

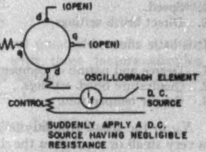
(OPEN)
d
q
(OPEN)
OSCILLOGRAPH ELEMENT
CONTROL
i_f
D.C. SOURCE
SUDDENLY APPLY A D.C. SOURCE HAVING NEGLIGIBLE RESISTANCE

Figure 12b. Circuit for obtaining Figure 12a

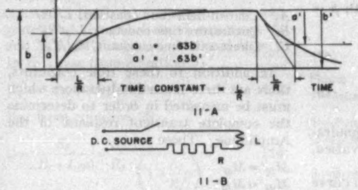
b
a
a'
b'
a = .63b
a' = .63b'
L/R
TIME CONSTANT = L/R
TIME
11-A
D.C. SOURCE
L
R
11-B

Figure 11a and b. Method of obtaining time constant for any linear inductive circuit

in terminal voltage of the quadrature circuit with quadrature current, when that circuit is opened at any point (see Figure 4a and b).

The slope of the quadrature regulation curve is $\partial V_q'/\partial i_q$. V_q' may be obtained from equation 31:

If $p = 0$ and $i_d = 0$,

$$N_{qf}i_f - R_q'i_q = V_q' \tag{37}$$

The slope of the quadrature regulation curves are given by equation 37 by taking the partial derivative:

$$-R_q' = \frac{\partial V_q'}{\partial i_q} \tag{38}$$

The slope then, is

$$-R_q' \text{ or } -(R_q+R_s+N_{qq}+N_{qs}) \tag{39}$$

It should be noted that the slope not only is affected by the ohmic resistance of the circuit, but includes the generated voltage terms N_{qq} and N_{qs}. N_{qq} can be adjusted in value by the quadrature brush setting.

The form of the quadrature regulation curves is affected by

1. Speed.
2. Quadrature–axis brush setting.
3. Copper temperature.

It is not affected by

1. Direct-axis brush settings.
2. Degree of compensation.

Compensation Characteristic Curves

As the name indicates, the compensation characteristic curves show the degree and nature of the compensation in the machine. The points for the curve are taken by reading the open-circuit quadrature voltage while varying the current through the direct armature circuit and compensating winding in series (see Figure 5a and b).

The slope of the curves is $\partial V_q'/\partial i_d$. The value of this derivative may be found from equation 31 by making $p = 0$ and $i_q = 0$.

$$N_{qf}i_f - N_{qd}'i_d = V_q' \tag{40}$$

Differentiating gives

$$\frac{\partial V_q'}{\partial i_d} = -N_{qd}' = -(N_{qd}-N_{qc}) \tag{41}$$

The form of the compensation characteristic curves is affected by

1. Degree and nature of compensation.
2. Speed.

It is little affected by

1. Direct brush settings.
2. Quadrature brush settings.
3. Copper temperature.

Direct – Quadrature Saturation Curve

The direct–quadrature saturation curve shows the variation of direct-axis open-circuit voltage with quadrature current (see Figure 6a and b). Its slope may be found from equation 32 with $p = 0$.

$$-N_{df}i_f + N_{dq}'i_q - R_d'i_d = V_d' \tag{42}$$

Taking the derivative gives

$$N_{dq}' = \frac{\partial V_d'}{\partial i_q} \tag{43}$$

The form of the direct-quadrature saturation curve is affected by speed. It is little affected by

1. Degree and nature of compensation.
2. Direct brush settings.
3. Quadrature brush settings.
4. Copper temperature.

Direct-Control Saturation Curve

The direct-control saturation curve shows the variation of direct-axis open-circuit voltage with control current (see Figure 7a and b). Its slope may be found from equation 42. By taking the partial derivative with respect to i_f, we have

$$-N_{df} = \frac{\partial V_d'}{\partial i_f} \tag{44}$$

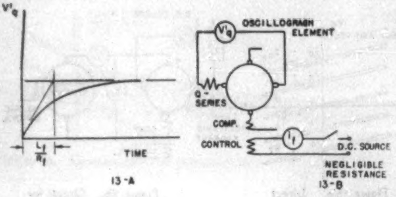
V'q
OSCILLOGRAPH ELEMENT
Vq
Q-SERIES
COMP.
CONTROL
i_f
D.C. SOURCE
NEGLIGIBLE RESISTANCE
TIME
$\frac{L_f}{R_f}$
13-A
13-B

Figure 13a and b. Alternative method for measuring control-field time constant

The form of the direct-control saturation curve is affected by

1. Speed.
2. Direct brush settings.

It is little affected by

1. Degree and nature of compensation.
2. Quadrature brush settings.
3. Copper temperature.

N_{df} in the usual Amplidyne generator is very small or zero when the direct-axis brushes are on neutral, since the control fields are wound so as to produce direct flux only.

TOTAL SATURATION CURVE

The total saturation curve is a plot of direct-axis no-load voltage against control current, with the quadrature circuit closed (see Figure 8a and b). The slope of the curve may be obtained from equation 33 with $p = 0$.

$$V_d' = E_f\left(\frac{N_{qf}N_{dq}' - R_q'N_{df}}{R_fR_q'}\right) + i_d\left(\frac{\Delta}{R_fR_q'}\right) - V_q'\left(\frac{N_{dq}'}{R_q'}\right) \tag{45}$$

or, since $E_f/R_f = i_f$,

$$V_d' = i_f\left(\frac{N_{qf}N_{dq}'}{R_q'} - N_{df}\right) + i_d\left(\frac{\Delta}{R_fR_q'} - V_q'\frac{N_{dq}'}{R_q'}\right)$$

Taking the partial derivative of equation 45 with respect to i_f, we find the slope of the total saturation curve to be

$$\frac{\partial V_d'}{\partial i_f} = \frac{N_{qf}N_{dq}'}{R_q'} - N_{df} \tag{46}$$

Note that the second term is the slope of the direct-control saturation curve. The other term is ordinarily much greater.

The form of the total saturation curve is affected by

1. Speed.
2. Quadrature brush settings.
3. Copper temperature.

It is little affected by

1. Degree or nature of compensation.
2. Direct brush settings.

DIRECT-REGULATION CURVE

The direct-regulation curve expresses the relation between direct-axis terminal voltage and direct-axis current, as all other currents in the system are held constant (see Figure 9a and b). Its slope may be found from equation 32 with $p = 0$.

$$-N_{df}i_f + N_{dq}'i_q - R_d'i_d = V_d' \tag{47}$$

$$\frac{\partial V_d'}{\partial i_d} = -R_d' \tag{48}$$

The curve is taken by holding quadrature current constant while i_d is varied, with $i_f = 0$.

The form of the direct-regulation curve is affected by

1. Speed.
2. Direct brush settings.
3. Copper temperature.

It is little affected by

1. Degree and nature of compensation.
2. Quadrature brush settings.

TOTAL REGULATION CURVE

The total regulation curve shows the variation of direct-axis terminal voltage with direct-axis current (see Figure 10a and b). Its slope may be found from equation 45 by taking the partial derivative with respect to i_d:

$$\frac{\partial V_d'}{\partial i_d} = \frac{\Delta}{R_fR_q'} \tag{49}$$

But, when $p = 0$ in equation 33,

$$\Delta = -R_fR_q'R_d' - N_{qd}'N_{dq}'R_f \tag{50}$$

Then, with equation 50 in equation 49,

$$\frac{\partial V_d'}{\partial i_d} = -\left(R_d' + \frac{N_{qd}'N_{dq}'}{R_q'}\right) \tag{51}$$

The form of the total regulation curve is affected by

1. Speed.
2. Degree and nature of compensation.
3. Quadrature brush settings.
4. Direct brush settings.
5. Copper temperature.

Transient Characteristics

SUMMARY

The principal time constants of the Amplidyne are:

A. Control-field time constant, L_f/R_f
B. Quadrature time constant, L'_q/R_q'
C. Direct-axis time constant, R_d'/L_d'

In addition to these time constants, there are three mutual inductances which must be measured in order to determine the complete transient response of the Amplidyne. These are:

$M_{fq}' = M_{qf}'$
$M_{df}' = M_{fd}'$
$M_{dq}' = M_{qd}'$

CONTROL-FIELD TIME CONSTANT

Equation 30, with $i_q - i_d = 0$ describes the rise of i_f with time after a field voltage E_f is applied. Solving, we have

$$i_f = \frac{E_f}{R_f + L_fp} = \frac{E_f}{R_f}\cdot\frac{1}{\left(1 + \frac{L_f}{R_f}p\right)} \tag{52}$$

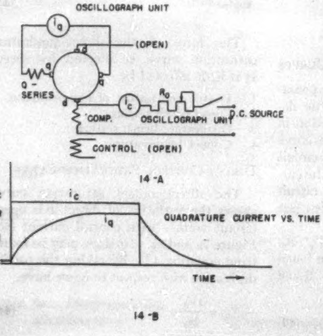
OSCILLOGRAPH UNIT
I_q
(OPEN)
q
d
Q-SERIES
I_c
R_0
COMP.
OSCILLOGRAPH UNIT
D.C. SOURCE
CONTROL (OPEN)
14-A
i_c
OR
i_q
i_c
i_q
QUADRATURE CURRENT VS. TIME
TIME
14-B

Figure 14a and b (left). Quadrature time constant and circuit for measuring

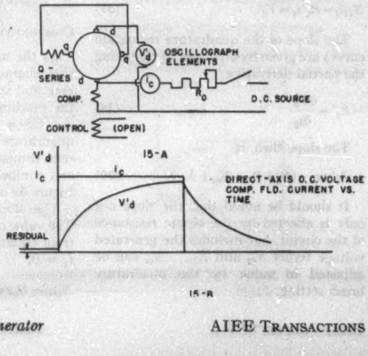
d
q
V_d
OSCILLOGRAPH ELEMENTS
Q-SERIES
I_c
R_0
COMP.
D.C. SOURCE
CONTROL (OPEN)
15-A
V'd
i_c
i_c
V'd
RESIDUAL
DIRECT-AXIS D.C. VOLTAGE COMP. FLD. CURRENT VS. TIME
15-B

Figure 15a and b (right). Alternative method for obtaining quadrature time constant

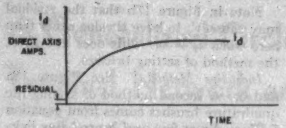

Figure 16a. Direct time constant

Control field (not shown) is open

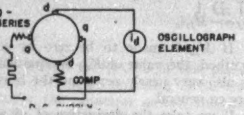

Figure 16b. Circuit for measuring direct time constant

The value of the time constant, L_f/R_f may be found by the simple method of suddenly applying E_f to the control field, and reading the rise of i_f with time. If the time constant of decay is also desired, the field may be supplied from a voltage divider whose resistance is low compared to that of the field (see Figure 12a and b). The oscillogram, Figure 12a may be analyzed to find the time constant L_f/R_f.

Another method of finding the time constant, L_f/R_f in certain cases is suggested by the solution of equations 30 and 31 for V_q' when $i_d = 0$ and $i_q = 0$. In this case from equation 31:

$$V_q' = (N_{qf} + M_{qf}'p)i_f \tag{53}$$

But from equation 30,

$$i_f = \frac{E_f}{(R_f + L_f p)} = \frac{E_f}{R_f} \cdot \frac{1}{\left(1 + \frac{L_f}{R_f}p\right)} \tag{54}$$

Then, from equations 53 and 54,

$$V_q' = \frac{E_f}{R_f} \cdot \frac{N_{qf} + M_{qf}'p}{1 + \frac{L_f}{R_f}p} \tag{55}$$

Now, where the quadrature brushes are on neutral and no quadrature fields are used which have magnetic coupling with the control field,

$$M_{qf}' = 0 \tag{56}$$

In this case

$$V_q' = \frac{E_f}{R_f} N_{qf} \cdot \frac{1}{1 + \frac{L_f}{R_f}p} \tag{57}$$

The time constant of rise of V_q' is then that of the control field, within the assumptions of this analysis. The circuit of Figure 13 may be used to determine L_f/R_f.

This second method is such that, if eddy-current and hysteresis effects introduce any measurable time delays, they are included as increases in the effective control-field time constant. Thus the entire delay between the application of a control voltage and the generation of a quadrature voltage is measured.

QUADRATURE TIME CONSTANT

Equation 31, with $i_f = 0$, and $V_q' = 0$ relates i_q to i_d. Solving, we have

$$i_q = i_d \frac{N_{qd}' + M_{qd}'p}{R_q} \cdot \frac{1}{1 + \frac{L_q'}{R_q'}p} \tag{58}$$

If the magnetic circuits of the Amplidyne are such that the quadrature and direct axis are not coupled, $M_{qd}' = 0$. If the current i_d flows through the compensating field only, it becomes i_c and N_{qd}' is replaced by $-N_{qc}$. Then we have

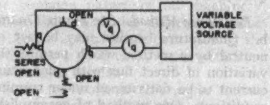

Figure 17a. Circuit for quadrature-brush setting by resistance method

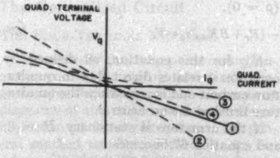

Figure 17b. Interpretation of curves for quadrature-brush setting by resistance

1—Armature stationary
2—Brushes off neutral in direction of rotation—armature rotating
3—Brushes off neutral against direction of rotation—armature rotating
4—Parallel to 1—brushes on neutral—armature rotating

$$i_q = i_c \frac{N_{qc}}{R_q'} \cdot \frac{1}{1 + \frac{L_q'}{R_q'}p} \tag{59}$$

Thus, the value of the time constant, L_q'/R_q' may be found by applying instantaneously a constant current i_c and reading the rise of quadrature current (see Figure 14 a and b).

For accurate results in this test,

$$R_0 \geqq 10 L_c \cdot \frac{R_q'}{L_q'} \tag{60}$$

It may be more convenient in some cases for the rise of V_d' to be recorded rather than the rise of i_q. In this event, the time constant, L_q'/R_q' may be found by applying an instantaneous current i_c and recording the transient values of V_d'. The equation for V_d' in differential form may be found from equation 32 with $i_f = 0$ and $i_d = 0$. If we have assumed that M_{qd}' is zero, then M_{dq}' must also be zero, and

$$V_d' = N_{dq}' i_q \tag{61}$$

Then, using equation 59 gives

$$i_q = i_c \frac{N_{qc} N_{dq}'}{R_q'} \cdot \frac{1}{1 + \frac{L_q'}{R_q'}p} \tag{62}$$

See Figure 15a and b. Here, again, it is necessary for reasonable accuracy that

$$R_0 \geqq 10 L_c \frac{R_q'}{L_q'} \tag{63}$$

The measured quadrature time constant will vary with those factors affecting R_q' (see the section, "Quadrature Regulation Curves").

DIRECT TIME CONSTANT

If, in equation 32,

$$i_f = V_d' = 0$$

$$i_d = i_q \cdot \left[\frac{(N_{dq}' - M_{dq}'p)}{R_d'}\right] \cdot \left[\frac{1}{1 + \frac{L_d'}{R_d'}p}\right] \tag{64}$$

If, as before, M_{dq}' is negligible, we have

$$i_d = i_q \left[\frac{N_{dq}'}{R_d'}\right] \cdot \frac{1}{\left(1 + \frac{L_d'}{R_d'}p\right)} \tag{65}$$

Thus, if V_d' is reduced to zero by short-circuiting the direct-armature circuit through the compensating circuit with control current zero, the time constant which regulates the response of direct-axis current is L_d'/R_d'. If a constant i_q is applied instantaneously, i_d will rise with a time constant L_d'/R_d' (see Figure 16a and b). The direct time constant will vary with those factors affecting R_d' (see the section, "Direct Regulation Curves").

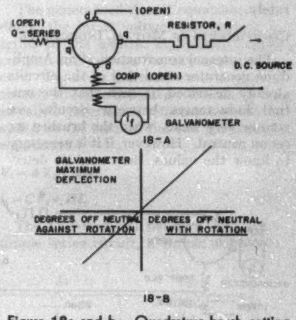
(OPEN)
d
(OPEN)
Q - SERIES
q
q
RESISTOR, R
d
COMP (OPEN)
D. C. SOURCE
I_f
GALVANOMETER
18-A
GALVANOMETER MAXIMUM DEFLECTION
DEGREES OFF NEUTRAL AGAINST ROTATION
DEGREES OFF NEUTRAL WITH ROTATION
18-B

Figure 18a and b. Quadrature-brush setting by inductive method

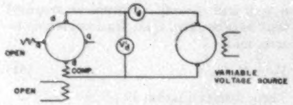

Figure 19a. Circuit for direct-brush setting by resistance method

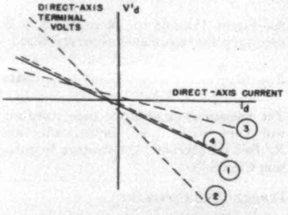

Figure 19b. Interpretation of curves for direct-brush setting by resistance method

1—Armature stationary
2—Brushes off neutral in direction of rotation—armature rotating
3—Brushes off neutral against direction of rotation—armature rotating
4—Parallel to 1—brushes on neutral—armature rotating

For a reasonable accuracy, in Figure 16a,

$$R \geq 10 L_q \frac{R_d'}{L_d'} \tag{66}$$

If the direct axis is well compensated, L_d'/R_d' will be quite small and may, for that reason, be difficult to measure accurately.

Coefficients of Mutual Inductance

The internal construction of an Amplidyne generator consisting of the circuits already described, is such that the mutual inductances between circuits are zero or very small, when the brushes are set on neutral. However, if it is necessary to know the values, they may be determined by applying a sinusoidal voltage to one circuit and reading the induced open-circuit voltages in the others with the armature stationary. The frequency should be sufficiently low that eddy current and hysteresis effects will not introduce important errors. Under certain conditions the brushes will allow circulating currents to flow by short-circuiting armature turns; hence it is wise to raise all brushes not needed during mutual measurement.

Commutation

Brush Setting

Quadrature Brushes

Resistance Method. See Figure 17a and b. Quadrature brushes may be set on neutral by a method which permits the variation of direct flux with quadrature current to be determined under running conditions. One method of accomplishing this is suggested by examination of equation 18. If we make all currents zero except i_q, we have, for steady state ($p = 0$).

$$-(R_q + BK_{dq})i_q = V_q \tag{67}$$

K_{dq} for this equation, as defined by equation 6 relates direct flux to quadrature current and is zero when the quadrature brushes are on neutral.

If the armature is stationary, $B = 0$, and equation 67 becomes

$$-R_q i_q = V_q \tag{68}$$

Then we have, for the machine running,

$$\frac{\partial V_q}{\partial i_q} = -(R_q - BK_{dq}) \tag{69}$$

and for the stationary machine

$$\frac{\partial V_q}{\partial i_q} = -R_q \tag{70}$$

If we find the effective resistance of the quadrature-armature circuit both running and stationary, and if we set the brushes so that these two resistance values are equal, the brushes must be on neutral.

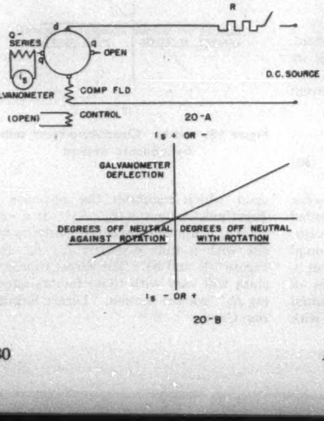

20-A

20-B

Figure 20a and b. Direct-brush setting by inductive method

Note in Figure 17b that the residual may cause V_q to have a value other than zero when $i_q = 0$. This does not affect the method of setting brushes.

Inductive Method. See Figure 18a and b. A second method of setting the quadrature brushes comes from equation 7, since direct-flux and control-flux linkages are zero under approximately the same conditions. In equation 7, with all currents except i_q at zero, we have:

$$\psi_f = -M_{fq} i_q \tag{71}$$

If M_{fq} is made to be zero by some method, the value of K_{dq} in equation 69 is also very nearly zero, and the brushes are on neutral.

If we take the derivative of ψ_f with time, we have the induced voltage in the control field as i_q varies:

$$p\psi_f = -M_{fq} p i_q \tag{72}$$

With the machine running, a plot can be made of galvanometer deflection (see Figure 18b) against brush position, as the switch is closed. When the brush position is such that the swing is nearly zero for repeated closing of the switch, the quadrature brushes are on neutral.

Direct Brushes

Resistance Method. See Figure 19a and b. The setting of the direct brushes may be made by a method similar to method 1 for the quadrature brushes. Thus, from equation 48 we get, for the armature rotating at steady state ($p = 0$):

$$\frac{\partial V_d'}{\partial i_d} = -R_d' = -[R_d + R_c + B(K_{qd} - K_{qc})] \tag{73}$$

If the compensating winding is symmetrical about the direct axis, $K_{qc} = 0$. We then have

$$\frac{\partial V_d'}{\partial i_d} = -(R_d + R_c + BK_{qd}) \tag{74}$$

When the armature is stationary,

$$\frac{\partial V_d'}{\partial i_d} = -(R_d + R_c) \tag{75}$$

In this test, the compensating and commutating fields are included in the measurements of effective drop, since their inclusion reduces nonlinear effects such as saturation and poor commutation.

Inductive Method. A second method of setting the direct brushes is similar to

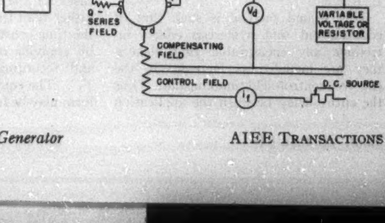

Figure 21. Circuit for black-band commutation tests

method 2 for the quadrature brushes. This method can be used when the Amplidyne generator is equipped with a quadrature series field (see Figure 20a and b).

From equation 9, if all currents except i_d are zero, we have

$$\psi_s = M_{sd} i_d \tag{76}$$

Then, differentiating gives

$$p\psi_s = M_{sd} p i_d \tag{77}$$

By reasoning similar to that used for method 2 for quadrature brushes, we may say that, when M_{sd} is zero, the direct brushes are on neutral. If the direct-brush position is such as to produce minimum deflection, the brushes are on neutral.

BLACK-BAND COMMUTATION TESTS

Although the assumption is made in this paper that the commutating field has been adjusted to give good commutation, a black-band commutation test may be run to check this. The circuit for the test is shown in Figure 21.

The interpretation of the results of the black-band test is the same as for any d-c generator and need not be discussed here.

References

1. DYNAMOELECTRIC AMPLIFIER FOR POWER CONTROL, E. F. W. Alexanderson, M. A. Edwards, K. K. Bowman. AIEE TRANSACTIONS, volume 59, 1940, pages 937–9.

2. DESIGN CHARACTERISTICS OF AMPLIDYNE GENERATORS, Alec Fisher. AIEE TRANSACTIONS, volume 59, 1940, pages 939–44.

3. AMPLIDYNE: A NEW TOOL OF MANY USES, F. Mohler. *Iron and Steel Engineer*, September 1940.

4. STEADY-STATE THEORY OF THE AMPLIDYNE GENERATOR, Troy D. Graybeal. AIEE TRANSACTIONS, volume 61, 1942, October section, pages 750–6.

A Generalized Circle Diagram for a Four-Terminal Network and Its Application to the Capacitor Single-Phase Motor

J. G. TARBOUX
FELLOW AIEE

THE MAIN PURPOSE of this paper is to present an operating circle diagram for the capacitor motor, showing that the input-current vector follows a circular envelope, as the mechanical shaft power is varied. A secondary aim is to review the theory of the generalized four-terminal network, thereby developing circle-diagram equations which can be applied to any linear network which delivers its output power into a variable impedance of constant power factor. This generalized method of approach can be applied quite readily to the three-phase induction motor, obtaining the same results which now are available in practically all textbooks on a-c machinery. The same point of view can be extended to single-phase motors, the capacitor motor being a good example. Considerable work still remains to be done in order to make the single-phase circle diagram as useful as the one commonly used for three-phase motors,[1] but the author believes that the generalized treatment offered in this paper may be a step in the right direction.

From the point of view of the teacher of a-c machinery the generalized method is quite worth while, in that it emphasizes the common nature of all machinery, rather than particular differences. This method of approach has been used by the author for a good many years with very encouraging results.

Since the work of this paper follows this generalized point of view, the review of this theory is given first, followed by its specific application to the capacitor motor.

The Generalized Circuit

THE FOUR-TERMINAL NETWORK

Undoubtedly the three-phase induction-motor equivalent circuit and circle diagram are the most widely understood diagrams of this nature which are found in electric-machinery literature. The general method usually adopted in the development of this circle diagram is first to present the equivalent motor network, which in its initial form is a T circuit as shown in Figure 1. Quite often this T circuit is converted into a cantilever circuit by connecting the shunt or exciting impedance $\mathbf{Z}_0$ directly to the input terminals. This step somewhat reduces the amount of analytical work without introducing appreciable errors in the general results.

Several suggestions of a generalized method of analyses have been presented from time to time. In 1930, Gabriel Kron[2] presented a generalized theory of electric machinery based upon energy content and energy utilization. In his paper he considers an electric machine as a device which receives energy and through a process of energy storage and energy transmission finally delivers a part of the total input energy into a load.

A similar development is presented in this paper following, however, the circuit point of view. The idea of a generalized four-terminal network is not new. It has been used extensively by the transmission-line engineer to include transformers and alternators as well as transmission lines. In general, therefore, a four-terminal network is defined as any electric circuit composed of resistances, inductances, and capacitances, so connected that there is only one point of energy input and only one point for energy output. For normal analytical treatment it is customary to assume that this network is linear and bilateral.

From the energy point of view the capacitor motor, as well as the three-phase induction motor, corresponds to a four-terminal network; the electric power input being supplied to the input or sending-end terminals while the output energy is in mechanical form. This point of view corresponds to that suggested by Mr. Kron[2] in 1930. The basic problem, therefore, is to represent the mechanically absorbed power by an equivalent electrical impedance element, and to incorporate in the network a suitable circuit which represents the electrical and magnetic features of the motor.

The generalized circuit equations must define the input voltage and current in terms of the electric equivalent output current and voltage for any type of circuit. Figure 2 indicates such a general circuit, which is defined by the use of the so-called generalized constants $\boldsymbol{A}$, $\boldsymbol{B}$, $\boldsymbol{C}$, and $\boldsymbol{D}$ in the form of the two generalized equations:

$$\boldsymbol{V}_1 = \boldsymbol{A}\boldsymbol{V}_r + \boldsymbol{B}\boldsymbol{I}_r \tag{1a}$$

$$\boldsymbol{I}_1 = \boldsymbol{C}\boldsymbol{V}_r + \boldsymbol{D}\boldsymbol{I}_r \tag{1b}$$

The four-terminal network may be a simple series circuit, a simple shunt im-

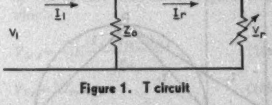

Figure 1. T circuit

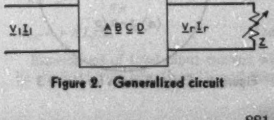

Figure 2. Generalized circuit

Paper 45-93, recommended by the AIEE committee on electric machinery for publication in AIEE TRANSACTIONS. Manuscript submitted August 5, 1944; made available for printing March 12, 1945.

J. G. TARBOUX is professor of electrical engineering, the University of Tennessee, Knoxville, Tenn.

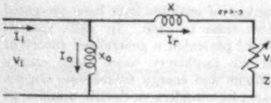

Figure 3. Cantilever circuit

pedance, a T circuit as used for transformers and three-phase (per phase) induction motors, or any other combination of resistances, inductances, and capacitances. Each particular type of network has its own particular constants, $\mathbf{A}$, $\mathbf{B}$, $\mathbf{C}$, and $\mathbf{D}$. These may be obtained directly from basic circuit analyses applied to the particular circuit involved. Example solutions are available in a good many textbooks on network theory including the author's.[3]

Simple Circuit Circle Diagram

As an example consider the simple circuit of Figure 3, composed of an inductive reactance X_o in parallel with a series element of inductive reactance X and variable load impedance $\mathbf{Z}$. The total current of such a circuit is

$$\mathbf{I}_1=\mathbf{I}_o+\frac{\mathbf{V}_1}{\mathbf{Z}+jX} \tag{2}$$

Three cases are considered, namely,

(*a*). Resistance load, $\mathbf{Z}=R\underline{/0}$.

(*b*). Resistance and inductance load of constant power factor, $\mathbf{Z}=R\underline{/\phi}$, $\phi=$constant.

(*c*). Resistance and capacity load of constant power factor, $\mathbf{Z}=R\overline{/\phi}$, $\phi=$constant.

Case a. Resistance Load. Equation 1 becomes

$$\mathbf{I}_1=\mathbf{I}_0+\frac{\mathbf{V}_1}{R+jX} \tag{3}$$

For $R=0$ (load short-circuited) the load current is equal to $\mathbf{V}_1/jX$. This current will lag the voltage vector $\mathbf{V}_1$ by 90 degrees, as indicated by the length BC of Figure 4a. The total current input to the circuit of Figure 3 is given as AC of Figure 4a. As the load takes on positive values of resistance, the load-current vector will follow a circle locus CDB,[2] the load current being zero for $R=$infinity (open circuit) at point B. For negative resistances the load-current vector will follow the lower half of the circle locus, the point B corresponding to positive or negative infinite resistance. The total current is equal to the vector sum of the shunt current $\mathbf{I}_o$ and load current $\mathbf{I}_r$ as given by the vector $\mathbf{AD}$ in Figure 4a.

Case b. Resistance and Inductance Load. Equation 2 is modified to the following:

$$\mathbf{I}_1=\mathbf{I}_0+\frac{\mathbf{V}_1}{Z\underline{/\phi}+jX}=\mathbf{I}_0+\frac{\mathbf{V}_1\overline{/\phi}}{(Z+X\sin\phi)+jX\cos\phi} \tag{4}$$

The results of this expression are indicated by Figure 4b in which the circle diameter is equal to $(\mathbf{V}_1\overline{/\phi})\div(jX\cos\phi)$. It will be noticed that the distance $BC=\mathbf{V}_1/jX$. As before the load-current vector follows a circle locus, a particular point being shown at D, the total circuit input current being equal to AD.

Case c. Resistance and Capacity Load. Equation 2 now is modified to the form,

$$\mathbf{I}_1=\mathbf{I}_0+\frac{\mathbf{V}_1}{Z\overline{/\phi}+jX}=\mathbf{I}_0+\frac{\mathbf{V}_1\underline{/\phi}}{(Z-X\sin\phi)+jX\cos\phi} \tag{5}$$

The graphical representation of this case is similar to that under "Open-Circuit Current" and is shown in Figure 4c.

The results of Figures 4a, b, and c will be found to be similar to Figures 3b, 3c, and 3d presented by Mr. Kron,[2] except that his diagrams represent energy distribution instead of currents.

The results of equations 2, 3, 4, and 5 could have been obtained directly from the generalized equations 1, as will be demonstrated.

Development of Generalized Circle Diagram Equations[5]

Dividing equation 1b by 1a and considering that $\mathbf{V}_r=\mathbf{I}_r\mathbf{Z}$ gives:

$$\mathbf{I}_1=\mathbf{V}_1\left(\frac{\mathbf{CZ}+\mathbf{D}}{\mathbf{AZ}+\mathbf{B}}\right) \tag{6}$$

It also can be shown[4] that $\mathbf{AD}-\mathbf{BC}=1$, for linear bilateral networks. Multiplying numerator and denominator of equation 6 by $\mathbf{A}$, and substituting $\mathbf{AD}=\mathbf{BC}+1$, and rearranging the result yields

$$\mathbf{I}_1=\frac{\mathbf{C}}{\mathbf{A}}\mathbf{V}_1+\frac{\dfrac{\mathbf{V}_1}{\mathbf{A}^2}}{\dfrac{\mathbf{B}}{\mathbf{A}}+\mathbf{Z}} \tag{7}$$

To illustrate the application of equation 7 it now will be applied to the circuit of Figure 3. The generalized constants for this particular circuit are easily found to be

$$\mathbf{A}=1,\ \mathbf{B}=jX,\ \mathbf{C}=\frac{1}{jX_o},\quad \mathbf{D}=1+\frac{X}{X_o}$$

Therefore, when these results are substituted into equation 7 it is found that

$$\mathbf{I}_1=\frac{\mathbf{V}_1}{jX_o}+\frac{\mathbf{V}_1}{\mathbf{Z}+jX}$$

which is seen to be the same as equation 2, as $\mathbf{I}_o=\dfrac{\mathbf{V}_1}{jX_o}$.

In the general equation 7, let $\mathbf{Z}=R\underline{/\phi}$, as was done in equation 4, then

$$\mathbf{I}_1=\frac{\mathbf{V}_1}{\mathbf{Z}_{so}}+\frac{\mathbf{V}_e}{(R+r)+jx} \tag{8}$$

in which

$$\mathbf{Z}_{so}=\frac{\mathbf{A}}{\mathbf{C}};\quad \mathbf{V}_e=\frac{\mathbf{V}_1}{\mathbf{A}^2}\overline{/\phi}\ \text{and}\ \ \frac{\mathbf{B}}{\mathbf{A}}\overline{/\phi}=r+jx$$

The first term of equation 8 is recognizable as the network current with the load impedance $R=$infinity. This current is shown as the length OA of Figure 5.

The most important deduction which can be obtained from equation 8 and referred to in the example of Figures 3 and 4 (proof of which has been indicated[4]) is that the fraction

$$\mathbf{I}_{ee}=\frac{\mathbf{V}_e}{(R+r)+jx}$$

represents a family of vector currents, so long as $\mathbf{V}_e$ and x are constant while $R+r$ or merely R take on all possible values from minus infinity to positive infinity.

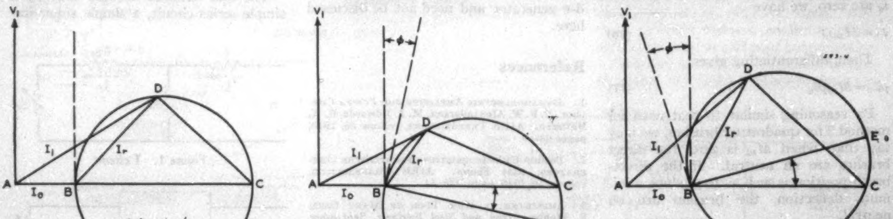

Figure 4. Circle diagrams for Figure 3

This result is indicated in Figure 5, the diameter of the circle being shown by the line AB. The total input current I_1 is represented by the vector $\mathbf{od}$, the point d being free to move along the circumference of the circle as the value of R, or load impedance is changed. Thus it follows that equations 7 or 8 may be referred to as one form of generalized circle-diagram equation.

The point B for $R+r=0$ cannot be realized, unless R is made negative. For $R=0$ the operating point would fall somewhere on the upper part of the circumference such as at E. The total current vector $\mathbf{OE}$ corresponding to a value of $R=0$, is obviously the total current with the receiver terminals short-circuited.

Another form of circle-diagram equation may be obtained from equation 6 by dividing numerator and denominator of that expression by $\mathbf{Z}$ and utilizing the following identities:

$$\mathbf{Y}=\frac{1}{\mathbf{Z}} \text{ and } \mathbf{BC}=\mathbf{AD}-1$$

thus giving the result,

$$\mathbf{I}_1=\frac{\mathbf{D}}{\mathbf{B}}\mathbf{V}_1-\frac{\frac{\mathbf{V}_1}{\mathbf{B}^2}}{\frac{\mathbf{A}}{\mathbf{B}}+\mathbf{Y}} \qquad (9)$$

which may be simplified to

$$\mathbf{I}_1=\frac{\mathbf{V}_1}{\mathbf{Z}_{sc}}+\frac{\mathbf{K}_e}{(G+g)+jb} \qquad (10)$$

where

$$\mathbf{Y}=\frac{1}{\mathbf{Z}}=Y/\underline{\phi};\ \mathbf{Z}_{sc}=\frac{\mathbf{B}}{\mathbf{D}};$$

$$\mathbf{K}_e=-\frac{\mathbf{V}_1/\underline{\phi}}{\mathbf{B}^2};\ \text{and } \frac{\mathbf{A}}{\mathbf{B}}/\underline{\phi}=G+g$$

The first term $\mathbf{I}_{1B}=\mathbf{V}_1/\mathbf{Z}_{sc}$ corresponds to the value of equation 10 for $G=$ infinity or $R=0$ of equation 8, since $G=1/R$. Thus this first term represents the input current for a short-circuited load and must be represented by the vector $\mathbf{OE}$ of Figure 5. The second term of equation 10, namely,

$$\mathbf{I}_{eB}=\frac{\mathbf{K}_e}{(G+g)+jb}$$

represents a family of vector currents, so long as $\mathbf{K}_e$ and b are constant while $G+g$ or merely G take on all possible values from minus infinity to positive infinity. This result also is shown in Figure 5, the circle diameter being shown as EF.

Thus, equations 7 and 9 may be defined correctly as the circle-diagram equations of a four-terminal network when loaded with a variable impedance $\mathbf{Z}=R/\underline{\phi}$ of constant power factor. The difference in the two expressions is found in the nature of the first terms of each equation, namely,

$$\mathbf{I}_{1s}=\frac{\mathbf{C}}{\mathbf{A}}\mathbf{V}_1=\frac{\mathbf{V}_1}{\mathbf{Z}_{so}}=\text{input current with open-circuited load}$$

and

$$\mathbf{I}_{1B}=\frac{\mathbf{D}}{\mathbf{B}}\mathbf{V}_1=\frac{\mathbf{V}_1}{\mathbf{Z}_{sc}}=\text{input current with short-circuited load}$$

Though equation 7 and 9 are referred to as the generalized circle diagrams, actual applications must be made from the modified forms of equations 8 and 10.

The application of these generalized circle-diagram equations to the solution of motors, normally would be carried out in the following order:

(*a*). First, an equivalent circuit is obtained from an analysis of the particular problem. With the three-phase induction as an example, this would mean that the standard T circuit first must be evolved.

(*b*). The second step would call for the determination of the four generalized constants **A**, **B**, **C**, and **D**. This step is relatively simple for T or cantilever circuits of the type of Figures 1 and 3.

(*c*). The last step involves merely a proper substitution of these constants in the general forms of equations 7 and 9, modified to the forms of equations 8 and 10.

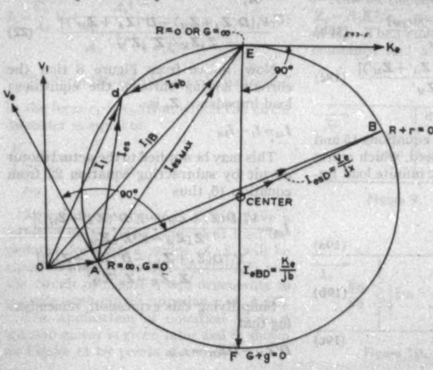

Figure 5. Circle diagram of four-terminal network

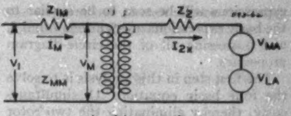

A—Main winding

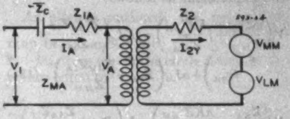

B—Auxiliary winding

Figure 6. Schematic circuit diagram of capacitor motor

In more complicated cases it might be more desirable to convert the basic laws of the motor into the forms of equations 7 and 9 without attempting to establish an equivalent circuit. This is the method of approach which is followed in this paper.

The Capacitor Motor

INPUT CURRENTS

The capacitor motor offers a more complicated problem because of the lack of a relatively simple equivalent circuit, such as the T circuit of the three-phase induction motor. The analyses which follow, therefore, will not begin with an equivalent circuit, but rather with the fundamental cross-field expressions as developed by Puckstein and Lloyd,[6,7] which according to the notation adopted in this paper are as follows:

$$\mathbf{V}_1=\mathbf{Z}_{MM}(\mathbf{I}_M-\mathbf{I}_{2xe})+\mathbf{I}_M\mathbf{Z}_{1M} \qquad (11a)$$

$$\mathbf{V}_1=\mathbf{Z}_{MA}(\mathbf{I}_A-\mathbf{I}_{2ye})+\mathbf{I}_A(\mathbf{Z}_{1A}+\mathbf{Z}_c) \qquad (11b)$$

$$\mathbf{Z}_{MM}(\mathbf{I}_M-\mathbf{I}_{2xe})+\frac{K}{a}[j\mathbf{Z}_{MA}(\mathbf{I}_A-\mathbf{I}_{2ye})+\mathbf{I}_{2ye}X_{2A}]-\mathbf{I}_{2xe}\mathbf{Z}_{2M}=0 \qquad (11c)$$

$$\mathbf{Z}_{MA}(\mathbf{I}_A-\mathbf{I}_{2ye})-aK[j\mathbf{Z}_{MM}(\mathbf{I}_M-\mathbf{I}_{2xe})+\mathbf{I}_{2xe}X_{2M}]-\mathbf{I}_{2ye}\mathbf{Z}_{2A}=0 \qquad (11d)$$

These equations refer to a double coupled circuit with the additional effect of two sets of speed voltages as illustrated by the circuit diagram of Figure 6, in which

$$\mathbf{V}_{MA}=-jK\frac{(\mathbf{I}_A-\mathbf{I}_{2ye})\mathbf{Z}_{MA}}{n_A} \qquad (12a)$$

$$\mathbf{V}_{LA}=K\mathbf{I}_{2y}X_2 \qquad (12b)$$

$$\mathbf{V}_{MM}=jK\frac{(\mathbf{I}_M-\mathbf{I}_{2xe})\mathbf{Z}_{MM}}{n_M} \qquad (12c)$$

$$\mathbf{V}_{LM}=-K\mathbf{I}_{2x}X_2 \qquad (12d)$$

Expressions of total input current will be obtained from equations 11, and these expressions will be seen to be similar to the basic expressions of equations 7 and 9, and possessing all of the circle-diagram properties.

The first step in this analysis is to solve the four basic equations 11 simultaneously, thereby eliminating the two rotor currents I_{2xe} and I_{2ye}. This will lead to two expressions as follows:

$$V_1\left(\frac{a\mathbf{Z}_{SM}}{\mathbf{Z}_{MM}}+j\frac{K\mathbf{Z}'_{SA}}{\mathbf{Z}_{MA}}\right)=jK\mathbf{I}_A\left(\frac{\mathbf{Z}'_{SA}\mathbf{Z}_{1T}}{\mathbf{Z}_{MA}}+jx_{2A}\right)+a\mathbf{I}_M\left(\mathbf{Z}_{2M}+\frac{\mathbf{Z}_{SM}\mathbf{Z}_{1M}}{\mathbf{Z}_{MM}}\right) \quad (13a)$$

$$V_1\left(\frac{\mathbf{Z}_{SA}}{\mathbf{Z}_{MA}}-j\frac{aK\mathbf{Z}'_{SM}}{\mathbf{Z}_{MM}}\right)=\mathbf{I}_A\left(\mathbf{Z}_{2A}+\frac{\mathbf{Z}_{SA}\mathbf{Z}_{1T}}{\mathbf{Z}_{MA}}\right)-jaK\mathbf{I}_M\left(\frac{\mathbf{Z}'_{SM}\mathbf{Z}_{1M}}{\mathbf{Z}_{MM}}+jx_{2M}\right) \quad (13b)$$

In the foregoing expressions as well as in later developments, it was found convenient to introduce a certain number of abbreviating terms. These are defined elsewhere in this paper under the title, "Symbols and Notation."

With the necessary substitutions, the two voltage equations 13 become

$$V_1(a\mathbf{D}+jK\mathbf{D}')=jK\mathbf{I}_A\mathbf{Z}'_A+a\mathbf{I}_M\mathbf{Z}_M \quad (14a)$$

$$V_1(\mathbf{D}-jaK\mathbf{D}')=\mathbf{I}_A\mathbf{Z}_A-jaK\mathbf{I}_M\mathbf{Z}'_M \quad (14b)$$

Solving these two equations for $\mathbf{I}_M$ and $\mathbf{I}_A$ leads to the following:

$$\mathbf{I}_M=\frac{V'[(\mathbf{D}\mathbf{Z}_A-K^2\mathbf{D}'\mathbf{Z}'_A)+jaKr_{2M}]}{\mathbf{Z}_A\mathbf{Z}_M-K^2\mathbf{Z}'_A\mathbf{Z}'_M} \quad (15a)$$

$$\mathbf{I}_A=\frac{V_1[(\mathbf{D}\mathbf{Z}_M-K^2\mathbf{D}'\mathbf{Z}'_M)-jaKr_{2M}]}{\mathbf{Z}_A\mathbf{Z}_M-K^2\mathbf{Z}'_A\mathbf{Z}'_M} \quad (15b)$$

The total current obviously is equal to the sum of $\mathbf{I}_M$ and $\mathbf{I}_A$, thus

$$\mathbf{I}_1=\frac{V_1[\mathbf{D}(\mathbf{Z}_A+\mathbf{Z}_M)-K^2\mathbf{D}'(\mathbf{Z}'_A+\mathbf{Z}'_M)]}{\mathbf{Z}_A\mathbf{Z}_M-K^2\mathbf{Z}'_A\mathbf{Z}'_M} \quad (16)$$

BLOCKED-ROTOR CURRENTS OF CAPACITOR MOTOR

A special case of interest is that of blocked rotor. The individual winding currents and the total current can be found by putting

$K=N/N_S=0$

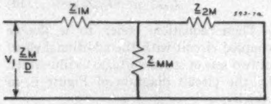

A—Main winding

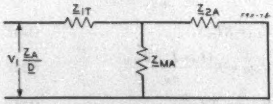

B—Auxiliary winding

Figure 7. Circuits for equations 17a and 17b

and utilizing the identities listed under "Symbols and Notation."

Thus equations 15 and 16 become

$$\mathbf{I}_{MB}=\frac{V_1\mathbf{D}}{\mathbf{Z}_M}=\frac{V_1}{\mathbf{Z}_{1M}+\dfrac{\mathbf{Z}_{2M}\mathbf{Z}_{MM}}{\mathbf{Z}_{SM}}} \quad (17a)$$

$$\mathbf{I}_{AB}=\frac{V_1\mathbf{D}}{\mathbf{Z}_A}=\frac{V_1}{\mathbf{Z}_{1T}+\dfrac{\mathbf{Z}_{2A}\mathbf{Z}_{MA}}{\mathbf{Z}_{SA}}} \quad (17b)$$

$$\mathbf{I}_{1B}=\frac{V_1\mathbf{D}(\mathbf{Z}_A+\mathbf{Z}_M)}{\mathbf{Z}_A\mathbf{Z}_M}=\frac{V_1\mathbf{D}}{\mathbf{Z}_1} \quad (17c)$$

where

$\mathbf{Z}_1=\dfrac{\mathbf{Z}_A\mathbf{Z}_M}{\mathbf{Z}_A+\mathbf{Z}_M}=$ the equivalent impedance of $\mathbf{Z}_A$ and $\mathbf{Z}_M$ in parallel.

The impedance terms

$$\frac{\mathbf{Z}_M}{\mathbf{D}}=\mathbf{Z}_{1M}+\frac{\mathbf{Z}_{2M}\mathbf{Z}_{MM}}{\mathbf{Z}_{SM}} \text{ and } \frac{\mathbf{Z}_A}{\mathbf{D}}=\mathbf{Z}_{1T}+\frac{\mathbf{Z}_{2A}\mathbf{Z}_{MA}}{\mathbf{Z}_{SA}}$$

are recognizable as the looking-in impedances of two T circuits as shown in Figure 7.

Equations 17a and 17b are quite valuable in that they indicate the nature of the motor circuit, at least during blocked condition. Each winding corresponds to a standard short-circuited coupled circuit or transformer, and these two composite circuits are connected in parallel.

CAPACITOR MOTOR CURRENTS AT SYNCHRONOUS SPEED

Let it first be emphasized that a capacitor motor cannot operate at synchronous speed unless it is driven mechanically by some suitable prime mover.

However, the current drawn by the motor under such conditions can be obtained by putting $K=N/N_s=1$ in equations 15 and 16, thus

$$\mathbf{I}_{MS}=\frac{V_1[(\mathbf{D}\mathbf{Z}_A-\mathbf{D}'\mathbf{Z}_A')+jar_{2M}]}{\mathbf{Z}_A\mathbf{Z}_M-\mathbf{Z}_A'\mathbf{Z}_M'} \quad (18a)$$

$$\mathbf{I}_{AS}=\frac{V_1[(\mathbf{D}\mathbf{Z}_M-\mathbf{D}'\mathbf{Z}_M')-jar_{2M}]}{\mathbf{Z}_A\mathbf{Z}_M-\mathbf{Z}_A'\mathbf{Z}_M'} \quad (18b)$$

$$\mathbf{I}_{1S}=\frac{V_1[\mathbf{D}(\mathbf{Z}_A+\mathbf{Z}_M)-\mathbf{D}'(\mathbf{Z}_A'+\mathbf{Z}_M')]}{\mathbf{Z}_A\mathbf{Z}_M-\mathbf{Z}_A'\mathbf{Z}_M'} \quad (18c)$$

OPEN-CIRCUIT CURRENTS

A third special case of equations 15 and 16 is that for infinite speed, which corresponds to the equivalent infinite load impedance.

Thus for $K=$ infinity

$$\mathbf{I}_{MO}=\frac{V_1\mathbf{D}'}{\mathbf{Z}_M'} \quad (19a)$$

$$\mathbf{I}_{AO}=\frac{V_1\mathbf{D}'}{\mathbf{Z}_A'} \quad (19b)$$

$$\mathbf{I}_{1O}=\frac{V_1\mathbf{D}'(\mathbf{Z}_A'+\mathbf{Z}_M')}{\mathbf{Z}_A'\mathbf{Z}_M'} \quad (19c)$$

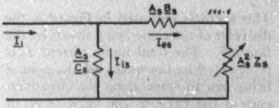

Figure 8. Equivalent circuit

CIRCLE DIAGRAM FROM SYNCHRONOUS-SPEED CURRENT, OR K=1

The general theory of the circle diagram of a three-phase induction motor was discussed in the first part of this paper. The circle diagram equation was shown to be

$$\mathbf{I}_1=\frac{\mathbf{C}_s}{\mathbf{A}_s}V_1+\frac{\dfrac{V_1}{\mathbf{A}_s^2}}{\dfrac{\mathbf{B}_s}{\mathbf{A}_s}+\mathbf{Z}_s} \quad (20)$$

in which $\mathbf{Z}_s$ represents the equivalent circuit load resistance which replaces the mechanical output of the motor.

The subscript s is used in this equation in order to distinguish the present constants from similar values used later.

Rearranging equation 20 gives

$$\mathbf{I}_1=\frac{\mathbf{C}_s}{\mathbf{A}_s}V_1+\frac{V_1}{\mathbf{A}_s\mathbf{B}_s+\mathbf{A}_s^2\mathbf{Z}_s} \quad (21)$$

This form of the four-terminal network equation is valuable in that it indicates that the total input current is equal to the sum of two currents: a constant current and a variable current. Furthermore equation 21 suggests an equivalent circuit of two parallel branches having impedances

$$\frac{\mathbf{A}_s}{\mathbf{C}_s} \text{ and } (\mathbf{A}_s\mathbf{B}_s+\mathbf{A}_s^2\mathbf{Z}_s)$$

as illustrated by the circuit of Figure 8.

Let the constant current $\mathbf{I}_{1S}$ of Figure 8 and equation 21 represent the motor current at synchronous speed, namely equation 18c, thus

$$\mathbf{I}_{1S}=\frac{\mathbf{C}_s}{\mathbf{A}_s}V_1=\frac{V_1[\mathbf{D}(\mathbf{Z}_A+\mathbf{Z}_M)-\mathbf{D}'(\mathbf{Z}_A'+\mathbf{Z}_M')]}{\mathbf{Z}_A\mathbf{Z}_M-\mathbf{Z}'_A\mathbf{Z}'_M} \quad (22)$$

Now, notice from Figure 8 that the current flowing through the equivalent load impedance $\mathbf{Z}_s$ is

$$\mathbf{I}_{es}=\mathbf{I}_1-\mathbf{I}_{1S}$$

This may be applied to the actual motor circuit by subtracting equation 22 from equation 16, thus

$$\mathbf{I}_{es}=\frac{V_1[\mathbf{D}(\mathbf{Z}_A+\mathbf{Z}_M)-K^2\mathbf{D}'(\mathbf{Z}_A'+\mathbf{Z}_M')]}{\mathbf{Z}_A\mathbf{Z}_M-K^2\mathbf{Z}'_A\mathbf{Z}_M'}-\frac{V_1[\mathbf{D}(\mathbf{Z}_A+\mathbf{Z}_M)-\mathbf{D}'(\mathbf{Z}'_A+\mathbf{Z}_M')]}{\mathbf{Z}_A\mathbf{Z}_M-\mathbf{Z}_A'\mathbf{Z}_M'}$$

Simplifying this expression, remembering that

$$\mathbf{D}'\mathbf{Z}_M-\mathbf{D}\mathbf{Z}_M'=r_{2M}$$

and

$$D'\mathbf{Z}_A-D\mathbf{Z}_A'=a^2r_{2M}$$

we have

$$I_{es}=\cfrac{V_1}{\cfrac{(\mathbf{Z}_A\mathbf{Z}_M-\mathbf{Z}_A'\mathbf{Z}_M')\mathbf{Z}_A'\mathbf{Z}_M'}{(\mathbf{Z}_A\mathbf{Z}_A'+a^2\mathbf{Z}_M\mathbf{Z}_M')r_{2M}}+\cfrac{(\mathbf{Z}_A\mathbf{Z}_M-\mathbf{Z}_A'\mathbf{Z}_M')^2}{(\mathbf{Z}_A\mathbf{Z}_A'+a^2\mathbf{Z}_M\mathbf{Z}_M')r_{2M}(1-K^2)}} \tag{23}$$

Combining equations 22 and 23 we have a result of the form of equation 21 which also complies with the equivalent circuit of Figure 8, provided that

$$\frac{\mathbf{C}_s}{\mathbf{A}_s}=\frac{D(\mathbf{Z}_A+\mathbf{Z}_M)-D'(\mathbf{Z}_A'+\mathbf{Z}_M')}{\mathbf{Z}_A\mathbf{Z}_M-\mathbf{Z}_A'\mathbf{Z}_M'} \tag{24a}$$

$$\mathbf{A}_s\mathbf{B}_s=\frac{\mathbf{Z}_A'\mathbf{Z}_M'(\mathbf{Z}_A\mathbf{Z}_M-\mathbf{Z}_A'\mathbf{Z}_M')}{(\mathbf{Z}_A\mathbf{Z}_A'+a^2\mathbf{Z}_M\mathbf{Z}_M')r_{2M}} \tag{24b}$$

$$\mathbf{A}_s^2\mathbf{Z}_s=\frac{(\mathbf{Z}_A\mathbf{Z}_M-\mathbf{Z}_A'\mathbf{Z}_M')^2}{(\mathbf{Z}_A\mathbf{Z}_A'+a^2\mathbf{Z}_M\mathbf{Z}_M')r_{2M}-(1-K^2)} \tag{24c}$$

$$\mathbf{A}_s=\frac{\mathbf{Z}_A\mathbf{Z}_M-\mathbf{Z}_A'\mathbf{Z}_M'}{\mathbf{Z}_A\mathbf{Z}_A'+a^2\mathbf{Z}_M\mathbf{Z}_M'} \tag{24d}$$

$$\mathbf{Z}_s=\frac{\mathbf{Z}_A\mathbf{Z}_A'+a^2\mathbf{Z}_M\mathbf{Z}'_M}{(1-K^2)r_{2M}} \tag{24e}$$

From which:

$$\mathbf{B}_s=\frac{\mathbf{Z}_A'\mathbf{Z}_M'}{r_{2M}} \tag{24f}$$

$$\mathbf{C}_s=\frac{D(\mathbf{Z}_A+\mathbf{Z}_M)-D'(\mathbf{Z}_A'+\mathbf{Z}_M')}{\mathbf{Z}_A\mathbf{Z}_A'+a^2\mathbf{Z}_M\mathbf{Z}_M'} \tag{24g}$$

Now let

$$\mathbf{Z}_s=\frac{R_s}{1-K^2}\,\underline{/\phi_s}=\text{equivalent load impedance}$$

where

$$\frac{R_s}{1-K^2}=\text{absolute value of }\mathbf{Z}_s$$

Equations 22 and 23 can be combined into a form similar to equation 20, thus

$$I_1=\frac{\mathbf{C}_s}{\mathbf{A}_s}V_1+\cfrac{\cfrac{V_1}{\mathbf{A}_s^2}\,\underline{/\phi_s}}{\cfrac{\mathbf{B}_s}{\mathbf{A}_s}\,\underline{/\phi_s}+\cfrac{R}{1-K^2}} \tag{25}$$

The term $(\mathbf{B}_s\div\mathbf{A}_s)\underline{/\phi_s}$ may be expressed in the form r_s+jx_s, from which the circle diameter is equal to

$$\cfrac{\cfrac{V_1}{\mathbf{A}_s^2}\,\underline{/\phi_s}}{jx_s}$$

At synchronous speed, K will have a value of unity. The equivalent load impedance for such a value of K will be equal to infinity, as $\mathbf{Z}_s=R_s/(1-K^2)$ and the circuit of Figure 8 will degenerate to a single open-circuit impedance of $\mathbf{A}_s/\mathbf{C}_s$.

The application of equation 25 to a specific motor is given later and is shown in Figure 11 by points *A* and *B*.

Circle Diagram for Open-Circuit Current, or $K=\pm$Infinity

At infinite operating speed or $K=\pm$ infinity, the input current was found by equation 19c to be:

$$I_{10}=\frac{D'(\mathbf{Z}_A'+\mathbf{Z}_M')}{\mathbf{Z}_A'\mathbf{Z}_M'}V_1 \tag{26}$$

If this current is subtracted from the total motor current of equation 16, we obtain the following

$$I_{eo}=\cfrac{V_1}{-\cfrac{\mathbf{Z}_A\mathbf{Z}'_A\mathbf{Z}_M\mathbf{Z}'_M}{(\mathbf{Z}_A\mathbf{Z}'_A+a^2\mathbf{Z}_M\mathbf{Z}'_M)r_{2M}}+\cfrac{K^2(\mathbf{Z}'_A\mathbf{Z}'_M)^2}{(\mathbf{Z}_A\mathbf{Z}'_A+a^2\mathbf{Z}_M\mathbf{Z}'_M)r_{2M}}} \tag{27}$$

Putting $K=\pm$infinity in equation 27 will result in a value of zero for the current I_{eo}, thus suggesting an open-circuited load. The combination of equations 26 and 27 represents a cantilever circuit as shown in Figure 9.

The constants of this circuit are, from equations 26 and 27,

$$\frac{\mathbf{C}_o}{\mathbf{A}_o}=\frac{D'(\mathbf{Z}'_A+\mathbf{Z}'_M)}{\mathbf{Z}'_A\mathbf{Z}'_M} \tag{28a}$$

$$\mathbf{A}_o\mathbf{B}_o=-\frac{\mathbf{Z}_A\mathbf{Z}'_A\mathbf{Z}_M\mathbf{Z}'_M}{(\mathbf{Z}_A\mathbf{Z}'_A+a^2\mathbf{Z}_M\mathbf{Z}'_M)r_{2M}} \tag{28b}$$

$$\mathbf{A}^2_o\mathbf{Z}_o=\frac{K^2(\mathbf{Z}'_A\mathbf{Z}'_M)^2}{(\mathbf{Z}_A\mathbf{Z}'_A+a^2\mathbf{Z}_M\mathbf{Z}'_M)r_{2M}} \tag{28c}$$

$$\mathbf{A}_o=-\frac{\mathbf{Z}'_A\mathbf{Z}'_M}{\mathbf{Z}_A\mathbf{Z}'_A+a^2\mathbf{Z}_M\mathbf{Z}'_M} \tag{28d}$$

$$\mathbf{Z}_o=\frac{(\mathbf{Z}_A\mathbf{Z}'_A+a^2\mathbf{Z}_M\mathbf{Z}_M')K^2}{r_{2M}} \tag{28e}$$

$$\mathbf{B}_o=\frac{\mathbf{Z}_A\mathbf{Z}_M}{r_{2M}} \tag{28f}$$

$$\mathbf{C}_o=\frac{D(\mathbf{Z}'_A+\mathbf{Z}'_M)}{\mathbf{Z}_A\mathbf{Z}'_A+a^2\mathbf{Z}_M\mathbf{Z}'_M} \tag{28g}$$

$$\mathbf{D}_o=\frac{1+\mathbf{B}_o\mathbf{C}_o}{\mathbf{A}_o}=\frac{D(\mathbf{Z}_A+\mathbf{Z}_M)}{r_{2M}} \tag{28h}$$

Now let the equivalent load impedance $\mathbf{Z}_o=R_oK^2\underline{/\phi_o}$, where R_o=absolute value of $\mathbf{Z}_o$. Then equations 26 and 27 can be combined and arranged in the form of the generalized circle-diagram law (see equation 20) as follows:

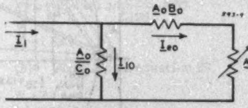

$\underline{A}_o\underline{B}_o$
893-9
$\underline{I}_1$
$\underline{I}_{eo}$
$\frac{\underline{A}_o}{\underline{C}_o}$
$\underline{I}_{10}$
$\underline{A}_o^2\underline{Z}_o$

Figure 9. Equivalent circuit

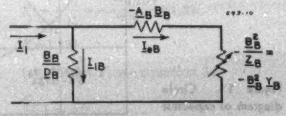

$-\underline{A}_B\underline{B}_B$
893-10
$\underline{I}_1$
$\underline{I}_{eB}$
$\frac{\underline{B}_B}{\underline{D}_B}$
$\underline{I}_{1B}$
$-\frac{\underline{B}_B^2}{\underline{Z}_B}=$
$-\underline{B}_B^2\underline{Y}_B$

Figure 10. Equivalent circuit

$$I_1=\frac{\mathbf{C}_o}{\mathbf{A}_o}V_1+\cfrac{\cfrac{V_1}{\mathbf{A}^2_o}\underline{/\phi_o}}{\cfrac{\mathbf{B}_o}{\mathbf{A}_o}\underline{/\phi_o}+R_oK^2} \tag{29}$$

As already outlined, the term $\frac{\mathbf{B}_o}{\mathbf{A}_o}\underline{/\phi_o}$ may be expanded into rectangular form r_o+jx_o, from which the circle diameter becomes equal to

$$\cfrac{\cfrac{V_1}{\mathbf{A}^2_o}\,\underline{/\phi_o}}{jx_o}$$

The application of equation 29 to a specific motor is outlined later and is shown by points *C* and *D* of Figure 11.

Circle Diagram From Blocked-Rotor Currents, or $K=0$

Equation 9 is another form of the circle diagram law for a four-terminal network, in which the first term represents the input current for short-circuit receiver or blocked-rotor condition of the motor. The entire equation represents a cantilever circuit as shown in Figure 10.

Equation 9 is of the form

$$I_1=\frac{\mathbf{D}_B}{\mathbf{B}_B}V_1+\cfrac{V_1}{-\mathbf{A}_B\mathbf{B}_B-\cfrac{\mathbf{B}^2_B}{\mathbf{Z}_B}} \tag{30}$$

or

$$I_1=I_{1B}+I_{eB} \tag{31a}$$

or

$$I_{eB}=I_1-I_{1B} \tag{31b}$$

We are now ready to apply equation 31 to the capacitor motor and determine whether or not a circle diagram is applicable.

The block-rotor motor current is given by equation 17c. This current should be subtracted from the total current of equation 16 as indicated by equation 31b, thus

$$I_{eB}=\cfrac{V_1}{\cfrac{\mathbf{Z}_A\mathbf{Z}'_A\mathbf{Z}_M\mathbf{Z}'_M}{(\mathbf{Z}_A\mathbf{Z}'_A+a^2\mathbf{Z}_M\mathbf{Z}'_M)r_{2M}}-\cfrac{(\mathbf{Z}_A\mathbf{Z}_M)^2}{K^2(\mathbf{Z}_A\mathbf{Z}'_A+a^2\mathbf{Z}_M\mathbf{Z}'_M)r_{2M}}} \tag{32}$$

It will be noticed that equation 32 has all of the properties of a circle diagram, as it is similar to the previous two circle-diagram equations. Comparing this result with the general form of equation 30, it is apparent that

$$\frac{\mathbf{D}_B}{\mathbf{B}_B}=\frac{D(\mathbf{Z}_A+\mathbf{Z}_M)}{\mathbf{Z}_A\mathbf{Z}_M} \tag{33a}$$

$$\mathbf{A}_B\mathbf{B}_B=\frac{\mathbf{Z}_A\mathbf{Z}'_A\mathbf{Z}_M\mathbf{Z}'_M}{(\mathbf{Z}_A\mathbf{Z}'_A+a^2\mathbf{Z}_M\mathbf{Z}'_M)r_{2M}} \tag{33b}$$

$$\frac{\mathbf{B}^2{}_B}{\mathbf{Z}_B}=\frac{(\mathbf{Z}_A\mathbf{Z}_M)^2}{K^2(\mathbf{Z}_A\mathbf{Z}'_A+a^2\mathbf{Z}_M\mathbf{Z}'_M)r_{2M}} \tag{33c}$$

$$\mathbf{Y}_B=\frac{1}{\mathbf{Z}_B}=\frac{r_{2M}}{K^2(\mathbf{Z}_A\mathbf{Z}'_A+a^2\mathbf{Z}_M\mathbf{Z}'_M)}=\frac{1}{\mathbf{Z}_o} \quad \text{(see equation 28e)} \tag{33d}$$

$$\mathbf{B}_B=\frac{\mathbf{Z}_A\mathbf{Z}_M}{r_{2M}}=\mathbf{B}_o \quad \text{(see equation 28f)} \tag{33e}$$

$$\mathbf{A}_B=-\frac{\mathbf{Z}'_A\mathbf{Z}'_M}{\mathbf{Z}_A\mathbf{Z}'_A+a^2\mathbf{Z}_M\mathbf{Z}'_M}=\mathbf{A}_o \quad \text{(see equation 28d)} \tag{33f}$$

$$\mathbf{D}_B=\frac{\mathbf{D}(\mathbf{Z}_A+\mathbf{Z}_M)}{r_{2M}}=\mathbf{D}_o \quad \text{(see equation 28b)} \tag{33g}$$

Now, let equation 30 be changed to the form

$$\mathbf{I}_1=\frac{\mathbf{D}_B}{\mathbf{B}_B}\mathbf{V}_1+\frac{\dfrac{\mathbf{V}_1}{\mathbf{B}^2{}_B}}{-\dfrac{\mathbf{A}_B}{\mathbf{B}_B}-\mathbf{Y}_B}$$

And finally, by putting

$$\mathbf{Y}_B=\frac{G_B}{K^2}\underline{/\phi_B}$$

$$\mathbf{I}_1=\frac{\mathbf{D}_B}{\mathbf{B}_B}\mathbf{V}_1+\frac{\dfrac{\mathbf{V}_1}{\mathbf{B}_B}\overline{/\phi_B}}{-\dfrac{\mathbf{A}_B}{\mathbf{B}_B}\overline{/\phi_B}-\dfrac{G_B}{K^2}} \tag{34}$$

Computations also have been carried out for the circle diagram as outlined above, and it is seen that all three methods give the same final diagram. This last method is illustrated by points *E* and *F* of Figure 11.

EXAMPLE SOLUTION OF CIRCLE DIAGRAM FOR A CAPACITOR MOTOR

The following data are taken from reference 7, page 390.

General Data. A four-pole one-fourth-horsepower 60-cycle 110-volt capacitor motor with core loss equal to 24 watts and friction and windage loss 13 watts is used.

Main Winding.

$\mathbf{Z}_{1M}=2.02+j2.79=3.45\ \underline{/54.1}$

$jX_{MM}=j66.8=66.8\ /90$ (core loss neglected)

Auxiliary Winding.

$\mathbf{Z}_{1A}=7.13+j3.22=7.83\ \underline{/24.35}$

$jX_{MA}=j92.9=92.9\ \underline{/90}$ (core loss neglected)

$\mathbf{Z}_c=9-j172$

$\mathbf{Z}_{1T}=\mathbf{Z}_{1A}+\mathbf{Z}_c=16.13-j168.78=169.\ \overline{/84.5}$

$a=\dfrac{n_A}{n_M}=1.18,\ a^2=1.39$

The core loss of 24 watts is taken into account by estimating the resistive element of the magnetizing impedances. It was shown by Puchstein and Lloyd that the main-winding magnetizing current is 1.51 amperes. If it is assumed that the core loss is divided equally between the two windings, the exciting resistance may be estimated as

$$R_{MM}=\frac{12}{1.5^2}=5.3 \text{ ohms}$$

The corresponding resistance in the auxiliary winding is

$R_{MA}=1.39\times 5.3=7.47$

Finally

$\mathbf{Z}_{MM}=5.3+j66.8=67.1\underline{/85}$

$\mathbf{Z}_{MA}=7.47+j93=93.5\underline{/85}$

Rotor Circuit.

$\mathbf{Z}_{2M}=4.12+j2.12=4.62\underline{/27.25}$

$\mathbf{Z}_{2A}=5.74+j2.95=6.43\underline{/27.25}$

The solution follows the definitions as outlined under "Symbols and Notation," the results of which are substituted in equations 24, 28, and 33.

$$\mathbf{Z}_{SM}=\mathbf{Z}_{MM}+\mathbf{Z}_{2M}=5.3+j66.8+4.12+j2.12 =9.42+j68.92=69.7\underline{/82}$$

$$\mathbf{Z}_{SM}'=\mathbf{Z}_{MM}+jx_{2M}=5.3+j66.8+j2.12 =5.3+j68.92=69.0\underline{/85.5}$$

$$\mathbf{Z}_{SA}=\mathbf{Z}_{MA}+\mathbf{Z}_{2A}=7.47+j93+5.74+j2.95 =13.21+j95.95=97\underline{/82}$$

$$\mathbf{Z}'_{SA}=\mathbf{Z}_{MA}+jx_{2A}=7.47+j93+j2.95 =7.47+j95.95=96.0\underline{/85.5}$$

$$\mathbf{D}=\frac{\mathbf{Z}_{SM}}{\mathbf{Z}_{MM}}=\frac{\mathbf{Z}_{SA}}{\mathbf{Z}_{MA}}=\frac{69.7\underline{/82}}{67.1\underline{/85}}=\frac{97\underline{/82}}{93.5\underline{/85}} =1.04\overline{/3}$$

$$\mathbf{D}'=\frac{\mathbf{Z}_{SM}'}{\mathbf{Z}_{MM}}=\frac{\mathbf{Z}_{SA}'}{\mathbf{Z}_{MA}}=\frac{69.0\underline{/85.5}}{67.1\underline{/85}}=\frac{96.0\underline{/85.5}}{93.5\underline{/85}} =1.03\underline{/0.5}$$

$$\mathbf{Z}_M=\mathbf{D}\mathbf{Z}_{1M}+\mathbf{Z}_{2M}=1.04\overline{/3}\times 3.45\overline{/54.1}+ 4.12+j21.12$$

$$\mathbf{Z}_M=6.38+j4.88=8.04\underline{/37.5}$$

$$\mathbf{Z}_M'=\mathbf{D}'\mathbf{Z}_{1M}+jx_{2M}=1.03\underline{/0.5}\times 3.45\underline{/54.1}+j2.12$$

$$\mathbf{Z}_M'=2.08+j4.99=5.4\underline{/66.5}$$

$$\mathbf{Z}_A=\mathbf{D}\mathbf{Z}_{1T}+\mathbf{Z}_{2A}=1.04\overline{/3}\times 169\overline{/84.5}+ 5.74+j2.95$$

$$\mathbf{Z}_A=11.83-j172.05=172.1\overline{/86.1}$$

$$\mathbf{Z}_A'=\mathbf{D}'\mathbf{Z}_{1T}+jx_{2A}=1.03\underline{/0.5}\times 169\overline{/84.5}+ j2.95$$

$$\mathbf{Z}_A'=16.7-j170.75=171\overline{/84.4}$$

Additional terms required are as follows:

$$\mathbf{Z}_A\mathbf{Z}_A'=172.1\overline{/86.1}\times 171\overline{/84.4} =29{,}400\overline{/170.5}=-29{,}000-j4{,}850$$

$$a^2\mathbf{Z}_M\mathbf{Z}_M'=1.39\times 8.04\underline{/37.5}\times 5.4\underline{/66.5} =60.3\underline{/104}=-14.45+j58.5$$

$$\mathbf{Z}_A\mathbf{Z}_A'+a^2\mathbf{Z}_M\mathbf{Z}'_M=-29{,}014-j4{,}792 =29{,}200\overline{/170.5}$$

$$\mathbf{Z}_A\mathbf{Z}_M=172.1\overline{/86.1}\times 8.04\underline{/37.5} =1{,}380\overline{/48.5}=915-j1{,}032$$

$$\mathbf{Z}_A'\mathbf{Z}_M'=171\overline{/84.4}\times 5.4\underline{/66.5}=923\overline{/17.9} =876-j285$$

$$\mathbf{Z}_A+\mathbf{Z}_M=11.83-j172.05+6.38+j4.88= 18.21-j167.17=168\overline{/83.7}$$

$$\mathbf{Z}_A'+\mathbf{Z}_M'=16.7-j170.75+2.08+j4.99 =18.78-j165.76=167\overline{/83.5}$$

$$\mathbf{D}(\mathbf{Z}_A+\mathbf{Z}_M)=1.04\overline{/3}\times 168\overline{/83.7} =174\overline{/86.7}=8.96-j173.5$$

$$\mathbf{D}'(\mathbf{Z}_A'+\mathbf{Z}_M')=1.03\underline{/0.5}\times 167\overline{/83.5} =172\overline{/83}=19.2-j171.8$$

$$\mathbf{D}(\mathbf{Z}_A+\mathbf{Z}_M)-\mathbf{D}'(\mathbf{Z}_A'+\mathbf{Z}_M')=-10.24- j1.7=10.3\overline{/169}$$

$$\mathbf{Z}_A\mathbf{Z}_M-\mathbf{Z}_A'\mathbf{Z}_M'=915-j1{,}032-876+j285 =39-j747=747\overline{/87}$$

With the foregoing detail computations available we now may develop the specific circle diagrams as follows: taking $\mathbf{V}_1=110\underline{/90}$ as the reference vector.

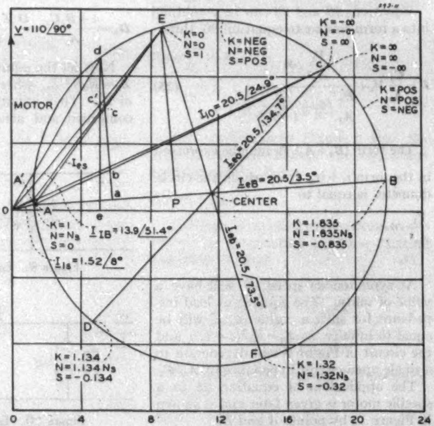

Figure 11. Circle diagram of capacitor motor

Synchronous-Speed $(K=1)$. The equivalent circuit is that of Figure 8 in which according to equations 24

$$\mathbf{A}_S=\frac{747\overline{/87}}{29{,}200\overline{/170.5}}=0.0256\underline{/83.5}$$

$$\mathbf{A}_S^2=0.000655\underline{/167}$$

$$\mathbf{B}_S=\frac{923\overline{/17.9}}{4.12}=224\overline{/17.9}$$

$$\mathbf{C}_S=\frac{10.3\overline{/169}}{29{,}200\overline{/170.5}}=0.000353\underline{/1.5}$$

$$\mathbf{Z}_S=\frac{29{,}200\overline{/170.5}}{4.12(1-K^2)}=\frac{7{,}080}{1-K^2}\overline{/170.5}$$

$$\frac{R_S}{1-K^2}=\frac{7{,}080}{1-K^2}$$

$$\mathbf{I}_{1S}=\frac{\mathbf{C}_S\mathbf{V}_1}{\mathbf{A}_S}=\frac{0.000353\underline{/1.5}\times110\underline{/90}}{0.0256\underline{/83.5}}=1.52\underline{/8}$$

$$\frac{\mathbf{V}_1\underline{/\phi_S}}{\mathbf{A}_S^2}=\frac{110\underline{/90}\,\underline{/170.5}}{0.000655\underline{/167}}=168{,}000\underline{/93.5}$$

$$\frac{\mathbf{B}_S\underline{/\phi_S}}{\mathbf{A}_S}=\frac{224\overline{/17.9}\,\underline{/170.5}}{0.0256\underline{/83.5}}=8{,}750\underline{/69.1}$$

$$=3{,}120+j8{,}200$$

$$\text{Diameter of circle}=\frac{168{,}000\underline{/93.5}}{8{,}200\underline{/90}}$$

$$=20.5\underline{/3.5}$$

From the value of I_{1S} and the diameter, it is possible to locate points A and B on the circle diagram of Figure 11.

Open-Circuit Current $(K=\pm\textit{Infinity})$. The equivalent circuit is that of Figure 9 in which according to equations 28

$$\mathbf{A}_o=-\frac{923\overline{/17.9}}{29{,}200\overline{/170.5}}=0.0316\overline{/27.4},$$

$$\mathbf{A}_o^2=0.001\overline{/54.8}$$

$$\mathbf{B}_o=\frac{1{,}380\overline{/48.5}}{4.12}=335\overline{/48.5}$$

$$\mathbf{C}_o=-\frac{172\overline{/83.5}}{29{,}200\overline{/170.5}}=0.00589\overline{/92.5}$$

$$\mathbf{Z}_o=\frac{29{,}200\overline{/170.5}K^2}{4.12}=7{,}080K^2\overline{/170.5}$$

$$R_oK^2=7{,}080K^2$$

$$\mathbf{I}_{1o}=\frac{\mathbf{C}_o\mathbf{V}_1}{\mathbf{A}_o}=\frac{0.00589\overline{/92.5}\times110\underline{/90}}{0.0316\overline{/27.4}}$$

$$=20.5\underline{/24.9}=18.6+j8.65$$

$$\frac{\mathbf{V}_1\underline{/\phi_o}}{\mathbf{A}_o^2}=\frac{110\underline{/90}\,\underline{/170.5}}{0.001\overline{/54.8}}=110{,}000\overline{/44.7}$$

$$\frac{\mathbf{B}_o}{\mathbf{A}_o}\underline{/\phi_o}=\frac{335\overline{/48.5}\,\underline{/170.5}}{0.0316\overline{/27.4}}=10{,}600\underline{/149.4}$$

$$=-9{,}150+j5{,}360$$

$$\text{Diameter of circle}=\frac{110{,}000\overline{/44.7}}{5{,}360\underline{/90}}$$

$$=20.5\overline{/134.7}$$

The values of I_{1o} and diameter previously given now are used to locate points C and D of Figure 11. The diameter as computed is seen to check with previous calculations.

Blocked Rotor Current $(K=0)$. The equivalent circuit is that of Figure 10. According to equations 33 the constants $\mathbf{A}_B$ and $\mathbf{B}_B$ are equal to the constants $\mathbf{A}_o$ and $\mathbf{B}_o$ of the case outlined under "Open-Circuit Current."
Thus

$$\mathbf{A}_B=\mathbf{A}_o=0.0316\overline{/27.4}$$

$$\mathbf{B}_B=\mathbf{B}_o=335\overline{/48.5},\ \mathbf{B}_B^2=112{,}000\overline{/97}$$

$$\mathbf{D}_B=\mathbf{D}_o=\frac{174\overline{/87.1}}{4.12}=42.2\overline{/87.1}$$

And

$$\mathbf{C}_B=\mathbf{C}_o=0.00589\overline{/92.5}$$

$$\mathbf{Z}_B=\mathbf{Z}_o=7{,}080K^2\overline{/170.5}$$

$$\mathbf{Y}_B=\frac{1}{7{,}080K^2}\underline{/170.5}=\frac{0.000141}{K^2}\times$$

$$\underline{/170.5},\ \phi_B=\underline{/170.5}$$

$$\frac{G_B}{K^2}=\frac{0.000141}{K^2}$$

$$\mathbf{I}_{1B}=\frac{\mathbf{D}_B\mathbf{V}_1}{\mathbf{B}_B}=\frac{42.2\overline{/87.1}\times110\underline{/90}}{335\overline{/48.5}}=13.9\underline{/51.4}$$

$$\frac{\mathbf{V}_1\overline{/\phi_B}}{\mathbf{B}_B^2}=\frac{110\underline{/90}\,\overline{/170.5}}{112{,}000\overline{/97}}=0.000981\underline{/16.5}$$

$$-\frac{\mathbf{A}_B\overline{/\phi_B}}{\mathbf{B}_B}=-\frac{0.0316\overline{/27.4}\,\overline{/170.5}}{335\overline{/48.5}}$$

$$=0.0000944\underline{/30.6}$$

$$=0.0000811+j0.000048$$

$$\text{Diameter of circle}=\frac{0.000981\underline{/16.5}}{0.000048\underline{/90}}$$

$$=20.5\overline{/73.5}$$

The values of I_{1B} and diameter just given now are used in locating points E and F of Figure 11.

Points B, D, and F of Figure 11 correspond to the following values of K:

(*a*). Point B, see equation 25.

$$\frac{R_S}{1-K^2}+r_s=0$$

or

$$K^2=1+\frac{R_s}{r_s}=1+\frac{7{,}080}{3{,}120}=3.37$$

$$K=1.835$$

(*b*). Point D, see equation 29.

$$R_oK^2+r_s=0$$

or

$$K^2=-\frac{r_s}{R_o}=-\frac{-9{,}150}{7{,}080}=1.29$$

$$K=1.134$$

(*c*). Point F, see equation 34.

$$\frac{G_B}{K^2}+g_B=0$$

Or

$$K^2=-\frac{G_B}{g_B}=-\frac{-0.000141}{0.0000811}=1.74$$

$$K=1.32$$

GENERAL SUMMARY OF CIRCLE DIAGRAM

It is worth while at this stage to examine the circle diagram of Figure 11. First, it will be noticed that Figure 11 is similar to the circle diagram of a three-phase induction motor and also to the circle diagram of a straight single-phase motor.

Point A corresponds to synchronous-speed operation. The unit can turn only at synchronous speed if driven mechanically. However, the stator magnetic field still must be supplied from the stator input current $\mathbf{I}_{1S}$.

Proceeding around the circle in a clockwise manner, the motor speed is seen to decrease, until blocked rotor is reached as indicated by point E, where $K=0$, or slip$=1$. Thus the motor region of the circle is limited to the arc AE.

From point E to point C, the rotor is indicated as operating in a direction reverse to that for straight motor action (arc AE). This action can take place only by the driving force of an external prime mover or a mechanical load which has become a prime mover. Since the stator still is drawing power from the a-c supply circuit, it appears that the motor now is acting as an energy-absorption device. At point C the speed is infinity in the reverse direction to normal motor action.

Returning to point A and proceeding counterclockwise around the circle, we notice that K becomes steadily greater than unity, indicating operation above synchronous speed, the rotor turning in the same direction as that for regular motor action. Infinite speed again is obtained at point C, approached in a counterclockwise fashion. This lower region of the circle corresponds to generator action.

Several other papers have been presented on some phase of the current loci for the capacitor motor. One such paper[8] is devoted to starting conditions only, whereas others[9,10] analyze the design effects produced by possible variations of capacitive reactance and turns ratio. The present paper presents an operating circle diagram for the capacitor motor and develops a general circle-diagram technique which can be applied to many cases. The general technique has been presented by Professor Karapetoff[11] for the case of a T circuit representing a three-phase induction motor. The author[5] has developed the same result by considering a generalized four-terminal network of which the T circuit is a special case.

Since any four-terminal network can be represented by an equivalent T circuit and since the circle diagram of Figure 11 possesses all of the general properties outlined by Professor Karapetoff,[11] it is reasonable to expect that the circle diagram of Figure 11 may be used as the basis for obtaining a rather complete set of operating data.

To obtain the operating characteristics from Figure 11[8,11] it is first necessary to draw a sufficiently large number of lines from the circle and perpendicular to the diameter *AB*, such as *ad* or *EP*. The motor section of Figure 11 is shown in more detail in Figure 12. The circle envelope of the vector $\boldsymbol{I_{es}}$ applies to a simple equivalent series circuit with applied voltage equal to $\boldsymbol{V_e}=(\boldsymbol{V_1}\div\boldsymbol{A_s}^2)\underline{/\phi_s}$ and impedance $(\boldsymbol{B_s}\div\boldsymbol{A_s})\underline{/\phi_s}+(R_s\div[1-K^2])$ (see equation 25) and illustrated by the circuit sketch of Figure 12. From equation 25 and the data previously worked out

$$I_{es}=\frac{168.\underline{/93.5}}{3.12+\dfrac{7.08}{1-K^2}+j8.2}$$

Power is absorbed by the two resistances of this circuit, namely, $R_1=3.12$ ohms and $R_{2e}=7.08\div(1-K^2)$ ohms, the total power being proportional to the inphase component of current as illustrated by the lines *ad*. For zero speed or $K=0$, the two resistances are $R_1=3.12$ ohms and $R_2=7.08$ ohms or a total of 10.2 ohms. Thus at $K=0$, the total absorbed power is proportional to the length $PE=10.05$ amperes.

The point *M* can be obtained in two ways. From previous analysis it was shown that line *AC* represents the value of I_{es} for $K=$ infinity, under which condition the resistance $R_{2e}=0$. The intersection of line *AC* and line *PE* (Figures 11 and 12) thus determines the point *M*. Point *M* also may be obtained by making the ratio EM/MP equal to the ratio 7.08/3.12. Thus it follows that $EM=6.95$ amperes, while $MP=3.07$ amperes.

For any operating point *d*, the circuit resistance can be expressed as $R_e+R_1+R_2$, where $R_1+R_2=3.12+7.08=10.2$ ohms, from which $R_e=7.08K^2\div(1-K^2)$ or $K^2=R_e\div(R_e+7.08)$. The power absorbed by these three resistances (R_e, R_1, and R_2) will be proportional to the lengths *cd*, *ab*, and *bc* of Figure 12, from which it follows that

$$K^2=\frac{cd}{bd}\text{ or }K=\sqrt{\frac{cd}{bd}} \tag{35}$$

From Figure 12 it is possible to obtain certain operating characteristics as follows:

Gross output $=V_1(cd)$ watts
Equivalent rotor copper loss $=V_1(bc)$ watts
Rotor input $=V_1(bd)$ watts
Stator input $=V_1(de)$ watts
(*de* is taken parallel to vector $\boldsymbol{V_1}$)
Ratio of operating to synchronous speed,

$$K=\sqrt{\frac{cd}{bd}}$$

Input current $=Od$ amperes

Power factor in per unit $=\dfrac{de}{Od}$.

The net power output and net efficiency may be approximated by introducing line $A'E$ (Figure 11) where A' represents the no-load operating current on the circle. The line $A'E$ may be drawn as a straight line without introducing appreciable error. Then from Figure 11

Net power output $=V_1(c'd)$ watts

Net efficiency in per unit $=\dfrac{c'd}{de}$

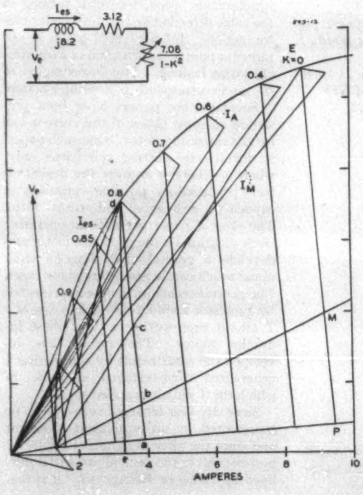

Figure 12. Motor circle diagram

To test the accuracy of this analysis, detailed calculations have been carried out for several items, followed by a check of the results against the circle diagram.

Stator currents I_M and I_A were obtained from equations 15. These results are indicated in Figure 12 and are seen to check with the circle envelope.

Other items which were calculated are: Rotor equivalent currents I_{2xe} and I_{2ye} by equations 11a and b.

Equivalent mutual impedance voltages $\boldsymbol{V_M}$ and $\boldsymbol{V_A}$ (back electromotive forces) as follows:

$$\boldsymbol{V_M}=\boldsymbol{V_1}-\boldsymbol{I_M}\boldsymbol{Z_{1M}}\text{ and }\boldsymbol{V_A}=\boldsymbol{V_1}-\boldsymbol{I_A}\boldsymbol{Z_{1T}}$$

Rotor input watts,

$$W_R=V_MI_{2xe}\cos(V_M,I_{2xe})+V_AI_{2ye}\cos(V_A,I_{2ye})$$

Torque in synchronous watts,

$$W_{ST}=aV_MI_{2ye}\sin(V_M,I_{2ye})+\frac{V_A}{a}I_{2xe}\sin(V_A,I_{2xe})$$

Torque in pound-feet,

$$T=7.04\frac{W_{ST}}{N_S}$$

Rotor copper losses,

$$I^2{}_{2xe}r_{2M}+I^2{}_{2ye}r_{2A}$$

All of these results were in agreement with similar data obtained from the circle diagram, with the exception of the torque For balanced polyphase motor the torque is proportional to the distance *bd*, but in the case at hand the two windings are considerably unbalanced with the result that no method has been found to indicate torque on the circle diagram.

Finally, the assumed values of *K* used in the detailed calculations were checked by equation 35. The resultant motor characteristics are shown in Figure 13. All were determined from the circle diagram of Figure 12 with the exception of torque, stator copper loss, and core loss.

Conclusion

The mathematical material of this paper may appear to be somewhat formidable. However, the circle diagram (Figures 11 and 12) can be obtained from a combination of test and computed data as follows:

(*a*). Point *A* corresponds practically to no-load operation.

(*b*). Point *E* can be obtained from a blocked rotor test.

(*c*). Point *C* must be computed according to equations 19. For general work it is possible to take $D'=1$, with the simplification of $\boldsymbol{Z_M}'=\boldsymbol{Z_{1M}}+jx_{2M}$ and $\boldsymbol{Z_A}'=\boldsymbol{Z_{1T}}+jx_{2A}$.

(*d*). Points *A*, *E*, and *C* are sufficient to determine the circle. Other details then are carried out as indicated in Figure 12.

In conclusion let it be stated that the incentive for this paper has been the de-

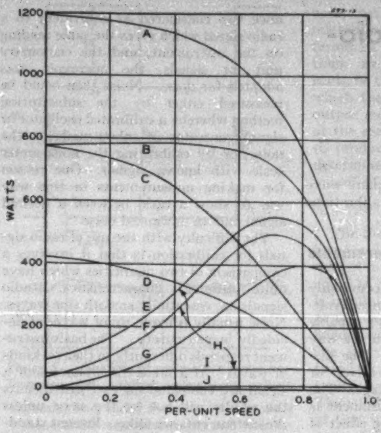

Figure 13. Operating characteristic

A—Total input
B—Power transferred to rotor
C—Rotor copper loss
D—Stator copper loss
E—Total
F—Main winding
G—Output
H—Torque power
I—Auxiliary winding
J—Core loss

sire to obtain a basic generalized circuit point of view which can be applied to the classroom. It is believed that this aim has been at least partially fulfilled. The author will be doubly gratified if this paper should in a small way also find some application to commercial design.

Symbols and Notation

All complex quantities such as vectors and impedances are indicated in boldface italic type such as $\boldsymbol{I}$ or $\boldsymbol{Z}$. Absolute values are indicated, I or Z, in lightface italic.

$\boldsymbol{V}_1$ = input voltage of four-terminal network

$\boldsymbol{V}_r$ = output voltage of four-terminal network

$\boldsymbol{V}_M = \boldsymbol{V}_1 - \boldsymbol{I}_M\boldsymbol{Z}_{1M} = \boldsymbol{Z}_{MM}(\boldsymbol{I}_M - \boldsymbol{I}_{2xe})$ = main-winding mutual voltage

$\boldsymbol{V}_A = \boldsymbol{V}_1 - \boldsymbol{I}_A\boldsymbol{Z}_{1T} = \boldsymbol{Z}_{MA}(\boldsymbol{I}_A - \boldsymbol{I}_{2ye})$ = main-winding mutual voltage

$\boldsymbol{W}_R$ = rotor input power in watts

W_{ST} = torque in synchronous watts

$\boldsymbol{I}_1$ = input current of four-terminal network

$\boldsymbol{I}_r$ = output current of four-terminal network

$\boldsymbol{A}, \boldsymbol{B}, \boldsymbol{C}, \boldsymbol{D}$ = four-terminal network generalized constants

$\boldsymbol{Z}$ = complex impedance

n_M = number of main-winding stator turns (assume rotor as having one turn)

n_A = number of auxiliary-winding stator turns (assume rotor as having one turn)

$\frac{n_A}{n_M} = a$, generally greater than one

$\boldsymbol{Z}_{1M}$ = leakage impedance of main stator winding

$\boldsymbol{Z}_{1A}$ = leakage impedance of auxiliary stator winding

$\boldsymbol{Z}_c$ = external impedance of auxiliary stator winding

$\boldsymbol{Z}_{MM}$ = mutual impedance of main stator winding

$\boldsymbol{Z}_{MA}$ = mutual impedance of auxiliary stator winding

$\boldsymbol{V}_1$ = applied stator voltage

$\boldsymbol{I}_M$ = total main-winding stator current

$\boldsymbol{I}_{\phi M}$ = exciting main-winding stator current

$\boldsymbol{I}_{2xe} = \boldsymbol{I}_M - \boldsymbol{I}_{\phi M}$ = rotor x-axis current referred to main winding

$\boldsymbol{I}_A$ = total auxiliary-winding stator current

$\boldsymbol{I}_{\phi A}$ = exciting auxiliary-winding stator current

$\boldsymbol{I}_{2Ye} = \boldsymbol{I}_A - \boldsymbol{I}_{\phi A}$ = rotor Y-axis current referred to auxiliary winding

$\boldsymbol{Z}_{2M}$ = rotor-circuit leakage impedance referred to main winding

X_{2M} = rotor-circuit leakage reactance referred to main winding $= x_2 n_M{}^2$

$\boldsymbol{Z}_{2A}$ = rotor-circuit leakage impedance referred to auxiliary winding

X_{2A} = rotor-circuit leakage reactance referred to auxiliary winding $= x_2 n_A{}^2$

$\boldsymbol{I}_{2x}$ = rotor current in x axis (main winding) $= -\boldsymbol{I}_{2xe} n_M$

$\boldsymbol{I}_{2Y}$ = rotor current in Y axis (auxiliary winding) $= -\boldsymbol{I}_{2Ye} n_A$

$\boldsymbol{Z}_2$ = rotor leakage reactance $= \frac{\boldsymbol{Z}_{2A}}{n_A{}^2} = \frac{\boldsymbol{Z}_{2M}}{n_M{}^2}$

X_2 = rotor leakage reactance in either axis $= \frac{x_{2M}}{n_M{}^2} = \frac{X_{2A}}{n_A{}^2}$

$\frac{\boldsymbol{Z}_{MM}}{n_M{}^2}$ = mutual impedance of main winding referred to rotor

$\frac{\boldsymbol{Z}_{MA}}{n_A{}^2}$ = mutual impedance of auxiliary winding referred to rotor

ϕ_M = main-winding magnetic flux

ϕ_A = auxiliary-winding magnetic flux

ϕ_{M1} = rotor, main-winding leakage flux

ϕ_{A1} = rotor, auxiliary-winding leakage flux

$\boldsymbol{V}_{MA}$ = main-winding rotor speed voltage due to flux ϕ_A

$\boldsymbol{V}_{LA}$ = main-winding rotor speed voltage due to leakage flux ϕ_{A1}

$\boldsymbol{V}_{MM}$ = auxiliary-winding rotor speed voltage due to flux ϕ_M

$\boldsymbol{V}_{LM}$ = auxiliary-winding rotor speed voltage due to leakage flux ϕ_{M1}

$K = \frac{N}{N_s}$ = ratio of actual rotor speed to synchronous speed

A few identities and certain other simplifications which are used in the paper are tabulated as follows:

$$\boldsymbol{Z}_{SM} = \boldsymbol{Z}_{MM} + \boldsymbol{Z}_{2M},\ \boldsymbol{Z}_{pM} = \boldsymbol{Z}_{MM} + \boldsymbol{Z}_{1M}$$

$$\boldsymbol{Z}_{SA} = \boldsymbol{Z}_{MA} + \boldsymbol{Z}_{2A},\ \boldsymbol{Z}_{pA} = \boldsymbol{Z}_{MA} + \boldsymbol{Z}_{1T}$$

$$\boldsymbol{Z}_{SM}' = \boldsymbol{Z}_{MM} + jx_{2M},\ = \boldsymbol{Z}_{SM} - r_{2M}$$

$$\boldsymbol{Z}_{SA}' = \boldsymbol{Z}_{MA} + jx_{2A} = \boldsymbol{Z}_{SA} - r_{2A}$$

$$\boldsymbol{Z}_{SA} = a^2\boldsymbol{Z}_{SM},\ \boldsymbol{Z}_{SA}' = a^2\boldsymbol{Z}_{SM}',\ \boldsymbol{Z}_{MA} = a^2\boldsymbol{Z}_{MM}$$

$$\boldsymbol{D} = \frac{\boldsymbol{Z}_{SM}}{\boldsymbol{Z}_{MM}} = \frac{\boldsymbol{Z}_{SA}}{\boldsymbol{Z}_{MA}},\ \boldsymbol{D}' = \frac{\boldsymbol{Z}_{SM}'}{\boldsymbol{Z}_{MM}} = \frac{\boldsymbol{Z}_{SA}'}{\boldsymbol{Z}_{MA}}$$

$$\boldsymbol{D}' = \boldsymbol{D} - \frac{r_{2M}}{\boldsymbol{Z}_{MM}} = \boldsymbol{D} - \frac{r_{2A}}{\boldsymbol{Z}_{MA}}$$

$$\boldsymbol{A}_M = \frac{\boldsymbol{Z}_{pM}}{\boldsymbol{Z}_{MM}},\quad \boldsymbol{A}_A = \frac{\boldsymbol{Z}_{pA}}{\boldsymbol{Z}_{MA}}$$

$$\boldsymbol{Z}_M = \frac{\boldsymbol{Z}_{SM}\boldsymbol{Z}_{1M}}{\boldsymbol{Z}_{MM}} + \boldsymbol{Z}_{2M} = \boldsymbol{D}\boldsymbol{Z}_{1M} + \boldsymbol{Z}_{2M}$$

$$\boldsymbol{Z}_A = \frac{\boldsymbol{Z}_{SA}\boldsymbol{Z}_{1T}}{\boldsymbol{Z}_{MA}} + \boldsymbol{Z}_{2A} = \boldsymbol{D}\boldsymbol{Z}_{1T} + \boldsymbol{Z}_{2A}$$

$$\boldsymbol{Z}_M' = \frac{\boldsymbol{Z}_{SM}'\boldsymbol{Z}_{1M}}{\boldsymbol{Z}_{MM}} + jx_{2M} = \boldsymbol{D}'\boldsymbol{Z}_{1M} + jx_{2M} = \boldsymbol{Z}_M - \boldsymbol{A}_M r_{2M}$$

$$\boldsymbol{Z}_A' = \frac{\boldsymbol{Z}_{SA}'\boldsymbol{Z}_{1T}}{\boldsymbol{Z}_{MA}} + jx_{2A} = \boldsymbol{D}'\boldsymbol{Z}_{1T} + jx_{2A} = \boldsymbol{Z}_A - \boldsymbol{A}_A r_{2A}$$

$$\boldsymbol{D}'\boldsymbol{Z}_M - \boldsymbol{D}\boldsymbol{Z}_M' = r_{2M},\ \boldsymbol{D}'\boldsymbol{Z}_A - \boldsymbol{D}\boldsymbol{Z}_A' = r_{2A} = a^2 r_{2M}$$

References

1. ALTERNATING CURRENT MACHINERY (book), A. F. Puchstein, T. C. Lloyd. John Wiley and Sons, Inc., New York, N. Y. Chapter 25.

2. GENERALIZED THEORY OF ELECTRIC MACHINERY, Gabriel Kron. AIEE TRANSACTIONS, volume 49, 1930, pages 666–85.

3. INTRODUCTION TO ELECTRIC POWER SYSTEMS (book), J. G. Tarboux. The International Textbook Company. Pages 93–4.

4. Reference 3. Pages 72–3, equation 126.

5. A-C MACHINERY (book), J. G. Tarboux. Volumes I and II (mimeograph).

6. THE CROSS-FIELD THEORY OF THE CAPACITOR MOTOR, A. F. Puchstein, T. C. Lloyd. AIEE TRANSACTIONS, volume 60, 1941, February section, pages 58–61, equations 1, 2, 3, and 4.

7. Reference 1 (second edition). Equations 483, 489, 496, and 501.

8. STARTING WINDINGS FOR SINGLE-PHASE INDUCTION MOTORS, C. G. Veinott. AIEE TRANSACTIONS, volume 63, 1944, June section, pages 288–94.

9. CURRENT LOCI FOR THE CAPACITOR MOTOR, Thomas C. McFarland. AIEE TRANSACTIONS, volume 61, 1942, March section, pages 152–6.

10. TURN RATIO OF THE CAPACITOR MOTOR, Thomas C. McFarland. AIEE TRANSACTIONS, volume 62, 1943, pages 802–8.

11. EXPERIMENTAL ELECTRICAL ENGINEERING (fourth edition), Karapetoff, Dennison. John Wiley and Sons, Inc., New York, N. Y. Volume II, chapter 48, pages 407–23.

A Study of Wave Shapes for Radio-Noise-Meter Calibrations

C. W. FRICK
ASSOCIATE AIEE

THIS PAPER presents the results of a theoretical and experimental study directed toward obtaining better agreement between measurements made with different radio-noise meters and proposes a modification of the present method of calibration. The need for work on this subject was pointed out in a paper[1] of which the writer was coauthor, presented before the Institute in 1943. Earlier papers[2-4] have described the development of the radio-noise meter and methods of calibration.

It is the practice at the present time to use radio-frequency sine waves for calibrations and to control within close limits certain instrument characteristics considered as essential.[5] It is presumed that instruments will be designed to come within these limits, but the problem of adequately demonstrating this by test has not been solved satisfactorily. Also, the checking of components or parts of the circuit which determine these essential characteristics does not preclude the possibility of errors due to other characteristics which are not essential but may be present and may vary among different instruments.

In the previous paper it was suggested that calibrating waves of representative shape and equivalent frequency might be standardized, as for instance square waves and sawtooth waves. It might then be specified that for a given magnitude of applied voltage of these waves the readings of instruments must not differ by more than a stated amount. Difficulties previously encountered in producing waves suitable for this purpose which can be reproduced and which remain fixed were overcome in this investigation.

Practical means were found for utilizing a simple type of wave such as the square wave for calibration purposes. This makes it unnecessary to produce pulsed radio-frequency or other waves sometimes used which require complicated apparatus. The simple square wave is known to produce audible effects similar to continuous noise as produced by commutator motors, gas-discharge devices, and so forth. The square wave is analyzed and utilized for calibrations in tests described in this paper.

Basis of Radio-Noise Measurements

The term *radio noise* as commonly used[5] refers to electric disturbances (voltage, current, or field intensity) capable of exciting a radio receiver in such a way as to produce acoustic noise. The disturbance as applied to a receiver or measuring instrument is a voltage. The function of the measuring instrument is to evaluate the noise-producing effect of the disturbance. A curve of the instantaneous voltage, the voltage wave, would not be sufficient, because the noise value depends also on certain apparatus characteristics which are essential to the reception of radio signals and certain characteristics associated with the conversion of the signals to sound and the effect on the ear. For waves of definite shape and frequency the noise effect is proportional to voltage. For different waves the noise effect depends upon shape and frequency as well as voltage. It would appear that the measuring instrument should be a voltmeter associated with a network which, in the case of continuous noise, gives a reading proportional to the noise effect. As a practical approach to this objective a basic instrument has been set up which includes the elements of a representative radio receiver and a particular arrangement of detector circuit and a voltmeter.

It is necessary to calibrate the basic instrument in definite units so that different measurements can be compared. Two disturbance voltages are considered as equal radio noises if they produce equal indications on the instrument. If a disturbance of known noise value had been available in the beginning it could have been used as a standard for calibrating the instrument. Since there was no noise of known value, attention was directed to radio signals as a possible means of establishing a calibration of the instrument. For calibration purposes a noise disturbance was considered as equivalent to a radio signal which gives the same reading on the instrument, and the customary unit for signals, the microvolt, was adopted for noise. Noise then could be measured either by the substitution method whereby a calibrated oscillator or signal generator is substituted for the noise, or by calibrating the noise-meter scale with known signals. One reason for making measurements in this way was to show a ratio between a desired signal and an unwanted noise.

The difficulty with the use of radio signals for calibration is that it involves a comparison of two quantities which have quite different characteristics. Radio signals are essentially smooth sine waves. Noise usually is made up of waves of decidedly jagged variety. The basic instrument responds differently to the two kinds of waves. If a noise disturbance and a signal are compared on two instruments the results will not be the same unless the instruments are alike. Present standards[5] aim to make all noise meters alike within practical limits. While noise meters have been produced according to these standards which give reasonably good results, the control of instrument characteristics does not remove the cause of the difficulty. The thing that is really needed is *a reference wave* of known noise value.

The possibility of using a simple wave shape, such as a square wave, is demonstrated in this paper. The steep wave fronts of such a wave are representative of the jagged character noise waves. When this wave, which must be completely defined as to shape, is applied to a basic noise meter with defined characteristics, the output voltage can be calculated by a method determined in this investigation and evaluated in the present units, microvolts. This method takes the essential instrument characteristics[5] into account but does not involve nonessential characteristics that may be present in actual noise meters. When so evaluated, the reference wave can be used to measure noise by the substitution method or to calibrate the noise-meter scale in place of the radio signals now employed.

The proposed method of calibration takes the basic instrument characteristics into account in the initial evaluation of the reference wave. From then on the measurements are essentially comparisons of the effects of known and unknown noises on the same instrument. Instrument differences have much less

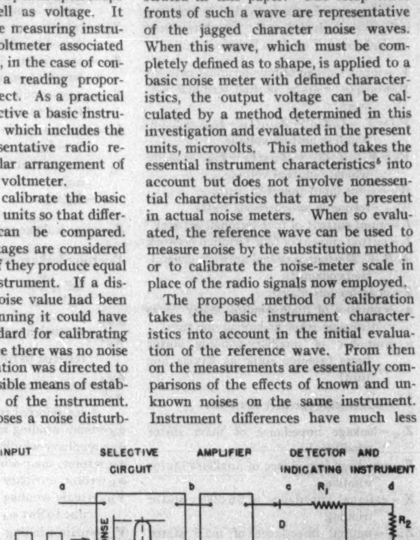

Figure 1. Functional diagram of radio-noise meter

Paper 45-146, recommended by the AIEE committees on communication and instruments and measurements for publication in AIEE TRANSACTIONS. Manuscript submitted May 15, 1945; made available for printing July 23, 1945.

C. W. FRICK is in the general engineering and consulting laboratory, General Electric Company, Schenectady, N. Y.

The author expresses his indebtedness to Mrs. Fern Green who conducted the experimental work which contributed in a large measure to the contents of this paper.

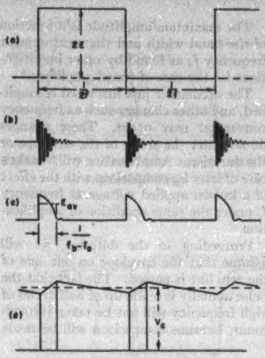

Figure 2. Analysis of radio-noise-meter performance with applied square-wave voltage

Curves *a*, *b*, *c*, and *d* show the voltage wave shape at the respective points in Figure 1

influence on these comparisons than on comparisons between signals and noises.

The development of the method and its application will now be described. The plan of investigation was as follows:

(*a*). Development of a method of evaluating the noise-producing effect of square wave and other generators in terms of the units employed in radio-noise measurements.

(*b*). Application of the method of evaluation to available wave generators.

(*c*). Comparison of noise-meter calibrations on the square-wave basis with calibrations on the present signal generator basis.

(*d*). Comparison of measurements of radio noise made with different noise meters when calibrated with the proposed square wave and when calibrated with radio signals.

(*e*). Comparison of measurements of radio noise made with a radio receiver and output meter calibrated with the square wave with measurements made with a radio-noise meter.

Development of Method of Evaluating the Noise-Producing Effect of a Reference Wave

The relation between the applied square-wave voltage and the noise value in microvolts involves the transformations which take place between the noise-meter input terminals and the indicating instrument. These transformations may be summarized as follows:

1. Frequency selection.
2. Amplification.
3. Detection.
4. Indication.

The four steps are illustrated by the functional diagram of Figure 1 which includes all the essential elements of the basic noise meter. To determine the desired relation a square wave is applied to the terminals and the various transformations are calculated. This procedure leads to the evaluation of the indication which the square wave produces on the output meter. The number of microvolts at the measurement frequency necessary to produce the same indication is then determined, which is the desired "noise value" of the square wave.

ANALYSIS OF SQUARE WAVE

The theoretical square wave to be analyzed is illustrated by Figure 2a. It consists of pulses of amplitude $2E$ and width equal to half the period. The wave front is infinitely steep. Either the ascending or the descending wave front produces a sudden change in the voltage applied to the instrument. The input circuit is tuned to pass a certain frequency f_o (actually a narrow band of frequencies). The sudden change sets up an oscillation at that frequency which has the appearance of Figure 2b. In other words, the square wave is changed to a series of oscillations. A similar effect can be observed by connecting a square-wave generator to a band-pass filter tuned to a considerably higher frequency and connecting the output to an oscilloscope.

The first step in the analysis is to calculate the oscillation. One way to do this is to express the applied wave as a Fourier series and perform certain operations which will be described. The series for the wave to be analyzed is

$$e=E+\frac{4E}{\pi}[\sin \omega t+(1/3)\sin 3\omega t+\ldots+(1/n)\sin n\omega t+\ldots] \quad (1)$$

Table I. Indirect Determination of Equivalent Steepness of Wave Front, Square Wave Generator 1

2.0 Volts Peak to Peak, Fundamental Frequency 60 Cycles

Measurement Frequency, Megacycles	Noise-Meter Reading, Microvolts	Calculated Square-Wave Noise Value, Microvolts	Ratio of Reading to Square-Wave Value	Equivalent Steepness t_e
0.2	5,600	5,650	0.99	1.00×10^{-7}
0.35	3,100	3,170	0.98	0.86
0.6	1,700	1,850	0.92	1.08
0.8	1,370	1,390	0.99	0.25
1.0	1,050	1,110	0.94	0.57
1.5	630	740	0.85	0.63
2.0	430	555	0.78	0.63
3.0	230	370	0.62	0.67
5.0	78	222	0.35	0.88
8.0	27	139	0.19	1.05
11.0	13	101	0.13	1.13
15.0	10	74	0.14	0.80
Average				0.80×10^{-7}

t_e = time in which voltage change is equal to 63 per cent of the peak-to-peak value on an exponential front

where

E = crest value of alternating component of wave
f = fundamental frequency of wave
$\omega=2\pi f$
n = any odd integer

As a first approximation it is assumed that all frequencies within the narrow range f_a to f_b are passed without change and all other frequencies are cut off. Therefore, we multiply all terms of equation 1 which represent frequencies between f_a and f_b by 1.0 and all the other

Table II. Comparison of Radio-Noise-Meter Calibrations on Square-Wave Generator and on Sine-Wave Signal Generator

Measurement Frequency f_o, Megacycles	Square-Wave Voltage E	Square-Wave Calibration Value, Microvolts; Noise Meters A, B, and C	Sine-Wave Signal Generator Calibration at f_o, Microvolts; Noise Meters A	B	C	Per-Cent Difference Between Calibrations; Noise Meters A	B	C
0.6	0.05	89	100	89	108	+12	0	+21
	0.1	178	210	174	185	+18	− 2	+ 4
	0.3	535	560	490	460	+ 5	+ 8	−14
	0.5	890	950	930	580	+ 7	+ 4	−35
	0.8	1,420	1,400	1,500	1,050	− 1	+ 6	−26
	1.0	1,780	1,760	1,900	1,300	− 1	+ 7	−27
	2.0	3,560	3,500	2,800	2,700	− 2	−21	−24
1.0	0.05	50	52	62	82	+ 4	+24	+64
	0.1	99	110	134	148	+11	+36	+50
	0.3	297	310	410	380	+ 4	+39	+28
	0.5	497	500	720	550	0	+45	+11
	0.8	792	800	800	750	+ 1	+ 1	− 5
	1.0	990	1,030	1,000	960	+ 4	+ 1	− 3
	2.0	1,980	2,100	2,000	1,900	+ 6	+ 1	− 4
2.0	0.05	20	12	22	34	−38	+10	+70
	0.1	39	33	44	61	−15	+13	+57
	0.3	117	120	140	178	+ 3	+20	+52
	0.5	195	240	230	290	+ 5	+18	+49
	0.8	312	330	360	440	+ 6	+17	+41
	1.0	390	410	460	500	+ 5	+18	+28
	2.0	780	880	980	970	+13	+26	+24
Average						+ 2.2	+12.9	+17.2

Fundamental frequency of square wave 60 cycles; $t_e=0.8\times10^{-7}$ second (see Figure 7).
Noise meter *A* represents one make; *B* and *C* represent two different models of another make.

terms by zero. This gives an equation containing as many terms as the number of harmonics passed. In the case of the square wave the number of terms is equal to the band width divided by twice the fundamental frequency since only odd harmonics appear. The next operation is to combine these terms as described in detail in Appendix I. The equation resulting from this procedure is

$$e' = \frac{4E}{\pi}\,\frac{f_b-f_a}{2f_o}\,\frac{\sin\pi(f_b-f_a)t}{\pi(f_b-f_a)t}\,\sin\,(2\pi f_a t+\phi) \quad (2)$$

where

f_a = lower frequency passed by selective circuit

f_b = upper frequency passed by selective circuit

f_o = measurement frequency which is midway between f_a and f_b

ϕ = phase angle, defined in Appendix I

An examination of equation 2 shows that it represents an oscillation such as Figure 2b. The term

$$\frac{\sin\pi(f_b-f_a)t}{\pi(f_b-f_a)t}$$

is of particular interest because it defines the shape of the envelope. The value of this term is 1.0 when $t = 0$ and zero when $t = 1/(f_b - f_a)$ and multiples of that value. Since the amplitude after the first zero is not more than one fifth of the initial amplitude, it will be assumed for simplicity that the oscillation ends at the first zero.

The maximum amplitude is a function of the band width and the measurement frequency f_o as found by other investigations for the case of tuned amplifiers.[6]

The oscillation just discussed is amplified, and other changes such as frequency conversion may occur. These changes do not alter the shape of the envelope or the duration. Amplification will be taken care of later by comparison with the effect of a known applied voltage at frequency f_o under the same condition of amplification.

Proceeding to the detector, we will assume that the envelope on one side of the zero line is passed. The fact that the pulse actually is made up of half cycles of high frequency will not be taken into account, because comparison will be made

Table III. Comparison of Radio-Noise-Meter Calibrations on Square-Wave Generator and on Sine-Wave Signal Generator

Noise Meter *B*

Measurement Frequency f_o, Megacycles	Square-Wave Voltage E	1st Calibration 60 Cycles* (From Table II)			2nd Calibration 120 Cycles*			3rd Calibration 400 Cycles*		
		Square-Wave Calibration Value, Microvolts	Signal-Generator Calibration at f_o, Microvolts	Per-Cent Difference	Square-Wave Calibration Value, Microvolts	Signal-Generator Calibration at f_o, Microvolts	Per-Cent Difference	Square-Wave Calibration Value, Microvolts	Signal-Generator Calibration at f_o, Microvolts	Per-Cent Difference
0.6	0.05	89	89	0	125	140	+12	175	220	+26
	0.1	178	174	− 2	250	250	0	350	370	+ 6
	0.3	535	490	+ 3	755	680	−10	1,060	1,000	− 6
	0.5	890	930	+ 4	1,250	1,270	+ 2	1,760	1,710	− 3
	0.8	1,420	1,500	+ 6	2,000	1,900	− 5	2,820	3,000	+ 6
	1.0	1,780	1,900	+ 7	2,500	2,300	− 8	3,520	3,600	+ 2
	2.0	3,560	2,800	−21	5,000	3,700	−26	7,040	6,400	− 9
1.0	0.02							39	66	+69
	0.05	50	62	+24	70	103	+47	99	150	+52
	0.1	99	134	+36	140	190	+36	196	290	+48
	0.3	297	410	+39	420	538	+27	590	800	+36
	0.5	497	720	+45	700	1,000	+43	985	1,420	+44
	0.8	792	800	+ 1	1,120	1,150	+ 3	1,560	2,200	+41
	1.0	990	1,000	+ 1	1,400	1,420	+ 1	1,960	2,700	+38
	2.0	1,980	2,000	+ 1	2,800	2,900	+ 4			
2.0	0.02							15	19	+27
	0.05	20	22	+10	28	35	+25	39	51	+31
	0.1	39	44	+13	55	63	+15	77	100	+30
	0.3	117	140	+20	165	190	+15	230	300	+30
	0.5	195	230	+18	275	320	+16	390	500	+28
	0.8	312	360	+17	440	530	+20	620	800	+29
	1.0	390	460	+18	550	630	+15	770	960	+25
	2.0	780	980	+26	1,100	1,360	+24			
Average				+12.9			+12.2			+26.2

* Fundamental frequency of square wave equal to the value given; $t_e = 0.8\times10^{-7}$ second for all these frequencies (see Figure 7).

Table IV. Comparison of Measurements With Different Radio-Noise Meters Calibrated According to Proposed and Present Methods

Test Sample	Measurement Frequency f_o, Megacycles	Noise Value, Microvolts					Per Cent Above or Below Average				Range Max to Min Per Cen
		Square-Wave Calibration; Noise Meter		Signal-Generator Calibration at f_o; Noise Meter			Square-Wave Calibration; Noise Meter		Signal-Generator Calibration; Noise Meter		
		A	B	A	B	Average	A	B	A	B	
D-c motor	0.6	280	300	310	270	290	+ 7	− 7	− 3	+ 3	14
	1.0	574	590	630	790	646	− 3	+22	−11	− 9	33
	2.0	2,140	2,480	2,500	2,300	2,355	+ 6	− 2	+ 6	+ 5	15
D-c generator	0.6	2,670	3,920	2,500	2,600	2,923	− 9	+33	−15	+11	48
	1.0	2,760	3,660	2,400	3,100	2,980	− 7	+23	−19	+ 4	42
	2.0	663	700	740	890	748	−11	− 6	− 1	+19	30
Gas-discharge device	0.6	900	924	920	900	911	− 1	+ 2	+ 1	− 1	3
	1.0	218	208	250	270	237	− 8	−12	+ 6	+14	26
	2.0	98	98	90	82	92	+ 6	+ 6	− 2	−11	17
Spark gap	0.6	768	845	990	865	867	−11	− 3	+15	0	26
	1.0	1,450	1,360	1,600	1,290	1,425	+ 2	− 5	+13	− 9	22
	2.0	1,083	1,050	1,300	1,360	1,198	− 2	−13	+ 9	+13	26

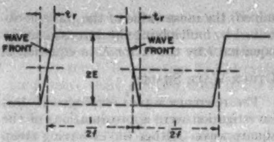

Figure 3. Approximately square wave—trapezoidal shape

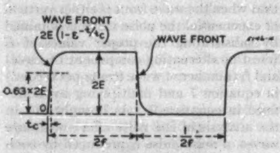

Figure 4. Approximately square wave—exponential wave front

with a rectified wave which is also made up of half cycles of frequency f_o. The detector output produced by the square wave is considered as a series of pulses of initial amplitude $\frac{4E}{\pi}\frac{f_b-f_a}{2f_o}$ and duration $\frac{1}{f_b-f_a}$ as shown in Figure 2c. The fundamental frequency of this wave is $2f$, since there is one pulse for each wave front and there are two wave fronts in each cycle of the square wave. Later in the analysis the average ordinate of the pulse will be employed. This average is approximately 0.59 times the initial value as demonstrated in Appendix I.

With reference again to Figure 1, the pulses passed by the detector D charge the capacitor C through the resistor R_1. The values of R_1 and C determine the charging time constant. Because of the brief duration of the pulse the discharge through R_2, which is chosen to give a relatively slow discharge rate, is negligible during the charging period. At other times the unidirectional characteristic of the detector prevents discharge except through the resistor R_2, so that the values of R_2 and C determine the discharging time constant. Also, the current through R_2 may be used to actuate the voltmeter M which measures the voltage across the capacitor C to be used as a measure of the noise output.

Table V. Summary of Comparison of Measurements With Different Radio-Noise Meters Calibrated According to Proposed and Present Methods

Measurement Frequency f_o, 0.6 to 2.0 Megacycles

Test Sample	Number of Measurements	Per-Cent Difference Between Noise Values Obtained With Noise Meters A and B: Square-Wave Calibration	Per-Cent Difference Between Noise Values Obtained With Noise Meters A and B: Sine-Wave Signal-Generator Calibration at f_o
D-c motor	27	13	19
D-c generator	27	26	18
Gas-discharge device	27	7	15
Spark gap	13	7	13
All	94	14	17

Next in order is the calculation of the voltage which the square wave produces across the capacitor C. Each pulse increases the capacitor voltage by an amount ΔV_c. The analysis in Appendix I shows that the increment of voltage is given by the formula:

$$\Delta V_c=\frac{A(E_{avg}-V_c')}{(f_b-f_a)R_1C} \quad \text{approximately} \qquad (3)$$

where

E_{avg} = average voltage of pulse
V_c' = voltage on capacitor
A = amplification factor

Then the capacitor discharges through R_2 for a period t_s which is the time interval between one pulse and the next. During this time the voltage is reduced by an amount ΔV_c^1 which is given by the following approximate formula derived in Appendix I:

$$\Delta V_c'=\frac{V_c'}{f_sR_2C} \qquad (4)$$

where

$$f_s=\frac{1}{t_s}$$

The capacitor voltage builds up to a steady-state value V_c for which the increment ΔV_c and the decrement $\Delta V_c'$ are equal. Putting these quantities equal to each other in equations 3 and 4 and solving for V_c' which in this case is equal to V_c, we obtain

$$V_c=\frac{A\,E_{avg}}{\frac{(f_b-f_a)R_1C}{f_sR_2C}+1} \qquad (5)$$

It remains to determine the voltage V of the sine wave of frequency f_o which will produce the same voltage V_c on the capacitor. This voltage passes through the initial stage without change. The detector passes half waves of sine shape to the capacitor C which charges the capacitor to the peak value. When the capacitor voltage is V_c the rms value of the applied voltage is

$$V=\frac{V_c}{\sqrt{2}A}\times10^6 \text{ microvolts} \qquad (6)$$

where A is the amplification factor, which is the same as in the case of the harmonics of the square wave and cancels out in making the substitutions which follow.

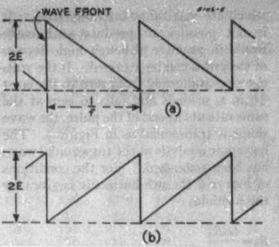

Figure 5. Sawtooth waves

Replacing V_c by the value given by equation 5 for the square wave, combining the constant terms, and expressing the result in microvolts, we obtain the following equation:

$$V=0.265E\frac{f_b-f_a}{f_o\times10^{-6}}\times\frac{1}{\frac{(f_b-f_a)R_1C}{f_sR_2C}+1} \text{ microvolts} \qquad (7)$$

where

E = crest value of alternating component of wave
f_s = number of steep wave fronts per second

This equation gives the "noise value" of a wave of crest voltage E having f_s wave fronts per second, as indicated on a noise meter of specified band width and detector-circuit time constants. The accepted values[5] of the last three factors are 10,000 cycles for the band width f_b-f_a (see Appendix I), ten milliseconds for the charging time constant R_1C, and 600 milliseconds for the discharging time constant R_2C. With this information and an additional factor, to be derived next, which allows for the small but appreciable slope of the actual wave front, a square wave can be evaluated and used to calibrate radio-noise meters. It may be noted that for a square wave of given voltage and frequency the noise value depends on the frequency f_o to which the noise meter is tuned which is called the measurement frequency in this paper.

Effect of Steepness of Wave Front

The wave shape analyzed in the preceding discussion involved wave fronts

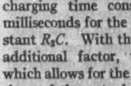

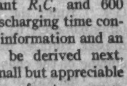

Figure 6a (left). Voltage wave shape of generator 1—conventional square-wave generator

Figure 6b (right). Voltage wave shape of generator 2—developmental square-wave generator for radio-noise calibrations which are vertical or infinitely steep. It is not possible to produce such wave fronts in practice although high degrees of steepness can be attained. If the voltage rises uniformly from zero to the crest $2E$ in t_r seconds and falls to zero at the same rate at the end of the pulse, the wave shape is trapezoidal as in Figure 3. The harmonic analysis of the trapezoidal wave has been published.[7] For the conditions of Figure 3 the nth harmonic is given by the formula:

$$E_n=\frac{4EK_1}{\pi n}$$

where

$$K_1=\frac{\sin \pi f_o t_r}{\pi f_o t_r}$$

t_r = time of voltage change negative-to-positive, or positive-to-negative peak

f_o = harmonic or measurement frequency which is n times the fundamental frequency f of the wave

n = order of harmonics

It may be seen by comparison with equation 1 that the amplitude of the nth harmonic of the trapezoidal wave is K_1 times the amplitude of the corresponding harmonic of the square wave. The factor K_1 is a function of rate of rise and harmonic frequency.

Actual wave generators do not produce the sharp corners shown in Figure 3, because of the presence of resistance, capacitance, and inductance in the apparatus circuits. When the shape is controlled by resistance and capacitance the wave front is exponential as in Figure 4. The time required for a change in voltage equal to $(1-\epsilon^{-1})$ times the peak-to-peak voltage (approximately 63 per cent of the peak-to-peak voltage) measured from the beginning of the change will be designated as t_c. One way to treat this case is to set up equations to represent the curve and apply the usual Fourier analysis. This is done in Appendix II. The value of the nth harmonic is given by the formula:

$$E_n=\frac{4EK}{\pi n} \tag{9}$$

where

$$K=\frac{1}{\sqrt{1+4\pi^2 f_o^2 t_c^2}}$$

f_o = harmonic or measurement frequency

t_c = time required to change voltage 63 per cent of peak-to-peak value

Another approach is to consider the wave generator as equivalent to a square-wave-voltage source applied to a resistance R in series and a capacitance C shunted across the output, having such values that the time constant of the circuit RC is equal to t_c. The nth harmonic voltage (frequency f_o) is equal to the square-wave harmonic from equation 1 multiplied by the ratio of the capacitor impedance $1/2\pi f_o C$ to the total impedance $\sqrt{\left(\frac{1}{2\pi f_o C}\right)^2+R^2}$. Putting $RC = t_c$ we obtain the formula

$$E_n=\frac{4E}{\pi n}\,\frac{1}{\sqrt{1+4\pi^2 f_o^2 t_c^2}}$$

which is the same as equation 9.

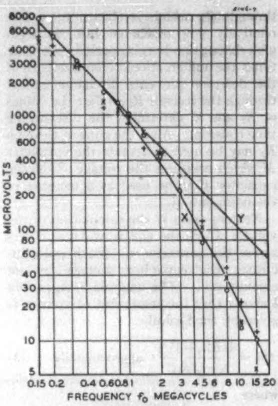

Figure 7. Radio-noise value of reference wave produced by generator 1

Curve X—Calculated noise for exponential shape, Figure 4. 1.0-volt crest of alternating component, 60-cycle fundamental frequency, equivalent steepness $t_c = 0.8\times10^{-7}$ second

Curve Y—Corresponding curve for theoretical square wave, Figure 2a. Test points obtained with radio-noise meters A, B, and C calibrated with a signal generator at frequency f_o

Test points
- O Noise meter A
- × Noise meter B
- + Noise meter C

The effect of inductance L in series with R can be allowed for by adding an inductance term to the total impedance giving

$$\sqrt{\left(2\pi f_o L-\frac{1}{2\pi f_o C}\right)^2+R^2}$$

Then

$$E_n=\frac{4E}{\pi n}\,\frac{1}{\sqrt{[4\pi^2 f_o^2 (L/R)t_c-1]^2+4\pi^2 f_o^2 t_c^2}} \tag{10}$$

Critical damping is obtained when $L = (^1/_4)\,R^2C$. When the inductance is less than this, the harmonics are approximately equal to those given by equation 9 which neglects the effect of inductance.

When the front of the wave produced by the generator is known to be exponential and the value of t_c has been determined, the noise value of the wave is obtained by multiplying the values given by equation 7 by the factor K in equation 9.

OTHER WAVE SHAPES

The reference waves employed in this investigation were approximations of the square wave. Other waves having steep fronts would serve the purpose equally well, for instance the sawtooth waves a and b of Figure 5. Waves of this type are analyzed in Appendix III which shows that when the wave front is either vertical or exponential the noise value is obtained by substituting the proper values of E (crest of alternating component of wave) and f_s (number of wave fronts per second) in equation 7 and multiplying by K defined in equation 9. As brought out in the analysis of the noise effect of square waves, a noise pulse is produced by each steep wave front. Such wave fronts are also present in the sawtooth waves of Figure 5. Two waves, whether square or sawtooth-shaped, will produce the same noise when the time between successive wave fronts is the same, the peak-to-peak voltage is the same, and the wave fronts are of the same shape.

ANALYSIS OF WAVE GENERATORS

Two generators designated as 1 and 2 were analyzed with a view to utilizing them as calibrators for radio-noise meters. The wave shapes produced were substantially square, as shown by the oscillograms of Figure 6. A mechanically operated generator, number 3, was tried but was not satisfactory because of the action of the contacts. This generator is included in the discussion.

WAVE GENERATOR 1

This generator was an all-purpose square-wave generator which produced negative pulses. For this analysis the pulse width was made equal to half the interval between pulses, the voltage was adjusted to two volts (one volt crest of alternating component E) and the fundamental frequency was adjusted to 60 cycles.

The noise value of this wave was calculated from the analysis given in the

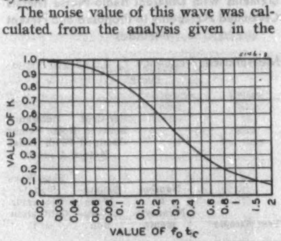

Figure 8. Factor K for wave with exponential front, Figure 4

Amplitude of harmonic of frequency f_o is equal to square-wave harmonic multiplied by K

preceding part of this paper for 1.0 megacycle, a frequency commonly used in noise measurements. By substitution of 1.0 volt for E in equation 7, 120 cycles for f_s since there are two wave fronts in each cycle of the square wave, and the values of band width (ten kilocycles) and time constants (10 and 600 microseconds) for the present noise meter, a noise value of 1,110 microvolts was obtained. The noise meter used in the test, designated as A, read 1,050 microvolts which was remarkably close to the calculated value. This would seem to indicate that the wave was "square," but readings at higher frequencies showed a definite falling off, apparently in accordance with equation 9.

Determination of the steepness of wave front was somewhat difficult in this case, because the voltage was too low to operate a high-speed oscillograph and because the generator circuit could not readily be reduced to a simple form that could be analyzed. Work of other investigators[8,9] suggested that the noise meter might be used as a harmonic analyzer. It would pass groups of harmonics instead of separate harmonics as in the usual harmonic measurements, but the preceding analysis indicates that the noise-meter reading taken on the wave at any frequency would be proportional to the amplitude of the harmonic of that frequency. Proceeding along these lines a set of readings was taken with the noise meter, given in the second column of Table I. These readings were compared with the calculated square-wave values in the third column which indicated that a value of time of rise t_c equal to 0.8×10^{-7} second would apply reasonably well. This figure was obtained by putting the ratio in the fourth column equal to the factor K in equation 9 and then calculating t_c as indicated in the table. The value of t_c seemed consistent with some oscillograph measurements previously reported which indicated that the crest was reached in about half a microsecond.

Curve X of Figure 7 shows the calculated noise using the value of t_c derived from this analysis. Curve Y shows the square-wave values for comparison. Readings are shown which were taken with the noise meter already referred to, A, and two noise meters, B and C, of a different make. All readings are reasonably consistent with the curve X. For convenience in calculating curves such as this, a curve giving values of K is shown in Figure 8.

A standard for calibration should be independent of noise meters and signal generators which in this case were employed to get started. Nevertheless, it seemed reasonable to use this generator as a bench mark in the laboratory to try out this method of calibration. Voltage, frequency, and pulse width were measured. The generator was enclosed, the wiring permanent, and external connections as short as possible, and so it seemed reasonable to expect that the wave shape would be fixed. The results shown on Figure 7 have been duplicated a number of times over a period of several months which seems to verify this conclusion.

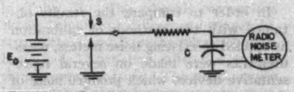

Figure 9. Equivalent circuit for wave generators 2 and 3

Table VI. Comparison of Measurements With Radio-Noise Meter and With Radio Receiver Calibrated According to Present and Proposed Methods

		Sine-Wave Signal-Generator Calibration at f_0; Noise Value, Microvolts				Square-Wave Calibration; Noise Value, Microvolts				
			Receiver*				Receiver*			
Test Sample	Measurement Frequency, Megacycles	Noise Meter	a	b	c	Noise Meter	a	b	c	Max Difference, Per Cent
D-c motor	0.6	160	250	400	525	147	138	130	130	12
	1.0	380	450	800	1,240	274	274	245	255	11
	2.0	5,800	4,300	15,000	15,500	8,300	8,700	9,000	5,700	41
Gas discharge	0.6	480	500	1,400	1,640	346	328	346	346	5
	1.0	310	330	790	900	198	217	178	198	20
	2.0	40	45	75	104	21	21	19	19	10

Noise meter B used in this test.

* Receiver audio tone control set at three different points: *a*, *b*, *c*.

Signal generator modulated 30 per cent for receiver calibration.

The generator was used for calibrations in the following manner. To calibrate by the substitution method the generator was substituted for the noise being measured and the voltage adjusted to give the same reading of the noise meter. The noise per volt from Figure 7 multiplied by the generator voltage gives the required noise value. To check the noise-meter scale at a given point the desired microvolt value was divided by the microvolt value at 1.0 volt from Figure 7 to obtain the required generator voltage.

Wave Generator 2

Generator 2 was a developmental square-wave generator designed to produce waves similar to those of generator 1. The tests reported here were intended to explore the possibilities of this type of generator as applied to noise-meter calibrations, and not to represent tests on a fully developed unit. The wave was produced by an electronic switch such as employed in multivibrators. This switch was synchronized with the 60-cycle supply to obtain a 60-cycle square wave. The crest of the alternating voltage was measured with an electronic voltmeter.

An analysis of the actual circuit showed that for the purpose of determining the wave shape the generator could be represented by the equivalent circuit of Figure 9. E_o represents a source of constant voltage equal to the peak-to-peak voltage of the square wave, and S represents an instantaneous switch which alternately applies full voltage and zero voltage (equivalent to a perfect square wave) to the R-C circuit. This produces a voltage across the capacitor C similar to that in Figure 4. The time of rise to 63 per cent of full voltage or of drop to 37 per cent of full voltage, t_c, is equal to the time constant RC. The resistance and capacitance which were effective in this equivalent circuit were measured giving R = 1,500 ohms and C = 50 micromicrofarads. By using these constants a value $t_c = 0.75 \times 10^{-7}$ was obtained.

Inductance would tend to round off the sharp corners in Figure 4 at the beginning of charge and discharge. The series inductance effective in the equivalent circuit of Figure 9 was measured and found to be about 1.0 microhenry. Substituting this value with the other constants in equation 10 shows that the effect of inductance is negligible.

The equivalent source voltage E_o in Figure 9 was not adjustable. The square-wave voltage applied to the noise meter was adjusted to desired values by means of a capacitor potential divider which was part of the capacitance C. The value of 50 micromicrofarads included the divider. The full voltage was measured with a thermionic voltmeter and divided by the measured ratio of the divider.

With this information curves giving noise values can be plotted which do not involve radio-frequency signal generators nor any particular noise meter. If the curves do not change when the same voltage is maintained, the generator can be used as a noise standard. The tests that were made, while not refined to the last degree, indicate that the device is very promising.

The curve on Figure 10 was calculated from the data given in the preceding paragraphs. The crest voltage was 1.13 volts at the output of the potential divider. This gave very nearly the same curve as X in Figure 7 for generator 1. Readings taken with the two noise meters A and B are plotted as in the previous test. In this case the test data are compared with calculations which are entirely independent of noise-meter measurements. The agreement is about as good as in the case of generator 1. Still better agreement

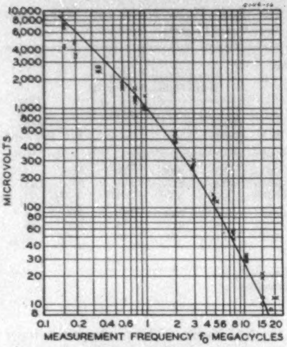

Figure 10. Radio-noise value of wave produced by generator 2

1.13-volt crest of alternating component, 60-cycle fundamental frequency, $t_c = 0.75 \times 10^{-7}$ second (see Figure 4)

Test points
O Noise Meter *A*
X Noise Meter *B*

undoubtedly could be obtained by taking further precautions. For instance, at the lowest frequencies noise meter *B* read low as compared with the test on generator 1. This was due probably to the effect of the noise-meter impedance when tuned to these frequencies. This would have to be corrected. In another test, shown on Figure 11, the noise meter was connected across a larger value of capacitance to get lower voltage (0.16 volt), and the readings were normal. Part of the wiring was temporary, but there was no indication of the results being critical to changes which occurred between one test and another. Also on Figure 10 two sets of readings are shown for each noise meter. These readings were taken with different tubes, and no significant changes are indicated.

This calibrator could be constructed as a small compact unit powered and controlled as to frequency from 60-cycle circuits. It would be used in a similar manner to the signal generators now employed.

WAVE GENERATOR 3

This generator was an attempt to use a mechanical vibrator for the switch *S* in Figure 9. A battery was used to supply the voltage E_o. The resistance *R* was 100 ohms, and the capacitance *C* was 0.00111 microfarad. When these values were used the calculated value of t_c was 1.11×10^{-7} second. The noise-meter readings were approximately 30 per cent below the calculated curve over the whole frequency range. This seemed to indicate that the steep part of the wave front was about 70 per cent of the full voltage. Observation on the screen of an oscilloscope showed a slow build-up before the steep wave front, evidently due to light contact at first. Also, the capacitor appeared to discharge appreciably while the contact was moving from one side to the other. It may be noted that the electronic switch in generator 2 gave results which checked with the noise-meter readings. This test demonstrates that switches such as mechanical vibrators are too slow for the purpose. However, the curve of microvolts versus frequency was of the shape predicted from the circuit constants.

Calibrations Made With Square Waves as Compared With Sine-Wave Signal-Generator Calibrations

Several tests were made to determine how the calibrations of existing noise meters made with the proposed reference wave would compare with the calibrations by the present method. Three noise meters of different makes designated as *A*, *B*, and *C* were tested. *B* and *C* were different models of the same make. The reference wave, an approximately square wave at 60 cycles, was obtained from wave generator 1 already described.

The method of test was as follows: The noise meter under test was tuned to one of the selected measurement frequencies (0.6, 1.0, or 2.0 megacycles) and connected to the square-wave generator. The generator voltage was adjusted to 1.0 volt which gave the noise value shown by curve *X* on Figure 7 at the measurement frequency. This showed what the instrument would read when calibrated on the proposed square wave. Then without changing the noise-meter adjustment a sine-wave signal generator, properly tuned, was substituted for the square-wave generator. The signal-generator voltage was adjusted to obtain the same scale deflection of the noise meter as before. The indicated output voltage of the signal generator showed what the noise meter would read when calibrated by the present method. This procedure was repeated at other values of square-wave voltage and at other measurement frequencies. These tests are summarized in Table II wherein the third column shows square-wave calibration values, and the next three columns (one for each instrument) show sine-wave signal-generator calibration values. Percentage differences between the two calibrations are indicated in the last three columns.

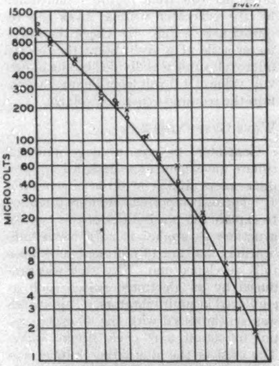

Figure 11. Radio-noise value of wave produced by generator 2

0.16-volt crest of alternating component, 60-cycle fundamental frequency, $t_c = 0.75 \times 10^{-7}$ second (see Figure 4)

Test points
O Noise meter *A*
× Noise meter *B*

With reference to the averages in Table II it may be noted that the differences between square-wave and sine-wave calibrations were 2.2, 12.9, and 17.2 per cent for instruments *A*, *B*, and *C*, respectively. The apparently close check in the case of instrument *A* may have resulted for the use of this instrument to obtain part of the data from which the noise curve for the square wave (curve *X* of Figure 7) was plotted. The general average, about ten per cent, is considerably better than the accuracy expected of noise meters at the present time. Also, the accuracy of radio-frequency signal generators is involved which is about eight per cent at these frequencies.

Similar tests were made on one noise meter, instrument *B*, using square waves at 120 and 400 cycles. Table III shows the data together with the 60-cycle values from Table II. Percentage differences are shown as in the previous table. The averages are 12.9, 12.2, and 26.2 per cent, respectively, for 60, 120, and 400 cycles. The figures for 400 cycles seem to indicate that the wave front was slightly steeper at that frequency for which a correction could be made.

Comparison of Measurements Made With Different Noise Meters Calibrated With Square-Wave and With Sine-Wave Signal Generators

In order to compare the results obtained with two methods of calibration as applied to existing noise meters, measurements were made on several representative devices which produce noise of the continuous type. Readings were taken with the two instruments of different designs, designated as *A* and *B*. Each noise meter was connected to the device and a reading obtained. The square-wave generator (number 1) was substituted, and a calibration was made as already described. The radio-frequency signal generator was then substituted and another calibration made. Four values of noise (two for each instrument) were obtained in each measurement. Theoretically, if the two noise meters were identical and had the standardized selectivity and time constants, all four values would have been the same. Actually the differences were not unduly large.

Table IV shows sample measurements on a commutator motor, a commutator generator, a gas-discharge device operated on a 60-cycle circuit, and a small sphere gap connected to the ungrounded side of a 60-cycle high-voltage circuit. The four noise values obtained in each measurement and their average are shown, as well as the percentage above or below the average for each value. In addition, the percentage difference between maximum and minimum is indicated for each measurement. This was not over 50 per cent.

The whole group of tests, which includes 94 measurements similar to those of Table IV, made at 0.6, 1.0, and 2.0 megacycles, is presented graphically in Figures 12, 13, 14, and 15, which show percentages above and below the average. The measurements are arranged in order of percentage difference between maximum and minimum, the smallest difference on the left and the largest on the right. The connecting lines indicate the instrument and method of calibration. The noises being measured were subject to continuous fluctuations of the order of 20 per cent which probably accounts for irregular variations of that magnitude. The two methods of calibration as applied here appear to work about equally well.

The data presented in Figures 12 through 15 were averaged in the following manner to obtain an over-all difference between the two instruments on each calibration basis given in Table V. For each measurement the percentage difference between the noise values as determined by instruments *A* and *B* on the square-wave basis was calculated. These percentage values were averaged for each device and for all the measurements. This procedure was repeated, using the noise values obtained on the radio-frequency signal-generator calibration basis. The average percentage values for each device and the general averages are shown in Table V. The over-all comparison shows 14-per-cent difference between instruments *A* and *B* on the reference-wave basis and 17-per-cent difference on the signal-generator basis. The small margin is in favor of the reference-wave method.

On further examination of the agreement between instruments when calibrated with the square wave, as indicated in Table V, it may be noted that the order of agreement with respect to devices was gas-discharge device, spark gap, motor, and generator. In the operation of the first two devices breakdown accompanied by a steep wave front occurs on the rise of voltage during each half cycle of the 60-cycle supply. Thus the 60-cycle reference noise should match the actual noise quite well. The motor and the generator produce steep wave fronts when brushes pass from bar to bar at a rate depending upon the number of bars and the speed. Under such conditions the reference noise might not match the actual noise quite so well, but the results are at least as good as those obtained with the sine-wave signal-generator calibrations. Some further improvement might be made by using a reference-wave frequency which corresponds more nearly to the actual noise, for instance, square waves of higher fundamental frequency.

Table VII. Summary of Comparison of Measurements With Radio-Noise Meter and With Radio Receivers Using Square-Wave Calibrations

Measurement Frequency f_a 0.6 to 2.0 Megacycles

	Noise Meter and Receiver Calibrated on Wave Generator 1		Noise Meter and Receiver Calibrated on Wave Generator 2	
Test Sample	Number of Measurements	Difference Between Noise Values, Per Cent	Number of Measurements	Difference Between Noise Values, Per Cent
D-c motor	7	7	5	18
D-c generator	8	13	6	32
Gas-discharge device	7	13	7	19
Spark gap	7	11	3	20
All	29	11	21	21
Average difference between noise values with noise meter and with receiver				15

Generator 1—Conventional square-wave generator, fundamental frequency 60 cycles.

Generator 2—Special developmental square-wave generator for calibration purposes, fundamental frequency 60 cycles.

Comparison of Measurements Made With Radio Receivers and With Radio-Noise Meters

A number of tests were made wherein readings were taken with a radio receiver and with a radio-noise meter for the purpose of comparing the results. The audio amplifier of the receiver was connected to the proper value of resistance for maximum audio output, and a vacuum-tube voltmeter was connected to the output terminals to indicate the noise effect. The noise meter was used in the usual manner. Detailed measurements on two devices which produce noise, a d-c motor and a gas-discharge device, are shown in Table VI. Readings were taken with the noise meter designated as instrument *B*, using the procedure already described. Two calibrations were made, one on a sine-wave signal generator and the other on the square-wave generator designated as number 1. Measurements then were

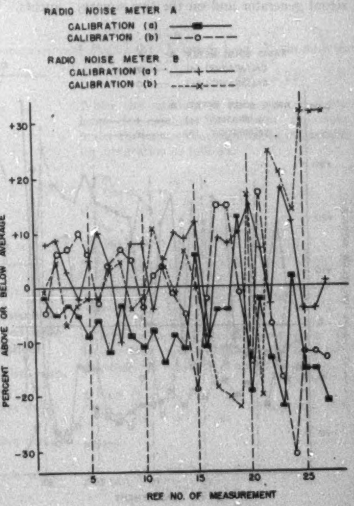

Figure 12. Comparison of measurements on d-c motor with different radio-noise meters and different methods of calibration

Tests arranged in order of difference between maximum and minimum readings

Calibration a made on square-wave generator 1

Calibration b made on sine-wave signal generator made with the receiver by the substitution method. The receiver was tuned to the desired measurement frequency and connected to the device under test. The receiver gain control was adjusted to give a measurable output voltage. Without changing the receiver adjustments the sine-wave signal generator with 30-per-cent modulation was substituted for the device and its voltage adjusted to give the same receiver output voltage. The microvolt value was read from the signal generator. The square-wave generator then was substituted and its output adjusted to give the same receiver output voltage. The noise value for this calibration was obtained from the crest voltage and the noise curve X of Figure 7.

In order to cover different receiver conditions the adjustments, particularly the tone control which was found to be critical, were changed and another measurement made at the same measurement frequency. This was followed by a third measurement with a different adjustment. The noise value as determined by the receiver when calibrated on the sine-wave signal generator varied by as much as three to one with different adjustments. On the other hand, the noise value as determined by the receiver when calibrated on the square-wave generator was substantially the same for all adjustments and agreed with the noise meter within the present measurement accuracy of about 40 per cent.

Additional measurement data were obtained on the four test samples, the motor, the generator, the gas-discharge device, and the spark gap. Readings were taken with the noise meter designated as A. Calibrations were made on a sine-wave signal generator and on the two square-wave generators 1 and 2 which produced similar waves. Readings taken with the receiver were calibrated on the two square-wave generators but not on the sine-wave signal generator, since that method of calibration was unreliable as already indicated. The five noise values obtained in each measurement were averaged. Figures 16 to 19 inclusive show for each measurement the percentage by which each individual reading is above or below the average. The graphs are similar to Figures 12 through 15. A large majority of the points are within the plus or minus 20 per cent range.

In order to show an over-all comparison between receiver measurements and noise-meter measurements percentage differences were computed and averaged. These percentages apply to comparable readings with the receiver and the noise meter both calibrated on the same reference wave. The general average was 15-per-cent difference. The percentage differences obtained on the four devices tested, using each of the two square-wave generators for calibration, are shown in Table VII. All of these figures are within the present accuracy of noise measurements. The results were a little more consistent with wave generator 1 than with generator 2, probably because the former was of permanent construction, while the latter was assembled for test purposes, and insufficient precautions were taken to eliminate incidental errors.

This test demonstrates quite effectively the necessity for calibrating waves which have the essential characteristics of radio noise. Without such a standard no correlation can be established between receiver measurements and noise-meter measurements. Use of these waves enables significant measurements to be made with receivers when needed. Besides a suitable wave, it is necessary to have an accepted standard for the noise meter to which all measurements are referred. The present specification of band width and detector time constants is sufficient.

Conclusions

1. The accuracy of radio-noise measurements can be materially improved by calibrating the instrument on waves having the essential characteristics of noise instead of on sine waves.

2. The wave proposed for use as described herein is a 60-cycle substantially square wave with adjustable voltage zero to 20 volts peak to peak, 63 per cent of the change between opposite peaks taking place in 0.075 microsecond, plus or minus 20 per cent, on a curve of exponential shape. This wave is intended for calibrations at measurement frequencies between 0.15 and 20 megacycles.

3. It is practical to build generators which produce such a wave of defined shape that remains fixed. These generators can be used as standards for calibrating noise meters.

4. Radio-frequency sine waves do not have all the essential characteristics of radio noise and therefore are not adequate for calibration purposes. Of course it is true that if all noise meters were identical as to circuits and had the same amplification factor for sine waves and noise, check results would be obtained on all instruments. However, this does not result necessarily in values which properly represent the noise levels.

5. The proposed method of calibration can be put into effect without changing the present noise meters and measurement technique. It requires only the use of a standardized wave generator in place of the

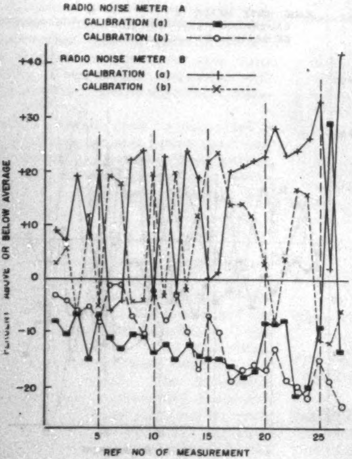

Figure 13 (left). Comparison of measurements on d-c generator with different radio-noise meters and different methods of calibration (see subcaption of Figure 12)

Figure 14 (right). Comparison of measurements on gas-discharge device with different radio-noise meters and different methods of calibration (see subcaption of Figure 12)

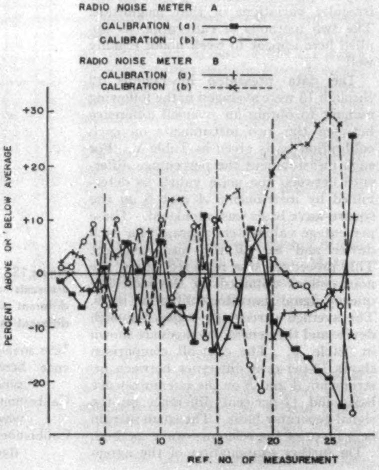

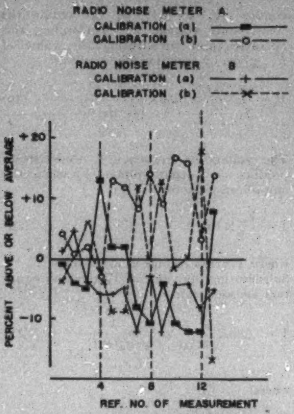

Figure 15. Comparison of measurements on spark gap with different radio-noise meters and different methods of calibration (see subcaption of Figure 12)

radio-frequency signal generators now employed.

6. Tests indicate that the proposed square-wave generator can be used with radio receivers to measure radio noise.

7. The calibration method is applicable to any range of measurement frequencies, but different waves may be required for different ranges. The upper frequency for which a given wave is effective depends upon the steepness of the wave front. Greater steepness is necessary when higher ranges of frequency are to be covered.

8. The results of this study apply to noises of the continuous type. A study of noises of the intermittent or pulse type along similar lines would be desirable.

Appendix I. Analysis of Effect of a Square Wave on the Radio-Noise Meter

This appendix contains the analysis from which a relation between amplitude and frequency of the square wave and noise output in terms of the accepted radio-noise meter was derived. Let a square wave as defined in Figure 2a be applied to a noise meter shown schematically in Figure 1. For the purpose of this analysis the square wave is represented by the Fourier series

$$e = E + \frac{4E}{\pi}[\sin \omega t + (1/3)\sin 3\omega t + (1/5)\sin 5\omega t + \ldots + (1/n)\sin n\omega t + \ldots] \quad (11)$$

The noise-meter input is frequency selective. Figure 20 shows a typical selective curve. In this analysis the effect of selectivity is represented by multiplying each term of equation 11 by the ordinate of the curve. Since the terms are additive, we use the ordinates of the rectangle between f_a and f_b which has the same area as the area under the actual curve (carried out to about 0.05 on the scale of ordinates) instead of those of the actual curve. This amounts to multiplying all the terms by 1.0 where $n\omega$ lies between $2\pi f_a$ and $2\pi f_b$ and multiplying all other terms by zero. f_a and f_b are the lower and upper frequencies determined by the equivalent rectangular selectivity curve.

Performing this operation we obtain an equation of m terms. If the measurement frequency f_0 midway between f_a and f_b is many times the fundamental frequency f, all m terms have approximately the same amplitude which is equal to $\frac{4E}{\pi}\frac{f}{f_0}$ wherein $\frac{f}{f_0}$ is used in place of $(1/n)$. The equation of the output voltage of the selective circuit is

$$e' = \frac{4E}{\pi}\frac{f}{f_0}[\sin \omega_0 t + \sin(\omega_0 t + \beta) + \sin(\omega_0 t + 2\beta) + \ldots + \sin(\omega_0 t + m\beta)] \quad (12)$$

where

$$m = \frac{f_b - f_a}{2f}$$

$$\beta = 4\pi f t$$

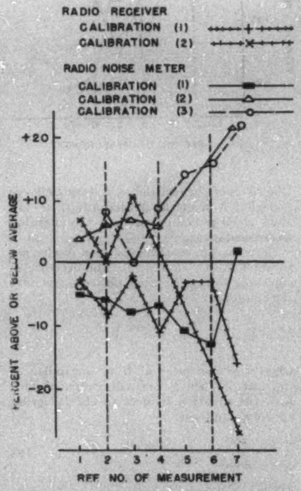

Figure 16. Comparison of measurements on d-c motor with radio-noise meter and radio receiver using square-wave calibrations

Tests arranged in order of difference between maximum and minimum readings

Calibration 1 made with square-wave generator 1

Calibration 2 made with square-wave generator 2

Calibration 3 made with sine-wave signal generator

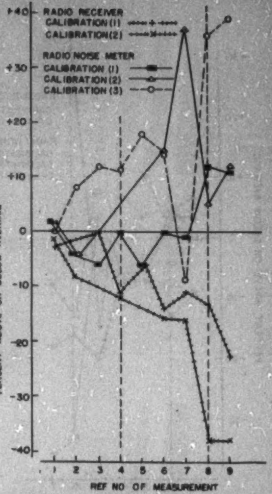

Figure 17. Comparison of measurements on d-c generator with radio-noise meter and radio receiver using square-wave calibrations (see subcaption of Figure 16)

This equation may be written

$$e' = \frac{4E}{\pi}\frac{f}{f_0}[\sin \omega_0 t(\cos 0 + \cos \beta + \cos 2\beta + \ldots + \cos m\beta) + \cos \omega_0 t(\sin 0 + \sin \beta + \sin 2\beta + \ldots + \sin m\beta)] \quad (13)$$

or

$$e' = \frac{4E}{\pi}\frac{f}{f_0}\sqrt{\left(\sum_{s=0}^{s=m}\cos \beta s\right)^2 + \left(\sum_{s=0}^{s=n}\sin \beta s\right)^2} \times \sin(\omega_0 t + \phi) \quad (14)$$

When the number of terms, m, is fairly large (for example 20 or more) the term under the square-root sign can be evaluated by integration as follows:

$$\int_0^m \cos \beta s\, ds = \frac{\sin m\beta}{\beta}$$

$$\int_0^m \sin \beta s\, ds = \frac{1 - \cos m\beta}{\beta}$$

$$\sqrt{\left(\frac{\sin m\beta}{\beta}\right)^2 + \left(\frac{1 - \cos m\beta}{\beta}\right)^2} = m\frac{\sin m\beta/2}{m\beta/2}$$

Substituting this for the term under the square root sign in equation 14 and substituting the values of m and β we obtain

$$e' = \frac{4E}{\pi}\frac{f_b - f_a}{2f_0}\frac{\sin \pi(f_b - f_a)t}{\pi(f_b - f_a)}\sin(\omega_0 t + \phi) \quad (15)$$

where

$$\phi = \tan^{-1}\frac{1 - \cos 2\pi(f_b - f_a)t}{\sin 2\pi(f_b - f_a)t}$$

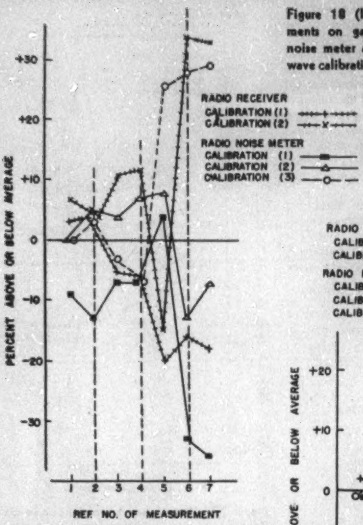

Figure 18 (left). Comparison of measurements on gas-discharge device with radio-noise meter and radio receiver using square-wave calibrations (see subcaption of Figure 16)

Figure 19 (below). Comparison of measurements on spark gap with radio-noise meter and radio receiver using square calibrations (see subcaption of Figure 16)

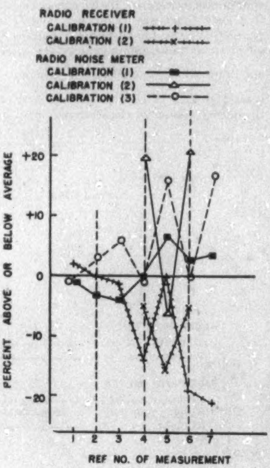

The output of the amplifier is obtained by multiplying equation 15 by the amplification factor A which may be taken as 1.0 in the analysis which follows.

The average value of the envelope of this curve between the beginning and the first zero is given by the equation:

$$E_{\text{avg}}=\frac{4E}{\pi}\frac{f_b-f_a}{2f_o}\frac{1}{\pi}\int_0^{\pi}\frac{\sin\theta}{\theta}d\theta$$

where

$$\theta=\pi(f_b-f_a)t$$

Substituting

$$\frac{1}{\pi}\int_0^{\pi}\frac{\sin\theta}{\theta}d\theta=1-\frac{\pi^2}{3\cdot3!}+\frac{\pi^4}{5\cdot5!}-\frac{\pi^6}{7\cdot7!}+\ldots$$

which is approximately equal to 0.59, we obtain

$$E_{\text{avg}}=\frac{4E}{\pi}\frac{f_b-f_a}{2f_o}\times0.59 \qquad (16)$$

If the capacitor C in the detector circuit shown in Figure 1 has been charged to voltage V_c' the average current during the pulse is

$$I_c=\frac{E_{\text{avg}}-V_c'}{R_1}\text{ approximately}$$

The increment of charge due to the pulse is equal to the average current multiplied by the time of the pulse. Equation 15 shows that the pulse is approximately equivalent to a voltage E_{avg} lasting $1/(f_b-f_a)$ seconds. Since the increment of charge is equal to ΔV_cC we have

$$\Delta V_c=\frac{E_{\text{avg}}-V_c'}{(f_b-f_a)R_1C}\text{ approximately} \qquad (17)$$

The effect of the resistance R_1 during charge is negligible since the discharging time constant is large compared with the charging time constant.

Between pulses the capacitor discharges through R_2 at a slow rate. The decrease in capacitor voltage between pulses is given by the equation:

$$V_c'-V_c''=V_c'\left(1-\epsilon-^{\frac{t_s}{R^2C}}\right)$$

where t_s = time interval from one pulse to the next. When t_s is small compared with R_2C, the equation reduces to the following approximate form:

$$\Delta V_c'=\frac{V_c'}{f_sR_2C} \qquad (18)$$

where

$$\Delta V_c'=V_c'-V_c''$$

$$f_s=\frac{1}{t_s}$$

A steady state is reached when the increment given by equation 17 becomes equal to the decrement given by equation 18. If we put the capacitor voltage V_c' in equations 17 and 18 equal to the steady-state voltage (average) V_c, which is large compared with the voltage increment, and equate $\Delta V_c'$ to ΔV_c, we can obtain the steady-state voltage V_c. Performing this operation and substituting the value of E_{avg} given by equation 16, we obtain

$$V_c=\frac{4E}{\pi}\frac{f_b-f_a}{2f_o}\times0.59\times\frac{1}{\frac{(f_b-f_a)R_1C}{f_sR_2C}+1} \qquad (19)$$

The voltage of frequency f_o necessary to produce an output voltage V_c when the amplification factor is 1.0 is

$$V=\frac{V_c}{\sqrt{2}}\times10^6 \qquad (20)$$

where V = rms voltage in microvolts

Substituting the value of V_c given by equation 19, we obtain

$$V=0.265E\frac{f_b-f_a}{f_o\times10^6}\times\frac{1}{\frac{(f_b-f_a)R_1C}{f_sR_2C}+1} \qquad (21)$$

where

V = noise value in microvolts
E = crest voltage of alternating component of wave
f_o = measurement frequency, cycles
f_s = number of steep wave fronts per second
f_b-f_a = band width, cycles
R_1C = charging time constant, seconds
R_2C = discharging time constant, seconds

This is the desired relation between the square-wave voltage and the noise output indicated by an ideal noise meter having the characteristics stated. In the case of the square wave the value of f_s is twice the fundamental frequency, because there are two steep wave fronts in each cycle.

Appendix II. Analysis of Wave With Exponential Front

When the front of the wave of Figure 2a is exponential instead of vertical, the wave has the shape shown by Figure 4, which is approximately square when the exponential curve is very steep. The curve of Figure 4 may be represented mathematically by subtracting from the equation of the square wave an exponential term at the beginning of the pulse of Figure 2a and adding thereto an exponential term at the end. In the case of the waves being studied, the exponential term is reduced to practically zero in a small fraction of a cycle of the wave.

Taking the origin at point O on the left in Figure 4, the curve may be represented by the following equations:

$$y=2E(1-\epsilon^{-\alpha\theta})0\leq y\leq\pi$$

$$y=2E\epsilon^{-\alpha(\theta-\pi)}\pi\leq y\leq2\pi$$

where

$$\theta=2\pi ft$$

$$\alpha=\frac{1}{2\pi ft_c}$$

t_c = time of rise to $(1-\epsilon^{-1})\times$amplitude
f = fundamental frequency of wave

This curve will be represented by the Fourier series:

$$y=E+a_1\sin\theta+a_2\sin 2\theta+a_3\sin 3\theta+\ldots+a_n\sin n\theta+\ldots+b_1\cos\theta+b_2\cos 2\theta+b_3\cos 3\theta+\ldots+b_n\cos n\theta+\ldots$$

Evaluating the coefficients a_n and b_n in the usual manner, we obtain

$$a_n=\frac{2E}{\pi}\left[\frac{1}{n}-\frac{n}{\alpha^2+n^2}(\epsilon^{-\pi\alpha}+1)\right](1-\cos n\pi)$$

$$b_n=\frac{2E}{\pi}\left[\frac{\alpha}{\alpha^2+n^2}(\epsilon^{-\pi\alpha}+1)\right](1-\cos n\pi)$$

The term $1-\cos n\pi$ is equal to 2 for odd values of n and zero for even values of n. The value of $\pi\alpha$ is large compared with 1.0 when the wave front is steep so that the term $\epsilon^{-\pi\alpha}$ is practically zero. Substituting these values and combining the terms, we obtain

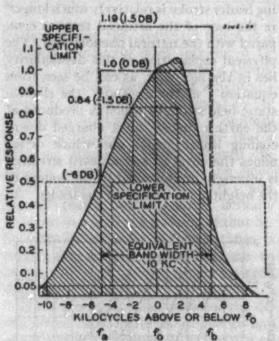

Figure 20. Example of radio-noise-meter selectivity curve

$$\sqrt{a_n^2+b_n^2}=\frac{4E}{\pi n}\,\frac{\alpha\sqrt{\alpha^2+n^2}}{\alpha^2+n^2}$$

where n = any odd integer

It may be noted that the harmonics are equal to the corresponding square-wave harmonics multiplied by a factor which will be represented by K

where

$$K=\frac{\alpha\sqrt{\alpha^2+n^2}}{\alpha^2+n^2}$$

If we put f_0/f in place of n and substitute the value of α given under the equations for the curve, this reduces to

$$K=\frac{1}{\sqrt{1+4\pi^2f_0^2t_c^2}}$$

where f_0 = harmonic frequency or measurement frequency

Values of K are plotted against f_0t_c in Figure 8.

Appendix III. Analysis of Sawtooth Waves

In this appendix the method of analysis described in Appendix I and Appendix II is applied to the sawtooth-type wave. The Fourier series for the wave shown in Figure 5a is

$$e=E+\frac{2E}{\pi}\left(\sin\omega t+\frac{1}{2}\sin 2\omega t+\ldots+\frac{1}{n}\sin n\omega t+\ldots\right)$$

and the series for the wave shown in Figure 5b is

$$e=E-\frac{2E}{\pi}\left(\sin\omega t+\frac{1}{2}\sin 2\omega t+\ldots+\frac{1}{n}\sin n\omega t+\ldots\right)$$

where n is any integer. These equations are similar to the equation for the square wave, but they contain the term $2E$ instead of $4E$, and there are twice as many harmonics in the band width so that the number of terms m in equation 12 is equal to the band width divided by the fundamental frequency. If t_2 represents the interval between wave fronts as before, we arrive at the same equation as 21 in Appendix I. In this case the factor f_2 which is $1/t_2$ is equal to the fundamental frequency of the wave instead of twice the fundamental frequency, because there is only one steep wave front in each cycle of the sawtooth wave. For a given amplitude of wave and time interval between wave fronts, the noise value is the same for either the square or the sawtooth shape.

When the wave front is exponential as in Figure 4, the multiplying factor K derived in Appendix II is used. This factor is the same, because the modification of the wave front is equivalent to adding or subtracting an exponential term to the equation defining the square or sawtooth wave. If the wave front in Figure 5a is exponential instead of vertical, the curve may be represented by the following equation:

$$y=2E\left(1-\frac{\theta}{2\pi}-\epsilon^{-\alpha\theta}\right)\Big]_0^{2\pi}$$

where

$$\alpha=\frac{1}{2\pi f t_c}$$

f = fundamental frequency of wave

t_c = time of rise to 63 per cent of full amplitude

The coefficients of the terms in the Fourier series given in Appendix II are as follows when it is assumed that $\epsilon^{-\pi\alpha}$ is zero:

$$a_n=\frac{2E}{\pi}\left(\frac{1}{n}-\frac{n}{\alpha^2+n^2}\right),\quad b_n=\frac{2E}{\pi}\,\frac{\alpha}{\alpha^2+n^2}$$

$$\sqrt{a_n^2+b_n^2}=\frac{2E}{\pi n}\,\frac{\alpha\sqrt{\alpha^2+n^2}}{\alpha^2+n^2}$$

Putting f_0/f in place of n in the last term and substituting the value of α already given, this reduces to

$$\sqrt{a_n^2+b_n^2}=\frac{2E}{\pi n}\,\frac{1}{\sqrt{1+4\pi^2f_0^2t_c^2}}$$

in which the last term is the same as K in Appendix II.

References

1. MEASUREMENTS PERTAINING TO THE CO-ORDINATION OF RADIO RECEPTION WITH POWER APPARATUS AND SYSTEMS, C. M. Foust, C. W. Frick. AIEE TRANSACTIONS, volume 62, 1943, June section, pages 284–91.

2. THE RADIO-NOISE METER AND ITS APPLICATION TO MEASUREMENT OF RADIO INTERFERENCE, C. R. Barhydt. *General Electric Review*, April 1933, pages 201–05.

3. THE MEASUREMENT OF RADIO-NOISE INTERFERENCE, C. J. Franks. Radio Manufacturers Association *Engineer*, November 1938.

4. INSTRUMENTS AND METHODS OF MEASURING RADIO NOISE, C. V. Aggers, Dudley E. Foster, C. S. Young. AIEE TRANSACTIONS, volume 59, 1940, March section, pages 178–92.

5. METHODS OF MEASURING RADIO NOISE, 1940, report of Joint Co-ordination Committee on Radio Reception of Edison Electric Institute, National Electrical Manufacturers Association, and Radio Manufacturers Association. Edison Electric Institute publication *G9*, National Electrical Manufacturers Association publication 107, Radio Manufacturers Association *Engineering Bulletin* 32.

6. INTERNAL DISCHARGES IN DIELECTRICS, A. E. W. Austen, W. Hackett. *Journal* of the Institution of Electrical Engineers (London, England), volume 91, August 1944, part I, page 298.

7. REFERENCE DATA FOR RADIO ENGINEERS (book), Federal Telephone and Telegraph Company, New York, N. Y., page 166.

8. SOME ANALYSES OF WAVE SHAPES USED IN HARMONIC PRODUCERS, F. R. Stansel. Bell System *Technical Journal*, volume 20, July 1941, pages 331–9.

9. THE COMMUNICATIONS RECEIVER AS A WAVE ANALYZER, Arnold Peterson. *General Radio Experimenter*, volume 18, January 1944, pages 1–4.

The Frequency of Occurrence and the Distribution of Lightning Flashes to Transmission Lines

R. H. GOLDE
ASSOCIATE AIEE

A STUDY of Franklin's correspondence on the subject of electricity shows his clear perception of the proper function of a lightning conductor; he also discusses such still controversial problems as bonding and the relative advantages of vertical rods and horizontal wire systems. On the other hand, no direct reference* as to the protective ratio of a vertical conductor could be found in his papers. Although this question was raised shortly after the introduction of the lightning conductor and has been discussed ever since, no general agreement so far has been reached. In what follows, this problem will be investigated from a new angle, and it will be shown to be even more involved than has been recognized hitherto.

The results obtained from this investigation will be applied to a calculation of the frequency of occurrence of direct lightning flashes to transmission lines, and it also will be seen that it is now possible to predict the distribution of direct flashes between the various elements of an overhead transmission line. Finally, it will be shown that a correlation exists between the frequency of occurrence of flashes to earth and the thunderstorm activity over the district involved.

The Protective Range of a Lightning Conductor

Present State of Knowledge

A survey of the vast technical literature† on the protective ratio of a lightning conductor shows that in the course of 170 years this ratio has been stated to be about 10:1, and less than 1:1, with all possible intermediate values being put forward at some time or other. All these investigations can be subdivided according to their methods of approach into three distinct categories,[2] that is, statistical, experimental (by model), and geometrical.

Statistical observations are based on the collection of actual occurrences of lightning flashes close to lightning conductors, or equivalent structures. The inherent difficulty in this method lies in the great variability of the number and intensity of thunderstorms over any district and the resulting necessity of long-term observations. Furthermore, unless visually observed and immediately reported, lightning flashes are noted only if they produce lasting damage. Since experience shows that only a small fraction of all flashes to earth prove destructive in the afore-mentioned sense it is not surprising to find these wide discrepancies in the alleged minimum values for the protective ratios under consideration.

Model tests, while almost as old[3] as the lightning conductor itself, came greatly to the forefront with the introduction of the surge generator. Their justification is stated to be found in the similarity of the artificial spark and the natural lightning discharge.[4] However, before this assumption can be accepted, a brief discussion of the lightning discharge and its simulation under laboratory conditions may be helpful.

From the present state of knowledge of the mechanism of the lightning stroke,[5] as developed mainly by Schonland,[6] it may be taken as established that the normal lightning leader stroke begins to develop unaffected by the characteristics of the soil beneath or the conditions near the earth surface. Instead it is mainly guided towards earth by local space charges of opposite polarity beneath the cloud which are caused by point discharge from the earth surface and the distribution of which should be determined mainly by the prevailing wind. Throughout this stage of the progression of the leader stroke, which occurs with an average velocity of about 3×10^7 centimeters per second, that is, with only a small fraction of the velocity of the electricity in an overhead line, electric charges of opposite sign to that lowered in the lightning channel flow in the earth towards the region underneath the leader, and a continuous increase of the electrostatic-field strength at the surface of the earth ensues. Now, only when this field strength reaches a magnitude sufficient to produce an upward-streamer discharge from an earthed object, should there be exerted a final directive effect on the downward-leader stroke, and it is possibly only at this stage that the precise point to be struck is determined.

According to the evidence produced by records obtained with rotating cameras,[7,4] the development of artificial spark discharges of conventional dimensions, while fundamentally similar, differs from the foregoing case in that the streamer discharge which rises from the earth or from an earthed object to meet the downcoming leader stroke is relatively much longer[8] in the case of the artificial tests as compared with the natural phenomenon. The physical explanation of this dissimilarity lies in the fact that, as can be seen from equation 7 of the appendix, the electrostatic-field strength which is produced at the earth's surface by a charged downcoming leader stroke and which determines the onset of any upward streamer is inversely proportional to the square of the height of the charge on the leader. As has first been shown by Meek,[9] this implies that, with increasing gap length, the negative downward leader has to approach increasingly nearer to the earth electrode before an upward streamer is initiated, so that the latter covers a progressively smaller proportion of the total gap.

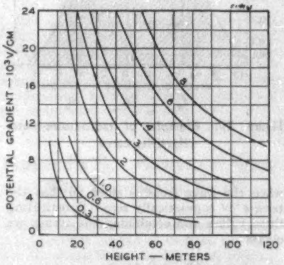

Figure 1. Variation of potential gradient at earth surface with height of tip of leader channel above ground and for varying charges on leader channel

The figures against the curves denote the charge on the leader stroke in coulombs

Since laboratory streamers from earthed electrodes invariably bridge a greater portion of the total gap than in the natural lightning case, it follows that model lightning conductors or similar structures produce a protective effect which is too large.

Geometrical considerations with a view

---

* Indirect evidence as to Franklin's opinion on this question is given later.

† The historically minded reader will find ample references to earlier work in books[1] on this subject.

Paper 45-141, recommended by the AIEE committee on power transmission and distribution for publication in AIEE Transactions. Manuscript submitted February 10, 1945; made available for printing July 9, 1945.

R. H. Golde is senior technical assistant with the British Electrical and Allied Industries Research Association, London, England.

The author is indebted to the British Electrical and Allied Industries Research Association for permission to publish this paper.

Table I. Flashes to Earth Close to Tall Earthed Metal Conductors

Height of Earthed Conductors, m	Distance of Flash to Earth, m	Protective Ratio Less Than
430	500	1.16
	600	1.40
	750	1.74
	750	1.74
	800	1.86
	800	1.86
	850	1.98
520	1,000	1.92
900	1,000	1.11
	1,000	1.11
	1,000	1.11
	1,150	1.28
	1,150	1.28
	1,150	1.28
1,000	1,200	1.20

to determining the protective range of a lightning conductor were introduced by Peek.[10] According to the state of knowledge at his time, he assumed a lightning stroke to develop in a field equal to the breakdown strength of air in a uniform field, and this led him to believe that a lightning stroke to earth followed the shortest possible line between the cloud and the object to be struck. As it is now known[11] that a lightning stroke actually develops in a field of a fraction of that believed to be necessary in former times, it follows that Peek's assumptions are no longer valid and that the protective radii deduced by him are again too large.

If the preceding description of the development of a lightning discharge and of any upward streamers from earth or an earthed object is accepted, it must be emphasized that lightning strokes vary in their characteristic parameters, and it is therefore to be expected that the range of protection afforded by a lightning conductor may vary in some similar manner. This then constitutes a departure from present conceptions and from previous investigations which were mainly confined to determining the *minimum* value of the protective radius. The problem under discussion can therefore be restated as an inquiry into the *average* protective ratios of a lightning conductor and of the various earthed parts of a transmission system and their possible variation with the parameters of the lightning discharge.

APPROXIMATE CALCULATION OF THE PROTECTIVE AREA

With a view to determining the protection afforded by a lightning conductor, the lightning leader stroke, as it progresses towards earth, should be regarded as a charged conductor which, according to the laws of electrostatics, determines the field strength at the earth's surface within its sphere of influence.* Now reasons have been given elsewhere[5] for assuming the charge density along the leader channel to be highest at its tip, and to decrease according to an exponential law towards the cloud (see equation 5 of the appendix). With some reasonable assumptions as to the exponential factor, the electrostatic field which is produced at the earth's surface around the leader stroke then can be calculated as a function of the total charge distributed along the leader channel, and of the instantaneous height of the tip of the leader stroke above earth. This calculation is given in the appendix in which equation 9 gives the field strength in volts per centimeter underneath the down-coming leader stroke as a function of the charge on the leader channel, the instantaneous height of the tip of the leader stroke, the height of the cloud center which is taken as 2.5 kilometers, and the horizontal distance between the point of observation and the projection of the leader channel.

For a point directly underneath the leader stroke, the field strength is given by equation 10 of the appendix, and this enables the field strength produced directly below the leader stroke to be calculated as a function of the instantaneous height of the tip of the leader, and for varying values of the charge q_0 deposited along the channel. The results are plotted in Figure 1.

Once this set of curves is obtained, the question now arises as to the field strength at which upward streamers may be expected to develop from the earth's surface. There are no data available on this value, but for a rough estimate the following arguments may be used. In a uniform field the initiating breakdown strength is 30,000 volts per centimeter, and in a long nonuniform gap the average breakdown strength, calculated as the ratio of flashover voltage over distance, is known to be of the order of 5,000 volts per centimeter. The condition pertaining to the earth's surface should lie between these two values, and, if it is considered that the surface is not an ideal plane but is covered by grass blades, stones, or other irregularly shaped materials, an average figure of 10,000 volts per centimeter for the initiation of upward discharges may be reasonable. Once a local discharge has started, it will develop rapidly into an upward streamer, owing to the influence of the highly charged tip of the leader stroke and the availability of the accumulated charge in the earth, the gradual collection of which during the leader process has been described.

Table II. Number of Flashes to Safe Harbor–Westport–Takoma Line

	1935	1936	1937	1938	1939
Estimated by ERA†	119	107	101	56	117
Estimated by Waldorf	115	108	87	54	118

† British Electrical and Allied Industries Research Association.

If the afore-mentioned value is accepted, the point where the 10,000-volt-per-centimeter line crosses the individual charge curves in Figure 1 represents the height above earth to which the down-coming leader stroke must proceed before streamers from the earth's surface can be expected to develop under normal conditions.

As can be seen from Figure 1, this height increases with increasing charge of the leader channel, so that the length of any upward-streamer discharges from earth should depend on the intensity of the lightning stroke. For an average charge of one coulomb distributed along the leader channel, the height of the leader tip at which a field strength of 10,000 volts per centimeter is produced at the earth's surface is seen to be about 17 meters. While there are no observational data available to prove or disprove this value, it is interesting to note that it corroborates an earlier conclusion[8] from photographic evidence as to the short length of any possible upward streamers from the earth's surface.

A further interesting conclusion to be drawn from Figure 1 is that the leader of an average lightning stroke to a point on the earth's surface may proceed below the level height of an average tower of say 20 to 25 meters height, before the precise point *ultimately* to be struck is determined. It therefore may be assumed that, under average conditions, the lowest level from which a lightning leader stroke may be "attracted" to strike a lightning conductor or transmission tower lies as low down as the level of the conductor or tower top itself. That such sudden changes in the direction of the leader stroke may in fact occur can be seen from photographs collected and discussed by B. Walter[12] and also from Figure 2 which shows a direct stroke to a wireless mast.[13]

If it thus is agreed that the lowest

Figure 2. Lightning flash to a wireless mast[13]

---

* This neglects the electrostatic field strength due to the predischarge field. This, however, amounts to only a few per cent of the field strength required to produce a streamer discharge from earth.

height h_1 at which a flash to a tower may occur in preference to a flash to earth is given either by the height obtained from Figure 1 at 10,000 volts per centimeter, or the height of the structure itself, whichever is the higher, equation 9 can be evaluated. The resulting curves are plotted in Figure 3, which gives the field strengths produced by the downcoming leader stroke at the heights discussed and for various stroke intensities as a function of the horizontal distance y.

Strictly speaking, the values calculated from equation 9 and plotted in Figure 3 apply to a space which is undisturbed by any conducting objects. In the presence of such an object, for example, a lightning conductor or tower, zero potential is impressed on its tip, and the field distribution is varied from the undisturbed condition. Similarly the field strength, which was found to exist at the surface of the earth, is by no means uniform in a vertical direction. Nevertheless, as a first approximation it may be permissible to assume that the field strength at the top of a lightning conductor is given by equation 9 and Figure 3.

The field strength at which streamers may develop from an earthed structure, such as a lightning conductor, also cannot be stated at present with accuracy. As mentioned, the mean breakdown strength of the longest gaps investigated, about two meters, is about 5,000 volts per centimeter, and this value appears to decrease slowly but steadily with increasing distance. On the other hand, it is now known that a lightning stroke occurs in an average field of a few hundred volts per centimeter. If we start from these two extremes, it may appear reasonable to adopt as a first estimate a value of 3,000 volts per centimeter for the field strength capable of producing streamers from lightning conductors or similar structures.

It follows that the distances y at which the horizontal line drawn through 3,000 volts per centimeter in Figure 3 crosses the individual charge curves represent the corresponding protective radii of a lightning conductor or similar structure.

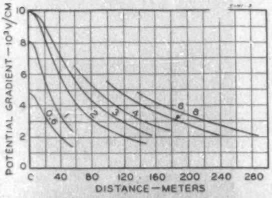

Figure 3. Variation of potential gradient with horizontal distance from leader channel and for varying charges on leader channel

The figures against the curves denote the charge on the leader stroke in coulombs

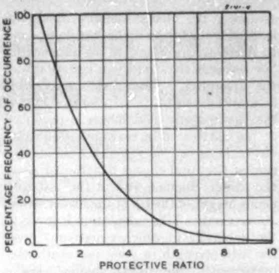

Figure 4. Protective ratios of a lightning conductor 20 meters high

Figure 3 then permits several interesting conclusions to be drawn. It has been shown elsewhere[5] that the magnitudes of lightning currents are proportional to the charges deposited along the leader channel and that an average current of 20 kiloamperes corresponds to about one coulomb. A distribution curve of the frequency of occurrence of lightning currents of varying amplitude should, therefore, provide a direct indication of the frequency distribution of the distances protected by a lightning conductor.

Before, however, any of the published curves showing the frequency distribution of lightning currents can be accepted, the limitations of these curves should be recognized clearly. Thus, it has been shown[14] that the great number of curves based either on the algebraical summation of the tower currents affected by one flash or on the summation of tower and earth wire currents nearest the point struck are misleading owing to the phase difference between the current components which are discharged through towers and earth wire, respectively. Two sets of curves[15] which are based on magnetic-link measurements in lightning rods on the top of transmission towers and on the summation of earth-wire currents, while more correct, suffer from the limitation of this and most other magnetic-link installations of being unable to record currents below five to ten kiloamperes. Since this paper was drafted, a further curve has been published[16] which is based on the highest component currents discharged through structures of varying heights, and this curve has the advantage of extending the current range down to a few hundred amperes. On the other hand, there is reason to believe that the amplitude of a lightning discharge depends to some extent on the height of the structure struck. Furthermore, the protective range of an earthed structure is determined by the charge distribution of and therefore by the resulting current in the first component stroke of a multiple-discharge flash, and, while this is known to carry in most cases the highest current, this is not always the case. If, despite these limitations from the present viewpoint, this last mentioned curve be accepted as a true distribution curve of the amplitude of the first stroke of a lightning flash, Figure 4 can readily be derived as showing the frequency variation of the protective ratio* of a lightning conductor or earthed structure of about 20 to 25 meters height. It thus can be seen that the protective ratio varies with the current intensity of lightning discharges** and the range protected is seen to vary between a few and about 200 meters, that is, a protective ratio from less than one to about ten.

For the purpose of the present investigation the most important conclusion to be drawn from Figure 3 is the average value of the radius protected by an earthed structure. As mentioned, the average charge of a leader stroke is about one coulomb, and Figure 3 shows that, for a structure of about 20 to 25 meters height, the distance protected amounts to about 45 meters. It thus can be said that such a structure has an average protective ratio of about 2, and this value will be used for subsequent considerations.

COMPARISON WITH FIELD OBSERVATIONS

As has been shown, the protective ratio of a lightning conductor can no longer be regarded as a constant figure which, apart from the ordinary vagaries of the spark discharge, is determined merely by the position of the tip of the lightning channel relative to the lightning conductor; instead, it is now recognized to vary over a considerable range, according to the intensity of the lightning stroke. In order to prove this statement by means of field observations, a great number of cases would be required in which the distance of the point struck from a nearby lightning conductor should be given in conjunction with the current amplitude of the first component stroke. Such data are not available.

Now, whereas the possibility of a lightning flash striking at a great distance from a lightning conductor is self-evident, it appears that there still exists some doubt as to the possibility of a direct stroke within distances of less than two or three times the height of the lightning conductor.† However, a survey of the literature will readily furnish instances of flashes within protective ranges smaller than those mentioned. It is impossible to enumerate these cases, and it must be sufficient to refer to the relevant literature. But to give a few examples, the oldest and one of the most famous cases[19] may be mentioned; this bears a particular interest, owing to the fact that the lightning-conductor system involved had been installed as the result of a report given by four eminent scientists, one of whom was Benjamin Franklin. Figure 5 shows a sketch of a British Government building at Purfleet which was struck and slightly damaged, as indicated, in 1777. The lightning conductor was found to be in perfect condition and well earthed, and the ratio of the distance of the corner struck from the conductor to the latter's height above the height of the point struck can be determined at 1.63:1. As this installation had Franklin's approval, it may be assumed that he regarded the whole building to be within the protective zone of the lightning conductor; but it may be significant to mention that the slight damage caused to the building tends to suggest a rather weak flash, and this may account for the low protective effect of the lightning conductor in this particular instance.

---

* From the new conception of the protective range it follows that the frequency distribution of occurrence of lightning currents should differ in strokes to open country and to different types of earthed metal structures. This matter is being further investigated, but the effect has been neglected in the present account.

** Bruce[17] predicted a variation of the zone of protection with the intensity of the lightning current from his theory on the mechanism of the lightning discharge.

†Thus the latest code of the Bureau of Standards[18] takes the radius of the base of the protected cone as two to four times the conductor height.

Among more modern observations, Walter[20] plotted, on a map of the old part of Hamburg, the situation of houses which had succeeded in insurance claims owing to damage from lightning in the course of the period from 1912 to 1932. As can be seen from Figure 6 there exist among the 25 buildings damaged four cases in which the buildings were situated within distances of less than twice the height of nearby church steeples above them.

Again, in the course of some lightning investigations in Russia,[21] apparently with test balloons, which were kept flying at various heights in conducting connection with earth, several strokes were noted at distances between one and two times the height of the earthed conductors. The results of the observations are given in Table I from which the lowest protective ratio indicated is seen to be less than 1.11, even with the great heights of the conductors involved. While the present account is intended to be limited strictly to lower structures, these observations certainly confirm the occurrence of flashes within distances which often are regarded as safe.

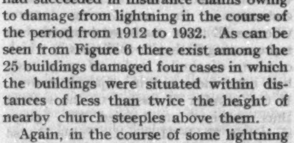

Figure 5. Sketch of building struck by lightning in 1777

Table III. Frequency of Flashes to Transmission Lines

Name of Line	Figure	Length, Miles	Span Length, Feet	Area "Covered," Square Miles	Number of Flashes Experienced	Years of Observation	Flashes Per Square Mile Per Year
Safe Harbor–Westport–Takoma	9b	91.8	1,050	4.60	698	8	19.0
Safe Harbor–Perryville	9d	32.5	1,000	2.21	365	8	20.6
Holtwood–York	9c	22.8	660	0.95	190	7	28.5
Holtwood–Coatesville	9e	29.4	650	1.17	253	7	30.9

That similar conditions may obtain for transmission lines can be shown by observations[22] on two parallel transmission lines, the approximate dimensions of which are given in Figure 7. The lower wood-pole line which was erected in 1920 suffered no outage during its first four years of service. In 1924 the parallel higher steel-pole line was built and, in the course of the subsequent $20^1/_2$ years six outages were experienced* on the wood-pole line. This, then, clearly indicates that the wood-pole line is not completely protected by the earth wire of the higher line, so that the protective ratio of this particular earth wire is, under certain conditions, less than 1.5:1.

The few examples quoted should suffice to show that the low protective ratios suggested by Figure 4 do not disagree with observations.

Areas Covered by the Various Elements of a Transmission Line

If we revert to the average area protected by a lightning conductor as derived, this can be applied directly to the case of a steel tower which represents a pointed earthed structure and which, therefore, may be taken to protect, on an average, a circle round its base, the radius of which is equal to twice the tower height.

The case of an ordinary overhead earth wire cannot be based strictly on the foregoing considerations; for, whereas the tower has always pronounced corners or points from which distinct streamers may readily develop, an earth wire is a smoother and more uniform conductor which can be expected to produce, under the influence of the approaching leader channel, a corona envelope over a certain length of its surface. The more uniform field distribution which results should increase the total field strength required to produce a distinct point discharge which, after having been once initiated, will draw all the charge from the neighboring parts of the earth wire up to itself and thus develop into an upward streamer. In the absence of experimental data it can merely be argued that the area "covered" by an earth wire should be smaller than that protected by the tower, and as a first estimate a value of 1.5 will be accepted for the subsequent calculations. An earth wire thus will be deemed to collect, on an average, all flashes likely to fall on an area which is given by the product of its length, and a width equal to three times the average height of the earth wire above ground, the latter being taken as 80 per cent of the tower height.

The conditions governing discharges from phase wires are different again. A phase wire is insulated from earth, and, even in the case of a system with earthed neutral point, it is earthed only over a transformer which may be very distant from the point to be struck. The charges required to build up the streamer discharges which are readily available in an earth wire, therefore, in the case of a phase wire, may have to be transported over several miles of line and cannot often be expected to be available readily during the few microseconds constituting the last step of the downward-leader stroke.† This difficulty further should reduce the area covered by a phase wire, and the protective ratio may be assumed to be equal to unity, so that a phase wire without earth-wire protection may be assumed to be struck, on an average, by all those flashes which originate above an area given by the product of its length, and a width equal to twice the average height of the phase conductor above earth. This average height is again taken to be 80 per cent of the height of the phase wire at the tower.

The foregoing considerations now make it possible for the areas to be calculated which are, on an average, covered by various types of transmission systems. To differentiate between the areas covered by towers and earth or phase wires, respectively, it is assumed, as shown in Figure 8, that the conductors cover the span up to the point at which their protective areas intersect the protective circles of the towers. If we assume now

h_t = height of tower
h_e = average height of earth wire above earth
h_p = average height of phase wire above earth
b_e = horizontal distance between earth wires
b_p = horizontal distance between outermost phase wires
l = span length

---

* According to information supplied by A. E. Davison of the Hydro-Electric Power Commission of Ontario.

† This leads to the interesting conclusion that the liability of phase wires to receive a direct hit should increase with decreasing distance from an earthed transformer. For systems with earthed neutral points, this consideration gives further emphasis to the importance of improved protection against direct strokes over the first few spans from a station.

the areas covered by each span of a transmission line may be determined as follows:

(*a*). Line without earth wire:

$$4h_t^2\pi+(l-2\times 2h_t)(b_p+2h_p)$$
$$=4h_t^2\pi+(l-4h_t)(b_p+2h_p) \quad (1)$$

(*b*). Line with one earth wire:

$$0.9\times 4h_t^2\pi+(l-2\times 1.6h_t)2\times 1.5h_o$$
$$=3.6h_t^2\pi+(l-3.2h_t)3h_o \quad (2)$$

(*c*). Line with two earth wires:

$$0.8\times 4h_t^2\pi+(l-2\times 1.5h_t)(b_o+2\times 1.5h_o)$$
$$=3.2h_t^2\pi+(l-3h_t)(b_o+3h_o) \quad (3)$$

In these expressions the first term signifies the area covered by the transmission tower, and the second term that covered by the phase or earth wires, respectively. It follows that the proportion of flashes likely to fall on the conductors in mid-span and on the towers can be found readily by the quotient of the two terms considered.

Expressions 1 to 3 thus enable the probable number of flashes to any type of transmission line to be calculated if the line dimensions and the number of flashes to earth over a given area are known, and they also give an indication of the distribution of flashes between towers and mid-span.

DISTRIBUTION OF POINTS STRUCK ON A TRANSMISSION LINE

In what follows the foregoing developed expressions are employed to calculate the probable average distribution of flashes to various parts of a transmission system. The results obtained then are compared with relevant published information, and it may be mentioned that the examples discussed constitute, to the best of the author's knowledge, all the statistical material available.

Ratio of Flashes to Phase Wires and Towers on Lines Without Earth Wire. From what has been said, this ratio can readily be found by dividing the second term of equation 1 by the first term. For an average medium-voltage line which may be operated without earth wire, the following numerical values may apply:

h_t = 50 feet
h_p = 35 feet
b = 20 feet
l = 500 feet

This gives a ratio for flashes to the phase wires in mid-span over flashes to towers of 0.86. According to German statistics[23] obtained on 170 kilometers of 6 to 16 kv and 80 kilometers of 100-kv lines, 103 flashes to the phase wires were observed as against 143 flashes to towers on lines without earth wire. This gives a ratio of 0.72 which is lower than the value calculated. The discrepancy possibly may be explained by the lack of knowledge of the correct dimensions of the lines involved, but it also may be due to the fact that the German statistics did not succeed in noting all cases of flashes to phase wires at mid-span. Since no indication is given as to the method by which flashes to phase wires which did not produce flashover were recognized, the foregoing uncertainty cannot be eliminated.

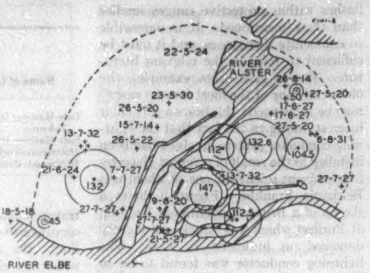

Figure 6. Damage caused by lightning in old part of Hamburg[30] during 1912 to 1932

+ Building damaged by lightning

● Tower; inner circle denotes height of tower minus 25 meters; outer circle has twice that distance

Ratio of Flashes to Earth Wire and Towers on Lines With One Earth Wire. For an average high-voltage line with one earth wire the following dimensions may be assumed:

h_t = 80 feet
l = 800 feet

From equation 2 the ratio of flashes likely to hit the earth wire at mid-span to those hitting a tower is found to be 1.44. German observations of 516 cases on high-voltage lines give 42 per cent of all flashes striking the towers and 58 per cent the earth wire in mid-span, that is, a ratio of 1.38. If we consider that the correct dimensions of the lines involved were again unknown, the agreement appears satisfactory.

Ratio of Flashes to Earth Wires and Towers on Lines With Two Earth Wires. For this case two sets of relevant observations are available, and these will now be discussed.

The essential dimensions of the Wallenpaupack–Siegfried line[24] are given in Figure 9a, to which need only be added the average span length of 1,110 feet. As the tower is of the portal type, equation 3 has to be slightly modified. The calculation, however, should be readily followed if the numerical evaluation of the ratio to be determined is given as follows:

$$\frac{(1{,}110-3\times 80)(23+3\times 0.8\times 80)}{3.2\times 80^2\pi+45\times 3\times 80}=2.48$$

Of 23 well-defined flashes to that part of the line which is equipped with double earth wires, six were found to have occurred to towers and 17 to spans, that is, a ratio of 2.83. With regard to the small number of cases observed, the agreement between calculated and observed values is satisfactory.

The second set of data applies to the 220-kv Safe Harbor–Westport–Takoma Line[25] of the Pennsylvania Water and Power Company.* The essential dimensions of that line, which has an average span length of 1,050 feet, are given in Figure 9b. The calculation of the ratio of flashes to mid-span and towers, identical with that for the preceding line, gives

$$\frac{(1{,}050-3\times 84)(42.25+3\times 0.8\times 84)}{3.2\times 84^2\pi+42.25\times 3\times 84}=2.39$$

No analysis as to the ratio of hits to earth wires and towers was published by Waldorf, but it previously had been made by the author for a different purpose by counting all those cases as flashes to towers where sufficiently high currents were measured in one tower with smaller currents in the neighboring towers, whereas all those cases were regarded as representing flashes to mid-span in which currents of similar order of magnitude had been measured in adjacent towers. If the number of flashes to the system thus obtained are totaled, the figures shown in Table II result. Table II also shows the numbers given in Waldorf's own estimate, the basis of which is not accurately known. The agreement is good enough to regard the present analysis as sufficiently substantiated.

It can be shown that a lightning discharge of a given intensity which causes a certain current to be discharged through a tower which it strikes directly produces a current discharge of roughly half that amplitude through the two neighboring towers in the case of its striking in mid-span. In order to obtain a consistent basis for analysis, the ratio of the number of flashes to the earth wires in mid-span to that of flashes to towers is based on minimum values of tower currents of five kiloamperes in the first and ten kiloamperes in the second case. The numbers thus obtained are 252 and 102 flashes, respectively. This suggests a ratio of 2.47 as against the calculated value of 2.39, an agreement which again can be regarded as satisfactory.

It thus may be said that on an average medium-voltage line without earth wire the towers may be expected to experience slightly more direct strokes than the phase wires in mid-span. With installation of earth wires and increasing span lengths, the number of direct strokes to an earth wire increases rapidly until, for a line with two earth wires and long spans, the earth wires may be subjected to $2^1/_2$ times as many direct flashes as the towers.

---

* The author is indebted to S. K. Waldorf of that company for putting the magnetic-link records of this and other lines at his disposal.

EFFECT OF THE INSTALLATION OF EARTH WIRES

From the earlier assumptions as to the areas protected by a phase wire and by an earth wire, respectively, it follows that the addition of an earth wire to an existing line should cause an increase in the number of flashes to the system. This effect might be checked numerically in the practical case of a line which was operated over a number of years without and later with earth wires. Such a line is the 66-kv Holtwood–York line of the Pennsylvania Water and Power Company, the performance of which may now be analyzed.

The type of tower used on this line is shown diagrammatically in Figure 9c. During its original operation without earth wires the line, which has an average span length of 660 feet would be expected, from equation 1, to cover the following area per span:

Area covered by tower $4\times75^2\pi=70{,}600$ square feet

Area covered by phase wire $(660-4\times75)(19+2\times0.8\times65)=44{,}300$ square feet

This suggests a ratio of flashes to mid-span to those striking the towers of 0.63. Now between 1925 and 1935 the number of single-circuit flashovers recorded on this line[26] amounted to 101, or 9.2 per year. If it be assumed that all these flashovers were due to flashes to phase wires, an assumption which should not be far from actual facts, owing to the high average footing resistance of 133 ohms which would favor double-circuit flashovers in the case of flashes to towers, the number of flashes to towers would be expected from the preceding striking ratio to be 14.7 per year. Actually 112 double-circuit flashovers or 10.2 flashovers per year have been recorded from which it might be concluded that about 30 per cent of the flashes to towers did not cause back flashover.

Towards the end of August 1935 two earth wires were added to the existing line, and in order to reduce the high footing resistances continuous counterpoise wires were installed. With this arrangement the area covered by every span of these lines becomes

Area covered by tower $0.85\times4\times75^2\pi+3\times11\times75=62{,}500$ square feet

Area covered by earth wires $(660-3\times75)(11+3\times0.8\times75)=83{,}100$ square feet

which suggests 1.33 times as many flashes to mid-span as to towers. As can be seen from the foregoing figures the area covered by the mid-span has been increased by the addition of the earth wires by a factor of 1.87 and the area covered by the towers reduced by a factor 0.88. This leads to an expectation of

$9.2\times1.87=17.2$ flashes per year to mid-span

and

$14.6\times0.88=12.9$ flashes per year to towers

or a total of 30.1 flashes to the complete system per year, which agrees well with the 190 flashes recorded[23] by means of magnetic links in seven years of operation, that is, 27.2 flashes per year.

The foregoing calculations lead therefore to the conclusion that the addition of the two earth wires increased the total number of flashes to the system from 23.9 to 30.1 per year, that is, an increase of 26 per cent. It may be added that the distance between these two earth wires is exceptionally small, and that a distance of more normal dimensions would have raised this figure higher. However, the increase in the number of flashes to the system does not involve an increased number of flashovers on the line. On the contrary, the installation of earth wires not only should prevent any direct strokes to phase wires in mid-span but also may have an additional beneficial effect in reducing the number of strokes to towers.

Frequency of Lightning Flashes

NUMBER OF FLASHES TO TRANSMISSION LINES

As has been mentioned equations 1 to 3 enable the number of flashes to a transmission line to be calculated if the number of flashes to earth over the area affected is known. Conversely, if the number of flashes to a transmission line is known, equations 1 to 3 provide the means of determining the local number of flashes to earth.

Such statistical data are available for four lines of the Pennsylvania Water and Power Company, some of which already have been discussed. As the method of calculation of the area protected by the various elements of a transmission line should be clear from the various instances already given, it may be sufficient to give the final results of the calculations. The dimensions of the lines involved, are given in Figure 9, and the results obtained in Table III.

The foregoing four lines of widely varying construction thus indicate figures between 19.0 and 30.9 flashes per square mile per year. Though these lines are operated by the same company, it is interesting to note that their isokeraunic levels vary markedly. Thus the isokeraunic levels for the first three lines considered are stated[26] to be 39, 42, and 62, respectively. A figure for the fourth line could not be found in the literature, but, owing to its proximity to the Holtwood–York line, it may be assumed to have the same value of 62. If the numbers of flashes calculated are plotted against the isokeraunic level, the crosses given in Figure 10 result. These points in the absence of further data clearly suggest a linear variation of the frequency of flashes to earth with the isokeraunic level, and this assumption is represented by the straight line drawn in Figure 10.

It may be worth mentioning that the isokeraunic level as defined does not necessarily give a measure of the severity of the storm in a certain region. This severity may well depend on the contour of the landscape, and great variation in the number of discharges to earth may result on that account. However, as the number of days with thunder heard is the only standard figure which is universally available, it must at present be accepted as the basis of reference. Furthermore, with regard to the many assumptions involved in the calculations given, it appears reasonable to adopt the straight-line law in Figure 10 until further data may be available.

Reference may be made to McCann's recent account[16] (which came to hand only after this paper had been drafted) of the number of direct lightning flashes to 19 fire towers and similar structures of about 100 feet height with an average of 2.7 years of observation. For an isokeraunic level of 40, Figure 10 suggests an average of 20 flashes per square mile per year, and this leads to an expectation of 4.6 flashes during the period covered. Actually ten flashes were noted, but this discrepancy may be due to one or more of the following three factors:

1. The few years of observation may have caused more than the average number of flashes to earth.
2. The fire towers may be situated on ex-

Table IV. Frequency of Faults on Lines Without Earth Wire

Name of Line	Figure	Area "Covered," Square Miles	Number of Faults Experienced	Years of Observation	Flashes Per Square Mile Per Year	Isokeraunic Level
Wallenpaupack–Siegfried	9a	1.35	138	8	12.8	35
Turner–Logan[33]	9g	1.52	55	3	12.1	54
34/*K*[39]	9h	1.16	233	10	20.0	65
34/*O*[39]	9i	2.42	339	10	14.0	65

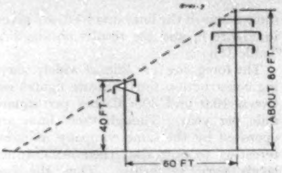

Figure 7. Diagram of Nipigon lines of the Hydro-Electric Power Commission of Ontario

posed hills which would increase their effective height above ground and therefore their susceptibility to flashes.

3. The currents involved may have been greater than average.

These data therefore do not invalidate Figure 10 from which it may be concluded that the number of flashes to earth per square mile per year is roughly equal to one half of the figure for the isokeraunic level of the area involved.

NUMBER OF FLASHOVERS ON TRANSMISSION LINES

In view of the few transmission lines discussed in the preceding section, for which the number of lightning hits is accurately known, an attempt now will be made to obtain further evidence from field observations in support of the curve given in Figure 10. There appear to exist two methods of approach:

1. **From data on lines fitted with protector tubes with counting devices.**
2. **From steel tower lines without earth wires.**

In both cases the numbers of flashovers registered depend on the average tower-footing resistances of the lines involved, so that the following analysis should provide some minimum figures for the number of flashes to earth, with the deviation of numbers of flashovers from that of actual flashes to the system increasing with decreasing footing resistances.

In the first category mentioned, statistical data on the number of operations of protector tubes are available[27] for the 132-kv Roanoke–Danville line of the American Gas and Electric Service Corporation. The total area covered by this line (Figure 9f) amounts to 3.31 square miles with a ratio of area covered by the earth wire as against that covered by towers of 1.98. The total number of tube operations including external flashovers of the tubes in the course of four years was found to be 426. Now this figure cannot be taken as equal to the number of flashes to the line since flashes to an earth wire in mid-span may be expected, in view of the high average footing resistance of the line of 67.3 ohms, to produce tube operation on both the adjacent towers. These two relations, that is, the ratio of flashes to mid-span and tower and the assumption that the total number of tube operations is equal to the sum of the number of flashes to towers and twice the number of flashes to mid-span, enable the total number of flashes to be found. This then gives 170 flashes to mid-span as against 86 flashes to towers or, with the data given, 12.8 flashes per square mile per year to mid-span, and 6.5 flashes per square mile per year to towers, that is, a total of 19.3 flashes per square mile per year to earth.

As already explained, this latter number should be regarded as a minimum value, since even with the high average footing resistance of 67.3 ohms, a few flashes may not cause a back flashover. In order to indicate this "minimum" character the result is plotted in Figure 10 against the isokeraunic level of the line of 34 as a point with a vertical arrow pointing upwards.

As to the second category, that is, steel-tower lines without earth wires, four lines can be analyzed. The results obtained are given in Table IV and plotted in Figure 10, the fact of their being minimum values being indicated by upward arrows.

As previously mentioned, high footing resistances should produce small differences between the minimum values calculated and the curve shown in Figure 10, whereas low footing resistances should cause considerable deviations. The average footing resistances for the three lines given in Table IV in combination with Figure 10 clearly conform with this prediction, and it may also be expected that line 34/*K* has a higher average earthing resistance than line 34/*O*, though both may be expected to be moderate.

In this connection it may also be interesting to analyze further the information available for the Turner–Logan line, though its operation of only three years without earth wire is rather too short to permit of any generalization. If the curve shown in Figure 10 is accepted as correct, the area under consideration should, with its isokeraunic level of 54, be subjected to 26 flashes to earth per square mile per year. Now a calculation of the areas covered by the phase wires in mid-span and the towers, respectively, suggests a ratio of 1.29 flashes to phase wires for every flash to a tower, so that altogether the phase wires should be struck annually by 14.6 flashes, and the towers by 11.4 flashes.

Actually the three years' record of the Turner–Logan line shows an average of

16 single-circuit flashovers per year.
2.3 double-circuit flashovers per year.

If it be assumed that all 14.6 flashes to phase wires produce single-circuit flashovers, the flashes to towers should be expected to cause per year:

2.3 double-circuit flashovers, or 20.2 per cent.
1.4 single-circuit flashovers, or 12.3 per cent.
7.7 cases without flashovers, or 67.5 per cent.

In view of the average footing resistance of 10.9 ohms, this result appears not unreasonable.

FREQUENCY OF LIGHTNING FLASHES TO EARTH

The results obtained in the preceding sections are at least not in contradiction to the frequency curve given in Figure 10. Whereas it appears therefore desirable to obtain some additional direct information about the number of flashes to earth, a survey of the technical and meteorological literature leads to the surprising result that there do not appear to exist any long-term counts of flashes to earth.

Indirect information can be obtained from two series of investigations with the point discharge recorder in England, from the number of buildings struck or of trees damaged by lightning, and from the number of human casualties. This material is discussed in an investigation which soon will be published in the *Quarterly Journal* of the Royal Meteorological Society, London, where it is shown that all the methods named are open to objection and in fact cannot be expected to provide more than minimum values.

With regard to this lack of data, an attempt was made to obtain the information required for England by means of a census to which the author's colleagues and a number of undergraduates of Cambridge University were subjected. The method adopted and the result obtained by this census are described in detail in the afore-mentioned publication. It must suffice to state here that a total of 254 persons (including all the author's 142 colleagues and a random selection of 112 undergraduates) with a total experience covering more than 4,000 years were asked to report all cases of close lightning flashes within their memory. With every precaution in the analysis being taken, a figure of about six flashes per square mile per year was deduced, areas involved being England proper with a pronounced bias towards the southern half and the area around London. The average isokeraunic level of this area may be stated

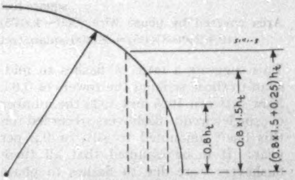

Figure 8. Protective ranges of towers and earth wires

to be about 14, and this result appears to fit well the curve suggested in Figure 10.

Discussion of Results

In assessing the results obtained it should be kept in mind that the present investigation represents the first attempt to put the problem of the protective range of a lightning conductor or a similar structure on a physical basis.

Now the numerical evaluation of the solution of the problem suggested herein entails two basic assumptions, namely, as to the initiating field strength for upward streamers from ordinary ground and from an earthed metal structure. The numerical values estimated were shown to lead to an average protective ratio which appears reasonable. Similarly, from field data on the frequency of flashes to transmission lines, numbers of flashes to earth are suggested which at least appear to be in no disagreement with the evidence available.

The question now arises as to the best method to obtain actual information on the field strength which is required to initiate upward-streamer discharges. If the possibility of future experimental and field work which it is hoped may be undertaken is omitted, some relevant information is available in a recent paper by Bruce[11] in which it is shown that the ordinary law for the current discharge from a pointed conductor:

$$i=cE^2 \qquad (4)$$

in which

i = the discharge current in amperes
c = a constant
E = the potential of the discharge point in volts

is apparently also applicable to the case of the lightning discharge.

From this theory of the lightning discharge Bruce deduces that a self-propagating discharge develops when the current in the initial streamer discharge reaches a value of about one ampere, that is, the transition current from a glow to an arc discharge. Accepting this current value and for a value of 3,000 volts per centimeter adopted earlier for the initiating field strength from an earthed metal conductor of 20 meters height, the constant c is found from equation 4 to be 2.78×10^{-14} as against $c = 2.5 \times 10^{-13}$ derived by Bruce. While the agreement is not perfect, it is good enough to suggest that further investigation of the factor c might provide the missing link in a more accurate calculation of the field strength required to produce streamer discharges. In addition, when the variation of the factor c with the height of the earthed conductor and with polarity has been determined, the combination of the data with the methods suggested in this investigation should render the question of the protective effects of high conductors and allied problems readily calculable.

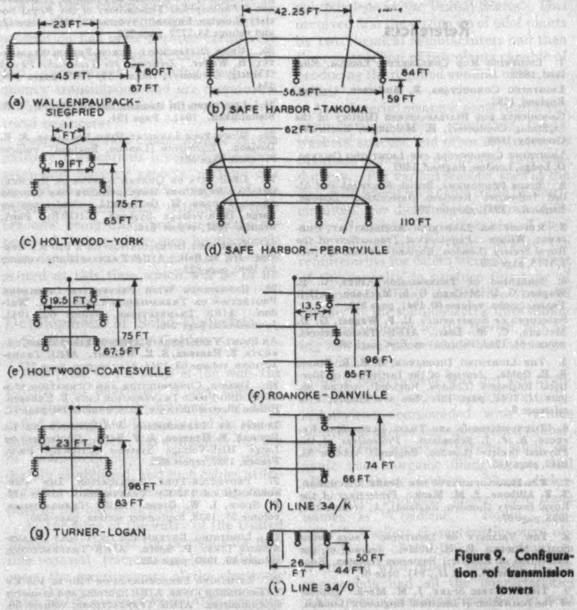

Figure 9. Configuration of transmission towers

Conclusions

While no finality can be claimed for the numerical results obtained in this investigation, owing to the inherent uncertainty of some assumptions which had to be made, it is felt that the methods developed herein throw new light on the problem of the protective range of a lightning conductor and related questions. With this limitation in mind the following conclusions can be drawn:

(*a*). A method has been evolved for calculating the protective range of a lightning conductor or a similar structure.

(*b*). With numerical assumptions as to the field strength required to initiate an upward streamer from open ground and from a pointed earthed conductor, the average protective range of a lightning conductor of ordinary height is found to be about 2.

(*c*). The protective ratio is shown to vary with the intensity of the lightning current, such that it increases with increasing amplitude of the lightning current.

(*d*). The distribution of direct strokes between transmission towers and earth wires or between towers and phase wires in cases of lines without earth wires has been determined. An indication also is given of the increase in the number of flashes to a system, due to the addition of earth wires. Calculated values are shown to agree with field observations.

(*e*). The number of lightning flashes to earth is given as a function of the isokeraunic level of the district.

(*f*). By reversing the procedure underlying items *d* and *e*, the number of probable flashes to a transmission line and their distribution between various parts of the line can now be calculated if the isokeraunic level of the district is known.

(*g*). Suggestions are made as to further investigations to correlate the method developed herein with the physical phenomena governing the initiation of streamer discharges.

Appendix. Calculation of the Earth's Potential Gradient Underneath a Leader Stroke

Reasons have been given elsewhere[5] for assuming the charge density Q_h at any height of a leader channel h above earth to decrease towards the cloud according to the exponential law:

$$Q=Q_0\epsilon^{-\beta h} \qquad (5)$$

where Q_0 is the charge density at ground level and β a constant of about 10^{-6}. With relation 5 the total charge q_0 deposited along the leader channel before it contacts earth becomes

$$q_o = Q_o \int_0^{h_2} \epsilon^{-\beta h} dh = \frac{Q_o}{\beta}(1-\epsilon^{-\beta h_2})$$

where h_2 is the height of the cloud charge. Taking this latter as 2.5×10^5 centimeters the total charge is seen to be approximately

$$q_o \approx \frac{Q_o}{\beta} \qquad (6)$$

Now the potential gradient at a plane under the influence of a point charge q, at a height h above the plane, is

$$e = \frac{2hq}{(h^2+y^2)^{3/2}} \text{ electrostatic units} \qquad (7)$$

where y is the horizontal distance between the point of observation and the projection of the point charge. If q be measured in coulombs equation 7 becomes

$$e = \frac{1.8 \times 10^{12} hq}{(h^2+y^2)^{3/2}} \text{ volts per centimeter}$$

Thus the potential gradient produced by a leader channel, the top of which is at height h_1 above earth becomes

$$e = 1.8 \times 10^{12} Q_o \int_{h_1}^{h_2} \frac{h\epsilon^{-\beta h}}{(h^2+y^2)^{3/2}} dh$$

and with equation 6

$$e = 1.8 \times 10^{7} q_o \int_{h_1}^{h_2} \frac{h\epsilon^{-\beta h}}{(h^2+y^2)^{3/2}} dh \qquad (8)$$

If we remember that

$$\epsilon^{-\beta h} = 1 - \beta h + \frac{\beta^2 h^2}{2!} - \frac{\beta^3 h^3}{3!} + \frac{\beta^4 h^4}{4!} \cdots$$

and with Dwight's "Tables of Integrals," the solution of expression 8 can be written in form of a converging series

$$e = 1.8 \times 10^{7} q_o \Big\{ -\frac{1}{a} - 10^{-5}\Big[-\frac{h}{a} + \log(h+a)\Big] + \frac{10^{-10}}{2}\Big(a + \frac{y^2}{a}\Big) - \frac{10^{-15}}{6}\Big[\frac{ha}{2} + \frac{y^2 h}{a} - \frac{3y^2}{2}\log(h+a)\Big] + \frac{10^{-20}}{24}\Big(\frac{1}{3}a^3 - 2y^2 a - \frac{y^4}{a}\Big) - \frac{10^{-25}}{120}\Big[\frac{h^5}{4a} - \frac{5y^2h^3}{8a} - \frac{15y^4 h}{8a} + \frac{15y^4}{8}\log(h+a)\Big] + \frac{10^{-30}}{720}\Big[\frac{a^5}{5} - y^2a^3 + 3y^4 a + \frac{y^6}{a}\Big] - \cdots\cdots \Big\}_{h_1}^{h} \text{ volts per centimeter} \qquad (9)$$

where $a = \sqrt{h^2+y^2}$

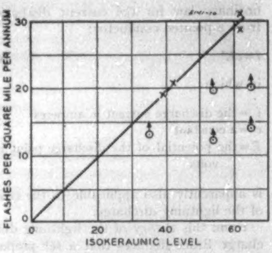

Figure 10. Variation of number of flashes per square mile per year with isokeraunic level

Directly underneath the leader stroke, that is, for $y=0$ or $a=h$, the gradient becomes then

$$e_o = 1.8 \times 10^{7} q_o \Big[-\frac{1}{h} + 10^{-5}(1 - \log 2h) + \frac{10^{-10}}{2} h - \frac{10^{-15}}{12} h^2 + \frac{10^{-20}}{72} h^3 \ldots \Big]_{h_1}^{h_2} \text{ volts per centimeter} \qquad (10)$$

References

1. Lightning Rod Conference, London, England, 1882.

Lightning Conductors, **R. Anderson**, London, England, 1885.

Geschichte des Blitzableiters (History of the Lightning Conductor), **H. Meidinger**, Karlsruhe, Germany, 1888.

Lightning Conductors and Lightning Guards, **O. Lodge**, London, England, 1892.

2. Surge Phenomena, British Electrical and Allied Industries Research Association, London, England. 1941, chapter 20.

3. Report on Lightning Accident at Purfleet, **Wilson**. *Philosophical Transactions* of the Royal Society (London, England) volume 68, part 1, 1778, page 239.

4. Shielding of Transmission Lines, **C. F. Wagner, G. D. McCann, G. L. MacLane**. AIEE Transactions, volume 60, 1941, page 313.

Shielding of Substations, **C. F. Wagner, G. D. McCann, C. M. Lear**. AIEE Transactions, volume 61, 1942, February section, page 96.

5. The Lightning Discharge, **C. E. R. Bruce, R. H. Golde**. *Journal* of the Institution of Electrical Engineers (London, England), volume 88, part *II*, 1941, page 487. See also chapter 1 of reference 2.

6. Thunderstorms and Their Electrical Effects, **B. F. J. Schonland**. *Proceedings* of the Physical Society (London, England), volume 55, 1943, page 445.

7. The Development of the Spark Discharge, **T. E. Allibone, J. M. Meek**. *Proceedings* of the Royal Society (London, England), *A*, volume 166, 1938, page 97.

8. The Validity of Lightning Tests with Scale Models, **R. H. Golde**. *Journal* of the Institution of Electrical Engineers (London, England), volume 88, part *II*, 1941, page 67.

9. The Electric Spark, **J. M. Meek**. *Journal* of the Institution of Electrical Engineers (London, England) volume 89, part I, 1942, page 335.

10. Lightning, **F. W. Peek**. AIEE Transactions, volume 50, 1931, page 1077.

11. The Initiation of Long Electrical Discharges, **C. E. R. Bruce**. *Proceedings* of the Royal Society (London, England), *A*, volume 183, 1944, page 228.

12. Von wo ab Steuert der Blitz auf Seine Einschlagstelle zu?, **B. Walter**. *Zeitschrift für Technische Physik* (Leipzig, Germany), volume 18, 1937, page 105.

13. Gewitterschutz von Grossendeanlagen, **W. Peters**. *Elektrische Nachrichten-Technik* (Berlin, Germany), volume 14, 1937, page 24.

14. Magnitudes of Lightning Currents, **R. H. Golde**. *Nature* (London, England), volume 151 1943, page 421.

15. Lightning Investigation on 132-Kv Transmission System of the American Gas and Electric Company, **I. W. Gross, G. D. Lippert**. AIEE Transactions, volume 61, 1942, April section, page 178.

16. The Measurement of Lightning Currents in Direct Strokes, **G. D. McCann**. AIEE Transactions, volume 63, 1944, pages 1157–64.

17. The Protection of Structures Against Lightning, discussion by **C. E. R. Bruce**. *Journal* of the Institution of Electrical Engineers (London, England), volume 90, part I, 1943, page 522.

18. Code for Protection Against Lightning, Bureau of Standards, handbook *H* 21, Washington, D. C., 1937.

19. Report of the Committee Appointed by the Royal Society to Consider a Method of Securing the Powder Magazines at Purfleet, **H. Cavendish, W. Watson, B. Franklin, J. Robertson**. *Philosophical Transactions* of the Royal Society (London, England), volume 63, 1773, page 42, and volume 68, 1777, page 232.

20. Über Blitzschutz durch Fernblitzableiter, **B. Walter**. *Zeitschrift für Technische Physik* (Leipzig, Germany), volume 14, 1933, pages 118, 254.

21. Lightning (in Russian, second edition), **I. S. Stekolnikoff**. 1941. Page 194.

22. Wood-Pole Lines at High Voltages, **A. E. Davison**. *Electrician* (London, England), volume 71, 1938, page 461.

23. Résultats de Quatre Années de Recherches au Sujet des Emplacements des Chutes de la Foudre, **H. Grunewald**. Conference on Large High-Voltage Systems (CIGRE), Paris, France, 1937, report 316.

24. Lightning Investigation on a 220-Kv System—*III*, **E. Bell**. AIEE Transactions, volume 59, 1940, page 822.

25. Experience With Preventive Lightning Protection on Transmission Lines, **S. K. Waldorf**. AIEE Transactions, volume 60, 1941, June section, page 249.

An Eight-Year Investigation of Lightning Currents, **E. Hansson, S. K. Waldorf**. AIEE Transactions, volume 63, 1944, May section, page 251.

26. Design, Construction and Operation of a Lightning-Proof Transmission Line, **E. Hansson**. Edison Electric Institute, 1938, number *F*6, page 11.

Lignes de Transmission à l'Épreuve de la Foudre, **E. Hansson, A. F. Bang**. Conference on Large High-Voltage Systems (CIGRE), Paris, France, 1937, report 338.

27. Protector-Tube Application and Performance on 132-Kv Transmission Lines—*II*, **P. Sporn, I. W. Gross**. AIEE Transactions, volume 57, 1938, September section, page 520.

28. Lightning Experience on 132-Kv Transmission Lines, **P. Sporn**. AIEE Transactions, volume 49, 1930, page 432.

29. Lightning Performance of 110- to 165-Kv Transmission Lines, AIEE lightning and insulator subcommittee. AIEE Transactions, volume 58, 1939, June section, page 294.

Report of Conference on Radio-Frequency Cables

I. The Development of Radio-Frequency Cables in the United States

J. H. NEHER
MEMBER AIEE

THE EXTENSIVE PART played by electronic equipments in the recent war has occasioned the rapid development of a number of component parts which were not available in satisfactory form at the outset. One of the more important of these developments is that of solid-dielectric flexible radio-frequency cables for internal wiring and interconnections between component parts of equipment.

While these cables have been developed specifically for war requirements and their production has been devoted exclusively toward this end, they are capable of general applications involving radio-frequency transmission and are therefore a subject of considerable interest to electrical engineers.

Despite the fact that, because of the military applications involved and their attendant security aspects, nothing can be said about the specific end use of the cables and equipments with which they are now being used, nor can certain aspects of their performance be discussed; considerable information can be presented at this time which will be of interest.

Development of Solid-Dielectric Radio-Frequency Cables

Just prior to the start of the war, the British had developed a new material, polyethylene, or "polythene," as they called it, and had investigated its use in submarine cables. Its suitability for use in radio-frequency cables was immediately established, and such cables utilizing this dielectric played an important part in the battle of Britain.

At the time of the entry of the United States into the war the demands for flexible coaxial transmission-line cable to meet the requirements of the electronic equipments needed were supplied for the most part by England and Canada with the aforementioned polyethylene cables. But the quantities required for our programs soon exceeded the capacity of the facilities thus available, and domestic sources had to be developed. Through the foresightedness and efforts of Commodore J. B. Dow, director of electronics, the Navy immediately sponsored the production of polyethylene in the United States. This involved first the setting up of pilot plants by two chemical manufacturers and then the construction of two plants capable of producing the required amount of the material.

As an interim measure, some equipment used flexible cables employing beads, washers, spacers, and other separators to maintain concentricity of the two conductors. For various reasons, such as the ease with which such cable could be short-circuited, low dielectric breakdown, difficulty of maintaining constancy of electrical characteristics, and because the requirements for cables were far in excess of the capacity to produce this type of transmission line, these were replaced rapidly by the solid-dielectric lines similar to those supplied by the British, but using new insulations which had been compounded here.

Since polyethylene was not yet available, these depended primarily on polyisobutylene compounded with various additional agents such as cyclized rubber, polystyrene, waxes of various kinds, organic and inorganic filling agents and other synthetic rubbers. These dielectrics were produced under such trade names as "Copolene," "Radol," "Intelin." Various characteristics were obtained, each of which was an advantage if coupled with others, but none of the compounds had all the characteristics which were considered necessary to meet the requirements of the military equipments.

Early in 1943 small quantities of locally produced polyethylene became available, and a committee was set up to co-ordinate the research work done by the various cable manufacturers on the methods of handling the material. As it was necessary to obtain the greatest amount of information about each bit of material allotted to each user, it was agreed among the participating cable manufacturers, laboratories, and raw-material producers that all information gained as to methods of operation, methods of cooling, methods of testing, and so forth, would be pooled for the mutual benefit of all concerned. This spirit of co-operation was of great help in reducing the time necessary to produce good cable with minimum waste of the then very scarce material.

By the summer of 1943 polyethylene was available in sufficient quantities, and sufficient experience with its handling had been gained by the cable manufacturers working with the committee to permit all of the required radio-frequency cables to be manufactured with it. Over 115,000,000 feet of polyethylene coaxial cable have since been manufactured.

The Army-Navy Radio-Frequency-Cable Co-ordinating Committee

The development of solid-dielectric radio-frequency cables in the United States has been accomplished through the combined efforts of the various cable and chemical manufacturers at the request of the Services.

Early in 1943 the Bureau of Ships in co-operation with the Signal Corps and the War Production Board set up in the Radio Division a special section to handle the research, development, co-ordination, and standardization of radio-frequency cables and associated fittings, not only for the Navy, but for the Army as well. Representatives of the Army were assigned to duty with the section which functioned as the "Army-Navy Radio-Frequency-Cable Co-ordinating Group."

In order to create a more effective organization, the Signal Corps Standards Agency and the Bureau of Ships reorganized the co-ordinating group in March of 1944. Since a primary function of the group was the co-ordination of the services and industry toward more complete standardization of radio-frequency trans-

---

Paper 45-145, sponsored by the AIEE committee on communication with the co-operation of the Army-Navy Radio-Frequency-Cable Co-ordinating Committee and recommended by the AIEE committee on communication for publication in AIEE TRANSACTIONS. Manuscript submitted April 6, 1945; made available for printing July 20, 1945.

J. H. NEHER is commander, United States Naval Reserve, Washington, D. C., and was formerly chairman of the Army-Navy Radio-Frequency Co-ordinating Committee.

mission-line components, the Signal Corps Standards Agency took cognizance over the Signal Corps part of the group by action of the Chief Signal Officer. The group was then known as the Army–Navy Radio-Frequency-Cable Co-ordinating Committee and was composed of a minimum number of full-time permanently assigned members designated by the Signal Corps Standards Agency and the Bureau of Ships. The committee now meets in continuous session at the Bureau of Ships with a Bureau of Ships officer as chairman and a representative from the Signal Corps and the Bureau of Ships.

The committee has authority to carry out for the Signal Corps and the Bureau of Ships the following duties:

(*a*). Co-ordinate the activities of the Army, the Navy, and industry with respect to the research, development, and testing of radio-frequency transmission lines and associated fittings.

(*b*). Prepare and issue specifications and revisions thereof covering radio-frequency transmission lines and fittings and recommend to the interested contracting agencies and bureaus waivers of any provisions of these specifications.

(*c*). Prepare and issue approved standard lists of radio-frequency transmission lines and fittings and issue waivers thereto.

(*d*). Designate testing laboratories, supervise tests, procure samples, analyze test data, and issue type approvals.

The co-ordinating group and later the co-ordinating committee carried on the arrangements previously begun concerning the production of polyethylene in the United States. The group prepared and issued the Army–Navy Standard List of Cables of October 18, 1943, and later a revision of this list dated October 15, 1944. This list reduced the number of radio-frequency cables in service equipments and recommended cables designed on the basis of universal application to cover all requirements.

The committee had been responsible for the preparation and issuance in July 1944 of the joint Army–Navy specification *JAN-C*-17 covering radio-frequency cables. The specification covers all radio-frequency cables on the standard list and is used almost exclusively by all procurement agencies, both services, and private industry, as the procurement specification for radio-frequency cables.

International Standardization

Work is under way toward the establishment of international standards for radio-frequency cables. In view of basic design differences among equipments in use in the United States, Great Britain, and Canada, such work must be considered in the light of a long-range program. Its importance in the future, however, should not be overlooked.

II. General Characteristics of Polyethylene

J. W. SHACKLETON

NONMEMBER AIEE

IT IS THE AIM, or at least the hope of most research workers to achieve perfection—and this is a commendable aim—but the more practical man, while waiting for the panacea, is inclined to go to work with materials at hand—to improvise perhaps.

So it is with the plastics industry and those which utilize plastics.

Since no plastic possesses all of the good characteristics which may be desired, a manufacturer selects, for a given use, that plastic which has properties indispensable for his needs, and then designs the manufactured article to minimize the disadvantages of its less desirable properties. With polyethylene this task is somewhat simplified, since the resin offers an unusual number of extraordinary properties. Slade and Crafton of the Okonite Company in a paper presented before the May 1944 Chicago meeting of the Society of the Plastics Industry have pointed out that, of 23 properties of interest to their particular industry, polyethylene could be rated excellent in 18 and good in 4 of these properties. These are summarized in Table I.

The outstanding properties of polyethylene, upon which it is expected that many important uses will be based, are its flexibility and toughness over a wide range of temperature, its light weight, its unusually good resistance to water and to penetration by moisture, its chemical inertness, and its excellent electrical properties.

The fact that ethylene can be polymerized has been known for many years, but the products of early experiments were of relatively indefinite molecular size, and were liquid oily resins or brittle solids. The work of Fawcett and Gibson, in England, on the effect of high pressures on chemical reactions, including those of polymerization, led to the development of solid polymers of ethylene and of practicable methods of manufacturing them.

Polythene is a generic name applied by Imperial Chemical Industries, Ltd., and adopted by E. I. du Pont de Nemours and Company to cover polymers of ethylene suitable for use in plastics. It is not a trade name. Polythene and the chemical term polyethylene may be considered interchangeable.

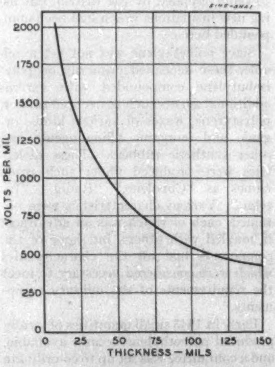

Figure 1. Dielectric strength of polythene, compression-molded

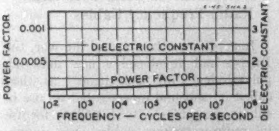

Figure 2. Dielectric constant and power factor of molded polythene

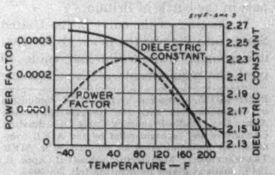

Figure 3. Dielectric constant and power factor (3 megacycles) of polythene versus temperature

---

J. W. Shackleton is with E. I. duPont de Nemours and Company, Wilmington, Del.

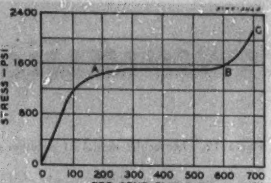

Figure 4. Typical stress—strain data for injected molded polythene in tension

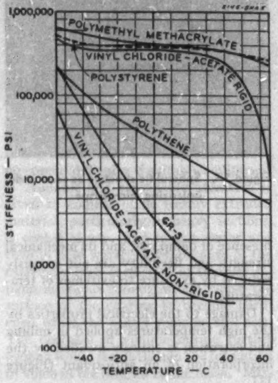

Figure 5. Stiffness versus temperature, ASTM D-747

The essentially saturated chain hydrocarbons in this category range from semisolid to solid, according to their average molecular size, and differ in details of physical and chemical properties. A picture of the molecular model of polythene is shown in Figure 13. The chemical formula of polythene is given below in which the nonpolar structure should be noted:

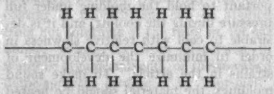

$$-\overset{H}{\underset{H}{C}}-\overset{H}{\underset{H}{C}}-\overset{H}{\underset{H}{C}}-\overset{H}{\underset{H}{C}}-\overset{H}{\underset{H}{C}}-\overset{H}{\underset{H}{C}}-\overset{H}{\underset{H}{C}}-$$

The polymer developed especially for dielectric applications to wire and cable has an average molecular weight in the vicinity of 18,000 to 20,000. Like others of greater molecular weight, this product is tough, flexible over a wide range of temperatures, including even very low temperatures, translucent, and normally white in color. Its structure, as would be expected, results in unusual resistance to water and chemicals, and its nonpolar nature leads to characteristic electrical properties, such as extremely low power factor and low dielectric constant, with high resistivity and dielectric strength.

Figure 6. Refractive-index – temperature curves of polythene, polyisobutylene, and natural rubber

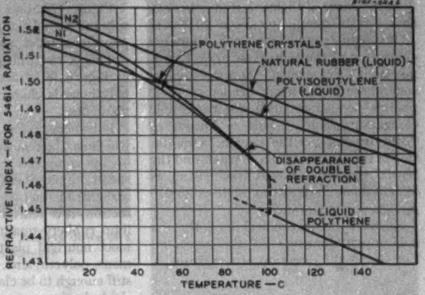

Figure 7 (below). Variation of density of polythene with temperature

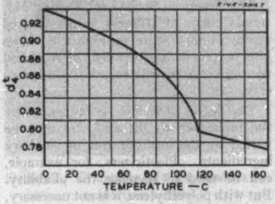

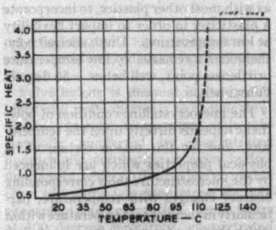

Figure 8. Specific heat of polythene versus temperature

The breakdown strength of compression-molded samples of polythene is shown in Figure 1. There will be variance between these values and those obtained with extruded specimens however.

The constancy of specific inductive capacity and power factor with changes in frequency is shown in Figure 2. Note that data are given for frequency values only up to 100 megacycles.

Characteristic curves for the change of power factor and dielectric constant with temperature are shown in Figure 3. These data are based on work carried out by W. A. Yager of the Bell Telephone Laboratories, and confirmed by our Arlington laboratories.

Polythene is a microcrystalline plastic, which contains, however, some amorphous material. Its mechanical behavior resembles in many respects that of nylon and other quasicrystalline polymers. The arrangement of its microcrystalline components, or crystallites, may vary considerably according to the source and treatment of the sample. In polythene which has not had special pretreatment, the crystallites tend to occur in a structure of spherulitic type which on X-ray examination shows a random distribution of crystallites. It consists largely of spherulites which are radial or tangential aggregates of crystallites having, under ideal conditions, a gross structure of spherical shape. The spherulitic structure is best seen under the polarizing microscope (Figure 14).

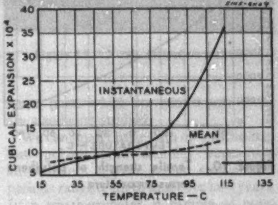

Figure 9. Thermal coefficient of cubical expansion of polythene

Figure 15 shows an X-ray photograph of a polythene specimen. This pattern is characteristic of a crystalline material.

The size of the spherulites can be varied by thermal treatment. By shock cooling, for example, a sheet can be made to contain only a few spherulites large enough to be resolved by the ordinary microscope. Such sheets are more flexible and more nearly transparent than ones which have been slowly cooled. In annealed films the spherulites may measure 20 microns or more in size.

If tension is applied to a test specimen of polythene sheeting at ordinary temperature, the elongation during the first phase of the stretching, up to about 100 per cent, is substantially reversible. When the tensile stress exceeds a certain critical value, a second phase of stretching occurs, up to about 600–700 per cent, in which a permanent orientation of the crystallites takes place, and the specimen necks down as cold drawing proceeds.

In the curve of Figure 4, it may be seen that for stresses up to about 10,000 to 12,000 pounds per square inch a nominal elongation of the sample occurs. This is an elastic phenomenon. At a stress value somewhere in the neighborhood of 1,600 pounds per square inch an irreversible elongation occurs. This is known as "cold drawing" of the sample. Orientation of the spherulites takes place, and the tensile strength of cold-drawn samples of polythene may run as high as 25,000 pounds per square inch.

Figure 16 shows the necking down of a cold-drawn filament. Polaroid examination shows the direction of the strain.

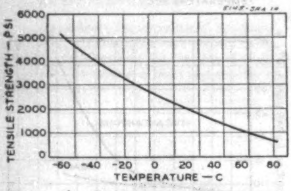

Figure 10. Tensile strength of polythene versus temperature

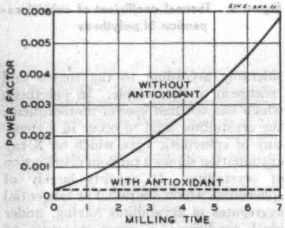

Figure 11. Power factor of polythene versus milling time

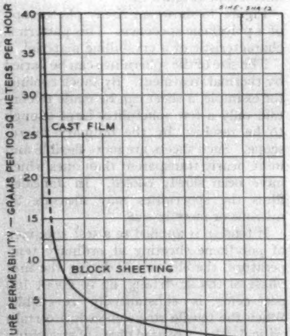

Figure 12. Moisture permeability versus sheet thickness, cellophane method

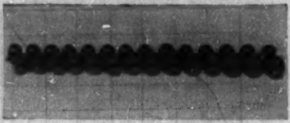

Figure 13. Molecular model of polythene

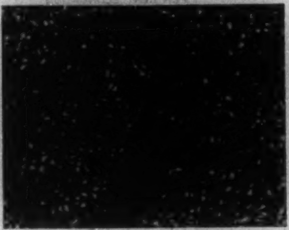

Figure 14. Spherulitic structure as seen under polarizing microscope

Figure 17 shows the orientation of the spherulites in a cold-drawn sample of polythene under a polarizing microscope.

The X-ray diffraction pattern shown in Figure 18 of a cold-drawn sample of polythene is characteristic of orientated filaments.

Polythene is a thermoplastic resin which can be readily molded by injection or by compression; extruded to form sheets, films, fibers, tubes and the like; and extruded on wire and cable. In thin sections it is nonrigid, without having the limp rubbery quality that characterized most nonrigid plastics. In thick specimens, polyethylene, on the other hand, is stiff enough to be classed among the more rigid plastics.

The American Society for Testing Materials curve of stiffness values plotted against temperature in Figure 5 shows how polythene lies between the rigid and nonrigid plastics with regard to this property.

The degree of rigidity is influenced by the molecular weight and also may be varied by the incorporation of auxiliary ingredients. Plasticizers, for example, can be used to increase the pliability. But with polyethylene, it is not necessary, as with most other plastics, to incorporate a plasticizer in order to impart flexibility at low temperatures. Unplasticized polythene has a remarkably low temperature brittleness point, well below −50 degrees Fahrenheit.

The microcrystalline condition of polythene depends directly upon the temperature, and for this reason certain of its physical properties which are influenced by the microstructure show corresponding distinct changes with temperature, particularly in the range of temperature within which there is a transition from crystalline to amorphous in liquid condition. Thus in Figure 6 in the range 80 to 100 degrees centigrade there occurs a change in index of refraction which is evidently due to the disappearance of a certain crystalline phase by solution of fusion, but the polarizing microscope demonstrates the persistence of some crystalline structure up to about 112 degrees centigrade beyond which the relationship of refractive index to temperature becomes a straight line. Analogous phenomena are indicated by curves showing the variation of density, specific heat, and coefficient of thermal expansion (Figures 7, 8, and 9). The variation of tensile strength with temperature is shown in Figure 10.

Polythene has very largely replaced all other materials in the insulation of wires for radio-frequency use. This is primarily on account of its outstanding dielectric properties—a power factor below 0.0005 and a dielectric constant of 2.2–2.3 at frequencies between 60- and 10-degree cycles. But, in addition, its insensitivity to moisture protects its electrical properties. It is substantially unimpaired in the presence of dampness, and its mechanical strength and flexibility are not seriously reduced by exposure to extremes of temperature.

Damage to the electrical properties by the high temperatures applied in milling and extrusion is entirely avoided by the incorporation of an antioxidant (Figure 11).

By the incorporation of pigments or colors, polythene insulating compound may be colored to provide identification of circuits.

The unusually large coefficient of thermal expansion of polythene must be considered in the design of equipment for molding and for extrusion. The compression-molding technique is rather simple, but certain precautions must be observed.

Light pressures are applied during the heating cycle, but it is particularly important to hold the molding under full pressure during the cooling, and it is desirable to cool with relative slowness in order to minimize the development of strains in the article. To make sound moldings, the material should be heated to at least 120 degrees centigrade, but temperatures above 160 degrees centigrade should be avoided because they cause the article to adhere to the mold. An external lubricant may be applied to the surface of the mold to facilitate the removal of the molded article.

Polyethylene can be handled also in standard automatic-injection molding equipment with cylinder temperatures of 175–260 degrees centigrade (350–500 degrees Fahrenheit, and die temperatures usually in the vicinity of 60 degrees centigrade (140 degrees Fahrenheit). The channels from the heating cylinder to the

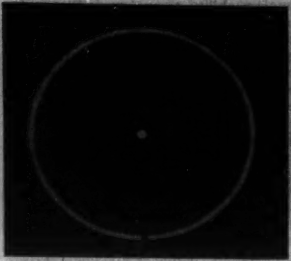

Figure 15. X-ray picture of a polythene specimen

mold must be of ample cross section to ensure the transmittal of pressure to the material in the cavity to compensate for its shrinkage as it cools.

The extrusion of polyethylene involves no special difficulty if suitable equipment is available and reasonable attention is given to control. The freshly extruded material, particularly in heavy sections, is cooled slowly, first in hot water and then in cold water, since, because of the extremely high coefficient of thermal expansion, rapid cooling would cause the surface of the coating to become hardened while the center remains still soft. The decrease in volume during further cooling would result then in the formation of voids in the interior of the mass. Mixtures of polyethylene with polyisobutylene can be extruded similarly but with less care in the cooling, because the exterior does not become so rigid when cooled.

Sheeting of polyethylene in various thicknesses can be made by calendering or by extrusion, or by forming a block attached to a bedplate and slicing it, as is done in the manufacture of the pyroxylin plastics. Massive polythene is readily machined with wood- or metal-working tools.

Waterproof and chemically resistant coating of polyethylene can be applied from hot solutions of the resin in, for example, xylene, or from dispersion in water or organic solvents, or the so-called flame-spraying process or by "hot-melt" dip technique. A solution in xylene should be prepared at a temperature of at least 80 degrees centigrade, preferably 100 degrees centigrade or more, and should be kept hot during its application. A film applied from solution or dispersion should be either dried at a temperature above 100 degrees centigrade or fused after it has been dried, to ensure a continuous and adherent film.

Films of polyethylene can be joined by heat sealing, and massive polyethylene can be welded satisfactorily if care is taken to prevent excessive oxidation. For patching and welding, a mixture of polyethylene with polyisobutylene is more satisfactory than polyethylene alone.

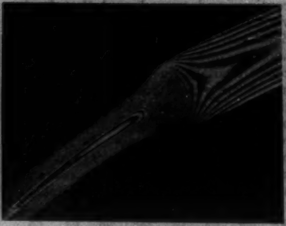

Figure 16. Illustration of necking down of a cold-drawn filament

Figure 17. Orientation of the spherulites in a cold-drawn sample

Polyethylene is unusual in its insolubility and in its inertness to chemical reagents. At room temperature, it is substantially unaffected by concentrated hydrochloric sulphuric, or even hydrofluoric acid, while nitric acid has no visible effect but ultimately does impair the tensile strength and elongation. In 24 hours at 100 degrees centigrade, concentrated hydrochloric acid, 50 per cent caustic soda solution, dilute nitric acid, and dilute sulphuric acid have no effect, while concentrated sulphuric acid causes some charring. The only common solvents which will affect polyethylene at room temperature are the chlorinated hydrocarbons, for example, carbon tetrachloride and trichloroethylene, and to a lesser extent the aromatic and aliphatic hydrocarbons in general. These solvents at room temperature tend to swell the plastic but do not usually dissolve it. Unfortunately this sensitivity to hydrocarbons prevents the use of polyethylene in parts which will be immersed in high-octane gasoline. It should be noted, however, that brief contact with gasolines, and the other solvents which attack polyethylene, generally does not harm the material.

Polyethylene is reported to be fungus-resistant. It is not attacked by salt water, and its use as an insulation on submarine cable and in other applications where contact with salt water has deleterious effects on other materials is being investigated. Protective coatings for metal parts which corrode in salt water are also being studied.

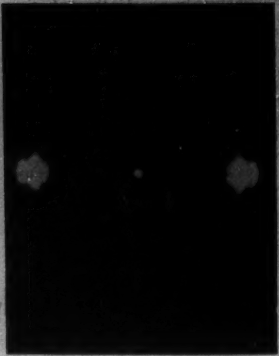

Figure 18. X-ray defraction pattern

We can report little data on weathering, but polyethylene samples containing antioxidants appear to be stable over periods ranging up to and over two years. In a weatherometer, a sample of polyethylene exposed for 200 hours shows no loss in flexibility and appears to be unchanged. This would be equivalent to several years exposure, although we realize that such data are not infallible and are subject to question.

Thus far, the available supplies of poly-

Table I. Summarized Comparison of Properties‡

Property	Polyethylene	Polystyrene	Polyisobutylene	Rubber†
Dielectric strength	E*	E	G	G
Volume resistivity	E	E	E	G
Dielectric constant	E	E	E	G
Power factor	E	E	E	G
Temperature stability of dielectric properties	E	E	E	E
Tensile strength	G	E	P	E
Modulus of elasticity	E	E	P	G
Elongation	E	P	E	E
Flexibility	G	P	E	E
Hardness	G	E	P	G
Impact strength	E	P	E	E
Resistance to cold flow	E	E	P	E
Distortion temperature	E	F	P	E
Brittle temperature	E	P	E	E
Nonflammability	P	P	P	P
Specific gravity	E	E	E	E
Low water absorption	E	E	E	G
Low permeability	E	G	G	F
Chemical resistance	E	E	E	P
Solvent resistance	G	P	P	F
Ozone resistance	E	E	E	P
Sunlight resistance	E	E	E	P
Heat resistance	E	E	E	G

* E = excellent, G = good, F = fair, P = poor.

† Refers to practical insulating compounds in general.

‡ See reference 1.

ethylene have been used in the production of items urgently needed by the Armed Forces, almost altogether in the field of electrical insulation. The material is available in production quantities only by specific authorization of the War Production Board under conservation order *M*-300, schedule 60, but small quantities for experimental purposes may be obtained on proper application.

After the war it is expected that the use of polyethylene in electric equipment will continue and expand, and that further varieties and modifications of it will be developed to meet specific needs. In addition, however, once the material becomes available in quantity for civilian uses, there will be many fields of application in which its unusual combination of properties will make it valuable. Its good resistance to chemicals and solvents points to its utility in chemical equipment in the manufacture of battery parts and as a coating and gasketing material. Its impermeability to moisture, Figure 12, indicates a broad utility in containers and the packaging of electrical and other goods, foods, and so forth. In this field it may be used as sheeting, as molded containers, or as an impregnant or coating of paper.

Reference

1. Polyethylene, a New Dielectric for Cables, H. C. Crafton, Jr., H. B. Slade. The Okonite Company.

III. Polyethylene as Cable Insulation

C. S. MYERS
NONMEMBER AIEE

A. E. MAIBAUER
ASSOCIATE AIEE

IN THE SPRING of 1942, the United States Navy requested Carbide and Carbon Chemicals Corporation to produce polyethylene resin, required for one of the most urgent war applications, coaxial-cable insulation. Prior to that time, the laboratories of its associated company, The Linde Air Products Company, had done some experimental work with high-pressure synthesis, and they proceeded to apply this knowledge to the making of polyethylene resin. A year from the date that the experimental work was started for the Navy, a plant had been built and was producing at 180 per cent of the rated capacity. In the short space of two years, all the problems on development, engineering, and operation of the plant were brought to a point where the Navy's requirements for coaxial-cable insulation could be met. The vital role which this insulation plays in military operations undoubtedly will be brought to light at cessation of hostilities.

In this discussion, an attempt will be made to review some of the important properties of polyethylene resin and to point out some that are of particular interest to the electrical engineer. It will be confined to the polyethylene resin now used widely in commercial coaxial-cable production. This resin has a molecular weight of 18,000–20,000, as determined by a modified Staudinger solution-viscosity method, described by Kemp and Peters of Bell Telephone Laboratories,[1] and it will be referred to as *D*-55 grade. Those interested in detailed properties of other molecular-weight resin grades can find a complete discussion in the paper on "Polyethylene" by C. S. Myers[2]. However, in order to fix the material under discussion, Figure 1 illustrates the flow-height dependence of polyethylene and polyisobutylene on the average molecular weight. Flow heights were obtained using the Williams' plastometer operated at 130 degrees centigrade. Standard *D*-55 resin has an average Williams flow height of 55 mils between allowable limits of 50 and 60 mils. Resins of other grades, plasticity-wise, are designated accordingly.

The flow height of both polyethylene and polyisobutylene shows a direct relationship with the average molecular weight for the range indicated by these curves. The resin under discussion is on the lower portion of the curve.

The following seven points have been chosen as being of sufficient interest to the electrical engineers to justify further comment:

1. Electrical properties.
2. Heat deformation.
3. Pliability.
4. Dimensional tolerances.
5. Homogeneity.
6. Low specific gravity.
7. Stabilizers.

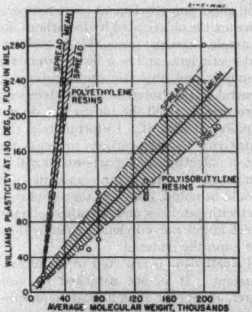

Figure 1. Williams plasticity versus average molecular weight of polyethylene resins and polyisobutylene resins

The electrical properties of polyethylene have been widely discussed and appear in several technical publications. The power factor of commercial production averages about 0.0003, and the dielectric constant about 2.3. These values are independent of either frequency or temperature. The electrical engineer has always regarded quartz as an ideal insulation, and it is interesting to note that a resin which has electrical properties approaching those of quartz is now available in commercial quantities and is being applied to wire under practical commercial conditions. The addition of stabilizer to polyethylene does not markedly change the constancy of its electrical properties with either temperature or frequency.

To give some idea of the temperature-load deformation, the following data are presented on two types of tests:

1. The United States Navy mandrel test.
2. A micrometer dial-gauge test for comparison.

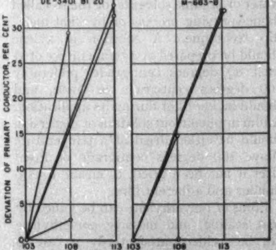

Figure 2. Heat deformation on coaxial cables

C. S. Myers and A. E. Maibauer are with Bakelite Corporation, Mr. Myers in the plant at Bound Brook, N. J., and Mr. Maibauer in the sales development department, New York, N. Y.

Figure 2 shows curves based on data taken on an *RG*-8/*U* cable insulated with stabilized *D*-55 resin, known as *DE*-3401 natural. This cable has a diameter over the dielectric of 0.285 inch and an outside diameter over jacket and braid of 0.405 inch. A length of cable complete with braid and jacket, equal to 30 times the diameter over the jacket, is placed on a mandrel whose diameter is ten times the outside diameter of the cable. Eight-pound weights are attached to the ends of the cable, and the assembly is kept at a specified temperature for $7^1/_2$ hours. At the end of this time, the deviation of the central conductor is noted. In the data shown, the test was run at 103, 108, and 113 degrees centigrade. At 103 there was no conductor deviation; at 108 the two samples tested showed a wide variation, whereas at 113 degrees centigrade the deviation was between 30 and 35 per cent. The curves indicate that, although no deviation was observed at 103 degrees centigrade, a critical range begins at about 108, and at 113 the values are quite high.

Figure 3 shows data obtained using a dial gauge with a $^3/_8$-inch foot and a number-14 solid copper wire with a 0.030-inch wall insulation. Tests were made using both 500- and 1,000-gram loads and two resin insulations, one the standard grade and the other having a flow height of 100 mils. With a 500-gram load, deformation of the standard-grade resin does not change appreciably until a temperature of 100 degrees centigrade is reached, at which point deformation increases sharply. With the 1,000-gram load, the rate up to 100 degrees centigrade is somewhat higher. For the other resin, the break point is raised only slightly, about three degrees centigrade.

Polyethylene is in itself a pliable resin, and does not require the addition of plasticizer. It is therefore, a relatively homogeneous material, and the usual problems, such as plasticizer volatilization and effect of plasticizer on electrical properties, are not present. It might be well to add a word here on stiffness. The stiffness of a plastic is used to define its resistance to elastic deformation. It is not simply related to the ability of the material to withstand fracture under impact conditions. This latter property is measured by its brittle temperature. The brittle temperature of polyethylene *ED*-3401 natural is below −70 degrees centigrade. Thus, polythylene is pliable over a wide temperature range and is similarly resistant to impact over the same temperature range.

Figure 4 is a plot of log stiffness versus temperature for polyethylene resins and a vinyl plasticized resin. The vinyl resin plasticized with 21-per-cent dioctyl phthalate shows about the same stiffness at room temperature as polyethylene. As the temperature is lowered, however, the plasticized vinyl resin increases in stiffness much more rapidly than the polyethylene. The more highly plasticized vinyl-resin compound is much more flexible at room temperature, but its stiffness increases very quickly also as the temperature is lowered with the difference between it and polyethylene decreasing until at −60 degrees centigrade the stiffness is about equal.

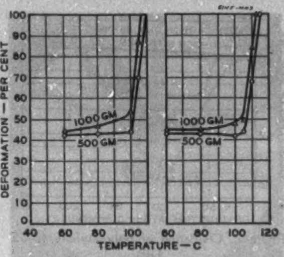

Figure 3. Per-cent deformation versus temperature American Wire Gauge number-14 solid wire, 30-mil insulation

DE-3401 natural: 60-mil flow, 10-minute preheat, 10-minute load

DEM-682 natural: 100-mil flow, 10-minute preheat, 10-minute load

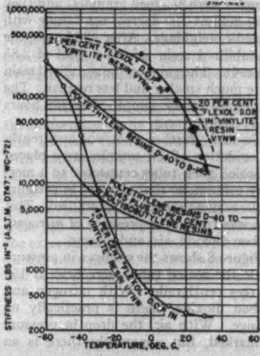

Figure 4. Stiffness–temperature comparison of plasticized Vinylite resin *VYNW* and polyethylene resins, average values

The stiffness of polyethylene resins has been found to be essentially independent of resin grade in the range of 40 to 145 mils flow height.

Addition of 50-per-cent polyisobutylene to polyethylene lowers the stiffness in the whole temperature range. The curve is the same general shape as for polyethylene alone.

Properties 4, 5, and 6 will be mentioned briefly:

A coaxial cable is an accessory to precision equipment and as such requires smaller dimensional tolerances which are not so essential in other types of cable insulation. A high degree of dimensional uniformity is possible at wire extrusion rates, which are commercially satisfactory when using polyethylene.

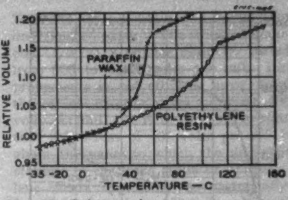

Figure 5. Relative volume versus temperature

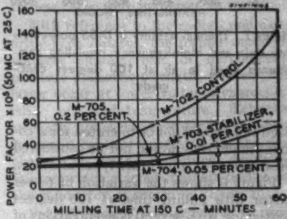

Figure 6. Milling stability of *D*-55 resin versus stabilizer concentration

In connection with dimensional tolerances, however, it is extremely important in the design of forming equipment, such as dies and molds, to keep in mind the relatively high-expansion coefficient of polyethylene.

Figure 5 shows data published by Clash and Rynkiewicz,[3] which illustrate change of relative volume of polyethylene with temperature. Starting with a relative volume of 1, at 0 degree centigrade, the volume changes slowly up to about 60 degrees centigrade, where the rate of change begins to increase much faster until the softening temperature of approximately 115 degrees centigrade is reached. At this temperature, the transition interval ends and the variation becomes linear and is also smaller than at temperatures immediately below it.

It is well to stress, in passing, the low specific gravity of polyethylene which is 0.92. In effect, this results in a larger volume per pound with lower insulation costs. For certain types of applications there is also an important weight advantage.

The subject of stability of polyethylene at elevated temperatures has been given much attention. For coaxial-cable insulation, it is essential that the power factor does not change after aging at elevated temperatures. However, it is important to keep in mind that the data to be shown were taken under greatly accelerated conditions and that, while the changes in power factor of the unstabi-

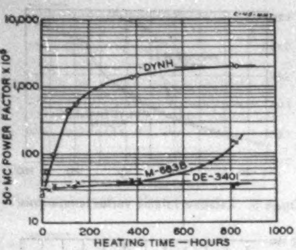

Figure 7. Thermal stability of *D*-55 polyethylene resin and high-frequency insulating compounds aged in air at 100 degrees centigrade

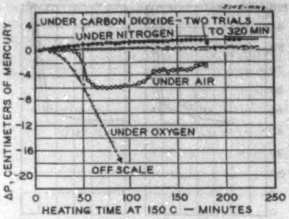

Figure 8. Oxidation of polyethylene (*D*-55 test)

Table I. Oxidation of Polyethylene Aged at 100 Degrees Centigrade and Weighed Periodically

Materials: Approximately $^5/_{16}$-Inch Granular

Heating Period at 100 C, Hours	Per Cent Change in Weight: D-55 Resin, Sample 1	D-55 Resin, Sample 2	DE-3401 Natural Compound, Sample 1	DE-3401 Natural Compound, Sample 2
1	−0.02	−0.008	−0.008	−0.01
3	−0.014	−0.004	0	−0.008
27	+0.054	+0.042	−0.006	−0.004
96	+0.67	+0.72	+0.18	+0.156
264	+2.25	+2.25	+0.090	+0.074
432	+2.85	+2.85		+0.168

lized resin could not be tolerated for a coaxial cable, they would not be considered prohibitive for some other types of cables.

Figure 6 shows the variation of power factor with milling time at 150 degrees centigrade with several concentrations of the standard stabilizer. After one hour milling at 150 degrees centigrade the unstabilized resin shows a sharp rise in power factor from approximately 0.00022 to 0.00144. In the presence of 0.01-per-cent stabilizer, this increase is sharply retarded but is still significant. Concentrations of 0.05- and 0.2-per-cent stabilizer show that the electrical deterioration has been practically arrested over the milling period studied.

Figure 7 shows the change in power factor with continued heating at 100 degrees centigrade. The unstabilized resin shows a sharp increase up to 400 hours after which it appears to level off. *DE*-3401 natural, containing 0.2 per cent of the standard stabilizer, shows practically no change after 800 hours. Since these curves were drawn, this test has run to 2,000 hours, and there is still no tendency for the stabilized resin to reflect a power-factor increase.

Table I illustrates weight gains of stabilized and unstabilized samples. The samples were $^5/_{16}$-inch granules, and they were held at 100 degrees centigrade with periodic weighings. After 432 hours, the unstabilized resin gained a total of 2.85 per cent. The gains on the stabilized resin were much smaller and less regular. The total gain in one sample after 432 hours was 0.168 per cent.

To study further what was apparently an oxidation effect, samples were placed in sealed glass tubes connected to a mercury column, so that changes in pressure in the sealed tubes could be studied. This test was run in the presence of nitrogen, carbon dioxide, air, and oxygen.

Figure 8 shows the changes in pressure while the sealed tubes were held at 150 degrees centigrade. With nitrogen and carbon dioxide, there is practically no change. With air, the drop in pressure is marked, but apparently there is an equilibrium point followed by a pressure rise. The drop in the oxygen curve indicates an appreciable oxygen absorption. A possible explanation for the air curve is that an equilibrium point is reached because of the limited amount of oxygen available. The reaction products, on further heating, probably account for the expansion which follows. It is believed that, if the oxygen curve could have been carried further, it too ultimately would assume a shape similar to the air curve.

This discussion has brought together several of the more important properties of polyethylene which are of interest to engineers. It is hoped that by giving these particular properties emphasis, the cable engineer will be in a better position to design cables to meet the various service requirements.

References

1. **Kemp, Peters.** *Industrial and Engineering Chemistry*, volume 33, 1943, pages 1106–12.
2. **C. S. Myers.** *Modern Plastics*, August 1944, page 103.
3. **Clash, Rynkiewicz.** *Industrial and Engineering Chemistry*, volume 36, March 1944, page 279.

IV. Dielectric Strength of Polyethylene

WM. A. DEL MAR
FELLOW AIEE

POLYETHYLENE is a particularly interesting material with which to study dielectric strength because of the remarkable uniformity of results obtainable, a characteristic which differentiates it from other dielectrics used for wires and cables. This uniformity, however, exists only if the material is free of mechanical stress.

As with other dielectrics, the dielectric strength of polyethylene, that is, the volts per unit thickness, is a function of the thickness, and is much higher for thin walls than for thick ones. This difference is more marked at low than at high temperatures, as indicated by the figures in Table I based on short-time 60-cycle tests.

There is a sharp break in dielectric strength at a little below 100 degrees centigrade. Thus a cable with 120 mils of insulation maintained a dielectric strength of 500 volts per mil (average stress) from 30 degrees centigrade to nearly 100 degrees centigrade but had only about 200 volts per mil dielectric strength at 110 degrees centigrade. This drop was even more pronounced with thin sheets. Thus a ten-mil sheet having 1,700 volts per mil at 30 degrees centigrade, had only 500 volts per mil at 110 degrees centigrade.

This characteristic is not peculiar to polyethylene but is common to most plastics as their softening point is approached.

Polyethylene bears a curious resemblance in its characteristics to oil-impregnated-paper insulation, owing partly to the fact that their coefficients of thermal expansion are about the same, and partly to the fact that impregnated-

---

Wm. A. Del Mar is chief engineer, Habirshaw Cable and Wire Division, Phelps Dodge Copper Products Corporation, Yonkers, N. Y.

paper insulation is virtually oil thickened with paper, whereas polyethylene is an oil product thickened by polymerization.

Longitudinal expansion of cable insulation is usually limited by friction to the amount of expansion of the copper conductor, which is about one tenth of that of the polyethylene. The greater part of the volume expansion, therefore, is taken up by radial expansion, which reveals itself by separation of the insulation from the conductor, by pressure against any outer covering, and by the introduction of mechanical stresses.

The resultant void between conductor and insulation is liable to be the seat of discharges which, if maintained, will lead to failure.

Like oil-impregnated paper, polyethylene may fail either by direct puncture or by dendritic discharges. The latter occur when a void of considerable thickness exists at the conductor surface.

Several years ago, some experimental data were published in England by F. Fernie, tending to show that impregnated-paper cables fail, on short-time voltage test, when a certain stress (about 250 volts per mil is attained at *the outer* surface of the insulation, whereas the current view at that time was that failure should occur at a certain critical stress at the inner surface of the insulation. Neither theory can be said to have been proved owing to the uneven dielectric strength of oil-impregnated-paper insulation.

Table I. Dielectric Strength of Polyethylene

Thickness of Sheet, Mils	Volts Per Mil	
	30 C	90 C
10	1,700	1,300
20	1,200	1,050
40	900	850
60	750	700
80	600	550

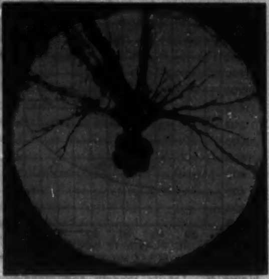

Figure 1. Dendritic failure in polyethylene

However, in the case of polyethylene, the uniformity of the material is so great that the two theories can be compared with considerable accuracy. Thus six cables of widely different dimensions made with some of the first American polyethylene failed at internal stresses from 720 to 2,300 volts per mil, whereas the external stresses ranged only from 200 to 280 volts per mil, the average value of 230 volts per mil being not far from the 250 volts per mil obtained in England for impregnated paper. The stress at diameter (1/2.72) × outside diameter varied from 600 to 1,420 volts per mil. Improvements in polyethylene have raised the critical exterior stress to about 400 volts per mil. It is of interest to note that this stress of 400 volts per mil is about the value to which the dielectric strength of the same grade of polyethylene sheets approaches asymptotically, for thicknesses above 100 mils. Nine of these cables had woven-wire outer electrodes; three were immersed in water.

With reference to the radial- and dendritic-type failures, the former occur at voltages characteristic of normal-temperature dielectric strength, whereas the latter occur at lower voltages characteristic of high-temperature dielectric strength, indicating that dendritic failure is caused by heat generated by the discharges in voids. A typical dendritic failure, which started at an air pocket on the conductor, is shown in Figure 1.

Polyethylene is very sensitive to pressure caused by local restraint against radial expansion. This is also characteristic of impregnated paper, although to a less degree. Breakdowns under these conditions have occurred at stresses as low as 60 volts per mil. Polyethylene is also very sensitive to tension such as occurs at sharp bends.

The d-c dielectric strength of polyethylene sheets is very high, being of the order of 6,000 volts per mil for thickness from 14 to 28 mils at room temperature. This is of the order of five or six times the 60-cycle dielectric strength.

V. Properties of Different Polyethylenes

W. J. CLARKE
NONMEMBER AIEE

AT THE PRESENT TIME the manufacturers of polyethylene in the United States are producing but one grade of the material for radio-frequency dielectric purposes, and this standard grade is covered by a Bureau of Ships specification. In England on the other hand the material produced by the Imperial Chemical Industries under the trade name Alkathene has been commercially available in various grades for the cable industry. The British classify their polyethylene according to a plasticity (melt-viscosity) index based on the amount of material at 190 degrees centigrade which flows through an orifice of arbitrary size under a definite pressure. The smaller the ICI plasticity index, the higher is the average molecular weight of the polyethylene. The British have commonly used for their radio-frequency cable a moderately low-molecular-weight grade known as Alkathene 20, and in order to improve its extrudability and low-temperature mechanical properties it has been their practice to modify the polyethylene slightly by the addition of some high-molecular-weight polyisobutylene. The highest-molecular-weight grades of polyethylene are the toughest forms of the material, but they are also not entirely satisfactory from the standpoint of smooth uniform diameter extrusion on wire. The standard American product represents a compromise between practical extrudability and good mechanical properties over the widest possible temperature range. It is superior to the polyisobutylene-modified British cable insulation chiefly in respect to very low-temperature impact and bend resistance and to deformation resistance at relatively high service temperatures, approaching 100 degrees centigrade.

The plasticity of the American polyethylene is measured by means of a parallel plate device known as the Williams plastometer. The Williams plasticity index is the thickness in mils of a two-cubic-centimeter specimen after being subjected to a five-kilogram load for three minutes at a test temperature of

---

W. J. Clarke is with the Bell Telephone Laboratories, Inc., New York, N. Y.

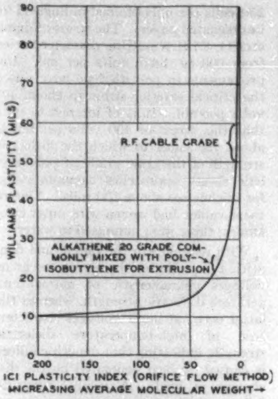

Figure 1. Comparison of British and American plasticity indices for polyethylene

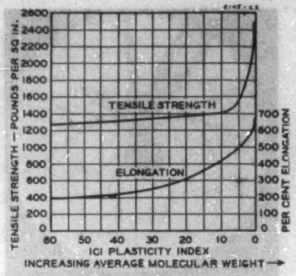

Figure 2. Tensile strength and elongation versus plasticity index

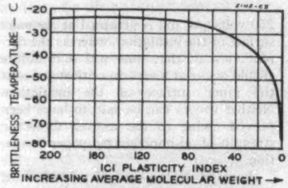

Figure 3. Brittleness temperature versus plasticity index

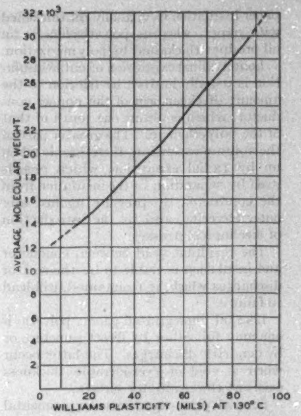

Figure 4. Average molecular weight by dilute-solution viscosity method versus Williams plasticity at 130 degrees centigrade, five-kilogram load, two-cubic-centimeter specimen for three minutes

130 degrees centigrade. The relationship between the British and American methods of measuring the plasticity of polyethylene is shown in Figure 1.

The physical properties of polyethylene at normal temperatures correlate approximately with the plasticity of the material in the melted state. As the complexity of the material increases, that is, as the average molecular weight goes up, such properties as tensile strength and elongation increase and the temperature at which the polyethylene becomes brittle under sharp impact is substantially lowered, as shown in Figures 2 and 3.

The intermolecular forces acting between the nonpolar hydrocarbon chains of polyethylene, both in the crystalline and amorphous regions of the material, are not large. These forces vary considerably with temperature, as is the case in all thermoplastic polymers. For example the tensile strength averages 1,800 pounds per square inch at 25 degrees centigrade but varies over the range of 0 degree centigrade to 100 degrees centigrade from over 3,000 pounds per square inch to about 200 pounds per square inch.

The brittleness temperature, as a rule an inherent characteristic of high-polymeric materials, shows a marked decrease as the average hydrocarbon chain length increases. The brittleness temperature of recent commercial lots of the radio-frequency-cable grade of polyethylene is exceptionally low when compared to most other plastics; in fact it is frequently below the minimum temperature to which it is practical to lower the test bath in the laboratory (that is, below about −65 degrees centigrade).

One would expect certain properties of the solid ethylene polymers not to change appreciably with variations in the molecular complexity of the material, for example:

1. Specific gravity.
2. Hardness (indentation, scratch, and so forth).
3. Water absorption.
4. Flammability.
5. Resistance to degradation by heat and ultraviolet light (stabilizer present).
6. Thermal conductivity, coefficient of expansion.
7. Machinability.
8. Resistance to alkalies, acids, and most organic chemicals.

Slight differences may exist in certain other properties however. The radio-frequency-cable grade of polyethylene is controlled as closely as is commercially practical between stated plasticity limits (see Figure 4 which shows the relation-

Table I. Differences in Properties of Commercial Polyethylenes*

	Sample			
	1	2	3	4
Average molecular weight (dilute-solution viscosity method)	17,800	20,300	21,650	23,800
Fractionation data				
Average molecular weight below 10,000, per cent	5.2	11.2	11.2	17.0
Average molecular weight between 10,000 and 20,000, per cent	78.8	21.0	42.8	13.7
Average molecular weight over 20,000, per cent	16.0	67.8	46.0	69.3
Softening temperature, degrees centigrade (plastic point)	111	108	108	105
Tensile strength, 25 degrees centigrade, pounds per square inch	1,900	1,670	1,900	1,470
Elongation	570	520	590	490
Brittleness temperature, degrees centigrade	<−65	<−65	<−65	−45 (−33 to −50)
Impact strength, Izod, foot-pounds				
at +25 degrees centigrade	>4	>4	>4	>4
at −10 degrees centigrade	0.4		0.7	0.1
at −36 degrees centigrade	0.2		0.1	<0.1
Deformation under load† at 98 degrees centigrade				
Deformation in 48 hours, per cent	9.7	14.4	21.2	39.9
Elastic recovery in 7 hours, per cent	5.6	8.8	9.9	12.0
Dielectric loss at 25 degrees centigrade				
Power factor at 50 megacycles	0.00030		0.00025	0.00030
Power factor at 1,330 megacycles	0.00054	0.0005	0.00035	0.00040
Power factor at 3,000 megacycles	0.00049		0.00030	0.00043

* All of approximately the same order of Williams plasticity at 130 degrees centigrade.

† 224 pounds per square inch pressure (at start) on cylindrical specimens (0.25 inch diameter by 0.31 inch height).

ship between plasticity and average molecular weights), but even in this rather narrow range of 50 to 60 slight variations in the average molecular weight and molecular species distribution may occur. This is characteristic of all synthetic high-polymeric materials. These variations, however small, are of importance to the cable manufacturers who may have to adjust extrusion temperatures and speeds accordingly. They may also have some bearing on the characteristics of the insulation, especially in its physical properties. In Table I is shown a series of four polyethylenes all of approximately the radio-frequency-cable-grade plasticity range. They were selected merely to illustrate possible variation and are not necessarily representative of current production.

The molecular-weight measurements were made by the dilute-solution viscosity method originated by Staudinger and commonly employed in the investigation of polymeric materials. No attempt is made to discuss the details of this work except to say that the measurements were made at 80 degrees centigrade in tetralin as a solvent. The results show that the average molecular weight of this series varies from 17,800 to 23,800.

In addition to the determination of the average molecular weight of the material as received from the manufacturer, an attempt was made to separate the samples into fractions of varying average molecular weight according to their solubility in carbon tetrachloride at different temperatures. Although a number of fractions were obtained, the results for convenience have been summarized in the table to show the percentage of the original material below 10,000 in average molecular weight, the percentage between 10,000 and 20,000, and the percentage over 20,000. It is not meant to infer that there has been a sharp separation of molecular species, that is, long and short chains. Nevertheless the characteristic distributions have been indicated.

Some of the physical properties may be seen to vary with the average molecular weight of the original polyethylenes, but the distribution data show more clearly why there are certain differences in the mechanical characteristics. Sample 1 represents a fairly narrow-band polyethylene with 78.8 per cent lying between 10,000 and 20,000 in average molecular weight. This material is high in softening temperature, tensile strength, and impact strength at low temperatures; and low in brittleness temperature and in deformation under load and elastic recovery at 98 degrees centigrade.

Polyethylenes 2 and 3 have somewhat different and broader distributions of their molecular species, which are reflected in various properties. Polyethylene 4 has the highest average molecular weight and a still different distribution. The high percentage of relatively short-chain molecules lowers the softening temperature (plastic point) and tensile properties. It also results in a higher brittleness temperature for the material, and the brittleness data seem to vary over a wider-than-normal temperature range. The weakening effect of the low-molecular-weight portion shows up also in the higher deformation of this sample at 98 degrees centigrade under load. The gradual increase in the elastic recovery after deformation with molecular weight may be due to the complexity of the molecular structure, that is, to a mechanical intertwining of the long straight hydrocarbon chains, or it may be an indication of an occasional chemical cross-linking between hydrocarbon chains to form a soft rubbery gel structure.

The dielectric losses of these samples at various frequencies differ slightly, but there does not appear to be any definite correlation with the molecular-weight data. The reason for this is probably that the samples are from different sources. When polyethylenes from only one source are considered, there appears to be a slight but definite decrease in power factor with an increase in average molecular weight, which is most noticeable at the higher frequencies.

The development of polyethylene has been rapid, spurred on by the need for the material in the war. It is impossible to say yet what the ideal molecular-weight distribution should be in a polyethylene coaxial-cable insulation. The present standard grade appears to be a very satisfactory material.

The slight differences existing in the properties of commercial lots of polyethylene will undoubtedly be gradually eliminated as greater knowledge of the material is gained and the polymerization process is further controlled.

Summary of Discussion on Polyethylene

After the presentation of the various prepared discussions on polyethylene a period of informal discussion followed from the floor. In response to a question regarding the hope of increasing the service range of polyethylene to higher temperatures, Doctor Shackelton stated that such an extension of the service range would to some degree be realized as the producers obtain better control over the molecular weight distribution, chain branching, cross-linking, and so forth, of polyethylene.

Mr. Rosch (Anaconda Wire and Cable) asked how the nature of the dielectric breakdown of polyethylene-insulated conductors compared with that of rubber-insulated conductors. Mr. Del Mar replied that no corona cracking has occurred with polyethylene, such as usually happens with rubber. Mr. Merrill (Phelps Dodge) added that it is the intrinsic dielectric strength of polyethylene that governs the breakdown rather than the cable construction. Tests were made on cables with copper braid and with lead on the outside and on cables under water, results being all about the same. An important point is the size of the void space around the center conductor where the corona discharge first occurs. Breakdown studies at higher frequencies than 60 cycles have not yet been made.

Mr. Cooper (du Pont) pointed out that, although polyethylene is essentially nonpolar, it is the small amount of polar constituents which accounts for the slight but definite power factor of the material. Mr. Yager (Bell Telephone Laboratories) stated that the dielectric losses in polyesters, polyamides, vinyl derivatives, vulcanized rubber, and polyethylene differ only in the matter of degree. The losses are due to rotational displays of polar groups of side chains, polar groups on the chain, or polar bridges cross-linking the long molecules. It is doubtful if much loss can be attributed to the stabilizer added to polyethylene, since it would not be free to rotate at high frequencies in such a viscous medium. More than likely in the case of polyethylene some oxidation occurs (from the oxygen catalyst used in the polymerization or from subsequent processing and handling of the material). The power factor-versus-frequency curve indicates a maximum dispersion at ultrahigh frequencies, which means that the internal friction must be low. Mr. Warner (Federal Telephone and Radio) called attention to a British paper by W. Jackson (and J. S. A. Forsyth) presented before the Institution of Electrical Engineers last year which showed that the dielectric losses in polyethylene may be largely ascribed to the formation first of —OOH groups, which are subsequently broken down to —OH groups attached to the hydrocarbon structure.

In answer to a question from Doctor Odarenko, Mr. Clarke stated that unmodified polyethylene was chosen as the cable dielectric in this country because of the exceptional combination of mechanical and electrical properties over the widest possible temperature range. Whether polyethylene will replace other coaxial-cable dielectrics after the war will be determined by economic considerations and the relative usefulness of other materials over this temperature range.

VI. Radio-Frequency-Cable Manufacturing Methods

T. M. ODARENKO
MEMBER AIEE

THE METHODS and processes currently used in the manufacture of radio-frequency low-loss semiflexible cables are the outcome of combined closely co-ordinated efforts of research institutions, raw-material producers, and cable manufacturers. In this manner it has proved possible, in a remarkably short time, to arrive at the manufacturing methods capable of turning out many types of high-frequency cables, which are subject to severe operating requirements, with the available equipments and man power in quantities sufficient to meet the everchanging war needs. Incidentally, the methods developed for high-frequency cables proved directly applicable and most useful, in the production of other plastic cables such as submarine cables, radio hookup wires, and Army field wires.

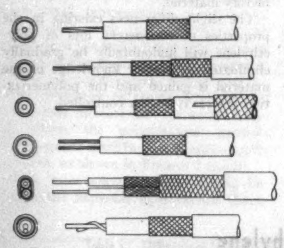

Figure 1. Basic types of coaxial cables

Of the large number of standard and experimental high-frequency low-loss cables which have determined the present manufacturing methods, most are of the so-called coaxial type, although some dual lines as well as twin-coaxial pairs are used. These basic types are shown in Figure 1. Fundamentally, a single conductor, or a pair of conductors, is embedded in the primary dielectric, over which a braid is applied. A jacket is provided for mechanical protection and for protection against the ingress of moisture, oils, gasoline, and the like. Frequently, particularly for the Navy use, an additional armoring braid is served over the jacket. Where shielding is of importance, a second braid is used under the jacket.

The problem of a cable manufacturer, then, is to build up the afore-mentioned structures, utilizing the known characteristics of the raw materials involved. These are: polyethylene for the primary insulation, various synthetic resins for the jacket, copper wires for the central conductors and braid, steel or aluminum for the armor. Where the requirements of the ultimate use demand them, copper-clad steel wires and silver- or tin-coated wires are also used.

The normal sequence of operations evolved to build up the structure of high-frequency cables is:

1. Extrusion.
2. Braiding.
3. Jacketing.
4. Armoring.

These operations have to be controlled very closely in order to meet the narrow tolerances of physical and electrical characteristics of the produced cables, which are dictated by the conditions of ultimate use of cables. Thus, simple in principle as the high-frequency-cable manufacturing processes are, they call for highly trained operators, a constant and close engineering supervision, and faultlessly performing equipments. The high-frequency low-loss transmission lines are still, therefore, the blue-blooded members of the cable and wire family.

Extrusion Equipments

The first and the most critical operation is the application of polyethylene around the central conductor or conductors. This is done universally by extrusion, and the basic equipment used for the purpose in the United States is a plastic extruder. Figure 2 shows a schematic cross-section of such extruder. This consists of a feed, a plasticizing chamber with a masticating screw, a head, and a die. A jacket is provided to control the temperature of different parts of the extruder by means of circulating oil. The general appearance of a plastic extruder is not unlike that of a conventional rubber extruder. There are, however, some important differences.

Unvulcanized rubber stocks of the type long used for wire-insulating purposes required comparatively little mechanical working to bring them to the proper consistency for extrusion, and this consistency often was obtained by prewarming

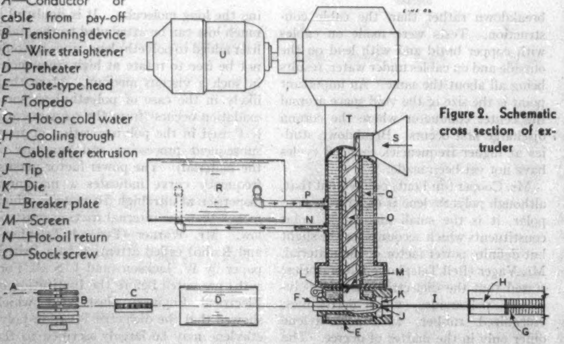

Figure 2. Schematic cross section of extruder

A—Conductor or cable from pay-off
B—Tensioning device
C—Wire straightener
D—Preheater
E—Gate-type head
F—Torpedo
G—Hot or cold water
H—Cooling trough
I—Cable after extrusion
J—Tip
K—Die
L—Breaker plate
M—Screen
N—Hot-oil return
O—Stock screw
P—Hot-oil feed
Q—Hot oil in extruder barrel
R—Oil-heating and storage tank
S—Hopper feed for extrusion material
T—Extruder
U—Motor

T. M. ODARENKO is products-line manager, Federal Telephone and Radio Corporation, Clifton, N. J.

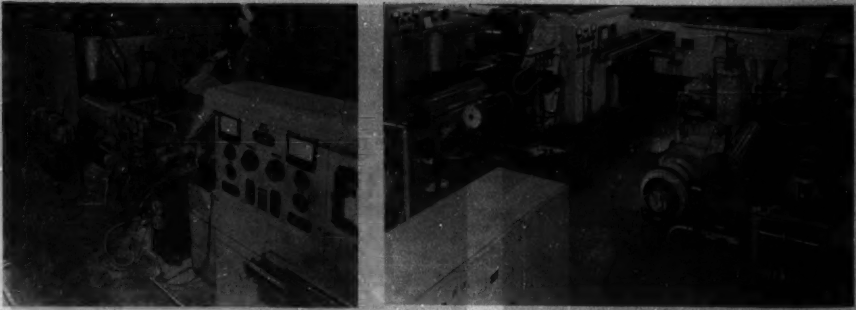

Figures 3 (left) and 4 (right). Two general views of extruder

on a two-roll mill. Consequently, the tubing machine acted primarily as a conveyor and as a device to build up sufficient pressure to form the rubber around the wire. A steam-heated short barrel machine with a deep-cut worm having a single thread of uniform pitch was found to give optimum delivery and product uniformity.

With the thermoplastic materials, however, a considerably greater mechanical working was required to bring the material to the proper extrusion consistency. Higher temperatures were essential, and the temperature build-up had to be accomplished primarily by internal frictional working. To accomplish this it was found desirable to increase the length of the worm and barrel by approximately 50 per cent, to add a breaker plate, backed up by steel-wire screens, at the end of the barrel, and to alter the worm design.

The breaker plate, a steel disk with a multitude of small-diameter holes, backed up by one or more wire-mesh screens, serves to hold the material back in the worm until, by the churning action of the worm and slippage of material between the thread surfaces and the cylinder wall, the material is brought to the proper plastic state. It is further broken down in passing through the screens and breaker plate and re-fuses in the crosshead into a mass of thoroughly plasticized material.

By extending the length of the worm additional time was obtained for the afore-mentioned plasticizing action. By using a single-lead narrow-depth thread of decreasing pitch, improved frictional working and pressure build-up was obtained. The worm, in addition, is water-cooled to prevent excessive temperature rise, with consequent thermal decomposition of the plastic material and sticking or burning on the worm.

Oil heating of the barrel jacket sections has been found to be more practical than high-pressure steam-heating methods, the oil being pump-circulated through the system from electrically heated storage tanks. Actually, with most thermoplastic materials, it has been found that the barrel sections need only be heated to bring the machine to the proper temperature, and that once extrusion has started sufficient heat is developed by the frictional working of the material so that either the oil circulation in those sections must be turned off, or the temperature of the circulating oil must be reduced to the point where oil acts as a cooling medium. Proper temperature balance is obtained by adjustment of oil circulation at the breaker plate, barrel sections, and head, and water circulation through the worm.

The head and die design of the plastics extruder is extremely important. The main problem is one of providing streamlining of all parts, minimum volume of cavity, and elimination of "dead spots" or pockets where material may lie stagnant and decompose.

Figures 3 and 4 show a general view of a plastic extruder. This is a so-called number-2 extruder, with the diameter of the screw about $3^1/_4$ inches. Plastic extruders come in various sizes, and those used in the United States vary from number 1, the smallest machine with the screw diameter of $1^1/_2$ inches to number 5, the diameter of the screw of which is eight inches. Most of the extruders in use are number 2 and number 4.

EXTRUDER ACCESSORY EQUIPMENTS

Originally it was thought that the extruder was the most important part for the high-quality extrusion. Now it is generally recognized that the successful manufacture of radio-frequency transmission lines will be found to depend as much on the design of extruder accessory equipment as on the design of the extruder itself. Because of the necessity for extremely close diameter control, the wire pay-off and take-up mechanisms must provide smooth actions over a wide range of speeds, free from jerks. This has necessitated careful design of frictioning devices, drive mechanisms, capstans, and reel traverse mechanisms. Electromagnetic drives with automatic electronic controls are coming into use, but much remains to be accomplished in this field.

A representative setup of extrusion equipments is shown in Figure 5. This involves a pay-off mechanism, a tensioning device, a wire straightener, a preheater, an extruder, a cooling trough, a capstan, a take-up mechanism, and various control devices.

POLYETHYLENE EXTRUSION

In the United States, polyethylene is universally fed into the extruder cold,

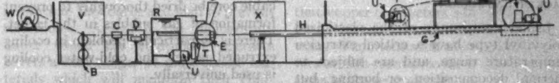

Figure 5. Schematic layout of extruder line

B—Tensioning device
C—Wire straightener
D—Preheater
E—Gate-type head
G—Hot or cold water
H—Cooling trough
R—Hot-oil tank and heaters
S—Hopper feed for extrusion material
T—Extruder
U—Motor
V—Power-control panel
W—Pay-off
X—Operator's control panel
Y—Take-up
Z—Printing machine
A1—Sparker
B1—Footage indicator
C1—Capstan

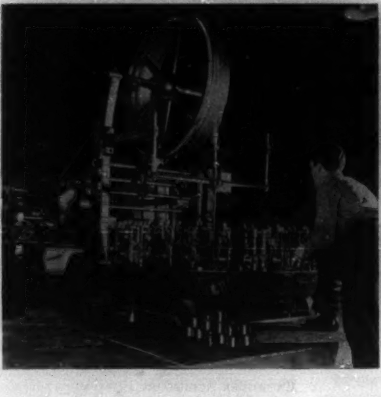

Figures 6 (left) and 7 (above). Two basic types of braiding machine

Figure 8. Winding machine

and for this reason it is supplied to the manufacturers in granulated form. It is plasticized by the mechanical working of the extruder worm and its extrusion temperature is kept around 310–320 degrees Fahrenheit.

Because of its rather sharp softening point, around 240 degrees Fahrenheit, and a comparatively high rate of volume expansion in the temperature range between the softening point and the room temperature, it has been found necessary to provide a careful control of the cooling rate.

If the extruded cable is chilled suddenly, the material will set rigidly on the outside, and on subsequent internal cooling, will shrink away from the center conductor forming voids of air spaces in which corona can take place at relatively low voltages. This is prevented by the use of a long cooling trough with a carefully controlled water-temperature gradient from approximately 200 degrees Fahrenheit at the input end to room temperature or lower at the capstan. Similarly, it is desirable to preheat the conductor as it enters the extruder head to assure removal of moisture and prevent chilling of the polyethylene at the conductor. Moisture in any form will cause bubbles or vapor formations in the extruded product.

JACKET EXTRUSION

Jacket compounds of the plasticized polyvinyl type have a critical extrusion temperature range, and are subject to thermal decomposition, or burning, but can be extruded at appreciably higher speeds than polyethylene. They do not have a sharp melting point but soften gradually over a wide temperature range, the extrusion temperature being on the order of 320–350 degrees Fahrenheit. They can be fed to the extruder cold in granular or continuous strip form, although frequently they are preheated on a two-roll mill and hot strips from the mill are fed directly to the machine. In this manner most of the mechanical work is done beforehand, and somewhat greater extrusion speeds are obtained.

It is imperative that the jacketing material be free from moisture and that the cable core be dried thoroughly to prevent formation of gas bubbles in the jacket. There is no particular problem in cooling extruded jacket, and cold-water cooling is used universally.

Wire Braiding and Winding

The braid, or braids, in case of specially shielded cables, and the armor are applied by means of wire braiders.

Two basic types of braiding machines are available for copper and other wire-braiding operations (Figures 6 and 7). One type is the so-called figure-eight type, wherein two sets of bobbin carriers revolve in opposite directions in grooves in a horizontal plate, weaving in and out in a figure-eight pattern. This type is made by the New England Butt Company of Providence, R. I., and the Textile Machine Works of Reading, Pa., and is a relatively slow machine. The other type is manufactured by the Wardwell Machine Company of Central Falls, R. I., and is a considerably faster machine and by far the more popular type. This machine contains bobbins mounted on two heads which revolve in opposite directions at speeds up to approximately 100 revolutions per minute, the wires from the bobbins on one head being deflected around the bobbins of the second head in the proper manner to form a basket weave.

Most of the problems in wire braiding arise from improperly wound bobbins.

Anywhere from 2 to 12 or more individual wires must be wound onto the bobbin, depending on the cable diameter and desired lay and coverage. Unless these wires are wound with equal tensions, slack or excessive tautness will develop in one or more strands during the braiding operation, causing breakage or loops in the braid. Thus, the bobbin winding operation is of extreme importance.

Winding machines made by the Universal Winding Machine Company of Providence, R. I., have been found suitable for this type of work. One type is shown in Figure 8. Many types of tensioning devices and methods of payoff from the individual wire spools have been tried. No entirely satisfactory system has been developed, and this problem requires constant attention.

Manufacturing Tolerances

Tolerances on the dielectric and conductor diameters must be kept quite narrow in order to maintain the variation in characteristic impedance within the permissible limits. In order to keep a plus or minus two-ohm tolerance on the impedance of 52 ohms, it can be proved that neither the central conductor nor the dielectric diameter may vary from its nominal value by more than plus or minus 2.5 per cent. In actual practice it has been found possible to maintain the diameter of extruded polyethylene to about two per cent. ASTM tolerances on most sizes of copper wire are less than 2.5 per cent, and the normal variations in effective dielectric constant do not contribute more than a few tenths of an ohm to the impedance variations, so that in general it is possible to maintain the over-all impedance characteristics within the specified limits. A certain amount of difficulty has been experienced with tolerances of the center conductors, particularly of small sizes or stranded. It has been found, also, that care must be taken during extrusion in order to prevent drawing down of the conductor wire. And, again, this problem is more severe with smaller sizes of conductors.

Summary of Discussion on Cable Manufacture

Following the description of the manufacturing methods used in the United States for production of high-frequency cables for communication purposes, the informal discussion centered on the following specific problems: difference in extrusion methods in the United States and Great Britain; differences in the tolerance requirements of high-frequency cables in the United States and Great Britain; the fundamental reasons for cold-water and hot-water cooling of the extruded core of polyethylene; the need for long lengths in cooling troughs; and the cleanliness requirements in high-frequency cable plants. Greenfield, Wyatt, Warner, Clarke, Shackleton, Sheldon, and Rosch participated in these discussions.

The discussion revealed that there exists a difference of opinion as to the best over-all cooling procedure for polyethylene cores of high-frequency cables, and as to the importance of segregation of high-frequency-cable production units from the synthetic-rubber wire and cable plants. The general procedure in this country is to house the high-frequency-cable production facilities in an isolated unit within the cable plant, and to use slow-cooling or annealing process in the manufacture of the polyethylene core of high-frequency cables.

The discussion brought out the fact that the differences in the production methods in the United States and in Great Britain are the results of the fundamental differences in the historical approach to the manufacturing problem, which are further accentuated by the differences in the equipments available in the two countries.

VII. General Considerations in Radio-Frequency-Cable Design

J. F. WENTZ
MEMBER AIEE

OUR PROBLEM in designing cables for high frequencies is somewhat different in detail from that which we have had in the past, but basically it comes down to these two facts:

1. What materials have we to work with?
2. What requirements do we have to meet?

If the line is many thousand miles long, obviously our main consideration is loss. If it is only a few feet the primary consideration may be matching the impedance to the source and load to prevent reflections. Again, if the temperature under which the equipment operates covers a wide range, we must choose materials which will maintain their characteristics well. Sometimes just plain mechanical stresses in bending or vibration will determine the kind of design we finally select. In this, as in all design work, we pick the best compromise between the conflicting requirements.

By design we mean determining the dimensions using the best materials so that the requirements are met.

I think we can assume in our discussion that copper conductors and polyethylene insulation are the materials we must work with. Variations such as silvered conductors or high-resistance wires will be exceptions to the general rule.

So let us consider the simple case of a solid-dielectric coaxial cable of given diameter to connect two equal impedances with minimum loss. If we were working at voice frequencies, we would find the added a-c resistance of the center conductor changing as the square of the frequency, but above the kilocycle range the reactance inside the metal forces the current to the outer surface, and we find it

---

J. F. Wentz is high-frequency transmission engineer, systems department, Bell Telephone Laboratories, Inc., New York, N. Y.

changing more nearly as the square root of the frequency. In this region up to some megacycles, it is quite possible on paper to design a stranded or braided conductor which has lower effective resistance than a solid one, but the strands soon get very fine, and problems of manufacture and handling multiply, so that stranding with a view to uniform distribution of current over the cross section of the wire rarely proves in. Certainly in the ultra-high-frequency and very high-frequency ranges we concede that the conductor with the minimum periphery is the best design and go to a stranded conductor only because of flexibility requirements. In this case it is found that a few large strands are better than many fine ones.

If we look at the transmission equations, we find the impedance of a long cable is the square root of L/C, and the attenuation is proportional to R and square root of C/L. The capacity and inductance are proportional to the logarithm of the diameter ratio of the outer and inner conductors, and so, without listing all the formulas, suffice it to say that we can proportion the conductors to get the desired impedance and, by making them large enough, get the loss down to reasonable amounts.

The real design problems come when we get down to the fine points of the structure. Let us take the distribution of the losses in the various components and study them individually to see where we may be able to compromise so as to use less material or get a better product.

Figure 1 shows the three component losses of a line made up of solid-copper inner conductor, polyethylene insulation, and copper-braid outer conductor. It happens to be the standard *RG*-18/*U* radio-frequency cable.

The inner and outer conductor contribute about equal amounts in the case of *RG*-18/*U*, each of them varying about as the square root of the frequency. The dielectric loss, however, goes up about directly with the frequency, and so, even with polyethylene, which has an extremely low power factor, this component becomes a predominating factor at the very high frequencies.

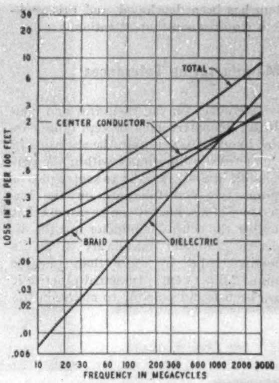

Figure 1. Distribution of losses in a typical *RG*-18/*U* cable

Starting on the outside we can do various things to the braid to reduce its resistance. The currents try to flow longitudinally since they encounter larger reactance if they follow the strands; therefore, the longer the lay of the strands, the lower the resistance. Of course, the cable gets stiffer as the length of lay is increased, and so again a compromise between the mechanical and electrical requirements forces us to a fairly short-lay braid. Where a second braid is used, the outer one, in general, can be of shorter lay, since most of the current remains on the inside. When the cable is flexed, the contacts between strands change, and, if the copper is dirty or corroded, the resistance may vary considerably. Silver plating the strands tends to keep this resistance more constant and usually reduces it as well because of the better contacts.

Going now to the dielectric, we dimension it primarily to obtain the proper impedance and must take the loss which the material produces. The ratio of outer to inner diameter is about 3.6 which gives an impedance of about 52 ohms. With this ratio the inner-conductor diameter is determined for a given-size cable, and the volume of dielectric is fixed. The absolute value of the loss due to the insulation is independent of the dimensions and is now determined by the power factor of the polyethylene, and we can do no more about reducing it.

In general, the best electrical performance is obtained at the very high frequencies with solid inner conductors. Without putting such a cable together, we can calculate what the impedance and losses should be, but when we make it we run into such things as variable contact in the strands of the conductors and voids in the dielectric that make the losses different from what we expected. By separating the component losses, we can work on them to determine how to improve the whole.

There are many special requirements besides loss and impedance which determine particular designs. For instance, for cables which transmit high powers, the heat generated in the inner conductor must be dissipated through the dielectric. Here the power rating is determined by the temperature the dielectric will stand. If the voltages are high, corona may form at sharp points on the conductors, and small strands may produce a very inferior cable. In some applications high losses instead of low ones are desired for padding, especially in cords for test equipment. For this purpose, high-resistance wires may be used, and then the distribution of losses is quite different.

So far we have considered only the coaxial type. In certain applications balanced conductors are needed. Then the current distribution in the shield is quite different, and the proximity effect of one conductor on the resistance of the other is large. There are formulas for calculating the losses and impedance of such cables, and the procedure, while more complicated, is the same as for the coaxial case.

Some of these problems are of more interest than others, and we have asked a number of engineers to take up specific ones and discuss them in more detail. These and other design problems will be brought out.

VIII. Losses in Radio-Frequency-Cable Components

G. L. RAGAN
NONMEMBER AIEE

DIELECTRICS may be described by means of a complex dielectric constant:

$$k\text{ comp}=k'-jk''$$

Here k' is the ordinary dielectric constant associated with the component of current out of phase with the applied voltage. k'' is associated with the inphase component of current and hence represents a loss of power. The ratio of these two components is called the loss tangent:

$$\tan\delta=\frac{k''}{k'}$$

For small values this tangent is approximately equal to the power factor. For dielectrics commonly used in cables, tangent delta is usually much less than 0.01. In such cases, the wave length in the cable is well approximated by the usual formula:

$$\lambda_c\cong\frac{\lambda_o}{\sqrt{k'}}$$

The losses in a dielectric may be due either to a true dielectric conductivity or to polarization effects in the molecule. In either case, one can ascribe the losses to an actual or to an equivalent conductivity:

$$\sigma_{di}=\frac{1}{60}\,\frac{k''}{\lambda_o}=\frac{1}{60}\,\frac{\tan\delta}{\lambda_o}\,k'\text{ mhos per centimeter}$$

The dielectric losses are expressible in the following alternative forms:

$$\alpha_{di}=27.3\sqrt{k'}\,\frac{\tan\delta}{\lambda_o}\text{ decibels per centimeter}$$

$$=27.3\,\frac{\tan\delta}{\lambda_c}\text{ decibels per centimeter}$$

$$=27.3\tan\delta\text{ decibels per wavelength in cable}$$

It should be noted that the dielectric loss is independent of the dimensions of the cable and dependent only on the characteristics of the dielectric itself.

For the coaxial line made of simple coaxial cylinders, the characteristic impedance is given by the familiar expression:

$$Z_o=\frac{138}{\sqrt{k'}}\log\frac{b}{a}$$

Here a is the radius of the inner conductor and b that of the outer conductor. Where the center conductor is stranded and the outer conductor is a braid, effective values for a and b must be used. The losses for the case of simple coaxial cylinders are

$$\alpha_i=\frac{23.8}{Z_o}\,\frac{1}{a}\left(\frac{\rho_a}{\lambda_o}\right)^{1/2}\text{ decibels per centimeter}$$

$$\alpha_o=\frac{23.8}{Z_o}\,\frac{1}{b}\left(\frac{\rho_b}{\lambda_o}\right)^{1/2}\text{ decibels per centimeter}$$

If

$$\rho=\rho_a=\rho_b$$

$$\alpha_{cu}=\frac{23.8}{Z_o}\left(\frac{1}{a}+\frac{1}{b}\right)\left(\frac{\rho}{\lambda_o}\right)^{1/2}$$

ρ_a and ρ_b are the resistivities of the metals of which the inner and outer conductors are made. Here again the situation is complicated by stranding of the center conductor or braiding of the outer conductor. In each equation, a factor must be introduced to adjust for this effect. The braid factor is particularly important. The braid factor is usually expressed as the ratio of the loss due to the actual braid as compared to that due to a copper tube as outer conductor.

The total attenuation of a cable is the sum of that due to copper and that due to dielectric:

$$\alpha=\alpha_{cu}+\alpha_{di}$$

The frequency dependence of these deserves special attention:

$$x=c_1f^{1/2}+c_2f$$

Both losses increase with frequency but at different rates. c_1 and c_2 are constants. c_1 depends on the size, material, and construction of the conductors. c_2 depends on the dielectric constant and power factor of the dielectric.

Since the copper losses vary less with frequency it is clear why *RG*-21/*U* cable with a resistance wire of nichrome for its center conductor makes a good attenuating cable.

As an example of the application of the principles and equations here described, a comparison is given of calculated and measured losses for a specific cable: *RG*-14/*U*. The losses due to dielectric, inner conductor, and outer conductor are shown as calculated from the data given in the table. The measured curve, the heavy line, is also shown. The sum of dielectric and copper losses is shown by the six circled points. The agreement is seen to be fair at the higher frequencies but rather poor at the lower frequencies. Here the calculated points show too high a loss. This is probably due to the fact that the braid factor is not a constant but depends on frequency. It is known that the braid factor is smaller at the lower frequencies. A braid factor of about two would bring the 100-megacycle point into agreement with the observations.

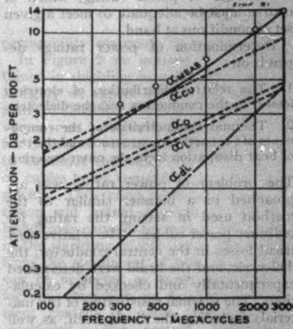

Figure 1. Comparison of calculated and measured losses for a specific cable *RG*-14/*U*

⊙ Points are calculated
RG-14/*u*
$a=0.051$ inch
$b=0.185$ inch

$Z_o=52\Omega$
$k'=2.25$
$\tan\delta=0.00037$
Braid factor = 4.0

G. L. RAGAN is with the Radiation Laboratory, Massachusetts Institute of Technology, Cambridge, Mass.

IX. Radio-Frequency-Cable Power Ratings and Stability

M. C. BISKEBORN
ASSOCIATE AIEE

SUPPLEMENTING the fundamental principles of the design of radio-frequency coaxial cable as reviewed by Mr. Wentz, there are certain details of sufficient interest to justify some additional amplification. A factor of considerable importance to the successful use of radio-frequency cable for many applications is the matter of power rating, which of course must be adequate to meet a given set of conditions at hand.

Determination of power ratings depends on

1. The relative distribution of electrical losses, in the conductors and the dielectric.
2. Thermal conductivities of the components of the particular structure and the rate of heat dissipation from the outer covering.

The problem of power rating was approached in a manner similar to the method used in setting the rating for ordinary power cables. The relative electrical losses in the central conductor, the dielectric, and the braid were determined experimentally and checked by calculation. The thermal resistivities of the materials including the braid itself, as well as the jacket, were measured on a number of samples. The particular structure involved, namely that of the coaxial, determined the relation between the thermal resistivities of the materials and the thermal resistance to the flow of heat from the inner conductor to the outer conductor. As is well known to power-cable engineers, the thermal resistance to the radial flow of heat through a coaxial structure is proportional to the product of the thermal resistivity and the logarithm of the diameter ratio familiar to impedance and capacitance calculations.

The limiting factor which dictates design considerations is the maximum allowable temperature of the dielectric itself at its hottest point. In a coaxial cable the hottest point in the dielectric is at the surface of the central conductor. Estimates of suitable power ratings, therefore, were made with a predetermined maximum temperature for the hot point in the dielectric with some factor of safety in the choice of the maximum allowable temperature to which the dielectric (polyethylene) may be subjected. It is of interest to note that, from the standpoint of temperature rise at the surface of the central conductor, the loss in the dielectric, being distributed in the manner peculiar to coaxial structures, is equivalent to one-half the total dielectric loss concentrated at the surface of the central conductor itself.

Unless the attenuation of a coaxial cable is fairly stable with time and temperature, a rating of the maximum allowable power in the cable is comparatively meaningless. Also, instability invites possible failure due to the establishment of a vicious circle in case the dissipation of power causes undue increase in loss. Fortunately the design and manufacture of cables having remarkable stability has been achieved.

In order to obtain a knowledge of design factors affecting stability, an investigation of the losses in the central conductor and the braid was begun early in 1941, at which time test equipment for direct measurement of the electric parameters was available only in the low-megacycle region. It is evident that stability is a function of the magnitude of the absolute losses in the two conductors; hence, the losses should be kept as low as practicable. It was soon discovered, for example, that an improperly designed braid could have a resistance factor many times that of an equivalent copper tube. For comparison purposes, therefore, the copper tube was chosen as a standard of reference for which high-frequency metallic losses may be computed with greater accuracy than it is possible to make measurements. Investigation disclosed that, as would be expected, braids having a long lay are better than short-lay braids. Also, braids having large conductors are superior, indicating that the consequent reduction in number of contacts is desirable. A 1/1 type of braid weave was found to be slightly better than the 2/2 type of weave. Coverage or fullness of braids is also of importance, and it was found that overcrowding of the wires in a strand is undesirable from the standpoint of resistance factor as well as shielding effect. Metals having inherently low contact resistance possess merits over those of high contact resistance. This of course indicates that current flow in a braid is not only along the wires themselves but also through the contacts between the wires. As would be expected from this consideration, the pressure holding the wires in contact with each other enters into the ultimate losses in the structure. This dictates the desirability of a tight braid and of a jacket having capabilities of exerting some pressure over-all.

Early in this work it also was found that the factors which affected the quality of a braid from the standpoint of loss were also pertinent in the design of central conductors. Since the flexibility demanded the use of multiple conductors rather than a solid conductor, which may be considered ideal electrically, numerous designs having multiple strands were tried. As in the case of braids, it was found that an improperly designed multiple conductor could produce losses greatly in excess of those obtained with a solid conductor of such size as to give the same capacitance as the multiple conductor under consideration. Fortunately a simple multiple conductor consisting of six wires stranded around one was found very satisfactory when properly assembled, and particularly when constructed of metals having inherently low surface-contact resistance. A comparison of resistance factors for several braids and central conductors demonstrating the effect of design variables is shown in Table I.

In the considerations just mentioned the optimum electrical design has been emphasized. Unfortunately, mechanical requirements are often in conflict with electrical requirements, and the final design must be a compromise between the two. Length of lay of braids and stranding lay of center conductors are good examples. The mechanical characteristics of various braid and center-conductor designs were determined by handling and flexing tests. As a result of this work, well-balanced designs were arrived at in which the braid and the center conductor would withstand approximately the same amount of handling. This applies particularly to cables intended for service involving appreciable flexing.

After factors related to the general design of braids and central conductors have been examined, it is of interest to note what results have been obtained in practice, in regard to the stability of the at-

Table I. Comparison of Resistance Factors for Braids and Central Conductors

0.39-Inch-Inside-Diameter Braids		
Length of lay	$3\frac{1}{4}$ inch	3.8
	$2\frac{1}{4}$ inch	4.3
Wire size	Number 30 American Wire Gauge	3.8
	Number 34 American Wire Gauge	4.1
Coverage	85 per cent full	4.1
	105 per cent full	5.3
Weave	1/1	3.8
	2/2	4.1
Surface metal	Silver	3.1
	Copper	3.8
	Lead alloy	4.9
Central Conductors		
Single solid-copper wire		1.0
7 silvered-copper wires stranded 6 around 1		1.1
7 copper wires stranded 6 around 1		1.3
19 copper wires stranded 12 around 6 around 1		6.6

M. C. Biskeborn is a member of the technical staff, Bell Telephone Laboratories, Inc., New York, N. Y.

tenuation with time, temperature, and flexing. In order to determine the degree of stability which has resulted from the design work already discussed, a number of cables have been under test for about 100 days at a top temperature approaching 200 degrees Fahrenheit. During this time, periodic returns to room temperature were made. Also, certain cables were subjected to flexing in combination with temperature cycles. In the case of cables which embody the features which make for stability, the maximum deviation in attenuation from the initial value for all conditions of temperature and flexing has not exceeded about ten per cent. Special cables of the high-loss type have shown even less variation than ten per cent.

X. Shielding Characteristics of Radio-Frequency Cables

R. G. FLUHARTY
NONMEMBER AIEE

THE PROBLEM of cable shielding from the standpoint of this discussion involves keeping energy inside or outside the cable. Shielding serves other useful purposes such as ground protection around high-voltage circuits.

Greater and greater emphasis on circuit isolation is becoming necessary. This increased emphasis is due to several factors, such as the need for greater sensitivity in receivers, the increasing number of equipment types with its consequent filling of the frequency spectrum, and the closer and closer proximity in which these equipments are being operated.

From the standpoint of energy lost from a given equipment the amount that escapes through a single braided coaxial cable is negligible. However, when a transmitter operates near a receiver of another equipment this leakage power becomes very important. Even though the two are not operating on the same frequency, interference to the receiver can and does occur. Many equipments, not necessarily only electronic but electronic as well, are inherently noise generators. These require adequate shielding to protect surrounding equipment from interference.

A theory of shielding is discussed in Bell Laboratories Record, March 1936. In this article S. Schelknoff considers the energy spreading radially outward from a cable. He considers this as being composed of an electric field parallel to the wire and a magnetic vector at right angles to the wire and the radial line. The shielding effectiveness is found to be due to two factors:

1. Reflection at surfaces of changing impedance.
2. Penetration losses in the shield itself.

Figure 1 shows characteristics radial impedance as a function of frequency for different materials. It is noticed that for low frequencies magnetic materials may have higher impedances than air. Table I shows experimental data verifying the theory. This work has been done for solid materials, but the same attack is useful for braids. For frequencies up to 1 megacycle, the effect seems to be the same as for solid materials, and above, the braids start having effect.

Other experimental work has been carried out using well-shielded sources and loads with a cable between. In this comparative shielding, measurements are made of the voltage developed across the outside of the cable. An example of such results is shown in Figure 2 where the voltage is measured across four feet of cable with the same inside noise source being used for different numbers and types of braids. The cable is electrically the same as *RG25/U* and *RG64/U*. These measurements were made at Bell Telephone Laboratories, and similar types are used by other manufacturers of shielding. Conduit has been made which is at least 12 decibels better than solid copper tube 0.035 inch in thickness at Titeflex.

In these designs the primary criteria has been skin depth.

$$d = 5{,}030\frac{e}{\mu f}$$

d = depth of penetration (centimeters) $\left(\frac{1}{e}\text{th of surface value}\right)$

μ = permeability of material

f = frequency

Marked improvements are being gained by the use of higher-resistance higher-permeability materials for outer shields.

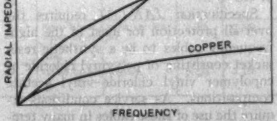

Figure 1. Characteristic radial impedance as a function of frequency for different materials

In Figure 2 we noticed the gain obtained in shielding in using more braids. Roughly we expect 40 decibels improvement in shielding when using two braids versus one. Experience shows the effectiveness of various two-shielded cables to be about the same (the armor braid on cables being considered an additional shield). Differences between shield separation and actual contact of the two braids may cause differences of two to one in the shielding effectiveness. However, from the standpoint of interference this can be neglected as there are coupling factors over which we do not have sufficient control to make this difference significant. For certain applications more braids may be necessary, but two shields are usually employed. For power circuits two are usually required and three or four more may be required. For receiver circuits operating in noise fields two are often needed and requests have been made for three.

It is important to point out that cable termination is another source of trouble. Many examples have occurred wherein blame has been laid to cable shielding for interference when the actual cause was poor braid termination. It is necessary to have very low-resistance terminations for both braids. These also should main-

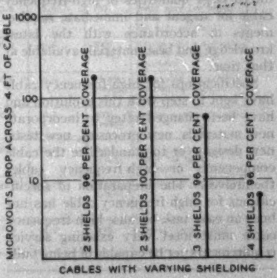

Figure 2. Gain obtained in shielding by using more braids

R. G. FLUHARTY is with the Radiation Laboratory, Massachusetts Institute of Technology, Cambridge, Mass.

tain shielding around the end of the cable, and the low resistance should be maintained around this circumference at as many points as possible.

Experience, not engineering knowledge, is about all that is available in this field, and a great deal more research is needed. Most of the development work upon cable shielding (outside of the telephone communications field) has been done by the people concerned with airplane-ignition shielding. The techniques used have been of the second type outlined. These have been useful and practical, but the experimental approach used to to confirm Schelknoff's theory should be more productive. For example, better shielding will be required upon many airplane equipments where weight considerations will require the best shielding designs possible.

Table I. Calculated and Measured Losses

Material	Thickness Mils	Frequency Kilocycles	Calculated Loss, Attenuation	Reflection	Total, Decibels	Measured Loss, Decibels
Copper	16	80	15.1	27.6	42.7	43.7
		150	20.7	31.3	52.0	52.1
Aluminum	18	80	13.3	26.5	39.8	39.8
		150	18.2	29.2	47.4	47.6
Zinc	18	80	9.3	23.4	32.7	32.0
		150	12.7	26.1	38.8	38.5
Lead	86	80	22.5	17.5	40.0	40.3
		150	30.8	22.0	52.8	52.3

XI. Types of Radio-Frequency Cables and Specifications

E. E. SHELDON
MEMBER AIEE

AN OUTLINE has been given of the electrical and mechanical principles that determine the design of high-frequency cable.

The application of these principles to formulate correct design procedure and correct designs for high-frequency cable has necessitated the closest co-operation among equipment designers, equipment users, research and testing laboratories, and cable manufacturers. The contributions of these varied groups has resulted in a continual and desirable evolution of high-frequency-cable design and manufacturing techniques during the last few years. Hundreds, and perhaps thousands, of different high-frequency cables have been submitted to laboratories by high-frequency cable manufacturers, to equipment designers, and to service agencies for test, evaluation, and trial installations. At every stage of this evolution cable manufacturers have produced large quantities of high-frequency cable for urgent and immediate requirements in accordance with the latest knowledge and best materials available at that time.

Specifications for high-frequency cable have kept in step with this evolution and have been changed often to incorporate new materials, new processes, new tests, new designs, or to standardize the cable components or high-frequency cables themselves. The preparation of specifications for high-frequency cable has not been an easy task because high-frequency cable must meet very exacting service requirements yet be capable of being built with available cable manufacturing equipment.

The Army–Navy Radio-Frequency Coordinating Committee has produced two aids to users and manufacturers of high-frequency cable:

1. "Joint Army–Navy Specification *JAN-C*-17 for Coaxial Cables."
2. "Army–Navy Standard List of Radio-Frequency Cables."

This joint Army–Navy specification *JAN-C*-17 completely outlines the field of high-frequency cable as far as any questions may arise which concern the high-frequency cable manufacturer.

The specification incorporates industry standards already existent, such as American Society for Testing Materials standards, wherever possible to specify the requirements for the components, such as the copper conductors.

In addition *JAN-C*-17 describes the construction of high-frequency cables in detail, specifies the allowable tolerances, and lists the test procedures necessary for type approval, for engineering data, or to check any production lot. Over 42 high-frequency cables appear in these specifications. Each of these types of high-frequency cable is identified by an *RG* number, such as *RG-5/U*, *RG-6/U*, or *RG-8/U*.

Specification *JAN-C*-17 requires the over-all protection for most of the high-frequency cables to be a synthetic resin jacket consisting of polyvinyl chloride or copolymer vinyl chloride–vinyl acetate compositions. As service conditions require the use of these cables in many temperatures, the jacketed cable is sampled and tested often during production for cold-temperature flexibility. The dimensional requirements also are very strict to facilitate the use of these cables with connectors. A few of these cables utilize a thin polyethylene jacket over all.

The high-frequency cables range in size from the smallest cable, the *RG-58/U*, which has an outside diameter of 0.195 inch and weighs only 2.5 pounds per 100 feet to the *RG-20/U* which has an outside diameter of 1.195 inches maximum and a weight of 92.5 pounds per 100 feet.

The "Army–Navy Standard List of Radio-frequency Cables" primarily serves the user of high-frequency cable. This list includes the 30 standard cables, the use of which is allowed in new electronic equipments for Army–Navy use. The 30 cables are grouped and classified by their most important characteristic.

Figure 1 shows the "Army–Navy Standard List of Radio-Frequency Cables" issue of October 15, 1944. The information presented not only includes the physical dimensions and construction but also the nominal electrical characteristics. The cables are divided into groups.

Group one consists of 12 cables with an impedance of 50 to 55 ohms and group two of five cables with an impedance of 70 to 80 ohms. The cables in these two groups are built in accordance with conventional high-frequency cable practice, that is a central copper conductor, polyethylene dielectric, either one or two copper shielding braids, synthetic resin jacket, and in some instances a basket-weave steel armor over all.

Groups three and four include the *RG* high-frequency cables which can be considered as special high-frequency cables.

E. E. Sheldon is in the wire, cable, and conduit engineering department, General Electric Company, Bridgeport, Conn.

ARMY-NAVY STANDARD LIST OF R.F CABLES

15 OCTOBER 1944

CLASS OF CABLES		ARMY NAVY TYPE NUMBER	INNER CONDUCTOR	DIELEC. MATERIAL (1)	NOMINAL DIAMETER OF DIELECTRIC (INCHES)	SHIELDING BRAID	PROTECTIVE COVERING	NOMINAL OVERALL DIA. (IN.)	WEIGHT POUNDS/FT.	NOMINAL IMPEDANCE OHMS	NOMINAL CAPACITANCE MMF/FOOT.	MAXIMUM OPERATING VOLTAGE RMS	REMARKS
50-55 OHMS	Single Braid	RG-58/U	20 A.W.G. Copper	A	0.116	Tinned Copper	Vinyl	0.195	0.025	53.5	28.5	1900	General purpose small size flexible cable
		RG-8/U	7/21 A.W.G. Copper	A	0.285	Copper	Vinyl	0.405	0.106	52.0	29.5	4000	General purpose medium size flexible cable
		RG-10/U	7/21 A.W.G. Copper	A	0.285	Copper	Vinyl (Non-contaminating) and Armor	(Max.) 0.475	0.146	52.0	29.5	4000	Same as RG-8/U armored for Naval equipment
		RG-17/U	0.188 Copper	A	0.680	Copper	Vinyl (Non-contaminating)	0.870	0.460	52.0	29.5	11,000	Large high power low attenuation transmission cable
		RG-18/U	0.188 Copper	A	0.680	Copper	Vinyl (Non-contaminating) Armor	(Max.) 0.945	0.585	52.0	29.5	11,000	Same as RG-17/U armored for Naval equipment
		RG-19/U	0.250 Copper	A	0.910	Copper	Vinyl (Non-contaminating)	1.120	0.740	52.0	29.5	14,000	Very large high power low attenuation transmission cable
		RG-20/U	0.250 Copper	A	0.910	Copper	Vinyl (Non-contaminating) Armor	(Max.) 1.195	0.925	52.0	29.5	14,000	Same as RG-19/U armor for Naval equipment
	Double Braid	RG-55/U	20 A.W.G. Copper	A	0.116	Tinned Copper	Polyethylene	(Max.) 0.206	0.034	53.5	28.5	1900	Small size flexible cable
		RG-5/U	16 A.W.G. Copper	A	0.185	Copper	Vinyl	0.332	0.087	53.5	28.5	2000	Small microwave cable
		RG-9/U	7/21 A.W.G. Silvered Copper	A	0.280	Inner-Silver Coated Copper Outer-Copper	Vinyl (Non-contaminating)	0.420	0.150	51.0	30.0	4000	Medium size, low level circuit cable
		RG-14/U	10 A.W.G. Copper	A	0.370	Copper	Vinyl (Non-contaminating)	0.545	0.216	52.0	29.5	5500	General purpose semi-flexible power transmission cable
		RG-74/U	10 A.W.G. Copper	A	0.370	Copper	Vinyl (Non-contaminating) Armor	0.615	0.310	52.0	29.5	5500	Same as RG-14/U armor for Naval equipment
70-80 OHMS	Single Braid	RG-59/U	22 A.W.G. Copperweld	A	0.146	Copper	Vinyl	0.242	0.032	73.0	21.0	2300	General purpose small size video cable
		RG-11/U	7/26 A.W.G. Tinned Copper	A	0.285	Copper	Vinyl	0.405	0.096	75.0	20.5	4000	Medium size, flexible video and communication cable
		RG-12/U	7/26 A.W.G. Tinned Copper	A	0.285	Copper	Vinyl (Non-contaminating) and Armor	0.475	0.141	75.0	20.5	4000	Same as RG-11/U armored for Naval equipment
	Double Braid	RG-6/U	21 A.W.G. Copperweld	A	0.185	Inner-Silver Coated Copper Outer-Copper	Vinyl (Non-contaminating)	0.332	0.082	76.0	20.0	2700	Small size video and I.F. cable
		RG-13/U	7/26 A.W.G. Tinned Copper	A	0.280	Copper	Vinyl	0.420	0.126	74.0	20.5	4000	I.F. cable
Cables of Special Characteristics	Twin Conductor	RG-22/U	2 Cond. 7-#18 A.W.G. Copper	A	0.285	Single-Tinned Copper	Vinyl	0.405	0.107	95.0	16.0	1000	Small size twin conductor cable
		RG-57/U	2 Cond. 7/21 A.W.G. Copper	A	0.472	Single-Tinned Copper	Vinyl	0.625	0.225	95.0	16.0	3000	Large size twin conductor cable
	High Attenuation	RG-21/U	16 A.W.G. Resistance Wire	A	0.185	Inner-Silver Coated Copper Outer-Copper	Vinyl (Non-contaminating)	0.332	0.087	53.0	29.0	2700	Special attenuating cable with small temperature coefficient of attenuation
	High Impedance	RG-65/U	No. 32 Formex F Helix Dia. 0.128 in.	A	0.285	Single-Copper	Vinyl	0.405	0.096	950	44.0	1000	High impedance video cable. High delay
Low Capacitance	Single Braid	RG-62/U	22 A.W.G. Copperweld	A	0.146	Copper	Vinyl	0.242	0.0382	93.0	13.5 Max. 14.5	750	Small size low capacitance air-spaced cable
		RG-63/U	22 A.W.G. Copperweld	A	0.285	Copper	Vinyl	0.405	0.0832	125	10.0 Max. 11.0	1000	Medium size low capacitance air-spaced cable
	Double Braid	RG-71/U	22 A.W.G. Copperweld	A	0.146	Inner-Plain Copper Outer-Tinned Copper	Polyethylene	0.250	0.0457	93.0	13.5 Max. 14.5	750	Small size low capacitance air-spaced cable for I.F. purposes
Pulse Applications	Single Braid	RG-26/U	19/0.0117 Tinned Copper	D	(2) 0.308	Tinned Copper	Synthetic Rubber and Armor	(Max.) 0.525	0.189	48.0	50.0	8000 (Peak)	Medium size pulse cable armored for Naval equipment
		RG-27/U	19/0.0185 Tinned Copper	D	(2) 0.455	Single-Tinned Copper	Vinyl and Armor	(Max.) 0.675	0.304	48.0	50.0	15,000 (Peak)	Large size pulse cable armored for Naval equipment
	Double Braid	RG-64/U	19/0.0117 Tinned Copper	D	(2) 0.308	Tinned Copper	Neoprene	0.495	0.205	48.0	50.0	8000 (Peak)	Medium size pulse cable
		RG-25/U	19/0.0117 Tinned Copper	D	(2) 0.308	Tinned Copper	Neoprene	0.565	0.205	48.0	50.0	8000 (Peak)	Special twisting pulse cable for Naval equipment
		RG-28/U	19/0.0185 Tinned Copper	D	(2) 0.455	Inner-Tinned Copper Outer-Galvanized Steel	Synthetic Rubber	0.805	0.370	48.0	50.0	15000 (Peak)	Large size pulse cable
Twisting Application	Single Braid	RG-41/U	16/30 A.W.G. Tinned Copper	C	0.250	Tinned Copper	Neoprene	0.425	0.150	67.5	27.0	3000	Special twist cable

NOTES:
1. Dielectric Materials
   - A Stabilized Polyethylene
   - C Synthetic Rubber Compound
   - D Layer of Synthetic Rubber Dielectric Between Thin Layers of Conducting Rubber
2. This Value is the Diameter Over the Outer Layer of Conducting Rubber

Figure 1

That is their physical construction varies considerably from the conventional construction just described to attain different electrical characteristics.

The twin conductor cables, an attenuating cable, a high-impedance cable, and three low-capacitance cables are listed in these two groups. The capacitance of these semisolid low-capacitance cables is about one half of the capacitance of equivalent solid dielectric high-frequency cables.

Groups five and six show the *RG* high-frequency cables insulated with synthetic rubber insulation. These are the only cables in the "Army–Navy Standard List of Radio-Frequency Cables" utilizing synthetic-rubber insulations rather than polyethylene. The pulse cables and a flexible rubber-insulated cable are included in these two groups.

XII. Design Considerations of High-Frequency Twin-Conductor Cable

E. W. GREENFIELD
MEMBER AIEE

THERE ARE a large number of cases in which it is required to transfer electric power at high frequencies by means of twin-conductor cable. For example, high-power transmitting dipole antennas require twin-conductor cable capable of operating at high voltage and high frequency with minimum losses. So, too, do the dipole receiving antennas require twin cable, but with somewhat different working characteristics. Measuring circuits also very often require twin cable and, in general, whenever a circuit source of balanced power, neither side of which is at ground potential, must be transmitted by wire, a twin- or duplex-conductor cable will be utilized. Conversion of coaxial circuits to balanced twins may also be desirable to obtain better shielding.

Design considerations for twin-conductor cable involve much the same problems and limitations as for coaxial cable. However, the mathematics for the twin is far more complicated, and, in fact, there are no exact solutions available for any but the most simple of configurations. This comes about, of course, as a result of nonuniform distribution of electric and magnetic fields and, in the case of the unshielded twin, refraction of the electric field at the dielectric boundaries.

Broadly speaking, there are about eight principal factors which are required to guide the designer before he can solve his twin-conductor-cable problem. These are:

1. Maximum operating *frequency* range.
2. Required *impedance*.
3. Maximum permitted *unbalance*.
4. Maximum *power* transfer.
5. Maximum permitted *loss*.
6. Maximum operating *voltage*.
7. Ambient *temperature* range.
8. Mechanical conditions of *installation*.

Unfortunately, in a presentation of this limited nature there is insufficient time to discuss all of the afore-mentioned factors. It is suggested, therefore, that we first examine the procedures for evaluating characteristic impedance, since these generally are a fundamental requirement, and then discuss losses in twin-conductor cable.

In the megacycle frequency range, characteristic impedance is for all purposes equal to the square root of the ratio of inductance to capacitance.

The calculation of inductance for equal round-conductor twins presents no great problem. At high frequency the internal inductances of each conductor certainly can be neglected. However, when the conductor radii are not small as compared to their separation the mutual actions between currents in the two wires cause "proximity" effect which is a further distortion of the current distribution, so that the assumption of cylindrical sheets is not admissible. At high frequency for nonmagnetic materials then:

$$L = 0.281 \log \frac{a-r}{r} \text{ millihenry per 1,000 feet} \quad (\text{for } a \gg r) \qquad (1)$$

and

$$L = 0.281 \log \left[\frac{a + (a^2 - 4r^2)^{1/2}}{2r} \right] \text{millihenry per 1,000 feet (for } r \text{ appreciable as compared to } a) \qquad (2)$$

where

r = conductor radius
a = separation of conductor axis

In these equations for inductance the kinds of conductor and dielectric material, so long as they are nonmagnetic, are of little importance. So also is the shape of the surrounding dielectric and to some extent the question as to whether the cable has or has not a shield over the dielectric.

On the other hand, the evaluation of capacitance for a twin-conductor cable is definitely not simple. The kind of dielectric material, its shape and extent, and the presence or absence of a grounded shield over all are all equally as important as conductor size and separation. For equal round conductors symmetrically located within a cylindrically shaped uniform dielectric having a conducting shield over all there are available a number of more or less rigorous expressions for capacitance. That due to Russell and independently to Breisig is given as follows:

$$\text{Capacitance between conductors} = \frac{3.68 \times 10^{-3} \epsilon}{\log \left(\frac{2a}{d} \cdot \frac{D^2 - a^2}{D^2 + a^2} \right)} \text{ microfarads per 1,000 feet} \qquad (3)$$

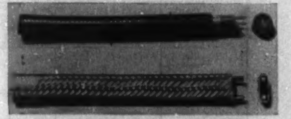

Figure 1. Two types of shielded twin ultra-high-frequency cables

Characteristic impedance about 100 ohms

Figure 2. A group of unshielded twin ultra-high-frequency cables

The lower two have a characteristic impedance of approximately 200 ohms
The upper one has a characteristic impedance of approximately 300 ohms

---

E. W. GREENFIELD is head of the electrical laboratory, engineering department, Anaconda Wire and Cable Company, Hastings-on-Hudson, N. Y.

Table I. Capacitance of Twin-Conductor Cable

Cable Description						Capacitance at 1,000 Cycles Per Second, Micromicrofarads Per Foot			
						Measured		Computed	
Shape	Major Axis, Inch	Minor Axis, Inch	Conductor Separation, Inch	Conductor Diameter, Inch	Insulating Material	Braid Shielded	Unshielded	Shielded Case Using Equation 3	Unshielded Case Using Equation 4
Round	0.288	0.288	0.101	0.046	Polyethylene	16.05		16.0	
Oval	0.550	0.217	0.380	0.085	Polyethylene	19.7	7.5	19.7	9.28
Oval	0.315	0.142	0.205	0.034	Polyethylene	15.0	7.2	14.4	11.8

where

a = separation of conductor axis

d = conductor diameter

D = diameter of insulation

ϵ = dielectric constant of insulating material.

Equation 3 neglects "proximity" effect which, as in the case of inductance, will modify the resulting capacitance when the conductor size is greater than about one-tenth their separation. When proximity effect is taken into account, it will be found to decrease inductance (see equation 2) but to increase capacitance. However, for all practical twin-conductor designs, it is not necessary to take "proximity" effect into the equations, since the error by not doing so is by far the least among the other uncertainties present. For example, in an open two-wire line one inch in separation, the conductor diameters can be as much as half the line separation and yet will give only an error of −5 per cent when proximity is neglected.

Capacitance of shielded twin cables which are not circular in section cannot be computed in any systematic manner. However, it is found that for the usual oval shielded-type twin cable as used by the Signal Corps equation 3 can be used to give a close estimate of the capacitance between conductors. All symbols are used as given in the equation with the exception that D is taken as the oval's major axis width. For so-called "flat" constructions the foregoing procedure gives values which are too great and is not recommended.

For unshielded twin cables, capacitance computations cannot be made with any certainty at all. Although for design purposes it is valid to assume ground far away, conditions of operation often bring grounded objects adjacent to the cable and in fact may cause considerable unbalance between conductors. To get a first-hand approximation, one can calculate the capacitance between conductors assuming ground remote and an infinite extent of dielectric as follows:

$$C=\frac{3.68\times10^{-3}\epsilon}{\log\frac{a-r}{r}}\text{ microfarads per 1,000 feet} \quad (4)$$

where

a = separation of conductor axis

r = conductor radius

ϵ = dielectric constant

Equation 4 will yield values which are anywhere from 15 to 75 per cent too high depending on the size and shape of the cable. Table I gives capacitance design data on a number of shielded and unshielded twin cables. These twins and others are pictured in Figures 1 and 2.

It follows that in all but the simplest cases one cannot lay out the final twin-cable design for characteristic impedance, but from preliminary approximations an experimental cable must be made and measured for conformity to desired values.

Summary of Discussion on Cable Design

This discussion was entirely on shielding. It was brought out that most radio-frequency shielding studies have been on coaxial cables. In balanced circuits requirement must be placed on the balance if the shield provided is to be effective. Balanced systems for shielding must be transformed to unbalanced ones to use the present line of connectors. An article on this subject was published in *Electrical Communication*,[1] 1945.

It was pointed out that an important problem in getting proper shielding is good bonding of the outer conductor and the shield of apparatus.

Armor acts as shielding, and in the *RG-26/U* it is about equivalent to the extra copper layer on *RG-25/U*. Semiconducting jackets are ineffective as shields because the conductivity is too low.

Reference

1. Special Aspects of High-Frequency Flexible Balanced Cables, N. Marchand. *Electrical Communication*, volume 22, 1945, number 3, page 193.

XIII. Methods of Electrical and Mechanical Testing of Radio-Frequency Cables at the Naval Research Laboratory

J. M. MILLER
NONMEMBER AIEE

THE FOLLOWING methods of electrical and mechanical testing are in general use at the Naval Research Laboratory for the type-approval testing of radio-frequency cables submitted by the various manufacturers and for special tests. Many of the methods originated at this laboratory.

Measurement of Attenuation

Naval Research Laboratory Method for the Frequency Range of the Order of 100 to 400 Megacycles

This method is in general use by cable manufacturers and combines the advantages of accuracy, simplicity, speed, and wide range of applicability. The method is applicable to cables of any size or characteristic impedance of both the concentric and twin-conductor varieties. It does not require the application of connectors to the sample under test and employs a low-voltage low-power oscillator.

The equipment consists of an oscillator unit, a vacuum-tube voltmeter unit, and nonreactive coupling loops which are used to terminate the cable under test. The oscillator unit uses a type-955 acorn triode in a tunable lumped oscillator circuit contained in a small metal box. A tunable circuit is also mounted on the box, partly inside and partly outside. The inside portion is loosely coupled to the oscillator, while the exterior portion is arranged so that it can be coupled magnetically with other circuits. The vacuum-tube voltmeter employs a type-9005 diode in a similar box. The input circuit of the diode is tunable and runs outside of the box so as to permit also magnetic coupling with other circuits. The nonreactive coupling loops are each a single turn of heavy wire with a small capacitor in series to compensate for the inductance of the loop. A loop is soldered on each end of the cable between the center conductor and braid in the case of concentric cable or between the two conductors in the case of twin-conductor cable. The two ends of the cable under test are brought to within about a foot and a half of each other, and the braid is well grounded to a common metal plate.

In making the measurement, the oscillator unit is first coupled directly to the voltmeter circuit. Loose coupling being used, the circuits are tuned to resonance. Then, by moving the boxes, the coupling is increased until the maximum voltmeter reading is obtained. This corresponds with the well-known critical or optimum coupling of resonant circuits. Next, utilizing the nonreactive coupling loops, the oscillator unit is coupled through the cable under test to the voltmeter unit, and the coupling of each unit is adjusted for a second maximum voltmeter reading. These adjustments automatically terminate the cable in its characteristic impedance, and the power in the voltmeter in the second step is equal to that in the first, excepting for the power loss in the cable under test. Hence the ratio of these two powers gives the attenuation.

Originally the voltmeter tubes were calibrated for voltage at 60 cycles, and the attenuation was calculated from the ratio of the voltage readings. The method was of sufficient accuracy to be very useful for several years in the development and production testing of radio-frequency cables. However, comparison with results obtained by the Bell Telephone Laboratories in the investigation reported upon by C. C. Fleming indicated that the Naval Research Laboratory results were 10 to 15 per cent high. Investigation showed that the error resulted from variations in impedance with voltage in the measurement diode, due to transit time, which produced variations in impedance in the voltmeter tuned-input circuit, so that power ratios did not correspond exactly with voltage-squared ratios. Looser coupling of the diode to its tuned input circuit minimized the error but with the inconvenient requirement of more power in the oscillator unit. A method of calibration was developed, using a piston-type mutual-inductance attenuator which gives a calibration, at the frequency of the measurement, of voltmeter circuit power plotted with an arbitrary decibel scale, against voltmeter deflection. The difference in decibel readings for the two deflections observed in the measurement gives directly the attenuation of the cable in decibels. Complete agreement with Bell Laboratory results are now obtained.

Preferred Method for Frequencies of the Order of 1,000 Megacycles

In the first step of this method, about 100 feet of the cable under test is included in a series circuit comprising the oscillation generator, variable attenuator, test cable, and receiver. "Lossy" cable is also included to isolate the various elements, and the cable under test is terminated with matching stub tuners. With a low setting of the variable attenuator, the tuners are adjusted for the best output of the receiver. A short length of similar cable then is substituted for the long length, and, without readjustment of the stub tuners, the attenuator setting is increased until the same receiver output is obtained. The difference in the attenuator settings measures the attenuation corresponding to the change in cable length. A piston-type mutual-inductance attenuator is convenient for this test.

Method for Frequencies of the Order of One Megacycle

This method is essentially a measurement of resistance, conductance, inductance, and capacitance per unit length using a Q meter or the equivalent. A length of cable short relative to one eighth of a wave length is employed. With the far end short-circuited, the cable is first inserted in series in the Q-meter circuit; the change in Q reading and tuning capacitance giving the resistance and inductance of the cable sample. With the far end open, the cable is connected across the tuning capacity of the Q meter; the change in Q reading and tuning capacitance giving the conductance and the capacitance of the sample. If we assume that the cable length to be short enough so that the current is substantially uniform in the first case and the voltage uniform in the second case, the quantitites R_1, G_1, L_1, and C_1 per unit length are obtained by dividing by the length. The error due to this assumption is in the direction of giving too high values for these quantities. A first-order correction can be applied by reducing the L_1 and C_1 values by the same percentage that the tangent of the electrical angle ($\tan 2\pi l/\lambda$) exceeds the angle in radians ($2\pi l/\lambda$), where l is the length of the cable and λ the wave length in the cable. The R_1 and G_1 values should be reduced by twice this percentage. The attenuation is given by

$$\text{Att(db/100 ft)} = 4.343l\left(\frac{R_1}{Z_0} + G_1 Z_0\right)$$

where

$$Z_0 = \sqrt{L_1/C_1}$$

The term $G_1 Z_0$ is frequently negligible

J. M. Miller is with the Naval Research Laboratory, Washington, D. C.

particularly at the lower frequencies, with the smaller cables, and with low-loss insulations.

METHOD EMPLOYING RESONANT CABLE LENGTHS

This laboratory has employed for about four years a method of deriving the attenuation from the measurement of the effective resistance of antiresonant lengths of cable which has been of particular value in certain applications. An odd number of quarter wave lengths short-circuited at the far end, or an even number of quarter wave lengths open-circuited, can be employed. Generally in this laboratory the measurements have been made in the range of 100 to 300 megacycles on short lengths of cable using special impedance measuring equipment. The Q-meter has also been used down to frequencies as low as two megacycles with about 100 feet of cable. At such a low frequency, it is desirable to parallel the Q-meter capacitor with another variable capacitor of about 1,500 micromicrofarads capacitance. The measurement is made by interpolation between several values of resistors which are substituted for the cable across the tuning capacitor of the Q meter. Type F, IRC, ceramic resistors are suitable for this purpose having very low frequency corrections up to values of 20,000 ohms and a frequency of 50 megacycles.[1] The attenuation is given by

$$\text{Att(db/100 ft)} = 26{,}500\,\frac{Z_0}{lR_r}$$

where

Z_0 = characteristic impedance of cable
l = total length of cable in centimeters
R_r = measured resonant resistance

The method is particularly applicable to very low low-loss cables such as large-diameter gas-filled lines and at the higher frequencies to measure short lengths of cable. For example, the braid resistance factor is determined by measuring a short length of cable with the braid and then replacing the braid by copper foil.

Determination of Velocity of Propagation and Characteristic Impedance

The velocity of propagation is given by the frequency and length of a resonant length of cable. The method generally in use by this laboratory and the cable manufacturers for polyethylene cables employs a cable length of 1.5 meters which is three quarters of a wave length at approximately 100 megacycles and is series resonant when open-circuited at the far end. The near end is terminated with a noninductive loop tunable about 100 megacycles by a small variable trimmer capacitor. The system is loosely coupled to an oscillator which is varied in frequency about 100 megacycles until resonance is indicated by a dip in a grid meter. The loop is then short-circuited on itself and the trimmer adjusted until the loop itself is in resonance with the oscillator. The loop is again made to terminate the cable and the oscillator readjusted for resonance with the system. Several repetitions of this procedure result in the loop, the cable, and the oscillator, each individually being tuned accurately to the same frequency f. If the cable length is 1.5 meters, the velocity of propagation in the cable in per cent of the velocity in free space is given by

$$V\ \text{(per cent)} = {}^2/_3 f; \quad f \text{ in megacycles}$$

Based upon this method, W. A. McCool of this laboratory originated a so-called *VP* meter adapted for rapid testing, in which the tunings of the loop circuit and the oscillator circuit are tracked and controlled by a single dial. When the test cable is inserted in the loop circuit, resonance occurs and is indicated at only one position of the dial which can be calibrated to read velocity of propagation directly.

The characteristic impedance $\sqrt{L_1/C_1}$ is usually derived from the velocity of propagation $1/\sqrt{L_1C_1}$ and capacitance of the cable. If C is the capacitance of the 1.5-meter length of cable in micromicrofarads, the characteristic impedance is given by

$$Z_0 = \frac{600{,}000}{V\text{(per cent)} \times C}$$

This assumes low-loss cable. The capacitance measurement may be made at 1,000 cycles to one megacycle.

At the lower frequencies, the velocity of propagation and characteristic impedance will differ somewhat from the high-frequency values owing to current penetration into the conductors. The values can be computed from L_1 and C_1 as determined in the section, "Method for Frequencies of the Order of One Megacycle."

Corona-Initiation Tests

The method of testing at this laboratory for the initiation of corona at high voltage is described in another part of the paper by Ensign D. C. Depackh.

Mechanical Tests

FLOW TESTS AT ELEVATED TEMPERATURE

A not very scientific but practical test for flow of the dielectric in cables at elevated temperature was developed by this laboratory and adopted in Army–Navy specifications. A 12-inch length of cable is prepared so as to expose one inch of the inner conductor at each end. Weights specified for each cable size are attached to the inner conductor at the ends. The cable is then draped over a circular mandril of specified size in an oven with the weights hanging free and tending to cause the inner conductor to cut through the dielectric. For polyethylene dielectric the temperature is raised to 98 degrees centigrade for seven hours. Any displacement of the inner conductor is observed by an X-ray picture or by slicing the cable and is strictly limited in the specifications.

COLD BEND TEST

A standard length of cable is cooled and bent over a standard mandril, and observation for possible failure is made. In general the cause of failure is cracking of the jacket. In the case of a plasticized polyvinyl jacket the test is effected at −50 degrees centigrade.

TWIST TESTS

The cable is repeatedly twisted under conditions simulating the most severe practical application until failure occurs generally caused by rupture of the inner conductor or braid.

Reference

1. Miller, Salzberg. *RCA Review*, April 1939, page 486.

XIV. Electrical Tests Over a Range of Frequencies

C. C. FLEMING
NONMEMBER AIEE

PARTLY at the request of the Navy Department, during 1942 the Bell Telephone Laboratories became actively involved in a program of measurement of electric-transmission characteristics of radio-frequency cables. There was greatest interest in improvement of the precision of attenuation measurements. At that time, the state of the art was such that spot measurements had been made at various isolated frequencies, but little if any wide-range data had been obtained on any one cable sample. Since the resistance of a cable braid and the power factor of the dielectric were almost always in doubt, we had no adequate check of the precision of specific measurements on a specific set.

We therefore sought to develop means for measuring attenuation over as wide a frequency range as possible and to let the smoothness of a curve through the measured points be one of the criteria of precision. It was realized that it would be necessary to use many test sets, each of which would be useful in only a restricted range of frequencies. However, we have gone through this procedure and find that we can plot smooth curves of attenuation against frequency over a range of 20 to 3,000 megacycles. Concurrently, other work has been proceeding on evaluation of the shunt and series losses in cables. Therefore, with the aid of certain measurements or reasonable assumptions as to components, we are now able to add up attenuation components to check within a few per cent a smooth curve drawn through measured points.

We have investigated many methods of utilization of standing wave phenomena, but have found that the method of most general value is that of measuring the insertion loss of a cable sample which has considerable attenuation at the frequency of test. In a sense this is a brute-force method requiring test samples of long length. At frequencies above 100 megacycles, however, it is generally possible to restrict test samples to lengths of the order of 100 or 200 feet.

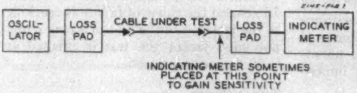
OSCIL-LATOR
LOSS PAD
CABLE UNDER TEST
LOSS PAD
INDICATING METER
INDICATING METER SOMETIMES PLACED AT THIS POINT TO GAIN SENSITIVITY

Figure 1. (left) Generalized setup for insertion-loss tests

Figure 1 shows the essential elements of any setup for measuring insertion loss. It is assumed either that the indicating meter is calibrated in decibels or that it includes a variable attenuator calibrated in decibels. "Reference" and "measure" readings are taken, respectively, without and with the cable under test in circuit, and the cable attenuation is determined by subtraction. It may be noted that two loss pads are shown. If the loss-pad cables closely matched the impedance of the cable under test, and if the cable connectors introduced no impedance irregularity, it would be possible to eliminate one of the isolating pads, and still read true attenuation differences on the indicating meter. However, since we cannot be certain of these factors at high frequencies, it is our general practice to provide as good a termination as possible on each side of the cable under test. Note also that if the indicating meter is placed ahead of the second loss pad, the sensitivity requirement of the indicating device is reduced.

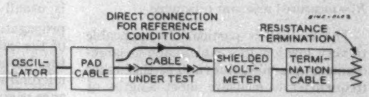

Figure 2. Shielded voltmeter set

Range, Mc	Preferred Cable Attenuations	
	Test Cable	Pad and Termination
20–50	10 db at 50 mc	7 db at 50 mc
140–420	10 db at 400 mc	20 db at 400 mc

This principle is utilized in our shielded voltmeter set, a block diagram of which is shown in Figure 2. The equipment is so named in order to distinguish it from a Naval Research Laboratory test set which operates in a similar frequency range, but which utilizes coupling loops external to the oscillator and voltmeter. The shielded voltmeter consists of a type-9004 diode vacuum tube mounted on a short section of air-dielectric coaxial line of impedance about equal to that of the cable under test and enclosed in a completely shielded copper box. Rectified current is read on a sensitive microammeter calibrated in decibels. In the range of 140 to 420 megacycles for which the set was originally designed, we have used a General Radio 757*A* oscillator. This type is now unavailable, but is reported to have been replaced by the 857*A*. The same diode voltmeter may be used in the region of 20 to 50 megacycles by provision of a suitable oscillator and loss pads. In this range we have used an oscillator of special design built around a type *HY*-615 vacuum tube. The probable precision of attenuation measurements on the shielded voltmeter is conservatively rated at ±5 per cent.

Most of the standard radio-frequency cables have a characteristic impedance in the region of 50 or 75 ohms. For both the shielded voltmeter and the heterodyne detector sets to be described later, sets of pads of both impedances have been provided. For each measurement the pads more closely matching the cable under test are used. For 50-ohm measurements, we have standardized on type-*N* connectors; and for 75-ohm measurements, Holmdel connectors. It is understood that 75-ohm type-*N* connectors will be available in the near future. As a further refinement of impedance matching, the shielded voltmeter is provided with inner conductors of different diameters, one of which is inserted for 50-ohm tests, the other for 75-ohm tests.

At higher frequencies, it has appeared desirable to read attenuation differences on a variable attenuator operating at a frequency considerably lower than that of test. This has been accomplished by utilization of the double-detection or heterodyne-detection systems of Figure 3. The method has been used in the regions of 1,100 and 3,000 megacycles, but may be extended to any part of the radio-frequency spectrum in which oscillators are available. In different frequency ranges, it is in general also necessary to change the design of the crystal converter to tune at the desired frequency.

Two oscillators with frequencies 60 megacycles apart are introduced into an International type of crystal converter; the beat oscillator directly, and the signal oscillator through isolating loss pads and the cable under test. The difference frequency product is fed into a 60-megacycle intermediate-frequency system consisting of a variable attenuator, high gain amplifier, rectifier, and indicating meter. The decibel difference between conditions of constant indicated output, with and without the test cable in circuit, is read on the 60-megacycle variable attenuator. The probable precision of results is about ±3 per cent. To achieve linearity of conversion of voltage ratios in the signal

---

C. C. FLEMING is with the Bell Telephone Laboratories, Inc., New York, N. Y.

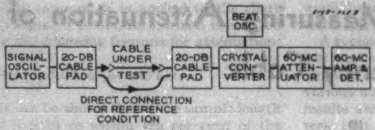

Figure 3. Heterodyne detector for 3,000 or 1,100 megacycles

Test cable should have 15–30 decibels loss

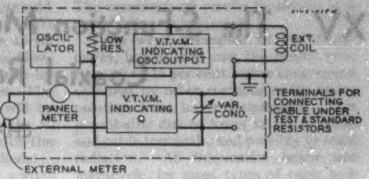
OSCIL-LATOR
LOW RES.
V.T.V.M. INDICATING OSC. OUTPUT
EXT. COIL
PANEL METER
V.T.V.M. INDICATING Q
VAR. COND.
TERMINALS FOR CONNECTING CABLE UNDER TEST & STANDARD RESISTORS
EXTERNAL METER

Figure 4. (right) Q meter for cable tests at 100 megacycles

Velocity, impedance, and attenuation

circuit to voltage ratios in the 60-megacycle circuit, that is, to insure decibel-for-decibel conversion, it is necessary that the crystal operate at essentially the same point of its characteristic at both "reference" and "measure" conditions. This is accomplished by taking two precautions regarding voltage level differences:

1. The beat oscillator must be sufficiently powerful to "bias" the crystal at some significant current value, in this case about 1.2 milliamperes.

2. At the crystal, the level of the signal voltage should at all times be at least 25 decibels below the voltage from the beat oscillator.

Oscillators at 1,100 and 3,000 megacycles are of special design. At 1,100 megacycles, type-*GL*-446 Lighthouse tubes are used in resonant cavities. These are specialized triodes with elements of cylindrical structure. At 3,000 megacycles, a velocity-modulated type is used.

We have commonly used one other test method which does not fall in the insertion loss category. This is the use of a *Q* meter to measure cable samples of relatively short physical length which resonate electrically at about 100 megacycles. The cable characteristics determined by the method are velocity ratio, characteristic impedance, and attenuation at about 100 megacycles. Theoretical considerations and comparison measurements indicate that, if the structure of a polyethylene cable does not vary with length, velocity and impedance are effectively constant between 100 megacycles and 3,000 megacycles. The necessary measured quantities to be observed on a test sample are: physical length, electrical length, resonant frequency, effective resistance at resonance, and capacitance at a low frequency such as 1,000 cycles per second.

A Boonton 170*A* *Q* meter is shown schematically in Figure 4. It is apparent that the device is essentially a variable-oscillator, tunable series-resonant circuit, and a device indicating the peak voltage (or *Q*) across the variable capacitor at resonance. The cable sample, which is connected across the variable capacitor, is commonly of electrical length equal to a multiple of half wave lengths, and is left open-circuited at the far end. For instance a test sample of *RG*-8/*U* cable is about $3^1/_4$ feet long, a half wave length open-circuited. In some cases a test sample may have electrical length of an odd number of quarter wave lengths, with the far end short-circuited. In all instances, the junction between the test cable and the *Q* meter occurs at a high-impedance point on the resonant cable.

The resonant frequency is determined by finding the frequency at which the setting of the variable capacitor for resonance is the same with and without the test cable in circuit. From the physical and electrical lengths and the resonant frequency, the velocity ratio is calculated. From these data and a measurement of capacitance at 1,000 cycles per second by any standard method, the characteristic impedance is calculated.

The equivalent resonance resistance of the cable sample is determined by comparison of the relative *Q* of the cable with that of a number of International Resistance Company type-*F* resistances in the range of the value of resistance of the cable. To increase precision, the values of relative *Q* are read on an external meter of 10 or 30 microamperes full-scale sensitivity. It has been determined that the resistance of these type-*F* resistors under 10,000 ohms remains constant from direct current to 100 megacycles. Therefore, it is found convenient to measure the resistors on a standard Wheatstone bridge at direct current, and to plot a curve of meter deflection against d-c resistance. On this curve the value of resistance of the cable may be spotted. From the measured resistance and the previously measured quantities, the cable attenuation at the resonant frequency is calculated. For 50-ohm cables, the precision is within ±5 per cent.

It should be emphasized that use of the foregoing procedure places no dependence on absolute values read on the *Q* indicating meter and the variable-capacitance dial of the *Q* meter. Owing to the inductance of internal leads and other more obscure parasitic effects, it appears that at 100 megacycles the absolute capacitance and *Q* indicated by commercial *Q* meters may be seriously in error and that the error may vary considerably between different instruments. On the other hand, assumption of the constancy of resistance of the type-*F* resistors appears to be well justified by tests at the Naval Research Laboratory, Bell Telephone Laboratories, and elsewhere. Moreover, the attenuation results obtained by the resistance-comparison method lie very nicely on curves of attenuation against frequency.

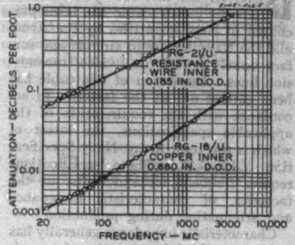

Figure 5. Attenuation of *RG*-18/*U* and *RG*-21/*U* cables

All the methods described have been used to determine the measured attenuation values plotted in Figure 5. The curves of attenuation against frequency drawn through the measured points are in close agreement with the results of theoretical analysis. Some degree of engineering judgment is required in making such comparisons, but it is possible to calculate closely enough to enable a test engineer to maintain a critical attitude toward test results. The curves of Figure 5 may be considered as examples. The curve for *RG*-21/*U* cable is very nearly a straight line with slope of 0.5. This result is in accord with the concentration of attenuation in the high-resistance-alloy inner conductor, the attenuation component of which varies as the square root of frequency. Considering the curve for *RG*-18/*U* cable, it may be noted that the slope of the curve increases with frequency. This is caused by the dominance at lower frequencies of conductor losses which vary about as the square root of frequency, and by the increasing percentage contribution at higher frequencies of dielectric loss which varies about as the first power of frequency. As to absolute magnitude of attenuation, the *RG*-18/*U* cable, by virtue of its comparatively large size and solid-copper inner conductor, has much lower attenuation than *RG*-21/*U* at all frequencies. By means of reasoning, similar but more laborious in extent, the details of configuration of measured curves may be evaluated theoretically.

XV. The *S*-Function Method of Measuring Attenuation of Coaxial Radio-Frequency Cable

CHANDLER. STEWART, JR.
NONMEMBER AIEE

DURING the last few years coaxial radio-frequency cable has been purchased in large quantities by the Army and the Navy for use in aircraft and surface vessels as radio and video transmission lines. Inspection of this cable has been carried out at the factories in accordance with the requirements of the applicable specifications, the latest of which is the Joint Army–Navy Specification *JAN-C*-17. These specifications require frequent measurements, at the factories, of characteristic impedance and attenuation during production.

Characteristic impedance generally has been determined from results of capacitance and velocity of propagation tests on samples of cable approximately five feet long. Accuracy of measurements by this method easily can be kept to within one per cent.

Attenuation measurements generally have been made at one or more frequencies such as 100 megacycles or 400 megacycles, by a method involving samples approximately 100 feet long. It has been shown by a series of comparison tests that results of measurements by this method on different equipments and at different laboratories may vary by as much as 20 per cent on one sample. This can be attributed partially to the use of nonstandard equipments and to the highly skilled technique required in making the measurements.

Another method of measuring the attenuation, known as the *S*-function method, is here described. This method has been found to be simpler, faster, and more convenient than any other in general use. Also, it requires samples which are shorter and whose lengths are less critical than do other methods so far proposed. For example, the best length of *RG-8/U* cable for a 100-megacycle test is 11 inches. Although a knowledge of the characteristic impedance is required, an error in its value generally will not affect adversely the attenuation results, which is in contrast to some methods using resonant lengths of cable, which are subject to errors in direct proportion to the relative error in the supplied value of the characteristic impedance. This method, however, is limited by the design of available equipment to frequencies from about 1 to 100 megacycles.

Table I. Comparison of Results of Measurements by Various Government and Commercial Laboratories of Attenuation of a Sample of *RG-8/U* Cable

Method	Laboratory	N at 100 Megacycles (in Decibels Per 100 Feet)
1	*E*	1.65
1	*S*	2.32
2	*E*	2.01
2	*T*	2.13
	B	2.0
3(d = 19 inches)	*S*	2.14
3(d = 38 inches)	*S*	2.17
3(d = 59 inches)	*S*	2.14
4	*S*	2.13

Method 1, described in the *General Electric Review* for September 1941, employs diode voltmeter at the ends of a cable sample which is terminated in its own characteristic impedance.

Method 2, one most commonly employed at radio-frequency-cable factories, uses tuned circuits to couple the cable to an oscillator and a diode voltmeter.

Method 3, described in the January 1945 *Proceedings* of the Institute of Radio Engineers, employs short resonant lengths of cable whose impedances are measured by a *Q* meter with an inductance connected.

Method 4 is the *S*-function method.

To measure attentuation of a cable sample by the *S*-function method, the approximate length of sample is determined by the formula:

$$d_0 = \frac{144V}{f_{mc}} \text{ feet} \qquad (1)$$

where

V = relative velocity of propagation

f_{mc} = test frequency in megacycles

Next, the sample is short-circuited at one end and trimmed at the other end for connection to the *Q* meter. The *Q* meter is operated in the usual manner for testing coils, and values of f, Q, and C are recorded. M is determined from the formula:

$$M = 2\pi 10^{-6} f_{mc}\, C_{mmf}\, Z_0 \qquad (2)$$

where

f_{mc} = test frequency in megacycles

C_{mmf} = capacitance dial setting micromicrofarads

Z_0 = characteristic impedance in ohms

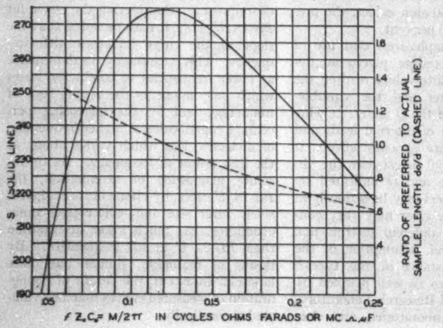

Figure 1. *S*-function curve for determining attenuation

Plot of $S = \dfrac{2{,}000 \log_{10}\epsilon}{M + 1/M + 1/\text{arccot } M}$ (solid line), and $d_0 \div d = 0.923/\text{arccot } M$ ratio of preferred to actual sample length (dashed line)

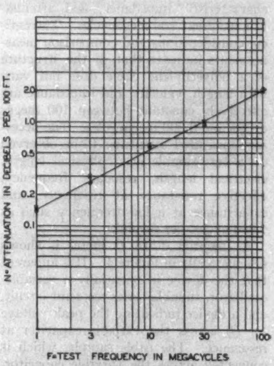

Figure 2. Results of attenuation measurements on radio-frequency cable *RG-7/U* by the *S*-function method (Θ) compared with engineering data listed in Joint Army–Navy Specification *JAN-C*-17, paragraph *E*-3 (X)

CHANDLER STEWART, JR., is with the Aircraft Radio Laboratory, Army Air Technical Service Command, Wright Field, Dayton, Ohio.

This value of M is applied to the chart in Figure 1 to obtain S, which is inserted in the following formula for attenuation:

$$N = \frac{S}{Qd} \text{ decibels per 100 feet} \qquad (3)$$

It can be shown that if the sample length d is held to within ten per cent of the length d_0, prescribed by equation 1, a ten-per-cent error in Z_0 will cause less than two-per-cent error in attenuation N, and likewise a 20-per-cent error in Z_0 will cause less than a six-per-cent error in N.

Also, it can be shown that, if M as calculated is held to within ten per cent of M_0, a 20-per-cent error in M (which would be due mainly to error in Z_0) would cause less than a four-per-cent error in N.

A typical sample of coaxial cable, about 200 feet long, was tested at several Government and commercial laboratories by various methods at 100 megacycles. The results are listed in Table I. It will be seen that the result obtained by the S-function method agrees closely with the average of the results of other methods.

In Figure 2, results obtained on a sample of *RG-7/U* cable at frequencies from 1 to 100 megacycles by the S-function method have been plotted and compared with nominal values listed in the Joint Army–Navy Specification *JAN-C-17*. The measurement results lie almost in a straight line on log paper.

Tests were attempted at 200 megacycles, but in each case the results were from 10 to 15 per cent higher than values obtained by other methods or by extrapolation from lower frequencies. This is probably due to losses in the Q meter and cable terminals, and possibly to some radiation. At frequencies below one megacycle, for most types of cable now in use, the Q values are too low to read accurately. Consequently, it is recommended that for presently available equipment this method be limited to frequencies from 1 to 100 megacycles.

XVI. Corona-Initiation Measurements on Polyethylene and Rubber Cables

D. DEPACKH
NONMEMBER AIEE

IN THE MAIN, cable corona is considered as being due to the presence of minute air voids within the body of the dielectric or adjacent to the inner or outer conductor. That this hypothesis is justified is well established by examination of cables in which corona is known to occur and by the experimental behavior of cables under test; their performance is identical with that of a capacitance-shunted gap in series with another capacitance, the whole being shunted by a large capacitor whose capacitance is equal to that of the cable under test. The gaps and their associated capacitances are basically microscopic circuits whose effects are to be measured by detection circuits capable of responding to macroscopic phenomena.

In order that such measurements may be carried out, it is necessary to transform the physical discharge into an electrically measurable quantity and to eliminate from the detecting circuit the component due to the applied voltage, whose amplitude is in general enormously greater than the corona-discharge amplitudes to be measured. This transformation can be effected in a variety of ways. Series detection involves the transformation of the discharge into a current; when this current passes through a small impedance in series with the cable, a voltage drop is created which may be measured by an oscilloscope or other device. In the case of shunt detection the minute change of voltage across the cable is measured by connecting the detecting circuit to the high-potential side of the cable through a capacitor of sufficient insulating strength to withstand the applied voltage without corona of its own. Again, the detecting circuits themselves may differ. In a series circuit, for example, the applied voltage component may be eliminated by bridge-balancing methods, in which a corona-free capacitor and associated impedance are made one side of a bridge of which the cable and its series impedance to ground are made the other side. The bridge then is unbalanced by corona occurring in the cable arm; this can be detected by an oscilloscope suitably connected.

Also, use may be made of the fact that the discharge in air at normal pressure has frequency components extending to hundreds of megacycles; that is, the breakdown process itself is exceedingly rapid. Thus the applied voltage component may be eliminated by using amplifying systems designed to have high gain over a band of frequencies not including the high-voltage components.

The problem in the case of 60-cycle sine-wave initiation measurements is a relatively simple one, and most of the methods already outlined have been used at one time or another in the measurement of corona-initiation point in these cables. Thus, the original method of detection used by the Bell Telephone Laboratory consisted of a shunt detector and a rather narrow-band selective amplifier operating around one megacycle per second. In their tests a loudspeaker is used by detection and audio amplification of these components. An oscilloscope also can be used with this system; this gives better resolving power and ability to discriminate against various interference. If adequate provision is taken against interference, the loudspeaker method is adequate and is in fact used in many cases.

The Naval Research Laboratory employs a series detector in a bridge circuit for 60-cycle measurements. The oscilloscope is used and the bridge itself provides some balancing effect against external interference. Since the balancing capacitor cannot be made precisely identical with the cable, it is in general possible to balance completely in both amplitude and phase for only one frequency. Therefore, since there are harmonics present, although only to a very small extent, in the applied voltage, these can be balanced only imperfectly. In general, however, harmonics can be kept well below corona level. Use of the bridge permits separation of effects of corona in different parts of the system by their characteristic appearance on the oscilloscope trace. It further permits, by virtue of its acceptance of all frequencies up to the limit of the oscilloscope, of some knowledge of the type of discharge by observation of characteristic oscilloscope patterns.

D-c pulse measurements have been carried out at the Naval Research Laboratory by similar methods. Pulses of varying recurrence rates have been used; pulse lengths have been employed of the order of 10^{-6} seconds, in which rise and decay times were kept negligible compared with pulse length. A series circuit

---

D. dePackh, an ensign in the United States Naval Reserve, is with the Naval Research Laboratory, Washington, D. C.

combining the principles of bridge balancing and selective amplification was used in these determinations. Since the applied voltage in this case contained frequency components up to a very high order, it was impossible to obtain complete elimination of the applied voltage, even by a combination of these two methods. Since the duration of these components is short, however, and is confined to the region in the immediate vicinity of the rise and fall of the voltage, satisfactory indications can be obtained by using video-amplifier constants such that the trace is not obscured for more than an insignificant fraction of the total time.

It has been found that for relatively lossless cables, such as those using polyethylene dielectric, there is a ratio of nearly exactly two between the pulse corona point and the 60-cycle sine-wave corona point. This has been largely independent of pulse wave form and length and apparently is explained by the fact that in the case of sine-wave corona in the steady state it is the peak-to-peak value of the voltage which determines the corona point. For lossy cables, of which rubber pulse cables furnish an example, this ratio is somewhat less than two; this is the result of the fact that the simple two-capacitor and gap equivalent circuit does not hold accurately for cables of this type. If the perfect capacitors are replaced by capacitances of known shunt leakage, the analysis predicts a ratio of less than two, depending on the amount of loss.

The preparation of the cable itself for corona measurements is an important process. The essential thing is to prevent the ends of the cable from producing spurious corona the effect of which would be to give an incorrect corona point, lower than the true one. The first of the techniques used with the object of avoiding this spurious corona was employed by the Bell Telephone Laboratory and consisted of the use of *aquadag* under the ends of the braid of the sample under test; the end of the braid itself was covered with rubber tape to exclude as much of the air as possible. This process required considerable time and skill for the preparation of a sample and was always subject to some uncertainty with regard to the completeness of the exclusion of the air from the ends. Another early technique was the use of guard rings by the Naval Research Laboratory; the bridge method is such that, if guard rings are used and are returned to the same side of the circuit as the balancing capacitor, then the effect of corona to these rings will be in the opposite direction on the oscilloscope trace to that corresponding to true cable corona. Although this technique is a theoretically valid one, it suffers from the severe practical disadvantage that the guard-ring corona amplitude on the screen is so great that extreme difficulty is encountered in discerning the effect of cable corona, particularly if it occurs at a high voltage.

At present almost universal use is made of oil-immersion techniques. With reasonable care they give no trouble and well-reproducible results up to corona levels now encountered in cables, and the preparation of a sample requires only a fraction of the time and skill required by earlier methods. Rubber cables also may be tested by this technique, since the deterioration of the rubber is not great if the period of immersion is short. Testing rubber cables by other methods is extremely difficult since the insertion of guard rings and the proper application of corona-sealing compounds is greatly complicated by the layer of "conducting" rubber placed adjacent to the outer conductor. Moreover any corona occurring in the neighborhood of the ends of the cable produces rapid failure of the dielectric in this region. Oil immersion is therefore almost indispensable in the testing of this type of cable.

This covers briefly the general methods and techniques used in corona-initiation measurements on polyethylene and rubber cables. Many problems remain to be solved, such as dependence of corona point and life of cables on frequency and in general under varying conditions of applied voltage. Work is going forward on all these tests, and it is probable that many of these questions will be cleared up in the not too distant future.

XVII. A Corona Voltmeter

A. E. WIDMER
ASSOCIATE AIEE

THIS INSTRUMENT was designed and built in an attempt to obtain an absolute low-voltage standard of corona. It consists of a three-inch-long coaxial cylindrical electrode system, the center conductor of which is a 0.013-inch stainless-steel wire. The outer conductor consists of a brass cylinder accurately drilled and finished bored on a lathe to 0.1505 inch diameter. The concentricity of the wire is accurately established by capacitance measurements.

The dimensions were chosen in order to give an ionization point well below the ionization point of any of the usual sizes of coaxial cable. This instrument then may be placed in parallel with a cable sample and the corona discharge point determined in this way by the corona detecting device under normal working conditions.

Knowing atmospheric pressure and temperature, we can determine the ionization voltage of the coaxial cylinder standard as follows:

$$g=31\delta\left(1+\frac{0.308}{\sqrt{\delta r}}\right) \text{ (kilovolts per centimeter (maximum)}$$

$$g=\frac{KVP}{r\log_e\frac{D}{d}}$$

δ = density factor

$$\delta=\frac{3.92\times\text{centimeters of mercury}}{273+t\text{ degrees centigrade}}$$

$$KVP=gr\log_e\frac{D}{d}$$

$$KVP=\frac{31}{\sqrt{2}}\delta\left(1+\frac{0.308}{\sqrt{\delta r}}\right)\quad r\log_e\frac{D}{d}$$

Calculated value of corona voltage at 76 centimeters of mercury 27.7 degrees centigrade = 2,930 volts rms.

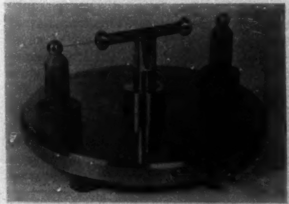

Figure 1. Low-voltage corona standard

A. E. WIDMER is with the Anaconda Wire and Cable Company, Hastings-on-Hudson, N. Y.

Measured value of corona voltage using the Anaconda internal corona detector = 2,850 volts rms.

The corona voltage standard may be used for two purposes:

1. It indicates whether any given discharge detector is operating properly as to voltage calibration.

2. It provides, at its corona voltage point, a standard volume of ionization which, if measured in terms of millivolts output of the bridge, filter, and amplifier combination, can be used to determine and maintain the sensitivity of the discharge detecting equipment constant.

Reference

1. **Dielectric Phenomena**, F. W. Peek.

Summary of Discussion on Cable Testing

Doctor Greenfield stated that the corona standard is of value in setting the amplification to the same level at all times. Ensign Depackh estimated that the Naval Research Laboratory voltage readings are accurate to less than half of one per cent. Doctor Odarenko asked whether anyone was studying corona effects at frequencies higher than 60 cycles. Ensign Depackh answered that, at the Naval Research Laboratory, continuous-wave equipment is under construction for corona studies at voltages up to 40 kv and at spot frequencies in the range from 10 kilocycles to 100 megacycles per second. Also equipment is being made for observations at microwaves.

The Dielectric Strength and Life of Impregnated-Paper Insulation—IV

Discussion and author's closure of paper 45-58 by J. B. Whitehead and J. M. Kopper, presented at the AIEE winter technical meeting, New York, N. Y., January 22–26, 1945, and published in AIEE TRANSACTIONS, 1945, April section, pages 171–7; earlier discussion published in AIEE TRANSACTIONS, 1945, pages 477–9.

A. E. W. Austen (nonmember; The British Electrical and Allied Industries Research Association, Greenford, Middlesex, England): This discussion refers to the recent paper by J. B. Whitehead and J. M. Kopper, "The Dielectric Strength and Life of Impregnated-Paper Insulation—IV," much of which is concerned with discharges in insulation. A clear understanding of the basic mechanism of internal discharges is essential in considering the sensitivity of detecting apparatus and in interpreting results. The present writer and a colleague have stated their view[1] as follows: "A gas-filled hole in solid insulation forms a capacitor with a second capacitor, formed by the solid dielectric, in series with it. The remaining sound dielectric is represented by a large capacitance in parallel. When the voltage on the whole capacitor attains a value such that the gas in the hole breaks down, the voltage on the void decreases suddenly to a low value, the discharge is extinguished, and the void again becomes insulating. The whole capacitor thus appears to have lost charge and the voltage on its terminals will be of the form of a unit function." There is much evidence which supports this view and none, as far as is known to the writer including the early work of Paine, which conflicts with it. Thus it is only when the test capacitor itself forms, or is connected to a resonant circuit of frequency not large compared with that of the detecting device that the disturbances due to discharges will appear to be of any particular frequency. Such terms as "the range of dominant frequencies of the gaseous discharge in cable insulation" used by Whitehead and Kopper are, therefore, in the writer's opinion, meaningless.

The apparatus used by Whitehead and Kopper appears from their Table I to be very insensitive. Thus if the solid dielectric in series with their artificial gaps be taken as of thickness 0.1 centimeter and dielectric constant 4, the size of discharge per square centimeter of 0.014-centimeter air gap would be $4{,}000\text{x}10^{-12}$ coulomb, which gave a deflection of less than one division. Sensitivities of $2\text{x}10^{-12}$ coulomb, that is, more than 1,000 times greater, are readily attained and commonly used. The conclusion that the apparatus detects "the first occurrence of gaseous ionization" is probably unjustified, as indeed the authors themselves state in the body of their paper.

Whitehead and Kopper appear to tend to the view that any voltage which produces discharges will lead ultimately to breakdown, so that, if the long-time breakdown voltage is of interest, it is the voltage which first produces discharges which should be measured. The measurement of time to breakdown in the short-time region is a measure of the relative ability of the constituents of the different dielectric samples to withstand severe discharges for short times, and it by no means follows that such ability is associated with a high discharge voltage and hence high long-time breakdown voltage.

It has been found in our laboratory that in well-impregnated paper no discharges were detected (and since the sensitivity was high it is believed that none occurred) up to a high stress at which there was a sudden onset of large discharges; discharges then persisted down to a very much lower stress, of order one sixth the ignition stress and recovery occurred only after some hours rest. In the opinion of the writer this behavior is characteristic of discharges in a gas bubble not present initially, but resulting from breakdown of oil. In the absence of such observations or some other evidence, doubt is felt about Whitehead and Kopper's assertion that their specimens were completely free from voids. The initial presence of voids could account for all the observations, since it is to be expected that both the denser paper and more viscous oil would correspond to poorer impregnation, larger voids, lower long-time breakdown voltage, and, if the stress–life curves do not cross at longer times, the lower breakdown voltages observed.

Reference

1. Internal Discharges in Dielectrics: Their Observation and Analysis, **A. E. W. Austen, W. Hackett.** *Journal* of the Institution of Electrical Engineers (London, England), volume 91, part I, 1944, page 298.

J. M. Kopper: The model circuit of Austen and Hackett to depict a gas-filled hole in solid insulation is reasonable and will have an action similar to that of a glow-discharge oscillator, its frequency being determined by the size of the void, rate of voltage rise across the void, and other constants of the dielectric circuit. At breakdown of the gas in the void the voltage on the whole capacitor, in the form of a unit function, will produce a transient current in the entire circuit of which the dielectric is a part. Breakdown of the gas in voids of various sizes will result in the application to the remainder of the circuit of unit functions at varying intervals in the power-frequency cycle. The total internal discharge in the insulation then will appear to have a conglomerate group frequency, which has been found to be in the range 4,000 to 10,000 cycles per second.[1] As the tests reported upon were carried out at stresses several times those used in normal cable operation, ionization, once started, reached formidable proportions in a comparatively short time. The purpose of the ionization recorder was to detect the stage in the test at which the ionization leading to rapid breakdown began, and then to follow the variation of the ionization up to failure.

The sensitivity of the apparatus using the recording milliammeter was $4{,}200 \times 10^{-12}$ coulomb per scale division. (In Figures 3 and 4 of the paper the recorder reading should be multiplied by 50 to get the deflection in scale divisions.) Had the galvanometer (sensitivity 120 megohms) used in a previous investigation[2] been employed in this study, the sensitivity of the equipment would have been 1.75×10^{-12} coulomb per millimeter deflection at a scale distance of one meter.

This study was directed only to the question of high- versus low-density paper. The superiority of the low-density paper over the high-density paper for both a light and a heavy oil was shown in these tests, in which a high stress was applied rapidly with resulting breakdown in a few minutes or hours; this same superiority was shown in earlier relatively long-time step-voltage tests.[3] The object of the short-time tests was to avoid running a sample for years at stresses around 60 volts per mil, at which stresses Whitehead and Terwilliger found the beginnings of internal discharges in oils. Whitehead and Shaw[2] studied internal discharges in samples similar to the ones in this test in the region of 90–750 volts per mil. Our apparatus was a recording method for a particular approach to the break down problem, making it possible to detect the beginning of extremely damaging discharge and to know when to remove stress from a sample of insulation in order to obtain a partial failure of 5 to 75 per cent of the insulation wall.

As for the degree of impregnation, a number of specimens were opened after appearance of the smallest trace of ionization, with no evidence of gas or failure or at most only a single spot of carbon or traces of wax along the edge of the paper tape. Any traces of air that might have remained after evacuation at two millimeters mercury pressure would have been readily absorbed by the oil. The influence on the degree of impregnation for both oil viscosity and paper density has been shown to be small in an earlier paper of this series.[3] The explanation of the results is in much evidence that failure begins in the oil channels, and in the fact that the stress in these channels increases with increasing paper density, owing to the differences in the values of dielectric constant in paper and in oil. A strictly rational explanation of the greater electric strength under certain conditions of cable insulation made up of papers of two different densities over that of paper of a single density is given by Whitehead.[4]

References

1. Oscillations Due to Ionization in Dielectrics and Methods of Their Detection and Measurement, **J. T. Tykociner, H. A. Brown, E. B. Paine.** *Bulletin* 259 Engineering Experiment Station, University of Illinois, Urbana, Ill.

2. The Detection of Initial Failure in High-Voltage Insulation, **J. B. Whitehead, M. R. Shaw.** AIEE Transactions, volume 60, 1941, June section, page 267.

3. The Dielectric Strength and Life of Impregnated Paper Insulation,—III, **J. B. Whitehead.** AIEE Transactions, volume 61, 1942, August section, page 618.

4. Oil Stresses in Impregnated-Paper Insulation, **J. B. Whitehead.** AIEE Transactions, volume 64, 1945, August section, page 555.

A Generalized Circle Diagram for a Four-Terminal Network and Its Application to the Capacitor Single-Phase Motor

Discussion and author's closure of paper 45-93 by J. G. Tarboux, published in AIEE TRANSACTIONS, 1945, pages 881-9.

Edward Bretch (Century Electric Company, St. Louis, Mo.): In a squirrel-cage motor the magnetic flux becomes substantially constant and rotary at and near synchronism, irrespective of whether the primary excitation is symmetrical polyphase, capacitor, or single phase. It is thus evident that the synchronous squirrel cage exerts an equalizing effect on the flux whereby an unbalanced or varying primary magnetomotive force produces a constant synchronous flux. Professor Tarboux accounts for the constant synchronous flux produced by the unbalanced capacitor excitation by the cross-flux theory of the single-phase squirrel-cage motor. This theory does not seem to visualize clearly how a constant flux is developed from a varying primary magnetomotive force.

The theory of the single-phase squirrel-cage motor includes two separate and distinct problems as follows:

1. The action of a squirrel-cage rotor in a field that is single phase, alternating at standstill, developing into a constant-rotary field at synchronism.

2. The forces and actions that change the single-phase alternating field at standstill into a constant-rotary field at synchronism. Stated another way, how a constant synchronous flux is derived from a varying magnetomotive force.

The first problem has been logically treated and practical formulas developed that check by test. However, in the second problem an attempt to apply the formula developed by the cross-flux theory stating that the quadrature flux varies directly with the speed, results in contradiction. Tests show that not only does the quadrature flux not increase with the speed above synchronism, but that it really decreases with overspeed. Thus the straight-line relation between rotor speed and quadrature flux assumed in the cross-flux theory does not exist.

The cross-flux theory is based on the erroneous assumption that two stationary single-phase alternating fluxes in time and space quadrature combine vectorially into a rotary flux. The fallacy of this assumption can be illustrated by considering the actions of the cathode-ray oscillograph. If a single cathode beam is acted on simultaneously by two equal alternating electromotive forces in time and space quadrature, their forces combine vectorially and cause the beam to trace a circle. However, if the two electromotive forces are exerted individually on two separate beams, causing the beams to move in time and space quadrature, and the two beams are superimposed on the same screen, under these conditions the figure traced by the two beams is not a circle, but two straight lines at right angles. So it is with magnetomotive forces and fluxes. If two equal alternating magnetomotive forces in time and space quadrature act simultaneously on a single flux, their forces combine vectorially and produce flux rotation. However, if the two magnetomotive forces are exerted individually to set up two separate alternating fluxes in time and space quadrature, these two fluxes will not then combine into a rotary flux. To produce a rotary flux the alternating magnetomotive forces in time and space quadrature must combine vectorially and act on a single flux. The vectorial combination takes place in the magnetomotive forces and not the fluxes. Magnetomotive forces are forces and combine according to the laws of forces. Fluxes are energies and do not follow the laws of forces but the laws of energy. While two stationary alternating magnetomotive forces in time and space quadrature combine into a rotary magnetomotive force, two stationary alternating fluxes in time and space quadrature do not combine into a rotary field. Thus in any squirrel-cage motor, whether single phase, capacitor, or polyphase, there is at synchronism but one flux, a constant rotating one. Therefore, at synchronism there can be no stationary single-phase flux component for the rotor conductors to cut across as assumed in the cross-flux theory.

While it is impossible to resolve a rotary field into two stationary single-phase components, it is interesting to consider this assumption and see where it leads. In the cross-flux theory it is assumed that the rotor currents generated by the speed action of rotor conductors cutting across the stationary alternating main or transformer flux lag approximately 90 time degrees. The electromotive force developed in the rotor conductors by speed action is in position to set up a flux at right angles to this assumed transformer flux. However, at synchronism with the rotor current lagging 90 time degrees, the rotor will move 90 space degrees during the time it takes the 90-degree lagging current to build up, so that when the rotor magnetomotive force appears it will have moved 90 space degrees from the quadrature position into a position of opposition to the main flux. This shifting action of the magnetomotive force is observed in the a-c generator and confirms the 90-degree space shift of the rotor magnetomotive force with 90-degree lagging rotor currents. Thus, it is physically impossible for uncommutated rotor currents generated by speed action to develop a cross flux that is in both time and space quadrature with the main flux, as assumed in the cross-flux theory.

The failure to recognize and take into account the fundamental differences between magnetomotive forces which represent forces and follow the laws of forces and fluxes which represent energies and follow the law of conservation of energy, and also the failure to recognize and take into account the fact that at synchronism the phase shift of the rotor magnetomotive force due to lagging uncommutated rotor currents is in space as well as in time result in confused reasoning and the illogical conclusions embodied in the cross-flux theory of the single-phase squirrel-cage motor.

J. G. Tarboux: Edward Bretch has called attention to some of the limitations of the cross-field theory as applied to the single-phase motor. His comments are well made. The author had no intention of developing any new basic theory; instead he used generally accepted laws (see reference 6 of the paper) as a starting point (see equations 11) and from these he has evolved a circle-diagram envelope for the current vectors.

There is no doubt that the criticisms offered by Mr. Bretch are correct. There are many other limitations to the circuit point of view as applied to electric machinery, particularly of the type studied in this paper. The standard circle diagram of the ordinary three-phase squirrel-cage motor is not absolutely correct. Any circle diagram of this type implies that all of the circuit parameters of the network are absolutely constant in magnitude. This is hardly ever true. Motor impedances change considerably between zero and synchronous speed, owing to different degrees of magnetic saturation and sometimes the effect of skin effect. The presence of harmonics of magnetomotive force and flux will also further complicate the analyses.

Considering the several sources of error, including those suggested by Mr. Bretch, it is quite gratifying to see how closely some of the operating characteristics of the capacitor motor, as obtained from the circle diagram, check true operating data. The lower half of the diagram, corresponding to oversynchronous speeds, is of no particular importance.

Rewinding Commutator-Type Traction Armatures

Discussion and authors' closure of paper 45-91 by N. J. Greene, D. E. Stafford, and C. Gentilini, published in AIEE TRANSACTIONS, 1945, August section, pages 563-9.

R. A. Hutchins (nonmember; General Electric Company, Erie, Pa.): We find that this is a well-written article on a timely subject, and believe that the detailed suggestions in general may be followed with good results.

COMMUTATORS

I do not consider that the authors have given sufficient emphasis to the need of thoroughly cleaning of commutator slots for the new coil leads. The satisfactory soldering of armature-coil leads to the commutator segments can only be obtained provided the surface of the copper in the commutator slot is free of all foreign matter and is not oxidized. After commutator slots have been thoroughly cleaned, they should be coated with a rosin alcohol flux.

V-RING MICA PROTECTION

The use of Fiberglas braid over the outside surface of the V-ring mica which projects beyond the commutator is recommended. Some operators have found that a flashover which carries across this bead ring does a lot more damage to the bead ring if it has been built up with Fiberglas braid and varnish than one made up of cotton cord that had been filled with varnish. There is some question as to whether an operator should make the change from the cotton cord with varnish, which has been used successfully for many years, to the Fiberglas braid.

BINDING OF ARMATURES

It is recommended that, "To reduce commutation voltage and band losses, a nonmagnetic band wire is desirable on higher-speed traction armatures. In the rebanding of armatures the operator should not make use of nonmagnetic binding wire unless the manufacturer's design specified its use. If steel binding wire were used for the core bands and compensation adjusted for the same, a change to nonmagnetic binding wire would affect the characteristics of the machine and such a change might result in unsatisfactory performance.

R. Beeuwkes (Chicago, Milwaukee, St. Paul, and Pacific Railroad Company, Seattle, Wash.): I consider that the authors of this paper have omitted reference to several important factors in rewinding commutator-type traction motors. These factors are as follows:

1. There has been no mention of suitable meggering tests during the process of dipping and drying armatures in order to determine progress of drying and enable the workmen to know when drying is complete after any particular dip so that the next step of procedure may be started.

2. No reference is made to turn tests for armature coils. These tests, where construction of coil permits, gives additional assurance that the insulation within the coil is in proper shape.

3. No reference is made to infrared lamps for drying armatures.

4. No mention is made of high-potential tests for commutators or armatures after repairs are completed.

5. Manufacturing companies, the Milwaukee Railroad, and, I presume, others, consider that the use of pure tin only in soldering coil ends to risers is, for various reasons, important, even though other solders are used in soldering bands and the like.

6. Slots in armature risers should be thoroughly cleaned before soldering is proceeded with.

J. W. Teker (General Electric Company, Schenectady, N. Y.): The subject of rewinding traction motor armatures, as a result of the rapid increase in the use of Diesel-electric motive power, is of timely interest to the great number now actively engaged in directing the maintenance of this equipment. The authors have organized and presented this subject in clear and excellent form.

Apparatus returned from the grueling punishment of actual service is worthy of the best engineering scrutiny. Often, thought-provoking evidence is disclosed, the proper analysis of which not only aids the operator in making correction, but is an important consideration for the designer as well.

An apparently simple detail such as securing the ends of the binding wire, presents a number of problems and various solutions. The method shown by Figures 6 and 7 in the paper can be improved and also simplified by anchoring both the start and finish ends of the band to the same tie clip. The ends of the wire are then linked together by a common tie passing under the main body of the band. This arrangement is less likely to slip or slide apart during a moment of excessive overload sufficient to cause solder to be melted and thrown off the band.

While tinned copper or soft-steel material is adequate for intermediate band clips, Superascoloy (18-8) is preferable for the anchor clip. This material offers greater resistance to the tearing through of the hook formed on the end of the wire when the full stress of the band falls upon it when unsoldered.

When an anchor clip of greater strength is required, it is preferable to use two pieces together rather than a single piece of double thickness to permit easy manipulation when forming and pulling tight the loops of the clip.

With reference to the "Guide for Armature Rewinding Materials," we are not in agreement with the type of varnish recommended by the authors for railway application.

The black synthetic varnishes are an improvement over the older asphaltic varnishes, but the black pigment is still a carbonaceous material which has the effect of lowering the arc resistance and probably the oil and heat resistance of the synthetic base. Synthetic varnishes used, either clear or colored, with a mineral pigment are in our opinion preferable to the black synthetic varnishes.

A. E. Ganzert (nonmember; Chicago, Rock Island, and Pacific Railway Company, Chicago, Ill.): It is desirable to finish grind commutators at as near normal operating speed as possible.

We have found it desirable to pull the equalizer windings down into place with a temporary band before applying the main winding.

We have found a fixture with slots, corresponding to the slots in the commutator riser, of material advantage in winding armatures with two piece coils. This arrangement insures all coils lying in their proper position during the entire winding operation and overcomes the crowding and attendant abuse of coils which might occur if the back ends of the coils are not held in a fixed position during the winding operation.

During the winding operation we have set up a schedule of taking insulation-to-ground readings and applying a high-potential test to ground during various stages of the winding operation. With this practice any defects are located before the winding is completed, with the result that it is often possible to remedy the defect with relatively little expense and labor, whereas, if the testing is not done until the winding is completed, it would frequently be necessary to remove a considerable portion of the windings. While this is rather obvious, I have known cases where complete windings have been removed, owing to a defect in the bottom conductors which would have been located before the top coils were put in place, had a progressive scheme of testing been used.

W. I. Conant (nonmember; Illinois Terminal Railroad Company, Decatur, Ill.): We have one thing to suggest; that is, in the analysis of failures, we would recommend you stress card records as the first step important to making a correct analysis of each armature.

Without these card records we would have been unable to maintain our armatures economically.

N. J. Greene, D. E. Stafford, and C. Gentilini: The authors thank the several contributors for their discussions. Comments from men having had long experience in traction-motor design and maintenance are most valuable and appreciably broaden the coverage of this paper.

Anchoring the starting and finishing ends of the band wire to the same clip, as cited by Mr. Teker, is simpler and preferable from the standpoint of minimizing loosening of the bands, should the solder melt. However, multiple tie clips over the starting and finishing turns of the band have other advantages:

1. They afford some anchorage in addition to that realized by a single tie clip over which the ends of the band wire are hooked.

2. Staggering the starting and finishing ends makes possible the use of an extra turn of band wire within the same band width.

3. It is the practice in some rewinding shops to start the band with three tie clips at both the starting and finishing end, insisting that two clips on each end be locked, and thus giving the operator one free tie-clip break per end without having to replace the entire band.

The 18-8 stainless steel for the tie clips as cited by Mr. Teker minimizes the hazard of tearing and should always be used for tie clips.

The black synthetic varnish referred to in the table, "Guide for Armature Rewinding Material," refers to modern reactive-type synthetic resins: that is, resins that react with vegetable drying oils in the presence of heat to form a totally new material having the original characteristics of neither the resins nor of the drying oils. Tests on varnishes of this type indicate that the black color does not lower the arc resistance and that the black varnish is fully as resistant to heat as the clear varnish and very nearly as oilproof.

The use of a megger for tests during process of dipping and baking to determine progress of drying as mentioned by Mr. Beeuwkes is good. Normally, after establishing a baking cycle for a particular armature, a time schedule suffices for repeat armatures.

Testing for quality of insulation between turns in multiturn coils both before and after installing in the armature is good practice. A recent AIEE technical paper[1] gives an interesting description of a relatively new surge testing method for checking turn-to-turn insulation.

Mention is made in this paper of test voltages with reference to commutator ground and bar-to-bar testing.

Pure tin solder has been generally accepted as standard for soldering coil leads to commutator risers, and, under the heading of "Solders" in the "Guide for Armature Rewinding Materials," 100-per-cent tin is listed along with 95-per-cent tin–5-per-cent antimony, and high-temperature alloy. Pure tin has a liquefaction and solidification point of 450 degrees Fahrenheit, which makes it more difficult to use than 95-per-cent tin and 5-per-cent antimony, which alloy has a slight plastic range and some preferred mechanical properties. Also, the melting point of tin is often too low to meet certain conditions where alloys melting at 550 degrees Fahrenheit are available and do the job.

Infrared lamps are used frequently and successfully for baking varnishes on armature windings. They are one of several forms of heat that produce satisfactory results.

The importance of a card record in connection with analyzing each armature failure as cited by Mr. Conant is a prime requisite to good maintenance, and the authors agree that its importance cannot be stressed too much.

The discussion by Mr. Ganzert injects a number of new thoughts, all of which are very important to proper armature maintenance, and the addition of these items materially adds to the completeness of this paper. The authors particularly favor the graduated voltage testing of the several parts of the armature assembly as work progresses.

The emphasis given by Mr. Hutchins to proper preparation of the commutator risers, along with his additional thoughts for providing satisfactory lead to commutator soldered joints, are valuable additions.

Glass braid thoroughly pretreated and properly coated with commutator enamel has been used extensively for the past five years over commutator mica V-ring projection, and to the authors' knowledge the glass braid has not contributed to a flashover. This, however, is believed to be a function of the varnish treatment whether glass- or cotton-wrapped.

Mr. Hutchins' calling attention to the hazard of a change from magnetic to nonmagnetic banding wire is important, and such a change should not be made without thorough engineering analysis of its effect on commutation.

REFERENCE

1. WINDING-FAULT DETECTION AND LOCATION BY SURGE-COMPARISON TESTING, G. L. Moses, Earl F. Harter. AIEE TRANSACTIONS, volume 64, 1945, July section, pages 499–503.

Winding-Fault Detection and Location by Surge-Comparison Testing

Discussion and authors' closure of paper 45-94 by G. L. Moses and Earl F. Harter, published in AIEE TRANSACTIONS, 1945, July section, pages 499–503.

C. M. Foust and **N. Rohats** (General Electric Company, Schenectady, N. Y.): This paper is another of the growing number of favorable reports on the multiple-surge method of testing with the winding-insulation tester. The authors of this discussion pioneered the multiple-surge method some years ago, were impressed with its usefulness, and proceeded steadily with a wide range of applications. Three instruments, the oscillograph electric-transient analyzer, the recovery-voltage analyzer, and the winding-insulation tester are now in general use and have been reported in the technical literature. In addition, modifications of the winding-insulation tester have been applied to good advantage in the field of aircraft magneto and armature testing. Other applications have been made to limited extent.

G. L. Moses and Earl F. Harter have done well in reviewing applications already made and several new ones. Their paper emphasizes fault detection and location particularly, and these functions often are performed quite conveniently with the winding-insulation tester. However, it should be pointed out that the tester serves primarily to very great advantage as a timesaver for all-around high-potential testing of winding or coil insulation. It made available for the first time a high-potential test which stresses turn-to-turn, coil-to-coil, and major insulation in terms of stresses encountered in service. Experience has shown that the use of the winding-insulation tester has contributed to improved field performance of equipments and coils in important measure.

The connections of Figures 1C and 1D for d-c armature testing are satisfactory for small or medium-sized armatures. For larger ones which have equalizer connections, we have found it necessary to increase the surge-generator capacitance, to use concentric leads to minimize the reactance drop, and to test from bar to bar in order to get about 1,000 volts per coil. This is about as high as the commutator will permit without flashing over.

For stator testing Figure 1E showing the use of an exploring coil is quite interesting. However, it involves some extra inconvenience in placing the coils which would have to be done quite carefully to insure the same degree of coupling for both.

Figure 8 showing measurement of coil-to-coil voltage directly would seem to be subject to some errors due to the isolating transformer. The voltage measured would be reduced somewhat by the parallel impedance, although this might be negligible with fair-sized test pieces. The isolating transformer itself would seem to be quite a design problem if fidelity is important. It may be that in most cases of this kind the coil voltage would be the information wanted and not the exact wave shape. Of course, if it is assumed that coil voltages only and not wave shapes are required, then direct calibrations of transformer ratio could be made for each wave shape used. However, our experience has been that it is important to look at the applied wave shape in many cases.

The multiple-surge method is firmly established for surge analysis of circuits, fault detection and location, and high-potential testing. Advantages already demonstrated suggest extended usefulness, and it seems fair to say that we have here a tool worthy of more general attention. Because the multiple-surge method in some places has displaced older methods, and because it has added new technique, consideration should be given to a proper place for it in instrument-and-measurement and test standards.

REFERENCE

1. INSULATION TESTING OF ELECTRIC WINDINGS, C. M. Foust, N. Rohats. AIEE TRANSACTIONS, volume 62, 1943, April section, pages 203–06.

G. L. Moses and **Earl F. Harter:** As stated in the discussion by C. M. Foust and N. Rohats the authors reviewed the experience previously reported in their reference 1, which discussed only the testing of three-phase motor stators. The value of the multiple-surge test as a quick check on internal insulation of many types of coils and windings was recognized by the authors. The tester disclosed by Foust and Rohats is, however, nearly always strictly limited to fault detection. It was discovered, furthermore, that even fault detection was impossible in large windings having many parallel circuits, because inherent minor dissymmetries between phases caused more fault indication than did a short-circuited turn and often even a short-circuited coil. Refer to Figure 4B. Since the location of faults is often almost as important as their detection, the authors believe that means for locating as well as detecting faults should be provided in the test equipment if it is to be generally useful.

New circuits were accordingly devised and incorporated in our surge-comparison tester to permit fulfillment of both these requirements. The chief example of this described in the paper included the exploring coils mentioned by the discussers. Apparently this method, Figure 1E, has not been tried by the discussers as the adjustment of the exploring coils is not particularly critical. The coils are merely placed in the bore and moved around rapidly one revolution for each phase, giving a test which is both simple and positive. The fault is not only detected but also exactly located at the same time. On the subject of exploring coil use it may also be revealed that this same technique made possible the testing of a group of large synchronous motors while they were completely assembled with rotors and covers in place.

The circuit of Figure 8 was used, as suggested by the discussers, merely to obtain the relative voltage maximums between the coil taps. Since these maximums all occurred at the same time after application of the surge, wave shapes were neglected.

There is evidently complete agreement that the multiple-surge-comparison tester will become an excellent tool for the engineer, manufacturer, and repairman. The authors believe that the field of usefulness of the device should be extended by the addition of means for detecting and locating faults in all common types of windings. The authors concur with the suggestion of Foust and Rohats that multiple-surge testing be recognized by inclusion in instrument and test standards.

Chemical Contamination as Causes of Electrical-Insulation Failure

Discussion and authors' closure of paper 45-97 by C. H. Braithwaite, Jr., and G. L. Moses, published in AIEE TRANSACTIONS, 1945, August section, pages 580–3.

Alvah Small (Underwriters' Laboratories, Inc., Chicago, Ill.): In regard to the subhead, "Carbon-Dioxide-Type Fire Extinguishers," the text under this subhead seems to apply exclusively to the foam type of fire extinguisher, whereas the subhead suggests that only the carbon-dioxide type is being discussed.

C. H. Braithwaite, Jr., and **G. L. Moses:** In reply to Alvah Small's comment, the use of the subhead "Carbon-Dioxide-Type Fire Extinguishers," is unfortunate. The extinguishing properties of foamite are due mainly to the carbon dioxide evolved. However, those extinguishers often referred to as "carbon-dioxide extinguishers" which contain liquefied carbon dioxide under pressure are not a possible source of contamination. The carbon-dioxide snow emitted when these are used does not contain harmful electrolytes and would be permissible for use near varnish tanks.

Precision Testing of Electric Tachometers

Discussion and author's closure of paper 45-100 by M. A. Princi, published in AIEE TRANSACTIONS, 1945, July section, pages 504-08.

T. H. Long (C. G. Conn Ltd., Elkhart, Ind.): The equipment described by Mr. Princi would seem to represent the ultimate in convenience and precision for high-production testing of electric tachometers.

For field testing, however, a very simple equipment may be built around a precise frequency-measuring instrument having an adequate range, such as our chromatic stroboscope.[1,2] This chromatic stroboscope is calibrated in terms of the chromatic (musical) scale, and has a frequency range from 31.772 to 4,066.8 cycles per second and a precision throughout the range of 0.05 per cent of reading. Such an equipment may comprise a tachometer generator driven by a variable-speed motor, with a tone wheel generator to provide frequencies within the range of the chromatic stroboscope. An equipment of this sort has been used for several years at Wright Field for tachometer testing.

In some work done here in connection with automatically regulating the speed of a one-half-horsepower 7,500-rpm motor from a 500-cycle-per-second supply considerable difficulty was encountered owing to hunting. This difficulty was attributed to the use of a solid field structure. I would like to inquire whether lamination of the field structure of the d-c motor was found to be either necessary or expedient in the equipment described.

Some further information would be appreciated on the full-scale calibration procedure. In adjusting the strength of some small magnets to a fraction of one-per-cent tolerance, we have rotated them end over end at a constant speed near a pickup coil and measured the voltage induced in that coil while bringing up a permanent magnet to knock the rotating magnet down to the proper strength. This works, but when the permanent magnet is removed there is a change in the induced-voltage reading amounting to between one and two per cent (depending on the magnet) which occasionally leaves the magnet strength outside the tolerance limits and requires repetiton of the magnetizing and knockdown steps. It would seem that the same hysteresis effect (if that is what it is) should show up while the tachometer is still in the test stand and that it would be more serious there. We found that a different mechanical arrangement reversed the direction of this effect without changing the magnitude appreciably and concluded that a second possible cause was field distortion, but have not found time for checking the matter.

REFERENCES

1. THEORY OF THE CHROMATIC STROBOSCOPE, Robert W. Young, Allen Loomis. *Journal* of the Acoustical Society of America, volume 10, October 1938, pages 112-18.

2. AN ADJUSTABLE TUNING-FORK FREQUENCY STANDARD, O. Hugo Schuck. *Journal* of the Acoustical Society of America, volume 10, October 1938, pages 119-27.

M. A. Princi: The full-scale calibrating procedure is similar to that employed in calibrating d-c indicating instruments. An alternating field is produced by the knockdown coil and controlled manually by means of a variac. There does exist a small error in the full-scale indication of the instrument after the knockdown field is removed. This appears to be due to a component of torque produced by the knockdown field tending to make the instrument read high. However, this effect is taken into account in the calibrating operation and, with a little skill, does not result in overcompensation.

The method described by Mr. Long suggests the possibility of a measurement error due to the location of the pickup coil. The pickup coil indication, essentially, may be due to the modulating effect of the magnet under test on the steady-state field of the magnet used for knockdown. This would result if the pickup coil were located to link the field of the magnet used for knockdown and the magnet under test. This effect would be minimized if the pickup coil were located at right angles to the field of the magnet used for knockdown. Attention is invited to my reference 1 in which additional information on magnets and their testing is given.

Our experience has not indicated the need for a laminated field structure in the d-c driving motor. Hunting, of course, is a function of other constants of the system, and, therefore, the scheme described by Mr. Long may not be directly comparable.

REFERENCE

1. BRAKING MAGNETS FOR WATT-HOUR METERS, I. F. Kinnard, J. H. Goss. AIEE TRANSACTIONS, volume 60, 1941, pages 431-9.

Analysis and Design of a D-C Selsyn System

Discussion and author's closure of paper 45-101 by Joseph Manildi, published in AIEE TRANSACTIONS, 1945, July section, pages 512-16.

R. W. Votaw and **P. G. Cushman** (both of General Electric Company, Schenectady, N. Y.): D-c Selsyn systems have been built and used in sizes ranging from a very small indicating unit weighing a few ounces to a large torque amplification and transmission unit weighing 55 pounds. The smaller types were described in "A D-C Telemeter or D-C Selsyn for Aircraft" by R. G. Jewell and H. T. Faus.[1]

As stated by the author they are used where an a-c source of power is not available or conveniently furnished, or where it is possible to use a receiver with a permanent-magnet rotor and thus eliminate two of the five wires which must go to the receiver in a conventional a-c Selsyn system.

However, they have another characteristic, that of torque amplification, which accounts for many of their applications, especially in the larger sizes. In an a-c Selsyn system, the amount of receiver torque obtained is equal to the mechanical torque impressed on the transmitter shaft, but in a d-c Selsyn system the transmitter requires only enough torque to move the brushes, and the receiver torque may be many times greater.

At least three different types of transmitter have been used. The first type is the uniformly wound toroidal potentiometer discussed in the subject paper. The second type operates by varying the series resistance inserted in each stator line and suitably reversing the polarity of each stator phase. The third type is a modification of the first with nonlinear resistance variation.

As is pointed out in the paper, the first type is subject to the disadvantages of an inherent electrical error of 1.1 degrees and to a variation of receiver torque gradient as the transmitter is revolved. In addition, such a transmitter requires an exhorbitant amount of power, compared with the power furnished the receiver stator. This becomes a very serious limitation on their practical use where large torques must be produced, as is necessary for the positioning of Diesel engine governors, and the like.

The second type of transmitter, at least in theory, can eliminate all the disadvantages already set forth. The power consumed in the transmitter varies from zero at one transmitter position to 13.4 per cent of the receiver stator power at a position 30 electrical degrees from this. There is no inherent error and no variation in receiver torque gradient. However, the required resistance gradient for such a transmitter varies so greatly that it has been used only for the larger units and with discrete steps or taps.

The third class includes the particular nonlinear potentiometer whose equations are developed by the author. For the particular variation given, the inherent electrical error is eliminated, but the variation in receiver torque gradient remains the same as for the linear transmitter. This is a serious limitation in many applications.

As a matter of fact, there are an infinite number of possible variations in the transmitter resistance gradient which will eliminate the inherent error. There is, however, only one of these which also will eliminate the variation in receiver torque gradient.

In a paper now in preparation, it is planned to give equations for the operation of d-c Selsyn systems at standstill and under rotation, and to give the derivation of the equations for the resistance gradients of transmitters of the second and third types mentioned.

Equation 23 of the paper appears to be incorrect. The factor $1/\sqrt{2}$ should be 0.55. This error arises because in the second equation of Appendix II a factor of 1/2 should appear with the term, $R_1^{-1/2}(KR_1+1)$.

REFERENCE

1 A D-C TELEMETER OR D-C SELSYN FOR AIRCRAFT R. G. Jewell, H. T. Faus. AIEE TRANSACTIONS, volume 61, 1942, June section, pages 314-17.

Joseph Manildi: The author wishes to express appreciation for the informative elaboration on the field of application and types of d-c Selsyn systems submitted by Mr. Votaw and Mr. Cushman.

Further appreciation is expressed for pointing out a numerical error in the derivation submitted in Appendix II and the consequent error in equation 23. However, the factor of $1/\sqrt{2}$ should not be changed to 0.55 as indicated by Mr. Votaw and Mr. Cushman but should be changed to 0.86. By rectifying the error pointed out in the second equation of Appendix II, the determining equation for $K'R_1$ becomes

$$3(K'R_1)^3-11(K'R_1)^2+3(K'R_1)+1=0$$

This equation has two positive roots, namely $K'R_1=0.52$ and $K'R_1=3.35$. The latter value, when substituted in equation 20 gives a negative value for R_2 and hence must be discarded. Using $K'R_1=0.52$ changes equation 22 to read

$$R_1=0.52(E^2/30P)$$

$$120R_1=\text{resistance per leg}=2.08\frac{E^2}{P}$$

and substitution of this value in equation 20 changes equation 23 to $R_2=0.86R_1$. Equations 22′ and 23′ remain unchanged.

A further error, not affecting the results, is noted in Figure 4. The middle resistance value should be $90(R_1R_2/R_1+R_2)$.

Basic Concepts of Moving-Magnet-Instrument Rotors

Discussion of paper 45-90 by Lewis I. Mendelsohn, published in AIEE TRANSACTIONS, 1945, July section, pages 529–34.

J. R. Macintyre (General Electric Company, West Lynn, Mass.): Mr. Mendelsohn has prepared an excellent treatise on the subject, and his paper should prove very valuable to instrument designers.

The use of the torque-to-weight ratio when applied to moving magnet instruments, as in Figures 11A and B, deserves further discussion to explain its significance. A general use of the term torque-to-weight ratio is not strictly correct, since it is the ratio of rate of change of torque to weight that actually determines instrument performance. The rate of change of torque of course must be measured at the point of equilibrium of the moving system.

In moving-coil instruments the torque-versus-deflection relationship is linear, and hence the rate of change of torque is constant. Under these conditions the 90-degree torque measurements are proportional to the rate of change of torque, and the 90-degree torque-to-weight ratio is a direct criterion of performance. The torque of these instruments, by convention, is measured at a deflection of 90 degrees from the point of equilibrium, and instrument designers are cognizant of the torque-to-weight factor based on this measurement. In moving-magnet instruments, however, the torque is not a linear but rather a sine function. The more fundamental concept of the rate of change of torque therefore must be employed to compare the performance of moving-magnet and moving-coil instruments.

The torque relationships of conventional moving-coil and moving-magnet instruments are shown in the following two equations:

$$T_{MC}=K\frac{2\theta}{\pi} \tag{1}$$

$$T_{MM}=K\sin\theta \tag{2}$$

K = gram-millimeters torque at $\pi/2$ radians deflection from equilibrium

θ = radians deflection from equilibrium

The rate of change of torque at the point of equilibrium (that is, $\theta=0$) can be determined by taking the first derivative of each equation as follows:

$$\frac{dT_{MC}}{d\theta}=K\frac{2}{\pi}\text{ gram-millimeters per radian}$$

$$\frac{dT_{MM}}{d\theta}=K\cos\theta\text{ gram-millimeters per radian}$$

At $\theta=0$ the rate of change of torque of the moving-coil instrument is $2K/\pi$ and K for the moving-magnet instrument. In other words the rate of change of torque at zero angle for the moving-magnet instrument is $\pi/2$ times that of the moving-coil instrument, although they both have the same measured torque (K) at 90 degrees.

With this in mind the torque-to-weight ratios shown in Figures 11A and B of Mr. Mendelsohn's paper should be multiplied by $\pi/2$ when applied to moving-magnet-instrument design. Under these conditions they will compare directly with conventional moving-coil 90-degree torque-to-weight ratios.

Governor Requirements for Aircraft Alternator Drives

Discussion and author's closure of paper 45-85 by W. K. Boice and L. G. Levoy, Jr., published in AIEE TRANSACTIONS, 1945, July section, pages 534–40.

Stanley J. Mikina (Westinghouse Electric Corporation, East Pittsburgh, Pa.): The authors might have pointed out that the analysis of speed governors controlling variable-ratio transmissions differs radically from that characterizing central-station or industrial governors in that the variable-ratio control is theoretically strictly analogous to a voltage regulator, since the ratio governor stability is substantially independent of the alternator and drive inertia. In the conventional speed-governed system, the rotational inertia of the prime mover and coupled machines is of paramount importance in determining governor stability.

In the case of a voltage regulator, a voltage error from the set voltage initiates a sequence of actions that produces a compensating output-voltage change. Similarly, in the case of these aircraft alternator drives, an alternator-speed deviation from set speed initiates a sequence of actions that result in a compensating output-speed change. In a conventional governor system, on the other hand, an output-speed error causes first a change in the prime-mover torque, which change in torque then works principally against the inertia of the rotating parts of the prime mover and coupled machinery to re-establish the required output speed. Mathematically speaking, for the same number of time delays in the governor system, the variable-ratio governor can be described by a differential equation one order *lower* than the differential equation for a conventional governor system. The variable ratio is thus much easier to stabilize, and operation with much lower "speed droop" is possible than with conventional governors.

It may be well to qualify the authors' calculations of rates of change of ratio for different output accelerations with the following reservations: For example, a statement is made that a rate of ratio change of 0.005 per second corresponds to a rate of alternator-speed change of 13.5 rpm per second. It is important to recognize that this figure is correct only when the input speed is constant. Thus, let

$$w_iR=w_o \tag{1}$$

where

w_i = input speed to transmission

R = transmission ratio

w_o = output speed

Then

$$\frac{dw_o}{dt}=w_i\frac{dR}{dt}+R\frac{dw_i}{dt} \tag{2}$$

For the case cited, $R=2.22$, $w_i=2{,}700$ rpm and $dR/dt=0.005$ per second. Hence

$$\frac{dw_o}{dt}=2{,}700\times0.005=13.5\text{ rpm per second} \tag{3}$$

Thus, the authors' result is correct only when $R(dw_i/dt)$ is zero, that is, when the input speed is constant.

H. B. Bunce (Westinghouse Electric Corporation, East Pittsburgh, Pa.): In their conclusions the authors have listed slip in the transmission, a drooping speed-load characteristic introduced by the governor, and a rate of governor response proportional to the speed error, as beneficial in maintaining synchronism during transients caused by engine accelerations. It is worth noting that slip or droop in the drives is detrimental to maintenance of synchronism during system faults, and, unless it proves necessary to provide more slip to maintain synchronism during engine accelerations (which does not seem likely with the overrunning clutch), the slip and droop should be limited to that necessary for load division.

When a fault occurs which is unsymmetrically located with respect to two generators, the resulting load difference will cause a difference in the speeds of the two machines. The greater the amount of slip or droop the generator drives have, the greater this speed difference will be and the faster the machines will tend to pull out of step.

Also governor response proportional to speed error will cause the two machines to pull out of step faster if both machines are accelerating or decelerating. If one machine is accelerating and the other deceleruting, a governor response proportional to speed error will be more beneficial than a constant rate of response.

The authors have assumed in their analysis that the impedance between generators is negligibly small, which would eliminate the possibility of an unsymmetrical fault location and consequent loss of synchronism. If this were the case, the slip in the drives would have no detrimental effect. This assumption is not justified for airplanes now being designed for a-c auxiliary power. In a particular system the impedance between generators is of such magnitude to cause loss of synchronism for either a double-line-to-ground fault or a three-phase fault if the drives have any inherent slip or droop.

L. G. Levoy, Jr.: We are pleased to note the interest which Mikina and Bunce exhibit in this study.

With reference to Mr. Mikina's discussion, the simplified differential equations which he proposes are valid only when slip is neglected. Although slip is not introduced intentionally, it is always present in a hydraulic drive, and even a small amount has a beneficial influence as shown in the paper.

With regard to the rate of ratio change, the statement referred to in the paper is correct without the qualifications which Mr. Mikina believes necessary. The calculation referred to gives the relation between rate of ratio change and corresponding rate of alternator-speed change at a given speed as stated. This relation is established by the geometry of the drive only. Mr. Mikina's calculation (equation 2) merely expresses the simple relation showing the rate of change of output speed when the input speed and ratio are changing simultaneously, but this does not influence the calculation for the coefficient showing the relation between rate of ratio change and rate of alternator-speed change. The result given in the paper is correct for the assumed input speed and is valid at this point even when the input speed is changing.

With reference to Mr. Bunce's discussion, both slip and droop are limited in practice. Slip is made as small as possible to obtain high efficiency. Droop is limited to a value which provides satisfactory load division, particularly during periods of transient acceleration of one or more of the driving engines.

In a practical case, the impedance between generators is much smaller than the internal impedance of the generators themselves. Consequently, the performance of the system is not materially influenced by the assumed fault location between machines.

We do not share Mr. Bunce's pessimism concerning loss of synchronism in event of a double-line-to-ground fault or a three-phase fault, because in the systems with which we are concerned such faults will be removed quickly from the circuit by circuit protection which is provided. It is not possible to state categorically whether or not any particular fault will cause loss of synchronism unless the duration of the fault is considered, as well as its location, condition of loading of the system, and any speed changes of the engines which may be occurring simultaneously. Many industrial systems are successfully operated in parallel with much higher-percentage impedance between generators than will be encountered in the proposed aircraft systems.

Governor response proportional to indicated speed error (within design limits) is correct in direction and magnitude to restore normal conditions, regardless of whether the machines are accelerating or decelerating. The indicated speed error is the sum of the actual speed error and the apparent error indicated by the droop circuit. In the case of a four-generator system operating normally, if one or two engines begin to accelerate, the corresponding generators will advance in angle and take more load, and the remaining generators, therefore, will take less load. Thus, the indicated error will signal the governor on the accelerated machines to reduce ratio, and on the other machines to increase ratio slightly, thereby restoring equilibrium. Similarly, the deceleration of an engine tends to make its corresponding alternator drop load which signals its governor to advance ratio while the remaining machines receive more load and their governors signal for reduced ratio, again restoring equilibrium.

At the time this paper was written, all work was based on theoretical analyses, since neither drives nor governors were available. Since then, a complete two-generator system has been set up and tested using two 450-horsepower radial-type gasoline engines. Each engine was connected to drive a governed continuously variable-ratio drive unit which in turn was directly connected to a 30-kw 40-kva 120Y/208-volt three-phase 400-cycle aircraft-type generator. Synchronizing, parallel operation, load division, and system stability with various types of loads and faults on the system have been explored, as well as many other conditions. These tests confirm previous calculations and show that it is normally possible to ride through all types of circuit faults without loss of synchronism when adequate circuit protection is provided.

A 400-Cycle Aircraft Motor

Discussion and author's closure of paper 45-87 by G. O. Schwandt, published in AIEE TRANSACTIONS, 1945, July section, pages 508-12.

B. B. Ramey (Black and Decker Manufacturing Company, Towson, Md.): I have read with considerable interest the paper by G. O. Schwandt on the 400-cycle aircraft motor, as I have had many years of experience in applying high-frequency motors of 180 cycles to portable electric tools. This development began about 1924 and was established pretty well commercially by 1926. It would have been better if a higher frequency of 240 to 300 cycles had been chosen as it would have resulted in slightly less weight for the motors and greater portability.

I can realize that there would be special requirements in connection with aircraft use which would make the problem of developing a motor for that service much more difficult than for portable tools. While portability is essential, it is not necessary to get a certain weight limit in the case of both tools and the frequency changer or generator as is the case on aircraft. Efficiency and power factor are always of considerable import in connection with induction motors but for portable tools not so important as in the case of motors for aircraft.

The high lock-rotor torque required on some of the aircraft motors make the matter of cooling much more difficult, owing to the increased heat in the rotor. This is another factor that was not encountered in the portable tool field.

In referring to Figure 3 it seems to me that the ventilation arrangement could be improved by not having the fan on the rotor at the inlet end, as this will tend to stir up the air locally and interfere with through-draft action, especially since there is such a limited space for the through draft to flow in. I have found also that on small motors such as this where the dimensions are so small, ventilating openings through the rotor and the stator are liable to do more harm than good. The magnetic material sections are reduced, making it necessary to hold the flux value down and limit the possible output of the motor. The openings are necessarily so small that it is impossible to get a fan that will pull any appreciable amount of air through these openings against the resistance that is encountered.

I believe that, in general, omitting the ventilating openings and arranging to draw air over the outside of the stator will result in less motor weight for a given output and better cooling.

I would be interested in knowing what grade of magnetic material was used and what gauge. In connection with the 180-cycle motors mentioned, satisfactory results have been obtained using electrical grade sheet of 29 gauge.

H. J. Braun (Westinghouse Electric Corporation, Lima, Ohio): In his attempt to cover a rather broad field Mr. Schwandt, of necessity, has had to sort and sift his material. He has done this job well. There is one point that is quite often neglected or, if thought of, does not receive the consideration that it deserves. This point is the variation of torque with combined variations of frequency and voltage. Although Mr. Schwandt mentions this, he does not give any numerical values.

On the basis of the worst conditions as cited in Mr. Schwandt's paper, the torques will vary as shown in Table I of this discussion. The values as given in the table are in per cent of the rated torque of the motor.

While it is unlikely that the unfavorable conditions of voltage and frequency will occur simultaneously, provision must be made for these extremes.

Table I

	Standard Voltage, Standard Frequency	High Voltage, Low Frequency	Low Voltage, High Frequency
Maximum torque	200	232	172
Starting torque	160	185	124

G. O. Schwandt: Certain fundamentals must be observed when designing any ventilation system. One is that sufficient air-flow area must be supplied so that the quantity of air flow is adequate to absorb the motor losses with a reasonable amount of air temperature rise. For aircraft motors which must operate at high altitudes, this reasonable value of air temperature rise is less than for motors operating at normal altitudes only. Therefore, the quantity of air flow must be greater. In regard to the size and placement of ventilation openings, it is fundamental that the greatest heat-transfer surface area per unit of air-flow area be used consistent with tooling and construction limitations. Both space and weight are conserved by a multiplicity of small ventilation paths rather than a few larger ones. This is done because the fewer larger airflow paths do not offer adequate heat-transfer surface.

In regard to the ventilation openings through the rotor, they cost nothing in the way of flux density. They do furnish additional air-flow area and cooling surface. They also lighten the motor, since the material removed is excess material as far as the magnetic design is concerned.

The small fans at each end of the rotor serve to increase the air velocity over the end turns. This increased velocity over the end turns more than offsets the disturbance created in the ventilating system. It is possible that these beneficial results will not exist in ventilation systems other than that used. Extreme care must be taken in the arrangement of fans in series to avoid considerable difficulty.

In regard to the magnetic material, our investigation, while incomplete, indicates that best results can be obtained by using a $3^1/_2$-per-cent silicon iron 0.014 inch thick.

H. J. Braun, in discussing the subject paper, has prepared an interesting table showing the percentage variations in motor torques due to pre-established variations allowed in the proposed 400-cycle aircraft electric system. The values given by Mr. Braun apply only to a specific motor design. Probably they are nearly correct for most designs that would be practical.

If the electrical constants of the motor are known it is possible to determine the internal torques by the following commonly used formula:

$$T_2=\frac{PV_1^2}{4\pi f_1}\left[\frac{S_{r_2}}{(r_1s+r_2)^2+s^2(x_1+x_2)^2}\right]$$

where

T_2 = internal torque per phase in pound-ft.

P = number of poles

V_1 = applied voltage

f_1 = applied frequency in cycles

s = slip at which torque is to be determined

r_1 = primary resistance in ohms per phase

r_2 = secondary resistance in ohms per phase

x_1 = primary leakage reactance in ohms per phase at rated frequency

x_2 = secondary leakage reactance in ohms per phase at rated frequency

Calculating values of breakdown and locked-rotor torques at voltages and frequencies within the range of expected variations permits obtaining percentage values in terms of rated full-load torque.

When one uses this formula it should be remembered that the reactance constants change in direct proportion to the applied frequency. It appears that Mr. Braun neglected this change in reactance constants when preparing his table.

Statistical Tools for Controlling Quality

Discussion and authors' closure of paper 45-99 by Joseph Manuele and Casper Goffman, published in AIEE TRANSACTIONS, 1945, July section, pages 524–8.

C. C. Craig (nonmember; University of Michigan, Ann Arbor, Mich.): As always in Mr. Manuele's discussions of the applications of statistical methods to the control of quality the exposition is clear and forceful. It has too the merit which the more academic statistician finds difficult to achieve—of being written in language which carries conviction to practical-minded shop people.

From my point of view as a mathematical statistician who has interested himself in quality-control methods there are two comments I should like to make. The first has to do with the relation between the use of a frequency tabulation with its average and standard deviation and the control chart as a means of getting and maintaining control over a variable-quality characteristic, say a dimension on a machined part.

Suppose a control chart is being kept by taking samples of five pieces produced consecutively at hourly intervals and plotting individual readings. What is being done is essentially comparing the variability one sees during the short period it takes to produce five pieces, during which time conditions will show little if any change with the variation that is taking place from hour to hour. If this latter variation is unduly large compared with the former, the indication is that the process is not stable but is jumping around in a way that ought to be corrected to get the best quality. It is therefore quite important that an estimate of variability be obtained which contains only very short-run fluctuation. I am sure that Manuele and Goffman have in mind, when they recommend a preliminary examination of 50 pieces in a frequency tabulation to locate the center of the process and to measure the variability, that the 50 pieces should be produced in an interval of time short in comparison with the one they will use later for periodic samples of five. My teaching experience has shown that this point is very frequently missed. The beginner may get his 50 pieces by putting together for his frequency tabulation ten hourly samples of five each. If the process was in control during this ten-hour stretch, he will be able to detect future lapses from control. But if the process was not that good, he is a good deal less likely to detect the fact then or later.

My second point has to do with the example of the analysis of variance Manuele and Goffman have used to illustrate the fact that this method frequently may be quite valuable in the control of quality.

Table I

Source	Sum of Squares	Degrees of Freedom	Estimated Variance
Between columns (cutters)	0.00056983	3	0.00018994
Between rows (cams)	0.00020683	5	0.00004137
Error (within same cutter and cam)	0.00006317	15	0.000004211
Totals	0.00083983	23	

When, as in the present case the total variance is analyzed into two components, it may be noted that the interpretation of the results is substantially the same as that for a control chart for averages. It is seen that there is variation in results from the same cutter which is measured by the variance within columns. This means that, if all four cutters are identical, there still will be variation between the averages of six pieces from each cutter. The question is whether this latter variance, between columns, is clearly larger than one would expect in view of the within-column variance. If it is, the indication is that the cutters are working to different average thicknesses.

But the authors remark that there also may be differences among the six cams. If this is true, unless one knows that cam differences are no more than chance differences between averages of four, then the variance between columns should be compared, not with the variance one gets on the same cutter alone, but with the variance one gets on the same cutter and cam. This is readily done with but little additional calculation as is explained in a number of textbooks. In Table I, I will merely give the results of the analysis of the variance into three components instead of two. Now to answer the question as to the reality of cutter differences we form the ratio $189.94 \div 4.211 = 45.11$ which is nearly three times as large as the one the authors used. We can now also answer the same question for cam differences. The ratio $41.37 \div 4.211 = 9.82$ with five and 15 degrees of freedom is significant not only at the one-per-cent level but even at the 0.1-per-cent level.

The authors can object perfectly correctly that their two-component analysis did show that there were differences between cutters. But suppose it had happened that the between-cam sum of squares was twice as large as that between cutters. Then the ratio to test the cutter effect would have been on a two-component analysis

$$\frac{189.94}{(569.83\times 2+63.17)\div 20}=3.16$$

which is just significant on the five-per-cent level. If in the present case interest had been centered on cam differences only, a two-component analysis for that would have given for the test ratio $41.37 \div 35.17 = 1.176$ which is not significant at all.

Of course, the authors were limited by time and the necessity of not making the dose of statistics too large for one swallow. I hope it is clear that I am not criticizing a fine presentation. My anxiety is that of the teacher who is afraid that beginners reading this paper will think they have the answers before they even understand the questions fully.

C. Bradner Brown (Naval Ordnance Laboratory, Washington, D. C.): This is an excellent paper which all engineers engaged in production and design would do well to study. It has been my experience that design engineers too often do not appreciate the significance of statistical variation both in the component parts used and in the performance of the ultimate product.

If design engineers would consider the performance to be expected from a new design in terms of the statistical variation to be expected in production, more reasonable specifications could be placed on component parts and less headaches would be encountered in going to full-scale production from research samples. Too often the performance of production items is disappointing when compared to handmade preproduction samples. In most cases this can be traced to lack of appreciation of the role played by statistical variation in manufacture. It is particularly noticeable in the case of complex electronic units. A thorough familiarity with statistical practices in quality control by the design engineer will result in better products and a more realistic attitude of performance to be expected from new designs.

Irwin S. Hoffer (nonmember; Temple University, Philadelphia, Pa.): Three statistical tools are described in this paper: the frequency distribution, the control chart, and the analysis of variance.

The control chart is the most efficient and the fundamental device for controlling quality during production. In the opinion of the reviewer, the best results are secured by accumulating samples of four or five pieces each until about 20 samples have been secured. The control chart for averages and for ranges then can be produced, and the presence of assignable causes can be determined. If the system is in control, an estimate can be made of the standard deviation of individual measures in the system. From these results it can be determined whether the system is operating within specifications, whether the proper level of quality is being secured, or whether too wide a distribution of individual pieces within the samples is appearing in the production process. It is believed that this procedure is fundamental.

In this paper, the statement is made that "the control chart for individual measurements has advantage over the control charts for average and ranges, that control-chart limits may be considered to be the limits within which the process is actually producing." It is believed that the procedure I have outlined will yield the same results. It is true that, according to the procedure outlined, an estimate only of the standard deviation of individual pieces is secured. It must be remembered, however, that if this standard deviation is based on a frequency distribution of individual pieces, the result will be only an estimate and will be subject to sampling fluctuations because in the instance cited in the paper the frequency distribution was based on a sample of 50 pieces. Moreover, this is usually the case; that is, a sample of the production is used as a basis for the construction of the frequency distribution.

In case, however, that a body of data is available, based on individual measurements which cannot be distinguished with respect to sequence of occurrence, a frequency distribution of such data will be helpful in determining the character of the quality that is being obtained and may be used as a standard point in setting up a control system. Otherwise, the standard control-chart technique will yield the same information as an analysis based on individual measurements.

The third technique which is described in this paper, the analysis of variance, is very helpful in cases like the one cited. It may be observed, however, that a repetition of the test or analysis of variance would be required at intervals if there is any indication that assignable causes have entered the system.

In summary then, at the beginning of the process, secure sufficient data for the installation of the control chart for averages and ranges. Determine whether assignable causes are present in the system. If they do exist, have them eliminated and calculate new values for the grand average and the average range. From these, test the centralization and the distribution in the entire system. The frequency series is not needed to answer these questions. The analysis of variance is helpful in cases like the one mentioned. Other techniques which may be applied in specific instances are correlation and chi square. The authors of this paper are to be commended for bringing this discussion to the attention of those interested in the development of statistical tools for controlling quality.

Martin A. Brumbaugh (nonmember; *Industrial Quality Control;* Buffalo, N. Y.): The use of statistical technique to obtain and maintain control of dimensions in the shop, to introduce precision in commercial inspection, and to catalog and assess responsibility for assembly faults is one of the important industrial advances introduced widely during this war. The authors of this paper have made a contribution to the literature on this subject in two major directions:

1. The explanation of fundamental method is so lucidly presented that a few pages suffice to tell the complete story of the use of statistical methods in the machine shop.
2. The approach should dispel permanently the criticism occasionally offered that these techniques are too complicated for the practical shop man to use.

The statistical background of control procedure lies in the properties of the frequency distribution and two measures, the average and the variability (standard deviation). The operating instrument is the control chart with these two measures used to segregate a constant system of causes or natural variability of a machine process from intermittent or assignable causes. A controlled process with variability consistent with design tolerances is the signal to the engineer to keep hands off the process. Lack of control due to assignable causes is the signal to the engineer to start corrective action to eliminate sources of trouble which are now producing or will produce scrap, rework, repair, and salvage. If orthodox inspection procedure can be likened to locking the stable after the horse is stolen, statistical quality control can be likened to the installation of a burglar alarm.

The explanation of the use of analysis of variance by means of an example is the best way of making this technique for dealing with related variability available to the practicing engineer who has neither the time nor the desire to master statistical textbooks. Mastery of Figure 10 and Table III of the paper is all that is required to make full industrial use of these statistical tools.

R. F. Bisbee (nonmember; Westinghouse Electric Corporation, Mansfield, Ohio): I like the presentation of statistical fundamentals and the illustrated examples very much. After reading the article, the reader is not confused by an excess of mathematical terminology and formulas.

I believe this paper could be used by the average man as a training text and he could apply the simplified methods to his own work without necessity for outside help.

P. M. Dickerson (nonmember; Westinghouse Electric Corporation, Bloomfield, N. J.): It has often been said that the development of science has far surpassed the development of politics and government. The same may be said of the high degree of development of statistical-methods theory for quality control, compared to the actual application of statistical methods by factory personnel in the various fields of manufacturing. I personally feel that more emphasis by writers on the subject of quality control should be placed, as Mr. Manuele has, on the practical applications of statistics for quality control to specific situations encountered in manufacturing. Many manufacturing men have been educated in statistical methods for quality control, but far fewer have found practical ways of applying these methods. People interested in quality control will want more papers like this one.

Mr. Manuele mentions that "statistical tests exist for symmetry, but one is often able to judge by sight whether or not a given frequency distribution is sufficiently symmetrical for purpose of controlling quality." To keep this paper in the practical trend of thought which distinguishes it, I would suggest that actual samples of curves be given to illustrate satisfactory and unsatisfactory normal curves.

Mr. Manuele states that the control chart for individual readings has a distinct advantage over the control charts for averages and ranges. I might point out that there is a disadvantage in that a significant change in range may not be noticed when individual readings are plotted, as recommended by Mr. Manuele. The disadvantage, however, may often be offset by the simplicity of Mr. Manuele's method of plotting individual readings. In other words, theoretically, the chart for averages and ranges gives more information, but for practical considerations a chart for individual readings may be preferred because of its simplicity. The practical advantage just mentioned is stressed by Mr. Manuele in the next few paragraphs.

The particular examples used by Mr. Manuele immediately appear significantly different and might not require calculation to reveal the fact. However, this in no way affects the thought contained in the paper. My suggestion is that perhaps an example could have been used in which there existed a significant difference, but not an apparent difference.

I hope that more writers, in this field can be persuaded to cover the subject from the standpoint of practical applications, rather than pure theory and generalizations. I believe that advances in quality control will surely be aided more, now, by practical thinking than by additional theory.

Eugene L. Grant (nonmember; Stanford University, Stanford University, Calif.): The AIEE subcommittee on applications of statistical methods is to be commended on securing these three interesting papers. The contrasting applications of the Shewhart control chart which they contain are evidence of the broad usefulness of this powerful statistical technique. All of the three control charts illustrated serve the two purposes of process control and acceptance inspection. Mr. Taylor's Figure 7 applies to the results of destructive tests of samples of the actual product being controlled, that is, suspension insulators. The control charts of weld quality shown in Figures 5 and 6 of the paper by Hobson, Inglis, and McCants also apply to destructive tests, in this case made on test specimens intended to be representative of the welds on the commercial product. The control charts given by Manuele and Goffman apply to measured dimensions; if, in this type of situation, the control chart shows continuous control at a satisfactory level, it is possible to substitute actual measurements on a sample of product for 100-percent inspection with go and not-go gauges.

Publicity given to many successful applications of statistical quality control in recent years has resulted in consideration of these methods for use in many manufacturing plants. Two common objections to the introduction of the methods are "Our raw materials are too variable" and "We make such a variety of different designs." Mr. Taylor's paper contains answers to these two objections. He points out that the variability in raw materials in insulator manufacture is an additional reason for the use of statistical methods rather than a reason for avoiding the statistical approach. He also shows how, because of the similarity in raw materials and manufacturing operations of the many different insulator types, a good measure of quality control can be obtained by the maintenance of control charts on a few major types.

Mr. Taylor does a skillful job of introducing electrical engineers to statistical concepts by the use of electrical analogies. His illustrations of different types of nonnormal distributions, with his explanation of the physical reason for each departure from normality, provides a good antidote to the easy assumption sometimes made that all quality characteristics of manufactured product have normal distributions. His comments are particularly valuable on the relationship between the frequency distribution of the quality characteristic and the possible good or bad effect of proof load testing on product quality.

A particularly important topic for the AIEE Standards committee is introduced by Mr. Taylor's critical remarks about specifications as they are commonly written and administered. The acceptance or rejection of each lot separately on the basis of whether or not any item in a small sample falls below a specified minimum is, as he states, certainly uneconomical and often unfair. Recently progress has been made toward writing acceptance specifications which recognize the evidence of a manufacturer's quality history as recorded in a control chart, as well as the evidence of the small sample from the current lot. Typical of these are the acceptance procedures for armor plate and steel castings developed by the Ordnance Department of the United States Army. These might well serve as models for writing of acceptance specifications in the postwar period.

In general, Mr. Taylor's paper is packed with concise statements of general principles, each well illustrated. It is an outstanding contribution to the literature of statistical quality control.

The application described by Hobson, Inglis, and McCants is typical of many in which the use of the control chart for routine process control must be preceded by an extensive program of production research aimed at standardization of variables previously subject to control of the operator. Similar studies in the California aircraft industry with respect to spotwelding of thin sheets of various aluminum alloys also have led to the use of the Shewhart control chart to assure uniform quality. Subgroups of three are used here also; the control-chart variable has been the test strength of welded coupons in simple shear, in contrast to the more complicated quality index described for torsional shear tests of spotwelds of heavy steel.

Manuele and Goffman, in their brief description of the grinding operation on bars of rectangular stock, give an excellent example of the use of the control chart as a basis for trouble shooting on machining operations.

In explaining their Figures 5 and 6, they mention the fact that the man in the shop is likely to confuse control limits on a chart for averages with the specification limits applying to individual items of product. This is a common experience wherever the control chart is introduced and has led to numerous schemes to avoid the troubles created by this misunderstanding. One common scheme is the use of a chart such as Figure 5 of the paper which shows individual measurements.

The writer believes that this is the wrong way to solve the problem; the true control chart such as Figure 6 is a much more reliable basis for process control because of its much greater sensitivity to shifts in process average and process dispersion. Another and better way to avoid the confusion between specification limits and control-chart limits is to plot the control chart for the sum of the numbers in the subgroup rather than for their average; as the control limits for subgroup totals appear to be numbers unrelated to the specification limits, they are not misinterpreted. The ideal way to avoid misinterpretation, although not always practicable, is for everyone who uses the control chart to understand *why* the limits are not comparable. An important rule to contribute to this understanding is *never* to show specification limits on a control chart for averages; such limits are an invitation to the man in the shop to become confused. This rule has been violated in Figure 6.

As pointed out by Manuele and Goffman, occasions sometimes arise when analysis of variance may help in solving manufacturing problems. However, the application of this time-consuming technique to the data of Table IV seems unnecessary; it should be reasonably obvious from inspection of Table IV that there are significant differences among the cutters. For each of the six cams, cutter 4 gives the highest value, cutter 3 the next highest, and the value for cutter 2 is always equal to or greater than that for cutter 1.

J. Manuele and **Casper Goffman**: Professor Craig is correct when he assumes that the preliminary sample of 50 pieces is taken during a short interval of time. As a matter of fact, the 50 pieces are taken as produced consecutively—one after the other. We do not recommend taking hourly samples and then lumping these together to accumulate a sample of 50 pieces. In many instances, the production order would be completed before the same would be accumulated. Therefore, we take the first 50 pieces produced at the beginning of the order. This may be over a period of 15 or 20 minutes.

The second point raised by Professor Craig has to do with the method used by the authors in presenting the example on analysis of variance. We know that given K factors a design can be made so that the total variance of a characteristic can be subdivided into the variance due to each factor and the variance due to the interaction between any subset of factors. The variance due to the interaction between all K factors is known as the error term. One can determine which factors and which interactions affect significantly the characteristic in question by comparing them with the error term.

In the example cited by the authors the case of one factor was considered; namely, the cutter number. The error term for this case is the within-cutter variance. Since the authors also identified parts with respect to cam number, a two-factor analysis of variance could have been made as Professor Craig has pointed out. Of course, the two-factor analysis makes more complete use of the data and may accordingly reveal differences not shown by the one-factor analysis. However, for the particular intention, the one-factor analysis seems adequate.

Application of Quality Control to Resistance Welding

Discussion of paper 45-98 by L. S. Hobson, R. S. Inglis, and R. P. McCants, published in AIEE TRANSACTIONS, 1945, August section, pages 573–5.

G. M. Reed (General Electric Company, Philadelphia, Pa.): The quality control of resistance welding as described in AIEE technical paper 45-98 has been a functional part of the steel fabrication shop of the General Electric Company switchgear equipment division for the past two years.

When it was proposed it was endorsed wholeheartedly, being recognized as a necessary tool by which a continued high standard of weld quality in switchgear structures could be insured.

The technical data of the weld characteristics obtained daily make it possible to record weekly trend charts to establish the following major controls:

1. Detection of unfavorable quality deviations in sheet, plate, and structural steels, by analysis from a material standpoint.
2. Detection of undesirable machine performances before they become critical and affect the quality of the finished product, by analysis from an equipment standpoint.
3. Provision of a continuous record of operator performance which not only is of value to the supervisor but also is an incentive to the operator himself.
4. Good quality from the start, assured by making test specimens after each machine setup and before production welding.

In this shop a large variety of steel having different degrees of weldability is used. This necessitates the use of many different scales in plotting weld quality on the control chart. The shop personnel, when discussing control limits, face an unnecessary complication in that they must associate the different weld-quality numbers with the control limits for each grade of steel. It has been proposed to the authors of this paper that a system of "process-control numbers" common to all steels be used for plotting data and for factory discussion purposes. A conversion table has been worked out whereby the quality-control operator can readily convert weld-quality numbers to process-control numbers. This will require the use of only one plotting scale when plotting data. The process-control number will be indicative of weld quality with respect to the control limits, irrespective of the grade of steel being welded. The necessary steps are being taken to incorporate this into the control system.

Eugene L. Grant (nonmember; Stanford University, Stanford University, Calif.): For discussion, see page 951.

Statistical Methods Applied to Insulator Development and Manufacture

Discussion of paper 45-89 by J. J. Taylor, published in AIEE TRANSACTIONS, 1945, July section, pages 495–9.

H. A. Adler (Commonwealth Edison Company, Chicago, Ill.): The method of analysis of endurance test data based on Figures 10 and 11 of the paper is extremely interesting. The author is to be complimented for having devised an ingenious method of evaluating test results for properties with a pronounced time dependence. There are a number of materials showing such a time characteristic for some of their properties. Impregnated-paper insulation of power cables, for example, has a dielectric breakdown strength which is a power function of the time to breakdown.

Further elaboration of Figures 10 and 11 by Mr. Taylor probably would have increased their interest and value and made their meaning clearer to engineers unfamiliar with probability analysis.

In a simplified way, Figures 10 and 11 seem to show the following:

1. If a number of samples are subjected to a constant test load A below the average ultimate strength, most of the samples will fail after an interval for which the corresponding most probable strength value equals A.

2. If the samples show a maximum deviation in strength of $\pm d$ for any duration, then, if a continuous load A is applied, failures may occur between a minimum duration which corresponds to a breakdown value of $A-d$ and a maximum duration which corresponds to a breakdown value of $A+d$.

3. It appears from the foregoing that a great spread in life of a number of samples subjected to a constant load may be due either to a wide spread in test results, that is, in a large value d, or to a very pronounced time characteristic, that is, a rapid increase with life for small decreases in load. This statement may be clearer if it is amplified somewhat. For example, the test results plotted on Figure 10, are based on a uniform test load for all samples of 80 per cent of the average short-time strength of a large number of similar insulators. Actually this average 80-per-cent value may be 98 per cent of the actual strength of one insulator and only 62 per cent of that of another one. Then, with the average 80-per-cent load applied to one insulator, a short life would be obtained, whereas a long life would be obtained on another one. Figure 10 shows that the results for 15 insulators fall within the expected load-life characteristics of the insulator and that the variation in life is no greater than should be expected.

It is possible to evaluate the spread in test results independent of the time effect if the breakdown–time relation is known. In this case, the breakdown values may be evaluated on the basis of a common equivalent time. This method has been widely used in the cable industry and should be applicable also in other fields.

Eugene L. Grant (nonmember; Stanford University, Stanford University, Calif.): For discussion, see page 951.

A New Outdoor Air Switch and the Principles Involved in Its Design

Discussion and authors' closure of paper 45-112 by H. W. Graybill and J. S. Ferguson, published in AIEE TRANSACTIONS, 1945, August section, pages 583–6.

A. H. Powell (General Electric Company, Philadelphia, Pa.): The authors are to be congratulated on the excellent manner in which they have summarized the problems involved in the designing of outdoor high-voltage switches. The outdoor air switch is often considered a minor part of station equipment compared with circuit breakers and transformers, but this is not entirely the case, for continuity of service is also dependent upon the switches and the proper functioning of them.

The paper presents an interesting discussion concerning contacts in outdoor switches, and the authors of this paper have come to the conclusion that braids for carrying the current around the hinge end of a switch should be eliminated and a direct contact substituted. In contrast to this conclusion, it is suggested that the elimination of additional moving-contact surfaces, with the resultant decrease in maintenance and reduction in switch resistance, may justify the use of braids at the hinge end of the switch. Thinking of a solid conductor as the fundamentally ideal current-carrying circuit, a switch which must open the circuit preferably should have no more than one joint or contact point. This, in general, can be accomplished only by using braids around the hinge of the blade. Such basic design has been followed for many years by several manufacturers of outdoor air switches. It is a fact that braids of suitable material properly designed have proved very reliable in service over a long period of time.

In the switch described in this paper, two questions come to mind regarding its construction. First, methods of adjustment to compensate for variables in interphase pipes, obstructions such as ice at the contact end, and misalignment apparently are lacking, and this may cause trouble in installation and maintenance. It is one thing to set up for test a three-pole high-voltage switch in ideal surroundings using every facility needed and obtain satisfactory operation. It is another thing to mount the switches on a steel structure high above the ground, with attendant variables in spacing, alignment, operating pipes, and the like. Means for adjusting the blade position with reference to the operating cranks and contact end of the switch would seem to be essential.

Second, it may be that ice at the contact would prevent the blade from closing, and the force available at the operating crank for breaking ice does not appear adequate. Movement of the blade during the final travel of the blade is directed by the operating arm designated as *c*, of Figure 3 of the paper. As clearly shown by Figure 4, as well as by suitable mathematics, there is considerable force exerted on the operating arm in an upward direction if the blade or mechanism housing encounters ice. If we assume that the arm is sufficiently sturdy to prevent breakage, there may be a certain resulting deflection in the arm and, of course, considerable pressure on the slot in which the end of the arm operates. Because the contact end of the switch blade is at some distance from the hinge, especially in the higher voltages, any variations in the slot or deflection of the arm is magnified to such an extent that poor contact may result.

The questions which have been raised concerning trouble-free installation and operation of the air switch described in this paper appear real. However, satisfactory performance can only be determined after trials under operating conditions over a period of time.

C. S. Beattie and **S. C. Killian** (Delta-Star Electric Company, Chicago, Ill.): The authors are to be commended for presenting a very interesting paper on an old and widely discussed subject. Analysis of the paper indicates that no attempt has been made to discuss new technical ideas but merely to describe a new switch design. The facts presented as applying to this switch have been known and applied to switch design by several switch manufacturers for years.

Vertical-break rotating insulator switches employing the dual-blade motion described have been available for over 20 years. The elimination of shunts, gears, cranks, and exposed levers on the hinge end of an outdoor switch also was accomplished years ago.

The authors have made an excellent survey of the difficulties inherent in the design of an outdoor air switch. Set out in the weather, often in exceptionally bad atmospheres, this piece of equipment is expected to perform its duties over long periods of time with little or no maintenance, though coated with corrosion or severely iced. Since the function performed is simple, it seems to almost everyone that air-break switch design should be simple. Such is far from the case. A long and painful evolution has brought forth the present line of equipment, and ingenious mechanisms without end have been designed in order to create that extra movement of the switch blade as described by the authors. This is the ice-breaking, corrosion-breaking, or contact-pressure-releasing motion as compared to the simple raising or lowering of the blade. Into that motion is usually built the success or failure of the switch. Contact design and contact materials are also features of major importance.

We have found that the argument advanced by the authors for line contacts against point contacts is not necessarily true from a practical standpoint, and we have largely abandoned the use of the line in favor of the point. It is recognized that the ability of a line to conduct heat away is superior to that of a point. However, it is difficult to get the line to lie flat against another surface so as to produce a full line contact. On heavy equipment of this nature mounted under all sorts of disadvantageous conditions where final assembly and adjustment often is made by the installation crew, it is next to impossible to align contacts of the line type. Owing to this they therefore approach point contacts. We have found it worth-while to admit that we could not obtain perfect line contacts, and therefore, use point contacts and design them with sufficient points and sufficient material at the points to preclude any danger of burning under fault conditions.

We have not found that the softer contact materials such as silver and copper are subject to galling, provided they are properly chosen from a physical, chemical, and electrical viewpoint. As a matter of fact, we find that some of the harder alloys gall much more than softer alloys under certain contact configurations and pressures. Since the authors do not mention what contact pressures they are using, the findings cannot be compared. Silver is superior as a contact metal to any of the copper alloys when subjected to the intensely corrosive atmospheres of many of our powerhouses and large industrial installations. So long as copper is used, the high-resistant oxides of copper will be present unless some means is devised of reducing them in the contact itself.

Complete laboratory tests backed up by years of actual service under the most severe atmospheric conditions have proved that silver to copper contacts are both feasible and desirable on high-pressure switches. By proper selection of materials and careful design, it is possible to retain the high-conductivity advantages of silver and copper and eliminate the necessity of using low-conductivity alloys. The retention of the high-conductivity materials greatly aids the contact in absorbing high fault currents.

H. W. Graybill and **J. S. Ferguson:** The question of braided shunts versus contacts at the hinge is, of course, not a new one, and opinion on the subject varies as widely among operators as among manufacturers. However, a poll of operating companies has indicated that, while shunts are acceptable for rural areas, particularly if switches are operated infrequently, the elimination of shunts is considered desirable in urban areas and essential near steel mills and chemical plants. It is true that a solid conductor is fundamentally ideal for current-carrying purposes. Unfortunately, the braided shunt does not approach the solid conductor in corrosion resistance. Consider, for example, a solid conductor one inch in diameter and a braid composed of enough 0.010-inch wires to give the same cross section. When corrosion has penetrated to a depth of five mils, as may happen in two to five years, the one-inch conductor remains comparatively unaffected, but the ten-mil wires are completely destroyed.

The number of joints or contact points in the switch is not, in itself, a matter of prime importance. The important characteristic is the temperature rise of the switch resulting from the resistance of the joints. It may be pointed out, however, that a braid generally introduces four joints: one at each end between the ferrule and the surface to which it is bolted, and one at each end between the braid and the ferrule. Unlike the contacts described in the paper, these joints have no rubbing action to keep the contact surfaces clean and bright; hence the resistance of these joints after several years' exposure to the weather may be higher than that of a moving contact.

The alignment of line contacts mentioned by Beattie and Killian is indeed no simple problem. Line contacts must be designed carefully if full line contact is to be obtained. They should either be so arranged that the contact pressure assures self-alignment (as is the case with the internal contacts described in the paper) or so that contact alignment is a simple matter. The one-piece break jaw used on the new switch aligns itself when the mounting bolts are loosened with the blade in the closed position, owing to its spring pressure and the clearance in the mounting bolt holes. When the jaw is aligned in this manner, the minimum number of contacts theoretically possible is two on each side—twice as effective as a single point on each side. Actually, our experience shows that uniform line contact is obtained with tooled pieces. Even if the alignment operation were omitted or neglected, the worst condition that would result would be a single-point contact on each side of the blade.

Mr. Powell has raised the question of adjustments necessary to assure proper and uniform operation of the three poles of the switch. The details of these adjustments were not described in the paper because only the conventional interphase pipe length and operating mechanism adjustments are necessary on installation. Adjustments possible, but not required in the field, are as follows: The blade can be rotated with respect to the fork, and the arm can be rotated with respect to the operating lever. In addition, in higher-voltage switches there is an adjustment to slightly raise or lower the blade in the closed position. As a result of these adjustments and careful tooling, all pole units have identical mechanical characteristics when leaving the factory.

Tests have proved the adequacy of the design to close in on a half inch of ice on the break jaw without undue effort or strain on the switch. A survey of the operating experience of utilities shows that one-half inch is about the maximum thickness of ice coating encountered in the United States. The switch can be closed with heavier coatings of ice by closing the blade rapidly once or twice to shatter the ice at the jaw. Because of the high mechanical advantage available for rotating the blade, the switch can be opened when covered with even more than one-half inch of ice. Switches of this type, some of which have been in service over three years, have shown very satisfactory performance in this respect.

Lightning Investigations on 33-Kv Wood-Pole Lines

Discussion and authors' closure of paper 45-115 by F. E. Andrews and G. D. McCann, published in AIEE TRANSACTIONS, 1945, November section, pages 768–77.

B. C. Sherwood and E. H. Grosser, Jr. (Commonwealth Edison Company, Chicago, Ill.): Since our company operates similar lines in territory adjacent to that covered in Andrews and McCann's investigation, their findings on the lightning performance of 33-kv wood-pole lines are of particular interest to us. Tripouts per 100 miles of line per year due to lightning on lines with ground wire, with protector tubes on the top phase at every pole, and on unprotected lines were found by them to be in the ratio 1.0, 1.4, and about 15, respectively. Our experience indicates performance ratios of similar order. For example, based on 28.5 miles of 33-kv wood-pole lines on the Commonwealth Edison system, the records of tripouts due to lightning in 1944 showed the following *relative* outage rates for different types of lightning protection: overhead ground wire 1.0; protector tubes (either on the top phase wire at each pole for lines in triangular configuration, or on the top phase wire on alternate poles for lines in double-circuit vertical configuration) 1.4; unprotected lines, about 8. This shows good agreement with the Andrews–McCann data, although the actual outage rates for our comparatively short lines were somewhat higher on a 100-mile-per-year basis.

One line, later converted to double-circuit construction, formerly had a triangular conductor arrangement with a protector tube on the top phase wire at each pole. Three-phase protection was provided only at corner poles where vertical configuration was generally used. Over a period of five years, this line had a perfect lightning performance record. Before the initial installation of protector tubes was made on this line, which runs through an open section of the city with negligible shielding from buildings or the surrounding terrain, lightning damage was severe and persistent. The improved performance with protector tubes is thus particularly significant in view of the severity of exposure shown in its early operation.

The protective scheme with a tube on the top phase conductor at alternate poles of double-circuit construction deserves some mention. The obvious arrangement from the standpoint of best protection for the number of tubes used would involve two protector tubes on every other pole, that is, at the top phase wire of each line. However, if the top conductors on the two lines are of different phases, and connected to the same station bus, as was the case here, such an arrangement runs the risk of phase-to-phase short-circuits. Hence it was necessary to accept the lower insulation level imposed by the presence of the ground lead to the protector tube for all poles rather than for the protected poles only, as would apply with two tubes on every other pole. At corners the ground lead is spaced away from the pole, but this was not believed to be necessary at tangent structures, particularly for the 150-foot pole spacing involved. Reasonably good performance has been shown for this construction over one lightning season.

The matter of protector-tube maintenance is of some concern in the consideration of protective methods. In order to find how seriously the tubes on our 33-kv system were eroded, a number of tubes were removed from random locations early this year for inspection and measurement of bore diameters. Some of these tubes had been in service since 1938. Of 56 protector tubes inspected, only three had bore diameters exceeding the manufacturers' recommended limit of 125 mils over the nominal diameter. The average increase for all tubes checked was 27 mils, indicating a reasonably large remaining useful life. All tubes removed were cleaned and repainted before reinstallation.

J. H. Hagenguth (General Electric Company, Pittsfield, Mass.): The paper presents valuable data applying to lightning performance to medium-voltage wood-pole lines. There are several questions and comments with regard to a few particular items.

What statistical data are available on the unshielded line with regard to the number of unguyed poles flashed over simultaneously with one or more guyed poles? Were there any cases where only the guyed poles flashed to ground?

What damage occurs to the wood poles from the lightning discharge? Is it necessary to remove the poles? What is the estimated current amplitude on unguyed structures as estimated from the damage produced?

In Table III of the paper the total number of direct strokes is given for the protected lines with an average density of 130 strokes per mile per year. Is it possible to give similar figures for the 25.4 miles of unshielded line on which the special inspections were made? Likewise, the tripout rate on this section would be of interest for comparison.

In Figure 5A of the paper the currents measured on both ends of a one-mile stretch were 11,000 and 12,000 amperes, respectively. Three wood poles next to one measuring station were also flashed over. It would seem that the total lightning stroke current must have been of considerable amplitude to produce 12,000 amperes current flow about one mile away. On steel-tower lines the current in ground wires after a few spans reduces to a few thousand amperes. It is therefore surprising to see such a high current amplitude at pole 369.

In Figure 6 of the paper, which shows the mechanism of the direct stroke, the implication is made that on contact with the conductor, a current wave is formed with amplitudes ranging between 1 and 160 kiloamperes. In the example a crest current of 25,000 amperes is assumed to produce 6,250 kv on the conductor unless flashover occurs. It occurs to me that the stroke currents before flashover should be of an entirely different order of magnitude, ranging from a few hundred to perhaps a maximum of 10,000 amperes and are due to the downward leader. The charges on the conductor should not increase these values materially. Only after contact is made with the ground by flashover should the higher-amplitude currents occur. I would expect that the voltage relations from conductor to ground, therefore, should be different from those shown in Figure 6. I would be interested in the authors' comments concerning this situation.

F. E. Andrews and G. D. McCann: The supplementary data supplied by Sherwood and Grosser provide a valuable addition to those given in the paper. Of particular interest is the splendid record of their line equipped with a protector tube on the top-phase wire.

In regard to Mr. Hagenguth's first question, statistical data are not available on the unshielded line concerning the number of unguyed poles flashed over simultaneously with one or more guyed poles. This could not be determined from the preliminary visual inspections, and insufficient data have so far been obtained from the detailed study on the short section of line to determine statistical curves. There have however been some cases where only one guyed pole appears to have been involved in the flashover.

The damage which occurs to the wood poles from the lightning discharge varies widely from small slivers between the ridge irons and crossarm to large lengthwise sections the entire length of the pole. In some cases the pole is so badly split that it will not hold the attachments, and replacement is required. No estimates have been made of current amplitude from the amount of splintering.

The 25.4 miles of unshielded line inspected is part of a 60-mile line with a large amount of type-VII (Table II) construction in addition to the type-I construction inspected. Since a large part of the unprotected section has not been equipped with surge-recording devices, no data are available on stroke density to unprotected lines. Since line tripouts could not be segregated to the different line sections, the tripout rate of this section is not available.

Mr. Hagenguth refers to the stroke mechanism pictured in Figure 6 of the paper, stating that the magnitude of the stroke current should be influenced by whether or not flashover occurs to ground. The authors agree that if a line with abnormally high insulation to ground were struck, as high crest-stroke current would probably not be reached as would be the case with flashover to ground on the front of the current wave. This however does not affect the general nature of the stroke mechanism as pictured by Figure 6.

New Transmission-Line Diagrams

Discussion and author's closure of paper 45-126 by A. C. Schwager and P. Y. Wang, published in AIEE TRANSACTIONS, 1945, September section, pages 610–15.

Felix Cecchetti (Rural Electrification Administration, St. Louis, Mo.): Though time does not permit a more thorough analysis of the subject, it is believed that the following general comments may be of some benefit.

The authors offer a simplification of the diagrams now in use for the calculation of power and impedances at either end of a transmission line, once the other values are given and the line constants are known. The simplification of a technical problem is always welcome and this one certainly meets the needs of the transmission-line designers. However, if a more detailed explanation of certain analytical expressions, integrated by typical cases, were included in the presentation, this new method may be more convincing in its practical applications, and more useful to a larger group of transmission engineers. It would be easier, for instance, to understand the limitations in the use of the impedance diagram for relaying problems if the authors were more explicit in their reference to the problems involved in actual design.

Further, it would be particularly interesting to know under what conditions voltage ratio and power angle are "not essential," as referred to in the second paragraph of the paper.

A. C. Schwager: Felix Cecchetti points out that a more detailed explanation of the derivations and additional examples would have helped to make the paper accessible to a larger number of engineers. Available space and time limited the paper essentially to proofs of the existence of certain new diagrams. It is hoped that more detailed studies by transmission specialists will follow.

With regard to the question as to when the knowledge of the power angle is not essential; this could be the case with charts whose range is limited initially to normal operating conditions.

Oil Stresses in Impregnated-Paper Insulation

Discussion and author's closure of paper 45-103 by J. B. Whitehead, published in AIEE TRANSACTIONS, 1945, August section, pages 555–7.

Wm. A. Del Mar (Phelps Dodge Copper Products Corporation, Yonkers, N. Y.): Doctor Whitehead presents an approximate theoretical analysis which purports to show that a cable of higher dielectric strength may be obtained by grading the paper density, using higher density paper for the inner layers. The method used in this analysis is admittedly approximate and might be of value if the author could show that it approximates experimental results with a fair degree of accuracy. Without such comparison, it is not apparent what value may be attached to the analysis.

Unfortunately a paper cable is not such a simple thing as Doctor Whitehead assumes for mathematical study. Paper has not only thickness and density but also a shrinkage coefficient, a modulus of elasticity, and other physical properties which do not enter into this approximate treatment. Paper tapes are not laid simply one on another, as in Doctor Whitehead's formulas, but are heated, dried, and impregnated. High- and low-density papers differ in these unconsidered characteristics.

I have found experimentally that if low-density paper is placed over high-density paper, the overlying layer will not hug the inner layers but the two types of paper will tend to separate. This is shown clearly by the styrene wafers of a paper by Wyatt, Smart, and Reynar, in Figure 10 of that paper for example. On the other hand, if the high-density paper is put outside and the low-density paper inside, the overlying layer will hug the inner layers tightly because it is possible to make high-density paper with greater elasticity and shrinkage. Cables of the latter type exhibit much less dendritic damage than those of the former type, under equal long applied voltages. They exhibit no difference in the Association of Edison Illuminating Companies' "life test."

The Whitehead formula, moreover, is a very artificial one, as it takes no account of the deflection of the electric field by irregularities in dielectric constant. I prefer to use a formula by E. B. Baker which appears in a letter to the editor[2] and which takes the deflection of lines of force into account. It gives entirely different results, as I pointed out in my discussion of the Whitehead and Kopper paper.[3] The graded cable, it will be seen, shows higher stress in the oil than the ungraded cable, and this agrees with my observations of what actually happened in the large number of cable samples tested and examined in the Habirshaw laboratories to check the grading theory.

REFERENCES

1. MECHANICAL UNIFORMITY OF PAPER-INSULATED CABLES, K. S. Wyatt, D. L. Smart, J. M. Reynar. AIEE TRANSACTIONS, volume 57, 1938, March section, pages 141–54.

2. Letter to the Editor on POTENTIAL AVAILABLE FOR GASEOUS DISCHARGE IN INSULATION VOIDS, Edward B. Baker. ELECTRICAL ENGINEERING, February 1934, page 363.

3. Discussion by Wm. A. Del Mar of THE DIELECTRIC STRENGTH AND LIFE OF IMPREGNATED-PAPER INSULATION—IV. AIEE TRANSACTIONS, volume 64, 1945, pages 477–9.

J. B. Whitehead: Mr. Del Mar apparently has failed to grasp several facts.

There has been much difference of opinion and much conflicting informal experimental evidence as to the influence of the use of high-density paper in cable insulation. My paper is a theoretical analysis showing how such contradictory evidence and opinion might be explained.

The paper states plainly that the analysis does not purport to cover the influence of gas pockets either original or subsequent. Solid-type cables are subject to all the relations given in the paper, but such cables usually are vulnerable at stresses much lower than those discussed in the paper.

The radial stress at the center of the longitudinal section of an oil channel or paper gap is independent of the width of the gap. The wider the gap the lower the space rate at which the stress falls off from the central constant value because of the fringing of stress lines at the outer edges of the gap.

The Baker formula to which Mr. Del Mar clings so tenaciously is not applicable to the conditions in an oil channel. (See closure to previous paper on impregnated paper.)[1]

The statements made by Mr. Del Mar in his third paragraph are interesting, and experimental data in support would be more so, but they are scarcely pertinent to the present discussion in that they deal with the presence of gas pockets. However, assuming that his cable behaves as claimed, it in no sense invalidates my treatment of the graded cable. It only means that he has elevated the gaseous ionization voltage and so narrowed the usual gap between values of gaseous ionization and critical oil-stress voltages.

An error in my computation of the quantity G, equation 13 of the paper, has been brought to my attention. The value of K_p, the dielectric constant of impregnated paper was taken as K_{ab}, and then as K_{bc}, the measured values for the respective papers when assembled as impregnated specimens.

Correcting this error, we find $G_a = K_{ab}/K_o$ for the denser paper and $G_b = K_{bc}/K_o$ for the lighter paper.

Making the appropriate corrections in Figures 1 and 3 of the paper, the horizontal dotted line for E_{oa}, all D paper, is raised in both figures to the value 2.04 on the scale of ordinates. In Figure 1 the approximate curve for E_{oa} is the diagonal, from lower left to upper right, of the rectangle formed by the two dotted lines and the vertical lines, $b/a = 1$ and 3. In Figure 3 the curve for E_{oa} is the diagonal from upper left to lower right of the same rectangle.

The conclusions of the paper should read as follows:

1. As given in the paper.

2. The use of both high- and low-density paper with the former inside as in a "graded" cable results in a voltage gradient, E_a at the surface of the conductor, which is lower for any proportion of the denser paper than that when either paper is used alone. However, the gradient in the oil channels or paper gaps, at the surface of the conductor, is always greater than in the case when the less dense paper is used alone.

If the denser paper is outside, E_a is always higher than for either paper used alone, and the gradient E_{oa} in the oil channels is always greater than in the case when the less dense paper is used alone.

Reference

1. Closure by J. B. Whitehead to The Dielectric Strength and Life of Impregnated-Paper Insulation. AIEE Transactions, volume 64, 1945, page 479.

Synchronous Starting of Generator and Motor

Discussion and authors' closure of paper 45-119 by C. Concordia, S. B. Crary, C. E. Kilbourne, and C. N. Weygandt, Jr., published in AIEE TRANSACTIONS, 1945, September section, pages 629–34.

I. C. Benson (nonmember; Electric Machinery Manufacturing Company, Minneapolis, Minn.): The paper entitled "Synchronous Starting of Generator and Motor" by Concordia, Crary, Kilbourne, and Weygandt presents many interesting curves showing the relationships among the various pertinent parameters. These data undoubtedly will prove useful in obtaining the optimum results for starting one synchronous machine by means of a second machine operating as a generator.

On several occasions of difficult starting, I have decelerated the generator (with field excitation on) down to about 15 per cent of normal speed. Then, with field excitation on the motor, and the motor connected to the generator, the motor has started rotating. As soon as the motor accelerated to substantially the operating speed of the generator, the generator speed was increased gradually to the desired speed. Undoubtedly, this method of starting requires less power from the generator prime mover, but I am wondering if the same curves can be utilized when starting at such a low speed wherein the effect of friction and breakaway is much reduced.

The test checks given in the paper prove the calculated results to a high degree and the appendix sets up the torque equations—all in a useful manner for future use.

C. Concordia, S. B. Crary, C. E. Kilbourne, and C. N. Weygandt: In regard to Mr. Benson's remarks about starting the motor with the generator at 15-per-cent speed, this method should be considerably different from the starting of both machines from rest simultaneously, even though the motor is excited continuously. With the generator at 15-per-cent speed, the motor starting torque should depend principally upon its amortisseur winding, rather than on the synchronizing-torque characteristics. There are acting on the motor:

1. An induction-motor torque caused by the generator excitation acting on the motor amortisseur.

2. A (negative) braking torque caused by the motor excitation acting on the line and armature resistances.

3. An induction-motor torque caused by the motor excitation acting on the generator amortisseur.

The relative magnitudes of these torque components will determine whether it is better to have the motor excited or unexcited during the first part of the starting period.

One would expect the total energy from the generator prime mover to be smaller when the full start is made in synchronism, since there is then considerably less dissipation of energy in the amortisseur windings. There is, of course, no exact and sharp boundary between regions to be classified as primarily synchronous or primarily induction-motor starting, but it would seem that the primarily synchronous region would exist for initial generator speeds no higher than two or three per cent.

Impulse-Failure-Detection Methods as Applied to Distribution Transformers

Discussion and authors' closure of paper 45-129 by H. C. Stewart and J. E. Holcomb, published in AIEE TRANSACTIONS, 1945, September section, pages 640–4.

J. H. Hagenguth (General Electric Company, Pittsfield, Mass.): It is gratifying to note that the authors have made a determined effort to evaluate present and proposed methods of failure detection during impulse test. It is of great interest that the experiences on distribution transformers are of similar character as those found in power transformers; namely, that very little reliance can be placed on bubbles, smoke, noise in tank, and normal-frequency excitation, as far as failure detection is concerned. In addition, even comparison of applied-voltage-wave shapes apparently is a very unsatisfactory means for detecting failures in these units. It is, therefore, of greatest value that the neutral-impedance method for measuring the current at the grounded end of the winding subjected to impulse has shown such excellent results even in detecting turn-to-turn short circuits. This simplifies the problem of failure detection greatly, since generally similar methods now are available which cover the entire field of distribution and power transformers, and the test procedure therefore can be standardized for the whole range of transformers.

The neutral-current method has been used during commercial impulse tests on approximately 50 power transformers. The experience gained indicates that the method is extremely sensitive. As a matter of fact, it is almost too sensitive, since it even has indicated corona streamers in the impulse circuit external to the transformer and small sparks on crossed ground wires. So far, any failures which occurred were detected by both the current and the voltage wave, although in no case was the decision that the transformer had failed based on the current wave alone. However, the greater sensitivity of the current method has substantially helped in the decision of determining whether or not failure had occurred, when used in combination with the comparison of the reduced and 100-per-cent voltage waves.

I heartily agree with the authors that a demonstration of the ability of electric apparatus to withstand impulse tests is of little value unless adequate failure detection methods are used; that is, methods which will detect all failures. Unless these failures are detected and repaired, the margin of demonstrated transformer insulation strength above protective levels, as outlined in ASA Transformer Standards, is not obtained.

Although in service a failure of the winding will be detected only when follow current occurs and therefore the transformer has to be taken off the line, it is hardly justifiable to pass a transformer on test even though the damage done during the test is of such order that it is difficult to detect, and follow current, bubbles, and smoke do not occur. Such a procedure permits an arbitrary decision by the manufacturer as to what constitutes a successful test, so that a damaged transformer may be said to have passed the test and then be shipped. This damage in test then may be the actual cause of ultimate failure of the transformer in the field after some years of service by a gradual increase in the damage over a period of years by corona resulting from continuous normal-frequency excitation and repeated surge applications at the level permitted by protective equipment. In such a case, the failure, although due to undetected damage on impulse test, would be charged to some other cause or perhaps called indeterminate.

H. C. Stewart and J. E. Holcomb: Since this paper was written, more experience has been gained in the use of method 8. Corona oscillations were not superimposed on the impulse current wave even though corona was observed on the circuit external to the transformer under test. One thing which helps to explain this difference from the power transformer tests in J. H. Hagenguth's discussion is the difference between the two shunts. The pure-resistance shunt is strictly linear and gives a true picture of the current wave without any distortion. This is not true of the parallel capacitance and resistance shunt. A typical shunt of

Table I. Summary of Impulse Tests

Transformer Rating		Failure Indicated by:				
Kva	Volts	Method 1	Method 8	60-Cycle Oscillogram	Smoke and Bubbles	Type of Failure
1½	7,200	No	Yes	Yes†	No	Layer failure
3	7,200	No	Yes	Yes†	No	One-half high-voltage coil
3	7,200	No	Yes	Yes†	No	Not located
3	7,200	No	Yes	No	Yes	Layer failure
3	7,200	No	Yes	No	No	One-half high-voltage coil
5	2,400	Yes (?)	Yes	No	No	Layer failure
100	2,400*	No	Yes	No	No	Not located
100	2,400*	No	Yes	No	No	Turn failure
200	2,400	Yes	Yes	No	Yes	High-voltage coil to low-voltage coil
200	2,400*	No	Yes	No	No	Turn failure

*Faults first detected by low-frequency tests but they immediately burned clear and could not be repeated.

†Magnetic oscillograms taken after at least ten more impulses were applied. (After failure was first detected with method 8.) Consequently, the resistance to follow current of the impulse failure path was considerably weakened.

0.01 microfarad and 8,000 ohms is used to illustrate this statement in the following example:

$$Z=\frac{R}{\sqrt{1+(2\pi fCR)^2}}=\frac{8{,}000}{\sqrt{1+(502.4\times10^{-6}f)^2}}$$

If a natural frequency for the transformer of 50 kilocycles is assumed:

$$Z=\frac{8{,}000}{\sqrt{1+(502.4\times10^{-6}\times50\times10^{3})^2}}$$
$$=319 \text{ ohms}$$

The higher-amplitude corona frequencies are of the order of magnitude of one megacycle or even higher. When $f=1\times10^6$ cycles per second:

$$Z=\frac{8{,}000}{\sqrt{1+(502.4\times10^{-6}\times10^{6})^2}}=16 \text{ ohms}$$

where

Z = total impedance of the shunt
R = resistance of the shunt
C = capacitance of the shunt
f = frequency of a particular current component

Consequently, the distortion caused by the corona current would be quite small because of the shunt's low impedance to high-frequency currents.

Since an impulse wave is really a combination of many superimposed frequencies, this reasoning can be used to explain the use of the parallel capacitance and resistance shunt. The front of a 1½x40-microsecond impulse wave corresponds roughly to a 200-kilocycle frequency and the tail of the wave to a much slower frequency. Consequently, by using a nonlinear shunt of this kind, reasonable amplitudes are observed on the oscillographic trace.

It is reasonable to assume that superimposed high-frequency oscillations will not appear on the crest of impulse waves applied to small distribution transformers, as they do with power transformers, because the oscillation frequencies of distribution transformers are lower in general. Consequently a change in this frequency due to a fault cannot be readily observed even though it is superimposed on the applied wave, for it is of approximately the same order of magnitude as the slower components of the applied wave. The amplitude of the higher-order harmonics appears to be quite small, probably because they are shunted to ground through the high ground capacitances. Calculations of this type show that shunts used for measuring the neutral current may be different for various types of winding construction, and discrimination must be used to select the most suitable method for each transformer under test.

The neutral-impedance method has been used to confirm turn failures, caused by mechanical defects, which occurred during the standard low-frequency tests but which immediately cleared by burning off the fault, so that when commercial low-frequency tests were repeated, there was no indication of any defect in the transformer. Also further impulse tests, using method 8, have been made on experimental designs of distribution transformers.

Table I of this discussion summarizes additional impulse tests where the faults were confined to coil interior. In four of the tests, the only method which indicated a fault was method 8. It appears that the effectiveness of method 1 and the 60-cycle oscillograms as failure-detection devices varies considerably with the different transformer designs, but method 8 seems to be equally effective for all the transformers tested.

Guides for Operation of Transformers, Regulators, and Reactors

Discussion of paper 45-130 by the AIEE transformer subcommittee, published in AIEE TRANSACTIONS, 1945, November section, pages 797–805.

F. A. Lane (American Gas and Electric Service Corporation, New York, N. Y.): While it may seem desirable to formulate some procedure for gauging the capabilites of transformers, regulators, reactors, and other apparatus over and above their nameplate ratings, it is felt that the material in the paper under discussion is of a highly theoretical nature. In large degree all of the reasoning seems to be based on assumptions supplemented here and there by theoretical considerations. After certain conclusions are reached which, in some instances at least, are wholly derived from a succession of assumptions, it is proposed to apply those to transformers having measuring devices which in themselves are anything but perfect. I have in mind the fact that the generally accepted temperature devices on transformers today do not measure any definite temperature. The thing that they do measure is again something that, based upon a chain of assumptions and theoretical considerations, is supposed to simulate a condition somewhere in the transformer, the location never being definitely understood.

It seems to me that in the face of this an attempt is being made to formulate firm rules which cannot by any stretch of the imagination be any more substantial than the bases on which they are established. My conclusion is that the discussion serves a very useful purpose from a theoretical standpoint, but it has no place in practical application until it can have been demonstrated that there is something more to it than mere theoretical derivation based on assumption.

It seems to me that, aside from these objections, the procedure which must be followed by anyone trying to apply these rules practically is far too complicated for any but a very limited group of people. It requires too much time. For the most part the cumbersome nature of the procedure will cause it to be ignored.

As I understand from a footnote of the paper, the material therein is to be presented to the American Standards Association for inclusion as a part of the proposed revision of transformer Standards. Unfortunately, although under the subtitle "Scope" it is stated that these guides cover general recommendations, the issue is clouded by reason of the fact that later on the reader is cautioned that before he follows these recommendations he had better take the whole matter up with the manufacturer and get his advice and recommendations. Thus at the very start serious doubt is brought into the mind of the reader that the authors themselves are inclined to take the recommendations very seriously.

At another point it is stated that the data in reference to the aging of insulation at different temperatures have been obtained in laboratory tests in which the decrease in mechanical strength has been measured. There may be a definite relationship between mechanical strength and electrical strength. That is not demonstrated, however, and to accept data on mechanical strength as a basis for arriving at the conclusions in this paper seems to me to be erroneous.

At another point in the paper it is pointed out that judgment and experience are important in determining what overloads transformers may be subjected to. This paper, however, attempts to set up definite rules which would tend to eliminate the factor of judgment and experience.

There are many other points in this paper which could be pointed out as being somewhat inconsistent with other parts of the paper.

A question raises itself with regard to the inclusion of these recommendations as part of the American Standards Association transformer Standards, as to what the manufacturers' attitude is going to be toward them. Is it going to be the policy of the transformer manufacturer to guarantee that his product will perform consistently with these rules? Is he going to attempt to design his transformer so that when operated in accordance with these rules the result will be as might be predicted from the rules? If this material is to become part of the Standards it would seem logical that this should be the case.

To sum up, it appears to me that the paper is valuable from the standpoint that it discusses various theoretical considerations with regard to the overloading of transformers and other electric equipment. It ought to take its place as a contribution to the general fund of knowledge on this point. I think, however, that it has not been demonstrated that this subject has been developed to a point where definite rules can be set forth which will work satisfactorily in everyday life. It appears to me that a great deal more work needs to be done. Something more definite is necessary before final conclusions of a workable nature can be arrived at. In short, I feel that this should not be a part of the transformer Standards.

Symmetrical Components as Applied to the Single-Phase Induction Motor

Discussion and author's closure of paper 45-102 by F. W. Suhr, published in AIEE TRANSACTIONS, 1945, September section, pages 651–6.

W. V. Lyon and **Charles Kingsley, Jr.** (Massachusetts Institute of Technology, Cambridge, Mass.): We are glad to see Mr. Suhr's paper on the method of two-phase symmetrical components applied to the analysis of single-phase induction motors.

The method of symmetrical components is a revolving-field theory and has many features in common with the revolving-field theory developed in Mr. Morrill's classic paper.[1] The principal difference is that Mr. Morrill considers the split-phase motor as two single-phase motors in the same frame with their windings in quadrature, each component motor producing a forward and a backward revolving field. Thus, four revolving fields have to be considered. When analyzed by the method of symmetrical components, the currents in the two stator phases are resolved into two symmetrical sets of components whose magnetomotive forces produce respectively a resultant forward and a resultant backward revolving field, and only these two fields need be considered. We believe, as does Mr. Suhr, that the method of symmetrical components gives a clearer concept of the physical phenomena than do either the revolving-field theory of Mr. Morrill's paper or the cross-field theory.

Although, as Mr. Suhr says, the basic principles on which the analysis of his paper is founded were published a number of years ago,[2,3] the paper should be a useful contribution to the literature in the field of single-phase induction-motor theory in that it gives further publicity to the symmetrical-component concept, summarizes the earlier general analyses, and derives a number of useful relations for special cases.

REFERENCES

1. THE REVOLVING FIELD THEORY OF THE CAPACITOR MOTOR, W. J. Morrill. AIEE TRANSACTIONS, volume 48, April 1929, pages 614–29.

2. ANALYSIS OF UNSYMMETRICAL MACHINES, W. V. Lyon, Charles Kingsley, Jr. ELECTRICAL ENGINEERING, volume 55, May 1936, pages 471–6.

3. APPLICATIONS OF THE METHOD OF SYMMETRICAL COMPONENTS (book), W. V. Lyon. McGraw-Hill Book Company, Inc., New York, N. Y., 1937, pages 342–51.

Edward Bretch (The Century Electric Company, St. Louis, Mo.): This timely paper recognizes the need for improvement in single-phase squirrel-cage-motor theory. To one who has spent many years with single-phase motors and has attempted to reconcile the conventional rotary-flux and cross-flux theories with each other, as well as with tests, the need for this action is evident. As these theories were proposed 50 years ago when experience with induction motors, particularly single phase, was rather limited, it is time they were clarified and co-ordinated into a single logical theory in the light of 50 years of progress. Neither of these theories recognizes the vital distinction between a magnetomotive force and a flux thus resulting in confusion and misunderstanding regarding the physical actions within the single-phase motor.

A magnetic flux represents energy while a magnetomotive force represents force only. Fluxes therefore follow the laws of energy while magnetomotive forces follow the laws of forces. Magnetomotive forces being forces combine vectorially into a resultant that depends on the space angle at which the components act. Fluxes, on the other hand, being energies combine arithmetically irrespective of the space angle at which the components merge.

Both the rotary-flux and cross-flux theories are based on the erroneous assumption that instantaneous fluxes combine vectorially in the same manner that magnetomotive forces do which results in the aforementioned confusion and misunderstanding.

For example, the assumption made in the rotary-flux theory that two similar constant rotary fluxes, rotating simultaneously and oppositely in the same space, combine vectorially into a single-phase alternating resultant flux, is disproved by placing two similar polyphase windings in the same core slots and then attempting to excite these windings simultaneously for opposite rotation. Logical considerations likewise discredit this assumption. The energy stored in a constant rotary flux is constant as the flux does not vary with its position, speed, or direction of rotation. As the stored energy in a constant rotary flux is constant, the combined energy of any two constant rotary fluxes also is constant. As the combined energy of any two constant rotary fluxes is constant while that of a single-phase alternating flux varies between zero and a maximum twice in each cycle, a single-phase alternating flux cannot possibly be the resultant of two constant rotary fluxes.

It appears that Mr. Suhr applies this same oppositely rotating-vector line of reasoning that is applied to the magnetic circuit in the rotary-flux theory, only in his case it is applied to the electric circuit. As phase M is a single-phase winding, it is capable of responding only to a single-phase electromotive force. Irrespective of what components may be included in V_M, V_M is their combined resultant, is single phase, and is the only electromotive force impressed on phase M. Consequently I_M is the only current in phase M. Similar conditions prevail in phase S.

It appears that by injecting these various arbitrary and fictitious factors, designated by the plus and minus subscripts, the mathematical expressions become so complicated and involved (see equations 45–50 of the paper) that they develop no clear conception of the physical actions they are presumed to disclose and clarify. However, the move to modernize single-phase squirrel-cage-motor theory is overdue. The distinction between a magnetomotive force, which is a force following the laws of forces, and a flux, which is energy following the laws of energy, should be recognized definitely. Also the corollary that instantaneous fluxes do not combine vectorially, as magnetomotive forces do, likewise should be recognized definitely. When this is done the physical actions within the single-phase squirrel-cage motor become as clear and as easily understood as those of the transformer or d-c motor.

Mr. Suhr's paper is a move in the right direction. Fifty years of development and experience should serve to clarify the situation so that the two controversial single-phase-motor theories can be co-ordinated into a comparatively simple and logical theory that clearly depicts the physical actions that take place in the single-phase squirrel-cage motor.

F. W. Suhr: The author wishes to thank Professors Lyon and Kingsley for their interest in this paper and for their comments which further amplify the conclusions given.

Admittedly some of the equations derived are quite formidable as Mr. Bretch points out. Following the line of reasoning he indicates, using fluxes and magnetomotive forces, it does not appear that the mathematical treatment could be simplified as fluxes are functions of currents which, in turn, are functions of the electrical constants of resistances, reactances, and the applied voltage. A paper covering the proposed theory should be of general interest.

Response Time and Lag of a Thermometer Element Mounted in a Protecting Case

Discussion and author's closure of paper 45-133 by W. N. Goodwin, Jr., published in AIEE TRANSACTIONS, 1945, September section, pages 665–70.

R. W. Lohman (War Production Board, Portland, Oreg.): In the paper by W. N. Goodwin which was presented to the Institute in June 1945, the author discusses the time lag of the temperature-sensitive resistance element which is introduced by the protective case in which such elements are generally placed. The following notes refer to methods employed by the writer to reduce such time lag, especially on thermometers required to withstand high hydrostatic pressure.

A Design for Minimum Time Lag

The type of thermometer described in the following was designed for use in oil wells filled with drilling mud, wherein the bottom hydrostatic pressure, in a well 15,000 feet deep, may be of the order of 10,000 pounds per square inch, and wherein such thermometers are used for logging temperature-depth curves during passage from the bottom to the top of the well at speeds up to 150 feet per minute.

Evidently, to withstand such collapsing pressure a closed protective case would have to be of such thickness that it would seriously decrease the rate of heat flow therethrough.

Therefore, in general, the subject design employs a thin inner tube in which is cut a spiral groove, and in which groove the temperature-sensitive wire is wound, double, so that both ends thereof may be brought out at one end of the groove. The grooves are then coated with oil, and a tightly fitting and also thin outer tube is forced over the inner tube. The container for the resistance element is, therefore, not in effect a closed vessel, but is open to fluid pressure at both ends, and consequently is not subjected to hydrostatic collapsing pressure. The ends of the resistance element are passed through a bushing, *A*, Figure 1, in the inner tube, and on out through a small bore tube, *B*, which is soldered into a boss on the inner circumference of the inner tube. Figure 2 shows a complete thermometer mounted on its Bakelite thermal insulating support, *A*, and also shown is the exterior steel tubing shield, *B*, for the mechanical protection of the instrument during its travel in the well.

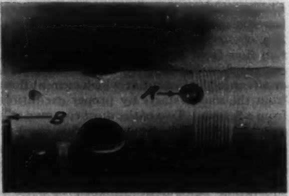

Figure 1. The one-inch-by-eight-inch silver-tube thermometer, showing the grooves containing the wire, the leadout bushing at *A*, and the leadout tube at *B*

It will be seen that in a thermometer of this design heat flow will take place to the outer semicircumference of each turn of wire from the outer tube, and simultaneously, to the inner semicircumference of each turn of wire from the inner tube, since the ambient fluid passes through the bore of the inner tube and at the same time longitudinally along the outer surface of the outer tube, thus transferring about twice the quantity of heat to the resistance wire per unit of time that would be possible with only an outer closed tube (if in the latter case no thermal insulation within the single tube is assumed).

Table I

Temperature, Degrees Centigrade	Viscosity
20	1.005
30	0.800
95	0.299

The containing tubes may be of silver or copper, preferably the former, for the reasons set forth in the following paragraphs.

Thermal Diffusivity

The term, thermal diffusivity, is equivalent to the expression, temperature conductivity, which latter is comparable to electrical conductivity, that is to say, the capacity of a material to conduct temperature (or electricity).

Now, with reference to the afore-mentioned thermometers, the rate at which temperature is conducted across the container, which is supplied with heat on one side (say from the ambient fluid), and (say) cooled on the other side by the resistance element, is chiefly determined by the temperature conductivity or thermal diffusivity, of the material of the container.

Therefore, the material of the container should be selected *not* on the basis of its thermal conductivity, but on the value of its thermal *diffusivity*.

While the thermal conductivity of silver and copper are very nearly the same, as shown in the following data, the thermal diffusivity of silver is about 50 per cent higher than that of copper.

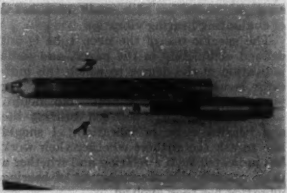

Figure 2. The two silver tubes soldered together, assembled on a Bakelite thermal insulator at *A*, and at *B* the $1^3/_4$-inch-outside-diameter-by-16-inch-long exterior steel shield

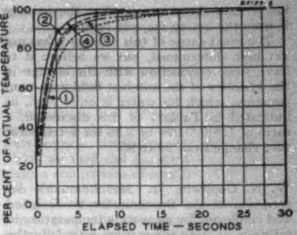

Figure 3. Curves showing the time lag of copper- and silver-tube resistance thermometers during heating and cooling cycles

Curve 1—Copper-tube container, from 98 to 26 degrees centigrade

Curve 2—Copper-tube container, from 26 to 98 degrees centigrade

Curve 3—Silver-tube container, from 98 to 26 degrees centigrade

Curve 4—Silver-tube container, from 26 to 98 degrees centigrade

The thermal diffusivity of a material may be expressed as follows:

Thermal diffusivity $= k/c\rho$

where

	At 18–25-C	
	For Silver	For Copper
k = thermal conductivity in gram-calories per second per degree difference per one centimeter thickness, per square centimeter	1.006	0.918
c = specific heat	0.059	0.0917
ρ = density in grams per cubic centimeter	10.6	8.89

In the Smithsonian physical tables the thermal diffusivity of silver is given as 1.737, and that of copper as 1.133, or a ratio of 1.533, or about 50 per cent greater for silver than for copper, which would indicate the selection of the former material for the container tubes.

It will be seen from Figure 3 which shows measured time-lag curves, that this theory is approximately confirmed, for, whereas say ten seconds are required for the copper-tube thermometers to reach a given temperature, the silver tubes reach the same temperature in about one third to three fourths of the time, or say 5 and 7.5 seconds, respectively.

Differences in Response Time

The author states, just preceding equation 2 in his paper, that the response of a given thermometer is the same whether it is being subjected to a heating or to a cooling cycle. From an examination of the curves in Figure 3, it will be seen that the response for the thermometer described, when either a silver- or copper-tube container thermometer is passed from a cold to a hot bath, is faster than the response when the passage is from the hot to the cold bath.

The exact cause of this difference has not yet been determined, but we believe it to have some connection with the change in the viscosity of the ambient fluid with temperature, which for water is quite high, as indicated in Table I of this discussion, a ratio of 1.005/0.299 or 3.36 for a temperature change from 20 to 95.

W. N. Goodwin, Jr. Mr. Lohman's description of the thermometer he designed and employed for measuring temperature in oil wells, is very interesting, especially the ingenious construction he uses to decrease response time and prevent damage by the large hydrostatic forces encountered in deep wells.

Mr. Lohman calls attention to two points of considerable practical value which, although considered in the writer's analysis, were not referred to specifically, as was the case with other interesting results, because of lack of space.

Attention is called to the reduction in response time by using metals having a small value of the product of density and specific heat. This is shown in the writer's paper in the time constants t_1, t_2, t_m, and t_o all of which are directly proportional to the product referred to, ms, since for a particular design m is directly proportional to density. To take Mr. Lohman's example, comparing silver with copper, the product of the density and specific heat for copper is $8.89 \times 0.0917 = 0.815$, and for silver it is $10.6 \times 0.059 = 0.626$. The ratio of this product for copper to that for silver is 1.3; that is, all the time constants for copper will be 1.3 times as large as those for silver.

The effect of the product of density and specific heat upon response time is shown by equation 1 of the writer's paper. Since the time constants t_1, t_2, t_m, and t_o are all affected alike by the product ms, if all the parts are constructed of the same material, then obviously P is not affected and is independent of the kind of material. The only quantity which changes the equation, and consequently the response time is t_o in the dimensionless quantity t/t_o.

The response time t, therefore, is directly proportional to the time constant t_o and consequently to the product ms. It follows from this that the response time for copper would be 1.3 times that which it would be if silver were used.

The thermal conductivity of the metal parts was not considered in the writer's paper, since the thermal resistance through the thin metal case is small in comparison to the thermal contact resistance in series with it, between the metal and the cooling medium. For example; for a water contact with copper, the thickness of the copper case, to have the same thermal resistance as the contact resistance, would be 35 centimeters, computed from the conductivity of copper and the convection coefficient $h_1 = 0.109$ for water, given in Table I of the paper. It is also for this reason that thermal diffusivity which includes conductivity cannot be used as a measure of response time, as suggested by Mr. Lohman.

Mr. Lohman refers to the fact, experimentally determined, that the response time of a thermometer when it is heated by placing it in hot water, is less than when it is cooled in cold water. He correctly assumes that at least a part of this may be the result of variation in the coefficient of viscosity, although this does not account for the large difference shown in Mr. Lohman's curves. It is suspected that experimental errors may account for part of the difference. The free convection coefficient h_1 is approximately inversely proportional to the fourth root of the viscosity. The values given in Table I of the paper are for room temperature, 25 degrees centigrade. Since, as Mr. Lohman points out, the viscosity of water at 100 degrees is 0.284 and at 25 degrees centigrade is 0.887, the ratio is 3.12. The fourth root of $3.12 = 1.33$ which is approximately the inverse ratio of the convection coefficient h_1 and the direct ratio of the time constant, t_1, when cooling from 100 to 25 degrees centigrade to the convection coefficient and time constant when heating from 25 to 100 degrees centigrade. The differences in response time for these two conditions can be found by the equations, or by interpolation of the curves in Figure 3 of the paper. The value of P for 100 degrees centigrade is computed to be 0.55, against 0.491 at 25 degrees centigrade, from which it is found that the time required for the thermometer to reach one-half its final value when heating from 25 to 100 degrees centigrade is approximately 90 per cent of that required when cooling from 100 to 25 degrees centigrade. When the value of the convection coefficient, h_1, is constant, then the heating and cooling curves are alike, but reversed, as stated in the paper.

A Tachometer–Accelerometer–Vibrometer for Instrument-Gyroscope Testing

Discussion and authors' closure of paper 45-105 by R. M. Laurenson and T. H. Long, published in AIEE TRANSACTIONS, 1945, August section, pages 593–6.

M. A. Princi (General Electric Company, Lynn, Mass.): The equipment described by the authors for measuring the coast time, and therefore the adjustment of gyroscope rotor bearings, represents an advancement over manual methods of accomplishing this operation. An equivalent contribution seems to be the use of a qualitative means of evaluating bearing vibration.

The specific use of the neon tube is not defined completely in the paper, and some indication of the degree to which this indicator is used as a measure of the bearing vibration would be helpful. No doubt, some relation exists between bearing life and bearing noise or vibration. I should like to ask the authors whether their work has indicated such a relation and whether a more quantitative measurement of bearing vibration has been evolved.

T. H. Long and **R. M. Laurenson:** The use of the neon lamp as a quantitative means of evaluating bearing vibration was not described in detail as our experience was confined to our own factory production line where it turned out to be unnecessary. The neon-lamp circuit was used in the original design because it looked like a good idea (and undoubtedly was at that time).

Then it was found that, with the electronic wattmeter type of balancing machines used, trouble was caused in balancing the two-pound rotor if the ball-bearing track on either of the cone bearings was as much as 0.0001 inch out of round. By holding the variation from a true circle to less than 0.000025 inch (as measured by a method that did not necessarily get all of it) we were able to balance these rotors quite consistently to within 0.33×10^{-6} inch-ounce in two or three drills per side and our vibration troubles disappeared.

Of course there were still rejections for ball dents but these were recognized so readily by the sound quality that there was no occasion for any other test.

Our gyroscope manufacturing experience was limited to the horizon type which has a pronounced case resonance that may exert a masking effect on significant vibrations. At least we were not able to get co-ordination between bearing noise and life.

Selsyn Design and Application

Discussion of paper 45-123 by T. C. Johnson, published in AIEE TRANSACTIONS, 1945, October section, pages 703–08.

F. O. Stebbins (General Electric Company, Schenectady, N. Y.): The author of this paper has described practically all of the important uses for Selsyns in which the Selsyn operates to indicate or control position. For approximately ten years Selsyns have also been used to advance or retard the phase position of voltages to control voltage and power[1] (F. O. Stebbins and C. W. Frick, "Output Waveshapes of Controlled Rectifiers," AIEE TRANSACTIONS, 1934, September section), and may be applied with static inverters, static frequency changers, nonsynchronous ties between power systems, and the like. Their use in controlling voltage and power in substations will be briefly described.

Current flows from the anode to the cathode of a thyratron (grid-controlled mercury-arc rectifier) only when the anode is positive with respect to the cathode and the grids have the proper excitation at the start of the flow of current. The grids cannot stop current flow from the rectifier anode once this current flow has started. They can retard or advance the instant at which current flow from the anode starts by proper excitation from a Selsyn. Two of the most common applications for Selsyns used in this manner have been on railway systems and in chemical plants.

A railway company wanted new rectifier substation equipment designed in such a manner that the breakers did not open in case of a short circuit on the system. Instead, by means of Selsyn control, the output voltage of the rectifier was reduced at a predetermined overload to an amount such that the substation output was limited when a short circuit occurred. As the result, with the occurrence of a short circuit, enough power was left available in the railway system to enable trains and cars to move out of dangerous locations (railroad crossings, street intersections, and the like). Without Selsyn control the trains and cars would be left in these locations until the short circuit was removed and power was returned. If the breakers were locked in and the station closed on the short circuit, feeders, trolley wire, and the like might be damaged while the trains were moving with the short circuit still in effect.

In a chemical plant Selsyns are used in conjunction with current regulators to maintain balanced loads on the different mercury-arc rectifiers feeding power to banks of electrolytic cells. Additional Selsyns also are employed in large chemical plants to control a battery of mercury-arc rectifiers, each of which has its own Selsyn control.

The Selsyns used in these applications generally are adapted from three-phase wound-rotor induction motors of one-horse power rating or more. For multiphase mercury-arc rectifiers, it is required that the Selsyns have either special stators wound for the number of rectifier phases, work with special transformers or enough Selsyns be used to control all the rectifier phases.

Industrial Control: Heating of Shunt-Motor Starting Resistors

Discussion and author's closure of paper 45-125 by G. F. Leland and L. T. Rader, published in AIEE TRANSACTIONS, 1945, October section, pages 695–9.

G. W. Heumann (General Electric Company, Schenectady, N. Y.): Design of resistors is limited by the premise that the resistor used on a given control application must not exceed a temperature rise as stipulated by standards recognized by the industry. The temperature rise depends on a number of factors, such as size and physical properties of the resistor, conditions of ventilation, magnitude of current carried, and time during which current is carried.

Starting resistors carry current intermittently. During each start the resistor heats and during intervening standstill periods it cools. Heating is a function of the energy dissipated during each start, in other words, the watt-seconds lost in the resistor during each start. The ultimate temperature which a resistor will attain thus is governed by the watt-seconds per start and the relationship between on-time and off-time. The authors have developed an analytical method by which the watt-seconds per start can be calculated for varying load conditions of a given motor. It is interesting to note that the new method obtains results which are quite different from values of dissipated energy calculated by the conventional method heretofore employed. It is the purpose of this discussion to point out this difference.

The conventional method of calculation is based on the assumption that during the starting period a constant rms value of current flows in the resistor. In accordance with the National Electrical Manufacturers Association Industrial Control Standard IC4–10, this current has been assumed to be 125 per cent of full-load current. In Figure 1 of this discussion the solid lines indicate a constant current of 1.25 I_{FL} flowing during switching-time interval t_1. The broken line represents the actual current, varying between an initial current peak I_0 (assumed to be $2I_{FL}$ for this comparison) and final current I_1 at the end of period t_1, which can be calculated from the formulas and curves given in the paper.

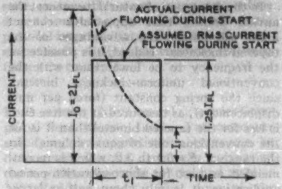

Figure 1. Comparison of methods of calculating watt-seconds dissipated in resistor

t_1 = switching time
I_{FL} = motor full-load current
I_0 = initial starting current
I_1 = current at end of switching time

Let us now consider the five-horsepower motors, which are used in the examples cited in the paper. Although the two motors have different speed and drive different mechanical loads, the conventional method makes no allowance for this but is based solely on current and resistance. Normal or 100 per cent resistance, which would produce starting torque equal to full-load torque, would be

$$R=\frac{V}{I_{FL}}=\frac{230}{20}=11.5\text{ ohms}$$

As the examples are based on the assumption that starting current is to be twice full-load current, and as internal motor resistance is assumed to be ten per cent, the external motor starting resistance is

$$R_1=0.4\times R=4.6\text{ ohms}$$

Table I

t_1 Seconds	E_1 Watt-seconds	E_2 Watt-seconds	E_1/E_2
2	5,750	5,920	0.97
4	11,500	6,950	1.65
6	17,250	7,160	2.40
8	23,000	7,220	3.19

Table II

t_1 Seconds	E_1 Watt-seconds	E_2 Watt-seconds	E_1/E_2
0.172	495	567	0.87
0.344	989	686	1.44
0.516	1,484	744	2.00

If we call E_1 the energy dissipated per start, assuming $1.25I_{FL}$ flowing during the starting period, we have

$$E_1=(1.25I_{FL})^2\times R\times t_1=2{,}875\times t_1\text{ watt-seconds}$$

In example 1 of the paper the time constant is calculated as two seconds and the watt-seconds dissipated in the resistor, which we shall call E_2, are given. Table I gives a comparison of energy calculated by the two methods.

Considering the case of example 2, the paper gives the time constant as 0.172 seconds. The energy E_2 dissipated in the resistor is as follows:

$$\begin{aligned}E_2&=4.62\times WR^2\times N^2\times 10^{-4}\times M\\&=4.62\times 10\times 556^2\times 10^{-4}\times M\\&=1430\ M\text{ watt-seconds}\end{aligned}$$

Multiplying factor M can be taken from Figure 9 of the paper, using $a=0.25$. For various amounts of switching time t_1, the dissipated energy calculated by the conventional method and by the authors' method is shown in Table II.

These comparisons indicate that the dissipated energy, calculated under the assumption of an rms current of 125 per cent full-load current, differs from the energy calculated by the authors' method, taking into consideration load conditions. This is especially true with switching times of twice time constant or higher. Load conditions are an important factor. Thus it becomes evident that the number of starts to which a given resistor can be subjected within a given period of time varies considerably with the character of the load.

Additional work will have to be done to relate the dissipated energy to temperature rise of a given resistor. It would be a great help to the control designer to establish a relationship between load conditions and permissible starts per unit of time which would produce a certain temperature rise.

G. F. Leland: G. W. Heumann states in his discussion that the control designer would welcome a method of establishing resistor designs in terms of load conditions and starts per unit of time for a given temperature rise.

The method of analysis presented in our paper yields results that make possible a method of rating resistors in starts per minute. This can be seen best from equation 22a of the paper. This equation is

$$E=J\Omega^2\frac{R_1}{R}\left[2-2.27b+0.761b^2\right]$$

which can be rewritten in terms of y as shown in Figure 6 of the paper.

Therefore

$$E=J\Omega^2y$$

which, in the practical system, is

$$E=\frac{4.62WR^2N^2}{10^4}y\text{ watt-seconds}$$

As E is the energy for each start, and if there are a starts per minute, the energy per minute becomes

$$Ea=\frac{4.62WR^2N^2}{10^4}ay\text{ watt-seconds}$$

Continuous watts of W_2 for 60 seconds will give an equivalent amount of energy input into the resistor. Therefore, if these two quantities are equated, we obtain

$$60W_2 = \frac{4.62WR^2N^2}{10^4}ay \text{ watt-seconds}$$

or

$$a = \frac{60W_2 \times 10^4}{4.62WR^2N^2y} = \text{starts per minute}$$

This shows that a given physical resistor, whose size is proportional to W_2, will have a rating which will vary inversely as the product of WR^2N^2 and inversely as the load function y.

It is evident therefore that duty-cycle curves can be obtained, including all of the variables of system.

Tapered-Thickness Bimetal

Discussion and author's closure of paper 45-120 by William B. Elmer, published in AIEE TRANSACTIONS, 1945, September section, pages 661–5.

E. K. Clark (nonmember; Westinghouse Electric Corporation, Mansfield, Ohio): We have reviewed this paper and wish to compliment the author on a job very well done.

We have very little to comment on this paper, inasmuch as it is a somewhat new step in the production and use of bimetal, and many of the production and fabrication problems are not yet clear. However, we should like to offer the following:

Assuming that tapered bimetal would be manufactured with the taper running transversely to the strip, we would suspect that we would have great difficulty in controlling cross curvature. This is one physical factor in bimetals over which we have found we must exercise rigid control in order to maintain trouble-free production and uniform operations.

We certainly agree with the theory established by the paper that the tapered form of bimetal will provide the most economical ratio of material to work and that there may be many other advantages, such as thermal mass being concentrated at the base or supported end, favorable vibration rates for slow-acting thermostats, and others.

John E. Ryan (nonmember; General Electric Company, Schenectady, N. Y.): The author's thorough analysis, with its results conveniently expressed in deflection, economy, and frequency coefficients, points out facts which were known, at least qualitatively, to early pioneers in the bimetal field. Difficulties encountered in economically producing straight strips with optimum grain direction caused the idea to be laid aside. We would be much interested in knowing more about the new process which, the author states, can produce tapered thickness at negligible increase in cost, since most of the advantages disappear if material saving cannot outweigh increased fabrication expense.

In the discussion of natural frequency, the author admits that appreciable contact mass will defeat the advantages of the tapered thickness. Indeed, it is possible for the frequency to be lower than with the conventional uniform-thickness bimetal, since the spring constant (force per unit displacement), as measured at the free end, is less for the tapered bimetal than it is for the conventional one of equal volume. In the range of $R=0.1$ to 0.2, which is recommended as best for short-vibration-period application, it is only about half as large. For the extreme case where the kinetic energy of the contact is much larger than that of the bimetal proper, the natural frequency of the system is only about 70 per cent as great as for the conventional bimetal of equal volume. This, of course, is an exaggeration of the practical case, but it serves to illustrate the extent to which attached masses can affect the author's results.

A treatment of stresses would have made this already comprehensive paper complete. Fortunately, the thermal stresses in an unloaded bimetal are independent of thickness; hence, tapering causes no difficulty there. Stresses due to external loading are less for the tapered bimetal than for the uniform-thickness one of equal volume, since the former approaches the condition of a uniform-strength beam with a greater section modulus at the clamped end; this is a definite advantage.

William B. Elmer: Mr. Ryan evidently has drawn the mistaken inference that this paper pretends to give out as new information all of the qualitative results therein presented. As far as the author has been able to determine, however, most of the quantitative relationships given have never been developed before, and this somewhat laborious task was undertaken in order to determine what exact economic justification might inhere in the tapered-thickness construction. In passing, it may be of interest to relate the curious fact that a United States patent was granted as late as 1939 on the tapered-bimetal construction in which the chief claims read on a specific range of ratios that completely missed the most efficient value of all. In view of such recent misconceptions the work represented by this paper appears well justified.

The method of manufacturing the material comprises no significant innovations: the most important fact is that the cost has been definitely determined, as stated in the paper, as being a negligible factor compared to the performance of the material.

Mr. Ryan's statements in regard to the frequency of strips with appreciable contact masses contain the misconception that the spring constant (stiffness) *decreases* during a constant-volume (and constant-deflection) transition of a bimetal strip from flat to tapered. On the contrary it can be shown readily that the stiffness during such a transition is represented as a function of taper ratio by the expression:

$$\frac{F}{\delta} = K\frac{2C_T^2C_{Ft}}{(1+R_t)}$$

in which the stiffness *increases* and does not fall below the original value for flat strip until the taper ratio has fallen to less than $R_t=3$ or 4 per cent. It is an interesting coincidence that the form economy as shown in Figure 3 of the paper also can be used directly as a measure of the stiffness of a bimetal strip during a constant-volume constant-deflection transition of taper ratio R_t from unity to zero. This appears obvious when one reflects that form economy is measured by stiffness alone when volume and deflection are held constant. It is therefore clear that Mr. Ryan is wrong in stating that the frequency of a tapered-thickness strip of $R=0.1$ to 0.2 is less than that of a uniformly thick strip of equal volume. It is also obvious that, if the spring constant of the strip is greater, the frequency will be greater, for any given contact weight, and can never reach a value of 70 per cent as claimed by Mr. Ryan, even with zero contact mass, until the ratio R_t reaches the unusably small value of about two per cent.

Resistance and Capacitance Relations Between Short Cylindrical Conductors

Discussion of paper 45-138 by F. L. ReQua, published in AIEE TRANSACTIONS, 1945, October section, pages 724–30.

L. M. Perrin (Public Utilities Commission, San Francisco, Calif.): This paper makes a useful contribution in a field inadequately covered in the past.

To illustrate, large water rheostats for generator test loads are still improvised by trial and error methods, just as uncivilized peoples build bridges. Such methods are wasteful in direct costs, and in the case of generator tests, the delay occasioned adds to the overhead item of interest during construction at its maximum rate. The formulas of this paper enable the engineer to predetermine the dimensional requirements of such rheostats, thereby realizing important savings, both direct and indirect.

Liquid rheostats are merely one field of application of the formulas presented in this paper. It is to be hoped that papers or discussions including experimental data on capacitance relations will be made available. Also, the use of liquid rheostats, in which resistance is utilized to simulate other electrical quantities under investigation, should be a subject for profitable discussion.

Ferroinductance as a Variable Electric-Circuit Element

Discussion and author's closure of paper 45-121 by J. D. Ryder, published in AIEE TRANSACTIONS, 1945, October section, pages 671–8.

C. Concordia (General Electric Company, Schenectady, N. Y.): I should like first to point out that, contrary to the statement of the author, equation 1 of this paper is not in any sense a basic defining relation for inductance. In case of purely inductive circuits containing iron the really basic relations are

1. Voltage e is proportional to time rate of change of flux linkage ψ

$$e = K d\psi/dt \tag{1}$$

2. Flux linkage ψ is some function of current i

$$\psi = \psi(i) \tag{2}$$

Any definition of inductance that one chooses now may be made, as mentioned in the author's reference 1. All are on an equal footing, and the only reason for preferring one over the other must be utility for the specific purpose at hand. Actually, there is considerable reason for preferring none and instead using directly the basic relations of voltage, flux linkage, and current. This is especially true since in many cases more than one electric circuit is involved, and under these circumstances the treatment of the problem in terms of the inductance $L = e/(di/dt)$ also becomes rather involved. In this paper there is, for example, a discussion of effective resistance, but it should be pointed out that the presence of an effective resistance different from the coil circuit resistance usually means that there are in reality coupled circuits (one consisting of current paths in the iron), and attempts to disregard this may lead to misleading results, since usually current and flux have different transient behaviors. On the other hand, it is usually possible to set up the problem in relatively simple form if the flux linkage relations are used directly.

If one must use an inductance it is belived that the definition

$$L = \psi/i \tag{3}$$

is the best. The great virtue of this definition is that it is suitable to the important general case wherein the flux linkage is also a function of the position of some moving element in the magnetic circuit. If, for example, the inductance is not a function of the coil currents at all but is only a function of position as may be the case in a rotating electric machine, a contactor, or the armature or torque motor of a mechanical voltage regulator, and if one then calculates the inductance from the physical dimensions in the usual way for each position, one naturally finds an inductance which fits the equation

$$e = \frac{-d}{dt}(Li) \tag{4}$$

In view of the basic relation 1 this inductance is defined by equation 3 of this discussion, not by equation 1 of the paper. It would seem a great pity to regard equation 1 of the paper as basic when it fails to fit so common a case.

The foregoing is not intended to disparage the author's attempt to arrive at a workable analytical expression for inductance, as we believe that such an attempt and the results obtained are very much worth while. However, we could not resist the temptation to comment on the philosophy upon which this analysis apparently is based. There unfortunately have been several papers in the last few years that have contained similar statements which seem to us to confuse derived mathematical relations with basic physical laws, and we believe that the engineer should distinguish carefully between these two concepts.

F. D. Olney, Jr. (General Electric Company, Fort Wayne, Ind.): The constants specifying the magnetization curve can be determined directly from the saturation curve without resorting to trial and error as Mr. Ryder suggests. The slope of the tangent to the saturation curve well above the knee is equal to the constant C, while the constant B_n is equal to 1/1.57 multiplied by the flux density at the intercept of this tangent with the ordinate through the origin. (The factor 1.57 is the value of the gudermannian for large values of the independent variable.) The constant a then is evaluated from the line drawn with maximum slope through the origin and tangent to the saturation curve by the relation

$$a = \frac{(\text{maximum slope}) - C}{B_n}$$

Mention is made of the Rader and Litscher equation which is used to match the magnetization curve, and the statement is made that this equation "is impossible for use for circuit analysis." It would have been more precise to state that the Rader and Litscher equation is useful in the analysis of magnetic apparatus, whereas the present paper is concerned with the analysis of electric circuits containing magnetic apparatus such as motors. There is a real difference here, since the Rader and Litscher equation makes use of flux density as the independent variable so that the ampere-turns required may be found directly by integration, whereas the use of the gudermannian by Mr. Ryder makes such an integration impractical. Thus each of these mathematical tools is useful only in a certain area, and as yet a generally applicable representation of the saturation curve has not been presented.

In connection with the author's equation 13 the statement is made that the second term (containing C) is the value of the inductance if the iron is removed, leaving an air core. If this were true, the value of the constant C always would be 3.2 in English units, and thus independent of the material used. This is not the case, since for the two examples used, the value of C was 180 and 6,200 for Hipersil and Nicaloi respectively.

J. D. Ryder: The author has not tried to force the use of any particular equation for inductance as a basic equation. For the purposes of the paper and the type of magnetic circuit being discussed the author feels his equation 1 is sufficiently fundamental and makes use of quantities which are measurable. No attempt was made in the paper to discuss inductance in any other form of magnetic circuit in which the area, turns, or length of circuit, change.

The author fails to understand the preference for equation 3 of the discussion. This equation is limited to linear magnetic materials and so has no great application in electric machinery and none in the field of ferroreactors discussed by the paper.

The work reported in the paper was directed toward a very large class of iron-cored circuits, types in very common usage, and it was not intended that the results obtained be applied directly to other fields. Consequently definitions were stated as basic to the paper, not necessarily basic in general.

The constructive comments of Mr. Olney are very helpful. The method of obtaining the constants C and B_n had not occurred to the author, although he realized the meaning of C. This will simplify considerably the calculation of these constants. The author is unable, by use of Mr. Olney's expression for a, to obtain the values of a used for various steels, the values given by the formula being low. It may be that the values of a given by Mr. Olney's formula would produce satisfactory fitting of the curves. The author would like to see the derivation of this formula.

As to Mr. Olney's point 2, the Rader and Litscher expression was rejected primarily because it was not an odd function, thereby preventing its use for negative currents. This is also true of many other expressions proposed.

In regard to point 3, Mr. Olney is quite correct, and a statement to that effect was inadvertently omitted. The attempt was made to emphasize the fact that equation 13 fitted the physical facts qualitatively. Since constant C is used to warp slightly the gudermannian portion of the magnetization curve, then the constant term is not that quantitatively expected for an air-core coil.

Line Drop Produced by Resistance Welders

Discussion of paper 45-104 by R. L. Longini, published in AIEE TRANSACTIONS, 1945, September section, pages 619–23.

D. L. Whitehead (Westinghouse Electric Corporation, East Pittsburgh, Pa.): Mr. Longini has made a definite contribution toward a better understanding of light flicker as caused by various types of welder loads. He points out certain welder characteristics that contribute to light flicker and indicate methods of eliminating or reducing their effects.

In equation 1 of his paper Mr. Longini gives a method for calculating line regulation. This equation gives the per cent voltage drop on the line supplying the welder. In many cases welders are supplied through a delta-y transformer connection, providing four-wire service on the secondary winding, with the single-phase welder connected line-to-line and lighting circuits connected line-to-neutral. The problem then arises as to the determination of the regulation on the lighting circuits caused by the line-to-line fluctuating welder load. This problem could be solved by simple application of Kirchoff's laws using the entire three-phase circuit constants. However, if the welder and other loads are supplied simultaneously, the method becomes quite laborious. This type of problem is solved readily by the method of symmetrical components. The welder load can be considered as a line-to-

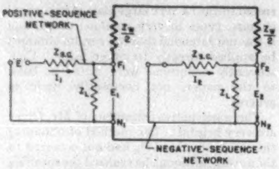

Figure 1. Positive- and negative-sequence equivalent circuits for a single-phase load supplied line-to-line on an otherwise balanced system

E = line-to-neutral supply voltage
$Z_{s.c.}$ = short-circuit or system impedance as measured on the load side of the transformer
Z_L = equivalent balanced load impedance. Line-to-neutral ohms
Z_w = equivalent welder-load impedance in ohms
I_1 = positive-sequence line current
I_2 = negative-sequence line current
E_1 = line-to-neutral positive-sequence voltage $= E - I_1Z_{s.c.}$
E_2 = line-to-neutral negative-sequence voltage $= O - I_2Z_{s.c.}$

line fault through an impedance equal to the equivalent welder load impedance and solved accordingly. The equivalent circuit for a single-phase welder supplied line-to-line and other balanced line-to-neutral, or equivalent line-to-neutral loads, supplied simultaneously is shown in Figure 1 of this discussion.

This circuit can be solved quite easily for the positive- and negative-sequence currents which in turn will give the positive- and negative-sequence voltage drops. It should be noted that $Z_{s.c.}$ includes the system impedance up to the point where the voltage is to be determined. The a or reference phase voltage then will be given by

$$E_a = E_1 + E_2 \tag{1}$$

and for the other two phases

$$E_b = a^2E_1 + aE_2 \tag{2}$$

and

$$E_c = aE_1 + a^2E_2$$

where

$$a = -0.5 + j0.866$$

and

$$a^2 = -0.5 - j0.866 \tag{3}$$

In Figure 1 the positive- and negative-sequence voltages are shown at the balanced-load points. The line-to-neutral voltages at any other point can be determined in the same manner.

C. N. Clark (Duquesne Light Company, Pittsburgh, Pa.): This paper, with its excellent comparison of characteristics for several types of resistance-welding systems, should be of considerable value to utility engineers in providing an adequate power supply for welding loads.

It is interesting to note that welder controls are now available for direct operation from 2,300-volt circuits. With reference to the voltage of the supply line, we often have found it necessary to extend the 11,000-volt or 22,000-volt circuits and transform to 220 volts or 440 volts at the customer's plant in order to limit the regulation to reasonable values at the welder or to prevent objectionable lighting flicker for adjacent customers.

When a small welder is located near a large distribution substation, the regulation of the 2,300-volt circuit usually will be small compared with the regulation of the distribution transformer. However, when a large welder is located several miles from the substation, the regulation of the 2,300-volt circuit may be several times as large as the regulation of the distribution transformer, depending upon the size of the 2,300-volt conductors.

As mentioned by the author, the regulation of the power system varies widely with changes in power factor of the welding load at a given location. For locations near a large distribution substation, the maximum regulation of an uncorrected power system may occur when the power factor of the welding is as low as 40 per cent.

When small conductors are used on a 2,300-volt circuit to supply a welder located several miles from the distribution substation, the maximum regulation of the power system may occur at power factors as high as 90 per cent. Under this latter condition, a part of the gain through improving the power factor of the load would be lost because of the increased voltage drop per ampere for the power system at the higher power factor.

It would be interesting to see the effect on the curves in Figure 4 of the paper by assuming a power line with the higher power factors frequently encountered on long distribution circuits with small conductor sizes.

The use of series-capacitor systems and low-frequency systems appears to have a number of advantages under certain conditions. However, in view of higher costs than for equivalent uncorrected systems, a thorough investigation of all factors should be made before purchasing new equipment. Particular attention should be given to the matter of lighting flicker when considering the low-frequency system.

When the Welding Load Outgrows the Distribution Power Supply

Discussion and authors' closure of paper 45-118 by C. N. Clark and C. M. Stearns, published in AIEE TRANSACTIONS, 1945, September section, pages 645–8.

R. L. Longini (nonmember; Westinghouse Electric Corporation, East Pittsburgh, Pa.): This paper is an excellent outline of the problem and cures of regulation and light flicker resulting from resistance welding. The main contribution of the paper is its approach to the problem. The authors make it possible to analyze each installation and, if the analysis shows that trouble will result, they suggest a number of possible cures. It is a relief from the all too prevalent demand by some power companies that *all* welders be power-factor corrected or that *all* loads be balanced on the three phases. In fact, the authors have explained why, in some cases, it is more economical and less trouble will result from loading one phase rather than dividing the load among the three phases.

This particular point is worth elaborating for no other reason than to point clearly to a rather common misapprehension. When a plant has a number of single-phase welders, it is usually most economical and less likely to cause trouble to have all welders supplied from one single-phase transformer than to divide the load among the three phases. If the load is divided up with one third of the transformers supplied by each phase, little use can be made of diversity between welders. The three-phase transformer bank would probably be oversize to cut down regulation. When all are supplied from one phase, the single-phase transformer usually can be designed from thermal considerations only. The regulation will be better, and even light flicker may be improved, as the single phase does not have any larger pulses of power drawn from it than do the three phases in the other arrangement.

From a power-company point of view it is frequently better to balance the load on three phases by balancing one plant against another rather than requiring each plant to draw a balanced load itself. Each case, however, should be treated individually rather than made to conform to some hard and fast rules which may prove costly and of little or no use.

H. E. Smith (Commonwealth Edison Company, Chicago, Ill.): Mr. Clark and Mr. Stearns have presented a thorough discussion of a subject which is of vital interest to the power-supply industry as well as to the welder users and manufacturers. The following discussion is offered in the hope that the experiences and practices of the Commonwealth Edison Company may be of help to engineers interested in this subject.

The guide for permissible primary-voltage fluctuation on the Chicago system for a welder installation is expressed in the form of a curve passing through 0.9 volt at one per second, 1.4 volts at one per minute, and 2.6 volts at three per hour. In establishing limits for this purpose, it should be remembered that welder installations often are made at several points on the same primary feeder, with the cumulative result that fluctuations of any given magnitude may occur much more frequently than indicated on the curve. The use of a curve in preference to the tabulation used by the Duquesne Light Company is believed to result in a more equitable application of the design limits at various frequencies.

It is suggested that considerable emphasis be placed on the use of three transformers (corrective method *B*) instead of single-phase installations. General experience indicates that welder loads are most frequently encountered in industrial areas, where the three-phase load can be combined with the welder supply. If we use the example cited in the paper, a 75-kva transformer connected single phase or a 50- and two 25-kva transformers connected three phase might normally be adequate from a regulation standpoint for a 150-kva welder load. The same welder could be connected to a bank of three 100-kva transformers carrying 300 kva of balanced three-phase motor load, with a resultant maximum of twice full load on the heaviest-loaded transformer. If we assume the same transformer characteristics, the transformer regulation in this case without adding any capacity for the welder would be the same as that on one 75-kva transformer, and slightly better than on one 50- and two 25-kva units, since the use of two smaller transformers in series to carry one third of the load involves a voltage shift in the primary neutral of the bank.

If the 150-kva welder load used as an example is operated on a 25-per-cent duty cycle, the 75-kva transformer or the 50- and two 25-kva three-phase bank would be carrying full load thermally. However, if we assume the 300-kva motor load on the bank of three 100-kva transformers operates at a power factor of 75 per cent, and the 150-kva welder load operates on the same bank at a power factor of 60 per cent, the peak demands will be approximately 199, 140, and 128 kva on the three phases, and the corresponding thermal equivalent loads will be 132, 112, and 108 kva. Thus, from a thermal standpoint, the increase in load caused by the welder will be only 52 kva.

It is believed that the application of series capacitors to welders justifies serious consideration by power-supply companies and by manufacturers. Where the reactance of the supply circuit is a major factor, the correction afforded by the capacitor is doubly effective in that it reduces the current drawn and also reduces the voltage drop per ampere of load. In a recent application figured in our company, the calculated drop was reduced approximately 50 per cent by correcting from 55-per-cent to 98-per-cent power factor. The improvement possible by such installations may eliminate the necessity of investing many thousands of dollars in an extension of a higher-voltage system.

In conclusion, it is hoped that manufacturers will devote increasing attention to the development of three-phase and of storage-type welders, as these types of equipment appear to offer considerable relief to the harassed engineer who spends considerable time figuring out what to do "When the Welder Load Outgrows the Distribution Power Supply."

C. N. Clark: The discussions by Mr. Smith and Mr. Longini on the relative merits of serving welding loads from single-phase or three-phase transformer installations show that each method has its advantages under certain conditions.

Where the three-phase power load in an industrial plant is small, the total transformer kilovolt-amperes often can be minimized by supplying the welding load from a separate single-phase transformer and service. A check should be made, however, of the voltage fluctuation affecting the adjacent lighting loads supplied from adjacent transformers connected to the same distribution circuit.

For industrial plants using large amounts of three-phase power, the lowest total transformer kilovolt-amperes may be required when supplying both welding and power loads from a common three-phase transformer bank and service.

This method provides relatively low overall voltage regulation and results in lower values of voltage fluctuation on the distribution circuit than would be obtained if the welding load were supplied through a single-phase transformer connected from phase to neutral on the primary side.

Design of Induction-Heating Coils for Cylindrical Nonmagnetic Loads

Discussion and authors' closure of paper 45-107 by J. T. Vaughan and J. W. Williamson, published in AIEE TRANSACTIONS, 1945, August section, pages 587–92.

N. R. Stansel (General Electric Company, Schenectady, N. Y.): A valuable feature of this paper is the presentation of experimental data in support of the theoretical study. Measured values are essential for engineering progress.

Another viewpoint of the subject is the consideration of an assembly for induction heating as a form of transformer, see reference 3 of the paper.

The rate of heat development in the load is,

$$P_a=\frac{e^2r_a}{Z^2} \text{ watts} \tag{1}$$

e = the applied voltage

r_a = the resistance of the path of the current in the load, that is, the secondary resistance, ohms

Z = the effective impedance of the circuits of the assembly, ohms

SOLID CYLINDRICAL LOADS

The equations for the circuit values of an assembly with a solid cylindrical charge (or load) are given in reference 3.

HOLLOW CYLINDRICAL LOADS

The equation for the secondary resistance, see reference 1 of this discussion, is

$$r_a=\frac{\sqrt{2}\pi\rho_a N^2\Delta M}{l} \text{ ohms} \tag{2}$$

ρ_a = the resistivity of the material of the charge, ohm-centimeter cube

N = number of turns in primary coil

l = length of coil, centimeters. A condition is that the length of the load be equal to or greater than the length of the coil

Δ = the index ratio of the corresponding solid cylindrical load, see reference 3

M = the resistance function

$$M=\left[\frac{(\sinh 2\Phi+\sin 2\Phi)+2\kappa^2(\sinh 2\Phi-\sin 2\Phi)+2\kappa(\cosh 2\Phi-\cos 2\Phi)}{(\cosh 2\Phi-\cos 2\Phi)+2\kappa^2(\cosh 2\Phi+\cos 2\Phi)+2\kappa(\sinh 2\Phi+\sin 2\Phi)}\right] \tag{3}$$

Φ = the index ratio of a hollow cylindrical load

$$\Phi=\frac{t}{\sqrt{2}p_a} \tag{4}$$

t = wall thickness, centimeters

p_a = the reference dimension, see reference 3

$$\kappa = \text{the factor } \frac{\sqrt{2}p_a}{(a-t)} \tag{5}$$

a = the outside radius of the load, centimeters

For values of $\Phi \geqslant 1.50$ the value of M is unity.

Equation 2 is on the long-coil basis; that is, a length of load much greater than its diameter. If the load does not meet this condition, a shortness correction must be applied. Reche[2] has published extensive tables of these corrections. Those values are for ratios of diameter and length 1.0 to 0.20 inclusive and air-gap ratios up to and including 2.0. It has been found that Reche's values check reasonably well with measured values.

The ratio of the resistance of a hollow cylindrical load and the corresponding solid cylindrical load is

$$\frac{r_a \text{ tube}}{r_a \text{ solid}}=\frac{M}{\sqrt{2}F_r} \tag{6}$$

F_r = the resistance function for solid cylinders

Thus for values of $\Phi \geqslant 1.5$ the resistances of hollow cylindrical loads are the same as those of the corresponding solid cylindrical loads.

ELECTRICAL EFFICIENCY

A peculiar electrical feature of the hollow cylindrical load is that with frequency considered as a variable in equation 2 the efficiency of the transformation from electric energy to heat reaches its maximum value with a certain frequency in each case. Thereafter, with increasing frequency the efficiency decreases and becomes the same value as that of the solid cylindrical load for $\Phi \geqslant 1.50$.

BASE FREQUENCY, f_B

This term defines the value of frequency given by the equation.

$$f_B=\frac{44\times 10^8\times\rho_a}{(a-t)t} \tag{7}$$

For the conditions $t<<p_a$ and $t/a<<1.0$ this equation gives the value of frequency with which the maximum efficiency is obtained. Many loads in practice, such as those cited in the paper, do not meet these conditions and the frequency for maximum efficiency is somewhat higher than given by equation 7.

Hence, generally, the base frequency for a hollow cylindrical load is the lowest desirable frequency for that service. However, with high load-resistivity values there is more freedom in the use of frequencies below the base frequency than with low load-resistivity values, such as those of aluminum and copper.

There is not much to be gained in efficiency by the use of a frequency above the base frequency. This leads to the statement that the frequency for a hollow cylindrical load should be the standard frequency nearest the base frequency with a preference for a standard frequency above the base frequency.

REFERENCES

1. THE POWER LOSS AND ELECTROMAGNETIC SHIELDING DUE TO THE FLOW OF EDDY CURRENTS IN THIN CYLINDRICAL TUBES, C. W. Oatley. *Philosophical Magazine*, volume 22, 7th series. 1936, pages 445–53.

2. THEORETICAL AND EXPERIMENTAL INVESTIGATION OF THE CORELESS INDUCTION FURNACE, K. Reche. *Wissenschaftliche Veroffentlichungen aus den Siemëns-Werken* (Berlin, Germany), volume 12, 1933, pages 1–33.

J. T. Vaughan and **J. W. Williamson:** As stated in Appendix II, no shortness correction is required if the ratio of outside diameter of the load to inside diameter of the coil is sufficiently near unity. To prove this, apply Ampere's integral law over the path $ABCD$ in Figure 1. Where $H \times dl$ is the scalar product of magnetic intensity and incremental displacement,

$$\oint \mathbf{H} \cdot \mathbf{dl} = 4\pi I_L$$

For sufficiently high ratios of diameter to reference depths of inductor coil and load, the number of lines of flux inside the load or coil copper is usually insufficient to produce an appreciable magnetic field outside the coil or between coil conductors. The number of lines of flux in the air gap could be made vanishingly small by reducing the area between the inside of the coil and outside of the load. Consequently, a limiting condition may be approached such that

$$\int_A^B \mathbf{H} \cdot \mathbf{dl} = 4\pi I_L$$

as

$$\frac{a_0}{d_2} \rightarrow \infty$$

and

$$\frac{a_0}{d_1} \rightarrow \infty$$

Since the distance between A and B is approximately L/N,

$$\frac{HL}{N} = 4\pi I_L$$

or

$$H = \frac{4\pi NI}{L}$$

as for an infinitely long coil; thus no shortness corrections are needed. Reche overlooks this fact. Also, he does not tabulate correction factors for coils of length greater than 2.5 times the inside diameter. Additional complications would be involved in applying his theory to longer coils. Despite these limitations, Reche's work probably constitutes the only attempt rigorously to derive corrections for coil shortness to date. As such it is worthy of consideration by all those interested in the subject.

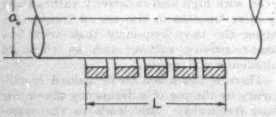

Figure 1. Inductor coil and load

Equation 30 of the paper gives the frequency for maximum efficiency when the wall thickness of the load is less than 0.13 of the load outside diameter. This equation when written in the notation used by Mr. Stansel becomes

$$f_B = \frac{44 \times 10^6 \times \rho_a}{\left(a - \frac{t}{2}\right)_t}$$

This is comparable to Mr. Stansel's equation 7.

The S-Function Method of Measuring Attenuation of Coaxial Radio-Frequency Cable

Discussion and author's closure of paper 45-134 by Chandler Stewart, Jr., published in AIEE TRANSACTIONS, 1945, September section, pages 616–19.

H. J. McCreary (Automatic Electric Company, Chicago, Ill.): The paper presents a very concise and simplified technique for obtaining the inherent characteristic constants most useful in transmission calculations and is based upon the coaxial cable of the continuous-insulator type using polyethylene. No mention or measurements are made of those types using beaded supports for the central wire, either of ceramic or plastic materials.

Where the beaded type of coaxial cable is used I presume that the d would be made an even integral number of bead sections. Errors of measurement would occur, no doubt, because of fringing capacitative effects, radiation losses, and so forth.

In equation 17 of the paper,

$$N = \frac{\left(\frac{1}{Q} + P\right) 2{,}000 \log_{10} \epsilon}{d\left(M + \frac{1}{M} + \frac{1}{\cot^{-1} M}\right)} \tag{17}$$

To simplify this an arbitrary constant S called the S function is assigned to the value (equation 18 of the paper)

$$S = \frac{2{,}000 \log_{10} \epsilon}{M + \frac{1}{M} + \frac{1}{\cot^{-1} M}} \tag{18}$$

This is substituted into equation 17 thus reducing this equation to

$$N = S \frac{\left(\frac{1}{Q} + P\right)}{d} \tag{19}$$

In order to simplify the determination of S when M is known, equation 18 of the paper is plotted in the curve of Figure 6 of the paper. However, although the values along the Y axis are S, the values along the X axis are not M but the more convenient value $\frac{M}{2}\pi$ since

$$M = \frac{Z_0}{X_{sc}}$$

and

$$X_{sc} \text{ is assumed} = \frac{1}{2\pi f C_0}$$

$$M = \frac{Z_0}{\frac{1}{2\pi f C_0}}$$

$$\frac{M}{2\pi} = Z_0 f C_0$$

Chandler Stewart, Jr.: As far as I know, no attempt has been made to apply this method of measurement to coaxial cables employing beaded supports. On first thought, I would agree with Mr. McCreary that a sample length of an integral number of bead sections would be desirable. Errors undoubtedly would be introduced by the cable capacitance not being evenly distributed but, in most cases, I believe these would be less than the errors inherent in the instrument. I do not believe that radiation losses would be any greater in beaded cable than in cables employing solid dielectric; in either case they are certainly negligible compared to the ohmic and dielectric losses.

Statistics as an Aid to Engineering Judgment in the Manufacture of Lightning-Arrester Blocks

Discussion and author's closure of paper 45-132 by Casper Goffman, published in AIEE TRANSACTIONS, 1945, September section, pages 607–10.

Martin A. Brumbaugh (nonmember; The University of Buffalo, Buffalo, N. Y.): This paper provides an excellent illustration of the employment of statistical technique in segregating causes of rejection of manufactured product. The methods used are quite independent of the particular application which the author has selected.

Correlation between tests is valuable on two counts:

1. Where inspection cost can be eliminated as in the example given.
2. Where nondestructive testing can be substituted for destructive, thus saving material.

The nondestructive substitute is often simpler, affording additional advantage.

The section of this paper dealing with "Effect of Molding Technique" would be strengthened by including a statement that the statistic referred to is the ratio of squared successive differences to variance. (I assume that this is correct.) The chi-square test is clear enough, but a restatement of the conclusions would help.

The use of the t distribution to determine from small samples that aging, temperature, and mold clearance are assignable causes of variation in electrical characteristics of the blocks is precisely the information that process engineering must have in order to write a manufacturing specification that will provide for control of these causes of variability. At the same time the variance analysis tells the engineer that his variability does not arise from the positions of the blocks in the ovens.

The final test reported suggests, although the data are not adequate to prove, that the greatest cause of product variability is variation in initial blending. I presume that the matter stands as follows: without control of blending of the mixture, good blocks will be accidental; with control of blending, good blocks can be assured by proper attention to the causes of significant variability entering the manufacturing process.

W. Edwards Deming (nonmember; Bureau of the Budget, Washington, D. C.): It is pleasing to see the spread of interest in statistical methods, exemplified by Mr. Goffman's paper. However, it is not necessary to test the line in Figure 3 or even to draw any line at all, to see that regression is indicated. Statistical tests made in cases so obvious only serve to alienate the statistician from the ranks of his fellow scientists.

The chi-square test on the five batches, made in the section entitled "Effect of Molding Technique . . ." is not trustworthy with only three degrees of freedom. Small samples give as good control as large samples over errors of the first kind, namely rejecting a perfectly good hypothesis, but they give very poor control over errors of the second kind, which is to accept a false hypothesis. Personally, I should hesitate to draw any conclusion at all from the value of chi square equal to 13.04, because of the small number of degrees of freedom. One possibly might conclude with justification that this value of chi square points toward the need of further investigation, but even there I dare say that a plot of the batches showing means and individual values would disclose much more information. The dangers of the use of statistical tests, particularly with small samples, have been publicized by numerous writers.

The same kind of comment should be offered with regard to the test made in the following section, and the next one as well.

Harold Hotelling (nonmember; Columbia University, New York, N. Y.): Mr. Goffman's paper uses effectively and accurately a number of statistical techniques to accomplish a great economy in a manufacturingand inspection problem. The possibilities of this kind of thing are very great and go far beyond what has generally been suspected.

The problem of detecting trends in the data of Figure 4 I should have attacked in a somewhat different way by fitting a polynomial of degree not exceeding the fourth to each of the batches of data. Probably a straight line fitted by least squares would have been sufficient in each case to demonstrate a significant trend. This test will, I think, usually be found more sensitive and efficient than the statistic used.

C. C. Craig (nonmember; University of Michigan, Ann Arbor, Mich.): This paper is an unusually interesting one of its kind since it contains in small space a variety of applications of statistical methods which give information of practical value concerning the manufacture of a single article. Furthermore, the statistical methods themselves show an unusual variety, and they give an idea of the resources a statistician equipped beyond the very beginnings of statistical theory has at his disposal. Mr. Goffman belongs to a rather small group in industry who has acquired such equipment.

I regret that Mr. Goffman could not have used more space to explain more fully the nature and meaning of some of the statistical tests he employed. It would prehaps have taken too much space to sketch all the numerical calculations to enable the general reader to follow them, but specific page references to books and articles where detailed explanations and fully worked out problems are found would be useful. Mr. Goffman's illustrations are worth being fully understood. I will confine my comments on specific points to two or three where I believe they will be helpful.

It is stated that it is desirable to "know the correlation between these voltages," but no estimate of this correlation is given. Instead the linear regression equation obtained from the data, for Y on X is given though the reader is left to infer what Y and X represent. A reader with an acquaintance with curve fitting will know that the origins for X and Y are taken at their respective means, but he may wonder about the scale. In Figure 3 the slope of the regression line is nearly 0.6 instead of 0.5 on the scale used there (if we assume that X and Y are measured on the horizontal and vertical scales, respectively). That the regression is highly significant means that the correlation, which can be calculated from the given sums of squares to be about 0.83, is also highly significant. That these sample values are highly significant means that the true long-run values are with a high degree of certainty not zero, but this information is considerably less than knowledge of what these long-run values are. Of course, we can never determine by any number of observations the exact values of these quantities, but we can by increasing the number of observations place with confidence these true values within smaller and smaller intervals. In the present case with 30 observations it is possible by a well-known method to place the true value of this correlation in the interval 0.59 to 0.93 with a confidence measured by the statement that 99 times in 100 an interval arrived at in this way will contain the true value.

Many readers with some familiarity with statistical methods will not recognize the quantity δ^2/σ^2 and would appreciate at least a brief statement of its meaning and a specific reference to von Neumann's paper and to the one which follows it in which the tables used are found.[1]

Likewise a specific reference to Rider's book (page 102) will be helpful to readers who wish to learn more about the chi^2 test used.

There is a quite proper objection to the way the data are used in making a retest on the effect of baking temperature on blocks. All the 32 observations should be used in calculating the second t. Would it not be equally defensible, since the t on the first 16 observations was too small to be quite conclusive, to pick out the four pairs from the first 16 which will give the largest t and base one's conclusion on them? In the present case one is safe only by being sure that the t based on all the equally valid observations will be large enough. It is pretty obvious that it will be (3.104 actually), but the correct procedure is to calculate this t instead of the second one found here.

It will be seen that my remarks contain little real criticism, for little is called for. Mr. Goffman is to be congratulated on the job he has done, and I hope a considerable number of readers will give his examples the close study they deserve.

REFERENCE

1. TABULATION OF THE PROBABILITIES FOR THE RATIO OF THE MEAN-SQUARE SUCCESSIVE DIFFERENCE TO THE VARIANCE, B. I. Hart, John von Neumann. *Annals of Mathematical Statistics*, volume 13, 1942, pages 207–14.

Louis C. Young (nonmember; Westinghouse Electric Corporation, Springfield, Mass.): In general, Mr. Goffman has demonstrated the many ways in which statistical tests may be used to form engineering conclusions, without requiring an exhorbitant amount of physical test data. A particularly good example of this is to be found in the test of the effect of baking temperature on blocks; the number of test data initially obtained in the study proved inadequate and were consequently reinforced only by the approximate number of data necessary to prove the significance of the 75-degree variation.

In the same example, there is some possibility of misinterpreting the conclusion, that oven temperature should not be allowed to vary by as much as 75 degrees. If a baking test had been conducted under a temperature variation of 50 degrees and with a larger number of samples and test data for both this condition and that of standard baking temperature, it is quite probable that a significant difference in "maximum rise" could have been demonstrated with equal facility. The pertinent fact in this case is that the 75-degree variation is related to practical circumstances and that an average measure of its effect on "maximum rise" has been obtained, together with the assurance that this "maximum-rise" difference is not accidental, but real.

In the section dealing with the effect of molding technique, on the other hand, there is some question as to the validity of the conclusion that the variables of shop molding practice affect the volt-ampere characteristics of the blocks. Although this is probably true, the most direct proof would appear to lie in a comparison of the laboratory-molded batch results with any single one of the batches molded in the shop; the conclusion in that case might be amplified in terms of the type of shop practice involved in the specific batch considered. Otherwise, it is possible that the only variable of shop molding practice which affects the volt-ampere characteristics is the factor of aging which was deliberately introduced into the experiment.

In reviewing the trends in Figure 4, it is interesting to note that the average "maximum rise" of batch *D* appears to be slightly higher than the stable values being reached in the trends of batches *B* and *C*. If this apparent tendency is real, it has a direct bearing upon the uncontrolled manufacture of batch *D*, as against the partially controlled manufacture of batches *B* and *C*; this would seem to warrant further investigation.

J. S. Ferguson (Westinghouse Electric Corporation, East Pittsburgh, Pa.): The exacting performance requirements imposed on lightning-arrester valve elements demand that they be uniform and of highest quality. A great deal of attention has been given by design engineers to the problem of manufacturing these elements.

For many years process controls and test procedures have been in use which give assurance that elements of doubtful quality will not be built into arresters but will be rejected. Until recently a method was lacking for finding the important causes of occasional deviations from standard quality.

Doctor Goffman's methods of analysis and controlled experiment have proved extremely valuable in determining certain variables in the process that must be watched closely and others that affect the quality only slightly. Statistical analysis of day-to-day test results permits a continual check on the important factors in the process and also helps identify probable causes when elements fail to pass tests. Corrective measures thus can be adopted with a minimum of delay.

One of the results of Doctor Goffman's work has been a substantial increase in the severity of the final test, thus insuring a higher quality of valve element.

H. F. Dodge (Bell Telephone Laboratories, Inc., New York, N. Y.): This paper presents results of a study of the variables affecting the electrical characteristics of lightning-arrester blocks, illustrating how statistical methods can serve practically as an aid to judgment regarding sources of variation within a manufacturing process. To the engineer not versed in statistical methods and terminology, the paper is probably too condensed for general comprehension. It does, however, get across the idea that there are available statistical tools with which the engineer might profitably become acquainted. It is believed that the average engineering reader would have gotten a great deal more from the article, had there been included more explanation of the statistical symbols and tests used, particularly had the author made reference to specific sources, including even the page numbers of the references, for each of the statistical tests employed. The engineer is noted for his desire for specific knowledge so that he can "go and do likewise."

The analyses make use of a number of new methods—not merely some of the more usual statistical tests. For instance, use is made of the statistic δ^2/σ^2, which is treated in several interesting articles presented in the *Annals of Mathematical Statistics* in 1941. In this connection only one reference is cited, and it is felt that it would have been helpful to include reference to other contemporary papers on the subject, particularly "The Mean-Square Successive Difference" by J. von Neumann, R. H. Kent, H. R. Bellinson, and B. I. Hart, *Annals of Mathematical Statistics*, volume 12, pages 153–62, since this is somewhat less mathematical and presents the basis for some of the methods actually used.

Since the average reader is not likely to be familiar with the new terminology and methods, a brief description of the statistic δ^2/σ^2 and the two terms used in this ratio would have been helpful. The numerator δ^2, for example, is based on the square of successive differences of individual observed values when they are arranged in order, perhaps with respect to time.

That part of the paper which relates to the "Effect of Baking Temperature on Blocks" would not appear to have provided a conclusive result. An initial test with relatively small samples does not show a significant difference in terms of the significance criterion used, but a retest, likewise with small samples, *does* show a significant difference. Although the author draws a conclusion from the results of the second test only, it would appear that the point was "not proved" on the basis of the total data presented—that, in fact, more tests are needed for a decision. In any situation of this kind, the whole picture may be changed from a practical point of view if other information, either qualitative or quantitative, but not mentioned in the text, contributes to the decision.

For those whose appetites may be whetted by the practicalness of statistical methods in handling the particular types of problems outlined in the paper, it is suggested that the author would undoubtedly be glad to provide more detailed technical information to any who have manufacturing problems of a like character.

Casper Goffman: The author will not attempt to answer Doctor Deming's general remarks but will confine his comments to the specific items mentioned.

The main point made by Doctor Deming is in regard to the use of small samples. Doctor Deming says it is proper to use small samples when errors of the first type can be made but not when errors of the second type can be made. The author believes that in each case considered in the paper the only type of error that could have been made is of the first type. The hypothesis was always the null hypothesis, and the conclusion was in each case to reject the hypothesis. Hence the type of error which could have been made was to reject a good hypothesis. This is an error of the first type.

Regarding the wisdom of performing the test of regression in Figure 3, the author's experience has been that the type of error most often made is to assume trends or differences when they actually do not exist. It is precisely in cases where the engineer believes he can arrive at a conclusion merely by glancing at data that he should be educated of the danger of such practice. In any case what may seem to be an obvious trend to one man may not be to another. Moreover, what may seem to be an obvious trend to some people may not actually be a trend at all. For this reason, the author advocates the practice of applying statistical tests in all cases where important decisions are to be made unless of course unreasonable expenditures are involved. How can this point of view alienate the statistician from the scientist?

Optimum Air Gap for Various Magnetic Materials in Cores of Coils Subject to Superposed Direct Current

Discussion and author's closure of paper 45-149 by V. E. Legg, published in AIEE TRANSACTIONS, 1945, October section pages 709–12.

R. C. Taylor (Western Union Telegraph Company, New York, N. Y.): This valuable paper is notable for the wide variety of materials and superposed conditions which are discussed. I would like to ask the author for some discussion of the range associated with the typical curves. This would permit a designer to consider the limiting cases he is likely to encounter, also show to what extent the properties of various materials may overlap. As the author notes in his reference 2, the permeabilities are subject to considerable variation. Of course the derivatives with respect to flux density also have manufacturing variations which, fortunately for the designer, often partially compensate in the various formulas of the paper. For instance, increased μ_r usually is associated with increased μ and, consequently, their difference does not vary as much as if they tended in opposite directions. Similarly, increased μ_r is associated with increased $d\mu_r/dB$ with corresponding beneficial effect on the stability of the quotient.

It has been our experience that optimum air-gap spacers at the lower flux densities are thin enough to require some degree of individual adjustment and accurate predetermination of spacer thickness is not as valuable as it would be otherwise.

Figure 2 of the paper shows two different areas in the magnetic circuit and, consequently, two polarizing flux densities will exist. For such construction some alteration of the formulas would be required. Perhaps the simplest would be the use of a fictitious l and corresponding u, v, w and α to keep the reluctance at its true value and a corresponding intermediate value of B.

Donald W. Howe, Jr. (nonmember; Worcester Polytechnic Institute, Worcester, Mass.): Mr. Legg has presented answers to many of the problems encountered by the designer of iron-cored inductors. While there is no question of the desirability of knowing the "optimum air gap," there are many other factors which the practical designer must consider in selecting the "best" air gap. I would like to discuss a few of these.

In a production run of a competitive stock inductor using E, I laminations, the optimum gap to be used first was determined in the laboratory by tests on the first few samples. Spot checks on the finished item showed a variation of ±50 per cent in inductance. An investigation yielded the following causes:

1. Variations in gap length impossible to eliminate in mass production.
2. Variation in steel characteristics.
3. Variation in gap length due to mechanical shocks after assembly.
4. Variations in effective gap length due to the fringing flux finding low reluctance paths in brackets or case.

The variation in L due to the first three of these causes can be reduced by using a gap large enough so that the major portion of the effective reluctance is in the air. A subsequent production run of a similar item was kept inside a ±ten-per-cent tolerance by using about twice the optimum gap. Another run with a ± five-per-cent tolerance was made possible by using F laminations with a gap three times optimum in the center leg where the fringing flux could get into no trouble. In both cases, the saving in labor offset the cost of extra material.

Mr. Legg's equations are based on the assumption that inductance is independent of variations in the amplitude of the alternating current. In many instances this may be far from true. Where constancy of inductance over a wide range of alternating and direct current is required, the optimum gap is not necessarily the best gap. A larger gap will minimize the effect of variations in steel permeability. It is interesting to note that if L varies, we cannot use the familiar relation

$$e=L\frac{dI}{dt}$$

but we must use

$$e=N\frac{d\phi}{dt}$$

Substituting L for $\frac{N\phi}{I}$ and performing the indicated differentiation, we get

$$e=L\frac{dI}{dt}+I\frac{dL}{dt}$$

The effect of this somewhat neglected second term has been found particularly evident in circuits carrying transients or square waves.

V. E. Legg: In reply to the discussions by Donald W. Howe, Jr., and R. C. Taylor, it should be pointed out that a mathematical derivation of "optimum" conditions is convenient only when the basic assumptions are kept simple. Such derivations of ideal cases are often useful in laying out a new project, or in assaying a completed product. However they do not profess to include such variations as nonuniformity of magnetic material, permeability dependance on a-c flux density, mechanical inaccuracy of gap length, or magnetic shunting through the frame or case. These details must remain as problems for design and manufacturing control. But the mathematics warns that, for instance, although inductance uniformity of product may be found to be obtained by use of two or three times optimum air gap, it entails sacrifices in coil characteristics such as lowered inductance, increased resistance, or increased size. The adjustment of such conflicting desires, and provision for unforeseen variables, often tax the designer's ingenuity or judgment.

In reference to Mr. Taylor's remarks about Figure 2 of the paper, it is usual to design the shell-type core so that the cross-sectional areas of the two side paths add up to equal that of the center leg, effectively.

A Study of Wave Shapes for Radio-Noise-Meter Calibrations

Discussion and author's closure of paper 45-146 by C. W. Frick, published in AIEE TRANSACTIONS, 1945, pages 890–901.

Arthur Bessey Smith (Automatic Electric Laboratories, Inc., Chicago, Ill.): This paper seems to me to be timely and very much needed. Those who for years have been working in the field of radio interference, its measurement and suppression, have been handicapped by the broad zone of doubt in all the measurements, which is even worse than the unavoidable deviations in the measurement of magnetism, admittedly so much worse than most electrical measurements. It is to be hoped that the square wave will perform equally well in the hands of other investigators, so that it may come to be commonly accepted.

Certainly all can agree with the objective: "a reading proportional to the noise effect." Standing between the electric circuit and the radio listener is the loud-speaker. Early loud-speakers differed very much in their response to differing audible frequencies, so that the audible frequency electromotive force applied to them was not much of a criterion of the loudness emitted into the air. It is believed that modern loud-speakers have very largely overcome this difficulty, so that radio noise may be rated by detected electromotive force with reasonable assurance that the effect on the listener will be proportional.

In 1938 we made tests on a multivibrator device as a signal generator for calibrating a radio-noise meter. The results were not encouraging. There was great lack of uniformity even through the broadcast band.

The author's description of shock excitation is very fitting, though he did not use that term. Even without the application of the Fourier series, the operation of the steep wave front on a tuned circuit is understandable. In fact, to many it is an easier concept than the Fourier series, though it does not take in the zone of frequencies which the meter circuit will pass.

It would have helped the presentation materially if the author had given the basic circuit of the best square-wave generator. It is to be hoped that this will shortly be done.

Wave generator 3, the vibrating metallic contact, seems to deserve further study. The evidence of slow fall of resistance excites our curiosity. What was the structure of the vibrator? How was it driven? What metals were used for contacts? What form did they have? What contact pressure did they attain? It seems to me that from the radio-frequency standpoint this deserves further investigation. Also it should be done as an adventure in pure physics if for no other reason.

Durward J. Tucker (Station WRR, Dallas, Tex.): Quite often the radio engineer has occasion to measure radio noise. As the author points out, numerous instruments are available for measuring such noise, but, unfortunately, an agreement between measurements made with different radio-noise meters is not always to be had. He attributes this disagreement partially to the method of calibration used for the various radio-noise meters. Particularly does he attribute the disagreement to the difference in wave shapes encountered. It has been the general practice to use the sine wave for the calibration of such instruments, but the author has shown, by practical data and theoretical data, that such a basis of calibration is not altogether satisfactory. By additional theoretical and practical data Mr. Frick has shown that utilization of the square wave for the calibration of radio-noise meters is a satisfactory solution to the problem.

The paper contains a thorough mathematical analysis of the square wave.

The paper is well written and contains much valuable information for those concerned with problems of radio-noise measurements and is heartily recommended, especially to broadcast engineers and others especially interested in radio-communication work.

C. W. Frick: The author wishes to thank Doctor A. B. Smith and Mr. D. J. Tucker for their helpful discussions. As to square-wave generators, it seemed better to state the characteristics of the wave rather than the details of the generator. This was done in the paper in item 2 of the conclusions. Square-wave generators are available, and, whenever one of them is found to provide a wave of acceptable shape and in addition is portable and sufficiently rugged for general calibration purposes, it can be used. Also various circuits that will produce square waves are described in the literature of the subject. Some recent information may be found in a recent paper.[1]

The vibrating-contact wave generator 3 was made up from parts of a vibrator inverter normally used to obtain alternating voltage from a six-volt battery. The magnet coil was connected to an independent 60-cycle circuit to drive the vibrator. It was believed desirable to call attention in the paper to the fact that this generator, which had mechanical contacts, was not successful. For general information a study of the causes of the trouble such as Doctor Smith suggests would be desirable. However, it was not needed in this investigation, because the desired result was accomplished by other means.

REFERENCE

1. MULTIVIBRATOR CIRCUITS, M. V. Kilbert, Jr., A. F. Inglis. *Proceedings*, Institute of Radio Engineers, volume 33, August 1945, page 534.

Lightning Arresters for Distribution Apparatus

Discussion and authors' closure of paper 45-147 by Edward Beck and A. D. Forbes, published in AIEE TRANSACTIONS, 1945, October section, pages 719–24.

E. R. Whitehead (Duquesne Light Company, Pittsburgh, Pa.): The authors are to be commended for their objective presentation of the relative performance characteristics of valve-type and expulsion-type lightning arresters for distribution apparatus.

The writer is in agreement with the authors that, on the whole, modern valve-type arresters provide the better protection for old transformers. If the impulse strength of the old transformers is unknown, however, there is still considerable uncertainty regarding the quality of protection obtained.

The Duquesne Light Company impulse tests all 2,400-volt distribution transformers sent to the central shop for reconditioning. The test consists of an application of a full wave at 45 kv of standard shape to each primary terminal, followed by an application of the same wave to the gapped secondary neutral. To date, over 3,000 units have been tested with a rejection rate of approximately 6 per cent. Tested transformers re-enter service with a certified level of 45 kv, and the margin of protection afforded by the protection scheme can be estimated readily.

The dependence of the quality of protection upon arrester location and method of grounding generally is realized, but little harm will be done by emphasizing this fact. Impulse tests were made recently on full-size models of distribution transformer pole-top construction to determine the relative merits of practicable designs. With valve-type arresters mounted on the transformer arm and the arrester ground lead directly connected to the tank and gapped to the secondary neutral, a maximum current of 26 kiloamperes could be discharged. Under these conditions, the impedance voltage across the transformer was 32 kv after an initial peak of 57 kv lasting less than 0.1 microsecond.

There was no evidence of transformer breakdown under these conditions. Upon substitution of a modern expulsion-type arrester, however, the transformer lead punctured and bushing flashover occurred. Replacement of the valve-type arrester restored protection, despite the punctured lead.

Other tests have provided evidence that the expulsion arrester will withstand repeated heavy discharges better, and therefore is preferable when the insulation level is set suitably. The permanence of such a co-ordinated insulation level continues to be a matter of concern to distribution engineers, and in this connection it may be mentioned that our impulse tests at 60 kv on new modern transformers have shown a failure rate of from one to 2.4 per cent, depending upon the exclusion or inclusion of an "epidemic" of failures in transformers of small kilovolt-ampere rating.

J. W. Bennett and **F. R. Longley** (Western Massachusetts Electric Company, Springfield, Mass.): We would like to suggest that at this time the industry take a new look at the most important characteristics of the distribution arrester: Its *IR* drop during discharge and its time-lag curve during spark-over. The *IR* drop should be small and the time-lag curve should be flat.

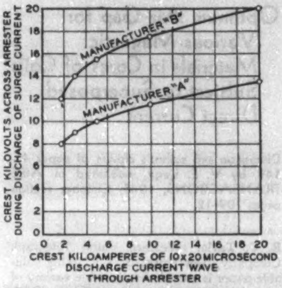

Figure 1. Comparison of discharge surge current *IR* drops across two three-kilovolt distribution lightning arresters of different manufacture

Now that interconnection of the primary arrester ground terminal with the transformer secondary neutral has become an accepted practice, the distribution arrester has become a far more dependable device for the protection of distribution transformers, and the arrester's protective characteristics thus have taken on a renewed importance.

With interconnection, the arrester's spark-over voltage and *IR* drop are the only surge voltages impressed across the transformer's insulation and they alone determine the margin of lightning protection.

The margin of protection is the difference between the impulse insulation strength of the transformer and the surge voltage across the arrester. The margin is a variable. It will vary with the magnitude of the arrester surge current, with the age and make of the transformer, and with the condition of the transformer insulation. After spark-over, the surge voltage across the arrester is, of course, its surge current *IR* drop.

Figure 1 of this discussion shows the surge discharge *IR* drops of two three-kilovolt distribution arresters of different manufacture. Each make is used widely. Note that the drop across the arrester of manufacturer *B* is about 50 per cent larger than that of manufacturer *A*.

As interconnection is applied to transformers of progressively older design, we reach a point where the margin of protection disappears. As the arrester with the smallest surge voltage drop will provide the largest margin of protection, it will provide protection for the largest number of the older transformers and will insure the minimum surge voltage strain on the insulation of all transformers.

Prior to the use of interconnection, the surge voltage across the arrester was often the least part of the surge voltage on the transformer and the arrester's protective characteristics may have been less important than now. We suspect that the older practice of noninterconnection, using a pole ground only, often left the distribution transformer with little or no protection.

Of course, when the transformer is designed to co-ordinate with an arrester of large *IR* drop, protection will be obtained, but it will be at the cost of a further increase in transformer insulation or an encroachment on the margin of protection. If the margin of protection is reduced, we are confronted with the question: Will the transformer be protected throughout its life as its insulation deteriorates in service? We note a new tendency to increase transformer loadings and thus accelerate the rate of insulation deterioration.

Turning to the expulsion-type arrester, we note that it has a very small IR drop but a poor time-lag characteristic which curves up like that of a standard rod gap. This may be seen in Figure 5 of the paper. The time-lag curve for the rupture of transformer insulation is relatively flat, similar to that of a sphere gap, or of a valve-type arrester.

To secure lightning protection of the transformer, it is essential that the time-lag curve of the arrester spark-over be, at all points, below the time-lag curve of the transformer insulation puncture. As the time-lag curves of the expulsion arrester and of transformer puncture are of different shapes, it is hard to keep them from crossing, especially at times of less than about one microsecond where the steep front and reflected waves operate. A comparison of the time-lag curves of a rod gap, a sphere gap, and an insulation barrier is illustrated in Figures 2 and 3 of a former AIEE paper.[1] Note that the sphere gap will protect the insulation while the rod gap will not. The curves for sphere gaps and valve-type arresters are quite similar.

We would consider a small IR drop and a flat (or nearly flat) time-lag curve to be the two arrester characteristics of supreme importance for they are the measure of the ability of the arrester to do its job which is to protect its transformer (or other apparatus). We would term them the primary qualities for they always must be smaller than the transformer insulation strength or the arrester is not an arrester; and the smaller they are, the better the arrester.

There are also, of course, other essential arrester qualities which must be included after the primary qualities first have been provided. These qualities are permanence of characteristics and ease of maintenance. We would term them secondary qualities. They are achieved by such qualities as high surge current discharge capacity, freedom from gap corrosion and contamination, protection of the valve material from harmful contamination, freedom from communication interference, low probability of failure, and easily seen evidence of failure if it does occur.

Concerning arrester failures during surge discharge, we believe that a small number of these can be tolerated provided the damaged arrester leaves evidence of failure that can be seen readily by inspection from the ground. When an arrester fails during discharge it, at the same time, protects its transformer against that particular surge. If easily seen by inspection, the damaged or destroyed distribution arrester can be replaced quickly and cheaply. If such an occurrence is infrequent, we would regard it as we would a fuse, to be replaced after it has destroyed itself in performing its protective duty. Until the damaged arrester is replaced, its transformer will be without protection against ensuing surges, and occasionally a transformer may be damaged by such a surge, but if the number of arrester failures is small a few arrester replacements and perhaps an occasional transformer replacement will be minor items in the maintenance schedule.

On the other hand, if the distribution arresters have a high rate of failure and frequently ground the circuit, without clearly showing visible evidence of having failed, they will impose an unequivocally intolerable operating condition upon the distribution system and burden upon the maintenance crew.

To summarize, we suggest that in the selection of distribution arresters, especially if they are to be installed on any and all distribution transformers without discrimination among make, age, location, and condition of insulation, they be chosen for small IR drop and flat time-lag curve provided their secondary qualities, as previously described, are judged to be satisfactory. We feel that the importance of these two characteristics often is overlooked or slighted and that, in view of the practice of interconnection of older transformers requiring the maximum possible protection, the arrester's protective characteristics have assumed an increased importance.

We would consider the four most important qualities of the distribution arrester to be:

1. Small surge current IR drop.
2. Flat time-lag curve.
3. Ease of maintenance.
4. Permanence of operating characteristics.

Distribution arresters are available with the afore-mentioned qualities 1 and 2 that compare favorably with station-type arresters of the same voltage rating, though their surge current discharge capacities are smaller. Most well-known makes, if of modern design, possess qualities 3 and 4.

REFERENCE

1. Co-ordination of Insulation, V. M. Montsinger, W. L. Lloyd, Jr., J. E. Clem. AIEE Transactions, volume 52, 1933, pages 417–27.

W. H. Hatch (Public Service Company of Northern Illinois, Chicago, Ill.): This paper by Beck and Forbes is a clear concise exposition of the merits of the valve and expulsion type of arresters, and as such is a good answer to the question the authors pose in their introduction "The question arises why both persist." Several thoughts it evoked in the minds of some engineers of an operating utility are listed herein. This utility uses both types of arresters and the remarks should be considered as applying principally to 3-kv arresters used on 2,400–4,160-volt Y feeders.

1. Line lockoutproof performance is claimed for both types of arresters. It is not known whether this term is intended to include blowing of sectionalizing fuses. Although this claim for expulsion-type arresters will be accepted generally, many operating people will be skeptical of the valve arrester's ability in this respect, based on experience with earlier designs. Performance of "dropouts" or disconnecting features has been erratic. As it is acknowledged that deterioration of the valve element will occur in some cases, dropout operation must be expected. Accordingly, dependent on magnitude of accompanying fault current, oil circuit breakers or sectionalizing fuse operation may follow.

2. The fact that both arresters will meet the 65,000-ampere AIEE test successfully demonstrates that both types are capable of withstanding the majority of surges to which they are exposed. However, one or both types may have the ability to withstand the even greater surges which occasionally occur. Field observation of both failed and intact arresters lead us to believe that the expulsion-type arrester has considerably greater capacity than the valve type. In these observations, the areas of "burns" produced on gap electrodes by natural lightning have been compared with areas of "burns" produced by impulse generators with similar currents. As judged by these burns, the expulsion arresters appeared to have passed considerably larger lightning currents successfully than had the valve arresters.

3. Published data on frequency of occurrence of surges of great magnitude through distribution arresters are rather sketchy, and the field observations described in the preceding lead us to the belief that distribution arresters are subjected to larger currents more frequently than is believed generally. Furthermore, existing data may not apply too well to the expulsion arrester because of its lower impedance. It would seem that some field data on discharge currents through expulsion arresters would be valuable.

4. Old distribution transformers are widely thought to have impulse strength below the standards established about 1932. There can be no proof on a comparable basis as impulse testing seldom was done previous to this time. Based on the fact that a great number of failures of old transformers attributed to lightning were actually lead and bushing failures, we are of the opinion that—except for the leads and bushings—transformers built from about 1920 to 1932 were not particularly deficient in impulse strength. It is our opinion that by overinsulating the leads (that is, providing the lead with insulation greater than that of present-day transformers) together with other reconditioning and sealing, we obtain performance almost as good as modern transformers, and also that we obtain ample protection from expulsion arresters.

5. It appears from the paper that some expulsion arresters may be limited in application by a maximum current interrupting capacity less than the fault current available on some systems. It is our understanding that expulsion arresters (and expulsion fuses) have a certain "current-limiting ability" that is, measured fault current has been observed as less than calculated fault current at high values. This is attributed to arc impedance, which is substantially the total impedance offered when expulsion arresters are connected directly across a large source. If this is correct, it would appear that the expulsion arrester generally is not limited in application by available fault current.

6. A possible advantage of the expulsion arrester which is not discussed is the ability to withstand system overvoltages. This paper states "in fact, excessive system voltage may be its (the valve-type arrester) chief enemy." We also have understood that system overvoltage as low as that which may result from neutral displacement (about 4,160 volts on a 3-kv arrester) may suffice to damage some arresters. As 3-kv arresters have 60-cycle breakdown voltage of the order of 4–12 kv, this appears reasonable. Expulsion arresters, having corresponding values of 18–25 kv, should be affected less by system disturbances. This

would seem to offer promise of fewer failures from these sources.

7. Operating people who work their feeders "hot" with rubber goods require that all energized equipment within reach be covered readily by rubber goods. Valve-type arresters inherently fulfill this requirement well, but expulsion arresters require added precautions. The grounded bracket of some expulsion arresters also requires special precautions. These facts are impeding the general acceptance of expulsion arresters.

The author's comments on these points, particularly those founded on supposition and limited field observation, would be very interesting.

E. C. Starr (Oregon State College, Corvallis, Oreg.): From the point of view of the operating engineer, this paper presents a very clear and useful comparison between valve and expulsion types of lightning arresters. One point not discussed however is the very rapid rate of decay of voltage across the transformer when protected by the expulsion arrester. This point is brought out in Figures 4a and 4b of the paper. The maximum rate of decay in Figure 4b is approximately five times the maximum rate of rise on the wave front.

As the chopped-wave and front-of-wave tests have as their purpose the testing of turn insulation, it appears that more severe duty is imposed on this insulation by the action of the expulsion arrester in applying the equivalent of a reversed steep-front wave than is imposed by the actual tests. Additional comment by the authors on this point would be appreciated.

H. F. Ostman (Union Electric Company of Missouri, St. Louis): The authors have brought out and discussed very effectively the more important points to be considered in determining the desirability of using the valve-type versus the expulsion-type arresters. There are some questions, however, that occur to us that have not been touched on.

First, in showing the margin of protection on the front-of-wave test in Figure 4b of the paper, a margin of 52 kv results with the expulsion arrester based on a rate of rise of 330 kv per microsecond.

1. Is this rate of rise considered representative of what might be expected in the field? It is our feeling that the insulation levels of lines in this class now are being built to values that will allow much steeper rates of rise without flashover of other equipment with consequent narrowing down of the margin.

2. The effect of lead distance between arrester and protected equipment would appear to be a factor that should be given consideration in choosing the type of arrester to be used. For instance, with conventional transformers a 10-foot distance between arrester and transformer on 13.2-kv lines would not be unusual. If steeper rates of rise than is shown occur, an additional margin must be considered to take care of the lead length. This would appear to make the valve-type arrester more attractive because of its inherent lower breakdown value and consequent greater margin of safety.

3. A point that we have questioned is the variation in breakdowns that actually will be experienced between individual arresters from any given lot. For instance, are the breakdown values shown in Figure 4 of the paper for both types of arrester the maximum for these makes or will there be an appreciable difference between individual arresters both above and below the values shown? Also, how do the two types of arresters compare in the inherent control that can be built into them from this viewpoint? This consideration may affect further the margin shown.

Secondly, in the case of very heavy surge currents at high rates of rise, will the valve-type arrester on the front of the wave control the voltage as shown or will it tend to overshoot appreciably? If this is a factor, do the authors have any data indicating the magnitude of surge currents necessary before this phenomenon becomes noticeable?

Edward Beck and **A. D. Forbes:** The authors are very gratified by the number of opportune discussions provoked by their paper. We recognize that the subject is controversial; this was one of the reasons for the paper. It was hoped that the experience and points of view of the users of lightning arresters would be expressed, as they have been. The discussions appear to substantiate the conclusion drawn at the end of the paper.

In answer to Mr. Hatch, to the best of our knowledge the statement made in the paper regarding lockoutproof performance is correct as applied to the arresters discussed. It is recognized that on other older types of valve arresters lockouts have occurred to annoying degrees. The valve arrester discussed in the paper has been in use for eight years. No cases of line lockout have been brought to our attention. We have concluded, therefore, that none has occurred.

In the matter of surge current capacity we again are speaking of modern arresters such as those discussed in the paper. The paper states that expulsion arresters surpass the earlier valve arresters in surge current capacity. It also states that for long low current discharges it is the authors' opinion that the expulsion arrester has greater discharge capacity than the valve. The probabilities of occurrence of discharges of various magnitudes and shapes thus enter into the picture and it is our opinion that the answer will be found with additional experience on modern arresters of both types and publication of this experience. In general, we believe that Mr. Hatch's statement is correct

We agree that more data on the character of the currents discharged by both expulsion- and valve-type arresters in the field under comparable conditions of installation are needed. In some data previously published on discharges through distribution arresters discharges through expulsion arresters are included. The best data available to date on expulsion devices are those of Figure 11 of a paper by F. E. Andrews and G. D. McCann.[1] While these data were collected on high-voltage tubes installed on a 33-kv line, they are indicative of the currents to be expected. It is the authors' opinion based on experience with various arrester designs that higher currents than so far measured do occur occasionally, and this has been mentioned in earlier AIEE papers,[2-4] but unfortunately the data accumulated to date are not sufficient to indicate their probability accurately. Theoretically, if we accept the conclusion that a lightning stroke injects a certain current into a system, the currents discharged by the two types of arrester should not vary by very much. The Andrews and McCann paper also reports that several tubes may discharge during one disturbance.

Mr. Hatch's comments on the reconditioning of old transformers is of considerable interest especially as his opinions seem to be borne out substantially by the actual testing experience as described by Mr. Whitehead. We feel, however, that overinsulating the leads above the level used on modern transformers would not serve any useful purpose and would not in any way compensate for a lack of adequate insulation in the transformer proper. It is necessary that both the transformer winding and the leads have adequate strength as a failure will take place at the weakest point regardless of how strong the stronger points may be.

In answer to Mr. Hatch's comments on application limitations, some expulsion arresters are not limited in application by available fault current. There are some, however, for limited application, which have a stated fault current restriction. Tubes for high-voltage systems definitely are limited in this respect.

In regard to the effects of system overvoltage, it is true that the usually higher 60-cycle spark-over voltage of the expulsion-type arresters tends to make the expulsion arrester less affected by system disturbances. However, the spark-over voltage alone cannot be used as a criterion of the risks; the arrester also must be able in the emergency to clear the system overvoltage should the arrester be discharged by a surge during the interval when the overvoltage exists. The use of arresters rated at more than 4,160 volts is the only assurance of proper performance in the case mentioned.

In reply to Mr. Starr, with respect to decay of voltage, it is true that the expulsion-type arrester produces a more rapid rate of decay. It is also true that in some transformer designs this more rapid rate of decay imposes more severe duty on the turn-to-turn insulation. It should be noted, however, that American Standards Association standards have been established for chopped-wave withstand tests as well as full-wave tests for transformers. This chopped-wave test not only covers the ability of the transformer to withstand the rise in voltage but also the decay of voltage. Thus transformers meeting the ASA standards are required to have strength ample to withstand the conditions mentioned.

Mr. Whitehead's comments are very interesting particularly as they tie in very closely with Mr. Hatch's fourth point.

We think it desirable to state that we understand through verbal discussions with Mr. Whitehead that the pole-top tests which he describes were made on old transformers which presumably did not have the impulse strength of modern new transformers. We think it is fortunate that utilities now are able to make surge tests of this type so that the industry is not dependent entirely on the investigation of manufacturers but can draw also on the experience and experiments made by the users of apparatus.

Replying to Mr. Ostman, in the tests illustrated by the oscillogram of Figure 4b of the paper, the test wave was chosen on the basis of what the authors consider might be a suitable front-of-wave withstand test for a distribution transformer of the 15-kv insulation class. It shows that the arresters co-ordinate with the transformer insulation strength. Waves of different rates of rise occur in service. Not much data are available yet on the rates of rise of voltage on distribution systems. It is thought from theoretical considerations,[1,5] that during the development of the stroke and just after the stroke contacts the system, the voltage rises more gradually than later. This would mean that on distribution systems where the spark-over levels of the arresters are low the rate of rise of voltage to arrester spark-over might be lower than on high-voltage systems. We suspect that many surges are less steep and that a limited few may be more steep than is shown in Figure 4b of the paper. However, in any case, as pointed out in the paper, transformer insulation has a rising characteristic at short times and the test shown in Figures 4a and 4b indicates that the spark-over voltages of the arresters are below the withstand strength of the transformer. Moreover, the many years of excellent experience with the *CSP* transformer gives further evidence of the validity of the conclusions drawn from Figures 4a and 4b.

As indicated by Figure 4b of the paper, there exists a comfortable margin between the spark-over voltage of the expulsion arrester and the strength of the transformer. Thus, some overshoot of voltage at the transformer resulting from "lead effect" would be permissible, especially as it would be of extremely short duration.

Regarding the variations in breakdown that may be expected in production lots, we would comment as follows. An AIEE paper on distribution lightning arrester performance characteristics[6] states that for valve arresters the tolerance permitted by any one manufacturer does not exceed 25 per cent. Sampling tests on production of valve arresters discussed in the paper indicate that the large proportion will have breakdowns as shown in the figures, with an occasional few that may deviate by the established tolerance. Impulse tests on each distribution arrester are not economically feasible at present. Similar performance data for expulsion arresters have not yet been published by the AIEE. Sampling tests on De-ion arresters indicate that they have quite consistent breakdowns in the region indicated in the paper. In the valve arrester discussed in the paper, the control is exercised by 60-cycle tests on the arrester in addition to control of manufacturing tolerances on parts. In the De-ion arrester the control is exercised by the mechanical assembly and manufacturing tolerances on parts.

In the case of very high surge currents at high rates of rise, the voltages on the valve arrester will be higher than shown in the figures of the paper. The paper calls attention to the fact that, on a 9-kv distribution valve arrester with a 65,000-ampere discharge, which has a steep rate of rise of current, the voltage peak may be 70 kv. The peak is of short duration and has subsided before the crest of the current discharge is reached. There is an effect of rate of rise of current on the peak voltage developed across the valve element. Just where it begins is difficult to say. There is some indication in the oscillogram of Figure 4b of the paper. The volt–time characteristic at 20,000 amperes has a slight hump of short duration which does not appear in the volt–time curve for the 5,000-ampere discharge. The peak of this hump occurs before 10 microseconds, which is the time at which the crest of the discharge current is reached. It is, therefore, probable that this is an effect of rate of rise of current.

We believe that the thoughts expressed by Mr. Bennett and Mr. Longley in their discussion are in substantial agreement with the thoughts expressed in our paper. It appears to us, however, that if transformers with impulse levels as low as intimated by Bennett and Longley in their reference to their Figure 1 are kept in service, then numerous difficulties may be expected regardless of the type of lightning protection. In this connection we wish to refer to another discussion, that of Mr. Whitehead. Possessors of impulse-testing equipment, the Duquesne Light Company has set up certain standards for the impulse strength of reconditioned transformers. Evidently this company considers this level (45 kv for 2,400-volt transformers) the minimum for their standards of service. However, if a lower level than that mentioned by Mr. Whitehead in his discussion were satisfactory for his company's service standards the figure surely would not have been set at 45 kv. The need for greater margins than those that might be inferred from the discussion of Bennett and Longley and their reference to Figure 1 of their discussion is indicated thereby. In considering the transformer cut-out and arrester as a pole-top assembly, it is our opinion that even with the interconnection there are factors such as spark-over, lead lengths, and rate of rise of discharge current that influence the voltage at the transformer. Mr. Whitehead's discussion appears to corroborate this and to indicate that under the varying conditions of installation and duty the degree of protection to the transformer is not related directly to the single factor shown in Figure 1 of the discussion and used by Bennett and Longley to draw their conclusions.

It is true that there is a new trend to increase transformer loadings. The practice appears on the average to be well justified economically even though the rate of insulation deterioration may be somewhat accelerated. In this respect the completely self-protected transformer fills a real need as the heavier loadings can be carried without the same danger to the transformer insulation.

References

1. Lightning Investigations on 33-Kv Wood-Pole Lines, **F. E. Andrews, G. D. McCann.** AIEE Transactions, volume 64, 1945, November section, pages 768–77.

2. Lightning Currents in Field and Laboratory, **P. L. Bellaschi.** AIEE Transactions, volume 54, 1935, August section, pages 837–43.

3. Surge Protection of Distribution Systems, **J. K. Hodnette, L. R. Ludwig.** AIEE Transactions, volume 56, 1937, June section, pages 683–8.

4. Lightning and Lightning Protection on Distribution Systems, **R. C. Bergvall, Edward Beck.** AIEE Transactions, volume 59, 1940, August section, pages 442–9.

5. Discussions by **J. E. Clem** and **K. B. McEachron** of Co-ordination of Power Transformers for Steep-Front Impulse Waves, **V. M. Montsinger.** AIEE Transactions, volume 57, 1938, April section, pages 189–90.

6. Distribution-Type Lightning-Arrester Performance Characteristics, AIEE committee. AIEE Transactions, volume 61, 1942, March section, page 132.

Phase-Comparison Carrier-Current Relaying

Discussion and authors' closure of paper 45-148 by A. J. McConnell, T. A. Cramer, and H. T. Seeley, published in AIEE TRANSACTIONS, 1945, December section, pages 825–33.

S. L. Goldsborough and **H. W. Lensner** (Westinghouse Electric Corporation, Newark, N. J.): The phase-comparison carrier relaying system described is similar in its fundamentals to the system previously described.[1] However, the detailed method of utilizing the fundamentals is sufficiently different to involve the application of the relay in somewhat of a welter of mathematical formulas, as is evidenced by the numerous appendixes.

The recurrent[2] fallacy which assumes that a 3-phase fault can be distinguished accurately from single- and double-phase-to-ground faults by the operation of three overcurrent elements did, indeed, simplify the situation down to the many rules and regulations set forth in the paper. Nevertheless, as is well known in the art, fault current in many instances does flow on all three phase wires during single-phase and two-phase-to-ground faults. In actual service there should be many cases where the overcurrent relays operate at only one end of the section to distort the network. Under this condition positive, negative, and zero sequence components of the fault current will appear at one end, and only negative and zero sequence components will be present at the other end. There also will be cases where the overcurrent relays operate at both ends of the line section, thus introducing another set of conditions which should be taken into consideration. When the overcurrent relays operate on single-phase or two-phase-to-ground faults, the network output no longer is represented by the relatively simple expression

$$E=K_c(-j\sqrt{3}I_2+KI_0)$$

on which the formulas in the appendixes are based, but is given by the expression

$$E=K_c(ka-a)I_1+K_c(ka^2-a)I_2+K_0kKI_0$$

It would seem that an application of this relaying system made on the basis of the formulas in the appendixes and which came near the limits would be very likely to operate incorrectly in the cases where the overcurrent relays operate on ground faults. It appears, therefore, that the application with this contingency in mind should be checked. It would be interesting to witness the result of extending the mathematical analysis to include this case.

It is difficult to see how the system as described could be expected to ride through an out-of-step condition without tripping. During this condition it definitely is expected that the overcurrent relays at both ends of the line section will pick up and drop out each slip cycle. However, it cannot be reasonably expected that the action of the relays at opposite line terminals will be synchronized exactly in timing within the limits set by the operating time of the tripping relay. No matter how accurately the pickup of the overcurrent relays is adjusted, it surely can be expected that the relays at one end of the line section will pick up or drop out at least 2.5 cycles before or after the relays at the other end. Consequently, there will be positive sequence filter output at one end and no output at the other end for a time sufficient to permit tripping. This possibility of incorrect tripping occurs not only during definite out-of-step conditions, but on all synchronizing surges which reach the pickup value of the overcurrent relays.

The same condition exists for remote external 3-phase faults where the current hovers around the pickup value of the relays. The three overcurrent elements at one terminal might pick up, but perhaps only one or two of them would operate at the other terminal. Operating voltage would be applied to the one comparer tube, but no restraining carrier signal would be received to prevent an incorrect operation of the trip relay. For internal 3-phase faults, some of the simplicity of the scheme is lost, since operation of five mechanical relay elements is necessary before the trip circuit is completed.

REFERENCES

1. A NEW CARRIER RELAYING SYSTEM, T. R. Halman, S. L. Goldsborough, H. W. Lensner, A. F. Drompp. AIEE TRANSACTIONS, volume 63, 1944, August section, pages 568-72.

2. Discussion by S. L. Goldsborough of DISTANCE RELAY PROTECTION FOR SUBTRANSMISSION LINES MADE ECONOMICAL. AIEE TRANSACTIONS, volume 62, 1943, page 978.

William L. Vest, Jr. (Western Massachusetts Electric Company, Springfield, Mass.): In 1933 the Western Massachusetts Electric Company installed 26 line terminals of carrier relays. This relay equipment for phase and ground protection at one terminal consisted of 6 relays and associated control devices having a total of 12 contacts of which 8 were used for tripping and/or carrier control. A panel space of 7 square feet was required to mount this equipment. In 1942 2 additional sets of carrier relay equipment were installed. At that time all the equipment for one line terminal was in one case and consisted of at least 12 different elements, with some 26 contacts in use, of which 19 were used for tripping and/or carrier control. A panel space of 4$^1/_2$ square feet was required.

The relay device described in this paper occupies 2$^2/_3$ square feet of panel space, has only six moving parts and six contacts, of which only two are used for tripping and/or carrier control. The moving parts are simple plunger or telephone-type relays. Incidentally, the earlier carrier installation required that the carrier current transmitter–receiver be installed as near to the line coupling device as possible, whereas today this equipment may be installed indoors adjacent to the relay equipment, which facilitates the installing, testing and maintenance procedures.

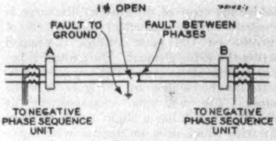
1φ OPEN
FAULT TO GROUND
FAULT BETWEEN PHASES
A
B
TO NEGATIVE PHASE SEQUENCE UNIT
TO NEGATIVE PHASE SEQUENCE UNIT

Figure 1

Thus we see a remarkable improvement and simplification of equipment in the 12-year period since our initial installation in 1933.

In 1928 A. S. Fitzgerald first stated the ideal qualifications for an ideal carrier relay system and described a scheme which would accomplish this. The succeeding developments did not follow all the earlier criteria, and it is only in the past few years that comparison of current at the two ends of the line has come to the fore. In that time three schemes have been described, of which the one described in the paper under discussion is the third. All arrive at the same result, but by different methods, and we of the relay protection field now have several schemes available.

In the practical application of the equipment described here, the authors give certain limits of operation, and methods of determining these limits. However, such limits involve the usual faults. What effect would a fault such as shown in Figure 1 have on the voltages derived from the network sequences at each end; that is, would the phase angle of the two voltages be such to indicate an internal fault, or would there be enough shift due to the difference in secondary phase currents to indicate an external fault? It might be argued that a fault such as indicated in Figure 1 never would happen. That might be true of a new line, but, when these relays are applied to lines which have low insulation levels and already have seen years of service, then anything can happen and usually does.

This paper describes a product which has been laboratory tested, probably with solid faults. It is hoped that by now some of these devices have been installed, and the authors can give us some data on actual operating experience, particularly where arcing between conductors occurs, such as during electrical storms.

The tripping time of the relays installed in 1933 was in the order of 4–6 cycles. Following this, the trend was downward to 1 cycle, and now this relay has tripping time of approximately 2$^1/_2$ cycles. It appears that this time is necessary and is a function of the comparer tube circuit. What are the prospects of this time being reduced to the 1-cycle time previously attained?

A. F. Drompp (nonmember; The Detroit Edison Company, Detroit, Mich.): The authors have done a very creditable job on a subject of considerable interest. Phase-comparison carrier-current pilot relaying in a simplified form, such as is described in this paper, would find a much wider field of application than the conventional directional carrier schemes now in general use.

From the operating companies' standpoint, it is gratifying to see the renewed interest in this field, and it is hoped that experience with this scheme will prove it to be a thoroughly satisfactory simple carrier-current pilot relaying system. The system described in this paper as well as several other systems which have been announced in the past, seem to offer good possibilities, although, in our opinion, this type of relaying is still in the developmental state.

A carrier pilot relay system that does not require a potential source overcomes two of the major drawbacks that have retarded the extensive use of carrier-current relaying; namely, cost and complexity. The primary factor now remaining is the one of proving the reliability and accuracy of such schemes. For this reason the absence of data in this paper, indicating the performance of the scheme under laboratory or field tests, is particularly disappointing.

Considerable effort has been put into the mathematical analysis of the sequence filter and its output. We would like to have seen the vacuum-tube control circuits analyzed equally thoroughly, especially with reference to safety factors and limits in the application of this scheme.

In a control system involving the coordination of vacuum-tube circuits, such as in this case, ample margins must be allowed between the values at which the component parts function. While the authors point out the effect of the normal variations in such things as control voltage and differences in fault current magnitude at the two terminals on the operating characteristics of the scheme, it appears that other changes in these characteristics may show up in field tests. Such a condition might arise when the protected line is carrying fault currents for an external fault. These currents may be of sufficient magnitude and phase to initiate tripping, but tripping is prevented by the blocking feature at the load end. If at this time a transient, caused perhaps by solenoid discharge, is imposed upon the control bus, some tubes may be shock-excited into momentary conduction sufficient to pick up a relay and permit the trip circuit to become energized. It may be that the scheme easily could be altered to overcome this possibility, but relay engineers would be relieved if they could be assured of this.

The simplified drawing, Figure 5, shows the fault detector and trip relays picked up directly through a vacuum tube. A short circuit between tube elements, tube deterioration or shock-excitation possibly could cause a tube to conduct and result in false tripping. Experience with the conventional-type carrier has indicated that it is desirable to have a contact in these circuits which will verify the existence of a fault on the line and thus prevent tripping on tube failures.

The use of negative-phase-sequence plus weighted zero-phase-sequence filter appears to have certain advantages. However, the necessity for using the three overcurrent relays introduces a complication in the application of this scheme. The paper does not explain in its discussion of operation what could be expected if, as is possible, a fault external to the protected line should draw current of such magnitude through the line that these overcurrent relays at one terminal would pick up, but those at the other end would not. In that case, the filters would not be similar, and there seems to be a possibility of false tripping. A study of the system suggests that settings could be so co-ordinated between the overcurrent relays and the fault detector at both terminals that the current required to pick up the overcurrent relays always would be greater than that required to pick up the fault detector. However, this means pyramiding settings and co-ordinating vacuum-tube circuits to work together within narrow limits. The solution to the completely successful application of this scheme seems to be a detailed study of a multitude of possibilities and the selection of a setting from these results. It was hoped that the advent of these inherently selective schemes would ease the burden of such lengthy analysis. That hope apparently is not realized in this scheme.

Whether desirable or not from the standpoint of the relay engineer, operating companies are faced more and more with the necessity of providing adequate protection for three-ended transmission lines or for tapped lines. It is this sort of thing that quite often presents a difficult or even insurmountable problem for orthodox relay systems to meet. The authors have given us no inkling that this problem can be solved by their system and if so whether or not the additional complication still would permit the usual tolerances between fault detector and trip settings to be applied.

In the paragraph on page 827 concerning the phase-sequence network, it is not clear which quantity is rotated through 60 degrees. Neither is it self-evident how the two constants K_c and K_a (equation 18) can be made equal. A statement explaining this more fully would be appreciated. The drawings of this part of the scheme require considerable study and some correction to reconcile them with the text of the paper.

More detailed information on the method of testing this equipment would be of considerable interest. The inclusion of reliable and easily operated test facilities in the relay units is a very desirable feature.

A. J. McConnell, T. A. Cramer, and H. T. Seeley: Mr. Drompp notes the lack of performance data during laboratory or field tests. Of course, laboratory tests using an artificial transmission line were made, but such tests are difficult to report upon, except to state that correct operation was obtained with all types of internal and external faults, including faults during out-of-step conditions. Field tests are scheduled to be made in December 1945.

The excitation network was stressed in the paper because of early work on phase-comparison relaying[1] which showed that blind spots can occur if not properly guarded against. Compared with the means of excitation, the vacuum-tube circuits present a relatively simple problem. Past experience indicated that suitable reliability could be obtained by observing the following rules:

1. Use simple circuits employing a minimum of vacuum tubes for each function.
2. Use vacuum-tube types which have a proved record, and apply them within the manufacturer's rating.
3. Use only high-vacuum types.
4. Avoid tubes with extreme power sensitivity.
5. Use circuits which compensate for changes in d-c supply voltage.

Difficulty from control-bus voltage surges can be experienced even in the absence of vacuum tubes. The best possible insurance against such trouble is to eliminate the surges by avoiding a potential supply drawn through an inductance which may also carry a current subject to rapid change. In practice certain arrangements of conductors in steel conduits can cause difficulty. However, the equipment employs the following safeguards against inadvertent operation during control voltage surges:

1. The operating voltage applied to the comparer screen grid is limited.
2. The restraining voltage on the comparer control grid is independent of d-c control voltage (simple diode rectifier).
3. Tube types having high power sensitivity are avoided to reduce the possibility of spurious oscillations caused by shock excitation.
4. Devices which operate on instantaneous peak values (thyratron inverters, trigger tubes, and the like) are avoided.

In regard to short circuits between tube elements, experience has indicated that tube handling is the principal cause. The a-c testing means provided with the equipment provides a simple check after replacing tubes.

Extra fault-detector contacts may be added external to the phase-comparison equipment if desired. The manufacturer's dilemma is indicated by the fact that one discusser suggests more contacts while another commends him for reduction of the number of contacts.

Mr. Drompp is correct in surmising that the fault-detector setting is higher than that of the phase-overcurrent relays. Thus, at the pickup level of a fault detector, all six phase-overcurrent relays (three at each line terminal) are sure to be picked up. Unfortunately, this fact was not made clear in the paper. (This also explains the question raised by Mr. Goldsborough and Mr. Lensner in regard to out-of-step blocking.) Pyramiding of settings, for the reason given, is necessary in all carrier-current schemes using the overcurrent principle. Figure 10 of the paper indicates that the fault detector can be set just about as accurately as a plunger-type overcurrent relay.

Mr. Drompp's expressions "detailed study of a multitude of possibilities" and "lengthy analysis" appear to be somewhat pessimistic. The only current values necessary are those required for the simplest overcurrent relays with these values inserted in relatively simple formulas. Given the current values, all necessary computations can be made in less than one-half hour.

The equipment is not applicable, in its present form, to 3-terminal lines, except in a relatively few special cases. For general 3-terminal line applications, its use would be somewhat questionable for various reasons, among which is the fact that its pickup current would have to be doubled. The reason for this is that on an external fault the terminal with the total current must be blocked by at least one of the remaining terminals, which can, in the limit, have one half of the total current. Thus, the pickup of the relay at the terminal carrying the total current must be twice the normal value in order to insure a current level at one of the remaining terminals capable of sending an adequate blocking signal.

Regarding the penultimate paragraph of Mr. Drompp's discussion, the voltage, E_C, corresponding to the phase a current is shifted 60 degrees in the lagging direction in accordance with equation 13, Appendix II (by means of resistor $R3$ and capacitor $C1$). K_c and K_a' are made equal by adjustment of $R2$, that is, by making E_c and E_C equal under balanced 3-phase conditions.

The a-c test switches at each line terminal have five positions marked *out*, *off*, *nor*, *off*, and *in*. When the test switch at each line terminal is in the *in* position, test currents simulating an internal fault flow in the two equipments, and both trip lamps should light. With one test switch in the *in* position and the other in the *out* position, one of the test currents is reversed relative to the other, simulating an external fault, and neither trip lamp should light. Proper sequence co-ordination is obtained via the carrier-current test telephone. This test roughly checks practically every circuit, tube, and relay in the equipments at both line terminals.

Figure 1 of Mr. Vest's discussion presents a problem not at all unique to the relay engineer. It so happens that with the conditions of Figure 1, correct relay operation would be obtained, but it is not at all difficult to conceive similar conditions during which correct operation would not seem to result. Granted that "anything can happen," would it not be reasonable to consider the probability? For example, in Mr. Vest's illustration it is practically impossible for the condition shown to come about on a sound line in the few cycles necessary for relay operation. Let us assume that the fault began as a phase-to-phase fault with one conductor burning open and one of the open wires dropping on the ground. Before this could happen, the relays would have operated on the phase-to-phase fault. (In fact with the relay speed involved, it is highly improbable that the conductor would burn open.)

In regard to the operating time, the phase-comparison system at low multiples of pickup is already as fast as conventional systems. It may be that operating experience with the present conservative design will justify additional risks to reduce the time at high multiples of pickup to the same low level now achieved with the other systems.

The "recurrent fallacy" injected by Mr. Goldsborough and Mr. Lensner appears to result from a misunderstanding of the purpose of the three overcurrent elements. Their purpose is not "to distinguish accurately a 3-phase fault from single- and double-phase-to-ground faults," but rather to assure that there is a network output during an internal 3-phase fault. During any unbalanced fault capable of operating all 3-phase-overcurrent relays, the negative-phase-sequence current or the 0-phase-sequence current will far outweigh the positive-phase-sequence current (introduced by the operation of all three overcurrent relays). The magnitude of the positive-phase-sequence output, relative to the negative or zero-phase-sequence output, is chosen purposely to limit the phase shift to a value insufficient to cause tripping.

---

[1] Reference 1 of the paper.

Electric Drives for Steam-Electric Generating-Station Auxiliaries

(45-151)

Power Systems for Auxiliary Drives in Steam-Electric Stations

(45-150)

Auxiliary-Power Supply for Generating Stations

(45-152)

Central-Station Auxiliary-Drive Motors for Constant and Adjustable Speed

(45-153)

Modern Practice in Power-Plant Auxiliary Equipment and Systems

(45-168)

Discussion and authors' closures of papers published as follows in AIEE TRANSACTIONS, 1945:

45-151 by Wm. R. Brownlee and J. E. Elzi, November section, pages 741–5.

45-150 by J. B. McClure and S. I. Whittlesey, December section, pages 844–51.

45-152 by V. E. McCallum, October section, pages 693–5.

45-153 by Hal Gibson, November section, pages 746–50.

45-168 by H. N. Muller, Jr., December section, pages 868–72.

F. W. Gay (Public Service Electric and Gas Company, Newark, N. J.): Figure 4 of Mr. Brownlee's and Mr. Elzi's paper indicates that the motor inrush current will diminish with the duration of the interruption down to zero time. Figure 1 of the discussion indicates that this may not be true. Figure 4 of the paper also indicates that the duration of the inrush current increases very little with duration of the power interruption. Our tests show a steady increase in duration of surge current with duration of the power interruption. In our tests a power interruption of 5-seconds duration is followed by a surge of 170-cycles duration. Further investigation of the subject is indicated to clear up these discrepancies.

Figure 1 shows an oscillograph for a power interruption of 50-cycles duration. This curve is interesting in showing the voltage decay on the auxiliary power bus after it is disconnected from the service transformer. It is calculated that the deceleration would have amounted to approximately one-half-cycle displacement in 12 cycles, had the machines been loaded fully; that is, if power were restored in 12 cycles, it would catch the decaying bus voltage directly out of phase and at approximately three fourths of its full value. After a power off time of about 24 cycles the bus could be reclosed with minimum disturbance, since the decaying bus voltage again would be inphase with the service voltage; but again at about 36 cycles the bus voltage would be out of phase and still would have a value about 20 per cent of normal. It would seem safest to delay the reclosing until the voltage on the disconnected bus has decayed to substantially zero.

Paper 45-150 as a whole is well written and covers the subject in an excellent manner.

Conclusion 2 is that the direct connection of auxiliary power transformers to the generator leads is a preferred method of power supply. There is little doubt that, when the use of powdered fuel in any station is less than about 30 per cent of the station capacity, this method will prove satisfactory under most operating conditions. When the percentage capacity of generation employing powdered fuel becomes great in any station, it is necessary to safeguard the auxiliary power supply against system disturbances to prevent the possibility of fire extinguishment with attendant delay in starting and possible explosion.

Two methods of safeguarding the auxiliary power supply against system disturbances are available:

(*a*). Trip the generator from the bus in case of sustained low system voltage.

1. If a shaft end exciter is used, tests would indicate that a sustained low voltage for 5 seconds is permissible before tripping.
2. If a motor generator excitation system is used and the time delay is more than about 3 seconds, a very large flywheel will have to be used with the motor generator exciter set. In either case auxiliary power motors should be purchased with pull-out torques sufficient to operate continuously at 70 per cent of normal auxiliary bus voltage. With such oversize auxiliary power motors no attention need be paid to sustained low bus voltage, provided the auxiliary bus voltage is not lower than 70 per cent.

(*b*). An alternative solution to protect against sustained system faults is the use of a separate generator connected to the shaft of the main unit to supply the essential auxiliaries. When such an auxiliary power generator is used, sustained low system voltage has no appreciable effect on the auxiliary power system.

Since high-pressure condensing turbines at 3,600 rpm are available in capacity greater than the capacity of the available generator, the use of an auxiliary power generator makes possible the adding of the auxiliary power requirement to the maximum available generator size to obtain a larger unit.

With the shaft-driven auxiliary generator there will be no need to trip the generator from the line following a sustained fault, even though the generator may go out of step with the system. The generator may be restored to synchronism by reducing the steam flow to the turbine. The required reduction in steam flow (whether automatic or by hand) for any sustained low voltage should be in proportion to the voltage reduction and will be greater for machines of low short-circuit ratio.

Experience has shown that, when the reduction in steam flow is automatic, the restoration should be manual, as the local load reduction in per cent due to low voltage will be greater than the voltage drop in per cent and the load returns slowly to its normal value over a period of 10 to 15 minutes.

C. A. Harrington (Cleveland Electric Illuminating Company, Cleveland, Ohio): The conclusions expressed in paper 45-151 are substantially the same as those which have been observed in the design of generating plants for the Cleveland area during the past several years. The authors have given a clear and concise statement of principles, which, in our experience, have seemed to work out quite successfully. The following comments relate to details rather than to the general conclusions.

Although across-the-line starting is regarded as standard practice with us, as with others, we sometimes find that we have particular motors which do not stand up satisfactorily under the heavy stresses imposed by such procedure. This occurs despite the fact that the motors were designed and sold for full-voltage starting. In such cases it seems better to provide reduced-voltage starting equipment than to be confronted with frequent burnouts of the motor windings. In a few other cases reduced voltage is used in order to avoid faster acceleration of the driven equipment than is wanted.

The authors mention the use in some instances of two separate motors for obtaining high and low speeds for boiler draft fans. Our practice has been to install for this purpose a two-speed motor, which requires less space but is subject to the disadvantage that, if there is a failure of either winding of the motor, the whole drive is lost for perhaps an extended period.

Of considerable interest are the tests made to determine drops in motor voltage as a function of transmission-line fault duration, and speed loss in various auxilia-

Figure 1

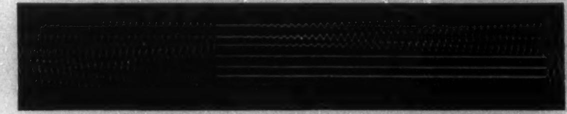

ries as related to length of interruption. The curve in Figure 4 which indicates that reacceleration of load can be accomplished in not more than 0.23 second, regardless of the length of the preceding coasting period, is rather surprising. It seems inconsistent with the ball-mill characteristic as shown in Figure 3, which shows that the mill would be stalled completely at the end of 4 seconds and that more than 2 seconds are required to bring it up to speed. Obviously, the authors are using the term "inrush current" in a different sense than accelerating current.

Clarification would be helpful with reference to the statement that "standard starters....are not suitable for motors in an interlocked scheme because the auxiliary switch on the contactor would start the tripping sequence of the other motors....." Is not that just what is wanted? In Cleveland we have had no difficulty in connecting standard industrial contactors and/or latched-in circuit breakers to achieve any of the usual forms of cascade control.

R. J. Cooper (Georgia Power Company, Atlanta, Ga.): The authors of paper 45-151 have presented a very thorough coverage of the subject and the conclusions drawn are easily justified.

As our experience has demonstrated the reliability and economy of the all-electric drives for station auxiliaries, we are entirely in sympathy with the main points brought forward by the authors.

As early as 1929 when one of our main steam-electric generating stations was being designed, it was thought justifiable to install duplicate station service transformers served from the generator bus to supply the electrically driven auxiliaries. At that time one steam-driven boiler feed pump (the only steam-driven auxiliary) was installed. In later years when the second unit was installed, the steam-driven pump was removed in favor of a spare motor-driven pump. This plant now has 3 60,000-kw units with no steam-driven auxiliaries. Interconnections between station service busses also eliminated the need of spare transformers.

In 1941 the first unit of another plant was installed with no steam-driven auxiliaries. Other units were installed following the same general scheme shown in Figure 1 of the paper, until at present we operate 3 40,000-kw units at this location with all-electric drive auxiliaries.

Various types of speed control are in use including wound rotor variable speed motors, variable speed hydraulic couplings, and two-speed (double wound) motors.

On a system which includes many long transmission lines and interconnections and on which undervoltage protection is not used, the necessity for motors designed for across-the-line starting is easily recognized.

The tests outlined to ascertain the possibility of the flame being extinguished in the boilers as a result of momentary voltage disturbances should be of interest to many plant operators. These tests tend to set at ease the minds of those inclined to doubt the value of co-ordinated control and relay schemes used in connection with applications of this kind.

Although there are many opinions as to the proper type of relay protection to be used in this type of service, we have had very satisfactory service from either induction-type overcurrent relays with instantaneous devices, or thermal-type relays with instantaneous devices. Care should be taken in the selection of a relay with a curve to parallel the heating curve of the motor, if protection for thermal overloads is desired. Our experience has led us to advocate protection that will operate for locked rotor currents, regardless of the risk involved during normal starting. If boiler operators are cautioned as to the risk, no serious delays result from unnecessary tripping during starting. In unit-type plants this small amount of restarting time will not delay getting the unit in service. As is stated in the paper, there has been too much tendency to use standard industrial type devices for the protection of 440-volt motors.

Surely we can afford to advocate all-electric drives in these days when others have learned to place so much dependence on the many uses of electricity.

John Finlaw (Philadelphia Electric Company, Philadelphia, Pa.): A review of paper 45-150 indicates a thorough understanding on the part of the authors of the requirements of a steam-electric station for auxiliary power drive and the need of careful design.

The increasing number of large pulverized-fuel-burning steam generators and turbine generators using large motors on auxiliaries such as fans, mills, pumps, and the like demands a liberally designed auxiliary power system and a positive power source available to restart the station in event of a total shutdown that affects turbine and boiler auxiliaries.

When a reliable outside source of power is available to the main station bus, then this power source and one from the generator leads usually is considered adequate. A house turbine generator supplemented by transformer supply from the main bus also provides a reliable source of energy for the auxiliary power system.

The auxiliary power transformers may be considered as reliable as the auxiliary equipment cable system.

Metal-clad bus structures are desirable for cleanliness and safety as well as reliability. This justifies the single-bus system. A well-designed bus should be sectionalized and the auxiliary equipment circuits distributed on the bus sections, and the bus setup should be operated to minimize the extent of auxiliary equipment interruption in the event of a power source failure.

The auxiliary power system relay design requires careful study and application. Relay reliability is just as essential on the station auxiliary power system as on the station main power system.

J. M. Geiger (Buffalo Niagara Electric Corporation, Buffalo, N. Y.): The authors of paper 45-150 are to be congratulated on the thoroughness with which they have studied their subject which is evidenced by the broad scope of their paper and the logical conclusions stated therein.

The writer is in accord with the opinion that the auxiliary power can be obtained to advantage from the generator terminals. It should be recognized that any electric power system, or a part thereof, is vulnerable to shutdown, regardless of the source of boiler auxiliary power. To minimize this possibility attention must be given to adequate sectionalizing of the system to produce voltage buffers, in the nature of current limiting reactors, impedance of transformers and lines, and so forth, and, in case of sustained low frequency or voltage, a prearranged program of dropping load be followed. If these precautions are taken, auxiliary power from the generator terminals is warranted.

From the writer's experience a 575-volt auxiliary power system possesses all of the advantages of a 460-volt system plus the saving and convenience of smaller cables and conduit. A reduction of 25 per cent in motor current is an appreciable amount. There has not been any difficulty or delay in obtaining 550-volt motors and control.

The writer is inclined to establish 200 horsepower (and sometimes less) in place of 250 horsepower for the maximum size motor on a 575-volt system upon giving effect to over-all cost and judgment. Here again the smaller conduit required by the 2,300-volt motor is a factor.

The writer agrees with the conclusion that a dual-voltage system should be considered where the transformer capacity is 1,500 kva or greater. For large boilers some advantage may be obtained in splitting the auxiliaries into two groups each supplied by a separate transformer. In this case a careful check of the voltage drop, consequent to starting a large motor, should be made for its effect upon voltage relays and synchronous motors, the latter now being used to drive air compressors for soot blowing. Smaller transformers, even though the quantity would be larger, are often desirable from a practical standpoint, because their size permits greater choice of location within the plant. The relative cost of using a single 5,000-kva transformer and 100,000-kva switchgear versus 2 2,500-kva transformers and 50,000-kva switchgear is about a standoff.

The manufacturers have made impressive strides in the development of control equipment for powerhouse motors. The 600-volt air circuit breakers with built-in overload and short-circuit protection have provided a long felt need. At times it is necessary to cascade these circuit breakers, in which case a few cycles delay in the instantaneous trip of the backup circuit breaker would assist in tripping selectivity. Some of the 600-volt air circuit breakers on the market are by no means reliable, and considerable improvement in performance is in order. The building of ordinary magnetic motor controllers into unit substations for the small miscellaneous motors is noted with satisfaction.

L. B. Stirling (The Shawinigan Water and Power Company, Montreal, Quebec, Canada): The use of the main station bus as a source of auxiliary power supply in a station such as Mr. McCallum has in mind almost certainly will insure that power for the auxiliaries will be available under all conditions. The reliability of such service decreases, however, in proportion to the size, the interconnection, and the subdivision of the main units and circuits. In any case this service is subject to the disturbances which occur on the main system, and these may result in the stoppage of some important auxiliary at the time when the entire station staff is occupied in locating a fault and restoring service. It is a great satisfaction to the operating staff to have a completely independent source of auxiliary power which can be relied upon to be unaffected by any fault or disturbance occurring on the main power system.

E. I. Gallagher (Philadelphia Electric Company, Philadelphia, Pa.): The author of paper 45-168 is to be complimented for the way in which he discusses the important electrical features of auxiliary equipment in modern power stations. Auxiliary drives and controls, as pointed out by the author, demand maximum reliability. The large steam generators and turbogenerators in the plant of today are usually large in capacity and of themselves very reliable, having to stay in service months at a time without shutdown; therefore, the auxiliaries, their supply systems, and controls should be just as reliable.

The discusser believes that the simplicity of the squirrel-cage induction motor with across-the-line starting is one of the reasons that the auxiliary drives are so reliable. Failures due to insulation are very rare in these motors. If the silicone varnishes will increase the life of the equipment, it will be a worth-while improvement, but the allowable operating temperatures of the present-day motors seem sufficiently high, unless lubricating oils are found that will withstand the higher temperatures. The ambient temperatures to which induced-draft fan motors are subjected may be lower than the motors used to drive forced-draft fans or boiler feed pumps.

Motor bearings of the sleeve type generally are better adapted than any other bearing to long continuous service. The only complaint about the sleeve bearing is that the inner seal is hard to maintain, with the result that oil is syphoned out of the bearing and deposited on the windings, thereby allowing dust particles (that ordinarily might go through) to collect, clogging up air passages and also causing deterioration of the insulation.

Anything that will reduce the noise level in all power plant equipment will be welcomed by the operator.

For cranes, coal handling equipment, or any of the other auxiliaries that are of intermittent operation, the wound rotor induction motor has proved very satisfactory, but for equipment which has to operate for long periods the hydraulic coupling (even with the extra bearings and cooling water) is more reliable.

Metal-clad switchgear with safety interlocking features has proved very satisfactory and with improvements in ventilation and safe removal of switching units will, I am sure, be most reliable.

Circuit breakers of all types are generally satisfactory, but I am in accord with the author in replacing oil with air. Except for the smaller and less important circuits, fuses should not be used for the reasons given by the author. Power distribution systems with which I have had experience are all of the radial design, and they have proved very reliable and are much simpler than any of the network systems. The engineer, when designing the power distribution system for station auxiliaries, knows very definitely the ultimate capacity and character of load and need not worry about future additions, as all new generating equipment installed will have its own power distribution system with the necessary ties. Simplicity is a long step toward reliability.

In conclusion the discusser thinks the author has given us an understandable paper pointing the way to greater reliability in power plant auxiliaries.

W. E. Sholl (Duquesne Light Company, Pittsburgh, Pa.): The ability of a power station to deliver power to the outgoing feeders depends so much on the performance of its auxiliary system that papers 45-150, 45-151, 45-152, 45-168, and 45-153 are read with great interest.

From these papers it is seen that we are all aiming at designing an ideal auxiliary system which has, as Mr. McCallum has so aptly expressed it, the maximum reliability together with safety of personnel, flexibility, simplicity of operation, ease of maintenance, and reasonable cost. In general practice it does not seem that the ideas of the different designers vary a great deal, although here and there one will have a somewhat different opinion from the others.

One point on which the Duquesne Company apparently went contrary to the ideas of most of the writers arose when the Frank R. Phillips station was designed. We chose a shaft-driven auxiliary generator for a source of supply in addition to a transformer bank fed from the system. This was done after a review of experiences with the auxiliary systems in the company's other stations which included all methods mentioned in the papers, such as,

(*a*). Separately driven steam station generators.
(*b*). Transformers connected to station busses.
(*c*). Transformers connected to generator leads.
(*d*). Shaft-driven station generators.

The aim has been to supply our auxiliaries with two reliable sources of power, which will not be subjected to the same voltage disturbances at the same time. This is accomplished by the use of transformers in certain stations where enough reactance is present between the sources of supply to the transformers, so that a voltage disturbance on one source is reflected in a much lesser degree to the other source. Since this principle could not be achieved because of the location on the system of the Frank R. Phillips station, the company believes it was justified in selecting the shaft-driven generator as a second source of supply.

We are in very close agreement with the authors in the choice of bus voltages, size of motors, and groupings. The Duquesne Company's classification of motors follows very closely the table in the appendix of Mr. Brownlee and Mr. Elzi's paper. Some consideration has been given to a network system, but there has been hesitation about adopting one.

In the boiler room, instead of having all the auxiliaries of one boiler on one group and those of the other boiler on the other group, half the auxiliaries of the two boilers have been put on one group and half on the other group. The operators prefer losing partial capacity on two boilers to losing one boiler completely.

Another feature in which the company seems to stand alone is in the use of the automatic transfer system. There can be a great difference of opinion concerning such a system. However we like it, incorporate it in our designs, and believe that it is quite convenient for normal transfers and that it has served us well during system disturbances.

It is interesting to note that the various writers stress the use of air circuit breakers for their auxiliaries. We are pleased to say that through the development of the air circuit breaker and dry-type transformers there is no oil in any electric equipment in the Phillips power station.

In the papers relay protection came in for considerable comment. One of the main objects of an adequate relay protective system is to disconnect a faulty piece of equipment from service with no disturbance to the rest of the system. In another case it may be desirable to remove an overloaded auxiliary from service before it does become faulted. These operations can be handled very well with instantaneous and inverse time limit relays. The correct relay setting for each auxiliary is very important.

The papers also cover other interesting subjects such as types of bearings, class of insulation, adjustable speed drives, and others. Our concluding comment will deal with the adjustable speed drives. In recent installations we have used magnetic couplings for driving the forced- and induced-draft fans. The operating men are very well satisfied with this type of drive and prefer it to any of the other types which have been discussed.

Patrick Henry Adams (Public Service Electric and Gas Company, Newark, N. J.): Papers 45-151, 45-150, 45-152, 45-168, and 45-153 seem to cover the selection of voltage, bus arrangement, and some types of equipment that are available. As to source of power for auxiliaries, great stress is laid on the transformer as the lowest in cost and most economical to operate.

Many years of experience with the transformer as the source of auxiliary power have accumulated, and the record of service reliability established is relatively good. There have been, however, occasional shutdowns of a unit or a station caused by sustained low voltage due to failure of protective relays to function as prescribed.

The care required to prevent explosions in the furnaces of boilers using pulverized fuel has developed a desire for a source of auxiliary power for boiler auxiliary drives that is free of the effect of system electric disturbances. The house generator is being used to provide this added reliability, but in most of the recent installations instead of using a separate prime mover it is connected to the shaft of the main unit to retain the operating economy of the large turbine and also attain as low first cost as possible.

The reliability of the house generator is such that a relatively slow speed motor generator set can be used for excitation of the main generator as well as the auxiliary unit. This type of exciter should help eliminate many of the troubles experienced with exciters driven from the shaft of the main unit, which include failures of commutator, brushes, brush rigging, soldered joints, couplings, gears, bearings, and many other parts that may be affected when this appendage is connected directly or geared to the main unit.

In the paper by McClure and Whittlesey the operation of auxiliary power systems ungrounded is indicated as the general practice. This brings before us the question, why has this practice been continued on such an important part of the system while at the same time the company has been busily engaged in providing a neutral ground in all other parts?

It would seem that here on a small scale is the same opportunity for arcing grounds to create similar trouble to that induced by them in the transmission and distribution parts of the system. It also would seem that a neutral ground on the auxiliary system would serve a useful purpose.

There are failures from phase to ground which occur and are indicated by the ground detectors, but these are difficult to locate, and frequently a second phase-to-ground fault develops before the first is located and cleared. The second phase-to-ground fault, probably caused by high phase-to-ground voltage, may occur on the same or any other circuit connected to the bus and produces a phase-to-phase short circuit which may take out one circuit or more.

A neutral ground arranged to prevent excessive phase-to-ground voltage and give sufficient current to ground to operate ground relays, either on the individual circuits or on the supply to a bus section, may serve to simplify the protective system in use. In some cases differential relays have been used on large motors supplied from an ungrounded system. These relays do not protect against single phase-to-ground faults, as they require more current to unbalance them than is available from a small ungrounded system such as that supplying station auxiliaries.

It would appear that a review of this subject is warranted. One method of providing an inexpensive protective ground for isolated delta systems uses three small distribution transformers connected Y-delta with the Y point solidly grounded and a current limiting resistor in one corner of the 240-volt delta.[1] The size of the distribution transformers, and resistance can be selected to give the ground current desired.

REFERENCE

1. DELTA SYSTEMS GROUNDED THROUGH HIGH RESISTANCE, A. A. Johnson. *Electrical World*, March 3, 1945, page 99.

William S. Peterson (Department of Water and Power, City of Los Angeles, Calif.): Since papers 45-151, 45-150, 45-152, 45-168, and 45-153 all apply to the same general subject, the following comments are applicable to the group rather than directed to any one paper.

The Department of Water and Power's new steam plant located in the Harbor District and designated as the Harbor Steam Plant was placed in operation in 1943. The design of the auxiliary power system for this plant closely follows the trends outlined in these papers. All auxiliaries are electrically driven with the exception that one boiler feed pump and one fuel-oil service pump are provided with steam-driven drives in addition to the motor drives. All auxiliary motors are constant-speed squirrel-cage induction type operated either from 2,300 volts or 440 volts 3 phase, depending upon the size. Economic studies made by the Department engineers indicated that motors in excess of 200 horsepower should be supplied at the higher voltage. All motors are of the across-the-line starting type and can be started and carry full load for 3 minutes at 70 per cent rated voltage. This requirement was incorporated in the design because low-voltage conditions are most likely to occur under conditions of quick pickup and maximum load.

The construction of this plant represents an unusual feature not ordinarily encountered. The plant serves a dual purpose in that it normally is operated as a stand-by source of power in case of failure of the main hydroelectric source from Boulder Dam and also is designed to furnish substitute energy during low water years. The operation as a stand-by plant imposes the requirements of picking up load from 5,000 to 75,000 kw instantaneously. This demand entails a change of draft fan speed from 60 rpm to 1,440 rpm within an interval of 14 seconds. On the other hand the operation of the plant as an energy source during low water years requires that fan speeds be maintained at constant values over a wide range of speeds, depending upon load conditions. Extensive studies by the Department engineers indicated that the best method of meeting these variable conditions for the draft fans was the use of a variable voltage d-c drive. This was adopted, therefore, for both the forced- and induced-draft fans in this plant.

The power supply for the auxiliaries is taken from the generator leads through a transformer to the 2,300-volt bus. A house turbine-driven generator is being installed to provide a stand-by source for the auxiliary system independent of outside system disturbances. In addition a 2,300-volt service from the outside distribution system is brought into the plant to provide a means of starting the plant cold.

Reliability of modern switchgear equipment has permitted the use of single bus installation on both the 2,300- and 440-volt systems. These busses, however, are sectionalized, and the duplicate auxiliaries are divided between the two sections in such a manner that one section of bus may be taken out of service and still permit operation of the plant at a somewhat reduced capacity.

Due to the complete satisfaction of the auxiliary system as it is designed for the first unit, it is intended that this system be duplicated for the second unit now in the process of installation.

H. D. Braley, J. G. Noest, and R. L. Webb (Consolidated Edison Company of New York, Inc., New York, N.Y.): It has been our opinion for some time that the subject of central station auxiliary supply and drives justifies the attention of the AIEE, and it is gratifying to see five papers on this general subject.

It seems clear from all of the papers that there is general agreement on the basic requirements for the "essential" auxiliaries and the manner of the supply thereto. It also would appear that there is fairly good agreement on the relative order of importance of principal requirements with reliability ranking first and simplicity second. To these may be added the following in whatever order may suit the circumstances and individual judgment:

3. Flexibility.
4. First cost.
5. Low maintenance.
6. Economical operation.
7. Good relay protection.

The manner in which these objectives are attained often is a matter of considerable difference of opinion, as illustrated in the papers and also by actual practice. It may be advantageous, therefore, to examine some of the elements which constitute the various requirements in order to establish a clear appraisal of their worth. This will be limited principally to the elements of reliability. We are in hearty agreement with two statements in the papers, namely, "the reliability of a station can be no better than the reliability of its auxiliaries," by McClure and Whittlesey and "Nowhere else on the entire system is the requirement of reliability so great compared with the investment in equipment involved," by Muller.

The principal elements of reliability are found in the construction and design of the equipment which best adapts it to meet the service conditions with a minimum of trouble. These may be discussed profitably with respect to the specific items composing the auxiliary system.

SOURCE OF AUXILIARY POWER

In respect to the source of auxiliary power supply we feel that the generator bus is the most reliable source since

(*a*). By design it is the least vulnerable to electric failure.

(*b*). It may draw its power directly from more than one generator and from tie feeders to other stations.

(*c*). It does not depend on any one particular generator, being in service to supply auxiliary power.

SERVICE VOLTAGES

We note that the authors of the papers appear to be in agreement regarding the use of 2,300 volts for larger auxiliary motors, and we agree with them. However, we observe a distinct difference of opinion regarding the service voltage for small auxiliaries. The McClure–Whittlesey and Brownlee–Elzi papers favor the use of 480 volts, excluding consideration of 220 or 208 volts by implication. The McCallum paper refers to use of 208 volts.

In the last ten years we have made plant extensions amounting to over 500,000 kw where motors of 100 horsepower and under are supplied at 120–208 volts. In these installations reasonable first cost of switching was obtained by use of safety switches with X or Z fuses at the load centers where high interrupting duty is required and National Electrical Code fuses, where fault currents are lower. The use of 120–208 volts permits the same load centers to be used for station lighting and allows the use of standard 500-kva and 1,000-kva network transformer units. Spare transformers are continuously available in case of failure. Use of standard network voltage permits interconnection of the station low-voltage system with the street network which provides support to the station system in case of transformer or feeder failure. The use of 120-208 volts, therefore, may be profitably employed where local conditions justify its use.

We believe also that a single transformation should be made from the bus voltage to the service voltage. Double transformations as shown in the McClure–Whittlesey, Brownlee–Elzi, and Muller papers results in buying the low-voltage transformer capacity twice, once in the low-voltage transformer and again in the 2,300-volt transformer. There is undoubtedly some sacrifice in reliability, for the same reason.

TRANSFORMERS

We foresee increasing use of air-cooled transformers for station auxiliary power supply at primary voltages ranging up to 15 kv, and in 3-phase ratings up to 5,000 kva or higher. Instead of providing 100 per cent reserve transformer capacity for each main unit, we believe a common reserve power supply for several groups of motors should be adequate. We also foresee the use of transformers grouped at load centers to form unit substations for auxiliary power supply.

SWITCHGEAR

We suggest that design of metal-clad unit substations be directed towards the development of units suitable for use under unfavorable service conditions such as prevail in turbine room basements and boiler rooms. The service generally will require dust-tight and watertight housings.

This equipment would eliminate the need for construction and ventilation of special switch houses in the boiler house and would permit location of the power supply directly at the load center.

Low-voltage switchgear such as safety switches, motor starting contactors, control stations, and so forth, should be provided with watertight and dust-tight enclosures where installed in boiler and turbine rooms. Only a portion of this equipment of such construction is available today.

In locating switchgear units, care should be taken to avoid high ambient temperature locations which are encountered in boiler rooms. In no case should switchgear be located in hazardous areas, such as adjacent to ash sluiceways.

Motor-starting metal-clad switchgear for 2,300-volt service, employing oil immersed contactors with high thermal capacity and current limiting fuses, offer attractive possibilities for some motor applications, particularly for the smaller motor sizes of 100 to 200 horsepower where short-circuit protection by other means would be difficult or disproportionately costly.

MOTORS

There seems to be general agreement that line-start squirrel-cage induction motors are in favor for a majority of the drives due to their reliability, simplicity, and ease of maintenance. While this motor is a comparatively simple machine by comparison with other types of rotating electric apparatus, there are a number of important factors which are of major importance in maintaining a high degree of reliability which have not been sufficiently emphasized.

Only brief reference has been made to the type of enclosure, although dripproof or splashproof construction is recommended for locations subject to dripping or splashing water.

For some time motor manufacturers have offered special impregnation of windings suitable for boiler room service. At best this is a poor substitute for totally enclosed motors, nor is it proof against insulation erosion from cinders, coal dust, or fly ash.

Reference has been made to modern stations being clean, free from dust, dirt, and the like. We aspire to see such a plant.

Our experience has been that no special impregnation treatment is proof against a thorough drenching from condensed steam, as a result of a burst high-pressure boiler tube, or erosion from cinders and fly ash. We have lost motors too many times to have any false illusions. These have included 2,300-volt motors driving forced-draft and induced-draft fans, and ranging from 200 to 1,000 horsepower. One instance involved a brand-new 1,000-horsepower 2-winding 3-speed induced-draft fan motor with specially treated windings to resist moisture and cinder erosion. In passing it may be observed that the losses suffered as a result of the motor failure involves not only cost of the repair job but also the increment cost in operating boilers at lower efficiency. The latter figure readily may exceed the cost of the motor repairs.

The use of splashproof motors has not offered a satisfactory solution either. They have given as much, or more, trouble as dripproof motors. The velocity of the intake cooling air is high, as a result of a relative small intake opening. The intake is usually so close to the floor that dirt, water, oil, and other foreign materials are picked up from the foundation or floor and drawn into the motor.

In one installation of 2 700-horsepower splashproof motors, driving overfire forced-draft fans, the ventilating ducts became plugged with coal dust, and the motor failed from overheating, after being in service for a relatively short period.

As a consequence of many motor failures in boiler rooms and turbine room basements in several plants, wherever practicable, only totally enclosed 55 degrees centigrade rise sleeve-bearing motors with full class *B* insulation are being used in such location. Freedom from trouble and the attendant expense more than compensates for the added first cost of the motors.

BEARINGS

Only brief reference is made to the use of antifriction bearings. There is no question but that this type of bearing is well adapted and should be used for some purposes. For example, in vertical motors and other similar applications where thrust load must be carried, and for general use where the duty is light to moderate and the air is reasonably clean.

Experience with such bearings on horizontal-shaft motors used for heavy-duty service and where clean air is notable by its absence has been decidedly unsatisfactory. As a consequence only sleeve bearings are used on motors of 15 horsepower and above where the duty is of the so-called essential class.

WINDINGS

Other factors of importance in maintaining a high level of reliability in across-the-line start motors are thorough bracing of stator coil end connections, firm wedging of windings in slots, and moderate starting currents. On speed-changing motors this is particularly important, as for example induced-draft fan drives where speed-changing operations may occur several times each day. High currents and loose windings soon result in winding failures as a result of copper crystallization at coil-to-coil splices at the coil ends, or chafing of insulation. The use of silver-bearing copper serves to minimize crystallization failures because of its superior fatigue resistance.

Well-designed rotors also contribute materially to the motor's reliability. Motor squirrel-cage windings normally operate at fairly high temperatures, and as a consequence considerable stress is placed on the joint between rotor bar and the short-circuiting ring due to expansion and contraction.

One of the most common causes of rotor failures is breaking of rotor bars near the brazed joint to the ring. This is often the result of crystallization of the copper in the brazing operation. Breakage of the brazed joint also may result from a poor design of the joint—notably in double-cage windings where two different size bars are welded to the ring. The use of oxygen-free copper is recommended, since this serves to eliminate the brittleness resulting from crystallization in the welding operation.

We note Mr. Muller's reference to silicone impregnated class *B* winding insulation. It is understood that silicone varnish is highly resistant to moisture as well as to high temperatures. We are not informed on its resistance to dust and cinder abrasion and its resistance to contact with oil. We are attempting to learn how these new materials will stand up in power plant service and have at present 1 300-horsepower totally enclosed squirrel-cage motor and 1 800-horsepower wound-rotor splashproof motor wound with class *B* insulation using silicone impregnation. The smaller motor is used to drive a salt water pump, and the larger one drives a boiler feed pump. Both were placed in operation in 1945 and we, therefore, have no operating experience to submit at this time.

RELAY PROTECTION

It is not the intent to discuss here various types of relays, as these are well known, but rather the type of protection. Where unit type boiler turbo-generator installations are employed, relay protection becomes a simple problem indeed. Instantaneous overcurrent short-circuit protection alone will suffice for most motors. Motors subject to overloads or stalling, such as those driving pulverizer mills, belt conveyors, and so forth, should be provided with thermal overload protection. The rotor winding is normally the weakest part of the squirrel-cage rotor under stalled condition.

Instantaneous undervoltage devices have no place in the power station. In some instances time delay undervoltage relays should be used where undervoltage protection is essential for safety. One example is that on powdered-fuel installations, where introduction of fuel into an incandescent combustion chamber after a temporary shutdown may result in a disastrous explosion.

Reference has been made to the use of automatic "throw-over" or transfer switches for guarding against loss of power supply. Such devices doubtlessly have many useful applications, but we do not favor their use in power plants to protect against loss of capacity or against damage to equipment. In striving to design these devices to function under all foreseeable conditions, the control becomes so elaborate that the throw-over device itself establishes a new maintenance problem of its own. The provision of the necessary reserve in auxiliaries, if somewhat more costly, provides the maximum degree of reliability and incidentally permits removal of equipment from service for maintenance purposes without reduction in capacity.

A word of caution may be in order in regard to the application of relay protection to a small capacity circuit which is served from a bus which can supply relatively high current under short-circuit conditions. An example is a 5,000-kva 2,300-volt 3-phase transformer supplying a bus to which a 60-horsepower or 100-horsepower motor circuit is connected. A normal reactance transformer may deliver upward of 25,000 amperes on a 3-phase short circuit. This is 1,000 to 1,600 times the motor full load current. In such a case it may be a question as to whether the relay current transformer or the relay itself would be the first to explode. A case of this kind would require either a reactor to limit the fault current to a value that would be normal for such a circuit or a special current transformer design whose primary winding has sufficient short-circuit thermal capacity to withstand the fault current and a magnetic circuit designed to saturate at 10 or 20 times normal flux in order to limit the secondary current to a safe value.

Relay protection of motors operating at 440 or 208 volts involves certain considerations not encountered at 2,300 volts. At these service voltages, there are of course many small motors, some of which require only manual control, and others must be provided with electrically operated switches for interlocking or other control purposes.

Even though the transformer banks used to supply the power busses are much smaller than used at the higher voltages, the same general problem of high short-circuit current and selectivity often develop.

The air circuit breaker situation is such that it is practically impossible to maintain selectivity at currents in excess of 10 or 12 times the circuit breaker rating, because there is no circuit breaker commercially available today which will be guaranteed to meet its rated interrupting capacity unless it is provided with a direct-acting instantaneous-trip device. We refer to Table V in the McClure-Whittlesey paper for confirmation of this. In other words, if it is desired to provide delayed action on tripping of an air circuit breaker at 25,000-amperes short-circuit current to obtain selective operation with another circuit breaker or fuse, it is necessary to buy a circuit breaker with a 50,000-ampere interrupting capacity to permit use of time delay at 25,000 amperes. This has forced employment of fuses in order to obtain selectivity.

Fuses developed by the Edison Company, with which the writers are associated, for network service can interrupt approximately 50,000 amperes at 208 volts and thus provide a means of obtaining selectivity with NEC branch circuit fuses where the fault current may be 10,000 amperes or less.

Wm. R. Brownlee and J. A. Elzi: We are pleased to note the interest in this subject as evidenced by the very good discussions that have been presented and the valuable information included. The principal divergence of opinion centers around methods of power supply to station auxiliaries, automatic transfer schemes, and so forth, with special attention to the transient characteristics of the over-all system.

Mr. Gay's discussion indicates a longer duration of the inrush current when a motor (or motors) is transferred from one circuit to another than is indicated by Figure 4 of the paper. His oscillogram shows an inrush current lasting for about 0.4 second after an interruption of some 52 cycles. These values are not difficult to reconcile, since Mr. Gay's oscillogram shows a noticeable reduction in station power bus voltage when the motor is re-energized, with a gradual recovery lasting through the inrush period. This would indicate that the motor (or motors) had been re-energized from a high reactance source such as a house generator. In contrast, in our tests the station power bus voltage was restored to normal within 1 or 2 cycles after transfer. This illustrates another advantage of supplying station auxiliaries from low reactance sources instead of from small generators.

Mr. Gay and also Mr. Harrington wish to have a further explanation of the very small change in maximum inrush current for moderate lengths of interruption of station power voltage. The data given in Figure 4 extend to a period of interruptions of approximately only 5 seconds, and undoubtedly this curve would bend upward for longer periods of time. As mentioned in the paper, the inrush current given in this figure is a composite value for all of the motors associated with one boiler. As can be seen from Figure 3, the speed of some of the motors is reduced very little during this period of time, whereas other motors, such as the pulverizer, slow down very rapidly. The influence of the pulverizer motor is obscured by the small decrease in speed of the other large motors. This also illustrates the difficulty of attempting to time the transfer periods so as to avoid energizing the motors with their induced voltages substantially out of phase with the bus voltage. No mechanical or electrical difficulties have been experienced in transferring at a speed of 18 cycles. Some of the tests indicated a short (1/2 cycle) peak of current at the instant of transfer of about 50 per cent greater than the inrush current after 2 cycles.

Mr. Harrington has asked clarification of the control and switching schemes as influenced by safety interlocking. For example, if a standard starter were used for the 480-volt-driven exhauster, a momentary voltage disturbance might cause this contactor to open. A latched-in relay can cause the contactor to reclose at the end of the disturbance, so that the operation of the exhauster itself might not be affected. However, the auxiliary switch on the exhauster contactor in this case would disconnect the main pulverizer motor (2,300-volt driven), and flame extinction would result. Therefore, the exhauster motor should be controlled by an air circuit breaker or latched-in contactor, so that the interlocking scheme will not be initiated by a momentary disturbance.

We are glad to have Mr. Cooper's further confirmation on the need of co-ordinating the control against voltage surges and on the desirability of improvements in industrial type control devices. We agree that locked rotor protection is highly desirable and hope for improvements in methods of obtaining it.

We note that Mr. Braley, Mr. Noest, and Mr. Webb apparently experienced a discouraging number of motor failures and have attributed this to the presence of cinders, coal dust, and flyash, with the result that only totally enclosed motors are used for most applications in spite of their recognized disadvantages. The number of failures of either motor insulation or bearings attributable to the presence of such foreign matter in the atmosphere has been negligible, and we have no indication that open motors with power plant insulation are not entirely satisfactory.

They also advocate the use of time delay undervoltage protection for safety purposes with powdered-fuel installations. We do not agree that such protection is necessary or desirable but strongly prefer instead the use of devices responding to the driven quantity (such as air flow in the pulverizer duct). These more direct devices also will guard against failures other than failure of power supply such as broken shafts, damaged couplings, mechanical damage to driven equipment, and so forth, which also could require the interlocking system to function.

Mr. Adams and Mr. Sholl both advocate the use of house generators in order to avoid voltage disturbances originating on the transmission system, and it is mentioned that occasionally protective relays have failed to function as prescribed. It is believed that other requirements make it absolutely necessary that transmission systems be guarded against disturbances of such length as would interfere with station auxiliary service. Experience has shown that disturbances of such extreme length usually will result in widespread system separations, loss of load, the isolation of certain sections of the system with too little generation, and the like, which are so serious that they must be guarded against, regardless of what source of power is chosen for station auxiliaries. After this is accomplished successfully, the transformer system of station auxiliary supply may be made entirely reliable.

J. B. McClure and S. I. Whittlesey: The authors wish to thank all those who have submitted discussions on this paper and are pleased to note that, in general, there is reasonable agreement on this subject. This means that auxiliary power systems now can be laid out with a reasonably consistent pattern—which is based largely on the use of radial systems and the application of factory-assembled equipments.

It is particularly gratifying to note that Mr. Geiger agrees with the transformer capacities at which the dual-voltage system should be adopted. However, Mr. Geiger seems to favor the 575-volt system instead of 460 volts, and there probably never will be a unanimous opinion on this point. Two considerations which favor the use of 460 volts should be emphasized. Namely first, the 460-volt system results in a more conservative application of 600-volt equipment; and second, 460 volts is considered a more practical voltage for the smaller motors, and this voltage in conjunction with single-phase 120-volt motors permits a practical solution of the small motor applications without introducing another voltage. The subject of cascading was mentioned briefly, and for applications of this type it is considered important to design the auxiliary power system so that selective tripping of circuit breakers is obtained with practical ratings.

Mr. Gay has indicated that the presence of a shaft auxiliary generator could be used to encourage the practice of prolonging out-of-step operation of the main generator. The decision as to when an out-of-step generator should be relieved of this type of operation should not necessarily depend on the source of auxiliary power. It is generally advantageous in any case of out-of-step operation of a generator to isolate it, either alone or with its portion of the system load, in order to save the system undue disturbance, to prevent an increasingly worse system condition, and to protect the machine from any possible damage. Experience has indicated that it is not good procedure to permit out-of-step operation of generator for any appreciable length of time.

Mr. Finlaw properly emphasized the need for two reliable auxiliary power sources, particularly where pulverized fuel is used, and in addition emphasized the advantages which might be derived from proper sectionalizing of the auxiliary power bus.

Mr. Scholl's successful experience with automatic transfer of auxiliary power sources should encourage increased consideration of this feature. The division of auxiliaries for one boiler onto two different busses can be indulged in only when the boiler is large enough to justify providing the boiler with divided auxiliaries. One other solution is to establish a bus section for each group of auxiliaries, and in this way the auxiliary power for two boilers may be kept separate, thereby increasing the operating simplicity.

Mr. Peterson describes an auxiliary power system with three power sources. This apparently is necessitated by unique operating requirements, since the steam station is to be used primarily as a stand-by source for hydroelectric power, and thus it may require availability of full auxiliary power during periods of sustained low system voltage.

Mr. Adams has implied that a motor-driven exciter set can be used successfully only with a separate auxiliary power supply from either a shaft or house generator. Modern high speed clearing of system faults has appreciably reduced the duration of system disturbances through which auxiliary power systems must continue to operate. Thus, it is believed that in most cases a properly designed motor-driven exciter set can be used successfully with a properly designed auxiliary power system, regardless of the power source finally chosen. The question of whether or not auxiliary power systems should be grounded is primarily a matter which must be determined from operating experience. The experience with grounded auxiliary systems to date has been rather limited.

Mr. Braley, Mr. Noest, and Mr. Webb have indicated that double transformation may sacrifice some reliability. Transformers, in general, are recognized as having high reliability, and experience indicates that two in series still give successful performance. The main advantage for two transformations is simplicity of operation, since all the power for both voltages is brought to the higher voltage bus.

The problem of obtaining selectivity with available equipment is always present and is more pronounced at 230 volts than at 460 volts. This is another reason why a 460-volt system is preferable to a 230-volt system. This problem was recognized and certain general application rules for obtaining selectivity at the lower voltage were given in the paper including:

(*a*). Co-ordination of transformer secondary and feeder circuit breaker rating.

(*b*). Co-ordination of feeder circuit breaker ratings with individual combination magnetic starter ratings.

The problem of providing adequate protection for the smaller 2,300-volt motors can be avoided largely by establishing a higher minimum rating for 2,300-volt motor applications. This higher minimum rating becomes more practical as the voltage of the lower voltage system is increased and should have been listed as another advantage of the 2,300–460-volt system.

It is noted that the use of fuses is suggested to provide selectivity. It is generally desirable to supplement the use of fuses with a thermal overload device in order to decrease the chance of continued single-phase operation of a motor due to the blowing of one fuse.

V. E. McCallum: The comments on the paper, "Auxiliary-Power Supply for Generating Stations," are by those who believe that some other source of power in conjunction with the main bus, as a stand-by source of power, is a more reliable auxiliary power service. In each station where these other schemes are employed, the stations are a large part of a small system or have a special function to perform.

Undoubtedly the same procedure cannot be applied to these stations as to one on a large closely interconnected system, where the station is supported by several transmission lines.

It is the author's belief that stability and reliability can be built into the main power system and station busses, which will provide more satisfactory service than can be obtained with an independent auxiliary power system.

W. E. Sholl suggests connecting one half of the auxiliaries of each of two boilers to one power bus, and the other half of these same two boilers to a second power bus. This arrangement seems to imply that there must be two sets of auxiliaries for the same function of each boiler, which in itself is a more expensive and complicated design. Also, with this arrangement the loss of one power group may shut down either boiler if there is only one of the two auxiliaries operating at that moment. The tendency to cross-connect and interconnect seems to have no advantage and some disadvantages. Experience has shown that simple, well-insulated, and well-installed power equipment is very dependable and that the addition of a complicated automatic switching sequence may only weaken the reliability of the installation.

H. N. Muller, Jr.: The author is very pleased by the several discussions presented on this paper and on the group forming the present symposium as a whole. These discussions are distinctly of a confirming and complementary nature and help materially in completing the over-all picture of modern practice in auxiliaries and their supply.

The remarks by Mr. Gallagher confirm, almost point by point, the items taken up in the original paper. The comments on radial versus network systems of power supply add to the over-all picture, and the variance from opinions expressed in the paper can be explained, since the discusser, operates an excellent radial supply in the stations with which he is personally associated.

Mr. Braley, Mr. Noest, and Mr. Webb point out the general agreement expressed by the authors of all papers in the symposium. Their additional comments on source of power, voltage selection, use of air in circuit breakers and transformers, motor design, and so forth all are worth while, particularly for the detail they add. Of particular note is the discussion of specific causes for motor failures, these not being covered in the symposium papers. These discussers, as well as Mr. Adams, Mr. Peterson and Mr. Sholl, all bring up the point of source of power for auxiliary systems. It appears that this is one of the more controversial aspects of station design today, so that the discussions on this point are particularly pertinent.

Mr. Sholl's remarks about the complete absence of oil in electric equipment in the Phillips Power station should be emphasized. This trend was pointed out in the author's original paper, and such confirmation is appreciated.

The Frequency of Occurrence and the Distribution of Lightning Flashes to Transmission Lines

Discussion and author's closure of paper 45-141 by R. H. Golde, published in AIEE TRANSACTIONS, 1945, pages 902–10.

J. H. Hagenguth (General Electric Company, Pittsfield, Mass.): The author is to be complimented on his attempt to give us a basis for calculating the protective cone and the number of strokes to transmission lines from physical considerations. There are a few points which need elaboration.

One of the author's assumptions is an estimated field strength of 3,000 volts per centimeter capable of producing streamers from lightning conductors or similar structures. Table I of this discussion shows some average field strength values for rod gaps at different spacings up to 30 feet. It will be noted that even at 30-feet spacing, the average field strength is of the order of 5,500 volts per centimeter. Also, doubling of the spacing from 15 to 30 feet results in a decrease in field strength from 5,680 to 5,580, or a drop of 1.8 per cent. If this same rate were maintained, a field strength of 5,150 volts per centimeter would result at 100-feet separation. However, while the drop in field strength as the spacing is increased from a few inches to a few feet is quite rapid; for greater increase in spacing, the relative drop becomes much slower, indicating that the average field strength at 100 feet is of the order of 5,400 volts per centimeter. All these values are based on the positive critical impulse flashover of rod gaps where spark-over occurs at 5 microseconds for the shorter gaps and at 10 to 20 microseconds for the larger gaps. Since, in the stepped-leader process, we are dealing with relative short-time intervals between individual steps[1] (31 to 91 microseconds) and the increase in length of the leader stroke per step varies between 33 and 600 feet, a value of at least 5,000 volts per centimeter should be more appropriate to cause streamer formation from a grounded object projecting from the earth's surface.

Other assumptions or approximations are the statements, "the magnitudes of lightning currents are proportional to the charges deposited along the leader channel" and "an average current of 20 kiloamperes corresponds to about one coulomb." Doctor K. B. McEachron has shown (reference 2, Figure 9) that the charge in current peaks measured oscillographically at the Empire State Building varies approximately directly with current amplitude beginning at about 8 kiloamperes, and his value of 1.1 coulombs in a 20-kiloampere stroke checks quite closely the author's value. (The abscissa values of Figure 9 of reference 2 should be divided by 10 to give the correct values.) However, in this figure, only that part of the charge in the current peak was considered, where the current wave has decayed to half value. Therefore, if it is considered that the current wave is a function of the charge in the leader stroke, the total charge laid down would be much greater—of the order of twice that given in the Figure 9 of the reference.

Furthermore, I do not believe that charges in current peaks necessarily are representative of charges laid down in the leader. For instance, many of Doctor Schonland's photographs[3] show a rather abrupt termination of high luminosity after a relatively short time—of the order of 10 microseconds—as the return stroke progresses toward the cloud. This would indicate a very short tailed current wave. On the other hand photographs taken at the Empire State Building and in Pittsfield never exhibit any such rapid changes in luminosity, the intensity of the photograph being practically uniform over thousands of feet of stroke length. This latter condition indicates a long tail wave. In my opinion the difference in the two conditions is caused by phenomena at the ground end of the stroke. In Doctor Schonland's case, the ground resistance is presumably very high, prohibiting large readily available charges at the ground terminus of the stroke, while in the aforementioned photographs, the ground resistances are much lower, and, particularly in the case of the Empire State Building, relatively large charges can be concentrated before and easily can be supplied after contact has been made. This is substantiated further by the analysis made by Malan and Collens[3] in which many of the photographs definitely indicate flow of charges from the cloud toward the ground in the later stages of the stroke mechanism.

Table I. Critical Spark-over of Rod Gaps With Positive-Polarity Impulse Waves

Spacing, Feet	Spark-over Voltage, Kilovolts	Average Gradient, Volts Per Centimeter
0.83	195	7,680
1.67	345	6,800
3.34	650	6,430
6.67	1,250	6,170
8.35	1,540	6,070
15	2,600	5,680
30	5,100	5,580

Table II. Lightning Strokes to Transmission Lines

Line	Flashes Per Mile Per Year	Iso-keraunic Level
Safe Harbor–Westport*	0.95	30
Safe Harbor–Perryville*	1.40	42
Holtwood–York*	1.20	62
Holtwood–Coatesville*	1.20	62
33-kv wood-pole lines*	1.2 to 1.36	25–45

*From Mr. Golde's paper.

The charges in the leader stroke, however, should not be affected by ground conditions. Thus, it is still very doubtful that a direct, general connection exists between charges in current peaks and charges in the leader stroke. There is some probability that there is a proportionality between current crest and leader charge in practical installations with relatively good ground connections.

From the foregoing it can be postulated that the average field strength required is 5,000 volts per centimeter, which, when translated in the author's Figure 4, would result in an average protective ratio of 1.6. If, further, the charge in an average leader stroke is considered—two coulombs as compared to the author's value of one coulomb—then a protective ratio of about 2 results.

Therefore, it is apparent that rather large changes in the assumptions made change the author's Figure 4 to only a small degree.

I would suggest a different title for Figure 4. From the author's own words, this represents a curve which shows the ratios of attraction, and "attraction ratio" or "collection ratio," therefore, would be better names, because they correlate the charge in a leader stroke with the distance of the stroke from a point where a streamer can just begin to form from the point. This, however, does not necessarily mean that the stroke will contact the point and, therefore, the protection ratio should be less than that shown. Further, this ratio is presupposed on a cone whose base radius is equal to the height of the point times the protective ratio. On the basis of the theory given in the paper, protection for any other points within this cone is not necessarily provided, because the protected point also is subjected to the field of the leader stroke, and therefore, may start streamers of its own. This is probably the reason why in some instances even a 1:1 cone is violated. The author's theory, which shows considerable merit once the actual values are known, therefore, would enable calculations to be made with good accuracy to obtain the real protection provided by a lightning-conductor system in installations where great risk is involved.

From the point of view of practical protecting practice of houses, a cone of 2, 4, and even greater base radius has been found satisfactory, particularly where the protected building is relatively low. In installations where great risk is involved, a 1:1 cone is obviously preferred.[4,5]

The author's calculations concerning the relative strokes to towers, line wires, and earth wires, apparently check very well with observed values. Likewise, Figure 10 of this paper definitely seems to indicate a direct correlation between the isokeraunic level and the strokes per square mile as computed from four lines where good records were kept of all flashes to lines and towers.

On the other hand statistics also simply indicate that strokes to transmission lines occur at a rate of approximately 1.2 strokes per mile per year (see Table II) in regions where the isokeraunic level ranges between 25 and 65. Therefore, not too much emphasis should be placed on such calculations.

In Pittsfield, with an isokeraunic level of 25, photographs taken during night storms only and only of lightning striking within an area of 0.162 square miles where the point of ground contact could be established definitely, showed an average stroke density of 45 (range from 19 to 68 strokes per square mile per year and a total of 22 strokes) strokes per square mile per year. This is a minimum value, as strokes during daylight storms are not included. This investigation extended over three years. This does not compare well with 12 strokes per square mile per year from Figure 10 of the paper. In order to arrive at a similarly high stroke density from transmission line calculations, the attraction ratio would have to be much less than that assumed by the author.

However, the basic approach to the problem shown in the paper is definitely in the right direction and should lead to a better theoretical understanding of the protective problem.

REFERENCES

1. PROGRESSIVE LIGHTNING, II, B. F. J. Schonland, D. J. Malan, H. Collens. *Proceedings* Royal Society of London, England, Series A, number 197, volume 152, November 1935, pages 595–625.

2. LIGHTNING TO THE EMPIRE STATE BUILDING, II, K. B. McEachron. AIEE TRANSACTIONS, volume 60, 1941, September section, pages 885–90.

3. PROGRESSIVE LIGHTNING, III., D. J. Malan, H. Collens. *Proceedings* Royal Society of London, England, Series A, number 909, volume 162, 1937, pages 175–203.

4. LIGHTNING PROTECTION. United States Army Ordnance Department Safety Bulletin number 70, June 1943.

5. CODE FOR PROTECTION AGAINST LIGHTNING, PART III. National Bureau of Standards Handbook, H40, 1945.

6. THE MEASUREMENT OF LIGHTNING CURRENTS IN DIRECT STROKES, G. D. McCann. AIEE TRANSACTIONS, volume 63, 1944, pages 1157–64.

E. Hansson (Pennsylvania Water and Power Company, Baltimore, Md.): The third sentence of the third paragraph under "Frequency of Lightning Flashes" in Mr.

Golde's paper, reads: "Thus the isokeraunic levels for the first three lines considered are stated to be 39, 42, and 62, respectively," the figures having been taken from a paper written by A. F. Bang and E. Hansson in 1937. The figures actually represent the number of storms passing over the lines, as reported by patrolmen and others to the operators at the stations. What is commonly known as the isokeraunic level of the territory in which the lines are located is from 30 to 32, as reported by the United States Weather Bureau. Unfortunately, the paper from which Mr. Golde obtained his information does not refer the figures to any specific line, thus he got the wrong impression. Actually, the number 39 should refer to Figures 9(d), 42 to 9(c), and 62 to 9(b).

W. W. Lewis (General Electric Company, Schenectady, N. Y.): In a footnote of Mr. Golde's paper is the statement that the latest "Code for Protection Against Lightning" (Bureau of Standards Handbook H21, 1937) takes the radius of the base of the protective cone as two to four times the conductor height.

It has been customary for some years in the United States to protect power stations and substations on the basis of overhead ground wires or masts with a protective ratio not exceeding 2. On the other hand it has been customary to protect powder magazines and similar structures with a protective ratio not exceeding 1, and during World War II most of the powder magazines and similar structures were so protected.

Recently Part III of the "Code for Protection Against Lightning" was revised and issued as part of Bureau of Standards Handbook H40 (1945). In this the cone of protection afforded by rods or masts is assumed to have a radius of base equal to their height in important cases, or up to twice the height in less important cases.

R. H. Golde: I am glad that, despite his detailed comments, Mr. Hagenguth has recognized the main purpose of the paper under discussion, namely, to present a physical approach to the problem of the protection afforded by an earthed structure. Actually it is stated in the paper that no finality is claimed for numerical results.

Turning to the individual points raised by Mr. Hagenguth, I am afraid I cannot accept his arguments in favor of a value of about 5,000 volts per centimeter for the estimated field strength capable of producing upward streamers from a lightning conductor. If the numerical flashover values given in his Table I were interpolated to the dimensions of the lightning discharge, that is, about 2.5 kilometers, a field strength of several thousand volts per centimeter would result, whereas it now is known[1,2] that the lightning discharge requires no more than about 200 volts per centimeter. Omitting any discussion on the possible effect of the energy of a surge generator on the propagation of the resulting spark discharge, the difference between laboratory test results and natural discharges can be described as follows.

The flashover values quoted by Mr. Hagenguth are based on 1.5×40-microsecond impulse waves in which, according to his statement, the breakdown occurs after some 10 to 20 microseconds, that is, well on the tail of the applied wave. In nature, on the other hand, the tip of the lightning conductor is subjected to a gradually increasing field which lasts for some 0.01 second (the time of propagation of the leader stroke) and which increases rapidly during the formation of the last dart leader until breakdown occurs, the time lag being, in 90 per cent of the cases, between 50 and 90 microseconds.[3] Both these factors, that is, the gradually increasing field strength and the longer time during which the voltage is applied in the natural discharge, clearly tend to reduce the breakdown field strength below the value determined under laboratory conditions. This argument, in addition to those given in the paper, led to the adoption of a value of 3,000 volts per centimeter.

The basis for the correlation of a lightning current of 20 kiloamperes with a charge on the leader stroke proper of 1 coulomb is given in an earlier paper.[1] This charge covers the whole of the average current wave apart from that responsible for the possible continuous current flow between multiple component strokes which is drained from the clouds. It is not surprising that Doctor McEachron's results show about twice this charge, since the presence of the tall metallic Empire State Building is bound to influence the charge distribution—and incidentally the resulting current wave form—in the manner suggested by Mr. Hagenguth himself.

Thus there seems to be no reason to alter the original assumption as to the average charge in a stroke to an earthed object of small height. In addition, Mr. Hagenguth's suggestion that the duration of the luminosity in the return channel is indicative of the duration of the high-current discharge has been corrected earlier.[1] Instead, the height of the luminous channel is likely to be related to the presence or otherwise of downward branches from the main channel. However, it is noted that Mr. Hagenguth agrees with the proposed proportionality between current crest and leader charge in installations with good earthing conditions, and this after all covers the practical installations discussed in the paper.

I am very glad to learn that it has been American practice to adopt in recent years a smaller protective range than used to be advocated in the technical literature, and I am grateful to Mr. Lewis for drawing my attention to the new version of the "Code for Protection Against Lightning" which, however, was issued after this paper had been submitted. In this connection I agree with Mr. Hagenguth that a different title might have been preferable for Figure 4. A lightning conductor should prevent strokes to earth within the distances indicated by that figure; earthed metal objects within this zone which protrude from earth may give rise to streamers of their own and be liable to a direct stroke. However, strokes to earth proper near tall structures have been reported, and it appears that these can be explained only by the theory put forward which links the protective zone with the severity of the lightning stroke.

It is unfortunate that I seem to have been misled by the figures for the storm frequencies of the lines of the Pennsylvania Water and Power Company. This certainly alters the points shown in Figure 10—which before was almost too good to be true—but it does not affect the trend of the curve. However, fundamentally more important seems to be the implication contained in Mr. Hansson's comment that over one line with an isokeraunic level of between 30 and 32 an average of no less than 62 storms were noted to have passed by visual observation. This statement confirms the attitude adopted in the paper that the isokeraunic level should be replaced by a better unit which should take into account the frequency and the severity of thunderstorms.

Without further information, it is impossible to say whether Mr. Hagenguth's rather startling figure for the number of strokes to earth over a small area in Pittsfield may be similarly affected by the inadequacy of the isokeraunic level. If it is remembered that his figure of 45 strokes per square mile per year is a minimum value which may well be considerably too low, this high frequency is difficult to explain even if the three years on which his count is based produced an exceptionally high local lightning activity. Of course, if the area involved contained one or more structures of such great height as to cause upward strokes, as in the case of the Empire State Building, the figure would cease to be relevant from the present viewpoint.

As Mr. Hagenguth refers to the attraction ratio of a transmission line, it seems pertinent to add here some information obtained since this paper was submitted. In a recent account[4] the number of protector tube operations are given which occurred on a 3-phase transmission line with horizontal configuration. From data kindly submitted by J. A. Rawls the number of single-phase tube operations could be obtained, which are undoubtedly due to direct strokes to the corresponding phase wires (as against multiphase operations which involve cases of back flashovers from the phase struck). The numbers obtained are 35 operations on the two outer conductors and 4 operations on the center conductor, or 89.7 per cent and 10.3 per cent respectively. The simple theory of the width of the zone of attraction proposed in the paper gives 88.4 per cent for the two outer and 11.6 per cent for the center conductor.

REFERENCES

1. See reference 5 of the paper.
2. See reference 11 of the paper.
3. THUNDERSTORMS AND THEIR ELECTRICAL EFFECTS, B. F. J. Schonland. *Proceedings*, Physical Society, London, England, volume 55, 1943, page 445.
4. PROTECTOR TUBES MINIMIZE OUTAGES, J. A. Rawls. *Electrical World*, volume 122, 1944, page 102.

Sag and Tension Calculations for Cable and Wire Spans Using Catenary Formulas

Discussion and author's closure of paper 45-144 by John F. Nash and John F. Nash, Jr., published in AIEE TRANSACTIONS, 1945, October section, pages 685–92.

E. L. Peterson (American Gas and Electric Service Corporation, New York, N. Y.): The calculation of sag problems for overhead wires, involving as it does the determination of tension and deflection values under various conditions of temperature and loading, always has been a somewhat tedious process. This is true for calculations based on the parabola as well as for those based on the catenary. The latter seldom were used for short- and medium-span lines until the publication of Martin's tables which greatly reduced the labor involved in using the catenary functions.

The authors' new approach to this problem should be of further assistance to engineers in solving sag problems as the solutions can be obtained without trial-and-error operations and with a saving of time over previous analytical methods.

C. H. Wagner (American Gas and Electric Service Corporation, New York, N. Y.): This paper presents a new approach to the problem of calculating sags and tensions by making use of factors evolved from the fundamental equations of the catenary. It gives accurate results for hillside spans as well as level spans.

One advantage of the authors' method is that in figuring initial sags an initial modulus of elasticity is not required. Also, their method of figuring the amount of permanent set is probably more accurate than the one normally used as the permanent set value they use is found from the average tension in the span.

It is interesting to compare the authors' method with Martin's method for the case where it is necessary to limit the stringing tension at 60 degrees Fahrenheit to 35 per cent of the ultimate strength of the conductor. For example, this limitation applies to dead-ended span lengths of 243 to 403 feet for number 2 three-strand copper under conditions of medium loading with maximum final loaded tension at 15 degrees Fahrenheit limited to 60 per cent and final unloaded tension at 60 degrees Fahrenheit limited to 30 per cent. As the stringing or initial conditions are known, the stringing sags can be found in the usual way without difficulty by using either method. The calculation of final sag and tension values presents somewhat of a problem as the correct value of permanent set necessary to get from the initial conditions to the final conditions depends on the unknown final conditions.

Using Martin's method this can be done by means of trial and error, as follows: For any given span length under consideration, determine the 60 degree Fahrenheit initial unstressed length factor using the basic tension of 35 per cent of conductor ultimate tensile strength and the initial modulus of elasticity. Guess at a value of permanent set to use which corresponds to a tension somewhere between 35 per cent and 60 per cent of conductor ultimate tensile strength and add this to the 60 degree Fahrenheit initial unstressed length factor. This then will be the value of the 60 degree Fahrenheit final unstressed length factor from which it is possible to calculate the maximum resultant tension under final conditions. This must be repeated until a resultant tension is found that will correspond closely to the permanent set used in the calculation. Both the resultant tension and the 60 degrees Fahrenheit final tension must be checked to see if they are still within the limits set by the National Electrical Safety Code.

In using the authors' method the procedure can be essentially the same but, of course, the mechanics are quite different. It must be kept in mind that the permanent set will be based on an average tension in the span; in this case the average tension will be made up of the maximum resultant tension at the supports (factor T) and the horizontal tension at the vertex (factor F). Calculations can be made as follows: For the span length under consideration determine the Y value and Z value, as described in the paper, from the basic tension T (35 per cent of the conductor ultimate tensile strength). Guess at a value of permanent set (based on the unknown factors F and T) and add it to the Z value (60 degrees Fahrenheit initial condition). This will give the new Z value (60 degrees Fahrenheit final condition) from which factor F and factor T would be found, as described in the paper. But factors F and T then must be averaged to determine whether the correct value of permanent set was chosen.

It seems to me that Table I of the paper, as far as the calculation of sags where supports are at the same elevation is concerned, would be much easier to use if it were made up on the basis of a full-span length (X multiplied by two) rather than on a basis of one-half-span length. In other words, I would prefer having two tables; one for level-span calculations based on full-span length, and one for hillside-span calculations based on distance X. The reason I recommend this change is that in calculating level spans the value of span length would be remembered better during calculations and, therefore, would be easier to use and less liable to error than the value of one-half-span length. The present Table I of the paper could be changed to this new basis easily by dividing all of the functions by two.

The authors' mention that their method eliminates the trial-and-error assumptions involved in a portion of Martin's method. This disadvantage has been overcome for all but exceptionally long-span lengths by charts of Martin's tables called "Sag Calculating Charts" recently issued by the Copperweld Company. However, a thorough study of the authors' paper will show that once a person becomes familiar with the formulas in their method many different kinds of problems in sags and tensions can be worked out quickly and accurately.

Marsh F. Beall (nonmember; Bonneville Power Administration, Portland, Oreg.): The authors have made a valuable contribution to the literature on sag and tension calculations using catenary equations. They have pointed out several of the peculiarities of the catenary equation, such as the relation between support tension, horizontal component of cable tension, and sag. These peculiarities of the catenary equation, if understood, are very useful in design and are not adequately covered in most textbooks on the subject. Most textbooks are written on the basis that a book is not complete academically unless it contains a statement of the equation of a catenary curve; but engineers never will use it and so a complete discussion of catenary sag and tension equations is not justified. The authors of the paper have given a comprehensive treatment of the theory of catenary equations and have called attention to many properties of the catenary curve which are very useful to the designing engineer.

Table I of the paper, which describes unit values of the catenary functions, is very useful in computation of sags and tensions where a conductor is sagged in accordance with a "basic" or "ruling" span. The table may be used for computation of a dead-end span if the V function is known.

For accurate computation of sags and conductor elevations at various points in a hillside span, it is necessary that the location of the low point of sag be known. The authors have derived an equation for finding the low point of sag which is applicable to spans in which the horizontal component of tension or the V function is a known quantity. The authors have derived their equation by use of the exponential forms of the catenary equation.

The writer, working independently, also has derived an equation for finding the location of the low point of sag in a hillside span. The authors' equation 3,

$$\frac{D}{V}=\cosh\frac{X_L+L}{V}-\cosh\frac{X_L}{V}$$

is the same as one derived by the writer. The writer derived his equation for finding the low point of sag by use of hyperbolic trigonometric functions. The step-by-step derivation and the final equation is as follows (see Figure 1):

Let

y_A = ordinate of point A
y_B = ordinate of point B
l = length of span
D = difference in elevation between points of support

$$y_A=V\cosh\frac{x}{V}$$

and

$$y_B=V\cosh\left(\frac{x+l}{V}\right) \tag{1}$$

$$y_B-y_A=D \tag{2}$$

$$D=V\cosh\left(\frac{x+l}{V}\right)-V\cosh\frac{x}{V} \tag{3}$$

$$\frac{D}{V}=\cosh\left(\frac{x+l}{V}\right)-\cosh\frac{x}{V} \tag{4}$$

$$\frac{D}{V}=\cosh\frac{x}{V}\cosh\frac{l}{V}+\sinh\frac{x}{V}\times\sinh\frac{l}{V}-\cosh\frac{x}{V} \tag{5}$$

$$\frac{D}{V}=\cosh\frac{x}{V}\left(\cosh\frac{l}{V}-1\right)+\sinh\frac{x}{V}\sinh\frac{l}{V} \tag{6}$$

$$\cosh\frac{x}{V}=\sqrt{1+\sinh^2\frac{x}{V}} \tag{7}$$

$$\frac{D}{V}=\sqrt{1+\sinh^2\frac{x}{V}}\left(\cosh\frac{l}{V}-1\right)+\sinh\frac{x}{V}\sinh\frac{l}{V} \tag{8}$$

$$\sqrt{1+\operatorname{snh}^2\frac{x}{V}}\left(\cosh\frac{l}{V}-1\right)=\frac{D}{V}-\sinh\frac{x}{V}\sinh\frac{l}{V} \tag{9}$$

Square both sides of equation 9.

$$\left(1+\sinh^2\frac{x}{V}\right)\left(\cosh\frac{l}{V}-1\right)^2=\left(\frac{D}{V}\right)^2-2\left(\frac{D}{V}\right)\sinh\frac{x}{V}\sinh\frac{l}{V}+\sinh^2\frac{x}{V}\sinh^2\frac{l}{V} \tag{10}$$

$$\left(\cosh\frac{l}{V}-1\right)^2+\sinh^2\frac{x}{V}\left(\cosh\frac{l}{V}-1\right)^2=\left(\frac{D}{V}\right)^2-2\left(\frac{D}{V}\right)\sinh\frac{x}{V}\sinh\frac{l}{V}+\sinh^2\frac{x}{V}\sinh^2\frac{l}{V} \tag{11}$$

$$\sinh^2\frac{x}{V}\left[\left(\cosh\frac{l}{V}-1\right)^2-\sinh^2\frac{l}{V}\right]+\sinh\frac{x}{V}\left[\frac{2D}{V}\sinh\frac{l}{V}\right]+\left[\left(\cosh\frac{l}{V}-1\right)^2-\left(\frac{D}{V}\right)^2\right]=0 \tag{12}$$

$$\cosh^2\frac{l}{V}-\sinh^2\frac{l}{V}=+1 \tag{13}$$

$$\sinh^2\frac{x}{V}\left[-2\left(\cosh\frac{l}{V}-1\right)\right]+\sinh\frac{x}{V}\left[\frac{2D}{V}\sinh\frac{l}{V}\right]+\left[\left(\cosh\frac{l}{V}-1\right)^2-\left(\frac{D}{V}\right)^2\right]=0 \tag{14}$$

Equation 14 is a quadratic equation with sinh x/V as the variable. Solving by the quadratic formula:

$$\sinh\frac{x}{V}=\frac{-\frac{2D}{V}\sinh\frac{l}{V}}{2\left[-2\left(\cosh\frac{l}{V}-1\right)\right]}\pm\frac{\sqrt{\left[\frac{2D}{V}\sinh\frac{l}{V}\right]^2-4\left[-2\left(\cosh\frac{l}{V}-1\right)\right]\times\left[\left(\cosh\frac{l}{V}-1\right)^2-\left(\frac{D}{V}\right)^2\right]}}{2\left[-2\left(\cosh\frac{l}{V}-1\right)\right]} \tag{15}$$

$$\sinh\frac{x}{V}=\frac{D}{2V}\left[\frac{\sinh\frac{l}{V}}{\left(\cosh\frac{l}{V}-1\right)}\right]\pm\sqrt{\frac{4\left(\frac{D}{V}\right)^2\sinh^2\frac{l}{V}+8\left(\cosh\frac{l}{V}-1\right)^3-8\left(\frac{D}{V}\right)^2\left(\cosh\frac{l}{V}-1\right)}{16\left(\cosh\frac{l}{V}-1\right)^2}} \tag{16}$$

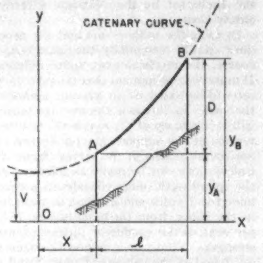

Figure 1. Hillside span between supports *A* and *B*, span length = *l*

Other dimensions used in derivation of equation for low point of sag in a hillside span are shown in figure

Simplification of equation 16 leads to equation 17 which is used for computation of the value of x, the distance from the low point of sag of support.

$$\sinh\frac{x}{V}=\frac{D}{2V}\left[\frac{\sinh\frac{l}{V}}{\left(\cosh\frac{l}{V}-1\right)}\right]\pm\sqrt{\left(\frac{D}{2V}\right)^2+\frac{1}{2}\left(\cosh\frac{l}{V}-1\right)} \tag{17}$$

Numerical computations of a design problem, using either the authors' or the writer's equation for determination of the low point of sag in a hillside span, yield results which check. An item of only minor importance is the fact that in computation for the low point of sag, use of the authors' equation requires the use of a logarithmic table in addition to the table of hyperbolic functions required for computation by use of the writer's equation.

Since equation 17 of this discussion is derived from a quadratic equation, there will be two roots, or two values of x. If the low point of sag is outside the span, the difference of the two values of x equals the span length.

If the low point of sag is inside the span, the sum of the two values of x equals the span length.

The foregoing relations may be used as a test to determine whether the low point is inside or outside the given span.

REFERENCE

1. HOW TO DETERMINE LOW POINT OF SAG WITHOUT USE OF A TEMPLATE, **Marsh F. Beal.** *Electrical World*, March 17, 1945.

John F. Nash: There are several very practical uses for the calculation methods of this paper. The writer uses these methods to prepare standard tables of sags and tensions for various types of wires and cables in general use. These tables each are prepared on the basis of a basic (ruling) span with the sags and tensions at that span, and the sags for related spans (same dead-end section) calculated for each of the related loading conditions assumed. These standard tables afford a quick source of design information and furnish the necessary data for making standard celluloid design templates used for locating structures.

There are several specific special uses for these procedures.

Tensions in existing spans can be calculated easily as shown in the following problem (slide-rule values):

Span length = 460 feet (level span)
Observed sag = 15.00 feet
Conductor size = number 2 bare hard drawn copper
Loading, one half inch ice, no wind = 1.074 pounds per foot

Therefore

$S/X=15.00/230=0.06520$
From Table I, $Y/X=7.74553$
$Y=7.74553\times230=1{,}782$
$T=1{,}782\times1.074=1{,}913$ pounds

As breaking strength of cable is 3,003 pounds, per cent loading is 1,913/3,003 × 100 = 63.7 per cent.

A span with uneven supports can be studied as follows:

1. Determine deflection of vertex below each support, S_u and S_L.
2. Let X_u be distance from vertex to upper support and X_L distance from lower support.
3. Solve for tension at upper support starting with S_u/X_u as in the foregoing (Table I of the paper) and for tension in lower support in like manner starting with S_L/X_L.

By a similar procedure by determining V/X, the horizontal longitudinal component of tension can be obtained in any span (level or hillside).

It should be noted that in the foregoing solutions, the size, type, strength of cable, or temperature does not enter the problem.

Transmission and distribution lines generally are designed and built on the basis of a ruling span and an assumed tension in that span for the expected loading. The tensions (at support) in related spans of other lengths (same dead-end section) vary from the design tension. It is often advisable to know how long an occasional span can be without too much increase in tension. The following is this type of calculation:

Conductor, number 2 bare hard drawn copper = 3,003 pounds ultimate
Loading, one half inch ice, eight-pound wind = 1.074 pounds per foot
Tension in basic (ruling) span = 60 per cent of ultimate = 1,801.8 pounds
Basic span = 500 feet
Sag for basic span = 18.90 feet
(from standard tables prepared by this method)
Sag for 800-foot span (related to basic) (standard tables) = 48.52 feet

Formula:

$T=F+SR$

For the basic span

$1{,}801.8 \text{ pounds}=F+(18.9\times1.074 \text{ pounds})$
$F=1{,}801.8-20.3$
$F=1{,}781.5$ pounds

Therefore, for the 800-foot span,

$T=1{,}781.5 \text{ pounds}+(48.52\times1.074 \text{ pounds})$
$T=1{,}833.6$ pounds

Per cent of ultimate (800-foot span)

$= 1{,}833.6/3{,}003 \times 100 = 61$ per cent
(slide-rule values)

It is interesting to note the divergence of sag values for a conductor when the per cent cable tension is varied.

Sample problem (slide-rule values):

Conductor, number 2 bare hard drawn copper = 3,003 pounds ultimate
Loading = 1.074 pounds per foot
Basic span = 500 feet

(*A*). Tension 50 per cent of ultimate:

$T = YR$ or $Y = T/R = 1{,}501.5/1.074 = 1{,}398$
$Y/X = 1{,}398/250 = 5.595$

By interpolation from Table I of the paper:

$S/X = 0.091135$
Sag $= 0.091135 \times 250' = 22.78$ feet

(*B*). Tension 60 per cent of ultimate:

$Y = 1{,}801.8/1.074 = 1{,}678$
$Y/X = 1{,}678/250 = 6.71$
$S/X = 0.0755298$
Sag $= 0.0755298 \times 250' = 18.88$ feet

(Standard-table value calculated by machine = 18.90 feet)

(*C*). Tension 70 per cent of ultimate:

$Y = 2{,}102.1/1.074 = 1{,}959$
$Y/X = 1{,}959/250 = 7.835$
$S/X = 0.064476$
Sag $= 0.064476 \times 250' = 16.12$ feet

While catenary calculations generally are used for transmission work involving long-span work, number 2 copper with a medium-length span was selected in the foregoing problems to illustrate the use of this method in distribution work.

It is interesting to note the relationship of tension at support, horizontal component of tension, and loading on structures in hillside spans. Reference is made to the problem illustrated as Case II of the appendix of the paper.

Note that in the 2,000-foot-level-span problem $T = 3{,}556.00$ pounds or 60 per cent ultimate and $F = 3{,}270.36$ pounds or 55.1 per cent ultimate.

However, in Case II,

T(upper support) $= Y_u R = 3{,}753.46$ pounds or 63.3 per cent ultimate

Determine loading on upper structure as follows:

Structure loading $= \sqrt{(T_u)^2 - (F)^2} =$ 1,842.10 pounds

(This loading is in the direction of the resultant plane. If the problem is solved for loading without wind the result would be vertical loading.)

T (lower support) $= Y_L R = 3{,}271.73$ pounds

Determine uplift on lower structure as follows:

Uplift $= \sqrt{(T_L^2) - (F)^2} = 94.66$ pounds
(in plane of resultant in this case)

It should be noted that in this problem the tension at the upper support exceeds the design value and is the tension to be found in a span of 2,588.72 feet (related to the 2,000-foot basic span).

In the foregoing calculation the obtained results hold for either a dead-ended span or a suspension span, providing the V value is the same.

These calculations illustrate why it is advisable in mountain work to select a basic span such that the horizontal distance from the vertex to upper support does not greatly exceed one half the basic span.

The following comment is offered with respect to C. H. Wagner's discussion of the paper. Mr. Wagner refers to the limiting of conductor stringing tensions to 35 per cent of the ultimate tensile strength, a condition which has to be watched under light loading conditions with medium-sized or large conductors, and under heavy loading conditions with large conductors on short-span construction. The methods outlined by Mr. Wagner are, of course, the accurate procedure when it is advisable to design exactly to the 35 per cent string limitation. This condition does not occur often with long-span heavy-loading construction, but when it does occur the writer prefers to reduce the design loaded tension and recalculate to values where the stringing tension at 60 degrees Fahrenheit does not exceed 35 per cent and the final conductor only tension at 60 degrees Fahrenheit is not more than 25 per cent of ultimate.

It is perfectly feasible to prepare Table I of the paper based on span length rather than on X values. Possibly this would be advisable for engineers who prefer to deal in span lengths; however, as written, Table I serves both for level and hillside spans. Reference to the table's footnote also shows that Table I can serve as a table of hyperbolic sine and cosine values.

In reference to Marsh F. Beall's discussion, Mr. Beall states that Table I is very useful in computing sags and tensions where a conductor is sagged in accordance with a basic span, and that the table may be used also for computing dead-end spans if the V function is known. A dead-end span is calculated in the same manner as a basic span. The calculations can be based on either a desired tension at support T value, or a horizontal component value F. In either case V is determined readily and is used along with Y values to secure sags and tensions at other conditions for the basic or dead-end span. Related spans (to the basic span) are calculated in the same manner for designs starting with established T or F values.

Parallel Operation of Main-Engine-Driven 400-Cycle Aircraft Generators

Discussion and author's closure of paper 45-158 by L. G. Levoy, Jr., published in AIEE TRANSACTIONS, 1945, December section, pages 811–16.

E. P. Barlow (nonmember; The Glenn L. Martin Company, Baltimore, Md.): A review of Mr. Levoy's paper supplemented by limited observation of actual performance on test, indicates that the equipment and system described offer very encouraging possibilities within their range of application. Where proper installation requirements actually can be met, agreement is expressed with the author's conclusion that this system is feasible for the supplying of electric power in large aircraft.

It is understood that installations of this remotely mounted engine-driven alternator system have been made experimentally on two types of airplanes, both of the pusher design with the propellers mounted aft of the wings instead of forward as in conventional tractor types. In the pusher type, with the main engines submerged in the wings, the airplane designer has relatively more space, greater accessibility to the power-drive pads and greater freedom of design in properly installing the drive and generator units, as compared with the cramped conditions in the crowded nacelles of tractor-type airplanes. Installations possessing the favorable features of pusher aircraft designs appear to offer the most advantageous type of application for this remote flexible drive alternator system.

On the other hand, in conventional tractor types of aircraft, especially those using the larger engines where demands for high-capacity electric-power sources are most generally encountered, installation of remotely mounted engine-driven equipment as described in this paper often presents practically insurmountable difficulties from an airplane designers point of view. With engines in some cases over ten feet long, necessary auxiliaries and nacelle structure immediately around and behind the engine always seriously interfere with, and usually prevent the design of, a reliable and satisfactory installation. A complete lack, or unsuitable location, of the necessary high-capacity power-take-off pads on the engine, and the lack of a dependable and serviceable flexible drive adaptable to a configuration requiring bends, offsets, or right angle drives, also complicate any contemplated use of this system. As an example, in one instance on a twin-engine airplane, where the need for large-capacity generators made possible use of this system appear advantageous, consideration was given to extending the flexible drive directly through the engine oil tank. However, because of difficulties in obtaining properly located take-off pads of adequate capacity on the engine and the impossibility of providing an accessible location for the variable-ratio drive and alternator without unacceptable changes in the airplane structure, a practical installation could not be made, and the application was abandoned.

The conditions encountered in this instance are not extreme, but rather are typical of the majority of the present and currently proposed conventional aircraft designs. Even on the larger airplanes, the problems of installing engine-driven equipment are always critical. Present indications are that, with jet engines now in process of development and application, conditions in this respect may be aggravated rather than relieved.

Consequently, though the equipment and system under discussion may be found entirely satisfactory in itself and for some types of installation, the difficulties of making a practical installation within the confines of present-day conventional airplane designs seem to preclude the possibility of extensive use of the system proposed. For such applications demanding high-capacity electric-power sources consideration of some other means of driving the large generators required appears necessary. One possible type of drive is the small auxiliary gas turbine which offers prospective advantages of reliability, flexibility, light weight, ease of installation and maintenance, and operating economy in over-all airplane performance; advantages which definitely warrant full investigation and study and possible intensive development.

H. Tyler Marcy (Massachusetts Institute of Technology, Cambridge, Mass.): The control for parallel operation of main-engine-driven 400-cycle aircraft generators first was discussed with me by Professor Charles Kingsley, Jr. of Massachusetts Institute of Technology in connection with a training program he was organizing for officers of the Army Air Corps. At that time I suggested a technique of control which seemed to have possibilities and which now seems pertinent discussion to Mr. Levoy's paper.

The problem of synchronization and operation of synchronous generators is essentially a positional problem, when the motion of the generator rotors is being studied. If two generators are in approximate mechanical synchronization before electrical connection in a parallel circuit, then the electric transient is minimized following their electrical connection. The ability of the system to divide the load properly and to withstand transient load conditions is also a problem of mechanical synchronization of the generator rotors. In the system described the speed of the rotors was controlled and the problem of angular synchronization of the rotors made possible by the use of a speed droop combined with a freewheeling device. The variation I would propose for discussion is to control directly the position of the generator rotors. As one author previously expressed it, the system then would control position in motion at synchronous speed.

There is no mystery in accomplishing the control of generator-shaft position. The measuring device geared to the generator shaft would be a "synchro" instead of a tachometer. A small auxiliary "master," comprising a battery-driven governed motor driving a transmitter synchro and possibly a small generator for synchro excitation, would direct the system. The control circuit would be essentially the same. The synchro stators all would be connected together and the rotor of the transmitter synchro excited. The voltages from the receiver synchro rotors then would be sent through a phase-sensitive rectifier to an electromechanical control of a hydraulic pilot valve. This would initiate action through the hydraulic transmission to maintain the receiver synchro voltage at zero. As the receiver synchro rotor voltages are kept near zero by the control systems, all the generator rotors are in mechanical synchronization. This follows from the unique character of synchro voltage systems, providing initial alignment has been made at assembly of the synchro rotors and the generator rotors.

Complete evaluation of the relative merits of the two systems cannot be made easily by one not familiar with aircraft-electric-system practice. In the proposed system the load torque might cause an angular droop of the generator rotors with respect to their no-load synchronous position, but there would be no change in speed and therefore no change in frequency with load. Constancy of frequency is a function only of the regulation of the small director motor which is unaware of load torques. However, it is likely to be more expensive of control equipment and require more nearly optimum performance of the components, but the constancy of frequency may make it worthwhile.

H. B. Bunce and **J. C. Cunningham** (Westinghouse Electric Corporation, East Pittsburgh, Pa.): The reactive-load droop and real-load boost Mr. Levoy proposes is a desirable method of obtaining reactive load division in that it would avoid the complication and vulnerability of the control wires and auxiliary contacts necessary for the differential scheme. If the voltage droop for reactive current and the voltage rise for in-phase current were made equal, the two effects would cancel for a 0.707 power-factor load. Based on a-c system loads now contemplated, such a setting would not cause more than about one per cent decrease in generator voltage for the majority of motor-starting conditions, and at normal running loads the rise in generator voltage would not over compensate for the line drop to principal load centers by more than about one per cent.

The main disadvantage of this scheme is that the reactive kilovolt-ampere is affected proportionately by any unbalance in real power. There may be a large real power differential between generators on this system because of governor error during engine transients. For example, refer to Figure 13. The power output oscillates in magnitude as much as 250 per cent load during this engine transient. With differential reactive division and no resistance compensation the total load on the accelerated machine would swing from 40 $(30+J26.5)$ kva (assuming 75 per cent load power factor) to 79.4 $(75+J26.5)$ kva. If a scheme with equal reactive droop and resistive rise were used and the exciter were fast enough to follow the real load changes, the load on this machine theoretically would swing to $100(75+J66.2)$ kva. The load on the other machine should be $(-15-J13.2)$ which indicates that it would be freewheeling and its excitation would be approximately zero. Actually the regulator and exciter would not follow such fast load changes, but an idea can be obtained as to the influence of real load upon reactive load with such a scheme. The increase in generator loading is less disturbing than the reduction in pull-out torque which would result from the reduced excitation.

In spite of these two possible disadvantages, this scheme should be investigated thoroughly because of the greater vulnerability of the differential scheme.

The star bus of Figure 6 is unsatisfactory for isolated operation. Provision for emergency isolated operation for certain military airplanes has been specified.

Figure 11 shows a voltage dip of four per cent with two 750-watt Amplidyne sets starting. It may be pointed out that voltage dips from two to four times this value would occur when starting the motors for wing flaps, landing gear, or motor generator sets from two generators.

D. W. Exner (Westinghouse Electric Corporation, Lima, Ohio): Mr. Levoy has presented some interesting test data showing performance, under certain conditions, of the particular equipment which he has helped to develop. This activity is a part of the 400-cycle aircraft-power program for large airplanes which was initiated by the Army Air Forces some years ago and has been pursued actively by the Air Forces and the various electrical manufacturers.

Because of lack of space Mr. Levoy has been able to show only a limited number of oscillograms. Unfortunately he has not chosen films representative of maximum conditions by which the ultimate effectiveness of the system could be evaluated. All of the films shown were taken at less than full rated load which is 40 kva, 120 volts line-to-neutral, 75-per-cent power factor, and 111 amperes. To judge by his voltage traces, his voltage and current scales are in instantaneous values. These alternators have five-minute 150-per-cent load and five-second 200-per-cent load ratings. Thus the test conditions shown are under weak-field conditions where a heavy surge of excitation may be supplied by the regulators when needed. Under conditions of heavier initial load greater voltage dips and longer disturbance must be expected.

In actual operation under emergency conditions it will be necessary at times to synchronize an incoming machine with one or more alternators which are heavily overloaded. Such a case might follow a nuisance trip during combat. Under this condition an automatic full-voltage synchronizing equipment will have especial merit in reducing the disturbance shown on a reduced scale in Figure 9 of the paper.

Figure 13 shows conditions at partial load with the input to the constant-speed drive accelerating at approximately 1,500 rpm per second. Since these drives are designed for use with engines having a 3 : 1 step up to the power take-off shaft, this represents an engine acceleration rate of only about 500 rpm per second, which is quite low. As mentioned in my 1943 paper[1], information from one of the engine manufacturers stated that engine acceleration rates of 3,000 rpm per second may be found in normal operation, with abnormal rates of 3,500 rpm per second being possible under certain combat conditions. These figures amount to some six times faster an acceleration rate than that shown in Figure 13. Since this film shows a peak load at the start of approximately $2^1/_3$ times the initial average load, there may well be some doubt as to the adequacy of response speed at heavier loads and much higher engine acceleration rates.

The advantage of a differential reactive-current equalizer circuit is the fact that the regulated voltage is not affected appreciably by variations in system reactive load. The droop type of equalizer combined with voltage boost proportional to kilowatt load, as proposed by Mr. Levoy, could maintain constant voltage if the load power factor were constant. Load charts for the larger airplanes show a large number of small motors with power factors as low as 0.6 and a few large motors of ten horsepower or more with power factors of 0.8 or higher. In addition there are sizable operational and combat loads of essentially 1.0 power factor. Heavy motor-starting loads accentuate this variation. Hence there may be important changes in load power factor during normal operation which could produce objectionable variations in regulated voltage if the droop type of equalization were used. Certain important military loads require good voltage regulation for satisfactory performance. Aside from the question of voltage regulation, the foregoing scheme is deficient in its ability to divide reactive load properly under conditions of kilowatt load surges between machines during governor deviations. If it were possible to find a single bus point at which total system load could be measured, this method would attain the object desired. Unfortunately this cannot be done, because loads are tapped off several bus sections. A summation circuit using separate current transformers at each alternator would reestablish the interconnections which Mr. Levoy desires to eliminate. If then we provide individual voltage boost proportional to the real load of each alternator, the alternator excitation will be affected by variations in governor operation such as shown in Figures 12 and 13. This may be expected to have detrimental effects on stability because of reduction of synchronizing torque during power surges between alternators. Considerable further study and testing need to be done before such a change can be accepted.

The first part of Mr. Levoy's paper reviews and summarizes the main points brought out in references 1 and 2 of this discussion. However, he has given an excellent description of some of the subsequent development work and presented preliminary oscillograph data which has great value. Tests on this system are being continued by the Air Forces and the manufacturers.

In closing, I am interested in the electronic means which Mr. Levoy mentions for driving an alternator. I assume he meant to refer to the electronic-frequency-changer development.

REFERENCES

1. PARALLEL OPERATION OF AIRPLANE ALTERNATORS, D. W. Exner. AIEE TRANSACTIONS, volume 62, 1943, December section, pages 755–60.

2. Closure of discussion on reference 1. AIEE TRANSACTIONS, volume 62, 1943, page 993.

J. G. Hutton and **P. F. Desch** (nonmember, General Electric Company, Schenectady, N. Y.): The author is to be congratulated on his very effective presentation of a broad subject in a comparatively limited article. In spite of the termination of hostilities the publication of the paper is timely, and a definite contribution to the field of aircraft electrical engineering.

Though much overshadowed by such spectacular achievements as the atomic bomb and radar, the development of an a-c electric system will be of great benefit in the success of a weapon for peace in the form of long-range military and civil aircraft.

Since the writing of the paper some 100 hours of operational experience has been gained on the developmental two-generator systems. Much has been learned about the various pieces of apparatus in the system, and this knowledge can be of great assistance when flight testing begins. Production units of the variable-ratio transmissions are being received, and performance and life tests are being carried out.

In his discussion of the governor-droop circuit, illustrated in Figure 4 of the paper, the author mentions a five-per-cent frequency droop at full load; on the developmental circuit this can be adjusted at will. By test it was found that the load division between two paralleled alternators was somewhat erratic for speed regulations of less than five per cent at full load. The setting at five per cent gave equal load division under all steady-state conditions.

The use of individual cross-current compensation on the voltage regulators for reactive-load division now is being studied to determine its suitability for an aircraft electric system. The value of the load and power factor may vary considerably during a flight. Such conditions may lead to a varying voltage. Except for the complicated switching of the reactive-division control circuits, when operating the generators nonparallel, the method of differential cross-current compensation has worked very well on the developmental system, and the voltage has been held within practical limits.

It is hoped that flight test data soon will be forthcoming. Success of the tests should see a rapid increase in the use of a-c electric systems for large aircraft.

W. M. Green and **A. F. Pelster** (Captains, United States Army Air Corps, Wright Field, Dayton, Ohio): The author is to be congratulated for writing a very explanatory paper. The Army Air Forces has been working on this development since 1942, and its findings substantiate the greater part of Mr. Levoy's paper.

Several points mentioned are open for discussion and probably will not be satisfactorily answered until further tests, including actual flight operation, are made.

Figure 6 of the author's paper shows a star or synchronizing bus arrangement. This system is not being employed thus far on military airplanes using the 200–115-volt system. Instead a ring-bus arrangement, or variation thereof, is being used, as indicated in Figure 1 of this discussion. Each system has certain advantages and disadvantages. The star-bus arrangement has the main disadvantage of preventing parallel operation completely in case of a fault on any part of the bus.

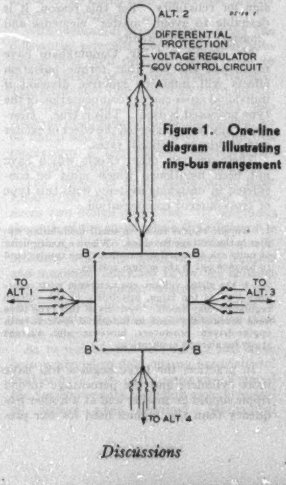

Figure 1. One-line diagram illustrating ring-bus arrangement

The author feels that a complete reactive-load-division circuit for a four-alternator circuit with bus tie circuit breakers would be unduly complicated. Such a circuit for the bus arrangement of Figure 1 is shown in Figure 2 of this discussion. This circuit differs from Figure 6 of the author's paper only in that an auxiliary contact on each bus tie circuit breaker connects between each corner of the reactive circuit and a star point. This scheme will allow proper reactive-load division under any condition including two sets of two alternators operating in parallel.

The differential-current circuit is being employed along with the ring bus on military aircraft for two reasons:

(a). Load power factor has no influence on system voltage.

(b). A rather steep droop characteristic to reactive current is necessary to maintain proper stability with the inherent system. In case the power factor of the system remains constant over the load range, it is possible to design an inherent system in the regulator such that constant output voltage can be maintained at that one power factor. In the present stage of development of the a-c system on military aircraft, the variation of power factor with load is not accurately known.

In regard to the author's paragraph on "Operating Experience," tests made in the A-C Laboratory, Wright Field, prove rather conclusively that full-voltage synchronizing will be employed in military aircraft. In a test made in the A-C Laboratory on synchronizing of alternators driven by variable output speed test stands rated at 75 horsepower, 52 oscillographs were taken. Two alternators of different manufacture were used, and approximately half of the pictures were taken at full voltage and half with the field circuit closing simultaneously with the circuit breaker. In all cases it was attempted to have the voltage 180 degrees out of phase when synchronizing. Of the 52 pictures, there were seven reversals of exciter polarity obtained. All reversals occurred when the field circuit was closed simultaneously with the closing of the circuit breaker.

Full-voltage random synchronizing is not satisfactory because of the excessive system disturbance when a 180-degree phase displacement exists. The afore-mentioned tests were probably more severe than the tests run at the General Electric Company, because the Army Air Forces tests were conducted without the aid of the freewheeling elements. However, none of the oscillograms shown to the undersigned indicate that the freewheeling element operated during the synchronizing tests.

L. G. Levoy, Jr.: I am pleased to note the interest in this paper as indicated by the various discussions.

Mr. E. P. Barlow has brought out a very important point; namely, the necessity of incorporating this drive in an airplane within structural and space limitations available.

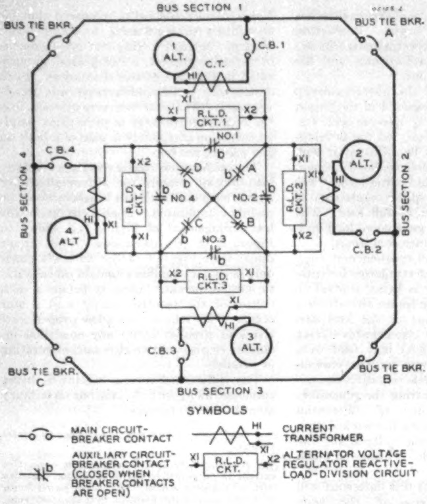

Figure 2. Reactive-load-division circuit

It is realized that many such problems will be encountered in practice, and it will be up to the ingenuity of the aircraft designers to incorporate this equipment in a manner which makes it superior to other ways of doing the job. There is no justification for using alternating current on an airplane, unless the total installation and performance can be proved to be superior to other means of accomplishing the required results.

One way of easing the critical installation problem to which Mr. Barlow refers is to design a split unit in which the pump element is located directly on the engine, and the hydraulic motor element and generator can be located someplace else in the airplane. Such a unit now is being considered for certain applications. The disadvantage of this method is that it introduces a hydraulic transmission system which is undesirable. It also increases weight and reduces efficiency.

Installation problems are beyond the scope of this paper. It was intended to give an idea of the present state of the art, so that aircraft designers could study this system more effectively and compare it with other systems.

The installations to which Mr. Barlow refers now are being made but have not been flight tested, so that no data are yet available concerning their performance.

I agree that a small reliable lightweight gas turbine drive would be a desirable development, and several companies are working on this project. However, to date no completely satisfactory drive of this nature has appeared on the market. Some aircraft manufacturers have been considering the use of two auxiliary gas-turbine-driven alternator units on a four-engine airplane. It should be noted that the variable-ratio drive as now proposed for such systems offers four-engine reliability. This factor must be considered in comparing weights and evaluating reliability.

With regard to the method of synchronization and load division described by Mr Marcy, it is undoubtedly true that such a system can be made to function. However, the principal disadvantage of this type of system is that of vulnerability. Loss of the auxiliary "master" would put the entire system out of order. Such a system would not be tolerated on a military airplane, and it is questionable for commercial aircraft for the same reason. In a well-designed system loss of any single circuit or generator should permit the other machines to function normally. It is considered that this is an important consideration and that damage in one part of the system never should be communicated to another part of the system. This is an essential principle of system design for reliability. For this reason, it is desirable to avoid "master" elements and "master" control circuits.

Mr. Bunce and Mr. Cunningham have mentioned the fact that torque pulsation effects will influence reactive division if individual cross-current compensation of the type proposed is used. This is true. However, they have neglected the effect of exciter and regulator response rates.

There are two other effects which have not been mentioned which must be considered in designing systems with this type of cross-current compensation.

1. Torque ripples result in small modulation ripples in the voltage envelope. Where a multiplicity of units are operated in parallel, these ripples tend to balance out in the system voltage.

2. If the rising-voltage characteristic with resistance load is too large, instability in the voltage regulators may result. Systems of this type have been successfully used in industrial systems with engine-driven generators, however, and warrant study for aircraft application.

In practice, the large engines will have more cylinders and the percentage torque ripple should be smaller and at a higher frequency than the engines used for our preliminary tests. Both of these factors tend to help this situation.

The individual cross-current compensation system should be studied when the actual aircraft-engine characteristics and system loads are known, to determine whether or not it can be built to operate successfully in practice. The reward for successful application of this system is a lessened vulnerability, since loss of any one reactive-division circuit affects only that generator and is not communicated to other generators on the system.

The star bus, or modification thereof, has certain advantages over the ring bus for example, but discussions of its use are meaningless unless specific aircraft system requirements are considered. The illustration used in the paper was included primarily to show how differential cross-current compensation is provided.

It is obvious that larger voltage dips will be encountered when starting larger motors, and also that the dips will be smaller on a four-generator system. The magnitude and duration of the dips is of interest, however. This problem is not peculiar to a-c systems. Existing d-c aircraft systems tolerate severe dips. For example, on the *B*-29 d-c system with one half of the generators operating and a battery, starting the drive motors to run the same Amplidynes would result in a momentary dip of approximately ten per cent.

Naturally these effects have to be evaluated in practice, and, if found excessive, they must be limited by step starters or increase in system stiffness by increased capacity to bring the effect within acceptable limits.

Mr. Exner has commented that we have not shown films covering tests under maximum overload conditions. As stated in the paper, the drives which were available at the time this paper was written were early designs which were limited both in speed range and load. Consequently, it was deemed advisable to get data under reasonable load conditions which could be obtained with available drives and thereby provide information for design of the new drives. New designs of drives are now available, and they will be tested over the entire range of conditions.

Regarding acceleration rates, we have tested up to the maximum rates available with our test equipment, consisting of aircraft-type engines rated 450 horsepower, with no load other than the variable-ratio drives and alternators. We found that the system performed satisfactorily, and the maximum acceleration rate which we obtained was 3,240 rpm per second at the input to the drive. Higher acceleration rates were simulated by switching blocks of resistance in and out of the governor circuits for response tests. It will be interesting to see if the high acceleration rates mentioned by Mr. Exner will be obtained in practice.

Regarding the method of cross-current compensation, it is expected that the load power factor will vary widely. It may well be, however, that the extremes of power factor go with certain light-load conditions, in which case the influence on the voltage level would be small. Full load to heavy overload conditions may show a much smaller power-factor range, in which case the proposed method of cross-current compensation could provide very satisfactory voltage levels. Study of this on an actual system should be made to eliminate the vulnerability of the differential scheme if possible. The use of a summation circuit described by Mr. Exner is unacceptable for the reason which he points out.

In describing the various means of obtaining substantially constant frequency power on aircraft, the first five methods listed in the paper under the heading refer to possible driving means for the conventional alternators when driven from variable-speed engines on an airplane. The last two methods refer to other means of providing substantially constant frequency power, using variable-speed direct-connected generators. There are a number of such systems, several of which were described in reference 1. For example, it is possible to generate variable-frequency constant potential alternating current, rectify, and invert to constant-frequency constant-potential alternating current. Such a scheme probably would use electronic frequency changers, and equipments of this general type are the electronic means to which reference was made.

Referring to the discussion by Captain Green and Captain Pelster, the principal objection to the differential cross-current scheme is its vulnerability, which is a result of its complication. Small wires run between the voltage regulators and circuit breakers of different units. An open circuit in one of these wires may cause improper operation of all other units on the system. This difficulty can be avoided to a certain extent by using multiple circuits, but this increases difficulty of checking circuits on routine maintenance. Aside from this problem, the differential cross-current scheme is very good.

One simple way of eliminating the difficulty caused by exciter polarity reversal is to use a small polarized relay with its actuating circuit across the exciter armature and its contacts connected in the voltage-regulator stabilizing circuit in such a way that, regardless of exciter polarity, the system operates correctly. This method was tested and found to function perfectly, regardless of the method of synchronizing used. Exciter polarity reversals did not disturb the system operation in any way when this polarized relay was used.

If manual full-voltage synchronizing is adopted, this operation will require rather close attention from the flight engineer. If automatic full-voltage synchronizing is adopted, a substantial increase in complexity and weight of the system will result. For these reasons, no voltage synchronizing with polarized relays to eliminate effects of exciter polarity reversal looks attractive. It is recommended that these various methods be tried on a ground setup, and this experience should point the way to the best method for use in aircraft.

If Captain Green and Captain Pelster will inspect the oscillogram shown as Figure 9 in my paper, they will see a case where the incoming machine freewheels for an instant during the synchronization. This is indicated by the fact that the power trace goes negative just before the machine pulls into step. As explained in the paper, the drive input torque does not go negative, because, while the generator is freewheeling, the drive losses are supplied by the input shaft.

The initial disturbance when synchronizing 180 degrees out of phase is the same whether or not the generators are equipped with freewheeling devices. The duration of the disturbance is greater if freewheeling is not used. Tests made without freewheeling are less realistic, as free wheeling will be used in the variable-ratio drives intended for use in aircraft. Some tests were made without freewheeling devices, but these were not shown, as they were of less general interest than those selected for use in this paper.

Constant-Speed Drives for Aircraft Alternators

Discussion and author's closure of paper 45-163 by C. J. Breitwieser, published in AIEE TRANSACTIONS, 1945, November section, pages 763–8.

H. D. Else (Westinghouse Electric Corporation, Lima, Ohio): The need for a substantially constant-speed power source for aircraft generator drives has been recognized for a number of years, and an enormous amount of effort has been expended in attemping to work out a satisfactory solution of the problem. With d-c equipment such a source is highly desirable. Except for electronic conversion, the use of some such device with an a-c system is mandatory.

Mr. Breitwieser has described in detail the functioning of two types of variable-ratio transmissions for connecting a main-engine take-off shaft with the alternator, and has discussed several other possibilities. He has pointed up two near axioms for obtaining good efficiency:

1. The device must be a torque converter rather than a pure slip-loss mechanism.
2. In a two element device, the differential principle in which the elements interchange function at some predetermined speed, should be employed.

It is the writer's opinion, however, that even with continued development, the values of efficiency and weight suggested by Mr. Breitwieser will not be realized. In fact, it has been a major achievement to arrive at the rather high values that already have been obtained.

With hydraulic arrangements using the differential principle, the cylinders are subjected to a fluid pressure proportional to torque whether or not there is fluid transfer. This introduces a slip loss at all input speeds. The mechanism described includes two stages of continuously operating gearing, an oil pump and a governor drive. With this mechanism a zero-transfer efficiency between 85 per cent and 90 per cent is good.

The change in input speed range from 1,000–3,000 rpm to 500–3,000 rpm introduces two design difficulties. It lengthens the ends of the curve where the efficiency is dropping, due to large fluid transfer. It probably shifts the point of zero transfer and maximum efficiency below the cruising speed of the airplane; otherwise the function-reversing mechanism must travel a much greater distance in one direction than in the other.

As to weight, the best values that have been achieved to date on any experimental devices have been of the order of 0.8 pound per horsepower not including governors and oil coolers when required. Mechanical apparatus is designed on the basis of safe stresses and pressures, and the established values must not be exceeded. Electrical apparatus is designed on thermal considerations and 100 per cent overload for several seconds ordinarily does not produce a failure. Thus, a generator rated 30 kw with 5-second 100 per cent overload capacity requires a transmission designed for at least 95 horsepower. On this basis the weight of a torque converter without coupling, cooling, and governor is more than 2.5 pounds per rated kilowatt.

Numerous other types of variable-ratio transmissions have been considered and experimental work has been carried on. Slip-loss devices, mechanical, fluid, or electrical, combined with multistage gearing have relatively good efficiencies. Friction drives employing cones or toroids might be used. Flash boilers and turbines utilizing exhaust heat are possible. Impulse or kinetic-type converters using liquids or gases are impractical without means of changing the angle of the input blading. A mechanical-electrical transmission has been described under the name "Electrogear."[1] None of these mechanisms appears to offer any advantages over the Sundstrund design.

Recent developments in main drives, however, have focused attention on the possibilities of the gas turbine. A small fuel-fed unit, independent of the main power plant, has many advantages over drives coupled to the main units. Not the least of these is the fact that failure or shutting down of a main unit does not affect the electric system. When the airplane is on the ground, the electric system can be operated with all main plants idle. The battery carried on the airplane need be only large enough to start one of the small turbines. Control of the electric system is simplified greatly for the reason that the power of the turbine and the alternator are substantially equal and the unit has excellent inherent regulation.

Fuel economy is not good, particularly at light loads, but, when cruising, only one unit need be in operation. With main-engine drives the airplane is continuously subjected to the light-load losses of all the converters and generators, even though one unit is capable of supplying the cruising requirements. The design limitations of a constant speed gas turbine are thermal. Consequently, the capacity need not greatly exceed the rating of the alternator. Transient overloads will not damage the apparatus and the rotational energy of high operating speed will clear electrical faults without undue sag in frequency.

Economical combinations of cabin supercharger and alternator turbine are possible. It may prove advisable to make the power unit large enough to handle both functions with interstage bleeding of the compressor. The exhaust from the fuselage would, naturally, be fed back to the compressor thus obtaining interstage cooling at no added over-all cost. To take care of the change in altitude the supercharging stages might be by-passed at low altitude and brought into operation when required by means of clutches. Another possibility is to supercharge by means of a separate variable-speed unit, turbine or otherwise, and feed from the cabin to the alternator turbine. On transport and commercial airplanes the air requirements of the cabin appear to be ample for the alternator turbines. On combat airplanes they are probably inadequate.

With the low fuel-air ratio of gas turbines, the carbon monoxide content of the exhaust may be low enough to permit its use without a heat exchanger for deicing.

Very little data are available on weight and economy of small-size gas turbines. In larger sizes weights are below 0.5 pound per horsepower, and fuel rates are of the order of 0.6 pound per horsepower hour. Allowing for greater relative weight of accessories, it would seem possible to build a 150-horsepower unit with a weight of 0.75 pound per horsepower. The fuel rate might be as high as 0.9 pound per horsepower hour. A conjecture as to size is 10 inches in diameter and the tube 5 to 8 feet in length.

REFERENCE

1. THE "ELECTROGEAR"—A NEW ELECTRO-MECHANICAL VEHICLE DRIVE, **Ernest Weber.** AIEE TRANSACTIONS, volume 60, 1941, July section, pages 770–7.

G. C. Crom (Army Air Forces, Wright Field, Dayton, Ohio): In the author's discussion on "Requirements for a Constant Speed Drive" he fails to remember that while the speed of the engine may vary from 500 rpm to 3,000 rpm, the accessory pad varies from 1,500 rpm to 9,000 rpm because of the 3:1 step-up gear ratio in the engine. This step-up ratio cuts down the ratio variation of the drive to 3:1 at low speed and 2:3 at high speeds. This does not improve the problem, but it does change the picture of what the drive must do.

The situation in regard to constant speed drives, whose development was sponsored by the Army Air Forces, as of October 1, 1945, is as follows:

(*a*). The Chrysler mechanical constant speed drive failed after about three weeks testing, seemingly due to unbalanced centrifugal forces at high speed. This project has been temporarily abandoned.

(*b*). Two of the Sundstrund hydromechanical constant speed drives in the experimental form operated satisfactorily for about 250 hours. The production form has had to overcome a number of difficulties, but two units are now under test by the General Electric Company at Schenectady, and a schedule of production has been adopted. This device weighs about 80 pounds. Governors and control details are not yet finished, depending on operating tests.

(*c*). Two additional hydromechanical drives are undergoing tests at the manufacturers. These devices seem to operate satisfactorily and soon will be shipped to Wright Field for further tests, but the weights are large, and they may not be suitable for installation in an aircraft.

(*d*). A form of constant speed drive that is entirely hydraulic is being developed by another manufacturer but has not yet been released. This has a weight of around 80 pounds and can be separated into two parts if desired as it is entirely hydraulic.

(*e*). Other types are under study by the Army Air Forces. These involve both mechanical and electromechanical forms, and in each case show evidence of having a low weight.

C. J. Breitwieser: The problem of securing adequate electric power at low or idling engine speeds, and on the ground when the main power plants are shut off, is a serious one. Mr. Else, in his comments, has indicated that to increase the input speed range of a constant speed drive from 1,000–3,000 rpm to 500–3,000 rpm may cause a loss in efficiency and increased fluid transfer may increase the weight and size of the drive. He has suggested the possibility of using a gas turbine auxiliary power plant.

As Mr. Else has pointed out, this type of generator drive has many interesting possibilities. Unfortunately, the gas turbine has a relatively constant rate of fuel consumption regardless of load. This results in excessive specific fuel consumption during the major portion of the flight. This situation may be improved somewhat by using a multiplicity of units operating only the portion of the units as required by the load demand. There is, however, a limit to how far it is practical to go in this direction, since the smaller units are generally less efficient and have higher weight per horsepower; also the installation and operation are more complicated for a greater number of units.

Considering an airplane of the size in which an a-c system would be used and operating at long-range conditions the gas turbine does not show up very favorably. For example, on a 20-hour flight, with an assumed fuel efficiency of 0.8 pound per horsepower hour at normal rated load and with a proportionate increase of specific fuel consumption at the same rate, as in the operation of modern large gas turbines for light loads—and integrating a representative load curve of an airplane with a 120-kw peak demand over the flight—the gas turbine would require approximately 1,850 pounds of fuel as contrasted with 360 pounds of fuel for alternators driven from the main engines through constant speed drives. It is assumed that the specific of the main engines will vary from 0.43 to 0.47 and the efficiency of the constant speed drive will be 75 per cent. This gives a direct fuel weight difference of 1,490 pounds which multiplied by the fuel, oil ratio of 1.5 for the airplane (additional fuel and oil required to carry an extra pound) results in a net increase of more than a ton in weight. This is by far too great a weight price to pay for the advantages of a separate gas-turbine-driven auxiliary power plant.

It is quite probable that some combination of main-engine-driven alternators and gas-turbine auxiliaries may be the ultimate answer. If the input speed range of the constant speed drive is reduced, its weight and efficiency may be improved, and they would be used on the lighter loads over the long range, whereas on the ground and at engine idling conditions the gas turbine would supply the system.

Whereas the use of the additional power capacity of a separate gas-driven turbine for cabin supercharging will improve the overall performance of the turbine, it still does not show up favorably in comparison with a bleed system from the main engines. With the exception of very limited emergency situations, the main engines are required to deliver rated horsepower only at take-off, and during the time at which the cabin supercharging demands will be made, will have a large reserve capacity and consequently no additional prime mover capacity is required. Also the main engines usually are operating at optimum fuel economy at the times cabin supercharger capacity is required. On the basis of supercharging being required for half the time of the afore-mentioned airplane and an assumed turbine efficiency of 0.9 pound per horsepower hour, the gas-turbine auxiliary would cost more than half a ton net weight increase, neglecting the weight cost of the additional equipment of the turbine installation.

Drives of a type similar to the hydraulic units described in this paper are being used in main-engine-driven superchargers. The British have developed a drive of this type in which the governor is an integral part of the design and can be used on regular lubricating oil from the main engine. This design saves the weight of an added governor and oil sump and cooler.

A few years ago the best aircraft electric motors weighed 6 pounds per hosepower; today we have motors less than 1$^{1}/_{2}$ pounds per horsepower. With a basic weight of prototype constant speed drives of 0.8 pound per horsepower today, the writer cannot help but remain optimistic and believe that in the very near future we shall have constant speed drives of less than 1 pound per kilowatt.

Resonant-Circuit Constant-Current Regulators

Discussion of paper 45-165 by G. M. Kevern, published in AIEE TRANSACTIONS, 1945, December section, pages 807–10.

H. Weichsel and **W. R. McCarty** (Wagner Electric Corporation, St. Louis, Mo.): This paper brings out the important part which the resonant-circuit constant-current regulator has played during the war by supplying adjustable constant alternating current for brightness control of airport approaches and runway lighting. It points out that the great success obtained by this system of lighting resulted in its adoption as standard by the Army Air Forces, the Army, the Navy, and the Civilian Aeronautics Administration.

A number of constant-current resonant circuits were originated by Boucherot in the year 1891. They all consisted of choke coil and capacitor combinations delivering with a constant alternating-voltage supply a constant alternating current regardless of the load circuit impedance. These circuits produced constant a-c output current without the use of moving coils. Three of the Boucherot combinations are given by Figure 1, A and B, and Figure 2. The former two are L connections, the latter is known as the monocyclic square. The L connections, if supplying a noninductive load circuit, draw leading or lagging input currents, depending upon whether Figure 1, A or B, is used. The monocyclic square draws unity power-factor input current when the load circuit is noninductive. But for lagging output current the input current is leading, and for leading output current the input current is lagging.

Steinmetz (see reference 2 of paper), as cited by Mr. Kevern, determines by imaginary quantity calculations the characteristics of the different Boucherot circuits.

The afore-mentioned original circuits were unsuitable for practical use for reasons to be discussed below. Furthermore, in those early days capacitors were unreliable and very expensive.

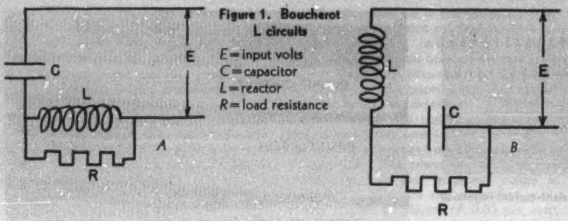

Figure 1. Boucherot L circuits

E = input volts
C = capacitor
L = reactor
R = load resistance

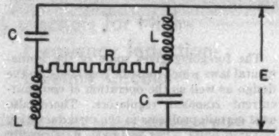

Figure 2. Boucherot bridge circuit, monocyclic square

E = input volts
C = capacitor
L = reactor
R = load resistance

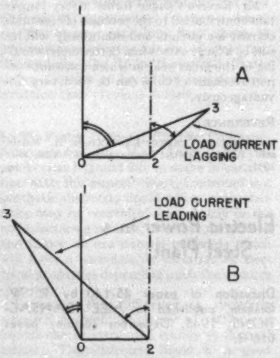

Figure 3. Effect of load power factor on the value of the load current when an output transformer is used

0–1 = output voltage of square
0–3 = constant amperes of square
0–2 = magnetizing current of output transformer
2–3 = useful load current

The monocyclic square, discussed so far, uses two choke coils, each having its own iron core. Tests and theory proved the superiority of a single iron circuit with two separate but equal windings, each acting as a choke coil. This arrangement gives greater operating stability and decreased weight and cost. The single-core two-winding choke coil has equal voltage across the terminals of each choke coil. The same current flow, however, is not essential in both windings, but the vectorial sum of their ampere turns must equal the magnetizing ampere turns required to produce the desired voltage across said windings. This forced equality of choke-coil voltages results in great stability of the monocyclic square. This constitutes a decided improvement over the original monocyclic circuit.

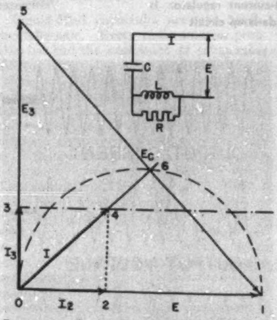

Figure 4. Circle diagram for Boucherot L circuit

0–1 = constant input voltage
0–5 = voltage across reactor L
5–1 = voltage across capacitor C
0–2 = current in reactor L
0–3 = constant current in load resistance R
0–4 = current in capacitor C equal to input current

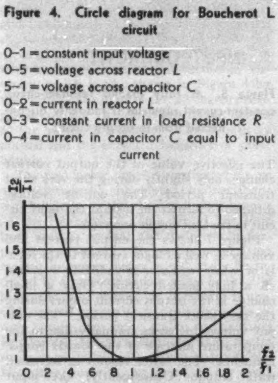

Figure 5. Change of output current of a monocyclic square with change of frequency

f_1 = normal operating frequency
f_2 = abnormal operating frequency
I_1 = output current at frequency f_1
I_2 = output current at frequency f_2

The described Boucherot circuits are undesirable from the operator's point of view, because the output circuits and the input circuits are electrically interconnected. Thus either a two-coil output transformer or a two-coil input transformer ahead of the constant-current regulator is essential.

The original Boucherot and Steinmetz circuits have the serious shortcoming of delivering an extremely high output voltage to an open-circuited load circuit. Said voltage can be limited to a desired value by designing the core of the output transformer for a magnetizing current, at aforesaid desired voltage, equalling the output current of the monocyclic square proper.

In the beginning of the year 1938, Young and Haug, Inc. installed at Lake Geneva a resonant-circuit constant-current regulator for series-lamp street lighting which contained the improvements just discussed. It also contained a very unique nonarcing switching arrangement which eliminated the large oil circuit breaker essential with moving-coil regulators.

Several similar installations were furnished by that company. After the middle of 1939 the Wagner Electric Corporation agreed to build these units and published suitable sales information in the middle of 1940. In the beginning of 1940, this company learned about the great desirability of brightness control for airport approaches and runway lighting circuits, the solution of which appeared at that time difficult if not impossible.

Said company submitted to the director of the equipment laboratories at Wright Field a number of solutions proposed by H. Weichsel using the monocyclic square. One of them employed, between the input terminals of the monocyclic square and the supply line, a transformer provided with taps for adjusting the voltage impressed on the monocyclic square to values corresponding to constant output currents required for the desired brightness control.

Upon said laboratories' request, a sample unit including runway control was built. It was tested by them, and its characteristics were found to be satisfactory. They placed it in actual service in the early part of 1941. This, to the best of our knowledge, was the first constant-current regulator of the resonant type arranged for brightness control. It was the guide for all units produced for this purpose thereafter. As a result of practical experience with this first installation, several improvements were incorporated in the later units without altering the principle of operation. For instance, for later units the laboratories specified their standard switches and relays and omitted the special nonarcing switch supplied with the sample unit.

The characteristics of constant-current regulators are not generally known. For this reason, some of them are discussed below.

A monocyclic-square unit built with a single-core two-winding choke coil has a kilovolt-ampere apparatus efficiency (utility factor) not exceeding 1/1.5 = 66.6 per cent, meaning that for each kilovolt-ampere output two capacitors of a combined rating of at least one kilovolt ampere and a single-core two-winding choke coil equivalent to a two-coil transformer rating of at least one-half kilovolt ampere are required. If input and output transformers are used, the total value of apparatus kilovolt amperes is increased by the kilovolt-ampere values of these transformers.

The constancy of the output current is very high for any of the Boucherot circuits,

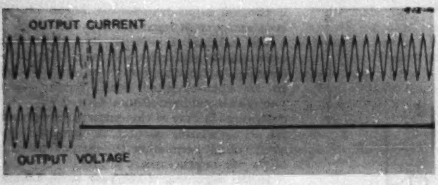

Figure 6. Load circuit of a resonant-circuit constant-current regulator is suddenly short-circuited

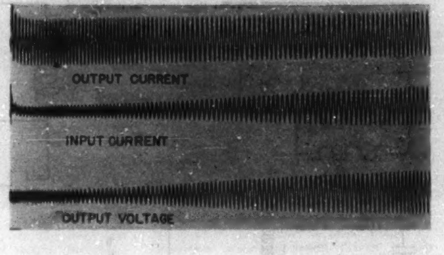

Figure 7 (right). A resonant-circuit constant-current regulator is suddenly switched on a fully loaded Mazda-lamp circuit

provided the input voltage is held constant. If an input and an output transformer are used, the constancy of the output current is decreased as a result of the input-transformer-voltage regulation and the change in current transformation ratio caused by the magnetizing current of the output transformer. The magnetizing current increases with increasing output load. Thus the output current is somewhat less at full load than at no load (load circuit short-circuited). For these reasons the Air Forces permitted a current variation of plus or minus two per cent.

The highest constancy of the output current occurs for noninductive or slightly capacitive loads. Heavy inductive constant power-factor loads decrease the ratio of full-load current to the short-circuited current (no load). But constant power-factor capacitive loads increase said ratio, and it may reach undesirable values for extremely capacitive loads. Figure 3, A and B, explain said relations.

An inductive or capacitive output load not only effects the constancy of the output current but also effects the voltages on the capacitors and reactors of the monocyclic square. For inductive loads the capacitor voltages are higher and the reactor voltages are lower than for noninductive loads of the same kilovolt amperes. For capacitive loads, the capacitor voltages decrease, and the reactor voltages increase.

Calculations based on the analytic methods developed by Steinmetz are very accurate. However, in practice a quicker inside view of the operating characteristics is obtained by vector diagrams and particularly by so-called circle diagrams. Figure 4 shows a circle diagram for an L-connected circuit. This diagram together with diagrams for a monocyclic square and other special cases appeared in a paper by H. Weichsel.[1]

Mr. Kevern touched in his paper on the effect of frequency changes on the output current. He cites a test on a regulator operating at 50 and 60 cycles.

The theoretical relation between the output current and impressed frequency for a monocyclic square without input and output transformers is given by Figure 5. With input voltage held constant, the output current varies only slightly over a very large range of frequencies. It is a simple matter to consider the effect of input and output transformers if used.

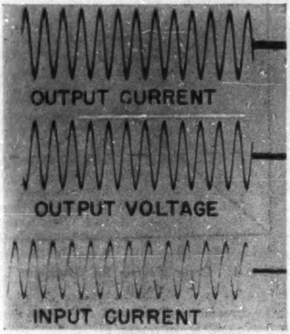

Figure 8. A fully loaded resonant-circuit constant-current regulator is suddenly disconnected from its supply circuit

Figure 6 shows the change in useful output current and voltage when the useful load circuit is suddenly short-circuited. The effective value of the output current changes only slightly during the very short transient period. The output voltage dropped to zero at the instant the short circuit in the load circuit occurred.

Figure 7 shows the output current and voltage as well as input current to the regulator when regulator is suddenly switched on a fully loaded circuit. Only a small change in the output current occurs during the very short transient period. The output voltage increases gradually due to the temperature increase of the Mazda lamps' filaments. The latter results in increased watt output. Consequently, the input current to the regulator increases nearly proportional with the output voltage.

Figure 8 represents, in the two upper pictures, the output current in the useful load circuit when the unit is suddenly disconnected from its supply circuit. The lower picture shows the corresponding input current to the regulator. The complete absence of oscillations or transients is noteworthy.

The opening of the input circuit of a fully loaded monocyclic square results in only a small arc, contrary to the experience when opening the input circuit of moving-coil transformers. This difference is partly brought about by the high power factor of the input current to a monocyclic square, whereas the input circuit to a moving-coil transformer is highly inductive.

The foregoing gives some of the fundamental laws which must be considered in the design as well as the operation of constant-current resonant regulators. There also exist certain problems in the manufacturing of these units. For instance, it is readily realized that neither the required capacitors nor the reactors can be manufactured to exactly the specified values. Theoretical study carried out on this very subject has shown that, in spite of said manufacturing variations, it is possible by suitable means to obtain a surprisingly high degree of constancy of the output current.

Mr. Kevern's paper forms a very important contribution to the problem of constant-current a-c circuits and doubtlessly will result to a large extent in a better understanding of the great field in which constant-current resonant circuits can be used very advantageously.

REFERENCE

1. CONSTANT-CURRENT REGULATORS, H. Weichsel. Wagner Electric Corporation, St. Louis, Mo., 1941.

Electric Power in a Steel Plant

Discussion of paper 45-140 by R. W. Graham, published in AIEE TRANSACTIONS, 1945, December section, pages 816–8.

C. G. Archibald (Westinghouse Electric Corporation, Buffalo, N. Y.): This paper presents in a condensed form the problems involved and the methods pursued by Mr. Graham and his associates in solving a very difficult problem in continuity of service. This paper shows that very thorough studies have been made of the system load requirements, the method of relaying, switching, and other problems associated with large load in a very small area, handling processes that require the highest degree of continuity.

The magnitude of this load may call to your attention that this is no small load; being, on the order of the amount of power consumed by central station load at peak, by a city of 350,000 to 400,000 population. However, it does have two unusual features about it that makes it a more interesting load. These are—first, the very high load factor from 24-hour operation, on the order of 70 to 75 per cent; and second, practically unity power factor at all times.

The solution of operating problems by using fast relaying (both phase and ground), and sectionalizing of the plant, with double feeds wherever possible, appears to be the most economical and practical method of rapid sectionalizing and maintenance of continuity to critical loads.

If all industrial plants placed an equal amount of emphasis on their electrical engineering problems, and solving these as well as this property has, greatly improved service would be maintained.

Capacitors for High-Frequency Induction-Heating Circuits

Discussion and authors' closure of paper 45-157 by F. M. Clark and M. E. Scoville, published in AIEE TRANSACTIONS, 1945, November section, pages 791–6.

Philip Bliss (The New Britain Machine Company, New Britain, Conn.): The writers have presented the problems of timing capacitors for high-frequency industrial use very well. The new oil and new method of construction make a much smaller, neater capacitor than those in present use employing mineral oil dielectric. Incidentally, the 15-kw industrial heater shown appears to be of far superior construction than previous models.

L. W. Foster (General Electric Company, Schenectady, N. Y.): There are two points that I should like to make in connection with this paper. First, Lectronol is a synthetic dielectric liquid whose characteristics may be controlled very closely in the manufacturing process; whereas mineral oil and castor oil are natural materials which will have a considerable variation in electrical properties depending upon their source of supply.

Secondly, the difference in dielectric strength at high frequency of solids and liquids can be attributed mainly to thermal effects. The dielectric liquid is a good thermal insulator but in the case of the parallel-plate capacitor free circulation is possible, therefore, hot spots will not be readily formed. In the case of solid insulation like styrene or mica the hot spot-temperature may be very high compared to the capacitor case temperature, therefore, the solid dielectric will have lower breakdown strength than the equivalent liquid dielectric because heat cannot be transmitted rapidly enough through the solid dielectric material.

L. J. Berberich (Westinghouse Electric Corporation, East Pittsburgh, Pa.): Every manufacturer of high-frequency heating equipment, during the war especially, has felt the need for a capacitor suitable for application in this type of equipment. Messrs. Clark and Scoville have presented a very satisfactory solution to this problem in the liquid-filled capacitor which promises to hold its own even in the postwar period when an abundant mica supply is again expected. Our analysis of the problem led us to the same conclusion reached by Messrs. Clark and Scoville; namely, that a liquid-filled capacitor should be the solution. We want to emphasize, even more strongly than the authors of the paper have, that liquid impregnated paper, despite its enviable record as a dielectric in low-frequency capacitors, is completely unsuited for high-voltage operation in the range from 100 kilocycles to 1 megacycle. The power factor of impregnated paper[1] in this frequency range is from 20 to 50 times the somewhat arbitrarily chosen maximum of 0.05 per cent which appeared feasible for this type of capacitor.

Liquid-filled capacitors are not fundamentally new. Every radio amateur probably has had the experience of submerging air capacitors in oil to cure breakdown difficulties. We agree with the authors that mineral oil, however, is not satisfactory for this application chiefly because its dielectric constant is so low that the size of the capacitor for a given rating would be larger than even the compressed gas capacitors which have come into use in the last few years. This meant that the solution had to be in a polar liquid whose dielectric constant is at least twice that of mineral oil. Lectronol obviously is such a polar liquid. We would add to the requirements for the liquid listed in the paper, that it must have a sufficiently low viscosity so that the increase in loss due to rotating dipoles is not serious in the frequency and temperature ranges of operation. Evidence of this type of loss is given in Figure 4 of the paper at frequencies above one megacycle. This loss is lowered at a given frequency by an increase in temperature because of a reduction in viscosity, which is also shown in Figure 4 by the relative positions of the 25 degree centigrade and the 75 degree centigrade curves at the higher frequencies. This is entirely normal and the expected behavior of polar liquids.

The first polar liquid investigated by us was mixture of chlorinated hydrocarbons which belong to the class of liquids known as the "Askerels." This liquid has long been used as coolant and dielectric in fireproof transformers. By proper purification means the power factor could easily be reduced to a reasonably low value in the 100 kilocycles to 1 megacycle operating range. Chlorinated aromatic hydrocarbons, as is well known, are quite stable to oxidation and have a dielectric strength at 60 cycles superior to that of oil. When tested at 400 kilocycles, however, we found, to our great surprise, that the dielectric stability is extremely poor. We further observed what we believe to be a new phenomenon.

This observation was made by placing the liquid in a test gap similar to the one used by authors, and applying 2,000 to 5,000 volts in the frequency range from 200 to 800 kilocycles with the gap separation set at from 0.5 to 0.75 inch. Within a short time after the application of high-frequency voltage, one or more scintillating streamers were observed as they progressed gradually under the liquid from one electrode to the other. Within a very short time after the first streamers bridged the gap, numerous other streamers appeared. The electrode gap and the region surrounding it gradually became filled with more streamers, and finally the field configuration of the gap was beautifully outlined with scintillating lines of light. The liquid eventually darkened and became so hot due to increased losses that it boiled. Carbon was formed, resulting in complete destruction of the liquid within a very few minutes, without breakdown in the usual sense. The higher the frequency, the lower the voltage necessary to produce this phenomenon. We have never developed a satisfactory explanation for this marked instability of chlorinated hydrocarbons in a high-frequency field. We would like to ask the authors if they have also observed this phenomenon, and, if so, would they venture an explanation.

This poor stability is not only characteristic of the chlorinated hydrocarbons but is also true of certain hydrocarbon phosphates, nitrated hydrocarbons, and some other polar liquids. Esters of certain dibasic organic acids as well as a few other liquids, on the other hand, were found to be quite stable. As a matter of fact, it was found that if a substantial portion of a stable ester is added to the unstable chlorinated hydrocarbon, the streamer formation could be temporarily inhibited. However, later long-time tests indicated that if appreciable quantities of chlorinated hydrocarbons are present in the mixture, instability always eventually results. Finally, of course, the chlorinated hydrocarbons were eliminated and a liquid developed which has very similar properties to those for the liquid described in the paper.

REFERENCE

1. CHARACTERISTICS OF CHLORINATED IMPREGNANTS IN D-C PAPER CAPACITORS, L. J. Berberich, C. V. Fields, R. E. Marbury. AIEE TRANSACTIONS, volume 63, 1944, pages 1173–9.

C. V. Fields (Westinghouse Electric Corporation, East Pittsburgh, Pa.): The authors have apparently developed a well integrated radio-frequency capacitor which is a definite contribution to both the capacitor and the high-frequency heating arts.

After trying a number of solid and composite dielectrics we, too, were forced to revive the liquid-filled capacitor which has long been dormant, primarily for lack of a suitable liquid. In addition to studying various liquids, we have encountered several interesting design problems touched on lightly by the authors.

In testing various liquids, it was found that even those considered suitable for use in radio-frequency capacitors show glowing and bubble formation prior to breakdown. If there are any sharp points in the structure, the stress may be such as to cause these phenomena to take place even at working stresses. Thus it is necessary to round all metal parts adjacent to stressed liquid not only to increase the ultimate breakdown, but also to insure stability in normal operation.

The authors seem to imply that the bushing losses are large compared with the capacitor dielectric loss, which at 1,000 kva and 0.0001 power factor would be 100 watts. We should not expect that the two bushings would have more than a fraction of this loss. It is obvious, however, that a suitably compact bushing for such voltages and currents at these frequencies must not only be liquid filled but must be designed with particular regard to the generation and elimination of heat. The problem is greatly simplified by the use of Zircon porcelain[1] which not only has very low power factor, but also has high thermal shock resistance and high strength. A permanently sealed liquid-filled Zircon bushing has been shown capable of carrying 175 amperes at 6,000 volts and 500 kilocycles without water cooling. It appears to us that the avoidance of water cooling is worth while since the difficulty of obtaining both a low and a high voltage source of water for the capacitors is surely an imposition on the radio-frequency generator designer.

The bushing described is apparently filled from the main body of liquid in the capacitor. If cooling water of perhaps as low as 10 degrees centigrade were turned on for some time before voltage is applied it would appear that the liquid might contract sufficiently to lower the level in the bushing to a dangerous point.

REFERENCE

1. Low Loss Ceramics, R. Russell, L. J. Berberich. *Electronics*, volume 17, pages 136–42.

C. B. Hemming (United States Plywood Corporation, New Rochelle, N. Y.): I believe that the authors are extending themselves a bit in including dielectric heating as a field which will benefit from the availability of Lectronol capacitors. With the trend to higher and higher frequencies in dielectric heating large condensers are of little value except for blocking purposes. There are other obvious reasons why in dielectric heating any types but air and vacuum condensers are undesirable in tuned circuits.

As far as induction heating is concerned, the paper appears to be completely valid and very important. The elimination of cellulose sheet insulation is practical, noteworthy, and appropriate.

A minor refinement could be added in the first paragraph of page 793. The reason why the dielectric strength of insulating liquids do not deteriorate so rapidly with the increasing frequencies may not be generally known and might be interesting to the reader.

The last paragraph on page 795 cannot be emphasized too much.

I am not thoroughly grounded in the policies of AIEE, but as long as Lectronol is a proprietary substance or mixture, the paper has a little bit the flavor of advertising, which possibly detracts from its force. However, on the other hand, I have no good suggestion for correcting the situation.

F. M. Clark and M. E. Scoville: The authors greatly appreciate the comments and interest expressed in their new capacitor. The use of a liquid as the sole dielectric in a power capacitor is not fundamentally new, as stated by Doctor Berberich. The development of an hermetically sealed capacitor for application at high voltage and high frequency does, however, represent a departure from past engineering practice. It is gratifying, therefore, to find that our developmental work and practical application are supported by the results of investigations by others.

In the long series of studies which culminated in the development and application of the capacitor liquid described, we have observed many unexpected dielectric phenomena associated with the use of high-frequency voltages. Prominent among these phenomena was the behavior of the chlorinated liquids. We have found that these liquids possess many of the qualifications necessary for use as dielectrics at high frequency. Their use, however, is limited to the lower voltages for as the voltage applied is increased, scintillating streamers appear, carbon is formed due to the decomposition of the liquid and the dielectric ultimately fails with the passage of a power arc. In this respect our experience parallels that reported by Doctor Berberich. Our new liquid, however, shows none of this hazardous behavior even under high-frequency voltage application which approaches the ultimate breakdown value.

We have not encountered any of the difficulties described by Mr. Fields. The possibility of liquid contraction, of course, has been factored in the design of the capacitor case used. The flexible construction of the case prevents void formation in the bushing at the lower temperatures, as well as the accumulation of excessive pressures at the higher temperatures of operation.

Mr. Hemming asks for an explanation of why the dielectric strength of liquids is more stable than that shown by solids as the frequency of the test voltage is raised. It is a general characteristic of liquids that their dielectric strength is less affected by changing test conditions than solids even at 60 cycle voltages. As suggested by Mr. Foster this greater stability in liquids is usually associated with their greater freedom from accumulated heat effects. It is, therefore, suggested that the same freedom from heat accumulation in liquids is responsible for their remarkably high dielectric strength at the higher frequencies of test.

Maintenance of Good Brush Performance

Discussion of paper 45-164 by W. G. Kalb, published in AIEE TRANSACTIONS, 1945, December section, pages 819–25.

G. U. Dautrich (General Electric Company, Hartford, Conn.): The subject of Mr. Kalb's paper is a timely one. During the last four or five years, the electrical maintenance departments in many plants have been understaffed. This meant that close attention to such items as brush performance could not be given. Also, with many machines operating nearly 24 hours per day, there was little opportunity to correct many obvious troubles, unless danger of an immediate shutdown was apparent.

Undoubtedly, in the coming postwar years, much closer attention will be given to the over-all efficiency of the operation of electric machinery, in which brush performance plays a vital part in many machines.

Mr. Kalb has covered the subject quite logically, as:

1. He has indicated the points to be given attention both in design and original starting of a machine, such as, grade and size of brush, brush pressure, spacing, and location of neutral. Observance of these items insures that a machine will get off to a good start.

2. The paper emphasizes various items of preventive maintenance, once the machine is in service, such as, attention to sparking, formation of good film, cleaning of the commutator, and presence of contaminating gases in the air.

3. Mr. Kalb has covered quite thoroughly the symptoms indicating the presence of trouble, diagnosis of the possible causes, and various methods of correction.

I do not know whether there is, at present, any manual being published, which covers the subject in this manner; but, if not, it would seem that this paper could well serve as the basis for a service manual, for the use of electrical maintenance men, which could be of real value in helping an electric equipment user to obtain maximum performance from his machines.

D. Ramadanoff (National Carbon Company, Cleveland, Ohio): In this paper the author has given an excellent summary of the factors affecting good brush performance. Of particular significance is the curve in Figure 8 showing the relation of brush pressure on the rate of brush wear. In field applications where commutator peripheral speeds are high, or machine vibrations pronounced, it is better to have the brush pressure above, rather than below or at the optimum range. This is particularly true in aircraft generators and motors, where vibration and high commutator peripheral speeds are present at the same time.

It may be of interest to point out, however, that the curve in Figure 8 is an idealized curve and that the region in the neighborhood of minimum rate of brush wear is a region of uncertainty in which individual brush-wear measurements are not reproducible.

In the second paragraph under the heading of "Criteria of Good Brush Performance," we wish to point out that bright surface on worn commutator can be obtained with nonabrasive brushes and dustless atmosphere if, for instance, small amounts of chlorine gas are present in the air. Chlorine gas causes periodic stripping of the commutator film, copper-picking by the cathode brushes, and this, in turn, causes commutator wear which gives it bright surface appearance.

Wear on the commutator surface in the form of threading can be caused also by copper-picking by the cathode brushes, which, in turn, is caused by the stripping of the commutator film due to alternate high and low brush-current densities.

W. R. Appleman (Master Electric Company, Dayton, Ohio): I had the pleasure of attending the meeting of the motor and control technical discussion group of the Dayton Section, AIEE, when Mr. Kalb presented the paper which has since been revised in its present form for publication.

It was my opinion during the talk, and again in reading the present paper, that Mr. Kalb has done an exceptionally thorough and clearly stated job of analyzing for practical use the problem, "Maintenance of Good Brush Performance."

The manufacture of $27^1/_2$-volt d-c rotating equipment for wartime aircraft, where the speed of rotation was usually 6,000–12,000 rpm, and where high altitudes presented additional problems, has brought about an appreciable amount of additional knowledge in the brush field. I was glad to see that

Mr. Kalb referred to these data in his talk and in his paper.

It might be well to mention that intimacy of contact between brushes and commutator has a decided effect on radio interference produced and that increasing the brush pressure above the limits usually set as the optimum is sometimes necessary to meet the latest radio interference requirements.

Dielectric Strength and Protection of Modern Dry-Type Air-Cooled Transformers

Discussion and authors' closure of paper 45-156 by P. L. Bellaschi and Edward Beck, published in AIEE TRANSACTIONS, 1945, November section, pages 759-63.

J. H. Hagenguth (General Electric Company, Pittsfield, Mass.): The experience with dry-type transformers in unexposed locations, where overvoltages do not occur, has been very satisfactory. The authors apparently are quite satisfied that a dry-type transformer can be protected successfully in the field with available lightning arresters when connected to exposed overhead circuits. Actually, the demonstrated margin between test voltage of a transformer of the 15-kv insulation class, 50 to 54-kv full wave from Table I of the paper, and the arrester *IR* protective level of a 15-kv arrester which is 50 kv at 3,000 amperes from Table III of the paper, is exceedingly slim. Tests presumably were made at room temperature on new transformers in a clean atmosphere. The operating temperature of the insulating air in air-cooled transformers will be of the order of 80 degrees centigrade to 120 degrees centigrade, or an average of about 100 degrees centigrade. The breakdown voltage of air decreases with relative air density. Relative air density decreases with increasing temperature as given by the equation

$$\delta=\frac{0.392b}{273+t}$$

b = barometric pressure in millimeters
t = temperature in degrees centigrade

Therefore, the transformer should have a demonstrated strength at 25 degrees centigrade at least 25 per cent higher than the arrester protective level in order to withstand the surge voltages permitted by the arrester at an air temperature of 100 degrees centigrade if it is to be used on exposed circuits.

The effect of dust particles collecting in the transformer, particularly where the atmosphere contains conducting paints or metal particles, also will result in lowering of the insulation strength. The effect of aging of insulation because of operating temperature, deterioration because of careless cleaning, and so forth, probably cannot be evaluated at this time but should result in lowered breakdown strength.

All these factors perhaps are not very important when transformers are used in protected locations where overvoltages do not occur. In exposed circuits, however, where overvoltages must be expected to occur and arrester discharge currents may greatly exceed 3,000 amperes—the highest current listed in Table III—the application of the dry-type transformer is definitely inferior to the liquid-filled transformer because of the very low margin between demonstrated strength and protective level. The latter has a demonstrated margin of 70 per cent to 80 per cent above the protective level and is not subjected to contamination like some dry-type transformers.

There are a few questions with regard to the impulse tests. Mr. Bellaschi has pointed out in a previous paper[1] that failures in liquid-filled transformers during impulse tests can be discovered readily by means of smoke and bubbles. This means will not be available when testing a dry-type transformer. Of course, in this type of transformer, the casing can be removed and the windings can be observed. However, it would take quite a few observers to watch the complete coil stack for coil-to-coil failures and to be certain that such failures did not occur. Removal of the case would not result in a correct test as the strength of the windings and leads to the grounded case would not be demonstrated. Furthermore, the mere presence of the large ground plane might lower the impulse flashover voltage of some of the insulating parts.

Perhaps normal frequency excitation would help in this case because in air 60-cycle follow current can be established more readily than in liquid-filled transformers where follow current practically never occurs even though impulse failure occurs every time a surge is applied.

It would be interesting to know what method the authors have developed to positively identify a coil-to-coil failure. This failure-detection problem is particularly intriguing because failures probably occur on the tail of the chopped wave or a steep-front wave. The steep tail of these waves is the most damaging part of the impulse test in this type of transformer. In liquid-filled transformers, the damage produced by the chopped wave persists and can be detected on application of the full wave[2] even if smoke or bubbles cannot be seen. In dry-type transformers, failure produced by the chopped wave very frequently will not reoccur on application of the full wave and, therefore, a failure occurring during chopped wave test, unless seen by the most careful visual inspection or indicated by power follow current, readily could be overlooked and the damaged transformer shipped. Thus, it would be good practice to omit chopped-wave tests until positive failure-detection methods are developed for this type of transformer.

The authors mention a test to flashover of the insulation on a 350-kva transformer without causing any ill effect to the transformer. Presumably these tests were made with simultaneous normal frequency excitation and perhaps follow current was established. The resulting burrs on previously smooth metal surfaces would be expected to lower subsequent flashover voltages.

The choice of positive polarity for dry-type transformers would seem correct and is formulated as such in the American Standard Association's Standard C57.2-10.116.

The choice of protective methods as shown in Figure 8 of the paper follows closely those recommended for the protection of rotating machinery[3,4] and so should be the best available for the purpose.

REFERENCES

1. Impulse Testing, a Power-Transformer Routine, P. L. Bellaschi. *Westinghouse Engineer*, May 1945, pages 67–70.

2. Progress in Impulse Testing of Transformers, J. H. Hagenguth. AIEE Transactions, volume 63, 1944, pages 999–1005.

3. Protection of Rotating A-C Machines Against Traveling Wave Voltages Due to Lightning, W. J. Rudge, R. W. Wieseman, W. W. Lewis. AIEE Transactions, volume 52, 1933, pages 434–40.

4. Protecting Machines From Line Surges, J. F. Calvert. AIEE Transactions, volume 53, 1934, January section, pages 139–46.

F. J. Vogel (Illinois Institute of Technology, Chicago, Ill.): The dry-type transformer is not a new device as there always has been a demand for a transformer without oil for use in buildings. They usually were limited to class-*A* insulation in the earlier days, but the use of fire-resistant or fireproof transformers with class-*B* insulation is of more recent origin. As such, the dry type is a rival of the Askarel-filled units, which are also fireproof but not necessarily explosion-proof. However, the Askarel-filled units should have higher impulse strength than the dry type. Actually, there are no data available, to my knowledge, regarding the impulse strength of barriers and insulation assemblies or transformers in Askarel. Dry-type transformers seem to be limited to 15,000-volt circuits for economical reasons based on insulation clearances, and it is possible that Askarel-insulated units also are limited as compared with oil-insulated ones.

There are some statements in the paper which seem a little questionable. One is that switching surges are relatively slow. There are several papers which have been published previously contradictory to this. These papers have reference to data obtained on systems and on the interrupting ability of breakers. However, this is not in my opinion important provided the surge magnitude is low. It is a subject worthy of more consideration although apparently the steepness of switching surges has not been a practical cause of trouble.

Another questionable statement is that positive polarity is generally more severe than negative. In the case of the oil-insulated transformer studies, typical insulation assemblies were made and breakdown data obtained for both polarities. In the paper, impulse ratios are assumed, and even a shape of time-lag curve, by means of the oscillograms in the paper's Figure 5. It is interesting that the leads provided protection for the windings, as it once was hoped that the bushings would do for oil-insulated apparatus. It would be a good principle of design but, nevertheless, the time-lag curve of the winding insulation is not established. As these tests all were made with positive polarity, it is not certain that exactly similar results would be obtained with negative polarity. The winding strength probably is not affected as much by polarity as the lead insulation which leads to a situation similar to that in oil-insulated transformers.

From a practical standpoint, the procedure of determining what the arrester will do, and then that the transformer can be protected by the arrester, seems sound. I think that the authors have demonstrated the value of the protective system by means of the "combined test." Also, the required levels of the transformer from the arrester standpoint can be established, and seem reasonable, even if not based on fundamental transformer-insulation data. The methods of arrester application are not new but are an extremely valuable addition to the paper.

P. L. Bellaschi and **Edward Beck:** Mr. Vogel has raised the point as to whether switching surges may attain a severity in the front duration comparable to impulse voltages. It would take this discussion far afield to review, even in part, the subject of system overvoltages. We may call attention to typical data in previous papers.[1,2] From these and similar records it can be seen that in power systems transient voltages seldom exceed a few kilovolts per microsecond. Stiffer overvoltages might occur under unusual conditions such as might be produced by forced quenching of the arc prior to current zero. The fact remains that system overvoltages rarely, if ever, are found to attain a severity comparable to impulse voltages (Figure 5 of the paper) and, provided dry-type transformers are designed to meet the impulse levels designated, switching surges in general present no problem. Operating experience sustains this conclusion.

With reference to Mr. Vogel's second question, the data in Table I of the paper give permissible test values at long, short, and very short impulses. Inasmuch as the same relative margins are present to breakdown voltage, the data in the tabulation represent the volt–time characteristic of the insulation. Tests conducted on models likewise bear out the impulse ratios reported in the paper. Test experience has demonstrated that the withstand strength is lower for positive than for negative waves.

Dielectric tests have been applied to dry-type transformers at room temperature and at temperatures corresponding to full-load operating conditions. It long has been appreciated that temperature does affect air density and air density affects strength, but the relations are not as simple or as much as Mr. Hagenguth would indicate. For instance, the impulse strength does not drop in direct proportion to air density, nor is it affected by usual dust and dirt accumulations. Contamination and other unusual service conditions would affect this as they affect other apparatus; bushings of oil-immersed transformers, insulators, and so forth.

The impulse levels of the dry-type transformer are determined by the economics of design. No claim is made that the impulse strengths are comparable to oil-immersed apparatus. In addition to the fundamental data on insulation, impulse levels proposed, and types of arresters and methods of protection recommended, that is, when the apparatus is required for applications on circuits quasi-exposed or exposed, the paper presents comprehensive verification impulse tests which should stand as reasonable confirmation of the soundness of the recommendations. Furthermore, it should be noted that these tests were conducted on 15-kv insulation, and that 15-kv arresters were used. For other classes of insulation and arresters the relative margins are even more favorable. There is also the further possibility of lower rated arresters as on systems with solidly grounded neutral.

A comparison to be valid has to be all embracing. The modern dry-type transformer hardly can be compared to the oil-immersed entirely on the basis of impulse strength. To mention one important factor, the latter does not fulfill the same requirements insofar as fire and explosion hazards are concerned. Perhaps the askarel-filled transformer might be compared to the dry-type transformer. If this were done such factors and limitations as Mr. Vogel has set forth, and others too, of necessity would come to the fore in the over-all comparison. The wide applications to this day of nearly 1,500,000 kva of dry-type power transformers is ample and clear evidence that industry has drawn the comparison and has assigned relative merits to each type of apparatus. The future alone will tell whether dry-type transformers may find even wider application, as on exposed circuits.

In the matter of impulse testing, many dry-type transformers have been impulse tested at recommended levels and all were found satisfactory. In tests intentionally carried to the point of ultimate strength, no difficulties have been found in observing the failure.

REFERENCES

1. TRANSIENT RECOVERY-VOLTAGE CHARACTERISTICS OF ELECTRIC-POWER SYSTEMS, H. P. St. Clair, J. A. Adams. AIEE TRANSACTIONS, volume 61, 1942, September section, pages 666–9.

2. TRANSIENT RECOVERY VOLTAGES AND CIRCUIT-BREAKER PERFORMANCE, R. C. Van Sickle. AIEE TRANSACTIONS, volume 61, 1942, November section, pages 804–13.

Wound- and Dummy-Rotor Methods of Quality Control and Trouble Shooting of Induction-Motor Windings and Cores

Discussion of paper 45-166 by P. H. Trickey, published in AIEE TRANSACTIONS, 1945, December section, pages 842–4.

R. F. Munier (The Emerson Electric Manufacturing Company, St. Louis, Mo.): Mr. Trickey has been very thorough in his treatment of the subject, particularly in his consideration of the determination of stator iron loss.

It is believed that a comparison of open-circuit reactance values would be of interest, with the results of dummy-rotor tests being contrasted with data from no load synchronous speed tests. There appear to be several factors which might cause the two values to differ.

Mr. Trickey, of course, confines his consideration of the wound-rotor method to quality control and trouble shooting. It might be noted that the procedure could be of value in the determination of design information that is impossible to obtain in other ways.

As an example of this, for fractional-horsepower motor designs there is a number of methods [illegible] holding stator core laminations together and of retaining the core in the frame structure, all of which result in different amounts of core loss. In general, it is not possible satisfactorily to carry through calculations which will take account of the effects of these various methods. Several of the many instances of this nature are the following:

(*a*). The use of rivets to hold laminations together, or of a key to hold laminations in alignment.

(*b*). Difference in pressure for holding laminations together, and the amount of flare that may exist at the radially inner part of the laminations, resulting from the method of assembly.

(*c*). Difference of insulation between laminations.

(*d*). The inclusion of a steel band directly around the outside of the laminations.

(*e*). The use of square or partially squared laminations.

(*f*). The inclusion of support rings or bands at the ends of the stator core for the purpose of preventing lamination flare.

By the use of a wound rotor, calibrated for various values of flux per pole, the stator core losses for the different methods of construction could be determined in such a manner as to make the data available for design work. The actual yoke flux of any stator core that was being tested could be determined by winding a search coil around the stator core through a stator slot halfway between the center lines of adjacent opposite poles set up by the wound rotor. The voltage induced in this coil could be used for calculating the flux through the yoke. If the stator core should be held together by rivets, or if there should exist other construction details that would cause the core-loss reading to vary with the angular position of the wound rotor, it is believed that a rather accurate value for core loss could be obtained for machines with revolving fields if an average were determined from a series of readings with the rotor moved about five electrical degrees between the successive readings.

Statistical Methods in the Development of Apparatus Life Quality

Discussion of paper 45-142 by Enoch B. Ferrell, published in AIEE TRANSACTIONS, 1945, October section, pages 700–03.

Casper Goffman (nonmember; Westinghouse Electric Corporation, East Pittsburgh, Pa.): This article illustrates the value of a rational plan of collecting data and of drawing conclusions. Generally, the engineer works in a hit-or-miss way and, therefore, often makes incorrect statements about the performance of a product.

Mr. Ferrell has blended rigorous statistics with practical experience in such a way as to obtain a plan which may be duplicated readily by engineers who have similar problems. On the other hand, the indirect manner used by the author makes the paper rather difficult to read.

The Self-Inductance of a Toroidal Coil Without Iron

Discussion and author's closure of paper 45-159 by H. B. Dwight published in AIEE TRANSACTIONS, 1945, November section, pages 805–06.

Thomas James Higgins (Illinois Institute of Technology, Chicago, Ill.): Professor Dwight's solution is most instructive and interesting. It seems desirable to mention that equations 1, 2, and those pertinent to the present case are derived for coils comprised of current sheets wrapped around cores. A winding consisting of fine wire closely wrapped around the entire core well approximates a current sheet. But, if the winding is of very coarse wire, or is loosely wrapped, the value calculated from the afore-mentioned formulas will differ more or less from the actual value of the inductance. The gratifying agreement between the calculated and measured values of the test coil indicates that the equations will furnish sufficiently accurate values for the windings usually encountered in practice.

The writer is desirous of learning why the coil of Figure 1 is not of uniform thickness and on what particular device such a winding is used.

L. K. Hedding (Union Switch and Signal Company, Swissvale, Pa.): The method employed for solving this problem is well worth noting. While at first glance the mathematics of the paper may appear to be quite involved, actually the equations are set up for the most part by utilizing simple proportionalities to establish the relationship between the various dimensions of the coil. These same equations are solved readily by applying the most elementary knowledge of integral calculus. Professor Dwight has performed an excellent job in taking what appears to be a complicated problem and solving it in a straightforward simple manner.

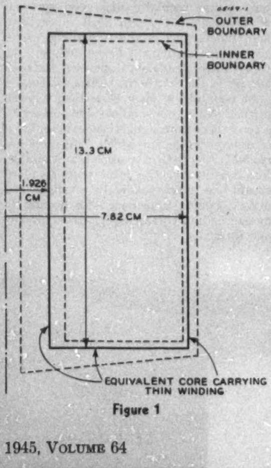

Figure 1

The fundamental principle upon which the solution is based is that for air the value of flux density at any point is numerically equal to field intensity at that point. Nearly all of the paper is devoted to deriving equations for evaluating total flux linkages in various parts of the winding itself in terms of known coil dimensions. This serves as a reminder to many of us that the formulas usually employed for calculating inductance, which involve only the dimensions of the core or form on which the coil is wound, may not always give the desired answer with sufficient accuracy.

In summary, Professor Dwight is to be commended, perhaps not so much because he has given us some formulas which did not exist previously, as on the fact that he took time to show, by a specific example, how a problem of this type may be solved using only the most elementary principles of mathematics and magnetic circuits.

Walther Richter (Allis-Chalmers Manufacturing Company, West Allis, Wis.): Professor Dwight's paper will be a welcome addition to the collection of formulas dealing with the subject of mutual and self inductance; this addition will be most useful to radio and communication engineers who deal with air core inductances and who must have a high degree of precision in their calculations.

To those of us who have to deal with problems of this kind only occasionally, the presentation of an accurate treatment, such as given in Professor Dwight's paper, affords an opportunity to check our rough and approximate methods against the accurate method; such a procedure shows how much error can be expected from approximations and the direction in which it will occur.

From this point of view then let us ask how we would have calculated the inductance of the toroidal coil described in the example before the accurate treatment presented in this paper was at our disposal.

The coil treated in the example has 1,680 turns. If the cross section of the wire were very small, we could wind this coil in a single layer around the core of the cross section wxh, as given in Figure 1 of Professor Dwight's paper. The inductance of such a single-layer toroidal coil then would be given by equation 1 in the paper. It is evident that the inductance obtained in this manner will be smaller than the actual one. The preceding analysis placed all the turns in the position occupied by the innermost layer of the actual coil; we also could make a new nonmagnetic core with a cross section equal to the cross section of the completed actual toroid and then wind the 1,680 turns on this core, which would place the winding in the position occupied by the outer turns of the actual coil. This obviously would give us an inductance larger than that of the actual coil. Therefore, there must exist a cross section somewhere between these two limits which, if wound with 1,680 turns, will give us the same self-inductance as the actual coil. The first reaction of the practical engineer probably will be to place the infinitely thin winding along a path halfway between the innermost and outermost layer. However, since the problem is one of flux linkages, that is, each layer not only adds to the magnetic flux but also to the induced voltage, such a position would result in too large an inductance. On the basis of a treatment given by Roters[1] it was decided to consider the winding concentrated at a distance 1/3 of the total winding thickness from the innermost layer; in other words, to the dimension w are added $t_1/3$ on the inside and $t_4/3$ on the outside. In a similar way, there is added 1/3 of the average of t_2 and t_3 to the dimension h on top as well as at the bottom. With these assumptions the equivalent core takes the shape indicated in the accompanying figure. Application of equation 1 to this core results in

$$\begin{aligned} L &= 2\times 13.3\times 1{,}680^2\times \mathit{ln}\,\frac{7.82}{1.926}\\ &= 2\times 13.3\times 1{,}680^2\times \mathit{ln}\ 4.06\\ &= 26.6\times 1{,}680^2\times 1.4012\\ &= 105.2\times 10^6 \text{ abhenrys}\\ &= 0.1052 \text{ henry} \end{aligned}$$

This figure is seen to agree with the result of the accurate formula within approximately 3.5 per cent. For most practical purposes this accuracy probably would be sufficient, giving us the comforting thought that our approximate calculations would not have carried us too far astray.

REFERENCE

1. ELECTROMAGNETIC DEVICES (book), Roters. Pages 98–9.

Robert F. Field (General Radio Company, Cambridge, Mass.): In answer to Professor Higgins' questions, it may be stated that the wire density is not the same on the inside and outside of the coil, because of the difficulties encountered in filling the center nearly full of wire. This coil is of such a shape as to have for a toroid a maximum ratio of inductance to d-c resistance for a given weight of copper wire and was built to check this fact.

H. B. Dwight: The approximate computation described by Mr. Richter is a very reasonable one, and it is interesting to see how well it results in the case of the practical example.

Control of Load, Frequency, and Time of Interconnected Systems

Discussion and author's closure of paper 45-139 by C. K. Duff, published in AIEE TRANSACTIONS, 1945, November section, pages 778–86.

J. M. Sharpe (Shawinigan Water and Power Company, Montreal, Quebec, Canada): While automatic control of frequency is generally preferable, and in some cases even may be essential, it is sometimes possible to obtain satisfactory results with manual control. At certain of our generating stations which have to control frequency for relatively short intervals, we have found that by extending the "synchronizing-motor" controls from the bench or control board to push buttons on the operator's desk, the frequency can be maintained within plus or minus 0.1 cycle of the normal 60-cycle value.

L. B. Stirling (Shawinigan Water and Power Company, Montreal, Quebec, Canada): C. K. Duff's description of the frequency-regulator characteristics brings out an interesting point regarding the sensitivity of the equipment. The continuous frequency fluctuation which he speaks of is generally too rapid to correct by the regulation of large hydroelectric units, and an attempt to make such a correction possibly will aggravate the condition and certainly will result in excessive wear of the speed-changing mechanism of the governor. The method described in the paper of making the regulator sensitive only to the integrated frequency error is a satisfactory way of avoiding this trouble, but a similar result can be obtained more readily by giving the regulator a dead band of slightly greater magnitude than the average frequency fluctuation. This method has the advantage that the regulator comes into action immediately when the frequency deviation exceeds the limits of the dead band instead of being delayed until the accumulated error reaches the predetermined value. Admittedly, this method of control will permit a slight time error to accumulate but, in practice, it has been found that this time drift is very small and can be corrected readily by occasional readjustment of the frequency setter dial.

William S. Peterson (Water and Power Department, City of Los Angeles, Calif.): Our experience with this equipment dates back to October 1936, when the first units in the Boulder Power Plant were placed in service. These large units with their high values of WR^2, sensitive governors, and precise equipment for the control of load, frequency, and time made possible a degree of system regulation which previously was considered impractical.

In the matter of tie-line load control, our problems have been relatively simple as, with one exception, all interconnections are with comparatively small systems which have little effect upon main-system regulation. In the single case of the interconnection with another large system, the tie-line capacity is sufficiently large to permit the use of manual control with satisfactory results.

In the matter of frequency and time control, the problems have been more difficult. This is because of the critical nature of service to motion-picture and radiobroadcasting studios, rubber and textile plants, and similar industries. In this we have achieved a high degree of success and our standards are much higher than those mentioned by C. K. Duff as existing on the Ontario system. Our normal frequency variations have a band width of one-tenth of a cycle on a 60-cycle basis, or a maximum and minimum of 60.05 and 59.95 cycles. The time control is equally close, and the maximum daily deviation in any 24-hour period seldom exceeds two-tenths of one second.

These results were attained by careful tests to determine and use the maximum practical sensitivity of the governors and time-frequency control apparatus. The first step was to adjust the governors to obtain the minimum band width of frequency that could be obtained under all conditions of loading without excessive movements of the servo motors on the turbines. Next it was necessary to adjust the frequency controllers to match this characteristic band width and prevent its deviation from a straight line on a graphic chart. This matching of characteristics was found to be very important as there is a tendency to try to use the high sensitivity of the controller to compensate for the lower sensitivity of the governor.

An important aid in the maintenance of close time adjustment is an audio-frequency oscillator and a synchronous-motor-driven contactor. With this device it is possible to obtain a system beat note for check with the Arlington beat note at regular intervals. This leads to much closer adjustment than could be accomplished by any visual means when dealing with fractions of a second.

The whole subject of frequency and time control in large systems is taking on increased importance. Interconnections with other systems, water and fuel economy, changing load schedules, and other factors all have a disturbing influence on the regulation of frequency and time. These matters should receive careful attention if close regulation is to be obtained.

C. K. Duff: On isolated systems or systems without low-capacity ties to other large systems, it is possible to regulate frequency by control extended to the operator's desk, in the manner described by J. M. Sharpe. This would require a frequency indicator with high precision and expanded scale easily readable from the operator's desk as a guide to frequency control. In spite of close attention, time drift would occur inevitably, although the average frequency otherwise might be acceptable.

If the system has tie lines to one or more other large systems it will be found difficult to regulate the load on such ties closely if frequency is controlled manually. Control of generators on both sides of the tie must be closely co-ordinated in order to avoid swings in frequency and tie-line load. In such cases automatic control has been found virtually indispensable.

L. B. Stirling compares the integrating-type regulator described in the paper with a type which operates on a measurement of instantaneous frequency deviations which exceed a fixed dead band made wide enough to cover the inherent uncontrollable frequency fluctuations of the system. The latter type usually has one or two seconds mechanical time delay in the measuring element. For frequency deviations outside the dead band it may deliver corrective impulses of a duration proportional to the instantaneous deviation and repeated at uniform time intervals until frequency recovers within the range of the dead band. The integrating type produces impulses of nearly equal duration, spaced at intervals which are inversely proportional to the average deviation, however small that may be. For example, an average deviation of one tenth of one per cent will produce an impulse at the end of 20 seconds and at intervals of 20 seconds as long as the deviation exists; for one fifth of one per cent deviation the time is ten seconds; for one half of one per cent, four seconds; and so on, with a minimum time of one second. For small deviations the integrating type will "wait and see" if the deviation will be averaged out by a swing in the other direction. On large sudden deviations the integrating type can be just as fast as the other, but either type will operate satisfactorily for frequency control. Time control is automatic in the regulator described in the paper, but automatic time correction can be added to the other type, thus relieving the operator of the need for making manual adjustments.

William S. Peterson draws attention to the necessity for adjustment of governors to their best possible performance before adding a frequency controller. This is an important practical point which has been crowded out in the presentation of principles based upon ideal governor performance.

Frequency and time deviations cited by Mr. Peterson are extremely small as everyday operating experience. These results are attainable only by use of a sensitive frequency-time regulator plus good governor performance and careful load supervision, with maintenance of ample spinning reserve generating capacity. As stated in the paper, reserve capacity sometimes has been lacking on the Southern Ontario system.

In maintaining such close time control, neither visual nor audible comparison of seconds-beat time signals is adequate, but a recording device, on which differences are readable to 1/100 of a second, is desirable. For consistency, the local time standard should be correspondingly precise, and means should be provided for accurately measuring and correcting its errors at suitable intervals.

Report of the Board of Directors

THE BOARD OF DIRECTORS of the American Institute of Electrical Engineers presents herewith to the membership its 61st annual report, for the fiscal year ending April 30, 1945. A general balance sheet showing the condition of the Institute's finances on April 30, 1945, together with other detailed financial statements, is included herein. This report contains a brief summary of the principal activities of the Institute during the year, more detailed information having been published from month to month in *Electrical Engineering*.

BOARD OF DIRECTORS' MEETINGS

The board of directors held five meetings during the year, four in New York, N. Y., and one in St. Louis, Mo. Two executive committee meetings were held.

Information regarding many of the more important activities of the Institute which have been under consideration by the board of directors and the AIEE committees is published each month in the section of *Electrical Engineering* devoted to Institute activities.

PLACES VISITED BY PRESIDENT POWEL

Alabama
Alabama Section, Birmingham

California
Los Angeles technical meeting
San Diego Section
San Francisco Section

Connecticut
Connecticut Section, New Haven

District of Columbia
Washington Section

Illinois
Chicago Section

Indiana
Central Indiana Section, Indianapolis
Fort Wayne Section
South Bend Section

Iowa
Iowa Section, Des Moines

Kentucky
Louisville Section

Louisiana
New Orleans Section

Maryland
Maryland Section, Baltimore

Massachusetts
Boston Section
Lynn Section
Worcester Section

Missouri
St. Louis Section

Montana
Montana Section { Butte
Great Falls

Nebraska
Nebraska Section, Omaha

New York
New York Section, New York
Winter technical meeting, New York
Niagara Frontier Section, Buffalo
Rochester Section
Ithaca Section

Ohio
Cincinnati Section
Cleveland Section
Columbus Section
Dayton Section
Toledo Section

Oklahoma
Oklahoma City Section
Tulsa Section

Oregon
Portland Section

Pennsylvania
Philadelphia Section
Pittsburgh Section

Rhode Island
Providence Section

Tennessee
Memphis Section

Texas
North Texas Section, Dallas
South Texas Section, San Antonio

Washington
Seattle Section
Spokane Section

Canada
Toronto Section

Mexico
Mexico Section

ANNUAL MEETING

The annual business meeting of the Institute was held Monday morning, June 26, 1944. The annual report of the board of directors for the fiscal year which ended April 30, 1944, was presented in abstract by the national secretary. In the absence of W. I. Slichter, national treasurer, H. H. Henline, national secretary, presented the treasurer's report. The report of the committee of tellers upon the election of officers for the year beginning August 1, 1944, was presented, and President-Elect Powel responded to his introduction with a brief address. Presentation of national prizes for papers presented in 1943 was made.

In addition to the presentation of the Lamme Medal to Arthur H. Kehoe, vice-president, Consolidated Edison Company of New York, Inc., the Faraday Medal of the Institution of Electrical Engineers, Great Britain, was presented by A. P. M. Fleming, Metropolitan-Vickers Electrical Company, Ltd., Manchester, England, and local honorary secretary of the AIEE for Great Britain, to Irving Langmuir, associate director of research, General Electric Company, Schenectady, N. Y., for "his outstanding contributions to electrical science." The meeting was concluded with the presidential address by N. E. Funk.

NATIONAL TECHNICAL MEETINGS

Three national technical meetings were held during the year, and a brief report on each follows:

Summer Technical Meeting. The 60th summer technical meeting was held in St. Louis, June 26–30, 1944. In addition to the annual business meeting and the conference of officers, delegates, and members, there were 28 sessions and conferences with approximately 90 technical papers and 31 conference papers. A joint luncheon meeting with the St. Louis Electrical Board of Trade featured Lieutenant Colonel T. B. Holliday, United States Army Air Forces, Wright Field, Dayton, Ohio, who gave an address entitled, "Aviation and the Electrical Engineer." The Circle Club of St. Louis sponsored a luncheon with members of the board of directors and headquarters staff as guests.

The general session was a fitting occasion to commemorate three important anniversaries in the electrical-engineering profession—the 60th anniversary of the AIEE, the 100th anniversary of the Morse telegraph, and the 40th anniversary of the International Electrical Congress, which met in St. Louis in 1904. Following the celebration of these anniversaries an address entitled "The Engineer's Present and Future Responsibilities" was delivered by William McClellan, AIEE past president and chairman of the board, Union Electric Company of Missouri, St. Louis. The registration at this meeting was 1,142.

Pacific Coast Technical Meeting. The 32d Pacific Coast technical meeting was held in Los Angeles, Calif., August 29–September 1, 1944, as the Los Angeles technical meeting, with a registration of 561. Because of the wartime situation, this meeting was largely on a local basis, and was devoted predominantly to electric equipment for military aircraft. There were 15 technical sessions on aircraft electrical developments with 58 papers and four sessions on other subjects. In the general session, J. M. Gaylord, vice-president District 8, presided, and the speakers were Brigadier General Donald F. Stace and C. A. Powel, president, AIEE, who spoke on "The Engineer and His Future." At a luncheon meeting Lieutenant Colonel Holliday gave his address on "Aviation and the Electrical Engineer."

Winter Technical Meeting. The 33d winter technical meeting was held in New York, January 22–26, 1945, with a program including 21 technical sessions, at which 80 papers were presented, and ten informal conferences. "Research and Its Effect on Winning the War" was the subject of an address by J. Carlton Ward, Jr., Fairchild Engine and Airplane Corporation, New York, at the general session. Other features of this session were presentation of the Alfred Noble prize to W. R. Wilson, General Electric Company, Schenectady, and presentation of an Honorary Member certificate to Dugald C. Jackson, AIEE past president and professor emeritus of Massachusetts Institute of Technology, Cambridge. A smoker was the only entertainment event. The registration at this meeting was 1,718.

As has been the custom in recent years, a joint evening session was held with the Institute of Radio Engineers, which was meeting concurrently in New York. The first portion of this session consisted of the presentation of the Edison Medal to E. F. W. Alexanderson, consulting engineer, General Electric Company, Schenectady, N. Y. The second portion was an address delivered by Captain J. B. Dow, United States Navy, Washington, D. C., entitled "The Navy Electronics Program and Some of Its Past, Present, and Future Problems."

DISTRICT TECHNICAL MEETING

North Eastern District Technical Meeting In compliance with the recent wartime ban on conventions this meeting, which was

Table I. Section and Branch Statistics

	For Fiscal Year Ending April 30					
	1940	1941	1942	1943	1944	1945
Sections						
Number of Sections	70	72	72	73	73	73
Number of meetings held	701	703	647	598	738	884
Total attendance	91,949	92,554	78,254	66,111	83,120	96,346
Branches						
Number of Branches	121	123	124	125	125	125
Number of meetings held	1,346	1,163	946	942	755	547
Total attendance	64,972	52,285	37,785	38,227	24,768	17,132

scheduled to be held in Buffalo, N. Y., April 25–26, 1945, was canceled.

SECTIONS

1. Section Programs. The Sections generally have been following a program of carrying on a reasonable amount of activity which will be most useful to their members and to their local communities. Considerable effort has been made to retain the diversified interest of the older members, as well as to attract new and younger members. Many programs have been devoted to air transportation, various phases of instrument manufacture and their application, the theory and application of electronics, communications, and other subjects closely related to the war effort. In December 1944 a letter was sent to all Sections calling attention to the advisability of properly expanding Section activities so as to create additional interest in AIEE within the Section territory. Several methods which are being most successfully used in this expansion were described. It was pointed out that it is expected that the individual Sections will select those additional activities which will bring to their Section the greatest benefits for the most economical expenditure of their available funds.

2. Sections-Committee Organization. Because of the increasing volume of the Sections committee work, the committee was organized at the beginning of the year into two groups. The planning group, consisting of six members, initiates and develops all plans of the committee. The promotional group consists of ten members located geographically on a District basis, making it possible for its members to handle most of the promotional work individually with the Sections. Most of the material used by the promotional group is sent to each member, who in turn supplements it with his personal knowledge of local conditions before contacting the Sections in his District. Close contact also is maintained between the promotional group member and the vice-president of the District. It is believed that this organization provides for closer relations between District officers and the Sections committee.

3. Section Finance. In co-operation with the finance committee of the Institute, plans were formulated to provide certain increases in appropriations to all Sections and additional increases to those operating subsections and technical groups. This new plan of Section appropriations was adopted by the board of directors at a meeting held on November 2, 1944. As a result of these increased appropriations, many Sections have been able to expand their programs of activities.

4. Technical Groups. The development of technical groups is a very important part of the plan to retain the diversified interest of the older members and to attract new members. As a result of the increased interest in the formation of these groups, the supply of the folder "Technical Groups," which was prepared by the Sections committee in January 1944, was exhausted. A revised edition of this folder was made available for distribution in January 1945. The Sections committee, through its promotional group, is making individual contacts with those Sections where there is a possibility of the successful operation of these technical groups. The possibility of forming groups on electronics, instruments and measurements, and communications have been particularly encouraged in this manner. The sections committee promotional group has also been supplying individual Sections with reports on examples of the successful operation of these technical groups. The value of such groups operated within the Section is becoming more generally recognized throughout the country. The number of these groups in active operation has increased from 27 to 51 during the year and consideration is being given by many Sections to the operation of additional groups.

5. Co-operation With Other National Committees. Certain features of the sections committee program have been closely coordinated with the finance committee of the Institute and the national membership committee. The chairman of each national committee has also been contacted in an effort to obtain the co-operation of these committees in giving active support on the development and operation of technical groups within the Sections. The members of these technical committees, working within their individual Sections, can encourage the development of technical groups corresponding to the work of their committees. They can also assist such technical groups with information on suitable programs and other information of an operating nature. In this manner, the technical committees may broaden the scope of their activities and at the same time materially assist on the technical group program of the sections committee. Several technical committees have participated actively in this program during the year, and it is believed that this work of these committees will serve as a pattern for future exploration of this field of committee cooperation, which should prove quite beneficial to the Institute in future years.

6. Subsections. Subsection operation is a valuable means of accomplishing a very important objective of the Institute by providing additional meeting places at which papers on electrical-engineering subjects may be presented and discussed. With all the territory in the continental United States allotted to the Sections, the next logical step forward in the development of Section activities is the formation of Subsections or additional centers of electrical-engineering influence. Many opportunities exist for members in remote areas of a Section territory to participate in Section activities through the development of Subsections in these areas. Subsection operation is becoming more popular each year as its advantages are more widely recognized. The number of Subsections in actual operation has been increased from 6 to 12 during the year, and several additional Subsections are in process of being formed. The Sections committee has assembled information on 43 widely distributed locations where the Sections involved are considering Subsection operation. The promotional group of the Sections committee is encouraging Sections to consider the opportunities which exist for the formation of many additional Subsections in cities which are located long distances from the regular Section meeting places. Examples of successful Subsection operation are being furnished individual Sections to give encouragement to this effort. The original Sections committee folder, "Subsections," has been rearranged and completely revised, so that it contains the latest information on the organization and operation of Subsections. This revised folder was made available for distribution in January 1945.

7. Changes in Section Territory. The following changes in Section territory were made during the year:

The assignment of the territory of the Canadian Maritime Provinces of New Brunswick, Nova Scotia, and Prince Edward Island to the Montreal (Quebec) Section was approved by the board of directors on May 25, 1944. It is believed that the assignment of this territory to the Montreal Section will lead to subsection operation in each of these Provinces.

Seven counties in the States of Indiana and Michigan in the territories of the Chicago (Ill.), Fort Wayne (Ind.), and Michigan Sections were transferred to the South Bend (Ind.) Section on approval of the board of directors on June 29, 1944. This transfer was made with the approval of all the Sections concerned in order to provide the South Bend Section with a more balanced territory.

Upon the request of a group of members at Lima, Ohio, Allen County, Ohio, was transferred from the territory of the Toledo (Ohio) Section to the territory of the Dayton Section by approval of the board of directors on January 25, 1945. This transfer had the approval of the Fort Wayne Section, and was made because the interests of the group involved were more comparable with the interests of the Dayton Section. It is quite probable that this transfer will result in Subsection operation at Lima.

The transfer of Auglaize County, Ohio, from the territory of the Fort Wayne Section to the territory of the Dayton Section was approved on February 27, 1945, by the executive committee of the Institute. This transfer was made with the approval of the Sections and the vice-presidents concerned, in order to make the territory of the Dayton Section continuous with newly acquired

Allen County. District boundary lines were changed in this transfer by removing Auglaize County from District 5 and including it in District 2.

8. Simplified Report on Section Activities. A simplified report form on Section activities was prepared and distributed to all Sections at the close of the season's activities in June 1944. A total of 71 reports were returned. This information was compiled and distributed to all Sections on a consolidated report, which provided an analysis of major activities and organization of all Sections. This report provided much information of value to the new officers in laying out their Section programs for the year. All vice-presidents, District secretaries, and the chairmen of all national committees also were sent copies of this report. Due to the wide acceptance of this report, it is planned to continue this feature at the close of the present operating year.

9. Section Operation and Management. Due to the cancellation of the summer technical meeting of the Institute, on account of the war emergency, the usual delegates meetings will not be held this year. Many plans have been considered as a substitute for these delegates meetings. It is recognized generally that any plan arranged will fall short of providing the information, enthusiasm, and inspiration which the delegates gain by the personal contacts made at the delegates meetings. The substitute plan suggests a District meeting in each District, to be held as early in the fall of 1945 as practicable. This should be at least a full-day meeting, with the morning session devoted exclusively to a clinic on Section operation and management. The vice-president of the District would conduct the clinic, and it is planned to have a representative of the Sections committee on hand at each meeting to assist in the discussions. An outline of suggested subjects, together with some information on each of these subjects, is being prepared by the Sections committee as an aid to each vice-president in conducting these clinics. Such a plan will leave the afternoon for the regular business meeting of the District committee. Some Districts also are arranging for the Section at the host city of the District meeting to hold a Section meeting on the evening of the District meeting, so that the visiting delegates could attend. Such a Section meeting would be devoted to subjects which would be most suitable for such an occasion.

10. Committee Meetings. As a result of the restrictions on travel, only one meeting of the committee was held during the year. This meeting was held on January 24, in New York during the winter technical meeting with an attendance of 26. At this meeting the entire Sections committee program was reviewed, and plans were discussed for the remaining portion of the year. Minutes of this meeting were distributed to all vice-presidents, District secretaries, and Section chairmen. Due to the nature of the Sections committee work, many of the activities of the committee are conducted by means of correspondence.

STUDENT BRANCHES

Much of the effort of the committee on Student Branches during the current year has been toward modification of the pattern of Student Branch operation. This pattern was one of proved success in normal times, but required revision to meet wartime conditions.

Student Branches, with surprisingly few exceptions, have been able to carry on during this year as in the past, but with activity and procedure limited by the more exacting obligations of Army and Navy training and other war activities. In general, the operations of individual Branches have been reasonably successful and satisfactory.

The principal omission of this year has been that of District conferences, both those held in connection with Institute conventions and independently. At a meeting of this committee, with some 30 present, held on January 23, 1945, during the AIEE winter technical meeting, it was voted after very careful study and discussion to follow the spirit of the Office of Defense Transportation restrictive travel order and to cancel all student conferences, rather than adopt a substitute program, such as that of holding a larger number of smaller gatherings, which came within the numerical limitation of the order. Later, the Institute canceled District meetings, such as that at Buffalo, in connection with which a number of student conferences were to be held.

During the year, this committee has worked with the other founder societies in exchange of information and improvement procedure through a joint committee on student activities, and has co-operated with Engineers Council for Professional Development and Society for the Promotion of Engineering Education as there was opportunity.

Particular effort has been devoted this year to the extension of Student Branch activity to every Student Member, with the slogan: "Every member working on some committee." This has been pushed to the letter devising new committees and activities to make sure that every Student Member has some part to play toward accomplishing the important Institute responsibility of developing leaders—executive as well as technical.

Toward this same end, particular emphasis has been placed on programs sponsored and carried on by the students themselves, with specific recommendations from this committee on possible symposia, joint meetings, discussion meetings under student leaders, and industrial orientation sessions presented by students with auxiliary outside help.

Table I gives information on Branch meetings in the past six years, and Table IV contains data on Student Members in the past seven years.

EMPLOYMENT CONDITIONS

The committee on collective bargaining and related matters completed a comprehensive report which was approved in principle by the board of directors. Its release for publication has been deferred by the committee with the hope that the report might be published simultaneously by several engineering societies.

Three members of this committee represent the Institute on a joint committee on the economic status of the engineer.

General Committees

FINANCE COMMITTEE

During the past fiscal year there has been a substantial gain in revenue as a result of the steady growth of Institute membership and an increasing interest in Institute publications. These important factors, together with others set forth in the detailed financial statements which appear with this report, account for the excess of income over expenditures.

Concessions to members serving in the various branches of the Armed Forces and merchant marine have been more than offset by the increase in dues revenue resulting from membership growth. Inactive status had been arranged on request for 2,259 members as of May 1, 1945, a figure comparable with 1,835 in 1944 and 771 in 1943.

All expenditures have been in accordance with the budget approved by the board of directors for carrying on effectively the activities of the Institute. The continuing favorable condition of finances has permitted assignment of $25,000 to the retirement system for members of the headquarters staff to meet the requirements of an increase in the allowance for prior services. An additional sum of $42,000 was transferred to the reserve capital fund, and $3,268 was placed in the Member-for-Life fund. All of these amounts have been invested in appropriate securities.

Schedule I presents a summary of the securities owned by the Institute and the value of these as of April 30, 1945. It will be noted that approximately 63 per cent of the investments for the reserve capital fund is in United States Government bonds. The market value of other securities is extremely favorable, and the entire schedule has had the continuing approval of investment counsel with respect to both individual items and diversification.

The Institute has for many years adhered to the policy of budgeting Institute expenditures within the total of anticipated revenue, estimated on a conservative basis. This has insured a sound financial condition at all times, exceptionally so at present because of the influence of the increase in membership and other factors previously mentioned. The opportunity thus has been afforded to strengthen the reserve fund and provide for the continuance at a proper level of essential Institute activities in those years when income may be reduced below an essential amount as a consequence of economic conditions or other at present unpredictable developments.

TECHNICAL-PROGRAM COMMITTEE

Technical Meetings. With the cancellation of the spring District meeting, only three technical meetings—the summer, Los Angeles, and winter—were held during the year. The total registered attendance at these three meetings was 3,415, which exceeded the total registration of 3,030 for the three corresponding meetings of the previous year and represents a 12.7-per-cent increase in attendance. More technical papers were presented, and more technical sessions were held than at any time during the past five years. Statistics are given in Table II covering the five-year period. In recognition of the importance of the aircraft industry on the Pacific Coast, the program for the Los Angeles meeting included 15 aircraft sessions and 58 papers on electrical applications to aircraft in addition to four sessions outside the aircraft field. Notwithstanding the limitation on attendance by distant members

Table II. Statistics of Technical Programs for Last Five Years

	For Fiscal Year Ending April 30				
	1945	1944	1943	1942	1941
Number of national technical meetings	3	3	3	3	3
Number of District technical meetings	0	2	2	3	2
Registration at national meetings and District meetings	3,415	3,880	3,497	4,274	4,339
Number of papers presented	250	196	168	182	195
Number of papers recommended for *Transactions*	224	153	141	152	167
Estimated number of pages required for printing papers in *Transactions*	1,286	875*	886*	807*	932*
Average length of papers recommended for *Transactions* (pages)	5.74	5.72	6.28	5.3	5.72
Number of technical sessions	64	53	44	50	46
Number of technical conferences	15	24	24	23	18

* Partly estimated.

Table III. Statistics on Meetings

	Registration Attendance	Number of Papers	Number of Transactions Papers	Estimated Number of Pages	Number of Sessions	Number of Conferences
Technical Meetings						
St. Louis	1,142	89	85	514	21	5
Los Angeles	561	74	60	348	20	
New York	1,712	87	79	424	23	10
	3,415	250	224	1,286	64	15
Aircraft Sessions						
St. Louis		17			4	
Los Angeles		58			15	
New York		9			2	
		84			21	

Per cent aircraft papers recommended for *Transactions* = $\frac{84}{224} = 37.5$

imposed by the acute travel congestion, a registration of 561 represented the highest ever obtained for a Pacific Coast meeting.

Wartime Programs. In accordance with the wartime policy adopted by the board of directors, the committee has continued to give preference to papers which aid in the war effort. In addition to the Los Angeles program, the St. Louis meeting program had four aircraft sessions, with 17 papers, and the New York meeting had two aircraft sessions, with nine papers. Of the total number of papers recommended for the AIEE *Transactions* 37.5 per cent were in the field of air transportation.

In the industrial field papers of aid to war work have come to the fore. Some of these papers have dealt with industrial-plant distribution systems and power recovery from airplane-engine testing, electric equipment for the propeller milling machine, industrial control, electric welding, and induction and high-frequency dielectric heating. The latter subject has many wartime applications, particularly in the synthetic products industries.

General Sessions. The general sessions have continued to deal with the broader aspects of the profession, at the summer technical meeting with the commemoration of three important anniversaries, at the winter technical meeting with the effect of research on the war.

Technical Conferences. Although technical conferences held have been fewer than during previous years, several conferences have presented subject matter important in the war effort. At the winter technical meeting, conferences were held on the subjects of wartime practices on distribution systems and their effect on system operation and future designs, air transportation, high-frequency dielectric heating, and high-frequency cables. The latter conference was an all-day meeting sponsored with the co-operation of the Army–Navy Radio-Frequency Cable Co-ordinating Committee, Lieutenant Commander John H. Neher presiding.

Committee Policies. The cancellation of all Institute and District meetings scheduled in 1945 following the winter meeting necessitated the adoption of a modified plan for the technical programs which normally would have been scheduled for those meetings. Under the new plan papers will be presented by publication with preprints made available and discussion submitted in writing as in the past. The papers for the year will be arranged in three programs for the spring, summer, and fall. The general plan was approved by the executive committee on February 27.

To minimize time and travel the committee has continued the policy of the past year, holding one meeting in the fall and another in the spring. The fall meeting was attended by 79.3 per cent of the committee members or duly appointed representatives, as compared with an attendance of 76.6 per cent for the corresponding meeting of the previous year. Much of the work has been conducted through correspondence.

PUBLICATION COMMITTEE

As in previous wartime years, war problems continued to hold first place in the Institute's technical publications during the year. Expected developments in the postwar period also received attention through the medium of a special series of articles appearing monthly in *Electrical Engineering*, beginning with the May 1944 issue and continuing through the entire year. Publication policies and procedures remain unchanged. Although the wartime ban on meetings, which became effective February 1, 1945, will have considerable influence on the handling of technical-program papers and discussions, it necessitated no change in publication procedure, and publication of this material will continue as scheduled insofar as approved papers and discussions are available.

Restrictions on magazine paper continued as in the preceding year, allowing the use in *Electrical Engineering* of 75 per cent (on a tonnage basis) of the paper used during the calendar year 1942, plus a token increase in quota of four tons annually granted by the War Production Board in June 1944 (present annual quota with this increase—112 tons). Further restrictions were imposed which resulted in the use of a lighter-weight paper. This lighter stock, of course, allows more pages of material to be published within the same tonnage limitations. The following tabulation shows the approximate number of words published in the three major divisions of *Electrical Engineering* during the years 1940–44.

Year	News	General-Interest Articles	Transactions Sections (Technical Papers)
1940	332,000	275,000	587,000
1941	426,000	296,000	517,000
1942	445,000	270,000	653,000
1943	357,000	266,000	546,000
1944	323,000	265,000	702,000

In accordance with present publication policies, the 1944 *Transactions* volume contains all approved 1944 technical papers and related discussions. Two semiannual "Supplements to *Electrical Engineering*—Transactions Section" were produced, on the usual limited-edition advance-order basis, containing

1. Technical papers that could not be accommodated in the monthly Transactions sections of *Electrical Engineering.*
2. All approved discussions.

The greatly expanded technical-paper program during 1944 required publication in the *Transactions* of a correspondingly expanded amount of papers and discussions. The total number of *Transactions* pages for the year was 1,558 as compared with 1,044 for 1943. Of this total, 1,272 pages were technical papers, 778 pages of which were included in the 12 monthly Transactions sections of *Electrical Engineering*; comparable figures for 1943 were 816 and 634 pages, respectively. Thus, the proportion of the year's technical-program papers included in *Electrical Engineering* in 1944 was less than in previous years, although more pages of such material were published therein than in previous years.

After an attempt to obtain a substantially increased quota of magazine paper in order to include more of the 1944 technical papers in *Electrical Engineering* had failed several additional economies in the use of paper were adopted. In the general section, the size of type was reduced and a three-column format adopted in place of the former two-column arrangement. At the same time, in the Transactions section the spacing between lines was reduced. It is believed that these economies will not impair seriously the readability of the material.

As an additional measure to conserve magazine paper, the annual index pamphlet for 1944 (covering both *Electrical Engineering* and *Transactions*) was not published as a second section of one of the monthly issues. Copies of the index were distributed to all members of all technical committees and to all subscribers to both *Electrical Engineering* and the supplements. Copies were made available to all others without charge upon written request.

Advance pamphlets of approved technical papers were produced as required by the technical-program committee for the national and District meetings held during the year and for discussion by mail during the spring of 1945 after the cancellation of meetings. The booklet, "Information for Authors," was reprinted, the previous supply having become exhausted. Although the present edition is somewhat out of date, revision was deferred so as to avoid having the booklet out of stock over an extended period. Revision is planned within the next year.

Publication of the quarterly AIEE *Bulletin* for Institute members in the armed services and the merchant marine, initiated in June 1943, was continued throughout the year. This consists of a four-page pamphlet and includes news of the Institute and related items that are considered of interest to these members. More than 2,000 copies of each issue now are being produced and distributed to members on all the fighting fronts.

Governmental censorship regulations were maintained during the year, although the procedure was changed. The censorship regulations now are applied entirely on a voluntary basis by the staff, and only material that is considered censorable is submitted to the Office of Censorship for advance review. Advance proofs of publications intended for export no longer are required, although all publications exported still are subject to inspection by the postal censors. As in the past, full co-operation has been extended to, and has been received from, the Office of Censorship.

MEMBERSHIP COMMITTEE

The Institute membership has continued its upward trend, and attained a total of 23,072 as of April 30, 1945. This compares with a total of 21,407 as of April 30, 1944. A net increase of 1,665 has been obtained in comparison with the net increase in 1943–44 of 1,246, and it is the largest increase in any one year in the history of the Institute with exception of the year 1920–21.

A total of 2,259 persons now are maintaining an "inactive status" because of military service or residence in Allied countries with which financial transactions are difficult. This is an increase of 424 over that of last year. There are, however, only 902 members in arrears for dues for the fiscal year ending April 30, 1945, as against a total of 1,288 last year. Incidentally, this is the lowest number of members in arrears at the end of any fiscal year for over 18 years and represents only 3.8 per cent of the total membership.

Tables IV, V, VI, VII and VIII outline certain statistical data relative to membership matters.

Table IV gives the data relative to the various grades of membership in the Institute, the additions, the deductions, and the net changes for the year 1944–45. In every instance, with the exception of the matter of deaths, the figures are on the favorable side. The number of members dropped represents a decrease of 323. The number of those reinstated or re-elected represents a gain of 65. The number of new members qualified represents a gain of 29. The number of transfers represents a gain of 88. The membership is divided as follows:

Member Grade	Per Cent
Honorary	0.03
Fellow	3.96
Member	27.03
Six-Year Associate	30.19
Associate	38.79
	100.00

The Member and Associate grades have increased 0.73 and 0.39 per cent, respectively, while the six-year Associate and Fellow grades have decreased 1.01 and 0.11 per cent, respectively. The six-year Associate grade of membership continues to be a large source of possible transfer to Member grade.

Table V shows a decline in applications from "Student Members" which is continuing as against the upward trend in applications from "All Others." No direct comparison between this table and Table VI can be made, since not all applications received during the fiscal year are acted upon before the close of the fiscal year.

Table VI gives the data on the number of applications received for Student membership. Prior to 1945, this group was known as Enrolled Students. It will be noted the "New Applications" have started an upward trend and that there has been a marked reduction in the downward trend of "Renewals." These favorable results were entirely unexpected.

Table VII is a record of the total membership of the Institute by years since 1884 and is given for information purposes.

Table VIII is the customary listing of the deaths of AIEE members as reported in *Electrical Engineering*. By this means the membership committee makes a record of the completed careers of those members taken from the ranks by the Great Reaper.

The preparation of additional material for use by the membership committee generally in interesting persons in membership in the Institute is being undertaken. This is the result of information obtained from various sources indicating a need in that direction.

As a result of requests from Section membership committee chairmen and others, a plan was introduced for sending a reprint

Table V. Number of Applications Received From Student Members and From All Others

Year Ending April 30	Students	All Others	Total
1945	249	2,179	2,428
1944	466	1,908	2,374
1943	783	1,431	2,214
1942	971	1,031	2,002
1941	887	1,011	1,898
1940	911	918	1,829
1939	849	872	1,721

Table VI. Number of Student Members as of April 30

Year	New Applications	Renewals	Total
1945	2,326	2,287	4,613
1944	2,242	2,656	4,898
1943	2,512	3,200	5,712
1942	2,585	3,377	5,962
1941	2,351	3,188	5,539
1940	2,525	2,992	5,517
1939	2,271	2,971	5,242

Table IV. Membership Statistics for Fiscal Year Ending April 30, 1945

	Honorary Members	Fellows	Members	Six-Year Associates	Associates	Subtotals	Totals
Membership April 30, 1944	6	872	5,632	6,659	8,238		21,407
Additions							
New members qualified			252		1,749	2,001	
Former members reinstated or re-elected		1	139	83	143	366	
Subtotals		1	391	83	1,892	2,367	
Transfers	1	67	396	873		1,337	
Totals	1	68	787	956	1,892	3,704	
Deductions							
Died	1	19	44	52	10	126	
Resigned		3	19	59	42	123	
Dropped		3	51	189	210	453	
Subtotals	1	25	114	300	262	702	
Transfers		1	67	352	917	1,337	
Totals	1	26	181	652	1,179	2,039	
Net changes		42	606	304	713	1,665	
Membership April 30, 1945	6	914	6,238	6,963	8,951		23,072

Table VII. Record of AIEE Membership

Year	Total May 1	Year	Total May 1	Year	Total May 1
1884	71	1905	3,460	1925	17,319
1885	209	1906	3,870	1926	18,158
1886	250	1907	4,521	1927	18,344
1887	314	1908	5,674	1928	18,265
1889	333	1909	6,400	1929	18,133
1890	427	1910	6,681	1930	18,003
1891	541	1911	7,117	1931	18,334
1892	615	1912	7,459	1932	17,550
1893	673	1913	7,654	1933	17,019
1894	800	1914	7,876	1934	15,230
1895	944	1915	8,054	1935	14,269
1896	1,035	1916	8,202	1936	14,600
1897	1,073	1917	8,710	1937	15,308
1898	1,098	1918	9,282	1938	16,078
1899	1,133	1919	10,352	1939	16,605
1900	1,183	1920	11,345	1940	17,213
1901	1,260	1921	13,215	1941	17,886
1902	1,549	1922	14,263	1942	18,944
1903	2,229	1923	15,298	1943	20,161
1904	3,027	1924	16,455	1944	21,407
				1945	23,072

of the postings in *Electrical Engineering* to each applicant for membership whose name appears therein, together with a statement from the membership committee outlining the time elements to be expected prior to the taking of final action on the application by the board of directors. This plan, while introducing some additional expenditure for membership activity, is considered to be justified, since the applicant is kept informed of the progress of the application and a record of the actual posting of applicant's name is given the applicant.

These membership data are almost entirely without an unfavorable aspect. It is for that reason that there is a considerable degree of satisfaction in presenting them. All of this has been made possible by the splendid response from the individual members of the Institute, the intensive continuous effort of the Section membership committee personnel, the membership committee District vice-chairmen, and the other members of the national membership committee.

BOARD OF EXAMINERS

The board of examiners held 12 meetings during the past year, averaging about $2\frac{3}{4}$ hours each, and acted upon 4,693 cases divided as shown in Table IX. The number of cases for both direct admission and transfer to Member and Fellow grades has been showing a steady increase during the past two years, the increase being 28 per cent in 1943–44, and 23 per cent this past year.

In 1943 a subcommittee was appointed to study the constitutional requirements for Fellow grade. Following conferences with the committee on constitution and bylaws, which also had those requirements under consideration, a final report was submitted this year and approved by the board of directors. The recommendations are now out to letter ballot of the membership. As finally submitted, no changes in substance of requirements are recommended, the proposed alterations and rearrangements of wording being for clarification only.

COMMITTEE ON MEMBERS-FOR-LIFE FUND

This committee was authorized by the board of directors in January 1944, and appointed by the president, to administer the fund established at the same time by turning into it all monies received from the members for life who voluntarily continue to pay their accustomed annual dues, even though no longer obligated to do so. The fund and its proceeds are to be used only for such special purpose or purposes as will aid the attainment of the objectives of the Institute.

After considering many possible applications of this fund, the one finally agreed upon was the payment of the expenses to the summer convention of the winners of the District awards, formal announcement of the details of which was made in the February 1945 issue of *Electrical Engineering*.

COMMITTEE ON CONSTITUTION AND BYLAWS

During the year the committee submitted a number of proposals for amendments to the constitution and to the bylaws. On June 29, 1944, the board of directors approved an amendment to the constitution eliminating the word "national" from the titles of officers and names of committees and meetings wherever it occurred.

On January 25, 1945, the board of directors approved amendments to the constitution

1. Improving the wording of Article III, Section 10, as regards references for an applicant for admission or transfer.
2. Clarifying and putting in more concise wording Section IV, Article II, covering the requirements for the grade of Fellow.

At the January 25, 1945 meeting, the

Table VIII. Deaths of AIEE Members Reported in "Electrical Engineering"

Name	Date of Election	Date of Death	Grade at Death	Obituary Notice in "Electrical Engineering"	Name	Date of Election	Date of Death	Grade at Death	Obituary Notice in "Electrical Engineering"
Albert, J. C.	A '10	Jan. 16, '45	M	Apr. '45, p. 164	Levy, C. C.	A '33	June 5, '44	A	July '44, p. 272
Armstrong, A. H.	A '98	May 31, '44	M	Aug. '44, p. 317	Lewis, D. L.	A '25	July 28, '44	A	Oct. '44, p. 386
Atkins, C. G.	A '01	Oct. 20, '44	M	Feb. '45, p. 78	Lincoln, P. M.	A '95	Dec. 20, '44	F	Feb. '45, p. 76
Ball, J. D.	A '11	Feb. 10, '45	F	Apr. '45, p. 163	Louttit, W. C.	M '31	July 9, '44	M	Sept. '44, p. 343
Ballantine, Stuart	M '42		M	Oct. '44, p. 386	Lovewell, E. B.	M '43	Nov. 1943	M	July '44, p. 272
Behr, Leo	A '29	June 25, '44	A	Dec. '44, p. 450	Manson, G. K.	A '09	Jan. 6, '45	F	Apr. '45, p. 163
Bergman, S. R.	A '04	Nov. 25, '44	A	Jan. '45, p. 41	Marshall, A. C.	A '14	Feb. 9, '45	F	Apr. '45, p. 163
Betts, Philander	A '96	Feb. 6, '45	F	Mar. '45, p. 126	Merrick, F. A.	A '07	Oct. 26, '44	A	Dec. '44, p. 450
Binford, J. T.	A '23	July 10, '44	A	Oct. '44, p. 386	Meyer, J. F.	A '08	Oct. 30, '44	M	Mar. '45, p. 126
Bliss, W. L.	A '94	Dec. 5, '44	F	Feb. '45, p. 78	Mowbray, W. J.	A '03	July 4, '44	F	Sept. '44, p. 343
Braden, N. S.	A '09	Sept. 27, '44	M	Dec. '44, p. 450	Newman, W. L.	M '35	Oct. 31, '44	M	Feb. '45, p. 78
Brown, H. A.	A '16	Feb. 25, '45	M	Apr. '45, p. 163	Northup, V. E.	A '39	Feb. 4, '44	A	June '44, p. 236
Campbell, John	A '04	Mar. 6, '44	A	May '44, p. 193	O'Donnell, C. E.	A '32	Oct. 3, '44	A	Dec. '44, p. 450
Cansfield, C.E.	A '25	July 23, '44	A	Sept. '44, p. 343	Oklund, A. L.	A '35	Aug. 19, '44	M	Nov. '44, p. 416
Carpenter, L. S.	A '20	Apr. 20, '44	A	July '44, p. 272	Pearson, E. R.	A '06		M	June '44, p. 236
Coffin, Leroy	A '37	Nov. 16, '44	M	Feb. '45, p. 78	Peterson, J. A.	A '37	July 13, '44	A	Oct. '44, p. 385
Cole, C. E.	A '27	Mar. 19, '44	A	July '44, p. 272	Pierce, D. A.	A '21	June 28, '44	M	Oct. '44, p. 386
Courad, L. L.	A '36	Apr. 6, '44	M	July '44, p. 272	Powell, F. H.	A '08	Dec. 11, '43	A	May '44, p. 193
Copeland, C. A.	A '97	Aug. 18, '44	F	Nov. '44, p. 415	Pratt, L. W.	A '38	Oct. 3, '44	A	Dec. '44, p. 450
Cox, E. H.	A '41	July 6, '44	A	Oct. '44, p. 386	Price, R. D.	A '44	June 24, '44	A	Sept. '44, p. 343
Crumley, T. R.	A '19	Oct. 5, '44	A	Feb. '45, p. 78	Osborne, L. A.	A '93	Aug. 18, '44	F	Oct. '44, p. 386
Darrall, S. S.	A '41	Sept. 1943	A	July '44, p. 271	Randall, K. C.	A '02	Dec. 4, '44	M	Mar. '45, p. 127
Davis, C. M.	A '43	Apr. 27, '44	A	July '44, p. 272	Reber, H. L.	A '03	Nov. 1, '44	F	Jan. '45, p. 41
Dey, N. A.	A '36	Aug. 8, '44	A	Nov. '44, p. 416	Roberts, C. J.	A '22	June 26, '44	A	Dec. '44, p. 450
Downing, P. M.	A '98	Dec. 11, '44	F	Feb. '45, p. 77	Rosenthal, L. W.	A '02	Jan. 8, '45	F	Feb. '45, p. 77
Edwards, J. B.	A '29	Feb. 5, '44	A	May '44, p. 193	Sands, H. S.	A '06	Dec. 13, '44	M	Feb. '45, p. 77
Eglinton, W. M.	A'03	Aug. 4, '43	A	July '44, p. 271	Sanford, W. J.	A '23	Dec. 23, '43	A	July '44, p. 272
Elliott, D. A.	A '28	July 31, '44	A	Sept. '44, p. 343	Schattner, Ernest	A '06	Feb. 13, '44	M	May '44, p. 192
Escher, Henry	A '37	June 16, '44	A	Dec. '44, p. 450	Schoonmaker, C. F.	A '12	Feb. 20, '44	M	May '44, p. 192
Fuqua, H. E.	A '42	Feb. 23, '44	A	Oct. '44, p. 385	Schou, Theodore	M '14	Nov. 16, '44	M	Feb. '45, p. 78
Gardner, J. H.	A '25	Oct. 11, '44	M	Dec. '44, p. 450	Scott, C. F.	A '92	Dec. 17, '44	HM	Jan. '45, p. 41
Gill, J. H.	A '12	June 16, '44	A	Aug. '44, p. 317	Sinks, A. T.	A '36	Aug. 3, '44	M	Oct. '44, p. 386
Gobel, F. C.	A '05	Sept. 16, '44	A	Mar. '45, p. 127	Skone, R. C.	A '19	Aug. 14, '44	M	Oct. '44, p. 386
Grant, L. T.	A '99	July 15, '44	M	Nov. '44, p. 415	Smith, H. L.	M '36	Apr. 7, '44	F	July '44, p. 272
Gray, C. D.	A '02	Mar. 29, '44	F	May '44, p. 193	Smith, J. B.	A '24		M	June '44, p. 236
Green, D. C.	M '26	July 2, '44	M	Nov. '44, p. 416	Stockman, E. O.	A '39		A	Dec. '44, p. 450
Greene, C. E.	M '31	Mar. 8, '44	M	May '44, p. 193	Tadlock, W. L.	A '29	Nov. 27, '44	M	Feb. '45, p. 77
Gremillion, B. X.	M '41	May 28, '44	M	Aug. '44, p. 317	Teach, F. A.	A '24	Oct. 25, '44	M	Feb. '45, p. 78
Henry, Maxwell	M '32	Apr. 7, '44	M	June '44, p. 236	Teker, Louis	A '26	June 11, '44	A	Aug. '44, p. 318
Hjort, Alf	M '21	Dec. 12, '44	M	Feb. '45, p. 77	Tower, L. W.	A '36		A	Nov. '44, p. 416
Hough, H. W.	A '08		M	June '44, p. 236	Troy, M. O.	A '08	Mar. 13, '44	M	May '44, p. 192
Hubbard, F. A.	M '23	Nov. 6, '44	M	Jan. '45, p. 41	Turnock, H. C.	A '16	June 4, '44	M	Oct. '44, p. 385
Huber, H. L.	M '23	Feb. 4, '45	M	Mar. '45, p. 126	Varney, Theodore	A '05	Oct. 2, '44	A	Feb. '45, p. 78
Hubley, G. W.	A '94	Apr. 8, '44	F	June '44, p. 236	Vergilio, J. L.	A '41	Oct. 17, '44	A	Mar. '45, p. 127
Hughes, G. A.	A '17	Sept. 9, '44	A	Mar. '45, p. 127	Warren, H. M.	A '03	Feb. 3, '45	A	Apr. '45, p. 163
Humm, D. L.	A '41	Apr. 10, '44	A	July '44, p. 272	Whitaker, S. E.	A '96	Aug. 10, '44	M	Nov. '44, p. 415
Hurlbert, F. W.	A '04	Dec. 4, '44	A	Feb. '45, p. 78	Willison, J. W.	M '26	Dec. 16, '44	M	Mar. '45, p. 127
Jackson, W. A.	A '18	June 1, '44	M	Aug. '44, p. 318	Wilson, A. M.	A '09	Aug. 23, '44	M	Mar. '45, p. 127
Jeffery, J. A.	M '20	Dec. 26, '44	M	Feb. '45, p. 77	Winslow, C. G.	A '02	Mar. 9, '44	A	May '44, p. 193
Karle, R. D.	A '40	July 27, '44	A	Oct. '44, p. 386	Wood, H. G.	A '23	Apr. 4, '44	M	June '44, p. 236
Kay, W. deY.	A '16	Jan. 31, '44	A	July '44, p. 272	Woodward, A. C.	A '18	July 17, '44	A	Oct. '44, p. 386
Kelsch, R. S.	A '02	Feb. 4, '45	F	Apr. '45, p. 163	Wright, M. L.	A '25	Aug. 9, '44	A	Nov. '44, p. 416

board of directors also approved the following amendments to the bylaws

1. Sections 51, 52, 53, 54, 55, 56, 57, 60 and 64, changing the designation "Enrolled Student" to "Student Member."

2. Section 65, changing the title of "committee on electrical machinery" to "committee on electric machinery" to conform to the American Standard, "Definitions of Electrical Terms."

The committee has under consideration a proposal for amending Section 51 of the bylaws to define "a university or technical school of recognized standing" in terms of the ECPD accrediting program.

The committee also is considering the matter of amending Section 27 of the bylaws to give the board of directors proper backing for its action in eliminating the 1945 summer meeting at the request of the Office of Defense Transportation.

COMMITTEE ON PLANNING AND CO-ORDINATION

The most important matter on which this committee took action was that brought about by the request of the Office of Defense Transportation that all conventions or meetings at which the out-of-town attendance would be greater than 50 people should be canceled, unless the war effort would be injured by the elimination of the meeting. After thorough consideration of all the activities affected, the committee was unanimous in recommending to the board that both the summer technical meeting and the North Eastern District meeting be canceled. This action was taken with the understanding that the technical committees would continue to secure papers, publish preprints, and obtain discussions so that the technical work of the Institute could be carried forward in much the same manner as though the papers actually would be presented in fact. Because of the possibility of change in conditions, the committee did not recommend the cancellation of the Pacific Coast technical meeting.

The board of directors referred to this committee the problem of obtaining more satisfactory publicity for Institute activities. Due to its action in recommending the cancellation of meetings, the committee considered it unwise to attempt to pursue this subject any further at present and recommended to the board that the matter be held in abeyance until conditions were more favorable.

The finance committee presented a resolution which was suggested for adoption by the board of directors to extend the period for Student Members in the Armed Forces and the merchant marine to continue on the inactive basis, which was to replace a similar resolution expiring January 28, 1945. The committee unanimously voted to recommend the adoption of this resolution to the board.

The board took affirmative action on all the recommendations of this committee except that for the Pacific Coast technical meeting, which was referred to the executive committee for further action.

COMMITTEE ON RESEARCH

Research under the auspices of the committee on research continues to be hampered by the fact that substantially all of the research facilities normally devoted to fundamental projects which would usually be fostered by this committee still are devoted to urgent war projects arranged by Government war agencies. The activities of the committee therefore are devoted largely to the preparation of a postwar research program which could be put into effect rapidly, as soon as normal conditions are restored. All the AIEE technical committees are informed of this program, and suggestions have been requested. Information on the procedure by which projects are formulated and presented to the Engineering Foundation for sponsorship and support was given to the technical committee representatives.

At the January meeting of the committee on research, it was recommended that the lists of research projects prepared in 1934, 1935, and 1937 be brought up to date with the revisions of the original subjects to take account of the progress made in the meantime and new projects added as suggested by present knowledge. It was proposed further that these lists be given broader circulation by having them distributed not only to heads of engineering departments in the colleges but also by sending them to engineering experiment stations and commercial and industrial research stations, which are frequently desirous of undertaking research on fundamental problems. Copies also should be available to interested persons other than those listed, and notice of the availability of the lists should be published in *Electrical Engineering*.

COMMITTEE ON SAFETY

Two meetings were held by the committee on safety during the past year, the first of which was a breakfast meeting during the summer technical meeting in St. Louis on June 26, 1944. At this meeting emphasis was placed on the importance of the committee's efforts to promote interest in safety educational work and safety procedure in the Student Branches, and steps were taken to bring together the points of view of the Counselors and others who might give helpful suggestions in this connection. Professor Albrecht Naeter accepted sponsorship for this activity and subsequently submitted a report which will be used in carrying the matter forward. There was a general discussion of the following items:

1. Electrical hazards to farm animals, on which W. B. Buchanan, a member of the committee on domestic and commercial applications, was submitting a paper at the June 29 session.

2. Static electricity, on which subject the committee will at an appropriate time arrange for a conference discussion at a technical meeting.

3. The report on fatalities in the electric-light-and power industry as prepared by the Edison Electric Institute accident prevention committee.

The chairman called attention to the report which was made by the conference committee on operating-room hazards of the National Fire Protection Association to the 48th annual meeting of that association held in Philadelphia, Pa., May 8–11, 1944. This report appears on pages 74 to 88 in part 2 of the *Quarterly* of the NFPA dated April 1944. W. Weinerth represented the chairman at this meeting.

The second meeting was held during the winter technical meeting in New York, on January 23, 1945. Thirty-seven members and guests were present. At this meeting, Cecil K. Drinker, professor of physiology, School of Public Health, Harvard University, presented an important discussion of the subject "The Use of Drugs in Resuscitation from Electric Shock." C. F. Dalziel, a member of the committee, and now technical aid, National Defense Research Committee, summarized for the committee the research work on electric shock carried on under his direction at the University of California, Berkeley. There was a general discussion of the subject of grounding of circuits operating at voltages in excess of 150 volts from the standpoint of hazard to personnel. The chairman announced that arrangements had been made with the editor of *Electrical Engineering* to have a news column appear under the heading "Safety Notes" whenever suitable material was available, with the expectation that this eventually would be a regular feature.

Table IX. Applications for Admission and Transfer, 1944–1945

Applications for Admission		
Recommended for grade of Associate	1,682	
Re-elected to the grade of Associate	140	
Not recommended	2	
		1,824
Recommended for grade of Member	353	
Re-elected to the grade of Member	27	
Not recommended	65	
		445
Applications for Transfer		
Recommended for grade of Member	419	
Not recommended for grade of Member	15	
		434
Recommended for grade of Fellow	63	
Not recommended for grade of Fellow	0	
		63
Students		
Recommended for enrollment as Students		1,927
Total		4,693

The annual meeting of the National Fire Waste Council which was held in Philadelphia on April 13 was attended by R. L. Lloyd, who represented the chairman and the Institute. The appointment of an official executive committee of the Council was authorized. The committee on safety will consider ways in which it may be helpful in promoting the Council's objectives and will submit suggestions through the Institute's representatives.

Standards

STANDARDS COMMITTEE

Due to restrictions placed on wartime travel, the Standards committee held only two meetings. The work of the committee itself, as well as its many co-operating committees and subgroups, however, has been prosecuted actively by correspondence and by conferences of local groups.

An indication of the widening scope of AIEE standardizing activities is illustrated in the list of the following projects appearing on the standards agenda since the last report: "Guiding Principles for the Specifications of Service Conditions," "Guiding Principles for the Selection of Test Voltages," "Test Code for Low-Frequency, D-C, and Impulse Testing," "Preferred Standards for Large 3,600 Rpm Condensing-Type Turbine Generators," "Standard Specifications for Generators for Large 3,600 Rpm Condensing-Type Turbine Generators," and, finally, standardization of aeronautical electric equipment.

Among the AIEE and American standards, revisions of which were consummated during the year, were: "Automatic Stations," "Lightning Arresters," "Insulator Tests," "Fuses Above 600 Volts," "Test Code for Synchronous Machines," and "General Standards for Wires and Cables."

Due largely to shifts brought about by wartime conditions, it has been necessary to make a large number of new appointments of Institute representatives serving on various sectional committees of the American Standards Association.

Participation by the Institute in the development of fundamental electrical standards in the aeronautical field is rapidly going forward under the control of the committee on air transportation, and guidance of an Institute liaison representative, with such other interested groups as the Society of Automotive Engineers, the National Aircraft Standards Committee, the Army Air Forces, the Bureau of Aeronautics, and National Electrical Manufacturers Association. Several subcommittees of the committee on air transportation are projected, and one of these on aircraft electric rotating machinery has completed a proposed standard which is now in process of publication.

In view of the widespread interest in the subject of application of statistical methods in engineering and manufacturing, the Standards committee appointed a subcommittee to explore the possible applications in the Institute's field and to ascertain the reaction of the membership.

In order to reach a conclusion, the subcommittee has set down a plan of work for the coming year embracing the following activities:

1. An educational program including:

(*a*). A series of short technical articles developing the subject from first principles.

(*b*). Articles describing special applications of statistical methods.

(*c*). The sponsoring of conferences and technical sessions and of the presentation of papers at Section, District, and national meetings.

(*d*). General articles addressed primarily to executives, pointing out the advantages of statistical methods.

2. A study of applications in Institute test codes and Standards.

3. Applications in the electrical utility fields.

4. Co-operation with Joint Committee on Application of Statistical Methods in Engineering and Manufacturing.

5. Keeping in touch with developments in which the Institute might properly co-operate.

UNITED STATES NATIONAL COMMITTEE OF THE INTERNATIONAL ELECTROTECHNICAL COMMISSION

During the past year, as in the preceding war years, the work of the International Electrotechnical Commission and the United States National Committee has remained in a state of suspension. It is not contemplated that work will be resumed until after the peace is concluded.

At its annual meeting on November 10, 1944, the United States National Committee re-elected E. C. Crittenden, president; L. F. Adams, vice-president; and H. S. Osborne, vice-president and treasurer.

During the year there was set up a United National Standards Co-ordinating Committee, with the national standardizing bodies of Great Britain, Australia, Canada, New Zealand, South Africa, Brazil, China, France, and the United States as members. Offices have been set up in London, England, under the direction of C. Le Maistre, who is also general secretary of the IEC, and in New York under the direction of H. J. Wollner. Participation in the United Nations Standards Co-ordinating Committee is limited to those countries which are participating on a positive scale in the war effort of the United Nations. A number of proposals for international standardization work have been made, and the work of the committee can now be considered to be well under way. The committee was organized with the understanding that it would operate for only two years, leaving the form of future international organization to be determined later.

Technical Committees

COMMITTEE ON AIR TRANSPORTATION

The past year has been a period of major activity in the field of aircraft electric applications. A large number of technical papers were presented at three national meetings, and an extensive program has been undertaken in respect to aircraft electrical standards.

At the 1944 summer meeting in St. Louis, four of the technical sessions were devoted to aircraft subjects; a total of 17 papers were presented.

At the Pacific Coast technical meeting in Los Angeles, in August, aircraft electrical subjects and technical sessions occupied the dominant place. Fifteen of the technical sessions were concerned with aircraft problems, and 58 technical papers were presented and discussed.

At the winter technical meeting in New York, aircraft electrical problems occupied an important part of the program, and, in view of the restriction on the total number of papers and sessions which could be handled, there were two technical sessions at which nine papers were presented and one conference session covering the general problems of application of electric devices to military and commercial aircraft.

The committee met twice during the year on the occasions of the Los Angeles and New York technical meetings.

A "Report on Proposed Standard for Aircraft D-C Apparatus Voltage Ratings" was approved by the committee and recommended for publication for one year's trial use. This report has been in the process of preparation for the past two years, and, although some further revisions are probable, it is believed that adherence to the recommendations will result in improved operation of electric equipment in aircraft.

During the year, the committee has been in close contact with the SAE, NASC, NEMA, AAF, and the Navy Bureau of Aeronautics to assist in the formulation of appropriate technical standards. To carry out this work, four subcommittees were formed with assignments as follows:

1. *Aircraft Electric System Subcommittee.* To prepare an informative type of report on "Fundamental Characteristics of Aircraft Electric Systems." This subcommittee has made considerable progress in the preparation of a comprehensive outline and already has received from various sources some draft contributions.

2. *Aircraft Electric Control and Protective Devices Subcommittee.* To prepare electrical standards and test codes covering aircraft control and protective devices to aid in the rating, testing, and application or evaluation as such for aircraft service.

3. *Aircraft Wire and Cable Subcommittee.* The preparation of electrical standards and test codes covering the rating and testing and application of aircraft wires and cables

4. *Aircraft Electric Rotating Machinery Subcommittee.* The preparation of electrical standards, tests, codes, and definitions for aircraft electrical rotating machinery. Immediate attention is being given by this subcommittee to the formulation of a suitable test code for aircraft d-c machines.

Consideration is being given to the formation of a subcommittee on brushes and brush test codes sponsored jointly by the committee on electric machinery and the committee on air transportation. It is believed that such a group can render worth-while service.

COMMITTEE ON AUTOMATIC STATIONS

The committee on automatic stations held two meetings during the year, one in Buffalo following the summer technical meeting, and one in New York during the winter technical meeting.

One of the principal matters discussed at these meetings concerned the revision of the "American Standard for Automatic Station Control, Supervisory and Telemetering Equipments, *C*37.2." The work of revising this Standard now has been completed, and it has been submitted to the AIEE Standards committee for approval.

The committee has sponsored papers on supervisory control and telemetering equipment and is continuing its efforts to bring before the Institute papers which will be of value to the engineering profession.

During the January meeting, plans were formulated for a conference session on automatic or supervisory control of high-voltage air switches and on automatic control of large capacitor banks. There appears to be considerable interest in these subjects, but on account of the present curtailment of travel it does not appear feasible to arrange this conference at the present time.

The committee is represented on several joint subcommittees and is participating in their work. The joint subcommittee on power system application of carrier current is undertaking several projects which should provide valuable information in this field. A report of the work of the sectional committee (*C*67) on preferred voltages under 100 was presented at the winter meeting of the committee on automatic stations by its representative and was given careful consideration. The committee on automatic stations also has appointed full representation on the joint subcommittee on telemetering. This subcommittee is working under the sponsorship of the committee on instruments and measurements.

COMMITTEE ON DOMESTIC AND COMMERCIAL APPLICATIONS

The committee has been enlarged to a total of 21 members, and two more subcommittees have been formed in addition to the three that were formed last year. Those formed this year are the subcommittee on laboratory projects, and the subcommittee on load characteristics. The other three subcommittees are on electrical hazards to farm animals, farm applications, and wiring.

The work of the two new subcommittees has been devoted since their inception entirely to organization, as practically all of the members have been too involved in vital war work to devote much time to committee activity.

The committee on domestic and commercial applications was formed just prior to the war with the purpose of propagating, more fully than had previously been done, the activities judged to be within its scope by the AIEE. It has been most unfortunate that the extreme pressure of war activities on the part of most of its members has precluded more vigorous pursuit of the domestic and commercial problems that confronted the committee. Excellent ground work has been laid, and conclusion of hostilities in the European theater of operation again will free some of the membership for committee work. At the conclusion of the war the committee should be in an excellent position to advance fully and rapidly with the original intent and purpose.

COMMITTEE ON ELECTRIC MACHINERY

Meetings of the main committee were held in June 1944 and January 1945, and one meeting of the subcommittee chairmen was held in October. The chairman attended the meetings of standards and technical-program committees during the year.

The committee has sponsored many sessions of interesting papers on the several technical programs and has held several conference sessions. Particular interest was shown this year in the subjects of temperature measurements and standards. Also, much interest was shown in the subject of machine insulation, particularly in the new silicone materials.

The synchronous-machine test code, which was passed on to the Standards committee, now has been approved and is ready for publication.

The questions of temperature measurements by thermocouple and by resistance were discussed at length in conference papers. The data on a-c machines were summarized in two papers, and it is hoped that this material soon can be presented to the Standards committee.

Similar data on d-c machines are being collected by the d-c subcommittee, but it is believed that further tests by interchanging machines between manufacturers is necessary before any conclusions can be drawn.

Several new items have come up for consideration by the d-c subcommittee, the problem of testing for stray-load loss, and the proposal that a test code for brushes be worked out jointly with the committee on air transportation.

The transformer subcommittee held two meetings during the year, one in Cleveland, Ohio, on October 27, 1944, and one in New York on January 23, 1945. The complete revision of the ASA "Guide for Operation of Transformers and Regulators *C*57.3" was completed and now is awaiting publication. It will be presented to the ASA sectional committee at the proper time. A revision of the data in ASA Standards, *C*57.1 and *C*57.2 on impulse testing has been practically completed. Several changes in the above ASA Standards were agreed to and passed on to the ASA sectional committee.

The co-ordinated study of life of transformer insulation is continued. Temperature gradients, hot-spot temperatures, and insulation strength of dry-type transformers are receiving consideration. A working group is considering the accuracy requirements for voltage-regulator control devices as well as operation of regulators above rating. The thermal capability of regulators on a reclosing cycle also is being studied.

The subcommittee on industrial control has sponsored a number of papers and has made a start on the study of standards for control devices.

COMMITTEE ON ELECTRIC WELDING

Two meetings of the committee were held, one in Cleveland, October 18, 1944, and one in New York, January 23, 1945. The discussions dealt with standards, particularly those concerning ASA Standards *C*52 on resistance-welding and arc-welding machines and the sponsoring and preparation of papers for technical sessions. The committee has assigned two of its members to assist with the preparation of arc-welding standards under the arc-welding subcommittee of *C*52, and has offered similar assistance for the resistance-welding subcommittee, as soon as active work is started by this subcommittee.

Two technical sessions were sponsored by the committee, one in St. Louis in June 1944, at which three technical papers and one conference paper were presented, and one in New York in January 1945, at which three technical papers and one conference paper were presented. The technical program in New York in January was confined to arc-welding subjects, and it was planned to sponsor a resistance-welding program for the 1945 summer technical meeting in Detroit. With the cancellation of that meeting, some of the original papers planned still will be written and presented as part of the technical-paper program, with discussions by mail, and others will be postponed until a later date.

COMMITTEE ON ELECTROCHEMISTRY AND ELECTROMETALLURGY

Most of the work of the committee during the year was carried on by correspondence, small conference groups, and meetings of two very active subcommittees. Work of the committee has been limited during the war period. Details of new developments may be released later.

The subcommittee on voltage transients in arc-furnace circuits presented a paper on "Voltage Transients in Arc-Furnace Circuits" at the summer technical meeting in St. Louis. This was published as technical paper 44-99 and was read by the chairman of the subcommittee, J. E. Hobson. E. R. Whitehead became chairman in December 1944. At a meeting of the subcommittee held in Pittsburgh, Pa., on January 19, 1945, E. W. Boehne of the General Electric Company, gave a report and a very interesting discussion of his findings on overvoltages caused by circuit interruptions. F. J. Vogel of the Illinois Institute of Technology has been doing laboratory research on overvoltages in transformer secondary circuits, and he gave a report on the progress of this work. A survey of protective measures is in progress but was not advanced far enough at the time of the meeting to justify a report. An outline of desirable future action for the committee was drawn up.

The subcommittee on metallic rectifiers held two meetings, and reported considerable progress on a rectifier bibliography. It was expected that some time in April 1945 a preliminary draft would be collected, completed, and sent out to the membership. A list of proposed definitions for metallic rectifiers has been proposed. A full-day session was held with Army and Navy Air Corps and Signal Corps officers in discussing special tests for rectifiers suitably protected for use in high humidity. Considerable progress has been made, and a series of co-operative tests at various plants are being undertaken to establish standard methods of tests as well as means of finding approved methods of protection. Some of the government procurement specifications will be incorporated in the new standards when they are drafted.

The committee is represented on the new joint subcommittee on induction and dielectric heating.

COMMITTEE ON ELECTRONICS

The committee has been active in soliciting and promoting papers on electronic subjects. Both the winter technical meeting and *Electrical Engineering* had a satisfactory percentage of such papers.

This year at the winter technical meeting, as an experiment, the available papers on the subject of electronics were distributed to other committees whose sessions covered the subjects involved. This was done to increase the number of papers on electronics presented to the membership.

As an activity of the joint subcommittee on induction and dielectric heating, the committee on electronics took an active part in organizing and conducting an informal technical conference on the subject of dielectric heating. This was well attended, which indicated that such conferences form a useful medium of promoting various aspects of electronics among the members of the Institute.

Two subcommittees of the committee have been active during the year. A working group of the subcommittee on electronic standards has had a number of meetings and is making excellent progress on the matter of nomenclature, and letter and graphical symbols. The object here has been to define electronic devices, particularly those outside of the radio field.

The subcommittee on mercury-arc rectifiers has been renamed the power electronics subcommittee, and has been engaged actively in the preparation of standards for mercury-arc power converters. The standards will cover definitions (rectifier names and letter symbols), standards (ratings and bases for acceptance tests), test code, operating guide and standards for rectifier transformer. This subcommittee also has organized a working group to prepare a report on "Inductive Co-ordination of Rectifier Equipment."

The scope of technical papers that can be obtained at the present time is restricted because of the war program, but it is believed that a sufficient number can be made available to keep this subject active and well represented at possible future technical meetings and in the pages of *Electrical Engineering* and the *Transactions.*

COMMITTEE ON INDUSTRIAL POWER APPLICATIONS

The main project of the committee was the completion of the report on "Electric-Power Distribution for Industrial Plants." The report was presented at one of the technical sessions at the 1944 summer technical meeting in St. Louis, and was approved for publication by the board of directors. A first issue of 10,000 copies was printed and released in January 1945. It already has been sold out completely, and a second printing of 10,000 copies since has been approved. Plans are being developed for the translation of the report into Spanish and Portuguese by the International General Electric Company and Westinghouse Electric International Company for distribution by these companies in Central and South America.

This report is in the form of a manual of 100 printed pages, 8 by 11 inches in size, in flexible binding. It contains in condensed form the basic information needed by an electrical engineer or industrial architect to design an industrial power-distribution system. It is neither a code, nor a standard but is intended to promote the use of sound engineering principles in the design of such a system and the selection of equipment for it.

A subcommittee has been appointed to assemble and edit suggestions for revisions of the report, in preparation for a future second edition.

At the 1944 summer technical meeting, the committee sponsored, jointly with the committee on electronics and the committee on power transmission and distribution, a technical session for the presentation of five related papers on the use and design of electronic power converters. Another session was devoted to the presentation of two papers on the control and switching of shunt capacitors, a conference paper discussing electrical facilities of an important war plant, and a discussion of the afore-mentioned committee report.

An organization meeting was held of members of the newly created subcommittee on inductive and dielectric heating and members of the sponsoring committees, the committees on electronics, electrochemistry and electrometallurgy, and industrial power applications. J. J. Orr, chairman of this subcommittee, has surrounded himself with a highly representative group of men, all interested and active in the developments in high-frequency heating.

At the 1945 winter technical meeting in New York, the committee sponsored the presentation of eight technical papers in two technical sessions, and a conference session devoted to a discussion of industrial system and apparatus voltage ratings. Speakers represented the utilities, electric-machinery manufacturers, and the industrial power user. The conference was well attended and developed a great deal of interest.

Another conference session was sponsored by the subcommittee on inductive and dielectric heating. This session too was very well attended, confirming the great interest of electrical engineers in developments in this modern field. The very fine start made by the new subcommittee gives promise of fine practical achievements in coming years in a field which is so new that few, if any, standards have yet been developed.

A luncheon meeting of members of the main committee was used to lay plans for the coming year. The increasing importance of co-ordinated drives in industrial processes is recognized by the committee, and special efforts will be made to stimulate the presentation of papers dealing with such installations.

COMMITTEE ON INSTRUMENTS AND MEASUREMENTS

In spite of the restrictions of the war, which prevent the publication of many potential papers, the number of papers approved by the committee for the winter technical meeting was greater than could be accommodated on the program. Also, although handicapped by duties imposed by the war, the members of the committee have advanced many projects, particularly those in the fields of definitions and standards.

At the summer technical meeting two papers sponsored by the committee were presented, one on a method of measuring dielectric properties at ultrahigh frequencies and the other on high-frequency cable design and testing. At a session of the winter technical meeting, four papers in widely diverse fields were presented, one on a method of improving bushing current transformers by superposing third-harmonic frequency excitation on the core, one on a modulated high-frequency-system method of telemetering developed for the City of Seattle, Wash., one on the dynamic measurements of electromagnetic devices such as subrelays, and the fourth on a compact portable instrument for measuring insulation resistance in the field with direct current at high voltage. A fifth paper sponsored by the committee on an electronic interval timer for arc duration was presented at the session on industrial control.

The committee is finding that the employment of electronic circuits and devices for making measurements is increasing rapidly, and several of the new members appointed to the committee in the past year were selected because of their proficiency in the electronic field.

The subcommittees have been active, particularly in making several additions and changes in the definitions of electrical terms in preparation for some future revision of the present "American Standard Definitions of Electrical Terms" and in bringing into agreement the definitions relating to watthour meters in that volume, the "Meterman's Handbook," and the "Code for Electricity Meters." A former report on a proposed Standard 40 for recording instruments is being brought to the status of a standard, and a draft is being circulated for review among Institute members and others who have interest in such a standard. Considerable progress has been made in the preparation of the master test codes for both resistance and temperature measurements. The subcommittee on ultrahigh-frequency measurements has in preparation an article for *Electrical Engineering* on recent developments in measurements in the ultrahigh-frequency field. The subcommittee on dielectric measurements in the field has compiled a bibliography on the subject and now is preparing a report on the methods now available for such measurements together with their scope.

For some time past there has been no permanent committee or subcommittee in the Institute to which matters concerning instrument transformers could be readily referred. Hence, during the past year, the committee on instruments and measurements has established a permanent subcommittee on instrument transformers, on which are representatives of widely diversified interests. The formation of this subcommittee was facilitated by the close co-operation of the AIEE committee on protective devices and the ASA subcommittee on instrument transformers. In view of the rapid expansion of the field of industrial control the name and the scope of the subcommittee on that subject have been changed to subcommittee on electrical servomechanisms and follow-up devices. Also, if a new committee on industrial control devices is authorized by the Institute, the committee on instruments and measurements desires representation thereon, since a large number of industrial control devices depend on measuring devices to initiate their operation.

In accordance with a request from the National Roster of Scientific and Specialized Personnel of the War Manpower Commission, the committee has submitted to it a statement of the duties, skills, and functions of those engaged in the instrument and measurement field.

The committee also has been requested to co-operate with the Sections committee in the formation of technical groups on instruments and measurements in the different Sections, through the activity of committee members in their own Sections and by assisting in supplying speakers on subjects in the instrument and measurement field. The committee already has taken action through letters and other material sent to its members and by making available to Section chairmen the names of members of the committee in their Section. In the Boston Section such a technical group is already in active operation.

COMMITTEE ON LAND TRANSPORTATION

A joint meeting of the committee on land transportation and the oil and gas power group of the railroad division of the American Society of Mechanical Engineers was held on November 29, 1944, in New York. Papers were presented at this meeting on the subject of gas-turbine locomotives, covering developments in Switzerland and in the United States and the present status and prospects for future developments of the gas turbine as a propulsion unit for road locomotives. The meeting was very well attended, and interest in the subject was pronounced.

On the morning of January 25, 1945, during the winter technical meeting in New York, a meeting of the committee was held to discuss various subjects to be brought before the committee members. The technical papers already available were reviewed, and additional papers to be obtained on subjects of interest and value along lines covered by this committee were discussed. In the afternoon the committee sponsored a technical session at which the four papers presented were received with a great amount of interest, and extensive discussion resulted.

Three technical papers have been made available for use in the spring technical-paper program.

In the interest of keeping travel to a minimum under present transportation conditions, no additional committee meetings have been scheduled.

COMMITTEE ON PRODUCTION AND APPLICATION OF LIGHT

No technical sessions or conferences were sponsored by the committee during the year, and a conference tentatively planned for the summer meeting has been abandoned with the cancellation of this meeting.

A meeting of the committee was held at Institute headquarters on January 23, 1945, with a substantial number of the members in attendance.

The report of the subcommittee on preferred characteristics of electric power for lighting has been prepared, and, in accordance with recommendation made at the January committee meeting, will be referred to other interested technical committees for comments and suggestions.

COMMITTEE ON MARINE TRANSPORTATION

During the year, four new members were added to the committee. All of these new members are associated with prominent organizations, and their time is occupied completely with marine electrical matters. They are very helpful to the committee, and their enthusiasm has aided in a more critical review of the existing standard.

The committee had one all-day meeting, and four two-day meetings. The attendance at all the meetings has been excellent, despite the fact that all the members are overloaded with war work.

In accordance with the custom of the committee, the 93 pages of the 1940 edition of Standard 45 have been subdivided into eight sections and assigned to an equal number of subcommittees. These subcommittees have reviewed critically the 1940 edition and reported their findings to the committee. This has been a very laborious and time-consuming task, for the rapid development of marine electric installations during this quantity production of ships and increased uses of electric power, including electronic devices, has necessitated many revisions to keep abreast of the changing conditions. In addition these revisions have been necessitated by the greatly increased use of a-c distribution systems through the ship and the increased number of electrically propelled vessels.

COMMITTEE ON POWER GENERATION

The two major projects of the committee have been practically completed. The joint subcommittee with ASME has prepared a specification for steam-turbine governors, which has been issued on a trial basis. This work is being extended to other kinds of prime movers.

Another project in which the committee on power generation has participated actively was the preparation of standards for 3,600-rpm steam-turbine generators for sizes 10,000–60,000 kw. This work is virtually completed, and it is expected that the recommended specification will be issued on a trial basis this year.

The technical sessions sponsored by the committee during the summer technical meeting in St. Louis and the winter technical meeting in New York were devoted to diverse subjects of interest to the committee and general membership of the Institute.

A well-attended and quite successful technical conference was held at the last winter meeting on the subject of central-station auxiliaries.

The plans of the committee for the immediate future include a symposium on hydroelectric systems, a series of papers on excitation systems, in addition to further contributions on the subject of central-station auxiliaries.

COMMITTEE ON POWER TRANSMISSION AND DISTRIBUTION

A meeting of the subcommittee chairmen was held in October 1944, and a full meeting of the committee was held at the winter technical meeting in New York in January 1945.

Technical Meetings. At the summer meeting in St. Louis in June 1944, the committee sponsored two technical sessions. One session dealt with general transmission and distribution problems, and the other with cables. At the winter meeting in New York in January 1945, the committee sponsored three technical sessions, and one conference session. The technical sessions dealt with lightning and protective relaying, supervisory control and stability, and cables. The conference was on the subject of wartime practices on distribution systems, and consisted of four conference papers and discussion.

Subcommittee Activities. The distribution subcommittee and stations subcommittee devoted their principal activities to arrangements for the conference session, which was sponsored jointly by the two subcommittees.

The general systems subcommittee is planning a conference session on the factors involved in serving kilowatt and kilovar and the effect on the rate structure.

The transmission subcommittee through its working group on towers, poles, and conductors is sponsoring papers dealing with modern trends in wood-pole structure design. The working group on cables is arranging papers on cable temperatures and also is planning a review of duct heating constants. The working group on lightning and insulators is collecting material for an addition to the lightning reference book covering the period 1934 to 1944. Work also is proceeding on a report on predicting lightning performance of transmission lines. During the year, "AIEE Standard 41, Insulator Tests," sponsored by this group was published as "ASA Standard C29.1."

COMMITTEE ON PROTECTIVE DEVICES

One meeting of the executive committee was held in the fall, at which time all of the subcommittees were organized and the work outlined for the year. One meeting of the full committee was held in January to review progress reports by the subcommittees and to get suggestions from all members about the future program.

The committee sponsored ten technical papers at the 1944 summer meeting, four at the Pacific Coast meeting and 11 at the winter meeting. Plans are being made to continue the preparation of technical papers, particularly those having an important bearing on wartime developments or practices.

Activities of the subcommittees may be summarized as follows:

Circuit Breaders, Switches, and Fuses. Standard 25, covering fuses above 600 volts, was approved and sent to the Standards committee with the recommendation that it should be published as an approved standard.

Standard 20, covering low-voltage air circuit breakers, has been worked on diligently through the year. The wide interest and broad field of use of this apparatus has encouraged much discussion of the material in the proposed revision.

A draft of a Standard on "Reclosing Devices for Distribution Circuits" has been completed by the working group.

On Standard 22, "Air Switches," no active work is being done. A working group is collecting data and comments that may lead to suggesting revisions.

Standard 27, "Switchgear Assemblies," was reviewed by a working group, which reported that "the standards as issued in August 1942 do not require any action looking toward revision at this time."

There has been no activity looking toward a revision on Standard 19, "Power Circuit Breakers."

Items recommended for continuing by future committees are:

(*a*). Study of the calculating of short-circuit currents for low-voltage circuits.

(*b*). Revision of methods used for rating power circuit breakers.

(*c*). Derating factors for air circuit breakers on reclosing service.

Some engineers feel that air circuit breakers need not be derated as severely as oil circuit breakers when used on reclosing service.

Lightning-Protective Devices. The eighth draft of the proposed AIEE Standard for expulsion-type distribution arresters was sent to members of the subcommittee for final approval March 2, 1945.

Two of the projects, namely, industry performance characteristics of high-voltage protector tubes and rod-gap characteristics have been delayed until a suitable industry standard for impulse testing has been set up.

A survey was started in co-operation with the committee on electric machinery to determine the success of present methods used for lightning protection of rotating a-c machines, covering both protected and unprotected machines.

The performance data of expulsion-type distribution arresters are being secured from all manufacturers and will be published as a committee report giving the range of performance values available.

Fault-Current-Limiting Devices. The working group revising Standard 32 for "Neutral Grounding Devices" has been very active, but much still remains to be done.

The working group on "Present-Day Grounding Practices" is well organized to prepare a report of interest and value in connection with postwar conversions and new construction. Steps have been taken to enlist the aid and support of other technical committees interested.

Relays. This working group has prepared a bibliography for the preceding year and has distributed this to members of the relay subcommittee. This is a continuing program and is of considerable value in keeping all interested members up to date.

Generator Protection. This working group has been studying various phases of the subject and conducted a conference session at the winter technical meeting. It is expected the working group ultimately will prepare a report on recommended practices.

Current Transformers. A working group is preparing a report on the use of current transformers having a secondary current rating of less than five amperes which will indicate where these can be used to advantage and will include a discussion of application and limitations.

Protection of Powerhouse Auxiliaries. A working group is preparing a questionnaire for limited circulation prior to issuing a report on present practices.

Transformer Protection. A working group was organized during the year to study various American and foreign practices and to prepare a report.

Instrument Transformer Standards for Relays. At the request of the ASA committee on transformers, a draft of a report has been completed recommending material for a proposed ASA section on instrument transformers.

National Electrical Code. A small working group has been working closely in co-operation with the committee on revision of the "National Electrical Code," and has made a number of recommendations, some of which have been adopted. This activity has been terminated.

Distribution Circuit Protection. A working group has just been organized to study the effect of distribution-circuit construction on the protection that can be obtained.

COMMITTEE ON APPLICATIONS OF ELECTRICITY TO THERAPEUTICS

The committee held no meetings during the year, as all of the members are engaged in war work. The members have, however, corresponded.

The war has resulted in the development of much new equipment which should prove valuable in the field of electrical therapy. Among the new developments are apparatus for determining the relaxation of muscles, for the production of very high-voltage cathode rays and for X rays at new wave lengths. Equipment is available for producing X rays at any voltage up to 100,000,000. This new equipment will be available for experimental therapy following the cessation of hostilities. There is evidence that the new rays may be of value in treating certain diseases.

It is the expectation of the committee that there will be a considerable and important development in the field of electrical therapeutics following the war.

Awards

COMMITTEE ON AWARD OF INSTITUTE PRIZES

Four Institute prizes and seven District prizes were awarded for papers presented during the calendar year 1943. As explained previously, the decrease in the number of District prize awards from that reported several years earlier is due to the effect of the training programs in the various colleges. No District prize for Branch paper was awarded during the academic year ending June 30, 1944.

A number of the technical papers were of a high order, and a choice between leading papers worthy of award was very close in several of the classifications. Two honorable mentions were made in the class of best paper prize and one honorable mention in the class of initial paper prize. The committee gratefully acknowledges the aid received from the technical committees and their reviewers in nominating and grading the large number of papers considered for the awards.

EDISON MEDAL

The Edison Medal, awarded by a committee composed of 24 members of the Institute, was presented for 1944 to E. F. W. Alexanderson, consulting engineer, General Electric Company, Schenectady "for his outstanding inventions and developments in the radio, transportation, marine, and power fields." The presentation took place January 24, 1945, during the winter technical meeting. The medal may be awarded annually for "meritorious achievement in electrical science, electrical engineering, or the electrical arts."

LAMME MEDAL

The Lamme Medal committee awarded the medal for 1944 to S. H. Mortensen, chief electrical engineer, Allis-Chalmers Manufacturing Company, Milwaukee, Wis., "for his pioneer work in the development of self-starting synchronous motors and for his contributions to the development of large hydraulic and steam-turbine-driven generators." Arrangements are being made for the presentation of the medal at the annual business meeting in New York, June 27, 1945. The medal may be awarded annually to a member of the AIEE "who has shown meritorious achievement in the development of electric apparatus or machinery."

JOHN FRITZ MEDAL

The John Fritz Medal board of award, composed of representatives of the American Society of Civil Engineers, American Institute of Mining and Metallurgical Engineers, ASME, and AIEE, awarded the 40th medal, for 1944, to John L. Savage, consulting engineer, for his "superlative public service in conceiving and administering the engineering of mammoth dams, both in America and beyond the seven seas."

HOOVER MEDAL

The Hoover Medal was established through a trust fund created by a gift from Conrad N. Lauer and is to be awarded periodically "to a fellow engineer for distinguished public service" by a board representing the ASCE, AIME, ASME, and AIEE. The seventh medal, for 1944, was awarded to Ralph E. Flanders, president, Jones and Lamson Machine Company, Springfield, Vt.

ALFRED NOBLE PRIZE

This prize, established in 1929, consists of a certificate and a cash award from the income of a fund contributed by engineers and others to perpetuate the name and achievements of Alfred Noble, past president of the ASCE, and of the Western Society of Engineers. It may be made to a member of any of the co-operating societies, ASCE, AIME, ASME, AIEE, or WSE, for a technical paper of particular merit accepted by the publication committee of any of these societies, provided the author, at the time of such acceptance, is not over 30 years of age. The award for 1944 was presented to W. R. Wilson, General Electric Company, Pittsfield, Mass., for his paper "Corona in Aircraft Electric Systems as a Function of Altitude."

CHARLES LE GEYT FORTESCUE FELLOWSHIP COMMITTEE

A fellowship amounting to $400 was awarded to Morton M. Astrahan, a student of Northwestern University and a veteran of the present war. Mr. Astrahan will undertake graduate work in the field of electronics at the California Institute of Technology starting in the fall of this year. The award is to cover expenses for the second semester as Mr. Astrahan will receive aid from the Veterans' Administration for the first semester.

Joint Activities

UNITED ENGINEERING TRUSTEES, INC.

This organization manages property and funds held jointly by the four founder societies, including the Engineering Societies Building, the Engineering Societies Library, and the endowment funds of the Engineering Foundation.

The building is fully occupied by engineering organizations, and additional space is needed both for offices and for meetings. Therefore, there has been a renewal of planning for the future adequate housing for engineering societies, and various types of projects are under serious consideration.

Increased revenue from meeting halls and the reduction of interest paid to the societies to token payments produced a small credit balance for the year ended September 30, 1944.

An abstract of the annual report for the year ended September 30, 1944, appeared in *Electrical Engineering* for February 1945, page 82.

ENGINEERING FOUNDATION

The Engineering Foundation was established in 1914 as a joint organization of the four societies, ASCE, AIME, ASME, and AIEE, for "the furtherance of research in science and engineering, and the advancement in any other manner of the profession of engineering and the good of mankind."

Each research project supported by it is under the sponsorship of one of the founder societies.

During the year 1944–45, work on five projects has been continued, and three new projects were initiated. The small number of each reflects the lessened demand for Foundation support caused by extensive government support of all types of research of probable importance to the war effort and the withdrawal of research personnel from the educational institutions to serve in war activities.

The Welding Research Council sponsored jointly by the AIEE and the American Welding Society has been in operation eight years. Its work is carried on by eight research committees. The principal accomplishment during the year 1943–44 was the development of a better understanding of the fundamentals of weldability and weld stresses.

An abstract of the annual report for the year ended September 30, 1944, appeared in *Electrical Engineering* for February 1945 pages 82–4.

ENGINEERING SOCIETIES LIBRARY

The Engineering Societies Library was formed by combining the separate libraries of the ASCE, AIME, ASME, AIEE, and preparing a composite card catalogue.

Special services rendered by the library include: photoprints, searches, abstracts, translations, bibliographies, book loans by mail.

Wartime conditions have prevented the usual growth in the book collection and greatly increased the demand for photostat prints and for other services.

An abstract of the annual report for the year ended September 30, 1944, appeared in *Electrical Engineering* (Feb '45, p 84–5).

EMPLOYMENT SERVICE

Operating as an incorporated nonprofit organization, the Engineering Societies Personnel Service, Inc., assists members of the Founder Societies desiring to secure new positions and employers searching for engineers. Nonmembers may receive such assistance when positions available cannot be filled by members.

Offices are operated in New York; Boston, Mass.; Detroit, Mich.; Chicago; and San Francisco, Calif.; with the co-operation of the Engineering Societies of New England in Boston, the Engineering Society of Detroit in that city, the Western Society of Engineers in Chicago, and the Engineers Club of San Francisco in that city.

For several years, the service has been on a self-supporting basis, but the prevailing scarcity of engineers available for new positions has reduced the number of placements. A record of registration and placements during the past year is given in Table X.

Table X. Analysis of Employment Service

	Men Registered						Men Placed					
Month	New York	Chicago	San Francisco	Detroit	Boston	Total	New York	Chicago	San Francisco	Detroit	Boston	Total
1944												
May	88	17	64	21	18	208	23	9	25	7	8	72
June	95	25	73	24	11	228	31	12	18	5	7	73
July	69	26	54	17	14	180	21	8	18	4	6	57
August	95	29	69	23	13	229	20	9	24	4	6	63
September	89	30	59	22	10	210	25	6	27	[illegible]	4	71
October	73	30	65	19	11	198	30	3	16	9	6	64
November	77	24	65	23	17	206	25	13	23	11	3	75
December	75	14	55	16	5	165	18	5	18	4	7	52
1945												
January	71	12	65	10	2	69	21	6	15	4	3	49
February	61	28	35	11	10	145	21	14	15	5	3	58
March	76	27	49	25	9	186	26	6	20	9	2	63
April	84	23	47	20	8	182	22	11	18	6	4	61
Total	953	285	696	231	128	2206	283	102	237	77	59	758

ENGINEERS' COUNCIL FOR PROFESSIONAL DEVELOPMENT

This council, organized in 1932 to engage in activities leading toward the enhancement of the professional status of the engineer, includes three representatives of each of the eight participating organizations, which are the ASCE, AIEE, ASME, and AIME, the SPEE, the National Council of State Boards of Engineering Examiners, and the Engineering Institute of Canada. Its principal activities have been carried on by four committees: student selection and guidance, engineering schools, professional training, and professional recognition.

One of the principal accomplishments during the year which ended on September 30, 1944, was the development of a plan for accrediting technical Institutes. This will be administered by a subcommittee of the committee on engineering schools which has administered the accrediting of engineering college curricula.

A revised general reading list for junior engineers was approved, progress was made in the preparation of a manual for junior engineers, and continuing progress was reported in the measurement and guidance program.

Although, due to wartime programs, few inspections of engineering curriculums have been made, plans are being made for the reappraisal of all curriculums after the war.

A comprehensive report on the activities during the year ended September 30, 1944, was published in *Electrical Engineering* for December 1944, pages 452–4.

JOINT CONFERENCE COMMITTEE

This committee, composed of the presidents, immediate past presidents, and secretaries of the Founder Societies and the American Institute of Chemical Engineers, considered topics of interest to the societies.

The committee serves in an advisory capacity, making occasional recommendations to the societies on matters of interest to all.

RADIO TECHNICAL PLANNING BOARD

This joint advisory body, organized in 1943, will formulate recommendations on the technical future of radio developments for submission to the Government, industry, and the public.

Initial member bodies in addition to the AIEE are: Radio Manufacturers Association; Institute of Radio Engineers; American Institute of Physics; American Radio Relay League; F M Broadcasters, Inc.; International Association of Chiefs of Police; National Association of Broadcasters; and National Independent Broadcasters. The board includes one representative of each member organization.

The work is carried on mainly by 13 technical panels, which have prepared many comprehensive reports.

REPRESENTATIVES

A complete list of the more than 30 joint activities in which the Institute is represented appears in the Year Book and in the September issue of *Electrical Engineering* each year.

Appreciation

With grateful recognition of the extent and effectiveness of the activities and the large increase in membership during the past year, the board of directors expresses its deep appreciation and thanks to the national committees, and the District, Section, and Branch officers for their generous contributions of energy and time, despite the adverse conditions, and to the members in general for their continuing interest and participation in Institute affairs.

Respectfully submitted for the board of directors.

H. H. HENLINE
National Secretary

May 29, 1945

HASKINS & SELLS
CERTIFIED PUBLIC ACCOUNTANTS

1 EAST 44TH STREET
NEW YORK

May 18, 1945

American Institute of Electrical Engineers,
33 West 39th Street, New York.

Dear Sirs:

We have examined the balance sheet of the American Institute of Electrical Engineers, and schedule of securities owned, as of April 30, 1945, and the related statements of cash receipts and disbursements of operating and restricted funds for the year ended that date, have reviewed the accounting procedures of the Institute, and have examined its accounting records and other evidence in support of such financial statements. Our examination was made in accordance with generally accepted auditing standards applicable in the circumstances and included all auditing procedures we considered necessary, which procedures were applied by tests to the extent we deemed appropriate in view of the system of internal control.

In our opinion, the accompanying balance sheet, schedule of securities owned, and statements of cash receipts and disbursements fairly present, respectively, the financial condition of, and securities owned by, the Institute as of April 30, 1945, and its recorded cash receipts and cash disbursements for the year ended that date, in conformity with generally accepted accounting principles and practices applied on a basis consistent with that of the preceding year.

Yours truly,

(Signed) HASKINS & SELLS

AMERICAN INSTITUTE OF ELECTRICAL ENGINEERS

(Incorporated in New York)

Balance Sheet, April 30, 1945

Exhibit A

ASSETS		
Property Fund Assets:		
One-fourth interest in physical properties of United Engineering Trustees, Inc.:		
Land, buildings, and equipment (less depreciation and renewal reserve)	$369,974.15	
Funded depreciation and renewal reserve	128,474.33	
Total	$498,448.48	
Equipment:		
Library—volumes and fixtures—estimated value	36,366.37	
Office furniture and fixtures (less reserve for depreciation, $26,047.47)	11,395.49	
Works of art, etc.	3,001.35	
Cash—proceeds from redemption of mortgage certificate	612.91	
Total property fund assets		$ 549,824.60
Restricted Fund Assets:		
Securities—at cost, less reserve, $7,372.65 (quoted market value, $398,266.61)—Schedule 1	$359,259.96	
Cash (Exhibit C)	35,064.88	
Accrued interest receivable	89.75	
Total restricted fund assets		394,414.59
Operating Fund Assets:		
Cash (not including $1,295.18 for Federal taxes withheld from employees) (Exhibit B)	$ 77,206.09	
Accounts receivable:		
Members—for dues (less reserve, $5,700.00)	6,114.11	
Advertisers	6,729.00	
Miscellaneous	3,544.12	
Accrued interest receivable	4,309.52	
Inventories:		
Transactions, etc.	1,048.50	
Electrical Definitions	4,388.40	
Work in process (May issue of *Electrical Engineering*, etc.)	7,706.26	
Text and cover paper	6,799.68	
Badges	1,589.34	
Total operating fund assets		119,435.02
Total		$1,063,674.21

LIABILITIES		
Property Fund Reserve		$ 549,824.60
Restricted Fund Reserves:		
Reserve Capital fund	$371,392.58	
Life Membership fund	8,427.63	
Member for Life fund	3,268.71	
International Electrical Congress of St. Louis Library fund	5,748.05	
Lamme Medal fund	4,456.66	
Mailloux fund	1,120.96	
Total restricted fund reserves		394,414.59
Operating Fund Reserves, Liabilities, Etc.:		
Accounts payable	$ 22,485.83	
Deferred income:		
Dues received in advance	3,200.10	
Entrance fees and dues advanced by applicants for memberships	1,136.68	
Subscriptions to publications received in advance	13,771.06	
Miscellaneous (including unallocated receipts)	967.25	
Operating fund reserves	77,874.10	
Total operating fund reserves, liabilities, etc.		119,435.02
Total		$1,063,674.21

AMERICAN INSTITUTE OF ELECTRICAL ENGINEERS

Statement of Cash Receipts and Disbursements of Operating Fund for the Year Ended April 30, 1945

Exhibit B

Cash on Deposit With The National City Bank of New York, May 1, 1944 (not including $1,079.42 for Federal taxes withheld from employees)		$ 53,749.13
Receipts:		
Dues (including $113,688.00 allocated to *Electrical Engineering* subscriptions)	$247,017.36	
Advertising	108,173.90	
Transactions subscriptions	7,832.37	
Electrical Engineering subscriptions	19,825.13	
"Electrical Definitions"	935.25	
"Electric-Power Distribution for Industrial Plants"	7,803.80	
Miscellaneous publications (preprints, Standards, *Electrical Engineering* supplement, etc.)	25,299.78	
Students' fees	10,848.85	
Entrance fees	17,159.03	
Membership badges	4,088.06	
Transfer fees	2,908.00	
Interest and dividends on investments of Restricted Capital fund	10,037.77	
Miscellaneous	178.63	
Total receipts		462,107.93
Total		$515,857.06
Disbursements:		
Publication expense:		
Electrical Engineering	$112,263.90	
Transactions	10,154.47	
Year Book	4,682.86	
Miscellaneous publications (preprints, Standards, "Industrial Plants" report, *Electrical Engineering* supplement, etc.)	27,156.68	
Institute meetings	16,159.00	
Institute Sections	48,358.49	
Institute Branches	2,748.23	
Finance committee	629.29	
Headquarters committee	184.09	
Membership committee	9,059.91	
Standards committee	11,365.60	
Forward	$242,762.52	$515,857.06
Total (forward)		$515,857.06
Disbursements (forward)	$242,762.52	
Technical committees	838.20	
Retirement system AIEE—normal contribution (see Exhibit C for payment of $25,000.00, special contribution from Reserve Capital fund)	5,074.35	
Radio Technical Planning Board	1,000.00	
Traveling expenses:		
Geographical Districts:		
Executive committees	4,731.57	
Vice-presidents	793.92	
Branch counselors and chairmen	2,045.97	
President's appropriation	1,245.09	
AIEE representatives	176.92	
Board of directors	5,655.16	
National nominating committee	1,138.68	
Administrative expenses	58,302.06	
Geographical Districts—Branch paper prizes	353.29	
Institute prizes, national	409.00	
American Co-ordinating Committee on Corrosion	25.00	
American Standards Association	1,500.00	
United Engineering Trustees, Inc.:		
Building assessment	17,813.56	
Library assessment	11,006.20	
Engineers' Council for Professional Development	1,700.00	
Engineering Foundation Project—welding research	250.00	
National Committee State Board Engineering Examiners	350.00	
International Committee on Illumination	30.00	
John Fritz Medal	50.00	
National Fire Protection Association—Dues	60.00	
Membership badges	4,585.47	
Legal services	250.00	
Committee on collective bargaining and related matters	691.40	
Office furniture and fixtures, and repairs	5,313.33	
Edison Medal committee	230.57	
Transfers:		
To Reserve Capital fund	67,000.00	
To Member for Life fund	3,268.71	
Total disbursements		438,650.97
Cash on Deposit With The National City Bank of New York, April 30, 1945 (not including $1,295.18 for Federal taxes withheld from employees)		$ 77,206.09

AMERICAN INSTITUTE OF ELECTRICAL ENGINEERS

Statement of Cash Receipts and Disbursements of Restricted Funds for the Year Ended April 30, 1945

Exhibit C

	Restricted Funds						
	Reserve Capital Fund	Member for Life Fund	Life Membership Fund	International Electrical Congress of St. Louis Library Fund	Lamme Medal Fund	Mailloux Fund	Total Restricted Funds
Cash on Deposit With The National City Bank of New York and Various Savings Banks, May 1, 1944	$ 27,676.29		$2,827.14	$401.80		$1,104.34	$ 32,009.57
Receipts:							
Interest on bonds			$ 125.00	$130.00	$ 240.00		$ 495.00
Interest on bank balances			43.56			$ 16.62	60.18
Proceeds from sale of securities	$ 8,535.00				4,200.00		12,735.00
Transfer from operating fund	67,000.00	$3,268.71					70,268.71
Life membership fees			845.66				845.66
Total receipts	$ 75,535.00	$3,268.71	$1,014.22	$130.00	$4,440.00	$ 16.62	$ 84,404.55
Total	$103,211.29	$3,268.71	$3,841.36	$531.80	$4,440.00	$1,120.96	$116,414.12
Disbursements:							
Purchase of securities	$ 51,624.89				$4,253.78		$ 55,878.67
Retirement system AIEE—contribution to meet the requirements of an increase in the allowance for prior services of the headquarters staff	25,000.00						25,000.00
Transfer to operating fund			$ 460.57				460.57
Engrossing certificate					10.00		10.00
Total disbursements	$ 76,624.89		$ 460.57		$4,263.78		$ 81,349.24
Balance on Deposit With The National City Bank of New York and Various Savings Banks, April 30, 1945	$ 26,586.40	$3,268.71	$3,380.79	$531.80	$ 176.22	$1,120.96	$ 35,064.88

AMERICAN INSTITUTE OF ELECTRICAL ENGINEERS

Securities Owned, April 30, 1945

Schedule 1

	Principal Amount of Bonds or Number of Shares of Stock	Restricted Funds				
		Reserve Capital Fund	Life Membership Fund	International Electrical Congress Library Fund	Lamme Medal Fund	Total Restricted Funds
Railroad Bonds:						
Atlantic Coast Line, First Consolidated 4%, due 1952	$ 4,000.00				$4,253.78	$ 4,253.78
Baltimore & Ohio, Pittsburgh, Lake Erie & West Virginia System 4%, due 1951	10,000.00	$ 6,450.00				6,450.00
Chicago & Erie Railroad Company 5% first mortgage, due 1982. Registered	1,000.00	1,105.00				1,105.00
New York Central Railroad Company 4% series A consolidated mortgage, due 1998	10,000.00	6,100.00				6,100.00
St. Louis-San Francisco Railway Company 5% prior lien mortgage series B, due 1950 (certificates of deposit). Registered, Stamped	6,000.00*	5,497.50*				5,497.50*
Total railroad bonds		$ 19,152.50			$4,253.78	$ 23,406.28
Public Utility Bonds:						
New York & Queens Electric Light & Power Company 3½% first and consolidated mortgage, due 1965	10,000.00	$ 11,000.00				$ 11,000.00
United States Government Bonds:						
Treasury Savings bonds series D, due July 1, 1949	10,000.00	$ 7,644.00				$ 7,644.00
Treasury Savings bonds series D, due January 1, 1950	10,000.00	7,500.00				7,500.00
Treasury bonds 2%, due 1950/48	77,000.00	78,130.94				78,130.94
Treasury bonds 2%, due 1950, Registered	3,000.00	3,060.94				3,060.94
Treasury bonds 2½%, due 1968/63	20,000.00	15,000.00	$5,000.00			20,000.00
Treasury bonds 2½%, due 1972/67	6,300.00	1,100.00		$5,200.00		6,300.00
Treasury bonds, 2½%, due 1972, Registered	3,500.00	3,516.41				3,516.41
Defense bonds series F, due June 1, 1953	34,000.00	25,160.00				25,160.00
Defense bonds series G, 2½%, due December 1, 1954	18,000.00	18,000.00				18,000.00
War Savings Bonds series G, 2½%, due September 1, 1955	40,000.00	40,000.00				40,000.00
War Savings Bonds series G, 2½%, due 1956	17,000.00	17,000.00				17,000.00
Total United States Government bonds		$216,112.29	$5,000.00	$5,200.00		$226,312.29
Capital Stocks:						
American Can Company	60 shares	$ 4,988.40				$ 4,988.40
American Telephone & Telegraph Company	50 shares	8,183.65				8,183.65
Atchison, Topeka & Santa Fe Ry. Company—Preferred	150 shares	13,035.46				13,035.46
Boston Edison Company	200 shares	4,927.50				4,927.50
Commonwealth Edison Company	200 shares	7,580.68				7,580.68
Consolidated Natural Gas Company	11 shares	221.92				221.92
Eastman Kodak Company	35 shares	4,768.23				4,768.23
E. I. du Pont de Nemours & Company	50 shares	7,982.07				7,982.07
General Electric Company	130 shares	4,463.80				4,463.80
General Motors Corporation	100 shares	4,235.53				4,235.53
International Harvester Company	100 shares	5,030.50				5,030.50
International Match Realization Co., Ltd. voting trust certificates for capital shares of International Match Corporation	6 shares*	1,875.15*				1,875.15*
Ohio Edison Co. 4.40% preferred stock	150 shares	15,727.50				15,727.50
Sears Roebuck & Company	100 shares	6,014.97				6,014.97
Standard Oil Company of New Jersey	200 shares	9,601.26				9,601.26
Union Carbide & Carbon Corporation	100 shares	7,277.42				7,277.42
Total capital stocks		$105,914.04				$105,914.04
Total		$352,178.83	$5,000.00	$5,200.00	$4,253.78	$366,632.61
*Less reserve in full for securities considered to be of doubtful value		7,372.65				7,372.65
Total Securities, Less Reserve		$344,806.18	$5,000.00	$5,200.00	$4,253.78	$359,259.96

Officers and Committees for 1945–46

Officers

President

WILLIAM E. WICKENDEN Cleveland, Ohio
(Term expires July 31, 1946)

Junior Past Presidents

NEVIN E. FUNK Philadelphia, Pa.
(Term expires July 31, 1946)

CHARLES A. POWEL East Pittsburgh, Pa.
(Term expires July 31, 1947)

Vice-Presidents

District
1 R. T. HENRY Buffalo, N. Y.
3 J. F. FAIRMAN New York, N. Y.
5 M. S. COOVER Ames, Iowa
7 R. W. WARNER Austin, Tex.
9 C. B. CARPENTER Portland, Ore.
(Terms expire July 31, 1946)

2 E. S. FIELDS Cincinnati, Ohio
4 H. B. WOLF Charlotte, N. C.
6 L. M. ROBERTSON Denver, Colo.
8 F. F. EVENSON San Diego, Calif.
10 F. L. LAWTON Montreal, Quebec
(Terms expire July 31, 1947)

Directors

K. L. HANSEN Milwaukee, Wis.
W. B. MORTON Philadelphia, Pa.
W. R. SMITH Newark, N. J.
(Terms expire July 31, 1946)

C. M. LAFFOON East Pittsburgh, Pa.
C. W. MIER Dallas, Tex.
S. H. MORTENSEN Milwaukee, Wis.
(Terms expire July 31, 1947)

P. L. ALGER Schenectady, N. Y.
M. J. McHENRY Toronto, Ontario
D. A. QUARLES New York, N. Y.
(Terms expire July 31, 1948)

J. M. FLANIGEN Atlanta, Ga.
J. R. NORTH Jackson, Mich.
WALTER C. SMITH San Francisco, Calif.
(Terms expire July 31, 1949)

Treasurer

W. I. SLICHTER New York, N. Y.
(Term expires July 31, 1946)

Secretary

H. H. HENLINE New York, N. Y.
(Term expires July 31, 1946)

Local Honorary Secretaries

AUSTRALIA—V. J. F. Brain, Department of Public Works, Bridge Street, Sydney, N.S.W.

BRAZIL—Richard H. Bowles, Sao Paulo Tramway Light and Power Company, Sao Paulo

ENGLAND—A. P. M. Fleming, Metropolitan-Vickers Electric Company, Trafford Park, Manchester

FRANCE—A. S. Garfield, 45 Bd. Beausejour, Paris, 16E

INDIA, NORTHERN—V. F. Critchley, 11 Bahawalpur Road, Lahore, Punjab

INDIA, SOUTHERN—N. N. Iengar, The Tata Power Co. Ltd., Bombay House, Bruce Street, Fort Bombay

NEW ZEALAND—P. H. Powell, Canterbury College, Christchurch

SWEDEN—A. F. Enstrom, Ingeniorsvetenskrapsakademien, Stockholm 5

TRANSVAAL, SOUTH AFRICA—W. Elsdon-Dew, P.O. Box 4563, Johannesburg

General Committees

Executive

W. E. Wickenden, *chairman*, Case School of Applied Science, Cleveland 6, Ohio
P. L. Alger R. T. Henry
J. F. Fairman W. I. Slichter
N. E. Funk W. R. Smith

Board of Examiners

Alexander Maxwell, *chairman*, Edison Electric Institute, 420 Lexington Ave., New York, N. Y.
E. D. Doyle, *vice-chairman*, Leeds & Northrup Co., 4901 Stenton Ave., Philadelphia 44, Pa.
H. E. Farrer, secretary, AIEE, 33 W. 39th St., New York 18, N. Y.
P. H. Adams A. E. Knowlton
R. W. Atkinson G. M. Laffoon
R. H. Barclay J. J. Pilliod
Robin Beach R. C. Roe
F. E. D'Humy M. F. Skinker
C. W. Franklin I. A. Terry
I. W. Gross H. M. Trueblood
L. F. Hickernell H. H. Weber
Sidney Withington

Code of Principles of Professional Conduct

D. D. Ewing, *chairman*, Purdue University, Lafayette, Ind.
Harry Barker Dugald C. Jackson
E. S. Fields S. H. Mortensen
E. H. Flath Wm. M. Piatt

Constitution and Bylaws

Mark Eldredge, *chairman*, 2110 Spencer Road, Silver Spring, Md.
Reginald L. Jones C. T. Sinclair
T. G. LeClair Walter Charles Smith
I. Melville Stein

Edison Medal

Appointed by the president for term of five years

J. T. Barron R. E. Doherty, *chairman* J. V. B. Duer
(Terms expire July 31, 1946)
F. D. Newbury D. C. Prince W. E. Wickenden
(Terms expire July 31, 1947)
C. R. Freehafer C. A. Powel David Sarnoff
(Terms expire July 31, 1948)
O. E. Buckley A. E. Knowlton H. E. Strang
(Terms expire July 31, 1949)
C. V. Christie Zay Jeffries Harold Pender
(Terms expire July 31, 1950)

Elected by Board of Directors from its own membership for term of two years

P. L. Alger M. S. Coover S. H. Mortensen
(Terms expire July 31, 1946)
J. R. North D. A. Quarles H. B. Wolf
(Terms expire July 31, 1947)

Ex officio

W. E. Wickenden, president
W. I. Slichter, treasurer
H. H. Henline, secretary

Finance

W. R. Smith, *chairman*, Public Service Electric & Gas Co., 80 Park Place, Newark 1, N. J.
J. F. Fairman D. A. Quarles

Charles LeGeyt Fortescue Fellowship

A. R. Stevenson, Jr. H. W. Tenney
(Terms expire July 31, 1946)
J. M. Gaylord R. T. Henry, *chairman*
(Terms expire July 31, 1947)
Joseph W. Barker Ernst Weber
(Terms expire July 31, 1948)

Lamme Medal

Robin Beach O. B. Blackwell C. M. Laffoon
(Terms expire July 31, 1946)
W. A. Del Mar John C. Parker, *chairman* Philip Sporn
(Terms expire July 31, 1947)
H. L. Hazen V. M. Montsinger G. A. Waters
(Terms expire July 31, 1948)

Headquarters

T. F. Barton, *chairman*, General Electric Company, 570 Lexington Ave., New York 22, N. Y.
H. H. Henline W. R. Smith

Members-for-Life Fund

F. M. Farmer, *chairman*, 2 East End Avenue, New York 21, N. Y.
C. R. Beardsley R. C. Muir
E. H. Colpitts F. D. Newbury
N. E. Funk W. S. Rodman
R. W. Sorensen

Membership

L. F. Howard, *chairman*, American Tel. & Tel. Co., 195 Broadway, New York 7, N. Y.
F. S. Bacon W. J. Lyman
Tomlinson Fort L. C. Miller
W. C. Fowler E. G. D. Paterson
P. H. Hughes D. B. Perry
A. W. Janowitz J. R. Riley
C. W. La Pierre R. W. Warner

District Vice-Chairmen
Wm. F. Cotter (1) A. M. Spaulding (6)
E. P. Yerkes (2) E. B. Robertson (7)
Richard F. Ham (3) Robert R. Richey (8)
W. J. Miller (4) H. C. Glase, Jr. (9)
E. W. Stone (5) Thomas Ingledow (10)

Ex officio
Chairmen of membership committees of all Sections

Planning and Co-ordination

J. F. Fairman, *chairman*, Consolidated Edison Company of New York, Inc., 4 Irving Place, New York 3, N. Y.
P. L. Alger M. D. Hooven
G. W. Bower T. G. LeClair
W. P. Dobson H. S. Osborne
Mark Eldredge W. R. Smith
H. H. Henline C. F. Wagner

Prizes, Award of Institute

M. D. Hooven, *chairman*, Public Service Electric & Gas Co., 80 Park Place, Newark 1, N. J.
C. S. Rich, *secretary*, 33 W. 39th St., New York 18, N. Y.
J. W. Barker J. J. Pilliod
H. W. Bibber H. E. Strang
F. A. Cowan C. F. Wagner
L. A. Kilgore R. J. Wiseman
J. D. Miner H. B. Wolf

Publication

C. F. Wagner, *chairman*, Westinghouse Electric Corporation, East Pittsburgh, Pa.
M. S. Coover John Mills
H. H. Henline J. J. Orr
B. M. Jones H. H. Race
G. A. Van Brunt

Publicity

E. E. Dorting, *chairman*, New York City Transit System, I.R.T. Div., 2545 Seventh Ave., New York 30, N. Y.
M. D. Hooven A. J. Koetsler
A. E. Knowlton C. F. Wagner

Research

J. W. Barker, *chairman*, Columbia University, New York 27, N. Y.
P. L. Alger E. L. Moreland
G. T. Harness G. M. L. Sommerman

J. A. Hutcheson
W. A. Lewis
C. G. Suits
V. K. Zworykin

Safety

L. F. Adams, *chairman*, General Electric Company, Schenectady 5, N. Y.
Robin Beach, *vice-chairman*, 32 Court St., Brooklyn 2, N. Y.
A. B. Smith, *secretary*, Bayberry Lane, Darien, Conn.
C. S. Bowden
M. M. Brandon
Allan B. Campbell
C. F. Dalziel
W. P. Dobson
John Grotzinger
F. L. Kemp
W. B. Kouwenhoven
R. L. Lloyd
A. C. Muir
Albrecht Naeter
W. T. Rogers
W. R. Smith
H. W. Tenney
E. E. Turkington
Wesley Weinerth
H. B. Williams

Sections

G. W. Bower, *chairman*, Public Service Electric & Gas Co., 80 Park Place, Newark 1, N. J.
R. M. Pfalzgraff, *vice-chairman*, American Viscose Corp., Wilmington 99, Del.
A. C. Muir, *secretary*, Berwind-White Coal Mining Co., 1138 Commercial Trust Bldg., Philadelphia 2, Pa.
O. C. Brill
M. S. Coover
W. E. Enns
Carl W. Evans
F. F. Evenson
H. P. Heafer
V. P. Hessler
W. R. Hough
Frederick Krug
F. L. Lawton
T. M. Linville
E. T. Mahood
R. G. Porter
C. S. Purnell

Ex officio

Chairmen of Sections

Standards

W. P. Dobson, *chairman*, Hydro-Elec. Power Commission Laboratory, 8 Strachan Ave., Toronto, Ont.
Reginald L. Jones, *vice-chairman*, Bell Telephone Laboratories, Inc., 463 West St., New York, N. Y.
H. E. Farrer, *secretary*, AIEE, 33 W. 39th St., New York 18, N. Y.
R. C. Bergvall
J. E. Clem
C. M. Gilt
R. T. Henry
T. B. Holliday
Alexander Maxwell
A. C. Monteith
S. H. Mortensen
J. R. North
M. S. Oldacre
E. B. Paxton
F. B. Silsbee
Gordon Thompson

Ex officio

Chairmen of working and co-ordinating committees of the Standards committee
Chairmen of AIEE technical committees
Chairmen of AIEE delegations on other standardizing bodies or sole representatives thereon
President, U. S. National Committee of the International Electrotechnical Commission

Student Branches

E. W. O'Brien, *chairman*, Southern Power & Industry, 1020 Grant Building, Atlanta 3, Ga.
M. M. Cory
H. L. Davis, Jr.
A. G. Ennis
T. G. LeClair
Everett S. Lee
Walter Charles Smith
E. M. Strong
R. G. Warner
C. R. Wischmeyer

Ex officio

Student Branch Counselors

Technical Program

M. D. Hooven, *chairman*, Public Service Electric & Gas Co., 80 Park Place, Newark, N. J.
S. H. Mortensen, *vice-chairman*, Allis-Chalmers Mfg. Co., Milwaukee 1, Wis.
C. S. Rich, *secretary*, AIEE, 33 W. 39th St., New York 18, N. Y.
O. E. Buckley
G. R. Canning
I. S. Coggeshall
F. A. Cowan
Frank Thornton, Jr.
C. C. Whipple
T. A. Worcester

Ex officio

J. F. Fairman, *chairman*, committee on planning and co-ordination
L. F. Adams, *chairman*, committee on safety
W. P. Dobson, *chairman*, Standards committee
Chairmen of all technical committees

Transfers

L. T. Blaisdell, *chairman*, General Electric Company, 4966 Woodland Ave., Cleveland 4, Ohio
B. D. Hull, *vice-chairman*, Southwestern Bell Telephone Co., 1010 Pine St., St. Louis 1, Mo.
D. E. Moat, *secretary*, Leeds & Northrup Co., 1800 Keith Bldg., Cleveland 15, Ohio
E. A. Crellin
A. E. Knowlton
K. B. McEachron
M. J. McHenry

Special Committee

Registration of Engineers

C. R. Beardsley, *chairman*, N.Y.C. Department of Commerce, 60 Broadway, Room 1404, New York 4, N. Y.
A. T. Campbell
N. E. Funk
N. B. Hinson
T. G. LeClair
K. B. McEachron
H. O. Murphy
W. H. Stueve
M. B. Wyman

Technical Committees

Air Transportation

J. D. Miner, *chairman*, Aviation Engg. Dept., Westinghouse Electric Corporation, Lima, Ohio
F. M. Roberts, *vice-chairman*, Industrial Engg. Division, General Electric Co., Schenectady 5, N. Y.
H. E. Keneipp, *secretary*, Engg. Dept., Westinghouse Electric Corp., P.O. Box 989, Lima, Ohio
J. W. Allen
W. L. Berry
C. J. Breitwieser
H. R. Brown
J. B. Coleman
R. W. Gemmell
R. M. Heintz
T. B. Holliday
Charles Kingsley, Jr.
John Maxian
R. A. Millermaster
J. D. Murray
J. R. North
O. F. Olsen
S. H. Orowski
M. H. Peairs
W. A. Petrasek
E. G. Ports
H. F. Rempt
R. A. Rugge
M. L. Schmidt
Raymond A. Smith
K. R. Smythe
T. J. Tanner
A. F. Trumbull
F. H. Walker
F. O. Wisman

Subcommittee Chairmen

W. S. Hay, Aircraft Wire & Cable
R. H. Kaufmann, Aircraft Electric Systems
R. A. Millermaster, Aircraft Electric Control and Protective Devices
M. L. Schmidt, Aircraft Electric Rotating Machinery

Automatic Stations

J. A. Elzi, *chairman*, Commonwealth & Southern Corporation, Jackson, Mich.
G. S. Whitlow, *vice-chairman*, Union Electric Co. of Missouri, 315 N. 12th Blvd., St. Louis, Mo.
G. S. Lunge, *secretary*, General Electric Company, Schenectady 5, N. Y.
J. A. Adams
F. F. Ambuhl
Harris Barber
G. W. Bean
W. A. Derr
J. M. Flanigen
E. E. George
I. T. Knight
Perry Peterson
C. F. Publow
M. E. Reagan
T. A. Taylor
J. H. Vivian
E. A. Williams, Jr.
C. E. Winegartner

Basic Sciences

J. G. Brainerd, *chairman*, Moore School of Electrical Engineering, University of Pennsylvania, Philadelphia, Pa.
K. W. Miller, *vice-chairman*, Elec. Engg. Div., Armour Research Foundation, 55 West 34th Street, Chicago 16, Ill.
J. D. Tebo, *secretary*, Bell Telephone Laboratories, Inc., 463 West Street, New York 14, N. Y.
R. W. Ager
Charles Concordia
Harvey L. Curtis
A. V. Eastman
L. O. Grondahl
C. R. Hanna
H. L. Hazen
N. S. Hibshman
Jesse E. Hobson
M. J. Kelly
Wm. A. Lewis
F. C. Lindvall
M. G. Malti
Brian O'Brien
G. W. Penney
H. W. Price
Walther Richter
W. J. Seeley
M. F. Skinker
James J. Smith
F. G. Tappan
G. S. Timoshenko
R. W. Warner
Ernst Weber

Communication

J. J. Pilliod, *chairman*, American Tel. & Tel. Company, 195 Broadway, Room 1833, New York 7, N. Y.
I. S. Coggeshall, *vice-chairman*, Western Union Telegraph Co., 60 Hudson Street, New York 13, N. Y.
H. I. Romnes, *secretary*, American Tel. & Tel. Co., 195 Broadway, New York 7, N. Y.
H. A. Affel
A. L. Albert
R. B. Beetham
H. H. Beverage
H. M. Bollinger
J. D. Booth
F. B. Bramhall
J. L. Callahan
J. W. Campbell
C. B. Carpenter
John L. Clarke
J. B. Coleman
F. A. Cowan
Harold Dangerfield
H. J. Dible
H. C. Dillingham
L. J. Dunnewold
Melville Eastham
H. E. Ellithorn
H. M. Engh
E. B. Fowler
D. G. Geiger
E. E. George
C. G. Grimes
S. B. Ingram
C. B. Jolliffe
I. J. Kaar
H. E. Jones
J. W. Kidder
M. L. Lehman
L. R. Mapes
Ralph G. McCurdy
C. W. Mier
Lee M. Moore
H. H. Nance
H. H. Newell
L. G. Pacent
J. G. Patterson
Haraden Pratt
John B. Russell
Arthur Bessey Smith
Rothwell E. Smith
W. B. Stephenson
T. DeWitt Talmage
H. M. Turner
Mead Warren
Wm. Comings White
E. P. Yerkes
F. C. Young

Subcommittee Chairmen

J. D. Booth, Power Line Carrier
I. J. Kaar, Sound Recording & Reproducing
L. G. Pacent, Hearing Aids
Arthur Bessey Smith, Testing of Telephone Transmitters and Receivers
H. M. Turner, Quick and Slow Acting Relays

Domestic and Commercial Applications

M. K. Brody, *chairman*, McCall's Test Rooms, 444 Madison Ave., New York 22, N. Y.
W. F. Ogden, *vice-chairman*, Edison General Electric Appliance Co., Inc., 5600 W. Taylor Street, Chicago 44, Ill.
Carl W. Evans, *secretary*, Electrical South, 1020 Grant Building, Atlanta, Ga.
L. F. Adams
R. U. Berry
D. K. Blake
M. M. Brandon
A. C. Bredahl
W. B. Buchanan
H. R. Cummins
L. R. Gamble
R. R. Herrmann
C. H. Leatham
F. W. Linder
L. W. McCullough
M. J. McHenry
H. E. Metz
H. P. Seelye
G. C. Tenney
Gordon Thompson
Wesley Weinerth

Subcommittee Chairmen

W. B. Buchanan, Electrical Hazards to Farm Animals
H. R. Cummins, Laboratory Projects
C. H. Leatham, Farm Applications
W. F. Ogden, Load Characteristics
Wesley Weinerth, Wiring

Education

H. W. Bibber, *chairman*, Union College, Schenectady 8, N. Y.
A. L. Abert
M. S. Coover
G. F. Corcoran
E. E. Dreese
W. L. Everitt
M. C. Hughes
E. B. Kurtz
E. A. Loew
O. D. Montgomery
J. A. Northcott, Jr.
R. G. Porter
Claire W. Ricker
L. M. Robertson
H. H. Skilling
R. W. Sorensen
J. G. Tarboux
B. R. Teare, Jr.
George B. Thomas
C. E. Tucker
C. E. Tuites
E. A. Walker
R. W. Warner
A. R. Zimmer

Electric Machinery

L. A. Kilgore, *chairman*, Westinghouse Electric Corporation, East Pittsburgh, Pa.
J. F. Calvert, *vice-chairman*, Northwestern Technological Institute, Evanston, Ill.
E. H. Alexander
Sterling Beckwith
Theodore Braaten
F. S. Brown
B. M. Cain
A. M. deBellis
G. T. Harness
F. E. Harrell
C. B. Hathaway
J. K. Hodnette
R. A. Hopkins
W. R. Hough
E. K. Kane
F. P. Kaspar
H. H. Kerr
C. E. Kilbourne
T. C. Lloyd
R. C. Moore
T. H. Morgan
M. S. Oldacre
F. D. Phillips
C. P. Potter
L. M. Robertson
M. L. Schmidt
W. C. Sealey
H. D. Sill
H. R. Sills
B. Van Ness, Jr.
C. G. Veinott

Subcommittee Chairmen

Sterling Beckwith, Synchronous Machinery
F. S. Brown, Transformer
A. M. deBellis, Insulation
W. R. Hough, D-C Machinery
C. E. Kilbourne, Test Code Co-ordinating
T. C. Lloyd, Induction Machinery

Electric Welding

G. W. Garman, *chairman*, General Electric Co., 1 River Road, Schenectady 5, N. Y.
E. H. Vedder, *vice-chairman & secretary*, Westinghouse Electric Corp., East Pittsburgh, Pa.
C. A. Adams
R. C. Bouse
E. M. Callender
C. M. Chute, Jr.
C. N. Clark
W. E. Crawford
J. W. Dawson
G. H. Fett
K. L. Hansen
W. F. Hess
C. E. Humble
J. Harold Lampe
C. I. MacGuffie
C. L. Pfeiffer
Sam Shiozawa
C. E. Smith
W. Spraragen
L. K. Stringham
B. L. Wise
M. Zucker

Electrochemistry and Electrometallurgy

J. Elmer Housley, *chairman*, Aluminum Company of America, P. O. Box 465, Alcoa, Tenn.
M. F. Skinker, *vice-chairman*, 112 North Mountain Ave., Montclair, N. J.
W. C. Kalb, *secretary*, National Carbon Co., Inc., Carbon Products Div., P.O. Box 6087, Cleveland 1, Ohio
J. V. Alfriend, Jr.
F. T. Chesnut
L. H. Fletemeyer
J. G. Ford
L. O. Grondahl
W. E. Gutzwiller
J. E. Hobson
J. B. Hodtum
W. B. Kouwenhoven
F. L. Lawton
D. H. Levy
R. M. Pfalzgraff
T. R. Rhea
F. O. Schnure
W. R. Schofield
N. R. Stansel
E. R. Whitehead

Subcommittee Chairmen

L. O. Grondahl, Metallic Rectifier
E. R. Whitehead, Voltage Transients in Arc Furnace Circuits

Electronics

W. R. G. Baker, *chairman*, General Electric Co., Electronics Dept., Thompson Road, Syracuse, N. Y.
L. C. F. Horle, *vice-chairman*, 90 West St., New York, N. Y.
W. G. Dow, *secretary*, University of Michigan, Ann Arbor, Mich.
C. T. Burke
R. S. Burnap
L. L. Call
W. R. Clark
C. J. Crowdes
A. V. Eastman
W. J. Field
William Fraser
A. P. Godsho
C. C. Herskind
S. B. Ingram
J. P. Jordan
L. A. Kilgore
D. D. Knowles
O. W. Livingston
H. L. Palmer
J. H. Palmer
G. W. Penney
W. H. Pickering
D. A. Quarles
M. E. Reagan
E. T. Sherwood
Thomas Spooner
B. F. Tellkamp
J. T. Thwaites
F. N. Tompkins
H. M. Turner
D. C. Ulrey
E. H. Vedder
Wm. Comings White
C. H. Willis
H. Winograd

Subcommittee Chairmen

R. S. Burnap, Nomenclature, Definitions, Letter and Graphical Symbols
L. E. Call, X-Ray Tubes
L. C. F. Horle, Tube Standards in Liaison with JETEC
J. P. Jordan, Electronic Heating
D. D. Knowles, Electronic Tube
O. W. Livingston, Electronic Control
G. W. Penney, Electronic Precipitation
Thomas Spooner, Electronic Standards
H. M. Turner, AIEE-IRE Liaison
E. H. Vedder, Electronic Welding
W. C. White, Papers Solicitation and Contact with Electronic Technical Groups in the Sections
C. H. Willis, Electronic Power Converters

Industrial Control Devices

E. U. Lassen, *chairman*, Cutler-Hammer, Inc., 315 N. 12th St., Milwaukee 1, Wis.
J. D. Leitch, *vice-chairman*, Electric Controller & Mfg. Co., 2700 E. 79th St., Cleveland 4, Ohio
E. F. Mekelburg, *secretary*, Square D Co., Industry Controller Div., 4041 N. Richards St., Milwaukee 12, Wis.
E. H. Alexander
W. J. Fleming
G. H. Garcelon
K. L. Hansen
Richard W. Jones
W. W. Miller
T. B. Montgomery
J. W. Picking
L. T. Rader
L. A. Watson
G. O. Wilms

Subcommittee Chairmen

J. D. Leitch, Standards for Industrial Electronic Control

Industrial Power Applications

Herbert Speight, *chairman*, Westinghouse Electric Corporation, 40 Wall St., New York 5, N. Y.
D. D. Douglass, *vice-chairman*, Chevrolet—Gear & Axle Div., General Motors Corp., 1840 Holbrook Ave., Detroit 12, Mich.
L. A. Umansky, *secretary*, General Electric Co., Industrial Engg. Dept., Schenectady 5, N. Y.
E. L. Bailey
D. L. Beeman
D. E. Bivins, Jr.
Philip Bliss
G. A. Caldwell
E. L. Carlson
F. W. Cramer
W. H. Dickinson
A. B. Emrick
E. S. Fields
S. F. French
J. S. Gault
John Grotzinger
S. Headman
K. W. John
C. A. Johnson
Royce E. Johnson
A. C. Muir
J. J. Orr
J. S. Parsons
L. C. Peterman
Ralph Randall
Hugh L. Smith
T. D. Thomas
E. E. Turkington
John M. Webb
C. C. Whipple
R. T. Woodruff

Subcommittee Chairmen

Philip Bliss, Machine Tool & Process Drives
C. C. Whipple, Industrial Voltage Requirements

Instruments and Measurements

Truman S. Gray, *chairman*, Massachusetts Institute of Technology, Cambridge 3, Mass.
E. D. Doyle, *vice-chairman*, Leeds & Northrup Co., 4901 Stenton Ave., Philadelphia 44, Pa.
C. T. Burke, *secretary*, General Radio Co., 30 State St., Cambridge, Mass.
P. A. Borden
H. H. Brauer
A. L. Brownlee
L. A. Bruckmyer, Jr.
D. T. Canfield
A. D. Colvin
A. B. Craig
C. L. Dawes
F. C. Doble
W. N. Eddy
J. L. Fuller
W. N. Goodwin, Jr.
A. J. Grant
E. I. Green
I. W. Gross
C. M. Hathaway
R. D. Hickok
G. B. Hoadley
I. F. Kinnard
W. G. Knickerbocker
A. E. Knowlton
H. C. Koenig
Everett S. Lee
J. T. Lusignan
D. A. Quarles
H. C. Rankin
C. W. Ricker
A. R. Rutter
F. B. Scott
F. B. Silsbee

Subcommittee Chairmen

Gordon S. Brown, Electrical Servomechanisms & Follow-up Devices
A. L. Brownlee, Dielectric Measurements in the Field
L. A. Burckmyer, Jr., Master Test Code for Temperature Measurements
C. T. Burke, Ultra-High-Frequency Measurements
C. L. Dawes, Definitions
W. G. Knickerbocker, Watthour Meters
A. E. Knowlton, Revision of Standard No. 40 (Recording Instruments)
H. C. Koenig, Revision of C-39 (Electrical Indicating Instruments)
J. T. Lusignan, Revision of Standard No. 4
H. C. Rankin, Instrument Transformers
F. B. Silsbee, Master Test Code for Resistance Measurements

Land Transportation

W. A. Brecht, *chairman*, Transportation Engineering, Westinghouse Electric Corporation, East Pittsburgh, Pa.
P. H. Hatch, *vice-chairman*, N.Y.N.H. & H.R.R. Co. Van Nest Shops, 1610 Matthews Ave., New York 60, N. Y.
J. G. Inglis, *secretary*, Toronto Transportation Comm., 35 Yonge St., Toronto, Ont., Canada
J. C. Aydelott
R. Beeuwkes
L. W. Birch
H. F. Brown
D. M. Burckett
C. M. Davis
Llewellyn Evans
E. B. Fitzgerald
J. E. Gardner
H. C. Griffith
W. S. H. Hamilton
G. S. Hoard
Fraser Jeffrey
L. C. Josephs
Paul Lebenbaum
P. A. McGee
W. B. Morton
Timothy H. Murphy
J. A. Noertker
A. G. Oehler
R. G. Thring
F. W. Willcutt

Light, Production and Application of

S. G. Hibben, *chairman*, The Westinghouse Lamp Division, Bloomfield, N. J.
I. A. Yost, *vice-chairman*, Westinghouse Electric Corp., 1216 West 58th Street, Cleveland, Ohio
C. L. Dows, *secretary*, General Electric Company, Nela Park, Cleveland, Ohio
James F. Angier
D. W. Atwater
O. W. Holden
W. C. Kalb
H. E. Mahan
Preston S. Millar
G. T. Minasian
R. C. Putnam
Harris Reinhardt
E. M. Strong
R. W. Warner
C. C. Whipple

Marine Transportation

W. H. Reed, *chairman*, Bruce Electric Company, 196 West Houston Street, New York 14, N. Y.
O. A. Wilde, *vice-chairman*, Sun Shipbuilding & Dry Dock Co., Chester, Pa.
W. N. Zippler, *secretary*, Gibbs & Cox, Inc., 1 Broadway, New York 4, N. Y.
E. C. Alger
R. A. Beekman
H. C. Coleman
P. J. DuMont
J. B. Feder
A. R. Gatewood
L. M. Goldsmith
H. F. Harvey, Jr.
W. R. Hight
J. E. Jones
A. Kennedy, Jr.
C. Lynn
V. M. Mayer
S. N. Mead
W. B. Morton
I. H. Osborne
E. M. Rothen
C. Stansbury
E. H. Stivender
G. O. Watson

Subcommittee Chairmen

E. C. Alger, Communications and Alarms
R. A. Beekman, Power Generation; Publicity, Personnel, and History
H. C. Coleman, Switchboards and Controls
J. B. Feder, Power Application
H. F. Harvey, Jr., Distribution
W. R. Hight, Navigation Equipment
A. Kennedy, Jr., Wires and Cables
O. A. Wilde, Fittings and Appliances
W. N. Zippler, Editing

Power Generation

A. J. Krupy, *chairman*, Commonwealth Edison Company, 72 West Adams St., Chicago 90, Ill.
H. A. Dryar, *vice-chairman*, Philadelphia Electric Co., 1000 Chestnut Street, Philadelphia 5, Pa.
M. J. Steinberg, *secretary*, Consolidated Edison Co. of N. Y., Inc., 4 Irving Place, New York 3, N. Y.
C. P. Almon, Jr.
M. H. Arndt
A. D. Caskey
C. A. Corney
R. P. Crippen
John J. Dougherty
J. H. Foote
A. H. Frampton
Frazer W. Gay
W. D. Hardaway
H. L. Harrington
C. T. Hughes
Fraser Jeffrey
C. B. Kelley
C. M. Laffoon
C. W. Mayott
H. N. Muller, Jr.
W. S. Peterson
G. M. Pollard
H. B. Reynolds
G. B. A. Skrotzki
H. D. Taylor
Robert Treat
W. R. Way
W. F. Wetmore

Subcommittee Chairmen

C. P. Almon, Jr., Hydro-Electric Systems
A. J. Krupy, Central Station Auxiliaries
H. N. Muller, Jr., Excitation Systems
M. J. Steinberg, Prime Mover Governors

Power Transmission and Distribution

R. J. Wiseman, *chairman*, The Okonite Company, Passaic, N. J.
E. V. Sayles, *vice-chairman*, Consumers Power Co., Jackson, Mich.
I. W. Gross, *secretary*, American Gas & Elec., Service Corp., 30 Church Street, New York 7, N. Y.
Dean W. Alden
D. L. Beeman
D. K. Blake
C. D. Brown
H. W. Clark
Harold Cole
S. B. Crary
H. A. Dambly
A. E. Davison
W. A. Del Mar
Robert D. Evans
J. M. Gaylord
Herman Halperin
Edwin Hansson
K. E. Hapgood
E. R. Hendrickson
J. E. Hobson
J. B. Hodtum
E. K. Huntington
J. T. Lusignan
W. D. Maddrey
E. McCormack
R. B. Miller
Lee M. Moore
E. W. Oesterreich
J. S. Parsons
L. M. Robertson
H. B. Robinson
S. J. Rosch
F. E. Sanford
R. V. Sanford
S. E. Schultz
A. E. Silver
E. V. Smith
Philip Sporn
E. C. Starr
O. W. Titus
J. J. Torok

H. E. Kent
A. A. Kroneberg
W. W. Lewis
H. M. Trueblood
C. F. Wagner
Loyd T. Williams
H. E. Wulfing

Subcommittee Chairmen

Harold Cole, Distribution
E. K. Huntington, Stations
W. W. Lewis, Transmission
C. F. Wagner, General Systems

Protective Devices

H. E. Strang, *chairman*, General Electric Company, 1 River Road, Schenectady 5, N. Y.
H. W. Collins, *vice-chairman*, Detroit Edison Company, 2000 Second Ave., Detroit 26, Mich.
H. D. Braley, *secretary*, Consolidated Edison Co. of New York, Inc., 4 Irving Place, New York 3, N. Y.
O. E. Charlton
William Deans
H. W. Haberl
W. A. Lewis
H. J. Lingal
F. R. Longley
J. R. North
H. V. Nye
H. H. Rudd
W. J. Rudge
J. H. Vivian

Subcommittee on Relays

W. A. Lewis, *chairman*
E. L. Michelson, *secretary*
C. E. Asbury
J. C. Bowman
W. R. Brownlee
J. E. Clem
G. B. Dodds
F. S. Fehr
S. Goldsmith
E. L. Harder
V. J. Hayes
L. F. Kennedy
E. W. Knapp
S. C. Leyland
H. F. Lindenmuth
W. E. Marter
M. S. Merritt
J. H. Oliver
C. E. Parks
H. R. Paxson
F. C. Poage
G. A. Powell
E. G. Ratz
K. N. Reardon
C. L. Smith
W. K. Sonneman
J. J. Tesar
H. Vivian
C. A. Woods

Subcommittee on Circuit Breakers and Assembled Switchgear

H. J. Lingal, *chairman*
A. E. Anderson
H. W. Collins
William Deans
H. W. Haberl
J. R. North
H. V. Nye
M. S. Oldacre

Subcommittee on Fault Limiting Devices

F. R. Longley, *chairman*
J. E. Clem
G. B. Dodds
W. W. Eberhardt
R. D. Evans
E. T. B. Gross
F. H. Hollister
P. A. Jeanne
H. E. Kent
A. A. Kroneberg
W. A. Lewis
W. W. Lewis

Subcommittee on Switches, Fuses and Insulators

H. H. Rudd, *chairman*
H. D. Braley
O. E. Charlton
F. R. Ford
A. H. Powell
H. L. Rawlins
G. V. Smith
J. C. Woods

Subcommittee on Lightning Protective Devices

W. J. Rudge, *chairman*
E. W. Beck
F. M. Defandorf
T. H. Mawson
W. E. Rushlow
A. H. Schirmer
H. R. Stewart
E. R. Whitehead

Therapeutics, Applications of Electricity to

W. B. Kouwenhoven, *chairman*, The Johns Hopkins University, Baltimore 18, Md.
W. D. Coolidge, *vice-chairman*, 1480 Lenox Road, Schenectady 8, N. Y.
W. R. Smith, *secretary*, Public Service Electric & Gas Co. 80 Park Place, Newark 1, N. J.
Lloyd L. Call
F. B. Claussen
Roy Kegerreis
H. D. Moreland
H. C. Rentschler

Joint Technical Subcommittees

Carbon Brushes

V. P. Hessler, *chairman*, University of Kansas, Lawrence, Kans.
H. R. Brown
J. V. Dobson
H. M. Elsey
H. E. Keneipp
T. M. Linville
E. A. Lapham
J. R. North
Dimiter Ramadanoff
E. R. Summers

Induction and Dielectric Heating

J. J. Orr, *chairman*, United States Rubber Company, 1230 Sixth Ave., New York 20, N. Y.
E. L. Bailey
R. M. Baker
Philip Bliss
O. E. Bowlus
F. T. Chesnut
W. J. Cotton
W. E. Dungan
J. T. Hodtum
J. P. Jordan
C. J. Madsen
H. B. Osborn, Jr.
K. Pinder
G. W. Scott, Jr.
Howard Somes
V. E. Trouant
W. M. Urbain
P. D. Zottu

Telemetering

(Appointees of Automatic Stations Committee)

G. S. Lunge, *chairman*, General Electric Company, Schenectady 5, N. Y.
E. E. George
A. P. Peterson
M. E. Reagan
T. A. Taylor
J. H. Vivian
G. S. Whitlow

(Appointees of Instruments and Measurements Committee)

P. A. Borden
E. C. Brown
C. K. Duff
J. T. Logan
Edward Lynch
W. E. Phillips
A. R. Rutter
G. M. Thynell

Power System Applications of Carrier Current

Philip Sporn, *chairman*, American Gas & Elec. Service Corp., 30 Church St., New York 7, N. Y. (Power Transmission and Distribution Committee)
J. D. Booth (Communication Committee)
L. F. Kennedy (Protective Devices Committee)
G. S. Lunge (Automatic Stations Committee)

Members-at-Large

J. C. Bowman
R. C. Ericson
J. D. Laughlin
S. C. Leyland
D. M. MacGregor
R. J. Mahler
J. A. Parrott
M. E. Reagan
F. M. Rives
S. B. Smith
T. D. Talmage
M. J. Thrasher
H. M. Trueblood
E. M. Wood

Institute Representatives

Aeronautical Electrical Equipment Standardization

J. R. North, Liaison Representative with NASC and SAE

Committee on Standard Commodity Classification or Index

E. B. Paxton

Industry Committee on Interior Wiring Design

M. M. Brandon L. C. Peterman

Joint Committee for Development of Statistical Applications in Engineering and Manufacturing

W. P. Dobson

Alfred Noble Prize Committee, ASCE

Robin Beach

Am. Assn. for the Adv. of Science, Council

J. W. Barker I. Melville Stein

American Committee on Marking of Obstructions to Air Navigation

J. W. Campbell I. W. Gross

American Coordinating Committee on Corrosion

H. S. Phelps J. M. Standring, Jr., *Alternate*

American Research Committee on Grounding

C. T. Sinclair

American Standards Assoc., Standards Council

W. P. Dobson R. T. Henry H. S. Osborne

Alternates

H. E. Farrer E. B. Paxton J. J. Pilliod

American Year Book, Advisory Board

H. H. Henline

Charles A. Coffin Fellowship and Research Fund Committee

W. E. Wickenden

Committee of Apparatus Makers and Users, NRC

L. F. Adams

Action and Advisory Committee on Construction, Committee for Economic Development

Gano Dunn

Consultative Committee on Engineering (Advisory to the War Manpower Commission)

John Castlereagh Parker

Electrical Standards Committee, ASA

H. E. Farrer A. C. Monteith J. J. Pilliod

Alternates

W. P. Dobson E. L. Moreland E. B. Paxton

Engineering Foundation Board

L. W. Chubb F. M. Farmer

Engineering Societies Monographs Committee

F. M. Farmer W. I. Slichter

Engineering Societies Personnel Service, Inc.

H. H. Henline

Engineers' Council for Professional Development

M. S. Coover Everett S. Lee E. C. Stone

Hertz Award Committee

M. S. Coover

Hoover Medal Board of Award

H. H. Barnes, Jr. H. S. Osborne
John Castlereagh Parker

John Fritz Medal Board of Award

Nevin E. Funk
Harold S. Osborne
C. A. Powel
W. E. Wickenden

Joint Conference Committee of Founder Societies and A.I.Ch.E.

W. E. Wickenden H. H. Henline C. A. Powel

Library Board, United Engineering Trustees, Inc.

N. S. Hibshman
H. H. Henline, *ex-officio*
G. L. Knight
D. A. Quarles

Marston Medal Board of Award

Harry B. Gear

National Bureau of Engineering Registration, Advisory Board

C. R. Beardsley

Nat'l Fire Protection Assoc., Electrical Committee

L. F. Adams W. Ralph Smith, *Alternate*

National Fire Waste Council

L. F. Adams Wills Maclachlan

Nat'l Research Council, Division of Engineering & Industrial Research

W. B. Kouwenhoven

National Technological Advisory Committee

John Castlereagh Parker

Quarterly of Applied Mathematics

J. G. Brainerd

Radio Technical Planning Board

H. A. Affel

Research Procedure Com., Engg. Foundation

William A. Lewis

United Engineering Trustees, Inc.

W. H. Harrison C. R. Jones Everett S. Lee

U. S. National Committee of the International Commission on Illumination

J. W. Barker Robin Beach S. G. Hibben

U. S. National Committee of the International Electrotechnical Commission

H. E. Farrer A. C. Monteith J. J. Pilliod

Alternates

W. P. Dobson E. L. Moreland E. B. Paxton

Washington Award Commission

H. B. Gear L. R. Mapes

World Power Conference, Executive Committee of U. S. National Committee

W. B. Wickenden

Geographical District Executive Committees

	District	Chairman (Vice-President, AIEE)	Secretary (District Secretary)	Chairman, District Committee on Student Activities
1	North Eastern	R. T. Henry, 303 Electric Bldg., Buffalo, N. Y.	Victor Siegfried, American Steel & Wire Co., Worcester 7, Mass.	R. G. Porter, Northeastern University, Boston, Mass.
2	Middle Eastern	E. S. Fields, Cincinnati Gas & Electric Co., 4th & Main Sts., Cincinnati, Ohio	A. A. Johnson, Westinghouse Electric Corporation, East Pittsburgh, Pa.	P. X. Rice, Pennsylvania State College, State College, Pa.
3	New York City	J. F. Fairman, Consolidated Edison Co. of New York, Inc., 4 Irving Place, New York 3, N. Y.	C. S. Purnell, Westinghouse Electric Corporation, 40 Wall St., New York 5, N. Y.	D. H. Wright, Pratt Institute, Brooklyn, N. Y.
4	Southern	H. B. Wolf, Duke Power Company, Charlotte 1, N. C.	C. B. Galphin, 2312 Greenway, Charlotte 4, N. C.	Otto Meier, Jr., Duke University, Durham, N. C.
5	Great Lakes	M. S. Coover, Iowa State College, Ames, Iowa	N. C. Pearcy, Public Utilities Engg. & Service Corp., 231 S. LaSalle St., Chicago 4, Ill.	J. A. Northcott, University of Notre Dame, Notre Dame, Ind.
6	North Central	L. M. Robertson, Public Service Co. of Colorado, Denver, Colo.	H. F. Gidlund, Public Service Co. of Colorado, Denver, Colo.	O. E. Edison, University of Nebraska, Lincoln, Nebr.
7	South West	R. W. Warner, University of Texas, Austin, Tex.	S. R. Friedsam, 3612 Bonnie Road, Austin, Tex.	M. C. Hughes, A. & M. College of Texas, College Station, Tex.
8	Pacific	F. F. Evenson, 600 E. Harbor St., P. O. Box 1710, San Diego, Calif.	Walter L. Bryant, Univ. of Calif. Div. of War Research, U. S. Navy Radio & Sound Laboratory, San Diego 52, Calif.	W. H. Pickering, California Institute of Technology, Pasadena, Calif.
9	North West	C. B. Carpenter, Pacific Tel. & Tel. Co., 730 S. W. Oak St., Portland 5, Oreg.	C. C. Boozier, Westinghouse Electric Corporation, 309 S. W. Sixth Ave., Portland 4, Oreg.	E. W. Schilling, Montana State College, Bozeman, Mont.
10	Canada	F. L. Lawton, Aluminum Co. of Canada Ltd., 1700 Sun Life Bldg., Montreal, Que.	D. M. Farnham, Quebec Hydro-Elec. Commission, 107 Craig St. West, Montreal, Que.	

NOTE: Each District executive committee includes also the chairmen and secretaries of all Sections within the District, and the District vice-chairman of the AIEE membership committee.

Sections of the Institute

(As of January 1, 1946)

Name	District	When Organized	Membership Aug. 1, 1945	Chairman	Secretary	Secretary's Address
Akron	2	Aug. 12, '20	105	M. B. Rankin	F. J. Ilse	795 West Market St., Akron 3, Ohio
Alabama	4	May 22, '29	37	F. C. Weiss	Robert S. Morrison	Westinghouse Electric Corp., 1406 Comer Bldg., Birmingham 3, Ala.
Arizona	8	Mar. 22, '41	60	Charles A. Rollins	E. A. Gissel	Central Arizona Light & Power Co., Phoenix, Ariz.
Beaumont	7	June 27, '45	61	Harold McIntosh	N. C. Spencer	2555 North St., Beaumont, Texas
Boston	1	Feb. 13, '03	673	F. S. Bacon, Jr.	R. E. Muehlig	Westinghouse Electric Corp., 235 Old Colony Ave., Boston, Mass.
Central Indiana	5	Jan. 12, '12	147	S. C. Leibing	E. G. Hinshaw	Indiana Bell Telephone Co., 240 N. Meridian St., Indianapolis, Ind.
Chicago	5	1893	959	J. F. Calvert	L. R. Janes	Public Service Co. of Northern Ill., 72 West Adams St., Chicago 3, Ill.
Cincinnati	2	June 30, '20	161	F. W. Willey	Paul H. Goodell	4817 Section Avenue, Cincinnati 12, Ohio
Cleveland	2	Sept. 27, '07	423	V. A. Diggs	R. W. Loehr	Westinghouse Electric Corp., 1216 West 58th St., Cleveland 1, Ohio
Columbus	2	Mar. 17, '22	90	N. J. Greene	Oliver Johnson	Westinghouse Electric Corp., 85 East Gay St., Columbus 15, Ohio
Connecticut	1	Apr. 16, '21	384	Vincent J. Hayes	Elmer G. Horton	Westinghouse Electric Corp., P. O. Box 1817, New Haven 8, Conn.
Dayton	2	June 9, '43	243	F. S. Himebrook	W. A. Dynes	312 Lonsdale Ave., Dayton 9, Ohio
Denver	6	May 18, '15	209	Louis A. Goalby	Leroy R. Patterson	Public Service Co. of Colorado, Denver, Colo.
East Tennessee	4	Sept. 2, '36	288	C. P. Almon, Jr.	S. E. Lyons	Tennessee Valley Authority, Power Bldg., Chattanooga, Tenn.
Erie	2	Jan. 11, '18	73	Harold S. Ogden	Wilbur C. Brown	General Electric Co., East Lake Road, Erie, Pa.
Florida	4	Jan. 28, '31	125	P. J. Carlin	C. H. Summers	Florida Power & Light Co., Miami, Fla.
Fort Wayne	5	Aug. 14, '08	107	E. G. Downie	L. L. Ray	General Electric Co., 1635 Broadway, Fort Wayne 2, Ind.
Georgia	4	Jan. 14, '04	145	Carl W. Evans	Robert O. Loomis	Georgia Power Co., Atlanta 1, Ga.
Houston	7	Aug. 7, '28	143	S. C. Commander	H. Lee Miller	Houston Lighting & Power Co., P. O. Box 1700, Houston 1, Texas
Illinois Valley	5	June 30, '45	47	F. E. Dace	R. P. Johnson	2511 W. Forrest Hill Ave., Peoria 5, Ill.
Iowa	5	June 29, '29	85	John A. Green	Wallace L. Cassell	Iowa State College, Ames, Iowa
Ithaca	1	Oct. 15, '02	72	N. L. Platt	W. H. Erickson	School of Elec. Engg., Cornell University, Ithaca, N. Y.
Kansas City	7	Apr. 14, '16	149	A. F. Hartung	J. E. Murray	J. E. Murray & Co., 1805 Grand Ave., Kansas City 8, Mo.
Lehigh Valley	2	Apr. 16, '21	188	L. Z. Ludorf	A. L. Price	173 South Church St., Hazleton, Pa.
Los Angeles	8	May 19, '08	718	Earl S. Condon	H. D. Strong	General Electric Co., P. O. Box 2830 Terminal Annex, Los Angeles 54, Calif.
Louisville	4	Oct. 15, '26	75	S. H. Gates	L. W. Anderson	647 Starks Bldg., Louisville 2, Ky.
Lynn	1	Aug. 22, '11	210	C. B. Fontaine, Jr.	Mark A. Princi	19 Clifton Ave., Marblehead, Mass.
Madison	5	Jan. 8, '09	81	Carl C. Crane	Bernhard C. Lueders	532 Oak St., Baraboo, Wis.
Mansfield	2	Mar. 6, '39	63	C. L. Lisle	H. E. Edwards	Westinghouse Electric Corp., Mansfield, Ohio
Maryland	2	Dec. 16, '04	417	J. L. Hildebrandt	Edwin Hansson	Penn. Water & Power Co., 1409 Lexington Bldg., Baltimore 1, Md.
Memphis	4	May 22, '30	94	J. A. Crisman	W. R. Moyers, Jr.	3480 Macon Rd., Memphis, Tenn.
Mexico	3	June 29, '22	181	F. A. Nava	Oscar R. Enriquez	Ave. Chapultepec 281-6, Mexico, D. F. Mexico
Michigan	5	Jan. 13, '11	436	L. W. Clark	G. M. Chute	General Electric Co., 700 Antoinette St., Detroit 2, Mich.
Milwaukee	5	Feb. 11, '10	408	G. W. Clothier	E. T. Sherwood	Globe Union, Inc., 900 E. Keefe Ave., Milwaukee 1, Wis.
Minnesota	5	Apr. 7, '02	133	Leroy A. Griffith	John H. Merriman	Northern States Power Co., 15 South Fifth St., Minneapolis 2, Minn.
Montana	9	June 24, '31	71	F. E. Gardiner	E. W. Williams	715 W. Galena St., Butte, Montana
Montreal	10	Apr. 16, '43	237	John J. Dougherty	Harold H. Remine	Quebec Hydro Elec. Commission, Montreal, Que., Canada
Muscle Shoals	4	Feb. 18, '38	19	W. E. Lindemann	Ernest L. Bishop	76 F St., Village 1, Wilson Dam, Ala.
Nebraska	6	Jan. 21, '25	48	M. L. Burgess	I. M. Ellestad	Northwestern Bell Tel. Co., Omaha, Neb.
New Mexico-West Texas	7	Mar. 7, '40	57	Robert C. Dickson	John F. Armstrong	3219 Altura Blvd., El Paso, Texas
New Orleans	4	Dec. 8, '33	159	Wm. Stone Leake	S. L. Kennedy	Louisiana Power & Light Co., Metairie, La.
New York	3	Dec. 10, '19	3,949	J. L. Callahan	W. J. Barrett	New Jersey Bell Telephone Co., 540 Broad St., Newark 2, N. J.
Niagara Frontier	1	Feb. 10, '25	198	J. M. Geiger	John D. Hershey	General Electric Co., 1 West Genessee St., Buffalo 2, N. Y.
North Carolina	4	Mar. 21, '29	137	Otto Meier, Jr.	J. O. Kimrey	Duke Power Co., 112 North Mangum St., Durham, N. C.
North Texas	7	May 18, '28	199	R. W. Roessler	H. K. Doyle	Dallas Power & Light Co., Dallas, Texas
Oklahoma City	7	Feb. 16, '22	109	W. A. Kitchen	H. E. Brashear	Southwestern Bell Tel. Co., Oklahoma City, Okla.
Philadelphia	2	Feb. 18, '03	925	C. T. Pearce	W. R. Clark	Leeds & Northrup Co., 4901 Stenton Ave., Philadelphia 44, Pa.
Pittsburgh	2	Oct. 13, '02	693	C. M. Skooglund	J. B. Hodtum	Allis-Chalmers Mfg. Co., N. S. Station, Pittsburgh 12, Pa.
Pittsfield	1	Mar. 25, '04	201	M. E. Scoville	J. C. Russ	Power Transformer Engg. Dept., General Electric Co., Pittsfield, Mass.
Portland	9	May 18, '09	228	O. A. Demuth	W. Morgan Allen	Pacific Tel. & Tel. Co., 730 S. W. Oak St., Portland, Oreg.
Providence	1	Mar. 12, '20	104	Carleton H. Parker	George E. Andrews	Narragansett Electric Co., Melrose St., Providence, R. I.
Rochester	1	Oct. 9, '14	133	Ernest B. Kempster	George R. Town	Stromberg-Carlson Co., 100 Carlson Rd., Rochester 3, N. Y.
St. Louis	7	Jan. 14, '03	346	Harry B. Seybt	R. C. Horn	1820 Telephone Bldg., 1010 Pine St., St. Louis 1, Mo.
San Diego	8	Jan. 18, '39	102	R. R. Richey	G. E. Jenner	861 Sixth St., San Diego 12, Calif.
San Francisco	8	Dec. 23, '04	776	D. I. Anzini	H. E. Becker	Westinghouse Electric Corp., 1 Montgomery St., San Francisco 4, Calif.
Schenectady	1	Jan. 26, '03	654	P. H. Light	B. H. Caldwell	Motor & Gen. Engg. Div., General Electric Co., Schenectady 5, N. Y.
Seattle	9	Jan. 19, '04	303	E. B. Hansen	George M. Palo	1707 Bigelow Ave. North, Seattle 9, Wash.
Sharon	2	Dec. 11, '25	149	A. D. Forbes	C. W. Miller	840 Mayfield Rd., Sharpsville, Pa.
South Bend	5	Feb. 26, '41	70	C. D. Highleyman	John C. Learman	1245 North Meade St., South Bend, Ind.
South Carolina	4	Mar. 2, '40	56	F. T. Tingley	J. L. Weeks	South Carolina Elec. & Gas Co., Columbia, S. C.
South Texas	7	May 23, '30	56	N. Bernard Gussett	Robert M. Eichuer	General Electric Co., 1014 Transit Tower, San Antonio, Texas
Spokane	9	Feb. 14, '13	106	J. F. Gogins	H. C. Glaze, Jr.	General Electric Co., 421 Riverside Ave., Spokane 8, Wash.
Springfield	1	June 29, '22	60	Byron N. Durfee	Fred G. Webber	9 Federal Court, Springfield, Mass.
Syracuse	1	Aug. 12, '20	149	C. E. H. Von Sothen	L. J. Audlin	Central N. Y. Power Corp., 300 Erie Blvd. West, Syracuse 2, N. Y.
Toledo	2	June 3, '07	67	F. C. Helwig	Walter M. Campbell	2145 Central Grove Ave., Toledo, Ohio
Toronto	10	Sept. 30, '03	400	A. H. Frampton	J. F. Moore	Dunlop Tire & Rubber Goods, 870 Queen St., E., Toronto, Ont., Canada
Tulsa	7	Oct. 1, '37	81	P. E. Gentry	L. F. Rylander	Public Service Co. of Oklahoma, 600 So. Main St., Tulsa, Okla.
Urbana	5	Nov. 25, '02	38	E. A. Reid	C. A. Kenner	308 Elec. Engg. Lab., University of Illinois, Urbana, Ill.
Utah	9	Mar. 9, '17	77	L. Dale Harris	John A. McDonald	General Electric Co., P. O. Box 779, Salt Lake City, Utah
Vancouver	10	Aug. 22, '11	109	J. P. Fraser	G. K. Haspel	1992 41st Ave., West, Vancouver, B. C., Canada
Virginia	4	May 19, '22	136	J. A. Rawls	C. H. Smoke	1523 Holland Ave., Norfolk 5, Va.
Washington	2	Apr. 9, '03	726	E. T. Walker	L. H. Cleary	1022—20th St. N. W., Washington 6, D. C.
West Virginia	2	Apr. 9, '40	50	W. E. Vellines, Jr.	R. F. Norwood	1400 Bridge Road, Charleston 3, West Virginia
Wichita	7	Sept. 16, '37	86	H. Kenneth Hentzen	Hugh E. Hartman	Kansas Gas & Electric Co., 201 N. Market St., Wichita 1, Kans.
Worcester	1	Feb. 18, '20	59	A. L. Duna	G. W. Bibber	Heald Machine Co., New Bond St., Worcester 6, Mass.
Total Sections	75		19,913			
Subsections						
Albuquerque (New Mexico–West Texas Section)				R. W. Tapy	W. F. Hardgrave	College of Engineering, University of New Mexico, Albuquerque, N. M.
Arrowhead (Minnesota Section)				H. Carpenter	R. H. Holmes	Duluth Missabe & Iron Range Ry. Co., 400 Wolvin Bldg., Duluth, 2 Minn.
Charleston (South Carolina Section)				D. H. Davis	M. G. Toole	P. O. Box 42, Navy Yard, Charleston, S. C.
Charlotte (North Carolina Section)				G. O. Bason	E. R. Davis	Duke Power Co., Charlotte, N. C.
Fresno (San Francisco Section)				R. D. Likely	George A. Collins	San Joaquin Light & Power Div. Pacific Gas & Elec. Co., Fresno, Cal.
Great Falls (Montana Section)					D. A. Johnson	Mountain States Tel. & Tel. Co., 401 First Ave., N., Great Falls, Mont.
Hamilton (Toronto Section)				J. M. Somerville	W. J. Porter	Canadian Westinghouse Co., Hamilton, Ontario, Can.
Hampton Roads (Virginia Section)				J. H. Berry	W. G. Gardner	14 Claremont Ave., Hampton, Va.
Lake Charles (New Orleans Section)				A. D. Hargroder	G. V. Cooper	Cities Service Refining Corp., Tutwiler Refinery, Lake Charles, La.
Lancaster–York (Maryland Section)				R. W. Larson	J. L. Stauffer	Penna. Power & Light Co., Griest Bldg., Lancaster, Pa.
Little Rock (Memphis Section)				M. E. Crippen	J. A. Hunter	Box 2100, Little Rock, Ark.
Niagara Falls (Niagara Frontier Section)				G. A. Zehr	C. R. Staker	203 79th St., Niagara Falls, N. Y.
Ottawa (Montreal Section)				B. G. Ballard	J. H. Simpson	National Research Council, Ottawa, Ontario, Can.
Panhandle (North Texas Section)				J. G. Ausman	D. H. Hickey	Capitol Hotel, Amarillo, Texas
Rock River Valley (Madison Section)				R. E. Schuette	Royce E. Johnson	Barber-Colman Company, Rockford, Ill.
Sacramento (San Francisco Section)				W. E. Camp	E. A. McGinty	Pacific Gas & Electric Co., 1314 29th St., Sacramento 16, Calif.
Saginaw Valley (Michigan Section)				E. L. Kirk	W. F. Gakle	Kuhlman Electric Co., Bay City, Mich.
Wilmington (Philadelphia Section)				R. G. Rudrow	Henry Evans	Delaware Power & Light Co., 600 Market St., Wilmington, Del.
Zanesville (Columbus Section)				J. G. Tankovich	A. J. Baker	Ohio Power Co., Zanesville, Ohio

Student Branches of the Institute

(As of January 1, 1946)

Name and Location	District	Counselor (Member of Faculty)	Chairman	Secretary
Akron, Univ. of, Akron, Ohio	2	A. J. Fairburn	Wm. F. Nelson	Leonard L. Katz
Alabama Polytechnic Inst., Auburn, Ala.	4		Barry Graves	Ed Stevenson
Alabama Univ. of, University, Ala,	4	W. J. Miller	Wm, Bess	J. R. Humphries
Alberta, Univ. of, Edmonton, Alberta, Can.	10	R. E. Phillips	T. A. Sissons	R. E. McClary
Arizona, Univ. of, Tucson, Ariz.	8	J. C. Clark		
Arkansas, Univ. of, Fayetteville, Ark.	7	W. B. Stelzner	J. M. Strabala	Austin Bollen
British Columbia, Univ. of, Vancouver, Can.	10	W. B. Coulthard	Kenneth Broe	J. D. Sansum
Brooklyn, Poly. Inst. of, Brooklyn, N. Y.	3	A. B. Giordano	Ralph Norton	T. LoGiudice
Brown Univ., Providence, R. I.	1	F. N. Tompkins	R. W. Carpenter	L. O. Heizer
Bucknell Univ., Lewisburg, Pa.	2	George Irland	C. Hellie	H. W. Morse
Calif. Inst. of Tech., Pasadena, Calif.	8	W. H. Pickering	Reed Nixon	Orison Wade
Calif. Univ. of, Berkeley, Calif.	8	P. L. Morton	W. Kummer	Don Lebell
Carnegie Inst. of Tech., Pittsburgh, Pa.	2	D. L. Trautman, Jr.	B. L. Schwartz	R. D. Teasdale
Case School of Applied Science, Cleveland, Ohio	2	P. L. Hoover	T. C. Sidlow	K. L. Walko
Catholic Univ. of America, Washington, D. C.	2		Wm. Hsiao	A. L. Burgess
Cincinnati, Univ. of, Cincinnati, Ohio	2	A. C. Herweh		
Clarkson College of Tech., Potsdam, N. Y.	1	A. R. Powers	A. Jacobson, Jr.	James Cooper
Clemson Agri. College, Clemson, S. C.	4	F. T. Tingley	J. Antonakos	L. P. Thomas, Jr.
Colorado State Col. of A. & M. Arts, Fort Collins, Colo.	6	F. B. Beatty		
Colorado, Univ. of, Boulder, Colo.	6	Platt Wicks	E. J. Fox	L. J. Mason
Columbia Univ., New York, N. Y.	3	W. A. LaPierre	J. D'Annunzio	W. H. Glick
Connecticut, Univ. of, Storrs, Conn.	1	G. S. Timoshenko	R. Spencer	E. Foerch
Cooper Union, New York, N. Y.	3	E. E. Shelton	N. Austern	Barney Reiffen
Cornell Univ., Ithaca, N. Y.	1	B. K. Northrop	A. D. Sutherland	W. G. Papsco
Delaware, Univ. of, Newark, Del.	2	M. G. Young	F. B. Cummins	W. J. Monaghan, Jr.
Denver, Univ. of, Denver, Colo.	6	F. H. McClain		
Detroit, Univ. of, Detroit, Mich.	5	H. O. Warner	Ralph Trese	V. Benaglio
Drexel Inst. of Tech., Philadelphia, Pa.	2	E. O. Lange		
Duke Univ., Durham, N. C.	4	Otto Meier, Jr.	R. M. Dunaiski	E. A. Madlon
Florida, Univ. of, Gainesville, Fla.	4	E. F. Smith	Paul Davis	
George Washington Univ., Washington, D. C.	2	M. K. Akers	Dave Carlson	B. L. Dunfee
Georgia School of Tech., Atlanta, Ga.	4	H. B. Duling		
Harvard Univ., Cambridge, Mass.	1	J. P. Newton	John C. Fisher	N. J. Cancilla
Idaho, Univ. of, Moscow, Idaho	9	J. Hugo Johnson	George Walsh	Herman Tilly
Illinois Inst. of Technology, Chicago, Ill.	5	T. J. Higgins	N. C. Vojta	W. C. Bachtel
Illinois, Univ. of, Urbana	5	E. A. Reid	R. B. McKinstry	John Reigle
Iowa State Col., Ames	5	B. S. Willis		
Iowa, Univ. of, Iowa City	5	E. B. Kurtz	Harry Carlson	J. F. Cuba
Johns Hopkins Univ., Baltimore, Md.	2	F. Hamburger, Jr.		
Kansas State Col., Manhattan	7	R. G. Kloeffler	C. A. Stewart	G. A. Sites
Kansas, Univ. of, Lawrence	7	G. A. Richardson		
Kentucky, Univ. of, Lexington	4	Brinkley Barnett	J. M. Hisle	Marie Kemper
Lafayette Col., Easton, Pa.	2	Morland King		
Lehigh Univ., Bethlehem, Pa.	2	J. L. Beaver		
Louisiana State Univ., Baton Rouge	4	A. K. Ramsey	E. B. McNeil	Julian S. Johnston
Louisville, Univ. of, Louisville, Ky.	4	M. C. Northrup	R. A. Cunningham	Geraldine Hardy
Maine, Univ. of, Orono	1	W. J. Creamer		
Manhattan College, New York, N. Y.	3	R. T. Weil	John Meenagh	Alfred Hughes
Marquette Univ., Milwaukee, Wis.	5	E. W. Kane	W. Cavagnaro	Thomas Bursh
Maryland, Univ. of, College Park	2	L. J. Hodgins	Wm. Talbott	Walter Beam
Mass. Inst. of Tech., Cambridge	1	D. P. Severance	N. A. Spiesberger	W. H. Turner
Michigan Col. of Mining & Tech., Houghton	5	G. W. Swenson	K. J. Kinsman	J. G. Liadis
Michigan State Col., East Lansing	5	M. M. Cory	Howard Cloyde	Leon C. Durfey
Michigan, Univ. of, Ann Arbor	5	J. S. Gault	Fred Gehring	Belle Sperling
Milwaukee School of Engg., Milwaukee, Wis.	5	E. L. Wiedner	R. Weliky	Charles Austin
Minnesota, Univ. of, Minneapolis	5	J. H. Kuhlmann		
Mississippi State Col., State College	4	H. C. Simrall		
Missouri School of Mines & Met., Rolla	7	F. H. Frame		
Missouri, Univ. of, Columbia	7	M. P. Weinbach	Oliver Weiss	Bill Spencer
Montana State Col., Bozeman	9	E. W. Schilling	B. D. Nolan	J. W. Heidt
Nebraska, Univ. of, Lincoln	6	O. E. Edison	J. R. Wallin	F. K. Ishii
Nevada, Univ. of, Reno	8	S. G. Palmer		
Newark Col. of Engineering, Newark, N. J.	3	J. C. Peet		
New Hampshire, Univ. of, Durham	1			
New Mexico State College, State College	7	H. A. Brown		
New Mexico, Univ. of, Albuquerque	7	R. W. Tapy		
New York, Col. of the City of, New York, N. Y.	3	Harry Baum	D. Goldstein	N. Yudewitz
New York Univ., New York, N. Y.	3	P. C. Cromwell		
(Day Division)				
(Evening Division)			R. L. Rocamora	F. J. Putallaz
North Carolina State Col., Raleigh	4	L. M. Keever	J. W. Chadwick	P. L. Snow
North Dakota State Agri. Col., Fargo	5	H. S. Dixon		
North Dakota, Univ. of, Grand Forks	5	C. W. Rook		
Northeastern Univ., Boston, Mass.	1	R. G. Porter	Richard Harris	John Rackliffe
Northwestern Univ., Evanston, Ill.	5	R. E. Beam		
Norwick Univ., Northfield, Vt.	1			
Notre Dame, Univ. of, Notre Dame, Ind.	5	J. A. Northcott		
Ohio Northern Univ., Ada	2		A. S. Burdick	W. Robert Wiener
Ohio State Univ., Columbus	2	E. E. Kimberly	H. D. Zink	Leo C. Bennett
Ohio Univ., Athens	2			
Oklahoma A. & M. College, Stillwater	7	A. Naeter		
Oklahoma, Univ. of, Norman	7	C. L. Farrar		
Oregon State Col., Corvallis	9	A. L. Albert	A. A. Armstrong	R. D. Robinson

Student Branches of the Institute

(As of January 1, 1946)

Name and Location	District	Counselor (Member of Faculty)	Chairman	Secretary
Pennsylvania State Col., State College	2	P. X. Rice	J. G. Wiley	C. B. Appleman
Pennsylvania, Univ. of, Philadelphia	2	C. D. Fawcett	B. B. Bycer	W. W. Weinstock
Pittsburgh, Univ. of, Pittsburgh, Pa.	2	R. C. Gorham	Carl Nielsen	Wm. Bilka
Pratt Institute, Brooklyn, N. Y.	3	D. H. Wright	E. J. Matus	Robert Kahn
Princeton Univ., Princeton, N. J.	2	W. C. Johnson	E. G. Zuercher	H. L. Stern
Puerto Rico, Univ. of, Mayaguez, P. R.	3	M. Wiewall, Jr.	H. M. Barcelo	H. R. Vega
Purdue Univ., Lafayette, Ind.	5	R. B. Marshall	F. E. Pritscher	P. H. Ward
Rensselaer Polytechnic Inst., Troy, N. Y.	1	E. D. Broadwell	Aubrey Mitchell	T. B. Brown
Rhode Island State Col., Kingston, R. I.	1			
Rice Institute, Houston, Texas	7	M. V. McEnamy	Wm. H. Newman	R. C. Wheatley
Rose Polytechnic Inst., Terre Haute, Ind.	5	C. C. Knipmeyer	J. A. Doerffler	B. E. Rumble
Rutgers Univ., New Brunswick, N. J.	3	P. S. Creager	Fred Lott	H. Bartron
Santa Clara, Univ. of, Santa Clara, Calif.	8	W. J. Warren		
South Carolina, Univ. of, Columbia	4	Samuel Litman	P. Pfannebecker	E. B. Winn
South Dakota State Col., Brookings	5	W. H. Gamble	LeRoy Dehnert	L. E. Reynolds
South Dakota State School of M. & T., Rapid City	6	E. E. Clark	D. G. Robertson	L. E. Tingley
Southern California, Univ. of, Los Angeles, Calif.	8	P. S. Biegler	Niel Nichols	Warren Parsons
Southern Methodist Univ., Dallas, Texas	7	R. L. Biesele, Jr.		
Stanford Univ., Stanford University, Calif.	8	H. H. Skilling	E. D. Regan	
Stevens Inst. of Technology, Hoboken, N. J.	3	W. L. Sullivan		
Swarthmore Col., Swarthmore, Pa.	2			
Syracuse Univ., Syracuse, N. Y.	1	C. W. Henderson		
Tennessee, Univ. of, Knoxville, Tenn.	4	J. G. Tarvoux	R. G. Ely, Jr.	T. H. Landrum
Texas A. & M. Col., College Station, Texas	7	M. C. Hughes	L. L. Lea	G. O. Hughes, Jr.
Texas Tech. Col., Lubbock, Texas	7	W. F. Helwig	Ben Logan	Irene Knowles
Texas, Univ. of, Austin	7	A. W. Straiton	A. W. Brun	W. A. Rees
Tufts College, Medford, Mass.	1	A. H. Howell	W. G. Cranton	J. W. Patterson
Tulane Univ., New Orleans 15, La.	4	M. G. Zervigon	C. G. Lob	A. C. Buxton
Union Col., Schenectady 5, N. Y.	1	H. W. Bibber	J. W. Vorndran	R. H. Brennan
Utah, Univ. of, Salt Lake City	9	O. C. Haycock	Karl L. Brown	D. Freebairn
Vanderbilt Univ., Nashville, Tenn.	4	S. R. Schealer	L. E. Rawls	H. J. Browne
Vermont, Univ. of, Burlington	1	E. R. McKee		
Villanova Col., Villanova, Pa.	2	H. S. Bueche	B. L. Price	L. Fallon
Virginia Military Inst., Lexington, Va.	4	J. S. Jamison		
Virginia Polytechnic Inst., Blacksburg	4	Claudius Lee	Bill Williams	M. S. Postman
Virginia, Univ. of, Charlottesville, Va.	4	L. R. Quarles	Wm. F. Stein	L. R. Jones
Washington, State College of, Pullman	9	H. F. Lickey	Earl Anderson	Frank Hekel
Washington, Univ. of, Seattle	9	R. E. Lindblom	R. J. Ringlee	J. P. Goodfellow
Washington, Univ., St. Louis, Mo.	7	D. A. Fischer	H. G. Lazarus	Wm. C. Milks, Jr.
West Virginia Univ., Morgantown, W. Va.	2			
Wisconsin, Univ. of, Madison, Wis.	5	G. F. Tracy	G. D. Keppert	Eugene Daniels
Worcester Polytechnic Inst., Worcester, Mass.	1		Frank Weeks	D. G. Lewis
Wyoming, Univ. of, Laramie, Wyo.	6	R. O. Trueblood	Donald E. Hull	D. M. Evans
Yale University, New Haven, Conn.	1	A. G. Conrad	J. C. Dorfman	B. C. Stevens

Total Branches.......................................125

Number of Enrolled Students November 1, 1945.........3,186